

## 1001

**Impairment of Mitochondrial Respiration Promotes Survival of Hypoxic Chondrocytes *In Vivo*.** Qing Yao<sup>\*1</sup>, Edward LaGory<sup>2</sup>, Laura Mangiavini<sup>1</sup>, Jiarui Hu<sup>1</sup>, Christophe Merceron<sup>1</sup>, Krishna Vemulapalli<sup>1</sup>, Mohd Parvez Khatn<sup>1</sup>, Zachary Tata<sup>1</sup>, Amato J. Giaccia<sup>2</sup>, Ernestina Schipani<sup>1</sup>. <sup>1</sup>University of Michigan, United States, <sup>2</sup>Stanford University, United States

Oxygen (O<sub>2</sub>) is not only an indispensable metabolic substrate in various enzymatic reactions including mitochondrial respiration but also a regulatory signal that controls stability and activity of the transcription factor Hypoxia Inducible Factor-1α (HIF-1α), a key mediator of the cellular adaptation to low O<sub>2</sub> tension (hypoxia). The fetal growth plate is avascular and has an inner hypoxic region. Along those lines, we provided genetic evidence that HIF-1α is a survival factor for hypoxic chondrocytes *in vivo*. However, how HIF-1α controls cell survival in the inner hypoxic region of the developing growth plate is still unknown. Notably, viable chondrocytes at the periphery of HIF-1α null growth plates are considerably more hypoxic than controls, and their extreme hypoxia is not the consequence of the reduced availability of O<sub>2</sub> to the growth plate. Therefore, we hypothesized it had to be the consequence of increased O<sub>2</sub> consumption. Our hypothesis is in line with the well-documented ability of HIF-1α to impair mitochondrial respiration *in vitro*. To test our hypothesis, we conditionally deleted Mitochondrial Transcription Factor A (TFAM) in mesenchymal cells of the limb bud using the PRX1-Cre transgenic mouse. In addition, we generated double mutant mice that lack both TFAM and HIF-1α in the same cells. Of note, TFAM is not a downstream target of HIF-1α; however, it regulates expression of numerous enzymes of the mitochondrial respiratory chain. Analysis of TFAM mutant mice showed that oxidative phosphorylation is dispensable for differentiation of mesenchymal cells into chondrocytes and for chondrocyte survival. However, it is required for timely differentiation of proliferative chondrocytes into hypertrophic cells. More importantly, loss of TFAM fully corrected the abnormal shape of mutant growth plates lacking HIF-1α and prevented both the severe hypoxia and the massive death of HIF-1α null chondrocytes. Therefore, loss of HIF-1α causes cell death of growth plate chondrocytes by increasing O<sub>2</sub> consumption. Our findings imply that activation of oxidative phosphorylation is detrimental for the survival of hypoxic tissues. Hence, they constitute a paradigm shift since they demonstrate that, distinct from what has been reported in the context of well-oxygenated tissues, impairment of mitochondrial respiration is an indispensable requirement for survival of hypoxic cells.

**Disclosures:** Qing Yao, None.

## 1002

**PiT1/Slc20a1-mediated endoplasmic reticulum homeostasis and cell survival in growth plate chondrocytes.** Greig Couasnay<sup>\*1</sup>, Nina Bon<sup>1</sup>, Claire-Sophie Devignes<sup>2</sup>, Sophie Sourice<sup>1</sup>, Arnaud Bianchi<sup>3</sup>, Joelle Veziers<sup>1</sup>, Pierre Weiss<sup>1</sup>, Sylvain Provot<sup>4</sup>, Jerome Guicheux<sup>1</sup>, Sarah Beck-Cormier<sup>5</sup>, Laurent Beck<sup>1</sup>. <sup>1</sup>INSERM U1229, University of Nantes, France, <sup>2</sup>INSERM 1132, Paris Diderot University, France, <sup>3</sup>CNRS UMR 7365, University of Lorraine, France, <sup>4</sup>INSERM U1132, Paris Diderot University, France, <sup>5</sup>INSERM U1132, University of Nantes, France

The mineralization of the skeleton requires large amounts of calcium and phosphate that are eventually deposited on the extracellular matrix of mineralizing chondrocytes and osteoblasts. The sodium-phosphate cotransporter PiT1/Slc20a1 is thought to provide the skeleton's phosphate needs during this process, although evidence is still missing. Gathering physiological evidence of a role of PiT1 in skeletal mineralization has been hampered by the embryonic lethality of mice lacking *PiT1*.

In the present study, we generated and characterized a chondrocyte-specific and temporally-controlled *PiT1* deficient mouse model to determine its role in growth plate chondrocytes. *PiT1* ablation by tamoxifen injection shortly after birth (at P3) generated a rapid (48h post-tamoxifen injection) and massive cell death in the hypoxic center of the growth plate. Interestingly, we observed that the vast majority of PiT1 protein was expressed in the ER compartment of chondrocytes, whereas expression at the plasma membrane was hardly detectable. We showed that PiT1 deletion led to an uncompensated ER stress illustrated by ER morphological changes and increased *Chop* expression. We showed that *PiT1* expression was up-regulated rather than down-regulated under ER stress conditions, a feature only shared by genes involved in Unfolded Protein Response (UPR)-related events. *PiT1* expression was regulated by the three main UPR transcription factors (ATF4, XBP1 and ATF6), further illustrating that *PiT1* is an UPR-regulated gene.

Using a yeast two-hybrid screen strategy, we identified the protein disulfide isomerase (Pdi) ER chaperone as a PiT1 binding partner and showed that loss of *PiT1* decreases Pdi reductase activity. The PiT1-dependent ER stress was associated with an intracellular retention of aggrecan and pro-angiogenic factor Vegf-A. Importantly, Vegf-A intracellular retention was rescued by expressing a transport-deficient mutant of PiT1 in *PiT1*-deficient primary chondrocytes. This important finding argues against a major role of PiT1-driven phosphate transport function in the observed ER phenotype and is consistent with its weak expression at the plasma membrane. Altogether, our data uncover a novel and transport-independent role of PiT1 in endochondral ossification, disclosing PiT1 as a regulator of ER homeostasis in chondrocytes, which expression is necessary for maintenance of growth plate chondrocyte survival.

**Disclosures:** Greig Couasnay, None.

## 1003

**HIF Prolyl Hydroxylase 2 Controls Chondrocyte Metabolism and Affects Endochondral Ossification.** Steve Stegen<sup>\*1</sup>, Kjell Laperre<sup>1</sup>, Guy Eelen<sup>2</sup>, Gianmarco Rinaldi<sup>3</sup>, Sophie Torrekens<sup>1</sup>, Sarah-Maria Fendt<sup>3</sup>, Peter Carmeliet<sup>2</sup>, Geert Carmeliet<sup>1</sup>. <sup>1</sup>Clinical and Experimental Endocrinology, KU Leuven, Belgium, <sup>2</sup>Angiogenesis and Vascular Metabolism, Vesalius Research Center, VIB/KU Leuven, Belgium, <sup>3</sup>Cellular Metabolism and Metabolic Regulation, Vesalius Research Center, VIB/KU Leuven, Belgium

Centrally localized chondrocytes in the developing growth plate require HIF-1α signaling to maintain cell viability. Mechanistically, these cells are considered to adapt their metabolism to survive and function within this avascular environment, but how chondrocytes respond to oxygen scarcity to preserve the anabolic process of endochondral ossification remains unknown.

Here, we identify the HIF prolyl hydroxylase 2 (PHD2) oxygen sensor as a central gatekeeper of chondrocyte metabolism and cartilage matrix. PHD2-deficient chondrocytes increase aerobic glycolysis to counteract the decreased glucose oxidation-dependent energy production, but this HIF-1α-dependent metabolic rewiring results in a hypometabolic state without affecting viability. Accordingly, loss of PHD2 reduces energy expenditure by two pathways: first, by decreasing proliferation, explaining why bones are shorter in PHD2 conditional knockout mice (*Phd2<sup>chon</sup>*); second, by diminishing global protein translation and thereby collagen synthesis. However, adaptations in glutamine metabolism promote collagen proline hydroxylation, making the cartilaginous matrix more resistant to degradation and this leads to more cartilage remnants and increased bone mass in *Phd2<sup>chon</sup>* mice. To prove the specific contribution of the altered glutamine and glucose metabolism, we pharmacologically blocked the rate-limiting enzymes. Inhibition of glutaminase (GLS) reduces the level of metabolites necessary for collagen hydroxylation, thereby decreasing cartilage remnants and the increased bone mass in mutant mice. On the other hand, normalization of glucose oxidation in *Phd2<sup>chon</sup>* mice with dichloroacetic acid (DCA) corrects the hypometabolic state and, consequently, matrix synthesis. Due to the persisting adaptations in glutamine metabolism, DCA-treated *Phd2<sup>chon</sup>* mice display accumulation of cartilage remnants and bone mass, whereas blocking GLS in these mice completely normalizes the cartilage and bone phenotype to the level of wild-type mice.

Together, chondrocytic PHD2 coordinates bone growth and matrix production by regulating glutamine and glucose metabolism in the avascular growth plate during endochondral ossification.

**Disclosures:** Steve Stegen, None.

## 1004

**Therapeutic Targeting of GPCR Gbetagamma-GRK2 Signaling in Osteoarthritis.** Elijah Carlson<sup>\*</sup>, Eric Schott, Heather Le Bleu, Monaliza El-Quadi, John Ketz, Reyad Elbarbary, Michael Zuscik, Fadia Kamal. University of Rochester, United States

Osteoarthritis (OA) is a debilitating disease of the joints that involves progressive cartilage degeneration, with no available therapy. Chondrocytes acquire an aberrant hypertrophic phenotype in OA leading to cartilage degeneration. G protein-coupled receptors (GPCRs) are widely expressed on chondrocytes, and activation of the GPCR-Gα has been shown to maintain chondrocytes in a non-hypertrophic state. In pathological conditions, increased activation of GPCR-Gβγ and its increased interaction with GPCR kinases (GRK2 particularly) lead to GPCR desensitization and dampened Gα signaling. Importantly, we recently reported the therapeutic efficacy of inhibiting Gβγ-GRK2 in several diseases, but its role in OA is unknown. Our preliminary data show that GRK2 expression is elevated in chondrocytes of human OA cartilage and in a posttraumatic OA mouse cartilage. Thus, we *hypothesize* that Gβγ-GRK2 signaling drives chondrocyte hypertrophy (CH) and its inhibition attenuates OA progression.

**Methods:** We determined the role of articular chondrocyte GRK2 signaling in CH and cartilage degeneration in OA using a tamoxifen-inducible conditional chondrocyte GRK2 knockout (GRK2-KO) mouse. Then, using wild type mice, we determined the therapeutic efficacy of Gβγ-GRK2 inhibition in OA using novel and FDA approved pharmacological inhibitors of Gβγ-GRK2. OA was induced by surgical destabilization of the medial meniscus (DMM) in 3 months old mice. GRK2-KO or drug treatment was initiated 8 weeks post-DMM until 12 weeks when mice were sacrificed. Articular cartilage structural changes were evaluated via Saf-O-Fast green staining, histomorphometry, OARS scoring and microCT. Molecular events were examined using immunofluorescent staining for CH markers, and TUNEL staining for apoptosis.

**Results:** We found that conditional GRK2-KO and pharmacological Gβγ-GRK2 inhibition exert chondroprotective effects, evidenced by reduced OARS score and preserved articular cartilage area and chondrocytes number, attenuated expression of the CH markers MMP-13 and ADAMTS-5, and reduced articular chondrocyte apoptosis. Finally, in corroborating experiments, we found that inhibition of Gβγ-GRK2 signaling in mouse ATDC5 cells and in *ex vivo* cultures of human cartilage explants led to attenuated CH.

**Conclusion:** Our findings (i) suggest that Gβγ-GRK2 signaling is a driver of CH in OA, and (ii) identify novel and FDA approved agents with Gβγ-GRK2 inhibitory effect as a novel therapeutic strategy for OA.

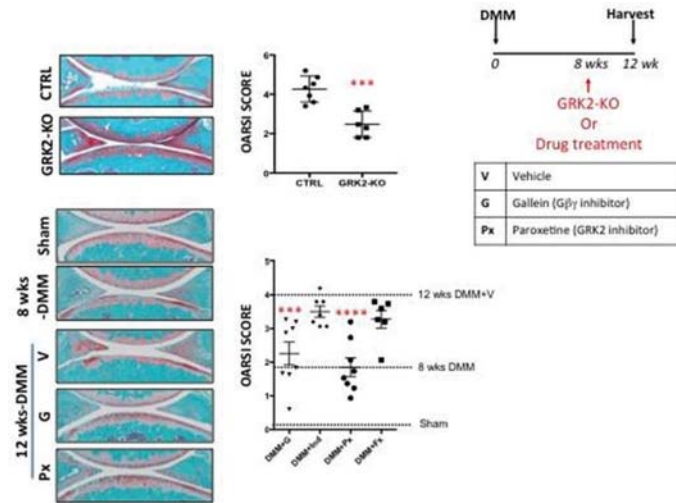


Figure 1

**Disclosures:** Elijah Carlson, None.

## 1005

**Fat Talks to Bone.** Wei Zou<sup>\*1</sup>, Nidhi Rohatgi<sup>1</sup>, Yan Zhang<sup>1</sup>, Charles Harris<sup>2</sup>, Steven L. Teitelbaum<sup>3</sup>. <sup>1</sup>Department of Pathology and Immunology, Washington University School of Medicine, United States, <sup>2</sup>Division of Endocrinology, Metabolism and Lipid Research, Department of Medicine, Washington University School of Medicine, United States, <sup>3</sup>Department of Pathology and Immunology; Division of Bone and Mineral Diseases, Department of Medicine, Washington University School of Medicine, United States

While obesity has long been considered beneficial for skeletal health recent studies suggest the opposite. Thus, despite its demographic importance, the influence of fat on bone remains enigmatic. Although controversial, studies of the effect of fat-produced molecules, such as leptin and adiponectin, indicate these selected adipokines impact bone. Adipose tissue is, however, a complex organ and there is little mechanistic insight as to how fat, per se, and which variety of fat, regulates the skeleton. Such information is clinically relevant as individuals with a predominance of visceral fat, as attends the metabolic syndrome, are osteopenic whereas subcutaneous and brown fat may positively influence bone mass. To address this issue we generated mice completely lacking visceral, subcutaneous and brown fat by cross-mating DTA<sup>flax/flax</sup> with Adiponectin Cre mice. The product has no visible body fat and virtually undetectable circulating adipocyte specific adipokines. As expected from their lipotrophic state, these “fat free” (FF) are insulin resistant and have fatty liver disease. Despite the hypogonadal state of FF mice, trabecular bone volume is markedly enhanced (400-500%) in both long bone and vertebrae with a significant increase in cortical thickness. The increased bone mass in FF mice is due to robust osteoblastic bone formation, determined by tetracycline double labeling. Unexpectedly in face of its marked osteosclerosis, osteoclasts in FF mice are also greatly enhanced although their resorptive capacity is compromised. This observation raises the possibility that the abundance of FF bone reflects, at least in part, osteoclast-mediated osteoblast recruitment. Most importantly, the skeletal phenotype of FF mice is completely rescued by transplantation of adipocyte precursors (MEFs) or various fat depots (visceral, subcutaneous and brown adipose tissue), suggesting adipocyte products, but not specific adipocyte type (BAT or WAT), regulates bone growth. Our observations establish that fat signals to bone and decreased adiposity may greatly enhance bone mass, challenging the concept that obesity improves skeletal health. Our study provides the first direct evidence that fat regulates bone homeostasis.

**Disclosures:** Wei Zou, None.

## 1006

**Forebrain neuronal ApoE regulates Trabecular Bone Mass in Mice in a super-ordinated Fashion and opposite to the Effect of Osteoblast ApoE on Bone.** Tobias Schmidt<sup>\*1</sup>, Christian Schlein<sup>2</sup>, Brigitte Müller<sup>2</sup>, Jörg Herren<sup>2</sup>, Andreas Niemeier<sup>3</sup>. <sup>1</sup>Department of Osteology and Biomechanics, University Medical Center Hamburg Eppendorf, Germany, <sup>2</sup>Institute of Biochemistry and Molecular Cell Biology IBMZ, University Medical Center Hamburg-Eppendorf, Hamburg 20246, Germany, Germany, <sup>3</sup>Department of Orthopaedics, University Medical Center Hamburg-Eppendorf, Hamburg 20246, Germany, Germany

### Objective

Next to its classical role in lipoprotein metabolism, apoE has long been known to be involved in the regulation of energy metabolism, bone metabolism and neurodegenerative diseases. Globally *ApoE*-deficient mice are lean, less prone to diet-induced obesity and diabetes and display high bone mass phenotype. Human *APOE* isoforms differentially regulate bone mass in mice. The exact molecular mechanisms and cell types through which apoE regulates energy metabolism and bone mass remain unclear at present. The goal of this study was to understand through which cell types apoE regulates bone mass in mice.

### Methods

Conditional inactivation of the mouse *ApoE* gene in C57Bl/6 mice via the Cre loxP system in osteoblasts (*Runx2cre*), osteoclasts (*Lysmcre*) and forebrain neurons (*Nkx2.1 cre*). Skeletal analysis by native x-ray,  $\mu$ CT, histomorphometry and analysis of bone turnover markers. Standard serum analysis of lipoprotein and glucose metabolic parameters, including oral glucose tolerance tests (OGTT) and oral fat tolerance tests (OFTT), as well as the induction of metabolic stress by high fat diet feeding (HFD) for 20 weeks.

### Results

Conditional knockout strains were characterized by standard procedures, revealing the expected cell-type specific deletion patterns. Osteoclast specific deletion of *ApoE* in female mice resulted in no apparent bone phenotype, while *ApoE* deletion in osteoblasts produced an unexpected age-dependent low bone mass phenotype in females. While three months old skeletons displayed no abnormalities, at six months of age lumbar vertebral and distal femoral trabecular bone mass were significantly reduced and osteoclast numbers and surface as well as resorption (urinary DPD) were significantly increased. There was no remarkable phenotype in any of the above mentioned measures of lipid or glucose metabolism, body weight and lean mass was normal. Most notably, forebrain neuronal deletion reproduced rather the global *ApoE* ko metabolic and bone phenotypes in that there was reduced obesity under the influence of HFD and high trabecular bone mass in lumbar vertebrae and distal femur in 6 months old animals.

### Conclusions

Forebrain neuronal *ApoE* regulates trabecular bone mass and adipose tissue mass in a super-ordinated fashion and is opposite to the effect of osteoblast apoE on bone mass. Next to leptin, apoE is evolving as a molecule with divergent CNS and peripheral effects in bone mass regulation and energy metabolism.

**Disclosures:** Tobias Schmidt, None.

## 1007

**Conditional deletion of the glucocorticoid receptor in osteoprogenitors inhibits lipid storage by BMSC-derived osteoblasts *in vitro* but promotes marrow fat *in vivo* following caloric restriction.** Jessica Pierce<sup>\*</sup>, Kehong Ding, Jianrui Xu, Paul Bernard, Kanglun Yu, Carlos Isales, Xingming Shi, Meghan McGee-Lawrence. Medical College of Georgia, Augusta University, United States

Aging promotes fatty infiltration of body tissues and a concomitant decline in organ health and function. In the bone marrow, fat storage is driven by a number of factors, including genetic and epigenetic predisposition/modifications, hormones, diet, and drug therapies (e.g., glucocorticoids). As fat accumulates in the bone marrow with age, bone density and strength decrease. We recently showed that osteoblastic expression of Hdac3 may play a role in this process: Hdac3 expression decreases with aging and inhibits lipid storage in bone marrow stromal cell (BMSC)-derived osteoblasts, and young Hdac3-deficient mice have high marrow fat and low bone mass like aged wildtype (WT) mice. This mechanism likely involves glucocorticoid signaling, as Hdac3 represses the transcription of 11 $\beta$ -hydroxysteroid dehydrogenase type 1 which activates glucocorticoids and drives lipid storage in BMSC-derived osteoblasts. Caloric restriction results in decreased BMD and increased marrow fat, much like that seen with aging and Hdac3 depletion. Because little is known about the biological reasons for fatty infiltration in bone marrow, we sought to directly test the role of the glucocorticoid receptor (GR) in caloric restriction-induced fat storage within osteoblasts and in the bone marrow. We hypothesized that deletion of the GR in a caloric restriction model would inhibit lipid storage and marrow fat and promote increased bone mass. GR<sup>flm</sup> mice were crossed with Osx1-Cre mice to generate GR conditional knockout mice (GR-CKO) and Cre-negative WT controls (6 mo old, n=4/group). BMSC-derived osteoblasts from GR-CKO animals demonstrated decreased lipid storage (~80%) and more matrix formation *in vitro* as compared to WT mice as hypothesized. Surprisingly, however, histological analysis of the tibia revealed that GR-CKO mice had more marrow fat (+130% adipocyte area / tissue area) and lower cortical bone mass in the femur (-11%) than WT mice following 6 weeks of caloric restriction. These data illustrate potential differences that may be governed by differences in the role of physiological vs pharmacological levels of glucocorticoids or compensatory hormonal changes following *in vivo* loss of the GR. This work highlights the complexities of the role of the GR in bone turnover, BMSC biology, and marrow adiposity under varying physiologic conditions.

**Disclosures:** Jessica Pierce, None.



## 1008

**PPAR $\gamma$  in Inflammation and Aging.** Raysa Rosario\*, Babak Baban, Mark Hamrick, Carlos Isales, Xing-Ming Shi, Augusta University, United States

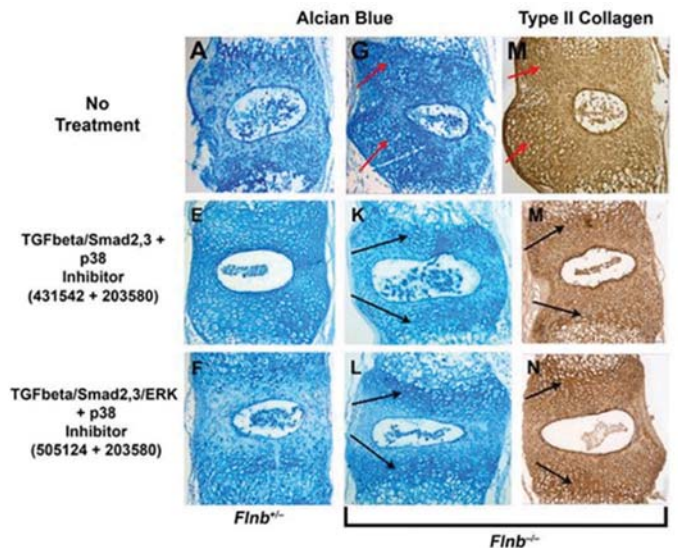
Aging is a state of chronic low grade inflammation (inflammaging). With advancing age, bone mass decrease and marrow fat increase (fatty marrow). Adipose tissue is an endocrine organ and produces large amounts of adipokines and inflammatory cytokines which may have profound impact on stem cell differentiation and functions. Peroxisome proliferator-activated receptor-gamma (PPAR $\gamma$ ) is a key transcription factor absolutely required for adipocyte differentiation both in vitro and in vivo. Since marrow fat and bone-forming osteoblasts share a common mesenchymal progenitor cell (MSC), we hypothesized that bone-specific PPAR $\gamma$  inactivation, which blocks marrow fat formation, may reduce or eliminate marrow fat-generated inflammatory cytokines, increases the availability and activity of osteoblasts, and improves immune function, thereby reducing the pace of bone loss in aging. To test this hypothesis we generated PPAR $\gamma$  conditional knockout mice and examined the effects of PPAR $\gamma$  deficiency on bone and immune cell profiles. uCT analysis showed that deficiency of PPAR $\gamma$  increased bone volume (BV/TV), trabecular number (Tb.N) and reduced trabecular spacing (Tb.Sp). The bone protective effect of PPAR $\gamma$  deficiency became more significant in older mice. ELISA and Luminex Multiplex Immunoassays showed that serum levels of adiponectin, resistin and leptin were all decreased significantly in PPAR $\gamma$  KO mice regardless of age. Levels of these adipokines were significantly higher in female PPAR $\gamma$ -floxed control mice than that in males, but no difference were observed between females and males in PPAR $\gamma$  KO mice. mRNA levels of inflammatory cytokine genes such as TNF- $\alpha$ , IL-1 $\beta$ , and IL-6 were decreased significantly in cultured marrow stromal cells of PPAR $\gamma$  KO mice. Contrary to our predictions, limited preliminary data suggested that deficiency of PPAR $\gamma$  may increase T cell proliferation, enhance the state of inflammation and shifting of immune cells from lymphoid towards myeloid cell populations. These data establish a critical role of PPAR $\gamma$  in age-related skeletal and immune dysfunctions.

**Disclosures:** Raysa Rosario, None.

## 1009

**Inhibition of post-receptor TGF $\beta$ /BMP signaling activation rescues disc degeneration in *Flnb*<sup>-/-</sup> Spondylarthritis Synostosis murine model.** Jennifer Zieba\*, Kimberly Forlenza<sup>2</sup>, Kelly Heard<sup>2</sup>, Jorge Martin<sup>2</sup>, Lukas Balek<sup>3</sup>, Michaela Kunova Bosakova<sup>3</sup>, Pavel Krejci<sup>3</sup>, Deborah Krakow<sup>2</sup>. <sup>1</sup>Baylor College of Medicine, United States, <sup>2</sup>University of California, Los Angeles, United States, <sup>3</sup>Masaryk University, Czech Republic

Spondylarthritis synostosis (SCT) is an autosomal recessive disorder characterized by progressive fusions of the thoracic and lumbar vertebrae, as well as carpal and tarsal bones, and results from nonsense mutations in the gene Filamin B (*FLNB*). *FLNB* is known to stabilize actin 3-dimensional structure while also acting as a signaling scaffold by interacting with multiple signal transduction systems, yet the disease mechanisms for SCT remain unresolved. Utilizing a *FLNB* global knockout mouse, we previously showed that the vertebral fusions in SCT result from intervertebral disc (IVD) degeneration/ossification of the annulus fibrosus (AF) and this degeneration partly results from alterations in the TGF $\beta$ /BMP signaling pathway. In this study, cultured AF cells were used to further elucidate the role of *FLNB* within the TGF $\beta$ /BMP pathway. In the absence of *FLNB*, the mouse IVD undergoes full mineralization and trabecular bone formation. This eventual mineralization is initially instigated by increased TGF $\beta$  canonical, BMP non-canonical, and Smad 1 nuclear activity. In a series of *in vitro* experiments, we show that *FLNB* interacts with inhibitory Smads 6 and 7 (iSmads) to attenuate TGF $\beta$ /BMP signaling. Loss of *FLNB* inhibits the normal function of iSmads causing increased TGF $\beta$  receptor activity and decreased Smad 1 ubiquitination. Through the use of small molecule inhibitors in an *in vitro* whole spine culture model, we modulated specific components of the TGF $\beta$ /BMP pathway based on our *in vitro* AF cell results in order to rescue the degenerative phenotype and design a more specific treatment for SCT and disc degeneration. By inhibiting canonical and non-canonical TGF $\beta$ /BMP pathway activity, the increased proteoglycan and Type II collagen secretion typically seen in *Flnb*<sup>-/-</sup> degenerating discs was diminished and ECM integrity was restored to the IVD. The most effective rescues resulted from inhibiting TGF $\beta$  canonical and/or noncanonical in combination with p38 post-receptor signaling activation. The results showed that a delicate balance in TGF $\beta$ /BMP signaling cascades needs to be maintained within the AF ECM and that biological therapies focused on more specific post-receptor components of the TGF $\beta$ /BMP signaling have the ability to rescue early disc degeneration/collapse. It is our hope that these discoveries will further the field of IVD research and bring about new possible treatments for disc degeneration and congenital vertebral fusion disorders.



Combined TGF $\beta$  and p38 inhibition rescues degenerative phenotype in cultured *Flnb*<sup>-/-</sup> murine IVDs

**Disclosures:** Jennifer Zieba, None.

## 1010

**Phenotypic study of a novel mouse model for Crouzon syndrome with acanthosis nigricans.** Maxence Cornille\*, Roman H Khonsari<sup>1</sup>, Morad Bensidhoum<sup>2</sup>, Federico Di Rocco<sup>3</sup>, Laurence Legeai-Mallet<sup>1</sup>. <sup>1</sup>INSERM U1163, France, <sup>2</sup>UMR CNRS 7052, France, <sup>3</sup>Lyon hospital, France

Crouzon syndrome with acanthosis nigricans (CAN) is a rare craniosynostosis characterized by a premature fusion of the coronal sutures of the skull, midface hypoplasia and acanthosis nigricans. CAN syndrome is caused by a single point mutation (A391E) localized in transmembrane domain of FGFR3 gene. This mutation causes an increased ligand-independent activation of the receptor. In order to understand bone formation in CAN syndrome, we generated the first mouse model for this condition thanks to ubiquitous Cre-LoxP system for the murine *Fgfr3* gene.

Macroscopic analyses of mutant mice (*Fgfr3*A385E/+ and *Fgfr3*A385E/A385E) and its control littermate were done from E16.5 embryos to newborn and adult animals. We performed morphological, X-rays analyses and alizarin and alcian blue staining of the skeleton. We completed these morphological analyses using micro-computed tomography (uCT) scanners. Membranous ossification was assessed using osteoblast cultures from newborn mice calvaria.

*Fgfr3*A385E/+ and *Fgfr3*A385E/A385E adult mutant mice exhibited mild craniofacial anomalies with incomplete penetrance. While no premature fusion of sutures was observed, significant reduction of length and skewing of the maxillary bone could be seen on mutants. Interestingly, osteoblasts culture from *Fgfr3*A385E/+ calvaria presented significant decreased alizarin red and alkaline phosphatase staining, suggesting a decreased mineralization. Appendicular skeleton did not present anomalies in mutants. Immunostaining for Collagen type X showed normal hypertrophic zone in the growth plate cartilage. The expression of *Fgfr3*A385E in the cartilage did not alter chondrogenesis.

Mild phenotype observed on CAN mice resemble to the phenotype observed on Muenke syndrome mouse model, another FGFR3 gain-of-function related-craniosynostosis. We showed that the A385E mutation modifies mineralization of osteoblasts in vitro thus indicating membranous ossification disruption in CAN syndrome. Further analyses in progress will permit to extend the characterization and the physiopathology of the CAN syndrome and the role of the FGFR3 gene in skull and craniofacial development.

**Disclosures:** Maxence Cornille, None.

## 1011

**Absence of pannexin-1 in osteocytes leads to high bone mass due to distinct cellular mechanisms in cancellous versus cortical bone, and in young versus old mice.** Rafael Pacheco-Costa\*, Emily Atkinson<sup>1</sup>, Julian Dilley<sup>1</sup>, Hannah Davis<sup>1</sup>, Carmen Herrera<sup>2</sup>, Roger Thompson<sup>2</sup>, Teresita Bellido<sup>1</sup>, Lilian Plotkin<sup>1</sup>. <sup>1</sup>Indiana University School of Medicine, United States, <sup>2</sup>Hotchkiss Brain Institute, Department of Cell Biology and Anatomy, University of Calgary, Canada

High osteocyte apoptosis, as in aging, triggers osteoclast recruitment by mechanisms not completely known. In immune cells, apoptosis results in opening of Pannexin1 (Pnx1) channels, which release ATP, an osteoclastogenic factor. However, whether this also occurs in osteocytes is unknown. To examine Pnx1 role in osteocytes, *Pnx1*<sup>fl/fl</sup>

were mated with 8kbDMP1-Cre to generate Pnx1<sup>Δot</sup> mice. BMD in Pnx1<sup>Δot</sup> mice (n=10) is higher starting at 2-3 months of age (3.5% femur, 5-7% spine, and 3.5% total BMD) compared to Pnx1<sup>fl/fl</sup> littermate controls (n=9). Vertebra  $\mu$ CT analysis shows increased BV/TV (9%) and TbTh (6%) in 4-mo Pnx1<sup>Δot</sup> mice. Higher cancellous MAR and unchanged MS/BS (or NOB/BS) leads to 24% higher BFR/BS. This increase is not due to reduced sclerostin protein levels, which are unchanged in serum or bone lysates. NOC/BS and OcS/BS do not change. Thus, increased cancellous bone in the absence of osteocytic Pnx1 is due to enhanced bone formation. Cortical thickness is 3.5% higher, and NOC/BS, OcS/BS, and ES/BS are 27-30% lower on femur endocortical surface, likely due to lack of osteoclastogenic signals from Pnx1-deficient osteocytes. Further, serum CTX is 14% lower in Pnx1<sup>Δot</sup> mice. Osteoclast precursor marker (CD14/CD11b) expression is lower in bone marrow cells of Pnx1<sup>Δot</sup> mice and MCSF/RANKL induced less osteoclasts and lower expression of osteoclastic genes, suggesting that osteocytic signals released via Pnx1 channels are required for osteoclast lineage commitment. Pnx1 deletion in 4-mo Pnx1<sup>Δot</sup> mice and in adenoCre-treated Pnx1<sup>fl/fl</sup> calvaria bones do not increase osteocyte apoptosis, as shown by active caspase3 staining and by apoptosis-related gene (CHOP, Foxo3, p27) expression, respectively; and, serum ATP is not changed in Pnx1<sup>Δot</sup> mice. We next tested the effect of pharmacological Pnx1 inhibition with mefloquine (MFQ, 5mg/kg/d/14d). MFQ reduces serum ATP levels and NOC/BS in 21-mo old WT mice, which exhibit higher prevalence of osteocyte apoptosis than 3.5-mo young mice. MFQ also increases cancellous BFR in old mice. Our results suggest that osteocytic Pnx1 deletion increases bone mass by different cellular mechanisms in cancellous vs cortical bone and inhibits osteoclastogenesis by apoptosis-induced ATP release-independent and dependent means in young vs old mice, respectively. We propose that osteocytic Pnx1 channels restrain bone formation and increase bone resorption, raising the possibility of using Pnx1 inhibitors to treat low bone mass conditions.

**Disclosures:** Rafael Pacheco-Costa, None.

## 1012

**Induction of the Hajdu Cheney Syndrome Mutation in B-cells Alters B-cell Allocation but not Skeletal Homeostasis.** Archana Sanjay<sup>\*1</sup>, Jungeun Yu<sup>1</sup>, Lauren Schilling<sup>1</sup>, Christopher Schoenherr<sup>2</sup>, Aris Economides<sup>2</sup>, Ernesto Canalis<sup>1</sup>. <sup>1</sup>UConn Health, United States, <sup>2</sup>Regeneron Pharmaceuticals, Inc., United States

Hajdu Cheney syndrome (HCS) is a rare genetic disorder characterized by severe osteoporosis and driven by autosomal-dominant mutations in exon 34 of *NOTCH2* that give rise to deletions of the PEST domain, which is required for the degradation of NOTCH2. The mutations result in the expression of a truncated and stable protein and NOTCH2 gain-of-function. Mice harboring a *Notch2* mutation that replicates the one found in HCS have marked osteopenia due to increased bone resorption. In addition, *Notch2HCS* mutant mice have a 3 to 5 fold increase in splenic marginal zone B-cells and a proportional decrease in follicular B-cells. Whether Notch2 activation in the spleen and altered B-cell allocation are responsible for the skeletal phenotype is not known. Antibodies to the negative regulatory region (NRR) of Notch2 (10 mg/Kg, Genentech) administered twice a week for 4 weeks to 1 month old *Notch2HCS* mutant or control littermate mice reversed the differential B-cell allocation and the osteopenia of *Notch2HCS* mutant mice confirming their dependency on Notch2 activation. To determine whether Notch2 activation in B-cells was responsible for alterations in splenic B-cell allocation and the osteopenic phenotype of *HCS* mutants, a conditional by inversion (COIN) HCS allele of *Notch2* was used. In this model, Cre recombination generates a permanent *Notch2<sup>ΔPEST</sup>* allele expressing a transcript where the sequences coding for the PEST domain and 3'-untranslated region are replaced by a STOP codon and a polyadenylation signal. As such, the *Notch2<sup>ΔPEST</sup>* mouse replicates the mutations found in HCS in a tissue-specific manner. *CD19-Cre* drivers were crossed with *Notch2<sup>COIN</sup>* mice to generate *CD19* cell specific *Notch2<sup>ΔPEST</sup>* or control littermate mice. There was an increase in marginal zone B-cells in *CD19<sup>Cre</sup>;Notch2<sup>ΔPEST</sup>* mice recapitulating the splenic phenotype of global *Notch2HCS* mutant mice. However, *CD19<sup>Cre</sup>;Notch2<sup>ΔPEST</sup>* mice did not exhibit an obvious skeletal phenotype. Moreover, splenectomies of *Notch2HCS* global mutant mice did not reverse their osteopenic phenotype. These results suggest that changes in splenic B-cell allocation by Notch2 have limited influence on basal skeletal homeostasis. In conclusion, these studies demonstrate that Notch2 activation determines B-cell allocation; this might explain the inflammatory reaction and acro-osteolysis, but not the osteoporosis, of HCS.

**Disclosures:** Archana Sanjay, None.

## 1013

**Antiresorptives Compromise Bone's Material Composition Predisposing to Atypical Femoral Fractures.** Cherie Chiang<sup>\*1</sup>, Roger Zebaze<sup>2</sup>, Hanh Nguyen<sup>3</sup>, Yu Peng<sup>4</sup>, Maria Zanchetta<sup>5</sup>, Peter Ebeling<sup>6</sup>, Ego Seeman<sup>7</sup>. <sup>1</sup>Austin Hospital, Australia, <sup>2</sup>Department of Medicine, Austin Health, Australia, <sup>3</sup>Department of medicine, Monash University, Australia, <sup>4</sup>Straxcorp.com Pty Ltd, Australia, <sup>5</sup>IDIM, Instituto de Diagnóstico e Investigaciones Metabólicas, Buenos Aires, Argentina, Argentina, <sup>6</sup>Medicine, Monash University, Australia, <sup>7</sup>Department of Medicine, Austin Health, Australia

Background Anti-resorptive therapies slow bone remodeling. The less renewed bone becomes more fully mineralized predisposing to brittleness and micro-damage.

The perception of risk of atypical femoral fractures (AFF) is a disincentive to the uptake of antiresorptives even though the risk of typical fragility fractures is much higher without treatment.

Methods To determine whether women treated with antiresorptives with AFFs could be identified we quantified bone microstructure using high resolution peripheral computed tomograph and StrAx1.0 in 49 women with AFFs treated with antiresorptive therapy, 60 women similarly treated remaining AFF-free, and 342 pre- and 55 postmenopausal healthy women. Deviation in cortical porosity and matrix mineral density (MMD) from the young normal mean was quantified using a Material Fracture Score (MFS).

Results Women with AFF had 0.88 SD lower cortical porosity but \_\_\_ SD higher MMD than treated women without AFFs (p<0.05). MMD was 0.27±0.13 SD, p=0.04 higher than premenopausal women and \_\_\_ SD higher than the other postmenopausal groups (p < 0.001). these abnormalities were captured in the MFS was 1.42±0.18 SD higher than postmenopausal women (p <0.0001) and distinguished women with AFFs from treated peers; area under curve of 0.74 (C.I. 0.65 – 0.84, p < 0.001) and OR 7.5 (95%CI 3.1-18.2, P < 0.0001). The corresponding figures when identifying AFFs patients from treatment naïve peers were an AUC of 0.7 (C.I. 0.6 – 0.8, p < 0.001) and Odds Ratio of 5.7 (CI 2.5-12.9, P < 0.0001)

Conclusions Quantification of bone microstructure identifies women with atypical fractures and may help to reassure those at low risk.

**Disclosures:** Cherie Chiang, None.

## 1014

**Screening for atypical femur fractures using extended femur scans by DXA.** Denise van de Laarschot<sup>\*</sup>, Sandra Smits, Sanne Buitendijk, Merel Stegenga, M. Carola Zillikens. Bone Center, Erasmus MC, Netherlands

Atypical femur fractures (AFFs) are a rare but serious complication associated with the use of antiresorptive drugs such as bisphosphonates. Assessment of incomplete AFFs on extended femur scans by Dual X-ray Absorptiometry (DXA) may prevent the development of complete fractures.

The aim of this study was to evaluate the potential of extended femur scans by DXA as a screening tool for incomplete AFFs. From June 2014 until September 2016 extended femur scans were routinely performed in all consecutive patients undergoing DXA scanning who had used bisphosphonates or denosumab at any given moment in the previous year. When "beaking" was found, defined as a localized periosteal or endosteal thickening of the lateral cortex, a radiograph of the femur was performed to confirm incomplete AFF.

Beaking was detected in 12 out of 282 patients (4.3%) with extended scans of both femora. In nine patients (3.2%) beaking corresponded with the radiological presence of incomplete AFFs, of whom four already had an X-ray made because of a previous complete AFF of the other leg. Five patients (1.8%) were newly diagnosed with six yet unknown incomplete AFFs. No additional X-ray was performed in two patients because of loss of follow-up. Beaking was explained by known soft tissue calcifications in one patient. The positive predictive value of beaking on extended femur scan was 83.3% in our study.

Three cases in whom the new diagnosis of incomplete AFF has affected medical and surgical treatment are further discussed to illustrate the relevance of early detection.

We conclude that extended femur scans by DXA can detect incomplete AFFs in patients on antiresorptive treatment and should therefore be considered a clinically relevant screening tool since early identification of AFFs has therapeutic consequences.

**Disclosures:** Denise van de Laarschot, None.

## 1015

**Characterization of > 100 Patients with Atypical Femur Fractures: The Quebec Atypical Femur Fracture Registry.** Suzanne Morin<sup>\*1</sup>, Michelle Wall<sup>2</sup>, Etienne Belzile<sup>3</sup>, Laetitia Michou<sup>4</sup>, Louis-Georges Ste-Marie<sup>5</sup>, Edward Harvey<sup>1</sup>, Prism Schneider<sup>6</sup>, Sonia Jean<sup>7</sup>, Jacques Brown<sup>3</sup>. <sup>1</sup>McGill University, Canada, <sup>2</sup>Research Institute of the McGill University Health Center, Canada, <sup>3</sup>Laval University, Canada, <sup>4</sup>Centre de Recherche du CHU de Quebec, Canada, <sup>5</sup>University de Montreal, Canada, <sup>6</sup>University of Calgary, Canada, <sup>7</sup>Institut national de santé publique du Quebec, Canada

Background: Atypical femur fractures (AFF) are a rare subset of atraumatic subtrochanteric and diaphyseal fractures associated with prolonged use of antiresorptive agents. Their pathophysiology remains unclear.

Methods: Since 2012, a collaborative network of Quebec (Canada) clinicians identify and refer consenting men and women, 45 years and older, with AFF to the Quebec AFF Registry for clinical and radiographic data collection. In addition, 2D-3D X-Ray EOS scans for femur geometry assessment were done in a subset of subjects. Descriptive statistics are presented and compared to data from reference populations: 1) men and women with femur fractures in Quebec; 2005-2008 and 2) for geometric parameters, data from Chaibi, Y. 2011 and Than, P. 2012.

Results: We have registered 102 participants (women 93%) with AFF (Table). Most were Caucasian (95%) and 69.5 [9.3] years at the time of AFF. All were exposed to BPs with an average cumulative duration of 10.4 [4.5] years. There were 154 fractures (77 complete) among the 102 participants; 71% experienced prodromal pain. Fifty-two participants had bilateral fractures, of which 87% were documented to be at concordant



sites on the femora. AFF were more common in the diaphysis (68%) than at the subtrochanteric site. Use of proton pump inhibitors (52%), hormone therapy (9%) and raloxifene (6%) was higher than in the Quebec population. In women (N=37) who underwent EOS scans femoral neck shaft angle (125.9 [5.2] °), varus deformity at the knee (-2.2 [4.2] °), femur bowing (-3.6 [3.49] °) and hip knee shaft angle (7.98 [2.3] °) confirmed varus anatomy at the hip and accentuated bowing of the femur compared to reference data. Forty-five participants used teriparatide post-AFF. In patients who underwent surgery (N= 85), subtrochanteric AFF were most often treated with long cephalomedullary nails, whereas diaphyseal AFF treatment was variable. Patients with unilateral complete AFF showed greater improvement in functional performance 6 months post-surgical fixation compared to patients with unilateral incomplete AFF without surgical fixation.

Conclusions: Significant differences are apparent in AFF subjects compared to reference populations. Furthermore, variance amongst orthopedic and medical practices may impact functional recovery in these patients. Through comprehensive data collection (including saliva specimens) the Quebec AFF Registry aims to provide new data towards the understanding of AFF pathogenesis.

**Table Clinical Characteristics of Participants in Quebec Registry AFF**

Characteristics	AFF N=102
Age years (SD)	69.5 (9.3)
Women n (%)	94 (93)
Height (cm) mean (SD)	157.7 (7.6)
Weight (kg) mean (SD)	68.3 (12.5)
BMI (kg/m <sup>2</sup> ) mean (SD)	27.4 (4.5)
Race/Ethnicity n (%)	
Caucasian	97 (95)
Asian	5 (5)
Previous Fracture n (%)	58 (57)
Family History n (%)	
Osteoporosis	43 (42)
Parental hip fracture	17 (17)
Other family member hip fracture	15 (15)
Supplement Dosage mean (SD)	
Vitamin D (UI/d)	1087 (997)
Calcium (mg/d)	779 (334)
Biochemistry Serum mean (SD)	
PTH (pmol/L)	73
Alkaline Phosphatase (U/L)	85
Osteocalcin (µg/L)	50
TSH (mIU/L)	67
C-telopeptide (µg/L)	60
25-OH Vitamin D (nmol/L)	88
Bone Mineral Density mean (SD)	
Femoral Neck (g/cm <sup>2</sup> )	81
T-score	87
Lumbar Spine (g/cm <sup>2</sup> )	83
T-score	88
Mechanism of Injury n (%)	
Bone broke without fall	67 (66)
Fall from standing height	33 (32)
Prodromal Pain	
Present n (%)	72 (71)
Length of time (months) mean (SD)	10.3 (13.4)
Fractures n (%)	
Total	154
Bilateral	52 (51)
Complete	77 (50)
Incomplete	77 (50)

Table: Clinical Characteristics of Participants in Quebec AFF Registry

Disclosures: Suzanne Morin, Amgen, Grant/Research Support.

## 1016

**Evaluation of Invasive Oral Procedures and Events in Women With Postmenopausal Osteoporosis Treated for up to 10 Years With Denosumab: Results From the Phase 3 FREEDOM Open-label Extension.** Nelson B Watts<sup>1</sup>, Peter W Butler<sup>2</sup>, Neil Binkley<sup>3</sup>, John T Grbic<sup>4</sup>, Michael McClung<sup>2</sup>, Antonette Tierney<sup>2</sup>, Rachel B Wagman<sup>2</sup>, Xiang Yin<sup>2</sup>. <sup>1</sup>Mercy Health, United States, <sup>2</sup>Amgen Inc., United States, <sup>3</sup>University of Wisconsin School of Medicine and Public Health, United States, <sup>4</sup>Columbia University, United States, <sup>5</sup>Oregon Osteoporosis Center, United States

Purpose: Antiresorptive therapy use is associated with osteonecrosis of the jaw (ONJ), an infrequent but serious adverse event. Positively adjudicated ONJ in the denosumab (DMAB) clinical trial program is rare (between ≥1 and <10 per 10,000). Completion of the 7-year FREEDOM Extension study (EXT) permitted an in-depth assessment of the risk factors and observed invasive oral procedures and events (OPEs; eg, dental implants, tooth extraction, natural tooth loss, scaling or root planing [extensive subgingival cleaning]) in the clinical trial setting.

Methods: In the randomized, placebo-controlled FREEDOM study, women received DMAB 60mg or placebo SC every 6 months for 3 years. Patients who missed

≤1 dose of investigational product and completed the Year-3 visit were eligible to participate in the 7-year open-label EXT to receive DMAB, regardless of original treatment assignment in FREEDOM. Women who reached the EXT Year-3 visit were asked to chronicle their history of invasive OPEs since the start of the EXT through Year 2.5, as well as oral events (including jaw surgery) in the prior 6 months. The oral event questionnaire was then administered every 6 months through the end of the EXT.

Results: During the EXT, the overall ONJ rate was 5.2 per 10,000 patient-years. The majority of women (79%; 3591/4550 patients) participated in the survey. Over the EXT, 1621 (45.1%) reported at least one invasive OPE; the incidence of five individual OPEs were similar between groups (Table). There were 12 confirmed cases of ONJ among women who participated in the survey (11 had OPE and one did not) and one additional case in a woman who did not complete the survey. ONJ incidence was 0.7% (11/1621 patients) in women reporting invasive OPEs and 0.05% (1/1970 patients) in women reporting no invasive OPEs. Of the 12 ONJ cases with survey results, one outcome was unknown due to consent withdrawn, one was ongoing at the end of study, and 10 resolved with treatment.

Conclusions: Nearly all cases of ONJ observed in this study occurred after a reported invasive OPE, yet while invasive OPEs were common in this group of DMAB-treated women with postmenopausal osteoporosis, ONJ incidence was low. The actual number of invasive OPEs may be underestimated due to limited capture of OPEs in medical charts and possible recall bias in patients with events that occurred in the first 2.5 years of the EXT. ONJ is an adverse event of interest that continues to be monitored in DMAB pharmacovigilance activities.

	7-year FREEDOM Extension		
	Cross-over (N = 1731)	Long-term (N = 1860)	All (N = 3591)
Age at EXT baseline in years, mean (SD)	74.3 (4.9)	74.4 (4.8)	74.3 (4.8)
Any invasive oral procedure or event, n (%)	795 (45.9)	826 (44.4)	1621 (45.1)
Scaling or root planing	503 (29.1)	531 (28.5)	1034 (28.8)
Tooth extraction	434 (25.1)	458 (24.6)	892 (24.8)
Dental implant	100 (5.8)	112 (6.0)	212 (5.9)
Natural tooth loss	72 (4.2)	75 (4.0)	147 (4.1)
Jaw surgery*	16 (0.9)	17 (0.9)	33 (0.9)

N = Number of patients who received ≥1 dose of investigational product in the EXT and responded to ≥1 oral event questionnaire related to the EXT

n = Number of patients with an OPE

\*Collected in the oral event questionnaire every 6 months; therefore, jaw surgery in the first 2.5 years of the EXT was not captured

Table: Invasive OPEs during the EXT for patients who completed at least one oral event questionnaire

Disclosures: Nelson B Watts, Shire, Grant/Research Support.

## 1017

**Sustained IKKβ activation in postnatal chondrocytes accelerates the onset of age-associated murine osteoarthritis.** Sarah Catheline\*, Christopher Dean, Michael Zuscik, Brendan Boyce, Jennifer Jonason. University of Rochester Medical Center, United States

Osteoarthritis (OA) is a degenerative joint disease that affects all tissues within synovial joints. Advanced age is an important risk factor for development of OA, and age-associated chronic, low-grade inflammation is now recognized as a likely contributor to disease. We have found that wild-type (WT) C57BL/6 mice show progressive activation of canonical NF-κB signaling within articular chondrocytes as they age and by 27 months exhibit an OA-like phenotype, consisting of loss of proteoglycan staining within the articular cartilage as well as synovial and meniscal hyperplasia. Given that increased IKKβ/NF-κB signaling is implicated in the pathogenesis of many age-associated diseases, we hypothesize that activation of this pathway in postnatal chondrocytes will be sufficient to accelerate the onset of OA. We generated chondrocyte-specific IKKβ gain-of-function (GOF) mice by combining the *Acan-CreER<sup>T2</sup>* knock-in allele with the *ROSA-Ikk2ca* allele to obtain overexpression of constitutively active IKKβ in chondrocytes. Following tamoxifen administration at 2 months of age, IKKβ GOF mice develop a phenotype strikingly similar to the age-associated joint pathology seen in WT mice, but at a markedly accelerated rate, suggesting that IKKβ GOF enhances spontaneous OA development. Chondrocyte-specific targeting invoked phenotypic changes in the cartilage, but also in synovium and meniscus tissues not targeted by *Acan-CreER<sup>T2</sup>*, suggesting that chondrocytes can have paracrine effects on adjacent tissues. IKKβ GOF mice show decreased SOX9 and increased COL10A1 expression in articular chondrocytes, and increased MMP13 expression, TUNEL-positive cell numbers and Alizarin red staining within the menisci. Micro-CT analyses confirmed enhanced meniscal mineralization in IKKβ GOF mice. *In vitro*, IKKβ GOF primary chondrocytes had significantly increased expression of *Mmp3*, *Cxcl1*, *Mmp13*, *Il-6*, *Ccl20*, and *Cox-2*, all genes associated with a senescence-associated secretory phenotype (SASP), which is characterized by high levels of pro-inflammatory cytokines, chemokines, matrix metalloproteinases, and growth factors. In addition, SASP-associated gene levels were higher in joint cartilage from aged WT mice than from young WT mice. Our findings define a novel link between NF-κB signaling and SASP in chondrocytes during aging that can accelerate the development of OA.

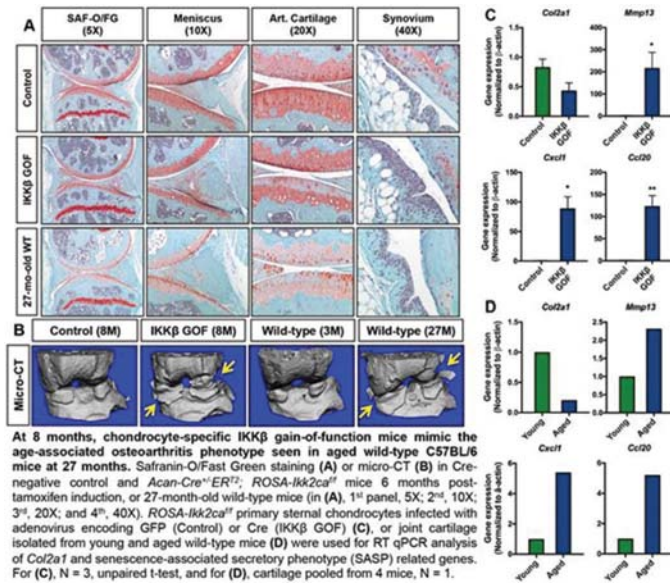


Figure 1

Disclosures: Sarah Catheline, None.

## 1018

**Multi-photon laser scanning microscopy reveals reduced angiogenesis and PDGFR $\beta$ -expressing mesenchymal progenitors in long bone fracture callus of aged mice.** Hengwei Zhang<sup>1</sup>, Jianguo Tao<sup>1</sup>, Longze Zhang<sup>1</sup>, Rana Gupta<sup>2</sup>, Edward Schwarz<sup>1</sup>, Brendan Boyce<sup>1</sup>, Lianping Xing<sup>1</sup>. <sup>1</sup>University of Rochester, United States, <sup>2</sup>University of Texas Southwestern Medical Center, United States

Fracture healing is often impaired in the elderly because of reduced osteogenesis and angiogenesis, which involve PDGFR $\beta$  signaling. PDGFR $\beta$  is expressed by a subset of mesenchymal progenitors that give rise to osteoblasts and pericytes. However, the precise time when the PDGFR $\beta$  cells are required is not known due to lack of longitudinal imaging methods to monitor dynamic changes of angiogenesis and cells in mouse long bones. To address this we: 1) developed a multi-photon laser scanning microscopy (MPLSM) protocol to visualize and assess blood vessels and PDGFR $\beta$  cells in fracture callus; and 2) determined the requirement of PDGFR $\beta$  cells during the early stages of fracture healing. Young (3-month-old) and aged (20-month-old) C57/B6 male mice received tibial fracture surgery and subjected to MPLSM at the fracture site of the same leg on day 3, 10, 21 longitudinally. Blood vessels and PDGFR $\beta$  cells in the callus area were visualized following i.v. injection of Dextran-Texas Red and FITC-anti-PDGFR $\beta$  antibody, respectively. MPLSM showed markedly increased vessel volume and PDGFR $\beta$  cells in young mice on d3, which peaked at d10, and decreased by d21, which decreased in aged mice at all time points (Vessel vol  $\times 10^{-3} \text{ mm}^3$ :  $73 \pm 11$  vs.  $6.3 \pm 1.2$  d3;  $380 \pm 72$  vs.  $22 \pm 5$  d10;  $120 \pm 32$  vs.  $8.6 \pm 3.4$  d21; PDGFR $\beta$  cell  $\times 10^4/\text{mm}^2$ :  $200 \pm 80$  vs.  $10 \pm 2$  d3,  $2600 \pm 46$  vs.  $500 \pm 10$  d10,  $40 \pm 20$  vs.  $30 \pm 20$  d21). Since MPLSM revealed increased PDGFR $\beta$  cells in callus of young mice at d3-d10 and this increase was significantly reduced in aged mice, we investigated the effects of PDGFR $\beta$  cell depletion on fracture healing during this time. PDGFR $\beta$ -rTA;TetO-DTA mice were treated with Doxycycline for 2d to deplete PDGFR $\beta$  cells, followed by tibial fracture surgery. Mice were sacrificed on d4, d10 and d14 post-fracture. PDGFR $\beta$  cells and blood vessels in callus were examined by IHC. Compared to saline control, Dox-fed mice had significantly decreased PDGFR $\beta$  cells/total cells at d4 (%:  $9.6 \pm 2.6$  vs.  $0.3 \pm 0.2$  d4;  $34 \pm 3$  vs.  $22 \pm 5$  d10;  $37 \pm 3$  vs.  $27 \pm 4$  d14), reduced vessel area at all time points ( $\text{mm}^2$ :  $20 \pm 8$  vs.  $6 \pm 3$  d4;  $140 \pm 30$  vs.  $60 \pm 20$  d10;  $190 \pm 20$  vs.  $110 \pm 10$  d14), and decreased woven bone area ( $1.5 \pm 0.3$  vs.  $0.9 \pm 0.2 \text{ mm}^2$ ) and cartilage area ( $0.25 \pm 0.08$  vs.  $0.09 \pm 0.05 \text{ mm}^2$ ) at d14. Thus, MPLSM can be used to assess dynamic changes of angiogenesis and osteogenesis in murine long bones during fracture healing. In addition, PDGFR $\beta$  cells are required for efficient fracture healing, and their numbers are limited in older mice.

Disclosures: Hengwei Zhang, None.

## 1019

**Bone Marrow Mesenchymal Cells Deficient in TRAF3 Attract RANKL-expressing B Cells via CXCL12/CXCR4 Signaling to Contribute to Age-related Bone Loss.** Jinbo Li<sup>1</sup>, Zhenqiang Yao<sup>1</sup>, Lianping Xing<sup>1</sup>, Brendan Boyce<sup>1</sup>. URM, United States

Low-grade chronic inflammation of aging is associated with increased RANKL/NF- $\kappa$ B-mediated bone resorption and osteoporosis. To investigate the cellular sources of

RANKL in bone marrow (BM) and bone during aging, we flow-assayed BM and bone-digested cells (BDCs) from 3-month-old mice. We found that B cells comprised  $70 \pm 4\%$  of RANKL<sup>+</sup> cells in BM, with the absolute number of RANKL<sup>+</sup> B cells ( $33 \pm 15 \times 10^4$ ) being significantly higher than RANKL<sup>+</sup> CD4 T cells ( $2 \pm 1 \times 10^4$ ) and mesenchymal stromal cells (MSCs,  $0.4 \pm 0.1 \times 10^4$ ) in BM and osteoblasts (OBs,  $0.04 \pm 0.03 \times 10^4$ ) in BDCs. Most RANKL<sup>+</sup> B cells were B220<sup>high</sup> (86 $\pm$ 3%) and IgM<sup>+</sup> (90 $\pm$ 3%), with ~80% RANKL<sup>+</sup> B cells enriched in the CD19<sup>+</sup>B220<sup>high</sup>IgM<sup>+</sup> subpopulation, which was higher in BM from 18-month than from 3-month-old mice ( $49 \pm 17\%$  vs.  $25 \pm 9\%$ ). TNF receptor-associated factor 3 (TRAF3) negatively regulates NF- $\kappa$ B signaling and could limit RANKL-mediated bone resorption during aging. We found that TRAF3 protein levels in OB and OC lineage cells decrease in mouse bone with age. To investigate the role of TRAF3 in bone during aging, we generated mice with TRAF3 conditionally deleted in osteoclast (OC) lineage (using Lys-M Cre) and OB/mesenchymal (using Prx-1 Cre) cells. We found that both TRAF3 conditional knockout (cKO) mice developed early onset osteoporosis with increased bone resorption. Prx-1 cKO mice had increased RANKL expression in BM cells and significantly increased frequency of BM CD19<sup>+</sup>B220<sup>high</sup>IgM<sup>+</sup> B cells, a recirculating B subpopulation, which can be recruited to BM by CXCL12/CXCR4 signaling. *Cxcl12* mRNA levels in MSCs were increased 7-fold and CXCL12 protein levels were increased 16-fold in BM cells from aged mice, which also had a 2-fold increase in CXCL12<sup>+</sup> MSCs. Prx-1 cKO mice had ~30-fold higher *Cxcl12* mRNA levels in MSCs and significantly more CXCL12<sup>+</sup> cells in their tibial metaphyses than control mice. In line with these findings, the frequency of CXCR4<sup>+</sup> CD19<sup>+</sup>B220<sup>high</sup>IgM<sup>+</sup> B cells was significantly higher in BM from aged than young mice and from Prx-1 cKO than control mice. These data suggest that CD19<sup>+</sup>B220<sup>high</sup>IgM<sup>+</sup> B cells may be the predominant RANKL-expressing population in BM promoting OC formation during aging as TRAF3 levels fall, and that TRAF3 deletion in OB progenitors causes CXCR4<sup>+</sup>CD19<sup>+</sup>B220<sup>high</sup>IgM<sup>+</sup> B cell accumulation in BM via enhanced CXCL12/CXCR4 signaling. We propose that inhibition of TRAF3 degradation in MSCs and of CXCR4<sup>+</sup> CD19<sup>+</sup>B220<sup>high</sup>IgM<sup>+</sup> B cell recruitment to BM could prevent age-related osteoporosis.

Disclosures: Jinbo Li, None.

## 1020

**Serum Amyloid A3 (SAA3) Causes Age-Related Bone Loss.** Shilpa Choudhary<sup>1</sup>, Siu-Pok Yee<sup>2</sup>, Douglas Adams<sup>1</sup>, Renata Rydzik<sup>1</sup>, Joseph Lorenzo<sup>1</sup>, Carol Pilbeam<sup>1</sup>. <sup>1</sup>UConn Musculoskeletal Institute, UConn Health, United States, <sup>2</sup>Department of Cell Biology, UConn Health, United States

SAA is a family of apolipoproteins (SAA1-4) that respond acutely to inflammation in both humans and mice and whose function is unclear. SAA3 is the major inducible SAA in mice. We have shown that secretion of SAA3 can be induced by PTH in osteoclast lineage cells via RANKL in osteoblasts if cyclooxygenase (COX) 2-produced prostaglandins are present. The current study examined the impact of SAA3 on aging bone loss using young (4 mo) and old (18 mo) WT and SAA3 knockout (KO) CD-1 male mice. In young mice, *Saa3* mRNA was barely detectable in tibial bone, SAA3 protein was undetectable in serum, and no difference was seen in any measured parameter between WT and SAA3 KO mice. Absence of SAA3 was not compensated by increased *Saa1* or *Saa2* in young or old mice. In the old mice, *Saa3* mRNA was increased 300-fold in tibiae and SAA3 was elevated in serum. Femur and lumbar bone mineral density (BMD, DXA) was decreased (18-24%) in old WT mice but not in old KO mice. Femur trabecular bone volume fraction (BV/TV,  $\mu$ CT) was decreased 82% in old WT mice but only 56% in old KO mice, resulting in BV/TV being 2.4-fold greater in old SAA3 KO mice compared to WT mice. There was a trend for cortical area and thickness to decrease with age only in WT femurs. Aging of WT mice was associated with a 38% decrease in PINP, a serum marker of bone formation, and a 112% increase in CTX, a marker of bone resorption. In old mice, PINP was 34% greater in KO than in WT mice, and CTX was 29% lower in KO than in WT mice. Serum PTH was elevated similarly (1.8-fold) in old WT and KO mice. Gene expression associated with osteogenesis (*osteocalcin*, *Igf1* and *Wnt10b*) was reduced more with age in WT than in KO tibiae. *Sost* and *cFos* expression were unaffected by age or genotype. *Cox2* mRNA was elevated (3.4-fold) similarly in old WT and KO tibiae. The *Rankl/Opg* ratio increased with age and was 3.3-fold greater in old WT tibiae than in KO. Expression of senescence-related genes, *p16<sup>Ink4a</sup>* and *p21*, and pro-inflammatory cytokine genes, *Il1 $\beta$* , *Il6* and *Tnfa*, was markedly elevated in old WT compared to KO tibiae. In summary, SAA3 increased with age and promoted trabecular bone loss and expression of pro-inflammatory and cellular senescence genes. Preserved bone in aged SAA3 KO mice was associated with increased bone formation and decreased bone resorption markers. Promotion of age-related bone loss is novel for SAA3 and suggests SAA could be a target for new therapies to treat age and inflammation-related bone loss.



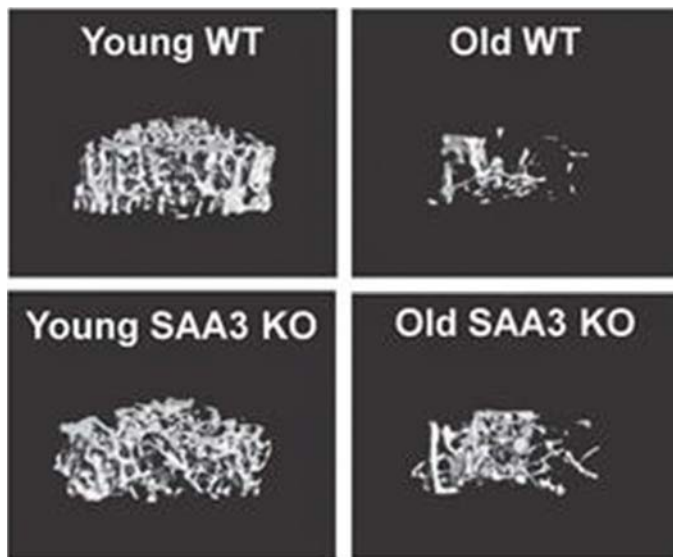


Figure 1

Disclosures: Shilpa Choudhary, None.

## 1021

**The NAD<sup>+</sup> Precursor Nicotinamide Riboside Reverses the Age-dependent Decline of NAD<sup>+</sup> and Osteoprogenitor Differentiation.** Ha-Neui Kim\*, Han Li, Srividhya Iyer, Aaron Warren, Stavros Manolagas, Maria Almeida. University of Arkansas for Medical Sciences and Central Arkansas Veterans Healthcare System, United States

The loss of bone mass with old age is due to a decrease in osteoblast number and bone formation and is associated with a decline in osteoprogenitor proliferation and number. The forkhead box O (FoxO) transcription factors attenuate Wnt signaling and the proliferation of osteoprogenitors, and thereby the supply of matrix synthesizing osteoblasts. The NAD<sup>+</sup> dependent Sirtuin1 (Sirt1) deacetylates FoxOs and inhibits their binding to  $\beta$ -catenin; and it also deacetylates  $\beta$ -catenin. Both of these mechanisms promotes osteoblastogenesis. However, the relevance of these interactions to skeletal aging has not been elucidated. Be that as it may, a decline in NAD<sup>+</sup> with age decreases Sirt1 activity and contributes to the dysfunction of several tissues. Here, we examined whether the NAD<sup>+</sup>/Sirt1/FoxO signaling pathway is altered in osteoblast progenitors from old mice. Cultured bone marrow stromal cells from 22 month-old mice exhibited decreased levels of NAD<sup>+</sup> as compared to cells from 6 month-old mice. Acetylation of FoxO1 was also increased in cells from old mice while the levels of Sirt1 (determined by Western Blot) were unaltered. The osteoblastogenic potential of the cell from the old mice was severely reduced after 21 days in culture, as determined by Alizarin Red staining. Addition 0.5 or 1 mM of the NAD<sup>+</sup> precursor nicotinamide riboside (NR) increased NAD<sup>+</sup> levels in cells from both young and old mice. NR also decreased the acetylation of both FoxO1 and  $\beta$ -catenin and increased the total levels  $\beta$ -catenin in cells from old mice. Consistent with these effects, NR increased the osteoblastogenic capacity of cells from old mice, but had no effect in cells from young mice. To determine the cause of the decreased NAD<sup>+</sup> levels with age in osteoprogenitors, we measure the expression of Nampt and CD38, two enzymes that are critical for NAD<sup>+</sup> generation and degradation, respectively. The mRNA levels of Nampt were unaffected by age in bone marrow stromal cells, but the levels of CD38 were increased. Moreover, the expression of Nampt increased 2-fold, while CD38 decreased 8-fold with osteoblast differentiation between 1 and 21 days of culture. Together, these findings suggest that the decrease in bone formation caused by old age may be accounted for by intrinsic defects in osteoblast progenitors that cause a decrease in NAD<sup>+</sup> and inhibition of Sirt1 activity. NAD<sup>+</sup> repletion with precursors such as NR may, therefore, represent a therapeutic approach to age-associated osteoporosis.

Disclosures: Ha-Neui Kim, None.

## 1022

**Maternal genotype has life-long effects on bone mass, shape and strength in *Dmp1Cre.Pthlh<sup>fl/fl</sup>* mice.** Niloufar Ansari<sup>1</sup>, Narelle McGregor<sup>1</sup>, Christopher S Kovacs<sup>2</sup>, Jonathan H Gooi<sup>3</sup>, T John Martin<sup>1</sup>, Natalie A Sims<sup>1</sup>. <sup>1</sup>St. Vincent's Institute of Medical Research, Australia, <sup>2</sup>Memorial University of Newfoundland, Canada, <sup>3</sup>The University of Melbourne, Australia

Local production of parathyroid hormone-related protein (PTHrP, gene name *Pthlh*) by osteoblasts and osteocytes is critical for normal bone formation. Although global *Pthlh* gene ablation is neonatal lethal, heterozygous *Pthlh* null mice and mice with conditional deletion of PTHrP in osteoblasts were both osteopenic by 12 and 6 weeks of age, respectively, due to a low level of bone formation. We have previously reported that *Dmp1Cre.Pthlh<sup>fl/fl</sup>* (*fl/fl*) mice with conditional deletion of PTHrP in late osteoblasts and osteocytes also exhibit low trabecular

bone mass and impaired bone formation, as well as reduced bone strength. That study was carried out on mice from heterozygous parents (*fl<sup>het</sup>*) to exclude any effect of parental genotype. Herein, we studied the influence of parental genotype on the skeleton.

When *Dmp1Cre.Pthlh<sup>fl/fl</sup>* mice were generated from homozygote parents (*fl<sup>hom</sup>*) and compared to cousin-bred *Dmp1Cre+* controls (*w/w*), they showed a phenotype opposite to the low bone mass observed in *fl<sup>het</sup>* mice. At 14, 16 and 26 weeks of age, *fl<sup>hom</sup>* mice had higher trabecular bone volume (~40% greater than control at all three time points,  $p < 0.01$ ) and greater trabecular number (~30% greater than control at all three time points,  $p < 0.01$ ) in femora and L5 vertebrae ( $n=9-10$ /group). They exhibited no change in cortical thickness or bone strength, but both male and female *fl<sup>hom</sup>* mice had significantly wider femora in both mediolateral and anteroposterior dimensions at all ages examined (~11% higher at 26 weeks of age).

Since maternal milk PTHrP levels have been reported to contribute to offspring bone mass, we extracted genomic DNA from tissues of adult female *fl/fl* and *w/w* mice, and found that *Pthlh* was excised not only in long bones and calvariae, but also in mammary glands of *fl/fl* mice. This indicates that the *Dmp1Cre* transgene directs Cre-mediated recombination in the mammary gland. To determine whether low PTHrP levels in maternal milk might lead to the greater bone width in *fl<sup>hom</sup>* offspring, we collected bones from 12 day-old suckling mice from both homozygous and heterozygous parents ( $n=6$ /group). At this age, *fl<sup>het</sup>* exhibited normal bone width, and as observed in adult mice, *fl<sup>hom</sup>* bone width was significantly greater.

These results indicate that maternal PTHrP controls trabecular bone mass, bone geometry and strength, not only of neonatal offspring, but also of adult *Dmp1Cre.Pthlh<sup>fl/fl</sup>* mice. We suggest this may result from a reduction in milk PTHrP levels.

Disclosures: Niloufar Ansari, None.

## 1023

**Palmitoleoylation of WNTs is a Major Determinant of Both Trabecular and Cortical Bone Mass in Mice.** Thomas Funck-Brentano\*<sup>1</sup>, Karin Nilsson<sup>1</sup>, Petra Henning<sup>1</sup>, Ulf Lerner<sup>1</sup>, Antti Koskela<sup>2</sup>, Juha Tuukkanen<sup>2</sup>, Robert Brommage<sup>1</sup>, Sofia Movérare-Skrtic<sup>1</sup>, Claes Ohlsson<sup>1</sup>. <sup>1</sup>Centre for Bone and Arthritis Research, Institute of Medicine, Sahlgrenska Academy, University of Gothenburg, Sweden, <sup>2</sup>Unit of Cancer Research and Translational Medicine, MRC Oulu and Department of Anatomy and Cell Biology, University of Oulu, Finland

Palmitoleoylation of WNTs by the enzyme Porcupine is essential for WNTs cell trafficking and signaling through the binding to Frizzled receptors. NOTUM is an extracellular WNT lipase, removing palmitoleic acid from WNTs and thereby abolishes its activity. We recently showed that *Notum<sup>-/-</sup>* mice have increased cortical bone thickness and that pharmacological inhibition of Notum increases cortical but not trabecular bone mass. The aim of this study was to evaluate the role of Porcupine-mediated palmitoleoylation of WNTs for trabecular and cortical bone mass. As *Porcn<sup>-/-</sup>* mice display embryonal lethality, we used Porcupine inhibitors (PORCN\_I) to determine the role of Porcupine for bone mass in adult mice.

Twelve-week-old female mice were treated for three weeks by oral gavage with two different PORCN\_I (LGK974 at 3 [LGK\_Lo] or 6 mg/kg [LGK\_Hi] or C59 at 10 mg/kg, Selleckchem), a NOTUM inhibitor (30 mg/kg, Lexicon) or vehicle ( $n=10$  per group). All treatments were well tolerated. DXA analyses revealed that total body BMD was dose-dependently decreased by PORCN\_I while it was increased by NOTUM inhibition. Cortical thickness at the femurs diaphysis measured by  $\mu$ CT was also dose-dependently decreased by PORCN\_I (LGK\_Lo:  $-16.5 \pm 1.8\%$ ; LGK\_Hi:  $-19.6 \pm 0.9\%$ ; C59:  $-8.9 \pm 1.1\%$ ,  $p < 0.001$ ) and increased by NOTUM inhibition ( $+12.5 \pm 1.9\%$ ,  $p < 0.001$ ). Vertebral trabecular bone volume fraction was substantially decreased by PORCN\_I (LGK\_Lo:  $-29.5 \pm 3.9\%$ ; LGK\_Hi:  $-37.8 \pm 3.7\%$ ; C59:  $-18.3 \pm 2.3\%$ ,  $p < 0.001$ ) but unchanged by NOTUM inhibition.

Three point bending of the tibia demonstrated that maximum load at failure was reduced by PORCN\_I, in line with cortical thickness changes. Mechanistic studies revealed that Porcupine inhibition substantially increased bone resorption (LGK\_Hi vs vehicle, serum CTX  $+39.8 \pm 11.0\%$ ,  $p < 0.01$ ) and slightly reduced bone formation (serum PINP  $-23.3 \pm 6.7\%$ ,  $p < 0.05$ ). An increased bone resorption was supported by increased *Cathepsin K* mRNA levels ( $+84.8 \pm 11.3\%$ ,  $p < 0.001$ ) and *Rankl/Opg* ratio ( $+54.3 \pm 18.9\%$ ,  $p < 0.05$ ) in cortical bone.

In conclusion, palmitoleoylation of WNTs by Porcupine is a major determinant of both trabecular and cortical bone mass. As NOTUM regulates cortical but not trabecular bone mass, we propose that depalmitoleoylation by NOTUM mainly occurs in cortical bone. In addition, our findings suggest that Porcupine inhibitors, under development for cancer treatment, may have deleterious skeletal side-effects.

Disclosures: Thomas Funck-Brentano, None.

## 1024

**Loss of TIEG expression results in defective skeletal muscle structure and function with associated impairment of mitochondrial biogenesis.** Malek Kammoun\*<sup>1</sup>, Vladimir Veksler<sup>2</sup>, Jerome Piquereau<sup>2</sup>, Gisele Bonne<sup>3</sup>, Isabelle Nelson<sup>3</sup>, Philippe Pouletaut<sup>1</sup>, Molly Nelson Holte<sup>4</sup>, Malayannan Subramaniam<sup>4</sup>, Sabine Bensamoun<sup>1</sup>, John Hawse<sup>4</sup>. <sup>1</sup>Université de Technologie de Compiègne, France, <sup>2</sup>University of Paris-Sud, France, <sup>3</sup>UPMC University Paris, France, <sup>4</sup>Mayo Clinic, United States

TGF $\beta$  inducible early gene-1 (TIEG), also known as KLF10, is a member of the Krüppel-like family of transcription factors that regulates gene expression in multiple

cell and tissue types. Loss of TIEG expression in mice is known to alter osteoblast, osteoclast and osteocyte function and result in a low bone mass phenotype in female animals. Furthermore, altered expression of TIEG, as well as polymorphisms in the TIEG gene, are associated with osteoporosis in humans. Although TIEG is most well-known for its roles in modulating bone homeostasis, this transcription factor is also highly expressed in skeletal muscle tissue. In light of emerging data demonstrating that cross-talk between muscle and bone is critical for normal function of both tissues, we sought to comprehensively characterize the impact of TIEG deletion on skeletal muscle. Loss of TIEG expression resulted in hyperplasia and hypertrophy of both slow and fast twitch muscle fibers. Histochemical analyses demonstrated a lack of succinate dehydrogenase activity, and decreased COX and menadione staining, in TIEG KO soleus muscle. These phenomena were also observed, but to a lesser degree, in TIEG KO EDL muscle. Transmission electron microscopy revealed that deletion of TIEG results in muscle disorganization, smaller sarcomeres and absence of I bands. Furthermore, decreased mitochondrial numbers and changes in mitochondrial shape were also identified in TIEG KO mice suggesting impaired mitochondrial biogenesis. Indeed, complex I, COX and citrate synthase activities were significantly lower in TIEG KO soleus muscle while only complex I was lower in TIEG KO EDL muscle. Interestingly, when TIEG KO mice were subjected to treadmill exercise, they tired more quickly than WT controls confirming an essential role for TIEG in skeletal muscle biology. These characteristics resemble human diseases associated with exercise intolerance. Therefore, TIEG KO mice are an ideal model system to study the cellular and molecular mechanisms controlling mitochondrial function and muscle metabolism which pertains to multiple muscle related diseases and disorders. These findings, in combination with past studies on the skeleton, implicate TIEG as a critical mediator of cross-talk between muscle and bone.

**Disclosures:** Malek Kammoun, None.

## 1025

**The Calcium-Sensing Receptor, a Class C GPCR, Spatially-Directs G-protein Selectivity via Endosomal Signaling.** Caroline Gorvin<sup>1</sup>, Angela Rogers<sup>1</sup>, Benoit Hastoy<sup>1</sup>, Andrei Tarasov<sup>1</sup>, Morten Frost<sup>1</sup>, Asuka Inoue<sup>2</sup>, Michael Whyte<sup>3</sup>, Patrik Rorsman<sup>1</sup>, Aylin Hanyaloglu<sup>4</sup>, Gerda Breitwieser<sup>5</sup>, Rajesh Thakker<sup>1</sup>. <sup>1</sup>University of Oxford, United Kingdom, <sup>2</sup>Tohoku University, Japan, <sup>3</sup>Shriners Hospital for Children, United States, <sup>4</sup>Imperial College London, United Kingdom, <sup>5</sup>Geisinger Center, United States

The calcium-sensing receptor (CaSR) is a class C G-protein coupled receptor (GPCR) that utilizes  $G_{\alpha_{q/11}}$ ,  $G_{\alpha_{i/o}}$  and  $G_{\alpha_{12/13}}$  to mediate multiple signaling effects including activation of intracellular calcium ( $Ca^{2+}$ ) release and mitogen-activated protein kinase (MAPK) pathways, membrane ruffling, and inhibition of cAMP production. Loss-of-function mutations of CaSR and  $G_{\alpha_{11}}$  cause familial hypocalcemic hypercalcaemia (FHH) types 1 and 2, respectively, while mutations in the adaptor protein-2  $\sigma$ -subunit (AP2 $\sigma$ ), that is critical for clathrin-mediated endocytosis, cause FHH3. The AP2 $\sigma$  mutations, which all affect the Arg15 residue, decrease CaSR-mediated  $Ca^{2+}$  release despite increased CaSR cell surface expression. To explain this paradox, we hypothesized that endosomal sustained signaling may contribute to CaSR-dependent G-protein pathways, and that AP2 $\sigma$  mutations disrupt CaSR internalization, leading to reduced availability of CaSR at endosomes. Using HEK293 cells stably expressing AP2 $\sigma$ -WT or the 3 FHH3-associated AP2 $\sigma$ -mutants, and Epstein-Barr virus transformed lymphoblastoids from FHH3 patients with an Arg15Cys mutation, we demonstrated that AP2 $\sigma$  mutations impair  $Ca^{2+}$  release, reduce MAPK signaling and membrane ruffling, and impair cAMP responses. Total internal reflection fluorescence microscopy showed these AP2 $\sigma$  mutations reduce CaSR internalisation by prolonging CaSR residency time at clathrin-coated pits and/or vesicles. Furthermore, studies in CRISPR-Cas generated  $G_{\alpha_{q/11}}$ -depleted HEK293 cells revealed that CaSR insertion at plasma membranes, and its internalization, rely on a signal from the  $G_{\alpha_{q/11}}$  pathway. The dynamin-inhibitor dyngo and a dominant-negative mutant of Rab5, which is required for early endosome maturation, were used to test luciferase reporter responses of the MAPK target serum-response element (SRE) in HEK293 cells stably expressing CaSR, to investigate the hypothesis that the CaSR signal may be enhanced by receptor internalization, which would mediate sustained signaling. SRE reporter activity was found to be sustained and this response required intact internalization and was derived from an endosomal source. Furthermore, the sustained signal was shown to be mediated by  $G_{\alpha_{q/11}}$  signaling, and impaired by AP2 $\sigma$ -Arg15 mutants. Our studies demonstrate that FHH3-associated AP2 $\sigma$  mutations impair CaSR internalization, thereby reducing endosomal sustained signaling, and thus are associated with loss-of-function by multiple CaSR signaling pathways.

**Disclosures:** Caroline Gorvin, None.

## 1026

**Extracellular vesicles (EVs) are biological and therapeutic tools in osteoblast communication.** Alfredo Cappariello<sup>1</sup>, Alexander Loftus<sup>1</sup>, Argia Ucci<sup>1</sup>, Maurizio Muraca<sup>2</sup>, Nadia Ricci<sup>1</sup>, Anna Teti<sup>1</sup>. <sup>1</sup>University of L'Aquila, Italy, <sup>2</sup>University of Padova, Italy

A new mechanism of intercellular communication is represented by EVs, complex phospholipid bilayer bordered structures sized 50-1000 nm. EVs shuttle bioactive molecules to target cells, including mRNAs, miRNAs and proteins, and are involved in physiologic and pathologic processes. To investigate the EV-shuttled communication between bone cells, we isolated EVs from primary mouse osteoblast conditioned media

( $3.03 \pm 0.79$  mg), increasing their yield by  $10^{-8}$  M rhPTH(1-34) ( $4.05 \pm 1.19$  mg,  $p=0.0405$ ). By FACS we sorted  $16.67 \pm 1.93\%$  events showing intact membrane and canonical EV size and ultrastructure. Osteoblast EVs shuttled exogenous fluorescent probes to naïve osteoblasts, monocytes and endothelial cells.  $97.1 \pm 0.26\%$  EVs contained RNAs transferred to target osteoblasts. Their mRNA cargo displayed an osteoblast-like signature, including *colla1*, *colla2* and *sparc* transcripts.  $53.95 \pm 3.48\%$  EVs carried RANKL, with their rate increasing to  $63.6 \pm 4.20\%$  after PTH treatment ( $p=0.037$ ). *In vitro*, EVs increased osteoclast size (fold: 1.2 more nuclei,  $p=0.027$ ; 2.2 wider area,  $p<0.05$ ) and prolonged their lifespan in a RANKL-dependent manner, while *rankl*<sup>-/-</sup> EVs failed to sustain osteoclast survival (10.35fold,  $p=0.0047$ ). EVs loaded with zoledronate and dasatinib shuttled the drugs to osteoclasts, inducing cell death as efficiently as the free drugs. EVs targeted *ex vivo* mouse calvaria incubated with CMFDA-loaded EVs, showing a vesicular pattern of fluorochrome integration in bone cells. *In vivo*, we injected i.p. 30000 FACS-sorted RANKL-positive EVs in 5 day-old CD1 pups and observed a fast uptake of EV-shuttled fluorochrome in bone, peaking at 1.5 hours from injection and declining thereafter to a lower plateau in 24 hours. To investigate the impact of RANKL-positive EVs on osteoclastogenesis, we injected 4 day-old *rankl*<sup>-/-</sup> mice i.p. with 30000-120000 RANKL-positive EVs/mouse, every other day for 5 times. Tibia sections revealed TRAcP-positive cells in EV-treated *rankl*<sup>-/-</sup> mice, which were instead totally absent in vehicle-treated mice. TRAcP-positive areas steadily increased with escalating EV densities (PBS: ND; 30000EVs,  $398.92 \pm 54.97 \mu m^2$ ; 60000EVs,  $810.17 \pm 169 \mu m^2$ ; 120000EVs,  $2403.91 \pm 932.30 \mu m^2$ ,  $p<0.05$ ), indicating EV density-dependent osteoclastogenic potential. Our data demonstrate that EVs are physiologically involved in inter-cellular communication between bone cells, contribute to the pro-osteoclastic effect of RANKL and represent a potential means for targeted therapeutic delivery.

**Disclosures:** Alfredo Cappariello, None.

## 1027

**The Senolytic ABT263 Eliminates Senescent Osteoprogenitors in Old Mice.** Ha-Neui Kim<sup>1</sup>, Srividhya Iyer<sup>1</sup>, Jianhui Chang<sup>2</sup>, Li Han<sup>1</sup>, Aaron Warren<sup>1</sup>, Stavros Manolagas<sup>1</sup>, Robert Jilka<sup>1</sup>, Charles O'Brien<sup>1</sup>, Daohong Zhou<sup>2</sup>, Maria Almeida<sup>1</sup>. <sup>1</sup>University of Arkansas for Medical Sciences and Central Arkansas Veterans Healthcare System, United States, <sup>2</sup>University of Arkansas for Medical Sciences, United States

The accumulation of senescent cells causes age-related diseases and curtails longevity. Osteoprogenitors decline with age in mice and exhibit several markers of cellular senescence including cell cycle arrest and expression of the senescence associated secretory phenotype (SASP). These changes are associated with activation of p53 and increased levels of the cell cycle inhibitor p21, the transcription factor GATA4 and stimulation of NF- $\kappa$ B, which are markers of senescence. In human IMR-90 fibroblasts, GATA4 increases IL-1 $\alpha$  which in turn stimulates NF- $\kappa$ B and the SASP. Moreover, GATA4 functions independently of p16 and p53 to promote cell senescence. On the other hand, removal of senescent cells with the senolytic drug ABT263 rejuvenates the aged hematopoietic and muscle stem cells in aged mice. However, the role of GATA4 or the effects of ABT263 in senescent osteoprogenitors remain unknown. To directly assess the effects of GATA4 in osteoprogenitors, we inserted a plasmid expressing GATA4 into a retroviral vector and infected newborn calvaria cells or bone marrow-derived primary stromal cells obtained from 3-month-old C57BL/6J mice. Overexpression of GATA4 increased the expression of p21 and decreased proliferation, as determined by BrdU incorporation, and abrogated osteoblastogenesis. GATA4 also caused an 80-fold increase in IL-1 $\alpha$  and other elements of the SASP including RANKL and MMP13. To test whether ABT263 eliminates senescent osteoprogenitors in vivo, we administered 40 mg/kg body weight ABT263 (or vehicle) by daily i.p. injections for 5 days to 24-month-old female mice. Bone marrow stromal cells from the femurs were cultured in the presence of osteogenic medium for 10 days to collect mRNA and for 21 days to assess their osteoblastogenic capacity. Cells from mice treated with ABT263 had decreased transcript levels of TNF- $\alpha$ , IL-1 $\alpha$ , and RANKL compared to cells from mice treated with vehicle. In addition, ABT263 improved the osteoblastogenic capacity of the cultures, as determined by alizarin red staining. Together, our findings indicate that an increase in GATA4 in osteoprogenitors of old mice contributes to cell senescence, and expression of the SASP. Removal of such senescent cells with senolytic agents like ABT263 may represent a novel therapeutic approach to involutional osteoporosis.

**Disclosures:** Ha-Neui Kim, None.

## 1028

**Characterization of long- and short-range compositional and mechanical bone tissue heterogeneity in patients with atypical femoral fractures.** Ashley Lloyd<sup>1</sup>, Emma Luengo<sup>1</sup>, Carmen Ngai<sup>1</sup>, Amy Cao<sup>1</sup>, Joseph Lane<sup>2</sup>, Eve Donnelly<sup>1</sup>. <sup>1</sup>Cornell University, United States, <sup>2</sup>Hospital for Special Surgery, United States

Heterogeneity of bone tissue properties is an important indicator of altered bone quality. However, the effect of heterogeneity on fracture resistance is controversial, as studies have shown opposite trends: increased nanomechanical heterogeneity is an intrinsic toughening mechanism, but can also act as a stress riser. Thus, the objective of this study is to examine bone tissue from women with differing histories of long-term bisphosphonate (BP) treatment and atypical femoral fractures (AFFs) to differentiate the competing effects of bone tissue heterogeneity on whole-bone fracture resistance.



Biopsies of proximal femoral bone were obtained during fracture repair or total hip arthroplasty from postmenopausal women with and without history of long-term BP treatment, and with or without history of typical and atypical femoral fracture (+BP Atyp n=12; +BP Typ n=10; -BP Typ n=11; +BP Nonfx n=5; -BP Nonfx n=12). Bone composition was assessed with Fourier transform infrared imaging (FTIRI) and Raman imaging. Nanomechanics were assessed with nanoindentation. Spatial maps of each property were used to measure long- and short-range heterogeneity through the full width at half maximum (FWHM) of the distribution, and the initial slope of the variogram.

Cortical bone from patients with AFFs had narrower distributions of hardness compared to that from BP-naïve non-fracture patients (-31%,  $p=0.02$ ). Similarly, in Raman imaging, cortical bone from patients with AFFs had narrower distributions of crystallinity compared to that from BP-naïve non-fracture patients (-34%,  $p=0.03$ ). Conversely, in FTIRI, cortical bone from patients with AFFs had a wider distribution of collagen maturity compared to that from patients with typical fractures (+112%,  $p=0.01$ ). However, FTIRI variogram analysis revealed that cortical bone from patients with atypical fractures had less short-range heterogeneity of crystallinity (+122% vs. +BP Typ,  $p=0.03$ ) and collagen maturity (+19% vs. -BP Nonfx,  $p=0.04$ ).

At small length-scales (measured with Raman, nanoindentation, and variograms of FTIRI) tissue from patients with AFFs had decreased heterogeneity. At larger length-scales (measured through FWHM of FTIRI) the heterogeneity increased. These results are consistent with the hypothesis that while microscale heterogeneity toughens bone, larger-scale heterogeneity could be detrimental as a stress riser, leading to different optimal levels of heterogeneity for fracture resistance at differing length scales.

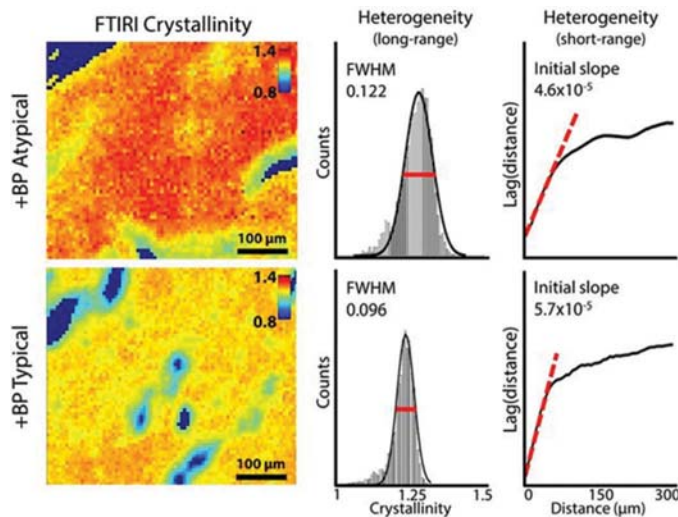


**Fig. 1:** FTIRI crystallinity in two women with history of BP-treatment, with atypical femoral fracture (+BP Atypical) or typical fragility fracture (+BP Typical). While the atypical fracture patient has greater long-range heterogeneity, the short-range heterogeneity is reduced

Figure 1: Long- and short-range heterogeneity of FTIRI crystallinity

**Disclosures:** Ashley Lloyd, None.

## 1029

**Life-long genetic Pyk2 deletion or short-term pharmacologic inhibition of Pyk2 prevents the increase in resorption by glucocorticoids and preserves bone mass and strength by promoting osteoclast apoptosis.** Amy Y. Sato\*, Meloney Gregor, Kevin McAndrews, Keith W. Condon, Lilian I. Plotkin, Teresita Bellido. Indiana University School of Medicine, United States

Mice lacking Pyk2, a kinase of osteoclast podosomes, are protected from resorption and bone loss induced by glucocorticoids (GC). However, the mechanism by which Pyk2 deficiency overrides GC-induced resorption and whether pharmacologic inhibition of Pyk2 also blocks GC effects is unknown. We addressed these questions using skeletally mature mice (4 mo) with global deletion of Pyk2 (KO) or WT mice treated with PF-431396 (PF), a Pyk2 kinase inhibitor. KO and WT littermates were implanted with pellets of 2.1 mg/kg/d prednisolone or placebo for 4wks; and WT mice were injected with PF (10mg/kg, 5x/wk) or vehicle for 2wks, starting 3d before pellet implantation. GC increased osteoclast number and circulating TRAP5b in both WT and KO mice; and increased osteoclast surface and circulating CTX in WT but not in KO mice. Osteoclasts in GC-treated WT mice were fully attached to bone surfaces whereas in KO mice were only partially attached, explaining the mismatch between osteoclast number vs surface; and KO mice exhibited a 3.2-fold increase in osteoclasts in the marrow. Further, the CTX/TRAP5b ratio was reduced in KO mice 0.6-fold vs WT indicating impaired activity of individual osteoclasts and explaining the mismatch between circulating TRAP5b vs CTX levels. In addition, osteoclasts on bone or in the marrow in KO mice exhibited 5- or 62-fold increase in apoptosis, respectively, vs WT. Also, osteoclasts generated *in vitro* from KO-derived marrow precursors exhibited 11-fold increased apoptosis vs WT; and GC partially reduced osteoclast apoptosis induced by alendronate in WT but not in KO cultures. These findings demonstrate that Pyk2 deficiency triggers

cell autonomous apoptotic effects and negates survival GC actions in osteoclasts. Moreover, the PF inhibitor prevented GC-induced increase in osteoclast surface and CTX, but not in TRAP5b. PF also increased marrow osteoclasts by 2-fold and marrow apoptotic osteoclasts by 2.4-fold in both placebo and GC-treated mice. Further, KO mice were protected from GC-induced decreased vertebral BV/TV, TbTh, and mechanical properties (ultimate force and toughness). PF also prevented GC-induced reductions in distal femur TbTh, and midshaft BA/TA and CtTh. These findings reveal that life-long genetic Pyk2 deletion or short-term pharmacologic inhibition of Pyk2 promotes osteoclast apoptosis and detachment from bone surfaces, thus prevailing over the increase in osteoclasts and protecting from bone loss and fragility induced by GC.

**Disclosures:** Amy Y. Sato, None.

## 1030

**Bone-Targeted Pharmacological Inhibition of Notch Signaling Decreases Resorption and Induces Bone Gain in Skeletally Mature Mice.** Jesus Delgado-Calle\*, Matthew E. Olson<sup>1</sup>, Jessica H. Nelson<sup>1</sup>, Emily G. Atkinson<sup>1</sup>, Kevin McAndrews<sup>1</sup>, Lifeng Xiao<sup>2</sup>, Frank H. Ebetino<sup>2</sup>, Robert K. Boeckman Jr<sup>2</sup>, G. David Roodman<sup>3</sup>, Teresita Bellido<sup>1</sup>. <sup>1</sup>Anatomy and Cell Biology, Indiana University School of Medicine, United States, <sup>2</sup>Department of Chemistry, University of Rochester, United States, <sup>3</sup>Department of Medicine, Indiana University School of Medicine, United States

Notch signaling plays a critical role in cell-to-cell communication among bone and bone marrow cells under physiological conditions and it favors growth and survival of cancer cells in bone. However, genetic manipulation of this pathway results in different bone phenotypes depending on the Notch component (ligands, receptors, target genes), the cell lineage, or differentiation stage being targeted; and the skeletal phenotypes result from combined developmental and postnatal effects. To dissect the effect of global inhibition of Notch signaling in the mature skeleton, we synthesized a Notch inhibitor by linking the  $\gamma$ -secretase inhibitor GSI-XII to an inactive bone-targeting molecule (BT). BT-GSI-II was thus designed to direct the conjugate to bone where the linker is cleaved near osteoclasts, thus releasing GSI. *In vitro*, the control unconjugated GSI decreased Notch target gene expression (Hes1) but BT-GSI had no effect. However, when both GSI and BT-GSI were preincubated at low pH to mimic the acidic conditions in resorption sites, equal inhibition of Notch target gene expression was observed. *Ex vivo*, both GSI and BT-GSI (non-preincubated) similarly decreased Hes1/5 expression in whole bone organ cultures that reproduce conditions in the bone microenvironment. We next administered for 2wks BT-GSI (5µg/g, 3xwk) or vehicle (DMSO) to 4-month old female mice. Mice treated with BT-GSI exhibited decreased Hes7 expression in bone, but not in brain or gut, compared to vehicle-treated mice. Further, BT-GSI did not increase the expression in the gut of Apsidin, a biomarker of gastrointestinal toxicity. BT-GSI-treated mice exhibited higher total (3%), femoral (4%), and spinal (7%) BMD compared to control mice. Moreover, BT-GSI decreased serum CTX by 40% and upregulated Opg mRNA expression in bone, thus decreasing the Rankl/Opg ratio. In contrast, serum PINP, the expression of osteoblast markers, Wnt target genes, or Sost remained unchanged by BT-GSI. These findings demonstrate that short-term pharmacological inhibition of Notch signaling in skeletally mature mice inhibits bone resorption and favors bone gain. Because BT-GSI shows bone specific Notch inhibition and lack of gut toxicity, it should circumvent the deleterious side effects that limit the use of this class of inhibitors in patients. Thus, BT-GSI is a promising approach to treat skeletal diseases characterized by bone loss, including those caused by cancer in bone.

**Disclosures:** Jesus Delgado-Calle, None.

## 1031

**Circulating MiR-338 and MiR-3065 as Novel Diagnosis and Treatment Markers for Postmenopausal Osteoporosis by Attenuating Estrogen-dependent Runx2 and Sox4 Regulation on Osteoblast Differentiation.** Chujiao Lin\*, Huan Liu, Zhi Chen. State Key Laboratory Breeding Base of Basic Science of Stomatology (Hubei-MOST) and Key Laboratory for Oral Biomedicine of Ministry of Education (KLOBM), School and Hospital of Stomatology, Wuhan University, China

**PURPOSE:** Osteoporosis is a major public health threat for the large population around the world, especially in postmenopausal women, greatly increasing the risk of bone fracture. However, more biomarkers for early diagnosis and treatment have not been intensively investigated. The "druggable" microRNAs (miRNAs) especially the mature miRNAs have been reported to be stably detectable in serum functioning as potent biomarkers in many diseases including osteoporosis. In the current study, we are trying to evaluate the role of circulating miR-338-3p and miR-3065-5p, locating in the opposite DNA strand, in patients with postmenopausal osteoporosis and investigate their diagnostic and prognostic value. **METHODS:** qPCR was performed to evaluate serum miR-338-3p and miR-3065-5p levels in mice and human. Using gain- and loss-of-function experiments to confirm the effect of miR-338-3p and miR-3065-5p on osteogenic differentiation of BMSCs. Also, miR-338-3p and miR-3065-5p inhibitor was injected into the mice by tail vein to investigate the therapeutic effects of inhibition of circulating miR-338 cluster on postmenopausal osteoporosis. Wild type and miR-338-knockout MC3T3 *in vitro* co-culture system was employed to elucidate one possible function of secretory miR-338 and miR-3065 on osteoblast differentiation. In the end,

RNA-seq, ChIP-qPCR and luciferase reporter assay were employed to investigate the up- and downstream factors of *miR-338-3p* and *miR-3065-5p* during osteoblast differentiation. RESULTS: We observed that *miR-338-3p* and *miR-3065-5p* decreased significantly during osteoblast differentiation *in vitro*, and overexpression of these two miRNAs inhibited osteoblast differentiation. Similarly, in postmenopausal osteoporosis patients and mice models both serum *miR-338-3p* and *miR-3065-5p* were highly enriched compared with healthy controls ( $P < 0.001$ ). Conversely, silencing these miRNAs in ovariectomized (OVX) mice ceased osteoporosis progression with more bone formation and bone mass comparing with untreated OVX mice, though less than those in sham mice. Co-culture experiments showed osteoblast maker genes were down-regulated when *miR-338* cluster knockout cell line was induced by the medium of wild type MC3T3 cell line. RNA-seq showed both *miR-338-3p* and *miR-3065-5p* can target and deactivate the positive-effectors on osteoblast differentiation, including *Runx2* and *Sox4*. Moreover, ChIP-qPCR and epistasis assay revealed that estrogen-dependent *Runx2* and *Sox4* can directly inhibit the expression of both miRNAs. CONCLUSIONS: The present study shows secretory *miR-338-3p* and *miR-3065-5p* serve as novel potential diagnostic and treatment markers. Mechanistically, we elucidate a novel positive-feedback loop with *Runx2*, *Sox4*, *miR-338* and *miR-3065* maintaining the physiological status of osteoblast, under the regulation of estrogen.

Disclosures: Chujiao Lin, None.

## 1032

**Teriparatide treatment decreases cortical bone material strength index (BMSi) assessed by impact microindentation in postmenopausal women.** Joy Tsai<sup>1</sup>, Linda Jiang<sup>1</sup>, Mary Bouxsein<sup>2</sup>, Benjamin Leder<sup>1</sup>. <sup>1</sup>Massachusetts General Hospital, United States, <sup>2</sup>Beth Israel Deaconess Medical Center, United States

**Background:** Bone strength is determined by bone mass, microarchitecture and intrinsic tissue material properties. Impact microindentation is an *in vivo* minimally invasive technique developed to assess the tissue-level properties of cortical bone at the mid-tibia. In the lead-in phase of an ongoing RCT, we assessed the short-term effects of two different doses of teriparatide on cortical bone properties of the tibia by impact microindentation.

**Methods:** 62 osteoporotic postmenopausal women ages 52-83 were assigned to receive 3 months of 20-mcg or 40-mcg of daily teriparatide (TPTD20 and TPTD40). Subjects were excluded if they had ever used IV bisphosphonates (BPs) or oral BPs in the past 6 months. The change in the bone material strength index (BMSi) was assessed at the mid-tibia by impact microindentation (Osteoprobe, ActiveLife Scientific) at 0- and 3-months.

**Results:** 33 and 29 women were randomized to the teriparatide 20-mcg and 40-mcg groups, respectively. Three subjects in TPTD20 and 4 subjects in TPTD40 groups did not undergo a 2nd micro-indentation procedure. Baseline clinical characteristics, including BMD at the hip and spine, were similar in the 2 treatment groups. Baseline BMSi was also similar in the two groups ( $82.1 \pm 8.3$  in TPTD20,  $83.2 \pm 10.1$  in TPTD40;  $P=0.661$ ). After 3 months of daily TPTD, BMSi decreased by  $-4.8 \pm 10.7\%$  in TPTD20 ( $P=0.011$  versus baseline) and by  $-7.0 \pm 15.5\%$  TPTD40 ( $P=0.011$  versus baseline), with no significant between group differences ( $P=0.552$ ) (Fig 1). When the full cohort is assessed irrespective of dose assignment, BMSi decreased by  $-5.8 \pm 13.0\%$  ( $P<0.001$ ). All subjects tolerated the microindentation procedure well and there were no complications related to the procedure.

**Conclusions:** Three-months of teriparatide administration significantly decreases cortical bone properties of the tibia, as assessed by impact microindentation. Notably, the variability in measurements may have limited our ability to detect a dose response relationship. Although the determinants of BMSi are incompletely understood, the observed reduction in BMSi may reflect teriparatide-induced stimulation of periosteal bone formation that is not fully mineralized. Moreover, these changes are consistent with the early effects of teriparatide on BMD at peripheral sites comprised of predominantly cortical bone. The assessment of BMSi after longer-term therapy is needed to better evaluate the effects of teriparatide on BMSi in a clinical context.

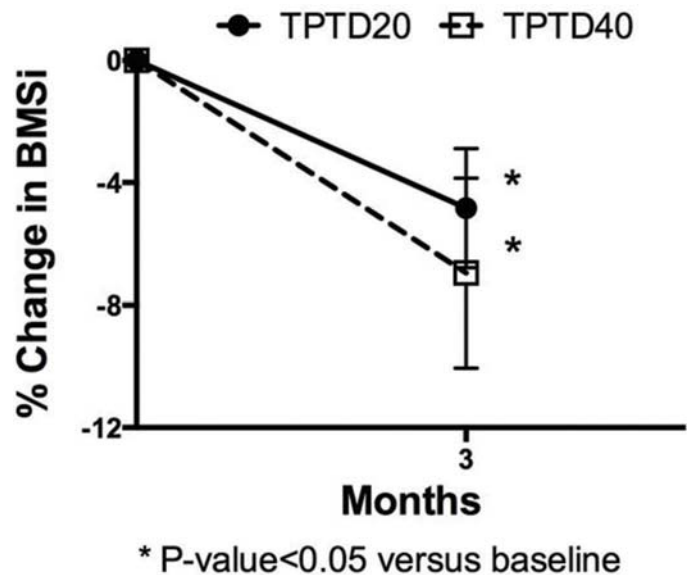


Figure 1: Mean (SEM) percent change in BMSi from baseline. \*P-value<0.05 versus baseline.

Disclosures: Joy Tsai, None.

## 1033

**Denosumab Treatment in Women with Osteoporosis Rapidly Prevents Deterioration in Trabecular Microstructure at the Distal Tibia.** Bin Zhou<sup>1</sup>, Ji Wang<sup>1</sup>, Ego Seeman<sup>2</sup>, Arkadi Chines<sup>3</sup>, Yifei Shi<sup>3</sup>, Andrea T Wang<sup>3</sup>, X Edward Guo<sup>1</sup>. <sup>1</sup>Bone Bioengineering Laboratory, Department of Biomedical Engineering, Columbia University, United States, <sup>2</sup>Austin Health, University of Melbourne, Australia, <sup>3</sup>Amgen Inc., United States

**Purpose:** Trabecular bone strength is determined by its plate and rod microstructure. Age- and menopause-related microstructural deterioration occurs because of unbalanced and rapid remodeling on the surfaces of plates and rods. The resulting thinning, perforation, and loss of connectivity compromise bone strength out of proportion to the bone loss producing this deterioration (Burr *JBRM* 1997). Denosumab (Dnab) treatment rapidly reduces bone remodeling and resorptive activity of osteoclasts at the time of administration. Individual Trabecula Segmentation (ITS) distinguishes individual trabeculae and quantitates plate and rod microstructure (eg, volume, number, thickness; Liu *JBRM* 2008). Here, we quantify the effect of Dnab treatment on trabecular plate-rod microstructure using ITS analyses and whole bone stiffness using finite element (FE) analyses.

**Methods:** This post-hoc analysis assessed postmenopausal women with low bone mass randomized to placebo (PBO) or Dnab 60 mg Q6M from a phase 2 study. Subjects were required to have lumbar spine or total hip BMD T-score between -2.0 and -3.0 at baseline. We quantified the effect of treatment on microstructure and whole bone stiffness using ITS and FE analyses at baseline and 12 months. Individual ITS and FE parameters at the distal tibia were expressed as a percent change from baseline (LS mean with 95% CI) at month 12 using an ANCOVA model adjusting for age, BV/TV, and baseline parameter value.

**Results:** This analysis included 164 subjects (82 PBO, 82 Dnab). Baseline characteristics were similar between groups: mean (SD) age 61 (6) years, BMI 27.1 (4.7) kg/m<sup>2</sup>, years since menopause 13 (7), and BMD T-scores -2.4 (0.4) at the lumbar spine and -1.2 (0.7) at the total hip. At the distal tibia, Dnab treatment prevented deterioration in or improved all microstructural parameters compared with PBO (Table). Dnab treatment increased plate number and thickness compared with baseline and prevented the increase in rod number and thinning seen in the PBO group. Plate to rod ratio, a marker of microstructural integrity, decreased significantly in the PBO group compared with baseline and was preserved in the Dnab group. Trabecular stiffness also increased in the Dnab group relative to PBO.

**Conclusions:** In postmenopausal women with low BMD, Dnab treatment prevents the rapid deterioration of trabecular microstructure at the distal tibia, resulting in preservation of bone strength.



Table. Percent Change in ITS and FE Parameters at the Distal Tibia From Baseline to Month 12

Parameter	% Change From Baseline <sup>a</sup>		Difference From Placebo <sup>a</sup>	
	LS Mean	95% CI	LS Mean	95% CI
pBV/TV				
Placebo (N = 68)	-1.4	(-3.4, 0.5)		
Denosumab 60 mg Q6M (N = 71)	3.4*	(1.5, 5.3)	4.9*	(2.1, 7.6)
rBV/TV				
Placebo (N = 68)	5.4*	(2.8, 7.9)		
Denosumab 60 mg Q6M (N = 71)	1.5	(-1.0, 3.9)	-3.9*	(-7.4, -0.3)
Trabecular stiffness				
Placebo (N = 68)	-1.7	(-4.1, 0.8)		
Denosumab 60 mg Q6M (N = 71)	2.3	(-0.1, 4.8)	4.0*	(0.5, 7.5)
pTb.N (plate number)				
Placebo (N = 68)	0.1	(-0.4, 0.6)		
Denosumab 60 mg Q6M (N = 71)	0.5*	(0.0, 0.9)	0.4	(-0.3, 1.0)
rTb.N (rod number)				
Placebo (N = 68)	2.6*	(1.4, 3.8)		
Denosumab 60 mg Q6M (N = 71)	0.5	(-0.7, 1.6)	-2.1*	(-3.8, -0.5)
pTb.Th (plate thickness)				
Placebo (N = 68)	0.1	(-0.2, 0.3)		
Denosumab 60 mg Q6M (N = 71)	0.7*	(0.5, 1.0)	0.7*	(0.3, 1.0)
rTb.Th (rod thickness)				
Placebo (N = 68)	-1.2*	(-1.7, -0.6)		
Denosumab 60 mg Q6M (N = 71)	-0.2	(-0.7, 0.4)	1.0*	(0.2, 1.8)
P-R (ratio of plates to rods)				
Placebo (N = 68)	-4.9*	(-8.9, -0.9)		
Denosumab 60 mg Q6M (N = 71)	3.6	(-0.3, 7.5)	8.5*	(2.9, 14.1)
Whole stiffness				
Placebo (N = 68)	-0.4	(-1.7, 0.9)		
Denosumab 60 mg Q6M (N = 71)	3.1*	(1.9, 4.4)	3.5*	(1.7, 5.4)

\*  $p < 0.05$ <sup>a</sup> Based on an ANCOVA model adjusting for age, BV/TV and endpoint value at baseline

ITS: individual trabecular segmentation; FE: finite element; LS: least squares; CI: confidence interval; BV: bone volume; TV: total volume; Q6M: every 6 months

Table: Percent Change in ITS and FE Parameters at the Distal Tibia From Baseline to Month 12

Disclosures: Bin Zhou, None.

## 1034

**Vertebral and Nonvertebral Fracture Risk in Subgroups of Patients Receiving Teriparatide in Real-World Clinical Practice: Integrated Analysis of Four Prospective Observational Studies.** Stuart Silverman<sup>\*1</sup>, Bente Langdahl<sup>2</sup>, Saeko Fujiwara<sup>3</sup>, Kenneth Saag<sup>4</sup>, Nicola Napoli<sup>5</sup>, Satoshi Soen<sup>6</sup>, Damon Disch<sup>7</sup>, Fernando Marin<sup>8</sup>, Hiroyuki Enomoto<sup>9</sup>, John Krege<sup>10</sup>.

<sup>1</sup>Cedars-Sinai/UCLA Medical Center and OMC Clinical Research Center, United States, <sup>2</sup>Arhus University Hospital, Denmark, <sup>3</sup>Health Management and Promotion Center, Japan, <sup>4</sup>University of Alabama at Birmingham, United States, <sup>5</sup>University Campus Bio-Medico, Italy, <sup>6</sup>Department of Orthopaedic Surgery and Rheumatology, Kindai University Nara Hospital, Japan, <sup>7</sup>Eli Lilly and Company, United States, <sup>8</sup>Lilly Research Centre, United Kingdom, <sup>9</sup>Eli Lilly Japan K.K., Japan, <sup>10</sup>Eli Lilly and Company, United States

Purpose: Although the phase 3 teriparatide (TPTD) fracture prevention trial showed significant reductions in clinical vertebral fracture (CVF) and nonvertebral fracture (NVF), real-world evidence regarding the effects of TPTD in subgroups of patients is limited. Our goal was to report the rate of CVF and NVF with TPTD in subsets of patients from four integrated real-world observational studies.

Methods: Data from DANCE (USA), EFOS and EXFOS (Europe), and JFOS (Japan) prospective, observational studies of ambulatory women (n=8117) and men (n=710; no response=1) with osteoporosis receiving subcutaneous TPTD 20 µg/day for 18 to 24 months (mo) as prescribed during real-world practice were integrated. During treatment with TPTD, CVF and NVF fracture rates at 0–6 months (a reference period) were compared to 6-month to end of dosing (>6 mo). Subgroups were diabetes, glucocorticoids, rheumatoid arthritis, previous bisphosphonates, previous hip fracture, previous vertebral fracture, female gender, and age ≥75 yrs, and comparison was to those patients not in these subsets using a piecewise exponential model for the first occurrence of fracture to evaluate rates.

Results: Data for 8828 patients with ≥1 assessment on treatment showed that 92% were women, mean age was 71 years, and median treatment with TPTD was 1.6 years. For the full cohort, NVF, CVF, and clinical and hip fractures, per 100 patient-years were significantly lower in the >6 mo vs 0–6 mo reference period by 50, 43, 62, and 56%, respectively. The effects of TPTD on CVF and NVF over time were statistically consistent in all subgroups; age interaction  $P=0.07$  for CVF where patients in both age groups had significantly reduced CVF over time and for all other interactions  $P>.11$ . Regardless of the time period, patients in the glucocorticoid and previous vertebral fracture subgroups had significantly higher risk of CVF, and patients in the rheumatoid arthritis, previous hip fracture, previous vertebral fracture, and female subgroups had significantly higher risk of NVF; age, diabetes, and previous bisphosphonate showed no significant effect on CVF or NVF. In all analyses, fracture risk significantly decreased

from 0–6 to >6 mo (except NVF by gender where only women had a significant reduction).

Conclusions: The present integrated posthoc results show a statistically consistent decrease in clinical vertebral and nonvertebral fracture risk during teriparatide treatment in important subgroups of real-world patients.

Disclosures: Stuart Silverman, Eli Lilly and Company, Grant/Research Support.

## 1035

**Medication Persistence and Risk of Fracture among Female Medicare Beneficiaries Diagnosed with Osteoporosis.** Jiannong Liu<sup>\*1</sup>, Haifeng Guo<sup>1</sup>, Richard Barron<sup>2</sup>, Lionel Pinto<sup>2</sup>. <sup>1</sup>Minneapolis Medical Research Foundation, United States, <sup>2</sup>Global Health Economics, Amgen Inc., United States

While persistence with osteoporosis (OP) medications (meds) is well-documented, little evidence links persistence to outcomes. Using Medicare 100% OP patient data, we examined the association between overall OP med persistence and fracture risk in female Medicare beneficiaries diagnosed with OP. A companion abstract (Liu et al, 2017) focuses on methodological considerations and treatment-specific differences in fracture among persistent users.

Female Medicare beneficiaries who were diagnosed with OP, initiated OP meds (bisphosphonates, denosumab, teriparatide, raloxifene, and calcitonin) in 2009-2011, were aged ≥66 years and covered by Medicare Parts A, B, and D for ≥1 year before the OP med initiation date (index date) were included. Patients with Paget's disease of bone, hypercalcemia, or cancer were excluded. Patients were followed from the index date to the earliest of death; diagnosis of Paget's disease, hypercalcemia, or cancer; loss of Medicare coverage; 18 months of follow-up; or end of 2012. Persistent use was defined as continuous use (no gap ≥60 days) for ≥1 year. The outcome was closed or pathologic fracture. To assess the effect of persistence on fracture risk, accounting for differences between persistent and non-persistent users, a difference-in-difference analysis was performed at the log scale of fracture rate using a Poisson regression model with months 1-6 before the index date as the reference period. To minimize regression-to-the-mean issues and recognizing that treatment effects are usually delayed, a sensitivity analysis was performed with months 7-12 before the index date as the reference period and follow-up starting from month 4.

In all, 294,369 patients were included, 32.9% in the persistent group. Fracture rates were high in the 6 months before the index date (see table), and decreased 74.4% for persistent and 61.6% for non-persistent users during follow-up. In the sensitivity analysis, rates during follow-up decreased 38% from the reference period for persistent users and increased 18.4% for non-persistent users. Poisson regression model results showed that, regardless of reference period, persistent use of OP meds better reduces risk of fracture ( $p<0.0001$ ). Results were similar for hip and vertebral fractures.

Persistent use of OP meds is associated with reduced risk of fracture. Despite this benefit, most patients are non-persistent and may require interventions that improve overall med persistence.



Table: Treatment Effect: Persistent OP Medication Users vs Non-persistent Users

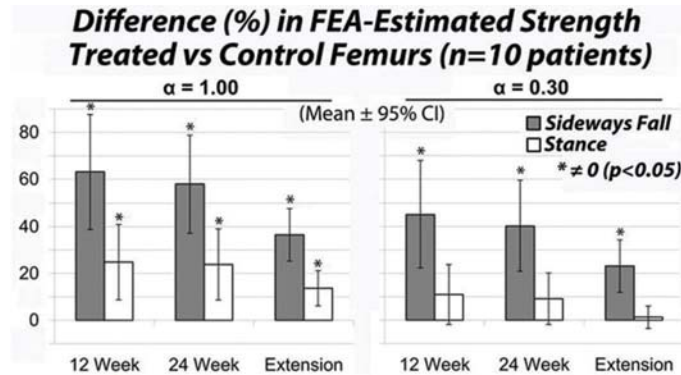
Disclosures: Jiannong Liu, None.

## 1036

**FEA-Estimated Proximal Femur Strength Increases Through 5-7 Year Follow-up in Osteoporotic Women Treated with a Local Osteo-Enhancement Procedure Involving Injection of a Resorbable, Triphasic Calcium-based Implant Material.** Tony Keaveny<sup>\*1</sup>, David Lee<sup>2</sup>, Dominique Favell<sup>3</sup>, Ronald Hill<sup>3</sup>, James Howe<sup>3</sup>, Bryan Huber<sup>4</sup>, Mary Boussein<sup>5</sup>. <sup>1</sup>University of California, Berkeley, United States, <sup>2</sup>O.N. Diagnostics LLC, United States, <sup>3</sup>AgNovos Healthcare, United States, <sup>4</sup>Copley Hospital, United States, <sup>5</sup>Harvard University, United States

Hip fragility fractures are catastrophic, costly, and are associated with high mortality rates. One new investigational treatment to lower hip fracture risk uses a minimally-invasive local osteo-enhancement procedure (LOEP) to inject a unique, resorbable, triphasic calcium sulfate/calcium phosphate implant material (AGN1) into the proximal femur with the intent of increasing femoral strength by regenerating bone lost due to osteoporosis. An IRB-approved clinical study was conducted to evaluate the biomechanical performance of the injected proximal femurs of 12 post-menopausal osteoporotic women (age range 56-89; right/left hip BMD T-scores:  $-3.0 \pm 0.7$  and  $-3.1 \pm 0.5$ ; mean  $\pm$  SD). For each patient, the left femur was injected and the right served as an untreated control. Hip CT scans were taken pre-operatively and at 12 and 24 weeks, and for 10 patients at 5–7 years. The CT scans were used to conduct patient-specific, non-linear Finite Element Analysis (FEA) to non-invasively estimate hip strength in simulated sideways fall and stance loading conditions (O.N. Diagnostics, Berkeley, CA).

For the newly regenerated bone tissue in the implant area, we applied a scale factor assuming either 100% ( $\alpha=1.0$ ) or, more conservatively, 30% ( $\alpha=0.30$ ) of the new tissue performed as normal load-bearing bone. Regardless of assumed scale factor, femoral strength in sideways fall was substantially higher in treated than control femurs at all follow-up visits (Figure). At 5–7 years, the treatment effect persisted as the treated femurs showed a  $36.5 \pm 14.5\%$  ( $\alpha=1.0$ ,  $p < 0.001$ ) and  $23.1 \pm 14.6\%$  ( $\alpha=0.30$ ,  $p < 0.01$ ) increase in sideways-fall strength relative to control femurs. The effects were smaller for stance loading and were statistically significant when all new tissue was assumed to be normal load-bearing bone ( $\alpha=1.0$ ). Mechanistically, at early time points newly formed bone adjacent to the implant area provided additional pathways through which load was transferred. As a result, there appeared to be newly generated integrated load-bearing bone tissue within the original implant area through the 5–7 year follow up. These results suggest that local osteo-enhancement of the proximal femur using AGN1 in osteoporotic women can substantially increase proximal femoral strength for a sideways fall and that this benefit is apparent soon after treatment and persists for at least 5–7 years.



Figure

Disclosures: Tony Keaveny, AgNovos Healthcare, Consultant.

## 1037

**Gsz Is Required for Craniofacial Bone Formation by Regulating Hedgehog Signaling in a Hedgehog Ligand Independent Manner.** Ruoshi Xu\*, Yingzi Yang, Sanjoy Khan. Department of Developmental Biology, Harvard School of Dental Medicine, 188 Longwood Ave. Boston, MA 02215, USA, United States

Gsz, the stimulatory G-protein alpha subunit that is encoded by GNAS gene in human and couples to G protein coupled receptors (GPCR), plays a crucial role in bone formation. GNAS activation mutations cause craniofacial hyperostosis and fibrous dysplasia, while GNAS loss of function causes craniosynostosis in progressive osseous heteroplasia. Previously, we have shown in both mouse and human that Gsz inhibits Hedgehog (Hh) signaling during osteoblast differentiation by promoting Gli3 repressor formation. It is known that Indian Hedgehog (Ihh) is required for long bone formation, not for craniofacial bone formation. Therefore, the role of Hh signaling in craniofacial bone formation remains unclear. Here, we show that Hh signaling is activated in the forming craniofacial bone where Gsz regulates Hh signaling activities in a Hh ligand independent way. We have generated a conditional gain of function allele of Gnas that allows expression of activated Gsz ( $Gsz^*$ ) in progenitor cells of the forming parietal bone by crossing with the Prx1Cre line. We found  $Gsz^*$  expression delayed intramembranous bone formation and dissolution of cartilage in sutures and fontanel. The mutant parietal bone exhibited discontinuous pattern and increased porosity by histological, immunohistochemistry and microCT analyses. Molecularly, we found that Hh signaling was severely downregulated by  $Gsz^*$  expression as revealed by analysis of Hh target gene expression. Conversely, by crossing the floxed loss of function Gsz allele with the Prx1Cre line, we found that the suture was closed prematurely due to accelerated osteoblasts differentiation, disorganized mature bone formation with enlarged bone marrow cavities, all of which were caused by increased Hh signaling. Furthermore, we found that loss of one Ptc1 allele could enhance the phenotypes of loss of Gnas function in mice. We therefore conclude that Gsz is a previously unknown regulator of craniofacial bone formation in both human and mice by regulating Hh signaling. Our work further indicates that understanding the cross-talk between GPCR-Gsz and Hh signaling will provide significantly new insight in the regulation of craniofacial bone formation and homeostasis. Such knowledge will be critical for diagnosis and therapeutic intervention of cranial malformation and craniosynostosis.

Disclosures: Ruoshi Xu, None.

## 1038

**Notch signaling activity identifies an early perichondrial population of skeletal progenitor cells in endochondral bone development.** Yuki Matsushita\*, Sunny Wong<sup>2</sup>, Noriaki Ono<sup>1</sup>. <sup>1</sup>University of Michigan School of Dentistry, United States, <sup>2</sup>University of Michigan Medical School, United States

The perichondrium is an essential component of fetal endochondral bone development, providing the source for a variety of skeletal cells such as chondrocytes, osteoblasts and marrow stromal cells. The first osteoblast precursors expressing an *osterix* (*Osx*) are formed in the perichondrium, which have the capability to translocate into the nascent ossification center. However, the characteristics of early perichondrial cells prior to the commitment to the osteoblast lineage have not been elucidated. Notch signaling is essential for maintaining skeletal progenitor cells by repressing Runx2 transcription activities (Hilton et al., 2008). In this study, we hypothesize that Notch signaling is activated in early perichondrial cells. First, to visualize Notch signaling activity, we took advantage of a Notch signaling reporter strain expressing a histone 2B (H2B)-bound Venus protein under a C promoter binding factor 1 (CBF1) promoter (CBF1:H2B-Venus). Venus<sup>bright</sup> cells were consistently found in a pattern surrounding the fetal cartilage template, specifically localized in the Sox9-negative region of the perichondrium including the groove of Ranvier. Second, to study fates of Notch-responsive perichondrial cells, we utilized *Hes1-creER* knock-in allele that activates an *R26R*-tdTomato reporter in a tamoxifen-dependent manner. Tomato<sup>+</sup> cells were found in the same pattern as Venus<sup>bright</sup> cells at 24 hours after tamoxifen injection. In the epiphysis, *Hes1*<sup>+</sup> perichondrial cells at E10.5 (*Hes1*-E10.5) became round and proliferating chondrocytes at the fetal stage, and continued to contribute to columnar chondrocytes postnatally. In contrast, *Hes1*-E12.5 cells only became periarticular round chondrocytes that failed to contribute to columnar chondrocytes. *Hes1*-E14.5 cells only became chondrocytes in the postnatal articular cartilage. In the metaphysis, both *Hes1*-E10.5 and *Hes1*-E12.5 cells became *Coll*(2.3kb)-GFP<sup>+</sup> osteoblasts, osteocytes and leptin receptor (LepR)<sup>+</sup> stromal cells in postnatal bone marrow. In contrast, a majority of *Hes1*-E14.5 cells became endomucin (Emcn)<sup>+</sup> sinusoidal endothelial cells. Therefore, these findings indicate that Notch activity identifies two distinct early perichondrial progenitor populations, including epiphyseal chondroprogenitors preceding Sox9 expression at E10.5 and diaphyseal osteo-stromal progenitors preceding *Osx* expression at E12.5 and earlier. Notch activity later than E14.5 predominantly marks the endothelial lineage.

Disclosures: Yuki Matsushita, None.

## 1039

**Resting Zone of the Growth Plate Harbors a Unique Class of Skeletal Stem Cells.** Noriaki Ono\*, Koji Mizuhashi<sup>1</sup>, Henry Kronenberg<sup>2</sup>, Wanida Ono<sup>1</sup>. <sup>1</sup>University of Michigan School of Dentistry, United States, <sup>2</sup>Massachusetts General Hospital / Harvard Medical School, United States

Skeletal stem cells regulate bone growth, maintenance and repair by providing diverse cell types including chondrocytes, osteoblasts and bone marrow stromal cells. The emerging model postulates a distinct type of skeletal stem cells that supports explosive bone growth in early life. However, the identity of such skeletal stem cells *in vivo* is unknown. We hypothesize that resting chondrocytes in the postnatal growth plate represent a unique type of skeletal stem cells. To test this hypothesis, we generated tamoxifen-inducible *PTHrP-creER* bacterial artificial chromosome (BAC) transgenic mice to perform *in vivo* lineage-tracing experiments. *PTHrP-creER*; *R26R*-tdTomato mice were pulsed with a low-dose tamoxifen injection (0.25mg) at postnatal day 6 (P6), when the resting zone is distinctly formed in the growth plate. Shortly after the pulse, tdTomato<sup>+</sup> chondrocytes were found exclusively within the resting zone and were mostly resistant to EdU incorporation, suggesting that our *PTHrP-creER* line could specifically mark resting chondrocytes. These P6-pulsed *PTHrP-creER*<sup>+</sup> resting chondrocytes stayed within the resting zone for the first week of chase, then formed columnar chondrocytes starting from the second week of chase. These cells became hypertrophic chondrocytes first, and further became *Cxcl12*-GFP<sup>+</sup> reticular stromal cells (CAR cells) and *Coll*(2.3kb)-GFP<sup>+</sup> osteoblasts in the metaphyseal bone marrow below the growth plate. *PTHrP-creER*<sup>+</sup> resting chondrocytes continued to establish columnar chondrocytes for at least one year within the growth plate. Importantly, no tdTomato<sup>+</sup> cells were noted in tamoxifen-untreated controls at any time point. To test if resting chondrocytes meet the criteria for skeletal stem cells, we harvested growth plate chondrocytes from *PTHrP-creER*; *R26R*-tdTomato mice shortly after the pulse and cultured these cells at a clonal density *in vitro*. Individual PTHrP<sup>+</sup> cells robustly formed tdTomato<sup>+</sup> colonies, some of which further formed secondary colonies upon transferring to a new well. These tdTomato<sup>+</sup> cells generated Alcian Blue<sup>+</sup> chondrocyte spheres in pellet culture, and gave rise to *Coll*(2.3kb)-GFP<sup>+</sup> osteoblastic cells and *Cxcl12*-GFP<sup>+</sup> reticular cells under inductive conditions in monolayer culture. Taken together, our findings provide the evidence that resting chondrocytes expressing *PTHrP* behave as skeletal stem cells, revealing the multilineage differentiation potential of the chondrocyte lineage.

Disclosures: Noriaki Ono, None.



## 1040

**A Novel Cell Population Contributing to Appositional Growth of Growth Plate in Postnatal Mice.** Yu Usami<sup>1\*</sup>, Aruni Gunawardena<sup>2</sup>, Noelle Francois<sup>2</sup>, Hajime Takano<sup>2</sup>, Satoru Otsuru<sup>3</sup>, Masahiro Iwamoto<sup>4</sup>, Wentian Yang<sup>5</sup>, Satoru Toyosawa<sup>1</sup>, Motomi Enomoto-Iwamoto<sup>4</sup>. <sup>1</sup>Osaka University, Japan, <sup>2</sup>Children's Hospital of Philadelphia, United States, <sup>3</sup>Nationwide Children's Hospital, United States, <sup>4</sup>University of Maryland Baltimore, United States, <sup>5</sup>Brown University, United States

The Wnt/ $\beta$ -catenin signaling is a one of most critical pathways that regulate post-natal development and growth of cartilage and bone. Previous reports have shown that osteoprogenitors in the developing long bones can be identified as Wnt-responsive cells with the use of *Axin2*CreERT2:ZsGreen (ACG) mouse system. In this study, we used this ACG system to study chondroprogenitors during epiphyseal growth. Three days after tamoxifen injection at P6, the strongly labeled ZsGreen-positive cells (ACG cells) were found inside the Ranvier's groove (RG) -the perichondrium at the border between growth plate (GP) and articular cartilage- and the outer layer of cells in GP facing the RG in the long bone (Fig. A). The similar distribution of the ACG cells was found in ribs and vertebrae. The ACG cells show chondro-osteoprogenitor characteristics as determined by FACS and the *in vitro* cultures. The ACG cells were rapidly expanded and incorporated into the ~1/4 outer portion of GP and the lateral side of articular cartilage by 5 weeks after tamoxifen injection (Fig. D) and remained there even 9 weeks after tamoxifen injection when the skeletons mature. The ACG cells were also sporadically distributed to the top layer of the GP and expanded longitudinally, making a columnar colony in the center portion of GP. The ACG cells in the most outer layer of GP were distinguished from other ACG cells in GP by the flat shape, no or faint sox 9 staining, strong alpha 5 integrin staining and slow-cell cycling (Fig. B). They are also distinguished from the ACG cells in RG by positive labeling in the *Col2*CreER:ZsGreen (*Col2*CG) system, but no labeling by the *Ctsk*Cre:ZsGreen (*Ctsk*CG) system that tags the RG cells. The 1/4 outer portion of GP was mostly labeled by *Col2*CG system, induced at P6, but only sparsely by the *Ctsk*CG system, indicating that the chondrocytes in the outer GP are not dominantly originated from the RG. Ablation of  $\beta$ -catenin by *Axin2*CreERT2 system at P6 induced ectopic chondrogenic cells in the RG (Fig. E-F, arrowheads) and deformity of GP while ablation of  $\beta$ -catenin by the *Col2*CreER system induced deformity of GP without ectopic chondrogenesis in the RG. The findings indicate that GP chondrocytes are supplied by two distinct niche: one, a novel population, resides in most outer region of GP facing the RG and is responsible for lateral appositional growth of GP; other is the top layer of the GP supplying cells in the center portion of GP.

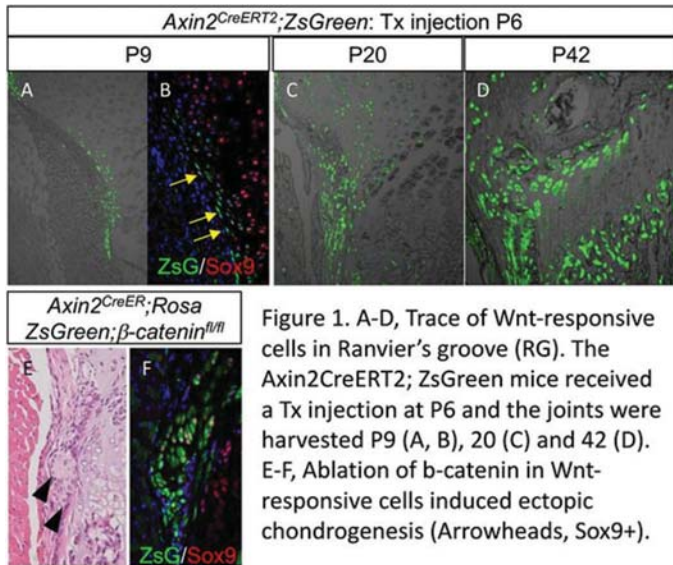


**Figure 1. A-D, Trace of Wnt-responsive cells in Ranvier's groove (RG). The *Axin2*CreERT2; ZsGreen mice received a Tx injection at P6 and the joints were harvested P9 (A, B), 20 (C) and 42 (D). E-F, Ablation of  $\beta$ -catenin in Wnt-responsive cells induced ectopic chondrogenesis (Arrowheads, Sox9+).**

Appositional growth of growth plate by Wnt-responsive cells

**Disclosures:** Yu Usami, None.

## 1041

**Involvement of 24,25-dihydroxyvitamin D during the endochondral phase of bone fracture repair in mice.** Corine Martineau\*, Roy-Pascal Naja, Abdallah Hussein, Bachar Hamade, Alice Arabian, René St-Arnaud. Shriners Hospitals for Children - Canada, Canada

Bone fracture repair is a complex process occurring in 3 broad stages: 1) an inflammatory phase, during which a hematoma is formed and cells are recruited at the fracture site; 2) a healing phase, during which the fracture gap is bridged by fibrocartilaginous tissue that is subsequently mineralized through endochondral and intramembranous ossification; 3) a remodeling phase, during which the callus is progressively replaced by true lamellar bone. The vitamin D axis has been shown to be beneficial to this process in

some instances, but in several studies the data remain inconclusive. This project focuses on a metabolite of the vitamin D catabolic pathway, 24,25-dihydroxyvitamin D [24,25-(OH)<sub>2</sub>D], shown to be upregulated in a model of fracture repair in chicken along with its metabolic enzyme, 25-hydroxyvitamin D-24-hydroxylase (CYP24A1). Our team has found that mice deficient for *Cyp24a1* show a significant, reproducible impairment in callus formation, which leads to poor biomechanical properties in the healed bones. This impairment culminates 18 days post-fracture, largely corresponding to the endochondral ossification phase of callus formation. These defects can be corrected by exogenous administration of 24,25-(OH)<sub>2</sub>D, but not by the hormonally active 1 $\alpha$ ,25-dihydroxyvitamin D. We measured a smaller callus volume and cartilage surface, as well as higher osteoclast number in the callus tissue from *Cyp24a1*-null mice. Gene expression monitoring using callus tissue from *Cyp24a1*-null mice identified FAM57B2 as a potential effector of the 24,25-(OH)<sub>2</sub>D effect. We have found that FAM57B2 produces lactosylceramide (LacCer) in response to 24,25-(OH)<sub>2</sub>D. We therefore generated a chondrocyte-specific *Fam57b*-deficient mouse strain (*Col2-Fam<sup>FL</sup>*). *Col2-Fam<sup>FL</sup>* mice exhibit the same callus formation defect during fracture repair than *Cyp24a1*-deficient mice. *In vivo* rescue experiments with LacCer or 24,25-(OH)<sub>2</sub>D confirmed the involvement of the FAM57B2 pathway in bone fracture repair, as both compounds are efficient in restoring bone quality in *Cyp24a1*-null mice, yet only LacCer rescued the *Col2-Fam<sup>FL</sup>* mouse model. Both the *in vitro* data and *in vivo* rescue experiments support the existence of a novel pathway influencing bone repair through LacCer production upon allosteric binding of 24,25-(OH)<sub>2</sub>D to its effector FAM57B2. A better understanding of this pathway could yield original approaches to ameliorate current fracture healing therapies.

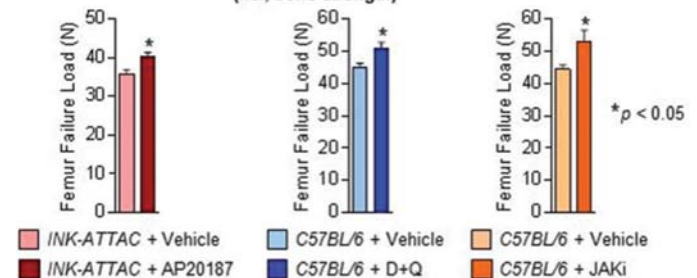
**Disclosures:** Corine Martineau, None.

## 1042

**Causal Role of Senescent Cells in Mediating Age-Related Bone Loss.** Joshua Farr\*, Megan Weivoda, Ming Xu, David Monroe, Jad Sfeir, Mikolaj Ogronik, Nathan LeBrasseur, Matthew Drake, Robert Pignolo, Tamar Tchkonja, James Kirkland, Sundeep Khosla, Mayo Clinic, United States

Accumulation of DNA damage and other cellular stressors cause proliferating as well as terminally differentiated, non-dividing cells to undergo senescence, characterized by increased expression of the cell cycle inhibitor, *p16<sup>INK4a</sup>*, along with profound morphological changes. In addition, senescent cells can produce the senescence-associated secretory phenotype (SASP), consisting of pro-inflammatory cytokines, chemokines, and extracellular matrix-degrading proteins, which have deleterious paracrine and systemic effects. Indeed, even a relatively low abundance of senescent cells (~10-15%) is sufficient to cause tissue dysfunction. Here, we investigate a role for senescent cells in age-related bone loss using 3 strategies: 1) reducing senescent cell burden using mice expressing the *INK-ATTAC* "suicide" transgene via drug (AP20187)-inducible caspase-8 driven by the senescence-associated *p16<sup>INK4a</sup>* promoter; 2) clearing senescent cells by administering previously validated "senolytic" compounds (dasatinib + quercetin) that specifically kill senescent cells without affecting proliferating or quiescent, differentiated cells; or 3) inhibiting the SASP production by senescent cells using a JAK inhibitor (JAKi). In old (20-22 month) mice with established bone loss, 2-4 month treatment with each of these interventions improved bone mass, microarchitecture, and strength (Figure). The beneficial effect of targeting senescent cells was due to suppression of bone resorption with either maintenance (trabecular bone) or an increase (cortical bone) in bone formation. *In vitro* studies demonstrated that senescent cell conditioned medium impaired osteoblast mineralization and enhanced osteoclast progenitor survival, leading to increased osteoclastogenesis; the latter effect was abrogated by pre-treatment of the senescent cells with the JAKi. The specificity of these interventions to aging was demonstrated by the absence of any skeletal effects in response to these interventions in young (7-12 month-old) mice. Collectively, these data establish a causal role for senescent cells in bone loss with aging. Because eliminating senescent cells and/or inhibiting their SASP also improves cardiovascular function, enhances insulin sensitivity, and reduces frailty, the efficacy of this approach to prevent age-related bone loss reveals a novel treatment strategy for osteoporosis via targeting a fundamental aging mechanism to thereby simultaneously treat multiple age-related co-morbidities.

**Figure. Micro-finite element analysis ( $\mu$ FEA)-derived failure load (i.e., bone strength)**



**Figure**

**Disclosures:** Joshua Farr, None.

## 1043

**The soluble form of RANKL contributes to cancellous bone remodeling in adult mice but is dispensable for ovariectomy-induced bone loss.** Jinhu Xiong\*, Keisha Cawley, Marilina Piemontese, Yuko Fujiwara, Ryan Macleod, Joseph Goellner, Haibo Zhao, Charles OBrien. University of Arkansas for Medical Sciences, United States

RANKL is produced as an integral membrane protein but can be cleaved to produce a soluble form (sRANKL). Cell culture studies suggest that the membrane-bound form is required for osteoclast formation. However, transgenic mice over-expressing sRANKL or mice injected with sRANKL exhibit increased resorption. Here we sought to determine the relative importance of membrane-bound versus sRANKL by creating mice that produce only the membrane-bound form. To do this, we generated a series of RANKL constructs lacking increasing amounts of the extracellular stalk region, which contains all known cleavage sites, and tested their resistance to MMP14, a protease that exhibits potent RANKL shedase activity. All of the deletions reduced shedding of RANKL in an in vitro assay. We then selected the longest mutant and tested its ability to support osteoclast formation when expressed in NIH-3T3 cells, which do not express endogenous RANKL. NIH-3T3 cells expressing this mutant supported osteoclastogenesis to levels similar to cells expressing full-length RANKL. We then used the CRISPR/Cas9 system to introduce this mutation into the endogenous RANKL gene (*tnfrsf11*) in mice. Mice homozygous for this mutation, designated RANKL<sup>sr</sup>, displayed normal tooth eruption, lymphocyte numbers, and lymph node development. Soluble RANKL was completely undetectable by ELISA or Luminex assay in either blood or bone marrow plasma from RANKL<sup>sr</sup> mice, but was easily detected in these fluids from WT littermates. Bone mass and architecture were analyzed at 5 wk, 3 mo, and 8 mo of age by microCT. No differences were observed between RANKL<sup>sr</sup> mice and WT littermates at 5 wk. At 3 mo, female RANKL<sup>sr</sup> mice had high cancellous bone volume in the spine and femur compared to WT littermates. At 8 mo, both male and female RANKL<sup>sr</sup> mice displayed high cancellous bone volume in the spine and femur. Histological analysis of 3 mo mice revealed that osteoclast number was low in cancellous bone of RANKL<sup>sr</sup> mice compared to WT littermates. We also examined the role of sRANKL in the bone loss caused by estrogen deficiency. Ovariectomy caused similar amounts of bone loss, and increased osteoclast number to a similar extent, in RANKL<sup>sr</sup> and WT mice. However, sRANKL remained undetectable by ELISA or Luminex in the ovariectomized RANKL<sup>sr</sup> mice. These results demonstrate that sRANKL contributes to osteoclast formation and bone remodeling in adult mice but not to the pathological bone resorption caused by estrogen deficiency.

**Disclosures:** Jinhu Xiong, None.

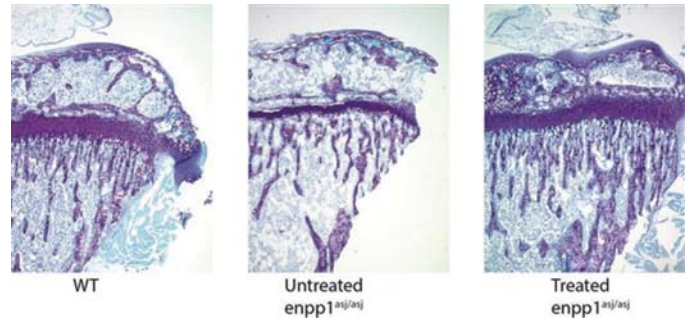
## 1044

**ENPP1 Enzyme Replacement Prevents Bone Loss and Corrects Fracture Susceptibility in a Murine Model of Autosomal Recessive Hypophosphatemic Rickets Type 2.** Mark Horowitz\*, Dillon Kavanagh, Xiaofeng Li, Tracy Nelson, Steven Tommasini, Demetrios Braddock. Yale University School of Medicine, United States

Humans with *ENPP1* loss of function develop a rare disease called Generalized Arterial Calcification of Infancy (GACI), characterized by extensive and often life-threatening calcification of the large and medium sized arteries as well as soft tissues. About 60-70% of GACI patients die within the first 6 months of life regardless of intervention. If affected individuals reach the age of 6 months they are likely to survive but will invariably develop elevated FGF23 and a phosphate wasting rickets, an evolution of their disease known as Autosomal Hypophosphatemic Rickets type 2 (ARHR2). The bone disease in ARHR2 can be severe and symptomatic, leading to repeated fractures of the long bones, rachitic skeletal deformities and impaired growth and development. Therapeutic interventions to address these complications include the use of phosphate and calcitriol, but carry the risk of iatrogenic new onset calcinosis in the kidneys, heart, liver and articular cartilage that may be life threatening in these patients.

We recently described an enzyme replacement therapy (ERT) preventing vascular calcification and death in the GACI *enpp1*<sup>asj/asj</sup> mouse. To understand the effects of ERT on the skeletal abnormalities in the ARHR2 phase of the disease, *enpp1*<sup>asj/asj</sup> mice (2 weeks-old) were injected daily with ENPP1-Fc or vehicle (8mg/kg of body wt) for 3 weeks and compared to age-matched untreated *enpp1*<sup>asj/asj</sup> mice and wild-type littermate controls.

The tibial growth plate of untreated *enpp1*<sup>asj/asj</sup> mice was approximately 50% smaller than controls measured histologically, although the orderly columns of chondrocytes remained intact (Figure). Untreated *enpp1*<sup>asj/asj</sup> mice had a marked loss of trabecular bone with a decrease in trabecular number and a concomitant increase in trabecular spacing as compared to controls measured by micro-CT. Importantly, they also had significant cortical bone loss with a decrease in cortical thickness and an increase in endosteal circumference and cortical porosity. The femurs of untreated *enpp1*<sup>asj/asj</sup> mice were weaker and less stiff compared to controls as measured by 3-point bending. Conversely, treatment with ENPP1-Fc ERT prevented the growth plate deficiency, trabecular and cortical bone loss and restored biomechanical strength and stiffness to that of controls. Our findings have important implications for the treatment of patients with ARHR2 and provide *in vivo* evidence of a role for *ENPP1* in other bone loss diseases.



ENPP1-Fc ERT of *enpp1*<sup>asj/asj</sup> Bone Defects

**Disclosures:** Mark Horowitz, Inozyme, Consultant.

## 1045

**Accelerated Aging in 1,25-Dihydroxyvitamin D Deficiency and the Role of Oxidative Stress and Cellular Senescence.** Lulu Chen\*<sup>1</sup>, Renlei Yang<sup>1</sup>, Wei Zhang<sup>1</sup>, Jie Chen<sup>1</sup>, Wanxin Qiao<sup>1</sup>, Li Mao<sup>1</sup>, David Goltzman<sup>2</sup>, Dengshun Miao<sup>1</sup>. <sup>1</sup>Nanjing Medical University, China, <sup>2</sup>McGill, Canada

There is increasing evidence that vitamin D may play an important role in the process of aging, however, it is unclear what the exact mechanism of action is. In this study, *1α(OH)ase*<sup>-/-</sup> mice and their wild-type littermates, after weaning, were injected subcutaneous with vehicle or 1,25(OH)<sub>2</sub>D<sub>3</sub> thrice weekly or were fed a rescue diet with or without supplementation with the antioxidant NAC. Compound mutant mice with homozygous deletion of both *p16* and *1α(OH)ase* or compound mutant mice homozygous for *1α(OH)ase* deletion and heterozygous for *p53* deletion were also generated. The life span of all models was monitored and their phenotypes were compared using histopathological and molecular techniques. Homozygous *1α(OH)ase*<sup>-/-</sup> mice survived on average for only 3 months and demonstrated aging phenotypes including skin atrophy. Mechanistically, increased multi-tissue oxidative stress and DNA damage, down-regulated *Bmi1* and up-regulated *p16*, *p53* and *p21* expression levels, reduced cell proliferation and induced cell senescence and senescence-associated secretory phenotype (SASP) were observed. Dietary supplementation of *1α(OH)ase*<sup>-/-</sup> mice which normalized serum calcium and phosphorus, prolonged their average life span to more than 8 months with reduced multi-tissue oxidative stress and cellular senescence, however, only slightly improved skin atrophy and osteoporosis. Supplementation with exogenous 1,25(OH)<sub>2</sub>D<sub>3</sub> or with combined calcium/phosphate and NAC prolonged the average life span of *1α(OH)ase*<sup>-/-</sup> mice to more than 16 months and nearly 14 months, respectively, and largely rescued their aging phenotypes including skin atrophy and osteoporosis by inhibiting oxidative stress, DNA damage, cell senescence and SASP, and stimulating cell proliferation. Homozygous ablation of *p16* prolonged the average life span of *1α(OH)ase*<sup>-/-</sup> mice on the rescue diet from 8 months to 16 months and largely rescued their skin atrophy and osteoporosis by enhancing cell proliferation, reducing cell senescence and SASP. Heterozygous ablation of *p53* prolonged the average life span of *1α(OH)ase*<sup>-/-</sup> mice on a normal diet from 3 months to 6 months and partially rescued skin atrophy by enhancing cell proliferation and reducing cell apoptosis. This study suggests that 1,25(OH)<sub>2</sub>D<sub>3</sub> deficiency accelerates aging by increasing oxidative stress and DNA damage, activating *p16/Rb* and *p53/p21* signaling, inhibiting cellular proliferation and inducing cellular senescence and SASP.

**Disclosures:** Lulu Chen, None.



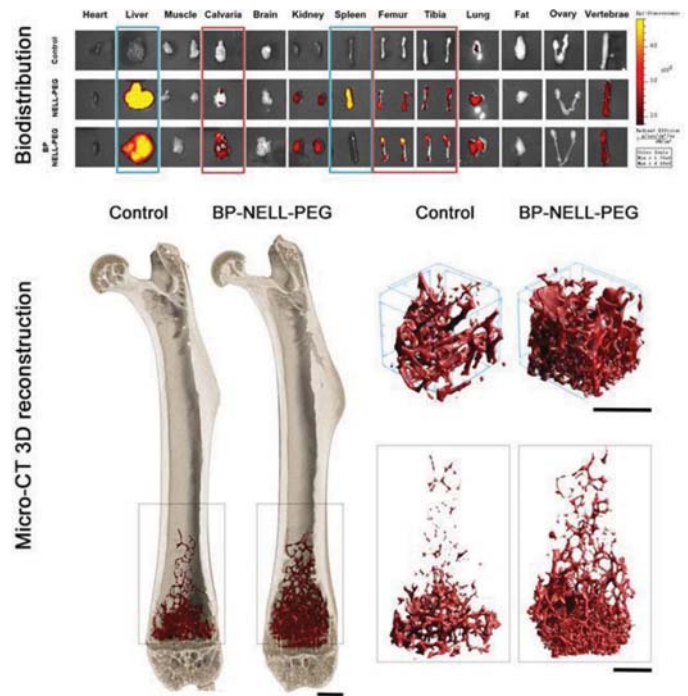
**A New Bone Seeking Anabolic Protein, Bisphosphonate-Modified NELL-PEG, Can Effectively Reverse Osteoporosis by Systemic Administration.** Yulong Zhang<sup>\*1</sup>, Jiayu Shi<sup>2</sup>, Jin Hee Kwak<sup>3</sup>, Justine Tanjaya<sup>4</sup>, Mengliu Yu<sup>2</sup>, Pin Ha<sup>5</sup>, Chenchao Wang<sup>3</sup>, Dan Pan<sup>2</sup>, Eric Chen<sup>2</sup>, Xinli Zhang<sup>2</sup>, Chia Soo<sup>6</sup>, Benjamin Wu<sup>7</sup>, Kang Ting<sup>8</sup>. <sup>1</sup>Division of Advanced Prosthodontics, School of Dentistry, UCLA; Department of Bioengineering, UCLA, United States, <sup>2</sup>Division of Growth and Development, Section of Orthodontics, School of Dentistry, UCLA, United States, <sup>3</sup>Division of Growth and Development, Section of Orthodontics, School of Dentistry, UCLA; Department of Orthodontics, College of Dentistry, Yonsei University, United States, <sup>4</sup>Division of Growth and Development, Section of Orthodontics, School of Dentistry, United States, <sup>5</sup>Orthopaedic Hospital Department of Orthopaedic Surgery and the Orthopaedic Hospital Research Center, UCLA, United States, <sup>6</sup>Orthopaedic Hospital Department of Orthopaedic Surgery and the Orthopaedic Hospital Research Center, UCLA; Division of Plastic and Reconstructive Surgery, Department of Surgery, David Geffen School of Medicine, UCLA, United States, <sup>7</sup>Division of Advanced Prosthodontics, School of Dentistry, UCLA; Weintraub Center for Reconstructive Biotechnology, School of Dentistry, UCLA; Department of Bioengineering, UCLA, United States, <sup>8</sup>Division of Growth and Development, Section of Orthodontics, School of Dentistry, UCLA; Orthopaedic Hospital Department of Orthopaedic Surgery and the Orthopaedic Hospital Research Center, UCLA, United States

Osteoporosis (OP) is the most common metabolic bone disease that is silent, but intensely debilitating and financially burdening to Americans. Currently available therapies for OP have limited clinical applications due to off-target effects. NELL-1 is a potent osteogenic and anti-resorptive cytokine that is newly being investigated as an OP therapy. Recently, we have successfully enhanced its circulation half-life in mice by PEGylation (NELL-PEG). In this study, we aimed to enhance NELL-PEG's bone-specificity in order to reduce off-target effects while preserving therapeutic potential, by conjugating it with non-effective bisphosphonate (BP, alendronate).

NELL-1 was first PEGylated, followed by conjugation with BP at a non-effective dose to enhance the bone-seeking potency. *In vitro*, the modification degree of BP-NELL-PEG was measured by fluorometric assay, while bone-binding affinity was tested on hydroxyapatite (HA) powder. Bioactivity was tested by ALP and AR staining on cultured osteoblasts. *In vivo*, biodistribution of BP-NELL-PEG in organs was imaged by IVIS Lumina II optical imaging at 48h post-intravenous injection in mice. Finally, BP-NELL-PEG's therapeutic efficacy in reversing OP was examined in ovariectomy (OVX)-induced osteoporotic mice. 5mg/kg BP-NELL-PEG or BP-BSA was intraperitoneally injected every 2 weeks for 8 weeks (n=6/group). Biweekly DEXA was performed to monitor dynamic BMD. Post-harvest, microCT, histology and IHC were performed.

After conjugation, the molar ratio of BP to NELL-1 was 3:1. Impressively, the HA-binding affinity was significantly improved from 20.1% to 64.9% by BP modification. Bioactivity assay confirmed preserved osteogenic function of NELL-1. Biodistribution test showed significantly enhanced protein retention in bone tissues (up to 80%) and significantly reduced retention in off-target organs (liver and spleen) in BP-NELL-PEG group (Figure). Furthermore, biweekly injection of BP-NELL-PEG showed significantly increased BMD and BV/TV (by over 15%) compared to BP-BSA by week 8 (Figure), confirmed by histology.

In sum, BP modification of NELL-PEG has significantly increased its bone-specificity while retaining the pro-osteogenic potency. These exciting findings not only demonstrate BP-NELL-PEG's potential as a powerful and safe systemic therapy for OP, but also present BP modification as an ideal platform to enhance the safety profile of other protein-based skeletal therapeutics to be developed for systemic use.



BP-NELL-PEG changed distribution pattern and reversed osteoporosis in OVX mice

**Disclosures:** Yulong Zhang, None.

## 1047

**Efferocytosis of Apoptotic Prostate Cancer Cells Induces Inflammation and Accelerates the Growth of Surviving Cancer Cells in Bone.** Hernan Roca<sup>\*1</sup>, Jacqueline Jones<sup>2</sup>, Marta Purica<sup>1</sup>, Savannah Weidner<sup>1</sup>, Amy Koh<sup>1</sup>, Robert Kuo<sup>1</sup>, John Wilkinson<sup>1</sup>, Yugang Wang<sup>1</sup>, Stephanie Daignault-Newton<sup>1</sup>, Kenneth Pienta<sup>3</sup>, Todd Morgan<sup>1</sup>, Evan Keller<sup>1</sup>, Jacques Nör<sup>1</sup>, Lonnie Shea<sup>1</sup>, Laurie McCauley<sup>1</sup>. <sup>1</sup>University of Michigan, United States, <sup>2</sup>Troy University, United States, <sup>3</sup>Johns Hopkins University School of Medicine, United States

Bone is a preferred shelter for disseminated prostate cancer cells and provides a supportive microenvironment for the growth of metastasis. Tumor progression and therapies induce cell death that is cleared mainly through phagocytosis (efferocytosis) by macrophages. The purpose of this study was to determine the impact of macrophage efferocytosis on prostate cancer growth in bone. Co-cultures of macrophages with fluorescence (CFSE+)-labeled apoptosis-inducible prostate cancer cells (RM1-iCasp9) were used to show that cancer cells were engulfed by bone marrow macrophages (F480+/CD11b+) when apoptosis was induced with a dimerizer ligand AP20187 (AP). Similarly, when these cells were implanted in mice via intra-tibial injection and treated with AP for two days, increased CD11b+/CFSE+ cells were observed by flow cytometric analysis of bone marrow. Macrophages engulfing apoptotic cancer cells activated the expression of inflammatory cytokines including CXCL5, CCL5 and IL6. Inflammatory cytokine production also occurred when macrophages efferocytosed other apoptotic epithelial cells but not apoptotic bone marrow stromal cells, osteoblasts, or primary bone marrow cells from the bone marrow microenvironment. Analysis of bone marrow macrophages co-cultured with apoptotic cancer cells showed that efferocytosis induced the activation of Stat3 and p65-NF- $\kappa$ B. Furthermore, inhibition of Stat3 or p65-NF- $\kappa$ B phosphorylation did not affect efferocytosis *in vitro* but mitigated the expression of inflammatory cytokines in macrophages. An *in vivo* syngeneic tumor model was used in which RM1-iCasp9 were implanted via intra-tibial injection and treated with vehicle or AP. Micro-CT analysis of tibiae revealed increased bone resorption in the tibiae where the apoptosis of cancer cells was induced as compared with controls, suggesting accelerated tumor growth mediated by efferocytosis. In human prostate cancer skeletal metastasis patients, isolated peripheral blood monocytes were more efferocytic compared to non-cancer patient monocytes and CD68+/CD14+/CD16+ mononuclear cells were increased in cancer versus normal (non-cancer) controls. Furthermore, the pro-inflammatory CXCL5 serum levels were higher in metastatic patients relative to localized prostate cancer or normal patients. Altogether these findings suggest that inflammation accelerates tumor growth in bone induced by the myeloid phagocytic clearance of apoptotic cancer cells.

**Disclosures:** Hernan Roca, None.

## 1048

**Loss of TGFBR2 in osteoblasts increases PTH1R and promotes prostate cancer bone metastasis.** Xiangqi Meng\*, Alexandra Vander Ark, Zachary Madaj, Galen Hostetter, Xiaohong Li. Van Andel Institute, United States

TGF- $\beta$  plays a central role in prostate cancer (PCa) bone metastasis, and it is crucial to understand how its signaling contributes to that process. TGF- $\beta$  signaling occurs through ligands binding to the TGF- $\beta$  type II receptor (TGFBR2). To study the bone cell-specific role of TGF- $\beta$  signaling, we used knockout (KO) mouse models having deletion of the *Tgfr2* gene specifically in osteoblasts (*Tgfr2<sup>Col1CreERT</sup>* KO) or in osteoclasts (*Tgfr2<sup>LysMCre</sup>* KO). PCa cells (PC3 or DU145 cells) were intracardially or intratibially injected into the *Tgfr2<sup>Flox</sup>* mice or their respective KO littermates. Immunohistochemistry was used to profile TGFBR2 expression in a PCa patient bone metastasis tissue microarray (TMA). Western blots, a cytokine array, *in vivo* rescue studies, and *in vitro* co-culture studies were also used.

We found that PCa-induced bone lesion development was promoted in the *Tgfr2<sup>Col1CreERT</sup>* KO mice, but inhibited in the *Tgfr2<sup>LysMCre</sup>* KO mice, relative to their respective *Tgfr2<sup>Flox</sup>* littermates. In the PCa patient TMA, we found loss of *Tgfr2* expression in the cancer-associated osteoblasts (CAOBs) in 21 out of 33 bone metastatic tissues. We next performed the mechanistic studies using the *Tgfr2<sup>Col1CreERT</sup>* KO mouse model. We found *Tgfr2* loss in osteoblasts increased parathyroid hormone receptor 1 (PTH1R) upon PC3-derived parathyroid hormone-related protein (PTHrP) stimulation. This was associated with up-regulation of pCREB, a transcription factor of PTH1R downstream signaling. *In vivo*, one of the pCREB targets, basic fibroblast factor (bFGF), was found unbiasedly increased in cancer-associated osteoblasts and was shown to mediate increased PC3 bone lesion development in *Tgfr2<sup>Col1CreERT</sup>* KO mice tibiae. *In vitro*, bFGF had no effect on PC3 cell proliferation, but promoted osteoclastogenesis and inhibited osteoblastogenesis from bone marrow cells. Our studies suggest that TGFBR2 loss in osteoblasts up-regulates the PTHrP/PTH1R signaling and promotes PCa bone metastasis in part through bFGF.

Conclusions: TGF- $\beta$  signaling in osteoblasts inhibited, but in osteoclasts promoted, PCa bone lesions. TGFBR2 is frequently lost in the CAOBs of PCa bone metastatic tissues. This loss increases PTH1R upon PCa-derived PTHrP stimulation and activates downstream signaling, which promotes PCa bone metastasis at least in part through bFGF.

**Disclosures:** Xiangqi Meng, None.

## 1049

**N-cadherin in Extra-Skeletal Osterix (Osx) Positive Cells Modulates Tumor Growth Independently of Cell-Cell Adhesion.** Francesca Fontana\*<sup>1</sup>, Biancamaria Ricci<sup>2</sup>, Jingyu Xiang<sup>3</sup>, Xinming Su<sup>3</sup>, Giulia Leanza<sup>1</sup>, Roberta Faccio<sup>2</sup>, Katherine Weilbaecher<sup>3</sup>, Roberto Civitelli<sup>1</sup>. <sup>1</sup>Division of Bone and Mineral Diseases, Washington University, United States, <sup>2</sup>Department of Orthopaedic Surgery, Washington University, United States, <sup>3</sup>Division of Molecular Oncology, Washington University, United States

Tumor growth and metastases are dependent on interactions between cancer cells and the local environment. The cell-cell adhesion molecule N-cadherin (Ncad), present in osteogenic cells, has been proposed as a molecular dock for tumor cells to engraft to bone marrow, thus forming the metastatic "pre-osteolytic" niche. To test this biologic model, we conditionally deleted the Ncad gene (*Cdh2*) in osteolineage cells using *Osx-cre* (*Cdh2* cKO). Despite absence of Ncad, bone marrow stromal cells isolated from *Cdh2* cKO mice remained capable of engaging in direct cell-cell interactions with breast tumor cells, assessed by stroma-induced chemoresistance and gap junctional intercellular communication (by cell-to-cell transfer of fluorescent probes); demonstrating that lack of Ncad does not compromise cell-cell adhesion. Neither spontaneous colonization of bone by tumor cells from primary PyMT-BO1 mammary or subcutaneous tumors, nor growth of intratibially-injected tumor cells was altered in *Cdh2* cKO mice. Surprisingly, subcutaneous tumors grew larger in *Cdh2* cKO relative to control littermates; and intratibial injection of PyMT-BO1 cells produced higher number and size of lung metastases in mutant mice. Cell tracking experiments using the Ai9 reporter driven by *Osx-cre* revealed the presence of *Osx*+ and *Ncad*+ cells in breast tumor stroma (2-5% of total), and also, unexpectedly, in a small population (0.1-0.2%) of lung cells of non-tumor bearing mice. Consistently, we found *Osx* mRNA expressed in the adherent, fibroblast-enriched stroma fraction of subcutaneous tumors from B16-F10 melanoma and Lewis Lung Carcinoma cells. Flow cytometry revealed the presence of *Osx*+ cells in the mammary fat pad and subcutaneous tissue, in addition to lungs of non-tumor bearing mice. Enhanced tumor growth was also seen in *Cdh2* cKO mice treated with doxycycline until after weaning to suppress *Osx-cre* and *Cdh2* recombination and exclude targeting of perinatal, definitive mesenchymal stem and progenitor cells. Hence, these extraskeletal *Osx*+ cells are resident soft tissue cells that express an osteogenic gene and affect tumor growth. The function of such "tumor niche" cells in normal physiology remains to be determined. Contrary to expectations, our results indicate that Ncad is indeed involved in the modulation of cancer growth and metastasis, but in a cell-cell adhesion independent fashion, via actions in previously undescribed *Osx*+ cells present at extraskeletal sites.

**Disclosures:** Francesca Fontana, None.

## 1050

**Re-Expression of Estrogen Receptor Alpha in Osteosarcomas Leads to Osteoblast Differentiation.** Susan Krum\*, Gustavo Miranda-Carboni, Maria Angeles Lillo Osuna. University of Tennessee Health Science Center, United States

Osteosarcoma is a malignant transformation of normal osteoblasts or osteoblast precursors. Normal osteoblasts express ERalpha; however, a 2008 study demonstrated that 0/28 osteosarcoma tumors showed expression of estrogen receptor alpha (ERalpha) by immunohistochemistry (1). The mechanism and consequences of ERalpha silencing in the transition from osteoblast to osteosarcoma is not understood. It is thought that sex hormones play a role in the onset of the disease, as more boys than girls get osteosarcoma and the cancer develops at the time of puberty. Because girls are less likely to get osteosarcoma, estrogens may be protective of osteosarcoma. Promoter DNA methylation of ERalpha is common in osteosarcomas, preventing osteoblast differentiation. Several osteosarcoma cell lines and 18 patient derived xenografts had no expression of ERalpha. We hypothesized that re-expression of ERalpha would induce osteoblast differentiation and halt proliferation. To this end, ERalpha was over-expressed in osteosarcoma cell lines (U2OS and 143B) and indeed, proliferation is significantly reduced, while alkaline phosphatase expression and activity, which is an osteoblast differentiation marker, is increased. To re-express ERalpha the DNA methylation inhibitor deoxyazacytidine (DAC), alone, or in combination with the histone deacetylase inhibitor suberoylanilide hydroxamic acid (SAHA), was used to treat 143B and U2OS cells and ERalpha expression was increased, along with osteoblast differentiation markers, including alkaline phosphatase. Addition of 17-estradiol (E2) further increased the differentiation of the cells. DAC was also used to treat mice *in vivo* with orthotopic injections of 143B cells. Tumor size and metastasis were decreased in mice treated with DAC. Together, these experiments suggest that the FDA-approved DNA methylation inhibitor DAC can be used to treat osteosarcoma patients to decrease proliferation and induce osteoblast proliferation.

1. Dohi O, Hatori M, Suzuki T, Ono K, Hosaka M, Akahira J, et al. Sex steroid receptors expression and hormone-induced cell proliferation in human osteosarcoma. Cancer science. 2008;99(3):518-23.

**Disclosures:** Susan Krum, None.

## 1051

**Atp6v1c1 Enhances Breast Cancer Growth by Activating the mTORC1 Pathway and Bone Metastases by Increasing V-ATPase Activity.** Matthew McConnell\*<sup>1</sup>, Shengmei Feng<sup>2</sup>, Lianfu Deng<sup>2</sup>, Guochun Zhu<sup>2</sup>, Dejun Shen<sup>1</sup>, Selvarangan Ponnazhagan<sup>1</sup>, Wei Chen<sup>1</sup>, Yi-Ping Li<sup>1</sup>. <sup>1</sup>University of Alabama at Birmingham, United States, <sup>2</sup>Shanghai Institute of Traumatology and Orthopaedics, China

ATP6v1c1 mediates the assembly of the V0 and V1 domains of Vacuolar-type H<sup>+</sup> ATPase (V-ATPase) involved in breast cancer growth and metastasis. Recently, it has been found that mTORC1, which plays important roles in the regulation of cell growth, cell proliferation, and transcription in all eukaryotes, senses lysosomal amino acids through an inside-out mechanism that requires the V-ATPase. However, the mechanism underlying how ATP6v1c1 activates cancer growth and metastasis remains unknown. In this study, we showed that ATP6v1c1 is highly expressed in human breast cancer cells. Our data revealed that silencing Atp6v1c1 in metastatic 4T1 mouse breast cancer cells (4T1) severely impairs 4T1 cell proliferation, migration, and metastasis and inhibited mTORC1 pathway activation stimulated by amino acids. We demonstrated that local inoculation of Atp6v1c1-depleted 4T1 mouse mammary tumor cells (4T1) in mouse femurs significantly inhibited tumor size and the severity of osteolytic lesions. Atp6v1c1 knockdown inhibited the co-localization of mTOR and Lamp-1, and prevented mTOR signaling activation stimulated by amino acids in 4T1 cells. Atp6v1c1 knockdown in human breast cancer MDA-MB-231 cells reduced the cell proliferation as much as 80% with dose response effect and attenuated mTORC1 pathway activation stimulated by amino acids, but has no effect on AKT pathway activation, and ERK1 pathway activation. Impaired cell proliferation and attenuated mTORC1 pathway activation stimulated by amino acid also were observed in MCF-7, MDA-MB-231, and MDA-MB-435s cancer cells. Importantly, the reduced cell proliferation and impaired mTORC1 pathway activation stimulated by amino acid were not observed in the untransformed, but immortalized, cell line C3H10T1/2. Bioinformatics data analysis shows that Atp6v1c1 is overexpressed or amplified in 34% of all 963 human breast cancer cases. Impressively, surviving rate was one fold lower in the cases with Atp6v1c1 gene overexpressed or amplification compared with the cases with Atp6v1c1 gene with normal gene expression and gene copy number. Our study reveals a the mechanism by which Atp6v1c1 facilitates cancer growth and metastasis through its function in both V-ATPase activation and mTOR pathway activation in a cancer cell specific manner, which may provide a novel therapeutic target for breast cancer treatment.

**Disclosures:** Matthew McConnell, None.



## 1052

**Active human immune system induces more severe osteoblastic bone reaction in a humanized mouse model of breast cancer bone metastasis.** Tiina E Kähkönen<sup>\*1</sup>, Mari I Suominen<sup>1</sup>, Jussi M Hallen<sup>1</sup>, Azusa Tanaka<sup>2</sup>, Michael Seiler<sup>2</sup>, Jenni Bernoulli<sup>1</sup>. <sup>1</sup>Pharmatest Services Ltd, Finland, <sup>2</sup>Taconic Biosciences, United States

Skeleton is a common site for metastasis in many cancers, and bone metastases cause high mortality in patients. Bone microenvironment changes tumor properties and induces drug resistance, and efficacy of new cancer therapies should be confirmed in bone metastasis models to reduce the currently very high failure rates in clinical trials due to poor efficacy. Immunotherapies have proven efficacy on primary tumors in preclinical studies. Bone provides an essential and natural site for testing immunomodulators, as bone marrow is the reservoir of hematopoietic stem cells (HSC), the precursors of immune cells. We have studied effects of functional human immune system on growth of experimental bone metastases to provide a validated platform for efficacy testing of immunotherapies.

Female CIEA NOG® mice were engrafted with human CD34+ HSCs, whose maturation was confirmed by measuring human CD45+ cells. The resulting humanized mice (huNOG: HSCFTL-NOG-F) and immunodeficient NOG mice were given an intratibial injection of BT-474 (ER+, PR+, HER2+) human breast cancer cells, and tumor-induced bone changes were monitored for 8 weeks by radiography. Changes in bone mineral deposit and bone volume were measured by dual X-ray absorptiometry (DXA) and micro-computed tomography (μCT) in tumor-bearing tibias. Immune-related organs and tumor-bearing tibias were analyzed for differentiated human immune cells, CTLA-4 and PD-L1.

Tumor-induced osteoblastic new bone growth was observed in all tumor-bearing tibias. Bone lesions were larger in huNOG mice compared to NOG mice, exhibiting more severe phenotype. Osteoblastic bone growth was accompanied with increased bone mineral density in huNOG mice, which correlated with increased cortical and trabecular bone volumes. Strong expression of CD3, CD4, CD8, CD20, and CD45 was observed in immune-related organs in the huNOG mice, indicating a high prevalence of active human immune cells. CD45-positive tumor-infiltrating lymphocytes (TILs) and CD4-positive T-helper cells were observed in the tumors. PD-L1 was expressed in the tumor and no CTLA-4 expression was observed.

Our results demonstrate that immune cells enhanced the tumor-induced osteoblastic bone reaction. These findings highlight the importance of the bone-tumor-immune cell interactions and demonstrate that humanized mouse models provide a novel platform for preclinical testing of cancer immunotherapies, particularly for therapies targeting cancers that often metastasize to bone.

**Disclosures:** Tiina E Kähkönen, None.

## 1053

**History of fractures for prediction of a future fracture in individuals from the general population.** Claudia Beaudoin<sup>\*1</sup>, Sonia Jean<sup>1</sup>, Lynne Moore<sup>2</sup>, Philippe Gamache<sup>1</sup>, Louis Bessette<sup>3</sup>, Louis-Georges Ste-Marie<sup>4</sup>, Jacques P. Brown<sup>3</sup>. <sup>1</sup>Institut national de santé publique du Québec, Canada, <sup>2</sup>Université Laval, Canada, <sup>3</sup>CHU de Québec Research Center, Canada, <sup>4</sup>Université de Montréal, Canada

**Background:** Occurrence of a fragility fracture in adult life is a major risk factor for a future fracture and appears in all fracture risk estimation tools. However, while the characteristics of prior fractures such as number, site and time since last fracture have been reported to influence subsequent fracture risk, they are generally not considered in estimation tools. **Objective:** To assess the contribution of number, site and time since last fracture for prediction of hip and major osteoporotic fractures (wrist, forearm, elbow, humerus, femur, hip, and spine) (MOF). **Method:** A retrospective cohort study was performed using administrative data from the Quebec Integrated Chronic Disease Surveillance System. The study population comprised all men and women aged 66 and older registered under the Quebec public drug insurance plan in 2004-2005 not treated or not compliant with osteoporosis medication (MPR ≤ 75%) in the previous year. Eligible individuals were followed from 2004-2005 to 2013-2014. Fractures were identified using a previously validated algorithm with high positive predictive values and sensitivities at all sites except vertebrae. Time until a first hip fracture or MOF were modeled using proportional hazard models while taking account of the competing risk of mortality. Adjusted risk ratios (RR [95% CI]) were calculated to quantify the contribution of history of fracture, fracture site, number of prior fractures, and time since last fracture. To compare the predictive ability of the predictors, area under the ROC curve will also be provided. **Results:** Of the 759,734 individuals included in the analysis, 32,975 (4.3%) suffered a hip fracture and 59,960 (7.9%) suffered a MOF. A prior fracture at any site increased the risk of hip fracture (RR [95% CI] = 1.5 [1.5-1.6]) and MOF (RR [95% CI] = 1.6 [1.6-1.7]). Contribution of history of fracture varied slightly between sites of prior fractures (Table). Risk of hip fracture increased little (RR from 1.5 to 1.6) with the number of prior fractures while risk of MOF increased considerably (RR from 1.6 to 2.3). Interestingly, the effect of prior fractures persists until at least 8 years and varies little with time. **Conclusion:** Time since last fracture and site contribute little to the prediction of hip or MOF. The number of prior fractures seems to contribute to the prediction of MOF, and its inclusion in estimation tools should be considered.

Predictor	Category	Risk ratio [95% confidence interval]*					
		Humerus, shoulder	Wrist, forearm, elbow	Hip, femur	Foot, ankle, tibia, fibula	MOF	Any site
Prior fx	No	1.0 (ref)	1.0 (ref)	1.0 (ref)	1.0 (ref)	1.0 (ref)	1.0 (ref)
	Yes	1.8[1.7-1.9]	1.5[1.5-1.6]	1.4[1.3-1.5]	1.3[1.3-1.4]	1.7[1.6-1.7]	1.6[1.6-1.7]
Number of prior fx	0	1.0 (ref)	1.0 (ref)	1.0 (ref)	1.0 (ref)	1.0 (ref)	1.0 (ref)
	1	1.8[1.7-1.9]	1.6[1.5-1.6]	1.4[1.4-1.5]	1.3[1.3-1.4]	1.7[1.6-1.7]	1.6[1.6-1.7]
	≥2	2.1[1.6-2.8]	1.5[1.2-1.9]	1.2[0.9-1.5]	1.4[1.2-1.7]	**	***
Time since last fx (years)	No fx	1.0 (ref)	1.0 (ref)	1.0 (ref)	1.0 (ref)	1.0 (ref)	1.0 (ref)
	≤1	1.9[1.7-2.1]	1.6[1.4-1.7]	1.2[1.1-1.4]	1.3[1.2-1.5]	1.6[1.5-1.7]	1.6[1.6-1.7]
	>1-5	1.8[1.7-1.9]	1.5[1.4-1.6]	1.5[1.4-1.6]	1.3[1.2-1.4]	1.7[1.7-1.8]	1.7[1.6-1.7]
	>5-8	1.6[1.5-1.8]	1.6[1.5-1.7]	1.4[1.2-1.5]	1.4[1.3-1.5]	1.7[1.6-1.8]	1.6[1.5-1.7]

MOF: major osteoporotic fracture (wrist, forearm, elbow, humerus, femur, hip, and spine)

fx: fracture

\* adjusted for age, sex, obesity, weight loss, chronic obstructive pulmonary disease (proxy for smoking), major oral glucocorticoid use, rheumatoid arthritis, diabetes, alcohol abuse, admission in a long-term care facility, and treatment for osteoporosis

\*\* 2 vs 0: 1.8[1.7-2.0], ≥3 vs 0: 1.9[1.5-2.5]

\*\*\* 2 vs 0: 1.9 [1.7-2.0], ≥3 vs 0: 2.3 [2.0-2.6]

Table: Contribution of number, site and time since last fracture for prediction of MOF

**Disclosures:** Claudia Beaudoin, None.

## 1054

**Jump Muscle Power in Octogenarian Men is Related to Prospective Recurrent Falls but not Fall Injuries Over One Year: Osteoporotic Fractures in Men (MrOS) Study.** Elsa Strotmeyer<sup>\*1</sup>, Paolo Caserotti<sup>2</sup>, Stephanie Harrison<sup>3</sup>, Mary Winger<sup>1</sup>, Robert Boudreau<sup>1</sup>, Peggy Cawthon<sup>3</sup>, Kristine Ensrud<sup>4</sup>, Eric Orwoll<sup>5</sup>, Jane Cauley<sup>1</sup>. <sup>1</sup>University of Pittsburgh, United States, <sup>2</sup>University of Southern Denmark, Denmark, <sup>3</sup>California Pacific Medical Center Research Institute, United States, <sup>4</sup>University of Minnesota, United States, <sup>5</sup>Oregon Health and Science University, United States

Lower-extremity muscle power (force\*velocity) may be an independent determinant of falls and fall injury compared to muscle strength and physical performance. In 1,196 men (age 83.7±3.7 years; 9% minorities), we measured peak power (Watts/kg body weight), force (Newton/kg body weight) and velocity (m/s) at peak power from the best of 3-5 weight-bearing countermovement leg extensions ("jump") assessed on a force plate at the 2014-16 Osteoporotic Fractures in Men (MrOS) clinic visit. Exclusions for jump test were due to health or inability to attempt test. Incident falls and fall injuries (fracture, head injury, sprain/strain, bruise, bleeding, or other injury type) were self-reported every 4 months for 1 year after exam. Jump measures per SD were examined as predictors of recurrent (≥2) falls without injury (N=92) or any fall injury (N=187) in multinomial logistic regression models vs. referent group of 0-1 falls without injury. Dynamometry measured grip strength (kg/kg body weight). Physical performance included 400m walk completion (sec), 6m usual walk (m/s), 5 repeat chair stands (#/sec), and short physical performance battery score (SPPB; 0-12). Men with incident recurrent falls or fall injury self-reported more falls in 1 year prior to exam vs. referent group of 0-1 falls without injury (67% and 60% vs. 25%; p<0.01). Men with incident recurrent falls or fall injury had lower jump peak power (19.6±5.0 and 20.0±5.3 vs. 21.1±5.4 W/kg; both p<0.05) and force (16.2±1.5 and 16.5±2.1 vs. 16.8±2.0 N/kg; p<0.05 recurrent falls only) but not velocity (1.19±0.3 and 1.20±0.3 vs. 1.24±0.3 m/s; both ns) vs. men with 0-1 falls without injury. In multivariate models, lower peak power and lower force at peak power were related to higher OR of recurrent falls vs. referent (Table). When added to the Table models, grip strength or performance measures were not associated with either recurrent falls or fall injury. Lower power, but not force, had a borderline association for fall injury. Velocity was not related to recurrent falls or fall injury. Future follow-up will evaluate individual type of fall injury as events accumulate. In conclusion, jump power and force were more strongly associated than grip strength and other performance measures with incident recurrent falls in community-dwelling older men. Jump power may predict fall outcomes and should be investigated in additional older populations.

Table. Jump peak power, force and velocity at peak power by SD:  
Multivariate multinomial logistic regression OR\* for incident recurrent falls without injury and any fall injury vs. 0-1 falls without injury (referent).

	OR (95%CI), Recurrent falls without injury (N=92)	OR (95%CI), Any fall injury (N=187)
Peak power per SD lower (W/kg)	<b>1.36 (1.04, 1.76)</b>	1.20 (0.99-1.47)
Force per SD lower (N/kg)	<b>1.36 (1.06, 1.76)</b>	1.09 (0.90-1.31)
Velocity per SD lower (m/s) <sup>†</sup>	1.19 (0.92-1.53)	1.16 (0.96-1.40)

\*All models adjusted for age, race, site, and height with adjustment for other lifestyle factors, medications, and medical conditions if  $p < 0.10$ : fall history in past year, fall-related medications, MI, Parkinsons disease, and total hip BMD (fall injury models only). <sup>†</sup>Additional adjustment for weight did not change results.

Table

Disclosures: Elsa Strotmeyer, None.

## 1055

**Fracture Risk Among 122,205 Cancer Patients: A Population-Based Cohort Study from Manitoba, Canada.** Harinder Singh<sup>\*1</sup>, Saeed Al-Azazi<sup>2</sup>, Lin Yan<sup>2</sup>, Lisa Lix<sup>2</sup>, Piotr Czaykowski<sup>1</sup>, Beatrice Edwards<sup>3</sup>, William Leslie<sup>2</sup>.  
<sup>1</sup>University of Manitoba, Cancercare Manitoba, Canada, <sup>2</sup>University of Manitoba, Canada, <sup>3</sup>MD Anderson Cancer Center, United States

Background: Prior studies have primarily assessed osteoporosis-related fracture risk among patients with breast or prostate cancer. Data are limited on occurrence of fractures and their risk factors for other cancers.

Aim: To estimate fracture burden for different cancers and determine predictors of fracture risk among cancer patients.

Methods: We linked population-based data (cancer registry, health administrative data, population registry) from Manitoba, Canada to identify cancer cases and matched controls, covariates and fracture events. Individuals with a first cancer diagnosis (excluding non-melanoma skin cancer) between 1987 and 2013 was matched with up to 4 individuals without a cancer diagnosis by age, sex and area of residence on the date of cancer diagnosis (index date). Individuals were followed for fracture occurrence, death, migration or end of the study (March 31, 2015). Previously validated algorithms were used to identify hip, clinical vertebral, forearm, and humerus fractures (collectively designated as "major fractures" [MF]). Fracture incidence rates and incidence rate ratios (IRRs) were calculated for MF overall and by fracture site for all cancer cases and then stratified by cancer site. For individuals with cancer, competing risk time-to-event analysis (competing event=death) was used to assess cancer-specific and general risk factors associated with time to first fracture.

Results: 122,255 cancer cases and 460,040 matched controls without cancer (median age 63 years; 55% women) were followed for a median of 15 years (IQR 8-22). Fracture incidence rates were slightly lower among cancer cases than controls (IRRs <1) more than 1 year before diagnosis. Fracture incidence increased after cancer diagnosis and remained elevated 5-10 years after diagnosis (Table). In stratified analyses, MF risk was significantly increased beyond 5 years for colorectal, breast, prostate, lung, urinary tract, multiple myeloma/non-Hodgkins lymphoma, other hematological and head/neck cancers. Independent predictors of MF among cancer patients included female sex, increasing age, cancer type, cancer stage, Charlson co-morbidity index score, rheumatoid arthritis, prior MF, alcohol/substance abuse and prolonged glucocorticoid exposure.

Conclusions: Fracture risk remains increased for up to 10 years after cancer diagnosis, and this is seen for most cancer diagnoses. Risk factors for fracture are similar to traditional risk factors in the non-cancer population.

Years before (-) or after (+) cancer diagnosis	Hip	Wrist	Humerus	Spine	Major Fracture
-10 to -5	0.76 (0.69,0.85)	0.99 (0.92,1.06)	0.92 (0.83,1.02)	0.96 (0.87,1.05)	0.92 (0.88,0.96)
-5 to -1	0.68 (0.64,0.72)	1.00 (0.95,1.05)	0.97 (0.91,1.04)	0.97 (0.91,1.03)	0.91 (0.88,0.93)
-1 to 0	0.80 (0.71,0.90)	0.97 (0.85,1.11)	1.20 (1.03,1.39)	1.65 (1.48,1.85)	1.10 (1.03,1.17)
0 to +1	0.90 (0.81,1.00)	0.95 (0.82,1.11)	1.33 (1.15,1.55)	1.73 (1.53,1.95)	1.15 (1.08,1.23)
+1 to +5	1.07 (1.01,1.12)	1.11 (1.04,1.18)	1.27 (1.18,1.36)	1.45 (1.37,1.55)	1.19 (1.15,1.23)
+5 to +10	1.22 (1.13,1.32)	1.17 (1.07,1.29)	1.39 (1.24,1.56)	1.46 (1.32,1.61)	1.28 (1.22,1.34)

Table: Fracture Incidence Rate Ratios (95% CIs) by Time Before/After Index Date

Disclosures: Harinder Singh, None.

## 1056

**High imminent vertebral fracture risk in smokers and COPD patients with a prevalent or incident vertebral fracture.** Mayke J. van Dort<sup>\*</sup>, Piet P.P.M. Geusens, Johanna H.M. Driessen, Elisabeth A.P.M. Romme<sup>4</sup>, Frank W.J. M. Smeenk<sup>4</sup>, Emiel F.M. Wouters, Joop P.W. van den Bergh. <sup>1</sup>Department of Internal Medicine, NUTRIM School of Nutrition and Translational Research in Metabolism, Maastricht University Medical Center+ (MUMC+), Netherlands, <sup>2</sup>Department of Internal Medicine, Rheumatology, Maastricht University Medical Center+ (MUMC+), Netherlands, <sup>3</sup>CAPHRI Care and Public Health Research Institute, NUTRIM School for Nutrition and Translational Research in Metabolism, Department of Clinical Pharmacy and Toxicology, Maastricht University Medical Center+ (MUMC+), Netherlands, <sup>4</sup>Department of Respiratory Medicine, Catharina Hospital, Netherlands, <sup>5</sup>Department of Respiratory Medicine, Maastricht University Medical Centre+ (MUMC+), Netherlands, <sup>6</sup>Department of Internal Medicine, VieCuri Medical Centre, Venlo and Department of Internal Medicine, NUTRIM School of Nutrition and Translational Research in Metabolism, Maastricht University Medical Center+ (MUMC+), Netherlands

Purpose – Patients with chronic obstructive pulmonary disease (COPD) have a high risk of vertebral fractures (VFs), but the incidence of VFs is unknown. Therefore, the aim of this study was to determine the incidence of new or worsening VFs in COPD patients and smoker controls.

Methods – COPD subjects (with GOLD stage 2, 3 or 4) and smoker controls from the ECLIPSE study with complete set of chest CT scans at baseline and after one and three years follow-up in order to evaluate the thoracic and first lumbar vertebrae were included. In case of a VF on the three year follow-up scan a detailed VF assessment of the previous CT scans was performed using SpineAnalyzer software. VFs were scored according to the method described by Genant as mild, moderate or severe.

Main outcome measure was the percentage of patients with new or worsening VFs between T1 and L1 during one and three years.

Results – In 1248 subjects (mean age of 61 years, 764 males, 1008 subjects with COPD, 258 (20.7%) with ≥1 VFs at baseline) the cumulative incidence of a VF during the first year was 10.1%, and 24.1% during three years. After correction for age and sex, the prevalence and incidence of VFs was similar between smokers and COPD gold stages, but dependent on baseline or incident VFs.

In the first year, the risk of a VF was 29.8% in subjects with a baseline VF compared to 5.0% in the absence of a baseline VF (HR: 5.5, 95%CI: 3.8-7.9) and 58.5% versus 15.0% after three years (HR: 3.6, 95%CI: 2.9-4.6) after correction for age, sex and presence of COPD.

The risk of an incident VF during three years increased with the number (50.4% after one baseline VF, 68.4% after ≥2 baseline VFs) (see Figure 1) and severity of baseline VFs (54.6 after baseline grade 1 VF, 75.8% after baseline grade 3 VF,  $p < 0.001$  for both trends).

In subjects who had a first or new or worsening VF during the first year, the risk of subsequent fracture was 56.3% during the next two years.

Conclusions - More than half of smokers and COPD subjects with a prevalent or incident VF sustain a subsequent VF during the next three years, and even more in the presence of multiple or severe VFs at baseline. This high imminent fracture risk indicates the need for immediate treatment of smokers and COPD patients with a prevalent or incident VF, with medication that has been shown to reduce the risk of VF at short term.

## New or worsening VFs

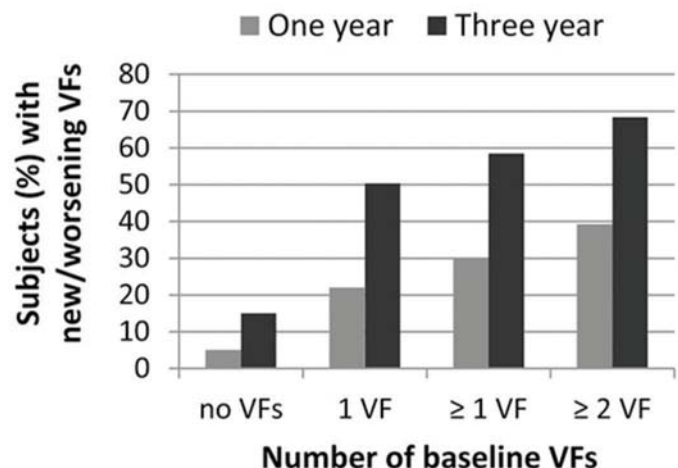


Figure 1: Subjects with new or worsening VFs in one and three years

Disclosures: Mayke J. van Dort, None.



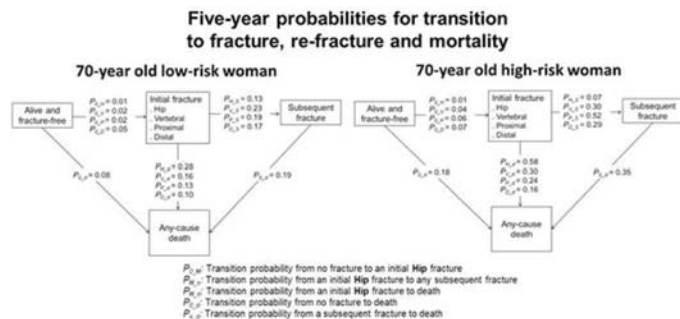
**Transition to re-fracture and mortality in the elderly: An individualized risk assessment tool for fracture and its outcomes from two large population-based prospective cohort studies.** Thach Tran<sup>\*1</sup>, Dana Bliuc<sup>1</sup>, Hanh Pham<sup>1</sup>, Tineke van Geel<sup>2</sup>, Jonathan D Adachi<sup>3</sup>, Claudie Berger<sup>4</sup>, Joop van den Bergh<sup>5</sup>, John A Eisman<sup>6</sup>, Piet Geusens<sup>7</sup>, David Goltzman<sup>4</sup>, David A Hanley<sup>8</sup>, Robert G Josse<sup>9</sup>, Stephanie M Kaiser<sup>10</sup>, Christopher S Kovacs<sup>11</sup>, Lisa Langsetmo<sup>12</sup>, Jerilynn C Prior<sup>13</sup>, Tuan V Nguyen<sup>14</sup>, Jacqueline R Center<sup>15</sup>. <sup>1</sup>Garvan Institute of Medical Research, Australia, <sup>2</sup>Maastricht University, Research school of CAPHRI, Netherlands, <sup>3</sup>McMaster University, Canada, <sup>4</sup>McGill University, Canada, <sup>5</sup>Maastricht University Medical Center, Research School Nutrim; VieCuri Medical Centre of Noord-Limburg, Netherlands, <sup>6</sup>Garvan Institute of Medical Research; Clinical School, St Vincent's Hospital; Faculty of Medicine, UNSW Sydney; School of Medicine Sydney, University of Notre Dame, Australia, <sup>7</sup>Maastricht University Medical Center, Research School CAPHRI; University Hasselt, Biomedical Research Institute, Netherlands, <sup>8</sup>University of Calgary, Canada, <sup>9</sup>University of Toronto, Canada, <sup>10</sup>Dalhousie University, Canada, <sup>11</sup>Memorial University, Canada, <sup>12</sup>School of Public Health, University of Minnesota, United States, <sup>13</sup>Department of Medicine and Endocrinology, University of British Columbia, Canada, <sup>14</sup>Garvan Institute of Medical Research; Faculty of Medicine, UNSW Sydney, Canada, <sup>15</sup>Garvan Institute of Medical Research; Clinical School, St Vincent's Hospital; Faculty of Medicine, UNSW Sydney, Canada

Existing fracture risk assessment models are not designed to predict fracture-associated consequences. We aimed to develop an individualized predictive model for trajectories from no fracture to specific types of initial fracture, re-fracture and mortality according to different comorbidity risk profiles using a multistate Markov model. The potential effect of treatment on fracture and its outcomes was not yet included.

There were 11,000 people (70% women) aged 67.5 ( $\pm 9$ ) years from Dubbo Osteoporosis Epidemiology Study and Canadian Multicentre Osteoporosis Study. Incident fracture was identified from X-ray reports and questionnaires, and death ascertained through contact with a family member or obituary review.

During a median follow up of 12.5 years (IQR: 5.8, 15.0), 2,500 individuals fractured (28/1,000 person-years in women, 15/1,000 person-years in men), 700 re-fractured [65/1,000 person-years (women), 44/1,000 person-years (men)] and 2,800 died [2.1/100 person-years (women), 4.4/100 person-years (men)]. The mean age of initial fracture, re-fracture and mortality was 75 ( $\pm 5$ ), 78.5 ( $\pm 8$ ) and 81 ( $\pm 9$ ) years, respectively. Predictive models included age, BMD, prior falls, prior fracture and comorbidities. A 70-year old low-risk woman (defined as T-score = -1.5 with no comorbidities) would have a 10% chance of sustaining a fracture in 5 years; this was increased to 19% for a similarly aged high-risk woman (T-score = -2.5 with history of falls, prior fracture, cardiovascular disease and diabetes). The more severe the initial fracture, the more the comorbidities added to post-fracture mortality risk resulting in lower subsequent re-fracture risk. Thus a 70-year old low-risk woman with an initial hip fracture would have a probability of 13% of re-fracture and 28% of dying within 5 years compared with 7% re-fracture and 58% mortality probability for a similarly aged high-risk woman. By contrast, comorbidities added more to re-fracture risk given the lower overall mortality risk for initial distal fractures. Thus a low and high-risk woman with an initial distal fracture would have re-fracture probabilities of 17% and 29%, and mortality probabilities of 10% and 16%, respectively. Similar patterns were found for men.

This study used a novel, robust technique to develop predictive models for individualization of progression to fracture and its outcomes which will allow informed decision making about risk and thus treatment on an individual basis.



Five-year transition risk to fracture, re-fracture and mortality

**Disclosures:** Thach Tran, None.

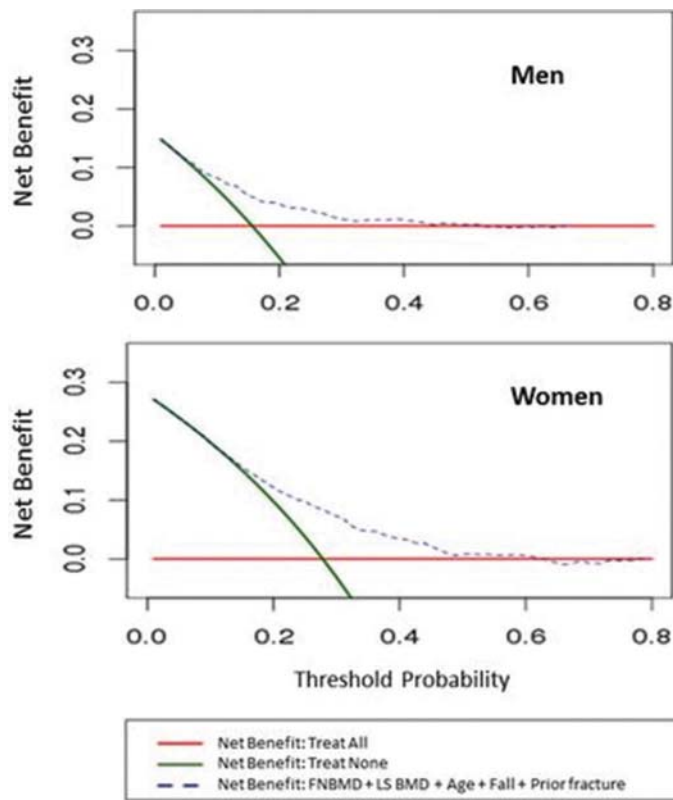
**Determination of Risk Threshold for Osteoporosis Therapy: A Decision Curve Analysis Approach.** Thao P. Ho-Le<sup>\*1</sup>, Jackie R. Center<sup>2</sup>, John A. Eisman<sup>3</sup>, Hung T. Nguyen<sup>4</sup>, Tuan V. Nguyen<sup>5</sup>. <sup>1</sup>Centre of Health Technologies, FEIT, University of Technology Sydney, Australia, <sup>2</sup>Bone Biology Division, Garvan Institute of Medical Research; St Vincent Clinical School, UNSW, Australia, Australia, <sup>3</sup>Bone Biology Division, Garvan Institute of Medical Research, NSW; St Vincent Clinical School, UNSW, Australia; School of Medicine, Sydney University of Notre Dame, Australia, Australia, <sup>4</sup>Centre of Health Technologies, Faculty of Engineering and Information Technology, University of Technology, Sydn, Australia, <sup>5</sup>University of Technology, Sydney; Bone Biology Division, Garvan Institute of Medical Research, NSW; St Vincent Clinical School, UNSW; School of Public Health and Community Medicine, UNSW; School of Medicine, Sydney University of Notre Dame, Australia

**Aim:** Although predictive models are available for fracture risk assessment, there is no scientifically derived threshold of fracture risk for the identification of "high risk" individuals. In this study, we employed a decision curve analysis (DCA) approach to determine the risk of fracture that is optimally suitable for the treatment of osteoporosis.

**Method:** The study was part of the Dubbo Osteoporosis Epidemiology Study that involved 2188 women and 1324 men aged 60 years and above who have been followed up to 20 years. At baseline, bone mineral density (BMD) and clinical risk factors were obtained. During the follow-up period, the incidence of fractures and mortality was ascertained. Three mortality-adjusted models for predicting fracture risk were considered: (1) Model I included age and femoral neck BMD; (2) Model II included age, femoral neck BMD, history of fracture and falls; (3) Model III had factors in Model II plus lumbar spine BMD. The mortality-adjusted fracture risks were corrected for potential over-fitting by using a 10-fold cross-validation analysis. For each model and each predicted probability of fracture, the clinical net benefit was assessed as the benefits (true positives) over the harms (false positives), with weights assigning to true positives and false positives are derived from the threshold probability of the outcome. The optimal threshold was defined as the point that yields the highest net benefit.

**Results:** In women, compared with the strategy of treating everyone, treating those with 5-yr predicted total fracture risk >20% yielded the greatest benefit (Model III). However, women with 10-yr predicted fracture risk >28% can also be beneficial from a treatment. For hip fracture, Models II and III showed that treating women with 5-yr risk of 4% or 10-yr risk of 6% will yield the greatest benefit. In men, the greatest benefit was achieved at the threshold of 10% for 5-year risk of total fracture or 15% for 10-yr risk. For hip fracture in men, model II showed the best benefit at 2% and 3% for 5-yr risk and 10-yr risk, respectively.

**Conclusion:** Thus, we propose that individuals with 5-yr fracture risk of greater than 10% (for men) and greater than 20% (for women) be considered "high risk" and may be indicated for treatment. For 10-yr prediction, the optimal threshold of fracture risks for treatment indication are >15% for men and >28% for women.



Decision curves for Model III to predict 10-year fracture risk in the elderly

**Disclosures:** Thao P. Ho-Le, None.

## 1059

**Selective requirement of the histone methyltransferase Ezh2 in distinct mesenchymal lineages during skeletal development.** Amel Dudakovic<sup>1</sup>, Emily Camilleri<sup>1</sup>, Deepanwita Pal<sup>2</sup>, Sonia Rozario<sup>3</sup>, Christopher Paradise<sup>1</sup>, Roman Thaler<sup>1</sup>, Meghan McGee-Lawrence<sup>4</sup>, Elizabeth Bradley<sup>1</sup>, Gary Stein<sup>5</sup>, Martin Montecino<sup>6</sup>, Jennifer Westendorf<sup>1</sup>, Ronen Schweitzer<sup>2</sup>, Emi Shimizu<sup>3</sup>, Andre van Wijnen<sup>1</sup>. <sup>1</sup>Mayo Clinic, United States, <sup>2</sup>Shriners Hospital for Children, United States, <sup>3</sup>Rutgers School Dental Medicine, United States, <sup>4</sup>Augusta University, United States, <sup>5</sup>University of Vermont Medical School, United States, <sup>6</sup>Universidad Andrés Bello, Chile

Epigenetic control by enhancer of zeste homolog 2 (Ezh2), a histone 3 lysine 27 (H3K27) methyltransferase, is critical for skeletogenesis. Ezh2 suppresses osteogenic differentiation, while facilitating adipogenic differentiation. Inhibition of Ezh2 enhances bone formation, but conditional loss of Ezh2 in uncommitted mesenchymal cells (Prx1-Cre) yields skeletal patterning defects, including shortened forelimbs, craniosynostosis and clinodactyly. Here, we examine Ezh2 function in committed lineages using tissue-specific Cre drivers that mediate loss of Ezh2 in bone (Ox-Cre), cartilage (Col2a1-Cre) or tendon (Scx-Cre). We show these drivers bypass patterning abnormalities observed with deletion of Ezh2 in mesenchyme (Prx1-Cre). Loss of Ezh2 in bone (Ox-Cre) results in low trabecular bone mass in young mice (3 week) by microCT. However, Ox-Cre cKO mice exhibit accelerated bone formation thereafter and the low bone mass phenotype resolves when animals enter adulthood (8 and 12 weeks). Remarkably, loss of Ezh2 in cartilage (Col2a1-Cre) does not result in cartilage defects, yet microCT analysis reveals low trabecular bone density in young mice (4 week), which normalizes in adults. Interestingly, Ezh2 loss in chondrocytes upregulates expression of osteogenic genes (e.g., Sp7, Bglap, and Ibsp), but joint development proceeds normally without inducing hypertrophy, osteophytes or osteoarthritis. Early loss of Ezh2 in Prx1-Cre mice disrupts proper tendon formation, but tendon-specific loss of Ezh2 (Scx-Cre) does not alter tendon structure or collagen organization. Hence, Ezh2 loss only generates tendon phenotypes that are secondary to defects in skeletal patterning, but is dispensable in the tendon lineage. Following up on previously observed cranial abnormalities (i.e., premature suture fusion) in Prx1-Cre mice, microCT and SEM revealed dental phenotypes. Loss of Ezh2 enhances enamel and dentin as reflected by high intrinsic electron density, a characteristic of enamel hyper-mineralization, although keyhole-shaped enamel rods and dentinal tubules are normal. This phenotype is paralleled by up-regulation of mRNA markers for ameloblasts (e.g., Ambn, Enam and Amelx) and odontoblasts (Dsp) in incisors. Thus, Ezh2 loss early in mesenchymal cells alters skeletal patterning, but loss of Ezh2 at later developmental stages indicates that Ezh2 is dispensable for tendon development, but important for suppression of mineralization in bone, cartilage and dental tissues.

**Disclosures:** Amel Dudakovic, None.

## 1060

**Ubiquitin-specific protease 34 regulates osteogenic differentiation of mesenchymal stem cells.** Yuchen Guo<sup>1</sup>, Mengyuan Wang<sup>2</sup>, Shiwen Zhang<sup>3</sup>, ChenChen Zhou<sup>3</sup>, Yunshu Wu<sup>3</sup>, Liang Xie<sup>4</sup>, Ling Ye<sup>4</sup>, Qianming chen<sup>5</sup>, Quan Yuan<sup>4</sup>. <sup>1</sup>author, China, <sup>2</sup>teammate, China, <sup>3</sup>workmate, China, <sup>4</sup>mentor, China, <sup>5</sup>teacher, China

The osteogenic differentiation of mesenchymal stem cells (MSCs) is governed by multiple mechanisms. Studies have given evidence that ubiquitin-dependent proteolysis system mediated protein degradation is critical for the differentiation of MSCs. However, the role of ubiquitin-specific proteases (USPs) family is largely unknown. Here we reported USP34 as a previously unrecognized regulator of osteogenic differentiation.

First, we treated human MSCs with a combination of BMP2 and Wnt3a, and profiled expression of 54 known USPs members. RT-qPCR revealed that USP34 is one of the top 5 USPs induced by the treatment. Next, we knocked down these five genes by siRNA and found that only depletion of USP34 reduced the intensity of ALP staining and formation of mineralized nodules. Moreover, knockdown of USP34 also inhibited the expression of osteogenic mark genes, such as *DLX5*, *RUNX2* and *SP7*. To verify the *in vitro* findings, We generated stable USP34 knockdown MSCs using lentiviruses expressing shRNA, and implanted them with  $\beta$ -TCP carriers into immunocompromised mice subcutaneously. H&E staining showed that USP34-depleted cells formed much less bone tissues compared with the scrambled shRNA MSCs.

Next, we generated *Usp34* flexed mice using CRISPR/Cas9 and bred them with *Prx1-Cre* mice to delete *Usp34* from MSCs.  $\mu$ -CT analysis of the distal femoral metaphysis showed decreased bone mineral density (BMD) and trabecular bone volume (BV/TV) in *Prx1-Cre; Usp34<sup>fl/fl</sup>* mice compared with their *Usp34<sup>fl/fl</sup>* littermates. Histomorphometric analyses revealed that osteoblast number (N.Ob/B.Pm) of those mice was significantly reduced, while osteoclast number (N.Oc/B.Pm) remained invariant. The mineral apposition rate (MAR) and bone formation rate (BFR/BS) were lower than the controls. Moreover, the serum levels of bone formation marker PINP were reduced in those mice, while bone formation marker CTX were unchanged. We also isolated the bone marrow MSCs from those mice and confirmed the inhibited osteogenic potential *in vitro*.

Mechanically, we found that USP34 binds with RUNX2 and regulates its stability through deubiquitylation.

Overexpression of Runx2 in *Prx1-Cre; Usp34<sup>fl/fl</sup>* MSCs by adenoviruses rescued the impaired osteogenic differentiation *in vitro* and recovered the capability of bone formation *in vivo*.

In summary, our data indicate that USP34 is a previously unknown regulator of osteogenic differentiation.

**Disclosures:** Yuchen Guo, None.

## 1061

**Identification of novel periosteal skeletal stem cells.** Shawon Debnath<sup>1</sup>, Alisha Yallowitz<sup>1</sup>, Jason Mc Cormick<sup>1</sup>, Tuo Zhang<sup>1</sup>, Yeon - Suk Yang<sup>2</sup>, Yifang Liu<sup>1</sup>, Sarfaraz Lalani<sup>1</sup>, Srushti Kittane<sup>3</sup>, Hwanhee Oh<sup>1</sup>, Jae Hyuck Shim<sup>4</sup>, Matthew Blake Greenblatt<sup>1</sup>, Ren Xu<sup>1</sup>. <sup>1</sup>Weill Cornell Medical College, Cornell University, United States, <sup>2</sup>University of Massachusetts Medical School, United States, <sup>3</sup>New York University, United States, <sup>4</sup>University of Massachusetts Medical College, United States

The periosteum is a thin mesenchymal layer present on the outside of bone that makes a unique contribution to bone health, playing a critical and unique role in adaptation to mechanical loading, fracture healing and responses to some osteoanabolic drugs. However, the identity of the stem cell giving rise to periosteal mesenchyme is currently unclear. Using microdissection of the periosteum together with a 16-color flow cytometry panel and a Cathepsin K (CTSK)-cre activated reporter, we have identified a novel population of periosteal stem cells (PSCs) in both long bones and calvarial sutures. These PSCs fulfill formal criteria for stemness in terms of displaying clonal multipotency, self-renewal capacity *in vivo* and *in vitro*, and in terms of sitting at the apex of a differentiation hierarchy. Consistent with the physiologic lack of marrow recruitment to the periosteal surface, when transferred into the kidney capsule of secondary hosts, PSCs undergo intramembranous bone formation without recruitment of hematopoietic elements, and PSCs lack expression of cell surface markers such as Leptin R, CD146, and CD140 $\alpha$  that have been previously reported as markers of mesenchymal cells with the capacity to support hematopoiesis. PSCs display self-renewal capacity in an *in vitro* mesenchymal assay or an *in vivo* serial transplantation assay. PSCs have a physiologic contribution to bone formation, as ablation of PSC-derived osteoblasts through CTSK-cre mediated conditional deletion of a gene essential for osteoblast differentiation, osterix (SP7), results in greatly increased cortical bone porosity while preserving endosteal trabecular bone mass. PSCs are also essential for fracture healing, as they show robust expansion after fracture, and mice with a CTSK-cre mediated osterix deletion show impaired fracture healing. Transcriptome characterization shows that PSCs bear a distinct transcriptional profile from both their derivatives and from other skeletal stem cells with a similar surface immunophenotype. Lastly, empiric identification of mesenchymal cell types present in bone by single cell RNA sequencing identifies a cellular population with a transcriptional profile consistent with PSCs. Taken together, PSCs are a bona fide stem cell population specialized to meet the physiologic demands of the periosteum that are distinct from other skeletal stem cell types. This finding suggests that bone contains multiple pools of skeletal stem cells that each display distinct functional specialization.

**Disclosures:** Shawon Debnath, None.



1062

**Identification of osteoprogenitor cells in the mouse periosteum.** Francesca V Sbrana<sup>\*1</sup>, Danka Grcevic<sup>2</sup>, Jessica Funnell<sup>3</sup>, Ivo Kalajzic<sup>1</sup>, Brya Matthews<sup>1</sup>. <sup>1</sup>UConn Health, United States, <sup>2</sup>University of Zagreb, Croatia, <sup>3</sup>Binghamton University, United States

The periosteum is a major source of cells involved in fracture healing, but the identity of osteoprogenitors in the periosteum is undefined. We have utilized  $\alpha$ SMA as a marker of osteochondroprogenitor cells in the periosteum following fracture. To identify and trace  $\alpha$ SMA+ cells we used  $\alpha$ SMACreERT2 combined with Ai9 tdTomato reporter (SMA9 mice) and mature osteoblasts were identified by Col2.3GFP expression.

Flow cytometry analysis of intact bones confirmed that CD45-  $\alpha$ SMA+ cells were very rare in the bone marrow and endosteum, but comprised 0.5-2% of cells in the periosteum of adult mice.  $\alpha$ SMA+ cells in periosteum showed enrichment of progenitor markers CD51, CD90 and PDGFR $\alpha$  compared to the total CD45- population, but had less CD105. In addition, there were large differences in the frequency of progenitor markers in different bone tissue compartments. Sca1 and PDGFR $\alpha$  were expressed in 15% of CD45- periosteum cells while they are present on <2% of cells in the bone marrow and endosteum.

In order to evaluate if the  $\alpha$ SMA-labeled population in the periosteum contains long-term progenitors, tibia fractures were generated in SMA9/2.3GFP mice treated with tamoxifen 6 or 2 weeks prior to fracture, or on the day of fracture.

60% of callus osteoblasts are  $\alpha$ SMA-labeled when tamoxifen is given the day of fracture. This decreases to 40% or 20% when labeled 2 or 6 weeks prior to fracture, compared to <2% without tamoxifen.  $\alpha$ SMA labeled fewer chondrocytes initially (30%), but showed a similar trend of reduced labeling after longer tracing periods.  $\alpha$ SMA+ periosteal cells isolated from intact bones formed more CFU-F than total CD45- cells, but few CFU-ALP. Following transplantation in a calvarial defect,  $\alpha$ SMA+ cells expanded but did not form bone. In contrast,  $\alpha$ SMA+ cells isolated after injury showed enhanced CFU-F and CFU-ALP formation.

Our lineage tracing studies indicate that the majority of osteoprogenitors involved in fracture healing express  $\alpha$ SMA. A subset of these cells remain capable of contributing to osteoblasts after 6 weeks indicating long-term progenitor potential.  $\alpha$ SMA+ cells do not show osteoprogenitor characteristics when isolated from intact periosteum, but show improved in vitro growth and differentiation following injury. Overall, the periosteum is highly enriched for the majority of stem cell markers evaluated compared to bone marrow and endosteum, confirming previous observations that it is rich in progenitor cell populations.

**Disclosures:** Francesca V Sbrana, None.

1063

**Gli1 Is A Common Lineage Marker For Osteogenic Mesenchymal Progenitors.** Yu Shi<sup>\*1</sup>, Guangxu He<sup>2</sup>, Wen-Chih Lee<sup>1</sup>, Jennifer McKenzie<sup>1</sup>, Matthew Silva<sup>1</sup>, Fanxin Long<sup>1</sup>. <sup>1</sup>Department of Orthopedic Surgery, Washington University School of Medicine, United States, <sup>2</sup>Department of Orthopedic Surgery, The Second Xiangya Hospital, Central South University, China

Bone formation in mammals begins in the embryo and continues throughout life, thus requiring continuous production of osteoblasts. Although osteoblast differentiation is extensively studied, the upstream mesenchymal progenitors are not well understood. Recent work has identified several genes marking cell populations that contribute to osteoblasts in the mouse, but a common identifier for all osteogenic mesenchymal progenitors remains elusive. Here, by lineage-tracing Hedgehog (Hh)-responsive cells expressing Gli1 in fetal or postnatal mice, we discover that Gli1+ cells progressively produce osteoblasts in all skeletal sites examined. Most notably, in postnatal growing mice, a pool of Gli1+ cells residing immediately below the growth plate, which we term "metaphyseal mesenchymal progenitors" (MMP), is essential for cancellous bone formation in endochondral bones. Most MMP express the mesenchymal marker Pdgfra but not the preosteoblast marker Osx (also known as Sp7), and differentiate in vivo into osteoblasts, bone marrow adipocytes, as well as the leptin receptor-positive (Lepr+) bone marrow stromal cells (BMSC) previously shown to generate osteoblasts in adult mice. Disruption of Hh signaling via genetic deletion of Smo impairs both proliferation and osteoblast differentiation of MMP. Removal of  $\beta$ -catenin causes MMP to favor adipogenesis, resulting in severe osteopenia coupled with increased marrow adiposity. Moreover, the number of MMP declines with aging and correlates with an age-dependent cancellous bone loss in the mouse.

Finally, Gli1 also marks in postnatal mice a progenitor population contributing to both chondrocytes and osteoblasts during fracture healing. Overall, Gli1 is a common lineage marker for osteogenic mesenchymal progenitors contributing to both normal bone formation and fracture repair.

**Disclosures:** Yu Shi, None.

1064

**Hox genes regulate adult osteoprogenitor cell fate decisions.** Vivian Bradaschia-Correa<sup>\*</sup>, Anne Marie Josephson, Shane Neibert, Devan Mehta, Philipp Leucht, NYU School of Medicine, United States

The adult periosteum serves as a niche for skeletal stem cells, and its contribution to fracture healing and bone regeneration is well documented (Colnot 2009). All bones in

the skeleton possess regenerative features and share a similar histological architecture, however, their embryonic origins are diverse: the appendicular skeleton develops from the mesoderm, while the craniofacial bones, except the parietal bones, are derived from the neural crest. With notable exceptions, the embryonic origin determines their differential expression of Hox genes, transcriptional factors that vary along the cranial-caudal axis to regulate the anterior-posterior positional patterning during development (Mallo et al. 2010). Previous studies have identified a superior regenerative potential of craniofacial osteoprogenitor cells (OPCs) to appendicular OPCs (Leucht et al. 2008). Here, we employed RNAseq analysis to interrogate OPCs from four distinct anatomic locations (Fig. 1A). We hypothesized that embryonic Hox gene expression is maintained into adulthood, provides a transcriptional signature that best differentiates between craniofacial and appendicular OPCs, and that Hox gene expression regulates adult OPC fate decisions. Hierarchical cluster analysis (Fig. 1B.1), PCA (Fig. 1B.2) and MA plot analysis (Fig. 1B.3,4) revealed that OPCs negative for Hox gene expression contain 5390 differentially expressed genes compared to Hox-positive OPCs, showing for the first time that on a transcriptional level, OPCs from the craniofacial skeleton and the appendicular skeleton present two distinct cell populations.

While the embryonic function of Hox genes is well characterized (Mallo et al. 2010), their role in adult cells is not clearly defined yet. Here, we used siRNA and antisense oligonucleotide (ASOs) to knockdown epigenetic regulators of Hox expression in adult periosteal OPCs in vitro and then assessed their differentiation potential. Hox knockdown in Hox-expressing tibial OPCs resulted in a more osteogenic and less adipogenic cell fate, demonstrating that Hox gene expression is crucial for adult OPC cell fate decisions (Fig. 1C).

This study provides evidence that embryonic Hox gene expression is maintained into adulthood, where one of its functions is to regulate OPC cell fate decisions. Epigenetic manipulation can be utilized to target and manipulate Hox gene expression, which may provide potential therapeutic opportunities with the goal to improve fracture healing.

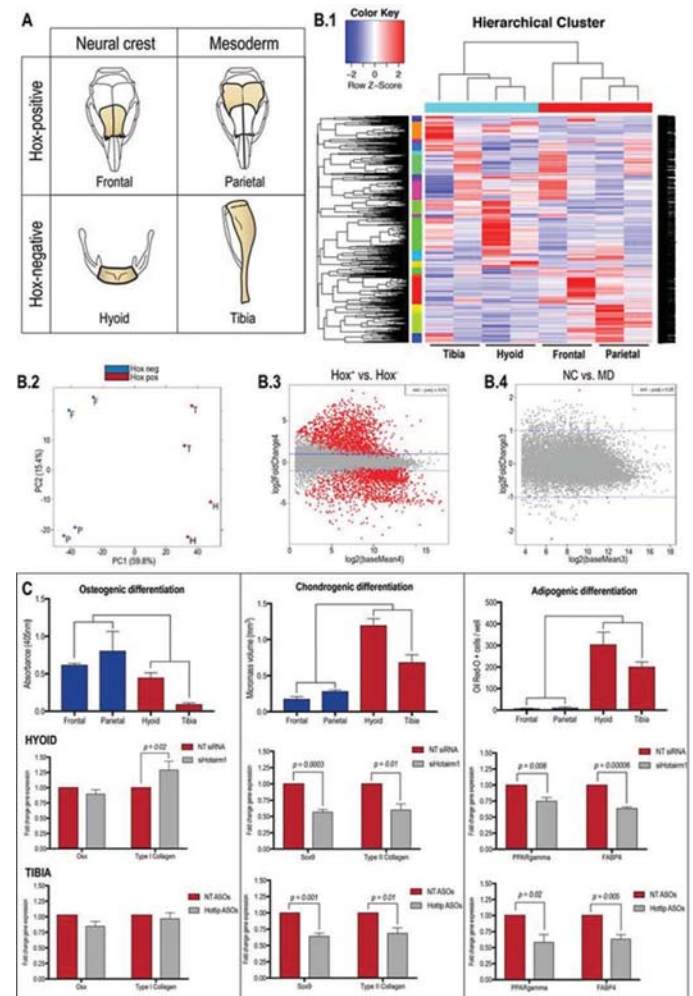


Figure 1

**Disclosures:** Vivian Bradaschia-Correa, None.

## 1065

**Long-term administration of rhPTH(1-84) results in marked and sustained improvements in skeletal indices by bone histomorphometry in hypoparathyroidism.** Mishaela Rubin\*, Natalie Cusano, Zhou Hua, Ruksana Majeed, Beatriz Omeragic, David Dempster, John Bilezikian. Columbia University, United States

rhPTH(1-84) is available for the treatment of hypoparathyroidism (HYPO), yet the skeletal effects of long-term treatment are unknown. We studied histomorphometric changes during long-term PTH treatment in HYPO (n=14) subjects in comparison to euparathyroid controls (Ct; n=45). rhPTH(1-84) treatment extended over 6-10 (mean  $8.2 \pm 1$  [SE]) years. HYPO (age  $45.9 \pm 5$  yrs; 10 female; duration  $16 \pm 5$  yrs) underwent tetracycline-labeled transiliac crest bone biopsies at baseline (HYPO-BL) and after long-term rhPTH(1-84) treatment (HYPO-LT). Mineralizing surface was higher by 23-fold (HYPO-BL:  $0.34 \pm 0.1$  to HYPO-LT:  $7.84 \pm 2.0\%$ ,  $p=0.003$ ) surpassing Ct levels (Ct:  $4.33 \pm 0.48\%$ ,  $p=0.02$  vs HYPO-LT); bone formation rate also was higher, by 19-fold (HYPO-BL:  $0.0026 \pm 0.001$  to HYPO-LT:  $0.0487 \pm 0.01 \text{ } \mu\text{m}^2/\text{um/d}$ ,  $p=0.01$ ) but did not differ from Ct (Ct:  $0.033 \pm 0.004$ ,  $p=0.19$  vs HYPO-LT). Cancellous bone volume was greater (HYPO-BL:  $19.6 \pm 1.7$  to HYPO-LT:  $29.18 \pm 10.6\%$ ,  $p=0.006$ ) exceeding Ct (Ct:  $19.8 \pm 0.66\%$ ,  $p<0.001$  vs HYPO-LT). Trabecular number also was greater (HYPO-BL:  $1.77 \pm 0.1$  to HYPO-LT:  $2.48 \pm 0.3 \text{ } \#/\text{mm}$ ,  $p=0.01$ ) surpassing Ct (Ct:  $1.74 \pm 0.05 \text{ } \#/\text{mm}$ ,  $p<0.001$  vs HYPO-LT), while trabecular separation was lower (HYPO-BL:  $474.0 \pm 41$  to HYPO-LT:  $321.4 \pm 51 \text{ } \mu\text{m}$ ,  $p=0.01$ ) becoming lower than in Ct (Ct:  $484.7 \pm 19.6 \text{ } \mu\text{m}$ ,  $p<0.001$  vs HYPO-LT). Trabecular width did not change (HYPO-BL:  $111.7 \pm 8$  to HYPO-LT:  $116.0 \pm 8$ ,  $p=0.4$ ) and did not differ from Ct (Ct:  $114.8 \pm 3$ ,  $p=0.83$  vs HYPO-LT). The changes in trabecular microstructure were accompanied by intra-trabecular tunneling. Cortical porosity increased (HYPO-BL:  $6.3 \pm 2$  to HYPO-LT:  $9.5 \pm 1\%$ ,  $p=0.05$ ) exceeding Ct values (Ct:  $4.77 \pm 0.36$ ,  $p=0.01$  vs HYPO-LT). The results indicate profound and sustained changes in dynamic and structural indices during long-term management of HYPO with rhPTH(1-84). To our knowledge, they represent the first histomorphometric data reflecting such a long period of continuous treatment with rhPTH(1-84) or any other PTH for any disease. For HYPO, the results have implications for clinical outcomes such as reduced fracture risk, the data for which are still needed.

**Disclosures:** Mishaela Rubin, Shire Pharma, Consultant.

## 1066

**Teriparatide Compared with Risedronate and the Risk of Fractures in Subgroups of Postmenopausal Women with Severe Osteoporosis: The VERO Trial.** Piet Geusens\*<sup>1</sup>, Fernando Marin<sup>2</sup>, David L Kendler<sup>3</sup>, Luis Russo<sup>4</sup>, Cristiano AF Zerbini<sup>5</sup>, Susan Greenspan<sup>6</sup>, Salvatore Minisola<sup>7</sup>, Alicia Bagur<sup>8</sup>, Peter Lakatos<sup>9</sup>, Enrique Casado<sup>10</sup>, Astrid Fahrleitner-Pammer<sup>11</sup>, Jan Stepan<sup>12</sup>, Eric Lespessailles<sup>13</sup>, Rüdiger Moericke<sup>14</sup>, Jean Jacques Body<sup>15</sup>, Pedro López-Romero<sup>2</sup>. <sup>1</sup>Maastricht University Medical Center, Netherlands, <sup>2</sup>Lilly Research Center Europe, Spain, <sup>3</sup>University of British Columbia, Canada, <sup>4</sup>Centro de Analises e Pesquisas Clínicas LTDA, Brazil, <sup>5</sup>Centro Paulista de Investigação Clínica, Brazil, <sup>6</sup>Osteoporosis Center, University of Pittsburgh, United States, <sup>7</sup>Policlinico Umberto I, Italy, <sup>8</sup>Centro de Osteopatías Comlit, Argentina, <sup>9</sup>Semmelweis University Medical School, Hungary, <sup>10</sup>Hospital Parc Tauli, Spain, <sup>11</sup>Division of Endocrinology, Medical University of Graz, Austria, <sup>12</sup>Institute of Rheumatology, Faculty of Medicine 1, Charles University, Czech Republic, <sup>13</sup>Regional Hospital of Orleans, France, <sup>14</sup>Institut Préventive Medizin & Klinische Forschung, Germany, <sup>15</sup>CHU Brugmann, ULB, Belgium

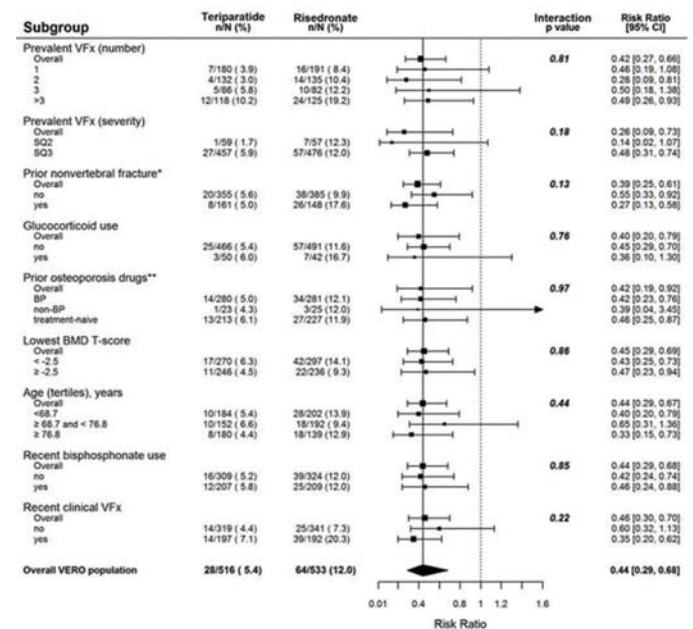
**BACKGROUND:** The VERO trial was an active-controlled fracture endpoint clinical trial that recruited postmenopausal women with low bone mass and prevalent vertebral fractures (VFX). We have reported that the risk of new vertebral and clinical fractures [a composite of clinical VFX and non-vertebral fragility fractures (NVFFx)] in patients randomized to teriparatide (TPTD) compared with those randomized to risedronate (RIS) was reduced by 56% and 52% respectively ( $p<.001$  for each), with a non-significant reduction in NVFFx (34%,  $p=0.1$ ). Here we present subgroup analyses on fracture data across pre-specified subgroups.

**METHODS:** Postmenopausal women with at least 2 moderate or 1 severe VFX and low bone mass (BMD T-score  $\leq -1.5$ ) were randomized (1:1) to sc daily TPTD 20  $\mu\text{g}$  or oral weekly RIS (35 mg) in a double-blind, double-dummy 2-year trial. Homogeneity of the treatment effect on the primary endpoint (new VFX fractures), and two key gated secondary fracture endpoints (clinical fractures, NVFFx) were investigated by logistic and Cox proportional hazards regression models (including treatment-by-subgroup interaction). Subgroups were evaluated for age, ethnicity, number and severity of prevalent VFX, prevalent NVFFx, significant glucocorticoid (GC) use, prior osteoporosis therapies, clinical VFX in the year before entering the study, recent bisphosphonate (BP) use, and baseline BMD T-score.

**RESULTS:** 1,360 women were randomized and treated (680 in each arm). Mean age was 72.1 years, 97.3% were Caucasian. The mean (SD) number of prevalent VFX was 2.7 (2.1), 55.4% had a BMD T-score  $<-2.5$  (lowest value measured at spine or hip), 36.5% a recent clinical VFX, 42.8% a prior NVFFx, 43.2% were osteoporosis drugs naïve, 39.3% were recent BP users, and 9.3% were taking GC at a prednisone-equivalent dose  $>5\text{mg/day}$ .

Due to the low number of non-Caucasians, the analyses by ethnicity were not feasible. The risk reduction of TPTD vs RIS for new VFX, clinical fractures, and NVFFx did not significantly differ in any of the subgroup analyses (treatment-by-subgroup interaction  $p>0.1$ ) (see Figure for the primary study endpoint).

**CONCLUSION:** In postmenopausal women with severe osteoporosis, the effect of TPTD vs RIS was consistent among the various predefined subgroups, with no evidence to conclude that the treatment effect was heterogeneous across the different categories of the subgroups in reducing the risk of new vertebral and clinical fractures.



Forest Plot for New Vertebral Fractures

**Disclosures:** Piet Geusens, Pfizer, Abbott, Eli Lilly and Company, Amgen, MSD, Roche, UCB, BMS, Novartis, Grant/Research Support.

## 1067

**A randomized, double-blind, placebo-controlled trial of denosumab in postmenopausal women undergoing cementless total hip replacement.** Hannu Aro\*<sup>1</sup>, Sanaz Nazari-Farsani<sup>2</sup>, Mia Vuopio<sup>3</sup>, Kimmo Mattila<sup>3</sup>. <sup>1</sup>Turku University Hospital and University of Turku, Finland, <sup>2</sup>University of Turku, Finland, <sup>3</sup>Turku University Hospital, Finland

**Purpose:** In total hip replacement (THR) of postmenopausal women, structural changes of the proximal femur may cause short-term migration of uncemented femoral stems, detectable by radiostereometric analysis (RSA). Transient migration has been found to delay, albeit not prevent, osseointegration. Osteoporotic women are also prone to periprosthetic bone loss (as much as 30%) during the first months. Denosumab inhibits osteoclastic bone resorption and has an influence on intracortical femur remodeling. Our primary objective was to investigate whether denosumab is effective in preventing periprosthetic bone loss in postmenopausal women during the first year after THR. The secondary objective was to investigate whether denosumab reduces femoral stem migration and enhances implant osseointegration and thereby promotes functional recovery.

**Methods:** This randomized, double-blinded, placebo-controlled trial enrolled 65 consecutive postmenopausal women with defined inclusion and exclusion criteria (ClinicalTrials.gov NCT01926158). The patients randomly received subcutaneous injections of denosumab 60 mg or placebo every 6 months, starting one month before cementless THR. Dual-energy X-ray absorptiometry of periprosthetic bone mineral density (BMD) and model-based RSA of stem migration were performed within 3 days after surgery and repeated at 12, 22 and 48 weeks. Gait analysis, pedometer-measured walking activity, analysis of bone turnover markers and clinical scoring (HHS, WOMAC, Rand-36, short BPI) were performed preoperatively and at each visit.

**Results:** Denosumab prevented ( $p<0.001$ , linear mixed effects model) periprosthetic bone loss in denosumab-treated patients (mean age  $69.1 \pm 5.2$  yrs,  $n=33$ ) compared with placebo-treated patients (mean age  $69.1 \pm 5.9$  yrs,  $n=32$ ). Periprosthetic BMD (Gruen 7) decreased by -5.3% (95% CI -2.1 - -8.6) in denosumab group and by -18.2% (95% CI -14.9 - -21.5) in placebo group within 48 weeks (Fig. 1). RSA showed no significant intergroup differences in 3D stem migration (translation and rotation). There were no significant differences in parameters of functional recovery. Serum CTX decreased by -77.3% (95% CI -61.6 - -93.0) and PINP by -23.8% (95% CI -8.3 - -39.2) in denosumab-treated patients already at 12 weeks ( $p<0.001$  compared with controls).

**Conclusion:** Denosumab was efficient in the maintenance of periprosthetic bone mass but did not enhance implant osseointegration and functional recovery of patients.



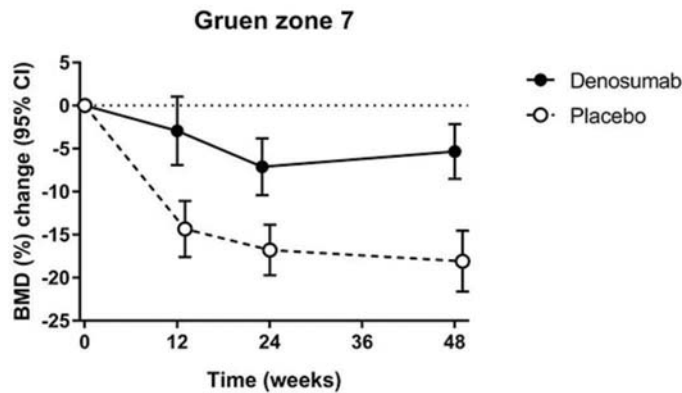


Figure 1

Disclosures: Hanmu Aro, Amgen Inc., Grant/Research Support.

## 1068

**Negligible Long-Term Effects on Bone Density after Four years of Treatment with Two Intensive Combination Strategies, including initially High dose Prednisolone, in Early Rheumatoid Arthritis patients: The COBRA-light Trial.** Merel JJ Lucassen<sup>1</sup>, Marieke M ter Wee<sup>1</sup>, Nicole PC Koniijn<sup>2</sup>, Debby den Uyl<sup>2</sup>, Maarten Boers<sup>2</sup>, Willem F Lems<sup>2</sup>. <sup>1</sup>VU University medical center, department of Epidemiology and Biostatistics, Netherlands, <sup>2</sup>Amsterdam Rheumatology and immunology center, location VU University medical center, Netherlands

**Introduction.** Combinatietherapie Bij Reumatoide Artritis (COBRA)-light therapy (methotrexate and initially 30mg/day prednisolone) has proven to be non-inferior to COBRA therapy (methotrexate, sulfasalazine and initially 60mg/day prednisolone) in the first year of treatment of early rheumatoid arthritis (RA) patients.(1)

**Objective.** This study assessed changes in bone mineral density (BMD) after four years in early RA patients initially randomized to one year of COBRA or COBRA-light therapy.

**Methods.** In the open-label, randomised, non-inferiority trial patients were assigned to COBRA or COBRA-light therapy. After one year, treatment was at the discretion of the treating rheumatologists. BMD was measured at baseline, after one, two and four years at total hip, femoral neck, and lumbar spine.

**Results.** Of the 162 original patients, 157 agreed to a follow-up visit after an average of four years (with a range from 34 to 74 months) and were analysed; 68% were female; mean (SD) age at follow up 52 (13) years. Four patients had outliers; these data were not taken into account. In the COBRA-light group, 11% of the patients used bisphosphonates after four years; the mean cumulative prednisolone dosage was 2.6gr (IQR 1.9 to 5.9) and 49% of the patients had minimal disease activity (DAS44<1.6). In the COBRA group, these numbers were 10%, 3.2gr (IQR 2.5 to 6.2) and 49%, respectively. The mean decline in BMD was slightly (but not significantly) larger in the COBRA-light group (-3.3% at total hip; -3.7% at femoral neck; -0.5% at lumbar spine), even when corrected for bisphosphonates, cumulative dosage of prednisolone and disease activity (Table), compared to the COBRA group (-1.7% at total hip; -3.0% at femoral neck; -1.0% at lumbar spine). The decline in bone was negligible small, but significantly different between baseline and after four years at total hip for both therapies and at femoral neck for COBRA-light.

**Conclusion.** In modern management of RA, one year of (initially high) glucocorticoid treatment has negligible long-term effects on bone.

1. Ter Wee, MM, den Uyl, D, Boers, M et al. (2014). Intensive combination treatment regimens, including prednisolone, are effective in treating patients with early rheumatoid arthritis regardless of additional etanercept: 1-year results of the COBRA-light open-label, randomised, non-inferiority trial. *Annals of the rheumatic diseases*, 74 (6), 1233-40.

Table. BMD of COBRA-light trial patients at four years of follow up

	COBRA-light				COBRA				GEE analyses	
	Baseline	T4	Bone Loss Absolute	% of baseline	Baseline	T4	Bone Loss Absolute	% of baseline	Mean difference	95% CI
Total Hip	0.96 (0.13)	0.93 (0.14)	-0.03 (0.05)	-3.3	0.95 (0.15)	0.94 (0.15)	-0.02 (0.05)	-1.7	-0.00	-0.04 - 0.05
									-0.00*	-0.04 - 0.05
									-0.00**	-0.04 - 0.05
Femoral Neck	0.88 (0.12)	0.85 (0.13)	-0.03 (0.05)	-3.7	0.90 (0.16)	0.88 (0.17)	-0.03 (0.06)	-3.0	-0.02 *	-0.06 - 0.03
									-0.01 **	-0.05 - 0.04
Lumbar Spine	1.10 (0.15)	1.10 (0.16)	-0.01 (0.08)	-0.5	1.13 (0.19)	1.12 (0.20)	-0.01 (0.08)	-1.0	-0.03	-0.08 - 0.03
									-0.03 *	-0.08 - 0.03
									-0.02 **	-0.08 - 0.03

GEE analysis: COBRA-light vs COBRA. Outcomes are given as mean (SD) unless stated otherwise. BMD is given in g/cm<sup>3</sup>.

\*Adjusted for percentage of bisphosphonate users.

\*\*Adjusted for percentage of bisphosphonate users, cumulative prednisolone dosage (gr) and percentage of patients with minimal disease activity (DAS44<1.6) after four years.

BMD, Bone Mineral Density; T4, measurement after 4 years; GEE, Generalized Estimating Equations; CI, Confidence Interval; SD, Standard Deviation

Table. BMD of COBRA-light trial patients at four years of follow up

Disclosures: Merel JJ Lucassen, None.

## 1069

**The Effect of Bisphosphonates on Mortality Risk Reduction is Partly Mediated Through a Reduction in the Rate of Bone Loss.** Dana Bliuc<sup>1</sup>, Thach Tran<sup>1</sup>, Tineke van Geel<sup>2</sup>, Jonathan Adachi<sup>3</sup>, Claudie Berger<sup>4</sup>, Joop van den Bergh<sup>5</sup>, John A. Eisman<sup>6</sup>, Piet Geusens<sup>2</sup>, David Goltzman<sup>7</sup>, David A. Hanley<sup>8</sup>, Robert G Josse<sup>9</sup>, Stephanie M Kaiser<sup>10</sup>, Christopher S Kovacs<sup>11</sup>, Lisa Langsetmo<sup>12</sup>, Jerilynn C Prior<sup>13</sup>, Tuan V. Nguyen<sup>1</sup>, Jacqueline R Center<sup>14</sup>. <sup>1</sup>Osteoporosis and Bone Biology Program, Garvan Institute of Medical Research, Australia, <sup>2</sup>Maastricht University Medical Center, Research School CAPHRI, Care and Public Health Research Institute, Netherlands, <sup>3</sup>Department of Medicine, McMaster University, Canada, <sup>4</sup>CaMos National Coordinating Centre, McGill University, Canada, <sup>5</sup>Maastricht University Medical Center, Research School Nutrim, Department of Internal Medicine, Subdivision of Rheumatology, Netherlands, <sup>6</sup>Osteoporosis and Bone Biology Department, Clinical Translation and Advanced Education, Garvan Institute, Clinical School, St Vincent's Hospital, Faculty of Medicine UNSW Australia, School of Medicine, University of Notre Dame, Australia, <sup>7</sup>Department of Medicine, McGill University, Canada, <sup>8</sup>Department of Medicine, University of Calgary, Canada, <sup>9</sup>Department of Medicine, University of Toronto, Canada, <sup>10</sup>Department of Medicine, Dalhousie University, Canada, <sup>11</sup>Faculty of Medicine, Memorial University, Canada, <sup>12</sup>School of Public Health, University of Minnesota, United States, <sup>13</sup>Department of Medicine and Endocrinology, University of British Columbia, Canada, <sup>14</sup>Osteoporosis and Bone Biology Program, Garvan Institute of Medical Research, Clinical School St Vincent's Hospital, Faculty of Medicine, UNSW Australia, Australia

**Background.** Bisphosphonates, potent anti-resorptive agents that reduce bone turnover, have been found to be associated with mortality risk reduction. Accelerated bone loss is, in itself, an independent predictor of mortality risk but the relationship between bisphosphonates, bone loss and mortality is unknown.

**Objective:** To determine whether the association between bisphosphonates and mortality is mediated by a reduction in the rate of bone loss.

**Setting and study design:** Nested case-control study of bisphosphonate users (BP) and non-users (NoRx) matched by age, gender and time of treatment, from the population-based Canadian Multicentre Osteoporosis Study. Fracture and mortality data were collected prospectively (1996-2011). Co-morbidities, medication and life-style factors were collected yearly and BMD at baseline, years 3 (for those aged 40-60), 5 and 10. Rate of bone loss was calculated using linear regression.

**Main outcome measure:** percent mortality risk associated with BP mediated by a reduction in the rate of bone loss obtained using causal mediation analysis. Three models were examined: association between 1) BP and survival 2) BP and rate of bone loss and 3) BP, bone loss and survival.

**Results:** There were 1631 pairs of BP and matched NoRx in women and 310 in men. BP was associated with significant mortality risk reduction in women [HR, 0.63 (95% CI, 0.53- 0.74)] but not men [HR, 0.91 (95% CI, 0.67-1.25)] after adjusting for confounders. The rate of bone loss was significantly higher in NoRx compared to BP in both sexes [Women: mean (sd) -0.59 (1.14)%/year and -0.05 (1.20)%/year; p<0.0001 and men: -0.36 (0.86)%/year and -0.16 (1.39)%/year; p=0.06]. Given that mortality risk reduction was not statistically significant in men, possibly related to small sample size, the causal mediation analysis was only carried out for women. When BP and rate of bone loss were simultaneously added to the survival model, the association between BP and mortality decreased [HR 0.74 (0.63-0.87)]. Mediation analysis indicated that 35% (20-55%) of the BP association with mortality was mediated by a reduction in the rate of bone loss.

**Conclusions:** Decreased rate of bone loss and BP use were significantly associated with decreased mortality risk in women. Approximately a third of the association of BP

with mortality was mediated by a reduction in the rate of bone loss. This finding has important implications for mechanistic studies of the effect of anti-resorptives on survival.

**Disclosures:** Dana Blünc, None.

## 1070

**Safety and Efficacy of Denosumab Among Subjects in the FREEDOM Extension Study With Mild-to-Moderate Chronic Kidney Disease (CKD).** Aaron Broadwell<sup>1</sup>, Peter R Ebeling<sup>2</sup>, Edward Franek<sup>3</sup>, Stefan Goemaere<sup>4</sup>, Rachel B Wagman<sup>5</sup>, Xiang Yin<sup>5</sup>, Susan Yue<sup>5</sup>, Paul D Miller<sup>6</sup>. <sup>1</sup>Rheumatology and Osteoporosis Specialists, United States, <sup>2</sup>Monash University, Australia, <sup>3</sup>Mossakowski Medical Research Centre, Polish Academy of Sciences, Poland, <sup>4</sup>Ghent University Hospital, Belgium, <sup>5</sup>Amgen Inc., United States, <sup>6</sup>Colorado Center for Bone Research, United States

**Purpose:** As renal function may decline with age, it is important to understand the safety and efficacy of therapeutic agents for postmenopausal osteoporosis (PMO) in patients with age-related renal insufficiency, as well as the effect these agents may have on intrinsic renal function. We assessed the safety and efficacy of denosumab (DMAb) in subjects with different levels of renal function and changes in renal function over time who participated in the FREEDOM Extension study.

**Methods:** Subjects were grouped based on baseline (BL) estimated glomerular filtration rate (eGFR) normalized to body surface area and calculated using the MDRD study equation. Change in eGFR subgroup from BL to last on-study visit for each subject was assessed and summarized. The annualized rates of new vertebral fractures (VFX), non-VFX, and adverse events (AEs) were assessed for the subgroups of subjects with normal renal function (eGFR ≥ 90 mL/min) or mild (eGFR = 60-89 mL/min; CKD stage 2) or moderate (eGFR = 30-59 mL/min; CKD stage 3) renal insufficiency. These outcomes were evaluated for both the long-term (up to 10 years DMAb treatment) and crossover (up to 7 years DMAb treatment) arms.

**Results:** The majority of subjects in the long-term (1969/2343; 84%) and crossover (1781/2206; 81%) arms had mild or moderate renal insufficiency (CKD stage 2 or 3) prior to receiving DMAb. Few subjects (n=4 long-term; n=5 crossover) had an eGFR = 15-29 mL/min (CKD stage 4) at BL; none had CKD stage 5. Most subjects (1325/1969 [67%] long-term; 1216/1781 [68%] crossover) with BL CKD stage 2 or 3 had relatively stable renal function, remaining within the same CKD subgroup at the last on-study visit. Less than 1% of subjects progressed from CKD stage 2 or 3 to CKD stage 4; no subjects initiated renal replacement therapy. The incidence of new VFX was similar among subjects with normal eGFR or CKD stage 2 or 3 in both the long-term (Figure) and crossover (data not shown) arms. The percentage of subjects reporting serious AEs was similar among the renal subgroups for both the long-term (54% normal GFR; 52% CKD stage 2; 57% CKD stage 3) and crossover (43% normal GFR; 42% CKD stage 2; 45% CKD stage 3) arms.

**Conclusions:** The safety and efficacy of DMAb did not substantially differ among subjects with mild-to-moderate renal insufficiency. Furthermore, long-term exposure to DMAb does not appear to have a meaningful effect on renal function in women with PMO.

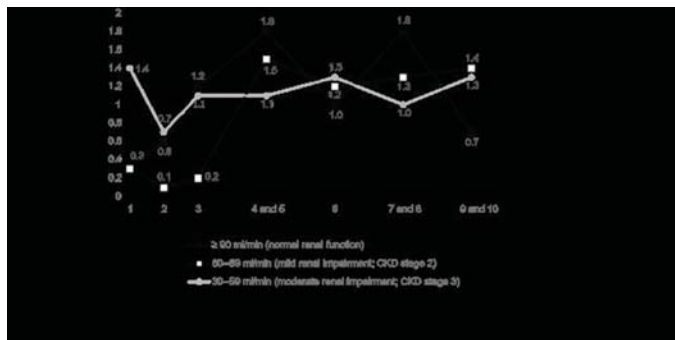


Figure: Annualized Incidence Rate of New VFX for the Long-Term Treatment Arm

**Disclosures:** Aaron Broadwell, Janssen, Grant/Research Support.

## 1071

**Continued Fracture Risk Reduction After 12 Months of Romosozumab Followed by Denosumab Through 36 Months in the Phase 3 FRAME (Fracture study in postmenopausal women with osteoporosis) Extension.** E Michael Lewiecki<sup>1</sup>, Rajani V Dinavahi<sup>2</sup>, Marise Lazaretti-Castro<sup>3</sup>, Peter R Ebeling<sup>4</sup>, Jonathan D Adachi<sup>5</sup>, Akimitsu Miyauchi<sup>6</sup>, Evelien Gielen<sup>7</sup>, Cassandra E Milmont<sup>2</sup>, Cesar Libanati<sup>8</sup>, Andreas Grauer<sup>2</sup>. <sup>1</sup>New Mexico Clinical Research & Osteoporosis Center, United States, <sup>2</sup>Amgen Inc., United States, <sup>3</sup>Federal University of São Paulo, Brazil, <sup>4</sup>Monash University, Australia, <sup>5</sup>McMaster University, Canada, <sup>6</sup>Miyauchi Medical Center, Japan, <sup>7</sup>University Hospitals Leuven, Belgium, <sup>8</sup>UCB Pharma, Belgium

### Background

Romosozumab (Romo) is a monoclonal antibody that binds sclerostin with a dual effect, increasing bone formation and decreasing bone resorption. In the primary analysis of the multicenter, double-blind, FRAME (NCT01575834) study of postmenopausal women aged 55-90 with osteoporosis (T-score ≤ -2.5 at total hip [TH] or femoral neck), Romo significantly reduced vertebral and clinical fracture risk vs placebo (Pbo) at 12 months (M).<sup>1</sup> A continued 75% new vertebral fracture and 33% clinical fracture relative risk reduction was observed at 24M in patients who initially received Romo, despite all patients receiving denosumab (DMAb) after 12M. BMD showed rapid and robust increases with Romo at the spine and hip, and these increases continued on transition to DMAb.<sup>1</sup>

### Methods

In FRAME, patients received Pbo or Romo SC monthly for 12M, followed by open-label DMAb SC every 6M for 12M. Here, we report results through 36M after a further 12M of open-label DMAb. Key endpoints included patient incidence of new vertebral, clinical (nonvertebral plus symptomatic vertebral), and nonvertebral fracture, and BMD.

### Results

Of the 7180 women enrolled, 5743 (80%) completed the 36M study (2892 Pbo followed by DMAb; 2851 Romo followed by DMAb). Through 36M, fracture risk reduction was observed for new vertebral, clinical, nonvertebral, and other predefined fracture endpoints in patients who received Romo followed by 24M of DMAb vs Pbo followed by 24M of DMAb (Table). At 36M, BMD continued to increase in the Romo followed by DMAb group to 18.1% (lumbar spine) and 9.4% (TH) (Figure). The mean differences in BMD in patients who received Romo in the first 12M compared with those initially on Pbo remained significant over the entire 36M ( $P < 0.001$ ). Adverse events were generally balanced between groups; no additional positively adjudicated cases of AFF or ONJ were reported since reporting the 24M data.<sup>1</sup>

### Conclusions

In postmenopausal women with osteoporosis, Romo followed by DMAb was well tolerated and reduced new vertebral, clinical, and nonvertebral fracture risk vs Pbo followed by DMAb for 24M. BMD continued to increase in both groups. BMD in patients treated with Romo in the first 12M remained significantly higher than in those who initially received Pbo despite all patients receiving DMAb for 24M, underscoring the important foundational effect of Romo. The sequence of Romo followed by DMAb will be a promising treatment regimen for postmenopausal women with osteoporosis.

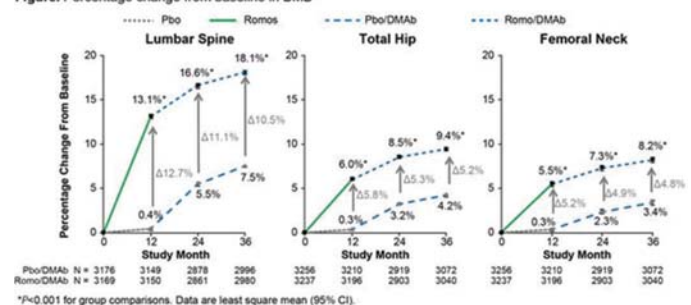
<sup>1</sup>Cosman NEJM 2016

Table. Summary of fracture endpoint results through month 36

Fracture Category	Incidence n/N1 (%)		RRR (%)	P Value
	Pbo/DMAb N = 3591	Romo/DMAb N = 3589		
New vertebral fracture	94/3327 (2.8)	32/3327 (1.0)	66	<0.001
Clinical fracture	196/3591 (5.5)	143/3589 (4.0)	27	0.004
Nonvertebral fracture	178/3591 (4.9)	139/3589 (3.9)	21	0.039
Major nonvertebral fracture	138/3591 (3.8)	100/3589 (2.8)	27	0.015
Major osteoporotic fracture	147/3591 (4.1)	103/3589 (2.9)	30	0.006
Multiple new or worsening vertebral fracture	20/3327 (0.6)	2/3327 (<0.1)	90	<0.001
New or worsening vertebral fracture	94/3327 (2.8)	33/3327 (1.0)	65	<0.001
Clinical new or worsening vertebral fracture	26/3591 (0.7)	5/3589 (0.1)	81	<0.001
Hip fracture	31/3591 (0.9)	18/3589 (0.5)	41	0.071

N = number of subjects randomized; n/N1 = number of subjects with fractures/number of subjects in the analysis set. DMAb = denosumab; Pbo = placebo; RRR = relative risk reduction; Romo = romosozumab.

Figure. Percentage change from baseline in BMD



\*P < 0.001 for group comparisons. Data are least square mean (95% CI).

### Fracture and BMD Results

**Disclosures:** E Michael Lewiecki, Amgen, Lilly, Merck, Grant/Research Support.



## 1072

**Effects of Romosozumab in Postmenopausal Women With Osteoporosis After 2 and 12 Months: Bone Histomorphometry Substudy.** Pascale Chavassieux<sup>\*1</sup>, Roland Chapurlat<sup>1</sup>, Nathalie Portero-Muzy<sup>1</sup>, Pedro Garcia<sup>2</sup>, Jacques P. Brown<sup>3</sup>, Stéphane Horlait<sup>4</sup>, Cesar Libanati<sup>5</sup>, Rogely Boyce<sup>6</sup>, Andrea Wang<sup>6</sup>, Andreas Grauer<sup>6</sup>. <sup>1</sup>INSERM UMR 1033, Université de Lyon, France, <sup>2</sup>Hospital Universitario de Monterrey, Mexico, <sup>3</sup>CHU de Quebec Research Centre and Laval University, Canada, <sup>4</sup>Amgen, France, <sup>5</sup>UCB BioPharma, Belgium, <sup>6</sup>Amgen Inc., United States

Purpose: Romosozumab, a humanized sclerostin antibody, increases bone formation, reduces bone resorption, increases BMD, and reduces fracture risk. This study evaluated the effects of romosozumab after 2 (M2) and 12 (M12) months on bone tissue by histomorphometry in postmenopausal women with osteoporosis from the randomized, double-blind, placebo-controlled FRAME trial.

Methods: Patients received romosozumab 210 mg or placebo monthly for 12 months and underwent transiliac bone biopsies at M2 and M12. Patients evaluable for histomorphometry included 29 (14 placebo, 15 romosozumab) with quadruple fluorochrome labeling (double fluorochrome labeling at baseline [M0] and before M2) at M2, and 70 (31 placebo, 39 romosozumab) with double fluorochrome labeling at M12. Continuous variables were summarized using median (Q1, Q3). Within-subject paired comparison between M0 and M2 were based on Wilcoxon signed rank test and between-group comparisons at M2 and M12 were based on Wilcoxon rank sum test.

Results: After 2 months of romosozumab when compared to M0, BFR/BS significantly increased in cancellous bone ( $3.4 \mu\text{m}^3/\mu\text{m}^2/\text{yr}$  at M0,  $12.5 \mu\text{m}^3/\mu\text{m}^2/\text{yr}$  at M2;  $p<0.001$ ) and endocortical bone ( $14.1 \mu\text{m}^3/\mu\text{m}^2/\text{yr}$  at M0,  $52.3 \mu\text{m}^3/\mu\text{m}^2/\text{yr}$  at M2;  $p<0.001$ ). No significant change was observed in the placebo group in cancellous bone ( $3.1 \mu\text{m}^3/\mu\text{m}^2/\text{yr}$  at M0 and  $5.2 \mu\text{m}^3/\mu\text{m}^2/\text{yr}$  at M2;  $p=0.24$ ) or endocortical bone ( $18.7 \mu\text{m}^3/\mu\text{m}^2/\text{yr}$  at M0 and  $15.2 \mu\text{m}^3/\mu\text{m}^2/\text{yr}$  at M2;  $p=0.34$ ). Over this period, BFR/BS increased by 328% for romosozumab vs 79% for placebo ( $p=0.007$ ) in cancellous bone and 233% vs -34% for endocortical bone ( $p<0.001$ ). Changes in MS/BS in cancellous and endocortical bone generally mirrored the changes in BFR/BS. Romosozumab did not affect cortical BFR/BS at M2 or M12, whereas cancellous BFR/BS was decreased at M12 compared with placebo (Table). At both M2 and M12, resorption indices (ES/BS) were decreased in cancellous and endocortical bone. The overall changes observed with romosozumab through the first 12 months resulted in significant increase in bone mass (BV/TV), trabecular thickness, and wall thickness (all  $p\leq 0.03$ ). Qualitative evaluation showed normal bone structure and quality.

Conclusion: Romosozumab produced an early, significant bone forming effect and a sustained decrease in bone resorption. At M12, cancellous bone turnover was reduced. These changes in bone formation and resorption were associated with significantly increased bone mass and improved microstructure.

	Month 2 median (Q1, Q3)			Month 12 median (Q1, Q3)		
	Placebo (N = 14)	Romosozumab (N = 15)	p-value	Placebo (N = 31)	Romosozumab (N = 39)	p-value
Cn-BV/TV (%)	12.3 (10.9, 17.0)	15.5 (9.0, 19.1)	0.98	11.4 (9.4, 15.5)	15.4 (11.0, 20.1)	0.03
Cn-Tb.Th (µm)	99.5 (85.8, 133.4)	105.9 (95.8, 125.4)	0.35	102.0 (86.1, 125.2)	132.0 (101.9, 158.4)	0.006
Cn-W.Th (µm)	31.7 (30.4, 33.9)	31.6 (30.7, 33.6)	0.91	29.5 (27.8, 32.3)	31.8 (30.8, 34.1)	0.014
Cn-MS/BS (%)	2.3 (0.7, 3.1)	5.6 (3.7, 8.4)	0.002	3.0 (0.9, 5.4)	0.6 (0.0, 2.2)	0.004
Cn-BFR/BS (µm <sup>3</sup> /µm <sup>2</sup> /year)	5.2 (2.9, 7.2)	12.1 (7.3, 16.1)	0.004	6.8 (2.7, 13.2) <sup>a</sup>	1.6 (0.9, 6.5) <sup>a</sup>	0.014
En-MS/BS (%)	7.0 (3.3, 9.9)	24.6 (16.0, 31.5)	<0.001	3.6 (1.0, 8.9)	1.9 (0.2, 7.6) <sup>a</sup>	0.25
En-BFR/BS (µm <sup>3</sup> /µm <sup>2</sup> /year)	15.2 (11.0, 21.2) <sup>a</sup>	52.3 (33.7, 64.9)	0.001	10.1 (3.9, 19.2) <sup>a</sup>	6.4 (1.4, 15.0) <sup>a</sup>	0.18
Ct-MS/BS (%)	4.6 (1.4, 8.5)	8.2 (5.0, 10.6)	0.077	4.4 (2.2, 8.3)	6.0 (3.4, 9.9) <sup>a</sup>	0.25
Ct-BFR/BS (µm <sup>3</sup> /µm <sup>2</sup> /year)	16.7 (7.1, 26.1) <sup>a</sup>	19.2 (13.1, 32.0)	0.41	13.4 (4.1, 20.6)	13.9 (6.3, 28.6) <sup>a</sup>	0.38
Cn-ES/BS (%)	3.4 (1.9, 4.5)	1.8 (0.9, 3.2)	0.02	2.9 (2.0, 4.5)	1.1 (0.5, 1.7)	<0.001
En-ES/BS (%)	6.3 (3.3, 7.7)	1.6 (0.6, 3.5)	0.003	4.1 (3.0, 6.5)	0.5 (0.2, 1.2) <sup>a</sup>	<0.001

<sup>a</sup>Dynamic parameters for samples with single label were imputed. Includes subjects with evaluable histomorphometry data at each time point. Between-group p-values based on the Wilcoxon rank sum test. <sup>a</sup>ns = 27; <sup>b</sup>ns = 26; <sup>c</sup>ns = 37; <sup>d</sup>ns = 12; <sup>e</sup>ns = 29; <sup>f</sup>ns = 13; <sup>g</sup>ns = 35; <sup>h</sup>ns = 38.

Cn: cancellous; BV: bone volume; TV: tissue volume; Tb.Th: trabecular thickness; W.Th: wall thickness; MS: mineralizing surface; BS: bone surface; BFR: bone formation rate; En: endocortical; Ct: intracortical; ES: eroded surface.

Table: Between-group Comparison of Histomorphometry Parameters at Months 2 and 12

Disclosures: Pascale Chavassieux, None.

## 1073

**Ten-year Continued Nonvertebral Fracture Reduction in Postmenopausal Osteoporosis With Denosumab Treatment.** S Ferrari<sup>\*1</sup>, P Butler<sup>2</sup>, DL Kendler<sup>3</sup>, PD Miller<sup>4</sup>, C Roux<sup>5</sup>, AT Wang<sup>2</sup>, RB Wagman<sup>2</sup>, EM Lewiecki<sup>6</sup>. <sup>1</sup>Geneva University Hospital, Switzerland, <sup>2</sup>Amgen Inc., United States, <sup>3</sup>University of British Columbia, Canada, <sup>4</sup>Colorado Center for Bone Research, United States, <sup>5</sup>Paris Descartes University, France, <sup>6</sup>New Mexico Clinical Research & Osteoporosis Center, United States

Purpose: Treatment with denosumab (DMAb) for 3 years significantly reduces the incidence of nonvertebral fractures (NVFx; Cummings *NEJM* 2009). While there are limited data describing the benefit/risk of long-term reduction in bone remodeling, recent findings show that subjects receiving DMAB for up to 7 years experience further decreases in NVFx risk (Ferrari *OI* 2015). To better characterize this observation,

we evaluated the reproducibility of the 7-year findings in the FREEDOM Extension (EXT) cross-over (XO) group and assessed long-term fracture rates with 10 years of DMAB treatment in the EXT long-term (LT) group.

Methods: During FREEDOM, subjects were randomized to placebo or DMAB 60 mg Q6M for 3 years. Subjects who missed  $\leq 1$  dose could enroll in the 7-year EXT, when all subjects received open-label DMAB 60 mg Q6M; LT subjects could receive up to 10 years of DMAB and XO subjects up to 7 years. The NVFx rate in the first 3 years of DMAB was compared with 1) years 4-7 in LT and XO groups separately and combined, and 2) years 4-10 in the LT group. Adjusted rate ratios (RR, 95% CIs) between observational periods were computed by generalized estimating equation Poisson regression.

Results: Of 5928 subjects eligible for the EXT, 4550 (77%) enrolled (N=2343 LT; N=2207 XO). Baseline characteristics at FREEDOM and EXT and % subjects who completed EXT were balanced between groups. The NVFx rate (95% CI) in the LT group was 1.98 per 100 subject-years (1.67-2.34) during the first 3 years of DMAB treatment and 1.54 (1.29-1.83) during years 4-7 (RR 0.79,  $p=0.046$ ; Table). To confirm this observation, the NVFx rate in the XO group was 2.37 (1.97-2.84) during the first 3 years of DMAB treatment and 1.52 (1.24-1.87) during years 4-7 (RR 0.65,  $p=0.002$ ). The NVFx rate in the combined LT + XO group was 2.15 (1.90-2.43) during the first 3 years and 1.53 (1.34-1.75) during years 4-7 (RR 0.72,  $p<0.001$ ). The LT group showed a NVFx rate of 1.44 (1.24-1.66) during years 4-10 (RR 0.74,  $p=0.008$ ). For 6089 subjects exposed to DMAB in FREEDOM or EXT, the rate of bone safety events (ONJ or AFF) was 4.2 per 10,000 subject-years.

Conclusions: Compared with the first 3 years of DMAB treatment, a longer duration of DMAB therapy was associated with a further decrease in NVFx rate through 10 years. Long-term reduction in bone remodeling is not only associated with continued increases in BMD (Bone ASBMR 2016), but also with a favorable benefit/risk profile for bone.

Table. Comparison of Nonvertebral Fracture Rates up to 10 Years of Denosumab Treatment

	First 3 Years of DMAB Treatment	Years 4-7 of DMAB Treatment	Years 4-10 of DMAB Treatment
<b>Long-term Subjects (N = 2343)</b>	140 Fractures	126 Fractures	184 Fractures
Fracture Rate (95% CI)	1.98 (1.67–2.34)	1.54 (1.29–1.83)	1.44 (1.24–1.66)
Rate Ratio (95% CI)	[Referent]	0.79 (0.62–1.00)	0.74 (0.60–0.93)
p-value		$p = 0.046$	$p = 0.008$
<b>Cross-over Subjects (N = 1731)</b>	123 Fractures	91 Fractures	
Fracture Rate (95% CI)	2.37 (1.97–2.84)	1.52 (1.24–1.87)	
Rate Ratio (95% CI)	[Referent]	0.65 (0.50–0.86)	
p-value		$p = 0.002$	
<b>Long-term and Cross-over Subjects Combined (N = 4074)</b>	263 Fractures	217 Fractures	
Fracture Rate (95% CI)	2.15 (1.90–2.43)	1.53 (1.34–1.75)	
Rate Ratio (95% CI)	[Referent]	0.72 (0.61–0.86)	
p-value		$p < 0.001$	

N = number of subjects who completed FREEDOM (ie, completed their 3-year visit and did not discontinue IP), did not miss >1 dose of IP in FREEDOM, and who enrolled in the Extension. In addition, cross-over subjects completed 3 years of the extension and did not miss >1 dose of DMAB during the first 3 years of the Extension. Fracture rates and rate ratios were obtained using generalized estimating equation Poisson models; fracture rates are per 100 subject-years. Rate ratios relative to the first 3 years of DMAB treatment were adjusted for age, total hip BMD T-score, weight, and history of nonvertebral fracture. In addition, the treatment group variable was included in the model for the combined analysis only.

Table. Comparison of Nonvertebral Fracture Rates up to 10 Years of Denosumab Treatment

Disclosures: S Ferrari, Agnovos, Amgen, Radius, UCB, Consultant.

## 1074

**Sustained Fracture Risk Reduction with Sequential Abaloparatide/Alendronate: Results of ACTIVEExtend.** Henry G Bone<sup>\*1</sup>, Felicia Cosman<sup>2</sup>, Paul D Miller<sup>3</sup>, Gregory C Williams<sup>4</sup>, Gary Hattersley<sup>4</sup>, Ming-yi Hu<sup>4</sup>, Lorraine A Fitzpatrick<sup>4</sup>, Socrates Papapoulos<sup>5</sup>. <sup>1</sup>Michigan Bone and Mineral Clinic, United States, <sup>2</sup>Helen Hayes Hospital and Columbia University, United States, <sup>3</sup>Colorado Center for Bone Research, United States, <sup>4</sup>Radius Health, Inc., United States, <sup>5</sup>Leiden University Medical Center, Netherlands

Introduction: ACTIVE was a study of 2463 postmenopausal women with osteoporosis who were randomized 1:1:1 to abaloparatide (ABL), blinded placebo (PBO), or open-label teriparatide. ABL significantly reduced vertebral, nonvertebral, clinical, and major osteoporotic fractures compared to PBO. In ACTIVEExtend, the ABL and PBO arms were switched to alendronate (ALN) 70 mg weekly for two years.

Methods: The extension enrolled 558 women who had completed ACTIVE in the ABL group and 581 in the placebo group. Vertebral and nonvertebral fractures, all clinical fractures regardless of the level of trauma, and major osteoporotic fractures (upper arm, wrist, hip, or clinical spine) were adjudicated as pre-specified fracture endpoints. The Genant semi-quantitative scale was used for vertebral fracture assessment. Fracture risk reduction was measured from the beginning of ACTIVE to the end of ACTIVEExtend (18 months of ABL or PBO, 1 month for consent, and 24 months of ALN treatment for a total of 43 months).

Results: Five of 544 evaluable women (0.9%) in the ABL followed by ALN (ABL/ALN) group had at least 1 new vertebral fracture vs 32/568 (5.6%) in the PBO followed by ALN group (PBO/ALN), an 84% relative risk reduction ( $p<0.0001$ ).

For nonvertebral fractures, there was a 39% risk reduction with ABL/ALN (n=27/558, 5.0%) compared to PBO/ALN (n=45/581, 8.0%; p=0.038). For all clinical fractures, there was a 34% risk reduction in the ABL/ALN group compared to the PBO/ALN group (p=0.045). For major osteoporotic fractures, there was a 50% risk reduction with the ABL/ALN group compared to the PBO/ALN group (p=0.011). The Kaplan-Meier curves for nonvertebral, clinical, and major osteoporotic (Figure) fractures showed early and sustained separation between the ABL/ALN and PBO/ALN groups.

Among women with no new vertebral fractures during 18 months of ACTIVE, 2 in the ABL/ALN group vs 13 in the PBO/ALN group experienced new vertebral fractures during the extension phase alone.

The incidence of AEs was similar for both arms, with a safety profile consistent with ALN treatment and no cases of AFF or ONJ.

Conclusions: Administration of abaloparatide for 18 months followed by alendronate resulted in persistent risk reduction for vertebral, nonvertebral, clinical, and major osteoporotic fractures compared to placebo followed by alendronate. Although both groups received alendronate therapy, the effects of abaloparatide during ACTIVE were maintained during ACTIVEExtend.

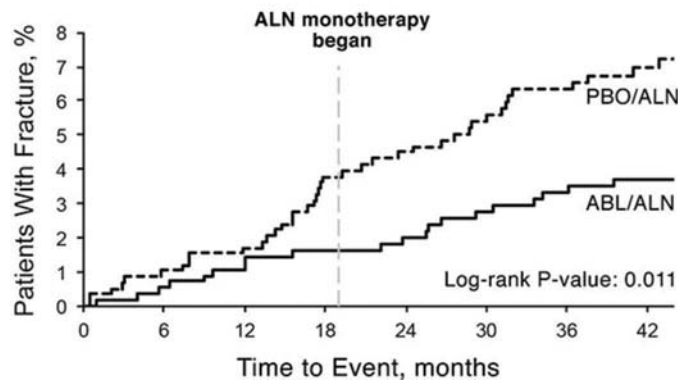


Figure: Time to event of major osteoporotic fractures.

Disclosures: Henry G Bone, Amgen, Consultant.

## 1075

**Comparison of BMD Changes and Bone Turnover Levels 3 Years After Bisphosphonate Discontinuation: FLEX and HORIZON Studies.** Tiffany Kim<sup>1</sup>, Douglas Bauer<sup>2</sup>, Anne Schafer<sup>1</sup>, Felicia Cosman<sup>3</sup>, Dennis Black<sup>2</sup>, Richard Eastell<sup>4</sup>. <sup>1</sup>University of California, San Francisco, and the San Francisco VA Health Care System, United States, <sup>2</sup>University of California, San Francisco, United States, <sup>3</sup>Helen Hayes Hospital, West Haverstraw, and Columbia University, New York, United States, <sup>4</sup>University of Sheffield, United Kingdom

An ASBMR task force recommended considering a drug holiday for certain women treated for  $\geq 5$  years with alendronate (ALN) or  $\geq 3$  years with zoledronic acid (ZOL), with reassessment 2-3 years later. However, there is little evidence about drug holiday management and differences in bone loss. Our goal was to compare BMD changes and bone turnover in the placebo extension arms of 2 key bisphosphonate trials.

In the Fracture Intervention Trial Long-term Extension (FLEX), women who had taken a mean of 5 years of ALN were randomized to placebo or continued ALN for 5 more years. Similarly in the HORIZON Pivotal Fracture Trial (HORIZON-PFT) extension, women who had 3 years of ZOL were randomized to placebo or continued ZOL for 3 more years. We analyzed the placebo groups. In both trials, total hip (TH) BMD changes from extension years 0 to 3 were categorized into those exceeding and those below the approximate least significant change (LSC; 4%). For the bone marker PINP (Roche Elecsys), year 3 levels were categorized into 3 groups: below, within, or above a target range of 16.3-36.0 ng/mL. This target range corresponds to the lower half of the reference interval for young, healthy women.

At extension baseline, the mean TH T-score was -2.0 for both studies. PINP geometric means (ng/mL) were 23.1 in FLEX and 21.1 in the HORIZON-PFT (p=0.07). After 3 years of placebo, 25.2% of those in FLEX and 18.7% of those in the HORIZON-PFT extension had total hip BMD loss  $\geq$  LSC (p=0.02) (Figure 1). At year 3, 42.0% of FLEX subjects and 24.6% of HORIZON-PFT extension subjects had PINP levels above the target range (p<0.01) (Figure 1). In total, 53% of FLEX subjects and 34% of HORIZON-PFT extension subjects had either total hip BMD loss exceeding LSC or PINP levels above the target range.

In conclusion, a high proportion of women had unsuppressed bone turnover or BMD decline in the placebo extension arms. This supports the ASBMR task force's recommendation to reassess risk 3 years after drug discontinuation. Finally, the effect of ZOL on BMD appears to be more potent and persistent than the effect of ALN. Evidence from the placebo arms of these extension trials may help guide the management of drug holidays.

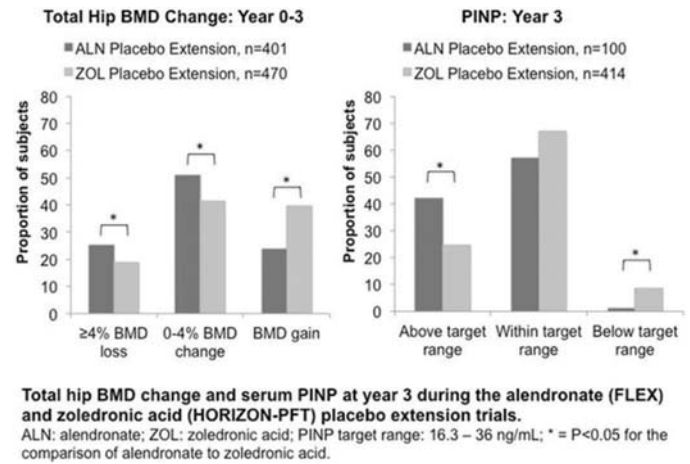


Figure 1

Disclosures: Tiffany Kim, None.

## 1076

**The Crucial p53-Dependent Oncogenic Role of JAB1 in Osteosarcoma Pathogenesis.** William Samsa<sup>\*</sup>, Lindsay Bashur, Murali Mamidi, Alexander Miron, Robin Elliott, David Danielpour, Guang Zhou. Case Western Reserve University, United States

Osteosarcoma (OS) is a highly malignant, most common primary bone cancer that mostly affects actively growing bones, and ranks amongst the leading causes of cancer mortality in adolescents. Therefore, elucidating the molecular mechanism of OS pathogenesis and metastasis is essential for better diagnostics and treatment outcomes. As a potential oncogene, Jun activation domain binding protein 1 (JAB1), also known as COP5/CSN5, is amplified and overexpressed in many cancers and has very recently emerged as a novel, specific target for cancer treatment. JAB1 regulates the DNA damage repair pathway, is implicated in chemotherapy and radiotherapy resistance, and is a negative regulator of p53 activity. Thus, we hypothesize that JAB1 controls OS tumorigenesis through p53-dependent mechanisms. We show by immunostaining that JAB1 was overexpressed in 75% of human OS patient biopsy samples and was associated with poor prognosis. Moreover, shRNA mediated JAB1 knockdown in human OS cell lines 143B and LM7 reduced tumor proliferation, colony formation, and motility. To determine the JAB1-mediated transcriptome in OS, we conducted RNA-sequencing in JAB1-depleted human 143B cells. We found 1756 differentially expressed genes, of which 75% were downregulated, solidifying the role of JAB1 as a transcriptional coactivator. Furthermore, we identified distinct alterations in key processes involved in cancer, including cell-cell adhesion, cell division, mRNA splicing, regulation of mRNA stability, rRNA processing, translation initiation, and positive regulation of apoptosis. To determine whether JAB1 overexpression promotes bone tumorigenesis in vivo, using a 2.3kb Col1a1 promoter we generated a novel mouse model in which JAB1 is overexpressed specifically in differentiating osteoblasts on a p53<sup>+/+</sup> background. While Col1a1-JAB1 transgenic mice did not develop any tumors, double transgenic Col1a1-JAB1; p53<sup>+/+</sup> mice develop spontaneous OS formation around 11 months of age, confirming an in vivo role for JAB1 in OS tumorigenesis. Histological analysis of these tumors showed poorly differentiated OS with hypercellularity and the presence of osteoid formation, along with invasion of tumor cells into the surrounding muscle and fat. In conclusion, by conducting RNA-sequencing and by using a new mouse model, we uncovered a distinct JAB1-governed regulatory network and an in vivo, p53-dependent role for JAB1 in OS formation. Thus, JAB1 is an attractive target for OS treatment.

Disclosures: William Samsa, None.

## 1077

**Mice with adipocyte-specific deficiency in protein phosphatase 5 (PP5) have high bone mass due to bone anabolic activity of marrow adipocytes.** Lance Stechschulte<sup>\*</sup>, Andrew Hendrix, Edwin Sanchez, Beata Lecka-Czernik. University of Toledo, United States

We have showed previously in three different animal models that adipocytes (AD) of beige phenotype secrete factors which are anabolic for bone, however we did not prove unequivocally that marrow AD of beige phenotype support bone formation. We have also showed that PP5 phosphatase reciprocally regulates PPAR $\gamma$  and RUNX2 activities through controlling a status of serine phosphorylation, and that mice with total deficiency in PP5 are characterized with high bone mass and increased energy metabolism. Peripheral AD of these mice have characteristics of beige phenotype with increased expression of genes for energy production. To test AD contribution to the regulation of bone mass, we developed mice model with PP5 deficiency specifically in cells of AD lineage by crossing PP5<sup>fl/fl</sup> with Adip<sup>Cre</sup> animals. As expected, Adip<sup>Cre</sup>PP5<sup>fl/fl</sup> mice have increased energy metabolism and insulin sensitivity. Interestingly, they also have high



bone mass due to increased bone formation. Osteoblasts (OB) isolated from endosteal surface are highly activated with increased expression of *Dlx5*, *Osx*, *Ocn*, *Wnt10b*, and genes associated with mineral matrix formation. Osteocytes (OT) isolated from cortical bone of Adip<sup>Cre</sup>PP5<sup>fl/fl</sup> mice do not differ from WT in expression of *Sost* and *Dkk1* suggesting their less likely contribution to increased bone formation in Adip<sup>Cre</sup>PP5<sup>fl/fl</sup> mice. As expected, adiponectin was not expressed in the endosteal OB and cortical OT, while PP5 expression was not affected in these cells in Adip<sup>Cre</sup>PP5<sup>fl/fl</sup> mice. Indeed, PP5 deficiency in cells of AD lineage did not affect OB differentiation from primary bone marrow cells (PBMC), however they were characterized with increased expression of beige AD markers including *Ucp1* and *Prdm16*, while decreased expression of white AD markers including *Lpl*, *CD36*, and *Tcf21*. To test whether PBMC derived from Adip<sup>Cre</sup>PP5<sup>fl/fl</sup> mice secrete bone anabolic activities, we cultured WT PBMC (recipient cells) in the presence of conditioned media (CM) collected from cultures of Adip<sup>Cre</sup>PP5<sup>fl/fl</sup> PBMC (donor cells). We found that CM from donor cells induced expression of OB-specific markers in recipient cells indicating that donor cells secrete pro-OB factors. Indeed, an analysis of donor cells showed significant upregulation of expression of *Wnt10b*, *Bmp4*, and *Igf1bp2*, factors known for their bone anabolic activity. These findings prove that marrow cells of AD lineage may acquire phenotype resembling beige AD producing bone anabolic factors.

**Disclosures:** Lance Stechschulte, None.

## 1078

**Cancellous Bone Volume Fraction and Mineral Content Contribute Differently to Mechanical Behavior in Type 2 Diabetic and Non-diabetic Men.** Heather Hunt<sup>1</sup>, Ashley Torres<sup>1</sup>, Pablo Palomino<sup>1</sup>, Rehan Saiyed<sup>2</sup>, Karen King<sup>3</sup>, Joseph Lane<sup>2</sup>, Christopher Hernandez<sup>1</sup>, Eve Donnelly<sup>1</sup>. <sup>1</sup>Cornell University, United States, <sup>2</sup>Hospital for Special Surgery, United States, <sup>3</sup>University of Colorado Anschutz Medical Campus, United States

Men with type 2 diabetes mellitus (T2DM) have an increased fracture risk compared to non-diabetic (NDM) men, even after accounting for bone mineral density (BMD), suggesting T2DM affects bone quality independently of BMD. Two proposed mechanisms for bone quality changes are the accumulation of advanced glycation endproducts (AGEs) and altered bone turnover. The goal of this study was to compare the microarchitectural, mechanical, and compositional properties of cancellous bone from men with and without T2DM.

Femoral neck specimens were retrieved from men undergoing total hip arthroplasty for osteoarthritis. Men with a T2DM diagnosis were allocated to the T2DM group (n=23, age=65±8, preoperative HbA1c=7.1±1.0), and the remainder were designated as NDM controls (n=23, age=61±8, HbA1c=5.5±0.4). Cylindrical cores were excised, imaged with microCT, and uniaxially compressed to 3% strain. Adjacent tissue was used for the compositional testing of FTIR spectroscopy to measure the mineral:matrix ratio (MM), carbonate:phosphate ratio (CP), collagen maturity (XLR), and crystallinity (XST) in homogenized KBr pellets; a fluorescence assay to assess total AGE content; and HPLC to quantify the enzymatic collagen crosslinks hydroxylsypyrinoline (HP) and lysylpyridinoline (LP) and the AGE pentosidine (Pen). Student's t-tests were performed using a 0.05 significance level. Multiple linear regressions were used to evaluate the effects of microarchitecture and composition on mechanical properties.

Bone volume fraction (BV/TV), MM, and Pen were greater in T2DM compared to NDM specimens (+30%, p<0.05; +8%, p<0.05; +60%, p<0.05). No differences in total AGEs, enzymatic crosslinking (XLR, HP, LP), or mineral properties (CP, XST) were observed between groups. Modulus, yield stress, and resilience were greater in T2DM compared to NDM specimens (+99%, p<0.05; +107%, p<0.05; 121%, p<0.05).

The microarchitecture and compositional measures indicated T2DM specimens had more Pen and more mineralized trabeculae compared to controls. This is consistent with AGE accumulation and increased tissue mineral content due to reduced bone turnover with T2DM. BV/TV and MM were strongly correlated with mechanical outcomes, and when combined with Pen and AGEs, these parameters explained 56-93% of the outcome variable (Table 1). Moreover, the effects of BV/TV and MM towards mechanical properties varied by group, indicating T2DM contributes differently to mechanical behavior.

**Table 1:** Coefficient of determination (R<sup>2</sup>) for single and multiple linear regressions of selected microarchitectural and compositional properties with mechanical properties.

Microarchitectural or Compositional Property	Modulus (MPa)	Yield Stress (MPa)	Ult. Strain (%)	Ult. Stress (MPa)	Resilience (kPa)	Tough. to Ult. Strain (kJ/m <sup>3</sup> )	Tough. to 3% Strain (kJ/m <sup>3</sup> )
BV/TV	0.78 ***	0.72 ***	0.24 **	0.81 ***	0.70 ***	0.79 ***	0.83 ***
MM	0.26 ***	0.27 ***	0.13 #	0.53 ***	0.27 ***	0.57 ***	0.26 ***
Group + BV/TV + Group*BV/TV	0.82 ***	0.76 ***	0.43 **	0.89 ***	0.77 ***	0.85 ***	0.88 ***
Group + MM + Group*MM	0.34 **	0.35 **	0.26 #	0.60 ***	0.34 **	0.63 ***	0.34 **
Group + BV/TV + MM + Group*BV/TV + Group*MM	0.90 ***	0.84 ***	0.49 *	0.94 ***	0.80 ***	0.91 ***	0.91 ***
Group + BV/TV + MM + Group*BV/TV + Group*MM + Pen + AGEs	0.91 ***	0.86 ***	0.56 *	0.96 ***	0.82 ***	0.93 ***	0.91 ***

BV/TV = bone volume fraction; MM = FTIR mineral to matrix ratio; Group = T2DM or NDM; Pen = pentosidine; AGEs = total fluorescent AGEs; Tough = toughness; Ult = ultimate. # indicates p < 0.10; \* p < 0.05; \*\* p < 0.01; \*\*\* p < 0.001.

**Figure 1:** Full multiple linear regression model fits (Group + BV/TV + MM + Group\*BV/TV + Group\*MM + Pen + AGEs) of selected mechanical properties versus BV/TV and MM by group. (A) and (C) demonstrate that the relationships between modulus and ultimate stress with bone volume fraction for T2DM and NDM groups are different (Group\*BV/TV p<0.05). Similarly, (D) demonstrates that the relationship between ultimate stress and MM is different between groups (Group\*MM p<0.05). In contrast, (B) shows similar trends of MM with modulus between groups.

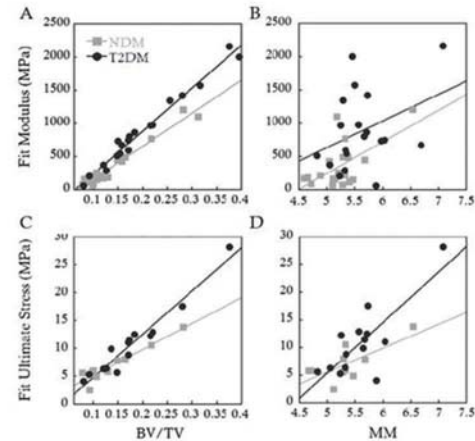


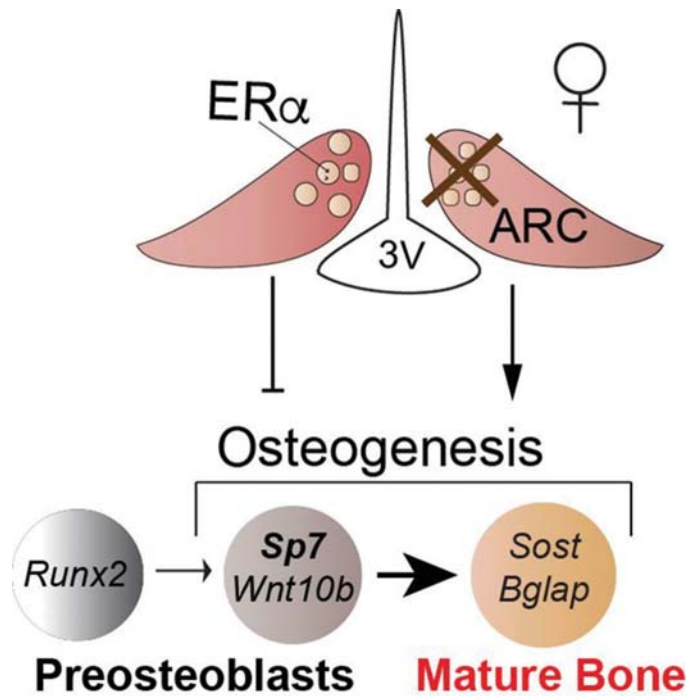
Table 1 and Figure 1.

**Disclosures:** Heather Hunt, None.

## 1079

**Disrupting Central Estrogen Receptor  $\alpha$  Signaling in the Arcuate Nucleus Produces a Dramatic Increase in Bone Mass and Strength.** Candice Herber<sup>1</sup>, William Krause<sup>1</sup>, Corey Cain<sup>1</sup>, Liping Wang<sup>1</sup>, Edward Hsiao<sup>1</sup>, Robert Nissenson<sup>1</sup>, Aaron Fields<sup>1</sup>, Stephanie Correa<sup>2</sup>, Holly Ingraham<sup>1</sup>. <sup>1</sup>University of California, San Francisco, United States, <sup>2</sup>University of California, Los Angeles, United States

Central estrogen signaling in females balances energetic needs of metabolism with reproduction. Two regions within the hypothalamus, the arcuate (ARC) and ventromedial ventrolateral hypothalamus (VMHvl) express estrogen receptor alpha (ER $\alpha$ ) and mediate estrogens effects on body weight and energy balance. Using a new genetic mouse model that eliminates all ER $\alpha$  in both the ARC and VMHvl (*Esr1<sup>Nkx2-1Cre</sup>*), we report the expected sex-dependent metabolic phenotypes without changes in food intake. Unexpectedly, *Esr1<sup>Nkx2-1Cre</sup>* females exhibit a stunning increase in trabecular bone mass of ~500% with an average BV/TV (%) of 60. Increased bone volume correlated with an elevation in trabecular number (Tb. N) from 4 to 12 (1/mm) in controls and mutants, respectively and increased trabecular thickness (Tb. Th) from 40µm in controls to over 60µm in mutants. Increases in bone density begin as early as 4 wks of age and persist in older females. Impressively, 33 wk old female mutants display increases in bone strength of nearly 200% as determined by an L5 crush test or a 3-point bend test of the femur. We confirmed the central origin of this bone phenotype by stereotactically guided AAV2-Cre driven deletion of ER $\alpha$  in the ARC of older *Esr1<sup>fl/fl</sup>* females. This remarkable bone phenotype exceeds that of other mouse models (SOST KO) and persists in ovariectomized females. Elevated *Sp7* (*Osx*) levels suggest that the increased bone formation in mutant females results from an expansion of pre-osteoblasts. Furthermore, female mutants exhibit an increase in bone formation rate (BFR) with no changes in resorption measured by TRAP staining and circulating catecholamines. Our findings establish a paradoxical role of central estrogen signaling as a major repressor of bone metabolism. We propose that this novel female brain-bone axis exists to divert calcium and energy stores away from bone building when reproductive energy demands are high. Breaking this axis, as in our genetic and viral ER $\alpha$  knockout models, results in abnormally dense, strong bones. Future efforts to define the precise mechanisms underlying this neuro-skeletal connection might identify new targets for preventing age-related bone loss.



Schematic of Central ERalpha Regulation of Bone Mass

Disclosures: Candice Herber, None.

## 1080

**Rapid-Throughput Skeletal Phenomics in Zebrafish.** Matthew Hur<sup>1\*</sup>, Charlotte Gistelink<sup>2</sup>, Philippe Huber<sup>1</sup>, Jane Lee<sup>1</sup>, Marjorie Thompson<sup>1</sup>, Adrian Monstad-Rios<sup>1</sup>, Claire Watson<sup>1</sup>, Sarah McMenamin<sup>3</sup>, Andy Willaert<sup>4</sup>, David Parichy<sup>5</sup>, Paul Coucke<sup>6</sup>, Ronald Kwon<sup>1</sup>. <sup>1</sup>University of Washington, United States, <sup>2</sup>Ghent University, Belgium, <sup>3</sup>Boston College, United States, <sup>4</sup>Ghent University, United States, <sup>5</sup>University of Virginia, United States, <sup>6</sup>University of Ghent, Belgium

Genome wide association and sequencing studies have identified a large number of loci associated with human bone mineral density and other osteoporosis-related traits. These loci have implicated a vast number of candidate causal target genes whose skeletal functions are unknown, and for which mutant mice are unavailable. The challenges in screening for loss-of-function phenotypes on a large-scale represents the primary barrier to identifying causal gene targets underlying genetic risk factors for osteoporosis, and consequently, to translating these genetic risk factors into new therapeutics. In this project, we developed a rapid-throughput, highly sensitive workflow to test the *in vivo* impact of genes on adult skeletal health by exploiting the amenability of zebrafish to large-scale gene mutation and whole-body phenomic analysis. We developed microCT-based methods and a segmentation algorithm, FishCuT, that enable rapid (<5min/fish), in-depth phenotypic profiling of the axial skeleton of adult zebrafish at the whole-body scale (Fig 1). Using FishCuT, we analyzed ~20,000 different phenotypic data points, comprising one of the largest phenotypic analyses of the adult vertebrate skeleton performed to date. We demonstrate the potential for phenomic patterns to confer heightened sensitivity, with similar specificity, in discriminating mutant populations compared to analyzing individual vertebrae in isolation, even when the latter is performed at higher resolution. We identify new skeletal phenotypes in zebrafish models of Osteogenesis Imperfecta (*bmp1a*<sup>-/-</sup> and *plod2*<sup>-/-</sup>), as well as in a zebrafish model of thyroid stimulating hormone receptor (*tshr*) hyperactivity (*opallus*). Finally, we develop phenome-based allometric models and show that they are able to discriminate mutant phenotypes masked by alterations in growth. This study advances the use of zebrafish as a rapid, high-content model of musculoskeletal health, develops methods to rapidly map gene-to-phenome relationships in a large number of zebrafish mutant populations, and clarifies relationships between zebrafish and human skeletal genotypes and phenotypes.

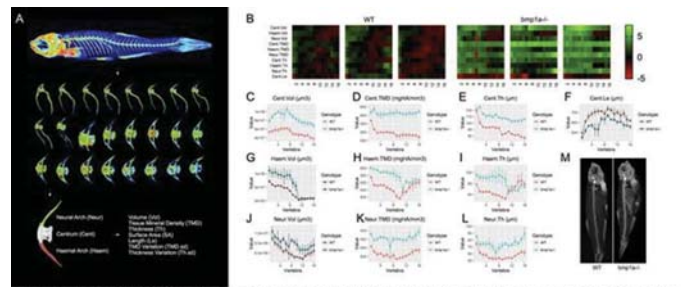


Figure 1. Schematic of workflow. (A) Using whole-body microCT scans, FishCuT isolates individual vertebrae, segments each vertebra into three elements, and compiles traits in each element. (B) Standard scores are computed and arranged into "skeletal barcodes" that facilitate data visualization. (C-L) Traits in *bmp1a*<sup>-/-</sup> mutants plotted as a function of vertebra. Those with a significant difference are colored in a lighter coloring scheme. (M) Max intensity projection of microCT scans.

Figure 1

Disclosures: Matthew Hur, None.

## 1081

**Fracture Risk Indices from DXA-Based Finite Element Analysis Stratify Incident Fracture Risk Independently from FRAX: The Manitoba BMD Registry.** William Leslie\*, Shuman Yang, Andrew Goertzen, Lisa Lix, Yunhua Luo. University of Manitoba, Canada

**Background:** Finite element analysis (FEA) is a computational method to predict the behavior of materials under applied loading. We developed a software tool that automatically performs FEA on dual energy x-ray absorptiometry (DXA) hip scans to generate site-specific fracture risk indices (FRIs) that reflect the likelihood of hip fracture from a sideways fall. This longitudinal study examined associations between FRIs and incident fractures.

**Methods:** Using the Manitoba BMD Registry, femoral neck (FN), intertrochanteric (IT) and subtrochanteric (ST) FRIs were automatically derived from 13,978 anonymized DXA scans (Prodigy, GE Healthcare) in women and men age 50 years and older (mean age 65 years). Baseline covariates and incident fractures were assessed from population-based data. We compared *c*-statistics for FRIs vs femoral neck BMD alone and FRAX probability computed with BMD. Cox regression was used to estimate hazard ratios (HRs) and 95% confidence intervals (95% CIs) for incident hip, major osteoporotic fracture (MOF) and non-hip MOF adjusted for relevant covariates including age, sex, femoral neck BMD, FRAX probability, FRAX risk factors and hip axis length (HAL).

**Results:** During mean follow up 6 years there were 268 subjects with incident hip fractures, 1003 with incident MOF and 787 with incident non-hip MOF. All FRIs gave significant stratification for hip fracture (*c*-statistics FN-FRI: 0.76, 95% CI 0.73-0.79, IT-FRI 0.74, 0.71-0.77; ST-FRI 0.72, 0.69-0.75) though these were slightly lower than for FN BMD alone (0.78, 0.75-0.80) and FRAX hip probability (0.82, 0.80-0.84). FRIs continued to predict hip fracture risk even after adjustment for age and sex (HR FN-FRI 1.89, 95% CI 1.66-2.16; age, sex and BMD (1.26, 1.07-1.48); FRAX probability (1.30, 1.11-1.52); FRAX probability with HAL (1.26, 1.05-1.51); and individual FRAX risk factors (1.32, 1.09-1.59) (TABLE). FRIs also predicted MOF and non-hip MOF, but the prediction was not as accurate as for hip fracture.

**Summary:** Automatically-derived femoral neck, intertrochanteric and subtrochanteric FRIs are associated with incident hip fracture independent of multiple covariates, including FN BMD, FRAX probability and risk factors, and HAL. Our data suggest that DXA-based FEA has matured to the point where widespread clinical testing is warranted. Development of other FEA models would be needed to improve prediction of non-hip MOF.

Outcome	Adjustments	Femoral neck FRI HR per SD (95% CI)	Intertrochanteric FRI HR per SD (95% CI)	Subtrochanteric FRI HR per SD (95% CI)
Hip Fracture	Age, sex	1.89 (1.66-2.16)	1.77 (1.58-1.98)	1.69 (1.50-1.91)
Hip Fracture	Age, sex, BMD	1.26 (1.05-1.51)	1.27 (1.08-1.49)	1.18 (1.02-1.38)
Hip Fracture	FRAX with BMD	1.30 (1.11-1.52)	1.31 (1.14-1.49)	1.27 (1.10-1.45)
Hip Fracture	FRAX with BMD, HAL	1.26 (1.07-1.48)	1.33 (1.16-1.53)	1.26 (1.09-1.44)
Hip Fracture	FRAX risk factors	1.32 (1.09-1.59)	1.25 (1.07-1.47)	1.16 (1.00-1.35)
MOF	FRAX with BMD	1.22 (1.13-1.31)	1.34 (1.25-1.44)	1.23 (1.15-1.32)
Non-hip MOF	FRAX with BMD	1.13 (1.03-1.23)	1.28 (1.19-1.38)	1.18 (1.09-1.27)

Table. Adjusted hazard ratios (HRs with 95% CIs) for fracture prediction from FRIs.

Disclosures: William Leslie, None.



## 1082

**FRAX for Fracture Prediction Shorter and Longer Than Ten Years: The Manitoba BMD Registry.** William Leslie<sup>1</sup>, Sumit Majumdar<sup>2</sup>, Suzanne Morin<sup>3</sup>, Lisa Lix<sup>4</sup>, Helena Johansson<sup>5</sup>, Anders Oden<sup>5</sup>, Eugene McCloskey<sup>5</sup>, John Kanis<sup>5</sup>. <sup>1</sup>University of Manitoba, Canada, <sup>2</sup>University of Alberta, Canada, <sup>3</sup>McGill University, Canada, <sup>4</sup>Lisa.Lix@umanitoba.ca, Canada, <sup>5</sup>University of Sheffield Medical School, United Kingdom

**Background:** FRAX<sup>®</sup> estimates 10-year probability of major osteoporotic fracture (MOF) and hip fracture. We examined whether FRAX accurately predicts MOF and hip fracture outcomes over intervals shorter and longer than ten years.

**Methods:** Using a population-based clinical registry for Manitoba, Canada, we identified 62,275 women and 6,455 men 40 years and older with baseline dual-energy X-ray absorptiometry hip scans and FRAX scores. Incident MOF and hip fracture were assessed up to 15 years from population-based data. We assessed agreement between estimated fracture probability from 1 to 15 years using linearly rescaled FRAX scores and observed cumulative fracture probability with competing mortality. The gradient of risk for FRAX probability and incident fracture was examined overall and for 5-year intervals.

**Results:** FRAX without and with BMD consistently predicted incident MOF and hip fracture for all time intervals in both women and men. There was no attenuation in the gradient of risk (hazard ratio [HR] per SD) for MOF prediction even for years >10 in women (HR/SD without BMD 2.15, 95% CI 1.96-2.35; with BMD 2.24, 95% CI 2.05-2.45) or men (HR/SD without BMD 2.55, 95% CI 1.47-4.41; with BMD 2.15, 95% CI 1.44-3.22). Gradient of risk was slightly lower for hip fracture prediction in years >10 (HR/SD with BMD in women 4.40, 95% CI 3.71-5.22; in men 3.18, 95% CI 1.55-6.54) vs years <5 (in women 5.29, 95% CI 4.71-5.95; in men 4.58, 95% CI 3.14-6.68), though HRs remained high and CIs overlapped. Strong linear agreement was seen in the relationships between observed vs predicted (rescaled) FRAX probabilities from 1 to 15 years ( $R^2$  0.95-1.00). Among women there was near-perfect linearity in MOF predictions with and without BMD (Figure). Deviations from linearity, with a slightly higher observed than predicted MOF probability, were most evident in the first years following a fracture event and after 10 years for hip fracture prediction in women using FRAX with BMD. Simulations showed that results were robust to large differences in fracture rates (0.1 to 2-fold), and moderate differences in mortality rates (0.5 to 1.5-fold).

**Conclusions:** FRAX predicts incident MOF and hip fracture up to 15 years, and could be adapted to predict fracture over time periods shorter and longer term than ten years in populations with fracture and mortality epidemiology similar to Canada.

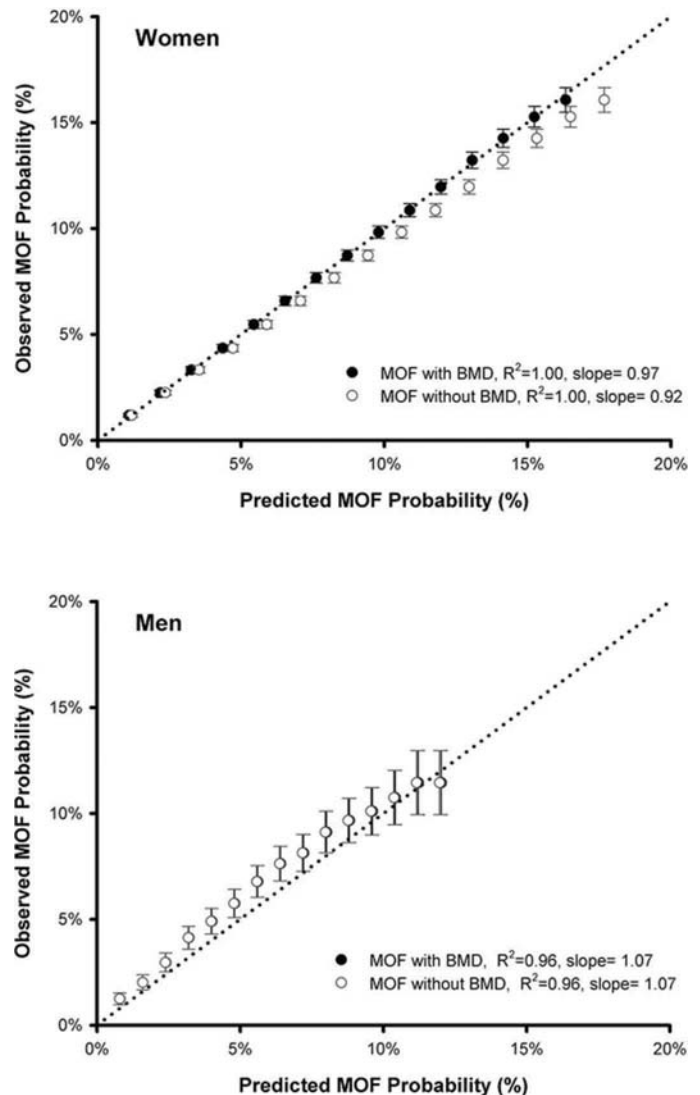


Figure: Calibration for observed vs predicted fracture probability for MOF, from 1 year to 15 years.

**Disclosures:** William Leslie, None.

## 1083

**The ROSE study: Risk-stratified Osteoporosis Strategy Evaluation Effectiveness of a two-step population based osteoporosis screening programme using FRAX<sup>®</sup>: A randomised prospective population-based study.** Katrine Hass Rubin<sup>1</sup>, Teresa Holmberg<sup>2</sup>, Mette Juel Rothmann<sup>2</sup>, Kim Brixen<sup>3</sup>, Mikkel Højberg<sup>2</sup>, Jeppe Gram<sup>2</sup>, Michael Bech<sup>2</sup>, Claus Glüer<sup>4</sup>, Reinhard Barkmann<sup>4</sup>, Anne Pernille Hermann<sup>2</sup>. <sup>1</sup>OPEN - Odense Patient Data Explorative Network, Denmark, <sup>2</sup>University of Southern Denmark, Denmark, <sup>3</sup>Odense University Hospital, Denmark, <sup>4</sup>University of Kiel, Germany

Despite the increasing burden of osteoporotic fractures in aging populations, systematic population-based screening for Osteoporosis is still controversial and not widely adopted. Even though BMD T-score < -2.5 is well-established as a diagnostic criterion for Osteoporosis, the sensitivity and specificity in fracture prediction is low. The aim of the ROSE study was to investigate the effectiveness of a two-step population based osteoporosis screening programme using FRAX<sup>®</sup> based on self-administered questionnaire to select women for DXA followed by the standard osteoporosis treatment according to National guidelines.

**Method:** a random sample of 34,229 women aged 65-80 years were randomized to either screening or control group before invitation to participate and stratified according to area of residence and age. The inclusion of the woman was ongoing from February 2010 to November 2011.

The intervention included two steps: 1) Fracture risk assessment, and 2) DXA assessment in participants with a FRAX estimate of  $\geq 15\%$ . Further work up and treatment initiation was handled by the GP in accordance with the National clinical pathway. Follow-up data on fracture incidence were drawn from national registries

together with information on sociodemographic data and prescriptions. The study was event-driven and aimed at 1500 major osteoporotic fractures in the control group.

Results: A total of 3416 fractures were observed during a median follow-up of 4.8 years. 1697 in the intervention group and 1719 in the control group ( $p=0.83$ ). In the intervention group antiosteoporotic treatment was recommended in 1236 women, while only 986 (80%) started treatment. In spite of this, a per protocol analysis comparing the 5009 women, who accepted DXA, to the 7026 women in the control group, who had a FRAX-score  $\geq 15\%$ , we found a significant fracture reduction (8.1% vs 9.3%,  $p=0.03$ ).

Conclusion: This study revealed no overall significant differences after 5 years of follow-up in the incidence of fractures between the current regime and the two-step screening program.

**Disclosures:** *Katrine Hass Rubin, None.*

## 1084

**Radius Microarchitecture Measured By HRpQCT Predicts Incident Fragility Fracture In The Subset Of Women With Moderately Decreased BMD – The QUALYOR Cohort.** Mathilde Prorol<sup>1</sup>, Blandine Merle<sup>2</sup>, Emmanuelle Vignot<sup>1</sup>, Jean-Baptiste Pialat<sup>3</sup>, Anne-Marie Schott<sup>4</sup>, Pawel Szulc<sup>4</sup>, Eric Lespessailles<sup>5</sup>, Roland Chapurlat<sup>4</sup>. <sup>1</sup>Hôpital Edouard Herriot, France, <sup>2</sup>INSERM, France, <sup>3</sup>Centre Hospitalier Lyon Sud, France, <sup>4</sup>INSERM U1033, France, <sup>5</sup>CHR d'Orléans, France

The majority of fragility fracture occurs in women not classified as osteoporotic according to their areal bone mineral density (BMD). The goal of this study was to test the value of microarchitecture measured by High Resolution peripheral Quantitative Computed Tomography (HRpQCT) to predict fragility fracture risk in the particular subset of those women with moderately decreased areal BMD.

In the QUALYOR (QUALité osseuse LYon Orléans) prospective cohort, we have enrolled 1,579 post-menopausal women aged 50 years or older, with a T-score at the hip or spine between -1.0 and -3.0. At baseline, we measured hip and spine areal BMD with Hologic Discovery A and microarchitecture by HRpQCT at the distal radius (XtremeCT, Scanco). We have also collected clinical risk factors for fracture. Participants have been followed-up prospectively, while incident vertebral fractures were detected by annual VFA and non vertebral fractures were ascertained by radiographs or surgical reports. The risk of incident fracture has been modelled using Cox proportional hazards models. Reclassification techniques such as the IDI (Integrated Discrimination Improvement) and the method of areas under the Harrell's curve have also been used to quantify the improvement of the fracture prediction by microarchitectural variables.

The mean age at baseline was 65.9 years old. The mean T-score at the femoral neck was -1.56 and was -1.24 at the spine. We observed 125 women with one or more fragility fractures, with a fracture incidence of 7.9% over an average follow-up time of 3.6 years. After adjustment for age, weight and BMD at the femoral neck, the HR for fracture was 1.38 [1.18-1.61] per SD decrease in the trabecular number, with a significant improvement compared with a basic clinical-densitometric model including {age, weight, BMD} ( $p < 0.0001$  with IDI and  $p = 0.045$  with area under the Harrell's curve). The other microarchitectural variables were also significant predictors of fracture, with HRs ranging from 1.19 [1.08-1.32] for trabecular spacing to 1.46 [1.22-1.74] for bone volume fraction.

We conclude that in a group of postmenopausal women with moderately decreased areal BMD, microarchitecture measured by HRpQCT at the radius identified women at higher risk for fracture, with an improvement compared with classical risk factors.

**Disclosures:** *Mathilde Prorol, None.*

## 1085

**Measures of physical performance or function, but not appendicular lean mass, predict new fractures independently of FRAX probability: Findings from MrOS.** Nicholas Harvey<sup>1</sup>, Anders Odén<sup>2</sup>, Eric Orwoll<sup>3</sup>, Jodi Lapidus<sup>4</sup>, Timothy Kwok<sup>5</sup>, Magnus Karlsson<sup>6</sup>, Björn Rosengren<sup>6</sup>, Sten Ljunggren<sup>7</sup>, Cyrus Cooper<sup>1</sup>, Peggy Cawthon<sup>8</sup>, John Kanis<sup>9</sup>, Claes Ohlsson<sup>2</sup>, Dan Mellström<sup>2</sup>, Helena Johansson<sup>10</sup>, Eugene McCloskey<sup>9</sup>. <sup>1</sup>MRC Lifecourse Epidemiology Unit, University of Southampton, United Kingdom, <sup>2</sup>Centre for Bone and Arthritis Research (CBAR), Sahlgrenska Academy, University of Gothenburg, Sweden, <sup>3</sup>Oregon Health & Science University, United States, <sup>4</sup>Department of Public Health and Preventive Medicine, Division of Biostatistics, Oregon Health and Science University, United States, <sup>5</sup>Department of Medicine & Therapeutics and School of Public Health, The Chinese University of Hong Kong, Hong Kong, <sup>6</sup>Clinical and Molecular Osteoporosis Research Unit, Department of Clinical Sciences Malmö, Lund University and Department of Orthopedics, Skane University Hospital, Sweden, <sup>7</sup>Department of Medical Sciences, University of Uppsala, Sweden, <sup>8</sup>Department of Epidemiology and Biostatistics, University of California, United States, <sup>9</sup>Centre for Metabolic Bone Diseases, University of Sheffield, United Kingdom, <sup>10</sup>Institute for Health and Aging, Catholic University of Australia, Australia

There is evidence that measures of muscle mass, strength and function might differentially predict risk of incident fractures. An important question for clinical assessment

is whether such indices are independent of FRAX probability. We investigated, across the 3 Osteoporotic Fractures in Men (MrOS) Study cohorts (MrOS Sweden, Hong Kong and USA), whether measures of physical performance/ function and appendicular lean mass by DXA predicted incident fractures in older men, independently of FRAX probability. Available information at baseline included falls history, clinical risk factors for falls and fractures, femoral neck BMD, and calculated FRAX probabilities. An extension of Poisson regression was used to investigate the relationship between time for 5 chair stands, walking speed over 6m, grip strength, appendicular lean mass (ALM), FRAX probability [major osteoporotic fracture (MOF) with femoral neck BMD], and incident fracture. All associations were adjusted for age, time since baseline and cohort, and are reported as hazard ratio (HR) for first incident fracture per SD increment in predictor. Information on physical performance/ function measures and FRAX probability was available for: 4138 men in USA (mean age 73.4 years); 1732 men in Sweden (mean age 75.3 years); and 1661 men in Hong Kong (mean age 72.3 years). Mean follow-up time ranged from 8.8 to 10.9 years. Across all cohorts, greater time for 5 chair stands, and lower walking speed, grip strength and ALM were associated individually with greater risk of incident fracture (any), MOF (hip, clinical vertebral, wrist, proximal humerus), or hip fracture. Since associations were similar for each fracture type, those for MOF are presented. Whilst ALM was not associated with incident fracture after adjustment for FRAX probability, associations with the other three measures remained robust. Thus HR/SD for MOF after adjustment for FRAX probability: Time for 5 chair stands [HR: 1.26 (95%CI: 1.19, 1.34)]; walking speed [HR: 0.86 (95%CI: 0.80, 0.93)]; grip strength [HR: 0.84 (95%CI: 0.77, 0.91)]; ALM [HR: 0.99 (95%CI: 0.91, 1.08)]. In conclusion, measures of physical performance or function, but not appendicular lean mass, predict incident fractures independently of FRAX probability. Although these findings suggest that such risk factors may usefully add to fracture risk assessment, further investigation will be required to clarify their role in the clinic.

**Disclosures:** *Nicholas Harvey, None.*

## 1086

**Women Identified at High Risk of Hip Fracture based on FRAX are Responsive to Appropriate Osteoporosis Management: Results from the SCOOP Study of Population Screening.** Eugene McCloskey<sup>1</sup>, Nicholas Harvey<sup>2</sup>, Helena Johansson<sup>1</sup>, Lee Shephstone<sup>3</sup>, Elizabeth Lenaghan<sup>3</sup>, Cyrus Cooper<sup>4</sup>, John Kanis<sup>1</sup>, and the SCOOP Study Investigators<sup>5</sup>. <sup>1</sup>Centre for Metabolic Bone Diseases, University of Sheffield, United Kingdom, <sup>2</sup>MRC Lifecourse Epidemiology Unit, University of Southampton, United Kingdom, <sup>3</sup>University of East Anglia, United Kingdom, <sup>4</sup>MRC Lifecourse Epidemiology Unit, United Kingdom, <sup>5</sup>The SCOOP Study, United Kingdom

Targeting of treatment in interventional studies to reduce osteoporotic fractures has usually been based on low BMD and/or prior fracture rather than the absolute risk of fracture, e.g. as assessed using FRAX probabilities. The recently completed primary-care based SCOOP screening study targeted treatment to those at highest hip fracture risk using FRAX. We wished to examine the impact of the screening intervention on hip fracture risk according to baseline FRAX hip fracture probability.

The SCOOP study comprised a two-arm randomised controlled trial in women aged 70 to 85 years comparing a screening programme versus usual management. In the screening arm, treatment was recommended in women identified to be at high risk of hip fracture by FRAX (including BMD). Age-dependent intervention thresholds were used ranging from 5.24% in 70-74 year olds to 8.99% hip fracture probability in 85 year olds.

Of 12 483 eligible participants, 6233 women were randomised to screening, with treatment recommended in 898 (14.4%); amongst these, anti-osteoporosis medication had been prescribed in over 70% by 6 months. In the screening arm, the number of incident hip fractures was lower than that in the control arm (218 vs 164) reflecting a 28% reduction in hip fracture risk (hazard ratio 0.72, 95%CI 0.59 to 0.89,  $p=0.002$ ). As treatment was targeted to those at highest risk, the effect on hip fracture increased significantly with baseline FRAX hip fracture probability ( $p=0.021$  for interaction); for example at the 10<sup>th</sup> percentile of baseline FRAX hip probability (2.6%), hip fractures were not significantly reduced (HR 0.93, 0.71-1.23) but at the 90<sup>th</sup> percentile (16.6%), there was a 33% reduction (HR 0.67, 0.53-0.84). The 10<sup>th</sup>, 50<sup>th</sup> and 90<sup>th</sup> percentile values of baseline hip fracture probability in the high risk group and the associated hazard ratios for incident hip fracture are shown in the Table.

Women identified to be at high fracture risk based on FRAX hip fracture probability are responsive to appropriate osteoporosis management. Community-based screening using the FRAX tool is feasible and effective.

Percentile	Baseline hip fracture probability (%)	HR (95% CI)
10	7.8	0.82 (0.66-1.03)
50	14.6	0.70 (0.57-0.87)
90	32.8	0.46 (0.28-0.73)

Effect of treatment at percentiles of baseline hip fracture probability in the high risk group.

**Disclosures:** *Eugene McCloskey, None.*



## 1087

**Osteoblasts are a major source of circulating Dickkopf-1 which is responsible for bone loss due to glucocorticoids in female mice.** Juliane Colditz<sup>1\*</sup>, Sylvia Thiele<sup>1</sup>, Ulrike Baschant<sup>1</sup>, Christof Niehrs<sup>2</sup>, Lynda Bonewald<sup>3</sup>, Lorenz Hofbauer<sup>1</sup>, Martina Rauner<sup>1</sup>. <sup>1</sup>TU Dresden, Germany, <sup>2</sup>Uni Heidelberg, Germany, <sup>3</sup>Indiana University School of Medicine, United States

Glucocorticoids (GC) are effective drugs in the treatment of inflammatory diseases. However, their use is limited by negative effects on bone strength. Dickkopf-1 (Dkk-1) is a potent Wnt inhibitor and altered in various metabolic and inflammatory bone diseases. Our project tested the hypothesis that the deletion of Dkk-1 specifically in osteoblasts or osteocytes contributes to the pathogenesis of GC-induced bone loss (GIO). Thus, we used mice with a deletion of Dkk-1 predominantly in osteoblasts (Ox cre) and in late osteoblasts/osteocytes (Dmp1 cre).

For phenotypic analysis, 12 wk old female and male mice were examined (n=5-9). Female Dkk-1<sup>OxCre</sup> mice showed a 4-fold increase in bone volume/total volume (BV/TV) compared to cre-negative controls. Furthermore, the trabecular number was increased by 59%, while the trabecular separation decreased by 38%. Cortical thickness and density were not changed. The deletion of Dkk-1 in osteoblasts had a significant impact on circulating Dkk-1 as Dkk-1<sup>OxCre</sup> mice had markedly lower Dkk-1 serum levels (-77%) compared to controls, whereas Dkk-1 serum levels were not changed in Dkk-1<sup>Dmp1Cre</sup> mice. However, Dkk-1<sup>Dmp1Cre</sup> mice also showed a significant increase in the BV/TV (2-fold), the trabecular number (+33%), and the cortical thickness (+9%) while the separation was reduced (-26%). Histomorphometric assessment underlined these results as the mineral apposition rate and the bone formation rate were increased in both mouse lines. Male Dkk-1<sup>OxCre</sup> and Dkk-1<sup>Dmp1Cre</sup> mice showed the same trends concerning bone volume, but failed to reach significance.

To test for GIO, slow-release pellets containing 7.5 mg prednisolone or placebo were subcutaneously implanted into 24 wk old female mice for 4 weeks. Dkk-1<sup>OxCre</sup> mice were protected from GIO in the spine and the femur, while Dkk-1<sup>Dmp1Cre</sup> mice were only partially protected. At the femur, Dkk-1<sup>Dmp1Cre</sup> mice lost a similar amount of bone as control mice (Co: -64%; cKO: -44% BV/TV), whereas in the spine, Dkk-1<sup>Dmp1Cre</sup> mice were protected from the negative impact of GCs.

In summary, osteoblasts from female mice may be a major source of secreted Dkk-1, which has an autocrine effect on osteoblastic bone formation. Moreover, Dkk-1 produced by osteoblasts is involved in the pathogenesis of GIO to a greater extent than osteocytes and suggests that Dkk-1 may be a useful target to treat GIO in humans. The mechanisms responsible for the gender differences remain to be investigated.

**Disclosures:** Juliane Colditz, None.

## 1088

**BMPs and Activins regulate bone mass through the competition of shared type 2 receptors.** Shek Man Chim<sup>\*</sup>, Laura Gamer, Vicki Rosen, Department of Developmental Biology, Harvard School of Dental Medicine, United States

A balance between BMP and Activin/TGF $\beta$  signaling contributes to tissue homeostasis in a wide variety of biological contexts. In the skeleton, BMP signaling induces bone formation, while Activin/TGF $\beta$  signaling generally inhibits bone formation. BMPs and Activins signal via complexes containing both type 1 and type 2 receptors. BMPR2 is a unique type 2 receptor for BMPs, while the type 2 receptors ACVR2A and ACVR2B are shared between BMPs and Activins. We previously demonstrated that loss of BMPR2 in skeletal stem cells (Bmpr2 f/f; Prx1-Cre) leads to a high bone mass phenotype in adult mice by selectively impairing Activin signaling. These results allowed us to postulate that increased BMP utilization of ACVR2A/B comes at the expense of Activin signaling. Here we continue to examine the interplay between BMPs and Activins in bone by generating two new mouse models: mice lacking ACVR2B in skeletal progenitor cells (Acvr2b f/f; Prx1-Cre = Acvr2b cKO); and mice lacking both ACVR2B and BMPR2 in the same skeletal progenitors (Acvr2b f/f; Bmpr2 f/f; Prx1-Cre = dcKO). We found that Acvr2b cKO mice have normal bone mass while dcKO mice have significantly increased bone mass that is greater than the increase observed by removing Bmpr2 alone. Western blot analyses of bone lysates from these mice demonstrate that pSmad2 levels were greatly reduced in dcKO mice but unchanged in Acvr2b cKO mice, while pSmad1/5/8 levels were unchanged. Next, we investigated the competition between BMPs and Activins for shared type 2 receptors *in vitro*. Western blot analyses demonstrated that Activin-induced pSmad2 levels were reduced by co-treatment with BMP2 in bone marrow stromal cells lacking only BMPR2 or both ACVR2B and BMPR2. Our findings suggest that removal of BMPR2 forces BMPs and Activins to compete for shared type 2 receptors and this competition is intensified when ACVR2B is further removed and only ACVR2A remains. From these studies, we conclude that a balance between BMP and Activin signaling contributes to the maintenance of adult bone mass through a complex mechanism involving competition for ACVR2A/B, the type 2 receptors shared by BMPs and Activins. As circulating Activin levels increase with age and in patients with inflammatory diseases, physiological states where reduced bone mass is observed, we believe that differential utilization of type 2 receptors for BMP and Activin plays a fundamental role in bone mass regulation in the adult skeleton.

**Disclosures:** Shek Man Chim, None.

## 1089

**Increased Ca<sup>2+</sup> signaling through altered CaV1.2 L-type Ca<sup>2+</sup> channel activity promotes bone formation and prevents estrogen deficiency-induced bone loss.** Chike Cao<sup>\*</sup>, Yinshi Ren<sup>2</sup>, Anthony J. Miranda<sup>2</sup>, Adam Barnett<sup>1</sup>, Douglas Rouse<sup>3</sup>, Se Hwan Mun<sup>4</sup>, Kyung-Hyun Park-Min<sup>4</sup>, Amy L. McNulty<sup>2</sup>, Farshid Guilak<sup>5</sup>, Courtney M. Karner<sup>2</sup>, Matthew J. Hilton<sup>2</sup>, Geoffrey S. Pitt<sup>6</sup>. <sup>1</sup>Ion channel Research Unit, Duke University Medical Center, United States, <sup>2</sup>Department of Orthopaedic Surgery, Duke University Medical Center, United States, <sup>3</sup>Department of Lab Animal Resources & Rodent Surgical and Genetic Services, Duke University Medical Center, United States, <sup>4</sup>Arthritis and Tissue Degeneration Program, Hospital for Special Surgery, United States, <sup>5</sup>Department of Orthopaedic Surgery, Washington University Medical Center, United States, <sup>6</sup>Cardiovascular Research Institute, Weill Cornell Medicine, United States

A G406R gain-of-function mutation in the *CACNA1C* gene, encoding the cardiac CaV1.2 L-type calcium channel, causes the multi-organ disorder Timothy syndrome (TS), characterized by cardiac arrhythmias and developmental abnormalities. G406R reduces channel inactivation and increases Ca<sup>2+</sup> flux into the cell. Here, we exploit the mutant channel in bone formation and bone remodeling.

Using a CaV1.2 *lacZ* reporter mouse we observed that CaV1.2 was highly expressed in the perichondrium/periosteum during skeletogenesis and in proliferating chondrocytes and BMSCs postnatally, suggesting important roles for endogenous CaV1.2 channels during skeletal development and homeostasis. Expression of the TS-mutant CaV1.2 channel (*Rosa26-CaV1.2<sup>TS</sup>*) driven by *Prx1-Cre*, *Col2a1-Cre* or *2.3Colla1-Cre* dramatically enhances bone mass, whereas expression of the wild type channel (*Rosa26-CaV1.2<sup>WT</sup>*) has no effect. This indicates that abnormal channel behavior—and not just overexpression—is necessary to increase bone mass. Using dynamic histomorphometry and TRAP staining, we observed an increase in osteoblast activity and fewer osteoclasts from CaV1.2<sup>TS</sup> mutant long bones. Furthermore, in primary bone marrow stromal cell (BMSC) cultures, qPCR analyses revealed that CaV1.2<sup>TS</sup> enhances *Rumx2*, *Sp7*, *Alpl*, *Ibsp* and *Bglap* gene expression. Von Kossa staining confirmed the enhanced osteogenic differentiation and mineralization of CaV1.2<sup>TS</sup>-expressing BMSCs. In contrast, inhibition of CaV1.2 activity by nifedipine (10  $\mu$ M) or diltiazem (10  $\mu$ M) decreased BMSCs mineralization. Gene expression analyses also demonstrated that CaV1.2<sup>TS</sup> decreased the *Rankl/Opg* ratio, whereas the CaV1.2 blockers nifedipine or diltiazem increased the *Rankl/Opg* ratio. These data indicate that Ca<sup>2+</sup> signaling through the CaV1.2 channel interfered with osteoblast-mediated osteoclastogenesis via the OPG/RANKL pathway. Moreover, postnatal induction of CaV1.2<sup>TS</sup> in *Sp7*-lineage cells markedly increased bone formation and *Sp7-CaV1.2<sup>TS</sup>* mice were protected from bone loss induced by ovariectomy (OVX). Dynamic histomorphometry and TRAP staining revealed enhanced bone formation and reduced bone resorption in *Sp7-CaV1.2<sup>TS</sup>* OVX mice compared to WT OVX mice. Taken together, these studies demonstrate that increased Ca<sup>2+</sup> signaling through CaV1.2<sup>TS</sup> promotes osteoblast differentiation and inhibits osteoclast formation. Our results suggest that enhancing CaV1.2 signaling may be a novel and effective therapeutic strategy for treating osteoporosis.

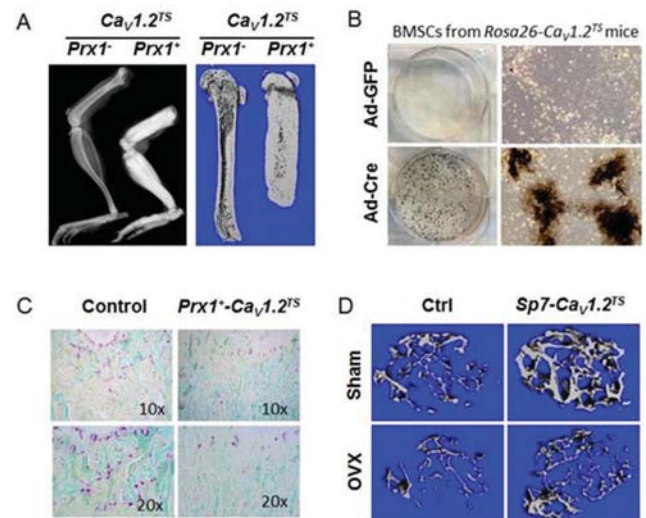


**Fig.1A: CaV1.2<sup>TS</sup> channel promotes bone formation in vivo;**  
**Fig.1B: CaV1.2<sup>TS</sup> channel enhances osteoblast differentiation;**  
**Fig.1C: CaV1.2<sup>TS</sup> channel decreases osteoclast differentiation;**  
**Fig.1D: Postnatal induction of CaV1.2<sup>TS</sup> in Sp7-lineage cells increases bone formation and protects bone loss induced by ovariectomy (OVX).**

CaV1.2TS promotes bone formation and prevents estrogen deficiency-induced bone loss

**Disclosures:** Chike Cao, None.

## 1090

**Osteoclast-secreted Cthrc1 Regulates Bone Remodeling through Waif1, a Receptor on Stromal/Osteoblastic Cells.** Yukihiro Kohara<sup>\*1</sup>, Kazuhiko Matsuoka<sup>2</sup>, Masako Ito<sup>3</sup>, Kyoji Ikeda<sup>1</sup>, Sunao Takeshita<sup>1</sup>. <sup>1</sup>National Center for Geriatrics and Gerontology, Japan, <sup>2</sup>Development and Disease Group, Cancer Cell Biology Programme, Spanish National Cancer Research Centre, Spain, <sup>3</sup>Medical Work-Life-Balance Center, Nagasaki University Hospital, Japan

In the previous study (JCI 2013) we identified collagen triple helix repeat containing 1 (Cthrc1) as a secreted protein of active bone-resorbing osteoclasts that stimulates differentiation of marrow stromal cells toward osteoblasts. Further, osteoclast-specific Cthrc1 conditional KO (cKO) mice exhibited impaired bone mass recovery after acutely induced bone resorption by Rankl injections, providing *in vivo* evidence for Cthrc1 as a coupling factor. However, the mechanisms of Cthrc1 action in stimulating osteoblastogenesis remained to be elucidated.

In this study we have biochemically identified Wnt-activated inhibitory factor 1 (Waif1) as a cell surface receptor of Cthrc1, using a Cthrc1-affinity column and membrane fractions of stromal ST2 cells followed by LC-MS/MS. Waif1 mRNA was expressed mainly in bone and brain but not in other tissues, revealing an identical expression pattern with that of Cthrc1. Cthrc1 binding to Waif1 elicited activation of PKC $\Delta$ -ERK-Rac1 pathway, thereby stimulating osteoblastic differentiation. Suppression of Waif1 mRNA expression by shRNA in ST2 cells did not only reduced Cthrc1 binding but also abolished ALP activity and mRNA expression of osteoblast marker genes, such as Col1a1 and Runx2, induced by Cthrc1 stimulation. Osteoblast lineage-specific Waif1 cKO mice showed unexpectedly a high bone mass phenotype as assessed by 3D micro CT analysis. Histomorphometric analysis revealed that not only bone formation but resorption was reduced in Waif1 cKO mice, suggesting that the high bone mass was due to impaired bone resorption. In fact, the expression of Rankl mRNA was decreased in the bone of Waif1 cKO mice, assessed by RT-PCR, compared with wild type control; deletion of Waif1 in ST2 cells by CRISPR/Cas9 resulted in a decreased Rankl expression, and co-cultures of calvarial osteoblastic cells from Waif1 systemic KO mice with normal macrophages showed impaired osteoclastogenesis, demonstrating that Waif1 surface expression is required for Rankl expression and osteoclastogenesis. Most importantly, osteoblast lineage-specific Waif1 cKO mice exhibited impaired bone mass recovery after Rankl injections, phenocopying osteoclast-specific Cthrc1 cKO mice. These results provide evidence for Waif1 on stromal/osteoblastic cells as a receptor of osteoclast-secreted Cthrc1, and suggest that Waif1 serves an important coupling function of bone resorption to formation.

**Disclosures:** Yukihiro Kohara, None.

## 1091

**Deletion of Menin Early in the Osteoblast Lineage Leads to Increased Bone Resorption, and Reduced Bone Mass and Strength in Adult Mice.** Jad Abi-Rafeh<sup>\*1</sup>, Ildi Troka<sup>1</sup>, Lucie Canaff<sup>1</sup>, Marie-Claude Faugere<sup>2</sup>, Thomas L. Clemens<sup>3</sup>, Geoffrey N. Hendy<sup>1</sup>. <sup>1</sup>McGill University, Canada, <sup>2</sup>University of Kentucky, United States, <sup>3</sup>Johns Hopkins University, United States

Mutations in the *MEN1* tumor suppressor gene cause the Multiple Endocrine Neoplasia type 1 disorder. Menin, the *MEN1* gene product, is expressed in many tissues, including osteoblasts, where its normal function remains poorly understood. Here, we examined the role of menin at earlier stages of the osteoblast lineage through conditional knockout of the *Men1* gene in mice using the Cre-LoxP recombination system: *Prx1-Cre;Men1<sup>fl/f</sup>*, *Osx-Cre;Men1<sup>fl/f</sup>* and *OC-Cre;Men1<sup>fl/f</sup>* represent the deletion of menin in the osteochondroprogenitor, osteoblast progenitor and mature osteoblast, respectively. Skeletal phenotyping performed at 6 months demonstrated significantly reduced body weight, BMD and femur length in the *Prx1-Cre;Men1<sup>fl/f</sup>* and *Osx-Cre;Men1<sup>fl/f</sup>* strains. By 3-dimensional micro-CT imaging, all three strains of knockout mice showed decreased trabecular bone volume, altered trabecular structure, and decreased cortical bone thickness. Femur stiffness and ultimate force were reduced in *Prx1-Cre;Men1<sup>fl/f</sup>* mice assessed by 3-point bending test. Primary calvarial osteoblasts of all strains of knockout mice were deficient in mineralization as assessed by Alizarin red staining, and had altered gene expression profiles. Osteoblasts from heterozygous (*Osx-Cre;Men1<sup>fl/f</sup>*) mice were intermediate in this respect. Serum biochemistries were unaffected. By contrast, whereas *OC-Cre;Men1<sup>fl/f</sup>* mice exhibited reduced numbers of osteoblasts, increased osteocyte density and decreased osteoclast number, *Prx1-Cre;Men1<sup>fl/f</sup>* and *Osx-Cre;Men1<sup>fl/f</sup>* mice had marked increases in osteoclast number and unaltered number of osteoblasts. This is consistent with *in-vitro* and *in-vivo* findings of increased RANKL/OPG mRNA ratios supporting increased osteoclastogenesis signalled by the osteoblasts/osteocytes in these earlier menin knockout models. We conclude that osteoblast menin plays a crucial role in bone development and maintenance on bone mass *in-vivo*, and may serve as a potential gain-of-function therapeutic target for low bone mass disorders such as osteoporosis. Haploinsufficiency of osteoblast menin may contribute to the more severe bone phenotype of the hyperparathyroidism of *MEN1* patients relative to that of sporadic primary hyperparathyroidism.

**Disclosures:** Jad Abi-Rafeh, None.

## 1092

**Gata4 directly controls osteoblast differentiation via Runx2.** Aysha Khalid<sup>\*</sup>, Alexandria Slayden, Chanel Perry, Gustavo Miranda-Carboni, Susan Krum. University of Tennessee Health Science Center, United States

GATA4 is a zinc-finger transcription factor that is essential in various tissues, such as heart, kidneys, intestine and more recent studies showed that it also has a role in bone mineralization. Previously we have shown that *in vivo* deletion of *Gata4*, driven by Cre-recombinase under the control of the Col1a1 2.3 kb promoter (conditional knockout, cKO), results in perinatal lethality, decreased trabecular bone properties, and abnormal bone development in newborn (P0) mice. Herein, we demonstrate that GATA4 regulates *Runx2* expression in osteoblasts *in vivo* and *in vitro* and helps open the chromatin to enable *Runx2* gene expression. mCT analysis of femur and tibia of 14-week-old mice showed significantly reduced values for trabecular bone properties, suggesting *Gata4* is necessary for maintaining normal bone phenotype. However, deleting *Gata4* did not have any effect on cortical bone. Quantitative PCR analysis revealed higher expression of *Gata4* in trabecular bone vs. cortical bone, suggesting a role of *Gata4* in maintaining normal trabecular bone mass. Analysis of cDNA of bone marrow mesenchymal stem cells from wild type controls (WT) and cKO mice differentiated for 14 days in osteogenic media demonstrated significant reduction of *Gata4* and *Runx2* gene expression along with reduced Alizarin Red staining in osteoblasts from cKO mice as compared to WT. Gene expression levels determined by qPCR for *Gata4* and *Runx2* were also reduced in primary calvarial cells infected with lentivirus expressing shRNA directed to *Gata4* (shGATA4), as compared to a negative control (shC). To determine if *Runx2* is a direct target of GATA4, ChIP was performed, and we identified that GATA4 is recruited to the two *Runx2* promoters and an enhancer region. Furthermore, when *Gata4* is knocked down, the chromatin at the *Runx2* region is not open, as detected by DNase assays and ChIP with antibodies to the open chromatin marks H3K4me2 (histone 3 lysine 4 dimethylation) and H3K27ac (histone 3 lysine 27 acetylation) and closed chromatin mark H3K27me2 (histone 3 lysine 27 trimethylation). Together the data suggest that GATA4 binds near the *Runx2* promoter and enhancer, helps open the chromatin to regulate *Runx2* expression and subsequent bone mineralization.

**Disclosures:** Aysha Khalid, None.

## 1093

**Twice Daily Injection of Inverse Agonist for Constitutively Active Parathyroid Hormone Receptor Ameliorates the Bone Phenotype in Col1-Jansen's Mice.** Hiroshi Noda<sup>\*1</sup>, Hiroshi Saito<sup>1</sup>, Monica Reyes<sup>1</sup>, Braden A Corbin<sup>1</sup>, Jun Guo<sup>1</sup>, Michael Armanini<sup>1</sup>, Daniel Brooks<sup>2</sup>, Janaina S Martins<sup>1</sup>, Mary L Bouxsein<sup>2</sup>, Marie B Demay<sup>3</sup>, Harald Jueppner<sup>3</sup>, Thomas J Gardella<sup>3</sup>. <sup>1</sup>Endocrine Unit, Massachusetts General Hospital, United States, <sup>2</sup>Endocrine Unit, Massachusetts General Hospital and Beth Israel Deaconess Medical Center, United States, <sup>3</sup>Endocrine Unit, Massachusetts General Hospital and Harvard Medical School, United States

Jansen's metaphyseal chondrodysplasia (JMC) is a rare disease caused by heterozygous activating mutations in the parathyroid hormone receptor-1 (PTHr). Patients with JMC exhibit short stature, limb deformities, impaired mobility, and dysregulation of blood calcium and phosphate levels; defects which arise, in large part, from perturbations in processes of bone development and bone turnover. There is no treatment option that directly targets the underlying molecular defect. Inverse agonists are ligands that bind to constitutively active receptors and reduce their basal signaling levels. An inverse agonist that targets constitutively active mutant PTH receptors of JMC could theoretically be used as a treatment for the disease. N-terminally truncated PTH and PTHrP analogs have been identified that function as inverse agonists on mutant PTHRs of JMC when tested in cell-based cAMP assays. These *in vitro* findings led us to examine whether such an inverse agonist could correct the bone/mineral ion defects seen in a mouse model of JMC. We thus used transgenic mice that express the PTHr-H223R allele via the Col1a1-promoter specifically in osteoblasts (C1HR-mice), and thus exhibit high bone turnover rates as well as excess bone accrual (Calvi et al. 2001 J.C.I.). One-week old C1HR or WT littermate mice were injected twice-daily, SC, for 17 days with either vehicle or the inverse agonist [L11,dW12,W23]-PTHrP(7-36) (IA1) (500 nmol/kg), at which point the mice were sacrificed for analysis (n = 8-10/group). Micro-CT analysis of femurs revealed significant positive effects of IA1 injection in C1HR mice (P vs. vehicle < 0.05) on total bone-length, as well as on distal bone volume (BV/TV-%) and mid-region medullary bone area (BA/TA-%). H&E histology further revealed reductions in the excess trabecular bone in metaphyseal area of the tibia. IA1 treatment also significantly reduced blood levels of CTX1 in C1HR mice, which were elevated in the vehicle-treated C1HR mice relative to vehicle-treated wild-type mice. RT-PCR analyses of femoral mRNA indicated that IA1 reduced expression of PTHrP-target genes in osteoblasts, including RANKL. The results thus suggest that twice-daily administration of a PTHrP-based inverse agonist by SC injection can ameliorate at least some of the bone metabolism defects that occur in this osteoblast-specific mouse model of JMC.

**Disclosures:** Hiroshi Noda, Chugai Pharmaceutical Co., Ltd., Other Financial or Material Support.



## 1094

**Development of blocking monoclonal antibodies against ALK2, which is a type I receptor for BMPs.** Takenobu Katagiri<sup>1</sup>, Shinnosuke Tsuji<sup>2</sup>, Sho Tsukamoto<sup>1</sup>, Satoshi Ohte<sup>1</sup>, Kengo Kumagai<sup>1</sup>, Kenji Osawa<sup>1</sup>, Kiyosumi Takaishi<sup>2</sup>, Kensuke Nakamura<sup>3</sup>, Yoshiro Kawaguchi<sup>3</sup>, Jun Hasegawa<sup>3</sup>. <sup>1</sup>Division of Pathophysiology, Research Center for Genomic Medicine, Saitama Medical University, Japan, <sup>2</sup>Rare Disease & LCM Laboratories, R&D Division, Daiichi-Sankyo Co., Ltd., Japan, <sup>3</sup>Modality Research Laboratories, Biologics Division, Daiichi-Sankyo Co., Ltd., Japan

Fibrodysplasia ossificans progressiva (FOP) is a rare autosomal-dominant disorder characterized by heterotopic endochondral bone formation in soft tissues, such as skeletal muscle, tendon and ligament. Substitution mutations of ALK2, one of seven type I transmembrane serine/threonine kinase receptors of transforming growth factor- $\beta$  family including bone morphogenetic proteins (BMPs), were found in patients with FOP. The mutant ALK2 associated to FOP are gain-of-function mutations, because they induce phosphorylation of Smad1/5 and activate BMP-specific signaling without adding ligands. Thus, various inhibitors for ALK2, such as kinase inhibitors, a Smad inhibitor and RNA interference, were developed for FOP to prevent heterotopic ossification. Recently, we developed novel rat monoclonal antibodies of ALK2, which specifically bound to the extracellular domain of ALK2. The antibodies inhibited BMP signaling of human, monkey, canine and mouse ALK2 but did not rat ALK2 in HEK293A cells. In addition, these antibodies inhibited osteoblastic differentiation of mouse C2C12 myoblasts in response to exogenous BMP stimulation and the ligand-induced intracellular signaling in HEK293A cells expressing mutant ALK2 associated with FOP. We analyzed crystal structure of the antibody-ALK2 extracellular domain complex and identified the amino acid residues critical for their interaction. Moreover, the antibodies inhibited heterotopic bone formation induced by BMP implantation in skeletal muscle in mice. These findings indicate that our monoclonal antibodies against ALK2 are specific inhibitors of ALK2 in vitro and in vivo and a potential novel therapeutic for FOP.

**Disclosures:** Takenobu Katagiri, Daiichi-Sankyo Co., Ltd., Grant/Research Support.

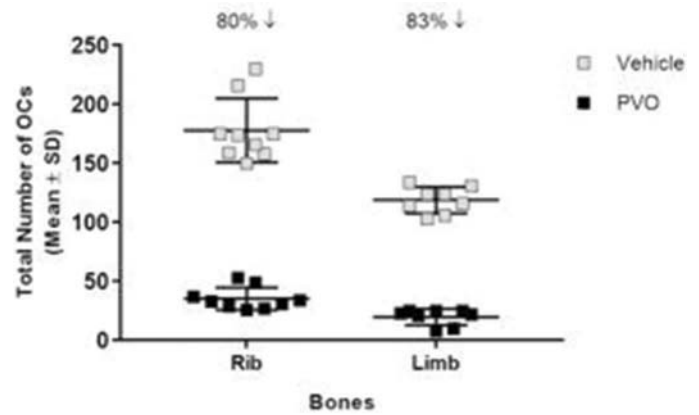
## 1095

**Efficacy of Palovarotene Oral Treatment on Prevention of Osteochondroma Formation in the Fsp1-Ext1<sup>CKO</sup> Mouse Model of Multiple Osteochondromas.** Toshihiro Inubushi<sup>1</sup>, Isabelle Lemire<sup>2</sup>, Michael Harvey<sup>2</sup>, Yu Yamaguchi<sup>1</sup>. <sup>1</sup>Sanford Burnham Prebys Medical Discovery Institute, United States, <sup>2</sup>Clementia Pharmaceuticals Inc., Canada

Multiple osteochondromas (MO), also known as multiple hereditary exostoses, is an autosomal dominant rare disease caused by loss-of-function mutations in *EXT* genes and is characterized by the development of osteochondromas (OCs) that often restrict movement and physical function. Currently there is no approved pharmacologic treatment for MO. OCs originating proximal to an active growth plate exhibit typical endochondral ossification, which comprises a growth plate-like cartilaginous cap overlying a bony base. Recent preclinical evidence suggests a functional role of enhanced BMP signaling in the pathogenesis of MO. Palovarotene (PVO) is an orally bioavailable retinoic acid receptor gamma (RAR $\gamma$ ) selective agonist, presently in Phase 2 clinical development for another rare bone disease. In mouse models, PVO potently inhibits chondrogenesis and prevents heterotopic ossification (HO) by affecting inflammatory elements and decreasing BMP signaling.

We evaluated the efficacy of orally administered PVO for preventing OCs in a Fsp1-Ext1<sup>CKO</sup> mouse model of MO. This novel model, based on Ext1 ablation targeted to the perichondrium, develops bony protrusions in bones of the limbs, ribs, and vertebrae consistent with the histological features of OCs in humans, and displays rib cage deformity and swelling of the chondro-osseous junction that are also consistent with clinical features of MO. In this study, Fsp1-Ext1<sup>CKO</sup> mice (N=9 per group) were treated by daily oral gavage at a 2.6 mg human equivalent dose of PVO or vehicle for 28 consecutive days starting at day 14 postpartum. At the end of treatment, whole-mount skeletal preparations were prepared from each animal, in which OCs were identified and counted on each rib (12 left, 12 right) and long bones (right and left humerus, radius, ulna, femur, tibia, fibula) under a dissection microscope.

The total number of OCs (mean  $\pm$  SD) at the rib and long bones in vehicle controls was 178  $\pm$  27 and 119  $\pm$  11, respectively. PVO daily treatment at a human equivalent dose of 2.6 mg significantly reduced ( $p < 0.0001$ ) the total number of OCs at the rib bones (35  $\pm$  10, 80% decrease) and at the long bones (20  $\pm$  7, 83% decrease) in Fsp1-Ext1<sup>CKO</sup> mice. Swelling of the chondro-osseous junction at the rib bones and the deformity of the rib cage were also considerably reduced by PVO daily treatment. These results suggest potential beneficial therapeutic effects of PVO in MO.



Efficacy of Oral PVO Treatment on Prevention of OC Formation in the Fsp1-Ext1<sup>CKO</sup> Mouse Model of MO

**Disclosures:** Toshihiro Inubushi, Clementia Pharmaceuticals Inc., Grant/Research Support.

## 1096

**The Musculoskeletal Effects of Soluble Activin Receptor Type IIB (sActRIIB-mFc) in the G610C Osteogenesis Imperfecta Mouse Model.** Youngjae Jeong<sup>1</sup>, Salah Daghlas<sup>1</sup>, Marybeth Brown<sup>2</sup>, Ferris Pfeiffer<sup>3</sup>, Yixia Xie<sup>4</sup>, Mark Dallas<sup>4</sup>, R. Scott Pearsall<sup>5</sup>, Sarah Dallas<sup>4</sup>, Charlotte Phillips<sup>1</sup>. <sup>1</sup>Department of Biochemistry, University of Missouri, United States, <sup>2</sup>Department of Biomedical Sciences and Physical Therapy Program, University of Missouri, United States, <sup>3</sup>Department of Bioengineering, University of Missouri, United States, <sup>4</sup>Department of Oral and Craniofacial Biology, University of Missouri, United States, <sup>5</sup>Acceleron Pharma, Inc., United States

Osteogenesis Imperfecta (OI) is a heritable connective tissue disorder characterized by compromised biomechanical integrity in type I collagen containing tissues, such as bone. Current treatments for OI include anti-resorptive drugs or surgical intervention, both of which have limited success. Thus identifying alternative therapeutic options is critical. Bone is mechanosensitive and can respond and adapt to external stimuli. Muscle mass and contractile force are some of the largest physiological loads that bone experience during their life. Muscle growth is regulated by myostatin, a member of TGF- $\beta$  superfamily, which signals through the activin receptor type IIB (ActRIIB) to regulate downstream gene transcription levels. Deficiency in myostatin leads to increased muscle and bone mass. The heterozygote *G610C* (+/*G610C*) OI mouse has a glycine to cysteine substitution in position 610 of the pro $\alpha$ 2(I) collagen chain, which results in the same genetic and mild/moderate OI type I/IV phenotype as 64 individuals in an Old Order Amish kindred with reduced bone mineral density. As a strategy to induce muscle growth in +/*G610C*, we utilized a soluble activin receptor type IIB fusion protein (sActRIIB-mFc, Acceleron Pharma) to inhibit ligand (myostatin, GDF-11, activin) binding to the endogenous cellular ActRIIB thereby altering the downstream signaling pathways. In the following study the effects of sActRIIB-mFc on the muscle and bone properties of +/*G610C* mice were evaluated. At 2 months of age, bi-weekly treatments of vehicle [Tris-Buffered Saline] or sActRIIB-mFc (10mg/kg) were given for 8 weeks to WT and +/*G610C* mice. At 4 months of age, skeletal muscle force was measured by *in-situ* muscle contractile testing prior to sacrifice. We demonstrated increases in body weight and hindlimb skeletal muscle weights with sActRIIB-mFc treatment without altering absolute contractile force regardless of genotype. By  $\mu$ CT analyses, sActRIIB-mFc treated mouse femurs exhibited improved trabecular and cortical microarchitecture regardless of genotypes. By histomorphometric analyses, periosteal bone formation rate was increased regardless of genotypes. Lastly, biomechanical testing of torsional loading to failure demonstrated increased torsional ultimate strength in sActRIIB-mFc treated WT and +/*G610C* mouse femurs. Our results suggest that sActRIIB-mFc may provide a new therapeutic option in OI by improving bone microarchitecture to increase bone biomechanical strength.

**Disclosures:** Youngjae Jeong, None.

## 1097

**Increasing Muscle Mass by GDF Ligand Trap Treatment Improves Bone Geometry in a Mouse Model of Severe Osteogenesis Imperfecta.** Josephine T. Tauer\*, Frank Rauch. Shriners Hospital for Children - Montreal, Canada

**Objective:** Osteogenesis imperfecta (OI) is mainly characterized by bone fragility but also by reduced muscle mass and function. Muscle mass and bone mass are closely linked, wherefore an intervention that increases muscle mass should also increase bone mass. Here we investigated the effect of a novel GDF ligand trap (Acceleron Pharma) on skeletal muscle mass and bone properties in a mouse model of severe dominant OI, the *Col1a1*<sup>Jr/Jr</sup> mouse.

Methods: Starting at an age of 8 weeks, GDF ligand trap (3 mg or 10 mg per kg body mass) or vehicle was injected subcutaneously twice per week for 4 weeks into male OI and wild-type (WT) mice.

Results: At baseline, OI mice had 20% lower body mass than control littermates. This difference persisted during the intervention as WT and OI cohorts exhibited a similar dose-dependent increase in body mass during GDF ligand trap treatment. Injections of GDF ligand trap led to a dose-dependent increase in muscle mass of quadriceps and gastrocnemius in WT and OI cohorts (Figure 1). In WT, GDF ligand trap also increased soleus weights (by 19 % and 26 %) and EDL weights (by 26 % and 73 %) in a dose-dependent manner. In OI cohorts, GDF ligand trap increased soleus and EDL weights as well, but both dosages almost to the same extent. GDF ligand trap injections had no effect on heart muscle mass or liver mass. Concerning bone unit, GDF ligand trap had no effect on femoral length in WT and OI mice but improved trabecular bone volume in the distal femoral metaphysis of WT mice (Figure 1). However, GDF ligand trap treatment resulted in a significantly increased mid-diaphyseal periosteal diameter in OI mice only (Figure 1), leading to an improved polar moment of inertia.

Conclusion: GDF ligand trap increases muscle mass and seem to improve diaphyseal bone geometry in a model of severe OI, representing a new therapy option for severe OI.

**Figure 1. Muscle-bone unit in WT (□) and OI (■) mice after treatment with a novel GDF ligand trap.** Data are shown as mean ± SEM; Veh: vehicle; a:  $p < 0.001$  vs veh-treated WT or OI mice, b:  $p < 0.01$  veh-treated WT vs veh-treated OI

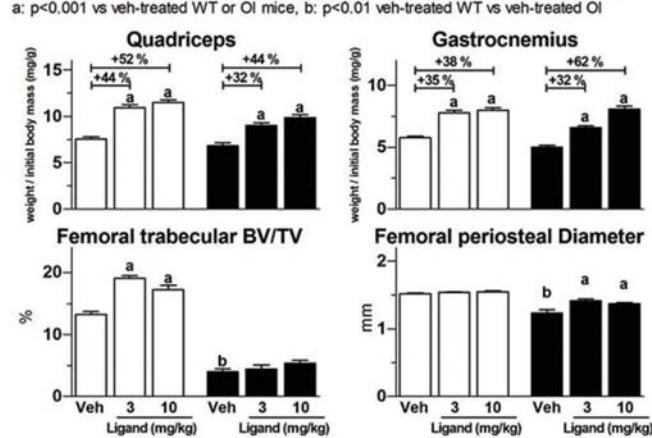


Figure 1

Disclosures: Josephine T. Tauer, None.

## 1098

### Inverse Agonist Infusion Mitigates Bone Remodeling Abnormalities in the Col1-PTHrH223R mouse model of Jansen's Metaphyseal Chondrodysplasia.

Jun Guo\*, Hiroshi Noda, Monica Reyes, Michael Armanini, Janaina Martins, Dan Brooks, Mary Bouxsein, Marie Demay, Harald Jueppner, Thomas J Gardella. Massachusetts General Hospital, United States

Jansen's metaphyseal chondrodysplasia (JMC) is a rare disease caused by dominant activating mutations in the parathyroid hormone receptor-1 (PTHrH1). Patients with JMC exhibit short stature, limb deformities, impaired mobility, hypercalcemia and increased phosphate excretion. These defects can be attributed in large part to effects of excessive PTHrH1 signaling on bone development and bone turnover. There is currently no treatment option that directly targets the underlying molecular defect. Inverse agonists are ligands that bind to a constitutively active receptor and reduce its basal level of signaling. An inverse agonist that targets the constitutively active mutant PTHrH1 receptors of JMC could, in theory, be used to treat this disease. N-terminally truncated PTHrH1 and PTHrH1 analogs containing the dTrp(W)12 substitution are known to function as inverse agonists on mutant PTHrH1s of JMC when tested in cell-based cAMP assays. These in vitro findings led us to examine whether such an inverse agonist could correct the bone growth/remodeling defects seen in the Col1a1-PTHrH1-H223R mouse JMC model (C1-HR mice). These mice express the PTHrH1-H223R allele predominantly in osteoblasts, and thus exhibit excessive bone accrual and high rates of bone turnover (Calvi et al. 2001 J.C.I.). C1-HR or WT littermate mice were infused via Alzet mini pump from post-natal day 14 to day 28 with either vehicle or the inverse agonist [L11,dW12,W23]-PTHrH1(7-36) (300 nmol/kg/day; n = 8-10 per group). The mice were then sacrificed for analysis (micro-CT and histomorphometry of femurs, qRT-PCR of femoral mRNA; H&E histology of tibia; blood CTX1). The analyses so far confirm significantly increased bone volumes and bone turnover rates, as well as increased expression of bone related genes (ALP, Col1a, iBSP, OCN, MMP9 and RANKL), in vehicle-treated C1HR mice, as compared to vehicle-treated WT mice. More importantly, they reveal a significant rescue effect of the inverse agonist on most of the investigated bone parameters that were altered in the C1-HR mice. The results thus suggest that administration of a PTHrH1(7-36)-based inverse agonist can effectively counter-act the deleterious effects that the constitutively active PTHrH1-H223R allele has on processes of bone formation and remodeling.

Disclosures: Jun Guo, Chugai Pharmaceutical Co. Ltd., Grant/Research Support.

## 1099

### Daily PTH (1-34) Administration Preserves Bone Structure and Enhances Bone Turnover after Severe Immobilization-induced Bone Loss. Lauren Harlow\*, Karim Sahbani<sup>1</sup>, Jeffry Nyman<sup>2</sup>, Christopher Cardozo<sup>1</sup>, William Bauman<sup>1</sup>, Hesham Tawfeek<sup>1</sup>. <sup>1</sup>James J. Peters VA Medical Center, United States, <sup>2</sup>Vanderbilt University School of Medicine, United States

Immobilization as a result of complete spinal cord injury (SCI) is associated with rapid bone loss that progresses to severe osteoporosis. This study determined whether daily PTH administration would reduce bone loss after acute SCI. Thus, 20 week old wild type female mice underwent sham or SCI by complete spinal cord transection at thoracic segments T9-10. Human PTH (1-34) (80 µg/kg/day) or vehicle was injected subcutaneously daily starting on the day of surgery and continued for 30 days when animals were sacrificed. Tibias and femurs were isolated and examined by micro-computed tomography scanning (micro-CT) and histology; serum markers of bone turnover were measured using biochemical assays. Micro-CT analysis of proximal tibial metaphysis revealed that the SCI/vehicle animals exhibited 49% and 18% reduction in trabecular bone volume/total volume and trabecular thickness, respectively, compared to sham/vehicle controls. Furthermore, analysis of femoral mid-shaft region showed that the SCI/vehicle group had 15% lower cortical thickness and 16% higher cortical porosity than sham/vehicle counterparts. Interestingly, PTH administration to SCI animals improved bone structure and architecture by restoring 78% of fractional bone volume, increasing connectivity to 366%, and lowering structure model index (higher plate/rod structure ratio) by 10% compared to sham/vehicle animals. PTH favorable effects were also evident on the cortical bone of the SCI animals by attenuating cortical bone loss to only 5% and completely preventing the SCI-associated increase in cortical porosity. Dynamic and static histomorphometry evaluation of femurs of immobilized SCI/vehicle animals demonstrated a marked 49% and 38% decline in osteoblast and osteoclast number/tissue area, respectively, and 35% reduction in bone formation rate. In contrast, PTH treatment of SCI animals preserved osteoblast and osteoclast number and enhanced bone formation rate ( $P=0.003$ ) to levels that were similar to or higher than sham/vehicle able-bodied animals. Furthermore, PTH-treated SCI animals had higher levels of both bone formation ( $P=0.0001$ ) and resorption markers ( $P=0.01$ ) than either SCI or sham/vehicle groups. In summary, daily PTH administration improves bone structure and promotes bone turnover in severely immobilized SCI animals. These findings suggest that intermittent PTH receptor activation is an effective therapeutic approach to preserve bone integrity after severe immobilization.

Disclosures: Lauren Harlow, None.

## 1100

### The GABA<sub>B1</sub>R Is A Critical Promoter of PTH Secretion in Ca<sup>2+</sup>-deficient and Hyperparathyroidism States. Amanda Herberger\*, Jenna Hwong<sup>1</sup>, Hanson Ho<sup>1</sup>, Alfred Li<sup>1</sup>, Zhiqiang Cheng<sup>1</sup>, Frederic Jean-Alphonse<sup>2</sup>, Chia-Ling Tu<sup>1</sup>, Jean-Pierre Vilardaga<sup>2</sup>, Wenhan Chang<sup>1</sup>. <sup>1</sup>University of California, San Francisco, United States, <sup>2</sup>University of Pittsburgh School of Medicine, United States

Parathyroid cells (PTCs) play a central role in maintaining a steady Ca<sup>2+</sup> concentration in extracellular fluids by secreting parathyroid hormone (PTH). Lowering serum [Ca<sup>2+</sup>] promotes PTH secretion, whereas small increases in serum [Ca<sup>2+</sup>] inhibit PTH secretion by activating the calcium-sensing receptor (CaSR) and its downstream Gq/11 signaling. Ca<sup>2+</sup>-deficiency or rescued CaSR expression in PTCs produces hyperparathyroidism (HPT) of different etiologies, but the mechanisms underlying the PTH hypersecretion in those conditions are unclear. PTCs express type B GABA receptor 1 (GABA<sub>B1</sub>R), another member of family C GPCRs, which physically interacts with the CaSR and alters its signaling response in HEK-293 cells transfected with those receptor cDNA. To delineate the physiological actions of GABA<sub>B1</sub>R and its associated downstream signaling responses, we studied the impact of PTC-specific GABA<sub>B1</sub>R KO and the effects of GABA<sub>B1</sub>R agonist, baclofen, on serum PTH and mineral homeostasis in mice and PTH secretion from the parathyroid glands (PTGs) cultured from the mice. We found that: (1) GABA<sub>B1</sub>R forms heteromeric complexes with the CaSR in native mouse and human PTCs; (2) in HEK-293 cells co-expressing GABA<sub>B1</sub>R and CaSR, baclofen markedly reduces CaSR-mediated Gq activation; (3) injection of baclofen acutely increases serum PTH levels in mice; (4) activation of GABA<sub>B1</sub>R by baclofen promotes PTH secretion in cultured PTGs by increasing their maximal secretory rates at low [Ca<sup>2+</sup>] and reducing the ability of high [Ca<sup>2+</sup>] to suppress PTH secretion (a right-shifted Ca<sup>2+</sup> set-point); (5) mice with selective deletion of GABA<sub>B1</sub>R in their PTCs develop hypoparathyroidism and hypocalcemia and are unable to increase serum PTH levels in responses to a chronic low-Ca<sup>2+</sup> diet; and (6) concurrent KO of GABA<sub>B1</sub>R reverses the HPT and hypercalcemic phenotypes of PTC-specific CaSR KO mice. Our data not only support a critical role for the GABA<sub>B1</sub>R in promoting PTH secretion in Ca<sup>2+</sup>-deficient and HPT states, but also a new paradigm that CaSR/GABA<sub>B1</sub>R heteromers and CaSR/CaSR homomers stimulate distinct signal responses that counterbalance each other as such to render PTCs able to sense and, more importantly, respond to changes in [Ca<sup>2+</sup>]<sub>e</sub> within a small physiological range.

Disclosures: Amanda Herberger, None.



## 1101

**Osteocalcin Has Anti-Geronic Functions in the Brain.** Lori Khramian\*, Arnaud Obri, Gerard Karsenty. Columbia University Medical Center, United States

Osteocalcin regulates anxiety, spatial learning, and memory. Considering the steep decrease in circulating osteocalcin levels observed before mid-life in all species tested, this observation raises the question of whether osteocalcin might be an anti-geronic factor for the brain. To address this question, we asked if osteocalcin is necessary for the recently-described beneficial effect on cognition of plasma from young mice, when delivered to older mice. Anxiety-like behaviors were analyzed using the dark to light transition test and the elevated plus-maze test, and hippocampal memory was assessed through the novel object recognition task. Sixteen month-old WT mice that received plasma from 3-month-old (young) WT mice were significantly less anxious and had improved hippocampal-dependent memory compared to 16-month-old (aged) WT mice receiving plasma from aged WT mice. In contrast, neither anxiety nor memory was improved in aged WT mice receiving plasma obtained from young *Osteocalcin*<sup>-/-</sup> (*Ocn*<sup>-/-</sup>) mice. To rule out a developmental component to this effect of young plasma, aged WT mice were injected with plasma from young *Ocn*<sup>-/-</sup> mice that had been supplemented with mouse osteocalcin. This injection reduced anxiety and improved memory to the same extent as young plasma. These results prompted us to ask if osteocalcin would be sufficient to reduce anxiety and improve cognition in older WT mice. This was tested by delivering vehicle or osteocalcin to 10- or 14-month-old WT mice, peripherally and continuously, for two months. We observed that osteocalcin significantly decreased anxiety-like behavior and markedly improved spatial learning and memory in older mice. At the mechanistic level, multiple findings indicated that brain-derived neurotrophic factor (BDNF), a marker of hippocampal-dependent memory formation, is regulated by osteocalcin signaling in the brain. First, BDNF accumulation was increased in hippocampi of aged WT mice receiving plasma from young WT mice but not in hippocampi of aged mice receiving plasma from young *Ocn*<sup>-/-</sup> or from aged WT mice. Second, BDNF accumulation in the hippocampus was increased in old WT mice receiving plasma from *Ocn*<sup>-/-</sup> mice supplemented with osteocalcin. Third, BDNF accumulation was increased in the hippocampi of WT mice injected peripherally with osteocalcin. Taken together, these results identify osteocalcin as an anti-geronic factor that can alleviate age-related cognitive decline.

**Disclosures:** Lori Khramian, None.

## 1102

**The Effects of Systemic Hedgehog Pathway Activation on Aged Fracture Healing.** Jennifer McKenzie\*<sup>1</sup>, Clayton Maschhoff<sup>1</sup>, Xiaochen Liu<sup>1</sup>, Nicole Migotsky<sup>1</sup>, Matthew Silva<sup>1</sup>, Michael Gardner<sup>2</sup>. <sup>1</sup>Washington University in St. Louis, United States, <sup>2</sup>Stanford University, United States

The healing potential of the skeleton diminishes with aging, which presents a significant clinical problem given the age-related increase in fractures. The role of the Hedgehog (Hh) pathway in adult skeletal healing is not well understood, but recent studies have indicated it may be a potential therapeutic target. We sought to determine the effects of pharmacological Hh pathway activation on fracture repair in a healing-challenged model. We hypothesized that activation of the hedgehog pathway, using a drug that activates the Smo receptor, improves fracture healing in an elderly mouse model. This animal study was approved by our IACUC. We performed daily dosing of either Hh agonist (Hh-Ag) or vehicle in more than 100 C57Bl/6 female mice at 18 months (NIA), an age when healing is delayed. The right femur was fractured in 3-point bending and the healing callus evaluated at post operative day (POD) 7 to 21 using a variety of assays (n= 3-11/group). We first confirmed that Hh-Ag increased hedgehog signaling in the callus: Pth1 and Gli1 expression were up ≥ 2-fold compared to control at POD7 and 10 (p<0.05). Evaluation of radiographs showed accelerated healing in the agonist group: 39% of Hh-Ag femurs exhibited full union at POD14, compared to 0% of vehicle femurs (p<0.05). By POD21, femurs in both groups were fully bridged radiographically although the Hh-Ag group had a larger callus volume by microCT. Vascular perfusion at POD7 revealed significantly less vessel volume in the callus of Hh-Ag mice, but by POD14 there was significantly more vessel volume compared to vehicle (p<0.05). At POD10 expression of chondrogenic markers Sox9 and Acan was lower in Hh-Ag femurs compared to vehicle, consistent with increased vasculature at POD14 and suggesting more rapid conversion of cartilage to bone. Importantly, at POD21 maximum torque of the fractured femurs in the Hh-Ag group averaged about 90% of their contralateral (intact) control value, whereas the vehicle group averaged ~50% of intact (p<0.05, Figure). In summary, pharmacological treatment with a Hh agonist led to a modest improvement in fracture healing in old mice, with evidence of earlier radiographic bridging, larger callus volume and increased vessel volume, as well as increased mechanical strength. These results provide pre-clinical support for the concept that the Hh pathway could be a biological target for fracture healing stimulation in challenging clinical situations.

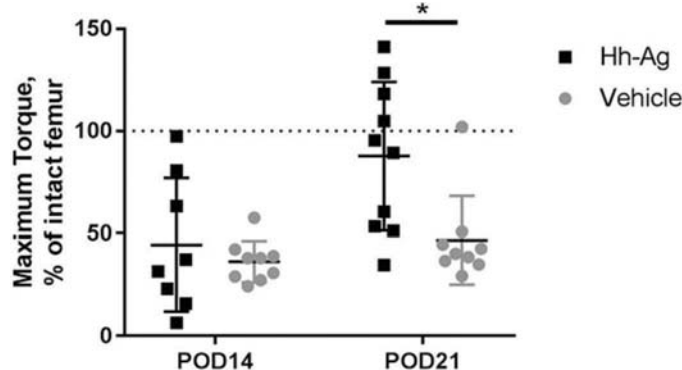


**Figure.** Hh-Ag treatment improved torsional strength to level of intact femur at POD21. \*p<0.05

**Torsion Figure**

**Disclosures:** Jennifer McKenzie, None.

## 1103

**Loss of deoxyribonuclease 1 impairs renal phosphate reabsorption and increases serum fibroblast growth factor 23 in mice.** Daniela Egli-Spichtig\*<sup>1</sup>, Martin Zhang<sup>1</sup>, Carsten A Wagner<sup>2</sup>, Farzana Perwad<sup>1</sup>. <sup>1</sup>University of California San Francisco, United States, <sup>2</sup>University of Zurich, Switzerland

Actin polymerization plays an important role in endocytotic retrieval of sodium dependent phosphate co-transporter IIa (NaPi-IIa) from the brush border membrane (BBM) of renal proximal tubules; a key mechanism in the maintenance of normal plasma phosphate levels. Deoxyribonuclease 1 (Dnase1) interacts with monomeric actin to inhibit polymerization. We have shown that renal *Dnase1* gene expression is upregulated by low phosphate diet and downregulated by fibroblast growth factor 23 (FGF23) in normal mice. Whether FGF23 downregulates *Dnase1* to facilitate endocytotic retrieval of NaPi-IIa is unknown. To determine whether regulation of *Dnase1* gene expression by FGF23 plays a role in phosphate homeostasis, we administered FGF23 to wild type (WT), early growth response 1 knockout (*Egr-1* KO) and *Fgf23* KO mice. A single intraperitoneal injection induced *Egr-1* gene expression in the kidney and rapidly recruited *Egr-1* to a regulatory region located 7.7kb upstream of the *Dnase1* gene transcription start site at 1 hour, and suppressed gene expression by 47% at 5 hours after FGF23 treatment in WT mice. The suppressive effect of FGF23 on *Dnase1* gene expression was diminished in *Egr-1* KO mice. In *Fgf23* KO mice we found a 2-fold increase in *Dnase1* gene expression which increased further with low phosphate diet. Administration of FGF23 fully reversed the up-regulation of renal *Dnase1* mRNA in *Fgf23* KO mice and abolished the effect of low phosphate diet. These studies demonstrate that FGF23 transcriptionally downregulates renal *Dnase1* gene expression in part via *Egr-1*-dependent mechanisms and overrides the stimulation of *Dnase1* by low phosphate diet. Next, we characterized phosphate homeostasis in *Dnase1* KO mice. At 6 weeks, the appearance and kidney function were normal but *Dnase1* KO mice displayed significantly decreased plasma phosphate levels and reduced renal BBM NaPi-IIa abundance compared to WT mice. Plasma FGF23 levels were significantly increased in *Dnase1* KO while *Fgf23* expression in bone was unchanged. Interestingly, at 12 weeks, *Dnase1* KO mice did not display any difference in parameters of phosphate homeostasis until challenged with low phosphate diet; plasma FGF23 increased 2-fold with a trend toward decreased plasma phosphate. In conclusion, FGF23 regulates renal *Dnase1* gene expression and loss of *Dnase1* impairs renal phosphate reabsorption and increases plasma FGF23 levels under conditions of phosphate deprivation and increased phosphate need in young mice.

**Disclosures:** Daniela Egli-Spichtig, None.

## 1104

**1,25-dihydroxyvitamin D treatment impairs renal FGF23 signaling in the Hyp mouse model of XLH.** Janaina Da Silva Martins\*, Eva S. Liu, Marie B. Demay. Endocrine Unit Massachusetts General Hospital, Harvard Medical School, United States

Hyp mice exhibit increased circulating levels of FGF23, renal phosphate wasting and impaired activation of vitamin D. 1,25-dihydroxyvitamin D (1,25D) treatment normalizes body weight and PTH, increases serum phosphate (Pi) and improves bone histomorphometry in Hyp mice, despite a >15 fold increase in bone FGF23 mRNA vs Hyp control and >100 fold increase vs WT controls. This suggests that 1,25D impairs FGF23 signaling.

1,25D treatment of Hyp mice leads to increased cortical bone mRNA expression of FAM20C, a protein that phosphorylates FGF23, promoting its cleavage. However, 1,25D treatment does not increase C-terminal FGF23 cleavage products in the circulation or in cortical bone. Thus, studies were undertaken to examine the effects of 1,25D

on the FGF23 signaling pathway in the kidneys of Hyp mice treated with 175 pg/g 1,25D for 1 hour, 18 hours or 4 days.

1,25D increased renal mRNA expression of  $\alpha$ Klotho without altering expression of FGFR1c, 3 and 4. Consistent with the increase in FGF23/  $\alpha$ Klotho, expression of FGF23 target genes, c-Fos and EGR1, as well as pERK1/2 was enhanced in Hyp mice treated with 1,25 D at all time points examined. Thus, 1,25D enhances rather than attenuates renal FGF23 signaling in Hyp mice despite decreasing renal phosphate excretion.

In spite of this apparent increase in FGF23 signaling in 1,25D treated Hyp mice, an increase in expression of sodium-dependent phosphate co-transporter 2a (Npt2a) is observed in Western analyses of brush border membrane proteins, in immunohistochemistry of renal proximal tubules and in kidney mRNA.

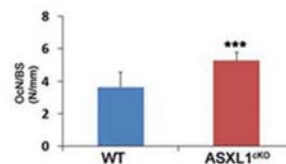
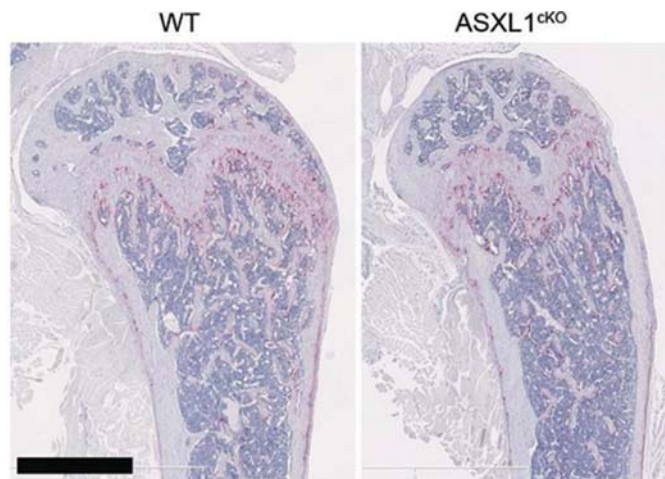
Brush border membrane location of Npt2a is regulated by interactions with the scaffold protein, Sodium-hydrogen exchanger regulatory factor 1(NHERF1). To examine Npt2a/NHERF1 interactions, NHERF1 was immunoprecipitated from kidney lysates and the immunoprecipitated proteins were subjected to Western analyses. A dramatic decrease in Npt2a protein was observed in the samples from control Hyp mice vs those of WT mice. Treatment of Hyp mice with 1,25D for 1 hour, 18 hours or 4 days increased immunoprecipitation of Npt2a by the NHERF1 antibody. Thus, 1,25D enhances Npt2a/NHERF1 interactions in Hyp mice, leading to increased renal phosphate reabsorption despite increasing circulating FGF23 and FGF23/FGFR signaling.

**Disclosures:** Janaina Da Silva Martins, None.

## 1105

**ASXL1 epigenetically suppresses osteoclast formation by methylating NFATc1.** Nidhi Rohatgi\*, Wei Zou, Tim Chen, Tim Chen, Yousef Abu-Amer, Steven Teitelbaum, Washington University in St. Louis, United States

Mammalian ASXL1 is an ETP protein which activates or retards transcription by modifying histone methylation. ASXL1 is a particularly relevant protein as inactivating mutations are commonly associated with myeloid malignancies and are a marker of aggressive disease. The negative impact of mutated ASXL1 on myelodysplasia likely reflects epigenetic transcriptional activation of leukemia-promoting genes in hematopoietic progenitors. Given that ASXL1 is indispensable for myeloid differentiation, we asked if it also regulates the osteoclast. Thus, we mated ASXL1(f/f) mice with those expressing Lysozyme M-Cre to delete ASXL1 in all osteoclast lineage cells. ASXL1-deficient precursors formed significantly more osteoclasts than their littermate controls when exposed to M-CSF and various doses of RANKL ( $p < 0.01$ ). Differentiation markers for osteoclastogenesis, were also increased as much as 10-fold in ASXL1-deficient cells. In keeping with increased osteoclastogenesis, deletion of ASXL1 in myeloid cells results in osteoporosis with decreased BMD and BV/TV in the KO animals ( $p < 0.001$ ) that co-incides with a significant increase in osteoclast number per bone surface ( $p < .001$ ). In addition, serum Trap5B and medium CTX levels were elevated in KO group attesting for increased osteoclast number. Osteoclast differentiation involves of a network of transcription factors, many of which are regulated epigenetically. We therefore asked, if ASXL1 modulates osteoclast differentiation by maintaining a balance between positive and negative epigenetic regulators. In fact, ASXL1 deficiency results in reduction of transcriptional repressor, H3K27me3, which enriches the NFATc1 promoter. Demethylation of H3K27me3 on NFATc1 thereby greatly enhances expression of the osteoclastogenic transcription factor and abundance of the bone resorptive cell. Because the histone demethylase, Jmjd3, promotes osteoclast formation by demethylating NFATc1-associated H3K27, it presented as a reasonable candidate to mediate the osteoclastogenesis of ASXL1<sup>lysM</sup> mice. Supporting this posture, Jmjd3 expression increases 40-fold in ASXL1-deficient osteoclasts. Most importantly, Jmjd3 knockdown in ASXL1<sup>lysM</sup> osteoclast precursors reduces NFATc1 expression and in consequence, arrests osteoclast formation. Thus, in addition to promoting myeloid malignancies, ASXL1 deficiency promotes osteoclastogenesis and osteoporosis, exerting its inhibitory effects by blunting repressive histone methylation of NFATc1.



Histomorphometric analysis of WT and ASXL1 tibias

**Disclosures:** Nidhi Rohatgi, None.

## 1106

**RIP140 in Osteoclast Precursors Regulates Bone Homeostasis, Growth and Osteoclast Activity.** Bomi Lee<sup>\*1</sup>, Urszula T Iwaniec<sup>2</sup>, Russell T Turner<sup>2</sup>, Yi-Wei Lin<sup>1</sup>, Bart L Clarke<sup>3</sup>, Li-Na Wei<sup>1</sup>, Anne Gingery<sup>4</sup>. <sup>1</sup>Department of Pharmacology, University of Minnesota Medical School, United States, <sup>2</sup>Skeletal Biology Laboratory, College of Public Health and Human Sciences, Oregon State University, United States, <sup>3</sup>Division of Endocrinology, Diabetes, Metabolism, and Nutrition, United States, <sup>4</sup>Department of Orthopedics Mayo Clinic, United States

Macrophages play a critical role in maintenance of bone homeostasis. We have shown that RIP140 (receptor interacting protein 140, nrip1) acts as a regulatory switch in macrophage M1/M2 polarization. Macrophage polarization typically defines tissue homeostasis with M1 tissue destructive inflammation and M2 wound healing and tissue regeneration. Recent work has determined that osteoclasts typically express an M2 profile. In mice, lowering macrophage-specific RIP140 expression levels reduces M1 macrophages, increases M2 macrophages, prevents high fat diet-induced insulin resistance, and enhances insulin sensitivity and white adipose tissue browning even under a high fat diet. However macrophage progenitor specific RIP140 knockdown (mΦRIP140KD) mice exhibit an osteopenic cancellous phenotype due to increased bone resorption and decreased bone formation. The loss of RIP140 in osteoclast precursors resulted in a significant increase in osteoclast differentiation. Treatment of primary osteoblasts with mΦRIP140KD primary osteoclast conditioned media significantly reduced markers of osteoblast expression including Runx2, Sp7, and Alpl indicating a potential uncoupling of osteoclasts and osteoblasts. Formation of RIP140/TR4 complex and gain-of-function studies showed that RIP140 protein and its transcriptional partners are targeted for degradation upon RANKL treatment via upregulation of Nfatc1, Csk and Acp5. Additionally we have previously shown that Syk, a nonreceptor tyrosine kinase, targets RIP140 protein ubiquitination and degradation in M1-polarized macrophages. When Syk was inhibited in osteoclasts RIP140 protein degradation was reduced as was osteoclast differentiation gene expression. Syk has been shown to be an important kinase in mature osteoclast cytoskeletal organization. Our data reveal for the first time that Syk may have an additional early regulatory role in osteoclast differentiation. Additionally we noted tibia length was significantly reduced in the mΦRIP140KD animals, which may have some important implications for normal bone growth. Together these data show that RIP140 in osteoclast precursors is an important regulator of osteoclast activity, bone homeostasis and growth. These data suggest that changes in the osteoclast/macrophage microenvironment alter bone formation.

**Disclosures:** Bomi Lee, None.



## 1107

**PGC1 $\beta$  Stimulates Osteoclast Function But not Formation via Mitochondrial Biogenesis and Activation.** Yan Zhang<sup>\*1</sup>, Nidhi Rohatgi<sup>2</sup>, Deborah V. Novack<sup>3</sup>, Joel Schilling<sup>4</sup>, Steven L. Teitelbaum<sup>3</sup>, Wei Zou<sup>2</sup>. <sup>1</sup>Department of Pathology and Immunology, Washington University School of Medicine, St. Louis, MO 63110, USA; Center for Translational Medicine, the First Affiliated Hospital of Xi'an Jiaotong University, Xi'an, Shaanxi 710061, People's Republic of China, United States, <sup>2</sup>Department of Pathology and Immunology, Washington University School of Medicine, St. Louis, MO 63110, USA, United States, <sup>3</sup>Department of Pathology and Immunology; Division of Bone and Mineral Diseases, Department of Medicine, Washington University School of Medicine, St. Louis, MO 63110, USA, United States, <sup>4</sup>Cardiovascular Division, Department of Medicine, Washington University School of Medicine, St. Louis, MO 63110, USA, United States

Peroxisome proliferator-activated receptor gamma coactivator 1- $\beta$  (PGC1 $\beta$ ) is a transcriptional coactivator that regulates energy metabolism by stimulating mitochondrial biogenesis. Previous studies using global and Tie2-Cre conditional knockout mice reported that PGC1 $\beta$  is essential for osteoclast (OC) differentiation. This conclusion is inconsistent, however, with the normal OC number in PGC1 $\beta$ -/- mice. To determine the role of PGC1 $\beta$  in OCs, we generated LysM-Cre conditional knockout mice in which PGC1 $\beta$  is exclusively deleted in myeloid lineage cells (PGC1 $\beta$ <sup>LysM</sup>). Challenging previous reports, differentiation of PGC1 $\beta$ <sup>LysM</sup> OC precursors is unaltered. However, OC function is impaired as manifest by cytoskeletal disorganization including a complete absence of actin rings and resorptive pits on bone as well as failure to form ruffled membranes. The OCs of PGC1 $\beta$ <sup>LysM</sup> mice are normal in number but their ability to attach to bone is compromised. In consequence PGC1 $\beta$ <sup>LysM</sup> OCs are hypermobile resulting in increased contact with mononuclear precursors and a giant phenotype. These deficits in OC function double bone mass of PGC1 $\beta$ <sup>LysM</sup> mice. Rac and c-Src activation are unaltered in PGC1 $\beta$ <sup>LysM</sup> OCs establishing PGC1 $\beta$  organizes the OC cytoskeleton in a non-canonical manner. In this regard, mitochondrial biogenesis and number, expression of mitochondrial respiratory chain proteins and oxygen consumption rates are decreased in the PGC1 $\beta$ -deficient OCs. Importantly, arrest of mitochondrial biogenesis using specific inhibitors mimics the cytoskeletal phenotype of PGC1 $\beta$ <sup>LysM</sup> OCs. Further confirming mitochondrial regulation, PGC1 $\alpha$ , which also enhances mitochondrial respiration, rescues OC size and actin ring formation. G protein-coupled receptor kinase interacting protein 1 (GIT1) regulates mitochondrial biogenesis in OCs and is diminished in those lacking PGC1 $\beta$ . Importantly, GIT1 transduction rescues mitochondrial and cytoskeletal abnormalities of PGC1 $\beta$ <sup>LysM</sup> OCs indicating it mediates PGC1 $\beta$ 's mitochondrial- and cytoskeletal-stimulating properties. Thus, PGC1 $\beta$  is essential for OC function but not differentiation and OC cytoskeletal organization is mitochondria-mediated.

**Disclosures:** Yan Zhang, None.

## 1108

**Igfl Derived from Osteoclasts Regulates Bone Formation via Signaling through EphrinB2/EphB4.** Yasuhiro Ohata<sup>\*1</sup>, Gabriel M Pagnotti<sup>2</sup>, Jolene J. Windle<sup>3</sup>, G. David Roodman<sup>4</sup>, Noriyo Kurihara<sup>1</sup>. <sup>1</sup>Indiana University, Medicine/Hematology-Oncology, United States, <sup>2</sup>Indiana University, Medicine/Endocrinology, United States, <sup>3</sup>Human and Molecular Genetics, Virginia Commonwealth University, United States, <sup>4</sup>Indiana University, Medicine/Hematology-Oncology; Roudebush VA Medical Center, United States

We reported that Igfl derived from osteoclasts (OCLs) induced EphrinB2 on OCLs and bound EphB4 on osteoblasts (OBs) to induce bidirectional signaling that enhances bone formation. Further, OCLs expressing measles virus nucleocapsid protein (MVNP), a model of Paget's disease, expressed higher levels of Igfl compared to wild type OCLs (JCI 2016). To determine the role of OCL-derived Igfl *in vivo*, we generated mice with targeted deletion of Igfl in OCL (TRAP-Cre(+) - Igfl<sup>fllox/fllox</sup> mice (TC(+)-Igfl)) and TRAP-Cre(-) - Igfl<sup>fllox/fllox</sup> mice (TC(-)-Igfl) as controls. TC(+)-Igfl mice were 25% smaller by body weight than TC(-)-Igfl mice, and the BV/TV ratio of their femurs was significantly decreased as compared to TC(-)-Igfl mice at 5 months of age. We then confirmed that Igfl knockdown was not decreased in liver, a major source of Igfl that also expresses TRAP. Igfl levels in liver were similar in TC(+)-Igfl and TC(-)-Igfl mice at the protein and mRNA levels as assayed by Western blot, ELISA and qPCR. Further, TRAP expression levels in liver were almost undetectable compared to OCLs as assessed by Western blot. We then measured serum levels of Igfl-1 in TC(+)-Igfl and control mice by ELISA. Interestingly, the mean of serum Igfl levels of TC(+)-Igfl mice vs. TC(-)-Igfl mice were 8 $\pm$ 3 vs 14 $\pm$ 5 ng/ml, respectively. These results suggest that Igfl from OCL may contribute to serum Igfl levels. We then examined Igfl expression levels in purified OCLs from TC(+)-Igfl mice and TC(-)-Igfl mice. Igfl expression was undetectable in OCLs from TC(+)-Igfl mice as compared to TC(-)-Igfl mice. Further, Igfl levels in 48 hours media conditioned by purified OCLs from TC(+)-Igfl mice and TC(-)-Igfl mice were 100 vs 225 pg/ml, respectively. OCLs formation by OCL-precursors from TC(+)-Igfl mice treated with 50 ng/ml of RANKL was decreased by 50% compared with TC(-)-Igfl mice. As expected, ephrinB2 levels on TC(+)-Igfl OCL were much lower compared with TC(-)-Igfl mice. In contrast,

Igfl-receptor levels on OBs derived from TC(+)-Igfl or TC(-)-Igfl mice were not significantly different. However, expression levels of Runx2, Osterix, ALP, EphB4 and Col-1 in OBs from TC(+)-Igfl mice were decreased compared to TC(-)-Igfl OBs ( $p < 0.05$ ). These results suggest that Igfl derived from OCLs contributes bone formation *in vivo* to induce bidirectional signaling via ephrinB2/EphB4 *in vivo*.

**Disclosures:** Yasuhisa Ohata, None.

## 1109

**Intravital imaging of osteoclasts *in vivo* reveals cellular recycling as a novel cell fate mechanism.** Michelle McDonald<sup>\*1</sup>, Pei Ying Ng<sup>2</sup>, Danyal Butt<sup>1</sup>, Karman Pathmanandavel<sup>1</sup>, Mate Biro<sup>3</sup>, Rachael Terry<sup>1</sup>, Weng Hua Khoo<sup>1</sup>, Sindhu Mohanty<sup>1</sup>, Marija Simic<sup>1</sup>, Ryan Chai<sup>1</sup>, Julian Quinn<sup>1</sup>, Jessica Pettitt<sup>1</sup>, David Abi-Hanna<sup>3</sup>, Rohit Jain<sup>4</sup>, Wolfgang Weninger<sup>4</sup>, Paul Baldock<sup>1</sup>, Michael Rogers<sup>1</sup>, Robert Brink<sup>1</sup>, Nathan Pavlos<sup>2</sup>, Peter Croucher<sup>1</sup>, Tri Phan<sup>1</sup>. <sup>1</sup>The Garvan Institute, Australia, <sup>2</sup>University of Western Australia, Australia, <sup>3</sup>University of New South Wales, Australia, <sup>4</sup>Centenary Institute, Australia

Osteoclasts are commonly defined as terminally differentiated polykaryons, with a lifespan of days to weeks, during which time they resorb bone, before undergoing apoptosis. This linear model of osteoclast fate has been formulated primarily through examination of osteoclasts *in vitro* and static histological analyses. Using a novel intravital imaging methodology we directly imaged the intact endocortical surface of the tibia in live mice, allowing visualisation of the dynamic behaviour of osteoclasts *in vivo* to reveal a previously unappreciated cell plasticity and alternative cell fate.

We showed that, in the steady-state, multi-nucleated LysM<sup>+</sup>Blimp-1<sup>+</sup>Osteosense<sup>+</sup>, Cathepsin K<sup>+</sup>, osteoclasts exhibit a stellate structure forming syncytial networks on the endosteal bone surface. Activation of bone resorption by treatment with soluble RANKL (sRANKL) induced rapid (within 20 minutes) retraction of cellular processes, causing loss of cell-to-cell contact and syncytial networks. Subsequently, these activated osteoclasts were visualised undergoing cell fusion and, unexpectedly, cell fission. Daughter cells were observed to refuse with parent cells or other nearby osteoclasts, in a novel process we have termed osteoclast recycling. This was blocked by treatment with osteoprotegerin-Fc fusion protein (OPG-Fc), which reversibly inhibits RANKL. However, rather than undergo apoptosis, small round LysM<sup>+</sup>Blimp-1<sup>+</sup> cells persisted after OPG-Fc treatment. Critically, 3-4 weeks following OPG-Fc treatment withdrawal recycling osteoclasts re-fused to form networks of active enlarged LysM<sup>+</sup>Blimp-1<sup>+</sup>Osteosense<sup>+</sup> osteoclasts, similar to those seen following sRANKL treatment.

These data demonstrate that intravital imaging of the intact endosteal bone surface in the tibia can be used to study osteoclast dynamics *in vivo* and that rather than a simple linear cell fate osteoclasts can also recycle their cellular constituents. Osteoclast recycling therefore not only provides a new paradigm for understanding the behaviour of these cells in their *in vivo* physiological niche, but also explains the paradoxical acceleration of bone loss and vertebral fractures observed upon discontinuation of the anti-RANKL therapeutic agent Denosumab that is used to treat patients with osteoporosis and metastatic bone disease.

**Disclosures:** Michelle McDonald, None.

## 1110

**FRAME Study: The Foundation Effect of Rebuilding Bone With One Year of Romosozumab Leads to Continued Lower Fracture Risk After Transition to Denosumab.** Felicia Cosman<sup>\*1</sup>, Daria B Crittenden<sup>2</sup>, Serge Ferrari<sup>3</sup>, Aliya Khan<sup>4</sup>, Nancy Lane<sup>5</sup>, Kurt Lippuner<sup>6</sup>, Toshio Matsumoto<sup>7</sup>, Cassandra E Milmont<sup>2</sup>, Cesar Libanati<sup>8</sup>, Andreas Grauer<sup>2</sup>. <sup>1</sup>Helen Hayes Hospital, West Haverstraw, and Columbia University, United States, <sup>2</sup>Amgen Inc., United States, <sup>3</sup>Geneva University Hospital, Switzerland, <sup>4</sup>Oakville Medical Centre, Canada, <sup>5</sup>UC Davis Medical Center, United States, <sup>6</sup>Osteoporosis Poliklinik, Inselspital, Bern University Hospital and University of Bern, Switzerland, <sup>7</sup>University of Tokushima, Japan, <sup>8</sup>UCB Pharma, Belgium

Purpose: Romosozumab (Romo), a sclerostin antibody, has a dual effect of increasing bone formation and decreasing bone resorption. In the FRAME study, one year of Romo treatment resulted in large BMD increases at the lumbar spine and total hip versus placebo (PBO); the differences between groups remained after all subjects transitioned to denosumab (DMAb) during the second year of study (Cosman *NEJM* 2016). Here, we further characterize the BMD gains during the FRAME study and the effect of building bone with Romo on fracture risk reduction upon transition to DMAb.

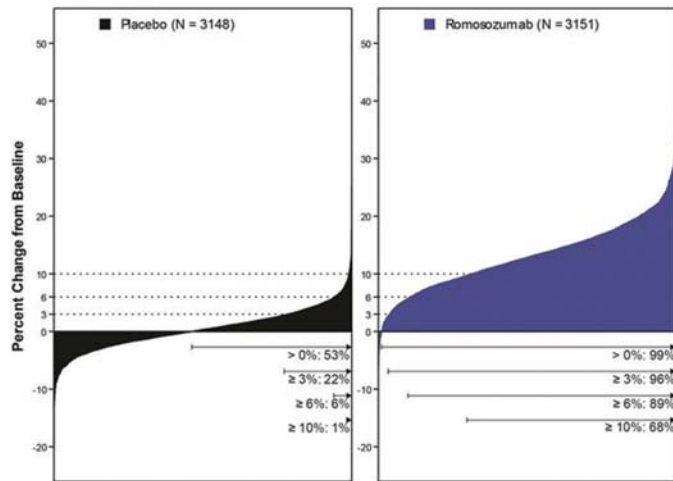
Methods: Subjects in FRAME (NCT01575834) were randomized to receive Romo 210 mg QM or PBO for 12 months, after which all subjects received DMAb 60 mg Q6M for an additional 12 months. Endpoints for the current analysis were mean change from baseline in BMD T-score, percent of subjects with a BMD gain, and subject incidence of fractures in the second year of the study, including new vertebral, clinical (nonvertebral plus symptomatic vertebral), and other fracture categories.

Results: There were 7180 subjects in the study (N=3589 Romo, N=3591 PBO). At month 12, mean change from baseline in lumbar spine BMD T-score was 0.88 for Romo and 0.03 for PBO; at month 24, after both treatment groups received DMAb in the

second year, the mean change from baseline was 1.11 for Romo/DMAb and 0.38 for PBO/DMAb. At the total hip, the mean changes were 0.32 for Romo and 0.01 for PBO at month 12, with month-24 changes of 0.45 for Romo/DMAb and 0.17 for PBO/DMAb. 99% of subjects in the Romo group showed some increase in BMD at month 12, with 89% achieving  $\geq 6\%$  gains in lumbar spine BMD (Figure). Administration of Romo during the first year led to relative risk reductions in fractures between groups during the second year, despite both groups receiving DMAb in year two, with reductions of 81% for vertebral fractures ( $p < 0.001$ ), 32% for clinical fractures ( $p = 0.052$ ), and 39% for major osteoporotic fractures ( $p = 0.034$ ).

Conclusions: Romo resulted in substantial T-score increases after one year; upon transition to DMAb, gains in both groups were similar, resulting in unprecedented BMD gains after treatment with Romo followed by DMAb. As a result of one year of Romo before transition to DMAb, fracture rates were substantially reduced during year two, when subjects in both groups received DMAb. The data support the clinical benefit of rebuilding the skeletal foundation with Romo treatment before transition to DMAb.

Figure. Percent Change in Lumbar Spine BMD From Baseline to Month 12 by Individual Subject



N = Number of subjects with values at baseline and at least one post-baseline visit at or before month 12. Data are percent change in lumbar spine BMD from baseline to month 12 by individual subject. N's included subjects with baseline and  $\geq 1$  postbaseline measurement; missing data were imputed by last observation carried forward. X-axis represents each individual subject. Dotted horizontal lines reflect 3%, 6%, and 10% BMD gain from baseline to month 12. Lines with arrowheads below the X-axis represent the percent of subjects with the indicated BMD gains ( $> 0\%$ ,  $\geq 3\%$ ,  $\geq 6\%$ , and  $\geq 10\%$ ). BMD, bone mineral density.

Figure. Percent Change in Lumbar Spine BMD From Baseline to Month 12 by Individual Subject

**Disclosures:** Felicia Cosman, Amgen, Eli Lilly, Merck, Radius, Other Financial or Material Support.

## 1111

**Denosumab Reduced Bone Remodeling, Eroded Surface, and Erosion Depth in Cortical Bone of Iliac Crest Biopsies From Postmenopausal Women in the FREEDOM Trial.** Roland Chapurlat<sup>1</sup>, Nathalie Portero-Muzy<sup>1</sup>, Jean-Paul Roux<sup>1</sup>, Stephane Horlait<sup>2</sup>, David Dempster<sup>3</sup>, Andrea Wang<sup>2</sup>, Rachel Wagman<sup>2</sup>, Pascale Chavassieux<sup>1</sup>. <sup>1</sup>INSERM UMR 1033, Université de Lyon, France, <sup>2</sup>Amgen Inc., United States, <sup>3</sup>Columbia University, United States

Denosumab (DMAb), a RANKL inhibitor, reduced the risk of vertebral, hip, and nonvertebral fractures in the FREEDOM trial of postmenopausal women with osteoporosis compared with placebo (PBO).<sup>1</sup> Bone histomorphometry of iliac crest bone biopsies collected during FREEDOM showed that DMAb reduced trabecular remodeling parameters, including eroded surface per bone surface (ES/BS).<sup>2</sup> We now report the effects of DMAb vs PBO on cortical bone histomorphometry from iliac crest bone biopsies obtained during FREEDOM.

A total of 112 biopsies were evaluable for cortical bone histomorphometry, including 67 obtained at month 24 (37 PBO, 30 DMAb) and 45 at month 36 (25 PBO, 20 DMAb). Both cortices were analyzed, if available. Endocortical (Ec) ES/BS, osteoclast surface (Oc.S/BS) and erosion depth (E.De) were assessed by an automatic-interactive method.<sup>3</sup> Cortical porosity and Ec wall thickness (W.Th) were measured. Dynamic remodeling parameters were assessed for Ec, periosteal, and intracortical envelopes.

The Ec structural variables, Oc.S/BS, ES/BS, and mean and maximal E.De, were significantly lower in the DMAb group vs PBO at months 24 and 36 (Table). There were no significant differences between DMAb and PBO groups for W.Th, cortical porosity, or cortical thickness. No extensive search for cortical fluorochrome labels was done, unlike prior trabecular analyses,<sup>2</sup> and cortical labels in at least one cortical envelope were observed in 13 (43%) and 10 (50%) of DMAb biopsies at months 24 and 36, respectively. Though envelope-specific dynamic bone formation and remodeling parameters could not be reliably assessed, the overall labeling findings indicate that DMAb markedly reduced cortical bone turnover.

These data are consistent with the mechanism of action of DMAb, which inhibits osteoclasts throughout the skeleton. Lower Ec eroded surfaces with DMAb may reflect inhibited bone resorption and refilling of resorption spaces. Reduced cortical labeling and bone formation indices with DMAb may reflect refilling of resorption spaces that were present before fluorochromes were administered, and reduced activation of new remodeling sites. Reduced E.De is a novel finding for DMAb that may contribute to increased bone strength by reducing Ec bone loss and structural vulnerabilities associated with deep resorption cavities.

1. Cummings SR, et al. *N Engl J Med*. 2009;361:756.
2. Reid IR, et al. *J Bone Miner Res*. 2010;25:2256.
3. Roux C, et al. *Bone*. 1995;17:153.

Parameter	Month 24		Month 36	
	PBO (n = 37)	DMAb (n = 30)	PBO (n = 25)	DMAb (n = 20)
Ec.Oc.S/BS (%)	0.26 (0.00, 0.59)	0.00 (0.00, 0.00)*	0.14 (0.00, 0.22)	0.00 (0.00, 0.00) <sup>1</sup>
Ec.ES/BS (%)	4.39 (3.26, 7.60)	1.59 (1.01, 2.17)*	3.53 (1.92, 5.32)	1.39 (0.67, 3.52) <sup>1</sup>
Maximum Ec.E.De (µm)	16.45 (12.88, 21.61)	11.43 (9.00, 13.11)*	17.40 (12.13, 21.01)	14.04 (6.92, 15.99) <sup>1</sup>
Mean Ec.E.De (µm)	10.26 (8.32, 13.34)	7.10 (6.03, 8.69)*	10.14 (7.39, 12.87)	7.91 (4.94, 9.65) <sup>1</sup>
Mean Ec.W.Th (µm)	32.41 (31.16, 33.83)	32.39 (31.68, 34.52)	32.11 (30.48, 33.05)	31.82 (29.30, 33.41)
Cortical thickness (µm)	749.3 (572.0, 904.9)	753.6 (521.3, 1022.0)	689.7 (478.7, 920.4)	605.8 (491.0, 799.3)
Cortical porosity (%)	6.43 (4.56, 9.34)	5.90 (3.83, 8.12)	5.42 (3.77, 7.42)	6.37 (4.39, 7.88)

Data represent median (Q1, Q3); n = number of subjects evaluable for cortical bone histomorphometry

\* $P < 0.0001$ , <sup>1</sup> $P < 0.05$ , Wilcoxon rank sum test (DMAb vs PBO).

Table: Summary of Cortical Histomorphometry Parameters at Months 24 and 36

**Disclosures:** Roland Chapurlat, Amgen, Janssen, Radius, Sandoz, UCB, Consultant.

## 1112

**Prospective, randomized, double-blind, placebo-controlled trial to evaluate efficacy and safety of zoledronic acid for the treatment of bone marrow lesions - ZoMARS.** Lothar Seefried<sup>1</sup>, Jasmin Baumann<sup>1</sup>, Franca Genest<sup>1</sup>, Anke Heidemeier<sup>1</sup>, Rainer Meffert<sup>2</sup>, Franz Jakob<sup>3</sup>. <sup>1</sup>Clinical Trial Unit, Orthopedic Institute, University Wuerzburg, Germany, <sup>2</sup>Department of Trauma, Plastic, Reconstructive, and Hand Surgery, University Hospital Wuerzburg, Germany, <sup>3</sup>Orthopedic Center of Musculoskeletal Research, University of Wuerzburg, Germany

**Background:** Bone marrow lesions (BML) are defined areas of deteriorated bone structure and metabolism, characterized by excessive water signal within the trabecular bone and marrow space on MR imaging. BML occur as a consequence of various conditions, all being associated with an imbalance of mechanical loading capacity and actual forces applied. There is no approved treatment for this condition. Bisphosphonates are known to improve bone stability in osteoporosis and other bone disorders and have been used off-label to treat this disorder.

**Methods:** Randomized (2:1), double-blind, placebo-controlled Phase III trial to assess efficacy and safety of single dose Zoledronic acid (ZOL446) 5mg i.v. plus Vitamin D vs placebo plus Vitamin D in 48 patients with bone marrow lesions. Primary efficacy endpoint was reduction of edema volume six weeks after treatment as assessed by MRI. Secondary endpoints included reduction of pain (VAS, Pain Disability Index) and quality of life (Clinicaltrial.gov; NCT01348269).

**Results:** At six weeks after treatment, bone marrow edema volume was sig. reduced by 64.53% in patients randomized to Zoledronic acid (n=34) while in the placebo group, there was an average increase by 14.43% (p 0.007). A decrease of bone marrow edema was observed for >75% of patients receiving ZOL446 and for 50% of the patients receiving placebo. Pain level (VAS + PDI) was also improved with ZOL446 as compared to placebo at 6 weeks but levels converged after 12 weeks of follow-up. Six SAE occurred in five patients, none of them being related to study drug. Most frequent AE related to ZOL446 were headache (n=13 pat), pain in extremities (n=11) and fatigue (n=10).

**Conclusions:** Single-dose Zoledronic acid 5mg i.v. plus Vitamin D may enhance resolution of bone marrow lesions within 6 weeks along with reduction of pain as compared to Placebo and Vitamin D supplementation. Convergence of pain levels at 12 weeks after treatment were most likely due to spontaneous healing in the placebo group. Treatment-emergent AE were in line with known side effects of intravenous bisphosphonates.

**Disclosures:** Lothar Seefried, Novartis, Grant/Research Support.



## 1113

**PTH(1-34) for Surgical Hypoparathyroidism: A 2 year Prospective, multicentric, Open-Label Investigation of Efficacy and Quality of Life.** Andrea Palermo<sup>1</sup>, Assunta Santonati<sup>2</sup>, Gaia Tabacco<sup>1</sup>, Daria Maggi<sup>1</sup>, Claudio Pedone<sup>3</sup>, Daniela Bosco<sup>2</sup>, Spada Antonio<sup>2</sup>, Bruno Raggiunti<sup>4</sup>, Doris Tina<sup>4</sup>, Silvia Manfrini<sup>5</sup>, Fabio Vescini<sup>6</sup>. <sup>1</sup>Department of Endocrinology and Diabetes, University Campus Bio-Medico, Italy, <sup>2</sup>Department of Endocrinology, San Giovanni Addolorata Hospital, Italy, <sup>3</sup>Unit of Geriatrics, University Campus Bio-Medico, Italy, <sup>4</sup>Department of Endocrinology, Hospital San Liberatore Atri, Italy, <sup>5</sup>Department of Endocrinology and Diabetes, University Campus Bio-Medico, Italy, <sup>6</sup>Department of Endocrinology and Diabetes, Santa Maria della Misericordia Hospital, Italy

**Purpose:** Many studies have demonstrated that PTH(1-84) and PTH(1-34) replacement therapy were able to reduce the required total daily dose of calcium/calcitriol and restore normocalcemia in hypoparathyroid subjects. As all PTH(1-34) trials were conducted on small cohorts including subjects with hypoparathyroidism of various etiologies, the aim of our study was to investigate the effects of 24 months of PTH(1-34) treatment in a homogeneous cohort of adult subjects with postoperative hypoparathyroidism. Furthermore, for the first time, we tested the hypothesis that PTH(1-34) therapy can improve the quality of life (QOL).

**Methods:** This was a 2-year prospective, multicentric, open-label study. Between June 2013 and September 2014, we enrolled 42 subjects (34 females, 8 males, age range 34-77) with post-surgical hypoparathyroidism. Subjects were instructed to self-administer a sc, twice-daily 20 mg injection of PTH(1-34). At baseline and after 3, 6, 12, 18 and 24 months of treatment, calcium and vitamin D supplementation requirements, serum calcium, phosphate, creatinine, alkaline phosphatase, uric acid, and 24-hour urinary calcium excretion were evaluated. At baseline and after 6, 24 months of treatment, QOL was evaluated by the Rand 36-Item Short Form Health Survey (SF-36) covering eight domains of physical and mental health.

**Results:** The mean serum calcium levels increased from baseline to 3 months (7.6 mg/dl vs. 8.9 mg/dl,  $P < 0.001$ ) and remained stable at 12 and 24 months (8.9 mg/dl at both time points). At the same time, there was a decrease in mean calcium supplementation from 4174 mg/d at baseline to 897 mg/d at 24 months ( $P < 0.001$ ) and in mean vitamin D supplementation from 0.8 mcg/d at baseline to 0.4 mcg/d at 24 months ( $P < 0.001$ ). Phosphate levels decreased from 4.3 mg/dl at baseline to 4.1 mg/dl at 3 months ( $P = 0.08$ ) and then remained stable until the end of the follow-up (4 mg/dl at 24 months), whereas alkaline phosphatase increased from 76 U/l at baseline to 157 U/l at 24 months ( $P < 0.001$ ). Data from the SF-36 showed a significant improvement in the mean scores of all domains ( $P < 0.001$ ). Adverse events led to the discontinuation of PTH(1-34) in 3 subjects (2 myalgia, 1 gastroenteritis).

**Conclusion:** This is the largest study that demonstrates the efficacy of PTH(1-34) in the treatment of patients with postsurgical hypoparathyroidism, and, for the first time, it shows that PTH(1-34) may improve the mental and physical health in hypoparathyroid subjects.

**Disclosures:** Andrea Palermo, None.

## 1114

**Effectiveness of a Private, Orthopedic Practice-Based Osteoporosis Management Program for Prevention of Recurrent Fractures.** Kathleen A. Taylor<sup>\*1</sup>, Andre B. Araujo<sup>1</sup>, Li Wang<sup>2</sup>, Natalie N. Boystov<sup>1</sup>, Ginger S. Haynes<sup>1</sup>, Shivani Pandya<sup>2</sup>, Debra L. Sietsema<sup>3</sup>, Douglas Faries<sup>1</sup>, Onur Baser<sup>4</sup>, Clifford B. Jones<sup>3</sup>. <sup>1</sup>Eli Lilly and Company, United States, <sup>2</sup>STATINMED Research, United States, <sup>3</sup>The CORE Institute, United States, <sup>4</sup>Columbia University, Center for Innovation and Outcomes Research, Department of Surgery, United States

**Purpose:** Evaluate the impact of an osteoporosis (OP) management service (MS) operated by a private, regionally-based orthopedic practice in the Midwestern US on the recurrent fracture rate and other aspects of OP patient management. **Methods:** Patients (pts) >65y residing in MI with any fragility fracture of the hip, pelvis, femur, upper limbs, lower limbs, upper body, unspecified non-vertebral (NV) or vertebral during 01APR10-30SEP14 were retrospectively identified from the 100% Medicare database. Fracture was defined as an inpatient hospital stay with a primary/secondary discharge diagnosis for specified fracture sites (discharge date defined as fracture date); or ≥2 outpatient medical claims ≤90 days (d) apart for specified fracture sites (first fracture claim date defined as fracture date). Pts seen by the OP MS within 90d of fracture date were considered as exposed and were identified by linking healthcare provider National Provider Identifiers with the National Plan and Provider Enumeration System. Pts who did not seek care at this facility but had a physician visit within 90d of fracture date were considered as unexposed. The date of the follow-up fracture care visit in exposed and unexposed groups was the index date. Pts were required to have continuous enrollment for Medicare part A and B for 90d pre-index (baseline) period and were followed until earliest of death, health plan disenrollment, or study end (31DEC14) to evaluate the recurrent fracture rate, OP medication use, and BMD assessment. Healthcare resource utilization (HCRU) and costs were evaluated in a subset of pts with 12 mos follow-up. Propensity score matching (PSM) with caliper 0.01 was used to balance differences in baseline patient characteristics. **Results:** There were 1,306 exposed and 123,815 unexposed pts with significant differences in baseline variables, including a greater proportion of hip/pelvis/femur and vertebral but fewer NV fractures among the exposed. Table 1 shows outcomes in the PSM population (N=1304 in each group).

The recurrent fracture rate was significantly lower; time to recurrent fracture was significantly longer; rates of OP medication use, BMD assessment, and 12mo HCRU and costs were significantly higher in exposed vs. unexposed pts. **Conclusion:** An OP MS operated by a private, regionally-based orthopedic practice not situated within an integrated health system effectively reduces recurrent fractures, possibly through prompt delivery of improved patient care.

**Table 1. Outcomes in the follow-up period among fracture patients exposed to an OP management service operated by a private, regionally-based orthopedic practice compared to propensity score matched\* fracture patients who were not exposed to this service.**

Clinical Outcomes	Exposed (N=1,304)		Unexposed (N=1,304)		P-value†
Recurrent fracture rate [N, IR (95%CI)†]	522	300 (275,327)	605	381 (352,412)	<.0001
Among index hip fracture patients [N, IR (95%CI)†]	190	284 (247,328)	241	446 (393,506)	<.0001
Time to first recurrent fracture [days; mean (SD)]	280.6	(306.5)	221.7	(260.1)	.0006
OP Medication [N, IR (95% CI)†]	325	160 (144,179)	209	93 (81,107)	<.0001
BMD test [N, IR (95% CI)†]	721	562 (523,605)	243	110 (97,124)	<.0001
HCRU and costs (during 12mo follow-up period)	Exposed (N=906)		Unexposed (N=904)		P-value‡
Number of visits [mean (SD)]					
Inpatient Visits	0.7	(1.2)	0.6	(1.2)	.0846
Outpatient Hospital Visits	11.2	(9.9)	9.8	(9.8)	.0017
Outpatient Office Visits	21.5	(14.7)	20.7	(16.4)	.2458
Pharmacy Visits	21.2	(24.2)	18.4	(22.3)	.0121
Healthcare costs [mean, (SD)]					
Inpatient Costs	\$9,889	(\$19,612)	\$7,703	(\$20,188)	.0196
Outpatient Hospital Costs	\$3,106	(\$5,344)	\$3,153	(\$4,899)	.8463
Outpatient Office Costs	\$3,025	(\$4,604)	\$2,979	(\$4,590)	.8295
SNF Costs	\$2,883	(\$5,098)	\$1,970	(\$4,922)	.0001
DME Costs	\$715	(\$1,829)	\$589	(\$1,365)	.0966
HHA Costs	\$2,314	(\$3,524)	\$2,408	(\$3,953)	.5945
Hospice Costs	\$254	(\$2,880)	\$698	(\$5,082)	.0224
Pharmacy Costs	\$3,132	(\$7,054)	\$2,208	(\$5,121)	.0015
Total Costs¶	\$25,319	(\$27,336)	\$21,709	(\$28,361)	.0059

Abbreviations: IR – Incidence Rate; CI – Confidence Interval; SD – Standard Deviation; OP – Osteoporosis; BMD – Bone mineral density; HCRU – Healthcare resource utilization; SNF – Skilled Nursing Facility; DME – Durable Medical Equipment; HHA – Home Health Agency

\* Patients in the exposed group were matched with those in the unexposed group with the closest propensity score based on the following baseline characteristics: age group, race, gender, SES score, Charlson comorbidity score, comorbid conditions (Cerebrovascular disease, Depression/bipolar disorders, Diabetes mellitus, Kidney disease, Rheumatoid arthritis, dementia), site of first fracture, physician specialty for first fracture, time from fracture date to index date, OP medication, BMD test, any outpatient office visit, index year, fractures with trauma/cancer, Paget's disease or treatments for Paget's disease.

† Incidence rate per 1,000 person years and 95% confidence interval

‡ Testing the null hypothesis of no difference between exposed and unexposed cohorts using Poisson regression for IRs and chi-square test for proportions.

¶ Total costs = inpatient + outpatient hospital (including emergency department) + outpatient office + SNF + DME + HHA + Pharmacy costs

Table 1

**Disclosures:** Kathleen A. Taylor, Eli Lilly and Company, Grant/Research Support.

## 1115

**The Fracture Panorama in Children and Adolescents - A Register-based Study of 3.5 Million Person-years in Sweden 1999-2010.** Daniel Jerrhag<sup>\*1</sup>, Magnus Karlsson<sup>1</sup>, Martin Englund<sup>2</sup>, Bjorn Rosengren<sup>1</sup>. <sup>1</sup>Clinical and Molecular Osteoporosis Research Unit, Department of Orthopedics and Clinical Sciences, Lund University, Skane University Hospital Malmö, Sweden, Sweden, <sup>2</sup>Clinical Epidemiology Unit, Orthopedics, Department of Clinical Sciences Lund, Lund University, Lund, Sweden and Clinical Epidemiology Research and Training Unit, Boston University School of Medicine, Boston, MA, USA, Sweden

**Purpose**

Even though childhood fractures are common, epidemiological data from recent decades are sparse. Childhood fractures are associated to factors such as activity pattern, physical function, risk taking behavior and bone strength but also low peak bone mass (determinant of osteoporosis in old age) and high adult fracture risk. By examining time trends in childhood fracture epidemiology, it may thus be possible to gain insights into future fragility fracture burden.

**Methods**

By use of official in- and out-patient registry data of children and adolescents (≤ 20 years) in the Skåne region, Sweden we ascertained fractures and estimated age- and sex-specific rates and time-trends from year 1999 to 2010 (3.5 million person-years [py]). For estimation of temporal trends, we used Poisson regression of annual direct age-standardized incidence rates (with the average population during the examined years as standard population) and included 95% confidence intervals (CI) to describe uncertainty.

**Results**

We found 71,525 fractures during the examination period (3.5 million py) which correspond to an overall fracture incidence of 205 per 10,000 py (254 in boys and 155 in girls). From year 1999 to 2010, the total annual number of fractures increased by 37% (from 4,732 to 6,500) while the population at risk increased by 7.4% (from 282,383 to 303,169). The total age adjusted incidence increased statistically significantly by 2.6%

per year (CI 2.4, 2.8), quite similar for different fracture types and for boys and girls. The most common fracture types were in decreasing order, wrist (27% of overall fractures), hand (23%), foot (9%) and elbow fractures (7%). We found an overall appendicular to axial fracture ratio of 11:1 (boys 9:1, girls 13:1). The overall boy to girl fracture ratio was 1.7:1. All fracture types were more common in boys than in girls except proximal humerus fractures (boy to girl ratio 0.8:1). Skull fractures (2.9:1) followed by femur diaphysis and scapular fractures (both 2.8:1) were the fracture types with highest boy to girl ratio.

#### Conclusions

The increasing overall and type specific fracture rates are a major concern in themselves but may also have implications for the future adult fracture burden if the higher fracture risk follows the individuals into adulthood. The origin of the upturn may include a more sedentary lifestyle of the computer and screen generation but further research is needed and should focus on reversal of the trends.

**Disclosures:** Daniel Jerrhag, None.

## 1116

**Femoral Stress Index Is Prominently Associated With Risk Of Fracture In Children Of School Age.** Olja Grgic<sup>\*1</sup>, Carolina Medina-Gomez<sup>2</sup>, Katerina Trajanoska<sup>3</sup>, Thomas J Beck<sup>4</sup>, Carola M Zillikens<sup>5</sup>, Vincent W V Jaddoe<sup>6</sup>, Eppo B Wolvius<sup>7</sup>, Fernando Rivadeneira<sup>8</sup>. <sup>1</sup>EMC, Generation R, EMC, Internal Medicine, EMC, Maxillofacial Surgery, Rotterdam/NL, Netherlands, <sup>2</sup>EMC, The Generation R Study Group, EMC, Internal Medicine, EMC, Department of Epidemiology, Netherlands, <sup>3</sup>EMC, Internal Medicine, EMC, Department of Epidemiology, Netherlands, <sup>4</sup>Department of Radiology, The Johns Hopkins University School of Medicine, Baltimore, USA, United States, <sup>5</sup>EMC, Internal Medicine, Netherlands, <sup>6</sup>EMC, The Generation R Study Group, Netherlands, <sup>7</sup>EMC, The Generation R Study Group, 3EMC, Oral & maxillofacial surgery, special dental care and orthodontics, Netherlands, <sup>8</sup>EMC, The Generation R Study Group, EMC, Internal Medicine, Netherlands

**Background:** Previous studies indicate that about half of boys and one fourth of girls suffer a fracture before the age of 16 years. Low total body BMD (TB-BMD) is an established risk factor for fractures in children. However, bone strength depends not only on bone mass and density, but also on the structural geometry of bones. The aim of our study was to evaluate skeletal determinants of fracture risk in healthy children of school age. Specifically, we examined the association between total body BMD in the whole cohort, and in a subset, the influence of a geometry-derived femoral stress index (FSI) on risk of fracture.

**Methods:** This study (n=3,633, 49.4% males) is embedded in the Generation R Study, a prospective multiethnic pregnancy/birth cohort in Rotterdam, The Netherlands. Total body and hip scans were measured using the same densitometer (GE-Lunar iDXA) at a mean age of 6.2 years. Hip DXA scans of participants (n=1,851) underwent hip structural analysis (HSA) with derivation of FSI. This stress index models bending and axial forces acting on the femoral neck due to loading, considering bone length levers and corrected for lean mass fraction. Fractures occurring at any skeletal site before a mean age of 9.8 years (SD 0.3) were assessed using questionnaire reports. Odds of fracture were estimated from logistic regression models adjusted for sex, age, weight and ethnicity.

**Results:** Fractures occurred in 521 children (14.3%), with no significant difference between sexes (OR boys = 1.04, 95% CI 0.84-1.28; P=0.74). One SD decrease in TB-BMD was associated with 26% higher risk of fracture at a mean age of six (OR=1.26, 95% CI 1.10-1.44; P=0.001) and 43% higher risk at a mean age of nine (OR=1.43, 95% CI 1.24-1.62; P=4.26x10<sup>-7</sup> years). In participants with HSA, fractures were observed in 251 children (13.7%), with similar odds per SD decrease in TBLH-BMD (OR: 1.28 95% CI 1.05-1.56; P=0.01); femoral neck BMD (OR=1.23 95% CI 1.06-1.43; P=0.005) and narrow neck BMD (OR= 1.26 95% CI 1.08-1.46; P=0.005). The FSI showed the strongest association with fracture, where every SD increment in FSI resulted in 28% increased odds of fracture (OR: 1.28 95% CI 1.13-1.45; P=0.0001). After inclusion of the FSI in the multiple regression models none of the BMD variables remained significant.

**Conclusions:** The stress index, constitutes a biomechanical assessment of bone that captures fracture propensity in young children at least as effectively as femoral and total body BMD.

**Disclosures:** Olja Grgic, None.

## 1117

**Fractures Prospectively Recorded in Healthy Children and Adolescents Are Predictive of Radial Peak Bone Mass and Strength Fragility in Females but not in Males.** Thierry Chevalley<sup>\*1</sup>, Jean-Philippe Bonjour<sup>1</sup>, Marie-Claude Audet<sup>1</sup>, Fanny Merminod<sup>1</sup>, Bert van Rietbergen<sup>2</sup>, Rene Rizzoli<sup>1</sup>, Serge Ferrari<sup>1</sup>. <sup>1</sup>Division of Bone Diseases, Geneva University Hospitals and Faculty of Medicine, Switzerland, <sup>2</sup>Department of Biomedical Engineering, Eindhoven University of Technology, Netherlands

**Background and Purpose:** Fractures frequently occur in healthy children and adolescents. These fractures result from trauma of various severities. Mechanistically, they may be due to a transient fragility occurring mainly during pubertal maturation. Moreover, these fractures could reflect an intrinsic fragility that could be maintained until the end of bone growth. In this report we investigate whether the predictability of

prepubertal fragility to reduced bone resistance in young adulthood would be similar in males than in females.

**Participants and Methods:** We prospectively followed healthy females (n=124) and males (n=152) enrolled in two prospective studies from prepuberty (age: 7-8 years) to young adulthood (age: 20-23 years). At 20-23 years, in both genders areal bone mineral density (aBMD) were assessed by DXA in radial metaphysis and diaphysis. At that time, microarchitecture and mechanical resistance were assessed by HR-pQCT and  $\mu$ FEA, respectively, in distal radius.

**Results:** In females 42 sustained at least one fracture (FX) i.e. 33.9%, while 82 remained free of fracture (NO-FX). In males the corresponding numbers were 90 FX, i.e. 59.2%, and 62 NO-FX. The corresponding percentage of subjects experiencing at least one forearm fracture was 52% (22/42) and 51% (46/90) in females and males, respectively. In adult females (mean age 20.4 years) significant lower forearm aBMD was recorded in FX vs. NO-FX and at the distal radius, this difference was associated with significant deficit in trabecular microstructure and strength (see Table). In adult males (mean age 22.6 years) none of the same radial variables were lower in FX as compared to NO-FX (see Table).

**Conclusions:** These two prospective studies carried out in 276 healthy individuals examined from prepuberty to their early twenties in the same clinical setting and using the same technical tools for bone assessment, highlight a striking gender difference in the predictability of fracture occurring during growth for the risk of bone fragility in adulthood. In healthy girls, fractures during childhood and adolescence appear to predict future bone fragility unlike those sustained by boys.

**Comparison of DXA, HR-pQCT and  $\mu$ FEA Z-Scores of Radius Variables Measured in Healthy Female and Male Adults Who Sustained (FX) or Not (NO-FX) Fractures During Growth**

	Females			Males		
	FX	NO-FX	P <sup>1</sup>	FX	NO-FX	P <sup>1</sup>
<b>DXA Data</b>	n=42	n=82		n=90	n=62	
Metaphysis (mg/cm <sup>2</sup> )	-0.32 (0.89)	0.16 (1.02)	0.011	0.05 (1.04)	-0.07 (0.94)	0.482
Diaphysis (mg/cm <sup>2</sup> )	-0.35 (0.99)	0.17 (0.96)	0.006	0.05 (1.04)	-0.07 (0.94)	0.479
<b>HR-pQCT &amp; <math>\mu</math>FEA Data</b>	n=42	n=82		n=85	n=61	
D Trab (mg HA/cm <sup>3</sup> )	-0.33 (0.78)	0.16 (1.06)	0.022	0.05 (1.00)	-0.07 (1.01)	0.467
BV/TV (%)	-0.33 (0.78)	0.16 (0.96)	0.021	0.05 (1.00)	-0.07 (1.01)	0.464
Tb.Th (μm)	-0.34 (0.83)	0.17 (1.02)	0.014	0.09 (0.94)	-0.13 (1.08)	0.189
Stiffness (kN/mm)	-0.32 (0.92)	0.16 (1.01)	0.023	0.11 (1.00)	-0.16 (0.98)	0.117
Failure Load (N)	-0.31 (0.91)	0.16 (1.01)	0.028	0.11 (1.00)	-0.16 (0.98)	0.103

All values are mean Z-scores (SD). Females and Males were aged 20.4 (0.6) and 22.6 (0.7) years, respectively. D trab: trabecular volumetric density. BV/TV: trabecular bone volume fraction. Tb.Th: trabecular thickness. Z-score of either females or males are calculated from the individual absolute values. P<sup>1</sup> and P<sup>2</sup> probability levels for difference in radial variables between the number of subjects sustaining or not a fracture during growth in females and males, respectively.

Table

**Disclosures:** Thierry Chevalley, None.

## 1118

**A genome-wide association meta-analysis implicates adrenal steroidogenesis in the process of skeletal maturation.** Alessandra Chesi<sup>\*1</sup>, Olja Grgic<sup>2</sup>, Carolina Medina-Gomez<sup>2</sup>, Shana E. McCormack<sup>1</sup>, Diana L. Cousminer<sup>1</sup>, Jonathan A. Mitchell<sup>1</sup>, Heidi J. Kalkwarf<sup>3</sup>, Joan M. Lappe<sup>4</sup>, Vicente Gilsanz<sup>5</sup>, Sharon E. Oberfield<sup>6</sup>, John A. Shepherd<sup>7</sup>, Andrea Kelly<sup>1</sup>, Soroosh Mahboubi<sup>1</sup>, Katerina Trajanoska<sup>2</sup>, Vincent Jaddoe<sup>2</sup>, Andre G. Uitterlinden<sup>2</sup>, Eppo B. Wolvius<sup>2</sup>, Babette S. Zemel<sup>1</sup>, Struan F.A. Grant<sup>1</sup>, Fernando Rivadeneira<sup>2</sup>. <sup>1</sup>The Children's Hospital of Philadelphia, United States, <sup>2</sup>Erasmus MC, Netherlands, <sup>3</sup>Cincinnati Children's Hospital Medical Center, United States, <sup>4</sup>Creighton University School of Medicine, United States, <sup>5</sup>University of Southern California Los Angeles, United States, <sup>6</sup>Columbia University Medical Center, United States, <sup>7</sup>University of California San Francisco, United States

**Objective:** Advanced or delayed physiological age can influence significantly health and disease processes. Physiological age can be assessed through several parameters, typically with skeletal age (SA) determined on carpal bones. We performed the first genome-wide association study (GWAS) meta-analysis to identify genetic determinants of skeletal maturation in children of school age.

**Methods:** Two cohorts were included in this study, the Generation R Study (GENR), a multiethnic birth cohort in Rotterdam, The Netherlands, (N=3510 children; mean age=9.79±0.33), and The Bone Mineral Density in Childhood Study (BMDCS; N=1048; mean age=11.34±1.79, range: 8 to 13y). Bone age was assessed on hand images using the Greulich and Pyle method by a pediatric radiologist or endocrinologist (BMDCS) and one trained observer (GENR). Standardized residuals of SA were calculated separately for boys and girls in both cohorts and used as outcomes in all further association analyses. Participants were genotyped with Illumina BeadChip technology using HumanHap 610K (GENR) and Human OmniExpressExome (BMDCS) arrays. Both studies were imputed to the 1000GP reference panel. Association between genotypes and SA was tested using linear regression in GENR, and linear mixed models in BMDCS. All models were corrected for age, BMI (and 10 genomic PCs in GENR).



The fixed-effects inverse variance method implemented in METAL was used for the meta-analysis. Genome-wide significance (GWS) was set at  $P < 5 \times 10^{-8}$ .

Results: In GENR, a GWS signal was identified mapping to *CYP11B1* on 8q24.3 (synonymous variant; rs6410;  $\beta = 0.15$ ;  $P = 2.8 \times 10^{-10}$ ), and three suggestive signals mapped to 9q21.32 (intergenic; rs1246290;  $\beta = 0.125$ ;  $P = 8.5 \times 10^{-7}$ ), 7p12.3 (intergenic; rs189058183;  $\beta = -0.85$ ;  $P = 3.6 \times 10^{-7}$ ) and 21q21.1 (intergenic; rs380807;  $\beta = -0.85$ ;  $P = 6.7 \times 10^{-7}$ ). Significant evidence of replication was observed in BMDCS for the first two signals (*CYP11B1*;  $P = 0.008$ ; 9q21.32;  $P = 0.05$ ). After meta-analysis only the *CYP11B1* signal achieved GWS ( $P = 1.1 \times 10^{-11}$ ).

Conclusion: We identified one novel locus robustly associated with SA containing *CYP11B1*. Mutations in *CYP11B1* cause congenital adrenal hyperplasia, a disorder presenting with precocious puberty and short stature among other clinical manifestations. These findings potentially implicate a role for adrenal steroidogenesis in the process of pediatric skeletal maturation, opening new avenues to investigate normal skeletal maturation and bone health in general.

**Disclosures:** Alessandra Chesi, None.

## 1119

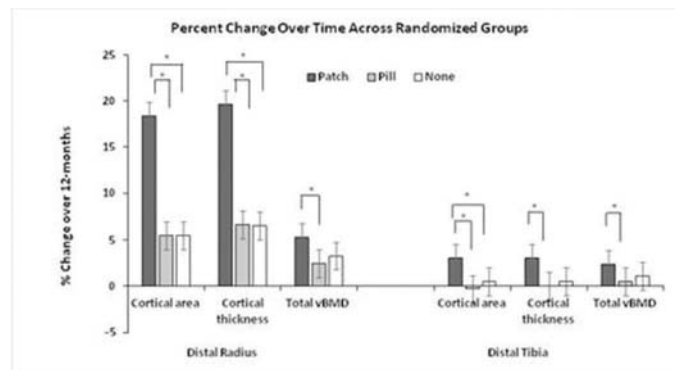
**Transdermal 17- $\beta$  Estradiol has a Beneficial Effect on Bone Parameters Assessed using HRpQCT Compared to Oral Ethinyl Estradiol-Progestosterone Combination Pills in Oligo-amenorrheic Athletes: a Randomized Controlled Trial.** Kathryn Ackerman\*, Meghan Slattery, Vibha Singhal, Charumathi Baskaran, Karen Campoverde Reyes, Alexander Toth, Hang Lee, Mary Boussein, Anne Klibanski, Madhusmita Misra. Massachusetts General Hospital, United States

Objective: Normal weight oligo-amenorrheic athletes have impaired bone parameters, including cortical and trabecular volumetric BMD (vBMD), geometry and microarchitecture compared to eumenorrheic athletes and non-athletes, associated with a higher risk of stress fracture. Data are lacking regarding the impact of estrogen administration on these parameters in young women. Given the impact of these data on informing decisions regarding hormone replacement, we determined the effect of estrogen administration via transdermal versus oral routes on skeletal outcomes in young normal-weight oligo-amenorrheic athletes engaged in weight bearing activity of the lower extremities.

Methods: 75 oligo-amenorrheic athletes 14-25 years old were randomized to receive either (i) a 100 mcg 17-beta estradiol transdermal patch with cyclic micronized progesterone (PATCH), or (ii) a 30 mcg ethinyl estradiol oral pill with 0.15 mg desogestrel (PILL), or (iii) no estrogen (NONE). All participants received calcium and vitamin D supplementation. Bone vBMD, geometry and microarchitecture were assessed at the distal radius and tibia at baseline and 12-months using high resolution peripheral quantitative computed tomography. Multivariate analyses were used to determine differences among groups after controlling for age, height, race and ethnicity.

Results: Mean age was  $19.7 \pm 2.8$  years, and BMI  $20.5 \pm 2.1$  kg/m<sup>2</sup>. Randomized groups were comparable for age, BMI and most bone parameters at baseline. Over 12 months, at the radius, compared to the PILL and NONE groups, the PATCH group demonstrated an increase in cortical area ( $p = 0.02$  and  $0.06$  respectively) and cortical thickness ( $p = 0.03$  and  $0.09$  respectively) after controlling for covariates. At the tibia, compared to the PILL and NONE groups, the PATCH group had an increase in cortical area ( $p = 0.007$  and  $0.09$  respectively) and decrease in trabecular area ( $p = 0.025$  and  $0.042$  respectively). Compared to the PILL group, the PATCH group also had an increase in cortical thickness ( $p = 0.023$ ), trabecular meta-vBMD ( $p = 0.034$ ), trabecular number ( $p = 0.043$ ), and total vBMD ( $p = 0.009$ ). The figure shows percent change over time in cortical area and thickness and total vBMD across randomized groups. Weight changes over 12 months did not differ among groups.

Conclusion: These data demonstrate beneficial effects of transdermal 17-beta estradiol over oral ethinyl estradiol on bone parameters in adolescent and young adult oligo-amenorrheic athletes.



Figure

**Disclosures:** Kathryn Ackerman, None.

## 1120

**Probiotics Induce Bone Anabolism Via A Regulatory T Cells-Wnt10b Mediated Pathway.** Abdul Malik Tyagi\*, Mingcan Yu, Trevor Derby, Jau-Yi Li, Jonathan Adams, Rheinallt M. Jones, Roberto Pacifici. Emory University, United States

Probiotics, defined as viable microorganisms that confer health benefits, have been shown prevent ovariectomy induced bone loss by decreasing bone resorption, but the effects of probiotics in eugonadic conditions and their mechanism of action are largely unknown. To investigate this matter, 10-week-old conventionally raised mice were treated for 4 weeks with vehicle or the well-studied probiotics *L. rhamnosus* GG (LGG) at the dose of  $1 \times 10^9$  total bacteria 5 times/week. In vivo and in vitro mCT measurements revealed that LGG induced a significant increase in trabecular BV/TV (+26% in the spine and +37% in the femur) by stimulating bone formation. Mechanistic studies revealed that LGG increased the number of bone marrow (BM) regulatory T cells (Tregs), an immunosuppressive population that derives from naive CD4+ T cells. In turns, Tregs induced the release of the osteogenic Wnt ligand Wnt10b by BM CD8+ T cells. Wnt10b caused the activation of Wnt signaling in osteoblastic cells, leading to increased osteoblast proliferation and differentiation, and increased bone formation. Attesting to the relevance of Tregs, in vivo blockade of Treg expansion by treatment with anti CD25 Ab prevented the bone anabolic activity of LGG. Additional mechanistic studies revealed that Tregs increased the expression of membrane bound TGF $\beta$ , which activates SMAD signaling in nearby CD28+ T cells. Moreover, Tregs block CD28 signaling in BM CD8+ cells by downregulating the costimulatory molecules CD80/86 on antigen presenting cells via their surface receptor CTLA4. Western blots and ChIP assays revealed that Tregs promoted the binding of NFAT1 and SMAD3 to a NFAT/SMAD-activated promoter site that stimulates Wnt10b gene expression in CD8+ T cells. In summary, the probiotic LGG is a potent bone anabolic agent that stimulates bone formation via Treg/Wnt10b dependent pathway that leads to the activation of Wnt signaling in osteoblasts. These data demonstrate that nutritional supplementation with the probiotic LGG may provide a novel therapeutic strategy for increasing bone mass and preventing osteoporosis.

**Disclosures:** Abdul Malik Tyagi, None.

## 1121

**Prebiotic Alteration of the Gut Microbiome Rescues Impaired Fracture Healing in Obesity.** Christopher Farnsworth\*, Ashlee MacDonald<sup>2</sup>, Eric Schott<sup>1</sup>, Jun Zhang<sup>3</sup>, Alex Grier<sup>4</sup>, Cheryl Ackert Bicknell<sup>5</sup>, Steven Gill<sup>6</sup>, Hani Awad<sup>7</sup>, Michael Zuscik<sup>7</sup>, John Ketz<sup>8</sup>, Robert Mooney<sup>9</sup>. <sup>1</sup>Department of Pathology and Center for Musculoskeletal Research, University of Rochester Medical Center, United States, <sup>2</sup>Department of Orthopedic Surgery, University of Rochester Medical Center, United States, <sup>3</sup>Center for Musculoskeletal Research, University of Rochester Medical Center, United States, <sup>4</sup>Department of Microbiology and Immunology, University of Rochester Medical Center, United States, <sup>5</sup>Department of Orthopaedic Surgery and Center for Musculoskeletal Research, United States, <sup>6</sup>Department of Microbiology and Immunology, United States, <sup>7</sup>Department of Orthopedic Surgery and Center for Musculoskeletal Research, United States, <sup>8</sup>Department of Orthopedic Surgery, United States, <sup>9</sup>Department of Pathology and Center for Musculoskeletal Research, United States

Purpose: Obesity is a risk factor for delayed fracture healing and fibrous non-union. We have published that high fat (HF) diet-induced obesity in mice leads to delayed tibial fracture repair, possibly through an obesity-induced systemic proinflammatory state that impacts the differentiation of osteoprogenitors during healing. It has been established that the altered gut microbiome in obesity influences systemic inflammation. Since specific prebiotics, including the undigestible fiber oligofructose (OF), can restore a healthy gut microbiome and suppress the systemic inflammation of obesity, we hypothesize that supplementing the HF diet with OF will rescue the impaired fracture healing in obese mice.

Methods: Lean and HF diet-induced obese mice were supplemented with OF or a control fiber (cellulose), and tibia fractures were surgically induced 2 weeks later. Mice were continued on supplements until sacrifice at 21 days post-fracture, with fecal samples collected pre- and post-OF for analysis of microbial abundance by 16S rDNA sequencing. Micro-CT imaging and histomorphometry analysis of stained tissue sections supported study of callus architecture.

Results: Obese mice had larger fracture calluses based on histomorphometry (Fig. 1B and 1E) and microCT. This tissue phenotype included a marked increase in callus adiposity (Fig. 1A), with significant increases in % adipocyte area (Fig. 1F) and adipocyte number (Fig. 1G). In mice provided OF, callus architecture, size and adiposity were normalized to those of lean mice (Fig. 1A-1D), with reduction in % adipocyte area (Fig. 1F), and adipocyte number (Fig. 1G). The rescue by OF corresponded with a profound shift in the gut microbiome. *Bifidobacterium pseudolongum*, a species associated with decreased inflammation, was lost in obesity but rescued by OF (Fig. 1H). Conversely, proinflammatory species that were increased in obesity, including *Lactobacillus helveticus* and *Staphylococcus sciuri*, were reduced by OF.

Conclusion: We demonstrate for the first time that manipulation of the gut microbiome impacts fracture healing. Data suggest that impaired fracture repair in obesity is linked to an inflammatory process driven by an altered gut microbiome that can be addressed by restoring a healthy microbial profile using dietary prebiotics. Prebiotics

may be a simple candidate treatment for a clinical problem that is without a globally accepted therapeutic strategy short of aggressive endocrine and surgical interventions.

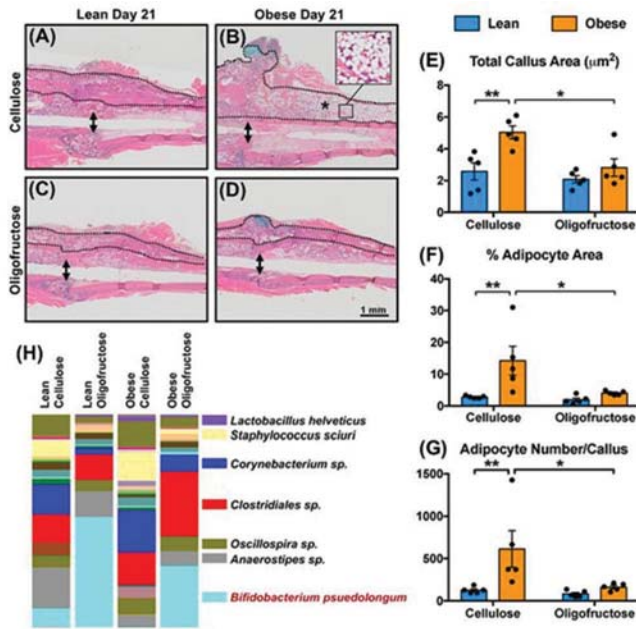


**Fig. 1: OF rescue of impaired fracture healing in obese mice is associated with restoration of a healthy gut microbial profile.** (A-D) Representative sections for each experimental group reveal increased callus size and adiposity at 21 days post-fracture, with rescue of these phenotypes in OF-supplemented mice. Arrows denote the fracture site, the dotted line outlines the callus, the asterisk demarcates an area crowded with adipocytes, and the box and inset shows a zoomed view of adipocytes. (E-G) Histomorphometry revealed increased total callus area and adiposity and correction of this phenotype in mice supplemented with oligofructose (\* $p < 0.05$ , \*\* $p < 0.01$ ,  $N = 5-6$ , ANOVA with a Tukey's multiple comparison post-test). (H) rDNA sequencing analysis reveals changes in gut microbial species, with *B. pseudolongum* (light blue) lost in obesity/T2D and restored with OF-supplementation.

Figure 1

**Disclosures:** Christopher Farnsworth, None.

## 1122

**GDF11 impairs bone remodeling and regeneration.** Weiqing Liu<sup>1</sup>, Liyan Zhou<sup>1</sup>, Chenchen Zhou<sup>1</sup>, Shiwen Zhang<sup>1</sup>, Xing Liang<sup>1</sup>, Ling Ye<sup>1</sup>, Qianming Chen<sup>1</sup>, Beate Lanske<sup>2</sup>, Quan Yuan<sup>1</sup>. <sup>1</sup>State Key Laboratory of Oral diseases, West China School of Stomatology, Sichuan University, China, <sup>2</sup>Division of Bone and Mineral Research, Harvard School of Dental Medicine, United States

Osteoporosis is an age-related disease that affects millions of people. Growth differentiation factor 11 (GDF11) is a secreted member of the TGF- $\beta$  superfamily, which has been proposed to be a long-sought rejuvenating factor. However, this notion was recently challenged, arguing that GDF11 increases with age and adds to age-related comorbidity and frailty. Notwithstanding, *Gdf11* KO mice displayed a skeletal anterior-posterior patterning disorder. However, the role of GDF11 in postnatal bone remodeling is not well described.

Initially, we observed that, in 9-week-old young adult mice, GDF11 treatment led to lower trabecular bone volume in distal femur metaphysis and reduced cortical thickness in mandible. Histomorphometric analyses revealed a significant increase in osteoclast number and a decrease in osteoblast number, meanwhile, the mineral apposition rate and bone formation rate were diminished in rGDF11 treated mice. Moreover, serum levels of bone resorption marker CTX significantly increased, while bone formation marker PINP dropped in rGDF11 treated mice.

Given its controversial role in aging, we sought to investigate its effect in 18-month-old aged mice and found similar results.

In addition, we established two bone defect healing models, 1.0 mm cortical defects in bilateral distal femurs and two subcritical-sized symmetrical defects in calvaria. Injection of rGDF11 impairs bone regeneration in both defects. Moreover, rGDF11 treatment compromises the fixation of titanium implants inserted into the distal end of femurs in both young and aged mice.

To elucidate the molecular mechanism, we performed microarray and found that GDF11 upregulated TGF- $\beta$  pathway associated gene expression. ChIP assay showed that rGDF11 induced the recruitment of both Smad2/3 and c-Fos to the binding region of *Nfatc1* in bone marrow-derived macrophages. Moreover, the abundance of acetylated histone at the Runx2 binding site of osteocalcin promoter was decreased in rGDF11-treated BMSCs.

Finally, we evaluated the potential therapeutic effect of GDF11 blocking. Injection of GDF11 neutralizing antibody successfully prevented the bone loss in ovariectomized mice, and increased the trabecular bone volume in aged mice.

In summary, GDF11 decreases bone mass and impairs bone regeneration by inhibiting osteoblast differentiation and stimulating RANKL-induced osteoclastogenesis via TGF- $\beta$  pathway. Blocking GDF11 function might be a potential treatment of osteoporosis.

**Disclosures:** Weiqing Liu, None.

## 1123

**1,25-Dihydroxy Vitamin D Prevents Tumorigenesis by Inhibiting Oxidative Stress and Inducing Tumor Cellular Senescence.** Renlei Yang<sup>1</sup>, Lulu Chen<sup>1</sup>, Wanxin Qiao<sup>1</sup>, Xiaoqin Yuan<sup>1</sup>, Shui Wang<sup>1</sup>, David Goltzman<sup>2</sup>, Dengshun Miao<sup>1</sup>. <sup>1</sup>Nanjing Medical University, China, <sup>2</sup>McGill University, Canada

Human epidemiological studies suggest that 1,25(OH)<sub>2</sub>D<sub>3</sub> deficiency might increase cancer incidence, however, no spontaneous tumors have to date been reported in 1,25(OH)<sub>2</sub>D<sub>3</sub> or vitamin D receptor deficient mice. We examined spontaneous tumor formation in 1 $\alpha$ (OH)ase<sup>+/+</sup>, 1 $\alpha$ (OH)ase<sup>-/-</sup> and wild-type mice, which were injected with vehicle or 1,25(OH)<sub>2</sub>D<sub>3</sub> thrice weekly or fed a diet to normalize their serum calcium and phosphorus, with or without supplementation with the antioxidant NAC. 1 $\alpha$ (OH)ase<sup>-/-</sup> and wild-type mice were also subcutaneously transplanted with TM40D mammary tumor cells. Tumor tissues were analyzed and compared using histopathological, cellular and molecular techniques. Spontaneous tumors were found in 6 of 52 (11.5%) 1 $\alpha$ (OH)ase<sup>+/+</sup> mice on a normal diet between 13-20 months of age and in 5 of 21 (23.8%) 1 $\alpha$ (OH)ase<sup>-/-</sup> mice on a rescue diet that survived over 12 months. The pathological diagnosis of the 11 spontaneous tumors included breast cancer, squamous-cell skin cancer, soft tissue sarcoma, hepatocellular carcinoma, granulocytic sarcoma, endometrial stromal tumor, gastrointestinal stromal tumor and pulmonary adenocarcinoma. No spontaneous tumors were found in age-matched wild-type mice or 1 $\alpha$ (OH)ase<sup>-/-</sup> mice with 1,25(OH)<sub>2</sub>D<sub>3</sub> or NAC supplementation. In spontaneous tumor tissues compared with the paraneoplastic tissues, SOD2 levels were reduced, the percentages of cells positive for  $\gamma$ -H2AX and Ki67 were increased, and c-Fos, RAS, c-Met and Bmi1 were up-regulated while p16, p21 and p27 were down-regulated. Levels of serum hepatocyte growth factor, a ligand of c-Met, were dramatically increased in 1 $\alpha$ (OH)ase<sup>-/-</sup> mice, as found by a protein array approach and confirmed by ELISA. We also demonstrated that 1,25(OH)<sub>2</sub>D<sub>3</sub> deficiency accelerated allograft tumor initiation and growth by increasing oxidative stress and DNA damage, activating oncogenes, inactivating tumor suppressor genes, stimulating malignant cell proliferation and inhibiting their senescence; in contrast, supplementation with exogenous 1,25(OH)<sub>2</sub>D<sub>3</sub> or NAC, or knock-down of the Bmi1 oncogene, largely rescued the phenotypes of allograft tumors. Our results indicate that 1,25(OH)<sub>2</sub>D<sub>3</sub> prevents tumorigenesis by inhibiting oxidative stress and DNA damage, reducing tumor cell proliferation and inducing tumor cell senescence. This study provides evidence to support the findings from human epidemiologic studies, suggesting that active vitamin D deficiency can increase cancer incidence.

**Disclosures:** Renlei Yang, None.

## 1124

**A comparison of the efficacy and side effects of an active site and ectosteric inhibitor of Cathepsin K in mouse.** Preety Panwar<sup>1</sup>, Kamini Srivastava, Dieter Bromme. University of British Columbia, Canada

Cathepsin K (CatK) is a major drug target for the treatment of osteoporosis. Several CatK inhibitors have been evaluated in clinical trials but despite their *in vivo* antiresorptive efficacies none of them have been approved because of side effects. Recently, the further development of Odanacatib (ODN), the most advanced CatK inhibitor in osteoporosis trials, was discontinued because of increased risk in stroke and skin complications. Active site-directed inhibitors such as ODN block the entire activity of CatK that might be vital to other pathways whereas ectosteric inhibitors specifically block only the disease relevant activity like the collagenase activity of CatK. Our hypothesis is that the various side effects seen in CatK clinical trials are due to the undesired inhibition of regulatory CatK activities and can be avoided when only the collagenase activity of the protease is blocked. The present study compared the effects of an ectosteric collagenase-specific inhibitor (T06) and ODN, a pan-CatK activity inhibitor, on bone and various organs in a mouse model. T06 (40 mg/kg) and ODN (20 mg/kg) were given orally at their antiresorptive active concentration every day for 10 weeks and the histological alterations in heart, aorta, lungs, skin, brain, and bones were investigated. The inhibitor treatment had no effect on body weight and the overall agility of the mice. However, all ODN-treated mice revealed hair loss in the neck, breast, and leg areas beginning after 10 days whereas T06 treated mice did not show any hair/skin alterations during the entire treatment period. Both inhibitors showed increased BMDs and comparable increases in trabecular bone parameters demonstrating the antiresorptive activity of both compounds in mice. However, the ODN-treated mice group revealed increased TGF- $\beta$  concentrations and ECM components in skin, lungs, and heart when compared to the T06 group. This may suggest ODN-induced TGF- $\beta$ -mediated fibrotic events in these organs and explaining some of the side effects seen in clinical trials. In conclusion, ectosteric inhibitors such as T06, represent a viable alternative to active site-directed protease inhibitors which all have been plagued by side effects, which have been previously developed as antiresorptive CatK drugs.

**Disclosures:** Preety Panwar, None.





## 1128

**HIV and Vertebral Fractures: a Systematic Review and Metanalysis.** Melissa Premaor<sup>\*1</sup>, Thales Ilha<sup>1</sup>, Rafaela Copes<sup>1</sup>, Fabio Comim<sup>1</sup>, Juliet Compston<sup>2</sup>. <sup>1</sup>Federal University of Santa Maria, Brazil, <sup>2</sup>University of Cambridge, United Kingdom

The survival of HIV-positive individuals has increased with the advent of antiretroviral therapy. Furthermore, the range of comorbidities they exhibit has changed. Vertebral fractures have been reported more frequently and at an early age in these subjects. This study aims to assess the frequency of spine fractures in HIV-positive men and women aged over 18 years. We performed a systematic review of randomized controlled trials (RCTs), cohort studies, cross-sectional studies, and case-control studies. The study protocol is registered with the International Prospective Register of Systematic Reviews (PROSPERO) under the number CRD42016048702. Studies evaluating either morphometric or clinical vertebral fractures were included. The search strategy included the following descriptors: "Spinal Fractures"; "Fractures, Bone"; "HIV"; "Acquired Immunodeficiency Syndrome"; and "Anti-Retroviral Agents" in the databases PubMed, BIREME, EMBASE, and the Cochrane Library. Additionally, some studies were selected from the reference lists of the included articles. We considered studies written in any language and with no publication date limits. In total 458 studies were found, of which 60 were duplicates. After screening the title and abstracts, 53 studies remained. Of these, 28 were excluded due to lack of outcome, inadequate study design, or redundant publication. The prevalence of all vertebral fractures in 14 studies with 10,691 subjects (41.5% women, age range 31 to 72) was 11.2% (CI 4.9% to 23.5%); in studies that evaluated only morphometric fractures (n=9), the prevalence was 21.1% (CI 14.1% to 30.4%). The incidence of vertebral fractures in 10 studies with 95,476 person/years (25.4% women, age range 18 to 72) was 2.1 per 1000 person/years (95% CI 0.9 to 5.0). The odds ratio (OR) for vertebral fractures in HIV-positive compared to HIV-negative subjects is shown in figure 1. The OR (95% CI) was 2.17 (1.30 to 3.65). In conclusion, HIV-positive subjects are at higher risk of vertebral fractures when compared with HIV-negative subjects. Hence, vertebral imaging should be considered in HIV-positive individuals, especially in those with risk factors for fracture, such as low BMD, height loss, kyphosis or glucocorticoid therapy.

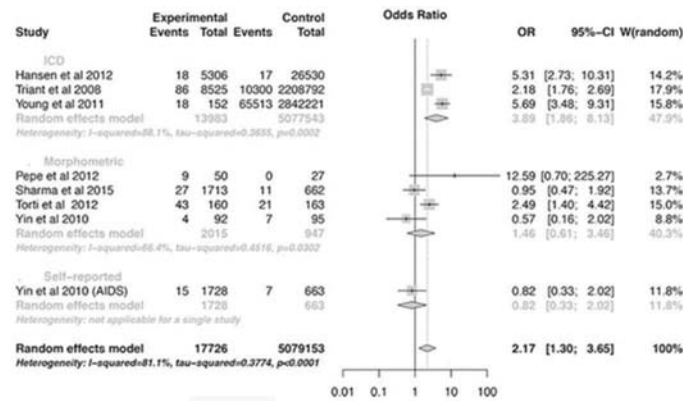


Figure 1: Forest plot of vertebral fracture risk estimates on HIV-positive subjects

**Disclosures:** Melissa Premaor, None.

## 1129

**Trends in Mean Femoral Neck Bone Mineral Density Among Individuals Aged 30 or Older in the United States, 2005-2006 through 2013-2014.** Yingke Xu<sup>\*1</sup>, William Donald Leslie<sup>2</sup>, Qing Wu<sup>1</sup>. <sup>1</sup>University of Las Vegas, Nevada, United States, <sup>2</sup>University of Manitoba, Canada

**Background:** Bone mineral density (BMD) is a major predictor of osteoporotic fracture. Data from the National Health and Nutritional Examination Survey (NHANES) has shown that osteoporosis prevalence in the US declined between 1988-1994 and 2005-2006. As well, US Medicare data indicates that a declining trend in hip fracture may have plateaued in 2013-2014. However, whether there has been a corresponding change in BMD trajectory for the US population in recent years is unknown. Therefore, we examined BMD trends among US adults from 2005-2006 to 2013-2014, overall and within sex, race and age subgroups. **Methods:** We used femur neck BMD data from the last four NHANES cycles (2005-2006 to 2013-2014) in subjects aged 30 or older. Although the densitometers and software of BMD measures were updated during its history, the update has no impact on femoral neck BMD measures. Mean BMD was estimated for each survey year, overall and by sex, age and race subgroup. Sample weights, which account for the unequal selection probabilities, were used for all analyses. Standard errors employed to construct confidence intervals were estimated using Taylor series linearization. Orthogonal contrasts were used to test for significant between-group differences, with Bonferroni adjustment for multiple comparisons. SAS version 9.3 (SAS Institute Inc) was used for analyses. **Results:** Overall mean BMD for the first three NHANES cycles was stable ( $p>0.25$ ), but significantly decreased in 2013-2014, from  $0.821 \text{ g/cm}^2$  to  $0.788 \text{ g/cm}^2$  ( $p<0.0001$ ). Although mean BMD in men was higher than in women in each survey cycle, similar BMD trends were observed for both sexes and only declined in the last cycle, from  $0.862 \text{ g/cm}^2$  to  $0.816 \text{ g/cm}^2$  for men ( $p<0.0001$ ), and from

$0.794 \text{ g/cm}^2$  to  $0.761 \text{ g/cm}^2$  for women ( $p=0.0005$ ). Non-Hispanic Blacks had the highest mean BMD within each age and sex subgroup, and no significant change was observed in mean BMD across the four survey cycles in Non-Hispanic Black men or women. Stable mean BMD for the first three cycles with a significant decline in 2013-2014 was seen in all other race subgroups, in all age subgroups in men, and in women aged 50-69 years. **Summary:** Mean femoral neck BMD in US men and women was stable from 2005-2006 to 2009-2010, but declined in 2013-2014, overall and within most subgroups. Further studies are warranted to explain this recent BMD decline.

**Table.** Mean Femoral Neck BMD Among Individuals Aged 30 or Older in the United States, 2005-2006 through 2013-2014

Mean BMD (g/cm <sup>2</sup> )	2005-2006	2007-2008	2009-2010	2013-2014	p-value *
<b>Overall</b>	0.821(0.811-0.830)	0.825(0.817-0.833)	0.827(0.820-0.833)	0.788(0.779-0.796)	<0.0001
<b>Men</b>	0.853(0.845-0.862)	0.857(0.850-0.865)	0.862(0.853-0.870)	0.816(0.803-0.830)	<0.0001
<b>Age group</b>					
30-49	0.890(0.877-0.903)	0.887(0.874-0.900)	0.895(0.884-0.906)	0.852(0.832-0.871)	0.002
50-69	0.822(0.805-0.839)	0.829(0.818-0.841)	0.826(0.811-0.841)	0.797(0.780-0.815)	0.03
70	0.756(0.724-0.789)	0.771(0.754-0.789)	0.771(0.752-0.791)	0.717(0.697-0.738)	0.05
<b>Race</b>					
Hispanic*	0.869(0.853-0.887)	0.885(0.869-0.901)	0.877(0.862-0.892)	0.843(0.827-0.859)	0.01
NH-White	0.841(0.831-0.852)	0.846(0.836-0.855)	0.851(0.840-0.862)	0.799(0.781-0.818)	0.0002
NH-Black	0.934(0.919-0.949)	0.919(0.894-0.941)	0.949(0.928-0.971)	0.905(0.884-0.927)	0.15
NH-Other	0.843(0.799-0.888)	0.832(0.803-0.862)	0.811(0.784-0.838)	0.797(0.775-0.820)	0.04
<b>Women</b>	0.789(0.777-0.799)	0.795(0.786-0.805)	0.794(0.786-0.802)	0.761(0.750-0.772)	0.0005
<b>Age group</b>					
30-49	0.842(0.832-0.853)	0.843(0.828-0.858)	0.848(0.838-0.857)	0.825(0.811-0.839)	0.08
50-69	0.749(0.735-0.763)	0.755(0.744-0.767)	0.741(0.730-0.753)	0.728(0.713-0.745)	0.02
70	0.644(0.631-0.658)	0.685(0.669-0.702)	0.674(0.654-0.693)	0.644(0.618-0.670)	0.78
<b>Race</b>					
Hispanic*	0.831(0.815-0.847)	0.820(0.795-0.845)	0.819(0.807-0.833)	0.780(0.757-0.803)	<0.0005
NH-White	0.773(0.762-0.783)	0.782(0.774-0.791)	0.776(0.766-0.786)	0.744(0.727-0.762)	0.0037
NH-Black	0.866(0.849-0.884)	0.873(0.857-0.889)	0.898(0.873-0.923)	0.856(0.838-0.873)	0.85
NH-Other	0.786(0.764-0.807)	0.762(0.737-0.787)	0.761(0.729-0.793)	0.724(0.699-0.750)	0.0023

\*Hispanic includes Mexican American and Other Hispanic

\*p-values were calculated by orthogonal contrasts

Table for Trends in Mean Femoral Neck Bone Mineral Density Among Individuals Aged 30 or Older in the

**Disclosures:** Yingke Xu, None.

## 1130

**African Ancestry-Specific Genetic Variants for Bone Mineral Density Determination.** Michelle S. Yau<sup>\*1</sup>, Yi-Hsiang Hsu<sup>1</sup>, Allison Kuipers<sup>2</sup>, Ryan Price<sup>3</sup>, Aude Nicolas<sup>3</sup>, Salman Tajuddin<sup>3</sup>, Samuel Handelman<sup>4</sup>, Liubov Arbeeve<sup>5</sup>, Alessandra Ches<sup>6</sup>, Ching-Ti Liu<sup>7</sup>, Fredrick Kinyua<sup>1</sup>, Wen-Chi Chou<sup>1</sup>, David Karasik<sup>1</sup>, Roby Joehanes<sup>1</sup>, Serkalem Demissie<sup>7</sup>, L. Adrienne Cupples<sup>7</sup>, Babette Zemel<sup>6</sup>, Struan Grant<sup>6</sup>, Joanne M. Jordan<sup>5</sup>, Rebecca Jackson<sup>4</sup>, Michele Evans<sup>3</sup>, Tamara Harris<sup>3</sup>, Joseph M. Zmuda<sup>2</sup>, Douglas P. Kiel<sup>1</sup>. <sup>1</sup>Hebrew SeniorLife, Harvard Medical School, United States, <sup>2</sup>University of Pittsburgh, United States, <sup>3</sup>National Institute on Aging, United States, <sup>4</sup>The Ohio State University, United States, <sup>5</sup>Thurston Arthritis Research Center, UNC, United States, <sup>6</sup>Children's Hospital of Philadelphia, United States, <sup>7</sup>Boston University School of Public Health, United States

Genetic studies of bone mineral density (BMD) have been conducted primarily in populations of European ancestry (EUR), revealing at least 56 independent loci for BMD. Despite differences in BMD between ethnic groups, there are few genetic studies of BMD in populations of African ancestry (AFR). We conducted a meta-analysis to determine whether variants in 56 known BMD loci were associated with BMD in AFR populations.

We included 4,967 individuals from six cohorts: Tobago Bone Health Cohort, Health Aging and Body Composition Study, Healthy Aging in Neighborhoods of Diversity across Life Study, Women's Health Initiative, Johnston County Osteoarthritis Project and the Bone Mineral Density in Childhood Study. Genome-wide genotyping was available for all cohorts except Tobago, where we directly genotyped selected tag SNPs for known BMD loci. Studies imputed genotypes to the most current 1000G reference panel (Phase 3) and had DXA readings for femoral neck (FN) and lumbar spine (LS) BMD. We conducted a fixed effects meta-analysis for SNP associations with FN and LS BMD, adjusting for sex, age, age<sup>2</sup>, weight, and genetic principal components to adjust for potential population stratification. Threshold for statistical significance was  $P<8.93 \times 10^{-4}$  after Bonferroni correction (0.05/56).

Mean age ranged from 12 - 73 years and about half of all individuals were women. Of 56 known BMD loci, variation at 26 was significantly associated with FN BMD and 27 with LS BMD (Table 1). Effect sizes were 0.01 to 0.11, consistent with magnitudes from EUR genetic studies. Most variants observed had much higher frequencies in AFR compared to EUR and in many instances, were rare/monomorphic in EUR. Only two variants (in *C6orf97* and *WNT16*) previously observed in a EUR study of BMD (GEFOSII) were genome-wide significant. Associations with lead BMD variants reported in EUR did not meet statistical significance.

We identified variants in 36 of 56 known BMD loci that were not previously reported in EUR genetic studies, possibly due to differences in allele frequencies between AFR and EUR. Several variants were unique to AFR populations. Variants in *C6orf97* and *WNT16* that were previously associated with BMD in EUR suggest a shared causal



locus that can be fine-mapped by taking advantage of shorter haplotype blocks in AFR populations. Our findings of ancestry-specific BMD variants underscores the importance of studying genetic factors in different racial groups.

Table 1. Lead FN and LS BMD genetic variants ( $P < 8.93E-4$ ) in African ancestry cohorts may be ancestry specific

Gene	Locus	Lead SNP	MAF in AFR	Beta	SE	P	Direction	MAF in 1000G EUR	P-value, GEFOSII EUR
<b>Femoral Neck BMD</b>									
GPR177	1p31.3	rs115656347	0.29	-0.05	0.02	7.21E-04	-----	< 0.01	NA
ZBTB40	1p36.12	rs1320597	0.31	0.04	0.01	8.42E-04	+++++	< 0.01	NA
PKDCC	2p21	rs113154109	0.27	-0.03	0.01	5.88E-04	-----	< 0.01	NA
GALNT3	2q24.3	2-166539611	0.01	-0.07	0.02	8.03E-05	----7+	< 0.01	NA
KIAA2018	3q13.2	3-113531846	0.29	-0.10	0.02	2.45E-05	-----	< 0.01	NA
MEPE	4q22.1	rs34891747	0.37	-0.02	0.00	1.04E-04	-----	0.23	NA
MEF2C	5q14.3	5-88292322	0.04	-0.04	0.01	5.09E-04	-7-7-	< 0.01	NA
CDKAL1	6p22.3	rs144898890	0.30	-0.03	0.01	3.61E-04	-----	< 0.01	NA
C6orf97	6q25.1	rs3020332	0.50	-0.01	0.00	1.84E-05	-----	0.47	2.16E-14
STARD3NL	7p14.1	rs1721399	0.33	0.02	0.00	4.10E-05	+++++	0.22	6.82E-03
WNT16	7q31.3	rs2536180	0.20	0.01	0.00	8.57E-05	+++++	0.45	4.65E-10
TNFRSF11B	8q24.12	rs73319661	0.46	0.01	0.00	5.32E-05	+++++	< 0.01	NA
MPP7	10p11.23	rs7916711	0.31	-0.02	0.01	4.61E-04	-----	0.06	NA
LINC7	11p14.1	rs116960959	0.29	0.07	0.02	2.70E-05	+++++	0.05	NA
DCDC5	11p14.1	rs288463	0.48	0.01	0.00	2.11E-04	7++++?	0.49	3.63E-02
LRP5	11q13.2	rs115647152	0.31	-0.02	0.01	1.73E-04	+++++	< 0.01	NA
AKAP11	13q14.11	rs5803130	0.23	-0.01	0.00	7.07E-04	-----	0.43	NA
RPS8KA5	14q32.12	rs61989780	0.30	-0.05	0.01	3.68E-05	-----	0.09	NA
AXIN1	16p13.3	rs115928687	0.37	0.02	0.00	7.01E-04	+++++	0.05	NA
C16orf38	16p13.3	rs1535324	0.13	-0.02	0.00	1.41E-04	-----	0.03	NA
FOX1	16q24.1	rs12919935	0.34	-0.02	0.01	7.93E-04	7-----	0.11	2.99E-01
SMG6	17p13.3	17-2008377	0.01	-0.07	0.02	5.55E-05	-----	0.02	NA
MAPT	17q21.31	rs80189278	0.32	0.08	0.02	7.92E-04	++++?	0.07	NA
TNFRSF11A	18q21.33	rs17069904	0.43	0.02	0.01	2.47E-04	7+++?	0.11	2.23E-01
GPATCH1	19q13.11	rs149111272	0.35	-0.02	0.00	2.42E-04	-----	< 0.01	NA
FAM9B	Xp22.31	rs12863157	0.36	0.02	0.00	1.40E-05	+7+???	0.28	NA
<b>Lumbar Spine BMD</b>									
ZBTB40	1p36.12	rs114268461	0.31	0.04	0.01	3.63E-04	+++++	< 0.01	NA
CTNNA1	3p22.1	rs191434156	0.29	0.08	0.02	5.36E-04	+++++	< 0.01	NA
KIAA2018	3q13.2	3-113371563	0.28	-0.11	0.03	2.43E-04	-----	< 0.01	NA
LEKR1	3q25.31	3-156503022	0.47	0.02	0.00	5.12E-05	+++7+	0.03	NA
GPR177	4q22.1	rs141259826	0.07	-0.02	0.01	6.14E-04	-----	< 0.01	NA
MEPE	4q22.1	rs112057797	0.39	0.02	0.00	5.44E-04	+++++	< 0.01	NA
CDKAL1	6p22.3	rs4710973	0.43	-0.01	0.00	1.21E-04	-----	0.40	NA
RSPO3	6q22.32	rs201098206	0.02	-0.06	0.01	2.28E-05	-----	< 0.01	NA
C6orf97	6q25.1	rs143390228	0.29	-0.07	0.02	1.33E-05	-----	0.04	NA
WNT16	7q31.3	rs35883000	0.47	-0.01	0.00	5.38E-04	-----	0.33	NA
XKR9	8q13.3	8-72033197	0.30	-0.08	0.02	3.82E-04	-----	< 0.01	NA
TNFRSF11B	8q24.12	rs1389544	0.47	0.02	0.00	6.37E-05	++++?	< 0.01	NA
MPP7	10p11.23	rs71523600	0.10	-0.02	0.01	4.48E-04	-----	0.11	NA
MBL2	10q21.1	10-54430008	0.01	-0.07	0.02	6.56E-04	-----	< 0.01	NA
DCDC5	11p14.1	rs192640864	0.29	-0.05	0.01	7.06E-05	-----	< 0.01	NA
LRP5	11q13.2	rs3781589	0.31	-0.02	0.01	3.81E-04	+++++	< 0.01	NA
ERC1	12p13.33	rs11061817	0.07	-0.03	0.01	3.39E-04	-----	0.13	NA
SP7	12q13.13	12-53641681	0.42	0.01	0.00	4.20E-04	+++7-	0.41	NA
C12orf23	12q23.3	rs149110561	0.30	0.04	0.01	6.63E-04	+++++	< 0.01	NA
AKAP11	13q14.11	rs114703306	0.29	0.03	0.01	3.39E-04	+++++	< 0.01	NA
MARCK3	14q32.32	rs116543673	0.30	0.03	0.01	8.15E-04	+++++	< 0.01	NA
C16orf38	16p13.3	rs960467	0.40	0.02	0.00	2.97E-05	+++++	< 0.01	NA
FOX1	16q24.1	rs191080821	0.29	-0.07	0.02	1.39E-04	-----	0.23	NA
C17orf53	17q21.31	17-42227903	0.29	-0.07	0.02	7.63E-04	-----	< 0.01	NA
TNFRSF11A	18q21.33	rs160003873	0.29	0.06	0.02	3.73E-04	+++++	< 0.01	NA
GPATCH1	19q13.11	rs73585909	0.47	-0.02	0.00	2.59E-05	-----	0.10	NA
FAM9B*	Xp22.31	rs12863157	0.36	0.02	0.01	1.81E-04	+7+???	0.28	NA

Abbreviations: AFR=African Ancestry, EUR=European Caucasians, FN=femoral neck, LS=lumbar spine, MAF=minor allele frequency, NA=Not tested in GEFOSII, P=P-value

Table 1. Lead FN and LS BMD genetic variants in African ancestry cohorts may be ancestry specific

Disclosures: Michelle S. Yau, None.

## 1131

**Activation of PI3K in the myeloid lineage induces bone loss and confers myeloproliferative neoplastic potential due to the increase in myeloid derived suppressor cells.** Jungeun Yu\*, Laura Doherty, Evan Jellison, Ernesto Canalis, Archana Sanjay, U Conn Health, United States

Myeloproliferative neoplasms are characterized by increased proliferation and expansion myeloid lineages. Phosphoinositide 3-kinases (PI3Ks) are involved in tumorigenesis however their role in inducing myeloid neoplasms is not known. We examined the requirement of the p110a catalytic subunit in myelopoiesis using p110a conditional mice where the ROSA26 allele harbors constitutively active p110 (p110a<sup>CA</sup>) preceded by a loxP flanked STOP cassette (R26Stop<sup>FL</sup>p110a<sup>CA</sup>). To activate PI3K in the myeloid lineage, R26Stop<sup>FL</sup>p110a<sup>CA</sup> mice were bred with the LysM Cre<sup>+/+</sup> mice. Activation of PI3K led to a 6-fold increase in phospho-AKT levels in bone marrow macrophages (BMMs) derived from p110a<sup>CA</sup> mice. While the body weight of p110a<sup>CA</sup> mice was comparable to control littermates, there was significant splenomegaly and hepatomegaly, increased

vasculogenesis, increased numbers of neutrophils in peripheral blood and accumulation of erythrocytes under the skin upon activation of PI3K. In vitro proliferation of p110a<sup>CA</sup> BMMs was augmented in response to m-CSF. Flow cytometric analysis of bone marrow showed that compared to control, p110a<sup>CA</sup> mice had 2.0-fold increase in CD11b<sup>+</sup> monocytes, CD11b<sup>+</sup>F480<sup>+</sup> macrophages and CD11b<sup>low</sup>CD115<sup>+</sup> osteoclast precursors. In spleen-derived myeloid populations from p110a<sup>CA</sup> mice, a 2.5-fold increase was found in CD11b<sup>+</sup>Ly6G<sup>+</sup>SSC<sup>int</sup> neutrophils and CD11b<sup>+</sup>Ly6G<sup>+</sup>SSC<sup>hi</sup> eosinophils compared to control mice. The number of CD3<sup>+</sup>T and B220<sup>+</sup>B and CD11c<sup>+</sup>dendritic cells were comparable between the two genotypes. Myeloid derived suppressor cells (MDSCs) are derived from tumor-bone marrow environment and can differentiate into functional osteoclasts influencing bone resorption. Flow cytometric analysis showed that the bone marrow and spleen of p110a<sup>CA</sup> mice harbored 1.5 fold more granulocytic and 2 fold more monocytic MDSCs. Micro Ct and histomorphometric analysis of femurs from 10 week old p110a<sup>CA</sup> female mice showed decreased bone volume and 2 fold increase in osteoclast numbers and 1.75 fold increase in eroded surface/bone surface, but no changes in osteoblast numbers. Increased osteoclast formation and bone resorption was confirmed in *in vitro* cultures. Cumulatively, these results indicate that enhanced PI3K signaling increases myelopoiesis and augmented MDSC proliferation contributing to enhanced osteoclastogenesis and bone loss. These data suggests that the dysregulation of PI3K signaling is responsible for myeloproliferative neoplasms.

Disclosures: Jungeun Yu, None.

## 1132

**A Novel Osteolineage-derived Cancer-Associated Fibroblast Population In Primary Tumors Expresses DKK1 And Enhances Tumor Growth.** Biancamaria Ricci\*, Francesca Fontana<sup>2</sup>, Sahil Mahajan<sup>1</sup>, Danielle Ketterer<sup>1</sup>, Roberto Civitelli<sup>3</sup>, Roberta Faccio<sup>4</sup>. <sup>1</sup>Washington University-School of Medicine, Department of Orthopaedic Surgery, United States, <sup>2</sup>Washington University-School of Medicine, Department of Medicine-Bone and Mineral Division, United States, <sup>3</sup>Washington University-School of Medicine, Department of Medicine-Bone and Mineral Division, United States, <sup>4</sup>Washington University-School of Medicine, Department of Orthopaedic Surgery, United States

We recently described that mice bearing extra-skeletal tumors have increased levels of the Wnt/ $\beta$ -catenin inhibitor DKK1 in circulation and in the bone marrow fluid. DKK1 acts as a strong immune suppressive factor, inducing the expansion of immature myeloid suppressor cells that inhibit T cell responses during tumor progression. Indeed, DKK1 neutralization reduces tumor growth by restoring anti-tumor immune responses. We found that DKK1 is expressed in the tumor mass, but also and at higher levels in bone of mice bearing orthotopic B16 melanomas, Lewis Lung carcinomas (LLC) or PymT breast carcinomas. In bone, DKK1 is highly expressed by osteoblasts (OBs) and osteocytes, but not by bone marrow cells. To identify the cell population within the tumor mass responsible for DKK1 production at tumor site, we separated the tumor adherent fraction, enriched in cancer-associated fibroblasts (CAFs) and analyzed DKK1 mRNA levels relative to the rest of the tumor. CAFs express abundant DKK1, but also, unexpectedly, two OB-specific markers Osterix (Osx) and osteocalcin. To determine whether these previously unidentified Osx<sup>+</sup> cells among CAFs are the DKK1-producing cells, we used the doxycycline-sensitive Osx-Cre model to activate the TdTomato (TdT) reporter in vivo. Doxycycline was administered until weaning to prevent Osx-Cre activation in perinatal mesenchymal stem cells and, at 8 weeks of age, mice were inoculated with B16, LLC or PymT tumors. We found that 3-9% cells in the tumor mass were TdT<sup>Osx+</sup>, and also expressed the fibroblast markers, Fsp-1 and Vimentin. Importantly, DKK1 mRNA was significantly higher in TdT<sup>Osx+</sup> than in TdT<sup>Osx-</sup> cells, suggesting that this sub-population is involved in DKK1 production at tumor site. To determine the role of TdT<sup>Osx+</sup> cells in tumor progression, we co-injected these cells isolated from primary B16 tumors with B16 cells into WT mice. Results showed an enhanced tumor growth relative to mice injected with tumor cells alone. Finally, flow cytometry analysis revealed the presence of TdT<sup>Osx+</sup> cells in bone marrow (15.3 $\pm$ 5.06%) and, surprisingly, also in circulation (16 $\pm$ 4.5%) of tumor bearing mice, suggesting that these Osx<sup>+</sup> CAFs might be mobilized from the bone microenvironment. In summary, we have identified a novel population of CAFs that express osteolineage markers and contribute to DKK1 production and tumor growth. Osx<sup>+</sup> cells may represent a new platform for targeting the stroma with the purpose of inhibiting cancer growth.

Disclosures: Biancamaria Ricci, None.

## 1133

**Evaluating the Role of Osteoblast-Specific Stabilization of  $\beta$ -catenin in Leukemia Initiation and Progression.** Mitchell McDonald\*, Cassandra Diegel<sup>1</sup>, Galen Hostetter<sup>1</sup>, Roderick Bronson<sup>2</sup>, Bart Williams<sup>1</sup>. <sup>1</sup>Van Andel Research Institute, United States, <sup>2</sup>Harvard Medical School, United States

Bone cells have a complex relationship with the adjacent bone marrow, where signals from the skeleton can trigger the differentiation and proliferation of bone marrow stem cell populations. Wnt signaling is important in stem cell differentiation and proliferation and plays an integral role in bone development and homeostasis. Recently, osteoblasts have been implicated in pre-leukemic conditions in mice; specifically, activating mutations of  $\beta$ -catenin in osteoblasts have been reported to induce acute myeloid leukemia

(AML) with mice succumbing to the disease by six weeks of age. These findings, suggesting that a modification within an osteoblast could lead to AML and other myelodysplastic syndromes (MDS), are novel and important in the bone field as Wnt agonists are currently being developed to treat various bone diseases. We wanted to independently validate the phenotype as it could affect potential treatments for a large population of patients.

We generated mice carrying the osteoblast-specific activating mutations of  $\beta$ -catenin by crossing mice carrying an osteoblast-specific Cre-recombinase (2.3kb *Col1 $\alpha$ 1*-promoter) with mice carrying alleles of  $\beta$ -catenin that contain loxP sites flanking its third exon which contains the GSK3 $\beta$  regulatory phosphorylation sites. Upon Cre-mediated recombination in osteoblasts,  $\beta$ -catenin is no longer able to be repressed in the absence of Wnt ligand, creating a constitutively active form of the protein. In our hands, mutant mice are osteopetrotic, with diminished amounts of bone marrow in the femurs while exhibiting stunted growth and no teeth. Surprisingly, analysis of peripheral blood and histological analysis of various tissues at multiple ages do not provide evidence of leukemogenesis or other dysplastic syndromes. In addition, mutant animals can live to be well over a year of age (Figure 1). Potential explanations for discrepancies from previously published work include slight differences in genetic background, genetic drift associated with Cre-drivers, or differences in housing or other aspects of the environment.

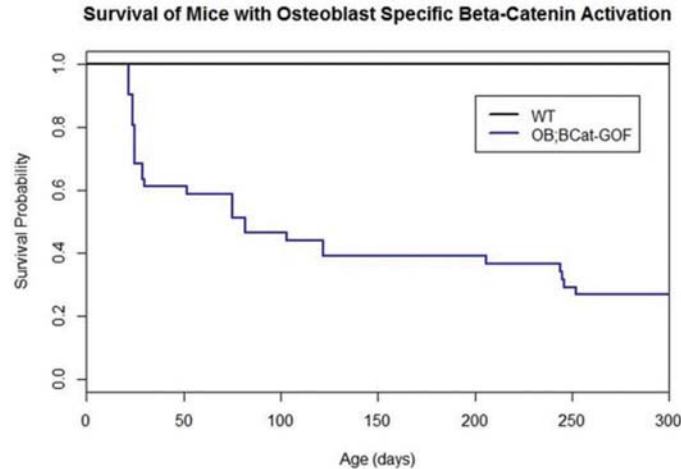


Figure 1

Disclosures: Mitchell McDonald, None.

## 1134

**Notch2 pathway and breast cancer cellular dormancy. A role for osteoblasts.** Mattia Capulli\*, Dayana Hristova, Zoe Valbret, Ronak Arjan, Antonio Maurizi, Alfredo Cappariello, Nadia Rucci, Anna Teti. University of L'Aquila, Italy

One fifth of breast cancer (BrCa) patients experience recurrences after >5 years of disease-free survival. In bone, BrCa cells (BrCaCs) may stop proliferating and enter a state of cellular dormancy. Long-Term Hematopoietic Stem Cells (LT-HSCs) display similar quiescent status, therefore, we hypothesize that dormant BrCaCs mimic LT-HSCs and exploit their medullary niche. We developed a mouse model of bone BrCaC dormancy by injecting the human osteotropic BrCaCs, MDA-MB-231 (MDA), into the tibias (IT) of athymic mice and selecting tumor-negative mice 4 weeks thereafter. In overt tumor-free tibias, we observed isolated cytokeratin<sup>+</sup> MDA (43±24 N/mm<sup>2</sup>). Time-course experiments showed a sub-population of MDA to progressively reach the endosteal surface within 1 week (p=0.02) and stay cell cycle arrested up to 1 month after IT injection. Confocal imaging showed non-proliferating (Ki67<sup>-</sup>) MDA preferentially bound to Spindle-shaped N-cadherin<sup>+</sup> Osteoblasts (SNO), previously associated with the LT-HSC niche. Accordingly, in vivo competition assay, the engraftment of HSCs declined with the increase of co-injected MDA (p=0.037; R=0.28). In vitro, sorted SNO, but not SNO-depleted osteoblasts (NON SNO), impaired MDA proliferation (-91%; p<0.02) and clone formation (-70%; p<0.05). Cultured SNO exhibited ~78% less ALP activity, reduced osteoblast markers expression, impaired mineralization and lack of actin stress fibers vs NON SNO. MDA bound to SNO shared the notch pathways with LT-HSC. Selective silencing of Notch1-4 led us to narrow-down to Notch2 the candidate signaling implicated in BrCaC dormancy. Sorted Notch2<sup>+</sup> MDA (9% of MDA population) overexpressed the LT-HSC stemness markers Sca-1, CXCR4 and cKit (+5.37; +1.34; +123-fold, respectively vs Notch2<sup>-</sup>; p<0.001). In vitro, Notch2-specific siRNA and the  $\gamma$ -secretase inhibitor, dibenzazepine (DBZ), induced MDA proliferation on SNO (+1.83fold; p=0.04 and +1.75fold; p=0.03), achieving the rate of MDA on NON SNO. In vivo, single Notch2<sup>+</sup>/cytokeratin<sup>+</sup> MDA bound to SNO were Ki67<sup>+</sup>. A single injection of 4.8mg/kg DBZ in our mouse model of BrCaC-dormancy increased the mean distance of MDA from the endosteal surface (+2.1fold; p=0.0002) and amplified liver metastases (+2.5fold; p=0.04), while both acute and chronic inflammation induced by LPS administration were ineffective. Key results were confirmed in 4T1 mouse BrCaCs. This study opened a new direction for understanding the molecular mechanisms governing BrCaC dormancy.

Disclosures: Mattia Capulli, None.

## 1135

**Metabolic reprogramming in breast cancer bone metastases via PKC- $\zeta$  regulated crosstalk of serine biosynthesis and autophagy regulation.** Manish Tandon\*, Ahmad Othman, Jitesh Pratap. Rush University Medical Center, United States

The ability to alter metabolism to improve cell survival is a key attribute of cancer metastases. Here, our results corroborate that protein kinase C zeta (PKC- $\zeta$ ) deficiency promotes glutamine dependence in glucose-addicted metastatic breast cancer MDA-MB-231 cells. The PKC- $\zeta$  is one of the two members of the atypical PKC family of isoenzymes (aPKCs) which is implicated in tumor suppressive functions. We compared parental and bone metastases-derived MDA-MB-231 cells for alterations in metabolism-related gene expression. In an array of genes related to metabolism and growth factor signaling, we identified more than seven-fold downregulation of PKC- $\zeta$  gene expression levels in bone-derived MDA-MB-231 cells. We validated this decline in PKC- $\zeta$  gene expression and confirmed the downregulation of PKC- $\zeta$  protein levels. Our results show that glucose uptake, expression of glucose transporter type 4, GLUT4, and glycolysis is reduced in bone-derived MDA-MB-231 cells compared to parental cells. Interestingly, an increased dependence on glutamine upon glucose withdrawal for cell adhesion and proliferation was observed in the bone-derived cells. Since PKC $\zeta$  deficiency promotes glutamine utilization via the serine biosynthetic pathway, we examined glutamine metabolism associated genes. The levels of serine biosynthesis pathway genes, phosphoserine phosphatase (PSPH), phosphoserine aminotransferase (PSAT1) and phosphoglycerate dehydrogenase (PHGDH) showed potent induction following glucose deprivation. The PHGDH upregulation was inhibited by ectopically expressing wild type but not mutated PKC- $\zeta$  in glucose-deprived conditions. The previously reported interaction of PKC- $\zeta$  with p62/SCSTMI1 (sequestosome1) suggested that PKC- $\zeta$  could also be important for induction of autophagy upon glucose deprivation. Therefore, we examined autophagy upon ectopic PKC- $\zeta$  expression by measuring levels of autophagy marker protein LC3B. The ectopic PKC- $\zeta$  expression showed reduced basal LC3B-II levels compared to the control cells suggesting a crosstalk between autophagy pathway and serine biosynthesis. Taken together, our results support metabolic plasticity in breast cancer cells undergoing bone metastases.

Disclosures: Manish Tandon, None.

## 1136

**CD8<sup>+</sup> T Cells Increase Osteolytic Bone Metastases from Breast Cancer in Mice.** Danna Arellano-Rodriguez\*, Andrea Verdugo-Meza<sup>1</sup>, Florian Drescher<sup>1</sup>, Felipe Olvera-Rodriguez<sup>2</sup>, Patricia Juarez<sup>1</sup>, Pierrick Fournier<sup>1</sup>. <sup>1</sup>Biomedical Innovation Dept., CICESE, Mexico, <sup>2</sup>Instituto de Biotecnología, UNAM, Mexico

Bone metastases are incurable and new treatments need to be explored. Immunotherapy to activate or enhance the immune response against cancer cells has led to promising advances. However a potential limiting factor for its application in bone metastases is the ability for T cells to increase bone resorption, which would fuel the vicious cycle of bone metastases.

To characterize the effect of T cells on bone metastases and select a proper syngeneic model, we tested different mouse cancer cells and found that the breast cancer cells 4T1 had both high expression of MHC class I necessary for CD8<sup>+</sup> T cell activation and T cell infiltration in bone metastases. When inoculated in the left cardiac ventricle of immunocompetent Balb/C mice, 4T1 caused osteolytic metastases detected on x-rays (5.3±1.3mm<sup>2</sup>). When inoculated in Balb/C SCID mice lacking T and B cells, 4T1 caused less osteolysis (1.5±0.3mm<sup>2</sup>, p<0.01). Histology confirmed that mice with a functional immune system had significantly less bone area and increased tumor burden and number of osteoclasts at the tumor/bone interface. We used then a treatment with antibodies against CD4 or CD8 to deplete T cells. Co-treatment with anti-CD4 and CD8 depleted all CD3<sup>+</sup> T cells and decreased the osteolysis of 4T1 metastases (-38%, p<0.05). Depletion of CD4<sup>+</sup> T cells only had no effect on osteolysis while specific depletion of CD8<sup>+</sup> T cells decreased 4T1 osteolysis area (-42%, p<0.05).

To characterize the effect of T cells on osteoclasts, CD3<sup>+</sup> T cells were isolated from the bone marrow of mice with or without bone metastases using cell sorting. In contrast with *in vivo* data, T cells from bone metastases suppressed osteoclast formation *ex vivo*. However this effect was due to the *ex vivo* activation of T cells with anti-CD3 and CD28 antibodies, consistent with decreased levels of *Rankl* and increased expression of anti-osteoclastic *Ifng* and *Il4* mRNA in activated T cells. When gene expression was measured after cell sorting, *Ifng* mRNA was not detected and levels of pro-osteoclastic *Rankl* and *Tnfa* were higher in T cells from 4T1 bone metastases when compared to splenic T cells, suggesting that T cells in bone were not activated. Accordingly in the bones of metastatic mice, there was an increase of myeloid derived suppressor cells that suppress T cell activation.

These results suggest that unactivated CD8<sup>+</sup> T cells increase bone metastases and their activation by immunotherapy could be used for the treatment of bone metastases.

Disclosures: Danna Arellano-Rodriguez, None.



## 1137

**Anabolic PTH Signaling Activates the Canonical Notch Pathway in Osteocytes to Restrain Bone Resorption and Facilitate Bone Gain.** Jesús Delgado-Calle\*, Jessica H. Nelson, Matthew E. Olson, Kevin McAndrews, Emily G. Atkinson, Xiaolin Tu, Teresita Bellido. Anatomy and Cell Biology, Indiana University School of Medicine, United States

Intermittent and chronic elevation of parathyroid hormone (PTH) have anabolic and catabolic effects in the skeleton, respectively. However, the mechanisms underlying these paradoxical effects remain unknown. PTH regulates the expression of the Notch ligand Jagged1 in bone cells. Yet, whether PTH regulates other Notch components and the role of Notch in the skeletal actions of the hormone is unclear. We report that expression of Notch components (receptors, ligands, and target genes) is elevated in bones from transgenic mice with a constitutively active PTH receptor in osteocytes (caPTH1R<sup>On</sup>) and in WT mice exposed to anabolic regimen of PTH (100ng/g/day; 4wks). In contrast, chronic endogenous elevation of PTH did not change the expression of Notch-related genes. Notch activation by anabolic PTH was absent in mice lacking PTH1R in osteocytes or overexpressing the Wnt antagonist SOST in osteocytes (DMP1-SOST), demonstrating that intermittent, but not chronic, PTH elevation, activates Notch by direct actions in osteocytes and through a mechanism downstream of Sclerostin down-regulation. To dissect the contribution of canonical Notch signaling in osteocytes to the bone gain in caPTH1R<sup>On</sup> mice, we genetically deleted the canonical Notch transcription factor RBPjk in osteocytes (with Dmp1-8kb-Cre) in WT and caPTH1R<sup>On</sup> and generated WT, caPTH1R<sup>On</sup>, RBPjk<sup>On</sup>, and caPTH1R<sup>On</sup>;RBPjk<sup>On</sup> littermates. Mice lacking RBPjk in osteocytes exhibited a reduction of ~50% in RBPjk mRNA expression in calvarial bone, regardless of whether they express or not the caPTH1R transgene. At 6 months, WT and RBPjk<sup>On</sup> mice exhibited no differences in BMD, cortical or cancellous bone volume, and markers of bone formation and resorption, suggesting that osteocytic canonical Notch signaling is dispensable for bone homeostasis. In contrast, caPTH1R<sup>On</sup>;RBPjk<sup>On</sup> mice exhibited 5% lower total BMD, decreased femoral cortical bone area (-9%), and reduced L5 cancellous BV/TV/ (-16%) and trabecular thickness (-30%) compared to control caPTH1R<sup>On</sup> mice. Moreover, caPTH1R<sup>On</sup>;RBPjk<sup>On</sup> mice displayed increased serum CTX (40%) and higher Rankl mRNA expression, thus increasing the Rankl/Opg ratio in bone. However, the increase in circulating PINP and Sost down-regulation observed in caPTH1R<sup>On</sup> mice remained unchanged in caPTH1R<sup>On</sup>;RBPjk<sup>On</sup> mice. We conclude that anabolic PTH receptor signaling activates the canonical Notch pathway in osteocytes, which in turn, restrains bone resorption and facilitates bone gain.

**Disclosures:** Jesús Delgado-Calle, None.

## 1138

**The extra-large G protein alpha-subunit (XL $\alpha$ s) mediates FGF23 production by maintaining FGFR1 expression and MAPK signaling in bone.** Qing He\*<sup>1</sup>, Cumhur Aydin<sup>2</sup>, Marc Wein<sup>1</sup>, Jordan Spatz<sup>1</sup>, Regina Goetz<sup>3</sup>, Moosa Mohammadi<sup>3</sup>, Antonius Plagge<sup>4</sup>, Paola Pajevic Divieti Pajevic<sup>5</sup>, Murat Bastepe<sup>1</sup>. <sup>1</sup>Endocrine Unit, Department of Medicine, Massachusetts General Hospital and Harvard Medical School, United States, <sup>2</sup>Department of Endodontics, Gülhane Military Medical Academy, Turkey, <sup>3</sup>Department of Biochemistry & Molecular Pharmacology, New York University School of Medicine, United States, <sup>4</sup>Department of Cellular and Molecular Physiology, Institute of Translational Medicine University of Liverpool, United Kingdom, <sup>5</sup>Department of Molecular & Cell Biology, Boston University School of Dental Medicine, United States

FGF23 is a bone-derived phosphaturic hormone, the excess or deficiency of which leads to a variety of diseases. Molecular mechanisms governing FGF23 production are poorly understood. The extra-large G $\alpha$ -subunit (XL $\alpha$ s) is a variant of the stimulatory G protein  $\alpha$ -subunit (G $\alpha$ s), which mediates the actions of PTH, another phosphaturic hormone shown to stimulate FGF23 production. XL $\alpha$ s can mimic the cellular actions of G $\alpha$ s when overexpressed, but its unique actions, as well as its roles in mineral metabolism, remain unclear. We found that XL $\alpha$ s is expressed in osteocytes and osteoblasts during early postnatal development. At postnatal day 10, XL $\alpha$ s knockout (XLKO) mice exhibited hyperphosphatemia (11.43 $\pm$ 0.43 vs. 10.23 $\pm$ 0.21 mg/dl in WT) and hypocalcemia (1.41 $\pm$ 0.02 vs. 1.46 $\pm$ 0.01 mmol/l in WT), as well as significantly increased 1,25(OH) $_2$ D levels (224.82 $\pm$ 3.49 vs. 142.51 $\pm$ 4.02 pmol/L in WT). Quantitative RT-PCR analysis of whole kidneys from XLKO pups revealed a 2.6-fold increase in Cyp27b1 and a 1.9-fold increase in Cyp24a1 mRNA levels compared to WT littermates. We also observed increased expression of sodium phosphate co-transporter Npt2a in XLKO renal brush-border membranes. Consistent with these findings, serum FGF23 levels were significantly reduced in XLKO pups (204.40 $\pm$ 10.50 vs. 398.68 $\pm$ 10.14 pg/mL in WT). FGF23 mRNA levels in XLKO femurs were also significantly reduced (34.79 $\pm$ 5.98% of WT levels), along with a reduction in FGFR1 mRNA levels (31.05 $\pm$ 2.83% of WT levels). XLKO bones showed reduced total and phospho-FRS2 $\alpha$ , as well as phospho-ERK1/2 levels. Injection of a stable FGF23 mutant (FGF23<sup>R176Q/R179Q</sup>) into XLKO mice normalized Pi levels (saline-injected WT: 12.07 $\pm$ 0.10 mg/mL; saline-injected KO: 13.64 $\pm$ 0.16 mg/mL; FGF23-injected WT: 10.53 $\pm$ 0.17 mg/mL; FGF23-injected KO: 11.62 $\pm$ 0.23 mg/mL), and significantly decreased renal Cyp27b1 mRNA levels. CRISPR/Cas9-mediated knockout of XL $\alpha$ s in a murine osteocytic cell line (Ocy454) significantly decreased FGF23 (14.81 $\pm$ 2.11% of control) and FGFR1 mRNA levels (26.79 $\pm$ 2.63% of control), as well as the level of phospho-ERK1/2. Moreover, transcriptional activation of FGFR1 expression through

CRISPR/Cas9 Synergistic Activation Mediator resulted in elevated FGF23 mRNA levels in WT Ocy454 cells (3.56 $\pm$ 0.29 fold over control) and rescued the reduced FGF23 expression in XLKO Ocy454 cells (3.45 $\pm$ 0.27 fold over control). Our findings indicate that XL $\alpha$ s promotes FGF23 production in bone by maintaining FGFR1 expression and MAPK signaling.

**Disclosures:** Qing He, None.

## 1139

**A Novel Distal Enhancer of the Mouse Fgf23 Gene Mediates the Inflammation- and CKD-induced Expression of FGF23.** Melda Onal\*, Alex Carlson, Mark Meyer, Benkusky Nancy, Seong Min Lee, Hillary St. John, John Wesley Pike. University of Wisconsin - Madison, United States

Inflammation induces Fibroblast Growth Factor 23 (FGF23) production. Consistent with this, elevated FGF23 levels have been associated with inflammatory markers in various diseases including chronic kidney disease (CKD). However, molecular mechanisms underpinning the elevated Fgf23 transcription in response to inflammation are unknown. Herein, we show that inflammation increases FGF23 mRNA levels in both bone and non-osseous tissues, including several tissues that normally do not express FGF23. To discover transcriptional regulatory elements of the Fgf23 gene, we utilized chromatin immunoprecipitation followed by DNA sequencing (ChIP-seq) in the IDG-SW3 osteocyte cell line and other bone cell lines. Utilizing ChIP-seq analysis of enhancer associated histone modifications such as H3K9 acetylation and H3K4 methylations, we identified a potential enhancer of Fgf23 gene distal to its transcriptional start site. We utilized the genome-editing CRISPR-Cas9 system to delete this potential enhancer from the mouse genome, producing an FGF23 distal enhancer knock-out (FGF23eKO) mouse strain. Compared to their wild type littermates (WT), FGF23eKO mice exhibited FGF23 expression slightly lower in bone, but drastically lower (>85%) in thymus and spleen without changes in the circulating intact FGF23 (iFGF23) compared to WT mice, confirming that under normal conditions bone is the major source of FGF23 production. Moreover, lack of this enhancer blunted FGF23 induction as a result of acute inflammation induced by a single injection of lipopolysaccharides (LPS), IL1 $\beta$  or TNF $\alpha$  in bone and non-osseous tissues in a tissue-specific manner. This transcriptional effect resulted in a blunting of the inflammation-induction of the circulating iFGF23 levels in the FGF23eKO mice as well. To address whether transcriptional regulation of FGF23 by this enhancer contributed to high FGF23 levels in CKD, we fed FGF23eKO and WT mice control or oxalate diet for one week. In this diet-induced model of CKD, FGF23 mRNA levels increased in kidney, thymus and bone in WT mice, while these increases were completely prevented in the FGF23eKO mice. However, FGF23eKO mice showed a blunted CKD-induced increase in circulating iFGF23 levels compared to WT mice. Taken together these results suggest that high levels of biologically active intact form of FGF23 observed in CKD are a result of both increased Fgf23 transcription mediated via this novel distal enhancer as well as decreased cleavage of FGF23.

**Disclosures:** Melda Onal, None.

## 1140

**Collagen Dynamics During the Process of Osteocyte Embedding and Mineralization.** Lora A. McCormick\*<sup>1</sup>, LeAnn M. Tiede-Lewis<sup>1</sup>, Eleanor C. Ray<sup>1</sup>, Youngebo Lu<sup>2</sup>, Sarah L. Dallas<sup>1</sup>. <sup>1</sup>University of Missouri, Kansas City, United States, <sup>2</sup>Texas A&M University College of Dentistry, United States

The processes of bone formation, remodeling and repair are dynamic, involving cell migration and embedding, ECM assembly and bone resorption. Using live cell imaging we have shown that osteoblast assembly of ECM proteins such as fibronectin and collagen is highly dynamic and is integrated with cell motility. We have also shown that the osteoblast to osteocyte transition involves arrest of cell motility and dendrite extension and retraction that may regulate positioning of the embedding cell. To further understand how osteocytes differentiate and embed we have generated mice co-expressing a Dmp1-Cre inducible TdTomato (TdTom) reporter with GFP $^{tpz}$ -tagged collagen to allow dual imaging of osteocytes and collagen matrix dynamics.

Live imaging in mineralizing primary calvarial cell cultures showed that the Dmp1-Cre/TdTom transgene turned on in early bone nodule forming regions, demarcated by foci of concentrated GFP-collagen bundles that were structurally distinct from the surrounding collagen. Dmp1-TdTom cells were post-mitotic, primarily arising by cells switching on TdTom rather than division of TdTom cells. The GFP-collagen fibrils showed considerable motion, including global (tissue-level) motions, suggesting coordinated cell layer movement, and local fibril motions mediated by cell-generated forces. In early (d6-8) cultures, prior to mineralization, TdTom cells were highly motile, moving freely in and out of the forming bone nodule with a small number of TdTom cells embedded in collagen, constraining their motion (av. velocity 3.1  $\pm$  0.3  $\mu$ m/h). Three apparent mechanisms for embedding of TdTom cells in collagen were seen. In some cases, a TdTom motile cell moved into an already formed "collagen lacuna" in the developing nodule, became stationary and developed dendrites. In other cases, motile TdTom cells were trapped and immobilized in collagen fibril networks newly assembled around the cell. Alternatively, some cells switched on TdTom in situ within a forming lacuna. In mineralizing (d12-14) cultures, we observed contraction of collagen fibril networks prior to mineralization. The av. cell velocity was significantly reduced (1.8 $\mu$ m/h  $\pm$  0.3, p < 0.01 vs. d6-8), with many TdTom cells immobilized in the

mineralizing nodule and motile TdTom cells actively migrating towards the nodule to become incorporated. These data provide new insight into the dynamic process of osteocyte embedding and suggest multiple mechanisms for osteocyte entrapment in collagen matrix.

**Disclosures:** Lora A. McCormick, None.

## 1141

**Osteocyte intrinsic TGF $\beta$  signaling in regulates bone quality through perilacunar remodeling.** Neha S. Dole<sup>\*1</sup>, Courtney M. Mazur<sup>1</sup>, Claire Acevedo<sup>1</sup>, Justin P. Lopez<sup>1</sup>, David A. Monteiro<sup>1</sup>, Tristan W. Fowler<sup>1</sup>, Bernd Gludovatz<sup>2</sup>, Flynn Walsh<sup>3</sup>, Robert O. Ritchie<sup>2</sup>, Khalid S. Mohammad<sup>4</sup>, Tamara Alliston<sup>1</sup>. <sup>1</sup>Department of Orthopaedic Surgery, University of California San Francisco, United States, <sup>2</sup>Materials Science Division, Lawrence Berkeley National Laboratory, United States, <sup>3</sup>Department of Materials Science and Engineering, University of California Berkeley, United States, <sup>4</sup>Department of Medicine, Indiana University School of Medicine, United States

Bone quality, like bone mass, is an important determinant of bone resistance to fracture, but an incomplete understanding of the cellular and molecular mechanisms controlling bone quality has limited the ability to target it therapeutically. TGF $\beta$  signaling is one of the few molecular pathways known to affect bone quality, but its cellular target is unknown. Since osteocyte perilacunar remodeling (PLR) has been associated with changes in bone quality, we tested the hypothesis that TGF $\beta$  regulates bone quality via osteocyte PLR.

Using TGF $\beta$  receptor type I inhibitor (T $\beta$ RI-I) we systemically inhibited TGF $\beta$  signaling *in vivo* and found a coordinated repression of key PLR enzymes, including MMP13, MMP14, and Cathepsin K (CTSK). Absence of TGF $\beta$  also caused a severe deterioration of osteocyte lacuno-canalicular network (LCN) integrity and these impaired PLR hallmarks strongly suggested of TGF $\beta$ 's regulatory role in PLR. Additionally, we found that TGF $\beta$  induced PLR gene expression in MLO-Y4 osteocyte-like cells, and reduced their intracellular pH, which is a functional measure of PLR. This indicated that TGF $\beta$  modulated PLR in an osteocyte-intrinsic manner. We tested this hypothesis *in vivo* using a novel osteocyte specific TGF $\beta$  receptor type II-deficient (T $\beta$ RII<sup>ocyl-/-</sup>) mouse model. Similar to the T $\beta$ RI-I administered mice, T $\beta$ RII<sup>ocyl-/-</sup> also exhibited a stark reduction in expression of PLR enzymes and osteocyte LCN connectivity compared to wild-type littermates. Thus, our data show that TGF $\beta$  regulates osteocyte mediated PLR.

Using flexural strength tests and nanoindentation, we tested whether osteocyte-intrinsic TGF $\beta$  signaling is sufficient to regulate bone quality. Despite high trabecular bone mass and normal cortical bone mass, T $\beta$ RII<sup>ocyl-/-</sup> bones showed reductions in yield strength, bending modulus and tissue elastic modulus, suggesting a defect in bone quality. During *in situ* fracture toughness testing, T $\beta$ RII<sup>ocyl-/-</sup> bones showed a 65% reduction in fracture toughness due to unchecked crack propagation. SEM analysis of crack propagation revealed that T $\beta$ RII<sup>ocyl-/-</sup> bone has inferior extrinsic toughening mechanisms with significantly shorter crack paths, less branching and uncracked ligament bridging relative to WT bone. These data implicate osteocytes as an essential target of TGF $\beta$  in the control of bone quality. Collectively, this study reveals the novel role of osteocyte-intrinsic TGF $\beta$  in the control of PLR and the importance of PLR in the regulation of bone quality.

**Disclosures:** Neha S. Dole, None.

## 1142

**Sclerostin antibody administration increases the Numbers and Differentiation of Osteoblast Precursors *in Vivo*.** Sophia Trinh<sup>\*1</sup>, Deepak Balani<sup>1</sup>, Rogely Boyce<sup>2</sup>, Henry Kronenberg<sup>1</sup>. <sup>1</sup>Endocrine Unit, Massachusetts General Hospital and Harvard Medical School, Boston, MA, United States, <sup>2</sup>Amgen, Inc, United States

Sclerostin antibody (Scl-Ab) increases trabecular and cortical bone mass in animals by modeling-based bone formation. The increase in bone formation is, initially due to activation of bone lining cells, however the effect of Scl-Ab on osteoprogenitors (OPs) and the contribution of OPs to the increase in bone formation *in vivo* is unclear. In Sox9-creERT mice, shortly after tamoxifen administration, Rosa26-TdTomato reporter expression is observed in chondrocytes and perichondrial and endosteal cells and some cells in the primary spongiosa. After a prolonged chase, the TdTomato label is found in mature osteoblasts and adipocytes. We hypothesized that this system could be used to study the effects of anti-Sclerostin antibody on early cells of the osteoblast lineage *in vivo*. To investigate the early effects of Scl-Ab on OPs, 6-8 week old triple transgenic mice carrying Sox9-creERT; Rosa26-TdTomato reporter, and osteocalcin (Ocn)-GFP received a single dose of 2 mg tamoxifen. After 24h, Scl-Ab (100 mg/kg) or vehicle (Veh) was administered once weekly by subcutaneous injection. Mice were euthanized 3, 7 and 21d post-tamoxifen injection. Femurs were utilized for flow cytometry and tibiae were processed for histology. To quantify the rate of proliferation and apoptosis in osteoblast precursors, mice were injected with EdU, 6 hours before sacrifice or tomato+ cells were stained with Annexin V, respectively. Flow cytometry analysis showed a time dependent increase of TdTomato+ cells on day 3, 7 and 21. After 3d there were no TdTomato/GFP double-positive cells, suggesting that no TdTomato+ cell had differentiated into Ocn-GFP+ osteoblasts yet. After 7 and 21d, in Scl-Ab-treated mice, TdTomato+ cells were increased 3-fold compared with Veh. Assessment of tomato+ cells

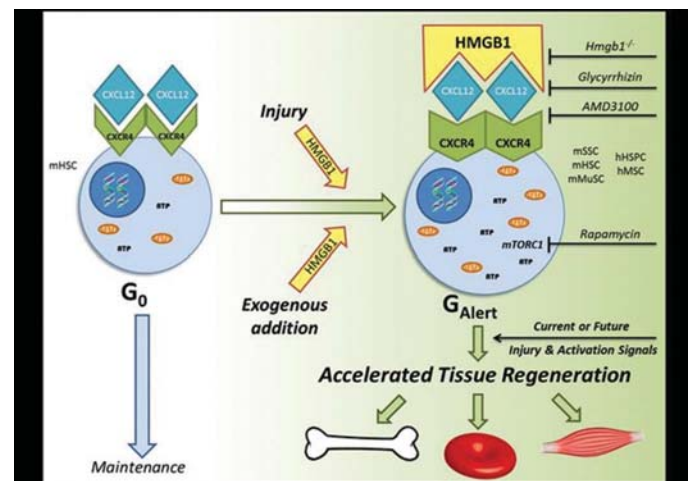
using epifluorescent/ confocal microscopy was consistent with the observations from flow cytometry. After 3w of antibody injections, tomato/GFP+ cells were increased 4-fold in Scl-Ab-treated mice compared with Veh and were distributed throughout the metaphyseal and diaphyseal regions. On day 7, Scl-Ab led to both increase in the rate of proliferation and suppression in the rate of apoptosis of tomato+ cells. These data suggest that administration of Scl-Ab significantly increases the number of tomato-positive cells in mice early in treatment by increasing proliferation and decreasing apoptosis. Over time, tomato+ cells become Ocn-GFP expressing osteoblasts contributing to the increased bone formation.

**Disclosures:** Sophia Trinh, None.

## 1143

**HMGB1 accelerates regeneration of multiple tissues by transitioning stem cells to G<sub>Alert</sub>.** Geoffrey Lee<sup>\*1</sup>, Ana Isabel Espirito Santo<sup>1</sup>, Stefan Zwingenberger<sup>2</sup>, Emilie Venereau<sup>3</sup>, Lawrence Cai<sup>4</sup>, Thomas Vogl<sup>5</sup>, Marc Feldmann<sup>1</sup>, Marco Bianchi<sup>6</sup>, Nicole Horwood<sup>1</sup>, James Chan<sup>1</sup>, Jagdeep Nanchahal<sup>1</sup>. <sup>1</sup>The Kennedy Institute of Rheumatology, University of Oxford, United Kingdom, <sup>2</sup>Department of Orthopaedics, University Hospital Carl Gustav Carus at Technische Universität Dresden, Germany, <sup>3</sup>Chromatin Dynamics Unit, Division of Genetics and Cell Biology, San Raffaele Scientific Institute, Italy, <sup>4</sup>Faculty of Medicine, UNSW Australia, Australia, <sup>5</sup>Institute of Immunology, University of Münster, Germany, <sup>6</sup>Chromatin Dynamics Unit, Division of Genetics and Cell Biology, San Raffaele University and Scientific Institute, Italy

Whilst stem cell therapy has been successful for some haematological disorders, considerable challenges remain for enhancing the repair of solid organs. Targeting endogenous cells overcomes many of the hurdles associated with exogenous stem cell therapy. Our objective was to identify the factor that transitions endogenous quiescent G<sub>0</sub> stem cells to an 'alert' phase thereby enhancing regeneration in multiple tissues, including bone, muscle and blood. Alarmins are endogenous molecules released upon tissue damage and are major triggers of the immune response. We hypothesised they may have a role in tissue repair, and found the alarmin HMGB1 accelerated tissue regeneration in various systems by transitioning particular stem cell types to G<sub>Alert</sub>. Alarmins were elevated post-fracture in both human and murine blood samples. *In vitro* screening of candidate alarmins with human bone marrow-derived mesenchymal stromal cells (MSCs) showed that in response to osteogenic media, only pre-treatment with the native fully reduced form of HMGB1 improved osteogenic differentiation. Next, using *in vivo* microCT and biomechanical analysis, we found that exogenous addition of HMGB1 accelerated fracture healing via the CXCL12-CXCR4 axis. To confirm our findings we generated conditional *Hmgb1*<sup>-/-</sup> mice and used small molecule inhibitors. Analysis of cell cycle kinetics, cell size, ATP levels, mitochondrial DNA, and mTORC1 dependency revealed this was due to HMGB1 transitioning the murine skeletal stem cell to G<sub>Alert</sub>. This effect also extended to murine muscle and haematopoietic stem cells, as well as human haematopoietic stem and progenitor cells and MSCs. HMGB1 also accelerated recovery in murine models when administered at the time, or 2 weeks before skeletal, muscle or haematopoietic injury. In summary, HMGB1 accelerates the regeneration of multiple tissues whose cells it transitions to G<sub>Alert</sub>, even if it is administered prior to injury, and only in response to injury. We have identified a novel physiologically dynamic and adaptive pathway, and therapeutic target, that accelerates the physiological regenerative response to current or future injuries, and could conceivably accelerate healing in any tissue that relies on repair from cells that express CXCR4 and can transition to G<sub>Alert</sub>. Moreover our findings highlight that the HMGB1-G<sub>Alert</sub> pathway has broad potential therapeutic applications, such as in trauma, chemotherapy, and elective surgery.



HMGB1-G(Alert) Graphical Abstract

**Disclosures:** Geoffrey Lee, None.



## 1144

**USP34 is required for BMP2 signaling and bone regeneration.** Mengyuan Wang\*, Shiwen Zhang, Yuchen Guo, Weiqing Liu, Yuan Wang, Liang Xie, Junjun Jing, Xuedong Zhou, Quan Yuan. State Key Laboratory of Oral diseases, West China Hospital of Stomatology, Sichuan University, Chengdu 610041, China., China

The Ubiquitin-specific protease 34 (USP34) is a member of deubiquitylases, which mediate the removal and processing of ubiquitin. Accumulating evidences indicate that the balance of protein ubiquitylation orchestrates many fundamental cellular processes. Our previous study showed that USP34 regulates the osteogenic differentiation of MSCs, however, the underlying mechanism is unclear.

To this end, we knocked down USP34 in human MSCs using siRNA and performed RNA-Sequencing after osteogenic induction. Depletion of USP34 increased the expression of 508 genes and decreased the expression of 391 genes. KEGG pathway analysis indicated that USP34 primarily regulated the expression of genes associated with TGF- $\beta$ /BMP signaling pathway. To verify this observation, we first performed BRE luciferase assay and revealed that knockdown of USP34 restricted BMP2-induced response. We then isolated the bone marrow MSCs from *Prx1-Cre;Usp34<sup>fl/fl</sup>* mice and stimulated with 100ng/ml BMP2. Both western blot and RT-qPCR revealed that deletion of *Usp34* significantly blunted the expression of Sp7 induced by BMP2. Meanwhile, the ALP activity and calcium mineralization were decreased after a prolonged BMP2 treatment. Next, we sought to investigate the *in vivo* function of USP34 in BMP2-induced bone formation by calvarial injection. Subcutaneous injection of BMP2 (twice daily for 5 days) onto the calvariae of *Prx1-Cre;Usp34<sup>fl/fl</sup>* mice induced markedly less bone than *Usp34<sup>fl/fl</sup>* littermate controls. Additionally, calvarial organ culture showed that BMP2 induced less sub-periosteal bone formation in *Prx1-Cre;Usp34<sup>fl/fl</sup>* calvariae. Since BMP2 activity is indispensable for the initiation of fracture healing, we performed mid-diaphyseal femur fractures. MicroCT and histological analyses showed significantly decreased trabecular bone formation in the marrow cavity of *Prx1-Cre;Usp34<sup>fl/fl</sup>* as compared to *Usp34<sup>fl/fl</sup>* controls. Furthermore, we sought to determine whether *Usp34* deficiency could have the same effect on bone regeneration of femoral cortical bone defects induced by drill hole injury. After a 2-week healing, the cortical gaps in *Usp34<sup>fl/fl</sup>* control mice were almost completely bridged, while those in *Prx1-Cre;Usp34<sup>fl/fl</sup>* were partially filled. The BMD and BV/TV of the mineralized callus of *Prx1-Cre;Usp34<sup>fl/fl</sup>* were significantly lower as compared to the control mice. In conclusion, our data demonstrated that USP34 is required for BMP2-induced response and bone regeneration.

**Disclosures:** Mengyuan Wang, None.

## 1145

**The CaSR Is A Critical Mediator of Chondrocyte Trans differentiation into Osteoblastic Lineage and Bone Fracture Repair in Mice.** Zhiqiang Cheng\*, Alfred Li, Fuqing Song, Jiali Wang, Xiaodong Liu, Amanda Herberger, Jenna Hwong, Dolores Shoback, Chia-Ling Tu, Wenhan Chang. UCSF, United States

Emerging evidence support direct transformation of chondrocytes into osteoblasts (OBs), namely chondro-to-osteo differentiation, in growth plate and bone fracture (Fx) callus. Previous studies of chondrocyte-specific calcium-sensing receptor (CaSR) knock-out (KO) mice confirmed non-redundant roles of the receptor in promoting chondrocyte terminal differentiation in growth plate and OB survival in bone. Here we defined the role of chondrocyte CaSR in mediating chondro-osseous differentiation and overall Fx repair by examining the impact of CaSR KO in calluses of mice subjected to unfixed tibial Fx. Adult tamoxifen(Tam)-induced cartilage-specific CaSR KO mice and control (Cont) littermates were subjected to 5 daily injections of Tam starting one day before Fx to induce CaSR gene KO or serve as Cont, respectively. Their cartilaginous and bony calluses were analyzed at day 10 and 28 post-Fx by  $\mu$ CT and histomorphometry for skeletal parameters; fluorescent tdTomato-labeling cell-tracking for the chondro-osseous differentiation; and histology for apoptosis. At day 10 post-Fx, the sizes of KO calluses were significantly increased by  $\approx 50\%$  vs Cont by  $\mu$ CT and histomorphometry (see Table; TV), along with an increase ( $\approx 50\%$ ) in total cartilage fraction (CV/TV) and a decrease ( $\approx 40\%$ ) in the ratio of mineralized cartilage volume over CV (MCV/CV), indicating delayed terminal differentiation and reduced mineralizing function in CaSR-deficient chondrocytes. As a result, we observed significant reductions in bone fraction (BV/TV), thickness (Th), and mineral density (BMD) in the KO vs Cont calluses during the osteogenic phase of repair at day 28 post-Fx. For cell tracing experiments, the KO and Cont mice were bred with mice carrying Rosa26-tdTomato alleles, which were activated in chondrocytes at day 4-6, along with gene KO, by 3 daily Tam injections. At day 10 post-Fx, we observed robust tdTomato signals in chondrocytes in soft calluses and growth plates of KO and Cont mice. In support of chondro-osseous differentiation, we observed substantial numbers (see Table) of tdTomato-positive OBs in bony calluses of Cont mice at day 28 post-Fx. However, the numbers of tdTomato-labeled OBs were significantly reduced by 75%, along with increased apoptotic cell number, in KO vs Cont calluses. Together, our data support a critical role for the CaSR in mediating chondro-osseous differentiation of chondrocytes, survival of the resulting OBs, and overall bone Fx repair.

10 d	uCT			Histomorphometry		
	TV mm3	BV/TV %	BMD mg/cm3	TV mm3	CV/TV %	MCV/CV %
Cont	7.7 $\pm$ 2.4	14.3 $\pm$ 2.1	665 $\pm$ 20	4.1 $\pm$ 0.8	30.6 $\pm$ 5.2	46.9 $\pm$ 7.5
KO	11.8 $\pm$ 4.8*	15.9 $\pm$ 5.0	675 $\pm$ 16	6.0 $\pm$ 1.8*	46.5 $\pm$ 14.4*	26.7 $\pm$ 8.8*

28 d	BV/TV %	Tb.Th um	BMD mg/cm3	21 d	
				Cont	tdTomato (+) OB #
Cont	51.3 $\pm$ 6.2	129 $\pm$ 19	1052 $\pm$ 20		141 $\pm$ 41
KO	44.4 $\pm$ 9.2*	108 $\pm$ 22*	1023 $\pm$ 33*	KO	39 $\pm$ 14*

\*p<0.05 vs Control

Table

**Disclosures:** Zhiqiang Cheng, None.

## 1146

**Osteoprogenitor directed overexpression of Notch signaling improves bone fracture healing.** Sanja Novak\*, Emilie Roeder, Brya G Matthews, Liping Wang, Douglas J Adams, Ivo Kalaic. Uconn Health, United States

Notch signaling is a key player in osteogenic differentiation and bone healing. We hypothesize that an increase in Notch signaling could regulate the expansion, migration and differentiation of mesenchymal progenitor cells to modulate the fracture healing process. We utilized an inducible mouse model to overexpress the Notch1 intracellular domain (NICD1) in osteoprogenitor cells using  $\alpha$ SMACreERT2 transgenic mice ( $\alpha$ SMACreERT2/Rosa-NICD1) during fracture healing.

The effects of NICD1 overexpression on fracture healing were assessed in male 8-9-week-old mice. Closed femoral fractures with internal fixation were generated in both experimental mice, and Cre-littermate controls, and Cre activity was induced by tamoxifen injections (days 0, 2, 4 post-fracture). Increased Notch signaling was confirmed by increased expression of Hes1 and Hey1 mRNA in the callus of  $\alpha$ SMACre<sup>+</sup>NICD1 mice seven days post fracture and in isolated periosteal progenitor cell (PPC) culture. PPCs overexpressing NICD1 had increased proliferation and migration compared to controls. Notch overexpression reduced osteogenic differentiation, evidenced by reduced von Kossa staining and lower expression of osteocalcin and bone sialoprotein.

Furthermore, we completed *in vivo* evaluation of healing parameters including assessing cartilage and bone volume histologically 7, 10 and 14 days after fracture. Mice with targeted NICD1 overexpression showed increased mineralized content 14 days after fracture than the control mice (p<0.01).

MicroCT analysis collected three weeks post-fracture demonstrated that the overexpression of NICD1 increased callus bone mass (p<0.05) with no changes in callus volume. Torsion testing showed increased strength and stiffness (p<0.001) in the callus 3 weeks post fracture in mice overexpressing NICD1. The  $\alpha$ SMACre<sup>+</sup>NICD1 mice also had increased bone strength and stiffness of the contralateral intact femur compared to controls (p<0.05) suggestive of the positive effects of the Notch overexpression on bone remodeling.

This is the first study showing that increased Notch signalling following fracture has an anabolic function and leads to increased bone mass and improves biomechanical properties of the fractured femur. Modulating Notch signaling could ultimately lead to development of therapies that could improve bone healing process and may be beneficial to the patients with osteoporosis.

**Disclosures:** Sanja Novak, None.

## 1147

**Static Preloading: A Previously Unrecognized Inhibitor of Bone Anabolism.** Sundar Srinivasan\*, Danica Balsiger, Philippe Huber, Brandon Ausk, Steven Bain, Edith Gardiner, Ted Gross. University of Washington, United States

It is well recognized that dynamic loading serves as an anabolic stimulus for bone while static loading alone is either ignored or is catabolic. However, dynamic lower limb loading during human exercise is achieved in the context of static loading (e.g., standing between exercise repetitions). Further, all animal models of skeletal loading utilize static preloading (SPL: a constant static load upon which dynamic loading is superimposed) in order to enable stable dynamic loading. The magnitude of SPL that has been implemented *in vivo* varies widely, even for the same model. For example, in the predominant model used to study trabecular bone adaptation (i.e., murine tibia axial compression), the SPLs typically range from -0.5 to -2.0 N, which are substantially larger than the forces encountered during normal ambulation (-0.1 N). Interestingly, the literature also suggests that the lower the SPL, the smaller the dynamic loading magnitude required to induce an anabolic response. We therefore hypothesized that SPL mitigates bone anabolism induced by dynamic mechanical loading. We tested this hypothesis in a newly developed mouse model that enables stable off-axial dynamic loading of the murine tibia but can be utilized with SPLs as small as 0.01 N (Fig 1a). The right tibiae of adult female BALB/c mice (4 Mo) were subjected to dynamic loading (-3.5 N, 50 c/d, 10 s rest, 3 d/wk, 3 wk) superimposed upon either a -0.05, -0.5 or -1.5 N SPL (n = 6, 4, and 8/grp, respectively). Mice were calcein labeled (d 10, 19) and sacrificed at d 22. The morphology of the proximal tibia metaphysis of loaded and contralateral tibia were assessed by mCT (SCANCO VivaCT 40), and bone formation at the mid-shaft by dynamic histomorphometry. We found that the dynamic loading regimen, when superimposed on a very small SPL (-0.05 N), increased trabecular BV/TV and mid-shaft p.BFR vs contralateral tibiae. In contrast, increasing the SPL to -0.5 N mitigated this

anabolic response. Further, we found that a -1.5 N SPL was catabolic for trabecular bone and significantly reduced  $rp.BFR$  (vs -0.05 N SPL; Fig 1b, c). While preliminary, these data suggest that SPLs are a previously unrecognized, but critical inhibitor of bone's anabolic response to dynamic loading. We believe that this ubiquitous aspect of activity based loading may underlie, in part, why skeletal loading regimens have sometimes produced equivocal results in both pre-clinical models and human exercise trials.

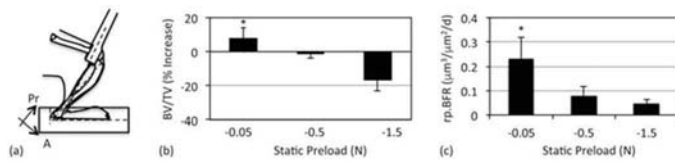


Fig 1: Static preloading mitigates bone response to dynamic loading. With the right foot placed in a heel restraining footbed and the right hind limb oriented as during the heel-strike phase of walking, controlled loads were applied to the distal femur, thereby placing the tibia-fibula in off-axial loading (a). SPL of -0.05 N resulted in increased metaphyseal BV/TV (b) and  $rp.BFR$  at the tibia mid-shaft (c); \*  $p < 0.05$  vs -1.5 N SPL.

Figure 1

Disclosures: Sundar Srinivasan, None.

## 1148

**Mx1-labeled Tendon Stem/Progenitor Cells in Paratenon Contribute to Tendon Regeneration and Repair in vivo.** Yannis Hara\*, Hamilton Wang, Brendan Lee, Dongsu Park. Department of Molecular Human Genetics, United States

Tendon and ligament injuries are the most common types of sports injuries, but slow and incomplete recovery of damaged tissues remains a major clinical challenge. In particular, the in vivo origin of tendon repairing cells and the underlying mechanism involved in their activation and differentiation are essentially unknown. We have recently developed a new method to track endogenous tendon cells and their stem/progenitor cells during tendon repair in living animals. Using intravital imaging techniques in combination with a newly developed dual reporter lineage-tracing animal model (Mx1-Cre; Rosa-Tomato; Scleraxis-GFP), we defined that interferon-inducible Mx1 promoter (a known skeletal stem cell marker) can label a subset of Scleraxis-GFP+ tendon cells and paratenon cells where the endogenous tendon stem/progenitor cells are present. Further, immunohistochemical and fluorescence-activated cell sorting (FACS) analysis showed Mx1-labeled paratenon cells (tomato+) are distinct from Scleraxis-GFP+ tendon cells and specifically express stem cell markers, such as CD105, CD146 and CD200. Sequential in vivo imaging of patella tendon injury revealed that Mx1-labeled paratenon cells rapidly appear at damaged sites during the first few days after injury. Subsequently, they proliferate and differentiate into Sox-GFP expressing tendon cells. When sort Mx1-labeled paratenon cells, transplant into wild-type tendon injury, and track them by intravital imaging, we found that Mx1-labeled cells successfully engraft, proliferate and contribute to tendon healing. Complementary in vitro studies show that this population differentiates by treatment with TGFβ. Taken together, our data indicate that tissue-resident tendon progenitor cells are abundant in the paratenon layer and can be labeled with Mx1 expression. These Mx1-labeled tendon progenitors represent a major source of new tendon cells and contribute to tendon regeneration after injury.

Disclosures: Yannis Hara, None.

## 1149

**Extracellular Vesicle-Mediated Cell-Cell Communication in Bone and Potential Role in Muscle-Bone Crosstalk.** Kun Wang\*, LeAnn Tiede-Lewis<sup>1</sup>, Lora McCormick<sup>1</sup>, Nuria Lara<sup>1</sup>, Andrew Keightley<sup>1</sup>, Nicholas Farina<sup>2</sup>, Jian Huang<sup>3</sup>, Jane Lian<sup>2</sup>, Marco Brotto<sup>3</sup>, Lynda Bonewald<sup>4</sup>, Sarah Dallas<sup>1</sup>. <sup>1</sup>University of Missouri, Kansas City, United States, <sup>2</sup>University of Vermont, United States, <sup>3</sup>University of Texas at Arlington, United States, <sup>4</sup>Indiana University, United States

A recent paradigm in cell-cell communication involves cell shedding of extracellular vesicles (EV) that deliver a cargo of proteins, mRNAs and miRNAs to target cells, altering their function. Using mice expressing a membrane-targeted GFP in osteocytes, we previously showed that embedding osteocytes shed EV and that osteocytes may release EV into the circulation. EV from late differentiated IDG-SW3 osteocyte-like cells (SW3) stimulated osteoblast-to-osteocyte differentiation and their composition was altered by PTH. To further characterize the osteocyte EV cargo, determine if hormones such as PTH can modify EV and their function and determine if EV play a role in muscle-bone signaling crosstalk, multiple approaches were used.

Western blotting and proteomic analysis of EV from late SW3 cells revealed an EV proteome of >800 proteins that was enriched for known EV markers and contained osteocyte markers E11, PHEX, sclerostin & RANKL and proteins involved with membrane fusion/exocytosis, motility/neurite outgrowth, mineralization and ECM assembly. Profiling of miRNAs (Affymetrix 4.0) in control and PTH-treated SW3 cells identified >500 miRNAs in the EV and >650 in the cell layer with 105 miRNAs increased in PTH vs. control EV. Principal component analysis showed differential miRNA partitioning between the EV and cell layer. Application of EV from PTH treated SW3 cells downregulated SOST expression in "naïve" cells that were not exposed

to PTH, suggesting the ability of EV to propagate PTH responses to other cells. Intravital imaging of osteocytes and vasculature in Dmp1-memGFP mice showed osteocytes extending dendrites towards blood vessels and releasing EV near the lumen, supporting our prior observations of osteocyte EV in the circulation and suggesting their potential to affect distant organs. The potential role of EV in muscle-bone crosstalk, was next examined. Live cell imaging showed EV release by C2C12 myogenic cells, with C2C12 myoblasts releasing 2-fold more EV than C2C12 myotubes. Treatment with C2C12 myotube but not myoblast EV increased Wnt/β-catenin signaling in MLO-Y4 cells, which has a known role in maintaining osteocyte viability. Confocal microscopy showed internalization of C2C12 EVs by MLO-Y4 cells, which altered their gene expression and conferred expression of muscle related mRNAs MyHC, MyoG, & MyoD. These data support an important role for osteocyte EV in regulation of bone cell function and suggest a role for EV in muscle-bone crosstalk.

Disclosures: Kun Wang, None.

## 1150

**Glutaminase is necessary for the maintenance and specification of mesenchymal stem cells.** Yilin Yu\*, Leyao Shen<sup>1</sup>, Fanxin Long<sup>2</sup>, Courtney Karner<sup>3</sup>. <sup>1</sup>Department of Orthopedic Surgery, Duke University, United States, <sup>2</sup>Department of Orthopedic Surgery, Washington University School of Medicine, United States, <sup>3</sup>Departments of Orthopedic Surgery and Cell Biology, Duke University, United States

Mesenchymal stem cells (MSC) are thought to provide a continuous supply of mature osteoblasts throughout life. However, under certain conditions, the MSC population can become incorrectly specified or is not maintained, resulting in reduced osteoblast formation, bone mass, and in severe cases osteoporosis. Recent work has focused on defining cell markers of the MSC population, however little is known about the molecular mechanisms regulating MSC maintenance or specification. Glutamine metabolism has emerged as a critical regulator of many cellular processes in diverse systems. In addition to direct incorporation in polypeptide chains, glutamine is an important oxidative fuel, a precursor of non-essential amino acids, nucleotides, and glutathione. The enzyme glutaminase (GLS) catalyzes the deamination of glutamine to form glutamate, the rate-limiting first step in glutamine metabolism. Here we demonstrate GLS is required for the maintenance and differentiation of bone marrow MSCs. Genetic deletion of a conditional (floxed) *Glsl* allele (*Glsl<sup>flp</sup>*) in bone marrow MSCs using either *Prx1Cre* or *LeprCre* significantly reduces bone mass in vivo due to decreased osteoblast numbers and bone formation. Colony forming unit assays demonstrate that osteoblast depletion is due to a significant reduction of MSCs in the bone marrow as well as altered specification of MSCs favoring the adipocyte lineage. Conversely, *Glsl* deletion in specified preosteoblasts using *Sp7Cre*, resulted in reduced bone mass due to diminished bone formation with no effect on MSCs or osteoblast numbers. In contrast, *Glsl* ablation in mature osteoblasts using either *Col1 (2.3kb) Cre* or *BglapCre* had no effect on bone mass, MSCs, osteoblast numbers or bone formation. Importantly, GLS activity declines with age in wild type mice and significantly correlates with depletion of bone marrow MSCs and reduced bone mass observed with aging. Collectively, these data illustrate a biphasic role for GLS and glutamine metabolism during osteoblast differentiation. First, GLS is required for the normal maintenance and osteoblast specification of MSCs. Later, GLS acts in specified osteoblasts to promote differentiation and bone formation while being dispensable in mature osteoblasts. Thus, stimulating GLS activity may provide a valuable therapeutic approach to maintain and expand bone marrow MSCs in aged individuals and enhance osteoblast specification and activity to repair or regenerate bone in many human bone diseases.

Disclosures: Yilin Yu, None.

## 1151

**The identification of TGFβ-induced osteoclast factors that couple bone resorption to bone formation.** Megan Weivoda\*, Ming Ruan<sup>1</sup>, Christine Hachfeld<sup>1</sup>, Glenda Evans<sup>1</sup>, Stephanie Youssef<sup>1</sup>, Rachel Davey<sup>2</sup>, Jeffrey Zajac<sup>2</sup>, Brendan Lee<sup>3</sup>, Jennifer Westendorf<sup>1</sup>, David Monroe<sup>1</sup>, Sundeep Khosla<sup>1</sup>, Merry Jo Oursler<sup>1</sup>. <sup>1</sup>Mayo Clinic, United States, <sup>2</sup>University of Melbourne, Australia, <sup>3</sup>Baylor, United States

Matrix-embedded TGFβ is released and activated by osteoclasts and contributes to the coupling of bone resorption to bone formation. These processes are uncoupled in mice with impaired osteoclast TGFβ signaling (*Tgfr2<sup>ocKO</sup>*) suggesting that TGFβ promotes coupling in part through the induction of osteoclast derived "coupling factors". To identify TGFβ-induced coupling factors we performed RNA-Seq of mature osteoclasts treated with vehicle or 1ng/mL TGFβ; we then evaluated candidate coupling factor target gene expression in freshly isolated bone marrow mesenchymal progenitors (MPs) from WT or *Tgfr2<sup>ocKO</sup>* mice. RNA-Seq revealed that *Wnt1* and *Wnt7b* were the most highly upregulated secreted factors in response to TGFβ (51 and 125 fold, respectively). Other significantly upregulated factors included *Wnt10b*, *Osm*, *Ephb2*, *Notch4*, *Ngf*, *Il10*, and *Bmp1*. Evaluation of *Tgfr2<sup>ocKO</sup>* MP gene expression showed a significant increase in osteoblast genes *Bsp*, *Colla1*, *Colla2*, *Osx*, and *Ocn*. Together with published data showing decreased osteoblast number in *Tgfr2<sup>ocKO</sup>* mice, this suggests that impaired osteoclast TGFβ signaling prevents osteoblast differentiation, leading to increased bone marrow osteoblast progenitors. Consistent with TGFβ inducing osteoclast Wnt expression, *Tgfr2<sup>ocKO</sup>* MPs exhibited reduced canonical Wnt target gene expression (*Lef1*, *Postn*, *Fra1*, *Opg*). In addition, Notch (*Lfng*, *Hey1*) and



Ngf (*Ier3*, *Cxcr4*, *Egr2*) target genes were significantly reduced. Because mutations to Wnt1 cause low bone mass in humans and Wnt1 is the second most highly upregulated TGF $\beta$ -induced secreted factor, we investigated the effect of osteoclast-specific Wnt1 deletion on bone (*CtskCre; Wnt1<sup>fl/f</sup>*). 22 week female Wnt1<sup>OcKO</sup> femurs exhibited significantly reduced BV/TV with reduced Conn.D and increased SMI, and histomorphometry revealed significantly reduced BFR/TV and a trend for reduced osteoblast number (n=6). Similar to Tgfb<sup>OcKO</sup> MPs, MPs isolated from the Wnt1<sup>OcKO</sup> showed increased expression of osteoblast genes (*Osx*, *Ocn*), along with reduced canonical Wnt target gene expression (*Ccn1*, *Lef1*, *Postn*, *Fra1*). In contrast, Wnt1<sup>OcKO</sup> MPs exhibited increased TGF $\beta$  and Notch target gene expression. These data are consistent with a paradigm in which TGF $\beta$  induces Wnt expression by osteoclasts in order to couple bone resorption to bone formation. Furthermore, additional factors secreted by osteoclasts are disrupted in Tgfb<sup>OcKO</sup> and may contribute to the more severe uncoupling in these mice.

**Disclosures:** Megan Weivoda, None.

## 1152

**Deletion of Androgen Receptor in Neurons Accelerates the Age-Related Loss of Cortical Thickness in Male Mice.** Ferran Jordi<sup>\*1</sup>, Michael Laurent<sup>2</sup>, Rougin Khalil<sup>1</sup>, Nari Kim<sup>1</sup>, Vanessa Dubois<sup>3</sup>, Ludo Deboel<sup>1</sup>, Dieter Schollaert<sup>1</sup>, Geert Carmeliet<sup>1</sup>, Brigitte Becallonne<sup>1</sup>, Frank Claessens<sup>1</sup>, Dirk Vanderschueren<sup>1</sup>. <sup>1</sup>KU Leuven, Belgium, <sup>2</sup>UZ Leuven, Belgium, <sup>3</sup>inserm, France

The central nervous system (CNS) modulates bone metabolism and is a target for sex steroid actions. Previous findings reveal that central estrogenic signaling in female mice inhibits bone mass. A similar CNS-mediated action on male bone has not been proved so far for the androgen receptor (AR). To this end, we knocked out AR in the nervous system of AR floxed male mice expressing a tamoxifen-inducible CreER under the control of the neuronal promoter Thy. Both 6-week-old neuronal-ARKO (N-ARKO) and littermate control mice were gavaged with tamoxifen (190 mg/kg) for 2 days. Tamoxifen but not vehicle induced a substantial loss of AR mRNA levels in Thy1-CreER-positive regions (cerebral cortex:~80%; hippocampus:~90%; brainstem:~75%) but not in the hypothalamus (Thy-CreER-negative) of N-ARKO mice. Expression of non-neuronal AR (tibia and muscle) remained unaffected. Body weight, serum leptin and tibia length were unaltered in 36-week-old male N-ARKO mice. However, microCT analysis of tibia and femur revealed a significant reduction (~6%) in both cortical thickness and area of N-ARKO mice. Regarding trabecular bone, N-ARKO mice showed a diminished trabecular thickness in both long bones as well as in L5 vertebra. The skeletal effects of neuronal ARKO were not observed in young adult male mice (16 weeks) and were not due to a decreased physical activity behavior, as assessed by voluntary wheel running. Despite serum T levels were comparable between genotypes, N-ARKO mice displayed a 40% increase in the weight of seminal vesicles (SV), which is a well-established bio-indicator of androgenic activity. To discard a role for an altered gonadal axis in the phenotype of N-ARKO mice, we repeated the previous experimental design but performing orchiectomy (ORX) and replacement with dihydrotestosterone (DHT) at 16 weeks of age. As in our previous experiment, ORX+DHT-treated N-ARKO mice displayed a significant reduction in cortical thickness compared to controls at 36 weeks. Unexpectedly, the SV weight of N-ARKO mice still showed a 20% increase vs. controls, thereby suggesting a role for central AR in the regulation of male reproductive accessory glands. To summarize, the selective inactivation of neuronal AR accelerates the loss of cortical thickness associated to ageing in male mice. We provide evidence for the first time that androgens act via the CNS to maintain cortical bone integrity.

**Disclosures:** Ferran Jordi, None.

## 1153

**The Epigenetic Regulator CXXC Finger Protein 1 is Required for Mesenchymal Progenitor Cell Function and Skeletogenesis.** Diana Carlone<sup>\*1</sup>, Lijie Jiang<sup>1</sup>, David Skalnik<sup>2</sup>, Ernesto Canalis<sup>3</sup>, David Breault<sup>1</sup>. <sup>1</sup>Boston Children's Hospital, United States, <sup>2</sup>IUPUI School of Science, United States, <sup>3</sup>UConn Health, United States

Skeletal development, remodeling and regeneration are dependent on the activity of mesenchymal progenitor cells (MPCs). Recent data have implicated epigenetics in the regulation of MPC function with links to altered bone formation in both mice and humans. Precisely how epigenetics controls MPC activity and function, including the ability of MPCs to participate in bone formation, remains less clear. Here, we investigate the role of CXXC finger protein 1 (Cfp1), a component of the Setd1 histone methyltransferase complex and a critical epigenetic regulator of histone and cytosine methylation. Previously, we showed that Cfp1 is required for progenitor/stem cell proliferation and differentiation in other tissues, though its mechanism(s) of action have not been established. To investigate its role in MPC action, we over-expressed Cfp1 in the murine mesenchymal progenitor cell line, ST-2. Increased cell growth and survival was observed in the presence of excess Cfp1 as compared to controls. However, these cells exhibited reduced osteogenic and adipogenic differentiation. Further analysis revealed a 40-60% decrease in bone morphogenetic protein (BMP)-2/Smad signaling in Cfp1 over-expressing cells via activation of ERK/Mapk mediated Smad4 inhibitory phosphorylation, implicating this factor as an important upstream regulator of signaling pathways critical for proper MPC self-renewal and differentiation. To determine whether Cfp1 is required for MPC contribution to the skeleton in vivo, we next conditionally deleted Cfp1 from MPCs during mouse development using Prx1-Cre. Conditional knockout (cKO) mice died shortly after birth and displayed a complete

lack of forelimbs, implying a profound defect in MPC function. Hindlimbs developed but were severely stunted, suggesting Cfp1 acts in a limb-specific manner to regulate MPCs during skeletogenesis. Further analysis of cKO hindlimbs revealed an abnormal growth plate with reduced proliferation and accelerated hypertrophy as well as defects in digit number, ossification and joint formation. Together, these data show Cfp1 is an essential regulator of skeletal patterning and bone formation, through augmentation of cellular signaling, such as the BMP pathway, to control progenitor cell maintenance and differentiation. Further, the limb-specific impact of Cfp1 deficiency highlights the intricate nature of the epigenetic regulatory network on mammalian development.

**Disclosures:** Diana Carlone, None.

## 1154

**Burosumab (KRN23), a Fully Human Anti-FGF23 Monoclonal Antibody for X-linked Hypophosphatemia (XLH): Final 64-Week Results of a Randomized, Open-label Phase 2 Study of 52 Children.** Michael Whyte<sup>\*1</sup>, Anthony Portale<sup>2</sup>, Erik Imel<sup>3</sup>, Annemieke Boot<sup>4</sup>, Wolfgang Högl<sup>5</sup>, Agnès Linglart<sup>6</sup>, Raja Padidela<sup>7</sup>, William van't Hoff<sup>8</sup>, Meng Mao<sup>9</sup>, Alison Skrinar<sup>10</sup>, Emil Kakkis<sup>10</sup>, Javier San Martin<sup>10</sup>, Thomas Carpenter<sup>11</sup>. <sup>1</sup>Shriners Hospital for Children, United States, <sup>2</sup>UCSF School of Medicine, United States, <sup>3</sup>Indiana University School of Medicine, United States, <sup>4</sup>University of Groningen, Netherlands, <sup>5</sup>Birmingham Children's Hospital, United Kingdom, <sup>6</sup>Hôpital Bicêtre, France, <sup>7</sup>Royal Manchester Children's Hospital, United Kingdom, <sup>8</sup>Great Ormond Street Hospital, United Kingdom, <sup>9</sup>Ultragenyx Pharmaceutical Inc., United States, <sup>10</sup>Ultragenyx Pharmaceutical Inc, United States, <sup>11</sup>Yale University School of Medicine, United States

In children with XLH, FGF23-mediated hypophosphatemia impairs skeletal mineralization and causes rickets. Investigational product burosumab (KRN23) binds to, and inhibits, circulating FGF23. In our Phase 2 study, 52 children with XLH (ages 5-12 years,  $\leq$  Tanner 2, at baseline [BL]) were randomized to receive burosumab biweekly (Q2W) or monthly (Q4W) by SC injection titrated (maximum 2 mg/kg) to achieve age-appropriate fasting serum phosphate (Pi) concentrations. Radiographs of wrists and knees were assessed by: i) the Thacher Rickets Severity Score (RSS) based on the degree of metaphyseal and growth plate abnormalities, and ii) the Radiographic Global Impression of Change based on a 7 point scale (RGI-C; -3= severe worsening; +2= substantial healing; +3= complete healing). In this first trial of burosumab in children with XLH, all participants have reached the Week 64 endpoint.

Rachitic disease was evident at BL (mean [SD] RSS 1.8 [1.1]) despite prior treatment with oral Pi/active vitamin D for a mean of ~7 years before enrollment. Fasting serum Pi increased in all subjects from BL (mean [SD]: 2.33 [0.356] mg/dL) to normal levels (3.16 [0.432] mg/dL; mean increase 0.84 [0.46] mg/dL;  $p < 0.0001$ ; normal range: 3.2 to 6.1 mg/dL), and was more stable with Q2W dosing. Neither hyperphosphatemia nor hypercalcemia occurred in any child. Serum alkaline phosphatase decreased by a mean of 98 (76) U/L ( $p < 0.0001$ ). RSS scores improved in both Q2W and Q4W groups and overall (Table), with greater improvement observed in children with more severe rickets at BL (RSS  $\geq 1.5$ , n=34). RGI-C indicated improved rickets in all groups. Substantial healing (RGI-C  $\geq +2$ ) occurred in most children with RSS  $\geq 1.5$  treated Q2W (82.4%; n=17) and Q4W (70.6%; n=17) (Table). Growth velocity increased from 5.35 cm/year in the 2 years before BL to 5.91 cm/year ( $p=0.0376$ ). Mean standing height Z score increased from -1.89 (1.0) at BL to -1.73 (1.0) (mean change: +0.15 [0.30],  $p < 0.0001$ ). Most treatment-related adverse events (AEs) were mild with transient injection site reactions (37%) being most common. One child experienced a serious AE (hospitalization for fever/muscle pain that resolved in a day) and continues in the extension study. No clinically meaningful changes occurred in serum or urine Ca and serum iPTH levels. Burosumab, a novel treatment that inhibits the biological activity of FGF23, improved serum phosphorus and rickets and was generally safe and well tolerated in children with XLH.

**Table. Rickets (Assessed by RSS and RGI-C) in Children with XLH After 64 Weeks of Burosumab Treatment**

	Q2W	Q4W	Overall
<b>RSS Total Score</b>			
Overall <sup>a</sup>			
Baseline, mean (SD)	1.92 (1.172)	1.67 (0.999)	1.80 (1.086)
Week 64, mean (SD)	0.81 (0.601)	0.94 (0.516)	0.88 (0.559)
LS mean change <sup>b</sup>	-1.00 (p<0.0001)	-0.84 (p<0.0001)	-0.92 (p<0.0001)
Higher RSS Subgroup (RSS ≥1.5) <sup>c</sup>			
Baseline, mean (SD)	2.62 (0.781)	2.29 (0.561)	2.46 (0.689)
Week 64, mean (SD)	1.00 (0.559)	1.03 (0.572)	1.01 (0.557)
LS mean change <sup>b</sup>	-1.44 (p<0.0001)	-1.44 (p<0.0001)	-1.44 (p<0.0001)
<b>RGI-C Global Score</b>			
Overall <sup>a</sup> , mean (SD)	+1.62 (0.809)	+1.53 (0.761)	+1.57 (0.779)
p value <sup>b</sup>	p<0.0001	p<0.0001	p<0.0001
Higher RSS Subgroup (RSS ≥1.5 <sup>c</sup> , mean (SD)	+2.08 (0.323)	+1.88 (0.456)	+1.98 (0.402)
p value <sup>b</sup>	p<0.0001	p<0.0001	p<0.0001
<b>Substantial Healing by RGI-C<sup>d</sup></b>			
Overall <sup>a</sup>	57.7% (15/26)	50.0% (13/26)	53.8% (28/52)
Higher RSS subgroup (RSS ≥1.5) <sup>c</sup>	82.4% (14/17)	70.6% (12/17)	76.5% (26/34)

Note: Negative change in RSS score indicates reduced rickets severity; positive RGI-C score indicates improvement of rickets. <sup>a</sup>Q2W, N = 26; Q4W, N = 26; Overall, N = 52. <sup>b</sup>Least squares (LS) mean, LS mean change, and p value per generalized estimation equation models, which included visit, regimen, visit by regimen as factors, and RSS total score at baseline as a covariate, with exchangeable covariance structure. <sup>c</sup>Q2W, N = 17; Q4W, N = 17; Overall, N = 34. <sup>d</sup>Percent (n/N) with RGI-C global score ≥ +2.

Table

Disclosures: Michael Whyte, Ultragenyx Pharmaceutical Inc., Grant/Research Support.

## 1155

**The Fracture, Osteoporosis, and CT Utilization Study (FOCUS) — Utilizing Pre-existing CT to Assess Risk of Hip Fracture in a Large Real-world Clinical Setting.** Annette Adams<sup>1</sup>, Heidi Fischer<sup>1</sup>, David Kopperdahl<sup>2</sup>, David Lee<sup>2</sup>, Dennis Black<sup>3</sup>, Mary Bouxsein<sup>4</sup>, Shireen Fatemi<sup>5</sup>, Sundeeep Khosla<sup>6</sup>, Eric Orwoll<sup>7</sup>, Ethel Siris<sup>8</sup>, Tony Keaveny<sup>2</sup>. <sup>1</sup>Department of Research & Evaluation, Kaiser Permanente Southern California, United States, <sup>2</sup>O.N. Diagnostics, LLC, United States, <sup>3</sup>Department of Epidemiology and Biostatistics, University of California San Francisco, United States, <sup>4</sup>Center for Advanced Orthopedic Studies, Beth Israel Deaconess Medical Center & Harvard Medical School, Endocrine Unit, Massachusetts General Hospital, United States, <sup>5</sup>Endocrinology, Southern California Permanente Medical Group, United States, <sup>6</sup>Mayo Clinic, United States, <sup>7</sup>Oregon Health & Science University, United States, <sup>8</sup>New York-Presbyterian Hospital, United States

Analysis of pre-existing clinical computed tomography (CT) hip scans to measure both DXA-equivalent BMD and finite element analysis-derived bone strength — termed here “biomechanical CT analysis” (BCT) — could potentially increase the number of people identified at high risk of hip fracture. Here, we evaluated the validity of this approach in a large real-world clinical setting, using a case-cohort analysis of pre-existing de-identified medical-record data, having new hip fractures as the outcome. Our full cohort included 111,694 patients aged ≥ 65 from 11 Kaiser Permanente Southern California (KPSC) hospitals, who had an abdominal or pelvic CT between 01/01/2006 and 12/31/2014, no fragility hip fracture before the CT, and a DXA within three years of the CT. The case-cohort included a sex-stratified randomly sampled subcohort and all cases with available medical-record data; from this, we defined the cases as those with a first hip fracture through 09/30/2015 (1340 women, 619 men) and the controls as a randomly selected approximately equal number without hip fracture; about 60% of the cohort was confirmed treatment-naïve for osteoporosis. Scans were de-identified at KPSC, sent to O.N. Diagnostics for BCT analysis using the VirtuOst software (blinded to fracture status), and results returned to KPSC for statistical analysis. Scans for 82% of the cohort provided BCT data. Sex-stratified weighted Cox proportional hazards analyses indicated that hip BMD and femoral strength from BCT were strongly associated with hip fracture, particularly for treatment-naïve patients (Table 1). As expected, the hazard ratios for DXA- and BCT-based hip BMD were similar, whereas the hazard ratios for both BCT measurements were higher than for clinical (hip/spine) DXA, significantly so for the women. For BCT, using established thresholds for osteoporosis (BMD T-score ≤ -2.5) and fragile bone strength (strength ≤ 3000 N women; ≤ 3500 N men), sensitivity for 5-year hip fracture for the treatment-naïve patients increased by 22% (0.55 to 0.67) and 26% (0.43 to 0.54) for the women and men, respectively, when bone strength was added to BMD (specificity decreased by 8–9%), reflecting fracturing patients with fragile bone strength who did not have BMD-defined osteoporosis. Taken together, these results demonstrate that in real-world practice, BCT analysis of routine clinical hip CT scans can be used to identify patients at high risk of hip fracture, including some without osteoporosis.

**Bone Strength and DXA-equivalent BMD for BCT.** Age- and race-adjusted Hazards Ratio (full cohort and only treatment-naïve patients); DXA BMD also shown.

	WOMEN			MEN		
	N	HR	95% CI	N	HR	95% CI
<b>BCT:</b>						
Hip BMD T-score	2157	2.18	(1.87–2.54)	967	3.12	(2.35–4.14)
Femoral Strength	2157	2.76	(2.25–3.39)	967	2.84	(2.20–3.66)
<b>Treatment-naïve patients:</b>						
Hip BMD T-score	1082	2.72	(2.24–3.32)	534	3.93	(2.46–6.26)
Femoral Strength	1082	3.81	(2.90–5.01)	534	3.37	(2.27–5.01)
<b>DXA:</b>						
Hip BMD T-score	2151	1.80	(1.53–2.13)	962	2.74	(2.15–3.49)
Clinical BMD T-score	2151	1.63	(1.43–1.86)	962	2.29	(1.80–2.91)

N is the combined number of cases and controls for all patients with complete BMD and strength data from BCT (~ 82% of the full cohort). Treatment-naïve confirmed from reliable medical record of prescription use, only available for a subset of patients from 2009 or later. “Hip” uses the lower of the femoral-neck and total-hip areal BMD measurements. “Clinical” uses the lower of the hip and (total) spine areal BMD measurements. HR is the increased risk per decrease in one sex-pooled SD.

Table 1

Disclosures: Annette Adams, Amgen, Grant/Research Support.

## 1156

**The Risk of Fracture among men with Sarcopenia, Obesity, their combination Sarcopenic Obesity, and men with neither condition: the MrOS Study.** Rebekah Harris<sup>1</sup>, Elsa Strotmeyer<sup>1</sup>, Robert Boudreau<sup>1</sup>, Jennifer Brach<sup>1</sup>, C. Kent Kwoh<sup>2</sup>, Nancy Lane<sup>3</sup>, Eric Orwoll<sup>4</sup>, Ann Schwartz<sup>5</sup>, Peggy Cawthon<sup>5</sup>, Jane Cauley<sup>1</sup>. <sup>1</sup>University of Pittsburgh, United States, <sup>2</sup>University of Arizona, United States, <sup>3</sup>University of California- Davis, United States, <sup>4</sup>Oregon Health & Science University, United States, <sup>5</sup>University of California- San Francisco, United States

The co-existence of sarcopenia and obesity act concomitantly to increase the risk of negative health outcomes. This combination may conceptually increase fracture risk through increased risk of falls and negative influences on bone mineral density. We examined fracture risk among men with sarcopenia alone, obesity alone, sarcopenic obesity, and men with neither condition. We hypothesized that men with sarcopenic obesity will have the highest risk of fracture in comparison to the other groups. Community-dwelling older men (N=5,994; age 73.1 ± 5.5 years; mean BMI = 26.9 kg/m<sup>2</sup>; 89% white) were enrolled in the Osteoporotic Fractures in Men Study (MrOS) at 6 clinical sites. We defined sarcopenia based on the European Working Group definition which includes cut points for physical performance measures. Appendicular lean mass and total body fat were measured by DXA. Low lean mass was defined using the residuals approach of Newman et al which corrects appendicular lean mass for height and fat mass and the 20<sup>th</sup> percentile of the distribution of residuals was used as the cut point. Performance measures included in the definition were slow gait speed (<0.8 m/s) and weak grip strength (<30 kg). Obesity was defined using a cut-point of 30% body fat. Participants were classified into 4 mutually exclusive groups based on their sarcopenia and obesity status: no sarcopenia/obesity (n=4357, 73.2%); obesity alone (n=1304, 21.9%); sarcopenia alone (n=164, 2.8%); and sarcopenia and obesity (n=128, 2.2%). Participants were followed on average for 7.5 years for incident fractures by tri-annual post-cards confirmed by radiographic report.

Cox proportional hazards models were used for incident fracture and classified as either: any clinical fracture, major osteoporotic fracture, hip, spine, or wrist fractures. Men with no sarcopenia or obesity were considered the referent population. Men with sarcopenic obesity had a 1.9 increased risk of any fracture and 3.1 risk of spine fracture as compared to men without either condition independent of important covariates including BMD. Men with sarcopenia alone also demonstrated a 1.6 increased risk of any fracture and 2.0 increased risk of hip fracture. These relationships may vary by site (Table). We conclude that sarcopenia, alone or in combination with obesity, may increase the risk for all clinical fractures in older men.

Table 1. Risk of Fracture by Body Composition by fracture site; fully adjusted models

Type	Referent	Obese	Sarcopenia	Sarcopenic Obesity
	HR	HR (95% CI)	HR (95% CI)	HR (95% CI)
Any Fracture	1.0	1.09 (0.92 – 1.30)	1.60 (1.05 – 2.45)*	1.87 (1.23 – 2.82)*
MOF	1.0	1.05 (0.82–1.35)	1.50 (0.89 – 2.54)	1.60 (0.90 – 2.84)
Hip	1.0	0.96 (0.66 – 1.41)	1.98 (1.04 – 3.78)*	1.08 (0.43 – 2.68)
Spine	1.0	1.13 (0.70 – 1.84)	1.28 (0.39 – 4.25)	3.09 (1.18 – 8.14)*
Wrist	1.0	1.65 (0.85 – 3.21)	1.28 (0.16 – 9.90)	1.14 (0.15 – 8.91)

All models adjusted for site, race, age, femoral neck bone mineral density, history of diabetes, health rating, use of benzodiazepines, use of osteoporosis medication, use of selective serotonin reuptake inhibitors, history of falls, physical activity. MOF: major osteoporotic fracture.\* indicates p-value <0.05.

Table 1: Risk of Fracture by Body Composition by fracture site; fully adjusted models

Disclosures: Rebekah Harris, None.



## 1157

**Physical performance, osteoporosis and vitamin D in elderly African-American women - the PODA trial and bone density loss.** Jeannette Owusu, MD\*, Mageda Mikhail, MD, Melissa Fazzari, PhD, Ruban Dhaliwal, MD, Subhashini Katumuluwa, MD, Albert Shieh, MD, Ayesha Ashraf Anwarullah, MD, Gianina Usera, M.D., Alexandra Stolberg, MD, Louis Ragolia, PhD, John Aloia, MD. Winthrop University Hospital, United States

**Purpose:** The purpose of this study was to determine whether maintenance of serum 25(OH)D levels above 75 nmol/L was effective in preventing bone density loss in healthy older African-American (AA) women. We previously showed that 2,000 IU of vitamin D3 per day did not influence bone density loss in AA postmenopausal women over a one-year period. The current study was designed to examine the effect of 25(OH)D levels at a higher level (>75 nmol/L) in an older AA population over a prolonged period (3 years).

**Method:** We conducted a randomized, double-blind, placebo controlled trial. 626 women were assessed for eligibility; of these, 366 were excluded. 130 were randomized to each group. There were 31 drop-outs from the vitamin D group and 38 from the placebo group; 98 completed 36 months in the treatment group vs. 93 in the placebo group. The dose of vitamin D3 was adjusted at each visit if needed by a research pharmacist. Calcium intake was adjusted to 1,200 mg/day through diet or supplements in all participants. Bone mineral density measurements were performed every 6 months using Hologic QDR 4500.

**Results:** Mean age was 68.5±4.9 years. The average dose was 3490±1465 IU of vitamin D3/day and the average serum 25(OH)D was 94±36 nmol/L compared to 51.7±20 in the placebo group. Serum 25(OH)D concentration was maintained at >75 nmol/L in 90% of the active group. The total femur (primary outcome) declined by -1.69% (-2.39, -0.98) in the treatment group compared to -2.47% (-3.06, -1.88) in the placebo group. The femoral neck BMD% change from baseline was -1.28% (-2.2, -0.37) in the D group compared to -2.01% (-2.99, -1.04) in the control group. The 1/3 radius decline was -1.68% (-2.29, -1.07) for the D group compared to -1.5% (-2.21, -0.79) for the contrast group. Significant changes in BMD were observed at other sites over time, but these changes were similarly consistent between groups. Serum carboxy-terminal collagen crosslinks (CTX) did not decline but both treatment groups showed a decline in PTH and bone specific alkaline phosphatase. No adverse events associated with vitamin D were observed.

**Conclusion:** These findings of ineffectiveness of vitamin D at doses maintaining serum 25(OH)D above 75 nmol/L in preventing bone loss in older AA women extend our previous findings of lack of effect of 2,000 IU/day in postmenopausal AA women. There is no evidence to support vitamin D intake greater than the recommended RDA by the Institute of Medicine in this population.

**Disclosures:** Jeannette Owusu, MD, None.

## 1158

**Relationship between femoral strength from QCT-based finite element analysis and femoral BMD before and after treatment: An Analysis from the FNIH Bone Quality Project.** Mary L. Bouxsein<sup>1</sup>, Tony M. Keaveny<sup>2</sup>, David C. Lee<sup>2</sup>, Sundeep Khosla<sup>3</sup>, Anne de Papp<sup>4</sup>, Richard Eastell<sup>5</sup>, Li-Yung Lui<sup>6</sup>, Douglas C. Bauer<sup>7</sup>, Dennis M. Black<sup>7</sup>. <sup>1</sup>Harvard Medical School, United States, <sup>2</sup>O.N. Diagnostics, LLC, United States, <sup>3</sup>Mayo Clinic College of Medicine, United States, <sup>4</sup>Merck & Co., Inc., United States, <sup>5</sup>University of Sheffield, United Kingdom, <sup>6</sup>California Pacific Medical Center, United States, <sup>7</sup>University of California, San Francisco, United States

The goal of the FNIH Bone Quality Study is to evaluate biochemical and imaging-based biomarkers for their use as potential surrogate endpoints in order to decrease the size, duration and cost of future trials of new osteoporosis therapies. To evaluate these biomarkers, we have attempted to collect data from all clinical trials in osteoporosis. The study database has individual data from over 23 trials, including ~150,000 subjects. QCT-based finite element analysis (FEA) of the hip is promising as a biomarker as it utilizes 3D volumetric data to accurately estimate femoral strength. Unfortunately, while we have DXA results from about 100,000 subjects, limited QCT data have been collected. We obtained the hip QCT scans from 297 subjects in 3 placebo-controlled RCT's (2 bisphosphonate, 1 denosumab), and reanalyzed the scans using standardized software (O.N. Diagnostics, Berkeley, CA) to estimate femoral strength by FEA. Here we determine the association between BMD and femoral strength at baseline and follow-up, and between the change in femoral neck (FN) or total hip (TH) BMD and change in femoral strength during the study. We found that the mean % changes in femoral strength were larger than the mean % changes in femoral BMD for both the treated and placebo (PBO) groups (Table 1). The change in femoral strength was strongly correlated to the change in FN and TH BMD ( $r^2=0.64$  to  $r^2=0.73$ ). Interestingly, the slope of the FN BMD vs. FEA-strength regression was significantly steeper for the treated than the PBO group ( $p=0.01$ ), suggesting that the FN BMD achieved after treatment may underestimate the femoral strength achieved after treatment. This observation suggests that structural re-arrangement of bone mass following treatment may contribute to fracture reduction beyond changes in BMD.

Altogether, these results support the potential value of FEA-strength as a surrogate that could be used in future trials of new osteoporosis medications. However, a definitive

validation of the relationship of FEA strength to fracture reduction requires more QCT-FEA data from trials with fracture endpoints.

Treatment	Duration	N	Placebo		Treated	
			ΔFEA Strength (%)	ΔFN BMD (%)	ΔFEA Strength (%)	ΔFN BMD (%)
Zoledronate	36 mo	155	-3.3 ± 6.1	-1.4 ± 3.8	1.7 ± 7.4	1.6 ± 3.8
Denosumab	36 mo	81	-1.0 ± 5.5	-1.6 ± 2.9	5.4 ± 4.3	2.6 ± 1.9
Ibandronate	12 mo	61	-1.7 ± 3.1	-0.83 ± 2.1	2.2 ± 4.3	0.39 ± 2.4

Table 1

**Disclosures:** Mary L. Bouxsein, Amgen, Grant/Research Support.

## LB-1159

**A Phase 3 Randomized, 24 Week, Double-Blind, Placebo-Controlled Study Evaluating the Efficacy of Burosumab, an Anti-FGF23 Antibody, in Adults with X-Linked Hypophosphatemia (XLH).** Karl Insogna<sup>1</sup>, Karine Briot<sup>2</sup>, Erik Imel<sup>3</sup>, Peter Kamenický<sup>4</sup>, Mary Ruppe<sup>5</sup>, Anthony Portale<sup>6</sup>, Thomas Weber<sup>7</sup>, Pisit Pitukcheewanont<sup>8</sup>, Hae Il Cheong<sup>9</sup>, Suzanne Jan De Beur<sup>10</sup>, Yasuo Imanishi<sup>11</sup>, Nobuaki Ito<sup>12</sup>, Robin Lachmann<sup>13</sup>, Hiroyuki Tanaka<sup>14</sup>, Diana Luca<sup>15</sup>, Christina Theodore-Oklota<sup>16</sup>, Matt Mealiffe<sup>17</sup>, Javier San Martin<sup>16</sup>, Thomas O. Carpenter<sup>1</sup>. <sup>1</sup>Yale University School of Medicine, United States, <sup>2</sup>CHU Paris Centre - Hôpital Cochin, France, <sup>3</sup>Indiana University Department of Medicine, United States, <sup>4</sup>Université Paris-Sud, Service d'Endocrinologie et des Maladies de la Reproduction, Hôpital de Bicêtre, France, <sup>5</sup>Houston Methodist Hospital, United States, <sup>6</sup>UCSF Medical Center, United States, <sup>7</sup>Duke University Medical Center, United States, <sup>8</sup>Children's Hospital Los Angeles, University of Southern California Keck School of Medicine, United States, <sup>9</sup>Seoul National University Hospital, Korea, Democratic People's Republic of, <sup>10</sup>Johns Hopkins University, United States, <sup>11</sup>Osaka City University Graduate School of Medicine, Japan, <sup>12</sup>The University of Tokyo Hospital, Japan, <sup>13</sup>University College of London Hospital, United Kingdom, <sup>14</sup>Okayama Saiseikai General Hospital, Japan, <sup>15</sup>Ultragenyx Pharmaceutical Inc., United States, <sup>16</sup>Ultragenyx Pharmaceutical, Inc, United States, <sup>17</sup>Ultragenyx Pharmaceutical, Inc., United States

In adults with XLH, hypophosphatemia is caused by inappropriately elevated circulating fibroblast growth factor 23 (FGF23) levels, leading to persistent osteomalacia, musculoskeletal pain, stiffness, pseudofractures, osteoarthritis, enthesopathy and muscle dysfunction. Burosumab, an investigational fully human monoclonal antibody, binds FGF23 and inhibits its activity. Here we report data from the first 24 wks of an ongoing, Phase 3, double-blind, multicenter study investigating the efficacy and safety of burosumab in adults with XLH (Table). Eligible patients (pts) had serum phosphorus (Pi) levels <2.5 mg/dL and skeletal pain (validated pain score ≥4). Pts (N=134) were randomized 1:1 to receive burosumab 1mg/kg or placebo (PBO) subcutaneously every 4 wks for 24 wks. At baseline, groups were comparable for sex, age, and disease severity. A significantly greater percentage of burosumab-treated pts (94.1%) attained the primary endpoint of mean serum Pi levels above the lower limit of normal at the midpoint of the dosing intervals through wk 24 compared with PBO-treated pts (7.6%). For secondary endpoints, burosumab-treated pts had significantly greater improvements in WOMAC stiffness compared with PBO-treated pts and there were strong trends toward greater improvements in WOMAC physical function and BPI pain severity with burosumab. Furthermore, burosumab-treated pts demonstrated substantial increases in markers of bone formation (PINP) and resorption (CTX). Fracture healing was evaluated radiographically using a baseline skeletal survey and follow-up target x-rays of regions identified with active fractures/pseudofractures (Fx/PFx). At baseline, 91 and 65 active Fx/PFx were present in 38 and 32 pts in the PBO and burosumab group, respectively. A greater percentage of baseline Fx/PFx were fully healed with burosumab (36.9%) compared with PBO (9.9%) at wk 24. Serious AEs were reported in 2 pts from each group, none of which were drug-related. There were no meaningful changes from baseline, or differences between groups, in serum or urine calcium, serum iPTH, or nephrocalcinosis severity scores. The overall safety profile of burosumab was similar to PBO; 12% of pts in each group experienced an injection site reaction. In sum, compared with PBO, burosumab was well tolerated, restored serum Pi homeostasis, reduced stiffness, improved physical functioning, and increased markers of bone remodeling with consequent improved healing of Fx/PFx in adults with XLH.

Table: Changes in Serum Phosphorus, Patient Reported Outcomes, and Skeletal Health in Adults with XLH at Week 24

	Change from Baseline		
	PBO (n = 66)	Burosumab (n = 68)	P Value
Serum Phosphorus Across the Midpoint of the Dose Intervals through week 24: Absolute Change from Baseline, mg/dL Percentage of Patients Above LLN, %	0.16 ± 0.03 7.6	1.21 ± 0.06 94.1	<0.0001
	Least Square Mean ± SE		
Stiffness, by WOMAC	0.25 ± 3.13	-7.87 ± 3.04	0.0122
Physical Function, by WOMAC	1.79 ± 2.72	-3.11 ± 2.55	0.0478
Worst Pain, by BPI Q3	-0.32 ± 0.22	-0.79 ± 0.21	0.0919
Serum P1NP, ng/mL	-1.00 ± 8.69	60.93 ± 8.63	<0.0001
Serum CTX, pg/mL	17.33 ± 47.26	207.58 ± 51.36	<0.0001
Active Fracture/Pseudofracture Healed at Week 24: Odds Ratio Burosumab vs PBO (95% CI)	7.76 (2.56, 23.49)		0.0004

All data is presented as least square mean ± SE from GEE modeling except the following: GLIMMIX model estimate odds ratio (active fracture/pseudofracture), absolute mean change (serum Pi above LLN), and percentage (patients achieving serum Pi above LLN). The number of patients in each analysis ranged from 61-66 for placebo and 63-68 depending on available samples.  
BPI Q3, Brief Pain Inventory Questionnaire 3; LLN, lower limit of normal; WOMAC, Western Ontario and McMaster Universities Osteoarthritis Index.

**Disclosures:** Karl Insogna, Ultragenyx Pharmaceutical Inc., Grant/Research Support.

## LB-1160

**Mortality after a recent clinical fracture before and after the introduction of a Fracture Liaison Service.** Caroline E Wyers\*, Lisanne Vranken, Johanna H Driessen, Irma JA de Bruin, Piet PM Geusens, Robert Y van der Velde, Heinrich MJ Janzing<sup>4</sup>, Sjoerd Kaarsemaker<sup>5</sup>, John A Eisman<sup>6</sup>, Joop PW van den Bergh<sup>1</sup>. Maastricht UMC+, NUTRIM, Department of Internal Medicine; VieCuri Medical Center, Department of Internal Medicine, Netherlands, <sup>2</sup>Maastricht UMC+, NUTRIM, CAPHRI, Department of Clinical Pharmacy and Toxicology; Utrecht Institute of Pharmaceutical Sciences, Division of Pharmacoepidemiology and Clinical Pharmacology, Netherlands, <sup>3</sup>Maastricht UMC+, CAPHRI, Department of Internal Medicine subdivision of Rheumatology; University of Hasselt, Netherlands, <sup>4</sup>VieCuri Medical Center, Department of Surgery, Netherlands, <sup>5</sup>VieCuri Medical Center, Department of Orthopedic Surgery, Netherlands, <sup>6</sup>Garvan Institute of Medical Research, Clinical Translation and Advanced Education, Australia, <sup>7</sup>Maastricht UMC+, NUTRIM, Department of Internal Medicine; VieCuri Medical Center, Department of Internal Medicine; University of Hasselt, Netherlands

**Purpose:** Only a few studies present mortality as an outcome associated with Fracture Liaison Services (FLS). The aim of this study is to evaluate the risk of mortality within 3 years after a clinical fracture (fx) in patients visiting the emergency department (ED) before and after the introduction of the FLS.

**Methods:** Historical cohort study of all consecutive patients aged 50-90 years with a fx presenting at the ED of VieCuri MC (Venlo, the Netherlands). From 2005 to 2007, only usual fx treatment procedures were followed (pre-FLS). From 2008 to 2013 (post-FLS), besides fx treatment, patients were screened by a nurse to receive an invitation for osteoporosis evaluation at the FLS. Patients were invited with a radiographically confirmed, diagnosed and treated fx, and living in the referral area of the hospital. Patients with cranial, facial, finger or toe fx, osteomyelitis, metastasis, peri-prosthetic fx, Paget's disease or multiple myeloma were excluded. In case of multiple ED visits for fx, only the first fx was taken into account for the pre-FLS or post-FLS period respectively. Fx were categorized based on the location as hip, major (pelvis, proximal humerus or tibia, vertebral, multiple rib, distal femur), minor (all other). Data on mortality were obtained by the national obituary database. In the post-FLS group, patients who were unable or unwilling to visit the FLS were included in the analysis. The risk for mortality within 3 years after fx was analyzed using multivariable Cox regression models adjusted for age, sex and fx location. Sensitivity analyses were performed with follow-up starting at 45 days (invitation date) and 125 days (date FLS visit) after fx.

**Results:** In total, 2653 patients were included in the pre-FLS period (72% women, mean age 69 yrs, 56% minor, 28% major and 16% hip fx) and 6415 in the post-FLS period (69% women, mean age 69 yrs, 54% minor, 32% major and 14% hip fx). Mortality decreased significantly from 16.6% to 14.6% (p=.015). After adjustments, patients in the post-FLS period had a significantly lower mortality risk (HR: 0.80; 95%CI: 0.71-0.90). Mortality risk was not affected by changing the start of follow-up (45 days HR: 0.82 95% CI: 0.72-0.93); 125 days HR: 0.81 95% CI: 0.71-0.93).

**Conclusion:** Mortality risk 3 years after a recent clinical fracture was reduced by 20% after the introduction of the FLS. It needs to be further clarified which part of the FLS care might be associated with this reduction in mortality.

**Disclosures:** Caroline E Wyers, None.

## LB-1161

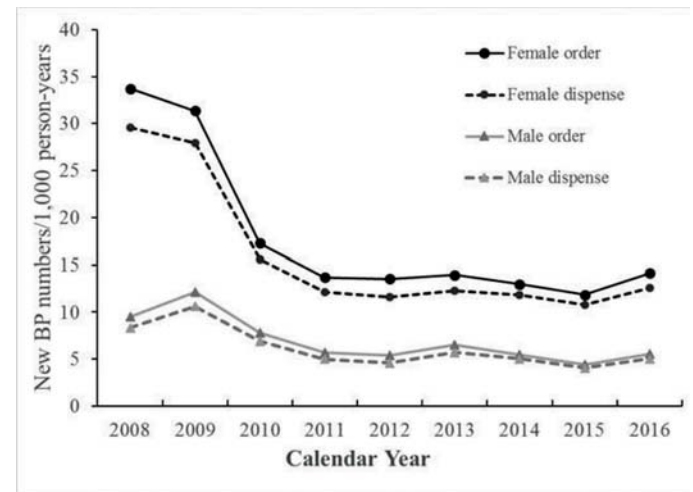
**Trends in Bisphosphonate Orders and Pharmacy Disposes, 2008-2016.** Annette Adams\*<sup>1</sup>, Hui Zhou<sup>1</sup>, Lei Qian<sup>1</sup>, Dennis Black<sup>2</sup>, Kristi Reynolds<sup>1</sup>. <sup>1</sup>Kaiser Permanente Southern California, United States, <sup>2</sup>University of California San Francisco, United States

**Purpose:** To estimate annual rates of new bisphosphonate (BP) orders and pharmacy dispenses in a large, integrated healthcare delivery system over a 9-year period.

**Methods:** This retrospective cohort study included women and men aged ≥50 years who were members of Kaiser Permanente Southern California during the years 2008-2016, and who had pharmacy benefits and had a full year of continuous health plan enrollment for the year of cohort entry. Subjects were excluded if they had evidence of prior anti-osteoporosis medication use, metastatic cancer, chronic kidney disease, Paget's disease, osteogenesis imperfecta, hypophosphatasia, or primary hyperparathyroidism. Numerators for the annual rates were the numbers of: 1) new orders for oral BP, and 2) new dispenses of oral BP. The denominator, annual person-years (p-y), was determined from enrollment data. Annual rates per 1000/p-y and percent changes were estimated.

**Results:** The overall annual rate of BP orders declined from 21.5 orders/1000p-y in 2008 to 9.8/1000p-y in 2016, a percent change (95% CI) of -54.2% (-55.5 to -53.0%). Orders for women declined from 33.7/1000p-y to 14.2/1000p-y, a -58.0% change (-59.3 to -56.7%), whereas orders for men went from 9.5/1000p-y to 5.6/1000p-y, a -41.4% change (-44.5 to -38.1%). Orders declined most dramatically among women aged <65 years (-71.8% change (-73.4 to -70.1%)). Rates declined sharply during 2008-2011 (-55.2% change (-57.0 to -53.8%)), then appeared to level off between 2011-2016 (+2.0% change (-1.2 to +5.4%)), except among the younger women and men, whose rates continued to decline substantially: -32.8% (-37.2 to -28.0%) for women <65 years and -39.4% (-46.5 to -31.3%) for men <70 years. Dispenses of BP also declined overall, going from 18.9/1000p-y to 8.8/1000p-y (-53.3% (-54.7 to -52.0%)). Again the steepest declines were observed during the period 2008-2011 (-54.7% (-56.2 to -53.2%)), while rates leveled off or even increased in 2011-2016 (+3.1% (-0.3 to +6.7%)), except among the youngest patients, where rates continued to decline: -34.8% (-39.4 to -29.9%) for women and -38.9% (-46.6 to -30.1%) for men.

**Conclusion:** Large declines in both orders for and dispenses of BP have been observed over the past several years. That orders and dispenses appear to be declining in parallel suggests that both care providers and patients are reducing their use of these medications. Intervention efforts aimed at increasing BP use should target both providers and patients.



**Disclosures:** Annette Adams, None.

## LB-1162

**A Randomized Alendronate-Controlled Trial of Romosozumab: Results of the Phase 3 ARCH Study (Active-controlled fraCture study in postmenopausal women with osteoporosis at High risk).** Kenneth G Saag\*<sup>1</sup>, Jeffrey Petersen<sup>2</sup>, Maria Luisa Brandi<sup>3</sup>, Andrew Karaplis<sup>4</sup>, Mattias Lorentzon<sup>5</sup>, Thierry Thomas<sup>6</sup>, Judy Maddox<sup>2</sup>, Michelle Fan<sup>2</sup>, Paul Meisner<sup>7</sup>, Andreas Grauer<sup>2</sup>. <sup>1</sup>University of Alabama, United States, <sup>2</sup>Amgen Inc., United States, <sup>3</sup>University of Florence, Italy, <sup>4</sup>McGill University, Canada, <sup>5</sup>University of Gothenburg and Sahlgrenska University Hospital, Sweden, <sup>6</sup>CHU de Saint-Étienne, France, <sup>7</sup>UCB Pharma, Belgium

The bone forming agent romosozumab (Romo) was previously shown to reduce vertebral and clinical fractures in postmenopausal women with osteoporosis. Here we report the efficacy and safety results of the ARCH study (NCT01631214).

This multicenter double-blind study enrolled postmenopausal women age 55-90 years with osteoporosis and high fracture risk, defined as a BMD T-score ≤ -2.5 at



total hip [TH] or femoral neck [FN] and either  $\geq 1$  moderate/severe or  $\geq 2$  mild vertebral fractures, or a BMD T-score  $\leq -2.0$  at TH or FN and either  $\geq 2$  moderate/severe vertebral fractures or a history of a recent hip fracture. Subjects were randomized 1:1 to 210mg Romo SC QM or 70mg alendronate (ALN) PO QW for 12 months, followed by open label 70mg ALN PO QW in both groups. Primary endpoints were subject incidence of new vertebral fracture through 24 months and clinical fracture through the primary analysis (PA). PA was performed when  $\geq 330$  clinical fractures had occurred and all subjects had completed the month 24 visit. Nonvertebral fracture at the PA was a secondary endpoint, as was BMD at the lumbar spine, TH, and FN at months 12 and 24. Hip fracture was evaluated as an additional secondary endpoint.

4093 women (mean age 74, mean TH T-score  $-2.8$ ) were randomized to Romo or ALN. 12 months of Romo prior to ALN vs ALN alone significantly reduced new vertebral, clinical, nonvertebral, and hip fractures (Table). Treatment with Romo also significantly increased BMD at all sites measured, at months 12 and 24 vs ALN alone (Table). Overall adverse events were balanced between groups. During the open label ALN period, 6 subjects (2 Romo; 4 ALN) were positively adjudicated for AFF and 2 subjects (1 Romo; 1 ALN) for ONJ. Cardiovascular (CV) serious adverse events (SAEs) were independently adjudicated; at 12 months the subject incidence was 2.5% in the Romo group vs 1.9% in the ALN group with cardiac ischemic events at 0.8% vs 0.3% and cerebrovascular events at 0.8% vs 0.3%, respectively.

In postmenopausal women with osteoporosis, Romo 210mg QM followed by ALN significantly reduced new vertebral, clinical, nonvertebral, and hip fracture risk vs ALN alone, suggesting that in osteoporotic patients at high risk for fracture, a treatment regimen starting with Romo followed by ALN leads to superior fracture risk reduction over ALN alone. An observed imbalance in CV SAEs compared with ALN was not seen in the previous placebo-controlled 7180-patient FRAME study and is currently being evaluated.

Efficacy Table		Relative Risk Reduction	Nominal P value	Adjusted P value	
Subject Incidence of Fracture (%)					
ALN 70mg QW / ALN 70 mg QW N=2047 <sup>a</sup>	Romo 210mg QM / ALN 70 mg QW N=2046 <sup>b</sup>				
New vertebral Fx <sup>c</sup>	8.0	4.1	50%	P<0.001	P<0.001
Clinical Fx <sup>d</sup>	13.0	9.7	27%	P<0.001	P<0.001
Nonvertebral Fx <sup>e</sup>	10.6	8.7	19%	P=0.037	P=0.040
Hip Fx <sup>f</sup>	3.2	2.0	38%	P=0.015	NA <sup>g</sup>

BMD Percent Change From Baseline (%) <sup>h</sup>		Nominal P value	Adjusted P value	
ALN 70mg QW / ALN 70 mg QW N=1757 <sup>a</sup>	Romo 210mg QM / ALN 70 mg QW N=1750 <sup>b</sup>			
ALN 70mg QW	ALN 70 mg QW			
Lumbar spine	5.0	13.7	P<0.001	P<0.001
Month 12	7.2	15.3	P<0.001	P<0.001
Month 24	2.8	6.2	P<0.001	P<0.001
Total hip	3.5	7.2	P<0.001	P<0.001
Month 12	1.7	4.9	P<0.001	P<0.001
Month 24	2.3	6.0	P<0.001	P<0.001

<sup>1</sup>Based on a combination of Hochberg, fixed sequential, and group sequential testing procedures which included the primary and selected secondary endpoint comparisons to be compared to a significance level of 0.05. <sup>2</sup>N=number of subjects randomized. <sup>3</sup>Incidence of fracture through month 24. <sup>4</sup>Incidence of fracture through primary analysis. <sup>5</sup>Multiplicity adjustment not applicable for hip fracture because it was not part of sequential testing strategy. Data are shown as least squares means based on ANCOVA models. <sup>6</sup>N=number of subjects with a baseline and  $\geq 1$  post-baseline value. ALN=alendronate, Fx=fracture, Romo=romosozumab.

**Disclosures:** Kenneth G Saag, Amgen, Merck, Consultant.

## LB-1163

**A Novel Mouse Model of Fibrous Dysplasia Reveals Both Cell autonomous and Non Cell-autonomous Function of *Gs*<sup>R201H</sup> Mutation.** Sanjoy Khan<sup>1</sup>, Prem Yadav<sup>1</sup>, Yingzi Yang<sup>1</sup>, Gene Elliot<sup>2</sup>. <sup>1</sup>Harvard School of Dental Medicine, United States, <sup>2</sup>National Human Genome Research Institute, United States

Fibrous dysplasia (FD, OMIM#174800) is a crippling skeletal disease caused by activating mutations of the GNAS gene, which encodes the stimulatory G-protein *Gs*. FD could result in severe adverse conditions such as bone deformity, fracture, severe pain in the bone, leading to functional impairment and wheelchair confinement. So far there is no cure as the molecular and cellular bases of FD remain largely unknown. The lack of appropriate animal models has severely hampered the advancement of molecular and cellular understanding of FD. Currently available transgenic mouse lines could not precisely model the disease, as in these models, the activated *Gs* is expressed from a different genomic locus driven by an artificial promoter. To this end, we have successfully generated a novel knock-in mouse line in which the mouse *Gnas* mutation corresponding to a human FD mutation (R201H) has been conditionally knocked into the mouse *Gnas* locus. When crossed with early osteochondro progenitor and osteoblast specific Cre lines (Prx1-Cre and Osx-Cre respectively), the mutant mice developed FD, phenotypically similar to human FD; deformed bone with abnormal trabeculae and the marrow space is replaced with fibrotic tissue. We observed that the bone formation in mutant mice was developmentally delayed due to delay in chondrocyte differentiation. The isolated mutant BMSCs were impaired of differentiating into osteoblasts. Mutant BMSCs exhibit upregulation of Wnt/ $\beta$ -catenin signaling similar to human BMSCs isolated from FD patients. Reducing Wnt/ $\beta$ -catenin signaling by deleting one copy of *Lrp6* in Osx-Cre;*Gnas* mutant mice, partially rescues the phenotype. Furthermore, using inducible Sox9CreER line, we found that mosaic expression of mutant *Gs* (due to low dose of tamoxifen) activates Wnt/ $\beta$ -catenin signaling in mutant cells cell-autonomously

but induces fibrotic response in both cell-autonomous and non cell-autonomous manner. Taken together, our novel knock-in model shows that expression of FD causing *Gs* mutation exactly replicates human FD in vivo and the *Gs* mutation plays a key role in both cell-autonomous and non cell-autonomous fibrosis leading to FD.

**Disclosures:** Sanjoy Khan, None.

## LB-1164

**Advanced Glycation End-Products (AGEs) Associated with Altered Gene Expression in Bone Strength Candidate Genes.** Ellen Quillen<sup>1</sup>, Anne Sheldrake<sup>1</sup>, Jeremy Glenn<sup>1</sup>, Jaydee Foster<sup>1</sup>, Laura Cox<sup>1</sup>, Daniel Nicoletta<sup>2</sup>, Todd Bredbenner<sup>2</sup>. <sup>1</sup>Texas Biomedical Research Institute, United States, <sup>2</sup>Southwest Research Institute, United States

Skeletal fragility is common among individuals with type II diabetes, despite high bone mineral density. One hypothesis to explain this apparent contradiction is that extended hyperglycemic states cause protein glycation in the bone resulting in advanced glycation end products (AGEs) and altered protein conformations, compromising normal function. AGEs are thought to influence intracellular signaling and gene expression as well as releasing free radicals and pro-inflammatory molecules.

To test the influence of AGE levels on gene expression of osteometabolic gene, serum pentosidine, an AGE biomarker, was measured in triplicate from serum samples collected at necropsy for 65 baboons using a human pentosidine ELISA kit from MyBioSource. No work was done on living animals and no animals were euthanized specifically for this study. Total RNA was extracted from white blood cells collected at necropsy and mRNA libraries were generated using the KAPA Stranded mRNA-Seq kit for sequencing on the Illumina HiSeq2500. Reads were aligned to the *Papio anubis* genome using the STAR aligner, normalized to read counts per sample, and converted to a log-fold scale. Welch's t-tests were used to identify bone strength candidate genes with significantly different transcript abundance between 25 baboons with low concentrations of pentosidine (644.45 $\pm$ 211 pmol/mL; 9 males; mean 18.6 years) and 25 baboons with high concentrations of pentosidine (1458.25 $\pm$ 283 pmol/mL; 10 males; mean 18.4 years).

Ten genes are differentially expressed ( $p < 0.05$ ). *CREG1* (two transcripts), *ADIPOR1*, *BACE2*, and *FZD5* are downregulated in the higher pentosidine group relative to the low pentosidine group; *FGFRL1*, *PTGER2*, *ACVR1*, *IL1A*, *ITGA2*, and *BMPRI1* are upregulated. Broadly, these genes fit into three functional domains: *CREG1*, *PTGER2*, *ADIPOR1* are involved in bone cell growth, differentiation, and repair. Within this category, *ACVR1* and *BMPRI1* are specifically involved in the bone morphogenic protein pathway. *IL1A* has been implicated in inflammatory bone loss. *FGFRL1* and *ITGA2* are preferentially expressed in collagen-containing tissues.

Altered regulation of gene expression associated with increased circulating AGEs is a promising means of identifying biological mechanisms explaining the influence of hyperglycemia on bone strength. In our study, five of these genes – *CREG1*, *FGFRL1*, *IL1A*, *BACE2*, and *FZD5* – were further associated with femur demineralization, density, or shape characterized by microCT.

**Disclosures:** Ellen Quillen, None.

## LB-1165

**Osteocytes express a unique transcriptome that underpins skeletal homeostasis.** Scott Youtlen<sup>1</sup>, Paul Baldock<sup>1</sup>, Victoria Leitch<sup>2</sup>, Julian Quinn<sup>1</sup>, Nenad Bartonicek<sup>3</sup>, Ryan Chai<sup>1</sup>, John Eisman<sup>1</sup>, J.H. Duncan Bassett<sup>2</sup>, Graham Williams<sup>2</sup>, Peter Croucher<sup>1</sup>. <sup>1</sup>The Division of Bone Biology, Garvan Institute of Medical Research, Australia, <sup>2</sup>Molecular Endocrinology Laboratory, Department of Medicine Imperial College London, United Kingdom, <sup>3</sup>Centre for Clinical Genomics, Garvan Institute of Medical Research, Australia

Osteocytes are pivotal regulators of skeletal homeostasis, communicating between the bone-cell lineages to coordinate activity. However, little is known of the pattern of coding and non-coding genes expressed by these cells, as the skeleton is frequently omitted from large-scale efforts to map tissue-specific transcriptomes. We hypothesised that osteocytes express a unique transcriptome, defining key signalling-pathways used to orchestrate bone turnover and skeletal homeostasis. Transcriptome-sequencing was performed on total-RNA extracted from osteocytes isolated from the tibiae, femora, humeri and calvariae of 16-week-old CB57BL6/NTac mice (n=8). De novo transcriptome-assembly was performed and gene-expression quantified. Osteocytes expressed a repertoire of ~12000 genes common across all bone types, 1197 of which were more than 4-fold enriched in osteocytes relative to bone marrow, thereby defining an osteocyte transcriptome signature. Osteocytes derived from different anatomical locations could be distinguished by unique patterns of homeobox-gene expression, including *Hoxc* and *Hoxd* clusters, and *Pitx1*. Of the ~880 lncRNAs expressed within osteocytes, 52 were present in the signature, including novel lncRNAs with osteocyte-restricted expression. In addition to highly enriched osteocyte genes such as *Sost*, *Mepe* and *Dmp1*, more than 80% of signature genes had not previously been annotated with a skeletal function in the Gene Ontology database. The osteocyte signature was highly enriched for pathways regulating axonal guidance, suggesting that osteocytes have repurposed neuronal pathways to control networking functions and facilitate intercellular communication between osteocytes and bone-cell lineages. Genes known to cause skeletal dysplasia were significantly enriched in the osteocyte signature ( $p=4.9E-16$ ), including more

than 80% of genes known to cause Osteogenesis Imperfecta, suggesting the signature may prove valuable in identifying causal variants for unexplained skeletal conditions by acting as a filter for patient genomic data. This study has defined the osteocyte transcriptome and provided important insights into the molecular pathways that control osteocyte biology and skeletal disorders.

**Disclosures:** Scott Youtten, None.

## LB-1166

**Osteocalcin signaling in the liver favors de novo gluconeogenesis.** Paula Mera\*, Subrata Chowdhury, Gerard Karsenty. Columbia University, United States

Even though osteocalcin (OCN) favors proliferation of pancreatic  $\beta$ -cells and insulin secretion, acute injection of OCN do not cause hypoglycemia in the mouse. We hypothesized that this paradoxical observation could indicate that OCN favors liver gluconeogenesis (GNG). In support of this idea we observed that in a pyruvate tolerance test (PTT) GNG was lower in *Ocn*<sup>-/-</sup> mice than in wild-type (WT) littermates. In order to dissect the putative function of OCN in the liver in a mouse model that would not display any of the metabolic abnormalities otherwise seen in *Ocn*<sup>-/-</sup> mice, we generated mice lacking the OCN receptor, *Gprc6a*, in cells of the liver (*Gprc6a*<sup>Albumin</sup><sup>-/-</sup>). Analyses of these mutant mice through a PTT established that OCN signals in the liver favors GNG. At the molecular level, gene expression performed in the liver of *Gprc6a*<sup>Albumin</sup><sup>-/-</sup> and control mice revealed that the expression of *Pepckc*, a gene encoding the enzyme phosphoenolpyruvate carboxykinase (PEPCK) that is necessary for GNG, was significantly decreased in *Gprc6a*<sup>Albumin</sup><sup>-/-</sup> livers when compared to control ones. Conversely, acute injection of OCN causes an increase in the expression of *Pepckc* in the liver of WT mice. Exercise is a physiological situation in which the liver increases GNG, using as a precursor lactate produced by skeletal muscle. Since circulating OCN levels markedly rise during exercise we asked whether OCN signalling in the liver favours GNG during exercise. To that end we used infusion of stable isotopes to trace liver glucose fluxes in *Gprc6a*<sup>Albumin</sup><sup>-/-</sup> and control mice during acute exercise. In full support of the regulation of *Pepckc* by OCN, this experiment showed that the flux from oxaloacetate to phosphoenolpyruvate, a reaction catalyzed by PEPCK, is decreased in *Gprc6a*<sup>Albumin</sup><sup>-/-</sup> mice during exercise. We next used real-time PCR to identify the cells targeted by OCN signalling in the liver. Surprisingly, this analysis showed that *Gprc6a* is not expressed in hepatocytes but rather in a population of non-parenchymal cells that expresses epithelial markers. Of note, these cells express *Pepckc* and markers of cholangiocytes, which are the epithelial cells of the bile duct. These results, broaden our understanding of the roles of OCN in the regulation of glucose homeostasis, indicate that, as in skeletal muscle, OCN exerts functions in the liver that are opposite to those of insulin and suggest that cholangiocytes are implicated in the regulation of liver GNG.

**Disclosures:** Paula Mera, None.



## FR0001

**The Trabecular Bone Score is associated with bone mineral density, markers of bone turnover and prevalent fracture in patients with chronic kidney disease stages 5 and 5D.** Jasna Aleksova<sup>\*1</sup>, Samantha Kurniawan<sup>2</sup>, Grahame Elder<sup>3</sup>. <sup>1</sup>Centre for Endocrinology and Metabolism, Hudson Institute of Medical Research; School of Clinical Sciences, Monash University, Australia, <sup>2</sup>The University of Notre Dame, Australia, <sup>3</sup>Department of Renal Medicine, Westmead Hospital; Osteoporosis and Bone Biology Division, Garvan Institute of Medical Research, Australia

**Background:** Declining renal function carries increased risks for fracture, but bone mineral density (BMD) is less predictive of fracture risk for patients with chronic kidney disease mineral and bone disorders (CKD-MBD) than for the general population. The trabecular bone score (TBS) is a novel gray-level textural metric obtained from lumbar spine dual-energy X-ray absorptiometry (DXA) images that provides a surrogate measure of bone microarchitectural integrity. TBS is complementary to BMD and can independently predict fracture risk in certain populations.

**Aim:** To assess the association of TBS to epidemiological, clinical, DXA, radiological and laboratory measures in patients with CKD stages 5/5D undergoing kidney and simultaneous pancreas kidney (SPK) transplantation.

**Methods:** 147 patients underwent immediate pre-transplant laboratory testing, followed by a DXA, lateral spine X-ray and comprehensive structured history within 4 weeks of transplantation. Associations of the TBS to demographic data, fracture history, prevalent vertebral fracture, BMD by DXA and laboratory variables were assessed. Multivariable linear regression models were used to identify factors predictive of the TBS.

**Results:** Of 147 patients with CKD stages 5/5D, 60% were male and the mean age was 48±13 yrs. Diabetes mellitus (DM) was present in 36% (27% type 1, 9% type 2 DM), 46% had prior fractures and 42% non-vertebral fractures. The mean TBS was 1.345 ± 0.125 and was lower in SPK compared with kidney-only transplant recipients (1.292 vs. 1.364, p=0.001). The TBS correlated significantly to BMD at the spine, hip and forearm sites, to body mass index (BMI) and inversely to parathyroid hormone (PTH) and alkaline phosphatase (ALP), but not to age, gender or dialysis vintage. In multivariable logistic regression models, TBS was significantly associated with prevalent non-vertebral fracture (p=0.045) but not vertebral fractures.

**Conclusion:** To our knowledge, this is the largest study to assess associations of the TBS in patients with CKD stages 5/5D undergoing transplantation. TBS correlated to BMD at all sites, to BMI, PTH and ALP and was associated with non-vertebral fractures. These findings suggest that TBS may assist in identifying CKD patients at increased fracture risk.

**Disclosures:** Jasna Aleksova, None.

## FR0003

**Retrospective Evaluation of Solid Tumor Patients with PTH-Independent Hypercalcemia and their Response to Bisphosphonates or Denosumab.** Tariq Chukir<sup>\*1</sup>, Yi Liu<sup>2</sup>, Azeez Farooki<sup>3</sup>. <sup>1</sup>New York Presbyterian Hospital - Weill Cornell, United States, <sup>2</sup>Hospital for Special Surgery, United States, <sup>3</sup>Memorial Sloan Kettering, United States

**Background:** PTH-independent hypercalcemia of malignancy is mediated through different mechanisms: humoral hypercalcemia of malignancy which is caused by secretion of parathyroid hormone related peptide (PTHrP), local osteolytic lesions and calcitriol-mediated hypercalcemia. Calcitriol-mediated hypercalcemia is uncommon in solid tumors and has not been well characterized.

**Objective and Design:** We undertook a retrospective record review from 1998-2016 to quantify and further characterize patients at our institution with solid tumors who had PTH-independent hypercalcemia. We aimed to assess whether different mechanisms of hypercalcemia are associated with different response to treatment. We also aimed to assess whether factors e.g. calcitriol, PTHrP, hypophosphatemia and osteolytic lesions are associated with refractory hypercalcemia.

**Results:** A total of 81 cases were eligible and classified into 4 groups: 1) patients with elevated PTHrP and calcitriol (n=25), 2) patients with elevated calcitriol (n=8), 3) patients with elevated PTHrP (n=30), and 4) patients without elevated calcitriol or PTHrP (n=18). There was no difference in age, gender, renal function, 25 OH vitamin D level and corrected calcium among the groups. PTHrP was higher in patients with elevated PTHrP and calcitriol compared to patients with only PTHrP elevation (126.9±83.8 vs 87.7±62.7, p<0.0001). Calcitriol was significantly higher in patients with elevated calcitriol alone compared to patients with elevated calcitriol and PTHrP (137.9±66.8 vs 88.4±29.3, p<0.0001). Patients with elevated calcitriol with or without elevated PTHrP had higher proportion of refractory hypercalcemia. Forty eight percent of all patients had incomplete response including refractory and relapsing (n=42). Patients with refractory hypercalcemia had significantly higher calcitriol (69.7±50.4 versus 35.5±42.9, P=0.032) and PTHrP (98.0±86 versus 62.2±60.5, P=0.035) levels as well as lower phosphorus levels (2.5±0.7 versus 2.96±1.1 mg/dl, P=0.015). The number of cases with bone metastasis and survival rate was similar in the complete and incomplete response groups.

**Conclusion:** Calcitriol-mediated hypercalcemia is more common than previously thought and may have important clinical implications for refractory hypercalcemia. A higher proportion of patients with elevated calcitriol were refractory to treatment.

**Disclosures:** Tariq Chukir, None.

## FR0004

**Phenotype assessment of adult offspring carriers of the SQSTM1/P392L mutation in familial forms of Paget's disease of bone.** Mariam Dessay<sup>\*1</sup>, François Jobin Gervais<sup>1</sup>, Andréanne Samson<sup>1</sup>, Jacques P. Brown<sup>2</sup>, Laëtitia Michou<sup>2</sup>. <sup>1</sup>CHU de Québec-Université Laval research centre, Canada, <sup>2</sup>Division of rheumatology and research centre, CHU de Québec-Université Laval, Canada

**Purpose:** Paget's disease of bone (PDB) is a common bone disorder. In the French-Canadian population, the SQSTM1/P392L mutation was involved in 46% of familial forms. In New-Zealand, the emergence of PDB in offspring inheriting SQSTM1 mutations was reported to be delayed by a decade compared to their parents. We aimed at assessing the phenotype of offspring carriers of this mutation in our French-Canadian cohort.

**Methods:** We reviewed research records from adult offspring carriers of this mutation aged <80 years and their affected parent. In parents, we collected data on sex, age at diagnosis, number of affected bones, total serum alkaline phosphatase levels (ALPs) expressed as a ratio to the midpoint to normal range. PDB extended phenotype assessment relying on tALPs, total body bone scan and skull and pelvis radiographs, was performed in offsprings at inclusion in 1996 to 2009. In 2016, we started an extended phenotype reassessment of these offsprings by bone scan and pelvis and skull radiographs, if not done during the past 8 years.

**Results:** We studied 97 adult offsprings in 16 different kindreds: 53.6% were men, mean age was 60.34±9.8 years (range 37 to 79). The offsprings originated from 58 affected parents. Parents mean age at diagnosis was 60.2±11.6 years (range 43 to 91). They had 6.5±5.2 affected bones and tALPs were 6.5±11.4. Phenotyping of offsprings at inclusion, at a mean age 44±10 years, provided tALPs at 0.98±0.30. Total body bone scans, performed at 45±10 years, were negative for PDB in 70% of cases and uncertain in 30%. Radiographs, performed at 46±11 years, were uncertain in 4.70% at the skull and 1.5% at the pelvis. Preliminary results of the phenotypic update in 22 offsprings, now aged of 60±11 years old, provided positive bone scan in four (18%) participants. Radiographs were positive at the skull (n=4) and/or at the pelvis (n=3). Overall six offsprings, including 3 men, now have a PDB phenotype with both positive bone scan and radiographs in 84% of them, over 16±4.6 years. At diagnosis, they were aged of 40, 40, 58, 64, 74 and 75 years old, respectively. Half of them were younger than their parent age at diagnosis. 34% had a polyostotic PDB.

**Conclusions:** 27% of offspring carriers of the SQSTM1/P392L mutation developed a clinical phenotype of PDB. Interestingly, half of them were aged of less than 60 years old. These results suggest the utility of a follow-up with bone scan and radiographs for healthy carrier of this mutation.

**Disclosures:** Mariam Dessay, None.

## FR0007

**Primary Hyperparathyroidism: Role of Impaired Cerebrovascular Function in Cognitive Symptoms.** Melissa Sum<sup>\*</sup>, Yunglin Gazes, Bucovsky Mariana, Colon Ivelisse, Kevin Slane, Arindam RoyChoudhury, Minghao Liu, Yu-Kwang Tay, Randolph Marshall, Ronald Lazar, Shonni Silverberg, Marcella Walker. Columbia University Medical Center, United States

We previously reported cognitive dysfunction in primary hyperparathyroidism (PHPT) reversible with cure (PTX) and showed that PTH levels are associated with vascular stiffness. We hypothesized that PTH-dependent intracerebral vascular dysfunction may impair blood flow and cognition in PHPT. Women with PHPT (N=20) undergoing PTX underwent cognitive testing, functional magnetic resonance imaging (fMRI) and transcranial Doppler to measure intracerebral vasomotor reactivity (VMR) pre- and 6 months post-PTX. PHPT were compared to normative control data at baseline. PHPT cases (mean age±SD, 65±7yrs) had mild PHPT (calcium 10.6±0.5mg/dl, PTH 93±42pg/ml) and normal mean vitamin D (39±14ng/ml), renal and thyroid function. Baseline mood and age-, gender- and education-adjusted Z-scores for visuospatial memory, verbal memory and motor speed were normal. VMR was worse in PHPT vs. 9 controls (3.2±0.9 vs. 4.2±1.1% mmHgPCO<sub>2</sub>, p=0.03), but not associated with PTH (r=0.28, p=0.43) or calcium (r=0.32, p=0.36) levels. On fMRI, PHPT had reduced neuronal activation in the cerebellum during matrix reasoning (t=32, k=179 voxels, p<0.001) and increased activation in the cingulate gyrus (t=14, k=26, p<0.001) vs. 18 age- and gender-matched controls. Activation in PHPT inversely correlated with PTH in the cingulate gyrus (r=-0.77, t=14, k=26), positively correlated with PTH in the frontal gyrus (r=0.84, t=15, k=21) and positively correlated with calcium in the caudate (r=0.87, t=14, k=62) and frontal gyrus (r=0.79, t=14, k=24), all p<0.0001. After PTX (n=15), visual memory (-0.07±1.56 vs. 0.61±1.78, p=0.03), verbal fluency (-0.16±0.94 vs. 0.31±1.26, p=0.03), motor speed (-0.56±1.23 vs. 0.2±1.2, p=0.03) and mood (12±10 vs. 8±6, p=0.04) improved, while VMR did not change (n=8; 3.4±0.9 vs. 3.7±1.0, p=0.52). Post-PTX, activation was reduced during both non-verbal abstraction [Inferior parietal lobe (t=14.35, k=222) and temporal gyrus (t=8.10, k=93), all p<0.001] and verbal memory [Middle frontal gyrus (t=8.54, k=20), lingual gyrus (t=6.74, k=20), and Insula (t=8.08, k=79), all p<0.001]. In summary, preliminary data suggest that PHPT may be associated with lower VMR. Cure of PHPT was associated with improvements in some aspects of cognition and mood. Brain activation in areas involved in decision-making and executive function also exhibited change. Further work is needed to determine if VMR ultimately improves post-PTX and whether it contributes to underlying cognitive changes in PHPT.

**Disclosures:** Melissa Sum, None.

## FR0008

**Fracture risk in Dialysis and Kidney Transplantation patients: A Systematic Review.** Aboubacar Sidibé<sup>1</sup>, David Auguste<sup>2</sup>, Catherine Fortier<sup>3</sup>, Sonia Jean<sup>4</sup>, Lynne Moore<sup>5</sup>, Louis-Charles Desbiens<sup>3</sup>, Yue Pei Wang<sup>6</sup>, Fabrice Mac-Way<sup>3</sup>. <sup>1</sup>Centre de Recherche du CHU de Québec, Hôpital Hôtel-Dieu de Québec, Division of Nephrology, Endocrinology and Nephrology Axis, Faculty of Medicine, Department of Social and Preventive Medicine, Laval University, Quebec Canada, Canada, <sup>2</sup>Centre de Recherche du CHU de Québec, Hôpital Saint-Sacrement, Faculty of Medicine, Department of Social and Preventive Medicine, Laval University, Quebec Canada, Canada, <sup>3</sup>Centre de Recherche du CHU de Québec, Hôpital Hôtel-Dieu de Québec, Division of Nephrology, Endocrinology and Nephrology Axis, Faculty and Department of Medicine, Laval University, Quebec Canada, Canada, <sup>4</sup>Institut National de Santé Publique du Québec, Medicine Faculty, Department of social and preventive medicine, Laval University, Quebec Canada, Canada, <sup>5</sup>Centre de Recherche du CHU de Québec, Hôpital de l'Enfant-Jésus, Traumatology Axis, Medicine Faculty, Department of Social and Preventive Medicine, Laval University, Quebec Canada, Canada, <sup>6</sup>CHU de Québec Research Center, Hôtel-Dieu de Québec Hospital, Division of Nephrology, Endocrinology and Nephrology Axis, Faculty and Department of Medicine, Laval University, Quebec Canada, Canada

**Background:** Chronic kidney disease (CKD) is associated with an increased risk of fracture and cardiovascular mortality. The risk of fracture in hemodialysis (HD), peritoneal dialysis (PD) and kidney transplantation (KT) patients is higher when compared to the general population. However, there exist a knowledge gap concerning which group has the highest risk of fracture. We aimed to compare the risk of fracture in HD, PD and KT populations.

**Methods:** We conducted a systematic review of observational studies evaluating the risk of fracture in HD, PD or KT patients with or without a comparator. Eligible studies were searched using MEDLINE, Embase, Web of Science, and Cochrane Library from their inception to January 2016. We also searched the grey literature. Incidence rates and proportions of fracture in individual studies were pooled together to estimate the mean fracture risk according to the site of fracture. Prevalence estimates were pooled separately.

**Results:** We included 46 studies from 2641 abstracts that evaluated the risk of fracture in HD, PD and KT populations. The mean incidence rate of any fracture was 20.74 (IQR: 16.93 to 25.60) and 45.83 (IQR: 9.87 to 76.86) for 1000 person-years in HD (5 studies) and KT patients (8 studies), respectively. The mean incidence rate of hip fracture was 10.42 (IQR: 8.90 to 11.47) in HD, 4.60 (IQR: 3.47 to 6.25) in PD, 2.90 (IQR: 2.25 to 3.55) in KT and 13.65 (IQR: 5.70 to 21.60) in dialysis (HD + PD) for 1000 person-years from 6, 3, 4 and 4 studies, respectively (Figure 1a). The mean prevalence of any fracture was 23.90 % (IQR: 12.50 to 38.46) in HD and 28.39 % (IQR: 17.00 to 44.08) in KT, from 6 and 3 studies. The mean prevalence of vertebral fracture was 21.72 % (IQR: 12.50 to 38.56) in HD (7 studies) and 19.16 % (IQR: 9.10 to 28.81) in KT (5 studies), (Figure 1b). Three studies reported a higher risk of hip fracture in HD as compared to PD population (HR=1.31 (95% CI: 1.01 to 1.70), 1.52 (95% CI: 1.09 to 2.12) and 1.67 (95% CI: 1.53 to 1.83)). One study reported a higher risk of hip fracture in KT compared to dialysis population (HR=1.34 (95% CI: 1.12 to 1.61)). We found only one study that compared the risk of fracture in these three groups, which did not observe a statistical difference (Figure 2).

**Conclusion:** HD patients seem to have a higher risk of hip fracture than PD patients. There were insufficient studies to draw conclusions on the difference in risk of fracture between dialysis and kidney transplant populations.

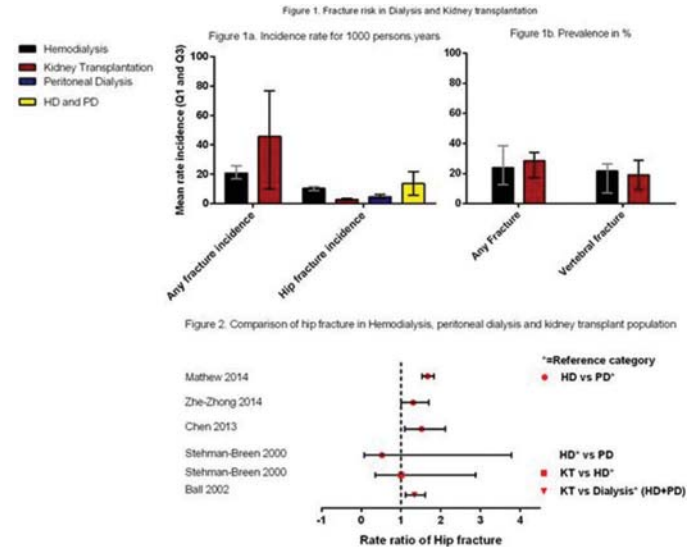


Figure 1 and 2

**Disclosures:** Aboubacar Sidibé, None.

## FR0011

**Alendronate Treatment Does Not Influence Resistance to Damage Accumulation in Femoral Cortical Bone in Hound Dogs.** Daniel Brooks<sup>\*</sup><sup>1</sup>, Dimitrios Psaltos<sup>1</sup>, Katherine Lo<sup>1</sup>, Robert Urban<sup>2</sup>, Sehanie McCarthy<sup>2</sup>, Deborah Hall<sup>2</sup>, Thomas Turner<sup>2</sup>, Mary Boussein<sup>1</sup>. <sup>1</sup>Beth Israel Deaconess Medical Center, United States, <sup>2</sup>Rush University Medical Center, United States

Although the mechanisms underlying atypical femoral fractures (AFF) are unknown, clinicians and patients are concerned about long-term use of bisphosphonates (BP) and their possible association with AFF. There is a common hypothesis that BPs reduce the ability of cortical bone to resist damage accumulation and subsequently increase the risk of AFF. To test this hypothesis, we determined the effect of 12 or 18 months alendronate (ALN) treatment on bone microarchitecture and mechanical properties of femoral cortical bone in large dogs. Skeletally-mature male hound dogs (29.7 ± 3.3 kg, range: 24 to 36 kg) were assigned (n=10 /gr) to: 1) Control, 12 mo; 2) Control, 18 mo, 3) ALN, 12 mo, or 4) ALN, 18 mo. Dogs received daily ALN-filled gelatin capsules at a clinically relevant dose (0.2mg/kg/day) or identical capsules filled with lactose. At study end, cortical beams (2 x 2 x 30 mm) were cut from the cranial, medial and lateral aspect of the femoral diaphysis of each dog and assessed using: 1) monotonic 4-pt bending, 2) cyclic damage accumulation testing, and 3) reference point indentation (RPI, 10 N for 20 cycles, Biodent, ActiveLife Scientific). For the damage accumulation testing, we cyclically loaded the beams in 4-pt bending with incrementally greater displacements (from 75% to 200% yield displacement in 25% increments) to induce tissue damage. Following each damage cycle, we computed the secant stiffness and calculated the percent stiffness degradation relative to baseline stiffness (Tommasini et al 2005). We used two-way ANOVA and unpaired t-tests to test for effects of ALN treatment. Results: Treatment duration did not influence the outcomes, thus results are presented for both time points combined (Table 1). ALN treatment did not alter any 4-pt bending properties (apparent bending modulus, strength, post-yield displacement, or toughness). ALN treatment also did not significantly influence the ability of cortical bone to resist stiffness degradation during cyclic damage accumulation testing. There were also no differences in the tissue level mechanical properties that were measured with RPI. In conclusion, we found that treatment of adult male hound dogs with clinically relevant doses of ALN did not influence the tissue level mechanical properties of femoral cortical bone nor alter the ability of cortical bone to resist damage accumulation.



Table 1. Effect of ALN treatment on femoral cortical bone tissue-level mechanical properties in hound dogs (mean  $\pm$  SD)

	ALN (n = 19)	CON (n = 20)	p-value
<b>Monotonic 4-pt Bending (Cortical beam from medial aspect)</b>			
Bending Modulus (GPa)	17.66 $\pm$ 1.59	17.71 $\pm$ 1.45	0.930
Flexural Strength (MPa)	132.8 $\pm$ 10.7	129.6 $\pm$ 10.9	0.369
Post-yield Displacement (mm)	2.572 $\pm$ 0.787	2.659 $\pm$ 0.597	0.702
Toughness to maximum force (mJ/mm <sup>3</sup> )	0.788 $\pm$ 0.359	0.762 $\pm$ 0.338	0.822
Toughness to yield (mJ/mm <sup>3</sup> )	0.097 $\pm$ 0.027	0.093 $\pm$ 0.022	0.558
Toughness to fracture (mJ/mm <sup>3</sup> )	1.100 $\pm$ 0.359	1.056 $\pm$ 0.279	0.672
Post-yield toughness to fracture (mJ/mm <sup>3</sup> )	1.003 $\pm$ 0.363	0.963 $\pm$ 0.278	0.706
<b>Reference Point Indentation (Cortical beam from cranial aspect)</b>			
Total Indentation Distance ( $\mu$ m)	86.58 $\pm$ 3.79	89.15 $\pm$ 5.68	0.101
Indentation Distance Increase ( $\mu$ m)	12.18 $\pm$ 1.17	12.90 $\pm$ 1.24	0.066
Average Creep Indentation Distance ( $\mu$ m)	1.51 $\pm$ 0.09	1.57 $\pm$ 0.11	0.092
Average Energy Dissipated ( $\mu$ J)	35.3 $\pm$ 2.16	36.61 $\pm$ 3.1	0.128
Average Unloading Slope (N/ $\mu$ m)	0.54 $\pm$ 0.05	0.55 $\pm$ 0.05	0.417
Average Loading Slope (N/ $\mu$ m)	0.42 $\pm$ 0.03	0.42 $\pm$ 0.03	0.712
<b>Damage Accumulation Testing (Cortical beam from lateral aspect)</b>			
Stiffness degradation (%) after 100% Yield loading	12.4 $\pm$ 4.4	11.9 $\pm$ 4.5	0.737
Stiffness degradation (%) after 150% Yield loading	46.3 $\pm$ 11.4	40.3 $\pm$ 13.1	0.146
Stiffness degradation (%) after 200% Yield loading	79.1 $\pm$ 9.2	77.3 $\pm$ 16.7	0.688

Table 1

**Disclosures:** Daniel Brooks, Merck, Grant/Research Support.

## FR0012

**Parathyroid Hormone (PTH) increased rod-shaped trabeculae and maintained modulus of cancellous bone before fatigue failure.** Julia T. Chen<sup>\*1</sup>, Remy Walk<sup>1</sup>, Shefford Baker<sup>1</sup>, G. Elizabeth Pluhar<sup>2</sup>, Adele Boskey<sup>3</sup>, Christopher Hernandez<sup>1</sup>, Marjolien van der Meulen<sup>1</sup>. <sup>1</sup>Cornell University, United States, <sup>2</sup>University of Minnesota, United States, <sup>3</sup>Hospital for Special Surgery, United States

Clinically parathyroid hormone (PTH), the only-FDA approved anabolic osteoporosis treatment, decreases fracture risk by 10% [Neer et al. 2001]. In animal models, PTH increases cancellous bone volume [Jike et al. 1999], but its effect on bone tissue composition and mechanics is unknown, particularly under cyclic loading experienced during normal function. We hypothesized that PTH would increase compressive strength and preserve mechanical properties during cyclic fatigue loading through architectural and compositional changes.

To produce osteopenia, 13 mature ewes underwent ovariectomy and were fed a metabolic acidosis diet for one year. In the second year, sheep were injected with PTH (PTH, n=7, 5 $\mu$ g/kg/day SQ) or saline (VEH, n=6). In each animal two cancellous samples were taken from the distal femur: one for monotonic loading and one for cyclic fatigue loading. Samples were submitted to microCT scanning to evaluate microarchitecture. The number and volume fraction of rod- and plate-like trabeculae were determined using individual trabecular segmentation [Liu et al. 2008]. Then specimens were failed in compression to determine cancellous bone strength. Cyclic loading (max. normalized stress=0.004) was applied to failure (2.5% apparent strain). Energy dissipation and modulus reduction were evaluated during cyclic loading, and fatigue life was determined (Nf, number of cycles of failure). Cancellous tissue mechanics and composition were analyzed by nanoindentation and Raman spectroscopy.

Compressive strength and fatigue life were not different between PTH and VEH. However, PTH-treated samples experienced less energy dissipation and reduction in modulus before fatigue failure than VEH (Fig 1). PTH increased the number and volume fraction of rod-type trabeculae and decreased the volume fraction of plate-like trabeculae. The increased fraction of rods explained 50% of the variation in cyclic energy dissipation. In addition, mineralization decreased, while nanoindentation modulus and mineral crystallinity increased with PTH. Considering both alterations in architecture and composition, the increased fraction of rods and decreased mineralization explained 74% of the variation in energy dissipation.

Not all osteoporosis-related fractures are caused by a single overload. Our finding show that PTH alters microarchitecture and material properties to improve maintenance of mechanical properties following cyclic loading.

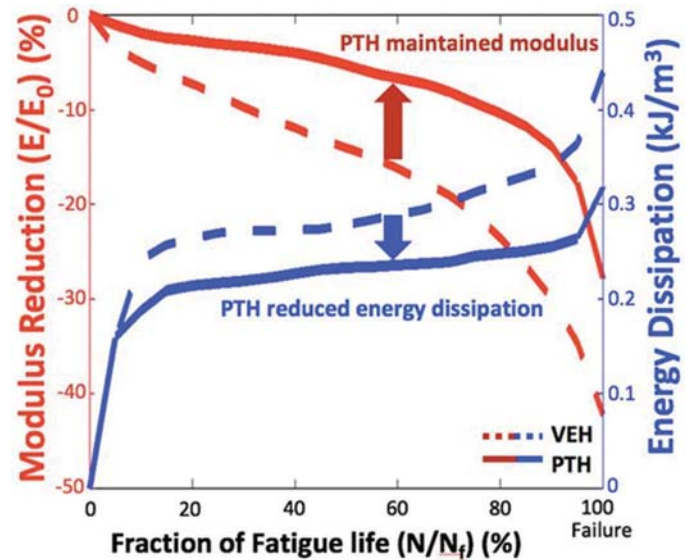


Figure 1: PTH maintained modulus (red) and experienced less energy dissipation (blue)

**Disclosures:** Julia T. Chen, None.

## FR0014

**Effects of Progressive Glycemic Derangement on Bone Tissue Composition in Postmenopausal Women.** Jared Pearl<sup>\*1</sup>, Nicholas Miller<sup>1</sup>, Jing Han Zhang<sup>1</sup>, Heather Hunt<sup>1</sup>, Kendall Moseley<sup>2</sup>, Eve Donnelly<sup>1</sup>. <sup>1</sup>Cornell University, United States, <sup>2</sup>Johns Hopkins University School of Medicine, United States

Individuals with type 2 diabetes mellitus (T2DM) have 10-year hip fracture risks greater than those of non-diabetics despite comparable bone mineral density (BMD). This observation suggests that progressive glycemic derangement may cause BMD-independent changes in bone quality. In this study, our objective was to assess the association between different states of glucose intolerance and bone tissue composition.

Iliac crest biopsies were collected from postmenopausal women ages 55-80 years allocated to three groups based on oral glucose tolerance testing: normal glucose tolerance (NGT, n=32), impaired glucose tolerance (IGT, n=12), and T2DM (n=13) (Table 1). Three cortical and three trabecular regions of ~400  $\mu$ m x 400  $\mu$ m on each of three sections per biopsy were scanned using Fourier transform-infrared imaging. The distribution of pixel values within each image was assessed for four parameters: mineral:matrix, carbonate:phosphate, collagen maturity, and crystallinity.

Tissue mineral content increased with progressive states of glycemic derangement, as evidenced by greater mean values of mineral:matrix in the IGT group. Specifically, cortical bone had greater mean mineral:matrix in the IGT vs. the NGT group (+6.5%, p = 0.0226; Fig. 1a). Furthermore, the distributions of trabecular mineral:matrix were narrower in the T2DM vs. the NGT group (-11.7%, p = 0.0457; Fig. 1d). Cortical and trabecular tissue from the T2DM group had wider distributions of crystallinity vs. that from the NGT group (+16.3%, p = 0.0168, Fig. 1c; +11.8%, p = 0.0219, Fig. 1d, respectively). The distributions of crystallinity values in the IGT group were also wider vs. the NGT group in trabecular bone (+16.8%, p = 0.0317), and trended toward being wider in cortical bone (+15.9% p = 0.0843). No other differences in tissue properties were observed.

Greater cortical mineral content, as well as narrower distributions of trabecular mineralization, were observed in bone tissue from individuals with worsening glycemic derangement. Because bone mineral content increases with tissue age (time since bone formation), these observations support prior observations that T2DM inhibits bone remodeling. However, the wider distributions in crystallinity in the IGT and T2DM groups compared to the NGT group are inconsistent with this interpretation; these more complex effects of impaired glycemic control on mineral properties require further investigation.

Table 1: Patient demographics.

Characteristic	NGT (n=32)	IGT (n=12)	T2DM (n=13)	IGT % difference vs. NGT	T2DM % difference vs. NGT
Age (years)	64.3 ± 6.9	65.6 ± 4.2	64 ± 5.1	2.02	-0.47
Height (cm)	161.0 ± 6.77	166.3 ± 5.58	156.6 ± 13.8	3.29	-2.73
Weight (kg)	77.7 ± 14.1	94.1 ± 19.1	92.5 ± 16.1	21.1	19.05
BMI (kg/m <sup>2</sup> )	30.01 ± 5.51	33.75 ± 5.00	34.1 ± 12.18	12.46	13.63
HbA1c	5.75 ± .27	6.02 ± .30	9.22 ± 2.03	4.7	60.35
Fast GLC (mg/dL)	90.1 ± 12.2	94.2 ± 9.86	N/A	4.55	N/A
120 Min GLC (mg/dL)	103.7 ± 24.5	158.5 ± 26.0	N/A	52.84	N/A

Values shown as means ± standard deviation. Significant differences (p<0.05) by ANOVA with Tukey post hoc are bolded.

**Figure 1:** FTIR properties (MinMatrix = mineral:matrix, CP = carbonate:phosphate, XLR = collagen maturity, XST = crystallinity) reported as image pixel distribution (a) means for cortical bone, (b) means 1 trabecular bone, (c) full widths at half maximum (FWHM) for cortical bone, and (d) full widths at half maximum for trabecular bone; \* p < 0.05, # p < 0.1. Bar heights and error bars indicate raw mean and 95% confidence intervals, respectively.

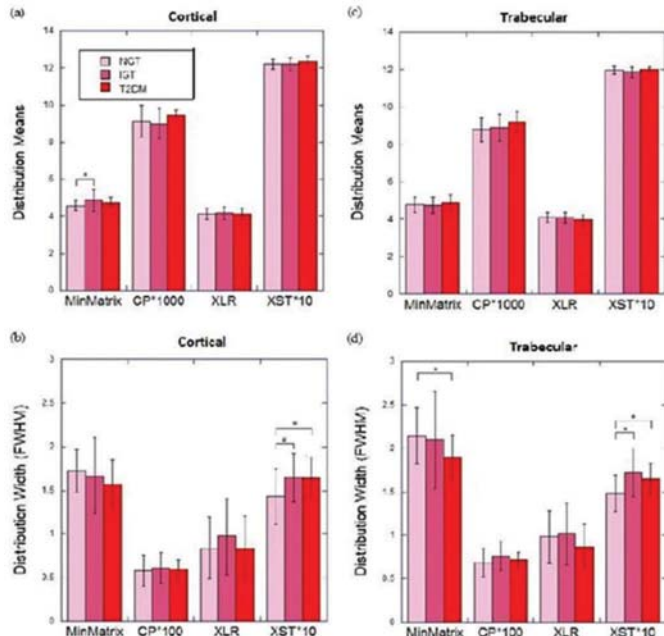


Figure 1, Table 1

Disclosures: Jared Pearl, None.

## FR0017

**Peak Trabecular Bone Microarchitecture But Not Bone Mass Predicts Rate of Estrogen-Deficiency-Induced Bone Loss.** Yihan Li\*, Wei-Ju Tseng, Chantal de Bakker, Hongbo Zhao, X. Sherry Liu. University of Pennsylvania, United States

Reduced estrogen levels during menopause lead to accelerated bone remodeling, resulting in low bone mass and increased fracture risk. Peak bone mass is a significant predictor of postmenopausal osteoporosis. However, it is not clear whether rates of postmenopausal bone loss depend on peak bone mass and bone microarchitecture. To establish this relationship, we used *in vivo*  $\mu$ CT to longitudinally track tibial bone changes in 62 rats (4-5 mo old) from 0 to 4 wks post-OVX.

Bone volume fraction (BV/TV) decreased 56% over 4 wks post-OVX. There was no correlation between baseline BV/TV and % decrease in BV/TV. Among all the baseline bone microarchitecture parameters, only trabecular thickness (Tb.Th) showed a trend of correlation with the extent of post-OVX bone loss ( $r = -0.21$ ,  $p = 0.097$ ). Stepwise multiple linear regressions suggested that the combination of baseline Tb.Th and connectivity density (Conn.D) was an important predictor for % decrease in BV/TV, Tb.Th, Tb spacing (Tb.Sp) and Conn.D (adjusted  $r = 0.36-0.66$ , Table 1).

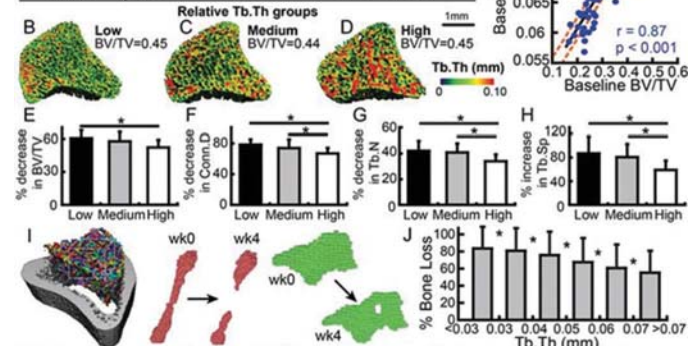
To further examine the influence of Tb.Th regardless of BV/TV on OVX bone loss, rats were stratified by the relative baseline Tb.Th (adjusted by BV/TV) into 3 groups: Low, Medium, and High relative Tb.Th (Fig 1A-D). No difference of baseline BV/TV was found among the 3 groups. In contrast, bone loss rate was 15% lower in the High and 5% lower in the Medium compared to the Low relative Tb.Th group, respectively (Fig 1E). Similar results were found for % decrease in Conn.D, Tb number (Tb.N), and Tb.Sp (Fig 1F-H). Next, we used individual trabecular dynamics (ITD) analyses to track bone loss that occurred in each individual trabecula based on precisely aligned pre- and post-OVX  $\mu$ CT images (Fig 1I). 11,862 trabeculae from 24 rats were analyzed and categorized to 6 groups based on their Tb.Th (Fig 1J). ANOVA test showed significant difference between all Tb.Th groups, suggesting thicker trabeculae led to less bone loss.

Moreover, trabeculae that went through connectivity deterioration (Fig 1I) had 14% lower Tb.Th than trabeculae that remained intact post-OVX.

In summary, the extent of OVX bone loss was affected by peak bone microarchitecture, most notably the trabecular thickness. Thicker trabeculae are less likely to be disconnected or perforated in response to OVX, resulting in less degree of bone loss. Given the same bone mass (BV/TV), a trabecular bone phenotype with thin trabeculae may be a risk factor toward accelerated postmenopausal bone loss.

**Table 1:** Correlation coefficients ( $r$ ) and independent baseline predictors by stepwise multiple linear regression for % decrease in trabecular parameters. Minus sign indicates negative correlation. \* $p < 0.05$ , \*\* $p < 0.01$ , \*\*\* $p < 0.001$ .

% decrease	$r$	Adjusted $r$	Independent predictors
BV/TV	0.39	0.36	-Tb.Th*, Conn.D*
Tb.Th	0.66	0.64	Conn.D*, Tb.Th*
Tb.Sp	0.47	0.44	-Conn.D*, Tb.Th*
Tb.N	0.46	0.44	-Tb.Th*, Tb.N*
SMI	0.26	0.22	-SMI*
Conn.D	0.67	0.66	-Tb.Th*, Conn.D*



(A) Linear regression of baseline BV/TV and Tb.Th to stratify data into 3 relative Tb.Th groups. (B-D) Representative trabecular bone images and (E-H) % changes in bone parameters in Low, Medium, and High relative Tb.Th groups. (I) Schematics of individual trabecular dynamics analysis; (J) % bone loss in individual trabeculae stratified by thickness. \*:  $p < 0.05$

Figure 1

Disclosures: Yihan Li, None.

## FR0020

**Zoledronate and Mechanical Loading Treatments During Simulated Weightlessness: Cancellous Structure and Osteocellular Responses.** Ryan T. Scott\*, Joshua Alwood<sup>2</sup>, Mohit Nalavadi<sup>3</sup>, Sulekha Anand<sup>4</sup>, Yasaman Shirazi-Fard<sup>2</sup>, Alesha Castillo<sup>5</sup>. <sup>1</sup>NASA Ames Research Center, San Jose State University, United States, <sup>2</sup>NASA Ames Research Center, United States, <sup>3</sup>Blue Marble Space Institute of Science, United States, <sup>4</sup>San Jose State University, United States, <sup>5</sup>New York University, United States

Astronauts using high-force resistance exercise as an in-flight countermeasure to weightlessness-induced bone loss, present with both elevated formation and resorption biomarkers. The bisphosphonate zoledronate is a candidate countermeasure for space-flight due to its substantial anti-resorptive potency and long half-life. We asked, are there negative side effects to bone when exercise, weightlessness, and zoledronate combine? We developed an integrated model mimicking mechanical strain of exercise via tibial cyclical loading in skeletally mature C57BL/6 mice (male, 16 weeks old), treated 3 days prior to study commencement with one dose of zoledronate (45 $\mu$ g/kg) or a saline vehicle, and subjected to 3 weeks of hindlimb unloading to simulate weightlessness or normal ambulation. Right tibiae of anesthetized mice were axially compressed *in vivo* 60 cycles/day, to 9N (+1200 periosteal  $\mu$ strain), 3 days/wk, for 3 weeks. Left tibiae served as within-subject, non-compressed controls. Microcomputed tomography determined structural changes and histomorphometry determined osteoclast- and osteoblast-relevant surfaces. A multivariate ANCOVA mixed model was used ( $\alpha$  of 0.05), with a random effect accounting for the within-subject treatments for the tibiae. Focusing on the cancellous compartment of the proximal tibial metaphysis, zoledronate increased the amount of cancellous bone volume (+32%), and caused a reduction of osteoclast surface (-45%), compared to vehicle. Surprisingly, zoledronate reduced mineralizing surface (-40%) and bone formation rate (-54%), indicators of osteoblast activity, compared to vehicle. Unloading reduced cancellous bone volume (-31%), reduced the mineralizing surface (-38%), and reduced bone formation rate (-50%), all compared to normally ambulating subjects. Compared to the non-compressed left tibiae, cyclical loading increased cancellous bone volume (+15%), mineralizing surface (+20%), and bone formation rate (+24%). Unique interactions were observed with zoledronate blunting the gains from cyclical loading in cancellous bone volume. Unloading also had an interaction with cyclical loading, preventing increases in bone formation rate. These data suggest either exercise is less effective or the kinetics of formation are slower during simulated weightlessness. Zoledronate was an effective countermeasure of weightlessness-induced bone loss, though each rendered exercise-related mechanical loading less effective in cancellous tissue.

Disclosures: Ryan T. Scott, None.



## FR0023

**Mechanical stimulus upregulates IGF-1 levels, restores bone mass and microarchitecture on both non-fractured and fractured femurs in diabetic rats.** Ariane Zamarioli<sup>\*1</sup>, Maysa Campos<sup>2</sup>, João P. B. Ximenez<sup>3</sup>, Raquel A. Silva<sup>4</sup>, José B. Volpon<sup>2</sup>. <sup>1</sup>Medical School of Ribeirão Preto, University of São Paulo, Brazil, <sup>2</sup>Medical School of Ribeirão Preto, Brazil, <sup>3</sup>School of Pharmaceutical Sciences of Ribeirão Preto, Brazil, <sup>4</sup>School of Dentistry of Ribeirão Preto, Brazil

The aim of this study was to assess the effects of mechanical stimuli on the bone quality and fracture healing in diabetic and non-diabetic rats. For this, 112 female Wistar rats (200±10g) were assigned to four groups: (1) SHAM, (2) sham with vibration therapy (SHAM+VT), (3) diabetes mellitus (DM), and (4) DM+VT. Diabetes was induced with a single intravenous injection of streptozotocin. Thirty days after diabetes induction, animals underwent closed bone fracture at the right mid-femur, followed by surgical stabilization of bone fragments. Three days after bone fracture, DM+VT and SHAM+VT rats were subjected to whole-body vibration therapy (50 Hz, 3x/wk, 20 minutes). On days 14 and 28 post-fracture (representing two distinct phases of normal bone healing: soft and hard bone callus formation, respectively), the rats were euthanized, blood was collected for serum bone marker analysis, and both femurs were collected for micro-computed tomography and histological analysis in order to assess bone quality (left femur) and fracture healing (right femur). Diabetes led to a dramatic impairment of both bone quality and fracture healing in both end-points assessment (with a time-dependent feature). The level of circulating IGF-1 was significantly reduced in diabetic rats (-93%). However, vibration therapy significantly increased the IGF-1 level by 839%. The CTX-I level was increased by 1385% in diabetic rats. Vibration therapy significantly decreased the RANK-L level by 19% in diabetic rats. Vibration therapy also decreased the RANK-L level by 20% in the sham rats, but without statistical significance. In intact bone, diabetes caused detrimental changes in bone microarchitecture (reduced BV by 90%, BV/TV by 87%, TbN by 85% and Conn.D by 77%). VT was effective at ameliorating trabecular microarchitecture (augmented BV by 494%, BV/TV by 386%, TbN by 394% and Conn.D by 233%).

In bone healing, diabetes caused a delay in cell proliferation; 81% in callus volume and 69% in callus mineralization. VT was effective at improving fracture healing by accelerating osteogenic and chondrogenic cell proliferation at the fracture callus (Fig 1), thus increasing callus volume by 52%. We concluded that diabetes had detrimental effects on both non-fractured bone quality and fracture healing. Vibration therapy was very effective at counteracting the significant disruption in bone metabolism, mass and microarchitecture on both non-fractured and fractured femurs of diabetic rats.

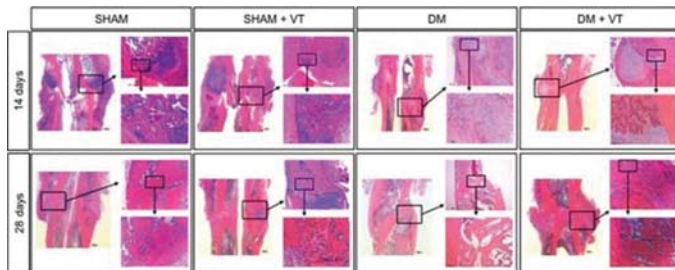


Figure 1. Histological slides of fractured femurs stained with HE (magnification 12.5, 50, and 200x)

**Disclosures:** Ariane Zamarioli, None.

## FR0027

**Maternal gestational vitamin D supplementation alters perinatal *RXRα* DNA methylation: findings from the MAVIDOS trial.** Elizabeth Curtis<sup>\*1</sup>, Nevena Krstic<sup>2</sup>, Eloise Cook<sup>2</sup>, Stefania D'Angelo<sup>1</sup>, Sarah Crozier<sup>1</sup>, Rebecca Moon<sup>3</sup>, Robert Murray<sup>2</sup>, Emma Garratt<sup>2</sup>, Paula Costello<sup>2</sup>, Nicholas Bishop<sup>4</sup>, Stephen Kennedy<sup>5</sup>, Aris Papageorgiou<sup>5</sup>, Inez Schoenmakers<sup>6</sup>, Robert Fraser<sup>7</sup>, Saurabh Gandhi<sup>7</sup>, Ann Prentice<sup>8</sup>, Kassim Javaid<sup>9</sup>, Hazel Inskip<sup>1</sup>, Keith Godfrey<sup>10</sup>, Christopher Bell<sup>11</sup>, Karen Lillycrop<sup>2</sup>, Cyrus Cooper<sup>12</sup>, Nicholas Harvey<sup>10</sup>. <sup>1</sup>MRC Lifecourse Epidemiology Unit, University of Southampton, United Kingdom, <sup>2</sup>Institute of Developmental Sciences, University of Southampton, United Kingdom, <sup>3</sup>MRC Lifecourse Epidemiology Unit, University of Southampton; Paediatric Endocrinology, University Hospitals Southampton NHS Foundation Trust, United Kingdom, <sup>4</sup>Academic Unit of Child Health, Sheffield Children's Hospital, University of Sheffield, United Kingdom, <sup>5</sup>Nuffield Department of Obstetrics and Gynaecology, John Radcliffe Hospital, University of Oxford, United Kingdom, <sup>6</sup>MRC Elsie Widdowson Laboratory; Department of Medicine, Faculty of Medicine and Health Sciences, University of East Anglia, United Kingdom, <sup>7</sup>Sheffield Hospitals NHS Trust, University of Sheffield, United Kingdom, <sup>8</sup>MRC Elsie Widdowson Laboratory, United Kingdom, <sup>9</sup>National Institute for Health Research (NIHR) Biomedical Research Centre, University of Oxford, United Kingdom, <sup>10</sup>MRC Lifecourse Epidemiology Unit, University of Southampton; NIHR Southampton Nutrition Biomedical Research Centre, University of Southampton and University Hospital Southampton NHS Foundation Trust, United Kingdom, <sup>11</sup>MRC Lifecourse Epidemiology Unit, University of Southampton; Institute of Developmental Sciences, University of Southampton, United Kingdom, <sup>12</sup>MRC Lifecourse Epidemiology Unit, University of Southampton; National Institute for Health Research (NIHR) Biomedical Research Centre, University of Oxford, United Kingdom

Evidence is accumulating of associations between perinatal epigenetic markers and offspring bone mass. We have previously demonstrated associations between perinatal DNA methylation at the retinoid-X-receptor- $\alpha$  (*RXRα*) locus and offspring bone mass in the Southampton Women's Survey mother-offspring cohort, and shown that this may be mediated by maternal vitamin D status. *RXRα* is known to play a key role in the nuclear action of 1,25(OH)<sub>2</sub>-vitamin D.

We tested the hypothesis that maternal supplementation with vitamin D during pregnancy in a randomised controlled trial setting would lead to altered perinatal DNA methylation at the *RXRα* locus.

The Maternal Vitamin D Osteoporosis Study (MAVIDOS) is a multicentre, double-blind, randomised, placebo-controlled trial of 1000IU/day cholecalciferol or matched placebo from 14 weeks gestation until delivery. Umbilical cord tissue from the fetal side was collected at birth and frozen at -80°C (n=436). Pyrosequencing was used to carry out in-depth DNA methylation analysis at 10 CpG sites within the *RXRα* promoter. The CpG sites were selected on the basis of those previously analysed in the observational Southampton Women's Survey mother-offspring cohort.

Independent t-tests were used to assess the differences in methylation between the treatment groups.

Statistically significant ( $p \leq 0.05$ ) differences in methylation at the *RXRα* region of interest were observed between the cholecalciferol supplemented and placebo group at 4 of 10 CpG sites. Overall, *RXRα* methylation levels were significantly lower in the umbilical cord from offspring of cholecalciferol supplemented mothers: e.g. at *RXRα* CpG 5, mean difference in % methylation between the supplemented and placebo groups was -2.1% (n=433, 95% CI -3.7 to -0.3,  $p=0.02$ ). We have previously demonstrated in vitro, using electrophoretic mobility shift assays, that methylation in this region leads to reduced transcription factor binding. Therefore, the reduced methylation observed in the cholecalciferol supplemented group may be associated with an upregulation of 1,25(OH)<sub>2</sub>-vitamin D signalling.

These findings support previous observational results and provide new evidence that maternal gestational supplementation with cholecalciferol leads to altered perinatal epigenetic marking. Such results inform potential mechanistic pathways linking maternal 25(OH)-vitamin D status to offspring bone mass, and may yield novel biomarkers of future bone development.

**Disclosures:** Elizabeth Curtis, None.

## FR0029

**Multiple fractures in children is related to cortical bone dimensions.** Dana L. Duren<sup>\*1</sup>, Emily V. Leary<sup>1</sup>, Dan G. Hoernschemeyer<sup>1</sup>, Laura L. Tosi<sup>2</sup>, Richard J. Sherwood<sup>1</sup>. <sup>1</sup>University of Missouri, United States, <sup>2</sup>Children's National Medical Center, United States

Reduced bone strength during childhood and adolescence is a well-described risk factor for fracture. And, putting aside contemporary debates on risk-taking behaviors influencing child fracture rates, it has also been suggested that children who sustain multiple fractures may have even lower bone mass than their single fracture peers. We sought to test the hypothesis that children who sustain more than one fracture during

childhood differ in bone structure than their peers with no or only one fracture. Our sample consisted of longitudinal data on midshaft cortical bone measures from the second metacarpal on left hand-wrist radiographs from 948 children participating in the Fels Longitudinal Study. Numbers of children per group were: 356 boys and 368 girls with no fracture; 88 boys and 61 girls with a single fracture; 48 boys and 27 girls with two or more fractures. Median number of observations per child was 21, and ages ranged from 0-18 years. We modeled each bone trait (bone width, cortical thickness, polar moment of inertia, and cross-sectional area/bone length) using a fifth order polynomial with fixed effects and random subject-specific effects to account for repeated measures. Girls and boys were analyzed separately. Children of both sexes with multiple fractures exhibited reduced means for each bone measure at some time across childhood. Bone cross-sectional area over length showed the greatest separation between groups, with the multi-fracture group exhibiting an average of 4.1% reduction across ages in boys, and 5.2% reduction across ages in girls. When the models were constructed using skeletal age rather than chronological age, differences between groups were reduced. Results of this study support previous research indicating reduced bone mass in children with multiple fractures, and extend the conclusions to include that the reduction in bone mass may be explained in part by altered bone and cortical dimensions. The role of skeletal maturity status in this relationship is worth further analysis as it could provide a further assessment tool for pediatric fracture risk.

**Disclosures:** Dana L. Duren, None.

## FR0031

**Frequency of vigorous physical activity predicts bone strength accrual during adolescence.** Leigh Gabel<sup>\*1</sup>, Lindsay Nettlefold<sup>1</sup>, Heather Macdonald<sup>1</sup>, Heather McKay<sup>2</sup>. <sup>1</sup>Centre for Hip Health and Mobility, Canada, <sup>2</sup>University of British Columbia, Canada

**Purpose:** The link between physical activity (PA) and bone strength is irrefutable; however, we do not know the precise PA prescription (i.e., frequency and total volume) for optimal accrual of bone strength during growth. Thus, we aimed to examine the influence of vigorous PA (VPA) bout frequency on bone strength accrual across adolescence, independent of total volume of VPA.

**Method:** We acquired high-resolution peripheral quantitative computed tomography scans of the distal tibia (8% site) and applied finite element analysis to estimate bone strength in compression (failure load, F.Load, N) in 309 adolescents (9–20 years at baseline) over a maximum of 4 years. We measured VPA [total volume (min/day) and bout frequency < 5 min in duration (bouts/day)] annually using accelerometers (ActiGraph GT1M). We aligned participants on maturity offset (years from age at peak height velocity) and fit a mixed effects model adjusting for maturity, sex, ethnicity, tibia length, lean body mass and VPA (volume and bout frequency).

**Results:** Average volume of VPA (min/day) and VPA bout frequency (# bouts per day of VPA < 5 min in duration) declined across adolescence, from approximately 14 and 20 min/day and 35 and 42 bouts/day in girls and boys, respectively, at 2 years prior to APHV to 6 and 8 min/day and to 8 and 11 bouts/day in girls and boys, respectively, at 7 years post-APHV. Both VPA total volume and bout frequency were positively associated with F.Load across adolescence. However, VPA volume did not predict F.Load after accounting for VPA bout frequency. Participants in the upper quartile of VPA bout frequency (~33 bouts/day) had 10% (500 N; 95% CI: 112 to 889;  $p = 0.012$ ) greater F.Load across adolescence compared with participants in the lowest quartile (~9 bouts/day) (Figure). Each additional daily bout of VPA was associated with 21 N greater F.Load, independent of total volume of VPA.

**Conclusion:** Consistent with results from classic animal loading models, VPA bout frequency was a stronger predictor of bone strength at the distal tibia in adolescent girls and boys as compared with total volume of VPA. Further, despite significant declines in VPA in girls and boys, our findings suggest the influence of VPA bout frequency on F. Load is consistent across adolescence. Public health guidelines for bone strength may be best served by encouraging frequent, short bouts of VPA.

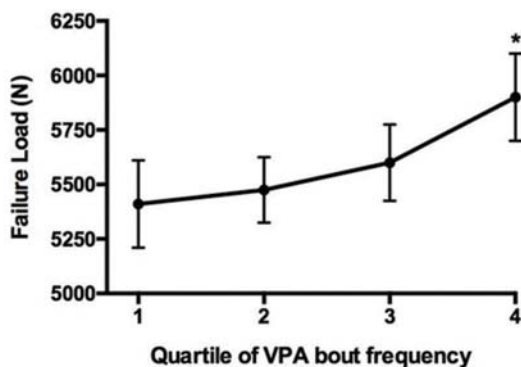


Figure. Relationship between failure load (N) and quartiles of vigorous physical activity (VPA) bout frequency. Estimated marginal means (95% confidence interval) from mixed effects model adjusted for maturity offset, sex, ethnicity, tibia length, lean body mass and total volume of VPA. Cut points for quartiles were 9, 20 and 33 bouts/day. \* $p = 0.012$  compared with quartile 1.

Figure

**Disclosures:** Leigh Gabel, None.

## FR0032

**Does Peak Bone Mass Coincide with Peak Bone Strength?** Erik Lindgren<sup>\*</sup>, Bjorn Rosengren, Magnus Karlsson, Department of Clinical Sciences and Orthopaedics, Lund University, Malmö, Sweden

**Purpose:** DXA estimated areal bone mineral density (aBMD) is gold standard to determine peak bone mass (PBM) and diagnose osteoporosis. aBMD is also the most used trait to estimate the ability of bones to withstand outer forces and fractures. Most studies infer that hip PBM in men occurs as early as age 16-19 years. However, the unit (g/cm<sup>3</sup>) states that aBMD have an inverse relationship with bone size. Bone size is also, independently of the amount of bone mineral, a predictor of bone strength and fracture risk. The question then arises - is PBM really the time at which also bone strength is the highest? Why the bones ability to withstand outer forces in an evolutionary perspective should start to decline at such an early age is difficult to understand.

**Materials and methods:** We measured bone traits in the left femoral neck (FN) by DXA in a cross-sectional study of 1,052 population-based men aged 18-28 years. We registered aBMD (g/cm<sup>3</sup>), bone mineral content (BMC; g) and bone area (cm<sup>2</sup>). We used ANOVA to evaluate statistical significant differences in traits between one-year age groups and Pearson correlation coefficient to evaluate correlation between traits and age.

**Results:** We found the highest aBMD value (PBM) at age 19 years. There were statistically significant differences between one-year age groups in FN aBMD, BMC and bone area (all  $p < 0.05$ ). However, while there from PBM until age 28 were negative correlations between age and aBMD ( $r = -0.12$ ;  $p < 0.001$ ) and age and BMC ( $r = -0.07$ ;  $p < 0.05$ ), there was a positive correlation with age and bone area ( $r = 0.06$ ;  $p < 0.05$ ). That is, the amount of bone minerals declined from age 19 to 28 while bone size increased during the same period.

**Conclusions:** We conclude that hip peak bone mass (PBM) in men cannot per se be regarded as the time with the highest hip bone strength, since bending strength of a tubular bone is related to the fourth power of the radial distance.

**Disclosures:** Erik Lindgren, None.

## FR0033

**Plate-like trabeculae increase with age and lean mass in healthy girls at the distal tibia.** Deborah Mitchell<sup>\*1</sup>, Signe Caksa<sup>2</sup>, Amy Yuan<sup>2</sup>, Mary Bouxsein<sup>2</sup>, Madhusmita Misra<sup>3</sup>, Sherri-Ann Burnett-Bowie<sup>2</sup>. <sup>1</sup>Pediatric Endocrine Unit, Massachusetts General Hospital, United States, <sup>2</sup>Endocrine Unit, Massachusetts General Hospital, United States, <sup>3</sup>Pediatric Endocrine and Neuroendocrine Units, Massachusetts General Hospital, United States

**Background:** Childhood is a critical window for bone accrual and microarchitecture development. Previous data suggest that changes in trabecular bone parameters are relatively modest across late childhood and adolescence in girls. We hypothesized that trabecular morphology would change across this period, becoming more plate-like and thereby conferring increased strength and fracture resistance. We further hypothesized that trabecular morphology would correlate with body composition.

**Design and methods:** We conducted a cross-sectional study of 86 healthy girls ages 9-18 years. Skeletal maturity was assessed with bone age x-ray. We measured body composition by DXA and used HR-pQCT to measure volumetric bone density and microarchitecture at the distal tibia. Individual trabecula segmentation (ITS) was used to assess trabecular morphology.

**Results:** Trabecular bone volume fraction (BV/TV) tended to increase with bone age ( $R = 0.20$ ,  $p = 0.065$ ). In comparison, plate-like BV/TV increased significantly ( $R = 0.41$ ,  $p < 0.001$ ), while rod-like BV/TV decreased significantly ( $R = -0.28$ ,  $p = 0.008$ ) with bone age. The increase in plate BV/TV was driven by increases in plate number ( $R = 0.24$ ,  $p = 0.026$ ) as well as by plate size including both thickness ( $R = 0.52$ ,  $p < 0.001$ ) and surface area ( $R = 0.43$ ,  $p < 0.001$ ). To examine the associations of body composition with trabecular morphology, we used multivariable modeling with bone age, lean mass, and fat mass as predictors. In this model, lean mass was positively correlated with plate BV/TV (partial  $R = 0.24$ ,  $p = 0.028$ ) and plate thickness (partial  $R = 0.28$ ,  $p = 0.010$ ), while fat mass was negatively correlated with plate thickness (partial  $R = -0.23$ ,  $p = 0.039$ ) and surface area (partial  $R = -0.26$ ,  $p = 0.019$ ). In addition, fat mass positively correlated with rod BV/TV (partial  $R = 0.31$ ,  $p = 0.004$ ) and rod number (partial  $R = 0.33$ ,  $p = 0.002$ ) and negatively correlated with rod length (partial  $R = -0.41$ ,  $p < 0.001$ ).

**Conclusions:** Between the ages of 9 to 18, despite only modest increases in BV/TV, trabecular morphology changes significantly in healthy girls, with an estimated 61% increase in plate BV/TV and 21% decrease in rod BV/TV at the distal tibia. Lean mass independently correlates with plate parameters, expected to confer strength, while fat mass correlates with smaller plates and more numerous and shorter rods. These data suggest that increased lean mass in youth promotes bone strength while increased fat mass may be associated with maladaptive microarchitecture.

**Disclosures:** Deborah Mitchell, None.



## FR0034

**Increased FGF23 in chronic kidney disease results from osteocyte maturation delay.** Renata C Pereira<sup>1</sup>, Barbara Gales<sup>1</sup>, Katherleen Noche<sup>2</sup>, Isidro I Salusky<sup>1</sup>, Katherine Wesseling-Perry<sup>1</sup>. <sup>1</sup>David Geffen School of Medicine at UCLA, Los Angeles, California, United States of America, United States, <sup>2</sup>University of California, United States

Increased bone FGF23 expression co-occurs with mineralization defects in pediatric CKD patients. FGF23-expressing osteocytes are located at the trabecular periphery, where young osteocytes reside. We hypothesized that increased bone FGF23 expression reflects impaired osteocyte maturation in CKD. We thus evaluated plasma FGF23 levels (C-terminal, Immutopics) as well as osteocyte-specific FGF23 and e11/gp38 (a marker of young osteocytes) expression in bone biopsies from 32 CKD patients aged 2-25 years. Bone turnover was high (n=15); normal (n=10); or low (n=7). Osteoid volume was increased in 25% of pre-dialysis and in 50% of dialysis patients. Immunohistochemical staining for FGF23 (anti-human FGF23 (225-244) (Immutopics)) was quantified in 5µm trabecular bone sections by counting numbers of FGF23-expressing osteocytes; co-localization of FGF23 and e11/gp38 (ab25, Abcam) was performed by immunofluorescence. Plasma FGF23 levels and numbers of FGF23-expressing osteocytes were increased in all patients (Figure A). Numbers of FGF23-expressing osteocytes correlated with plasma C-terminal FGF23 in dialysis (r=0.70, p<0.01), but not in pre-dialysis, patients. FGF23 co-localized with e11/gp38 (Figure B). Co-localization with e11/gp38 suggests that FGF23 expression is a characteristic of young osteocytes. The tight correlation between numbers of young, FGF23-expressing, osteocytes and circulating FGF23 values in dialysis patients suggests that increased circulating FGF23 concentrations reflect increased numbers of young osteocytes. Renal FGF23 clearance likely contributes to the lower circulating FGF23 levels and their imperfect correlation with bone FGF23 expression in pre-dialysis patients. Thus, osteocyte maturation delay may contribute to excess FGF23 levels and may also explain the co-occurrence of skeletal mineralization defects in the CKD population.

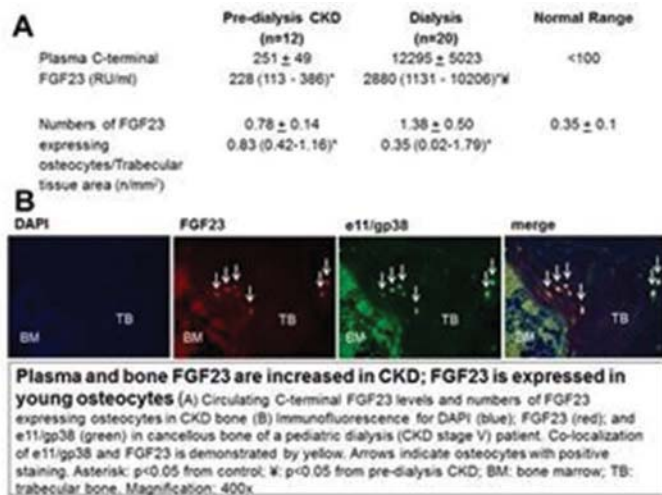


Figure A

**Disclosures:** Renata C Pereira, None.

## FR0037

**Effects of Sclerostin Depletion on Hematopoietic Stem Cells.** Cristine Donham<sup>1</sup>, Gabriela Loots<sup>2</sup>, Jennifer Manilay<sup>3</sup>, Aris Economides<sup>4</sup>. <sup>1</sup>University of California Merced, United States, <sup>2</sup>Lawrence Livermore National Laboratories, United States, <sup>3</sup>University of California, Merced, United States, <sup>4</sup>Regeneron Pharmaceuticals, United States

There is a deficit in current understanding of how interactions between hematopoietic stem cells and cells in their microenvironment result in changes in stem cell behavior. Our overall goal is to define the molecular mechanisms that guide the behavior of long-term HSCs (LT-HSCs) after exposure to an irregular bone marrow (BM) niche. Sclerostin (Sost) is a secreted Wnt antagonist protein that is important for bone homeostasis, as demonstrated by the increased bone mass that is observed in Sost-knockout (KO) mice. As Wnt signaling is also important for LT-HSC maintenance and self-renewal, we hypothesized that loss of Sost in the bone microenvironment would influence LT-HSCs. To test this hypothesis, we performed serial hematopoietic progenitor transplantation assays and utilized congenic CD45.1 and CD45.2 alleles to track donor and host-derived hematopoiesis in wild-type (WT) and KO recipient mice. We observed that LT-HSCs derived from WT CD45.1+ progenitors were expanded in frequency in WT CD45.1+ @ KO CD45.2+ mice (WT @KO) compared to WT CD45.1+ @ WT CD45.2+ (WT@WT) recipients. Serial transplantation of hematopoietic progenitors from WT@KO mice into secondary WT hosts demonstrated continued expansion of the LT-HSCs, even though Sost expression in the microenvironment was replenished. This permanence in LT-HSC expansion suggests that the Sost-depleted

microenvironment induces epigenetic changes in LT-HSCs. In support of this idea, our preliminary studies indicate that global DNA methylation in KO LT-HSCs is lower than WT controls, and expression of positive regulators of DNA methylation, *Tet2* and *Dnmt1*, is decreased. Transcriptome profiling by RNA-Seq to identify other gene expression differences between WT and KO LT-HSCs and changes in LT-HSC gene expression after transplantation into WT and KO microenvironments is planned. We have also investigated whether exposure of hematopoietic progenitors to KO microenvironments influences their differentiation, and our data suggest that the KO bone marrow niche tends to favor hematopoietic differentiation to the myeloid lineages. Taken together, our data indicate a role for Sost in the bone marrow niche in the regulation of LT-HSC self-renewal, proliferation and differentiation, which could be used towards clinical applications such as ex vivo HSC expansion and directed differentiation of HSCs to specific hematopoietic lineages.

**Disclosures:** Cristine Donham, None.

## FR0038

**Targeting the Endosteal Niche in Myelodysplasia and Acute Myeloid Leukemia.** Marta Galán-Diez<sup>1</sup>, Govind Bhagat<sup>1</sup>, Julie Teruya-Feldstein<sup>2</sup>, Azra Raza<sup>1</sup>, Elin Berman<sup>3</sup>, Stavroula Koustini<sup>1</sup>. <sup>1</sup>Columbia University, United States, <sup>2</sup>Mount Sinai, United States, <sup>3</sup>Memorial Sloan Kettering Cancer Center, United States

It has been shown that an activating mutation of  $\beta$ -catenin in osteoblasts (*Ctnnb1*<sup>CAosb</sup> mice) is sufficient to initiate the development of MDS with rapid progression to AML, through upregulation of *Jagged1* expression in osteoblasts and subsequent activation of Notch signaling in hematopoietic cells (HSCs). The disease is cell-autonomous and associated with clonal evolution at the cytogenetic level. These findings are relevant to human disease since more than 30% of patients with MDS/AML show increased  $\beta$ -catenin activation and *Jagged1* expression in their osteoblasts and increased Notch signaling in HSCs. We examined the efficacy of a monoclonal mouse anti-human *Jagged1* antibody (JAG1-Ab) as a therapeutic agent for osteoblast-induced MDS/AML. JAG1-Ab binds to the EGF2/EGF4 domains of human, mouse and rat *Jagged1* with EC50<0.066nM (11ng/ml) and inhibits in a dose-dependent manner, induced Notch-signaling with IC50<6nM (1µg/ml). Single administration pharmacokinetic analysis in mice at 3mg/kg body-weight (BW) showed maximum blood concentration (6.26µg/ml) at 24hr, and a terminal half-life of 36hrs. Organ dysfunction or toxicity was not observed at concentrations as high as 30mg/kg BW for 5 weeks. The efficacy of weekly subcutaneous administration of 3mg/kg BW was examined in *Ctnnb1*<sup>CAosb</sup> leukemic mice. Administration of JAG1-Ab at post-natal day 8 -a time at which MDS/AML has developed- prevented anemia, neutrophilia and lymphocytopenia. Circulating blasts disappeared from the blood within 2-weeks following JAG1-Ab administration (2 doses) and the increase in the long-term repopulating HSC progenitors -the leukemia initiating population- was reversed. Myeloid differentiation was restored and the percentage of mature myeloid population increased indicating myeloid maturation. Dysplastic features seen in the marrow, spleen and liver of *Ctnnb1*<sup>CAosb</sup> mice were absent in JAG1-Ab-treated mice and normal trilineage hematopoiesis was established. As a result, JAG1-Ab prevented lethality of *Ctnnb1*<sup>CAosb</sup> mice and progressively increased BW for the entire period that the treatment was maintained (12 weeks). Upon treatment-termination, blast reappeared in the blood within 7 weeks with subsequent development of full-blown AML-phenotype leading to lethality within 14 weeks. These results suggest that blocking *Jagged1* signaling between osteoblasts and HSCs efficiently treats osteoblast-induced MDS/AML in mice and may have a therapeutic application in patients with MDS and AML.

**Disclosures:** Marta Galán-Diez, None.

## FR0040

**Deletion of TIEG in CD4+ T-cells results in a sexually dimorphic bone phenotype.** Malayannan Subramaniam<sup>1</sup>, Abdulrahman Saadalla<sup>1</sup>, Molly Nelson Holte<sup>1</sup>, Megan Weivoda<sup>1</sup>, Merry Jo Oursler<sup>1</sup>, Khashayarsha Khazaei<sup>1</sup>, Russell Turner<sup>2</sup>, Urszula Iwaniec<sup>2</sup>, John Hawse<sup>1</sup>. <sup>1</sup>Mayo Clinic, United States, <sup>2</sup>Oregon State University, United States

TGF $\beta$  inducible early gene-1 (TIEG), also referred to as KLF10, was originally discovered in human osteoblasts and has been shown to play important roles in mediating osteoblast, osteoclast and osteocyte function. TIEG is known to regulate TGF $\beta$ , BMP, estrogen and Wnt signaling in bone and altered expression of TIEG, as well as polymorphisms in the TIEG gene, are associated with osteoporosis in humans. More recently, TIEG has been implicated as a critical modulator of CD4+ T-cell development and function demonstrating that this transcription factor also plays important roles in regulating inflammation and immune cell function. For these reasons, as well as the known roles of the immune system in regulating bone metabolism and skeletal homeostasis, we sought to examine the effects of CD4+ T-cell specific deletion of TIEG (TIEG TKO) on the mouse skeleton. Characterization of 3-month-old WT (CD4-cre) and TIEG TKO mice using pQCT and micro-CT analyses surprisingly revealed a sexually dimorphic phenotype characterized by increased bone mass in TIEG TKO male mice but decreased bone mass in TIEG TKO female mice relative to WT littermates. Interestingly, histomorphometric analyses revealed no significant changes in osteoclast perimeter per bone perimeter between WT and TIEG TKO male mice, but instead nearly a doubling in osteoblast perimeter. These effects were accompanied by increased numbers of CD4+ Treg cells in the bone marrow of male mice with no changes

in Treg numbers observed in female TIEG TKO mice. However, significant increases in osteoclast precursors, as defined by CD11b-low, cFms+ monocytes, were observed in the bone marrow of TIEG TKO female mice but not in male mice relative to WT littermates. Consistent with this, co-culture of female TIEG TKO Treg cells with osteoclast precursors isolated from WT mice resulted in increased osteoclast differentiation *in vitro* compared to co-culture with Tregs isolated from WT mice. In naive CD4+ T-cells, deletion of TIEG resulted in decreased expression of the osteoclastogenic factors, CCL3, RANKL and TRAF6 in male mice, but increased expression in female mice. These findings are the first to describe a sexually dimorphic bone phenotype that results from loss of function of a transcription factor in T-cells and identifies TIEG as a novel osteoimmunological factor that differentially regulates bone metabolism in males and females potentially through sex steroid specific effects on CD4+ T-cells.

**Disclosures:** Malayannan Subramaniam, None.

## FR0041

**Erythropoietin regulates bone marrow stromal cell differentiation.** Sukanya Suresh<sup>\*1</sup>, Luis Fernandez De Castro Diaz<sup>2</sup>, Soumyadeep Dey<sup>1</sup>, Pamela Robey<sup>2</sup>, Constance Noguchi<sup>1</sup>. <sup>1</sup>Molecular Medicine Branch, National Institute of Diabetes and Digestive and Kidney Diseases, National Institutes of Health, United States, <sup>2</sup>Skeletal Biology Section, National Institute of Dental and Craniofacial Research, National Institutes of Health, United States

Erythropoietin (EPO), made in kidneys is essential for erythroid differentiation into red blood cells. Functional EPO-receptor (EPOR) present on non-erythroid cells suggests systemic effects exerted by EPO. Bone marrow (BM) is the primary site of EPO stimulated erythropoiesis and BM stromal cells (BMSCs), progenitors for osteoblasts and bone marrow adipocytes (BMAT), express EPOR. Hence, we assessed the role of EPO signaling in BMSC differentiation to determine potential consequences of EPO on bones and BMAT.

Micro-Ct scans of femurs of transgenic mice (Tg6) with chronic EPO overexpression (hematocrit ~85%) showed a 60% reduction in trabecular bone mineral density (BMD), fewer trabeculae and extensive loss of BMAT. Tg6 mice had more osteoclasts in their femurs and less bone morphogenetic protein (Bmp2 and Bmp6) levels in BM. Tg6 mice also exhibited decreased osteogenic and adipogenic cells in BMP2 induced ectopic ossicles. Acute EPO treatment in wild type (wt) C57BL/6J mice (1200 IU/kg of EPO for ten days) induced similar phenotypic changes as in Tg6 mice, except for the increase in osteoclasts seen in Tg6 mice with chronic EPO overexpression. This suggests that increased osteoclastogenesis could be due to an increase in Tg6 macrophages that give rise to osteoclasts or due to an intrinsic change in the activity of Tg6 BMSCs, based on the fact that BMSCs are major regulators of osteoclast formation.

Mice with EPOR deletion die *in utero* due to severe anemia. Therefore, to assess the role of endogenous EPO in bones and BMAT, we used transgenic mice with EPOR expression restricted to erythroid cells ( $\Delta$ EPOR). These mice had a 40% reduction in trabecular BMD, fewer trabeculae and increased BMAT. Unlike wt mice, EPO treatment in  $\Delta$ EPOR mice did not further reduce bones despite achieving a similar hematocrit suggesting that the reduced bones seen with elevated EPO is independent of erythropoiesis. BMSCs isolated from wt, Tg6 and  $\Delta$ EPOR mice were adsorbed into collagen sponges and transplanted into immunocompromised mice to develop into a bone marrow organ. Tg6 BMSCs expressing EPO had less differentiation into osteogenic cells and adipocytes.  $\Delta$ EPOR BMSCs not expressing EPOR formed ectopic bones with reduced osteogenic cells but with increased adipocytes.

We report that endogenous EPO is essential for the lineage commitment and differentiation of BMSCs, while aberrant EPO levels result in impaired differentiation disrupting bone and marrow homeostasis.

**Disclosures:** Sukanya Suresh, None.

## FR0044

**CXCL14 Is a Pro-Bone Metastatic Chemokine with CXCR4 Dependent and Independent Actions.** Diondra Harris<sup>\*1</sup>, Alexander Dowell<sup>2</sup>, Katrina Clines<sup>1</sup>, Hyun Sik Moon<sup>1</sup>, Charlotte Cialek<sup>1</sup>, Alexander Smith<sup>1</sup>, Hui Jiang<sup>1</sup>, Colm Morrissey<sup>3</sup>, Shi Wei<sup>2</sup>, Riley Brien<sup>1</sup>, Euisik Yoon<sup>1</sup>, Yu-Chih Chen<sup>1</sup>, Kathryn Luker<sup>1</sup>, Gary Luker<sup>1</sup>, Gregory Clines<sup>1</sup>. <sup>1</sup>University of Michigan, United States, <sup>2</sup>University of Alabama at Birmingham, United States, <sup>3</sup>University of Washington, United States

Chemokines function as crucial links between tumor cells and the metastatic environment, promoting proliferation, migration and invasion through multiple signaling pathways. The chemokine CXCL14 was identified in a screen for prostate cancer bone metastatic factors. The expression of CXCL14 in prostate cancer bone metastasis was investigated using a human prostate cancer tissue microarray. CXCL14 expression was significantly higher in bone metastases compared to normal prostate, benign prostatic hypertrophy, primary prostate cancer, and metastases to lymph nodes and soft tissues (H-score  $p < 0.0001$ ). These data suggested that the bone metastatic environment increases CXCL14 prostate cancer expression after metastasis to the skeleton. Investigations were performed to understand the biology of CXCL14 as a pro-metastatic prostate cancer chemokine. Compared to vehicle control, CXCL14 stimulated *in vitro* scratch assay migration (38 vs. 69 RUs,  $p < 0.001$ ) and transwell cellular matrix invasion (0.38 vs. 0.62 RUs,  $p < 0.001$ ) of the human prostate cancer cell line ARCaP<sub>M</sub>, and promoted expression of

epithelial-to-mesenchymal transition-associated genes (*SLUG*, *SNAIL*, *TWIST*) in ARCaP<sub>M</sub> and PC-3 prostate cancer cells. Moreover, CXCL14 rapidly activated MAPK and PI3K/AKT signaling pathway proteins. Controversy as to whether CXCR4 is a CXCL14 chemokine receptor was next investigated in this study. Using a validated click beetle green luciferase complementation assay that detects  $\beta$ -arrestin 2-dependent recruitment to the CXCR4 receptor, CXCL14 did not activate  $\beta$ -arrestin 2-dependent CXCR4 signaling. Furthermore, a physical interaction of CXCL14 with CXCR4 or CXCR7 was not detected using a sensitive luminescent complementation assay. Despite the lack of a CXCL14/CXCR4 interaction, CXCL14-activated migration was dependent on CXCR4 as demonstrated using a novel microfluidic cell migration assay. Together, these data suggested that CXCL14 interacts with an unidentified chemokine receptor that may have cooperative actions with CXCR4. This investigation thus identified CXCL14 as a novel prostate cancer pro-bone metastatic chemokine and may represent an appealing target for the treatment of prostate cancer bone metastasis.

**Disclosures:** Diondra Harris, None.

## FR0045

**CaMKK2 Inhibition as a "Dual-Hit" Strategy against ADT-Induced Osteoporosis and Bone-Metastatic Prostate Cancer.** Ushashi Dadwal<sup>\*1</sup>, Eric Chang<sup>1</sup>, Justin Williams<sup>1</sup>, Austin Pucylowski<sup>1</sup>, Khalid Mohammad<sup>2</sup>, Theresa Guise<sup>2</sup>, Uma Sankar<sup>1</sup>. <sup>1</sup>Department of Anatomy and Cell Biology, Indiana University School of Medicine, United States, <sup>2</sup>Division of Endocrinology and Metabolism, Department of Internal Medicine, Indiana University School of Medicine, United States

Androgen deprivation therapy (ADT), as the standard treatment for prostate cancer (PCa), contributes to significant decreases in bone mass, predisposing the patient to increased fracture risk and a diminished quality of life. Established anti-resorption therapies though effective do not stimulate new bone growth. Hence, there is a critical need for anabolic therapies that reverses treatment-induced bone loss in patients.

Recently, Ca<sup>2+</sup>/calmodulin-dependent protein kinase kinase 2 (CaMKK2) was shown to play a role in both the anabolic and catabolic pathways of bone remodeling. Pharmacological inhibition of CaMKK2 using STO-609 protects against in ovariectomy-mediated and age-associated bone loss in mice. Further, whereas CaMKK2 is not expressed in the normal prostate, it is highly over-expressed in prostate cancer and thought to be regulated by the androgen receptor. *In vitro* studies have shown that its inhibition suppresses the growth and migration of PCa cells. We observed that CaMKK2 inhibition suppresses the size of 3-D spheroids formed by the androgen-independent cell line C4-2 but not those of the androgen-dependent cell line PC3. However, the exact downstream mechanism by which CaMKK2 regulates PCa growth remains unknown.

Based on these preliminary data, we hypothesize that inhibition of a single target, CaMKK2, will result in the therapeutic alleviation of two chief complications in advanced-stage PCa, i.e., bone metastatic tumor burden and ADT-induced bone loss. To replicate ADT-induced bone loss we performed sham or bilateral orchiectomy (ORX) on pretreated (saline/STO-609) 5-week-old male athymic nude mice (n=15 per cohort). Tri-weekly intraperitoneal (i.p.) injections were continued for 9 weeks (saline/STO-609). Micro-computed tomography analyses indicated a prevention of ORX-induced bone loss in STO-609 treated mice compared to saline treated controls (3-fold,  $p < 0.05$ ). Additionally, two weeks after surgery, sham and ORX mice were intra-tibially injected with C4-2B cells. Radiographic and histomorphometric analyses reveal a decrease in C4-2B-initiated bone lesions in STO-609 treated mice compared to the saline treated cohorts. Taken together, our studies represent a highly novel and unique approach in the treatment of advanced-stage PCa.

**Disclosures:** Ushashi Dadwal, None.

## FR0046

**Cancer cell-derived microRNA induces osteoblastic phenotype in bone metastasis microenvironment.** Kyoko Hashimoto<sup>\*1</sup>, Satoko Sunamura<sup>1</sup>, Hiroki Ochi<sup>1</sup>, Toru Fukuda<sup>2</sup>, Atsushi Okawa<sup>3</sup>, Mitsuru Futakuchi<sup>4</sup>, Shu Takeda<sup>5</sup>, Shingo Sato<sup>1</sup>. <sup>1</sup>Department of Physiology and Cell Biology, Graduate School and Faculty of Medicine, Tokyo Medical and Dental University, Japan, <sup>2</sup>Department of Foodscience, Tokyo Seiei College, Japan, <sup>3</sup>Department of Orthopaedic Surgery, Graduate School and Faculty of Medicine, Tokyo Medical and Dental University, Japan, <sup>4</sup>Department of Molecular Toxicology, Graduate School of Medical Sciences, Nagoya City University, Japan, <sup>5</sup>Division of Endocrinology, Toranomon Hospital Endocrine Center, Japan

Bone is one of favorite metastasis organs for cancer cells and bone metastatic lesions are classified broadly into two types; osteoblastic or osteolytic phenotype. In bone metastasis microenvironment, cancer cells interact with osteoblasts or osteoclasts, leading to osteoblastic or osteolytic bone metastasis. However, secreted factors from cancer cells for the modification of the bone cells has not been defined. Micro RNAs (miRNAs) have an important role in regulating cell proliferation, migration and differentiation. In addition, it has been recently revealed that miRNAs are transported via exosomes from cells to cells as an intercellular communication tool. In this present study, we hypothesized that secreted miRNAs from cancer cells define osteoblastic or osteolytic phenotype in bone metastasis microenvironment.



We firstly examined the expression profile of miRNAs in exosomes secreted from seven human cancer cell lines; four prostate carcinoma cell lines osteoblastic metastasis-inducing cells, and one breast cancer and two myeloma cell lines as osteolytic metastasis-inducing cells. Based on the results of miRNA microarray, we identified eight human miRNAs highly expressed in exosomes isolated from prostate cancer cell lines. Next, to study the effect of the identified human miRNAs on osteoblast differentiation, immortalized human mesenchymal stem cells (hMSCs) were transfected with each miRNA mimics, and the transfected cells were cultured in osteogenic differentiation medium. ALP activity assay and mineralization assay revealed that the overexpression of hsa-miR-940 significantly promoted the osteoblast differentiation of hMSCs. Furthermore, to investigate whether hsa-miR-940 has an ability to induce osteogenic tumorigenesis *in vivo*, a hsa-miR-940-overexpressing breast cancer cell line (MDA-MB-231-miR-940) was established, and the cells were transplanted on the calvarial bones of immunodeficient mice. MDA-MB-231 is commonly known as osteolytic metastasis-inducing cell line. However, surprisingly, MDA-MB-231-miR-940 cells formed tumors with lots of osteoblastic lesions. Further histological analysis showed that the cellular origin of newly formed bones, was the host MSCs, suggesting that hsa-miR-940 secreted from the transplanted cancer cells induce osteoblastic differentiation of host cells.

In conclusion, we identified hsa-miR-940, which was highly secreted by prostate cancer, as a crucial inducer of osteoblastic bone metastasis.

**Disclosures:** Kyoko Hashimoto, None.

## FR0047

### Gfi1 Modulation of SphK1 Maintains Growth and Survival of Myeloma Cells.

Daniela N. Petrusca<sup>\*1</sup>, Cheolkyu Park<sup>2</sup>, Colin Crean<sup>2</sup>, Denise Toscani<sup>3</sup>, Judith Anderson<sup>2</sup>, Rebecca Silberman<sup>2</sup>, G. David Roodman<sup>4</sup>. <sup>1</sup>Indiana University, Department of Medicine/Hematology-Oncology, United States, <sup>2</sup>Department of Medicine/Hematology-Oncology, Indiana University School of Medicine, United States, <sup>3</sup>Myeloma Unit, Dept. of Clinical and Experimental Medicine, University of Parma, Italy, <sup>4</sup>Department of Medicine/Hematology-Oncology, Indiana University School of Medicine and Rodebush VA, United States

Multiple myeloma (MM) is an incurable hematologic disease caused by the accumulation of malignant plasma cells in the bone marrow and is characterized by osteolytic lesions in the majority of patients. We previously reported that Growth independent factor 1 (Gfi1) is upregulated in bone marrow stromal cells (BMSC) in MM and causes suppression of osteoblast differentiation. We also found that Gfi1 is increased in the majority of CD138<sup>+</sup> cells from MM patients and cell lines. We hypothesize that Gfi1 plays a central role in MM regulating cell growth and survival in part by modulating SphK1 levels, a known modulator of cancer progression and SIP "inside-out" signaling, through modulation of plasma membrane channel spinster 2 (SPNS2). Therefore, we determine the effect of knock down (KD) or overexpression (o/e) of Gfi1 in MM cells on their growth and survival and the contribution of SphK1 and SPNS2 to these effects.

Effects of Gfi1 KD in MM cell survival were assessed by transduction of MM cells with pLKO.1-puro lentivirus encoding Gfi1 or a non-mammalian shRNA. The anti-apoptotic effects of Gfi1 o/e were tested by transduction of MM cells with pUC2 lentivirus encoding Gfi1 or the empty vector.

We found that SphK1 mRNA is highly expressed in CD138<sup>+</sup> cells from MM patients and cell lines compared with normal donors and that Gfi1 protein levels correlated with expression of active SphK1. Microenvironmental factors in MM (IL-6 and SIP), hypoxia and adhesive interactions with BMSC further increased Gfi1 and SphK1 mRNA and protein levels and enhance viability in MM cells. KD of Gfi1 caused a profound decrease of SphK1 at the mRNA and protein levels and decreased SPNS2 mRNA levels in MM cells, while inhibiting the growth and inducing apoptosis of MM cells. Gfi1 overexpression had the opposite effects on SphK1 and SPNS2 levels and conferred a survival advantage to MM cells compared to control cells. These data suggest that Gfi1 regulates MM growth in part by enhancing expression and activity of SphK1 and facilitating SIP release through modulating its specific channel levels.

Taken together, our results suggest that Gfi1 may act as a key regulator of MM growth and survival in part through modulation of SphK1 and facilitating the release of SIP, its bioactive sphingolipid metabolite. SIP may then act in an autocrine and paracrine manner. Therefore, targeting Gfi1 may be a novel therapeutic strategy for MM patients.

**Disclosures:** Daniela N. Petrusca, None.

## FR0051

### HDAC inhibitors promote LIFR expression and tumor dormancy in breast cancer cells that home to the bone.

Miranda Sowder<sup>\*1</sup>, Vera Mayhew<sup>1</sup>, Samuel Doovema<sup>1</sup>, Rachelle W Johnson<sup>2</sup>. <sup>1</sup>Vanderbilt University, United States, <sup>2</sup>Vanderbilt University Medical Center, United States

Breast cancer cells often metastasize to the bone, where they may enter a dormant state. Our laboratory previously found that leukemia inhibitor factor receptor (LIFR) promotes breast cancer dormancy. Specifically, when LIFR is lost, breast cancer patient survival is reduced and human MCF7 tumor cells down-regulate a number of pro-dormancy genes and become proliferative and bone destructive *in vivo*. Histone deacetylase 2 (HDAC2) is predicted to bind to the LIFR in the UCSC genome browser, suggesting that HDACs may directly regulate LIFR expression; however, specific knockdown of HDAC2 does not enhance LIFR expression, indicating compensation by other HDACs. LIFR expression on breast cancer cells can be stimulated

(>7-fold, p<0.01) using the FDA-approved pan-HDAC inhibitor valproic acid (VPA; 1-10mM), leading to significant upregulation of pro-dormancy genes (*TSP1*, *TPM1*, *p27*, *AMOT*, *P4HA1*, *MIR190*, *PDCD4*, *SELENBP1*, *QSOX1*; up to 3.8-fold, p<0.05-0.0001). Based on these findings, we hypothesized that LIFR is epigenetically down-regulated in breast cancer and that HDAC inhibitors (HDACi) may be used to induce LIFR expression and maintain tumor cells in a dormant state. To test this, we treated MCF7 breast cancer cells, which we and others have proposed as a model of tumor cell dormancy *in vivo*, with FDA-approved HDACi (romidepsin, panobinostat, vorinostat) or HDACi in phase II clinical trials (entinostat) for treatment of breast and other tumor types. All HDACi significantly induced LIFR mRNA levels (2.9-6.1-fold, p<0.05-0.002) after 6-12 hours of treatment in MCF7 cells and dramatically increased LIFR protein levels in both MCF7 and aggressive MDA-MB-231 bone metastatic cells by 24 hours (12.4-14.4-fold). HDACi also increased mRNA levels of several dormancy-associated genes including *AMOT*, *TGFB2*, *IGFBP5*, and *p27* (up to 5.5-fold, p<0.05-0.0001), suggesting that multiple HDACi may be effective at inducing tumor cell dormancy. Together, these data indicate that HDACi induce LIFR expression and stimulate a pro-dormancy gene panel. Studies to elucidate the epigenetic mechanism by which LIFR is regulated and to determine whether HDACi can prevent outgrowth of dormant tumor cells *in vivo* and/or revert aggressive breast cancer cells into a dormant state are currently in progress. Importantly, these studies may have clinical implications for the use of HDACi as a means to activate a pro-dormancy program and maintain breast cancer cells in a chronic dormant state.

**Disclosures:** Miranda Sowder, None.

## FR0052

### TAK1 inhibition impairs myeloma cell-bone marrow interaction to reduce myeloma tumor growth and bone destruction.

Junpei Teramachi<sup>\*1</sup>, Masahiro Hiasa<sup>2</sup>, Asuka Oda<sup>3</sup>, Hirofumi Tenshin<sup>4</sup>, Ryota Amachi<sup>4</sup>, Takeshi Harada<sup>3</sup>, Shingen Nakamura<sup>3</sup>, Hirokazu Miki<sup>3</sup>, Itsuro Endo<sup>3</sup>, Tatsuji Haneji<sup>3</sup>, Toshio Matsumoto<sup>6</sup>, Masahiro Abe<sup>3</sup>. <sup>1</sup>Department of Histology and Oral Histology, Tokushima University, Japan, <sup>2</sup>Department of Biomaterials and Bioengineering, Tokushima University, Japan, <sup>3</sup>Department of Hematology, Endocrinology and Metabolism, Tokushima University, Japan, <sup>4</sup>Department of Orthodontics and Dentofacial Orthopedic, Tokushima University, Japan, <sup>5</sup>Division of Transfusion and Cell Therapy Medicine, Tokushima University Hospital, Japan, <sup>6</sup>Fujii Memorial Institute of Medical Sciences, Tokushima University, Japan

Multiple myeloma (MM) has a unique propensity to develop and expand almost exclusively in the bone marrow and generates destructive bone disease. MM cell adhesion to bone marrow stromal cells (BMSCs) via VLA-4-VCAM-1 confers cell adhesion-mediated drug resistance (CAM-DR) along with induction of bone destruction. We and others reported that MM cells constitutively overexpress Pim-2 as an anti-apoptotic mediator, which was further upregulated through interaction with bone marrow stromal cells (BMSCs) or osteoclasts (OCs). The MM cell cocultures in turn induced Pim-2 in BMSCs and OCs to impair osteoblastogenesis and stimulate osteoclastogenesis, respectively. We identified TGF- $\beta$ -activated kinase-1 (TAK1) as an upstream mediator responsible for the Pim-2 induction in these types of cells, which can serve as a pivotal therapeutic target for MM growth and bone destruction. The present study was undertaken to clarify the therapeutic impact of TAK1 inhibition on MM-bone marrow interaction. The phosphorylation of TAK1 was upregulated in MM cells and also induced in BMSCs after both types of cells were cocultured. The expression of VCAM-1, a VLA-4 ligand, and IL-6 production were substantially upregulated along with induction of RANK ligand and Pim-2 in BMSCs after the cocultures. However, treatment with the TAK1 inhibitor LLZ1640-2 (LLZ) dose-dependently reduced the VCAM-1 expression by BMSCs, and impaired MM cell adhesion onto BMSCs. Importantly, LLZ potentially suppressed the Pim-2 expression to induce apoptosis in MM cells in cocultures with BMSCs or OCs, while reducing RANK ligand expression and IL-6 production by BMSCs. TAK1 inhibition by LLZ or siRNA also reduced VEGF production by MM cells and their expression of BCMA and TACI, receptors for BAFF and APRIL. Furthermore, LLZ was able to abolish TNF- $\alpha$ -induced NF- $\kappa$ B, p38MAPK and ERK activation and IL-6-induced STAT3 activation in MM cells. Finally, treatment with LLZ markedly suppressed MM tumor growth and prevented bone destruction in mouse MM models with intra-tibial injection of 5TGM1 MM cells. These results collectively demonstrate that TAK1 plays a critical role in MM cell-bone marrow interaction and that TAK1 inhibition effectively impairs the MM cell-bone marrow interaction to suppress MM tumor growth with drug resistance, bone destruction and angiogenesis. Therefore, TAK1 inhibition appears to be a promising therapeutic option targeting bone marrow microenvironment as well as MM cells.

**Disclosures:** Junpei Teramachi, None.

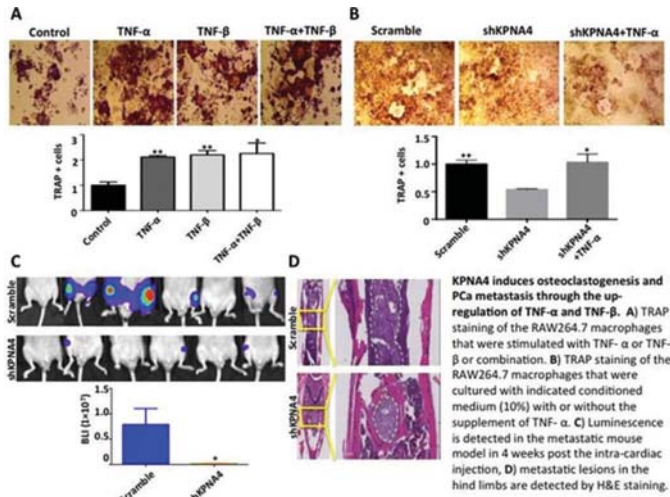
## FR0054

### KPNA4 modulates osteoclastogenesis during the skeletal metastasis of prostate cancer.

Jian Yang<sup>\*</sup>, Liang Luo, Ruohan Zhang, Yuqi Guo, Xin Li. New York University College of Dentistry, United States

Karyopherin Subunit Alpha 4 (KPNA4) is one of the major members of soluble nuclear importer superfamily, it activates NF $\kappa$ B signaling by the nuclear transportation of p50 and p65, the subunits of NF $\kappa$ B. We recently show that this molecule is over-expressed in the prostate cancer (PCa) cells and positively correlated the pathological

stage and Gleason score of PCa. These findings imply that KPNA4 might be involved in the progression, especially the bone metastasis of PCa. Bone is the major metastatic site and the primary lethal cause of PCa patients. To date, the role of KPNA4 in the regulation of bone environment during PCa bone metastasis remains unclear. Our study demonstrates that KPNA4 overexpression is associated with the cytoplasmic accumulation and extracellularly releasing of NFkB related cytokines including TNF $\alpha$  and TNF $\beta$  from PCa cells. Quantitative PCR array data show that the knockdown of KPNA4 suppresses the expression of inflammatory cytokines in general. The change of inflammatory cytokines in the bone microenvironment could directly impact on the bone destruction and PCa metastasis. Indeed, using TRAP staining we have shown that the conditioned medium of PCa cells with KPNA4 knockdown is less capable of inducing osteoclastogenesis *in vitro*. In contrast, the condition medium from KPNA4 overexpression PCa cells stimulates osteoclastogenesis and the stimulation is reduced by the KPNA4 siRNA. Further, using the intra-cardiac metastatic mouse model we show that stable knockdown of KPNA4 significantly reduces the number of osteoclasts and attenuates bone metastatic lesions *in vivo*. These findings support that KPNA4 overexpression in PCa could stimulate bone resorption during the skeletal metastasis. In summary, our data provide solid evidence on the role of KPNA4 in facilitating PCa bone metastasis by activating the NFkB-TNFs signaling. Thus, KPNA4 is a promising therapeutic target for treating skeletal metastatic PCa.



Data

Disclosures: Jian Yang, None.

## FR0055

**Effect of Bone Allograft in Multiple Myeloma Spine Surgeries.** Meera Mohan<sup>\*1</sup>, Samant Rohan<sup>1</sup>, Amy Buros<sup>1</sup>, Daisy Alapat<sup>1</sup>, Jerry Walters<sup>1</sup>, Thomas G Pait<sup>1</sup>, Nancy A. Ghaleb<sup>1</sup>, Sharmilan Thanendrarajan<sup>1</sup>, Frits van Rhee<sup>1</sup>, Faith Davies<sup>1</sup>, Gareth Morgan<sup>1</sup>, Carolina Schinke<sup>1</sup>, Larry J. Suva<sup>2</sup>, Maurizio Zangari<sup>1</sup>. <sup>1</sup>University of Arkansas for Medical Sciences, United States, <sup>2</sup>Texas A&M University, United States

Multiple myeloma (MM) is characterized by the clonal proliferation of plasma cells in the bone marrow associated with extensive osteolytic bone lesions which represent an independent factor for mortality and morbidity. Bone lesions are present in approximately 70% of patients at time of diagnosis; skull, spine, rib cage and pelvis being the most commonly involved disease sites. MM is the most common primary tumor of the spine and surgical intervention is indicated with spinal instability or compressive lesions. Approximately 10% of patients present with significant invasion of the spinal cord causing neurological impairment necessitating surgery, while 55-70% of patients have vertebral compression fractures. During decompression of the bony and ligamentous spinal structures that may be compressing neural elements, the cortex is frequently removed to prepare for fusion. Allograft is then packed on top of these exposed surfaces for fusion and in specific cases in conjunction with metal implants used to fill bone lytic defects.

Following IRB approval the UAMS Myeloma data base was retrospectively interrogated for patients who underwent various neurosurgical interventions. From 1996 to 2017, 127 subjects underwent neurosurgical intervention. A subset of patients with isolated spinal lytic lesions were identified and followed with serial imaging, 3 months after surgery. Median age was 60 years with 71% of the subjects being male and 6/28 patients (21%) were high risk by gene expression profile 70 score. 8/28 patient had clinical and/or radiological evidence of spinal cord compression. 20/28 patients received high dose chemotherapy followed by autologous stem cell transplant after surgical management. One patient received radiation at the site of the lesion before surgical intervention. Remineralization within the lytic lesion site was observed in 16/28 (57%) patients. Bone allograft was used in all the patient to achieve adequate fusion/stabilization of the vertebrae. We have previously reported significant remineralization of lytic pelvic lesions in MM following high dose chemotherapy and autologous stem cell transplant. In this analysis a significant percentage 57% of patients were undergoing remineralization at the site of a lytic spinal lesion. Radiological evidence of facet joint fusion was seen in more than

75% of the subjects. The mechanism leading to remineralization remains unknown, but immobilization with good spinal fusion followed by high dose chemotherapy and autologous stem cell transplant likely promotes new bone deposition.

Baseline Patient Characteristics	Allograft Neurosurgery Patients
Age: Mean (Minimum to Maximum)	60 (38 – 85)
Male	20 / 28 (71%)
LDH $\geq$ 190 U/L	8 / 28 (29%)
Albumin $<$ 3.5 g/dL	20 / 28 (71%)
B2M $\geq$ 3.5 mg/L	9 / 28 (32%)
Creatinine $\geq$ 2.0 mg/dL	0 / 28 (0%)
Platelet Count $<$ 150 $\times 10^3$ /L	5 / 28 (18%)
GEP70 High Risk	6 / 28 (21%)
GEP70 CD-1 Subgroup	1 / 28 (4%)
GEP70 CD-2 Subgroup	5 / 28 (18%)
GEP70 HY Subgroup	7 / 28 (25%)
GEP70 LB Subgroup	1 / 28 (4%)
GEP70 PR Subgroup	10 / 28 (36%)
GEP70 MF Subgroup	1 / 28 (4%)
GEP70 MS subgroup	0 / 28 (0%)
IgA Isotype	3 / 28 (11%)
IgG Isotype	11 / 28 (39%)
IgD Isotype	0 / 28 (2%)
Nonsecretory Isotype	1 / 28 (4%)
Light Chain Isotype	7 / 28 (25%)

Table 1

Disclosures: Meera Mohan, None.

## FR0058

**Periosteal chondrogenesis and temporal dynamics of BMP2-induced middle phalanx regeneration in the adult mouse.** Lindsay Dawson<sup>\*1</sup>, Ling Yu<sup>2</sup>, Mingquan Yan<sup>2</sup>, Connor Dolan<sup>2</sup>, Ken Muneoka<sup>2</sup>. <sup>1</sup>Texas A & M University, United States, <sup>2</sup>Texas A&M University, United States

The successful mammalian regeneration response is restricted to amputation of the distal digit tip, the terminal phalanx (P3). The mouse digit regeneration response is amputation-level specific; proximal amputations fail to elicit regeneration, instead culminating in scar formation and bone truncation. The adjacent skeletal element, the middle phalanx (P2), functions as a model system to investigate regenerative failure and as a site to test approaches aimed at enhancing regeneration. P2 amputation initiates a dynamic tissue repair response characterized by inflammation, periosteal-derived cartilaginous callus formation, woven bone callus formation, and secondary bone remodeling. We report that targeted exogenous BMP2 functions to transition the scarring event of P2 into a robust bone regeneration response.

Several combinations of P2 amputation(s) and BMP2 or BSA XeroGel treatment were performed; treatment (1) after wound closure with or without intact periosteum (9 days post amputation (DPA)), (2) after bone healing (24 DPA), and (3) after bone healing, P2 stump re-injury, and wound healing (33 DPA). Bone regeneration was quantified using MicroCT. Digits assayed via histology and immunohistochemistry.

Exogenous BMP2 induces P2 regeneration mediated by transient cartilaginous callus formation distal to the amputation plane. BMP2 initiates regeneration during the cartilaginous phase of P2 bone repair, yet fails to induce regeneration in the absence of the periosteum, or after the cartilage has been remodeled to bony callus. We provide evidence that a temporal component associated with wound maturation exists in P2 induced regeneration, termed the 'regeneration window', in which cells are transiently responsive to signals after amputation. Re-injury of the scarred P2 stump functions to reinitiate bone repair, therefore re-opening the 'regeneration window' and thus recreating a regeneration-permissive environment that is response to exogenous BMP2 treatment.

These findings indicate that amputation initiates a regenerative response that is not realized (regenerative potential) but can be triggered with targeted BMP2 treatment. As the wound matures to a scarring response, BMP2-responsiveness declines, but can be re-activated by re-injury. The periosteal requirement for BMP2-induced regeneration suggests that the 'regeneration window' is linked to dynamic changes associated with the cartilaginous phase of P2 bone healing.

Disclosures: Lindsay Dawson, None.

## FR0060

**Chondrocyte PTH1R Signaling is Essential for Articular Cartilage Maintenance and Protection Post-trauma.** Fadia Kamal<sup>\*1</sup>, Eric Schott<sup>1</sup>, Elijah Carlson<sup>1</sup>, Monaliza El-Quadi<sup>1</sup>, Heather Le Bleu<sup>1</sup>, Matthew Hilton<sup>2</sup>, Jennifer Jonason<sup>1</sup>, Michael Zuscik<sup>1</sup>. <sup>1</sup>University of Rochester, United States, <sup>2</sup>Duke University School of Medicine, United States

Previously, we found in a preclinical model of posttraumatic OA (PTOA) that rPTH treatment resulted in chondroregeneration, this was associated with elevated Jagged-1 expression in articular chondrocytes. Whether this effect is directly through



articular chondrocyte PTH1R is unknown, and the potential dependence of this effect on Jagged-1/Notch pathway is uninvestigated.

**Hypothesis:** PTH1R signaling maintains articular chondrocytes in a non-hypertrophic state and protects against de novo and injury-induced cartilage degeneration, in part via Jagged-1.

**Methods:** Three sets of experiments were performed using a TM-inducible conditional deletion model to delete PTH1R in chondrocytes: First, we examined the role of articular chondrocyte PTH1R deletion in cartilage homeostasis. Second, we assessed the impact of PTH1R deletion on PTOA progression. Third, we established the role of articular chondrocyte PTH1R deletion in the chondroregenerative effect of rhPTH. PTOA was induced by surgical destabilization of the medial meniscus (DMM) in 3 month old mice and knee joints were harvested 12 weeks post-DMM. Conditional PTH1R deletion with or without rhPTH treatment were initiated 8 weeks following DMM and continued until 12 weeks. Further, we administered PTH /vehicle to DMM mice with conditional Jagged-1-KO. In all these studies, articular cartilage structural changes were evaluated via Saf-O-Fast green staining, histomorphometry, OARSI scoring and  $\mu$ CT. Molecular events were examined using immunofluorescent staining.

**Results:** Loss of PTH1R in articular chondrocytes led to spontaneous cartilage degeneration and increased expression of the matrix degrading enzymes (MMP-13 and ADAMTS-5). Following DMM, PTH1R-KO mice showed a more aggressive OA phenotype characterized by almost complete loss of uncalcified articular cartilage, lower numbers of articular chondrocytes, increased MMP-13 and ADAMTS-5 expression. The chondroregenerative effect of rhPTH was lost in PTH1R-KO mice indicating that this effect is mainly exerted through articular chondrocyte PTH1R signaling. Importantly, loss of Jagged-1 in articular chondrocytes led to the loss of rhPTH chondroregenerative effect.

**Conclusion:** Our data show that PTH1R is a key regulator of articular chondrocytes, maintaining them in a non-hypertrophic state both at baseline and following injury; and that the therapeutic effect of rhPTH in PTOA is dependent on i) chondrocyte PTH1R signaling, and ii) downstream Jagged-1/Notch pathway.

**Disclosures:** Fadia Kamal, None.

## FR0061

**Ghrelin Protects against Osteoarthritis through Interplaying with Akt and NF- $\kappa$ B Signaling Pathways.** Weiwei Li<sup>1</sup>, Wenhan Wang<sup>2</sup>, Yunpeng Zhao<sup>1</sup>.  
<sup>1</sup>Shandong University Qilu Hospital, China, <sup>2</sup>Shandong University, China

Osteoarthritis is a common chronic degenerative disease characterized by degeneration in the joints and subsequent destruction of cartilage and bone. Ghrelin is a recently discovered neuropeptide with anti-inflammatory actions, while it is unknown whether ghrelin is involved in OA.

Human primary chondrocyte were collected from patients with osteoarthritis, and expression pattern of ghrelin was assessed through Western blot, IHC as well as cell immunostaining. Besides, human chondrocyte was stimulated with IL-1 $\beta$ , and exogenous ghrelin alleviated disorganization of metabolism mediated by IL-1 $\beta$ . Moreover, a surgically induced OA model was established in wild type mice as we have previously reported (Zhao Y, et al, Annals of the Rheumatic Diseases, 2015). Thereafter, the mice were administered with ghrelin or PBS through intraperitoneal injection. Severity of inflammation as well as degeneration in the joints was determined by measuring the levels of various inflammatory cytokines and degeneration associated molecules through Western blot, ELISA and real time PCR. Additionally, potential underlying mechanisms, including Akt and NF- $\kappa$ B signaling pathways, were assessed.

As a result, ghrelin was detected in cartilage and primary chondrocyte, as measured by IHC (Fig. 1A), Western blot (Fig. 1B) as well as cell immunostaining (Fig. 1C). Furthermore, ghrelin attenuated destruction of cartilage structure (Fig. 1D-1E) as well as osteophyte formation (Fig. 1F) in surgically induced mice models. Moreover, ghrelin diminished the levels of MMP-13 and ADAMTS-5 (Fig. 1G), and downregulated the production of various inflammatory cytokines including IL-6, TNF- $\alpha$ , iNOS and COX-2 (Fig. 1H-1I). In cultured primary human chondrocyte, ghrelin maintained the expression of critical matrix determined by GAG synthesis (Fig. 1J) and collagen 2 expression level (Fig. 1K) in stimulation of IL-1 $\beta$ . Moreover, IL-1 $\beta$  mediated suppression of Akt signaling pathway was antagonized by ghrelin administration, and MK2206, a specific Akt inhibitor, markedly abolished anabolic function of ghrelin (Fig. 1L-1O). Additionally, activation of NF- $\kappa$ B signaling was inhibited by ghrelin (Fig. 1P-1Q).

In this study, ghrelin appears to be protective in disorganization of chondrocyte metabolism and degeneration of cartilage, which might rely on its interaction with Akt and NF- $\kappa$ B signaling pathways. This is a clue for the assessment of ghrelin as a potential therapeutic approach to the treatment of OA.

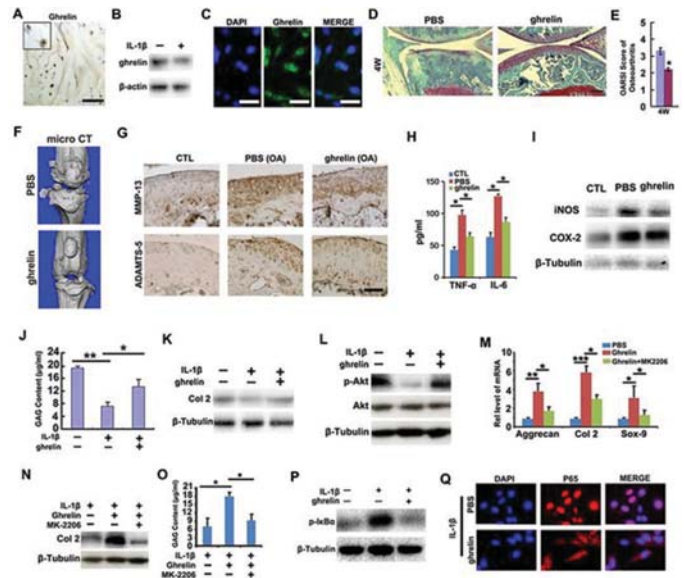


Figure 1

**Disclosures:** Weiwei Li, None.

## FR0063

**Global and Chondrocyte-specific Deletion of FGF2 Contribute to Trauma-induced Osteoarthritis.** Patience Meo Burt<sup>1</sup>, Liping Xiao<sup>1</sup>, Siu-Pok Yee<sup>2</sup>, Brya G. Matthews<sup>3</sup>, Marja Marie Hurley<sup>1</sup>. <sup>1</sup>Department of Medicine/Endocrinology, School of Medicine, Uconn Health, United States, <sup>2</sup>Department of Cell Biology, Uconn Health, United States, <sup>3</sup>Department of Reconstructive Sciences, School of Dental Medicine, Uconn Health, United States

Osteoarthritis (OA) is the most common degenerative joint disease, but the molecular mechanisms that contribute to its initiation and progression are not well defined. Studies showed that global Fgf2 knockout (*Fgf2*<sup>-/-</sup>) mice spontaneously develop severe and accelerated OA by 6 months of age. However, it is unclear whether it is the absence of FGF2 in cartilage or bone that contributes to OA development. Since FGF2 may be chondroprotective, we posit that global *Fgf2*<sup>-/-</sup> mice and chondrocyte-specific FGF2 knockout mice will develop OA following tibial compression loading compared to their WT littermates, and joints from *Fgf2*<sup>-/-</sup> mice will have modifications of gene expression of pathways involved in hypertrophic chondrocyte signaling before the OA phenotype occurs. To examine if changes in these genes are occurring before *Fgf2*<sup>-/-</sup> mice develop OA, total RNA was isolated from the knees at 2 months old and qPCR analysis showed significant increases in genes involved in chondrocyte hypertrophy including Adamts5, Elk1, Ihh, Il-1 $\beta$ , Nfkb1, Bmp2, Bmp4, BMPR1a, Hif2a, and Igf-1 in *Fgf2*<sup>-/-</sup> mice compared to WT. We also generated a novel inducible chondrocyte-specific Fgf2 knockout mouse (Col2creERT2<sup>tg/+</sup>:Fgf2<sup>fl/fl</sup>), which were subjected to tamoxifen induction at 2 months old, followed by tibial loading 2 weeks later using our novel noninvasive mechanical loading model. Mice were sacrificed 2 weeks after loading, and x-ray, microCT, Safranin-O staining, and immunohistochemistry were performed. Chondrocyte-specific Fgf2 knockout mice expressed FGF2 protein in bone but not articular cartilage. Loaded right knees of Col2creERT2<sup>tg/+</sup>:Fgf2<sup>fl/fl</sup> mice showed osteophyte formation, joint space narrowing, sclerotic bone, eroded surface, fraying of cartilage, decreased superficial layer of cartilage and loss of proteoglycan content compared to the controls (Fig. 1). Expression of the degradative enzyme, MMP13, was enhanced in loaded right knees of Col2creERT2<sup>tg/+</sup>:Fgf2<sup>fl/fl</sup> mice compared to left and control mice (Col2creERT2<sup>tg/+</sup>:Fgf2<sup>fl/fl</sup>). These results indicate that signaling pathways involved in hypertrophic chondrocytes are enhanced in phenotypically normal joints from young *Fgf2*<sup>-/-</sup> mice, implying that these pathways are initiating OA. Chondrocyte-specific deletion of Fgf2 *in vivo* leads to OA after mechanical loading. This data suggests that the presence of FGF2 in cartilage is vital for joint homeostasis and its absence leads to chondrocyte hypertrophy and OA development.

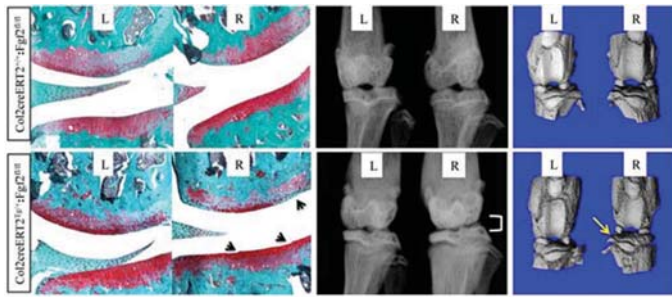


**Fig. 1: Chondrocyte-specific FGF2 knockout mice develop an OA phenotype following tibial loading.** L=left non-loaded control knee, R=right tibial loaded knee; arrows=fibrillated cartilage; bracket=joint space narrowing; yellow arrow=erosion/pitting.

Figure 1

**Disclosures:** Patience Meo Burt, None.

## FR0064

**Actions of PTHrP, HDAC4, and SIK3 to Regulate Chondrocyte Hypertrophy.** Shigeki Nishimori\*, Marc N. Wein, Henry M. Kronenberg. Endocrine Unit, Massachusetts General Hospital and Harvard Medical School, United States

**Background:** Parathyroid hormone-related protein (PTHrP) inhibits chondrocyte hypertrophy. We demonstrated that PTHrP represses phosphorylation of Histone Deacetylase (HDAC) 4 at the 14-3-3 binding sites and induces subsequent nuclear translocation of HDAC4 in vivo (submitted). In the nucleus, HDAC4 blocks Myocyte Enhancer Factor 2 (MEF2) that drives chondrocyte hypertrophy.

**Methods:** SIK3 also influences chondrocyte hypertrophy (Sasagawa, Development, 2012). SIK2 and SIK3 phosphorylate HDAC4 and HDAC5 at the 14-3-3 binding sites in vitro (Walkinshaw, JBC, 2013). To investigate if SIK3 might work on the PTHrP signaling pathway in chondrocytes, we generated the double knockout (KO) mouse of SIK3 and HDAC4 or that of SIK3 and PTHrP. We also studied the acute effects of a SIK inhibitor, YKL-05-099 (Sundberg, ACS Chem Biol, 2016) in vivo.

**Results:** The Col2-Cre: SIK3 conditional KO (SIK3-cKO) mouse shows a long proliferating chondrocyte (PC) region (distance from the top of the growth plate to the beginning of hypertrophic chondrocytes), probably due to delayed chondrocyte hypertrophy (200% of WT, proximal tibial growth plate at birth). By deleting the HDAC4 gene in the SIK3-cKO mouse, stepwise shorter PC regions were observed at birth (SIK3-cKO: HDAC4-cKO=140% of WT, Double cKO=63 % of WT), consistent with the idea that HDAC4 acts downstream of SIK3 to delay chondrocyte hypertrophy.

The PTHrP-KO mouse dies immediately after birth from respiratory failure due to abnormal rib chondrocyte hypertrophy. Surprisingly, the SIK3-cKO: PTHrP-KO mouse survives after birth. The double KO mouse exhibits normal rib chondrocytes and has a longer PC region at birth (135% of WT, PTHrP-KO=40% of WT). This result is consistent with the model that PTHrP works by blocking SIK3 action. The double KO mouse can't survive after weaning due to lack of teeth eruption.

Injection of YKL-05-099 to pregnant mice by 4 daily injections from E15.5 to E18.5 rescues the PTHrP-KO mouse partially to avoid perinatal death. Administration of YKL-05-099 to the SIK3-cKO mouse also extends the PC region with delayed separation of hypertrophic regions, suggesting that other SIK proteins (SIK1 or SIK2) may control chondrocyte hypertrophy in the SIK3-cKO mouse.

**Conclusions:** These genetic and pharmacologic studies suggest that PTHrP may act on chondrocytes through a SIK-HDAC4 pathway.

**Disclosures:** Shigeki Nishimori, None.

## FR0065

**Osteoglycin, an Osteoblast-derived Regulator of Bone Mass and Glucose Homeostasis.** Nikki Lee\*, Herbert Herzog<sup>1</sup>, Paul Baldock<sup>2</sup>. <sup>1</sup>Neuroscience Division, Garvan Institute of Medical Research, Australia, <sup>2</sup>The Division of Bone Biology, Garvan Institute of Medical Research, Australia

**Purpose:** Increasing evidence suggests that bone plays an active role in regulating glucose homeostasis through both osteocalcin-dependent and osteocalcin-independent mechanisms. We previously demonstrated that neuropeptide Y signals specifically in the osteoblast to regulate glucose homeostasis, through an osteocalcin-independent pathway. Loss of neuropeptide receptor from early, but not late, osteoblasts altered whole-body glucose homeostasis, by modulating insulin secretion and insulin action. We have now identified osteoglycin, a proteoglycan secreted by osteoblasts, as an endocrine mediator of this pathway.

**Methods:** Osteoglycin knockout mice (Ogn<sup>-/-</sup>) were generated using CRISPR/Cas9 to disrupt the first exon of the osteoglycin gene, and we examined bone and glucose homeostasis.

**Results:** These mice display an anabolic bone phenotype with significant increases in femur length, femoral BMD and BMC, and cancellous bone volume. Ogn<sup>-/-</sup> mice have no difference in body weight or adiposity; however, they have elevated serum glucose and impaired glucose clearance during a glucose tolerance test (GTT), associated with

increased insulin levels, indicating suppressed insulin action in Ogn<sup>-/-</sup>. This effect is enhanced when the mice have been fed a high fat diet.

Exogenous osteoglycin improved glucose tolerance. We pre-treated wildtype mice with osteoglycin (3ug/kg i.p.) prior to a GTT: Serum glucose was significantly reduced at the start and throughout the GTT, whilst insulin levels were higher at the start of the GTT but then returned to baseline earlier than controls, indicating enhanced insulin action. Insulin-induced Akt phosphorylation in muscle was significantly enhanced by osteoglycin pre-treatment, suggesting that osteoglycin improves insulin action in target tissues, as well as insulin secretion.

Furthermore, in a cohort of type-2 diabetic patients, serum osteoglycin levels were significantly lower compared to both lean and obese/overweight but insulin-sensitive patients. Serum osteoglycin was also markedly reduced in obese wild type mice fed a high fat diet, compared to lean, chow-fed controls.

**Summary and Conclusions:** These data highlight the importance of bone-derived factors in the regulation of whole body glucose balance. Specifically, they identify osteoglycin as a novel factor capable of regulating bone and glucose homeostasis and suggest osteoglycin as a novel platform for the development of treatments for type-2 diabetes.

**Disclosures:** Nikki Lee, None.

## FR0070

**Vitamin K<sub>2</sub>-Induced Carboxylation of Osteocalcin and Matrix Gla Protein Improves Bone and Lipid Metabolism in Overweight Children.** Mary Ellen Fain\*, Celestine Williams<sup>1</sup>, Allison Jasti<sup>1</sup>, Reda Bassali<sup>2</sup>, Catherine Davis<sup>2</sup>, Norman Pollock<sup>2</sup>. <sup>1</sup>Georgia Prevention Institute, Medical College of Georgia, Augusta University, United States, <sup>2</sup>Department of Pediatrics, Medical College of Georgia, Augusta University, United States

Limited evidence suggests that vitamin K-dependent proteins, osteocalcin (OC) and matrix Gla protein (MGP), play a beneficial role in bone and cardiovascular health. The vitamin K-OC-MGP relationship is based on the notion that vitamin K is required to carboxylate inactive OC and MGP for activation, which in turn, influences skeletal and cardiovascular conditions. Thus, manipulation of circulating vitamin K provides a model for testing the hypothesized link between carboxylation of OC and MGP with bone and lipid metabolism. We investigated dose-response effects of vitamin K<sub>2</sub> (menaquinone-7) supplementation on OC and MGP carboxylation and markers of bone and lipid metabolism in children at risk for cardiovascular disease (CVD). Associations between changes in carboxylation in OC (uncarboxylated OC; uOC) and MGP (dephosphorylated-uncarboxylated MGP; dp-ucMGP) and changes in bone and lipid metabolism were also determined. Twenty-one overweight children aged 8-17 years were randomly assigned to daily vitamin K<sub>2</sub> of 45-μg or 90-μg or placebo for 8 weeks. At baseline and posttest, fasting blood samples were measured for uOC, dp-ucMGP, procollagen-type 1-amino-propeptide (PINP; bone formation marker), C-telopeptide (CTX; bone resorption marker), receptor-activator-nuclear-factor-κB-ligand (RANKL; promoter of osteoclast differentiation/activation), osteoprotegerin (OPG; inhibitor of bone resorption and regulatory factor in vascular calcification by binding to RANKL—higher OPG levels are associated with an increased risk of CVD events and vascular damage), and lipids (triglycerides [TG], total cholesterol [TC], HDL-cholesterol [HDL-C], and LDL-cholesterol [LDL-C]). After 8 weeks, there were significant linear downward dose-response trends for uOC, dp-ucMGP, OPG, TG, TC, and LDL-C (all  $P$ -trend $\leq 0.03$ ). Conversely, significant linear upward dose-response trends were observed for PINP and RANKL/OPG (both  $P$ -trend $\leq 0.04$ ). No effect of vitamin K<sub>2</sub> on CTX, RANKL, or HDL-C was observed. Multiple linear regression adjusting for age, sex, and race revealed that change in dp-ucMGP was positively associated with changes in OPG, TG, and LDL-C, and inversely related to PINP and RANKL/OPG (all  $P\leq 0.04$ ). Change in uOC was positively correlated with changes in TG and LDL-C, but negatively associated with change in PINP (all  $P<0.05$ ). In overweight children, vitamin K<sub>2</sub>-induced carboxylation of OC and MGP demonstrated beneficial dose-response effects on bone and lipid metabolism. In addition, the increase in bone formation along with the decrease in OPG might reflect an increase in OPG binding to RANKL. This could explain the effects of vitamin K<sub>2</sub> on bone and lipids, providing further evidence of the bone-vascular relationship.

**Disclosures:** Mary Ellen Fain, None.



## FR0073

**Suppression of undercarboxylated osteocalcin after acute prednisolone ingestion is associated with impaired post-exercise insulin sensitivity and attenuated mTOR protein signaling.** Lewan Parker\*<sup>1</sup>, Andrew Garnham<sup>2</sup>, Glenn McConell<sup>1</sup>, Nigel Stepto<sup>1</sup>, David Hare<sup>3</sup>, Elizabeth Byrnes<sup>4</sup>, Peter Ebeling<sup>5</sup>, Ego Seeman<sup>6</sup>, Tara Brennan-Speranza<sup>7</sup>, Itamar Levinger<sup>1</sup>. <sup>1</sup>Clinical Exercise Science Research Program, Institute of Sport, Exercise and Active Living (ISEAL), Victoria University, Melbourne, Australia, Australia, <sup>2</sup>School of Exercise & Nutrition Sciences, Deakin University, Melbourne, Australia, Australia, <sup>3</sup>University of Melbourne and the Department of Cardiology, Austin Health, Melbourne Australia, Australia, <sup>4</sup>PathWest QEII Medical Centre, Perth, Australia, Australia, <sup>5</sup>Department of Medicine, School of Clinical Sciences, Faculty of Medicine, Nursing and Health Sciences, Monash University, Australia, Australia, <sup>6</sup>University of Melbourne and the Department of Endocrinology, Austin Health, Melbourne, Australia, Australia, <sup>7</sup>Department of Physiology, Bosch Institute for Medical Research, University of Sydney, Sydney, Australia, Australia

Purpose. Glucocorticoid (GC) treatment impairs bone formation, undercarboxylated osteocalcin (ucOC) and insulin sensitivity. The effects of acute GC ingestion on post-exercise insulin sensitivity in humans are unclear. We investigated whether attenuation of ucOC, by a single dose of prednisolone, is associated with impaired post-exercise insulin sensitivity and skeletal muscle insulin protein signaling.

Methods. Nine healthy males (Age:  $28 \pm 2$  years; BMI:  $24 \pm 1$ ; Mean  $\pm$  SEM) were randomly allocated in a double-blinded cross-over design to a single dose of either 20 mg of prednisolone or placebo, ~7 days between trials. Twelve hours after capsule ingestion, after an overnight fast, participants performed a session of high-intensity interval exercise (4 x 4-minute cycling intervals at 90-95% HRpeak, 2-minute active recovery periods). The homeostatic model assessment (HOMA2-IR) was used to assess basal insulin resistance and the euglycaemic hyperinsulinaemic clamp (EHC) was used to assess insulin sensitivity 3 hours after exercise. Serum ucOC, and skeletal muscle AS160<sup>Thr642</sup>, Akt<sup>Ser473</sup> and mTOR<sup>Ser2481</sup> protein signaling, were measured at baseline and post-EHC (~5 hours post-exercise).

Results. Compared to placebo, prednisolone treatment decreased ucOC at baseline ( $-24 \pm 2\%$ ,  $p < 0.001$ ) and post-EHC ( $-18 \pm 2\%$ ), which coincided with increased HOMA2-IR at baseline ( $107 \pm 27\%$ ,  $p < 0.001$ ) and decreased post-exercise insulin sensitivity ( $-34 \pm 5\%$ ,  $p < 0.001$ ). Lower baseline serum ucOC was associated with greater HOMA2-IR ( $r = -0.54$ ,  $p < 0.05$ ) and lower post-exercise insulin sensitivity ( $r = 0.72$ ,  $p < 0.01$ ). Prednisolone ingestion significantly impaired ( $p < 0.05$ ) the insulin stimulated increase in skeletal muscle AS160<sup>Thr642</sup> (~50%), Akt<sup>Ser473</sup> (~61%) and mTOR<sup>Ser2481</sup> (~59%) protein phosphorylation, which were significantly correlated ( $p < 0.01$ ) with lower serum ucOC ( $r = 0.64$ ,  $r = 0.71$  and  $r = 0.61$ , respectively).

Conclusions. The suppression of ucOC with a single dose of prednisolone is associated with impaired post-exercise insulin sensitivity and attenuated skeletal muscle insulin and mTOR protein signaling. These findings provide novel evidence and potential mechanisms for the role of ucOC in post-exercise insulin sensitivity in humans.

**Disclosures:** Lewan Parker, None.

## FR0074

**Improving Mitochondrial Function via CypD Genetic Deletion Promotes BMSC Osteogenicity and Fracture Repair.** Brianna Shares\*, Laura Shum, Roman Eliseev. University of Rochester, United States

Bone marrow stromal (a.k.a. mesenchymal stem) cells (BMSC) are multipotent progenitors that can differentiate into osteoblasts, adipocytes, and chondrocytes. As BMSCs undergo osteogenic differentiation they upregulate use of their mitochondria and oxidative phosphorylation (OxPhos). Our data and the literature indicate that active mitochondria are required for osteoblast differentiation. Our lab is investigating if strategies aimed at improving mitochondrial OxPhos are effective in stimulating bone formation especially in pathological settings (aging and fracture). One such strategy is inhibition of opening of a non-selective mitochondrial pore called the mitochondrial permeability transition pore (MPTP). MPTP opening is the most common mechanism of mitochondrial dysfunction. Cyclophilin D (CypD) is a genetically proven positive regulator of the MPTP. Recently, our lab showed that protecting the mitochondria by genetic removal of CypD protected against age-related bone loss in mice. However, the role of CypD during osteogenic differentiation in physiological and pathological settings has not been fully elucidated. To uncover the role of CypD during osteogenic differentiation, we isolated BMSCs from CypD KO and wild-type littermates to perform osteoinduction. BMSCs from CypD KO mice showed enhanced osteogenic potential as shown by mRNA and protein expression and staining for mineralization. We also performed an ectopic bone formation assay by subcutaneously implanting BMSCs from CypD KO and wild-type littermates into nude mice. Cells from CypD KO mice produced larger ossicles, further indicating their increased osteogenic potential. Next, to uncover the role of CypD in a pathological setting, tibial fractures were done on both CypD KO and wild-type littermates. At 0, 14, and 35 days post-fracture, blood and bones were collected. Both fractured and unfractured tibiae were analyzed via biomechanical testing and uCT. Blood serum was analyzed for levels of PINP, a bone formation marker. We observed that CypD KO mice show enhanced fracture healing in regards to bone biomechanical parameters and bone formation post-fracture when compared to wild-type littermates. This work shows that improving mitochondrial function via CypD genetic

deletion induces BMSC towards the osteogenic lineage and promotes the bone fracture healing process, further highlighting the importance of mitochondria for bone formation.

**Disclosures:** Brianna Shares, None.

## FR0075

**Glucose metabolism and insulin release are impaired under conditions of excess TGF- $\beta$  mediated high bone turnover.** Trupti Trivedi\*<sup>1</sup>, Jenna Regan<sup>1</sup>, Sarah Tersey<sup>2</sup>, Sutha John<sup>1</sup>, Yun She<sup>1</sup>, Sreemala Murthy<sup>1</sup>, Xu Cao<sup>3</sup>, Khalid Mohammad<sup>1</sup>, Theresa Guise<sup>1</sup>. <sup>1</sup>Division of Endocrinology, Department of Medicine, Indiana University, United States, <sup>2</sup>Department of Pediatrics, Indiana University School of Medicine, United States, <sup>3</sup>Department of Orthopedic Surgery, Johns Hopkins University School of Medicine, United States

Bone loss and/or type 2 diabetes increases the risk of pathological fractures, muscle weakness and obesity. We have shown that TGF- $\beta$  released from the bone matrix during resorption can act systemically to cause skeletal muscle weakness. Given that circulating TGF- $\beta$  and other bone-derived factors can potentially signal in different tissues, we explored the significance of bone-to-pancreas signaling using a mouse model of Camurati-Engelmann disease (CED), a rare bone diaphyseal dysplasia associated with high bone turnover. Mice expressing a bone-directed CED mutation exhibit high bone resorption, increased circulating TGF- $\beta$ , fractures, and muscle weakness. Since TGF- $\beta$  can impair insulin secretion, we hypothesized that the high bone turnover and increased systemic TGF- $\beta$  in CED mice would cause hyperglycemia due to impaired insulin secretion from pancreatic  $\beta$ -cells. Forty-five-week old control and CED mice were fed either high fat diet (HFD) or low fat diet (LFD) for 15 weeks, mimicking the conditions of aging, high bone resorption, and obesity. Our data show that HFD CED mice have higher fat mass compared to HFD control ( $p < 0.001$ ) suggesting that high bone resorption and release of bone-derived factors exacerbate the effects of diet-induced obesity. Compared to HFD controls, HFD CED mice had significant glucose intolerance ( $p < 0.01$ ) and mild insulin resistance. Isolated pancreatic  $\beta$ -cells from HFD CED mice showed significantly less insulin secretion ( $p < 0.05$ ) in response to glucose stimulation, indicating impaired metabolic-secretion coupling. In contrast, there were no differences in glucose tolerance, insulin sensitivity, insulin secretion, or fat mass between control and CED mice on LFD. Muscle specific force in HFD CED mice was significantly lower compared to HFD control ( $p < 0.001$ ). The muscle specific force for CED LFD was lower compared to control but was not as reduced as that seen with the HFD. This implies that muscle weakness in the setting of CED-induced high bone turnover is sensitive to the added insult of diet-induced obesity and its associated metabolic complications. Overall, our data indicate that a state of high bone turnover (with excess TGF- $\beta$ ) adversely affects both glucose and fat metabolism and impairs insulin secretion by pancreatic  $\beta$ -cells. Future studies will be directed at understanding the mechanisms of bone-energy cross-talk to develop therapeutic targets in conditions of bone loss associated with diabetes, obesity, and age related sarcopenia.

**Disclosures:** Trupti Trivedi, None.

## FR0076

**Par1/Mark3 functions in osteoblasts to coordinate bone mineral density and body mass.** Qian Zhang\*<sup>1</sup>, Gina Calabrese<sup>2</sup>, Angela Verado<sup>1</sup>, Larry Mesner<sup>2</sup>, Thomas Clemens<sup>1</sup>, Charles Farber<sup>2</sup>. <sup>1</sup>Johns Hopkins University, United States, <sup>2</sup>University of Virginia, United States

Genome-wide association studies (GWASs) have identified thousands of loci associated with complex diseases; however, little progress has been made identifying the responsible genes. Through an analysis of GWAS data we identified SNPs on Chr14q32.32 associated with both bone mineral density (BMD) and body mass index (BMI). To identify the responsible gene we used an innovative network-based strategy to predict that *MARK3*, a conserved serine/threonine kinase known to regulate cellular bioenergetics, was causal and regulated BMD through a role in osteoblasts. To determine if *Mark3* is the causal gene we characterized the phenotypes of mice lacking the gene globally (*Mark3*<sup>-/-</sup>) or selectively in osteoblasts (*Mark3*<sup>oc-cre/-</sup>). Male 12-week-old mice from both mutant cohorts had identical femoral morphometry characterized by progressively increased BMD exclusively in the cortical compartment; biomechanical measurements indicated that femurs from the KO mice were also stronger than controls. *Mark3*<sup>oc-cre/-</sup> mice fed a normal chow diet had normal postnatal growth and body weight. However, when challenged with a high fat diet mutant mice gained less weight than controls and exhibited increased glucose tolerance and insulin sensitivity. Resistance to weight gain and glucose intolerance when fed a high fat diet was also seen in mice lacking *Mark3* globally strongly suggesting that the metabolic phenotype was secondary to an intrinsic function of *Mark3* in the osteoblast. To begin to explore the mechanism underlying osteoblast autonomous actions of *Mark3* we examined the impact of loss of function of *Mark3* in primary osteoblasts. In wild type osteoblasts, *Mark3* mRNA was high early in undifferentiated cultures and declined as cells matured. Primary osteoblasts lacking *Mark3* exhibited increased mineralization at 14 days assessed by alizarin compared to controls. Analysis of expression of candidate genes known to influence osteoblast differentiation revealed a marked suppression of Jagged 1, a ligand for the Notch effector Hes1. Interestingly, signaling through Jagged1-Notch has previously been proposed as a selective regulator of the cortical bone compartment (Bone 91, 2016 64-74). Together, our studies demonstrate that *Mark3* functions intrinsically in osteoblasts possibly through the Notch-Hes effector pathway to control

cortical bone development and impacts global metabolism. These findings further support *MARK3* as a genetic determinant of bone mass and metabolism in humans.

**Disclosures:** Qian Zhang, None.

## FR0077

**Absence of ASXL2 only in Myeloid Lineage Cells Prevents Obesity while Increasing Bone Mass.** Wei Zou<sup>\*1</sup>, Nidhi Rohatgi<sup>1</sup>, Jesse Williams<sup>1</sup>, Hua Pan<sup>2</sup>, Terri Pietka<sup>3</sup>, Nada A Abumrad<sup>3</sup>, Samuel Wickline<sup>2</sup>, Gwendalyn J Randolph<sup>1</sup>, Steven L Teitelbaum<sup>4</sup>. <sup>1</sup>Department of Pathology and Immunology, Washington University School of Medicine, United States, <sup>2</sup>University of South Florida Morsani College of Medicine, United States, <sup>3</sup>Department of Internal Medicine, Division of Nutritional Science, Washington University School of Medicine, United States, <sup>4</sup>Department of Pathology and Immunology; Department of Internal Medicine, Division of Bone and Mineral Diseases, Washington University School of Medicine, United States

Profound weight loss, such as that attending bariatric surgery, is complicated by osteoporosis and enhanced fracture risk. On the other hand, congenital lipodystrophy is often associated with increased bone mass. We have noted that global deletion of the *ETP* gene, *ASXL2*, arrests osteoclastogenesis and promotes lipodystrophy, attended by profound insulin resistance. To determine if the osteoclastogenic properties of *ASXL2* are cell autonomous, we conditionally deleted its gene in myeloid lineage cells. Confirming cell autonomy, osteoclast formation is arrested and bone mass significantly increased in the resultant (*ASXL2*<sup>LysM</sup>) mice. Given the relationship of bone mass and adipogenesis, we fed *ASXL2*<sup>LysM</sup> mice a high fat diet (HFD). Whereas WT mice increase weight by 50% in 8 weeks, surprisingly those with *ASXL2* deleted only in myeloid cells, are completely resistant to weight gain despite similar activity, food intake and fecal fat. Accounting for their resistance to obesity, basal energy expenditure is increased 45% in *ASXL2*<sup>LysM</sup> mice. As expected, HFD WT mice are insulin resistant and have elevated levels of free fatty acids while those with myeloid-depleted *ASXL2* exhibit no metabolic abnormalities. Importantly, whereas fat-residing macrophages of WT mice are predominantly M1 (pro-inflammatory), those of *ASXL2*<sup>LysM</sup> are largely M2 (pro-immune) polarized. Brown adipose tissue (BAT), which is the prime mediator of thermogenic energy expenditure, is protected from HFD-induced lipid accumulation in *ASXL2*<sup>LysM</sup> mice and attesting to increased BAT activation, the mutant animals are resistant to cold exposure. The increased energy consumption by HFD *ASXL2*<sup>LysM</sup> BAT is confirmed by documentation that glycolytic function and mitochondrial respiration are significantly increased. Fatty acid oxidation also appears accelerated in *ASXL2*<sup>LysM</sup> BAT as manifest by enhanced PET-determined palmitate uptake and augmented expression of key lipolytic enzymes as well as tyrosine hydroxylase and  $\beta$ 3 adrenergic receptors. While white adipose tissue contains no evidence of developing a BAT phenotype ("beiging") oxidative phosphorylation complex expression is increased, indicative of enhanced mitochondrial function. Suggesting therapeutic potential, suppression of macrophage *ASXL2* expression via nanoparticle-based siRNA delivery, prevents HFD induced obesity. Our data indicate diet-induced obesity and weight loss-associated osteoporosis may be prevented by exclusive targeting of macrophages.

**Disclosures:** Wei Zou, None.

## FR0078

**Similar increase in bone resorption and decrease in bone mass but opposite effects in osteocytic gene expression in female versus male mice with FMR1 deletion, a model of fragile X syndrome.** Hannah M. Davis<sup>\*1</sup>, Rafael Pacheco-Costa<sup>1</sup>, Alexandra Aguilar-Perez<sup>1</sup>, Carmen Herrera<sup>1</sup>, Greg Smith<sup>2</sup>, Joaquin Lugo<sup>2</sup>, Lilian I. Plotkin<sup>1</sup>. <sup>1</sup>Indiana University School of Medicine, United States, <sup>2</sup>Baylor University, United States

Fragile X syndrome (FraX), an X-linked disease, is the cause of 5% of the autism spectrum disorder cases. Scoliosis is present in some FraX patients and both humans with FraX and mice lacking FMR1 (KO), a model for FraX, exhibit craniofacial abnormalities. However, the rest of the skeleton has not been studied. We now report that FMR1 is expressed in bone preparations, and in osteoblasts, osteocytes and osteoclasts. Hemizygous male KO (x/y), homozygous female KO (x/x) and WT 2-month-old mice of both sexes were used. FMR1 deletion did not alter femur length (14.7±1.0 and 14.4±1.1mm for male and 14.7±0.3 and 14.7±0.5mm for female WT and KO mice, respectively).  $\mu$ CT analysis showed that vertebra cancellous BV/TV was significantly reduced (9%) with low TbTh (10%) in KO female mice. Similar decrease in BV/TV (12%) with low TbN (9%) and high TbS (8%) were found in KO male mice. Further, bone material density was slightly, but significantly decreased in both male and female mice. This change in material density could be due to an increase in bone remodeling, resulting in newer, less mineralized bone, or to a defect in bone mineralization. Consistent with the first possibility, CTX measured in whole tibia bone lysates was 72% higher in KO female mice compared to WT controls. Osteoclastic gene (CatK and CalR) and RANKL expression was high, and OPG was low in female KO mice compared to WT mice. Female FMR1 x<sup>+</sup>/x<sup>-</sup> mice exhibited a similar, but more modest bone phenotype possibly due to X-inactivation mosaicism, with 60% increase in bone CTX levels. Male KO mice showed a tendency towards higher CTX levels, without reaching significance, and higher RANKL/OPG ratio without changes in osteoclastic genes in bone. While similar

osteoclastic gene phenotype and increased DKK1 and ALP levels were found in both sexes, opposite effects of FMR1 deletion were detected in osteocytic genes. Thus, E11 was lower and Sost was higher in females, and the genes were respectively increased and decreased in male KO mice. Further osteocalcin and collagen1a1 were only decreased in female mice. In summary, FMR1 deletion results in low bone mass and high bone resorption in both sexes, but might have different effects in osteoblast-osteocyte transition in female versus male KO mice. This evidence, together with studies showing defective dendrite formation in FMR1-deficient neurons, raise the possibility of a role of FMR1 in osteocytogenesis in a sex specific manner.

**Disclosures:** Hannah M. Davis, None.

## FR0080

**MicroRNA miR-204 and miR-211 Control Runx2 Expression and Regulate Bone Mass.** Jun Li<sup>\*1</sup>, Jian Huang<sup>1</sup>, Lan Zhao<sup>1</sup>, Ge Zhang<sup>2</sup>, Guang-qian Zhou<sup>3</sup>, Andre J. van Wijnen<sup>4</sup>, Di Chen<sup>1</sup>. <sup>1</sup>Department of Orthopedic Surgery, Rush University Medical Centre, United States, <sup>2</sup>Institute for Advancing Translational Medicine in Bone & Joint Diseases, Hong Kong Baptist University, China, <sup>3</sup>Department of Medical Cell Biology and Genetics, Shenzhen Key Laboratory and the Center for Anti-Ageing and Regenerative Medicine, Shenzhen University Medical School, China, <sup>4</sup>Department of Orthopedic Surgery, Mayo Clinic, United States

We previously demonstrated that microRNAs, miR-204/-211, play a key role in regulation of Runx2 expression and MSC differentiation. In this study we further determine the role of miR-204/-211 in bone formation using *in vivo* approach. 1) We generated miR-204 antagonist (sponge) transgenic mice (*Sponge*<sup>Prx1</sup>) by breeding *pCALL2-miR-204-sponge* mice (generated in our lab) with *Prx1-Cre* mice. We found that BV was significantly increased (31%) in 2-month-old *Sponge*<sup>Prx1</sup> mice. Consistent higher trabecular number and lower trabecular separation were also observed in *Sponge*<sup>Prx1</sup> mice. We then isolated BMSCs from *Sponge*<sup>Prx1</sup> mice and found that a) Runx2 protein levels, ALP and Alizerin red staining, and expression of *Osx* (4-fold), *Alp* (13-fold), *OPN* (7-fold) and *OC* (3-fold) were significantly increased. b) MSC population (CD45/CD29<sup>+</sup>/CD105<sup>+</sup>/Sca1<sup>+</sup> cells) was increased in *Sponge*<sup>Prx1</sup> mice. c) NGF and pAKT expression was significantly increased and the expression of CDK inhibitors, including *p16* (88%), *p21* (60%), *p27* (38%), and *p57* (95%), was significantly decreased in BMSCs derived from *Sponge*<sup>Prx1</sup> mice. These findings suggest that MSC proliferation and differentiation were accelerated in *Sponge*<sup>Prx1</sup> mice. 2) We then generated miR-204/-211 double KO mice (*dmiR*<sup>Prx1</sup>) by breeding *miR-204*<sup>lox/lox</sup> and *miR-211*<sup>lox/lox</sup> mice (generated in our lab) with *Prx1-Cre* mice. Similar results on Runx2 upregulation, MSC expansion, osteoblast differentiation, and bone mass increase were observed in *dmiR*<sup>Prx1</sup> double KO mice. 3) We transfected anti-miR-204 antagonist into human MSCs. Upregulation of osteoblast marker genes, *Osx* (>10-fold) and *SATB2* (2-fold), and down-regulation of chondrocyte marker genes, *Sox9* (70%), *Sox5* (75%), *Sox6* (80%), and *Col2a1* (40%) were observed 7 days after transfection of anti-miR-204 in human MSCs. 4) To explore the therapeutic potential of miR-204, we delivered anti-miR-204 antagonist into 6-month-old female C57BL/6 mice by (Asp-Ser-Ser)<sub>6</sub>-liposome via tail vein injection. (Asp-Ser-Ser)<sub>6</sub>-liposome could specifically deliver miRNA to the bone surface. The  $\mu$ CT analysis showed that BV and BMD in proximal tibiae (BV: 26%; BMD: 22%), distal femora (BV: 29%; BMD: 19%), and vertebrae (L4) (BV & BMD: 23%) were significantly increased 6-weeks after anti-miR-204 administration (n=4-6). These results suggest that anti-miR-204 could be potentially used for the treatment of osteoporosis and other bone loss associated diseases.

**Disclosures:** Jun Li, None.

## FR0081

**Use of the CRISPR/dCas9::KRAB system to suppress gene expression as an alternative to conditional gene deletion.** Ryan Macleod<sup>\*</sup>, Charles OBrien. University of Arkansas for Medical Sciences, United States

The Cre/LoxP system is widely used to delete or activate genes in specific cell types. A significant limitation of this approach is that many, if not all, Cre driver strains exhibit Cre recombinase activity in multiple cell types. This off-target activity often goes unrecognized but may confound interpretation of results. Thus, there is a need for new approaches to reduce or elevate expression of a gene of interest *in vivo*. The CRISPR/Cas9 system is a bacterial adaptive immune system, components of which have been modified for use as a method of gene editing. In this system, the Cas9 nuclease is targeted to a specific DNA sequence by a single guide RNA (sgRNA) complementary to the target sequence. Recently, the system has been modified for use as a modulator of gene expression rather than gene editing. The modified system, known as CRISPR interference (CRISPRi), uses a sgRNA to guide a transcriptional repressor to the start-site of a gene of interest to suppress expression of that gene. The repressor consists of a catalytically inactive Cas9 fused to a Krüppel Associated Box (KRAB) repressor domain (dCas9::KRAB). Here we tested the efficacy of CRISPRi to suppress the RANKL gene *in vitro* as a prelude to studies in mice. Previous studies have shown that targeting dCas9::KRAB to within 100 bp of the transcription start-site leads to effective suppression. We introduced the Cas9::KRAB coding sequence into UAMS-32 stromal cells using a lentiviral vector and then tested three different sgRNAs that were complementary to different sequences within 100 bp of the RANKL transcription start-site. A sgRNA complementary to GFP cDNA was used as a control. The sgRNAs were introduced into UAMS-32-dCas9::KRAB cells using a second lentiviral vector. One of



the three sgRNAs reduced RANKL mRNA in UAMS-32 cells by more than 80 percent, compared with cells expressing the GFP sgRNA. The protein kinase A (PKA) pathway is a potent stimulator of RANKL transcription. We used dibutyl-cAMP to activate PKA in UAMS-32 cells and found that the same sgRNA that suppressed basal RANKL transcription also suppressed stimulated levels by more than 50 percent. This approach is easily modifiable to suppress other genes of interest simply by targeting loci with different sgRNAs. Moreover, by expressing the dCas9::KRAB coding sequence under the control of cell type-specific promoters, this system may be useful for examining the function of a gene of interest in specific cell types in mice.

**Disclosures:** Ryan Macleod, None.

## FR0084

### Regulation of phalangeal joint development by ACVR1 in fibrodysplasia ossificans progressiva. O. Will Towler<sup>\*1</sup>, Frederick S. Kaplan<sup>1</sup>, Eileen M. Shore<sup>2</sup>.

<sup>1</sup>Center for Research in FOP and Related Disorders, Department of Orthopaedic Surgery, Perelman School of Medicine, University of Pennsylvania, United States, <sup>2</sup>Center for Research in FOP and Related Disorders, Departments of Orthopaedic Surgery and Genetics, Perelman School of Medicine, University of Pennsylvania, United States

Fibrodysplasia ossificans progressiva (FOP; OMIM #135100), caused by enhanced activity of the bone morphogenetic protein (BMP) type 1 receptor ACVR1, is a genetic disease of heterotopic ossification accompanied by laterally deviated great toes and impaired digit joint mobility. Normal joint development during embryogenesis requires that BMP signaling is reduced at the site of the future joint. Therefore, we hypothesized that the increased signaling by the mutant ACVR1 receptor escapes inhibition in the developing joint, resulting in malformation and dysfunction.

We used a conditional knock-in mouse model (MGI:5763014) with the FOP ACVR1 R206H mutation to examine digit and joint formation *in vivo*. *Acvr1*<sup>floxR206H/+</sup> mice crossed to mice harboring a universally expressed doxycycline-responsive Cre driver (*R26-rtTA;tetO-Cre*) or a limb-specific Cre (*Prrx1-Cre*) exhibit stunted hindlimb first digits similar to FOP patients. Although effects on first digits were most pronounced, we determined that multiple digits were affected and showed delayed digit development during embryogenesis. To investigate the three-dimensional patterns of BMP pathway signaling in mutant vs. control limbs, we performed 3D whole-mount pSmad1/5 immunohistochemistry and imaging of embryonic mouse limbs over time. Unrestricted BMP signaling throughout the digit rays of mutant animals at critical times for joint formation (E12.5 and E13.5) revealed that BMP pathway activity from the mutant receptor was insufficiently inhibited in the joint space. To confirm that the phenotype is primarily one of altered joint tissue development, we activated the mutation only in joint progenitor cells using *Gdf5-Cre* and found this activation was sufficient to produce the joint and digit phenotype. Histological analyses revealed interphalangeal chondrocyte proliferation, supporting that the phenotype is due to improper spatiotemporal activation of a chondrogenic pathway in the joint space by BMP pathway signaling through the mutant ACVR1 receptor.

These data provide new insight into the critical regulation of BMP signaling activity in early digit development, and into the roles of ACVR1 in digit and joint formation. This is the first investigation of the development of the unique and characteristic malformed great toes of FOP, and it establishes altered BMP pathway signaling in joint tissue cells and joint formation as culpable for the disease phenotype.

**Disclosures:** O. Will Towler, None.

## FR0085

### Mutation Correction in OI iPSC Restores Bone Formation. Xiaonan Xin<sup>\*1</sup>, Mark Kronenberg<sup>1</sup>, Li Chen<sup>1</sup>, Zhihua Wu<sup>1</sup>, Liping Wang<sup>1</sup>, Xi Jiang<sup>2</sup>, David Rowe<sup>1</sup>, Alexander Lichter<sup>1</sup>. <sup>1</sup>UConn Health, United States, <sup>2</sup>University of Pennsylvania, United States

We have reported that iPSC from a type III/IV osteogenesis imperfecta (OI) patient with a glycine substitution point mutation in the COL1A1 gene produce substantially less bone than iPSC from control subjects in an *in vivo* mouse calvarial defect model. Instead, these cells produced substantial amounts of adipose tissue, which had not been seen with control cells. We reported using CRISPR/Cas technology to produce a mutation-corrected clone, #88, that does not show secondary mutations near the mutation correction site or loss of heterozygosity of the COL1A1 gene. We now show that the mutation corrected cells produce greatly increased bone compared to the original mutant cells as demonstrated by skull X-rays. Histological analysis with human specific antibodies and mouse osteoblast specific GFP shows that the osseous tissue was produced by human cells, which also didn't produce adipose tissue. Thus the mutation-corrected cells produce tissue that closely resembles tissue created by control iPSC, with a normal bone producing phenotype. We did not detect mutations in several potential off-target cleavage sites for the CRISPR guide RNA that we used in the correction of clone #88. The next phase of our goal of utilizing iPSC-derived human osseous and cartilage tissue as a diagnostic tool for studying genetic disorders affecting bone and cartilage is to develop methods for performing RNA expression studies. One approach uses laser capture microdissection (LCM) of formalin-perfusion fixed, non-decalcified and cryoembedded tissues. Protocols have been developed for capturing specific tissue types from mineralized and collagen rich regions without contamination from adjacent tissues. Recovery of 10-50 pg of total RNA from these fragments allows for efficient amplification by SPIA technology for analysis by PCR and RNAseq. A second approach uses enzymatic digestion of a freshly dissected tissue implant to liberate cells for FACS

sorting. Using Col2.3RFP to identify human osteoblasts and Col3.6GFP to exclude mouse contamination, intact RNA from human osteoblasts can be purified and amplified for analysis. Because genetic background affects disease severity, one advantage of developing the iPSC model is the ability to perform a comparison of mutant and mutation corrected cells in the same genetic background. Thus the possibility for appreciating a personalized disease mechanism and even drug optimization is a future application of this platform.

**Disclosures:** Xiaonan Xin, None.

## FR0087

### Identification of anabolic bone genes using whole genome sequencing in high bone mass families. John Eisman<sup>\*1</sup>, Peter Croucher<sup>2</sup>, Paul Baldock<sup>2</sup>, Tuan Nguyen<sup>2</sup>, Robert Brink<sup>2</sup>, Daniel Hesselton<sup>2</sup>, Sing Nguyen<sup>2</sup>, Mohammad Moni<sup>2</sup>, Scott Youlten<sup>2</sup>. <sup>1</sup>Garvan Institute of Medical Research; School of Medicine Sydney, University of Notre Dame Australia; St Vincents Hospital; UNSW Sydney, NSW, Australia, Australia, <sup>2</sup>Garvan Institute of Medical Research, Australia

Bone mineral density exhibits strong heritability in family and twin-based studies. This has been the focus of large-scale international genome-wide association studies (GWAS) that have identified genetic loci associated with bone mass but only explain a small proportion (<10%) of the heritability, suggesting that new approaches to identifying the genes that control skeletal mass are required.

We hypothesized that whole genome sequencing (WGS) in families, in which high bone mass segregates as a dominant trait, will identify novel rare variants of large effect size for bone mass providing insight into bone biology and targets for anabolic therapies.

In our large, extended families with high bone mass in the Dubbo Osteoporosis Epidemiology cohort, we have applied WGS followed by selection based on variant rarity, likely functional impact, familial segregation, followed by expression in osteocyte-specific transcriptome and signal in large-scale international bone GWAS data to identify informative gene variants.

In a 5-member sub-unit of one of the large families, WGS identified >7 million variants. These were narrowed to 1.2 million rare (<1%) coding and non-coding genetic variants and then to 513 genes based on projected high functional impact and then to 167 genes based on family-segregation criteria. Of these, 8 genes showed consistent osteocyte-specific expression and two are close to GWAS peaks in the GEFOS international bone genetics consortium. One of these genes has been reported to have a high bone mass phenotype in knockout mice. The variants in these two genes, that encode major amino acid changes expected to materially change protein function and/or folding, are in regions and encoded proteins that are highly conserved from human to lamprey. These are being examined by gene editing in mouse and zebrafish.

These initial studies are 'proof-of-principle' that the strategy of WGS in Mendelian families can identify rare genetic variants as major contributors to high bone mass/density within families and potentially identify novel genes and pathways in bone biology.

**Disclosures:** John Eisman, None.

## FR0089

### Genetic Prediction of Lifetime Risk of Fracture. Thao P. Ho-Le<sup>\*1</sup>, Jackie R. Center<sup>2</sup>, John A. Eisman<sup>3</sup>, Hung T. Nguyen<sup>1</sup>, Tuan V. Nguyen<sup>4</sup>.

<sup>1</sup>Centre of Health Technologies, FEIT, University of Technology Sydney, Australia, <sup>2</sup>Bone Biology Division, Garvan Institute of Medical Research; St Vincent Clinical School, UNSW, Australia, Australia, <sup>3</sup>Bone Biology Division, Garvan Institute of Medical Research; St Vincent Clinical School, UNSW, Australia; School of Medicine, Sydney University of Notre Dame, Australia, <sup>4</sup>University of Technology, Sydney; Bone Biology Division, Garvan Institute of Medical Research, NSW; St Vincent Clinical School, UNSW; School of Public Health and Community Medicine, UNSW; School of Medicine, Sydney University of Notre Dame, Australia

**Aim:** Residual lifetime risk of fracture (RLRF) is the probability of sustaining a fracture during the individual's remaining lifetime. There is a high variation in RLRF between individuals, and we hypothesize that the variation is partly due to genetic factors. Several genetic variants have been identifying to be associated with bone mineral density (BMD). This study sought to develop a genetic profiling of BMD-associated genetic variants for predicting the lifetime risk of fracture for men and women.

**Methods:** This population-based prospective study involved 1326 men and 2189 women aged 60 years at study entry (1989-1992). The individuals have been followed continuously for up to 20 years. During the follow-up period, the incidence of fragility fractures was ascertained from X-ray reports. The incidence of mortality was also ascertained. Femoral neck bone mineral density (BMD) was measured by dual-energy X-ray absorptiometry. A polygenic risk score (GRS) was created by summing the weighted number of risk alleles for each single-nucleotide polymorphism (SNP), with the weight being regression coefficients associated with BMD. The RLRF from the age of 60 was estimated by survival analysis taking into account the competing risk of death.

**Results:** During the 20-year follow-up period, 667 women (31%) and 239 men (18%) had sustained at least one fracture. After adjusting for competing risk of death, the RLRF for women and men from age 60 was 36% (95% CI, 34-39%) and 21% (95% CI, 18-24%),

respectively. Greater GRS was significantly associated with higher lifetime risk of fracture. Among women with GRS>4.24 (median), the RLRf was 42% (95% CI, 35-47%) which was 1.17-fold greater than average. Among men with GRS>4.24, the RLRf 24% (95% CI, 19-28%), which is 1.14-fold greater than the average. For hip fracture, the mortality-adjusted residual lifetime risk was 10% (95% CI, 8-12%) for women and ~5% (95% CI, 3-6%) for men. Higher GRS was associated with higher lifetime risk of hip fracture: 15% (95% CI, 9-20%) for women and 6% (95% CI, 3-9%) for men. Importantly, the association of GRS and RLRf was independent of femoral neck BMD.

Conclusion: A genetic profiling of BMD-associated genetic variants is associated with the residual lifetime risk of fracture in men and women. The finding raises the possibility of personalized fracture risk assessment by using an osteogenomic profile.

**Disclosures:** Thao P. Ho-Le, None.

## FR0090

**A Whole Genome Association Meta-Analysis Study Identifies Novel Loci Associated with Bone Microarchitecture Assessed by HR-pQCT independent of aBMD.** Yi-Hsiang Hsu<sup>\*1</sup>, Fredrick Kinyua<sup>2</sup>, Ching-Ti Liu<sup>3</sup>, Maria Nethander<sup>4</sup>, Emmanuël Biver<sup>5</sup>, Elizabeth J. Atkinson<sup>6</sup>, Elisabeth Sornay-Rendu<sup>7</sup>, Claire Watson<sup>8</sup>, Andy Kin On Wong<sup>9</sup>, Shreyasee Amin<sup>10</sup>, Elise Lim<sup>3</sup>, Michelle Yau<sup>11</sup>, Laiji Yang<sup>2</sup>, Eric Lespessailles<sup>12</sup>, Roby Joehanes<sup>13</sup>, Kerry Broe<sup>2</sup>, Jonathan D. Adachi<sup>14</sup>, Serkalem Demissie<sup>3</sup>, David Karasik<sup>2</sup>, Blandine Merle<sup>15</sup>, Dan Mellström<sup>16</sup>, L. Adrienne Cupples<sup>3</sup>, Brent Richards<sup>17</sup>, David Goltzman<sup>18</sup>, David A. Hanley<sup>19</sup>, Steven K. Boyd<sup>20</sup>, Mary L. Bouxsein<sup>21</sup>, Ronald Y. Kwon<sup>8</sup>, Mattias Lorentzon<sup>22</sup>, Claes Ohlsson<sup>23</sup>, Pawel Szulc<sup>24</sup>, Serge Ferrari<sup>25</sup>, Roland D. Chapurlat<sup>24</sup>, Sundeep Khosla<sup>10</sup>, Douglas P. Kiel<sup>13</sup>. <sup>1</sup>HSL Institute for Aging Research, Harvard Medical School, Broad Institute of MIT and Harvard, United States, <sup>2</sup>Institute for Aging Research, Hebrew SeniorLife, United States, <sup>3</sup>Biostatistics, Boston University School of Public Health, United States, <sup>4</sup>University of Gothenburg, Sweden, <sup>5</sup>University of Geneva, Switzerland, <sup>6</sup>Mayo Clinic, United States, <sup>7</sup>INSERM and University of Lyon, France, <sup>8</sup>Musculoskeletal Systems Biology Lab, Orthopaedics and Sports Medicine, University of Washington, United States, <sup>9</sup>Toronto General Research Institute, University Health Network and McMaster University, Canada, <sup>10</sup>Mayo Clinic College of Medicine, United States, <sup>11</sup>Institute for Aging Research, Hebrew SeniorLife and Department of Medicine, Beth Israel Deaconess Medical Center and Harvard Medical School, United States, <sup>12</sup>University of Orleans, France, <sup>13</sup>Institute for Aging Research, Hebrew SeniorLife and Harvard Medical School, United States, <sup>14</sup>Charlton Medical Centre, McMaster University, Canada, <sup>15</sup>INSERM, University of Lyon, France, <sup>16</sup>Univ of Gothenburg, Sweden, <sup>17</sup>Lady Davis Institute and Department of Human Genetics, McGill University, Canada, <sup>18</sup>Departments of Medicine and Physiology, McGill University, Canada, <sup>19</sup>Cumming School of Medicine, University of Calgary, Canada, <sup>20</sup>University of Calgary, Canada, <sup>21</sup>Beth Israel Deaconess Medical Center, Harvard Medical School, United States, <sup>22</sup>Sahlgrenska University Hospital, Sweden, <sup>23</sup>Center for Bone and Arthritis Research at the Sahlgrenska Academy, Sweden, <sup>24</sup>INSERM and University of Lyon, Hospital E. Herriot, France, <sup>25</sup>Geneva University Hospital, Switzerland

Bone microarchitecture assessed by high resolution peripheral quantitative computed tomography (HR-pQCT) has been reported to be heritable even after adjusting for DXA-based areal BMD (aBMD), and has been associated with fracture risks. Genetic studies of these phenotypes may reveal unique, novel genes that contribute to skeletal integrity not identifiable in previous genome-wide association studies of aBMD. Thus, our objective was to conduct a whole genome association study with the largest samples collected.

We performed and expanded our whole genome association meta-analysis on both rarer functional variants and common variants in 5,692 adult Caucasians obtained from 7 cohort studies (Framingham Study, Mayo Clinic, GeReCo, Lyon OFELY, Lyon STRAMBO, MoS Sweden and GOOD Study) and replicated associated SNPs in 2,100 independent samples (CaMoS and Lyon Qualyor studies). HR-pQCT (XtremeCT, Scanco Medical AG) phenotypes were assessed (Table 1). All studies were genotyped by SNP chips and whole genome imputation to ~40 million SNPs was performed based on the Haplotype Reference Consortium. We used either linear regression or mixed-effects model (family-based) for single SNP-phenotype associations. Additive genetic effect models were applied and adjusted for age, sex, weight and genetic ancestry. For less common variants (MAF < 1%), we performed gene-based Optimal SKAT test in each study. Meta-analysis was performed to combine association results.

Of the 17 genome-significant loci (386 SNPs with  $p < 5 \times 10^{-8}$ ), 12 were not reported by previous aBMD GWAS meta-analyses: *SIX2*, *PNPT1*, *chr4q35.2*, *KCNIP1*, *chr5q11.2*, *chr7q31.31*, *CSMD1*, *NRG1*, *PTHLH-CCFC91*, *FAM155A*, *C3* and *FMN2* loci. The majority of these loci were specifically associated with  $\mu$ FEA-FL, TtAr, CtTh, TbSp, TbN or CtBMD. The most significantly associated SNP, rs10254825, was associated with  $\mu$ FEA-FL ( $p=2.6 \times 10^{-22}$ ) and associated with all fracture risks. The remaining 5 loci (*ZBTB40*, *SPTBN1*, *MEF2C-AS1*, *WNT16-FAM3C* and *AKAP11-TNFSF11*) were previously reported by aBMD GWAS and are associated with multiple HR-pQCT phenotypes at both radius and tibia (e.g., TbBMD, TtBMD, TbSp).

Our findings suggest that the genetic control of bone microarchitecture may provide additional insights into the pathogenesis of skeletal integrity not available from aBMD. Genome editing in zebrafish using the CRISPR/Cas9 on selected genes from the novel loci is underway to dissect the potential functional involvement in bone biology.

**Table 1 Selected HR-pQCT Measurements at Both Distal Radius and Tibia for Whole Genome Association Meta-Analyses**

Measurement	Abbreviation
Trabecular density	TbBMD
Trabecular number	TbN
Trabecular thickness	TbTh
Trabecular separation	TbSp
Cross sectional area	TtAr
Total density	TtBMD
Cortical thickness	CtTH
Cortical porosity	CtPo
Cortical Density	CtBMD
Failure load from $\mu$ FEA	$\mu$ FEA-FL

Table 1

**Disclosures:** Yi-Hsiang Hsu, None.

## FR0092

**Genetic Profiling of Decreased Bone Mineral Density in an Independent Sample of Caucasian Women.** Xiangxue Xiao<sup>\*</sup>, Darius Roohani, Qing Wu. University of Nevada, Las Vegas, United States

Background: Genetic risk of osteoporosis and low Bone mineral density (BMD) in healthy populations is still unclear, especially in Caucasian women, the most vulnerable group. Genomic Wide Scans for Female Osteoporosis Gene Study (GWSFO) is a cohort that has never been involved in any BMD-associated Single Nucleotide Polymorphism (SNP) discovering study. Therefore, GWSFO is an ideal independent data source for examining genetic risk in a healthy sample. As the phenotypic risk factors are variable, while the genes remain constant, uncovering the underlying genetic risk of healthy individuals will help identify susceptible subjects for preventive interventions. Aims: 1) To examine the distribution of risk alleles in healthy Caucasian women; and 2) To examine the association of Genetic Risk Score (GRS) and BMD in a sample of healthy Caucasian women. Methods: Genotype data of GWSFO, which included 1209 unrelated healthy US Caucasian women over 18 years of age, was acquired through dbGap. Genotype imputation was conducted at the Michigan Imputation Server, using HRC Reference Panel. Based on a recent well-powered, genome-wide association study (GWAS) meta-analysis, a total of 62 BMD-associated SNPs was included for analysis. Weighted GRS of both femoral neck (FN\_GRS) and lumbar spine (LS\_GRS) for each individual were calculated. We examined the distribution of unweighted GRS (UW\_GRS). The magnitude of association between GRS and BMD at the lumbar spine and femoral neck was assessed by multiple linear regression, with age, weight, and height as covariates. SAS 9.4 was used for data analysis. Results: The UW\_GRS ranged from 27 to 56. Half of the women in this sample carried 66% risk alleles, which indicated that an apparent “healthy” population may have a substantially high genetic risk of low bone mass and thus of osteoporosis. Regression analysis indicated that for a given age and weight, higher GRS was significantly associated with decreased BMD at both the lumbar spine ( $p < 0.0001$ ) and the femoral neck ( $p = 0.0046$ ). For a one unit increase of GRS, the BMD at the spine and the hip decreased  $\sim 0.09$  g/cm<sup>2</sup> and  $0.06$  g/cm<sup>2</sup>, respectively. A sensitivity analysis was conducted after excluding excessive alcohol or tobacco users, and the results were similar. Conclusions: A substantially large percentage of healthy Caucasian women have a high genetic risk of osteoporosis. In healthy Caucasian women, GRS was significantly associated with BMD.



**Table.** Association between Genetic Risk Score (GRS) and BMD: Results of Multiple Linear Regression Analysis

BMD sites and covariates	Regression Coefficient (SE)	p
<b>Hip total BMD</b>		
Age	-0.003 (0.0003)	<0.0001
Weight	0.004 (0.0003)	<0.0001
Femoral neck GRS	-0.059 (0.0206)	0.0046
<b>Spine total BMD</b>		
Age	-0.002 (0.0003)	<0.0001
Weight	0.003 (0.0003)	<0.0001
Height	0.002 (0.0006)	0.0016
Lumbar spine GRS	-0.091 (0.0180)	<0.0001

Table

**Disclosures:** Xiangxue Xiao, None.

## FR0095

**Lack of Fibroblast Growth Factor-23 (Fgf23) signaling improves cardiac function in a murine model of acute myocardial infarction.** Kristopher Ford\*, Svetlana Slavic, Flora Klinger, Flora Klinger, Marlies Dolezal, Ute Zeitz, Karolina Hilse-Koller, Elena Pohl, Reinhold G Erben, Olena Andrukhova. Department of Biomedical Sciences University of Veterinary Medicine, Austria

Circulating fibroblast growth factor-23 (FGF23) is increased in experimental myocardial infarction (MI). FGF23 is bone-derived hormone acting through its co-receptor Klotho on phosphate homeostasis and vitamin D metabolism. Clinical studies have suggested an association between FGF23 and the development of left ventricular (LV) hypertrophy and cardiac dysfunction. Here, we explored the hypothesis that FGF23 may be causally linked to the progression of cardiac dysfunction post-MI, using a mouse model lacking either Fgf23 or Klotho in addition to a non-functioning vitamin D receptor (VDR). To normalize mineral homeostasis in VDR mutants, all mice were maintained on a rescue diet enriched with calcium, phosphorus and lactose. Three-month-old, male, wild-type (WT), VDR<sup>Δ/Δ</sup>, Klotho<sup>-/-</sup>/VDR<sup>Δ/Δ</sup> (Klotho/VDR) and Fgf23<sup>-/-</sup>/VDR<sup>Δ/Δ</sup> (Fgf23/VDR) compound mutants were subjected to permanent ligation of the left descending coronary artery. One week post-MI, MI was confirmed by decreased fractional shortening and left ventricular (LV) chamber dilation as measured by echocardiography. Aortic and cardiac catheterization was performed as a terminal procedure, either 2 or 8 weeks post-MI for monitoring of arterial pressure and of LV contraction and relaxation. As expected, circulating Fgf23 was significantly increased in all MI animals. LV contraction and relaxation was improved in Fgf23/VDR and in Klotho/VDR mice compared to WT and VDR mutant mice post-MI. Serum levels of the pro-inflammatory cytokines IL-1β and TNF-α were reduced in Fgf23/VDR MI animals compared to all other genotypes. Similarly, mRNA expression of IL-1β in the non-ischemic myocardium remained at Sham level only in Fgf23/VDR and Klotho/VDR animals post-MI. The MI-induced collagen degradation in the non-ischemic myocardium was lowest in Fgf23/VDR and Klotho/VDR mice. Furthermore, Fgf23/VDR MI animals showed an improved collagen I/III ratio, relative to WT and VDR controls. *In vitro*, co-treatment of primary cardiac fibroblasts with recombinant FGF23 (rFGF23) and IL-1β increased expression of pro-fibrotic markers, collagen I and α-smooth muscle actin in an additive fashion, compared to rFGF23 or IL-1β treatment alone. Our data indicate that absence of Fgf23 signaling improves cardiac remodeling and contractile function following experimental MI through the regulation of cardiac pro-inflammatory and pro-fibrotic signaling pathways, underscoring the potential importance of the heart-bone-axis.

**Disclosures:** Kristopher Ford, None.

## FR0096

**Inflammation, not Phosphate or Anemia, Stimulates the Initial Rise in FGF-23 at the Onset of Chronic Kidney Disease.** Jackie Fretz\*, Xiuqi Li, Tracy Nelson, Karin Finberg. Yale School of Medicine, United States

FGF-23 has arisen as an early biomarker of renal dysfunction, but at the onset of chronic kidney disease (CKD) data suggest that it may be produced independent of the parathyroid hormone (PTH), 1,25(OH)<sub>2</sub> Vitamin D<sub>3</sub> signaling axis. It has been observed that iron status is inversely correlated to the level of circulating FGF-23, and improvement in iron bioavailability within individual patients correlates with a decrease in FGF-23. To determine whether iron bioavailability was regulating FGF-23 production in early CKD we profiled the changes in iron homeostasis that accompany the onset of a mouse model of congenital CKD. Conditional deletion of Ebf1 from renal stroma using Foxd1-cre exhibit a highly penetrant and temporally reproducible CKD pathology. These mice present with phosphate wasting (P14), albuminuria (P21), leukocyturia (P24), glomerulosclerosis (P28) and hematuria (P30). We profiled the sequential presentation of indicators of renal dysfunction (NGAL, IL-6, TGF-β, TNF-α, CRP, IL-1β, activin B), phosphate imbalance (PTH, serum phosphate, phosphaturia), and regulators of iron bioavailability and transport (serum iron, hepcidin, transferrin, erythrocyte counts, Epo, and splenic erythropoiesis) to identify the events that initiate osteocytic production of FGF-23 during the onset of CKD. We report here that elevations in circulating intact-FGF-23 coincide with the earliest indicators of renal dysfunction

(P14), and precede changes in serum phosphate or iron homeostasis. Hypophosphatemia is present at P21, anemia (assessed by erythrocyte counts and hemoglobin content) was not significantly altered until P24. Splenomegaly arose at P28. Serum Epo was normal until disease was well established, at P28, but was preceded by transferrin loss in the urine (P21), and elevations in Epo-transcript levels within the kidney (P14). Serum PTH was not changed within the first month. Instead, production of inflammatory markers from the kidney and systemic elevation of these in the circulation matched the induction of FGF-23. The ability of these cytokines to induce FGF-23 from osteocytes was confirmed on bone chips in culture. We conclude that early CKD resembles a situation of primary FGF-23 excess mediated by inflammation. Elevations in FGF-23 occur weeks prior to imbalances in iron or phosphate homeostasis. Additionally, the precise and reproducible timing of CKD progression in the Ebf1-CKO mouse provides a novel model to investigate and separate these early events.

**Disclosures:** Jackie Fretz, None.

## FR0098

**Phosphorylation of S122 in ERα Is Important for the Skeletal Response to Estrogen Treatment in Male Mice.** Karin Gustafsson\*, Helen Farman<sup>1</sup>, Sofia Movérare-Skrtic<sup>1</sup>, Vikte Lionikaite<sup>1</sup>, Jianyao Wu<sup>1</sup>, Petra Henning<sup>1</sup>, Sara Windahl<sup>1</sup>, Klara Sjögren<sup>1</sup>, Andree Krust<sup>2</sup>, Pierre Chambon<sup>2</sup>, Claes Ohlsson<sup>1</sup>, Marie Lagerquist<sup>1</sup>. <sup>1</sup>Centre for Bone and Arthritis Research at Institute of Medicine, Sahlgrenska Academy at University of Gothenburg, Sweden, <sup>2</sup>Departement of Functional Genomics, Institut de Génétique et de Biologie Moléculaire et Cellulaire, Collège de France, Université de Strasbourg, France

It is well established that estrogen has positive effects on bone, not only in females, but also in males. Estrogen receptor-α (ERα), the main mediator of bone-protective estrogenic effects, is widely subjected to posttranslational modifications (PTMs), which can affect cellular responses to estrogen in a tissue specific manner by influencing the function of ERα and its interactions with other proteins. The phosphorylation site S122 in ERα has been shown, *in vitro*, to modulate ERα transcriptional activity, but the *in vivo* role of this PTM site for the skeleton in males is unknown. Our aim was therefore to investigate if phosphorylation of S122 in ERα is involved in ERα-mediated bone effects in male mice. To this end, we used mice with a point mutation in S122 (S122A) and wild-type (WT) littermates as controls. Twelve-week-old mice were orchidectomized and treated with estradiol (E2, 16 ng/day/mouse) or placebo for four weeks. At termination tibiae and vertebrae (L5) were dissected and analysed using high-resolution μCT.

E2 treatment increased cortical thickness in tibia both in WT (+59.7±4.2%, p<0.001) and S122A (+45.4±2.6%, p<0.001) males. Interestingly, the E2 response on cortical thickness was significantly decreased in the S122A mice compared to WT mice (-24.0±4.4%, p<0.05, interaction p-value from two-way-ANOVA analysis). Trabecular bone volume fraction (BV/TV) in vertebrae (L5) was increased after E2 treatment in both WT (+110.5±12.2 %, p<0.001) and S122A (+76.5±5.7%, p<0.001) mice. Importantly the estrogen response on trabecular BV/TV was also decreased in S122A mice compared to WT mice (-30.8±5.1% p<0.05, interaction p-value from two-way-ANOVA analysis). Our results demonstrate that phosphorylation of S122 is important for the E2 effect in both trabecular and cortical bone in male mice.

In conclusion, the S122 phosphorylation site is involved in the skeletal response to E2 treatment and this finding is the first *in vivo* proof of a physiological role of phosphorylation of ERα in male mice.

**Disclosures:** Karin Gustafsson, None.

## FR0099

**Anabolic bone effects of soluble Frizzled1, 2 and 7 receptors in mice.** Hisashi Hasegawa\*, Kengo Yamawaki<sup>1</sup>, Takuya Murakami<sup>1</sup>, Kenji Nagao<sup>1</sup>, Makoto Kakitani<sup>2</sup>, Kazuma Tomizuka<sup>2</sup>. <sup>1</sup>Nephrology Research Laboratories, Kyowa Hakko Kirin Co.,Ltd., Japan, <sup>2</sup>Innovative Technology Laboratories, Kyowa Hakko Kirin Co.,Ltd., Japan

Genetic studies in humans and mice have shown that the Wnt signaling positively regulates bone mass through a variety of mechanisms. Activation of Wnt signaling is triggered by the binding of secreted Wnt proteins to cysteine rich domain (CRD) at the amino terminus of Frizzled (Fzd) receptors and low-density lipoprotein receptor-related protein 5 or 6 (LRP5/6) co-receptors. Because of the complexity of this signaling in which there are 19 Wnt ligands and 10 Fzd receptors, the role of each Fzd-Wnt combination in bone metabolism has not been elucidated by using conventional "loss of function" approaches including knockout mouse models. Ligand trapping with soluble receptors is considered to be an alternative "loss of function" approach to study ligand/receptor interactions. Maintaining circulating soluble Fzd receptors at a high level in mice could allow for the simultaneous trapping of multiple Wnt ligands, thereby providing new information into the biology of Wnt signaling.

Here, we demonstrate that adult-specific systemic over-expression of Fzd1, 2 or 7 CRD/modified human IgG1 Fc domain fusion protein in transgenic mice resulted in remarkable increase in bone volume (BV/TV), respectively (Figure). Enhancement of bone formation was also confirmed in 8-week-old mice administrated with recombinant Fzd2-Fc, accompanying the increase of osteoblast numbers. It is noted that no change in osteoclast numbers was observed. Thus, Fzd2-Fc positively influence bone formation through enhancing osteoblast differentiation and/or proliferation. Since *in vitro* studies

showed that the Fzd2-Fc protein inhibited Wnt3a-induced beta-catenin signal, although precise molecular mechanism remains unclear, it is presumed that trapping of multiple Wnt ligands by Fzd1/2/7-Fc in vivo shifted the balance of Wnt signaling toward anabolic state in bone metabolism.

Taken together, these findings demonstrated that Fzd1/2/7-Fc fusion proteins are potent inducers of bone formation and could be novel therapeutic candidates for treating bone related disorders.

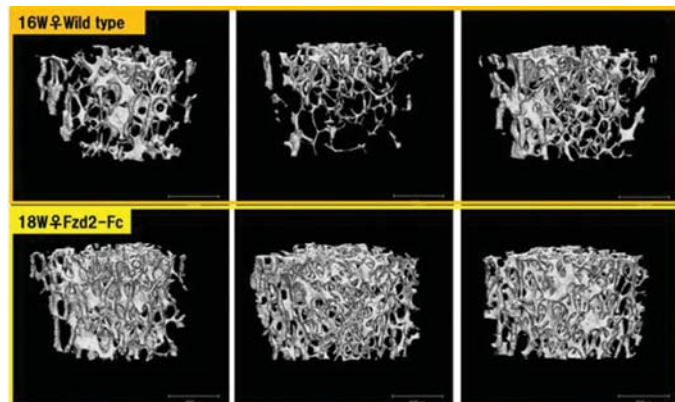


Figure micro-CT of the distal femur metaphysis

**Disclosures:** Hisashi Hasegawa, None.

## FR0100

**Androgens Inhibit Renal Calcium and Phosphate Transporters Independent of Bone Resorption Through AR-mediated Effects.** Rougin Khalil<sup>1</sup>\*, Michaël Laurent<sup>2</sup>, Na Ri Kim<sup>1</sup>, Ferran Jordi<sup>1</sup>, Frank Claessens<sup>3</sup>, Brigitte Decallonne<sup>1</sup>, Dirk Vanderschueren<sup>1</sup>. <sup>1</sup>Laboratory of Clinical and Experimental Endocrinology, KU Leuven, Belgium, <sup>2</sup>Center for Metabolic Bone Diseases, Geriatrics Department, University Hospitals Leuven, Belgium, <sup>3</sup>Laboratory of Molecular Endocrinology, KU Leuven, Belgium

Several studies suggest that sex steroids play a role in the regulation of renal calcium ( $\text{Ca}^{2+}$ ) and phosphate ( $\text{PO}_4^{3-}$ ) homeostasis. The kidney strongly expresses the androgen receptor (AR) but previous studies in orchidectomized (ORX) male mice have revealed contradictory results on renal  $\text{Ca}^{2+}$  handling. Furthermore, it remains unknown whether sex steroid deficiency regulates renal mineral transporters directly or indirectly by inducing skeletal mineral efflux.

We hypothesized that the kidney AR regulates renal  $\text{Ca}^{2+}$  and  $\text{PO}_4^{3-}$  homeostasis, independent of androgen effects on bone resorption. Therefore, we performed ORX on 18 weeks old male mice (ORX vs SHAM), treated with vehicle, testosterone (T, aromatizable into estradiol) or dihydrotestosterone (DHT, non-aromatizable). At 1 and 2 weeks after ORX, urine (metabolic cages) and serum was collected. Two weeks after ORX kidneys and intestines were taken for qPCR analysis of  $\text{Ca}^{2+}$  and  $\text{PO}_4^{3-}$  transporter gene expression. Trabecular bone loss was analyzed by vertebra microCT.

ORX induced hypercalciuria at 1 (increase of 102%,  $p < 0.0001$ ) and 2 (increase of 44%,  $p < 0.05$ ) weeks after ORX, while serum and urinary  $\text{PO}_4^{3-}$  remained unchanged. An upregulation of renal  $\text{Ca}^{2+}$  (TRPV5, calbindin 9K, calbindin 28K, PMCA, NCX1) and  $\text{PO}_4^{3-}$  transporters (NaPi-IIc, PiT1, PiT2) was observed, while intestinal expression levels were not affected by ORX. These changes were independent of PTH, FGF23 and 1,25-dihydroxyvitamin D and inhibited similarly by T and DHT treatment, suggesting that these effects were mediated via the AR.

In order to study whether these changes were due to direct effects on the kidney or due to sex steroid deficiency-induced bone loss, we treated sham operated and ORX male mice with vehicle or antiresorptive risedronate. MicroCT of the vertebrae showed significant trabecular bone loss of 22% ( $p < 0.05$ ) only 2 weeks after ORX. ORX combined with bisphosphonate therapy abolished trabecular bone loss and the early hypercalciuric phase, indicating that this  $\text{Ca}^{2+}$  flux was due to increased bone loss. Interestingly however, the upregulation of renal  $\text{Ca}^{2+}$  and  $\text{PO}_4^{3-}$  transporters was independent of the effects on bone resorption.

In conclusion, sex steroid deficiency upregulated renal  $\text{Ca}^{2+}$  and  $\text{PO}_4^{3-}$  transporters, independent of the effects on bone resorption. This upregulation was mediated through androgenic action of T. Further studies on the effects of sex steroids on the kidney and its mineral metabolism are warranted.

**Disclosures:** Rougin Khalil, None.

## FR0102

**Conditional Silencing of IL-17 Receptor in Osteocytes Blocks the Bone Catabolic Activity of Continuous PTH Treatment by decreasing osteocytic RANKL production.** Jau-Yi Li<sup>1</sup>\*, Jonathan Adams, M.N. Weitzmann, Roberto Pacifici. Emory University, School of Medicine, United States

Hyperparathyroidism in humans and continuous PTH treatment (cPTH) in mice stimulate bone resorption and cause bone loss by regulating RANKL production by osteocytes (OCYs) and bone marrow (BM) cells. RANKL produced by OCYs is critical for cPTH induced bone loss and directly PTH targeting of OCYs is required for RANKL production by these cells. However, other studies have shown that cPTH increases the production of the osteoclastogenic cytokine IL-17 by BM TH17 cells. IL-17 is also critical for cPTH induced bone loss because treatment with IL-17 Ab or global silencing of IL-17R prevents the bone loss induced by cPTH. Together these data suggest that targeting of OCYs by both PTH and IL-17 is required for cPTH to stimulate RANKL production by OCYs. To investigate this hypothesis, we generated conditional KO mice (IL-17RA<sup>ΔOCY</sup>) lacking the expression of IL-17RA in osteocytes (and late osteoblasts). These mice were generated by crossing C57BL/6 IL-17RA fl/fl mice with C57BL/6 8kb DMP1-Cre mice. 16 weeks old 17RA<sup>ΔOCY</sup> mice and fl/fl controls were infused with vehicle or cPTH (80mg/kg/day delivered by osmotic pumps) for 2 weeks. cPTH induced a ~9% loss of cortical bone volume and a ~31% loss of trabecular bone volume (as measured by  $\mu\text{CT}$ ) in fl/fl mice. By contrast, there was no bone loss in 17RA<sup>ΔOCY</sup> mice. Moreover, cortical and trabecular thickness were more substantially decreased in fl/fl mice than in 17RA<sup>ΔOCY</sup> mice. Mechanistic studies revealed that cPTH increased serum levels of CTX (a marker of bone resorption) in fl/fl mice but not in 17RA<sup>ΔOCY</sup> mice. Conversely, cPTH increases serum P1NP (a marker of bone formation) in all strains. Importantly, cPTH increased the expression of RANKL mRNA in OCYs purified at sacrifice in fl/fl mice but not in 17RA<sup>ΔOCY</sup> mice. In summary, the data confirm that OCYs are critical for the bone catabolic activity of cPTH, however our findings support the novel hypothesis that PTH regulates the activity of OCYs both directly and through IL-17. Specifically, our findings demonstrate that IL-17 is a PTH-induced upstream cytokine that stimulates OCY production of RANKL by increasing the sensitivity of OCYs to cPTH.

**Disclosures:** Jau-Yi Li, None.

## FR0104

**Parathyroid Hormone Increases EphrinB2/EphB4 of Osteoclast/Osteoblast Coupling Factor in Primary Hyperparathyroidism Model.** Yuki Nagata\*, Yasuo Imanishi, Daichi Miyaoka, Noriyuki Hayashi, Tomomi Maeda, Masanori Emoto, Masaaki Inaba. Osaka City University Graduate School of Medicine, Department of Metabolism, Endocrinology, and Molecular Medicine, Japan

Primary hyperparathyroidism (PHPT) is an endocrine disorder characterized by hypercalcemia with an inappropriate normal or high parathyroid hormone (PTH) level. Patients with PHPT displayed both a high bone turnover state and cortical bone loss. Since bone remodeling is composed of the coordination of bone resorption and bone formation performed by osteoclast (OCL) and osteoblast (OB), the investigation of bone resorption/formation coupling regulated by PTH offers key insights for treatments of osteoporosis. However, the mechanisms responsible are still unclear. EphrinB2 and EphB4 were recently identified as key bidirectional coupling factors for OCL and OB. EphrinB2 on OCL enhances OB differentiation and bone formation through specific interactions with EphB4 on OB, while EphB4 on OB suppresses OCL differentiation and bone resorption through EphrinB2 on OCL. To determine if EphrinB2 and EphB4 play a role on bone remodeling in the PHPT, we examined their alterations in PHPT mice. We found that expressions of EphrinB2 on OCL and EphB4 on OB were increased in bone tissue of PHPT mice, compared to WT mice. OCL derived from bone marrow cells of PHPT mice and PTH (50  $\mu\text{g/kg/day}$  for 5 days) injected mice also increased EphrinB2 expression, compared to OCL derived from WT mice. We then investigated its mechanism in vitro using primary culture of OCL and OB. EphrinB2 expression was increased in mature OCL treated with RANKL, compared to OCL precursor. We next tested if PTH ( $10^{-7}\text{M}$ ) treatment affects the expressions of EphrinB2 on OCL and EphB4 on OB. PTH did not change EphrinB2 expression in OCL, while it increased EphB4 expression on OB as well as RANKL. Importantly, PTH increased not only OCL formation but also EphrinB2 and EphB4 expressions in the co-culture of OCL and OB. OCL formation were also increased by OB conditioned medium (CM) cultured with PTH, compared to OB CM without PTH, and it was decreased by EphB4-Fc (5  $\mu\text{g/ml}$ ). On the other hand, OB treated with EphrinB2-Fc (5  $\mu\text{g/ml}$ ) increased ALP staining and it was more enhanced by PTH. These results suggest that PTH enhances EphrinB2/EphB4 coupling factors to upregulate EphB4 on OB directly and EphrinB2 on OCL indirectly via increased RANKL on OB in bone tissue of PHPT. In addition, EphrinB2 on OCL promotes OB differentiation coordinately with PTH.

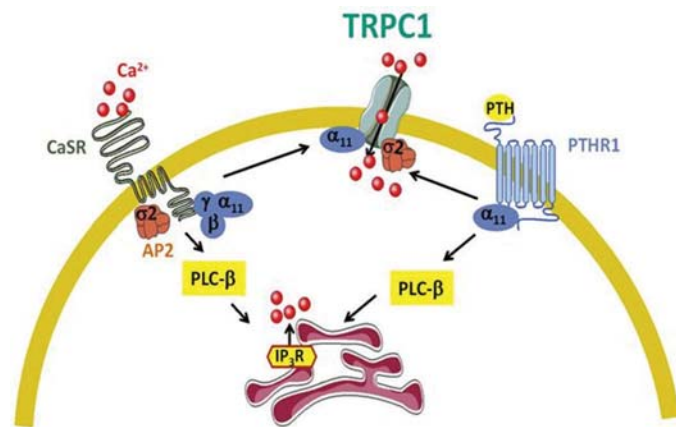
**Disclosures:** Yuki Nagata, None.



## FR0105

**Calcium Sensing Receptor and PTH Receptor responses are regulated by TRPC1 Ion Channel.** Marta Onopiuk<sup>1</sup>, Bonnie Eby<sup>2</sup>, Vasyl Nesin<sup>1</sup>, Peter Ngo<sup>1</sup>, Maria Luisa Brandi<sup>3</sup>, Wenhan Chang<sup>4</sup>, Mary Beth Humphrey<sup>1</sup>, Kai Lau<sup>2</sup>, Leonidas Tsiokas<sup>1</sup>. <sup>1</sup>Department of Cell Biology, University of Oklahoma Health Sciences Center, Oklahoma City, OK73104, USA, United States, <sup>2</sup>Department of Medicine, Division of Nephrology, University of Oklahoma Health Sciences Center, Oklahoma City, OK73104, USA, United States, <sup>3</sup>Università degli Studi di Firenze, CTO-SOD Malattie del Metabolismo Minerale e Osseo, Florence, Italy, <sup>4</sup>Department of Medicine, UCSF Endocrinology and Metabolism, UCSF, San Francisco, CA, USA, United States

Hyperparathyroidism resulting in abnormally high parathyroid hormone (PTH) and hypercalcemia can develop from parathyroid adenomas, hyperplasia secondary to severe renal disease, or due to genetic conditions such as in Familial Hypocalciuric Hypercalcemia (FHH). PTH secreted from parathyroid glands (PTG) is normally regulated by extracellular calcium activating the calcium sensing receptor (CaSR) leading to inhibition of PTH production and secretion. However, the mechanism by which activation of CaSR leads to suppression of PTH secretion in the PTG is not completely understood. In this study, we focus on the role of transient receptor potential channel 1 (TRPC1) in mediating the CaSR-induced suppression of PTH. Using *Trpc1*<sup>-/-</sup> and *Trpc1*<sup>+/+</sup> mice, we analyzed serum and urine indicators of calcium regulation and renal function. *Ex vivo* PTH secretion was measured on freshly isolated parathyroid glands. Isolated bones were analyzed by micro-CT and histomorphometry. PTH secretion and single cell  $\text{Ca}^{2+}$  imaging were conducted on the rat stable PTG cell line (PTH-C1). We found that *Trpc1*<sup>-/-</sup> mice have elevated levels of serum calcium and PTH and decreased urinary calcium excretion. PTG from *Trpc1*<sup>-/-</sup> mice show increased overall PTH secretion and a shift in the calcium set point. Overexpression of TRPC1 in the stable PTH-C1 cell line suppresses PTH secretion, while downregulation of TRPC1 leads to inability of these cells to suppress PTH secretion in response to high extracellular calcium concentrations. PTH-C1 cells depleted of endogenous TRPC1 show reduced  $\text{Ca}^{2+}$  influx in response to activation of CaSR. Surprisingly, despite the presence of hyperparathyroidism, aged *Trpc1*<sup>-/-</sup> mice have increased bone mass, reduced number of osteoblasts, and increased osteocyte apoptosis. Osteoblast precursors derived from *Trpc1*<sup>-/-</sup> mice show increased calcified bone nodule formation, secreted osteocalcin, and decreased proliferation. *Trpc1*<sup>-/-</sup> osteocytes have abnormal gene expression in response to PTH *ex vivo*. These data suggest that TRPC1 functions downstream of CaSR in the regulation of  $\text{Ca}^{2+}$  influx, which in turn can control the secretion of PTH from the PTG and further, they identify *Trpc1*<sup>-/-</sup> mice as a new mouse model for human FHH. Additionally, the increased bone mass of *Trpc1*<sup>-/-</sup> mice in the setting of hyperparathyroidism and hypercalcemia is likely due to altered CaSR and PTH receptor responses of osteoblasts and osteocytes.



Model of TRPC1 functioning downstream of CaSR and PTHR1

**Disclosures:** Marta Onopiuk, None.

## FR0109

**RNA-Seq Based Transcriptome Profiling and Transformation of Mature Osteoblasts into Bone Lining Cells during Bone Loss Induced by Mechanical Unloading.** A Ram Hong<sup>1</sup>, Kwangsoo Kim<sup>2</sup>, Jae-yeon Yang<sup>2</sup>, Ji-yeon Lee<sup>2</sup>, Kyoung Min Kim<sup>3</sup>, Jung Hee Kim<sup>1</sup>, Chan Soo Shin<sup>1</sup>, Sang Wan Kim<sup>4</sup>. <sup>1</sup>Seoul National University College of Medicine, Korea, Republic of, <sup>2</sup>Seoul National University Hospital Biomedical Research Institute, Korea, Republic of, <sup>3</sup>Seoul National University Bundang Hospital, Korea, Republic of, <sup>4</sup>Seoul National University College of Medicine, Seoul Metropolitan Government Boramae Medical Center, Korea, Republic of

**Background:** It is not fully elucidated cellular and molecular mechanisms by which mechanical unloading induce bone loss. To better understand the effect of mechanical unloading on bone loss, we investigated RNA-seq based transcriptome profiling combined with transformation of mature osteoblasts (Obs) into bone lining cells (BLCs) using a lineage tracing study.

**Methods:** Dmp1-CreERT2 mice were crossed with Rosa26R reporter mice to render targeted mature Obs and BLCs. Dmp1-CreERT2(+);Rosa26R mice were injected with 1 mg 4-OH-tamoxifen (4-OHTam) three times a week from postnatal 7 w. The animals underwent combination of 2U/100g botulinum toxin injection with left hindlimb tenotomy from 8 to 10 w. The animals were euthanized on 8, 9, 10 and 12 w (2 d, 2 w and 4 w after the last 4-OHTam, 4-6 mice in each group). We quantified the number and thickness of X-gal(+) cells on the periosteum of both femoral bones at each time. Furthermore, we also performed RNA-seq on pairs of femoral diaphyseal bones at each time for wild type male mice using the same experimental protocol.

**Results:** Mechanical unloading induced a significant decrease in femoral bone mass from 1 w till 4 w since unloading. On 2 d after the last 4-OHTam injection, many X-gal(+) cells were found in the periosteal surface of the femurs. On 2 w, a significant decrease in the number and a subtle change in the thickness were observed in left hindlimbs (mechanical unloading site) compared to right (number; right:  $10.9 \pm 0.8/\text{mm}$ , left:  $7.3 \pm 2.4/\text{mm}$ ,  $p < 0.05$ ; thickness; right:  $3.5 \pm 0.2 \mu\text{m}$ , left:  $2.9 \pm 0.2 \mu\text{m}$ ,  $p = 0.071$ ). On 4 w a decrease in the thickness was accelerated in left hindlimbs compared to right but the number was comparable (number; right:  $9.3 \pm 1.9/\text{mm}$ , left:  $8.1 \pm 1.1/\text{mm}$ ,  $p = 0.760$ ; thickness; right:  $2.7 \pm 0.2 \mu\text{m}$ , left:  $2.0 \pm 0.3 \mu\text{m}$ ,  $p < 0.05$ ). We identified 153 differentially expressed protein-coding transcripts between left hindlimbs and right. Majority of these genes were down-regulated at 2 w, which continued until 4 w. We clustered these genes according to the bone and muscle-specific expression based on published RNA-seq data.

**Conclusion:** The present findings support the hypothesis that mechanical unloading can accelerate the transformation of mature Obs into BLCs in early stage of bone loss *in vivo*. Furthermore, we provide a comprehensive database of mechanical unload-regulated genes in bone that is potentially useful to identify drug targets with dual action for osteoporosis and sarcopenia.

**Disclosures:** A Ram Hong, None.

## FR0110

**Effect of Estrogen Receptor and  $\beta$ -Catenin Signaling Activation on Mechanically Induced Bone Formation in Ovariectomized Mice.** Astrid Liedert<sup>\*</sup>, Claudia Nemitz, Anita Ignatius. University of Ulm, Germany

Dysfunctions of Wnt/ $\beta$ -catenin and estrogen receptor signaling resulted in impaired mechanotransduction and bone loss. Previous studies demonstrated the interaction of Wnt/ $\beta$ -catenin and estrogen receptor signaling in mechanotransduction *in vitro* and *in vivo*. In this study, we analyzed the effect of estrogen receptor and  $\beta$ -catenin signaling activation on mechanically induced bone formation in ovariectomized mice.

12-week-old mice were ovariectomized. 4 weeks later, an estrogen pellet was implanted and the right ulna was loaded for 2 weeks on 5 consecutive days. For  $\beta$ -catenin activation, the Gsk-3 $\beta$  inhibitor SB415286 was injected daily during the loading period. Mice receiving placebo pellets and vehicle injections were used as controls. Endocortical and periosteal bone formation rates (EcBFR, PsBFR) were calculated by bone histomorphometry, and bone structure was analyzed by microCT. Preosteoblastic cells were loaded by stretching in collagen type I precoated dishes. Estrogen, SB415286 and appropriate vehicles, respectively, were added to the medium 3 h before loading. Western blotting was performed using antibodies to key and target proteins of estrogen receptor and  $\beta$ -catenin signaling. Data were analyzed for significance (value  $p < 0.05$ ) using Wilcoxon and Mann-Whitney-U test. Animal experiments were approved by the National Ethics Committee.

Loading induced bone formation. At the endocortical surface, estrogen induced bone formation and acted additively with loading. At the periosteal surface, both estrogen and SB415286 enhanced mechanically induced bone formation in ovariectomized mice. When estrogen and SB415286 were administered together, the sensitizing effect on mechanically induced bone formation of each activator alone was abolished. Mechanical loading and treating of preosteoblastic cells with either estrogen or SB415286 resulted in activation of estrogen receptor and  $\beta$ -catenin signaling. Mechanical loading together with estrogen and SB415286 treatment abolished the effect on key proteins of estrogen receptor and  $\beta$ -catenin signaling of each activator alone.

The interaction of estrogen receptor and  $\beta$ -catenin signaling seems to be one mechanism that is involved in the regulation of bone mass homeostasis by mechanical loading. The interacting regulatory mechanism appears to be well suited to fine-tune protein expression in response to different loading conditions.

**Disclosures:** Astrid Liedert, None.

## FR0113

**Shared Molecular Mechanisms Contributing to PTOA in Loading-Mediated Injury Models.** Aimy Sebastian<sup>\*1</sup>, Jiun Chang<sup>1</sup>, Nicholas Hum<sup>1</sup>, Deepa Muruges<sup>1</sup>, Gabriela Loots<sup>1</sup>, Blaine Christiansen<sup>2</sup>. <sup>1</sup>Lawrence Livermore National Laboratories, United States, <sup>2</sup>UC Davis Medical Center, Department of Orthopedic Surgery, United States

Mechanical loading is thought to have both beneficial and detrimental effects on joint physiology. Excessive loading or loading causing injury (i.e., ligament rupture) can both contribute to the development of post traumatic osteoarthritis (PTOA). To better understand how different types of mechanical stress contribute to PTOA development we profiled load-induced gene expression changes in knee joints of 10 week old C57BL/6 male mice using 3 tibial compression loading regimens: high magnitude load without injury (HL; 15N), injury load resulting in anterior cruciate ligament rupture (ACLR; 12N) and cyclic loading without injury (CL; 8N magnitude applied at 4 Hz for 1200 cycles). Subsequently, we examined the transcriptional changes in loaded joints compared to contralateral joints using RNA sequencing (RNA-seq) at 1 day post loading. We identified 826, 47, and 28 genes differentially regulated in loaded joints (>1.5 fold change;  $p$ -value <0.05) in response to ACLR, CL and HL, respectively. ACL injury activated a large number of genes associated with the inflammatory response (57 genes), extracellular matrix organization (62 genes) and vasculature development (74 genes). Several inflammatory response related genes including *Serpina3n*, *Ccr5* and *C3ar1* were also activated by cyclic loading. Thirteen genes up-regulated in response to ACLR including *Mmp3*, *Timp1*, *S100a4*, *Serpina3n*, *Ccr5* and *Mt2* overlapped with genes activated by cyclic loading whereas none of the genes were affected in HL, suggesting that these genes may contribute to the shared mechanism of PTOA between these two loading based models of osteoarthritis. Only 1 gene, *Mybph*, was found differentially regulated in response to both HL and ACLR, suggesting that one single bout of mechanical stress is not sufficient to induce long term deleterious effects on joint physiology. The transcriptome level data generated in this study shows that ACLR had the largest impact on joint gene expression and high load without injury had minimal impact. This study sheds light on how different types of mechanical loading impact gene expression in the knee joint and suggests that ACLR and CL may mediate PTOA development by activating genes associated with inflammatory responses and cartilage degradation.

**Disclosures:** Aimy Sebastian, None.

## FR0114

**Cortical bone loss due to skeletal unloading in aldehyde dehydrogenase 2 gene knockout mice is associated with decreased expression of PTH receptors in osteocytes.** Takafumi Tajima<sup>\*</sup>, Kunitaka Menuki, Kayoko Okuma, Manabu Tsukamoto, Hokuto Fukuda, Yasuaki Okada, Kenji Kosugi, Akinori Sakai. Department of Orthopaedic Surgery, University of Occupational and Environmental Health, Japan, Japan

Purpose: Aldehyde dehydrogenase2 (ALDH2) is the enzyme which degrades and detoxifies acetaldehyde produced by alcohol metabolism. The inactive ALDH2 phenotype is prevalent in East Asians, and an association between this ALDH2 polymorphism and osteoporosis has been reported. In our previous study, we found that alcohol consumption resulted in decreased trabecular bone volume in *Aldh2* knockout (*Aldh2*<sup>-/-</sup>) mice compared with that in wild-type (*Aldh2*<sup>+/+</sup>) mice, and that climbing exercise did not increase trabecular bone mass in *Aldh2*<sup>-/-</sup> mice of growing phase. However, the effect of the *Aldh2* gene on the skeletal unloading remains unknown. The purpose of this study was to clarify the effect of *Aldh2* gene on bone metabolism in skeletal unloading. Method: 8-week-old male *Aldh2*<sup>-/-</sup> (KO) and *Aldh2*<sup>+/+</sup> (WT) mice were divided into the ground control (GC) group and the tail suspension (TS) group in each genotype for one week (KOGC, KOTS, WTGC, WTS). We measured bone mineral density (BMD) of the femur and lumbar using dual-energy X-ray absorptiometry. We assessed the femoral morphometry using peripheral quantitative computed tomography (pQCT), histomorphometry of femoral cortex, systemic bone chemical markers, cortical mRNA using quantitative RT-PCR, and cortical bone immunohistochemistry. Results: 1) A significant difference was not found in femoral BMD between WTGC and WTS, but BMD in KOTS was significantly lower than in KOGC. Lumbar BMD did not show significant differences among the four groups. 2) The results of pQCT revealed that the cortical bone density at the femoral diaphysis in KOTS was significantly lower than that in KOGC, whereas there was no significant difference between WTGC and WTS. Furthermore, the cortical bone area and the cortical thickness were significantly lower in KOTS compared to those in the other three groups. 3) Cortical histomorphometrical study revealed that endosteal and periosteal bone formation parameters in KOTS were significantly lower than that in KOGC. 4) The plasma level of osteocalcin in KOTS was significantly lower than that in KOGC. 5) There were significant decreases in bone formation signals such as collagen type1, osteopontin, osteocalcin, and PTH receptor in KOTS compared with those in KOGC. 6) Cortical bone immunohistochemistry revealed significant decreased expression of PTH receptors in osteocytes in KOTS compared with that in KOGC. Conclusion: Disruption of *Aldh2* gene resulted in decrease in cortical bone mass due to suppression of bone formation by skeletal unloading. The possible mechanism was decreased expression of PTH receptors in osteocytes.

**Disclosures:** Takafumi Tajima, None.

## FR0115

Withdrawn

## FR0119

**Unloaded Mice Treated with the Myokine Irisin Are Protected from Bone Loss and Muscle Atrophy.** Graziana Colaianni<sup>\*1</sup>, Luciana Lippo<sup>1</sup>, Paolo Pignataro<sup>1</sup>, Lorenzo Sanesi<sup>1</sup>, Giovanna Spiro<sup>2</sup>, Ilenia Severi<sup>3</sup>, Giovanni Passeri<sup>4</sup>, Giacomina Brunetti<sup>1</sup>, Umberto Tarantino<sup>5</sup>, Silvia Colucci<sup>1</sup>, Janne Reseland<sup>6</sup>, Roberto Vettor<sup>2</sup>, Saverio Cinti<sup>3</sup>, Maria Grano<sup>7</sup>. <sup>1</sup>Department of Basic Medical Science, Neuroscience and Sense Organs, University of Bari, Italy, <sup>2</sup>Department of Medicine-DIMED, Internal Medicine 3, University of Padova, Italy, <sup>3</sup>Department of Experimental and Clinical Medicine, Center of Obesity, United Hospitals, University of Ancona, Italy, <sup>4</sup>Department of Clinical and Experimental Medicine, University of Parma, Italy, <sup>5</sup>Department of Orthopedics and Traumatology, Tor Vergata University of Rome, Italy, <sup>6</sup>Department of Biomaterials, Institute for Clinical Dentistry, University of Oslo, Blindern, Norway, <sup>7</sup>Department of Emergency and Organ Transplantation, University of Bari, Italy

Irisin is a hormone-like myokine secreted from skeletal muscle in response to exercise. We previously demonstrated that treatment with recombinant Irisin (r-Irisin) in healthy mice improved cortical bone mass and geometry, supporting the idea that Irisin recapitulates some of the most important benefits of physical exercise on the skeleton and plays protective role on bone health. Here we show that treatment with r-Irisin prevented bone loss in hind-limb suspended mice when administered during suspension and induced recovery of bone mass when mice were injected after bone loss due to a suspension period of 4 weeks. By microCT analysis of femurs, we found that unloaded mice treated with vehicle showed, as expected, decrease of cortical (-4.1%;  $p$ <0.01) and trabecular (-39.1%;  $p$ <0.01) bone mineral density (BMD) with respect to control mice, whereas the unloaded mice injected with r-Irisin had no loss of cortical ( $p$ =0.69) and trabecular ( $p$ =0.10) BMD. Likewise, the dramatic decrease of the trabecular bone volume fraction (BV/TV) (-56.5% vs control mice;  $p$ <0.01) was prevented by r-Irisin therapy ( $p$ =0.11). In particular, r-Irisin treatment preserved trabecular number (Tb.N) and the fractal dimension, an index of optimal micro-architectural complexity of trabecular bone. Furthermore, when unloaded mice were treated with r-Irisin after they developed bone loss, the decrease of cortical (-3.3% vs control mice;  $p$ <0.01) and trabecular (-24.7% vs control mice;  $p$ <0.05) BMD was completely restored. Moreover, we also showed that r-Irisin treatment protects from muscle mass decline during unloading. Thus, unloaded mice treated with vehicle displayed a severe loss of muscle mass, as confirmed by ~63% decline of *vastus lateralis*/body weight ( $p$ <0.001) and ~33% decrease of fiber cross-sectional area ( $p$ <0.05) with respect to control mice. Conversely, Irisin-treated unloaded mice showed no loss of muscle weight ( $p$ =0.39) and similar fiber size ( $p$ =0.44) as those of control mice. Notably, the dramatic decrease in myosin type II expression (MyHC II) in *vastus lateralis* of unloaded mice ( $p$ <0.05 vs control mice) was completely prevented by r-Irisin treatment. If these results will translate to humans, they may support a promising clinical strategy for the prevention and treatment of both osteoporosis and sarcopenia, particularly applicable to those patients who cannot perform physical activity, as occurs during aging, immobility and microgravity in space flight missions.

**Disclosures:** Graziana Colaianni, None.

## FR0121

**Assessment of the Effect of two Myostatin Inhibitors on Body Composition using MRI and DXA in Non Human Primates.** Martin Guillot<sup>\*1</sup>, Sebastien Garipey<sup>1</sup>, Luc Tremblay<sup>2</sup>, Aurore Varela<sup>1</sup>. <sup>1</sup>Charles River Laboratories Montreal, Canada, <sup>2</sup>CIMS-CRCHUS, University of Sherbrooke, Canada

Myostatin growth and differentiation factor-8 is a negative regulator of skeletal muscle development. Specific inhibitors that block the myostatin signaling pathway are currently under development for the treatment of muscle diseases, inhibition of muscle atrophy, and anti-ageing therapies.

The objective of this study was to characterize the pharmacodynamic effects of two Myostatin inhibitors on muscle mass in cynomolgus monkeys using MRI and DXA. A Myostatin inhibitor analogue A (3 or 10 mg/kg/dose), a Myostatin inhibitor analogue B (positive control, 10 mg/kg/dose) or Phosphate Buffered Saline (PBS controls) were given by subcutaneous injection once weekly for 12 weeks to cynomolgus monkeys ( $n$ =4 males/group). Right and left hindlimb MRI scans (axial proton density) were acquired during predosing period (additional duplicate scanning done on 7 animals to assess reproducibility), and once on a non-dosing day during Weeks 8, 12, and 16, on all animals. A semi-automatic segmentation method was used for obtaining muscle volume. DXA whole body scans were acquired once prior to initiation of dosing and at end of dosing period (Week 12) for animals given PBS controls and Myostatin inhibitor analogue A at 10 mg/kg/dose.

Reproducibility was good with on average less than 4% difference between initial scan and the re-scan, with complete repositioning of both right and left rectus femoris volumes. At Weeks 8 and 12, administration of Myostatin inhibitor analogue A resulted in dose-dependent minimally to slightly higher increases in both right and left rectus femoris volume (+12 to +24%) compared to PBS controls. Administration of the positive control resulted in lower increases in both right and left rectus femoris volume (minimal increase, +9 to +11%). At Week 12, animals given 10 mg/kg/dose of Myostatin



inhibitor analogue A also presented a slightly higher increase in whole body lean mass (+14%). Following 4 weeks off-dose, animals given Myostatin inhibitor analogue A at  $\geq 3$  mg/kg/dose or the positive control presented persistent increases in both right and left rectus femoris volume (+10 to +18%).

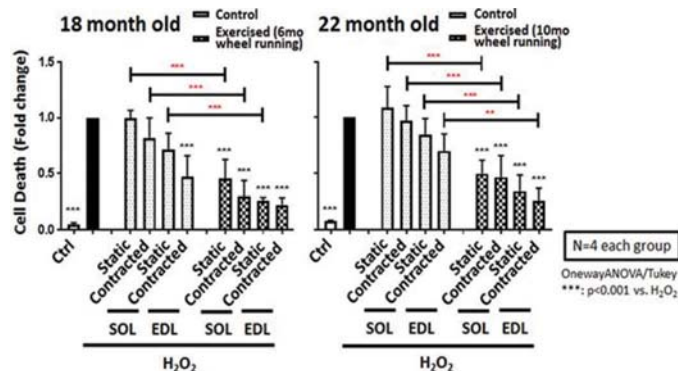
MRI provided an adequate and reproducible assessment of muscle volume in NHP to assess efficacy and safety of muscle changes. Myostatin inhibitor analogue A had significant persistent effects, increasing in lean mass that was adequately assessed using MRI in cynomolgus monkeys. Changes in the Myostatin inhibitor analogue A were slightly higher compared to positive control.

**Disclosures:** Martin Guillot, Charles River Laboratories, Other Financial or Material Support.

## FR0122

**Long-term physiologic exercise maintains the protective effects of muscle-secreted factors on osteocyte viability.** Yukiko Kitase<sup>\*1</sup>, Hong Zhao<sup>2</sup>, Jennifer Rosser<sup>3</sup>, Michael J. Wacker<sup>3</sup>, Julian Vallejo<sup>3</sup>, Marco Brotto<sup>4</sup>, Lynda F. Bonewald<sup>2</sup>. <sup>1</sup>Indiana University, United States, <sup>2</sup>Indiana University, United States, <sup>3</sup>University of Missouri-Kansas City, United States, <sup>4</sup>University of Texas at Arlington, United States

Exercise maintains both muscle and bone mass and evidence is accumulating that circulating factors released by muscle and bone support not only the musculoskeletal system, but overall health. Previously we have shown that soluble factors produced by contracted muscle, extensor digitorum longus (EDL) and soleus (SOL), from young, 5-6 mo, C57BL/6 mice protect osteocytes from cell death induced by glucocorticoids and reactive oxygen species. However, conditioned media (CM) from the muscle of old, 22-24 mo mice lost this capacity. Here we sought to determine whether exercise in aged mice would maintain the protective effects of muscle factors on osteocytes. Voluntary wheel running (VWR) was used since this most closely mimics normal physiologic exercise in contrast to exercise such as treadmill running, swimming or wire walking that induce stress and disrupt circadian rhythm. Female, 12 mo old mice were allowed access to wheels for 6 or 10 mo. Running activity was monitored on a daily basis revealing that mice run an average of 3.4-6.7 km/day. Although no significant differences ( $P < 0.05$ ) in body weight were observed, heart weight to body weight ratio was significantly increased in VWR compared to sedentary mice ( $5.0 \pm 0.2$  vs  $4.4 \pm 0.2$ ,  $n=7$ , for 6 mo;  $6.7 \pm 0.5$  vs  $5.0 \pm 0.4$ ,  $n=4$ , for 10 mo). While there was no difference in EDL muscle weight, there was a significant increase in SOL muscle weight in the VWR mice ( $10.2 \pm 0.5$  vs  $7.0 \pm 0.2$  mg,  $n=8$ , for 6 mo;  $8.1 \pm 0.6$  vs  $6.3 \pm 0.3$  mg,  $n=4$ , for 10 mo) and SOL muscle weight to body weight ratio ( $0.34 \pm 0.02$  vs  $0.20 \pm 0.01$ , 6 mo;  $0.3 \pm 0.02$  vs  $0.2 \pm 0.01$ , 10 mo). An increase in VWR compared to control SOL absolute force was observed ( $308 \pm 8$  vs  $229 \pm 10$  mN, for 6 mo;  $274 \pm 16$  vs  $223 \pm 9$  mN, for 10 mo) but no difference in EDL absolute force between VWR and control animals. However, CM (10%) from both EDL and SOL, static and contracted muscle from both 18 and 22 mo old exercised animals still possessed the capacity to protect MLO-Y4 osteocyte cells from apoptosis due to oxidative stress ( $0.3$  mM  $H_2O_2$ ) unlike secreted muscle factors from the sedentary mice (Figure). This suggests that exercise, but not necessarily a change in muscle size nor force correlates with production of osteocyte protective factors. These studies show that exercise can have beneficial effects even when initiated in the late adult stage and that exercise can maintain the production of muscle factors that protect osteocytes against oxidative stress.



Figure

**Disclosures:** Yukiko Kitase, None.

## FR0124

**An aging-associated decrease in periosteal osteoprogenitor populations accompanies attenuation of load-induced bone formation in mice tibiae.** Pamela Cabahug-Zuckerman<sup>\*1</sup>, Chao Liu<sup>1</sup>, Cinyee Cai<sup>2</sup>, Ian Mahaffey<sup>3</sup>, Stephanie Norman<sup>3</sup>, Whitney Cole<sup>3</sup>, Alesha Castillo<sup>1</sup>. <sup>1</sup>Dept of Mechanical and Aerospace Engineering, Tandon School of Engineering, and Dept of Orthopaedic Surgery, School of Medicine, New York University; Veterans Affairs New York Harbor Healthcare System, United States, <sup>2</sup>Dept of Orthopaedic Surgery, School of Medicine, New York University, United States, <sup>3</sup>Veterans Affairs Palo Alto Healthcare System, United States

Adult skeletal tissue responds to increasing mechanical stimulation by forming new bone to resist damage; however, aging can diminish mechanoresponsiveness and lead to bone loss and increased fracture risk. In pursuit of therapies to maintain healthy bone, we assessed age-associated changes in the periosteal osteoprogenitor cell population, and accompanying load-induced periosteal bone formation, cortical geometry, and trabecular microarchitecture. We hypothesized that aging mice have reduced osteogenic capacity in response to mechanical loading due to decreased osteoprogenitor cell numbers and reduced cellular proliferation. Right tibiae of 16-wk-old adult and 52-wk-old aged female,  $n=6$ , C57BL/6 mice were subjected to axial compression (5N, 2Hz, 60 cycles, 3 days/week) for two weeks, and cortical and trabecular bone assessed with micro-computed tomography and dynamic histomorphometry. Baseline periosteal cell number and nuclear morphology at tibial midshaft were quantified using two-photon imaging of intact DAPI-stained tibiae in adult and aged mice. In addition, acute periosteal responses were assessed in a separate group of adult and aged mice subjected to four consecutive days of strain-matched axial compression ( $1400\mu\epsilon$ , 120 cycles, 2Hz). In this group, cell proliferation and osteoprogenitor number were quantified in the periosteum by immunohistochemical staining of proliferating cell nuclear antigen and paired-related homeobox1 (Prrx1, osteoprogenitor marker) on transverse midshaft sections from loaded and non-loaded tibiae. A Student's t-test determined significance at  $p < 0.05$ . Two-weeks of loading resulted in increasing trends in Ct.Ar, Imin, pMOI, and measures of trabecular microarchitecture, though not significant in either age group. Age-related differences were detected in load-induced periosteal bone formation ( $p < 0.05$ ), which increased significantly in adults but not in aged. At baseline, adult mice exhibit greater periosteal cell number, nuclear area, and circularity (all  $p < 0.01$ ) than aged mice (Fig 1a). In the acutely loaded groups, both adult and aged tibiae responded with similar increases in periosteal cell proliferation, 140% and 111%, respectively (Fig 1b); however, Prrx1-positive cells are reduced by a third in aged midshaft tibiae (Fig 1c). We conclude that the aged-related attenuation of load-induced periosteal bone formation may be explained, in part, by decreased Prrx1+ osteoprogenitors residing in periosteal stem cell niche.

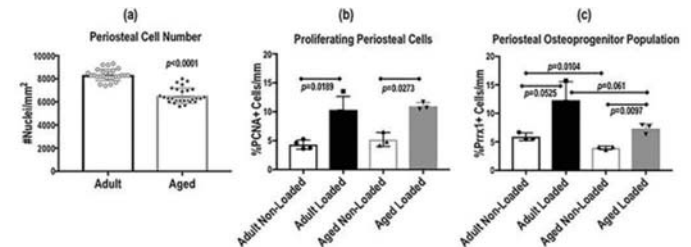


**Figure 1. Age-associated changes in mouse tibial periosteum.** (a) Overall periosteal cell number is reduced by 22% with aging. (b) Percentage of cells staining for proliferating cell nuclear antigen (PCNA), in both adult and aged baseline non-loaded and loaded groups. (c) Percentage of paired related homeobox1 (Prrx1), osteoprogenitor cells at baseline, in adult and aged non-loaded and loaded groups. At baseline, the aged osteoprogenitor population is reduced by 33% versus adult. Acute mechanical loading resulted in an increased osteoprogenitor cell number for both adult and aged groups.

Figure

**Disclosures:** Pamela Cabahug-Zuckerman, None.

## FR0125

**Osteoporosis and Muscle Atrophy: Is Vitamin D Receptor an Unknown Determinant?** monica celi<sup>\*</sup>, Manuel scimeca, Federica Centofanti, maurizio feola, annalisa botta, Umberto Tarantino. University of Rome Tor Vergata, Italy

### INTRODUCTION

Intracellular 1,25-dihydroxyvitamin D receptor (VDR) is expressed in human skeletal muscle tissues. However, it is unknown whether VDR expression *in vivo* is related to age or vitamin D status. Therefore, in this study we investigated the influence of age, muscle atrophy, main VDR polymorphism and vitamin D levels on the expression of the VDR in human muscle tissue of osteoporotic and osteoarthritis patients.

### MATERIALS AND METHODS

We performed a *vastus lateralis* muscle biopsy in 50 patients with osteoporosis (OP) undergoing surgery for fragility hip fracture and in 50 age-matched patients (age range, 60-85 years) undergoing arthroplasty for hip osteoarthritis (OA). The patients signed an informed consent form before participating in the study. Serum concentrations of 25-hydroxyvitamin D and 1,25-dihydroxyvitamin D were assessed at day of admission

to surgery. To evaluate fibers atrophy 250 muscle fibers per biopsy have been evaluated comparing minimum transverse diameter and cross-sectional area of type I and type II fibers for relative prevalence. Nuclear Expression of VDR were studied by counting 500 nuclei per specimen and person. Nuclear VDR expression, Type I and Type II fibers were identified by immunohistochemistry.

#### RESULTS

Morphometric analysis showed a significant difference in fiber type distribution between the two groups of patients. Mann-Whitney test displayed a significant difference in the nuclear expressions of VDR in OA group as compared to OP patients (OA  $212.10 \pm 11.85$ , OP  $84.73 \pm 7.29$ ,  $p < 0.0001$ ). In the univariate analyses, increased age was associated with decreased VDR expression ( $p = 0.004$ ), whereas there were no significant correlations between VDR expression and vitD levels. In particular, the nuclear translocation of VDR appeared age independent in OA group and not influenced by age in OP patients. On note, we also found a strictly association between the polymorphism of Cdx2 and FoxI gene and muscle fiber atrophy. Specifically, patients with Cdx2 polymorphisms associated to minor expression of VDR, and FOKI polymorphisms associated to minor activity of VDR, showed more than 50% of atrophic fibers.

#### CONCLUSION

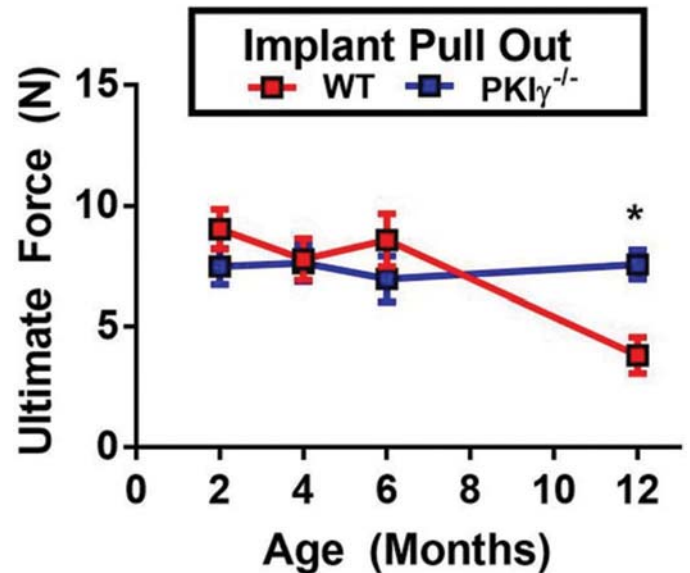
Older age was significantly associated with decreased VDR expression in osteoporotic patients, independent of serum vitD. Our results could lay the foundation for identification of patients potentially responsive to supplementation of vitamin D.

**Disclosures:** monica celi, None.

## FR0126

**Regulation of Protein Kinase A (PKA) by Protein Kinase Inhibitory (PKI $\gamma$ ) Reduces Osteogenesis in Aged Mice.** Bryan S. Hausman<sup>\*1</sup>, Xin Chen<sup>2</sup>, Hyonmin Choe<sup>3</sup>, Ozan Akkus<sup>4</sup>, Edward M Greenfield<sup>1</sup>. <sup>1</sup>Department of Orthopaedics, Case Western Reserve University, United States, <sup>2</sup>Gene Therapy Center, University of North Carolina at Chapel Hill, United States, <sup>3</sup>Department of Orthopaedics, Yokohama City University, Japan, <sup>4</sup>Departments of Biomedical Engineering and Orthopaedics, Case Western Reserve University, United States

Aging skeletal bone is characterized by decreased osteogenesis and increased adipogenesis resulting in bone loss and diminished repair capacity. We previously showed that PKI $\gamma$  terminates PTH-induced activity of the cAMP/PKA pathway in mesenchymal precursor cells. Thus, PKI $\gamma$  terminates primary PKA-response genes (*c-fos*, IL-6, and LIF) and thereby reduces osteogenesis and enhances adipogenesis. In this study, we generated and characterized PKI $\gamma$ <sup>-/-</sup> mice; both genders were viable, fertile, and indistinguishable by body weight from wild-type littermates. Compared with wild-type MEFs, PKI $\gamma$ <sup>-/-</sup> MEFs exhibited greater Fsk-induced nuclear PKA activity (3-fold,  $p < 0.001$ ) and expression of primary response genes (2- to 10-fold,  $p < 0.05$ ). However, upon differentiation into mature osteoblastic cells, the effects of PKI $\gamma$  deficiency were lost as wild-type and PKI $\gamma$ <sup>-/-</sup> MEFs responded similarly to FSK. Consistent with these findings, no differences between wild-type and PKI $\gamma$ <sup>-/-</sup> were detected in primary gene responses to PTH or Fsk by calvarial osteoblasts *in vitro* or to PTH in femoral osteoblasts *in vivo*.  $\mu$ CT of femora from 12-month old PKI $\gamma$ <sup>-/-</sup> mice revealed a modest elevation of cortical thickness ( $0.167 \pm 0.003$  vs  $0.157 \pm 0.003$  mm,  $n = 14-15$ ,  $p = 0.025$  in males;  $0.177 \pm 0.003$  vs  $0.166 \pm 0.003$  mm,  $n = 15$ ,  $p = 0.015$  in females) and bone area ( $0.88 \pm 0.02$  vs  $0.82 \pm 0.02$  mm<sup>2</sup>,  $p = 0.03$  in males;  $0.81 \pm 0.02$  vs  $0.77 \pm 0.02$  mm<sup>2</sup>,  $p = 0.09$  in females) that was not observed in 4- or 6-month-old mice. Similarly, trabecular BV/TV trended higher in 12-month old PKI $\gamma$ <sup>-/-</sup> mice ( $9.3 \pm 0.4$  vs  $7.7 \pm 0.7\%$ ,  $p = 0.08$  in males;  $2.3 \pm 0.2$  vs  $1.8 \pm 0.15\%$ ,  $p = 0.06$  in females) but not in younger mice. Based on the age dependency of the  $\mu$ CT results and the enhanced osteogenesis in PKI $\gamma$ <sup>-/-</sup> MEFs, we speculated that the decline in osteogenesis with aging would be lessened in PKI $\gamma$ <sup>-/-</sup> mice. We therefore investigated intramembranous bone formation 7 days after placing a uncortical titanium implant in the distal femoral metaphysis. Biomechanical pull-out testing showed the expected age-related decline in osteogenesis in wild-type but not in PKI $\gamma$ <sup>-/-</sup> mice [see figure]. As a result, osseointegration in 12-month old PKI $\gamma$ <sup>-/-</sup> males ( $n = 8$ ) was significantly greater than in 12-month old wild-type males ( $n = 13$ ): Ultimate Force ( $7.6 \pm 1.7$  vs  $3.8 \pm 2.7$  N,  $p = 0.02$ ) and Average Stiffness ( $6.7 \pm 1.6$  vs  $3.4 \pm 2.4$  N/m,  $p = 0.005$ ). Together, these results show that regulation of PKA by PKI $\gamma$  reduces osteogenesis both *in vitro* and in aged mice.



PKA reg by PKI $\gamma$  Osseointegration PullOut Ult Force

**Disclosures:** Bryan S. Hausman, None.

## FR0129

**Hydrogen Sulfide Epigenetically Attenuates Homocysteine Induced Bone Loss in CBS Deficient Mice.** Jyotirmaya Behera<sup>\*</sup>, Akash George, Kimberly Kelly, Suresh Tyagi, Neetu Tyagi. University of Louisville, United States

Hydrogen sulfide (H<sub>2</sub>S) is an important gasotransmitter produced during homocysteine (Hcy) metabolism through Cystathionine- $\beta$ -synthase (CBS) activity. However, it is not clear whether H<sub>2</sub>S plays a pivotal role in pathological bone loss during CBS deficiency. Therefore, we hypothesize that CBS is a novel molecular regulator in bone marrow (BM) cells which promotes bone development. Here we show that CBS deficient (CBS<sup>-/-</sup>) mice, which display a model of osteoporotic bone loss, exhibit decreased serum H<sub>2</sub>S levels as well as decreased BM CBS activity, the key H<sub>2</sub>S-generating enzyme. CBS deficiency causes an aberrant increase in total serum homocysteine (tHcy) levels. This increase in tHcy downregulates Histone Deacetylase 3 Activity (HDAC3), which controls osteogenic differentiation of murine BM and osteoporotic phenotype. Treatment with the H<sub>2</sub>S-donor GYY4137 (GYY) normalizes serum H<sub>2</sub>S in CBS<sup>-/-</sup> mice, decreases serum tHcy levels, increases bone formation and completely prevents the loss of bone mineral density (BMD) induced by CBS deficiency. Molecular studies revealed that H<sub>2</sub>S increases murine osteogenesis through increased production of ALP, RunX2, OSTERIX, OCN in the BM and decreases the expression of inflammatory cytokine and matrix-degrading genes (IL-6, MMP-9, MMP-13). This increased inflammatory cytokine production in CBS<sup>-/-</sup> mice further activates osteoclast differentiation and bone resorption via IL-6 signaling. This increased resorptive activity is further confirmed with immunostaining of tibia cross sections by TRAP-activity and increased osteoclast number in bone tissue of CBS<sup>-/-</sup> mice. Blockade of HDAC3 activation in CBS<sup>-/-</sup> mice by RGFP566 (HDAC3 Inhibitor) leads to the remodelling of histone landscapes in the genome, thereby accelerating histone acetylation through identifying the acetylated lysine residue in histone (H3K27ac) of chromatin. This eventually resulted in transcriptional activation of MMP-9, -13 and IL-6 gene expression causing osteolytic bone loss. In conclusion, we demonstrated that H<sub>2</sub>S produced during CBS activity controls osteoblast balance, osteoblast differentiation/mineralization and osteoclastogenesis via HDAC3 in a dependent manner during bone development. Furthermore, administration of H<sub>2</sub>S may provide a novel therapeutic treatment for diseases such as osteoporosis that arise due to H<sub>2</sub>S deficiencies. **Acknowledgement:** This work is financially supported from the National Institutes of Health grant AR-067667.

**Disclosures:** Jyotirmaya Behera, None.

## FR0130

**The Novel Role of PINCH in Skeletogenesis.** Xin Liu<sup>\*</sup>, Guozhi Xiao. SUSTech, China

PINCH is a LIM-domain-only adaptor that plays important roles in integrin activation and extracellular matrix adhesion and migration. Mammalian cells have two functional PINCH proteins, PINCH1 and PINCH2. To investigate the role of PINCH in skeletogenesis, we deleted PINCH1 expression in Prx1-expressing head and limb mesenchymal cells and PINCH2 globally. Loss of PINCH resulted in limb shortening and osteopenia due to impaired endochondral ossification without affecting the intramembranous ossification. The formation of the second ossification was delayed in the mutant mice. We ablated PINCH1 expression in type II collagen-expressing chondrocytes and PINCH2 globally. Mutant mice appeared to be normal at birth, but developed



a severe growth retardation and dwarfism postnatally. Majority of the mutant mice died within 4 weeks of age. Notably, chondrocyte-specific PINCH1 knockout or global PINCH2 knockout mice did not exhibit any obvious skeletal phenotypes. Collectively, these results suggest a functional redundancy between the two PINCH proteins during skeletogenesis. In vitro studies revealed that deletion of PINCH1 in ATDC5 cells by using the CRISPR/Cas9 technology dramatically increased the expression levels of type X collagen and MMP13, suggesting an increase in chondrogenic differentiation induced by the loss of PINCH protein. Furthermore, deleting PINCH1 up-regulated the protein level of transcription factor MEF2C. Finally, PINCH1 deletion disrupted actin cytoskeleton in ATDC5 cells and impaired cell adhesion. These results demonstrate an essential role for PINCH in regulation of chondrocyte function and skeletal development.

**Disclosures:** Xin Liu, None.

## FR0132

**Identifying A Novel Regulator Of Anabolic Bone Metabolism.** Yu Shao<sup>\*1</sup>, Kylie Jacobs<sup>2</sup>, James Hamilton<sup>3</sup>, Thomas M O'Connell<sup>4</sup>, Nickolay Brustovetsky<sup>3</sup>, Jeanette McClintick<sup>5</sup>, Ronald Wek<sup>5</sup>, Joseph Bidwell<sup>2</sup>. <sup>1</sup>Medical & Molecular Genetics, Indiana University School of Medicine, United States, <sup>2</sup>Anatomy & Cell Biology, Indiana University School of Medicine, United States, <sup>3</sup>Pharmacology & Toxicology, Indiana University School of Medicine, United States, <sup>4</sup>Otolaryngology & Head/Neck Surgery, Indiana University School of Medicine, United States, <sup>5</sup>Biochemistry & Molecular Biology, Indiana University School of Medicine, United States

Loss of the transcription factor *Nmp4* amplifies PTH-induced bone formation in mice. *Nmp4*<sup>-/-</sup> mesenchymal stem/progenitor cells (MSPCs) exhibit an accelerated and enhanced mineralization but expression of *Runx2* and *Sp7*, key regulators of osteoblast differentiation, are only modestly elevated. The greater secretory activity is supported in part by c-Myc-driven increased ribosome biogenesis and expansion of the endoplasmic reticulum capacity for processing protein. *Nmp4* binds to the regulatory regions of several hundred genes in the osteoblast genome that govern biosynthetic processes. Recent studies show that aerobic glycolysis is stimulated during osteogenesis and in response to PTH. Therefore we inquired whether *Nmp4* regulates metabolism. Cultures of expanded MSPCs were established from WT and *Nmp4*<sup>-/-</sup> mice. Cells were harvested for whole-transcriptome (RNA-seq) analysis at Day 3 (uncommitted cells) and at Day 7 (early osteogenesis) post-seeding. Ingenuity Pathway Analysis (IPA) was used to interpret the transcriptome data. Genome-wide *Nmp4* ChIP-seq analysis was performed using MC3T3-E1 cells. The Seahorse XFe24 flux analyzer was employed to perform mitochondrial stress tests comparing uncommitted WT and *Nmp4*<sup>-/-</sup> MSPCs. IPA of the transcriptome data identified glycolysis among the functions that exhibited significant perturbations in the *Nmp4*<sup>-/-</sup> cells. Loss of *Nmp4* strikingly elevated the expression of the glucose transporter *Slc2a1* and the lactate transporter *Slc16a3*. Several genes mediating the conversion of glucose to pyruvate exhibited significantly elevated expression in *Nmp4*<sup>-/-</sup> cells. Genes that regulate the switch between aerobic glycolysis and oxidative phosphorylation including *Hk2*, *Pkm*, *Pdk1*, and *Ldha* showed significantly higher mRNA levels in the *Nmp4*<sup>-/-</sup> cells. ChIP-seq revealed that *Nmp4* associates at or near the 5' regions of these genes. The mitochondrial stress test showed that under basal conditions *Nmp4*<sup>-/-</sup> MSPCs exhibited significantly increased respiration associated with oxidative phosphorylation, consistent with augmented ATP production, and a higher maximal respiration than WT cells. The *Nmp4*<sup>-/-</sup> cells exhibited a significantly larger spare respiratory capacity and higher non-mitochondrial oxygen consumption. *Nmp4*<sup>-/-</sup> cells showed a significantly elevated extracellular acidification rate, consistent with lactate release. We conclude that loss of *Nmp4* enhances both aerobic glycolysis and oxidative phosphorylation in osteoprogenitors.

**Disclosures:** Yu Shao, None.

## FR0133

**TSC1 Regulates Bone Marrow Stromal Cell (BMSC) Lineage Commitment.** Han Kyoung Choi<sup>\*1</sup>, Hebao Yuan<sup>2</sup>, Fang Fang<sup>1</sup>, Fei Liu<sup>1</sup>. <sup>1</sup>University of Michigan School of Dentistry, United States, <sup>2</sup>University of Michigan, United States

mTORC1 signaling plays important role in skeletal growth. Herein we deleted *Tsc1* in osterix-expressing cells using osterix-cre to further determine the role of TSC1/mTORC1 signaling in osteoblast progenitor cells. Similar to another report, MicroCT analysis showed that CKO mice had increased femoral cortical bone mass. Surprisingly, CKO mice had significantly reduced femoral trabecular bone mass compared to controls (Ox-Cre, CHet, and *Tsc1*<sup>+/f</sup>) ( $p < 0.05$ ,  $n = 10-19$ ) at one month. Histomorphometric analysis showed that CKO femur had significantly decreased osteoblast number but increased adipocyte and osteoclast number ( $p < 0.05$ ,  $n = 8-9$ ). In consistent with decreased osteoblastogenesis and increased adipogenesis in vivo, TSC1-null BMSCs had compromised osteoblastic differentiation but enhanced adipogenic differentiation showed by Alizarin Red and Oil Red staining respectively. qPCR showed that TSC1-null BMSCs had decreased expression of osteoblast differentiation genes (*Runx2*, *Osterix*, *Alpl*, *Bsp*, etc) but increased expression of adipocyte differentiation genes (*Ppar $\gamma$* , *Fabp4*, *Adiponectin*, etc.) ( $p < 0.05$ ,  $n = 4$ ). Mechanistically, TSC1 deletion caused decreased  $\beta$ -catenin protein level and decreased expression of canonical Wnt target genes (*Axin2*, *Lef1*, etc.) in both BMSCs and mouse embryonic fibroblasts (MEFs). Rapamycin treatment restored the  $\beta$ -catenin level in TSC1-null BMSCs and

MEFs. Furthermore,  $\beta$ -catenin level decrease in TSC1-null cells was not mediated through canonical  $\beta$ -catenin degradation pathway, evidenced by the increased protein level of inhibitory form of phospho-GSK3 $\beta$  (S9) and diminished  $\beta$ -catenin protein increase in response to Wnt3a treatment in TSC1-null BMSCs and MEFs. In addition, TSC1 deletion led to increased Notch1 protein level and Notch target gene (*Hey1* and *Jagged1*) expression. Since it was reported that Notch1 can mediate  $\beta$ -catenin degradation independent of GSK3 $\beta$ -dependent activity of  $\beta$ -catenin destruction complex, our data suggest that TSC1 may regulate  $\beta$ -catenin through this noncanonical pathway by modulating Notch1 protein level. Lastly, TSC1-null BMSCs had decreased autophagy shown by decreased LC3-II and decreased LC3-GFP puncta/cell in response to starvation; Notch1 level was decreased by autophagy activation under starvation or rapamycin treatment in BMSCs. Altogether, our data suggested that TSC1 is a cell fate determinant of BMSCs by modulating  $\beta$ -catenin level, possibly through regulating Notch1 level via its autophagy function.

**Disclosures:** Han Kyoung Choi, None.

## FR0135

**Identification of Murine Circulating CD34<sup>+</sup> OCN<sup>+</sup> Cells.** Ryan Kelly<sup>\*1</sup>, Lindsay McDonald<sup>2</sup>, James Cray<sup>1</sup>, Amanda LaRue<sup>2</sup>. <sup>1</sup>Medical University of South Carolina, United States, <sup>2</sup>Ralph H. Johnson Department of Veterans Affairs Medical Center, United States

Circulating osteoprogenitors are receiving increased attention for their potential in cell-based therapies, particularly in cases of bony repair. The origin of these cells is still controversial; as it is not known if adherent bone marrow (BM)-derived mesenchymal stromal cells (MSCs), the population thought to generate osteoblasts, circulate. Similarly, circulating osteoprogenitors likely originate in the BM, where they then must egress into circulation, suggesting they are non-adherent. The non-adherent BM fraction also harbors the hematopoietic stem cell (HSC) and its progeny. Although the current paradigm suggests MSCs form osteoblasts and HSCs form osteoclasts, a number of studies have shown that HSCs have osteogenic potential. Thus, circulating osteoprogenitors may be of hematopoietic origin. Due to limitations in the therapeutic use of MSCs and the latest findings suggesting MSCs act as medicinal signaling cells, studying other populations with osteogenic potential, including HSCs, is warranted. Previous work from other groups identified a circulating human osteoblastic population that expressed OCN and ALP, increased during fracture repair and pubertal growth, and formed mineralized colonies *in vitro* and bone *in vivo*. Interestingly, a subpopulation also expressed CD34, suggesting a hematopoietic/endothelial origin. Our study extends these findings by identifying circulating CD34<sup>+</sup>OCN<sup>+</sup> in mice by flow cytometry. These cells were confirmed to be of hematopoietic origin by use of the VavR double transgenic mouse model, in which any cell that expresses the global hematopoietic gene, Vav1, is permanently labeled with GFP. Using a murine non-stabilized tibial fracture model, we showed that circulating CD34<sup>+</sup>OCN<sup>+</sup> cells peak 3 weeks post-fracture, suggesting involvement in callus formation and early mineralization. In regards to therapeutic potential, these CD34<sup>+</sup>OCN<sup>+</sup> cells can be mobilized after 3 days of treatment with 10mg/mL AMD3100. Together, our data demonstrate a murine CD34<sup>+</sup>OCN<sup>+</sup> circulating population similar to that seen in humans. These cells are of hematopoietic origin, increase during fracture repair, and can be mobilized via AMD3100. We hypothesize that increasing CD34<sup>+</sup>OCN<sup>+</sup> cells will correlate with improved fracture healing outcomes. Studies are currently underway to test this hypothesis and further define these cells' phenotype and osteoblast potential.

**Disclosures:** Ryan Kelly, None.

## FR0136

**Transplantation of Human Skeletal Muscle-Derived Progenitor Cells Ameliorates Knee Osteoarthritis.** Shing-Hwa Liu<sup>\*</sup>, Chen-Yuan Chiu, Ding-Cheng Chan, Rong-Sen Yang. National Taiwan University, Taiwan, Province of China

**Introduction:** Osteoarthritis (OA) is a degenerative joint disorder ongoing cartilage destruction and inflammation. The therapeutic effect and mechanism of human skeletal muscle-derived progenitor cells (HSMPCs) on OA still remain unclear. Here, we investigated the therapeutic potential of HSMPCs on monosodium iodoacetate (MIA)-induced OA and streptozotocin (STZ)-induced diabetes-related OA in mice. **Methods:** Male ICR mice were used to develop MIA (1 mg/10  $\mu$ l, intraarticular injection, two months)-induced OA and STZ (100 mg/kg, intraperitoneal injection, one month)-induced diabetes-related OA. HSMPCs were isolated from rectus muscles of orthopedic surgery patients. HSMPCs (1x10<sup>5</sup> cells) were injected into the knee joint for 1 month after OA induction in both models. Histology of articular cartilage was determined by Safranin O/Fast green stain and Mankin scoring system. The cyclooxygenase (COX)-2 expression in the cartilage was determined by immunohistochemistry. **Results:** HSMPCs significantly prevented the progression of degenerative changes in the cartilage of MIA-induced OA mice (Figure 1A), including an obvious increase of total articular cartilage (TAC) thickness (about 59.26% increase,  $n = 5$ ,  $p = 0.01$ ; Figure 1B) and a decrease of fibrous cartilage (FC) thickness (about 72.9% decrease,  $n = 5$ ,  $p = 0.09$ ; Figure 1C). After four weeks post-transplantation, significant differences determined by Mankin OA scoring were shown among control, MIA, and MIA+HSMPCs groups (Total score:  $1 \pm 0$  in control,  $5.0 \pm 0.58$  in MIA,  $2 \pm 0.41$  in MIA+HSMPCs,  $n = 5$ ,  $p < 0.05$ ; Figure 1D). HSMPCs also exerted anti-inflammatory effects on the MIA-induced OA cartilage with a decline of COX-2 expression (Figure 1E). Similarly, HSMPCs could significantly reverse the reduction of TAC thickness and the elevation of FC thickness and Mankin OA scores in the cartilage of STZ-induced OA mice via COX-2 down-regulation ( $n = 5$ ,  $p < 0.05$ ). **Conclusion:** COX-2 is upregulated and is responsible for elevated production

of prostaglandins in the OA joint, and COX-2 inhibitor celecoxib has been shown to possess the chondroprotective effect in OA patients. STZ is known as a chemical inducer for type 1 diabetes, which also induce cartilage damage and inflammation. In this study, we found that HSMPCs ameliorated cartilage degeneration via COX-2 down-regulation not only in MIA-induced OA mice but also in diabetes-induced OA mice. These findings suggest that HSMPCs transplantation may apply as a potential therapeutic use of OA.

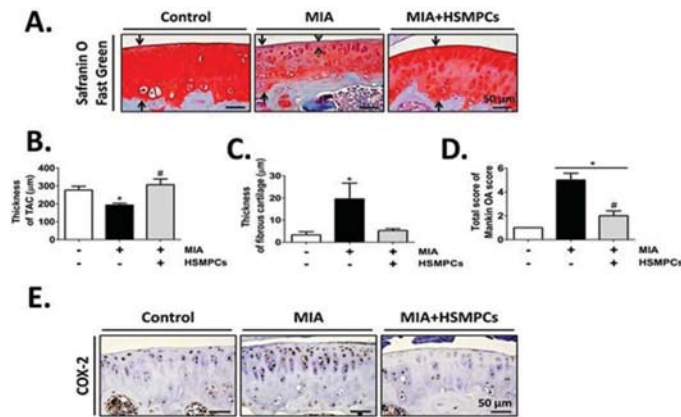


**Figure 1.** Intra-articular injection of human skeletal muscle-derived progenitor cells (HSMPCs) ameliorates cartilage degeneration via cyclooxygenase-2 (COX-2) down-regulation in monosodium iodoacetate (MIA)-induced osteoarthritis (OA) mice. Male ICR mice were intra-articularly injected with MIA (1 mg/10 μl saline)-induced OA for two months. HSMPCs ( $1 \times 10^5$  cells/10 μl saline) were singly injected into the knee joint for 1 month after OA induction. (A) Representative histology examined by Safranin O/Fast green staining; (B) Thickness of total articular cartilage (TAC); (C) Thickness of fibrous cartilage; (D) Quantification of histological analysis using the Mankin OA scoring system; (E) The expressions of COX-2 in the OA cartilage is determined by immunohistochemistry. In A, solid arrows indicate the thickness of articular cartilage. Dot arrows indicate the thickness of fibrous cartilage. Scale bar = 50 μm. All data are presented as mean±SEM for five independent experiments. \*,  $p < 0.05$  as compared with control group; #,  $p < 0.05$  as compared with MIA group.

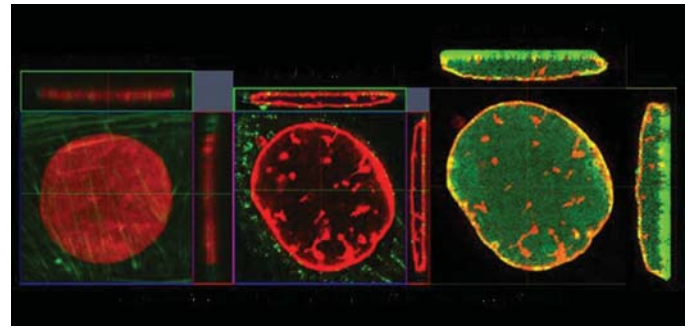
HSMPCs prevented the progression of degenerative changes in the cartilage of MIA-induced OA mice

**Disclosures:** Shing-Hwa Liu, None.

## FR0138

**Intranuclear actin assembly is critical for extracellular matrix mediated osteogenic differentiation of mesenchymal stem cells.** Jeyant Srinivas Sankaran<sup>1</sup>, Buer Sen<sup>1</sup>, Zhihui Xie<sup>1</sup>, Cody McGrath<sup>1</sup>, Maya Styner<sup>1</sup>, Rebekah Samsonraj<sup>2</sup>, Andre van Wijnen<sup>2</sup>, Janet Rubin<sup>1</sup>. <sup>1</sup>University of North Carolina, Chapel Hill, United States, <sup>2</sup>Mayo Clinic, United States

Nuclear actin, which has a role in gene expression, is a critical mediator of mesenchymal stem cell (MSC) fate selection. Nuclear actin is present in monomeric or polymeric (linear or branched) forms. We showed that polymerized forms of nuclear actin are necessary to the mechanism by which cytochalasin D stimulates MSC osteogenesis, requiring actin translocation and branching within the nucleus. Here, we hypothesized that intranuclear actin branching also plays a critical regulatory role in dictating MSC osteogenic lineage commitment under physiologic conditions. MSCs were grown in MEM growth medium or osteogenic O-medium (+ascorbate). Confocal microscopy revealed that the morphology of undifferentiated MSCs is starkly different from those exposed to O-medium: osteogenic MSCs had taller nuclei that stained more intensely for the nuclear structural protein, lamin B, which, in turn folded prominently along the inner leaflet of the nuclear membrane. Intense intranuclear phalloidin staining of F-actin and increased nuclear height was strongly suggestive of an intranuclear branched actin network. We tested whether actin branching was critical for osteogenic differentiation by inhibiting the branching enzyme complex, ARP2/3 with CK666. As expected, CK666 induced rapid adipogenesis, as reflected by a >10-fold increase in the adipogenic mRNA markers APN and FABP4. To overcome this strong adipogenic stimulus, and to accelerate osteogenesis, MSCs were cultured in O medium along with BMP2: BMP2 increased the osteogenic transcription factor, Osterix/SP7, by 4 fold at 3 days. Inhibition of actin branching completely prevented the rise in SP7. Linear actin filament formation, which precedes Arp2/3 guided branching in the nucleus, requires formins, and preventing their action halts cytochalasin D induced osteogenesis. Remarkably, siRNA knock down of the formin mDia1 increased Sp7 by 10-fold; at the same time mDia2, which is localized within the nucleus, increased by 2-fold, and actin branching factors (ARP2, ARP3) increased by 1.5-fold. Since mDia1 was predominantly localized to the cytoplasm during osteogenesis, the increased nuclear expression of mDia2 may accelerate intranuclear F-actin formation, resulting in osteogenesis. We propose that physiological osteogenesis requires the intranuclear presence of enzymes that control actin polymerization and alter nuclear morphology to activate previously silenced osteogenic genes.



Confocal microscopy images of undifferentiated and osteogenic MSCs

**Disclosures:** Jeyant Srinivas Sankaran, None.

## FR0139

**Conditional ablation of Prx1 expressing cells and haploinsufficiency of Prrx1 gene lead to impaired fracture healing.** Lai Wang<sup>\*</sup>, Alessandra Esposito, Joseph Temple, Ji Eun Han, Tieshi Li, Anna Spagnoli. Department of Pediatrics, Rush University Medical Center, Chicago, United States

The regenerative ability of bones after fracture implies the existence of adult progenitors. Paired-related homeobox 1 (Prx1), which is encoded by the *Prrx1* gene, is postnatally expressed in the periosteum and endosteum. Periosteal and endosteal cells have been reported as major sources of soft and bone callus in fracture repair. To determine the role of Prx1 and Prx1 expressing cells in fracture healing, we used two transgenic mouse approaches: 1) *Prx1CreER;R26DTA* mice to genetically ablate Prx1 expressing cells through toxicity of diphtheria toxin subunit A (DTA), the expression of which is activated via a tamoxifen-driven-cre expressed under the control of *Prrx1* gene; and 2) *Prx1CreER;Prrx1<sup>tm1bl/+</sup>* mice to conditionally and inducibly inactivate *Prrx1* gene. To the latter purpose, *Prrx1<sup>tm1al/+</sup>* mice, in which loxP sites flank *Prrx1* exon 2 which encodes the first half of the homeobox domain, were bred with *Prx1CreER* mice to generate *Prx1CreER;Prrx1<sup>tm1al/+</sup>* mice. Tamoxifen administration led to *Prx1CreER;Prrx1<sup>tm1bl/+</sup>*. In both transgenic mice, male mutant mice and their littermate controls were subjected to tibia fracture at postnatal age 10-12 weeks. 4-OH-tamoxifen was injected intraperitoneally 0.5mg/mouse/day for 6 days started two days before fracture. Mice were euthanized 14 days after fracture. Micro-computed tomography (micro-CT) analysis of the fractured tibias revealed that the volume of callus and soft tissue was decreased in *Prx1CreER;R26DTA* mice compared to their control littermates ( $1.000 \pm 0.214$  vs.  $0.736 \pm 0.222$  in callus, and  $1.000 \pm 0.236$  vs.  $0.657 \pm 0.263$  in soft tissue, data were normalized to total bone). *Prx1CreER;Prrx1<sup>tm1bl/+</sup>* mice also showed lower volume of callus and soft tissue compared to their control littermates ( $1.000 \pm 0.300$  vs.  $0.525 \pm 0.172$  in callus, and  $1.000 \pm 0.331$  vs.  $0.471 \pm 0.158$  in soft tissue). Quantitative real-time PCR of the tibia fracture callus samples showed decreases of mRNA expression of chondrogenic and osteoblastogenic markers (Sox9, Col2a1, Col10a1, Runx2 and Osterix) in *Prx1CreER;Prrx1<sup>tm1bl/+</sup>* mice compared to the samples from their control littermates ( $85.2 \pm 8.8\%$ ,  $50.3 \pm 11.7\%$ ,  $37.0 \pm 3.1\%$ ,  $67.1 \pm 7.9\%$ , and  $83.4 \pm 8.6\%$ , respectively), indicating a reduced cartilage and new bone formation in the fracture callus of *Prrx1* insufficient mice. These findings provide evidence that *Prrx1*+ cells and in particular their expression of *Prrx1* is crucial in promoting fracture healing by serving as multipotent progenitors.

**Disclosures:** Lai Wang, None.

## FR0140

**PDGFRβ signaling regulates osteogenesis of periosteal mesenchymal stem cells.** Xi Wang<sup>1</sup>, Brya G Matthews<sup>1</sup>, Jungeon Yu<sup>2</sup>, Archana Sanjay<sup>1</sup>, Danka Grcevic<sup>3</sup>, Ivo Kalajic<sup>1</sup>. <sup>1</sup>Uconn Health, United States, <sup>2</sup>Uconn Health, United States, <sup>3</sup>University of Zagreb, United States

Fracture repair is a complex process involving the release of growth factors, induction of signaling pathways and their interplay with stem cells. As an important progenitor pool, the periosteum plays an essential role for fracture healing. To understand the mechanisms regulating differentiation of MSCs within periosteum, we isolated and phenotyped cells from the early phases of fracture callus formation. Four days after fracture, over 50% of CD45<sup>+</sup> non-hematopoietic cells were PDGFRβ<sup>+</sup>. Using mesenchymal stem cell marker αSMA, we found the expression of PDGFRβ was highly enriched in progenitors, with about 90% αSMA<sup>+</sup> cells expressing PDGFRβ. FACS sorted PDGFRβ<sup>+</sup> cells from uninjured periosteum formed significantly more colonies than PDGFRβ<sup>+</sup> cells, indicating enrichment of progenitor cells.

We further investigated the regulation of PDGF/PDGFRβ signaling on periosteal progenitor cells (PPCs).

PPCs were isolated and treated with 10ng/ml PDGF-BB. We observed PPCs to be highly responsive to PDGF-BB with activation of multiple downstream signaling including the phosphorylation of Erk1/2, Akt, p38, and PLCγ1. This effect was mainly mediated through PDGFRβ, as cells with PDGFRβ knocked out, some of which still express PDGFRα, were not responsive to PDGF-BB.



Interestingly, PDGF-BB exerted an inhibitory effect on osteogenic differentiation, and dampened BMP2-induced osteogenesis of PPCs. Treatment of PPC with BMP2 activated canonical Smad signaling but this effect was reduced in the presence of PDGF-BB. Additionally, inhibition of PDGFR $\beta$  with a chemical inhibitor (su16f) rescued the inhibition of pSmad signaling as well as osteogenic differentiation of PPCs in vitro.

PDGFR $\beta$  is highly expressed in  $\alpha$ SMA labeled periosteal progenitor cells, therefore we conditionally deleted PDGFR $\beta$  using  $\alpha$ SMA-CreERT2 crossed with PDGFR $\beta$  flox/flox mice. We treated isolated PPCs with 4-OH Tamoxifen and induced the periosteal differentiation. ALP staining showed that PDGFR $\beta$  deficient cells exhibited significantly enhanced osteogenic differentiation in vitro.

We have demonstrated that PDGF, signaling through PDGFR $\beta$ , inhibits BMP2-induced differentiation of PPCs in vitro. In addition, PDGFR $\beta$  is widely expressed in progenitor cells that contribute to fracture healing in vivo.

**Disclosures:** Xi Wang, None.

## FR0141

**The fracture Callus is Formed by Progenitors of Different Skeletal Origins in a Site Specific Manner.** Yongmei Wang<sup>1</sup>, Faming Tian<sup>1</sup>, Lin Ling<sup>1</sup>, Wasima Mayer<sup>1</sup>, Ling Chen<sup>2</sup>, Misun Kang<sup>2</sup>, Sunita Ho<sup>2</sup>, Daniel Bikle<sup>1</sup>. <sup>1</sup>Endocrine Unit, University of California, San Francisco/San Francisco VA Health Care System, United States, <sup>2</sup>Bioengineering & Biomaterials Micro-CT and Imaging Facility, University of California, San Francisco, United States

Fracture (Fx) repair is a complex process. We evaluated repair following a mid diaphyseal Fx of the tibia in 3m old mice. We observed differences in the repair process at 3 different sites of the callus (Fig.1). Site1: intramembranous bone formation (IBF) developing from the outer layer of the periosteum of the cortex; site2: endochondral bone formation (EndoBF) developing within the bridge region of the Fx; site3: intramedullary bone formation (IMBF), within the marrow of the ends of broken bones. The origin of the progenitors and mechanism of progenitor differentiation involved at these sites was evaluated. We traced the cell fate of prx-1 expressing and type II collagen (Col.II) expressing cells in the mice by crossing tamoxifen (tam) regulated prx1cre-recombinase GFP (GFPprx1 cre) or tam regulated Col.II cre-recombinase (Col.II cre) with Rosa TdTomato (TdT) expressing mice. A unilateral closed mid tibial Fx was made in the mice. Tam was given 1 day prior to Fx. In the TdGFPprx1 cre mice, following tam administration but before fracture (day0) only GFP (prx1 positive cells, green) and TdT (activated prx1 positive cells, red) dual labelled cells (yellow) appeared in the periosteum. At day10 post Fx, TdT labeled cells (red) appeared in the periosteum and osteocytes embedded in the cortical bone distant to the Fx site. At this time point, dual labeled cells were observed in site1 and site2, but not in site 3. In contrast, in the TdCol.II cre mice, at day10 after Fx, TdT labeled cells appeared in site2, site3 as well as in the cortical bone of the fractured bone ends as osteocytes, but were observed neither in site1, nor in the periosteum and endosteum. Immunohistochemistry identified that in site2, TdCol.II labeled cells co-expressed with the osteoblast (OB) differentiation marker osteocalcin. Surprisingly, in the cortical bone, TdCol.II labelled osteocytes continuously expressed Col.II by IHC and co-expressed the stem cell marker Sox2 in site 2 but not site 1. In site3, the TdCol.II labelled cells no longer expressed Sox2, but expressed the osteocytic gene DMP-1. Our data indicate that during Fx repair, prx1 expressing osteochondroprogenitors from the periosteum contribute to IBF and EndoBF, but not IMBF. A sub set of Col.II expressing chondrocytes transdifferentiates into OBs and contributes to EndoBF in site2 but not site 1 or 3. In site 3 Col.II expressing osteocytes appear to reprogram, differentiate into OBs, and contribute to IMBF.

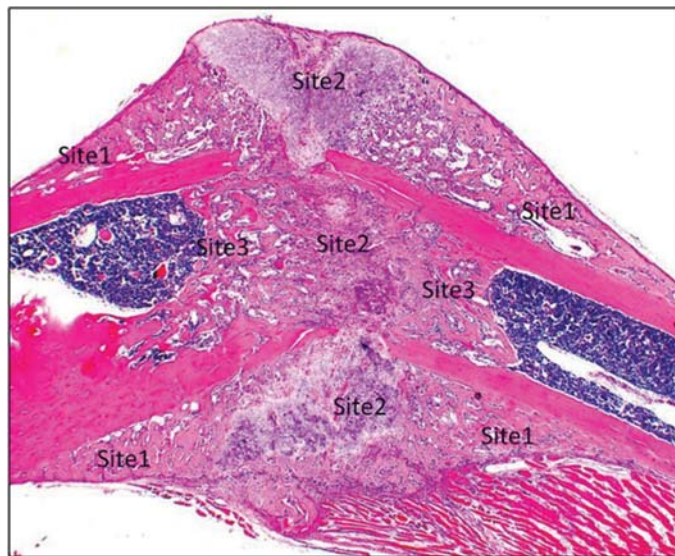


Figure 1

**Disclosures:** Yongmei Wang, None.

## FR0145

**Bone mineral density is related to proximal femur shape: findings from a cross-sectional study in middle aged women.** Monika Frysz<sup>1</sup>, Jenny Gregory<sup>2</sup>, Denis Baird<sup>3</sup>, Richard Aspdon<sup>2</sup>, Lavinia Paternoster<sup>1</sup>, Jonathan Tobias<sup>1</sup>. <sup>1</sup>School of Social and Community Medicine, University of Bristol, UK; MRC Integrative Epidemiology Unit at the University of Bristol, UK, United Kingdom, <sup>2</sup>Arthritis and Musculoskeletal Medicine, Institute of Medical Sciences, University of Aberdeen, UK, United Kingdom, <sup>3</sup>Musculoskeletal Research Unit, School of Clinical Sciences, University of Bristol, UK, United Kingdom

### Purpose

Epidemiological studies suggest an inverse association exists between osteoporosis and osteoarthritis (OA), the basis of which is unclear. In the present study, we investigated whether shared developmental influences on hip bone mineral density (BMD) and shape might contribute to this relationship, by (i) studying cross-sectional associations between hip BMD and hip shape in adult females, and (ii) investigating whether this association is causal using two-sample Mendelian randomization (MR) approach.

### Methods

Hip DXA scans were obtained in adult females from the Avon Longitudinal Study of Parents and Children (ALSPAC), a UK population based cohort. To quantify hip morphology, hip DXA images were analyzed using Shape software (Aberdeen, UK) based on a 53-point Statistical Shape Model (SSM). Principal component analysis was used to generate independent modes of variation (hip shape mode (HM) scores) for each image. We examined the associations of hip BMD with the top ten HMs, using multivariable linear regression adjusted for age, height, fat and lean mass. Summary level data from genome-wide association studies for femoral neck BMD and hip shape were used. Single nucleotide polymorphisms (SNPs)-exposure (BMD) effects were combined with SNPs-outcome (hip shape) effects using an inverse-variance weighted fixed-effects approach.

### Results

Data were available from 4298 females at mean age 48.1 (4.2) years. Observationally, hip BMD was positively related to a number of modes (table 1), including HM5 (standardized  $\beta$  0.129; 95% CIs [0.098, 0.160]  $p=7.5 \times 10^{-16}$ ), HM3 (0.161 [0.131, 0.192]  $p=5.1 \times 10^{-25}$ ) and HM7 (0.099 [0.070 – 0.128]  $p=2.3 \times 10^{-11}$ ) reflecting variation in femoral head size, and HM2 (0.122 [0.093; 0.151]  $p=4.3 \times 10^{-16}$ ) which reflects variation in femoral neck width. Higher HM2 score associated with BMD reflects narrower femoral neck. Using two-sample MR approach we found evidence for a causal relationship between BMD and HM2 (0.290 [0.100; 0.479]  $p=0.003$ ), consistent with observational associations, however no evidence of a causal association with other modes was found.

### Conclusion

Our results suggest that BMD is strongly associated with several components of hip shape, consistent with shared influences on risk of hip fracture and hip OA in later life. Causal pathway analysis suggested that factors determining BMD mediate alterations in HM2, whereas relationships between BMD and other hip shape modes reflect shared associations with other factors.

**Table 1** Observational associations between total hip BMD and top ten HMs in adult females from ALSPAC cohort

SD change in HM per 1 SD change in hip BMD and 95% Confidence intervals							
	Model 1			Model 2			
HM	estimate	95% CI	p	estimate	95% CI	p	
1	0.096	0.080 0.112	1.40E-31	0.094	0.076 0.111	4.10E-25	
2	0.032	0.005 0.060	0.02	0.122	0.093 0.151	4.30E-16	
3	0.144	0.116 0.171	2.40E-24	0.161	0.131 0.192	5.10E-25	
4	0.022	-0.002 0.045	0.07	0.019	-0.007 0.045	0.146	
5	0.070	0.042 0.098	1.40E-06	0.129	0.098 0.160	7.50E-16	
6	0.047	0.017 0.077	2.30E-03	0.046	0.013 0.079	7.10E-03	
7	0.050	0.023 0.076	2.20E-04	0.099	0.070 0.128	2.30E-11	
8	-0.023	-0.052 0.006	0.117	-0.002	-0.034 0.030	0.902	
9	-0.071	-0.099 -0.042	1.40E-06	-0.054	-0.086 -0.023	7.80E-04	
10	-0.008	-0.036 0.019	0.553	0.040	0.010 0.071	1.00E-02	

Abbreviations: HM (hip shape mode), CI (confidence interval). Table shows results of linear regression analysis between hip BMD and top ten HMs. Results are standard deviation change in HM per standard deviation increase in exposure, 95% CIs and p value. Model 1: adjusted for age, Model 2: additionally adjusted for height, lean and fat mass.

Table 1

**Disclosures:** Monika Frysz, None.

## FR0149

**Combining fractal- and entropy-based bone texture analysis for the prediction of Osteoarthritis: data from the Multicenter Osteoarthritis study (MOST).** Zsolt Bertalan<sup>1</sup>, Richard Ljuhar<sup>1</sup>, Stefan Nehrer<sup>2</sup>, Davul Ljuhar<sup>3</sup>, Astrid Fahrleitner-Pammer<sup>4</sup>, Hans-Peter Dimai<sup>4</sup>. <sup>1</sup>ImageBiopsy Lab, Austria, <sup>2</sup>Danube University Krems, Austria, <sup>3</sup>Braincon Technologies Research, Austria, <sup>4</sup>Medical University Graz, Austria

### INTRODUCTION:

Osteoarthritis (OA) is one of the leading causes of long-term pain and disabilities associated with musculoskeletal disorders. Effective treatment and disease-progression slowdown depend on early detection and quantification of risk. However, current disease parameters, like joint space width (JSW), have proven to be insufficient for the prediction of OA. The purpose of the present study was to investigate if combining

fractal- and entropy-based bone texture analyses with joint space width (JSW) and joint space area (JSA) may improve prediction of OA.

#### METHODS:

Conventional posterior-anterior (PA) knee radiographs of men and women were obtained from the Multicenter Osteoarthritis Study (MOST) database, which provides valuable information to identify and define modifiable biomechanical, bone and structural, nutritional, and other risk factors for future disease and progression of existing disease (1). Oriented fractal- and entropy based texture algorithms were developed, using state-of-the-art computer hardware and software as well as specific machine-learning algorithms. The selected subchondral area used for textural analyses included 4 regions of interest (ROI) in the proximal tibia and one on each condyle of the distal femur (Figure 1). Furthermore, JSW and JSA were assessed using newly developed and fully automated software.

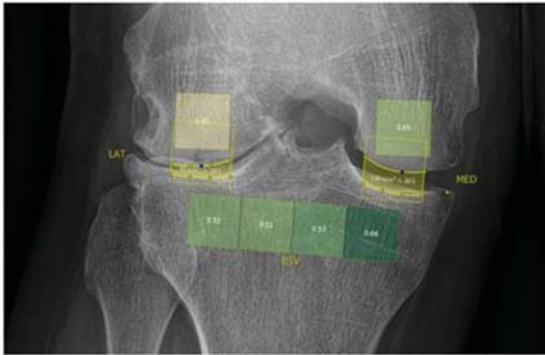
#### RESULTS:

1092 conventional knee radiographs obtained from one study center were screened for eligibility. Of these, a total of 574 radiographs (230 women, 344 men) met the inclusion criteria, i.e. Kellgren & Lawrence (KL) score of 0 at baseline. At month 84, 41 female and 79 male patients had developed KL $\geq$ 1, and 189 female and 265 male patients remained at KL0. Area-Under-the-Curve (AUC) for incident OA using JSW/JSA and clinical features was  $0.67\pm0.08$  for women, and  $0.61\pm0.1$  for men. In contrast, combining fractal/entropy-based texture, JSW/A and clinical features resulted in significantly improved AUC for women and men ( $0.80\pm0.07$  for women and  $0.69\pm0.1$  for men, respectively). To test whether these differences in predicting incident-OA were significant, we performed classifier comparison:  $t = 3.84$ ;  $p < 10^{-3}$  for women, and  $t = 3.38$ ;  $p < 10^{-3}$  for men.

#### CONCLUSION:

This study provides strong evidence, that a combination of fractal- and entropy-based textural analyses of plain subchondral bone radiographs together with JSW/A and clinical features is superior to JSW/A and clinical features alone in predicting incident OA in men and women.

1) <http://most.ucsf.edu/studyoverview.asp>



Feb 2017

© Image Biopsy Lab 2017

Selected Regions of Interest (ROI) for bone texture analyses

Disclosures: Zsolt Bertalan, None.

## FR0150

**Focal Thickening Of Femoral Head Cortical Bone Predicts Total Hip Replacement For Osteoarthritis.** Ilya Burkov<sup>\*1</sup>, Graham Treece<sup>1</sup>, Andrew Gee<sup>1</sup>, Thomas Turmezei<sup>2</sup>, Fjola Johannesdottir<sup>3</sup>, Sigurdur Sigurdsson<sup>4</sup>, Thor Aspelund<sup>4</sup>, Vilmundur Gudnasson<sup>4</sup>, Helgi Jonsson<sup>5</sup>, Kenneth Poole<sup>1</sup>.

<sup>1</sup>University of Cambridge, United Kingdom, <sup>2</sup>Addenbrooke's Hospital, Cambridge, United Kingdom, <sup>3</sup>Beth Israel Deaconess Medical Center, United States, <sup>4</sup>The Icelandic Heart Association, Iceland, <sup>5</sup>Landspítalinn University Hospital, Iceland

#### Objectives

To investigate the pathophysiology of osteoarthritis, baseline pelvic CT scans from 258 healthy participants in a large, prospective study were analysed with 3D cortical bone mapping (CBM). We aimed to discover whether 3D automatic measurements of focal bone thickening in contact areas of the femoral head could predict those people who would undergo total hip replacement (THR) for clinical osteoarthritis within 5 years. We also studied whether focal thickening and osteophyte burden were correlated, and whether focal thickening corresponded with sites of high habitual load during gait.

#### Methods

All cases who eventually underwent THR and two matched controls per case were selected from consented volunteers in the Age, Gene, Environment Susceptibility-Reykjavik Study. CBM was used to estimate and map the cortical thickness of the bone across the entire proximal femur semi-automatically. Parametric mapping (with the General Linear Model including shape and demographic covariates) was used to identify regional

differences in 3D cortical bone thickness between cases and controls. The colour maps produced allowed us to highlight systematic differences on a 3D canonical femur model. Model coefficients and receiver operating characteristic were used to determine the predictive ability of cortical thickness for THR.

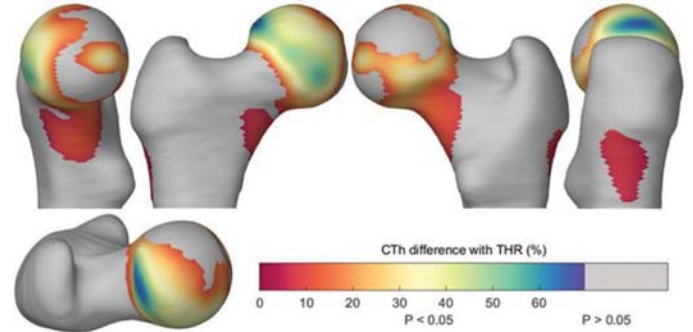
#### Results

A total of 258 individuals were included (mean age 74, range 67-89). Baseline scans of the relevant hip of the 74 men and women destined for eventual total hip replacement within

5 years showed a characteristic pattern of cortical bone thickening compared with the 184 controls. There was a statistically significant focal thickening antero-superiorly in contact areas, with up to 70% greater hip cortical thickness in those who needed a subsequent THR (figure). This thickening coincided with areas of high predicted contact pressure between acetabulum and femur during routine tasks (e.g. walking and sitting). The thickening also correlated with osteophyte load. For every standard deviation thicker than control in the focal region, the odds ratio for undergoing THR within 5 years was 4.4 (AUC of 0.81).

#### Conclusions

Men and women destined for total hip replacement for osteoarthritis have a pattern of femoral cortical bone thickening consistent with a 'wear' hypothesis of osteoarthritis, either through focal, structural cartilage degradation and subsequent osteophyte repair or a local structural bone response to habitual joint loading.



Figure

Disclosures: Ilya Burkov, None.

## FR0151

**Prevalence of Arthritis using a Job Exposure Matrix in Lower and Middle Income Countries: World Health Organization's Study on Global Ageing and Adult Health.** Brennan-Olsen Sharon<sup>\*1</sup>, Svetlana Solovieva<sup>2</sup>, Eira Viikari-Juntura<sup>3</sup>, Steven Bowe<sup>4</sup>, Paul Kowal<sup>5</sup>, Nirmala Naidoo<sup>5</sup>, Ilana Ackerman<sup>6</sup>, Anita Wluka<sup>6</sup>, Michelle Leech<sup>6</sup>, Richard Page<sup>4</sup>, Gustavo Duque<sup>7</sup>, Fernando Gomez<sup>8</sup>, Mohammadreza Mohebbi<sup>4</sup>. <sup>1</sup>University of Melbourne, Australian Institute for Musculoskeletal Science (AIMSS), Australia, <sup>2</sup>Finnish Institute of Occupational Health, Finland, <sup>3</sup>Finnish Institute of Occupational Health, Finland, <sup>4</sup>Deakin University, Australia, <sup>5</sup>World Health Organization, Switzerland, <sup>6</sup>Monash University, Australia, <sup>7</sup>University of Melbourne; Australian Institute for Musculoskeletal Science (AIMSS), Australia, <sup>8</sup>Facultad de Ciencias para la Salud Universidad de Caldas, Colombia

**Purpose:** In higher income countries, job-related stressors such as squatting and heavy lifting have been associated with increased arthritis risk. However, little is known about physical job stressors and prevalent arthritis in lower and middle income countries (LMICs). Using data from the World Health Organization Study on global AGEing and adult health (SAGE), we assessed prevalent arthritis across the job-related stressors of heavy physical work (HPW), kneeling/squatting (K/S), and heavy lifting (HL), using a sex-specific Job Exposure Matrix (JEM).

**Methods:** SAGE Wave 1 (2007-10) includes nationally-representative samples of adults ( $\geq 50$  yrs), plus smaller samples of those aged 18-49 yrs, from Ghana, India, Russia and South Africa for whom self-reported occupation was recorded and coded to the International Standard Classification of Occupations (ISCO) (n=21,514; 49.2% female). Arthritis was identified using a symptom-defined algorithm (current), and as self-reported doctor-diagnosed (lifetime). The SAGE and the JEM<sup>1</sup> were linked using the ISCO codes as linkage key. In multivariable analyses we investigated prevalent arthritis across job-related stressors, adjusted for age (10yr groups), sex and country. Multivariate logistic regression, adjusted for country were implemented to evaluate job-related stressors with self-reported and symptom-based arthritis prevalence after adjusting for sex and age.

**Results:** Job-related K/S was associated with symptom-defined arthritis (OR 1.41, 95% 1.21-1.65); significant factors included female sex, advancing age and country (all  $p \leq 0.002$ ). Similar associations were seen for HL (OR 1.42, 95%CI 1.22-1.66). Although associations between HPW and symptom-defined arthritis were in the same direction, this was not significant (OR 1.14, 95%CI 0.99-1.31).

For doctor-diagnosed arthritis, adjusted results were similar; job-related K/S was significantly associated with arthritis (OR 1.22, 95%CI 1.10-1.34), whilst a trend was



seen for HL (OR 1.02, 95%CI 0.93-1.11) and HPW (OR 1.05, 95%CI 0.97-1.14). Female sex, advancing age and country were significant in all models.

**Conclusions:** Symptom-defined arthritis was associated with job-related HL, and for both symptom-defined and doctor-diagnosed arthritis, associations were seen with job-related K/S after adjusting for age and sex. The novel application of a JEM enables us to investigate job-related stressors and arthritis in different LMICs using an internationally-comparable coding system.

**Disclosures:** Brennan-Olsen Sharon, None.

## FR0155

**MicroRNA 23a cluster Maintains BAF-PRC2 Epigenetic Equilibrium to Preserve Bone Mass in vivo.** Tanner Godfrey<sup>1</sup>, Benjamin Wildman<sup>1</sup>, Mohammad Rehan<sup>1</sup>, Harunur Rashid<sup>1</sup>, Mohammad Hassan<sup>1</sup>, Chris Lengner<sup>2</sup>, Ajmad Javed<sup>1</sup>. <sup>1</sup>School of Dentistry, University of Alabama, United States, <sup>2</sup>School of Veterinary Medicine Member, Institute for Regenerative Medicine University of Pennsylvania, United States

We hypothesized that the unstable state produced by either loss-of-function of SWI-SNF remodeling activity or gain-of-function of PRC2 chromatin modification is critical for bone formation and development. Recently, we observed that an increase in miR-23a cluster and Ezh2 (member of PRC2 complex) expression or a relative decrease in BAF45a expression is inhibitory to bone formation. Current studies do not have any insight on how epigenetic remodeling and modification of bone-specific chromatin are maintaining bone mass *in vivo*. To address the above queries *in vivo*, we created and studied an inducible anti-miR-23a cluster (miR-23aCl<sup>ZIP</sup>) knockdown mouse model, an activating chromatin remodeler, Baf45a conditional mouse line (Baf45a<sup>fl/fl</sup>) and Ezh2 conditional mouse line (Ezh2<sup>fl/fl</sup>) (a catalytic subunit of the PRC2/EED-EZH2 complex, which methylates Lys-27 of histone H3). MiR-23a cluster knockdown mice developed high cortical and trabecular bone. RNA sequencing from these mice displayed increased expression Baf45a and Runx2 essential for skeletogenesis and decreased expression of Ezh2, a chromatin repressor indispensable for skeletogenesis. Osteoblast-specific Baf45a deletion (Baf<sup>fl/fl</sup>, Ocn-Cre) significantly reduced cortical and trabecular bone. ChIP assays using miR-23a cluster knockdown and Baf<sup>fl/fl</sup> calvarial cells demonstrated that Baf45a guided remodeling led H3K27 acetylation of osteoblast-specific open chromatin. Similar ChIP assays using miR-23a cluster gain and loss of function cells revealed that miR-23a guided Ezh2 recruitment led H3K27 methylation of osteoblast-specific close chromatin. Furthermore, we observed that Baf45a decreased the suppressive activity of Ezh2 to promoters of bone essential genes, for osteogenesis. Together, our findings strongly suggest that miR-23a cluster connection with tissue specific BAF-PRC2 function, linked to bone homeostasis, is a unique regulatory mechanism. Thus, this mechanism will be vital to the genetic basis of bone development, growth and maintenance further. Understanding of this mechanism is pivotal for further studies to identify specific targets for future therapies, which protect bone loss.

### Conclusion: The epigenetic mechanism of bone formation in vivo

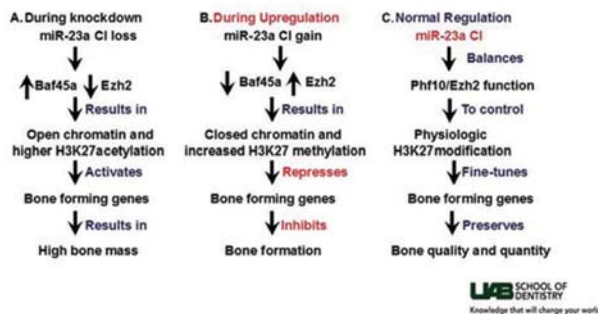


Figure 1

**Disclosures:** Tanner Godfrey, None.

## FR0157

**The in Vivo Roles of Osteoblast AMP-activated Protein Kinase in Skeletal Development.** Ippei Kanazawa<sup>\*</sup>, Ayumu Takeno, Ken-ichiro Tanaka, Masakazu Notsu, Toshitsugu Sugimoto. Shimane University Faculty of Medicine, Japan

**Background:** Bone and energy metabolism are closely associated with each other. AMP-activated protein kinase (AMPK) is a crucial regulator of energy and metabolic homeostasis. Previous *in vitro* studies have shown that AMPK plays important roles in osteoblast differentiation and mineralization. However, little is known about *in vivo* roles of osteoblast AMPK in bone development.

**Methods:** We conditionally inactivated *Ampr* in osteoblast (Ox)-expressing cells by crossing Ox-Cre mice with floxed AMPK $\alpha$ 1 (*Ampr*<sup>fl/fl</sup>) to generate mice lacking AMPK $\alpha$ 1 in osteoblasts (*Ampr*<sup>fl/fl</sup> mice). Micro-architecture of trabecular and cortical bone in distal femur was analyzed by micro-computed tomography (micro-CT) and histomorphometric analysis, and gene expression analysis was performed by real-time PCR in primary cultured osteoblasts from calvaria.

**Results:** Compared with the control mice, *Ampr*<sup>fl/fl</sup> mice displayed retardation of postnatal bone development although bone deformity was not observed at the birth. micro-CT analysis showed significant reductions in trabecular bone volume, cortical bone length and density, and increased cortical porosity in 8-week *Ampr*<sup>fl/fl</sup> mice. Surprisingly, histomorphometric analysis demonstrated that the number of osteoclasts was significantly increased, although the number of osteoblasts or bone formation rate was not altered. Moreover, loss of trabecular network connections and mass as well as shortened growth plate and reduced thickness of cartilage adjacent to the growth plate were observed in *Ampr*<sup>fl/fl</sup> mice, compared to the controls. In primary cultured osteoblasts, the expressions of alkaline phosphatase, type 1 collagen, osteocalcin, BMP-2, Runx2, and Osterix were significantly inhibited in the *Ampr*<sup>fl/fl</sup> osteoblasts, whereas the expression of RANKL and RANKL/osteoprotegerin ratio were significantly increased.

**Conclusion:** These findings indicated that osteoblastic AMPK plays important roles in bone development *in vivo*, and that deletion of AMPK in osteoblasts decreased osteoblastic differentiation and enhanced bone turnover by increasing RANKL expression.

**Disclosures:** Ippei Kanazawa, None.

## FR0158

**Murine model for type VI OI (*Serpinf1*<sup>-/-</sup>) reveals dynamic regulation of vascularization and mineralization in bone.** Heeseog Kang<sup>\*</sup>, Smriti Aryal A.C.<sup>1</sup>, Valentin David<sup>2</sup>, Aline Martin<sup>2</sup>, Susan Crawford<sup>3</sup>, Joan Marini<sup>1</sup>. <sup>1</sup>NIH, United States, <sup>2</sup>Northwestern University, United States, <sup>3</sup>NorthShore University, United States

Null mutations in *SERPINF1*, encoding Pigment Epithelium-Derived Factor (PEDF), cause type VI osteogenesis imperfecta (OI), a progressive deforming OI characterized by accumulation of unmineralized osteoid *in vivo* and delayed mineralization *in vitro*. An atypical form of type VI OI is caused by a p.S40L substitution in BRIL, the gene in which a 5'-UTR mutation causes type V OI. Demonstration of decreased PEDF in bone with BRIL p.S40L provided evidence of a connection between types VI and V OI. Prior to identification as the cause of type VI OI, PEDF was well-known for its potent anti-angiogenic effects, which depend on direct interaction of PEDF with collagen in matrix. Bone vascularization is crucial for bone modeling and remodeling, with endothelial cells secreting factors that affect osteoprogenitor differentiation. We utilized RNA-seq of differentiating *Serpinf1*<sup>-/-</sup> calvarial osteoblasts (OB), validated by RT-qPCR, whole animal vascular perfusion and type H endothelial cells (CD31<sup>+</sup>/Endomucin<sup>+</sup>) isolated from crushed LE long bone by FACS, to explore the relationship of bone vascularization and mineralization in OI. These studies revealed biphasic regulation of bone vascularization pathways by PEDF in osteoblasts. In PEDF-null cells, pro-angiogenic *VEGF* is elevated early in differentiation (3.5x increased vs. WT at Day 7). However, on Day 14 of differentiation *BMPER* (BMP-binding endothelial regulator, a protein which inhibits the BMP-mediated positive effect on VEGF transcription) is significantly increased in KO vs. WT OB, potentially compensating for VEGF elevation. *In-vivo*, PEDF deletion results in a significant increase in vessel density by 33% (P < 0.05) in the tibial periosteum of BaSO<sub>4</sub> perfused KO mice. In agreement, the number of type H ECs is increased in KO mice by 18% (P < 0.05), as are type H cell VEGF and VEGF receptor 2 transcripts, suggesting an overall pro-angiogenic effect. In contrast, decreased expression of osteoblastic markers of differentiation and mineralization *Sp7*, *Col1a1*, *Ibsp*, *Sost* and *Dmp1* was observed in KO cells. Interestingly, BRIL expression is also reduced, demonstrating reciprocity of the effects of BRIL on PEDF. In line with these findings, Alizarin Red staining of KO OB yielded a delay of mineralization at Week 2 but increased mineralization at Week 4 vs. WT. These results demonstrate complex regulation of vascularization and mineralization by *SERPINF1*/PEDF and we are exploring the potential interaction of these pathways.

**Disclosures:** Heeseog Kang, None.

## FR0160

**A novel osteoblast subpopulation initiates endochondral ossification by forming osteogenic capillaries.** Yukiko Kuroda<sup>\*</sup>, Ayako Sakamoto<sup>1</sup>, Masaki Yoda<sup>1</sup>, Yanlin Wu<sup>2</sup>, Hidekazu Takano<sup>2</sup>, Atsushi Momose<sup>2</sup>, Koichi Matsuo<sup>1</sup>. <sup>1</sup>Keio University School of Medicine, Japan, <sup>2</sup>Tohoku University, Japan

Mammalian skeleton largely consists of endochondral bones built by developmental replacement of cartilage with bone. Osteoblasts deposit bone matrix after chondroclasts have resorbed calcified cartilage matrix, but whether specialized osteoblasts initiate depositing bone matrix on the cartilage is unknown. Our previous study revealed that endochondral ossification progresses by forming "osteogenic capillaries" in the malleus, which is one of the auditory ossicles. Osteogenic capillaries are composed of endomucin-positive endothelial cells associated with osteoblasts, and the capillary lumens are narrowed as bone matrix is produced by osteoblasts around the capillaries. Here we report a novel type of osteoblast subpopulation presents the earliest in the cartilage after vascular invasion. These osteoblasts produce bone mineral matrix on calcified cartilage as visualized using synchrotron X-ray tomographic microscopy. Unexpectedly, they express alkaline phosphatase, Runx2, and osteocalcin at high levels, but express lower levels of the collagen  $\alpha$ 1(I) gene (*Col1a1*) than conventional osteoblasts. The lower *Col1a1* expression was at a promoter level and was confirmed by *in situ* hybridization and immunostaining. *Col1a1*<sup>low</sup> osteoblasts and endothelial cells form osteogenic capillaries in the ossifying malleus. Osteocalcin, but not alkaline phosphatase expression in *Col1a1*<sup>low</sup> osteoblasts was impaired in osteopetrotic mice suggesting that chondroclasts

are crucial for the maturation of *Col1a1*<sup>low</sup> osteoblasts. Despite the low *Col1a1* expression, bone mineral density of the malleus was higher than that of the femoral diaphysis, suggesting that compositional changes of bone matrix produced by *Col1a1*<sup>low</sup> osteoblasts may be responsible for the altered bone quality. Thus, *Col1a1*<sup>low</sup> osteoblasts are distinct from conventional osteoblasts, and lay down unusual bone matrix with reduced type I collagen  $\alpha 1$  chain on the cartilage surface. We propose that these cells be called "endochondral osteoblasts".

**Disclosures:** Yukiko Kuroda, None.

## FR0163

**WNT16 Overexpression Protects Against Glucocorticoid-Induced Bone Loss.** Karin Nilsson\*, Sofia Movérare-Skrtic, Petra Henning, Jianyao Wu, Karin Gustafsson, Matti Poutanen, Ulf Lerner, Claes Ohlsson. Centre for Bone and Arthritis Research, Institute of Medicine, Sahlgrenska Academy, University of Gothenburg, Gothenburg, Sweden

Therapeutic use of glucocorticoids (GCs) is a major cause of bone loss and fractures. Although the underlying pathogenic mechanisms involve both decreased bone formation and increased bone resorption, the molecular mechanisms responsible for the deleterious effects of GCs are only partially understood. Recently we demonstrated that endogenous WNT16 is a crucial physiological regulator of cortical but not trabecular bone while pharmacological overexpression of WNT16 by a transgene also increases trabecular bone mass (<sup>1</sup>Movérare-Skrtic, Nat Med, 2014, <sup>2</sup>Movérare-Skrtic, PNAS, 2015). This difference between the physiological and pharmacological role of WNT16 is most likely the result of high endogenous WNT16 expression in cortical but not trabecular bone.

Here, we hypothesize that disturbed WNT16 activity might be involved in the deleterious effects of GC in bone. We first observed that GC-treatment (7.6 mg/kg/day of prednisolone) decreased the *Wnt16* mRNA levels in bone of female mice (-56.4±6.1% compared to vehicle, p<0.01). We next evaluated if WNT16 overexpression protects mice against GC-induced bone loss by treating 12-week-old female *Obl-Wnt16* mice (WNT16 expression driven by the rat procollagen type I  $\alpha 1$  promoter) and WT littermates with a subcutaneous slow-release pellet of prednisolone (7.6 mg/kg/day) or placebo for 4 weeks. GC-treatment did not reduce the high *Wnt16* mRNA levels in the bone of *Obl-Wnt16* mice. DXA analyses revealed that GC-treatment decreased total body bone mineral density in WT mice (-3.92±1.2%, p<0.05), but not in *Obl-Wnt16* mice (+1.29±1.4%, non-significant, n.s.). We then evaluated the trabecular and cortical bone separately using  $\mu$ CT. GC-treatment significantly decreased trabecular bone volume fraction (BV/TV) of the femur in WT mice (-14.3±3.2%, p<0.05) but not in *Obl-Wnt16* mice (-6.5±3.1%, n.s.). Also, serum levels of the bone formation marker PINP, procollagen type I N-terminal propeptide, were strongly reduced by GC-treatment in WT mice (-50.3±7.0%, p<0.01) but not in *Obl-Wnt16* mice (-3.8±21.2%, n.s.). However, the cortical bone thickness in the mid-diaphyseal region of femur was reduced by GC-treatment in both WT mice (-14.8±1.6%, p<0.01) and *Obl-Wnt16* mice (-12.8±0.6%, p<0.01).

In conclusion, GC-treatment decreases *Wnt16* mRNA levels in bone and WNT16 overexpression protects against GC-induced trabecular but not cortical bone loss.

### References:

1. Movérare-Skrtic S, et al. *Nature Medicine* 2014; 20:1279
2. Movérare-Skrtic S, et al. *PNAS* 2015; 112:14972

**Disclosures:** Karin Nilsson, None.

## FR0166

**Transcriptional Coactivator JAB1 Promotes Osteoblast Differentiation and Postnatal Bone Formation.** William Samsa\*, Lindsay Bashur, Murali Mamidi, Guang Zhou. Case Western Reserve University, United States

JAB1, also known as COPS5/CSN5, is a part of the evolutionarily conserved COP9 signalosome complex that plays a vital role in the regulation of many signal transduction pathways. We previously showed that Jab1 regulates the master transcription factors Sox9, Runx2, and the BMP signaling pathway during chondrogenesis in a spatiotemporal-specific manner. Indeed, using a Col2a1-cre driver, the cartilage-specific Jab1-null mutants had severely impaired endochondral ossification with enhanced Runx2 expression and increased BMP signaling. Furthermore, when Jab1 was deleted in endochondral progenitor cells of the limb buds using a Prx1-cre driver, mice exhibited drastically shorter limbs and decreased Sox9 and BMP signaling activity. In this study, we hypothesize that Jab1 is also essential for osteoblast progenitor cell differentiation in vivo through the control of BMP signaling. Using ex vivo cultures of mouse calvarial osteoblasts, we altered Jab1 expression by either gene silencing or overexpression via adenovirus infection and examined the effect on osteoblast differentiation. We found that osteoblasts deficient in Jab1 had impaired osteoblast differentiation and mineralization, with decreased expression of osteoblast differentiation marker Osteocalcin and reduced von Kossa staining after 21 days in osteogenic medium. Furthermore, osteoblasts deficient in Jab1 had an altered response to BMP treatment, likely leading to an increased expression of non-canonical ERK1/ERK2 signaling. To determine the role of Jab1 in bone development in vivo, we knocked out Jab1 specifically in differentiating osteoblasts using a 2.3kb Col1a1-cre driver, but these mice had no gross phenotype. However, when we deleted Jab1 specifically in committed osteoblast progenitors using an Osterix-cre driver, these mutant mice appeared normal at birth but developed progressively severe dwarfism and all died prior to weaning. Histological analysis of

long bones from these mutant mice showed a decreased trabecular bone formation by postnatal day 2, and a smaller secondary ossification center by postnatal day 6. Furthermore, by postnatal day 18-21, the mutant epiphyseal growth plates had a reduced hypertrophic zone, drastically disintegrated secondary trabeculae, and altered bone compartment, hinting at defective hematopoiesis. In conclusion, Jab1 plays an important stage-specific role in postnatal bone development and homeostasis by positively regulating osteoblast differentiation.

**Disclosures:** William Samsa, None.

## FR0168

**Tgfr1 Controls Bone Remodeling and Anabolic Response to Parathyroid Hormone.** Hanna Taipaleenmäki\*, Hiroaki Saito<sup>1</sup>, Andreas Gasser<sup>1</sup>, Simona Bolamperti<sup>1</sup>, Miki Maeda<sup>1</sup>, Matthias Ring<sup>1</sup>, Yang Shi<sup>1</sup>, Levi Matthies<sup>1</sup>, Hartmut Schlüter<sup>2</sup>, Steven A. Johnsen<sup>3</sup>, Katharina Jähn<sup>1</sup>, Courtney L. Long<sup>1</sup>, Carl Haasper<sup>4</sup>, Thorsten Gehrke<sup>4</sup>, Vaibhav Saini<sup>5</sup>, Paola Divieti Pajevic<sup>5</sup>, Teresita Bellido<sup>6</sup>, Andre van Wijnen<sup>7</sup>, Khalid S Mohammad<sup>8</sup>, Theresa Guise<sup>8</sup>, Eric Hesse<sup>1</sup>. <sup>1</sup>Molecular Skeletal Biology Laboratory, Department of Trauma, Hand and Reconstructive Surgery, University-Medical Center Hamburg-Eppendorf, Germany, <sup>2</sup>Institute of Clinical Chemistry and Laboratory Medicine, University Medical Center Hamburg-Eppendorf, Germany, <sup>3</sup>Department of General, Visceral and Pediatric Surgery, Göttingen Center for Molecular Biosciences, University Medical Center Göttingen, Germany, <sup>4</sup>HELIOS ENDO Hospital Hamburg, Germany, <sup>5</sup>Department of Molecular and Cell Biology, Boston University, School of Dental Medicine, United States, <sup>6</sup>Department of Anatomy and Cell Biology, Indiana University School of Medicine, United States, <sup>7</sup>Department of Biochemistry and Molecular Biology, Department of Orthopedic Surgery, Mayo Clinic, United States, <sup>8</sup>Division of Endocrinology, Department of Medicine, Indiana School of Medicine, United States

Bone formation is often decreased during aging-related bone loss but can be activated by the intermittent administration of parathyroid hormone (PTH) to treat patients at advanced stages of osteoporosis. Bone is formed by osteoblasts, whose activity is controlled by signaling pathways and regulatory factors, including homeodomain proteins. To identify novel stimulators of bone formation, we performed an unbiased screen in mouse bone marrow stromal cells and identified the TG-interacting factor 1 (Tgfr1) among the most abundantly expressed homeodomain proteins. To determine the physiological role of Tgfr1 in bone, we generated mice with a germ-line deletion of Tgfr1 (*Tgfr1*<sup>-/-</sup>). In vitro culture revealed an impaired differentiation of *Tgfr1*<sup>-/-</sup> osteoblasts. Consistent with this finding, the number and activity of osteoblasts and the bone formation rate were decreased in tibiae of 8-week old *Tgfr1*<sup>-/-</sup> mice and in mice in which Tgfr1 was deleted within the osteoblast lineage using two different conditional knockout systems (*Osx1*- and *Dmp1*-Cre). Interestingly, despite an impaired bone formation, bone mass was unchanged due to a concomitant decrease in bone resorption, suggesting that Tgfr1 in osteoblasts supports osteoclast activity. To unravel the underlying mechanism, we performed unbiased SILAC and RNA-seq analyses and identified Semaphorin 3E (Sema3E) to be abundantly secreted by *Tgfr1*<sup>-/-</sup> osteoblasts. An in vitro co-culture system revealed that siRNA-mediated downregulation of Sema3E expression in *Tgfr1*<sup>-/-</sup> osteoblasts dose-dependently restored the reduced osteoclast differentiation. These data demonstrate that Tgfr1 is a novel factor that supports bone formation directly and bone resorption indirectly in a Sema3E-dependent manner. Due to its role in bone formation, we tested if Tgfr1 is implicated in the PTH pathway. Indeed, PTH-receptor signaling increased Tgfr1 expression in osteoblasts through the PKA-CREB pathway, which activated an AP1 regulatory element within the Tgfr1 promoter. In addition, PTH treatment failed to increase bone mass in *Tgfr1*<sup>-/-</sup> and *Dmp1*-Cre;*Tgfr1*<sup>fl/fl</sup> mice due to a persistent expression of sclerostin, which was decreased in the bones of control littermates. Furthermore, analysis of human bone specimen revealed that Tgfr1 expression is associated with a higher bone mass. In summary, our data establish Tgfr1 as a novel regulator of bone remodeling and PTH target gene that is necessary to elicit PTH bone anabolic action.

**Disclosures:** Hanna Taipaleenmäki, None.

## FR0169

**Cdk 1 is essential for bone formation and fracture repair.** Hiroyuki Inose\*, Akira Takahashi<sup>2</sup>. <sup>1</sup>Orthopedics, Japan, <sup>2</sup>Kyushu University, Japan

### Introduction

Bone remodeling, consisting of bone formation by osteoblasts and bone resorption by osteoclasts, is an essential process regulating bone mass and strength. So far, there have been many reports regarding the mechanism of osteoblast differentiation. While previous works have established the essential role of transcription factors, such as Runx2 and Osterix, in osteoblast differentiation, the regulatory mechanism of osteoblast proliferation remains unclear. The aim of our study was to investigate the role of cyclin dependent kinase1 (hereafter Cdk1) in bone metabolism.

### Methods and Results

As the differentiation of osteoblast-like MC3T3-E1 cells proceeded, the expression of Cdk1 gradually decreased. Knockdown of Cdk1 in MC3T3-E1 cells resulted in the



inhibition of the cell proliferation. While the treatment with parathyroid hormone (hereafter PTH) promoted the proliferation of osteoblasts, PTH failed to promote proliferation of osteoblasts stably knocked down Cdk1. Since conventional Cdk1 knock-out mouse leads to embryonic lethality, we generated osteoblast-specific Cdk1 knockout mouse (hereafter CKO mouse) using Osterix promoter. CKO mice exhibited significantly less bone volume than wild type (hereafter WT) mice at 12-week old. Bone histomorphometric analysis revealed significantly less mineral apposition rate and bone formation rate in CKO mice. Finally, to investigate the effect of Cdk1 on fracture repair, we employed a mouse femur fracture model. Whereas control mice had fracture healing at six weeks after the fracture, the CKO mice had impaired fracture healing.

#### Discussion and Conclusions

Though cell cycle regulatory proteins have been reported to be important for cell proliferation, no cell cycle regulatory protein has been shown to regulate osteoblast proliferation through cell specific loss of function experiments in vivo. Our data suggests that Cdk1 is essential for not only bone formation but also for fracture repair. Furthermore, our results suggested the involvement of Cdk1 in PTH signaling pathway.

**Disclosures:** Hiroyuki Inose, None.

## FR0170

**Bone loss in genetic Hfe-hemochromatosis is driven by the actions of Hfe in the osteoblasts and not by the excess of iron.** Maja Vujic Spasic\*. Institute of Comparative Molecular Endocrinology, Ulm University, Germany

Acquired and inherited iron overload disorders constitute an increasing public health problem worldwide. The most prevalent hereditary hemochromatosis (HH) disorder is caused by mutations in the *HFE* gene resulting in excessive iron absorption from the diet and iron deposition in tissues causing multiple organ damage and failure. Clinical data have raised a considerable attention to the correlation between massive iron overload in HH and the development of osteoporosis, however the exact mechanism leading to bone loss in HFE-HH is unknown.

The aim of our study was to unveil the cause of bone loss in Hfe-HH. More precisely, we questioned whether iron overload or selective actions of Hfe in bone cells contribute HH osteoporosis.

To address the contribution of iron to bone loss, we compared bone status between mice with constitutive (*Hfe*<sup>-/-</sup>) and selective hepatocytic *Hfe* deficiency, since these two models present similar systemic iron levels. Furthermore, the consequence of the lack of *Hfe* in osteoblasts was evaluated in constitutive *Hfe* knock-out and in mice with osteoblast-specific *Hfe* deletion.

We show that *Hfe*<sup>-/-</sup> mice develop osteoporosis with low bone mass and alteration of the microarchitecture in regard to control mice, contrasting the observations in hepatocyte-specific *Hfe*-deficient mice. These data imply that iron is not the central contributor in the development of osteoporosis in *Hfe*-HH. Furthermore, we show that lack of *Hfe* in osteoblasts, derived from constitutive and osteoblast-specific *Hfe*-deficient mice, greatly decreased alkaline phosphatase activity and the expression of several osteoblast-markers. The observed effect could be reverted by over-expressing *Hfe* in these cells. By contrast, the lack of *Hfe* in osteoclasts did not affect their functions thus excluding the contribution of *Hfe* in these cells to bone loss.

Our data highlight a previously unrecognized action of *Hfe* in bone metabolism being required for the osteoblast differentiation and bone integrity.

**Disclosures:** Maja Vujic Spasic, None.

## FR0172

**YAP and TAZ expression in mesenchymal progenitors versus mature osteoblasts and osteocytes plays distinct roles in osteoblastogenesis.** Jinhu Xiong\*, Priscilla Baltz, Charles O'Brien. University of Arkansas for Medical Sciences, United States

YAP (Yes associated protein) and TAZ (transcriptional co-activator with PDZ-binding motif) are related transcription cofactors that function in a redundant manner. In vitro studies suggest that high extracellular matrix rigidity enhances osteoblast differentiation by promoting YAP and TAZ nuclear translocation. TAZ is also required for bone formation in zebrafish. However, other in vitro studies show that YAP and TAZ suppress osteoblast differentiation. Here we sought to clarify the role of YAP and TAZ in osteoblast differentiation by deleting these genes from cells at different stages of the mesenchymal lineage in mice using *Prx1-Cre*, *Osx1-cre*, and *Dmp1-Cre* transgenes. Complete loss of YAP and TAZ in cells targeted by *Prx1-Cre* or *Osx1-Cre* caused embryonic lethality. However, mice with haploinsufficiency of YAP and complete lack of TAZ in mesenchymal progenitors (*Prx1-Cre*; *YAP*<sup>f/f</sup>; *TAZ*<sup>f/f</sup>) developed normally. At 5 weeks of age, *Prx1-Cre*; *YAP*<sup>f/f</sup>; *TAZ*<sup>f/f</sup> mice displayed high cancellous bone volume and elevated cortical thickness associated with an increased bone formation rate. We used suppression of the *Osx1-Cre* transgene by doxycycline to delete YAP and TAZ postnatally in osteoblast progenitors. Breeders and offspring were maintained on doxycycline-containing diet until one month of age and then kept on regular diet for an additional month before analysis. Histological analysis of vertebra at 2 months of age revealed increased osteoblast number in *Osx1-Cre*; *YAP*<sup>f/f</sup>; *TAZ*<sup>f/f</sup> mice compared to *Osx1-Cre* controls. Ex vivo culture of bone marrow cells from *Prx1-Cre*; *YAP*<sup>f/f</sup>; *TAZ*<sup>f/f</sup> or *Osx1-Cre*; *YAP*<sup>f/f</sup>; *TAZ*<sup>f/f</sup> mice revealed increased osteoblast differentiation, enhanced Wnt signaling, and increased Runx2 activity. Mice lacking both YAP and TAZ in cells targeted by the *DMP1-Cre* transgene were born at the expected frequency and had normal size. At 12 weeks of age, *DMP1-Cre*; *YAP*<sup>f/f</sup>; *TAZ*<sup>f/f</sup> mice exhibited low cancellous bone volume and cortical thickness associated with decreased osteoblast

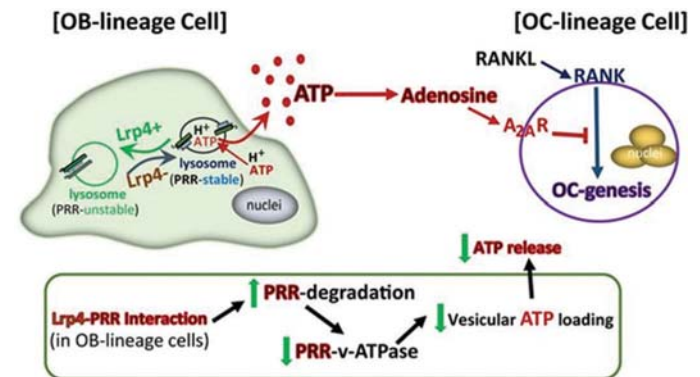
number and bone formation rate together with increased osteoclast number. Together, these results demonstrate that YAP and TAZ activity in mesenchymal progenitors inhibits their differentiation into osteoblasts whereas these factors expressed in mature osteoblasts and osteocytes promote osteoblast number and bone formation but suppress osteoclastogenesis. Moreover, and in contrast to zebrafish, TAZ expression in mesenchymal progenitors is dispensable for osteoblastogenesis in mice.

**Disclosures:** Jinhu Xiong, None.

## FR0173

**Osteoblastic Lrp4 Promotes Osteoclastogenesis by Regulating ATP Release and Adenosine-A<sub>2A</sub>R Signaling.** Lei Xiong<sup>\*1</sup>, Ji-Ung Jung<sup>2</sup>, Hao-Han Guo<sup>1</sup>, Jin-Xiu Pan<sup>1</sup>, Xiang-Dong Sun<sup>2</sup>, Lin Mei<sup>1</sup>, Wen-Cheng Xiong<sup>1</sup>. <sup>1</sup>Department of Neuroscience and Regenerative Medicine, and Department of Neurology, Medical College of Georgia; Charlie Norwood VA Medical Center, United States, <sup>2</sup>Department of Neuroscience and Regenerative Medicine, and Department of Neurology, Medical College of Georgia, United States

Bone homeostasis depends on the functional balance of osteoblasts (OBs) and osteoclasts (OCs). Each releases secreted factors that regulate the function of the other. Lrp4 (low-density lipoprotein receptor-related protein 4) is a transmembrane protein, which is mutated in patients with high bone-mass such as sclerosteosis and Van Buchem diseases. Loss of Lrp4 in OB-lineage cells increases bone-mass by elevating bone formation by OBs and reducing bone resorption by OCs. However, the underlying mechanisms remain unclear. To better understand how Lrp4-deficiency in OBs impairs osteoclastogenesis, we conditionally deleted Lrp4 in OB-lineage cells by using *Ocn-Cre* transgenic mice and floxed Lrp4 mice. BMMs from osteoblastic Lrp4 mutant mice or BMMs treated with conditioned medium (CM) of Lrp4-deficient OB-lineage cells showed reduced OC differentiation by using TRAP staining and FACS analysis. To identify the secreted factors that inhibit OC genesis, we analyzed the CMs of WT and Lrp4-deficient BMSCs and found increased levels of ATP and its derivative, pyrophosphate (PPi) and adenosine in extracellular compartments of Lrp4-deficient OB-lineage cells. Inactivation of adenosine-A<sub>2A</sub>R signaling by using SCH58261 treatment or A<sub>2A</sub>R knockout diminished receptor activator of nuclear factor  $\kappa$ B (RANK)-mediated osteoclastogenesis deficit and reduced trabecular bone mass in Lrp4<sup>Ocn-cko</sup> mice, demonstration a critical role for adenosine-A<sub>2A</sub>R signaling in the inhibition of OC genesis. In addition, Lrp4-deficient OB-lineage cells showed increased V-ATPase activity and vesicular acidification. Bafilomycin A1, an inhibitor of V-ATPase, could abolish increased vesicular ATP loading and release from Lrp4 mutant BMSCs, suggesting an enhanced V-ATPase-dependent ATP release. Further mechanistic studies indicated that Lrp4 interacted with pre-receptor (PRR), a component of V-ATPase. Lrp4 mutation in osteoblast-lineage cells stabilized PRR and thus increased PRR/V-ATPase-driven vesicular ATP release. Taken together, these results identify a mechanism by which osteoblastic Lrp4 controls osteoclastogenesis by regulating PRR/V-ATPase activity, reveal a cross talk between A<sub>2A</sub>R and RANK signaling in osteoclastogenesis, and uncover an unrecognized pathophysiological mechanism of high bone-mass disorders.



Model

**Disclosures:** Lei Xiong, None.

## FR0174

**Direct Reprogramming of Human Fibroblasts into Osteoblasts for Osteogenic Cell Therapy.** Kenta Yamamoto<sup>\*1</sup>, Toshihisa Kawai<sup>1</sup>, Tsunao Kishida<sup>2</sup>, Osam Mazda<sup>2</sup>. <sup>1</sup>Nova Southeastern University, United States, <sup>2</sup>Kyoto Prefectural University of Medicine, Japan

**Objective:** Osteoblasts (OBs) play a central role in remodeling the skeletal system through osteogenesis. However, such age/hormone-related osteolytic diseases as periodontitis or osteoporosis significantly reduce both activity and number of OB progenitors. An ideal cell therapy for predictable and efficient bone regeneration typically utilizes autologous stem cells or iPS cells. This approach is, however, limited by the number of available authentic stem cells as well as cost- and time-consuming procedures.

Therefore, we herein introduce a method of directly reprogramming human fibroblasts into functional OBs as a novel bone regenerative cell therapy.

**Methods:** Primary culture of human fibroblasts were developed from discarded gingiva and skin transfected with Runx2, Osterix (Osx), Oct4 and L-Myc genes using a retroviral or polycistronic plasmid vector, and then cultured in osteogenic medium. The resultant cells were tested *in vitro* for expressions of OB-specific genes, the production of calcified bone matrix, and the epigenetic status of the cells. Direct conversion of fibroblasts into OB-like cells, but without intermittent transformation into pluripotent stem cells, was also evaluated. To assess *in vivo* efficacy, the resultant cells were transplanted into critical-sized defect (CSD) created in femur of immunodeficient NOD/SCID mice.

**Results:** Gene transfection induced osteocalcin- and ALP-positive OB-like cells with a high degree of efficiency using retroviral vector, but less so using polycistronic plasmid vector. The resultant cells also produced mineralized bone matrix. Such reprogrammed OB-like cells demonstrated a genomic methylation status distinct from original fibroblasts, while, at the same time, displaying a gene expression profile similar to that of normal OBs, but excluding stem cell-related genes. These results suggest successful direct transformation of fibroblasts into OBs. Finally, using micro-CT and immunohistochemistry, it was determined that directly reprogrammed OBs facilitated efficient bone regeneration following transplantation into CSD.

**Conclusion:** For the first time, this technique allowed direct reprogramming of human somatic cells into OBs through transfection of defined genes, which solves many limitations associated with the using of autologous stem cells or iPS cells, including time and cost, potential carcinogenesis, and availability of vital mesenchymal stem cells from aged patient.

**Disclosures:** Kenta Yamamoto, None.

## FR0175

**Inactivation of Wnt Receptor Regulators, Rnf43 and Znf3, in Osteoblasts Augments Bone Mass.** Zhendong A. Zhong<sup>1\*</sup>, Cheryl N. Christie<sup>1</sup>, Mitch J. McDonald<sup>1</sup>, Nicole J. Ethen<sup>1</sup>, Cassandra R. Diegel<sup>1</sup>, Bart O. Williams<sup>2</sup>. <sup>1</sup>Van Andel Research Institute, United States, <sup>2</sup>Van Andel Research Institute, United States

Wnt signaling is one of the most important pathways that regulate bone development and homeostasis. Wnt receptors, known as Frizzled (Fzd), are engaged by Wnt ligands to activate canonical ( $\beta$ -catenin catenin-independent) pathways. However, Fzd has 10 identified isoforms with and TCF-dependent) pathways and non-canonical ( $\beta$ -compensatory functions in cell- and tissue-dependent manners, which makes it difficult to study this crucial Wnt pathway component.

Rnf43 and Znf3 (R/Z) are E3 ubiquitin ligases that ubiquitinate Fzds on the cell membrane and target them for degradation. Our initial findings implicate R/Z genes as sensitive targets of canonical Wnt signaling in a number of osteoblastic cell lines and primary calvarial cells; Rnf43 expression increased significantly with osteoblast maturation (> 300 fold by 21 days) while Znf3 slightly decreased with differentiation. The inactivation of R/Z genes in calvarial cells significantly increased the responses to Wnt stimulation in both canonical and non-canonical (YAP/TAZ activation) Wnt pathways, and accelerated osteoblast differentiation and mineralization *in vitro*.

We crossed osteoblast-specific Ocn (osteocalcin)- Cre mice to mice with Rnf43-flox and/or Znf3-flox alleles. Although body weight and size were not different, Z-only knockouts (Z-cKO) or R/Z double knockouts (R/Z-cKO) showed significantly increased bone mineral density (BMD) and bone mineral content (BMC) by whole-body dual-energy x-ray absorptiometry (DXA), compared to wild-type littermates. The increases in BMD/BMC between R-cKO and R/Z-cKO mice were comparable. Mice lacking R only (R-cKO) displayed normal bone phenotypes. Unexpectedly, microCT analysis of mutant femoral bones showed significantly lower BV/TV ratio in the metaphysis and decreased cortical bone thickness in the diaphysis. Interestingly, mid-shaft bone perimeter and bone perimeter/femur length ratio increased significantly in Z-cKO mice and increased even more dramatically in R/Z-cKO mice (Figure 1). Further comprehensive characterization of this mouse model is ongoing.

In conclusion, we identified R/Z as downstream Wnt targets and osteoblast differentiation markers. The inactivation of R/Z *in vitro* could potentiate Wnt activation and osteoblast differentiation, while R/Z knockouts *in vivo* caused a complex high-bone-mass phenotype. Future work will focus on dissecting how R/Z affects osteogenesis through canonical and non-canonical Wnt pathways.

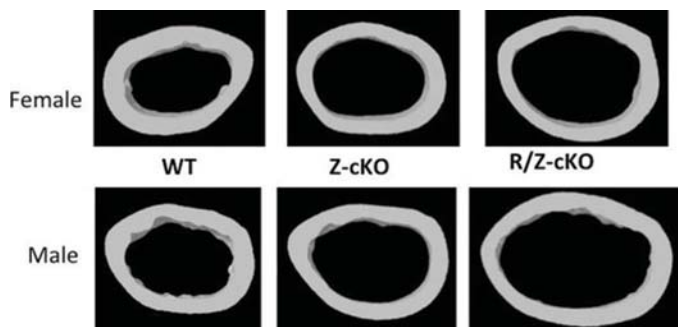


Figure 1

**Disclosures:** Zhendong A. Zhong, None.

## FR0176

**Osteoclast-specific TSC2 deletion increases bone mass via increasing CTHRC1 and bone formation by osteoblasts.** Nicola Alesi<sup>1\*</sup>, Julia F. Charles<sup>2</sup>, Elizabeth P. Henske<sup>1</sup>, David J. Kwiatkowski<sup>1</sup>, Haoming Liu<sup>2</sup>, Sabah Nobakhti<sup>3</sup>, Sandra J. Shefelbine<sup>3</sup>. <sup>1</sup>Division of Pulmonary and Critical Care Medicine, Department of Medicine, Brigham and Women's Hospital and Harvard Medical School, Boston, Massachusetts, USA, United States, <sup>2</sup>Division of Rheumatology, Allergy, and Immunology, Department of Medicine, Brigham and Women's Hospital and Harvard Medical School, Boston, Massachusetts, USA, United States, <sup>3</sup>Department of Mechanical and Industrial Engineering, Northeastern University, Boston, Massachusetts, USA, United States

Normal bone is remodeled by the actions of bone forming osteoblasts and bone resorbing osteoclasts (OC). The tuberous sclerosis complex (TSC) is a critical negative regulator of the mammalian target of rapamycin complex 1 (mTORC1) with two essential subunits, TSC1 and TSC2. mTORC1 integrates information about growth factor and nutrient availability to modulate cell function. To examine the function of TSC in OC, we crossed *Cathepsin K-Cre* (*Ctsk-Cre*) mice, where *Cre* is expressed in OC, with *Tsc2<sup>fl/fl</sup>* mice, to generate *Ctsk-Cre; Tsc2<sup>fl/fl</sup>* mice (subsequently denoted *Tsc2<sup>ΔOC</sup>*). Trabecular bone mass, cortical thickness, number of trabeculae, periosteal area and circumference are elevated by 1.5 to 2-fold in 3 mo old *Tsc2<sup>ΔOC</sup>* mice of both sexes. With aging, *Tsc2<sup>ΔOC</sup>* mice continue to accrue both trabecular and cortical bone.

We hypothesized that *Tsc2* deficiency compromises OC differentiation or function. However, *ex vivo* differentiation and resorptive function of OC derived from *Tsc2<sup>ΔOC</sup>* mice was indistinguishable from WT. OC function *in vivo* was also unaffected, as serum C-terminal telopeptide of type I collagen (CTX-I), an established marker of osteoclast resorptive activity, was similar in *Tsc2<sup>ΔOC</sup>* and WT mice at 3 and 9 mo of age. Thus, the *Tsc2<sup>ΔOC</sup>* high bone mass phenotype is not due to loss of OC function. In contrast, serum levels of procollagen type I N propeptide (PINP), a marker of osteoblast activity, is elevated approximately 2-fold in all groups of *Tsc2<sup>ΔOC</sup>* mice, suggesting that loss of TSC2 in OC stimulates bone formation. Three-point bending tests on *Tsc2<sup>ΔOC</sup>* femurs demonstrated increased mechanical strength, with increased stiffness and ultimate load. This suggests that the increased bone formation rate does not compromise bone biomechanical properties.

To address the molecular mechanism of the high bone mass phenotype in *Tsc2<sup>ΔOC</sup>* mice, we hypothesized that an OC-derived molecule capable of increasing osteoblast function was involved, and evaluated several candidates including CTHRC1 (collagen triple helix related containing 1), a secreted glycoprotein reported to be expressed by OC. CTHRC1 was increased in *Tsc2<sup>ΔOC</sup>* bone at both mRNA (11 fold) and protein level (3 to 5 fold). We conclude that mTORC1 may promote OC production of CTHRC1, thereby stimulating osteoblastic bone formation. These data suggest the involvement of osteoclasts in the pathogenesis and functional consequences of sclerotic bone lesions in TSC.

**Disclosures:** Nicola Alesi, None.

## FR0177

**Bone matrix components activate the NLRP3 inflammasome and promote osteoclast differentiation.** Yael Alippe<sup>1\*</sup>, Chung Wang<sup>1</sup>, Biancamaria Ricci<sup>2</sup>, Jianqiu Xiao<sup>3</sup>, Wei Zou<sup>4</sup>, Deborah Novack<sup>2</sup>, Yousef Abu-Amer<sup>2</sup>, Roberto Civitelli<sup>3</sup>, Gabriel Mbalaviele<sup>3</sup>. <sup>1</sup>Division of Bone and Mineral Diseases - Washington University School of Medicine, United States, <sup>2</sup>Department of Orthopaedic Surgery-Washington University School of Medicine, United States, <sup>3</sup>Division of Bone and Mineral Diseases-Washington University School of Medicine, United States, <sup>4</sup>Department of Pathology and Immunology-Washington University School of Medicine, United States, <sup>5</sup>Division of Bone and Mineral Disease-Washington University School of Medicine, United States

The NLRP3 inflammasome is responsible for the maturation of IL-1 $\beta$  in response to a variety of signals referred to as danger-associated molecular patterns (DAMPs), including those triggered by crystalline particulates. We tested the hypothesis that bone matrix components released during bone resorption function as DAMPs for the NLRP3 inflammasome and regulate osteoclast (OC) differentiation. Bone particles prepared from bovine cortical bones increased NLRP3 expression and IL-1 $\beta$  secretion (>25-fold over control). Notably, hydroxyapatite crystals, but not collagen I fragments activate the NLRP3 inflammasome, suggesting that the mineral phase of bone particles function as DAMPs for this inflammasome. Importantly, bone DAMPs dramatically enhanced osteoclastogenesis induced by M-CSF/RANKL in WT cells in NLRP3-dependent manner. To determine the relevance of these findings to bone homeostasis, we studied the impact of Nlrp3 deficiency on bones using 3 pre-clinical mouse models of high bone turnover: estrogen deficiency (bone indices measured 8 weeks post-surgery), sustained exposure to PTH (ALZET osmotic pump-mediated PTH infusion for 2 weeks) or RANKL (1  $\mu$ g/kg, once daily for 2 days). Despite comparable baseline volumetric bone mass (BV/TV) between WT and Nlrp3 deficient mice, hormonal or RANKL perturbations induce significant osteopenia in WT mice compared to Nlrp3 deficient mice (e.g., BV/TV: OVX, 31.78% $\pm$ 9.71 vs 11.71% $\pm$ 9.71; PTH infusion, 17.47% $\pm$ 4.21 vs 0.65% $\pm$ 3.97; RANKL administration, 5.6% $\pm$ 1.6 vs 1.80% $\pm$ 1.7). Consistent with the notion that osteolysis releases DAMPs from bone matrix, pharmacologic inhibition of bone resorption by zoledronate (40  $\mu$ g/kg, once weekly for 4 weeks prior to RANKL injection)



attenuates inflammasome activation in mice induced by this cytokine. Thus, signals originating from bone matrix activate the NLRP3 inflammasome in the osteoclast lineage, and may represent a bone-restricted positive feedback mechanism that amplifies bone resorption in pathologic conditions of accelerated bone turnover.

**Disclosures:** Yael Aliphe, None.

## FR0178

**MYC-dependent oxidative metabolism regulates osteoclastogenesis via nuclear receptor  $ERR\alpha$ .** Seyeon Bae\*, Min Joon Lee, Se Hwan Mun, Kyung-Hyun Park-Min. Hospital for special surgery, United States

Osteoporosis is a metabolic bone disorder with compromised bone strength and an increased risk of fracture. Inhibiting differentiation of bone-resorbing osteoclasts is an effective strategy for the treatment of osteoporosis. Prior work by our laboratory and others has shown that MYC promotes osteoclastogenesis *in vitro*, but underlying mechanisms are not well understood. In addition, the *in vivo* importance of osteoclast-expressed MYC in physiological and pathological bone loss is not known. Here, we demonstrate that deletion of *Myc* in osteoclasts increases bone mass and protects mice from ovariectomy-induced osteoporosis. Transcriptomic analysis revealed that MYC drives metabolic reprogramming during osteoclast differentiation and functions as a metabolic switch to an oxidative state. A new mechanism of MYC action is transcriptional induction of estrogen receptor-related receptor alpha ( $ERR\alpha$ ), a nuclear receptor that cooperates with the transcription factor NFATc1 to drive osteoclastogenesis. Accordingly, pharmacological inhibition of  $ERR\alpha$  attenuated ovariectomy-induced bone loss. Our findings highlight the importance of a novel MYC- $ERR\alpha$  pathway in physiological and pathological bone loss by integrating the MYC- $ERR\alpha$  axis to metabolic reprogramming during osteoclast differentiation.

**Disclosures:** Seyeon Bae, None.

## FR0180

**Regulation of Adhesion Signaling in Osteoclasts by Tetraspanin CD82.** Alexis Bergsma\*<sup>1</sup>, Bart Williams<sup>2</sup>, Cindy Miranti<sup>3</sup>. <sup>1</sup>Van Andel Institute Graduate School, United States, <sup>2</sup>Van Andel Institute, United States, <sup>3</sup>University of Arizona Cancer Center, United States

CD82 is a tetraspanin protein involved in molecular scaffolding and was recently identified as being upregulated during osteoclast differentiation (Crotti, T.N., et al., J Cell Physiol, 2011). To investigate the physiological consequences of CD82 loss on bone morphology and function, we generated a mouse model in which CD82 is globally deleted. Our data indicate that CD82 loss results in narrower and more fragile bones, and that this narrowing phenotype is due to simultaneous osteoblast and osteoclast dysfunction. Supporting our findings that CD82 affects the mesenchymal stem cell lineage in addition to the hematopoietic lineage, we've shown that loss of CD82 dramatically increases bone marrow adipogenesis. To further investigate the effect of CD82 loss on osteoclastogenesis without affecting the mesenchymal lineage, we generated a myeloid-specific mouse model of CD82 loss. Osteoclast adhesion to bone is essential for its bone resorbing function, yet the pathways involved in osteoclast adhesion haven't been wholly elucidated. Using primary cells from these mice *in vitro* osteoclast differentiation model, we show that osteoclasts lacking CD82 are super-fused up to 10x their normal size, and are characterized by dysregulated cellular polarization, adhesion, migration, and resorption on bone. We have evidence that these cytoskeletal abnormalities are due to defective Syk and Src signaling to Rac1 within at least two signaling axes; integrin  $\alpha v \beta 3$  and the c-type lectin-like receptor Clec2 along with its ligand, podoplanin, with the latter two having otherwise been unstudied in bone. These data recognize three proteins that are important for bone remodeling that have yet to be acknowledged as such. Future studies necessitate evaluation of the clinical significance of these pathways in the perspective of bone diseases and potential therapeutics in malignancies that localize to the bone.

**Disclosures:** Alexis Bergsma, None.

## FR0185

**miR-182 regulates osteoclastogenesis and bone remodeling in both physiological and pathological conditions.** Kazuki Inoue\*<sup>1</sup>, Christine Miller<sup>2</sup>, Gregory Vitone<sup>2</sup>, Mahmoud Elguindy<sup>2</sup>, Liang Zhao<sup>3</sup>, Baohong Zhao<sup>1</sup>. <sup>1</sup>Hospital for Special Surgery/Weill Cornell Medicine, United States, <sup>2</sup>Hospital for Special Surgery, United States, <sup>3</sup>Nanfeng Hospital, The Southern Medical University, China

As important regulators of multiple physiological and pathological processes, miRNAs have drawn increasing attention. We recently identified miR-182 as a positive regulator of osteoclast differentiation *in vitro* via inhibition of its targets, Foxo3 and Maml1. We furthermore generated conditional miR-182 transgenic and knockout mice to comprehensively elucidate the role of miR-182 *in vivo* as well as to dissect the underlying regulatory mechanisms of action. Deficiency of miR-182 (*miR-182<sup>fl/fl</sup>; LysMcre<sup>+</sup>*) in osteoclast precursors dramatically increased bone mass by suppressing osteoclast formation in mice. A transgenic mouse model of miR-182 (LSL-miR-182;*LysMcre<sup>+</sup>*) showed a complementary phenotype with markedly decreased bone mass and enhanced

osteoclast formation. In pathological settings, miR-182 deficiency drastically prevented TNF or LPS induced inflammatory osteoclast generation and bone resorption. Moreover, osteoporosis induced by ovariectomy (OVX) was significantly reversed by the lack of miR-182 in mice. When searching upstream regulators, we found that miR-182 expression was suppressed by RBP-J, a key negative regulator of inflammatory bone resorption. Strikingly, enhanced osteoclastogenesis and bone resorption due to RBP-J deficiency was completely abolished in the miR-182/RBP-J double knockout mice. Furthermore, ChIP and gene reporter assays demonstrated that RBP-J directly binds to miR-182 promoter and suppresses its expression. Thus, the suppression of miR-182 by RBP-J serves as an important mechanism that restrains TNF-induced osteoclastogenesis and bone resorption. Mechanistically, we performed genome-wide analysis of RNAseq data and found that miR-182 promoted the expression of key osteoclastogenic factors NFATc1 and Blimp1 by selectively and significantly suppressing endogenous IFN- $\beta$  mediated gene expression and autocrine feedback loop of osteoclast differentiation. Of note as a link to human diseases, miR-182 expression levels were significantly elevated in monocytes isolated from rheumatoid arthritis patients. Collectively, our data identify miR-182 as a novel positive regulator of osteoclastogenesis in both physiological and pathological conditions and provide a new mechanism for the regulation of osteoclastogenesis driven by the miR-182-IFN- $\beta$  axis and its mediated gene expression program. Targeting miR-182 and its downstream targets may represent an attractive therapeutic approach to prevent pathological bone destruction.

**Disclosures:** Kazuki Inoue, None.

## FR0187

**MMP14 Derived From Macrophages Mediates TRAP+ Osteoclast-independent Inflammatory Bone Destruction In c-Fos-deficient SH3BP2 Cherubism Mice.** Mizuho Kittaka\*<sup>1</sup>, Kotoe Mayahara<sup>2</sup>, Tomoyuki Mukai<sup>3</sup>, Tetsuya Yoshimoto<sup>1</sup>, Teruhito Yoshitaka<sup>1</sup>, Jeffery P Gorski<sup>1</sup>, Yasuyoshi Ueki<sup>1</sup>. <sup>1</sup>University of Missouri-Kansas City, School of Dentistry, United States, <sup>2</sup>Nihon University School of Dentistry, Japan, <sup>3</sup>Department of Rheumatology, Kawasaki Medical School, Japan

It is believed that tartrate-resistant acid phosphatase-positive (TRAP+) osteoclasts are the exclusive bone-resorbing cells responsible for focal bone destruction in arthritis. This consensus is based on previous results that osteoclast-free mice are completely protected against inflammatory bone destruction in TNF- $\alpha$  transgenic mice lacking c-Fos or in RANKL-deficient mice with serum-transfer arthritis. However, this paradigm may be re-evaluated as a result of our study showing that cells other than TRAP+ osteoclasts can resorb bone in a knock-in (KI) mouse model of cherubism (*Sh3bp2<sup>KIKI</sup>*), which develops autoinflammatory joint destruction due to a gain-of-function mutation in SH3BP2. MicroCT analysis revealed that c-Fos-deficient *Sh3bp2<sup>KIKI</sup>* mice at 12 weeks old still exhibit detectable bone erosion at the distal tibia in the absence of TRAP+ osteoclasts. M-CSF-dependent macrophages from fetal liver of the c-Fos-deficient *Sh3bp2<sup>KIKI</sup>* mice failed to differentiate to TRAP+ osteoclasts when stimulated with RANKL or RANKL/TNF- $\alpha$ . Resorption lacunae were filled with lesions containing a large number of F4/80+ macrophages. Levels of serum ICTP, a marker of bone resorption produced by MMPs, were elevated, while levels of serum CTX, a marker of resorption by cathepsin K, were not increased. Consistent with this result, MMP14 levels were increased in inflamed joints of the c-Fos-deficient *Sh3bp2<sup>KIKI</sup>* mice. Genetic ablation of M-CSF-dependent macrophages in the mice using *Csf1r*-floxed mice on an *Mx1-Cre* background suppressed the bone erosion and reduced MMP14 levels in the ankle joints. Expression levels of *Mmp14* in the macrophages were synergistically increased by gain-of-function of SH3BP2 and loss-of-function of c-Fos, which was mediated through the NF- $\kappa$ B pathway. Administration of NSC405020, an MMP14 inhibitor against the PEX domain, ameliorated the bone erosion. In contrast, *Sh3bp2<sup>KIKI</sup>* mice lacking RANKL failed to develop a noticeable amount of bone erosion. However, c-Fos deletion restored bone erosion to the RANKL-deficient *Sh3bp2<sup>KIKI</sup>* mice, suggesting that both gain-of-function of SH3BP2 and loss-of-function of c-Fos are required for the TRAP+ osteoclast-independent bone erosion. Together, these data provide the first genetic evidence that cells other than TRAP+ osteoclasts can cause focal bone destruction in arthritis and suggest that MMP14 is a key mediator conferring pathological bone-resorbing capacity on the c-Fos-deficient *Sh3bp2<sup>KIKI</sup>* macrophages.

**Disclosures:** Mizuho Kittaka, None.

## FR0188

**Tgfr1-Deficiency Attenuates Aging-Related Bone Loss through ERK1/2 Signaling in Osteoclasts.** Miki Maeda\*, Hiroaki Saito, Hanna Taipaleenmäki, Eric Hesse. Molecular Skeletal Biology Laboratory, Department of Trauma, Hand and Reconstructive Surgery, University-Medical Center Hamburg-Eppendorf, Germany

Activated bone resorption is a component of aging-related bone loss. We identified an increased expression of the homeodomain protein TG-interacting factor 1 (Tgfr1) during osteoclast differentiation, suggesting a functional role of Tgfr1 in osteoclast function and bone resorption. To test this hypothesis, we deleted Tgfr1 in the germline (*Tgfr1<sup>-/-</sup>*) and in the osteoclast lineage (*CatK-Cre;Tgfr1<sup>fl/fl</sup>*). Interestingly, 8-month old *CatK-Cre;Tgfr1<sup>fl/fl</sup>* mice were protected from aging-related decrease in bone mass due to a reduced osteoclast number and bone resorption. Furthermore, *in vitro* differentiation of bone marrow macrophages (BMMs) obtained from *Tgfr1<sup>-/-</sup>* or *CatK-Cre;Tgfr1<sup>fl/fl</sup>*

mice demonstrated a decreased number and size of osteoclasts, fewer and more shallow resorption pits, and a diminished expression of the osteoclast-related genes NFATc1 and Cathepsin K. These findings indicate that Tgfr1 promotes osteoclast differentiation and function in a cell-autonomous manner and establish Tgfr1 as a novel regulator of bone resorption. To elucidate the underlying molecular mechanism we performed signaling pathway analyses, which revealed a reduction of phosphorylated ERK1/2 in *Tgfr1*<sup>-/-</sup> BMMs. While the *de novo* phosphorylation of ERK1/2 in response to RANK-L and MCSF stimulation was comparable between wild-type and *Tgfr1*<sup>-/-</sup> BMMs, ERK1/2 was rapidly de-phosphorylated in the absence of Tgfr1. This suggests that Tgfr1 controls ERK1/2 activity by inhibiting the expression of a specific phosphatase. Indeed, expression analysis of several ERK phosphatases demonstrated an increased expression of the Protein Phosphatase 2A catalytic subunit isoform  $\beta$  (PP2A-C $\beta$ ) in *Tgfr1*<sup>-/-</sup> BMMs compared to control cells. Mechanistically, pharmacological inhibition of PP2A using Okadaic acid or targeted silencing of the specific C $\beta$  isoform using the GapmeR technology normalized the level of phosphorylated ERK1/2 in *Tgfr1*<sup>-/-</sup> BMMs. Furthermore, inhibition of PP2A activity restored the impaired differentiation of *Tgfr1*<sup>-/-</sup> BMMs, demonstrating that Tgfr1 promotes osteoclast differentiation in an ERK1/2-dependent manner. In summary, Tgfr1-deficiency in osteoclasts impairs ERK1/2 signaling thereby inhibiting osteoclast function and bone resorption. Thus, Tgfr1 is a novel regulator of bone remodeling with an important function in aging-related bone loss.

**Disclosures:** Miki Maeda, None.

## FR0191

**Collagen Type VI  $\alpha 2$  Chain Deficiency Causes Trabecular Bone Loss by Enhancing Osteoclast Differentiation.** Hai Pham\*, Ainnie Dar, Vardit Kram, Li Li, Tina Kilts, Marian Young. Craniofacial and Skeletal Diseases Branch, National Institute of Dental and Craniofacial Research, National Institutes of Health, United States

Type VI collagen is widely known for its role in muscular disorders, however its function in bone is still not well understood. Type VI collagen is composed of three  $\alpha$ -chains ( $\alpha 1$ ,  $\alpha 2$ ,  $\alpha 3$ ) that align in a triple helix that forms trimers that assemble into fibrils found in many musculoskeletal tissues. When we examined the expression of all three type VI chains by quantitative RT-PCR during fracture healing, we found that Col6a2 mRNA was highly upregulated at day 14 post-fracture. Using immunohistochemistry we confirmed that the collagen VI expression levels were induced in the callus of healing bones suggesting it could have a role in bone homeostasis. To determine the role of type VI  $\alpha 2$  in bone function we analyzed the trabecular bone from femora and vertebra in mice deficient in type VI  $\alpha 2$  (Col6a2 KO) at 3 months of age. DEXA analysis indicated a significant lower bone mineral density in Col6a2 KO mice. Additionally, micro CT analysis showed significant decreases in bone volume/tissue volume, trabecular bone number and bone mineral density in the Col6a2 KO compared to wild-type (WT) mice. To try to understand the cellular basis for the decreased bone mass, we isolated bone marrow stromal cells (BMSCs) from WT and Col6a2 KO mice and cultured them under osteogenic conditions. No significant differences in osteogenic differentiation could be observed. Similarly, no changes in osteogenesis were observed between WT and Col6a2 KO BMSCs when media was supplemented with 100 ng/ml of human Type VI collagen. These experiments indicate that neither gain nor loss of function of type VI collagen in murine BMSCs induced significant effects on osteogenesis in vitro. When we examined femora sections of the Col6a2 KO mice for the abundance of TRAP positive osteoclasts, we discovered that the mutant mice exhibited 2.4 times more osteoclasts compared to WT mice. Osteoclast precursors were then isolated from WT and Col6a2 KO mice bone marrow and induced to differentiate in vitro using a combination of RANKL and MCSF. Our data showed that cells from Col6a2 null mice generated more TRAP positive cells after induction. Moreover, media supplementation with human Type VI collagen in WT osteoclast differentiation cultures significantly decreased the number of TRAP positive cells. In summary, our data indicate that collagen type VI regulates trabecular bone mass by inhibiting osteoclast differentiation, and could be a new molecular drug target to prevent bone loss.

**Disclosures:** Hai Pham, None.

## FR0192

**Identification of the signals provided by osteoclasts to induce FoxP3 in T cells.** Elena Shashkova\*, Anna Cline-Smith, Grant Kolar, Macey Peterson, Suman Nellore, Rajeev Aurora. Saint Louis University, United States

Bone homeostasis is maintained by a balance between bone-forming and bone-resorbing activities of osteoblasts and osteoclasts, respectively. The recognition that cytokines produced by activated lymphocytes can perturb bone-remodeling cycle gave rise to the field of osteoimmunology, which studies crosstalk between skeletal and immune systems. We have recently described a new regulatory CD8 T-cell population (TcREG) that is induced by osteoclasts treated with low dose of receptor activator of nuclear factor kappa-B ligand (RANKL). TcREG suppress osteoclastogenesis, decrease the number of pro-inflammatory effector T-cells, and therefore decrease inflammation-induced bone loss and promote bone formation. Regulatory T-cells are characterized by expression of the transcription factor FoxP3. The aim of this study was to delineate the signals provided by osteoclasts that induce FoxP3. We show that osteoclasts signal through Notch1 and Notch4 receptors on CD8 T-cells. Notch4 is activated by Delta like ligand 4 (DLL4) expressed on mature osteoclasts. Notch1 is cleaved in response to T-cell receptor stimulation. Chromatin immunoprecipitation (ChIP) demonstrated

occupancy of Notch1 and Notch4 intracellular domains on RBPj-binding sites in the regulatory regions of FoxP3 gene. This indicates that osteoclasts trigger canonical RBPj-dependent Notch signaling in CD8 T-cells leading to induction of FoxP3. We show by ChIP-qPCR that NFkB p65 binds to FoxP3 promoter at (-13) bp site, which overlaps with Notch binding site. Inhibition of either Notch cleavage by  $\gamma$ -secretase inhibitor or NFkB signaling by IKK inhibitor prevented p65 binding to this site and suppressed expression of FoxP3. Therefore induction of FoxP3 in CD8 T cells requires cooperation between Notch and NFkB signaling pathways. We demonstrate that osteoclasts provide CD200 to activate NFkB in CD8 T-cells via interaction with CD200R. We show that engagement of co-stimulatory CD28 is not required for TcREG generation. Instead, we found that CD200R is co-localized with CD3 and phosphorylated Zap70 similarly to CD28. Finally, we demonstrate that three signals: TCR engagement, DLL4, and CD200 are necessary and sufficient to generate TcREG in the absence of osteoclasts. Furthermore, we show that same three signals induce FoxP3 in CD4 T cells. Therefore CD8 and CD4 T-cells share common mechanism of induction of FoxP3 expression.

**Disclosures:** Elena Shashkova, None.

## FR0193

**Critical role of Endothelin in Osteoclast Differentiation and Function.** Ji Su Sun\*<sup>1</sup>, Sueyoung Oh<sup>2</sup>, Dong Min Shin<sup>1</sup>, Inik Chang<sup>2</sup>. <sup>1</sup>Department of Oral Biology, BK21 PLUS Project, Yonsei University College of Dentistry, Korea, Republic of, <sup>2</sup>Department of Oral Biology, Yonsei University College of Dentistry, Korea, Republic of

Endothelin (ET) system comprises three 21-amino acid peptides, ET-1, -2, and -3 that activate two G-protein coupled receptors, ET receptor A (ET<sub>A</sub>) and B (ET<sub>B</sub>) and its two processing enzymes, endothelin converting enzyme (ECE)-1 and -2. The role of ET-1 via ET<sub>A</sub> activation in the regulation of osteoblastic function has been widely discussed. However, the information about ET-1 function in osteoclasts is limited and ambiguous despite the elevation of its plasma levels in patients of osteoporosis and Paget's disease of bone. Here, we show that the ET<sub>B</sub> activation by ET-1 stimulates osteoclast differentiation and function in both in vitro and in vivo. ET<sub>B</sub>, but not ET<sub>A</sub>, is expressed in both bone marrow-derived macrophages and mature osteoclasts, and its levels were greatly increased during the osteoclast differentiation by RANKL and M-CSF. ET-1 not only enhanced RANKL-induced osteoclast formation but also markedly increased the proportions of multinuclear cells through ET<sub>B</sub> receptor, whereas the proliferation of osteoclast precursors was unchanged by ET-1. Transient or permanent ET<sub>B</sub>-deficiency impaired multinuclear osteoclast formation and reduced bone resorptive activity, but the proliferation of osteoclast progenitors was not changed. ET<sub>B</sub> activated by ET-1 promoted migration of osteoclast progenitors. Mechanistically, ET-1 induced calcium oscillation and Pyk2 phosphorylation in an ET<sub>B</sub>-dependent manner. ET-1 stimulated the expression and nuclear translocation of NFATc1 via ET<sub>B</sub> which led to the induction of majority of osteoclastogenic genes particularly, MMP-9 and -13. Mice lacking osteoclast ET<sub>B</sub> or administering a specific inhibitor, BQ788 had increased bone mass and decreased bone resorptive activity in vivo. Finally, genetic ablation and pharmacological inhibition of ET<sub>B</sub> protected against the bone loss induced by ovariectomy and lipopolysaccharide challenge. Together, our findings reveal a critical role of endothelin in the regulation of osteoclast differentiation and bone mass. Furthermore, these results underline the potential utility of ET<sub>B</sub> as a new therapeutic target for anti-resorptive agent.

**Disclosures:** Ji Su Sun, None.

## FR0194

**Transgenic expression of TBK1 in Osteoclast Lineage Cells Increased Both Osteoclasts and Bone Formation.** Quanhong Sun\*<sup>1</sup>, Peng Zhang<sup>1</sup>, Juraj Adamik<sup>1</sup>, Mark Subler<sup>2</sup>, Jolene J. Windle<sup>2</sup>, Laëticia Michou<sup>3</sup>, Jacques P. Brown<sup>4</sup>, Noriyoshi Kurihara<sup>5</sup>, G. David Roodman<sup>5</sup>, David W. Dempster<sup>6</sup>, Kostas Verdelis<sup>7</sup>, Hua Zhou<sup>6</sup>, Deborah L. Galson<sup>1</sup>. <sup>1</sup>Department of Medicine, Hematology-Oncology Division, University of Pittsburgh Cancer Institute, The McGowan Institute for Regenerative Medicine, University of Pittsburgh, PA, USA, United States, <sup>2</sup>Department of Human and Molecular Genetics, Virginia Commonwealth University, Richmond, VA, United States, <sup>3</sup>Department of Medicine, Laval University, CHU de Quebec Research Center and Department of Rheumatology, CHU de Quebec, Quebec City, Canada, <sup>4</sup>Department of Medicine, Laval University, CHU de Quebec Research Center and Department of Rheumatology, CHU de Quebec, Quebec City, Canada, United States, <sup>5</sup>Department of Medicine, Hem-Onc Division, Indiana University, Indianapolis, IN, United States, <sup>6</sup>Regional Bone Center, Helen Hayes Hospital, Route 9W, West Haverstraw, NY 10993, USA, United States, <sup>7</sup>The Center for Craniofacial Regeneration, Department of Oral Biology, The McGowan Institute for Regenerative Medicine, University of Pittsburgh, Pittsburgh, PA, USA, United States

Paget's disease of bone (PDB) is a very common late-onset metabolic bone disease affecting 1 million Americans. Measles virus nucleocapsid protein (MVNP) expression in osteoclast (OCL) precursors along with mutation of the SQSTM1 (p62) gene contributes to the development of abnormally active OCL in Paget's disease in concert with aberrant excess woven bone formation. In addition, MVNP expression targeted to OCL



in transgenic mice induces pagetic-like lesions *in vivo* and OCL with a pagetic phenotype *in vitro*. We reported that MVNP activation of TBK1, an IKK family member, plays a critical role in mediating the effects of MVNP on OCL differentiation. Further, MVNP expression up-regulated TBK1 protein in BMM. Importantly, over-expression of TBK1 in BMM by lentiviral transduction generated pagetic-like OCL. Therefore, to assess if over-expression of TBK1 was sufficient to mimic the effects of MVNP in mice, we generated a new mouse model with TBK1 targeted to the OCL lineage (TG-TBK1). Analyses by microCT and histology revealed that the TG-TBK1 mice had increased osteoclast surface and trabecular width, which was associated with increased mineralizing surface, mineral apposition rate and bone formation rate. Thus osteoclast lineage-specific transgenic expression of TBK1 had profound effects on OCL and bone formation, which is characteristic of pagetic bone. Further, similar to TG-MVNP pre-OCL, TG-TBK1 pre-OCL have higher activated TBK1 and lower levels of optineurin (OPTN), which we previously reported is a negative regulator of TBK1 function and OCL formation. We found MVNP interacts with OPTN, and they both colocalize with TBK1 in bone marrow monocytes (BMM). Modulation of TBK1 activity by over-expression, shTBK1 lentiviral knockdown, or kinase inhibition reciprocally regulated OPTN levels. OPTN overexpression blocked MVNP or TBK1-induced p65 activation and IL-6 expression. Importantly, OPTN lentiviral transduction into BMM from wild type, TG-MVNP, and TG-TBK1 mice decreased RANKL-stimulated OCL formation and IL-6 expression. Conversely, OPTN knockdown in BMM increased OCL formation and IL-6 expression. These results indicate that OPTN is a negative regulator of OCL formation, and that MVNP alters the balance of TBK1 and OPTN in OCL lineage cells to generate pagetic OCL. Together, these data indicate that over-expression of TBK1 in osteoclast-lineage is sufficient to mimic MVNP pagetic effects.

**Disclosures:** *Quanhong Sun, None.*

## FR0197

**Deletion of the transferrin receptor 1 gene in murine osteoclasts attenuates mitochondrial metabolism and cytoskeletal organization and increases trabecular bone mass.** *Lei Wang*<sup>1</sup>, *Toshifumi Fujiwara*<sup>2</sup>, *Bin Fang*<sup>3</sup>, *Nukhet Aykin-burns*<sup>4</sup>, *Zhichang Zhang*<sup>5</sup>, *Xiaolin Li*<sup>5</sup>, *Michael L Jennings*<sup>6</sup>, *Stavros C Manolagas*<sup>7</sup>, *Jian Zhou*<sup>1</sup>, *Haibo Zhao*<sup>7</sup>. <sup>1</sup>Department of Orthopedics, First Affiliated Hospital, Anhui Medical University, China, <sup>2</sup>Department of Orthopedic Surgery, Kyushu University, Japan, <sup>3</sup>Department of Dermatology, University of Arkansas for Medical Sciences, United States, <sup>4</sup>Division of Radiation Health, Department of Pharmaceutical Sciences, University of Arkansas for Medical Sciences, United States, <sup>5</sup>Department of Orthopedics, Shanghai Jiao Tong University Affiliated Sixth People's Hospital, China, <sup>6</sup>Department of Physiology and Biophysics, University of Arkansas for Medical Sciences, United States, <sup>7</sup>Division of Endocrinology and Metabolism, Department of Internal Medicine, University of Arkansas for Medical Sciences, United States

The generation and function of osteoclasts (OCs) demand high energy, but the mechanisms by which they achieve that remain largely unknown. Iron plays a fundamental role in mitochondrial metabolism and the biosynthesis of heme as well as a cluster of mitochondrial iron-sulphur (Fe-S) containing proteins which are critical components of the respiratory complexes. Mammalian cells acquire iron through the uptake of transferrin (Tf), heme, and ferritins. In Tf-dependent pathway, Fe<sup>3+</sup>-loaded Tf binds to Tf receptor (TfR1) on the cell surface, and the complex is then internalized via endocytosis. Fe<sup>3+</sup> is released from Tf in endosomes and is reduced to Fe<sup>2+</sup> by the Steap family of ferredoxins before being transported to the cytoplasm by divalent metal transporter 1 (DMT1). The expression of TfR1, Steap4, and DMT1 are up-regulated during OC differentiation, whereas transporters of heme and ferritins remain unchanged or undetectable, suggesting that Tf-dependent iron uptake is the dominant pathway of iron acquisition during OC differentiation and activity. Moreover, iron chelation inhibits OC bone resorption and protects against bone loss induced by estrogen deficiency. To elucidate the role of cellular iron homeostasis in OCs, we generated TfR1 myeloid and mature OC deficient mice in C57BL/6J mixed background by crossing TfR1-floxed mice with LysM-Cre (FPNf/f;LysM-Cre) and Cathepsin K-Cre (FPNf/f;CTSK-Cre) mice, respectively. Both strains of mice had an over two-fold increase in trabecular bone mass in femurs of male and female mice as analyzed by  $\mu$ -CT. *In vitro* mechanistic studies revealed that loss of TfR1 totally abolished Tf-dependent iron uptake in monocytes and mature OCs as measured by a Tf-Fe<sup>59</sup> uptake assay. Cellular bioenergetics studies using the Seahorse Extracellular Flux analyzer demonstrated a 75% decrease in reserve respiratory capacity, a parameter indicating the difference between maximum and basal respiration, in TfR1-deficient OC precursors compared to control cells; whereas the oligomycin-sensitive ATP-linked respiration was similar between the two genotypes of OC precursors. TfR1-null monocytes differentiated OC normally. TfR1-deficient mature OCs, however, exhibited defective podosome-belt and actin-ring formation. From these results we conclude that TfR1-dependent iron uptake is critical for OC energy metabolism and cytoskeleton organization, but not for OC differentiation; and it is needed for OC bone resorption and bone homeostasis.

**Disclosures:** *Lei Wang, None.*

## FR0198

**Kindlin-2 in Osteocytes Controls Bone Remodeling.** *Huiling Cao*<sup>\*</sup>, *Guozhi Xiao*. SUSTech, China

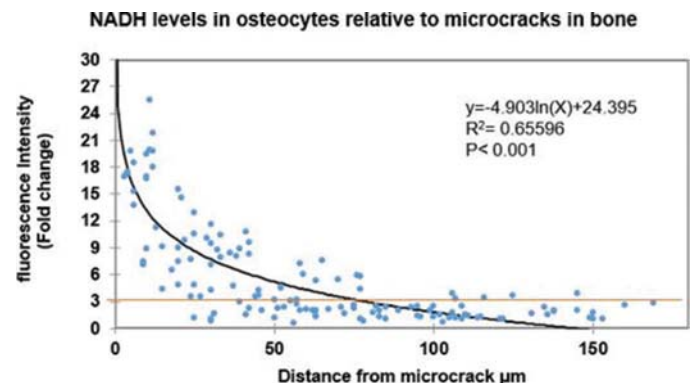
Bone mass is delicately controlled through bone remodeling, a process in which the osteoclast-mediated bone resorption closely couples with the osteoblast-mediated bone formation. Osteocytes embedded in the bone matrix play a critical role in regulation of bone remodeling; however, the underlying mechanism is largely unclear. Here we show that deleting Kindlin-2, a previously known focal adhesion molecule that activates integrin, in osteocytes by breeding the floxed *Kindlin-2* mice and the *Dmpl-Cre* transgenic mice resulted in a severe osteopenia. Specifically, bone parameters that decreased significantly in *Kindlin-2*<sup>Dmpl</sup> mice compared to control littermates were BV/TV by 84.4% ( $p = 0.00089$ ), Tb.N by 52.6% ( $p = 0.00142$ ), and Cort.Th ( $p = 0.03536$ ) by 10.2%; in contrast, Tb.Sp was significantly increased by 122.9% ( $p = 0.01954$ ). Furthermore, intermittent PTH-induced increase in bone mass was significantly decreased in *Kindlin-2*<sup>Dmpl</sup> mice with or without ovariectomy surgery. Interestingly, the restoration of bone loss induced by tail suspension was impaired in *Kindlin-2*<sup>Dmpl</sup> mice. Kindlin-2 ablation in osteocytes dramatically reduced bone formation rate (BFR), an *in vivo* indicator for osteoblast function, and promoted osteoclast formation in bone. We used CRISPR/Cas9 technology and deleted Kindlin-2 expression in MLO-Y4 osteocyte-like cells. Conditioned media (CM) from MLO-Y4 cells with Kindlin-2 deletion dramatically inhibited osteoblast differentiation gene expression and mineralization in murine MC3T3-E1 and primary osteoblast cultures and greatly promoted the formation of multinuclear osteoclasts in primary bone marrow monocyte cultures. Thus, we demonstrate that Kindlin-2 in osteocyte plays a critical role in controlling bone mass by modulation of osteoblast and osteoclast function.

**Disclosures:** *Huiling Cao, None.*

## FR0200

**Acute Increase in Osteocyte Oxidative Stress at Focal Microdamage Site in Bone.** *Dorra Frikha-Benayed*<sup>\*</sup>, *Jelena Basta-Plajkic*, *Robert J Majeska*, *Mitchell B Schaffler*. City College of New York, United States

At microdamage sites, there is more widespread of osteocyte apoptosis than can be accounted for by cells direct physical injury by microcracks. The cause of this apoptosis remains unknown. Local metabolic stress has been posited to be the major driver of osteocytes apoptosis spread around microcracks as microdamage in fatigued bone could disrupt canalicular integrity, altering fluid flow to and from osteocytes (1). Metabolic stress can be assessed by monitoring changes of mitochondrial NADH fluorescence *in situ*. In the current studies, we used this approach to test whether microcracks in cortical bone impair osteocyte mitochondrial oxidative function *in vivo*. Localized microcracks were placed *in vivo* at the 3rd metatarsal diaphyses of anesthetized 15-17 weeks female C57Bl/6 mice, using a recently reported indentation approach (2). Osteocyte NADH accumulation was monitored *in situ* by multiphoton microscopy (MPM) at 4 hours after damage placement (3). Evans Blue labeling *in vivo* was used to identify acutely damaged osteocytes at the microcrack sites. Mice were euthanized at the end of the imaging studies without recovery from anesthesia. All procedures were IACUC approved. Acutely damaged (Evans Blue labeled) osteocytes were few in number and seen only within 5 to 10  $\mu$ m of microcracks. Thus, acute cell injury resulting from microcracks in bone accounts for only a very small component of the overall cell death at microdamage sites in bone. In contrast, dramatically increased NADH levels (~15-fold intensity increase over baseline) were observed in osteocytes close to microcracks, indicating highly elevated mitochondrial oxidative stress levels in osteocytes surrounding microcrack in bone. Osteocyte NADH levels declined rapidly with distance from microcracks following an inverse logarithmic relationship (Fig 1) baseline level by approximately 100  $\mu$ m from the microcrack site. Thus, there is a zone surrounding microcracks in which osteocytes experience very high levels of oxidative stress. This zone corresponds to the localized region of osteocyte apoptosis seen around microcracks in bone (4). Acutely elevated cellular oxidative stress level is a well-established trigger for apoptosis, and is a likely trigger for the osteocyte apoptosis and bystander signaling responses that activate and regulate resorption of microdamage in bone. REF: 1) Tami et al, JBMR. 2002; 2) Kennedy et al, Bone 2017; 3) Frikha-Benayed et al, Bone, 2016; 4) Kennedy et al, Bone 2012.



NADH levels in osteocytes relative to microcracks in bone

**Disclosures:** *Dorra Frikha-Benayed, None.*

## FR0201

**Autoregulation of osteocyte through estrogen-miRNA-Sema3A-Nrp1 axis.** Mikihiro Hayashi<sup>1</sup>, Tomoki Nakashima<sup>2</sup>, Hiroshi Takayanagi<sup>3</sup>. <sup>1</sup>Department of Cell Signaling, Graduate School of Medical and Dental Sciences, Tokyo Medical and Dental University, Japan, <sup>2</sup>Department of Cell Signaling, Graduate School of Medical and Dental Sciences, Tokyo Medical and Dental University; Core Research for Evolutional Science and Technology (CREST), Japan Agency for Medical Research and Development (AMED), Japan, <sup>3</sup>Department of Immunology, Graduate School of Medicine and Faculty of Medicine, The University of Tokyo, Japan

Semaphorin 3A (Sema3A), which is highly expressed in osteoblast lineage cells, plays a critical role in controlling bone mass in mice. However, the mechanisms responsible for the regulation of Sema3A expression are still poorly understood. We found that Sema3A protein expression, but not mRNA expression, was increased by the inhibition of miRNA expression under the control of estrogen in osteoblast lineage cells. In addition, Sema3A is also expressed in neuronal cells, and it is unclear which of them are the major source of Sema3A for physiological bone remodeling in adult mice. Mice with a post-natal global deletion of Sema3A by *CAG-CreER* with tamoxifen administration, post-natal conditional deletion of Sema3A in osteoblast lineage cells by *Sp7-tTA-tetO-Cre* with doxycycline administration, and mesenchymal progenitor cell-specific deletion of Sema3A by using *Prrxl1-Cre* resulted in a significant reduction in trabecular bone volume. In contrast, *Sp7-tTA-tetO-Cre*-mediated Sema3A deletion in aged mice did not affect bone mass. We therefore generated osteocyte (and late osteoblast)-specific Sema3A null mice by crossing 10 kb *Dmp1-Cre* mice. Although *Dmp1-Cre<sup>+</sup> Sema3A<sup>fllox/Δ</sup>* mice had normal bone mass at 10 weeks of age, aged *Dmp1-Cre<sup>+</sup> Sema3A<sup>fllox/Δ</sup>* mice displayed markedly lower trabecular bone volume and cortical thickness compared to littermate control. These results suggest that osteocytes express Sema3A to maintain bone homeostasis, especially in aged mice. Notably, we found that the number of osteocytes was greatly reduced in aged *Dmp1-Cre<sup>+</sup> Sema3A<sup>fllox/Δ</sup>* mice. Indeed, the survival of differentiated, but not of undifferentiated IDG-SW3 cells, was increased by the treatment with Sema3A. The phenotype observed in *Dmp1-Cre<sup>+</sup> Sema3A<sup>fllox/Δ</sup>* mice was recapitulated in osteocyte (and late osteoblast)-specific *Nrp1* deficient/mutant mice, indicating that Sema3A signaling in osteocytes is essential to protect from osteocyte apoptosis *in vivo*. Furthermore, the administration of the stimulator of the Sema3A signaling pathway decreased bone loss after ovariectomy in osteoblast lineage-specific Sema3A knockout mice, whereas E2 treatment failed to protect from bone loss in osteoblast lineage-specific Sema3A knockout mice. These findings collectively suggest that osteocyte-derived Sema3A acts on osteocytes to maintain cell survival and bone homeostasis.

**Disclosures:** Mikihiro Hayashi, None.

## FR0202

**Changes in osteocyte calcium signaling *in vivo* due to estrogen withdrawal.** Karl Lewis<sup>1</sup>, Joyce Louie<sup>1</sup>, Samuel Stephen<sup>1</sup>, David C. Spray<sup>2</sup>, Mia M. Thi<sup>2</sup>, Zeynep Seref-Ferlenge<sup>2</sup>, Robert J. Majeska<sup>1</sup>, Sheldon Weinbaum<sup>1</sup>, Mitchell B. Schaffler<sup>1</sup>. <sup>1</sup>The City College of New York, United States, <sup>2</sup>Albert Einstein College of Medicine, United States

Bone has long been known to be sensitive to estrogen (E2)<sup>1-3</sup>. Osteocytes (OTs), the principal bone mechanosensors that are responsible for regulating bone tissue mass and organization, have E2 receptors. However, it not known if E2 levels *in vivo* affects their mechanosensitivity. In the present study, we investigated the effect of E2 withdrawal on OT Ca<sup>2+</sup> signaling events *in vivo* triggered by mechanical loading.

OT expression of the fluorescent Ca<sup>2+</sup> sensor GCaMP3<sup>4,5</sup> was achieved by crossing A138 mice (bearing the GCaMP3 gene behind a Lox-STOP-Lox codon<sup>6</sup>) with DMP1-Cre mice<sup>7</sup>. Ovariectomy (OVX) at age 16wk was used to deplete E2. OTs were studied at baseline, 2, & 28d post-OVX (n=6/group). For mechanical loading studies, anesthetized mice were placed in a custom device to permit 3-point bending of 3<sup>rd</sup> metatarsal bones while under observation using multiphoton microscopy. Bones were loaded under displacement control with an haversine waveform to strains of 250, 500, 1000, 2000 and 3000μ<sup>2</sup> at 1Hz. GCaMP3 signal was visualized during loading using a 40X magnification water immersion objective, 920nm excitation and 490-560nm band pass filter for detection. Time series images were acquired at mid-diaphysis. For each OT, pixel intensity values were collected in each frame before and during loading. Data were analyzed for number of responding cells (% responding, based on those exhibiting a >25% over baseline) and peak intensity. Statistical analyses were performed using SPSS software. All procedures were IACUC approved.

Number of Ca<sup>2+</sup> signaling OTs increased similarly with increasing mechanical strain similarly for both control and 2d post-OVX bones (Fig 1a, p>0.05, 2-Way ANOVA). Ca<sup>2+</sup> signaling intensity per OT was unchanged except at 3000μ<sup>2</sup> (Fig 1a, p<0.05, ANOVA). In 28d post-OVX, OT Ca<sup>2+</sup> signaling differed profoundly. OTs Ca<sup>2+</sup> signaling was effectively absent at strains lower than 1000μ<sup>2</sup>. At 2000μ<sup>2</sup>, OT Ca<sup>2+</sup> signaling was evident but the number of signaling cells was still reduced ~30% vs controls (Fig 1b) Only at 3000μ<sup>2</sup> were OT responses similar in long-term OVX and intact bones. Maximum intensity was not affected by OVX in any experiment.

We report here the first observations that loss of E2 effectively shuts down load induced OT Ca<sup>2+</sup> signaling *in vivo* at strain levels typical of normal activities (e.g. walking). These results have notable implications regarding bone loss and physical activity in postmenopausal osteoporosis.

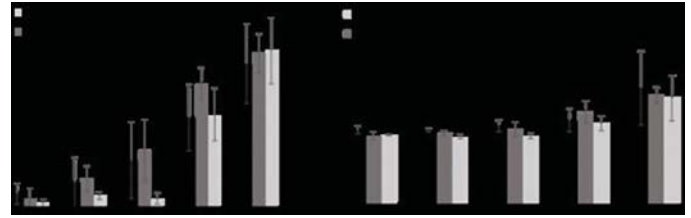


Figure 1

**Disclosures:** Karl Lewis, None.

## FR0205

**Unexpected decrease in osteoclast number and bone resorption with increased osteocyte apoptosis in the absence of osteocytic miR21.** Rafael Pacheco-Costa<sup>\*</sup>, Hannah Davis, Emily Atkinson, Julian Dilley, Carmen Herrera, Keith Condon, Mircea Ivan, Teresita Bellido, Lilian Plotkin. Indiana University School of Medicine, United States

Cx43 expression is decreased in bones from old mice; and osteocytic Cx43 deletion in Cx43<sup>Δot</sup> mice partially mimics the aging skeletal phenotype, with high osteocyte apoptosis, low bone miR21 expression, and increased osteoclast number and bone resorption on endosteal bone surfaces. miR21 can be transferred between cells and induces osteoblast and osteoclast differentiation. We showed that miR21 is released to the conditioned media of MLO-Y4 osteocytic cells and that apoptosis in Cx43-deficient MLO-Y4 cells is due to reduced miR21 expression. To test miR21 role in osteocytes *in vivo* we crossed miR21<sup>fl</sup> with 8kbDMP1-Cre mice to generate miR21<sup>Δot</sup> mice (n=10) and littermate miR21<sup>fl</sup> controls (n=10). miR21 expression is 46% lower and protein levels of the miR21 target gene phosphatase and tensin homolog (PTEN) are 67% higher in calvaria bones from 4-mo miR21<sup>Δot</sup> vs miR21<sup>fl</sup> mice. Female miR21<sup>Δot</sup> and miR21<sup>fl</sup> mice do not exhibit anatomical abnormalities with similar cartilage and mineralized bone distribution at birth. Body weight and total, spinal, and femoral BMD are not different between genotypes from 1-4 months of age. Bone microarchitecture, NOB/BS, OBS/BS, and BFR/BS are not changed, with 10% decrease in OcS/BS and ES/BS in cancellous bone in 4-mo miR21<sup>Δot</sup> mice. Osteocyte or osteoblast apoptosis was not altered in cancellous bone, similar to Cx43<sup>Δot</sup> mice. As expected, and similar to 5-mo Cx43<sup>Δot</sup> and 22-mo old WT mice, apoptotic active caspase3 positive osteocytes increase by 50% and marrow cavity area is 11% higher in the femur midshaft of miR21<sup>Δot</sup> vs miR21<sup>fl</sup> mice. But, unlike other conditions with high osteocyte apoptosis, which exhibit increased bone resorption, osteocytic miR21 deletion leads to 40% lower osteoclasts on femur endosteal surface and a 27% decrease in serum CTX, compared to controls. Serum RANKL levels are 47% higher in miR21<sup>Δot</sup> mice; and expression of osteoclast precursor markers CD14/CD11b is unchanged, but RANK expression is 76% lower in miR21<sup>Δot</sup> bones, suggesting defective osteoclast differentiation. miR21<sup>Δot</sup> mice also show lower BFR/BS (15%) on femur endocortical surface explaining the increase in marrow cavity area, and low serum PINP (18%) and ALP (26%) levels. In summary, osteocytic miR21 deletion increases apoptosis but, to our surprise, results in decreased bone resorption and formation. Our results suggest that miR21 can act as a mediator released by apoptotic osteocytes promoting osteoclast differentiation and bone resorption.

**Disclosures:** Rafael Pacheco-Costa, None.

## FR0208

**Finite Element Analysis of 3D-DXA Femur Reconstructions to Predict Hip Fracture.**

Luis Del Rio<sup>1</sup>, Carlos Ruiz<sup>2</sup>, Andy Luis Olivares<sup>2</sup>, Silvana Di Gregorio<sup>1</sup>, Simone Tassani<sup>3</sup>, Silvia Martinez-Pardo<sup>4</sup>, Mihail Gregorov<sup>4</sup>, Jérôme Noailly<sup>3</sup>, Miguel Angel Gonzalez<sup>3</sup>. <sup>1</sup>CETIR Grupo Medic, Spain, <sup>2</sup>Simulation, Imaging and Modelling for Biomedical Systems, Universitat Pompeu Fabra, Spain, Spain, <sup>3</sup>Simulation, Imaging and Modelling for Biomedical Systems, Universitat Pompeu Fabra, Spain, <sup>4</sup>Servicio reumatología, Hospital Universitarios Mutua de Terrassa, Spain

**Introduction:** The aim of this study was to validate 3D-DXA based finite element (FE) models to predict femoral strength in loading charge simulations, integrating patient-specific anatomic bone quality and biomechanical behavior information. The currently available 3D-DXA provides assessment of the hip geometry and spatial distribution of the trabecular and cortical BMD from a standard 2D DXA acquisition. **Materials and Methods:** We collected 128 DXA scans acquired with a DXA GE Prodigy in subjects older than 75 years. 73 of them suffered a recent hip fracture event (mean 9.5 days) and 55 without hip fracture (controls) were included. Proximal femur 3D models were generated using the software 3D-DXA (Galgó Medical). FE models were automatically generated by morphing a generic mesh to the patient-specific bone shape. Side fall effect was simulated by using a static peak load depending on patient mass and height. Local mechanical fields were calculated based on relationships between Young's modulus (E) and volumetric BMD for cortical and trabecular bone. Other variables as BMD, strain, stress, and strain energy density with potential discrimination power among fracture and non-fracture cases were analyzed through the ROC-AUC method. **Results and discussion:** The major principal stress (MPS) was the parameter



with the highest ROC-AUC values. For intertrochanteric fractures, it led to ROC-AUC values 28% and 18% higher than the values obtained with the volumetric BMD measured by DXA, when analyzed in the trabecular and cortical bone respectively. MPS results from a tradeoff between external loads and tissue deformation, by the distribution of the bone density and local stiffness values. For intertrochanteric and neck fractures, the ROC-AUC values for the MPS calculated at the trabecular bone of those fracture zones in all patients were 0.88 and 0.81, respectively. The ROC-AUC values for the MPS calculated at the cortical bone of the forehead mentioned fracture zones were 0.74 and 0.71. These results were similar to those previously reported using CT-based FE models, and suggest that the trabecular bone quality is particularly critical for proximal femur osteoporotic fractures, in general. Conclusion: 3D-DXA-based FE models of the femur provide descriptors with good to excellent sensitivity to hip fracture occurrence. Statistical analyses by type of fracture, tissue and gender are crucial to achieve accurate patient classification in the near future.

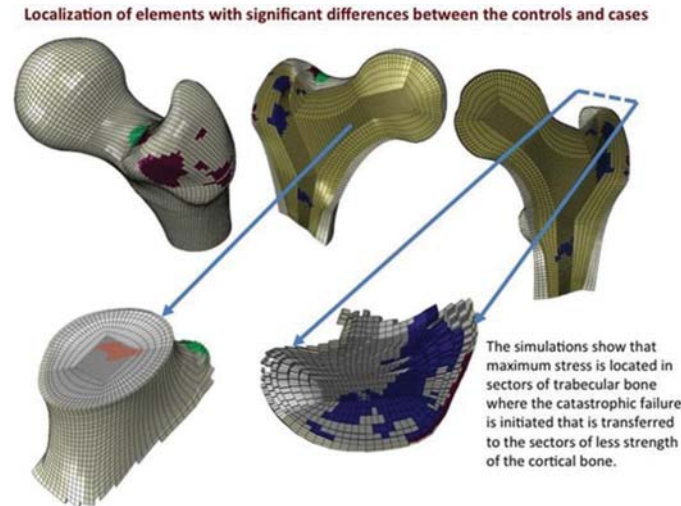


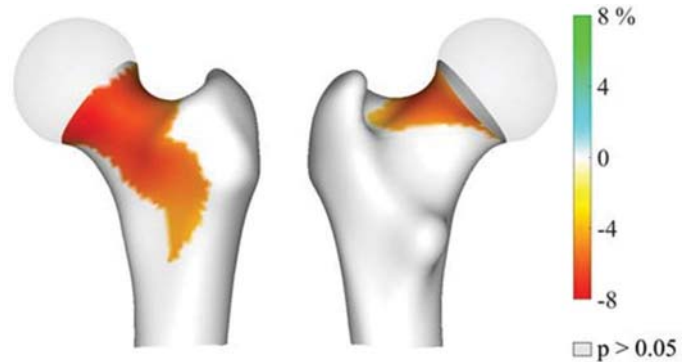
figure FEA 3D DXA

Disclosures: Luis Del Rio, None.

## FR0209

**Analyzing the cortical and trabecular bone of the femur of patients with vertebral fractures by 3D-DXA.** AM Galich<sup>1</sup>, L Humbert<sup>2</sup>, R Winzenrieth<sup>2</sup>, L Maffei<sup>1</sup>, V Premrou<sup>1</sup>, A Frigeri<sup>1</sup>, E Vega<sup>1</sup>. <sup>1</sup>Endocrinologist, Argentina, <sup>2</sup>Researcher, Spain

The purpose of this study was to analyze the cortical and trabecular bone of the femur of patients with prevalent vertebral fractures. 162 postmenopausal women were included in this study. A questionnaire was used to assess prevalent vertebral fractures. DXA analysis were performed at same site (Buenos Aires, Argentina) using a Prodigy scanner (GE Lunar, USA) and the software enCORE (version 16, GE Lunar). 3D analysis of the femoral cortical and trabecular bone were performed using the 3D-DXA software (version 2.4, Galgo Medical). 3D-DXA registers a 3D appearance model of the femoral shape and density onto the hip DXA scan to obtain a 3D subject-specific model of the femur of the patient and quantify the volumetric BMD (vBMD) and cortical thickness distribution. 29 subjects (Fx) had prevalent vertebral fractures, while 133 subjects (controls) had no history of major osteoporotic fracture. Mean age of participants was  $64.7 \pm 8.9$  years. No statistical difference was found between Fx subjects and controls ( $p = 0.425$ , Student's t-test). The body mass index of Fx group ( $23.7 \pm 2.9 \text{ kg/m}^2$ ) was lower, compared to controls ( $25.5 \pm 4.2 \text{ kg/m}^2$ ,  $p = 0.025$ ). aBMD measured at the total hip and neck by DXA was lower for Fx participants, compared to controls, although the differences between the two groups were not statistically significant ( $-0.035 \text{ g/cm}^2$ ,  $-4.3\%$ ,  $p=0.080$ ) for the total hip and ( $-0.034 \text{ g/cm}^2$ ,  $-4.3\%$ ,  $p=0.081$ ) for the neck. Significant differences were found for the cortical vBMD measured by 3D-DXA at the total hip ( $-2.1\%$ ,  $p=0.027$ ) and neck ( $-2.4\%$ ,  $p=0.026$ ). The cortical thickness at the total hip was lower for Fx participants ( $-3.5\%$ ,  $p=0.089$ ), although not statistically significant. A significant difference was found for the cortical thickness at the neck ( $-4.7\%$ ,  $p=0.042$ ). The trabecular vBMD at the total hip was lower for Fx participants ( $-7.9\%$ ,  $p=0.059$ ), although not statistically significant. A significant difference was found for the trabecular vBMD at the neck ( $-7.4\%$ ,  $p=0.043$ ). To conclude, differences in aBMD measured by DXA between Fx participants and controls at the neck and total hip were not statistically significant. 3D-DXA did show statistical differences at the neck (cortical thickness, cortical vBMD and trabecular vBMD) and at the total hip (cortical vBMD). 3D-DXA could potentially be used as a tool to assess the risk of fragility fracture at the hip in patients with prevalent vertebral fractures.



Hip cortical percentage

Disclosures: AM Galich, None.

## FR0211

**Prediction of Hip Fracture in Post-menopausal Women using Artificial Neural Network Approach.** Thao P. Ho-Le<sup>1</sup>, Jackie R. Center<sup>2</sup>, John A. Eisman<sup>3</sup>, Hung T. Nguyen<sup>1</sup>, Tuan V. Nguyen<sup>4</sup>. <sup>1</sup>Centre of Health Technologies, FEIT, University of Technology Sydney, Australia, <sup>2</sup>Bone Biology Division, Garvan Institute of Medical Research; St Vincent Clinical School, UNSW, Australia, Australia, <sup>3</sup>Bone Biology Division, Garvan Institute of Medical Research; St Vincent Clinical School, UNSW, Australia; School of Medicine, Sydney University of Notre Dame, Australia, <sup>4</sup>University of Technology, Sydney; Bone Biology Division, Garvan Institute of Medical Research, NSW; St Vincent Clinical School, UNSW; School of Public Health and Community Medicine, UNSW; School of Medicine, Sydney University of Notre Dame, Australia

**Introduction:** Hip fracture among post-menopausal women is one of the most serious health problems worldwide. It is very difficult to predict hip fracture because its risk is affected by multiple interactive risk factors. Although a number of statistical models have been available for predicting hip fracture risk, the level of discrimination is ranging from modest to good. In this study, we trained an artificial neural network (ANN) to predict ten-year hip fracture risk in women using clinical information in one cohort, and validated its predictive performance in another cohort.

**Methods:** This study involved 1167 women aged 60 years and above who were participants of the Dubbo Osteoporosis Epidemiology Study (DOES), which was designed as a prospective cohort study. The data for training (60%) and validation (40%) included age, bone mineral density (BMD), clinical factors, and lifestyle factors which had been obtained at entry time. The women had been followed up for up to 20 years, and during the period, the incidence of new hip fractures was ascertained from X-ray report. We built the multi-layer feed-forward neural networks in the training dataset using 5-fold cross-validation. The performance of model was then assessed in the test set, from which the sensitivity and specificity were evaluated and compared with other common machine learning approaches: k-nearest neighbours (KNN) and Support Vector Machine (SVM).

**Results:** The accuracy of model I (which included only lumbar spine and femoral neck BMD) with 7 hidden nodes yielded an accuracy rate of 79% in the training dataset, and 81% in the test dataset. The AUC for model I was 0.87. Model II (which included only non-BMD risk factors) yielded an accuracy of 86% in the training dataset and 84% in the test dataset. The AUC for model II was 0.92, significantly better than Model I. When BMD and non-BMD risk factors were combined in Model III, the accuracy was 86% in the training dataset and 87% in the test dataset. Compared with Model I and Model II, Model III had the highest AUC values (0.94). The KNN and SVM had the same sensitivity as ANN (81%), but the specificity and accuracy for KNN (79%) and SVM (82%) were lower than ANN.

**Conclusion:** These findings indicate that artificial neural network models are able to predict hip fracture more accurately than any existing statistical models, and that the model can help stratify individuals for complex medical decision making in the clinical setting.

Disclosures: Thao P. Ho-Le, None.

## FR0212

**Vertebral Fracture Discrimination for QCT, HR-QCT, and CTXA based DXA.** Lukas Huber<sup>\*1</sup>, Timo Damm<sup>1</sup>, Wolfram Timm<sup>2</sup>, Julian Ramin Andresen<sup>3</sup>, Claus-Christian Glüer<sup>1</sup>, Reimer Andresen<sup>4</sup>. <sup>1</sup>Section Biomedical Imaging, Department of Radiology and Neuroradiology, UKSH, Christian-Albrechts-Universität zu Kiel, Germany, Germany, <sup>2</sup>MINDWAYS CT, Austin, TX, USA, United States, <sup>3</sup>Medical School, Sigmund Freud University, Vienna, Austria, Austria, <sup>4</sup>Institute of Diagnostic and Interventional Radiology/Neuroradiology, Westkuestenlinikum Heide, Academic Teaching Hospital of the Universities of Kiel, Luebeck and Hamburg, Heide, Germany, Germany

## Objectives

Quantitative computed tomography (QCT) has long been regarded superior to DXA in discriminating patients with and without vertebral fractures [1]. However, most studies used single slice QCT. Fewer data is available for spiral QCT and high-resolution QCT (HR-QCT). We compared their performance with CTXA, i.e. DXA data calculated from QCT data obtained at the proximal femur [2][3].

## Methods

144 female patients (mean age 69 years, range 40–89) were examined for osteoporosis, 70 with at least one fractured vertebral body (cases) and 74 without fractures (controls). Clinical QCT/HR-QCT images of the spine (120kVp, 90–420mAs, slice thickness 0.8mm, reconstructed increment 0.4mm, in-plane pixel size 0.5–0.7mm) were evaluated using standard QCT software of the spine and CTXA of the hip used clinically (Mindways, Austin, TX, USA). Additional analysis of the QCT/HR-QCT images of the spine was performed using StructuralInsight (SI) our in-house CT software. Simultaneous calibration to mg/cc  $K_2HPO_4$  was performed. Vertebral fracture status was evaluated by an experienced radiologist (RA). Fracture discrimination was assessed in age-adjusted logistic regression models (per standard deviation) and ROC analysis (AUC) using JMP (SAS Institute, Cary, NC, USA). Following variables were investigated: mean bone mineral density (mean BMDspine) of 3 vertebral bodies (typically L1–L3), aBMD of the femoral neck (aBMDfn) and total proximal femur (aBMDhptot), both estimates from CTXA. Using SI, we investigated spinal BMD (typically L1), bone volume fraction (BV/TV), tissue mineral density (TMD), trabecular separation (Tb.Sp) and its standard deviation (Tb.Sp-SD) from an ellipse-shaped volume of interest (VOI).

## Results

See Table.

Combined model of BMD (L1) ( $p < 0.0001$ ) & Tb.Sp-SD (L1) ( $p < 0.0166$ ) with AUC = 0.901

## Summary &amp; Conclusion

DXA equivalent aBMD of the femoral neck and the total femur assessed by CTXA showed significant vertebral fracture discrimination. QCT based BMD resulted in odds ratios more than twice as high. Bone microstructure (Tb.Sp-SD) added further discriminatory power. These results demonstrate a potential for superior performance in vertebral fracture risk assessment.

## References

- [1] Wang X1, et al. J Bone Miner Res. 2012 Apr;27(4):808-16
- [2] Khoo BCC, et al. Osteoporos Int (2009) 20: 1539.
- [3] Cann CE, et al. PLoS One. 2014 Mar 17;9(3):e91904

All BMD in mg/cm<sup>3</sup>; aBMD in mg/cm<sup>3</sup>; Tb.Sp, Tb.Sp-SD in mm; mean±SD

Acquisition	Variable	Cases	Controls	p	sOR(95%CI)	AUC
CTXA	aBMDfn	0.54±0.10	0.69±0.13	<0.0001	3.4(2.0-5.9)	0.838
	aBMDhptot	0.61±0.12	0.79±0.15	<0.0001	4.3(2.4-7.6)	0.859
QCT	mean BMDspine	51.6±19.2	92.3±30.1	<0.0001	11.2(4.5-28.0)	0.891
HR-QCT	BMD (L1)	37.0±17.7	74.0±26.1	<0.0001	9.0(4.0-20.2)	0.890
	TMD (L1)	284.7±15.1	289.8±21.3	0.1115	1.5(0.9-2.4)	0.778
	BV/TV (L1)	0.007±0.012	0.036±0.054	0.008	6.5(1.6-25.9)	0.814
	Tb.Sp (L1)	10.3±3.9	6.8±3.8	0.0005	2.1(1.4-3.2)	0.815
	Tb.Sp-SD (L1)	1.9±0.6	1.6±0.6	0.0023	1.9(1.3-2.9)	0.800

Table Results

Disclosures: Lukas Huber, None.

## FR0214

**Associations of TBS and fractures differ among ethnicities: a study of NHANES 2005-2008.** Rajesh Jain<sup>\*</sup>, Tamara Vokes. University of Chicago Medicine, United States

**Background:** Trabecular bone score (TBS), a textural analysis of the lumbar spine image, has been shown to capture fracture risk. However, this has been reported in Caucasian populations (CA) with little or no information on associations of TBS with fractures in African Americans (AA) or Mexican Americans (MA). Recently, TBS data from the National Health and Nutrition Examination (NHANES) was publicly released. Thus, the aim of this study was to examine the association of TBS with self-reported history of fracture in AA and MA as compared to CA in a nationally representative sample.

**Methods:** This is a study of NHANES 2005-2008 data, for which BMD and TBS are available. T-scores were derived from young CA reference data for the hip (NHANES III) and spine (NHANES 2005-2008). Only subjects over 40 and with BMI 15-37 were analyzed, as that is the working BMI range for TBS. For the primary analysis, fractures

were excluded if due to severe trauma or if the location was the skull, fingers, toes, or unspecified. Due to the design of the questionnaire, hip, wrist, and spine fractures that occurred before age 50 were not evaluated for trauma, and the subjects reporting them (351 men, 141 women) were excluded from analysis—leaving 2045 women and 2094 men.

**Results:** Among 468 AA and 399 MA women, fracture history was less common than among 1,178 CA women (4.7% and 6.5% vs. 14.4%,  $p < 0.001$  for both). This was also true of 504 AA and 388 MA men as compared to 1,202 CA men (4.4% and 2.6% vs. 11.0%,  $p < 0.001$ ). For a given BMD or TBS category, AA and MA were less likely than CA to have history of fracture (see Figure 1, subgroups of <20 subjects omitted).

As BMD or TBS category worsened, CA women and men had clear stepwise increases in self-reported fractures ( $p < 0.001$  for trend, see Figure 1). In minorities, these trends were present but attenuated for TBS among AA women ( $p = 0.50$ ) and for both BMD and TBS among MA men ( $p = 0.18, 0.74$ ), possibly due to a low number of fractures. Including all fractures, regardless of age of occurrence or trauma, yielded similar trends for TBS in all subgroups, except for an attenuated trend in AA men ( $p = 0.54$ ).

**Conclusion:** Ethnicity and gender affected the association between TBS and history of prior fracture in a nationally representative sample. These findings suggest that TBS may need to be used differently in minority populations. Prospective fracture information is needed to precisely define how to apply TBS in non-Caucasians.

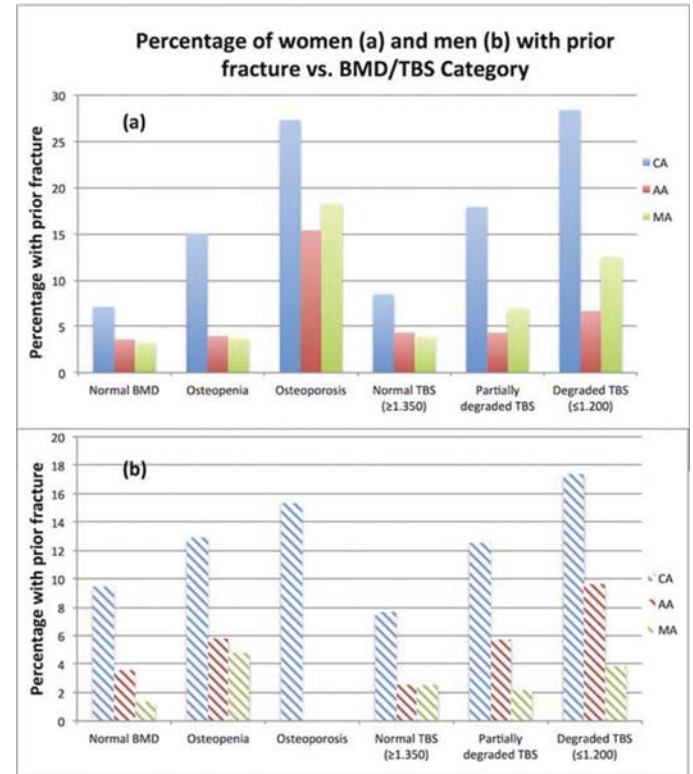


Figure 1

Disclosures: Rajesh Jain, None.

## FR0216

**Adding Cortical Porosity to Garvan or FRAX tools Improve Identification of Postmenopausal Women with Nonvertebral Fracture: The Tromsø Study.** Rita Kral<sup>\*1</sup>, Marit Osima<sup>2</sup>, Tove T Borgen<sup>3</sup>, Elin Richardsen<sup>4</sup>, Åshild Bjørnerem<sup>1</sup>. <sup>1</sup>Department of Obstetrics and Gynaecology, University Hospital of North Norway, Department of Clinical Medicine, UiT The Arctic University of Norway, Tromsø, <sup>2</sup>Department of Community Medicine, UiT The Arctic University of Norway, Tromsø, <sup>3</sup>Department of Orthopaedic Surgery, University Hospital of North Norway, Tromsø, Norway, <sup>4</sup>Department of Rheumatology, Vestre Viken Hospital Trust, Hospital of Drammen, Norway, <sup>5</sup>Department of Medical Biology, UiT The Arctic University of Norway, Tromsø, <sup>6</sup>Department of Pathology, University Hospital of North Norway, Tromsø, Norway, Norway

Despite of the importance of cortical bone for bone strength, neither Garvan nor Fracture Risk Assessment Tool (FRAX) take into account the cortical architecture. We tested whether adding cortical porosity or cortical thickness to existing Garvan or FRAX tools improve the identification of women with fragility fracture. This nested case-control study included 211 postmenopausal women aged 54-94 years with non-vertebral fractures and 232 controls from the Tromsø Study, Norway. We assessed Garvan and FRAX 10-year risk estimates for fragility fracture and quantified femoral subtrochanteric cortical porosity and thickness in CT images using StrAx1.0 software. Women with fracture had higher Garvan and FRAX estimates, higher cortical porosity



and thinner cortices than controls (all  $p < 0.001$ ). Per SD higher Garvan and FRAX estimates, higher cortical porosity and thinner cortices, odds ratio (95% CI) for fracture was 3.34 (2.40-4.67), 2.09 (1.64-2.67), 1.71 (1.38-2.11) and 1.79 (1.44-2.23), respectively. Cortical porosity and thickness remained associated with fracture adjusted for Garvan or FRAX estimates. When using Garvan threshold  $>25\%$  combined with cortical porosity ( $>80^{\text{th}}$  percentile) or cortical thickness ( $<20^{\text{th}}$  percentile), 52.6% and 50.2% of fracture cases were identified. FRAX threshold  $>20\%$  combined with cortical porosity or thickness identified 43.1% and 40.3%, respectively. Measurement of cortical porosity or thickness identified 17.1% and 14.7% additional fracture cases who were not identified using Garvan alone, and 21% and 17.5% additional fracture cases than FRAX alone. Fracture detection was improved, and developing a future tool combining clinical risk factors with cortical bone architecture may improve identification of patients who need preventive treatment.

**Disclosures:** Rita Kral, None.

## FR0217

**Are grade 1 vertebral fracture, fractures?** Brian Lentle<sup>1</sup>, Claudia Berger<sup>2</sup>, Linda Probyn<sup>3</sup>, Jacques P. Brown<sup>4</sup>, Lisa Langsetmo<sup>5</sup>, Ben Fine<sup>3</sup>, Kevin Lian<sup>1</sup>, Arvind Shergill<sup>3</sup>, Jacques Trollip<sup>1</sup>, Stuart Jackson<sup>6</sup>, William D. Leslie<sup>7</sup>, Jerilyn C. Prior<sup>1</sup>, Stephanie M. Kaiser<sup>8</sup>, David A. Hanley<sup>9</sup>, Angela M. Cheung<sup>3</sup>, Jonathan D. Adachi<sup>10</sup>, Tanveer Towheed<sup>11</sup>, K. Shawn Davison<sup>12</sup>, David Goltzman<sup>13</sup>. <sup>1</sup>University of British Columbia, Canada, <sup>2</sup>McGill University Health Centre- Research Institute, Canada, <sup>3</sup>University of Toronto, Canada, <sup>4</sup>Université Laval, Canada, <sup>5</sup>University of Minnesota, United States, <sup>6</sup>University of Alberta, Canada, <sup>7</sup>University of Manitoba, Canada, <sup>8</sup>Dalhousie University, Canada, <sup>9</sup>University of Calgary, Canada, <sup>10</sup>McMaster University, Canada, <sup>11</sup>Queens University, Canada, <sup>12</sup>University of Victoria, Canada, <sup>13</sup>McGill University, Canada

Using the Canadian Multicentre Osteoporosis Study, we compared 2 methods of vertebral fracture (VF) assessment: the Genant Semi-Quantitative tool (GSQ) and the Algorithm-Based Qualitative tool modified to include cortical buckling or breaks (mABQ).

Both methods graded fractures according to their apparent degree of vertebral height reduction similar to GSQ. A participant was categorized according to the highest grade assigned to his spine (T4-L4). Incident VF were defined as new or worsening VF. Analyses on overall VF scores were possible at baseline for 5319 and 5242 participants for GSQ and mABQ methods, respectively, and longitudinal analyses, for 3954 and 3930 participants for GSQ and mABQ methods, respectively. We used regression models (linear/logistic) with baseline BMD, incident VF and non-vertebral major osteoporotic fractures (NVMOF) as dependent variables to compare the groups: a) grade 1 GSQ (GSQ1) vs no GSQ VF, b) grade 1 mABQ (mABQ1) vs no mABQ VF, and c) mABQ1 vs GSQ1 alone (without mABQ signs). Models were adjusted for sex, age, height and BMI.

We found that 8.5% of participants had a GSQ1 and 83.6% had no GSQ VF, while 1.0% had mABQ1 VF and 93.3% had no mABQ VF. Participants with grade 1 VF, by either method, had lower mean BMD values at the spine, femoral neck and total hip compared with those with no VF. Adjusted femoral neck BMD estimates were  $-0.024 \text{ g/cm}^2$  (95% C.I.:  $-0.034$ ;  $-0.014$ ) for GSQ1 and  $-0.064 \text{ g/cm}^2$  ( $-0.092$ ;  $-0.036$ ) for mABQ1 compared to no VF. Participants with mABQ1 VF had lower L1-L4, femoral neck and total hip BMD than those with a GSQ1 VF alone (from  $0.047 \text{ g/cm}^2$  to  $0.073 \text{ g/cm}^2$ ). Participants with prevalent GSQ1 VF were associated with incident VF (GSQ1-GSQ3) compared to those without prevalent GSQ VF; but mABQ1 VF were more likely to be associated with incident VF (GSQ1-GSQ3) than GSQ1 VF (OR of 5.4 and 95% C.I.: 2.4; 11.9). The sample size was too small to examine incident mABQ VF in participants with grade 1 VF. GSQ1 VF was not associated with 15-year incident NVMOF compared to no GSQ VF. Participants with mABQ1 VF were more likely to have 15-year NVMOF than those with no mABQ VF (2.6 [1.3; 5.2]) and also than those with GSQ1 alone VF (2.5 [1.1; 5.3]).

Thus, prevalent grade 1 GSQ and mABQ VF were both associated with reduced BMD, and with incident GSQ VF but the associations were stronger with prevalent grade 1 mABQ, which were also associated with incident non-vertebral major osteoporotic fractures.

**Disclosures:** Brian Lentle, None.

## FR0218

**"Risk-Equivalent" T-score Adjustment Using Lumbar Spine Trabecular Bone Score (TBS): The Manitoba BMD Registry.** William Leslie<sup>1</sup>, Enisa Shevroja<sup>2</sup>, Helena Johansson<sup>3</sup>, Anders Oden<sup>3</sup>, Eugene McCloskey<sup>3</sup>, John Kanis<sup>3</sup>, Didier Hans<sup>2</sup>. <sup>1</sup>University of Manitoba, Canada, <sup>2</sup>Lausanne University Hospital, Switzerland, <sup>3</sup>University of Sheffield Medical School, United Kingdom

**Background:** Lumbar spine trabecular bone score (TBS) can be used to modify the output from FRAX to enhance fracture prediction. We explored an alternative approach for using TBS in clinical practice based upon a "risk-equivalent" offset adjustment to the bone mineral density (BMD) T-score.

**Methods:** Using the Manitoba BMD Registry, we identified 45,185 women age 40 years and older with body mass index 15-37  $\text{kg/m}^2$ , baseline DXA, lumbar spine

TBS and FRAX-based probabilities estimated with femoral neck BMD. Incident non-traumatic major osteoporotic fractures (MOF,  $n=3925$ ) were identified using population-based health services data during mean 7.4 years observation (335,910 person-years). Age- and BMI-adjusted Cox proportional hazards models were first used to estimate the risk for MOF from BMD T-score alone (separately for femoral neck, total hip, lumbar spine). TBS was then added to the model to estimate the BMD-independent effect on TBS on MOF risk, with inclusion of a multiplicative interaction term to account for the larger effect of TBS on fracture risk in younger individuals.

**Results:** TBS and all BMD measurements were independent predictors of MOF ( $p < 0.001$ ), and the age\*TBS interaction term was significant in all BMD models ( $p < 0.001$ ). From the relative risk gradients we calculated the BMD T-score offset that would reflect the equivalent risk from using BMD and TBS together. We tested our results by comparing TBS-adjusted FRAX probabilities with output from the FRAX algorithm when the "risk-equivalent" femoral neck BMD T-score was used as the BMD input to FRAX. There was a high level of agreement between MOF probability estimated from TBS-adjusted MOF FRAX probability (X-axis) and FRAX MOF probability using the "risk-equivalent" femoral neck T-score (Y-axis):  $r^2 = 0.98$ , slope = 1.02, intercept = -0.3 (Figure left). A similarly high level of agreement was also seen between hip fracture probability estimated from TBS-adjusted MOF FRAX probability (X-axis) and FRAX hip probability using the "risk-equivalent" femoral neck T-score (Y-axis):  $r^2 = 0.95$ , slope = 1.07, intercept = 0.0 (Figure right).

**Conclusion:** Lumbar spine TBS is a predictor of fracture, and the BMD-independent effect of TBS on fracture risk can be estimated as a simple offset to the BMD T-score. This approach may be helpful in regions where intervention guidelines are based upon BMD T-score rather than fracture probability.

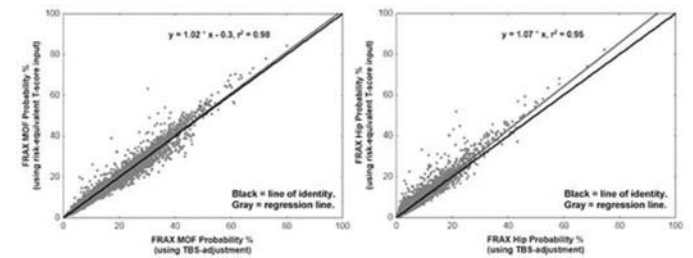


Figure: FRAX Probability using TBS adjustment vs. "risk-equivalent" T-score input.

**Disclosures:** William Leslie, None.

## FR0220

**Cost-effectiveness of a program to identify patients at high risk of hip fracture utilizing pre-existing CT scans in managed-care systems.** Maria Pisu<sup>1</sup>, David Kopperdahl<sup>2</sup>, Cora Lewis<sup>1</sup>, Michael Saddekni<sup>1</sup>, Kenneth Saag<sup>1</sup>, Tony Keaveny<sup>3</sup>. <sup>1</sup>University of Alabama Birmingham, United States, <sup>2</sup>O.N. Diagnostics, United States, <sup>3</sup>University of California Berkeley, United States

Management of osteoporosis is limited in part by the low number of patients tested diagnostically with DXA and a lack of information on bone quality. One way to help address this is to utilize pre-existing CT scans by re-analyzing them with biomechanical CT analysis (BCT), in which both DXA-equivalent BMD and finite element analysis-derived bone strength are measured. Here we assessed the cost effectiveness of this approach in a managed-care system. The hypothetical program at a single medical center was for 1,000 women who get a hip-containing CT for any medical reason during a single year, and who otherwise qualify for but have not had a recent DXA. Using Markov models, we assessed three cases: no screening for osteoporosis, screening with DXA at current rates (DXA), and one-time screening with BCT right after the CT. For the latter, the BCT analysis included both BMD and bone strength, but we also assessed measuring just BMD from the CT (CT-BMD). Outcomes were fractures averted and costs (2016 US\$), at an annual discount rate of 3%, over ten years. We considered scenarios where 25–90% of the 1000 women have the BCT test and varied the risk of hip fracture upwards from the 1995 rate for Medicare women. We assumed a 50% treatment rate for those testing positive, a 40% treatment efficacy for hip fracture for generic alendronate, and values of sensitivity and specificity from a prospective hip-fracture observational BCT study (44 sensitivity, 0.84 specificity for BMD, either for CT or DXA; 0.66 sensitivity, 0.71 specificity for BCT). Costs included \$200 for BCT; \$100 for CT-BMD or DXA; \$50 per patient for personnel to manage the program; one-year \$50,000 treatment cost of a hip fracture, plus \$10,000 the second year.

We found that all screening strategies avert fractures and were cost saving compared to no screening, except for the use of DXA in patients at the lowest fracture probability rate (Table). One-time testing with BCT and CT-BMD both produced better outcomes than typical DXA testing if 40% and 50%, respectively, of the CT scans were tested. BCT was always better than CT-BMD. If 90% of scans were tested with BCT, cost savings were substantial, particularly for higher-risk patients. Managed-care systems, which have a financial incentive to reduce the number of hip fractures, can feasibly implement standing-order BCT testing on all eligible patients. Our results suggest that doing so would both improve medical care and reduce healthcare spending.

Table: Hip fractures averted and cost savings for BCT, versus population risk and testing rate.

Test Strategy	Type	Rate (%)	5-Year Probability of Hip Fracture					5-Year Probability of Hip Fracture				
			0.04	0.05	0.07	0.09	0.11	0.04	0.05	0.07	0.09	0.11
			Hip Fractures averted per 1000 patients					Costs Savings per 1000 patients (in \$1000)				
DXA	8		1.0	1.2	1.7	2.2	2.7	-15	3	39	73	107
BMD-CT	25		0.6	0.7	1.0	1.2	1.5	70	98	155	211	265
BCT	25		0.8	1.0	1.3	1.7	2.0	91	134	217	299	379
BMD-CT	40		0.9	1.1	1.6	2.0	2.4	111	158	248	337	424
BCT	40		1.2	1.5	2.1	2.7	3.2	146	214	347	478	606
BMD-CT	50		1.1	1.4	2.0	2.5	3.0	139	197	310	421	530
BCT	50		1.5	1.9	2.6	3.4	4.1	183	267	434	598	757
BMD-CT	90		2.1	2.5	3.5	4.5	5.4	251	355	559	759	954
BCT	90		2.8	3.4	4.7	6.0	7.3	329	481	782	1076	1363

Cost Savings compared to no testing at all. DXA performed annually at a typical rate for diagnostic purposes; BCT is performed only once, for the proportion of CT scans denoted by the testing rate; BMD-CT is BMD measured from CT; BCT measures both BMD and finite element analysis-derived bone strength. Lowest value of probability of hip fracture based on 1995 Medicare rates.

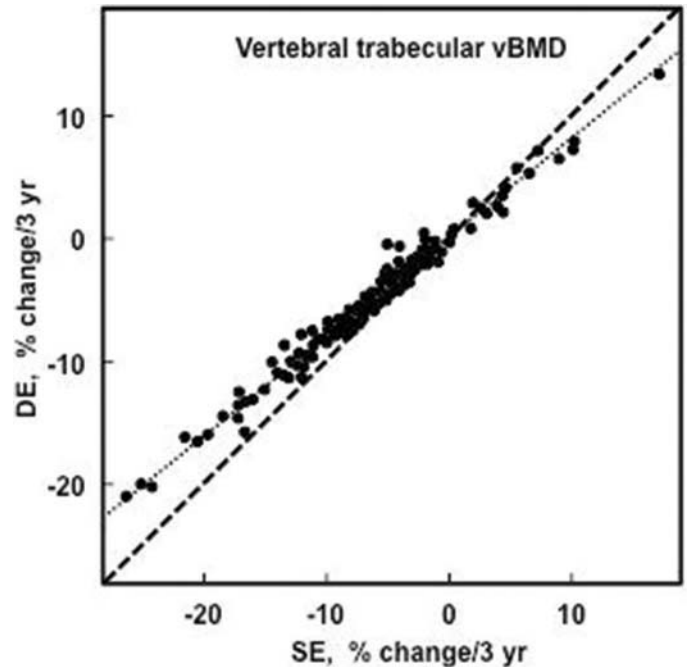
Table: Hip fractures averted and cost savings for BCT, versus population risk and testing rate

Disclosures: Maria Pisu, None.

## FR0222

**Changes in Bone Marrow Fat Overestimate Trabecular Bone Loss by Single-Energy Quantitated Computed Tomography.** Jad Sfeir\*, Matthew Drake, Elizabeth Atkinson, Jon Camp, Amanda Tweed, Louise McCready, Lifeng Yu, Mark Adkins, Shreyasee Amin, Sundeep Khosla, Mayo Clinic, United States

Central quantitative computed tomography (QCT) is increasingly used in clinical trials and practice to assess bone mass or strength and to evaluate longitudinal changes in response to drug treatment. Current studies utilize single-energy (SE) QCT scans, which may be confounded both by the amount of bone marrow fat at baseline and changes in marrow fat over time. However, the extent to which marrow fat changes either underestimate volumetric BMD (vBMD) measurements at baseline or under-/overestimate longitudinal changes remains unclear. To address this issue, 175 early postmenopausal women (mean age $\pm$ SD, 57 $\pm$ 3 yrs) underwent spine and hip QCT scans at baseline and 3 yrs using a 128-slice dual-source dual-energy (DE) scanner (SOMATOM Definition Flash, Siemens Healthcare, 100 kVp and 140Sn kVp). A tin filter was added to the 140 kVp beam to improve beam separation and DE performance. The scans were analyzed as either SE scans (100 kVp) or DE scans, with the latter accounting for bone marrow fat. At baseline, vertebral trabecular vBMD was (median) 18% lower (signed rank test  $P < 0.001$ ) while femur neck (FN) cortical vBMD was only 3% lower ( $P < 0.001$ ) when assessed by SE vs DE scanning. For trabecular bone at the spine, SE scanning overestimated the 3 yr rate of bone loss by 24% ( $P < 0.001$  vs DE rates of loss) but only by 10% for changes in FN cortical vBMD ( $P < 0.001$  vs DE rates of loss). In addition, as shown in the Figure, the deviation between SE and DE rates of bone loss in vertebral trabecular vBMD became progressively greater as the rate of bone loss increased. Thus, SE QCT scans underestimate trabecular vBMD and substantially overestimate rates of age-related bone loss due to ongoing conversion of red to yellow marrow. Further, the greater the rate of bone loss (and presumably the greater the accumulation of fatty marrow), the greater the overestimation of bone loss by SE scans. Conversely, the dramatic changes following some anabolic treatments in spine trabecular vBMD (e.g., 48% increase with PTH) as compared to more modest DXA changes (18%; NEJM 349:1215, 2003) may be due, at least in part, to PTH effects on reducing marrow fat (Cell Metab 25:661, 2017). In conclusion, longitudinal SE QCT changes in trabecular vBMD need to be considered with caution, particularly the marked "anabolic" effects of PTH (and perhaps other anabolic agents that may alter cell fate in the marrow), and future studies should validate these longitudinal changes with DE scans.



Figure

Disclosures: Jad Sfeir, None.

## FR0223

**Clinical Impact of Bone Microstructure Assessment by High Resolution Peripheral Quantitative CT Imaging in Adults with Recurrent Fractures and Normal or Near-Normal Bone Density.** Jad Sfeir\*, Bart Clarke, Robert Wermers, Robert Tiegs, Ann Kearns, Kurt Kennel, Sundeep Khosla, Matthew Drake, Mayo Clinic, United States

High resolution peripheral quantitative CT (HRpQCT) imaging for non-invasive *in vivo* evaluation of bone microarchitecture has been widely used in clinical research studies. Although HRpQCT can be a powerful diagnostic tool to evaluate bone microarchitecture in patients at increased fracture risk despite normal areal BMD (aBMD) by DXA, its clinical use remains limited. We aimed to assess bone volumetric BMD (vBMD) and microarchitecture in patients with recurrent fractures, and to evaluate the impact of HRpQCT-derived microarchitectural information on clinical care decisions.

Sixteen consecutive adult patients (13 women) with recurrent fragility fractures and normal or near normal aBMD consented to undergo HRpQCT imaging at the non-dominant radius and tibia using the Xtreme CT II device. For each variable, T- and Z-scores were calculated using normative population-based data from healthy subjects previously evaluated by HRpQCT in other ongoing research studies. All patients underwent clinical evaluation to exclude secondary causes of osteoporosis prior to enrollment.

Patients had a median age of 57.2 yrs (IQR, 53.9 – 62.8) with a median lowest aBMD T-score at any site of -1.25 (-1.62 to -0.95). Median vBMD T-scores at the tibia and radius were -1.33 (-2.46 to -0.78) and -2.03 (-2.60 to -0.82), respectively. Cortical indices appeared to account for the majority of the discrepancies between the clinical fractures and aBMD measurements. When compared to other measurements at the same site, median T-scores for tibial cortical vBMD [-2.74 (-4.17 to -0.23);  $p=0.0008$ ], radial cortical thickness [-2.92 (-3.89 to -1.89);  $p=0.0004$ ], and radial cortical porosity [1.34 (0.06 to 4.09);  $p=0.0004$ ] were significantly different. Further, trabecular bone score (TBS) values obtained retrospectively on 8 patients showed poor correlation with HRpQCT-derived trabecular measurements by linear regression ( $R^2=0.069$ ).

Following the generation of HRpQCT reports, clinical providers modified their treatment plan in 10/16 patients (62%), with 7 subjects initiated on a skeletal anabolic agent for impaired cortical microarchitectural parameters. In addition, 2 patients were assessed as having a relative contraindication to teriparatide due to markedly increased cortical porosity.

In patients with a higher fracture risk than that suggested by their aBMD, HRpQCT imaging provides clinically useful information regarding changes in cortical bone indices and implications for management.

Disclosures: Jad Sfeir, None.



## FR0224

**Urinary N-telopeptide as an Indicator of the Onset of Menopause-related Bone Loss in Pre- and Early Perimenopausal Women: Results from the Study of Women's Health Across the Nation (SWAN).** Albert Shieh<sup>\*1</sup>, Gail Greendale<sup>1</sup>, Jane Cauley<sup>2</sup>, Joan Lo<sup>3</sup>, Arun Karlamangla<sup>1</sup>. <sup>1</sup>UCLA, United States, <sup>2</sup>University of Pittsburgh, United States, <sup>3</sup>Kaiser, United States

Some investigators have suggested that the menopause transition (MT) represents a time-limited window to intervene and prevent rapid bone loss and permanent micro-architectural damage. However, the rapid phase of MT-related bone mineral density (BMD) decline begins around 1 year before the final menstrual period (FMP); we thus need to be able to identify women who have begun to experience this decline prior to substantial bone loss. Since the bone resorption marker, urinary N-telopeptide (U-NTX), begins to increase prior to the onset of rapid MT-related BMD decline, we hypothesized that U-NTX, measured in pre- or early perimenopause, could be used to predict whether a woman will lose bone over the next few years. U-NTX was measured in 42-52 year-old women in pre- or early perimenopause, at the baseline visit of the Study of Women's Health Across the Nation (SWAN). Lumbar spine (LS) and femoral neck (FN) BMD were measured by DXA (Hologic) at the baseline visit and during annual follow-up visits. Bone loss was said to have begun if the annualized rate of BMD decline during the 3-4 year period after U-NTX measurement was faster than the following thresholds based on site-specific least significant change for DXA-based BMD measurements: 1.23% per year in the LS and 1.93% per year in the FN. A total of 1,243 women had measurements of both U-NTX and BMD decline. Among these participants, after adjusting for relevant clinical covariates (MT stage, age, body mass index, race/ethnicity, SWAN study site) in multivariable modified Poisson regression, each standard deviation increment in U-NTX was associated with 14% greater risk of LS bone loss (RR = 1.14, p=0.02), but was not associated with risk of bone loss in the FN. The area under the receiver-operator curve for predicting LS bone loss was 0.73. We conclude that measurement of a bone resorption marker, such as U-NTX, in pre or early perimenopause may aid in early identification of women who will experience MT-related bone loss over the next few years.

**Disclosures:** Albert Shieh, None.

## FR0229

**Peripheral Arterial Disease Predicts Hip Fracture in Men. Results from the MrOS Sweden Study.** Tove Bokrantz<sup>\*1</sup>, Claes Ohlsson<sup>2</sup>, Mattias Lorentzon<sup>3</sup>, Magnus Karlsson<sup>1</sup>, sten Ljunggren<sup>4</sup>, Karin Manhem<sup>1</sup>, Dan Mellström<sup>5</sup>. <sup>1</sup>Department of Molecular and Clinical Medicine, Institute of Medicine, Sahlgrenska Academy, University of Gothenburg, Gothenburg, Sweden, <sup>2</sup>Centre for Bone and Arthritis Research (CBAR), Sahlgrenska Academy, University of Gothenburg, Gothenburg, Sweden, <sup>3</sup>Department of Geriatric Medicine, Institute of Medicine, Sahlgrenska Academy, University of Gothenburg, Gothenburg, Sweden, <sup>4</sup>Department of Medical Sciences, University of Uppsala, Uppsala, Sweden, <sup>5</sup>Department of Geriatrics, Institute of Medicine, Sahlgrenska Academy, Centre for Bone and Arthritis Research (CBAR) University of Gothenburg, Gothenburg, Sweden, Sweden

**Purpose** Peripheral Arterial Disease (PAD) has been related to bone loss and increased risk for incident fractures. The association between PAD and hip fracture risk in elderly men is uncertain.

**Population and methods** Ankle-brachial index (ABI) was assessed in the Swedish part of the MrOS (Osteoporotic fractures in Men) study (n=3014, average age 75.4 years). PAD was defined as ABI < 0.90. Incident fractures were assessed in computerized X-ray archives. The risk for hip fractures was calculated using Cox proportional hazard models. Areal bone mineral density (BMD) at hip sites and lumbar spine as well as lean and fat mass were assessed at baseline using DXA (Lunar Prodigy and Hologic QDR 4500). Standardized BMD was calculated. Hand grip strength was measured with a Jamar hand dynamometer and glomerular filtration rate (GFR) was calculated with serum cystatin C.

**Results** At baseline, 2893 men had an ABI measurement and PAD was found in 10.9 percent. The number of men with an incident hip fracture after 10 years of follow up was 186. Men with PAD were older and had reduced lean mass, BMD at all sites and hand grip strength while their body mass index and fat mass was normal. Men with PAD were more often current smokers (20 percent vs 7 percent), had more often diabetes type 2 (18 percent vs 7 percent) and had more often hypertension (49 percent vs 32 percent). GFR was also lower in men with PAD. Number of falls tended to be higher in men with PAD (p=0.09).

The hazard ratio (HR) for hip fracture among men with PAD was 1.70 (CI 1.14-2.54), adjusted for age and site. Additional adjustment for femoral neck BMD only marginally affected this association (HR 1.64; CI 1.10-2.45), suggesting that the association between PAD and hip fracture is not mediated via BMD. In a multivariate model, the HR for hip fracture in men with PAD was 1.53 (CI 1.01-2.31) adjusted for age, site, BMD, BMI, falls, hypertension, diabetes, current smoking, estimated GFR and hand grip strength.

**Conclusion** PAD predicts hip fracture independently of BMD in Swedish men. We propose that PAD might be a useful BMD independent risk marker for hip fractures in men.

**Disclosures:** Tove Bokrantz, None.

## FR0231

**Impact of Competing Risk of Mortality on Association of Cognitive Impairment with Risk Of Hip Fracture in Older Women: Results From the Study of Osteoporotic Fractures (SOF).** Susan Diem<sup>\*1</sup>, Tien Vo<sup>1</sup>, Lisa Langsetmo<sup>1</sup>, John Schousboe<sup>2</sup>, Kristine Yaffe<sup>3</sup>, Kristine Ensrud<sup>4</sup>. <sup>1</sup>University of Minnesota, United States, <sup>2</sup>Health Partners Research Foundation, United States, <sup>3</sup>University of California, United States, <sup>4</sup>Minneapolis Veterans Affairs Medical Center and University of Minnesota, United States

To determine the associations of mild cognitive impairment (MCI) and dementia with risk of hip fracture in women late in life with and without accounting for competing risk of mortality, we used data from 1483 women (mean age 87.6 ± 3.3 yrs) participating in the Year 20 (Y20) SOF exam. Cognitive function was categorized as normal, MCI, or dementia based on a comprehensive cognitive assessment. Participants were contacted every 4 months after Y20 to ask about hip fractures (confirmed by x-ray reports) and ascertain vital status (deaths verified by death certificates). Absolute probability of hip fracture by cognitive function category was determined using Kaplan-Meier survival curves and using cumulative incidence models with mortality as a competing risk (CICR). Similarly hazard ratios were calculated using Cox proportional hazards regression and Fine-Gray models considering death as a competing risk. During a mean follow-up of 5.6 yrs, 139 (9.4%) women sustained a hip fracture [incidence 16.8 (95% CI: 14.0-19.6)/1000 person-yrs] and 985 (66.4%) died [incidence 113.4 (95% CI: 106.4-120.5)/1000 person-yrs]. Using traditional survival analysis, the absolute probability of hip fracture at 5 years was higher for those with cognitive impairment: normal cognition, 7% [95% CI: 5-9%]; MCI, 11% [95% CI: 8-15%]; dementia 12% [95% CI: 7-17%]. When the competing risk approach (CICR) was used, these probabilities among women with cognitive impairment were substantially reduced: normal cognition, 6% [95% CI: 5-8%]; MCI, 9% [95% CI: 6-12%]; dementia, 8% [95% CI: 5-12%]. The difference in probabilities calculated by the 2 methods increased with increasing duration of follow-up. Among those with dementia, the Kaplan-Meier estimate at the end of follow-up (9.8 yrs) was 19% [95% CI: 9-32%] whereas the competing risk estimate was much lower at 9% [95% CI: 6-13%]. Similarly, use of models accounting for competing risk of death also attenuated the associations of MCI and dementia with hip fracture (Table 1). In conclusion, women with MCI and dementia late in life who survived were at increased risk of hip fracture. However, not taking into account the competing mortality risk among women with cognitive impairment markedly overestimated their absolute fracture probability and adjusted fracture risk. Guidelines regarding fracture risk assessment and use of drug treatment in older adults with cognitive impairment need to take into account the impact of the competing risk of death.

**Table 1. Traditional Cox Proportional Hazards Models\* and Fine-Gray Competing Risk Models for Association of cognitive status with hip fracture (Entire Cohort N=1483)**

Hip fracture (n=139)	Hazard Ratio (95% CI)			
	Normal (n=80)	MCI (n=36)	Dementia (n=23)	MCI/Dementia (n=59)
<b>Model 1†</b>				
Cox proportional model	(referent)	1.60 (1.07-2.39)	1.48 (0.92-2.39)	1.55 (1.10-2.20)
Fine-Gray model	(referent)	1.31 (0.88-1.96)	1.04 (0.65-1.65)	1.19 (0.85-1.68)
<b>Model 2‡</b>				
Cox proportional model	(referent)	1.49 (0.98-2.28)	1.42 (0.85-2.39)	1.48 (1.01-2.13)
Fine-Gray model	(referent)	1.28 (0.83-1.97)	1.10 (0.66-1.86)	1.21 (0.83-1.77)

\*Cox proportional hazards models do not account for competing risk of death

†adjusted for site, age and race

‡adjusted for site, age, race, education and multi-morbidity score and gait speed

Table 1

**Disclosures:** Susan Diem, None.

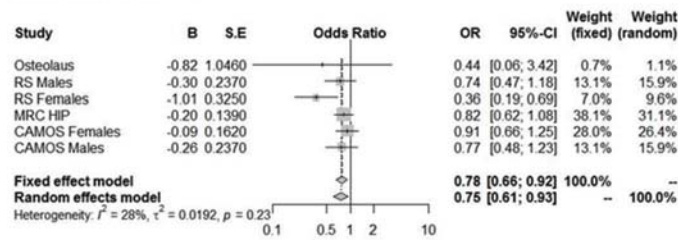
## FR0233

**Type 2 Diabetes Is Associated With Lower Prevalence Of Vertebral Fractures: A Meta-Analysis of Prospective Studies.** Fjorda Koromani<sup>\*1</sup>, Ling Oei<sup>1</sup>, Taulant Muka<sup>1</sup>, Enisa Shevroja<sup>2</sup>, Josje Schoufour<sup>1</sup>, Oscar Franco<sup>1</sup>, Carola Zillikens<sup>1</sup>, Eugene Mc Closkey<sup>3</sup>, William Leslie<sup>4</sup>, Olivier Lamy<sup>2</sup>, Edwin Oei<sup>1</sup>, Didier Hans<sup>2</sup>, Fernando Rivadeneira<sup>1</sup>. <sup>1</sup>Erasmus MC, Netherlands, <sup>2</sup>University of Lausanne, Switzerland, <sup>3</sup>University of Sheffield, United Kingdom, <sup>4</sup>University of Manitoba, Canada

**Background:** Paradoxically, individuals with type 2 diabetes (T2D) have increased risk of non-vertebral fractures despite having on average higher Bone Mineral Density (BMD) than non-diabetics. We aimed to assess the association between T2D and prevalent vertebral fractures (VFs). **Methods:** Participants of three population-based cohorts MRC HIP (n=5,165); Osteolaus (n=1410) and Rotterdam Study (RS) (n=5,874), with baseline data on T2D status, radiographic VFs, BMD and Trabecular Bone Score (TBS) derived from DXA or Hologic scans, were analysed together with published summary level data from the Camos Study (n=7,753). VFs in Osteolaus and RS were scored based on Genant's SQ method with cases defined as vertebral height reduction ≥ 26% and in CAMOS the threshold ≥ 20% was applied. In MRC HIP, VFs were scored based on McCloskey method which has similar sensitivity and specificity to grade 2-3 in Genant method. T2D status was derived from clinical records or based on glucose levels and treatment status. The association between T2D and VFs was assessed in each cohort, sex stratified, using logistic regression models adjusted for variables including age, BMI, anti-osteoporotic treatment, and either LS- or FN-BMD; in RS and

Osteolus models were additionally adjusted for TBS. Study estimates expressed as odds ratios were then combined in a fixed effect inverse variance meta-analysis. Results: The meta-analysis comprised 20,202 participants of which 1,243 (6.1%) were diagnosed with T2D among which 250 (20.1%) had suffered at least one VF. T2D cases had significantly higher LS- BMD or FN- BMD across all studies with a mean difference ranging from 0.025 to 0.135 g/cm<sup>2</sup> (p-value <0.001). TBS assessed in Osteolus and RS was 0.06 (p <0.001) to 0.02 (p=0.09) lower in diabetics than non-diabetics. After meta-analysis, T2D was associated with a lower prevalence of VFs (OR 0.78, 95% CI 0.66 to 0.92), independently of BMD levels. Conclusion: In contrast to the observed increased risk for non-vertebral fractures in individuals with T2D despite higher BMD, our findings indicate that the prevalence of vertebral fractures is significantly lower in individuals with T2D than in non-diabetics. The findings of our study are in line with the contention that the deleterious effect of T2D might be different in trabecular than in cortical bone. Yet, the mechanisms for the discordant effects of T2D on vertebral and non-vertebral fracture risk remain to be identified.

Fig.1. Meta- analysis of four prospective studies that assessed the association between T2D and prevalent vertebral fractures



Results of the meta-analysis of four cohorts that assessed the association between T2D and VFs

**Disclosures:** *Fjorda Koromani, None.*

## FR0234

### Prevalence and Characteristics of Atypical Periprosthetic Femoral Fractures.

Jean-Thomas Leclerc<sup>\*1</sup>, Laëticia Michou<sup>2</sup>, François Vaillancourt<sup>1</sup>, Stéphane Pelet<sup>1</sup>, David Simonyan<sup>3</sup>, Etienne Belzile<sup>1</sup>. <sup>1</sup>Division of orthopedic surgery, CHU de Québec-Université Laval, Canada, <sup>2</sup>Division of rheumatology, CHU de Québec-Université Laval, Canada, <sup>3</sup>CHU de Québec-Université Laval, research centre, Canada

**Purpose:** Bisphosphonates use has been associated to atypical femoral fractures (AFF) as defined by the ASBMR Task force criteria which currently exclude periprosthetic fractures. The prevalence and risk factors associated with AFF in patients with hip and knee replacements is unknown. The objectives of this study were to establish the proportion of atypical periprosthetic femoral fractures (APFF) in patients with hip and knee arthroplasties and to determine the clinical and radiological risk factors associated with this type of fracture.

**Methods:** A retrospective radiological review was conducted of all femoral fractures between January 1st, 2006, and March 31st, 2015, at our center. Patients who sustained a periprosthetic femoral fracture were identified and included in this study. We used the ASBMR Task force criteria to identify APFF and to establish their prevalence. Data from medical records and radiological assessments of the femoral anatomy, the characteristics of the fracture and the positioning of the prosthesis were collected. Descriptive statistics are presented and compared to non-atypical periprosthetic fractures data. Bivariate and multivariate analyses were performed to determine the characteristics and potential risk factors of APFF.

**Results:** The prevalence of APFF amongst periprosthetic femoral fractures was 8.3% (11/122). A strong association with bisphosphonates (p=0.0072) was observed as well as an increased risk of atypical fractures among alendronate users compared to risedronate users (p=0.0365). A transverse fracture (p<0.0001), a periosteal thickening of the lateral cortex at the fracture (p<0.0001), a unicortical fracture (p=0.0190), an increase in diaphyseal lateral cortical thickness (p=0.0461) and prodromal symptoms (p=0.0329) were associated to APFF. The type of hip or knee implant, the implant positioning and the femoral geometry did not appear to be risk factors for APFF.

**Conclusions:** Bisphosphonates use constitutes a major risk factor for APFF. The exclusion of periprosthetic femoral fractures from the ASBMR criteria should be reconsidered since they present clinical and radiological signs similar to those of AFF without an arthroplasty. Further studies are required to better define the healing potential of APFF.

**Disclosures:** *Jean-Thomas Leclerc, None.*

## FR0238

### Cathepsins B and S Are Novel Biomarkers for Bone Mineral Density: A Mendelian Randomization Study. John Morris<sup>\*1</sup>, John Kemp<sup>2</sup>, David Evans<sup>2</sup>, Brent Richards<sup>3</sup>. <sup>1</sup>Department of Human Genetics, McGill University, Canada, <sup>2</sup>The University of Queensland Diamantina Institute, Australia, <sup>3</sup>Department of Medicine, McGill University, Canada

Global osteoporosis prevalence continues to rise, motivating the need to identify bone-relevant biomarkers for earlier diagnosis and intervention therapies to reduce fracture risk. Cathepsins, a family of cysteine proteases, have been previously studied as drug targets to treat osteoporosis. However, drug development has ceased due to adverse side-effects caused by the pleiotropic effect of cathepsins in other important biological pathways. Despite this, cathepsins may still be useful biomarkers as many act on type I collagen and can be measured in blood plasma. The causality of biomarkers can be tested using Mendelian randomization (MR), a method that uses genetic determinants of a biomarker to provide an estimate of its effect on an outcome, greatly reducing bias due to confounding and reverse causation. Here, we used data on cathepsins from genome-wide association studies (GWAS) of blood plasma protein levels in 1,000 individuals from the Cooperative Health Research in the Region of Augsburg (KORA) study to estimate their effect on bone mineral density (BMD) using data from a GWAS of estimated BMD from the heel calcaneus in 142,487 individuals from the UK Biobank (UKBB) study (*unpublished*).

Instruments were defined as single nucleotide polymorphisms (SNPs) significantly associated with a cathepsin's plasma levels and mapping to the cathepsin's gene. We targeted SNPs associated with proteins that mapped directly to their genes to reduce possible pleiotropic effects of the SNPs on other genes. We identified, from the UKBB study, corresponding BMD effect estimates and standard errors for instruments and weighted these summary statistics by the effect estimates on a cathepsin. We calculated MR effect estimates ( $\beta_{MR}$ ), 95% confidence intervals (95% CI), and P-values from the weighted summary statistics to interpret the effect of cathepsins on BMD.

rs3947 and rs41271951 associated with and directly mapped to cathepsin B (*CTSB*;  $\beta = 0.52$ ;  $SE = 1.5 \times 10^{-27}$ ) and cathepsin S (*CTSS*;  $\beta = 0.97$ ;  $SE = 4.1 \times 10^{-46}$ ), respectively, in unit standard deviation changes of cathepsin plasma levels. In unit standard deviation changes of BMD, moderate association with BMD was observed for rs3947 ( $\beta = -0.020$ ;  $SE = 0.004$ ;  $P = 1.1 \times 10^{-7}$ ) and rs41271951 ( $\beta = 0.0149$ ;  $SE = -0.006$ ;  $P = 8.6 \times 10^{-3}$ ). MR analyses estimated a significant effect of cathepsin B on BMD ( $\beta_{MR} = -0.040$ ; 95% CI = [-0.054, -0.025];  $P = 8.4 \times 10^{-8}$ ) and a marginally significant effect of cathepsin S on BMD ( $\beta_{MR} = 0.015$ ; 95% CI = [0.003, 0.028];  $P = 0.013$ ), in unit standard deviation changes of BMD for each standard deviation increase of cathepsin plasma levels.

These data are consistent with circulating cathepsins B and S having causal effects on BMD, where increased levels of cathepsin B decrease BMD and increased levels of cathepsin S increase BMD. Our findings suggest that both cathepsins are suitable biomarkers for human bone biology.

**Disclosures:** *John Morris, None.*

## FR0241

### The association between type 2 diabetes mellitus, hip fracture, and post-hip-fracture mortality: a multi-state cohort analysis. Cristian Tebe<sup>\*1</sup>, Daniel Martinez-Laguna<sup>2</sup>, Cristina Carbonell-Abella<sup>3</sup>, Carlen Reyes<sup>3</sup>, Daniel Prieto-Alhambra<sup>4</sup>.

<sup>1</sup>Statistical Assessment Service at Bellvitge Biomedical Research Institute (IDIBELL), Spain, <sup>2</sup>GREMPAL Research Group (Idiap Jordi Gol Primary Care Research Institute) and CIBERFes, Universitat Autònoma de Barcelona, Spain, <sup>3</sup>GREMPAL Research Group, Idiap Jordi gol, CIBERFes and Universitat Autònoma de Barcelona, Spain, <sup>4</sup>Centre for Statistics in Medicine and Nuffield Department of Orthopaedics, Rheumatology, and Musculoskeletal Sciences (NDORMS), University of Oxford, United Kingdom

#### PURPOSE

Recent studies have suggested an increased hip fracture risk in patients suffering from type 2 diabetes (T2DM), whilst failing to model the effect of T2DM status on subsequent post-fracture mortality. We used novel multi-state cohort analyses to estimate the association between T2DM and the transitions to hip fracture, fracture-free death, and post-hip-fracture mortality.

#### METHODS

Design and participants Cohort including all subjects aged 65 to 80 years and with a recorded diagnosis of T2DM on 1/1/2006; and T2DM-free controls matched (up to 2:1) by year of birth, gender, and primary care practice.

Setting Primary care electronic medical records in the SIDIAP database ([www.sidiap.org](http://www.sidiap.org)), which contains data for >5.5 million subjects (>80% of the population) from Catalonia, Spain.

Exposure and follow-up primary care diagnosis of T2DM on 1/1/2006. Subjects were followed from then to study outcome (hip fracture or death) date, and then from hip fracture to death (where applicable).

Statistical Analyses Multi-state Cox regression models were fitted to estimate Hazard Ratios (HR) and 95% Confidence Intervals [95CI] for hip fracture, fracture-free death, and post-hip-fracture death according to T2DM status. Multivariable models were adjusted for age at T2DM diagnosis and at hip fracture respectively. All analyses were stratified by gender, which otherwise violated proportionality of hazards.



## RESULTS

A total of 44,796 T2DM and 81,221 matched controls (53% women, mean age 72 years old) were followed for a median of 8 years: 23,816 died without fracturing, and 3,308 broke a hip, of which 829 subsequently died (Figure 1). Median time to hip fracture was 4.7 years, with a median of 1.5 years from then to death. Adjusted HRs for fracture-free death were 1.40 [1.35-1.45] for men and 1.86 [1.79-1.94] for women. HRs for hip fracture were 1.30 [1.13-1.49] and 1.50 [1.38-1.62], whilst HRs for post-hip-fracture mortality were estimated at 1.30 [1.05-1.62] and 1.69 [1.42-2.01] in men and women respectively.

## CONCLUSION

T2DM patients are at a 30% (men) to 50% (women) increased risk of hip fracture, and at a 30% (men) to 70% (women) risk of dying after suffering such a hip fracture. The effect of T2DM on overall baseline (fracture-free) mortality was of a similar magnitude (40% higher for men, 85% for women) to that following a hip fracture.

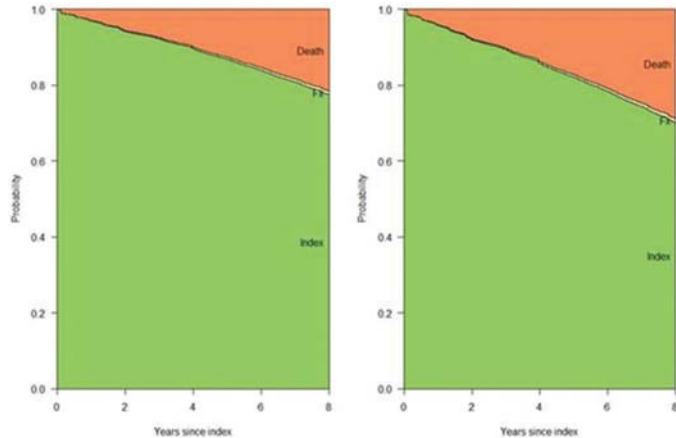


Figure 1: Stacked predicted probability of study outcomes (death, fx = hip fracture, and fracture-free survival) over 8 years.

**Disclosures:** Cristian Teb , Amgen, Other Financial or Material Support.

## FR0242

**Use of oral bisphosphonates and bone mineral density changes in moderate-severe (Stage 3B+) chronic kidney disease: an open cohort multivariable and propensity score analysis from Funen, Denmark.** Sanni Ali<sup>1</sup>, Martin Ernst<sup>2</sup>, Fergus Caskey<sup>3</sup>, Nigel Arden<sup>4</sup>, Yoav Ben-Shlomo<sup>3</sup>, Mads Nybo<sup>5</sup>, Katrine Hass Rubin<sup>2</sup>, Andrew Judge<sup>1</sup>, Cyrus Cooper<sup>1</sup>, M Kassim Javaid<sup>4</sup>, Pernille Hermann<sup>6</sup>, Bo Abrahamsen<sup>2</sup>, Daniel Prieto-Alhambra<sup>1</sup>. <sup>1</sup>Centre for Statistics in Medicine and Nuffield Department of Orthopaedics, Rheumatology, and Musculoskeletal Sciences (NDORMS), University of Oxford, United Kingdom, <sup>2</sup>OPEN, Department of Health, University of Southern Denmark, Denmark, <sup>3</sup>School of Social and Community Medicine, University of Bristol, United Kingdom, <sup>4</sup>Nuffield Department of Orthopaedics, Rheumatology, and Musculoskeletal Sciences (NDORMS), University of Oxford, United Kingdom, <sup>5</sup>Department of Clinical Biochemistry, Odense University Hospital, Denmark, <sup>6</sup>Department of Endocrinology, Odense University Hospital, Denmark

**PURPOSE** In addition to safety concerns, there is a paucity of data for oral bisphosphonates (oBP) to improve bone mineral density (BMD) in patients with moderate or severe chronic kidney disease (CKD). We linked all BMD measurements in the Funen area (pop 478,000, Denmark) to biochemistry, national health registries, and filled prescriptions to study the association between oBP use and BMD changes.

**METHODS** Design and participants Cohort including all subjects aged 40 years or older, with an estimated glomerular filtration rate of <45 (CKD stage 3B+), and with at least 2 BMD measurements 2 or more years apart. Previous users of oBP, and those with >1 year between closest renal and BMD measurement were excluded.

Setting Regional BMD database covering all DXA-based routine measurements in Funen, Denmark between 08/17/1999 and 02/23/2016.

Exposure, follow-up, and outcome Dispensation of oBP therapy was the main exposure. Subjects were followed from first BMD to the latest of subsequent ones. oBP non-users were identified using incidence density sampling with replacement. Outcome was annualized % change (relative to previous/baseline) in total hip BMD.

Statistical Analyses Multivariable linear regression models adjusted for age, sex, body mass index, baseline eGFR, fracture history, co-morbidities (Charlson index and renal problems), hospital contacts in previous year, and relevant treatment/s history (number of ATCs in previous year, use of steroids, aromatase inhibitors, anti-diabetics, etc.) were fitted to model BMD change according to oBP use. In addition, propensity scores (ps) were calculated using the same confounders, and linear regression stratified by ps deciles was used in a sensitivity analysis to minimise confounding by indication.

**RESULTS** Use of oBP was rare in this group of patients: 81 oBP users and 282 non-users with stage 3B+ CKD (as in the 1 year before DXA) were included. Whilst oBP users gained an average 0.59% total hip BMD per year, non-users lost an average 1.98% per annum. Multivariable adjusted mean difference was +1.81% (95%CI 0.99% to 2.63%),

which was enhanced in the ps adjusted analysis at +2.44% (1.80% to 3.07%) in favour of oBP users.

**CONCLUSION** In a cohort including >360 subjects with stage 3B+ CKD, use of oBP appears associated with a significant improvement of about 2% per year in total hip BMD. More data are needed on both anti-fracture effectiveness and safety of oBP therapy in moderate-advanced CKD patients.

**Disclosures:** Sanni Ali, None.

## FR0243

**Older Men Who Sustain a Hip Fracture Experience Greater than Expected Declines in Bone Mineral Density at the Contralateral Hip.** Alan Rathbun<sup>1</sup>, Jay Magaziner<sup>2</sup>, Michelle Shardell<sup>2</sup>, Laura Yerges-Armstrong<sup>3</sup>, Denise Orwig<sup>1</sup>, Gregory Hicks<sup>4</sup>, Marc Hochberg<sup>1</sup>. <sup>1</sup>University of Maryland School of Medicine, United States, <sup>2</sup>National Institute on Aging, United States, <sup>3</sup>GlaxoSmithKline, United States, <sup>4</sup>University of Delaware, United States

Men with hip fracture experience declining bone mineral density (BMD) in the year after hip fracture and are at risk of secondary fractures. However, the magnitude of BMD declines among men attributable to hip fracture is unknown and necessary to determine and improve post-fracture outcomes. The study aim was to ascertain whether rates of BMD change in men after hip fracture exceed those expected with aging using two existing prospective cohorts: the Baltimore Hip Studies 7<sup>th</sup> Cohort (BHS-7) and the Baltimore Men's Osteoporosis Study (MOST). BHS-7, conducted from 2006 to 2011, recruited older adults hospitalized for hip fracture (N=339) and had assessments within 22 days of hospitalization (baseline) and at 2, 6, and 12 months follow-up. MOST, conducted from 2000 to 2003, enrolled age-eligible men (N=694) from population-based listings and collected data at baseline and a second visit that occurred 10 to 31 months (mean=18 months) later. The combined sample (n=452) comprised Caucasian men from BHS-7 (n=89) and MOST (n=363) with at least 2 DXA scans and overlapping ranges of age, height, and weight. Mixed-effects models estimated individual rates of change in total hip and femoral neck BMD; annual percent declines ((slope/baseline BMD)\*100) were calculated. Annual percent BMD decline was regressed on cohort (BHS-7 versus MOST) using generalized linear models adjusted for age, height, weight, smoking, alcohol consumption, comorbidity, baseline BMD, and use of bone-active drugs (glucocorticoids, testosterone, bone-active drugs, calcium supplements). Adjusted cohort-specific BMD declines and corresponding between-group differences in change were estimated. Adjusted annual declines in total hip and femoral neck BMD were greater in BHS-7 participants than in MOST participants: -4.16% (95% confidence interval [CI]: -4.87, -3.46) and -4.90% (95% CI: -5.88, -3.92) versus -1.57% (95% CI: -2.19, -0.96) and -0.99% (95% CI: -1.88, -0.10), respectively (Figure 1). Statistically significant (P<0.001) between-group differences in change were -2.59% (95% CI: -3.26, -1.91) for total hip BMD and -3.91% (95% CI: -4.83, -2.98) for femoral neck BMD. Hip fracture in older men is associated with BMD declines at the contralateral hip that are many times faster than those expected from aging. Interventions to prevent excess bone loss in men after hip fracture may reduce the risk of secondary fractures.

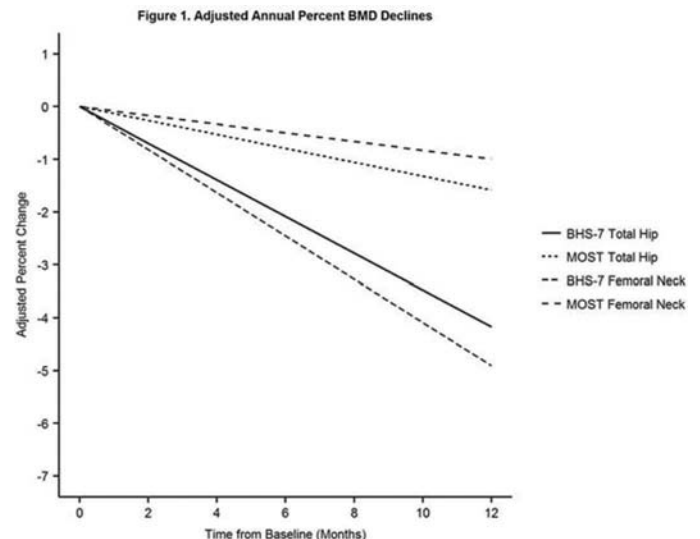


Figure 1: Adjusted Annual Percent BMD Declines

**Disclosures:** Alan Rathbun, None.

## FR0245

**The Utility of TBS-adjusted BMD T-score in the Vertebral Fractures Risk Estimation in the Postmenopausal Women of the OsteoLaus and the Rotterdam Studies.** Enisa Shevroja<sup>1</sup>, Fjorda Koromani<sup>2</sup>, William Leslie<sup>3</sup>, Berengere Aubry-Rozier<sup>4</sup>, Edwin Oei<sup>5</sup>, Olivier Lamy<sup>6</sup>, Fernando Rivadeneira<sup>7</sup>, Didier Hans<sup>6</sup>. <sup>1</sup>Center of Bone diseases, Bone and Joint Department, Lausanne University Hospital and Departments of Internal Medicine and Epidemiology, Erasmus MC, Rotterdam, The Netherlands, Switzerland, <sup>2</sup>Departments of Internal Medicine and Epidemiology, Erasmus MC, Rotterdam, The Netherlands, Netherlands, <sup>3</sup>Department of Internal Medicine, University of Manitoba, Winnipeg, Manitoba, Canada, Canada, <sup>4</sup>Center of Bone diseases, Bone and Joint Department, Lausanne University Hospital, Lausanne, Switzerland, Switzerland, <sup>5</sup>Department of Radiology, Erasmus Medical Center, Rotterdam, The Netherlands, Netherlands, <sup>6</sup>Center of Bone diseases, Bone and Joint Department, Lausanne University Hospital, Switzerland, <sup>7</sup>Departments of Internal Medicine and Epidemiology, Erasmus MC, Netherlands

Background: Lumbar spine (LS) trabecular bone score (TBS) can be used to modify the output from FRAX to enhance fracture prediction. Leslie et al. (ASBMR 2017) proposed an alternative approach for using TBS in clinical practice based upon a "risk-equivalent" offset adjustment to the bone mineral density (BMD) T-score. The aim of this study is to test whether the TBS-adjusted BMD T-score outperforms BMD T-score alone.

Methods: Our study included 3,168 women (age 46-99 y) from the OsteoLaus (N=1,317) and the Rotterdam (N=1,851) Studies. All women had DXA scans (Hologic Discovery or GE-Lunar Prodigy) of LS and femoral neck (FN). In total, 234 prevalent VF were identified using Genant's semi-quantitative approach (classified as grade 2 and 3) scored on DXA-VFA (OsteoLaus) or digital X-rays (Rotterdam). TBS-adjusted BMD T-score of FN or LS was calculated using the formulas provided by Leslie et al. (ASBMR 2017). The lowest BMD T-score and TBS-adjusted BMD T-score from FN and LS, were used for the statistical analysis. Estimates were derived from the basic logistic regression model adjusted for age, cohort effect and lowest BMD T-score. The improvement in VF risk prediction when adding the lowest TBS-adjusted BMD T-score to the basic model, was assessed by calculating the area under the curve (AUC) and the continuous overall net reclassification improvement (NRI) as well as the event (sensitivity) and the non-event (specificity) NRIs.

Results: Women who fractured were older, had lower BMD, TBS and TBS-adjusted BMD. The increased risks of prevalent VF for every SD decrease in the lowest BMD T-score and TBS-adjusted BMD T-score were 60%, OR=1.60, 95%CI (1.39;1.84); and 78%, OR=1.78, 95%CI (1.35;2.35), respectively. The AUCs for the basic model and the one adjusted for TBS-adjusted BMD T-score were 0.695, 95%CI (0.658;0.733) and 0.715, 95%CI (0.680;0.751), respectively, p=0.004. The NRI analysis showed an overall NRI of 0.20, 95%CI (0.16;0.23). An improvement of 20%, 95%CI (17;23%) was seen in the nonevent NRI, whereas the event NRI did not show any improvement, -0.6% (95% CI: -1.2;0.6%).

Conclusion: The result of this study illustrates how TBS contributes to VF risk assessment by increasing the specificity of the model without compromising the sensitivity. Pending evaluation in a larger prospective setting, this approach postulates itself as a helpful strategy to improve patient care in regions where intervention guidelines are based solely on the BMD T-score

**Disclosures:** Enisa Shevroja, None.

## FR0246

**Increased Mortality in Older Home-dwelling Men with High Serum Periostin Levels – the Prospective STRAMBO Study.** Pawel Szulc<sup>\*</sup>, Jean Charles Rousseau, Cindy Bertholon, Roland Chapurlat. INSERM UMR1033, University of Lyon, Hospices Civils de Lyon, France

Elevated tissular periostin expression and its higher serum levels are associated with a higher risk of relapse and death in cancer patients. However, although periostin is involved in many pathological processes, its link with mortality in general population is not clear. We studied the association of serum periostin with mortality in a cohort of 815 home-dwelling men aged 60-87 followed up prospectively for 8 years. Periostin was measured at baseline using ELISA (USCN). All-cause mortality (n=168) increased across the periostin quartiles (lowest: 16%, 17%, 19%, highest: 30%, p<0.005). After adjustment for age, BMI, lifestyle, co-morbidities, treatments, glomerular filtration rate, grip strength, and serum testosterone and high sensitivity C-reactive protein levels, higher serum periostin was associated with higher mortality (HR=1.30 per SD, 95% CI: 1.13–1.50, p<0.001). All-cause mortality was higher in the highest periostin quartile vs. three lower quartiles combined: HR=1.79, 95%CI: 1.29–2.48, p<0.001. Cancer mortality (n=69) increased across the periostin quartiles (6%, 5%, 8%, 14%, p<0.005). In the fully adjusted model, cancer mortality increased with periostin levels (HR=1.44 per SD, 95%CI: 1.16–1.79, p<0.001) and was higher in the highest quartile vs. three lower quartiles combined (HR=2.31, 95%CI: 1.41–3.78, p<0.001). The unadjusted link between cardiovascular mortality and periostin quartiles (n=55) was not significant (5%, 7%, 5%, 10%, p=0.15). By contrast, in the multivariable model, cardiovascular mortality was higher in the highest quartile vs. three lower quartiles combined: HR=1.93, 95%CI: 1.07–3.48, p<0.05. The mortality for other causes analyzed jointly (n=44) was not

associated with periostin levels in the unadjusted (5%, 5%, 6%, 6%, p=0.94) nor in the multivariable models (HR=1.22 per SD, 95%CI: 0.91–1.65, p=0.19). After exclusion of 106 men with prevalent neoplasms and 29 men who died during the first 2 years of the follow-up, all-cause and cancer mortality remained higher in the highest periostin quartile vs. three quartiles combined (25 vs. 15%, p<0.005 and 10 vs. 5%, p<0.05, respectively). The trends persisted in the fully adjusted model for all-cause mortality (HR=1.80, 95%CI: 1.21–2.65, p<0.005) and for cancer mortality (HR=2.12, 95%CI: 1.10–4.03, p<0.05). In conclusion, in older home-dwelling men, high serum periostin levels are associated with higher mortality, mainly cancer mortality, after adjustment for potential confounders.

**Disclosures:** Pawel Szulc, None.

## FR0247

**Does High Serum 25-Hydroxyvitamin D Prevent Falls in Older Women After All?** Kirsti Uusi-Rasi<sup>\*</sup>, Radhika Patil<sup>1</sup>, Saija Karinkanta<sup>1</sup>, Kari Tokola<sup>1</sup>, Pekka Kannus<sup>1</sup>, Christel Lamberg-Allardt<sup>2</sup>, Harri Sievänen<sup>1</sup>. <sup>1</sup>The UKK Institute for Health Promotion Research, Finland, <sup>2</sup>University of Helsinki, Finland

Previously, a 2-year randomized four-arm intervention trial (DEX) assessed the effects of exercise and vitamin D3 (20 µg/d) on falls in Finnish home-dwelling women aged 70 to 80 years. The trial showed that though the rate of all falls did not differ between groups, multimodal supervised exercise reduced the rate of medically-attended injurious falls. Vitamin D3 had no such effect.

Here we assessed the relationship between mean S-25(OH)D levels (6 to 24 months, mean of four measurements) and falls incidence in 387 women included in the analyses. Irrespective of the original randomization, participants were divided into quartiles based on mean S-25(OH)D levels; mean levels (SD) were 59.3 (7.2), 74.5 (3.3), 85.7 (3.5), and 105.3 (10.9) nmol/L, respectively. Mean baseline age and height were 74.2 years and 160 cm with no between-quartile differences. Mean body weight was 74 (12) kg in the two lowest quartiles, and 70 (11) and 71 (12) kg in the two highest quartiles respectively. Exercisers were equally distributed in each quartile, while most of the vitamin D supplemented women belonged to the two highest quartiles.

Falls were recorded with monthly diaries, and physical functioning (maximal isometric leg extensor strength, 5-times chair stand, walking speed and TUG) was assessed at baseline and 24 months. Falls during the first 6 months were excluded from the analyses.

Negative binomial regression was used to assess incidence rate ratios (IRRs) for falls and Cox-regression for hazard ratios (HR) for fallers. Generalized linear models were used to estimate between-quartile differences in physical functioning using age, height, weight, and baseline physical functioning as covariates, with the lowest S-25(OH)D quartile as reference.

There were 37% less falls in the highest quartile, while the two middle quartiles did not differ statistically significantly compared to the reference group. The IRRs (95% CI) for falls were 0.87 (0.62 to 1.22), 0.78 (0.55 to 1.10), and 0.63 (0.44 to 0.90) respectively, indicating lower incidence of falls with increasing mean S-25(OH)D levels. There were also 42% less fallers (HR 0.58; 0.40 to 0.83) in the highest S-25(OH)D quartile compared to the lowest. No between-quartile differences in physical functioning were found.

High S-25(OH)D was associated with the least rate of falls and fallers, while physical functioning showed no association.

**Disclosures:** Kirsti Uusi-Rasi, None.

## FR0248

**Older Men with Decreasing Hemoglobin Have a Higher Risk of Future Hip Fracture: The Cardiovascular Health Study.** Rodrigo J. Valderabano<sup>\*</sup>, Petra Buzkova<sup>2</sup>, Po-Yin Chang<sup>3</sup>, Neil A. Zakai<sup>4</sup>, Howard A. Fink<sup>5</sup>, John A. Robbins<sup>3</sup>, Joy Y. Wu<sup>1</sup>, Jennifer S. Lee<sup>6</sup>. <sup>1</sup>Division of Endocrinology, Stanford University School of Medicine, United States, <sup>2</sup>University of Washington, United States, <sup>3</sup>University of California, Davis, United States, <sup>4</sup>Department of Medicine and Department of Pathology and Laboratory Medicine, University of Vermont, United States, <sup>5</sup>GRECC, Veteran Affairs Health Care System, United States, <sup>6</sup>Division of Endocrinology, Stanford University School of Medicine and Palo Alto Veteran Affairs Health Care System, United States

Purpose: Hematopoiesis and bone health are linked. We previously found that anemia in older men is associated with increased risk of non-spine fracture (Fx) independent of BMD. We hypothesized that lower hemoglobin (Hgb) levels are associated with an increased risk of hip Fx in both older men and women.

Methods: The Cardiovascular Health Study is a prospective longitudinal cohort of 5,888 non-institutionalized, non-wheelchair bound men and women aged >65 years recruited during 1989-90 (first visit). We used data from 4,670 participants with available Hgb levels in the first visit and 1992-93 (second visit). Anemia at the second visit was defined as <13 g/dL for men and <12 g/dL for women (WHO criteria). Hgb change was annualized and divided into sex-specific quartiles. Incident hip Fxs were ascertained every 6 months after the second visit from self-reports and hospitalization records, and defined by ICD-9 codes. Cox proportional hazards modeling estimated the hazard ratios (HR) and 95% confidence intervals (CI) for incident hip Fx. Unadjusted; age, sex and race-adjusted; and fully adjusted (age, sex, race, height, weight, smoking, alcohol, bone



medication, steroids, physical activity score, self-reported health, heart disease) models were performed for participants with anemia (vs. without) and for participants in the quartile with the greatest Hgb loss (vs. others).

Results: 12.5% of women and 14.6% of men had anemia at the second visit. During a median follow-up of 12 years, men with anemia had higher hazards of hip Fx in the unadjusted model (HR 1.76; 95% CI 1.17-2.65); however, risk was attenuated in the fully adjusted model (HR 1.58; 95% CI 0.98-2.54). Men in the quartile with the greatest annualized Hgb loss ( $>0.36$  g/dL) had higher fully adjusted hazards of hip Fx (HR 1.59; 95% CI 1.10-2.31) than other men. Associations were not observed in women except for black women, in whom those with anemia had higher fully adjusted hazards of hip Fx (HR 4.38; 95% CI 1.41-13.55) than those without.

Conclusions: In this older cohort, men with the greatest Hgb loss had a 59% higher risk of subsequent hip Fx. Men with anemia had a similar higher risk of hip Fx, but the association was not statistically significant. Results were consistent with past work evaluating nonspine Fx. Decreasing Hgb may be an earlier marker of skeletal fragility than anemia. Study findings support further research evaluating the utility of Hgb measurement in sex-specific Fx risk assessment.

**Disclosures:** Rodrigo J. Valderrabano, None.

## FR0249

**Prediction of Incident Fragility Fractures in Women with Peripheral CT Imaging – One Slice is Often Enough: the CaMos Bone Quality Study.** Andy Kin On Wong<sup>\*1</sup>, Lauren Burt<sup>2</sup>, Eva Szabo<sup>1</sup>, Steven K. Boyd<sup>2</sup>, Shannon Reitsma<sup>3</sup>, Hana Gillick<sup>3</sup>, Hugo J.W. Fung<sup>4</sup>, Tiffany Yan<sup>5</sup>, Claudie Berger<sup>6</sup>, Heather Macdonald<sup>7</sup>, Leigh Gabel<sup>7</sup>, Maureen C. Ashe<sup>7</sup>, Danmei Liu<sup>8</sup>, Jerilynn Prior<sup>7</sup>, David A. Hanley<sup>2</sup>, Chantal Kawalilak<sup>9</sup>, Andrew Frank-Wilson<sup>10</sup>, Saija Kontulainen<sup>9</sup>, Shawn Davison<sup>11</sup>, Wojciech Olszynski<sup>9</sup>, George Ioannidis<sup>3</sup>, Christopher L. Gordon<sup>3</sup>, Colin E. Webber<sup>3</sup>, Karen A. Beattie<sup>3</sup>, Alexandra Papaioannou<sup>3</sup>, Lora Giangregorio<sup>12</sup>, Robert G. Josse<sup>13</sup>, Norma MacIntyre<sup>3</sup>, Tassos Anastasiades<sup>14</sup>, David Goltzman<sup>6</sup>, Angela M. Cheung<sup>1</sup>, Jonathan D. Adachi<sup>3</sup>, CaMos Bone Quality Study for the<sup>3</sup>.

<sup>1</sup>University Health Network, Canada, <sup>2</sup>University of Calgary, Canada, <sup>3</sup>McMaster University, Canada, <sup>4</sup>University of Toronto, Canada, <sup>5</sup>Ryerson University, Canada, <sup>6</sup>McGill University, Canada, <sup>7</sup>University of British Columbia, Canada, <sup>8</sup>Centre for Hip Health and Mobility, Canada, <sup>9</sup>University of Saskatchewan, Canada, <sup>10</sup>National Institute on Aging, United States, <sup>11</sup>University of Victoria, Canada, <sup>12</sup>University of Waterloo, Canada, <sup>13</sup>St. Michael's Hospital, Canada, <sup>14</sup>Queen's University, Canada

**Objective:** To compare single slice pQCT and 110 slice HR-pQCT-derived bone quality parameters' ability to predict fragility fractures (fx) in women. **Methods:** Women aged 60-85 years in the Canadian Multi-centre Osteoporosis Study (CaMos) at 6/9 study centres, each with access to pQCT, HR-pQCT or both had their non-dominant wrist and ankle imaged. Standard HR-pQCT settings were applied, acquiring 110 slices (voxel size: 0.082mm isotropic). For pQCT, pixel size was 0.200x0.200mm and a single (2.3±0.2mm) slice was obtained (10 mm/s) at the 4% distal radius and tibia. Standard, extended cortical, and finite element analyses were applied to HR-pQCT images. Scans with motion grades  $\geq 4$  were excluded. pQCT manufacturer software computed densitometric measures and microstructural analysis was completed using OsteoQ (ISS Inc). Risk factors for osteoporotic fx according to FRAX were captured at baseline. Annual follow-up was conducted to obtain information about deaths and incident fx (due to fall from standing height or less, excluding fingers, toes, face and skull, as ascertained radiographically). **Statistics:** Fine and Gray subdistribution hazard models evaluated the ability of bone quality parameters from either modality to predict fx, adjusting for competing risk of mortality. Models were adjusted for FRAX risk factors and for osteoporosis treatment. **Results:** In 806 women (mean age: 72.1±8.1 yr, BMI: 27.6±5.4kg/m<sup>2</sup>), 497 completed pQCT scans and 767 HR-pQCT scans; 393 completed both. Mean time to follow-up was 3.0±1.2 years. 75 participants sustained an incident fx and 25 died over this period. Trabecular measures at the radius more strongly associated with incident fx than at the tibia (Table I). Total BMD consistently predicted incident fx at both sites and on both modalities. Cortical BMD and measures of bone strength predicted fx well on HR-pQCT but not on pQCT. Although cortical thickness erred towards an association with incident fx, cortical porosity did not demonstrate an apparent association. In analyses examining participants who received scans from both modalities, similar fracture association patterns were observed. Effect sizes appeared larger for HR-pQCT measures, though only BV/TV at the radius showed significance. **Conclusions:** Total BMD at both sites and trabecular microstructure at the distal radius consistently predicted incident fx over 3 years in women 60 and over. A single pQCT slice may already be sufficient to yield such information.

**Table I. pQCT and HR-pQCT parameters' prediction of incident fragility fractures (fx) in women 60-85 years of age.** Manufacturer analyses were conducted for HR-pQCT and for densitometric measures on pQCT. Apparent bone microstructure from pQCT images was measured using OsteoQ software (Ingilis Software Solutions). HR = Hazard Ratio, expressed per standard deviation decrease in each parameter unless otherwise noted (\* = increase). FL= failure load. BSI= bone strength index. Other abbreviations as per ASBMR taskforce on standardization of bone structure and density nomenclature.

ULTRADISTAL RADIUS	HR-pQCT (110 slices, 0.082 mm isotropic voxel)			pQCT (1 slice, 0.200 x 0.200 x 2.0 mm voxel)		
Variables	HR	Lower CI	Upper CI	HR	Lower CI	Upper CI
CIPO*	0.80	0.55	1.18	N/A	N/A	N/A
FL/BSI	1.61	1.20	2.16	1.60	0.53	4.86
CITh	1.26	0.94	1.70	1.07	0.68	1.67
CIbMD	1.36	1.00	1.85	1.29	0.77	2.15
TbBMD	1.61	1.22	2.12	1.92	1.30	2.83
TIBMD	1.46	1.08	1.97	1.88	1.10	3.23
TIAr	0.98	0.69	1.37	0.97	0.86	1.10
TbAr	0.93	0.67	1.29	0.96	0.84	1.09
BV/TV	1.09	0.72	1.66	1.79	1.24	2.58
TbN	1.42	1.11	1.81	1.65	1.23	2.22
TbSp*	1.16	1.01	1.33	1.50	1.22	1.85
TbTh	1.44	0.99	2.09	1.51	1.05	2.17

	Censored 540			Fx 59	Deceased 23	Censored 375			Fx 40	Deceased 12
ULTRADISTAL TIBIA	HR-pQCT (110 slices, 0.082 mm)				pQCT (1 slice, 2.0 mm)					
	Variables	HR	Lower CI	Upper CI	HR	Lower CI	Upper CI			
CIPO*	0.94	0.62	1.41		N/A	N/A	N/A			
FL/BSI	1.44	1.08	1.93		0.88	0.63	1.22			
CITh	1.27	0.97	1.68		1.20	0.80	1.79			
CIbMD	1.21	1.00	1.47		1.36	0.89	2.08			
TbBMD	1.22	0.97	1.54		1.40	1.00	1.98			
TIBMD	1.28	1.00	1.63		1.59	1.02	2.47			
TIAr	0.81	0.57	1.15		0.69	0.43	1.11			
TbAr	0.79	0.55	1.12		0.67	0.41	1.08			
BV/TV	1.03	0.65	1.63		1.37	0.94	1.98			
TbN	1.13	0.85	1.49		1.28	1.04	1.58			
TbSp*	1.13	0.95	1.35		1.11	0.94	1.32			
TbTh	1.09	0.84	1.41		1.53	0.65	3.65			
	Censored 579	Fx 63	Deceased 24		Censored 439	Fx 39	Deceased 12			

Censored 540 Fx 59 Deceased 23 Censored 375 Fx 40 Deceased 12

Censored 579 Fx 63 Deceased 24 Censored 439 Fx 39 Deceased 12

Table 1

**Disclosures:** Andy Kin On Wong, None.

## FR0250

**Trends in Post-fracture Care for Manitoba, Canada 2000-2014: A Population-Based Analysis.** Yang Cui<sup>\*1</sup>, Shuman Yang<sup>2</sup>, Colleen Metge<sup>3</sup>, William Leslie<sup>2</sup>. <sup>1</sup>George & Fay Yee Centre for Healthcare Innovation, University of Manitoba, Canada, <sup>2</sup>University of Manitoba, Canada, <sup>3</sup>George & Fay Yee Centre for Healthcare Innovation, Canada

**Background:** A large body of research has consistently revealed a large gap in post-fracture secondary prevention at the population level. A province-wide post-fracture notification program was implemented in Manitoba, Canada after June 2010 based on successful results from a randomized controlled trial (June 2008 to May 2010, ClinicalTrials.gov NCT00594789), but its effectiveness at the population level is uncertain. Therefore, we examined trends in post-fracture care province-wide between 2000 and 2014.

**Methods:** Using population-based administrative data we identified incident major non-traumatic osteoporosis fractures (hip, forearm, humerus and clinical vertebral) in women and men aged 50 and older between April 1, 2000 and January 31, 2014. Those already receiving osteoporosis treatment, with recent DXA testing in nursing homes or with early post-fracture mortality were excluded. We ascertained the proportion with post-fracture intervention (DXA testing, new osteoporosis medication use, or either of the preceding) within one year. The Chi-square test was used to test for differences related to sex and age subgroups. The Cochran-Armitage test was used to examine for linear trend in care.

**Results:** A total of 21,141 fracture events occurred during the study period (4,293 hip, 8,334 forearm, 4,468 humerus, and 4,046 vertebral). The average age of the cohort was 69.9 (SD 12.2) and 70.9% were female. A higher proportion of women (vs men) and older (vs younger) patients received post-fracture interventions (Table,  $p < .01$ ). Post-fracture DXA testing increased significantly over time for all subgroups ( $p < .05$ ). Osteoporosis medication use remained stable after forearm and humerus fractures, with a significant decline for hip and vertebral fractures. Either post-fracture intervention (DXA testing or osteoporosis medication use) showed a significant increase over time for forearm and humerus fractures, but only a non-significant increase for hip and spine fractures.

**Summary:** After a successful randomized controlled trial, we found evidence that adopting a population-based post-fracture notification program led to sustained improvement in post-fracture DXA testing, but did not improve osteoporosis medication use. Most patients with a prior osteoporotic fracture still did not receive minimal post-fracture care.

HIPC File No. 2008/2009-16, Theme 4

ASBMR Sponsor: Yang Cui

**Table.** Percentage (95% CI) receiving post-fracture care after a major osteoporotic fracture

Year	DXA testing	Drug treatment	DXA testing or drug treatment
<b>Women &lt;65 years</b>			
2000-2004	16.9 (15.2-18.8)	11.0 (9.6-12.7)	21.2 (19.3-23.3)
2005-2009	25.4 (23.4-27.4)	10.2 (8.9-11.7)	28.8 (26.8-30.9)
2010-2014	31.8 (29.5-34.1)	10.2 (8.8-11.8)	34.1 (31.8-36.5)
<b>Women ≥65 years</b>			
2000-2004	10.4 (9.4-11.4)	24.3 (22.9-25.7)	28.5 (27.0-30.0)
2005-2009	15.2 (14.0-16.5)	21.0 (19.6-22.4)	29.4 (27.8-31.0)
2010-2014	22.0 (20.5-23.6)	21.7 (20.1-23.3)	33.8 (32.0-35.6)
<b>Men &lt;65 years</b>			
2000-2004	4.1 (2.9-5.6)	2.0 (1.2-3.1)	5.0 (3.7-6.6)
2005-2009	5.9 (4.6-7.6)	2.4 (1.6-3.6)	7.0 (5.5-8.7)
2010-2014	11.1 (9.1-13.4)	3.2 (2.1-4.6)	12.1 (9.9-14.4)
<b>Men ≥65 years</b>			
2000-2004	4.0 (2.9-5.3)	10.8 (9.1-12.8)	13.2 (11.3-15.3)
2005-2009	9.7 (8.1-11.5)	10.7 (9.0-12.6)	17.7 (15.6-20.0)
2010-2014	17.7 (15.4-20.2)	11.3 (9.4-13.4)	24.0 (21.4-26.7)

Figure 1

**Disclosures:** Yang Cui, None.

## FR0251

**Cost-effectiveness of a Bone Health Team for Screening and Treating Veterans at Risk for Fragility Fractures.** Karla Miller<sup>\*1</sup>, Jordan King<sup>2</sup>, Phillip Lawrence<sup>3</sup>, Richard Nelson<sup>1</sup>, Joanne LaFleur<sup>1</sup>, Grant Cannon<sup>1</sup>, Scott Nelson<sup>4</sup>. <sup>1</sup>Salt Lake City Veterans Affairs Medical Center and University of Utah, United States, <sup>2</sup>Kaiser Permanente Colorado, United States, <sup>3</sup>Roseman University of Health Sciences, United States, <sup>4</sup>Vanderbilt University Medical Center, United States

**Purpose:** To evaluate the cost-effectiveness of a bone health team (BHT) as a primary prevention service to screen, monitor, and treat Veterans at risk for fragility fractures compared to current clinical practice from the Veteran's Administration (VA) perspective over a lifetime.

**Methods:** We conducted this analysis by adapting a previously validated Markov microsimulation model of osteoporosis incidence and outcomes in the VA. The model was used to estimate fracture events, quality-adjusted life years (QALYs), and direct healthcare costs of using a BHT vs. current clinical practice. Model inputs were derived from national sources, published literature, and program estimates from the BHT. Uncertainty in model parameters was assessed by conducting one-way and probabilistic sensitivity analyses.

**Results:** In the base-case, the BHT was associated with a substantially higher proportion of patients with underlying osteoporosis or osteopenia diagnosed and treated with bisphosphonates (osteoporosis: 38% vs 6.9%, osteopenia: 25.5% vs 0.2%). This resulted in the BHT strategy being associated with a modestly lower fracture rate than current clinical practice. In probabilistic sensitivity analysis, the BHT was the dominant option; however, in all analyses, no meaningful differences were observed in life-time estimated costs, unadjusted survival, and QALYs between the prevention strategies.

**Conclusion:** A BHT appears to be a potentially cost-effective method for screening and treating US Veterans for osteoporosis compared to no intervention. Quality improvement programs addressing primary prevention of osteoporotic fractures provide a feasible, team-based, approach to this important problem, while unburdening the increasingly limited time and availability of primary care providers.

**Table 1.** Base-case Results (per patient average)

	Bone Health Team	No Bone Health Team	Difference
Costs (mean)	\$58,250	\$59,617	-\$1,367
Unadjusted life years (mean)	11.937	12.059	-0.122
QALYs (mean)	8.379	8.446	-0.068
<b>ICER</b>			
Costs/life year		\$20,190	
Costs/QALY		\$11,174	
<b>Treated</b>			
Percent with osteoporosis	38.0%	6.9%	31.1%
Percent with osteopenia	25.5%	0.2%	25.3%
# AEs/1000 treatment years	1.92	5.05	-3.122
Years of treatment (mean)	9.93	5.42	4.518
<b>Fracture Incidence (per 1,000 patient years)</b>			
Clinical Vertebral	15.399	16.587	-1.188
Hip	3.797	4.073	-0.276
Subclinical Vertebral	5.062	5.494	-0.432
Wrist	0.808	0.977	-0.169
Death	70.548	70.089	0.459
<b>Other (#/1000 patients)</b>			
Dependence	27.336	27.084	0.252
Nursing home placement	13.907	13.857	0.050

VABHTCEA Table Base Case Results

**Disclosures:** Karla Miller, None.

## FR0252

**Opportunistic Identification of Vertebral Fractures from Cross-Sectional Imaging and Impact on Fracture Liaison Services.** Emily Russell<sup>\*1</sup>, Emma Foweraker<sup>2</sup>, Kassim Javaid<sup>2</sup>. <sup>1</sup>Oxford Medical School, United Kingdom, <sup>2</sup>Oxford University Hospitals, United Kingdom

Opportunistic identification of vertebral fractures from CT scans provides an opportunity for earlier intervention and management in osteoporosis.

**Introduction:**

Up to 75% of vertebral fractures do not reach clinical attention. Identification of vertebral fractures is critical for effective secondary fracture prevention as they are associated with a 2.3x increase in future hip fracture. CT scans are a common investigation performed for a variety of clinical indications and provide an ideal platform for opportunistic identification. We tested the screening of CT scans in patients over the age of 50 for vertebral fractures.

**Methods:**

16,935 CT scans were performed in a UK region (population 620,000) over one year, in patients over the age of 50. We retrospectively analysed a representative sample of 321 scans for moderate or severe vertebral fractures using Optasia medical's ASPIRE™ service. This uses machine-learning to flag scans, with all images then over-read by an Optasia radiologist to confirm the presence of fracture. Where fractures were identified, radiologist reports were examined to look for mention of the fracture and suggestion of referral for further management. Patients were cross referenced with the local Fracture Liaison Service (FLS) to see how many patients were already known to services.

**Results:**

Of the 321 scans analysed, 53 (16.5%) moderate/ severe vertebral fractures were found by the ASPIRE system. 63% had been reported by the radiologists, although none recommended further secondary fracture prevention. The ASPIRE service identified 20 patients with previously undiagnosed vertebral fractures. The rate was higher in women (8.6%) vs men (4.1%). Of the newly identified vertebral fracture patients, 3 were already known to the FLS. If all new, unknown patients found by the ASPIRE service were appropriate for referral, this could mean an initial extra 886 patient referrals per year to the FLS in comparison to the 620 hip fractures seen by the FLS per year.

**Conclusion:**

Computer driven services have the potential to identify vertebral fractures with a greater sensitivity than radiologists when used opportunistically on CT scans taken for a variety of clinical indications. However, to reduce the burden of fractures, substantial service planning is required to account for the increase in referrals for secondary fracture prevention of at least 1.4 times the number of hip fractures in this locality.

**Disclosures:** Emily Russell, Optasia Medical, Other Financial or Material Support.



## FR0254

**Predictors of Near-Term Non-Vertebral Fracture in Elderly Women with Osteoporosis, Osteopenia, or a History of Fracture, Based on Data from the Canadian Multicentre Osteoporosis Study (CaMos).** Derek Weycker<sup>\*1</sup>, Jonathan Adachi<sup>2</sup>, David Goltzman<sup>2</sup>, Alexandra Papaioannou<sup>2</sup>, Tanveer Towheed<sup>2</sup>, Tassos Anastassiades<sup>2</sup>, Rich Barron<sup>3</sup>. <sup>1</sup>Policy Analysis Inc. (PAI), United States, <sup>2</sup>Canadian Multicentre Osteoporosis Study (CaMos), Canada, <sup>3</sup>Amgen, United States

Background: Fractures are a major cause of morbidity, mortality, and healthcare costs among elderly women. Assessment of their fracture risk has tended to focus on a long-term horizon and populations with a broad risk range. For a high-risk population (e.g., older women with osteoporosis, osteopenia, or a history of fracture), however, it may be more pertinent to patients, physicians, and payers to evaluate fracture risk over a shorter time horizon.

Methods: A retrospective repeated-observations design and data from the Canadian Multicentre Osteoporosis Study (CaMos)—an ongoing, Canada-wide, population-based, prospective cohort study with periodic exams—were employed. The study population comprised all women aged  $\geq 65$  years with osteoporosis (T-score  $\leq -2.5$  at total hip), osteopenia (T-score  $> -2.5$  and  $\leq -1.0$  at total hip), or history of (any) fracture (irrespective of T-score at total hip) at the Year 5 Exam and/or the Year 10 Exam; for each woman in the study population, each qualifying exam was considered as a separate observation in analyses. Non-vertebral fractures—defined as incident fractures of the ankle, clavicle, elbow, foot, hand, heel, hip, humerus, knee, lower leg, pelvis, rib, upper leg, or wrist—were ascertained over a 2-year period following each qualifying exam. Potential predictors of 2-year non-vertebral fracture were evaluated within a multivariate framework using a shared frailty model, and included demographic characteristics, anthropometric measures, bone mineral density, comorbidities, fracture/fall history, pain measures, mental/physical function, drug utilization, and quality of life.

Results: The study population included 3,228 women aged  $\geq 65$  years with osteoporosis, osteopenia, or a history of fracture who contributed a total of 5,004 observations. During the 2-year follow-up period, 6.0% of women had a non-vertebral fracture. Independent predictors of elevated 2-year risk of non-vertebral fracture included falls history, fracture history, poorer physical function/performance, and lower total hip T-score (Table).

Conclusions: Near-term fracture risk among women with osteoporosis, osteopenia, or a history of fracture is higher among those with a fracture history, falls history, poorer physical function/performance, and lower BMD. Careful consideration should be given to identifying this population so that those at elevated risk of near-term fracture may be targeted for the appropriate therapy.

Risk Factors	No. of Obs.	No. of Fr*	% Fr*	Multivariate Model: 2-Year Non-Vertebral Fracture**			
				HR	95% CI	UL	p-value
Falls in Past 12 Months							
$\geq 2$	524	52	9.9	1.75	1.25	2.43	0.001
0-1	4480	249	5.6	REF	—	—	—
Fractures (any) in Past 12 Months							
$\geq 1$	224	25	11.2	1.61	0.99	2.62	0.054
0	4780	276	5.8	REF	—	—	—
SF-36 Physical Component Summary Score							
Quintile 1 - Quintile 2 (7.1 - 42.0)	1989	165	8.3	1.81	1.40	2.33	<0.001
Quintile 3 - Quintile 5 (42.0 - 68.6)	2984	133	4.5	REF	—	—	—
Total Hip T-Score							
$\leq -3.5$	116	18	15.5	3.94	2.24	6.93	<0.001
$\leq -2.5$ to $> -3.5$	616	60	9.7	2.47	1.64	3.71	<0.001
$\leq -1$ to $> -2.5$	2467	130	5.3	1.40	0.98	2.01	0.067
$> -1$	996	38	3.8	REF	—	—	—

Obs: observations; Fr: fracture; HR: hazard ratio; CI: confidence interval; LL: lower limit; UL: upper limit; REF: referent group

\*Fractures during 2-year follow-up period

\*\*Only risk factors with p-value  $< 0.10$  were retained in the final multivariate model, which was estimated using 4,175 observations without missing data

Table 1

Disclosures: Derek Weycker, Amgen Inc., Grant/Research Support.

## FR0255

**Bone CYP27B1, CYP24A1 and Serum 25-Hydroxyvitamin D are Key Positive Factors for Trabecular Bone Architecture in Hip Fracture Patients.** Deepti Sharma<sup>\*1</sup>, Thomas Robertson<sup>2</sup>, Roumen Stamenkov<sup>3</sup>, Catherine Stapledon<sup>2</sup>, Gerald Atkins<sup>2</sup>, Peter Clifton<sup>1</sup>, Lucian Solomon<sup>2</sup>, Paul Anderson<sup>1</sup>, Howard Morris<sup>1</sup>. <sup>1</sup>University of South Australia, Australia, <sup>2</sup>The University of Adelaide, Australia, <sup>3</sup>Royal Adelaide Hospital, Australia

Although calcium and vitamin D supplementation is well known to reduce hip fracture risk, little is understood about the mechanism of how elevated serum 25-hydroxyvitamin D (25D) improves bone health. Previously, we have demonstrated the positive effects of serum 25D levels on bone structure in rodents, independent of serum parathyroid hormone (PTH) and 1 $\alpha$ ,25-dihydroxyvitamin D (1,25D) levels (1). As well, we have previously reported that the osteoblastic overexpression or deletion of 25-hydroxyvitamin D-1 $\alpha$  hydroxylase (CYP27B1) mouse models demonstrated that bone-derived 1,25D plays an anabolic role in bone formation. We now report the relationships between 25D and trabecular bone structure in humans. Intertrochanteric trabecular bone biopsies together with serum samples were collected from hip fracture

patients undergoing surgery for a hip replacement (70 females, 41 males). Trabecular bone structure was analysed by microCT (Skyscan 1076). Serum 25D, 1,25D and 1-84PTH were analysed by chemiluminescent immunoassay (Diasorin Liaison) and clinical data, including eGFR were collected from medical records. Serum 25D levels correlated positively with trabecular thickness ( $r = 0.209$ ,  $p < 0.05$ ) and negatively to the ratio of bone surface to bone volume (BS/BV) ( $r = -0.214$ ,  $p < 0.05$ ), both indicators of bone strength. However, no bone structural parameters were determined by either serum PTH or 1,25D levels. When accounting for gender, 19% of the variance in BS/BV is determined by 25D, bone CYP27B1 and CYP24A1 mRNA levels ( $P = 0.001$ ). Furthermore, bone CYP24A1 levels were not determined either by serum 1,25D or PTH levels. These data suggest that the supply of serum 25D and its synthesis and metabolism within bone play a greater role in determining bone architecture than serum PTH and 1,25D levels. These findings are the first data which provide clinical evidence that the positive effects of vitamin D on bone structure are through the supply and metabolism of 25D within bone.

1. Anderson et al JBMR 2008 23:1789-97.

2. Turner et al Osteoporosis Int 2011 22: S590-S591.

Disclosures: Deepti Sharma, None.

## FR0256

**Effect of Exercise Modality during Weight Loss on Hip and Spine Bone Mineral Density in Older Adults with Obesity.** Kristen Beavers<sup>\*1</sup>, Michael Walkup<sup>2</sup>, Walter Ambrosius<sup>2</sup>, Stephen Kritchevsky<sup>2</sup>, Leon Lenchik<sup>2</sup>, Sue Shapses<sup>3</sup>, Barbara Nicklas<sup>2</sup>, Anthony Marsh<sup>1</sup>, W. Jack Rejeski<sup>1</sup>. <sup>1</sup>Wake Forest University, United States, <sup>2</sup>Wake Forest School of Medicine, United States, <sup>3</sup>Rutgers University, United States

Purpose: To evaluate the long term effect of exercise modality during weight loss on bone mineral density (BMD) in older adults with obesity.

Methods: 188 older adults [66.9 $\pm$ 4.8 (SD) years, 70% women, 32% AA] with obesity (34.5 $\pm$ 3.7 kg/m<sup>2</sup>) and BMD at baseline were randomized to weight loss alone (WL; 7-10% baseline weight), WL+ aerobic training (WL+AT; 4 d/wk, 45 min/d, 12-14 RPE), or WL+ resistance training (WL+RT; 4 d/wk, 8 exercises, 3 sets, 10-12 reps at 75% 1 RM) for 18-months, with a 30-month follow-up assessment (i.e., no study contact between 18 and 30 months). Body mass and DXA-acquired total hip, femoral neck, and lumbar spine BMD were assessed at baseline, 6-, 18-, and 30-months. Overall treatment effect estimates were generated using a mixed model including group, time, and a group by time interaction and adjusted for gender, wave, baseline value of the outcome, and weight change.

Results: 138 (73%) participants completed the 18-month intervention, with 108 (58%) returning for the 30-month assessment. Median attendance to scheduled intervention sessions was  $> 67.5\%$  and total body weight was reduced in all groups ( $p < 0.01$ ), with both WL plus exercise groups experiencing greater overall weight loss than WL alone (WL+AT: -8.8 $\pm$ 0.8% and WL+RT: 9.2 $\pm$ 0.8% vs. WL: -5.4 $\pm$ 0.8%; both  $p < 0.01$ ). Baseline total hip, femoral neck, and lumbar spine BMD was 1.01 $\pm$ 0.13 g/cm<sup>2</sup>, 0.95 $\pm$ 0.12 g/cm<sup>2</sup>, and 1.28 $\pm$ 0.20 g/cm<sup>2</sup>, respectively. Reduction in total hip BMD was observed in all groups over time [WL: -0.025 (-0.031, -0.019) g/cm<sup>2</sup>; WL+AT: -0.022 (-0.028, -0.017) g/cm<sup>2</sup>; WL+RT: -0.018 (-0.023, -0.012) g/cm<sup>2</sup>], with a significantly different treatment effect between WL and WL+RT groups ( $p = 0.05$ ). Similarly, a marginally significant treatment effect was seen for femoral neck BMD when contrasting WL and WL+RT group estimates [WL: -0.011 (-0.020, -0.002) g/cm<sup>2</sup> vs. -0.000 (-0.009, 0.008) g/cm<sup>2</sup>;  $p = 0.06$ ]. Interestingly, lumbar spine BMD was increased in WL and WL+RT compared to WL+AT [WL: 0.015 (0.007, 0.024) g/cm<sup>2</sup>, WL+AT: -0.003 (-0.012, 0.005) g/cm<sup>2</sup>, WL+RT: 0.009 (0.000, 0.017) g/cm<sup>2</sup>, both  $p \leq 0.01$ ; see Figure 1].

Conclusion: RT, but not AT, modestly attenuates WL-associated BMD loss at the total hip and femoral neck. Results lend support for RT to be added to dietary WL to minimize WL-associated bone loss in the hip region. Future research is needed to identify strategies to fully prevent WL-associated BMD loss.

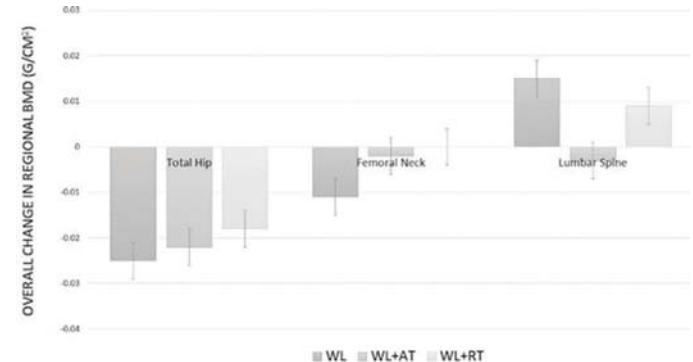


Figure 1: Overall change in regional BMD by group

Disclosures: Kristen Beavers, None.

## FR0258

**High Dairy Protein Intake is Associated with Greater Bone Strength Parameters at the Distal Radius and Tibia in Older Men: A Cross-sectional Study.** Lisa Langsetmo<sup>1</sup>, James Shikany<sup>2</sup>, Andrew Burghardt<sup>3</sup>, Peggy Cawthon<sup>3</sup>, Jane Cauley<sup>4</sup>, Eric Orwoll<sup>5</sup>, Douglas Bauer<sup>3</sup>, John Schousboe<sup>6</sup>, Brent Taylor<sup>7</sup>, Tien Vo<sup>1</sup>, Elizabeth Barrett-Connor<sup>8</sup>, Kristine Ensrud<sup>7</sup>.  
<sup>1</sup>University of Minnesota, United States, <sup>2</sup>University of Alabama, United States, <sup>3</sup>University of California, San Francisco, United States, <sup>4</sup>University of Pittsburgh, United States, <sup>5</sup>Oregon Health and Science University, United States, <sup>6</sup>Park Nicollet Clinic and Health Partners Institute, United States, <sup>7</sup>University of Minnesota and VA Health Care System, United States, <sup>8</sup>University of California, San Diego, United States

Previous studies have reported that the association between protein intake and fracture depends on the source (dairy, non-dairy animal, plant). Experimental studies have indicated that protein source has differential effects on markers of bone mineral metabolism, but the consequence for bone strength and effects on cortical vs. trabecular bone are unknown. Our objective was to determine the association of protein intake by source (dairy, non-dairy animal, plant) with bone strength and trabecular and cortical bone microarchitecture at weight bearing (tibia) and non-weight bearing (radius) skeletal sites among older men. We used data from 1016 men (mean 84.3 years) who attended the Year 14 exam of the Osteoporotic Fractures in Men (MrOS) study, completed a food frequency questionnaire (500-5000 kcal), were not taking androgen or androgen agonists and had high resolution peripheral quantitative computed tomography (HRpQCT) scans of the distal radius and/or distal tibia. Protein was expressed as % of total energy intake (TEI); mean±SD for TEI=1548±607 kcal and for total protein=16.2±2.9%TEI. We used linear regression with standardized HRpQCT parameters as dependent variables and adjusted for age, height, center, education, race/ethnicity, marital status, smoking, alcohol intake, physical activity level, corticosteroids use, supplement use (calcium and vitamin D), and osteoporosis medications. Increased dairy protein intake was associated with higher estimated failure load at the distal radius and tibia, as well as higher cortical and trabecular BMD, higher cortical thickness and area (but not cortical porosity) and lower total area (Table 1). Non-dairy animal protein was associated with higher cortical thickness, cortical area, and cortical BMD, and total BMD at the radius, but the remaining associations at the radius (including failure load) and those with all parameters at the tibia were not significant. Plant protein intake was not associated with any bone strength parameter. In conclusion, increased dairy protein intake was associated with higher failure load at both weight bearing and non-weight bearing sites and these associations were consistent with both cortical and trabecular bone strength parameters. In contrast, there was a more limited association between non-dairy animal protein and bone strength parameters. These results support a link between dairy protein intake and skeletal health but an intervention study is needed to evaluate causality.

**Table 1: The Association\* between Protein Intake by Source (Dairy, Non-dairy Animal, Plant) and High Resolution Peripheral Quantitative Computed Tomography Bone Strength Parameters**

Effect size (95% CI)	Dairy protein	Non-dairy Animal Protein	Plant protein
<b>Distal Radius</b>			
Failure load	<b>0.16 (0.07, 0.26)</b>	0.06 (-0.01, 0.13)	0.02 (-0.09, 0.13)
Area	<b>-0.10 (-0.19, -0.01)</b>	-0.04 (-0.10, 0.02)	-0.09 (-0.20, 0.01)
BMD	<b>0.20 (0.10, 0.30)</b>	<b>0.07 (0.00, 0.14)</b>	0.04 (-0.07, 0.15)
Trabecular BMD	<b>0.13 (0.03, 0.23)</b>	0.03 (-0.03, 0.10)	0.05 (-0.07, 0.16)
Cortical BMD	<b>0.19 (0.10, 0.29)</b>	<b>0.07 (0.01, 0.14)</b>	0.07 (-0.04, 0.18)
Cortical Thickness	<b>0.17 (0.07, 0.27)</b>	<b>0.08 (0.01, 0.15)</b>	-0.02 (-0.13, 0.09)
Cortical Area	<b>0.17 (0.07, 0.27)</b>	<b>0.08 (0.01, 0.15)</b>	-0.05 (-0.16, 0.06)
Cortical Porosity	-0.04 (-0.14, 0.07)	-0.02 (-0.09, 0.05)	-0.03 (-0.15, 0.09)
<b>Distal Tibia</b>			
Failure load	<b>0.12 (0.02, 0.21)</b>	-0.01 (-0.07, 0.06)	-0.01 (-0.12, 0.10)
Area	<b>-0.11 (-0.19, -0.03)</b>	-0.04 (-0.10, 0.01)	-0.06 (-0.15, 0.03)
BMD	<b>0.18 (0.08, 0.28)</b>	0.01 (-0.06, 0.07)	0.02 (-0.10, 0.13)
Trabecular BMD	<b>0.13 (0.03, 0.23)</b>	-0.01 (-0.08, 0.06)	0.08 (-0.03, 0.19)
Cortical BMD	<b>0.13 (0.04, 0.23)</b>	0.04 (-0.02, 0.11)	-0.02 (-0.13, 0.09)
Cortical Thickness	<b>0.14 (0.05, 0.24)</b>	0.00 (-0.06, 0.07)	-0.05 (-0.16, 0.06)
Cortical Area	<b>0.14 (0.04, 0.24)</b>	0.00 (-0.07, 0.07)	-0.08 (-0.20, 0.03)
Cortical Porosity	-0.01 (-0.11, 0.10)	-0.03 (-0.10, 0.04)	0.06 (-0.06, 0.18)

\*Effect size (beta coefficient with unit=SD) adjusted for age, height, center, education, race/ethnicity, marital status, smoking, alcohol intake, physical activity level, corticosteroids use, supplement use (calcium and vitamin D), and osteoporosis medications. Protein measured as percentage of total energy intake (TEI), SD=2.9% TEI.  
 Note: data in bold = p<0.05

Table 1

**Disclosures:** Lisa Langsetmo, None.

## FR0260

**Protein Intake and Bone Mineral Density- A Systematic Review and Meta-Analysis of Randomized Controlled Trials.** Marissa Shams-White<sup>1</sup>, Zhuxuan Fu<sup>1</sup>, Micaela Karlens<sup>1</sup>, Joachim Sackey<sup>1</sup>, Jian Shi<sup>1</sup>, Karl Inosoga<sup>2</sup>, Meryl LeBoff<sup>3</sup>, Sue Shapses<sup>4</sup>, Connie Weaver<sup>5</sup>, Taylor Wallace<sup>6</sup>, Mei Chung<sup>1</sup>.  
<sup>1</sup>Tufts University, United States, <sup>2</sup>Yale University, United States, <sup>3</sup>Harvard University, United States, <sup>4</sup>Rutgers University, United States, <sup>5</sup>Purdue University, United States, <sup>6</sup>George Mason University, United States

**Objective:** To conduct a systematic review and meta-analysis examining the effects of 1) high vs. low protein intake; 2) protein intake's synergistic effect with calcium or vitamin D; and 3) animal vs. plant protein intake on bone mineral density (BMD) and bone mineral content (BMC).

**Methods:** This is a sub-analysis of a larger systematic review. Searches were conducted in five databases through October 31, 2016. Randomized controlled trials (RCTs) at least one year in duration that compared high vs. low or animal vs. plant protein intake and reported total body (TB), total hip (TH), lumbar spine (LS) or femoral neck (FN) BMD or TB BMC outcomes in healthy adults were included. Strength of evidence (SOE) was rated for each outcome. Random-effects meta-analyses were performed when data were sufficient.

**Results:** Fourteen RCTs were included. Ten RCTs examined high vs. low protein in different populations; SOE was rated moderate for LS, TH and FN BMD outcomes and limited for TB BMD and BMC outcomes. Meta-analysis results suggest higher protein intake has a protective effect on LS BMD compared to lower protein, increasing BMD an average of 0.52% (N=5, pooled net % change = 0.52%, 95% CI: 0.06%, 0.97%), but no effect on TH or FN BMD (TH: N=7, 0.30%, 95% CI: -0.02%, 0.62%, FN: N=6, -0.14%, 95% CI: -0.60%, 0.32). Seven RCTs supplemented all groups with calcium and/or vitamin D, but none examined their interaction with protein. Four RCTs examined animal vs. isoflavone-rich soy protein (soy+) intake in postmenopausal women, of which two also compared them to isoflavone-poor soy protein. SOE was rated limited or inadequate for all outcomes. There were no significant differences between groups in BMD or BMC across studies, and no effect comparing animal vs. soy+ on LS, FN or TB BMD (LS: n=4, 0.24%, 95% CI: -0.80%, 1.28%; FN: n=3, 0.13%, 95% CI: -0.94%, 1.21%; TB: n=3, -0.24%, 95% CI: -0.81%, 0.33%). None of these meta-analyses showed statistical heterogeneity.

**Conclusions:** Results suggest that higher protein intake, rather than the source of protein, may have a small effect on attenuating BMD loss, but the effects were not consistent across BMD sites. RCTs were limited in number and quality; high vs. low protein RCTs were heterogeneous in doses and populations; and animal vs. soy protein RCTs in postmenopausal women may not be generalizable to other populations. More high quality, long-term RCTs are needed to clarify dietary protein's role on bone health.

**Disclosures:** Marissa Shams-White, None.

## FR0261

**Type of Sports Participation Modulates Risk For Low BMD in Athletes With Female Athlete Triad.** Adam Tenforde<sup>1</sup>, Kristin Sainani<sup>2</sup>, Jennifer Carlson<sup>2</sup>, Neville Golden<sup>2</sup>, Michael Fredericson<sup>2</sup>.  
<sup>1</sup>Spaulding Rehabilitation Hospital, Harvard University, United States, <sup>2</sup>Stanford University, United States

**Introduction:** Sports participation has known benefits for skeletal health, especially for athletes participating in jumping and high impact loading sports. In contrast, a subset of athletes primarily participating in non-weight bearing, endurance sports and sports emphasizing leanness has been observed to have impaired bone health and risk for fracture. The Female Athlete Triad (Triad) describes the interrelationship of energy availability, menstrual function and bone mineral density (BMD). Triad risk assessment score quantifies risk for athletes based on Triad risk factors. The interaction among components of the Triad risk assessment score and type of sports participation and BMD has not been previously described. *We hypothesize that athletes participating in high impact loading sports will have highest BMD and non-weight bearing, endurance and sports emphasizing leanness will have lowest BMD. The effects of sport loading will be reduced with greater Triad risk factors.*

**Methods:** A total of 239 athletes participating in 16 collegiate sports completed dual energy x-ray absorptiometry (DXA) scans to measure BMD Z-scores of the lumbar spine and total body. Each athlete had her height and weight measured to calculate body mass index (BMI). The remaining 4 risk assessment values were obtained from preparticipation examination. The Triad risk factors measured: history of eating disorder/disordered eating, low BMI (values <18.5 kg/m<sup>2</sup>), late menarche (age of first menstrual period ≥ 15), oligomenorrhea/amenorrhea (fewer than 9 periods in past 12 months), and prior stress reaction/stress fracture. Mean and standard error BMD Z-scores were determined for each sport. Univariate and multivariate regression analysis with adjustment for multiple comparisons were performed with P-value <0.05 as threshold of significance of Triad risk factors and between sports.

**Results:** Sports with lowest BMD Z-scores include water sports, endurance and lean sports: swimming/diving (-1.04±0.29), synchronized swimming (-1.04±0.37), and cross-country (-0.41±0.21). Sports with highest BMD Z-scores: gymnastics (1.25±0.32), volleyball (1.19±0.41), basketball (1.03±0.31), and softball (0.98±0.29). All Triad risk factors were associated with lower BMD Z-scores. Even after adjusting for Triad risk factors, however, the association between sports participation in specific sports to BMD persisted.

**Discussion:** Both type of sports participation and Triad risk factors influence BMD in athletes. However, type of sports participation modulates risk for impaired bone health associated with the Triad.

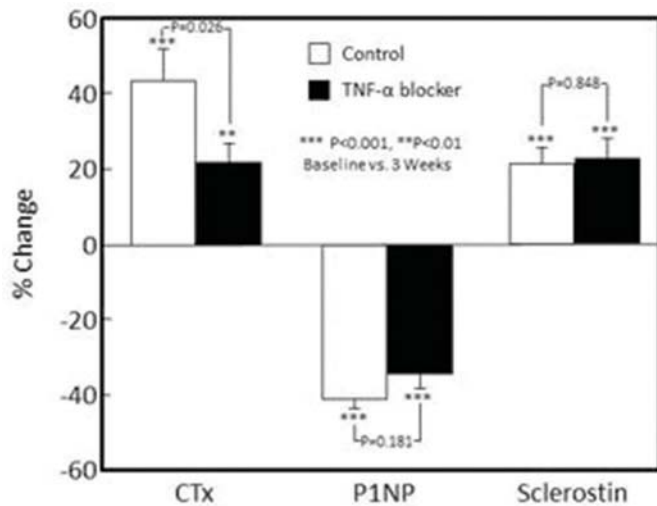
**Disclosures:** Adam Tenforde, None.



## FR0264

**Blocking TNF- $\alpha$  action does not prevent the increase in serum sclerostin levels following estrogen withdrawal in postmenopausal women.** Matthew Drake<sup>1</sup>, Frank Blocki<sup>2</sup>, Kim Hilgers<sup>2</sup>, Jennifer Fenske<sup>2</sup>, Brianne Thicke<sup>1</sup>, Joshua Farr<sup>1</sup>, Sundeep Khosla<sup>1</sup>. <sup>1</sup>Mayo Clinic, United States, <sup>2</sup>DiaSorin, United States

There is considerable evidence demonstrating that estrogen suppresses both circulating sclerostin levels as well as bone *SOST* mRNA levels in humans. However, the underlying mechanisms by which estrogen regulates sclerostin production remain unclear. A previous study in mice (BBRC 424:170, 2012) found that the number of sclerostin-positive osteocytes increased following ovariectomy, and this increase was prevented by treatment with estradiol or by a TNF- $\alpha$  blocker, suggesting that the increase in TNF- $\alpha$  following estrogen deficiency might mediate the increase in sclerostin. Consistent with these findings, a second study (Sci Transl Med 8:330ra35, 2016) showed that mice overexpressing TNF- $\alpha$  had a marked increase in sclerostin expression in osteocytes. These mouse data thus suggested that increased TNF- $\alpha$  production following estrogen deficiency may mediate the observed increase in sclerostin. To test this directly in humans, we reanalyzed serum samples from a previous study (JBMR 22:724, 2007) in which transdermal estradiol, 0.1mg/d, was administered for 60 days to 28 early postmenopausal women (mean age, 58.5 yrs). Estrogen treatment was discontinued, and the subjects were randomly assigned to receive 3 wk injections with 0.9% saline (control, n=13) or the TNF- $\alpha$  blocker, etanercept (n=15, 25 mg/twice weekly). As shown in the Figure, estrogen withdrawal led to 43% increase in serum CTx (panel A) and a 41% decrease in serum PINP (panel B) in the control women. Treatment with the TNF- $\alpha$  blocker attenuated the increase in serum CTx (panel A, 22% increase, P = 0.026 vs control) but not the decrease in PINP (panel B, 35% decrease, P = 0.180 vs saline). As shown in panel C, serum sclerostin levels, measured using a highly specific assay for intact sclerostin (Diasorin), increased similarly in the control (+22%) and TNF- $\alpha$  blocker-treated (+23%) women (P=0.848). Thus, in humans, acute estrogen withdrawal leads to increased bone resorption and decreased bone formation, along with an increase in serum sclerostin that is not prevented by TNF- $\alpha$  blockade. These findings are consistent with the conclusion that sclerostin may mediate the effects of estrogen in reducing bone resorption and maintaining bone formation, but in contrast to the murine models, the *in vivo* regulation of sclerostin by estrogen appears to be independent of TNF- $\alpha$  in humans.



Sclerostin Figure

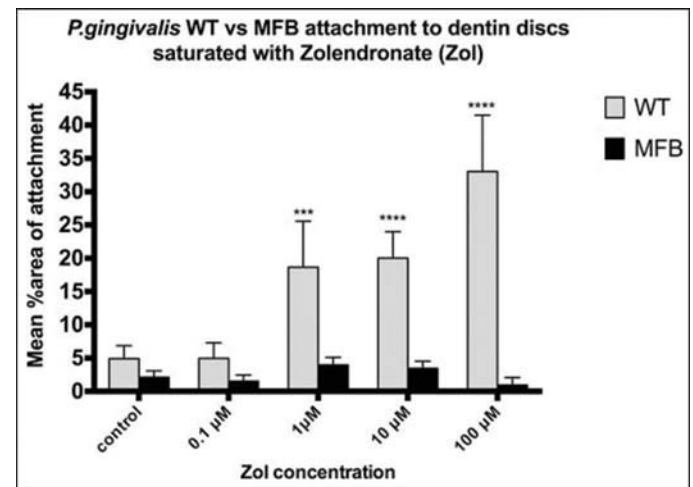
Disclosures: Matthew Drake, None.

## FR0265

**Interaction between *Porphyromonas gingivalis* (*P.gingivalis*) and Matrix Bound Bisphosphonates during Induction of Osteonecrosis.** Ranya Elsayed<sup>1</sup>, Ahmed Alawady<sup>2</sup>, Mohamed Meghij<sup>3</sup>, Pheba Abraham<sup>4</sup>, Mohamed Awad<sup>5</sup>, Christopher Cutler<sup>6</sup>, Mohammed Elsalanty<sup>7</sup>. <sup>1</sup>Oral Biology Dept., graduate school, Augusta University, United States, <sup>2</sup>university of florida college of dentistry, United States, <sup>3</sup>Departments of Oral biology and Periodontics, Augusta University, United States, <sup>4</sup>oral biology, Augusta University, United States, <sup>5</sup>Augusta University, United States, <sup>6</sup>professor and chair Dept. of periodontics, Associate dean for research, dental college of Georgia, Augusta university, United States, <sup>7</sup>Associate professor, Dental College of Georgia, Augusta University, United States

Previous studies have shown a strong association between periodontal disease and bisphosphonate related osteonecrosis of the jaw (BRONJ). The purpose of this study is to determine whether there may be synergy between matrix bound Zoledronate (Zol)

and a keystone pathogen in periodontitis; *P.gingivalis*, in BRONJ induction. Our aims were: 1) to examine whether matrix-bound Zol enhances *P.gingivalis* attachment and colonization to the bone via fimbrial interaction. 2) to investigate if *P.gingivalis* has a synergistic role in the BRONJ development *in vivo*. The adsorption of Zol on the dentin discs was assessed by fluorescent imaging of dentin discs treated with increasing doses of FRFP (far red fluorescent Pamidronate). Dentin discs were treated with different doses of nitrogen containing and non-nitrogen containing bisphosphonates and then attachment of *P.gingivalis* (WT381, MFBFimA-Mfa1-) as well as attachment of *Fusobacterium nucleatum* and *Streptococcus gordonii* to the discs was assessed using live and dead bacterial stain and imaging with confocal microscopy. Effect of Zol on *P.gingivalis* major and minor fimbriae (FimA and Mfa) was assessed using qPCR and western blot. Tibial defects were performed on bisphosphonate treated and control animals and then the defects were either sham injected or injected with *P.gingivalis* in Carboxymethyl cellulose (CMC), then healing of the defect was assessed both clinically and histomorphometrically. Our Results show a dose dependent increase in the fluorescent signal of the FRFP on the dentin discs confirming Zol adsorption. Confocal microscopy showed a significant increase in the attachment of WT *P.gingivalis* on the Zol treated discs than was on the control discs, and compared to their fimbrial mutant counterpart (p-value <0.001). qPCR showed an increase in fimbrial expression with high dose of Zol. Clinical evaluation showed a slower healing of tibial defects in rats with the *P.gingivalis* infection. In conclusion, *P.gingivalis* through its fimbrial adhesins may play an important synergistic role in development of BRONJ, as suggested by its preferential attachment to bisphosphonate modified alveolar bone. This emphasizes the vital role of matrix bound Zol in promoting BRONJ formation and also suggests a possible way to prevent BRONJ through chelation of Zol with EDTA.



graph showing attachment of WT vs MFB *P.gingivalis* to Zol-treated dentin discs

Disclosures: Ranya Elsayed, None.

## FR0267

**A Novel Strategy to Rescue Osteogenesis of Impaired Bone Marrow Stromal Cells in Diabetes.** Yuqi Guo<sup>\*</sup>, Jian Yang, Xin Li. New York University, United States

Diabetes mellitus is a group of chronic diseases characterized by high blood glucose levels. Over time, the widespread chronic disorder of diabetes mellitus adversely affects multiple organ systems, including bones. T2D patients have a higher risk of sustaining osteoporotic fractures than their non-diabetic counterparts, and fracture healing, including the nonunion of skeletal fractures, is usually impaired in diabetics. Despite its clinical importance, our understanding of the detrimental effects of hyperglycemia on bone marrow stromal Cells (BMSCs), a critical cell population essential for bone repair, remains limited.

We recently reported the deficiency of the respiration activity in T2D mouse bone marrow aspirate and BMSCs evidenced by the abnormal accumulation of many metabolites in the tricarboxylic acid (TCA). It indicates a mechanistic connection between metabolites and bone damage under diabetic conditions. Succinate is one of the most elevated metabolites in TCA cycle in T2D mouse bone marrow in our study and its elevation has been observed in other T2D models including human. The succinate accumulation indicates an insufficient succinate dehydrogenase (SDH) activity in BMSCs. We hypothesize that stimulation of SDH activity in BMSCs rescues osteogenesis in diabetes. In this study, we demonstrate that both lean and obese T2D mouse models exhibit impaired BMSC osteogenesis and delayed bone healing using various fracture models including 1) a femoral drill-hole defect model, 2) a radius osteotomy without fixation model and 3) a closed femoral fracture with intramedullary fixation model. Our results further demonstrate that high glucose culture decreases the SDH activity in human and mouse BMSCs which is associated with an impaired osteogenic capacity measured by CFU-ALP and Alizarin Red assays. Reset the SDH activity by metformin can rescue the reduction of osteogenesis and improve the bone healing process in diabetic mice.

Taken together, our study reveals a novel strategy to improve the osteogenesis of BMSCs under hyperglycemic conditions by stimulating SDH activity. This work will inspire further studies to explore whether the stimulations of SDH activity or the

respiration also influence other cellular procedures like angiogenesis, chondrocytogenesis, and osteoclastogenesis to improve fracture healing in diabetes.

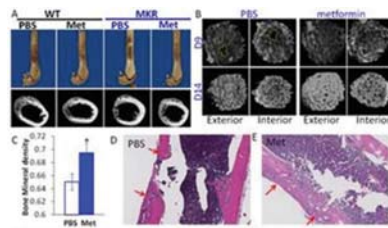


**Fig 1. Drill-hole bone repair model in WT and MKR mice.** A diameter of 0.8 mm (SEM=0.011 mm) drill injury has been given to the mouse right femur, 5 mm distal to the femur distal end. We reconstructed the cross-sections with a 9.7- $\mu$ m pixel size. CTan was used on the scanned images to generate the regions of interest and CTVis was used to generate 3D images with a 60-degree view angle and a (0, 0, 4) camera position. (A) Longitudinal and cross-section views of the drill-hole. (B) Exterior and interior views of the defect areas 9 or 14 days post-surgery. (C) A Volume of Interest (VOI) of the remodeling part (80x4 slides) at the injury site has been traced and binary analysis were carried to generate the Bone mineral density (BMD) on the remodeling tissue at the injury site. N=5; \* p<0.05, as indicated by a t-test. (D-E) H&E staining of the drilled area 14 days post-surgery. Red arrows indicate the drill-hole.

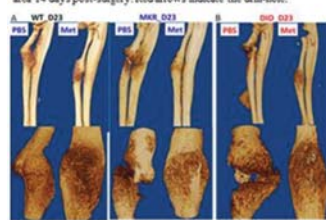


**Fig 3. Radius osteotomy without fixation on day 23 post-surgery.**  $\mu$ CT views of the radius and defects in A) WT and MKR and B) D10 mice treated with PBS or Met.

Data

**Disclosures:** Yuqi Guo, None.

## FR0268

**Type 2 Diabetes Impairs Insulin-Stimulated Blood Flow in Femur and Lumbar Vertebra of Hyperphagic OLETF Rats.** Pamela Hinton\*, Rebecca Dirkes, T. Dylan Olver. University of Missouri, United States

Recently, impaired bone vascular function represents a possible mechanism for the increased bone fragility and fracture risk associated with Type 2 diabetes (T2D). Impaired insulin-induced vasodilation, referred to as microvascular insulin resistance, in skeletal muscle and nervous tissue is associated with hallmark features of T2D including decreased skeletal muscle glucose uptake and neuropathy, respectively. Whether microvascular insulin resistance manifests in the bone vasculature, and contributes to increased bone fragility in the setting of T2D remains unknown. This study tested the hypothesis that T2D is associated with bone microvascular insulin resistance, indicated by decreased insulin-stimulated vasodilation and blood flow in the femur and lumbar vertebra. Four-week old, male Otsuka Long-Evans Tokushima Fatty (hyperphagic model of T2D) rats were randomized to either T2D (ad lib access to a chow diet) or CON (fed 70% of T2D intake) until sacrifice at 40 weeks of age. Blood flow to the femoral proximal epiphysis, distal epiphysis, diaphysis and marrow and to vertebrae (L4) was measured before (at 0 min) and during (at 60 min) a euglycemic hyperinsulinemic clamp (EHC) via infusion of fluorescent microspheres. The effects of T2D on insulin-stimulated blood flow were evaluated using a RM ANOVA with post hoc paired and independent sample t-tests; group differences in % blood flow were evaluated using Mann-Whitney U test. As expected, the hyperphagic T2D rats had significantly greater body weight, body fat and fasting glucose than CON. T2D rats had reduced whole body insulin sensitivity compared to CON, indicated by a lower glucose infusion rate required to maintain euglycemia during the EHC. Basal regional femoral and vertebral blood flow were similar among groups, but the blood flow response to insulin stimulation was depressed in the T2D compared to CON in the proximal and distal epiphyses and lumbar vertebra. Mean arterial pressure (MAP) was greater in T2D compared to CON and was reduced after insulin stimulation in both groups. However, the percent increases in vascular conductance (VC; blood flow/MAP) in the proximal and distal epiphyses were decreased in T2D compared to CON. Thus, attenuated insulin-stimulated increases in VC in T2D likely accounted for reduced blood flow relative to CON. In summary, the results of this study suggest that microvascular insulin resistance might play a causal role in diabetic bone fragility.

**Disclosures:** Pamela Hinton, None.

## FR0270

**MFG-E8 deficiency: A model of inflamm-aging associated bone loss robustly rescued by teriparatide.** Megan Michalski\*, Anna Seydel<sup>1</sup>, Erica Siimets<sup>1</sup>, Benjamin Sinder<sup>1</sup>, Amy Koh<sup>1</sup>, Kamran Atabai<sup>2</sup>, Jose Aguirre<sup>3</sup>, Hernan Roca<sup>1</sup>, Laurie McCauley<sup>1</sup>. <sup>1</sup>University of Michigan, United States, <sup>2</sup>University of California, San Francisco, United States, <sup>3</sup>University of Florida, United States

Multiple processes become less efficient with age, leading to chronic increases in pro-inflammatory cytokines, termed inflamm-aging. This process has been associated with osteoporotic- and autoimmune-associated bone loss. We hypothesized that crucial components of anti-inflammatory pathways are associated with age-related bone loss. Milk fat globule-EGF 8 (MFG-E8) is a glycoprotein that is pro-resolving, regulates apoptotic cell clearance and has recently been linked to autoimmune disease and skeletal homeostasis. The role of MFG-E8 in the skeleton was determined with age. Primary bone marrow stromal cell (BMSC) and osteoclast cultures from MFG-E8 deficient (KO) and C57BL/6 (WT) mice were used to assess mineralization and resorption. Skeletal phenotypes were analyzed at 6, 16 and 22wks in KO and WT. KO and WT (16wk) mice were administered intermittent PTH (iPTH) (50 $\mu$ g/kg/d x 6wks) or vehicle to assess therapeutic potential. Micro-CT, serum biomarkers, static and dynamic histomorphometry, complete blood counts, spleen weight, and flow cytometric (FACS) analysis of bone marrow populations were performed. KO and WT osteoblasts and osteoclasts from 6wk old mice displayed similar differentiation, mineralization and resorption. Adult (22wk) KO BMSCs had decreased mineralized nodules compared to WT controls. In vivo, similar parameters of trabecular bone were found in KO and WT mice at 6 and 16wks, whereas 22wk KO mice displayed significantly reduced trabecular bone. Cortical bone was similar in KO and WT at 6wks with significantly reduced cortical bone in 16 and 22wk KO vs. WT. Osteoclast number per bone surface was increased in 22wk KO vs. WT. Adult KO mice had decreased serum TRAcP 5b and increased serum CTX-I vs. WT. KO spleen weight/body weight was increased compared to WT and FACS analysis showed significantly increased myeloid cells (CD11b<sup>hi</sup>GR-1<sup>+</sup>) in KO vs. WT. Interestingly, iPTH-treated KO mice showed a robust anabolic response in trabecular bone volume (+122%), exceeding the response in iPTH-treated WT mice (+48%). These data suggest MFG-E8 plays an important role in bone loss with age. The strong anabolic response in KO demonstrates that iPTH therapy may be more effective in models of age-related bone loss and/or inflammatory states. These data give insight into the role of MFG-E8 in aging, provide a new model of age-associated bone loss, and suggest anabolic PTH may be a valuable therapeutic approach for autoimmune-associated skeletal disease.

**Disclosures:** Megan Michalski, None.

## FR0271

**Activin A Signaling Is Critical For Renal Osteodystrophy in the CKD-MBD.** Toshi Sugatani\*, Yi-Fu Fang<sup>1</sup>, Hartmut Malluche<sup>2</sup>, Keith Hruska<sup>1</sup>. <sup>1</sup>Department of Pediatrics, Nephrology, Washington University School of Medicine, United States, <sup>2</sup>Division of Nephrology, Bone and Mineral Metabolism, University of Kentucky, United States

Renal osteodystrophy (ROD) consists of the pathological abnormalities in the bone of patients with chronic kidney disease (CKD) and it is a component of the CKD-mineral bone disorder (CKD-MBD) syndrome which causes a high incidence of skeletal fractures and contributes to the high mortality rates associated with kidney diseases. The prevalence of osteopenia/osteoporosis in CKD patients exceeds that of the general population and is a major public health concern in patients with CKD. That CKD is closely associated with compromised bone health is widely accepted, yet the mechanisms underlying impaired bone metabolism in CKD are not fully understood. We found that systemic activin A, a homodimer of inhibin- $\beta$ A (Inhba), is remarkably increased in CKD mouse model, alport syndrome (AL) mice. AL mice had a high turnover ROD produced by significantly increased osteoclast number and function. Although osteoblast number was also increased, osteoblast function was not activated evidenced by a decrease in the bone formation rate per osteoblast. As a result, there was an increase in osteoid area. Treatment with RAP-011, a ligand trap for the activin receptor type 2A (ActR1A), led to an amelioration of these events, indicating that activin A may be contributor to a high turnover ROD caused by increased osteoclast activity in CKD, irrespective of PTH elevation in AL mice. Consistent with our *in vivo* studies, abundant evidence in cell culture have demonstrated that activin A is a required enhancer of RANKL-induced osteoclastogenesis. However, the molecular mechanisms of the activin A effect are unknown. We found that activin A regulates RANKL-induced osteoclastogenesis through reciprocal cooperation between Smad2 and c-Fos. In addition, lack of Inhba, ActR1A, or Smad2, in M-CSF-dependent bone marrow macrophages produced impaired RANKL-induced osteoclastogenesis. Co-culture studies demonstrated that both the autocrine and paracrine actions of activin A are critical in osteoclastogenesis. Taken together, the data suggest that activin A is a critical direct mediator of RANKL-induced osteoclastogenesis and CKD stimulated bone resorption and osteoblast dysfunction in AL mice. The elucidation of activin A biology in bone metabolism lead to increased understanding of mechanisms underlying compromised bone health caused by CKD and identification of a new therapeutic target.

**Disclosures:** Toshi Sugatani, None.



## FR0272

**Role of Progranulin in Skeletal Homeostasis in Female Mice.** Liping Wang\*, Theresa Roth, Robert Nissenson. San Francisco VA Medical Center, United States

Progranulin (PGRN) is best known as a glial protein whose deficiency leads to the most common inherited form of frontotemporal dementia. Recently, PGRN has been found to be an adipokine associated with diet induced obesity and insulin resistance. The role of PGRN in regulating skeletal homeostasis is not clear. We investigated this issue by comparing the skeletal phenotypes of 6 month old global PGRN knockout (KO) and wild type (WT) mice in a C57/B6 background. We found that fractional bone volume (BV/TV) in the distal femur was comparable in male KO and male WT mice. Strikingly, female KO mice displayed a 2-fold increase ( $p < 0.01$ ) in BV/TV compared to WT female mice. The increased cancellous bone in female KO mice was associated with increased trabecular number (30%,  $p < 0.001$ ) and decreased trabecular separation (26%,  $P < 0.001$ ). Female (but not male) KO mice also displayed a 108% increase ( $p < 0.001$ ) in bone formation rate and a 50% increase ( $p < 0.001$ ) in mineral appositional rate. Strikingly, KO mice of both genders displayed defects in bone resorption (decreased average erosion depth and decreased expression of cathepsin K and TRAP genes in cultured OCs). Inhibition of bone resorption and enhancement of bone formation in aging female mice by the loss of PGRN suggests that PGRN could mediate bone loss induced by estrogen deficiency. We thus performed ovariectomy (Ovx) on 4 month old KO and littermate WT mice. Five weeks after surgery, the Ovx WT mice displayed a significant decrease in trabecular BV/TV (%) in the third lumbar vertebra (L3) (Sham vs. Ovx:  $16.9 \pm 1.57$  vs.  $12.4 \pm 0.75$ ,  $p < 0.01$ ), whereas in Ovx KO mice estrogen depletion did not alter the L3 BV/TV (Sham vs. Ovx,  $21.1 \pm 1.7$  vs.  $19.1 \pm 1.8$ ,  $p > 0.05$ ). Moreover, trabecular BV/TV in L3 vertebrae in Ovx KO mice was much higher than that of age-matched Sham WT mice. PGRN deficiency had no effect on serum PINP, but resulted in a decrease in serum PYD by 39.4% ( $p < 0.001$ ) in Sham KO mice and by 48.2% ( $p < 0.0001$ ) in Ovx KO mice. Ovariectomy did not affect serum PINP and PYD in WT mice. RNA was extracted from the tibial diaphysis and real time PCR demonstrated that Sham KO mice had a higher expression of *Sp7* (2.2 fold,  $p < 0.05$ ), *Bglap2* (5.2 fold,  $p < 0.05$ ), *Tnfsf11* (10.5 fold,  $p < 0.05$ ), *Dmp1* (7.0 fold,  $p < 0.01$ ), *Sost* (8.0 fold,  $p < 0.001$ ), and *Wnt1* (10.3 fold,  $p < 0.05$ ) than Sham WT mice. However, these effects of PGRN deficiency on skeletal gene expression were abolished following Ovx. We conclude that PGRN serves to uncouple bone turnover in adult female bone by promoting bone resorption but suppressing the coupled increase in bone formation. Furthermore, PGRN mediates bone loss induced by Ovx by preventing bone formation from increasing to offset bone resorption.

**Disclosures:** Liping Wang, None.

## FR0275

**Effects of Endogenous Hypercortisolism on bone specific microRNA in bone tissue samples of patients with Cushing's disease.** Zhanna Belaya\*, Tatjana Grebennikova<sup>1</sup>, Alexey Nikitin<sup>2</sup>, Olga Brovkina<sup>2</sup>, Alexander Solodovnikov<sup>3</sup>, Liudmila Rozhinskaya<sup>1</sup>, Galina Melnichenko<sup>1</sup>. <sup>1</sup>Endocrinology Research Centre, Russian Federation, <sup>2</sup>Federal Research and Clinical Center FMBA, Russian Federation, <sup>3</sup>Ural State Medical Academy, Russian Federation

**Objective:** to evaluate the levels of microRNAs related to bone remodeling regulation in bone tissue samples from patients with Cushing's disease (CD).

**Materials and Methods:** patients with clinically evident and biochemically proven active CD and patients with hormonally inactive pituitary adenoma as a control group matched by age, sex and BMI were invited to participate. Bone samples were taken during transphenoidal adenomectomy from the base of the sella-turcica, immediately placed in lysis buffer (QIAzol) and subjected to homogenization. Total RNA isolation from bone tissue with on-column digestion of the genomic DNA was carried out with miRNeasy Mini Kit on the automatic station "QIAcube". Reverse transcription was carried out using a TaqMan Advanced miRNA cDNA Synthesis Kit. MicroRNA expression analysis was performed by Real-Time PCR on StepOnePlus instrument with TaqMan Advanced miRNA Assay.

**Results:** we enrolled 26 subjects (16 patients suffered from CD and 10 with hormonally inactive pituitary adenomas) in total 20 females and 6 males, the mean age was 42 years (confident interval (CI) 95% 37–47); BMI – 29 (CI95% 27–32) kg/m<sup>2</sup>. There were no significant difference between the groups. Mean 24h urinary free cortisol (UFC) levels in subjects with CD – 1159 (CI95% 725–1593) nmol/24h were significantly higher as compared to control group ( $p < 0.001$ ) in which 24hUFC was within a reference range (60–413 nmol/24h).

Hypercortisolism altered microRNA (miR) expression profiles in bone samples by statistically significant overexpression of miR210-5p, miR125b-5p, miR9-5p, miR328-5p, miR34a-5p, miR203a-5p, miR188-3p, and downregulation of miR135a-5p, miR211, miR31-5p, miR550a-5p, miR199a-5p, miR27a-5p, miR96-5p. The expression of miR155-5p, miR148a-3p, miR7g-5p, miR10b-5p, miR22-3p, miR230a-5p, miR100-5p, miR133a-5p, miR213-5p, miR550b-2-5p, miR320a were unchanged in subjects with CD as compared to control group.

**Conclusion:** Suppression of osteoblastogenesis in patients with endogenous hypercortisolism is explained in part by altered expression of miR which affect the mesenchymal stem commitment into a different lines namely chondrogenesis, adipogenesis.

**Disclosures:** This study was supported by the Russian Science Foundation (Russian Scientific Foundation 15-1530032)

**Disclosures:** Zhanna Belaya, None.

## FR0276

**Risk Factors of Fractures in Patients with Stage 3 Chronic Kidney Disease: Analysis of Cartagene.** Louis-Charles Desbiens\*, Aboubacar Sidibe<sup>1</sup>, Rémi Goupil<sup>2</sup>, François Madore<sup>2</sup>, Fabrice Mac-Way<sup>1</sup>. <sup>1</sup>CHU de Québec Research Center, L'Hôtel-Dieu-de-Québec Hospital, Endocrinology and Nephrology axis, Faculty and Department of Medicine, Laval University, Canada, <sup>2</sup>Centre de recherche de l'Hôpital du Sacré-Coeur de Montréal, Faculty and Department of Medicine, Montreal University, Canada

## Introduction

The association between end-stage renal disease and increased fracture risk is now well described. However, whether mild chronic kidney disease (CKD) is also associated with higher fracture risk is poorly known. We aimed to determine if mild CKD increases fracture risk vs general population. Secondary objectives were to evaluate whether bone mineral density (BMD) was associated with fracture and to compare the risk factors of fractures in mild CKD.

## Design and methods

Cross-sectional, retrospective and comparative study of the CARTaGENE cohort, a population-based survey of individuals aged 40 to 69 years old from the province of Quebec (Canada). Patients with KDIGO stage 3 CKD (eGFR between 30 and 60 ml/min/1.73m<sup>2</sup> as calculated by the CKD-EPI formula) were compared to controls (eGFR > 60 ml/min/1.73m<sup>2</sup>). Self-reported fractures were classified as osteoporotic (femur, hip, rib, vertebra, wrist, pelvis, sacrum) or total fractures. BMD was measured by calcaneal quantitative ultrasound at baseline. Fracture risk was adjusted for demographic, clinical, pharmacological and biochemistry parameters measured at baseline using multivariate logistic regression. To evaluate risk factors of fractures associated with CKD, stepwise multivariate regressions were performed after stratification for CKD.

## Results

Of the 20,004 CARTaGENE participants, 17,614 had eGFR > 30 ml/min/1.73m<sup>2</sup>, were not taking anti-resorptive therapy and had available data on fractures and BMD (656 stage 3 CKD and 16,958 controls, Figure 1). CKD patients (mean eGFR  $53 \pm 6$  ml/min/1.73m<sup>2</sup>) were older, had higher body mass index (BMI), more diabetes, cardiovascular disease, hypertension, smoking and a lower BMD t-score (Table 1). Total but not osteoporotic fracture risk was higher in CKD patients, but not when stratified by age groups and after adjustments for important covariables (Tables 2 and 3). In multivariate stepwise models after stratification for CKD status, BMD t-score and use of benzodiazepines were associated with total fracture in both groups. Total cholesterol levels and mean blood pressure vs age, smoking and BMI were also associated with fracture in CKD and control groups respectively (Table 4).

## Conclusion

Stage 3 CKD patients have a similar fracture risk but different risk factors of fracture compared to general population. Our results suggest that bone pathology in CKD is different from the general population even at an early stage of CKD.

Table 1. Population characteristics

	Control (n = 16,958)	CKD (n = 656)
<b>Demography</b>		
Age (years)	53±7	61±7**
Sex (Male)	8479 (50.0)	328 (50.0)
Body mass index	27±5	29±6
<b>Comorbidities</b>		
Diabetes mellitus	1,509 (8.9)	136 (20.7)**
Cardiovascular disease	967 (5.7)	91 (13.9)**
Treated hypertension	3,697 (21.8)	323 (49.2)**
Smoking	3,290 (19.4)	97 (14.8)*
<b>Biochemistry</b>		
eGFR (ml/min/1.73m <sup>2</sup> )	89±13	53±6**
Total cholesterol (mmol/L)	5.1±1.0	5.0±1.2*
<b>Bone parameters</b>		
T-Score	0.22±1.2	0.12±1.2*
Total fracture	2,052 (12.1)	119 (18.1)**
Osteoporotic fracture	678 (4.0)	35 (5.4)
Low BMD (T-score < -1.0)	2,120 (12.5)	97 (14.8)
<b>Medication</b>		
Statins	3,035 (17.9)	234 (34.1)**
Vitamin D supplementation	3,035 (17.9)	165 (25.2)**
Benzodiazepines	1,051 (6.2)	71 (10.9)**
RAAS blockers	2,595 (15.3)	241 (36.8)**
Beta-blockers	1,001 (5.9)	94 (14.4)**
Diuretics	1,034 (6.1)	119 (18.1)**
Calcium channel blockers	882 (5.2)	90 (13.7)**

Continuous variables are expressed as mean ± SD. Categorical variables are expressed as number (percentage).  
eGFR, estimated glomerular filtration rate; BMD, bone mineral density; RAAS, renin-angiotensin-aldosterone-system.  
\*  $p < 0.05$   
\*\*  $p < 0.001$

Table 2. Fracture risk stratified by age

Age (years)	Control (n = 16,958)	CKD (n = 656)	P
<b>Total fractures</b>			
40-50	391 (6.2)	5 (6.8)	0.83
50-60	880 (13.4)	32 (17.0)	0.15
60-70	774 (18.9)	82 (20.8)	0.33
<b>Osteoporotic fractures</b>			
40-50	112 (1.8)	1 (1.4)	0.79
50-60	271 (4.1)	8 (4.3)	0.93
60-70	289 (7.0)	28 (7.1)	0.95

Fractures are expressed as number (percentage).

Table 3. Factors associated with total fractures

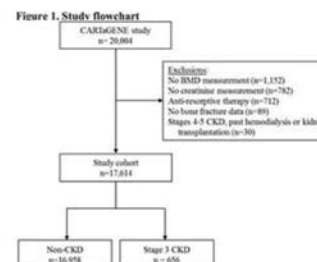
	RR	Low	High
Chronic Kidney Disease	1.111	0.888	1.391
Age**	1.054	1.046	1.061
BMI*	1.013	1.001	1.023
Cardiovascular disease*	1.312	1.070	1.669
Smoking**	1.247	1.103	1.411
Total cholesterol (per mmol/l)	1.038	0.909	1.185
BMD T-score	0.769	0.735	0.805
Mean arterial pressure (per mm Hg)	1.000	0.996	1.005
Statins	0.968	0.837	1.120
Vitamin D supplementation	1.047	0.925	1.183
Benzodiazepines*	1.303	1.093	1.553
RAAS blocker	0.926	0.799	1.073
Beta-blockers	0.877	0.713	1.079
Thiazide diuretics*	1.257	1.031	1.532
Calcium channel blockers	0.898	0.727	1.109

BMI, Body mass index; BMD, Bone mineral density; RAAS, Renin-angiotensin-aldosterone-system.  
Relative risks are calculated by logistic regression.  
\*  $p < 0.05$   
\*\*  $p < 0.001$

Table 4. Risk factors for total fractures in CKD and control

	RR	Low	High
<b>Non-CKD</b>			
Age (per year)	1.058	1.051	1.065
BMI	1.012	1.003	1.022
Smoking	1.224	1.087	1.378
T-score	0.769	0.736	0.804
Benzodiazepines	1.205	1.008	1.440
RAAS blocker	0.869	0.760	0.995
<b>CKD</b>			
Total cholesterol (per mmol/L)	1.267	1.046	1.534
T-score	0.687	0.566	0.834
Benzodiazepines	2.153	1.201	3.860
RAAS blocker	1.958	1.249	3.068
Mean arterial pressure (per mmHg)	1.022	1.003	1.042

BMI, Body mass index; RAAS, Renin-angiotensin-aldosterone-system.  
Relative risks are calculated by logistic regression in a stepwise forward model which included the following covariables: age, BMI, cardiovascular disease, smoking, total cholesterol, high-density lipoprotein, BMD T-score, Statins, Vitamin D, Mean arterial pressure, RAAS blockers, Benzodiazepines, Diuretics, Beta-Blockers, Calcium channel blockers



Annex

**Disclosures:** Louis-Charles Desbiens, None.

## FR0280

**Alendronate ameliorates the risk of urinary stone formation of astronauts on the International Space Station for 6 months.** Atsushi Okada<sup>1</sup>, Takahiro Yasui<sup>1</sup>, Kenjiro Kohri<sup>2</sup>, Toshio Matsumoto<sup>3</sup>, Adrian LeBlanc<sup>4</sup>, Jean Sibonga<sup>5</sup>, Elisabeth Spector<sup>6</sup>, Jeff Jones<sup>4</sup>, Jay Shapiro<sup>7</sup>, Thomas Lang<sup>8</sup>, Linda Shackelford<sup>5</sup>, Scott Smith<sup>5</sup>, Harlan Evans<sup>6</sup>, Joyce Keyak<sup>9</sup>, Hiroshi Ohshima<sup>10</sup>. <sup>1</sup>Department of Nephro-urology, Nagoya City University Graduate School of Medical Sciences, Japan, <sup>2</sup>Nagoya City University, Japan, <sup>3</sup>University of Tokushima Fuji Memorial Institute of Medical Sciences, Japan, <sup>4</sup>Baylor College of Medicine, United States, <sup>5</sup>NASA Johnson Space Center, United States, <sup>6</sup>KBRWyle, United States, <sup>7</sup>Kennedy Krieger Institute, United States, <sup>8</sup>UCSF, United States, <sup>9</sup>University of California at Irvine, United States, <sup>10</sup>Japan Aerospace Exploration Agency, Japan

**Backgrounds.** Increased risk of urinary stone formation during space flight has been reported. Pain attacks of stones during space flight can not only fail the mission but also threaten the lives of crews. The bisphosphonate study is a collaborative effort between NASA and JAXA to investigate the potential for preventing hypercalciuria-induced kidney stone formation caused by bone resorption associated with long-duration space-flight. In this study, we investigated the risk of kidney stone formation by measuring urine biochemistry of the astronauts on the *International Space Station (ISS)* for 6 months, and assessed whether bisphosphonate would ameliorate the risk.

**Methods.** Seventeen astronauts stayed on the *ISS* for 6 months were divided into two groups; the medication group (MED;N=7) who were administered oral alendronate, 70 mg/week, and the control group (CON;N=10) who exercised under a protocol using the advanced resistive exercise device (ARED). We used unpaired t-test for comparison between the groups, and paired t-test for chronological data.

**Results.** Urine volume significantly decreased and creatinine excretion increased in both groups after the initiation of space flight and recovered after the earth return. CON group showed increased urinary calcium excretion from the 15th day to 60th day of space flight, while no remarkable change was observed in MED group during space flight. Urinary NTX, DPD and PYD as bone resorption markers were significantly elevated in CON group during the space flight, which did not increase in MED group. In particular, urinary NTX of MED group remained significantly lower during the flight and until 30 days after returning to the earth as compared with CON Group. Urinary oxalate and uric acid excretion of CON group tended to be higher than in MED group during flight. Calculated renal stone risk including estimation of supersaturation of stone-forming compounds demonstrated increased risk of calcium oxalate, brushite and sodium urate stones in CON group but not in MED group.

**Conclusion.** The present results demonstrate that the astronauts staying on the *ISS* for a long time are exposed to high risk of kidney stone, especially calcium oxalate, associated with increased bone resorption, which is similar to the previous reports about space flight and long-term bed rest as an analog for space flight. It is suggested that alendronate is effective in preventing microgravity-induced bone mineral loss and kidney stone formation.

**Disclosures:** Atsushi Okada, None.

## FR0282

**Hip QCT for Assessment of Trabecular Bone Loss and Recovery after Space Flight: A Pilot Study.** Jean Sibonga<sup>1</sup>, Thomas Lang<sup>2</sup>, Harlan Evans<sup>3</sup>, Elisabeth Spector<sup>3</sup>. <sup>1</sup>NASA-Johnson Space Center, United States, <sup>2</sup>UCSF, United States, <sup>3</sup>KBRWyle, United States

Since the early 1990s, space flight-induced declines in measurements of areal bone mineral density (aBMD) have been serially documented by Dual-energy X-ray Absorptiometry (DXA). While DXA is limited by an areal measurement and inability to delineate trabecular (Tb) vs. cortical bone, Quantitative Computed Tomography (QCT) can assess volumetric bone mineral density (vBMD) in both compartments. QCT studies have shown rapid bone losses in the trabecular compartment of the hip after flight (averaging 2.3%/mo without effective countermeasures and as high as 4.0%/mo in some individuals) that were not detectable by DXA. The purpose of this pilot study was to demonstrate the use of QCT to augment standard DXA measurements of long-duration astronauts as a surveillance tool to monitor space flight bone loss and recovery. Methods: QCT and DXA scans of the left and right hip were obtained on 8 astronauts before ISS flight (duration 154 ± 23 days), approximately 1 week after flight and again at 1 year of recovery (R+1yr). All subjects exercised 6 days/wk using some combination of resistive exercise and aerobic exercise (i.e., cycle ergometer and treadmill). If a subject's R+1yr QCT Tb vBMD did not return to baseline (i.e., within established measurement error of 2.3%) in one or both hips, an additional QCT session was obtained at R+2yr. Results: For the overall group of n=8, mean %change in QCT Tb vBMD was -10.3% at R+1wk\* and -4.0% at R+1yr\*. For the subset requiring R+2yr testing (n=5), QCT Tb vBMD changes were: -12.7% at R+1wk\*, -6.3% at R+1yr\*, and -6.6% at R+2yr\*. Mean DXA aBMD changes for the n=8 group were: -2.4% at R+1wk\* and -0.8% at R+1yr. For the subset with R+2yr QCT testing, DXA aBMD changes were: -2.2% at R+1wk\* and -1.1% at R+1yr. While DXA total hip aBMD losses were modest and essentially recovered by R+1yr, QCT Tb vBMD losses were significantly larger and showed incomplete recovery in 5/8 subjects at R+1yr and 4/8 subjects at R+2yr. Mean QCT losses were similar between R+1yr and R+2yr and suggest only ~50% recovery in Tb vBMD at these time points. Conclusions: QCT assesses space flight changes in hip trabecular BMD that are (a) not detectable by DXA and (b) possibly irreversible in some

individuals. Lack of recovery at R+2yr may indicate a need for follow-up testing or clinical intervention to prevent premature osteoporosis/fragility fracture in this unique population (Orwoll et al. JBMR, 2013). \*p<0.05 by Student's paired T-test

**Disclosures:** Jean Sibonga, None.

## FR0286

**Predictors of Improvement in Bone Mineral Density after Celiac Disease Diagnosis.** Haley M. Zylberberg<sup>1</sup>, Benjamin Lebwohl<sup>1</sup>, Arindam RoyChoudhury<sup>2</sup>, Minghao Liu<sup>3</sup>, Marcella Walker<sup>4</sup>, Peter H.R. Green<sup>1</sup>. <sup>1</sup>Celiac Disease Center at Columbia University, College of Physicians and Surgeons, United States, <sup>2</sup>Mailman School of Public Health, Columbia University, United States, <sup>3</sup>Dept of Medicine Endocrinology Columbia University, College of Physicians and Surgeons, United States, <sup>4</sup>Division of Endocrinology, Columbia University, College of Physicians and Surgeons, United States

Low bone density is frequently found in patients newly diagnosed with celiac disease (CD), and improvement is variable. The purpose of this analysis was to assess changes in bone mineral density (BMD) by dual x-ray absorptiometry (DXA) at the lumbar spine, femoral neck, total hip, and one-third radius as well as clinical predictors of BMD changes after the diagnosis and treatment of CD.

Adult patients with CD who had serial DXA as part of their usual clinical care at the Celiac Disease Center at Columbia University Medical Center were included (N=103). We assessed within-person changes in BMD with paired t-tests. Multiple regression was utilized to assess baseline clinical and laboratory predictors of BMD improvement after diagnosis and treatment. Regression analysis was limited to 51 patients who had a complete set of clinical and laboratory predictors.

After a median follow-up of 21 months, lumbar spine BMD increased by 1.7±5.5% (p=0.006) after the diagnosis of CD. There was a similar trend at the total hip (1.6±6.3%, p=0.06), but no change at the femoral neck or one-third radius. Lower baseline serum calcium predicted a greater increase in lumbar spine BMD (B = -0.0470 g/cm<sup>2</sup>, p=0.002). At the hip, higher creatinine clearance (B=0.005, p=0.02) was associated with greater gains in BMD after the diagnosis of CD.

BMD increases at the lumbar spine after the diagnosis of CD and greater BMD improvement is associated with lower baseline serum calcium. These results suggest that those with the lowest calcium, which is likely a surrogate for the greatest malabsorption, may have the greatest potential for improvement in skeletal health after identification and treatment of CD.

	B estimate	Standard error	P-value	Overall Model R <sup>2</sup>
Lumbar Spine				
Intercept	0.3998	0.1773	0.03	R <sup>2</sup> =0.40, p=0.001
Age (per 10 years)	-0.005	0.006	0.4	
Weight (per 10 kg)	0.0041	0.009	0.7	
LS BMD (per 10g/cm <sup>2</sup> )	-0.179	0.740	0.8	
Calcium (per mg/dl)	-0.0470	0.0141	0.002	
Creatinine clearance (per 10 ml/min)	0.002	0.003	0.5	
Alkaline phosphatase (per 10 U/L)	0.002	0.002	0.2	
Male Sex	0.01780	0.0175	0.3	
Disease Duration (per 10 yrs)	0.0003	0.0003	0.3	
Diarrhea at presentation	0.0083	0.0137	0.6	
Race- White/Non-Hispanic	0.0185	0.0181	0.3	
Total Hip				
Intercept	0.0555	0.1257	0.7	R <sup>2</sup> =0.32, p=0.01
Age (per 10 years)	0.006	0.005	0.3	
Weight (per 10 kg)	-0.014	0.007	0.08	
Hip BMD (per 10 g/cm <sup>2</sup> )	0.244	0.505	0.6	
Calcium (per mg/dl)	-0.108	0.108	0.3	
Creatinine clearance (per 10 ml/min)	0.005	0.002	0.02	
Alkaline phosphatase (per 10 U/L)	0.002	0.001	0.11	
Male Sex	0.0242	0.0134	0.08	
Disease Duration (per 10 yrs)	0.0005	0.0003	0.07	
Diarrhea at presentation	0.0055	0.0102	0.6	
Race-White/Non-Hispanic	0.0195	0.0140	0.17	

Table: Predictors of Change in Bone Mineral Density at the Lumbar Spine and Total Hip

**Disclosures:** Haley M. Zylberberg, None.

## FR0287

**Long-term effects of bisphosphonate therapy: perforations, microcracks and mechanical properties.** Shaocheng Ma<sup>\*</sup>, Ulrich Hansen, Justin Cobb, Richard Abel. Imperial College, United Kingdom

Bisphosphonates (BP) are the frontline therapy for osteoporosis, which act by reducing bone remodeling to prevent bone loss, thinning of trabeculae and perforations caused by hyperactive osteoclasts; thereby maintaining microstructure. However, there



is growing concern that BP may over suppress remodeling resulting in the accumulation of microcracks. This paper aims to investigate the effect of BP on microstructure and mechanical properties.

Trabecular bone samples were harvested from femoral heads of 3 cohorts: a BP treated (alendronate 70mg/weekly) fracture group ( $n=8$ ), untreated fracture controls ( $n=8$ ) and healthy ageing non-fracture controls ( $n=5$ ). Mean ages respectively  $79.3 \pm 6.4$ ,  $77.8 \pm 3.4$  and  $77.8 \pm 4.9$  years were comparable (ANOVA  $F=0.523$ ,  $p=0.644$ ). Assessment of microdamage was performed using a particle accelerator synchrotron micro-CT system (Diamond Light Source, UK). Cylindrical cores ( $h$  10 and  $d$  7 mm) were drilled from the trabecular chiasma. The density and volume of both perforations and microcracks were measured at the center of the cores (away from drilling damage) using image analysis software (VG StudioMAX). Mechanical uniaxial tensile tests were carried out using standard rectangular samples ( $11 \times 2.8 \times 1$  mm) sectioned from the region immediately inferior to the cores. Stress-strain curves were examined to calculate the ultimate tensile strength and Young's Modulus, which were normalized according to trabecular bone volume. Microstructural and mechanical data were analyzed using non-parametric statistics i.e. Kruskal-Wallis.

Trabecular bone volume fraction in the non-fracture group ( $0.34 \pm 0.03$ ) was significantly higher ( $p=0.001$ ) than the untreated fracture group ( $0.24 \pm 0.03$ ) but not the BP-treated fracture group ( $0.29 \pm 0.07$ ). BP patients exhibited a significantly lower density ( $p=0.040$ ) and smaller volume ( $p=0.030$ ) of perforations than fracture controls, but significantly higher density and larger volume than non-fracture controls. BP patients exhibited a significantly higher density of microcracks ( $p=0.010$ ) and larger microcrack volume ( $p=0.001$ ) than both fracture and non-fracture controls. BP patients exhibited significantly lower normalized tensile strength ( $p=0.001$ ) and Young's Modulus ( $p=0.030$ ) than both fracture and non-fracture controls.

BP therapy seems effective at reducing perforations but may also cause microcrack accumulation, leading to a loss of microstructural integrity and consequently reduced mechanical strength.



Micro-cracks inside bone samples from patients treated with bisphosphonate

**Disclosures:** Shaocheng Ma, None.

## FR0290

**Denosumab Improves Glycemic Control of Type 2 Diabetic or Prediabetic Patients with Osteoporosis.** Chee Kian Chew\*, Sundeep Khosla, Robert Rizza, Jennifer Geske, Bart Clarke. Mayo Clinic, United States

**Introduction:** Denosumab (DMab) has been shown to stimulate human  $\beta$ -cell proliferation through inhibition of the RANKL pathway in mice. The primary aim of this study was to determine if DMab could improve glycemic control in T2DM or prediabetic (preDM) patients with osteoporosis.

**Study design:** This was a retrospective case control study of subjects aged 45 to 100 years with T2DM/preDM and osteoporosis treated at Mayo Clinic from 1/1/2009 to 7/13/2016. Subjects were divided into 3 groups based on osteoporosis treatment with DMab, oral or IV bisphosphonate (BP), or calcium and/or vitamin D (Ca/vitD) supplementation. Fasting plasma glucose (FPG), HbA1c and weight were assessed at baseline, 6 months, and 12 months after subjects started osteoporosis treatment. The primary endpoint was the change in HbA1c at 6 and 12 months. Secondary endpoints were the changes in FPG and body weight at 6 and 12 months. Linear regression models predicting change in weight, HbA1c, or FPG were adjusted for age, sex, BMI, duration of T2DM/preDM, and DM medication class to test for differences in the groups.

**Results:** There were 115 eligible subjects matched for age, sex, BMI, and duration of T2DM/preDM in each group of the study. Subjects in DMab group were older. There were no significant differences in sex, BMI, duration of T2DM/preDM, baseline HbA1c and baseline FPG between the groups. From 0-12 months, there were significant differences across treatment groups in change in HbA1c (Ca/vitD: 0.1%, BP: 0.3%, DMab: -0.3%;  $p$ -value = 0.003), and weight (Ca/vitD: -0.3kg, BP: 0.8kg, DMab: -2.5kg;  $p$ -value = 0.0003), but no significant difference in change in FPG. In DMab group, HbA1c decreased nonsignificantly by 0.2% at 6 months, but significantly by 0.3% at 12 months from baseline. This decrease remained significant after adjustment for age, sex, BMI, duration of T2DM/preDM, and diabetic treatments. There was a significant 0.3% increase in HbA1c at 12 months from baseline in BP group, and no change in Ca/vitD group. Compared with Ca/vitD group, there was significant weight reduction at 6 and 12 months from baseline (1.0kg and 2.5kg, respectively) in DMab group. There

was sustained weight loss at 12 months compared to 6 months. However, no weight loss effect was observed in BP group at any time point.

**Conclusion:** DMab has been demonstrated to be useful for treatment of osteoporosis, but it may also be beneficial for treatment of T2DM/preDM in patients with osteoporosis.

**Disclosures:** Chee Kian Chew, None.

## FR0292

**Rates of Mortality and Second Hip Fracture Following the Implementation of a Fracture Liaison Service (FLS): A Single Center Experience.** Vitaly Medvedovsky\*, Uri Yoel<sup>1</sup>, Lior Baraf<sup>1</sup>, Dayana Cohen<sup>1</sup>, Tamar Eshkoli<sup>1</sup>, Avital Blum<sup>1</sup>, Vera Polischuk<sup>1</sup>, Poliana Shamgar<sup>1</sup>, Michal Lamberger<sup>1</sup>, Dvora Lieberman<sup>1</sup>, Victor Novack<sup>1</sup>, Ethel Siris<sup>2</sup>, Merav Fraenkel<sup>1</sup>. <sup>1</sup>Soroka University Medical Center and the Faculty of Health Sciences, Ben-Gurion University of the Negev, Israel, <sup>2</sup>Columbia University Medical Center, United States

### Aims

It was our aim to assess rates of mortality and recurrent hip fracture after the implementation of a fracture liaison service (FLS) in patients with hip fracture at Soroka University Medical Center (SUMC) a tertiary university medical center.

### Methods

Patients over age 50 admitted to SUMC with hip fracture were offered an endocrinologist consultation and recommendation on treatment with anti-osteoporotic medication according to current international guidelines. Patients were subsequently assessed as to the acceptance of prescribed anti osteoporotic medication, recurrent hip fracture incidence following the index fracture, and mortality.

### Results

As of October 2016, 608 patients admitted to SUMC with hip fracture joined the FLS; mean age  $79.14 \pm 9.9$ , 73.9% females. Patients who died within 30 days of fracture were excluded from analysis ( $n=30$ ). 73% of patients who received endocrine consultation (inpatient or outpatient) compared to only 30% of those w/o endocrine consultation received anti-osteoporotic treatment. Among all treated patients 157 (44.6%) received Zoledronic acid, 73 (20.8%) Denosumab, 12 (3.4%) Teriparatide, and 110 (31.2%) received Oral Bisphosphonates. During follow up (median 10 months Q1:Q3, 4:18), 89 patients died. Patients who died were older (mean age  $82.86 \pm 9.08$  vs.  $78.02 \pm 9.89$ ,  $p$ -value < 0.001), and had higher rates of comorbidities including hypertension (61.8% vs 49.4%  $p=0.031$ ), CKD (16.9% vs. 7.6%  $p=0.005$ ), IHD 25.8% vs. 14.8%  $p=0.009$  and malignancy (7.9% vs. 2.3%  $p=0.012$ ). Cox Regression analysis, standardized for age and gender showed a HR 0.324 for death in those with and without medical treatment for osteoporosis ( $p < 0.001$ , CI 95% 0.202-0.505). During follow up 20 patients (3.3%) experienced second hip fracture, median time between first and second hip fracture was 161 days (Q1:Q3 66:341).

### Conclusions

Fracture liaison service following hip fracture in a single center medical setting is possible, efficacious and safe. Medical treatment for osteoporosis following hip fracture is associated with reduced mortality. Recurrent hip fractures within study period were very few not allowing to draw conclusions.

**Disclosures:** Vitaly Medvedovsky, None.

## FR0293

**A Phase 1, Subject- and Investigator blinded, Sponsor unblinded, Placebo-controlled, Randomized, 2 part, Sequential, Single Ascending Dose Study to Assess the Safety, Tolerability, Pharmacokinetics, and Pharmacodynamics of DS 1501a in Healthy Young Subjects and Healthy Postmenopausal Women.** Victor Dishy\*, Dongwoo Kang<sup>1</sup>, Vance Warren<sup>1</sup>, William Maxwell<sup>1</sup>, Benjamin Levinson<sup>1</sup>, Jarema Kochan<sup>1</sup>, Ling He<sup>1</sup>, Merav Baz-Hecht<sup>1</sup>, Chie Fukuda<sup>2</sup>, Junichi Koga<sup>2</sup>, Eisuke Tsuda<sup>2</sup>, Ko Watanabe<sup>2</sup>. <sup>1</sup>Daiichi Sankyo, Inc, United States, <sup>2</sup>Daiichi Sankyo, Inc, Japan

DS-1501a is a monoclonal antibody against siglec-15, a member of cell-surface receptors that recognize sialylated glycoconjugates and is highly expressed on osteoclasts. In vitro, anti-Siglec 15 antibody inhibited osteoclast fusion and bone-resorbing activity of mature osteoclasts. This first in human study assessed the safety, tolerability, pharmacokinetics and pharmacodynamics of single ascending subcutaneous doses of DS-1501a in healthy young subjects (Part A) and of a single dose of DS-1501a in healthy postmenopausal women (Part B). Subjects were followed for 12 weeks after dosing. In Part A, 45 subjects received DS-1501a at a dose range of 0.005 to 3 mg/kg and 15 subjects received placebo. In Part B, 9 postmenopausal women received a single dose of DS-1501a 1 mg/kg and 3 received placebo.

Maximum serum concentrations of DS-1501a were reached between 5 to 11 days post dose and mean T1/2 ranged from 11.4 to 23 days. There was no apparent difference in the T<sub>max</sub> or T1/2 between healthy young subjects and postmenopausal women.

TRACP-5b and CTX, decreased after DS-1501a compared to placebo in both Parts A and B in a dose related manner. Maximum decreases were reached 29 to 36 days post dose and were maintained up to 85 days at doses > 0.015 and 0.05 mg/kg for TRACP-5B and CTX respectively. In Part A, maximum percentage decreases from baseline, [mean (SD)], were 85%(16) for TRACP-5B and 70%(7) for CTX, at DS 1501a 1.5 mg/kg. In Part B, decreases were 56%(18.5) and 56%(7.5) for TRACP-5B and CTX respectively.

Levels of PINP, decreased only modestly by Day 85: maximum decrease 33%(9) at doses >0.15 mg/kg in Part A and 22%(9) in Part B. iPTH increased following all doses of DS-1501a in both study Parts. Peak increase was observed at 22 days post dose and trended down with time.

No apparent differences in mean PK or PD of DS-1501a were noted between subjects with (7) or without (47) anti-drug antibodies.

There were no deaths, drug-related serious adverse events or symptomatic hypocalcemia. Transient, asymptomatic elevations of serum creatine kinase were observed in 5 DS-1501a treated subjects in Part A and no subject in Part B. There were no clinically meaningful changes in numbers of circulating leukocyte subtypes or ex-vivo cytokine response of peripheral blood mononuclear cells to LPS.

In conclusion, single doses of DS-1501a resulted in sustained decreases of bone resorption biomarkers while having a modest effect on bone formation biomarkers.

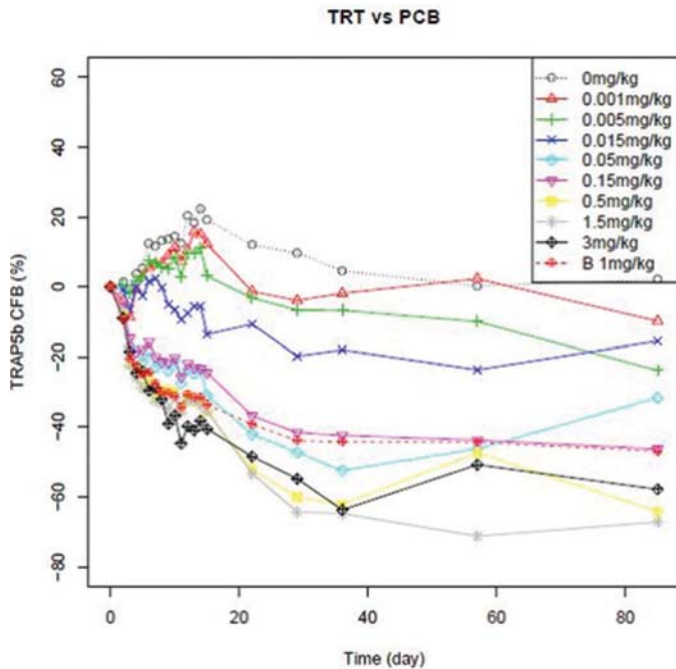


Figure 1

Disclosures: Victor Dishy, None.

## FR0295

**Factors affecting fracture location in atypical femoral fractures: a cross-sectional study with 147 patients.** Ji Wan Kim<sup>1</sup>, Jung Jae Kim<sup>2</sup>, Jae Suk Chang<sup>2</sup>, Jai Hyung Park<sup>3</sup>, Hyun Chul Shon<sup>4</sup>, Kwang Hwan Jung<sup>5</sup>, Chul-Ho Kim<sup>2</sup>, Seong-Eun Byun<sup>6</sup>, Chang-wug Oh<sup>7</sup>. <sup>1</sup>Haeundae Paik Hospital, Inje University, Korea, Republic of, <sup>2</sup>Asan Medical Center, University of Ulsan, Korea, Republic of, <sup>3</sup>Kangbuk Samsung Hospital, Sungkyunkwan University, Korea, Republic of, <sup>4</sup>Chungbuk National University Hospital, Korea, Republic of, <sup>5</sup>Ulsan University Hospital, Korea, Republic of, <sup>6</sup>CHA Bundang Medical Center, CHA university, Korea, Republic of, <sup>7</sup>Kyungpook National Hospital, Kyungpook National University, Korea, Republic of

**Introduction:** Many studies have tried to determine the characteristics of atypical femoral fractures (AFFs) through age-, sex-, and ethnicity-matched comparison with non-AFFs. However, we hypothesized that diaphyseal AFFs would have characteristics different from those of subtrochanteric AFFs. The aim of this study was to evaluate the clinical features of diaphyseal/subtrochanteric AFFs and determine the factors related to fracture location.

**Patients and Methods:** One hundred forty-seven patients with AFF were enrolled, 114 patients (78%) had a history of bisphosphonate use. Forty-nine patients (33%) had bilateral lesion, and 35% of patients had thigh pain. Patients were divided into two groups according to fracture location: 52 patients (35.4%) with subtrochanteric AFF and 95 patients (64.6%) with diaphyseal AFF. The patient demographics and fracture characteristics of the two groups were compared. Multivariate logistic regression analysis was used to adjust for variables related to fracture location.

**Results:** The patients in the diaphyseal AFFs group were older and had lower BMI, lower BMD, and larger lateral and anterior bowing. Multivariate analysis revealed that age greater than 65 years and low BMD were related with diaphyseal location. With greater lateral bowing angle, the AFF location was moved from the subtrochanteric area to the diaphyseal area.

**Conclusion:** This study demonstrated that patients with diaphyseal AFFs had different characteristics compared with those with subtrochanteric AFFs.

Disclosures: Ji Wan Kim, None.

## FR0298

**The effect of teriparatide on fracture healing of vertebral compression fracture in post menopausal women.** Seung Woo Suh<sup>1</sup>, Si Young Park<sup>2</sup>, Jae Young Hong<sup>1</sup>, Tae Wook Kang<sup>1</sup>. <sup>1</sup>Korea Univerisity Hospital, Korea, Republic of, <sup>2</sup>Korea University Hospital, Korea, Republic of

**Introduction:** Acute vertebral compression fractures cause severe back pain and need long time to heal. The progression of fracture or nonunion is not rare. The teriparatide is a synthetic parathyroid hormone which has been used as anabolic agent and treatment of osteoporosis.

It also can be used for promoting fracture healing in special condition. Periodic infusion of teriparatide enhances bone formation and increases bone strength. We evaluated the effect of periodic teriparatide infusion on fracture healing of acute vertebral compression fractures

**Methods:** A prospective study consisting of a review of case report form. We prospectively enrolled 84 postmenopausal women who had one or two acute painful vertebral compression fractures confirmed by MRI. All patients were treated conservatively. Among them, 32 patients were treated conservatively with teriparatide for at least 6 months (group I), and 52 were treated with antiresorptive agent (group II). VAS and ODI scores were assessed at each follow up until 1 year after trauma. We also measured radiographic changes, the degree of collapse progression.

**Results:** The progression of fractured vertebral body collapse was shown in both groups, but the degree of progression was significantly lower in group I than in group II. At the last follow-up, mean increments of kyphosis and wedge angle were significantly lower in group I. Clinical outcome measures were closely related with vertebral body collapse.

**Conclusion:** Periodic infusion of teriparatide might have many beneficial effect on acute vertebral compression fractures in postmenopausal women. Patients using teriparatide showed quicker symptomatic improvement and less collapsed vertebral body 1 year after trauma compared to patients using anti-resorptive agent.

Disclosures: Seung Woo Suh, None.

## FR0299

**Effect of fracture risk assessment on anti-osteoporosis medication use and adherence: Findings from the SCOOP Trial.** C. Cooper<sup>1</sup>, C. Parsons<sup>2</sup>, N. C Harvey<sup>1</sup>, L. Shepstone<sup>3</sup>, J. A. Kanis<sup>4</sup>, E. Lenaghan<sup>3</sup>, S. Clarke<sup>5</sup>, R. Fordham<sup>3</sup>, N. Gittos<sup>6</sup>, I. Harvey<sup>3</sup>, R. Holland<sup>3</sup>, A. Heawood<sup>5</sup>, N. Redmond<sup>5</sup>, A. Howe<sup>3</sup>, T. Marshall<sup>3</sup>, T.J. Peters<sup>5</sup>, D. Torgerson<sup>7</sup>, T.W. O'Neill<sup>8</sup>, E. McCloskey<sup>9</sup>. <sup>1</sup>MRC Lifecourse Epidemiology Unit, University of Southampton, United Kingdom, <sup>2</sup>RC Lifecourse Epidemiology Unit, University of Southampton, United Kingdom, <sup>3</sup>University of East Anglia, United Kingdom, <sup>4</sup>Centre for Metabolic Bone Diseases, University of Sheffield and Institute for Health and Ageing, Catholic University of Australia, United Kingdom, <sup>5</sup>University of Bristol, United Kingdom, <sup>6</sup>Queen Elizabeth Hospital, United Kingdom, <sup>7</sup>University of York, United Kingdom, <sup>8</sup>University of Manchester, United Kingdom, <sup>9</sup>Centre for Metabolic Bone Diseases, University of Sheffield, United Kingdom

We aimed, in the context of a large randomised controlled trial, to investigate the effect of a population based, primary care led fracture risk screening intervention, on initiation of anti-osteoporosis medications, and subsequent adherence. The 'Screening for prevention of fracture in older women' (SCOOP) study is a pragmatic RCT of screening for osteoporotic fracture risk compared with usual care in the UK. 12,483 women (70 to 85 years old), identified from primary care lists, were randomised to either fracture risk assessment using the FRAX tool +/-DXA BMD, with medication recommended via the primary care physician for those found to be at high risk of fracture, or to usual NHS care. Self-reported anti-osteoporosis medication use was obtained by postal questionnaire at 6, 12, 24, 36, 48 and 60 months after randomisation. Ordered logistic regression was used to investigate baseline determinants of adherence (defined as the percentage of study visits at which the participants reported taking anti-osteoporosis medication, following a positive report at the index visit). The mean (SD) age of the participants was 75.6 (4.2) years, with 6233 randomised to screening and 6250 to usual care (control group). At 6 months, 73.8% of participants who were classified at high fracture risk and completed the 6-month questionnaire, were taking anti-OP medication, compared with only 2% overall in the control group. Across all participants, 37.1% in the screening group on treatment at 6 months after randomisation were still treated at 60 months; the respective figure for the control group was 21.6%. For those participants commenced on treatment later during follow-up, rates of adherence at 60 months became increasingly similar between intervention and control participants (e.g. 70.3% vs 68.1% respectively at 60 months for treatment initiated at 48 months). Older age was associated with lower adherence [OR 0.96 (95%CI: 0.93, 0.98), p=0.001] and history of parental hip fracture with greater adherence [OR 1.68 (95%CI: 1.28, 2.20), p<0.001]. Active screening for fracture risk in older women leads to a marked increase in use of anti-osteoporosis medications, and greater adherence, in women at high fracture risk. These findings inform public health strategies aimed at reduction of fragility fractures.

Disclosures: C. Cooper, None.



## FR0300

**Prevalence of severe suppression of bone turnover (SSBT) in patients on long-term bisphosphonate (BP) therapy.** Shijing Qiu\*, Elizabeth Warner, Pooja Kulkarni, Mahalakshi Honasoge, Arji Bhan, Shiri Levy, George Divine, D. Sudhaker Rao, Henry Ford Hospital, United States

*In vivo* tetracycline labeling of bone is a gold standard marker to determine the rate of bone turnover (or bone remodeling). Severe suppression of bone turnover (SSBT) is commonly defined as complete absence of tetracycline labeling in cancellous bone. However, it is inappropriate to assume that bone with tetracycline labeling, no matter how little, as having normal bone turnover. In the current study, we developed reference range for bone turnover based on the results from healthy premenopausal women, the lower limit of which as the cutoff to define SSBT.

The bone turnover-related variables, including mineralizing surface (MS/BS, %), mineral apposition rate (MAR,  $\mu\text{m}/\text{day}$ ), bone formation rate (BFR/BS,  $\mu\text{m}^3/\mu\text{m}^2/\text{year}$ ) and activation frequency (Ac.f, /year), were determined in iliac bone biopsies obtained from 43 healthy premenopausal white women. The reference range was defined as a 95% interval with 2.5% of the values less than the lower limit and 2.5% were more than the upper limit. SSBT was defined when BFR/BS and/or Ac.f fell below the lower limit. The same measurements were performed on iliac bone biopsies from postmenopausal healthy women and from patients on long-term BP therapy (all postmenopausal) with and without atypical femur fracture (AFF). The results are shown in Table 1. Since wall thickness to calculate Ac.f may not be detected in some patients with BP exposure, we suggest BFR/BS as more appropriate variable to define bone turnover. In postmenopausal women, the prevalence of SSBT was < 5% in cancellous bone, and none in whole biopsy. In contrast, the prevalence of SSBT increased to approximately 60% in cancellous bone and 30% in whole biopsy in BP-treated patients, both of which were significantly higher than those in postmenopausal women. However, there was no significant difference in the prevalence of SSBT between BP treated patients with and without AFF.

In conclusion, this study confirms that BP exposure can significantly increase the risk of SSBT in postmenopausal women. Although the prevalence of SSBT was similar in BP-treated patients with and without AFF, a higher trend was seen in patients with AFF.

Table 1. The difference in SSBT prevalence among healthy postmenopausal women and BP treated patients with and without atypical femur fracture

	MS/BS %	MAR $\mu\text{m}$	BFR $\mu\text{m}^3/\mu\text{m}^2/\text{year}$	Ac.f /year
Reference Range (Premenopausal Women n = 43)				
Cancellous Surface	0.881 - 14.2	0.107 - 0.791	0.628 - 26.9	0.016 - 0.751
Combined Surface	1.41 - 12.5	0.107 - 0.847	0.689 - 29.8	0.019 - 0.727
Cancellous Surface				
HPMW	4/66 (6.06)	1/66 (1.52)	3/66 (4.55)	2/66 (3.03)
Patients with BP exposure	35/54 (64.8)	24/54 (44.4)	32/54 (59.3)	29/51 (56.9)
no AFF	22/34 (64.7)	14/34 (41.2)	19/34 (55.9)	19/34 (55.9)
with AFF	13/20 (65.0)	10/20 (50.0)	13/20 (65.0)	10/17 (58.8)
Combined Surface				
HPMW	1/66 (1.52)	0/66 (0)	0/66 (0)	0/66 (0)
Patients with BP exposure	28/54 (51.9)	12/54 (22.2)	16/54 (29.6)	13/48 (27.1)
no AFF	15/34 (44.1)	6/34 (17.6)	9/34 (26.5)	8/33 (24.2)
with AFF	13/20 (65.0)	6/20 (30.0)	7/20 (35.0)	5/15 (33.3)

HPMW: Healthy postmenopausal women. All variable rates in HPMW were significantly lower than those in patients with BP exposure.

Table 1

**Disclosures:** Shijing Qiu, NIAMS, Grant/Research Support.

## FR0301

**Effect of Denosumab Compared With Risedronate on Percentage Change in Lumbar Spine BMD at 12 Months in Subgroups of Glucocorticoid-treated Individuals.** K Saag\*<sup>1</sup>, N Pannacciuoli<sup>2</sup>, P Geusens<sup>3</sup>, J Adachi<sup>4</sup>, E Lespessailles<sup>5</sup>, J Malouf-Serra<sup>6</sup>, O Messina<sup>7</sup>, A Wang<sup>2</sup>, RB Wagman<sup>2</sup>, WF Lems<sup>8</sup>. <sup>1</sup>University of Alabama, United States, <sup>2</sup>Amgen Inc., United States, <sup>3</sup>Maastricht University, Netherlands, <sup>4</sup>McMaster University, Canada, <sup>5</sup>University Hospital Orleans, France, <sup>6</sup>Hospital San Pablo, Spain, <sup>7</sup>Cosme Argerich Hospital, Argentina, <sup>8</sup>VU University Medical Centre, Netherlands

Purpose: Glucocorticoid (GC)-induced osteoporosis (GIOP) remains the most common secondary cause of osteoporosis. We previously demonstrated that denosumab (DMAb) significantly increased lumbar spine (LS) BMD more than risedronate (RIS) at 12 mos in GC-treated individuals. Here, we explored the effects of DMAb and RIS on LS BMD in predefined subgroups to determine whether these factors affected the treatment effect.

Methods: This was a phase 3, randomized, double-blind, active-controlled study to evaluate DMAb vs. RIS in GC-treated individuals for 24 mos. Eligible subjects were women and men  $\geq 18$  yrs receiving GC therapy at a dose  $\geq 7.5$  mg prednisone daily or its equivalent for  $\geq 3$  mos or  $< 3$  mos prior to screening (GC-continuing [GC-C] and GC-initiating [GC-I], respectively). All subjects  $< 50$  yrs were required to have a history of

osteoporotic fracture. GC-C subjects  $\geq 50$  yrs were required to have a LS, total hip, or femoral neck T-score  $\leq -2.0$ ; or a T-score  $\leq -1.0$  with a history of fracture. Subjects were randomized 1:1 to SC DMAb 60 mg every 6 mos or oral RIS 5 mg daily for 24 mos. Subjects were to receive daily calcium ( $\geq 1000$  mg) and vitamin D ( $\geq 800$  IU). Effect of DMAb vs. RIS with respect to percentage change from baseline in LS BMD at 12 mos was determined in the GC-C and GC-I subpopulations and in 7 predefined subgroups that may influence treatment effect (gender, race, age group, baseline BMD T-score, geographic region, menopausal status, and baseline GC daily dose).

Results: A total of 795 subjects (505 GC-C and 290 GC-I) enrolled in the study. Baseline characteristics were balanced between treatment groups. As previously shown (Saag, ACR 2016), DMAb resulted in significantly greater gains in LS BMD at 12 mos compared with RIS for both the GC-C and GC-I subpopulations (Table). Results from all of the subgroups consistently demonstrated a greater increase in LS BMD at mo 12 with DMAb compared with RIS. A significant quantitative interaction was observed only in the gender analysis in the GC-I subpopulation. However, non-significant qualitative interaction testing indicated that there was no evidence that the direction of the DMAb effect differed by gender in this subpopulation.

Conclusion: DMAb consistently increased BMD more than RIS at the LS at 12 mos across 7 different subgroups of GC-treated individuals. DMAb has the potential to become a better treatment option for patients newly initiating or continuing GC who are at increased risk for fracture.

Table. Difference in Lumbar Spine BMD Percentage Change From Baseline at Month 12 (GC-C and GC-I Subpopulations)

	GC-C Subpopulation (N = 230 RIS / 228 DMAb)		GC-I Subpopulation (N = 133 RIS / 128 DMAb)	
	Difference (DMAb - RIS)	Interaction P value Qualitative (Qualitative)	Difference (DMAb - RIS)	Interaction P value Qualitative (Qualitative)
Overall Subpopulation	2.2 (1.4, 3.0)*	N/A	2.9 (2.0, 3.9)*	N/A
Gender				
Female	2.4 (1.5, 3.3)*	0.31	3.7 (2.5, 4.9)*	0.018 (0.50)
Male	1.3 (-0.3, 2.9)		1.2 (-0.4, 2.8)	
Race				
Caucasian	2.1 (1.2, 2.9)*	0.46	2.9 (1.9, 3.8)*	0.68
Not Caucasian	2.5 (0.2, 4.8)*		3.0 (-0.4, 6.3)	
Age Group				
< 60 years	1.9 (0.8, 3.1)*	0.57	2.7 (0.6, 4.8)*	0.57
$\geq 60$ years	2.3 (1.2, 3.5)*		3.1 (2.0, 4.2)*	
Baseline LS T-score				
$\leq -2.5$	2.4 (0.9, 3.9)*	0.40	3.8 (1.5, 6.0)*	0.081
$> -2.5$	2.0 (1.1, 2.9)*		2.5 (1.5, 3.5)*	
Baseline LS T-score				
$\leq -1.0$	2.2 (1.3, 3.2)*	0.55	3.5 (2.2, 4.9)*	0.18
$> -1.0$	1.3 (-0.2, 2.9)		2.0 (0.7, 3.2)*	
Geographic Region				
Europe	2.0 (1.0, 3.0)*	0.46	3.2 (2.1, 4.3)*	0.60
Non-Europe	2.5 (1.1, 3.8)*		2.6 (0.8, 4.3)*	
Menopausal Status				
Premenopausal	1.7 (-0.7, 4.1)	0.47	6.3 (1.9, 10.7)*	0.37
Postmenopausal	2.4 (1.4, 3.4)*		3.5 (2.2, 4.8)*	
Baseline GC Daily Prednisone-equivalent Dose				
7.5 - < 10 mg	2.9 (1.7, 4.1)*	0.37	3.1 (0.9, 5.4)*	0.98
$\geq 10$ mg	2.0 (1.0, 3.1)*		2.9 (1.8, 4.0)*	

N = Number of randomized subjects with a baseline and  $\geq 1$  postbaseline lumbar spine BMD measurement. \*DMAb compared with RIS p < 0.05

Table

**Disclosures:** K Saag, Amgen, Merck, Consultant.

## FR0302

**Credible Intervals of The Rates of Osteonecrosis of The Jaw (ONJ) In Patients Treated With Denosumab.** Abdulhazef Selim\*<sup>1</sup>, Paula Karabelas<sup>2</sup>, Ahmed Kaseb<sup>3</sup>. <sup>1</sup>Philadelphia College of Osteopathic Medicine (PCOM), United States, <sup>2</sup>Private Investigator, United States, <sup>3</sup>Department of Gastrointestinal Medical Oncology, M. D. Anderson Cancer Center, United States

Denosumab is a fully human IgG2 monoclonal antibody that binds and inhibits human RANKL. RANKL is essential for the formation, function, and survival of osteoclasts, thereby modulating calcium release from bone. In June 2010, the U.S. Food and Drug Administration (FDA) approved Denosumab for use in postmenopausal women with risk of osteoporosis, and for the prevention of skeleton-related events in patients with bone metastases from solid tumors. Denosumab treatment is associated with a sustained, and reversible reduction in bone turnover markers. However, given its brief post-market period, vigilance is advised regarding adverse events related to putative RANKL inhibition. Recently, multiple studies have established a relationship between ONJ and chronic antiresorptive therapy. Treatment options have been explored; however, severe cases of ONJ still require surgical removal of the affected bone. Given the widespread use of chronic antiresorptive therapy, the observation of an associated risk of ONJ should alert practitioners to re-evaluate the duration, frequency, and/or dose of Denosumab therapy.

A literature search was conducted to identify relevant studies that evaluated the safety of Denosumab. The search words included Denosumab[Title/Abstract] AND Clinical Trial[ptyp]. A total of 138 citations were retrieved. Of these, 131 studies were evaluated, with 101 studies excluded because of the following reasons: safety data was

not reported/ONJ was not specified, exclusion of patients at risk of ONJ, treatment combination, and previous exposure to any anti-resorptive therapy. The following data were extracted from 30 eligible studies (13 cancer, and 17 osteoporosis); number of patients, duration, and the cumulative number of patients with ONJ. Data were further analyzed using Bayesian simulation approach.

The data included 35,978 patients (27,360 osteoporotic patients, and 8,618 cancer patients). The average study duration was 2.3 years in the osteoporotic population, and 1.96 years in the cancer population. ONJ was seen in 0.07% (19 / 27,360) osteoporotic patients; and 1.3% (112 / 8,618) cancer patients. Posterior data demonstrated higher rates in the cancer population. In cancer patients, the credible interval was between 0.3% and 2.0%. However, markedly lower rates were seen in the osteoporosis population; 0.00% to 0.2%. This difference is translated into an odds ratio of 18.7 (CI: 11.5 - 30.4,  $P < 0.0001$ ). This higher risk could be attributed to the higher, frequent doses and potential interactions with concomitant chemotherapy used in the cancer patients. Therefore, further analysis is needed to investigate the relationship between the ONJ's risk and the dose/frequency used in various cancer patients. It remains of clinical interest to determine a clearer guideline for Denosumab's dose, and/or frequency to minimize or avoid ONJ's occurrence in certain populations.

**Disclosures:** Abdulhafez Selim, None.

## FR0303

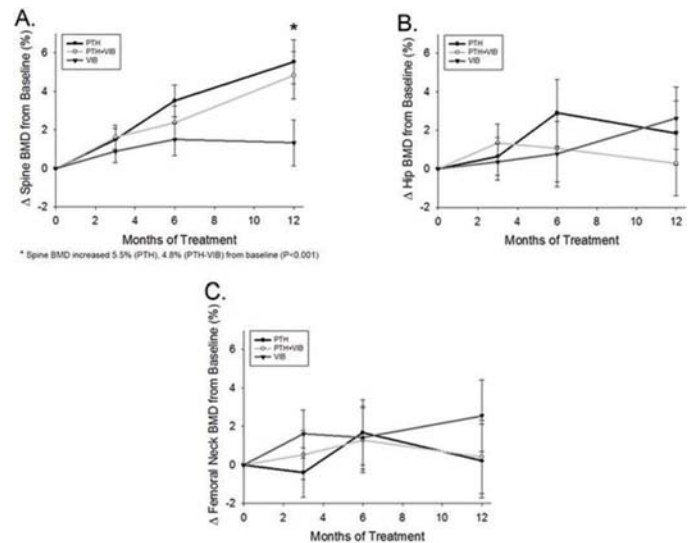
**The Effects of Teriparatide, Vibration and the Combination on Bone Mass, Architecture and Metabolism in Chronic Spinal Cord Injury.** Narina Simonian<sup>\*1</sup>, Brent Edwards<sup>2</sup>, Elaine Gregory<sup>1</sup>, Keith Gordon<sup>1</sup>, Rama Parachuri<sup>3</sup>, Ifaz Haider<sup>2</sup>, Karen Troy<sup>4</sup>, Thomas Schnitzer<sup>1</sup>. <sup>1</sup>Northwestern University, United States, <sup>2</sup>University of Calgary, Canada, <sup>3</sup>Edward Hines Jr. VA Hospital, United States, <sup>4</sup>Worcester Polytechnic Institute, United States

**Purpose:** Chronic spinal cord injury (SCI) with impaired weight-bearing results in bone loss in the lower extremities and an increased risk of fracture. In animal models, parathyroid hormone with mechanical loading has been shown to reverse bone loss. Herein, we investigated the effects of 12 months (m) of therapy with teriparatide (PTH), a recombinant form of parathyroid hormone with or without mechanical loading simulated via vibrating platform (VIB) in patients with chronic SCI to assess the effect on bone: mineral density, architecture and metabolism.

**Methods:** In a randomized, double-blind clinical trial we compared the effects of 12 m of PTH+VIB, PTH alone, and VIB alone. Changes in areal bone mineral density (aBMD) were assessed via DEXA at the spine, total hip, and femoral neck. Architectural changes (cortical, trabecular, volumetric BMD, volumetric bone mineral content, compressive stress index and bending stress index) were assessed at the femur and tibia via CT. Baseline studies were obtained and repeated at 3, 6 and 12 m of therapy. Changes in bone metabolism were assessed via serum bone markers: PINP, CTX, and BSAP. Statistical analysis included a repeated measure analysis to detect interactions of time by therapy. Interactions were followed by one-way ANOVA to examine the effect of time for each therapy.

**Results:** 60 subjects were enrolled, of those, 49 provided data which could be analyzed, and included 73.5% males, mean age  $39.5 \pm 12.9$  y,  $14.9 \pm 11.1$  y post SCI. An interaction of time by therapy was observed for aBMD at the spine ( $p=0.031$ ) with an effect of time for PTH and PTH+VIB ( $p<0.01$  for both). At 12 m, spine aBMD was 5.5% and 4.8% higher than at baseline for PTH and PTH+VIB, respectively ( $p<0.001$  for both). No interaction of time by therapy were observed for other DXA or any CT measurements and no significant changes with VIB alone. Bone markers showed a time by therapy interaction for CTX and PINP ( $p=0.037$ ,  $0.044$ ). Effect of time was only observed for PINP after PTH and VIB ( $p=0.027$ ,  $0.001$ ). At 12 m compared to baseline PINP was 125.8% higher in the PTH group and 21.3% lower in the VIB group ( $p=0.027$ ,  $0.001$ ).

**Conclusions:** PTH increased spine aBMD but had no effect on hip aBMD or lower extremity bone architecture after 12 m of treatment. Bone markers showed a robust response to PTH. VIB alone failed to increase aBMD, bone architecture or bone markers.



Graph

**Disclosures:** Narina Simonian, None.

## FR0305

**Combination treatment with teriparatide and denosumab improves spine trabecular microarchitecture in DATA-Switch: a randomized controlled trial.** Joy Tsai<sup>\*1</sup>, Linda Jiang<sup>1</sup>, Hang Lee<sup>1</sup>, Didier Hans<sup>2</sup>, Benjamin Leder<sup>1</sup>. <sup>1</sup>Massachusetts General Hospital, United States, <sup>2</sup>Lausanne University Hospital, Switzerland

**Background:** In postmenopausal women, 2-years of combined teriparatide (TPTD) and denosumab (DMAB) increases bone mineral density (BMD) more than either drug alone and switching from either combination or TPTD monotherapy to DMAB for an additional 2-years further increases BMD. Conversely, switching from DMAB to TPTD results in transient bone loss. The effects of these interventions on spine microarchitecture are unknown. **Methods:** In the DATA and DATA-Switch studies, 94 postmenopausal osteoporotic women were randomized to receive 24-months of TPTD (20-μg-daily), DMAB (60-mg-every-6-months), or both drugs. Then, women originally assigned to 24-months of TPTD received 24-months of DMAB whereas subjects originally randomized to 24-months of DMAB received 24-months of TPTD. Subjects who originally received both drugs, received an additional 24-months of DMAB alone. Trabecular bone score (TBS) of the spine was assessed blinded to treatment group using images extracted from 2-dimensional DXA spine scans at 0, 12, 24, 30, 36, and 48 months. **Results:** After 24 months, TPTD alone increased TBS by  $2.7 \pm 4.7\%$  ( $P=0.009$  vs. baseline), DMAB alone by  $1.8 \pm 5.0\%$  ( $P=0.118$  vs. baseline), and combination increased by  $4.5 \pm 6.7\%$  ( $P=0.017$  vs. baseline), with no significant between-group differences. In the 6-months after treatments were switched at month 24, TBS continued to increase in the combination-to-DMAB and TPTD-to-DMAB groups but changed by  $-1.1 \pm 4.0\%$  ( $P=0.238$  versus month 24) in the DMAB-to-TPTD group ( $P<0.05$  versus other groups). After 48 months, TBS increased by  $5.1 \pm 5.8\%$  ( $P<0.001$  versus baseline) in the TPTD-to-DMAB group, by  $3.6 \pm 4.2\%$  ( $P<0.001$  versus baseline) in the DMAB-to-TPTD group, and by  $6.1 \pm 4.7\%$  ( $P<0.001$  versus baseline) in the combination-to-DMAB group (no significant differences between groups). **Conclusions:** In postmenopausal women with osteoporosis, TPTD, DMAB, and combined therapy improved trabecular microarchitecture of the spine as assessed by TBS while the transition from DMAB-to-TPTD transiently decreased TBS. These findings support the potential of combination therapy in the treatment of postmenopausal osteoporosis and suggest that while the use of TPTD followed by DMAB improved spine trabecular microarchitecture, the use of DMAB followed by TPTD may have the opposite effects and likely should be avoided in high-risk patients.

**Disclosures:** Joy Tsai, None.



## FR0310

**MicroRNA-125b Derived from Osteoblasts Exerts its Anti-Osteolytic Effect through Targeting Preosteoclasts.** Faisal Ahmed<sup>1</sup>, Tomoko Minamizaki<sup>1</sup>, Shota Ito<sup>2</sup>, Nusrat Sarmin<sup>1</sup>, Chise Fujimoto<sup>1</sup>, Yuko Nakao<sup>2</sup>, Kotaro Tanimoto<sup>2</sup>, Shinji Hiyama<sup>3</sup>, Yuji Yoshiko<sup>1</sup>. <sup>1</sup>Department of Calcified Tissue Biology, Graduate School of Biomedical & Health Sciences, Hiroshima University, Japan, Japan, <sup>2</sup>Department of Orthodontics and Craniofacial Developmental Biology, Hiroshima University Graduate School of Biomedical & Health Sciences, Hiroshima, Japan, Japan, <sup>3</sup>Department of Oral Biology, Graduate School of Biomedical & Health Sciences, Hiroshima University, Japan, Japan

MicroRNAs (miRNAs) are involved in the regulation of gene expression and coordinate a broad spectrum of biological processes. Growing evidence indicates pivotal roles of miRNAs in the skeletal system. Previously we demonstrated that miRNAs are enriched in matrix vesicles secreted from osteoblasts and accumulates in bone matrix, of which miR-125b inhibits osteoclast formation by targeting the transcription repressor *Prdm1*, resulting in increased levels of *irf8* and *Mafk*, negative regulators of osteoclastogenesis. To determine the potential of osteoblast-derived miR-125b for a new target of clinical intervention, we generated transgenic (Tg) mice overexpressing miR-125b under the control of the human osteocalcin promoter. Overexpression of miR-125b in osteoblasts resulted in high bone mass with decreased number of osteoclasts. FACS analysis of bone marrow cells revealed that populations of c-Kit<sup>+</sup>CD115<sup>+</sup>CD11b<sup>low</sup> osteoclast precursor cells in Tg mice were less than those in wild type (WT) mice. In contrast, CD115<sup>+</sup>CD11b<sup>+</sup>F4/80<sup>+</sup> macrophages were more abundant in Tg mice than in WT mice. There were no changes in the numbers of T cells and B cells. Ex vivo analysis confirmed that bone marrow macrophages from either Tg mice or WT mice did not differentiate enough to osteoclasts, only when cocultured with Tg osteoblasts. Thus, osteoblast-derived miR-125b may act relatively selectively on osteoclast precursor cells. To confirm the roles of miR-125b in bone under pathological conditions, we studied the effect of ovariectomy (OVX) and neurectomy (NX) in WT and Tg mice. OVX caused weight gain equally in both genotypes, while OVX-dependent bone loss was significantly reduced by Tg mice. An increase in the number of TRAP<sup>+</sup> osteoclasts per bone perimeter (N. Oc/B.Pm) was obvious in WT mice with OVX but not Tg mice with and without OVX vs. sham-operated WT mice. Similar effects were observed in Tg vs. WT mice with and without NX. Further, we found that transfection of miR-125b mimic inhibited LPS-induced osteolysis in normal mice. Thus, our findings suggest that osteoblast-derived miR-125b inhibits bone resorption via the mechanism underlying transfer of osteoblast-derived miR-125b into osteoclast precursor cells and protect bone loss in mouse bone disease models. These data may provide a novel therapeutic target for osteolytic bone diseases.

**Disclosures:** Faisal Ahmed, None.

## FR0312

**Vitamin D deficiency promotes breast cancer invasion and metastasis through the regulation of the CXCR4/CXCL12 axis in the MMTV-PyMT mouse model.** Jiarong Li<sup>\*</sup>, Richard Kremer, McGill University, Canada

We previously demonstrated that administration of 25-hydroxyvitamin D (25OHD), in the PyMT mouse model of breast tumor progression, inhibits tumor initiation, growth and metastasis through the local activation of CYP27B1 to generate its active form 1,25(OH)2D. However, the mechanisms underlying vitamin D effects on metastasis remain elusive. The membrane bound receptor CXCR4 has been identified to play a major role in the metastatic process. Lung tissues secrete high levels of CXCL12 (SDF1), the ligand for CXCR4. Breast tumors express high levels of CXCR4 that can direct chemotaxis and invasive responses in target tissues.

To investigate potential mechanistic relationship between vitamin D and CXCR4/SDF1 axis we first examined the expression of SDF1 in lungs and expression of CXCR4 in the tumors of vitamin D deficient (fed a low D diet) and vitamin D replete (fed a normal D diet) mice as well as SDF1 in the lungs of VDR knockout mice. Next, we examined the development of lung metastasis in PyMT mice fed a low vitamin D diet and in mice where the CYP27B1 gene had been ablated. Primary tumors and metastatic tumors to lungs were examined by IF, qPCR and flow cytometry for EMT markers.

Mammary specific ablation of CYP27B1 in animals fed the low vitamin D diet had an earlier onset of metastatic tumor in lungs (57% vs 0% of 6-week-old mice) and a higher number and size of lung metastases ( $P < 0.05$ ) as compared to wild type animals fed a normal diet. Furthermore, EMT markers, Zeb1, Zeb2, Snail2, Twist1 and SMA were all significantly increased in CYP27B1 ablated tumors ( $P < 0.001$ ). In contrast, in vitro treatment of tumor cells isolated from PyMT tumors with 10<sup>-7</sup>M 1,25(OH)2D3 had decreased levels of EMT markers ( $P = 0.002$ ). Finally, SF expression in lungs from vitamin D deficient animals and from VDR knockout animals was increased by over 50% ( $P < 0.001$ ) as compared to vitamin D replete animals or wild type animals. SDF1 serum concentrations were also elevated in vitamin D deficient compared to vitamin D sufficient mice (527 $\pm$ 34 vs 350 $\pm$ 28 pg/ml  $P < 0.001$ ). Furthermore, CXCR4 expression was significantly increased in tumors from vitamin D deficient animals and CYP27B1 knockout mice compared to controls ( $P < 0.001$ ).

In summary, our results demonstrate that vitamin D is a strong regulator of the breast metastatic process through its regulation of the CXCR4/SDF1 axis and suggest that vitamin D sufficiency is necessary for targeting therapy directed against CXCR4 in breast cancer.

**Disclosures:** Jiarong Li, None.

## FR0313

**Exosomes Derived from Mesenchymal Stem Cells Promotes Osteogenesis and Angiogenesis during Hyperhomocysteinemia in Bone.** Neetu Tyagi<sup>\*</sup>, Jyotirmaya Behera, Kimberly E. Kelly, Kimberly E. Kelly, Akash George, Suresh Tyagi. University of Louisville, United States

It is critical that bone formation and angiogenesis are tightly coordinated during bone development, but the molecular regulator of such intercellular communication in the bone microenvironment is not well studied. Cystathionine- $\beta$ -synthase (CBS), an enzyme involved in the homocysteine (Hcy) metabolic pathway, plays a crucial role in osteoblast differentiation and mineralization. Therefore, we hypothesize that CBS is a novel molecular regulator in osteoblasts, which regulates vascularization during bone development in osteoblast derived exosomes. To test this hypothesis, we have used 16-18 week old, wild type (C57BL/6, WT) and CBS<sup>+/−</sup> mice in our study. Blocking CBS function by either inhibiting hydroxylamine (HA) or through CRISPR/Cas9 gene editing were the approaches utilized to prevent osteoblast differentiation. This was supported by studies using osteoblasts cultured from the bone marrow of CBS<sup>+/−</sup> mice. Exosomes of mesenchymal stem cell (MSC-Exo) derived osteoblasts, stimulated endothelial migration and angiogenesis, which was prevented by blocking CBS in osteoblasts using HA or the CRISPR/Cas9 gene editing approach. Importantly, miRNA sequencing results indicated that MSC-Exo identified novel miRNAs, including miR126, miR132 and miR21 which were present in control MSC-Exo, these results were shown to be involved in angiogenesis and osteogenesis. Immunostaining and metatarsal angiogenesis assay showed decreased vascularization in bone tissue of CBS<sup>+/−</sup> mice. However, the osteopenia phenotype was confirmed in CBS<sup>+/−</sup> mice by microCT analysis. CBS<sup>+/−</sup> mice also showed significantly reduced bone mineral density (BMD), reduced bone volume/tissue volume (BV/TV) and increased plasma tHcy levels compared to C57BL/6, WT mice. However, CBS<sup>+/−</sup> mice exhibited a significant increase in the number of TRAP-positive osteoclasts and higher levels of RANKL than C57BL/6, WT mice. Furthermore, real-time PCR and Western Blot analyses revealed significant decreases in Alkaline Phosphatase (ALP) and Runt-related transcription factor 2 (RUNX2) expression in CBS<sup>+/−</sup> mouse bone marrow cells. In conclusion, we demonstrate that CBS in osteoblasts is at the crossroad of osteoblast differentiation/mineralization and angiogenesis. These findings uncover the previously undefined molecular understanding of CBS that promotes angiogenesis and osteogenesis.

**Acknowledgement:** This work is financially supported from the National Institutes of Health grant AR-067667 NT.

**Disclosures:** Neetu Tyagi, None.

## FR0314

**The Deleterious Effects of IGF1 Signaling on the Development of Post-Traumatic Osteoarthritis.** Yongmei Wang<sup>\*</sup>, Faming Tian<sup>1</sup>, Alexis Dang<sup>2</sup>, Zara Butte<sup>2</sup>, Ling Chen<sup>3</sup>, Misun Kang<sup>3</sup>, Sunita Ho<sup>3</sup>, Daniel Bikle<sup>1</sup>. <sup>1</sup>Endocrine Unit, University of California, San Francisco/San Francisco VA Health Care System, United States, <sup>2</sup>Department of Orthopaedic Surgery, University of California, San Francisco/San Francisco VA Health Care System, United States, <sup>3</sup>Bioengineering & Biomaterials Micro-CT and Imaging Facility, University of California, San Francisco, United States

Stimulation of endochondral bone formation (endoBF) in the adult joint post trauma (PT) results in osteoarthritis (OA). Recent clinical studies showed that insulin like growth factor 1 (IGF1) signaling, a positive regulator of endoBF during skeletal development, may be involved in this process but the details remain unclear. To address this issue, we investigated the role of IGF1 signaling during PTOA development by deleting the IGF1 receptor (IGF1R) in articular chondrocytes (KO) (floxed IGF1R X Col.II-CreERT). To initiate PTOA, ACL rupture was made by a single bout of tibial compression overload (TCO) at 18 N in the KOs and their control littermates (CONs). Tamoxifen was given 1 day prior to TCO. The non-TCO and TCO knees from both CONs and KOs were obtained 3wks later.  $\mu$ CT images identified the damage in the articular surface of the CONs after TCO, but less damage was observed in the KOs. High-resolution X-ray tomography (X-CT) demonstrated that TCO increased porosity in the subchondral bone in the CONs but not KOs. Deletion of IGF1R decreased overall mineral density and increased the porosity in the subchondral bone of the uninjured knee of the KOs, but blunted the effects of TCO. 3wks after TCO, gait assessment (by DigiGait) showed that TCO resulted in decreased paw area (18%), loading rate (20%) and stance factor (15%) in the CONs compared with the non-TCO limb. These effects were abolished in the KOs, suggesting less pain and better functional recovery on walking in KOs compared to CONs. Safranin O /Fast Green staining revealed that in the CONs, TCO caused erosion of the articular cartilage and formation of osteophytes when compared with the non-TCO knee, but these effects were not observed in the KOs. Immunohistochemistry demonstrated that TCO induced MMP-13 production in the CONs, but not in the KOs. To test the effects of inhibition of IGF1R in chondrocytes in vitro, chondrocytes (ATDC5 cell line) were treated by DMSO or an IGF1R inhibitor (NVP-AEW541), then further treated with vehicle or IGF1. qPCR showed that the inhibitor (3  $\mu$ M) blocked IGF1 stimulated expression of MMP-9 (50%) and MMP-13 (60%) in chondrocytes. Our data indicate that IGF-1R signaling plays deleterious roles in the development of PTOA by promoting matrix metalloproteinase production to damage articular cartilage and subchondral bone. Inhibition of this pathway may lead to therapy that can prevent and/or treat PTOA.

**Disclosures:** Yongmei Wang, None.

## FR0316

**Parathyroid hormone (1-34) ameliorated knee osteoarthritis and function in rats by decreasing chondrocyte terminal differentiation and apoptosis via autophagy.** Chung-Hwan Chen<sup>\*1</sup>, Ling-Hua Chang<sup>1</sup>, Lin Kang<sup>2</sup>, Yi-Shan Lin<sup>1</sup>, Sung-Yen Lin<sup>3</sup>, Je-Ken Chang<sup>3</sup>, Shih-Tse Chen<sup>4</sup>, Mei-Ling Ho<sup>1</sup>. <sup>1</sup>Kaohsiung Medical University, Taiwan, Province of China, <sup>2</sup>National Cheng Kung University Hospital, Taiwan, Province of China, <sup>3</sup>Kaohsiung Medical University Hospital, Taiwan, Province of China, <sup>4</sup>National Taiwan University Hospital Hsin-Chu Branch, Taiwan, Province of China

Anterior cruciate ligament (ACL) tear usually leads to osteoarthritis (OA). However, parathyroid hormone (PTH) (1-34) was found to alleviate OA progression in a papain-induced OA model. Autophagy is a protective mechanism in normal cartilage, and its aging-related loss is linked with chondrocyte death and OA. Thus, we examined the roles of autophagy in PTH treatment on OA after ACL transection (ACLT). Thirty-six rats were randomized into three groups: control group, ACLT-induced OA (ACLT-OA) group, and OA with intra-articular PTH (1-34) treatment group. Knee function was evaluated by weight-bearing and treadmill tests. Cartilage matrix was determined by a histological evaluation of glycosaminoglycan (GAG), the OARSI score, apoptosis, and immunohistochemistry for collagen type II (Col II) and X (Col X), Indian hedgehog (Ihh) and autophagy-related proteins including mTOR, p62, LC3, and Beclin-1. Rats in the ACLT-OA group had significantly decreased weight-bearing and running tolerance. The histological results indicated that functional markers (GAG, Col II) and chondrocyte autophagy had decreased, but that the OARSI score, terminal differentiation markers (Col X, Ihh), and chondrocyte apoptosis had increased in the OA group. Additionally, PTH (1-34) treatment significantly improved weight-bearing and treadmill test scores, preserved functional markers (GAG, Col II), and reduced the OARSI score and terminal differentiation marker (Col X, Ihh). Finally, PTH (1-34) ameliorated chondrocyte apoptosis by regulating the expressions of autophagy-related proteins, through reducing mTOR and p62, and enhancing LC3 and Beclin-1. Reconstructive surgery after ACL rupture cannot prevent OA occurrence. Intra-articular PTH (1-34) treatment can alleviate OA progression after ACLT, and improve joint function and histological molecular changes. Possible mechanisms are reducing chondrocyte terminal differentiation and apoptosis, as well as increasing autophagy. ACL injury increases the risk of subsequent posttraumatic OA; this development, particularly after ACL rupture and reconstructive surgery, remains an unsolved problem. PTH (1-34) may be a candidate to delay the progression of OA after ACL injury in the future.

**Disclosures:** Chung-Hwan Chen, None.

## FR0317

**Effects of ferric citrate administration in a murine model of Chronic Kidney Disease.** Connor Francis<sup>\*1</sup>, Samantha Neuburg<sup>1</sup>, Claire Gerber<sup>1</sup>, Xueyan Wang<sup>1</sup>, Corey Dussold<sup>1</sup>, Lixin Qi<sup>1</sup>, Guillaume Courbon<sup>1</sup>, Aline Martin<sup>1</sup>, Myles Wolf<sup>2</sup>, Valentin David<sup>1</sup>. <sup>1</sup>Division of Nephrology and Hypertension, Department of Medicine, and Center for Translational Metabolism and Health, Institute for Public Health and Medicine, Northwestern University Feinberg School of Medicine, United States, <sup>2</sup>Division of Nephrology and Hypertension, Duke University, United States

**Background:** Disordered bone and mineral metabolism, including elevations of serum fibroblast growth factor 23 (FGF23), is a common complication of Chronic Kidney Disease (CKD). Excess FGF23 is strongly associated with cardiovascular disease, mortality, and progression of CKD. Hyperphosphatemia and iron deficiency, common among patients with CKD, are powerful stimuli of FGF23 production. This suggests that reducing dietary phosphate intake or absorption and increasing serum iron may lower FGF23 levels and improve clinical outcomes in CKD.

**Methods:** We tested the hypotheses that ferric citrate treatment will simultaneously correct iron deficiency and also bind to dietary phosphate in the Col4a3<sup>ko</sup> mouse model of progressive CKD. We fed 4 week-old wild-type (WT) and Col4a3<sup>ko</sup> (CKD) mice, a control (Ctr) or a 5% Ferric Citrate (FC) enriched diet for 6 weeks and performed biochemical, molecular and histological analysis of iron and mineral metabolism status.

**Results:** At ten weeks, Ctr-CKD mice showed impaired renal function and morphology, hyperphosphatemia and displayed signs of iron deficiency anemia as evidenced by low serum iron (99±12 vs 128±5 mg/dL) and hemoglobin (15±1 vs 19±1 g/dL) (p<0.05 vs WT). This was concomitant with a marked increase in both total (tFGF23) and intact FGF23 (iFGF23) serum levels, compared to WT (11426±2623 vs. 433±32 pg/mL and 7312±1749 vs. 207±57 pg/mL respectively, p<0.05). Consequently, 1,25Vitamin D levels were low (34±7 vs 143±45 pg/mL) and serum PTH markedly elevated (3676±755 vs 375±53 pg/mL) in Ctr-CKD mice (p<0.05, vs. Ctr-WT) resulting in increased bone turnover evidenced by a dramatic 30-fold increase in bone Cathepsin K (*Ctsk*) mRNA expression.

Ferric citrate supplementation decreased serum phosphate by 1.5 fold and increased serum iron by 1.6-fold in CKD (p<0.05, vs. Ctr-CKD). The correction of iron deficiency and serum phosphate levels, significantly reduced tFGF23 by 4-fold, iFGF23 and bone *Fgf23* mRNA by 3-fold (p<0.05 vs. Ctr-CKD). Consistent with decreased iFGF23, serum 1,25Vitamin D levels increased by 2-fold in FC-CKD mice (p<0.05 vs. Ctr-CKD). In addition, the FC diet decreased BUN (127±21 vs. 218±24 mg/dL), and bone *Ctsk* expression by 3 fold (p<0.05 vs. Ctr-CKD).

**Conclusion:** Our data show that FC administration in CKD mice reduces FGF23, slows the progression of CKD and attenuates CKD-related mineral and bone

alterations. This suggests that FC treatment might mitigate renal and bone injury in patients with CKD.

**Disclosures:** Connor Francis, None.

## FR0318

**A novel bone formation-sparing anti-resorptive agent, DS-1501a, increased BMD and bone biomechanical properties of cortical bone in ovariectomized cynomolgus monkeys.** Chie Fukuda<sup>\*</sup>, Akiko Okada, Tsuyoshi Karibe, Yoshiharu Hiruma, Seiichiro Kumakura, Eisuke Tsuda. R&D Division, Daiichi Sankyo Co., Ltd., Japan

DS-1501a, a humanized anti-Siglec-15 antibody, has been shown to reduce bone resorption with a minimal inhibition of bone formation *in vitro* and *in vivo* single administration studies with rats and monkeys. The aim of this study is to determine the effects of DS-1501a on bone turnover, BMD, and bone strength by repeated administrations in ovariectomized (OVX) monkeys.

**Methods:** Forty-two cynomolgus monkeys were ovariectomized and divided into three groups (9 years to 12 years old, n = 14/group). Five weeks after OVX, DS-1501a at doses of 0, 30 and 60 mg/kg was subcutaneously administered to the monkeys once every 4 weeks for 9 months. In month 0 (pre-dose), 3, 6, and 9, BMD of lumbar vertebrae (L3-L5) and cortical BMD of midshaft tibia were measured using DXA and pQCT, respectively. After completion of the 9-month administration, biomechanical tests of vertebral body (L5) and femur diaphysis were performed.

**Results:** DS-1501a significantly decreased serum TRACP-5b (~40%) from the pre-dose value. Serum BAP was also decreased by DS-1501a (~20%) to the value similar to that of pre-OVX. Lumbar spine and tibial cortical BMD were decreased by OVX. DS-1501a significantly increased both BMD at 3, 6, and 9 months after administration. In the lumbar spine compression testing, DS-1501a increased apparent strength compared with vehicle treatment. Interestingly, the beneficial effects of DS-1501a on bone strength were remarkable in cortical bone. In 3-point bending test using femur diaphysis, DS-1501a significantly increased not only structural property (stiffness, ~20%), but also material properties (ultimate stress, ~20%, modulus ~30%) compared with vehicle treatment. In these analyses, no major differences were found between the DS-1501a treatment groups. In correlation analysis on lumbar spine compression strength, strong positive significant correlations were observed between peak load and pQCT total BMC, and apparent strength and pQCT total BMD (r = 0.75 and 0.74). Correlation analysis on 3-point bending strength, showed significant positive linear relationships between peak load and pQCT cortical BMC (r = 0.95), and between ultimate stress and pQCT cortical BMD (r = 0.62).

In conclusion, DS-1501a suppressed bone resorption to the level lower than pre-dose level and bone formation to the pre-dose level, and prevented decreases in trabecular and cortical BMD, leading to subsequent increases in mechanical properties in OVX monkeys with 9-month treatment.

**Disclosures:** Chie Fukuda, Daiichi Sankyo Co., Ltd., Grant/Research Support.

## FR0319

**Anti-Siglec-15 antibody reduces bone resorption while maintaining bone formation in ovariectomized (OVX) rats and monkeys.** Chie Fukuda<sup>\*1</sup>, Eisuke Tsuda<sup>1</sup>, Akiko Okada<sup>1</sup>, Norio Amizuka<sup>2</sup>, Tomoka Hasegawa<sup>2</sup>, Tsuyoshi Karibe<sup>1</sup>, Yoshiharu Hiruma<sup>1</sup>, Nana Takagi<sup>1</sup>, Seiichiro Kumakura<sup>1</sup>. <sup>1</sup>R&D Division, Daiichi Sankyo Co., Ltd, Japan, <sup>2</sup>Department of Developmental Biology of Hard Tissue, Faculty of Dental Medicine, Hokkaido University, Japan

Sialic acid-binding immunoglobulin-like lectin (Siglec)-15 is expressed on the cell surface of mature osteoclasts (Oc). Anti-Siglec-15 antibody (Ab) has been shown to inhibit Oc fusion but did not inhibit formation of mononuclear Oc which are reported to have high potency to support bone formation. Therefore, it is expected that anti-Siglec-15 Ab reduces bone resorption while maintaining bone formation. The aim of this study is to examine this hypothesis using anti-Siglec-15 Ab, in rats and monkeys.

In a pharmacokinetics study, single administration (s.c. and i.v.) of DS-1501a, a humanized anti-Siglec-15 Ab, to F344 rats (12 weeks old, 0.25, 1, 4, and 16 mg/kg, n=4) and cynomolgus monkeys (3 to 6 years old, 0, 0.03, 0.3, 3, and 30 mg/kg, n=5) resulted in dose-dependent increases in C<sub>max</sub> and AUC in both species. Anti-drug antibodies were detected in approximately 70 % of the DS-1501a-treated monkeys, which were associated with sharp decreases in serum concentration of DS-1501a.

DS-1501a was administered once to F344 rats (12 weeks old, n = 10 or n = 4 for time course of TRACP-5b, s.c.) at dose levels of 0, 0.5, 0.75, 1, 2, and 4 mg/kg on 1 day after OVX. DS-1501a significantly suppressed TRACP-5b and urinary DPD/Cre in all groups, while DS-1501a decreased serum osteocalcin only at 2 mg/kg. DS-1501a completely prevented a decrease in BMD of the lumbar vertebrae at 4 weeks after administration in all groups.

DS-1501a was administered once to cynomolgus monkeys (8 to 14 years old, n = 8) at dose levels of 0, 0.3, 3, and 30 mg/kg on 5 weeks after OVX and bone turnover markers were monitored. DS-1501a at 30 mg/kg decreased TRACP-5b, urinary and serum NTx, urinary and serum CTX, with maximum decrease of 39%, 52%, 32%, 64% and 41%, respectively. On the other hand, DS-1501a had a mild effect on BAP with maximum decrease of 2%.

32A1, rat anti-Siglec-15 Ab, was administered (0, 1, 10 mg/kg, s.c.) once to OVX F344 rats (12 weeks old, n = 3) and bone histological analysis was performed. In tibial metaphysis, small and flattened TRACP(+) Oc were present. These Oc were attached to



the bone surface with fine cytoplasmic processes without forming typical clear zone, and did not form a ruffled border. These Oc were surrounded with many ALP(+) osteoblasts (Ob), indicating the possibility of cellular coupling between Oc and Ob.

In conclusion, DS-1501a was suggested to be a novel bone formation-sparing anti-bone resorptive agent for the treatment of osteoporosis.

**Disclosures:** Chie Fukuda, None.

## FR0320

**A Novel H<sub>2</sub>S-releasing Amino-Bisphosphonate Which Combines Bone Anti-Catabolic And Anabolic Functions.** Francesco Grassi<sup>\*1</sup>, Laura Gambari<sup>1</sup>, Gina Lisignoli<sup>2</sup>. <sup>1</sup>Lab RAMSES, Istituto Ortopedico Rizzoli, Italy, <sup>2</sup>Lab Immunoreumatologia e Rigenerazione Tissutale, Istituto Ortopedico Rizzoli, Italy

Purpose of the study.

It was recently described that the gasotransmitter H<sub>2</sub>S inhibits osteoclast development *in vitro* and stimulates osteogenic differentiation of human MSC *in vitro* and *in vivo*. Moreover, endogenous levels of serum H<sub>2</sub>S are significantly decreased in estrogen-deficient mice, suggesting that H<sub>2</sub>S-replacement therapy could be a novel therapeutic approach for osteoporosis. Based on the dual action exerted by H<sub>2</sub>S, we developed a H<sub>2</sub>S-releasing bisphosphonate compound, named DM-22, prototype of a novel family of hybrid molecules aiming at treating bone loss.

Methods.

DM-22 was synthesized upon chemical addition of an H<sub>2</sub>S-releasing moiety to the backbone of Alendronate.

H<sub>2</sub>S release was analyzed by amperometry and effects of DM-22 or Alendronate were investigated *in vitro* on human osteoclasts (OCs) and mesenchymal stromal cells (MSC). To test the effects on OCs, DM-22 was added to osteoclastogenic cultures of CD11b+ cells isolated from healthy donors; to test the effects on osteogenesis, MSC were stimulated with DM-22 for 14 days in the presence of osteogenic stimuli.

Gene expression of relevant osteogenic markers was analyzed by RT-PCR and LDH assay was used to assess cytotoxicity.

Results.

The incubation of DM22 at 1 mM in aqueous solution lead to a long-lasting release of H<sub>2</sub>S (peak concentration: 42 μM of H<sub>2</sub>S).

LDH assay revealed that DM-22 was devoid of toxicity at all the concentrations tested (1, 3.3, 10, 33 μM) both on OCs and MSC cultures. By contrast, equal concentrations of Alendronate lead to a dose-dependent cytotoxicity on CD11b+ cells starting at 10mM while induced significant cytotoxicity and the inhibition of proliferation on osteogenic MSC cultures at the high dose of 33μM.

DM-22 dose-dependently inhibited OCs differentiation reaching up to 40% relative inhibition in the total number of TRAP+ OC at 33 μM. Inhibition of OC activity was confirmed by pit assay. The parent drug Alendronate virtually abrogated OC differentiation by the concentration of 3.3 μM.

DM-22 dose-dependently increased mineral apposition, as revealed by Alizarin Red staining, compared to unstimulated MSC; moreover, DM-22 at the high concentration of 33μM led to a 3-fold increase in the mRNA expression of Collagen I and BSP. On the contrary, Alendronate significantly inhibited mineralization and the gene expression of osteogenic markers.

Based on these data, DM-22 is the first aminobisphosphonate to display both anti-resorptive and anabolic effect on bone cells.

**Disclosures:** Francesco Grassi, None.

## FR0324

**Pharmacokinetics of TransCon PTH in Rat and Cynomolgus Monkey: a Sustained-Release PTH Prodrug for Treatment of Hypoparathyroidism.** Susanne Pihl<sup>\*1</sup>, Mathias Krusch<sup>2</sup>, Lars Holten-Andersen<sup>1</sup>, Joachim Zettler<sup>2</sup>, Felix Cleemann<sup>2</sup>, Caroline Rasmussen<sup>1</sup>, Kennett Sprogø<sup>1</sup>, David Karpf<sup>3</sup>, Vibeke Miller Breinholt<sup>1</sup>. <sup>1</sup>Ascendis Pharma A/S, Denmark, <sup>2</sup>Ascendis Pharma GmbH, Germany, <sup>3</sup>Ascendis Pharma Inc., United States

Natpara (PTH1-84) is approved for subcutaneous injection as an adjunct to vitamin D and calcium in patients with hypoparathyroidism but has not demonstrated the ability to reduce the incidence of hypercalcemia, hypocalcemia, or hypercalciuria relative to conventional therapy, likely due to its relatively short half-life resulting in little-or-no exposure over at least 12 hours per day. Continuous infusion of teriparatide (PTH1-34) has proven superior to twice daily injections in clinical studies. Thus, a PTH product that provides continuous exposure with daily dosing could represent a major step forward in addressing a large unmet medical need. TransCon PTH is a prodrug releasing unmodified teriparatide via non-enzymatic hydrolysis of the proprietary TransCon Linker for the treatment of hypoparathyroidism.

TransCon PTH has been designed to maintain a normal, steady concentration of PTH in the blood stream. It is intended to address the fundamental limitations of short-acting PTH by providing infusion-like PTH blood levels.

TransCon PTH was administered to rat and cynomolgus monkeys in single dose bioavailability studies and in 28-day toxicology studies with daily dosing. The systemic concentrations of TransCon PTH and calcium were assessed at multiple time points following dosing.

TransCon PTH demonstrated good bioavailability in both rat and monkey. In both species, exposure to TransCon PTH increased in a dose proportional manner with

infusion-like pharmacokinetics observed at steady state. The TransCon PTH peak-to-trough ratios following 28 days of dosing was approximately 1.3 to 1.6 in monkeys (n = 6 to 10/group) and 1.1-1.3 in rats (n = 6/sampling time point).

The study in cynomolgus monkeys demonstrated a mean half-life of 34 hours after a single dose of TransCon PTH at 1 and 5 μg/kg (n = 3/group). After a single dose of TransCon PTH of 10 and 30 μg/kg in rats (n = 3/sampling time point), the PK profiles demonstrated a mean half-life of 28 hours. Overall the data suggests that once-daily administration of TransCon PTH could provide an infusion-like profile in humans.

The substantial extension of PTH half-life and the narrow peak-to-trough values may more closely mimic physiological levels of PTH observed in healthy individuals, and therefore maintain blood calcium levels while normalizing urinary calcium excretion.

**Disclosures:** Susanne Pihl, None.

## FR0325

**High-throughput Genetic Screens Reveal Targets of Nitrogen-containing Bisphosphonates.** Lauren Surface<sup>\*1</sup>, Zhou Yu<sup>1</sup>, Ji Woong Park<sup>2</sup>, Erin O'Shea<sup>3</sup>, Timothy Peterson<sup>2</sup>. <sup>1</sup>Harvard University, United States, <sup>2</sup>Washington University School of Medicine, United States, <sup>3</sup>Harvard University, Howard Hughes Medical Institute, United States

Nitrogen-containing bisphosphonates (NBP) are the standard of treatment for several bone diseases, including osteoporosis. While the use of these drugs is quite common, we still lack a clear mechanistic understanding of the process by which NBPs enter, traffic through, and affect their target cells. In addition, associations between the prolonged use of NBPs and the risk of atypical femoral fractures further emphasize the need for increasing the number of genes implicated in NBPs' action. To investigate this, we utilized two distinct high-throughput genetic screens to identify genes involved in NBP-induced cell death.

Our initial screen used a largely haploid human cell line (KBM7) to generate a library of retroviral gene trap mutants, and selected for clones which were resistant to cytotoxic levels of Alendronate, a common NBP. In this screen we identified a poorly characterized gene, which we termed TBONE1 (Target of Bisphosphonates, Nitrogen-containing). Our second screen used the recently developed CRISPR-based transcriptional inactivation technology, CRISPRi, where lentivirally introduced short guide RNAs (sgRNAs) recruit an inactive Cas9 fused to a transcriptional repressor to transcriptional start sites. In this CRISPRi based screen, we identified a large set of genes that when depleted confer either resistance or sensitivity to alendronate, including the above identified TBONE1. Confirming the utility of our screen, depletion of FPPS, the canonical target of NBPs, conferred sensitivity to Alendronate. We focused follow-up studies on TBONE1 and TBONE2, another poorly characterized gene amongst the most highly enriched resistance-conferring genes.

In cell based models, loss of TBONE1 or TBONE2 function results in selective resistance to NBP-mediated loss of cell viability and the prevention of NBP-mediated inhibition of prenylation. TBONE1 and TBONE2 are required for alendronate inhibition of osteoclast cell function, and TBONE1-deficient mice have impaired therapeutic responses to Alendronate in a model of postmenopausal osteoporosis. In addition, we investigated the mechanism by which TBONE1 and TBONE2 act molecularly, and find they are membrane proteins, likely involved in NBP uptake and endocytic trafficking through the lysosome. Our work adds key insights to the mechanistic action of NBPs and identifies a cadre of high-priority genes that may underlie differential responsiveness to NBPs.

**Disclosures:** Lauren Surface, None.

## FR0326

**Cyclic Treatment Regimen Rescues Parathyroid Hormone (PTH) Discontinuation-Induced Bone Loss and Microarchitecture Deterioration.** Wei-Ju Tseng<sup>\*</sup>, Hongbo Zhao, Wonsae Lee, Yang Liu, Yihan Li, Chantal de Bakkar, Ling Qin, X. Sherry Liu. University of Pennsylvania, United States

Despite the potent effect of intermittent PTH treatment on promoting new bone formation, BMD rapidly decreases upon PTH discontinuation. To uncover the mechanisms behind this adverse phenomenon, we first examined the changes in tibial bone microarchitecture in ovariectomized (OVX) rats by *in vivo* μCT. 18 4-mo-old rats underwent OVX surgery and developed osteopenia for 4 wks (50% reduction in BV/TV). Bone loss continued in VEH-treated rats (n=9) for 12 wks. In contrast, 3-wk PTH treatment (40 μg/kg, n=9) led to 97% and 27% greater BV/TV and Tb.Th, respectively, in the PTH vs. VEH group. Intriguingly, 1 wk after the withdrawal (wk 4), BV/TV and Tb.Th continued to show trends of improvement. Trends of bone deterioration appeared during the 2nd and 3rd wk of PTH withdrawal (wk 5 and 6), with a 28% decrease in BV/TV at wk 6 vs. wk 4 (Fig 1A). Histology (n=6/group) suggested that 3-wk PTH treatment led to 117% greater osteoblast # (Ob.N/BS) and 55% and 70% lower osteoclast # (Oc.N/BS) and adipocyte # (Adi.N/Ma.Ar), respectively, than VEH group. After 1-wk withdrawal from PTH, Ob.N/BS decreased 82% but remained 36% greater than VEH, and Oc.N/BS and Adi.N/Ma.Ar continued to be suppressed. 2 wk after PTH discontinuation, there was no remaining difference in Ob.N/BS and Oc.N/BS from VEH while Adi.N/Ma.Ar was 56% lower than VEH group (Fig 1BCD). The continuous anabolic window upon early withdrawal from PTH offers a new mechanism in support of a cyclic administration regimen with repeated cycles of on and off PTH treatment. Next, 3 treatment regimens were examined in OVX rats: VEH (n=3, 18-wk saline),

PTH-VEH (n=6, 9-wk PTH followed by 9-wk saline), and Cyclic PTH (n=7, 3-wk PTH followed by 3-wk saline, 3 cycles). In the PTH-VEH group, 9-wk PTH led to a 97% increase in BV/TV, followed by a 72% decrease after 9-wk discontinuation, with no difference from VEH group at wk 18. Similar trends were found for Tb.Th (Fig 2). In contrast, in the Cyclic PTH group, the first cycle of 3-wk PTH on and 3-wk off prevented reduction in BV/TV and led to a 33% increase in Tb.Th. BV/TV stabilized and Tb.Th continued to increase during the 2nd and 3rd cycles. At wk 18, BV/TV and Tb.Th in Cyclic PTH rats were greater than both PTH-VEH and VEH rats ( $p < 0.05$ , Fig 2AB). In summary, our study discovered a continuous anabolic window upon early withdrawal from PTH which allowed the cyclic treatment regimen to maximize the total duration and efficacy of PTH treatment on bone microarchitecture.

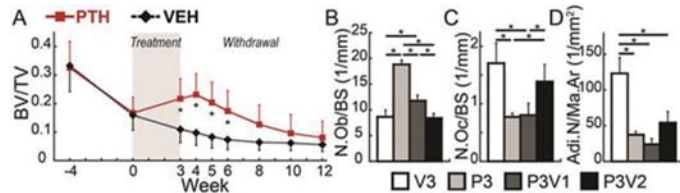


**Fig 1** (A) Changes in BV/TV in 12-wk VEH treated, and 3-wk PTH followed by 9-wk VEH treated OVX rats. (B-D) Comparisons in cellular activities among rats with 3-wk VEH (V3) and PTH (P3), and 3-wk PTH followed by 1- and 2- wk VEH treatments (P3V1 and P3V2). \* difference between treatment groups ( $p < 0.05$ ).

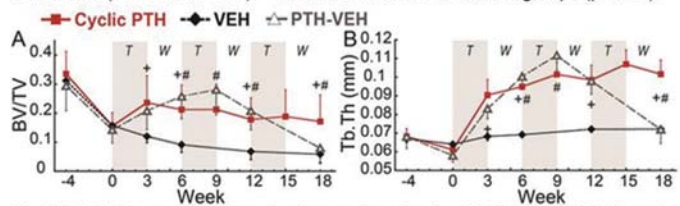


**Fig 2** (A-B) Changes in trabecular bone microstructure in VEH, PTH-VEH, and Cyclic PTH-treated OVX rats. + difference between Cyclic PTH and VEH groups ( $p < 0.05$ ). # difference between Cyclic PTH and PTH-VEH groups ( $p < 0.05$ ). T: Treatment, W: Withdrawal in the Cyclic PTH group.

A17018125-Fig

Disclosures: Wei-Ju Tseng, None.

## FR0331

### Effects of Burosumab (KRN23), a Fully Human Anti-FGF23 Monoclonal Antibody, on Functional Outcomes in Children with X-linked Hypophosphatemia (XLH): Final Results from a Randomized, 64-week, Open-label Phase 2 Study.

Thomas Carpenter<sup>\*1</sup>, Erik Imel<sup>2</sup>, Agnès Linglart<sup>3</sup>, Annemieke Boot<sup>4</sup>, Wolfgang Högl<sup>5</sup>, Raja Padidela<sup>6</sup>, William van't Hoff<sup>7</sup>, Anthony Portale<sup>8</sup>, Meng Mao<sup>9</sup>, Alison Skrinar<sup>10</sup>, Javier San Martín<sup>10</sup>, Michael Whyte<sup>11</sup>. <sup>1</sup>Yale University School of Medicine, United States, <sup>2</sup>Indiana University School of Medicine, United States, <sup>3</sup>Hôpital Bicêtre, France, <sup>4</sup>University of Groningen, Netherlands, <sup>5</sup>Birmingham Children's Hospital, United Kingdom, <sup>6</sup>Royal Manchester Children's Hospital, United Kingdom, <sup>7</sup>Great Ormond Street Hospital, United Kingdom, <sup>8</sup>University of California, San Francisco School of Medicine, United States, <sup>9</sup>Ultragenyx Pharmaceutical Inc., United States, <sup>10</sup>Ultragenyx Pharmaceutical Inc, United States, <sup>11</sup>Shriners Hospital for Children, United States

Children with XLH often have significant musculoskeletal symptoms and impaired mobility despite treatment with oral phosphate (Pi)/active vitamin D. In a Phase 2, open-label study, 52 children with XLH (ages 5-12 years) received burosumab (KRN23) subcutaneously biweekly (Q2W) or monthly (Q4W). At study entry, most had received oral Pi/active vitamin D (mean duration ~7 years). Rickets severity score (RSS), walking ability (six minute walk test [6MWT]), and patient-reported pain and functional ability (Pediatric Outcomes Data Collection Instrument [PODCI]) were assessed at baseline (BL) and up to Week 64 (Wk64). Data were analyzed for the entire cohort and after stratification by: i) rickets severity (defined as RSS  $< 0$  or  $\geq 1.5$ ), ii) walking impairment (defined as 6MWT  $< 80\%$  of predicted normal distance), and iii) level of functional impairment at BL (Global Functioning Scale score  $< 40$ ).

After 64 weeks of burosumab treatment, the six-minute walk distance (expressed as percent of predicted for age, gender, and height) increased from 80% to 85% for the full cohort. In subjects with greater walking impairment at BL, the mean increased from 68% to 79% (N=24). Similar improvements occurred in the Q2W and Q4W groups.

Using the PODCI, an instrument developed to measure functional ability, children treated with burosumab for 64 weeks experienced improved gross motor function and decreased pain. The 2 Global Function domains most compromised at BL were Pain/Comfort (P/C) and Sports/Physical Functioning (S/PF). Mean BL normative scores for the P/C and S/PF domains were 35 and 33, respectively, indicating pain and gross motor impairment approximately 1.5 SD below healthy mean values (normative mean score is 50; 1 SD = 10 points). Among subjects with greater disability at BL, the mean P/C score improved from 24 at BL to 38, and the mean S/PF score improved from 22 at BL to

37 after 64 weeks of treatment ( $p < 0.0001$  each, N=28). The Q2W and Q4W groups improved comparably in both the S/PF and P/C domains, and mean scores became closer to the normal range.

In children with XLH, pain, walking impairment, and compromised gross motor function were documented despite prior treatment with oral Pi/active vitamin D. Burosumab treatment was associated with substantial improvements in these key clinical outcomes, demonstrating the potential to improve health-related quality of life in pediatric XLH.

Disclosures: Thomas Carpenter, Ultragenyx Pharmaceutical Inc, Other Financial or Material Support.

## FR0334

### Efficacy and Safety of Palovarotene in Fibrodysplasia Ossificans Progressiva (FOP): A Randomized, Placebo-Controlled, Double-Blind Study.

Frederick S. Kaplan<sup>\*1</sup>, Edward C. Hsiao<sup>2</sup>, Genevieve Baujat<sup>3</sup>, Richard Keen<sup>4</sup>, Donna R. Grogan<sup>5</sup>, Robert J. Pignolo<sup>6</sup>. <sup>1</sup>The University of Pennsylvania, United States, <sup>2</sup>Institute of Human Genetics and the Division of Endocrinology & Metabolism, University of California, San Francisco, United States, <sup>3</sup>Laboratoire de Génétique Moléculaire, Institut de Recherche et Hôpital Necker-Enfants Malades, France, <sup>4</sup>The Royal National Orthopaedic Hospital (Stammore), United Kingdom, <sup>5</sup>Clementia Pharmaceuticals Inc., United States, <sup>6</sup>Geriatric Medicine & Gerontology, Mayo Clinic, United States

FOP is a rare, severely disabling disease characterized by episodic flare-ups and accumulation of heterotopic ossification (HO) in skeletal muscle and soft tissues. Progressive HO formation leads to restricted movement, physical disability, and early death. Palovarotene (PVO) is an orally bioavailable retinoic acid receptor gamma (RAR $\gamma$ ) agonist; RAR $\gamma$  agonists potentially impair heterotopic endochondral ossification by redirecting prechondrogenic mesenchymal stem cells to a nonosseous soft tissue fate. PVO demonstrated dose-dependent reductions in HO formation in various mouse models of FOP. This study evaluates whether PVO reduces HO formation in subjects with FOP.

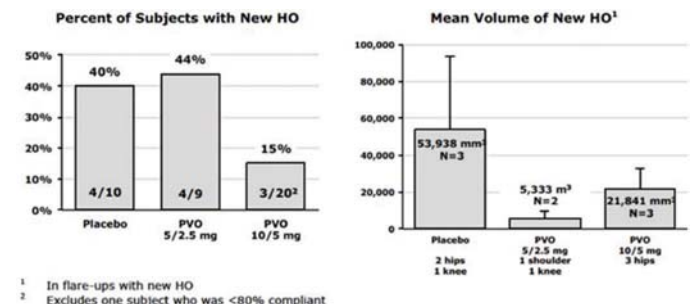
Forty FOP subjects (mean age=21 yrs; range=7-53 yrs; 45% males) were randomized 3:3:2 to the following PVO regimens within 7 days of flare-up onset: 10 mg for 2 weeks then 5 mg for 4 weeks (10/5 [N=21]); 5 mg for 2 weeks then 2.5 mg for 4 weeks (5/2.5 [N=9]); or placebo for 6 weeks (N=10). Change from baseline in HO (volume and incidence of new HO) at Week 12 was assessed on CT scans of the flare-up site. Pre-specified imaging interpretation procedures were blinded to treatment.

Sixty-five percent fewer subjects in the 10/5 group had new HO following a flare-up versus placebo (trend test  $p=0.0837$ ). In flare-ups with new HO, a 60% reduction in mean bone volume was observed in the 10/5 group versus placebo (Cohen's D=0.65) (see figure).

Dose-related increases in retinoid-associated adverse events (placebo: 60%; 5/2.5: 89%; and 10/5: 95%), primarily dermatologic in nature, were observed. The most common AE in all groups was dry skin. No subjects discontinued treatment or were dose de-escalated. No other safety signals were seen including clinical safety laboratory parameters or electrocardiograms.

In conclusion, this study indicates that 10/5 PVO lowered the incidence of new HO formation relative to placebo and 5/2.5 PVO. Although the data are limited due to the small sample size in this ultra-rare disease, the volume of new HO at comparable flare-up locations was lower in the 10/5 group than in the placebo group. Palovarotene was well tolerated at the doses administered. The results support continued evaluation of palovarotene as a potential treatment for FOP.

Acknowledgments: the authors wish to thank the FOP patient community and the clinical research teams for their participation and support of this study.



Effects of Palovarotene on Flare-up Incidence and Volume of HO

Disclosures: Frederick S. Kaplan, None.



## FR0336

**Transient Osteoporosis: Clinical Spectrum and Associated Risk Factors.** Anupam Kotwal\*, Daniela Hurtado, Jad Sfeir, Robert Wermers. Division of Endocrinology, Mayo Clinic, United States

Transient osteoporosis (TO) is a rare clinical syndrome characterized by acute joint pain, bone marrow edema (BME) on magnetic resonance imaging (MRI), periarticular osteopenia on X-ray, and usually spontaneous resolution within several months. We aimed at describing the natural history of TO and ascertain associated risk factors by retrospectively identifying adults diagnosed with TO at Mayo Clinic between 10/31/2001 and 11/1/2016. Adult patients with acute onset joint pain worsened by weight bearing and BME on MRI (Figure 1) were included; exclusion criteria were trauma, tumors, rheumatic diseases, avascular necrosis, infection or hyperesthesia. Over 15 years, 33 patients were identified (61% were males). Median age at diagnosis was 47 years (range 25-74) and median BMI was 28 kg/m<sup>2</sup> (20-45). Median time to diagnosis was 2 months (0.5 – 12) and median time to symptom resolution was 4 months (1 – 18). Most patients (78%) had at least one risk factor and 40% had two or more. The most frequent risk factor was low bone mineral density (BMD) in 13 (81%) of 16 patients investigated with DXA (39% of the entire cohort); 8 (62%) of those having low BMD at a site other than that involved by TO. The second most frequent risk factor was limb overuse in 10 (30%), followed by disorders of mineral metabolism in 9 (27% of all; most common being hypovitaminosis D). Bone turnover markers were normal in all patients with measurements (n = 7). Other risk factors included 8 (24%) patients who smoked >10 cigarettes/day, 7 (21%) with a previous episode of TO, and 2 females were pregnant. All had lower extremity involvement (hip 76%, knee 15% and ankle 9%). Clinical features included painful weight bearing (94%), limited mobility (94%), antalgic gait (64%) and tenderness to palpation (23%). All 7 patients that underwent bone scintigraphy had increased uptake. 29 (88%) were given crutches for offloading, 31 (94%) were given analgesics, 7 (21%) received a bisphosphonate, 1 received calcitonin nasal spray, and 3 (9%) had a surgical intervention performed. All patients had complete recovery without any sequelae. Our data suggests that TO affects middle age men more than women, primarily involves weight bearing joints, often takes several weeks to recognize and usually resolves with conservative management. The underlying etiology of TO remains unclear, however the common presence of risk factors and generalized decrease in BMD suggest that systemic factors may be important.

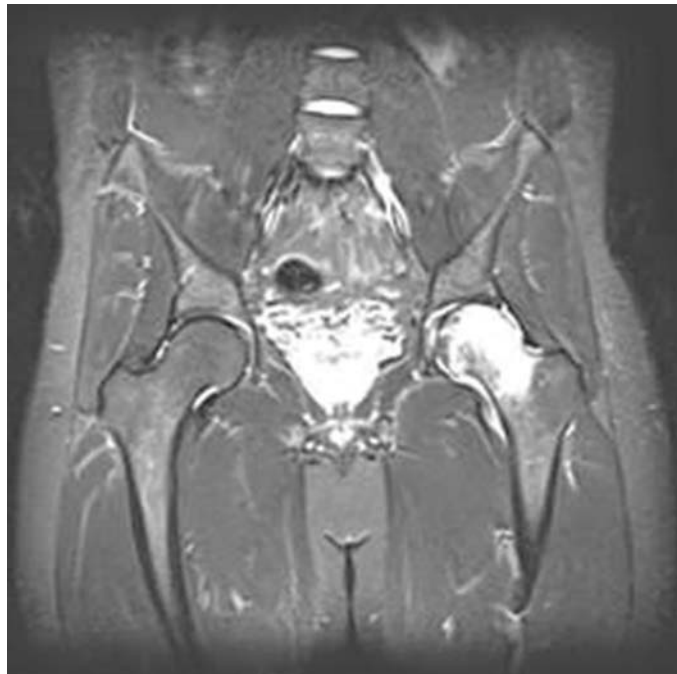


Figure 1: Diffuse bone marrow edema involving the left femur head and neck

**Disclosures:** Anupam Kotwal, None.

## FR0337

**Clinical, Biochemical and Genetic Features of 41 Families with Primary Hypertrophic Osteoarthropathy, and Their Therapeutic Response to Etoricoxib: Results from a 6 Months Prospective Clinical Intervention.** Shan-Shan Li\*, Jin-We He, Wen-Zhen Fu, Zhen-Lin Zhang. Metabolic Bone Disease and Genetics Research Unit, Department of Osteoporosis and Bone Diseases, Shanghai Jiao Tong University Affiliated Sixth People's Hospital, China

Primary hypertrophic osteoarthropathy (PHO) is a rare inherited disease caused by genetic defects in prostaglandin metabolism pathway; disturbed prostaglandin E2 (PGE2) catabolism resulting in increased PGE2 levels is suggested in the pathogenesis.

Forty-three patients with PHO were studied and 41 of them were treated. Mutations in HPGD gene, causing hypertrophic osteoarthropathy, primary, autosomal recessive 1 (PHOAR1; OMIM 259100), were identified in 7 patients, and mutations in SLC02A1 gene, causing hypertrophic osteoarthropathy, primary, autosomal recessive 2 (PHOAR2; OMIM 614441), were identified in 36 patients. Clinical phenotypes of PHO varied, ranging from mild isolated clubbing finger to severe pachydermia and disabling joint swelling, even within families. Circulating PGE2 metabolism features of PHOAR2 were different from those of PHOAR1. Different frequency and severity of pachydermia between the subgroups were also indicated. A percentage of PHOAR2 patients suffered from gastrointestinal hemorrhage, but this symptom was not observed in PHOAR1 subgroup. Clinical evidence highlighted essential role of sex hormones in prostaglandin transporter regulation with respect to PHOAR2 onset, although no significant associations of urinary PGE2 or PGE-M with sex hormones were identified. Treatment with Etoricoxib, a selective cyclooxygenase-2 inhibitor, was proved to be beneficial and safe. We detected its notable efficacy in decreasing urinary PGE2 levels in the majority of the enrolled patients during 6 months of intervention; assessed clinical phenotypes, including pachydermia, clubbing finger and joint swelling, were improved. We found no visible evidence of positive effect of Etoricoxib on periostosis. But significant links between urinary PGE2 and serum bone turnover markers indicated potential role of decreased PGE2 in periostosis management. This is the largest reported cohort of subjects genetically diagnosed with PHO. For the first time, we systematically investigate the biochemical and clinical differences between PHOAR1 and PHOAR2, and prospectively demonstrated the positive efficacy and safety of Etoricoxib for PHO patients.

**Disclosures:** Shan-Shan Li, None.

## FR0340

**Incidence of mutations in the *TNSALP*, *GGPS1* and *CYP11A1* genes in patients with atypical femoral fractures.** Pilar Peris\*<sup>1</sup>, Eva Gonzalez<sup>2</sup>, Sebastian Rodriguez<sup>3</sup>, Ana Monegal<sup>3</sup>, Ana Monegal<sup>3</sup>, Nuria Guañabens<sup>3</sup>.

<sup>1</sup>Rheumatology Department, Hospital Clinic. University of Barcelona, Spain, <sup>2</sup>Immunology Department. Hospital Clinic., Spain, <sup>3</sup>Rheumatology Department. Hospital Clinic, Spain

**Introduction:** Atypical femoral fractures (AFF) are an uncommon disorder often related to prolonged bisphosphonate (BP) treatment. Recently, isolated cases of AFF have been linked to mutations of Tissue Nonspecific Alkaline Phosphatase (*TNSALP*), as a clinical form of presentation of hypophosphatasia in adults. Moreover, mutations in the geranylgeranyl pyrophosphate synthase (*GGPS1*) enzyme which can be inhibited by BPs, and also in the enzyme of the cytochrome P450 superfamily (*CYP11A1*), the latter related to the metabolism of several drugs, have also been associated with the development of some cases of AFF. Therefore, the aim of this study was to analyse the incidence of *TNSALP*, *GGPS1* and *CYP11A1* gene mutations in patients with AFF as well as the clinical characteristics of these patients.

**Methods:** 17 women with AFF with a mean age of 68±10 years were included in the study. Sanger sequencing for the *TNSALP*, *GGPS1* and *CYP11A1* genes was performed in all patients to determine the presence of mutations and polymorphisms. Additionally, we analysed the ALP substrates (vitamin B6 and PEA), bone turnover markers, bone mineral density (BMD), previous antiosteoporotic treatment and the clinical characteristics of the patients and the fractures.

**Results:** 2/17 patients (12%) presented mutations: one in *TNSALP* (p.G288A) and the other in *CYP11A1* (p.R136H), both being heterozygote mutations. The patient with the *TNSALP* mutation presented an increase in the ALP substrates (vitamin B6 serum levels) with marginally decreased serum ALP levels while the patient with the *CYP11A1* mutation has a glucocorticoid-induced osteoporosis and was previously treated with BPs for only 3 years. All patients (17/17) had previously been treated with BPs (94% with alendronate) during 74±45 months, and nearly 50% also received glucocorticoids. The AFF was bilateral in 35% of cases, and most of these patients (76%) had had previous fragility fractures.

**Conclusions:** Mutations in either the *CYP11A1* or *TNSALP* gene may be related to the development of AFF in some patients treated with BPs. Evaluation of ALP substrates in patients with low ALP levels allows the identification of patients with hypophosphatasia. The role of *CYP11A1* mutations in AFF needs further study.

**Disclosures:** Pilar Peris, None.

## FR0342

**Risk of complications in hypoparathyroidism are associated with disturbances in calcium-phosphate homeostasis: a case-control study.** Line Underbjerg\*<sup>1</sup>, Tanja Sikjaer<sup>2</sup>, Lars Rejnmark<sup>3</sup>. <sup>1</sup>MD/Ph.D.-student, Denmark, <sup>2</sup>MD, Ph.D., Denmark, <sup>3</sup>Clinical professor, consultant, PhD, DMSc, Denmark

Only few data are available on indices affecting risk of complications in hypoparathyroidism. We aimed to assess risk of different complications using biochemical data from patients with verified hypoparathyroidism (N=431). We used a case-control design, comparing patients with hypoparathyroidism who had acquired the complication in question (cases) with hypoparathyroid patients without the complication (controls). Patients had an average age of 41 years at time of diagnosis (81% females) and a median disease duration of 12 years. The majority (88%) had hypoparathyroidism due to surgery, mainly following thyroidectomy for non-toxic goiter. More than 95% were on treatment with a daily supplement of calcium and/or activated vitamin D. Time-weighted serum levels of ionized calcium was median 1.17 (interquartile range [IQR]

1.14-1.21) mmol/L, phosphate 1.21 (IQR 1.11-1.32) mmol/L, and the calcium-phosphate product was 2.80 (IQR 2.51-3.03) mmol<sup>2</sup>/L<sup>2</sup>. Compared to an averages level of ionized calcium in the mid-tertile (1.16-1.19 mmol/L), patients in the lowest tertile (<1.16 mmol/L) had a significantly increased risk of developing cardiovascular diseases (OR 2.52; 95% CI, 1.08; 5.90). Serum phosphate levels above the median was associated with a significantly increased mortality (OR 2.76; 95% CI, 1.32; 5.80) and risk of infections (OR 1.77; 95% CI, 1.04; 3.01). Moreover, a calcium-phosphate product above median was associated with an increased mortality (OR 2.67; 95% CI, 1.27; 5.63) and risk of renal diseases (OR 1.71; 95% CI, 1.03; 2.86).

Forty-one percent of our patients had experienced one or more episodes of hypercalcemia which was associated with an increased mortality (1.76; 95% CI, 1.02; 3.05) and risk of infections (OR 1.86; 95% CI, 1.18; 2.93), as well as a borderline increased risk of cardiovascular- (OR 1.89; 95% CI, 0.99; 3.61) and renal- (OR 2.28; 95% CI, 0.92; 5.64) diseases.

In conclusion, although most of our patients had average (time-weighted) serum levels of calcium and phosphate within the normal range, phosphate levels and a calcium-phosphate product above the median was associated with a significantly increased risk of complications. Moreover, risk increased if calcium levels were in the lowest tertile as well as with episodes of hypercalcemia. Our data suggest that treatment of hypoparathyroidism should aim to keep serum levels of calcium and phosphate in the lower part of the reference interval.

**Disclosures:** Line Underbjerg, NPS pharmaceuticals, Shire, Speakers' Bureau.

## FR0343

**TransCon CNP, a Sustained-Release Prodrug of C-type natriuretic Peptide, exerts Positive Effects on Bone Growth in Juvenile Cynomolgus Monkeys and in a Mouse Model of Achondroplasia.** Vibeke Miller Breinholt<sup>1</sup>, Nabil Kaci<sup>2</sup>, Oliver Keil<sup>3</sup>, Susann Aderman<sup>3</sup>, Ulrich Hersel<sup>3</sup>, Maxence Cornille<sup>4</sup>, Martin Guillot<sup>5</sup>, Nancy Doyle<sup>5</sup>, Per Mygind<sup>1</sup>, Aurore Valera<sup>6</sup>, Kennett Sprogø<sup>1</sup>, Laurence Legèai-Mallet<sup>2</sup>. <sup>1</sup>Ascendis Pharma A/S, Denmark, <sup>2</sup>Imagine Institute, Denmark, <sup>3</sup>Ascendis Pharma GmbH, Denmark, <sup>4</sup>Imagine INstitute, France, <sup>5</sup>Charles River Laboratories, Canada, <sup>6</sup>Charles River Laboratories, France

No FDA-approved treatment options exists for achondroplasia (ACH), the most common form of dwarfism. C-type Natriuretic Peptide (CNP) has shown promising efficacy in both animal models and human subjects with ACH. TransCon CNP is a prodrug designed specifically to release free CNP at a slow rate, resulting in hemodynamically safe and efficacious drug levels, employing a weekly dosing regimen. The aim of these nonclinical studies was to compare the efficacy of the long-acting TransCon CNP to a daily administered CNP analogue in intact monkeys and in an animal achondroplasia model.

TransCon CNP was administered by daily injections to newborn mice harboring the *Fgfr3*<sup>Y367C/+</sup> mutation (5.6 mg CNP/kg/day, n = 9) for 14 days from immediately after birth and for 14 days and to juvenile cynomolgus monkeys (26-29 months at initiation of treatment) (n = 4/group) (up to 100 µg/kg/week) for 6 months. Body, tail, and selected long bones were measured in both models by radiography/µCT and/or with a caliper. H&E and Collagen X staining were performed on femoral bone from the ACH mice to address effects on the growth plate architecture.

In young, healthy cynomolgus monkeys, TransCon CNP induced a dose-related effect on tibia growth. TransCon CNP at 100 µg/kg/week demonstrated increased efficacy compared to daily vorosotide at a dose of 20 µg/kg/day and similar efficacy at one-third the dose. The administration of TransCon CNP to ACH mice resulted in positive effects on axial and appendicular bones. Collagen type X and H&E staining showed an improvement of the growth plate architecture compared to *Fgfr3*<sup>Y367C/+</sup> mice treated with vehicle. Also an increased naso-anal length, an increased size of the epiphysis and secondary ossification centers were observed.

In conclusion, TransCon CNP exerted growth promoting effects on long bones in both healthy animals and in a disease model of ACH; in the latter resulting in improved phenotypical appearance. These data support further development of TransCon CNP as a potential therapy for ACH; providing efficacious CNP levels with weekly administration.

**Disclosures:** Vibeke Miller Breinholt, None.

## FR0346

**Prevention of zoledronate-induced MRONJ in a mouse model of Bisphosphonate Displacement (BPD) prophylaxis therapy.** Akishige Hokugo<sup>1</sup>, Shuting Sun<sup>2</sup>, Yujie Sun<sup>3</sup>, Kenzo Morinaga<sup>3</sup>, Qingqing Wu<sup>3</sup>, Mark Lundy<sup>4</sup>, Charles McKenna<sup>5</sup>, Frank Ebetino<sup>2</sup>, Ichiro Nishimura<sup>3</sup>. <sup>1</sup>David Geffen School of Medicine at UCLA, United States, <sup>2</sup>BioVinc LLC, United States, <sup>3</sup>UCLA School of Dentistry, United States, <sup>4</sup>Indiana University, United States, <sup>5</sup>University of Southern California, United States

Medically-related osteonecrosis of the jaw (MRONJ) can be a serious concern, particularly for oral surgery patients who have received a nitrogen-containing bisphosphonate (NBP) drug to avoid skeletal complications and relieve bone pain due to multiple myeloma or metastatic bone cancer. We recently introduced the concept of bisphosphonate displacement (BPD) as a potential approach to prevent or treat BP-related MRONJ by displacement of active BP drug in the isolated jawbone compartment via appropriate local administration of a suitable inactive BP, which may also incorporate a fluorescent marker. Here we examine

this hypothesis by evaluating the prophylactic effectiveness of BV501001 in mouse model of zoledronate (ZOL)-induced MRONJ.

To assess the anti-prenylation activity of BV501001, J744.2 macrophages were treated with the compound at 10 and 100 µM. After 24 hours, cells were lysed, and unprenylated Rap1A and total Rap1 were detected by Western blotting and compared to controls. Whereas ZOL potently inhibits Rap1 prenylation in this assay, BV501001 had undetectable activity up to the higher concentration used.

Experimental ONJ was induced in adult female mice by iv injection of 500 µg/kg ZOL, followed by extraction of the maxillary left first molar. To evaluate the ONJ preventive effect of the displacement approach, BV501001 (250 µM), or saline vehicle were injected to the maxillary gingiva 1 day before extraction. Two weeks later, the disease control mice showed delayed healing consistent with an ONJ-like lesion. In contrast, mice treated with BV501001 exhibited nearly complete wound healing without signs of ONJ lesion development.

Oral mucosa cells were dissociated from maxillary gingiva tissues. Mice developing ONJ-like lesions demonstrated reduced CD45+CD3+ T cells and increased CD11b+GR1+ myeloid cells, which was normalized by BPD prophylaxis therapy.

Our results provide support for the proposal that local BPD prophylaxis prior to dental surgery can prevent or mitigate the induction of MRONJ associated with legacy NBPs accumulated in the jawbone after routine therapy, while preserving the therapeutic effect of NBPs at diseased skeletal sites.

**Disclosures:** Akishige Hokugo, None.

## FR0347

**Inflammation and increased osteoclastogenesis in osteogenesis imperfecta murine.** Ivo Kalajzic<sup>1</sup>, Emilie Roeder<sup>1</sup>, Xi Wang<sup>1</sup>, Hector Leonardo Aguila<sup>1</sup>, Sun Kyeong Lee<sup>1</sup>, Danka Grcevic<sup>2</sup>, Brya Matthews<sup>1</sup>. <sup>1</sup>UConn Health, United States, <sup>2</sup>University of Zagreb, Croatia

Osteogenesis imperfecta (OI) is a disease caused by defects in type I collagen production that results in brittle bones. While the pathology is mainly caused by defects in the osteoblast lineage, there is also elevated bone resorption by osteoclasts resulting in high bone turnover in severe forms of the disease. Consistent with high bone turnover, we observed dramatically elevated serum CTX in OIM mice (>500ng/ml compared to ~20ng/ml in WT) and found splenomegaly in all ages examined (up to 20 weeks of age).

Osteoclasts originate from hematopoietic myeloid cells, however changes in hematopoiesis have not been previously documented in OI. We evaluated hematopoietic lineage distribution and osteoclast progenitor cell frequency in bone marrow, spleen and peripheral blood of osteogenesis imperfecta murine (OIM) mice in comparison to their wild-type littermates by flow cytometry. In 7-week old male OIM animals, we identified a number of changes in hematopoietic cell frequency including expansion of the granulocyte-macrophage progenitor pool, increased myeloid lineage cells (CD11b<sup>+</sup>) in bone marrow and spleen, and reduced proportion of erythrocyte precursors (Ter119<sup>+</sup>) in the bone marrow coupled with increased frequency in the spleen. OIM spleens also showed an increased frequency of purified osteoclast progenitors (OCP, CD11b<sup>hi</sup>CD115<sup>+</sup>Ly6C<sup>hi</sup>). This phenotype is suggestive of chronic inflammation. Isolated osteoclast precursors from both spleen and bone marrow formed osteoclasts more rapidly than WT controls in vitro.

We found that serum TNFα levels were increased in OIM, as was IL1α in OIM females. We targeted inflammation therapeutically by treating growing animals with murine TNFR2:Fc, a compound that blocks TNFα activity. Anti-TNFα treatment marginally decreased spleen mass in OIM females, but failed to reduce bone resorption as determined by serum CTX, or improve BMD measured by DEXA or femoral bone parameters determined by µCT. Fracture rate in OIM animals was also unchanged, however fracture rate appeared to be higher in male mice than females.

We have demonstrated that OIM mice have changes in their hematopoietic system, and form osteoclasts more rapidly even in the absence of OI osteoblast signals. OIM mice have indications of chronic inflammation but therapy targeting TNFα did not improve disease parameters.

**Disclosures:** Ivo Kalajzic, None.

## FR0348

**Reduced autophagy increases OI severity in mice with Gly610 to Cys substitution in the triple helical region of the α2(I) collagen chain.** Elena Makareeva<sup>\*</sup>, Shakib Omari, Anna Roberts-Pilgrim, Laura Gorrell, Edward Mertz, Sergey Leikin. SPB, NICHD, NIH, United States

Glycine substitutions in the triple helical region of type I collagen are the most common mutations resulting in severe forms of osteogenesis imperfecta (OI). The G610C mouse (MGI:3711122) with a Gly610 to Cys substitution in the α2(I) chain produces moderately severe OI in heterozygous (het) and lethal OI in homozygous (hom) animals. Heterozygous animals exhibit significant variability of bone phenotype, which is a common feature of Gly substitutions. Our studies of G610C mice suggest that (a) osteoblast cell stress and malfunction caused by accumulation of misfolded procollagen inside the cell is a major factor in bone pathology, (b) cells degrade misfolded procollagen via a previously unknown autophagy pathway, and (c) osteoblast ability to adapt to the cell stress associated with procollagen misfolding contributes to the phenotypic variability of OI. We demonstrate that hypomorphic expression of an essential autophagy gene *Atg5* in *Atg5*<sup>flax/flax</sup> (MGI:3663625) mice with the heterozygous G610C mutation reduces the autophagy flux in osteoblasts and results in ~30% neonatal lethality and more severe bone malformations and fractures. Conditional



knockout of *Atg5* upon crossing with osteocalcin-Cre mice (MGI:2446069) further increases the frequency and severity of bone malformation without increasing the perinatal lethality, consistent with our observations of perinatal death being associated with deficient lung rather than bone development. Conditional *Atg5* knockout upon crossing with osterix-Cre mice (MGI:3689350) produces no live animals with the heterozygous G610C mutation and extremely severe skeletal deformities in dead newborn pups. Combined with our other observations, this study suggests that misfolded procollagen autophagy plays an important role in OI bone pathology. It appears to be at least partially responsible for variable severity of the same mutation in different individuals and might be targeted for therapeutic intervention.

**Disclosures:** Elena Makareeva, None.

## FR0349

**Enthesopathy in the Hyp mouse model of XLH is characterized by enhanced BMP and IHH signaling.** Eva Liu<sup>\*1</sup>, Janaina da Silva Martins<sup>2</sup>, Marie Demay<sup>3</sup>. <sup>1</sup>Brigham and Women's Hospital and MGH, United States, <sup>2</sup>Massachusetts General Hospital, United States, <sup>3</sup>Massachusetts General Hospital, Harvard Medical School, United States

X-linked hypophosphatemia (XLH) is characterized by elevated serum FGF23 levels, leading to hypophosphatemic rickets. A complication of XLH is enthesopathy, abnormal mineralization of bone-tendon attachment sites, which leads to pain and impaired mobility. The molecular markers and signaling pathways involved in XLH enthesopathy are poorly understood. Safranin O (Safo) staining of the Achilles tendon entheses in the Hyp mouse model of XLH reveals aberrant hypertrophic enthesopathy cells (HECs), which gradually expand from the entheses into the tendon d14 to d60. Wild type (WT) entheses, in contrast have no Safo positive cells d30. In contrast to WT entheses, the Hyp HECs exhibit alkaline phosphatase activity d75. Lineage tracing analyses demonstrate that both the WT and Hyp entheses cells originate from Sox9-ERt and Scleraxis(Scx)-Cre expressing cells. Furthermore, cells in the Achilles tendon entheses from both WT and Hyp mice exhibit immunoreactivity for the chondrocyte marker Sox9 and Scx-GFP, a marker of tenocytes.

Investigations were undertaken to identify signaling abnormalities that lead to the development of enthesopathy in the Hyp mice. BMP signaling induces phosphorylation of Smad 1/5 and promotes hypertrophy of chondrocytes. Consistent with increased BMP signaling, an expansion of pSmad 1/5 immunoreactive cells was observed in the HECs of the Hyp mice, accompanied by enhanced expression of the BMP target genes Noggin, Indian hedgehog (IHH) and Patched, a receptor and target of IHH signaling. Compared to WT, Hyp entheses were found to have increased expression of IHH target genes Runx2 and Gli1.

To assess whether enhancing 1,25 dihydroxyvitamin D (1,25D) or attenuating FGF23 action affects enthesopathy development, Hyp mice were treated with 1,25D or FGF23 blocking antibody (FGF23Ab) d2 to 30. Both therapies partially attenuated the development of enthesopathy, evidenced by a decrease in alkaline phosphatase activity and Patched immunoreactivity in HECs. However, 1,25D therapy was superior to FGF23Ab in decreasing Safo staining of the Hyp HECs.

Thus, the entheses cells of both WT and Hyp mice express markers of tenocyte and chondrocyte lineages. These studies implicate increased BMP and IHH signaling in Hyp HECs in the pathogenesis of the mineralizing enthesopathy observed with XLH. Despite increasing circulating FGF23 levels, 1,25D attenuates the development of enthesopathy in the Hyp mouse model of XLH.

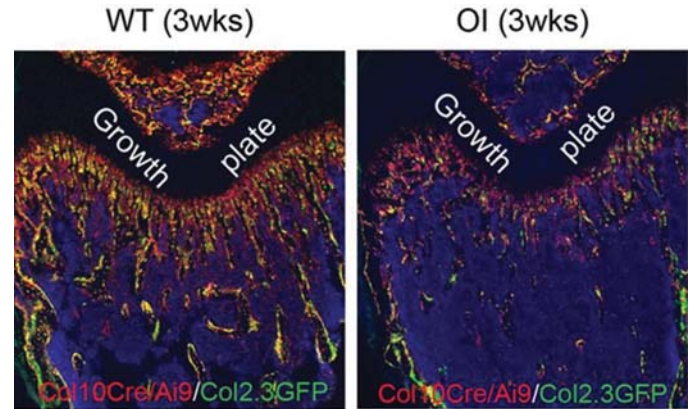
**Disclosures:** Eva Liu, None.

## FR0351

**Identification of the Mechanism Underlying Growth Deficiency in Osteogenesis Imperfecta.** Satoru Otsuru<sup>\*1</sup>, Adam Guess<sup>1</sup>, Kathryn Cheah<sup>2</sup>, Masahiro Iwamoto<sup>3</sup>, Edwin Horwitz<sup>1</sup>. <sup>1</sup>Center for Childhood Cancer and Blood Diseases, The Research Institute at Nationwide Children's Hospital, United States, <sup>2</sup>Department of Biochemistry, and Centre for Reproduction, Development and Growth, Li Ka Shing Faculty of Medicine, The University of Hong Kong, Hong Kong, <sup>3</sup>Department of Orthopaedics, University of Maryland School of Medicine, United States

Osteogenesis imperfecta (OI) is a genetic bone disease mostly caused by autosomal dominant mutations in one of two genes that encode type I collagen (Col1). Besides bone fragility, patients also exhibit impaired bone growth. However, no effective treatments currently address growth deficiency. The greatest obstacle in the development of such treatments is that the mechanism by which mutations in Col1 result in growth deficiency remains unknown. In our study, we found that G610C mice (a murine model of OI harboring a Col1a2 mutation) have elongated growth plate, especially in the hypertrophic zone, and decreased cell turnover. Given that late hypertrophic chondrocytes (late HCs) must be eliminated from the growth plate during bone growth, these findings led us to hypothesize that elimination of late HCs from the growth plate is suppressed in OI, resulting in impaired bone growth. To test this hypothesis we tracked the fate of HCs in G610C mice by generating novel quadruple transgenic strain from Col10a1-Cre knock-in mice, Ai9 reporter mice, Col1a1 2.3-GFP transgenic mice, and G610C mice. Triple transgenic mice without G610C mice served as non-OI controls. In these quadruple/triple transgenic strains, HCs and their progeny express red fluorescence, and osteoblasts/osteocytes express green fluorescence. Osteoblasts/osteocytes that are

derived from HCs fluoresce yellow. Histological evaluation of bones from 3-week old quadruple/triple transgenic mice demonstrated that the translocation of HCs from the growth plate to the metaphysis as well as the transdifferentiation of HCs into osteoblasts/osteocytes was significantly reduced in OI. TUNEL staining revealed that the OI growth plate had a small but statistically significant increase in apoptotic HCs. However, the increase seems too small to account for the reduction in HC-derived cells in the OI metaphysis. Moreover, our study showed that late HCs start expressing Col1, suggesting that mutated Col1 is expressed in late HCs in the OI growth plate. Interestingly, electron microscopic analyses revealed swollen endoplasmic reticulum (ER) in the growth plate HCs in G610C mice, suggesting that mutated Col1 induces ER stress in HCs, which is a major mechanism of osteoblast dysfunction in OI. Therefore, these results indicate that ER stress in HCs induced by mutated Col1 suppresses their translocation and transdifferentiation, resulting in reduced cellular turnover in the growth plate, leading to growth deficiency.



**Histological analyses of quadruple/triple Tg mice. These Tg mice showed HCs and their progeny in red, mature osteoblasts/osteocytes in green, and HC derived osteoblasts/osteocytes in yellow.**

Otsuru et al. Figure

**Disclosures:** Satoru Otsuru, None.

## FR0354

**SIRT1 SNPs Associated with Bisphosphonate-related Osteonecrosis of the Jaw (ONJ).** Guang Yang<sup>\*1</sup>, Taimour Y Langae<sup>1</sup>, Issam Hamadeh<sup>2</sup>, Joseph Katz<sup>3</sup>, Alberto Riva<sup>4</sup>, Jan S Moreb<sup>5</sup>, Yan Gong<sup>1</sup>. <sup>1</sup>Department of Pharmacotherapy and Translational Research and Center for Pharmacogenomics, College of Pharmacy, University of Florida, United States, <sup>2</sup>Cancer Pharmacology Department, Levine Cancer Institute, Charlotte NC, USA., United States, <sup>3</sup>Department of Oral Medicine, College of Dentistry, University of Florida, Gainesville FL, USA., United States, <sup>4</sup>Bioinformatics Core, Interdisciplinary Center for Biotechnology Research, University of Florida, Gainesville FL, USA., United States, <sup>5</sup>Department of Medicine, College of Medicine, University of Florida, Gainesville FL, USA., United States

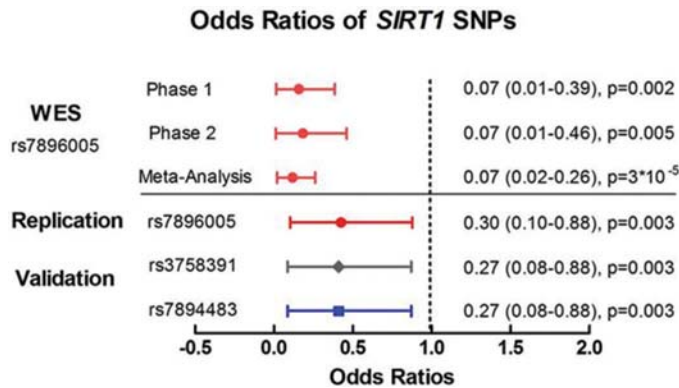
**Background:** Osteonecrosis of jaw (ONJ) is a rare and serious adverse drug side effect, mainly associated with the use of intravenous (IV) bisphosphonates (BPs). Current clinical practice guidelines recommend dental screening prior to therapy initiation as the only measure available for the prevention of BP related ONJ in high-risk individuals. The purpose of this study is to identify genetic variants associated with ONJ in patients treated with IV BPs (zoledronate or pamidronate) using a whole-exome sequencing (WES) approach followed by validation/replication process in an independent case-control study.

**Methods:** Exome-wide association analyses were performed in two phases in patients of European ancestry who were treated with IV BPs. Phase 1 included 46 multiple myeloma patients (23 individuals with ONJ and 23 age, gender and race-matched controls who did not develop ONJ after at least 24 months of IV BP treatment). In phase 2, 17 patients with solid tumors treated with IV BPs and developed ONJ were included. Multiple logistic regression analyses were performed adjusting for age, gender and principal components for ancestry (PCA). Meta-analysis was performed to estimate the combined odds ratio (OR) for ONJ. *In silico* analyses were performed to identify expression quantitative loci (eQTL) SNPs that are in high Linkage disequilibrium (LD) with the single nucleotide polymorphisms (SNPs). The associations of the potentially functional SNPs with BP related ONJ were verified in an independent case-control study of 48 patients of European ancestry treated with zoledronate or pamidronate (19 ONJ cases and 29 age, gender matched controls).

**Results:** The top signal in the meta-analysis was a Sirtuin1 (*SIRT1*) SNP (rs7896005) with an OR of 0.07 and 95% confidence interval (CI) of 0.02-0.26 ( $p=3 \times 10^{-3}$ ) (Figure). In the *in silico* functional analysis, two promoter region SNPs (rs7894483 and rs3758391) were identified to be in high LD with rs7896005 ( $r^2=0.76$ ,  $D'=0.86$ ) and are expression

quantitative loci (eQTLs) for *SIRT1* gene in whole blood in the GTEx database. The association of the original top SNP and the two promoter SNPs with ONJ were replicated/validated in an independent replication sample (Figure). The three-study meta-analysis p-value for rs7896005 is  $3.397 \times 10^{-7}$ .

Conclusions: Exome wide association studied identified the *SIRT1* SNP, rs7896005 which is in high LD with two eQTL SNPs (rs7358391 and rs7894483), as a potential genetic marker for BP related ONJ.



Figure

Disclosures: Guang Yang, None.

## FR0355

**Lateral Meningocele Syndrome Causes Marked Osteopenia.** Ernesto Canalis\*, Lauren Schilling, Stefano Zanotti. UConn Musculoskeletal Institute, UConn Health, United States

Lateral Meningocele (LMS) or Lehman Syndrome is a rare genetic disorder characterized by craniofacial developmental abnormalities, osteoporosis and neurological complications. LMS is associated with point mutations or short deletions in exon 33 of *NOTCH3* that lead to the translation of a truncated and stable protein product lacking sequences necessary for NOTCH3 degradation. As a consequence, a state of NOTCH3 gain-of-function ensues. Despite the skeletal manifestations reported in LMS, mechanisms underlying the bone loss are not known. To understand the disease process, we created a mouse model harboring a *Notch3* mutant allele reproducing the mutations found in subjects with LMS. A tandem termination codon was introduced into the mouse genome (6691-6696 ACCAAG>TAATGA) utilizing Crispr-Cas9 technology. The mutation leads to the creation of a truncated protein of 2230 amino acids (vs. 2318 in wild type) devoid of the PEST domain which is required for protein degradation. Sequences necessary for Notch3 transcriptional activity are preserved. The *Notch3* mutation was verified by DNA sequencing of founder and F1 mice. Notch target genes were induced in bone extracts from *Notch3LMS* mutant mice, demonstrating Notch signal activation in the skeleton. Male and female heterozygous *Notch3LMS* mice had pronounced cancellous and cortical bone osteopenia. Compared to littermate controls, microcomputed tomography of *Notch3LMS* mutants revealed a 35 to 60% decrease in cancellous bone volume associated with a reduction in trabecular number and decreased connectivity. Cortical thickness and area were decreased. Histomorphometry revealed a marked increase in osteoblast number (2-fold vs. control) and a modest increase in bone formation that was not sufficient to correct the osteopenic phenotype. *Notch3LMS* mice had a modest increase in osteoclast surface, and bone marrow macrophages had a greater capacity to form multinucleated osteoclasts in response to M-CSF and Rankl. Expression of Rankl mRNA was 3-fold higher in osteocyte-rich collagenase/EDTA digested femurs from *Notch3LMS* mice than controls without changes in osteoprotegerin expression. In conclusion, a genetically engineered *Notch3LMS* mutant mouse recreates aspects of the human disease and exhibits pronounced osteopenia due to an increase in osteoblasts with limited functional capacity and enhanced osteoclastogenesis.

Disclosures: Ernesto Canalis, None.

## FR0356

**Distinctive Impact of Peak Jump Power on the 3D Geometry of the Proximal Femur assessed by Asynchronous Quantitative Computed Tomography in Elderly.** Namki Hong\*<sup>1</sup>, Chang Oh Kim<sup>2</sup>, Yosik Youm<sup>3</sup>, Hyeon Chang Kim<sup>4</sup>, Yumie Rhee<sup>1</sup>. <sup>1</sup>Department of Internal Medicine, Severance Hospital, Endocrine Research Institute, Yonsei University College of Medicine, Korea, Republic of, <sup>2</sup>Division of Geriatrics, Department of Internal Medicine, Severance Hospital, Yonsei University College of Medicine, Korea, Republic of, <sup>3</sup>Department of Sociology, Yonsei University College of Social Sciences, Korea, Republic of, <sup>4</sup>Department of Preventive Medicine, Yonsei University College of Medicine, Korea, Republic of

Physical activity and weight-bearing exercise is associated with low hip fracture risk, affecting bone mineral density (BMD) as well as bone geometry of hip via localized bone adaptation. Countermovement jump power has emerged as a reliable assessment for muscle function, which demonstrated positive correlation with tibial bone geometry. However, it remains unclear whether the peak jump power is independently associated with BMD and geometry of the proximal femur in elderly.

Among 548 participants enrolled in Korean Urban Rural Elderly cohort in 2016, 534 subjects underwent computed tomography scan at pelvis and jumping mechanography test. Peak jump power relative to body mass (W/kg), volumetric BMD (vBMD) and bone geometry parameters of proximal femur, and mid-thigh muscle cross-sectional area (CSA) were measured. Subjects who could not jump due to muscle weakness, joint pain, recent fractures or surgery were grouped as non-jumpers as the most frail group.

Compared with subjects with higher jump power (N=224; ≥sex-specific median, 27.5 W/kg for men and 20.3 W/kg for women), non-jumpers (N=86) had older age (75.6 vs. 73.4 years), higher prevalence of women (80.2 vs. 64.3%), lower thigh muscle CSA (82.9 vs. 100.9cm<sup>2</sup>), more falls within last year (37.2 vs. 18.3%), and lower participation to moderate to vigorous physical activity (17.5 vs. 34.9%, P<0.05 for all). After adjustment for age, sex, height, and thigh muscle CSA, non-jumpers had significantly lower total hip vBMD (adjusted mean 240.8 vs. 254.1 mg/cm<sup>3</sup>), lower femur neck vBMD (252.3 vs. 266.7 mg/cm<sup>3</sup>) particularly at superior posterior quadrant (integral vBMD 120.2 vs. 131.6 mg/cm<sup>3</sup>), and higher buckling ratio (BR, 14.2 vs. 12.5, P<0.05 for all) compared to high jumpers. Among subjects who jumped (N=448), higher jump power (per 1 standard deviation increase, 5.8 W/kg) was robustly associated with greater integral vBMD (β=5.38, P=0.009) and cortical thickness (β=0.06, P=0.010) at superior posterior quadrant of femur neck, whereas the association was attenuated at other quadrants after adjustment for age, sex, height, thigh muscle CSA, regular exercise, and serum bone turnover markers.

In conclusion, peak jump power was positively associated with vBMD and cortical thickness of femur neck, particularly at superior posterior quadrant, independent of age, sex, height, and lower extremity muscle mass in community-dwelling elderly, suggesting the localized interplay between lower extremity muscle and bone.

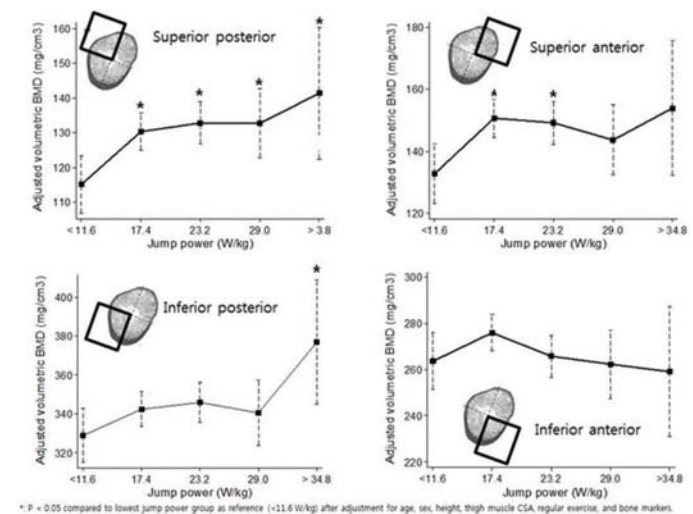


Figure 1: Distinctive impact of jump power on volumetric BMD of femur neck quadrants

Disclosures: Namki Hong, None.

## FR0357

**A Quantitative Frailty Index Predicts Falls and Fractures in 75y Old Community Dwelling Women – A 10 Year Longitudinal Study.** Kristina Akesson\*, Patric Bartosch, Linnea Malmgren, David Buchebner, Fiona E McGuigan. Lund University, Sweden

Background: Fragility fractures related to osteoporosis are a significant cause of disability, pain and reduced quality of life. With aging and the inevitable functional decline that goes with it, almost every second woman will suffer a fracture by the age of 80. One way of



preventing fractures may be identification of the frailest who are vulnerable to falls for targeted fracture management.

**Objective:** The aim of this study was i) to describe frailty over 10 years of follow-up in community-dwelling older women and ii) Describe the relationship between frailty, falls and fractures.

**Methods:** The OPRA cohort consists of 1044 women, all aged 75 at baseline and attended followup visits age 80 and 85. Falls occurring within the previous 12 months were recorded and prospective fractures continuously monitored. We created a frailty score of deficits in health using 13 key variables (including mobility, muscle strength, co-ordination, major diseases, polypharmacy). The index ranged from 0 (lowest) to 1 (highest). Frailty was analysed as a continuous variable or Q1 = lowest level of frailty; Q4 = highest level of frailty.

**Results:** Over 10-years frailty score increased from 0.17 at 75y; 0.24 at 80y to 0.32 at 85y – equivalent to an annual progression of 6-7%. The frailest women had poorer balance, lower muscle strength and higher polypharmacy (all  $p < 0.001$ ). Compared to the least frail group, more than three times as many women had falls in the highly frail group (14.2% vs 45.2%;  $p < 0.001$ ), a trend continuing across follow-up (80y: 26.8% vs 41%;  $p = 0.012$ ; 85y: 38.2% vs 63.6%;  $p = 0.017$ ). At 10-years hip, but not osteoporotic, fractures showed a stepwise increase across quartiles of frailty (Q1 8.4% vs Q4 16.1%,  $p = 0.007$ ). Frailty status influenced time-to-fracture, with the frailest women suffering a hip fracture on average 2-years earlier than the least frail women ( $p = 0.004$ ).

**Summary and Conclusions:** Assessment of frailty may be an important instrument in fracture management to prevent or minimise falls in community-dwelling older individuals.

**Disclosures:** Kristina Akesson, None.

## FR0358

**Greater abdominal adiposity is associated with lower muscle quality, but not with muscle strength or performance in men and women: The Framingham Study.** Robert McLean<sup>\*1</sup>, Xiaochun Zhang<sup>2</sup>, Shivani Sahni<sup>1</sup>, Thomas Trivison<sup>1</sup>, Marian Hannan<sup>1</sup>, Douglas Kiel<sup>1</sup>. <sup>1</sup>Hebrew SeniorLife Institute for Aging Research and Harvard Medical School, United States, <sup>2</sup>Hebrew SeniorLife Institute for Aging Research, United States

Age-related increases in fat mass may contribute to sarcopenia. One previous study suggests greater total fat mass is associated with lower muscle quality (strength per unit muscle mass) and accelerated loss of lean mass. Higher total fat mass is also associated with functional limitations and poor mobility, yet central adiposity may be an even stronger predictor. It is unclear if central adiposity or specific abdominal fat depots play a role in sarcopenia. The objective of this cross-sectional study was to determine the associations of overall adiposity (BMI), abdominal adiposity (waist circumference, WC) and abdominal visceral (VAT) and subcutaneous (SAT) adipose tissue volumes with grip strength, muscle quality and chair stand time among 1,173 participants (53% women) in the community-based Framingham Offspring cohort. VAT and SAT volumes (cm<sup>3</sup>) were assessed by multidetector CT imaging, and maximum grip strength (kg) by isometric dynamometer. Muscle quality (kg/kg) was calculated as grip strength divided by arm lean mass from DXA. Time (sec) required to rise from a chair 5x without using arms was recorded. Sex-specific linear regression was used to calculate the differences ( $\beta$ ) in grip strength, muscle quality and chair stand time associated with 1 SD greater BMI. BMI was highly correlated with WC ( $r \geq 0.89$ ), SAT ( $r \geq 0.74$ ) and VAT ( $r \geq 0.63$ ) in both sexes (all  $P < 0.01$ ), thus regression models for WC, VAT and SAT were calculated for separate BMI strata ( $< 30$  kg/m<sup>2</sup> vs.  $\geq 30$  kg/m<sup>2</sup>). Models adjusted for age, height, physical activity, smoking, and menopause status (women). Mean age was 60 years (range 36-83), mean BMI was 28 kg/m<sup>2</sup> (range 16-53). Higher BMI was associated with greater grip strength ( $\beta = 0.8$ ,  $P = 0.03$ ), lower muscle quality ( $\beta = -1.1$ ,  $P < 0.01$ ) and longer chair stand time ( $\beta = 0.4$ ,  $P < 0.01$ ) in women, and with lower muscle quality ( $\beta = -0.7$ ,  $P < 0.01$ ) and longer chair stand time ( $\beta = 0.4$ ,  $P < 0.01$ ) in men. WC, SAT and VAT were not associated with grip strength or chair stand time in either BMI group (Table). In women, higher WC, SAT and VAT were associated with lower muscle quality. In men, greater WC in both BMI groups and higher SAT in the BMI  $< 30$  group were associated with lower muscle quality. Although this study was limited by its cross-sectional design, results suggest that central adiposity and specific abdominal fat depots may contribute to age-related decline in muscle quality. Analyses are underway exploring adipocytokines as a possible mechanistic link.

Table. Multivariable-adjusted<sup>a</sup> linear regression coefficients (SE) for the difference in grip strength (kg), muscle quality (kg/kg) and chair stand time (sec) associated with a 1 SD increase in waist circumference (WC, inches), SAT (cm<sup>2</sup>) and VAT (cm<sup>3</sup>) by BMI group, among men and women in the Framingham Offspring cohort.

Outcome	Central adiposity	Men		Women	
		BMI $< 30$ kg/m <sup>2</sup> (n=385)	BMI $\geq 30$ kg/m <sup>2</sup> (n=164)	BMI $< 30$ kg/m <sup>2</sup> (n=454)	BMI $\geq 30$ kg/m <sup>2</sup> (n=170)
Grip strength	WC	-0.2 (0.8)	-1.2 (1.0)	0.5 (0.6)	-0.8 (0.9)
	SAT	-1.1 (0.8)	-1.6 (0.8)	-0.1 (0.5)	-1.4 (0.8)
	VAT	0.6 (0.6)	-0.3 (1.0)	0.6 (0.5)	-0.8 (0.6)
Muscle quality	WC	-0.7 <sup>b</sup> (0.1)	-0.4 <sup>c</sup> (0.2)	-0.7 <sup>b</sup> (0.2)	-1.0 <sup>b</sup> (0.2)
	SAT	-0.5 <sup>b</sup> (0.1)	-0.2 (0.1)	-0.7 <sup>b</sup> (0.1)	-0.8 <sup>b</sup> (0.2)
	VAT	-0.1 (0.1)	-0.1 (0.1)	-0.4 <sup>b</sup> (0.1)	-0.5 <sup>b</sup> (0.1)
Chair stand time	WC	0.3 (0.3)	0.7 <sup>c</sup> (0.3)	0.3 (0.2)	0.5 (0.3)
	SAT	-0.01 (0.2)	0.1 (0.3)	-0.1 (0.2)	-0.2 (0.3)
	VAT	0.1 (0.2)	0.03 (0.3)	0.3 (0.2)	0.2 (0.2)

<sup>a</sup>Adjusted for age, height, physical activity, smoking, and, in women, menopausal status.

<sup>b</sup> $P = 0.002$

<sup>c</sup> $P = 0.03$

Table

**Disclosures:** Robert McLean, None.

## FR0364

**Effect of Physical Activity on Frailty: A Secondary Analysis of the LIFE Randomized Controlled Trial.** Andrea Trombetti<sup>\*1</sup>, Mélanie Hars<sup>1</sup>, Fang-Chi Hsu<sup>2</sup>, Kieran Reid<sup>3</sup>, Timothy Church<sup>4</sup>, Thomas Gill<sup>5</sup>, Abby King<sup>6</sup>, Christine Liu<sup>7</sup>, Todd Manini<sup>8</sup>, Mary McDermott<sup>9</sup>, Anne Newman<sup>10</sup>, W. Jack Rejeski<sup>11</sup>, Jack Guralnik<sup>12</sup>, Marco Pahor<sup>8</sup>, Roger Fielding<sup>3</sup>.

<sup>1</sup>Division of Bone Diseases, Department of Internal Medicine Specialties, Geneva University Hospitals and Faculty of Medicine, Switzerland,

<sup>2</sup>Department of Biostatistical Sciences, Wake Forest School of Medicine, United States, <sup>3</sup>Nutrition, Exercise Physiology and Sarcopenia Laboratory,

Jean Mayer USDA Human Nutrition Research Center on Aging, Tufts University, United States, <sup>4</sup>Department of Preventative Medicine,

Pennington Biomedical Research Center, United States, <sup>5</sup>Department of Internal Medicine, Yale School of Medicine, United States, <sup>6</sup>Department of Health Research and Policy and Department of Medicine, Stanford

University, School of Medicine, United States, <sup>7</sup>Department of Medicine, Boston University School of Medicine, United States, <sup>8</sup>Department of Aging

and Geriatric Research, University of Florida, United States, <sup>9</sup>Department of Medicine and Preventive Medicine, Northwestern University, Feinberg

School of Medicine, United States, <sup>10</sup>Department of Epidemiology, Graduate School of Public Health, University of Pittsburgh, United States,

<sup>11</sup>Department of Internal Medicine, Wake Forest University and School of Medicine, United States, <sup>12</sup>Department of Epidemiology and Public Health,

University of Maryland School of Medicine, United States

Frailty, a state of increased vulnerability to stressor events, confers high risk for major negative outcomes, including disability and mortality. Limited evidence suggests that physical activity may help prevent frailty and associated negative outcomes in older adults; however definitive data from large, long-term, randomized trials are lacking. We aimed to determine whether a long-term structured, moderate-intensity physical activity program is associated with the risk of frailty and whether frailty status affects the reduction of major mobility disability observed with physical activity, in community-dwelling older people, using data from the Lifestyle Interventions and Independence for Elders (LIFE) trial.

The LIFE study was a multicenter, single-blind, randomized trial, conducted at eight field centers across the U.S., and who enrolled 1635 community-living participants aged 70-89 years with functional limitations. Participants were randomized to a structured, moderate-intensity physical activity program (n=818) that included aerobic, resistance, and flexibility training activities or a health education program (n=817) of educational workshops and upper extremity stretching exercises, and were followed for an average of 2.6 years. Frailty, as defined by the Study of Osteoporotic Fractures (SOF) index, was assessed at baseline, 6 months, 12 months, and 24 months. Major mobility disability was assessed for up to 3.5 years.

Over 24 months of follow-up, the risk of frailty was marginally reduced in the physical activity group compared with the health education group. The intervention was particularly beneficial on the chair rise criterion among the three criteria of the SOF index ( $P = 0.001$ ). The effect of the intervention on incident mobility disability did not significantly differ by frailty status at baseline ( $P$  for interaction=0.91).

A structured, moderate-intensity physical activity program appears to be only marginally associated with a reduced risk of frailty over two years among sedentary community-dwelling older adults. The beneficial effect of physical activity on incidence of major mobility disability does not differ between frail and non-frail individuals. Findings underline the feasibility and the importance of effective long-term community-based physical activity programs for vulnerable older adults.

**Disclosures:** Andrea Trombetti, None.

## SA0001

See Friday Plenary Number FR0001.

## SA0002

**Exome analysis of a large family with Familial Isolated Primary Hyperparathyroidism (FIHP) and multiple cancers.** Filomena Cetani<sup>1</sup>, Elena Pardi<sup>2</sup>, Simona Borsari<sup>2</sup>, Federica Saponaro<sup>2</sup>, Liborio Torregrossa<sup>3</sup>, Chiara Mazzanti<sup>4</sup>, Paolo Aretini<sup>4</sup>, Marco La Ferla<sup>4</sup>, Sara Franceschi<sup>4</sup>, Francesca Lessi<sup>4</sup>, Prospero Civita<sup>4</sup>, Claudio Marcocci<sup>2</sup>. <sup>1</sup>University-Hospital of Pisa, Italy, <sup>2</sup>Department of Clinical and Experimental Medicine, University of Pisa, Italy, <sup>3</sup>Department of of Surgical, Medical and Molecular Pathology and Critical Area, University of Pisa, Italy, <sup>4</sup>Fondazione Pisana per la Scienza ONLUS, Pisa, Italy

Familial Isolated Hyperparathyroidism (FIHP) is a hereditary disorder characterized by primary hyperparathyroidism (PHPT) with no evidence of other endocrine disorders. Germline *MEN1*, *CDC73* and *CASR* mutations have been identified, but the majority of FIHP has still unrecognized causes.

The aim of this study was to identify, by whole-exome sequencing, novel gene alterations in a large FIHP kindred.

The family's proband, her sister, brother and niece were affected by PHPT. The proband was negative at *MEN1*, *CDC73* and *CASR* gene mutations by Sanger analysis. The proband, her sister and niece were also affected by papillary thyroid carcinoma, the brother had Non-Hodgkin Lymphoma and bladder cancer. The proband had also a moderate colorectal polyposis and the niece a renal angiomyolipoma. We analyzed the proband, two affected and two healthy family's members with the Illumina NextSeq550 platform. The raw data were converted using Bcl2toFastq tools. Data analysis was performed by the SeqMule pipeline. The three affected individuals, but not the healthy relatives, shared 57 rare genetic variants. A more stringent filter related to genes involved in hereditary cancer detected one missense variant in the *APC* gene (V530A) in the three affected patients, subsequently confirmed by Sanger analysis. Moreover, the other affected relative and 2/15 healthy members carried the variant. The *APC* gene is involved in familial polyposis (FAP), an inherited disease marked by thousands colorectal polyps. The *APC* variant was predicted deleterious by three statistic model. Although the affected individuals don't have classical FAP features, the proband had the excision of two colonic polyps. We might speculate that the presence of non-truncating mutation could lead to a mild colonic phenotype, as showed in the attenuated FAP, characterized by the presence of <100 polyps. FAP tumor spectra is highly various, in about 2% of cases papillary thyroid carcinoma and bladder cancer have been reported.

**Disclosures:** Filomena Cetani, None.

## SA0003

See Friday Plenary Number FR0003.

## SA0004

See Friday Plenary Number FR0004.

## SA0005

**Relationship between muscle strength and bone mineral density in patients with class III obesity.** Florêncio Diniz-Sousa<sup>1</sup>, Giorjines Boppre<sup>1</sup>, Leandro Machado<sup>2</sup>, João Vilas-Boas<sup>2</sup>, Vitor Devezas<sup>3</sup>, John Preto<sup>3</sup>, Hugo Sousa<sup>3</sup>, José Oliveira<sup>1</sup>, Hélder Fonseca<sup>1</sup>. <sup>1</sup>CIAFEL, Faculty of Sport, University of Porto, Portugal, <sup>2</sup>CIFI2D, Faculty of Sport, University of Porto, Portugal, <sup>3</sup>Department of Surgery, Centro Hospitalar de São João, Portugal

**Purpose:** Lean mass has been suggested to be an independent predictor of total body, lumbar spine and hip bone mineral density (BMD) in overweight and obese patients. However, this relation has not been thoroughly investigated in extreme classes of obesity. Our purpose was to investigate the association between BMD and muscle strength, both absolute and relative to body weight and lean mass, in patients with class III obesity.

**Methods:** Sixteen patients with class III obesity (48.7±9.9 years, 47.6±1.8 kg/m<sup>2</sup> body mass index, 3 male and 13 female) were recruited between January 2016 and February 2017 from the obesity surgery consultation. BMD in the lumbar spine, lean mass and fat mass were measured by dual-energy X-ray absorptiometry (DXA). Muscle strength of the quadriceps and hamstrings was measured by isokinetic dynamometer during maximal dynamic concentric movement of the knee at 60°/s of angular velocity and between 0° (maximum knee extension) and 90° of flexion. Data were corrected for the gravity effect. The isokinetic peak torque was selected as a surrogate of muscle strength and was analyzed both in absolute terms and relative to body weight and lean mass. The Shapiro-Wilk test was used to verify the normality of the data distribution. The correlation between muscle strength and BMD was assayed by Pearson correlation coefficient. Patients were also divided in tertiles of muscle strength, and differences in BMD between tertiles were assayed by analysis of variance (ANOVA) with Bonferroni post hoc.

**Results:** Both absolute ( $r = 0.53$ ,  $p = 0.035$ ) and relative to body weight ( $r = 0.51$ ,  $p = 0.042$ ) peak knee flexion torque were shown to be significantly and positively correlated with lumbar spine BMD. Absolute and relative peak knee extension torque however, did not showed any significant correlation with lumbar spine BMD. Significant differences in the comparison of lumbar spine BMD between tertiles of relative to body weight peak knee flexion torque were also identified, with the groups of patients with higher strength displaying a significantly higher BMD ( $p = 0.016$ ).

**Conclusion:** Lumbar spine BMD displays a significant positive correlation with hamstrings muscle strength in patients with class III obesity.

**Disclosures:** Florêncio Diniz-Sousa, None.

## SA0006

**Incidence and Prevalence of Post-surgical Hypoparathyroidism in Korea.** Eunhyun Jee<sup>\*1</sup>, So Young Park<sup>2</sup>, Song Vogue Ahn<sup>3</sup>, Sihoon Lee<sup>1</sup>. <sup>1</sup>Gachon University School of Medicine, Korea, Republic of, <sup>2</sup>Cheil General Hospital, Dankook University College of Medicine, Korea, Republic of, <sup>3</sup>Yonsei University Wonju College of Medicine, Korea, Republic of

**Objective** The epidemiology of post-surgical hypoparathyroidism(hypoPT) in Korea is not known well. This study aimed to investigate the prevalence and incidence of post-surgical hypoPT in Korea.

**Methods** Health insurance claims data for patients with a diagnosis of post-surgical hypoPT were extracted from the database of the National Health Insurance Sharing Service (NHSS) provided by National Health Insurance Corporation (NHIC) in Korea which covers almost all Korean residents approximately 50 million in total including detailed files of the outpatient, emergency, inpatient and pharmacy treatment records from January 1, 2003 to December 31, 2015. Post-surgical hypoPT was identified using ICD-10-CM diagnostic codes as well as following neck surgery that necessitated treatment with calcium and/or vitamin D analog supplementation for more than 2 times a year.

**Results** During the study years, prevalence of post-surgical hypoPT increased from 0.0016% to 0.013%. The incidence (per 100,000) increased throughout the years from 3.02 (2.87-3.18) in 2008 to 6.07 (5.86-6.28) in 2014. However, the incidence dropped abruptly in the year 2015 to 3.24 (3.25-3.57). The incidence was generally low compared to the previous study performed in other countries potentially thanks to advances in surgical skills to localize and preserved the unaffected parathyroid gland(s).

**Conclusions** This study demonstrated a substantial increasing trend in post-surgical hypoPT prevalence during 2003-2014 in Korea but relatively lesser than other countries. The reason why the incidence was suddenly decreased in 2015 might be the recognition of thyroid cancer over-diagnosis issue leading inevitably to more surgical complications such as hypoPT.

**Disclosures:** Eunhyun Jee, None.

## SA0007

See Friday Plenary Number FR0007.

## SA0008

See Friday Plenary Number FR0008.

## SA0009

**Influence of obesity on Trabecular Bone Score remains after parathyroidectomy in Primary hyperparathyroidism.** Donovan Tay<sup>\*</sup>, Natalie Cusano, John Williams, Beatriz Omeragic, John Bilezikian. Columbia University Medical Center, Dept of Medicine Endocrinology, United States

Trabecular bone score (TBS) is an indirect measure of bone microstructure. Better bone microstructure is reflected as a more homogenous pixel variation and a higher TBS while inferior skeletal microstructure exhibits a more heterogeneous pixel variation and a lower TBS. The tertiles of TBS are: ≤1.2 (degraded); 1.20-1.35 (partially degraded); and ≥1.35 (normal). The influence of adiposity on skeletal microstructure in primary hyperparathyroidism (PHPT) is of interest because PTH influences osteoblast and adipocyte lineage. Although TBS is inversely related to BMI in subjects without PHPT, whether a relationship exists in PHPT and/or differs from what has been described among normal subjects is not known. If there is a difference between TBS among normal and obese subjects with PHPT, it is not known if such differences are affected by parathyroidectomy (PTX).

We studied 28 patients who underwent PTX. TBS was calculated from the L1-L4 DXA image (Hologic) using TBS iNspire®, version 2.1 software. Presence of diabetes mellitus, a BMI >37 or <15 kg/m<sup>2</sup> or current users of bisphosphonates or denosumab were excluded. The 2 groups were defined by the BMI threshold value of 30. Paired sample t-test was used for within group comparison of the TBS value at 5 time points while independent t-test was used for between group comparisons.

The cohort (mean age: 63±12yrs; PHPT duration: 5.5±6.8yrs) were mostly Caucasian (89%), female (71%) and postmenopausal (85%). At baseline, the mean TBS for the cohort was low at 1.27±0.11. There was a significant inverse relationship between baseline TBS and BMI ( $r = -0.458$ ,  $p = 0.019$ ). Non-obese patients had significantly higher TBS values than obese patients at all 5 time points (Baseline: 1.31±0.10 vs 1.21±0.09,  $p = 0.026$ ; 6m: 1.32±0.13 vs



1.21±0.09, p=0.024; 12m: 1.33±0.10 vs 1.21±0.08, p=0.004; 18m: 1.30±0.14 vs 1.18±0.06, p=0.036; 24m: 1.33±0.12 vs 1.18±0.06, p=0.005). There was no significant change in TBS after PTX up to 24m in the non-obese group. However, there was a significant decrease in TBS at 18m compared to 12m and a trend towards significant decrease in TBS at 24m compared to 12m in the obese group. How these changes relate to post-PTX changes in body composition, PTH, calcium and vitamin D levels remain to be elucidated.

We demonstrate for the first time that obesity is associated with reduced TBS in PHPT. These results may be accounted for, in part, by the actions of PTH on osteoblast and adipocyte lineage and function.

**Disclosures:** Donovan Tay, None.

## SA0010

**Hypophosphatemic Osteomalacia: a Diagnosis Often Overlooked.** Annegreet Veldhuis-Vlug<sup>\*1</sup>, Marlous Rotman<sup>2</sup>, Peter Bisschop<sup>1</sup>, Natasha Appelman-Dijkstra<sup>2</sup>. <sup>1</sup>Academic Medical Center Amsterdam, Netherlands, <sup>2</sup>Leiden University Medical Center, Netherlands

We present two patients (females aged 39 and 45), previously diagnosed with fibromyalgia and chronic back pain and treated by a psychiatrist, who were referred to our departments for a second opinion. Both women suffered from progressive bone pain and muscle weakness leading to wheelchair dependency. Physical examination showed proximal muscle weakness and abnormal reflexes of the lower extremities.

Biochemical analysis showed a low phosphate (0.5 and 0.2 mmol/L, ref 0.9-1.5mmol/L), high alkaline phosphatase activity (377 and 200 U/L) and normal calcium and parathyroid hormone concentrations. 24-hour urine collections showed excessive renal phosphate wasting. Radiological examination showed multiple fractures at the painful locations. These findings were consistent with a diagnosis of hypophosphatemic osteomalacia. Since in both cases there were no signs of underlying tubular disease, interfering drugs or congenital disease, tumor-induced osteomalacia was considered the most likely diagnosis. Indeed fibroblast growth factor-23 (FGF-23) concentrations were inappropriately elevated confirming FGF-23 overproduction. Both patients were treated with phosphate and 1,25 (OH) vitamin D supplementation which improved their symptoms.

FGF-23 producing tumors are of mesenchymal origin and express the somatostatin receptor and therefore a gallium-68-dotatate PET/CT scan was performed to localize the tumor. A gallium-68-dotatate positive lesion was identified in the left vastus medialis in patient A and in the sixth rib in patient B. After surgical resection of the tumors, phosphate concentrations normalized, providing curative treatment.

These cases illustrate the challenge in establishing the diagnosis tumor induced osteomalacia and underline the importance of phosphate measurements in chronic bone pain.

**Disclosures:** Annegreet Veldhuis-Vlug, None.

## SA0011

See Friday Plenary Number FR0011.

## SA0012

See Friday Plenary Number FR0012.

## SA0013

**Relationship between cortical and trabecular microstructure and estimated strength of vertebral bone: an ex vivo HR-pQCT study.** Ko Chiba<sup>\*</sup>, Narihiro Okazaki, Kazuaki Yokota, Kazuteru Shiraishi, Makoto Osaki. Nagasaki University, Japan

**Introduction:**

High Resolution peripheral Quantitative CT (HR-pQCT) is a useful tool for ex vivo scans of relatively larger bone samples up to 14cm of diameter, when compared with an experimental micro CT. The aim of this study is to investigate the relationship between cortical and trabecular microstructure and estimated strength of cadaveric human vertebral bones using HR-pQCT.

**Methods:**

Whole spines were extracted from two Japanese cadavers (76 and 81 years, female) and scanned by HR-pQCT (XtremeCT II, Scanco Medical, Switzerland) at the voxel size of 61µm. In a total of 42 vertebra (21 vertebra from 2 cadavers: 3rd to 7th cervical, 1st to 12th thoracic, and 1st to 4th lumbar vertebra), trabecular bone microstructure (two types of region of interest (ROI) : cylindrical and whole ROI) and cortical bone microstructure were measured. Estimated bone strength to vertical compression load was also calculated by the finite element method (TRI/3D-BON, Ratoc System Engineering Co., Ltd., Japan). The correlation between bone microstructure and estimated strength was analyzed.

**Results:**

Correlation coefficients between bone microstructure and estimated failure load were as follows: Cylindrical ROI: trabecular bone volume fraction (BV/TV) 0.40, trabecular thickness (Tb.Th) 0.57. Whole ROI: BV/TV 0.40, Tb.Th 0.63. Cortical bone: cortical thickness (Ct.Th): 0.69. (p<0.01)

**Conclusion:**

It is generally thought that the strength of vertebral bones depends mainly on trabecular bones, not on cortical bones. However, this study indicates the possibility that cortical

thickness serves as important a role as trabecular bones for the strength to vertical compression.

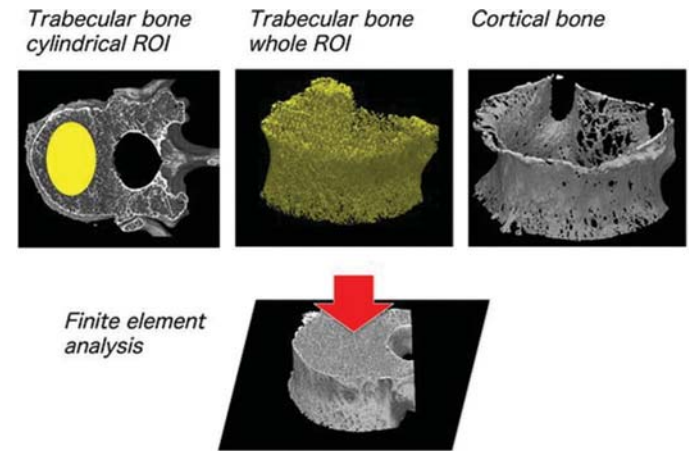


Figure 1

**Disclosures:** Ko Chiba, None.

## SA0014

See Friday Plenary Number FR0014.

## SA0015

**A Novel Measurement of Regional Bone Mineral Density Around the Pedicle Screw Using QCT Has a Positive Correlation with Screw Insertional Torque in Posterior Lumbar Fixation.** Koji Ishikawa<sup>\*</sup><sup>1</sup>, Tomoaki Toyone<sup>1</sup>, Toshiyuki Shirahata<sup>1</sup>, Yoshifumi Kudo<sup>1</sup>, Akira Matsuoka<sup>1</sup>, Hiroshi Maruyama<sup>1</sup>, Soji Tani<sup>2</sup>, Koki Tsuchiya<sup>1</sup>, Takashi Nagai<sup>1</sup>, Katsunori Inagaki<sup>1</sup>.

<sup>1</sup>Department of Orthopaedic Surgery, Showa University School of Medicine, Japan, <sup>2</sup>Department of Orthopaedic Surgery, Showa University School of Medicine, Tokyo, Japan, Japan

**Introduction:** Pedicle screw fixation system is the gold standard technique for spinal fusion in treating various spinal disorders. Despite the advantage of biomechanical stability, screw loosening is a common complication. In previous studies, pullout strength and screw insertional torque are correlated and it most importantly affected by bone mineral density (BMD). Although the density and structure of vertebral body is not homogeneous, no study has yet been conducted to evaluate the relationship between screw insertional torque and regional BMD around the pedicle screw *in vivo*.

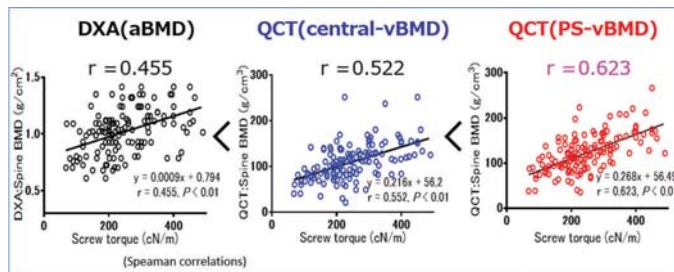
**Purpose:** The objective of this study was to investigate the feasibility of regional BMD around the pedicle screw before operation in patients undergoing transpedicular fixation.

**Study Design:** Prospective feasibility study on consecutive patients.

**Methods:** There were 16 men and 34 women, with an average age of 75.4 years (range, 64-84). These consecutive patients scheduled for transpedicular fixation was evaluated for BMD before operation, which was measured globally by DXA and regional BMD around the pedicle screw (PS-vBMD) using QCT. Of all, 190 screws (diameter: 7.5-8.5 mm, length: 40-45, inserted from L1 to L5) were eligible for this study and were analyzed to identify the factors contributing to the insertional torque. The following factors were investigated; age, pedicle diameter, screw diameter, screw length, bone turnover markers, DXA: spine and hip aBMD, and QCT: spine vBMD / PS-vBMD.

**Results:** The insertional torque exhibited significant correlations with each BMD measurement and showed a stronger correlation with PS-vBMD [DXA: TH-aBMD; (r=0.40, P<0.01), FN-aBMD; (r=0.42, P<0.01), spine-aBMD; (r=0.45, P<0.01), QCT: central-vBMD; (r=0.58, P<0.01), PS-vBMD; (r=0.64, P<0.001)](Figure). Multiple regression analysis showed that age, pedicle diameter, PS-vBMD were significant independent factors affecting screw insertional torque.

**Conclusion:** The preoperative measurement of PS-vBMD was technically feasible and reliably predictive of screw insertional torque during transpedicular fixation in a clinical setting. Larger studies are needed to define specific thresholds that indicate a need for additional technique to increase screw purchase.



Correlations between screw insertional torque and BMD measurement

**Disclosures:** Koji Ishikawa, None.

## SA0016

**Voluntary Jumping Exercise in Rats Prior to Unloading Prevents Unloading-related Bone Loss.** Scott Lenfest<sup>1</sup>, Jennifer Kosniewski<sup>1</sup>, Corinne Metzger<sup>2</sup>, Jessica Brezicha<sup>3</sup>, Jon Elizondo<sup>4</sup>, Amelia Looper<sup>4</sup>, Susan Bloomfield<sup>2</sup>, Harry Hogan<sup>5</sup>. <sup>1</sup>Texas A&M University Department of Mechanical Engineering, United States, <sup>2</sup>Texas A&M University Department of Health & Kinesiology, United States, <sup>3</sup>Texas A&M University Department of Biomedical Engineering, United States, <sup>4</sup>Texas A&M University College of Veterinary Medicine, United States, <sup>5</sup>Texas A&M University Departments of Mechanical Engineering and Biomedical Engineering, United States

Resistance exercise is an important component of in-flight countermeasures for mitigating microgravity-induced bone loss in astronauts. The hindlimb unloading rat model allows for ground-based study of skeletal effects due to simulated microgravity, but simulating exercise is more challenging in this animal model. Even so, voluntary resistance exercise through operant conditioning has been effective in enhancing bone properties of adult rats in recent studies [1,2]. The goal of our current study was to assess the efficacy of a voluntary jumping exercise (VJE) protocol that uses positive reinforcement.

Adult male rats (5 mo.) were placed in a custom jumping cage and trained over 5 weeks to jump onto a 10" platform. Rats were then assigned to aging control (AC, n=19), hindlimb unloading control (HU, n=8) or exercise (VJE, n=16) groups by body weight and jumping ability. VJE animals performed 30 jumps/d, 5 d/wk, for 4 wks at an average rate of 1 jump each 20-25 sec. After the 28d exercise period, HU and VJE animals experienced 28d of unloading. *In vivo* pQCT scans of the proximal tibia metaphysis (PTM) were taken before (d0) and after (d28) VJE pre-treatment, and at the end of HU (d56). Static cancellous histomorphometry (SCH) was performed on the proximal tibia metaphysis of bones harvested at the end of HU (d56).

For the PTM, 28 days of exercise resulted in significantly higher values in total BMC (+11.5%), total vBMD (+6.8%), cortical BMC (+12.5%), and cortical area (+10.5%) for the VJE group compared to AC. Cancellous vBMD also trended higher for VJE (8.5%) compared to AC. After 28 days of HU, the VJE group had significantly higher total BMC and cancellous vBMD (+14.3%, +25.5%, resp.) compared to HU, and neither were different from AC. Total vBMD for the VJE group also trended higher compared to both HU (+7.1%) and AC (+2.4%). SCH, performed on a subset of n=4 per group, demonstrated that cancellous bone volume and trabecular thickness were significantly lower for HU compared to AC (-22.7%, -26.4%, resp.), but VJE protected against these declines.

These data indicate that our new VJE protocol induces an anabolic bone response that conserved bone integrity, particularly in the cancellous compartment, during a subsequent period of disuse. These findings have important implications for situations when patients on bed rest or crew members aboard ISS are unable to exercise.

1. Swift et al. (2010) J Appl Physiol 109:1600.
2. Shirazi-Fard et al. (2014) Bone 66:296.

**Disclosures:** Scott Lenfest, None.

## SA0017

See Friday Plenary Number FR0017.

## SA0018

**Sex-Related Differences in Endplate Porosity and its Correspondence to Vertebral Strength.** Elise Morgan\*, Timothy Jackman, Amira Hussein, Cameron Curtiss. Boston University, United States

Epidemiological data suggest that the pathogenesis of vertebral fractures may not be the same between men and women. Recent evidence from biomechanical studies indicates that the vertebral endplate is critically involved in the mechanisms of vertebral fracture: the onset of endplate deflection during mechanical loading coincides with a pronounced drop in the ability of the vertebra to support loads and is associated with the local microstructure of the endplate region. The goal of this study was to investigate sex-related differences in the endplate microstructure and its correspondence to vertebral strength. Cadaveric, spine segments (T7-T9; 16 male, 12 female; mean+/-stdev in age = 72+/-11 years) were imaged via

quantitative computed tomography to measure integral BMD (In.BMD) and micro-computed tomography to measure endplate porosity and microstructural properties of the 5mm-thick layer of trabecular bone immediately underlying the endplate. The spine segments were compressed to failure in axial compression (n=14) or axial compression with anterior flexion (n=14). Each microstructural parameter was compared between sexes via a t-test and analysis of covariance (ANCOVA) with age and In.BMD as covariates. Regression analysis was used to examine the potential sex-dependence of a correspondence between vertebral compressive strength on endplate porosity. We found that endplate porosity was 19.3% higher (p=0.012), and that the trabecular degree of anisotropy (DA) was 5.0% higher (p=0.050), in female than in male vertebrae. The difference in endplate porosity between sexes persisted even after adjustment for In.BMD and age (Figure. 1), whereas the difference in trabecular DA did not. No sex differences in any other microstructural parameters (including trabecular BV/TV) were found (p>0.110). We found a strong trend towards a dependence of compressive strength of the vertebra on endplate porosity for both sexes (r<sup>2</sup>=0.507, p=0.060); however, the dependence tended to be stronger in female than male vertebra (p=0.060 for the interaction between sex and endplate porosity). In contrast, the dependence of vertebral compressive strength on In.BMD did not differ between sexes (p=0.670). These results indicate a sex-dependent, BMD-independent difference in microstructure specifically in a region that is biomechanically critical in the process of vertebral failure. Endplate porosity may be associated with the higher rates of vertebral fracture in women vs. men.

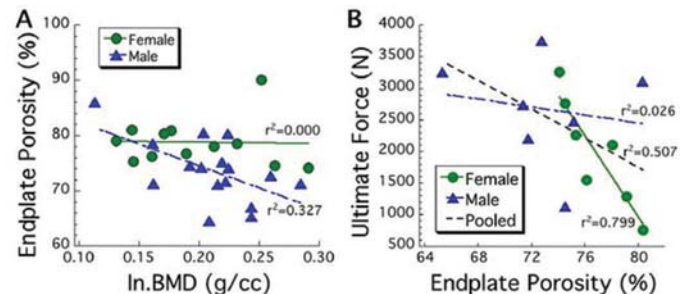


**Figure 1.** Endplate porosity is (A) higher in women than in men, even after adjustment for In.BMD and (B) more strongly associated with vertebral strength in women than in men.

Figure 1

**Disclosures:** Elise Morgan, None.

## SA0019

**Multiscale characteristics of toughness in Lrp5<sup>A214v/A214v</sup> mice.** Sabah Nobakhti\*, Sandra Shefelbine. Northeastern University, United States

**Introduction:** Bone is a multi-layered composite material with various toughness mechanisms acting at its different length scales. At the nanoscale, bone is composed of collagen and mineral crystals. Alterations in quantity/quality of the collagen and mineral at the nanoscale influences toughness in bone hierarchy. We hypothesized that bone with a higher mean elastic modulus has decreased fracture toughness, and elastic modulus heterogeneity promotes crack propagation toughness.

**Method:** It has been previously shown that Lrp5<sup>A214v/A214v</sup> model has a high bone mass phenotype and increased energy to failure compared to controls [1]. We chose this model (female, 8 weeks) and compared that with a standard C57BL/6 model (female, 10 weeks) in a multiscale analysis. At the nano-scale, we investigated crystal size with wide angle x-ray diffraction analysis on the humerus (n=5/group). At the micro-scale, we looked at mineral to matrix ratio by thermogravimetric analysis on humerus (n=5/group), degree of mineralization by quantitative backscattered scanning electron microscopy on tibia (n=5/group), and the elastic modulus by nano-indentation on tibia (n=1/group, more than 100 indents on the bone). Heterogeneity was characterized by histogram full width at half max (FWHM) for the degree of mineralization. At the whole bone level, fracture toughness resistance curve was characterized by notched three-point bending experiments on femurs (n=1/group).

**Results:** Initial resistance curve measurements indicated a reduction in fracture toughness but an increase in crack initiation and growth toughness in Lrp5<sup>A214v/A214v</sup> mouse compared to control (Fig. 1). Elastic modulus and degree of mineralization were significantly higher in Lrp5<sup>A214v/A214v</sup> mice compared to controls (Table 1). Material heterogeneity (FWHM) and the crystal size were not significantly different between the groups. Mineral to matrix ratio was significantly higher in Lrp5<sup>A214v/A214v</sup> compared to controls.

**Discussion:** Higher amount of mineral in Lrp5<sup>A214v/A214v</sup> bone would likely result in an increase in the degree of mineralization and higher elastic modulus. Initial crack resistance curve measurements confirmed that a higher mean elastic modulus results in decreased fracture toughness. The standard deviation of all the elastic modulus measurements was higher in Lrp5<sup>A214v/A214v</sup>, which could possibly explain the increase in crack growth toughness in this model.

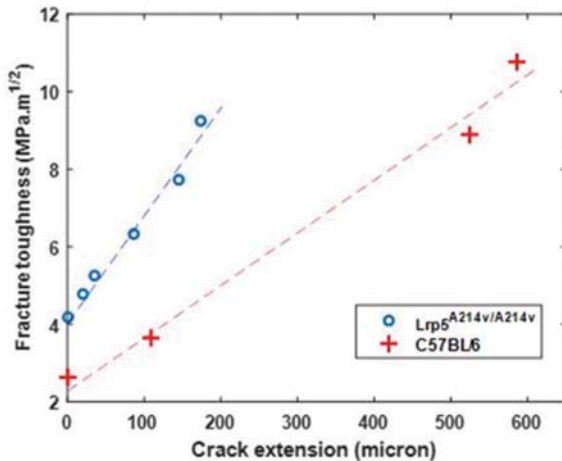
**References:**

- [1] Cui, Yajun, et al., Nature medicine, 2011.



Table 1- Results of the multiscale analysis.

Measurement	Lrp5 <sup>A214v/A214v</sup>	C57BL/6	Significance
Crystal size (nm)	13.8±1.3	15.0±0.3	n.s.
Mineral/matrix (mg/mg)	3.2±0.1	3.0±0.1	p < 0.05
Degree of mineralization (calibrated gray value)	179.2±1.8	170.0±3.1	p < 0.05
FWHM (calibrated gray value)	19.1±1.3	18.3±1.9	n.s.
Elastic modulus (GPa)	22.8±2.6	19.4±2.1	p < 0.01
Crack initiation toughness (MPa.m <sup>1/2</sup> )	4.2	2.7	-
Crack growth toughness (MPa.m <sup>1/2</sup> /micron)	0.03	0.01	-
Fracture toughness (MPa.m <sup>1/2</sup> )	9.3	10.8	-

Fig. 1- Crack resistance curve for Lrp5<sup>A214v/A214v</sup> and C57BL/6 bone

Multiscale analysis of toughness

Disclosures: Sabah Nobakhti, None.

## SA0020

See Friday Plenary Number FR0020.

## SA0021

Streptomycin attenuates the effects of electrical stimulation-induced muscle contraction on reducing trabecular bone loss in the early stages of disuse in old rats. Hiroyuki Tamaki<sup>1</sup>, Kengo Yotani<sup>2</sup>, Futoshi Ogita<sup>2</sup>, Hikari Kirimoto<sup>1</sup>, Kaishi Hayao<sup>1</sup>, Hideaki Takahashi<sup>1</sup>, Keigo Tamakoshi<sup>1</sup>, Atsuhiko Tsubaki<sup>1</sup>, Hideaki Onishi<sup>1</sup>, Norikatsu Kasuga<sup>3</sup>, Noriaki Yamamoto<sup>4</sup>. <sup>1</sup>Niigata University of Health and Welfare, Japan, <sup>2</sup>National Institute of Fitness and Sports in Kanoya, Japan, <sup>3</sup>Aichi University of Education, Japan, <sup>4</sup>Niigata Rehabilitation Hospital, Japan

Limb disuse due to denervation causes musculoskeletal atrophy, together with changes in the structural and functional profile of bone such as reduction in trabecular bone mass, impairment of bone architecture, and deterioration of bone strength. Findings from animal studies suggest that electrical stimulation (ES)-induced muscle contraction has multiple effects on reducing the muscle and bone loss caused by disuse. However, whether the effects of ES are associated with mechanosensors in bone tissue or with stimulated skeletal muscle mass remains unknown. We tested the hypothesis that streptomycin, a stretch-activated channel (SAC) blocker, can abolish the reduction in bone loss elicited by ES in old rats.

Direct ES was applied to the tibialis anterior (TA) muscle after sciatic denervation in 2.0-2.5 years old male rats divided into groups as follows: control (CON); denervation (DN); denervation with direct ES (DN+ES); and DN with ES treated with streptomycin (DN+ES+Str). ES was performed at an intensity of 16 mA and a frequency of 10 Hz for 30 min/day for 1 week. TA muscle weight was determined, and the metaphyseal trabecular regions of the tibiae were analyzed using 3D micro CT and histomorphometry.

Significant loss of trabecular bone in the tibiae and TA muscle was evident in the DN rats. Trabecular bone volume fraction (BV/TV), thickness (Tb.Th), connectivity density (Conn.D.), osteoid thickness (O.Th), and DMP1 immunoreactivity were greater in DN+ES compared with DN rats at 1 week after denervation. However, these parameters

were lower in the DN+ES+Str than in the DN+ES group, without the differences in TA muscle weight.

These findings suggest that ES-induced muscle contraction reduced trabecular bone loss, and that streptomycin treatment did not induce bone loss but did attenuate the effects of ES-induced muscle contraction on reducing the loss of disused bone in old rats.

Disclosures: Hiroyuki Tamaki, None.

## SA0022

Prediction of Distal Radius Failure Load Using Finite Element Modeling of Peripheral Quantitative Computed Tomography (pQCT-FE): A Validation Study. Hongyuan Jiang<sup>\*1</sup>, Dale L Robinson<sup>1</sup>, Saija Kontulainen<sup>2</sup>, James D Johnston<sup>2</sup>, Peter VS Lee<sup>1</sup>, John D Wark<sup>1</sup>, Matthew McDonald<sup>3</sup>. <sup>1</sup>The University of Melbourne, Australia, <sup>2</sup>University of Saskatchewan, Canada, <sup>3</sup>Department of Engineering, College of Engineering, University of Saskatchewan, Canada

**BACKGROUND** Finite element (FE) modeling based on peripheral quantitative computed tomography (pQCT-FE) has potential to estimate distal radius failure load non-invasively due to the volumetric and density distribution information acquired by pQCT. The objective of this study was to compare distal radius failure loads derived from biomechanical testing using cadaveric forearms with pQCT-FE estimates of bone mechanical properties.

**METHODS** Forty fresh-frozen cadaveric forearms were scanned at the distal end of radius (4% of length) using pQCT (Stratec XCT 3000). Specimens were then loaded to failure with either 15° inclination (n=21), which simulated bending and compressive loading experienced during a fall onto the outstretched hand, or no inclination (n=19), which simulated pure compressive loading. Peripheral QCT images were used to establish a cross-sectional FE model. Stiffness and strength of three loading cases were obtained from the FE models, including: compression, torsion and bending. Axial compression was simulated by a 0.01 mm displacement of the superior surface towards the inferior surface. Torsion was simulated by a 0.01° rotation of the inferior surface about the z-axis. Bending was simulated by a 0.01° rotation of the inferior surface about a bending axis aligned with inclination rotation axis.

**RESULTS** In specimens with 15° inclination, bone strength derived from FE analysis correlated well with experimental failure load ( $S_{compression}$ :  $r^2$  0.452;  $S_{torsion}$ :  $r^2$  0.570;  $S_{bending}$ :  $r^2$  0.615). In specimens with no inclination, moderate correlations were observed ( $S_{compression}$ :  $r^2$  0.264;  $S_{torsion}$ :  $r^2$  0.23;  $S_{bending}$ :  $r^2$  0.339).

**DISCUSSION** Our pQCT-FE model offered reasonable predictions of distal radius failure load acquired using experimental mechanical testing simulating a fall onto the outstretched hand associated with Colles' fracture. Future research will compare failure load with pQCT-FE analyses of the radial mid-shaft (radial diaphysis).

Table 1. Correlations between experimental failure load and pQCT-FE bone strength

	With 15° inclination		With no inclination	
	R <sup>2</sup>	p	R <sup>2</sup>	p
$S_{bending}$	0.615	<0.001	0.339	0.006
$S_{compression}$	0.452	<0.001	0.264	0.01
$S_{torsion}$	0.57	<0.001	0.230	0.02
$S_{bending}+S_{compression}$	0.616	<0.001	0.341	0.04
$S_{bending}+S_{torsion}$	0.621	<0.001	0.394	0.02
$S_{compression}+S_{torsion}$	0.568	0.001	0.268	0.09
$S_{bending}+S_{compression}+S_{torsion}$	0.625	0.001	0.406	0.06

Table 1: Correlations between experimental failure load and pQCT-FE bone strength

Disclosures: Hongyuan Jiang, None.

## SA0023

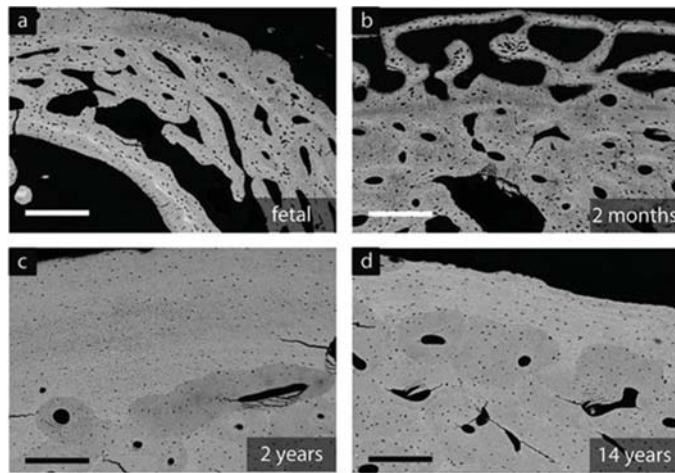
See Friday Plenary Number FR0023.

## SA0024

**Bone quality and mechanical competence during pediatric skeletal growth.**

Elizabeth Zimmermann<sup>1</sup>, Christoph Riedel<sup>1</sup>, Kilian Stockhausen<sup>1</sup>, Yuriy Chushkin<sup>2</sup>, Eric Schaible<sup>3</sup>, Felix Schmidt<sup>1</sup>, Bernd Gludovatz<sup>4</sup>, Eik Vettorazzi<sup>5</sup>, Frederico Zontone<sup>2</sup>, Klaus Püschel<sup>6</sup>, Michael Amling<sup>1</sup>, Robert Ritchie<sup>7</sup>, Björn Busse<sup>1</sup>. <sup>1</sup>Department of Osteology and Biomechanics, University Medical Center Hamburg, Germany, <sup>2</sup>European Synchrotron Radiation Facility, Grenoble, France, <sup>3</sup>Advanced Light Source, Berkeley, United States, <sup>4</sup>Lawrence Berkeley National Laboratory, United States, <sup>5</sup>Department of Medical Biometry and Epidemiology, University Medical Center Hamburg, Germany, <sup>6</sup>Department of Forensic Medicine, University Medical Center Hamburg, Germany, <sup>7</sup>Department of Materials Science and Engineering, University of California, Berkeley, United States

Thirty percent of children/adolescents experience a bone fracture. High fracture incidence was linked initially to cortical porosity (1); however, recent clinical studies find no correlation between cortical bone volume fraction and fracture risk (2,3). Thus, transitions in *bone quality* (i.e., structure, composition) may explain pediatric fracture risk. Here, bone quality was quantitatively investigated in a cross-sectional cohort between 22 weeks of gestation and 14 years from the mid-femoral diaphysis, allowing comparison between ages. Autopsy samples were separated into groups consisting of primary bone (fetal-1 year, n=4) or remodeled osteonal bone (2-14 years, n=4). The study was approved by the local Institutional Review Board. Histological sections were used to image bone structure, mineral distribution was measured with quantitative backscattered electron imaging (qBEI), collagen fiber orientation was imaged with polarized light microscopy and mechanical tests evaluated bone strength. The *primary bone* consisted of a porous scaffold of woven tissue (Fig. 1a,b). Comparatively, *remodeled bone* consisted of osteons with highly organized lamellae (Fig. 1c,d). Remodeled bone exhibited 29% greater cortical bone volume fraction (primary BV/TV = 0.73±0.06, osteonal BV/TV = 0.95±0.03, p=0.03) and 10% higher mineralization relative to primary bone (qBEI: primary CaMean = 22.3±1.2 CaWt%, osteonal CaMean = 24.5±0.5 CaWt%, p=0.03). These structural and compositional differences are associated with 160% larger stiffness (primary stiffness = 5.1±2.0 GPa, osteonal stiffness = 13.2±1.9 GPa, p=0.05) and 83% higher strength (primary strength = 73.5±18.1 MPa, osteonal strength = 134.3±20.4 MPa, p=0.05) in remodeled osteonal vs primary bone. Thus, higher bone volume fraction, osteonal organization and mineralization in *remodeled bone* enhance mechanical resistance. The limitations to the study include its cross-sectional design and unknown inter-individual differences, which may influence some observed differences. The implications of this study are that primary bone is inherently weaker than remodeled bone. As primary bone is present in the fetal/infantile skeleton and near sites of growth (i.e., growth plate), our results suggest primary bone quality during growth contributes to high fracture incidence in children/adolescents. (1) Parfitt, AM, Osteoporos Int, 3:382, 1994. (2) Määttä M, et al., Osteoporos Int, 26:1163, 2015. (3) Farr JN, et al., JBM, 29: 2193, 2014.



Transitions in bone mineralization from primary to osteonal bone

**Disclosures:** Elizabeth Zimmermann, None.

## SA0025

**Bone Strength and Microarchitectural Deficits in Children with Cystinosis.**

Andrew Burghardt<sup>1</sup>, Kyla Kent<sup>2</sup>, Jin Long<sup>2</sup>, Jessica Whalen<sup>2</sup>, Mary Leonard<sup>2</sup>. <sup>1</sup>University of California, San Francisco, United States, <sup>2</sup>Stanford University, United States

Children with cystinosis have numerous risk factors for impaired bone accrual. We used state-of-the-art quantitative imaging of bone microarchitecture (HR-pQCT) to measure trabecular and cortical microstructure and bone strength in children and adolescents (5-20yrs) with cystinosis. We enrolled 20 cystinosis patients and recruited

34 healthy age- and gender- matched controls. Distal radius and tibia HR-pQCT scans (XtremeCT II, Scanco Medical) were acquired 2 mm proximal to the proximal margin of the growth plate or remnant. Diaphyseal radius and tibia scans were centered at an offset from the same landmark, corresponding to 30% of limb length. Bone volumetric density and microstructure were measured using an automated image analysis pipeline optimized for pediatric scans. Micro-finite element analysis (μFEA) was applied to estimate bone strength. One-way ANOVA regression, adjusting for age and sex was used to test for differences in bone measures between cystinosis and healthy control groups. After correcting for age, and sex (Table 1 and 2), cystinosis patients had significantly lower bone strength, most prominently at the distal tibia (-25%, p<0.008) where smaller cross-sectional area, thinner cortices, and deficits in trabecular architecture were all significant. Smaller bone size was observed at all sites, suggesting a systemic lag in bone development (Figure 1). The addition of the corresponding limb length as a covariate to the ANOVA did not alter group-wise differences. Our findings indicate cystinosis subjects have significantly impaired bone strength and abnormal architecture at the weight-bearing tibia, and will consequently have an elevated lifetime risk of sustaining a fragility fracture.

**Table 1:**

	Distal Radius			Distal Tibia		
	CYST N	CTRL 18	p-value*	CYST 20	CTRL 34	p-value*
Total-Area	172±81	193±67	0.04	628±239	717±215	0.06
BMD	310±53	313±53	0.91	222±31	261±47	0.002
Ct.Ar	40±14	46±17	0.007	61±16	78±29	0.003
Ct.BMD	788±76	763±83	0.13	771±62	757±83	0.28
Ct.Po	0±0	0.01±0	0.003	0±0	0.01±0.01	0.003
Ct.Th	1.0±0.2	1.1±0.3	0.46	0.8±0.1	0.9±0.3	0.02
Tb.Ar	134±71	149±54	0.12	572±228	639±197	0.17
Tb.BMD	153±32	167±34	0.15	161±32	198±31	0.0002
BV/TV	0.2±0.05	0.23±0.05	0.09	0.23±0.04	0.28±0.05	0.0001
Tb.N	1.4±0.2	1.5±0.2	0.29	1.5±0.2	1.6±0.2	0.002
Tb.Th	0.21±0.02	0.22±0.02	0.08	0.23±0.02	0.25±0.02	0.009
Tb.1/N.SD	0.27±0.09	0.24±0.07	0.35	0.27±0.08	0.23±0.04	0.01
AppMod	1505±364	1660±315	0.13	1106±246	1479±412	0.0006
FailureLoad	2695±1076	3135±1564	0.08	6353±2189	8227±5044	0.08
Ct.LF.Dist	46±8	39±10	0.02	34±10	26±7	0.001

**Table 2:**

	Diaphyseal Radius			Diaphyseal Tibia		
	CYST N	CTRL 31	p-value*	CYST 20	CTRL 32	p-value*
Total-Area	65±20	81±24	<0.0001	233±76	279±68	<0.0001
BMD	820±101	855±78	0.06	704±61	707±76	0.83
Ct.Ar	53±15	69±21	<0.0001	165±56	203±58	0.0003
Ct.BMD	991±76	1017±52	0.01	967±55	960±51	0.59
Ct.Po	0.03±0.02	0.02±0.01	0.002	0.03±0.03	0.04±0.03	0.19
Ct.Th	2.7±0.5	3.1±0.6	0.0004	4.3±0.9	4.9±1.1	0.01
Tb.Ar	13.0±7.4	13.6±4.7	0.56	71±27	79±23	0.09
AppMod	7904±677	8442±691	0.002	7516±654	7709±681	0.22
FailureLoad	3219±1031	4243±1376	<0.0001	10116±3667	12388±4074	0.0006

**Fig 1.** 3D image showing the distribution of mineralization and cortical bone deficit in cystinosis patient (left) compared to age- and gender- matched control (right).



Tables 1 and 2, Figure 1

**Disclosures:** Andrew Burghardt, None.



## SA0026

**Incidence of Metabolic Bone Disease in Children Receiving Elemental Formula.** Ana Creo, MD<sup>\*1</sup>, Lisa Epp, RDN LD<sup>2</sup>, Julie Buchholtz, RDN LD<sup>3</sup>, Peter Tebben, MD<sup>1</sup>. <sup>1</sup>Mayo Clinic Department of Pediatric Endocrinology, United States, <sup>2</sup>Mayo Clinic Home Enteral Nutrition, United States, <sup>3</sup>Mayo Clinic Clinical Nutrition, United States

**BACKGROUND:** Many children develop milk protein intolerance necessitating elemental formula (EF) use. A recent multicenter survey described 51 children with hypophosphatemia and metabolic bone disease (MBD) while receiving EF (Neocate®)<sup>1</sup>. Our aim is to determine the incidence of MBD in children receiving Neocate®.

**METHODS:** We identified a retrospective cohort using an institutional enteral nutrition database. Children who received at least 75% of calories from Neocate® for at least 3 months were included. Children known to have a primary heritable condition causing abnormal mineral metabolism were excluded. Charts, laboratory tests, and radiographs were reviewed. Children were considered to have biochemical evidence of MBD if they had a low serum phosphorus and elevated alkaline phosphatase. Radiographic evidence was considered present if rickets or low trauma fractures were present.

**RESULTS:** 57 children were identified. Six children had either laboratory or radiographic results suggesting evolving or evident MBD (10.5%); four children had both laboratory and radiographic evidence of MBD (7.0%). Of the remaining 51 children without apparent MBD, 25 (49%) had no laboratory or radiographic studies while receiving EF, 16 (31.3%) had laboratory data only, 6 (11.7%) had radiographic data only, and 4 (7.8%) had both laboratory and radiographic data. Children with MBD had a mean nadir phosphorous of  $1.7 \pm 0.46$  mg/dL compared to children without MBD who had mean phosphorus nadir of  $4.2 \pm 1.3$  mg/dL ( $p=0.0016$ ) while on EF. Affected children had low urinary phosphorus, elevated alkaline phosphatase, and elevated 1,25 dihydroxyvitamin D. Of those with MBD, radiographs revealed 2 with rickets and 2 with fractures. All cases of MBD resolved after changing to an alternative formula and/or providing phosphorus supplementation.

**CONCLUSION:** 4 of 57 children who received Neocate® products in our institution developed clear evidence of MBD with 2 additional children with evidence of possible MBD for an overall incidence of 7-10%. Two of the cases were described previously in a multicenter survey. Those with MBD had low serum and urine phosphorous supporting the previously postulated mechanism of low phosphorous bioavailability.<sup>1</sup> Most children did not have complete laboratory and radiographic data suggesting a higher true incidence. Further work is needed to explore MBD incidence associated with this and alternate elemental formulas. 1) Bone 97(2017) 287-292.

**Disclosures:** Ana Creo, MD, None.

## SA0027

See Friday Plenary Number FR0027.

## SA0028

**Etiology Identification and Serum FGF-23 Measurement in Ten Patients with Fanconi Syndrome.** Juan Du\*, Cong Zhang, Qian-qian Pang, Yan Jiang, Ou Wang, Mei Li, Xiaoping Xing, Weibo Xia. Peking Union Medical College Hospital, Peking Union Medical College, Chinese Academy of Medical Sciences, China

#### Objectives

Fanconi syndrome is a rare cause of rickets in children. The feasibility of next generation sequencing has increased with greater availability and decreasing costs. The aim of this study was to detect gene mutations with Fanconi syndrome. Furthermore, few studies have investigated FGF-23 levels in patients with hereditary Fanconi syndrome. We also evaluated intact FGF-23 in patients with these patients.

#### Methods

10 patients from nine unrelated families have been involved in the study (median age 7; 6 male), who were diagnosed with Fanconi syndrome clinically. A custom panel carrying 13 genes for Fanconi syndrome, and 378 additional genes were sequenced on Illumina HiSeq2500 platform. All pathogenic mutations were confirmed using Sanger sequencing. Also, all exons of EHHADH and HNF4A were tested by direct sequencing, which were not include in the panel. Serum intact FGF-23 were measured by Elisa test (Kainos Lab, Tokyo, Japan).

#### Results

In the present study, we identified pathogenic mutations in all cases. Two patients were diagnosed with tyrosinemia, demonstrated by the compound heterozygous mutations in FAH, including 3 novel mutations. Two CTNS mutations were found in two siblings with cystinosis. One affected individual was found to be heterozygous for two missense mutations in URAT1, also exhibited Fanconi syndrome. One affected patient had CLCN5 R774X for Dent's disease. Two SLC4A1 gene mutations were verified eventually in three cases with distal renal tubular acidosis. We also identified HNF4A missense mutation (c.187C>T) in one patient. The results of Elisa test demonstrated that serum intact FGF-23 levels in all patients were extremely low. FGF-23 levels in 5 patients were below the lower limit of detection.

#### Summary & Conclusion

Targeted next-generation sequencing is a highly efficient way to detect mutations causing Fanconi syndrome. Patients with hereditary Fanconi syndrome-induced hypophosphatemia exhibited a reduction of intact FGF-23 in serum.

**Disclosures:** Juan Du, None.

## SA0029

See Friday Plenary Number FR0029.

## SA0030

Withdrawn

## SA0031

See Friday Plenary Number FR0031.

## SA0032

See Friday Plenary Number FR0032.

## SA0033

See Friday Plenary Number FR0033.

## SA0034

See Friday Plenary Number FR0034.

## SA0035

**Severe bone loss and multiple fractures in SCN8A-related epileptic encephalopathy.**

Tim Rolvien<sup>\*1</sup>, Sebastian Butscheidt<sup>1</sup>, Anke Jeschke<sup>1</sup>, Axel Neu<sup>2</sup>, Jonas Denecke<sup>2</sup>, Christian Kubisch<sup>3</sup>, Miriam Meisler<sup>4</sup>, Klaus Püschel<sup>5</sup>, Florian Barvencik<sup>1</sup>, Timur Yorgan<sup>1</sup>, Ralf Oheim<sup>1</sup>, Thorsten Schinke<sup>1</sup>, Michael Amling<sup>1</sup>.

<sup>1</sup>Department of Osteology and Biomechanics, University Medical Center Hamburg-Eppendorf, Germany, <sup>2</sup>Department of Neuropediatrics, University Medical Center Hamburg-Eppendorf, Germany, <sup>3</sup>Department of Human Genetics, University Medical Center Hamburg-Eppendorf, Germany, <sup>4</sup>Department of Human Genetics, University of Michigan, Ann Arbor, MI, USA, United States, <sup>5</sup>Department of Legal Medicine, University Medical Center Hamburg-Eppendorf, Germany

Mutations in the SCN8A gene encoding the neuronal voltage-gated sodium channel Nav1.6 are known to be associated with epileptic encephalopathy type 13. We identified a novel de novo SCN8A mutation (p.Phe360Ala, c.1078\_1079delTTinsGC, Exon 9) in a 6-year-old girl with epileptic encephalopathy accompanied by severe osteoporosis and multiple skeletal fractures, similar to two previous case reports. Skeletal assessment using dual energy X-ray absorptiometry (DXA), high-resolution peripheral quantitative computed tomography (HR-pQCT) and serum analyses revealed a combined trabecular and cortical bone loss syndrome with elevated bone resorption. Likewise, 2 week-old Scn8a-deficient mice displayed reduced trabecular and cortical bone mass, and histomorphometric quantification revealed increased osteoclast indices. Based on these findings the patient was treated with neridronate (2 mg/kg body weight administered every 3 months) for 24 months. Since no additional skeletal fractures were observed after initiation of the treatment, it is evident that the skeletal pathologies associated with SCN8A-mutations are caused, at least in part, by excessive bone resorption. Taken together, our data provide evidence for a negative impact of SCN8A mutations on bone mass, which can be positively influenced by anti-resorptive treatment.

**Disclosures:** Tim Rolvien, None.

## SA0036

**A Role for Apolipoprotein E in Fracture Healing.** Puvindran Nadesan<sup>\*1</sup>, Gurpreet Baht<sup>2</sup>. <sup>1</sup>Department of Orthopaedic Surgery, United States, <sup>2</sup>Duke Molecular Physiology Institute, Department of Orthopaedic Surgery, United States

The capacity for tissues to repair and regenerate diminishes with age. *In vivo* bone repair and *in vitro* differentiation of bone marrow stromal cells to osteoblasts is more efficient in young animals than old animals. The etiology of this discrepancy is not known. Our previous work used parabiosis and bone marrow transplantation to identify macrophages as a key cell type responsible for the aged phenotype. Secretome constituents of macrophages from young animals were able to rejuvenate aged bone healing. Apolipoprotein E (ApoE) was a protein identified as a key member of this secretome. ApoE is expressed and secreted by macrophages and its function was initially associated with transporting of fat-soluble molecules however ApoE has also been identified to have anti-inflammatory properties. Here we investigated the role of ApoE in bone fracture healing and in osteoblastic differentiation. Fracture healing was investigated using a stabilized tibial fracture model and assessed using  $\mu$ CT analysis, histological observation, and histomorphometry. Osteoblastic differentiation was assessed by adhering bone marrow aspirates to tissue culture plastic and using osteogenic media to induce cellular differentiation. ApoE protein levels in homeostatic bone and in 7-day fracture callus were lower in samples from aged (20-months old) mice than from young (4-months old) mice. Fracture healing in wildtype and ApoE<sup>-/-</sup> mice proceeded to

completion however, at 21 days post injury fracture calluses were smaller and hypermineralized in the ApoE<sup>-/-</sup> mice relative to wildtype. Histomorphometry confirmed enhanced bone deposition in ApoE<sup>-/-</sup> mice relative to wildtype mice. Enhanced bone deposition was unchanged with age (4-months old vs 20-months old) and with administration of high fat diet. Investigation of fracture calluses revealed there to be more inflammatory cells in the fracture calluses of ApoE<sup>-/-</sup> mice. From bone marrow aspirates, osteoblastic differentiation was enhanced in cultures from ApoE<sup>-/-</sup> mice as indicated by CFU-ALP and CFU-VK. Interestingly, the number of progenitor cells from ApoE<sup>-/-</sup> mice was diminished, as indicated by CFU-F. Modulation of cellular metabolism in cultures using 2-deoxy-glucose or etomoxir revealed ApoE<sup>-/-</sup> cells to have a greater reliance on glycolysis for energy. Together these data indicate a role for ApoE in inflammation and cellular metabolism during fracture healing and osteoblastic differentiation.

**Disclosures:** Puvindran Nadesan, None.

## SA0037

See Friday Plenary Number FR0037.

## SA0038

See Friday Plenary Number FR0038.

## SA0039

**Parathyroid Hormone Rescues Bone Loss and Marrow Fat Expansion Induced by Calorie Restriction.** David Maridas<sup>\*1</sup>, Elizabeth Rendina-Ruedy<sup>1</sup>, Ron Helderman<sup>1</sup>, Anyonya Guntur<sup>1</sup>, Victoria DeMambro<sup>1</sup>, Beate Lanske<sup>2</sup>, Daniel Brooks<sup>3</sup>, Mary Boussein<sup>3</sup>, Clifford Rosen<sup>1</sup>. <sup>1</sup>Maine Medical Center Research Institute, United States, <sup>2</sup>Harvard School of Dental Medicine, United States, <sup>3</sup>Beth Israel Deaconess Medical Center, United States

Recently, parathyroid hormone (PTH) receptor deletion in mice has been shown to result in the accumulation of marrow fat, whereas PTH prevents this expansion *in vitro*. Thus, we postulated that PTH could prevent the increase in marrow fat reported in the calorie-restricted mouse model of anorexia nervosa. Eight-week-old female C57BL/6J mice were fed either a control (AIN93M) diet (CTRL) or a 70% calorie restricted (CR) diet. The CR diet was formulated to have matching nutrients and minerals to the CTRL diet. At 12 weeks of age, CR and CTRL mice were injected daily with PTH (80µg/kg, CR/PTH or CTRL/PTH) or vehicle (CR/VEH or CTRL/VEH) for 4 weeks. An additional two cohorts of 8-week-old mice were CR and simultaneously injected (CR+PTH or CR+VEH) for 4 weeks. CR mice lost considerable amount of body weight compared to the CTRL mice with significant decreases in fat proportion, lean mass, aBMD and aBMC after 4 weeks of CR. Histological sections of tibias showed an increase in marrow fat in CR compared to CTRL. PTH injections significantly increased aBMD and aBMC in both CR/PTH and CTRL/PTH mice as well as in CR+PTH mice when compared with their respective controls. Interestingly, simultaneous injections had a much stronger effect on aBMD and aBMC than injections after calorie restriction. PTH did not affect fat proportion and lean mass when compared with VEH in any of the cohorts. µCT revealed that BV/TV from CR/VEH mice was not different from CTRL/VEH mice, yet PTH significantly increased BV/TV in CR/PTH and CR+PTH mice. Cortical fraction was considerably decreased in CR/VEH compared to CTRL/VEH. PTH injections also increased the cortical fraction in both CR/PTH and CR+PTH. Bone marrow fat was analyzed on histological sections of proximal tibias stained with hematoxylin-eosin. We observed increases in adipocyte density and size in CR mice compared to CTRL mice. Surprisingly, PTH did not change adipocyte density although there was a trending decrease in adipocyte size in CR/PTH. The opposite effect was observed in CR+PTH with a trending decrease in adipocyte density but no change in adipocyte size. Our results show that PTH can rescue bone loss in CR mice. Furthermore, our data suggest that PTH may reduce adipocyte size after CR. However, when PTH injections start with CR, PTH affects the density of adipocytes indicating both a differentiation inhibition and a lipolytic effect for PTH depending on the time of treatment.

**Disclosures:** David Maridas, None.

## SA0040

See Friday Plenary Number FR0040.

## SA0041

See Friday Plenary Number FR0041.

## SA0042

**PTH stimulation of osteoblasts protects against immunodeficiency.** Asuka Terashima<sup>\*1</sup>, Kazuo Okamoto<sup>1</sup>, Hiroshi Takayanagi<sup>2</sup>. <sup>1</sup>Department of Osteoimmunology, Graduate School of Medicine and Faculty of Medicine, The University of Tokyo, Japan, <sup>2</sup>Department of Immunology, Graduate School of Medicine and Faculty of Medicine, The University of Tokyo, Japan

Sepsis is a host inflammatory response to severe infection associated with high mortality. Over the past few decades, the incidence of sepsis has gradually increased. In spite of extensive basic research and clinical studies, there are currently no effective treatments for severe sepsis. The fact that anti-inflammatory agents failed to cure patients with sepsis prompted us to search for a novel therapeutic approach. The high mortality rate in sepsis is often caused by secondary infections due to immunosuppression mediated by persistent lymphopenia. We previously showed that sepsis rapidly suppressed osteoblastic bone formation and reduced the number of common lymphoid progenitors in the bone marrow as well as the peripheral T and B cell numbers without impairment of osteoclast function. Osteoblast-specific interleukin (IL)-7 conditional knock-out mice exhibited the lymphopenic phenotype together with a lower common lymphoid progenitor number, indicating that osteoblast-derived IL-7 supports common lymphoid progenitors in the bone marrow. Thus, we hypothesized that sepsis-induced lymphopenia can be treated by increasing osteoblasts. To test this, we administered the septic mice with intermittent parathyroid hormone (PTH), which is a potent accelerator of osteoblastic bone formation. The mCT and bone morphometric analyses demonstrated that the PTH treatment abrogated sepsis-induced bone loss. The PTH administration effectively increased the osteoblast surface, osteoid volume and bone formation rate even in the septic mice. Expression of both *Bglap* and *Il7* in CD31<sup>+</sup>CD45<sup>+</sup> cells from the septic bone marrow was increased by the PTH administration. IL-7 expression was detected mostly in osteocalcin-positive cells using immunofluorescent staining analysis. Importantly, the osteoblast stimulation successfully increased the T and B cell numbers in the septic mice. This study showed the potential of osteoblast as a therapeutic target for immunodeficiency which is observed during systemic inflammation like sepsis. The new approach targeting at osteoblasts, combined with acute stage treatments, may be beneficial for the improvement of sepsis outcomes.

**Disclosures:** Asuka Terashima, Noevir Co., Ltd., Grant/Research Support.

## SA0043

**Mesenchymal stem cells promote B cells to produce inflammatory factors under chronic inflammation.** Xichao Zhou<sup>\*1</sup>, Wen Sun<sup>2</sup>, Nida Meednu<sup>3</sup>, Hengwei Zhang<sup>1</sup>, Brendan F Boyce<sup>1</sup>, Jennifer H Anolik<sup>3</sup>, Lianping Xing<sup>1</sup>. <sup>1</sup>Department of Pathology and Laboratory Medicine, University of Rochester Medical Center, United States, <sup>2</sup>Department of Pathology and Laboratory Medicine, University of Rochester Medical Center; Nanjing Medical University, Nanjing 210029, People's Republic of China, United States, <sup>3</sup>Department of Medicine, Division of Allergy, Immunology and Rheumatology, University of Rochester Medical Center, United States

Mesenchymal stem cells (MSCs) have immune-modulatory effects on various immune cells, including B cells. Rheumatoid arthritis (RA) is an autoimmune disease with abnormalities in target tissues, including synovium, subchondral bone and bone marrow (BM). B cells play important roles in RA. However the association between MSCs and B cells in RA target tissue has not been well investigated. Using TNF-transgenic (Tg) and collagen-induced arthritis (CIA) RA mouse models and immunofluorescence (IF), we found that B cells are enriched in the subchondral and endosteal BM. These B cells were close to bone surfaces and adjacent to osteocalcin-negative MSCs and expressed high levels of pro-inflammatory factors, including TNF and CCL3. We hypothesize that MSCs positively regulate B cell functions in RA target tissues. To test this, we first examined the effect of MSCs on B cell proliferation and survival in co-cultures of WT BM CD19<sup>+</sup> B cells and bone-derived MSCs. MSCs did not increase B cell proliferation, but promoted B cell survival (% live B cells: 44±2 vs. 11±2% in B cell alone). Mature osteoblasts and osteoclast precursors had no effects on B cell survival. TNF pre-treated MSCs increased B cell survival by 1-fold compared to PBS-treated MSCs. We then examined the effect of MSCs on B cell production of these cytokines. MSCs markedly increased B cell expression of TNF by 10±2-fold and CCL3 by 4±0.6-fold, which was further increased in TNF-pre-treated MSCs (fold-increase: 1.7±0.3 for TNF, 1.5±0.15 for CCL3 vs. PBS). In addition, B cells co-cultured with TNF-pre-treated MSCs expressed higher levels of NF-κB RelA and RelB proteins (fold-increase: 4±2.1 vs. B cell alone for RelA; 4±0.52 vs. B cell alone for RelB). Next, transwell assays demonstrated that cell-cell contact was not required for the stimulatory effect of MSCs on B cells. Finally, RNA sequencing and pathway analyses of WT and TNF-Tg RA mouse MSCs revealed that several B cell-related signaling pathways, including B cell receptor/IL9 signaling, IL-15 and LPS-mediated pathways are elevated in TNF-Tg MSCs compared to WT MSCs. Thus, MSCs may promote B cell survival and activate B cells in RA target tissues to produce inflammatory factors likely via MSC secretory factors and involve NF-κB signaling. These studies indicate that MSCs contribute to the pathogenesis of RA by interacting with B cells.

**Disclosures:** Xichao Zhou, None.



**SA0044**

See Friday Plenary Number FR0044.

**SA0045**

See Friday Plenary Number FR0045.

**SA0046**

See Friday Plenary Number FR0046.

**SA0047**

See Friday Plenary Number FR0047.

**SA0048**

**Multiple Myeloma and Bone Marrow Adipose: Exploring An Unknown Relationship.** Michaela Reagan\*, Heather Fairfield, Clifford Rosen, Carolyne Falank, Maine Medical Center Research Institute, United States

**Purpose:** Multiple myeloma (MM) is a hematological malignancy that is characterized by clonal proliferation of transformed plasma cells within the bone marrow (BM) and severe bone disease. Although MM cells are initially sensitive to steroids, proteasome inhibitors, and chemotherapies, patients with MM eventually relapse with refractory disease. Because MM cells show a dependency on the BM microenvironment for survival and proliferation, and BM adipocytes (BMAs) demonstrate a unique, endocrine signaling capacity and lipid composition, it is likely that there is cross-talk between MM cells and BMAs. Unlike the influences of osteoblasts and osteoclasts, the effect of BMAs in MM is poorly understood. In fact, only a few studies have investigated the relationship between BMAT and cancer in general. *Based on our recent findings on BMAs, we hypothesized that BMAs induce drug resistance in MM cells.*

**Approach:** We generated BMAT from BM-derived stromal cells from mice (mBMAT) or humans (hBMAT) with adipogenic media. We performed direct and indirect co-culture experiments to study the effects of BMAT on MM proliferation and drug resistance. MM cells were cultured on, or with conditioned media (CM) from 3T3L1 white pre-adipocytes, or mouse or human BMAT with or without compounds (dexamethasone (dex), bortezomib (bort), or adiponectin). Adiponectin-KO mBMAT was also tested. MM drug resistance was assessed by bioluminescence imaging, MTT and apoptosis assays. We also developed a tissue-engineered 3-D BMAT-MM model using silk scaffolds and imaged these with confocal microscopy over 2 weeks.

**Results:** In contrast to prior reports, we found that adiponectin does not induce MM apoptosis and that BMAT does not typically affect MM proliferation. However, hBMAT rescued MM1S MM cells from dex-induced apoptosis. Moreover, OPM2 MM cells were resistant to bort when grown in direct, but not indirect, culture with hBMAT, suggesting that direct cell-cell adhesion signals drive this drug resistance. Our 3-D model also demonstrated destruction of BMAT through pathways that are currently unknown but may include apoptosis, lipolysis or lipophagy.

**Conclusions:** We found that, certain combinations of drugs and BMAT demonstrate drug resistance in MM cells. Drug resistant profiles were dependent on MM cells, MSC donor, and adipocyte lineage. We are currently investigating the mechanism(s) behind adipocyte-induced chemoresistance in MM and we are confirming our *in vitro* observations *in vivo*.

**Disclosures:** Michaela Reagan, None.

**SA0049**

Withdrawn

**SA0050**

**BSP Deficiency Reduces Osteolytic Bone Metastasis of Breast Cancer.** Yu Shi\*, Qisheng Tu, Jake Chen, Division of Oral Biology, Tufts University School of Dental Medicine, United States

**Introduction:** Bone sialoprotein (BSP) has a major role in bone metastasis of breast cancer. Previous studies have elaborated the mechanisms by which BSP enhances osteoclastogenesis, and tumor-derived BSP promotes breast cancer osteolytic metastasis. The purpose of this study is to reveal how BSP inhibits apoptosis of osteoclast precursor cells and to determine the role of endogenous BSP in breast cancer osteolytic metastasis. **Materials and Methods:** In vitro, RAW264.3 cells were treated with or without human recombinant BSP. DNA condensation, caspase activity assay, Quantitative Real Time-PCR, and immunoprecipitation analyses were used to determine the effects of BSP in osteoclast precursor cell survival and apoptosis. In vivo, osteoblast-specific BSP knockout (Ox-BSP-C57BL/6J) mice line and wild-type (C57BL/6J) mice line were treated with 4T1-12B (luciferase labeled) breast cancer cell intracardiac/intratibial inoculation. IVIS scan, radiographic analysis, micro-CT scan, H-E staining and TRAP staining were used to evaluate the bone metastasis and osteolytic lesion. **Results and Conclusions:** BSP has an anti-apoptotic effect in osteoclast precursor cells in apoptosis events mediated by Caspase. BSP inhibits cell apoptosis by mainly inhibiting Caspase-8 activity, which means that it achieve this effect by primarily

regulating the extrinsic apoptotic pathway. Co-IP experiments show that the inhibitory effect of BSP on the activity of Caspase-8 was related to the interaction between Caspase-8 and  $\alpha V\beta 3$ . Osteoblast-specific BSP knockout down-regulated the endogenous BSP level, especially in the metastatic niche, by which, both systematic metastasis and bone metastasis were inhibited. Meanwhile, endogenous down-regulated BSP level results in a smaller osteolytic bone lesion. Graphic shows the bone metastasis and osteolytic lesion in Ox-BSP-C57BL/6J mice (KO) and C57BL/6J mice (WT).

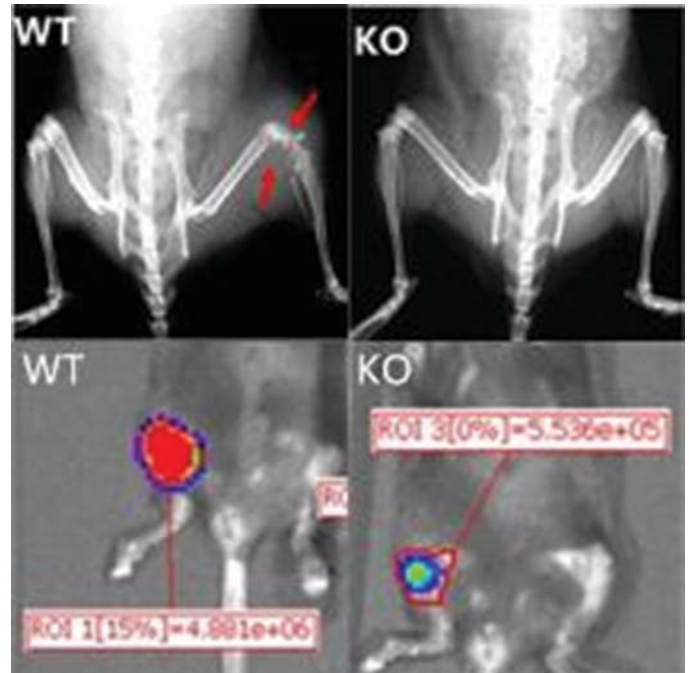


Figure: Bone Metastasis

**Disclosures:** Yu Shi, None.

**SA0051**

See Friday Plenary Number FR0051.

**SA0052**

See Friday Plenary Number FR0052.

**SA0053**

**MET/VEGFR/FMS signaling contributes prostate cancer-induced osteoclast differentiation and bone resorption.** Kenta Watanabe\*<sup>1</sup>, Michiko Hirata<sup>1</sup>, Tsukasa Tominari<sup>1</sup>, Chiho Matsumoto<sup>1</sup>, Hidenori Fujita<sup>2</sup>, Kazuhiko Yonekura<sup>2</sup>, Gillian Murphy<sup>3</sup>, Hideaki Nagase<sup>4</sup>, Chisato Miyaura<sup>1</sup>, Masaki Inada<sup>1</sup>. <sup>1</sup>Tokyo University of Agriculture and Technology, Japan, <sup>2</sup>Taiho Pharmaceutical Co., Ltd., Japan, <sup>3</sup>University of Cambridge, United Kingdom, <sup>4</sup>Kennedy Institute of Rheumatology, United Kingdom

The tyrosine kinase inhibitors that targeted to blockage of vascular endothelial growth factor (VEGF) receptor and hepatocyte growth factor (HGF) receptor MET signaling exhibits anti-tumor properties in xenografts of human gastric carcinoma (*Mol. Cancer Ther.* 2013). Although bone metastases frequently occur in prostate cancer patients, the role of VEGF receptor and MET in cancer-induced bone resorption is not known. Patients with advanced prostate cancer show sclerotic bone metastases, which cause chronic pain and pathologic fractures, however, the invasion of prostate cancer cells into bone tissues firstly induces bone destruction by increased osteoclast-mediated bone resorption. In this study, we have evaluated the efficacy of the tyrosine kinase inhibitor TAS-115 in preventing prostate cancer bone metastasis and bone resorption using human prostate cancer cell line (PC3). When PC3 cells were injected into proximal tibiae in nude mouse, severe trabecular and cortical bone destruction were detected with subsequent tumor growth. Oral administration of TAS-115 almost completely inhibited both PC3-induced bone loss and PC3 cell proliferation. In an ex vivo bone organ culture, PC3 cells induced osteoclastic bone resorption effectively suppressed by the treatment of TAS-115. In the culture of the bone marrow cells, M-CSF dependent macrophage differentiation and following RANKL-induced osteoclast formation were suppressed by adding TAS-115. FMS related receptor kinases such as ERK and Akt were also suppressed by the presence of TAS-115. FMS expression was only detected in macrophage and in osteoclast cell lineage. These results indicate that FMS tyrosine kinase signaling in host pre-osteoclasts/osteoclasts is critical for bone destruction induced by prostate cancer. Targeting of MET/VEGFR/FMS signaling is promising therapeutic candidate for the treatment of prostate cancer patients with bone metastasis.

Disclosures: Kenta Watanabe, None.

## SA0054

See Friday Plenary Number FR0054.

## SA0055

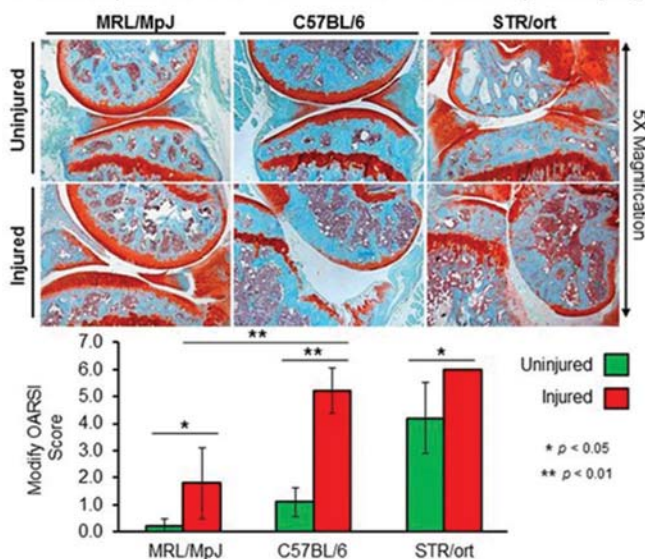
See Friday Plenary Number FR0055.

## SA0056

**Attenuation of Inflammatory Responses May be Critical in PTOA Development in MRL/MpJ and Str/ort Strains.** Jiun Chiun Chang<sup>\*1</sup>, Aimy Sebastian<sup>2</sup>, Deepa Muruges<sup>2</sup>, Sarah Hatsell<sup>3</sup>, Aris Economides<sup>3</sup>, Blaine Christiansen<sup>4</sup>, Gabriela Loo<sup>1</sup>. <sup>1</sup>Lawrence Livermore National Laboratories and University of California Merced, United States, <sup>2</sup>Lawrence Livermore National Laboratories, United States, <sup>3</sup>Regeneron Pharmaceuticals, United States, <sup>4</sup>University of California Davis Medical Center, United States

Anterior cruciate ligament rupture often results in post-traumatic osteoarthritis (PTOA) 10-20 years post injury. However, the mechanisms contributing to PTOA development have yet to be fully elucidated. To uncover the molecular events that promote PTOA pathogenesis and development, we profiled gene expression changes after non-invasive tibial compression overload injury inducing ligament rupture in the right knee joints of 10 week-old male mice from strains with varying susceptibility to PTOA: MRL/MpJ (resistant), C57BL/6 (moderately susceptible) and STR/ort (highly susceptible). Histological evaluation of injured joints at 12 weeks post injury (n=5 per strain) revealed extreme cartilage and tibial subchondral bone erosion in both STR/ort and C57BL/6, while minimal cartilage damage was observed in the MRL/MpJ (Figure). Subsequently, we examined transcriptional changes between intact injured and contralateral joints using RNA sequencing at 1-, 7-, and 14-days post injury. We identified 103, 141, and 68 differentially regulated genes (>1 fold) commonly changed in all three strains at 1-, 7-, and 14-days post injury, respectively. At 1-day post injury, we found several immune/inflammatory response related genes including *IL-1b*, *IL-6*, *IL-11*, *Ccl2*, *Ccl7*, *Cxcl1*, and *Cxcl5* were highly expressed in STR/ort compared to C57BL/6 and MRL/MpJ. Interestingly, *IL-1b*, *IL-6*, *Ccl2*, *Cxcl1*, and *Cxcl5* were largely attenuated by 7 days post injury in MRL/MpJ but remained elevated in STR/ort compared to C57BL/6. In addition, transcripts associated with catabolic enzymes including matrix metalloproteinase (MMPs) 2, 3, 12, and 14 were all upregulated by 7 and 14 days post injury for every strain. However, relative to injured joints, MRL/MpJ expression was significantly less than that of the C57BL/6 and STR/ort strains. Furthermore, *ADAMTS* (a disintegrin and metalloproteinase with thrombospondin motifs) 3, 4, 15, and 16 expression were lower in the injured joints of MRL/MpJ mice than those of C57BL/6 or STR/ort mice at 7 days post injury week and were further reduced by 14 days. Because many of the identified inflammatory genes are known to upregulate MMP and ADAMTS transcriptionally and post-transcriptionally, the PTOA-resistant phenotype of MRL/MpJs may be largely driven by attenuation of the immune response shortly after injury.

**Figure 1: MRL/MpJ revealed mild OA while C57BL/6 and STR/ort presented severe OA at 12 weeks post injury**



Figure

Disclosures: Jiun Chiun Chang, None.

## SA0057

### Global Analysis of Runx2 Regulated Genes During Chondrocytes Differentiation.

Haiyan Chen\*, Jessica Boni, Harunur Rashid, Mohammad Hassan, Amjad Javed. University of Alabama at Birmingham, United States

Runx2 transcription factor is essential for bone formation. To elucidate Runx2 regulatory control distinctive to chondrocyte cell population, we ablated Runx2 gene using Col2a-Cre mice. Runx2<sup>Ch-/-</sup> mice exhibited failed endochondral ossification and die shortly after birth. The progressive differentiation of chondroprogenitors to hypertrophic chondrocytes was absent in the Runx2<sup>Ch-/-</sup> mice. For a molecular understanding of failed endochondral ossification, we determined global changes in chondrocyte transcriptome. RNA was isolated from cartilaginous portions of hind limbs of E18 Runx2<sup>Ch-/-</sup> littermates. To control for contaminating non-skeletal tissue (blood, bone marrow, muscle), we performed limited enzymatic digestion on de-skinned limbs to clear the skeletal muscle and connective tissue. Bone shafts from metaphyseal to metaphyseal regions were then removed to obtain pure epiphyseal cartilage tissue. RNA integrity (RIN) is critical for obtaining meaningful gene expression data. Thus we determined RIN of three wild-type and three Runx2<sup>Ch-/-</sup> samples from independent litters. Only RNA samples with RIN values above 8.0 were used for RNAseq to allow for a valid comparison among RNA samples from different litters. Analysis of 23,529 genes showed that 2,498 genes are differentially expressed in Runx2<sup>Ch-/-</sup> cartilage. We compared gene profile of all three Runx2<sup>Ch-/-</sup> samples and find only 1,011 genes are common and consistently show 2-25-fold change in level of expression. Thus, failed chondrogenesis due to loss of Runx2 is associated with differential changes in 10% of chondrocyte transcriptome. Among the differentially expressed genes, 236 (23%) were increased and 775 (77%) decreased in the Runx2<sup>Ch-/-</sup> cartilage. It is important to note that during chondrogenesis and endochondral ossification, the induced genes would normally be inhibited and the set of suppressed genes would normally be activated by Runx2. The most common biological process that the genes belonged to were cellular, developmental, and the metabolic pathways. The most common protein classes that showed expression changes were receptor, ECM proteins, nucleic acid binding proteins, and enzymes. Experiments are in progress to validate top 50 genes that showed at least 25-fold increase or decrease expression and whether they are a direct target of Runx2. Together, our studies identified multiple novel targets of Runx2 that are expressed during chondrocyte differentiation and cartilage development.

Disclosures: Haiyan Chen, None.

## SA0058

See Friday Plenary Number FR0058.

## SA0059

### In vitro evidence for a role of the phosphatidylinositol-5-phosphatase SHIP2 in matrix mineralization.

Anais Fradet\*, Jamie Fitzgerald, Henry Ford Hospital - Bone and Joint Center, United States

SHIP2, encoded by the INPPL1 gene, is a mammalian phosphatase that dephosphorylates the lipid second messenger molecule phosphatidylinositol (3,4,5)P3. The role of SHIP2 in the regulation of insulin production and the control of obesity is well-studied. However, it is emerging that SHIP2 also has a major role in regulating skeletal development. We and others have shown that null mutations in INPPL1 cause Opsismodysplasia, a severe chondrodysplasia characterized by a delayed bone maturation. The mechanism by how the loss of an inositol phosphatase causes a major skeletal developmental defect is completely unknown. To assess whether SHIP2 is involved in mineralization, the effect of SHIP2 catalytic inhibitor, AS1949490, on chondrogenic and osteoblastic differentiation was evaluated.

For this study we used three different cell models, the ATDC5 chondrocyte differentiation model; the SaOs-2 osteoblast differentiation model; and an *ex vivo* mouse metatarsal culture model for studying endochondral ossification.

Inhibition of SHIP2 had no effect on cell differentiation in all three cell systems but the inhibitor reduced matrix mineralization in all models in a dose dependent manner. Mineralization process starts in matrix vesicles (MVs), which bud from mineralizing cells. MVs extracted from differentiated cells are able to mineralize *in vitro*. In contrast, MVs isolated from cells grown in the presence of the SHIP2 inhibitor failed to mineralize. Importantly, MVs are still able to mineralize when treated with the SHIP2 inhibitor only during the mineralization assay suggesting that SHIP2 acts to inhibit mineralization at a stage prior to hydroxyapatite crystal formation in MVs.

The main function of SHIP2 is to dephosphorylate PI(3,4,5)P3 to PI(3,4)P2. Immunohistochemistry studies on chondrocyte pellet sections confirm an accumulation of PI(3,4,5)P3 when the cells were treated with the SHIP2 inhibitor in a dose dependent manner. Since PI(3,4,5)P3 is implicated in membrane dynamics, our hypothesis is that the accumulation of PI(3,4,5)P3 in these cells could lead to a disorganization of the plasma membrane causing defective matrix vesicles, but this needs to be confirmed.

In conclusion, these results suggest that SHIP2 acts in the first steps of endochondral ossification, more precisely in the mineralization step but further investigations are needed to understand the exact role of SHIP2 in these process.

Disclosures: Anais Fradet, None.



## SA0060

See Friday Plenary Number FR0060.

## SA0061

See Friday Plenary Number FR0061.

## SA0062

**Epigenetic Regulation of Articular Chondrocytes by Vitamin C Involving Prolyl Hydroxylase Domain-containing Protein 2 (PHD2): Role of Vitamin C Deficiency in the Pathogenesis of Osteoarthritis.** Richard Lindsey\*, Shaohong Cheng, Sheila Pourteymoor, Catrina Godwin, Subburaman Mohan. VA Loma Linda Healthcare System, United States

Vitamin C (ascorbic acid, AA) deficiency leads to spontaneous fractures, and the AA effect on osteoblast differentiation via transcriptional regulation of osteon expression is well established. Additionally, AA exerts important effects on chondrocytes (CCs), and epidemiological studies have linked low AA intake with increased osteoarthritis (OA) risk. However, the mechanism of AA regulation of articular CCs remains largely unknown. Since chondrocyte-specific conditional knockout (cKO) of PHD2, a known mediator of AA, leads to an OA-like phenotype due to increased differentiation of articular cartilage (AC) progenitors, we predicted that the AC phenotype of AA deficient mice should mimic that of PHD2 cKO. Accordingly, we found AA-deficient *Gulo* mutant mice had significantly decreased AC area at the femur and tibia (21% and 15%, respectively,  $P < 0.05$ ) and significantly decreased (8%) AC width at the femur compared to AA-replete heterozygous littermates. Furthermore, *in vitro* treatment of cultured primary articular CCs with AA significantly increased mRNA expression of immature CC markers (aggrecan, Col2a1, sonic hedgehog, and clusterin) and decreased expression of a CC differentiation marker (Col10a1). Due to the recent finding that AA promotes demethylation of many gene promoters via activation of ten eleven translocases (TETs) in stem cells and because PHDs, like TETs, belong to a family of 2-oxoglutarate-dependent dioxygenases that depend on AA for their activities, we hypothesized that the biological effects of AA on articular CCs are in part due to TET- and/or PHD-mediated conversion of 5-methylcytosine (5-mC) to 5-hydroxymethylcytosine (5-hmC) in the promoter regions of target genes. All 3 TETs and all 3 PHDs are expressed in articular CCs at varying levels. However, AA treatment in articular CCs significantly increased expression of all TETs while PHD expression was largely unchanged. Treatment of cultured articular CCs with AA led to a significant 4.5-fold increase in 5-hmC content measured by ELISA compared to untreated cells. Furthermore, pharmacological inhibition of PHD2 with IOX2 decreased 5-hmC levels in the promoter regions of known AA chondrocyte target genes *HIF1α* and *VEGFα* in AA-treated articular CCs. Taken together, these data suggest that AA promotes transcription of target genes in part by PHD2-mediated epigenetic demethylation of DNA in articular CCs, and this mechanism should be exploited towards development of therapies for OA.

**Disclosures:** Richard Lindsey, None.

## SA0063

See Friday Plenary Number FR0063.

## SA0064

See Friday Plenary Number FR0064.

## SA0065

See Friday Plenary Number FR0065.

## SA0066

**Are Benefits from an 8-Month Exercise Intervention in Pre- and Peri-pubertal Children Maintained After 1 Year of Detraining? Follow-Up Data from the CAPO Kids Trial.** Belinda Beck\*, Benjamin Weeks, Rossana Nogueira. Griffith University, Australia

**Purpose:** The CAPO Kids trial was a school-based bone- and fat-targeted exercise intervention that improved bone, fat and physical performance in healthy pre- and peri-pubertal children (1,2). The aim of the current work was to determine if benefits of the CAPO Kids trial were maintained after twelve months of detraining.

**Methods:** The intervention involved block randomization of 9-11 year old children into either 8 months of 10 minutes thrice-weekly capoeira plus jumping exercise in addition to regular PE classes (EX), or regular PE classes alone (CON). Testing originally occurred at baseline (T1) and 8 months at the end of the intervention (T2) (previously reported; 1,2). Additional testing was conducted 1 year after withdrawal of the exercise program (T3). Measures included age of peak height velocity, weight, standing and sitting height, calcaneal broadband ultrasound attenuation (BUA) and stiffness index (SI) (Achilles, GE), waist circumference, resting heart rate, blood pressure, maximal vertical jump, and estimated maximal oxygen consumption. Between-group differences at each time point were determined by repeated measures ANCOVA, adjusting for change in anthropometrics, physical activity and calcium consumption.

**Results:** 240 of the 311 children in the original CAPO Kids trial (77% of initial follow-up sample) were remeasured at T3 (12.3±0.6 yrs); 155 EX and 85 CON. EX and CON increased BUA (EX: 5.6%,  $p \leq 0.001$ ; CON: 6.5%,  $p \leq 0.001$ ), SI (EX: 7.3%,  $p \leq 0.001$ ; CON: 5.2%,  $p \leq 0.001$ ), vertical jump (EX: +5.9% vs. CON: +6.3%,  $p = 0.054$ ) and estimated VO2 max (EX: 13.3% vs. CON: 12.1%;  $p = 0.197$ ), and reduced waist circumference (EX: -5.2%,  $p \leq 0.001$ ; CON: -5.6%,  $p \leq 0.001$ ) between T2 and T3 time points, with no between-group differences, reflecting normal growth and maintenance of exercise effects.

**Conclusion:** The benefits of an 8-month in-school bone- and fat-targeted exercise intervention to the bone, fat and physical performance of pre- and peri-pubertal children endured even after 12 months of detraining. Findings suggest even brief exposure to targeted exercise during the vital growing years can evoke benefits for metabolic and skeletal health in the longer term.

1. Nogueira RC, Weeks BK, Beck BR. An in-school exercise intervention to enhance bone and reduce fat in girls: the CAPO Kids trial. *Bone* 2014;68:92-9

2. Nogueira RC, Weeks BK, Beck BR. Targeting bone and fat with novel exercise for peripubertal boys: the CAPO kids trial. *Pediatr Exerc Sci* 2015;27(1):128-39

**Disclosures:** Belinda Beck, None.

## SA0067

**Circulating Fibroblast Growth Factor 23 Levels Decline Following Sleeve Gastrectomy.** Emma Billington\*<sup>1</sup>, Rinki Murphy<sup>2</sup>, Karen Callon<sup>2</sup>, Greg Gamble<sup>2</sup>, Michael Booth<sup>3</sup>, Ian Reid<sup>2</sup>. <sup>1</sup>University of Calgary, Canada, <sup>2</sup>University of Auckland, New Zealand, <sup>3</sup>Waitemata District Health Board, New Zealand

**Background:** Circulating levels of the bone-derived phosphaturic hormone fibroblast growth factor 23 (FGF23) have been positively associated with measures of adiposity such as body mass index (BMI) and fat mass in cross-sectional studies. To gain insight into the direction of causality of these associations, we evaluated the effect of weight loss on FGF23 levels in a cohort of individuals undergoing sleeve gastrectomy (SG).

**Methods:** Twenty-two adults with type 2 diabetes who underwent SG were assessed. Plasma intact FGF23 concentrations were determined at baseline and 12 months following SG using an ELISA (Immutopics, San Clemente, CA). Age, BMI, parathyroid hormone (PTH), calcium, 25-hydroxyvitamin D, and estimated glomerular filtration rate were also evaluated at baseline and 12 months after SG. Changes in FGF23 and other parameters were assessed using the Wilcoxon signed-rank test. Correlates of change in FGF23 were determined using Spearman's rank correlation test. Sex-specific analyses were also undertaken.

**Results:** The study cohort consisted of 22 individuals (9 females, 13 males) with median (IQR) age of 51 (43 to 54) years, BMI 40.9 (36.9 to 46.9) kg/m<sup>2</sup> and FGF23 66.2 (55.2 to 82.9) pg/mL. Changes in parameters following SG are outlined in Table 1. A significant reduction in median FGF23 (-12.4 pg/mL, 95% CI: -19.5 to 2.0,  $p = 0.005$ ) was observed within the entire cohort. Change in FGF23 was inversely associated with baseline glomerular filtration rate ( $r = -0.57$ ,  $p = 0.005$ ), but not with other baseline parameters. When each sex was considered separately, median change in FGF23 was significant in females (-17.9 pg/mL, 95% CI: -23.7 to 2.0,  $p = 0.02$ ) but not males (-4.3 pg/mL, 95% CI: -24.0 to 5.3,  $p = 0.2$ ). Median change in BMI was similar in females (-11.3 kg/m<sup>2</sup>, 95% CI: -10.8 to -6.2,  $p = 0.004$ ) and males (-10.6 kg/m<sup>2</sup>, 95% CI: -12.6 to -7.2). Change in FGF23 was positively correlated with change in BMI in females ( $r = 0.75$ ,  $p = 0.02$ ), but not in males ( $r = 0.04$ ,  $p = 0.9$ ).

**Conclusions:** FGF23 levels are reduced in the setting of significant weight loss following SG, implying that increased adiposity causes higher circulating FGF23 levels, and not the reverse. Changes in FGF23 following weight loss appear to be more marked in females than males, indicating that the association between adiposity and FGF23 may be mediated by sex-specific factors.

**Table 1.** Comparison of patient characteristics before and 12 months after sleeve gastrectomy in adults with type 2 diabetes (n=22)

Characteristic	Baseline	12 months	P-value
Weight (kg)	122.6 (110.4-139.4)	91.7 (79.0-99.9)	<0.0001
BMI (kg/m <sup>2</sup> )	40.9 (36.9-46.9)	30.0 (27.7-31.8)	<0.0001
FGF23 (pg/mL)	66.2 (55.3-82.9)	52.6 (42.3-72.5)	0.005
PTH (pmol/L)	4.9 (3.8-6.3)	3.5 (3.1-5.6)	0.009
Calcium (mmol/L)	2.33 (2.25-2.40)	2.30 (2.30-2.35)	0.6
25-hydroxyvitamin D (nmol/L)	34 (25-46)	74 (63-90)	<0.0001
eGFR (mL/min/1.73 <sup>2</sup> )*	107 (100-111)	108 (104-112)	0.8
Lumbar spine BMD (g/cm <sup>2</sup> )	1.28 (1.22-1.41)	1.24 (1.19-1.32)	0.0001

Data are presented as median (IQR); P-values are for changes from baseline to 12 months (Wilcoxon signed-rank test)

BMI = body mass index, FGF23 = fibroblast growth factor 23, PTH = parathyroid hormone, eGFR = estimated glomerular filtration rate, BMD = bone mineral density

\*eGFR calculated using the CKD-EPI equation

Table 1

**Disclosures:** Emma Billington, None.

## SA0068

**Cold stress challenge enhances NGF mRNA level in brown fat and testis and regulates BDNF and Osteocalcin mRNA in bone and brain of mice.** Claudia Camerino<sup>\*1</sup>, Elena Conte<sup>2</sup>, Adriano Fonzino<sup>2</sup>, Kejla Musaraj<sup>2</sup>, Roberta Caloiero<sup>2</sup>, Domenico Tricarico<sup>2</sup>. <sup>1</sup>Dept. of Biomedical Sciences & Human Oncology, University of Bari, Italy, <sup>2</sup>Dept. of Pharmacy – Drug Sciences, University of Bari, Italy

Energy metabolism regulates bone turnover while BAT activity is anabolic to bone. A significant correlation between NGF/BDNF/Osteocalcin (Ost) expression levels and their receptors was found in brain, BAT and bone, suggesting an homeostatic relation between them (Camerino et al., *Front. in Physiol.* 2016). We challenged this previous system investigating NGF and its receptors p75NTR and NTRK1, BDNF, Ost and its receptor GPRC6A mRNA from 3 months-old mice in bone, brain, BAT and testis during cold stress (CS). UCP-1 in BAT was used as positive control. Mice were divided into three groups: controls at room temperature (RT=25°C), CS for 6h and 5-days at T=4°C (N=15 mice). Mice were sacrificed and the mRNA interscapular BAT, bone, brain and testis were extracted. CS for 6h enhanced UCP-1 and NGF mRNA levels in BAT respectively by 2 and 1.5-fold vs controls, down-regulating p75NTR and NTRK1 genes. UCP-1 in BAT was up-regulated after 5-days of CS vs controls; NGF was not affected and its receptors were down-regulated. The p75NTR/NTRK1 receptor genes were not affected in bone and brain, while the mRNA level of the NGF gene was significantly enhanced in bone and unchanged in brain following 5 days CS. UCP1 increased in bone after 5 days CS. p75NTR mRNA increased by 0.76 and 0.83 folds, respectively, after 6h and 5-days of CS in testis vs controls, while NGF was unaffected. BDNF shows an opposite trend. BDNF mRNA increased by 9.5-fold in bone following 5-days of CS vs controls, and in brain by 0.6-fold after 6h, but not in BAT. BDNF decreased by 1 and 0.6 folds respectively after 6h and 5-days of CS in testis. Similarly, Ost mRNA increased by 16-fold in bone and 3-fold in BAT after 5-days of CS vs controls; its receptor was unaffected. GPRC6A is upregulated by 3-fold after 6h in brain, Ost was down-regulated by 0.33-fold; these were not affected after 5-days of CS. Ost/GPRC6A mRNA levels were not significantly affected in testis following CS. This study suggest that during cold stress in mice, UCP1 increase in BAT is associated with early NGF response in the same tissue, long-term potentiation of NGF in bone and NGF receptor in testis. UCP1 upregulation in bone is consistent with its protective effect on this organ. BDNF activity may exert bone and neuroprotective effects reducing its function on the reproductive tissue. Similarly to UCP1, Ost signaling is enhanced in bone and BAT while it may exert local neuroprotective effects through its receptor.

**Disclosures:** Claudia Camerino, None.

## SA0069

**FGF23 is associated with adiposity in dialysis patients: crosstalk between bone and adipose.** Janet Chiang<sup>\*1</sup>, George Kaysen<sup>2</sup>, Anne Schafer<sup>1</sup>, Kirsten Johansen<sup>1</sup>. <sup>1</sup>University of California, San Francisco, United States, <sup>2</sup>University of California, Davis, United States

FGF23 concentration rises throughout stages of CKD and can be extremely high in patients with ESRD. Evidence suggests that FGF23 may be involved in signaling between bone and adipose, but its role is uncertain. In a study in ESRD participants, FGF23 level was inversely associated with BMI. In a study with ob/ob mice, injections of leptin led to an increase in FGF23. To probe these apparently paradoxical results, we hypothesized that FGF23 would be associated with adiposity and the association would be explained in part by leptin. We performed univariate and multivariate logistic regression analyses using data from 611 participants in the ACTIVE/ADIPOSE cohort of prevalent hemodialysis patients. Mean age was 57±14 years, 39.5% were female, and the median time on dialysis was 2.85 years. Serum FGF23 concentration was measured by C-terminal ELISA. BMI and waist circumference were measured, and percentage fat was determined by bioelectrical impedance spectroscopy as a more direct assessment of adiposity. We found FGF23 to be inversely associated with BMI in univariate analyses and after adjusting for potential confounders, including age, race, gender, calcium, phosphorus, albumin, and time on dialysis (-0.69 kg/m<sup>2</sup> per pg/mL of FGF23, 95% CI -1.10, -0.30, p=0.001). FGF23 was also inversely associated with waist circumference (-1.20 cm, 95% CI -2.14, -0.26, p=0.01), and percentage fat (-0.01%, 95% CI -0.01, -0.003, p=0.001) in multivariate analyses. We explored the extent to which FGF23 was associated independently with visceral and non-visceral adiposity. FGF23 was not significantly associated with waist circumference after adjusting for fat mass but was inversely associated with fat mass after adjusting for waist circumference. We investigated the role of leptin in these relationships. Leptin was inversely associated with FGF23, and the association between FGF23 and BMI was attenuated when we adjusted for leptin (-0.18 kg/m<sup>2</sup>, 95% CI -0.48, 0.11, p=0.24), as was the association with waist circumference (-0.25cm, 95% CI -0.94, 0.44, p=0.48), and percentage fat (-0.002%, 95% CI -0.005, 0.002, p=0.31). We conclude that there is a negative association between FGF23 and adiposity that is mainly related to non-visceral adiposity and explained in part by leptin. This may be one mechanism through which high FGF23 levels contribute to mortality in dialysis patients given that higher fat mass is associated with better survival in this population ("obesity paradox").

**Disclosures:** Janet Chiang, None.

## SA0070

See Friday Plenary Number FR0070.

## SA0071

**The Phosphate Hypothesis: an expanding role for FGF23.** Robert Fredericks<sup>\*</sup>. Endocrine Associates, United States

The phosphate hypothesis has been formulated based on the assumption that phosphate is the foundation for the organization of energy in the manifestation of phenotypes. The signaling structure built upon this foundation engages Vitamin D metabolites and their receptors as an interface between systemic physiology and cellular metabolism. Health is then defined as the ability to appropriately adapt to changing environments that is both recorded in and modulated by the skeleton. Recent discoveries that FGF23 influences sodium, calcium and iron contribute to clarification of the roles of calcitropic hormones in the adaptive strategies evolved by nature.

Utilizing case-based discovery as a means to organize the data of others, including basic, translational and clinical disciplines, for the development of models depicting causal relationships that govern health, it was predicted that hepcidin, the target of hemochromatosis mutations, plays a central role in metabolic adaptations. The phenotypes of heterozygote carriers have not been characterized and are predicted by the models to be sexually dimorphic and variable over time while conferring both favorable and adverse consequences.

In the first 20 patients suspected to be carriers 15 were found. The expectation would be no more than 1 in 10 as seen in northern Europeans. This serves to validate the utility of causal modeling that contrasts with risk factor management as a means to organize data and formulate personalized strategies for interventions in metabolic bone diseases.

Recent observations that FGF23 is in a strong relationship with hepcidin suggests that the modeling of causal relationships based on the phosphate hypothesis and a general theory of metabolism that incorporates signals generated by glucose metabolism will be useful when considering personalization of interventions that modulate FGF23.

**Disclosures:** Robert Fredericks, None.

## SA0072

**Upregulation of Lipocalin 2 is a Protective Mechanism to Counteract Insulin Resistance.** Ioanna Mosialou<sup>\*</sup>, Steven Shikhel, Stavroula Kousteni. Columbia University, United States

Regulation of food intake is a recently identified endocrine function of bone that is mediated by Lipocalin 2 (LCN2). Osteoblast-secreted LCN2 suppresses appetite, induces satiety after feeding and decreases fat mass while improving glucose tolerance, insulin secretion and sensitivity. Circulating LCN2 levels are inversely correlated with body weight and glycated haemoglobin (HbA1c) in patients with type 2 diabetes. However, studies in humans have indicated a positive association of LCN2 with adiposity and insulin resistance. To dissect this apparent discrepancy, we examined the connection between LCN2 and insulin resistance in mouse models of obesity. We found that circulating LCN2 levels are 2-fold higher in 8 week-old obese, insulin resistant leptin-deficient (*Lepr<sup>ob/ob</sup>*) and leptin receptor-deficient (*Lepr<sup>db/db</sup>*) mice and 25% higher in mice placed on a high fat diet for 12-16 weeks. Due to the appetite suppressive function of LCN2, and its beneficial effects in insulin sensitivity, we examined whether the increase in LCN2 serum levels in *Lepr<sup>db/db</sup>* mice is a protective mechanism to counteract obesity and insulin resistance. siRNA against LCN2 was delivered as a complex with a polymer-based reagent (In vivo JetPei) to *Lepr<sup>db/db</sup>* mice by subcutaneous injections administered every 2 days for a total of 30 days. This regime decreased by 50% circulating LCN2 levels thus normalizing them to those of wild type mice. A 50% reduction in LCN2 serum levels, worsened the metabolic dysfunction of *Lepr<sup>db/db</sup>* mice. Hyperphagia increased by 24% and correlated with 50% increase in body weight gain and a corresponding 44% increase in gonadal fat pad weight. In addition, fasting blood glucose levels increased by 50%, and a higher impairment in glucose stimulated insulin secretion was observed as well as a trend towards a decrease in fed insulin levels. In contrast, treatment of *Lepr<sup>db/db</sup>* mice with recombinant LCN2 suppressed food intake by 16.5% and improved glucose tolerance and insulin sensitivity to levels similar to those of control *Lepr<sup>db/+</sup>* littermates. Body weight and gonadal fat were decreased and energy expenditure was increased in LCN2-treated *Lepr<sup>db/db</sup>* mice. These results support a protective role for LCN2 in obesity and insulin resistance. An overproduction of inflammatory cytokines, an excess of nutrients and possibly other factors may trigger LCN2 release as a compensatory response to combat the deleterious effects of obesity and insulin resistance.

**Disclosures:** Ioanna Mosialou, None.

## SA0073

See Friday Plenary Number FR0073.

## SA0074

See Friday Plenary Number FR0074.



**SA0075**

See Friday Plenary Number FR0075.

**SA0076**

See Friday Plenary Number FR0076.

**SA0077**

See Friday Plenary Number FR0077.

**SA0078**

See Friday Plenary Number FR0078.

**SA0079**

**The Skeletal Phenotype of Mice Deficient in Liver Fatty Acid Binding Protein-1 (L-FABP-1) is Increased Bone Marrow Fat and Bone Mass.** Claire Watson\*, Diarra Williams, Shannon Huggins, Alyssa Falck, Avery McIntosh, Friedhelm Schroeder, Ann Kier, Larry Suva, Dana Gaddy, Texas A&M University College of Medicine, United States

In the liver, Fatty Acid-Binding Protein-1 (L-FABP) allows for arachidonic acid (AA) and endocannabinoid degradation within the cytosol, as well as brings AA and endocannabinoids (EA) into the nucleus for lipolysis and fatty acid oxidation. Deleting L-FABP reduces hepatocyte fatty acid degradation, lipolysis and oxidation, leading to an accumulation of these fatty acids, AA and EA in the cytosol and systemic circulation, as well as an increase in whole body fat content. Since alterations in circulating AA resulting are known to elicit effects in peripheral tissues, we determined the skeletal phenotype of male and female mice lacking L-FABP by DEXA, microCT and serum markers, and examined bone marrow (BM) fat content, as well as ex vivo bone marrow cell differentiation. Similar to the expected increases in liver fat in L-FABP null mice, L-FABP deletion significantly increased BM fat content in the distal femur and proximal tibia of female mice (n=6-10/group for each genotype and gender). Although BM fat content was consistently increased in males compared with females of both genotypes, deletion of L-FABP in male mice did not significantly increase BM fat content. Surprisingly, BMD was significantly increased in the lumbar spine, distal femur and proximal tibia in male L-FABP null mice, as well as in the distal femur of female L-FABP null mice. MicroCT analyses of the proximal tibiae demonstrated that L-FABP-deficiency caused significant increases in trabecular bone volume, Tb.N. and Tb.Th. in both male and female mice. In addition, BMD in the middle third ROI of the femur, representing only cortical bone, as well as cortical CSA and thickness by microCT, increased only in male L-FABP null mice. Consistent with this increased bone mass, capacity of osteoclastogenesis in bone marrow cultures of L-FABP null mice was significantly reduced, suggesting decreased bone resorption in L-FABP null mice. Together, these data demonstrate increases in both bone marrow fat, as well as increases in bone volume, microarchitecture and geometry in both cortical and trabecular compartments and in both genders. While not surprising that, like liver fat content, BM fat content might also be increased by deletion of L-FABP, these studies represent the first demonstration of an increased bone mass phenotype in mice lacking L-FABP, and provide novel insight into the role of fatty acids and AA in the regulation of bone metabolism and bone mass.

*Disclosures: Claire Watson, None.***SA0080**

See Friday Plenary Number FR0080.

**SA0081**

See Friday Plenary Number FR0081.

**SA0082**

**What can be discovered by an unstructured screening of KOMP lines?** David Rowe\*<sup>1</sup>, Douglas Adams<sup>1</sup>, Renata Rydzik<sup>1</sup>, Li Chen<sup>1</sup>, Zhihua Wu<sup>1</sup>, Seung-Hyun Hong<sup>2</sup>, Gaven Garland<sup>3</sup>, Caibin Zhang<sup>1</sup>, Dong-Guk Shin<sup>2</sup>, John Sundberg<sup>3</sup>, Cheryl Ackert-Bicknell<sup>4</sup>. <sup>1</sup>University of Connecticut Health, United States, <sup>2</sup>University of Connecticut, United States, <sup>3</sup>The Jackson Laboratory, United States, <sup>4</sup>University of Rochester School of Medicine, United States

The International Mouse Phenotyping Consortium is generating Knockout (KO) lines in the C57BL/6N background. The 3 US phenotyping centers (KOMP) use whole body DXA to assess skeletal health. To date, we have examined 181 of these lines, as well as 33 sets of wildtype controls, using  $\mu$ CT quantitation of femoral and vertebral morphometry. Twenty strains had a low trabecular BV/TV fraction, while 31 strains have high values. These findings were frequently dimorphic by site (axial vs appendicular) and or sex. There

was no concordance between KOs identified by DXA and by  $\mu$ CT. The BV/TV measurement can be segmented into KOs with low, normal, or high trabecular compartment size (TV). Low TV and body weight often varied in the same direction irrespective of the BV/TV and in some cases evidence of a systemic disorder might explain the phenotype. Even excluding this category, the frequency of abnormal BV/TV suggests that over 2000 genes can potentially influence skeletal mass, which is consistent with the highly polygenic nature of bone mass. Selected KO lines with abnormal trabecular morphometry undergo a cryo-histological study to assess static, dynamic and cellular activity. Within the groups of low or high BV/TV, a pattern based on the osteoclast number and the corresponding osteogenic response is emerging, possibly reflecting the degree of inter-lineage coupling. For example, *Irf8* is a previously described low bone mass KO due to activated osteoclasts that does not induce an osteoblastic response. In contrast, *Htr1d*, a neuron-associated serotonin receptor, shows high osteoclast number in association with markers of high bone formation (high turnover). KO mice with high bone mass can demonstrate low osteoclast numbers without increased osteogenic activity (Rin3 and Elk1), probably due to impaired osteoclastogenesis. Other high BV/TV lines can have high osteoclast numbers and normal bone forming activity (Ocstamp) reflecting ineffective osteoclastic resorptive activity. Associating the literature with a specific KO line provides clues to the underlying basis for the altered bone volume and cellular dynamics. For example, *Elk1* and *Rin3* (a GWAS bone mass loci) are highly expressed in myeloid cells suggesting a direct cellular action on osteoclastic cells. These observation and more can be viewed at [www.bonebase.org](http://www.bonebase.org), which is designed to provide sufficient information for an investigator to obtain a specific KO line for detailed mechanistic experiments.

*Disclosures: David Rowe, None.***SA0083**

**TRAC: a Novel Gene Expression Quantification Method Compared to qPCR.** Francesco Rossignolo\*<sup>1</sup>, Stefano Fontana<sup>1</sup>, Jani Salmivaara<sup>2</sup>, Oona Kivelä<sup>2</sup>, Piia Tirola<sup>2</sup>, Hinnerk Boriss<sup>2</sup>. <sup>1</sup>Aptuit, Italy, <sup>2</sup>ValiFinn, Finland

TRAC (Transcript analysis by Affinity Capture) is a novel gene expression analysis technique that is utilizing multiplexing mRNA detection and high throughput sample processing. In TRAC, each target mRNA of interest is recognized by a specific fluorescence labeled ssDNA probe. Hybridization of probes and targets takes place in 96-well plate, after which the probe-transcript complexes are captured by streptavidin coated magnetic beads. Unbound material is washed off and the probes are eluted for detection and quantification by capillary electrophoresis. In this study we compared expression level measurements obtained from TRAC to the gold standard qPCR method (TaqMan). Specifically, we measured differential expression levels of CYP1A2, CYP2B6 and CYP3A4 of cryopreserved primary hepatocyte incubated with and without known inducers. Primary hepatocyte cells were treated with known CYP inducers omeprazole, phenobarbital, rifampicin, beta-naphthoflavone, dexamethasone and phenytoin. In qPCR analysis results were normalized using GAPDH. TRAC allows a broader set of housekeeping genes for normalization: YWHAZ, HPRT1, SDHA, UBC, GAPDH and B2M. Fold-changes of expression levels as response to the inducers were calculated relative to untreated cells. The cell culture work and TaqMan analysis was performed at Aptuit (Italy), while the TRAC analysis of the same sample material was done at ValiFinn (Finland).

We observed a strong correlation ( $R^2=0.9229$ ) between the results from TRAC and TaqMan. The coefficient of variation of the TRAC measurements was 8.6%, while the average coefficient of variation of TaqMan measurements was over 26%. We therefore conclude that the TRAC method, that doesn't rely on cDNA conversion and amplification, results in more precise results. Moreover, TRAC allows substantially higher levels of multiplexing that qPCR without any compromise in data quality.

*Disclosures: Francesco Rossignolo, None.***SA0084**

See Friday Plenary Number FR0084.

**SA0085**

See Friday Plenary Number FR0085.

**SA0086**

**Wnt signals control development of the periodontium.** Xue Yuan\*<sup>1</sup>, Yan Wu<sup>2</sup>, Yuan Zhao<sup>3</sup>, Kristy Perez<sup>1</sup>, G Pellegrini<sup>4</sup>, K Condon<sup>5</sup>, K McAndrews<sup>5</sup>, M Gregor<sup>5</sup>, Teresita Bellido<sup>5</sup>, Jill Helms<sup>1</sup>. <sup>1</sup>Stanford University, United States, <sup>2</sup>Stanford University & Stomatology Hospital of Chongqing Medical University, China, <sup>3</sup>Stanford University & Lanzhou University, United States, <sup>4</sup>Indiana University, United States, <sup>5</sup>Indiana University, United States

Teeth are anchored to the jawbones by the periodontium, a tripartite structure consisting of cementum, a periodontal ligament (PDL), and alveolar bone. Cementum is a bone-like material that covers the tooth root and provides an attachment site for the fibrous PDL; the other end of the PDL is tethered to alveolar bone of the socket. This arrangement provides a flexible attachment between the tooth and the jawbone, which allows for tooth movement in response to large bite forces. Our goal was to understand the molecular mechanisms responsible for generating and maintaining the tripartite

periodontium. To do so we focused on Wnt signaling because of its known function in controlling alveolar bone formation and in maintaining the PDL.

Mice expressing a dominant active  $\beta$ catenin in DMPI-expressed cells (e.g.,  $\text{d}\beta\text{cat}^{\text{Ox}}$  mice) and littermate controls were generated, along with  $\text{Wnt1CreR26RLacZ/+}$  mice to follow the fates of the cranial neural crest from which the periodontium arises. Mineralized tissues were analyzed by  $\mu\text{CT}$ , histology, enzymatic activity assays and immunohistochemistry. These analyses revealed that tooth eruption was perturbed in  $\text{d}\beta\text{cat}^{\text{Ox}}$  mice.

The eruption defect in  $\text{d}\beta\text{cat}^{\text{Ox}}$  mice was not due to an absence of osteoclast activity, as monitored by TRAP staining. Rather,  $\text{d}\beta\text{cat}^{\text{Ox}}$  teeth lacked a PDL. The PDL space was instead occupied by an overgrowth of cellular cementum and alveolar bone, which together resulted in a direct fusion of the tooth to the alveolar bone, a pathologic condition known as ankylosis. Our data suggest that a simple molecular switch, mediated by Wnt signaling, is responsible for creating the periodontium from a single population of cranial neural crest cells, and that sustained Wnt signaling in this locale is sufficient to replace the fibrous PDL with mineralized tissue.

**Disclosures:** Xue Yuan, None.

## SA0087

See Friday Plenary Number FR0087.

## SA0088

**Genome-Wide Association Study Identifies Three Novel Genetic Determinants of Dental Maturation.** Olja Grgic<sup>\*1</sup>, Carolina Medina-Gomez<sup>2</sup>, Brunilda Dhamo<sup>3</sup>, Katerina Trajanoska<sup>4</sup>, Strahinja Vucic<sup>3</sup>, Edwin M Ongkosuwo<sup>5</sup>, Vincent W V Jaddoe<sup>6</sup>, Andre G Uitterlinden<sup>7</sup>, Marjo-Riitta Jarvelin<sup>8</sup>, Nicholas Timpson<sup>9</sup>, David M Evans<sup>10</sup>, Eppo B Wolvius<sup>3</sup>, Fernando Rivadeneira<sup>11</sup>. <sup>1</sup>EMC, The Generation R Study Group, EMC, Internal Medicine, EMC, Oral & maxillofacial surgery, special dental care and orthodontics, Netherlands, <sup>2</sup>EMC, The Generation R Study Group, EMC, Internal Medicine, EMC, Department of Epidemiology, Netherlands, <sup>3</sup>EMC, The Generation R Study Group, EMC, Oral & maxillofacial surgery, special dental care and orthodontics, Netherlands, <sup>4</sup>EMC, Internal Medicine, EMC, Department of Epidemiology, Netherlands, <sup>5</sup>EMC, The Generation R Study Group, 3EMC, Oral & maxillofacial surgery, special dental care and orthodontics, Netherlands, <sup>6</sup>EMC, The Generation R Study Group, Netherlands, <sup>7</sup>EMC, The Generation R Study Group, 2EMC, Internal Medicine, Netherlands, <sup>8</sup>NFBC1966/Lifecourse Epidemiology, Imperial College London/U.K., United Kingdom, <sup>9</sup>ALSPAC/MRC Integrative Epidemiology Unit, Bristol University/U.K., United Kingdom, <sup>10</sup>ALSPAC/MRC Integrative Epidemiology Unit, Bristol University/U.K., Diamantina Institute, University of Queensland/AU, United Kingdom, <sup>11</sup>EMC, The Generation R Study Group, EMC, Internal Medicine, Netherlands

**Objectives:** Advanced or delayed physiological age may influence significantly health and disease processes. Physiological age can be estimated using several parameters including dental age (DA). Previous meta-analyses studying "Number of Teeth at 15 Months" (NT15M) and "Age at First Teeth Eruption" (AFTE) have identified 15 loci. We performed a genome-wide association study (GWAS) meta-analysis to identify genetic determinants in children of school age.

**Methods:** Discovery GWAS of DA was performed in the Generation R study, a multiethnic pregnancy cohort in Rotterdam, The Netherlands. We included 2,793 children with mean age 9.82 (SD=0.34) years. DA was determined from dental panoramic radiographs using the Demirjian method. Participants were genotyped with the HumanHap 610K platform, imputed to the 1000GP reference panel. Analysis was adjusted for age, sex, height, BMI and 20 genomic principal components; genome-wide significance (GWS) was set at  $P < 5 \times 10^{-8}$ . Replication of signals associated with DA was pursued using summary level results from the published GWAS meta-analysis of the ALSPAC and NFBC1966 studies ( $n=12,012$ ) studying NT15M and AFTE. Fisher's combined probability test weighted by sample size, implemented in METAL, was used for the combined meta-analysis.

**Results:** Top signals mapped to 16q12.2 (IRX5;  $P=1.1 \times 10^{-7}$ ) and 17p11.2 (SREBF1;  $P=9.1 \times 10^{-8}$ ) loci associated with advanced DA. Significant evidence for replication of both GWAS signals was observed in the previous NT15M meta-analysis (IRX5:  $P=2.7 \times 10^{-5}$  and SREBF1:  $P=0.001$ ). In the combined meta-analysis, the top-associated marker in the IRX5-region reached GWS ( $P=2.1 \times 10^{-9}$ ). Also, alleles of these markers associated with higher DA were nominally associated with earlier teeth eruption in the AFTE meta-analysis (IRX5:  $P=1.5 \times 10^{-5}$  and SREBF1:  $P=0.002$ ). Furthermore, after genome-wide meta-analysis we identified variants in three novel loci: 16q12.2 (IRX5;  $P=3.4 \times 10^{-9}$ ), 7p15.3 (IGF2BP3;  $P=2.87 \times 10^{-8}$ ) and 14q13.3 (PAX9;  $P=3 \times 10^{-8}$ );

**Conclusion:** We describe here three novel loci associated with dental development. These findings provide further understanding into the process of dental maturation in children from early infancy to late school age. Further, these novel loci implicate diverse pathways related to BMI, lipid metabolism, growth hormone/insulin-like growth factors and craniofacial development.

**Disclosures:** Olja Grgic, None.

## SA0089

See Friday Plenary Number FR0089.

## SA0090

See Friday Plenary Number FR0090.

## SA0091

**Correlations between Transcriptomic Gene Expression and Bone Phenotype in a Phosphate-Deficient, Mouse Fracture Healing Model.** Zi Jun Deng<sup>\*1</sup>, Amira Hussein<sup>1</sup>, Kyle Lybrand<sup>1</sup>, Deven Carrol<sup>1</sup>, Alexander Wulff<sup>1</sup>, Heather Matheny<sup>1</sup>, Brenna Hogue<sup>1</sup>, Serkalem Demissie<sup>2</sup>, Elise Morgan<sup>3</sup>, Louis Gerstenfeld<sup>1</sup>. <sup>1</sup>Boston University School of Medicine, United States, <sup>2</sup>Boston University School of Public Health, United States, <sup>3</sup>Boston University, United States

Previous studies have shown that dietary phosphate (Pi) deficiency leads to delayed fracture healing and impaired metabolic function. The goal of this study was to use a systems biology approach to identify correlations between callus transcriptome and callus phenotype. Femoral fractures were generated in three strains of male mice. Pi deficiency was initiated 2 days prior to fracture and maintained for 14 days after which mice were returned to normal diet. Controls were fed a normal diet. Microarray analysis of total callus RNAs was carried out over 35 days of healing. Analyses of variance with diet and time-points as the two factors identified  $n=11,037$  expressed genes that were either significantly different with respect to diet or with a significant diet\*time interaction. This gene group was then used for subsequent stages of the analysis. Callus microstructural properties were obtained at post-operative days 14, 21, and 35 ( $n=12$  per time-point/strain/diet) using micro-computed tomography. Weighted Gene Co-expression Network Analysis (WGCNA) was used to cluster the transcriptomic data based on expression levels for each diet group and to identify correlations between each cluster and the callus phenotypic properties. Within each diet group, genes that were positively and negatively correlated with callus phenotypic properties were analysed using Ingenuity Pathway Analysis software to identify their biological functions. Ten and fourteen unique clusters were found for the Pi and control groups, respectively. Cartilage development was up-regulated relative to non-fracture controls and was negatively correlated to callus mineralization in both diet groups. Bone-related functions were upregulated relative to non-fracture controls and were negatively correlated to callus mineralization in both diet groups; however, more bone-related functions were found in the Pi compared to the control groups. Vasculogenesis and angiogenesis-related functions were up-regulated relative to non-fracture controls and were negatively correlated to callus mineralization in both diet groups. The functions that were down-regulated relative to non-fracture controls and were positively correlated to callus mineralization were primarily immune related functions. These results indicate that dietary phosphate deficiency primarily affected bone-related functions such as differentiation of bone cells and osteoblastic-lineage.

**Disclosures:** Zi Jun Deng, None.

## SA0092

See Friday Plenary Number FR0092.

## SA0093

**Risedronate could reduce the glomerular basement membrane thickening in Pit-1 overexpressing transgenic rat.** Yohei Asada<sup>\*</sup>, Takeshi Takayanagi, Shogo Nakayama, Eisuke Tomatsu, Yasumasa Yoshino, Sahoko Sekiguchi-Ueda, Megumi Shibata, Atsushi Suzuki. Fujita Health University, Japan

Hyperphosphatemia is one of prognostic factors in CKD-MBD. We have previously reported type III Pi transporter-overexpressing transgenic rats (Pit-1TG) manifested decreasing bone mineral density and increasing proteinuria. Their glomerular epithelial cells showed increasing phosphate (Pi) uptake, decreasing number of foot processes, and thickened glomerular basement membrane. Therefore, the Pit-1TG is considered as a pathological model of nephrotic syndrome. Bisphosphonates given rapidly in high dose would induce adverse renal effect, could also inhibit Pi-induced vascular calcification according to atherosclerosis. In the present study, we investigated whether risedronate can reduce proteinuria due to chronic Pi overload in vivo.

**Methods:** Pit-1TG rats and their control rats at 5-weeks-old are divided into 4 groups: I, control rat without risedronate (C-C); II, control rat with risedronate (C-R); III, Pit-1TG rat without risedronate (TG-C); IV, Pit-1TG rat with risedronate (TG-R). The protocol of risedronate administration was 5  $\mu\text{g/kg}$  weight s.c. twice a week for 7 weeks. Their blood and urine for 24 hours after 12h-starvation were collected at 5, 8 and 12 weeks-old. Tissues for histological analysis were obtained at 8 weeks of age. The thickness of the glomerular basement membrane was measured between the foot processes and the glomerular endothelial cells.

**Results:** The body weight gain and serum Ca, Pi, and albumin levels in each group were same with each other. Proteinuria in TG-C group was significantly higher than that in C-C group ( $\text{TG-C}, 42.2 \pm 27.8 \text{ mg/day}$ ;  $\text{C-C}, 7.1 \pm 3.6 \text{ mg/day}$ ,  $p=0.037$ ). Risedronate treatment reduced proteinuria in TG-R group. In electron microscope analysis, the glomerular basement membrane thickening was found in TG-C group, and risedronate



reduced this pathological thickening in TG-R group (TG-R,  $206.1 \pm 75.1$  nm; TG-C,  $221.1 \pm 88.4$  nm,  $p=0.016$ ).

In conclusion, these findings suggest that risedronate could reduce adverse effect of P overload on glomerular basement membrane, which may improve barrier function in glomerulus in nephrotic syndrome.

**Disclosures:** Yohei Asada, None.

## SA0094

**Membrane Estrogen Receptor- $\alpha$  is Essential for Estrogen Signaling in Bone of Male Mice.** Helen Farman<sup>\*1</sup>, Karin Gustafsson<sup>1</sup>, Petra Henning<sup>1</sup>, Vikte Lionikaite<sup>1</sup>, Sofia Movérare-Skrtic<sup>1</sup>, Jianyao Wu<sup>1</sup>, Henrik Ryberg<sup>1</sup>, Ellis Levin<sup>2</sup>, Claes Ohlsson<sup>1</sup>, Marie Lagerquist<sup>1</sup>. <sup>1</sup>Centre for Bone and Arthritis Research at Institute of Medicine, Sahlgrenska Academy at University of Gothenburg, SE-41345 Gothenburg, Sweden, Sweden, <sup>2</sup>Division of Endocrinology, Departments of Medicine and Biochemistry, University of California, Irvine, Irvine, California, and the Long Beach VA Medical Center, Long Beach, CA, USA, United States

The importance of estradiol (E2) signaling via estrogen receptor  $\alpha$  (ER $\alpha$ ) for the regulation of bone mass in males is well established (1). ER $\alpha$  mediates estrogenic effects by translocating to the nucleus and there affecting gene transcription, but can also mediate effects via extra-nuclear actions by e.g. triggering cytoplasmic signaling cascades. The role of membrane-initiated ER $\alpha$  (mER $\alpha$ ) signaling for the estrogenic response in male mice is unknown.

To investigate the role of mER $\alpha$  signaling in male mice, we used a mouse model (NOER) with a point mutation (C451A), resulting in loss of ER $\alpha$  palmitoylation and thereby the trafficking of ER $\alpha$  to the plasma membrane is inhibited. 12-week-old NOER mice and WT littermates were used to investigate the role of mER $\alpha$  signaling in male mice.

We orchidectomized (ORX) 12-week-old male NOER and WT mice and treated them with either E2 ( $16.7$  ng-mouse<sup>-1</sup>.day<sup>-1</sup>) or placebo for four weeks. Dual X-ray absorptiometry (DXA) was used to analyze total body areal bone mineral density (aBMD) and computed tomography (CT) was used to analyze the cortical and trabecular bone parameters. Sex steroid levels in serum were analyzed by high sensitive GC-MS/MS (2).

Serum levels of testosterone were not altered in the male NOER mice compared with WT mice, demonstrating that the feed-back regulation of sex steroid levels was not disturbed. Gonadal intact male NOER mice had significantly decreased total body aBMD ( $-4.8 \pm 0.78\%$ ,  $p < 0.001$ ) compared to WT mice. As expected E2 treatment significantly increased the total body aBMD, trabecular BMD in the distal metaphyseal region of femur and cortical bone thickness in the diaphyseal region of femur in ORX WT mice. Importantly, the estrogenic responses were substantially decreased in ORX NOER mice compared with the estrogenic responses in ORX WT mice on total body aBMD ( $-43.4 \pm 10.1\%$ ,  $p < 0.01$ ), trabecular BMD ( $-54.9 \pm 7.9\%$ ,  $p < 0.001$ ), and cortical bone thickness ( $-41.2 \pm 6.7\%$ ,  $p < 0.01$ ).

In conclusion, membrane estrogen receptor- $\alpha$  is essential for estrogen signaling in both trabecular and cortical bone of male mice. Increased knowledge of estrogen signaling mechanisms in the regulation of the male skeleton may aid in the development of new treatment options for male osteoporosis.

### References

1. Vanderschueren et al. *Endocr Rev.* 2014;35(6):906-60.
2. Nilsson et al. *Endocrinology.* 2015;156(7):2492-502.

**Disclosures:** Helen Farman, None.

## SA0095

See Friday Plenary Program FR0095.

## SA0096

See Friday Plenary Program FR0096.

## SA0097

**A Calcium-Sensing Receptor (CaSR) Mutation Causes Hypocalcemia by Disrupting a Transmembrane Salt Bridge that Modulates  $\beta$ -arrestin Signaling.** Caroline Gorvin<sup>\*1</sup>, Valerie Babinsky<sup>1</sup>, Tomas Malinauskas<sup>1</sup>, Peter Nissen<sup>2</sup>, Anders Schou<sup>3</sup>, Christian Siebold<sup>1</sup>, E. Yvonne Jones<sup>1</sup>, Fadil Hannan<sup>4</sup>, Rajesh Thakker<sup>1</sup>. <sup>1</sup>University of Oxford, United Kingdom, <sup>2</sup>Aarhus University Hospital, Denmark, <sup>3</sup>Odense University Hospital, Denmark, <sup>4</sup>University of Liverpool, United Kingdom

The calcium-sensing receptor (CaSR) is a G<sub>q/11</sub>- and G<sub>i/o</sub>-protein-coupled receptor that signals via cytosolic calcium (Ca<sup>2+</sup>) and mitogen-activated protein kinase (MAPK) pathways to regulate extracellular calcium homeostasis. Furthermore, CaSR can activate MAPK pathways by interacting with the scaffold proteins  $\beta$ -arrestin-1 and  $\beta$ -arrestin-2. Studies of loss- and gain-of-function CaSR mutations, which cause familial hypocalcaemic hypercalcaemia type 1 (FHH1) and autosomal dominant hypocalcaemia

type 1 (ADH1), respectively, have revealed the CaSR to signal in a biased manner. Thus, FHH1 mutations may lead to signaling predominantly via MAPK, whereas ADH1 mutations preferentially enhance Ca<sup>2+</sup> responses. Here, we report a novel ADH1-associated Arg680Gly CaSR mutation, which led to identification of a structural motif that mediates biased signaling by CaSR. *In vitro* studies expressing the Arg680Gly CaSR mutation in HEK293 cells showed it to upregulate MAPK signaling without altering Ca<sup>2+</sup> responses. Moreover, this gain-of-function in MAPK activity occurred independently of G<sub>q/11</sub>, assessed using an inositol phosphate-1 (IP1) accumulation assay, and G<sub>i/o</sub>, assessed measuring serum-response element (SRE) luciferase reporter activity in the presence of the G<sub>i/o</sub> blocking agent pertussis toxin. Studies of SRE reporter activity in the presence of siRNAs targeting  $\beta$ -arrestin-1 and  $\beta$ -arrestin-2 showed that the increase in MAPK signaling by the Arg680Gly mutant was mediated by a non-canonical pathway involving  $\beta$ -arrestin scaffolding proteins. Homology modelling of the CaSR predicted that the Arg680 residue, which is located in transmembrane domain-3, could form a salt bridge with the side chain of neighbouring Glu767, or with the side chain of the more distantly located Glu837 residue. Studies replacing Glu767 and Glu837 with Arg767 and Arg837, that would be predicted to disrupt a salt bridge, revealed that Arg767 enhanced CaSR signaling via  $\beta$ -arrestin in a manner analogous to the ADH-mutant Arg680Gly, while Arg837 had no effect on signaling. Furthermore, an engineered double mutant of Glu680-Arg767, which was predicted to continue to form a salt bridge between residues 680 and 767, restored MAPK signaling to wild-type levels, and  $\beta$ -arrestin siRNA treatment had a similar effect on Glu680-Arg767 responses to those of wild-type CaSR. Thus, our results demonstrate that CaSR signals via  $\beta$ -arrestin and that the Arg680-Glu767 salt bridge is important for mediating signaling bias.

**Disclosures:** Caroline Gorvin, None.

## SA0098

See Friday Plenary Program FR0098.

## SA0099

See Friday Plenary Program FR0099.

## SA0100

See Friday Plenary Program FR0100.

## SA0101

**Estrogens decrease osteoclastogenesis in vitro by stimulating Bak/Bax-dependent apoptosis of early progenitors.** Ha-Neui Kim<sup>\*</sup>, Li Han, Aaron Warren, Stavros Manolagas, Maria Almeida, Robert Jilka. Division of Endocrinology and Metabolism, Center for Osteoporosis and Metabolic Bone Diseases, Central Arkansas Veterans Healthcare System, United States

Estrogens decrease osteoclast number and restrain resorption in cancellous bone, at least in part, by stimulating apoptosis. However, it is unclear whether they do so by inducing death of osteoclast progenitors, mature osteoclasts, or both; and the death program(s) involved remains unknown. Earlier evidence has established that RANKL prolongs the lifespan of both osteoclast progenitors and mature osteoclasts. Nonetheless, osteoclast survival is limited by both apoptotic and non-apoptotic death pathways that overcome the RANKL-induced pro-survival signals. Here, we have examined the impact of 17 $\beta$ -estradiol (E2) on the number and death of pre-osteoclasts vs mature osteoclasts generated from murine (C57BL/6J) bone marrow-derived macrophages stimulated with RANKL and M-CSF for 5 days – a time at which large multinucleated TRAPase-positive osteoclasts predominate. We report that the presence of 10 nM E2 for a 24 hour period during the 1<sup>st</sup>, 2<sup>nd</sup>, or 3<sup>rd</sup> day of culture, or during the entire 5 day period, caused a 2-3-fold fold reduction in the number of osteoclasts measured at the end of day 5. In contrast, exposure to E2 during the 4<sup>th</sup> or 5<sup>th</sup> day of culture had no effect on osteoclast number. E2 stimulated caspase-3 activity by 2-fold, as measured at the end of the first day of culture. This effect was abrogated in cultures of marrow progenitors lacking Bak and Bax – the two essential proteins for the mitochondrial apoptotic death pathway – isolated from Bak<sup>-/-</sup>;Bax<sup>fl/fl</sup>;LysM-Cre mice. Lack of Bak and Bax also prevented the reduction of osteoclast number that occurred in cultures maintained in the presence of E2 for 5 days. In line with the finding that addition of E2 during the late stages of culture had little effect on osteoclast number, addition of E2 to mature osteoclasts maintained in the presence of RANKL only modestly accelerated the death that occurred during the subsequent 4-5 days, as measured by caspase-3 activation. Furthermore, E2 failed to accelerate the death of mature osteoclasts lacking Bak and Bax. Taken together, these findings suggest that the decrease of osteoclast number by estrogens is due in part to activation of the mitochondrial apoptotic death pathway in osteoclast progenitors rather than mature cells. Moreover, these results corroborate evidence, reported elsewhere in this meeting, that the calcium binding protein S100A8, not FasL, is a likely gene target of the direct anti-resorptive effect of ER $\alpha$  signaling on cancellous bone.

**Disclosures:** Ha-Neui Kim, None.

## SA0102

See Friday Plenary Program FR0102.

## SA0103

**Discovery of the Genomic and Homeostatic Circuitry Controlling *Cyp27b1* Expression through *in vivo* Manipulation.** Mark Meyer<sup>1</sup>, Nancy Benkuský<sup>1</sup>, Seong min Lee<sup>1</sup>, Melda Onal<sup>1</sup>, Martin Kaufmann<sup>2</sup>, Glenville Jones<sup>2</sup>, John Wesley Pike<sup>1</sup>. <sup>1</sup>University of Wisconsin - Madison, United States, <sup>2</sup>Queen's University, Canada

The final hydroxylation of vitamin D<sub>3</sub> to form the active hormonal 1 $\alpha$ ,25(OH)<sub>2</sub>D<sub>3</sub> is completed by the cytochrome P450 enzyme CYP27B1 in the mitochondria of kidney cells. 1,25(OH)<sub>2</sub>D<sub>3</sub> functions together with the parathyroid hormone (PTH), and the phosphate sensing fibroblast growth factor 23 (FGF23) to maintain the normal physiologic levels of calcium and phosphate. All three hormones act in endocrine fashion to control the expression of the *Cyp27b1* gene in the kidney and conversely, they also regulate *Cyp24a1* gene expression which degrades 1,25(OH)<sub>2</sub>D<sub>3</sub>. *Cyp27b1* is also expressed in non-renal cells (NRC) and increases in expression during disease states or inflammation by an independent mechanism. Despite understanding the homeostatic fluctuations of *Cyp27b1* gene expression, a mechanism and genomic enhancer location for regulation of *Cyp27b1* by 1,25(OH)<sub>2</sub>D<sub>3</sub>, PTH, and FGF23 has remained elusive. In our studies, we utilized epigenetic and genetic ChIP-seq directed observations followed by CRISPR/Cas-mediated genome editing to eliminate several putative enhancer elements upstream of the *Cyp27b1* gene in mice that were unique to the kidney and, in part, the parathyroid gland. We have identified a CREB and VDR-bound enhancer that, when deleted, eliminated all PTH-mediated induction of *Cyp27b1*. A second VDR-bound enhancer deletion eliminated all FGF23-mediated and 1,25(OH)<sub>2</sub>D<sub>3</sub>-mediated repression of *Cyp27b1*. While both deletions decreased the basal expression of *Cyp27b1* transcript and protein, only the PTH enhancer deletion resulted in a striking biological and skeletal phenotype similar to the *Cyp27b1*-null mouse, whereas the FGF23 enhancer deletion resulted in a mouse with metabolite compensation for a mild skeletal phenotype. Dissection of the PTH enhancer resulted in mice with a distinct separation of basal repression and PTH induction activities. None of our genomic deletions affected NRC *Cyp27b1* basal expression or response to inflammation. Furthermore, CTCF occupancy helped define a topologically associated domain in which we found co-regulation of genes near *Cyp27b1* by these endocrine ligands and our deletions. These deletions in mice have exquisite consequences to mineral homeostasis and also highlight the importance of the homeostatic interplay with the expression of the degrading enzyme *Cyp24a1* for maintenance of circulating 1,25(OH)<sub>2</sub>D<sub>3</sub> levels. In summary, we have discovered the genomic enhancers unique for endocrine control of 1,25(OH)<sub>2</sub>D<sub>3</sub> production *in vivo*.

**Disclosures:** Mark Meyer, None.

## SA0104

See Friday Plenary Number FR0104.

## SA0105

See Friday Plenary Number FR0105.

## SA0106

**Estrogen via Estrogen Receptor Alpha Inhibits Mandibular Condylar Fibrocartilage Degeneration through Upregulation of Protease Inhibitors.** Jennifer Robinson<sup>\*</sup>, Paola Soria, Jing Chen, Helen Lu, Sunil Wadhwa. Columbia University, United States

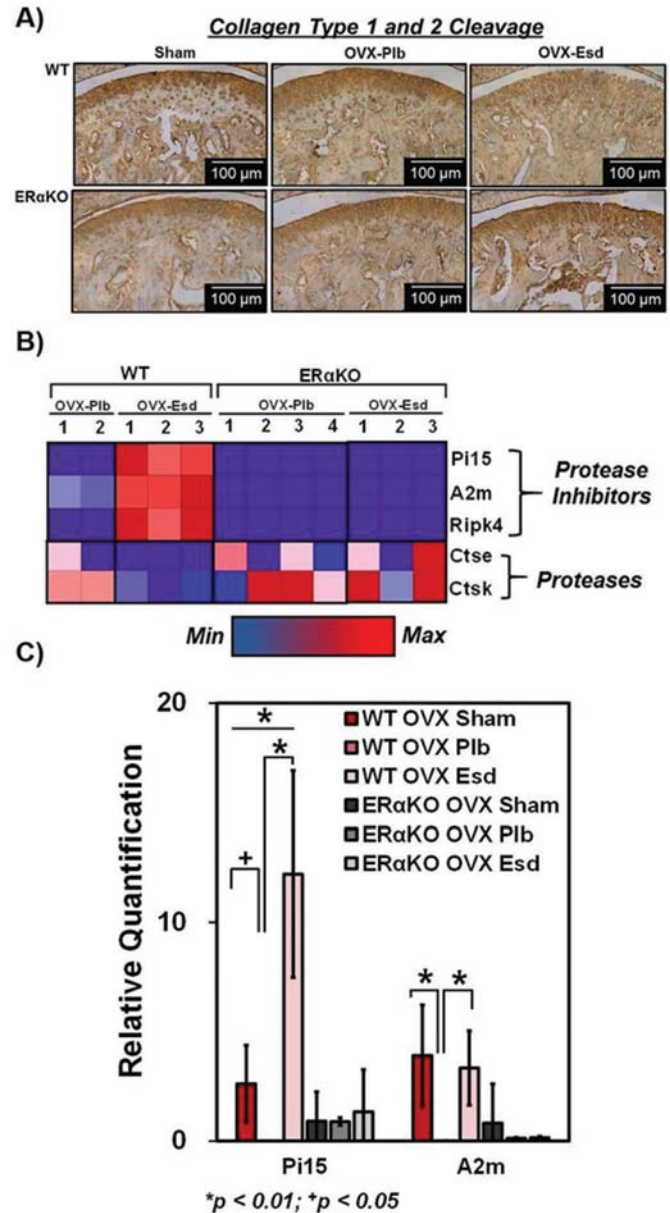
Temporomandibular joint degenerative disease (TMJ-DD) is marked by degradation of the extracellular matrix proteins and proteoglycans that promote joint function. The majority of patients afflicted with TMJ-DD are post-menopausal women suggesting estrogen's protective role in the disease process. In the growing mandibular condyle, estrogen is known to decrease cell proliferation and fibrocartilage thickness and play a role in chondrogenesis via estrogen receptor alpha (ER $\alpha$ ). However, the role of estrogen on mature condylar fibrocartilage is unknown. Thus, the goal of this work was to investigate the role of ER $\alpha$  on the homeostasis and degeneration of the mandibular condylar fibrocartilage in adult female mice.

To assess the role of estrogen via ER $\alpha$  on mandibular condylar fibrocartilage degradation, both a murine ovariectomy model and a mandibular explant model with estradiol treatment were employed. For the ovariectomy model, 13-week old female WT and ER $\alpha$ KO mice were either sham operated or ovariectomized and treated with placebo or estradiol for 4 weeks. The articular condylar fibrocartilage tissue was dissected for histology/immunohistochemistry (n=6), RNA sequencing (n=3), and relative gene expression analysis (n=6) of matrix proteins, proteases, and protease inhibitors. In the explant model, mandibles were extracted from 13-week old female WT mice and placed in culture with FBS-free media overnight. Following overnight incubation, mandibles were subjected to 0 M, 10<sup>-8</sup>M 17 $\beta$ -estradiol, and 10<sup>-6</sup>M 17 $\beta$ -estradiol treatment for 48 hours. Supernatant from cultures was harvested (n = 6) to assess protease activity via gelatin zymography and collagen cleavage utilizing a Col1/Col2 cleavage ELISA. Gene expression (n=6) of matrix proteins and proteases was also evaluated.

Estradiol treatment in both the ovariectomy and explant model resulted in decreased protease activity and decreased cleavage of collagen type 1 and 2 in WT but not in ER $\alpha$ KO mice (Figure 1A). RNA sequencing analysis revealed significant increases in protease inhibitor expression including PI15 and A2m and a corresponding decrease in proteases including cathepsins solely in WT samples (Figure 1B). Gene expression

analysis in both models confirmed a significant increase in PI15 and A2m with estradiol treatment solely in WT tissue (Figure 1C).

This study suggests estrogen via ER $\alpha$  protects the mandibular condylar fibrocartilage from protease degradation by upregulation of the protease inhibitors PI15 and A2m. Currently, a clinical trial is underway for the use of A2m to inhibit knee osteoarthritis providing an exciting translational pathway for this work. Future work is focused on determining the efficacy for PI15 and A2m in decreasing matrix degradation in a TMJ osteoarthritis murine model.



J. Robinson et al. Figure 1. Estrogen via ER $\alpha$  decreases condylar fibrocartilage matrix degradation by upregulating protease inhibitors PI15 and A2m. A) Immunohistochemistry of collagen type 1 and 2 cleavage shows estradiol decreases the amount of cleavage in WT but not ER $\alpha$ KO mice. B) Heat map illustrates RNA sequencing results of upregulation of protease inhibitors and downregulation of proteases with estradiol treatment in WT but not ER $\alpha$ KO mice. C) Gene expression analysis illustrates an increase in PI15 and A2m with estradiol treatment in WT but not ER $\alpha$ KO mice.

Figure 1

**Disclosures:** Jennifer Robinson, None.



## SA0107

**Ethnic Differences in the Diurnal Rhythms of Calcium and Phosphate Metabolism.**

Inez Schoenmakers<sup>\*1</sup>, Jean Redmond<sup>2</sup>, Landing Jarjou<sup>3</sup>, Bo Zhou<sup>4</sup>, Ann Prentice<sup>2</sup>, Tony Fulford<sup>5</sup>. <sup>1</sup>Medical Research Council (MRC) Human Nutrition Research, Cambridge, UK and Department of Medicine, University of East Anglia, Norwich, UK, United Kingdom, <sup>2</sup>Medical Research Council (MRC) Human Nutrition Research, Cambridge, UK, United Kingdom, <sup>3</sup>MRC Keneba, The Gambia, Gambia, <sup>4</sup>Department of Public Health, Shenyang Medical College, Shenyang, PR China, China, <sup>5</sup>MRC International Nutrition Group, London School of Hygiene and Tropical Medicine, London, UK, United Kingdom

**Objectives & Methods:** Ethnic differences exist in calcium (Ca), phosphate (P) metabolism and their regulatory hormones. These factors have a diurnal rhythm (DR) and may be influenced by eating patterns and other lifestyle factors known to differ between ethnic groups. Changes in DRs of Ca and P metabolism and PTH are associated with alterations in bone integrity. Ethnic differences in the DRs of Ca and P metabolism may contribute to differences in bone health between groups.

We have investigated healthy White-British (B), Mandinka-Gambian (G) and Han-Chinese (C) adults (60-75 years; n=91). Dietary intake of Ca and P were recorded by food diaries and fractional urinary Ca (F<sub>u</sub>Ca) and P (F<sub>u</sub>P) excretion was determined from fasting timed blood and urine samples. Blood ionised Ca (iCa), plasma P, parathyroid hormone (PTH) and C-terminal fibroblast growth factor 23 (C-FGF-23) and its co-factor  $\alpha$ Klotho were analysed in blood samples collected 4-hourly and urinary calcium and P excretion in 4-hourly collections during a 24h cycle. A random effects Fourier (trigonometric) regression with a 24h cyclic component was used to analyse the DRs. The coefficients of the Fourier terms were used to calculate the Coefficient of Cyclic Variation (CCV), a measure of the amplitude of the DR.

**Results:** Dietary intakes and F<sub>u</sub>Ca and F<sub>u</sub>P significantly differed between groups. The DRs of Ca and P metabolism were significant for all variables in all groups ( $P < 0.05$ ), except iCa in B. There were ethnic differences in the 24h mean for all variables except for iCa and  $\alpha$ Klotho (Table). The DRs of plasma P, and C-FGF-23 were unimodal with a night-time peak and a day-time nadir in all groups. In contrast, the peaks and nadirs of  $\alpha$ Klotho occurred during the night and day, respectively. PTH had 2 peaks in all groups. Urinary Ca and P excretion was low and unimodal in G and bimodal in B and C, with the lowest excretion rate uniformly occurring in the morning.

**Conclusion:** Despite differences in dietary intakes, renal handling and 24h mean concentrations, rhythmicity was maintained in all groups. The timing of the peaks and nadirs of markers of Ca and P metabolism was similar between countries and to those described in Western populations. This may indicate an innate DR which is conserved independent of external stimuli, whereas group differences in the overall 24h mean may reflect dietary and lifestyle influences.

Schoenmakers ASBMR 2017

Table: Daily dietary nutrient intakes, fasting fractional urinary Ca and P excretion and parameters of the DR of Ca and P metabolism								
Daily dietary nutrient intakes, fasting fractional urinary Ca and P excretion								
Group	B (n=30)	G (n=31)	C (n=30)	P <sup>†</sup>				
Dietary Ca mg/d	1076 (961, 1204) <sup>a, †</sup>	282 (240, 333) <sup>†</sup>	546 (467, 638)	<0.001				
Dietary P mg/d	1432 (1312, 1568) <sup>a, †</sup>	705 (638, 778) <sup>†</sup>	1158 (1084, 1237)	<0.001				
F <sub>u</sub> Ca %	0.91 (0.75, 1.09) <sup>a, †</sup>	0.37 (0.25, 0.55) <sup>†</sup>	1.07 (0.87, 1.32)	<0.001				
F <sub>u</sub> P %	13.3 (11.8, 15.0) <sup>a, †</sup>	6.6 (5.6, 7.9) <sup>†</sup>	12.3 (10.3, 14.8)	<0.001				
Parameters of the DR of Ca and P metabolism								
Fitted 24-hour mean (95% CI)					Amplitude, CCV % (95% CI)			
Group	B (n=30)	G (n=31)	C (n=30)	P <sup>†</sup>	B (n=30)	G (n=31)	C (n=30)	P <sup>†</sup>
iCa (mmol/L)	1.12 (1.11, 1.13)	1.14 (1.12, 1.15)	1.12 (1.12, 1.13)	>0.05	0.5 (0.01, 1.1)	1.0 (0.5, 1.7)	0.6 (0.1, 1.0)	>0.05
P (mmol/L)	1.12 (1.09, 1.16) <sup>†</sup>	1.10 (1.05, 1.15) <sup>†</sup>	0.98 (0.93, 1.03)	<0.001	5.2 (4.1, 6.2)	6.0 (4.7, 7.3)	6.0 (4.0, 7.9)	>0.05
PTH (pg/mL)	53 (46, 60) <sup>†</sup>	77 (67, 87) <sup>†</sup>	57(50, 63)	<0.001	4.1 (1.3, 6.9)	4.1 (1.2, 7.0)	7.4 (4.4, 10.4)	>0.05
C-FGF-23 (RU/mL)	116 (91, 123) <sup>a, †</sup>	151 (101, 201) <sup>†</sup>	79 (67, 91)	<0.001	11 (9, 13) <sup>a, †</sup>	18 (15, 22) <sup>†</sup>	7.4 (5.9, 9.1)	<0.001
αKlotho (pg/L)	647 (586, 709)	668 (568, 769)	712 (646, 778)	>0.05	2.9 (1.9, 4.0)	2.5 (1.4, 3.6)	1.9 (0.9, 2.8)	>0.05
uCa (mmol/4h)	0.67 (0.59, 0.76) <sup>a, †</sup>	0.19 (0.15, 0.22) <sup>†</sup>	0.56 (0.47, 0.65)	<0.001	40 (32, 47)	45 (35, 56) <sup>†</sup>	34 (24, 44)	<0.05
uP (mmol/4h)	3.89 (3.58, 4.20) <sup>a, †</sup>	1.28 (1.07, 1.48) <sup>†</sup>	2.73 (2.36, 3.11)	<0.001	37 (31, 44)	36 (26, 45)	38 (30, 46)	>0.05

<sup>†</sup> Differences in dietary intakes and urinary excretion of Ca and P were tested with one-way ANOVA/Scheffé. <sup>a</sup> Differences in the 24-hour mean were tested with regression using ethnicity as a categorical variable; b, c, g indicates significant differences between groups.

<sup>†</sup> group differences were tested with the z-test

<sup>†</sup> Differences in dietary intakes and urinary excretion of Ca and P were tested with one-way ANOVA/Scheffé; <sup>†</sup> Differences in the 24-hour mean were tested with regression using ethnicity as a categorical variable; b, c, g indicates significant difference between groups.

Table 1

**Disclosures:** Inez Schoenmakers, None.

## SA0108

**The influence of scaffold stiffness on murine fracture healing: an *in silico* study.**

Duncan Betts<sup>\*1</sup>, Esther Wehrle<sup>1</sup>, Gisela Kuhn<sup>1</sup>, Sandra Hofmann<sup>2</sup>, Ralph Müller<sup>1</sup>. <sup>1</sup>Institute for Biomechanics, ETH Zurich, Switzerland, <sup>2</sup>Institute for Biomechanics, ETH Zurich, Zurich, Switzerland, Department of Biomedical Engineering and, Institute for Complex Molecular Systems, Eindhoven University of Technology, Eindhoven, The Netherlands, Netherlands

The fracture healing process is mediated by mechanosensitive cells within the healing bone. A tissue engineered scaffold should create an optimal local mechanical environment for these cells and provide cues that encourage the bone to regenerate itself. In this study an *in silico* model is used to investigate the importance of scaffold stiffness in creating the necessary mechanical cues for cells within and around a scaffold. We hypothesised that scaffold stiffness will influence the amount of deformation in the local tissue and consequently the size of the viable volume in which bone can regenerate.

Data from a previous study was used, in which five female mice (C57BL/6) with stabilized femoral mid-shaft defects were scanned using *in vivo* micro-computed tomography (microCT) over 6 weeks. A specific level of strain energy density (SED) was found, that predicted 85±3% of bone formation in the first three post-operative weeks. In the present study, virtual scaffolds with a periodic cubic mesh of cylindrical struts were virtually implanted into the microCT images of the bone defects. The strut diameter was 42µm and periodicity was 210µm, resulting in a porosity of 75%. Scaffolds were filled with soft tissue with an elastic modulus 3MPa. The scaffold struts were adjusted that the bulk stiffness of the scaffold-soft tissue mixture was between 2.25MPa and 75MPa. This range was chosen as many biomaterials (PLGA, PCL, PLT, silk fibroin) fall in this range in the wet state. The mechanical environment was calculated using a microFE model. Soft tissue voxels with an SED value within the osteoinductive range were defined as part of a viable volume, and subsequently these volumes were compared in the case of a defect with a scaffold (blue volume in Fig. 1B) and empty defect (red volume in Fig. 1C): This ratio is the "viable volume fraction" (VVF).

A scaffold stiffness between 3 and 5 MPa was found to increase VVF above 100%, however values both higher and lower resulted in decreased VVF as seen in Fig. 1A. The VVF is more sensitive to changes below 3MPa compared to material stiffer than 5MPa.

Our findings indicate that, as with fracture fixation, stiff scaffolds shield the tissue from beneficial loading. Soft scaffolds allowed the soft-tissue to relax by storing deformation in the scaffold elements. Both cases result in a reduction of the VVF. In conclusion, a scaffold should not match the stiffness of bone but rather that of the early callus, nature's own scaffold.

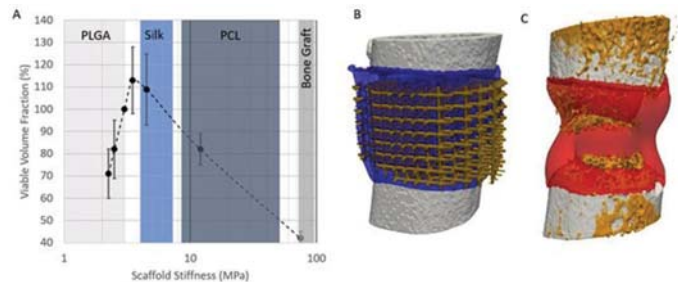


Figure 1: A) VVF vs. stiffness. B) Blue VVF with scaffold and C) VVF in empty defect

**Disclosures:** Duncan Betts, None.

## SA0109

See Friday Plenary Number FR0109.

## SA0110

See Friday Plenary Number FR0110.

## SA0111

**Microtubule-dependent regulation of a signaling relay that tunes the osteocyte mechanical load response.**

James Lyons<sup>\*1</sup>, Humberto Joca<sup>1</sup>, Robert Law<sup>2</sup>, Jaclyn Kerr<sup>1</sup>, Guoli Shi<sup>1</sup>, Ramzi Khairallah<sup>3</sup>, Konstantinos Konstantopoulos<sup>2</sup>, Christopher Ward<sup>1</sup>, Joseph Stains<sup>1</sup>. <sup>1</sup>University of Maryland, Baltimore, United States, <sup>2</sup>Johns Hopkins University, United States, <sup>3</sup>Myologica, LLC., United States

The molecular mechanisms by which bone cells sense and respond to mechanical cues to regulate bone mass are incompletely understood. In many tissues, the microtubule (MT) network is a critical element for mechanotransduction by altering cytoskeletal stiffness. MT detyrosination, a post translational modification of  $\alpha$ -tubulin, promotes interactions of MTs with other cytoskeletal proteins and increases cytoskeletal stiffness. We hypothesized that detyrosinated MTs are a critical driver of bone mechanotransduction by dynamically regulating cytoskeletal stiffness. By immunofluorescence, we observed abundant detyrosinated MTs in osteocyte cell processes and primary cilia, two putative osteocyte mechano-sensors. Using atomic force microscopy and western

blotting, we confirmed that the abundance of dephosphorylated MTs modulates cytoskeletal stiffness in OCY454 osteocyte-like cells. Taxol (1 $\mu$ M, 2h) increased dephosphorylated MTs and cytoskeletal stiffness, while parthenolide (PTL, 25 $\mu$ M, 2h) inhibited dephosphorylated MTs and decreased cytoskeletal stiffness. Using these pharmacologic agents to tune cytoskeletal stiffness through a dynamic range, we showed that dephosphorylated MTs and cytoskeletal stiffness regulate the mechano-responsive range at which osteocytes elicit a  $Ca^{2+}$  response (Fluo-4) and down regulate sclerostin following exposure to fluid shear stress (FSS). Further, we demonstrated that this FSS-induced downregulation of sclerostin protein requires  $Ca^{2+}$  influx. A screen of calcium channels in osteocytes suggested TRPV4 may be a source of FSS-activated  $Ca^{2+}$  influx. Inhibition of TRPV4 with GSK-219374 (10 $\mu$ M, 15min) or a TRPV4 specific siRNA both significantly blunted FSS-induced  $Ca^{2+}$  influx and sclerostin downregulation. Conversely, a TRPV4 agonist (GSK-1016790A, 10 $\mu$ M, 15min) decreased sclerostin levels, suggesting an important role for TRPV4 in osteocyte mechanotransduction. Finally, we have found that TRPV4 activation requires reactive oxygen species (ROS) generated by FSS-induced activation of the mechano-sensitive NADPH oxidase 2 (NOX2) enzyme. Inhibition of Nox2 with GP91ds-TAT (10 $\mu$ M, 30min) blocked the FSS-induced  $Ca^{2+}$  influx and sclerostin downregulation, and  $H_2O_2$  treatment (100 $\mu$ M, 30min), a ROS mimetic, reduced sclerostin protein abundance. These data reveal a novel signaling relay responsible for regulating the osteocyte FSS-activated  $Ca^{2+}$  influx and downregulation of sclerostin.

**Disclosures:** James Lyons, None.

## SA0112

**TIEG1 is a Critical Mediator of Wnt Signaling in Calcific Aortic Valve Disease.** Nalini Rajamannan\*. Mayo Clinic, United States

We have previously demonstrated that  $\beta$ -catenin plays an important in calcific aortic valve disease (CAVD). Recent studies indicate that TIEG1, a transcription factor known to play critical roles in osteoblast differentiation is also involved in the Wnt signaling pathway. Therefore, we sought to determine if TIEG1 participated in regulating Wnt signaling, in CAVD. Transfection of valvular interstitial cells with Lef1,  $\beta$ -catenin, and/or TIEG1 resulted in activation of the canonical Wnt signaling top-flash reporter construct, especially in combination. This finding was confirmed by the observation that TIEG1 and  $\beta$ -catenin co-localize with one another in the nucleus of VICs following stimulation with LiCl or treatment with TGF- $\beta$ , a cytokine known to induce TIEG1 expression and enhance osteogenic phenotypes. LiCl treatment of VICs increased thymidine incorporation in vitro. BMP-4 and Wnt3a in combination increased synthesis of alkaline phosphatase. Experimental hypercholesterolemia in Lrp5 null mice demonstrate an increase in TIEG1 expression and calcification in the aortic valve as compared to control. LiCl alone increases calcified atheroma in the aortic valve implicating a proof of principle for Wnt Signaling Taken together, these data implicate a novel role for TIEG1 in mediating Wnt signaling in CAVD.

**Disclosures:** Nalini Rajamannan, None.

## SA0113

See Friday Plenary Number FR0113.

## SA0114

See Friday Plenary Number FR0114.

## SA0115

**Low Magnitude Mechanical Signals Decrease Invasion and Expression of Osteolytic Factors in MDA-MD-231 Breast Cancer cells, with subsequent Suppression of Osteoclastogenesis.** Xin Yi<sup>1</sup>, Laura Wright<sup>1</sup>, Gabriel Pagnotti<sup>1</sup>, Jenna Reagan<sup>1</sup>, Gunes Uzer<sup>2</sup>, Clinton Rubin<sup>3</sup>, Khalid Mohammad<sup>1</sup>, Theresa Guise<sup>1</sup>, William Thompson<sup>1</sup>. <sup>1</sup>Indiana University, United States, <sup>2</sup>Boise State University, United States, <sup>3</sup>State University of New York Stony Brook, United States

Bone is a preferred site of breast cancer metastasis, with complications including pain, pathological fractures, muscle weakness, and death. The growth factor rich bone microenvironment supports cancer growth and invasion, while states of high bone turnover, such as estrogen depletion, perpetuate metastasis and bone lysis. Low-intensity vibration (LIV) stimulates bone formation. Furthermore, LIV restricts bone loss and tumor progression in models of multiple myeloma and ovarian cancer. Transmission of LIV signals requires connection between the actin cytoskeleton and the nucleus via the Linker of Nucleoskeleton and Cytoskeleton (LINC) complex. This study examined direct effects of LIV on human breast cancer cells, hypothesizing that LIV suppresses catabolic gene expression. Human MDA-MB-231 cells were exposed to LIV (90Hz, 0.3g) in twenty minute bouts once or twice a day in the presence or absence of TGF $\beta$ 1. Of the genes surveyed, only expression of PTHrP significantly decreased with once-daily LIV (2.54-fold,  $p<0.01$ ). In contrast, exposure to LIV twice-daily resulted in significant reduction of PTHrP (6-fold,  $p<0.001$ ), Ctgf (2.3-fold,  $p<0.05$ ), IL-11 (1.76-fold,  $p<0.001$ ), and Rankl (2-fold,  $p<0.05$ ) mRNA. With the exception of Rankl, significant ( $p<0.05$ ) reductions were also seen in the presence of TGF $\beta$ 1. Notably, with respect to PTHrP, twice-daily LIV resulted in over 2-fold greater reduction compared to once-daily LIV. Using transwell assays, a 3.6-fold ( $p<0.05$ ) decrease in MDA-MB-231 cell invasion was observed following LIV. Significant reductions in Mmp1 (4.2-fold,  $p<0.01$ ) and Mmp3 (2.73-fold,  $p<0.05$ ) mRNA were seen. Addition of conditioned media from

MDA-MB-231 cells, exposed to LIV, to RAW 264.7 macrophages reduced osteoclast formation by 3.47-fold ( $p<0.0001$ ). As previous work demonstrated that nucleocytoskeletal connectivity enabled transmission of LIV signals, we examined expression of LINC complex genes in response to LIV. Expression of Syne1 (1.83-fold,  $p<0.001$ ), Syne2 (2.63-fold,  $p<0.05$ ), Sun1 (2.28-fold,  $p<0.001$ ), and Sun2 (4.33-fold,  $p<0.05$ ) were significantly increased in MDA-MB-231 cells with twice-daily LIV, suggesting that these connections influence LIV signal transduction. These data show that application of LIV to MDA-MB-231 cells decreases invasion and production of osteolytic genes, with subsequent suppression of osteoclastogenesis. Thus, LIV may serve as a non-invasive intervention to suppress breast cancer metastasis and osteolysis.

**Disclosures:** Xin Yi, None.

## SA0116

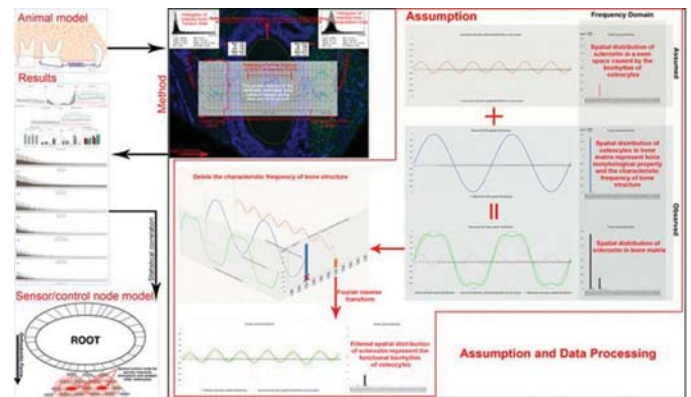
**Fast Fourier Transform Analysis Showed Morphological Change of Bone Structure and Change of Periodicity of Sclerostin Expression during Orthodontic Tooth Movement.** Ziyi Wang\*, Yoshihito Ishihara, Naoya Odagaki, Masahiro Nakamura, Ei Ei Hsu Hlaing, Hiroshi Kamioka. Okayama University, Japan

**Purpose:** To investigate the change of functional periodicity of osteocytes and the morphological change of bone structure during orthodontic tooth movement.

**Methods:** Expression of sclerostin (Scl), an osteocyte-expressed negative regulator of bone formation, and character of bone structure were investigated by immunofluorescence staining. A region of 128 x 310 pixels from the boundary of periodontal ligament were measured in both compression and tension side. In these two regions, counted the Scl positive cell and entire cell amount, produced averaged histogram of fluorescence intensity and averaged curve of fluorescence intensity along the orthodontic force direction (curve of spatial distribution of fluorescence intensity: CSD) from each side at each time point. Converted all CSD to frequency domain by fast Fourier transform (FFT), then averaged power spectrum density graph were produced. To reduce the influence of bone structure on spatial distribution of Scl expression, all peak power frequency of DAPI fluorescence CSD were subtracted from original Scl CSD. Then the filtered Scl CSD was produced by Fourier inverse transform. The difference of each frequency from each side at each time point was tested by multiple t test to detect the morphological change of bone structure (DAPI CSD of osteocytes), spatial distribution of Scl in bone matrix (original Scl CSD) and biorhythm of Scl expression (filtered Scl CSD).

**Results:** During orthodontic tooth movement: frequency of DAPI signal was increased on compression side, while decreased on tension side; original and filtered Scl CSD was changed in a certain pattern; and this pattern could be independent of Scl expression level. Spearman's rho and multiple linear regression showed that the percentage of Scl positive cells had association with frequency of original sclerostin CSD; the 95<sup>th</sup> and 5<sup>th</sup> percentile of fluorescence intensity of sclerostin had positive association with frequency of DAPI and negative association with filtered Scl CSD respectively.

**Conclusions:** Our results indicated that orthodontic force can induce the morphological change of bone structure (extend and compress), and maybe the osteocytes response to stimulation by a sort of biorhythm. The regulation of this biorhythm maybe a negative feedback system. Considering our previous study, we hypothesize that only few osteocytes wake for monitoring of stimulation in nature status.



Figure

**Disclosures:** Ziyi Wang, None.

## SA0117

**Loss of GORAB Leads to an Impaired Anabolic Cortical and Cancellous Bone Response to Mechanical Loading.** Haisheng Yang<sup>1</sup>, Anne Seliger<sup>2</sup>, Wing-Lee Chan<sup>2</sup>, Michael Thelen<sup>2</sup>, Uwe Kornak<sup>2</sup>, Bettina Willie<sup>3</sup>. <sup>1</sup>Beijing University of Technology, China, <sup>2</sup>Charité-Universitätsmedizin Berlin, Germany, <sup>3</sup>Shriners Hospital for Children-Canada, McGill University, Canada

Gerodermia osteodysplastica (GO) is a segmental progeroid disorder caused by loss-of-function mutations in the GORAB gene, associated with early onset osteoporosis and bone fragility [1]. A mouse model of GO (*Gorab*<sup>Prx1</sup>) was generated wherein the Gorab



gene was deleted in long bones. We observed an abnormal osteocyte morphology and a reduced and disrupted canalicular network in *Gorab<sup>Prx1</sup>* mice [2]. Given the crucial role of osteocytes in sensing mechanical signals and orchestrating adaptive bone remodeling, we hypothesized loss of *Gorab* would lead to an impaired anabolic response of cortical and cancellous bone to loading. In vivo cyclic compressive loading was applied to left tibiae of 10-week-old *Gorab<sup>Prx1</sup>* and littermate control (LC) mice for 2 weeks (+1200  $\mu$  at midshaft determined by strain gauging, 216 cycles/day at 4 Hz) and right tibiae served as internal controls. Load-induced changes in bone formation and resorption were quantified for both midshaft cortical and metaphyseal cancellous bone using in vivo microCT-based 3D time-lapse morphometry [3] and fluorochrome-based 2D histomorphometry. In LC mice, loading significantly enhanced bone formation responses, with the loaded limb having increased volume and surface area of newly formed bone compared to the control limb for the midshaft cortical (MV/BV<sub>day0-15</sub>: +741%, MS/BS<sub>day0-15</sub>: +174%) and metaphyseal cancellous bone (MV/BV<sub>day0-15</sub>: +189%, MS/BS<sub>day0-15</sub>: +82%)(Fig. 1). Loading significantly reduced resorbed bone volume and surface for metaphyseal cancellous bone in LC mice (EV/BV<sub>day0-15</sub>: -22%, ES/BS<sub>day0-15</sub>: -27%). Dynamic histomorphometry confirmed that both endocortical and periosteal bone formation rates increased with loading at the tibial midshaft in LC mice (Ec.BFR/BS: +240%, Ps.BFR/BS: +725%). In *Gorab<sup>Prx1</sup>* mice all bone formation and resorption parameters were not significantly different between the loaded and control limbs (Fig. 1). These results show that loss of *Gorab* leads to a complete absence of bone formation and resorption responses to mechanical loading for both cortical or cancellous bone. These data suggest the low bone mass phenotype of *Gorab<sup>Prx1</sup>* mice could be attributable in part to a loss in skeletal mechanoresponsiveness. Future strategies to treat GO disease could consider therapies to restore or enhance adaptive bone formation. References: [1] Hennies et al, 2008 *Nat Genet*, [2] Steiner et al. 2015 *JBM* 28 (Suppl 1), [3] Birkhold et al, 2014 *Bone*.

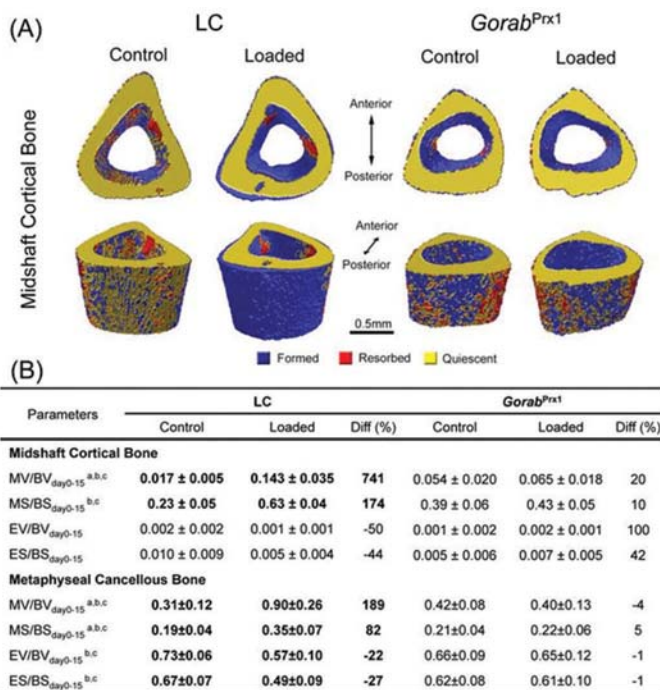


Fig. 1. (A) 3D in vivo time-lapse morphometry showing bone formation and resorption over 15 days of the loading experiment in the tibial midshaft. (B) Newly formed or resorbed bone volume (MV/BV<sub>day0-15</sub>, EV/BV<sub>day0-15</sub>) and surface area (MS/BS<sub>day0-15</sub>, ES/BS<sub>day0-15</sub>) over 15 days in control and loaded tibia of LC and *Gorab<sup>Prx1</sup>* mice. ANOVA: <sup>a</sup>genotype, <sup>b</sup>loading, <sup>c</sup>interaction between genotype and loading. Bold indicates difference between control and loaded limb (paired t-test).

Figure 1

Disclosures: Haisheng Yang, None.

## SA0118

**Effects of Low-intensity Aerobic Exercise and Activated Vitamin D, Alfacalcidol, on Blood Glucose, Bone, and Muscle in Diabetic Model Rats.** Manabu Akagawa\*, Naohisa Miyakoshi, Yuji Kasukawa, Hiroyuki Tsuchie, Yuichi Ono, Masazumi Suzuki, Tetsuya Kawano, Yusuke Yuasa, Itsuki Nagahata, Yoichi Shimada, Akita University Hospital, Japan

### Introduction

Diabetes mellitus causes secondary osteoporosis and muscle atrophy. Whether activated vitamin D, alfacalcidol (ALF), and exercise treatment inhibit osteoporosis and muscle atrophy in diabetic model rats was examined, along with their effects on the expressions of muscle-related genes.

### Methods

Twenty-week-old Otsuka-Long-Evans-Tokushima-Fatty rats were randomized into four groups (n=8-10): ALF group, orally treated with 0.1  $\mu$ g/kg/day ALF; Ex group, exercised by treadmill at 10 m/min, 60 min/day, 5 days/week; COMB group, treated with ALF and exercised by treadmill; and CNT group, treated with ALF vehicle and no exercise. ALF administration and/or exercise were continued for 2 or 6 weeks with measurements of blood glucose (BG) levels every 2 weeks. After sacrifice, the cross-sectional area (CSA) of tibialis anterior muscle fibers and total femoral bone mineral density (BMD) were measured. The relative quantities of MyoD, Pax7, Myogenin, REDD1, Atrogin-1, and MuRF-1 of soleus muscle were measured by real-time polymerase chain reaction assays.

### Results

#### 2-Week Group

BG and BMD showed no significant differences among the groups. CSAs were significantly larger in the ALF, Ex, and COMB groups than in the CNT group (all  $p < 0.0001$ ). MyoD expression was significantly higher in the COMB group than in the CNT group ( $p < 0.05$ ), and Atrogin-1 expression in the ALF group and MuRF-1 expressions in the Ex and COMB groups were significantly lower than in the CNT group (all  $p < 0.05$ ).

#### 6-Week Group

BG was significantly lower in the Ex and COMB groups than in the CNT group ( $p = 0.007$ ,  $p = 0.04$ , respectively). BMD was significantly higher in the ALF group ( $p < 0.0001$  vs CNT group,  $p = 0.0007$  vs Ex group) and the COMB group ( $p < 0.0001$  vs CNT group,  $p = 0.005$  vs Ex group) than in the CNT and Ex groups. CSAs were significantly larger in the ALF, Ex, and COMB groups than in the CNT group (all  $p < 0.0001$ ). REDD1 expression in the COMB group and Atrogin-1 expressions in the ALF and COMB groups were significantly lower than in the CNT group (all  $p < 0.05$ ).

### Discussion

A combination of alfacalcidol and exercise improved muscle volume from the early stage by stimulating the differentiation of muscle satellite cells and suppressing muscle catabolic genes. Improvements of BG, BMD, and muscle volume were observed as long-term effects of the combination therapy. Continuing suppression of muscle catabolic genes was also observed as a background to these long-term effects.

Disclosures: Manabu Akagawa, None.

## SA0119

See Friday Plenary Number FR0119.

## SA0120

**Postmenopausal Osteoporosis is Characterized by a Distinct Muscle Transcription Profile Which Can Be Markedly Changed Through Heavy-load Strength Training.**

Ole K. Olstad<sup>1</sup>, Sjur Reppe<sup>1</sup>, Håvard Wiig<sup>2</sup>, Nils Helge Kvamme<sup>2</sup>, Camilla Kirkegaard<sup>2</sup>, Truls Raastad<sup>2</sup>, Vigdis T. Gautvik<sup>3</sup>, Karl J. Kvernevik<sup>4</sup>, Tor P. Utheim<sup>1</sup>, Kaare M. Gautvik<sup>5</sup>. <sup>1</sup>Oslo University Hospital, Department of Medical Biochemistry, Norway, <sup>2</sup>Norwegian School of Sport Sciences, Department of Physical Performance, Norway, <sup>3</sup>University of Oslo, Institute of Basic Medical Sciences, Norway, <sup>4</sup>Lovisenberg Diakonale Hospital, Norway, <sup>5</sup>Lovisenberg Diakonale Hospital, Unger-Vetlesen Institute, Norway

Postmenopausal osteoporosis (OP) is recognized as a primary skeletal disease with a dominant genetic influence resulting in a continued bone loss causing skeletal fragility and risk for fractures. Muscular weakness and involution (sarcopenia) characteristic to these patients have been considered to be secondary to less physical activity and negative life style factors. The aim of the study was to explore whether the OP phenotype is linked to the muscle transcriptome and if heavy load strength training could influence muscle gene expression. Healthy (n=18) or OP women (n=17) age 55-80 years, whose bone transcriptome and BMD were known, were subjected to heavy load strength training for three months. Thigh muscle biopsies (*m. vastus lateralis*) were obtained prior to and after training and analyzed by global transcriptional profiling, muscle fiber immunohistochemistry and Western blot. Quantitative thigh computed tomography (CT) was used to measure changes in muscle size. Heavy load training improved muscle strength and size to a similar degree in patients as in healthy controls. Before training, healthy controls and OP women showed differences in fiber type distribution. Fiber cross sectional area only increased in type II fibers in healthy after intervention. Intervention resulted in reduced levels of HSP70 in both groups ( $p < 0.01$ ).  $\alpha$ -B-crystalline levels increased in OP ( $p < 0.05$ ), but was unchanged in healthy women. The skeletal muscle transcriptomes were subjected to principal component analysis. Healthy controls and OP women grouped to separate areas, indicating distinct muscular transcription profiles. After intervention, the average global transcript level rose by 1.4-fold in OP women compared to the control group. When pooling the two cohorts, 1069 mRNAs changed expression after exercise. Seventeen of these correlated to total Hip BMD T-score at  $FDR \leq 0.10$  with r-values ranging from -0.37 to -0.44. Several of the genes are also known to be associated with bone metabolism, e.g. FZD4 and IGF1. Ingenuity pathway analysis identified several over-represented pathways. The present study discloses marked molecular pathology in the muscular system of postmenopausal OP women as reflected by a changed transcriptome, protein expression and muscle fiber distribution. Heavy load strength training changed the muscle transcriptome, affecting genes that are also correlated to BMD. This study strongly suggests that postmenopausal OP is a primary musculo-skeletal disease

Disclosures: Ole K. Olstad, None.

## SA0121

See Friday Plenary Number FR0121.

## SA0122

See Friday Plenary Number FR0122.

## SA0123

**Bone morphogenetic proteins and myostatin: key mediators of Sarcopenia-Osteoporosis connection.** Umberto Tarantino\*, Maurizio Feola, Cecilia Rao, Monica Celi, Manuel Scimeca. University of Rome Tor Vergata, Policlinic Tor Vergata Foundation, Italy

### Background

Sarcopenia is an aging-induced generalized pathological condition characterized by loss of muscle mass and function. It is strongly associated to reduction of the global physical strength and poor quality of life, ultimately the patient experiences fall and fractures and is confined to bed with an increased risk of mortality. Osteoporosis (OP), osteoarthritis (OA) and sarcopenia are the most frequent musculoskeletal disorders affecting older people. Indeed, aging process is a factor involved in the loss of the functionality of both bone and muscle. The aim of this study was to test the hypothesis that the balance between BMPs and myostatin pathways regulates the age-related muscle degeneration in OP and OA patients. We investigated the relationship among the expression of BMP-2/4-7, myostatin and phosphorylated Smad1-5-8 and the muscle quality, evaluated in term of fibers atrophy and satellite cells activity.

### Methods

In this retrospective study, we collected 102 biopsies of vastus lateralis: 48 biopsies from patients who underwent hip arthroplasty for medial fragility fractures of the femur (OP) and 55 biopsies from patients who underwent hip arthroplasty for OA. Serial sections were used for morphometrical and immunohistochemical analysis (BMP-2/4-7, myostatin, Smad1-5-8, Pax7 and myogenin).

### Results

Morphometric data indicated an increase of the number of atrophic fibers in OP patients compare to OA. In line with these data, we found an high regenerative potential in muscle tissues of OA patients due to the significant amount of both Pax7 and myogenin positive satellite cells detected in OA group. In addition, our data showed the decrease of BMP2/4 and -7 expression in OP patients compared to OA group. Conversely, OP patients were characterized by high levels of myostatin expression. A different expression profile was also found for phosphorylated Smad1-5-8 between OP and OA patients. In particular, OP patients showed a low number of positive phosphorylated Smad1-5-8 nuclei.

### Conclusion

The identification of molecular pathways involved in the pathogenesis of sarcopenia open new perspective for the development of drugs able to prevent/treat the muscle impairment that occur in elderly. Results here reported, highlighting the role of BMPs and myostatin pathways in physio-pathogenesis of human sarcopenia, allow us to propose human recombinant BMP-2/7 and anti-myostatin antibodies as a possible therapeutic option for the sarcopenia.

**Disclosures:** Umberto Tarantino, None.

## SA0124

See Friday Plenary Number FR0124.

## SA0125

See Friday Plenary Number FR0125.

## SA0126

See Friday Plenary Number FR0126.

## SA0127

**Intermittent High Dietary Protein Feeding Is As Effective In Increasing Bone Mass As Continuous High Protein Diet.** Kehong Ding\*<sup>1</sup>, Priyanka Thakur<sup>1</sup>, Walter Ramsey<sup>1</sup>, Ying Han<sup>2</sup>, Jianrui Xu<sup>1</sup>, Qing Zhong<sup>1</sup>, Wendy Bollag<sup>1</sup>, Meghan McGee-Lawrence<sup>1</sup>, William Hill<sup>1</sup>, Xingming Shi<sup>1</sup>, Monte Hunter<sup>1</sup>, Mohammed Elsalanty<sup>3</sup>, Mark Hamrick<sup>1</sup>, Carlos Isales<sup>1</sup>. <sup>1</sup>Medical College of Georgia, United States, <sup>2</sup>Jiaotong University, China, <sup>3</sup>Augusta University, United States

Low dietary protein has been associated with increased longevity and beneficial aging effects comparable to caloric restriction. However, low protein diets are associated with bone loss. In contrast, it has been shown recently that high dietary protein is associated with lower hip fracture rates in elderly men. The present study compared the effects of low (8%) vs. high (28%) vs. intermittent (8% five days/28% two days) dietary protein on bone mass in an IACUC approved protocol. After feeding specified diets for eight weeks, aged (24-month-old male, N=6/group) mice were sacrificed and

bone analyzed by bone densitometry (DXA) and markers of bone turnover (PYD). At the end of eight weeks there were no statistically significant differences in body weights among the groups (35.1±2.5 (8%) vs. 36.7±2.4 (28%) vs. 35.4±3.6 (8/28%) grams; Mean ±SD grams). Mice on the high protein diets had significantly higher bone density than those on the low protein group. There were no differences in DXA measurements at the femur between the high protein and intermittent protein groups (0.0527±0.0031 vs 0.0572±0.0028 vs 0.0589±0.0042 gm/cm<sup>2</sup>; Mean±SD; 8% vs 28% vs 8/28%; p<0.03 8 vs 28% and p<0.01 8 vs 8/28%). Values for the markers of bone breakdown (PYD) were highest in the mice on a low protein diet (1.94±0.49 vs. 1.07±0.11 vs. 1.69±0.28 nmol/L; Mean±SD; p<0.001 8 vs. 28%). In conclusion, administration of dietary protein in an intermittent fashion may be a means of obtaining both the benefits associated with low and of high protein diets.

**Disclosures:** Kehong Ding, None.

## SA0128

**125-150 kDa TSP2 appears during post-natal endochondral ossification and is sensitive to matrix metalloproteinase inhibition.** Andrea Alford\*, Anita Reddy. University of Michigan, United States

The trimeric matricellular protein thrombospondin (TSP)-2 is highly expressed in the skeleton where it influences mesenchymal stromal cell (MSC) fate, angiogenesis and collagen fibrillogenesis. We documented two distinct species (200 and 125-150 kDa) of TSP2 in the femoral epiphyseal-metaphyseal region of male and female 1-2-month old C57/B6 mice. Here, we determined the age at which 125-150 kDa TSP2 is first detected. Femora and calvaria of neonatal (P1, P7 and P11; n= 9 per age) C57/B6 mice were subject to TSP2 immunoprecipitation and Western blot. Only 200 kDa TSP2 was detected in neonatal calvaria. The 125-150 kDa TSP2 isoform was first detected in femora at day 7 and consistently at day 11. At P8, P9 and P10, the 125-150 kDa isoform was enriched in the proximal epiphyses and femoral head, but it was not detected in diaphyses or distal ends. At 6 weeks of age, both TSP2 isoforms were detected in both proximal and distal ends, but the 200 kDa isoform was highly enriched in diaphysis. Neither TSP2-immunoreactive band was detected in tissues obtained from TSP2-/- mice. N-glycosidase F treatment of bone tissue protein extracts obtained from 6-week old mice shifted both TSP2 immunoreactive bands down, suggesting that differential glycosylation of a single protein does not account for the presence of two bands. Non-reducing SDS-PAGE and Western blot suggest that both isoforms are trimeric. 3D cultures of ST2 mesenchymal stromal cells contained both 125 and 150 kDa TSP2, while ADTC5 chondrocyte pellet cultures only contained 200 kDa TSP2. The broad-spectrum matrix metalloproteinase (MMP) inhibitor, GM6001, reduced levels of 125-150 kDa TSP2 in mineralizing primary marrow-derived osteoblast lineage cell cultures in a dose dependent fashion. After immunoprecipitation from the long bones of 6-week old WT mice, the 125-150 kDa region was isolated and subject to trypsin digestion and mass spectrometry. 8 peptides with TSP2 sequence identity were recovered, with coverage spanning amino acids 47-765. Together our data suggest that the appearance of 125-150 kDa TSP2 occurs via an MMP-dependent mechanism that is unique to the milieu of epiphyseal tissues undergoing post-natal endochondral growth and remodeling. We also hypothesize that the MMP-dependent cleavage event occurs downstream (C-terminal) of amino acid 765.

**Disclosures:** Andrea Alford, None.

## SA0129

See Friday Plenary Number FR0129.

## SA0130

See Friday Plenary Number FR0130.

## SA0131

**Thyroid hormone locally interacts with the Sympathetic Nervous System to control bone linear growth.** Manuela Rodrigues\*, Bianca Papi. University of Sao Paulo, Brazil

It is well known that thyroid hormone (TH) is essential for normal bone growth and development. However, the mechanisms by which TH regulates these processes are poorly understood. Recently, the sympathetic nervous system (SNS) was identified as a potent regulator of bone metabolism. In vivo studies by our group have shown that TH interacts with the SNS to regulate bone mass and structure, and that this interaction involves  $\alpha 2$  adrenoceptor ( $\alpha 2$ -AR) signaling. We have also identified the presence of  $\alpha 2A$ -,  $\alpha 2B$ -, and  $\alpha 2C$ -AR subtypes in the epiphyseal growth plate (EGP) of mice. In addition, we have found that mice with isolated gene deletion of  $\alpha 2A$ -AR and  $\alpha 2C$ -AR ( $\alpha 2A$ -AR-/- and  $\alpha 2C$ -AR-/-) show a disorganized EGP, smaller long bones and a delay in endochondral ossification (EO). Moreover, we have found that the EGP of  $\alpha 2A$ -AR-/- and  $\alpha 2C$ -AR-/- animals respond differently than those of wild-type (WT) animals, to TH excess and deficiency. These in vivo findings strongly suggest that TH also interacts with the SNS to regulate bone growth and development. Through a long bone organ culture system, the present study aims to investigate if TH interacts with the SNS directly in the skeleton, to regulate bone linear growth and if  $\alpha 2$ -AR is involved in this process. We evaluated the linear bone growth of the femur and tibia derived from WT and  $\alpha 2C$ -AR-/- neonate mice for 12 days. Treatment with 10-8 M triiodothyronine



(T3), for the whole culture period of twelve days, significantly decreased bone linear growth of both femur and tibia in WT animals, but not in  $\alpha 2C$ -AR-/- mice. To better examine EO, another approach was to analyze the organ culture of WT embryos (E15.5) treated for 6 days with 10-8 M T3, and/or with UK – an  $\alpha 2$ -AR agonist, and/or treated with YO – an  $\alpha 2$ -AR antagonist. We demonstrated that T3 increased the length of the ossified diaphysis of the tibia. On the other hand, YO decreased the length of the ossified diaphysis of the tibia and blocked the T3-induced increase in ossified diaphysis. As expected, T3 decreased the thickness of the reserve zone of the tibial EGP, whereas increased the thickness of the hypertrophic zone, confirming the well-known T3 effect of inducing growth plate chondrocyte terminal differentiation. On the other hand, YO increased the thickness of the reserve, proliferative and hypertrophic zones, but these YO effects were abolished in the presence of T3 (T3+YOH). These findings suggest that TH locally interacts with the SNS to control EO, the EGP morphophysiology and, therefore, the longitudinal bone growth.

**Disclosures:** *Manuela Rodrigues, None.*

## SA0132

See Friday Plenary Number FR0132.

## SA0133

See Friday Plenary Number FR0133.

## SA0134

**miR-146a Is An Endogenous Regulator of Both Hematopoiesis And Bone Mass.** Jennifer Geisler\*, Blake Eason Hildreth III, James Lee, Michael Ostrowski, Sudarshana Sharma, The Ohio State University, United States

MicroRNAs (miRNAs), non-coding RNAs, regulate cellular activity by binding to protein-coding RNAs, suppressing translation or causing RNA degradation. One microRNA, miR-146a, is a key regulator of inflammation and is a physiologic break on immune activity. In the skeleton, osteoclasts share a common progenitor with macrophages of the myeloid lineage within the hematopoietic hierarchy. miR-146a has, historically, been shown to negatively regulate osteoclast differentiation and function in vitro. Due to this finding, we wanted to investigate the role of miR-146a in bone biology and hematopoiesis in vivo. Two transgenic mouse models were used for this purpose: a knock-out (KO) mouse model with global deletion of miR-146a and a knock-in (KI) mouse model overexpressing miR-146a. Male and female mice were aged 6-7 months and, at necropsy, tissue samples were collected for phenotyping. Spleen and liver weights were obtained, femurs isolated for radiographic evaluation, and blood, spleens, and bone marrow collected for flow cytometric evaluation. In both male and female KO mice and male KI mice there was a significant increase in spleen weight compared to wild-type controls. Female KO mice had significantly greater liver weights. These findings suggest altered hematopoietic cell number and/or cellularity. KO mice had decreased bone density and KI mice had increased density, suggesting that miR-146a also negatively regulates osteoclast function in vivo. These findings indicate that miR-146a regulates both hematopoiesis and bone mass. Further phenotyping is ongoing to provide insight into the role of miR-146a in these processes.

**Disclosures:** *Jennifer Geisler, None.*

## SA0135

See Friday Plenary Number FR0135.

## SA0136

See Friday Plenary Number FR0136.

## SA0137

**Specification of Sclerotome Cells via Axial Skeletal Lineage Differentiation of Human Pluripotent Stem Cells.** Ryan Russell\*, Peter Maye, UConn Health, United States

A comprehensive understanding for directing pluripotent stem cells to mature, functional skeletal cell types remains essential for orthopaedic translational medicine. Our research employs a stepwise, embryonic differentiation strategy to produce skeletal progenitors via paraxial mesoderm and sclerotome intermediates. Such axial skeletal lineage derivatives possess vast therapeutic utility owing to a capacity to form mature cells including chondrocytes and osteoblasts.

We have exploited axial mesoderm signaling pathways by differentiating with WNT3a and CHIR99021 (WNT pathway stimulation), FGF2 (FGF stimulation), AGN193109 (retinoic acid receptor inhibition), and LDN193189 (BMP inhibition) to promote paraxial mesoderm formation, and with SAG (Hedgehog agonist) and LDN to promote subsequent sclerotome maturation. These strategies were tested on an H9 ESC *TBX6-mCherry/Ubiqutinin-C-Citrine* reporter line and an HDFA-YK27 iPSC *MEOX1-Citrine* reporter line to facilitate diagnostic analyses using fluorescent reporter expression.

Evaluation of paraxial mesoderm formation in H9-TBX6 cells revealed WNT3a +CHIR combined with AGN for 4 days resulted in a considerable increase in TBX6 reporter expression confirmed by FACS sorting: 26.9% TBX6<sup>+</sup> to <1% without AGN. Increased endogenous *TBX6* (26-fold), *Mesogenin* (30-fold), and *MEOX1* (18-fold) expression in the TBX6<sup>+</sup> sorted population was shown by RT-PCR, indicating strong paraxial mesoderm induction with comparable reporter and endogenous gene expression. YK27-MEOX cells were used to assess ensuing sclerotome specification. Primary factors (FGF2, WNT3a, CHIR, AGN) with delayed LDN, followed by SAG+LDN treatment were tested. Gene expression revealed an initial FGF+WNT+CHIR+AGN strategy resulted in a 10-fold increase in *PAX1* and 4-fold increase in *PAX9*, both key sclerotome markers, compared to FGF+CHIR alone, while including delayed LDN resulted in further enhancement of *PAX1* (23-fold) and *PAX9* (7-fold).

Specification of sclerotome from human stem cells was optimized by combined FGF and WNT stimulation with retinoic acid receptor and BMP inhibition during the paraxial mesoderm differentiation phase. Initial differentiation conditions appear to have a tremendous influence on downstream cell fate and may ultimately dictate therapeutic functionality. Thus, simulating embryonic lineage determination of the axial skeleton may afford a reproducible roadmap for generating several clinically relevant skeletal progenitor cell types.

**Disclosures:** *Ryan Russell, None.*

## SA0138

See Friday Plenary Number FR0138.

## SA0139

See Friday Plenary Number FR0139.

## SA0140

See Friday Plenary Number FR0140.

## SA0141

See Friday Plenary Number FR0141.

## SA0142

**The Power and Potential of Alternative Splicing to Dictate Stem Cell Fates in Bone.** Yuanyuan Wang\*<sup>1</sup>, Emad Bahrami-Samani<sup>2</sup>, Rene Chun<sup>3</sup>, John Adams<sup>3</sup>, Yi Xing<sup>2</sup>. <sup>1</sup>Bioinformatic Interdepartmental Graduate Program, University of California, Los Angeles, United States, <sup>2</sup>Department of Microbiology, Immunology and Molecular Genetics, University of California, Los Angeles, United States, <sup>3</sup>Department of Orthopaedic Surgery, University of California, Los Angeles, United States

Almost all multi-exonic genes in the human genome are subject to alternative splicing (AS) events. The production of multiple alternatively spliced variants from a single gene frequently occurs in a tissue-specific or developmental stage-specific manner. An unbiased analysis of the consequences of AS during the maturation of mesenchymal stem cells (MSC) in the bone marrow niche to their terminal fates has not been performed systematically. As such, the primary goal of this study is to comprehensively evaluate the consequences of AS in determining pathways taken by human MSCs as they differentiate towards a calcifying osteoblast or a fat-accumulating adipocyte. We performed global pairwise AS and gene expression comparisons among three ENCODE datasets: 1) primary MSC derived from the bone marrow (Homo sapiens; ENCSR000CUD); 2) osteoblasts derived from that MSC (Homo sapiens; ENCSR000CUF); and 3) adipocytes derived from MSC (Homo sapiens; ENCSR000CTZ). In the MSC:osteoblasts comparison 3,528 significant AS events were detected, among which 54% were of the skipped exon (SE) variety. Notably, there was no significant overlap between AS genes and differentially expressed genes (DEG) between MSC and osteoblasts. Among the AS events analyzed in three-way or pairwise comparisons, there were 1,064 differentially spliced genes. Included among these was the vitamin D receptor gene (*VDR*). There were two highly significant differential exon skipping events between MSC and osteoblasts in the *VDR*, both of which occurred in the regulatory, transfactor binding-rich 5'UTR. The fact that differences in AS were not accompanied by differences in DEG indicates an orthogonal function of gene expression and AS in osteoblast development. Splicing co-expression analyses revealed that: 1) changes in concordant binding proteins (RBP) gene expression, including the splicing factor *NOVA1*, were identified with AS; and 2) expression levels of several RBP were associated with 'exon inclusion' AS events. This suggests a potential regulatory function of RBPs in two key AS events in MSC-to-osteoblast differentiation. In sum, AS under the control of RBPs may affect bone formation by defining the differentiation direction of MSCs towards functional osteoblast or adipocyte.

**Disclosures:** *Yuanyuan Wang, None.*

## SA0143

**Conditional Knockout of FGF2 in Progenitor Cells in Mice is Associated with Impaired Periosteal Proliferation During Fracture Repair.** Liping Xiao<sup>1</sup>, Siu-Pok Yee<sup>1</sup>, Ivo Kalajic<sup>1</sup>, Maria Hurley<sup>2</sup>. <sup>1</sup>UConn Health, United States, <sup>2</sup>UConn Health School of Medicine, United States

Fibroblast growth factor 2 (FGF2) is decreased in aged human and aged mouse mesenchyme-derived progenitor cells (MDPCs) and FGF2 treatment increases their proliferation. Fgf2 heterozygote and knockout mice have impaired bone formation and impaired fracture healing associated with reduced periosteal cell proliferation. To target Fgf2 deficiency in progenitors in fracture repair, we generated a novel conditional deletion of Fgf2 using alpha smooth muscle actin Cre transgenic mice. [ $\alpha$ SMACreERT2Tg/+;Fgf2flox/flox (Fgf2cKO)] and  $\alpha$ SMACreERT2/+;Fgf2flox/flox (control, Ctrl) mice at 2-months of age were induced with tamoxifen (100ug/g) at day -1 to day 2 post fracture and harvested at day 3 post fracture. To detect recombination of the Fgf2 floxed alleles, we performed PCR to detect Fgf2 knockout specific DNA fragment and immunofluorescence for FGF2 protein (green) and  $\alpha$ SMA protein (red) on fractured femur sections. PCR showed the Fgf2ko fragment in callus from Fgf2cKO mice but not in non-fractured femur from the same mice (Fig1.A). Tissue sections from Ctrl mice showed robust double labeling (yellow, shown by arrows) for FGF2 and  $\alpha$ SMA within the periosteum. Fgf2cKO IF sections showed a complete depletion of FGF2 in  $\alpha$ SMA positive cells (Fig.1B). These data demonstrate that the FGF2 can be efficiently deleted in  $\alpha$ SMA expressing periosteal progenitors using  $\alpha$ SMACreERT2 mouse. Since FGF2 enhances periosteal cell proliferation that is important in fracture repair, we assessed whether fracture in Fgf2cKO mice was associated with decreased periosteal cell proliferation in the early post-fracture period. We performed femur fracture in 2-months-old Ctrl and Fgf2cKO female mice. Tamoxifen (TM, 1mg/10g body weight) was administered daily via ip injection for 4 continuous days starting at 1 day prior to fracture. On day 0, day 1, and day 2-post fracture, mice were injected with EdU (10ug/gram, IP) to assess nascent cell proliferation. Mice were sacrificed on post fracture day-3 and frozen sections of fractured femurs were stained for EdU and counterstained with DAPI to identify nuclei. We observed decreased labeling with EdU in cells of the periosteal surface of the cortical bone in Fgf2cKO compared with Ctrl mice (Fig. 1C). These data demonstrate that removal of FGF2 signaling within progenitors during early stage of fracture results in decreased cell proliferation in periosteum, and therefore highlights the importance of FGF2 signaling for fracture healing.

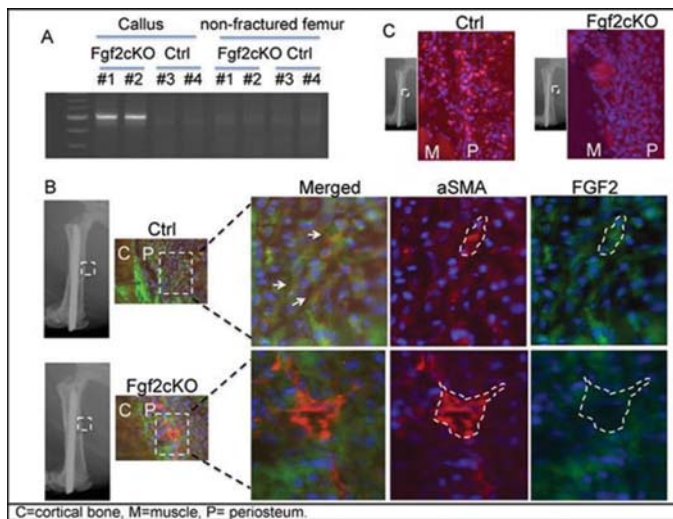


Fig.1

**Disclosures:** Liping Xiao, None.

## SA0144

**LOXL2 has a protective role in human and mouse cartilage in vivo.** Mustafa Tashkandi<sup>1</sup>, Saqer Alsager<sup>1</sup>, Weam Alshenibr<sup>1</sup>, Pushkar Mehra<sup>1</sup>, Mary B. Goldring<sup>2</sup>, Louis C. Gerstenfeld<sup>3</sup>, Manish V Bais<sup>1</sup>. <sup>1</sup>Boston University Henry M. Goldman School of Dental Medicine, Boston, MA, United States, <sup>2</sup>Weill Cornell Medical College, New York, NY, United States, <sup>3</sup>Boston University School of Medicine, Boston, MA, United States

Lysyl oxidase like-2 (LOXL2) is elevated during mouse fracture healing and promotes chondrocyte differentiation as shown in our previous studies. Recent data also showed that LOXL2 is expressed in the human knee, hip and TMJ-OA tissue section and LOXL2 overexpression inhibits IL-1 $\beta$ -induced phospho-NF- $\kappa$ B/p65 and TGF- $\beta$ 1 induced Erk1/2 phosphorylation and regulatory transcription factor network. The goal of this study is to evaluate if LOXL2 protects from osteoarthritis (OA) in human and mouse cartilage and identify the mechanism. All experiments were performed by relevant guidelines and regulations through Institutional Review Board and Institutional Animal Care and Use Committee (IACUC) approval. Human articular

chondrocytes Matrigel implants in nude mice and Chondrodysplasia (Cho) mice, which shows progressive OA-like changes starting from 3 months of age, were treated with adenovirus-LOXL2/Empty in respective groups. The extracted implants and knee joints were subjected to RNAseq analysis, staining and immunofluorescent analysis. Data analyses were performed using two way ANOVA with Bonferroni post-hoc analysis or Student's t-test. Matrigel constructs of primary chondrocytes from knee OA cartilage implanted in nude mice (n=5/condition) showed increased alcian blue and safranin-O staining representative of chondrogenesis and proteoglycan deposition compared to control vector treated implants in nude mice. Further, trichrome staining showed no evidence of mineralization by LOXL2 transduction. RNAseq analysis showed LOXL2 treated Matrigel implant decreased or unchanged expression of catabolic response such as MMP13 and VEGF-A whereas increased expression of genes related to an anabolic response such as SOX9, ACAN, and CSPG4 mRNA expression. LOXL2 increased the expression COL2A1 and inhibited phospho-smad2/3. Next, 12 and 20 weeks old Cho/+ mice (n=8/12/condition) treated with adenovirus-LOXL2 for another 16 weeks showed increased mRNA expression of Col2A1 whereas the reduction in expression of MMP13 and RANKL in knee joints compared to control. Thus, LOXL2 induces an anabolic response in human articular chondrocytes implants in nude mice and protective response in Cho/+ OA mouse models. This study has a translational significance because we showed for the first time that LOXL2 could have a potential protective function in human and mouse OA models in vivo and inhibits specific signaling pathways.

**Disclosures:** Mustafa Tashkandi, None.

## SA0145

See Friday Plenary Number FR0145.

## SA0146

**Novel Role of High Molecular Weight Fibroblast Growth Factor 2 and FGF23 in Osteoarthopathy in HMWtg Mice.** Maria Hurley<sup>\*</sup>, Patience Meo Burt, Liping Xiao. UConn Health, United States

Osteoarthopathy (OA) is prevalent in individuals with X-linked hypophosphatemia (XLH) and is a major cause of morbidity. High molecular weight FGF2 isoforms (HMWFGF2) are overexpressed in Hyp (mouse homolog of XLH) osteocytes, and similar to Hyp mice, HMWtg mice developed osteomalacia and severe OA associated with increased FGF23 in bone and serum. Importantly mice overexpressing low molecular weight FGF2 (LMWtg) in osteoblast lineage cells do not develop OA. Our goal is to determine how HMWFGF2 contribute to OA. Since HMWFGF2 but not LMWFGF2 transcriptionally regulates FGF23 that has recently been implicated in OA, we assessed FGF23 and OA markers in total RNA and protein extracted from whole knee joints of Vector, HMWtg and LMWtg mice. Significantly increased Fgf23, FGFR1, Runx2, ColX, Mmp13 mRNAs and increased pERK1/2 and pSMAD1/5/8 were found in articular cartilage of HMWtg but not LMWtg mice. To determine how HMWFGF2 contribute to OA, murine chondrogenic cells ATDC5 were stably transduced with retroviral constructs CMV/IRES/ eGFP (Vector), CMV/HMW Fgf2 /IRES/ eGFP, or CMV/LMW Fgf2 /IRES/eGFP and cultured in growth media (Day0) or differentiation media (Days 7-14) to assess chondrogenic and hypertrophic differentiation and to interrogate intracellular signaling pathways that may contribute to OA development. At Day 10, (Fig. 1A) alkaline phosphatase staining was increased in HMWATDC5 cultures compared with Vector and LMWATDC5 cultures. As shown in (Table.1) comparison of genes expression in Day0 undifferentiated cultures revealed more than 2-fold change in FGFR1c, Bmp2 and Hif12 $\alpha$  mRNA compared with Vector or LMWATDC5 cultures. At Day14, Bmp2 and Hif12 $\alpha$  mRNA was further increased in HMWATDC5 and there was a 4-fold increase in FGF23 mRNA compared with Vector and LMWATDC5 cultures. In contrast to HMWATDC5 cultures FGFR3 and Col2 mRNA was markedly increased in LMWATDC5 cultures at Day 0 and 14. Western blot (Fig. 1B) showed increased pERK42/44, pAKT, pJNK and pSMAD1/5/9 in HMWATDC5 cultures at Day 0 compared with Vector and at Day 14 both pERK44/42 and pJNK remained markedly elevated in HMWATDC5 cultures. There was increased pERK44/42 in LMWATDC5 cultures at Day 0 but not at Day 14. Our studies show increased FGF23/FGFR1/MAPK, PI3K/AKT and BMP/Smad1/5/8 in HMWATDC5 in undifferentiated and differentiated chondrocyte cultures supporting our hypothesis that HMWFGF2 isoforms contribute to OA via modulation of multiple downstream signaling pathways.



Table 1. mRNA expression in transduced ATDC5 cells

Day 0	Fgfr1c	Fgf23	Fgfr3	Col2	Bmp2	HIF2 $\alpha$
Vector	1.00	1.00	1.00	1.00	1.00	1.00
HMWTg	2.13	1.19	0.68	1.09	3.02	2.21
LMWTg	1.12	0.91	1.24	2.05	0.93	1.39
Day 14	Fgfr1c	Fgf23	Fgfr3	Col2	Bmp2	HIF2 $\alpha$
Vector	1.00	1.00	1.00	1.00	1.00	1.00
HMWTg	1.14	3.73	0.34	6.73	5.34	3.92
LMWTg	1.33	1.28	1.33	63.42	4.62	2.46

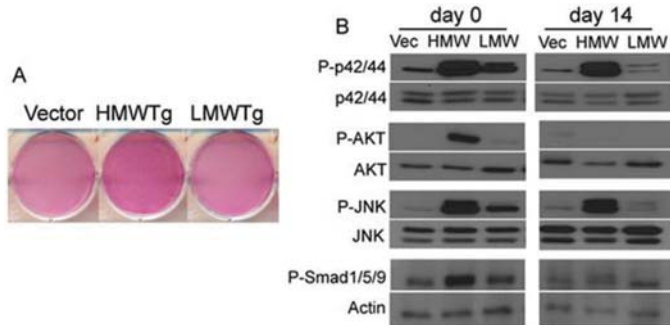


Table 1 and Figure 1

Disclosures: Marja Hurley, None.

## SA0147

**Age-related synovial lymphatic dysfunction is associated with the development of osteoarthritis.** Xi Lin\*, Richard D Bell, Edward M Schwarz, Brendan F Boyce, Lianping Xing. University of Rochester Medical Center, United States

The pathogenesis of osteoarthritis (OA) is strongly linked to aging, but the cellular and molecular mechanisms are incompletely understood. We reported decreased draining function of the synovial lymphatic system (SLS) in mice with post-traumatic OA (PTOA) using near-infrared lymphatic imaging, suggesting that insufficient SLS drainage of macromolecules (catabolic factors) and cells from synovium may contribute to PTOA pathogenesis. However, the detailed functional components of the SLS and their potential involvement in age-related OA have not been studied. We hypothesize that aging negatively affects these lymphatic functions: 1) "influx" into synovial lymphatic vessels, 2) "clearance" of synovial factors to draining lymph nodes (DLNs), and 3) overall "DLN capacity", defined as the molecules that remain in DLN. To test this, we performed intra-articular injections of Dextran-Texas Red (DEX) in young (Y, 3-month) and aged (A, 19-month) C57BL/6 male mice. IVIS imaging and whole slide imaging microscopy of the knee and DLN were performed 1, 6, 24, 48 hours after injection. Compared to young mice, aged mice had significantly reduced lymphatic influx (%DEX + area in synovium:  $1.7 \pm 0.8$  vs.  $5.1 \pm 2.4$  in Y,  $p < 0.01$ ), clearance (DEX signal intensity-arbitrary unit in knee:  $6.6 \pm 1.9$  vs.  $4.1 \pm 1.9$  ( $10^6$ ) in Y,  $p < 0.001$ ), and DLN capacity (DEX signal intensity-arbitrary unit in DLN:  $1.4 \pm 0.8$  vs.  $3.7 \pm 1.2$  ( $10^6$ ) in Y,  $p < 0.01$ ). As expected, aged mice had osteoarthritic changes, including cartilage matrix loss, cartilage surface fibrillation, meniscus hypertrophy, and higher OARSI scores ( $1.6 \pm 0.2$  vs.  $0.2 \pm 0.2$  in Y,  $p = 0.0009$ ). We investigated the cellular mechanisms of synovial macromolecule transfer and found that 34% of DEX+ cells in DLN, and 50% of DEX+ cells in synovium co-localized with F4/80+ macrophages. DEX+ cells were in close proximity to Lyve-1+ lymphatic vessels, but not endomucin+ blood vessels. Furthermore, fewer DEX+ cells were seen in aged DLNs (%DEX+/LN: 0.9 vs. 7.6 in Y,  $N = 2$ ). In conclusion, aged mice with OA have reduced SLS function including decreased lymphatic influx, clearance, and DLN capacity. The OA is more severe in aged mice than in young mice, and this may be due to impaired clearance of catabolic macromolecules from the synovium. Improving SLS may be a new therapeutic strategy to treat OA.

Disclosures: Xi Lin, None.

## SA0148

**Serum Levels of Tartrate-Resistant Acid Phosphatase 5b (TRACP-5b) and the Risk for the Radiographic Medial Knee Joint Space Narrowing in Men in Early Forties without Knee Pain -A Three Years Prospective Observational Study.** Muneaki Ishijima\*, Lizu Liu<sup>1</sup>, Mayuko Kinoshita<sup>1</sup>, Masashi Nagao<sup>1</sup>, Haruka Kaneko<sup>1</sup>, Ryo Sadatsuki<sup>1</sup>, Shinnosuke Hada<sup>1</sup>, Anwarjan Yusup<sup>1</sup>, Hitoshi Arita<sup>1</sup>, Jun Shiozawa<sup>1</sup>, Yoshinori Tamura<sup>1</sup>, Hirotaka Watada<sup>1</sup>, Kazuo Kaneko<sup>2</sup>. <sup>1</sup>Juntendo Univ. Graduate Sch. of Med., Japan, <sup>2</sup>Juntendo Univ. Graduate Sch. of Med.t, Japan

Osteoarthritis (OA) is a joint disease characterized by progressive degeneration of extra-cellular matrix (ECM), enhanced subchondral bone remodeling, osteophyte formation and synovial thickening. Healthy subchondral bone protects cartilage

from high peak stresses and possible matrix damage, suggesting that subchondral bone remodeling is involved in disease progression. Recent development of OA research has revealed that the degeneration and destruction of articular cartilage initiates earlier than it has been considered without pain. The aim of this prospective study was to investigate whether the baseline serum level of tartrate-resistant acid phosphatase 5b (TRACP-5b) was associated with the radiographic joint space narrowing (JSN) of the medial knee joint in men in early forties without radiographic knee OA and knee pain.

This prospective study was conducted by analyzing data of the Sportology Core Study underwent by our university. 87 healthy male volunteers (42.9 y in average) who didn't have any symptoms for knee pain and experience any traumatic episodes for the knee joints were enrolled in this study.

A standing, extended antero-posterior view radiograph of both knee were taken at the time of study entry and at 3-years of follow up. The presence of radiographic JSN is defined as a 0.3 mm or greater of JSN during 3-years of follow up. The BMD of lumbar spine (L2-L4) (LS-BMD) was measured using dual X-ray absorptiometry (DXA). The serum levels of TRACP-5b were measured by ELISA. The significance of the differences in the data was evaluated using the Mann-Whitney U-test. We examined the relation of tertiles of sTRACP-5b (using the lower tertile as the referent category) to the risk of the radiographic JSN using the logistic regression model.

The subjects were divided into two groups by the presence or absence of the radiographic JSN: the JSN during three year of follow-up was observed in twelve of 87 subjects (14%, JSN group), while it was not observed in the remaining 75 subjects (non-JSN group). The LS-BMD of JSN group at baseline ( $0.931 \text{ mg/kg}^2$ ) was significantly lower than those of non-JSN group at baseline ( $1.005 \text{ mg/kg}^2$ ,  $p < 0.01$ ). The sTRACP-5b of the subjects were negatively correlated with the LS-BMD at baseline ( $r: -0.316$ ,  $p = 0.003$ ). The sTRACP-5b of JSN group at baseline ( $326.9 \text{ mg/dl}$ ) were significantly higher in comparison to those of non-JSN group at baseline ( $280.8 \text{ mg/dl}$ ,  $p < 0.01$ ). When the subjects were divided into three groups according to the sTRACP-5b at baseline (T1, T2 and T3), the odds ratio (OR) for the JSN after 3-years of follow up in the upper tertile at baseline (T3) after adjustment for age and BMI was significantly higher than that in the lower tertile (T1) [OR: 10.5 (95% CI: 1.1 to 97.0),  $p < 0.05$ ]. In conclusion, the higher levels of sTRACP-5b were the risk for the radiographic medial JSN in men in early forties without knee pain.

Disclosures: Muneaki Ishijima, None.

## SA0149

See Friday Plenary Number FR0149.

## SA0150

See Friday Plenary Number FR0150.

## SA0151

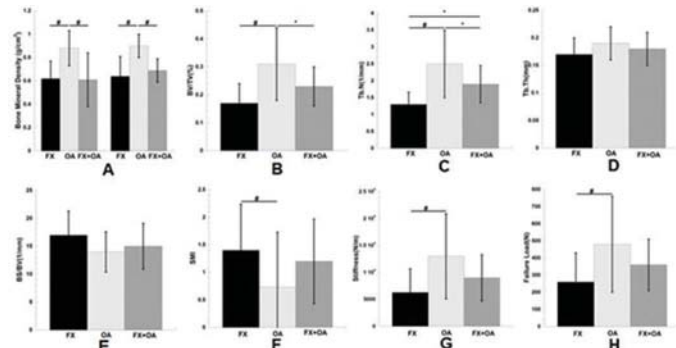
See Friday Plenary Number FR0151.

## SA0152

**Effects of Osteoporosis with Osteoarthritis on the Microstructure and Mechanical Properties of Subchondral Bone.** Xinhua Qu\*, Zhifeng Yu<sup>1</sup>, Xuqiang Liu<sup>2</sup>, Tingting Tang<sup>1</sup>. <sup>1</sup>Shanghai Key Laboratory of Orthopaedic Implants, Department of Orthopaedic Surgery, Shanghai Ninth People's Hospital, Shanghai Jiao Tong University School of Medicine, China, <sup>2</sup>The First Affiliated Hospital of Nanchang University, China

Osteoporosis and osteoarthritis are common degenerative diseases in clinic with the feature of different change of microstructure in subchondral bone. Osteoporosis and osteoarthritis often occur in the same patient. The relationship between osteoporosis and osteoarthritis has been controversial in many years. Controversy is focused on the sequential changes of subchondral bone. The aim of this research is to study the difference of microstructure and mechanical property of subchondral bone in osteoporosis and osteoarthritis patients, especially those osteoporosis patients with osteoarthritis. Fifty femur head were collected after total hip arthroplasty with the approval of all the patients. After all the patients were scanned by dual energy X-ray absorptiometry (DXA), they were divided into osteoarthritis group (OA group:  $n = 14$ ), osteoporotic fracture group (FX group:  $n = 19$ ), osteoporotic fracture with osteoarthritis group (FX+OA group:  $n = 17$ ). All femur head samples were scanned by micro computed tomography (Scanco  $\mu 80$ ). One virtual cylinders ( $\phi 5.4 \text{ mm}$ ,  $L 5.4 \text{ mm}$ ) were extracted from the reconstructed 3D image in the superior subchondral bone from the load-bearing area of the femoral head. Micro finite element ( $\mu \text{FE}$ ) model was generated from segment  $\mu \text{CT}$  images by transforming image voxel to an 8-node elastic brick model. Bone mineral density from DXA showed OA group has higher BMD than FX group and FX+OA group, no difference were found between FX group and FX+OA group (Fig. A). OA group has more BV/TV than FX group and FX+OA group (Fig. B). FX group has lower Tb.N than OA group and FX+OA group (Fig. C). There were no difference of Th.Th (Fig. D) and BS/BV among there three groups (Fig. E). FX group has the highest SMI than OA group, and no difference were found between FX group and FX+OA group (Fig. F). There was significant difference of stiffness and failure load between groups. OA group have higher stiffness than FX group with significant difference. FX+OA group have no difference with FX group and OA group (Fig. G,H). Our study found osteoarthritis most occurred in middle aged patient, while osteoporotic fracture happened in elderly patients. The subchondral bone of osteoporosis is mainly in the reduction of bone

volume and trabecular number, in contrast to that of osteoarthritis. For patients with osteoporosis combined with osteoarthritis, the subchondral bone is mainly in the increase in bone volume and trabecular number, but it does not affect the mechanical properties. On the other hand, the increase in the number of trabecular bone. The difference in mechanical properties among these groups in cancellous bone is attributed to different bone structure. Osteoarthritis provide cancellous bone a superior capacity to resist failure.



Bone mineral density, microstructure and mechanical property difference among groups

**Disclosures:** Xinhua Qu, None.

## SA0153

### Up-regulation of inhibitors of DNA binding/differentiation gene during alendronate-induced osteoblast differentiation. hoon choi<sup>1</sup>, heung yeol kim<sup>2</sup>.

<sup>1</sup>Department of Ob/Gyn, Inje university Sanggyepaik Hospital, Korea, Republic of, <sup>2</sup>Department of Ob/Gyn, College of Medicine, Kosin University, Korea, Republic of

**Aim:** Alendronate enhances bone morphogenetic proteins (BMP)-mediated osteoblast differentiation. A balanced regulation of inhibitors of DNA binding/ differentiation (Ids) plays an important role in BMP-induced osteoblast differentiation. However, there are no studies on the possible roles of Id genes in alendronate-induced osteoblast differentiation. This study investigated the effect of alendronate on the expression of Id genes in osteoblast differentiation.

**Methods:** C2C12 cells were treated with alendronate for various concentrations and time periods. For evaluation of alendronate-induced osteoblast differentiation in C2C12 cells, alkaline phosphatase (ALP) activity was measured. The expression of osteoblast differentiation markers such as ALP, type-1 collagen (Col 1), and osteocalcin (OCN), and the expression of Id-1 and Id-2 were measured by RT-PCR. In order to understand the mechanism underlying the regulation of Id genes, the promoter region of the Id-1 gene was identified. Database analysis of the promoter region for Id-1 using known consensus sequences identified several putative response elements, including CCAAT/enhancer-binding protein beta (C/EBPβ).

**Results:** Alendronate treatment significantly increased not only ALP activity but also expression of ALP, Col 1, and OCN, Id-1 and Id-2. C/EBPβ and alendronate cooperatively increased the promoter activity and expression of Id-1.

**Conclusion:** These results suggest that C/EBPβ-mediated Id-1 transcriptional activation may regulate alendronate-induced osteoblast differentiation of C2C12 cells.

**Disclosures:** hoon choi, None.

## SA0154

### Synergistic Effects of 1α,25-Dihydroxyvitamin D and 17β-Estradiol on Mesenchymal Stem Cells from Pre-pubertal Children. Jing Li<sup>1</sup>, Bonnie Padwa<sup>2</sup>, Shuanhu Zhou<sup>1</sup>, Julia Mullokandova<sup>3</sup>, Meryl LeBoff<sup>1</sup>, Julie Glowacki<sup>1</sup>. <sup>1</sup>Brigham and Women's Hospital, United States, <sup>2</sup>Boston Children's Hospital, United States, <sup>3</sup>Brigham and Women's Hospital, United States

Vitamin D is essential for mineral homeostasis and contributes to bone metabolism by stimulating osteoblast differentiation of mesenchymal stem cells (MSCs). In this study, we used MSCs from pre-pubertal girls and boys to test the hypothesis that 1α,25(OH)<sub>2</sub>D and 17β-estradiol have synergistic effects on these MSCs, and what mechanism is involved. With IRB approval, we isolated MSCs from discarded excess iliac marrow graft from 8 male and 8 female subjects (age 8.8-10.4 yrs) undergoing alveolar cleft repair. Excess plasma was available for hormone assays [25(OH)D, total testosterone, estradiol, estrone, DHEA-S, Growth Hormone, IGF-I]. Alkaline phosphatase (ALP) activity was used to measure osteoblast differentiation at day 7; alizarin red was used to measure matrix mineralization at day 21. RT-PCR was used for gene expression. All subjects were pre-pubertal based on their hormone levels. Serum 25(OH)D levels ranged from 13.1 to 30.3 ng/mL, with 75% below 20 ng/mL. Constitutive gene expression of VDR and ERA, b varied from subject to subject with no association with sex or serum chemistries. In osteoblastogenic medium, 1α,25(OH)<sub>2</sub>D3 (10 nM) increased ALP activity by 36% (p<0.05) in MSCs; 10 nM of E2 was not stimulatory but the combination of 1α,25(OH)<sub>2</sub>D3 and E2 increased ALP 151% (p<0.05 vs. control) and by

84.5% (p<0.05 vs. 1α,25(OH)<sub>2</sub>D3 alone). The combination of 1α,25(OH)<sub>2</sub>D3 and E2 significantly increased mineralization 11-fold, compared with either agent alone (p<0.05). Twenty-four hour treatment with 1α,25(OH)<sub>2</sub>D (10 nM) or E2 (10 nM) upregulated each other's receptor by as much as 6.4-fold for ERA and 2.9-fold for the VDR. In summary, 1α,25(OH)<sub>2</sub>D3 stimulated osteoblast differentiation and matrix mineralization of MSCs from pre-pubertal subjects, with a synergistic effect of E2, mediated by receptor levels, at least in part. These studies add new information about the regulation of human osteoblast differentiation, effects of 1α,25(OH)<sub>2</sub>D3 and E2 on MSCs, and the importance of vitamin D for skeletal health.

**Disclosures:** Jing Li, None.

## SA0155

See Friday Plenary Number FR0155.

## SA0156

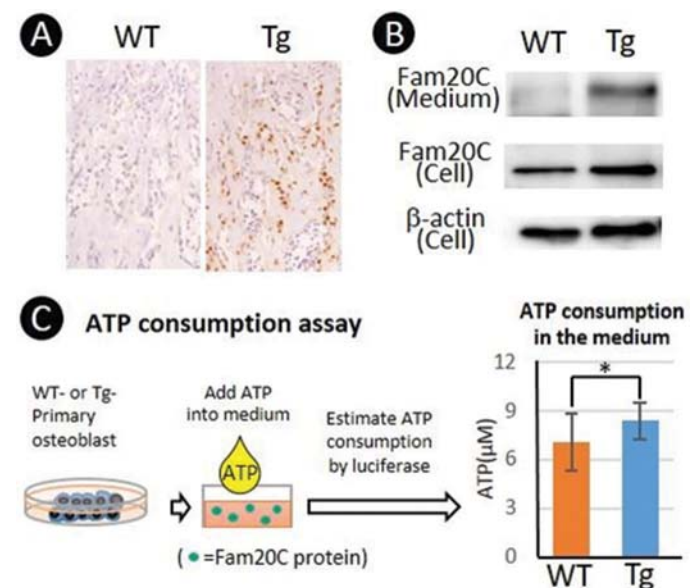
**Analysis of the role of Fam20C in Fam20C-transgenic mice.** Katsutoshi Hirose<sup>1</sup>, Yu Usami<sup>1</sup>, Sunao Sato<sup>1</sup>, Kaori Oya<sup>1</sup>, Toshihisa Komori<sup>2</sup>, Satoru Toyosawa<sup>1</sup>. <sup>1</sup>Department of Oral Pathology, Osaka University Graduate School of Dentistry, Osaka, Japan, <sup>2</sup>Department of Cell Biology, Unit of Basic Medical Sciences, Nagasaki University Graduate School of Biomedical Sciences, Nagasaki, Japan

[Background] Family with sequence similarity 20-C (Fam20C) is an evolutionary conserved molecule that is highly expressed in mineralized tissues. Recent studies identified Fam20C as Golgi-localized protein kinase, which phosphorylates secretory proteins with S-X-E/pS motifs, including small-integrin-binding ligand N-linked glycoproteins (SIBLINGs) family proteins. *In vitro* studies demonstrated that recombinant Fam20C can phosphorylate Dmp1 and osteopontin, which are important for bone formation. However, the role of Fam20C and phospho-proteins phosphorylated by Fam20C on bone formation is still unclear. In this study, we investigated the role of Fam20C on bone formation using osteoblast-specific Fam20C transgenic mice (Fam20C-Tg).

[Materials and methods] We generated the transgenic mice that Fam20C expression is driven by α2.3-kb pro-α1(I) collagen promoter, which is active in osteoblasts. Skeletal samples of Fam20C-Tg were analyzed *in vivo* and *in vitro*.

[Results and Discussion] In Fam20C-Tg, mRNA level of *Fam20C* at postnatal day 30 (P30) was approximately 30 - 40 fold higher than those in wild-type mice (WT). In Fam20C-Tg, Fam20C protein was highly accumulated in the Golgi area of the osteoblasts (Fig A). Western blot analysis revealed that Fam20C produced by the primary osteoblasts isolated from Fam20C-Tg, was highly secreted into the medium, compared to those of WT (Fig B). We confirmed the kinase activity of Fam20C expressed in Fam20C-Tg by estimating ATP consumption of the medium *in vitro* kinase assay (Fig C).

Histological analyses showed Fam20C-Tg had lesser trabecular bone volume compared to those of WT (P0, P3, P7, P30 and P90). μCT analyses revealed Fam20C-Tg had lesser cortical bone mineral density at P90, compared to those of WT. On the other hands, *in vitro* mineralization assay, the primary osteoblasts isolated from Fam20C-Tg increased induction of mineralization, compared to those of WT. Organ culture of femurs of Fam20C-Tg increased slight mineralization, compared to those of WT. These results indicate that Fam20C plays an important role in bone formation and mineralization.



HiroseK A17017989

**Disclosures:** Katsutoshi Hirose, None.



## SA0157

See Friday Plenary Number FR0157.

## SA0158

See Friday Plenary Number FR0158.

## SA0159

**Direct delivery of recombinant Pin1 protein rescued osteoblast differentiation of Pin1 deficient cells.** Woo Jin Kim<sup>\*</sup>, Hyun Mo Ryoo. Seoul National University, Korea, Republic of

Pin1 is a peptidyl prolyl cis-trans isomerase that specifically binds to the phosphoserine-proline or phosphothreonine-proline motifs of several proteins. We reported that Pin1 plays a critical role in the fate determination of Smad1/5, Runx2 and  $\beta$ -catenin that are indispensable nuclear proteins for osteoblast differentiation. Though several chemical inhibitors have been discovered for Pin1, no activator has been reported as of yet. In this study, we directly introduced recombinant Pin1 protein successfully into the cytoplasm via fibroin nanoparticle encapsulated in cationic lipid. This nanoparticle-lipid complex delivered its cargo with a high efficiency and a low cytotoxicity. Direct delivery of Pin1 leads to increased Runx2 and Smad signaling and resulted in recovery of the osteogenic marker genes expression and the deposition of mineral in Pin1 deficient cells. These result indicated that a direct Pin1 protein delivery method could be a potential therapeutics for the osteopenic diseases.

**Disclosures:** Woo Jin Kim, None.

## SA0160

See Friday Plenary Number FR0160.

## SA0161

**Connexins form distinct complexes with signaling machinery that differentially affect osteoblast signaling and gene expression.** Megan Moorer<sup>\*</sup><sup>1</sup>, Carla Hebert<sup>2</sup>, Joseph Stains<sup>3</sup>. <sup>1</sup>graduate student, United States, <sup>2</sup>lab technician, United States, <sup>3</sup>PI, United States

Intercellular communication between osteoblast and osteocytes by connexin43 (Cx43) gap junctions affects bone modeling and remodeling. The molecular details of what Cx43 communicates and how Cx43 affects bone are incompletely understood. Our recent work showed the requirement of the Cx43 C terminus (CT) for optimal osteoblast signaling and gene expression *in vivo* and *in vitro*, and the absence of the Cx43 CT in mice resulted in an osteopenic skeletal phenotype analogous to osteoblast conditional deletion of the entire Cx43 gene. These data imply that Cx43-containing gap junctions not only exchange signals, but also recruit signaling machinery to the Cx43 CT domain to optimally affect cell signaling, cell function, and bone acquisition. Additionally, different connexins have distinct effects on osteoblast signaling and function, with Cx43 and Cx45 having antagonistic roles. We hypothesized that the function of connexins are dictated not only by their permeability, but also by their protein-protein interactions. Amino acid sequence alignment of the Cx43 and Cx45 CT domains revealed 17.5% identity and 46.1% similarity, supporting the potential of different interactions with signaling machinery (i.e., interactomes). By co-immunoprecipitation (co-IP), our preliminary data show that Cx43 complexes with ERK, CAMKII, and  $\beta$ -catenin, and Cx43 overexpression enhanced the co-IP of these signaling proteins. In contrast, co-IP of a myc-tagged Cx45 results in minimal co-association of these signaling proteins. Further, when Cx45 is overexpressed forming heterotypic gap junctions with Cx43, the interactions of Cx43 with ERK, CAMKII, and  $\beta$ -catenin are reduced. These data suggest that Cx43 and Cx45 have different interactomes. To confirm the function consequences of these interactions, we used chimeric connexin proteins composed of portions of both Cx43 and Cx45 and examined downstream signaling and gene expression in osteoblasts. We found that, in general, both the Cx43 pore and Cx43 tail are required for optimal osteoblast signaling (e.g., MAPK,  $\beta$ -catenin) and gene expression (e.g., COL1A1, OCN, Osterix), as replacement of the Cx43 pore or tail domain with that of Cx45 was ineffective or inhibitory for connexin-dependent signaling and gene expression. In summary, these data imply that each connexin can differentially regulate downstream signaling and gene expression by local recruitment of distinct interactomes to each connexin's CT.

**Disclosures:** Megan Moorer, None.

## SA0162

**Proteomic comparison of extracellular vesicles secreted from osteogenic and vascular smooth muscle cells.** Sandeep Chaudhary<sup>\*</sup><sup>1</sup>, Victoria Smethurst<sup>2</sup>, Daisy Monier<sup>2</sup>, James Mobley<sup>1</sup>, Dobrawa Napierala<sup>2</sup>. <sup>1</sup>University of Alabama at Birmingham, United States, <sup>2</sup>University of Pittsburgh, United States

Extracellular vesicles (EV) is a broad term describing sub-micron size, lipid membrane-enclosed particles released from cells to the extracellular milieu. It has been demonstrated that a specific group of EV, termed matrix vesicles (MV), are deposited in the extracellular matrix by chondrocytes, osteoblasts and odontoblasts during the initiation of mineralization of the skeletal and dental tissues. Accordingly, it has been proposed that the biological function of MV is to facilitate the initiation of the mineralization process. This is further supported by studies showing that pathological mineralization of blood vessels is also promoted by EV released from vascular smooth muscle cells. The goal of this study was to compare the molecular composition of EV secreted during physiologic and pathologic mineralization and to compare protein composition of MV with EV released to cell culture medium. We also analyzed the protein composition of EV secreted from cells cultured under standard growth conditions and upon stimulation with elevated phosphate levels. We used liquid chromatography tandem mass spectrometry (LC-MS/MS) followed by Scaffold (Proteome Software) analyses to determine the protein composition of EV secreted by osteogenic cells (17IIA11 cell line) and vascular smooth muscle cells (MOVAS cell line, an *in vitro* model of pathological vascular calcification). A total of 8 groups of EV were analyzed: 1) MV from 17IIA11 cells in standard growth medium; 2) medium EV from 17IIA11 cells in standard growth medium; 3) MV from 17IIA11 cells treated with 10mM Na-Pi for 24h; 4) medium EV from 17IIA11 cells treated with 10mM Na-Pi for 24h; 5) MV from MOVAS cells in standard growth medium; 6) medium EV from MOVAS cells in standard growth medium; 7) MV from MOVAS cells treated with 5mM Na-Pi for 24h; 8) medium EV from MOVAS cells treated with 5mM Na-Pi for 24h. High levels of annexins and actin cytoskeleton proteins were detected in all analyzed groups of EV. Significant differences between MV isolated from the extracellular matrix and EV from conditioned medium in both 17IIA11 and MOVAS cells were identified, suggesting that these are two different populations of EV. Furthermore, we determined that phosphate changes the protein composition of EV.

**Disclosures:** Sandeep Chaudhary, None.

## SA0163

See Friday Plenary Number FR0163.

## SA0164

**Bone Structure and Function in Osteocalcin-null Rats on a High Fat Diet.** Aidi Niu<sup>\*</sup><sup>1</sup>, Jeffrey Nyman<sup>2</sup>, Lihua Zhou<sup>1</sup>, Laura Lambert<sup>1</sup>, Robert Kesterson<sup>1</sup>, Jayleen Grams<sup>1</sup>. <sup>1</sup>University of Alabama at Birmingham, United States, <sup>2</sup>University of Vanderbilt, United States

Obesity associated with a high fat diet (HFD) may increase the risk of certain fractures. Since osteocalcin is a negative regulator of bone formation in mice, we hypothesized osteocalcin knockout would be protective for bones in rats on a HFD.

Wild type (WT; n=14/sex) and osteocalcin knockout rats (KO; n=14-16/sex) were fed a normal chow or HFD for 21 weeks after weaning. Femurs were examined by  $\mu$ CT and three-point bending test; serum assays were performed.

At 6 months, animals on HFD gained more weight than those on chow in both sexes, and there was no difference based on genotype. Femur lengths were similar across the four groups in both sexes, but KO-chow males had a significantly lower total cross-sectional area (p=0.0410), endosteal circumference (p=0.0124), and moment of inertia (p=0.0247) when compared to WT-chow males. KO-chow males also had a significant increase in cortical bone area fraction (Ct. Ar/Tt. Ar) (p=0.0287), cortical thickness (p=0.0295), and trabecular tissue mineral density (p=0.0126) vs WT-chow. There was no difference in females. All parameters of cortical bone were unchanged in HFD vs chow animals within corresponding genotype. Decreased trabecular number (p=0.0083) and increased trabecular spacing (p=0.0081) were observed in KO-HFD males vs KO-chow males; there was no difference in WT males. In females, trabecular bone volume fraction (BV/TV) (p=0.0037) and number (p=0.0158) were significantly decreased in WT-HFD vs WT-chow, while there was no decrease in KO animals based on diet. The biomechanical tests showed that KO-chow femurs had lower peak moment for both male and female rats (p=0.0118 and p=0.0185, respectively), and KO-chow females had a significantly lower bending strength (independent of structure) compared to WT-chow (p=0.0053). There was no difference in rigidity across the groups in either sex. In serum analyses, PINP was higher in WT-HFD vs WT-chow males (p=0.0306), while KO-HFD females had decreased PINP vs KO-chow (p=0.0146). CTX-1 was unchanged across groups. TRAcP5b levels in males on a HFD were significantly increased vs controls on chow (WT, p=0.0053 and KO, p=0.0120). Females had no differences of serum TRAcP5b.

In conclusion, male and female rats had differential outcomes in bone structure and function to HFD and osteocalcin KO. The mechanism of these findings remains unclear and requires further study.

**Disclosures:** Aidi Niu, None.

## SA0165

**Alpha-lipoic Acid (ALA) Pre-treatment Specifically Prevents the Suppression of Lgr4 Expression by TGF-beta.** Chantida Pawaputanon na Mahasarakham\*, Yoichi Ezura, Masaki Noda. Tokyo Medical and Dental University, Japan

Lgr4 is an important regulator of multiple organ systems including skeleton. A deleterious mutation in human Lgr4 causes multiple organ failure including osteoporosis. Recently, we demonstrated that Lgr4 is necessary for osteoblast marker gene expression in MC3T3-E1 cells by siRNA transfection experiments, whereas its expression may be usually limited only at early differentiation status in standard culture condition. However, this preferential expression was modulated by multiple factors, including the BMP2 that transiently induces Lgr4 expression along with various osteoblastic marker genes, and the hydrogen peroxide that suppresses the Lgr4 expression in parallel with other osteoblastic marker genes. Here, we report that similar suppression could occur by TGF- $\beta$ , which is known to induce intracellular ROS in various cell types. Time-course experiments indicated that the effects of TGF- $\beta$  on Lgr4 suppression were similar to that mediated by hydrogen peroxide that requires about 10 hours after treatment. Possible mechanisms for the increased intracellular ROS may include the downregulation of the intrinsic antioxidants. We found that TGF- $\beta$  rapidly suppresses the Catalase gene expression in MC3T3-E1 cells. The possible link between the Lgr4 suppression by intracellular ROS and TGF- $\beta$  was supported by the experiments using anti-oxidants including alpha-lipoic acid (ALA) before adding TGF- $\beta$  and hydrogen peroxide. Although 4 hours of ALA pre-treatment at 0.5mM failed to prevent the TGF- $\beta$  mediated Lgr4 down-regulation, 24 hours of pre-treatment significantly prevented it. However, because it does not affect major osteoblast marker gene expression other than the premature Lgr4 suppression, the observed protection was regarded as specific in Lgr4 expression. Inhibitor experiments suggested that the suppression of osteoblast marker genes as well as Lgr4 expression may be mainly dependent on the Smad pathway but not largely on the MAPK pathways. These observations suggest that intracellular oxidation events are involved in the causes of Lgr4 suppression by TGF- $\beta$ .

**Disclosures:** Chantida Pawaputanon na Mahasarakham, None.

## SA0166

See Friday Plenary Number FR0166.

## SA0167

**Superior bone quality in MRL/MpJ mice is attributed to high bone formation and remodeling.** Xuving Sun\*, Xueqin Gao<sup>2</sup>, Aiping Lu<sup>2</sup>, Sarah Amra<sup>3</sup>, Xiaodong Mu<sup>4</sup>, Johnny Huard<sup>2</sup>, Charles Huard<sup>5</sup>. <sup>1</sup>Department of Orthopaedic Surgery, University of Texas Health Science Center at Houston; McGovern Medical School, Brown Foundation Institute of Molecular Medicine Center for Tissue Engineering and Aging, United States, <sup>2</sup>1.Department of Orthopaedic Surgery, University of Texas Health Science Center at Houston; McGovern Medical School 2. Brown Foundation Institute of Molecular Medicine Center for Tissue Engineering and Aging 3. Steadman Philippon Research Institute, United States, <sup>3</sup>1.Department of Orthopaedic Surgery, University of Texas Health Science Center at Houston; McGovern Medical School 2. Brown Foundation Institute of Molecular Medicine Center for Tissue Engineering and Aging, 3. Steadman Philippon Research Institute, United States, <sup>5</sup>Department of Orthopaedic Surgery, University of Texas Health Science Center at Houston; McGovern Medical School, United States

**INTRODUCTION:** The Murphy Roths large (MRL/MpJ) mice, with a remarkable capacity for cartilaginous healing, the bone characteristics of the mice were not well studied.

**METHODS:** 1. Femur, tibia, and spine from 2 and 4 month old C57BL/10J (10J), C57BL/6J (6J) and MRL/MpJ mice were collected and fixed, then subjected to microCT scanning. After decalcification and paraffin-embedding, osteocalcin staining for osteoblast (OB) and TRAP, cathepsin K (CatK) for osteoclast (OC) were performed. OB and OC number were quantified. Herovici's staining was performed to detect collagen type I. 2. Bone marrow were collected from the three groups, cells were cultured for different time points to allow osteoclastogenesis. TRAP staining was performed and RNA was extracted, osteoclastogenesis markers were detected with Q-PCR. **RESULTS:** 1. Lumbar spine 6 (L6): MRL/MpJ showed enhanced bone parameters compared to normal strains both in 2 and 4 month old mice, including higher trabecular bone volume (BV/TV), number (Th.N), thickness (Tb.Th.), BV density and lower separation. 2. Proximal tibia: For 2 month mice, MRL/MpJ showed higher BV/TV and Tb.Th. At 4 month, the BV density was higher than two normal strains. 3. Femur: MRL/MpJ exhibited increased cortical bone thickness and BV density both in 2 and 4 month old mice. 2. Herovici's staining indicated MRL/MpJ have higher density of collagen type I. 3. OB staining demonstrated at 2 month, more OB at L6 spine, but no difference for long bones. At 4 month, MRL/MpJ showed more OB in L6 spine, but not at proximal tibia and femur. 4. OC, both TRAP and CatK staining indicated more OC in L6 spine in

MRL/MpJ. At 2 month, no difference at proximal tibia and femur. Osteoclastogenesis is also higher in MRL/MpJ demonstrated by TRAP staining and osteoclastogenesis markers Acp-5, CatK, NFATC1. However, at 4 month, both staining demonstrated reduction in OC in the L6 spine of MRL/MpJ. The OC is also down regulated for proximal tibia and femur.

**CONCLUSION:** MRL/MpJ exhibited higher bone quality both in 2 and 4 month old mice than normal mice. Increased formation and bone remodeling at 2 month in MRL/MpJ was found as indicated by elevated OB and OC. However, at 4 month old, OB remained higher in MRL/MpJ, but OC decreased significantly, indicating osteogenesis remained active at an older age, which contribute to superior bone quality observed in MRL/MpJ. Further mechanism is needed to identify the factors that regulate superior bone quality in these mice.

**Disclosures:** Xuving Sun, None.

## SA0168

See Friday Plenary Number FR0168.

## SA0169

See Friday Plenary Number FR0169.

## SA0170

See Friday Plenary Number FR0170.

## SA0171

**Tsc1 Deletion Increases Craniofacial Bone Mass by Increasing Extracellular Matrix (ECM) Production and Enhancing Osteoblast Differentiation.** Xiaoxi Wei\*, Min Hu<sup>2</sup>, Han Kyoung Choi<sup>1</sup>, Andrea Alford<sup>3</sup>, Erin M.R. Bigelow<sup>3</sup>, Karl Jepsen<sup>3</sup>, Fei Liu<sup>1</sup>. <sup>1</sup>University of Michigan School of Dentistry, United States, <sup>2</sup>Jilin University School and Hospital of Stomatology, China, <sup>3</sup>University of Michigan Medical School, United States

We reported that mTORC1 activation by deleting *Tsc1* in neural crest derived cells increased craniofacial bone mass in *Tsc1<sup>fl/fl</sup>;P0Cre* (CKO<sup>P0Cre</sup>) mice. Herein, we further determined the impact and mechanism of *Tsc1* deletion in craniofacial bone acquisition. Histologically the mutant bone was well-organized with increased blood vessels. Ash weight assay showed that the ECM (organic) content significantly increased 13% but the water content significantly decreased 19% ( $p < 0.05$ ,  $n = 5$ ), while there was no change in mineral (ash) content in mutant frontal bone compared to control at 2m, indicating a significant increase in ECM production. In supporting the hypothesis that increased ECM content and cell density lead to hypoxia which in turn leads to increased angiogenesis, mRNA level of both hypoxia-inducible genes (*Hif1a*, *Hif2a*, etc.) and key angiogenesis genes (*Vegfs* and receptors) significantly increased in mutant bones ( $p < 0.05$ ,  $n = 3$  for all thereafter presented significant changes). In addition, mRNA level of proliferation marker genes (*Ki67*, *Pcna*, etc.) decreased about 70% but mRNA level of osteoblast differentiation genes (*Runx2*, *Osterix*, *Alpl*, *Bsp*, *Ocn*) significantly increased 1.6-6 folds in 2m mutant bone. Pathway analysis using RNASeq data showed that ECM/receptor interaction and focal adhesion are top altered pathways. There was significant increase in mRNA level of nearly all collagen genes, non-collagenous genes and most integrins expressed in osteoblast. FAK (Focal Adhesion Kinase) is a major ECM/integrin signaling mediator and we showed that FAK promotes osteoblast differentiation. FAK mRNA, protein and phospho-FAK (Ty397) were significantly increased in mutant bone, supporting the hypothesis that FAK signaling mediates the effect of *Tsc1* deletion on osteoblast differentiation. To determine the extent osteoblasts contributed to the bone phenotype in CKO<sup>P0Cre</sup> mice, we used *Osterix-Cre* to delete *Tsc1* postnatally from 2m to 5m. Micro-CT analysis showed that CKO<sup>OssCre</sup> mice at 5m had a significant increase in bone mass and tissue mineral density (TMD) of all craniofacial bones, including a 240% and 16% increase in frontal bone volume and TMD respectively at 5m. Thus, CKO<sup>OssCre</sup> mice largely reproduced the high bone mass phenotype in CKO<sup>P0Cre</sup> mice. Altogether, our data suggest that *Tsc1* deletion in osteoblasts increased craniofacial bone mass with increased ECM production and enhanced osteoblast differentiation, which may be mediated via enhanced FAK signaling.

**Disclosures:** Xiaoxi Wei, None.

## SA0172

See Friday Plenary Number FR0172.

## SA0173

See Friday Plenary Number FR0173.

## SA0174

See Friday Plenary Number FR0174.



**SA0175**

See Friday Plenary Number FR0175.

**SA0176**

See Friday Plenary Number FR0176.

**SA0177**

See Friday Plenary Number FR0177.

**SA0178**

See Friday Plenary Number FR0178.

**SA0179**

**Development of an ELISA for the quantification of human soluble Semaphorin 4D in plasma.** Anna Laber<sup>\*1</sup>, Gabriela Berg<sup>2</sup>, Gottfried Himmeler<sup>1</sup>. <sup>1</sup>The Antibody Lab, Austria, <sup>2</sup>Biomedica Medizinprodukte GmbH & Co KG, Austria

Semaphorin 4D or CD100 is a member of a family of transmembrane and secreted proteins that regulates key cellular functions and is involved in cell-cell communication. In bone, Semaphorin 4D is produced by osteoclasts and acts through its receptor Plexin-B1 on osteoblasts to inhibit their differentiation and motility. Cleavage of Semaphorin 4D near the cell membrane through matrix metalloproteinases leads to the biologically active soluble Semaphorin 4D (sSEMA4D) with a molecular weight of 120 kD consisting of 734 amino acids. Semaphorin 4D has emerged as a pharmacological target and as a potential biomarker of bone turnover that may assist in the management of bone diseases.

To gain a better understanding on the role of circulating soluble Semaphorin 4D (sSEMA4D) in humans we developed a specific assay that enables the accurate measurement of sSEMA4D in plasma samples. The assay utilizes two monoclonal anti-human Semaphorin 4D antibodies, both recognizing conformational epitopes on Semaphorin 4D. The epitopes have been mapped by overlapping constrained peptides and shown to involve amino acids AA30-AA34 and amino acids AA238-AA241, respectively.

Our results demonstrate that sSEMA4D can reliably be measured in various plasma preparations (EDTA, citrate, heparin) with a mean coefficient of variation of <8% between these matrices. Serum measurement of sSEMA4D showed in average a 3 fold higher concentration than plasma, indicating that the measurement of sSEMA4D in blood samples may be interfered by the in vitro release from platelets. Hence, the assay was optimized for human plasma samples only. The assay covers a wide calibration range between 0 to 2000 pmol/l and sSEMA4D EDTA-plasma concentrations in apparently healthy individuals are 239 +/- 59 pmol/l (n=44). Assay characteristics, such as precision, dilution linearity and spike/recovery as well as sample stability have been analysed and meet the international standards of acceptance. Our novel ELISA provides a reliable and accurate tool for the quantitative determination of soluble, biologically active Semaphorin 4D in human plasma samples.

*Disclosures: Anna Laber, None.***SA0180**

See Friday Plenary Number FR0180.

**SA0181**

**Phlpp1 Deficiency Reduces Bone Mineral Density by Enhancing M-CSF Responsiveness of Osteoclast Progenitors.** Anna M. Mattson<sup>\*</sup>, Jennifer J. Westendorf, Merry Jo Oursler, Elizabeth W. Bradley. Mayo Clinic, United States

Bone remodeling processes are disrupted in many diseases, including osteoporosis, periodontitis, tumor-induced bone disease and arthritis. Decreased bone mineral density in these conditions is often caused by enhanced osteoclast function. Phlpp1-deficient mice have diminished cancellous bone mineral density. Phlpp1 deficiency activates pathways that promote osteoclast activity, including Akt, PKC and Erk1/2 in the cytoplasm, and alters the epigenome by enhancing histone 3 (H3) phosphorylation and acetylation in the nucleus. The purpose of this study was to determine if Phlpp1 is a novel suppressor of bone resorption. We first show that osteoclast number and osteoclast surface per bone surface are 2- to 2.5-fold higher in Phlpp1 null mice as measured by histomorphometry. To assess cell autonomous effects of Phlpp1 deficiency on osteoclastogenesis, bone marrow macrophages were collected from WT or Phlpp1<sup>-/-</sup> mice and osteoclasts were then generated ex vivo with recombinant M-CSF and RANKL. Greater numbers of larger osteoclasts were obtained from bone marrow macrophages cultures from Phlpp1 null mice as compared to WT controls. To evaluate possible mechanisms for increased osteoclastogenesis and increased osteoclast size, we determined if Phlpp1 null osteoclast progenitors exhibited enhanced responses to RANKL and M-CSF. Pre-osteoclasts were treated with M-CSF and RANKL in the absence of serum. Mek1/2 phosphorylation decreased in WT cultures after 30 minutes, but was sustained by Phlpp1 null pre-osteoclasts. No change in NF-κB phosphorylation

was detected between WT and Phlpp1 null pre-osteoclasts. M-CSF binds c-fms, a receptor tyrosine kinase, to elicit Mek1/2 phosphorylation. C-fms expression was 3-fold higher in Phlpp1<sup>-/-</sup> pre-osteoclasts. Western blotting confirmed the increased c-fms levels in Phlpp1<sup>-/-</sup> osteoclast progenitor cells. In accordance with enhanced c-fms expression, Phlpp1<sup>-/-</sup> osteoclast cultures were hyper-responsive to M-CSF and showed elevated osteoclast numbers at all concentrations as compared to WT osteoclasts. Importantly, PHLPP1 levels decline in human bone with aging. These results demonstrate that suppression of Phlpp1 expression and/or activity reduces bone density and increases osteoclast numbers and size through enhanced M-CSF responsiveness.

*Disclosures: Anna M. Mattson, None.***SA0182**

**Diet-derived phenolic acids inhibit osteoclastogenesis and bone resorption through GPR109A.** Jin-Ran Chen<sup>\*</sup>, Oxana P. Lazarenko, Matthew E. Ferguson. Arkansas Children's Nutrition Center and the Department of Pediatrics, University of Arkansas for Medical Sciences, United States

Bone development and remodeling are coordinately regulated by both local paracrine molecules, as well as hormones travelling through the bloodstream. On the other hand, the human skeleton also requires an adequate supply of many different nutritional factors to optimize peak bone mass and minimize osteoporosis risk during aging. Food-based biologically active factors are usually referred to non-nutrient molecules, such as phytochemicals, and they may not only promote bone development but also protect bone from degeneration. Here we report effects of blueberry (BB) diet-derived phenolic acids, hippuric acid (HA) and 3-(3-hydroxyphenyl) propionic acid (3-3-PPA) on inhibiting osteoclastogenesis and bone resorption. In RAW 264.7 cell cultures, HA and 3-3-PPA, but not 3-4-PPA, dose-dependently inhibited RANKL (50 ng/ml)-induced osteoclastogenesis. HA and 3-3-PPA dose-dependently decreased osteoclast resorptive activity on a Corning Osteo Assay® surface 24-well plate (Corning Life Sciences, Corning, NY, USA). Using real-time PCR, we found that HA and 3-3-PPA significantly inhibited RANKL-induced gene expression specific for osteoclast differentiation and activity such as NFATc1, ITGB3, TRAP and CTR. We recapitulated the majority of our results using *ex vivo* cultures of non-adherent bone marrow hematopoietic osteoclast precursors, isolated from 4 week old wild type mice. However, we found that, in the presence of RANKL, osteoclast precursors from GPR109A<sup>-/-</sup> mice had significantly decreased differentiation potential to mature osteoclasts compared wild type animals. HA and PPA had no additional effects on inhibiting osteoclastogenesis and osteoclast resorptive activity in *ex vivo* cultures of osteoclast precursors from GPR109A<sup>-/-</sup> mice, compared to cells without HA or PPA treatments. This suggests an important role for GPR109A in BB-associated osteoclast regulation. To test this, we fed a BB diet to 4 week old wild type and GPR109A<sup>-/-</sup> mice (both genders) for 4 weeks. Bone analysis using micro-CT showed increased bone volume and trabecular number in GPR109A<sup>-/-</sup> mice compared to those from wild type mice. Bone resorption (bone marrow plasma CTX) significantly decreased by 35% in GPR109A<sup>-/-</sup> mice compared to wild type mice. Feeding BB diet to GPR109A<sup>-/-</sup> mice did not increase bone volume and trabecular number compared to animals without treatment. We conclude that HA and PPA may inhibit osteoclastogenesis through GPR109A. Supported by USDA-ARS Project #6026-51000-010-05S.

*Disclosures: Jin-Ran Chen, None.***SA0183**

**Phytoncide reduces differentiation and stimulates apoptosis of osteoclasts.** In-Jin Cho<sup>\*1</sup>, You Cheol Hwang<sup>1</sup>, In-Kyung Jeong<sup>1</sup>, Kyu Jeung Ahn<sup>1</sup>, Hyoun-Moo Park<sup>2</sup>, Ho-Yeon Chung<sup>3</sup>. <sup>1</sup>Kyung Hee Univ, Korea, Republic of, <sup>2</sup>Chung-Ang, Korea, Republic of, <sup>3</sup>Kyung Hee University, Korea, Republic of

A forest bathing trip involves visiting a forest for relaxation while breathing in volatile substances, called phytoncides (wood essential oils), which are antimicrobial volatile organic compounds derived from trees. Some studies have shown that phytoncide compounds have anti-inflammatory effects in mammalian cells. LPS-induced increases of TNFα, NFκB, and oxidative stress were attenuated by phytoncide-like compounds in macrophage cells, RAW264.7. In the present study, we hypothesized that phytoncide may modulate osteoclast differentiation and survival due to its activity on macrophage. Thus, we determined the effect of phytoncide in bone cells, osteoclasts and osteoblasts in vitro system. Phytoncide solution was provided from GNG Corporation (Kyoungki-do, Korea). The essential oil from freshly cut needles of Hinoki cypress (*Chamaecyparis obtusa*) was obtained by steam distillation using a manufactured apparatus with a condenser.

We evaluated the effects of phytoncide on osteoclast formation using bone marrow-derived macrophage and RAW 264.7 cells and osteoblast differentiation using MC3T3-E1 cells. Phytoncide significantly inhibited RANKL-induced TRAP-positive multinucleated cell formation in bone marrow-derived macrophages and RAW 264.7 cell cultures in a dose-dependent manner. The suppression of ERK, AKT, and p38 mitogen-activated protein kinases engaged by RANK were observed in Western blotting after phytoncide treatment in RAW 264.7 cells. Furthermore, phytoncide suppressed Bcl-2 and stimulated Bax protein expression in RAW 264.7 cells. Phytoncide significantly stimulated apoptosis in RANKL-induced RAW 264.7 cells in a dose-dependent manner. In contrast to the effect on osteoclasts, phytoncide increased ALP activities and bone nodule formation in MC3T3-E1 cell cultures. The expression of Bcl-2 protein was

increased, but the expression of Bax protein was decreased by phytoncide treatment in MC3T3-E1 cells.

These results demonstrate that phytoncide may cause anti-differentiation and pro-apoptosis in osteoclasts but stimulate osteoblasts and their activity.

**Disclosures:** In-Jin Cho, None.

## SA0184

**Lrrk1 regulation of actin assembly in osteoclasts involves serine phosphorylation of L-plastin.** Helen Goodluck<sup>\*1</sup>, Songqin Pan<sup>2</sup>, Sharon Morley<sup>3</sup>, Subburaman Mohan<sup>1</sup>, Weirong Xing<sup>1</sup>. <sup>1</sup>Musculoskeletal Disease Center, VA Loma Linda Healthcare System, United States, <sup>2</sup>Proteomics Core Facility, University of California, United States, <sup>3</sup>Department of Pediatrics; Department of Pathology and Immunology, Washington University School of Medicine, United States

Targeted knockout (KO) of leucine rich repeat kinase 1 (Lrrk1) in mice resulted in severe osteopetrosis, and patients with mutations in the Lrrk1 gene exhibited a phenotype of osteosclerotic metaphyseal dysplasia characterized by severe osteosclerosis confined to the metaphysis of the long and short tubular bones due to osteoclast dysfunction. To understand how Lrrk1 regulates formation of F-actin rings and podosomes in osteoclasts, we examined proteins that are differentially phosphorylated in the wild type and Lrrk1 deficient osteoclasts by metal affinity purification coupled LC/MS analyses. One of the candidates that we have identified by LC/MS is L-plastin, an actin bundling protein. We found that phosphorylation of L-plastin at serine (Ser) residues 5 and 7 was only present in wild type osteoclasts but not in Lrrk1 deficient cells. Western blot analyses with antibodies specific for Ser5 phosphorylated L-plastin confirmed the reduced L-plastin Ser5 phosphorylation in Lrrk1 KO osteoclasts. Based on the published *in vitro* findings that L-plastin regulates F-actin assembly and sealing zone formation in osteoclasts and macrophages via its Ser5 phosphorylation, we evaluated if targeted KO of L-plastin influences the skeletal phenotype in mice. MicroCT analyses revealed that trabecular bone volume (BV) of the distal femur was increased by 49% ( $P < 0.05$ ) in the 16-18 week old L-plastin KO females as compared to the wild type control mice. The ratio of BV to tissue volume (BV/TV) and connectivity density were increased by 48% and 55% (both  $P < 0.05$ ), respectively, in L-plastin KO mice. Based on these data, we conclude that: 1) targeted disruption of L-plastin increases trabecular bone volume, 2) the magnitude of increase is much smaller than that seen in Lrrk1 KO mice (50% vs. 400%), and 3) Lrrk1 phosphorylation of Ser5 of L-plastin may in part contribute to actin assembly in mature osteoclasts

**Disclosures:** Helen Goodluck, None.

## SA0185

See Friday Plenary Number FR0185.

## SA0186

**A Jumonji C(Jmj) domain-containing protein negatively regulates RANKL-mediated osteoclastogenesis.** Seon-Young Kim<sup>\*</sup>, Hye-Jin Kim, Do Won Jung, Jong-Wan Park, Yang-Sook Chun. Seoul National University College of Medicine, Korea, Republic of

The regulation of osteoclastogenesis is critical to maintain physiological bone homeostasis and prevent bone-destructive diseases. The nuclear factor of activated T-cells calcineurin-dependent 1 (NFATc1) plays an essential role in osteoclastogenesis, and its expression is induced during early osteoclastogenesis. On the other hand, the Jumonji C (JmjC) domain-containing protein (JHDM), a histone demethylase, catalyzes histone 3 lysine 9 and is involved in osteoblastic bone formation. However, the mechanism for regulation of the enzymatic activity of JHDM in osteoclastogenesis is not yet well known. Here, we show that JHDM is a key negative regulator during receptor activator of nuclear factor- $\kappa$ B ligand (RANKL)-induced osteoclastogenesis. The expression level of JHDM gradually decreased during osteoclastogenesis in bone marrow macrophages (BMMs) treated with RANKL. Down-regulated expression of JHDM strongly facilitated osteoclast formation together with induction of several osteoclast-specific genes such as TRAP, Oscar and CathepsinK. NFATc1 proteins are ubiquitinated and rapidly degraded during late stage osteoclastogenesis. Interestingly, overexpression of JHDM induces NFATc1 degradation during late stage osteoclastogenesis. Taken together, the present study demonstrated that JHDM is a post-translational co-repressor for NFATc1 that attenuates osteoclastogenesis.

**Disclosures:** Seon-Young Kim, None.

## SA0187

See Friday Plenary Number FR0187.

## SA0188

See Friday Plenary Number FR0188.

## SA0189

**OFS-1, a Sentinel Probe for Early Detection of Disease-induced Osteolysis by Multiple Myeloma in Humanized BLT Mice.** Kenzo Morinaga<sup>\*1</sup>, Akishige Hokugo<sup>2</sup>, Eric Richard<sup>3</sup>, Kimberly Hui<sup>3</sup>, Boris Kashemirov<sup>3</sup>, Charles McKenna<sup>3</sup>, Ichiro Nishimura<sup>1</sup>. <sup>1</sup>Weintraub Center for Reconstructive Biotechnology, UCLA School of Dentistry, United States, <sup>2</sup>Division of Plastic Surgery, David Geffen School of Medicine at UCLA, United States, <sup>3</sup>Department of Chemistry, Dornsife College of Letters, Arts and Sciences, USC, United States

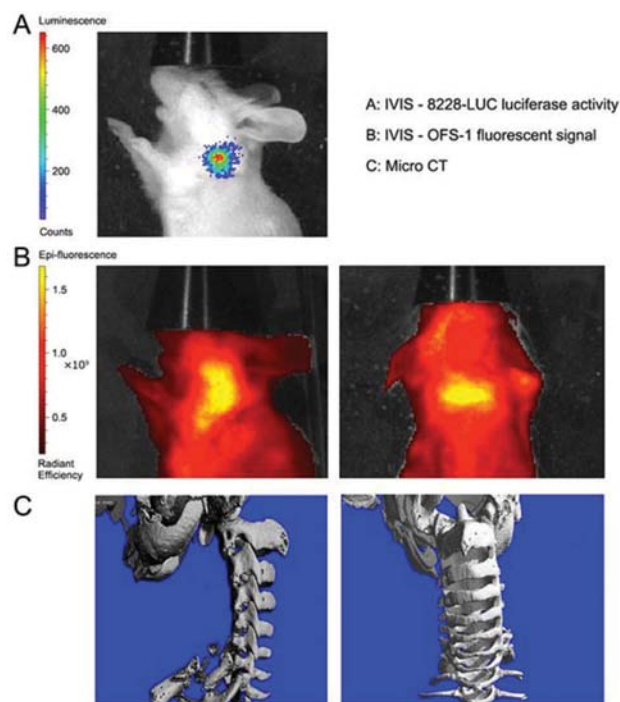
Multiple myeloma is the most frequent primary malignant neoplasm of the skeletal system and develops debilitating or life-limiting skeletal-related events. The pathological mechanism of disease-induced bone lesions is still unclear; however, the preferred initial diagnosis and staging of multiple myeloma remains the radiological skeletal survey detecting the characteristic osteolytic images.

Osteoclasts on the bone surface release hydrogen ions and cathepsin K (CTSK). CTSK is nearly exclusively secreted by osteoclasts and has an optimal enzymatic activity in acidic conditions for collagenolysis. Postulating that *in situ* detection of CTSK activity would allow identification of early stage multiple myeloma-induced osteolysis, we have synthesized a fluorescent compound linked to a Förster resonance energy transfer (FRET) quencher through a CTSK peptide substrate, and decorated with a bisphosphonate (BP) moiety for bone localization (OFS-1).

OFS-1 was activated *in vitro* by human CTSK, which was dose dependently inhibited by odanacatib. When human osteoclasts derived from CD14+ peripheral blood monocytes were cultured on Corning Osteo Assay plates pretreated with OFS-1, fluorescence was detected around the periphery of resorption pits as well as in the osteoclast cytoplasm. Osteoclasts co-cultured with 8226-LUC human multiple myeloma cells exhibited significantly increased OFS-1 activation.

We next developed an immune-competent multiple myeloma mouse model. Irradiated NSG immunodeficient mice were co-grafted with human CD34+ hematopoietic stem cells, liver and thymus (BLT mice), resulting in the complete humanization of immune regulatory and effector cells. Four weeks after intravenous injection of  $1.5 \times 10^6$  8226-LUC cells and three weeks after OFS-1 injection, BLT mice were subjected to *in vivo* imaging. 8226-LUC multiple myeloma cells were found engrafted at lumbar and cervical bones as well as femurs and tibia emitting different luciferase intensities. Strong fluorescence was detected at the 8226-LUC grafted sites, even with weak luciferase signal intensity.

OFS-1 thus appears to have potential as a novel detection system of early osteolysis activity induced by multiple myeloma and possibly other solid tumors affecting the skeletal system such as metastatic breast and prostate cancers.



Strong fluorescence was detected at the 8226-LUC grafted sites, even in an early osteolysis stage.

OFS-1 activation by Multiple myeloma

**Disclosures:** Kenzo Morinaga, None.



## SA0190

**Negative Regulation of Canine Osteoclastogenesis and *Mitf*-E Expression by Transforming Growth Factor- $\beta$ .** Masaru Murakami<sup>\*1</sup>, Kumiko Asai<sup>1</sup>, Fumie Shimokawa<sup>1</sup>, Masaharu Hisasue<sup>2</sup>, Masayuki Funaba<sup>3</sup>. <sup>1</sup>Laboratory of Molecular Biology, Azabu University School of Veterinary Medicine, Japan, <sup>2</sup>Laboratory of Veterinary Internal Medicine II, Azabu University School of Veterinary Medicine, Japan, <sup>3</sup>Division of Applied Biosciences, Kyoto University Graduate School of Agriculture, Japan

With longevity, the prevalence of osteoporosis, which occurs when the activity of osteoclast surpasses that of osteoblasts, has increased in dogs. However, limited information is available on canine osteoclastogenesis. We herein show culture conditions to induce osteoclasts from canine bone marrow cells, and identify factors affecting canine osteoclastogenesis. Tartrate-resistant acid phosphatase (Trap)-positive multinucleated cells were efficiently formed in a culture of bone marrow mononuclear cells with macrophage-colony-stimulating factor (M-CSF; 25 ng/mL) for 3 days and a subsequent culture in the presence of M-CSF (25 ng/mL) and soluble receptor activator of NF- $\kappa$ B ligand (RANKL; 50 ng/mL) for 4 days. These cells had bone-resorption activity, which was shown by a pit formation assay. In addition, real-time RT-quantitative PCR analysis revealed that expression of genes related to osteoclastogenesis or osteoclast function was up-regulated in cells treated with M-CSF and RANKL. We previously reported in a murine cell system that gene induction of the E isoform of microphthalmia-associated transcription factor (*Mitf*-E) was required and sufficient for osteoclastogenesis, while transforming growth factor- $\beta$  (TGF- $\beta$ ) enhanced RANKL-induced *Mitf*-E expression and osteoclastogenesis (Cell Biochem Funct, 32: 401, 2014). *Mitf*-E expression also increased during RANKL-induced osteoclastogenesis in canine cells. Forced expression of *Mitf*-E stimulated transcription of cathepsin K, a gene required for bone resorption by osteoclasts, which was shown by a luciferase-based reporter assays. However, unlike murine cells, TGF- $\beta$  inhibited osteoclastogenesis, which was verified by Trap staining and expression levels of osteoclast-related genes. In addition, TGF- $\beta$  down-regulated expression of *Mitf*-E during canine osteoclastogenesis. The results of the present study show that, consistent with murine cells, M-CSF and soluble RANKL enable canine bone marrow cells to differentiate into osteoclasts, and *Mitf*-E expression is induced during osteoclastogenesis. However, the role of TGF- $\beta$  in osteoclast formation is distinct between murine and canine cells, suggesting the necessity of analyses using canine cells to examine the factors affecting canine osteoclastogenesis.

**Disclosures:** Masaru Murakami, None.

## SA0191

**Collagen Type VI  $\alpha$ 2 Chain Deficiency Causes Trabecular Bone Loss by Enhancing Osteoclast Differentiation.** Hai Pham<sup>\*</sup>, Ainnie Dar, Vardit Kram, Li Li, Tina Kilts, Marian Young. Craniofacial and Skeletal Diseases Branch, National Institute of Dental and Craniofacial Research, National Institutes of Health, United States

Type VI collagen is widely known for its role in muscular disorders, however its function in bone is still not well understood. Type VI collagen is composed of three  $\alpha$ -chains ( $\alpha$ 1,  $\alpha$ 2,  $\alpha$ 3) that align in a triple helix that forms trimers that assemble into fibrils found in many musculoskeletal tissues. When we examined the expression of all three type VI chains by quantitative RT-PCR during fracture healing, we found that Col6a2 mRNA was highly upregulated at day 14 post-fracture. Using immunohistochemistry we confirmed that the collagen VI expression levels were induced in the callus of healing bones suggesting it could have a role in bone homeostasis. To determine the role of type VI  $\alpha$ 2 in bone function we analyzed the trabecular bone from femora and vertebra in mice deficient in type VI  $\alpha$ 2 (Col6a2 KO) at 3 months of age. DEXA analysis indicated a significant lower bone mineral density in Col6a2 KO mice. Additionally, micro CT analysis showed significant decreases in bone volume/tissue volume, trabecular bone number and bone mineral density in the Col6a2 KO compared to wild-type (WT) mice. To try to understand the cellular basis for the decreased bone mass, we isolated bone marrow stromal cells (BMSCs) from WT and Col6a2 KO mice and cultured them under osteogenic conditions. No significant differences in osteogenic differentiation could be observed. Similarly, no changes in osteogenesis were observed between WT and Col6a2 KO BMSCs when media was supplemented with 100 ng/ml of human Type VI collagen. These experiments indicate that neither gain nor loss of function of type VI collagen in murine BMSCs induced significant effects on osteogenesis *in vitro*. When we examined femora sections of the Col6a2 KO mice for the abundance of TRAP positive osteoclasts, we discovered that the mutant mice exhibited 2.4 times more osteoclasts compared to WT mice. Osteoclast precursors were then isolated from WT and Col6a2 KO mice bone marrow and induced to differentiate *in vitro* using a combination of RANKL and MCSF. Our data showed that cells from Col6a2 null mice generated more TRAP positive cells after induction. Moreover, media supplementation with human Type VI collagen in WT osteoclast differentiation cultures significantly decreased the number of TRAP positive cells. In summary, our data indicate that collagen type VI regulates trabecular bone mass by inhibiting osteoclast differentiation, and could be a new molecular drug target to prevent bone loss.

**Disclosures:** Hai Pham, None.

## SA0192

See Friday Plenary Number FR0192.

## SA0193

See Friday Plenary Number FR0193.

## SA0194

See Friday Plenary Number FR0194.

## SA0195

**Monocyte-Specific Knockout of *C/EBP $\alpha$*  Results in Osteopetrosis Phenotype, Blocks Bone Loss in Ovariectomized Mice and Reveals the Indispensable Function of *C/EBP $\alpha$*  in Osteoclast Differentiation and Function.** Jun Tang<sup>\*</sup>, Guochun Zhu, Joel Jules, Yi-Ping Li, Wei Chen. Department of Pathology, University of Alabama at Birmingham, United States

Age-associated osteoporosis in postmenopausal women due to estrogen deficiency is a major health problem, characterized by increase of osteoclastogenesis and osteoclast activity, and severe bone loss. Current treatment options are constrained by lower response rates and adverse side-effects. Despite osteoclast lineage commitment and differentiation been extensively studied, the mechanism by which transcription factor (s) control osteoclast terminal differentiation, activation and function remains unclear. *C/EBP $\alpha$*  has been reported as a key regulator in osteoclast cell lineage commitment. However, the role of *C/EBP $\alpha$*  in postnatal skeletal development has not been reported owing to lethality in *C/EBP $\alpha$ <sup>-/-</sup>* mice from hypoglycemia within 8 hours after birth. Herein, we generated conditional knockout mice by deleting the *C/EBP $\alpha$*  gene in OC precursors via LysM-Cre to examine its role in postnatal skeletal development. Radiological and histological analyses showed that *C/EBP $\alpha$ <sup>F/F</sup>* LysM-Cre mice exhibited a severe postnatal osteopetrosis due to impaired osteoclastogenesis and defective OC differentiation and activity. Furthermore, our *ex-vivo* osteoclast differentiation and function assays revealed that *C/EBP $\alpha$*  conditional deletion drastically abrogated OC differentiation, maturation, and activity while mildly repressed macrophage development. At the molecular level, Western blot and qPCR results showed that *C/EBP $\alpha$*  deficiency suppressed the expression of osteoclast function genes (e.g. Cathepsin K, *ATP6i*), osteoclast regulator genes (e.g. *c-fos*, *NFATc1*) and a gene that is common to both osteoclasts and macrophages (ie. PU.1). Consistently, our promoter activity mapping and ChIP assay identified numerous *C/EBP $\alpha$*  critical cis-regulatory elements on the Cathepsin K promoter which allow *C/EBP $\alpha$*  to drastically upregulate Cathepsin K during OC differentiation and activity. Notably, we show that *C/EBP $\alpha$*  deficiency can protect mice against ovariectomy-induced bone loss in a mouse model of osteoporosis, uncovering a central role for *C/EBP $\alpha$*  in osteolytic diseases. These results were further confirmed by extensive phenotypic and mechanistic studies using the osteoclast-specific *C/EBP $\alpha$ <sup>F/F</sup>* Ctsk-Cre mice. Collectively, these findings provide significant insights into *C/EBP $\alpha$* 's role as a regulatory molecule in osteoclast terminal differentiation, as well as its role in postnatal bone homeostasis, uncovering a potential effective target for osteoporosis therapy.

**Disclosures:** Jun Tang, None.

## SA0196

**Characterization of a Novel *TCIRG1* Mutation Responsible for a Mild Form of Autosomal Recessive Osteopetrosis.** Andrew Wang<sup>\*1</sup>, Ralph Zirngibl<sup>1</sup>, Joerg Krueger<sup>2</sup>, Roberto Mendoza<sup>3</sup>, Irina Voronov<sup>1</sup>. <sup>1</sup>Faculty of Dentistry, University of Toronto, Canada, <sup>2</sup>Department of Hematology, Hospital for Sick Children, Canada, <sup>3</sup>Division of Clinical and Metabolic Genetics, Hospital for Sick Children, Canada

Osteopetrosis is a group of diseases characterized by dense and brittle bones. Autosomal recessive osteopetrosis (ARO) is the most severe form of the disease and is caused by mutations that affect formation or function of osteoclasts, the bone resorbing cells. Mutations in the  $\alpha$ 3 subunit of the vacuolar type H<sup>+</sup>-ATPase (encoded by *TCIRG1* gene) are responsible for almost 50% of all ARO cases. We identified a novel *TCIRG1* mutation responsible for an unusually mild form of the disease. This mutation (c.630G>A) replaces the last nucleotide of exon 6 and, therefore, is predicted to affect *TCIRG1* splicing efficiency. Therefore, we decided to characterize this novel mutation and to examine the mechanisms leading to a mild form of osteopetrosis.

To characterize this novel mutation, first, we used peripheral blood monocytes from the patient (homozygous for the mutation, c.G630A/c.G630A), unaffected male sibling (non-carrier, +/+), unaffected female sibling (carrier, heterozygous for the mutation, +/c.G630A), and unaffected parent (carrier, heterozygous for the mutation, +/c.G630A) to differentiate osteoclasts *in vitro*. Cells were cultured with 20 ng/ml M-CSF and 100 ng/ml RANKL for 8 days, and then (1) fixed and stained for tartrate resistant acid phosphatase (TRAP), (2) lysed in RIPA buffer to measure protein expression by immunoblotting, (3) lysed in Trizol to analyze mRNA *TCIRG1* expression levels.

All three genotypes formed multinucleated TRAP positive osteoclasts; however, the c.G630A/c.G630A osteoclasts failed to resorb bone-like substrate when plated on Osteologic surface. *TCIRG1* mRNA expression levels were decreased in the c.G630A/c.G630 cells compared to the +/+ and +/c.G630A osteoclasts. *TCIRG1* protein levels were also decreased in the c.G630A/c.G630A patient-derived osteoclasts as determined by immunoblotting; however, the levels of another V-ATPase subunit, V1A, were not affected.

These results show that the c.G630A mutation in the affected patient leads to decreased *TCIRG1* protein and mRNA expression levels, indirectly confirming the original prediction that this mutation might affect splicing efficiency. Future

experiments will investigate the precise mechanisms involved, and will examine whether the c.G630A mutation affects only splicing efficiency or also results in exon skipping.

**Disclosures:** Andrew Wang, None.

## SA0197

See Friday Plenary Number FR0197.

## SA0198

See Friday Plenary Number FR0198.

## SA0199

**The role of osteocytes in regulating bone marrow fat: insight into large and small animal models of osteoporosis.** Thaqif El Khassawna<sup>1</sup>, Deeksha Malhan<sup>1</sup>, Diaa Eldin Daghma<sup>1</sup>, Sabine Stoetzel<sup>1</sup>, Stefanie Kern<sup>1</sup>, Fathi Hassan<sup>1</sup>, Katrin Susanne Lips<sup>1</sup>, Christian Heiss<sup>2</sup>. <sup>1</sup>Experimental Trauma Surgery, Faculty of Medicine, Justus-Liebig University of Giessen, Germany, <sup>2</sup>Department of Trauma, Hand and Reconstructive Surgery, University Hospital of Giessen - Marburg, Germany

Bone mechanosensation is mainly governed by osteocytes. However, their specific role in regulating homeostasis in diseased bone remains unclear. In this study we aim to explore the correlation of osteocyte morphology and brown adipocytes accumulation in bone marrow in osteoporotic sheep model. The study investigated the induction of osteoporosis after (month=M) 3M and 8M in 31 female merino-land sheep divided into four groups: control, ovariectomy (OVX), OVX with dietary limitation (OVXD), and OVXD with steroid injection (OVXDS). Dual-energy X-ray absorptiometry (DXA) revealed an increase in body fat in OVXDS (p-value  $\leq 0.05$  between the time points) and negatively correlated with Bone Mineral Density (BMD) with treatment progression. Only OVXDS showed significant BMD reduction from initial time point at 3M and 8M (p-value  $\leq 0.05$ , and 0.026, respectively). Beside the typical bone structural changes which hallmark the osteoporotic bone status, numbers of empty lacunae and adipocytes increased with treatment progression and severity. The direct influence of osteocytes was investigated through immunostaining BMP7, UCP1, PGC1 alpha, and PRDM16 with silver nitrate as counter staining. Our results showed for the first time the more frequent signal of all the mentioned proteins in spherical but not spindle shaped osteocytes which increased in numbers throughout the treatment. Interestingly, immunostaining signal increased corresponding to osteoporosis severity in the bone marrow area. However, in OVXDS group PRDM16 was highest after 3 months of treatment before becoming lower at 8 months in the adipocytes. This might indicate the phase where brown adipocytes start to lose their characteristics. The results draw a direct relation of bone marrow fat regulation through osteocytes. To associate PGC1 alpha and PRDM16 regulation through osteocytes with osteoporosis progression further animal models are being investigated. Therefore, Senile and pre-aged rat models are utilized with ovariectomy, dietary limitation and steroid treatment. Furthermore, serum analysis and bone panel qPCR analysis is currently in progress to understand the systemic alteration versus the region then cell specific alterations resulting from the treatment. Understanding the role of osteocytes in regulating fat metabolism might suggest cell specific therapeutic targeting to prevent osteoporotic fractures.

**Disclosures:** Thaqif El Khassawna, None.

## SA0200

See Friday Plenary Number FR0200.

## SA0201

See Friday Plenary Number FR0201.

## SA0202

See Friday Plenary Number FR0202.

## SA0203

**Osteocyte role in osteoporotic sheep model: cell-specific gene profiling.** Deeksha Malhan<sup>1</sup>, Diaa Eldin S. Daghma<sup>1</sup>, Sabine Stoetzel<sup>1</sup>, Stefanie Kern<sup>1</sup>, Fathi Hassan<sup>1</sup>, Katrin Susanne Lips<sup>1</sup>, Thaqif El Khassawna<sup>1</sup>, Christian Heiss<sup>2</sup>. <sup>1</sup>Experimental Trauma Surgery, Faculty of Medicine, Justus Liebig University of Giessen, Germany, <sup>2</sup>Department of Trauma, Hand and Reconstructive Surgery, University Hospital of Giessen-Marburg, Germany

Osteoporosis is a systemic skeletal disease characterized by lower bone mass. Cellular investigation shows imbalance in osteoblasts, osteoclasts, and osteocytes thereby increasing fracture risk. Understanding the behavior of cells during normal and diseased condition is crucial to develop therapeutic agents.

The current study aimed to unravel complex molecular regulation within osteocytes using sheep model of ovariectomy and multi-deficient diet administration. To investigate the targeted cells, the procedure for cell-picking and RNA isolation was optimized. RNA integrity and quality was appropriate for RNA sequencing.

The study utilized 31 Merino land sheep (average-age = 5.5years) randomly divided into four groups: Control, bilaterally ovariectomized (OVX), OVX and a calcium- and vitamin-D2/3-deficient diet (OVXD), and OVX, diet and corticosteroids (OVXDS). After 8 months, biopsy from lumbar vertebrae were collected and freeze embedded. Besides, rhodamine staining, silver staining, and immunohistochemical (IHC) stains were performed to investigate osteocyte network and proliferation activity. After freeze- sectioning, osteocytes were isolated using PALM laser system (Carl Zeiss AG, Jena, Germany). Total RNA was isolated to perform Next generation RNA-sequencing.

Rhodamine and silver staining showed the irregular arrangement of osteocytes in OVXDS group while osteocytes were well-arranged in control. IHC stain showed the high signal intensity of Ki-67 within the osteocyte vicinity. Ki-67 is known as the cell proliferation markers. Therefore, our study optimized LMD approach to study differential gene expression within osteocyte in osteoporotic sheep model. The established protocol was also successfully tested on osteoporotic rat model, and pseudoarthrosis human sample. Currently, processing of all samples and RNA sequencing are being carried out.

**Disclosures:** Deeksha Malhan, None.

## SA0204

**Profiling the composition of osteocyte pericellular matrix (PCM) in vivo and in vitro.** Jerahme Martinez<sup>1</sup>, Liyun Wang<sup>1</sup>, Shaopeng Pei<sup>1</sup>, Shubo Wang<sup>1</sup>, Ashutosh Parajuli<sup>1</sup>, Mary Farach-Carson<sup>2</sup>. <sup>1</sup>University of Delaware, United States, <sup>2</sup>The University of Texas Health Science Center at Houston School of Dentistry, United States

Osteocytes comprise the overwhelming majority of the cells in bone and play a crucial role in maintaining bone homeostasis and orchestrating bone's responses to mechanical loading. Increasing evidence indicates that the proteoglycan-rich osteocyte pericellular matrix (PCM) functions as a mechanical sensor to detect external loading signals. Previously, we identified perlecan/HSPG2, a large heparan sulfate proteoglycan, as a key component of the osteocyte PCM and demonstrated its importance for *in vivo* loading and unloading. In those studies, we used a perlecan-deficient mouse that mimics the human skeletal dysplasia Schwartz-Jampel Syndrome (SJS), which develops both osteoarthritis and osteoporosis. We hypothesize that perlecan is part of a mechanosensitive tethering complex in the osteocyte PCM that is disrupted in SJS. To test this hypothesis *in vivo* and *in vitro*, we first examined the tissue PCM composition, using a mass spectrometry-based glycoproteomic analysis of bone tissue extracts from both wild-type and perlecan-deficient mice. For comparison, we investigated the PCM produced by commonly used osteocyte cell lines, MLO-Y4 and IDG-SW3. To enrich PCM constituents prior to mass spectroscopy analysis, we metabolically labeled osteocyte-secreted sialylated glycoproteins using an azide-modified sugar, then isolated labeled products using dibenzocyclooctyl (DBCO) copper-free click chemistry. The results provide a comprehensive expression profile of native actively produced osteocyte PCM glycoconjugates, among which are novel candidate targets that, alone or in complex with perlecan, may be key components of the osteocyte's mechanosensing complex. This novel strategy provides a powerful launchpad from which to dissect the structure-function relationships of the glycoconjugate components of the load detecting complexes in osteocyte-rich bone.

**Disclosures:** Jerahme Martinez, None.

## SA0205

See Friday Plenary Number FR0205.

## SA0206

**Effects of Glucose Uptake Inhibition by Phloretin on Expressions of RANKL and Osteocalcin in Osteocytic MLO-Y4-A2 Cells.** Ayumu Takeno<sup>\*</sup>, Ipppei Kanazawa, Masakazu Notsu, Ken-ichiro Tanaka, Toshitsugu Sugimoto. Internal Medicine 1, Shimane University Faculty of Medicine, Japan

Background: Bone metabolism plays important roles in glucose homeostasis. It has been shown that osteocalcin regulates glucose homeostasis, and that the activity of osteocalcin requires its production by osteoblast lineage and decarboxylation by osteoclasts. Because osteocytes orchestrate bone remodeling by producing RANKL and sclerostin, osteocytes may be involved in glucose homeostasis. A recent study has shown that glucose transporter (GLUT) 1 is expressed in osteoblasts and that the deletion of osteoblast GLUT1 markedly decreased bone formation via AMP-activated protein kinase (AMPK) activation and exacerbates glucose tolerance. However, the roles of glucose uptake in expressions of RANKL, osteoprotegerin, and sclerostin as well as osteocalcin activity in osteocytes are unknown. Methods and results: We used MLO-Y4-A2, a murine long bone-derived osteocytic cell line, and confirmed that GLUT1 was expressed in MLO-Y4-A2 cells, but not GLUT2, 3, or 4. Furthermore, treatment with phloretin, a GLUT inhibitor, (10-100  $\mu$ M) significantly inhibited glucose uptake in the cells. Real-time PCR and Western blot showed that phloretin significantly and dose-dependently decreased the expressions of RANKL and osteocalcin, whereas osteoprotegerin and sclerostin were not affected. Because phloretin



activated AMPK, we investigated whether AMPK activation would modulate the RANKL and osteocalcin expressions. Coincubation of ara-A, an AMPK inhibitor, with phloretin significantly reversed the phloretin-induced decrease in osteocalcin expression, but not RANKL. In contrast, phloretin suppressed phosphorylation of ERK1/2, JNK, and p38 MAPK, and treatments with a JNK inhibitor SP600125, a p38 inhibitor SB203580, or a MEK inhibitor PD98059, significantly decreased the expressions of RANKL and osteocalcin. Conclusion: This study indicates that glucose uptake by GLUT1 is required for RANKL and osteocalcin expressions in osteocytes and that inhibition of glucose uptake decreases their expression through activation of AMPK and inhibition of MAPK pathways. These findings suggest that osteocytes may sense low glucose levels and contribute to maintain glucose levels by decreasing osteocalcin expression and RANKL-induced bone resorption, resulting in suppressing the activation of osteocalcin.

**Disclosures:** Ayumu Takeno, None.

## SA0207

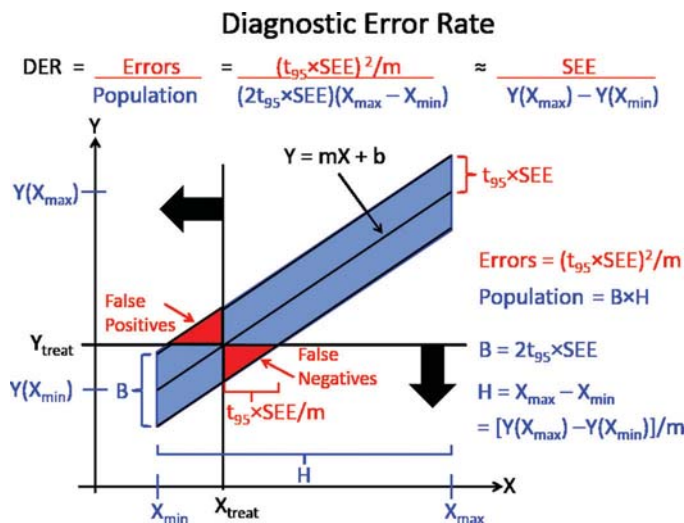
**Diagnostic Error Rates of Bone Mineral Density and Other Proxies for Bone Strength.** Lyn Bowman\*, Gabriel C. Hausfeld, Emily R. Ellerbrock, Jennifer M. Neumeyer, Tyler C. Beck, Maureen A. Dean, McKenzie L. Nelson, Anne B. Loucks. Ohio University, United States

**Purpose:** Osteoporosis is characterized by a decline in bone strength, but a patient's bone strength cannot be measured directly. So, osteoporosis is diagnosed in patients with T-scores of bone mineral density (BMD) below a threshold of -2.5. However, most such patients do not fracture, and most fractures occur in patients diagnosed as not osteoporotic. These unexpected outcomes drive healthcare costs. The purpose of this study was to assess the extent to which unexpected outcomes of osteoporosis treatment might be explained by the imperfect correlation of bone strength and BMD, and whether such outcomes might be reduced by other diagnostic methods.

**Methods:** When classifying bivariate observations of any Y and X relative to threshold values, imperfect correlation introduces false positive and false negative errors (See Figure). We defined the proportion of these errors in a population whose bone strength Y is predicted by proxy X as the Diagnostic Error Rate (DER) of that proxy. By statistical theory, geometry and algebra, we derived that, for any diagnostic threshold values,  $DER = SEE/(Y(X_{max}) - Y(X_{min}))$ , where SEE = the standard error of the estimate in the regression of Y on X, and Y(X<sub>max</sub>) and Y(X<sub>min</sub>) are the predicted values of the maximum and minimum values of X, respectively. We then searched the literature for regressions of human bone strength on BMD and other proxies. Because bones break as structures not materials, we considered only structural tests of bone strength measured directly by quasistatic mechanical testing (QMT). We also measured the bending strength, cortical porosity (CP), and bending stiffness (EI) of ulna bones in 35 cadaveric human arms from men and women ranging widely in age (17-99 yrs) and body mass index (BMI) (13-40 kg/m<sup>2</sup>).

**Results:** We found the following DER values: BMD = 15-24%, bone mineral content = 11-28%, quantitative computed tomography (QCT) with finite element analysis = 11-13%, peripheral QCT = 12-17%, reference point indentation = 36-42%, BMI = 28%, CP = 34-44%, EI = 5-8% by QMT and 7% noninvasively by cortical bone mechanics technology (CBMT). If only the lower half of the population (BMD T-scores <0) is considered for treatment, DER doubles. If only T < -1 is considered, DER is multiplied by 6.

**Conclusions:** Misallocation of patients to treatment by BMD is sufficient to account for all of the unexpected outcomes of osteoporosis treatment. CBMT may have the greatest potential for reducing these outcomes.



Figure

**Disclosures:** Lyn Bowman, None.

## SA0208

See Friday Plenary Number FR0208.

## SA0209

See Friday Plenary Number FR0209.

## SA0210

**Older Age and Higher Body Mass Index are Associated with more Microarchitectural Degradation in Trabecular Bone Score Compared to Bone Mineral Density.** Young Ho Shin\*, Hyun Sik Gong<sup>2</sup>. <sup>1</sup>Department of Orthopedic Surgery, Asan Medical Center, Korea, Republic of, <sup>2</sup>Department of Orthopedic Surgery, Seoul National University Bundang Hospital, Seoul National University College of Medicine, Korea, Republic of

**Purpose:** We identified Korean women over age 40 whose trabecular bone score (TBS) reflected relatively more microarchitectural degradation than did their BMD and evaluated whether age and body size were associated in these subjects.

**Methods:** We analyzed BMD and TBS in 1505 Korean women over age 40 who had no history of osteoporotic fractures or conditions that affect bone metabolism. We considered three groups to have TBS values that reflected relatively more microarchitectural degradation than did their BMD values: 1) normal BMD but partially degraded microarchitecture on TBS, 2) normal BMD but degraded microarchitecture on TBS, and 3) osteopenia but degraded microarchitecture on TBS. We compared subjects in these 3 groups with other subjects in age and body size, and used multivariate logistic regression to analyze the odds ratios (ORs) for the occurrence of more degraded microarchitecture on TBS than on BMD using age, height, weight, and body mass index (BMI).

**Results:** One hundred and twenty-seven subjects (8.4%) were found to have more microarchitectural degradation based on TBS than on BMD; these subjects were older (p = 0.026) and more obese (p < 0.001) than other subjects. Age (OR: 1.038; 95% CI: 1.017-1.058; p < 0.001) and BMI (OR: 1.244; 95% CI: 1.179-1.314; p < 0.001) were statistically significant on multivariate analysis for the occurrence of this feature.

**Conclusions:** Women with more microarchitectural degradation in TBS compared to BMD are older and have higher BMI than other subjects. Hidden microarchitectural deterioration may partially explain the increased fracture risk in old or obese people.

**Disclosures:** Young Ho Shin, None.

## SA0211

See Friday Plenary Number FR0211.

## SA0212

See Friday Plenary Number FR0212.

## SA0213

**Preliminary Computed Tomography (CT) Multi-scale Investigation of Cortical Bone Quality in Non-osteoporotic Males.** Randee Hunter\*, Amanda Agnew<sup>1</sup>, Michelle Murach<sup>1</sup>, Karen Briley<sup>2</sup>. <sup>1</sup>Skeletal Biology Research Laboratory; Injury Biomechanics Research Center, United States, <sup>2</sup>Wright Center for Innovation in Biomedical Imaging, United States

The purpose of this study is to investigate the impact of subject level variables (age and body size) on cross-sectional properties and bone mineral density along the length of the diaphysis of a weight bearing (tibia) and non-weight bearing (radius) bone. Quantifying the impact of these factors on the functional adaptation of human cortical bone and the site dependent co-variation of these traits for differing mechanical environments integrates a multiscale approach to bone quality. Bilateral tibiae and radii were excised from n=39 non-osteoporotic subjects (assessed via lumbar DXA T-scores <-2.5) ranging in age from 25 to 87 years old (mean of 63.9 ± 12.5 years). Whole bone computed tomography (CT) scans were acquired using a Philips Ingenuity 64 channel multi-slice system with resulting resolutions of 0.167mm for the radius and 0.335mm for the tibia. Cross-sectional parameters including cortical area (Ct.Ar) and section modulus (Z) were quantified for segment sites calculated relative to total length (mm) in the radius (30 and 50%) and tibia (38, 50 and 66%). Site-specific volumetric bone mineral density (vBMD) was calculated using Skyscan CTAn software (Bruker) and a QRM cortical phantom. Robustness was determined as cross-sectional total area (Tt.Ar) divided by total bone length thus representing a mixed geometry predictor of whole bone strength. Lastly, body size measurements were determined to be the individual's total mass (kg) multiplied by total bone length (Bm-Le). Linear regressions indicate neither age nor body size could predict any significant variation in bone quality parameters in the radius (p > 0.05). However, age demonstrates a weak but significant (p < 0.02; R<sup>2</sup> = 0.14-0.244) relationship with robustness at all tibia sites, and both age and body size are significantly related to vBMD (p < 0.05; R<sup>2</sup> = 0.13-0.24 and 0.12-0.18 respectively). Co-variation of these traits in both elements indicate cortical cross-sectional properties (Ct.Ar and Z) decrease from proximal to distal with functional compensation in the form of increasing vBMD. The results of this study support a more discriminate method of quantifying bone quality which considers functional adaptation as a hierarchical model that appears

to vary along the length of the bone and are differentially influenced by subject level variables. Future work will include dynamic mechanical testing to investigate the tangible effects of this variation on fracture risk.

**Disclosures:** Randee Hunter, None.

## SA0214

See Friday Plenary Number FR0214.

## SA0215

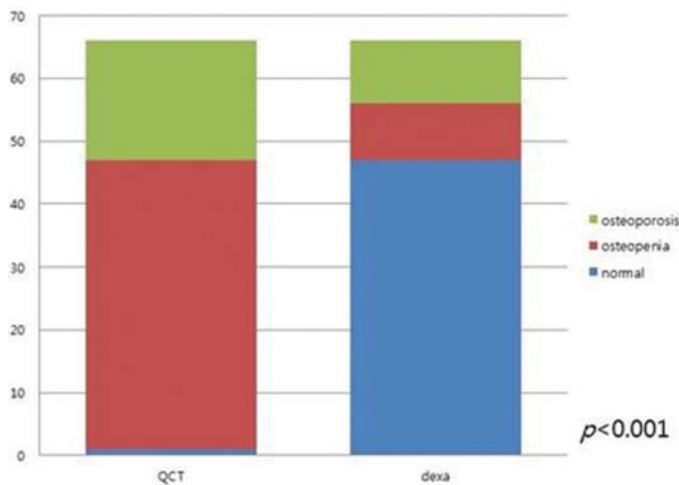
**A comparative study of evaluation of bone mineral density using DXA and QCT in the post-menopausal patients under thyrotropin suppressive therapy.** Yun Kyung Jeon<sup>\*1</sup>, Keunyoung Kim<sup>1</sup>, In Joo Kim<sup>1</sup>, Kyoungjune Park<sup>1</sup>, Myung-Jun Shin<sup>1</sup>, Tae Sik Goh<sup>2</sup>. <sup>1</sup>Pusan national University Hospital, Korea, Republic of, <sup>2</sup>Pusan National University, Korea, Republic of

**Purpose:** The objectives of this study were to examine the discrepancy in diagnosis of osteoporosis with central quantitative computed tomography (QCT) and dual energy X-ray absorptiometry (DXA) in postmenopausal women with papillary thyroid cancer.

**Materials and Methods:** A total 89 post-menopausal patients (mean age 60.12±7.06 years) who were under thyrotropin suppressive therapy after total thyroidectomy for papillary thyroid cancer were enrolled. All participants do not have bone metastasis and history of medication of bisphosphonate or selective estrogen receptor modulator with a preexisting diagnosis of osteoporosis. The areal BMD (aBMD) of lumbar spines were generated from DXA files. The volumetric BMD (vBMD) of lumbar spine was calculated with QCT.

**Results:** In 66 patients, the results were discordant results with using DXA and QCT. The patients whose T-score was normal with DXA (n=53) were shifted to osteopenia (n=36) or osteoporosis (n=11) with QCT. Among 16 patients who were diagnosed as osteopenia according to T-score of DXA, 8 patients were diagnosed as osteoporosis using QCT. There was a significant difference in diagnosis with osteoporosis and osteopenia when using DXA and QCT ( $p<0.001$ ) (Figure).

**Conclusion:** Discordances might exist in skeletal status category between DXA and QCT in postmenopausal women with thyrotropin suppressive therapy



Figure

**Disclosures:** Yun Kyung Jeon, None.

## SA0216

See Friday Plenary Number FR0216.

## SA0217

See Friday Plenary Number FR0217.

## SA0218

See Friday Plenary Number FR0218.

## SA0219

**Trabecular Bone Score and Fracture Risk Prediction in HIV and Hepatitis C Infection.** Roger Bedimo<sup>\*1</sup>, John Poindexter<sup>2</sup>, Beverley Adams-Huet<sup>2</sup>, Naim Maalouf<sup>2</sup>. <sup>1</sup>VA North Texas Health Care System, United States, <sup>2</sup>University of Texas Southwestern Medical Center, United States

**Background:** Both HIV and HCV infections are associated with higher osteoporotic fracture risk. Beyond decreased bone mineral density (BMD), microarchitectural changes might contribute to this increased risk.

**Methods:** We used a prospective, cross-sectional cohort of participants with either virologically suppressed HIV, untreated HCV, HIV/HCV co-infection or non-infected controls. We measured BMD and trabecular bone score (TBS), a non-invasive measurement of bone microarchitecture, by dual x-ray absorptiometry (DXA). We conducted analysis of covariance comparing BMD and TBS between groups, controlling for age, race, BMI and smoking. We evaluated predictors of BMD and TBS with linear regression, and calculated FRAX® scores without BMD (FRAX-noBMD), with BMD (FRAX-BMD), and with TBS included (FRAX-BMD-TBS).

**Results:** A total of 532 male subjects were included: 57 HIV/HCV co-infected, 174 HIV, 123 HCV and 178 controls. HIV and HCV infections were each independently associated with lower total hip BMD ( $p<0.001$  and  $p=0.002$  respectively), and lower femoral neck BMD ( $p<0.001$  and  $p=0.008$  respectively). Only HCV was associated with lower TBS score ( $p=0.004$ ), while HIV was not ( $p=0.08$ ). Among HCV infected patients (both mono- and co-infected), greater HCV viremia and the aspartate aminotransferase-to-platelet ratio index (APRI) score, a validated surrogate marker of liver fibrosis, were not associated with TBS. FRAX-BMD was significantly higher than FRAX-noBMD in HIV ( $p<0.01$ ), but not in HCV ( $p=0.24$ ). Conversely, FRAX-BMD-TBS was significantly higher than FRAX-BMD in HCV ( $p<0.01$ ), but not in HIV ( $p=0.94$ ).

**Conclusions:** The increased OF risk among HCV-infected individuals may be mediated by altered bone micro-architecture, as suggested by a lower TBS score. Further studies are needed to understand the mechanism(s) of lower TBS in HCV, and whether HCV treatment improves TBS. Addition of TBS to BMD increases fracture risk estimates among HCV and HIV/HCV patients, and might improve fracture risk prediction in HCV infection.

**Disclosures:** Roger Bedimo, Bristol Myers Squibb, Grant/Research Support.

## SA0220

See Friday Plenary Number FR0220.

## SA0221

**Normative Distribution of Multirow Detector CT-Based Bone Measures and their Relationships with Dual-Energy X-ray Absorptiometry-Based Measures.** Punam K Saha<sup>\*</sup>, Xiaoliu Zhang, Elena M Letuchy, Kathleen F Janz, Trudy L Burns, James C Torner, Steven M Levy. University of Iowa, United States

Imaging is important for planning intervention and for monitoring response to treatments aimed at reducing fracture risk among patients with osteoporosis. Recent advances in multirow detector CT (MDCT) technology produce high spatial resolution at ultra-low dose radiation and enable quantitative analysis of cortical and trabecular bone. The ultra-high speed scanning and long scan-length dramatically reduce motion artifacts and positioning errors. This abstract reports the normative distribution of MDCT bone measures and their relationships with dual-energy X-ray absorptiometry (DXA).

The distal tibia of healthy volunteers (N=324; age: 19.8±0.7 years; 178 females) from the Iowa Bone Development Study (IBDS) was imaged using a Siemens SOMATOM FLASH scanner at 120kV, 200mAs, pitch=1.0, 10cm FOV using the ultra-high resolution mode. Images were reconstructed at 0.2mm slice spacing and 0.12mm in-plane resolution.

A Gammex phantom was used to calibrate CT Hounsfield units into bone mineral density (BMD). Cortical bone (CB) measures were computed over 14-16% of tibia, while trabecular bone (TB) measures were obtained from 4-6% of tibia with a 30% peel. Whole-body, hip, spine, and left-leg DXA areal BMD measures were obtained on a Hologic Discovery A model densitometer.

Table 1a presents descriptive statistics of Age 19 IBDS participants and their MDCT and DXA outcomes. Although age and BMI for males and females were similar, significant sex differences were observed in body size (weight and height). There were significant sex differences for both MDCT and DXA outcomes. Regression analyses of MDCT outcomes adjusted for body size and sex show that sex is the most important predictor for most MDCT outcomes, and that body size differences between males and females do not account for sex differences. Table 1b shows that CB porosity has low correlation with DXA outcomes, while CB thickness has moderate correlation with all DXA outcomes except the spine; TB outcomes show moderate to high correlations with DXA outcomes, with relatively higher correlation for DXA outcomes at the hip and leg.

Sex differences should be accounted for while analyzing MDCT bone outcomes. MDCT TB outcomes show stronger correlation with DXA as compared to MDCT CB outcomes. Moderate correlations between MDCT and DXA outcomes suggest uniqueness of bone structural properties captured by MDCT measures as compared to DXA.

This study was funded by NIH grants: R01-AR054439, R01-DE012101, and UL1-RR024979.



**Table 1.** The normative distribution of MDCT-based bone measures and their relationships with DXA measures. (a) Descriptive statistics for Age 19 BDOS participants by sex (N=324). Each cell presents mean (std.) values. (b) Partial (weight- and height-adjusted) Spearman correlations for MDCT cortical and trabecular bone outcomes with DXA areal BMD. Column headings are MDCT variables, while row headings are DXA variables. Spearman correlations were separately computed for males and females. **Abbreviations:** CB: cortical bone; CB-poro: CB porosity; CB-Th: mean CB thickness; TB: trabecular bone; TB-vBMD: TB volumetric BMD; TB-tBMD: TB volumetric BMD contributed by transverse trabeculae; TB-pBMD: TB volumetric BMD contributed by trabecular plates; TB-NA-den: TB network area per-unit volume of TB region; TB-PW: mean TB plate-width; TB-Th: mean TB thickness; TB-Sp: mean trabecular spacing.

Variables	Males (n=146)	Females (n=178)
Scan-age (Y)	19.77 (0.74)	19.77 (0.69)
Height (cm)	180.2 (7.7)**	166.4 (6.9)
Weight (kg)	84.74 (19.90)**	70.64 (19.31)
BMI	26.05 (5.60)	25.44 (6.49)
<b>DXA aBMD</b>		
Whole-body	1.283 (0.099)**	1.165 (0.090)
Hip	1.174 (0.165)**	1.031 (0.132)
Spine	1.099 (0.119)**	1.054 (0.130)
Left leg	1.390 (0.125)**	1.205 (0.103)
<b>MDCT Cortical</b>		
CB-poro	0.219 (0.022)**	0.205 (0.042)
CB-Th (mm)	2.319 (0.269)**	2.006 (0.236)
<b>MDCT Trabecular</b>		
TB-vBMD (mg/cc)	1182.9 (27.7)**	1164.4 (32.1)
TB-tBMD (mg/cc)	360.4 (74.2)**	312.1 (86.3)
TB-pBMD (mg/cc)	1005.0 (103.1)**	928.2 (120.9)
TB-NA-den (mm <sup>3</sup> /mm <sup>3</sup> )	0.063 (0.013)**	0.050 (0.013)
TB-PW (micron)	1375.7 (300.2)**	1211.0 (315.9)
TB-Th (micron)	173.2 (24.9)**	161.6 (23.8)
TB-Sp (micron)	398.0 (63.9)**	439.6 (85.1)

\*p-value<0.05, \*\*p-value<0.01 for t-tests comparing males and females.

(b)

sex	Variable	CB-poro	CB-Th	TB-vBMD	TB-tBMD	TB-pBMD	TB-NA-den	TB-PW	TB-Th	TB-Sp
F	Whole-body	-0.08	0.39**	0.64**	0.61**	0.58**	0.64**	0.61**	0.53**	-0.57**
	Hip	-0.06	0.44**	0.61**	0.60**	0.56**	0.63**	0.58**	0.50**	-0.54**
	Spine	-0.08	0.29**	0.49**	0.46**	0.40**	0.46**	0.44**	0.36**	-0.43**
	Left leg	-0.07	0.60**	0.64**	0.65**	0.64**	0.69**	0.65**	0.61**	-0.57**
M	Whole-body	0.20*	0.41**	0.48**	0.48**	0.41**	0.55**	0.40**	0.36**	-0.50**
	Hip	0.08	0.41**	0.55**	0.54**	0.48**	0.59**	0.48**	0.43**	-0.53**
	Spine	0.17*	0.29**	0.34**	0.34**	0.30**	0.37**	0.26**	0.25**	-0.34**
	Left leg	0.18*	0.51**	0.57**	0.54**	0.52**	0.61**	0.52**	0.50**	-0.52**

\*p-value<0.05, \*\*p-value<0.01.

Table 1

Disclosures: Punam K Saha, None.

## SA0222

See Friday Plenary Number FR0222.

## SA0223

See Friday Plenary Number FR0223.

## SA0224

See Friday Plenary Number FR0224.

## SA0225

**TBS is associated with biomechanical properties of human vertebrae, ex-vivo.**

Doris Tran<sup>1</sup>, Franck Michelet<sup>1</sup>, Christophe Lelong<sup>1</sup>, Didier Hans<sup>2</sup>.

<sup>1</sup>Medimaps, France, <sup>2</sup>Center of Bone diseases, Bone & Joint Department, Lausanne University Hospital, Switzerland

**Objective:** The clinical utility of Trabecular Bone Score (TBS) to evaluate the risk for osteoporotic fracture has been widely recognized by the scientific community. To date only one study presented data on the relations between TBS and bone mechanical properties, with a relatively small sample size. The aim of this study was to evaluate the relations between TBS, BMD and mechanical properties of on a larger sample of human vertebra ex vivo.

**Method:** 52 vertebrae (L1 to L4) retrieved from 13 post-mortem human subjects (mean age 74.9 ± 8.2 yrs) were scanned with a DXA device (Prodigy, GE-Lunar) using water to simulate soft tissues around the bone. Bone texture was evaluated using TBS iNsite (Medimaps). BMD and TBS were computed over the same region of interest. Biomechanical testing was performed to measure failure load and stiffness of the vertebrae. The quasi-static compression tests were realized with a traction-compression device (INSTRON 55000, INSTRON).

Relations between TBS and mechanical properties were evaluated using Pearson correlation test. A multivariate analysis including both TBS and BMD was performed.

**Results:** 35 vertebrae remained included after exclusions due to BMD outlying values compared to the global distribution, arthrosis or vertebral fracture. Mean BMD, TBS, failure load and stiffness were 0.854±0.161 g/cm<sup>2</sup>, 1.561±0.098, 2351±1064 N, 4170±1260 N.mm<sup>-1</sup> respectively. Moderate but significant correlations (figure) were observed with failure load for BMD (r=0.65; p<0.0001) and for TBS (r=0.63;

p<0.0001). Stronger significant correlations were observed with stiffness for BMD (r=0.65; p<0.0001) and for TBS (r=0.73; p<0.0001).

In the multivariate analysis, both BMD and TBS remained significantly associated with the failure load (r=0.50, p=0.002 and r=0.47, p=0.005 respectively). The combined model explained 52.3% (r<sup>2</sup>-adjusted) of the failure load. The association with the stiffness also remained significant for BMD and TBS (r=0.49, p=0.004 and r=0.62, p=0.0001 respectively). The combined model explained 64.6% (r<sup>2</sup>-adjusted) of the stiffness.

**Conclusion:** The present study confirms on a larger sample the correlations between TBS and biomechanical properties of the lumbar spine and those results are independent of spine BMD. Both BMD and TBS characterize a significant part of the vertebral bone strength which may explain the ability of TBS in conjunction with BMD to improve the prediction of fracture risk in clinical practice.

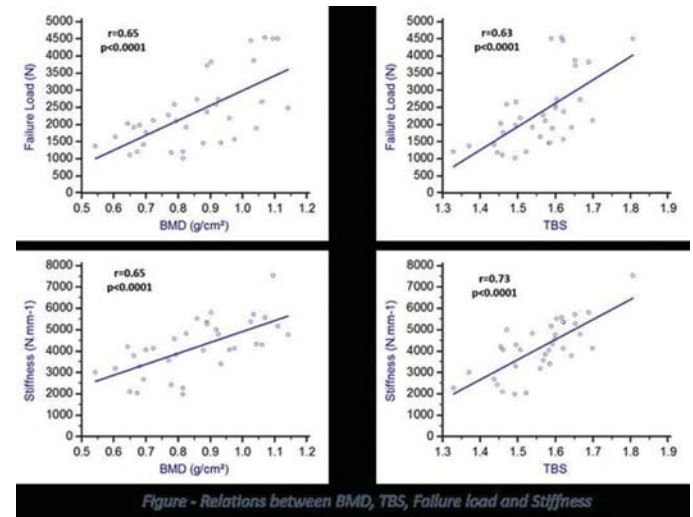


Figure 1: biomech compression

Disclosures: Doris Tran, Medimaps, Other Financial or Material Support.

## SA0226

**The Wards Region shows proportionately greater osteoporosis by DXA.**

Jingmei Wang<sup>\*1</sup>, Yun Sun<sup>2</sup>, Tom Sanchez<sup>3</sup>. <sup>1</sup>Department of Research and Development, Norland at Swissray, China, <sup>2</sup>Department of Radiology, Hospital of Tsinghua University, China, <sup>3</sup>Department of Research and Development, Norland at Swissray, United States

The area referred to as the Ward's Region of the Norland hip scan is said to be largely a storage site for calcium located in a region of the hip shielded from mechanical forces. If that is the case the results obtained in the Ward's Region may offer an insight into recent calcium balance for an individual. The current study compares results obtained in the AP Spine and Hip Scan Regions (Femur Neck, Trochanter, Wards and Total) to assess if Ward's mirrors results obtained in the other sites.

AP Spine and Hip scans from 201 subjects between 21 and 87 years of age were obtained on a Norland XR-800 scanner to assess the relationship between T-score results obtained on the AP Spine, Femur Neck, Trochanter, Wards and Total Hip. Relationship between T-score at the Ward's and the other sites were examined by regression analysis. Chi-square analysis then compared the occurrence of Normal and Osteoporotic findings in Wards and AP Spine, Femur Neck, Trochanter and Total Hip assessments to determine if Wards leads in the Osteoporotic findings.

Significant positive regressions were found between T-score results at Wards and AP Spine (y = 0.8448X + 1.0283; r = 0.6164; p<0.0001), Femur Neck (y = 0.6761x + 0.2766; r = 0.7860; p<0.0001), Trochanter (y = 0.976X + 0.9784; r = 0.8354; p<0.0001) and Total Hip (y = 0.9106X + 0.8356; r = 0.8568; p<0.0001). Comparing the number of subjects with a Normal Wards or AP Spine to the number of subjects with an Osteoporotic Wards or AP Spine by Chi-square Analysis (χ<sup>2</sup> = 12.73, P<0.001) shows significant difference in the proportions of subjects with an Osteoporotic Wards. Similar findings were seen when evaluating the Femur Neck (χ<sup>2</sup> = 18.03, P<0.001) with lesser findings—although still significant—being seen when evaluating the Trochanter (χ<sup>2</sup> = 3.79, P=0.05) or Total Hip (χ<sup>2</sup> = 9.16, P=0.003).

The data suggests that although T-score values obtained on these five sites are significantly correlated there clearly seem to be proportionately more osteoporotic findings at the Wards Region than seen at the AP Spine, Femur Neck, Trochanter and Total Hip. Given that bone mineral at the Wards may reflect storage calcium, this finding may suggest that subjects with a low Wards T-score may be demonstrating the consequence of a consistent negative calcium balance.

Disclosures: Jingmei Wang, None.

## SA0227

**Utilization of Trabecular Bone Score in Fracture Risk Assessment Tool (FRAX).** Li Hao Richie Xu\*, Alberto Cabo-Chan. University of Texas Southwestern Medical Center, United States

**Background:** Trabecular bone score (TBS) is a texture index derived from standard lumbar spine dual energy X-ray absorptiometry (DXA) images. A procedure to generate TBS-adjusted FRAX probabilities is more accurate than the standard FRAX tool, particularly for patients with FRAX probabilities around an intervention threshold. In this study, we examine the use of this TBS-adjusted model of predicting fracture risk in patients with osteopenia.

**Objectives:** To describe the impact of integrating TBS into FRAX when assessing whether to treat patients with osteopenia, and determine factors that contribute to a change in FRAX when TBS is added.

**Methods:** A retrospective chart review was conducted on osteopenia patients (T-score between -1.0 and -2.5) at a single specialty clinic who underwent DXA and TBS measurement from 2015 to 2016. Excluded were patients with chronic kidney disease, disuse osteoporosis, primary hyperparathyroidism, or on osteoporosis treatment (bisphosphonates, denosumab, teriparatide, or raloxifene). Demographic, historical, densitometric and laboratory characteristics at the time of DXA scan were assessed. FRAX for major osteoporotic fracture (FRAX-MOF) was calculated with and without TBS. FRAX-MOF of 20% was used as a cut-off for initiation of anti-osteoporosis medication in patients with osteopenia.

**Results:** 838 patients with osteopenia were included (83.9% female, 74.7% White, 13.6% African Americans). Mean age was 64.7 years, BMI 27.6 kg/m<sup>2</sup>, and T-score at femoral neck was -1.6. The mean TBS score was 1.3, and FRAX-MOF is 8.1%. Adding TBS to FRAX calculation reclassified 0.5% of osteopenic patients from FRAX-MOF < 20% to ≥ 20% (threshold for anti-osteoporosis medication use), and reclassified 0.4% of osteopenic patients from above to below this threshold. The change of FRAX-MOF with TBS inclusion was positively correlated with body weight in all 838 patients. Adding TBS to FRAX altered absolute risk of MOF by more than 3% (either positively or negatively in 70 patients (8.4% of patients with osteopenia)). Of these, 59 patients had increased FRAX-MOF by ≥ +3%, while 11 had decreased FRAX-MOF by ≤ -3%. Those patients with increased FRAX-MOF after TBS adjustment had higher BMI and body weight, but lower TBS, FRAX-MOF and lumbar BMD than those with decreased FRAX-MOF (Table 1).

**Conclusions:** TBS inclusion in FRAX-MOF calculation leads to re-classification of 0.8% of patients with osteopenia. TBS-FRAX is more likely to exceed FRAX without TBS in patients with higher body weight, whereas TBS-FRAX is more likely to be lower than FRAX without TBS in patients with lower body weight. This phenomenon could be due to inaccurate TBS measurement at extremes of body weight, or from true alteration in bone quality at these extremes of body weight.

FRAX-MOF range of change>3% with TBS			
	Increased w/ TBS	Decreased w/ TBS	P-value
<b>Sample Size</b>	59	11	
<b>Age, years</b>	68.5±6.9	73.9±8.5	0.07
<b>Females</b>	95%	100%	
<b>White, %</b>	92%	100%	
<b>Height, cm</b>	162.8±8.2	159.5±7.5	0.20
<b>Weight, kg</b>	86.7±17.8	62.2±7.1	0.00
<b>BMI, kg/m<sup>2</sup></b>	32.7±6.4	24.7±4.3	0.00
<b>Prev. Fracture</b>	0%	0%	
<b>Parent's Hip Fracture</b>	10%	64%	
<b>Smoker</b>	3%	0%	
<b>Steroid</b>	24%	45%	
<b>Rheumatoid Arthritis</b>	15%	36%	
<b>2nd Osteoporosis</b>	2%	9%	
<b>TBS</b>	1.05±0.1	1.4±0.07	0.00
<b>FRAX-MOF</b>	11.1±4.9	22±7	0.00
<b>FRAX-Hip</b>	2.3±2.5	9.1±7.3	0.01
<b>TBSFRAX-MOF</b>	15.2±4.6	18.2±6.9	0.19
<b>TBSFRAX-Hip</b>	3.1±2.8	8.2±6.8	0.03
<b>L2/L4BMD</b>	0.973±0.096	1.132±0.099	0.00
<b>L2/L4T</b>	-1±0.9	0.4±0.9	0.00
<b>FNBM</b>	0.685±0.081	0.67±0.063	0.50
<b>FNT</b>	-1.5±0.7	-1.6±0.6	0.67
<b>HipBMD</b>	0.844±0.093	0.826±0.083	0.52
<b>HipT</b>	-0.9±0.8	-1±0.7	0.74
<b>Rad13BMD</b>	0.632±0.312	0.721±0.364	0.89
<b>Rad13T</b>	-1.1±0.8	0.5±0.4	0.00

Table 1

**Disclosures:** Li Hao Richie Xu, None.

## SA0228

**Role of bone mineral density and trabecular bone score in the identification of bone fragility in postmenopausal women with vitamin D deficiency/insufficiency.** Mika Yamauchi<sup>1</sup>\*, Kiyoko Nawata<sup>2</sup>, Masahiro Yamamoto<sup>1</sup>, Toshitsugu Sugimoto<sup>1</sup>. <sup>1</sup>Internal Medicine 1, Shimane University Faculty of Medicine, Japan, <sup>2</sup>Health and Nutrition, The University of Shimane, Japan

**Objective:** Vitamin D deficiency/insufficiency (VitD D/I) is a risk factor for osteoporotic fractures. It has been reported that the majority of Japanese individuals meets the criteria for VitD D/I. Therefore, the aim of the present study was to elucidate the factors that are useful for identifying individuals with VitD D/I who are at high risk of fractures. The trabecular bone score (TBS) is an indicator of cancellous bone microstructure. A decrease in TBS is considered to be a risk factor for vertebral fracture that is independent of bone mineral density (BMD). However, the relationships between TBS and bone fragility caused by VitD D/I are unclear, and this study was conducted to elucidate these relationships. **Methods:** The subjects were 201 healthy postmenopausal women who had undergone osteoporosis screening. Serum levels of PTH, 25-hydroxyvitamin D [25(OH)D], P1NP, CTX were measured. The BMD of the lumbar (L) and femoral neck (FN) was measured using dual-energy X-ray absorptiometry, and the presence or absence of morphological vertebral fracture was determined. The presence or absence of non-vertebral fracture history was determined through physician interviews. **Results:** Mean values of age were 63.5±7.5 years. Osteoporotic fractures (vertebral and non-vertebral) were observed in 71 subjects. The mean values of measured variables were: 25(OH)D 16.0±4.2 ng/mL, P1NP 53.9±16.6 ng/mL, CTX 0.40±0.15 ng/mL, L-BMD: T-score -1.6±1.3, Z-score 0.3±1.1, FN BMD: T-score -1.5±0.8, Z-score 0.1±1.0 and TBS 1.313±0.728. Serum levels of 25(OH)D had significantly negative correlations with age and PTH, and significantly positive correlations with L and FN BMD and TBS. The fracture group had significantly lower levels of 25(OH)D as well as L and FN BMD and TBS (p<0.01). When subjects were classified into four groups based on 25(OH)D and L-BMD levels, the low 25(OH)D/low L-BMD group had a significantly higher proportion of fractures than the other groups. Furthermore, the low 25(OH)D/low TBS group had a significantly higher proportion of fractures than the high 25(OH)D/high TBS and low 25(OH)D/high TBS groups. Logistic regression analysis revealed that low 25(OH)D/low L-BMD as well as low 25(OH)D/low TBS were significant risk factors for fracture even after adjustments for age and BMI. **Conclusion:** Candidate indicators for identifying cases at high risk of fractures among postmenopausal women with VitD D/I include measurements of L-BMD as well as TBS in addition to 25(OH)D.

**Disclosures:** Mika Yamauchi, None.

## SA0229

See Friday Plenary Number FR0229.

## SA0230

**Factors Associated with Readiness for Adopting Osteoporosis Treatment Change.** Maria Danila<sup>1</sup>, Elizabeth Rahn<sup>1</sup>, Amy Mudano<sup>1</sup>, Ryan Outman<sup>1</sup>, Peng Li<sup>1</sup>, David Redden<sup>1</sup>, Fred Anderson<sup>2</sup>, Susan Greenspan<sup>3</sup>, Andrea LaCroix<sup>4</sup>, Jeri Nieves<sup>5</sup>, Stuart Silverman<sup>6</sup>, Ethel Siris<sup>7</sup>, Nelson Watts<sup>8</sup>, Sigrid Ladores<sup>1</sup>, Karen Meneses<sup>1</sup>, Jeffrey Curtis<sup>1</sup>, Kenneth Saag<sup>1</sup>.

<sup>1</sup>University of Alabama at Birmingham, United States, <sup>2</sup>University of Massachusetts Medical School, United States, <sup>3</sup>University of Pittsburgh, United States, <sup>4</sup>University of California at San Diego, United States, <sup>5</sup>Helen Hayes Hospital, United States, <sup>6</sup>Cedars-Sinai Medical Center, United States, <sup>7</sup>Columbia University Medical Center, United States, <sup>8</sup>Mercy Health Osteoporosis and Bone Health Services, United States

**Purpose:** Understanding factors associated with the readiness for adopting osteoporosis treatment change may inform the design of behavioral interventions to improve osteoporosis treatment uptake in women at high risk for fracture.

**Methods:** US women in the Global Longitudinal Study of Osteoporosis (GLOW) with prior self-reported fractures and not currently using osteoporosis therapy were eligible to participate in the Activating Patients at Risk for Osteoporosis (APROPOS) Study. Participants' readiness for behavior change was assessed using a modified form of the Weinstein Precaution Adoption Process Model (PAPM). We defined pre-contemplative participants as those who self-classified in the unaware and unengaged stages of PAPM. Contemplative participants were defined by the undecided, decided not to act, and decided to act stages of PAPM. Bivariate tests and stepwise multivariable logistic regression evaluated the following factors associated with these two levels of readiness for behavior change: sociodemographic characteristics, health literacy, self-reported history of depression and dementia, previous treatment for osteoporosis, whether participants had been told they had osteoporosis/osteopenia, and whether they had concerns about osteoporosis.

**Results:** A total of 2,684 women were enrolled in APROPOS. Participants were 95% Caucasian, with a mean(SD) age 74.9(8.0) years and 77% had some college education. Overall, 25% (N=544) self-classified in the contemplative stage of behavior change. Compared to women who self-classified as pre-contemplative, contemplative women were more likely to be concerned about osteoporosis (adjusted OR[aOR]=3.2, 95% CI 2.3-4.4) and to report prior osteoporosis treatment (aOR 4.3, 95% CI 3.1-6.0). Individuals who had been told they had osteoporosis had a 12.4 fold odds to be in the



contemplative group (95% CI 8.5-18.1), while those who had been told they had osteopenia had 4.1 fold odds to be in the contemplative group (95% CI 2.9-5.9).

Conclusion: Among women with high risk of future fracture, having been told by a health care provider that they had osteoporosis/osteopenia was independently associated with considering taking medications for osteoporosis. Our results suggest that in considering osteoporosis intervention design efficiency and effectiveness, women's recognition of a diagnosis of osteoporosis/osteopenia are critical components to be considered when attempting to influence stage of behavior transitions.

**Disclosures:** Maria Danila, None.

## SA0231

See Friday Plenary Program FR0231.

## SA0232

**Association of High-Resolution Peripheral Quantitative CT (HRpQCT) Bone Microarchitectural Parameters with Previous Clinical Fracture in Older Men: the Osteoporotic Fractures in Men (MrOS) Study.** Howard Fink<sup>1</sup>, Lisa Langsetmo<sup>2</sup>, Tien Vo<sup>2</sup>, Eric Orwoll<sup>3</sup>, John Schousboe<sup>4</sup>, Kristine Ensrud<sup>5</sup>. <sup>1</sup>GRECC, VA Health Care System, United States, <sup>2</sup>University of Minnesota School of Public Health, United States, <sup>3</sup>Oregon Health Sciences University, United States, <sup>4</sup>Park Nicollet Clinic, United States, <sup>5</sup>VA Health Care System, United States

Areal BMD is a strong predictor of fractures, but does not assess microarchitecture. HRpQCT assesses both volumetric BMD (vBMD) and trabecular and cortical microarchitecture, but past studies evaluating the association of HRpQCT parameters with fracture history have been small and often have performed limited adjustment for potential confounders.

We used data from 1789 men with evaluable HRpQCT scans (Scanco, Bruttisellen, Switzerland) from the MrOS Study Year 14 (Y14) exam to evaluate the association of distal radius and tibia microarchitectural parameters with a history of previous clinical fracture. The primary HRpQCT exposure variables were the finite element analysis (FEA) estimated failure loads for each skeletal site. Secondary exposure variables for each skeletal site were total vBMD, total bone area, trabecular vBMD, trabecular bone area, trabecular thickness, trabecular number, cortical vBMD, cortical bone area, cortical thickness, and cortical porosity. Clinical fractures were ascertained from triennial questionnaires between study baseline and Y14 exams and centrally adjudicated by blinded review of radiographic reports. We used multivariate-adjusted logistic regression to estimate the odds of a history of clinical fracture between baseline and Y14 per 1 SD decrement for each Y14 HRpQCT parameter (Table).

Men in the analysis cohort were a mean of 84.5 years of age at Y14, and 342 (19.1%) had experienced a confirmed clinical fracture between baseline and Y14. After multivariate adjustment, each SD decrement in Y14 FEA estimated failure load was associated with a 35% (radius) and 28% (tibia) higher likelihood of previous fracture (Table). Odds of previous fracture were significantly higher per 1 SD decrement for all cortical parameters except for cortical porosity. Most trabecular parameters were not independently associated with previous fracture.

In this cohort of older men, lower FEA estimated failure load and lower levels of all cortical parameters (except cortical porosity) were independently associated with greater odds of a history of clinical fracture within the previous 14 years, even after accounting for multiple fracture risk factors (see Table footnote). Future studies should explore associations of HRpQCT microarchitectural parameters with specific fracture types and with risk of incident fractures.

Table: Multivariate-adjusted\* odds of confirmed previous clinical fracture per 1 SD decrement in HRpQCT distal radius and tibia microarchitectural parameters (OR, 95% CI)

HRpQCT parameter	Distal Radius		Distal Tibia	
	1 SD decrement	Odds of previous clinical fracture per 1 SD HRpQCT parameter decrement	1 SD decrement	Odds of previous clinical fracture per 1 SD HRpQCT parameter decrement
FEA estimated failure load	1338.1 N	1.35 (1.14-1.61)	2934.3 N	1.28 (1.06-1.54)
Total vBMD	61.2 mg/cm <sup>3</sup>	1.22 (1.03-1.43)	55.2 mg/cm <sup>3</sup>	1.23 (1.04-1.47)
Total bone area	66.3 mm <sup>2</sup>	1.02 (0.88-1.19)	136.9 mm <sup>2</sup>	0.88 (0.75-1.04)
Trabecular vBMD	39.4 mg/cm <sup>3</sup>	1.16 (0.99-1.37)	38.1 mg/cm <sup>3</sup>	1.01 (0.86-1.18)
Trabecular bone area	68.3 mm <sup>2</sup>	0.97 (0.83-1.12)	145.7 mm <sup>2</sup>	0.84 (0.71-0.99)
Trabecular thickness	0.018 mm	1.03 (0.89-1.18)	0.023 mm	0.99 (0.86-1.14)
Trabecular number	0.21 mm <sup>-1</sup>	1.16 (0.99-1.35)	0.21 mm <sup>-1</sup>	0.96 (0.83-1.11)
Cortical vBMD	69.2 mg/cm <sup>3</sup>	1.18 (1.03-1.35)	80.8 mg/cm <sup>3</sup>	1.28 (1.11-1.49)
Cortical bone area	14.3 mm <sup>2</sup>	1.30 (1.11-1.54)	31.2 mm <sup>2</sup>	1.28 (1.10-1.52)
Cortical thickness	0.230 mm	1.23 (1.05-1.45)	0.335 mm	1.27 (1.09-1.47)
Cortical porosity	0.81%	1.06 (0.93-1.22)	1.65%	0.96 (0.85-1.09)

\*Multivariate models were adjusted for age, race, clinic site, height, weight, physical activity, smoking history, alcohol consumption, past falls, self-reported history of fractures between age 50 and MrOS baseline, and visit 4 total hip BMD

Table

**Disclosures:** Howard Fink, None.

## SA0233

See Friday Plenary Program FR0233.

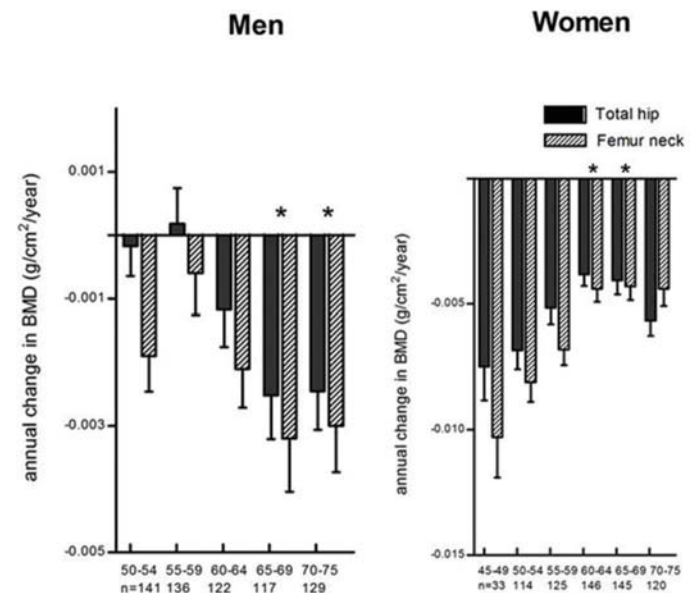
## SA0234

See Friday Plenary Program FR0234.

## SA0235

**Gender-different association between age-related body composition change and hip bone loss: Anung cohort study.** Ji Hyun Lee<sup>1</sup>, Jung Hee Kim<sup>1</sup>, Seo Young Lee<sup>1</sup>, A Ram Hong<sup>1</sup>, Hyung Jin Choi<sup>2</sup>, Sang Wan Kim<sup>3</sup>, Nam H. Choi<sup>4</sup>, Chan Soo Shin<sup>3</sup>. <sup>1</sup>Department of Internal Medicine, Seoul National University College of Medicine, Korea, Republic of, <sup>2</sup>Department of Anatomy, Seoul National University College of Medicine, Korea, Republic of, <sup>3</sup>Department of Internal Medicine, Seoul National University Hospital, Korea, Republic of, <sup>4</sup>Department of Preventive Medicine, Ajou University School of Medicine, Korea, Republic of

Bone loss is known to be associated with aging, weight loss, menopause and current smoking. However, the relative effect of lean mass (LM) and fat mass (FM) change on bone loss has not been well known. We investigated whether body composition change was associated with bone mineral density (BMD) change in Korean men and postmenopausal women. This is an ongoing prospective cohort study of BMD measurements at both 2007 and 2011 year at community-based Anung cohort. A total of 645 men aged over 50 years and 683 postmenopausal women were categorized according to longitudinal changes in BMD within 2007 and 2011. BMD change was categorized by 3 groups by using the standard deviation (SD) distance from the mean. The mean reduction in total hip (TH) BMD was -0.00785 for men and -0.01201 for women. Three groups were categorized-"maintained" BMD: slope >or=0; "expected" BMD loss: slope <-1 SD below mean. Bioelectrical impedance analysis was performed to evaluate body composition. The prevalence of osteoporosis was 9.8% in males and 22.1% in females. In multivariate logistic regression models including age, BMI, LM and FM mass loss, current smoking, total hip BMD, and regular exercise, significant predictors of hip bone loss was BMI and LM loss (BMI, OR = 0.91, 95% CI = 0.83-0.99; LM loss (> 9%), OR=3.14; 95% CI= 1.76-5.60) in men. In women, LM and FM loss (>1SD), baseline total hip BMD, year since menopause (YSM) under 3 years were associated with hip bone loss (LM loss (> 11%), OR=1.85, 95% CI=1.02-3.36; FM loss (> 7%), OR=2.44, 95% CI=1.28-4.65; TH-BMD, OR=2.87, 95% CI= 1.10, 7.53; YSM under 3 years OR=5.90, 95% CI=2.89-12.02). In conclusion, LM loss was an independent predictor of hip bone loss in both men and women. In postmenopausal women, percent of FM loss, TH-BMD, YSM under 3 years were also important risk factors for hip bone loss.



Annual change in TH and FN- BMD by 5-yr age groups among men and women

**Disclosures:** Ji Hyun Lee, None.

## SA0236

**Characteristics and Consequences of Hip Fracture in an Elderly Irish Population.** James Mahon<sup>1</sup>, Oisín Hannigan<sup>1</sup>, Georgina Steen<sup>1</sup>, Nessa Fallon<sup>1</sup>, Niamh Maher<sup>1</sup>, Aoife Dillon<sup>1</sup>, Geraldine McMahon<sup>2</sup>, Alison Reynolds<sup>3</sup>, Thomas McCarthy<sup>3</sup>, Irina Tomita<sup>1</sup>, Laura Clowry<sup>1</sup>, Ronan O'Toole<sup>1</sup>, MC Casey<sup>1</sup>, JB Walsh<sup>1</sup>, Kevin McCarroll<sup>1</sup>. <sup>1</sup>Osteoporosis and Bone Health Unit, St James's Hospital, Dublin 8, Ireland, <sup>2</sup>Department of Emergency Medicine, St James's Hospital, Dublin 8, Ireland, <sup>3</sup>Department of Orthopaedic Surgery, St James's Hospital, Dublin 8, Ireland

## Purpose

Osteoporosis prevalence increases with age and is responsible for significant morbidity and mortality in the elderly populations due to hip, vertebral and wrist fractures. We aimed to define the baseline characteristics of patients attending out University Hospital admitted with hip fracture and determine their length of hospital stay and mortality.

## Methods

We performed a prospective longitudinal observational study of patients admitted to our hospital with a diagnosis of fragility fracture of the hip from January 2014 to March 2015. Patients over 65 years of age were eligible for inclusion. We collected cross-sectional data on basic demographics, functional status and serum vitamin D levels at time of admission and followed patients up for a 12-month period after their initial fracture.

## Results

199 patients admitted with hip fracture; 161 patients recruited for follow-up. Mean age 80.5 years (SD 12.3); 108 female, 53 male. 96.3% of participants were community-dwelling and 3.7% were nursing home-dwelling. Baseline BMI was 22.7kg/m<sup>2</sup>. Mean serum vitamin D 58.3 nmol/litre (SD 34.1); mean estimated glomerular filtration rate (eGFR) 63.2 ml/min (SD 12.1). 10.6% had a prior diagnosis of osteoporosis and 76.4% of these patients were on treatment with an antiresorptive agent at the time of presentation. 22.3% of the entire cohort were on vitamin D supplements at the time of presentation. 3.1% of participants had a prior history hip fracture; 5.8% had a prior history of vertebral fracture and 13.1% had a prior history of wrist fracture. 51% had a history of falls in the previous 12 months and the median Rockwood Clinical Frailty Score was 5/9 (mildly frail). Median length of stay in hospital was 13 days (range 3-146 days); inpatient mortality was 1.84%. 12-month mortality was 22%.

## Conclusions

Patients presenting with hip fracture were a relatively elderly and frail population and had a significant length of hospital stay, which could increase the chances of complications such as hospital acquired pneumonia. In keeping with other studies, perioperative mortality following hip fracture was low, but one-year mortality is relatively high, highlighting the importance of osteoporosis screening and treatment in elderly frail patients. This is especially important in the context of the fact that a minority of participants had a prior diagnosis of osteoporosis before presentation with their fracture, implying a missed opportunity for

**Disclosures:** James Mahon, None.

## SA0237

**Bone-Formers and Bone-Losers in a 200yr old Archaeological Population.** Simon Mays\*. Historic England, United Kingdom

**Background.** Some recent studies suggest a positive association between the occurrence of osteophytes at articular margins and enthesophytes at ligamentous insertions, and that individuals who show these types of bone formation ('bone-formers') show a reduced tendency to lose skeletal mass in age-related osteoporosis. However, the validity of these generalisations continues to be debated. The current work is a contribution to this debate. It uses a collection of skeletons from an archaeological site in England. It tests the hypotheses that ossification into the anterior longitudinal ligament (ALL) in the thoracic spine is positively associated with peripheral bone mass and positively associated with hip osteophytes, once the effects of age and some other potentially confounding variables are controlled for.

**Methods.** Ossification into the ALL in the thoracic spine is scored from gross examination of vertebrae from 105 burials (age at death 40-92yrs) from an 18-19<sup>th</sup> century AD crypt at Christ Church Spitalfields, London. Peripheral bone status is measured using cortical index (CI) of the second metacarpal. Marginal osteophyte formation was recorded at the lunette surface of the acetabulum. The effects of age at death and sex are controlled for, as is number of thoracic vertebrae preserved (not all skeletons were complete). Logistic regression was used in analysis, with presence / absence of ALL ossification as the dependent variable and age, sex, number of thoracic vertebrae, metacarpal cortical index and hip osteophyte formation as the independent variables.

**Results.** Ossification into the ALL is associated with male sex, increasing age and is positively associated with metacarpal CI, but no association was found with hip osteophyte formation (Table). Decomposing CI into total and medullary widths and re-running the analysis suggests that ALL ossification - CI association reflects lesser age-related resorption at the endosteal surface in those showing ALL ossification.

**Conclusions.** The results support the hypothesis of a link between the presence of ossification into the ALL and a greater tendency toward conservation of peripheral cortical bone mass into old age. The link between ALL ossification and hip osteophytes was non-significant. Tendency toward ossification into the ALL may be associated with lesser resorption at the endosteal envelope rather than with subperiosteal deposition of bone around joints.

**Table.** Logistic regression analysis, with presence / absence of anterior longitudinal ligament ossification in the thoracic spine as the dependent variable, and age, metacarpal cortical index, sex, number of thoracic vertebrae preserved and hip osteophyte score as the independent (predictor) variables (N=105 individuals)<sup>1</sup>.

Variable	Coefficient (SE)	Wald	p	Odds ratio (95% conf. int.)
Age	0.072 (0.025)	8.13	0.004	1.074 (1.022-1.129)
CI	0.067 (0.030)	5.18	0.023	1.070 (1.009-1.133)
Sex	1.382 (0.485)	8.13	0.004	3.982 (1.540-10.299)
N. thoracic vert.	0.192 (0.184)	1.08	0.298	1.212 (0.845-1.738)
Hip osteophyte	0.227 (0.131)	3.01	0.083	1.255 (0.970-1.623)
Constant	-11.571 (3.443)			

<sup>1</sup> Age (years, given on coffin plate); CI = second metacarpal cortical index taken from antero-posterior radiographs, CI = 100 x (T-M)/T, where T=total width, M=medullary width (Dequeker, 1976); Sex (from name on coffin plate), coded 0=female, 1=male; N. thoracic vert, number of thoracic vertebrae preserved for inspection; Hip osteophyte, osteophyte score at acetabular rim and posterior horn of lunette surface, calculated as mean of variables 2 and 4 of Rissech et al. (2006) expressed on a ten-point scale. Constant, constant in logistic regression equation; Coefficient, coefficient for variable in logistic regression equation; Wald, Wald statistic evaluating the probability that the coefficient of the variable differs from zero; p, significance level of the Wald statistic. Odds ratio, change in odds of observing ALL ossification with unit increase in the independent variable.

## References

- Dequeker J. 1976. Quantitative radiology: radiogrammetry of cortical bone. *Br J Radiol* 49: 912-20.  
Rissech C, Estabrook G, Cunha E, Maligno A. 2006. Using the acetabulum to estimate age in males. *J Forensic Sci* 51: 213-229.

## Table

**Disclosures:** Simon Mays, None.

## SA0238

See Friday Plenary Number FR0238.

## SA0239

**Preceding and subsequent high- and low-trauma fracture patterns – A 13-year epidemiological study in females and males in Austria.** Christian Muschitz<sup>\*1</sup>, Roland Kocijan<sup>1</sup>, Andreas Baierl<sup>2</sup>, Rainer Dormann<sup>1</sup>, Xaver Feichtinger<sup>3</sup>, Judith Haschka<sup>1</sup>, Gabriela Katharina Muschitz<sup>4</sup>, Jakob Schanda<sup>5</sup>, Peter Pietschmann<sup>6</sup>, Heinrich Resch<sup>1</sup>, Hans Peter Dimai<sup>7</sup>. <sup>1</sup>St. Vincent Hospital - VINFORCE, Austria, <sup>2</sup>Department of Statistics and Operations Research, the University of Vienna, Austria, <sup>3</sup>AUVA Trauma Center Meidling - Department of Surgery, Austria, <sup>4</sup>Division of Plastic and Reconstructive Surgery, Department of Surgery, the Medical University of Vienna, Austria, <sup>5</sup>AUVA Trauma Center Meidling, Austria, <sup>6</sup>Department of Pathophysiology and Allergy Research, Center for Pathophysiology, Infectiology and Immunology, the Medical University of Vienna, Austria, <sup>7</sup>Department of Internal Medicine, Division of Endocrinology and Metabolism, the Medical University of Graz, Austria

**Purpose:** Little is known about the impact of the skeletal fracture site in conjunction with the severity of a past fracture (high- or low-trauma preceding fracture) and its effect on future fracture risk. **Methods:** Patients with de novo high- and low-trauma fractures admitted to seven large trauma centers across Austria between 2000 and 2012 were stratified into sex and different age groups. Kaplan-Meier estimates, cox proportional hazards regression models (HR) and likelihood calculations estimated effects of age, sex and the anatomic region on the probability of a subsequent fracture in the same patient. **Results:** 433,499 female and male patients at an age range from 0 to 100 years with 575,772 de novo high- and low-trauma fractures were included. In the age range of 54 – 70 years, subsequent fractures were observed in 16% of females and 12.1% of males. A preceding high-trauma fracture was associated with 12.9% of subsequent fractures, thereof 6.5% of high- and 6.4% of low-trauma in origin, usually at the hip, humerus or pelvis. The highest effect sizes were observed femur, humerus and thorax fractures with hazard ratios (HR) of 1.26, 1.18, and 1.14. After splitting into high-trauma preceding and subsequent low-trauma fractures the femoral neck (HR= 1.59), the female sex (HR=2.02) and age (HR=1.03) were discriminators for increased future fracture risk. **Conclusions:** Preceding high-trauma fractures increase the risk of future low-trauma non-vertebral fractures including hip. For each patient with a fracture, regardless of the severity of the trauma, osteoporosis should be taken into clinical consideration.

**Disclosures:** Christian Muschitz, None.



## SA0240

**Relationship between bone turnover and bone microstructure: an HR-pQCT study in healthy Japanese women.** Narihiro Okazaki\*, Ko Chiba, Kazuaki Yokota, Kazuteru Shiraishi, Makoto Osaki. Department of Orthopaedic Surgery, Nagasaki University Hospital, Japan

### Introduction

Previous studies have shown that bone microstructure weakens with age, but little has been reported on the influence of bone turnover. The present study aimed to investigate the relationship between bone turnover and bone microstructure in healthy Japanese women using high-resolution peripheral quantitative computed tomography (HR-pQCT).

### Methods

Subjects comprised 76 healthy Japanese women (mean age, 48.9 years; range, 21-87 years). The distal radius and tibia were scanned using HR-pQCT (XtremeCT II; Scanco Medical, Switzerland) with a voxel size of 61 µm, and the volumetric bone mineral density (vBMD) and parameters of bone microstructure were analyzed. We also measured serum levels of tartrate-resistant acid phosphatase-5b (TRACP-5b) as a marker of bone resorption, and total procollagen type I N-terminal propeptide (PINP) as a marker of bone formation, and analyzed relationships between bone turnover markers and bone microstructure after adjusting for age. The level of statistical significance was established at  $p < 0.01$ .

### Results

TRACP-5b showed a significant negative correlation with cortical vBMD (Ct.vBMD) and cortical thickness (Ct.Th) at the distal radius, and a significant negative correlation with Ct.vBMD and a positive correlation with cortical porosity (Ct.Po) at the distal tibia.

Total PINP showed a significant negative correlation with Ct.vBMD and Ct.Th at the distal radius, and a significant negative correlation with Ct.vBMD at the distal tibia.

TRACP-5b and total PINP did not correlate with trabecular vBMD or trabecular bone microstructure. In addition, a positive correlation was also observed between TRACP-5b and total PINP.

### Conclusions

Cortical vBMD and microstructure were deteriorated in cases with increased concentrations of markers for bone resorption and formation, even after adjusting for age. Women with increased bone resorption markers also showed increased bone formation markers. These findings suggest that increased bone turnover has a more detrimental effect on cortical bone than on trabecular bone.

**Disclosures:** Narihiro Okazaki, None.

## SA0241

See Friday Plenary Number FR0241.

## SA0242

See Friday Plenary Number FR0242.

## SA0243

See Friday Plenary Number FR0243.

## SA0244

**Rest-activity circadian rhythm and bone mineral density in older men.** Tara S Rogers\*<sup>1</sup>, Stephanie Harrison<sup>2</sup>, Christine Swanson<sup>3</sup>, Jane A. Cauley<sup>4</sup>, Elizabeth Barrett-Connor<sup>5</sup>, Eric Orwoll<sup>6</sup>, Katie Stone<sup>2</sup>, Nancy Lane<sup>7</sup>.

<sup>1</sup>Center for Musculoskeletal Health and Department of Internal Medicine, University of California at Davis, United States, <sup>2</sup>California Pacific Medical Center Research Institute, United States, <sup>3</sup>University of Colorado Anschutz Medical Campus, Division of Endocrinology, United States, <sup>4</sup>Department of Epidemiology, Graduate School of Public Health, University of Pittsburgh, United States, <sup>5</sup>University of California, San Diego, United States, <sup>6</sup>Bone and Mineral Unit, Oregon Health & Science University, United States, <sup>7</sup>Center for Musculoskeletal Health and Department of Internal Medicine, United States

Disrupted rest-activity circadian rhythm (RAR) patterns have been associated with poor health outcomes (e.g. diminished cognitive function & increased risk of dementia & falls). Bone turnover exhibits circadian variation; relationships between bone & RAR are emerging areas of research. We evaluated associations between RAR & total hip bone mineral density (BMD) in older men from the Osteoporotic Fractures in Men (MrOS) cohort. We hypothesized that weaker RAR patterns would be associated with lower BMD. MrOS is an ongoing prospective cohort study following ambulatory men  $\geq 65$  years ( $n=5994$ ) at 6 U.S. clinics (baseline enrollment 3/2000- 4/2002); participants for this analysis are from an ancillary study, Outcomes of Sleep Disorders in Older Men (MrOS Sleep). We included data from men who had technically adequate measures of RAR & BMD at Sleep Visit 1 (12/2003-3/ 2005) & BMD at Visit 3 (3/2007-3/2009) ( $n=2412$ ; mean age at Sleep Visit 1:  $75.7 \pm 5.2$  years). BMD was measured by DXA. Actigraphs (SleepWatch-O; Ambulatory Monitoring, Inc., Ardsley, NY, USA) worn on

the non-dominant wrist were used to collect circadian activity data over  $4.8 \pm 0.8$  consecutive 24-hour periods. An extension of the traditional cosine curve was used to fit RAR to the activity data. Six RAR parameters were evaluated: acrophase (time of peak activity), amplitude (rhythm strength), mesor (mean of activity fitted curve), F-statistic (rhythm robustness; overall circadian rhythmicity), alpha (daytime: nighttime activity ratio), & beta (daytime activity). Associations between RAR & BMD (Sleep Visit 1), and RAR &  $\Delta$ BMD (Sleep Visit 1-Visit 3) were assessed with generalized linear models. Covariates included age, clinic site, physical activity, race, comorbidity, body composition, smoking, alcohol, caffeine & urinary melatonin. Associations between F-statistic & BMD, and between F-statistic &  $\Delta$ BMD, were significant after adjusting for age & clinical site but not after further multivariate (MV) adjustment (Table). There were no consistent, significant associations between the other RAR variables & BMD or  $\Delta$ BMD (data not shown). Overall circadian rhythmicity of rest and activity (measured by F-statistic) was modestly associated with total hip BMD &  $\Delta$ total hip BMD; adjustment for covariates related to lifestyle, body composition & comorbidities attenuated these associations. These data suggest that RAR is not independently associated with BMD or  $\Delta$ BMD in older men.

**Table: Associations between overall circadian rhythmicity (F-statistic) and total hip BMD in older men**

F-statistic	BMD at Sleep Visit 1 (Age and Site adjusted)		BMD at Sleep Visit 1 (MV adjusted)		$\Delta$ BMD (Age and Site adjusted)		$\Delta$ BMD (MV adjusted)	
	LS Means (95%CI)	p-trend	LS Means (95%CI)	p-trend	LS Means (95%CI)	p-trend	LS Means (95%CI)	p-trend
Q1	0.96 (0.95, 0.98)	0.009	0.95 (0.94, 0.97)	0.688	-1.68 (-1.99, -1.36)	0.017	-1.55 (-1.87, -1.23)	0.127
Q2	0.96 (0.95, 0.98)		0.96 (0.95, 0.97)		-1.56 (-1.86, -1.26)		-1.57 (-1.87, -1.27)	
Q3	0.95 (0.94, 0.97)		0.96 (0.95, 0.97)		-1.24 (-1.53, -0.94)*		-1.26 (-1.55, -0.96)	
Q4	0.94 (0.93, 0.96)		0.95 (0.94, 0.96)		-1.22 (-1.52, -0.93)*		-1.30 (-1.59, -1.01)	

BMD MV model adjusted for body mass index, waist-hip ratio, diabetes, alcohol, caffeine, physical activity, depression  
 $\Delta$ BMD MV model adjusted for depression, hypertension, congestive heart failure  
 Q1 = reference category

Table

**Disclosures:** Tara S Rogers, None.

## SA0245

See Friday Plenary Number FR0245.

## SA0246

See Friday Plenary Number FR0246.

## SA0247

See Friday Plenary Number FR0247.

## SA0248

See Friday Plenary Number FR0248.

## SA0249

See Friday Plenary Number FR0200.

## SA0250

See Friday Plenary Number FR0250.

## SA0251

See Friday Plenary Number FR0251.

## SA0252

See Friday Plenary Number FR0252.

## SA0253

**Assessment of vitamin D status using Mitra<sup>TM</sup> volumetric absorptive micro-sampling (VAMS) device.** Jonathan Tang<sup>\*1</sup>, Holly Nicholls<sup>1</sup>, Nicole Ball<sup>1</sup>, John Dutton<sup>1</sup>, Isabelle Pic<sup>1</sup>, James Rudge<sup>2</sup>, Christopher Washbourne<sup>1</sup>, William Fraser<sup>1</sup>. <sup>1</sup>University of East Anglia, United Kingdom, <sup>2</sup>Neoteryx, United States

**Introduction:** The use of dried blood spot (DBS) sampling for general wellness assessment and in clinical diagnostics has gained popularity as a convenient and less invasive alternative to venous sampling. Collection of blood samples from a finger/heel prick using conventional filter paper suffers from variability in sample volume and spot sizes which undermine the quality of results. We describe the use of a volumetric absorptive micro-sampler (VAMS), called Mitra<sup>TM</sup> (Torrance, CA, USA) for measurement of 25OHD<sub>3</sub> and interpretation of vitamin D status according to current international guidelines.

**Method:** A liquid-chromatography mass spectrometry (LC-MS/MS) method was used for measurement of 25OHD<sub>3</sub> (Tang *et al.* ASBMR 2015, LB-MO0026). We compared results from patient samples (n=97) collected by VAMS and Whatman® 903 cards extracted as whole spot (wDBS) and sub-punches (spDBS) against plasma 25OHD<sub>3</sub> concentration. We investigated the volume displacement effects of haematocrit (Hct) on DBS 25OHD<sub>3</sub> measurements and described the use of DBS-to-plasma equivalence value (PEV) to allow accurate interpretation of vitamin D status.

**Results:** VAMS showed the best assay precision CV (<8.2%) compared to wDBS (<16.6%) and spDBS (<15.1%) across the assay range of 0.1-125 nmol/L, the least variability in recovery and lowest LLoQ (Figure 1). We observed a decrease in DBS 25OHD<sub>3</sub> concentration in proportion to the reduction in plasma volume and increase in packed cell volume. The displacement effect of Hct resulted in a strong but negatively biased correlation ( $r^2=0.893$ , -39.3%) between raw DBS values and plasma concentrations, that was dependent upon the level of Hct present in sample. We demonstrated the use of simple linear regression model to transform raw DBS values into PEVs. In a subsequent cohort of patient samples (n=70), PEV<sub>VAMS</sub> produced the most accurate interpretation of vitamin D status compared to PEV<sub>wDBS</sub> and PEV<sub>spDBS</sub>.

**Discussion:** We present data supporting the use of VAMS for measurement of 25(OH)D<sub>3</sub>, particularly in circumstances where venesection may be impossible or difficult and where sample volume may be limited. Although the recovery of analyte remains Hct-dependent, the use of DBS-to-plasma equivalence values improves the clinical applicability and broadens the utility of DBS as a sampling technique.

Intra assay	wDBS [25OHD <sub>3</sub> ] (nmol/L)	wDBS CV (%)	spDBS [25OHD <sub>3</sub> ] (nmol/L)	spDBS CV (%)	VAMS [25OHD <sub>3</sub> ] (nmol/L)	VAMS CV (%)
Sample 1	7.5	16.1	7.6	13.6	7.3	8.2
Sample 2	23.4	8.9	23.2	9.0	20.5	6.7
Sample 3	43.6	9.1	45.0	12.0	40.3	6.4
Sample 4	64.2	6.5	71.1	9.8	59.5	7.7
Inter assay						
Sample 1	10.6	16.6	12.2	15.1	10.9	7.4
Sample 2	57.7	6.9	62.7	7.5	64.8	7.1
Sample 3	82.0	3.6	93.3	8.3	91.3	7.0
Recovery						
average	92.8 (78.9-114.1)	5.3	103.3 (88.3-120)	5.5	100.0 (93.4-114.1)	2.9
Lower limit of quantitation						
LLoQ (nmol/L)	1.6		2.6		1.5	

Figure 1. Table of assay performance

Figure 1 Table of assay performance

**Disclosures:** Jonathan Tang, None.

## SA0254

See Friday Plenary Number FR0254.

## SA0255

See Friday Plenary Number FR0255.

## SA0256

See Friday Plenary Number FR0256.

## SA0257

**25-hydroxyvitamin D Levels, Bone Mineral Density and Vertebral Fractures In Patients With Type 2 Diabetes Mellitus.** María Lorena Brance<sup>\*1</sup>, Luis Agustín Ramírez Stieben<sup>2</sup>, Raquel Dobry<sup>2</sup>, Lilian Anca<sup>2</sup>, Adrián González<sup>2</sup>, María Isabel López<sup>2</sup>, Salvador Bayo<sup>2</sup>, Ariel Sánchez<sup>3</sup>, Lucas R. Brun<sup>4</sup>. <sup>1</sup>Centro de Reumatología de Rosario, Argentina, <sup>2</sup>Servicio de Endocrinología del Hospital Español, Argentina, <sup>3</sup>Centro de Endocrinología, Argentina, <sup>4</sup>Laboratorio de Biología sea. Facultad de Ciencias Médicas UNR, Argentina

25-hydroxyvitamin D (25OHD) has been associated with insulin resistance, metabolic syndrome (MS) and type 2 diabetes (DM2). In addition, DM2 patients showed an increased risk of fracture. The aim of this study was to evaluate 25OHD levels, bone mineral density (BMD) and vertebral fractures (VFX) in patients with DM2. An observational study with 209 patients with DM2 and 173 patients as control group (CG) over 18 years from Rosario city (32°52'18"S) Argentina were carried out from January to December 2016. Exclusion criteria: chronic renal or liver disease, cancer, autoimmune or connective diseases, or patients treated with glucocorticoids, anticonvulsants or vitamin D. The total 25OHD (ng/ml) was performed by chemiluminescence. The BMD (g/cm<sup>2</sup>) was determined by DXA (Lunar Prodigy). VFX were assessed by Genant classification. The results are expressed as mean±EE. Data distribution was analyzed using the Kolmogorov-Smirnov test and the comparison between groups was performed with parametric and non-parametric tests as appropriate. Results: The DM2 group consisted in 117 women and 92 men (60.9±0.7 years, 9.5±0.56 years of DM2 diagnosis, 75.7% with MS and 7.5±0.1% of HbA1c). The CG consisted in 152 women and 21 men with 62.6±1.2 years. The DM2 group showed higher BMI (CG= 27.1±0.4, DM2= 32.5±0.4 kg/m<sup>2</sup>, p<0.0001) and higher percentage of obese and overweight patients (chi<sup>2</sup> test, p<0.0001). BMD of postmenopausal women was significantly higher in DM2 (L1-L4: GC= 0.997±0.033, DM2= 1.129±0.033; femoral neck: GC= 0.782±0.013, DM2= 0.883±0.018). However the prevalence of VFX was significantly higher in DM2 (chi<sup>2</sup> test, RR: 3.09, p<0.0001). 25OHD was significantly lower in DM2 (GC= 24.0±0.6, DM2= 19.5±0.8, p<0.0001) without differences between patients with and without VFX. In DM2, a higher percentage of 25OHD deficiency was found (GC= 37.7%, DM2= 62.2%, p<0.0001). The 25OHD showed correlation with BMI (r= -0.28) and age (r= -0.20). The subgroup of patients with MS (n=156) showed significantly higher BMI and lower 25OHD (without MS= 22.0±1.4; with MS= 18.6±0.6). The triglyceride/HDL index, used as indirect marker of insulin resistance, was significantly higher in DM2 (GC= 1.5±0.1, DM2= 3.6±0.2) and correlated with HbA1c (r= 0.26) and 25OHD (r= -0.16). It is concluded that DM2 patients have lower 25OHD levels and higher prevalence of VFX despite better BMD. The subgroup of patients without MS showed higher levels of 25OHD similar to the CG.

**Disclosures:** María Lorena Brance, None.

## SA0258

See Friday Plenary Number FR0258.

## SA0259

**Higher dairy food intake favorably influences spine Quantitative Computed Tomography (QCT) bone measures in the Framingham Study.** Shivani Sahni<sup>\*1</sup>, Laura H. van Dongen<sup>2</sup>, Douglas Kiel<sup>1</sup>, Marian Hannan<sup>1</sup>. <sup>1</sup>Institute for Aging Research, Hebrew SeniorLife, Harvard Medical School, United States, <sup>2</sup>Wageningen University and Research Centre, Netherlands

Higher dairy food intake is associated with higher DXA-derived BMD. In post-menopausal women, higher dairy intake was linked with higher trabecular volumetric BMD (vBMD). Yet, few studies have addressed if dairy food intake is related to bone strength and size. We examined the association of dairy food intake with QCT measures at the L3 spine level in men and women from the Framingham Cohorts (Offspring and Generation 3). We also examined if these associations differed by age (≥50y) or by serum vitamin D (25-OH D <20, ≥20–<50; ≥50 ng/ml). We hypothesized that higher dairy food intake would be related with more favorable QCT bone measures especially in older men and women and in those with higher 25-OH D.

In this cross-sectional study, 1,522 men and 1,104 women [aged 32-81y, mean 50 (men); 55 (women)] had measures of dairy food intake (milk, yogurt, cheese, cream, milk +yogurt; milk+yogurt+cheese, serv./wk) from a FFQ, QCT vBMD (integral and trabecular, g/cm<sup>3</sup>), cross-sectional area (CSA, cm<sup>2</sup>) and 25-OH D (radioimmuno assay). Sex-specific multivariable linear regression was used to calculate the association of dairy food intake with each QCT measure adjusting for covariates (Table), and examined by age and 25-OH D levels.

Mean milk intake was 6±7 serv./wk in men and in women and mean total calcium intake (mg/d) was 905±451 (men) and 1180±584 (women). In men, higher intake of milk, milk+yogurt and milk+yogurt+cheese was related with higher integral and trabecular vBMD (Table). Further, higher cheese intake was related with higher CSA. In women, no significant results were seen except a positive association of cream intake with CSA. No associations were seen for other dairy foods. These associations appeared to be stronger in older men and in those with 25-OH D ≥20–<50 ng/ml. With 25-OH D ≥50 ng/ml, higher dairy food intake was related with lower integral and trabecular vBMD.

Higher dairy food intake may be beneficial for trabecular and integral vBMD in men and for bone size in men and women. Overall, benefit of dairy food intake on these spine bone measures appeared to be stronger in older men and those with 25-OH D ≥20–<50 ng/ml. Adverse effect of dairy foods with 25-OH D ≥50 ng/ml was unexpected and need



further investigation. Higher intake of total calcium in women and residual confounding by physical activity could explain sex differences. This is the first study to describe sex specific differences in volumetric spine indices.

Table. Association of dairy food intake (serv./wk) with spine (L3) cross-sectional area (CSA, cm<sup>2</sup>), and integral and trabecular vBMD (g/cm<sup>3</sup>) in the Framingham Offspring and Generation 3 cohorts.

Dairy food intake (serv./wk) <sup>1</sup>	Men (n=1,522)			Women (n=1,104)		
	$\beta$	SE	P value	$\beta$	SE	P value
<b>CSA</b>						
Milk	0.0024	0.004	0.58	0.0021	0.006	0.74
Yogurt	0.0009	0.018	0.96	-0.0293	0.018	0.11
Cheese	0.0144	0.007	0.05*	0.0230	0.013	0.08
Cream	-0.0023	0.028	0.93	0.1114	0.042	0.008*
Milk+Yogurt	0.0023	0.004	0.58	-0.0012	0.006	0.83
Milk+Yogurt+Cheese	0.0057	0.003	0.13	0.0030	0.006	0.59
<b>Integral vBMD</b>						
Milk	0.0003	0.001	0.006*	0.0001	0.001	0.42
Yogurt	0.0003	0.001	0.55	-0.0001	0.001	0.91
Cheese	0.0003	0.001	0.14	0.0001	0.001	0.61
Cream	0.0011	0.001	0.14	-0.0009	0.001	0.36
Milk+Yogurt	0.0003	0.001	0.006*	0.0001	0.001	0.47
Milk+Yogurt+Cheese	0.0003	0.001	0.001*	0.0001	0.001	0.37
<b>Trabecular vBMD</b>						
Milk	0.0002	0.001	0.06	0.0001	0.001	0.54
Yogurt	0.0005	0.005	0.34	-0.0002	0.001	0.66
Cheese	0.0003	0.001	0.08	0.0003	0.001	0.37
Cream	0.0010	0.001	0.23	-0.0003	0.001	0.75
Milk+Yogurt	0.0002	0.001	0.04*	0.0001	0.001	0.67
Milk+Yogurt+Cheese	0.0003	0.001	0.006*	0.0001	0.001	0.43

<sup>1</sup> Adjusted for age, BMI, energy intake (residual method), current smoking, calcium and vitamin D supplement use and current estrogen use (in women). Models for vBMD were additionally adjusted for height. \*P $\leq$  0.05 considered significant.

Table

**Disclosures:** Shivani Sahni, Dairy Management Inc., Grant/Research Support.

## SA0260

See Friday Plenary Number FR0260.

## SA0261

See Friday Plenary Number FR0261.

## SA0262

**Local glucocorticoid metabolism regulates the effects of therapeutic glucocorticoids on bone.** Chloe Fenton<sup>1</sup>, Craig Doig<sup>1</sup>, Karim Raza<sup>1</sup>, Gareth Lavery<sup>1</sup>, Mark Cooper<sup>2</sup>, Rowan Hardy<sup>1</sup>. <sup>1</sup>University of Birmingham, United Kingdom, <sup>2</sup>University of Sydney, Australia

Long-term exposure to elevated endogenous and therapeutic glucocorticoids is associated with high risk of osteoporosis and fracture. The 11 $\beta$ -hydroxysteroid dehydrogenase (11 $\beta$ HSD) enzymes mediate the actions of glucocorticoids in many tissues. The 11 $\beta$ HSD1 enzyme converts inactive endogenous glucocorticoids such as dehydrocorticosterone and cortisone, as well as therapeutic glucocorticoids such as prednisone, to their active counterparts corticosterone, cortisol and prednisolone. In contrast, renal inactivation of glucocorticoids by the 11 $\beta$ HSD2 enzyme generates a supply of inactive substrate for 11 $\beta$ HSD1 in vivo. We have previously demonstrated the presence of 11 $\beta$ HSD1 within bone and hypothesised that 11 $\beta$ HSD1 within osteoblasts regulates the effects of exogenous glucocorticoids on bone.

Mice with transgenic deletion of 11 $\beta$ HSD1 (11BKO) and their wild type (WT) littermates were treated for four weeks with the active murine glucocorticoid corticosterone (100 $\mu$ g/mL) or vehicle control delivered in drinking water. Upon completion, bone density and structure were analysed by microCT. Whilst serum corticosterone and body weights were increased and adrenal weights reduced in mice receiving corticosterone at four weeks, there were no significant differences between 11BKO and WT counterparts. No differences were evident in microCT parameters of bone volume to tissue volume (BV/TV), trabecular number (TN) and trabecular separation (TS) between WT and 11BKO mice given control drinking water (BV/TV: WT 8.6% $\pm$ 0.81 vs 11BKO 7.4% $\pm$ 1.3, NS; TN: WT 0.85 1/mm $\pm$ 0.093 vs 11BKO 0.77 1/mm $\pm$ 0.04, NS; TS: 669.8 $\mu$ m $\pm$ 72 vs 11BKO 706.8 $\mu$ m $\pm$ 92.8, NS). As expected, WT mice treated with corticosterone developed osteoporosis on the basis of decreased BV/TV and TN and increased TS. However, 11 $\beta$ HSD1 KO animals were almost completely protected against the effects of corticosterone (BV/TV: WT 5.31% $\pm$ 0.84 vs 11BKO 7.51% $\pm$ 1.31, P $\leq$ 0.05; TN: WT 0.65 1/mm $\pm$ 0.051 vs 11BKO 0.925 1/mm $\pm$ 0.044, P $\leq$ 0.05; TS: WT 1000.2 $\mu$ m $\pm$ 72.1 vs 11BKO 809.2 $\mu$ m $\pm$ 82.6, p=0.08).

These data indicate that local reactivation of glucocorticoids within osteoblasts contributes substantially to the development of glucocorticoid-induced osteoporosis.

**Disclosures:** Chloe Fenton, None.

## SA0263

**Disruption of Energy Metabolism in Postmenopausal Osteoporosis (PMO): Altered Fat Metabolism and Adipokines.** Kaare Gautvik<sup>1</sup>, Michael Prediger<sup>2</sup>, Yi-Hsiang Hsu<sup>3</sup>, Rachel Saunders<sup>4</sup>, Ole Olstad<sup>5</sup>, Marie Appleton<sup>4</sup>, Vigdis Gautvik<sup>6</sup>, Marco Ponzetti<sup>7</sup>, Yngve Bliksrud<sup>8</sup>, Nadia Rucci<sup>9</sup>, Mark Walker<sup>10</sup>, Anna Teti<sup>9</sup>, Dermot Neely<sup>11</sup>, Mark Birch-Machin<sup>4</sup>, Joseph Brain<sup>12</sup>, Sjur Reppe<sup>13</sup>, Harish Datta<sup>14</sup>. <sup>1</sup>Lovisenberg Diakonale Hospital, Unger-Vetlesen Institute, Oslo, Norway, <sup>2</sup>Blood Sciences, Royal Victoria Infirmary, Newcastle Upon Tyne, United Kingdom, <sup>3</sup>Institute of Ageing Research 1200 Centre Street, United States, <sup>4</sup>Institute of Cellular Medicine, Faculty of Medicine, Newcastle University, United Kingdom, <sup>5</sup>Oslo University Hospital, Department of Biochemistry, Norway, <sup>6</sup>University of Oslo, Institute of Basic Medical Science, Norway, <sup>7</sup>University of L'Aquila, Department of Biotechnological and Applied Clinical Sciences, Italy, <sup>8</sup>Oslo University Hospital, Department of Medical Biochemistry, Norway, <sup>9</sup>University of L'Aquila, Department of Biotechnological and Applied Sciences, Italy, <sup>10</sup>Institute of Cellular Medicine (Diabetes), Faculty of Medicine, Newcastle University, United Kingdom, <sup>11</sup>Blood Science (Biochemistry Section), The Newcastle Upon Tyne Hospitals, United Kingdom, <sup>12</sup>Harvard T.H. Chan School of Public Health, Department of Health Sciences, United States, <sup>13</sup>Lovisenberg Diakonale Hospital, Unger-Vetlesen Institute, Norway, <sup>14</sup>Institute of Cellular Medicine, Faculty of Medicine, Newcastle University and Pathology Department, James Cook University Hospital, United Kingdom

Pioneer animal studies suggest relationships between energy metabolism and osteoporosis, but its role in PMO is unclear. We report results of endocrine, metabolomics and bone-transcriptomics studies in Norwegian PMO fulfilling WHO criteria (n=27), healthy matched controls (n=39) and validation group (n=15)<sup>1</sup>. Transcriptome profiling of iliacal biopsies was by Affymetrix arrays and serum metabolites or hormones by LC-MS/MS, GC-MS or ELISA, respectively. PMO had lower age-adjusted BMI (means(SD) 22.3(2.9) vs 25.6(3.9); p<0.001) and lean body mass (38.5(5.1) vs 42.3 (4.6) kg; p<0.05) but without significant difference in fat mass (20.3(8.9) vs 25.6(9.0) kg; p<0.08). Plasma leptin had a positive correlation with BMI (p< 10<sup>-5</sup>) and fat mass (p<10<sup>-5</sup>) and mean total hip BMD T-score (p<8x10<sup>-4</sup>) and Z-score (p<0.03) and L1-L4 T-score (p<0.001) and Z-score (p<0.05). In contrast, adiponectin in PMO was higher (25.4(14.2) vs 17.3(6.34); (p<0.005) and showed negative correlation with L1-L4 T-score (p<0.01). Fasting lipid profile revealed PMO had lower serum triglycerides (1.1(0.3) vs 1.4(0.8) mM; p<0.05) with significant but weak positive correlation with total hip T- and Z-scores. Plasma lipoprotein a (Lp(a)), which is lowered by weight loss, showed strong positive correlation with BMD T-score and Z-score at all sites, strongest with spinal Z-score (p<4.0x10<sup>-4</sup>). PMO bone showed higher expression of genes associated fat metabolism and strong negative correlation between BMD and osteogenic genes were observed (ACSL3, FABP3, ACADM, ACADSB, and PPARA). Serum acetyl- and acylcarnitine (C14, C16 and C18) showed strong positive correlation with BMD. In PMO accumulation of serum 5 dicarboxylic fatty acids (2-4 fold higher in patients), oleamide (cannabinoid receptors agonist) and serotonin (5HT) was evident. LCN2 bone expression showed negative association with total femoral Z-score, but the serum levels were unaffected. Other alternative mechanisms, i.e., mitochondrial dysfunction and insulin resistance were excluded by RT-PCR Quantification of mitochondrial DNA damage and by analyses of plasma insulin and leptin:adiponectin, IGF and IGF:IGFBP3 ratio, respectively. In conclusion, PMO have elevated serum serotonin (5HT) and oleamide and exhibit marked changes in endocrine (leptin, adipokine), metabolic (fat metabolites, Lp(a) and triglycerides) and transcription profiles, suggesting a disrupted regulation of energy homeostasis. <sup>1</sup>Jemtland R et al. JMBR 2011, 26,1793-8.

**Disclosures:** Kaare Gautvik, None.

## SA0264

See Friday Plenary Number FR0264.

## SA0265

See Friday Plenary Number FR0265.

## SA0266

**Novel ELISA for the detection of circulating bioactive Sclerostin.** Jacqueline Wallwitz<sup>1</sup>, Elisabeth Gadermaier<sup>1</sup>, Gabriela Berg<sup>1</sup>, Venugopal Bhaskara<sup>2</sup>, Emilio Casanova<sup>3</sup>, Gottfried Himmeler<sup>1</sup>. <sup>1</sup>The Antibody Lab GmbH, Austria, <sup>2</sup>Medical University of Vienna, Austria, <sup>3</sup>Ludwig Boltzmann Institute for Cancer Research, Austria

Objective: Sclerostin is a 190-amino acid glycoprotein secreted by osteocytes and has emerged as a therapeutic target for treating osteoporosis. The core protein consists of a cystine-knot with three loops, whereas the second loop binds to the LRP5/6 complex of the Wnt signaling pathway and leads to the inhibition of bone formation. The development of an ELISA utilizing well-characterized and validated antibodies for the

measurement of putative bioactive circulating sclerostin may be helpful to further investigate sclerostin as a biomarker in the diagnosis of bone remodeling disorders and in the assessment of therapeutic effectiveness.

Methods: A sandwich immunoassay for the detection of the free bioactive circulating sclerostin in human serum and plasma samples was developed. The ELISA contains a monoclonal antibody for capture and a horseradish-peroxidase conjugated affinity-purified polyclonal anti-human sclerostin antibody for detection. Both antibodies were characterized and the overall assay performance was validated according to international quality guidelines.

Results: For characterization of the antibodies epitope mapping, kinetic studies and size exclusion chromatography were performed. The recombinant coating antibody recognizes a distinct epitope within the second loop of sclerostin, whereas the polyclonal detection antibody has five linear epitopes distributed throughout the molecule. Both antibodies have very good binding kinetics of  $k_{\text{dis}}$  of  $<1.0 \times 10^{-7} \text{ s}^{-1}$  for the monoclonal antibody and  $1.19 \times 10^{-5} \text{ s}^{-1}$  for the polyclonal goat antibody, respectively. The validation parameters like specificity ( $>80\%$  competition), accuracy (80-120% spike recovery), dilution linearity (80-120%) and precision ( $<10\%$  CV) are within the standards of acceptance.

Summary and Conclusion: This well-characterized ELISA provides a reliable and accurate tool for the quantification of bioactive sclerostin in human serum and plasma samples and may give a new perspective within the bone and mineral research field.

**Disclosures:** Jacqueline Walwitz, None.

## SA0267

See Friday Plenary Number FR0267.

## SA0268

See Friday Plenary Number FR0268.

## SA0269

**Smoking in men after peak bone mass acquisition is associated with faster trabecular bone loss.** Bruno Lapauw\*, Charlotte Verroken, Stefan Goemaere, Jean-Marc Kaufman, Hans-Georg Zmierzczak. Unit for Osteoporosis and Metabolic Bone Diseases, Department of Endocrinology, Ghent University Hospital, Belgium

Objective: The risk of osteoporosis is determined by the acquisition of peak bone mass during growth as well as by subsequent bone loss. Although smoking has been associated with a disturbed peak bone mass acquisition, its effects on subsequent changes in bone characteristics are poorly studied. We investigated whether smoking was a determinant of changes in DXA- and pQCT-derived bone parameters in cohort of healthy adult men.

Methods: 428 healthy men aged 25-45 years (mean  $34.9 \pm 5.3$ ) participated in a longitudinal, population-based sibling-pair study, with a mean follow-up of  $12.4 \pm 0.4$  years (range 11.2-13.6). Areal BMD (aBMD) was measured at the proximal femur and lumbar spine using DXA. Trabecular volumetric BMD (vBMD) was assessed at the distal radius, cortical vBMD and geometry at the radial and tibial shafts using pQCT. Smoking behaviour was assessed using a validated health questionnaire. Associations between baseline smoking behaviour (smoker vs. non-smoker) and changes in bone characteristics were evaluated using mixed-effects modeling.

Results: In the overall cohort, aBMD decreased by  $1.7 \pm 5.3\%$  at the lumbar spine,  $3.1 \pm 4.6\%$  at the total hip, and  $6.0 \pm 5.8\%$  at the femoral neck (all  $p < 0.001$ ). Trabecular vBMD decreased by  $1.6 \pm 2.7\%$  and trabecular area increased by  $1.6 \pm 3.7\%$  (both  $p < 0.001$ ). Cortical vBMD decreased by  $0.5 \pm 2.7\%$  ( $p < 0.001$ ) at the radius and  $0.2 \pm 1.6\%$  ( $p = 0.047$ ) at the tibia. Cortical area and peri- and endosteal circumferences increased by  $1.3 \pm 6.9\%$ ,  $5.7 \pm 5.9\%$  and  $11.9 \pm 12.1\%$  at the radius and by  $1.5 \pm 4.2\%$ ,  $3.3 \pm 3.1\%$  and  $6.2 \pm 7.3\%$  at the tibia (all  $p < 0.001$ ), respectively. Cortical thickness decreased at both the radius ( $-5.8 \pm 5.6\%$ ) and at the tibia ( $-2.5 \pm 7.1\%$ ; both  $p < 0.001$ ). Smoking at baseline was associated with a smaller increase in trabecular area and larger decreases in trabecular bone mineral content and vBMD in both unadjusted ( $p = 0.031$ ,  $p = 0.012$  and  $p = 0.047$ , respectively) and baseline age-, height- and weight-adjusted analyses ( $p = 0.038$ ,  $p = 0.009$  and  $p = 0.029$ ). In contrast, smoking at baseline was not associated with changes in aBMD or cortical bone geometry.

Conclusion: In healthy adult men, aBMD as well as trabecular and cortical vBMD start to decrease early after peak bone mass attainment, but these changes are at least in part offset by increases in bone size. Smoking is associated with a faster decline in trabecular bone mineral content and vBMD, but does not affect changes in aBMD or cortical bone geometry.

**Disclosures:** Bruno Lapauw, None.

## SA0270

See Friday Plenary Number FR0270.

## SA0271

See Friday Plenary Number FR0271.

## SA0272

See Friday Plenary Number FR0272.

## SA0273

**BMP2 Impaired Mineralization Potential in Primary Human Osteoblasts Isolated from Osteoporotic Patients.** Hilary Weidner\*, Anja Nohe<sup>1</sup>, Mark Eskander<sup>2</sup>, Debbie Dibert<sup>2</sup>. <sup>1</sup>University of Delaware, United States, <sup>2</sup>Christiana Care Hospital, United States

Signaling pathways that are impaired in patients with osteoporosis must be identified in order to develop new treatments for osteoporosis. Currently only a few are identified. Here we show that cells isolated from human femoral heads in osteoporotic patients have decreased mineralization. BMP2 or bone morphogenetic protein 2, is a crucial growth factor in bone development. Along with BMP7, BMP2 is known to induce osteoblast differentiation. BMP2 has also been approved for spinal infusion for anterior lumbar interbody fusion in order to promote bone growth. This would make BMP2 an obvious candidate for treatment for osteoporosis. Osteoporosis is a bone disease that is characterized by low bone density. This leads to deterioration of the bones, which ultimately increases the occurrences of fractures or breaks. BMP2 has been studied clinically for the treatment of osteoporosis, however long term use of BMP2 was actually shown to increase the risk of fracture, or increase osteoclast activity. Taking this prior knowledge into account human femoral heads were collected from Christiana Care Hospital in Newark, Delaware from patients undergoing hip hemiarthroplasty surgery. The patients were diagnosed with either osteoporosis or osteoarthritis. The specimens were X-rayed then cells were extracted and grown. The X-rays were analyzed and bone mineral density (BMD) was calculated. Within the osteoporotic population it was found that as the subject's age increases their BMD decreases however this decrease was more dramatic in the osteoporotic fractured population. Within the osteoarthritic population the BMD remained the same as age increased, so no relationship can be inferred. The X-rays helped to verify the decreased or deterioration of bone tissue within the osteoporotic patient pool. The grown cells were treated with BMP2, and a mineralization assays (Von Kossa) were conducted in order to measure cellular mineralization activity. Our lab has shown that treatment of BMP2 within the osteoporotic population had no effect. This would be the first time, to our knowledge, that extracted human osteoporotic cells had no mineralization response upon BMP2 stimulation. This could indicate that BMP pathway is disrupted in some way in patients diagnosed with osteoporosis.

**Disclosures:** Hilary Weidner, None.

## SA0274

**HPMA Copolymer Dexamethasone Conjugates Prevent Osteoporosis induced by Traumatic Brain Injury.** Gang Zhao\*, Xin Wei, Dong Wang. University of Nebraska Medical Center, United States

Traumatic brain injury (TBI) is a leading cause of death and disability around the world. Besides neuronal damage, traumatic brain injury could also induce osteoporosis as we found in mouse and reported clinically. The bone loss triggered by TBI will not only further influence the life quality but also is life threatening. With balance disorder which is common in brain injury patients, bone loss will put the patients at a higher risk of fracture. Patients may develop more severe second brain injury. Thus, the therapeutic strategy for TBI focusing on the injury itself is not enough. Strategies ameliorating the complication associated with TBI is needed. We proposed to utilize HPMA copolymer dexamethasone conjugates (P-Dex) in attenuating TBI and preventing osteoporosis.

Mice were randomly divided into 3 groups (severe TBI with saline treated, P-Dex treated and healthy mice). TBI was induced by controlled cortical impact with 0.75mm depth at 3.5 m/s. 5 mice from each group were sacrificed at designed time points up to 8 weeks. Femurs, tibias and lumbar vertebrae (L4-L6) were harvested for bone morphology and mineral density study to evaluate bone loss. Brains were harvested to evaluate P-Dex therapeutic efficacy on traumatic brain injury. IRDye® 800CW labeled P-Dex were administrated to evaluate P-Dex targeting property at 1 day, 3 days, 7 days and 2 weeks.

Preliminary data from micro-CT shows TBI-induced trabecular bone loss at distal femur from 2 weeks. Bone volume fraction dropped to ~40% 5 weeks post-TBI compared with healthy mice. Bone volume fraction in P-Dex treated group shows no significant difference from health group. From optical imaging study, we found P-Dex accumulated at the site of injured cortex as long as 7 days. Immunohistochemistry results showed P-Dex could inhibit the activation of microglia and reduce lipid peroxidation. Brain edema in P-Dex treated group was reduced by inhibiting the expression of Aquaporin 4. P-Dex could preserve neurons from degeneration after injury.

With these preliminary study, we could confirm osteoporosis developed after TBI. The therapeutic intervention P-Dex we proposed could attenuate the brain injury and prevent bone loss after TBI. HPMA copolymer dexamethasone conjugates would be a promising candidate in ameliorating traumatic brain injury and its complicated diseases.



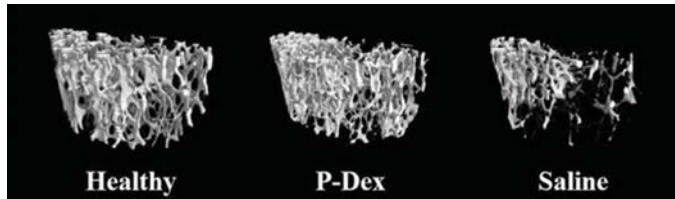


Figure 1. Representative 3D images of trabecular bone in distal femur from micro-CT at 5 weeks post-

**Disclosures:** Gang Zhao, None.

## SA0275

See Friday Plenary Number FR0275.

## SA0276

See Friday Plenary Number FR0276.

## SA0277

**Relationship between depression and anxiety and low bone mineral density in patients hospitalized with severe anorexia nervosa.** Julia Herrou<sup>\*1</sup>, Adrien Etcheto<sup>1</sup>, Sami Kolta<sup>1</sup>, Nathalie Godart<sup>2</sup>, Nicole Barthe<sup>3</sup>, Alain Daragon<sup>4</sup>, Yves Maugars<sup>5</sup>, Thierry Thomas<sup>6</sup>, Christian Roux<sup>1</sup>, Karine Briot<sup>1</sup>. <sup>1</sup>Cochin Hospital, Rheumatology Department, France, <sup>2</sup>INSERM U1178, Psychiatry Unit, Institut Mutualiste Montsouris, France, <sup>3</sup>Médecine Nucléaire, Centre Hospitalier de Bordeaux, France, <sup>4</sup>Rheumatology, CHU Rouen, France, <sup>5</sup>Rheumatology, CHU Nantes, France, <sup>6</sup>Rheumatology, CHU Saint Etienne, France

Depression, anxiety and obsessive-compulsive (OCs) symptoms are frequent during anorexia nervosa (AN). Low bone mineral density (BMD) is highly prevalent in AN. The aim of this study was to assess the relationships between depression, anxiety and low BMD in patients hospitalized with severe AN. We also assessed the relationships between these disturbances and the change in BMD over 1 year after the hospitalization.

From 2009 to 2011, 220 women with severe AN from 11 centers in France have been included in the study upon admission to inpatient treatment (cohort EVHAN, Evaluation of Hospitalization for AN). Global clinical state was evaluated by the Morgan and Russell Global Outcome Score (GOAS), depression, anxiety and OCs were measured using psychometric scales (Beck Depression Inventory, Maudsley Obsessive Compulsive Inventory, Hospital Anxiety and Depression, and Liebowitz Social Anxiety) at admission. BMD was measured by dual energy X ray absorptiometry during the hospitalization and 1 year after the discharge with centralized analysis. Low BMD was defined by Z score  $\leq -2$  (at least one site). The gain of BMD was defined by an increase in the BMD  $^3$  0.03g/cm<sup>2</sup> at spine or hip sites.

168 patients with severe AN had a BMD measurement at during hospitalization (mean age 20.7 (6.6 SD) years, mean AN duration 4.2 (4.5 SD) years, mean BMI of 14.1kg/m<sup>2</sup> (1.5 SD)). According to the BDI, the prevalence of patients with depression ( $\geq 20$ ) at the admission was 75%; 36% had an antidepressant treatment. 67% (n=109) of patients had a poor global status ( $\leq 6$ ) according to the GOAS. 52% (n=87) of patients had a low BMD. Univariate analysis showed a significantly association between GOAS score and a low BMD (OR 0.81 (0.67-0.97) p=0.02). A trend for an association was found between low BMD and BDI (p=0.06), LSAS (fear and social interaction) (p=0.07) and HAS (p=0.08). However, these associations were no significant in multivariate analysis adjusted on duration of illness, age, BMI and antidepressant treatment; lifetime lowest weight was the single determinant significantly associated with low BMD (OR=1.172 (1.04-1.33) p=0.008). 1-year BMD follow-up was available for 56 patients; 25 (45%) had a significant gain of BMD. There was no association between depression or anxiety scores at admission and gain in BMD in univariate and multivariate analyses.

This study confirms that half of a population of young females with severe AN has a low BMD. The main predictor of low BMD is the lifetime minimal BMI. There is a trend for an association between depression and anxiety scores and low BMD but these disturbances are not significant determinants of low BMD.

**Disclosures:** Julia Herrou, None.

## SA0278

**The Predictors for 24 Months Efficacy of Denosumab, an Anti-RANKL Antibody, on Osteoporosis in Rheumatoid Arthritis Patients from Japanese Multicenter Study (TBCRBONE).** Yuji Hirano<sup>\*1</sup>, Yasuhide Kanayama<sup>2</sup>, Kyosuke Hattori<sup>1</sup>, Nobunori Takahashi<sup>3</sup>, Naoki Ishiguro<sup>3</sup>, Toshihisa Kojima<sup>3</sup>. <sup>1</sup>Department of Rheumatology, Toyohashi Municipal Hospital, Japan, <sup>2</sup>Department of Orthopaedic Surgery and Rheumatology, Toyota Kosei Hospital, Japan, <sup>3</sup>Department of Orthopaedic Surgery, Nagoya University Graduate School of Medicine, Japan

**Purpose:** Although medication of rheumatoid arthritis (RA) has been improved, treatment of concomitant disease in RA patients, such as osteoporosis (OP), will be more important. Although denosumab (DMB), an anti-RANKL antibody, was approved for treatment of OP in Japan in 2013, clinical data is lacking in RAOP. The objectives of this study is to investigate the 24 months efficacy of DMB on RAOP and predictors of efficacy from multicenter registry study in Japan (TBCRBONE).

**Methods:** 71 female RAOP patients treated with DMB for 2 years were included. Bone mineral density of lumbar spine (LSBMD) and total hip (THBMD) and bone turnover markers (BTM: PINP and TRACP-5b) were measured at baseline and every 6 months to 24 months. Predictors of efficacy of DMB on RAOP were evaluated by investigating Spearman's rank correlation coefficient between %increase of LSBMD or THBMD and parameters (Baseline: BMD, BTM, prednisolone, age, RA duration, height, weight, body mass index and ADL(mHAQ)). %BMD increase at 6 months. Time averaged data: DAS28-CRP, SDAI, CRP, MMP-3, PINP and TRACP-5b). Time averaged data (ta data) was calculated as average of data at every 6 months.

**Results:** Baseline characteristics: Mean age was 70 years old. Mean RA duration was 17 years. Mean T-score were -2.4 (LSBMD), -2.6(femoral neck BMD) and -2.8 (THBMD). Mean DAS28-CRP was 2.7. 45% of cases had the past history of fracture. Mean FRAX was 28%. Daily teriparatide (dTPD) was used in 11 cases just before DMB treatment. %increase of LSBMD at every 6 months to 24 months was 4.5%-6.0%-7.6%-8.0% and significantly increased from baseline. %increase of THBMD at every 6 months to 24 months was 2.7%-3.3%-4.8%-7.6% and significantly increased from baseline. Mean %decrease in PINP were 36.8%-31.4%-23.4%-27.0% and mean % decrease in TRACP-5b was 31.1%-25.5%-20.1%-2.4%. Parameters significantly correlated with %increase of LSBMD at 24 months (correlation coefficient, p value) were baseline PINP (0.302, 0.012), baseline TRACP-5b (0.251, 0.039), baseline height (-0.267, 0.028), %increase of LSBMD at 6 months (0.645, <0.001), ta %change of PINP (-0.332, 0.010) and ta %change of TRACP-5b (-0.447, <0.001). Parameters significantly correlated with %increase of THBMD at 24 months were baseline PINP (0.305, 0.012), baseline TRACP-5b (0.294, 0.015), %increase of LSBMD at 6 months (0.339, 0.007), %increase of THBMD at 6 months (0.642, <0.001), ta %change of PINP (-0.432, 0.001) and ta %change of TRACP-5b (-0.392, 0.002). %increase of LSBMD at 24 months was not correlated with %increase of THBMD at 24 months.

**Conclusions:** DMB was effective in RAOP. Elevated bone turnover at baseline, good early response, and sustained decreased BTMs compared with baseline were suggested to be one of the predictors of the efficacy of DMB in RAOP. Efficacy of DMB was not influenced by inflammation status or RA disease activity.

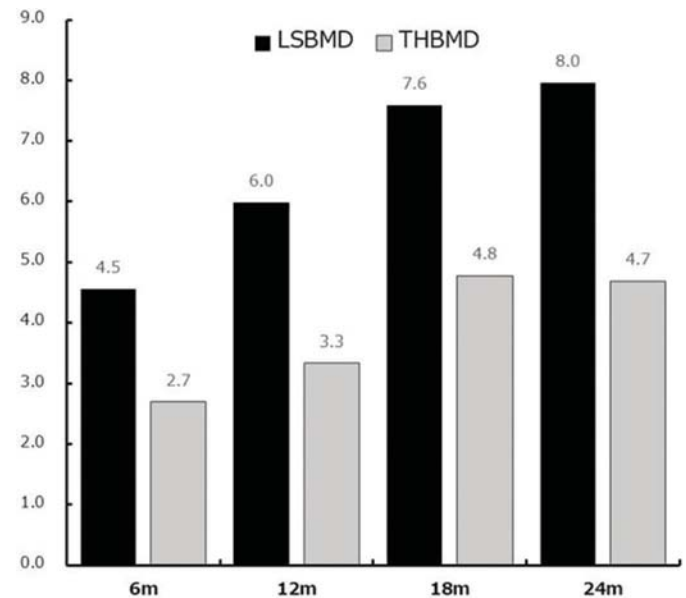


**Fig. Mean %increase of bone mineral density**

Figure: %increase of BMD

**Disclosures:** Yuji Hirano, None.

## SA0279

**Denosumab increased bone mineral density but did not affect trabecular bone score (TBS) during first year after kidney transplantation.** Shogo Nakayama<sup>1</sup>, Yasumasa Yoshino<sup>1</sup>, Izumi Hiratsuka<sup>1</sup>, Megumi Shibata<sup>1</sup>, Taihei Ito<sup>2</sup>, Hitomi Sasaki<sup>3</sup>, Midori Hasegawa<sup>4</sup>, Mamoru Kusaka<sup>3</sup>, Ryoichi Shiroyuki<sup>3</sup>, Takashi Kenmochi<sup>2</sup>, Yukio Yuzawa<sup>4</sup>, Kiyotaka Hoshinaga<sup>3</sup>, Atsushi Suzuki<sup>1</sup>.

<sup>1</sup>Division of Endocrinology and Metabolism, Department of Internal Medicine, Fujita Health University, Japan, <sup>2</sup>Department of Organ Transplant Surgery, Fujita Health University, Japan, <sup>3</sup>Department of Urology, Fujita Health University, Japan, <sup>4</sup>Division of Nephrology, Department of Internal Medicine, Fujita Health University, Japan

**Background:** Post kidney transplantation (KTx) patients are known to have high fracture risk mainly due to immunosuppression therapy such as glucocorticoid. Bisphosphonate (BP) should be a first-line drug for glucocorticoid-induced osteoporosis, but might affect renal function, especially when the glomerular filtration rate is low. Denosumab could be another candidate as anti-resorptive agents and is known to increase bone mineral density (BMD) in primary osteoporosis. However, volumetric increase of bone mass does not fully reflect bone strength. TBS is a novel technique to assess bone microarchitecture, and is considered to give additional information for bone strength. In the present study, we compared the change of BMD with that of TBS by the treatment with denosumab after KTx.

**Methods:** This observational study was done in Fujita Health University Hospital, and post-KTx patients were recruited (n=38, M/F=30/8, age 51 ± 21 years old) from 2014 to 2016. In 30 cases, denosumab was administered twice during first year after KTx. Serum samples were collected and lumbar and femoral neck BMD was measured soon after KTx, and at 6 and 12 months after first denosumab treatment. BMD was measured by Hologic Discovery®, and lumbar DXA image was reanalyzed by TBS iNsight® ver. 3.0.

**Results:** Denosumab significantly increased lumbar BMD ( $0.95 \pm 0.15 \text{ g/cm}^2$  at KTx;  $0.96 \pm 0.15 \text{ g/cm}^2$  at 6 months;  $0.98 \pm 0.16 \text{ g/cm}^2$  at 12 months), and femoral neck BMD ( $0.64 \pm 0.11 \text{ g/cm}^2$  at KTx;  $0.65 \pm 0.11 \text{ g/cm}^2$  at 6 months;  $0.66 \pm 0.12 \text{ g/cm}^2$  at 12 months). However, denosumab did not affect TBS score ( $1.33 \pm 0.07$  at KTx;  $1.33 \pm 0.08$  at 6 months;  $1.33 \pm 0.07$  at 12 months). Denosumab also decreased bone-specific alkaline phosphatase (BAP) and tartrate-resistant acid phosphatase form 5b (TRACP 5b). The change of lumbar TBS was not associated with either change of lumbar BMD, femoral neck BMD or any bone turn over marker.

**Conclusion:** Our results suggest that it seems unlikely that TBS could reflect the efficacy of denosumab better than BMD in early post-KTx patients.

**Disclosures:** Shogo Nakayama, None.

## SA0280

See Friday Plenary Number FR0280.

## SA0281

**Bilirubin and lithocholic acid induce osteocyte damage which may partially explain the development of osteoporosis in cholestatic disease.** Silvia Ruiz-Gaspá<sup>\*</sup>, Núria Guañabens, Andres Combaliá, Pilar Peris, Ana Monegal, Albert Parés. Liver and Metabolic Bone Diseases Units, Hospital Clínic, IDIBAPS, CIBERehd, University of Barcelona, Barcelona, Spain, Spain

Osteoblasts and osteoclasts are the cells involved in bone remodeling, which contribute significantly to the development of osteoporosis. However, little information is available on osteocytes, cells derived from osteoblasts, which play an important role in the regulation of bone remodeling. The influence of cholestasis on osteocytes, the most ubiquitous cells of the skeleton, is little known. Therefore, the aim of the study was to analyze the effect of increased molecules of cholestasis, such as bilirubin (Bil) and lithocholic acid (LCA), and the potential protective effect of ursodeoxycholic acid (UDCA) on the osteocyte function.

MLO-Y4 and MLO-A5 osteocyte lines treated at different times and concentrations with Bil, LCA, UDCA and serum from patients with normal and high bilirubin were used to determine: 1) Viability: WST colorimetric method; 2) Differentiation: quantification of alkaline phosphatase (ALP) activity; 3) Mineralization: Alizarin red staining quantification; and 4) Apoptosis: quantification of DNA fragmentation and caspase-3 activity.

LCA (100mM) and Bil (50mM) significantly decreased viability in MLO-Y4 from 72 hours (10%) and 48 hours (11%), respectively ( $p \leq 0.01$ ), and Bil decreased viability (49%) in MLO-A5 from 96 hours ( $p < 0.01$ ). High bilirubin serum also decreased viability (56%). Bil decreased ALP activity by 47% after 96 hours, under conditions of differentiation in MLO-Y4 ( $p \leq 0.01$ ). After 14 days, Bil was associated with a significant mineralization decrease, as high as 87%, in MLO-A5 ( $p \leq 0.02$ ). Moreover, Bil and LCA increased apoptosis in MLO-Y4, determined by DNA fragmentation (242% and 119%, respectively) and caspase 3 activity (190% and 251%, respectively) ( $p \leq 0.01$ ) after 24 hours. In contrast, in cells cultured with fetal bovine serum or serum from cholestatic patients treated with UDCA (100mM) increased viability after 72 hours (11%) and decreased the deleterious effects of LCA or Bil ( $p \leq 0.02$ ). UDCA increased ALP activity in MLO-Y4 after 72 hours under growth conditions ( $p = 0.018$ ), and after 24 hours under differentiation conditions ( $p \leq 0.01$ ).

Bilirubin and lithocholic acid have damaging consequences on osteocytic cells decreasing viability, differentiation and mineralization, and increasing apoptosis, effects

that are neutralized by the UDCA. These results indicate that substances retained in cholestasis impair osteocyte functions, and therefore may be involved in the pathogenesis of osteoporosis in cholestatic diseases.

**Disclosures:** Silvia Ruiz-Gaspá, None.

## SA0282

See Friday Plenary Number FR0282.

## SA0283

**The role of Trabecular Bone Structure Analysis in predicting Incidental Fractures in Rheumatoid Arthritis.** Ikuko Tanaka<sup>\*</sup><sup>1</sup>, Motokazu Kai<sup>2</sup>, Kunikazu Ogawa<sup>2</sup>, Shigenori Tamaki<sup>1</sup>, Mari Ushikubo<sup>3</sup>, Keisuke Izumi<sup>4</sup>, Kumiko Akiya<sup>3</sup>, Hisaji Oshima<sup>3</sup>. <sup>1</sup>Nagoya Rheumatology Clinic, Japan, <sup>2</sup>Mie Rheumatology Clinic, Japan, <sup>3</sup>Tokyo Medical Center, Japan, <sup>4</sup>Tokyo Medical Center, Jersey

**Background and purpose)** Rheumatoid Arthritis (RA) is known to cause the secondary osteoporosis. Recently, Trabecular Bone Structure (TBS) has been developed as a novel biomarker for evaluating primary osteoporosis. The purpose of this study was to clarify a role of TBS in RA induced secondary osteoporosis.

**Subjects and Methods)** Patients with Rheumatoid Arthritis at NAGOYA & MIE Rheumatology Clinic was subjected to this one-year longitudinal cohort study. The number of subjects was 120 (female 110; age 65±15 (mean ± SD); prednisolone (PSL) dosage at base line 3.8±2.8 mg/day; prevalent vertebral fracture (Genant, H. 1996) 20.7%). Lumbar bone mineral densities (L-BMD) were measured with Horizon (HOLOGIC). TBS values were calculated with TBS (medimaps). Incident vertebral fractures were analyzed with XP at thoracic and lumbar spines. Medications during this study were bisphosphonates (65%), denosumab (10%), and weekly teriparatide (10%).

**Results)** 1) The value of L-BMD (%Young Adult Mean; %YAM) at the base line was 81.5±10.6%, and that of TBS was 1.268±0.107. The rate of incident fractures during the follow-up period was 7.1%. 2) TBS was significantly c logistic regression analysis revealed that incident fractures could be predicted (87.1%) with L-BMD (per 5% decrease; OR 1.32; 95%CI 1.08-1.81;  $p < 0.01$ ), daily prednisolone dosages (per 1mg/day increase 1.17; 1.10-1.81;  $p < 0.01$ ), and the prevalent fractures (3.63; 1.33-9.89;  $p < 0.02$ ). When TBS data were added to the logistic regression analysis, TBS (1.78; 1.10-2.86;  $p < 0.02$ ) was extracted instead of L-BMD.

**Conclusions)** TBS analysis of the lumbar spine DXA data might be useful for prediction of incident fractures in Rheumatoid Arthritis.

**Disclosures:** Ikuko Tanaka, None.

## SA0284

**Risk factors for reduced bone mineral density in patients with rheumatoid arthritis.** Jun Hashimoto<sup>\*</sup><sup>1</sup>, Shoichi Kaneshiro<sup>2</sup>, Yoshio Nagayama<sup>3</sup>, Hideki Tsuboi<sup>2</sup>. <sup>1</sup>Osaka Minami Medical Center, Japan, <sup>2</sup>Osaka Rosai Hospital, Japan, <sup>3</sup>Nagayama Rheumatic/Orthopaedic clinic, Japan

**Objectives;** To evaluate risk factors for reduced bone mineral density (BMD) in patients with rheumatoid arthritis.

**Methods;** We examined 131 RA patients who were measured BMD at proximal femur using DXA (GE Healthcare PRODIGY) and performed a cross-sectional study between two groups; group(A), young adult mean (YAM) less than 70% and group(B), YAM above 70%. We investigated the factors which affected the BMD in RA patients among age, gender, body mass index (BMI), disease duration, RA disease classification (Steinbrocker classification), RA disease activity (patient VAS score, DAS 28-CRP, SDAI, the number of tender joints and swollen joints, CRP, MMP-3) and medications (MTX, biological agents, steroid) against RA.

**Results;** Among 131 patients, 67 cases were divided into group A and 64 cases into group B respectively. The average age was 74.5 ± 72.2 in group A, 69.8 ± 54.5 in group B ( $P = 0.001$ ). BMI was 20.0 ± 9.6 in group A, 22.6 ± 8.0 in group B ( $P < 0.001$ ). Disease stage was 2.67 ± 0.86 in group A, 2.33 ± 1.02 in group B ( $P = 0.04$ ). Disease class was 2.30 ± 0.45 in group A, 1.88 ± 0.37 in group B ( $P < 0.001$ ). Patient VAS score was 26.4 ± 455 in group A, 18.7 ± 353 in group B ( $P = 0.03$ ). There were significant differences between reduced BMD and those factors, however, there were no significant differences in gender, duration of disease, DAS 28-CRP, SDAI, tender joints, swollen joints, CRP, MMP-3, steroid dosage, use of biological products and MTX dosage.

**Conclusion;** In RA patients, elderly, low BMI, advanced stage/class and high level of patient VAS score were considered risk factors of reduced BMD.

**Disclosures:** Jun Hashimoto, None.



## SA0285

**Efficacy and safety of denosumab on post-kidney transplantation recipients.** Yasumasa Yoshino<sup>1</sup>, Shogo Nakayama<sup>1</sup>, Izumi Hiratsuka<sup>1</sup>, Megumi Shibata<sup>1</sup>, Taihei Ito<sup>2</sup>, Hitomi Sasaki<sup>3</sup>, Midori Hasegawa<sup>4</sup>, Ryoichi Shiroki<sup>3</sup>, Takashi Kenmochi<sup>2</sup>, Yukio Yuzawa<sup>4</sup>, Kiyotaka Hoshinaga<sup>3</sup>, Atsushi Suzuki<sup>1</sup>. <sup>1</sup>Division of Endocrinology and Metabolism, Department of Internal Medicine, Fujita Health University, Japan, <sup>2</sup>Department of Organ Transplant Surgery, Fujita Health University, Japan, <sup>3</sup>Department of Urology, Fujita Health University, Japan, <sup>4</sup>Division of Nephrology, Department of Internal Medicine, Fujita Health University, Japan

**Background:** Post kidney transplantation (KTx) patients are known to have high fracture risk especially during first year after KTx mainly due to immunosuppression therapy such as glucocorticoid. Bisphosphonate (BP) should be first-line drug for glucocorticoid-induced osteoporosis. However, the safety of BPs in the patients with chronic kidney disease is concerned, because BP might be some burden to the kidney function. Denosumab could be another candidate to prevent osteoporotic fracture, but its efficacy and safety after KTx is still uncertain. In the present study, we explored the efficacy and safety of denosumab during first year after KTx.

**Methods:** This observational study was done in Fujita Health University Hospital, and post-KTx patients were recruited (n=38, M/F=30/8, age 51 ± 21 years old) from 2014 to 2016. Among them, denosumab was administered twice during first year after KTx in 31 cases. The patients in denosumab-treated (Dmab) group took 0.25-1.0 mg/day of alfacalcidol or 400 IU/day of cholecalciferol.

**Results:** Among Dmab group, one male patient had stopped the treatment because of tuberculosis. The bone fracture was found in 2/31 cases in Dmab group, while 1/8 cases in control group. Lumbar and femoral neck BMD significantly increased in Dmab group, while femoral neck BMD decreased in the control group. Serum creatinine levels in Dmab group were stable as those in control group. There was no patient who suffered from clinical hypocalcemia.

**Conclusion:** Our results suggest that the treatment with denosumab would be safe and effective in post KTx patients.

**Disclosures:** Yasumasa Yoshino, None.

## SA0286

See Friday Plenary Number FR0286.

## SA0287

See Friday Plenary Number FR0287.

## SA0288

**Patients without prior zoledronic acid (ZOL) infusion show increased Trabecular Bones Score (TBS) after one year on denosumab (Dmab).** Mohammed Almohaya<sup>1</sup>, Naveen Sami<sup>2</sup>, Stephen Robertson<sup>2</sup>, David Kendler<sup>3</sup>. <sup>1</sup>King Fahad Medical City, Saudi Arabia, <sup>2</sup>Prohealth clinical research, Canada, <sup>3</sup>University of British Columbia, Canada

TBS is an indicator of vertebral architecture, independently predictive of fracture in treatment naïve patients. There are limited data concerning TBS utility in following patients on osteoporosis therapies. We retrospectively reviewed consecutive patients at an osteoporosis referral center either treatment naïve or after ZOL who were switched to Dmab. Lumbar spine (LS) DXA Bone Mineral Density (BMD) and TBS were measured at baseline and one year after switching to Dmab.

We studied 205 patients (176 females, 29 males). Their mean age was 65 years. Of them, 106 were treatment naïve and 99 patients had had prior ZOL, within the past 18 months. In the treatment naïve group, LS BMD increased 5.1% (0.709 g/cm<sup>2</sup> increasing to 0.747 g/cm<sup>2</sup>, p=0.0001). Mean TBS in treatment naïve was 1.303 at baseline, increased by 1.6% after one year (p=0.0007). In patients switched from ZOL, LS BMD increased 3.8% (0.708 g/cm<sup>2</sup> increasing to 0.736 g/cm<sup>2</sup>, p=0.0001); mean baseline TBS was 1.311 and after one year was 1.312 with no significant change (p=0.96). In the entire group, a weak correlation was observed between TBS and BMD (Pearson r=0.30 at baseline and r=0.25 after one year). [In the treatment naïve group there was a weak correlation between TBS and BMD (Pearson r = 0.39 at baseline and r=0.27 after one year). In the ZOL group there was also a weak correlation between TBS and BMD (Pearson r = 0.17 at baseline and r=0.21 after one year).

The weak correlation between TBS and BMD has previously been reported and may indicate the ability of TBS to evaluate bone architecture. We speculate that the improvement in TBS observed in treatment naïve patients may be indicative of architectural changes from filling in open remodelling space in patients with baseline high bone turnover. Prior ZOL would lead to low baseline remodelling with less potential for Dmab to fill in remodelling space and improve bone architecture. The similar improvement in BMD in both treatment naïve and ZOL patients after switching to Dmab may result from different mechanisms; in treatment naïve patients there may be bone formation during the resorption transient and after ZOL, increases in BMD likely relate mostly to increased mineralization.

**Disclosures:** Mohammed Almohaya, None.

## SA0289

**Changes in Bone Mineral Density (BMD): A Longitudinal Study of Osteoporosis Patients.** Sarah Berry<sup>1</sup>, Hao Zhu<sup>1</sup>, Thomas Trivison<sup>2</sup>, Alyssa B. Dufour<sup>1</sup>, John Caloveras<sup>3</sup>, Rich Barron<sup>3</sup>, Elizabeth Samelson<sup>1</sup>. <sup>1</sup>Hebrew SeniorLife, Institute for Aging Research, United States, <sup>2</sup>Hebrew SeniorLife, United States, <sup>3</sup>Amgen, United States

There is increasing interest in defining target BMD T-scores as a goal of osteoporosis drug treatment. However, there is little evidence to support this strategy. While treatments have been shown to improve BMD in clinical trials, less is known about changes in T-scores in clinical practice. We conducted a retrospective cohort study in osteoporosis patients to 1) describe frequency of transitions between T-score categories, and 2) quantify changes in BMD according to drug treatment.

Individuals included all patients from United Osteoporosis Centers (referral center in Gainesville, GA), who had two or more BMD tests at the femoral neck at least 1 yr apart, 1995-2015. We evaluated successive pairs of BMD tests to describe the distribution of transitions between T-score groups. We considered each BMD test as the unit of analysis and used generalized estimating equations to estimate mean change in BMD according to treatment, adjusting for age, sex, height, weight, baseline BMD, fracture, and follow-up time.

We included 1,232 patients (90% women, mean 66+10 yr, 33% prior fracture), who had 4,918 pairs of successive BMD tests. Mean time between BMD tests was 1.2 yr; range, 0.3 to 9.6 yr. Total follow-up time was mean 4.9 +3.3 yr. Mean baseline T-score was -2.04 + 0.87. 61% of participants received an IV bisphosphonate, 55% an oral bisphosphonate 28% denosumab, and 9% received no treatment at some point during the study, and the median number of different therapies was 2 (+1.2) per person.

Frequency of transition to an improved T-score category with a repeat BMD test was 41% when prior T-score ≤ -3.50, 30% for T-score -3.49 to -3.00, and 25% for T-score -2.99 to -2.50 (Table). 59% to 84% of repeat BMD tests remained in the same T-score category, and 9% to 20% of repeat BMD tests were in a lower T-score category. Adjusted mean BMD increased 0.0024 g/cm<sup>2</sup>/yr (95% CI, 0.0001 to 0.0048) with IV bisphosphonates and 0.0058 g/cm<sup>2</sup>/yr (95% CI, 0.0010 to 0.0106) with denosumab.

In clinical practice, we observed that 25% of patients with prior T-score -2.99 to -2.50 may achieve a potential target T-score >2.50 over an average follow-up of 1.2 yr. Additional studies are needed to determine the optimal time to repeat BMD testing and to determine whether therapies that achieve target T-scores reduce fracture risk. Future work considering changes in BMD over longer time periods and treatment persistence will complement the current findings.

	Repeat T-Score						
Prior T-Score	≤ -3.50	-3.49 to -3.00	-2.99 to -2.50	-2.49 to -2.00	-1.99 to -1.50	> -1.50	Total
≤ -3.50	<b>73 (59%)</b>	37 (30%)	9 (7%)	3 (2%)	1 (<1%)	0 (0%)	123
-3.49 to -3.00	36 (9%)	<b>257 (61%)</b>	117 (28%)	9 (2%)	2 (<1%)	0 (0%)	421
-2.99 to -2.50	4 (<1%)	97 (12%)	<b>506 (66%)</b>	188 (23%)	9 (1%)	4 (<1%)	808
-2.49 to -2.00	1 (<1%)	1 (<1%)	158 (12%)	<b>886 (68%)</b>	236 (18%)	12 (1%)	1,297
-1.99 to -1.50	2 (<1%)	2 (<1%)	7 (<1%)	219 (19%)	<b>747 (65%)</b>	175 (15%)	1,152
> -1.50	0 (0%)	0 (0%)	2 (<1%)	10 (<1%)	171 (15%)	<b>934 (84%)</b>	1,117
Total	116	397	799	1,315	1,166	1,125	4,918

Table

**Disclosures:** Sarah Berry, Amgen, Grant/Research Support.

## SA0290

See Friday Plenary Number FR0290.

## SA0291

**Retrospective-prospective Observational Study in rEal life treatment in Mexican patients with denosumAb queRY database.** Fidencio Cons<sup>1</sup>, Salomon Jasqui<sup>2</sup>, Carlos Salinas<sup>3</sup>, Amador E Macias<sup>4</sup>, Alfonso J Zarain<sup>5</sup>, Alfredo Reza<sup>6</sup>, Hugo D Pena<sup>7</sup>, Jorge Morales<sup>8</sup>, Lucio J Balcazar<sup>9</sup>, Jaime Elizondo<sup>10</sup>, Pilar de la Pena<sup>11</sup>. <sup>1</sup>Centro Investigacion Artritis y Osteoporosis, Mexico, <sup>2</sup>Clinica Osteoporosis Dr. Salomon Jasqui, Mexico, <sup>3</sup>Clinica Menopausia Dr. Carlos Salinas Dorantes, Mexico, <sup>4</sup>Centro Medico San Francisco, Mexico, <sup>5</sup>Centro de Clinaterio y Osteoporosis, Mexico, <sup>6</sup>Clinica Osteoporosis Dr. Alfredo Reza, Mexico, <sup>7</sup>Centro Diagnostico de Osteoporosis, Mexico, <sup>8</sup>Hospital Aranda de la Parra, Mexico, <sup>9</sup>Hospital Regional "Dr. Manuel Cárdenas de la Vega", Mexico, <sup>10</sup>Centro de Investigación Clínica, Mexico, <sup>11</sup>Clinica de Osteoporosis Dra. Pilar de la Pena, Mexico

**Purpose.** DMAb has been available in Mexico since Feb 2012 for the treatment of postmenopausal osteoporosis (PMOp). Understanding real-world effectiveness is of interest as patient populations may be more heterogeneous. We are reporting the Mexican experience in the treatment of PMOp with DMAb

**Methods.** This is a 48-month, multicenter, retrospective-prospective descriptive cohort study in Mexico. We create a database registry (web based) to collecting data from 11 different osteoporosis care centers from private practice. Primary indications for DMAb use, prior treatment, history of fractures (Fxs), yearly DXA scans at the same anatomical site lumbar spine (LS), femoral neck (FN) and total hip (TF) were

recorded. The 10-year probability of hip Fx and major osteoporotic Fx using FRAX was calculated at BL.

Results: 504 patients were recorded, age at baseline (BL) was  $67 \pm 12.9$  years old and 75% of them were  $>60$  years. As expected, BMD increased over time (Figure 1). Mean BMD at the LS increased from BL by 4.5, 5.7, 6.9 and 8.1% at years 1, 2, 3 and 4 respectively. At the FN, BMD increased from BL by 2.2, 3.6, 4.8 and 9.4% at years 1, 2, 3 and 4 respectively. At the TF, BMD increased from BL by 1.4, 4.3, 6.4 and 9.4% at year 1, 2, 3 and 4 respectively. Patients presented different levels of risk of Fx at baseline. The mean of 10-year probability of Fx using FRAX shows at baseline  $8.5 \pm 5.8$  for Major Osteoporotic Fx and  $2.8 \pm 3.4$  for Hip Fx using Mexican adjusted values at <http://www.shef.ac.uk/FRAX/>. Previous Fxs was present in 75 (14.8%) patients, 21 (4.1%) patients with  $>1$  Fx, and 410 (81.3%) patients without previous Fxs. Also, 16 (3.1%) patients developed Fxs during DmAb treatment with 9 (1.7%) at least 1 Fx and 7 with  $>1$  Fxs (1.3%). Secondary effects was reported in 9 (1.7%) of patients with skin rash (3) bone pain (2) blood pressure increase (1) tingling in legs (1) oral ulcers (1) and thrombocytopenia (1).

Conclusions. DmAb improved BMD in most patients in a real-world setting. Moreover, the changes observed in routine clinical practice were similar to the efficacy achieved in DmAb clinical trials. The clinical profile of Mexican PM women with Op using DmAb are similar to other populations and DmAb has shown to be as safe as it was shown in clinical registration studies.

This study received funding from: Amgen Inc.

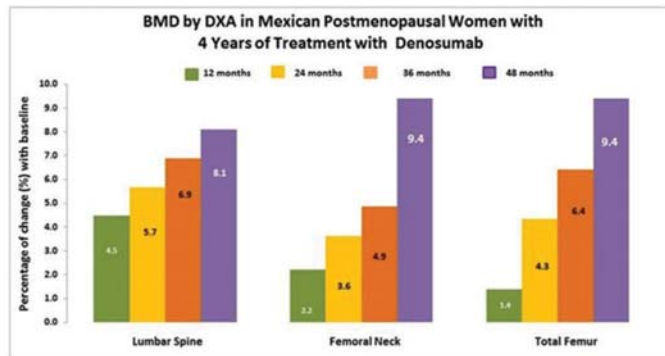


Figure 1

Disclosures: Fidencio Cons, None.

## SA0292

See Friday Plenary Number FR0292.

## SA0293

See Friday Plenary Number FR0293.

## SA0294

**The effect of once-weekly teriparatide administration on prevention of vertebral collapse in new thoracolumbar vertebral fractures – T-WRAP prospective randomized controlled study.** Satoshi Ikeda\*. Ken-Ai Memorial Hospital, Orthopedic Surgery, Japan

**Introduction:** Vertebral fracture often occurs in thoracolumbar region. It leads to kyphotic deformity and often causes delayed union. It is important to prevent vertebral collapse and achieve early fusion. The aim of this study is to examine the effect of once-weekly teriparatide on the vertebral collapse prevention and delayed union in new thoracolumbar vertebral fractures in comparison with once-weekly alendronate. In addition, we examined the characteristics between two agents for bone strength. **Methods:** This prospective randomized controlled study was conducted at twenty-five hospitals and clinics. Seventy-six patients with new thoracolumbar vertebral (T10-L2) fractures within 7 days from injury were randomized to either once-weekly teriparatide injection (TPID: 56.5µg/week, n = 40) or alendronate (ALN: 35mg/week, n = 36) group. Vertebral anterior height (A), middle height (C), and posterior height (P) were measured at 0, 1, 2, 4, 8, and 12 weeks. A/P, C/P, wedge angle (WA), and kyphosis angle (KA) both sitting and lying position were calculated at each time point. Moreover, delayed union was detected at 12 weeks. In addition, visual analog scale (VAS) and EQ-5D were measured at 0, 1, 2, 4, 8, and 12 weeks. **Results:** A/P and C/P were gradually decreased after injury. WA and KA were increased in both groups until 12 weeks. A/P and C/P on lying position in TPID group showed significantly higher values in comparison with those in ALN group ( $p < 0.05$ ). Delayed union rate did not differ between both groups (TPID: 28.3%, ALN: 35.9%). VAS value was decreased in both groups, but there was no significant difference between both groups. EQ-5D in TPID group showed significantly higher value in comparison with that in ALN group at 12 weeks ( $p < 0.05$ ). Change ratio of A/P and C/P depended on baseline lumbar BMD in ALN group ( $p < 0.01$ ), but did not in TPID group. We divided the subjects into three subgroups (higher, middle, and lower) based on baseline lumbar BMD and compared A/P and C/P between both groups. In the lower subgroup of baseline lumbar BMD, A/P and C/P in TPID group showed

significantly higher value in comparison with those in ALN group ( $p < 0.05$ ). **Conclusion:** In the patients with new thoracolumbar vertebral fractures, the effect of once-weekly teriparatide administration on the prevention of vertebral collapse did not depend on baseline lumbar BMD, especially in the lower subgroup of baseline lumbar BMD.

Disclosures: Satoshi Ikeda, None.

## SA0295

See Friday Plenary Number FR0295.

## SA0296

**Effects of 1-year treatment of anti-resorptive agents on trabecular bone score and hip geometry.** Ji Hyun Lee\*, Kyoung Min Kim<sup>1</sup>, Young Ji Kim<sup>1</sup>, Sunghwan Suh<sup>2</sup>, Su Jin Lee<sup>3</sup>, Sang Wan Kim<sup>4</sup>, Chan Soo Shin<sup>5</sup>. <sup>1</sup>Seoul National University Bundang Hospital and Seoul National University College of Medicine, Korea, Republic of, <sup>2</sup>Dong-A University Medical Center, Dong-A University College of Medicine, Korea, Republic of, <sup>3</sup>Division of Endocrinology, Department of Internal Medicine, National Health Insurance Service Ilsan Hospital, Korea, Republic of, <sup>4</sup>Boramae Hospital and Seoul National University College of Medicine, Korea, Republic of, <sup>5</sup>Seoul National University Hospital and Seoul National University College of Medicine, Korea, Republic of

**Objective** The effects of anti-resorptive agents on trabecular bone score (TBS) and hip geometry is unclear. The aim of this study was to investigate the effect of 1-year treatment of anti-resorptive agents on TBS and hip geometry in postmenopausal women with osteoporosis.

**Methods** We conducted a retrospective study including postmenopausal osteoporotic women who had performed annual dual-energy X-ray absorptiometry (DXA) evaluations at baseline and 1-year follow up. Bone mineral density (BMD)s, were measured using DXA (Hologic, discovery W). Each image from DXA were further analyzed using TBS iNsight for evaluating TBS values and APEX for measuring hip geometric parameters

**Results** A total of 247 women were finally included, 106 women who had not used any anti-resorptive drugs (No treatment-group), 44 women who had been treated with selective estrogen receptor modulators (SERMs, SERM-group), and 97 women who had been administered bisphosphonates (BPP-group) for 1 years. After adjustment for age and body mass index (BMI), baseline lumbar spine (LS)-BMD was significantly lower in BPP-group compared to No treatment-group or SERM-group. TBS and hip geometry were not different among the groups after adjusting for age, BMI, and total hip (TH) BMD. After 1-year treatment, changes in LS-BMD were significantly greater in BPP-group compared to No treatment-group or SERM-group, reaching +5.4% (in BPP-group) vs. +1.4% (in No treatment-group) vs. +1.8% (SERM-group) ( $P < 0.0001$ , respectively). In changes of TBS values after 1-year treatment, BPP-group provided significantly greater increment of TBS values compared to those of No treatment-group or SERM-group ( $1.7 \pm 4.2\%$  in BPP-group,  $-1.1 \pm 5.1\%$  in SERM group, and  $-0.6 \pm 5.7\%$  in No-treatment group,  $P < 0.001$ ). The proportion of subjects who showed reduction in TBS values of 5% or more was significantly lower in BPP-group compared to No treatment-group or SERM-group (4.1% in BPP group, 20.5% in SERM-group, and 13.2% in No treatment-group,  $P < 0.05$ ). Regarding the changes in hip geometric parameters, BPP-group also provided significantly greater increases in cross sectional area (CSA) and cortical thickness compared to those of other two groups group (CSA,  $2.1 \pm 8.0\%$  in BPP-group,  $-0.2 \pm 5.1\%$  in SERM-group, and  $0.01 \pm 4.91\%$  in No treatment-group; cortical thickness,  $1.2 \pm 8.8\%$  in BPP group,  $-1.9 \pm 5.9\%$  in SERM-group, and  $-1.1 \pm 6.0\%$  in No treatment-group,  $P < 0.05$ , respectively). The proportion of subjects who showed gain in CSA values of 5% or more was significantly higher in BPP-group compared to the other two groups (35.1% in BPP group, 6.8% in SERM-group, and 13.2% in No treatment-group,  $P < 0.05$ ).

**Conclusion** BPP treatment for one year showed beneficial effects on BMD and bone geometric parameters as well. Further longitudinal studies are needed to better clarify the differential effects of each anti-resorptive agents on TBS and hip geometry.

Disclosures: Ji Hyun Lee, None.

## SA0297

**Effect of Bisphosphonate and Teriparatide on Vertebral Bone Microarchitecture and Strength *In Vivo* Assessed by Clinical Computed Tomography.** Taro Mawatari<sup>1</sup>, Koichiro Kawano<sup>1</sup>, Shinkichi Arisumi<sup>1</sup>, Muneyuki Takahashi<sup>1</sup>, Satoshi Ikemura<sup>2</sup>, Satoshi Hamai<sup>2</sup>, Gen Matsui<sup>1</sup>, Takahiro Iguchi<sup>1</sup>, Hiroaki Mitsuvasu<sup>1</sup>, Shinya Kawahara<sup>1</sup>, Yasuhiro Nakashima<sup>2</sup>. <sup>1</sup>Hamanomachi Hospital, Japan, <sup>2</sup>Kyushu University, Japan

**Purpose:** Both anti-resorptives such as bisphosphonates and osteoanabolic agents increase bone mineral density (BMD) and reduce fracture risk, while underlying mechanisms are different. The purpose of this study was to clarify the effect of minodronate (MIN) and daily teriparatide (TPID) in vivo on the vertebral microarchitecture and strength estimated by finite element analysis (FEA).

**Methods:** MIN-treated (n=10,  $67.0 \pm 2.9$ yo) female osteoporosis patients, non-treated age-matched historical control (n=10,  $67.0 \pm 9.9$ yo), and TPID-treated (n=10,



69.6±8.3yo) female severe osteoporosis patients were retrospectively evaluated. Areal BMD (aBMD) scanned by DXA, and 3D data of 3<sup>rd</sup> lumbar spine scanned by quantitative computed tomography (qCT) at a spatial resolution of 351 x 351 x 500µm were repeatedly evaluated at baseline and 1 year later. Bone volume fraction (BV/TV), trabecular thickness (Tb.Th), trabecular number (Tn.N), and connectivity density (CD) were calculated by custom-made software. In addition, vertebral fracture load defined as the vertebral strength index was estimated by FEA (Mechanical Finder, Tokyo, Japan).

Results: After 1 year, non-treated control lost -2.9% of aBMD, the MIN group gained 6.3%, and the TPTD group gained 7.7%, while BV/TV changed -14.6%, +15.3%, and +73.3% respectively. Tb.Th and Tn.N in non-treated control were severely decreased over 1-year period (-4.7%, -10.0%, respectively), whereas MIN could reverse changes (+5.5%, +9.2%, respectively), and TPTD could further increase those parameters (+15.23%, +47.9%, respectively). CD, however, could be only improved by TPTD (-27.9%, -3.2%, and +57.8%, respectively). FEA revealed severe strength loss in the non-treated control and gain in the MIN and TPTD groups (-15.3%, +10.0%, and +49.9%, respectively).

Conclusions: In spite of the limited image resolution of clinical MDCT and limited number of cases, our *in vivo* human analysis could provide noninvasive assessment of trabecular bone microarchitecture. Our results indicate that evaluation of aBMD by DXA would underestimate both changes in bone microarchitecture and strength. Despite the apparent increase in bone volume by MIN, it might be difficult to restore trabecular connectivity. In order to prevent connectivity loss, earlier therapeutic intervention would be necessary before the connectivity has been lost, and TPTD might be able to re-establish connectivity.

**Disclosures:** Taro Mawatari, None.

## SA0298

See Friday Plenary Number FR0298.

## SA0299

See Friday Plenary Number FR0299.

## SA0300

See Friday Plenary Number FR0300.

## SA0301

See Friday Plenary Number FR0301.

## SA0302

See Friday Plenary Number FR0302.

## SA0303

See Friday Plenary Number FR0303.

## SA0304

**Teriparatide regains the bone of the patients who has failed in bisphosphonate therapy.** Katsuya Kanesaki<sup>\*1</sup>, Shinya Tanaka<sup>2</sup>, Hiromi Oda<sup>2</sup>. <sup>1</sup>Nagata orthopedic hospital, Japan, <sup>2</sup>Saitama medical university, Japan

The anti-bone-resorption drugs are used as a master drug for osteoporosis. According to the concept of goal-directed-treatment, there is need to change drug to another one when patient has fracture or does not increase in BMD during the therapy. Although the change from bisphosphonate to teriparatide is expected to increase in bone volume and improve bone structure, it is not easy to detect it by DXA. The objective of this study is to clarify the usefulness of the teriparatide to patients who had been failed in bisphosphonate therapy, by tracking the change of the BMD value from teriparatide to an anti-resorption drug after teriparatide.

This study was performed retrospectively. Patients who had changed from bisphosphonate to teriparatide and had changed again to anti-resorption drugs, bisphosphonates or denosumab, were included. The periods of the observation were 6, 12, 18, 24, 30 months after the start of teriparatide therapy and the rates of increases in BMD at lumbar spine and femoral neck at each points were recorded. The daily injection of teriparatide 20 µg / d had been continued for 2 years (dTPTD group; n = 15) and the weekly injection of teriparatide 56.5 µg / w had been continued for 1.5 years (wTPTD group; n = 11).

The increases of BMD values at lumbar spine in dTPTD group were 6.3% at 6 months, 5.9% at 12 months, 6.9% at 18 months, 8.81% at 24 months and 9.73% at 30 months (6 months after re-changing from teriparatide to anti resorption drugs). The increases at femoral neck were -1.6%, -0.27%, 4.7%, 6.8% and 3.9%, respectively. The patients in wTPTD group were re-changed therapy from teriparatide to an anti-resorption drug at 18 months. The increases of BMD value at lumbar spine in wTPTD group were 3.7%, 4.4%, 6.7%, 9.0% and 9.0% respectively. The increases at femoral neck were 0.78%, -1.2%, -0.45%, 2.1% and 1.1% respectively.

Conclusion; Both daily and weekly teriparatide followed by an anti-bone-resorption drug is useful for the patients who has had a fracture or has not had increase in BMD during bisphosphonate therapy.

**Disclosures:** Katsuya Kanesaki, None.

## SA0305

See Friday Plenary Number FR0305.

## SA0306

**Acute phase reactions after intravenous infusion of zoledronic acid in Japanese patients with osteoporosis: sub-analysis of the phase III (ZONE) study.** Tatsuhiko Kuroda<sup>\*1</sup>, Masataka Shiraki<sup>2</sup>, Satoko Ueda<sup>3</sup>, Yasuhiro Takeuchi<sup>4</sup>, Toshitsugu Sugimoto<sup>5</sup>, Toshitaka Nakamura<sup>6</sup>. <sup>1</sup>Corporate Research & development, Asahi Kasei Corporation, Japan, <sup>2</sup>Department of Internal Medicine, Research Institute and Practice for Involuntional Diseases, Japan, <sup>3</sup>Medical Affairs, Asahi Kasei Pharma Corporation, Japan, <sup>4</sup>Toranomon Hospital Endocrine Center, Japan, <sup>5</sup>Internal Medicine 1, Shimane University Faculty of Medicine, Japan, <sup>6</sup>Aoba Hospital, Japan

**Purpose** To investigate factors involved in acute phase reactions (APRs) in Japanese patients treated with once yearly intravenous administration of 5 mg zoledronic acid (ZOL) for 2 years, the relation between APRs and clinical parameters was studied.

**Methods** Post-hoc analysis focusing on APRs was performed using the data of the phase III study of zoledronic acid (ZONE study) in Japanese patients with primary osteoporosis. Patients having prior use of bisphosphonate were allowed to participate in the study after washout for more than 2 years. Patients with and those without APRs were compared for baseline characteristics. The change from baseline in bone turnover markers (BTMs) and bone mineral density (BMD) were also investigated and compared.

**Results** A total of 333 and 332 patients received ZOL and placebo, respectively in the ZONE study. In the ZOL group, 51.2% of patients developed APRs after the first infusion, and 12.6% after the second infusion. The mean age was younger in the patient with APRs (p = 0.031). Less patients in those with APRs had taken prior bisphosphonate (p = 0.016). At baseline, in the patients with APRs, significantly lower neutrophil/lymphocyte ratio (NLR; p<0.001), significantly higher levels of serum C-terminal telopeptide of type I collagen degradation products (CTX; p=0.011) and procollagen type I N-terminal propeptide (PINP; p=0.001) were observed. There were no significant differences in serum 25(OH) vitamin D levels at baseline. Stepwise multivariate regression analysis was performed using age, PINP, NLR, and previous bisphosphonate as the candidate variables. Age (p = 0.050), NLR (p = 0.001), and PINP (p = 0.002) were statistically significant, although previous bisphosphonate usage was not (p = 0.082).

Patients with APRs showed significantly higher increases from baseline in total hip BMD at 6 and 12 months compared with those without APRs, although no significant differences were observed in lumbar (L2-4) and femoral neck BMD. In terms of BTMs, patients with APRs demonstrated a significantly greater decrease from the baseline in the levels of CTX, PINP, serum bone specific alkaline phosphatase, and tartrate-resistant acid phosphatase 5b at almost all measurement time points.

**Conclusions** Patient profiles differed significantly for patients with and those without APRs. APRs were correlated to some clinical parameter of ZOL efficacy.

**Disclosures:** Tatsuhiko Kuroda, Asahi Kasei, Other Financial or Material Support.

## SA0307

**24-month follow up of teriparatide treatment in GIOP patients and postmenopausal osteoporosis after bisphosphonate treatment failure.** Vaclav Vyskocil<sup>\*1</sup>, Zuzana Zbozinkova<sup>2</sup>. <sup>1</sup>Charles university hospital, Bone disease center, Czech Republic, <sup>2</sup>Institute of Biostatistics and Analyses, Faculty of Medicine, Masaryk University, Czech Republic

The authors observed 109 patients treated with teriparatide (rh-PTH 1-34) out of which 70 were treated for GIOP (64.2%), 32 for postmenopausal osteoporosis bisphosphonate treatment failure (34.9%) and 1 (0.9%) for men osteoporosis. Patients were treated by a once-daily subcutaneous injection of 20 µg of teriparatide and with 600 mg calcium carbonate and 400 IU vitamin D.

There were 87 females (79.8%) and 22 males (20.2%). BMD of total hip, femoral neck, spine was measured at the beginning and after 6, 12, 18, and 24 months follow up. Vitamin D, sCa, uCa, PINP were measured at the same time interval. There were 37.6% of patients with at least single fracture at the beginning of the observation.

There were 2 patients with osteoporotic fractures during follow up. The first patient experienced 1 and the second patient experienced 2 fractures.

Statistical significance was evaluated by p value, statistical significance of differences in time by Wilcoxon pair test.

Statistically significant difference (p < 0.001) in vitamin D and sCa levels was achieved only after 6 months of observation. Despite of high compliance to treatment only 50 patients came to final blood and DXA testing, which is less than half of the original group.

Age (years)	
Median	64.4
5th percentile	40.8
95th percentile	80.7

Statistic

Disclosures: Vaclav Vyskocil, None.

## SA0308

**Cortical and trabecular compartments behavior in patients under bone treatments using 3D parameters obtained from DXA.** Renaud Winzenrieth<sup>\*1</sup>, Silvana Di Gregorio<sup>2</sup>, E. Bonel<sup>2</sup>, Ludovic Humbert<sup>1</sup>, M. Garcia<sup>2</sup>, Luis Del Rio<sup>2</sup>. <sup>1</sup>Galgo Medical, Spain, <sup>2</sup>CETIR Grup Mèdic, Spain

**Purpose:** The objective of the study was to assess longitudinal changes of different osteoporosis treatments on areal BMD and in volumetric BMD (integral, trabecular and cortical) and cortical thickness – as assessed using 3D reconstruction from DXA- at the proximal femur.

**Method:** We retrospectively analyzed 161 patients. We stratified the cohort by treatments: Naive of treatment (Naive, n=43), Alendronate (AL, n=54), Denosumab (Dmb, n=33) and PTH (n=31). From femoral DXA acquisition, in addition to areal BMD at total femur (aBMDTot) and at the neck (aBMDFN), volumetric trabecular and volumetric cortical BMDs (vBMDTrab & vBMDCort) as well as the average cortical thickness (CTh) were assessed using 3D DXA software (Galgo Medical, Spain). The follow-up changes from baseline were normalized at 24 months and evaluated in terms of percentage and in SD variations to normalize parameters. Paired tests were used to compare parameters at the end of the follow-up and at baseline.

**Results:** After 24 month (as presented table below), a non-significant decrease was observed for aBMDTot, aBMDFN and vBMDTrab (-0.55, -0.50 & -0.46%) in the naive group while a non significant increase was observed for vBMDCort and CTh parameters (+0.48 and +1.12%). Compared to baseline, significant improvement (p<0.001) have been observed in CTh (4.99 & 5.4%) and in vBMDTrab (5.7 & 6.9%) and vBMDCort (2.34 & 2.22%) as well as at aBMDTot (2.11 & 3.4%) for AL and Dmb treatment respectively. For PTH, a significant increase of 2.3% has been observed at aBMDFN only. This increase seems to be related to a trabecular increase as expressed by a borderline no significant vBMDTrab increase of 3.2% (p=0.052). It has been also observed a non significant decrease (-0.05%) of vBMDCort in these patients.

**Conclusion:** As expected, no changes have been observed in the naive group after 24 months of follow-up. As expected, significant increases were observed in both cortical and trabecular compartments in patients treated with AL and Dmb while an increase (trend) has been observed only in the trabecular compartment in patient under PTH. Further studies are needed to confirm these promising results.

	Treatments			
	Naive (n=43)	AL (n=54)	Dmb (n=33)	PTH (n=31)
Age (yrs)	61.8±9.2	62.2±6.5	66.4±7.3	69.2±8.3
BMI (kg/m <sup>2</sup> )	26.6±4.0	23.3±3.6	23.0±4.5	25.3±3.4
Changes observed after 24 months expressed in %±SEM (SD variation)				
Volumetric trabecular BMD	-0.46±1.04 (-0.03)	5.7±1.38 (0.19)**	6.9±2.4 (0.19)**	3.2±2.7 (0.11)
Volumetric cortical BMD	0.48±0.27 (0.06)	2.34±0.30 (0.47)**	2.22±0.48 (0.44)**	-0.05±0.63 (-0.008)
Average Cortical thickness	1.12±0.46 (0.01)	4.99±0.62 (0.04)**	5.4±0.37 (0.04)**	0.48±1.0 (0.008)
BMD at neck	-0.55±0.58 (-0.04)	1.12±0.34 (0.07)	3.0±0.33 (0.17)	2.3±1.05 (0.11)*
BMD at total Femur	-0.50±0.44 (-0.03)	2.11±0.49 (0.15)**	3.4±0.60 (0.22)**	0.99±1.11 (0.06)

Significant difference from baseline: \* p&lt;0.05, \*\* p&lt;0.001

Table

Disclosures: Renaud Winzenrieth, Galgo Medical, Other Financial or Material Support.

## SA0309

**Trabecular bone score and hip structural analysis in patients with atypical femoral fractures.** Sanne Buitendijk<sup>\*1</sup>, Denise van de Laarschot<sup>1</sup>, Sandra Smits<sup>1</sup>, Fjorda Koromani<sup>1</sup>, Fernando Rivadeneira Ramirez<sup>2</sup>, Thomas Beck<sup>3</sup>, M. Carola Zillikens<sup>1</sup>. <sup>1</sup>Bone Center, Erasmus MC, Netherlands, <sup>2</sup>Epidemiology, Erasmus MC, Netherlands, <sup>3</sup>Beck Radiological Innovations, United States

Bisphosphonate (BP) use has declined dramatically in recent years, partly because of fear of rare side effects like atypical femoral fractures (AFFs). It is therefore desirable to have a diagnostic method to identify those at risk of AFF in order to prevent this serious

complication. We compared trabecular microarchitecture and hip geometry between 30 patients with AFF and 141 controls of similar age and sex, using BPs. Trabecular Bone Score (TBS) and hip structural analysis (HSA) were used to assess trabecular microarchitecture and macroscopic hip geometry from DXA images of the lumbar spine and hip, respectively. General characteristics, TBS and HSA were compared between AFF patients and controls using student T-tests and chi-square statistics. Bone mineral density (BMD), TBS and HSA were corrected for confounders with analysis of covariance. AFF patients had significantly higher BMI than controls, had used BP longer and glucocorticoids and proton pump inhibitors more frequently. BMD T-score was significantly higher in AFF patients at the lumbar spine (p<0.001), but borderline at the femoral neck (p=0.050). TBS did not differ significantly between AFF patients and controls. Also, HSA at the femur shaft nor neck shaft angle differed between AFF patients and controls. At the narrow neck, AFF patients had lower endocortical diameter, lower buckling ratio and higher centroid position, consistent with a lower risk of classical fragility hip fractures. These findings, as well as higher BMD might be explained by the fact that the majority of AFF patients used BP to prevent glucocorticoid-induced osteoporosis. Based on our results, TBS and HSA do not appear to have value in detecting patients at risk of AFF.

Disclosures: Sanne Buitendijk, None.

## SA0310

See Friday Plenary Number FR0310.

## SA0311

**Serum exosome-mediated resistance to the intracrine actions of 25-hydroxy-vitamin D in human macrophages.** Rene Chun<sup>\*1</sup>, Carter Gottlieb<sup>1</sup>, Kathryn Zavala<sup>1</sup>, Albert Shieh<sup>2</sup>, Andrea Salinas<sup>1</sup>, Vahe Yacoubian<sup>1</sup>, Samya Konda<sup>1</sup>, Martin Hewison<sup>3</sup>, Philip Liu<sup>1</sup>, John Adams<sup>4</sup>. <sup>1</sup>Department of Orthopaedic Surgery, University of California, Los Angeles, United States, <sup>2</sup>Department of Medicine, University of California, Los Angeles, United States, <sup>3</sup>University of Birmingham, United Kingdom, <sup>4</sup>Departments of Molecular, Cell and Developmental Biology and Orthopaedic Surgery, University of California, Los Angeles, United States

Adverse disease outcomes and increased mortality in humans are associated with low circulating concentrations of 25-hydroxyvitamin D (25D), not low levels of the intracellularly-active hormone, 1,25-dihydroxyvitamin D (1,25D). This suggests that vitamin D-directed bioactions in some target cells are dependent on the cellular uptake of substrate 25D and cell autonomous expression of the CYP27B1- and CYP24A1-hydroxylases and vitamin D receptor (VDR). A good example of such intracrine regulation is the 25D-mediated induction of the antimicrobial cathelicidin (*CAMP*) gene expression in human macrophages. We used serum from age and sex-matched vitamin D-deficient white (n=11), black (n=11) or Hispanic (n=11) donors before and after vitamin D supplementation to raise serum 25D. Each serum sample was used to culture non-autologous, primary human adherent monocyte-macrophages. In vitamin D supplemented serum from white, but not black or Hispanic, donors elevated 25D levels were associated with increased expression of *CAMP* (p<0.001), suggesting that serum from black and Hispanic hosts bestowed resistance to intracrine induction of *CAMP* even in the face of similar levels of extracellular 25D. We theorized that resistance was due to factor(s) in the exosome fraction of serum; exosomes are circulating membrane enveloped microvesicles harboring non-organelle intracellular contents of the parent cell. To explore the possible role of exosomes in 25D resistance, the *CAMP* bioassay was conducted with a subset of black (n=6) and white (n=6) exosome-depleted sera, matched for total 25D level. Exosome-depleted serum from white and black donors significantly increased *CAMP* (p≤0.05) in macrophages. Exosome “add-back” to exosome-stripped serum abolished this increase. This pattern of exosome-mediated resistance was also observed with the *CYP24A1* gene also but not with three other 1,25D-responsive genes in macrophages, *TREMI*, *CDA* and *VDR*. Taken together these data suggest that serum exosomes may participate in trans-regulation of specific 1,25D-VDR responsive genes in human macrophages.

Disclosures: Rene Chun, None.

## SA0312

See Friday Plenary Number FR0312.

## SA0313

See Friday Plenary Number FR0313.

## SA0314

See Friday Plenary Number FR0314.



## SA0315

**Abaloparatide-SC Improved Cortical Bridging and Increased Callus Mass and Strength in a Rat Closed Femur Fracture Model.** Heidi Chandler\*, Allen Pierce, Jeffery Brown, Michael Ominsky, Gary Hattersley, Radius Health Inc, United States

Healing of long bone fractures involves endochondral and intramembranous bone formation, which together form a callus that achieves union, stabilization, and gradual recovery of bone strength. Endogenous PTHrP activates PTH1 receptors (PTH1R) at fracture sites to promote endochondral and intramembranous ossification, and exogenous PTH1R agonists including PTHrP have been shown to enhance fracture healing in animal models. We therefore studied the effects of abaloparatide (ABL), a selective PTH1R agonist, in a rat femur fracture model. Ninety-six 12-week-old male SD rats underwent a closed, internally stabilized fracture of the right femur. Treatment began the next day with daily sc ABL at 5 or 25 µg/kg/d (ABL5 and ABL25, n = 32/dose level) or with daily sc saline (VEH, n = 32). Sixteen rats from each group were necropsied after 4 and 6 weeks of healing, with 12 fractured femurs per group used for micro-CT and biomechanical testing and the other 4 femurs used for micro-CT and histology. Semi-quantitative histologic scoring of cortical bridging across the fracture gap showed significantly greater bridging in the ABL5 and ABL25 groups at week 4 compared with VEH controls. Histomorphometry at week 4 indicated significantly greater callus area in the ABL5 and ABL25 groups, which persisted at week 6 for the ABL25 group, compared to VEH. Micro-CT of fracture calluses showed that the ABL5 and ABL25 groups had significantly greater callus bone volume, bone volume fraction, and BMC at weeks 4 and 6, compared to VEH. Three-point bending tests at week 4 indicated that callus stiffness was 60% and 96% higher in the ABL5 and ABL25 groups, respectively (both p < 0.05 vs VEH). At week 6, callus stiffness was 112% higher in the ABL5 group (p < 0.05 vs VEH). Callus peak load was 77% higher in the ABL25 group at week 4 (p < 0.05 vs VEH), and remained numerically higher in both ABL groups at week 6 compared with VEH. Together these data suggest systemically administered ABL can enhance local healing in a rat closed femur fracture model.

**Disclosures:** Heidi Chandler, Radius Health, Other Financial or Material Support.

## SA0316

See Friday Plenary Number FR0316.

## SA0317

See Friday Plenary Number FR0317.

## SA0318

See Friday Plenary Number FR0318.

## SA0319

See Friday Plenary Number FR0319.

## SA0320

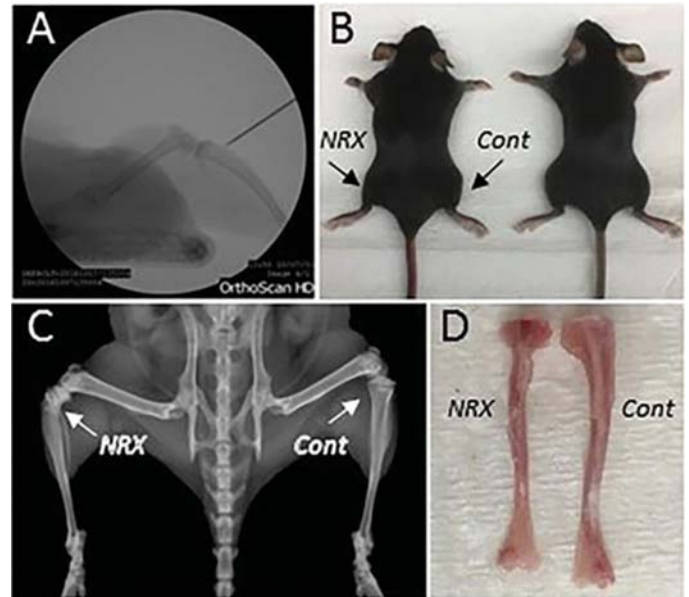
See Friday Plenary Number FR0320.

## SA0321

**Controlling Targeted Bone Growth by Retinoic Acid Receptor Gamma Agonist.** Masatake Matsuoka\*<sup>1</sup>, Kenta Uchibe<sup>2</sup>, Ivan Alferiev<sup>3</sup>, Joshua M Abzug<sup>1</sup>, Min Liu<sup>4</sup>, Motomi Enomoto-Iwamoto<sup>1</sup>, Michael Chorny<sup>3</sup>, Masahiro Iwamoto<sup>1</sup>. <sup>1</sup>Department of Orthopaedics, University of Maryland School of Medicine, United States, <sup>2</sup>Okayama University Graduate School of Medicine, Dentistry and Pharmaceutical Sciences, Japan, <sup>3</sup>Pediatrics, The Children's Hospital of Philadelphia, United States, <sup>4</sup>University of Pennsylvania School of Dentistry, United States

Pediatric long bone fractures require careful follow-up. Fractures in growth-plate (GP) or diaphysis could lead either inhibition or acceleration of bone growth, resulting in progressive growth imbalance, deformity and significant physical problems. Surgery is the only mean to correct substantial imbalance but the procedures are invasive and cause substantial burden to the child. Chronic exposure of excess vitamin A or retinoic acid (RA) causes early closure of the GP, leading to shortened bone. We have shown that one of retinoid receptor (RAR) isoforms-RAR $\gamma$ - is highly expressed in GP and responsible for the growth arrest in response to excess RA. Utilizing this knowledge, we explored feasibility of pharmaco-therapeutic approach for correcting imbalanced bone growth using RAR $\gamma$  ligands. Following oral administration of agonists for RAR isoforms or vehicle in P11 mice, only RAR $\gamma$  agonist, NRX204647 inhibited bone growth, 15% shorter body length at P18. The bony elements are proportionally shorter in the RAR $\gamma$ -treated group. Histological examination revealed that proximal tibial GP of RAR $\gamma$ -treated mice was transiently enlarged with an increase in width of hypertrophic zone and closed in 8 days whereas the samples treated with agonists for other RAR isoforms did not show such changes. Furthermore, NRX204647 treatment down-

regulated gene expression of *sox* families and cartilage matrices and up-regulated *MMPs* and *Rankl*, suggesting that the treatment facilitated transition of cartilage to bone by decreasing cartilage matrix production and increasing matrix degradation. Subsequently, local delivery of NRX204647 was tested to see if it restricted growth of the targeted bone. To ensure local and sustained delivery of the active drug, we entrapped NRX204647 in PLLA based *nano* particles (NRX-Nano) and injected it into the vicinity of the proximal GP of left tibiae of 3 week mice (A) following the approved IACUC protocol. Right tibiae received empty particles. NRX-Nano was injected every 7 days and the bone was analyzed at 5 week of age. The x-ray analysis detected narrowing of the GP in the NRX-Nano group (C). The length of the tibia became shorter in the treated group compared to the control (D). The results indicate that (1) RAR $\gamma$  plays an important role in regulation of longitudinal bone growth, (2) RAR $\gamma$  agonist-based pharmacological manipulation of the targeted bone growth is feasible and could potentially substitute invasive growth-restriction surgery.



figure

**Disclosures:** Masatake Matsuoka, None.

## SA0322

**Effects of Eldecalcitol and Ibandronate on Bone Mineral Density, Arthritis and Muscle Atrophy in Rats with Adjuvant-induced Arthritis.** Yuichi Ono\*, Naohisa Miyakoshi, Yuji Kasukawa, Manabu Akagawa, Masazumi Suzuki, Tetsuya Kawano, Itsuki Nagahata, Yusuke Yuasa, Yoichi Shimada, Department of Orthopedic Surgery, Akita University Graduate School of Medicine, Japan

**Introduction:** Rheumatoid arthritis (RA) is characterized by chronic inflammation of the synovium, progressive erosion of the articular cartilage and joint destruction. RA also causes secondary osteoporosis and muscle weakness. We examined whether a new vitamin D3 analogue, eldecalcitol (ELD), could inhibit osteopenia, arthritis and muscle atrophy in rats with adjuvant-induced arthritis (AIA), in comparison with bisphosphonate and ibandronate (IBN).

**Methods:** Eight-week-old male Lewis rats were randomized into five groups, with AIA in all four non-control groups: ELD group (oral administration of ELD at 30 ng/kg/day); IBN group (subcutaneous administration of 10 µg/kg IBN once every 2 weeks); ELD + IBN group (treated with ELD and IBN); vehicle group (treated with the vehicle of ELD and IBN); and control group (treatment with vehicle, without no AIA). Arthritis score and paw thickness were recorded once weekly. After 2 or 4 weeks, rats were sacrificed. Cross-sectional areas (CSAs) of left tibialis anterior muscle fibers, and bone mineral density (BMD) of the total femur and lumbar vertebrae 2-4 (lumbar spine, LS) were measured following administration.

**Results:** After 2 weeks, BMD of the femur and LS were significantly higher in the ELD group (p = 0.0044 and p = 0.0002, respectively) and ELD + IBN group (p < 0.0001 and p < 0.0001, respectively) than in the vehicle group. BMD of the LS was significantly higher in the ELD + IBN group than in the IBN group (p = 0.0188). After 4 weeks, BMD of the femur and LS were significantly higher in the IBN group (p = 0.0011 and p = 0.0007, respectively), ELD group (p < 0.0001 and p < 0.0001, respectively) and ELD + IBN group (p < 0.0001 and p < 0.0001, respectively) than in the vehicle group. BMD of the femur and LS were significantly higher in the ELD + IBN group than in the IBN group (p = 0.0052 and p = 0.0001, respectively). No significant differences in CSAs, arthritis score or paw thickness were seen in the four groups with AIA at 2 or 4 weeks.

**Conclusion:** ELD and IBN did not inhibit arthritis and muscle atrophy, but did inhibit bone loss. Treatment with the combination of ELD and IBN has additive effects on the inhibition of bone loss in AIA rats.

**Disclosures:** Yuichi Ono, None.

## SA0323

**Macrolactin A attenuates RANKL-induced osteoclastogenesis via MAPKs and NFATc1 signaling pathways in BMMs and promotes osteoblastogenesis through Runx2, BMP-2 and MAPKs signaling pathways in MC3T3-E1 cells.** Yunjo Soh<sup>\*1</sup>, Maresh Sapkota<sup>2</sup>, Liang Li<sup>2</sup>, Sewoong Kim<sup>2</sup>. <sup>1</sup>Department of Dental Pharmacology, School of Dentistry, Chonbuk National University, Korea, Republic of, <sup>2</sup>Department of Dental Pharmacology, School of Dentistry, Korea, Republic of

The inequality between bone resorption and bone formation leads to rheumatoid arthritis, osteoporosis and Paget's disease. The imbalance is caused by decreased bone formation over bone resorption. Osteoclasts are responsible for bone resorption; inhibition of osteoclast differentiation could lead to formation of osteogenesis. Numerous studies suggest that macrolactin A (MA) has powerful anti-inflammatory, anti-cancer and anti-angiogenic effects in various cell types. We investigate whether MA could inhibit bone loss and enhance bone formation. We used BMMs cells to study osteoclast activity and MC3T3-E1 cells for osteoblast activity *in-vitro*. MA suppressed TRAP+ multinucleated cells, bone resorption activity and F-actin ring formation in a concentration-dependent manner as well as a specific time point. Moreover, MA markedly suppressed RANKL-induced osteoclastogenic marker genes and transcription factors such as AKT, ERK 1/2, JNK, NFATc1 and c-Fos. Consistent with the *in-vitro* results, inflammatory bone loss in mice were recovered by MA. This study showed that MA not only repressed osteoclast differentiation via MAPKs and NFATc1 signaling pathways, but it also enhanced osteoblast differentiation and mineralization by up-regulating osteogenic marker genes and transcription factors. Therefore, MA could be an effective candidate for inhibition and management of osteoporosis, arthritis, and bone metastatic disease.

**Disclosures:** Yunjo Soh, None.

## SA0324

See Friday Plenary Number FR0324.

## SA0325

See Friday Plenary Number FR0325.

## SA0326

See Friday Plenary Number FR0326.

## SA0327

**Bone Structure and Bone Mineral Density in Growing Male Mice is Largely Unchanged when Calcium and Vitamin D is Fed at Levels Lower Than Those Present in the AIN93G Reference Diet.** C. Brent Wakefield<sup>\*1</sup>, Jenalyn L. Yumol<sup>1</sup>, Sandra M. Sacco<sup>1</sup>, Phillip J. Sullivan<sup>1</sup>, Elena M. Comelli<sup>2</sup>, Wendy E. Ward<sup>1</sup>. <sup>1</sup>Brock University, Canada, <sup>2</sup>University of Toronto, Canada

**Background:** Our group along with others use CD-1 mice to study the effects of nutritional interventions on bone development. While reference diets are used in these studies to ensure nutritional intake is standardized between and within research groups, there is evidence that the AIN93G reference diet contains excess calcium (Ca) and vitamin D (vit D) which may confound results. Considering males may require higher dietary Ca and vit D due to a greater rate of growth, females were studied separately. **Purpose:** To determine if a lower level of Ca and vit D than that in the AIN93G reference diet supports bone development in growing male CD-1 mice. **Methods:** Weanling male CD-1 mice were randomized to modified AIN93G diets containing either 100 IU vit D/kg diet (trial 1) or 400 IU vit D/kg diet (trial 2) within one of three Ca levels (3.5, 3, or 2.5 g/kg diet) or the reference AIN93G diet (REF) (1000 IU vit D and 5 g Ca/kg) from weaning to 4 months of age (N = 124). At 2 and 4 months of age, BMD and structural properties of the tibia were analysed using *in vivo* microcomputed tomography (SkyScan 1176). The 4<sup>th</sup> lumbar vertebrae (L4) were scanned *ex vivo* at 4 months of age. **Results:** In trial 1 (100 IU vit D/kg diet), at the proximal tibia, the 2.5 g Ca/kg group had lower trabecular thickness compared to the REF group, and cortical thickness was lower in the 2.5 and 3 g Ca/kg groups at the midpoint compared to the REF group (p<.05). In trial 2 (400 IU vit D/kg diet), at tibia midpoint, the 2.5 g Ca/kg group had lower (p<0.05) cortical thickness compared to the 3.5 g Ca/kg group. There were no differences in LV or for other trabecular or cortical bone measures at the tibia in Trial 1 or 2. **Conclusion:** When Ca levels were lowered to 2.5 or 3 g Ca/kg some tibia but not LV outcomes were compromised. Considering humans generally consume less Ca and vit D than what is recommended, it is possible that rodent research diets that do not contain higher levels of nutrients than needed may strengthen the extrapolation of results to the human scenario. Further research is needed to refine the level of Ca and vit D of reference diets that meets the needs for growth while also allowing other food components to be tested for their role in supporting healthy bone development.

**Disclosures:** C. Brent Wakefield, None.

## SA0328

**Enhancement of ghrelin signaling by Rikkunshi-To attenuates teriparatide-induced nausea in rats.** Kouichi Yamamoto<sup>\*1</sup>, Yukihiro Isogai<sup>2</sup>, Takayuki Ishida<sup>1</sup>, Keisuke Hagihara<sup>3</sup>. <sup>1</sup>Department of Medical Science and Technology, Division of Health Sciences, Graduate School of Medicine, Osaka University, Japan, <sup>2</sup>Medical Affairs Department, Pharmaceutical Business Administration Division, Asahi Kasei Pharma Corporation, Japan, <sup>3</sup>Department of Advanced Hybrid Medicine, Graduate School of Medicine, Osaka University, Japan

Teriparatide is clinically used for the treatment of osteoporosis; however, severe nausea is often observed in patients. Nausea is not a life-threatening symptom, but teriparatide-induced nausea is closely related with the persistence of teriparatide therapy. Rikkunshi-To (RKT), a Japanese traditional herbal medicine, has been prescribed for patients with various gastrointestinal (GI) symptoms because it improves the GI function via the potentiation of ghrelin secretion and its signaling pathway. In this study, we investigated the effects of RKT on the prevention of teriparatide-induced nausea in rats and the involvement of ghrelin in its therapeutic effect.

Nausea is defined as an unpleasant feeling in the upper gastrointestinal tract with an involuntary urge to vomit; thus, it is difficult to recognize whether laboratory animals feel nausea. We reported that stimuli causing nausea induced pica, a behavior characterized by eating non-nutritive materials, such as kaolin, in rats. Since we have confirmed that subcutaneous injection of teriparatide increased kaolin intake in rats<sup>1</sup>, the amount of kaolin intake was used as an index of nausea in rats. Rats were allowed free access to kaolin and a diet supplemented with or without RKT (1 %) for more than 2 weeks. On the day of the experiment, rats were subcutaneously administered teriparatide (400 µg/kg) and their kaolin intakes were measured for 24 hours. We examined the effect of teriparatide on alteration of the intestinal motility and plasma ghrelin levels in rats fed the diet supplemented with or without RKT. Furthermore, the effects of the ghrelin receptor antagonist ([D-Lys<sup>3</sup>]-GHRP-6, 200 nmol/rat) on the teriparatide-induced nausea and the intestinal motility were investigated.

Rats fed the diet supplemented with RKT did not show teriparatide-induced nausea, and this therapeutic effect was antagonized by pretreatment with the ghrelin receptor antagonist. Subcutaneous injection of teriparatide significantly suppressed the intestinal motility and plasma ghrelin levels in rats fed the normal diet; however, RKT recovered both motility and ghrelin levels. Furthermore, the ghrelin receptor antagonist reduced the effect of RKT to improve the intestinal motility.

These findings suggest that RKT is a potential treatment for teriparatide-induced nausea in patients, and that the enhancement of ghrelin signaling is involved in its therapeutic effect.

1. Yamamoto K. et al. Eur. J. Pharmacol. 764: 457-462, 2015.

**Disclosures:** Kouichi Yamamoto, None.

## SA0329

**PTH (1-34) prevents glucocorticoid-induced reduction in blood flow and bone formation.** Wei Yao<sup>\*1</sup>, Abhijit Chaudhari<sup>2</sup>, Yuan Lay<sup>1</sup>, Mie Jin Lim<sup>1</sup>, Alexander Kot<sup>1</sup>, Donald Kimmel<sup>3</sup>, Nancy Lane<sup>1</sup>. <sup>1</sup>UC Davis Medical Center, United States, <sup>2</sup>UC Davis, United States, <sup>3</sup>University of Florida, United States

Glucocorticoid (GC) excess reduces bone strength more than is explained by reduced bone mass and quality. Bone vasculature provides both hydration for bone tissue and nutrition to bone cells. Reduced bone strength caused by GC is associated with decreased bone vascular density. <sup>18</sup>F-fluoride Positron Emission Tomography/Computed Tomography (<sup>18</sup>F-PET/CT) scanning can measure blood flow (vascularity) and bone formation (turnover) *in vivo*. 0-15min post-injection (*early*), <sup>18</sup>F-uptake and location reflects blood flow. By 45-60min (*late*), <sup>18</sup>F-ions have exchanged with hydroxyl groups of hydroxyapatites to form fluorapatite at bone formation sites, meaning that <sup>18</sup>F-uptake and location then reflect bone formation activity. Our objective was to determine simultaneously the effect of GCs on bone vascular density and formation and whether an agent with pro-angiogenic properties (e.g., PTH[1-34]) prevents GC-induced reduced bone vascular density, as it prevents GC-induced reduced bone formation.

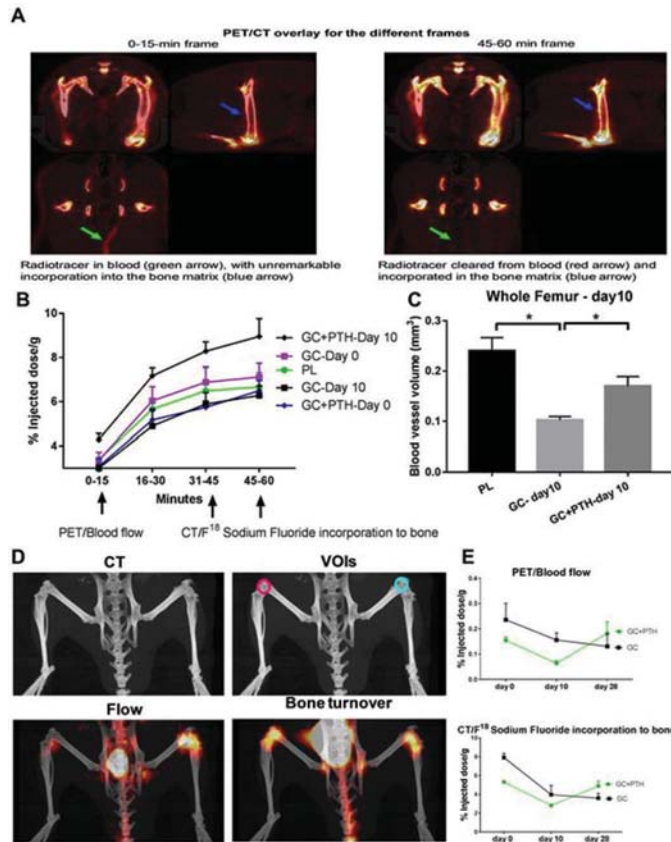
Two studies were done (N=3/grp). Study #1: 2-month-old male SD rats were treated for 10 days with placebo (PL), GC (methylprednisolone, 100 mg IP daily) or GC+hPTH (1-34) (20µg/kg 5d/wk). Study #2: 2-month-old Balb/c male mice were treated for 28 days with GC (dexamethasone, 4mg/kg/d PO), or GC+hPTH (1-34) (20µg/kg/d 5d/wk). Both hindlimbs were scanned for 60 minutes after administration of 10µBq of <sup>18</sup>F, at Day 0 and end of study. MicroFil was given just before necropsy and MicroCT was used to determine femoral bone volume (BV/TV) and vascular density (FVV).

Study #1: GC reduced BV/TV by 22% in rats; this change was prevented by PTH. GC caused *lower* early and late <sup>18</sup>F uptake in the long bone metaphyses than PL. Conversely, GC+PTH rats showed *greater* early and late <sup>18</sup>F uptake than GC only rats. The FVV data showed that blood vessel volume was reduced in GC rats than PL, but better in GC+PTH rats than GC only rats. Study #2: GC mice showed lower early and late <sup>18</sup>F uptake than PL at the distal femur. The GC+PTH group had *greater* early and late <sup>18</sup>F uptake than in GC mice than GC mice. Figure 1 is an axial view of lower extremity <sup>18</sup>F-PET/CT mouse scan.

In summary, *in vivo* <sup>18</sup>F-PET/CT imaging documented: a) GC-related reduced vascular density and bone formation, and b) hPTH prevention of GC-induced reduction



in bone vascularity and bone formation in two representative rodent models. The  $^{18}\text{F}$ -PET/CT vascularity data was confirmed by ex vivo studies of FVV.



PET-CT-GC

Disclosures: Wei Yao, None.

## SA0330

**Significance of DXA and HR-pQCT for the Diagnosis of Osteopetrosis (ADO II) – Establishment of a Diagnostic Threshold.** Sebastian Butscheidt<sup>1</sup>, Tim Rolvien<sup>2</sup>, Uwe Kornak<sup>3</sup>, Felix N. Schmidt<sup>4</sup>, Thorsten Schinke<sup>5</sup>, Michael Amling<sup>6</sup>, Ralf Oheim<sup>7</sup>. <sup>1</sup>SB, Germany, <sup>2</sup>TR, Germany, <sup>3</sup>UK, Germany, <sup>4</sup>FNS, Germany, <sup>5</sup>TS, Germany, <sup>6</sup>MA, Germany, <sup>7</sup>RO, Germany

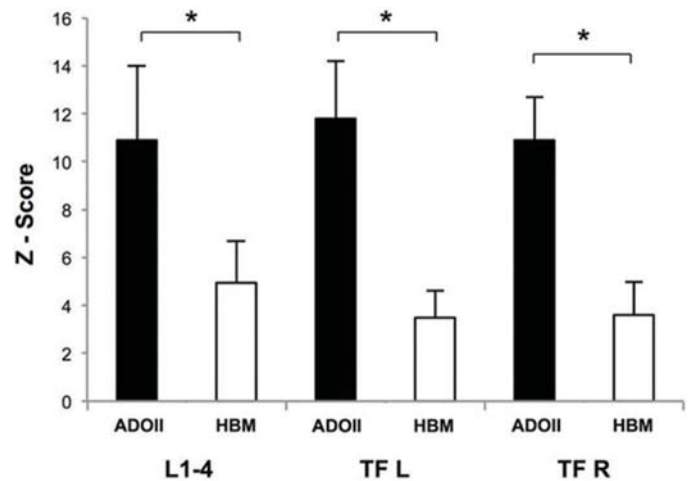
The main hallmark of skeletal dysplasias with high bone mass (HBM) is increased bone mineral density, visible in conventional radiographs and quantifiable by other radiographic methods. While one of the most common forms of HBM is CLCN7-related autosomal dominant osteopetrosis type II (ADO II), there is no consensus on diagnostic thresholds, as well as the correlation of bone mineral density with increased fracture risk.

We therefore wanted to assess whether CLCN7-osteopetrosis cases differ from a HBM CLCN7-negative control collective in terms of, bone mineral density, bone structure, and microarchitectural abnormalities.

13 patients meeting the criteria of HBM were included in this retrospective study. Osteologic assessment using dual-energy X-ray absorptiometry (DXA), high-resolution peripheral quantitative computed tomography (HR-pQCT) and serum analyses was performed. The presence of CLCN7 and/or other HBM gene mutations affecting bone mass were tested using a custom designed bone panel.

While a clear DXA threshold could be implemented for ADO II (DXA Z-score  $\geq 6.0$ ), the differences in bone microarchitecture were of lesser extent. All adult patients with ADO II suffered from elevated fracture rates independent from Z-score. In HR-pQCT, structural alterations, such as bone islets were found only inconsistently.

In cases of HBM, DXA represents the tool of choice in detecting patients with increased risk of inheritable high bone mass disorders. Microarchitectural bone alterations might represent local microfracture repair or accumulation of cartilage remnants due to impaired osteoclast function, but seem not to be correlated with fracture risk.



DXA Z-score in ADO II and HBM; \*p < 0.05

Disclosures: Sebastian Butscheidt, None.

## SA0331

See Friday Plenary Number FR0331.

## SA0332

**Diagnostic value of  $^{18}\text{F}$ -NaF PET/CT as an early marker in fibrodysplasia ossificans progressiva.** Elisabeth Eekhoff<sup>1</sup>, Esmée Botman<sup>1</sup>, Coen Netelenbos<sup>1</sup>, Pim de Graaf<sup>2</sup>, Pieter Raijmakers<sup>1</sup>. <sup>1</sup>VU University Medical Center (VUmc), Netherlands, <sup>2</sup>VU University Medical Center, Netherlands

Fibrodysplasia ossificans progressiva (FOP) is a rare genetic disease with a progressive course characterized by episodically local flare-ups, which often, but not always, may lead to heterotopic bone formation (HO).

Recently we showed that  $^{18}\text{F}$ -NaF PET/CT may be the first tool to predict progression of a flare up into new HO formation. This was demonstrated during a follow-up study in a patient with FOP who underwent a maxillofacial surgery, which is known to lead to activation of the disease with recurrence of HO.

In the present case study, we followed the course of a new spontaneous flare-up in a 19-year-old girl known with FOP with the aim to use and explore the efficacy of  $^{18}\text{F}$ -NaF PET/CT in early detection of spontaneous new HO formation.

Three weeks after the patient suddenly noticed a painful increasing swelling extending to her total right upper leg, the  $^{18}\text{F}$ -NaF PET/CT scan showed increased  $^{18}\text{F}$  uptake at a circumscribed location in the right distal lateral quadriceps muscle. On the CT scan however, no HO was detectable.

She was treated with high dosages of prednisolon and nonsteroidal anti-inflammatory drugs for several weeks, after which the pain and swelling slowly decreased, resulting in a knee contracture and wheel chair dependence.

After 7 months, when the flare-up had disappeared, the  $^{18}\text{F}$ -NaF PET scan showed no uptake anymore. However, on the CT scan maturing HO was visible, but only at the location where muscle  $^{18}\text{F}$  uptake had been increased before. Blood investigation did not show differences during this course of her disease.

In conclusion  $^{18}\text{F}$ -NaF PET/CT can predict the location of new HO formation early in the course of a spontaneous flare-up, underscoring the efficacy of  $^{18}\text{F}$ -NaF PET/CT as an important early marker of the disease.

Disclosures: Elisabeth Eekhoff, None.

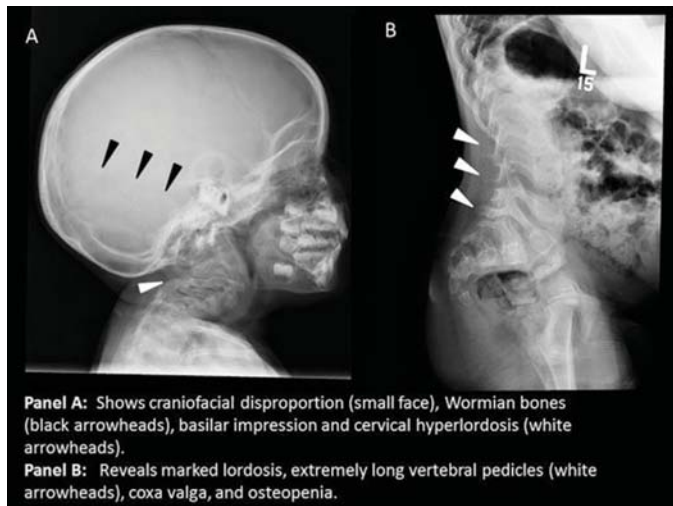
## SA0333

**New Skeletal Dysplasia Associated with a Heterozygous De Novo Mutation in MMP24.** Gary S. Gottesman<sup>1</sup>, William H. McAlister<sup>2</sup>, Angela Nenninger<sup>1</sup>, Rebecca Green<sup>3</sup>, Steven Mumm<sup>4</sup>, Michael P. Whyte<sup>4</sup>. <sup>1</sup>Shriners Hospital for Children - St. Louis, United States, <sup>2</sup>Mallinckrodt Institute of Radiology, Washington University School of Medicine, United States, <sup>3</sup>Springfield Clinic, United States, <sup>4</sup>Shriners Hospital for Children and Washington University School of Medicine, United States

We report a 4-year-old girl with an apparently unique skeletal dysplasia featuring short stature (Z-score -4.4), craniofacial disproportion, basilar impression, Wormian bones, cervical hyperlordosis, proximal thoracic kyphosis, wide spinal canal with extraordinarily long vertebral pedicles, protrusio acetabuli, coxa valga, and narrow femoral diaphysis (Figure). Social development was normal. Evaluations elsewhere did not identify a recognized disorder. She sustained at least 4 extremity fractures, and DXA bone mineral density (BMD) was low for chronologic age. Routine genetic metabolic screening including plasma amino acids, urine organic acids, acylcarnitine profile, serum

creatine kinase, as well as thyroid and growth hormone studies were normal. At our Research Center, comprehensive metabolic panel, markers of bone turnover, and serum PTH and 25(OH)-vitamin D levels were essentially normal. Elsewhere, molecular cytogenetic studies revealed a normal 46, XX karyotype, and chromosomal microarray analysis was unrevealing. Studies of mtDNA excluded mitochondrial disorders. However, trio exome sequencing (XomeDx, GeneDx, Gaithersburg, MD, USA) performed in 2015, was notable only for a de novo heterozygous variant of uncertain significance in the matrix metalloproteinase 24 gene [MMP24 (OMIM 604871)]. Analysis included variants in genes associated with short stature, increased susceptibility to fractures, gross motor delay and several other clinically-related findings. The *MMP24* missense mutation (c.1493 G>A, p.Arg498His), was considered a conservative amino acid substitution unlikely to impact protein secondary structure. However, the substitution involved a residue conserved across species. In silico analysis predicted that this variant was probably damaging to protein structure/function. No variants in *MMP24* have been associated with human disease.

MMPs are endopeptidases that degrade protein components of the extracellular matrix (ECM). MMP24 is expressed primarily in the rat central nervous system, but also richly in bone and kidney. MMP24, "membrane-type"-MMP, is reportedly shed from the plasma membrane as a soluble proteinase, with both cell bound and soluble roles in ECM modeling processes, especially in the murine brain and during embryonic development. Any role for MMP24 in our patient's apparently unique skeletal disorder is uncertain. We report her hoping to identify similar patients for exploration of the physiological role of MMP24.



Figure

Disclosures: Gary S. Gottesman, None.

## SA0334

See Friday Plenary Number FR0334.

## SA0335

**Bone Mineral Density but not Bone Microstructure is impaired in Adult Patients with Hypophosphatasia.** Roland Kocijan<sup>1</sup>, Ursula Renner<sup>1</sup>, Martin Kuzma<sup>2</sup>, Christian Muschitz<sup>1</sup>, Judith Haschka<sup>1</sup>, Daniel Kirchgörfer<sup>1</sup>, Juraj Payer<sup>3</sup>, Heinrich Resch<sup>1</sup>. <sup>1</sup>St. Vincent Hospital Vienna - Medical Department II, the VINforce study group, Austria, <sup>2</sup>Comenius University Faculty for Medicine, 5th Department of Internal Medicine, University Hospital Bratislava, Slovakia, <sup>3</sup>Comenius University Faculty of Medicine, 5th department of Internal Medicine, University Hospital Bratislava, Slovakia

### Purpose:

Hypophosphatasia (HPP) is a rare genetic bone disease caused by low levels of tissue non-specific alkaline phosphatase (AP) leading to defects in bone mineralization. Consequently HPP is characterized by stress fractures with poor healing, bone deformities and extra-skeletal manifestations. To date, no data regarding bone microstructure, one of the main components of bone strength, are available in HPP.

### Methods:

We investigated 6 adult patients with HPP (4 female, 2 male, mean age  $46.8 \pm 13.7$  years) and 6 healthy controls (4 female, 2 male, mean age  $46.4 \pm 9.3$  years, CTRL). Microstructure and volumetric bone mineral density (vBMD) were assessed by HR-pQCT (SCANCO Medical) at the ultra-distal radius and tibia in all subjects. Total, trabecular and cortical vBMD (mgHA/cm<sup>3</sup>) were evaluated. Microstructure analyses included the trabecular bone volume fraction (BV/TV), trabecular number (Tb.N, 1/mm), inhomogeneity of the trabecular network (Tb.I/N.SD, mm), trabecular thickness (Tb.Th, mm) and cortical thickness (Ct.Th, mm). BMD by DXA and DXL of the calcaneus as well as bone turnover markers (BTM) were measured in HPP patients. In addition, correlations between demographic data, AP, BMD and microstructure were carried out.

### Results:

AP was decreased in all HPP patients (mean  $17.2 \pm 10.1$  U/L). 83% of HPP patients have sustained low traumatic fractures in the past. A positive family history for HPP was found in 50% of HPP patients. Bone turnover markers, Calcium and Phosphate were in normal range in all HPP patients. Vitamin D deficiency ( $<30$  ng/ml) was found in 50% of HPP patients. HPP patients were significantly shorter ( $p=0.09$ ) and lighter ( $p=0.017$ ) compared to CTRL. Comparable trabecular and cortical bone microstructure were found in HPP and CTRL at both measuring sites. Trabecular vBMD but not total or cortical vBMD at the radius was lower in HPP than in controls (n.s.). The trabecular bone score (TBS, 1.401) was above the reference range ( $>1.200$ ) in all HPP patients. Low BMD at the lumbar spine ( $1.139$  m<sup>2</sup>, T-score -1.0) and femoral neck ( $0.850$  g/cm<sup>2</sup>, T-score -1.3) by DXA and DXL at the calcaneus ( $0.386$  g/cm<sup>2</sup>, T-score -1.8) were found in HPP patients. AP was not correlated to parameters of bone microstructure.

### Conclusion:

Trabecular and cortical bone microstructure as well as established bone turnover markers besides AP do not reflect the increased fracture risk in adult patients with HPP. BMD indicates the impaired mineralization in HPP.

Disclosures: Roland Kocijan, None.

## SA0336

See Friday Plenary Number FR0336.

## SA0337

See Friday Plenary Number FR0337.

## SA0338

**Asfotase alfa therapy heals recalcitrant bilateral pathologic femoral fractures in a patient with Hypophosphatasia after 1 year of treatment, that were previously non-healing up to 9 years.** Paul Miller, MD<sup>1</sup>, Deborah Aggers, CCRP<sup>2</sup>, Erin Carrithers, NP<sup>3</sup>, Philostratos Klidas, RPH, MRPharmS<sup>1</sup>, Jared R.H. Foran, MD<sup>4</sup>. <sup>1</sup>Colorado Center for Bone Research, United States, <sup>2</sup>Centura Health Physician Group Colorado Center for Bone Research, United States, <sup>3</sup>Centura Health Physician Group Colorado Center for Bone Research, United States, <sup>4</sup>Panorama Orthopedics, United States

Hypophosphatasia (HPP) is a rare bone disease with a prevalence of approximately 1 in 25,000. It is characterized by low serum Total Alkaline Phosphatase, elevated Vitamin B6, and skeletal manifestations including bone pain, pathologic fractures, poor fracture healing, and poor dentition.

The patient is a 61-year-old male who presented with a fragility fracture of the right femur in May 2006. Due to persistent pain and radiographic evidence of non-union he underwent intramedullary nailing 31 months later. Unfortunately, despite operative intervention he continued to have pain in his thigh and serial radiographs demonstrated continued non-union of the fracture.

In 2014 the patient sought the opinion of another orthopaedic surgeon. He now complained of left knee pain, as well as difficulty with gait and balance. Radiographs demonstrated a stress fracture of the left femoral diaphysis. The subject declined operative intervention, as he was dissatisfied with the lack of healing of the same issue on his contralateral femur fracture years before. As such, his orthopaedic surgeon referred him to Dr. Paul Miller at the Colorado Center for Bone Research due to suspicion of a metabolic bone problem.

The patient's medical history includes Diabetes Mellitus II, Hypertension, waddling gait, and poor dentition.

A complete laboratory work-up was completed and significant for the following:

- alkaline phosphatase: 6 U/l (normal range, 39 – 177 U/L)
- phosphorus: 5.5 mg/dl (normal range, <4.5mg/dl)
- vitamin B-6: > 100 ug/L (normal range, 5.3-46.7 ug/L)

Genetic testing confirmed the diagnosis of HPP with 2 mutations:

Heterozygous variant c.874C>A (p.Pro292Thr)  
Heterozygous variant c.1195G>A (p.Ala399Thr)

In March 2015 the patient initiated a course of teriparatide to assist with fracture healing. After 6 months he discontinued this treatment, as he was unable to tolerate the side effects of the drug.

In September 2015 he screened for the Alexion AA-HPP-405 protocol an Early Access Protocol for subjects to receive the now approved treatment for HPP asfotase alfa. As part of the screening work-up full body radiographs were obtained. The right femur fracture was still present despite the presence of an intramedullary nail. The left femur fracture was also still present and the subject was again offered surgery, which he declined. The subject received his first dose of asfotase alfa on October 22, 2015. His dosing regimen was 1 mg/kg six times weekly. Within 54 weeks of starting therapy, radiographs revealed interval healing of the left femur fracture. In February 2017 radiographs demonstrated complete healing of the right femur and near resolution of the left femur (see attached figure).

In conclusion this patient showed remarkable and rapid healing of chronic recalcitrant bilateral pathologic femur fractures with non-operative treatment with asfotase alfa 1 mg/kg six times weekly.





Images bilateral femur fragility fracture treated with asfotase alfa

**Disclosures:** Paul Miller, MD, Alexion Pharmaceutical, Inc, Grant/Research Support.

## SA0339

**Assessing Outcomes of Joint Replacement in Patients with X-Linked Hypophosphatemia.** Emily Mills\*, Louis Iorio, Carolyn Macica, Frank H Netter MD School of Medicine at Quinnipiac University, United States

X-linked hypophosphatemia (XLH) is the most common form of the heritable phosphate wasting disorders. As patients age, they report significant bone and joint pain and present with enthesophytes, osteoarthritis, and marginal osteophytes of the weight bearing joints. However, few studies have been conducted on pain associated with the arthropathies of XLH. One relatively undocumented approach to pain management with improved functionality is joint replacement surgery. In this study, our aim was to determine if patients with XLH benefit from hip or knee replacement surgery. We surveyed 25 patients from the United States (23), the United Kingdom (1), and Australia (1) using the Hip or Knee Osteoarthritis Outcome Score Physical Function Shortform (HOOS-PS or KOOS-PS), making this the largest study of joint replacement in patients with XLH. Herein we describe the patient-reported data. Patients were asked to estimate their symptoms before joint replacement and then asked to report their current symptoms. A total of 46 joint replacements were reported among the 25 patients. 17 were hip replacements and 28 were knee replacements. The mean HOOS-PS score, reported as mean  $\pm$  SD, before surgery was  $13.6 \pm 3.5$  and after surgery was  $4.9 \pm 4.3$  ( $p < .001$ ). The mean KOOS-PS score before surgery was  $17.7 \pm 4.6$  and after surgery was  $9.8 \pm 4.8$  ( $p < .001$ ). Joint replacement was reported to improve patient quality of life in 93.3% of patients. The average time since surgery was 7.07 years ( $0.5$ - $19.4$ ,  $\pm 4.54$ ), with one patient requiring revision surgery after 19 years. Because bone is of poor quality and patients present at a much younger age than the unaffected population, many surgeons are hesitant to perform joint replacement surgery in the XLH population due to concerns of replacement failure. Nonetheless, from these data, we conclude that joint replacement is a sufficient way to manage pain and increase function in patients with XLH. Additionally, we asked patients for medical records to analyze the surgical techniques and implants used in this population. Analysis of patient records thus far indicates that cemented implants and revision stems lead to better outcomes. However, we have not received all records and cannot yet draw any conclusions about the surgical techniques. It is our goal to report these additional findings in the future and propose a standard of care for these patients as it relates to joint replacement surgery.

**Disclosures:** Emily Mills, None.

## SA0340

See Friday Plenary Number FR0340.

## SA0341

**Negative Illness Perceptions are associated with impairments in Quality of Life in patients with Fibrous Dysplasia.** Marlous Rotman\*, Bas Majoor, Casper Quispel, Neveen Hamdy, Sander Dijkstra, Ad Kaptein, Natasha Appelman-Dijkstra. Leiden University Medical Center, Netherlands

**Introduction** Fibrous dysplasia (FD) is a rare bone disorder where healthy bone is being replaced by fibrous tissue. This can cause pain and pathological fractures but can be asymptomatic as well, with both outcomes leading to distinct differences between patients in Quality of Life (QoL). Illness perceptions are patients' thoughts and beliefs about their illness and its treatment and found to contribute to QoL. In this study we aimed to explore illness perceptions in patients with FD and to identify factors associated with these perceptions.

**Patient and Methods** A total of ninety-seven patients with FD completed the validated Illness Perception Questionnaire Revised (IPQ-R) and the Short Form-36 (SF-36). Data on age, gender, skeletal burden score (SBS), type of FD and biochemical parameters were retrieved and analysed for examining associations between illness perceptions and QoL via correlational analyses.

**Results** Significant differences in illness perceptions were observed between patients with subtypes of FD (monostotic/polystotic/MAS) concerning the domains: identity ( $p = 0.006$ ), timeline acute/chronic ( $p = 0.002$ ) and consequences ( $p < 0.001$ ). However, patients with craniofacial FD scored significantly higher in the consequences domain ( $18.8 \pm 5.7$ SD vs.  $15.6 \pm 5.6$ SD;  $p = 0.022$ ). High skeletal burden scores were associated with the IPQ-R domains consequences and psychological attributions (both  $p < 0.01$ ) and high levels of FGF-23 were associated with the identity domain and the consequences domain (both  $p < 0.01$ ). The IPQ-R domains identity, timeline acute/chronic, timeline cyclical, consequences, emotional representations, treatment control were all found to be significantly associated with different domains of QoL.

**Conclusion** This study demonstrates that illness perceptions are affected throughout the wide spectrum of fibrous dysplasia, that high SBS and high levels of FGF-23 are determinants of negative illness perceptions and lastly that negative illness perceptions are associated with impairments in quality of life. Managing maladaptive illness

perceptions in these patients might aid in improving coping, and thereby quality of life in patients with FD, especially in the severely affected patients.

**Disclosures:** Marlous Rotman, None.

## SA0342

See Friday Plenary Number FR0342.

## SA0343

See Friday Plenary Number FR0343.

## SA0344

**Serum Glycosylation Characterization of Osteonecrosis of the Femoral Head for Potential Biomarker Discovery.** Ting Song\*, Peng Chen<sup>2</sup>, Ziqi Li<sup>3</sup>, Wei He<sup>2</sup>, Carlito Lebrilla<sup>4</sup>. <sup>1</sup>Department of Chemistry, United States, <sup>2</sup>First Affiliated Hospital of Guangzhou University of Chinese Medicine, China, <sup>3</sup>Guangdong Provincial Hospital of Chinese Medicine, China, <sup>4</sup>Department of Biochemistry(School of Medicine), United States

Osteonecrosis of the femoral head (ONFH) is a recalcitrant and paralyzing disease often discovered in the end stage at the time of diagnosis, which is often performed by physical examination and diagnostic imaging. ONFH is typically caused by trauma or long-term steroid use. There are over 30 million patients in US taking steroids, and roughly 40% will develop ONFH. However, the exact pathophysiological process is not well understood. This study aims to examine the serum glycosylation alteration of ONFH using the state-of-the-art analytical tool to provide more analytical data for pathophysiology research and possibly biomarker discovery. A training set containing 27 serum samples from steroid induced ONFH patients and 25 from gender and age matched controls were collected and used. Glycosylation of whole serum and site-specific glycosylation of immunoglobulins are characterized using ESI-Q-TOF and ESI-Triple-Quadrupole via multiple reaction monitoring (MRM) respectively. The whole serum glycosylation analysis yielded 14 N-glycan compositions and MRM yielded 8 glycopeptides that were altered between cases and controls with statistical significance. The increase of the non-sialylated, non-fucosylated N-glycans and decrease of the fucosylated N-glycans are associated with the development of ONFH. Glycosylation is a post-translational protein modification that appears to be affected by ONFH. The results are consistent with recent reports that specific glycosylation profiles are related to various pathological states. Further studies with a testing set will provide validation of these potential markers.

**Disclosures:** Ting Song, None.

## SA0345

**ZNF687 gene is recurrently mutated in PDB patients from a geographic area of South Italy.** Giuseppina Divisato\*, Nadia Petrillo<sup>1</sup>, Federica Scotto di Carlo<sup>1</sup>, Teresa Esposito<sup>2</sup>, Fernando Gianfrancesco<sup>1</sup>. <sup>1</sup>Institute of Genetics and Biophysics, National Research Council of Italy, Italy, <sup>2</sup>Institute of Genetics and Biophysics, National Research Council of Italy; IRCCS INM Neuromed, Pozzilli, Italy, Italy

Paget's disease of bone (PDB) is a metabolic disorder, characterized by focal increases in bone turnover that result in deformities and fractures of the involved bones. Mutations in the *SQSTM1* gene, encoding the p62 protein, are the most common cause of PDB, and affect the NF $\kappa$ B pathway. Recently, a founder germline mutation (c.2810C>G) in the *ZNF687* gene has been identified as the cause of a severe form of PDB, complicated by Giant Cell Tumor of Bone (GCT). It was supposed that this mutation, located on an ancestral haplotype, only represented the genetic signature of PDB patients predisposed to develop Giant Cell Tumor (0.4%).

By literature revision, we previously highlighted that 45% of the worldwide GCT/PDB patients (117 cases) derive from Italy and that 80% of them originate from the geographic area of Avellino and neighbouring cities. Therefore, we hypothesized that PDB patients from this region are carriers of the *ZNF687* mutation and they develop GCT as a consequence of the longstanding disease.

In this study, we first collected a cohort of 30 unrelated PDB patients from this geographic area and then investigated the presence of *ZNF687* or *SQSTM1* mutations. Our analysis revealed that in these PDB patients the mutation in the *ZNF687* gene was present in 8 out of 30 patients (27%). Moreover, we disclosed the rare haplotype surrounding the *ZNF687* mutation in all patients, confirming the same ancestral origin. On the contrary, only 2 out of 30 patients (7%) were positive for *SQSTM1* mutation, carrying the most common one (P392L). All *ZNF687*-mutated patients presented polystotic PDB, with at least 3 affected sites ( $8.25 \pm 3$ ), whereas those mutated in *SQSTM1* both showed the monostotic form of the disease. Moreover, in *ex-vivo* studies, the *ZNF687* mutated patients also showed an enhanced osteoclastogenesis compared with the *SQSTM1* ones. Therefore, we disclosed that the severe phenotype of PDB patients of Avellino region is defined by this specific genetic signature, leading us to hypothesize their neoplastic degeneration in untreated condition.

In a parallel study, to uncover if the relationship between *ZNF687* mutation and GCT/PDB phenotype was only restricted to Avellino hot spot area, we also recruited three additional GCT/PDB patients, derived from different Italian Regions.

Our *ZNF687* targeted sequencing confirmed the causality of the c.2810C>G mutation, indicating a unifying scenario for all GCT/PDB patients.

**Disclosures:** *Giuseppina Divisato, None.*

## SA0346

See Friday Plenary Number FR0346.

## SA0347

See Friday Plenary Number FR0347.

## SA0348

See Friday Plenary Number FR0348.

## SA0349

Withdrawn

## SA0350

**Visualization of Immune Response During Initiation and Progression of Heterotopic Ossification in Mouse Model of Fibrodysplasia Ossificans Progressiva (FOP).** Kalyan Nannuru<sup>\*1</sup>, Johanna Jimenez<sup>2</sup>, LiQin Xie<sup>1</sup>, Lily Huang<sup>1</sup>, Xialing Wen<sup>1</sup>, Lili Wang<sup>1</sup>, Vincent Idone<sup>1</sup>, Andrew Murphy<sup>1</sup>, Sarah Hatsell<sup>1</sup>, Aris Economides<sup>1</sup>. <sup>1</sup>Regeneron Pharmaceuticals Inc, United States, <sup>2</sup>Regeneron Pharmaceutical Inc, United States

Fibrodysplasia ossificans progressiva (FOP) is a rare debilitating genetic disorder characterized by progressive heterotopic endochondral ossification of skeletal muscle and tendons. FOP results from missense mutations in the type I BMP receptor *ACVR1*, with the most common mutation altering Arg206 to His. FOP mutations alter the sensitivity of ACVR1 to Activin A from an antagonist to an agonist. We have previously shown that Activin A is necessary for driving heterotopic ossification (HO) in murine FOP (MGI:5763014, *Acvr1*<sup>R206H/Plen<sup>+</sup></sup>; *Rosa-CreER*<sup>T2</sup> mice) in part by showing that prophylactic inhibition of Activin A blocks HO. Natural histories of FOP patients indicate that HO is often associated with flare-ups, which might be due to a soft tissue injury or other inflammatory stimuli. In order to explore the role of inflammation in the initiation of HO in FOP mice, we visualized the homing of phagocytes to the site of injury. Phagocytes were tracked by intravenous administration of Exitron nano - radio dense nanoparticles that are readily taken up by phagocytes and hence enable monitoring of phagocyte homing by *in vivo*  $\mu$ CT. Phagocytes are recruited to the site of injury rapidly following the injury-inducing event, and remain in place for at least 4 days post-injury. By day 10, heterotopic bone arises at the site of injury, which results in obscuring of the signal by Exitron nano. However, phagocytes can also be tracked *in vivo* using probes that target myeloperoxidase (a marker of activated phagocytes) with chemiluminescence. Using this second imaging modality, we demonstrated sustained or increased inflammatory response correlates with HO lesion progression in FOP mice; in contrast, inflammation rapidly resolves in wild type mice. Our findings demonstrate that HO formation is preceded by an inflammatory response at the site of injury and that inflammation is sustained during the early stages of mineralization of the lesions. This data is consistent with the proposed model of how HO arises in FOP, i.e. that it is precipitated by inflammation-inducing events that result in the recruitment of phagocytes, and which in turn express Activin A, the key HO-inducing factor in FOP. The ability to mark the site of early HO-arising events using imaging modalities that are compatible with life, enables investigation of these early events in a longitudinal manner that can be coupled with *ex vivo* interrogations such as histology and gene expression profiling.

**Disclosures:** *Kalyan Nannuru, Regeneron Pharmaceuticals Inc, Other Financial or Material Support.*

## SA0351

See Friday Plenary Number FR0351.

## SA0352

**A Role for TGF- $\beta$  Signaling in Cherubism.** Tulika Sharma<sup>\*1</sup>, Yaling Liu<sup>1</sup>, Peter Maye<sup>1</sup>, Yasuyoshi Ueki<sup>2</sup>, Ernst Reichenberger<sup>1</sup>, Iping Chen<sup>1</sup>. <sup>1</sup>UConn Health, United States, <sup>2</sup>University of Missouri Kansas City, United States

Cherubism is a rare autosomal dominant craniofacial disorder affecting pre-pubertal children. It is characterized by multilocular lesions in the mandible and/or maxilla consisting of numerous giant osteoclasts and extensive fibrous-osseous tissue hyperplasia. Most cases of cherubism have gain-of-function point mutations in *SH3BP2*, a gene encoding for a cytoplasmic adaptor protein. Past generation and characterization of a murine animal model for cherubism revealed an over-reactive immune system and overproduction of TNF- $\alpha$ . Given excessive bone resorption and tissue hyperplasia, we have postulated that TGF- $\beta$  signaling may also have a fundamental role in the

presentation of this disease. In this study, we show that cherubism mice have elevated levels of latent form of TGF- $\beta$ 1 in their serum. Additionally, bone marrow stromal cultures derived from heterozygous and homozygous knock-in cherubism mice exhibited reduced osteogenic differentiation and spontaneous osteoclast formation compared to cultures derived from wild type littermates. However, reduction of TGF- $\beta$  signaling during osteoblast differentiation using type I receptor small molecule inhibitors (SB505124/EW-7197) or a pan-TGF- $\beta$  blocking antibody (1D11) rescued osteoblast differentiation of heterozygous and homozygous cherubic cultures. Interestingly, *Col1a1*-2.3-EGFP+ osteoblasts, which retained a fibroblastic cell morphology in cherubism cultures was able to adopt a more wildtype-like cuboidal cell morphology upon treatment with TGF- $\beta$  inhibitors. Finally, type I receptor antagonist treatment also resulted in a significant reduction in spontaneous osteoclast formation and appropriately adjusted the imbalance in RANKL and OPG. Collectively, these studies implicate an important role for TGF- $\beta$  signaling in the pathology of cherubism.

**Disclosures:** *Tulika Sharma, None.*

## SA0353

**Deletion of *B3glct* disrupts craniofacial and skeletal development in mice: a model for Peters Plus syndrome.** Sardar Uddin<sup>\*1</sup>, Richard Grady<sup>2</sup>, Diana Rubel<sup>2</sup>, Takashi Sato<sup>3</sup>, Hisashi Narimatsu<sup>3</sup>, Robert Haltiwanger<sup>4</sup>, David Komatsu<sup>1</sup>, Bernadette Holdener<sup>2</sup>. <sup>1</sup>Department of Orthopaedics, Stony Brook University, United States, <sup>2</sup>Department of Biochemistry and Cell Biology, Stony Brook University, United States, <sup>3</sup>National Institute of Advanced Industrial Science and Technology in Japan, Japan, <sup>4</sup>Complex Carbohydrate Research Center, University of, United States

Peters plus syndrome (PPS) is a rare genetic disorder characterized by eye abnormalities, short stature, distinctive facial features, and cognitive impairment. PPS is caused by a loss-of-function mutation in the beta-3-glucosyltransferase gene (*B3GLCT*). *B3GLCT* is an enzyme that adds glucose to fucose on thrombospondin type 1 repeats (TSRs), which are a characteristic domain of several secreted and cell-surface proteins including the ADAMTS (A Disintegrin and Metalloproteinase with Thrombospondin motifs) family of extracellular proteases. We have generated *B3GLCT* deficient mice to understand the role of *B3GLCT* in the developmental defects present in PPS. Homozygous null mice showed reduced neonatal viability, runting, doomed head, and variable hydrocephaly. MicroCT 3D reconstruction of the skulls showed a short, wide and domed skull with shortening of the jaw and separated cranial sutures in mutants (fig 1a). Bone quantity was assessed at the proximal tibia with microCT and showed a significant decrease in trabecular bone volume fraction (67%,  $p < 0.03$ ), connectivity density (85%,  $p < 0.01$ ), and thickness (24%,  $p < 0.05$ ), and as well as increased structure model index (31 %,  $p < 0.05$ ) in *B3GLCT* deficient mice relative to age-matched wild-types (fig 1b). Cortical bone analyses at the tibial mid-diaphysis did not show any differences. Femoral mechanical integrity was tested using three-point bending and showed decreased ultimate force in *B3GLCT* deficient mice. Histological analysis of tibial growth plates with Mason's trichrome staining showed a condensed proliferative zone, depleted hypertrophic zone, and reduction in metaphyseal ossification in *B3GLCT* deficient mice (fig 1c). Overall *B3GLCT* deficient mice are the first animal model of PPS to demonstrate a comparable phenotype to human patients. This study shows that *B3GLCT* deficiency impairs endochondral and intramembranous ossification and mineralization, leading to runted growth, separated cranial sutures, and mechanically compromised bone. Our data strongly suggest a role of *B3GLCT* in skeletal development, but systemic effects on bone growth such as impaired vascularization cannot be ruled out. Our future studies will specifically look at the association of *B3GLCT* with ADAMTS proteins and its role in the function of osteoblast and chondrocyte differentiation and function.

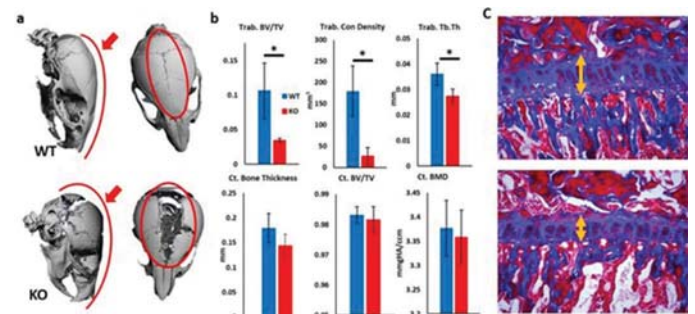


Fig1: *B3GLCT* deficient mice show a Peter plus syndrome-like phenotype: (a) a domed shaped skull wit

**Disclosures:** *Sardar Uddin, None.*

## SA0354

See Friday Plenary Number FR0354.



## SA0355

See Friday Plenary Number FR0355.

## SA0356

See Friday Plenary Number FR0356.

## SA0357

See Friday Plenary Number FR0357.

## SA0358

See Friday Plenary Number FR0358.

## SA0359

**Vitamin D Deficiency is Related with Altered Functional Performance and Diminished Muscle Mass but not with Falls in Older Ambulatory Women from Buenos Aires.** Beatriz Oliveri<sup>1</sup>, Sabrina Lucas<sup>2</sup>, Maria Gabriela Torres<sup>2</sup>, Claudia Martinez<sup>2</sup>, Felipe Silva Pavon<sup>2</sup>, Reynaldo Gomez<sup>2</sup>, Adriana Graciela Diaz<sup>2</sup>. <sup>1</sup>Laboratorio Osteoporosis y Enfermedades Metabólicas Oseas (INIGEM, UBA-CONICET), Argentina, <sup>2</sup>Division Endocrinología, Hospital de Clinicas-UBA, Argentina

**Purpose:** To investigate associations between vitamin D (VD) status and appendicular lean mass, physical performance, and falls in ambulatory postmenopausal women  $\geq 60$  years.

**Methods:** out of 321 ambulatory postmenopausal women  $\geq 60$  years who attended a community activity to evaluate risk factors for bone and muscle health at the University Hospital, 144 completed the questionnaire about falls in the last year, currently physical activity (scored as none, mild and moderate activity) and VD supplementation and performed the following: physical performance tests: 4-meter walking speed (WS) [(Normal value(NV) < 5 s), 3-meter Timed Get-Up-and-Go Test(NV  $\leq 10$  s) and Chair sit-to-stand test(NV < 11.2s). Grip strength was assessed by dynamometry (NV  $> 20$ kg) and appendicular lean mass by whole body Lunar DXA (adjusted by height<sup>2</sup>=ALM/ht<sup>2</sup>, NV  $> 5.67$ kg/m<sup>2</sup> and by BMI NV  $> 0.512$ ). Obesity was considered BMI  $> 30$ kg/m<sup>2</sup>. Sarcopenia was defined as low muscle mass plus any low physical performance test or low Grip strength. Albumin and 25OHD levels were measured (deficiency <20ng/ml, sufficiency  $\geq 20$ ng/ml).

**Results:** Women with age  $69.44 \pm 6.9$  yo, BMI of  $28.4 \pm 5.6$  kg/m<sup>2</sup> and ALM/ht<sup>2</sup>  $6.33 \pm 0.87$  kg/m<sup>2</sup> were analyzed. 25OHD levels were associated with VD supplementation ( $p < 0.0001$ ). Sixty percent of participants had 25OHD deficiency, of them 81% had one or more physical performance test altered. The 25OHD deficiency was associated with diminished ALM/ht<sup>2</sup> ( $p < 0.021$ ) and ALM/BMI ( $p = 0.052$ ), but not with falls. 25OHD levels correlated negatively with BMI ( $r = -0.313$ ,  $p < 0.0001$ ) and positively with ALM/BMI ( $r = 0.198$ ,  $p = 0.024$ ). Age correlated with worse physical performance tests and Grip strength ( $p < 0.0001$ ), and obesity with worse walking speed ( $r = 0.203$ ,  $p = 0.014$ ). Physical activity was only associated with better Chair sit-to-stand test ( $p = 0.042$ ), but not with muscle mass or Grip strength. Women with falls had abnormal Grip strength ( $p = 0.003$ ) and Walking speed ( $p = 0.012$ ) and diminished ALM/ht<sup>2</sup> ( $p = 0.09$ ).

**Conclusions:** Vitamin D deficiency was related with altered functional performance tests and diminished muscle mass but not with falls. Obesity and sedentarism showed a trend to worse physical performance tests, emphasizing the importance of correcting both factors in the elderly population.

**Disclosures:** Beatriz Oliveri, None.

## SA0360

**Efficacy of volumetric change of lumbar paraspinal & psoas muscle in spinal balance.** Jaewon Lee\*, Ye-Soo Park. Guri Hospital Hanyang University, Korea, Republic of

**Objective:** Lumbar degenerative kyphosis is closely associated with spinal sagittal imbalance and it makes low back pain and considered as a factor in a variety of spinal disorders. There are several studies about causes of spinal sagittal imbalance, but, they just reveal the risk factor, such as aging, illness, trauma, surgery. The present study was to determine the relationship between the sagittal imbalance and sarcopenia, especially cross sectional area (CSA) and fatty degeneration (FD) of muscle around the spine. **Methods:** This study is based on the patients over 60 years-old who had gone through standing lumbar spine radiograph and lumbar MRI, admitted to our hospital between June 2013 and June 2015. Patients with vertebral fractures, vertebral and paravertebral infection, and any history of having surgical procedure on vertebrae are excluded. Overall, 165 patients are included in this study, classified by three groups according to the distance from sagittal vertical axis to posterior end of upper end plate of sacrum. 38 patients were classified as group 1 (distance  $\geq 9$ cm), 50 and 53 patients as group 2 (distance 5-9cm) and group 3 (distance < 5cm), respectively. For measurement of CSA and FI of paraspinal muscles, five transverse T1W images of S1-S5 were obtained from PACS and measured with Adobe Photoshop 7.0®, by counting the number of pixels included in each selected muscle area. A variance analysis on average muscle surface

area of those five images was done with SPSS 19.0 Windows version (SPSS Inc., Chicago, IL, USA). Results: The average age of total patients was 69.1, average BMI was 22.57 and bone density was -2.34 (T-score). No significant differences were detected on ages, BMI, and bone density. Each correction coefficient of multifidus, erector spinae and psoas muscle was 0.80, 0.75 and 0.81, respectively. CSA of paraspinal muscles has significant differences between group I and III, II and III. Psoas has significant differences between all groups. FI has significant differences between all groups in multifidus and between I and III, II and III in erector spinae. But, psoas has no significance between three groups. Conclusion: Authors were able to detect significant muscle atrophy in the group with severe imbalance. And degeneration of paravertebral muscle has significant increased with sagittal imbalance. Effort for preventing weakness of muscle around spine might cause influence to alignment of spine.

**Disclosures:** Jaewon Lee, None.

## SA0361

**Severe hypoglycemia is associated with increased frequency of falls in individuals with type 1 diabetes.** Vrial Shah<sup>1</sup>, Mengid Wu<sup>2</sup>, Ruban Dhaliwal<sup>3</sup>, Mona Al Mukaddam<sup>4</sup>. <sup>1</sup>Barbara Davis Center for Diabetes, United States, <sup>2</sup>Jaeb Center for Health Research, United States, <sup>3</sup>SUNY Upstate Medical University, United States, <sup>4</sup>University of Pennsylvania, Perelman School of Medicine, United States

**Purpose:** Fracture risk in adults with type 1 diabetes (T1D) is high, even at young age, which cannot be explained by bone mineral density alone. Fall is one of the most important risk factors for osteoporotic fracture. Therefore, we employed the T1D Exchange Clinic Registry cohort to evaluate frequency of falls and factors affecting falls among middle aged and older adults with T1D. **Methods:** Participants aged  $\geq 55$  years with T1D were invited to complete an email-based detailed questionnaire on falls in the prior 12 months. Demographic, clinical, and fall-related information were gathered from the questionnaire; HbA1c was recorded from medical record data extraction. Results Of 1226 eligible participants, 435 (mean age  $64 \pm 6.5$  years, 57% females and 97% were Non-Hispanic whites) completed the survey (response rate 35.5%). Mean diabetes duration was 36 years with HbA1c of 7.3% (68% were reported on insulin pump and 46% were using continuous glucose monitors). Among the 435 participants, 126 reported at least one fall in the prior 12 months (29%) with 42% of these reporting fall in the house. Fall frequency in adults (55-64 years) with T1D and older adults ( $> 65$  years) were 26% and 32%, respectively ( $p = 0.16$ ). There was no significant difference in frequency of fall between female and male participants (31% vs. 26%,  $p = 0.33$ ). Of 126 participants who had a fall, 44% had injuries due to fall, 24% required medical attention and 13 participants reported fracture (10%). Figure 1(a) shows reported factors leading to falls; 23% of participants reported hypoglycemia (blood glucose  $< 70$  mg/dl) as a reason for their falls. In addition, 13% of participants who had fall reported occurrence of  $\geq 1$  episode of severe hypoglycemia (hypoglycemia that resulted in passing out, loss of consciousness, or seizure) in the three months prior to survey completion. Participants who experienced  $\geq 1$  episode of severe hypoglycemia in the past three months were more likely to fall compared to participants without reported severe hypoglycemia events (Odds ratio = 3.6;  $p$ -value  $< 0.001$  (Figure 1(b)). 41% of participants were fearful of falls. **Conclusion:** Falls are common among participants in the T1D Exchange. Hypoglycemia, a unique diabetes-related factor is attributed with nearly 23% of falls in this study. Further studies are needed to understand the contribution of falls to fracture risk in patients with T1D and to develop better approaches for fall prevention.

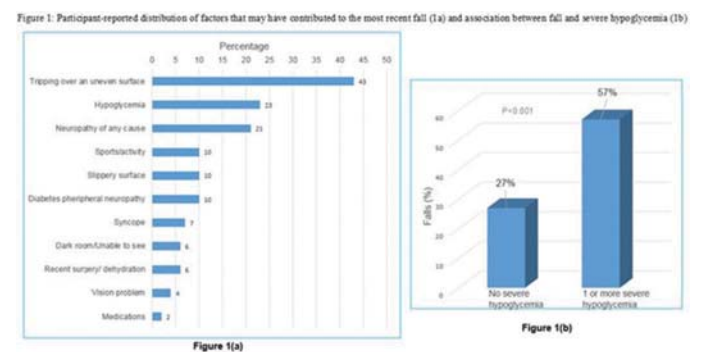


Figure 1

**Disclosures:** Vrial Shah, None.

## SA0362

**Is adiposity related to neuromuscular performance and musculoskeletal strength in community-dwelling older adults?** Harshvardhan Singh<sup>\*1</sup>, Zhaojing Chen<sup>2</sup>, Daeveol Kim<sup>3</sup>, Ryan Pohl<sup>4</sup>, Michael Bembien<sup>2</sup>, Debra Bembien<sup>2</sup>. <sup>1</sup>Department of Physical Therapy and Rehabilitation Science, University of Maryland School of Medicine, United States, <sup>2</sup>Department of Health and Exercise Science, University of Oklahoma, United States, <sup>3</sup>Department of Physical Education, Chonnam National University, Korea, Republic of, <sup>4</sup>Department of Kinesiology and Applied Physiology, University of Delaware, United States

Osteosarcopenic obesity syndrome (OSO) is defined as the simultaneous presence of: 1) osteopenia/osteoporosis, 2) sarcopenia, and 3) adiposity. It can lead to decreased mobility and increased susceptibility for osteoporotic fractures in older adults. There is evidence that age-related adiposity confers an increased susceptibility to sarcopenia in older adults; however, its relationship with muscle power is still unknown. Moreover, the relationship between adiposity and bone density/strength is still not clear. Community-dwelling older adults (n = 110, 55-75 years; men = 27, women = 83) were recruited from the Oklahoma City metropolitan area for this study. Jump power (JPow) and jump height (JHt) were assessed by jump test performance. %Body fat, relative skeletal muscle mass index (RSMI), total hip bone mineral density (BMD), femoral neck BMD, lumbar spine BMD, and cross-sectional moment of inertia (CSMI) were determined by DXA. Leg press strength and bilateral hip abduction strength were evaluated by one repetition-maximum testing. Grip strength was measured using a handgrip dynamometer and gait speed was measured using an 8-meter straight path marked with tape. Obesity was defined having a %body fat of more than 30% in men and 40% in women. Age- and gender-adjusted estimates showed that the obese group had lower jump power (Cohen's  $d = 0.4$ ,  $p = 0.014$ ), jump height (Cohen's  $d = 0.8$ ,  $p < 0.001$ ), leg press strength (Cohen's  $d = 0.8$ ,  $p < 0.001$ ), hip abduction strength (Cohen's  $d = 1.0$ ,  $p < 0.001$ ), and grip strength (Cohen's  $d = 0.7$ ,  $p = 0.008$ ). No group differences were found in BMD at any of the sites and CSMI of the hip. Obesity status was associated with 1) BMD status:  $\chi^2(1) = 4.55$ ,  $p = 0.033$ , and 2) sarcopenia status per the FNIH primary criterion,  $\chi^2(1) = 11.0$ ,  $p = 0.001$ . Age- and gender-adjusted correlations showed that %body fat was negatively associated with jump power ( $r = -0.274$ ,  $p = 0.004$ ), jump height ( $r = -0.580$ ,  $p < 0.001$ ), leg press strength ( $r = -0.490$ ,  $p < 0.001$ ), hip abduction strength ( $r = -0.601$ ,  $p < 0.001$ ), and grip strength ( $r = -0.613$ ,  $p < 0.001$ ). No relationship was found between gait speed and %body fat. Our results suggest that a higher %body fat is associated with decreased neuromuscular performance and muscle strength. Also, obesity was associated with osteopenia/osteoporosis and sarcopenia. The role of mitigating obesity in neuromuscular and musculoskeletal rehabilitation in older people requires further investigation.

**Disclosures:** Harshvardhan Singh, None.

## SA0363

**Frailty and Fracture Risk in Older Women.** Monica Tembo<sup>\*</sup>, Kara Holloway, Lana Williams, Sophia Sui, Sharon Brennan-Olsen, Mark Kotowicz, Sarah Hosking, Julie Pasco. Deakin University, Australia

**Purpose:** Frailty is characterized by age-related decline across various physiological systems including physical, psychological and social functioning. One adverse outcome of frailty is fracture. Currently there are numerous assessment tools that have been developed to assess frailty and these include the frailty phenotype and frailty index of deficit accumulation. This study aimed to investigate whether FRAX<sup>®</sup> scores could be used to identify frail and pre-frail individuals in a cohort of older women.

**Methods:** This cross-sectional study included 254 women aged 60-90 years enrolled in the Geelong Osteoporosis Study (GOS). Frailty was identified using a modified frailty phenotype index which segregated participants into frail, pre-frail or robust groups. FRAX (Aus) 10-year probabilities of major osteoporotic fracture (MOF) and hip fracture were calculated without BMD (n=254) and with BMD (n=229, n=25 excluded as no BMD results were available). We used Kruskal-Wallis test for non-parametric data to investigate differences between the three frailty groups.

**Results:** Of the 254 women with FRAX scores without BMD, 44 were frail, 137 pre-frail and 73 robust. For MOF, frail women had a higher median FRAX score (18.5 IQR 7.5-28.0) compared to pre-frail (7.8 IQR 3.9-15.0) and robust (6.2 IQR 3.65-11.0) ( $p < 0.001$ ). Similar results were observed for hip-FRAX scores; frail (9.5 IQR 2.5-14), pre-frail (2.7 IQR 0.9-6.6) and robust (1.9 IQR 0.9-4.7) ( $p < 0.001$ ).

When BMD was included in FRAX calculations, 37 women were frail, 124 were pre-frail and 68 were robust. For MOF, frail women had a higher median FRAX score (13.0 IQR 6.4-18.0) compared to pre-frail (6.0 IQR 3.2-10.0) and robust (4.9 IQR 3.2-8.5) ( $p < 0.001$ ). A similar pattern was observed for hip-FRAX scores; frail women had a higher median score (4.3 IQR 1.9-6.6) than pre-frail (1.5 IQR 0.4-3.6) and robust (1.0 IQR 0.5-2.8) ( $p < 0.001$ ).

**Conclusion:** Frail women had higher FRAX scores across all the groups compared to pre-frail and robust women. FRAX scores might be useful in the clinical setting for identifying older women at risk of being frail or pre-frail.

**Disclosures:** Monica Tembo, None.

## SA0364

See Friday Plenary Number FR0364.

## LB-SA0365

**A LC-MS/MS method for the diagnostic measurement of cAMP in plasma and urine.** Isabelle Picc<sup>\*1</sup>, John Dutton<sup>1</sup>, Sulaiman Al-Riyami<sup>1</sup>, Christopher Washbourne<sup>1</sup>, Inez Schoenmakers<sup>1</sup>, Hillel Galitzer<sup>2</sup>, Gregory Burshtein<sup>3</sup>, Phillip Schwartz<sup>3</sup>, Jonathan Tang<sup>1</sup>, William Fraser<sup>1</sup>. <sup>1</sup>University of East Anglia, United Kingdom, <sup>2</sup>Entera Bio Ltd, Israel, <sup>3</sup>Entera Bio Ltd., Israel

**Background:** Parathyroid hormone (PTH) plays a key role in calcium and phosphate homeostasis. Upon binding to its receptor, it signals via a second messenger, cyclic adenosine 3', 5' monophosphate (cAMP). Lack of increase in plasma and urinary cAMP concentrations in response to PTH are used as diagnostic markers for pseudohypoparathyroidism (PHP), a condition primarily associated with resistance to PTH (Ellsworth-Howard Test).

**Aims:** 1) Develop and validate a LC-MS/MS method for the quantification of cAMP in plasma and urine. 2) Investigate assay performance in a rat pharmacokinetic study investigating the response to an oral dose of PTH (1-34) and the response to subcutaneous (sc) PTH administration in a patient with suspected PHP.

**Method:** cAMP and <sup>13</sup>C<sub>5</sub>-cAMP internal standard were extracted from EDTA plasma using a weak anion exchange solid phase extraction. Chromatography was performed in positive electrospray ionisation mode, using a pentafluorophenyl column with a 10 mins 2% formic acid water:acetonitrile gradient. Transitions were m/z 330/136 for cAMP and 335/136 for <sup>13</sup>C<sub>5</sub>-cAMP. Over concentrations ranging from 4.6 (lower limit of quantification) to 293.5 nmol/L, the calibration curve was linear (mean curve fits of >0.95, 5 repeats) and intra- and inter-assay precisions were <12% and <8%, respectively. Spiked recovery was 98±5%.

**Application:** A single oral dose of 5 mg/kg PTH (1-34) or placebo was administered to Sprague-Dawley rats after an overnight fast. cAMP was analysed in EDTA samples obtained at baseline, prior to dosing and every 15 min for 1h and then hourly for another 3h after dosing. In the suspected PHP patient, urinary cAMP was measured after a standard 20µg sc injection of teriparatide (Forsteo).

**Results:** In rats, plasma PTH (1-34) and cAMP increased significantly within 15min of dosing, reaching peak values between 15 and 30 mins. PTH (1-34) concentration increased significantly by up to 6770-fold, although response to PTH (1-34) varied between animals. Plasma cAMP typically tripled, from 36.5±3.7 nmol/L at baseline to 108.9±26.3 nmol/L. Placebo had no effect.

Urine cAMP from the suspected PHP patient did not change significantly reflecting a lack of biological response to sc PTH (1-34) despite a significant increase in plasma PTH (1-34) (27.8 to 101.1 pmol/L).

**Conclusion:** The present method was robust and selective. It also showed utility in determining cAMP in biological systems and the ability to study the effect of drugs such as Forsteo.

**Disclosures:** Isabelle Picc, None.

## LB-SA0366

**Sleep Apnea and Bone Health in Mid-life Women.** W. P. P. Thu<sup>\*1</sup>, H. Y. Tng<sup>2</sup>, S. Logan<sup>1</sup>, Izzuddin M Aris<sup>1</sup>, J. A. Cauley<sup>3</sup>, E. L. Yong<sup>1</sup>. <sup>1</sup>Department of Obstetrics and Gynaecology, National University of Singapore, Singapore, <sup>2</sup>Department of Obstetrics and Gynecology, National University of Singapore, Singapore, <sup>3</sup>University of Pittsburgh, Graduate School of Public Health, Department of Epidemiology, United States

**Purpose:** Menopause is associated with a decline in bone health, with 40-60% reporting sleep disturbances. However, the relationship between these two remains controversial. A recent meta-analysis concluded that obstructive sleep apnea (OSA) was a risk factor for osteoporosis. However, a study of elderly patients found that intermittent hypoxia as measured by pulse oximetry was associated with improved bone mineral density (BMD). This study explored the relationship between OSA symptoms and BMD in midlife women.

**Methods:** Participants (n=1201) aged 45-69 years attending health checks at gynecologic clinics at National University Hospital, Singapore were recruited. Breathing discomfort, snoring and trouble staying awake from the Pittsburgh Sleep Quality Index (PSQI) and partner-witnessed apnea and snoring were assessed. Hip BMD was assessed with dual energy X-ray absorptiometry and classified into tertiles based on T-scores. Univariate analyses were performed across tertiles for sleep, demographic, and clinical measures. Variables with  $p < 0.1$  and reported to affect sleep apnea and bone health in medical literature were covariates. Multivariable ordinal regression assessed associations between sleep measures and BMD. To validate findings, we analyzed four OSA characteristics from the STOP questionnaire. Analyses were performed using SPSS version 20.0.

**Results:** Mean (SD) age and PSQI score were 56.3 (6.2) years and 5.44 (3.4) respectively. 68.5% (n=816) had partner reports, and 32.4% (n=264) had self-reported OSA. Univariate analyses revealed significant differences in medication use, ethnicity, age, diabetes, handgrip strength, body mass index (all  $p < 0.001$ ), physical activity and WHO Disability Assessment Schedule 2.0 (both  $p < 0.05$ ) across tertiles. Partner-witnessed apnea, snoring (both  $p < 0.01$ ) and self-reported breathing discomfort ( $p < 0.05$ ) were associated with higher tertiles. Factors associated with higher tertiles were partner-witnessed apnea (OR per SD increase = 1.36, 95% CI [1.01, 1.85]), handgrip strength (1.04 [1.02, 1.07]) and Indian ethnicity (1.80 [1.03, 3.13]). Age (0.90 [0.88, 0.92]) and diabetes (0.46 [0.27, 0.77]) were associated with lower hip tertiles. A high likelihood of OSA (OR = 1.42, [1.04, 1.93]) was associated with higher hip tertiles.

**Conclusion:** Intermittent hypoxia in OSA may confer a protective role in bone health in midlife women. Future research should explore the use of hypoxia-mimicking agents to improve bone health.

**Disclosures:** W. P. P. Thu, None.



## LB-SA0367

**Characterization of the bone healing process in rats with spinal cord injury.**

Mariana Butezloff<sup>1</sup>, Kelly Astolpho<sup>1</sup>, Vitor Correlo<sup>2</sup>, Rui Reis<sup>2</sup>, Jose Volpon<sup>1</sup>, Ariane Zamarioli<sup>1</sup>. <sup>1</sup>University of Sao Paulo, Brazil, <sup>2</sup>3B's Research Group, Biomaterials, Biodegradables and Biomimetics, University of Minho, Portugal

Bone fracture healing in spinal cord injured individuals are very controversial, with no consensus whether their bone calluses are smaller or larger than general population. The aim of this study was to investigate the bone healing in rats with spinal cord injury (SCI). Ten male Wistar rats with six weeks were divided into two experimental groups: (1) CON: control rats with bone fracture; (2) SCI: rats with spinal cord injury and bone fracture. SCI was performed as previously described. Ten days after SCI a fracture was created in the femoral diaphysis by closed method and immediately fixed by an intra-medullary nail. The right distal femur was shaved and then disinfected with 70% alcohol. Subsequently, rat's thigh was placed in a device especially manufactured to perform a closed fracture in the mid-femur. Immediately after fracturing bone, an incision was made parallel in the proximal extremity of the femur. A 1-mm-diameter Kirschner wire was introduced into the medullary canal in order to stabilize the bone fragments. Bone healing was observed for 14 days post-fracture. At the end of the experiment, animals were euthanized and the femurs were harvested and submitted to tridimensional micro-structure analysis ( $\mu$ CT), DEXA and histology at the bone callus. Our DEXA data showed that SCI rats exhibited bone calluses 30% less dense than those in control rats. Curiously, our  $\mu$ CT data strengthened the controversial results shown in literature. Bone callus in SCI rats presented larger volume (BV) than those in controls (+52%), whereas BV/TV was shown to be only 4% higher in SCI rats than in controls (Figure 1). This may be explained by our histological slides. Bone callus in SCI rats are shown to be mainly formed by an unorganized non-bony structure, when compared to control rats (Figure 2). Furthermore, we found that the level of separation within the tissue forming the bone callus in SCI rats is higher than in control. Therefore, although SCI rats may have a larger bone callus than control animals, we believe this tissue is less resistant and may fracture easier due to the delayed and abnormal bone healing formation. Our further molecular and mechanical analysis may provide substantial information to understand the mechanisms and mechanical features involved in these events.

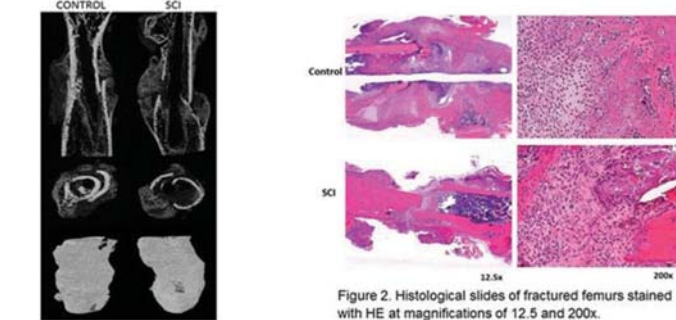


Figure 1.  $\mu$ CT images of bone callus, in sagittal and axial planes.

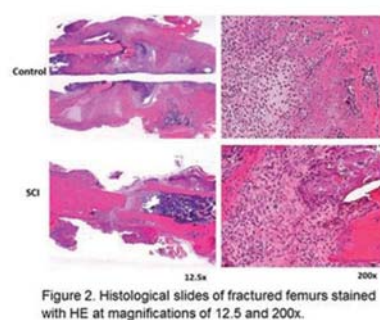


Figure 2. Histological slides of fractured femurs stained with HE at magnifications of 12.5 and 200x.

**Disclosures:** Mariana Butezloff, None.

## LB-SA0368

**Treatment-Related Changes in Bone Turnover and Fracture Risk Reduction in Clinical Trials of Anti-Resorptive Drugs: The FNIH Bone Quality Study.**

Richard Eastell<sup>1</sup>, Dennis Black<sup>2</sup>, Mary Bouxsein<sup>3</sup>, Li-Yung Lui<sup>4</sup>, Jane Cauley<sup>5</sup>, Sundeep Khosla<sup>6</sup>, Charles McCulloch<sup>2</sup>, Douglas Bauer<sup>2</sup>. <sup>1</sup>University of Sheffield, United Kingdom, <sup>2</sup>University of California, San Francisco, United States, <sup>3</sup>Harvard Medical School, United States, <sup>4</sup>California Pacific Medical Center, United States, <sup>5</sup>University of Pittsburgh, United States, <sup>6</sup>Mayo Clinic College of Medicine, United States

Few pooled analyses of anti-resorptive (AR) treatment trials, including bisphosphonate (BP) and selective estrogen receptor modulators (SERM), are available that relate short-term changes in bone turnover markers (BTMs) to fracture reduction. Such information would be useful to assess new ARs or novel dosing regimens before initiating large fracture trials.

In the FNIH Bone Quality project, we identified placebo-controlled fracture endpoint trials of osteoporosis treatments, and are in the process of collecting individual data from over 150,000 participants including serial BTMs if available, DXA, and fracture outcomes. We previously presented an analysis including bone-specific alkaline phosphatase (bone ALP) and N-telopeptide of type I collagen (NTX). We have now extended the number of trials and BTMs and in these new analyses include the data we received from 14 AR trials that included 2 bone formation markers (bone ALP and pro-collagen I N-propeptide (PINP)) and 2 bone resorption markers (N- and C-terminal telopeptide of type I collagen). Using the individual-level BTM results and incident fracture outcome data we performed a meta-regression relating the mean net effect of treatment on change in bone turnover (active minus placebo percent difference from

baseline after 3-12 mo.) to the log of study-wide fracture risk reduction and used linear regression to plot the best fitting line.

Separate analyses were performed for morphometric vertebral, non-vertebral and hip fractures. This analysis includes over 28,000 randomized participants from 11 BP and 3 SERM trials; change in bone ALP was available for over 16,000 participants and change in PINP was available for over 10,000. Fracture follow-up for incident vertebral and non-vertebral fracture ranged from 1-4 years. For vertebral fracture, the results showed a strong relationship between treatment-related bone ALP or PINP changes and vertebral fracture risk reduction ( $r^2=0.82$  and  $0.75$ ,  $p<0.02$ , respectively). Relationships were weaker and no longer statistically significant for non-vertebral ( $r^2=0.33$  and  $0.53$ ,  $p<0.10$ ) and hip fracture ( $r^2=0.17$  and  $0.43$ ,  $p>0.10$ ) outcomes. For all fracture types, relationships were weaker and non-significant for bone resorption markers. We conclude that short-term AR treatment-related changes in bone ALP and PINP strongly predict vertebral fracture treatment efficacy, but are not as strongly associated with non-vertebral or hip fracture treatment efficacy. These results suggest that change in the bone formation markers might be useful to predict the anti-vertebral fracture efficacy of new AR compounds or novel dosing regimens with approved AR drugs.

**Disclosures:** Richard Eastell, Amgen, AstraZeneca, Chronos, GSK, Immunodiagnostic Systems, Fonterra Brands, Ono Pharma, Lilly, Bayer, Janssen Research, Alere, CL Biosystems, Teijin Pharm, D-Star, Roche Diagnostics, Inverness Medical, Consultant.

## LB-SA0369

**Adaptive Vitamin D Metabolism at the Equator Can Predispose to Insufficiency in**

**Children of First Generation African Immigrants in the US.** Elwaseila Hamdoun<sup>1</sup>, Brandon Nathan<sup>1</sup>, Thereza Piloya-Were<sup>2</sup>, Zahra Mahamed<sup>1</sup>, Sarah Cusick<sup>1</sup>, Antoinette Moran<sup>1</sup>, Anna Petryk<sup>3</sup>, Muna Sunni<sup>1</sup>. <sup>1</sup>University of Minnesota, United States, <sup>2</sup>University of Makerere, Uganda, <sup>3</sup>University of Minnesota and Alexion Pharmaceuticals, Inc., United States

Skin pigmentation, vitamin D inactivation and genetic variation of vitamin D binding protein (DBP) are all possible adaptive vitamin D metabolism in African children at the equator. Relying on a total serum 25-hydroxyvitamin D (25OHD) level to assess for vitamin D sufficiency in this population of children who live in a more northern climate ignores their inherent differences and maladaptive vitamin D metabolism, and may therefore potentially misclassify their vitamin D status. The goal of this multi-center international cross-sectional observational study was to stringently define vitamin D status in Somali immigrants living in northern US. Healthy children aged 6 months to 7 years living in Minnesota (US-born of Somali descent,  $n=55$ ) or Uganda ( $n=95$ ) were enrolled. 25OHD and other vitamin D metabolites (24,25(OH)<sub>2</sub>D) were measured by immune-affinity extraction and liquid chromatography-tandem mass spectrometry. Parathyroid hormone (PTH) and hypocalcemia status were used as primary markers of vitamin D insufficiency. DBP haplotypes were determined. Compared to the Ugandan group, and despite superior nutritional status (vitamin D fortified milk intake), MN Somali children had lower 25OHD (23.7 vs 30.1 ng/mL;  $p<0.0001$ ) and calcium levels (9.1 vs 9.5 mg/dL;  $p<0.0001$ ), and higher PTH levels (47 vs 36 pg/mL;  $p<0.0001$ ). Ninety-one percent of the MN Somali participants had 25OHD levels  $<30$  ng/mL (vs 48% in Ugandans). Somalis had higher frequency (57% vs 14% in Ugandans;  $p<0.001$ ) of calcium in the lower level of normal even at 25OHD levels  $>20$  (American Academy of Pediatrics [AAP] cutoff for sufficiency) and this was not significantly different from the Somali group with 25OHD  $<20$  ng/mL ( $p=0.3$ ). The high-affinity allele Gc1f (which limits free forms of vitamin D) was the predominant DBP variant in both MN Somalis and Ugandans, but Somalis had a higher percentage of low serum calcium status. The Somali group had a higher level of vitamin D inactivation (greater 24,25(OH)<sub>2</sub>D, less 1,25(OH)<sub>2</sub>D levels,  $p<0.001$ ) despite having lower 25OHD levels raising a concern of maladaptive vitamin D metabolism and inherent susceptibility to vitamin D deficiency independent of limited cutaneous vitamin D synthesis as a result of darker skin tone. These results suggest that even at the AAP cutoff for sufficiency ( $>20$  ng/mL), clinically significant low 25OHD levels were common in Somali children in the northern US, who are yet misclassified as vitamin D sufficient. Also, while African children at the equator possess adaptive mechanisms to protect against excessive acquisition and utilization of vitamin D, but those same mechanisms may render them susceptible to insufficiency when migrating to high-latitude regions such as Minnesota.

**Disclosures:** Elwaseila Hamdoun, None.

## LB-SA0370

**Presence of Cyr61 in Native Bone Marrow-derived Extracellular Matrix Is Critical for Retention of Mesenchymal Stem Cell Properties.** Milos Marinkovic<sup>\*</sup>, Aaron Gonzalez, David Dean, Xiao-Dong Chen. UT Health San Antonio, School of Dentistry, United States

Previously, we reported that mouse and human bone marrow-derived mesenchymal stem cells (BM-MSCs) cultured on native decellularized extracellular matrix (ECM) made by BM stromal cells (BM-ECM) display enhanced attachment, proliferation, and retention of stem cell properties. Furthermore, BM-MSCs from aged mice or elderly human donors, displaying deficits in self-renewal and differentiation, can be restored by culture on BM-ECM synthesized by BM stromal cells from young animals (3 months old) or young human donors (18-23 years old). However, ECM loses its restorative capability with aging (i.e. old-ECM made by cells from 18-month old mice or  $>65$ -year old humans). Proteomic analyses of BM-ECM indicated that the matricellular protein, CCN1/Cyr61, was the only protein present in young- but not old-ECM. This study tests

the hypothesis that production of CCN1/Cyr61 by BM stromal cells declines with aging, altering the stem cell niche, and results in the loss of its ability to retain MSC properties. Here we specifically evaluate the effect of CCN1/Cyr61 on the responsiveness of MSCs to BMP-2 (an inducer of osteogenesis) and rosiglitazone (RGZ) (an inducer of adipogenesis) when maintained on CCN1/Cyr61-deficient young ECM (C61<sup>+</sup> young-ECM synthesized by RNAi-treated young cells) or CCN1/Cyr61-overexpressed old-ECM (C61<sup>+</sup>-old-ECM synthesized by adenovirus-treated old cells). Human young MSCs (passage 1) were maintained for 7 days on tissue culture plastic (TCP), young-ECM, C61<sup>+</sup> young-ECM, old-ECM, or C61<sup>+</sup>-old-ECM and then treated with BMP-2 (60ng/ml) or RGZ (1mg/ml) for 48 hrs. Runx2 and bone sialoprotein protein (BSP) expression were measured to assess BMP-2-responsiveness, while PPAR $\gamma$  (a marker of adipogenesis) expression was used to assess RGZ-responsiveness. Remarkably, young-MSCs, maintained on C61<sup>+</sup> young-ECM, lost all responsiveness to BMP-2 and RGZ; further, addition of exogenous CCN1/Cyr61 (100ng/ml) to the culture failed to rescue MSC responsiveness. In contrast, the ability of old-ECM to retain MSC responsiveness to BMP-2 and RGZ was rescued by addition of CCN1/Cyr61 (via adenoviral infection) during synthesis of old-ECM (C61<sup>+</sup>-old-ECM). These data strongly suggest that the presence of CCN1/Cyr61 in the ECM is critical for MSC differentiation, supporting our hypothesis. This study provides important information for developing a defined culture system for expanding large numbers of high-quality autologous MSCs for MSC-based therapies in the elderly.

**Disclosures:** Milos Marinkovic, None.

## LB-SA0371

**Disproportionally decreased volume and histopathologic changes in foetal growth plate following gestational hypoglycaemia in the rat: a corticosterone mediated effect?** Vivi Jensen<sup>\*1</sup>, Fiona McGuigan<sup>2</sup>, Kristina Åkesson<sup>2</sup>. <sup>1</sup>Novo Nordisk A/S, Lund University, Denmark, <sup>2</sup>Lund University, Sweden

**Background:** Maintaining glucose homeostasis during pregnancy is pivotal, as both maternal hyperglycaemia and hypoglycaemia may affect foetal development. Maternal hypoglycaemia typically results in foetal growth restriction, especially of the skeleton, reflected by decreased ossification and malformations including bent long bones.

**Purpose:** The primary aim of this study was to investigate the histological effects of gestational hypoglycaemia on foetal growth plates.

**Methods:** Non-diabetic rats received continuous intravenous infusion with insulin throughout gestation to induce persistent hypoglycaemia. On gestation day 20 foetuses were removed by caesarean section, measured and weighed. Foetal hind limbs were sampled (n=8-13 foetuses/group, 1 foetus/litter), sections of foetal tibiae examined histologically and volume of growth plate zones measured. Foetal and maternal plasma corticosterone was measured.

**Results:** Maternal hypoglycaemia decreased the total volume of foetal growth plates by 40%. This was reflected by decreased volumes of individual growth plate zones except the hypertrophic zone, which was unchanged. Additional, histopathologic changes in the central longitudinal growth plate were seen in all foetuses. These were characterised by a hypocellular area with increased chondrocyte cytoplasm and pyknotic nuclei. Dams and foetuses had increased corticosterone levels. Increased plasma corticosterone levels were considered to be a counter regulatory response to hypoglycaemia to increase hepatic glucose output.

As glucocorticosteroids are known to decrease growth plate size with relative sparing of the hypertrophic zone in animals as well as to induce hypoxia in long bone growth plates, it seems likely that the growth plate changes seen in the present study are a consequence of the increased plasma corticosterone level.

**Conclusion:** These results increase the knowledge of maternal hypoglycaemia on foetal skeletal development, most likely in part as a consequence of increased maternal corticosterone level. This could potentially play a role in foetal intrauterine growth restriction seen after maternal nutrient restriction.

**Disclosures:** Vivi Jensen, None.

## LB-SA0372

**Longitudinal genome-wide association analyses and heritability estimates of pediatric bone mineral density.** Diana Cousminer<sup>\*1</sup>, Alessandra Chesi<sup>1</sup>, Jonathan Mitchell<sup>1</sup>, Heidi Kalkwarf<sup>2</sup>, Joan Lappe<sup>3</sup>, Vicente Gilsanz<sup>4</sup>, Sharon Oberfield<sup>5</sup>, John Shepherd<sup>6</sup>, Andrea Kelly<sup>1</sup>, Shana McCormack<sup>1</sup>, Benjamin Voight<sup>1</sup>, Babette Zemel<sup>1</sup>, Struan Grant<sup>1</sup>. <sup>1</sup>Children's Hospital of Philadelphia, United States, <sup>2</sup>Children's Hospital Medical Center, United States, <sup>3</sup>Creighton University, United States, <sup>4</sup>Children's Hospital Los Angeles, United States, <sup>5</sup>Columbia University, United States, <sup>6</sup>University of California San Francisco, United States, <sup>7</sup>University of Pennsylvania, United States

**Background:** SNP heritability ( $h^2_{SNP}$ ) is an estimate of the trait variance attributed to genotyped genetic factors.  $h^2_{SNP}$  of bone mineral density (BMD) varies at different skeletal sites and with age, and assessments of  $h^2_{SNP}$  and genome-wide association studies (GWAS) have typically been performed using cross-sectional adult data. In contrast, systematic longitudinal assessment of  $h^2_{SNP}$  in the pediatric context has not yet been conducted. Thus, in this study we determined  $h^2_{SNP}$  estimates for BMD and bone mineral content (BMC) across various clinically important skeletal sites using

modeled longitudinal pediatric growth curves. We also performed GWAS to search for novel bone-related loci that impact growth across the trajectory of childhood growth.

**Methods:** In the multicenter, multiethnic Bone Mineral Density in Childhood Study (BMDCS) of healthy children aged 5 to 20 years old each with up to 7 annual measurements, we measured BMD and BMC of the spine, total hip, femoral neck, distal radius and total body less head in up to 1,876 boys and girls. GCTA Restricted Maximum Likelihood (GREML) was used to estimate  $h^2_{SNP}$  for Super Imposition by Translation and Rotation (SITAR)-modeled longitudinal growth parameters (*size*, *tempo*, and *velocity*) at each skeletal site with adjustment for population ancestry. Subsequently, sex and ancestry-specific standardized SITAR-modeled growth parameters were analyzed with GWAS using GEMMA, which also accounts for population ancestry.

**Results:**  $h^2_{SNP}$  was higher for the *size* parameter than for the *tempo* and *velocity* parameters, and estimates for *size* (ranging from 0.52 (SE=0.093,  $P=2.0 \times 10^{-8}$ ) for femoral neck BMD to 0.20 (SE=0.09,  $P=0.011$ ) for radius BMD) were comparable to previously published cross-sectional estimates. Subsequent GWAS analysis recapitulated the known signal at *CPED1* for female radius BMD, here associated with the radius *size* parameter, but also yielded a number of novel genetic signals associated with *size*, *tempo*, and *velocity* that varied across skeletal sites.

**Conclusions:** We report skeletal site-specific longitudinal estimates of  $h^2_{SNP}$  for pediatric BMD and BMC that are comparable to previous estimates but cover a more detailed skeletal resolution than previous studies and capture growth longitudinally. We find that  $h^2_{SNP}$  and the most prominent GWAS-implicated loci vary across skeletal sites. These results will eventually lead to the identification of genes and biological insights into our understanding of skeletal bone acquisition, vital to reducing later life osteoporosis risk.

**Disclosures:** Diana Cousminer, None.

## LB-SA0373

**Voxel-based morphometry of peripheral BMD in elderly men with recent excessive bone loss: the Osteoporotic Fractures in Men (MrOS) Study.** Julio Carballido-Gamio<sup>\*1</sup>, Jane A Cauley<sup>2</sup>, Dennis M Black<sup>3</sup>, Sharmila Majumdar<sup>3</sup>, Nancy E Lane<sup>4</sup>, Elizabeth Barrett-Connor<sup>5</sup>, Eric S Orwoll<sup>6</sup>, Andrew J Burghardt<sup>3</sup>. <sup>1</sup>University of Colorado, Denver, United States, <sup>2</sup>University of Pittsburgh, United States, <sup>3</sup>University of California, San Francisco, United States, <sup>4</sup>University of California, Davis, United States, <sup>5</sup>University of California, San Diego, United States, <sup>6</sup>Oregon Health & Science University, United States

Age-related bone loss is spatially non-homogeneous, varying according to a complex array of hormonal, physiological, genetic, and behavioral factors. Measurement of bone properties in anatomic regions most sensitive to clinical risk factors or outcomes could provide greater precision for fracture prediction and optimized targeting for interventions. In this study, we used Voxel-Based Morphometry (VBM), a class of image-driven computational anatomy techniques, to identify characteristic regions associated with excessive bone loss in elderly men participating in Visit 4 of the Osteoporotic Fractures in Men (MrOS) Study. We defined excessive bone loss (EBL) from Visit 3 to 4 (7.1 yrs) as >10% loss at the total hip or femoral neck by DXA. The tibia of these participants was imaged by HR-pQCT at Visit 4. The images were automatically segmented and shapes were spatially normalized to a common template, effectively aligning corresponding anatomical regions across the study population. These transformations were applied to voxel-based maps of homogenized volumetric bone mineral density (vBMD). Voxel-wise comparisons of vBMD between men with and without EBL were performed in the space of the template using general linear models with vBMD as the dependent variable, EBL status as the independent variable, and age, height, and weight as covariates. These comparisons yielded a Student's t-test statistical map (T-Map), which was corrected for multiple comparisons using the false discovery rate approach ( $q=0.05$ ). Of 1770 participants with HR-pQCT and DXA scans available, 1379 were successfully processed automatically for VBM: 241 participants with, and 1138 without EBL. Figure 1 summarizes the results of this study, where different views and cross-sections of the VBM T-Map indicate significant differences in vBMD across the entire tibia, between men with vs. without EBL. However, these differences were non-homogeneous, with the most prominent vBMD differences (red) observed in the intra- and endo-cortical regions, and in a peripheral region on the medial side of the medullary space. These observations suggest preferential bone loss in these regions are characteristic of men experiencing EBL. Targeted measurement of EBL-specific regions may provide greater fracture risk prediction. In the future, spatial parametric mapping of longitudinal intervention effects could be cross-referenced with our results to provide personalized treatment recommendations for men with EBL.



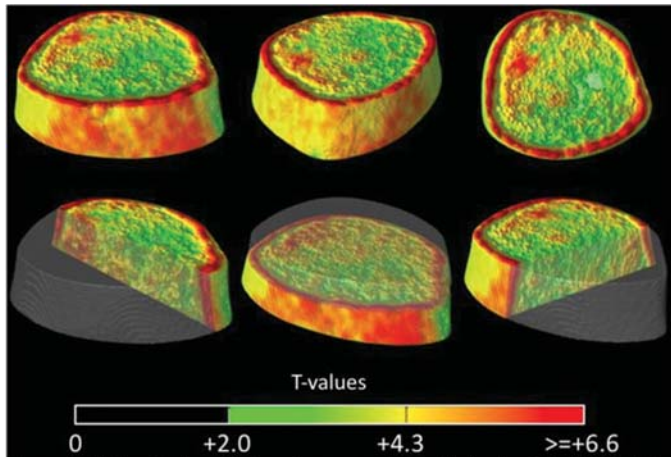


Figure 1. Different views (top) and cross-sections (bottom) of the VBM T-Map indicating significant voxel-wise differences of vBMD between subjects with and without EBL.

Disclosures: Julio Carballido-Gamio, None.

## LB-SA0374

**Intraflagellar transport protein is required for stem cell maintenance through regulating and coupling of FGF and Hh signaling.** Xue Yuan\*<sup>1</sup>, Xu Cao<sup>2</sup>, Shuying Yang<sup>3</sup>. <sup>1</sup>University of Stanford, United States, <sup>2</sup>Johns Hopkins School of Medicine, United States, <sup>3</sup>University of Pennsylvania, United States

Stem cells, capable of self-renewal and differentiation into multiple lineages, are essential for tissue development and homeostasis. A growing number of studies have showed that primary cilia, antenna-like structures projecting from cell surfaces are present on both embryonic and adult stem cells. Intraflagellar transport (IFT) proteins are essential for assembly of primary cilia and critical for transducing environmental cues and regulating cell behaviors. However, it is largely unknown about the role and mechanism of IFT proteins in the control of stem cell properties. Here, we revealed that dental pulp stem cells (DPSCs) express IFT80, which is required for controlling DPSCs proliferation and differentiation. Mice with odontoblast-specific deletion of *IFT80* show reduced DPSC proliferation in cervical loop, impaired molar root development and delayed incisor eruption. Decreased proliferation is associated with down-regulation of FGFR1 expression, leading to the disruption of FGF2-FGFR1-PI3K-AKT signaling in *IFT80*-deficiency DPSCs. Moreover, FGF2 enhances osteogenic differentiation through promoting Hedgehog (Hh) and bone morphogenetic protein 2 (BMP2) signaling. This coupling of FGF and Hh/BMP2 signaling was disrupted in *IFT80*-deficiency DPSCs, leading to impaired differentiation. The results provide the first evidence that IFT80 controls stem cell properties and tooth development through regulating and coupling FGF signaling and Hh/Bmp2 signaling pathways, demonstrating IFT proteins are likely new therapeutic targets for tooth and other tissue regeneration and treatment of various diseases.

Disclosures: Xue Yuan, None.

## LB-SA0375

**Anabolic Mechanism of Picolinic Acid action in Human Mesenchymal Stem Cells.** Lakshman Singh\*, Ahmed Al Saeidi, Ebrahim Bani Hassan, Gustavo Duque. University of Melbourne & Australian Institute for Musculoskeletal Science, Australia

Introduction: Picolinic acid (PA) is one of the end products of the kynurenine pathway with bone anabolic effect *in vitro*. However, the exact mechanism of its anabolic nature is not completely understood. In this study, we explored the potential mechanisms of action of PA in human mesenchymal stem cells (hMSCs).

Methods: hMSCs were cultured in osteogenic induction media in the presence of an osteogenic dose of PA (100 nM) or vehicle. Nitric oxide was determined by Greiss' reagent. Changes in beta catenin (nuclear and cytoplasmic) and GSK3 $\beta$  expression were determined by fluorescence microscopy and western blotting.

Results: No effect on nitric oxide was found by treatment with PA. In contrast, we found an increased expression of total beta-catenin and a concomitant decrease in GSK3 $\beta$  expression in hMSCs treated with an anabolic dose of PA. Beta catenin was expressed much earlier in time in PA treated cells as compared to vehicle treated cells, and also accumulated significantly in the nuclei of PA-treated cells. PA had a strong inhibitory effect on GSK3 $\beta$ , an effect that was more significant at later stages of differentiation.

Discussion: Our results suggest that the anabolic effect of PA on hMSCs is not carried out through its anti-oxidant effect observed in other cell types. The anabolic

effect of PA in hMSCs seems to be associated with changes in beta catenin, which could activate RUNX2 expression, a finding that we have already reported in the past<sup>1</sup>. In summary, we found a shift in beta-catenin expression kinetics in PA-treated hMSCs, indicating that elevated expression and stability of beta-catenin is involved in the action of PA as a strong bone anabolic.

References:

1. The Kynurenine Pathway of Tryptophan Degradation is Activated During Osteoblastogenesis. *Stem Cells* 2015;33:111-121.

Disclosures: Lakshman Singh, None.

## LB-SA0376

**Adult hip shape is influenced by variation in genes involved in endochondral bone formation: findings from a genome-wide association study followed by meta-analysis.** Denis Baird\*<sup>1</sup>, Jennifer Gregory<sup>2</sup>, Rebecca Barr<sup>2</sup>, Fiona Saunders<sup>2</sup>, Claudiu Giuraniuc<sup>2</sup>, Lavinia Paternoster<sup>3</sup>, Daniel Evans<sup>4</sup>, Benjamin Faber<sup>1</sup>, Benjamin Mullin<sup>5</sup>, Frederick Kinyua Kamanu<sup>6</sup>, Debbie Lawlor<sup>3</sup>, Scott Wilson<sup>5</sup>, Tim Spector<sup>5</sup>, Eric Orwoll<sup>7</sup>, Steven Cummings<sup>4</sup>, David Karasik<sup>6</sup>, Douglas Kiel<sup>6</sup>, Richard Aspden<sup>2</sup>, Jonathan Tobias<sup>1</sup>. <sup>1</sup>Musculoskeletal Research Unit, School of Clinical Sciences, University of Bristol, United Kingdom, <sup>2</sup>Arthritis and Musculoskeletal Medicine, Institute of Medical Sciences, University of Aberdeen, United Kingdom, <sup>3</sup>MRC Integrative Epidemiology Unit, University of Bristol, United Kingdom, <sup>4</sup>CPMC Research Institute, United States, <sup>5</sup>Department of Twin Research and Genetic Epidemiology, King's College London, London, United Kingdom, <sup>6</sup>Institute for Aging Research, Harvard Medical School Affiliate, United States, <sup>7</sup>Oregon Health and Science University, United States

Alterations in hip shape are thought to contribute to the risk of both hip osteoarthritis (OA) and hip fracture. To identify biological mechanisms contributing to hip shape, we performed a genome wide association study (GWAS) of its different components generated from hip DXA scans.

Hip shape modes were derived by statistical shape modelling using SHAPE software (University of Aberdeen), from hip DXA scans in ALSPAC (females only, n=3,111), Twins UK (mixed, n=4,047), Framingham (mixed, n=2,606), MrOS (male only, n=4,535), and SOF (female only, n=1,635) (total n=15,934). GWAS adjusted for age at scan and ancestry was conducted, using the top ten hip shape modes as outcomes, followed by fixed effects meta-analysis. A multiple correction threshold of  $p=5 \times 10^{-9}$  was defined as the cut-off for genome-wide significance. Genetic effects ( $\beta$ ) are expressed as a per SD change according to the minor allele.

Six genome-wide significant associations were observed with hip shape mode 1 (width: height ratio): rs2158915 (SOX9,  $\beta=0.065$ ,  $P=1.4 \times 10^{-26}$ ), rs1243579 (GSC-DICER1,  $\beta=0.058$ ,  $P=4.5 \times 10^{-14}$ ), rs10743612 (PTHrP,  $\beta=0.046$ ,  $P=3.6 \times 10^{-12}$ ), rs73197346 (RUNX1-MIR802,  $\beta=0.053$ ,  $P=5.4 \times 10^{-10}$ ), rs59341143 (NKX3-2,  $\beta=0.048$ ,  $P=1.1 \times 10^{-9}$ ) and rs6458443 (RUNX2,  $\beta=-0.035$ ,  $P=4.2 \times 10^{-9}$ ). Three associations were observed with hip shape mode 2 (superiorly displaced femoral head): rs1966265 (FGFR4,  $\beta=0.12$ ,  $P=3.9 \times 10^{-20}$ ), rs1542725 (HHIP,  $\beta=-0.070$ ,  $P=2.9 \times 10^{-9}$ ) and rs17725170 (near ADAMTS16,  $\beta=-0.078$ ,  $P=4.5 \times 10^{-9}$ ). rs2160442 in complete linkage disequilibrium (LD) with rs2158915 was also associated with mode 5 (narrower femoral head;  $\beta=-0.086$ ,  $P=6.1 \times 10^{-14}$ ). SOX9, PTHrP, NKX3-2, RUNX1, RUNX2 and FGFR4 have established roles in endochondral bone formation; SOX9 and NKX3-2 mutations cause abnormal joint morphology, and RUNX1 and RUNX2 skeletal abnormalities; the PTHrP locus was associated with hip OA in arcOGEN (OR=1.18,  $P=9.2 \times 10^{-7}$ ); both SOX9 loci were in moderate LD ( $r^2=0.4$ ) with rs7217932, previously associated with femoral neck BMD in GEFOS ( $\beta=0.03$ ,  $P=2 \times 10^{-11}$ ).

Adult hip shape appears to be influenced by genetic variation in genes involved in endochondral bone formation. Our results also suggest that hip shape variation resulting from these genetic influences contributes to the development of hip OA and osteoporosis.

Disclosures: Denis Baird, None.

## LB-SA0377

**Deficiency of Osteoblast Lineage-intrinsic *TSC1* leads to severe Endoplasmic Reticulum (ER) Stress in Osteoblasts and Compromised Osteogenesis.**Qi Han<sup>\*1</sup>, Xu Yang<sup>2</sup>, Qianming Chen<sup>3</sup>, Elia Beniash<sup>2</sup>, Hong-Jiao Ouyang<sup>4</sup>.<sup>1</sup>Department of Endodontics, College of Dentistry, Texas A&M University; State Key Laboratory of Oral Diseases, National Clinical Research Center for Oral Diseases, West China Hospital of Stomatology, Sichuan University, United States, <sup>2</sup>The Center for Craniofacial Regeneration, Department of Oral Biology, School of Dental Medicine, University of Pittsburgh, United States, <sup>3</sup>State Key Laboratory of Oral Diseases, National Clinical Research Center for Oral Diseases, West China Hospital of Stomatology, Sichuan University, China, <sup>4</sup>Department of Endodontics, College of Dentistry, Texas A&M University; The Charles and Jane Pak Center for Mineral Metabolism and Clinical Research, Department of Internal Medicine, the University of Texas Southwestern Medical Center, United States

Tuberous Sclerosis Complex 1 (TSC1) is an upstream negative regulator of the mammalian target of rapamycin pathway (mTOR), a central regulator of protein synthesis. We aimed to elucidate the physiological roles of TSC1 in regulating osteogenesis by generating and characterizing an osteoblast-specific *Tsc1* conditional knockout (CKO) mouse model.

*TSC1<sup>fl/f</sup>* and *Osterix-Cre+* mice were used to generate *TSC1<sup>fl/f</sup> Osterix-Cre+* (CKO) and *Tsc1<sup>+/+</sup> Osterix-Cre+* (Control; CTR). Age- and gender-matched 1-month-old female littermates were used in our studies. Micro-computed tomography (micro-CT) analyses of the cortical bone in the tibia demonstrated that *TSC1* CKO mice had an increased tissue volume, bone volume, bone volume fraction, apparent density, and porosity, but reduced tissue mineralized density, compared with CTR littermates. Consistently, H&E staining of the femurs of the same animals showed thickened but disorganized cortical bone. The results demonstrated compromised bone formation and mineralization in the absence of osteoblast *TSC1*.

Transmission electron microscopy (TEM) analyses of the proximal humeral heads showed that CTR osteoblasts contained multiple mitochondria and excessive ER networks with an average lumen width of about 100 nm. Moderately dilated ER lumens were found in osteoblasts, consistent with the active biosynthesis status of these secretory cells. In a drastic contrast, *TSC1*-deficient osteoblasts displayed numerous, severely dilated ER lumen. The widest ER lumen was  $196 \pm 11$  nm, versus  $314 \pm 27$  nm in the CTR and CKO osteoblasts, respectively. Furthermore, the number of dilated ER lumens ( $>200$  nm) in the CKO osteoblasts was significantly higher than that of the control group ( $p=0.019$ ). Similar observations were made in the osteocytes as well. Consistently, qRT-PCR analyses showed that *TSC1*-deficient bone tissues had increased gene expression of several ER stress markers, such as *xbp1-spliced*, and the ratio of *xbp1-spliced* in *total xbp1*. Immunohistochemical staining also showed an increased protein level of phospho-Eukaryotic Initiation Factor 2 alpha in the CKO bone tissues, compared with that of the CTR counterparts.

Taken together, these observations indicate that *TSC1* deficiency leads to an increased level of ER stress and consequently heightened activity of ER stress signaling in osteoblast lineage cells. It remains to be determined whether and how deregulated ER stress signaling contributes to *TSC1* deficiency-induced osteoporosis.

Disclosures: Qi Han, None.

## LB-SA0378

**Identification of a gene signature associated with elevated bone formation rate in aging mice.** Krista Jackson\*, Aaron Hudnall, Jonathan Lowery. Marian University College of Osteopathic Medicine, United States

Osteoporosis, a disease of low bone mass that results from bone resorption exceeding bone formation, places individuals at enhanced risk for fracture, disability, and death. There is an urgent and unmet need for novel targets in treating osteoporosis, requiring a better understanding of the endogenous mechanisms regulating bone formation. We reported that deletion of the *Bmpr2* gene in skeletal progenitor cells of mice causes substantially elevated bone mass in young adulthood due to increased bone formation rate (Lowery et al, 2015). As yet unpublished work indicates the age-related decline in bone mass of *Bmpr2* mutant mice is reduced approximately three-fold compared to control mice; quantification of serum bone turnover markers indicates this is caused by a sustained increase in bone formation rate to at least 35 weeks of age with no alteration in bone resorption. Here, we determine the gene signature associated with elevated bone formation rate using genome-wide transcriptome profiling in bones of 35-week-old control and *Bmpr2* mutant mice. Applying stringent criteria comparing the expression data to eight well-accepted housekeeping genes (*Ppib*, *Gapdh*, *Hprt*, *Tbp*, *Ppia*, *Gusb*, *Prkg1*, and *Ywhaz*), we found that, out of 24,980 exon-containing transcripts detected in both genotypes, 334 genes were up-regulated and 310 were down-regulated at least two-fold compared to controls. An additional 704 genes were detected in only one genotype. We refined this putative signature by performing transcriptome profiling in these animals at 55 weeks of age when bone formation rate is no longer elevated. This revealed that, of those genes altered at 35 weeks of age, 570 (88.5%) were either no longer up-regulated or down-regulated in *Bmpr2* mutant mice by 55 weeks of age. Bioinformatic analyses on this refined gene set indicates that elevated bone formation rate in *Bmpr2* mutant mice correlates with enrichment for genes containing binding sites for transcription factors associated with skeletal homeostasis, including FOXF1, SOX2, EGR1, E2F1, KLF4, CNOT3, STAT4, and FOXA1. Further, several genes corresponding

with osteoblast differentiation and activity, such as *Pak4* and *Pla2g4a*, the latter of which encodes cytosolic phospholipase A2 and whose deletion causes osteopenia, are up-regulated in *Bmpr2* mutant mice. Collectively, our findings provide insight into the mechanisms regulating age-related bone loss and highlight potential targets for therapeutic modulation of bone mass.

Disclosures: Krista Jackson, None.

## LB-SA0379

**Bone Mass is Increased in Female Mice Lacking Mitofusin2 (Mfn2) in Osteoclast Precursors under Basal and Pathologic Conditions.** Anna Ballard\*, Rong Zeng, Deborah Novack. Washington University in St. Louis, United States

Mitochondria exist in a highly dynamic network in many cell types, and disruption of factors that contribute to network remodeling is associated with a number of debilitating syndromes in humans. Mitochondrial transmembrane GTPase Mitofusin2 (Mfn2) is involved in the fusion of mitochondria to one another and the ER, as well as the initiation of mitochondrial autophagy. During osteoclast (OC) differentiation, mitochondrial copy number increases in parallel with Mfn2 expression. To investigate the role of Mfn2 in bone, we crossed mice bearing floxed Mfn2 alleles and Lysozyme M-cre to generate cohorts of ctrl (Mfn2<sup>+/+</sup>;LysM<sup>cre</sup>) and conditional knock out (cKO) (Mfn2<sup>fl/fl</sup>;LysM<sup>cre</sup>) animals. Basally, 2 mo cKO female mice display an increase in cortical thickness and tissue mineral density with normal trabecular mass via  $\mu$ CT analysis, whereas 4-5 mo cKO females lack cortical differences but have significantly increased trabecular bone mass (BV/TV) compared to ctrls by VivaCT ( $p<0.05$ ,  $n=9-19$  per group). At these ages, bone parameters in male cKO mice are not different from ctrls. No trabecular or cortical parameters are significantly different between groups when animals of either sex are aged to 10-12 mo ( $n=8-17$  per group). To address how Mfn2 deficient animals respond to OC activation, we injected RANKL I.P. into 2 mo old ctrl and cKO mice of both sexes 50 and 26 hrs prior to  $\mu$ CT analysis, a protocol that acutely induces trabecular but not cortical bone loss. In males, ctrl and cKO mice show a significant RANKL-induced decrease in femoral BV/TV (37 and 30%,  $n=9-11$  per group). While female ctrls also lose significant BV/TV when challenged with RANKL (40%), there is no significant effect of RANKL in the cKOs ( $n=7-10$  per group). This indicates that loss of Mfn2 is protective against induced osteolysis in a sex-dependent manner. Curiously, *in vivo* results are not replicated *in vitro*. While altered mitochondrial morphology by Mitotracker staining is apparent in OC cultures derived from 2 mo old cKO mice, no consistent change in OC formation or function is observed in either sex. We are continuing to investigate this discrepancy by modulating culture conditions to better recapitulate the bone microenvironment. Our Mfn2 results reveal an unexpected sexually dimorphic role of mitochondrial dynamics in OC biology. Further studies aim to determine the mechanism through which mitochondrial dynamics (fusion vs. mitochondrial autophagy) impact OC differentiation and/or function.

Disclosures: Anna Ballard, None.

## LB-SA0380

**Synthetic Human Beta-Defensin-3-C15 Peptide Inhibits Bone Resorption via Disrupting Podosome Belt Formation in Osteoclasts.** Ok-Jin Park<sup>\*1</sup>, Jiseon Kim<sup>1</sup>, Jue Yeon Lee<sup>2</sup>, Yoon-Jeong Park<sup>1</sup>, Kee-Yeon Kum<sup>1</sup>, Cheol-Heui Yun<sup>3</sup>, Seung Hyun Han<sup>1</sup>. <sup>1</sup>School of Dentistry, Seoul National University, Korea, Republic of, <sup>2</sup>Nano Intelligent Biomedical Engineering Corporation, Korea, Republic of, <sup>3</sup>Research Institute for Agriculture and Life Sciences, Seoul National University, Korea, Republic of

Human beta-defensin-3 (HBD3), which is secreted from cells in the skin, salivary gland, and bone marrow, exhibits antimicrobial and immunomodulatory activities. Its C-terminal end contains a 15-amino acid polypeptide (HBD3-C15) that is known to effectively elicit antimicrobial activity. Recently, certain antimicrobial peptides are known to inhibit osteoclast differentiation and, thus, we investigated whether HBD3-C15 hinders osteoclast differentiation and bone destruction to assess its potential use as an anti-bone resorption agent. HBD3-C15 inhibited RANKL-induced osteoclast differentiation and formation of resorption pits. In addition, HBD3-C15 disrupted the formation of RANKL-induced podosome belt which is a feature typically found in mature osteoclasts with bone-resolving capacity. HBD3-C15 down-regulated cortactin, cofilin, and vinculin, which are involved in the podosome belt formation. Furthermore, bone loss induced by RANKL was significantly reduced in a mouse calvarial implantation model that was treated with HBD3-C15. Similar inhibitory effects were observed on the osteoclast differentiation and podosome belt formation induced by *Aggregatibacter actinomycetemcomitans* lipopolysaccharide (AaLPS). Concordantly, HBD3-C15 attenuated the resorption in the calvarial bone of AaLPS-implanted mouse. Collectively, these results suggest that HBD3-C15 has an anti-bone resorption effect in developing osteoclasts, and that this occurs via its disruption of podosome belt formation. HBD3-C15 could be a potential therapeutic agent for the inhibition of bone destruction.

Disclosures: Ok-Jin Park, None.



## LB-SA0381

**Sclerostin Antibody Attenuates Morphological Alteration of Osteocytes in a Combined Ovariectomized and Concurrent Functional Disuse Rat Model.** Dongye Zhang<sup>\*1</sup>, Xiaofei Li<sup>1</sup>, Jiangmeng Han<sup>1</sup>, Nancy Rojas<sup>1</sup>, Yue-li Sun<sup>1</sup>, Minyi Hu<sup>1</sup>, Xiaodong Li<sup>2</sup>, Huazhu Ke<sup>3</sup>, Yi-Xian Qin<sup>1</sup>. <sup>1</sup>Stony Brook University, United States, <sup>2</sup>Amgen, Inc, United States, <sup>3</sup>UCB, Inc, United Kingdom

Osteoporosis and osteopenia are major health issues that mainly affect elderly people, women after menopause and immobilized patients. Our previous studies have proved that sclerostin antibody (Scl-Ab) can dramatically enhance bone formation and reduce bone resorption in a severe osteoporosis rat model with the combination of ovariectomy (OVX) and hindlimb immobilization (HLS). However, the mechanism in the cellular level is unclear. The objective of this study is to assess the effect of Scl-Ab on osteocytic morphology change in a combined OVX and HLS rat model via quantification of long- and short-axis and the ratio and osteocyte volume in midshaft cortical bone (Fig.1). Four-month-old virgin female SD rats were divided into 7 groups (n=11 per group): Sham+Veh, Sham+HLS+Veh, Sham+HLS+Scl-Ab, OVX+Veh, OVX+Scl-Ab, OVX+HLS+Veh, OVX+HLS+Scl-Ab. HLS was performed 2 weeks after sham or OVX surgery; and treatment was initiated at the time of HLS. Scl-Ab (25 mg/kg) or vehicle was subcutaneously injected twice per week for 5 weeks. Femurs were harvested at the end of study and embedded in PMMA and polished for SEM imaging. Cortical bone mid shaft osteocyte number per bone area was quantified under 1K magnification; the ratios between long axis and short axis of osteocytes were quantified under 2K magnification; osteocyte dendrite number and surface area were quantified under 5K magnification. Osteocyte dendrites width was quantified using 10K magnification. All the quantification was done by ImageJ. We have reported that multiple morphological and structural changes in osteocytes, including a decreased osteocyte density and reduced osteocyte dendrite number in HLS, OVX or the combination group and Scl-Ab's ability to abolish these unfavorable alterations. We continued our SEM analysis on osteocytes and discovered that the oval shape of osteocyte under HLS, OVX or HLS +OVX has been distorted toward a spindle-like shape, with relatively longer long axis and shorter short axis, assuming osteocyte has a perfect spheroid shape. The ratio between long- and short- axis showed an increased trend in OVX and HLS condition, but Scl-Ab inhibited these increases ( $p<0.001$ ,  $p<0.01$ , respectively; Fig.2 (a)). The volume decreased in HLS, OVX group, but Scl-Ab maintained osteocytes' volume in HLS condition ( $p<0.001$  Fig.2 (b)). It indicates that cortical bone responds to HLS and/or OVX and Scl-Ab treatment via multiple cellular mechanisms, including density of osteocyte, dendrite number and osteocyte shape. The change of osteocyte shape may imply an altered cytoskeleton system within osteocyte and a subsequent disruption of mechanosensing ability for osteocyte, which lead to bone loss macroscopically. These data suggest Scl-Ab's therapeutic potential could be related with its ability to maintain osteocyte's morphologic and structural changes induced by OVX, HLS or both.

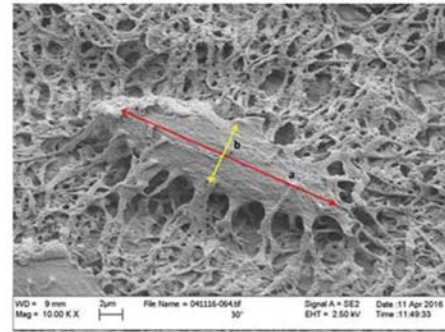


Fig.1. SEM images of a single osteocyte under 10K magnification. The red line represents the long axis a, the yellow line represents the short axis b, and the equation for volume:  $V = \frac{4}{3}\pi ab^2$

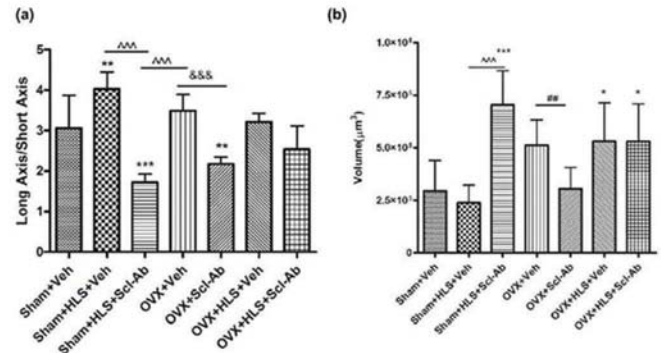


Fig.2. (a) Mean±SD values for the ratio between long axis and short axis of osteocytes. (\*\* $p<0.01$  vs. Sham+Veh; \*\*\* $p<0.001$  vs. Sham+Veh; \*\*\*\* $p<0.001$  and &&& $p<0.001$  vs. the indicated group). (b) Mean±SD values for the volume of osteocytes. (\*\* $p<0.01$  vs. Sham+Veh; \*\*\* $p<0.001$  vs. Sham+Veh; \*\*\*\* $p<0.001$ , &&& $p<0.001$  and ## $p<0.05$  vs. the indicated group).

Disclosures: Dongye Zhang, None.

## LB-SA0382

**Incidental Screening for Osteoporosis in the Presence of Contrast Agents Using No Dose Computed Tomography.** W. Timm<sup>\*1</sup>, J. K. Brown<sup>1</sup>, C.-C. Glüer<sup>2</sup>, R. Andresen<sup>3</sup>. <sup>1</sup>Mindways Software, Inc., United States, <sup>2</sup>Christian-Albrechts-Universität zu Kiel, Germany, <sup>3</sup>Westkuestenlinikum Heide, Germany

Dose-free extraction of bone status information with Asynchronous QCT from existing CT scans may help reduce under-diagnosis and under-treatment of osteoporosis. Spine and femur measurement bias induced by IV contrast agent and possible bias compensation require further investigation.

Patients were recruited receiving routine native, arterial, and portal phase (Imeron 350, Bracco Imaging Deutschland GmbH, Konstanz, Germany) CT scans (GE Revolution EVO, Waukesha, WI, USA). Bone mineral density was obtained from 48 patients (age 70.3 ± 12.7 years) from three vertebrae and the adjacent aorta, and from 33 patients (age 67.7 ± 12.5 years) at total hip and femoral neck regions using QCT Pro Asynchronous 3D Spine, Version 6.1 (Mindways Software, Inc., Austin, TX, USA) and QCT Pro Asynchronous CTXA Hip, respectively. Statistical Analysis was performed using GNU R 3.3.2 (R Foundation for Statistical Computing, Vienna, Austria).

Compared to the native phase, vertebral densities were significantly higher (arterial phase: 8.6 mg/ccm, sd=6.0 mg/ccm,  $p<0.001$ ; portal phase: 21.0 mg/ccm, sd=8.2 mg/ccm,  $p<0.001$ ). Contrast enhanced vertebral densities explained 96.7% (arterial phase) and 93.9% (portal phase) of the variation of native vertebral density. Density at the total hip (arterial and portal phase) and the femoral neck (arterial phase) was not significantly different between arterial and native scans, while significant differences were observed in the portal phase at the femoral neck (aBMD difference: mean 0.013 g/cm² (11.2% of a standard deviation)),  $p<0.01$ ; vBMD difference: mean 3.9 mg/ccm,  $p<0.001$ ). The use of a non-linear Generalized Additive Model and the inclusion of aortic density into the statistical predictive model for the spine resulted in a residual error of 3.7 mg/ccm (arterial phase) and 4.1 mg/ccm (portal phase), respectively.

For the spine, the improved results of the Generalized Additive Model including aortic density are suitable for the estimation of native BMD values from both arterial and portal vertebral densities. With the exception of a clinically non-significant difference in femoral neck density within the portal phase, hip measurements were not significantly different between contrast enhanced and native phases. Summarizing, this supports the application of asynchronous QCT for the purpose of incidental screening.

Disclosures: W. Timm, Mindways Software, Inc., Other Financial or Material Support.

## LB-SA0383

**Shape and Texture Modeling of Hip Bone Density for Fracture Discrimination.** John A Shepherd<sup>1</sup>, Amir Pasha Mahmoudzadeh<sup>1</sup>, Bo Fan<sup>1</sup>, Luke Chaplin<sup>2</sup>, Timothy Cootes<sup>2</sup>, Jane A Cauley<sup>3</sup>, Peggy Cawthon<sup>4</sup>, Steve Cummings<sup>5</sup>, Felix Liu<sup>1</sup>, Claudia Lindner<sup>2</sup>, Rachel Murphy<sup>6</sup>, Marjolein Visser<sup>7</sup>, Ann Schwartz<sup>1</sup>. <sup>1</sup>University of California, San Francisco, United States, <sup>2</sup>University of Manchester, United Kingdom, <sup>3</sup>University of Pittsburgh, United States, <sup>4</sup>California Pacific Medical Center, United States, <sup>5</sup>UCSF School of Medicine, United Kingdom, <sup>6</sup>National Institute on Aging Laboratory of Epidemiology and Population Sciences Bethesda MD USA, United States, <sup>7</sup>VU University Amsterdam Department of Health Sciences Amsterdam The Netherlands VU University Medical Center Department of Epidemiology and Biostatistics Amsterdam The Netherlands, Netherlands

**Objective:** The objective for this study was to determine whether the shape and texture of bone, fat and lean masses are independently associated with incident hip fracture after adjusting for other known risk factors.

**Methods:** Baseline hip bone density for the Health Aging and Body Composition Study (Health ABC) was measured on 2986 of 3097 participants using a Hologic system (Hologic Inc., Marlborough, MA). Participants were 70-79 years (50% male) at baseline. Scans were reanalyzed in two steps. First, the dual-energy attenuations were used to soft for the fat/lean masses outside the bone area. The fat/lean over the bone was approximated by interpolating the percent fat over the bone resulting in complete images of fat, lean, and bone mass. Second, these images were automatically annotated to outline the bone shape using a Random Forest approach. Shape and texture modeling was applied to each image resulting in a principal component (PC) description of the bone shape (PCS<sub>bone</sub>). The images for the entire population were then registered to the average shape using nonlinear warping techniques. Then the texture of the fat, %fat, lean, and bone (PCT<sub>fat</sub>, PCT<sub>%fat</sub>, PCT<sub>lean</sub>, PCT<sub>bone</sub>) was described again using PCs. Proportional hazards regression analyses were employed to determine the associations (Hazard Ratios, HR) of each PC to incident hip fracture, separately for men and women, after adjustment for age, race, femoral neck (FN) BMD, BMI, self-reported health alcohol use, smoking status and education.

**Results:** The baseline mean (standard deviation) of age was 74 ± 3 years and BMI was 26.7 ± 4.3 kg/m<sup>2</sup> respectively. During the 16-year follow-up period, 230 participants sustained a hip fracture (Table 1). To describe 95% of the variance took 14 PCs for bone shape, 73, 21, and 42 for bone, fat and lean textures respectively. After full adjustment, no bone shapes were significantly associated to fractures. However, PCTs for bone, fat and lean mass texture were independently associated with fracture. In men PCT<sub>bone</sub> 27, PCT<sub>fat</sub> 4, PCT<sub>%fat</sub> 1, 3, 5, and 16 remained in our model with HR(95%CI) &lt;math>= 0.45(0.31-0.65), 0.62(0.47-0.8), 1.7(1.23-2.34), 2.05(1.46-2.89), 0.63(0.49-0.81), 0.53(0.39-0.73), \text{ and } 1.39(1.07-1.81), \text{ respectively. In women, PCT}\_{bone} 1 \text{ and } 28, PCT\_{fat} 1 \text{ and } 20, PCT\_{lean} 10 \text{ were associated with fracture risk and HR(95\%CI) = 1.8(1.15-2.83), 1.27(1.02-1.57), 1.28(1.06-1.56), 1.27(1.07-1.51), 0.65(0.51-0.82), 0.79(0.64-0.96), \text{ respectively (Table 2). The addition of these PCs to the risk factors alone improved the AIC from 576 to 536 for men and 1169 to 1149 for women.}

**Conclusion:** The distribution of bone of the proximal hip and the surrounding fat and lean masses are independently related to hip fracture risk in older adults and may improve existing fracture risk models.

	Male										Female										
	Non-Fracture					Fracture					Non-Fracture					Fracture					
	N	Mean	SD	Min	Max	N	Mean	SD	Min	Max	N	Mean	SD	Min	Max	N	Mean	SD	Min	Max	
Age at Year 1 Clinic Visit	1351	73.7	2.9	69.0	80.0	285	74.5	2.7	69.0	80.0	1405	73.4	2.8	68.0	80.0	147	74.8	2.6	69.0	80.0	
White race, n (%)	1351					285					1405					147					
BMI, kg/m <sup>2</sup>	1351	27.0	3.9	14.9	64.2	80.0	26.7	3.4	17.6	36.5	1405	27.9	3.4	14.9	47.3	147	25.4	4.8	17.5	37.9	
Weight (kg)	1351	83.3	13.2	43.8	134.5	80.0	80.3	12.8	55.3	128.7	1405	75.1	14.6	55.3	128.2	147	64.7	12.4	38.8	86.2	
Age 10 standing height (cm)	1351	170.3	66.7	150.9	200.0	80.0	170.2	60.1	139.2	191.5	1405	159.5	62.3	138.9	190.9	147	159.6	52.1	148.9	170.0	
Alcohol Consumption	1349					80.0					1403					147					
No consumption last year		536	(39.7)				44	(7.3)				807	(58.2)				89	(61.9)			
Less than once per week		267	(19.7)				13	(4.3)				324	(23.2)				28	(19.7)			
3 - 7 times per week		536	(39.7)				22	(3.8)				211	(18.2)				28	(19.7)			
More than 3 per day		142	(10.6)				5	(1.8)				51	(3.6)				4	(2.7)			
Smoking status	1349					80.0					1403					147					
Never		388	(28.8)				27	(9.5)				802	(58.2)				87	(59.4)			
Current		150	(11.1)				7	(2.5)				137	(9.8)				17	(11.5)			
Former		813	(60.4)				46	(16.2)				464	(33.5)				43	(29.3)			
Completed years of education	1349					80.0					1403					146					
Less than high school		376	(27.8)				17	(6.3)				324	(23.2)				33	(22.5)			
High school graduate		237	(17.5)				22	(8.2)				340	(24.3)				40	(27.5)			
Postsecondary		736	(54.7)				44	(16.5)				527	(38.5)				55	(38.2)			
Fat or lean or total body	1351					80.0					1405					147					
Body Total BMD (g/cm <sup>3</sup> )	1349	0.8	0.1	0.5	1.3	80.0	0.8	0.1	0.5	1.3	1404	0.8	0.1	0.5	1.3	147	0.8	0.1	0.5	1.3	
Controlled each BMD	1349	0.8	0.1	0.5	1.3	80.0	0.8	0.1	0.5	1.3	1404	0.8	0.1	0.5	1.3	147	0.8	0.1	0.5	1.3	

\*p<0.05 \*\*p<0.001

Table 1: Demographic and BMD measurements by Fracture status For Cohort Data Set

**Disclosures:** John A Shepherd, None.

## LB-SA0384

**Bone Density During Lactation and After Weaning in African-American and Caucasian Women.** Marilyn Augustine<sup>1</sup>, Nayana Nagaraj<sup>2</sup>, Deborah Majchel<sup>2</sup>, Poonam Sood<sup>2</sup>, Robert Boudreau<sup>2</sup>, Jane Cauley<sup>2</sup>, Andrew Stewart<sup>3</sup>, Mara Horwitz<sup>2</sup>. <sup>1</sup>University of Rochester, United States, <sup>2</sup>University of Pittsburgh, United States, <sup>3</sup>Mount Sinai School of Medicine, United States

**Background:** Loss of bone from the maternal skeleton is necessary during lactation to provide adequate breast milk calcium. This process is mediated by parathyroid hormone-related protein in combination with low estrogen levels. After weaning, bone is usually rapidly regained.

Most studies of lactational bone metabolism have been done in Caucasians (C). There are well-documented differences between African-American (AA) and Caucasian bone metabolism. Our group has shown increased serum markers of bone turnover in both AA and C to a similar extent during 12 weeks of lactation. To our knowledge, this is the first study assessing changes in BMD during lactation in AA women.

**Methods:** This was a prospective paired cohort study comparing 29 AA and 29 C healthy postpartum women ages 21-45 who were exclusively breastfeeding. Study visits occurred at two weeks (baseline), 3 and 6 months postpartum and 6 months after weaning at which time a medical history, metabolic bone labs, and a BMD were obtained.

**Stats:** Generalized linear mixed models were used to assess the change over time and differences between races.

**Results:** AA and C lactating mothers were similar at baseline except the AA mothers were slightly younger and significantly heavier than the C women (age 30.52 vs 31.86, BMI 30.79 vs 26.49, respectively). Additionally, AA women had significantly higher baseline absolute BMD (g/cm<sup>3</sup>) compared to the C group at the lumbar spine (LS), total hip (TH), femoral neck (FN) and distal radius (DR) (LS 1.31 vs 1.15; TH 1.12 vs 0.99; FN 1.13 vs 1.00; DR 0.90 vs 0.85).

LS and TH BMD decreased in both groups at 3 and 6 months postpartum and returned to or exceeded baseline after weaning (Table 1). There was no difference between the groups at the LS but the loss at the TH was greater for the C group. The FN BMD also decreased significantly and similarly at 3 and 6 months postpartum for both groups. BMD returned to baseline in the AA group but remained significantly below baseline for the C group. DR BMD remained near baseline at all time points for the AA's, but decreased in the C women at 3 months (Table 1). Adjusting for BMI did not alter the results.

**Conclusion:** Despite baseline differences, BMD decreased at the LS, TH and FN during 6 months of lactation in both AA and C women. BMD returned to or exceeded baseline at all sites except for the C women at the FN. This is the first study comparing changes in bone density during lactation and weaning in AA and C women.

Table 1: Absolute change in BMD from baseline (g/cm<sup>3</sup>)

	3 month Mean (95% CI)	6 month Mean (95% CI)	6 months post-wean Mean (95% CI)	Racial differences for change over time p-value
<b>LS BMD</b>				
African American	-0.03(-0.04, -0.02)*	-0.03(-0.05, -0.01)**	0.02(-0.01, 0.04)	0.28
Caucasian	-0.03(-0.04, -0.02)*	-0.04(-0.05, -0.02)*	0.03(0.01, 0.05)*	
<b>FN BMD</b>				
African American	-0.02(-0.03, -0.01)*	-0.02(-0.03, -0.01)*	0.005(-0.03, 0.04)	0.075
Caucasian	-0.03(-0.03, -0.02)*	-0.05(-0.07, -0.04)*	0.03(-0.04, -0.01)*	
<b>Total Hip BMD</b>				
African American	-0.01(-0.02, -0.01)*	-0.02(-0.03, -0.01)*	0.002(-0.001, 0.01)	0.03
Caucasian	-0.02(-0.02, -0.01)*	-0.04(-0.05, -0.02)*	0.01(-0.02, 0.01)	
<b>Distal 1/3 Radius BMD</b>				
African American	-0.004(-0.01, 0.005)	-0.004(-0.01, 0.01)	-0.003(-0.02, 0.01)	0.73
Caucasian	-0.01(-0.02, -0.001)*	-0.004(-0.02, 0.01)	-0.004(-0.02, 0.01)	

\* p ≤ 0.0001 \*\* p ≤ 0.0002  
\* p ≤ 0.007 \*\* p ≤ 0.05

**Disclosures:** Marilyn Augustine, None.

## LB-SA0385

**Effect of Vitamin D Replacement on Maternal and Neonatal Outcomes - Preg-D Trial Protocol.** Marlene Chakhtoura<sup>1</sup>, Ghada El Hajj Fuleihan<sup>1</sup>, Cyrus Cooper<sup>2</sup>, Nicholas Harvey<sup>2</sup>, Anwar Nassar<sup>1</sup>, Maya Rahme<sup>1</sup>, Sara Ajjour<sup>1</sup>, Mariam Assad<sup>1</sup>, Myriam Chlela<sup>1</sup>, Joe Eid<sup>1</sup>. <sup>1</sup>American University of Beirut, Lebanon, <sup>2</sup>Southampton University, United Kingdom

**Introduction:**

The vitamin D recommended doses during pregnancy differ by organization, and are not evidence based. Our hypothesis is that in Middle Eastern pregnant women, at high risk of vitamin D deficiency, a vitamin D dose of 3,000 IU/day is required to reach a desirable maternal 25-hydroxyvitamin D [25(OH)D] level, and to positively impact infant bone mineral content (BMC).

**Methods:**

This is a blinded randomized controlled trial (BMJ Protocol). Pregnant women presenting to the OB-GYN clinics at AUB-MC and Bahman hospital are being approached. Eligible women are randomized to equivalent doses of cholecalciferol,



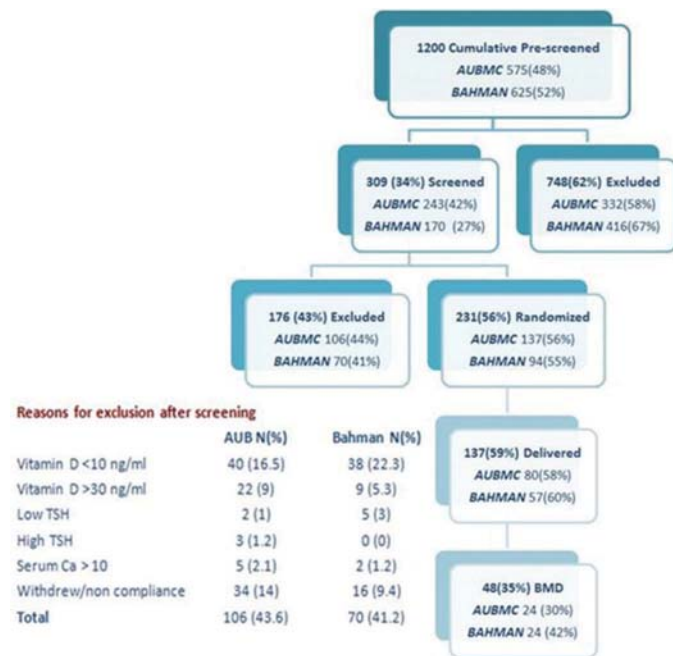
600 IU/d or 3,000 IU/d, from 15-18 weeks gestation until delivery. Maternal 25(OH)D and chemistries are assessed at baseline, and at delivery. Neonatal anthropometric variables are measured at birth, and bone mass assessed by DEXA at 1 month of age. 280 pregnant women are needed to demonstrate a significant difference in the proportion of women reaching a 25(OH)D level  $\geq 50$  nmol/L at delivery, and a difference in infant BMC of 6(10)g (90% power;  $\alpha=2.5\%$ ). The primary analysis is an intention-to-treat analysis of unadjusted results

#### Results:

The trial was launched in July 2015 and is ongoing. To-date, 1,200 pregnant women were pre-screened, 413 pregnant women were screened and 231 were eligible and enrolled (See Appendix). The mean ( $\pm$ SD) age is 30( $\pm$ 4.8) years, and the mean BMI is 24.5( $\pm$ 4) kg/m<sup>2</sup>. The 25(OH)D level at randomization differs by center, 14.7(5.8) ng/ml at Bahman Hospital (N=94) and 17.9(6.4) ng/ml, at AUB-MC (N=137) (P<0.001). 137 women have delivered so far. Consistent with the literature, there is a decrease in maternal serum calcium between visit 1 and delivery due to the dilution effect. 15 serious adverse events have been registered, none is related to vitamin D, and no hypercalcemia is reported. The drop-out rate is 10%. Protocol registered on clinicaltrials.gov (NCT02434380)

#### Conclusion:

This trial is the first to directly address the applicability of the Institute of Medicine vitamin D guidelines worldwide. Findings from our study will inform guidelines on vitamin D replacement in pregnant women in our region.



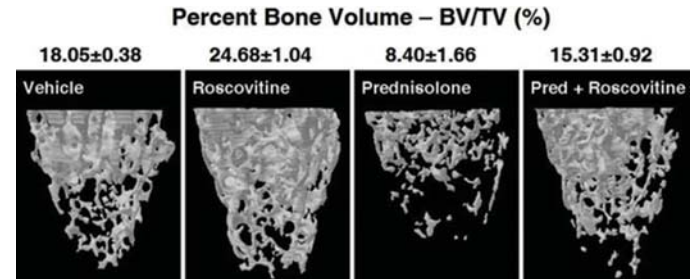
**Disclosures:** Marlene Chakhtoura, None.

## LB-SA0386

**Cyclin-dependent Kinase 5 Inhibits Osteoblast Differentiation to Regulate Bone Integrity.** Mubashir Ahmad<sup>\*1</sup>, Sabine Vettorazzi<sup>1</sup>, David Carro Vázquez<sup>1</sup>, Dilay Lai<sup>1</sup>, Torsten Kroll<sup>2</sup>, Maja Vuijc-Spasic<sup>1</sup>, Aspasia Ploubidou<sup>2</sup>, Johanna Pachmayr<sup>3</sup>, Jan Tuckermann<sup>1</sup>. <sup>1</sup>Institute for Comparative Molecular Endocrinology (CME), Ulm University, Germany, <sup>2</sup>Leibniz Institute for Age Research – Fritz Lipmann Institute (FLI), Germany, <sup>3</sup>Paracelsus Medizinische Privatuniversität, Institute of Pharmacy, Austria

Osteoporosis is characterized by low bone mass and altered bone microarchitecture, leading to increased risk of fractures, particularly in the aging population. Similar to age-related bone loss glucocorticoids (GCs), widely used to treat acute and chronic inflammatory diseases, lead to glucocorticoid-induced osteoporosis (GIO). GIO is quite reminiscent of the age-related osteoporosis characterized by low bone turnover. Currently available pharmacological agents to treat osteoporosis are antiresorptive and decrease the risk of fractures by stabilizing the bone mass but do not improve bone quality. Drugs favoring bone formation, such as intermittent PTH and sclerostin antibodies are costly. Therefore, small molecular compounds are needed for anabolic therapies that would enhance or facilitate bone formation by osteoblasts. To identify those novel targets for small molecule inhibitors, we performed an unbiased cell-based siRNA screen in primary cells using Alkaline Phosphatase (ALP) as a readout. This functional analysis screen led to the identification of cyclin-dependent kinase 5 (Cdk5) as a potent novel suppressor of osteoblast differentiation. Cdk5 siRNA knockdown or a drug inhibition with a specific inhibitor, roscovitine, enhanced ALP activity: 100% $\pm$ 1.87 (Non-Targeting siRNA) versus 371.90%  $\pm$ 47.43 (siCdk5) and 100% $\pm$ 3.86 (Vehicle) versus 156.64% $\pm$ 27.39 (Roscovitine), respectively. In addition, siRNA and Roscovitine both abrogated the deleterious effects of glucocorticoid treatment *in vitro*.

Furthermore, *in vivo* microCT analysis of femur from roscovitine-treated 13-week old female BALB/c mice revealed significantly higher bone mass (Fig. 1), as a consequence of higher trabecular thickness and trabecular number with respect to control. Thus, Cdk5 serves as a potential therapeutic target to treat osteoporosis. In addition, *in vivo* microCT analysis of prednisolone treated mice exhibited a decrease in bone mass (Fig. 1). Importantly, the combined treatment of prednisolone and roscovitine reduced the deleterious effect of prednisolone on bone mass (Fig. 1), suggesting an important role of Cdk5 in glucocorticoid-induced osteoporosis. In conclusion, we identified a novel suppressor of osteoblast differentiation, cyclin-dependent kinase 5, as a potential target for an anabolic therapy to treat osteoporosis, glucocorticoid-induced osteoporosis and other bone related disorders.



**Disclosures:** Mubashir Ahmad, None.

## LB-SA0387

**Examining the Longitudinal Changes in Trabecular vBMD in Individuals with a Chronic SCI.** Rasha El-Kotob<sup>\*1</sup>, Catharine Craven<sup>2</sup>, Lehana Thabane<sup>2</sup>, Alexandra Papaioannou<sup>3</sup>, Jonathan Adachi<sup>3</sup>, Lora Giangregorio<sup>1</sup>. <sup>1</sup>University of Waterloo, Canada, <sup>2</sup>Toronto Rehabilitation Institute, University Health Network, Canada, <sup>3</sup>McMaster University, Canada

**Purpose:** To determine whether trabecular volumetric bone mineral density (TrabvBMD) continues to decline in individuals with a chronic spinal cord injury (SCI).

**Methods:** Longitudinal changes in TrabvBMD were examined via a secondary analysis of data from a prospective observational study. Eligible participants were  $\geq 18$  years of age, had diverse levels of SCI (C2-T12 AIS A-D) and were at least 2 years post injury. Peripheral quantitative computed tomography (pQCT) scans were collected at the 4% tibia site at baseline, year-1, and year-2. The images were analyzed using the pQCT software (Stratec), the CALCBD mode was applied with contour mode 3, peel mode 2, outer threshold of 130 mg/cm<sup>3</sup>, and inner threshold of 400 mg/cm<sup>3</sup>. Repeated measures analyses of variance were performed to examine whether TrabvBMD (mg/cm<sup>3</sup>) changes between the study time points in the total sample and in subgroups of participants with complete and incomplete SCI.

**Results:** Seventy participants (50 men) with a SCI were recruited at baseline, with a mean (standard deviation [SD]) age of 48.8 (11.5) years, and duration of injury (DOI) of 15.5 (10.0) years. Most participants had tetraplegia (51%), motor complete injuries (64%), and reported bisphosphonate exposure (73%). TrabvBMD was not significantly different between baseline [140.1 (53.0)], year-1 [143.3 (55.8)] and year-2 [134.0 (51.2)], V=0.077, F (2,40)=1.674, p=0.200. Despite controlling for bisphosphonate use (yes/no) and DOI, there were no statistically significant mean group changes over two years [V=0.078, F (2,38)=1.618, p=0.212] in the total sample, or in subgroups of participants with complete (p=0.277) and incomplete injuries (p=0.627). The TrabvBMD changes ranged from -183.6 to 207.6 mg/cm<sup>3</sup> at year-1, and -188.2 to 76.4 mg/cm<sup>3</sup> at year-2. At year-2 (n=49), the mean TrabvBMD difference was -6.1 mg/cm<sup>3</sup> [95% CI (-18.0, 5.9)]; when compared to the least significant change (LSC) for TrabvBMD of  $\pm 10.45$  mg/cm<sup>3</sup>, an increase was observed in 5 participants (DOI:3-28 years) and a decrease in 7 individuals (DOI:2-14 years), with changes  $\leq$  LSC in 37 participants.

**Conclusion:** There were no significant differences between the study time points suggesting that TrabvBMD is maintained at the distal tibia, even after controlling for DOI. However, there was some inter-individual variability in BMD over time.

**Disclosures:** Rasha El-Kotob, None.

## LB-SA0388

**Oral bisphosphonate use and risk of acute kidney injury, gastrointestinal events and hypocalcaemia in patients with moderate-advanced chronic kidney disease: a population-based cohort study.** M Sanni Ali<sup>1\*</sup>, Fergus John Caskey<sup>2</sup>, Antonella Delmestri<sup>1</sup>, Daniel Dedman<sup>3</sup>, Nigel Arden<sup>4</sup>, Yoav Ben-Shlomo<sup>5</sup>, Bo Abrahamson<sup>6</sup>, Andrew Judge<sup>1</sup>, C Cooper<sup>7</sup>, M K Javadi<sup>8</sup>, Daniel Prieto-Alhambra<sup>1</sup>. <sup>1</sup>Centre for Statistics in Medicine and Nuffield Department of Orthopaedics, Rheumatology, and Musculoskeletal Sciences (NDORMS), University of Oxford, Oxford, UK, United Kingdom, <sup>2</sup>School of Social and Community Medicine, University of Bristol, Bristol, UK and UK Renal Registry, Bristol, UK., United Kingdom, <sup>3</sup>Clinical Practice Research Datalink, MHRA, United Kingdom, <sup>4</sup>Nuffield Department of Orthopaedics, Rheumatology, and Musculoskeletal Sciences (NDORMS), University of Oxford, Oxford, UK, United Kingdom, <sup>5</sup>School of Social and Community Medicine, University of Bristol, Bristol, UK UK Renal Registry, Bristol, UK., United Kingdom, <sup>6</sup>University of Southern Denmark, Odense, Denmark and Holbæk Hospital, Dept of Medicine, Holbæk, Denmark, Denmark, <sup>7</sup>Centre for Statistics in Medicine and Nuffield Department of Orthopaedics, Rheumatology, and Musculoskeletal Sciences (NDORMS), University of Oxford, Oxford, and MRC Lifecourse Epidemiology Unit, Southampton, UK, United Kingdom, <sup>8</sup>Centre for Statistics in Medicine and Nuffield Department of Orthopaedics, Rheumatology, and Musculoskeletal Sciences (NDORMS), University of Oxford, United Kingdom

## BACKGROUND

The risks and benefits of oral bisphosphonates (oBP) are unclear in patients with moderate to severe chronic kidney disease (CKD): while they could reduce fracture risk, some reports suggest they could worsen renal function.

## OBJECTIVES

To study the association between oBP use and the risk of acute kidney injury (AKI), gastrointestinal events (GIE) and hypocalcaemia in moderate-severe CKD.

## METHODS

**Design:** Cohort study including all subjects with an estimated glomerular filtration rate (eGFR) <45 (stage IIIB+ CKD) at age 50 years or older, with 1+ years run-in data available. Previous users of anti-osteoporosis drugs were excluded.

**Setting:** UK Primary Care computerised records in the Clinical Practice Research Datalink (CPRD) linked to Hospital Episode Statistics (HES) and Office for National Statistics (ONS) mortality data.

**Exposure/s:** GP prescriptions of oral bisphosphonates (oBP) were identified using CPRD medcodes. Treatment episodes (in BP users) were created by concatenating prescriptions until patients switched or stopped therapy (refill gap in prescriptions of 180+ days), or were censored (end of study or transfer out). A wash-out of 30 days was added to date of last prescription to account for carry-over effects.

**Outcome/s:** AKI leading to hospital admission, GIE (bleeding or ulcer/s), or hypocalcaemia leading to hospital admission.

**Statistical analyses:** Cox regression models were fitted to estimate Hazard Ratios (HR) and 95% Confidence Intervals (95CI) according to BP use after 1:5 matching on propensity scores (PS). Different PS models were constructed for each of the outcomes using a priori defined confounders including baseline demographic characteristics, co-morbidities and co-medications, previous fracture and hospital admissions in the previous year. Pre-specified interactions by gender, fracture history and CKD stage were tested.

## RESULTS

A total of 19,315 oBP users and 210,568 non-users were included, with 8846, 499 and 682 patients developing AKI, GI events and hypocalcaemia respectively during follow-up (Table 1). After PS matching, the HR for AKI, GIE and hypocalcaemia were 0.95 (95%CI 0.84 -1.07), 0.85(0.48, 1.52), and 1.11(0.77, 1.62), respectively. None of the interactions were significant.

## CONCLUSIONS

BP use is not associated with AKI, GIE or hypocalcaemia amongst patients with moderate to severe (stage IIIB+) CKD. More data are needed on the potential risks and benefits of BP therapy in this increasing population.

**Table 1. Crude incidence rates of acute kidney injury, gastrointestinal events or hypocalcaemia (N= Number of outcome events and IR= incidence rates).**

	oBP Users			Non Users		
	N	IR/100 Person years	95%CI	N	IR/100 Person years	95%CI
AKI-Hospital	387	0.99	0.14, 7.1	8459	0.94	0.12, 7.1
GI-Events	15	0.04	0.001, 721.35	484	0.05	0.001, 320.43
Hypocalcaemia	41	0.10	0.001, 49.18	641	0.07	0.001, 115.45

**Disclosures:** M Sanni Ali, None.

## LB-SA0389

**Bone Mineral Density Changes in Adherent Denosumab Treated Patients Over a 24 Months Period in Real Clinical Settings.** José Francisco Torres Naranjo<sup>1\*</sup>, Pedro Alberto García Hernández<sup>2</sup>, Claudia Flores Moreno<sup>2</sup>, Pilar De La Peña Rodríguez<sup>3</sup>, Hugo Gutierrez Hermosillo<sup>4</sup>, Roberto González Mendoza<sup>5</sup>, Alejandro Gaytán González<sup>5</sup>, Noe Albino González Gallegos<sup>6</sup>, Juan Lopez Y Taylor<sup>5</sup>. <sup>1</sup>Centro de Investigación Ósea y de la Composición Corporal, CIO, Mexico, <sup>2</sup>Servicio de Endocrinología, Hospital Universitario, UANL, Mexico, <sup>3</sup>De La Peña, Servicios Médicos de la Peña, Mexico, <sup>4</sup>Asociación Mexicana De Metabolismo Óseo Y Mineral, AC, Mexico, <sup>5</sup>Instituto de Ciencias Aplicadas a la Actividad Física y al Deporte, Universidad de Guadalajara, Mexico, <sup>6</sup>Departamento De Bienestar Y Desarrollo Sustentable, Centro Universitario del Norte, Universidad de Guadalajara, Mexico

The FREEDOM phase 3 study in postmenopausal women with osteoporosis reported that denosumab administration was effective for increasing bone mineral density (BMD) relative to baseline for 9.2% at lumbar spine (LS) and 4.8% at total hip (TH) after 36 treatment months. Those BMD gains were associated with a reduced risk of new vertebral fractures and non-vertebral fractures relative to placebo. However changes in BMD in real clinical settings has not been tested in México.

The purpose of this study is to evaluate the changes in BMD in adherent denosumab treated patients in a real clinical setting over a 24 months period.

## Methods.

A multi-center national open-label, non-randomized, observational study. All patients included were under the medical care of physicians in high performance Osteoporosis Medical Centers (OC) with expertise in osteoporosis diagnosis and management. OC conduct rigorous and reliable records protocols. OC have the facilities to perform high precision bone densitometry LSC <3% for all regions: lumbar spine (LS), total hip (TH) and femoral neck (FN).

The sample was composed of 160 women with postmenopausal osteoporosis (range 42-91 years old) adherent to treatment with denosumab 60 mg subcutaneously every 6 mo for 24 mo. No other inclusion criteria were applied.

BMD was measured with DXA for LS, FN and TH at baseline and months 6, 12, 18, 24 during treatment. Both, denosumab 60 mg SC injections and DXA scanners were applied and recorded at OC. Mean BMD change from baseline over 0-24 months and percent of subjects who achieved BMD changes below or above the LSC after 24 months were recorded.

## Results.

The means of BMD (gr/cm<sup>2</sup>) for LS and TH at baseline were 0.642 (±0.103) and 0.685 (±0.102), respectively. Similarly, 34% of our sample had at least 1 prevalent vertebral or non-vertebral fracture before treatment. The mean BMD increase after 24 months of treatment relative to baseline was 7.2% at LS, 4.0% and 3.7% at TH. Likewise, 76%, 62% and 62% of our sample observed a BMD increase above the LSC at LS FN and TH, respectively (Fig. 1). There was a decrease in BMD above LSC in 27% of our patients in any of the measurements during follow-up. Only 2% of patients experienced no change or decrease in BMD in two or more regions after 24 months of treatment.

## Conclusion.

Denosumab was effective for increasing BMD at LS, FN and TH in most of the postmenopausal women during a 24 months period of real clinical setting.

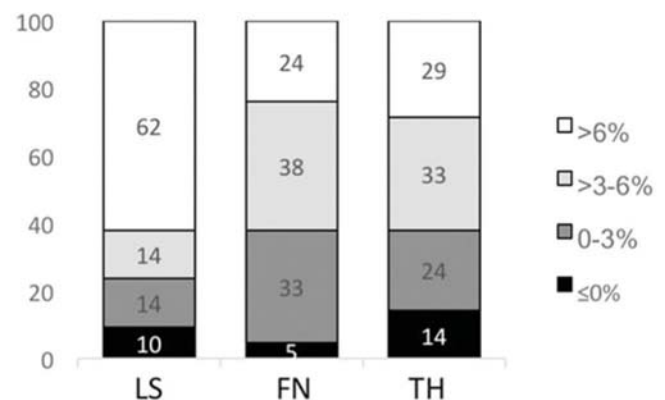


**Fig 1.** Percentage of subjects by bone mineral density (BMD) response category based on the BMD percent change from baseline to month 24 at the lumbar spine (LS), total hip (TH) and femoral neck (FN). Percentages annotated in the bars were rounded to whole numbers.

**Disclosures:** José Francisco Torres Naranjo, None.



## LB-SA0390

**Increased preosteoclast platelet-derived growth factor type BB secretion abrogates negative effect of prednisolone on skeletal angiogenesis.** Janet Crane\*, Shan Lyu, Xu Cao. Johns Hopkins University, United States

Skeletal angiogenesis is necessary for osteogenesis. Glucocorticoids, particularly at high doses associated with osteoporosis, decrease skeletal angiogenesis. In the present study, we dissected the mechanism of glucocorticoid impairment of skeletal angiogenesis directly on endothelial precursor cells (EPCs) and indirectly via paracrine preosteoclast platelet-derived growth factor type BB (PDGF-BB). As angiogenesis and osteogenesis are more abundant in young mice, we developed a young glucocorticoid-induced osteoporotic mouse model, injecting prednisolone 10 mg/m<sup>2</sup>/day intraperitoneally daily from 2 to 6 weeks of age. Wild type-prednisolone mice had decreased bone volume per tissue volume (BV/TV) and type H blood vessels. Tartrate-resistant acid phosphatase (TRAP) and PDGF-BB co-positive cells, which we have previously shown to induce type H vessel formation were also decreased in prednisolone- relative to vehicle-mice. Lineage tracing using an inducible Nestin-Cre<sup>ERT</sup>;YFP mouse showed that Nestin<sup>+</sup> cells in young mice differentiated into endothelial and osteoprogenitor cells, both of which were decreased in prednisolone-mice. In vitro culture of EPCs with prednisolone demonstrated a direct negative effect of glucocorticoids on angiogenesis with decreased tube formation and VEGF expression relative to vehicle EPCs; addition of PDGF-BB partially abrogated the effect. To evaluate the indirect role of preosteoclast secreted PDGF-BB, we utilized a Trap-Cre;Pdgfb<sup>fl</sup> mouse model. Pdgfb<sup>fl</sup> mice had lower BV/TV and type H blood vessels relative to controls (Pdgfb<sup>fl</sup>). Pdgfb<sup>fl</sup> prednisolone mice had an accelerated osteoporotic phenotype and decreased type H vessels relative to Pdgfb<sup>fl</sup> vehicle mice. These results demonstrate both direct and indirect effects of glucocorticoids on endothelial cells, reducing angiogenesis. Inhibition of cathepsin K can secondarily increase PDGF-BB in bone marrow. Therefore, to determine if manipulation of the indirect pathway could prevent glucocorticoid-induced osteoporosis, wild type mice were treated with vehicle, prednisolone or prednisolone plus L-235 (cathepsin K inhibitor). The phenotype of decreased type H vessels and BV/TV in the prednisolone only mice was prevented in the prednisolone plus L-235 mice. Thus, although prednisolone has both direct and indirect effects on bone vasculature, pharmacological manipulation of the indirect pathway can abrogate the negative consequences of glucocorticoids on osteogenesis.

**Disclosures:** Janet Crane, None.

## LB-SA0391

**Oral administration of an egg yolk-derived peptide promotes fracture healing in a mouse model.** Yoshiaki Kitaura\*, Utano Nakamura<sup>2</sup>, Maya Sakashita<sup>2</sup>, Motonori Yamaguchi<sup>2</sup>, Mujo Kim<sup>2</sup>, Ung-il Chung<sup>3</sup>, Shinsuke Ohba<sup>3</sup>. <sup>1</sup>Department of Bioengineering, The University of Tokyo, Japan, <sup>2</sup>Pharma Foods International Co., Ltd., Japan, <sup>3</sup>Center for Disease Biology and Integrative Medicine, The University of Tokyo, Japan

We recently found that oral administration of an egg yolk-derived peptide promoted bone formation and growth in growing rats, suggesting a potential of the peptide as a bone anabolic agent. The bioactive peptide was identified from proteolytic products of chicken egg yolk and generated by peptide engineering approaches; when orally administered, it is processed into smaller peptides and absorbed in the intestine. Here we report that oral administration of the egg yolk-derived bioactive peptide also promotes fracture healing in a mouse model. We created fractures by a transverse osteotomy in tibias of 8-week-old male C57BL/6J mice. Beginning on postoperative day (POD) 1, we orally administered the peptide (10 mg/kg/day, daily) to the mice for up to 56 post-operative days. Three-dimensional micro-computed tomography (3D-μCT) scanning was performed on POD 7, 11, 14, 28, 42, and 56 to assess the fracture healing. 3D-μCT analysis demonstrated that the callus volume was significantly higher in the peptide-administered group than in the vehicle-administered group on POD 11, 14, and 28. We next compared the callus quality of the two groups by quantifying: (1) the volume of callus grouped into bins of different levels of bone mineral density (BMD) and (2) the mechanical property of fractured sites with three-point bending tests. The peptide-administered group showed the higher volume of high BMD callus (850-1000 mg/cm<sup>3</sup>) than the vehicle-administered group on POD 14; the three-point bending test further revealed a trend towards higher mechanical strength of fractured sites in the peptide-administered group than in the vehicle-administered group on POD 14. In addition, when compared with the vehicle administration, the increase in callus volume by the peptide administration was comparable to that by intermittent administration of recombinant parathyroid hormone (1-34) (50 μg/kg/day, daily) on POD 14. Lastly, the peptide enhanced alkaline phosphatase activity in the osteogenic culture of MC3T3-E1 cells at 100 nM within 14 days of the culture compared with control; significant upregulation of *Id1* expression in the peptide-treated cells suggest the involvement of bone morphogenetic signaling in the peptide's effect. These data suggest that the oral administration of the egg yolk-derived bioactive peptide, which is a novel candidate for a bone anabolic agent, can be a facile strategy for managing fracture healing as well as bone quality itself.

**Disclosures:** Yoshiaki Kitaura, None.

## LB-SA0392

**Low Alkaline Phosphatase Levels: Could it be Hypophosphatasia?.** C. Tornero\*, P. Aguado<sup>1</sup>, S. Garcia<sup>1</sup>, J. A Tenorio<sup>2</sup>, P. Lapunzina<sup>2</sup>, K. Heath<sup>2</sup>, A. Buño<sup>3</sup>, J.M Iturzaeta<sup>3</sup>, I. Monjo<sup>1</sup>, C. Plasencia<sup>1</sup>, A. Balsa<sup>1</sup>, Centro de Investigación en Red de Enfermedades Raras (CIBERER)<sup>4</sup>. <sup>1</sup>Rheumatology. La Paz University Hospital., Spain, <sup>2</sup>Institute of Medical and Molecular Genetics (INGEMM). La Paz University Hospital., Spain, <sup>3</sup>Laboratory medicine. La Paz University Hospital., Spain, <sup>4</sup>H. Carlos III., Spain

**Background/Purpose:** Hypophosphatasia (HPP) is a rare disorder caused by mutations in *ALPL* (alkaline phosphatase liver type *ALPL* gene). Clinical presentation is variable and adult forms of the disease are usually milder than those affecting infants and children. It can be overlooked or misdiagnosed as chondrocalcinosis or osteoporosis, which can lead to erroneous therapeutic decisions. The primary objectives were to estimate the prevalence of patients with adult HPP, to analyze their clinical and functional characteristics and to compare these findings between the patients with or without mutations. **Methods:** In this cross-sectional study, 1,536,711 ALP measurements from 386,356 patients were evaluated between 2009 and 2015. Those having at least two values < 35 IU/l and none > 45 IU/l constituted the study population, a total of 427 patients were included. 31 were excluded because of secondary hypophosphatasemia and 13 were lost on follow-up. 108 patients were contacted by phone to fulfill a questionnaire about clinical manifestations and health assessment. Patients were divided into two groups according to whether or not they presented a positive (HPP GT+) or negative (HPP GT-) genetic test. **Results:** Demographic and clinical characteristics are shown in Table 1. Of the 108 patients evaluated, genetic results were available for 85: 47% (40/85) were found to have pathogenic mutations, five previously unreported with the remaining having variants of unknown significance. We identified compound heterozygous mutations in an adult patient diagnosed with infantile HPP and the rest were in heterozygosity and associated with a less severe phenotype. Nine patients carried mutations associated with odontohpp. A higher proportion of patients in the HPP GT+ group presented bone pain (80 v 46.7%, p=0.001), dental abnormalities (35 v 13.3%, p=0.01), premature dental loss (17.5 v 2.2%, p=0.02), metatarsal fractures (10.2 v 0%, p=0.047) and a higher risk of fracture assessed with FRAX (mayor: 3.3 ± 2.5 v 2.2 ± 1 and hip: 0.6 ± 1 v 0.2 ± 0.2, p= 0.02). Furthermore, there was a non-significant trend to present orthopedic surgery, chondrocalcinosis and peripheral fractures in this group. No differences were found in muscle weakness, vertebral fractures, calcific periarthritis, renal disease or necessity of analgesic medication. An elevation of serum phosphate was found in the HPP GT+ group (4.1 ± 0.8 v 3.6 ± 0.6, p=0.01). No differences were observed in pain assessment (Visual Analogue Scale) and the health questionnaire (HAQ). **Conclusion:** The diagnosis of HPP can be difficult and is often missed or delayed, particularly in adults. The prevalence of HPP in patients with low ALP values is high and although clinical presentation is milder in adults, it often presents with bone pain, dental abnormalities, dental loss and fractures. These data should promote a proactive attitude towards detection of adult HPP.

Characteristics	HPP GT + group N= 40	HPP GT -group N= 45	P value
<b>Demographic characteristics</b>			
Mean age $\pm$ DS, n/N	50,38 $\pm$ 15,17 (40/40)	44,53 $\pm$ 10,47 (45/45)	P = 0,04
Gender - Male, n/N (%) - Female n/N (%)	16/40 (40%) 24/40 (60%)	7/45 (15,6%) 38/45 (84,4%)	P = 0,01
Race - Caucasian, n/N (%) - Hispanic, n/N (%) - Black, n/N (%)	38/40 (95 %) 1/40 (2,5%) 1/40 (2,5%)	45/45 (100 %)	NS
<b>Clinical characteristics</b>			
Chronic bone pain, n/N (%)	32/40 (80 %)	21/45 (46,7%)	P = 0,001
Muscle weakness, n/N (%)	6/40 (15%)	3/45 (6,7%)	NS
Calcific periarthritis, n/N (%)	5/40 (12,5%)	3/45 (6,7%)	NS
Chondrocalcinosis, n/N (%)	2/39 (5,12%)	0/45 (0%)	p < 0,13
Peripheral fractures, n/N (%)	18/39 (46,2%)	13/43 (30,2%)	P < 0,14
Metatarsal fractures, n/N (%)	4/39 (10,2%)	0/43 (0%)	P = 0,047
Vertebral fractures, n/N (%)	3/37 (8,1%)	1/45 (2,2%)	NS
Dental abnormalities, n/N (%)	14/40 (35%)	6/45 (13,3%)	P = 0,01
Teeth loss, n/N (%)	7/40 (17,5%)	1/45 (2,2%)	P = 0,02
History of orthopedic surgery, n/N (%)	7/40 (17,5 %)	2/45 (4,4 %)	P = 0,051
Use of analgesic medication for pain, n/N (%)	25 /40 (62,5%)	23 /45 (51,1%)	NS
History of kidney disease, n/N (%)	5/39 (12,8%)	2/39 (5,12%)	NS
Risk of fracture (FRAX), n/N (%) Major Osteoporotic fracture: Hip fracture:	3,3 $\pm$ 2,5; (37/40) 0,6 $\pm$ 1; (37/40)	2,2 $\pm$ 1; (37/45) 0,2 $\pm$ 0,2; (37/45)	P = 0,02 P = 0,02
<b>Biochemical data</b>			
Alkaline phosphatase $\pm$ DS; (n/N)	21,6 $\pm$ 6,76; (38/40)	29,69 $\pm$ 3,4; (45/45)	P = 0,0001
Serum calcium $\pm$ DS; (n/N)	9,43 $\pm$ 0,4; (23/40)	9,27 $\pm$ 0,3; (25/45)	P < 0,14
Urine calcium $\pm$ DS; (n/N)	68,3 $\pm$ 44,1; (4/40)	123; (1/45)	NS
Serum phosphate $\pm$ DS; (n/N)	4,11 $\pm$ 0,78; (21/40)	3,57 $\pm$ 0,6; (24/45)	P = 0,01
Urine phosphorus $\pm$ DS; (n/N)	238,5 $\pm$ 354; (3/40)	(0/45)	
<b>Quality of life assessment</b>			
Visual analogic scale (VAS pain) $\pm$ DS; (n/N)	3,32 $\pm$ 2,3; (38/40)	2,34 $\pm$ 2,7; (45/45)	P = 0,08
Health assessment disability (HAQ) $\pm$ DS; (n/N)	0,18 $\pm$ 0,34; (40/40)	0,18 $\pm$ 0,4; (45/45)	NS

GS-9973-treated *Sh3bp2<sup>KI/KI</sup>* mice was 50% greater than non-treated control mice ( $0.18 \pm 0.02 \text{ mm}^3$  vs.  $0.12 \pm 0.02 \text{ mm}^3$ ,  $n = 4$ ,  $p < 0.05$ ). Histomorphometric analysis of liver tissue showed that GS-9973 administration significantly reduces total area of inflammatory infiltrates compared to non-treated *Sh3bp2<sup>KI/KI</sup>* mice ( $5.4 \pm 4.2\%$  vs.  $17.1 \pm 3.7\%$ ,  $n = 4$ ,  $p < 0.05$ ). Taken together, our results demonstrate that administration of a SYK inhibitor Entospletinib can ameliorate established cherubism phenotypes in mice, suggesting that anti-SYK therapy may be a future treatment option for cherubism patients who already have inflammatory lesions responsible for jawbone destruction.

**Disclosures:** Tetsuya Yoshimoto, None.

**Disclosures:** C. Tornero, Alexion Pharmaceuticals, Other Financial or Material Support.

## LB-SA0393

**Administration of a novel SYK inhibitor Entospletinib ameliorates fully established inflammation and bone destruction in adult cherubism mice.** Tetsuya Yoshimoto\*, Toshio Kondo, Mizuho Kittaka, Yasuyoshi Ueki. University of Missouri-Kansas City, United States

Cherubism is a genetic disorder of the craniofacial skeleton caused by gain-of-function mutations in the SH3-domain binding protein 2 (SH3BP2), which is characterized by the maxillary and mandibular bone destruction due to development of inflammatory lesions. Homozygous knock-in (KI) mouse model of cherubism (*Sh3bp2<sup>KI/KI</sup>*) develops macrophage inflammation that causes bone and joint destruction. While administration of a TNF- $\alpha$  blocker to neonatal *Sh3bp2<sup>KI/KI</sup>* mice prevented the disease, this therapy was not effective for adult *Sh3bp2<sup>KI/KI</sup>* mice and human cherubism patients who have lesions already. Since our recent study showed that genetic ablation of SYK in myeloid cells rescues *Sh3bp2<sup>KI/KI</sup>* mice from inflammation and bone destruction, we examined whether administration of a SYK inhibitor to adult cherubism mice can ameliorate fully developed cherubism symptoms. Entospletinib (GS-9973), which has greater selectivity for SYK than R406, diluted with DMSO was intraperitoneally injected into 10-week-old *Sh3bp2<sup>KI/KI</sup>* mice every day for 6 weeks (100 mg/kg), and treated *Sh3bp2<sup>KI/KI</sup>* mice were analyzed by microCT and liver histomorphometry. Survival rate of GS-9973-treated *Sh3bp2<sup>KI/KI</sup>* mice at 16 weeks old was 100% ( $n = 4$ ), while all vehicle-treated *Sh3bp2<sup>KI/KI</sup>* mice died during the treatment period ( $n = 4$ ). GS-9973 treatment improved the closure of eyelids associated with facial skin inflammation in all *Sh3bp2<sup>KI/KI</sup>* mice, which is typically seen in *Sh3bp2<sup>KI/KI</sup>* mice by 10 weeks old. MicroCT images showed that GS-9973 treatment suppresses bone erosion at elbow joints and calvariae in *Sh3bp2<sup>KI/KI</sup>* mice compared to non-treated *Sh3bp2<sup>KI/KI</sup>* mice. To quantify the level of rescue from focal bone loss, bone volume (BV) of calcaneus was compared to the BV of non-treated *Sh3bp2<sup>KI/KI</sup>* mice. The average BV in



## SU0001

**Primary hyperparathyroidism due to atypical adenoma: clinical, biochemical and histological features of an Italian cohort.** Filomena Cetani<sup>\*1</sup>, Federica Saponaro<sup>2</sup>, Marina Di Giulio<sup>2</sup>, Elena Pardi<sup>2</sup>, Simona Borsari<sup>2</sup>, Claudio Marcocci<sup>2</sup>. <sup>1</sup>University-Hospital of Pisa, Italy, <sup>2</sup>Department of Clinical and Experimental Medicine, University of Pisa, Italy

Primary hyperparathyroidism (PHPT) is mostly due to a benign parathyroid tumor (99%). Some have parathyroid "atypical adenomas", rare tumors with histological features of parathyroid cancer (PC) (fibrous trabeculae, thick fibrous bands, mitotic figures in parenchymal cells), without local invasion or metastasis.

We evaluated 20 patients with histological diagnosis of atypical adenomas, followed at our Institution.

Patients were 13 women and 7 males (mean age: 55±13 yrs). Nineteen patients had a sporadic PHPT and one a Familial Isolated PHPT (FIHP). At least one of the following symptoms was present in 8 (40%) patients: nephrolithiasis (n=8), clinical fragility fractures (n=1), neuropsychiatric symptoms (n=6). In the remaining patients (n=12) PHPT was asymptomatic. Osteoporosis (T score <-2.5 at any skeletal site by DXA), was detected in 8 (40%). Preoperative imaging was positive in 16 (80%) patients. The association with other tumors was recorded: papillary thyroid carcinoma (n=4), adrenal bilateral hyperplasia (n=1), breast cancer (n=1), Morton's neuroma (n=1). Biochemical tests at baseline were: albumin adjusted serum calcium 12.4±0.8 mg/dl, PTH 204 (160-277) pg/ml and 25OHD 13.4±7 ng/ml.

All patients underwent PTx at our Department. The histological diagnosis was of atypical adenoma (mean diameter 24±10.6 mm) with the following features: fibrous trabeculae in 2, thick fibrous bands in 13, capsular invasion infiltration in 7 and mitotic figures in 2.

All but one patients were cured after PTx and remained normocalcemic (mean follow-up 5 years). One patient, with apparently sporadic PHPT, had persistent hypercalcemia and he is in follow-up.

This study suggests that PHPT due to atypical adenoma is in about half of the cases symptomatic at diagnosis, it has a moderate-severe biochemical profile resembling that of PC, it is a sporadic disease and shows a benign prognosis in the majority of cases. We found an association with other tumors, that will be evaluated in further studies.

**Disclosures:** Filomena Cetani, None.

## SU0002

**Calbindin-D 9K mediates vascular calcification from high dose Vitamin D injection via blocking BMP signaling pathway.** Xiangguo Che<sup>\*1</sup>, Na-Rae Park<sup>1</sup>, Yu-Min Hong<sup>1</sup>, Min-Su Han<sup>1</sup>, Youn-Kwan Jung<sup>1</sup>, Yu-Rae Choi<sup>1</sup>, Xian Jin<sup>1</sup>, Goo Taeg Oh<sup>2</sup>, Shigeaki Kato<sup>3</sup>, Je-Yong Choi<sup>1</sup>. <sup>1</sup>Department of Biochemistry and Cell Biology, Korea Mouse Phenotype Consortium, BK21 PLUS, School of Medicine Kyungpook National University, Korea, Republic of, <sup>2</sup>Ewha Womans University, Korea, Republic of, <sup>3</sup>Department of Pharmacy, Iwaki Meisei University, Japan

Vascular calcification (VC) refers to the pathological deposition of calcium phosphate which related with cardiovascular diseases. Previously we established VC mouse model using high dose vitamin D injection subcutaneously and reported the essential roles of Runx2 and vitamin D receptor (Han MS et al., Functional cooperation between vitamin D receptor and Runx2 in vitamin D-induced vascular calcification. *PLoS One*, 8:e83584, 2013). In this study, we explored whether calcium binding protein Calbindin-D9K (Cabp9K), one of vitamin D dependent intracellular calcium transporting proteins, is involved in the VC using high dose vitamin D injection model. Expression of Cabp9K by vitamin D was induced in aorta and kidney. High dose vitamin D injection caused soft tissue calcification in blood vessels and kidney as expected in wild type (WT) mice. However, they were not observed in Cabp9K null mice. Hypervitaminosis D increased serum calcium level in WT, but not in Cabp9K null mice. Serum phosphate level did not change among mice. Expression of osteogenic markers like Runx2, osteopontin, and vitamin D receptor (VDR) was less upregulated in Cabp9K null mice than those of WT mice. In addition, expression of smooth muscle myosin heavy chain was decreased in WT mice, but not in Cabp9K null mice. Vitamin D treatment increased Cabp9K, Bmp2, phospho-Smad 1/5, VDR and Runx2 in vascular smooth muscle cells (VSMCs) derived from WT mice, but not in VSMCs derived from Cabp9K null mice. Collectively, these findings suggest that the protective effects of Cabp9K in the vascular calcification by high dose of vitamin D mediate serum calcium homeostasis and BMP signaling pathway.

**Disclosures:** Xiangguo Che, None.

## SU0003

**The Global, Prospective, Observational PARADIGM™ Registry for Patients With Chronic Hypoparathyroidism Was Expanded to Capture Recombinant Human Parathyroid Hormone, rhPTH(1-84), Use Under Routine Clinical Care.** Bart L. Clarke<sup>\*1</sup>, Maria Luisa Brandi<sup>2</sup>, John Germak<sup>3</sup>, Stefanie Hahner<sup>4</sup>, Pascal Houillier<sup>5</sup>, Olle Kampe<sup>6</sup>, Christian Kasperk<sup>7</sup>, Aliya Khan<sup>8</sup>, Michael A. Levine<sup>9</sup>, Michael Mannstadt<sup>10</sup>, Rebecca Piccolo<sup>11</sup>, Lars Rejnmark<sup>12</sup>, Dolores M. Shoback<sup>13</sup>, Tamara J. Vokes<sup>14</sup>, Neil Gittoes<sup>15</sup>. <sup>1</sup>Mayo Clinic Division of Endocrinology, Diabetes, Metabolism, and Nutrition, United States, <sup>2</sup>University Hospital of Careggi, Italy, <sup>3</sup>Shire International GmbH, Switzerland, <sup>4</sup>University of Würzburg, Germany, <sup>5</sup>Georges Pompidou Hospital and Paris Descartes University, France, <sup>6</sup>Karolinska Institutet, Sweden, <sup>7</sup>Medical University, Germany, <sup>8</sup>McMaster University, Canada, <sup>9</sup>Children's Hospital of Philadelphia, United States, <sup>10</sup>Massachusetts General Hospital and Harvard Medical School, United States, <sup>11</sup>Shire Human Genetic Therapies, Inc., United States, <sup>12</sup>Aarhus University Hospital, Denmark, <sup>13</sup>SF Department of Veterans Affairs Medical Center, University of California, United States, <sup>14</sup>University of Chicago Medicine, United States, <sup>15</sup>University of Birmingham, United Kingdom

PARADIGM™, a global, prospective, observational registry of patients with chronic hypoparathyroidism (HPT), began enrollment in 2013 to collect data on the natural history of chronic HPT (ClinicalTrials.gov NCT01922440). Since initiation, rhPTH(1-84) received US FDA approval and European EMA positive opinion (final authorization due mid-2017) for the treatment of HPT patients. The protocol for the registry (now an EMA-designated postmarketing commitment) was amended to capture rhPTH(1-84) use in HPT patients under routine clinical care (EUPAS16927).

Patient recruitment continues with a global enrollment goal of ≥900 patients, including ≥300 receiving rhPTH(1-84). Follow-up data collection on each patient is planned for ≥10 years. Patients with a diagnosis of HPT of ≥6 months are eligible for inclusion; exclusions include inability to provide informed consent, enrollment in any interventional study, or active PTH(1-34) therapy. Treatment regimens are determined by the patients' physician, per usual clinical practice, and can be conventional calcium/vitamin D supplements and/or rhPTH(1-84). Primary outcome variables are HPT lab tests, including renal function; renal and cardiovascular events; soft tissue calcification or bone fractures; presence of cataracts; and adverse events, including those considered to be related to rhPTH(1-84) treatment. Secondary outcome variables include health-related quality of life, disease-specific patient-reported measures, and hospitalizations and emergency room visits. Additional data to be collected include demographics, medical history, HPT management, and concomitant medications. Data are collected every 6 months and the database uploads are via electronic data capture. A steering committee reviews scientific reports and evaluates requests for analyses.

Prior to starting the new protocol, a registry data cut on December 1, 2016, was completed. 41 investigator sites and 492 patients (49±17 years of age; 30±9 kg/m<sup>2</sup> BMI) had been enrolled. Notably, 93% of patients reported ≥1 symptom within the previous 6 months despite prescribed conventional therapy of calcium (91%) and vitamin D (84%) (Table). Only 7% were recorded as receiving rhPTH(1-84) in a clinical trial setting (ie, data capture was prior to FDA approval).

Data from PARADIGM will provide physicians with needed information on the natural history of HPT in patients prescribed conventional treatment and in those prescribed rhPTH(1-84).

Patient Baseline Characteristics, n (%)	N=492
Most common causes of HPT	
Surgery*	370 (75)
Idiopathic	48 (10)
Genetic	35 (7)
Autoimmune	8 (2)
Received rhPTH(1-84) in a clinical trial	34 (7)
HPT conventional management	
Oral calcium	477 (91)
Active vitamin D	411 (84)
Symptom within past 6 months	
Any symptom	459 (93)
Most common symptoms†	
Fatigue	182 (40)
Paresthesia	139 (30)
Muscle twitching	110 (24)
Anxiety	92 (20)
*Thyroid, parathyroid, head/neck. †n=459.	

Table

Disclosures: Bart L. Clarke, Shire, Consultant.

## SU0004

**Influence of sedentary behavior and voluntary physical activity in bone mineral density in patients with class III obesity.** Florêncio Diniz-Sousa<sup>\*1</sup>, Giorjines Boppre<sup>1</sup>, Leandro Machado<sup>2</sup>, João Vilas-Boas<sup>2</sup>, Vitor Devezas<sup>3</sup>, John Preto<sup>3</sup>, Hugo Sousa<sup>3</sup>, José Oliveira<sup>1</sup>, Hélder Fonseca<sup>1</sup>. <sup>1</sup>CIAFEL, Faculty of Sport, University of Porto, Portugal, <sup>2</sup>CIFI2D, Faculty of Sport, University of Porto, Portugal, <sup>3</sup>Department of Surgery, Centro Hospitalar de São João, Portugal

**Purpose:** Both daily sedentary behavior (SB) and physical activity (PA), particularly vigorous physical activity, can influence bone mass. However, it is not known if this relationship is also valid in patients with severe obesity. Our purpose was to investigate the association between SB, PA and bone mineral density (BMD) in patients with class III obesity.

**Methods:** Sixteen patients with class III obesity [48.7±9.9 years, 47.6±1.8 kg/m<sup>2</sup> body mass index (BMI), 3 male, 13 female] were recruited between January 2016 and February 2017 from the obesity surgery consultation. Hip BMD (total and femoral neck) were measured by dual-energy X-ray absorptiometry (DXA). SB and PA were measured by an accelerometer worn at the waist for 1 week during the entire awake period. Non-wear time was defined as 90 min of consecutive zero counts. Patients with wear time <10 h/d, and <4 valid days were excluded from the analysis (n=2). Sedentary time (ST) and time spent at light PA (LPA), moderate PA (MPA) and vigorous PA (VPA) were defined as <200 counts per minute (cpm), 200 to 1645 cpm, 1646 to 3061 cpm and >3061 cpm, respectively. ST and PA intensities were expressed in minutes/day. Linear regression analyses were used to examine relationships between sedentary, light, moderate and vigorous PA and BMD parameters. Analyses were adjusted for sex, age and BMI.

**Results:** Patients spent 694.1±79.3 min/d in ST, 118.7±50.3 min/d in LPA, 19.7±10.2 min/d in MPA and 7.0±7.2 min/d in VPA. Only a significant association between LPA and femoral neck BMD was identified (r=0.64, p=0.015) and no association between ST, MPA and VPA and femoral neck BMD was detected. Total hip BMD was also not shown to be significantly associated with either ST or PA levels. Our linear regression model showed that, when adjusted for sex, age and BMI, 22% of the variance of femoral neck BMD was explained by LPA [model: sex (unstandardized β=0.049; p=0.545), age (unstandardized β=0.000; p=0.971), BMI (unstandardized β=-0.009; p=0.750)] and LPA (unstandardized β=0.001; p=0.031). The unadjusted linear regression model showed that LPA alone explained 35% of variance in femoral neck BMD (unstandardized β=0.001; p=0.015).

**Conclusion:** As the pattern of physical activity in patients with severe obesity is mainly composed of activities of light intensity, in these patients, femoral neck BMD variance is mostly explained by the time spent in LPA and not by activities of higher intensity.

Disclosures: Florêncio Diniz-Sousa, None.

## SU0005

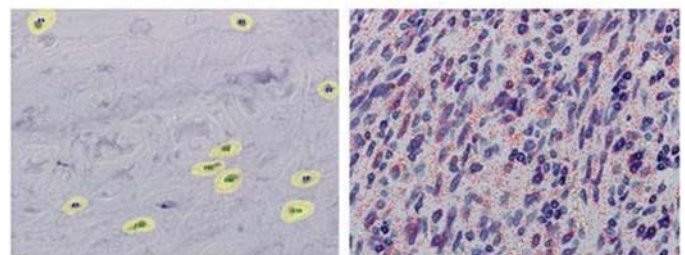
**Utility of the Somatostatin Receptor Scintigraphy and Systemic Venous FGF23 Sampling for the Identification of the Tumor Induced Osteomalacia causing FGF23 producing tumor, and New FGF23 Immunostaining System with High Sensitivity for the Differential Diagnosis.** Nobuaki Ito<sup>\*1</sup>, Minae Koga<sup>1</sup>, Yuka Kinoshita<sup>1</sup>, Masaki Katsura<sup>2</sup>, Miwako Takahashi<sup>2</sup>, Hiroshi Kobayashi<sup>3</sup>, Tetsuo Ushiku<sup>4</sup>. <sup>1</sup>Department of Endocrinology & Nephrology, University of Tokyo Hospital, Japan, <sup>2</sup>Department of Radiology, University of Tokyo Hospital, Japan, <sup>3</sup>Department of Orthopaedic Surgery Faculty of Medicine, University of Tokyo Hospital, Japan, <sup>4</sup>Department of Pathology, Graduate School of Medicine, The University of Tokyo, Japan

**Background:** FGF23 is the physiological phosphate regulating hormone which increase phosphaturia and decrease the serum 1,25D level. Tumor induced osteomalacia: TIO is caused by FGF23 excess producing tumor and which can only be curable when the causative tumor is surgically removed. The identification of TIO causing tumor could be sometimes very problematic because 1) the size of the tumor could be very small, 2) the causative tumor could be generated anywhere in the body, 3) the productivity of FGF23 should be determined in some way.

**Method:** In the current study, the consecutive 10 TIO patients from a single facility were subjected to the both somatostatin receptor scintigraphy (111In Pentetreotide or 68Ga DOTATOC PET/CT) and systemic FGF23 venous sampling and the utility of these tests in identifying the FGF23 producing tumor was analyzed.

**Result:** The mean age of the participants was 61.5 (from 28 to 82, male 6, female 4), the mean serum FGF23 level was 393.1 (107 ~ 1452) pg/mL. Somatostatin receptor scintigraphy and FGF23 sampling concertedly detected FGF23 producing tumor in seven patients. Six tumors were detected in the bone and one tumor was identified in the connective tissue. In the other three patients, there was no clue to localize the causative tumor with these two methods. These three patients are 29, 62 and 67 year-old when they were first diagnosed to suffer from TIO. There aren't affected relative members nor consanguineous marriage of the parents of the index cases. To determine if these three patients are truly suffering from TIO or have other FGF23-related hypophosphatemic diseases with germline mutation, the new FGF23 immunostaining system utilizing Phosphor Integrated Dot nanoparticles (PID) with very high sensitivity and specificity was developed in collaboration with Konica Minolta. This FGF23 immunostaining is sensitive enough to detect suppressed expression of FGF23 in non-affected bones in TIO patients. Therefore, this system would be helpful to differentially diagnose these three FGF23 related hypophosphatemic patients by demonstrating iliac bone biopsy.

FGF23 immunostaining with Phosphor Integrated Dot nanoparticles (PID)

FGF23-PID  
Normal Bone sample from femoral headFGF23-PID  
FGF23 producing bone tumor

FGF23 immunostaining-PID

Disclosures: Nobuaki Ito, None.

## SU0006

**An overview of the etiology, clinical manifestations, management strategies and complications of hypoparathyroidism from the Canadian National Hypoparathyroidism Registry (CNHR).** Aliya Khan<sup>\*1</sup>, Mohammed Almutairi<sup>1</sup>, Rafik El-Werfalli<sup>1</sup>, Adam Waldbillig<sup>1</sup>, Namrah Siraj<sup>1</sup>, Tayyab Khan<sup>1</sup>, Reema Shah<sup>1</sup>, Zubin Punthakee<sup>1</sup>, Adam Millar<sup>2</sup>, Manoela Braga<sup>1</sup>, JEM Young<sup>1</sup>. <sup>1</sup>McMaster University, Canada, <sup>2</sup>University of Toronto, Canada

The CNHR was formed in 2014 and enrolment of prevalent and incident cases began following approval by McMaster University ERB

Objective(s):

- identify the etiology and presenting symptoms of patients with hypoPTH
- evaluate current treatment practice in Canada
- compare parameters of calcium homeostasis amongst those developing complications of nephrolithiasis or nephrocalcinosis versus those without complications
- assess fracture risk in Canadian patients with hypoPTH

Material and Methods:

95 patients aged >18 years registered in the CNHR were reviewed as per the following inclusion criteria



1. Chronic HypoPTH (low PTH in the presence of low serum calcium total or ionized below normal reference range for at least 6 months prior to enrolment)

2. HypoPTH (including post surgery) requiring calcium/calcitriol replacement to maintain normal calcium (total or ionized calcium) for at least 6 months prior to enrolment

3. Pseudohypoparathyroidism with elevated PTH and low serum calcium (total or ionized) normal vit D and hyperphosphatemia

We reviewed etiology, clinical presentation, biochemical profile, management strategies, markers of skeletal health including fractures, bone mineral density (BMD), fracture risk and complications including nephrolithiasis/nephrocalcinosis, and basal ganglia calcification

Results: Most patients (66/95) had postsurgical hypoparathyroidism, followed by idiopathic/autoimmune disease (26/95) and pseudohypoparathyroidism (3/95). The mean age of onset was 41.1 years, with mean duration of follow-up of 2.4 years. Almost all patients were taking calcium supplements (91.6%); calcitriol was taken by 86.3% and 3 patients were receiving parathyroid hormone. Nephrolithiasis or nephrocalcinosis were present in 26.1% of treated patients despite a mean calcium phosphate product <4.4 mmol<sup>2</sup>/L<sup>2</sup>

Basal Ganglia calcification was present in 7 of the 23 patients reviewed

Hospitalization was required in 37 of the 95 patients for symptoms of hypocalcemia

Conclusion:

1. HypoPTH is associated with a significant disease burden and leads to hospitalization in a large number of patients

2. Renal complications were present in 26.6% of treated patients despite maintenance of a calcium phosphate product in the desired range (<4.4 mmol<sup>2</sup>/L<sup>2</sup>). The ideal calcium phosphate product needs to be reconsidered

3. Fracture risk was low in the absence of traditional osteoporosis risk factors

**Disclosures:** Aliya Khan, None.

## SU0007

**FRAX-based Intervention Threshold for Therapeutic Decision in Patients with End-stage Renal Disease on Maintenance Dialysis.** Jerzy Przedlacki<sup>1</sup>, Monika Wieliczko<sup>1</sup>, Jolanta Buczyńska-Chyl<sup>2</sup>, Piotr Kozmiński<sup>3</sup>, Paweł Żebrowski<sup>1</sup>, Ewa Wojtaszek<sup>1</sup>, Joanna Matuszkiewicz-Rowińska<sup>1</sup>, Study Group<sup>4</sup>. <sup>1</sup>Chair and Department of Nephrology, Dialysis and Internal Medicine, Medical University of Warsaw, Poland, <sup>2</sup>Dialysis Unit, Regional Specialist Hospital, Poland, <sup>3</sup>Fresenius Dialysis Center, Poland, <sup>4</sup>26 Dialysis Centers, Poland

Usefulness of FRAX in prediction of an increased bone fracture risk in patients with chronic kidney disease was described, however, it is not clear whether the FRAX-based threshold for pharmacological antifracture treatment used in osteoporosis (in Poland >10% for major bone fractures) is useful in patients with end-stage renal disease (ESRD) on maintenance dialysis. The aim of the study was to determine the optimal FRAX threshold for major bone fracture prediction, at which antifracture drug therapy could be considered. Our prospective, observational study included 742 ESRD patients (410 men and 332 women; 718 HD and 24 PD patients), aged 64.7±11.1 years from all 29 dialysis centers of mazovia region. Patients were treated accordingly to KDIGO guideline. FRAX (without DXA measurement) was calculated at the beginning of study. Observation lasted until the first low-energy major bone fracture or up to 2 years in patients without fracture. The following eligibility criteria to drug therapy were used: FRAX>10%, other decision-making levels of FRAX (>2 to >26%), age >65 years and information on previously broken major bones. During the 2-year observation 30 major bone fractures were diagnosed, including 13 hip and 9 clinically overt spine fractures. Five fractured patients had increased serum iPTH, 5 decreased, and 20 optimal iPTH (130-585 pg/ml) at the beginning of observation. On the basis of the examined criteria we could predict for: FRAX>10%: 9 of total 30 fractures (sensitivity 30.0%, specificity 91.8%; in total, with FRAX>10% 67 patients could be accepted for pharmacological treatment); for FRAX>5%: 21 fractures (sensitivity 70.0%, specificity 69.9%, 235 treated patients); age>65 years: 21 fractures (sensitivity 70.0%, specificity 56.9%, 328 treated patients); information on previous fracture: 9 fractures (sensitivity 30.0%, specificity 87.5%, 98 treated patients). Optimal iPTH did not guarantee antifracture efficacy and 20 patients with optimal iPTH suffered fractures suggesting the need for antifracture treatment. We conclude that in ESRD patients FRAX-based intervention threshold of >10% for major bone fracture risk, as in the general population, requires verification (for 2-year treatment at least). The adoption of a lower threshold, especially >5% seems more practical due to the sensitivity, specificity of the method, and the number of potentially treated patients. This is an open question if anabolic or antiresorptive medicine should be used.

**Disclosures:** Jerzy Przedlacki, None.

## SU0008

**Primary Hyperparathyroidism related to a Parathyroid Adenoma in a Patient with Familial Hypocalcemic Hypercalcemia.** Bridget sinnott<sup>\*1</sup>, Victoria Loseva<sup>1</sup>, David Terris<sup>1</sup>, Seth Kay<sup>1</sup>, Helena Spartz<sup>1</sup>, Robert Brennan<sup>2</sup>, Anthony Mulloy<sup>1</sup>. <sup>1</sup>Medical College of Georgia, United States, <sup>2</sup>Laurel Endocrine, United States

A 53 year old white male was referred for evaluation of progressive hypercalcemia and hyperparathyroidism. He had a prior diagnosis of Familial Hypocalcemic Hypercalcemia (FHH) with a heterozygous missense Calcium Sensing Receptor (CASR) gene mutation C2008G>C; p Gly670Arg. Baseline calcium and PTH were in the 11-12mg/dL (8.7-10.2mg/dl) and 18-40pg/ml (11.1-79.5pg/ml) ranges, respectively. A progressive increase in calcium and PTH levels over the prior three years was noted, with calcium levels recorded in 13-15mg/dl range and PTH levels ranging from 80-160pg/ml. Comorbidities included DM2, HTN and autoimmune hypothyroidism. Family history was negative for calcium disorders or endocrinopathies. On presentation to our clinic, he complained only of mild fatigue despite a calcium level 14.8mg/dL, PO4 level 1.0mg/dL (2.4-5.1) and PTH level 242.1pg/ml.

A thyroid ultrasound was remarkable for a circumscribed 1.4 x 0.5 x 0.7cm hypoechoic nodule in the posterior aspect of the right lobe of the thyroid gland, which demonstrated peripheral vascularity. This corresponded to a region of focal uptake at the posteromedial aspect of the right lower pole of the thyroid gland on SPECT-CT. Preferential cortical bone loss was noted at both the femoral neck and distal 1/3 radius on bone DXA.

A 4 gland surgical exploration revealed an enlarged right superior parathyroid gland which had the gross appearance and texture consistent with a parathyroid adenoma. Baseline intraoperative PTH level was 206pg/ml. Intraoperative PTH levels at 5 and 10 minutes following excision were 32.8 and 25.2pg/ml, respectively, confirming biochemical cure.

The post-operative course was complicated by minimal transient paresthesias which improved with calcium carbonate tablets. Pathology was remarkable for 0.42gm left superior parathyroid adenoma and the left superior and inferior parathyroid biopsies showed hypercellular parathyroid tissue. One week post-operative calcium, PTH and PO4 levels were 10.7mg/dL, 19pg/ml and 3.1mg/dL, respectively. These post-operative values were consistent with his baseline values prior to the development of a parathyroid adenoma.

FHH is a rare benign disorder characterized by a loss of function mutation in the calcium sensing receptor with baseline elevated calcium levels. It is important to establish this diagnosis to prevent unnecessary parathyroid surgery. The development of primary hyperparathyroidism in the setting of FHH has been described in the literature however it is exceedingly rare and it is unclear if this is coincidental or if there is a causative link between the two disorders.

**Disclosures:** Bridget sinnott, None.

## SU0009

**Occult Stones in Primary Hyperparathyroidism are Associated with Urinary Calcium Excretion, 1,25-Dihydroxyvitamin D Levels and Male sex.** Donovan Tay<sup>\*1</sup>, Minghao Liu<sup>1</sup>, Melissa Sum<sup>1</sup>, Leonardo Costa Bandeira<sup>1</sup>, Mariana Bucovsky<sup>1</sup>, Ivelisse Colon<sup>1</sup>, James Lee<sup>2</sup>, Shonni Silverberg<sup>1</sup>, Marcella Walker<sup>1</sup>. <sup>1</sup>Columbia University Medical Center, Dept of Medicine Endocrinology, United States, <sup>2</sup>College of Physicians and Surgeons, Columbia University, United States

Parathyroidectomy (PTX) is recommended for patients with asymptomatic primary hyperparathyroidism (PHPT) who have imaging evidence of nephrolithiasis or nephrocalcinosis. In order to determine the prevalence of, and risk factors for occult nephrolithiasis in PHPT, we conducted a prospective chart review of PHPT patients who had renal imaging from 11/2013-1/2017 as part of their clinical evaluation. Patients with a history of kidney stones after the diagnosis of PHPT or within 4 years before the diagnosis of PHPT were excluded. The cohort (n=87; age 64±11yrs) was mostly female (84%) and had mild PHPT (calcium 10.4±0.9 mg/dl, PTH 88±43 pg/ml, 25OHD 30±11 ng/ml). Renal imaging included ultrasound (47.1%), X-ray (38.8%), CT scan (12.9%) and MRI (1.2%). In the cohort, 51% had osteoporosis, 24% had a history of fracture and 60% met ≥ 1 criterion for PTX. Stones were identified in 18%. Stones were located in the renal pelvis, ureter and bladder. Of all stone formers (n=15), 73.3% had just one stone. Mean size was 7.0±4.3mm (range 2-21mm). Those with vs. without stones had higher urine calcium excretion (333±162 vs 204±104 mg/24h, p=0.02) and were more likely to be male (42.9% vs 12.7%, p<0.01). In those with 1,25-dihydroxyvitamin D (1,25OHD) levels (n=17), stone-formers had higher 1,25OHD (94±21 vs 67±20pg/ml, p=0.02). There was no difference in age, race, BMI, daily calcium or vitamin D intake, serum calcium, PTH, phosphate, 25OHD, renal function, BMD, or fracture history. In a logistic model not including 1,25OHD as a variable, urine calcium was a predictor (B=0.007, p=0.015) of nephrolithiasis adjusting for sex. Receiver operator curves indicated that urinary calcium and 1,25OHD had an area under the curve of 0.725 (p=0.14) and 0.850 (p=0.02) respectively; a 24hr urine threshold of >200mg/day provided a sensitivity of 83.3% and a specificity of 50.0% for presence of stones. A 1,25OHD threshold of >80pg/ml provided a sensitivity of 66.7% and a specificity of 80.0%. Occult nephrolithiasis is associated with higher urinary calcium and activated vitamin D levels as well as male sex. If confirmed with more data, our results suggest that a targeted screening approach in those with high urine calcium and/or activated vitamin D may be an appropriate screening algorithm.

**Disclosures:** Donovan Tay, None.

## SU0010

**Hypophosphatemic Osteomalacia Induced by Long-Term Low-Dose Adefovir Dipivoxil: Clinical Characteristics of 105 Cases.** Zhe Wei\*, Zhen lin Zhang, Metabolic Bone Disease and Genetic Research Unit, Department of Osteoporosis and Bone Diseases, Shanghai Jiao Tong University Affiliated Sixth People's Hospital, Shanghai, China, China

**Objective:** Adefovir dipivoxil (ADV) has been extensively used for the therapy of chronic hepatitis B in China. During the long term of clinical application, the use of ADV at a low dosage has already been found to be responsible for proximal renal tubular dysfunction and secondary hypophosphatemic osteomalacia. The objective of the study was to summarize the clinical characteristics of ADV-induced hypophosphatemic osteomalacia.

**Methods:** Clinical data of 105 ADV-induced hypophosphatemic osteomalacia patients were reviewed and summarized.

**Results:** From June 2008 to March 2017, 105 patients (M:F=63:42) were diagnosed with ADV-induced hypophosphatemic osteomalacia in Shanghai Sixth People's Hospital. The median age was 56.0 (46.0-62.0) years. All patients were chronically infected with hepatitis B, using ADV 10 mg/d for antiviral therapy. Clinical symptoms of osteomalacia appeared after 1.5-15.0 years of ADV use, the median interval was 6.0 years. "Muscle weakness, bone pain and difficulty in activities" were the main clinical manifestations. Laboratory tests showed hypophosphatemia [0.53(0.45-0.64) mmol/L], higher serum alkaline phosphatase [247(192-317)U/L], hypouricemia [121(95-139)umol/L], nondiabetic glycosuria (65/105), proteinuria (76/105) and metabolic acidosis (40/105). Bone turnover markers including serum osteocalcin (OC) and beta C-terminal cross-linked telopeptides of type I collagen ( $\beta$ -CTX) significantly increased. Imaging examinations mainly showed fracture and pseudofracture. The diagnosis of ADV-induced nephrotoxicity and hypophosphatemic osteomalacia was established. Withdrawing adefovir dipivoxil, supplement of calcitriol and calcium and adjusting acid-base with sodium bicarbonate were the main treatments. Elemental phosphate supplementation was not used for any patients. The average follow-up period was 10.9 (1-62) months. During the follow-up, clinical symptoms of most patients relieved in 3 months, serum phosphorus level of 87.1%(61/70) patients became normal in 6 months and the biochemical indicators gradually returned to normal in 12 months.

**Conclusions:** Treatment dose of ADV (10mg/d) could cause severe hypophosphatemic osteomalacia, mostly appear after long-term oral administration. Missed diagnosis and misdiagnosis occur frequently because of its non-specific clinical manifestations. Once correctly diagnosed and treated, the prognosis is usually satisfactory.

**Disclosures:** Zhe Wei, None.

## SU0011

**Quantifying Microdamage in Fatigue Loaded Cortical Bone Tissue.** Dan McDonald\*, Brad Hugenroth, Brett Rosauer, Robert Recker, Mohammed Akhter, Creighton University, United States

Microdamage in bone can accumulate following physiological loading and unloading and in the mechanical stresses of the activities of everyday life. The ability to assess and observe the development of microdamage in bone in three dimensions using non-invasive radiological imaging would greatly improve our understanding the role of microdamage in causing bone fragility. In this study we used MicroXCT-200 (Zeiss/Xradia) 3D imaging to quantify microdamage in bone tissue as it accumulates before and after various stages of fatigue loading. The aim of this study was to quantify microdamage magnitude in human tibial cortical bone following fatigue loading-related strength decline. Cortical specimens (n=10) from mid tibial shaft were obtained from a human cadaver donor. Each specimen was prepared to a standard size of 2mmx2mm cross section and 35mm in length with a notch (25% of the depth) in the center. Prior to initial stiffness testing and fatigue loading (3-point bending) each specimen was scanned at 2.5µm pixel resolution to quantify any existing microdamage and any subsequent microdamage after fatigue loading of 10%, 20%, and 40% stiffness/strength decline. The fatigue load profile was a sinusoidal wave function (4Hz) where 25N was the midpoint of the load and the amplitude was 20N. The volume and surface area of microdamage along with stiffness were determined (Figure-1). Both the microdamage volume and surface area increased significantly (\*P<0.05) at each event of stiffness decline (Figure- 2). In addition, there was a strong correlation between accumulation of microdamage (microcrack volume) and stiffness decline. This unique study of quantifying the micro crack volume at various stages of decline in strength helps to understand the relationship between bone fragility and accumulated micro-damage in bone tissue.

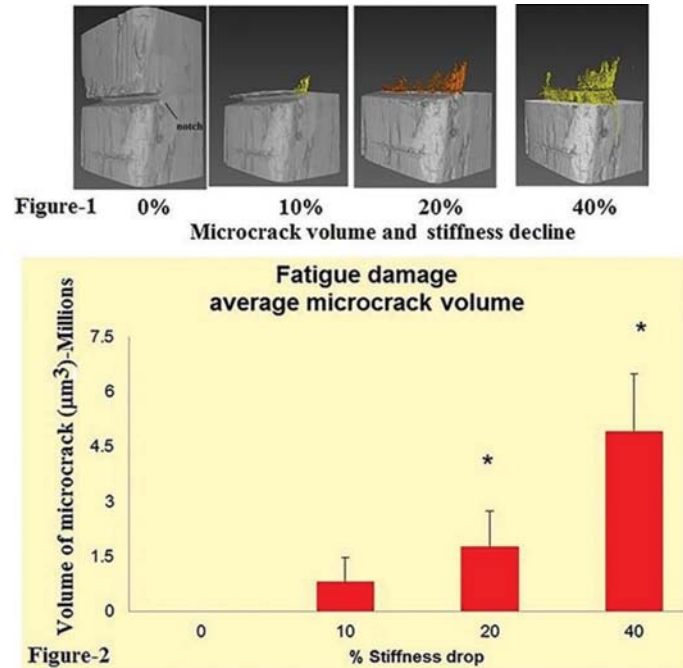


Figure 1 & 2: Microdamage volume and stiffness decline

**Disclosures:** Dan McDonald, None.

## SU0012

**Relating Cortical Bone Mechanics to Intracortical Pore Morphology, Distribution and Remodeling History within the Fibula Diaphysis.** Lydia Bakalova\*<sup>1</sup>, Christina Andreasen<sup>2</sup>, Jesper Thomsen<sup>3</sup>, Annemarie Bruel<sup>3</sup>, Ellen Hauge<sup>3</sup>, Birgitte Kiiil<sup>3</sup>, Jean-Marie Delaisse<sup>3</sup>, Thomas Andersen<sup>2</sup>, Mariana Kersh<sup>1</sup>. <sup>1</sup>University of Illinois at Urbana-Champaign, United States, <sup>2</sup>University of Southern Denmark, Denmark, <sup>3</sup>Aarhus University, Denmark

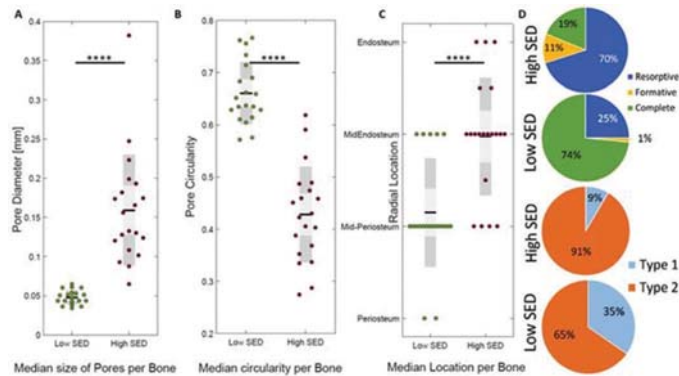
During aging and osteoporosis, the cortical bone becomes more porous, making it more fragile and susceptible to fractures. The aim of this study was to investigate the intracortical compression-induced strain energy distribution, and determine whether the intracortical pores associated with high strain energy density (SED) in the surrounding bone have a different morphology, distribution and remodeling history than pores with low SED.

The study was conducted on fibula diaphysis specimens from 20 patients undergoing a jaw reconstruction (age range 43-75 years, 14 men and 6 women). Specimens were plastic embedded, µCT-scanned and sectioned for histology. Pore size, circularity, and location with respect to the bone edges was quantified. Three-dimensional micro-finite element models of each specimen were tested in compression using a linearly elastic analysis, and the SED of the bone immediately surrounding the pores was calculated within a plane of interest corresponding to the histological sections. The statistical distribution of the SED of all pores, per sample, was used to identify high SED pores (SED > 1.5 times the interquartile range from the 75th percentile) and the remaining low SED pores.

Pores with high SED were larger ( $p \leq 0.0001$ ), less circular ( $p \leq 0.0001$ ), and were located closer to the endosteal edge of the cortex ( $p \leq 0.0001$ ) than low SED pores (Figure 1A-C). A detailed histological analysis of the remodeling events generating the pores revealed that the high SED pores compared to low SED pores had 13.3-fold higher odds of being a resorptive (70%) or formative (11%) pore rather than a completely remodeled pore ( $p \leq 0.0001$ ). Compared to the low SED pores, the resorption space associated with the high SED pores had 5.9-fold higher odds of overlapping with the pore of a preexisting osteon (type 2 pore - 91%) than having no overlap (type 1 pore - 9%) ( $p \leq 0.0001$ ).

Collectively, these data show that the high SED pores are enlarged irregular pores positioned closer to the endosteal surface of the cortex. These pores tend to be resorptive and overlap with the pore of a preexisting parent osteon, suggesting that these pores may originate from resorption within preexisting pores rather than from penetrative resorptions generating new pores. Overall, the study demonstrates a strong relationship between cortical bone mechanics and pore morphology, distribution and remodeling history in the human fibula.





Bakalova Cortical Bone Mechanics

Disclosures: Lydia Bakalova, None.

## SU0013

**Prolonged high repetition high force loading induces localized osteocyte apoptosis, increased CCN2 and sclerostin secretion, and increased RANKL-induced osteoclastogenesis and activity in rat radial bones.** Mary F Barbe<sup>1</sup>, Vicky Massicotte<sup>1</sup>, Alexandra M Monroy<sup>2</sup>, Steven N Popoff<sup>1</sup>. <sup>1</sup>Temple University Lewis Katz School of Medicine, United States, <sup>2</sup>University of Pennsylvania, United States

We have an operant model of upper extremity reaching and grasping in which detrimental bone remodeling is observed rather than beneficial adaptation when rats perform a high repetition high force (HRHF) task for 12 weeks. We sought to examine underlying mechanisms of this bone loss. We investigated the impact of HRHF task performance for 18 weeks (HRHF 18W, n=18) on young adult Sprague-Dawley, female, rat radial bones, compared to age-matched controls (C, n=24). Subsets of bones per group were examined using microCT, histomorphometry, immunohistochemistry, qPCR or ELISA. Serum was also collected and analyzed. HRHF rats performed at 4 reaches/min, at 55% of their maximum pulling force (1.22 Newtons) for 2 hours/day, in four 30 minute sessions, with 1.5 hours between sessions, 3 days/week, for 18 weeks. MicroCT analysis of the distal radial metaphysis demonstrated decreased trabecular bone volume, number and thickness, as well as increased trabecular separation and anisotropy, in HRHF compared to C rats. Anabolic indices (osteoblast numbers, osteoid volume, bone formation rate, and osteocalcin protein levels) were also decreased in this region of the bone in HRHF rats. These responses were concomitant with localized increases in catabolic indices (osteoclast numbers, osteoclast surface/bone surface, osteocyte apoptosis (TUNEL), RANKL mRNA expression, RANKL protein levels and immunoexpression by osteocytes, and RANKL/OPG mRNA ratios). CCN2/CTGF immunoexpression was increased in the trabecular bone matrix, a response thought to contribute to osteocyte apoptosis. Sclerostin had dichotomous changes, with decreased mRNA expression and immunoexpression in osteocytes, yet increased protein levels due to increased secretion and matrix deposition. In contrast, the only microarchitecture changes in mid-diaphyseal cortical bone of HRHF rats were modest increases in cortical porosity, concomitant with increased periosteal osteoclasts and CCN2, and decreased osteocalcin protein levels and SOST mRNA expression, compared to C rats. Serum sclerostin levels were similar between groups, yet serum RANKL and CTX1 levels were higher in HRHF rats. We can conclude that HRHF prolonged task performance leads to localized trabecular bone loss changes due to increased osteocyte apoptosis as a result of repeated high force loading, increased sclerostin secretion from apoptosing osteocytes, and increased RANKL-mediated osteoclastogenesis and activity.

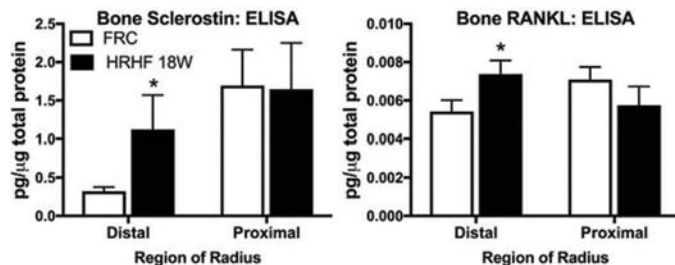


Figure 1

Disclosures: Mary F Barbe, None.

## SU0014

**Whole body vibration therapy triggers load-driven bone formation in adolescents with idiopathic scoliosis.** Patrik Christen<sup>1</sup>, Gianna Marano<sup>1</sup>, Yuk-Wai Wayne Lee<sup>2</sup>, Tsz-Ping Lam<sup>2</sup>, Ralph Müller<sup>1</sup>. <sup>1</sup>ETH Zurich, Switzerland, <sup>2</sup>The Chinese University of Hong Kong, China

Adolescent idiopathic scoliosis (AIS) is a spinal deformity that can lead to severe morbidity and mainly affects peripubertal girls. Using micro-finite element (micro-FE) models derived from high-resolution quantitative computed tomography (HR-pQCT) images, it has been shown that bone strength is significantly lower in AIS versus healthy control. Whole body vibration (WBV) therapy is a suggestive solution because pharmacological drugs are not recommended for the affected adolescents. Nevertheless, the effects of WBV therapy on bone mechanical integrity has not been investigated yet and therefore was the purpose of the present study.

HR-pQCT images of the distal tibia section scanned clinically in young AIS females using XtremeCT (Scanco Medical) were used from a previous study to derive micro-FE models. The WBV group (n=30) was standing on a low-magnitude high-frequency WBV plate (Juvant 1000 DMT, Juvant Medical, 32-37 Hz, 0.085 mm) for 20 min/day, 5 days/week for 12 months, whereas the AIS control group (n=24) was only observed. Imaging was performed at baseline and 12-month follow-up. Bone strength and local tissue loading were estimated using micro-FE analysis.

No significant differences were found in bone strength changes over 12 months between the AIS control and WBV group. However, the treatment group showed larger increases in bone strength in some patients, indicating that WBV therapy can have an effect. Treated patients showing a considerable increase in bone strength (upper third group, n=10) revealed a significant (p<0.01) decrease of local peak loading (98th percentile) after 12-month WBV (Fig. 1). In contrast, treated patients showing a considerable decrease in bone strength (lower third group, n=10) revealed a significant (p<0.01) increase of local peak loading (98th percentile). Furthermore, serological study showed that adequate vitamin D status could be a prerequisite for this bone formation as baseline levels were on average higher (48.1 versus 40.6 nmol/l, p=0.09) in the upper third group than in the lower third group.

This in-depth imaging analysis supports previous clinical observation of increased femoral bone density in AIS patients receiving WBV and suggests that WBV therapy might trigger load-driven bone formation in patients displaying a considerable increase in bone strength (upper third group). These patients also showed higher serum vitamin D levels, however, a larger cohort study is warranted to validate these findings.

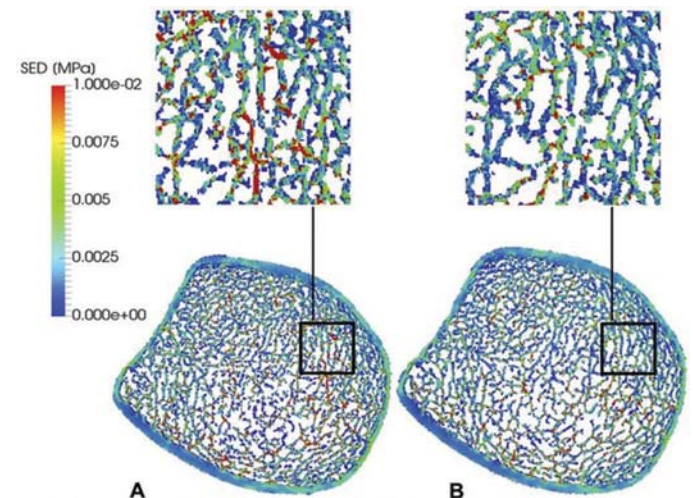


**Figure 1:** Local tissue strain energy density (SED) in the distal tibia of AIS patients at baseline (A) and after receiving 12-month whole body vibration (B) showing a considerable increase in bone strength (upper third group). Patients of this group revealed a significant (p<0.01) reduction in local peak loading (98th percentile) between baseline and follow-up.

Figure 1

Disclosures: Patrik Christen, None.

## SU0015

**The Decrease in Fracture Resistance with Aging in BALB/c Mice Involves Alterations to the Bone Matrix.** Amy Creecy<sup>1</sup>, Sasidhar Uppuganti<sup>2</sup>, Mathilde Granke<sup>3</sup>, Madeline Girard<sup>4</sup>, Siegfried Schlunk<sup>4</sup>, Paul Vozizyan<sup>5</sup>, Jeffry Nyman<sup>6</sup>. <sup>1</sup>Vanderbilt University, VA Tennessee Valley Healthcare System, United States, <sup>2</sup>Vanderbilt University Medical Center, VA Tennessee Healthcare System, United States, <sup>3</sup>Vanderbilt University Medical Center, VA Tennessee Valley Healthcare System, United States, <sup>4</sup>Vanderbilt University, United States, <sup>5</sup>Vanderbilt University Medical Center, United States, <sup>6</sup>Vanderbilt University, VA Tennessee Valley Healthcare System, Vanderbilt University Medical Center, United States

The age-related increase in fracture risk is disproportionate to the loss in areal bone mineral density. Thus, a decrease in bone quality with aging is thought to contribute to increased fracture risk among the elderly. To elucidate mechanisms by which deleterious changes in the bone matrix lowers fracture resistance, there is a need for a validated pre-clinical model that mimics the aging effects on human bone. After euthanizing BALB/c mice from a NIA colony, we analyzed bones from 6-mo adult males (n=20) and females (n=20) and 20-mo aged males (n=18) and females (n=18). Following  $\mu$ CT evaluations of the mid-shaft to determine structural properties and tissue mineral density (Ct.TMD), each hydrated femur was broken in 3pt bending (3 mm/min) to assess fracture resistance. Bound water was measured with non-destructive <sup>1</sup>H-NMR followed by crosslink measurements with HPLC on hydrolysates. Protein extracts from the left tibiae were analyzed by mass spectrometry. As expected, moment of inertia was higher at 20-mo than at 6-mo (male: p=0.002 and female: p<0.0001). Unexpectedly, cortical thickness decreased with age in males (p<0.0001), while it increased with females (p<0.0001). Tissue mineral density was higher for older mice, irrespective of sex (p<0.0001 for each). Independent of geometry, bending strength was lower with advanced aging for both males (p=0.0008) and females (p=0.003)(Fig. 1). Moreover, toughness was significantly less for the aged cortical bone (p<0.0001 for both sexes). Within the matrix, hydroxyllysyl-pyridinoline concentration (PYD) was higher for 20-mo than for 6-mo cortical bone (p<0.0001), and the pentosidine concentration (an AGE crosslink) was also higher with aging (p=0.0003). As for other post-translation modifications, significant age-related differences were found in the collagen  $\alpha$ 1 chain and in matrix-bound osteopontin. These included higher carboxy-methyl-modifications (CML) at specific lysine residues (p=0.015 and p=0.03, respectively) in old than in young bone. Bound water within the bone matrix was lower in older mice (p<0.0001). The increases in CML, PYD, and pentosidine with aging, along with the decrease in bound water, suggest that lower fracture resistance with aging in mice could be the result of changes to the organic matrix of bone, though an age-related increase in mineralization may also contribute. With similarities to human aging, the BALB/c mouse is suitable for studies into the age-related decrease in bone quality.

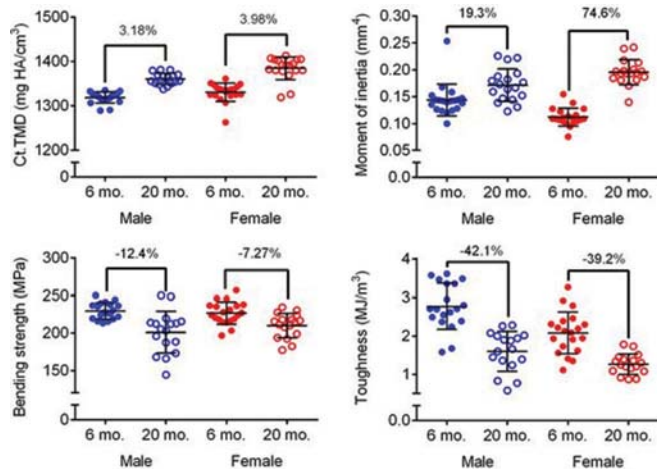


Figure 1: TMD and  $I_{min}$  are shown to be higher in aged mice for males (blue) and females (red), while bending strength and toughness are shown to be lower. Brackets indicate statistical differences between age groups. Numbers above brackets indicate the percent change from 6 mo. aged mice

Figure 1

Disclosures: Amy Creecy, None.

## SU0016

**Influence of Microcracks and Compositional Heterogeneity on Fracture Resistance of Cortical Bone.** Ahmet Demirtas\*, Ani Ural. Villanova University, United States

Several recent studies demonstrated an association between atypical femoral fracture and long-term bisphosphonate (BP) use for osteoporosis treatment. Due to BP treatment, bone undergoes mechanical alterations including reduced tissue composition

heterogeneity and increased microcrack density. The aim of this study is to investigate the effects of microcracks and tissue composition heterogeneity on the crack propagation behavior in human cortical bone by using finite element (FE) analysis.

A transverse microscopy image of cortical bone from the mid-diaphysis of a 58-year-old male donor tibia was converted to a 3D FE model (Fig. 1a, 1b). The fracture behavior of the model was investigated by modeling compact tension specimen tests (Fig. 1c) incorporating cohesive extended finite element method in the osteons and interstitial bone and by cohesive interface elements at the cement lines. Twelve simulations were performed on the model including homogeneous (HM) and heterogeneous (HT) material compositions, and four different microcrack distributions which were composed of 5 and 10 randomly distributed microcracks per unit area and 10 clustered microcracks per unit area. Fracture resistance was assessed by comparing the crack volume between the models.

The simulation results (Fig. 1d) showed that the crack volume was the highest in the model with no microcrack for both HM and HT material properties. Increasing the microcrack density resulted in lower crack volume in all models. The microcracks reduced the crack volume more in HM models compared to the HT ones (Fig. 1d-f). Comparison of the two different random distribution of microcracks demonstrated the influence of the location and size of microcracks on the crack growth behavior in cortical bone (Fig. 1d). In addition, clustered microcracks were not as effective in contributing to the fracture resistance as distributed microcracks (Fig. 1d, 1g, 1h).

In summary, the results showed that the microcracks enhance the fracture resistance of bone, however, their distribution and location significantly affect the fracture behavior. Microcracks influence the fracture resistance less when the tissue composition is more heterogeneous. These results provide new information on the interaction of microcracks, tissue heterogeneity and fracture resistance and may improve the understanding of the influence of mechanical changes due to prolonged bisphosphonate use on the fracture behavior of cortical bone.

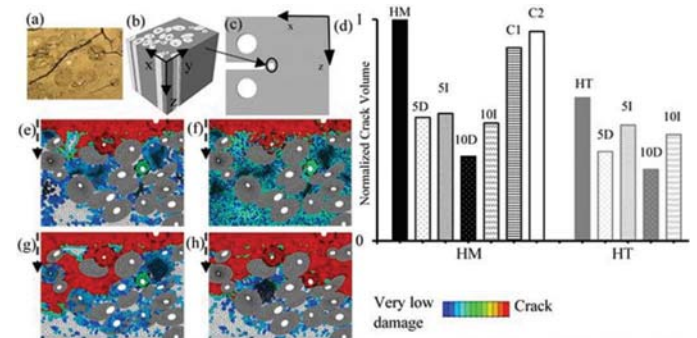


Figure 1: (a) A transverse microscopy image of human cortical bone from the mid-diaphysis of a 58-year-old male donor tibia. (b) 3D model of the transverse microscopy image in (a). (c) Finite element model of the CT specimen. The marked region shows the location where the microstructure cell was inserted. (d) Normalized crack volume of the models where the values are grouped by material composition as homogeneous (HM) with black color and heterogeneous (HT) with gray color. "5" and "10" shows the microcrack density. "D" and "I" represent the two different random distributions of microcracks. C1 and C2 represent the clustered MC models that are located around the edge and the center of the model, respectively. Representative planar crack growth views of (e) 10HMI, (f) 10HTI, (g) HM-C1 and (h) HM-C2.

Figure 1

Disclosures: Ahmet Demirtas, None.

## SU0017

**Characterization of a sandwich ELISA for the quantification of mouse periostin.** Elisabeth Gadermaier\*, Manfred Tesarz, Jacqueline Wallwitz, Gabriela Berg, Gottfried Himmler. The Antibody Lab GmbH, Austria

Purpose: Periostin (osteoblast-specific factor OSF-2) is an extracellular matrix protein which belongs to the FAS1 superfamily. It consists of a conserved N-terminus and a C-terminal region which is affected by alternative splicing leading to different periostin isoforms. In bone, periostin has a general function in homeostasis. It is upregulated in bone development and remodeling, and it acts on bone formation by increasing osteoblast function. To further study periostin in preclinical settings there is the need for a high-quality assay for quantification of periostin in mouse models.

Methods: We developed a sandwich ELISA employing polyclonal and monoclonal anti-periostin antibodies. Linear epitopes were mapped with microarray technology, and assay parameters like specificity, dilution linearity and spike recovery were assessed.

Results: The novel assay is calibrated with mouse periostin isoform 1. It employs only minimal amounts of mouse sera and plasma for the quantification of periostin. Linear epitopes are located in the fourth FAS1 domain for the monoclonal antibody, or distributed over the whole periostin sequence for the polyclonal antibody. All assay characteristics (specificity, dilution linearity, spike recovery) meet the standards of acceptance.

Conclusion: This novel mouse periostin ELISA provides a reliable and accurate tool for the quantification of mouse periostin in serum and plasma samples.

Disclosures: Elisabeth Gadermaier, None.



## SU0018

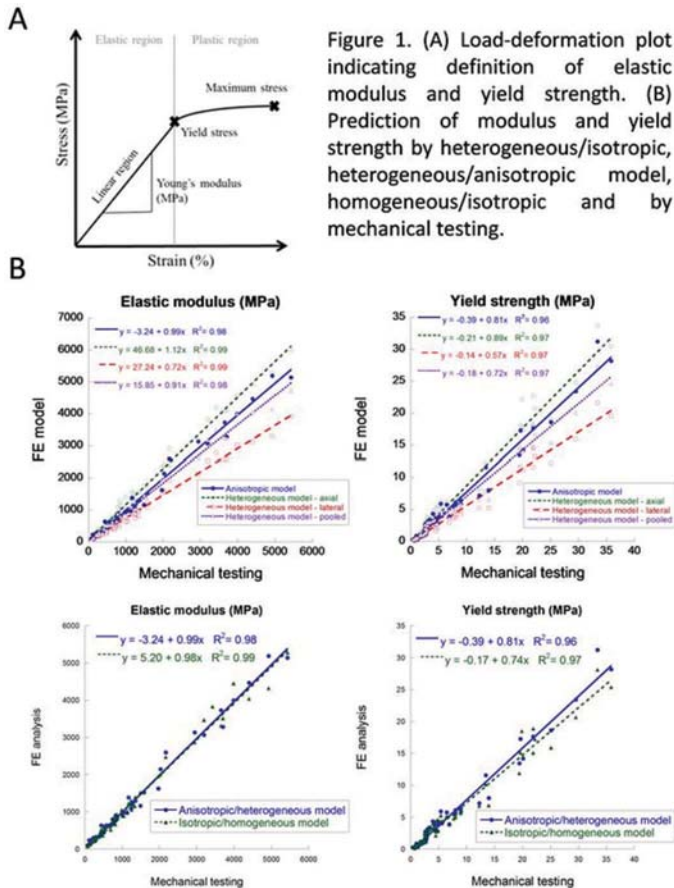
**Consideration of Tissue-Level Anisotropy and Heterogeneity Does Not Increase the Prediction Power of Apparent-Level Mechanical Properties.** Y. Eric Yu\*, Yizhong Hu, Xingjian Zhang, X. Edward Guo. Bone Bioengineering Laboratory, Department of Biomedical Engineering, Columbia University, United States

A key mechanical component of the skeleton, the trabecular bone is highly anisotropic and heterogeneous. Its complex lamellar structure gives rise to its differential modulus in the longitudinal and transverse direction of the fibers, and the non-uniform mineral distribution further adds spatial variance mechanically. The link between these tissue-level properties and apparent-level mechanics has never been established, due to the complicated microstructure and irregular morphology of trabecular bone. This study's objective was to assess the contribution of tissue-level anisotropy and heterogeneity to apparent-level bone mechanics.

Trabecular bone cores along the principal loading direction were harvested from human cadaveric tibiae (n=15) and proximal femur (n=15). Specimens were scanned using  $\mu$ CT, and thresholded images were converted to voxel-based  $\mu$ FE models. For each specimen, non-linear simulations of uniaxial compression with and without incorporation of experimentally determined anisotropy and heterogeneity were created. Young's modulus was determined using experimentally obtained TMD/modulus correlations, where TMD was converted from grayscale value based on density phantom calibration. Predictions of stiffness and strength from these models were compared to the corresponding mechanical testing results.

We found that comparing isotropic but heterogeneous models with different TMD/modulus correlations, while all models resulted in high correlation compared to mechanical testing results, axial trabecular moduli overestimated stiffness, while lateral moduli underestimated stiffness. Average moduli underestimated but improved bone stiffness prediction with slope approaching 1. Incorporating anisotropy in addition to heterogeneity, prediction of bone stiffness was highly correlated ( $R^2=.98$ ) and indistinguishable from (slope=0.99) mechanical testing calculations. The prediction, however, was not better than the simple isotropic/homogeneous model.

This study was the first to incorporate both anisotropy and heterogeneity into a  $\mu$ FE model using experimentally obtained Young's modulus of individual trabeculae. While inclusion of the mechanically obtained tissue-level Young's modulus closely predicted the mechanical properties, it did not improve the prediction power of the models, suggesting that the tissue-level heterogeneity and anisotropy are not as important predictors as morphological parameters for the apparent-level mechanical behaviors.



Figure

Disclosures: Y. Eric Yu, None.

## SU0019

**Bone Quality Assessment of Fresh Bone Using FTIR Imaging.** Teppei Ito<sup>\*1</sup>, Masahiko Takahata<sup>2</sup>, Tomohiro Shimizu<sup>2</sup>, Kyosuke Kanazawa<sup>1</sup>, Hiromi Kimura-Suda<sup>1</sup>. <sup>1</sup>Chitose Institute of Science and Technology, Japan, <sup>2</sup>Hokkaido University, Japan

Bone strength is determined by a combination bone mass (or bone mineral density, BMD) and bone quality. Therefore, bone quality assessment is very important for understanding of fracture risk in osteoporosis patients. Bone quality results from a combination of material properties and structure properties, including parameters such as rate of turnover, architecture/geometry, mineral-to-collagen matrix ratio and accumulation of microdamage, so that Fourier transform infrared (FTIR) imaging is a powerful tool for the assessment of bone quality. Generally, it requires poly(methyl methacrylate) (PMMA) embedding to prepare thin sections for FTIR imaging measurements. The PMMA embedding process takes more than two weeks, and may lead to denaturation of the bone. Development of an easy sample preparation technique is, therefore, needed for the clinical evaluation of fresh bone using FTIR imaging. We developed a method for preparing thin sections of fresh bone using a combination of frozen sectioning and polypropylene (PP) film as a bone substrate, and herein demonstrate that the combined use of thin PP film coated with glue (PP film + glue) as a substrate and the frozen sectioning procedure without denaturation of proteins by solvent or resin is particularly suited to the assessment of the bone quality of fresh calcified bone using FTIR imaging in transmittance mode. The bone quality of femoral thin sections prepared by the PMMA embedding procedure (RESIN-S) or frozen sectioning procedure (FROZEN-S) were evaluated by FTIR imaging. The mineral-to-matrix ratio and crystallinity in the RESIN-S sections were higher than those in the FROZEN-S sections, whereas the carbonate-to-phosphate ratio in the RESIN-S sections was lower than that in the FROZEN-S sections. The increase in the  $\text{PO}_4^{3-}$  band after PMMA embedding indicated dehydration during PMMA embedding. In addition, anisotropy of the PP film was negligible in FTIR imaging. Based on these results, we concluded that the combined use of PP film coated with glue and the frozen sectioning procedure without denaturation appears well suited to the assessment of the bone quality of fresh calcified bone using FTIR imaging.

Disclosures: Teppei Ito, None.

## SU0020

**Strain Magnitude Influences Structural Changes in the Radius of Healthy Adult Women.** Megan Mancuso\*, Joshua Johnson, Sabahat Ahmed, Karen Troy. Worcester Polytechnic Institute, United States

Prescribed exercise has been proposed as a means of increasing peak bone mass in premenopausal females<sup>(1)</sup>, but the importance of specific parameters related to mechanical stimulus is not well understood. Here, we used an upper-extremity compressive loading intervention<sup>(2)</sup> to investigate factors contributing to osteogenic response in the radius. Sixty-one healthy women (age  $29.3 \pm 5.7$  years) provided consent for this institutionally approved study. Subjects were assigned to a control (n=16), low (1800  $\mu\text{e}$ , n=21), or high strain magnitude (3600  $\mu\text{e}$ , n=24) group. The non-dominant (ND) arm was voluntarily cyclically loaded four times weekly for 12 months, and applied force was monitored using load cell signal recordings. Subject-specific forces were assigned using validated<sup>(3)</sup> finite element (FE) models relating applied force to energy-equivalent tissue strain. Clinical computed tomography (CT) scans of the ND forearm were performed at baseline and 12 months. Radius bone volume (BV), mineral density (BMD) and mineral content (BMC) were calculated for ultradistal and total regions extending 9.375 and 45 mm proximally from the subchondral plate. Values were calculated for the integral, trabecular, cortical and endocortical regions using previous methods<sup>(4)</sup>. Changes in CT parameters were compared between groups using linear regression with contrasts between each intervention group and the control group (Table 1). Average peak applied strain was  $1638 \pm 761 \mu\text{e}$  and  $2089 \pm 825 \mu\text{e}$  for the low (n=17) and high (n=19) groups. Structural changes in the ultradistal region did not increase linearly across groups ( $R^2 \leq 0.12$ ,  $p \geq 0.073$ ), but membership in the low intervention group was associated with improved integral BMC ( $p=0.041$ ), integral BV ( $p=0.034$ ), and trabecular BMD ( $p=0.023$ ). In the total region, strain magnitude was positively associated with increases in trabecular BMD ( $R^2=0.143$ ,  $p=0.046$ ), with a strong positive effect of membership in the low group ( $p=0.018$ ). Results suggest that 12 months of cyclic compressive loading at 1800  $\mu\text{e}$  produced modest improvements in bone structure, particularly within the trabecular compartment. Further analysis considering strain rate and distribution, as well as protocol compliance, may further explain the mechanism of structural adaptation to mechanical loading in healthy female bone.

[1] Babatunde (2012) Osteoporos. Int. [2] Troy (2013) J Orthop. Res. [3] Bhatia (2014) J. Biomech. [4] Edwards (2013) Osteoporos. Int.

**Table 1: Regression results for integral and trabecular bone mineral content (BMC, g), mineral density (BMD, g/cm<sup>3</sup>) and volume (BV, cm<sup>3</sup>) with model summary and standardized coefficients ( $\beta$ ) for contrasts with control group \* $p < 0.05$**

		Integral			Trabecular		
		BMC	BMD	BV	BMC	BMD	BV
Ultra	Model R <sup>2</sup>	0.10	0.01	0.11	0.04	0.12	0.05
	Low $\beta$	0.37*	0.09	0.39*	0.35	0.41*	0.27
	High $\beta$	0.22	0.10	0.23	0.16	0.20	0.12
Total	Model R <sup>2</sup>	0.02	0.01	0.03	0.10	0.14*	0.01
	Low $\beta$	-0.12	-0.02	-0.19	0.34	0.43*	-0.10
	High $\beta$	0.03	0.06	-0.07	0.32	0.34	-0.09

Table 1: Regression results for integral and trabecular bone

Disclosures: Megan Mancuso, None.

## SU0021

**The role of osteopontin in the mechanics of the bone across length-scales.** Sabah Nobakhti<sup>1</sup>, Baptiste Depalle<sup>2</sup>, Alexandra Porter<sup>2</sup>, Sandra Shefelbine<sup>1</sup>. <sup>1</sup>Northeastern University, United States, <sup>2</sup>Imperial College London, United States

**Introduction:** The role of osteopontin (OPN) in the mechanics of the mineralized collagen fibril and toughness in bone has been previously investigated [1]. It has been suggested that OPN acts as a glue and connects the mineralized collagen fibrils in bone [2], and lack of OPN results in bone brittleness [1]. The objective of this work was to investigate the multi-scale properties of bone in osteopontin knock-out (OPN<sup>-/-</sup>) compared to wild type (C57BL/6) mice to better understand factors that lead to reduced fracture toughness at the whole bone level.

**Method:** We measured: 1) size of the bone mineral crystals with wide angle x-ray diffraction analysis on the humerus (n=5/group), 2) mineral to matrix ratio with thermogravimetric analysis of the humerus (n=5/group); 3) degree of mineralization by quantitative backscattered scanning electron microscopy on tibia (n=5/group), 4) elastic modulus with nanoindentation on a grid of more than 100 indents on tibia (n=1/group), 5) collagen organization using transmission electron microscopy on demineralized sections of tibia (n=2/group).

**Results:** Crystal size and mineral to matrix ratio were not significantly different between OPN<sup>-/-</sup> and controls (Table 1). Degree of mineralization, characterized by the mode of gray level intensities in the qbSEM images, was significantly lower in OPN<sup>-/-</sup> compared to controls. Elastic modulus was not significantly different between the groups (p=0.2). Fibrils were disorganized in the OPN<sup>-/-</sup> and had regions of non-banded fibrous structure, contrasting the wildtype mice that showed collagen fibrils aligned with the longitudinal axis of the bone (Fig. 1).

**Discussion:** Unlike previous work [1], we found a decrease in degree of mineralization (qbSEM). The lower mineralization would likely explain the reduction of the elastic modulus in OPN<sup>-/-</sup> compared to controls (although it was not significant). Interestingly, lack of osteopontin results in a disorganized collagen matrix in bone, which has not previously been shown. Anisotropy plays a critical role in fracture toughness and therefore, unorganized fibrils may lead to brittleness of OPN<sup>-/-</sup> bone. This work indicates that mineral and collagen characteristics at the nano-scale influence the bone matrix properties at the micro-scale and toughness at the whole bone level.

### References:

[1] Turner, P., et al., Bone, 2010. [2] Poundarik, A., et al. PNAS, 2012.

Table 1- Results of the multiscale analysis.

Measurement	OPN <sup>-/-</sup>	C57BL/6	Significance
Crystal size (nm)	14.4±0.4	15.0±0.3	n.s.
Mineral/matrix (mg/mg)	3.0±0.1	3.0±0.1	n.s.
Degree of mineralization (calibrated gray value)	156.2±4.0	170.0±3.1	p = < 0.01
Elastic modulus (GPa)	18.2±1.2	19.4±2.1	n.s.

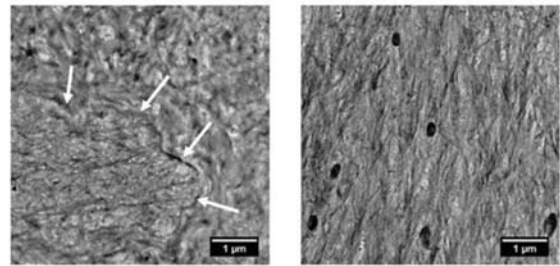


Fig. 1- Demineralized collagen structure in OPN<sup>-/-</sup> (left) and C57BL/6 (right) mice. White arrows show the regions of non-banded fibrous structure.

Multiscale analysis of bone mechanics

Disclosures: Sabah Nobakhti, None.

## SU0022

**Evaluation of a new bovine biomaterial to conduct bone healing.** Gretel Pellegrini<sup>1</sup>, Macarena Gonzalez-Chaves<sup>2</sup>, Francisco Duran<sup>3</sup>, Ricardo Orzuza<sup>4</sup>, Luciano Parodi<sup>5</sup>, Susana Zeni<sup>1</sup>. <sup>1</sup>Instituto de Immunología Genética y Metabolismo, Universidad de Buenos Aires-CONICET (INIGEM), Universidad de Buenos Aires, Facultad de Odontología, Cátedra de Bioquímica General y Bucal, Argentina, <sup>2</sup>Universidad de Buenos Aires, Facultad de Odontología, Cátedra de Bioquímica General y Bucal, Argentina, <sup>3</sup>Instituto de Immunología Genética y Metabolismo, Universidad de Buenos Aires-CONICET (INIGEM), Argentina, <sup>4</sup>Universidad de Buenos Aires, Facultad de Odontología, Cátedra de Bioquímica General y Bucal, Argentina, Argentina, <sup>5</sup>Comisión Nacional de Energía Atómica, División Bioterio. Centro Atómico Ezeiza, Argentina

Placing biomaterials to prevent resorption and preserve the integrity of alveolar ridges after invasive dental procedures is highly recommended. Bovine bone grafts are biocompatible and osteoconductive, allowing new bone apposition by osteoprogenitor cells. Developing new high quality biomaterials offer professionals an alternative option to obtain the most suitable solution for each individual patient. We evaluated and compared the effects of new bovine bone grafts Synergy Bone Matrix (SBM) [Odontit Implant System, Argentina] with Bio-Oss (BO) [Geistlich, Switzerland], recognized for its osteoconductive effects on the bone healing process in rabbits. We created a critical sized bone defect (CSBD) at both sides of mandibles and filled them with each biomaterial or remained unfilled (C: control). Animals were sacrificed at 4, 8 and 12 weeks. We assessed: clinical and biochemical systemic toxicity of lungs, kidney and liver pathology; bone formation and device resorption histomorphometrically; X-rays and compression and flexural biomechanical tests. None of the rabbits presented signs of systemic toxicity. C rabbits developed either fibrosis or adipose tissue independently of the time-period; new bone formation or remaining bone substitute amount did not show significant differences between SBM and BO (p=ns). CSBD in mandibles filled with both biomaterials exhibited radio-opacity indicating proper healing and gradual replacement of the bone grafts; no significant differences between SBM and BO were observed for elastic modulus (Mpa) [4 weeks: C: 13.34±1.23; BO: 47.83±4.82\*; SBM: 42.59±5.21\*. 8 weeks: C: 13.72±1.84; BO: 43.42±6.32\*; SBM: 46.61±4.45\*. 12 weeks: C: 14.61±3.1; BO: 50.57±15.7\*; SBM: 49.32±18.9\*]; shear modulus (Mpa) [4 weeks: C: 182.5±15.4; BO: 423.9±20.3\*; SBM: 425.6±25.7\*. 8 weeks: C: 185.4±12.1; BO: 397.8±30.5\*; SBM: 447.4±35.6\*. 12 weeks: C: 172.2±13.1; BO: 464.6±26.9\*; SBM: 473.1±32.4\*] and compressive strength (KgF/mm<sup>2</sup>) [4 weeks: C: 0.0595±0.0082; BO: 0.6407±0.0124\*; SBM: 0.6913±0.0110\*. 8 weeks: C: 0.0583±0.0098; BO: 0.6874±0.0115\*; SBM: 0.6816±0.0153\*. 12 weeks: C: 0.0694±0.0104; BO: 0.6983±0.0199\*; SBM: 0.6956±0.0178\*], while C group showed significantly lower values (\*p<0.001). Our findings show that both biomaterials are similar regarding bone regeneration, osteoconduction and newly formed bone quality. Therefore SBM can be used as an alternative biomaterial for the healing of bone defects.

Disclosures: Gretel Pellegrini, None.



## SU0023

**Sequential antiresorptive and anabolic treatment maintains cortical bone quality in an ovariectomized rat model.** Erik Taylor<sup>\*1</sup>, Xiaomei Yao<sup>2</sup>, Yong Wang<sup>2</sup>, Don Kimmel<sup>3</sup>, Mark Johnson<sup>2</sup>, Eve Donnelly<sup>1</sup>, Nancy Lane<sup>4</sup>. <sup>1</sup>Cornell University, United States, <sup>2</sup>University of Missouri-Kansas City, United States, <sup>3</sup>University of Florida, United States, <sup>4</sup>University of California Davis, United States

Antiresorptive and anabolic agents are used sequentially to treat osteoporosis, but their effects on bone quality are incompletely understood. Therefore, in this study, we compared cortical bone tissue composition from ovariectomized rats treated with multiple sequential treatment regimens.

Six-month-old female Sprague-Dawley rats were ovariectomized (OVXd) (N=40) or sham-OVXd (Sham, N=6). After 2 months, OVXd rats were given varying treatment sequences every 3 months for 9 months that included vehicle (V, saline 1 ml/kg/dose, 3x/wk SC), h-PTH 1-34 (P, 25 µg/kg/ 5x/wk SC), alendronate (A, 25 µg/kg/ dose, 2x/wk SC), and raloxifene (R, 5 mg/kg/dose 3x/wk by oral gavage) in groups corresponding to 6 treatments: VVV (N=6), AAA (N=4), RRR (N=5), PVV (N=5), AVA (N=5), APA (N=5), and RPR (N=4). After euthanasia, a mid-frontal section through the proximal third of the tibia was prepared, and 48-80 Raman spectra per tibia were collected within 20 µm of lacuni. Four parameters were calculated: the mineral:matrix ratio, carbonate:phosphate ratio, crystallinity, and collagen maturity.

Cortical tissue mineral content decreased in animals treated with PVV compared to that of the VVV control (-17.2%,  $p < 0.05$ ; Fig. 1A). The cortical collagen maturity increased in the RRR group relative to the VVV control (+10.5%,  $p < 0.01$ ; Fig. 1D). Cortical bone from the APA group had lower collagen maturity relative to RRR, AAA, and PVV (-12.0%,  $p < 0.01$ ; -9.8%,  $p < 0.05$ ; and -9.1%,  $p < 0.05$  respectively).

Overall, estrogen-deficient osteopenic female mature rats exposed to osteoporosis treatment sequences with both anti-resorptive and anabolic agents at 3-month intervals resulted in cortical tissue with lower mineral content relative to the VVV control. Suppression of resorption can increase tissue age, reflected by increased secondary mineralization and collagen maturity. The decrease in tissue mineral content in the PVV group reflects younger tissue age arising from recent bone formation. The decrease in collagen maturity with sequential anabolic and antiresorptive treatments in the APA group relative to monotherapies suggests that this treatment regime can decrease collagen maturity without increasing tissue mineral content. These results suggest that sequential anti-resorptive and anabolic treatments may improve cortical bone quality relative to monotherapies. Studies should be extended to human cortical bone biopsies to determine if these results can be translated to clinical care.

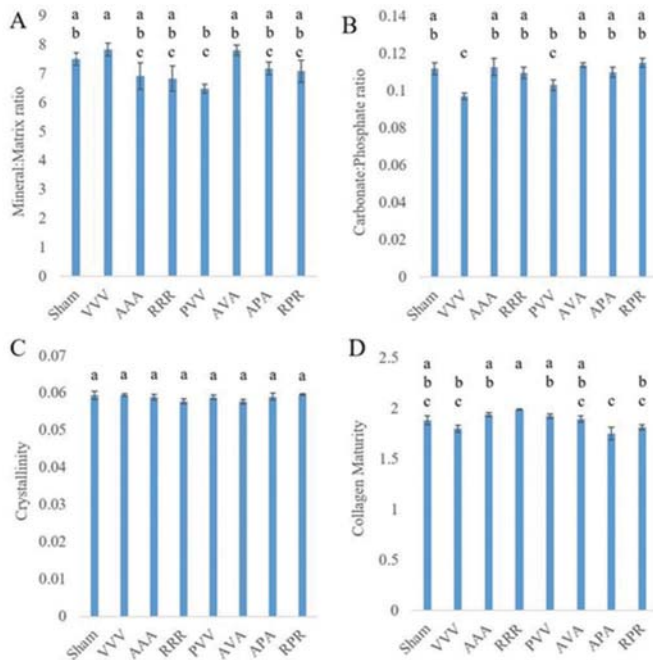


Figure 1. Raman mineral:matrix ratio (A), carbonate:phosphate ratio (B), crystallinity (C), and collagen maturity (D) outcomes for sequential and monotherapies with anti-resorptives and anabolic agents of PVV, RRR, AVA, APA, RPR, and AAA in rats with osteopenia; (P=PTH, V=vehicle, R= raloxifene, A=alendronate) levels not connected by same letter (a,b,c) are significantly different at  $p=0.05$  by ANOVA with Tukey post hoc.

Figure 1: Raman outcomes

Disclosures: Erik Taylor, None.

## SU0024

**Effect of Mineralized Collagen Fibril Orientation on Cortical Bone Fracture Resistance.** Yaohui Wang<sup>\*</sup>, Ani Ural, Villanova University, United States

Bone is a hierarchically structured composite material which exhibits different fracture mechanisms at each length scale. At the submicroscale, the bone is composed of mineralized collagen fibrils. At this scale, the fracture processes in cortical bone have not been extensively studied in the literature. In this study, a novel approach to simulate the submicroscale fracture response in cortical bone was developed incorporating finite element models of unit cells of mineralized collagen fibrils. The models with varying fibril orientations were utilized to assess the influence of the fibril network pattern on the fracture behavior in cortical bone at the submicroscale.

Four sets of fibril networks were generated using a MATLAB script with a plywood structure incorporating fibril orientations of  $0^\circ/90^\circ$ ,  $\pm 15^\circ$ ,  $\pm 30^\circ$ ,  $\pm 45^\circ$  (Fig. 1a). A fibril diameter distribution of  $100 \pm 5$  nm was used in all models. Both longitudinal and transverse tensile loading with respect to simmain fibril direction were applied to each model. Interfacial separation between the fibrils was represented by cohesive interface elements. Extended finite element (XFEM) cohesive fracture approach was applied to individual fibrils to account for fibril fracture. The material properties used in all the simulations were adapted from recent experimental data reported in the literature.

The simulation results showed that the interfacial separation dominates transverse loading as the interfaces are mostly perpendicular to the loading direction (Fig. 1b, 1d). The fibril fracture dominates longitudinal loading since the loading direction is approximately along the fibril direction (Fig. 1c, 1e). The yield and ultimate strength in longitudinal loading is higher than the transverse direction because the interface is much weaker than the fibril. With larger fibril orientation angles, fibrils deviate further from the main loading direction leading to an increase in the elastic modulus and strength in transverse loading (Fig. 1d) and a decrease in longitudinal loading (Fig. 1e).

In conclusion, this study introduced a new modeling method to simulate the submicroscale fracture behavior of bone using a novel model generation approach and fracture mechanics-based finite element modeling. The results demonstrate the importance of the orientation of mineralized collagen fibrils with respect to the loading direction in determining cortical bone fracture behavior at the submicroscale.

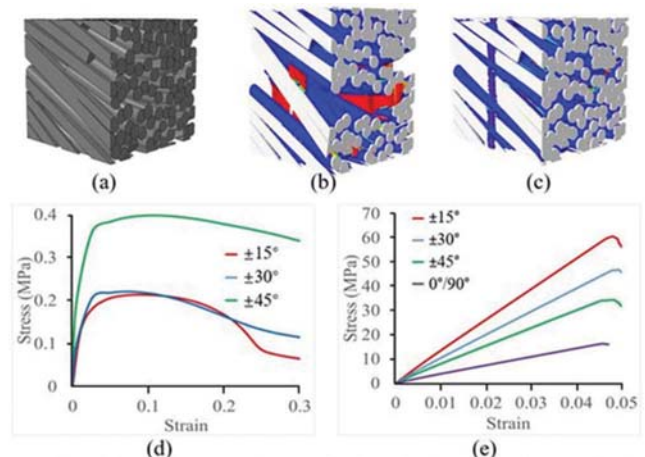


Figure 1: (a) A sample FE unit cell of mineralized collagen fibrils with  $\pm 30^\circ$  plywood fibril orientation. (b) Deformed shape of the model in (a) under transverse loading demonstrating fibril separation (denoted by red color). (c) Deformed shape of the model in (a) under longitudinal loading demonstrating fibril fracture (denoted by red color). Stress-strain curves for various fibril orientations under (d) transverse loading and (e) longitudinal loading.

Figure 1

Disclosures: Yaohui Wang, None.

## SU0025

**Impact of Skeletal Maturity Status on Height Trajectory During Childhood and Adolescence.** Melanie E. Boever<sup>\*</sup>, Emily V. Leary, Richard J. Sherwood, Dana L. Duren, University of Missouri, United States

Growth trajectories based on serial measures of height vary from child to child. Some children reach their adult height substantially earlier than others. Clinically, knowledge of a patient's growth trajectory can aid predictions of adult height and inform treatment planning, including timing and duration of interventions for skeletal conditions commonly treated during childhood. However, methods to determine a child's current status and future trajectory are often imprecise. Additional factors, such as skeletal maturity, relative skeletal age, and bony features, including the first sign of epiphyseal fusion, have the potential to improve predictions of a child's growth trajectory. To elucidate the relationship between skeletal development and growth potential, we assessed serial measurements of height from birth to adulthood in 488 children from the Fels

Longitudinal Study, all of whom were healthy and of European ancestry. Data were analyzed separately for boys and girls. Using a 5th order multi-level polynomial with fixed and random effects, we compared the overall growth models for children classified as “early, normal, or late” maturers based on relative skeletal age at the first sign of epiphyseal fusion in the third metacarpal. We also tested for group differences in mean age at three milestones of height attainment (60%, 90%, and 99% of adult height) using a one-way ANOVA containing a single observation per subject per milestone. Significant differences were found in age at the milestones of height attainment among the three maturational groups. Early maturing boys reached 60%, 90%, and 99% of adult height 4, 11, and 14 months earlier than average maturing boys. Early maturing girls reached 90% and 99% of adult height 13 and 16 months earlier than average maturing girls. Late maturing boys reached 60%, 90%, and 99% of adult height 4, 10, and 15 months later than average maturing boys. Late maturing girls reached 60%, 90%, and 99% of adult height 4, 10, and 14 months later than average maturing girls. Differences in growth trajectories among these three maturational groups provides novel insight into the etiology of height attainment, improving future treatment regimens for pediatric musculoskeletal disorders.

**Disclosures:** *Melanie E. Boeyer, None.*

## SU0026

### A School-Based Exercise Intervention Program from Tanner stage 1 until 5 Improves Composite Risk Score for Fracture in Both Genders. Felix Cronholm<sup>\*1</sup>, Magnus Dencker<sup>2</sup>, Björn Rosengren<sup>1</sup>, Magnus Karlsson<sup>1</sup>.

<sup>1</sup>Clinical and Molecular Osteoporosis Research Unit, Department of Orthopedics and Clinical Sciences, Lund University, Skåne University Hospital, Sweden, <sup>2</sup>Department of Physiology and Clinical Sciences, Lund University, Skåne University Hospital, Sweden

**Purpose:** Physical activity (PA) in childhood is associated with musculoskeletal benefits that may reduce fracture risk, but most PA studies have used single traits as end points thereby missing a possible effect of combined traits.

**Method:** In a cluster randomized controlled trial we increased PA in one school to 200 min/week (40 minutes moderate PA per school day) during the entire study period. Children in 3 control schools maintained Swedish standard of 60 minutes/week PA. We followed 89 boys and 51 girls from mean age 8 (all Tanner stage 1) to mean age 15 years (all Tanner stage 5) and registered incident fractures. At baseline and at follow-up we assessed 5 different musculoskeletal traits associated with fracture risk; Lean mass (LM; kg), lumbar spine bone mineral content (BMC; g) and bone area (cm<sup>2</sup>) by DXA; calcaneal bone quality as speed of sound (SOS; m/s) by quantitative ultrasound (QUS); muscle strength as knee flexion peak torque (PT; Nm) by a computerized dynamometer (Biodex®). For each trait in each individual we calculated gender specific Z-scores (number of standard deviations above or below the age predicted mean) by linear regression using the control cohort as reference population. We calculated a composite risk score for fracture as average Z-score of all measured traits for each individual. We evaluated group differences by ANCOVA adjusted for age and baseline trait value as well as composite risk score adjusted for baseline trait value. Data are reported as mean differences (95% CI) or proportions.

**Results:** At follow-up both intervention boys and intervention girls had better composite risk scores for fracture than their respective control groups (mean Z-score difference boys 0.3 (0.05, 0.6) and girls 0.4 (0.1, 0.8)). For absolute values at follow-up, we found no statistically significant differences between intervention and controls in boys for LM (p=0.24) and SOS (p=0.37) and in girls for LM (p=0.49) and PT (p=0.13). During the study period 19% of intervention children and 22% of control children sustained fractures.

**Conclusion:** When only using single traits as end points there is a risk not to appreciate overall PA effects as found in this long term PA intervention study. We however found a beneficial composite risk score for fracture in both genders indicating a possible usefulness for fracture risk estimations.

**Disclosures:** *Felix Cronholm, None.*

## SU0027

### Predictors of Stress Fractures in Adolescents Engaging in Weight-Bearing Exercise: Use of Peripheral Quantitative Computed Tomography versus Dual-Energy X-Ray Absorptiometry. Rachel L Duckham<sup>\*1</sup>, Shara R Bialo<sup>2</sup>, Jason Machan<sup>3</sup>, Peter Kriz<sup>4</sup>, Catherine M Gordon<sup>5</sup>.

<sup>1</sup>Institute for Physical Activity and Nutrition, Deakin University and Australian Institute for Musculoskeletal Sciences, St. Albans, Australia, <sup>2</sup>Division of Pediatric Endocrinology, Rhode Island Hospital/Hasbro Children's Hospital, Warren Alpert Medical School of Brown University, Providence, RI, United States, <sup>3</sup>Division of Biostatistics, Rhode Island Hospital, Warren Alpert Medical School of Brown University, Providence, RI, United States, <sup>4</sup>Division of Sports Medicine, Rhode Island Hospital, Warren Alpert Medical School of Brown University, Providence, RI, United States, <sup>5</sup>Division of Adolescent and Transition Medicine, Cincinnati Children's Hospital, Cincinnati, OH, United States

**Background:** Adolescence is a critical period for acquisition of peak bone mass. While 3.9% of adolescent girls report at least one stress fracture (FX), determining the

underlying cause can be difficult as many do not present with known risk factors. Given the high FX prevalence in adolescent girls, it is imperative to investigate the best predictive tools for these patients. The purpose of this study was to determine whether bone outcomes assessed with pQCT vs. DXA could predict a tendency to develop FX in a sample of adolescent athletes.

**Methods:** Twelve female adolescent athletes diagnosed with a lower extremity FX were compared with twelve healthy controls matched for age, race, sport, training, and postmenarcheal years. DXA was used to measure bone mineral density (BMD) and content of the total body, and lumbar spine. pQCT was used to assess bilateral tibia. At the metaphysis (3%), total density (ToD), trabecular density (TrD), trabecular area (TrA), and estimated bone strength in compression (BSIc); and at the diaphysis (38% and 66%), total bone area (ToA), cortical density (CoD), cortical area (CoA), estimated bone strength in torsion (SSI<sub>p</sub>), and peri- and endocortical and muscle area (MuA) were obtained. Cortical bone mass/density around the center of mass and marrow density (estimate of adiposity) were calculated using Image J software.

**Results:** BMD and content assessed by DXA showed no significant differences between case and control athletes. However, when assessed by pQCT, trabecular density at the 3% tibia was 54 to 56% (p<0.001) lower in the FX athletes injured and uninjured limb compared to controls. Marrow density at the 66% site was 1% (p<0.05) lower in the injured vs. uninjured leg in athletes, with no significant differences between cases and controls. There were no other significant differences in bone outcomes between the groups.

**Conclusions:** FX athletes show a greater tendency for lower trabecular density at the 3% tibia compared to controls suggesting at-risk athletes to have more pronounced differences in bone structure rather than BMD. Therefore, the assessment of bone structure with pQCT may better identify adolescent athletes at risk for FX compared to a DXA assessment alone.

**Disclosures:** *Rachel L Duckham, None.*

## SU0028

### Toll-Like Receptor 4 Activation Inhibits Osteoblastic Differentiation of Bone Marrow Stromal Cells and Decreases Bone Formation Following Ischemic Osteonecrosis. Gen Kuroyanagi<sup>\*</sup>, Naga Suresh Adapala, Harry K.W. Kim. Texas Scottish Rite Hospital for Children, United States

Legg-Calvé-Perthes disease is a pediatric form of ischemic osteonecrosis of the femoral head. It produces a severe femoral head weakening and collapse during healing due to increased bone resorption and decreased bone formation. Toll-like receptor 4 (TLR4) is a pattern recognition receptor found in immune and other cells that detects the presence of cell damage molecules called alarmins, and is known to stimulate the inflammatory Ikkinase- $\alpha$  (IKK $\alpha$ )-nuclear factor- $\kappa$ B (NF- $\kappa$ B) pathway. The activation of IKK $\alpha$ -NF- $\kappa$ B pathway has been shown to inhibit osteoblast differentiation by Runx2 suppression. The role of TLR4 activation on bone marrow stromal cells (BMSCs) following ischemic osteonecrosis has not been studied. We hypothesized that soluble factors in the necrotic bone inhibit osteoblastic differentiation of BMSCs through TLR4 activation. *In-vitro* and *in-vivo* experiments were performed to determine the effects of TLR4 activation on osteoblastic differentiation of BMSCs in a necrotic bone environment. We found that the soluble fraction of the necrotic bone extract prepared by a freeze thaw method dramatically inhibited alkaline phosphatase (ALP) and alizarin red staining (matrix mineralization) of pig BMSCs in osteogenic culture media (p<0.01), and suppressed the mRNA levels of Runx2, ALP and Osterix in a dose-dependent manner on qRT-PCR analysis (p<0.01). Necrotic bone extract treatment increased TLR4 expression in BMSCs (p<0.01) and phosphorylation of IKK $\alpha$  on Western blotting. TLR4 deletion by CRISPR-Cas9 or TLR4 inhibition using TAK242 inhibited IKK $\alpha$  phosphorylation, increased Runx2 gene expression, and rescued osteoblastic differentiation of BMSCs in the presence of soluble necrotic bone extract (p<0.01). Lastly, administration of TLR4 inhibitor TAK242 following surgical induction of ischemic osteonecrosis of distal femoral epiphysis in 12-week-old male mice (n=5/group) significantly increased bone volume % (saline=34.1  $\pm$  2.4 % vs. TAK242=41.4  $\pm$  2.5 %, p<0.01) on micro-CT analysis and significantly increased osteoblast number per bone surface (p<0.01) on Bioquant analysis at 4 weeks after surgery. Taken together, the findings indicate that TLR4 activation by soluble necrotic bone factors plays a critical role in the inhibition of osteoblastic differentiation of BMSCs following ischemic osteonecrosis. These findings suggest that TLR4 inhibition could be a potential therapeutic target to improve bone formation following ischemic osteonecrosis.



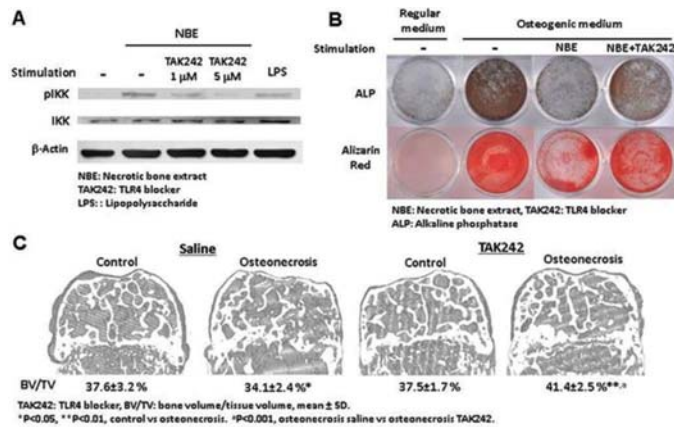


**Figure legend.**  
 A. Necrotic bone extract (NBE) stimulates phosphorylation of IKK (ser-176) through TLR4 activation.  
 B. TLR4 blockade (TAK242) rescues osteoblastic differentiation of BMSCs in NBE.  
 C. Micro-CT analysis of the distal femoral epiphysis of mice at 4 weeks following the induction of ischemic osteonecrosis.

Figure

**Disclosures:** Gen Kuroyanagi, None.

## SU0029

**In search of hypophosphatasia at two pediatric bone clinics in two Czech hospitals.** Stepan Kutilek\*. Dept. of Pediatrics, Klatovy Hospital, Czech Republic, Czech Republic

**Background:** Hypophosphatasia (HPP) is a rare disease (1:500 000 in Europe) which is a result of ALPL mutations leading to deficient activity of the tissue-nonspecific alkaline phosphatase isozyme (TNAP) and extracellular accumulation of inorganic pyrophosphate (PP<sub>i</sub>), a natural substrate of TNAP and potent inhibitor of mineralization. Characteristic HPP features are rickets or osteomalacia, and hypomineralization of teeth. Typically, HPP is characterized by low serum alkaline phosphatase activity (S-ALP). As physicians mostly focus on detection of high S-ALP, the low S-ALP is frequently overlooked.

**Results & Future directions:** In our hospitals in Klatovy and Pardubice, those patients with clinical signs of mild (i.e. childhood or adult) HPP and low S-ALP are referred to respective pediatric bone clinics by pediatric endocrinologists, nephrologists, rheumatologists. So far, two patients underwent genetic evaluation: A 4-year-old girl with craniofacial dysmorphism, hypotonia, mild psychomotor retardation and repeatedly low S-ALP (1.4  $\mu$ kat/L) was diagnosed as an asymptomatic HPP heterozygote for infantile HPP (ALPL mutation: ALPL c.571G>A). In another 4-year-old girl with epilepsy, short stature, dental caries, failure to thrive (-1.8 to -2SD body height Z-score; 3-10 centile), joint and bone pain, no fractures and S-ALP 1.4  $\mu$ kat/L (parents' S-ALP  $\leq$  1  $\mu$ kat/L) no ALPL mutations were found. Another 4 patients aged 5-23 years with history of stunted growth, dental caries, limb pain; low-energy trauma fractures with poor healing and low S-ALP 0.7-1.1-1.4  $\mu$ kat/L are currently being evaluated (phosphoethanolamine-PEA, pyridoxal phosphate-PLP, genetics). Furthermore, a retrospective screening program, in cooperation with departments of clinical biochemistry, to detect low S-ALP in pediatric patients and consequently to diagnose those children with HPP is under way in 10 hospitals in the Czech Republic. In the Klatovy (pop. 25 000) hospital a retrospective (2009-2016) screening of all S-ALPs in individuals <18 years of age revealed 1233 S-ALP evaluations. 25 patients had S-ALP <1.5  $\mu$ kat/L; out of those 5 patients had S-ALP <1.0  $\mu$ kat/L (0.78-0.98  $\mu$ kat/L). In Pardubice (pop. 90 000) hospital retrospective (2006-2016) screening of all S-ALPs in individuals <15 years of age revealed 8900 S-ALP evaluations. One patient has S-ALP 0.6  $\mu$ kat/L, 30 patients had S-ALP <1.0  $\mu$ kat/L. Meticulous assessment of those patients with low S-ALP is being performed.

**Disclosures:** Stepan Kutilek, None.

## SU0030

**Nutritional ricket - the Norwegian experience.** Haakon E. Meyer\*, Kristina Skram\*, Ingvill Almås Berge\*, Ahmed Madar\*, Hilde Johanne Bjørndal\*. <sup>1</sup>University of Oslo and Norwegian Institute of Public Health, Norway, <sup>2</sup>Department of Pediatrics, Oslo University Hospital, Norway, <sup>3</sup>Section for Preventive Medicine and Epidemiology, Department of Community Medicine, University of Oslo, Norway

**Objectives:** Poor vitamin D status is highly prevalent in many non-western immigrant groups living in western countries. This also applies to women of childbearing age. It is therefore a concern that rickets can emerge as a large problem in infants with immigrant background. However, population-based data on rickets are scarce, and in the current study we aimed to identify new cases of nutritional rickets in the Norwegian population during 2008-2012.

**Material and methods:** This register-based cohort study covered the total Norwegian population under the age of 5 from 2008-2012. In order to identify children with nutritional rickets, we retrieved information from the Norwegian Patient Registry on all patients with ICD10 diagnosis code E55.0 (active rickets). We managed to review 85% of the medical records at the treating hospitals for confirmation of the diagnosis. In order to identify individuals with rickets who had been given alternative diagnoses, we also identified patients with the diagnoses E55.9, E64.3 and E83.3.

**Results:** Nutritional rickets was confirmed in 42 patients under the age of five. Fifty-seven percent of the patients were boys and 86% were 1 to 2 years old when diagnosed. Mean 25-hydroxyvitamin D concentration was 17.9 nmol/l. Sixty percent of the patients had immigrant background from Asia, and 29% from Africa. In the total Norwegian child population under the age of 5, the incidence rate of rickets was estimated to be 0.3 per 10,000 person-years, whereas it was 3.1 per 10,000 person-years in those with an immigrant background from Asia or Africa.

**Conclusion:** In the period 2008-12, the incidence of nutritional rickets in Norway remained low. However, the vast majority of the patients had a non-western immigrant background.

**Disclosures:** Haakon E. Meyer, None.

## SU0031

**Established Adult Height Loci Operate in the Pediatric Setting to Influence Bone Mineral Density.** Jonathan Mitchell\*, Alessandra Chesl, Shana McCormack, Diana Cousminer, Heidi Kalkwarf, Joan Lappe, Vicente Gilsanz, Sharon Oberfield, John Shepherd, Andrea Kelly, Babette Zemel, Struan Grant. <sup>1</sup>Children's Hospital of Philadelphia, United States, <sup>2</sup>Cincinnati Children's, United States, <sup>3</sup>Creighton University, United States, <sup>4</sup>Children's Hospital Los Angeles, United States, <sup>5</sup>Columbia University, United States, <sup>6</sup>UCSF School of Medicine, United States

Osteoporosis is a complex disease that may have origins in childhood, necessitating the need to understand the genetics of bone accretion. The strongest pediatric areal bone mineral density (aBMD) genetic locus resides at 7q31.31 (CPED1-WNT16). Interestingly, variants near CPED1-WNT16 also influence adult height, and linear growth is an important dimension of bone accretion. Over 700 known genetic variants for adult height have been reported. We therefore aimed to determine the associations of height variants that are common (>5%), low frequency (1-5%), and rare (<1%) with pediatric aBMD.

We analyzed data from the Bone Mineral Density in Childhood Study, restricted to participants of European ancestry (N=1,298; 52% female). Dual energy X-ray absorptiometry was used to calculate spine, total hip, femoral neck and distal radius aBMD Z-scores, and total body less head bone mineral content (TBLH-BMC) Z-scores, adjusted for height. Genetic risk scores (GRS) for taller stature were calculated using: 1) 683 common height variants and 2) 83 low frequency or rare (LFR) variants. Both scores were standardized and weighted based on their effect size with adult height. Linear mixed models were used to test for association between each standardized GRS (beta= bone Z-score change per 1 SD increase in the GRS), as well as the individual variants (with Bonferroni correction for multiple comparisons), and the bone Z-scores. Age and sex interactions were tested.

As expected, the common-GRS and LFR-GRS were positively associated with height Z-score (beta=0.26,  $P=3.6 \times 10^{-22}$ ; and beta=0.10,  $P=1.1 \times 10^{-6}$ , respectively). In contrast, the common-GRS was negatively associated with bone Z-scores (e.g. TBLH-BMC: beta=-0.08,  $P=1.2 \times 10^{-4}$ ). The negative association was stronger among older adolescents ( $P$ -age interactions <0.05). No sex differences were observed. The LFR-GRS was not associated with bone Z-scores. At the individual variant level, a common height increasing allele near CPED1 associated with higher distal radius aBMD (stronger in females,  $P$ -sex interaction=7.9  $\times 10^{-4}$ ; and only among younger males,  $P$ -age interaction=1.4  $\times 10^{-4}$ ), while a common height increasing allele near PDE3A associated with lower spine aBMD (no sex or age differences). Six low frequency variants associated with bone Z-scores.

Our observations provide insight into the genetic regulation of the growing skeleton and could aid in developing more effective therapies for preventing and treating osteoporosis.

**Disclosures:** Jonathan Mitchell, None.

## SU0032

**Growth and Skeletal Effects in Children and Adolescents After Kidney Transplantation: A 3-Year Prospective Study.** Diana Swolin-Eide\*, Sverker Hansson, Per Magnusson. <sup>1</sup>Department of Pediatrics, Institute for Clinical Sciences, The Queen Silvia Children's Hospital, The Sahlgrenska Academy at Göteborg University, Göteborg, Sweden, <sup>2</sup>Department of Clinical Chemistry, Linköping University, Linköping, Sweden

**Purpose:** Children's bone health is an important issue and there are many factors and medical conditions that are associated with an increased risk of mineral bone disorder (MBD). Children and adolescents with chronic kidney disease (CKD) are at risk of developing CKD-MBD, because of the risk of long-term consequences such as growth retardation, low peak bone mass and fragility fractures. This study was designed to follow Swedish pediatric patients prospectively for 3 years after kidney transplantation regarding growth and skeletal development.

**Methods:** The study group comprised 13 patients (9 males), 4-15 years of age. Growth, bone mineral density (BMD) and markers of bone and mineral metabolism were investigated at start, and after 3, 12, 36 months after kidney transplantation.

**Results:** Median glomerular filtration rate was 63 (range 37–96) mL/min/1.73 m<sup>2</sup> after 3 years. The median height standard deviation score (SDS) increased from -1.7 to -1.1 after 3 years,  $p=0.0012$ , and median BMI SDS increased from -0.1 to 0.6 after 3 years,  $p=0.013$ , which implies that transplantation had a favorable outcome on growth. The fat mass percentage increased after transplantation (from median 12.9% to 27.4%),  $p<0.01$ , and total lean mass was unchanged after 3 months, but increased after 1 year and 3 years (from median 23.1 kg at baseline to 29.3 kg at 3 years),  $p<0.01$ . Total BMC increased at all time points in comparison with the initial values at study start,  $p<0.001$ . No change was observed for total BMD, calcaneal BMC and BMD over the study period. A delayed median bone age was found at start and after 3 years post-transplantation. Parathyroid hormone, phosphate and magnesium decreased at 3 months, and decreased further during the study period. The bone resorption markers tartrate-resistant acid phosphatase isoform 5b (TRACP5b) and carboxy-terminal cross-linking telopeptide of type I collagen (CTX) decreased initially after 3 months ( $p<0.05$ ), and remained stable throughout the study period. The bone formation markers alkaline phosphatase, intact amino-terminal propeptide of type I procollagen (PINP) and osteocalcin decreased initially, but successively increased over the study period.

**Conclusion:** This study demonstrates that height SDS and BMI SDS increased, along with the increased markers of bone formation that reveals a positive bone acquisition after kidney transplantation, which was reflected by the significant increase in total body BMC.

**Disclosures:** Diana Swolin-Eide, None.

## SU0033

**Effects of Crohn's Disease Fecal Microbial Transplant on Bone Mass of Germ-Free Mice Are Independent of Gastrointestinal Inflammation.** Francisco Sylvester\*, Anu Maharjan, Emily Bulik-Sullivan, Hong Yuan, Maureen Bower, Ian Carroll. University of North Carolina at Chapel Hill, United States

**Background:** Crohn disease (CD), a chronic inflammatory disorder of the gastrointestinal tract, is frequently associated with significant bone mass deficits from diagnosis, which persist even when CD is in clinical remission. **Aim:** We hypothesized that CD enteric microbiota reduces bone mass independently of intestinal inflammation. **Methods:** We performed fecal microbiota transfer (FMT) from a child with newly diagnosed, untreated CD and an unaffected age-matched healthy control (HC) into 6-week old germ-free (GF) wild type 129SvEvFv male mice. Four weeks post FMT, we measured bone mineral density (BMD), bone volume (BV), trabecular thickness (Tt), and trabecular number (Tn), cortical thickness (Ct), and cortical surface area (CArea) with  $\mu$ CT in the 3<sup>rd</sup> lumbar vertebra, femoral head and femur midshaft. We tracked weight daily and obtained colon length and histology post-sacrifice. We also analyzed the fecal microbiome of donor and recipient mice using 16sRNA and next-generation sequencing. **Results:** We observed no signs of colitis (no weight loss, no changes in colonic length or histological changes) after FMT. Results of  $\mu$ CT are summarized in the Table (mean  $\pm$  SEM). In femur head, mice that received FMT from CD compared to GF control had a significant decrease in Tn and Tt. In femur mid-shaft, there was a significant decrease in BMD and Ct in mice that received FMT from HC or CD relative to GF mice. BV in femur mid-shaft was lower in mice that received FMT from CD compared to HC. However, there were no significant changes in  $\mu$ CT readouts in L3 post HC or CD FMT. **Conclusion:** CD fecal microbiota affects femur trabecular and cortical bone, even in the absence of colonic inflammation. Responsible mechanisms may involve gut microbial metabolites or microbial molecular patterns that travel to bone via blood.

	Germ-free (GF)	Post-FMT HC	Post-FMT CD
<b>Femur mid-shaft</b>			
BMD (mg HA/ccm)	1153 $\pm$ 8.9	1119 $\pm$ 7.4, $p=0.0345$	1114 $\pm$ 9.2, $p=0.025$
BV/TV (%)	56.8 $\pm$ 1.4	51.4 $\pm$ 0.4, $p=0.0864$	48.6 $\pm$ 3.0, $p=0.014$
CT (mm)	0.23 $\pm$ 0.006	0.20 $\pm$ 0.002, $p=0.0011$	0.19 $\pm$ 0.005, $p=0.0002$
CArea (mm <sup>2</sup> )	4.2 $\pm$ 0.04	3.9 $\pm$ 0.08, $p=0.27$	3.9 $\pm$ 0.19, $p=0.19$
<b>L3</b>			
BMD (mg HA/ccm)	757 $\pm$ 10.9	762 $\pm$ 23.0, $p=0.98$	716.3 $\pm$ 15.6, $p=0.24$
BV/TV (%)	35.9 $\pm$ 3.0	27.5 $\pm$ 4.7, $p=0.27$	23.3 $\pm$ 3.8, $p=0.09$
Tt (mm)	0.05 $\pm$ 0.001	0.05 $\pm$ 0.003, $p=0.795$	0.04 $\pm$ 0.002, $p=0.2$
Tn	7.4 $\pm$ 0.5	7.1 $\pm$ 0.6, $p=0.94$	7.15 $\pm$ 0.55, $p=0.96$
<b>Femur head</b>			
BMD (mg HA/ccm)	792 $\pm$ 17.2	811 $\pm$ 21.9, $p=0.75$	765 $\pm$ 17.3, $p=0.61$
BV/TV (%)	22.6 $\pm$ 1.7	9.0 $\pm$ 3.0, $p=0.001$	4.6 $\pm$ 1.2, $p=0.0002$
Tt (mm)	0.05 $\pm$ 0.001	0.04 $\pm$ 0.003, $p=0.09$	0.03 $\pm$ 0.003, $p=0.001$
Tn	6.1 $\pm$ 0.3	5.0 $\pm$ 0.4, $p=0.060$	4.00 $\pm$ 0.2, $p=0.002$

Table

**Disclosures:** Francisco Sylvester, None.

## SU0034

**Bone deficits and discordance between lean mass and bone measures in ambulatory children with cerebral palsy.** Daniel Whitney\*<sup>1</sup>, Freeman Miller\*<sup>2</sup>, Melissa Ziegler<sup>1</sup>, Christopher Modlesky<sup>1</sup>, Chuan Zhang<sup>1</sup>. <sup>1</sup>University of Delaware, United States, <sup>2</sup>AI duPont Hospital for Children, United States

Children with cerebral palsy (CP) have low levels of physical activity and an under-developed musculoskeletal system. Whether the skeletal deficits in ambulatory children with CP exist across the skeleton and are related to fat and lean mass is unknown.

Nineteen ambulatory children with mild CP and 19 sex-, age- and race-matched typically developing children (controls) participated in this study. Dual-energy x-ray absorptiometry was used to assess body composition of the total body and the more affected (CP) or non-dominant (controls) extremities. Fat mass index (FMI) and lean mass index (LMI) were determined by dividing fat and lean mass of the total body, upper extremity and lower extremity by standing height squared. Independent t-tests were used to assess group differences in physical characteristics, FMI, LMI and bone measures. Multiple linear regression was used to determine group differences in the relationship of FMI and LMI with total body, upper extremity and lower extremity bone area, bone mineral content (BMC) and areal bone mineral density (aBMD) after adjusting for height.

Compared to controls, children with CP had a lower height percentile, total body BMC and aBMD and lower extremity bone area, BMC and aBMD (all  $p < 0.05$ ). LMI of the lower extremity was lower in children with CP compared to controls, but the difference was marginally insignificant ( $p = 0.054$ ). There were no group differences in total body bone area or upper extremity bone area, BMC or aBMD (all  $p > 0.05$ ). For every standard deviation increase in LMI in the group of children with CP, there was a blunted increase in BMC of the total body by 83 g and aBMD of the total body and upper extremity by 0.051 and 0.029 g/cm<sup>2</sup>, respectively (all  $p < 0.05$ ).

These findings suggest that ambulatory children with CP have skeletal deficits of the total body and lower extremity but not of the upper extremity. The skeletal deficits may be linked to a lower accretion of bone mineral with increasing lean mass but are unrelated to fat mass. The reason for the discordance between bone and lean mass in children with CP requires further investigation.

**Disclosures:** Daniel Whitney, None.

## SU0035

**CCL3 is Essential for Leukemia Progression but Dispensable for Homeostatic Hematopoiesis.** Rhonda Staversky\*, Mary Georger, Marian Ackun-Farmmer, Michael Becker, Danielle Benoit, Laura Calvi, Benjamin Frisch. University of Rochester, United States

**Background:** Hematologic malignancies remodel the bone marrow microenvironment (BMME), reducing support for normal hematopoiesis while increasing support for the malignancy. The chemokine CCL3 has been demonstrated to play a role in BMME dysfunction in multiple malignancies including myeloma, acute myelogenous leukemia (AML), chronic myelogenous leukemia (CML), and myelodysplastic syndrome.

**Methods/Results:** We utilized genetically altered mice with a global loss of CCL3 (CCL3KO) on a C57Bl/6 background. We used sorted hematopoietic stem and progenitor cells (HSPCs) from CCL3KO mice or wild type controls to generate 2 models of myelogenous leukemia, the BCR/ABL+Nup98/HoxA9 model of blast crisis CML (bcCML), and the MLL/AF9 model of AML. In the bcCML model, CCL3KO leukemic cells do not generate a leukemic disease when transplanted into naive WT recipient mice. In the AML model, the disease progression of CCL3KO leukemic cells is significantly delayed as compared to WT controls (WT vs. CCL3KO  $p<0.05$   $n=15$  mice/group). The small molecule maraviroc targets one of the receptors for CCL3, CCR5. We loaded maraviroc into micelle nanoparticles that are targeted to the BMME through the use of a tartrate-resistant acid phosphatase (TRAP) binding peptide. Following CCR5 inhibition in WT bcCML mice leukemic burden was decreased  $>2$  fold in the bone marrow, and alterations to the BMME were abrogated.

If CCL3 signaling is to be a viable therapeutic target in AML it must be specific to leukemic cells and not to normal hematopoiesis. To study this we sorted Lineage-Sca1 + Ckit+Flt3- (Flt3-LSK) bone marrow cells enriched for long term repopulating HSPCs (LT-HSCs) in order to establish stem cell activity on a per cell basis through competitive transplantation. Upon secondary transplantation, the true test of LT-HSC function, CCL3KO Flt3-LSK donor cells engrafted in recipient mice at a higher rate (2-way ANOVA,  $p<0.05$  over 16 weeks,  $n=8$  mice/group). These results confirm that CCL3KO mice maintain a functional LT-HSC population.

**Conclusions:** These results demonstrate that in multiple mouse models of myelogenous leukemia CCL3 plays an important, and in some cases, indispensable role in leukemogenesis, likely involving manipulation of the normal BMME. Importantly however, a long-term engrafting normal HSC population is clearly maintained even in the complete absence of CCL3 suggesting that anti-CCL3 therapy would be well tolerated by the benign hematopoietic system.

**Disclosures:** Rhonda Staversky, None.



## SU0036

**Disease stabilization in a lower-risk myelodysplastic syndrome (MDS) patient with activated beta-catenin upon All Trans-Retinoic Acid (ATRA) treatment.** Marta Galán-Díez\*, Abdullah Mahmood Ali, Miray Nilufer Cimsit, Can Ege Yalçın, Stavroula Kousteni, Azra Raza. Columbia University, United States

Myelodysplastic Syndrome (MDS) is a heterogeneous set of clonal stem-cell disorders characterized by ineffective hematopoiesis, variable cytopenias, genetic instability and propensity to progress to acute myeloid leukemia (AML). MDS prevalence is increasing due to aging of the general population and despite the fact that a fraction of lower-risk MDS patients benefit from approved therapies for a limited period of time, experimental therapies are often needed and allogeneic transplantation is the only curative-therapy for high-risk MDS. Here we report a patient with Refractory Cytopenia and Multilineage Dysplasia (RCMD) whose worsening thrombocytopenia stabilized in response to all All-Trans-Retinoic Acid (ATRA) treatment. A 70-year-old Caucasian male presented a white-blood cell count of 2.1 cells/ $\mu$ L, hemoglobin of 15.1 g/dL and 85,000 platelets/ $\mu$ L. Bone marrow (BM) biopsy showed normocellular marrow with 4% blasts and normal cytogenetics. The patient was followed without any treatment and during the follow-up he showed worsening thrombocytopenia. Repeated BM biopsies confirmed a low-risk RCMD diagnosis. When the patient's platelets count came down to 20,000, he was started on ATRA at a dose of 120 mg/ $m^2$ /day; the dose was subsequently adjusted due to side effects to every other two weeks. Patient's platelets fluctuated between 25,000 to 40,000 cells/ $\mu$ L. Two somatic alterations in genes recurrently mutated in AML, TET2 and SRSF2, were identified in his blood. The patient has been kept on ATRA for more than 3 years and shows a stabilized disease with almost complete remission. In view of reports that Retinoic Acid (RA) signaling through RA-receptor- $\alpha$  (RARA) inhibits  $\beta$ -catenin function, we analyzed  $\beta$ -catenin activity on BM aspirates of this patient pre-ATRA and post/on-ATRA. Interestingly, we found increased  $\beta$ -catenin activity in both CD34<sup>+</sup> cells and osteoblasts (Lin<sup>-</sup>, CD34<sup>+</sup>, RunX2<sup>+</sup>, OCN<sup>+</sup> cells) in the pre-therapy BM sample but not in the post/on-therapy ones, where  $\beta$ -catenin activation was completely downregulated. Our data suggest that the disease stabilization is due to ATRA treatment since the patient's platelet count was stabilized in parallel with the treatment and more importantly because the  $\beta$ -catenin activity was completely abrogated after it. This case report suggests the possibility of a larger trial using targeted-therapy with ATRA in patients with high  $\beta$ -catenin activity.

**Disclosures:** Marta Galán-Díez, None.

## SU0037

**Expression of CD38 and the Ectoenzymes of the Adenosinergic Pathways in Myeloma Bone Microenvironment: A Rational Basis for an Anti-CD38 Antibody Based Therapy for Myeloma-induced Osteoclastogenesis.** Denise Toscani\*, Federica Costa<sup>1</sup>, Antonella Chillemi<sup>2</sup>, Valeria Quarona<sup>2</sup>, Marina Bolzoni<sup>1</sup>, Valentina Marchica<sup>1</sup>, Rosanna Vescovini<sup>3</sup>, Cristina Mancini<sup>4</sup>, Eugenia Martella<sup>4</sup>, Fabrizio Accardi<sup>1</sup>, Alberto L. Horenstein<sup>2</sup>, Mario Pedrazzoni<sup>5</sup>, Franco Aversa<sup>6</sup>, Fabio Malavasi<sup>2</sup>, Nicola Giuliani<sup>1</sup>. <sup>1</sup>Myeloma Unit, Dept. of Medicine and Surgery, University of Parma, Italy, <sup>2</sup>Laboratory of Immunogenetics, Dept. of Medical Sciences and CeRMS, University of Turin, Italy, <sup>3</sup>Dept. of Medicine and Surgery, University of Parma, Italy, <sup>4</sup>Pathology, "Azienda Ospedaliero-Universitaria di Parma, Italy, <sup>5</sup>Internal Medicine, University of Parma, Italy, <sup>6</sup>Hematology and BMT Center, "Azienda Ospedaliero-Universitaria di Parma, Italy

Bone disease is the hallmark of multiple myeloma (MM) patients. CD38 is a receptor involved in cell-to-cell adhesion with a significant ectoenzyme activity. Moreover CD38 is critically involved in the osteoclast differentiation and development. A high expression of CD38 characterizes MM cells recently leading to develop human anti-CD38 monoclonal antibodies including Daratumumab (DARA) able to kill MM cells by immunomediated mechanisms. Currently, the expression profile of CD38 and its potential role in the alteration of the bone remodeling in MM patients are not known. The aim of this study was to define the expression profile of CD38 and the other ectoenzymes of the adenosinergic pathway as CD31, CD39, CD73 and CD203a by MM bone microenvironment. Then, the effect of DARA on osteoblast and osteoclast differentiation and activity was investigated.

Firstly, we performed immunohistochemical analysis on bone biopsies of a cohort of 37 patients with MM and 14 controls with monoclonal gammopathy of uncertain significance (MGUS). The same antigens were analyzed by flow cytometry on primary MM cells, mesenchymal stromal cells (MSC), osteoblasts (OB), monocytes and osteoclasts (OC). MM cells showed a high expression of CD38 and were positive for CD31, CD39, CD73 and CD203a at variable levels. CD38 was expressed by monocytes and early OC progenitors but not by OB, mature OC and MSC that were positive for CD73 and CD203a. Indeed, CD38 was lost during the human OC differentiation process. Based on these results, we tested the effect of DARA, in the presence or absence of *all-trans* retinoic acid, compared with human IgG isotype control, on OC differentiation from either CD138<sup>+</sup> cell fraction or purified MM bone marrow (BM) CD14<sup>+</sup> cells. We also investigated the effect of microvesicles isolated from a MM cell line treated with DARA or the human IgG isotype control, on OC differentiation and activity.

We found that DARA reacts with CD38 expressed by monocytes and its binding inhibits early *in vitro* osteoclastogenesis, OC activity and bone resorption from total mononuclear cells. Interestingly, *all-trans* retinoic acid treatment increased the inhibitory effect of DARA on OC formation. On the other hand any significant effect was

observed by MM-derived microvesicles suggesting that the anti OC effect of DARA was not mediated by this mechanism.

We conclude that DARA inhibits osteoclastogenesis, targeting monocytes and early OC progenitors giving the rationale for the use of an anti-CD38 antibody-based approach as treatment for MM-induced bone disease.

**Disclosures:** Denise Toscani, None.

## SU0038

**3D Tissue-Engineered Bone Constructs Direct Osteogenic Differentiation of human Mesenchymal Stem Cells.** Alyssa Merkel\*, Joseph Vanderburgh<sup>2</sup>, Shanik Fernando<sup>3</sup>, Scott Guelcher<sup>2</sup>, Julie Sterling<sup>1</sup>. <sup>1</sup>Center for Bone Biology, Vanderbilt University Medical Center, Nashville, TN. Department of Veterans Affairs, Tennessee Valley Healthcare System, Nashville, TN, United States, <sup>2</sup>Center for Bone Biology, Vanderbilt University Medical Center, Nashville, TN. Department of Chemical and Biomolecular Engineering, Vanderbilt University, Nashville, TN, United States, <sup>3</sup>Department of Chemical and Biomolecular Engineering, Vanderbilt University, Nashville, TN, United States

Properties of the bone microenvironment, including elastic modulus, porosity, and curvature, are known to regulate cell fate in a number of physiological processes, including bone remodeling, tissue repair, and disease progression. Previous work by our lab and others has shown that osteogenic differentiation and mineralization of mesenchymal stem cells (MSCs) are influenced by matrix rigidity and pore size. Biomimetic 3D *in vitro* systems recapitulating the bone microenvironment are critical for understanding the spatio-temporal dynamics of bone remodeling as well as how bone cells respond to mechanical and chemical signals. In order to test our hypothesis that surface curvature of trabecular bone regulates MSC proliferation, differentiation, and mineralization, we fabricated human bone mimicking 3D tissue engineered bone constructs (TEBCs) using a novel  $\mu$ CT/3D inkjet printing process. TEBCs were designed to recapitulate anatomical site-specific morphometric properties of trabecular bone for femoral head (FH), proximal tibia (PT), and vertebral body (VB). Furthermore, TEBCs were fabricated with nano-hydroxyapatite to mimic the physicochemical properties of bone. Human MSCs (hMSCs) were cultured on 3D TEBCs for up to 10 days and analyzed for osteogenic potential. Cells grown on PT-TEBCs had higher metabolic activity, as measured by MTS assay, compared to FH- and VB-TEBCs ( $p < 0.05$ ). Osteogenic differentiation of hMSCs was assessed by measuring expression changes of osteogenic genes (OPN, ALP) using qRT-PCR, and by ELISA for secreted osteocalcin (OCN) after 8 days in culture of osteogenic media. Expression of alkaline phosphatase significantly increased between days 3, 5, and 8 for PT- and VB-TEBCs ( $p < 0.05$ ) while a decrease was observed for FH-TEBCs. Additionally, we observed increased concentrations of secreted OCN at day 8 on VB-TEBCs compared to PT- and FH-TEBCs ( $p < 0.001$ ), suggesting that cells grown on convex constructs exhibit delayed osteogenic differentiation. Alizarin Red staining was used to measure mineralization of hMSCs cultured in osteogenic media for up to 10 days. Mineralization was observed between days 7 and 10 and increased with decreasing surface convexity. Taken together, these data demonstrate that site-specific properties of trabecular bone influence osteoblast activity, highlighting the need for anatomically relevant *in vitro* models that can potentially provide new precision medicine approaches to treating diseases of the skeleton.

**Disclosures:** Alyssa Merkel, None.

## SU0039

**Genetic Instability of the 2.3Colla1-Cre Transgenic Line reveals a threshold for leukemogenesis in a model of osteoblast-induced acute myeloid leukemia.** Ioanna Mosialou\*, Alvaro Cuesta-Dominiguez<sup>1</sup>, Julie Teruya-Feldstein<sup>2</sup>, Elin Berman<sup>3</sup>, Stavroula Kousteni<sup>1</sup>. <sup>1</sup>Columbia University, United States, <sup>2</sup>Mount Sinai, United States, <sup>3</sup>Memorial Sloan Kettering Cancer Center, United States

A growing body of evidence indicates that osteoblasts have a direct pathogenetic role in the development of myelodysplastic syndromes (MDS), acute myeloid leukemia (AML) and transformation of MDS to AML. Models of osteoblast-induced MDS or AML (OIAML) include  $\beta$ -catenin activation in osteoblasts inducing AML in mice and seen in more than 30% of MDS and AML patients; deletion of *Dicer1* in osteoblast progenitors leading to MDS in mice; Noonan syndrome mutation (PTPN11) in stromal cells driving MPN in mice; and Schwachman-Diamond syndrome mutation in stromal cells driving MDS in mice and predicting AML progression in patients. To further understand the mechanism of OIAML we examined whether a defined threshold of AML-inducing signal by osteoblasts is required for disease development. For this purpose we constitutively activated  $\beta$ -catenin in osteoblasts using three different lines of 2.3Colla1-Cre transgenic mice characterized by different recombination efficiencies in bone. Line 1, was the original line generated in 2002 in which recombination efficiency was 75%. Line 2 was the same original line in which after several inter-breeds we detected a reduction in recombination efficiency to 45%. Line 3 was recently raised from the original stock and had 75% recombination efficiency. Activation of  $\beta$ -catenin in osteoblasts using Line 1, as originally reported, led to the development of MDS which rapidly transformed to full-blown AML characterized by multi-organ infiltration with myeloid blasts, hematopoietic deregulation and lethality by 6 weeks of age. In contrast, activation of  $\beta$ -catenin in osteoblasts using Line 2 did not lead to AML development.

Mice remained healthy and when placed in powdered or gel-based diet survived until at least 8 months of age, the entire time they were observed. Activation of b-catenin in osteoblasts using Line 3 led to anemia, with the appearance of myeloid blasts, segmented neutrophils and Pelger Huet neutrophils in the blood, all features characteristic of a myeloid leukemia phenotype. These observations suggest that a minimal activation level of a key leukemogenic signal from the stroma, which commonly occurs in human disease, is required to initiate cancer development, and provides mechanistic insight into the formation and progression of preleukemic stem cells in AML and the transformation of MDS to AML. They also illustrate the importance of measuring the degree of recombination of any gene of interest when performing cell-specific gene deletion.

**Disclosures:** Ioanna Mosialou, None.

## SU0040

**Distribution of Nerve Fibers in Human Bone and their Association to Bone Remodeling Events and Vascular Structures.** Manasi Sayilekshmy<sup>1</sup>, Rikke Rie Hansen<sup>1</sup>, Jean-Marie Delaisse<sup>2</sup>, Lars Rolighed<sup>3</sup>, Anne-Marie Heegaard<sup>1</sup>, Thomas Levin Andersen<sup>2</sup>. <sup>1</sup>Department of Drug Design and Pharmacology, University of Copenhagen, Copenhagen, Denmark, <sup>2</sup>Department of Clinical Cell Biology, Vejle Hospital – Lillebaelt Hospital, Institute of Regional Health Research, University of Southern Denmark, Vejle, Denmark, <sup>3</sup>Department of Otorhinolaryngology, Aarhus University Hospital, Aarhus, Denmark, Denmark

Recent years, the concept that the central nervous system plays a role in the regulation of bone remodeling has become well established and several studies have now shown that the bone resorption and formation in animal models may be directly regulated by nerve fibers within the bone. However, little is known about local distribution of nerve fibers in the human bone. The aim of this study is to investigate the local distribution of nerve fibers in human bone and their association to both vascular structures and bone remodeling events on the bone surface.

The analysis of the local distribution of nerve fibers was conducted on transiliac bone biopsies from 16 patients with primary hyperparathyroidism, which has an increased extent of bone remodeling events. The nerve fibers were either double-immunostained with antibodies for PGP9.5 (protein gene product 9.5), a pan-neuronal marker, and TH (tyrosine hydroxylase), a marker for sympathetic nerve fibers, or double-immunostained for PGP9.5 or TH in combination with CD34, an endothelial marker, on serial 3.5-µm-thick sections. Adjacent sections were Masson trichrome stained to identify the remodeling events. The local densities of nerve fibers were estimated as numbers of nerve profiles per area (np/mm<sup>2</sup>).

Overall, the density of PGP9.5<sup>+</sup> nerve profiles was more than 8-fold higher in the intracortical pores than in the bone marrow or periosteum. In the intracortical pores, the TH<sup>+</sup> nerve profiles were twice as abundant as TH<sup>-</sup> nerve profiles. In all three compartments nearly all the nerve profiles were associated with vascular structures, which in the bone marrow were preferentially identified as large and small arterioles. In the bone marrow, both the PGP9.5<sup>+</sup> and TH<sup>+</sup> nerve profiles were denser within a 100µm distance to the bone surfaces than in the more distant bone marrow. In the bone marrow within 100µm of the bone surface the PGP9.5<sup>+</sup> and TH<sup>+</sup> nerves profiles were denser above remodeling surfaces than quiescent surfaces, and the PGP9.5<sup>+</sup> nerve profiles were denser above resorptive surfaces than formative surfaces.

Collectively, this study demonstrates that the nerve fibers in the human bone are highly associated with vascular structures and that the density of nerve fibers is exceptionally high in the pores of the cortical bone. Moreover, the study shows that the nerve density in the bone marrow is higher close to the bone surface, and even higher above remodeling events.

Thomas Levin Andersen and Anne-Marie Heegaard are co-senior authors

**Disclosures:** Manasi Sayilekshmy, None.

## SU0041

**T Cell-Derived IL-17A and IL-17F Drive Bone Formation from Human Periosteal Stem Cells: Implications for Enthesophyte Formation.** Mittal Shah<sup>1</sup>, Ash Maroof<sup>1</sup>, Rawiya Al-Hosni<sup>2</sup>, Panagiotis Gikas<sup>3</sup>, Neil Gozzard<sup>1</sup>, Stevan Shaw<sup>1</sup>, Scott Roberts<sup>1</sup>. <sup>1</sup>UCB Pharma, United Kingdom, <sup>2</sup>Institute of Orthopaedics and Musculoskeletal Science, United Kingdom, <sup>3</sup>The Royal Orthopaedic Hospital, United Kingdom

Purpose: The involvement of IL-17 signaling in bone pathology during spondyloarthritis (SpA) disease progression is poorly understood. Recently, IL-17-producing γδ-T cells have been associated with periosteal bone formation for fracture repair<sup>1</sup>; the periosteum is also implicated in pathologic bone formation in SpA<sup>2</sup>. As such, we investigated IL-17 signaling in the context of pathologic bone formation using a biomimetic human periosteum-derived stem cell (hPDSC) model of osteogenic differentiation.

Methods: hPDSCs were obtained through enzymatic digestion of periosteal biopsies from patients undergoing orthopedic surgery. Expanded cultures were treated with recombinant human IL-17A, IL-17F, or both for 96h and expression of gene markers evaluated. hPDSCs were also stimulated using a biomimetic protocol in combination with IL-17A and IL-17F, or human Th17 and γδ-T-cell supernatants (SNs). Antibodies with strong affinity to IL-17A, IL-17F, or bimekizumab (a humanized IgG1 mAb with strong affinity for both IL-17A and IL-17F) were used to define the role of these cytokines in the SNs. Expression of osteogenic markers and matrix mineralization was assessed to define *in vitro* bone formation.

Results: Under basal conditions IL-17A and IL-17F significantly up-regulated IL-6 expression and transiently enhanced the expression of RUNX-2. When IL-17 cytokines were combined in a biomimetic protocol, both IL-17A and IL-17F promoted osteogenic differentiation. Following 9 days' exposure, IL-17F enhanced expression of most osteogenic markers to a greater extent than IL-17A; however, less matrix mineralization was apparent with IL-17F. The SNs potentially enhanced hPDSC osteogenic differentiation and mineralization. While IL-6 expression and *in vitro* bone formation were blocked by neutralization of IL-17A or IL-17F individually, dual neutralization with bimekizumab exhibited the greatest effect on most tested parameters.

Conclusion: These data show that both IL-17A and IL-17F enhance *in vitro* osteogenic differentiation and bone formation from hPDSCs. We propose that IL-17A and IL-17F drive pathologic bone formation resulting in enthesophytes at the enthesis/periosteum interface. Current therapeutics have limited efficacy in blocking enthesophyte formation, hence inhibition of both IL-17A and IL-17F with bimekizumab offers an attractive strategy to prevent this debilitating feature of SpA.

### References

<sup>1</sup>Ono, *et al.* Nat Commun 2016;7:10928; <sup>2</sup>Lories, *et al.* Arthritis Res Ther 2009;11:221

**Disclosures:** Mittal Shah, UCB Pharma, Grant/Research Support.

## SU0042

**Role of Sirtuin 3 in Bone Homeostasis during Aging.** Liping Wang<sup>\*</sup>, Linh Ho, Theresa Roth, Robert Nissenon. San Francisco VA Medical Center, United States

Sirtuin 3 (Sirt3) is reported to play a positive role in maintenance of bone mass and a negative role in osteoclastogenesis in young mice. However, the role of Sirt3 in bone homeostasis during aging is not clear. We have characterized the bone phenotype of young (3 month old) and old (8 to 13 month old) adult male and female mice overexpressing Sirt3 (Sirt3Tg). Young Sirt3Tg mice had normal bone mass, but surprisingly µCT demonstrated that cortical thickness at the tibio-fibular junction was reduced by 8.6% (p<0.05) and histomorphometry showed a decrease of 50% (p<0.01) in fractional bone volume (BV/TV, %) at the distal femur in old male Sirt3Tg mice compared to littermate wild type (WT) controls. We have carried out skeletal phenotyping of 6 month old male Sirt3 KO mice. µCT demonstrated that Sirt3 gene deficiency did not alter the distal femoral BV/TV (WT vs. KO, 14.1±1.9 vs. 13.6±1.0). EchoMRI assessment demonstrated that deletion of Sirt3 gene did not significantly affect body weight (WT vs. KO, 33.1±4.1 vs. 31.2±2.4g), total body fat (WT vs. KO, 6.54±3.2 vs. 5.0±1.3g), or lean mass (WT vs. KO, 25.0±1.1 vs. 24.5±1.4g). To investigate the mechanism by which overexpressing Sirt3 causes bone loss in aging mice, we performed histomorphometry and found a significant increase in bone marrow (BM) adipocyte numbers (Sirt3Tg vs. WT, 92±6.0 vs. 11±0.1) and a 2.5 fold increase (p<0.05) in TRAP<sup>+</sup> cells in the tibia BM of old male Sirt3Tg mice, compared to age and sex matched WT mice. We also found that old male Sirt3Tg mice displayed enhanced adipogenesis of BM stromal cells (BMSCs) (2.9-fold vs. WT, p<0.05) and decreased proliferation of marrow progenitors (1.27 fold vs. WT, p<0.01) with no change in osteoblast differentiation *in vitro*. Overexpressing Sirt3 significantly increased mRNA levels of RANKL (2.8 fold, p<0.01) and SOD2 (1.6 fold, p<0.05) in osteoblasts, compared to WT BMSCs. Sirt3 overexpression also significantly increased the number of TRAP<sup>+</sup> cells (2 fold, p<0.01) derived from BM cells *in vitro* and increased the mRNA levels of TRAP (1.2 fold, p<0.05) and cathepsin K (1.3 fold, p=0.05) compared to WT cell culture. Western blot demonstrated that osteoclast progenitor cells derived from Sirt3Tg mice displayed increased phosphorylation of mTOR. We conclude that Sirt3 promotes age-related adipogenesis and osteoclastogenesis associated with bone loss. These findings identify Sirt3 as a potential target for the treatment of age-related osteoporosis.

**Disclosures:** Liping Wang, None.

## SU0043

**Soluble factors of prostate cancer cells induce bone pre-metastatic niche changes in mice with induced prostate tumors.** Juan A Ardura<sup>\*</sup>, Irene Gutierrez-Rojas, Luis lvarez-Carrión, Verónica Alonso. IMMA-Universidad San Pablo CEU. Madrid, Spain

Metastases are the leading cause of death by cancer. Recent studies have described pro-metastatic changes in organs where metastases later develop. It has been suggested that formation of a pre-metastatic niche by cross-talk communication between the tumor and the target organ favors circulating tumor cell colonization. The aim of our study was to analyze the effects of primary prostate tumors on the bone environment before the settlement and propagation of the metastases.

An *in vivo* pre-metastatic prostate cancer model based on the implantation of prostate adenocarcinoma TRAMP-C1 cells in immunocompetent C57BL/6 mice was used. One month after TRAMP-C1 cell implantation –a period of time sufficient for prostate tumor developing without bone metastases formation- histomorphometric parameters and bone markers were analyzed in femurs of mice with and without TRAMP-C1-induced prostate tumors. Also, we studied the effects of conditioned medium of murine TRAMP-C1 or human prostate tumor LNCaP cells on mouse osteocyte-like MLO-Y4 cells and human osteoblasts, respectively.

*In vivo*, primary prostate tumors exhibited osteomimetic features including increased Runx2, osterix, osteocalcin and RANK-L mRNA expression. Femurs of TRAMP-C1-induced tumor mice showed decreased trabecular thickness, trabecular separation,



eroded surface and number of osteoclasts/bone surface and an increase in trabecular number compared to non-tumor control mice. Other histomorphometric parameters were not significantly altered. Associated to histomorphometric changes, elevated immunolabeling of Runx2, osterix and sclerostin bone markers in femurs of TRAMP-C1-induced tumor mice compared to control mice were observed.

In vitro, Runx2 and osterix expression was induced in MLO-Y4 and human osteoblasts by conditioned medium of TRAMP-C1 and LNCaP cells, respectively.

These results suggest that secreted soluble factors of prostate tumorigenic cells induce changes in the bone environment before metastatic implantation.

**Disclosures:** Juan A Ardura, None.

## SU0044

**A novel tubulin inhibitor induces apoptosis of human osteosarcoma cells.** Yufan Chen<sup>\*1,3</sup>, Baohong Zhao<sup>2</sup>, Jingle Xi<sup>1,3</sup>, Liang Zhao<sup>1,3</sup>. <sup>1</sup>NanFang Hospital, China, <sup>2</sup>Cornell University, United States, <sup>3</sup>Nanfang Hospital, China

A novel class (2-amino-4-phenyl-4H-chromene-3-carboxylate) of inhibitors of tubulin assembly by modifying HA14-1 has been developed, which is a Bcl-2 inhibitor discovered by our group. One of these compounds, mHA11, showed in vitro cytotoxicity against osteosarcoma cells that were more potent and more stable than the backbone compound HA14-1.

**Objectives:** To explore the effect of a novel class of tubulin inhibitor, mHA11, on growth inhibition and apoptosis in human osteosarcoma cell lines MG-63 and HOS cells, and in HOS Xenograft models in nude mice.

**Methods:** MG-63 cells and HOS cells were treated with various concentrations of mHA11 and apoptosis was monitored via an MTT assay and Cell Counting kit 8 (CCK-8) assay as well as examined for morphological changes by inverted fluorescence microscopy and photography. Female BALB/c-nude mice with subcutaneous injection of HOS cells were randomized to be treated with mHA11 or saline by tail intravenous injection, and tumor volume of mice was monitored after injection.

**Results:** The survival rate of MG-63 cells and HOS cells treated for 24 to 72 hours with 1 µmol/l or more of mHA11 decreased significantly. The human osteosarcoma MG-63 cells and HOS cells were treated with mHA11 at 1 µmol/L of mHA11 for 24 hours and their morphological changes could be observed by inverted fluorescence microscopy and photography. The result of Cell Counting kit 8 (CCK-8) assay shows that the IC 50 values decline as the action time went by and finally between 0.6449 µmol/L to 0.6870 µmol/L after 48h in MG63 cells and between 0.3993 µmol/L to 0.4393 µmol/L after 48h in HOS cells. What's more, tumor volume of mice which treated with mHA11 were significantly smaller than those treat with saline. Further results would be achieved in this study.

**Conclusions:** A novel tubulin inhibitor induces apoptosis in human osteosarcoma cells in vitro and in vivo. This new tubulin inhibitor may be a potential option for the therapy of osteosarcoma. However, the effect of new tubulin inhibitor on osteosarcoma needs further study.

**Disclosures:** Yufan Chen, None.

## SU0045

**H3F3A mutation is responsible for the rare Giant Cell Tumor of the Clivus.** Giuseppina Divisato<sup>\*1</sup>, Federica Scotto di Carlo<sup>1</sup>, Maurizio Iacoangeli<sup>2</sup>, Teresa Esposito<sup>3</sup>, Fernando Gianfrancesco<sup>1</sup>. <sup>1</sup>Institute of Genetics and Biophysics, National Research Council of Italy, Italy, <sup>2</sup>Department of Neurosurgery, Umberto I General Hospital, Italy, <sup>3</sup>Institute of Genetics and Biophysics, National Research Council of Italy; IRCCS INM Neuromed, Italy

Giant Cell Tumor of Bone (GCT) is a locally aggressive primary bone tumor representing 5% of all bone tumors, and usually occurs at the epiphyses of the long bones of the appendicular skeleton with a tendency to recurrence. GCTs involving the skull account for less than 1% of all GCTs and those affecting the clivus, representing a surgery challenge, are extremely rare with only 10 cases reported in the literature. This tumor is characterised by malignant mesenchymal stromal cells and multinucleated osteoclast-like giant cells. Recently, we recruited a 55-year-old female with progressive headache and diplopia. Brain magnetic resonance imaging and an angio-computed tomography scan showed a large tumor mass involving the clivus and expanding into the sellar floor and the epistropheus that was surgically removed.

In order to reveal the genetic bases of Clival GCT, we performed targeted sequencing of GCT-related genes (H3F3A, H3F3B, IDH1, IDH2 and ZNF687) on the tumor tissues deriving from this patient and from a previously described case. This analysis revealed that both of them were positive for the p.Gly34Trp mutation in H3F3A gene. In parallel, the molecular analysis on peripheral blood revealed the absence of the mutation at germline level, confirming that H3F3A molecular defects only occurred at somatic level. Haematoxylin and eosin staining revealed that Clival GCT lesions resulted composed by a high-vascularized tissue that contained numerous multinucleated giant cells interspersed among spindle and ovoid cells.

In conclusion, we report for the first time that the rare Clival GCT is genetically defined by somatic mutations in the H3F3A gene, linking it to the conventional GCT. These results suggest the utility of the adjuvant therapy with Denosumab (already effective for GCTs) also in this tumor where its complete surgical resection is very difficult.

**Disclosures:** Giuseppina Divisato, None.

## SU0046

**Transcriptional plasticity of tRNA fragments and microRNAs can be remodulated in chondrosarcoma.** Darrell Green<sup>\*</sup>, William Fraser. University of East Anglia, United Kingdom

Chondrosarcoma is the second most common primary bone cancer after osteosarcoma and has no approved chemotherapy. We aimed to identify transcriptional plasticity of regulatory small RNAs during chondrosarcoma progression with the hypothesis that reprogramming transcriptional plasticity could have therapeutic potential. We used high definition adapters in next generation sequencing of resected chondrosarcoma tissue. Clinical and molecular data were obtained for 13 chondrosarcoma patients and 6 control participants who donated cartilage tissue after a neck of femur fracture resulted in resection of the femoral head. We then developed three dimensional models of human chondrosarcoma to perform loss of function and gain of function studies. We observed a modulated expression, by at least four-fold, of 30 tRNA fragments and 37 microRNAs during chondrosarcoma progression. We selected three tRNA fragments, tRF-Gly-TCC, tRF-Lys-CTT, tRF-Asn-GTT and three microRNAs, miR-140, miR-320a and miR-486 for further analysis based on their role in cancer and bone biology according to the literature. We found miR-140, a key molecule in embryonic bone development, is highly expressed in high grade tumours. We also found tRF-Gly-TCC is a tumour suppressor in which overexpression induces a novel tumour cell morphology and changes in gene expression. We profiled several genes linked to primitive mesenchymal cell proliferation, migration, hypoxia and malignant transformation in control and chondrosarcoma tissue and compared to tRF-Gly-TCC mimic treated models. Expression of HDAC4, a transcriptional suppressor, was high in treated models compared to control and cancer tissue. RUNX2, a key driver of bone cell proliferation was reduced to control levels in treated models when compared to cancer tissue that has a high expression. PTHLP, ANG, IHH had a very low expression in treated models when compared to control and cancer tissue. YBX1 expression was highest in treated models. We hypothesise overexpression of tRF-Gly-TCC, which contains a Y box binding protein 1 interaction motif, increases interaction with Y box binding protein 1 leading to inhibition of chondrosarcoma progression.

**Disclosures:** Darrell Green, None.

## SU0047

**PTHrP negatively regulates tumor cell dormancy in a PTHR1-independent manner.** Rachelle W Johnson<sup>\*1</sup>, Yao Sun<sup>2</sup>, Patricia WM Ho<sup>2</sup>, Natalie Sims<sup>2</sup>, T John Martin<sup>2</sup>. <sup>1</sup>Vanderbilt University Medical Center, United States, <sup>2</sup>St. Vincent's Institute of Medical Research, Australia

Parathyroid hormone-related protein (PTHrP) is expressed at high levels in breast cancer bone metastases compared to primary tumors. Human MCF7 breast cancer cells home to the bones of immune deficient mice following intracardiac inoculation, but do not grow well and stain negatively for Ki67, thus serving as a model of breast cancer dormancy in vivo. We have previously shown that PTHrP overexpression in MCF7s overcomes this dormant phenotype, causing them to grow as osteolytic deposits, and that MCF7 PTHrP-overexpressing cells showed significantly lower expression of genes associated with dormancy compared to vector controls (e.g. AMOT, P4HA1, H2BK, SELENBP1) by RNAseq and qPCR. Since early work showed a lack of cyclic AMP (cAMP) response to parathyroid hormone (PTH) in MCF7 cells, and cAMP is activated by PTH/PTHrP receptor (PTHR1) signaling, we hypothesized that the effects of PTHrP on dormancy in MCF7 cells occurs through non-canonical PTHR1-independent signaling. The data presented here confirms the lack of cAMP response in MCF7 cells to full length PTHrP and PTH(1-34) in a wide range of doses, while response to two known activators of adenylyl cyclase was present: calcitonin (100-fold max) and prostaglandin E2 (PGE2) (30-fold max). Moreover, whereas both calcitonin and PGE2 activate a cAMP Cre-luciferase reporter construct transfected into MCF7 cells, PTHrP and PTH had no effect. PTHR1 mRNA was detectable in MCF7 cells at a low level (30-50-fold lower than in osteoblastic cells with functional PTHR1), and was similarly found in 8 other human breast and murine mammary carcinoma cell lines. Although PTHrP overexpression in MCF7 cells changed expression levels of many genes (>2500 genes with >1-log2fold change, p<0.05), only 2/32 PTHrP-responsive cAMP / CREB genes (e.g. NR1P1, AREG) were significantly upregulated and PTHR1 was unaltered. We conclude that MCF7 breast cancer cells have no functional PTHR1. Thus changes in gene expression in response to PTHrP overexpression must therefore result from autocrine or intracrine actions of PTHrP independent of PTHR1, through signals emanating from other domains within the molecule, such as the nuclear localization sequence. These cells therefore offer a model with which to investigate the significance of non-canonical PTHrP actions.

**Disclosures:** Rachelle W Johnson, None.

## SU0048

**A potential JAB1-SOX9 link in chondrosarcoma pathogenesis.** Murali Mamidi<sup>\*1</sup>, William Samsa<sup>2</sup>, David Danielpour<sup>3</sup>, Guang Zhou<sup>4</sup>. <sup>1</sup>Department of Orthopaedics, Case Western Reserve University, United States, <sup>2</sup>Department of Orthopaedics, Case Western Reserve University, United States, <sup>3</sup>Case Comprehensive Cancer, Case Western Reserve University, United States, <sup>4</sup>Department of Orthopaedics, Department of Genetics and Genome Sciences, Case Comprehensive Cancer, Case Western Reserve University, United States

Chondrosarcoma (CS) is the second most common skeletal malignancy and extremely resistant to chemo-, and radio-therapies. Thus, novel therapies for CS are urgently needed. The evolutionarily conserved transcriptional co-factor JAB1 has emerged as a novel regulator in tumorigenesis. Overexpression of JAB1 occurs in various cancers and is associated with poor prognosis. However, the effects of JAB1 on cell proliferation, survival, apoptosis and cell cycle progression of CS, as well as the underlying mechanisms, are still obscure. In this study, for the first time, we demonstrated that shJAB1 knockdown (KD) led to decreased cell proliferation, decreased colony formation, and elevated apoptosis in two human CS lines, SW1353 and Hs819.T. The elimination of JAB1 significantly decreased mRNA and protein expressions of cell cycle regulators, including SKP2, p53, and p21, suggested that JAB1 might be involved in CS cell cycle progression and DNA damage repair. Neddylated CUL1 was also upregulated upon JAB1 deletion, suggesting that JAB1 is necessary for CUL1 ubiquitin ligase homeostasis through JAB1's deneddylation activity. Interestingly, ChIP assay confirmed that JAB1 bound to the promoter region of the cell cycle inhibitor INK4A. Furthermore, in CS, endogenous JAB1 interacted with SMAD1/5/8 but not with SMAD2/3, thus, JAB1 likely acts through BMP signalling. Revealingly, endogenous JAB1 bound with endogenous SOX9, RUNX2, RUNX3 and isocitrate dehydrogenase-2 (IDH2) in CS; in contrast, endogenous JAB1 did not interact with these same oncogenes in primary mouse rib chondrocytes. Recent human genetics study showed that the disruption in normal type II collagen biosynthesis, such as COL2A1 mutations, is a major contributor to CS pathogenesis. Indeed, the expression of SOX9, the chondrocyte master regulator and a potent oncogene, as well as its down-stream targets, COL2A1 and AGGRECAN, were markedly reduced upon shJAB1 KD in CS. Moreover, ChIP analysis showed JAB1's enrichment at chondrocyte-specific enhancer sites of *SOX9*, *COL2A1*, and *AGGRECAN* promoters, indicating that JAB1 might directly regulate chondrocyte differentiation in CS. In conclusion, our study supports the notion that JAB1 acquires a distinct pro-tumorigenic regulatory network with SOX9 to promote CS development.

**Disclosures:** Murali Mamidi, None.

## SU0049

**Roles of prostaglandin E2 in prostate cancer induced angiogenesis and bone metastasis.** Shosei Yoshinouchi<sup>\*1</sup>, Kenta Watanabe<sup>1</sup>, Tsukasa Tominari<sup>1</sup>, Michiko Hirata<sup>1</sup>, Chiho Matsumoto<sup>1</sup>, Takayuki Maruyama<sup>2</sup>, Masaki Inada<sup>1</sup>, Chisato Miyaura<sup>1</sup>. <sup>1</sup>Tokyo University of Agriculture and Technology, Japan, <sup>2</sup>Ono Pharmaceutical Co., Ltd., Japan

Prostaglandin E2 (PGE2) is associated with inflammatory bone destruction in various infectious immune responses. Metastasis of human prostate cancer to bone was promoted by prostaglandin E2, however, the effect of PGE2 on the migration of prostate cancer cells and the cancer induced angiogenesis is not known. In this study, we investigated the roles of PGE2 in bone metastasis associated angiogenesis and cancer cell migration using prostate cancer cells and endothelial cells. Using PC3 prostate cancer cells that are stably transfected with luciferase, we showed that the development of bone metastasis was accompanied by increased osteoclastic bone resorption, and that was abrogated by the treatment of EP4 receptor antagonist. Furthermore, the PC3 cell growth and its accompanied neo-vascularization were significantly attenuated by the treatment of EP4 antagonist. The in vitro cell growth of PC3 was not altered by the treatment of PGE2 and EP4 antagonist. When we analyze the migration activity of PC3 cells, the treatment of PGE2 promoted the cell migration and that was inhibited by treatment of EP4 antagonist. In the co-culture of PC3 and endothelial cells, we detected the PGE2 production associated endothelial tube formation with the mRNA expression of COX-2 and mPGES-1 in endothelial cells. Treatment of EP4 antagonist also attenuated the endothelial tube formation. These results indicated that both PC3 induced bone resorption and angiogenesis abrogated by the treatment of EP4 antagonist in vivo. The blockade of PGE-EP4 signaling inhibited prostate cancer induced neo-vascularization, motility of PC3 for cell migration and following bone resorption. EP4 antagonist is useful as therapeutic agents in advanced bone metastasized prostate cancer.

**Disclosures:** Shosei Yoshinouchi, None.

## SU0050

**Osteoblastic  $\beta 2$  Adrenergic Receptor Contributes to the Immunosuppressive Activity of Myeloid-Derived Suppressor Cells in the Metastatic Bone Microenvironment.** Hyo Min Jeong<sup>\*1</sup>, Eun Jung Lee<sup>1</sup>, Hye-Eun Kim<sup>1</sup>, Bo Yeon Seo<sup>1</sup>, Hyun-Ho Kim<sup>1</sup>, Yun-Jae Kim<sup>1</sup>, Hyun-Ju Lee<sup>1</sup>, Seok-Hyung Lee<sup>1</sup>, Young Mi Whang<sup>2</sup>, Serk In Park<sup>1</sup>. <sup>1</sup>Department of Biochemistry and Molecular Biology, Korea University College of Medicine, Korea, Republic of, <sup>2</sup>Chungang University, Korea, Republic of

We investigated how chronic psychological stress contributes to the progression of bone metastasis of prostate cancer patients, focusing on osteoblasts and a subset of immune-suppressive bone marrow cells termed myeloid-derived suppressor cells (MDSCs). We first confirmed that MC3T3E1 subclone 4 osteoblastic cells and murine femoral osteoblasts express  $\beta 2$ , but not  $\beta 1$  nor  $\beta 3$ , AR. Isoproterenol, a potent  $\beta$  agonist, treatment significantly increased many cytokines including, but not limited to, GM-CSF, IL-6, C-C chemokine ligand 2 (CCL2), etc. from osteoblasts by cytokine array assay. We subsequently identified that CCL2 expression was significantly induced by isoproterenol treatment *in vivo* and *in vitro* by quantitative PCR and ELISA. Lastly, we found that CD11b+Gr1+ MDSCs from the femoral bone marrow of isoproterenol-treated mice had significantly increased T cell suppressive activity compared with saline-treated controls. Collectively, our data suggest that chronic psychological stress contributes to prostate cancer bone metastasis via osteoblastic CCL2 and increased immunosuppressive activity of MDSCs.

**Disclosures:** Hyo Min Jeong, None.

## SU0051

**Differentiation capacity of osteosarcoma cells transformed by distinct oncogenic drivers.** Kirby Rickel<sup>\*1</sup>, Fang Fang<sup>1</sup>, Kaitlyn Dorn<sup>2</sup>, Jianing Tao<sup>3</sup>. <sup>1</sup>Sanford Research, United States, <sup>2</sup>Augustana University, United States, <sup>3</sup>Sanford Research & University of South Dakota, United States

Osteosarcoma (OS) is the most common type of primary bone malignant neoplasms, mainly affecting adolescents. Current treatment consists of a combination of surgery and chemotherapy. Once metastasis occurs, OS becomes resistant to chemotherapy and five-year survival rates are reduced from 70% to 30%. One key step in improving the treatment outcomes of OS is to enhance our understanding of the nature of bone cancer stem cells (CSCs), which represent the driving force behind drug resistance, cancer recurrence, and metastasis. Gene mutations in distinct pathways have been reported in human OS cases and have shown to result in distinct subtypes of murine OS. However, differentiation capacity of osteosarcoma cells transformed by distinct oncogenic drivers remains unknown. In this study, we established OS cell lines from mouse tumors engineered to recapitulate the features of human bone cancer. Those OS cells were transformed by either osteoblastic-specific Notch gain of function (Notch OS cells) or p53 loss of function (p53 OS cells) from a population of committed osteoblasts with limited proliferation ability. We found that Notch OS cells have a high adipogenic potential similar to mesenchymal stem cells, but display restricted osteogenic potential. In contrast, p53 OS cells have a high osteogenic potential but little adipogenic potential. Moreover, peroxisome proliferator-activated receptor gamma (PPAR-gamma) ligand, rosiglitazone, alone transdifferentiates Notch OS cells into adipocytes. Lineage tracing showed relative distribution of originating osteoblast cells of Notch OS and p53 OS in postnatal bone. Bioinformatics and protein analyses indicate a sustained activation of PI3K/AKT/mTOR pathway in Notch OS cells. Accordingly, Notch OS cells are sensitive to the treatment of rapamycin, the mTORC1 specific inhibitor. When treated with rapamycin, the adipogenic potential of Notch OS cells was reduced, suggesting a function of mTOR in the cell fate determination of Notch OS. These findings suggest that osteosarcoma cells transformed by distinct oncogenic drivers have different CSCs properties. Agents targeting OS CSCs and signaling pathways such as mTOR that maintain cancer cells have the potential to be used in increasing vulnerability to chemotherapy to manage recurrent and metastatic disease.

**Disclosures:** Kirby Rickel, None.

## SU0052

**Secreted Factors from the Dura Mater Promote Proliferation and Invasion of Prostate Cancer Cells via CXCR2 Activation.** Nicholas Szerlip<sup>\*1</sup>, Alexandra Calinescu<sup>1</sup>, Catherine Van Poznak<sup>2</sup>, Russell Taichman<sup>3</sup>, Greg Clines<sup>1</sup>. <sup>1</sup>University of Michigan School of Medicine, United States, <sup>2</sup>University of Michigan, United States, <sup>3</sup>University of Michigan School of Dentistry, United States

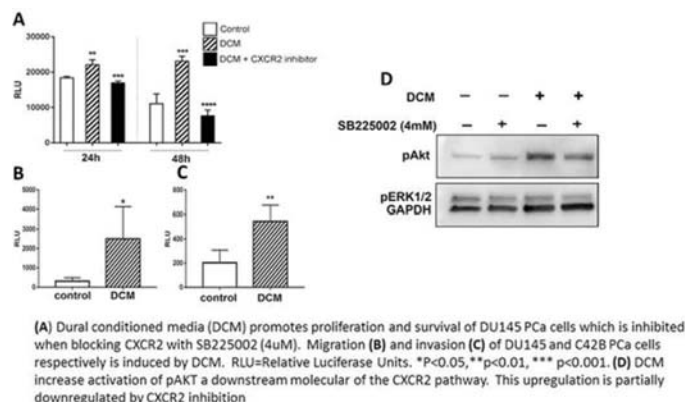
The spine represents the most common and debilitating site of metastatic spread of malignant disease. The cause of this preferential tumor growth in the spine is not understood. The dura mater, the outer layer of the meninges, surrounds and protects the spinal cord and is situated in close contact with the vertebrae. The dura is a dense connective tissue, made of collagen bundles and mainly fibroblasts. Numerous studies demonstrate that in the context of cancer, fibroblasts change their phenotype to become cancer-associated fibroblasts, which promote tumor invasion and progression. During development, the dura regulates morphogenesis in the underlying CNS tissue and in the



overlying bone cells, secreting molecules which promote the proliferation, migration and differentiation of precursor cells. We hypothesized that growth factors and cytokines produced by the dura promote tumor growth and dissemination, contributing to the high incidence of spinal metastatic disease.

To characterize the transcriptional activity of the dura, mouse dural fibroblasts were cultured either in isolation or in non-contact co-culture with human prostate carcinoma (PCa) cells. RNA was extracted and sequenced en masse. Analyses revealed high expression of many secreted molecules. Upon co-culture with PCa cells we observed an even further increase in expression of several secreted factors, with the highest increase in expression represented by the CXCR2 ligands CXCL5 (82 fold) and CXCL1 (12.8 fold). These changes in mRNA were also reflected at the protein level in ELISA analysis of co-culture supernatants. We treated PCa cells with dura conditioned media (DCM) and observed increased proliferation of DU145 PCa cells (2-fold,  $p=0.0003$ ), which was abrogated by a specific CXCR2 inhibitor. DCM also promoted increase in migration of DU145 cells ( $p=0.0374$ ) and invasion of C4-2B cells ( $p=0.0066$ ). In Western blot analyses we show that DCM activated the PI3K/AKT signaling pathway, and was partially abrogated by the CXCR2 inhibitor. In contrast, the CXCR2 inhibitor had no effect on the activation of the ERK pathway.

These data demonstrate that the dura produces bio-active molecules and that this secretory activity is increased in the presence of PCa cells. Secreted factors from the dura stimulate proliferation and invasion of PCa cells in vitro. This effect was abrogated in part by a CXCR2 inhibitor, supporting future investigations of this receptor in spine metastases.



Effect of Dural Cytokines on Prostate Cancer Cells

**Disclosures:** Nicholas Szerlip, None.

## SU0053

**Effects of the Anti-Estrogen Endoxifen on the Musculoskeletal System and Implications for the Tumor Microenvironment.** Laura Wright<sup>\*1</sup>, Jenna Regan<sup>1</sup>, Andrew Marks<sup>2</sup>, Khalid Mohammad<sup>1</sup>, Theresa Guise<sup>1</sup>. <sup>1</sup>Indiana University, United States, <sup>2</sup>Columbia University, United States

Adjuvant endocrine therapy is a standard treatment for postmenopausal women with ER-positive breast cancer. Unfortunately, between 25-50% of women treated with endocrine therapies develop musculoskeletal toxicities that result in treatment discontinuation. Previous studies in our laboratory demonstrated that aromatase inhibitor (AI) treatment caused bone loss and skeletal muscle weakness in mice, recapitulating effects observed in cancer patients. We also demonstrated that prevention of AI-induced osteoclastic bone resorption using a bisphosphonate attenuated ER-negative breast cancer bone metastases and improved muscle function. These preclinical findings highlight the bone microenvironment as a modulator of tumor growth locally and muscle function systemically. Because muscle weakness is also commonly reported in women treated with selective estrogen receptor modulators (SERMs), we compared musculoskeletal effects of AI with a bone-sparing SERM endoxifen in a non-tumor model. Endoxifen (Endx), an active metabolite of tamoxifen, is currently in phase I trials for ER+ advanced breast cancer and little is known of its effects on the musculoskeletal system. Mature female C57BL/6 mice underwent sham surgery or ovariectomy (OVX) and were treated daily with vehicle, the AI letrozole (Let), or Endx. After eight weeks, changes in cancellous and cortical bone indices were assessed by  $\mu$ CT and muscle contractility of the extensor digitorum longus (EDL) was measured *ex vivo*. Bone volume fraction (BV/TV) decreased by 50% in OVX-vehicle and OVX-AI mice ( $p<0.05$ ), whereas BV/TV increased threefold in Endx mice relative to sham-vehicle ( $p<0.0001$ ). Periosteal and endosteal expansion of cortical bone was inhibited by Endx evidenced by a decrease in medullary area, total cortical cross sectional area, and polar moment of inertia relative to sham- and OVX-vehicle ( $p<0.0001$ ). At the termination of the study, muscle-specific force was lower in OVX-Endx mice relative to OVX-vehicle and OVX-AI mice ( $p<0.05$ ), indicating that SERM-induced muscle weakness may be independent of bone resorption. Histological and biochemical assessment of skeletal muscle will be performed to determine a mechanism for muscle weakness in Endx-treated mice. Ongoing studies will determine how Endx-driven changes in cancellous and cortical bone morphology impact the mechanical strength of bone, and how these changes to the bone microenvironment impact breast cancer metastasis to the skeleton.

**Disclosures:** Laura Wright, None.

## SU0054

**miRNA-150, a novel regulator of post-traumatic osteoarthritis.** Asaad Al-Adlaan<sup>\*1</sup>, Fatima Jaber<sup>2</sup>, Nazar Hussein<sup>2</sup>, Fayeze Safadi<sup>1</sup>. <sup>1</sup>Northeast Ohio Medical University (NEOMED), United States, <sup>2</sup>School of Biomedical Sciences, Kent State University, United States

Osteoarthritis (OA) is a chronic joint disease causes irreversible damage to the articular cartilage resulting in loss of joint function and subchondral bone remodeling. There is no cure for OA and currently the available treatment like pain management, and joint replacement surgery is used to treat this disease. MiRNAs are small non-coding RNAs consist of 21-29 nucleotides which regulate gene expression by targeting the 3' untranslated region (UTR) leading to translation inhibition. In recent years, many studies showed that microRNAs could be a target for many diseases including OA. In this study, we examined the role of miRNA 150 in OA. First we examined the expression of miRNA150 in human OA cartilage and found that miRNA expression is significantly down regulated in damaged compared to undamaged cartilage. Next, we determined the role of miRNA 150 in IL-1beta-induced catabolic gene expression. Primary chondrocytes derived from WT and miRNA 150 KO mice were cultured with or without IL-1beta. Our data showed that IL-1beta treatment caused an increase in MMP-3, MMP-9, MMP-13, IL-6 expression while Sox9 and collagen type II expression was decreased compared to untreated control. MiRNA 150 null chondrocytes treated with IL-1beta showed lower levels of catabolic gene expression compared to WT IL-1beta treated cells. Next, we determined the contribution of miRNA 150 in a post-traumatic osteoarthritis model. WT and miRNA 150 null mice were subjected to DMM surgery. Histological evaluations of medial tibia plateau and medial femur condyle were graded by OARSI scoring system after 12 weeks of DMM surgery. Our results showed that the miRNA150 KO have less cartilage damaged evaluated by toluidine staining compared to the WT mice, suggesting that miRNA 150 contributes to the development of osteoarthritis. To determine mRNA targets by miRNA150 that might contribute to decrease cartilage damaged, we identified Gpnmb as a target mRNA by miRNA 150 at the 3'UTR. Gpnmb was initially discovered in our lab in bone that plays a role in bone homeostasis, however, the expression and function of Gpnmb in cartilage is unknown. Next, we determine the effect of recombinant Gpnmb on IL-1beta-induced catabolic genes in WT primary chondrocytes and found that Gpnmb treatment down regulated catabolic gene expression induced by IL-1-beta when compared to control. These data suggest that Gpnmb acts as a protective protein in osteoarthritis. Next, we assessed the contribution of Gpnmb in post-traumatic OA in vivo using the DMM model in Gpnmb mutant and WT mice. Gpnmb mutant showed severe cartilage damaged compared to WT mice, suggesting that Gpnmb has a protective role in OA. Work is underway to determine the mechanism by which Gpnmb acts as an anabolic factor to reduce cartilage damage and maintain cartilage homeostasis. Collectively, these data showed that inhibition of miRNA 150 or the treatment with rGpnmb will have beneficial therapeutic effects in post-traumatic OA.

**Disclosures:** Asaad Al-Adlaan, None.

## SU0055

**Lactosylceramide enhances chondrocytic differentiation.** Lilit Antonyan<sup>\*1</sup>, Corine Martineau<sup>2</sup>, René St-Arnaud<sup>2</sup>. <sup>1</sup>McGill University and Shriners Hospitals for Children - Canada, Canada, <sup>2</sup>Shriners Hospitals for Children - Canada, Canada

When studying bone healing in *Cyp24a1*-deficient mice, which cannot synthesize the vitamin D metabolite, 24,25-(OH)<sub>2</sub>D, we have measured a significant, reproducible impairment in callus formation during fracture repair. The callus formation defect can be corrected by exogenous administration of 24,25-(OH)<sub>2</sub>D. From the callus of *Cyp24a1*-null mice, we cloned *Fam57b2*, encoding a transmembrane protein that specifically interacts with 24,25-(OH)<sub>2</sub>D. Mice deficient for FAM57B2 in chondrocytes exhibit the same impaired callus formation during fracture repair than *Cyp24a1*-deficient mice, providing genetic evidence that FAM57B2 is an effector of 24,25-(OH)<sub>2</sub>D-mediated signaling during fracture repair. In addition to transmembrane motifs, FAM57B2 contains a domain related to acyl-CoA-dependent ceramide synthase, suggesting potential enzymatic activity. Ceramide serves as a substrate to produce glycosphingolipids through glucosylceramide and the key branching intermediate, lactosylceramide (LacCer). LacCer was shown to act as a signaling molecule that regulates several aspects of cellular function. We have measured 24,25-(OH)<sub>2</sub>D-dependent production of LacCer by FAM57B2, suggesting allosteric regulation of the enzymatic activity of FAM57B2 by the vitamin D metabolite. We hypothesized that LacCer acts as a second messenger molecule in chondrocytes to optimize fracture repair. To determine the potential effect of LacCer on chondrocyte differentiation and function, we used ATDC5 cells that differentiate into chondrocytes when cultured in media containing insulin, transferrin, and selenium (ITS). We treated ATDC5 cells with 10  $\mu$ M of LacCer and measured cellular responses. Treatment with LacCer reduced proliferation after 48 and 96 hours. LacCer had no effect on adhesion, apoptosis, or migration of ATDC5 cells. When assessing differentiation using gene expression monitoring by RT-qPCR, we measured a reproducible two-fold enhancement of the expression of the differentiation marker Type X collagen over the levels induced by ITS treatment alone. In ATDC5 cells stably transfected with an expression vector for *Fam57b2*, expression of Type II and Type X collagen was increased, and this was further stimulated by 24,25-(OH)<sub>2</sub>D treatment of the transfected cells. Our results show that *Fam57b2* expression and its enzymatic product LacCer enhance chondrocytic differentiation. Future experiments will aim to characterize the signalling pathways involved.

**Disclosures:** Lilit Antonyan, None.

## SU0056

**The role of TAK1 in postnatal articular cartilage homeostasis and OA pathogenesis.** Christopher Dean\*, Sarah Catheline, Jennifer Jonason. University of Rochester Medical Center, United States

TGF- $\beta$ -activated kinase 1 (TAK1) is a MAP3K that mediates non-canonical TGF- $\beta$ /BMP signaling as well as inflammatory cytokine signaling. During the embryonic period, TAK1 is essential for cartilage and joint development as deletion of *Tak1* in osteochondroprogenitor cells leads to severe chondrodysplasia with defects in both chondrocyte proliferation and maturation. During the early postnatal period, TAK1 is essential for normal development of the articular cartilage as deletion of *Tak1* in committed chondrocytes results in loss of SOX9 expression and subsequent reductions in proteoglycan and Type II collagen content within the articular cartilage extracellular matrix (ECM). Here, we designed experiments to determine the role of TAK1 in postnatal articular cartilage homeostasis as well as in osteoarthritis (OA) pathogenesis. Using the *Acan-CreER<sup>2</sup>; Tak1<sup>fl</sup>* mouse model, we induced deletion of *Tak1* at 2 months of age and investigated the effects on knee joints via histology at multiple time points up to 8 months of age. Surprisingly, loss of TAK1 did not affect the proteoglycan or collagen content of the articular cartilage ECM suggesting that, while TAK1 is essential for normal development of the articular cartilage, its presence is not required to maintain cartilage in skeletally mature joints. We next tested the effect of chondrocyte-specific TAK1 deficiency on the progression of OA pathogenesis following meniscal/ligamentous injury (MLI), an established murine model of post-traumatic OA (PTOA). Again, using the *Acan-CreER<sup>2</sup>; Tak1<sup>fl</sup>* mouse model, we induced deletion of *Tak1* at 2 months of age, performed MLI at 3 months of age, and harvested knee joints for histology 8 weeks following injury. Cartilage degradation appeared more severe in joints with chondrocyte-specific *Tak1* deletion and histomorphometry confirmed that areas of total, unmineralized, and mineralized tibial articular cartilage were significantly reduced in *Acan-Cre<sup>+/+</sup>ER<sup>2</sup>; Tak1<sup>fl</sup>* mice compared to Cre-negative control mice. Interestingly, IHC for MMP13 revealed more MMP13-positive cells in the articular chondrocytes of joints with TAK1 deficiency. While additional studies are required to define the mechanisms responsible for the accelerated progression of PTOA in the *Acan-Cre<sup>+/+</sup>ER<sup>2</sup>; Tak1<sup>fl</sup>* mice, our results suggest that TAK1 signaling in chondrocytes may inhibit cartilage loss following injury; a role potentially related to its anabolic function during cartilage development.

**Disclosures:** Christopher Dean, None.

## SU0057

**Involvement and therapeutic potential of Nell-1 in inflammatory arthritis.** Chenshuang Li\*<sup>1</sup>, Zhong Zheng<sup>1</sup>, Pin Ha<sup>2</sup>, Jie Jiang<sup>3</sup>, Wenlu Jiang<sup>4</sup>, Seungjun Lee<sup>5</sup>, Richard Song<sup>6</sup>, Bernard Boback<sup>1</sup>, Alireza Hourfar<sup>1</sup>, Eric Chen<sup>1</sup>, Cymbeline Cuiat<sup>7</sup>, Xinli Zhang<sup>8</sup>, Kang Ting<sup>8</sup>, Chia Soo<sup>3</sup>. <sup>1</sup>Division of Growth and Development, Section of Orthodontics, School of Dentistry, University of California, Los Angeles, United States, <sup>2</sup>Department of Cleft Lip and Palate Surgery, West China Stomatology Hospital, Sichuan University, China, <sup>3</sup>Department of Orthopaedic Surgery and the Orthopaedic Hospital Research Center, University of California, Los Angeles, United States, <sup>4</sup>State Key Laboratory of Oral Diseases, Department of Orthodontics, West China Hospital of Stomatology, Sichuan University, China, <sup>5</sup>Department of Chemistry and Biochemistry, University of California, Los Angeles, United States, <sup>6</sup>School of Dentistry, University of California, Los Angeles, United States, <sup>7</sup>Oak Ridge National Laboratory, United States, <sup>8</sup>Division of Growth and Development, Section of Orthodontics, School of Dentistry, University of California, United States

As the leading cause of disability, arthritis is estimated to cost more than \$100 billion annually. Unfortunately, current available treatments are not directly targeting the biological causes of arthritis, especially in the case of inflammatory arthritis such as rheumatoid arthritis, psoriatic arthritis, ankylosing spondylitis, juvenile idiopathic arthritis, and inflammatory osteoarthritis. Our previous studies showed that the pivotal osteogenic Neural EGFL like 1 (Nell-1) suppresses BMP2-induced inflammation during bone regeneration and plays critical roles in cartilage development and regeneration. Additionally, single nucleotide polymorphisms (SNPs) in Nell-1 are associated with ankylosing spondylitis and psoriatic arthritis. Here, we investigated the involvement and therapeutic potential of Nell-1 in inflammatory arthritis. In human arthritic samples obtained from patients undergoing hip or knee arthroplasty, immunostaining revealed that inflammation in the arthritic cartilage is accompanied by interruption of Nell-1's signal transduction. In mice, immunostaining and gene profiling showed that *Nell-1* haploinsufficiency not only disrupts chondrogenic differentiation and maturation, but also leads to significant inflammation of cartilage throughout their life. Moreover, aged *Nell-1<sup>+/-</sup>* mice exhibited more severe osteoarthritic alterations in histological observation and altered anabolic and catabolic marker expression in comparison with wild-type (WT) mice. Using a direct intra-joint IL1 $\beta$  injection model, we found more severe inflammation and cartilage degradation of knee joint in *Nell-1<sup>+/-</sup>* mice than that of WT mice. Meanwhile, administration of exogenous Nell-1 significantly reduced the inflammatory response and articular cartilage damages in IL1 $\beta$ -challenged WT and even *Nell-1<sup>+/-</sup>* mice. Excitingly, the lame walking observed in IL1 $\beta$ -challenged *Nell-1<sup>+/-</sup>* mice was rescued by Nell-1 application. Intriguingly, Nell-1 strongly repressed the IL1 $\beta$  or TGF $\beta$ 3 (another well-known growth factor contributing to inflammatory reactions in cartilage) induced inflammation of chondrogenic-committed ATDC5 cells, primary rabbit articular chondrocytes, and human chondrocytes isolated from both healthy and osteoarthritic sites of resected articular cartilage tissue. Collectively, our present

data revealed the nature of Nell-1 as a pro-anabolic factor involving pathogenesis of arthritis and a potential inflammatory combating factor in arthritis prevention and treatment.

**Disclosures:** Chenshuang Li, NIH-NIAMS, Grant/Research Support.

## SU0058

**Femurs versus Phalanges: differences in bone length are achieved by modulating the progression of growth plate senescence.** Julian Lui\*<sup>1</sup>, Youn Hee Jee<sup>1</sup>, Presely Garrison<sup>1</sup>, Shanna Yue<sup>1</sup>, Michal Ad<sup>1</sup>, Quang Nguyen<sup>1</sup>, Bijal Kikani<sup>1</sup>, Yoshiyuki Wakabayashi<sup>2</sup>, Jeffrey Baron<sup>1</sup>. <sup>1</sup>Section on Growth and Development, NICHD, United States, <sup>2</sup>DNA Sequencing and Genomics Core, NHLBI, United States

Increase in bone length results from chondrocyte proliferation and hypertrophy in the growth plate. Growth plate function is rapid in infancy but slows and eventually ceases with age due to a developmental program termed growth plate senescence. Bone size varies dramatically among bones at different anatomical locations. For example, human femurs are 20-fold longer than distal phalanges. To explore the underlying mechanisms, we compared growth plates of long bones (femurs and tibias) and short bones (metacarpals and phalanges) at multiple prenatal and postnatal ages in both mice and rats. We found that the shorter length of the short bones was due both to diminished growth plate chondrocyte proliferation and hypertrophy compared with the long bones at any given age. These differences in turn resulted from differences in the developmental program of growth plate senescence; senescence was more advanced in short bones than in long bones. This greater advancement involved multiple cellular developmental changes that occur with senescence, including decline in: height of overall growth plate, proliferative zone, and hypertrophic zone (all  $P < 0.001$ ); number of chondrocytes in resting zone, proliferative zone (per column) and hypertrophic zone (per column) (all  $P < 0.001$ ); and chondrocyte proliferation (measured by BrdU incorporation,  $P < 0.001$ ). This greater advancement in senescence also involved changes in gene expression, which were assessed by laser capture microdissection of proliferative and hypertrophic zones followed by RNA-seq. For genes that underwent significant increases in expression with age (1- vs 4 weeks) in proximal tibia, the expression was higher in 1-week phalanges than in 1-week tibias, and conversely, for genes that showed decreasing expression with age (1- vs 4-weeks) in tibia, expression was already low in phalanges at 1-week (mouse proliferative zone, Pearson's  $r = 0.388$ ; rat proliferative zone,  $r = 0.557$ ; mouse hypertrophic zone,  $r = 0.597$ ; rat hypertrophic zone,  $r = 0.599$ ; all  $P < 1E-40$ ), indicating greater advancement in the small bone. In further support of this hypothesis, the short bones underwent epiphyseal fusion earlier (mouse, age 3-4 weeks/w; rat, 8-12 w) than the long bones (remained unfused at last time points studied: mouse, 12 w; rat, 16 w). We conclude that the dramatic differences in length among bones in different anatomical locations is achieved in large part by modulating the progression of growth plate senescence.

**Disclosures:** Julian Lui, None.

## SU0059

**A novel 3D measurement of mouse joint subchondral bone plate reveals a positive correlation between its thickness and loading status due to altered Sclerostin amount at late osteoarthritis stage.** Xiaoyuan Ma<sup>\*1,2</sup>, Haoruo Jia<sup>1,2</sup>, Wei Tong<sup>1,2</sup>, Zhaochun Yang<sup>3</sup>, Robert Tower<sup>1,2</sup>, Kairui Zhang<sup>1,2</sup>, Wei-Ju Tseng<sup>1,2</sup>, X. Sherry Liu<sup>1,2</sup>, James H-C. Wang<sup>3</sup>, Lin Han<sup>4</sup>, Motomi Enomoto-Iwamoto<sup>1,2</sup>, Ling Qin<sup>1,2</sup>. <sup>1</sup>University of Pennsylvania, United States, <sup>2</sup>University of Pennsylvania, United States, <sup>3</sup>University of Pittsburgh, United States, <sup>4</sup>Drexel University, United States

Osteoarthritis (OA) is a whole joint disease involving changes not only in articular cartilage but also in neighboring tissues including subchondral bone. In the past, studying subchondral bone structure, particularly the thickness of subchondral bone plate (SBP), in mouse joints was unreliable due to its small size and 2D analysis approaches. In this study, we designed a novel protocol that transfers microCT images of mouse femoral condyle SBP into a 3D color map, in which the color at any position linearly corresponds to its thickness. This allows comparisons of SBP thickness among different anatomic sites (eg. anterior vs posterior and medial vs lateral) in a 3D manner. Using this method, we discovered that, in normal adult mice, SBP in the posterior region of a mouse distal femoral condyle is 2.0-fold thicker than that in the anterior region at both medial and lateral sites. The posterior region, but not the anterior region, of femoral condyle is in direct contact with tibial plateau and thus, is the area that undergoes load bearing and energy dissipation during joint motion. This result provided the first evidence that SBP thickness is positively correlated with the loading status. Thickening of SBP is an indisputable sign of late OA. We generated four mouse models with severe joint OA to study the SBP changes: cartilage-specific *Egfr* knockout (*CKO*) mice at 2 months after surgical destabilization of the medial meniscus (DMM), 1-year-old aged *Egfr* *CKO* mice, wild-type (*WT*) mice at 10 months after DMM, and *WT* mice at 4 months after DMM plus hemisection of the meniscus (DMMH) surgery. In all these late OA models, we observed that SBP sclerosis was only restricted to area under severely eroded articular cartilage. This was accompanied by elevated bone formation (more osteoblasts and higher bone formation rate) at the bone marrow side of SBP and a remarkable reduction of Sclerostin amount in osteocytes within SBP. Computational simulation of normal and OA knees demonstrated that focal mechanical stress on SBP under cartilage damage site is drastically increased by 48-fold at the late OA stage. Since mechanical loading is a



major regulator of Sclerostin, we conclude that loading-induced attenuation of Sclerostin within SBP followed by Wnt activation and elevation of bone formation along SBP at the bone marrow site is the major mechanism for SBP sclerosis associated with the late stage OA.

**Disclosures:** Xiaoyuan Ma, None.

## SU0060

**Activated FGFR3 Prevents Subchondral Bone Sclerosis During the Development of Osteoarthritis in Transgenic Mice with Achondroplasia.** Toshiaki Okura\*, Masaki Matsushita, Kenichi Mishima, Taisuke Seki, Naoki Ishiguro, Hiroshi Kitoh, Department of Orthopaedic Surgery, Nagoya University Graduate School of Medicine, Japan

**Objective:** Osteoarthritis (OA) is a degenerative joint disease, which affects not only articular cartilage but also subchondral bone. Fibroblast growth factor receptor 3 (FGFR3) is highly expressed in articular chondrocytes and contributes articular cartilage homeostasis. The purpose of this study is to investigate the histological and morphometric changes of articular cartilage during the development of OA specifically focused on morphology of the subchondral bone by employing transgenic mice with achondroplasia (*Fgfr3<sup>ach</sup>*) carrying a heterozygous gain-of-function mutation in *Fgfr3*.

**Methods:** Two OA models (spontaneously developed with age: the aging model, and surgically induced by destabilization of the medial meniscus: the DMM model) were established. Articular cartilage and subchondral bone of the knee joint were histologically and morphometrically compared between wild-type mice and *Fgfr3<sup>ach</sup>* mice in both OA models. Articular cartilage degeneration was scored according to the Osteoarthritis Research Society International (OARSI) scoring system. Several morphometric parameters including bone mineral density (BMD), bone volume/tissue volume (BV/TV), trabecular bone thickness (Tb.Th) in epiphysis of the proximal tibia, and subchondral bone thickness in the medial tibial plateau (Sb.Th med) were quantified by micro-computed tomography.

**Results:** In the aging model of wild-type mice, Sb.Th med was significantly increased at the age of 12 months compared with that of 18 weeks although there were no significant differences in the OARSI score between both age groups. On the other hand, Sb.Th med as well as the OARSI scores were unchanged between 18 weeks and 12 months old in *Fgfr3<sup>ach</sup>* mice. These results indicated that subchondral bone sclerosis occurred prior to cartilage degradation. In the DMM model, the OARSI score of the medial compartment was significantly lower in *Fgfr3<sup>ach</sup>* mice than in wild-type mice at 4 and 8 weeks after the surgery. BMD, BV/TV and Tb.Th in the epiphysis were increased in wild-type mice and unchanged in *Fgfr3<sup>ach</sup>* mice. Additionally, Sb.Th med was significantly larger in wild-type mice after the surgery.

**Conclusions:** Subchondral sclerosis, which preceded the cartilage degeneration, was inhibited in *Fgfr3<sup>ach</sup>* mice. Activated FGFR3 signaling prevented sclerotic changes of the subchondral bone and subsequent cartilage degeneration. Stimulation of FGFR3 signaling in the articular cartilage could be a potential therapeutic target for OA.

**Disclosures:** Toshiaki Okura, None.

## SU0061

**Phlpp Inhibitors Alter the Chondrocyte Epigenome and Promote Cartilage Regeneration.** Earnest Taylor\*, Elizabeth Bradley, Jennifer Westendorf. Mayo Clinic, United States

Osteoarthritis (OA) is a degenerative joint disease and leading cause of disability. Patients receive short-term treatments for pain and are advised to change their lifestyle or use mobility aids, but there are no FDA-approved disease modifying OA drugs (DMOADs) that slow or prevent disease progression. The protein phosphatase Phlpp1 is an effector of chondrocyte differentiation in vitro and Phlpp1 deficiency limits OA disease progression in mice. A Phlpp inhibitor also blocked injury-induced cartilage destruction and pain in vivo and is a potential DMOAD candidate. The goal of this study was to determine the molecular and epigenetic mechanisms by which two Phlpp inhibitors, NSC117079 and NSC45586, enhance cartilage matrix production in murine and human primary chondrocytes, cell lines and human OA cartilage explants. Phlpp1/2 dephosphorylate and inactivate proteins such as Akt, PKC and Erk1/2 in chondrocytes to arrest matrix production and induce apoptosis. Phlpp1 also modifies the epigenome by dephosphorylating histone 3 at serine 9, thereby repressing transcription. Phlpp inhibitors NSC117079 and NSC45586 increased phosphorylation of these substrates and downstream effectors in time- and concentration-dependent manners. Phlpp inhibition also augmented the post-translational modification of substrates in response to Igf1 and insulin. Functionally, the Phlpp inhibitors enhanced glycosaminoglycan production and the expression of aggrecan and Has2 in the majority of human cartilage explants. These data demonstrate that Phlpp1/2 are epigenomic modifiers in chondrocytes and that Phlpp inhibitors alter the chondrocyte epigenome and facilitate cartilage regeneration of explanted human OA articular cartilage.

**Disclosures:** Earnest Taylor, None.

## SU0062

**IGFBP-2 Mediated Effects of PTH on Bone and Cellular Respiration.** Victoria DeMambro\*, David Maridas<sup>1</sup>, Anyonya Guntur<sup>1</sup>, Elizabeth Rendina-Ruedy<sup>1</sup>, Gang Xi<sup>2</sup>, David Clemmons<sup>2</sup>, Clifford Rosen<sup>1</sup>. <sup>1</sup>Maine Medical Research Institute, United States, <sup>2</sup>University of North Carolina Chapel Hill, United States

IGF-I has been shown to be essential for the bone anabolic response to PTH through increases in glycolysis and to a lesser extent oxidative phosphorylation (OxPhos) in osteoblasts. Preliminary data in our lab has shown that PTH treatment also induces IGFBP-2 in addition to IGF-I. Thus we hypothesized that IGFBP-2 is also important for the peak anabolic response of PTH in bone. To test this hypothesis we treated Ovariectomized +/+ and *Igfbp2*-/- female mice for 4wks with 80ug/kg PTH (1-84). In vitro we utilized *Igfbp2* silenced (BP2si) and control MC3T3 cell lines and analyzed the effects of 24hr treatment of PTH (500ng/ml) on cellular bioenergetics at Day 0 and 7 of differentiation. In vivo PTH increased aBMC in both genotypes however these effects were blunted in the -/- mice (+/+ 20% vs. -/- 10%; p<0.05, 16 vs. 20wks). Structural analysis of the distal femur revealed PTH increased BV/TV in both genotypes, yet *Igfbp2*-/- femurs did not respond as robustly as controls (+/+ 90% vs. 75%; VEH vs. PTH) due to a suppression in the thickening of the trabeculae (+/+ 35% vs. -/- 24% -/-; VEH vs. PTH). Analysis of the cortical bone confirmed the blunted response to PTH in the *Igfbp2*-/- mice. Bones from +/+ mice treated with PTH exhibited a two fold increase in both *Igfbp2* and *Fgf23* expression confirming our earlier observations, and PTH signaling induction respectively. In vitro, control cells treated with PTH exhibited increased glycolysis at both D0 and D6 concurrent with increases in *Igf1*, *Glut1* and *Glut10* expression. BP2si cells at D0 had higher OxPhos and respiratory capacity with reduced glycolysis compared to control cells. By D6 near peak *Igfbp2* expression, BP2si cells exhibited reductions in OxPhos and increases in glycolysis. BP2si PTH treated cells had a similar switch from D0 to 6 in OxPhos/glycolysis. Paradoxically we observed that BP2si PTH treated cells had a greater glycolytic capacity than control PTH treated cells. Furthermore, at D6 we observed continuing increases in *Igf1* expression in the BP2si PTH treated cells only, suggesting that the suppression of the PTH effects in the *Igfbp2* -/- mice are not energy dependent. In summary, *Igfbp2*-/- females exhibit suppressed effects of PTH on bone. Preliminary studies have confirmed that PTH treatment induces glycolysis in MC3T3 cells in an IGF1 dependent manner. Further studies in calvarial osteoblasts derived from *Igfbp2* -/- mice are essential to confirm the role of IGFBP-2 in PTH induced glycolysis.

**Disclosures:** Victoria DeMambro, None.

## SU0063

**Changes in Visceral Fat and Android Fat over the Menopause Transition: Results from the Study of Women's Health Across the Nation (SWAN).** Gail Greendale\*, Mei-Hua Huang<sup>1</sup>, Carrie Karvonen-Gutierrez<sup>2</sup>, Joel Finkelstein<sup>3</sup>, Jane Cauley<sup>4</sup>, Kristine Ruppert<sup>5</sup>, Arun Karlamangla<sup>1</sup>. <sup>1</sup>Division of Geriatrics, Geffen School of Medicine at UCLA, United States, <sup>2</sup>School of Public Health, University of Michigan, United States, <sup>3</sup>Massachusetts General Hospital, United States, <sup>4</sup>Graduate School of Public Health, University of Pittsburgh, United States, <sup>5</sup>Epidemiology Data Center, University of Pittsburgh, United States

**Objective:** To discern the influence of the menopause transition (MT) on body composition, and describe: 1) the rate of change in visceral fat and android fat during the 10 years bracketing the final menstrual period (FMP); and 2) the independent associations of age at FMP and race with both types of fat and their rates of change during the MT.

**Methods:** In the Study of Women's Health Across the Nation (SWAN) UCLA study site, we measured visceral fat and android fat by DXA (Hologic) at baseline when participants were 42-52 years of age and pre- or early perimenopausal, and again in 11 follow up visits over 13 years. This analysis is restricted to the 73 white and 162 Japanese participants for whom an FMP date could be determined.

**Results:** Loess-smoothed curves illustrated that gains in visceral fat and android fat occurred primarily during the transmenopause: a 5.5-year period around the FMP, starting 2.5 years before and ending 3 years after the FMP. Piecewise-linear, mixed-effects regression models demonstrated that in white women, visceral fat increased by 152 g/year (p=0.002) and android fat by 383 g/year (p=0.049) during transmenopause, but neither changed significantly before or after the transmenopause (Table). Over the 5.5 year transmenopause, visceral fat increased by nearly 1 kg and android fat by 2 kgs, representing 11-fold and 3-fold increases, respectively. The annualized increase in visceral fat was slightly smaller (by 2.4 g per year, p=0.01) if the FMP occurred at a later age. Relative to whites, Japanese women had ~10% smaller increase in visceral fat (p=0.001) and ~15% smaller increase in android fat (p=0.001) during the transmenopause.

**Conclusions:** The MT has a large, unfavorable effect on visceral fat and android fat. Future work will explore potential inflammatory, metabolic, and skeletal effects of these striking MT-related increases in visceral and android fat.

### ACKNOWLEDGMENTS

The Study of Women's Health Across the Nation (SWAN) has grant support from the National Institutes of Health (NIH), DHHS, through the National Institute on Aging (NIA), the National Institute of Nursing Research (NINR) and the NIH Office of Research on Women's Health (ORWH) (Grants U01NR004061; U01AG012505, U01AG012535, U01AG012531, U01AG012539, U01AG012546, U01AG012553, U01AG012554, U01AG012495). The content of this article is solely the responsibility of the authors and does not necessarily represent the official views of the NIA, NINR, ORWH or the NIH.

Table: The influence of the menopause transition on visceral fat and android fat<sup>1</sup>

Participant characteristics	Type of fat	Value at FMP (grams)	Annualized slope (g/year) during each interval relative to date of the final menstrual period (FMP)		
			Prior to 2.5 y before FMP	2.5 y prior to 3 y after FMP (transmenopause)	More than 3 y after FMP
White referent <sup>2</sup>	Visceral	462.3	-9.26*	<b>152.06</b>	-38.51**
Effect of 1-y increase in age at FMP	Visceral	<b>20.16</b>	0.36	<b>-2.41</b>	0.71**
Association with Japanese race <sup>3</sup>	Visceral	<b>-72.5</b>	3.11**	<b>-15.36</b>	-4.00*
White referent	Android	1986.5	-87.10	<b>382.72</b>	76.50
Effect of 1-y increase in age at FMP	Android	<b>69.25</b>	2.14	-5.46	-1.82
Association with Japanese race <sup>3</sup>	Android	<b>-561.4</b>	7.30*	<b>-62.66</b>	12.46**

<sup>1</sup>Sample size = 73 White and 162 Japanese women. In addition to the 2 variables listed in table, model is adjusted for time-varying HT use. Slopes that are statistically significantly different from zero and statistically significant associations (p value < 0.05) are in **bold italic** font.

<sup>2</sup>The reference values are for white women whose age at FMP is 52.3 years (sample mean).

<sup>3</sup>Level (value at FMP) and slopes in Japanese obtained by adding the Japanese race effect estimate to the referent level and slopes.

\* 0.05 < p < 0.1 for difference in slope between this interval and the transmenopause.

\*\* p < 0.05 for difference in slope between this time interval and the transmenopause.

Table: The influence of the menopause transition on visceral fat and android fat

Disclosures: Gail Greendale, None.

## SU0064

**Identification of Novel Pleiotropic Variants Associated With Osteoporosis and Obesity Using Pleiotropy-informed Conditional False Discovery Rate.** Yuan Hu<sup>\*1</sup>, Xiang-Ding Chen<sup>1</sup>, Zhen Liu<sup>1</sup>, Shi-Shi Min<sup>1</sup>, Qin Zeng<sup>1</sup>, Hui Shen<sup>2</sup>, Li-Jun Tan<sup>1</sup>, Hong-Wen Deng<sup>2</sup>. <sup>1</sup>Hunan Normal University, China, <sup>2</sup>Tulane University, United States

**Aims:** Osteoporosis and obesity are two closely interrelated diseases. Genome-wide association studies (GWASs) have been successful in identifying loci associated with osteoporosis and obesity. However, the identified loci explained only a small fraction of the total genetic variance and the shared genetic determination between osteoporosis and obesity is largely unknown. The aim of this study was to identify novel and pleiotropic genetic variants associated with osteoporosis and obesity.

**Methods:** A pleiotropic conditional false discovery rate (cFDR) method was applied to three independent GWAS summary statistics of femoral neck bone mineral density (FN\_BMD, n = 53,236), body mass index (BMI, n = 224,459) and waist-hip ratio (WHR, n = 339,224). Next, weighted gene co-expression analysis (WGCNA) was performed to identify functional connections between novel pleiotropic genes and known osteoporosis/obesity susceptibility genes using transcriptomic expression datasets in bone biopsies (E-MEXP-1618) and adipocytes (GSE2508).

**Results:** We identified 39 SNPs significantly (cFDR < 0.05) associated with FN\_BMD, 147 SNPs significantly associated with BMI and 20 SNPs significantly associated with WHR. Of these loci, 7 loci, that is rs3759579 (MARK3), rs2178950 (TRPS1), rs1473 (PUM1), rs9825174 (XXYL1), rs2047937 (ZNF423), rs17277372 (DNM3), and rs335170 (PRDM6), showed significant pleiotropic effects on osteoporosis and obesity. By constructing gene networks for 152 osteoporosis related genes (14 novel and 138 known genes) using bone biopsy transcriptomic data, we found that the 7 pleiotropic genes were contained in two gene modules. Remarkably, ZNF423 was one of the highly connected intramodular hub genes and interconnected with 21 known osteoporosis related genes, such as JAG1 and EN1. Similarly, we found functional connections of ZNF423 with a large number of obesity related genes, including VEGFA, TMEM160 and 106 other obesity genes, when applying network analysis for 303 obesity related genes (25 novel and 278 known genes) in adipocyte gene expression data.

**Conclusions:** 7 pleiotropic genes were identified between osteoporosis and obesity. The findings provide new insight into genetic mechanisms of osteoporosis and obesity and enable us to gain a better understanding of the shared genetic determination between these two disorders.

Disclosures: Yuan Hu, None.

## SU0065

**Uncarboxylated osteocalcin attenuates the migration of vascular smooth muscle cells.** Kyoung Min Kim<sup>\*1</sup>, Min Ji Kang<sup>2</sup>, Ghayoung Lee<sup>2</sup>, Sung Hee Choi<sup>1</sup>, Soo Lim<sup>1</sup>, Hak Chul Jang<sup>1</sup>. <sup>1</sup>Seoul National University Bundang Hospital, Korea, Republic of, <sup>2</sup>Laboratory of Endocrinology, Biomedical Research Institute, Seoul National University Bundang Hospital, Korea, Republic of

Emerging evidences suggest extra-skeletal roles osteocalcin (OCN), and recent human studies have demonstrated negative associations between uncarboxylated osteocalcin (ucOCN) levels and parameters related to atherosclerosis. However, the roles of osteocalcin in atherosclerosis remain unknown. The aim of this study was to elucidate the effects of ucOCN in the development of atherosclerosis *in vitro*.

Rat aortic vascular smooth muscle cells (VSMCs) were treated with carboxylated OCN (cOCN, 1, 10, 50 ng/mL) or ucOCN (1, 10, 50 ng/mL). Platelet-derived growth factor (PDGF, 10 ng/mL) were treated for induction of VSMC migration, and migration level was measured using a scratch-wound healing assay. Protein expression and

phosphorylation were detected by western blot. Proliferation was assessed by CCK8 assay and apoptosis was measure by Annexin V.

GPRC6A, a putative receptor for OCN, was present in VSMCs, but not in endothelial cells. Treatment of ucOCN significantly suppressed PDGF-induced VSMC migration, whereas cOCN did not. On the other hand, the proliferation and apoptosis of VSMCs were not significantly affected by ucOCN administration. The PDGF-induced expression of phosphorylated p38 and ERK was abolished by treatment of ucOCN. We tested the expression levels of matrix metalloproteinase-2 (MMP-2), which is pro-migrating factor in development of atherosclerosis, and the expression of MMP-2 was significantly decreased by ucOCN treatment.

VSMC migration is critical step in development of atherosclerosis. Our results showed that ucOCN significantly reduced the VSMC migration. These studies highlight the potential anti-atherogenic effects of ucOCN, and ucOCN may be a promising candidate for the clinical therapy for atherosclerosis.

Disclosures: Kyoung Min Kim, None.

## SU0066

**Misty mice are resistant to high fat diet-induced bone loss and have improved insulin sensitivity.** Phuong Le<sup>\*1</sup>, Kathleen Bishop<sup>2</sup>, Katherine Motyl<sup>2</sup>, Daniel Brooks<sup>3</sup>, Mary Bouxsein<sup>3</sup>, Clifford Rosen<sup>2</sup>. <sup>1</sup>Maine Medical Center Research Institute, United States, <sup>2</sup>Maine Medical Center Research Institute, United States, <sup>3</sup>Beth Israel Deaconess Medical Center, United States

Diet related obesity and type 2 diabetes have become a major health concern resulting in increased skeletal fragility and poor skeletal health. Adipocytes interact with the skeletal homeostasis on multiple levels through modulating the inflammation to leptin signaling resulting in many types of metabolic syndromes and imbalances in glucose homeostasis. Bone loss has been observed in many high fat diet models suggesting and important connection between adipose tissue and bone remodeling. Misty mice (*m/m*) have a loss of function mutation in Dock7, a guanine nucleotide exchange factor, resulting in low bone mass, uncoupled bone remodeling, reduced bone formation, and reduced of preformed brown adipose tissue activity leading to compensatory increases in sympathetic nervous system (SNS) activity as well as browning of peripheral white adipose depots. In order to determine if the mutation of Dock7 in *m/m* was capable of preventing high fat-induced bone loss, wild type (+/+) and *m/m* mice were fed on either 10% Kcal (Lfd) or 58% Kcal (Hfd) for 13 weeks starting at 3 weeks old. The skeletal, adipogenic, and metabolic phenotype were assessed by DXA,  $\mu$ CT, and both glucose tolerance as well as insulin tolerance tests at 16 wks of age. *In vivo* abdominal scans were performed at 12 weeks of age. Only *m/m* on a Hfd showed a significant increase in total fat mass and lean mass when compared to *m/m* on a Lfd. These increases were not observed in +/+. Increases in inguinal fat pad and subcutaneous adipose tissue (SAT) volume were observed in both +/+ and *m/m*. However, *m/m* on a Hfd were protected against adipocyte hypertrophy. Despite *m/m* gaining as much total fat mass on Hfd, *m/m* displayed improved glucose tolerant and insulin sensitive compared to the +/+ on a Hfd suggesting that loss of Dock7 in the *m/m* model protects against high fat diet-induced metabolic syndromes. Analysis of the bone phenotype by DXA revealed decreased total aBMD as well as femoral aBMD, and a BMC in +/+ on a Hfd while no change was observed in *m/m* suggesting that loss of Dock7 in the Misty models is protective against high fat diet-induced bone loss. Furthermore, analysis of the femur by  $\mu$ CT indicated a reduction in Tb BV/TV (p = .016), Tb BMD (p = .035), and Conn. D (p = .018) in +/+ on hfd. However, no significant bone loss was observed in *m/m*. Taken together, these data suggest that loss of Dock7 in the Misty model is protective against many of the skeletal and metabolic consequences of obesity.

Disclosures: Phuong Le, None.

## SU0067

**Metabolomics of Osteoporosis in Southern Chinese.** Grace Koon Yee Lee<sup>\*</sup>, Ching-Lung Cheung. Department of Pharmacology and Pharmacy, the University of Hong Kong, Hong Kong

**Introduction:** Osteoporosis is a prevalent disease characterized by low bone mass and deterioration in microarchitecture and bone strength with consequent increased risk of fragility fracture. It is well-established that genetic factors, environmental factors and their interaction play a major role in osteoporosis development. In addition, metabolic pathways play a major role in age-related bone loss. The identification of bone mineral density (BMD)-associated metabolites through untargeted metabolomics analysis is important for elucidating disease aetiology.

**Materials and Methods:** Untargeted metabolomic profiling was performed in 340 and 291 participants from the Hong Kong Osteoporosis Study at the baseline and follow-up respectively. An extreme phenotype truncated case-control design was adopted for the baseline study; whereas a random cohort design was used for the follow-up study. BMD was measured using Dual-energy X-ray absorptiometry (DEXA). In total, 725 metabolites with known identity and missingness < 50% were included in the final analysis. Multivariable robust regressions were used to evaluate the association between metabolites and BMD, adjusting for age, sex, height, and weight. Analyses were conducted both in the baseline and follow-up study, followed by meta-analysis using inverse variance method. Multiple comparison was corrected using false-discovery rate (FDR) method.

**Results:** Among 725 metabolites, 9, 16, and 46 significant associations were observed for BMD at the lumbar spine, femoral neck, and total hip, respectively. Successful replication in the TwinsUK cohort was observed in some of the BMD-associated metabolites. The most associated metabolite was pyroglutamine for BMD at the lumbar spine (Beta=0.043 per SD change; FDR-corrected P=0.017) and femoral neck



(Beta=0.032 per SD change; FDR-corrected P=0.006); whereas urate was the most associated metabolite with BMD at the total hip (Beta=0.06 per SD change; FDR-corrected P=0.002). In addition, pathway analysis revealed that glycerophospholipid metabolism was significantly associated with BMD variation (FDR-corrected P=0.03).

Conclusion: Numerous metabolites, particularly related to glycerophospholipid, are found to be associated with BMD. It provides new biological evidence of the role of metabolite in bone health and these findings may implicate in clinical management of bone-related diseases.

**Disclosures:** Grace Koon Yee Lee, None.

## SU0068

**Body Composition and Glucose Metabolism in an Osteocalcin Knockout Rat Model with Diet Induced Obesity.** Aidi Niu\*, Laura Lambert, Lihua Zhou, Maria Johnson, Timothy Nagy, Robert Kesterson, Jayleen Grams. University of Alabama at Birmingham, United States

Osteocalcin has been reported to act as a hormone regulating energy and glucose metabolism in mice. Due to the greater similarity of the rat osteocalcin gene locus to that in humans, we generated an osteocalcin knockout rat model using CRISPR/Cas9 technology. We hypothesized the rat knockout model would recapitulate bone, but not metabolic phenotypes described for the osteocalcin deficient mouse model confounded by genome triplication.

Wild type (WT; n=14 male, n=14 female) and osteocalcin knockout rats (KO; n=14 male, n=16 female) received a normal chow or high-fat diet (HFD) for 21 weeks after weaning. Body composition determination by dual energy X-ray absorptiometry (DXA) and glucose and insulin tolerance tests (GTT & ITT) were performed.

At 6 months, when compared to chow controls, animals of both sexes on the HFD were significantly heavier (male, p=0.0002 and female, p=0.0003), with increased fat mass (male, p<0.0001 and female, p<0.0001), and unchanged lean mass (male, p<0.0001 and female, p<0.0001). There was no difference based on genotype. Fasting glucose was not affected by either genotype or diet in either sex. Male WT animals were more sensitive to the HFD based on GTT. Although there was a trend toward increased glucose intolerance for both WT and KO male animals on HFD vs chow based on GTT, it did not reach significance (AUC, p=0.0548 and p=0.0738, respectively); there was no difference based on genotype. There were no differences in insulin sensitivity in any of the male groups based on genotype or diet. For females on GTT, AUC in KO-HFD was significantly higher than in KO-chow (p=0.0283), indicating a decrease in glucose tolerance; there was no difference in WT-HFD vs WT-chow (p=0.5451). On ITT, KO-HFD females exhibited a trend toward lower inverse AUC (p=0.0719) when compared to KO-chow, but there was no difference based on genotype on the same diets.

Overall, in contrast to the mouse model of osteocalcin deficiency, there were no significant differences in the osteocalcin KO rats based on genotype. Male and female WT and KO rats had differential responses to HFD, with male KO rats being somewhat protected from the dysmetabolism of HFD and female KO rats being more sensitive to HFD. However, there were no significant differences in glucose tolerance or insulin sensitivity based on genotype on the same diet.

**Disclosures:** Aidi Niu, None.

## SU0069

**Relationship of BMP and Phosphate to Chondrocyte and Adipocyte Differentiation and Energy Consumption.** Takashi Noguchi\*, Amira Hussein, Louis Gerstenfeld. Boston University School of Medicine, United States

Introduction: Dietary phosphate deficiency have been shown to impair oxidative phosphorylation during fracture healing. Prior studies had also shown that murine chondrogenic ATDC5 cell cultures showed differences in energy consumption, mineralization and collagen production depending on phosphate availability. The goal of this study was to examine the effect of phosphate deficiency on commitment in stem cells.

Methods: Multipotential C3H10T1/2 murine cell line was expanded in growth medium ( $\alpha$ MEM with 10% FBS and 1% pc/sm). Once cells had achieved confluence (day 0) they were switched to differentiating media: ( $\alpha$ MEM with 5% FBS, plus 1X insulin- transferrin-selenium and 0.2mM ascorbate) containing full phosphate (Pi, 1mM) medium or low phosphate (Pi, 0.25mM). Half of the wells received 2uM BMP2 (+BMP), while the remaining wells did not have any BMP2 (-BMP). Gene expression levels for Adipocytes (UCP1, Pparg, Plin1) and cartilage Col2a1, Col10a, Aggrecan, were measured at days 0, 4 and 8. Total Lipid, protein, hydroxyl proline (HP) and DNA content were assessed. Oxygen Consumption Rate (OCR) was measured using Seahorse XF96 mitochondrial stress test.

Results: Col2a1, Col10, Aggrecan were significantly expressed at higher levels only in BMP2 treated cells (p<0.0001) independent of the Pi content of the medium. In contrast adipose genes were most significantly expressed in media minus BMP2. Interestingly in low phosphate media plus BMP adipose and cartilage differentiation appeared to be co-expressed while in the absence of BMP in low phosphate media adipose differentiation shifted from a white to a beige phenotype. The increased cartilage differentiation based on gene expression was associated with the increased accumulation of hydroxyproline. Levels of hydroxyproline showed a tight correlation to the overall oxygen consumption and energy production of the cells. Interestingly the low phosphate no BMP2 cultures showed an overall increased in respiratory capacity without increasing ATP production (p < 0.01) consistent a shift towards a beige fat phenotype.

Discussion: The results indicate that C3H10T1/2 cells were affected by phosphate concentration and BMP2 in differentiating medium. Phosphate deficiency led to a delay in cell differentiation to chondrocytes, while lack of BMP2 resulted in a preference for adipogenic cell fate. These data suggest that overall energy consumption is related to collagen production and the production of hydroxyproline.

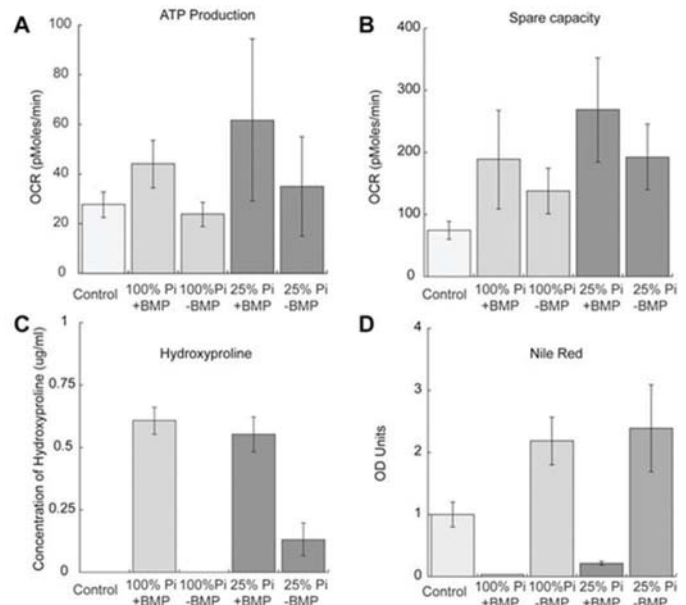


Figure 1

**Disclosures:** Takashi Noguchi, None.

## SU0070

**Mitochondria Play Different Roles in Age-Related vs Estrogen-Related Bone Loss.** Laura Shum\*, Brianna Shares, Roman Eliseev. University of Rochester, United States

Purpose: Our previous work underlined the importance of mitochondrial metabolism in osteoprogenitor differentiation and showed that preventing mitochondrial dysfunction can prevent age-related bone loss. The most common mechanism of mitochondrial dysfunction is through opening of the mitochondrial permeability transition pore (MPTP), regulated by Cyclophilin D (CypD). When the MPTP opens, energetic potential of the mitochondrial membrane dissipates, impairing mitochondrial function. Inhibition of CypD prevents the MPTP from opening, thus preserving mitochondrial function. Our previous work showed that CypD KO prevented age-related bone loss in mice. In the current study, we sought to determine if CypD KO also protects against bone loss associated with estrogen deficiency, and to elucidate the effects of estrogen on the metabolism of osteoprogenitors.

Methods: CypD KO mice and littermate controls underwent ovariectomy (OVX) at 3 mo and samples collected at 5 mo (8 wk post-OVX). Bones were imaged via microCT, DEXA scanning, and subjected to biomechanical testing. Cell culture experiments were performed with primary isolated bone marrow stem (aka stromal) cells (BMSCs), C3H10T1/2 BMSC-like cells, or MC3T3 osteoblast precursor cells.

Results: We found that body fat increased and bone mineral density decreased in both CypD KO and control mice after OVX. There were no significant changes in biomechanical parameters after OVX. Although there were some differences in microCT between the two groups, CypD KO mice were not significantly rescued from bone loss after OVX. In cell culture experiments, estrogen inhibited the MPTP in both C3H and MC3T3 cells. Estrogen depletion decreased mitochondrial membrane potential, which was rescued by pharmacological inhibition of CypD. Treatment with estrogen also increased mitochondrial metabolism in BMSCs.

Conclusion: Although CypD deletion protects against age-related bone loss in mice, it does not appear to protect against bone loss after OVX, adding to the literature that suggests the two phenomena are mechanistically distinct. This is not entirely unexpected as our previous work showed that CypD KO had no effect on osteoclasts and bone resorption. However, cell culture experiments suggest that there is still interplay between estrogen and mitochondrial metabolism, potentially due to a difference in estrogen effects systemically (OVX) and locally (*in vitro*). Further study is needed to elucidate these interactions.

**Disclosures:** Laura Shum, None.

## SU0071

**An Improved Energy Profile Predicts Favorable Bone Remodeling Dynamics in Amenorrheic Athletes.** Emily Southmayd\*, Nancy Williams, Mary Jane De Souza. The Pennsylvania State University, United States

In energy deficient exercising women, metabolic and gonadal steroid hormone adaptations to conserve energy may dysregulate bone turnover. Our purpose was to determine factors that predict change in bone turnover balance and rate during nutritional recovery from energy deficiency in amenorrheic exercising women (18-30yr, BMI  $20.8 \pm 0.3 \text{ kg} \cdot \text{m}^{-2}$ ) randomized to increase caloric intake (AM+Cal, n=19) or control (AM-C, n=21). Metabolic hormones (total triiodothyronine (TT<sub>3</sub>), leptin) and markers of bone formation (procollagen I intact N-terminal, P1NP) and resorption (C-terminal telopeptide, sCTX) were measured in serum. Bone balance and turnover rate were calculated using multiple of median scores of bone markers (bone balance =  $\text{MoM}_{\text{P1NP}} / \text{MoM}_{\text{sCTX}}$ ; turnover rate =  $\sqrt{(\text{MoM}_{\text{P1NP}} + (\text{MoM}_{\text{sCTX}})^2)}$ ). Body composition (fat and lean mass) and bone mineral density (BMD: total body, L1-L4 spine, femur) were assessed via DXA. Metabolic suppression was determined by comparing measured (indirect calorimetry) to predicted (Harris-Benedict) resting energy expenditure (mREE/pREE). All measurements were repeated at baseline, 6mo, and 12mo. Generalized linear mixed modeling identified predictors of change in bone balance, bone turnover rate, and BMD. Average BMI increased from 19.4 to 20.9  $\text{kg} \cdot \text{m}^{-2}$ , fat mass increased from 12.5 to 14.8 kg, and mREE/pREE increased from 0.83 to 0.93 in the AM+Cal group after the 12mo intervention. In the AM+Cal group, bone balance was positively predicted by BMI ( $\beta=0.061$ ,  $p=0.033$ ) and mREE/pREE ( $\beta=0.860$ ,  $p=0.28$ ); turnover rate was positively predicted by fat mass ( $\beta=0.115$ ,  $p=0.001$ ), TT<sub>3</sub> ( $\beta=0.018$ ,  $p<0.001$ ), and lean mass ( $\beta=0.046$ ,  $p=0.051$ ). Turnover rate negatively predicted ( $p<0.009$ ) L1-L4 z-score ( $\beta=-0.238$ ) and BMD ( $\beta=-0.040$ ). In the AM-C group, BMI and mREE positively predicted bone balance ( $\beta=0.056$ ,  $\beta=1.477$ ,  $p<0.009$ ); only fat mass predicted turnover rate ( $\beta=0.047$ ,  $p=0.036$ ). Bone balance and turnover rate did not predict BMD outcomes in the AM-C group. In amenorrheic exercising women, improved energy status after a 12mo refeeding intervention predicted shifts in bone balance to favor bone formation and increased turnover rate, but turnover rate negatively predicted lumbar spine BMD. The relationship between energetic factors, bone turnover, and BMD was not apparent in the AM-C group, underscoring the potent impact that changing energy status has on bone remodeling dynamics.

**Disclosures:** Emily Southmayd, None.

## SU0072

**Exercise Effect on Marrow Adipose Tissue, Metabolic and Skeletal Health in Lipodystrophic SEIPIN Deficient Mice.** Cody McGrath\*<sup>1</sup>, Zengying Wu<sup>2</sup>, Jeyant Srinivas Sankaran<sup>1</sup>, Buer Sen<sup>1</sup>, Zhihui Xie<sup>1</sup>, Martin Styner<sup>3</sup>, Xiaopeng Zong<sup>4</sup>, Weiqin Chen<sup>5</sup>, Janet Rubin<sup>1</sup>, Rosalind A. Coleman<sup>2</sup>, Maya Styner<sup>1</sup>. <sup>1</sup>Department of Medicine, Division of Endocrinology, University of North Carolina, United States, <sup>2</sup>Department of Nutrition, School of Public Health, University of North Carolina, United States, <sup>3</sup>Departments of Computer Science and Psychiatry, University of North Carolina, United States, <sup>4</sup>Biomedical Research Imaging Center, University of North Carolina, United States, <sup>5</sup>Department of Physiology, Medical College of Georgia at Augusta University, United States

Berardinelli-Seip congenital lipodystrophy (BSCL) is an autosomal recessive syndrome caused by loss of function in SEIPIN and characterized by impaired lipid storage leading to few adipocytes, decreased body fat, low leptin, hepatic steatosis and glucose intolerance. We asked whether decreases in marrow adipose tissue (MAT) quantity paralleled the white fat scarcity of SEIPIN deficiency. Further, we asked whether exercise, which induces bone formation while using marrow fat stores, could improve glucose tolerance and have salutary effects in bone in a BSCL mouse model. Twelve-week-old male global Bsc1 (SEIPIN)<sup>-/-</sup> mice on a C57BL/6 background and WT littermate controls were allocated to a voluntary running exercise intervention (WT-E, SEIPIN-E) or control groups (WT, SEIPIN) for 6 weeks (n=7/group). The weight of the WT group was  $29.9 \pm 3.0$  and the weight of the SEIPIN group was  $29.42 \pm 2.6$  (p=0.6) before exercise. After 6 weeks of running, WT mouse weight was 25% higher than SEIPIN (p<0.01). Running decreased the weight of WT mice by 22% compared to sedentary controls (p<0.01) but failed to attenuate weight in SEIPIN. Running trended to be 29% lower in SEIPIN-E compared to WT-E (p=0.061). Compared to SEIPIN mice, SEIPIN-E had improved glucose AUC in response to OGTT after 6 weeks of running, with a 17% decrease in peak blood glucose level (p<0.0001), but failed to normalize to glucose levels of WT mice. Trabecular BV/TV responded more vigorously to exercise in SEIPIN than in WT: a 28% increase in SEIPIN-E vs. SEIPIN (p<0.05) compared to a 9% increase in WT-E vs. WT (p=0.3109). Cortical bone microarchitecture did not differ between the groups. Bone quality (pMOI) was lower in SEIPIN-E vs. WT (-23% lower, p=0.077). MAT as measured by MRI decreased with exercise in WT-E by 4% (p value=0.79) but did not decrease in SEIPIN-E. Interestingly, MAT quantity in SEIPIN mice was similar to that found in WT-E. Liver triglyceride was 231% higher in SEIPIN vs. WT, and exercise attenuated this by 12% (p < 0.05). In conclusion, running exercise improved metabolic health and induced bone formation in SEIPIN mice. Surprisingly, MAT relative to bone volume in SEIPIN was similar to that found in WT, highlighting the uniqueness of this fat depot when compared to other adipose depots. Exercise-induced bone formation is possible even without attenuation in MAT in the setting of SEIPIN deficiency, highlighting the likelihood that SEIPIN mice use an alternative fuel source.

**Disclosures:** Cody McGrath, None.

## SU0073

**Zoledronic acid ameliorates thyroxine-induced loss of bone mass and strength but reverses improved glucose tolerance in male mice with exogenous hyperthyroidism.** Elena Tsourdi\*, Franziska Lademann, Ulrike Baschant, Holger Henneicke, Martina Rauner, Lorenz Hofbauer. Department of Medicine III and Center for Healthy Aging, Technische Universität Dresden Medical Center, Dresden, Germany, Germany

Objective: Hyperthyroidism in mice is associated with a low bone mass, an increased bone turnover, and an improved insulin sensitivity and glucose tolerance. Here, we explored the effects of a bisphosphonate-induced reduction in bone turnover on bone mass and strength and its subsequent effects on glucose tolerance in hyperthyroid mice.

Methods: Twelve-week-old C57BL/6 male mice were rendered hyperthyroid by adding L-thyroxine (T4) to the drinking water (1.2 µg/ml). Saline or 100 µg/kg zoledronic acid (ZOL) 1x/weekly were administered to hyperthyroid and control mice for 4 weeks. MicroCT analysis, dynamic histomorphometry, biomechanical testing, measurement of bone turnover markers and oral glucose tolerance tests were performed.

Results: Hyperthyroid mice displayed a lower trabecular bone volume at the spine (-42%, p<0.05) and the distal femur (-55%, p<0.05) compared to euthyroid controls. ZOL treatment of hyperthyroid mice increased trabecular bone volume at the spine by 2-fold as compared to PBS-treated hyperthyroid mice (p<0.01). Similar trends were seen for the femur. Trabecular bone stiffness at the lumbar vertebra was 63% lower in hyperthyroid mice (p<0.05), and was increased 2.7-fold (p<0.01) after ZOL treatment. Hyperthyroidism reduced ultimate load (-10%, p<0.05), while ZOL treatment led to a 22% increase (p<0.001). Bone turnover was increased in hyperthyroid mice based on increased CTX, P1NP, and osteocalcin serum levels, which were reduced to baseline after ZOL treatment. Hyperthyroid mice experienced a weight gain of 7.5% (p<0.05) and showed an improved glucose tolerance. Brown adipose tissue was increased in hyperthyroid mice (p<0.001) and treatment with ZOL didn't reverse this effect. While ZOL treatment did not influence body weight, blocking bone turnover completely mitigated the positive effect of hyperthyroidism on glucose tolerance.

Conclusion: Thus, anti-resorptive treatments are effective in preventing bone loss in hyperthyroidism. Moreover, our data suggest that the rate of bone turnover may contribute to glucose handling in hyperthyroid mice.

**Disclosures:** Elena Tsourdi, None.

## SU0074

**Irisin and its functional domain for stimulating the downstream signaling.** Dongdong Zhang\*, Myeongmo Kang, Hye sun Park, Zeyu Jin, Weontae Lee, Sung-Kil Lim. Yonsei University, Korea, Republic of

Irisin, a novel identified hormone secreted by skeletal muscle in response to exercise, plays a vital role in reprogramming white adipose tissue browning. Importantly, irisin was reported to enhance bone mass and strength. However, the domain which modulates receptor activation remains elusive yet. The previous study reported that the flexible loops of irisin lie on a hydrophobic face of the dimer, suggesting the regions as the potential candidate domain for interactions with other proteins. This work is to determine the function domain of irisin.

Point mutations in 55-58 and 106-108 region of irisin were applied to construct mutant irisins (m-irisins). Recombinant human irisin (WT-irisin) and its mutants were purified from E.coli expression system. Uncoupling protein 1 (UCP1) expression levels were detected by treating HIB1 cells with WT-irisin or m-irisins. We observed the cell proliferation activity by CCK-8 assay in MC3T3E1 preosteoblast cells after treatment with WT-irisin or m-irisins. The P38/ERK MAPK, AMPK and AKT signaling pathways were detected by using western blotting.

WT-irisin and m-irisins were successfully purified from E.coli. By western blotting analysis, the purified target proteins were human irisin protein. Both WT-irisin and 108 m-irisin stimulate phosphorylation of ERK, AMPK, AKT and P38. Treatment HIB1 cells with WT-irisin or 108 m-irisin significantly increased levels of the brown cell markers UCP1, however, WT-irisin significantly increased UCP1 levels compared with 108 m-irisin. Furthermore, WT-irisin rather than 108 m-irisin promoted osteoblasts proliferation.

These results indicated that the loop region (106-108) might be the functional domain of irisin related to the potential anabolic effects on bone.

**Disclosures:** Dongdong Zhang, None.



## SU0075

**Genetic Variation of Inbred Mouse Strains Uncovers Differences in Femur Strength Distinctly Influenced by Bone Matrix Composition.** Michael-John Beltejar<sup>\*1</sup>, Jun Zhang<sup>2</sup>, Dana A. Godfrey<sup>1</sup>, Renata Rydzik<sup>3</sup>, Olivia Hart<sup>3</sup>, Douglas J. Adams<sup>3</sup>, Cheryl L. Ackert-Bicknell<sup>1</sup>. <sup>1</sup>Center for Musculoskeletal Research, University of Rochester Medical Center, United States, <sup>2</sup>Department of Orthopedics, Zhejiang Provincial People's Hospital, China, <sup>3</sup>Department of Orthopaedic Surgery, University of Connecticut Health, United States

Osteoporosis is a disease characterized by progressive reduction in bone quantity and alterations in bone matrix quality. This often culminates in fractures that significantly alter quality of life and increase mortality risk. Although bone mineral density (BMD) is the current basis for surveillance, diagnosis, and therapy, it only captures 50% of fracture resistance because it minimally reflects contributions from bone shape and composition. Understanding the contributions of composition is necessary to develop novel and more comprehensive screening and treatment. The goal of this work was to determine how defined genetic variations in bone matrix quality results in altered bone strength. To accomplish this, we leveraged the genetic diversity of 7 inbred mouse strains. Three-point bending was used to measure flexural strength of femurs from 20-week old male mice. Moments of inertia for diaphyseal cross sections of femurs were measured using microCT. Tissue modulus and strength were calculated using beam theory. Areal BMD of the whole body was measured using DXA. Finally, matrix composition of humeri was assessed using Fourier-Transform Infrared Spectroscopy (FTIR). Differences among strains were determined by one-way ANOVA with a Student's T post hoc test with a Bonferroni correction. All of these determinants were highly reproducible within a strain, yet differed among strains, suggesting high heritability for these phenotypes. Multiple regression using parameters of composition (BMD, mineral: matrix, carbonate:phosphate, crystallinity) and geometric properties (I and I/c about ML axis) confirmed that whole-bone mechanical strength is predominantly determined by I/c, crystallinity and the mineral to matrix ratio (min:matrix). Tissue modulus is predominantly determined by crystallinity and min:matrix. Poignantly, contributions of aBMD to whole-bone strength is redundant. We then identified the main determinants of strength for each strain. For example, despite having lower BMD and geometrically smaller bones than B6, CAST femora have greater tissue strength, tissue modulus, and a mineral to matrix ratio, resulting in greater structural strength than B6 mice. This suggests that genetically regulated matrix properties might be involved in offsetting deficiencies of size and shape to produce femurs of similar structural strength. These genetic differences can now be exploited to identify the molecular pathways involved in governing structural bone strength.

**Disclosures:** Michael-John Beltejar, None.

## SU0076

**Cyclin D1-Driven Parathyroid Neoplasia is CDK4/6 Dependent in Transgenic Mice.** Jessica Costa-Guda<sup>\*1</sup>, Kristin Corrado<sup>2</sup>, Justin Bellizzi<sup>2</sup>, Robert Romano<sup>2</sup>, Elizabeth Saria<sup>2</sup>, Kirsten Saucier<sup>2</sup>, John Vu<sup>2</sup>, Madison Rose<sup>2</sup>, Samantha Cummins<sup>2</sup>, Samip Shah<sup>2</sup>, Cynthia Alander<sup>2</sup>, Sanjay Mallaya<sup>3</sup>, Andrew Arnold<sup>2</sup>. <sup>1</sup>University of Connecticut School of Dental Medicine, United States, <sup>2</sup>University of Connecticut School of Medicine, United States, <sup>3</sup>UCLA School of Dentistry, United States

Cyclin D1 (encoded by the *CCND1/PRAD1* oncogene) is an established driver of multiple human tumor types, including sporadic parathyroid tumors. In a subset of these, peri-centromeric inversion of chromosome 11 places the *CCND1* coding region adjacent to the *PTH* 5' regulatory region, resulting in high-level cyclin D1 overexpression; also, some parathyroid malignancies exhibit *CCND1* amplification. Cyclin D1 is a regulatory subunit that binds and activates its partner cyclin-dependent kinase (cdk4 or cdk6) in a holoenzyme complex that can phosphorylate and thereby inactivate the retinoblastoma protein pRB. However, a number of nonclassical, cdk-independent, functions of cyclin D1 with potential relevance to tumorigenesis have also been described. Indeed, a kinase-dead mutant form of cyclin D1 was shown to drive mammary tumorigenesis, with similar kinetics as wild-type cyclin D1, in transgenic mice. With the recent introduction of pharmacologic cdk4/6 inhibitors in cancer therapy, understanding the mechanisms by which cyclin D1 overexpression drives tumorigenesis is increasingly important. We therefore sought to determine if cyclin D1's role in driving parathyroid tumorigenesis is effected primarily through kinase-dependent or kinase-independent functions. An established mouse model of parathyroid neoplasia, driven by a *PTH-CCND1* transgene, mimicking the rearrangement found in human parathyroid tumors, and developing both biochemical hyperparathyroidism and hypercellular parathyroids with known kinetics, served as a control. We generated transgenic mice with a modified *PTH-CCND1* transgene, harboring a *CCND1* codon 112 mutation resulting in a lysine (K) to glutamic acid (E) substitution. This KE mutant cyclin D1 is unable to activate its partner kinases. Despite levels of cyclin D1 overexpression similar to controls, KE mutant mice did not develop biochemical hyperparathyroidism or parathyroid hypercellularity. These results suggest, in stark contrast to observations in mammary tissue, that in the parathyroid glands cyclin D1 acts predominantly through cdk-dependent mechanisms to drive tumorigenesis. Our findings highlight crucial tissue-specific differences in the mechanisms through which cyclin D1 drives tumorigenesis, which carry important implications for therapeutic intervention, and suggest that parathyroid cells may be more tumorigenically vulnerable to acquired genetic perturbations in cdk-mediated proliferation control compared with other tissue contexts.

**Disclosures:** Jessica Costa-Guda, None.

## SU0077

**Genotyping assays to distinguish bone-selective cre-driver mouse lines.** greig couasnay<sup>\*</sup>, christopher Frey, florent Elefteriou. Baylor college of medicine, United States

The use of genetic mutant mouse models, especially conditional KO mouse models, has become common practice in our field of research. Not only do we need to use such loss-of-function models to support solid mechanisms and conclusions, we also need to use several of them to manipulate genes in different tissues, development times, cells or stages of differentiation. The generation of these fantastic tools led to the expansion of cre lines available, and to the existence and sharing of multiple of them within and between laboratories.

These cre-deleter lines are in general genotyped with a generic set of primers amplifying the 'cre' transgene. Although convenient, this practice does not distinguish the increasing number of cre-deleter lines available within each laboratory or mouse room. Therefore, the inadvertent swap of cre mice between lines can go undetected, which can have disastrous consequences in term of result interpretations, productivity and cost.

We report here the design and validation of cre line-specific PCR primer sets designed to distinguish one cre-deleter line from the others, with a focus on cre lines used in the musculoskeletal field. Specificity was designed by the selection of a PCR amplicon spanning both the cre transgene and the promoter driving its expression. It was verified by negative amplification results in other cre lines and by sequencing of PCR products.

**Disclosures:** greig couasnay, None.

## SU0078

**Decreased bone strength induced by persistent activation of calcium-sensing receptor.** Itsuro Endo<sup>\*1</sup>, Bingzi Dong<sup>2</sup>, Yukiyo Ohnishi<sup>3</sup>, Takeshi Kondo<sup>3</sup>, Masahiro Hiasa<sup>3</sup>, Jumpei Teramachi<sup>3</sup>, Shinichi Aizawa<sup>4</sup>, Toshio Matsumoto<sup>5</sup>, Masahiro Abe<sup>3</sup>, Fukumoto Seiji<sup>5</sup>. <sup>1</sup>Department of Chronomedicine, Institute of Biomedical Sciences, Tokushima University Graduate School, Japan, <sup>2</sup>Department of Endocrinology, Affiliated Hospital of Qingdao University, China, <sup>3</sup>Department of Hematology, Endocrinology and Metabolism, Tokushima University, Japan, <sup>4</sup>Genetic Engineering Team, RIKEN Center for Life Science Technologies, Japan, <sup>5</sup>Fujii Memorial Institute of Medical Sciences, Tokushima University, Japan

Background: Calcium-sensing receptor (CaSR) is expressed in several tissues to regulate Ca homeostasis. Activating mutations of CaSR cause autosomal dominant hypocalcemia type 1 (ADH1). Patients with ADH1 show similar biochemical features of hypocalcemia with low PTH to patients with hypoparathyroidism. However, bone strength in patients with ADH1 has not been well studied. Previously, we have created knock-in mice of human activating mutant CaSR (KI mice) as model mice for ADH1. KI mice mimicked almost all the biochemical features of ADH1.

Methods: We assessed bone mineral density (BMD: total, cortical, cancellous) of whole femur, cortical area and perimeter of mid-shaft femur in female ADH1 mice aged 18-38 weeks. Breaking peak load was also evaluated by diaphysis 3-point bending test. The other side of the femur was stained using fuchsin and evaluated for both number and density of micro-cracks in bone.

Results: ADH1 mice showed significantly lower BMD, cortical area and perimeter of mid-shaft of femurs compared to those of age matched wild-type mice. The breaking peak load was also significantly lower in ADH1 mice. Micro-cracks were rarely detected in wild-type mice, while ADH1 model mice exhibited remarkable increase in the number and density of micro-cracks ( $p < 0.005$ ,  $p < 0.0005$ , respectively). In the analysis including both ADH1 and wild-type mice, there was a significant positive correlation between the peak load and total, cortical, cancellous BMD, cortical area or perimeter of femur. On the other hand, a significant negative correlation was observed between the peak load and micro-crack number or micro-crack density. In the analysis of ADH1 mice, negative relationship was still observed between the peak load and micro-crack number or micro-crack density. Furthermore, multivariate analysis revealed that total BMD and crack density were independently associated with peak load (both  $p < 0.05$ ) in ADH1 mice.

Conclusion: Increased micro-cracks cause decreased bone strength in ADH1 mice. These observations demonstrate that the fracture susceptibility might be increased in patients with ADH1.

**Disclosures:** Itsuro Endo, None.

## SU0079

**Bone compartment specific effects of long duration hypothalamic leptin gene therapy on osteopetrosis in leptin-deficient *ob/ob* mice.** Kenneth Philbrick<sup>\*1</sup>, Laurence Lindenmaier<sup>1</sup>, Amy Colagiovanni<sup>1</sup>, Dawn Olson<sup>1</sup>, Satya Kalra<sup>2</sup>, Adam Branscum<sup>1</sup>, Urszula Iwaniec<sup>1</sup>, Russell Turner<sup>1</sup>. <sup>1</sup>Oregon State University, United States, <sup>2</sup>University of Florida, United States

Delayed resorption of cartilage entrapped within bone matrix during growth occurs with low bone turnover and is a defining feature of juvenile osteopetrosis. Growing, leptin-deficient *ob/ob* mice exhibit a mild form of osteoclast-rich osteopetrosis. However, the extent to which the disease is (1) self-limiting or (2) reversible by leptin treatment is

unknown. To address the first issue, we performed histomorphometric analysis of femurs in growing 2-month-old and skeletally mature 4-month-old, 6-month-old, and 10-month-old male *ob/ob* mice. Ten-month-old *ob/ob* mice are near the end of their lifespan. In contrast to its absence in 6-month-old wild type mice, cartilage was present within cancellous bone (epiphysis) and cortical bone (diaphysis) in 6-month-old and 10-month-old *ob/ob* mice, suggesting that the osteopetrotic phenotype of *ob/ob* mice is present throughout life. To address the second issue, we randomized 2-month-old male *ob/ob* mice to one of three groups: (1) no treatment control, (2) recombinant adeno-associated virus encoding the gene for leptin (rAAV-leptin), or (3) recombinant adeno-associated virus encoding the gene for green fluorescent protein (rAAV-GFP). Mice in the latter two groups were implanted with cannulae in the 3rd ventricle of the hypothalamus and injected with the respective vectors. Following maintenance for 7 months, rAAV-leptin mice exhibited negligible cartilage and greater osteoclast and osteoblast perimeters within the distal femoral epiphysis compared to non-treated and rAAV-GFP-treated mice. The leptin-induced increases in bone turnover fully replaced cartilage with bone in the epiphysis. However, replacement of cartilage by bone was incomplete in the diaphysis, a site with low bone turnover. These findings (1) support the concept that leptin is critical for normal maturation of bone during growth and (2) demonstrate that osteopetrosis in *ob/ob* mice is bone compartment specific and reversible by long duration hypothalamic leptin gene therapy at skeletal sites capable of undergoing robust bone turnover.

**Disclosures:** Kenneth Philbrick, None.

## SU0080

**Combination Therapy with Anti-TGF-Beta Antibody and a Mutation in *Lrp5* Improves Trabecular Bone Properties In Mice with Osteogenesis Imperfecta.** Shannon Kaupp<sup>1</sup>, Alexander Robling<sup>2</sup>, Matthew Warman<sup>3</sup>, Christina Jacobsen<sup>4</sup>. <sup>1</sup>Boston Children's Hospital, United States, <sup>2</sup>Indiana University, United States, <sup>3</sup>Boston Children's Hospital/Harvard Medical School/Howard Hughes Medical Institute, United States, <sup>4</sup>Boston Children's Hospital/Harvard Medical School, United States

Osteogenesis Imperfecta (OI), a disorder most frequently caused by mutations in type I collagen, is characterized by increased skeletal fragility. Therapies are needed to reduce fractures and improve quality of life in patients with OI. Heterozygous missense mutations in the cell surface receptor, low-density lipoprotein receptor-related protein 5 (LRP5) increase bone mass and strength in humans and mice. TGF-beta signaling has emerged as an important regulator of bone mass and is known to be increased in OI. Treatment with a monoclonal antibody targeting TGF-beta improves bone density in mouse models of OI. We hypothesize that combination therapy for OI targeting both the TGF-beta and the LRP5 pathways will be more effective than either therapy alone.

We mated mice with a dominant *Lrp5* high bone mass (HBM)-causing knockin allele to a mouse model of moderate OI (*Col1a1*<sup>G610C</sup>). Offspring were randomly assigned to receive either monoclonal anti-TGF-beta antibody (1D11, Sanofi Genzyme) or a sham antibody (13C4, Sanofi Genzyme). We analyzed femoral bone density at 12 weeks of age by microCT, as well as femoral strength by 3-point bending analysis (N=7-10 per sex/genotype/treatment group). As expected, there was a significant increase in trabecular BV/TV in mice with an OI mutation treated with anti-TGF-Beta antibody (1D11) compared to littermates with an OI mutation who received control antibody (13C4), as well as a significant increase in trabecular BV/TV in mice with an OI allele and an *Lrp5* HBM allele compared to littermates with an OI allele alone ( $p < 0.05$ ). Male and female mice with both an OI allele and a HBM allele treated with 1D11 had significantly greater trabecular BV/TV, compared both to mice of the same genotype who received control antibody (13C4) and to mice with an OI allele alone who also received 1D11 ( $p < 0.05$ ). Similar increases in trabecular number and thickness were seen ( $p < 0.05$ ). However, no significant differences in cortical thickness or ultimate force were seen between mice with an OI allele and/or a HBM allele that received 1D11 compared to those who received control antibody (13C4). Notably, 1D11 treatment did not increase post-yield displacement in any animals with an OI allele. These results demonstrate treatment with TGF-beta antibody combined with an anabolic mutation in *Lrp5* has an additive effect in increasing trabecular bone density in OI, suggesting patients will benefit from combination therapy.

**Disclosures:** Shannon Kaupp, None.

## SU0081

**Clinical Spectrum and Unifying Pathomechanisms in Ectopic Connective Tissue Mineralization Disorders.** Qiaoli Li\*, Jouni Uitto. Department of Dermatology and Cutaneous Biology, Thomas Jefferson University, United States

Ectopic mineralization has been linked to several common clinical conditions with considerable morbidity and mortality. The mineralization processes, both metastatic and dystrophic, affect primarily the skin and vascular connective tissues. There are several contributing metabolic and environmental factors that make uncovering of the precise pathomechanisms of these acquired disorders exceedingly difficult. Several relatively rare heritable disorders share phenotypic manifestations similar to those in common conditions, and, consequently, they serve as genetically controlled model systems to study the details of the mineralization process in peripheral tissues. These heritable disorders are characterized by mineral deposition in the skin and vascular

connective tissues, as exemplified by pseudoxanthoma elasticum (PXE), generalized arterial calcification of infancy (GACI), and arterial calcification due to CD73 deficiency (ACDC), caused by loss-of-function mutations in the *ABCC6*, *ENPP1*, and *NTSE* genes, respectively. Studies in these diseases and their corresponding mouse models suggest a unifying pathomechanism relating to reduced plasma inorganic pyrophosphate/inorganic phosphate ratio in these disorders. This hypothesis is based on the notion that inorganic pyrophosphate serves as a powerful inhibitor of mineralization, whereas inorganic phosphate is a prominerization factor, and an appropriate inorganic pyrophosphate/inorganic phosphate ratio is critical for prevention of ectopic mineralization under homeostatic conditions. Reduced plasma pyrophosphate levels has raised the possibility of direct supplementation of inorganic pyrophosphate, or using stable, nonhydrolyzable pyrophosphate analogues, bisphosphonates, for treatment of these ectopic mineralization disorders. This concept is currently tested in both preclinical animal models and in patient clinical trials.

**Disclosures:** Qiaoli Li, None.

## SU0082

**Targeted Deletion of Claudin (*Cldn*)-12 Gene Inhibits Chondrocyte Differentiation and Increases Articular Cartilage Thickness.** Richard Lindsey\*, Weirong Xing, Patrick Aghajanian, Catrina Godwin, Sheila Pourteymoor, Subburaman Mohan. VA Loma Linda Healthcare System, United States

The claudin (Cldn) family comprises 24 members of 20–34 kDa tetraspan transmembrane proteins of tight junctions. In addition to their established canonical role as barriers controlling the flow of molecules in the intercellular space between cells, a distinct non-canonical role for Cldns is now emerging in which they serve as mediators of cell signaling. In our studies evaluating expression of all 24 *Cldn* family members during osteoblast (OB) differentiation, *Cldn-12* showed the largest decrease during *in vitro* OB differentiation. To study the role of *Cldn-12*, we developed mice with targeted deletion of exon2 for skeletal phenotype analysis. MicroCT analysis of femurs and tibiae of mice with targeted disruption of the *Cldn-12* gene and control littermates showed no significant genotype-specific differences in either cortical or trabecular bone parameters for either gender at 13 weeks of age. Immunohistochemistry revealed that while *Cldn-12* is expressed in both differentiating chondrocytes (CCs) and OBs of secondary spongiosa of 2-week old wild-type mice, its expression is restricted to differentiating CCs of the articular cartilage (AC) and growth plate in adult mice. Therefore, we determined the AC phenotype of *Cldn-12* knockout (KO) and control mice at 13 weeks of age. AC area at the knee was increased by 43% and 51% (both  $P < 0.05$ ), respectively, in *Cldn-12* KO females and males compared to gender matched controls. AC width was increased by 22% ( $P < 0.01$ ) in KO females and 16% ( $P = 0.06$ ) in KO males. Immunohistochemistry suggested reduction in the expression of differentiation marker Col10a1 and increased expression of articular CC marker lubricin in the AC of KO mice. In addition, mRNA expression of lubricin was increased by 50% ( $P < 0.05$ ) in primary cultures of articular CCs derived from KO mice compared to control mice. Studies on regulation of *Cldn-12* expression revealed that treatment with thyroid hormone, a known regulator of articular CC differentiation, increased expression of *Cldn-12* in epiphyseal CCs and ATDC5 CCs by 2–4-fold ( $P < 0.01$ ). In contrast, treatment with BMP-2 or vitamin C had no significant effect on *Cldn-12* expression in CCs. Based on these data, we propose a novel role for *Cldn-12* in regulating articular CC differentiation and AC thickness and that manipulation of *Cldn-12* signaling in articular CCs could be used as a therapeutic means to treat osteoarthritis.

**Disclosures:** Richard Lindsey, None.

## SU0083

**Assessment of genetics underlying the trabecular plate-rod ratio using whole exome sequencing.** Melissa Sum\*, Xiaolin Zhu, Minghao Liu, Edward Guo, David Goldstein, Marcella Walker. <sup>1</sup>Columbia University Medical Center, United States, <sup>2</sup>Columbia University, United States

Using high resolution peripheral quantitative computed tomography, we have shown that Chinese women have smaller bone size, but thicker and denser cortices and a higher trabecular plate-rod ratio (TPR) vs. white women. These features confer greater stiffness. TPR was the trait most highly associated with race. The study aim was to identify genetic variants associated with TPR using whole exome sequencing (WES). We conducted a genetic association analysis (N=65) with TPR as the phenotype using a gene-based collapsing linear regression approach focusing on rare variants (global variant allele frequency <5%) with predicted functional impact [missense, loss of function (LOF)]. We tested the genotype-phenotype association under a dominant model. Principle components (PCs) were generated from linkage disequilibrium-pruned SNPs and we adjusted for the top 10 PCs. A Bonferroni-corrected p-value of 2.5E-6 was considered significant assuming simultaneously testing 20,000 genes. Our results suggest an association ( $\beta = 1.3$ ,  $p = 6.91E-07$ ) between TPR and GPR84, a G-protein 7-transmembrane receptor, expressed in bone marrow and osteocytes. There were 3 qualifying GPR84 variants in 6 individuals. One missense variant, 12-54756528-A-G, was present in 3 Chinese women (2 hetero- and 1 homozygous) with high TPR (mean=2.529), while the other, 12-54757526-C-T, was present in 2 heterozygous Chinese women also with high TPR (mean=2.790). Both missense variants were predicted to likely be damaging with HumDiv score 1 by PolyPhen-2. The third, 12-54757167-G-C-G, was a frameshift variant present in one heterozygous white woman with low TPR (0.526). The results



suggest the missense variants could have a gain-of-function effect increasing TPR, while the frame-shift and presumably LOF variant may have an opposite effect decreasing TPR. We estimated that 70.89% of the Chinese/white difference in TPR can be explained by the cumulative frequency difference of GPR84 qualifying variants between races. Covariate-adjusted bone specific alkaline phosphatase ( $32.5 \pm 1.0$  vs.  $25.1 \pm 3.7$  U/L,  $p=0.065$ ) and collagen c-telopeptide ( $0.72 \pm 0.10$  vs.  $0.54 \pm 0.03$  ng/L,  $p=0.09$ ) tended to be higher, suggesting greater remodeling, in those with vs. without GPR84 variants. If the GPR84 association is confirmed, it may explain a large amount of variation in the TPR trait. These preliminary data show the feasibility and power of the WES-based approach to identify rare variants associated with bone microstructure.

**Disclosures:** Melissa Sum, None.

## SU0084

**An Orthologous Transcription Factor Network Modulated by PU.1 Bound Enhancers in Osteoclasts Predicts Bone Density.** Heather Carey\*, Blake Hildreth, Jennifer Geisler, Sankha Ghosh, Ramiro Toribio, Michael Ostrowski, Sudarshana Sharma. Ohio State University, United States

Genome wide association studies (GWAS) and model organism based mechanistic studies have been the two vital yet 'disconnected' arms of scientific approach in understanding the complex pathophysiological traits. The knowledge gained from both of these approaches independently have been instrumental in understanding as well as identifying therapeutic targets to several illnesses. In the study outlined here, we have attempted to combine functional genomics, mouse modeling and bone mineral density associated SNPs (BMD-SNPs) identified by the Genetic Factors for Osteoporosis Consortium (GEFOS) to identify SNPs that are more relevant in osteoclast (OC) lineage.

Osteoporosis is a complex disease that involves disrupted balance between bone-forming osteoblasts and bone-resorbing OCs. While most current therapies for osteoporosis are directed towards inhibiting OC function, studies 'linking' BMD-SNPs to regulatory networks in OC compartment are scarce. By integrating human ChIP-Seq data for the master transcriptional regulator of the myeloid lineage, PU.1, with BMD-SNPs from the GEFOS database, we identified PU.1 regulated genes associated with human BMD-SNPs and provide experimental evidence that these genes have an osteoclast-specific role.

In validation of our methodology, functional genomic analysis of these PU.1 BMD-SNP genes revealed OC differentiation as a significantly enriched process. Interestingly, transcriptional regulation was the most significant and most enriched molecular function in PU.1 BMD-SNP genes.

Although multiple transcription factors (TFs) have been shown to be essential for OC differentiation, their interplay remains largely unknown. To understand the mechanisms behind these observations, we utilized mouse models to delete PU.1 either in the entire myeloid lineage or specifically in OCs. In both models, deletion of PU.1 led to osteopenia and increased BMD, indicating that unrestrained PU.1 activity may contribute to the decrease in BMD observed in osteoporosis. Further, functional genomic analysis (ChIP-Seq and global gene expression profiling) in mice revealed that PU.1 is essential for the expression of genes necessary for OC function and that PU.1 controls a complex network of OC-lineage determining TFs, including Nfatc1, a key regulator of terminal OC differentiation. Most of these OC lineage determining TFs exhibited the hallmarks of superenhancers, requiring cooperative binding between PU.1 and the BET protein, BRD4, a recently identified potential target in osteoporosis therapy. Lastly, we determined that PU.1-dependent chromatin looping of an intronic enhancer is necessary for induction of the Nfatc1 in mice. In humans, a similar enhancer region at this respective locus contains a cluster of four PU.1 BMD-SNPs with a high degree of linkage disequilibrium.

**Disclosures:** Heather Carey, None.

## SU0085

**Identification of rare variants in young adults with idiopathic osteoporosis.** Corinne Collet\*, Agnes Ostertag<sup>1</sup>, Manon Riquebourg<sup>1</sup>, Marine Delecourt<sup>2</sup>, Giulia Tueur<sup>2</sup>, Thomas Funck-Brentano<sup>1</sup>, Philippe Orcel<sup>1</sup>, Jean-Louis Laplanche<sup>2</sup>, Martine Cohen-Solal<sup>1</sup>. <sup>1</sup>Inserm U1132 and hospital Lariboisiere, France, <sup>2</sup>Department of Biochemistry, hospital Lariboisiere, France

**Objective:** Idiopathic osteoporosis (OP) in young adults is an uncommon disorder with an unclear genetic cause. Several mutations have been described in population-based cohorts or in affected families in relation to bone mineral density (BMD) and fractures. Our aim was to analyze in a large cohort of young adult patients with primary osteoporosis the contribution of NGS target sequencing in identifying novel variants in previously reported genes.

**Methods:** We selected patients aged 20 to 55 years who were referred to the clinic for osteoporosis after exclusion of secondary causes. We included 122 patients with primary OP defined by spinal or hip bone mineral density (BMD, Z-score < 2.0 SD) associated or not to major OP fractures. Molecular screening was based on target sequencing approach including *ALPL*, *COL1A1*, *COL1A2*, *IFTIM5*, *LRP5*, *LRP6*, *PLS3*, *WNT1* and *WNT16*. In case of novel or very rare missense LRP5 variant, functional studies were performed by site-directed mutagenesis in Saos-2 cells line transfected with mutant LRP5 or WT for the analysis of Wnt pathway.

**Results:** Novel or rare mutations in *COL1A2*, *PLS3* and *WNT1* were identified at heterozygous level in 12 patients. No variant was found in 56 %. The p.Val667Met

variant was present in 24% in young osteoporotic patients (heterozygous frequency 4% in European general population). Moreover, 14 novel pathogenic heterozygous *LRP5* variants were identified with a frequency of 10 %. Compared to OP patients without mutations, carriers of p.Val667Met or novel variants in *LRP5* displayed a significantly lower spinal Z-Score ( $-2.63 \pm 0.8$  SD vs  $-3.12 \pm 0.9$  and  $-3.48 \pm 0.9$  SD,  $p < 0.001$ ) and a higher number of fractures (36% vs 50 and 75%,  $p < 0.001$ ). Site-directed mutagenesis in Saos-2 cells transfected with mutant *LRP5* showed reduced Wnt signalling suggesting the contribution of the mutation in bone failure.

**Conclusions:** NGS target sequencing is a powerful tool to identify genetic background in young osteoporotic patients. *LRP5* appears to be a major gene that could explain partly the BMD. A molecular screening in young adults could be useful in order to personalized treatment in future.

**Disclosures:** Corinne Collet, None.

## SU0086

**Genome-wide association study of extreme high bone mass identifies *NPR3* as a novel BMD-associated gene and highlights the contribution of common genetic variation to extreme BMD phenotypes.** Celia Gregson\*, Felicity Newell<sup>2</sup>, Paul Leo<sup>2</sup>, Lavinia Paternoster<sup>1</sup>, Mhairi Marshall<sup>2</sup>, Graeme Clark<sup>2</sup>, John Morris<sup>3</sup>, Bing Ge<sup>3</sup>, Xiao Bao<sup>2</sup>, Duncan Bassett<sup>4</sup>, Graham Williams<sup>4</sup>, Scott Youten<sup>5</sup>, Peter Croucher<sup>5</sup>, George Davey Smith<sup>1</sup>, David Evans<sup>6</sup>, John Kemp<sup>6</sup>, Matthew Brown<sup>2</sup>, Jon Tobias<sup>1</sup>, Emma Duncan<sup>2</sup>. <sup>1</sup>University of Bristol, United Kingdom, <sup>2</sup>Queensland University of Technology, Australia, <sup>3</sup>McGill University, Canada, <sup>4</sup>Imperial College London, United Kingdom, <sup>5</sup>The Garvan Institute of Medical Research, Australia, <sup>6</sup>University of Queensland, Australia

Generalised high bone mass (HBM), a mild skeletal dysplasia, has a prevalence of 0.18% amongst a UK-based DXA-scanned adult population. We hypothesized that extreme HBM is in part polygenic, explained by genetic variation in both established and novel BMD loci, novel loci with large effect being detectable within a rare population constituting the extremes of a quantitative phenotype.

Hence, we performed a quantitative trait genome-wide association study (GWAS) of adults with either extreme high or low BMD (Z-scores +1.5 to +9.3; n=1287 and -1.5 to -4.0; n=900) and tested association between SNPs and total hip and lumbar spine BMD Z-scores. We identified associations exceeding genome-wide significance between BMD and four loci: two established BMD-associated loci (5q14.3 containing *MEF2C* and 1p36.12 containing *WNT4*) and two novel loci: 5p13.3 containing *NPR3* (rs9292469; minor allele frequency [MAF] =0.33%), associated with lumbar spine BMD; and 11p15.2 containing *SPON1* (rs2697825; MAF=0.17), associated with total hip BMD. Both *Npr3* and *Spon1* have reported mouse models with altered skeletal phenotypes providing biological validation that these genes play a functional role in bone. It is thought that *NRP3* regulates endochondral ossification and hence skeletal growth, whilst *SPON1* alters TGF- $\beta$  regulated BMP-driven osteoblast differentiation. Rs9292469 (lying downstream of *NPR3*) was independently replicated in association with forearm BMD in GEFOS (n=32,965). We found *Spon1* was highly expressed in murine osteocytes from the tibiae, femora, humeri and calvaria, whereas *Npr3* expression was more variable.

We examined SNPs previously associated at GWAS significance level with DXA BMD and/or fracture in GEFOS; 49 were available in our imputed dataset. QQ (quantile-quantile) plots for p values for associations with total hip and lumbar spine BMD showed enrichment for genetic variation in these known BMD-associated SNPs (i.e. observed p values were much smaller than those expected), particularly SNPs at loci known to regulate endochondral ossification and Wnt signalling, suggesting that part of the genetic contribution to HBM is polygenic.

Our findings, from this most extreme truncate GWAS of BMD performed to date, validate the use of extreme BMD populations for genetic discovery and have identified potentially important anabolic bone regulatory pathways which warrant further study.

**Disclosures:** Celia Gregson, None.

## SU0087

**The response to antenatal cholecalciferol supplementation is associated with common vitamin D related genetic variants: findings from the MAVIDOS trial.** Rebecca Moon<sup>\*1</sup>, Nicholas Harvey<sup>2</sup>, Cyrus Cooper<sup>1</sup>, Stefania D'Angelo<sup>1</sup>, Elizabeth Curtis<sup>1</sup>, Sarah Crozier<sup>1</sup>, Sheila Barton<sup>3</sup>, Sian Robinson<sup>1</sup>, Keith Godfrey<sup>1</sup>, Nikki Graham<sup>4</sup>, John Holloway<sup>4</sup>, Nicholas Bishop<sup>5</sup>, Stephen Kennedy<sup>6</sup>, Aris Papageorgiou<sup>6</sup>, Inez Schoenmakers<sup>7</sup>, Robert Fraser<sup>8</sup>, Saurabh Gandhi<sup>8</sup>, Ann Prentice<sup>9</sup>, Hazel Inskip<sup>1</sup>, M Kassim Javaid<sup>10</sup>.  
<sup>1</sup>MRC Lifecourse Epidemiology Unit, University of Southampton, United Kingdom, <sup>2</sup>MRC Lifecourse Epidemiology Unit, United Kingdom, <sup>3</sup>MRC Lifecourse Epidemiology Unit, University of Southampton, United Kingdom, <sup>4</sup>Human Health and Development, Faculty of Medicine, University of Southampton, United Kingdom, <sup>5</sup>Academic Unit of Child Health, University of Sheffield, United Kingdom, <sup>6</sup>Nuffield Department of Obstetrics and Gynaecology, John Radcliffe Hospital, United Kingdom, <sup>7</sup>MRC Human Nutrition Research, United Kingdom, <sup>8</sup>Sheffield Hospitals NHS Trust, United Kingdom, <sup>9</sup>MRC Human Nutrition Research, United Kingdom, <sup>10</sup>NIHR Musculoskeletal Biomedical Research Unit, University of Oxford, United Kingdom

## Objectives

Maternal 25-hydroxyvitamin D [25(OH)D] status in pregnancy has been associated with offspring bone mass and muscle strength, suggesting optimization of maternal 25(OH)D level might be beneficial to long-term health. However, the response to gestational vitamin D supplementation is highly variable. 25(OH)D status does differ by single nucleotide polymorphisms (SNP) in genes related to vitamin D metabolism in non-pregnant adults, but the relationship with the response to antenatal vitamin D supplementation has not previously been examined. We assessed whether SNPs in *DHCR7* (7-dehydrocholesterol reductase in the skin), *CYP2R1* (25-hydroxylase), *CYP24A1* (24-hydroxylase) and *GC* (Vitamin D binding protein) were associated with the response to gestational cholecalciferol supplementation.

## Methods

MAVIDOS is a randomised double-blind placebo-controlled trial of 1000 IU/day cholecalciferol from 14 weeks gestation until delivery in women with a baseline 25(OH)D of 25-100nmol/l. Anthropometry, serum 25(OH)D (Diasorin Liaison), health and diet were assessed at 14 and 34 weeks gestation. Genotyping of rs12785878 (*DHCR7*), rs10741657 (*CYP2R1*), rs6013897 (*CYP24A1*) and rs2282679 (*GC*) was undertaken using KASP<sup>TM</sup> competitive allele-specific PCR (LGC Genomics, Hoddeston, UK). Multiple linear regression was performed using an additive model with the homozygous minor allele as the reference group (beta represents the change in outcome per additional major allele), adjusting for a number of previously identified determinants of 25(OH)D.

## Results

712 women (367 placebo, 345 cholecalciferol) were included (95.8% White ethnicity). Only rs12785878 (*DHCR7*) was associated with baseline 25(OH)D [ $\beta$ =4.1nmol/l (95% CI 2.2, 6.1),  $p$ <0.001]. Conversely, rs10741657 (*CYP2R1*) [ $\beta$ =-4.1nmol/l (95%CI -7.1, -1.2),  $p$ =0.006] and rs2282679 (*GC*) [ $\beta$ =4.4nmol/l (95%CI 1.2, 7.6),  $p$ =0.007] were associated with achieved 25(OH)D after supplementation, but rs12785878 and rs6013897 were not.

## Conclusion

Genetic variation in *DHCR7*, which encodes 7-dehydrocholesterol reductase in the cholesterol/vitamin D biosynthesis pathway in the skin appears to modify baseline 25(OH)D, whereas the response to antenatal cholecalciferol supplementation was associated with SNPs in *CYP2R1* and *GC*, which may alter 25-hydroxylase activity and vitamin D binding protein synthesis. Women with more risk alleles may require higher supplement doses to achieve vitamin D repletion in pregnancy.

**Disclosures:** Rebecca Moon, None.

## SU0088

**Genotype-phenotype Correlation Analysis in 419 Subjects with Germline *CDC73* Gene Mutations.** Jianhua Zhang<sup>\*</sup>, Bin Guan, James Welch, William F. Simonds, Yulong Li, NIH, United States

## Background:

Hyperparathyroidism-Jaw Tumor (HPT-JT) syndrome, a rare familial form of primary hyperparathyroidism, is associated with germline mutations in the *CDC73* gene (formerly known as *HRPT2*). HPT-JT patients can manifest parathyroid carcinoma, benign parathyroid disease (adenoma or hyperplasia), or clinically normal parathyroid function. Genotype-phenotype correlation in patients with *CDC73* germline mutation is currently unknown.

## Methods:

In this retrospective study, 419 subjects with germline *CDC73* mutations were analyzed. Among these subjects, 68 were from an NIH patient cohort and 351 were from previously published case reports/series. Based on whether the *CDC73* mutations predict significant protein structural changes, the subjects were divided into Major mutation group (nonsense, frame-shift indels, gross deletions/insertions or splice site mutations) and Minor mutation group (missense, in-frame indels or non-coding region mutations). The subjects were also categorized into three groups based on the protein domain(s) of parafibromin predicted to be affected by the mutation: affecting the N-terminal domain only (NTD), affecting the C-terminal domain only (CTD), and

affecting both the N- and C-terminal domains (N+CTD). Kaplan-Meier time-to-event analysis was used to compare risk of parathyroid carcinoma or hyperparathyroidism between groups.

## Results:

Most of *CDC73* mutations (87%) were major mutations, and the remainder (13%) were minor mutations. Majority of mutations were mapped to the exonic regions of *CDC73* gene encoding the N-terminal domain, but the most common protein alteration is loss of both N- and C-terminal domains of parafibromin as a result of frame-shift mutations or nonsense mutations. 77 subjects (18.4%) were diagnosed with parathyroid carcinoma, 252 subjects (60.1%) with benign parathyroid adenoma/hyperplasia, and 90 subjects (21.5%) with no evidence of parathyroid disease. Kaplan-Meier analysis showed that the subjects in major mutation group had a much higher risk of parathyroid carcinoma compared to those in minor mutation group (HR=13,  $P$ =0.0008), while no significant difference in risk of hyperparathyroidism was found between two groups. In addition, the subjects with only the NTD affected had a much lower risk of parathyroid carcinoma compared to those with only the CTD affected (HR=15.2,  $P$ =0.0016) or with both N+CTD affected (HR=10.0,  $P$ =0.0045), while no difference in risk of hyperparathyroidism was found among three groups.

## Conclusion:

Our study demonstrates a correlation between the genotypes of germline *CDC73* mutations and the risk of parathyroid carcinoma. Mutations that affect only the NTD of parafibromin confer less risk of parathyroid carcinoma than those that affect the CTD only or both N+CTD. These findings have direct implications for the clinical management and genetic counseling of patients with germline *CDC73* mutation.

**Disclosures:** Jianhua Zhang, None.

## SU0089

**Identification of new candidate markers crucial for fracture healing in mice.**

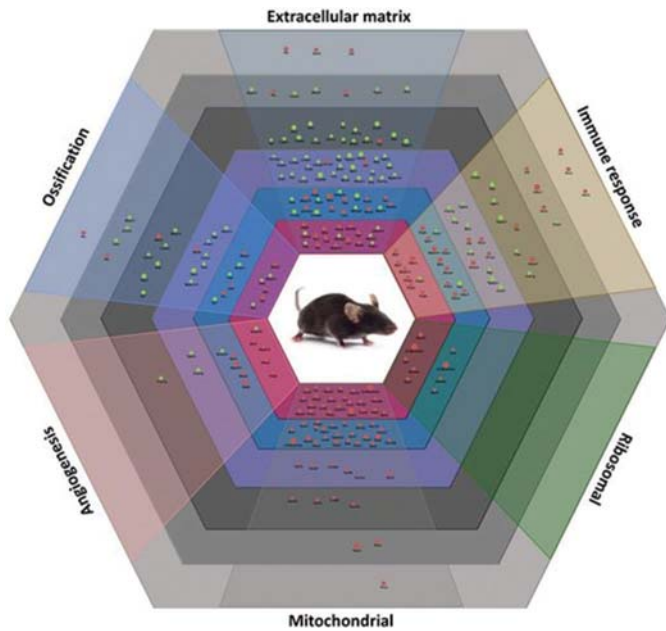
Deeksha Malhan<sup>\*1</sup>, Katharina Schmidt Bleek<sup>2</sup>, Georg N. Duda<sup>3</sup>, Christian Heiss<sup>1</sup>, Thaqif El Khassawna<sup>1</sup>. <sup>1</sup>Experimental Trauma Surgery, Faculty of Medicine, Justus Liebig University of Giessen, Germany, <sup>2</sup>Julius Wolff Institute and Center for Musculoskeletal Surgery, Charité - Universitätsmedizin, Germany, <sup>3</sup>Julius Wolff Institute and Center for Musculoskeletal Surgery, Charité - Universitätsmedizin Berlin, Germany, Germany

In clinical practice, non-unions or delayed healing cases are often treated using local or systemic therapeutic agents. The choice of therapeutics further relies on three main essential element of bone regeneration i.e. osteoinduction, osteoconduction, and osseointegration. However, the overlapping phases of fracture healing are not well understood. Furthermore, processes as angiogenesis, ossification, extracellular matrix, and immune response are variably regulated throughout bone formation. Therefore, we aim to identify novel candidate markers of bone healing to develop phase-directed treatment.

A closed standard mid diaphyseal fracture using intramedullary pin was created in eight week old male mice. Animals were sacrificed at (day = D) D3, D7, D10, D14, D21& D28 post fracture (N = 5 / time point) and D0 served as control. Whole genome transcriptome profiling was performed using Illumina  $\mu$ -array kit to unravel the complex molecular mechanism. Data normalization and qualitative analysis was performed using "R" language. Differentially expressed genes (DEGs) were obtained using fold-change (FC)  $\geq$  |2| and  $p$ -value  $\leq$  0.01. Gene ontology and pathway analysis was performed using NCBI-DAVID and KEGG, respectively. Histological analysis was performed to decipher the changes during bone healing.

Engineering a blueprint of differential regulation of normal healing is essential to define phase-specific markers. Such a blueprint will pinpoint genes deviating from the regular timeline. In this study, we curated a map for the overlapping biological processes between time points, which in turn represents the phases of bone healing. Interestingly, gene ontology showed the drastic downregulation among the mitochondrial and ribosomal genes during the early phase of healing. Genes like pyruvate dehydrogenase kinase 4 (Pdk4) and Ubiquitin B (Ubb) were significantly downregulated during the early phase of healing (Fig.1). Pdk4 encodes a mitochondrial protein and regulate glucose metabolism. The expression of Pdk4 is linked to the glucocorticoid and insulin sensitivity. Ubb performs a crucial role in the degradation of cellular components by proteasome. Furthermore, Ubiquitins are crucial for osteoclast mediated RANK-NF- $\kappa$ B signaling. Currently, we are investigating the role of mitochondrial and ribosomal genes during Wnt and MAPK pathway. Moreover, immunohistochemistry will be performed to mark the changes during bone healing. The current study can serve as a template for understanding the molecular mechanism underlying human genetic skeletal disorders.





An overview of DEGs from D3 (pink) until D28 (grey) involved in key biological processes

**Disclosures:** Deeksha Malhan, None.

## SU0090

**Osteocalcin signaling in peripheral organs inhibits the parasympathetic tone.** Julian Berger\*, Emilio Arteaga-Solis, Clio Meghir, Gerard Karsenty. Columbia University, United States

The regulation of bone formation by the sympathetic nervous system together with the regulation of catecholamine synthesis in the brain exerted by osteocalcin were the two reasons that led us to test whether osteocalcin also regulates the sympathetic tone in peripheral organs. Surprisingly however, we found that circulating catecholamine levels, urinary elimination of catecholamines and *Ucp1* expression in brown fat were indistinguishable between *Osteocalcin*<sup>-/-</sup> mice and control littermates thus ruling out that osteocalcin regulates the sympathetic tone in any significant manner in peripheral organs. In the course of this investigation we instead observed that the expression of three genes that encode enzymes needed for acetylcholine synthesis and recycling, *Choline acetyl transferase (Chat)*, *Choline transporter 1 (Cht1)* and *Vesicular acetylcholine transporter (Vcht1)*, was significantly increased in the retroperitoneal white adipose tissue, the heart, trachea, and lungs of *Osteocalcin*<sup>-/-</sup> mice. These results suggested the possibility that osteocalcin might be an endocrine inhibitor of the parasympathetic tone in peripheral organs. In support of this hypothesis we observed that cervical vagotomy that removes parasympathetic innervation to the lungs corrected the bronchoconstriction otherwise present in mice lacking osteocalcin or its peripheral receptor, *Gprc6a*. Moreover, circulating levels of gastrin a hormone whose secretion is regulated by the parasympathetic tone were significantly higher in *Osteocalcin*<sup>-/-</sup> and *Gprc6a*<sup>-/-</sup> mice than in their littermate controls. In view of these data and to establish that osteocalcin signaling in peripheral organs could affect the parasympathetic tone, we followed a two-step experimental strategy. First, we generated a *Gprc6a-Gfp* mouse model to establish a detailed map of the expression of this receptor. Analysis of these *Gprc6a-Gfp* mice revealed that *Gprc6a* is expressed in *Chat*-expressing parasympathetic neurons in the upper and lower airways, the cardiac ganglia, and ganglia of the retroperitoneal white. These results support the notion that osteocalcin signaling could inhibit the parasympathetic tone in these peripheral organs. Second, to define the importance of the osteocalcin regulation of acetylcholine synthesis and recycling in vivo we have generated mice lacking *Gprc6a* specifically in post-ganglionic parasympathetic neurons. Analysis of these mutant mice is ongoing and will be presented at the meeting.

**Disclosures:** Julian Berger, None.

## SU0091

**Pivotal role of Pit1/Slc20a1 and Pit2/Slc20a2 in phosphate-dependent MAPK/ERK1/2 signaling and FGF23 secretion in bone.** Nina Bon\*<sup>1</sup>, Annabelle Bourguin<sup>1</sup>, Greig Couasnav<sup>1</sup>, Sophie Source<sup>1</sup>, Jérôme Guicheux<sup>2</sup>, Sarah Beck-Cormier<sup>1</sup>, Laurent Beck<sup>1</sup>. <sup>1</sup>INSERM UMRS 1229 – Regenerative Medicine and Skeleton (RMeS), team Skeletal physiopathology and joint regenerative medicine (STEP), University of Nantes, School of Dental Surgery, France, <sup>2</sup>INSERM UMRS 1229 – Regenerative Medicine and Skeleton (RMeS), team Skeletal physiopathology and joint regenerative medicine (STEP), University of Nantes, School of Dental Surgery, CHU Nantes, Pôle Hospitalo-Universitaire 4 OTONN, France

In bone, the signaling function of phosphate (Pi) is illustrated among others by the Pi-dependent chondrocyte apoptosis, MAPK/ERK1/2 activation or FGF23 secretion. Contrary to the well-described PHO pathway in yeasts and bacteria in which Pi membrane transporters play a key role in Pi signaling, its mechanism in mammals is still unknown. Pit1 and Pit2 being the only high affinity Na-Pi cotransporters expressed in bone, we sought to investigate their role in ERK1/2 signaling and FGF23 regulation by a set of complementary *in vitro*, *in vivo* and *ex vivo* experiments.

First, we showed that the deletion of either Pit1 or Pit2 in osteoblasts (MC3T3) or chondrocytes (MC615) blunted the Pi-dependent ERK1/2 activation. This suggested that the presence of both PitTs was necessary for Pi signaling. Therefore, we addressed the possibility that Pit1 and Pit2 could hetero-oligomerize using a Bioluminescence Resonance Energy Transfer (BRET) approach. Our results demonstrated a basal interaction under normal (1mM) Pi concentration (dissociation constant 3.38±0.26). This interaction was enhanced when Pi concentration was increased to 3 and 10mM (2.90±0.15 and 2.14±0.20, respectively). In addition, we could rescue the lack of Pi-dependent ERK1/2 activation of Pit-depleted cells by overexpressing Pi-transport deficient mutants of PitTs, suggesting a dispensable role of their transport function in this process. Furthermore, we showed that Pi-dependent Pit1-Pit2 interaction was not affected in absence of sodium, a condition in which Pi transport is blunted. Altogether, our data strongly support that Pit1 and Pit2 are cooperating to mediate Pi signaling independently from Pi entry.

Regarding the Pi-dependent FGF23 regulation, we investigated the role of Pit2 using global knockout (KO) mice fed with a standard (0.55% Pi) or low-Pi diet (0.05% Pi) during one week. Although no difference in FGF23 serum level could be observed for the standard-Pi diet (4.34±0.39pM (control) vs 3.81±0.57pM (KO)), it was unexpectedly normal in Pit2 KO mice fed with low-Pi diet (1.44±0.15pM (control) vs 3.84±0.79pM (KO) p=0.001). We confirmed these results using *ex vivo* long bone diaphysis cultures. Our data demonstrate the requirement of Pit2 for bone autonomous Pi-dependent FGF23 secretion. Experiments regarding Pit1 are undergoing.

Taken together, these data illustrate the pivotal role of Pit1 and Pit2 in the Pi-sensing mechanism in mammals, which appears to be uncoupled from their Pi transport function.

**Disclosures:** Nina Bon, None.

## SU0092

**Synergistic Actions of VDR and CaSR in Mediating PTH Secretion and Mineral and Skeletal Homeostasis in Mice.** Amanda Herberger\*, Zhiqiang Cheng, Alfred Li, Jenna Hwong, Chia-Ling Tu, Daniel Bikle, Dolores Shoback, Wenhan Chang. University of California, San Francisco, United States

1,25hydroxyvitamin D (1,25D) and Ca<sup>2+</sup> are robust negative regulators of PTH secretion by acting on their respective receptors – VDR and CaSR – in parathyroid cells (PTCs), but whether these two receptors interact to modulate PTC functions remains unclear. Identification of VDR responsive element in the *CASR* gene promoter suggests that VDR may exert its action by altering the sensitivity of PTC to changes in [Ca<sup>2+</sup>]. To test this hypothesis and explore other synergistic actions of these two receptors, we compared serum PTH levels and mineral and skeletal phenotypes in mice with PTC-specific homozygous VDR knockout (VDR-KO), heterozygous CaSR KO (CaSR-Het), or combination (VDR-KO//CaSR-Het). We also studied their parathyroid glands (PTGs) to compare their maximal secretion rate (PTH-Max) and Ca<sup>2+</sup> set-points ([Ca<sup>2+</sup>] required to suppress 50% of PTH-Max) in culture. The VDR-KO produced moderate increases in serum Ca, PTH, and 1,25D levels and robust skeletal anabolism, as indicated by increased trabecular (Tb) bone fraction (BV/TV), number (Tb.N.), and/or thickness (Tb.Th.), as measured by micro-computed tomography (μCT), in distal femurs of both male and female mice (see Table). As we reported previously, heterozygous CaSR KO also produced moderate hypercalcemia and hyperparathyroidism (HPT) in both male and female mice, but only produced skeletal anabolism in male mice. Interestingly, VDR and CaSR double knockout synergistically increased serum PTH and 1,25D levels (≈2 fold over those in VDR-KO or CaSR-Het mice). These increases in PTH and 1,25D level were associated with reversion of the skeletal anabolism seen in the VDR-KO and CaSR-Het mice, suggesting a catabolic bone effect by PTH and/or 1,25D excess. In PTGs cultured from VDR-KO mice, we observed a significant increase in PTH-Max without altering Ca<sup>2+</sup> set-point, indicating little impact on Ca<sup>2+</sup>-sensing ability of the PTGs. In contrast, heterozygous CaSR KO significantly increased the Ca<sup>2+</sup> set-point (from 1.2 to 1.5 mM) in addition to an increase in PTH-Max. In the background of CaSR-Het KO, VDR KO further increased the Ca<sup>2+</sup> set-point (from 1.5 to 1.7 mM) and PTH-Max. Together our data suggest that VDR and CaSR interact synergistically to regulate PTH secretion, particularly in conditions with

CaSR-insufficiency in PTCs, and that only moderate increases in serum PTH levels produce skeletal anabolism.

	Serum			Bone			PTH Secretion	
	Ca (mg/dL)	PTH (pg/mL)	1,25-D (pM)	Tb. BV/TV (%)	Tb.N. (1/mm <sup>3</sup> )	Tb.Th. (μm)	PTH Max (pg/mL)	Ca set-point (mM)
<b>FEMALE</b>								
Control	9.7 ± 0.1	109 ± 10	236 ± 23	6.5 ± 0.2	2.3 ± 0.1	28 ± 0.3	452 ± 78	1.2
VDR-KO	10 ± 0.2	161 ± 10*	327 ± 45	9.5 ± 1*	2.6 ± 0.3	31 ± 1*	640 ± 60	1.2
CaSR-Het	10.8 ± 0.1*	177 ± 20*	244 ± 22	6.5 ± 0.5	2.3 ± 0.1	25 ± 1*	530 ± 86	1.5
VDR-KO/CaSR-Het	10.6 ± 0.2*	390 ± 79**	485 ± 56**	6.7 ± 0.4	2.3 ± 0.1	27 ± 1**	765 ± 54	1.7
<b>MALE</b>								
Control	9.8 ± 0.1	116 ± 8	234 ± 30	9.7 ± 0.4	3.6 ± 0.1	32 ± 1		
VDR-KO	10.2 ± 0.2*	179 ± 20*	291 ± 22	16.2 ± 1.2*	4.8 ± 0.5*	34 ± 3		
CaSR-Het	10.9 ± 0.2*	188 ± 19*	206 ± 21	12.2 ± 0.8*	4.9 ± 0.2*	38 ± 1*		
VDR-KO/CaSR-Het	10.8 ± 0.1*	248 ± 33*	471 ± 71**	11.8 ± 0.9*	3.6 ± 0.2*	30 ± 1**		

\* p < 0.05 vs. Control  
\*\* p < 0.05 vs. CaSR-Het

Table

Disclosures: Amanda Herberger, None.

## SU0093

**Chromatin Landscape and GCM2 Targets in the Parathyroids.** Youngsook Jung<sup>\*1</sup>, Wenping Zhao<sup>2</sup>, Ian Li<sup>3</sup>, Amira Barkal<sup>4</sup>, Richard Sherwood<sup>5</sup>, Cassianne Cohen<sup>6</sup>, Bryan Kestenbaum<sup>6</sup>, Sareh Parangi<sup>7</sup>, Brad E. Bernstein<sup>8</sup>, Charles B. Epstein<sup>9</sup>, Peter Park<sup>10</sup>, Michael Mannstadt<sup>3</sup>.

<sup>1</sup>Department of Biomedical Informatics, Harvard Medical School, United States, <sup>2</sup>Endocrine Unit, Massachusetts General Hospital, United States, <sup>3</sup>Endocrine Unit, Massachusetts General Hospital and Harvard Medical School, United States, <sup>4</sup>Brigham and Women's Hospital, Department of Medicine, Division of Genetics, United States, <sup>5</sup>Division of Genetics, Department of Medicine, Brigham and Women's Hospital and Harvard Medical School, United States, <sup>6</sup>Kidney Research Institute, Division of Nephrology, University of Washington, United States, <sup>7</sup>General and Endocrine Surgery, Massachusetts General Hospital and Harvard Medical School, United States, <sup>8</sup>Department of Pathology and Center for Cancer Research, Massachusetts General Hospital and Harvard Medical School, United States, <sup>9</sup>Epigenomics Program, Broad Institute, United States, <sup>10</sup>Department of Biomedical Informatics, Harvard University, United States

Parathyroid cells produce PTH, which is essential for maintaining normal calcium homeostasis and bone health. This highly specialized function is achieved by epigenetic mechanisms that regulate transcription.

Using human parathyroid tissue, we mapped global chromatin accessibility by DNase-seq profiling, predicted transcription factor (TF) binding sites by footprint analysis, and profiled genome-wide active and repressive histone marks by ChIP-seq. Using ChIP-seq, we also examined binding sites of GCM2, the parathyroid-specific TF that has emerged as the master regulator of parathyroid gland development with persistent expression in the adult parathyroids. We validated a subset of these enhancers through luciferase assays and linked SNPs, identified in a GWAS study of PTH levels in the population, to these functional elements.

We identified 17,819 active promoter and 93,373 enhancer regions of which 1,369 and 10,742, respectively, were parathyroid-specific. Also, we discovered 634 super-enhancers, some of which were located in genes with known important roles in the parathyroids such as CASR, MAFB, GATA3, GCM2, and PTH. We identified 4,158 GCM2 binding sites, primarily in active promoters and enhancers. The target genes of GCM2 were often predicted to be also bound by GATA3, MAFB, VDR, and BCL6 TF's. Functional validation of 13 parathyroid-specific enhancers in cell culture yielded a 2- to 40-fold increase in luciferase activity compared to vector alone for all tested enhancers. One parathyroid-specific enhancer element, which was also a target of GCM2, was located in the first intron of the calcium-sensing receptor and showed a 20-fold increase in luciferase activity. Strikingly, this enhancer overlapped with a GWAS variant recently identified in a genome-wide association study of blood PTH levels (Robinson-Cohen, JASN December 2016) and showed significant allelic imbalance of 3:1 from the GCM2 ChIP-seq reads.

These datasets provide powerful tools to analyze functional elements in the parathyroids, and link GWAS hits to functional elements and target genes. More broadly, knowledge of the chromatin landscape of parathyroids provides insights into the pathogenesis of common disease states of the parathyroid glands.

Disclosures: Youngsook Jung, None.

## SU0094

**The Calcium Binding Protein S100A8 is a Likely Gene Target of the Direct Anti-Resorptive Effects of ER $\alpha$  Signaling on Cancellous Bone.** Ha-Neui Kim<sup>\*1</sup>, Srividhya Iyer<sup>1</sup>, Li Han<sup>1</sup>, Haibo Zhao<sup>1</sup>, Charles O'Brien<sup>1</sup>, Robert Jilka<sup>1</sup>, Maria Almeida<sup>1</sup>, Stavros Manolagas<sup>1</sup>, Philippe Tesser<sup>2</sup>. <sup>1</sup>University of Arkansas for Medical Sciences, United States, <sup>2</sup>Centre de Recherche en Infectiologie, Canada

Characterization of the skeletal phenotype of mice with conditional deletion of the estrogen receptor (ER) $\alpha$  has revealed that the anti-resorptive effects of estrogens on cancellous bone result from ER $\alpha$  signaling on myeloid lineage cells (targeted by LysM-Cre). To elucidate ER $\alpha$  gene targets responsible for these effects, we isolated ER $\alpha$  deleted cells from our conditional mouse model and performed microarray analysis. The expression of Fas ligand, a purported target gene of estrogens in osteoclasts, was not altered in ER $\alpha$  deleted macrophages or mature osteoclasts; and in contrast to published findings by others, FasL<sup>gld/gld</sup> mice which lack functional FasL lost cortical and cancellous bone following OVX indistinguishably from FasL-intact controls. The highest up-regulated mRNAs in macrophages from ER $\alpha$ <sup>fl/fl</sup>;LysM-Cre mice, as compared to ER $\alpha$ <sup>fl/fl</sup> controls, encoded the abundant calcium binding proteins S100A8 and S100A9, which are produced primarily by neutrophils and monocytes and function intracellularly or in an autocrine or paracrine fashion via the Toll-like receptor 4 (TLR4). In agreement with the microarray data, 17 $\beta$ -estradiol (E2) decreased the S100A8 and S100A9 mRNAs in BM macrophages from wild-type mice. Macrophage proliferation and osteoclast generation were increased in BM macrophage cultures from wild-type C57Bl6 mice transduced with retroviral vectors expressing the murine S100A8, but not S100A9. Conversely, silencing S100A8, but not S100A9, decreased macrophage proliferation and increased their apoptosis and greatly attenuated osteoclast generation. S100A8 silencing also decreased RANKL-induced NF $\kappa$ B, but had no effect on NF- $\kappa$ B, c-Fos, or phosphorylated ERK, suggesting that consistent with its calcium-binding properties S100A8 attenuates osteoclastogenesis by regulating intracellular calcium. TLR4 silencing had no effect on any of these signaling cascades. Collectively, these results suggest that S100A8 is a target of the anti-resorptive effects of ER $\alpha$  signaling on cancellous bone. Furthermore, these findings support the notion that searching for ER $\alpha$  gene targets in ER $\alpha$ -deficient cells isolated from mice with cell-targeted deletions represents an advantageous and fruitful approach that establishes *a priori* that: a) these genes are expressed in cell targets that have been functionally validated in vivo and b) are contextually relevant to bone mass regulation in the whole animal.

Disclosures: Ha-Neui Kim, None.

## SU0095

**Circulating microRNA-203a is a novel biomarker for bone loss and response to anabolic therapy with PTH.** Roland Kocijan<sup>\*1</sup>, Elisabeth Geiger<sup>2</sup>, Susanna Skalicky<sup>2</sup>, Moritz Weigl<sup>2</sup>, Gabriele Leinfellner<sup>3</sup>, James Ferguson<sup>3</sup>, Patrick Heimel<sup>3</sup>, Heinz Redl<sup>3</sup>, Johannes Grillari<sup>4</sup>, Matthias Hackl<sup>2</sup>. <sup>1</sup>St. Vincent Hospital – Medical Department II, The VINFORCE Study Group, Academic Teaching Hospital of Medical University of Vienna, Austria, Austria, <sup>2</sup>TAmiRNA GmbH, Austria, <sup>3</sup>Ludwig Boltzmann Institute for Experimental and Clinical Traumatology, Austria, <sup>4</sup>Department of Biotechnology, BOKU - University of Natural Resources and Life Sciences, Vienna, Austria

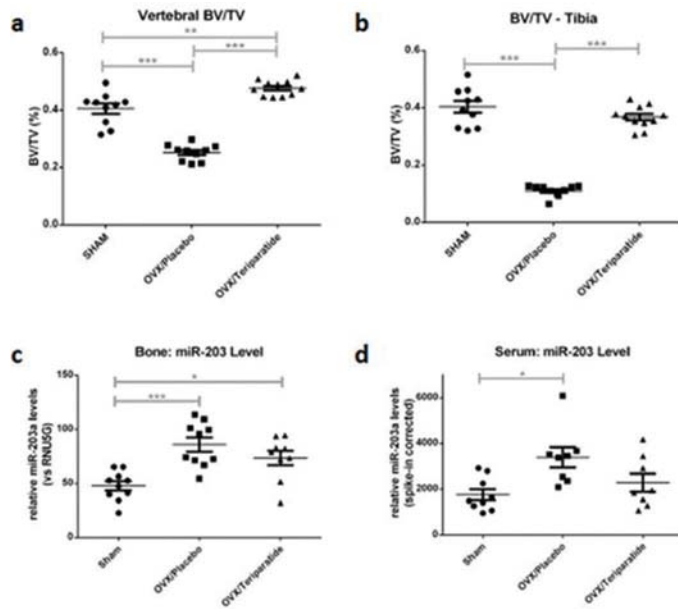
**Objective:** Circulating microRNAs (miRNAs) in serum have been proposed as novel biomarkers for osteoporosis. However, (i) changes in miRNA levels due to bone loss and bone modeling have not been investigated and, (ii) the association between miRNA levels in bone and serum remains unclear. The objective of this study was to analyze miRNA expression in bone tissue and serum in a pre-clinical model of postmenopausal osteoporosis.

**Methods:** Six-month old Wistar rats were randomized to ovariectomy (OVX, n=21) or sham-operation (n=10). After additional 8 weeks, OVX rats were randomized to placebo (n=10) or osteoanabolic treatment using recombinant PTH (teriparatide, n=11). Treatments were maintained for 12 weeks, and blood and microCT (tibia) analyses were performed in regular intervals. At week 20, bone tissue and serum were harvested and miRNA expression analysis and nanoCT at the tibia and the vertebrae were performed.

**Results:** Ovariectomy resulted in a significant decline of volumetric bone mineral density (vBMD, mgHA/cm<sup>3</sup>) at week 8 as well as deterioration of trabecular microstructure measured by nanoCT at week 20 (p < 0.0001). Treatment with teriparatide resulted in a significant improvement of BV/TV, Th.Th, and Tb.Sp at both tibia and vertebrae at week 20 (p < 0.0001). Accordingly, we observed major changes in microRNA expression in bone: ovariectomy resulted in a predominant up-regulation of miRNAs, while anabolic treatment showed the opposite effect. Using qPCR, significant up-regulation of miR-203a due to ovariectomy and down-regulation due to teriparatide-treatment was observed. Likewise, serum levels of miR-203a were found to increase following ovariectomy and reach baseline levels after 12 weeks of anabolic treatment.

**Summary and conclusion:** These results demonstrate that (i) microRNA expression in bone is significantly changed following ovariectomy and partially rescued due to anabolic treatment, and (ii) that miR-203a levels in bone and serum could be used to monitor bone loss and response to anabolic treatment.





miR-203a is regulated in bone and serum in response to ovariectomy and PTH treatment

**Disclosures:** Roland Kocijan, None.

## SU0096

**Mice lacking the DNA segment between -511 and -1423 bp, relative to the transcription start-site, of the endogenous murine *Tnfrsf11* (RANKL) gene display normal RANKL mRNA levels and bone mass.** Ryan Macleod<sup>1</sup>, Mark Meyer<sup>2</sup>, Jinhu Xiong<sup>1</sup>, Keisha Cawley<sup>1</sup>, Yu Liu<sup>1</sup>, Priscilla Baltz<sup>1</sup>, Melda Onal<sup>2</sup>, Nancy Benkusky<sup>2</sup>, Wes Pike<sup>2</sup>, Charles OBrien<sup>1</sup>. <sup>1</sup>University of Arkansas for Medical Sciences, United States, <sup>2</sup>University of Wisconsin-Madison, United States

Production of RANKL, encoded by the *Tnfrsf11* gene, is regulated by a variety of factors and hormones that control bone resorption. Transcriptional control of the murine *Tnfrsf11* gene has been studied by numerous laboratories. While some studies have identified important regulatory elements in the proximal promoter of this gene, others have identified elements that are located between 23 and 123 kilobases (kb) upstream from the transcription start site. The functional significance of several of these more distal elements has been demonstrated by deleting them from the mouse genome and observing significant changes in RANKL production and bone mass. The goal of the current study was to determine the functional significance of the DNA segment between -511 and -1423 basepairs (bp), relative to the transcription start site, by deleting this proximal promoter region from the endogenous mouse gene. This region has been reported by others to mediate responsiveness to 1,25-dihydroxyvitamin D3 (1,25D3), parathyroid hormone related protein (PTHrP), and the sympathetic nervous system. We used the CRISPR/Cas9 system to create mice lacking the DNA segment between -511 to -1423 bp and confirmed deletion by amplifying and sequencing the deletion junction. Male and female mice lacking this region (KO) were compared to wild type (WT) mice using serial measurement of bone mineral density (BMD) at 2, 4, and 6 months of age. Mice were euthanized at 6 months of age for flow cytometry counts of bone marrow hematopoietic cells and gene expression analyses of ex vivo primary bone marrow cultures. At all ages, there were no differences in BMD between WT and KO mice in the femur, spine, or total body. Flow cytometry revealed no differences between WT and KO mice cell counts of monocytes, T cells, B cells, or erythroid progenitors. Importantly, 1,25D3 stimulated RANKL mRNA to a similar extent in WT and KO bone marrow cultures. Since PTHrP and the sympathetic nervous system have both been shown to stimulate *Tnfrsf11* transcription via protein kinase A (PKA), we treated cultures with di-butyl cAMP to activate this enzyme, but observed similar stimulation of transcription in cultures from both genotypes. These results demonstrate that the region of the *Tnfrsf11* proximal promoter from -511 to -1423 bp is not required for physiological levels of *Tnfrsf11* production or for the responsiveness of this gene to 1,25D3 or factors that stimulate RANKL via PKA.

**Disclosures:** Ryan Macleod, None.

## SU0097

**Galectin-3 null mice are protected against cortical bone loss following gonadectomy.** Kevin Maupin<sup>1</sup>, Daniel Dick<sup>2</sup>, Bart Williams<sup>2</sup>. <sup>1</sup>Indiana University School of Medicine, United States, <sup>2</sup>Van Andel Research Institute, United States

Loss of bone mass occurs following the loss of sex hormone production due to menopause or castration. Thus, there is a need to identify novel targets to improve bone mass that are independent of sex hormone status. Galectin-3 (Gal3) is a chaperone protein which functions both intracellularly via protein-protein interactions and extracellularly by binding specific glycans on glycoproteins. Gal3-null mice have no major negative health phenotypes and are protected against fibrosis. Previously we observed that female Gal3-null mice had increased cortical bone mass during aging. Because the phenotype was only weakly observed in males, we hypothesized that sex hormones influence the bone phenotype of Gal3-null mice. To test this, we performed gonadectomy (GDX)  $\pm$  sex hormone rescue on male and female Gal3-null mice and compared them to their wild-type littermates.

Following GDX, both male and female Gal3-null mice had significantly greater cortical bone mass and improved geometry (MMI) following GDX compared to wild types, as measured by  $\mu$ CT. Sex hormone rescue revealed that cortical bone from Gal3-null mice was unresponsive to androgen and hyper-responsive to estrogen, which likely explains the sexual dimorphism we previously observed in sex hormone replete animals. However, while estrogen was able to suppress axial expansion in wild-type mice, estrogen only enhanced endocortical infilling in Gal3-null mice, suggesting that estrogen function on periosteal bone formation is altered in Gal3-null mice.

Previously we observed that during aging, the cortical expansion in Gal3-null femurs was coupled to reduced mechanical properties as assessed by 4-point bending. Following GDX, reduced mechanical properties were again observed in male Gal3-null femurs. Interestingly, the empty pellets used as controls for sex hormone rescue did not affect bone geometry compared to GDX alone, but the pellets did rescue mechanical strength in femurs from Gal3-null males. Taken together, these results suggest that the cortical expansion in Gal3-null mice is independent of tissue quality and that the reduced mechanical strength in Gal3-null bones can be rescued. This study identifies Gal3 to have both sex hormone dependent and independent roles in regulating cortical bone mass and quality. While further experimentation is necessary, our data provide further support for the development of Gal3 targeted therapies to improve bone mass during aging and in sex hormone deficient conditions.

**Disclosures:** Kevin Maupin, None.

## SU0098

**Genetic Background Influences Cardiac Phenotype in Murine Chronic Kidney Disease.** Samantha Neuburg<sup>1</sup>, Xueyan Wang<sup>1</sup>, Connor Francis<sup>1</sup>, Corey Dussold<sup>1</sup>, Lixin Qi<sup>1</sup>, Valentin David<sup>1</sup>, Myles Wolf<sup>2</sup>, Aline Martin<sup>1</sup>. <sup>1</sup>Division of Nephrology and Hypertension, Center for Translational Metabolism and Health, Northwestern University, Chicago, IL, USA, United States, <sup>2</sup>Division of Nephrology and Hypertension, Duke University, Durham, NC, USA, United States

An increased level of FGF23 is the earliest detectable sign of disordered mineral metabolism in chronic kidney disease (CKD), and a powerful risk factor for left ventricular hypertrophy (LVH), heart failure and death. Experimental models of CKD with elevated FGF23 and LVH are needed. We hypothesized that slower rates of CKD progression in the Col4a3<sup>KO</sup> mouse model of CKD would increase exposure to elevated FGF23 and promote development of LVH.

We studied congenic Col4a3<sup>KO</sup> and WT mice with either 75% 129X1/SvJ (129Sv) or 94% C57Bl6/J (B6) genomes. We compared Col4a3<sup>KO</sup> with advanced CKD: at 10 weeks in the 129Sv, 20 weeks in the B6 mice.

B6-Col4a3<sup>KO</sup> lived longer than 129Sv-Col4a3<sup>KO</sup> (22 $\pm$ 1 vs. 11 $\pm$ 1 weeks; p<0.05). Ten week-old 129Sv-Col4a3<sup>KO</sup> showed impaired renal function (BUN: 191 $\pm$ 39 vs. 34 $\pm$ 4 mg/dL), hyperphosphatemia (serum Pi: 14.1 $\pm$ 1.4 vs. 6.8 $\pm$ 0.3 mg/dL) and a 33-fold increase in serum FGF23 (p<0.05 vs. WT for each). At 20 weeks, B6-Col4a3<sup>KO</sup> showed a similar but milder phenotype with impaired renal function (BUN: 85 $\pm$ 17 vs. 24 $\pm$ 3 mg/dL), hyperphosphatemia (Pi: 8.9 $\pm$ 0.8 vs. 6.2 $\pm$ 0.4 mg/dL) and an 8-fold increase in FGF23 levels (p<0.05 vs. WT for each), consistent with slower rates of CKD progression. 20-week-old B6-Col4a3<sup>KO</sup> were the only ones that presented LVH (LV Mass: 125 $\pm$ 3 vs. 98 $\pm$ 6 mg; p<0.05 vs. WT) with  $\sim$ 2 to 4 fold increased mRNA expression of FGF receptor 4 (FGFR4) and markers of cardiac hypertrophy (ANP, BNP,  $\beta$ -MHC; p<0.05 vs. WT for each).

Slower CKD progression and longer survival are associated with development of LVH in B6-Col4a3<sup>KO</sup>, which can serve as a novel model of cardiorenal disease. Whether longer exposure to elevated FGF23 contributes to LVH in B6-Col4a3<sup>KO</sup> mice requires further study.

**Disclosures:** Samantha Neuburg, None.

## SU0099

**Functional Characterization of Small Molecule Antagonists/Inverse Agonists (JB-4250 and JB-4365) for the Parathyroid Hormone Receptor-1.** Hiroshi Noda\*<sup>1</sup>, Thomas J Gardella<sup>2</sup>. <sup>1</sup>Endocrine Unit, Massachusetts General Hospital, United States, <sup>2</sup>Endocrine Unit, Massachusetts General Hospital and Harvard Medical School, United States

Small molecule mimetics for the parathyroid hormone receptor-1 (PTHr1) hold interest both as potential therapeutics and as pharmacologic probes of receptor mechanisms, but few such ligands have been reported. The large size of the receptor surface area available for ligand contact likely challenges PTHr1 drug discovery efforts. PTH(1-34) thus interacts with the PTHr1 via a mechanism that involves docking interactions to the N-terminal extracellular domain (ECD) of the receptor as well as signaling interactions to the receptor's heptahelical transmembrane domain (TMD) region. Identifying sites in the PTHr1 used by any currently available mimetic ligand could facilitate future PTHr1 drug discover/design efforts. Several small-molecule antagonist compounds for the PTHr1 have been reported by the James Black Foundation (McDonald 2007 J Med Chem.), but their mechanisms of interaction have not been elucidated. We investigated these mechanisms for two of these small-molecules: JB-4250 and JB-4365. In membranes prepared from COS-7 cells expressing the PTHr1R, each compound dose-dependently displaced the binding of 125I-M-PTH(1-15) and 125I-PTH(1-34), but was more effective against the former versus the latter radioligand. In SaOS-2 cells endogenously expressing the human PTHr1, each compound dose-dependently antagonized the cAMP signaling responses induced by M-PTH(1-11) and PTH(1-34), and was more effective against M-PTH(1-11) than PTH(1-34). In transfected HEK-293 cells, each compound fully antagonized the cAMP signaling actions induced by M-PTH(1-11) on PTHr1-deINT, which lacks the ECD, and they also fully suppressed the high basal signaling activity mediated by PTHr1-Tether(1-9), in which residues 1-9 of PTH are tethered to the extracellular end of TMD helix-1. The compounds also dose-dependently reduced the basal cAMP signaling activities of two constitutively active mutant receptors, PTHr1-H223R and PTHr1-T410P. Thus, we have functionally localized the binding site for two small molecule antagonist compounds to the TMD region of the PTHr1, and more specifically to a portion of the TMD that mediates activation interactions with the PTH(1-9) agonist pharmacophore. We have also identified these compounds as the first small molecules that acts as inverse agonist ligands for constitutively active mutant PTHr1s that cause Jansen's chondrodysplasia. The TMD region of the PTHr1 thus contains a hot-spot that can be targeted for small-molecule binding.

**Disclosures:** Hiroshi Noda, Chugai Pharmaceutical Co., Ltd., Other Financial or Material Support.

## SU0100

**PTHrP(1-36) and Abaloparatide: Differential Regulators of Osteoblast Genes Compared with PTH(1-34).** Florante Ricarte\*, Carole Le Henaff, Alon Aminov, Ching-Yun Hsu, Nicola Partridge. New York University, United States

PTH (2-34), or teriparatide, remains the only FDA-approved osteoanabolic therapy for the treatment of osteoporosis. However, prolonged use of teriparatide causes levels of bone resorption markers to rise to that of formation, thus limiting its efficacy. This "anabolic window" justifies the search for therapies that maximize anabolism, without incurring the resorptive effects of teriparatide. Miller et al. (JAMA, 2026;316:722) describe the phase III trial results of abaloparatide (ABL), a novel analog of parathyroid hormone-related protein (PTHrP 1-34), where similar anabolic effects are observed, but a lesser stimulation of resorption is induced with ABL compared with teriparatide or placebo. The present study aims to elucidate the mechanisms that underlie the actions of PTHrP (1-36) and ABL in the osteoblast. Our work has shown that in primary murine calvarial osteoblasts, PTHrP (1-36) and ABL result in a significantly reduced cyclic AMP (cAMP) response compared with PTH (1-34). Subsequently, peak activation of protein kinase A (PKA) was achieved at 1-2.5min and dose response analyses reveal 1/2 max values of 1nM, 13nM, and 30nM for PTH (1-34), PTHrP (1-36), and ABL, respectively. These events resulted in the differential sub-cellular localization of the transcriptional repressor, histone deacetylase 4 (HDAC4), where PTH (1-34) led to its nuclear export, while PTHrP (1-36) and ABL did not. Inhibition of PKA by H-89 prevented the PTH (1-34)-induced exit of HDAC4, but did not affect the PTHrP (1-36)- or ABL-induced retention. Quantitative real-time PCR revealed differential expression of key osteoblastic genes, receptor activator of nuclear factor kappa-B ligand (RANKL) and transcription factor, c-fos, with PTH (1-34) treatment resulting in 3-fold greater RANKL expression and 2-fold greater c-fos expression compared with PTHrP (1-36) and ABL (n=9, p<0.05). Expression of other osteoblastic genes such as Sost, Runx2, and Mmp13 were similarly regulated by all three peptides. Based on the conditions where differential expression of RANKL was observed, cells were treated with 1nM PTH (1-34), PTHrP (1-36), or ABL for 4h and subjected to RNA-Sequencing (>1.5fold, FDR<0.05). Here, we report that PTH (1-34) regulates 1,607 genes, of which 1,019 are uniquely regulated. PTHrP (1-36) regulates 609 genes, of which 67 are unique. Lastly, ABL regulates 293 genes, of which 10 are unique. Ingenuity Pathway Analysis shows that the 238 genes commonly regulated by all three treatment groups are implicated in the cAMP/PKA signaling axis, but the 10 genes uniquely regulated by ABL are not. Taken together, these data suggest that PTHrP (1-36) and ABL are less effective in utilizing the cAMP/PKA axis and may employ signaling bias to achieve their downstream effects. This provides a possible explanation for the decreased resorptive effect of ABL compared with PTH (1-34) in the treatment of osteoporosis.

**Disclosures:** Florante Ricarte, None.

## SU0101

**Half-life of 25(OH) Vitamin D<sub>3</sub> is Not Influenced by Vitamin D Supplementation Dose.** Inez Schoenmakers\*<sup>1</sup>, Shima Assar<sup>2</sup>, Terence Aspray<sup>3</sup>, Ann Prentice<sup>2</sup>, Kerry Jones<sup>2</sup>. <sup>1</sup>MRC Human Nutrition Research, Cambridge, UK and Medical School, University of East Anglia, UK, United Kingdom, <sup>2</sup>MRC Human Nutrition Research, Cambridge, UK, United Kingdom, <sup>3</sup>Newcastle University, Institute for Cellular Medicine, Newcastle upon Tyne, UK, United Kingdom

There is wide variation in the dose-response to oral vitamin D and the increment in plasma 25(OH) Vitamin D (25(OH)D) decreases per unit vitamin D given. We hypothesised that this is related to increased 25(OH)D catabolism into predominantly 24,25 (OH)<sub>2</sub>D and is reflected in a shorter 25(OH)D half-life (25(OH)D<sub>3</sub> t<sub>1/2</sub>).

Design: 25(OH)D<sub>3</sub> t<sub>1/2</sub> was measured with a stable isotope (SI) technique in older (70y+) men and women in the UK during winter before (n=47; 0kIU) or after 9-10 months of supplementation (n=20, 24, 22 for 12k, 24k or 48k IU vitamin D<sub>3</sub>/month, respectively). Plasma concentrations of 25(OH)D<sub>2</sub>, 25(OH)D<sub>3</sub> (expressed as total 25 (OH)D), 24,25(OH)<sub>2</sub>D<sub>3</sub> and the SI labelled-25(OH)D<sub>3</sub> were measured by LC-MS-MS and 1,25(OH)<sub>2</sub>D by RIA.

Results: Plasma 25(OH)D<sub>3</sub> t<sub>1/2</sub> did not significantly differ before and after supplementation (P=0.35) and between groups with no apparent dose-response (ANOVA for group difference P=0.05); mean (SEM) 25(OH)D<sub>3</sub> t<sub>1/2</sub> was 20.3 (0.5), 22.6 (1.1), 20.6 (0.7) and 19.8 (0.6) days for 0, 12, 24 and 48kIU, respectively. Vitamin D supplementation was associated with a significantly higher plasma 25(OH)D [49 (4), 73 (5), 77 (3) and 97 (5) nmol/L; P<0.0001] and 24,25(OH)<sub>2</sub>D [3.1 (0.3), 7.1 (0.6), 7.1 (0.4) and 9.0 (0.6) nmol/L; P<0.0001] for 0, 12, 24 and 48kIU, respectively. Plasma 1,25(OH)<sub>2</sub>D concentrations were (geometric mean (95%CI)): 123 (69-220), 125 (68-234), 145 (88-241) and 143 (98-210) pmol/L (P=0.04). After supplementation, there was a significant increase in the ratio between the peak intensities of both 25(OH)D<sub>3</sub> and 24,25(OH)<sub>2</sub>D with two, as yet, unidentified peaks that shared the same mass transitions as 25(OH)D and 24,25(OH)<sub>2</sub>D, respectively.

Conclusions: Plasma 25(OH)D<sub>3</sub> t<sub>1/2</sub> was not influenced by vitamin D supplementation, despite higher plasma 24,25(OH)<sub>2</sub>D concentrations and thus 25(OH)D catabolism was proportional to its plasma concentration. This suggests that mechanisms other than 25- and 24-hydroxylation may be involved in the increased clearance of vitamin D at a high oral supply and in contrast to previous assumptions, 25(OH)D<sub>3</sub> t<sub>1/2</sub> may be closely regulated.

Funded by the UK Department of Health (PRP 024/0051) and UK MRC (programme U105960371).

**Disclosures:** Inez Schoenmakers, None.

## SU0102

**Inducible Androgen Receptor Inactivation Reveals an Essential Role of the Androgen Receptor for both Trabecular and Cortical Bone in Adult Male Mice.** Jianyao Wu\*, Petra Henning, Klara Sjögren, Sofia Movérare-Skrtic, Claes Ohlsson. Centre for Bone and Arthritis Research, Institute of Medicine, Sahlgrenska Academy, University of Gothenburg, Gothenburg, Sweden, Sweden

Previous studies evaluating the role of the androgen receptor (AR) for the skeleton and other androgen-responsive tissues have used mouse models with global or tissue specific lifelong inactivation of the AR. However, these mouse models have the AR inactivated already early in life and developmental effects may have confounded the described adult phenotype. To determine the role of the AR in adult mice, avoiding confounding developmental effects, we established a tamoxifen-inducible AR inactivated mouse model.

The AR (located on the X-chromosome) was conditionally ablated in adult male mice through tamoxifen-inducible Cre-mediated recombination using *CAG-CreER*; *AR<sup>fllox</sup>* mice. At 10 weeks of age, tamoxifen was administered i.p. for 4 consecutive days (50mg/kg/day). *AR<sup>fllox</sup>* mice did not have a bone phenotype and, therefore, tamoxifen-treated *CAG-CreER*; *AR<sup>fllox</sup>* mice (TAM-ARKO) were compared with tamoxifen-treated *CAG-CreER* mice (TAM-Cre) at 14 weeks of age.

TAM-ARKO mice had substantially lower AR mRNA levels in the bone compared with TAM-Cre mice (-76±3%, p<0.01). Efficient adult inactivation of the AR in the TAM-ARKO mice were supported by the weights of two androgen responsive tissues, seminal vesicles (-86.5±1.9%, p<0.001) and muscle levator ani (-60.6±3.7%, p<0.001) were substantially reduced compared with TAM-Cre mice. Serum testosterone levels were not affected in the TAM-ARKO mice, demonstrating that they had a normal feed-back regulation of serum sex steroids.

TAM-ARKO mice displayed lower total body bone mineral density compared with TAM-Cre mice (-3.1±1.0%, p<0.05).  $\mu$ CT analyses of the tibia revealed reduced diaphyseal cortical bone thickness (-7.2±2.0%, p<0.01) and metaphyseal trabecular bone volume fraction (BV/TV; -23.7±8.0%, p<0.05) in TAM-ARKO mice compared with TAM-Cre mice.

In conclusion, inducible adult AR inactivation reveals an essential role of the AR for maintenance of both the trabecular and cortical bone in adult male mice.

**Disclosures:** Jianyao Wu, None.



## SU0103

**The age-related changes of plasma 1,25-dihydroxyvitamin D levels and dietary phosphate responsiveness is associated with renal  $\alpha$ -Klotho gene expression, but not plasma PTH levels.** Hironori Yamamoto<sup>\*1</sup>, Ryouhei Yoshikawa<sup>2</sup>, Otoko Nakahashi<sup>2</sup>, Tomohiro Kagawa<sup>2</sup>, Mari Tajiri<sup>2</sup>, Shiori Fukuda<sup>2</sup>, Masashi Masuda<sup>2</sup>, Masayuki Iwano<sup>3</sup>, Eiji Takeda<sup>2</sup>, Yutaka Taketani<sup>2</sup>. <sup>1</sup>University of Jin-ai, Japan, <sup>2</sup>University of Tokushima, Japan, <sup>3</sup>University of Fukui, Japan

The FGF23/Klotho system down-regulates 1,25(OH)<sub>2</sub>D and Pi levels by suppressing expression of Cyp27b1, Npt2a and Npt2c, while promoting Cyp24a1 expression in the kidney. And, the  $\alpha$ -Klotho gene was also identified as an "anti-aging" gene when its disruption in mice was found to induce a phenotype that mimicked age-related symptoms, including atrophy of skin and muscles, osteoporosis, ectopic calcification. It has been reported that aging is associated with modification of several organ functions and homeostatic adaptation, including vitamin D and Pi metabolism. However, whether changes in  $\alpha$ -Klotho gene expression with age affect vitamin D metabolism is unclear. In this study, we investigated the relationship between various age-related changes, including renal  $\alpha$ -Klotho gene expression and vitamin D metabolism, and the responsiveness of dietary Pi using 1, 2 and 13 month-old mice fed a high Pi (HP) or low Pi (LP) diet. We found that plasma 1,25-dihydroxyvitamin D [1,25(OH)<sub>2</sub>D] levels were significantly lower in the HP group than the LP group for 1 and 2 month-old mice, but not 13 month-old mice. In addition, in the HP group plasma 1,25(OH)<sub>2</sub>D levels were decreased in 2 month-old mice relative to 1 month-old mice, but 13 month-old mice had higher levels than 2 month-old mice. In fact, plasma 1,25(OH)<sub>2</sub>D levels showed a significant correlation with renal Cyp27b1 and Cyp24a1 mRNA expression in the HP group. Interestingly, renal Klotho mRNA and protein levels were significant change with age. Furthermore, Klotho mRNA expression showed a significant negative correlation with plasma 1,25(OH)<sub>2</sub>D levels in the HP group. However, plasma PTH levels didn't have a significant correlation with plasma 1,25(OH)<sub>2</sub>D levels in the HP group, this result suggest that the FGF23/Klotho system might be more important than PTH on age-related changes in vitamin D metabolism. Our results suggest that age-related alterations in renal Klotho expression could affect the responsiveness of dietary Pi to vitamin D metabolism.

**Disclosures:** Hironori Yamamoto, None.

## SU0104

**Skeletal Unloading Induces Resistance to the Growth Hormone (GH) Anabolic Effect on Trabecular Bone in Mice.** Nikita Bajwa<sup>\*</sup>, Chandrasekhar Kesavan, Heather Watt, Subburaman Mohan. Musculoskeletal Disease Center, VA Loma Linda Healthcare System, United States

Novel regulatory axes between brain and bone have been recognized in recent studies. Accordingly, we recently demonstrated that repeated mild traumatic injury (TBI) to the brain exerts a significant negative effect on bone mass accretion in mice. Loss of physical activity and GH deficiency are common features in TBI patients that may contribute to bone loss. The pivotal importance of GH/IGF-I axis in bone cell mechanotransduction processes is well established. Therefore, we tested the hypothesis that GH treatment will rescue the hind limb unloading (UL)-induced skeletal deficit in TBI mice. Eighty-one 9-week old female C57BL/6J mice were randomly assigned to the following groups: Control-Sham-Vehicle (VH), Control-Sham-GH, Control-UL-VH, Control-UL-GH, TBI-Sham-VH, TBI-Sham-GH, TBI-UL-VH, and TBI-UL-GH. Mild TBI was induced experimentally using a weight drop model, once per day for four consecutive days. Unloading (right hind limb) and treatment (3 mg/day GH or vehicle) began two weeks after the first TBI episode and lasted for four weeks. Femur aBMD measured by DXA was reduced by 9% ( $p < 0.05$ ) on the left side (loaded) versus 18% ( $p < 0.05$ ) on the right side (unloaded) in TBI mice compared to control sham mice. Micro-CT analysis of the trabecular (Tb) bone at the secondary spongiosa of right tibia revealed that BV/TV was reduced by 15% ( $p < 0.01$ ), 70% ( $p < 0.0001$ ) and 75% ( $p < 0.0001$ ), respectively in the TBI-Sham-VH, Control-UL-VH and TBI-UL-VH mice compared to Control-Sham-VH group. GH treatment increased Tb BV/TV by 35% ( $p < 0.01$ ) in control mice, thus suggesting the effectiveness of GH dose used in this study. While GH treatment increased Tb bone mass in the TBI-Sham, Control-UL and TBI-UL groups, it rescued Tb deficit in the TBI-Sham (115% of Control-Sham-VH group) but not in the Control-UL and TBI-UL groups (55% and 45% of Control-Sham-VH group,  $p < 0.01$ ). Serum IGF-I was reduced by 11%, 25% and 16%, respectively in the VH treated TBI-Sham, Control-UL and TBI-UL groups. GH treatment increased serum IGF-I levels similarly in TBI-Sham, Control-UL and TBI-UL groups (114-118% of Control-Sham-VH group), thus suggesting the GH effect on liver IGF-I production was unaffected by skeletal unloading. Based on these data, we conclude that 1) skeletal unloading caused a greater trabecular BV/TV deficit than mild TBI alone, and 2) skeletal unloading-induced resistance to GH treatment locally in the bone but not distally in the liver.

**Disclosures:** Nikita Bajwa, None.

## SU0105

**Hindlimb Unloading (HU) Inhibits Regeneration of the Mouse Digit Tip.** Connor Dolan<sup>\*</sup>, Lindsay Dawson, Felisha Imholt, Tae Jung Yang, Rihana Bohkari, Ken Muneoka. Texas A&M University, United States

Prolonged mechanical unloading, such as astronauts experiencing microgravity, enhances skeletal degeneration, impairs wound healing, and disrupts stem cell proliferation and differentiation. Mice, as well as humans, are capable of regenerating the tips of their digits following injury. Digit tip regeneration following amputation of the distal tip of the terminal phalanx is a complex process that occurs through sequential stages, which include inflammation, histolysis, epidermal closure, blastema formation, and redifferentiation to replace the amputated structures. Surprisingly, the effect of mechanical unloading on mammalian digit regeneration is unknown, and was thus the focus of the current study.

Hindlimb unloading (HU), a well-established model of musculoskeletal disuse, was utilized for digit regeneration using three groups of 8 week old female C57Bl6 mice ( $n = 5$  mice/20 digits per group): 1) amputated (Amp) digit, non-HU mice were used as an amputation control, 2) non-amputated digit, HU mice were used as an HU control, and 3) amputated digit/HU (Amp/HU) mice as our experimental group. The distal tip of the terminal phalanx (P3) of the 2nd and 4th digits on both hindlimbs was amputated and mice placed in HU for 26 days. P3 bone volume was determined at weekly intervals using in vivo microCT for 26 days post-amputation (DPA), at which time mice were terminated, digits harvested, and assessed for wound closure using Mallory's Trichrome Stain. Multi-nucleated cathepsin K+ osteoclasts were quantified using immunohistochemistry.

At 26DPA, HU control digits had no bone loss indicating that the terminal phalanx is not a mechanically loaded bone. However, Amp/HU digits at 26DPA mice had significantly less bone volume relative to 0DPA (59.02%;  $P < 0.0001$ ) and compared to Amp/nonHU (49.1%;  $P < 0.0001$ ) and HU controls (46.4%;  $P < 0.0001$ ) controls at 26DPA. Wound closure complete in 100% of amputation control digits but was incomplete in 95% of Amp/HU digits ( $P < 0.0001$ ). Further, cathepsin K-positive cells were elevated in Amp/HU digits compared to amputation and HU control digits.

The absence of bone loss in HU control digits suggests that the P3 bone is not mechanically loaded. However, wound closure failure, increased bone degradation, and elevated cathepsin K+ osteoclasts indicate that HU completely inhibited digit tip regeneration. Therefore, we propose that endogenous regeneration of the digit tip is a mechanical load-dependent event.

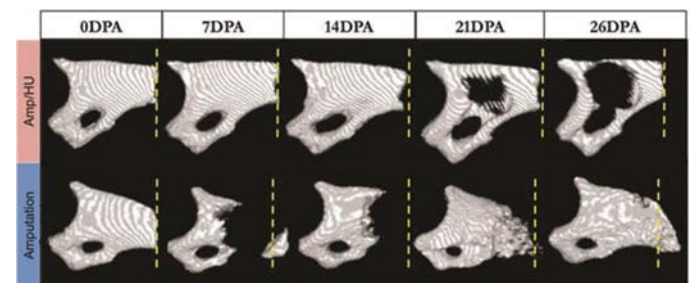


Figure 1

**Disclosures:** Connor Dolan, None.

## SU0106

**Particular adaptation of the human fibula to long-term exercise.** Laura Nociolino<sup>\*1</sup>, Gustavo Cointy<sup>1</sup>, Alex Ireland<sup>2</sup>, Sergio Lüscher<sup>1</sup>, Jose Ferretti<sup>1</sup>, Joern Rittweger<sup>3</sup>, Ricardo Capozza<sup>1</sup>. <sup>1</sup>Center of P-Ca Metabolism Studies (CEMFOC), National University of Rosario, Rosario, Argentina, <sup>2</sup>School of Healthcare Science, Manchester Metropolitan University, Manchester, UK, United Kingdom, <sup>3</sup>Division of Space Physiology, Institute of Aerospace Medicine, German Aerospace Center, Cologne, Germany, Germany

We have shown that cortical structure of human tibia and fibula respond differently to disuse, and fibula is adapted to resist bending/torsion rather than compression. Now we analyze the fibula response to long-term exercise. pQCT indicators of cortical mass (BMC, area), mineralization (vBMD), design (perimeters, moments of inertia -MIs-, buckling ratio -BR-) and strength (Bone Strength Indices, BSI's) were determined in serial scans of the fibula at 5% increments along the tibia length measured between the tibio-tarsal joint line and the proximal articular surface of the tibia (19 scans per individual) of 52 healthy men and women (26/26) aged 20-40 years who were either sedentary (13/13) or chronically trained in long-distance running (13/13).

Proximally, runners' fibula cross-sections were smaller, more elliptically shaped and more sagittally oriented, with lower total and cortical BMC and cortical area than controls. Distally, the sections were smaller and with thicker cortices than controls, especially in men. Cortical vBMD of runners' bones was slightly but significantly lower proximally and higher distally than in controls. The lateral-bending MI and BSI were lower in runners than in their controls throughout the bone. Both the torsion and A-P bending MI's and BR were lower in runners than controls only in the distal half. Adjustment of MI's values to bone length and/or body mass did not affect these results.

Strikingly, while the percent differences between runners and controls in lateral- and A-P-bending MI's and BSI's values decayed progressively toward the distal end of the bone (congruent with the smaller bone size), the BR values showed a parallel increase of bone resistance to buckling (congruent with the thicker cortices).

Within the limitations of its cross-sectional design, this study shows a particular response of the human fibula to its mechanical environment, which seems to comprise a striking compliance to bending or torsion after a chronic training in long-distance running. Those changes would have enhanced the fibula's contribution to fast-running optimization (elastic energy storing for muscles, tibio-talar joint widening), in spite of a general weakening of the bone in bending/torsion. However, bone resistance to failure in buckling would have been conveniently improved at its ultradistal end (the region most prone to fracture). This suggests that, in the studied conditions, the usage-derived strains may induce different changes in structural stiffness or strength in different regions of the fibula as a response to the same method of mechanical stimulation of the bone.

**Disclosures:** Laura Nocciolino, None.

## SU0107

**Bioactivation of poly(ester-urethane) scaffolds with platelet rich plasma to enhance cell recruitment in bone tissue engineering.** Géraldine Rohman<sup>\*1</sup>, Sophie Frasca<sup>2</sup>. <sup>1</sup>Team ITP - CSPBAT UMR 7244 CNRS – University Paris 13, France, <sup>2</sup>Institut de Recherche Biomédicale des Armées (IRBA), Département Soutien Médico-Chirurgical des Forces (SMCF), Unité de Biothérapie Ostéo-Articulaire (BOA), France

In bone tissue engineering, a small number of studies combined osteoconductive scaffolds, osteoinductive growth factors, and osteogenic cells since multicomponent approaches involved many questions that remain to be solved. With the aim to develop scaffolds able of recruiting cells, the present study focuses on the bio-activation of poly(ester-urethane) (PCLU) scaffolds with platelet rich plasma (PRP). In vitro and in vivo assays were performed. Porous cross-linked poly( $\epsilon$ -caprolactone urethane) PCLU scaffolds were prepared through a polyHYPE method. Scaffolds were sterilized by autoclave and bioactivated with PRP. For in vitro assays, human mesenchymal stem cells (hMSCs) were grown up to confluence. Thereafter, scaffolds were set down onto the cell sheet and maintained in culture medium for up to 35 days to achieve cell infiltration. Environmental scanning electron microscopy (ESEM) was employed to visualize hMSCs within scaffolds. For in vivo assays, scaffolds were implanted in 3 mm cavitary defects in Lewis rats' femoral bone. Bone reconstruction was monitored with micro computed-tomography and histology.

The in vitro study demonstrated that hMSCs were not able to migrate in PCLU scaffold, whereas the bio-activation with PRP has allowed the recruitment of cells. The in vivo assay showed that the bone regeneration has started after 15 days when PCLU was implanted in the defect, demonstrating osteo-inductive properties for this biomaterial. At the same time point, a better regeneration was found for bio-activated scaffold (PCLU+PRP).

PRP is an allogenic source of growth factors and extracellular matrix macromolecules susceptible to bio-activate tissue substitutes. Association of PRP with PCLU scaffolds is a promising approach, as it would be a simple and efficient method allowing the immobilization of a number of highly concentrated bioactive factors creating an osteogenic environment and impacting on bone regeneration. In addition to enhance cell recruitment within PCLU, PRP will promote cell adhesion and differentiation leading to an increase of new bone formation and vascularization. Deeper in vitro and in vivo investigations are underway to assess the efficiency of bio-activated PCLU scaffolds as graft substitute for the repair of bone defects.

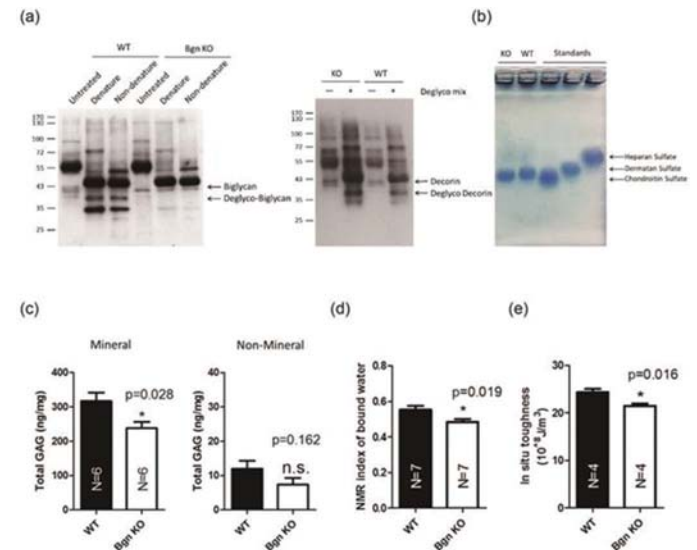
**Disclosures:** Géraldine Rohman, None.

## SU0108

**Biglycan Deficiency Impairs Bone Toughness through Reduced Bound Water in Bone Matrix.** Rui Hua<sup>\*1</sup>, Jie Bai<sup>1</sup>, Qingwen Ni<sup>2</sup>, Jean X. Jiang<sup>3</sup>, Xiaodu Wang<sup>1</sup>. <sup>1</sup>University of Texas at San Antonio, United States, <sup>2</sup>Texas A&M International University, United States, <sup>3</sup>UT Health Science Center at San Antonio, United States

Proteoglycans (PGs) are one of the structural non-collagenous proteins (NCPs) in the extracellular bone matrix, containing long unbranched glycosaminoglycans (GAGs) chains attached to core proteins. Previous studies show that PGs may play a pivotal role in sustaining the toughness of bone via retaining the bound water in the matrix in an in vitro model using human cadaveric bone samples. To further verify the mechanism, this study intended to examine the effect of PGs on the toughness of bone in vivo using a biglycan-deficient mouse model. Biglycan belongs to small leucine-rich proteoglycans (SLRPs) and is considered to be one of the major subtypes of PGs in bone matrix. In this study, wild-type and biglycan (Bgn) knockout (KO) mice were used and biochemical assays were performed to determine the amount and major subtype of GAGs in bone matrix. First, Bgn KO mice model were validated by immunoblotting with antibodies for Bgn and its related PGs, decorin (Dcn). In mineralized bone matrix, Bgn expression was totally abolished while the level of decorin was unaffected in the bone samples of Bgn knockout. Agarose electrophoresis showed that chondroitin sulfate was the major subtype of GAGs. Next, the level of GAGs was determined in both mineralized and non-mineralized bones. A significant decrease of GAGs amount was observed only in the mineralized compartment, but not in the non-mineralized compartment of Bgn KO mouse bone. Moreover, results from a novel nanoscratch test showed a significant

reduction in the in situ toughness of bone of Bgn KO mice compared to WT mice. In addition, low field NMR measurements exhibited that Biglycan deficiency had a significant effect on the amount of bound water in bone by an average reduction of 12.6%. Taken together, our results demonstrated that Bgn in bone matrix may play a pivotal role in retaining bound water in bone matrix, thus imparting the plasticity and toughness to bone.



Bgn Deficiency Impairs Bone Toughness through Reduced Bound Water in Bone Matrix

**Disclosures:** Rui Hua, None.

## SU0109

**Spatio-temporal Regulation of Sclerostin Expression and Dynamics in Alveolar Bone During Orthodontic Tooth Movement.** Naoya Odagaki<sup>\*</sup>, Yoshihito Ishihara, Ziyi Wang, Masahiro Nakamura, Ei Ei Hsu Hlaing, Hiroshi Kamioka. Okayama University, Japan

Sclerostin (Scl), a negative regulator of bone formation, represses bone formation and favors bone resorption by antagonizing canonical WNT signaling. Osteocytes are the primary source of Scl, the cells responsible for mechanosensing, and key regulators of bone remodeling and homeostasis. Although changes in Scl expression in osteocytes are known to affect bone formation and bone resorption, little is known about the influence of Scl towards bone remodeling caused by orthodontic tooth movement (OTM). We herein demonstrated the spatio-temporal pattern of Scl expression in alveolar bone and periodontal ligament (PDL) during OTM by cell unit and region unit.

Eight-week-old male ICR mice were loaded with coil spring for OTM. A spring delivering 10 grams of mechanical force was placed between the maxillary first molar and the incisors to move the first molar mesially for 0, 1, 5, 10 days, respectively. A region of 200 x 310 pixels from the boundary of PDL were measured in both compression and tension side. The number of cells and the distribution patterns of Scl expression were analyzed by immunofluorescence staining.

PDL contraction on the pressure side and its extension on the tension side were observed. The number of osteocytes on pressure side decreased significantly from day 1 to day 10. In the analysis of region unit, histogram and profile of fluorescence intensity showed that Scl expression in the alveolar bone was increased on pressure side, peaked at day 5 with gradually increased region of significance. This significance returned to values similar to control level only around the PDL-alveolar bone boundary at day 10. The intensity of Scl in PDL area on pressure side also increased compared to tension side. Conversely, the fluorescence intensity of Scl in the alveolar bone on tension side were decreased significantly only at day 1. In parallel with the region analysis, the ratio of Scl positive osteocytes on tension side didn't change significantly, whereas the positive ratio on pressure side was significantly increased on day 5, then the ratio was decreased to the initial value on day 10.

Taken together, our experimental system could be used to capture the dynamic spatio-temporal regulation of Scl expression and be determining the effect of OTM at high resolution. Our results suggested that the potential role of Scl in regulating alveolar bone remodeling in response to OTM possibly due to the different kind of mechanical stress induced to PDL.

**Disclosures:** Naoya Odagaki, None.



## SU0110

**Diverging Periosteal and Endosteal Modeling/Remodeling Under PTH and Mechanical Loading.** Samuel Robinson\*, Yizhong Hu, X. Edward Guo. Columbia University, United States

Mechanical loading and intermittent injections of parathyroid hormone (PTH) are both established stimulants of an anabolic response in bone, and have been shown to produce combined effects in some regions of both trabecular and cortical bone [1]. However, a characteristic of natural cortical bone growth is concurrent endosteal resorption and periosteal formation, a means of increasing resistance to bending without dramatically affecting total bone mass. Furthermore, bone adaptation can occur through either remodeling (resorption followed by formation) or modeling (uncoupled resorption or formation). With the possibility of both formation and resorption being affected by these treatments and adaptation occurring through either regime, we sought to more accurately characterize the response using dynamic *in vivo* morphometry. We treated C57BL/6 mice with daily injections of PTH and uniaxial tibia loading for 3 weeks, with an additional 2 weeks of injections and regular cage activity. Weekly micro-computed tomography scans of loaded and non-loaded limbs were registered between adjacent weeks using a custom algorithm to detect the quantity and location of formation and resorption events. The dynamic progression of formation/resorption at each voxel location was recorded to classify events as modeling or remodeling.

On the periosteal surface, anabolic modeling was significantly increased with loading and PTH, and the two-way interaction was significant. Correspondingly, catabolic modeling was significantly suppressed. However, on the endosteal surface the effect was reversed: loading led to significantly more catabolic modeling and less anabolic modeling. Despite an early endosteal anabolic response in the loaded groups, formation slowed and then decreased to levels below non-loaded controls. In its place, a significant progression of endosteal catabolic modeling ensued, independent of PTH treatment. Formation via remodeling decreased with load on the periosteal surface, potentially a result of the response being dominated by modeling, and did not differ among groups on the endosteal surface. Therefore, in total our data demonstrate surprisingly different bone dynamics on the endosteal and periosteal surfaces in response to load, some aspects of which are enhanced by PTH. The localized mechanical and biochemical environments that contribute to this divergence remain to be further investigated.

[1] Sugiyama et al., 2008, *Bone*

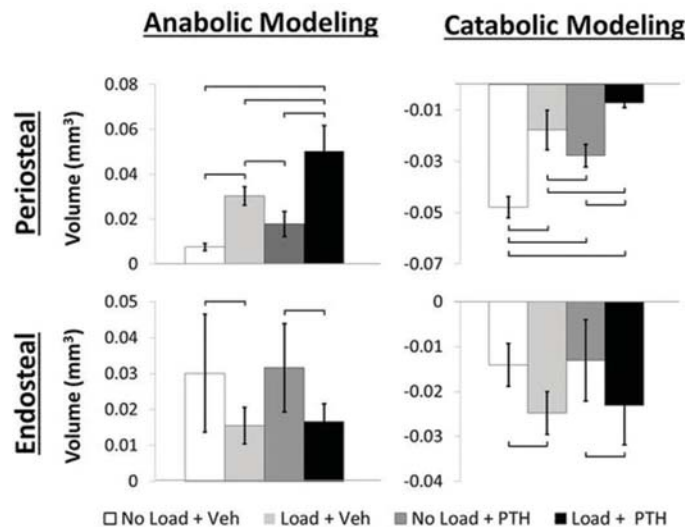


Figure 1

**Disclosures:** Samuel Robinson, None.

## SU0111

**Whole body vibration intervention: a randomized, prospective, controlled study in children with obesity.** Bojan Tubic\*, Rickard Zeilon<sup>2</sup>, Göran Wennergren<sup>1</sup>, Barbara Obermayer-Pietsch<sup>3</sup>, Staffan Mårild<sup>1</sup>, Jovanna Dahlgren<sup>1</sup>, Per Magnusson<sup>4</sup>, Diana Swolin-Eide<sup>1</sup>. <sup>1</sup>Department of Pediatrics, Institute of Clinical Sciences, Sahlgrenska Academy, Gothenburg University, The Queen Silvia Children's Hospital, Gothenburg, Sweden, Sweden, <sup>2</sup>Department of Internal Medicine, Sahlgrenska University Hospital, Gothenburg, Sweden, Sweden, <sup>3</sup>Division of Endocrinology and Metabolism, Department of Internal Medicine, Medical University of Graz, A-8036, Graz, Austria, Austria, <sup>4</sup>Department of Clinical Chemistry, Linköping University, Linköping, Sweden, Sweden

**Background:** The prevalence of obesity in the world has more than doubled since 1980. A low level of physical activity and a sedentary lifestyle are both regarded as two important contributors to obesity and low bone mass. Studies have demonstrated a

positive effect of whole body vibration (WBV) on insulin, fasting blood glucose, as well as on bone metabolism and muscle strength. New strategies are required to increase physical activity and improve metabolic profile in children with obesity. Our aim was to study the effect of WBV in children with obesity on: (i) biochemical markers of energy and bone metabolism; (ii) anthropometric measurements; (iii) muscle parameters; and (iv) the effect on calcaneal bone mineral density (BMD).

**Methods:** A randomized, prospective, controlled study in children with obesity. Thirty-six children with obesity, aged 7-17 years, were randomized to WBV (10 girls/6 boys) or as controls (8 girls/6 boys). WBV was performed on a Galileo Med Basic side-alternating vibration plate at 16-24 Hz three times/week for 12 weeks in a home setting, and study parameters were assessed at start and after 12 weeks. Leonardo Mechanography® Ground Reaction Force Plate (GRFP) was used to evaluate muscle parameters.

**Results:** Thirty children completed the study. The subjects performed WBV in mean 13 minutes/week according to logbooks and mean 11 minutes/week according to the actual Galileo data, in comparison to the expected 21 minutes/week. Adherence was 51% of the expected WBV-time. Sclerostin, bone-specific alkaline phosphatase and carboxy-terminal collagen crosslinks (CTX) decreased in the WBV group ( $p < 0.05$ ), but osteocalcin and insulin remained unchanged. Balance improved in the WBV group ( $p < 0.006$ ). No difference was found between the groups at study start, or after 12 weeks of WBV regarding age, height-standard deviation score (SDS), weight-SDS, body mass index (BMI), BMI-SDS, waist circumference or blood pressure. Muscle strength and calcaneal BMD did not differ between the two groups.

**Conclusions:** This WBV intervention study did not alter metabolic parameters, anthropometry, lower extremity muscle strength or calcaneal bone mass; however, the reduction of sclerostin implies that WBV therapy in children with obesity has direct effects on osteocytes, the key-players in bone mechanotransduction. The low adherence illustrates that "exercise", in the form of home-based WBV, is difficult to perform on a regular basis for children with obesity.

**Disclosures:** Bojan Tubic, None.

## SU0112

**Site-specific "rescue" of the age-impaired response to mechanical loading in tibiae of old mice.** Gabriel G Galea<sup>\*1</sup>, Peter J Delisser<sup>1</sup>, Lee Meakin<sup>1</sup>, Lance E Lanyon<sup>1</sup>, Joanna S Price<sup>2</sup>, Sara H Windahl<sup>3</sup>. <sup>1</sup>School of Veterinary Sciences, University of Bristol, United Kingdom, <sup>2</sup>Royal Agricultural University Cirencester, United Kingdom, <sup>3</sup>Centre for Bone and Arthritis Research, University of Gothenburg, Sweden

Bones' reduced ability to respond appropriately to functional loading could contribute to the pathogenesis of age-related bone loss. We have shown previously that aspects of the impaired osteogenic response of aged bone to mechanical loading are different between males and females (1), and that prior and concurrent disuse "rescues" the osteogenic response to loading in old female mice (2). The aim of the present study was to determine whether 'rescue', by sciatic neurectomy (SN)-induced disuse, of the osteogenic response to artificial loading also occurs in males.

19-month-old C57BL/6 mice were subjected to either sham surgery or SN. 4 days post-surgery, their right tibiae were subjected to short periods of axial mechanical loading, three times per week for 2 weeks (40 cycles, peak strain 2500  $\mu\epsilon$ ). Left limbs were used as internal controls (3). Bone architecture was analyzed by  $\mu$ CT. Site specificity analysis (SSA) (4) was used to map differences in bone architecture along the length of the tibiae.

Unlike the gender-specific difference seen in young mice, the adaptive response to loading in old mice was similar in old males and females at all sites along the tibia's length. Prior and concurrent disuse enhanced the loading-related increase in total cortical bone area 3-fold in old male mice, as previously reported in old females. However, the site where this 'rescue' is most prominent occurred more proximally in old males than females (20% compared with 37% site). In contrast to old females, disuse augmented the loading-related response in trabecular thickness of old males by 3-fold.

This study demonstrates that sex and site specific differences in the osteogenic response to loading seen in young mice are abrogated in old mice. Prior and concurrent disuse can, at least partly, rescue the age-related decline in the osteogenic responses to loading in males as it does in females, but there is an effect of sex on the site where the 'rescue' is most pronounced. It has been suggested that "rescue" derives from the effects of long periods of normal loading averaging with, and so reducing, the osteo-adaptive response to short periods of more error-related activity.

1. Meakin et al, JBMR, 2014
2. Meakin et al, Osteoporosis International, 2015
3. Sugiyama et al, Bone, 2010
4. Galea et al, Front Endocrinol, 2015

**Disclosures:** Gabriel G Galea, None.

## SU0113

### Substrate Stiffness Regulates Arterial-Venous Differentiation of Mouse Bone Marrow-Derived Endothelial Progenitor Cells via the Ras/Mek Pathway. Changyue Xue\*, Sichuan University, China

**Objective:** To investigate the effect of different degrees of substrate stiffness on the arterial-venous differentiation of mouse bone marrow-derived EPCs and provide methodologies to culture EPCs for use in tissue engineering.

**Methods:** A polydimethylsiloxane (PDMS)-based substrate capable of simulating the physiologically relevant stiffness of both venous (7 kPa) and arterial (128 kPa) tissue was developed. This substrate was then utilized to investigate the effects of changes in substrate stiffness on the differentiation of EPCs. Cell morphology and spreading area on PDMS substrates of varying degrees of stiffness were observed. Variations of arterial and venous markers in EPCs were detected using immunofluorescence, Western Blot and Polymerase Chain Reaction. Further molecular biology experiments were performed to identify the mechanotransduction pathway involved in this process.

**Results:** The mRNA and protein levels of the specific arterial endothelial cell marker ephrinB2 were found to increase, while the expression of the venous marker EphB4 decreased. The results also indicated that substrate stiffness regulates the arterial and venous differentiation of EPCs via the Ras/Mek pathway.

**Conclusions:** Substrate stiffness regulates the differentiation of EPCs. A venous lineage was obtained on soft substrates while an arterial lineage predominated on stiffer substrates. Substrate stiffness during EPC culture may serve as a factor to precisely control the differentiation level of EPCs in tissue engineering applications.

**Disclosures:** Changyue Xue, None.

## SU0114

### Undercarboxylated osteocalcin enhances basal and insulin-stimulated glucose uptake in mouse skeletal muscles *ex vivo*. xuzhu lin<sup>\*1</sup>, emma mcLennan<sup>1</sup>, lewan parker<sup>1</sup>, glenn mcConell<sup>1</sup>, xinmei zhang<sup>1</sup>, alan hayes<sup>1</sup>, tara brennan-speranza<sup>2</sup>, itamar levinger<sup>1</sup>. <sup>1</sup>Institute of Sport, Exercise and Active Living (ISEAL), Victoria University, Australia, <sup>2</sup>Department of Physiology and Bosch Institute for Medical Research, University of Sydney, Australia

Undercarboxylated osteocalcin (ucOC) improves insulin sensitivity in mice. Previously we found ucOC augmented the increase in insulin-stimulated glucose uptake in mice EDL muscle after *ex vivo* contraction. However, whether ucOC also directly enhances basal muscle glucose uptake and whether these effects are muscle-type specific are still not clear. We hypothesized that ucOC will increase glucose uptake in both EDL and soleus muscles, with or without the presence of insulin, via the activation of ERK.

EDL and soleus muscles from male C57BL/6 mice were isolated and split longitudinally. Samples were pretreated with the ERK inhibitor U0126 or DMSO vehicle, followed by 90 minutes treatment of ucOC or KHB buffer control. Insulin or control was added in the last 30 minutes. After the treatment, muscle glucose uptake and signaling proteins were assessed.

ucOC significantly increased basal (non-insulin stimulated) glucose uptake in both EDL (45.4%,  $p < 0.001$ ) and soleus (31.2%,  $p < 0.01$ ). It also enhanced basal phosphorylation levels of ERK2, mTOR, and AS160 and tended to increase basal levels of p-AKT ( $p = 0.074$ ). Treatment with U0126 reduced the ucOC-induced increase in basal glucose uptake in both muscles. The inhibitor also completely blocked the ucOC effects on the phosphorylation of AKT and AS160 in EDL, and attenuated these ucOC effects in soleus. ucOC significantly augmented insulin-stimulated glucose uptake (28.8%,  $p < 0.05$ ) and potentiated insulin-stimulated phosphorylation of ERK2, mTOR, AKT, and AS160 only in soleus. However, the ERK inhibitor had little impact on the ucOC effects on insulin-stimulated phosphorylation of AKT and AS160.

Taken together, we, for the first time, showed that ucOC can increase basal glucose uptake in both glycolytic and oxidative muscles in mice, and has insulin-sensitizing effect on oxidative muscle only. We also demonstrated that ucOC exerts the beneficial effects on basal muscle glucose uptake and mTOR-AKT-AS160 axis, at least in part, via ERK activation.

**Disclosures:** xuzhu lin, None.

## SU0115

### Low Intensity Vibrations increase strength, reduce fat, and improve glucose tolerance in mice with complete estrogen deprivation. Gabriel M. Pagnotti<sup>\*1</sup>, Laura E. Wright<sup>1</sup>, Jenna A. Regan<sup>1</sup>, William R. Thompson<sup>1</sup>, Khalid S. Mohammad<sup>1</sup>, Clinton T. Rubin<sup>2</sup>, Theresa A. Guise<sup>1</sup>. <sup>1</sup>IUPUI, United States, <sup>2</sup>Stony Brook University, United States

Post-menopausal, estrogen receptor-positive breast cancer patients treated with aromatase inhibitor (AI) experience deleterious effects on bone and muscle. Pharmacological agents which inhibit osteoclastic bone resorption are effective in preventing bone loss but may have adverse effects. Low intensity vibrations (LIV), a subtle mechanical signal that reintroduces the high-frequency elements of physical activity, have been demonstrated to safely preserve bone in two murine models of cancer, reduce adipogenesis, and upregulate muscle-bound satellite cell populations in ovariectomized (OVX) mice. We hypothesized that LIV could preserve bone mass and muscle strength

following complete estrogen deprivation. Twenty weight-matched, 4w female C57BL/6 mice were treated with LIV (90Hz, 0.35g, 1x/d) or sham-control (SH) for 4 weeks. After 4 weeks of LIV treatment, all mice were subjected to complete estrogen deprivation by OVX and treatment with aromatase inhibitor letrozole followed by another 22 weeks of LIV treatment. At 26w of treatment LIV-mice maintained a significantly ( $p < 0.001$ ) lower body weight in comparison to SH (untreated)-mice. Longitudinal body composition measurements for lean mass, fat mass and bone mineral density were assessed by DXA every 3 weeks and cortical (Ct) and trabecular (Tb) bone microarchitecture were assessed by *in vivo*  $\mu$ CT (resolution=19 $\mu$ m) every 4 weeks. Our data show that LIV-treated mice have significantly higher lean mass ( $p < 0.02$ ) and significantly lower fat mass ( $p < 0.0001$ ) compared to SH-treated mice as assessed by DXA. These findings were accompanied by a significant improvement in glucose intolerance in LIV-treated mice ( $p < 0.05$ ). Functional grip strength of LIV-treated mice was significantly higher compared to SH (31%;  $p < 0.04$ ). No difference in bone mineral density (BMD) between LIV-treated and SH-mice was observed as assessed by DXA. *In vivo*  $\mu$ CT analyses at the proximal tibia showed significant increases in Ct bone volume in LIV-treated mice as compared to the tibiae of SH-treated mice ( $p < 0.04$ ) but no differences in Tb bone volume were observed. Ct.BMD increased by 12% in LIV-mice relative to OVX but by just 7% in SH-mice. Taken together, our data suggest that LIV may be a novel means to protect and/or increase lean mass, reduce fat mass and improve glucose metabolism resulting from complete estrogen deprivation. Further, long-term studies may be required to test LIVs effects on bone loss associated with estrogen deficiency.

**Disclosures:** Gabriel M. Pagnotti, None.

## SU0116

### Muscle-Specific Vitamin D Receptor (VDR) Ablation Results in Reduced Grip Power and Altered Gene Expression Pattern in Mice. Maria Tsoumpra\*, Itsuro Endo, Shun Sawatsubashi, Yuichi Takashi, Seiji Fukumoto, Toshio Matsumoto. Tokushima University, Japan

1,25-dihydroxyvitamin D (1,25(OH)<sub>2</sub>D) is a calcium regulating hormone that exerts its tissue-specific biological actions through binding to its intracellular vitamin D receptor (VDR). A link of VDR implication in transcriptional down-regulation of myogenic factors during skeletal muscle development has been reported by our group (Endo *et al.* 2003) whereas *in vitro* studies on murine C2C12 muscle cells backed up the involvement of the biologically active metabolite 1,25(OH)<sub>2</sub>D<sub>3</sub> in proliferation, differentiation, and myotube formation (Girgis *et al.* 2014). However whether this postulated 1,25(OH)<sub>2</sub>D<sub>3</sub> effect on murine myogenic differentiation occurs as a direct VDR-dependent action remains unclear. We therefore aimed to elucidate the physiological effect of VDR on murine muscle function and differentiation. We generated a muscle specific VDR knockout mouse where VDR floxed targeted ablation is driven by myosin light chain (Mlc) Cre recombinase (Bothe *et al.* 2000). Grip power test indicated reduced grip power tendency in VDR<sup>lox/lox</sup>/Mlc<sup>Cre/+</sup> males versus their control littermates throughout our 5-10 week (wk) experimental period and was more prominently observed at 6<sup>th</sup> and 8<sup>th</sup> wk. In addition, qPCR studies demonstrated that VDR, MyoD and SERCA2A were downregulated in 10 wk gastrocnemius (Gast) and 8 wk tibialis anterior (TA) in homozygote males, but not in quadriceps or soleus, muscles less rich in fast fiber content. We then performed microarray studies on TA obtained from 8 wk mice to identify candidate genes that may be exerting a VDR direct effect in muscle. Of particular interest for follow up, *biglycan* (*Bgn*) and *calcium/calmodulin-dependent protein kinase I* (*CamK1*) genes were upregulated in both Gast and TA of 5 and 6 wk old homozygotes respectively, as confirmed via qPCR. We then sought to confirm the *in vitro* suppressive effect of 1,25(OH)<sub>2</sub>D<sub>3</sub> on these genes by induction of myogenesis in C2C12 cells via daily supplementation of Ham's-F12 medium and 1% horse serum with or without 1,25(OH)<sub>2</sub>D<sub>3</sub>. We clearly demonstrated that *Bgn* and *CamK1* expression was dose-dependently downregulated upon administration of 1,25(OH)<sub>2</sub>D<sub>3</sub> on day six where myotubes were clearly formed and maximal suppression was observed with 10 nM 1,25(OH)<sub>2</sub>D<sub>3</sub>. In the future we aspire to assess any possible link of CamK1 and Bgn in myogenic differentiation and muscle physiology.

**Disclosures:** Maria Tsoumpra, None.

## SU0117

### Muscle Paralysis Differentially Alters Expression of miR-206 and miR-133b. Leah Worton\*, Edith Gardiner, Ronald Kwon, Brandon Ausk, Steven Bain, Ted Gross. University of Washington, United States

Transient muscle paralysis via Botulinum toxin A (BTxA) induces muscle atrophy and profound bone resorption in the adjacent skeleton of a wide range of vertebrates. Interestingly, the focal catabolic influence of muscle paralysis is minimally derived from reduced skeletal loading, even though the rate and extent of bone loss exceeds that induced by sciatic neurectomy. In this context, it has recently been demonstrated that surgical denervation results in upregulation of the muscle bicistronic partner transcripts miRNAs -206 and -133b to guide neuronal and skeletal muscle regeneration. Although the effects of BTxA on muscle have been extensively explored, it is not known whether BTxA induced paralysis precipitates altered regulation of miRNA expression as with denervation. First, we confirmed that 2.0U/100g BTxA injected into the quadriceps of mice significantly reduced ipsilateral muscle mass by d28 (-47 $\pm$ 8% vs contralateral quadriceps). We then injected the right quadriceps of mice with 2.0U/100g BTxA followed by sacrifice at d7, 14, or 28 (n=4-6/grp). Naive mice were sacrificed at the same time points (n=10). We assessed the muscle miRNAs -206 and -133b and the non-muscle miRNA-29b in all ipsilateral and contralateral quadriceps. We then assessed a



panel of muscle mRNAs that included genes known to be altered by muscle dysfunction (*Myog*, *Myod* and *Myf5*) and targets of miR-206 (*Fgf1*) or miR-133b (*RhoA*, *Tgfb1*, *Egfr*). The non-muscle miR-29b was not altered by muscle paralysis. miR-206 expression was significantly upregulated by BTx injection compared to naïve quadriceps (6- and 9-fold for d14 and 28 respectively). In contrast, miR-133b was downregulated at all time-points (d7: -63%; 14: -61%; and 28: -72% vs naïve). Similar to other conditions of muscle dysfunction, we saw increased expression of muscle mRNAs *Myog*, *Myod* and *Myf5* in ipsilateral quadriceps. Consistent with miR-206 upregulation, target *Fgf1* was downregulated (d7: -77%; 14: -79%; 28: -70% vs naïve). Consistent with miR-133b downregulation, miR-133b target expression was upregulated (*RhoA*, *Tgfb1* and *Egfr*). From these data, we conclude that BTx induced muscle paralysis alters regulation of both miR-206 and miR-133b. However, in contrast with observations following denervation, miR-206 and miR-133b were differentially regulated. Given prospective downstream targets, this differential response holds potential to clarify the surprising severity of muscle paralysis induced bone loss.

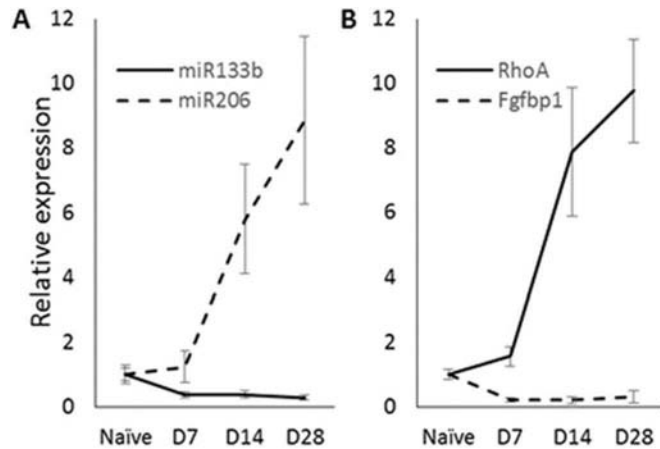


**Figure 1. BTx induced muscle paralysis differentially alters (A) miRNA-133b and -206 and (B) target mRNA expression in ipsilateral quadriceps relative to naïve mice.**

Figure 1

**Disclosures:** Leah Worton, None.

## SU0118

**Advanced Glycation End Products-Mediated  $\beta$ -enolase Is Involved in the Diabetes-Impaired Muscle Function.** Rong-Sen Yang<sup>\*1</sup>, Chen-Yuan Chiu<sup>2</sup>, Ding-Cheng Chan<sup>3</sup>, Shing-Hwa Liu<sup>2</sup>. <sup>1</sup>Department of Orthopaedics, College of Medicine, National Taiwan University, Taipei, Taiwan, Taiwan, Province of China, <sup>2</sup>Institute of Toxicology, College of Medicine, National Taiwan University, Taiwan, Province of China, <sup>3</sup>Superintendent's Office, National Taiwan University Hospital, Chu-Tung Branch, Taiwan, Province of China

**Introduction:** Advanced glycation end products (AGEs) are the etiology of several diabetic complications. Skeletal muscle is also a target of AGEs accumulation in diabetic animals. It has been reported that adult men with AGEs accumulation had lower muscle strength and power. However, the role of AGEs in the diabetic myopathy (muscle weakness or muscle wasting) still remains unclear. Moreover, muscle-specific enolase ( $\beta$ -enolase), a crucial glycolysis enzyme in the skeletal muscle, was developed as a marker for exercise-induced muscle damage. Here, we investigated whether the modulation of  $\beta$ -enolase is linked to AGE accumulation and AGEs-related impaired skeletal muscle function in diabetic mice.

**Methods:** Adult male ICR mice were intraperitoneally injected with streptozotocin (STZ, 100 mg/kg) to induce diabetes (a type 1 diabetes-like model). The expressions of AGEs and  $\beta$ -enolase in the soleus muscles were determined by immunohistochemistry. Moreover, the mouse skeletal muscle C2C12 cells were used to test the *in vitro* effect of AGEs. The protein expressions were determined by Western blotting.

**Results:** Results revealed that the accumulation of AGEs is accompanied by the existence of  $\beta$ -enolase in soleus muscles of STZ-induced diabetic mice (n=5; Figure 1). Lactate levels in diabetic muscles were also increased (n=5, p<0.05). Aminoguanidine, an inhibitor of AGEs formation, exhibited an obvious reduction in AGEs accumulation and  $\beta$ -enolase expression (n=5; Figure 1) and increased lactate (n=5, p<0.05) in soleus muscles of diabetic mice. To explore the action mechanism of AGEs on  $\beta$ -enolase expression, C2C12 cells were exposed to 10-100  $\mu$ g/mL AGEs in the growth media for 24 h. AGEs significantly and dose-dependently stimulated the expressions of  $\beta$ -enolase, receptor of AGEs (RAGE), and phospho-NF $\kappa$ B-p65, which could be reversed by RAGE neutralizing antibody (n=4, p<0.05).

**Discussion:** An increase of  $\beta$ -enolase has been found in marathon runners that the serum  $\beta$ -enolase is suggested to be more appropriate to relate to muscle damage. It has been found that the expression of  $\alpha$ -enolase is increased in the bladder smooth muscle of STZ-induced diabetic rats. The change of  $\beta$ -enolase in diabetic skeletal muscle still remains uncertain. The results of this study suggest that AGEs may up-regulate

$\beta$ -enolase expression via a RAGE-NF $\kappa$ B pathway, leading to induction of diabetic muscle symptom.

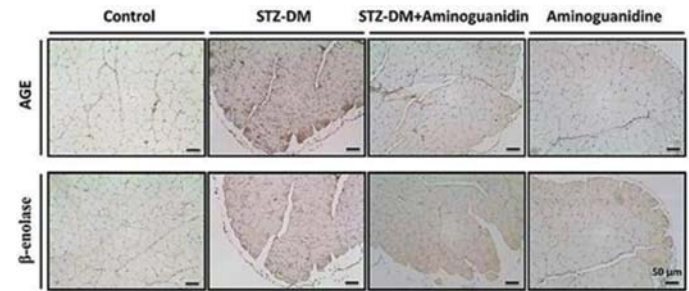


**Figure 1. The protein expressions of AGE and  $\beta$ -enolase in skeletal muscles of streptozotocin (STZ)-induced diabetic mice in the presence or absence of AGE formation inhibitor aminoguanidine. The expressions of AGE and  $\beta$ -enolase were determined by immunohistochemistry. Results shown are representative from five independent experiments.**

Figure 1

**Disclosures:** Rong-Sen Yang, None.

## SU0119

**Pin1 regulates skeletal muscle fusion through structural modification of Smad3 in linker region.** Rabia Islam<sup>\*1</sup>, Heeun Yoon<sup>2</sup>, Hye-rim Shin<sup>2</sup>, Han-sol Bae<sup>2</sup>, Bong-soo Kim<sup>2</sup>, Won-joon Yoon<sup>2</sup>, Kyung-Mi Woo<sup>2</sup>, Jeong-Hwa Baek<sup>2</sup>, Yun-Sill Lee<sup>2</sup>, Hyun-Mo Ryoo<sup>2</sup>. <sup>1</sup>Seoul National University, Bangladesh, <sup>2</sup>Seoul National University, Korea, Republic of

Myoblast fusion is critical for muscle growth, regeneration, and repair. We previously reported that the enzyme Peptidyl-prolyl cis-trans isomerase NIMA interacting 1 (Pin1) is involved in osteoclast fusion. The objective of this study was to investigate the possibility that Pin1 also inhibits myoblast fusion. Here, we show the increased number of nuclei in Pin1<sup>-/-</sup> mice muscle fiber compared to wild type mice. Moreover, we show that low dose of Pin1 inhibitor DTM treatment caused enhanced fusion in C2C12 cells. The R-Smads are well known mediators of muscle hypertrophy and hyperplasia as well as being substrates of Pin1. We found that Pin1 is crucial for maintaining the stability of Smad3. Our results show that Serine 204 within Smad3 is the key Pin1 binding site during inhibition of myoblast fusion, and both Tgf receptor and Erk mediated phosphorylation is required for the interaction of Pin1 with Smad3. These findings suggest that a precise level of Pin1 activity is essential for regulating myoblast fusion during myogenesis and muscle regeneration.

**Disclosures:** Rabia Islam, None.

## SU0120

**Mouse digit regeneration: a new model to study age-related regenerative decline.** Regina Brunauer<sup>\*</sup>, Ken Muneoka. Texas A&M University, United States

According to the UN World Population Ageing Report 2015, the global population of people older than 60 years will have doubled by 2050. To improve quality of life for the elderly, a better understanding of the aging process is crucial to prevent and treat age-related diseases. It is widely accepted that a gradual decline of regenerative capacity drives aging, but models to study *in vivo* regeneration are sparse and typically involve only one tissue type. Epimorphic regeneration such as limb regeneration in the salamander is accomplished by a concerted interplay of connective, nervous and bone tissue. Among vertebrates, epimorphic regeneration is perceived to be the exclusive domain of salamanders and fish, but also mammals are capable of regenerating lost appendages. This is exemplified by regeneration of amputated digit tips in mice and humans. Upon amputation, extensive bone histolysis driven by osteoclasts occurs, after which a blastema, an aggregate of undifferentiated cells, is generated, and intramembraneous osteogenesis results in a near-perfect regenerated digit bone. To establish if digit tip regeneration is affected by aging, we amputated hindlimb digits of young and aged mice. While the digit still regenerates in aged mice, we observed a delay in the onset of bone histolysis, and a decreased rate of bone redifferentiation. We hypothesize that in digit regeneration, aging inhibits osteoclast differentiation and limits stem cell availability, and we will test these hypotheses with the long-term goal to understand the mechanisms that interfere with successful regeneration in aging.

**Disclosures:** Regina Brunauer, None.

## SU0121

**Relative Age-related Decline in Trunk Muscle Density is Greater in Women than Men whereas Muscle Mass Declines Similarly in Both Sexes: the Framingham Study.** Fjola Johannesdottir<sup>1</sup>, Brett Allaire<sup>2</sup>, Dennis Anderson<sup>1</sup>, Elizabeth J. Samelson<sup>3</sup>, Douglas Kiel<sup>4</sup>, Mary Bouxsein<sup>1</sup>. <sup>1</sup>Harvard Medical School and Center for Advanced Orthopaedic Studies, Beth Israel Deaconess Medical Center, MA, USA, United States, <sup>2</sup>Center for Advanced Orthopaedic Studies, Beth Israel Deaconess Medical Center, MA, USA, United States, <sup>3</sup>Institute for Aging Research, Hebrew Senior Life and Harvard Medical School, United States, <sup>4</sup>Institute for Aging Research, Hebrew Senior Life, Department of Medicine Beth Israel Deaconess Medical Center and Harvard Medical School, MA, USA, United States

**Background:** Studies suggest that trunk muscle atrophy impairs physical function and increases the risk of disability and injury in older people. A better understanding of the effect of aging on trunk musculature may inform interventions to preserve mobility and reduce injury. Thus, we determined the relative age-related differences in muscle density and size of a comprehensive set of trunk muscles.

To do so we conducted a cross-sectional study in an age and sex stratified sample of 250 community-based men (n=125) and women (n=125) aged 40 to 90 years from the Framingham Offspring and Third Generation cohorts who underwent quantitative computed tomography (QCT) scans. QCT was used to measure muscle mass, estimated as cross-sectional area (CSA), and muscle density (Hounsfield units) at the T5-L4 vertebral levels for the following muscles: pectoralis major (PM), rectus abdominis (RA), serratus anterior (SA), latissimus dorsi (LD), trapezius (TR), external oblique (EO), erector spinae (ES), transversospinalis (TS), psoas major (PS), and quadratus lumborum (QL). Relative age-related differences in muscle mass and density were estimated from general linear regression models with adjustment for height and weight.

**Results:** With increasing age, the relative difference in muscle mass was similar in both sexes (p>0.05) except for rectus abdominis, where women had a greater age-related decrease compared with men (p=0.02). Rectus abdominis and pectoralis major showed the greatest age-related decrease in muscle mass. Notably, the relative age-related decrease in muscle density was greater among women than men. Specifically, muscle density in the latissimus dorsi, rectus abdominis, serratus anterior, external oblique, pectoralis major and psoas major decreased more rapidly in women (p<0.05, Fig. 1). Total trunk muscle mass declined by 7% per decade in both sexes, whereas average muscle density declined by 22% and 13% per decade in women and men, respectively.

**Conclusion:** Our findings indicate that the age-related differences cannot be generalized across all trunk muscles. Future studies should explore the possible reasons for the diversity in muscle changes, and in particular for the greater fatty infiltration of muscle in women than men with increasing age.

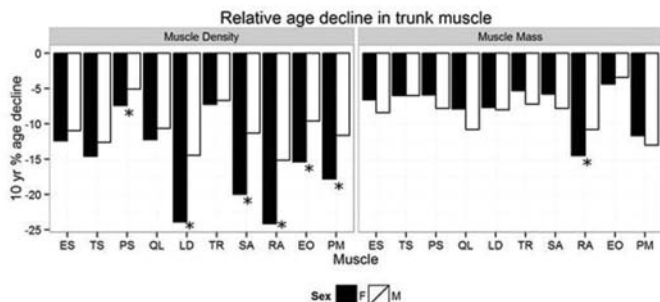


Figure 1: Relative age-related decline in trunk muscle density (left) and mass (right). \* Significantly different between men and women (p<0.05).

Figure 1

**Disclosures:** Fjola Johannesdottir, None.

## SU0122

**Changes in muscle strength and physical performance from midlife and bone health in early old-age: a 7-year follow up study of the MRC National Survey of Health and Development.** Kate Ward<sup>1</sup>, Stella Muthuri<sup>2</sup>, Adam Moore<sup>2</sup>, Judith Adams<sup>3</sup>, Cyrus Cooper<sup>1</sup>, Di Kuh<sup>2</sup>, Rachel Cooper<sup>2</sup>. <sup>1</sup>MRC Lifecourse Epidemiology, University of Southampton, United Kingdom, <sup>2</sup>MRC Unit for Lifelong Health and Ageing at UCL, United Kingdom, <sup>3</sup>Central Manchester University Hospitals Foundation NHS Trust, United Kingdom

There are few prospective data investigating how muscle strength and physical performance in adulthood may relate to later bone health. The aim of this study was to test associations between changes in grip strength and chair rise speed, measured from midlife, with bone outcomes in early old age in men and women from a British birth cohort study, the MRC National Survey of Health and Development.

At age 60-64y, 1583 (824 women) had assessments of bone including pQCT and DXA. Associations between four categories of 'change' in grip strength and chair rise speed (i.e. decline, stable-high, stable-low, reference (no meaningful decline) between ages 53 and 60-64 years and bone outcomes (radius: volumetric BMD, cross-sectional

area (CSA), medullary CSA; hip: aBMD, femoral neck cross-sectional moment of inertia (CSMI), total hip CSA) were tested using linear regression stratified by sex and adjusting for standardised height and weight. Results are presented as percentage mean [95%CI] differences in DXA- and pQCT outcomes when comparing each change category to the reference category.

**Grip strength:** Men in the stable-high category had significantly higher aBMD (hip 6.2%[2.1,10.2], femoral neck 6.8%[2.3,11.4] and larger radius CSA (5.7%[1.3,10.1]) than the reference category. The stable low category had smaller bones; radius CSA (-9.1% [-13.7,-4.4], medullary CSA (-16.4%[-28.2,-4.5]) hip CSA (-4.6%[-7.2,-1.9]). There were no significant differences in bone between those men who experienced decline and the reference category. In women, there were no significant differences in bone between the different change categories. **Chair-rise speed:** Men in the stable low category had significantly lower total radius vBMD and hip aBMD (-6.6%[-13.2,-0.1]; -5.7%[-10.5,-0.8]) and larger radii (8.9%[4.1,13.7]) with wider medullary cavities (16.2% [3.8,28.6]) than the reference category.

Changes in muscle force and performance in men were associated with bone health at age 60-64 years. The associations of the stable-high grip strength category with aBMD and bone size highlight the importance for bone health of achieving and maintaining 'peak' muscle strength during adulthood. In contrast, the associations of the stable-low grip strength and chair-rise categories with bone, suggest a trajectory to poorer bone health beginning at least as early as midlife. Midlife may provide an opportune time to intervene to prevent disability associated with sarcopenia and osteoporosis in later life.

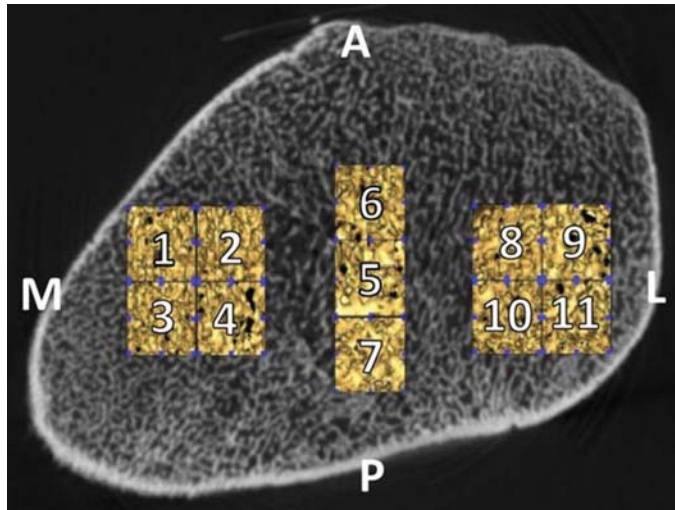
**Disclosures:** Kate Ward, None.

## SU0123

**Ontogenetic Patterning of Human Subchondral Bone Microarchitecture in the Proximal Tibia.** Jesse Goliath<sup>1</sup>, Timothy Ryan<sup>2</sup>, James Gosman<sup>1</sup>. <sup>1</sup>Department of Anthropology, The Ohio State University, United States, <sup>2</sup>Department of Anthropology, Center for Quantitative Imaging, Pennsylvania State University, United States

The objective of this study was to test the hypotheses that ontogenetic patterns of change in tibial subchondral trabecular and cortical bone microstructure are age and condyle site-specific due to differential loading associated with changing joint kinematics and body mass. HR-pQCT images were acquired for 31 human tibiae, ranging in age from 8 to 37.5 years. The skeletal samples are from Norris Farms #36 site, a cemetery associated with the Oneota culture, dating to A.D. 1300. Proximal epiphyses were digitally isolated for analysis as regions of interest (ROIs) using Avizo Fire 6.2 and 8.1.1. 3D resolution-corrected morphometric analysis of subchondral bone architecture was performed for 11 cubic volumes of interest (VOIs) using BoneJ. VOIs were positioned within and between the tibial condyles. The analysis of the subchondral cortical plate was accomplished through dual-threshold cortical masking. Ontogenetic patterns were quantified using eight parameters: bone volume fraction (BV/TV), trabecular thickness (Tb.Th), trabecular spacing (Tb.Sp), structure model index (SMI), connectivity density (Conn.D), degree of anisotropy (DA), trabecular number (Tb.N), and cortical thickness (Ct.Th) in the subchondral cortical plate. Kruskal-Wallis and Wilcoxon signed rank tests were used to examine the association between region, age, and each structural parameter. Findings in this study indicate that age-related changes in mechanical loading have heterogeneous effects on subchondral bone morphology within the proximal tibia. Specifically, there were significant differences in BV/TV ( $\alpha = 0.033$ ), Conn.D ( $\alpha = 0.001$ ), DA ( $\alpha = 0.012$ ), and Plate Ct.Th ( $\alpha = 0.000$ ) across age. With age, subchondral trabecular microstructure increased in bone volume fraction and degree of anisotropy, and decreased in connectivity density. In the plate, there is an age-related increase in thickness. When comparing condylar regions, only the degree of anisotropy significantly differed ( $\alpha = 0.004$ ) between medial and lateral condyles. Trabeculae in the medial condyle were more anisotropic than the lateral region. The differential response of subchondral bone to changing mechanical loads during growth and development serves as a powerful tool to evaluate the significance of mechanical loading on adult bone morphology. Understanding the spatial specifics of ontogenetic processes during subchondral bone development can offer insights into adult morphological variation in joint health and disease.





VOI Placement

**Disclosures:** Jesse Goliath, None.

## SU0124

### The Role of Discoidin Domain Receptor 2 in Craniofacial Morphogenesis.

Fatma Mohamed\*, Chunxi Ge, Nan Hatch, Abdulaziz Binraves, Renny Franceschi, University of Michigan School of Dentistry, United States

**Background:** Discoidin domain receptor 2 (DDR2), a receptor tyrosine kinase activated by fibrillar collagen, is essential for skeletal development. In humans, mutations in the DDR2 gene cause spondylo-meta-epiphyseal dysplasia (SMED), a rare, autosomal recessive disorder characterized by short stature, short limbs and craniofacial anomalies. In addition to dwarfism and major defects in bone formation in the axial and appendicular skeleton, Ddr2-deficient mice have distinct skull abnormalities including short snout, eye protrusions and shortened cranial length. The shortened skull phenotype suggests that Ddr2 regulates craniofacial morphogenesis. However, little is known about the role of DDR2 in craniofacial development. Purpose of this study is to uncover the role of Ddr2 in regulation of craniofacial morphogenesis using loss of function genetic studies. **Methods and Results:** Ddr2<sup>slie/slie</sup> mice used in our studies contain a spontaneous 150 kb deletion in the Ddr2 locus to produce an effective null. We analyzed knockout and wildtype (WT) littermates at different time points postnatally. LacZ staining of newborn and 3-month calvariae from Ddr2-lacZ knock-in mice showed  $\beta$  gal activity in cranial sutures and the resting zone of cranial base growth plates (synchondroses) and in bone marrow. Ddr2-null skulls had defects in cranial sutures and bone ossification as early as P0. At P14, the posterior frontal suture, which is normally closed at this age, remained strikingly wide open in mutant mice. Spatial expression of Ddr2 in suture mesenchyme suggests a role for Ddr2 in normal suture closure and cranial morphogenesis. Compared with WT littermates, Ddr2-null mice also showed abnormally enlarged synchondroses at the base of skull due to widening of resting and hypertrophic zones, as analyzed by histological quantification. The widened resting zone is likely due to delayed maturation as fewer chondrocytes in the resting zone undergo proliferation leading to a narrower proliferative zone and reduced chondrocyte proliferation, as confirmed by Ki67 antibody proliferation marker. The effect of Ddr2 loss on the hypertrophic zone, however, is possibly the result of diminished MMP13 signaling and impaired remodeling rather than differentiation or apoptosis. **Conclusion:** Together, these findings demonstrate the novel function of Ddr2 in regulating craniofacial bone growth; as well as emphasize the importance of identifying the etiologies of human genetic diseases causing defective cranial morphogenesis.

**Disclosures:** Fatma Mohamed, None.

## SU0125

**Postnatal ablation of Smad4 enhances endochondral ossification in epiphyseal growth plate.** Sho Tsukamoto\*<sup>1</sup>, Noriko Sekine<sup>1</sup>, Mai Kuratani<sup>1</sup>, Keigo Kumagai<sup>1</sup>, Shinya Tanaka<sup>2</sup>, Eijiro Jimi<sup>3</sup>, Hiromi Oda<sup>2</sup>, Takenobu Katagiri<sup>1</sup>. <sup>1</sup>Division of Pathophysiology, Research Center for Genomic Medicine, Saitama Medical University, Japan, <sup>2</sup>Department of Orthopedic Surgery, Saitama Medical University, Japan, <sup>3</sup>Division of Molecular Signaling and Biochemistry, Department of Health Improvement, Kyushu Dental University, Japan

The transforming growth factor- $\beta$  (TGF- $\beta$ ) family regulates cell proliferation and differentiation of skeletal cells, such as osteoblasts, osteoclasts and chondrocytes during embryonic development. The members consist of more than 30 members including TGF- $\beta$ s, activins, bone morphogenetic proteins (BMPs) and growth and differentiation factors (GDFs). They are classified into two subgroups due to intracellular signaling

pathways through phosphorylated Smad1/5 and Smad2/3, respectively. Smad4 is an essential coactivator of both Smad1/5 and Smad2/3. In the present study, we established a mouse line of tamoxifen (Tam)-inducible Smad4 conditional knockout (Smad4 cKO) by crossing Smad4-floxed mice with CAG-CreERT mice. To examine the role of the TGF- $\beta$  family in postnatal skeletal growth, the mice were injected with Tam at 10-w-old and kept for additional 3 weeks. The Smad4 cKO mice showed increased primary spongiosa in tibia and femur in micro-CT analysis. Bone histomorphometric analysis indicated that bone formation was increased in the mice. The numbers of osteocalcin-positive activated osteoblasts were increased in the primary spongiosa but not secondary spongiosa or cortical bone. Hypertrophic zone in the epiphyseal growth plates was expanded in the Smad4 cKO mice. Hypertrophic chondrocytes in the epiphyseal growth plate were stained with an antibody against phosphorylated Smad3. Chondrocytes were prepared from wild-type mice and were cultured in vitro in the presence of TGF- $\beta$ 1 or SB-431542, a specific small chemical inhibitor of TGF- $\beta$  receptor. Treatment with TGF- $\beta$ 1 suppressed chondrogenic differentiation. In contrast, treatment with SB-431542 increased the cell size and the gene expression related to chondrogenic differentiation. These findings suggest that the Smad4-dependent signaling of the TGF- $\beta$  family suppresses differentiation of chondrocytes in epiphyseal growth plate and reduces endochondral ossification in postnatal mice.

**Disclosures:** Sho Tsukamoto, None.

## SU0126

### Bone Renovation of the Mouse Neonatal Fibula into the Adult Skeleton.

Masaki Yoda\*, Yukiko Kuroda, Koichi Matsuo, Keio university school of medicine, Japan

Endochondral ossification is a process by which bone replaces cartilage templates. Growth plate-dependent endochondral ossification allows longitudinal growth of various bones including long bones, vertebrae, scapula, and the skull base, whereas growth plate-independent endochondral ossification occurs without changing shape and size as seen in the auditory ossicles. The primary ossification center of a long bone diaphysis also ossifies independently of growth plate during development, and the initial bony diaphysis usually disappears after postnatal cross-sectional growth. Here we report that neonatal mouse fibular cortex near the distal tibiofibular junction (hereinafter referred to as "distal fibula"), which have ossified growth plate-independently from the cylindrical cartilage, may partly persist into adult skeleton. First, we performed time-course fluorescent double labeling by subcutaneous injection on the day of birth and two days prior to sacrifice, and the tibia and fibula of labelled mice were made transparent at P9, P16, P23 etc with 1:2 benzyl alcohol:benzyl benzoate (BABB) treatment. A fluorescence stereo microscopic analysis revealed "the ossification area without growth plate involvement" in the distal fibula. In addition, histological analyses showed that the distal fibular cortex facing the tibia undergoes appositional growth on the periosteum towards tibia coupled with bone resorption on the endosteum. The fibular cortex facing away from the tibia showed endosteal bone formation eventually filling the bone marrow cavity except for the central canal. Whole-mount staining of fibula for the osteoclast marker TRAP also detected specific and continuous resorption surfaces on the opposite side of the osteogenic surfaces in the distal fibular cortex. Second, synchrotron X-ray tomographic microscopy of the adult distal fibula revealed the polarity of individual osteocyte lacuna indicative of the endosteal or periosteal appositional growth. These data suggest that adult distal fibula near the distal tibiofibular junction is a composite of neonatally ossified bone with bone formed by appositional growth, and bone resorption maintains its diameter of approximately 300 micrometers. In other words, growth plate-independent, cartilage template-derived bone can be renovated and survive into adulthood.

**Disclosures:** Masaki Yoda, None.

## SU0127

### Effects of human amniotic fluid stem cells and their conditioned medium on bone defect healing.

Mariangela Basile\*<sup>1</sup>, Paola Vizzarri<sup>2</sup>, Francesco Marchegiani<sup>2</sup>, Alexander C Lichtler<sup>1</sup>, Ivo Kalajic<sup>1</sup>, Roberta Di Pietro<sup>2</sup>.

<sup>1</sup>Uconn Health, United States, <sup>2</sup>Department of Medicine and Aging Sciences, Italy

Human amniotic fluid stem cells (hAFSCs) represent an attractive cell model for transplantation therapy. Although hAFSCs have been investigated for bone repair, the cellular distribution and the post-implantation fate and viability have not been verified. Furthermore, some authors demonstrated the vascularizing properties of hAFSCs conditioned medium (CM), but its role in regeneration of bone defects is still unknown. The aim of the study was to investigate whether hAFSCs and their CM could improve bone healing in vivo.

hAFSCs were obtained from routine clinical amniocentesis specimens and cultured *in vitro*. CM was collected after 48 h. For *in vivo* experiments a critical size (3.5 mm) calvarial defect was generated in NSG immunodeficient mice. hAFSCs were expanded *in vitro* and transfected with a lentiviral vector expressing a ubiquitously directed red fluorescent protein (Ub-Cherry). Transfected hAFSCs and hAFSCs CM were transplanted *in vivo* at the lesion sites after being loaded on HEALOS scaffold (cross-linked collagen fibers fully coated with hydroxyapatite) appropriately shaped to fit inside the defect. The calvarial defect was filled with the scaffold alone, 10<sup>6</sup> Ub-Cherry hAFSC, or hAFSC CM. Six weeks after implantation animals were sacrificed. Healing was evaluated by X-ray. Cellular engraftment was evaluated histologically by fluorescence microscopy, and then stained with haematoxylin-eosin to better analyze histological structures.

X-rays demonstrated the presence of mineralized tissue only in the defects loaded with the scaffold plus hAFSCs and, interestingly, plus hAFSCs CM. Light microscopy

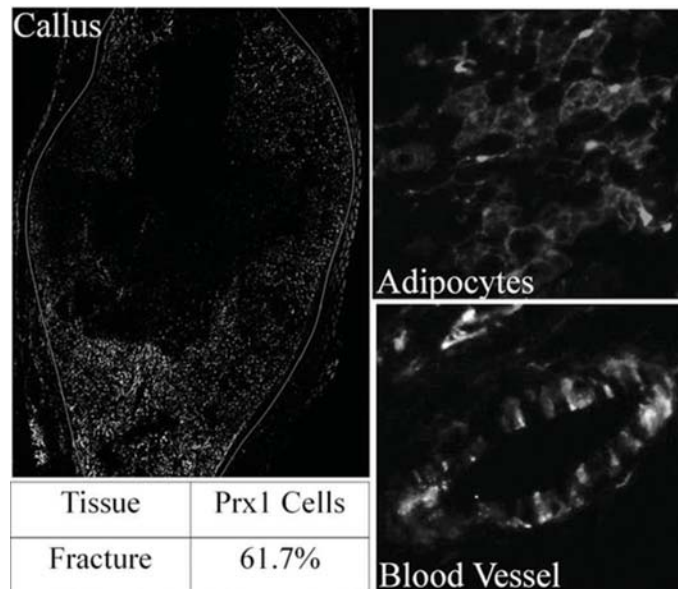
observations revealed a major fibrous reaction in mice specimens treated with the scaffold supplemented with hAFSCs and hAFSCs CM compared with mice treated with the cell-free scaffold. Our findings indicate that undifferentiated hAFSCs and their CM seeded on a collagen scaffold can contribute to new bone formation. These preliminary observations pave the way to the use of new bioengineered constructs of stem cell- and CM-collagen scaffold for correcting large cranial defects in animal models and human subjects.

**Disclosures:** Mariangela Basile, None.

## SU0128

**Prx-1 Embryonic Specification Is Retained in a Postnatal Regenerative Stem Cell Population that Gives Rise to Skeletal, Fat, and Vascular Tissues.** Beth Bragdon<sup>\*1</sup>, Andrew Bennie<sup>1</sup>, Jenny Lei<sup>2</sup>, Elise Morgan<sup>2</sup>, Louis Gerstenfeld<sup>1</sup>. <sup>1</sup>Boston University School of Medicine, United States, <sup>2</sup>Boston University College of Engineering, United States

Mesenchymal stem cell (MSC) is used to describe a population of adult stem cells that are multipotent and contribute to bone homeostasis and repair. However, this population of cells has not been identified *in vivo* and is recently suggested to be pericytes. A cell population conditionally expressing Prx1 previously shown to identify embryonic appendicular and calvaria tissues and postnatally associated with bone formation and repair was used for *in vivo* lineage tracking studies. Male and female mice aged 8-11 weeks were used in IACUC approved studies. Different models of postnatal bone formation were used: closed stabilized transverse femoral fracture, distraction osteogenesis (limb lengthening), and ectopic bone formation at appendicular and axial sites (limb, sternum, spine). Tamoxifen inducible Prx1 Cre ERT transgenic mice were crossed with B6.Cg-Gt(Rosa)26sor<tm14(CAG-tdTomato)Hze>/J mice to create Prx1/Ai14 reporter. Subsequently Prx1/Ai14 mice were crossed with B6.129S7-Rag1<sup>tm1Mom</sup>/J to create a transgenic reporter mouse allowing for the implantation of human demineralized bone matrix (DBM) to induce ectopic bone. Tamoxifen was administered and allowed to be washed out for at least 28 days or for only 3 days prior to surgery or ectopic bone induction in order to follow the specified population through postnatal bone formation. Under both homeostatic and short duration labeling conditions cell labeling was observed in differentiated osteoblasts and osteocytes in cortical and trabecular bone and cells on both periosteal and endosteal surfaces of both fore and hind limbs and cranium. Immunohistochemistry confirmed that adipocytes and smooth muscle cells in vessels within the muscle compartment of the appendicular skeleton were also labeled. Prx1 was induced in regenerative tissues after bone injury (fracture (see figure)) and distraction osteogenesis within the same lineages as seen under homeostatic labeling. Ectopic bone induced in response to DBM implantation in the limbs showed labelled cells differentiated into chondrocytes, osteoblasts, adipocytes, and vessel associated smooth muscle however ectopic bone induction at axial skeletal sites such as sternum and spine did not show labelled cells. These results suggest that Prx1 expression connotes a multi-potential postnatal MSC that retained its embryonic tissue specification and contributes to both postnatal homeostatic maintenance and tissue repair in response to injury.



Figure

**Disclosures:** Beth Bragdon, None.

## SU0129

**Transcriptional Heterogeneity During Lineage Specification Defines Human Musculoskeletogenesis.** Gabriel Ferguson<sup>\*</sup>, Benjamin Van Handel, Denis Evsenko. University of Southern California, United States

Tissue-specific gene expression defines cellular identity and function, but our current knowledge of early human development is limited, making the development of cell and tissue-based therapies a significant challenge. Here, we created a transcriptional profile of human skeletogenesis, generating expression data for 5 distinct cell types at a single stage of fetal development. Additionally, we profile pre-chondrocyte progenitors of the embryonic limb bud 5-6 weeks post conception (WPC), presumptive articular chondrocytes from the fetus 17 WPC, and adult articular chondrocytes in parallel with chondrocytes derived pluripotent stem cells at two distinct timepoints in the differentiation process. We defined tissue-specific gene modules which correctly segregated known lineage-specific genes. Application of these modules combined with chromatin state analysis showed broad similarities in gene expression patterns during cartilage specification both *in vitro* and *in vivo*, suggesting close mimicry of *in vivo* ontogeny. Taken together, these analyses provide new insight into human musculoskeletal development and provide a critical comparative resource for pluripotent stem cell differentiation.

**Disclosures:** Gabriel Ferguson, None.

## SU0130

**Actin Filament Associated Protein 1 (AFAP1) is required for osteogenic differentiation of mesenchymal stem cells.** Evan Frigoletto<sup>\*1</sup>, Holly Corkill<sup>1</sup>, Alben Gesheva<sup>2</sup>, Jess Cunnick<sup>1</sup>, John Arnott<sup>1</sup>, Youngjin Cho<sup>1</sup>. <sup>1</sup>Geisinger Commonwealth School of Medicine, United States, <sup>2</sup>University of Scranton, United States

Differentiation, survival, and function of mesenchymal stem cells (MSC) in bone formation are regulated by anabolic signals, including TGF- $\beta$ 1 and mechanical inputs, and the interplay and convergence occurring between these anabolic signaling pathways. Understanding the relationships among these anabolic inputs, their inherent points of signaling convergence within MSC and osteoblast has become an area of intense clinical interest with the ultimate goal of reversing clinical bone loss. Actin Filament Associated Protein 1 (AFAP1) is a scaffolding protein composed of numerous motifs and domains that enable the assembly of signaling complexes and integration of signaling molecules in subcellular compartments, affecting the location and crosstalk between these molecules. We have shown that the loss of AFAP1 in osteoblast lead to impaired proliferation and mineralization and that the loss of AFAP1 in mice lead to impaired skeletogenesis with significant reduction in bone volume. We recently generated osteoblast specific null AFAP1 mice (CKO) and discovered that newborn CKO mice show defects in intramembranous ossification and adult CKO mice show delayed mineralization in calvaria with the presence of irregularly shaped gaps in calvarial sutures. These results demonstrate that AFAP1 is important for normal skeletogenesis and strongly suggest potential defects in MSC growth and differentiation in the absence of AFAP1. To test the hypothesis that AFAP1 is required for osteogenic differentiation of MSC, we isolated MSC from bone marrow or cortical bones of the wild type control and AFAP1 null mice and assessed whether the osteogenic differentiation of MSC is affected. We similarly assessed the osteogenic, chondrogenic, and adipogenic differentiation of murine embryonic fibroblasts (MEFs) isolated from the wild type control and AFAP1 null mice. The loss of AFAP1 leads to altered morphology, delayed mineralization, and reduced osteogenic differentiation of MSC and MEFs without affecting either chondrogenic or adipogenic differentiation of these cells. In order to further elucidate AFAP1's role in the observed differentiation patterns of MSC, we looked to well-known anabolic input signals that modulate differentiation and survival of MSC. Wherein, we found the transduction of TGF- $\beta$ 1 and mechanical loading signals for Akt activation is specifically reduced in bone cells and MEFs in the absence of AFAP1. Akt is one of the key signaling molecules that can integrate multiple signaling inputs and relay these integrated signals to orchestrate transcriptional and translational networks that can fine-tune the growth and differentiation of MSC and osteoblasts. Therefore, these results suggest that AFAP1 may provide a point of signal convergence among these pathways to differentially activate Akt depending on the cellular context, such as in MSC differentiation and during osteoblast maturation.

**Disclosures:** Evan Frigoletto, None.

## SU0131

**Comparison of Genomic Enhancer and Enhancer RNAs Utilized by  $\alpha$ SMA Positive Bone Marrow Stromal Cells and  $\alpha$ SMA Positive Periodontal Stem/Progenitor Cells During Differentiation.** Stephen e harris<sup>\*1</sup>, Audrey Rakian<sup>1</sup>, Rebecca Neitzke<sup>1</sup>, Michael Rediske<sup>1</sup>, Marie a Harris<sup>1</sup>, Ivo Kalajic<sup>2</sup>, Jian q Feng<sup>3</sup>, Lynda f Bonewald<sup>4</sup>, Brian f Foster<sup>5</sup>, Jelica Gluhak-Heinrich<sup>1</sup>, Yong Cui<sup>1</sup>. <sup>1</sup>UTHSCSA, United States, <sup>2</sup>UCHC, United States, <sup>3</sup>TAMHSC, United States, <sup>4</sup>IU, United States, <sup>5</sup>OSU, United States

Postnatal deletion of the Bmp2 gene using  $\alpha$ SMA-CreERT2 results in a profound skeletal phenotype with reduced cross-sectional area in tibia and femur, reduction in cranial alveolar bone, and defects in cementogenesis and the periodontal ligament (PDL). To understand the Bmp2 function,  $\alpha$ SMA+ cells isolated from both bone



marrow (BMSC) and periodontium (PSC), were expanded on StemBio ECM matrix to maintain stem cell state for carrying out full transcriptome analysis. These cells, over 90% positive for  $\alpha$ SMA, were treated with rBMP2 for 24 hrs (early) or after 5-12 days of culture and differentiation/mineralization. Full transcriptome analysis of both coding and long-noncoding RNAs (lncRNAs) along with Chip-seq analysis with H3K27ac was performed. Enhancers (H3K27ac peaks) were mapped to within 100,000 bp to the nearest gene body that showed corresponding regulated expression. In BMSC, there were a total of 18,408 candidate enhancers identified, with 7,138 rapidly induced at 24hrs after rBmp2 treatment, and 5,865 selective for the differentiated state. In PSC, with 25,350 candidate enhancers, 4,187 are rapidly induced at 24hrs after rBMP2 treatment, and 5,906 enhancers selective for the differentiated state. 83% of these regulated enhancer regions have associated lncRNAs that are excellent candidates for enhancer RNAs involved in bone marrow stem cell to alveolar osteoblast to osteocyte differentiation or periodontal stem/progenitor cell differentiation to PDL to cementoblasts to cementocytes. By comparison of the gene transcripts and regulated enhancers in the BMSC and PSC system, a core regulatory gene-enhancer network was derived using the transcription factor binding sites in the enhancers and their regulated coding transcript levels. Selective gene-enhancer networks for BMSC versus PSC were identified. Using the IDG-CM6 periodontal progenitor/cementocyte cell line, complete coding and lncRNA transcriptome analysis was carried out at the progenitor state and at stages of cementocyte differentiation. Many of the coding and lncRNA overlap with the PSC system. For example, the Bmp2 gene with 6 induced enhancer regions with associated candidate eRNAs found in both the PSC and BMSC, was also found in the IDG-CM6 model. The IDG-CM6 system will now allow us to dissect out the function of selective enhancer-eRNA regions that are critical nodes in the gene transcript-enhancer networks using CRISPRi methods.

**Disclosures:** *stephen e harris, None.*

## SU0132

**The role of Hedgehog signaling in large-scale bone repair.** Stephanie Kuwahara\*, Francesca Mariani, Gage Crump, Sandeep Paul, Nikita Tripuraneni, Jason Hsieh, Monica Liu, Ashlie Munoz, Neel Hedge, Lynette Lester. USC, United States

Non-union fractures and the failure to naturally repair large bone injuries without surgery are still challenging clinical problems that lead to increased cost and lower quality of life. It is often thought that the process of regeneration involves the recapitulation of developmental programs. In our novel model for large-scale bone repair in the mouse, some aspects of bone development are recapitulated (the formation of a cartilage template for example), however the cells that make this cartilage are very different from developmental cartilage. The callus cells express both cartilage and bone-specific genes by RNA in situ hybridization and have other hybrid cartilage and bone properties. Although it is known that cells in the periosteum contribute to bone repair, how the periosteal cells build the repair callus made of these hybrid cells only in response to injury has remained unclear. Through genetic approaches, we show that Hh signaling is required for the generation of a full-thickness callus consisting of hybrid cells. Without abundant hybrid cells, repair is of poor quality and seems to favor direct ossification. Thus, the presence of a Hh signal may represent the critical switch between endochondral and direct ossification. Furthermore, our results indicate that enhancing the production of hybrid repair cells by stimulating the Hh pathway may lead to improved bone repair therapies.

**Disclosures:** *Stephanie Kuwahara, None.*

## SU0133

**Conservation of perivascular progenitor cell antigens and methods of isolation across mammalian species.** Carolyn Meyers\*<sup>1</sup>, Winters Hardy<sup>2</sup>, Paul Hindle<sup>3</sup>, Greg Asatryan<sup>2</sup>, Catherine Ding<sup>2</sup>, Mihaela Crisan<sup>3</sup>, Noah Yan<sup>1</sup>, Sonja Lobo<sup>2</sup>, Pei Liang<sup>2</sup>, Xinli Zhang<sup>2</sup>, Kang Ting<sup>2</sup>, Chia Soo<sup>2</sup>, Bruno Peault<sup>2</sup>, Aaron James<sup>1</sup>. <sup>1</sup>Johns Hopkins University, United States, <sup>2</sup>UCLA, United States, <sup>3</sup>University of Edinburgh, United Kingdom

**Background.** Human subcutaneous adipose tissue is a rich source of tissue resident mesenchymal progenitor cells (MPCs), commonly considered to share a perivascular residence. The interest in using CD146<sup>+</sup> pericytes and CD34<sup>+</sup> adventitial progenitor cells for tissue engineering has significantly increased. Previously, human perivascular progenitor cells from adipose tissue were observed to outpace conventionally derived MPCs in three pre-clinical models of bone regeneration. Here we report on several recent steps to advance the translation of a perivascular progenitor cell therapy, including derivation of PSC from canine and ovine tissues.

**Methods.** Subcutaneous adipose tissues were procured under IRB approval from human (n=131), ovine (n=4), and canine sources (n=12). Immunofluorescent identification of perivascular antigens was performed (CD34,CD146), followed by fluorescence activated cell sorting (FACS) of pericyte (CD45-CD31-CD146+CD34-) and adventitial progenitor cells (CD45-CD31-CD146-CD34+). Among culture propagated cells, cell surface marker characterization was performed by flow cytometry (CD31,CD34,CD44,CD45,CD90). Among representative samples, trilineage mesenchymal differentiation potential was examined *in vitro*, including osteogenic, chondrogenic, and adipogenic differentiation.

**Results.** Human, canine, and ovine vessels within adipose tissue show a remarkable conservation in markers of perivascular identity, using antibodies directed against

CD146 and CD34. Distinct perivascular subpopulations are identifiable in tissue sections (Fig A), and isolatable by fluorescence-activated cell sorting (Fig B). Cell yield and progenitor cell frequency are similar between human, canine, and ovine fat sources. Classic MPC markers are shared among perivascular progenitors of large mammals (e.g. CD44, CD90), and trilineage differentiation potential is a canonical feature of PSC independent of species of origin (osteogenic, chondrogenic, and adipogenic cell lineages). However, differences in baseline osteogenic potential are observed across species. These include a marked predilection for human perivascular progenitor cells to undergo osteogenic differentiation *in vitro* in comparison to other species.

**Conclusion.** Perivascular progenitor cells from adipose tissue are an abundant, uncultured cell source for future efforts in regenerative medicine. Perivascular progenitor cell markers, cell frequency, and multipotentiality appear conserved across large mammals.

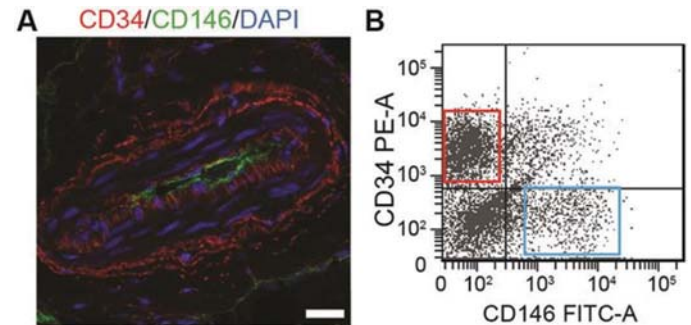


Figure 1

**Disclosures:** *Carolyn Meyers, None.*

## SU0134

**Validation of osteogenic properties of Cytochalasin D by high-resolution RNA-sequencing in human mesenchymal stem cells.** Rebekah Samsonraj\*<sup>1</sup>, Amel Dudakovic<sup>1</sup>, Christopher Paradise<sup>1</sup>, Buer Sen<sup>2</sup>, Allan Dietz<sup>1</sup>, Janet Rubin<sup>2</sup>, Andre van Wijnen<sup>1</sup>. <sup>1</sup>Mayo Clinic, United States, <sup>2</sup>University of North Carolina, United States

Adipose-derived mesenchymal stem cells (AMSCs) offer several advantages over other sources of MSCs, particularly in the ease of tissue harvest, isolation and expansion to generate sufficient cell numbers for therapy. Because AMSCs are generally considered to have relatively lower osteogenic potential than bone marrow-derived MSCs (BMSCs), it is important to design strategies that improve their ability to attain a mature osteoblastic phenotype. It has been previously established that cell stiffness and elasticity can influence lineage commitment of stem cells. Previous work on bone marrow-derived MSCs has shown that Cytochalasin D (CytoD), a fungal metabolite that disrupts actin polymerization and cytoskeleton integrity, promotes osteogenesis by inducing accumulation of intranuclear actin leading to bone-specific gene expression. We report that CytoD alters cell shape of proliferating cells but not confluent cells in both AMSCs and BMSCs. In AMSCs, CytoD enhances osteogenic differentiation by promoting alkaline phosphatase activity and mineralization, as well as the expression of osteogenic genes ALP, TGF $\beta$ 3, COL1A1 and SPARC. High-resolution RNA-seq analysis showed that CytoD upregulates HSD11B1, MTSS1, NPR1 and MCTP1 in AMSCs while downregulating TEAD4 and KLF2. A three-way comparison between human AMSCs, human BMSCs, and mouse BMSCs by RNA-seq analyses revealed significant upregulation of genes linked to extracellular matrix organization, cell adhesion and bone metabolism as well as PDGFR $\beta$  and VEGFR pathways, accompanied by a downregulation of nuclear and cell cycle-related genes. We also identified eight novel genes commonly upregulated across species and tissue source of MSCs, which are thought to play key roles in bone metabolism. Together, our study suggests that CytoD supports the acquisition of osteogenic phenotype by AMSCs and advances their therapeutic potential in bone tissue regeneration.

**Disclosures:** *Rebekah Samsonraj, None.*

## SU0135

**Biglycan Regulates the Proliferation and Differentiation of Periosteum-Derived Cells.** Reut Shainer\*, Megan Noonan, Vardit Kram, Tina Kilts, Marian Young. NIH, United States

Bone healing involves a complex sequence of physiological events resulting in the formation of new bone in the fracture area.

The periosteum, a thin membrane surrounding the bone, rapidly expands after fracture and is thought to be the source of progenitor cells needed for bone formation and repair. The periosteum-derived cells (PDCs) have the capability to differentiate into multiple skeletal phenotypes, suggesting they have stem cell-like properties.

The matrix proteoglycan biglycan (Bgn) is highly expressed in bone and cartilage formation, particularly during fracture healing, and yet its exact role in regulating bone repair is still unclear. Histological analysis of the tissues around the fracture site revealed the fracture induced thickened periosteum contains high levels of Bgn, suggesting it has a function there.

In the current study, we examined the role of Bgn in modulating PDCs differentiation potential using a novel 3D culture system. When PDCs were isolated from *Wt* and *Bgn* KO mice and expanded in culture, *in-vitro* proliferation assays showed that *Bgn* deficient cells proliferated faster than *Wt* controls. To test the differentiation potential of PDCs we tried to mimic the native environment of the cells by seeding PDCs from *Wt* and *Bgn* KO mice in a 3D cell culture system made of type I collagen (RAFT from Lonza). After seeding the RAFT structures with PDCs, they were then induced to undergo osteogenic and chondrogenic differentiation. Scanning electron microscopy (SEM) 3 weeks after differentiation revealed that the 3D *Bgn* deficient cell culture secreted enhanced levels of extra-cellular matrix (ECM) compared with the *Wt* samples, both in the osteogenic and the chondrogenic inducing media. Analysis of the 3D structures by histology and by immunohistochemistry staining showed there were high amounts of aggrecan in the ECM secreted by the *Bgn* KO cells, both in the cartilage and the bone differentiated samples.

**Disclosures:** Reut Shainer, None.

## SU0136

**Oleanolic Acid Enhances Mesenchymal Stromal Cell Osteogenic Potential by Inhibition of Notch Signaling.** Guangxi Wang<sup>\*1</sup>, Bing Shu<sup>2</sup>, Sheila Rogers<sup>1</sup>, Dollie Smith<sup>1</sup>, Massimo Morandi<sup>1</sup>, Shane Barton<sup>1</sup>, Yufeng Dong<sup>1</sup>. <sup>1</sup>LSU Health Sciences Center, United States, <sup>2</sup>Shanghai University of Traditional Chinese Medicine, China

Oleanolic acid (OA), a natural pentacyclic triterpenoid, has been shown to modulate multiple signaling pathways in a variety of cell lineages, but the mechanism(s) underlying OA-mediated mesenchymal stromal cell (MSC) osteogenic differentiation are not known. In this study, we examined the effects of OA on MSC osteogenic differentiation, and the involvement of Notch and BMP signaling. In bone marrow derived MSC cultures, OA treatment induced cell differentiation towards osteoblastic cells by showing enhanced Alkaline phosphatase (ALP) staining and osteogenic marker gene expression. In contrast, Notch reporter RBPJ luciferase activity and Notch target gene *Hes1* expression were significantly reduced in a dose dependent manner. Overexpression of Notch intracellular domain NICD to activate Notch signaling in OA-treated MSC cultures resulted in decreased ALP staining at day 7 when compared to control cells infected with GFP lentivirus (Fig. 1) suggesting that constitutive activation of Notch signaling in cells blocks OA-induced osteogenic differentiation. Furthermore, ALP activity and expression of osteogenic marker gene were significantly enhanced by combined treatment with OA and BMP2 when compared with either OA or BMP2 alone treated MSCs, indicating a synergistic effect between BMP2 and OA. Finally, Masson's Trichrome staining of tissue sections from the *in vivo* ectopic ossicle formation confirmed this synergistic effect by showing more enhanced bone matrix formation in transplantation of MSCs mixed with both BMP2 and OA. These results demonstrate that inhibition of Notch signaling is required for OA-induced MSC osteogenic differentiation that works parallel with BMP signaling to accelerate MSC differentiation into osteoblasts. Thus, OA is a promising bioactive agent that could be used for bone tissue regeneration.

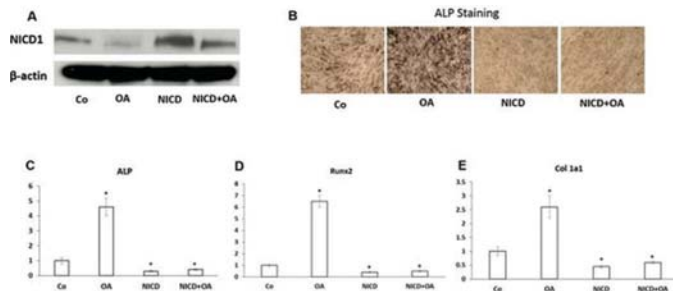


Figure 1: Notch signaling inhibits OA-induced osteogenesis in MSC culture

**Disclosures:** Guangxi Wang, None.

## SU0137

**Influences of Chronic Kidney Disease and Obesity on Vitamin D Metabolism and Action in Human MSCs.** Shuanhu Zhou<sup>\*</sup>, Fangang Meng, Jing Li, Meryl LeBoff, Julie Glowacki. Brigham and Women's Hospital, Harvard Medical School, United States

Two common clinical conditions are associated with dysregulated vitamin D metabolism and bone mass. In chronic kidney disease (CKD), there is impaired renal biosynthesis of  $1\alpha,25$ -dihydroxyvitamin D [ $1\alpha,25(\text{OH})_2\text{D}$ ] and low bone mineral density (BMD); in CKD there is elevated serum FGF-23, the osteocytic inhibitor of osteoblastogenesis. In Obesity there is low serum  $25$ -hydroxyvitamin D [ $25(\text{OH})\text{D}$ ] and high BMD in many sites; in Obesity there is increased serum leptin, secreted by adipocytes. Human mesenchymal stem cells (hMSCs) are targets of  $1\alpha,25(\text{OH})_2\text{D}$  action to enhance their differentiation to osteoblasts; they also express D-relevant genes and synthesize  $1\alpha,25(\text{OH})_2\text{D}$ . These findings suggest an autocrine/paracrine role for vitamin D in hMSC differentiation. There is growing interest in the regulation and function of extrarenal vitamin D hydroxylases. We examined the influence of CKD or obesity on

vitamin D metabolism and action in hMSCs. With IRB approval, we isolated human MSCs from discarded marrow from well-characterized, consenting subjects undergoing orthopedic surgery. Estimated glomerular filtration rate (eGFR) was determined according to the MDRD equation; Fat Mass Index (FMI) and BMD were measured by DXA. We conducted *in vitro* correlation analyses for constitutive gene expression and clinical features and *in vitro* treatments to test regulation of osteoblast differentiation by FGF-23 and by leptin. The FGF-23 receptor and Klotho co-receptor genes were expressed in hMSCs, the later being downregulated in cells from hemodialysis subjects compared with age/gender-matched controls. There was a wide range of constitutive expression of Klotho with statistically significant correlation with eGFR ( $p=0.019$ ). *In vitro*, rhFGF-23 significantly inhibited vitamin D stimulated osteoblastogenesis, and downregulated VDR, CYP27B1, and BMP-7. As expected, the cohort showed significant positive correlation for BMD with FMI and an inverse correlation for  $25(\text{OH})\text{D}$  with FMI. *In vitro*, rhLeptin increased osteoblastogenesis, BMP-7, and CYP27B1 and decreased  $24$ -hydroxylase, with a likely local increase in pro-osteoblastogenic  $1\alpha,25(\text{OH})_2\text{D}$ . Thus, leptin effects in hMSCs may protect the bone from low  $25(\text{OH})\text{D}$  in obese subjects. In sum, CKD and Obesity were associated with opposite effects on vitamin D metabolism in MSCs, which were replicated by FGF23 and Leptin inhibition and stimulation of osteoblastogenesis, respectively, both involving D-hydroxylases and BMP-7.

**Disclosures:** Shuanhu Zhou, None.

## SU0138

**Investigation of the relationship between susceptibility loci for hip osteoarthritis and DXA-derived hip shape in a population based cohort of middle-aged women.** Denis Baird<sup>\*1</sup>, Lavinia Paternoster<sup>2</sup>, Jennifer Gregory<sup>3</sup>, Benjamin Faber<sup>1</sup>, Richard Aspdon<sup>3</sup>, Jonathan Tobias<sup>1</sup>. <sup>1</sup>Musculoskeletal Research Unit, School of Clinical Sciences, University of Bristol, United Kingdom, <sup>2</sup>MRC Integrative Epidemiology Unit, University of Bristol, United Kingdom, <sup>3</sup>Arthritis and Musculoskeletal Medicine, Institute of Medical Sciences, University of Aberdeen, United Kingdom

**Objective:** To investigate whether osteoarthritis (OA) susceptibility loci, identified previously in patients with hip osteoarthritis also influence hip shape, we examined their associations with hip shape parameters derived from statistical shape modelling of hip DXA scans.

**Methods:** 31 hip OA loci were identified by literature search. Hip DXA scans were obtained from mothers of the Avon Longitudinal Study of Parents and Children study (mean 48 years). Overall hip shape was measured using SHAPE software from the University of Aberdeen; the upper femur and superior acetabulum were outlined, following which 10 independent hip shape modes were generated using principal component analysis. Three further shape models (each with five further shape modes) were constructed, capturing femoral head sphericity, cam deformity and superior joint space width. Associations between the selected OA SNPs and each hip shape model were examined using multivariate analysis (canonical correlation analysis). Correlation coefficients from modes showing significant contributions were subsequently used to annotate deviation from the mean shape.

**Results:** 3111 participants had genetic and hip shape data. Four SNPs were associated with hip shape at or below the  $P=2 \times 10^{-3}$  Bonferroni-corrected threshold, namely the intergenic *KLHDC5-PTHLH* rs10492367 (whole hip,  $P=10^{-3}$ ), *COL11A1* rs2615977 (superior joint space,  $P=5 \times 10^{-4}$ ), *DOTL1* rs12982744 (superior joint space,  $P=2 \times 10^{-3}$ ) and *COL11A1* rs4907986 (superior joint space  $P=7 \times 10^{-4}$ ) SNPs. The OA risk increasing allele for rs10492367 associated with whole shape influenced hip angulation (coxa vara), and the alleles for the three other SNPs associated with reduced lateral superior joint space. Regional association plots suggested a further independent signal within *COL11A1*; rs10047217 was also strongly associated with superior joint space ( $P=6 \times 10^{-6}$ ), which was partly, but not completely, attenuated following conditional analysis for rs2615977 and rs4907986 ( $P=0.02$ ).

**Conclusion:** OA susceptibility genes are associated with altered hip shape, including a tendency towards coxa vara and narrower supero-lateral joint space, which may explain their tendency to increase hip OA risk.

**Disclosures:** Denis Baird, None.

## SU0139

**Differences in bone and cartilage between women with ACL tears and uninjured age matched controls.** Jennifer Bhatla<sup>\*1</sup>, Andres Kroker<sup>1</sup>, Sarah Manske<sup>1</sup>, Carolyn Emery<sup>2</sup>, Steven Boyd<sup>1</sup>. <sup>1</sup>McCaig Institute for Bone and Joint Health, Department of Radiology, Cumming School of Medicine, University of Calgary, Calgary, Canada, Canada, <sup>2</sup>Sport Injury Prevention Research Centre, Faculty of Kinesiology, University of Calgary, Calgary, Canada, Canada

Anterior cruciate ligament (ACL) tears significantly increase the risk of early onset osteoarthritis (OA) leading to degradation of articular cartilage and bone in the joint. While the contribution of bone in OA development is unclear, evidence suggests that bone changes accompany cartilage degradation. This study aims to explore the relationship between subchondral compact bone thickness and cartilage thickness by comparing women with ACL tears at least 5 years post-injury to age matched uninjured controls.



Women with unilateral ACL tears that occurred prior to age 18 ( $\geq 5$  years post-injury, age 22-28,  $n=15$ ) and age matched controls were recruited from the Alberta PrE-OA cohort. Both knees were scanned in 1.5 T MRI (GE Optima) to image cartilage and HR-pQCT (XtremeCTII) to image bone. The images from the two modalities were registered to align 3D bony anatomy. Medial and lateral regions of interest (ROI) were defined as approximate weight bearing regions on the tibia and femur. ROIs were morphed using a non-rigid registration with a kappa statistic to a common shape and average thickness maps for each group were created (Fig 1). Paired t-tests compared contralateral to injured knees and unpaired t-tests compared contralateral and injured knees to controls. A Bonferroni correction for multiple comparisons was used.

Injured knees had 45% thicker (95%CI 24-67%,  $t=4.3$ ,  $p<0.001$ ) and contralateral knees 19% thicker (95%CI 4-33%,  $t=2.6$ ,  $p=0.049$ ) subchondral compact bone than control knees in the lateral femur only ( $n=13$  pairs; two pairs excluded due to motion artifact). Cartilage thickness did not differ between groups, although the medial and lateral tibia of injured and contralateral knees trended toward thicker cartilage than controls. There were no differences between left and right knees in controls nor between injured and contralateral knees in injured participants ( $p>0.1$ ).

Increased subchondral compact bone thickness in the lateral femur of both the injured and contralateral knees compared with controls suggests that bone changes may occur early on in the development of OA, and our approach detected significant bone changes prior to changes in cartilage morphology. It is hypothesized that increased compact bone thickness in the lateral femur of both injured and contralateral knees could result from a variety of factors including weight-bearing during gait or biological factors. A limitation is the historical cohort study design makes it difficult to infer change rather than differences between groups that may have predisposed some to ACL tears. As subchondral bone sclerosis is known to occur during OA development, establishing an understanding of early bone changes may have implications for treatment and prevention of OA.

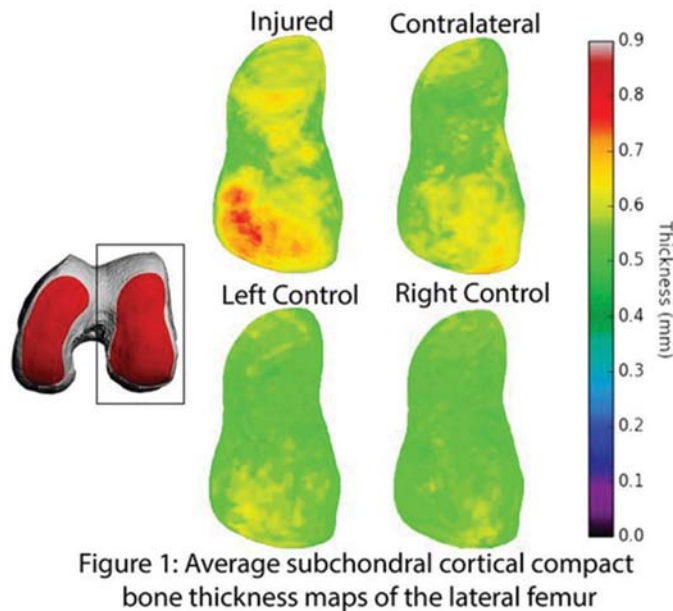


Figure 1

Disclosures: Jennifer Bhatla, None.

## SU0140

**Semiautomatic analysis of bone erosion volume by HR-pQCT in patients with rheumatoid arthritis.** Ko Chiba\*, Narihiro Okazaki, Kazuteru Shiraishi, Naoki Iwamoto, Atsushi Kawakami, Makoto Osaki. Nagasaki University, Japan

### [Introduction]

HR-pQCT is a high resolution CT dedicated to human extremities. It has been used mainly for osteoporosis, while in more recent years it has been applied to research in rheumatoid arthritis (RA).

The aim of this study is to develop a method to quantify the volume of erosions in RA patients semiautomatically using second generation HR-pQCT.

### [Methods]

Twenty patients with RA ( $70 \pm 8$  years, 15 female, 5 male) participated in this study. The second and third MCP joints were scanned using HR-pQCT (XtremeCT II, Scanco Medical, Switzerland) at the voxel size of  $61 \mu\text{m}$ .

The erosion volume was measured semiautomatically using the dedicated software (TRI/3D-BON, Ratoc System Engineering, Tokyo).

All concave regions on the bone surface around the MCP joints were extracted automatically by subtracting the bone region from the smoothed bone model. Erosions were selected manually by a medical doctor based on certain criteria. The volume of the erosions were measured by voxel counting.

### [Results]

In a total of 37 joints (3 joints were excluded due to severe deformities), 40 erosions were detected by HR-pQCT (phalanx side: 9 erosions, metacarpal side: 31 erosions). The average volume of the erosions was  $1.84 \text{ mm}^3$ , minimum  $0.08 \text{ mm}^3$ , and maximum  $16.3 \text{ mm}^3$ .

### [Conclusion]

The semiautomatic method to quantify the volume of erosions at MCP joints in RA patients by HR-pQCT was developed.

The determination as to whether the concave regions are pathological erosion or physiological concave, vascular channel or recess of osteophyte is occasionally difficult and should be performed by an experienced tester.



Figure 1

Disclosures: Ko Chiba, None.

## SU0141

**Hyperelastic Bone Composite: A Novel 3D-printed Biomaterial Ink used for Spinal Fusion.** Andrew Schneider<sup>1</sup>, Adam Jakus<sup>2</sup>, Gurmit Singh<sup>1</sup>, Karina Katchko<sup>1</sup>, Danielle Chun<sup>1</sup>, Joseph Weiner<sup>1</sup>, Ralph Cook<sup>1</sup>, Michael Schallmo<sup>1</sup>, Chawon Yun<sup>1</sup>, Soyeon Jeong<sup>1</sup>, Michael Newton<sup>3</sup>, Tristan Maerz<sup>3</sup>, Kevin Baker<sup>3</sup>, Ramille Shah<sup>2</sup>, Wellington Hsu<sup>1</sup>, Erin Hsu<sup>1</sup>. <sup>1</sup>Northwestern University Department of Orthopaedic Surgery, United States, <sup>2</sup>Northwestern University Department of Materials Science and Engineering, United States, <sup>3</sup>Orthopaedic Research Laboratory, Beaumont Health, United States

Pseudarthrosis occurs in 10-15% of patients who undergo spine fusion. Recombinant human bone morphogenetic protein-2 (rhBMP-2) is a biologic bone graft substitute (BGS) that elicits high fusion rates but is associated with serious adverse effects. Both DBM and synthetic ceramics have improved safety profiles over rhBMP-2, but have insufficient osteoinductivity, low structural strength and/or poor handling properties to serve as BGS. We have developed a unique biomaterial ink consisting of various hydroxyapatite (HA)-demineralized bone matrix (DBM) compositions to 3D-print Hyperelastic "Bone" composite (HBC) scaffolds. This study evaluates the capacity of these HBC scaffolds to serve as BGS in a rat posterolateral spine fusion (PLF) model.

Sixty Sprague-Dawley rats underwent L4-L5 PLF with placement of one of five HBC scaffolds. Each scaffold consisted of 30 vol.% poly(lactic-co-glycolic acid) (PLGA), a biodegradable polymer. The remaining 70 vol.% was composed of five varying ratios of HA:DBM particles (1:0, 3:1, 1:1, 1:3, or 0:1). At 8 weeks postoperative, successful fusion was evaluated using plain radiographs, manual palpation, and synchrotron microCT imaging and analysis. Fusion was assessed via manual palpation by 3 blinded investigators using an established scoring system: 0=no fusion, 1=unilateral fusion and 2=bilateral fusion. Spines with an average score  $\geq 1.0$  were considered fused.

Animals treated with the 3:1 composite had the highest fusion rate (92%) compared to all remaining groups (Figure 1B). The 3:1 composite group also had the highest average fusion score of 1.39 (1:3 group, 1.14; 1:1 group, 0.97; 1:0 group, 1.22; and 0:1 group, 0.78). Synchrotron microCT imaging conducted on the 1:0 and 3:1 groups (highest average fusion scores) demonstrated equivalent percentage of pores containing de novo bone formation (30% vs. 31% respectively,  $p=0.97$ ).

All composite variations of the HBC scaffolds had favorable handling properties relative to currently used forms of DBM or HA. Fusion scoring and microCT data suggest that a 3:1 HA:DBM ratio may represent the most potent iteration for spine fusion. Further modifications to the HBC scaffold architecture may improve its bone regenerative capacity. This study highlights HBC's potential to serve as a BGS that may overcome the limitations of currently used BGSs.

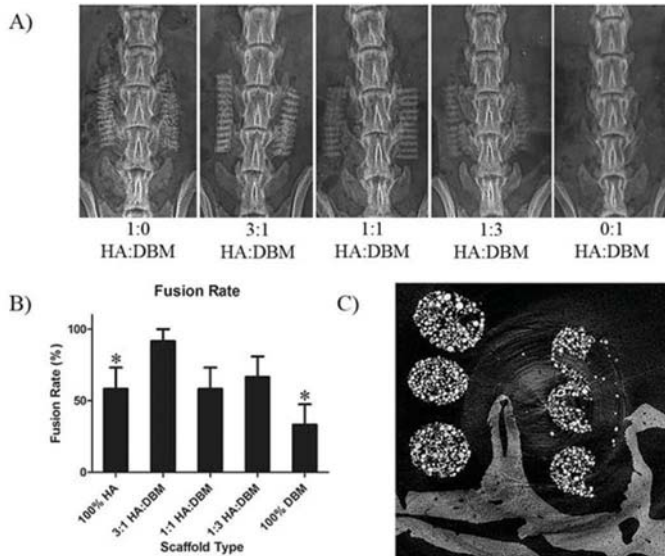


Figure 1. (A) Eight week post-op representative radiographs of the five 3D-printed scaffolds implanted. (B) Fusion rate (\* =  $p < 0.05$ ). (C) Representative synchrotron microCT depicting new bone forming around and within scaffold struts

Figure 1

Disclosures: Andrew Schneider, None.

## SU0142

**Association of Total 25-Hydroxyvitamin D Levels With Disease Activity In A Large Patient Cohort With Rheumatoid Arthritis.** Sofie Malmstroem<sup>\*1</sup>, Lars Rejnmark<sup>2</sup>, Jonathan Graf<sup>3</sup>, John B. Imboden<sup>3</sup>, Kara Lynch<sup>4</sup>, Dolores M. Shoback<sup>5</sup>. <sup>1</sup>Endocrine Research Unit, San Francisco Department of Veterans Affairs Medical Center, University of California, San Francisco and Department of Endocrinology and Internal Medicine, Aarhus University Hospital, Denmark, United States, <sup>2</sup>Department of Endocrinology and Internal Medicine, Aarhus University Hospital, Denmark, <sup>3</sup>Division of Rheumatology and Department of Medicine, Zuckerberg San Francisco General Hospital, University of California, San Francisco, United States, <sup>4</sup>Department of Laboratory Medicine, Zuckerberg San Francisco General Hospital, University of California, San Francisco, United States, <sup>5</sup>Endocrine Research Unit, San Francisco Department of Veterans Affairs Medical Center, University of California, San Francisco, United States

**PURPOSE:** In vitro 1,25-dihydroxyvitamin D suppresses production of pro-inflammatory cytokines by T-helper cells, a pathway that is implicated in the pathogenesis of rheumatoid arthritis (RA). Some studies but not all show an inverse correlation between disease activity and total serum 25-hydroxyvitamin D (25OHD) in RA patients. We aim to examine the correlation between total 25OHD levels and disease activity and cytokine levels in a multiethnic cohort of RA patients.

**METHODS:** Cross-sectional study on patients included in the UCSF RA cohort. Academic rheumatologists collected disease activity by DAS28 scores (a standardized assessment based on tender joint count, swollen joint count, erythrocyte sedimentation rate) and clinical information. Plasma samples for multiple cytokines and biomarkers were collected and measured by multiplex analysis. Total 25OHD was measured by liquid chromatography tandem mass spectrometry.

**RESULTS:** The study population (N=353, 87% women) had a median age of 57 (range 18-86) years, and is of multiethnic origin (38% Hispanic, 28% Asian, 9% African American, 23% Caucasian, 2% other). All patients fulfilled the 1987 American College of Rheumatology classification criteria for RA and 81% were rheumatoid factor positive and 81% had anti-cyclic citrullinated peptide antibodies. Disease activity scores according to DAS28 ranged from remission (20%) to low (19%), moderate (43%), and high (18%). Mean total 25OHD levels were 33.2 ( $\pm 16.4$ ) ng/ml. Total 25OHD correlated negatively with total DAS28 score ( $r = -0.168$ ,  $p < 0.01$ ). This was not changed by adjustment for age and gender ( $r = -0.120$ ,  $p = 0.02$ ). Total 25OHD and DAS28 differed significantly between ethnic groups with the highest total 25OHD and lowest DAS28 in Caucasians. Further analyses are in progress to assess associations between cytokines and 25OHD and disease activity.

**CONCLUSION:** This large, well-characterized, multiethnic RA cohort showed a negative association between total 25OHD levels and DAS28, after adjusting for age and sex. DAS28 and 25OHD levels differed significantly between ethnic groups. Whether optimization of vitamin D status may improve disease activity in RA needs further study.

Disclosures: Sofie Malmstroem, None.

## SU0143

**Inhibition of CaMKK2 attenuates subchondral bone remodeling in post-traumatic osteoarthritis model.** Elsa Mevel<sup>\*</sup>, Anthony Huls, Yong Li, Uma Sankar. Department of Anatomy and Cell Biology, Indiana University School of Medicine, Indianapolis Indiana, United States

Osteoarthritis (OA) is a highly prevalent rheumatology disease that lacks curative treatment. Subchondral bone remodeling plays a key role in the disease process. In skeletal cells,  $\text{Ca}^{2+}$  binds to calmodulin (CaM) and activates CaM-dependent protein kinases (CaMKs). Among these, the loss or inhibition of CaMKK2 protects mice from bone loss and from lipopolysaccharide or high-fat diet-induced inflammation. The aim of this study was to establish an innovative and clinically relevant approach in OA treatment by targeting CaMKK2.

The impact of CaMKK2 deficiency in articular cartilage physiopathology was evaluated in murine articular chondrocytes (MACs) stimulated by interleukin-1 ( $\text{IL-1}\beta$ ). Real-time PCR was used to monitor the expression of transcripts for inflammatory (iNOS, COX2, IL6) and catabolic (MMP2-9-13 and ADAMTS5) markers. The related inflammation products (nitric oxide (NO), prostaglandin  $\text{E}_2$  ( $\text{PGE}_2$ ), interleukin-6 (IL-6)) were also measured. We also evaluated whether loss or pharmacological inhibition of CaMKK2 would affect the development of OA using a destabilization of medial meniscus (DMM) model of post-traumatic OA. Wild type (WT) or *Camkk2*<sup>-/-</sup> mice (n=10 per group) were subjected to unilateral DMM or sham surgery. CaMKK2 inhibitor or saline solution were administered tri-weekly by intra-peritoneal injection for 8 weeks following surgery. Subchondral bone remodeling was evaluated by micro-computed tomography ( $\mu\text{CT}$ ) 8 weeks after surgery.

Data obtained in MACs revealed that  $\text{IL-1}\beta$  significantly increased the expression of inflammatory (iNOS, COX2, IL6) and catabolic (MMP2-9-13 and ADAMTS5) markers in WT MACs. In contrast,  $\text{IL-1}\beta$ -induced inflammatory and catabolic responses were significantly lower in *Camkk2*<sup>-/-</sup> MACs. Consistent results were obtained by measuring related inflammation products (NO,  $\text{PGE}_2$ , IL-6) in culture supernatants. The  $\mu\text{CT}$  analyses revealed significant increases in the total subchondral bone volume, tissue volume, tissue surface, bone surface trabecular thickness in DMM mice compared to sham-operated cohorts, indicating enhanced bone remodeling. These parameters were significantly diminished in CaMKK2 inhibitor-treated WT mice and/or *Camkk2*<sup>-/-</sup> mice, indicating that the loss or inhibition of CaMKK2 prevents the subchondral bone remodeling induced by DMM.

In conclusion, our study generated novel information on the role of CaMKK2 in OA pathogenesis and opens new avenues to design innovative therapeutic strategies against OA.

Disclosures: Elsa Mevel, None.

## SU0144

**The study of Bone Cells in osteoarthritis and other Factors that may contribute to a Progressive form of osteoarthritis.** Christine Schutz<sup>\*1</sup>, gerald atkins<sup>2</sup>. <sup>1</sup>University of Adelaide, Australia, <sup>2</sup>adelaide university, Australia

End-stage osteoarthritis (OA) is the major reason for knee and hip replacement surgery in Western countries. In 2014, the Australian Orthopaedic Association National Joint Replacement Registry (AOANJRR) recorded more than 54,000 total knee arthroplasties (TKA) performed. As OA affects other joints, the timeline of disease progression is attributed to in part by biomechanical influences but to a large extent the contributing factors are unknown. Since the discovery of Wnt signalling pathways in bone research, studies have focussed on understanding this complex network in both osteoporosis and, to a lesser extent, OA. Sclerostin is a Wnt signalling pathway antagonist produced by osteocytes and is a potent inhibitor of bone formation and key regulator of bone metabolism. Patients with end-stage OA in one joint are at risk of OA progression to other joints. In this study we examined a small cohort of patients undergoing TKA surgery for OA and compared patient factors (age, BMI, pain score and basal metabolic index), serum measures of 25-hydroxy vitamin, serum and synovial fluid sclerostin levels, and bone and cartilage histology, to determine if there are differences between non-progressor patients and those with progressive OA, which we defined as patients requiring surgery on another arthritic joint within 24 months of their initial TKA procedure.

**Results:** A total of 38 subjects were enrolled and provided consent for this study. Six patients were removed as they had evidence of rheumatoid arthritis. Of the remaining 32 subjects, 16 were males, mean age 65.9  $\pm$  SD 10.1 (P value 0.0136 (significant)) and 16 females, mean age 70.0  $\pm$  SD 10.1 (not significant). Sclerostin levels were higher in the males than the females (Male P 0.702 r 0.224) Female p 0.010 r 0.3871 (?), sclerostin Vitamin D (25OHD) levels ranged from 15.95- 90.75 nmol/L, with a mean of 49.14 nmol/L pre surgery. At 12 months post-surgery vitamin D levels were measured in only half the subjects but were slightly higher than preoperatively. Other factors such as Pain scores and BMI were also reviewed. Oxford Pain scores pre surgery were 19 Pre-surgery (poor with high pain severity) and at 12 months post-surgery pain scores were 40 (very little pain).

Of the 32 subjects, 37% reported undergoing other joint surgery for osteoarthritis (N contralateral knee = 5; N hips = 4; N other = 2; N Shoulder = 1). Of these patients, (the progressors) approximately 60% had evidence of denudation corresponding to OARSI grades 5 and 6, compared with 40 % in the group who reported no additional surgery. The non progressors showed more vertical fissures extending into the mid zone. Due to the progressive nature of the OA the 37 % return rate for additional joint surgery suggests that low sclerostin and Vitamin D levels may predict a more progressive form of OA.

Disclosures: Christine Schutz, None.



## SU0145

**Subchondral bone microstructure analysis by HR-pQCT: a new imaging marker for knee osteoarthritis.** Kazuteru Shiraishi\*, Ko Chiba, Narihiro Okazaki, Makoto Osaki. Nagasaki University, Japan

**Introduction:** Osteoarthritis (OA) is characterized by cartilage attrition, synovitis, and subchondral bone abnormality. We developed the method to analyze subchondral bone microstructure of OA knees using HR-pQCT (High Resolution peripheral Quantitative CT).

**Methods:** Ten knees with OA were investigated. 20mm width of proximal tibia was scanned by HR-pQCT (XtremeCT II, Scanco Medical, Switzerland) at the voxel size of 61  $\mu$ m and integration time of 100 ms. 5mm width of subchondral trabecular bone of the medial joint was extracted, divided into 4 subregions: anterior, center, posterior, and medial (figure). Trabecular bone microstructure at the each region was measured by the software.

**Results:** BV/TV (bone volume fraction) at the anterior, center, posterior, and medial regions were 29.5, 29.6, 15.5, 34.2% respectively. Tb.Th (trabecular thickness) were 285, 294, 245, 338  $\mu$ m. Tb.N (trabecular number) were 0.64, 0.58, 0.65, 0.61 /mm, and Conn.D (connectivity density) were 2.33, 2.38, 1.15, 2.48.

**Conclusion:** Subchondral bones were increased particularly at the medial region of the medial proximal tibia, composed of thickened and well-connected trabecular bones. Subchondral bone microstructure measured by HR-pQCT may become a new imaging marker for OA knees.

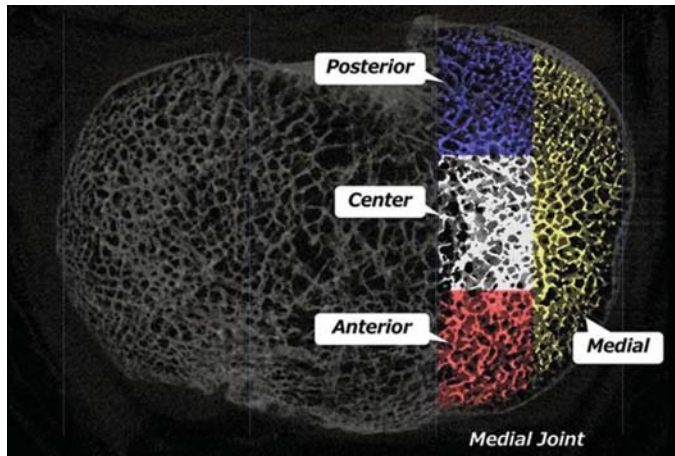


Figure 1

**Disclosures:** Kazuteru Shiraishi, None.

## SU0146

**Osteoporosis in those with Knee Osteoarthritis: Differences in Subchondral Bone Quality, Cartilage Thickness and Associations with Symptoms in the Osteoarthritis Initiative.** Andy Kin On Wong\*<sup>1</sup>, John A. Lynch<sup>2</sup>, Linda Probyn<sup>3</sup>. <sup>1</sup>University Health Network, Canada, <sup>2</sup>University of California at San Francisco, United States, <sup>3</sup>University of Toronto, Canada

**Methods:** Men and women in the Osteoarthritis Initiative (OAI) at visit 5 (36 months) were examined for osteoporosis (N=1483) using DXA (T-score at femoral neck  $\leq -2.5$ ), use of bisphosphonates within the last 5 years, or having experienced a fracture (non-ascertained at any site) within the last 36 months. Those with and without osteoporosis were compared in terms of subchondral bone quality (in a subset of N=289 using fast imaging with steady state precision (FISP) MRI at the proximal tibia, with 0.23 x 0.23 x 1.0 mm voxels), bone marrow lesion (BML) size, number and effusion (semi-quantitatively scored by a radiologist using the MRI Osteoarthritis Knee Score system; data at visit 3 (24 months)), as well as mean and weight-bearing region cartilage thickness, all using general linear models. Measures in the affected compartment were primarily used. Moderation analysis examined the relationship between symptoms (as measured by the Knee injury and Osteoarthritis Outcome Score (KOOS) and Western Ontario and McMaster Universities Arthritis Index (WOMAC)) and each of cartilage thickness and BML properties conditional upon the presence of osteoporosis. Results: A total of 15.2% (226/1483) of participants (825 women, 658 men, mean age: 64.4 $\pm$ 8.9yrs, BMI: 30.1 $\pm$ 4.9 kg/m<sup>2</sup>) were categorized as likely having osteoporosis (4.4% experienced a fracture within 36 months, 11.5% used bisphosphonates within 5 years, but none showed BMD T-score  $\leq -2.5$ ). The median duration of bisphosphonate use was 3 years (1,5). Those categorized as having osteoporosis had lower medial and lateral subchondral bone density and larger trabecular separation (all  $p < 0.01$ ). Cartilage thickness also appeared lower in this group but only by a small yet significant amount ( $p = 0.04$ ). While both BML properties and cartilage thickness correlated with knee-specific symptoms, osteoporosis was only a significant moderator for cartilage thickness' relationship with knee symptoms (Table I). Upon probing the interaction, those with osteoporosis showed no relationship between cartilage thickness and any measure of knee symptoms. Further examination of models that included both cartilage and BML properties revealed that BMLs explained knee pain better than cartilage thickness in those with osteoporosis.

**Conclusions:** Those with osteoporosis exhibit different subchondral bone and cartilage properties. The origin of symptoms in this sub-cohort may differ from those with knee osteoarthritis but without osteoporosis.

**Table I. Relationship between knee symptoms and cartilage thickness moderated by the presence of osteoporosis. All models adjusted for age, sex, body mass index, physical activity, and use of analgesics.**

Variable	With Osteoporosis (N=163)			Without Osteoporosis (N=843)			Intcn p
(Scores)	B	Lower CI	Upper CI	B	Lower CI	Upper CI	
Weight-Bearing Portion Cartilage Thickness (mm)							
KOOS knee pain	1.08	-1.85	4.01	3.23	2.00	4.46	0.366
KOOS symptoms	-0.43	-3.34	2.47	4.01	2.98	5.04	0.003
WOMAC Knee pain	-0.31	-0.88	0.26	-0.56	-0.80	-0.32	0.603
WOMAC Stiffness	0.01	-0.29	0.31	-0.33	-0.44	-0.23	0.060
WOMAC Global	-0.48	-3.19	2.23	-2.63	-3.71	-1.56	0.284
Mean Cartilage Thickness (mm)							
KOOS knee pain	-0.12	-9.96	9.73	6.45	2.54	10.35	0.392
KOOS symptoms	-4.13	-13.86	5.59	9.38	6.10	12.66	0.006
WOMAC Knee pain	-0.18	-2.09	1.73	-1.13	-1.89	-0.37	0.498
WOMAC Stiffness	0.42	-0.59	1.43	-0.79	-1.13	-0.45	0.042
WOMAC Global	-0.07	-9.17	9.02	-6.44	-9.83	-3.06	0.342

Table I

**Disclosures:** Andy Kin On Wong, None.

## SU0147

**Regulatory Networks Involving Ror $\beta$  and miR-219a-5p during Osteoblast Differentiation and in Age-related Bone Loss.** Ruben Aquino-Martinez\*, Joshua Farr, Brittany Negley, Andre van Wijnen, Sundeep Khosla, David Monroe. Mayo Clinic College of Medicine, United States

Osteoporosis and increased risk of fractures in the aging population is correlated with deterioration in quality of life and loss of autonomy. To improve the limited efficacy of current clinical therapies for osteoporosis, we investigate new molecular targets to stimulate bone accrual. We have recently reported that retinoic acid receptor-related orphan receptor beta (Ror $\beta$ ) is aberrantly upregulated in bone marrow-derived osteoprogenitor cells and in osteocytic bone fractions isolated from aged mice and humans, and that global deletion of Ror $\beta$  in mice inhibits age-related bone loss. We have also demonstrated that Ror $\beta$  expression is strongly reduced during normal osteoblastic differentiation and that constitutive Ror $\beta$  expression inhibits this process. These data suggest that Ror $\beta$  is an inhibitor of osteogenesis and that proper control of Ror $\beta$  expression is essential for the normal maintenance of osteoblast differentiation and in aging. Here, we investigated the interaction between Ror $\beta$  and a specific subset of microRNAs (miRs) to establish their roles in osteoblastic differentiation and in aging. To initially identify miRs that are strongly predicted to target Ror $\beta$ , we used the online target prediction database TargetScan to identify miR-219a-5p, 218-5p, 148a-3p and 135a-5p as potential Ror $\beta$ -regulating candidate miRs. To determine any potential involvement of these miRs in the regulation of Ror $\beta$  levels, MC3T3-E1 mouse osteoblastic cells were cultured in the presence of osteogenic media and assayed at multiple time points (0-14 days) for Ror $\beta$  and miR expression. As Ror $\beta$  levels decreased during the timecourse, the expression of all 4 miRs was upregulated, suggesting possible involvement in the suppression of Ror $\beta$  levels. To determine whether these miRs directly suppress Ror $\beta$  levels, MC3T3-E1 cells were transfected with each of the 4 miRs and Ror $\beta$  mRNA expression levels were evaluated. Although all 4 miRs suppressed Ror $\beta$  levels to some degree, the most significant inhibition was achieved by miR-219a-5p. Finally, the expression of these miRs was quantified in osteocytic bone fractions of young and old mice and a significant down-regulation ( $p < 0.001$ ) in miR-219a-5p was observed, concomitant with the increased Ror $\beta$  expression. Our findings thus demonstrate that miR-219a-5p is involved in the regulation of Ror $\beta$  levels during osteoblast differentiation and perhaps with aging.

**Disclosures:** Ruben Aquino-Martinez, None.

## SU0148

**Isoproterenol induces RANKL expression by activating NFAT and ATF4 in mouse osteoblastic cells.** Kyunghwa Baek\*<sup>1</sup>, Hyun-Jung Park<sup>2</sup>, Hyung-Ryong Kim<sup>3</sup>, Jeong-Hwa Baek<sup>2</sup>. <sup>1</sup>Gangneung-Wonju National University, Korea, Republic of, <sup>2</sup>Department of Molecular Genetics, Seoul National University School of Dentistry, Korea, Republic of, <sup>3</sup>Graduate School, DGIST, Korea, Republic of

Isoproterenol (ISO), a nonspecific beta-adrenergic receptor agonist is known to induce bone loss and increase of osteoclast action. Although ISO has been shown to increase receptor activator of NF-kappaB ligand (RANKL), the details of the regulatory mechanisms remain unclear. In the present study, we investigated the role of calcineurin/NFAT and cAMP/PKA pathways in ISO-induced RANKL expression in C2C12 and primary cultured mouse calvarial cells. ISO increased expression levels of RANKL

mRNA and protein and RANKL promoter reporter activity. ISO also promoted the phosphorylation of ATF4 and CREB and the transcriptional activity of NFAT. ISO-mediated RANKL expression was downregulated by the inhibitors of calcineurin and PKA. Mutations in CRE-like or NFAT-binding element suppressed ISO-induced RANKL promoter activity. ChIP analysis demonstrated that ISO increased the NFAT and ATF4-binding activity on the mouse RANKL promoter but not CREB-binding activity. Association of NFATc1 and ATF4 was not observed in co-immunoprecipitation study. Knockdown of NFATc1 or ATF4 blocked ISO-mediated RANKL expression. ATF4 knockdown also prevented ISO induction of NFATc1 expression. These results suggest that ISO-induced RANKL expression depends on the activation of NFAT and ATF4.

**Disclosures:** *Kyunghwa Baek, None.*

## SU0149

**Phlpp1 Regulates Osteoblast Differentiation and Maturation Through mTORC1.** Dana Begun\*, Elizabeth Bradley, Jennifer Westendorf. Mayo Clinic - Orthopedic Surgery, United States

Diseases of altered bone mass or density arise due to dysregulation of bone homeostasis. To better treat these disorders, a more thorough understanding is needed of the proteins that control anabolic and catabolic pathways. Phlpp1 (pleckstrin homology domain leucine-rich repeat protein phosphatase-1) is a Ser/Thr phosphatase that dephosphorylates and alters the activity of proteins crucial for bone metabolism. *Phlpp1* knockout mice have low cancellous bone mass and shorter femora. To assess the mechanisms behind the reduced bone, we harvested primary calvarial osteoblasts from *Phlpp1* knockout mice and their wild type littermates. In osteogenic medium, *Phlpp1* knockout osteoblasts produced less alkaline phosphatase and were less calcified than wildtype cell cultures. Phosphorylation of the Phlpp1 substrate Akt2 was increased in the knockout cultures. Akt2 is an upstream repressor of AMPK, which is responsible for phosphorylation of Raptor – a scaffold protein associated with mTOR in the mTORC1 complex – at Ser792. This phosphorylation of Raptor<sup>Ser792</sup> inhibits mTORC1 kinase activity. Importantly, Raptor<sup>Ser792</sup> was not phosphorylated in *Phlpp1* knockout cultures. To further test this relationship, we treated *Phlpp1* knockout and wildtype cells with rapamycin, a well-established inhibitor of mTORC1. Rapamycin increased p-Raptor<sup>Ser792</sup> in wildtype cells but not in the *Phlpp1* KO cells. We conclude that Phlpp1 may indirectly modulate mTORC1 activity to promote osteoblast maturation.

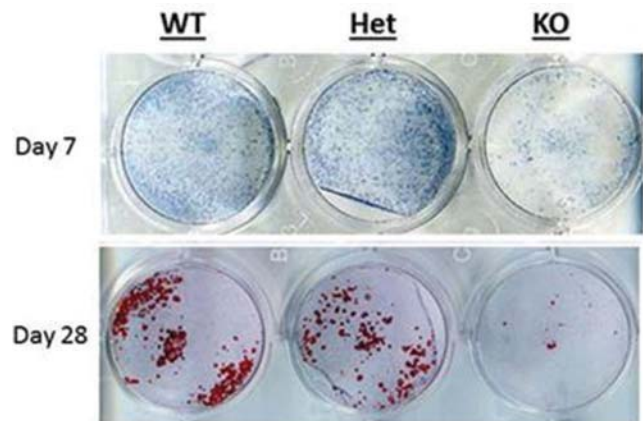


Figure 1 – Primary osteoblasts from *Phlpp1* WT, Het, and KO calvaria cultured 7 and 28 days in osteogenic media. Alkaline phosphatase staining (top) demonstrates reduced proliferation in the *Phlpp1* KO cells. Alizarin Red staining (bottom) is reduced in the KO cells compared to WT and Het.

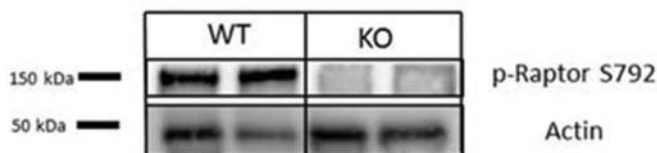


Figure 2 – Primary osteoblasts from WT and *Phlpp1* KO calvaria in growth media were harvested. Western blotting was conducted to assess relative levels of phosphorylation at Raptor's Ser792 site. *Phlpp1* KO cells show reduced ability to phosphorylate this site.

Figures

**Disclosures:** *Dana Begun, None.*

## SU0150

**Estrogen receptor-alpha participates in osteoblast mineralization through upregulating ATP synthesis by specifically inducing expressions of genomic mitochondrial complex genes and mitochondrial cytochrome c oxidase I and II genes.** Pei-I Lin\*, Mei-Hsiu Liao, Ruei-Ming Chen. Taipei Medical University, Taiwan, Province of China

Cellular levels of adenosine triphosphate (ATP) are closely related to osteoblast survival, proliferation, and mineralization. Previous studies have shown participation of estrogen receptors (ERs) in modulating ATP biosynthesis in epithelia and neurons. This study was aimed to investigate the roles of ERs in regulations of ATP synthesis and osteoblast mineralization and the possible mechanisms. Exposure of rat calvarial osteoblasts to estradiol caused significant improvement of cell mineralization. In parallel, estradiol increased mitochondrial complex I enzyme activity and cellular ATP amounts in primary osteoblasts. As to the mechanisms, treatment of human U-2 OS cells, derived from a female osteosarcoma patient, with estradiol did not affect cell viability but specifically augmented levels of ER- $\alpha$  without altering ER- $\beta$ . The results by confocal microscopy showed that exposure of U-2 OS cells to estradiol for 12 and 24 h triggered translocation of ER- $\alpha$  to nuclei from the cytoplasm. In comparison, estradiol stimulated ER- $\alpha$  translocation to mitochondria after exposure for 1 h. Analysis of a quantitative PCR array for genomic ATP synthesis-related genes revealed that estradiol induced 9 (11%) mitochondrial complex gene expressions in U-2 OS cells. Bioinformatic search showed existence of estrogen response elements in the 5'-promoter regions of mitochondrial cytochrome c oxidase (CO) I and II genes. After exposure to estradiol, RNA and protein levels of CO I and II in U-2 OS cells were sequentially induced. Consequently, estradiol increased levels of cellular ATP. Taken together, this study has shown that ER- $\alpha$  plays a critical role in improvement of osteoblast mineralization via stimulating cellular ATP levels by specifically inducing expressions of genomic complex genes and mitochondrial CO I and II genes. This study provides a novel insight into the underlying mechanism of postmenopausal osteoporosis.

**Disclosures:** *Pei-I Lin, None.*

## SU0151

**Differential Expressions of Osteoblast genes *in-vitro* under the influence of Recombinant Human Parathyroid Hormone (rhPTH) and Zoledronic acid (ZOL).** Vandana Dhiman\*, Sanjay Bhadada<sup>2</sup>, Sudhaker D. Rao<sup>3</sup>, D.K. Dhawan<sup>1</sup>. <sup>1</sup>Panjab University, India, <sup>2</sup>PGIMER, India, <sup>3</sup>Henry Ford Hospital, United States

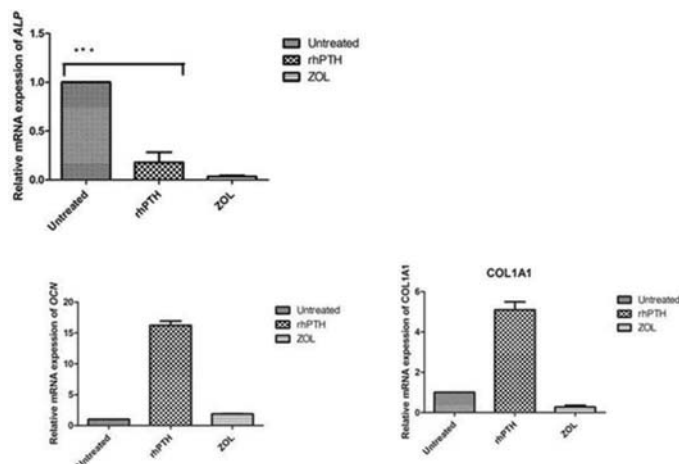
**Introduction:** Osteoblast cells are suitable model to explore the molecular mechanisms of osteo-anabolic and anti-catabolic therapies. rhPTH is a strong anabolic and ZA is strong prototypical anti-catabolic agent both which have been used widely for treatment of osteoporosis and other metabolic bone diseases. Recently, biopsy studies showed differential effects at the tissues level, but the molecular basis for their effects is not well understood. The purpose of the study was to explore the effect on osteoblast gene expressions in response to rhPTH and ZOL in osteoblast cell lines

**Methodology:** Human Osteosarcoma cells (U2OS) were treated with either 1  $\mu$ M of ZOL or 5  $\mu$ g rhPTH over 48 hours. A control group was treated with vehicle alone. The cells were analyzed for viability, and for expression of alkaline phosphatase (ALP), osteocalcin (OCN), and Col1A1 genes by measuring respective gene mRNAs by real time PCR. The results are expressed as fold change in relation to 18s house-keeping gene.

**Result:** Both rhPTH and ZOL showed significant decline in ALP expression ( $0.178 \pm 0.18$  and  $0.033 \pm 0.019$  fold decrease respectively) with no difference between them. OCN gene expression was significantly increased by rhPTH ( $16.23 \pm 1.17$  fold), but was unaffected by ZOL ( $1.872 \pm 0.058$  fold). COL1A1 gene expression was significantly increased by rhPTH ( $5.104 \pm 0.674$  fold) and was unaffected by ZOL ( $0.271 \pm 0.152$  fold), with significant difference between rhPTH and ZOL effects.

**Conclusion:** rhPTH and Zol have differential effects on osteoblast gene expressions. Further studies are needed to understand the implications of these differential effects





Graph 1

Disclosures: Vandana Dhiman, None.

## SU0152

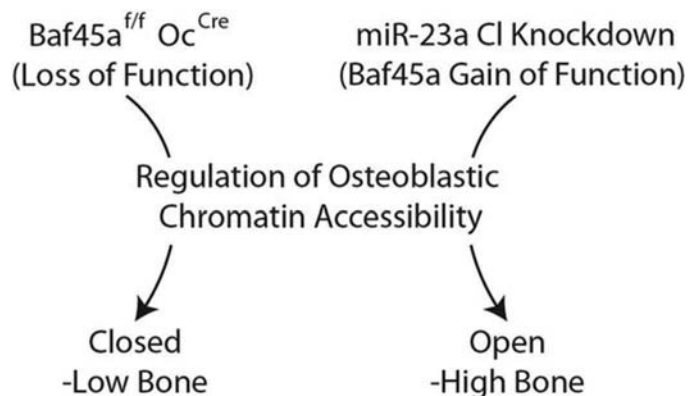
### Brg1 Associated Factor 45a chromatin remodeling is key for bone formation.

Tanner Godfrey<sup>1</sup>, Benjamin Wildman<sup>1</sup>, Mohammad Rehan<sup>1</sup>, Mohammad Hassan<sup>1</sup>, Chis Lengner<sup>2</sup>, Harunur Rashid<sup>1</sup>, Amjad Javed<sup>1</sup>. <sup>1</sup>University of Alabama at Birmingham, United States, <sup>2</sup>University of Pennsylvania, United States

The BAF chromatin remodeling complex (SWI/SNF) plays a critical role in the regulation of chromatin structure, a process which coordinates differentiation and maintains physiological function of a cell. To date, little is known of the mechanism or composition of an osteoblast-specific BAF complex. We have identified BAF45A, a subunit of BAF, to play a critical role in bone formation through the regulation of chromatin structure in osteoblasts. Additionally, we identified the miRNA-23a cluster (miR-23a CI) to regulate expression of Baf45a in osteoblasts, attenuating bone formation.

Previously we observed that in vivo knockdown of the miR-23a CI results in a robust increase in bone formation. RNA sequencing of miR-23a CI knockdown cells (miR-23a CI<sup>Zip</sup>) revealed a 17-fold upregulation of Baf45a. During the induction of osteogenesis, we found that expression of Baf45a and its recruitment to osteoblastic promoters increased as seen by RT-qPCR and ChIP respectively. We subsequently demonstrated that Baf45a acts as a positive regulator of osteoblastic promoters and gene expression through promoter-reporter, overexpression and knockdown strategies. Additionally, knockdown of Baf45a in miR-23a CI<sup>Zip</sup> cells resulted in the reversion of osteoblastic gene expression to the physiological state. Osteoblast-specific deletion of Baf45a (Osteocalcin Cre - Baf45<sup>fl/fl</sup> Ocn<sup>Cre</sup>) in 2-month-old mice resulted in decreased trabecular bone as seen by microCT and histomorphometry. ChIP analysis of osteoblastic promoters with Baf45a<sup>fl/fl</sup> OC<sup>Cre</sup> cells revealed decreased BAF45A occupancy and a six fold decrease in H3K27ac, a transcriptionally activating histone modification. In support, these trends were reversed in miR-23a CI<sup>Zip</sup> cells when levels of Baf45a are high. In order to reveal the osteoblast-specific BAF complex composition, we used a promiscuous biotin ligase fused to Baf45a. Thus far, we have identified Runx2 to be associated with Baf45a, and mass spectrometry analysis is now underway to determine the osteoblastic BAF complex composition.

These studies reveal Baf45a to be positive regulator of osteogenesis. Furthermore, loss of Baf45a leads to decreased bone formation through the disruption to osteoblast-specific chromatin structure. Additionally, the miR-23a CI acts as a key regulator of osteoblastic chromatin structure through the modulation of Baf45a expression. These results will provide valuable understanding for the development of treatments for low-bone-mass disorders.



Summary Schematic

Disclosures: Tanner Godfrey, None.

## SU0153

### An Epigenetic Switch Confers Pleiotropic Risk for Bone Mineral Density and Hyperglycaemia.

Yi-Hsiang Hsu<sup>1</sup>, Nicholas A Sinnott-Armstrong<sup>2</sup>, Isabel S. Sousa<sup>2</sup>, Elizabeth R Ruedy<sup>3</sup>, Richard Sallari<sup>2</sup>, Xing Chen<sup>4</sup>, Simon E Nitter Dankel<sup>5</sup>, Gunnar Mellgren<sup>5</sup>, Anyonya Guntur<sup>3</sup>, David Karasik<sup>6</sup>, Hans Hauner<sup>7</sup>, Clifford Rosen<sup>3</sup>, Douglas Kiel<sup>4</sup>, Melina Claussnitzer<sup>8</sup>. <sup>1</sup>Harvard Medical School and Broad Institute of MIT and Harvard, United States, <sup>2</sup>Broad Institute of MIT and Harvard, United States, <sup>3</sup>Center for Molecular Medicine, Maine Medical Center Research Institute, United States, <sup>4</sup>Institute for Aging Research, Hebrew SeniorLife and Harvard Medical School, United States, <sup>5</sup>University of Bergen, Norway, <sup>6</sup>Faculty of Medicine of the Galilee, Bar-Ilan University, Israel, <sup>7</sup>Else Kröner-Fresenius-Center for Nutritional Medicine, Technical University Munich, Germany, <sup>8</sup>Beth Israel Deaconess Medical Center, Harvard Medical School, United States

Recent studies suggest shared etiologies of skeletal and glycemic traits, but the underlying genetic factors remain unknown. We performed a bivariate genome wide association study (GWAS) analysis using summary statistics from GWAS meta-analyses for BMD and fasting glucose levels. We found a bivariate association at the ADCY5 locus (SNP rs56371916,  $p=1.9 \times 10^{-9}$ ). The SNP was found to be correlated with hyperglycemia (T allele) and low BMD (C allele). The 3q21.1 locus is repressed in progenitor cells for adipocytes and osteoblasts but contains an enhancer which activates during differentiation. Derepression is mediated by a conserved SREBP1 activator motif that was present in individuals with the major T allele (hyperglycaemia). However, those persons with the C allele fail to fully derepress because the SREBP1 motif is disrupted and this permits continued activity of the Polycomb-repressive complex 2 subunit EZH2. This failure to derepress results in downregulation of adenylate cyclase 5 (ADCY5) in both osteoblasts and adipocytes (2.7-fold,  $p=0.0007$  and 2.6-fold,  $p=0.0007$ , respectively). Network analysis revealed genes involved in lipid oxidation pathways and in osteoblast differentiation, respectively ( $p = 4.8 \times 10^{-6}$ ). The adipose progenitor derived osteoblasts isolated from 23 homozygous major T allele carriers and 18 individuals heterozygous for the low BMD minor C allele for rs56371916, ADCY5 downregulation leads to a cell-autonomous perturbation of fatty acid oxidation during early differentiation events ( $p=0.003$ ) and failure to differentiate ( $p=0.0014$ ), which was further supported through murine osteoblast expression profiling during differentiation. These data establish ADCY5-dependent lipid oxidation during early differentiation as an important factor in osteoblast development. In adipocytes, we demonstrated a decreased adrenergic lipolysis rate (1.9-fold,  $p=0.0012$ ) for the C allele, consistent with a lower serum glucose. CRISPR/Cas9 C-to-T editing of rs56371916 in patient derived cells restored ADCY5 activation by SREBP1, restored osteoblast differentiation programs, and accelerated lipolysis rate and glycerol release in adipocytes. Together, our bivariate GWAS analysis identified a pleiotropic risk locus that acts through the ADCY5 gene on bone and fat. In conclusion we have shown that rs56371916 alters lineage-specific Polycomb derepression, and forms the basis for the genetic correlation between low BMD and glucose levels.

Disclosures: Yi-Hsiang Hsu, None.

## SU0154

### A Graphene Oxide modified Shape Memory Polymer with Enhanced Physicochemical Properties and Osteoinductivity.

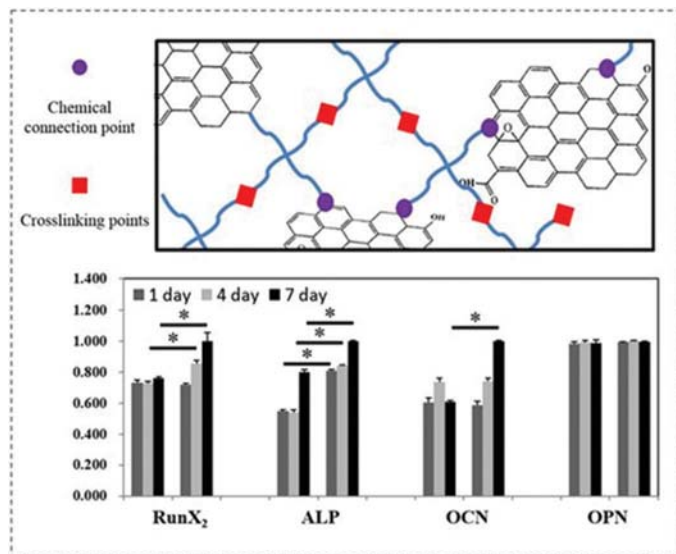
Qian Huang\*, Yunfeng Lin. Sichuan University, China

Objective: Shape memory polymers are intelligent materials that show great application value and potential in the machinery and electronics, aerospace, and many other areas. To manufacture biocompatible materials with shape memory properties is an appealing idea and worth studying.

Methods: In our study, we fabricated a composite by adding low content of graphene oxide (GO) in the photo crosslinking four-arm poly (ethylene glycol)-poly ( $\epsilon$ -caprolactone) (4A PEG-PCL). Various tests are used to characterize the morphology, physico-chemical properties and shape memory effects of the composite.

Results: As a result, The tensile strength and elastic modulus of the polymer is greatly improved by graphene oxide, which is not only attribute to the extremely high strength of graphene but also the interactions of chemical bond between the graphene oxide and the polymer. Considering the biological applications of the composite, cell experiments are conducted on clonal murine calvarial preosteoblast cell line (MC3T3-E1) and through the cell proliferation assay, fluorescent staining and morphology observation by the electron microscope. The 4A PCL-PEG/GO showed better cytocompatibility in the adhesion behavior and proliferation rate of MC3T3-E1. Additionally, expression of ossification genes, runt-related transcription factor (Runx2), alkaline phosphatase (ALP) and osteocalcin are up-regulated, which prove the better osteogenic differentiation ability of 4A PCL-PEG/GO.

Conclusion: With these results, It is expected that the GO have great potential in modifying the biosafe shape memory polymers with various excellent performance and broaden its applications in biomedical fields.



Figure

Disclosures: Qian Huang, None.

## SU0155

**Promotion of osteoblast differentiation and bone regeneration by a novel indene compound KR-34A through regulation of Bmp7 and Runx2.** Ju Ang Kim<sup>\*1</sup>, Young-Ae Choi<sup>1</sup>, Hye Jung Ihn<sup>1</sup>, Myung Ae Bae<sup>2</sup>, Hui-suk Yun<sup>3</sup>, Nack-Jeong Kim<sup>2</sup>, Hong-In Shin<sup>1</sup>, Eui Kyun Park<sup>1</sup>. <sup>1</sup>Department of Oral Pathology and Regenerative Medicine, School of Dentistry, Kyungpook National University, Korea, Republic of, <sup>2</sup>Korea Bio-Organic Science Division, Korea Research Institute of Chemical Technology, Korea, Republic of, <sup>3</sup>Powder & Ceramics Division, Korea Institute of Materials Science (KIMS), Korea, Republic of

In order to achieve efficient regeneration of the bone defect, enhancement of bone formation is critically necessary. However, a small chemical compound that can induce osteoblast differentiation has not been well documented for in vivo regeneration efficacy. Therefore, we screened chemical library to isolate an osteogenic compound and tried to validate stimulatory effects on osteoblast differentiation in vitro and bone regeneration in vivo.

The chemical library of the Korea Research Institute of Chemical Technology was screened to isolate compounds that increase alkaline phosphatase (ALP) activity, an early osteoblast differentiation marker, in MC3T3-E1 cells, and we found a novel indene compound KR-34A promoted osteoblast differentiation and mineral deposition of human BMSCs, mouse primary calvarial osteoblasts and MC3T3-E1 cells, and induced the expression of osteoblast differentiation marker genes, including Bmp7, Runx2, Alp, and Oc. KR-34A also induced phosphorylation of signaling molecules such as Akt, Mek, and Erk, and transcription factor Runx2 in MC3T3-E1 cells. On the other hand, KR-34A inhibited osteoclast differentiation by down regulation of Trap, Atp6v0d2, and Cathepsin k. These results suggest that KR-34A enhances osteoblast differentiation in vitro. Next, to examine the effect of KR-34A on bone regeneration in vivo, KR-34A was incorporated into magnesium phosphate (MgP) ceramics. The MgP ceramics containing KR-34A were implanted into calvarial defects (5 mm diameter), and bone regeneration was examined at 4 and 8 weeks later. At 8 weeks after implantation, bone volume was significantly increased in KR\_25 scaffold (134%) compared to control. Bone area was also significantly increased by 83% and 158% in KR\_5 and KR\_25 scaffolds, respectively. TRAP staining showed that osteoclast distribution was decreased by KR-34A at 4 weeks. In immunohistochemistry, the expression of Bmp7, Cd34, and Col1a1 was

increased in ceramic implanted area by KR-34A dose dependently. Collectively, our data suggest that KR-34A induces osteoblast differentiation through up regulation of Bmp7 and Runx2, and successfully promotes in vivo bone regeneration in combination with MgP ceramics.

Disclosures: Ju Ang Kim, None.

## SU0156

**A CK2/USP7/RUNX2 pathway mediates physiologic bone formation and heterotopic ossification.** Jung-Min Kim<sup>\*1</sup>, Xianpeng Ge<sup>1</sup>, Ren Xu<sup>2</sup>, Yeon-Suk Yang<sup>1</sup>, Na Li<sup>2</sup>, Odile Filhol-Cochet<sup>3</sup>, Brigitte Boldyreff<sup>4</sup>, Minkyung Song<sup>2</sup>, Matthew B. Greenblatt<sup>2</sup>, Jae-Hyuck Shim<sup>1</sup>. <sup>1</sup>Department of Medicine, University of Massachusetts Medical School, United States, <sup>2</sup>Weill Cornell Medical College, United States, <sup>3</sup>Institute de Recherches en Technologies et Sciences pour le Vivant/Biologie du Cancer et de l'Infection, Commissariat à l'Energie Atomique et aux Energies Alternatives Grenoble, France, <sup>4</sup>KinaseDetect ApS, Denmark

Osteogenesis is tightly controlled by a hierarchy of transcription factors in a defined temporal and spatial sequence, and dysregulation of this process causes clinically devastating skeletal disorders in human. How posttranslational mechanisms regulate bone formation remains an area of intense investigation. Here, we demonstrate that Casein Kinase 2 (CK2) is a key regulator of Runx2 protein stability essential for osteoblast development. Genetic deletion of b-subunit of CK2 in mesenchymal stem cells (*Ck2b<sup>flx</sup>*) abrogated skeletogenesis and its deletion in osteoprogenitors (*Ck2b<sup>ox3</sup>*) caused cleidocranial dysplasia (CCD), recapitulating the phenotypes observed in mice with impaired Runx2 function. Mechanistically, Runx2 phosphorylation by CK2 promotes recruitment of the deubiquitinating enzyme (DUB) USP7 and USP7 in turn stabilizes Runx2 by inhibiting its ubiquitin-dependent proteasomal degradation, which is required for BMP signaling. Using a mouse model of trauma-induced heterotopic ossification (HO), we provided proof of principles that inhibition of CK2 or USP7 ablated development of HO in vivo. Collectively, our results uncover a novel posttranslational mechanism of Runx2 regulation by CK2 and the CK2 pathway may represent an attractive therapeutic target to suppress ectopic bone formation in HO.

Disclosures: Jung-Min Kim, None.

## SU0157

**Red Rooibos Tea Increases Mineral Deposition by Osteoblasts in a Concentration-Dependent Manner.** Michael McAlpine<sup>\*</sup>, Wendy Ward, Adam MacNeil, William Gittings. Faculty of Applied Health Sciences, Brock University, Canada

Rooibos tea is not a traditional tea in that it is from *Aspalathus linearis* rather than *Camellia sinensis* but is thought to have similar benefits to bone health as traditional black or green tea due to its polyphenols. Our lab previously reported that the addition of green rooibos tea (GR) (1 or 10 µg/mL of polyphenols) increased mineral deposition by Saos-2 osteoblast cells. While there were no observed differences between the two concentrations in terms of the quantity of mineral deposited, of interest was whether red rooibos tea (RR), at lower doses than previously studied and more closely reflecting potential intakes through tea-drinking, also stimulates mineral deposition. RR was also of particular interest as it is oxidized, giving it a more flavorful taste profile and is less expensive; both aspects contribute to the fact that it is the more commonly consumed type of rooibos tea. The purpose of this study was to investigate a potential dose-response of RR on mineral deposition in the Saos-2 model. Cells were cultured and differentiated for 8 days at 37°C in 5% CO<sub>2</sub>. Following this, mineralization was induced for 5 days in the presence or absence of varying concentrations (0.1, 0.5, 0.75, 1, 2, 5, or 10 µg/mL) of RR polyphenols (in the absence of polyphenols, dH<sub>2</sub>O was added in equivalent volumes). RR loose leaf tea was steeped in distilled water at 96°C for 5 min. Total polyphenol content (TPC) was determined using Folin-Ciocalteu's reagent with Gallic acid as a standard. Mineralization content was measured using the alizarin red stain (n=6, where each 'n' represents an independent plating of four replicate wells that were averaged). TPC of RR was determined to be 21.8±4.7 mg of gallic acid equivalents/g. Addition of RR, regardless of concentration, increased (p<0.05) mineral deposition by osteoblasts. Mineral deposition increased (p<0.05) concurrently with the addition of higher concentrations of polyphenols (% of control, 126.5±14.4, 166.3±22.1, 185.5±23.2, 196.0±21.3, 222.6±23.9, 234.9±26.2, 243.9±26.3 at 0.1, 0.5, 0.75, 1, 2, 5, and 10 µg/mL respectively). These findings suggest that a concentration of red rooibos polyphenols as low as 0.1 µg/mL, attainable through consuming realistic amounts of RR, stimulates mineral deposition. Differential quantitative gene expression analysis, as well as cell viability measurements, are ongoing to elucidate potential molecular mechanisms and will be presented.

Disclosures: Michael McAlpine, None.



## SU0158

**Melatonin Increases Osteoblast Differentiation in Human Mesenchymal Stem Cells Derived from Bone Marrow and Adipose Tissue: implications for a role of MT2 melatonin receptors, MEK1/2, MEK5 and PPAR $\gamma$ .** Sifat Maria<sup>\*1</sup>, Fahima Munmun<sup>1</sup>, Rebekah Samsonraj<sup>2</sup>, Amel Dudakovic<sup>2</sup>, Andre van Wijnen<sup>2</sup>, Bruce Bunnell<sup>3</sup>, Matthew Burrow<sup>4</sup>, Paula Witt-Enderby<sup>1</sup>. <sup>1</sup>Duquesne University Graduate School of Pharmaceutical Sciences, United States, <sup>2</sup>Mayo Clinic Department of Orthopedic Surgery, United States, <sup>3</sup>Tulane University School of Medicine Department of Pharmacology, United States, <sup>4</sup>Tulane University School of Medicine Cancer Research Center, United States

One year nightly melatonin treatment increased bone mineral density (BMD) in mice equal in efficacy to one year estrogen/progesterone hormone therapy. In perimenopausal women (Melatonin Osteoporosis Prevention Study; MOPS; NCT01152580), melatonin renormalized bone marker turnover; in postmenopausal osteopenic women (Treatment of Osteopenia with Melatonin; MelaOst; NCT01690000), melatonin increased BMD, decreased total fat mass and increased lean body mass; and in postmenopausal women with osteopenia, melatonin added in combination with strontium citrate, vitamin D3 and vitamin K2 (Melatonin-micronutrients Osteopenia Treatment Study; MOTS; NCT01870115) increased BMD, PINP, and improved mood and sleep quality and in bone marrow- and adipose-derived mesenchymal stem cells, increased osteoblastogenesis. The mechanisms underlying these bone-protective actions of melatonin are unclear. Using two model systems—a human bone marrow-derived mesenchymal stem cell: peripheral blood monocyte co-culture (hMSC:hMC) or a human adipose-derived mesenchymal stem cell monoculture (hAMSC)—melatonin induced osteoblastogenesis, which was blocked in the presence of an MT2 melatonin receptor antagonist, 4P-P-DOT. Melatonin receptors were also detected in osteoblasts (hMSC- and hAMSC-derived) and in osteoclasts using 2-[<sup>125</sup>I]-iodomelatonin. Melatonin increased expression of pERK1/2 and RUNX2 but decreased PPAR $\gamma$  expression in MSC-derived osteoblasts. Melatonin in combination with PD98059 (MEK1/2 inhibitor), Bix02189 (MEK5 inhibitor) or SC-1-151, (dual MEK1/2 and 5 inhibitor) failed to induce osteoblastogenesis. These findings provide support for a role of MT2 melatonin receptors, MEK1/2/5 and PPAR $\gamma$  in modulating melatonin's effects on osteoblast differentiation and further support the use of melatonin for the prevention of osteopenia and osteoporosis.

**Disclosures:** Sifat Maria, None.

## SU0159

**Single-Cell RNA Sequencing Provides Molecular Dissection of Osteoblasts and their Adipogenic Potential.** Masashi Nakano<sup>\*1</sup>, Hirota Yoshioka<sup>2</sup>, Saki Okita<sup>3</sup>, Kotaro Tanimoto<sup>3</sup>, Katsuyuki Kozai<sup>4</sup>, Tomoko Minamizaki<sup>2</sup>, Yuji Yoshiko<sup>2</sup>. <sup>1</sup>Department of Calcified Tissue Biology, Department of Pediatric Dentistry, Graduate School of Biomedical & Health Sciences, Hiroshima University, Japan, Japan, <sup>2</sup>Department of Calcified Tissue Biology, Graduate School of Biomedical & Health Sciences, Hiroshima University, Japan, Japan, <sup>3</sup>Department of Orthodontics and Craniofacial Developmental Biology, Hiroshima University Graduate School of Biomedical & Health Sciences, Hiroshima, Japan, Japan, <sup>4</sup>Department of Pediatric Dentistry, Graduate School of Biomedical & Health Sciences, Hiroshima University, Japan, Japan

During bone formation processes, besides apoptosis, some osteoblasts are entrapped in bone matrix and become osteocytes, and others cover inactive bone surfaces as bone lining cells. It is thought that a subset of osteoblasts has potential to transdifferentiate into adipocytes under certain conditions. Thus, osteoblasts appear to comprise a heterogeneous cell population that may underlie the diversity in transcriptional profiles. To explore this hypothesis and its biological implications, osteoblasts were subjected to single cell RNA-sequencing. Osteoblasts were isolated by sequential digestion from calvariae of transgenic mice expressing the yellow fluorescence protein Venus under the control of the 2.3 kb *Col1a1* promoter. Of 96 Venus-positive (Venus<sup>+</sup>) single cells analyzed, 90 cell data sets were available for applications. In unsupervised hierarchical clustering analysis, Venus<sup>+</sup> single cells were categorized into two clusters, and one of which was further categorized into multiple subclusters. These two clusters showed a significant difference in the expression levels of 145 genes, such as, *Cfh*, *Cdkn1c*, and *Hist1h2bc*. Further approaches based on genes of interest among these, we categorized Venus<sup>+</sup> single cells into multiple osteoblast types. Focusing on adipogenic potential, the majority of Venus<sup>+</sup> single cells expressed genes involved in initial adipogenesis, including *Klf4*, *Cebpb*, and *Ebf1*. These cells, however, expressed the anti-adipogenic genes *Klf2* and *Klf3*. Notably, *Ppar $\gamma$*  and *Cebpa*, master transcription factors of adipogenesis, were detected in some of Venus<sup>+</sup> single cells, suggesting the adipogenic potential of osteoblasts. When cultured under osteogenic conditions, almost all Venus<sup>+</sup> cells showed nuclear staining of RUNX2, and a part of them were positive for PPAR $\gamma$  in the cytoplasm. In the presence of rosiglitazone, a synthetic ligand of PPAR $\gamma$ , nuclear distributions of these transcription factors dramatically changed from RUNX2 to PPAR $\gamma$  with accumulation of large lipid droplets. Thus, this is the first study demonstrating the diversity of osteoblasts from the viewpoint of gene expression at the single cell level. Our results suggest that a subset of osteoblasts showing mature phenotypes may have the potential to transdifferentiate into adipocytes in a PPAR $\gamma$ -dependent manner.

**Disclosures:** Masashi Nakano, None.

## SU0160

**The effect of ROCK inhibitor on bone remodeling.** Juri Nakata<sup>\*1</sup>, Yosuke Akiba<sup>2</sup>, Kaori Eguchi<sup>2</sup>, Jun Nihara<sup>3</sup>, Isao Saito<sup>3</sup>, Yoshito Kakiyama<sup>4</sup>, Makio Saeki<sup>4</sup>. <sup>1</sup>Division of Dental Pharmacology, Division of Orthodontics, Niigata University Graduate School of Medical and Dental Sciences, Japan, <sup>2</sup>Division of Bio-Prosthodontics, Niigata University Graduate School of Medical and Dental Sciences, Japan, <sup>3</sup>Division of Orthodontics, Niigata University Graduate School of Medical and Dental Sciences, Japan, <sup>4</sup>Division of Dental Pharmacology, Niigata University Graduate School of Medical and Dental Sciences, Japan

Bone homeostasis is tightly controlled by osteoblasts and osteoclasts which are involved in bone formation and resorption, respectively. To search chemical compounds which affect bone metabolism, we performed a chemical library screen for osteoclastic differentiation. RAW264.7 cells were induced osteoclastogenesis in MEM $\alpha$  containing 10% fetal bovine serum and 100 ng/ml RANKL in the presence of 5  $\mu$ M of each chemical compound for 5 days. TRAP-positive cells with more than three nuclei were counted as multinucleated mature osteoclasts. As a result, 8 activators and 7 inhibitors of osteoclastogenesis were isolated out of 378 compounds. Interestingly, two ROCK (Rho-associated coiled-coil forming protein kinase, Rho kinase) inhibitors, HA-1077 and Y-27632 were isolated as an activator of osteoclastogenesis. Rho kinase is a serine/threonine kinase and downstream target of the small GTPase Rho. It has been shown that ROCKs are involved in many aspects of cell motility, from smooth-muscle contraction to cell migration and cell-size regulation. To determine the effect of ROCK inhibitors on osteoblastic differentiation, MC3T3-E1 cells were cultured in MEM $\alpha$  containing 10 mM glyceric acid, 50  $\mu$ g/ml ascorbic acid, 10 nM dexamethasone in the presence of each ROCK inhibitor. The cells were fixed and stained with alizarin red S to evaluate the differentiation. Both of the inhibitors, HA-1077 and Y-27632 activated osteoblastogenesis. Also, similar effects were observed in murine bone marrow cells. To examine whether the ROCK inhibitors stimulate bone regeneration *in vivo*, critical-sized bone defects in rat calvaria were treated with atelocollagen sponge containing 5  $\mu$ M HA-1077 or Y-27632, and PBS was used as control. Micro CT analysis was performed after 3 weeks of the injections. The defect in calvaria was significantly recovered in the presence of each ROCK inhibitor compared with the control. Thus, our results suggest that inhibition of the activity of the ROCKs enhances bone remodeling.

**Disclosures:** Juri Nakata, None.

## SU0161

**YAP Promotes Osteogenesis and Suppresses Adipogenic Differentiation.** Jinxin Pan<sup>\*</sup>, Lei Xiong, Kai Zhao, Peng Zeng, Bo Wang, Xiao Yang, Wen-cheng Xiong. Augusta University, United States

YAP (yes-associated protein) is a key transcriptional factor that is negatively regulated by Hippo pathway, a conserved pathway for the development and size control of multiple organs. However, the exact function of YAP in bone remains unclear and controversial. Here we use Yap conditional knock out mice, YapOcn-Cre, to investigate YAP's function in OB-lineage cells in young adult mice, we provide evidences for a critical role of YAP in promoting osteogenesis, suppressing adipogenesis, and thus maintaining bone homeostasis. We also describe potential mechanism(s) by which YAP regulates osteogenesis.

KEY WORDS: YAP, Osteogenesis, Adipogenesis, Osteoporosis

**Disclosures:** Jinxin Pan, None.

## SU0162

**Interaction of bromodomain-containing proteins BRD2 and BRD4 with osteoblast transcription factor RUNX2 during osteoblast-lineage commitment.** Christopher Paradise<sup>\*1</sup>, Amel Dudakovic<sup>1</sup>, Roman Thaler<sup>1</sup>, Thomas O'Toole<sup>2</sup>, Pengfei Zan<sup>1</sup>, Andre van Wijnen<sup>1</sup>. <sup>1</sup>Mayo Clinic, United States, <sup>2</sup>Mayo Clinic, United Kingdom

Lineage commitment of multi-potent stem cells relies on the concerted expression of tissue-specific transcription factors and proteins. These changes in gene expression profiles are dictated by epigenetic mechanisms such as DNA methylation or post-translational histone modifications. Specifically, post-translational modifications of histone tails can serve as a "histone code" for gene transcription by inducing chromatin compaction, relaxation, and/or recruitment of transcriptional machinery. Epigenetic regulators, the enzymes that read, write, and erase histone tail modifications, are responsible for maintenance of this histone code and are therefore essential for altering gene expression and driving lineage commitment. Here, we investigated changes in gene expression by RNA-seq for mRNAs of 557 epigenetic regulators in 155 human-derived cell cultures with the aim of identifying osteoblast-specific epigenetic regulators. Comparing the average expression of epigenetic regulators in osteoblastic cells to the average expression in all other cells types, including embryonic stem cells, mesenchymal stem cells, and chondrocytes, generated a gene list of 155 differentially expressed epigenetic regulators in osteoblastic cells (115 up-regulated and 40 down-regulated). Remarkably, Bromodomain Containing 2 (BRD2), a member of the bromodomain family of proteins that recognize acetylated lysine residues, is significantly up-regulated

in the osteoblastic cells. In addition, previous studies have shown that BRD family members, in particular BRD4, control the expression of lineage-specific transcription factors, including RUNX2. To elucidate the role of the BRD2 and BRD4 during osteoblast differentiation, we performed knock-down studies (siRNA). We show that BRD2 depletion increases RUNX2 expression, while BRD4 loss suppresses RUNX2 expression. Similarly, JQ1, an inhibitor of BRD4, inhibits the expression of RUNX2 and suppresses osteogenic differentiation of MC3T3 cells as measured by RT-qPCR (e.g., Bglap, Ibsp, Alpl), alkaline phosphatase activity, and alizarin red staining. Our findings suggest that BRD2 and BRD4 are critical regulators of RUNX2 expression and control osteoblast differentiation.

**Disclosures:** Christopher Paradise, None.

## SU0163

**Role of HERPUD1 and ERAD activation during differentiation and mineralization of osteoblast *in vitro*.** Luan Americo-Da-Silva<sup>\*1</sup>, Jheimmy Diaz<sup>2</sup>, Mario Bustamante<sup>1</sup>, Georhan Mancilla<sup>1</sup>, Ingrid Oyarzún<sup>1</sup>, Mia Memmel<sup>1</sup>, Hugo Verdejo<sup>1</sup>, Clara Quiroga<sup>1</sup>. <sup>1</sup>División de Enfermedades Cardiovasculares, Facultad de Medicina, Pontificia Universidad Católica de Chile, Santiago, Chile & Advanced Center for Chronic Diseases (ACCDiS), Pontificia Universidad Católica de Chile, Santiago, Chile, <sup>2</sup>División de Enfermedades Cardiovasculares, Facultad de Medicina, Pontificia Universidad Católica de Chile, Santiago, Chile, Chile

Bone is a highly dynamic tissue whose integrity is the result of a balance among bone synthesis by osteoblasts and bone resorption by osteoclasts. The high secretion capacity of mature osteoblast requires a strict control of synthesis, quality control, traffic and secretion processes. The increase in protein synthesis demand induces Endoplasmic Reticulum (ER) stress, activation of unfolded protein response (UPR) and ER-associated degradation (ERAD).

ERAD is quality control mechanism that implies dislocation of unfolding proteins from ER lumen to cytosol and degradation by ubiquitin-proteasome system avoiding ER accumulation. UPR impairment have been related to bone physiopathology. However, in the osteoblast biology, ERAD, the quality control mechanisms and its regulators, is fully unknown.

HERPUD1 is an ER membrane protein and a key component of the ERAD multi-protein complex stability. The expression of HERPUD1 is strongly up-regulated by UPR and the lack of the protein has been related to ERAD dysfunction.

Our aim is to establish if HERPUD1 and the regulation of ERAD, play a role during the differentiation and maturation of osteoblasts. For this, pre-osteoblast MC3T3-E1 cell line, was differentiated in presence and absence of HERPUD1 for 3, 7 and 14 days. Osteoblast differentiation was evaluated through increase in calcium deposits, alkaline phosphatase (ALP) activity and expression of differentiation genetic markers (*runx2*, *osx*, *rankl* mRNAs). HERPUD1 levels was determined by qPCR and Western blot analysis. ERAD and proteasomal degradation activity was performed using GFP $\mu$  or CD3-YFP reporters.

Our results showed that during osteoblast differentiation the expression of HERPUD1 is increased since 12 h to 14 days. We observed that fluorescence of both reporters, GFP $\mu$  or CD3-YFP, was reduced during differentiation, confirming that ERAD and proteasomal degradation is activated during osteoblast maturation. The absence of HERPUD1 blocked the osteoblast mineralization *in vitro*, and significantly reduced the ALP activity as well the expression of *runx2*, *osx* and collagen 1. Whereas, HERPUD1 overexpression was sufficient to activate the whole osteoblast differentiation program (gene expression, ALP activity and mineralization).

In conclusion, HERPUD1 and ERAD are important to activate the osteoblast maturation program and could be a new target to understand the bone physiopathology.

**Disclosures:** Luan Americo-Da-Silva, None.

## SU0164

**Non-Mineralized and Mineralized Collagen Scaffolds induce Differential Osteogenic Signaling pathways in human mesenchymal Stem Cells.** Qi Zhou<sup>\*1</sup>, Xiaoyan Ren<sup>2</sup>, David Bischoff<sup>3</sup>, Daniel Weisgerber<sup>4</sup>, Dean Yamaguchi<sup>3</sup>, Timothy Miller<sup>2</sup>, Brendan Harley<sup>4</sup>, Justine Lee<sup>2</sup>. <sup>1</sup>UCLA and VA Great Los Angeles and Shandong University of China, United States, <sup>2</sup>UCLA and VA Great Los Angeles, United States, <sup>3</sup>VA Great Los Angeles, United States, <sup>4</sup>University of Illinois at Urbana-Champaign, United States

The instructive capabilities of extracellular matrix components in progenitor cell differentiation have recently generated significant interest in the development of bioinspired materials for regenerative applications. Previously, we described a correlation between the osteogenic capabilities of nanoparticulate mineralized collagen glycosaminoglycan scaffolds (MC-GAG) and an autogenous activation of Smad1/5 in the canonical bone morphogenetic protein receptor (BMPR) pathway with a diminished ERK1/2 activation when compared to non-mineralized scaffolds (Col-GAG). In this work, we utilize a canonical BMPR inhibitor, DMH1, and an inhibitor of the MEK/ERK cascade, PD98059, to characterize the necessity of each pathway for osteogenesis. While DMH1 inhibited Runx2 and BSPII gene expression of primary human mesenchymal stem cells (hMSCs) on MC-GAG, PD98059 inhibited BSPII expression on Col-GAG independent of Runx2 expression. DMH1 inhibited mineralization on both Col-GAG and MC-GAG, however, PD98059 only inhibited mineralized on Col-GAG. DMH1 inhibited both Smad1/5 phosphorylation and Runx2 protein expression,

whereas PD98059 inhibited ERK1/2 and JNK1/2 phosphorylation without affecting Runx2. Thus, activation of the canonical BMPR signaling is necessary for osteogenic differentiation and mineralization of hMSCs on Col-GAG or MC-GAG. The MEK/ERK cascade, intimately tied to JNK activation, is necessary for Runx2-independent osteogenesis on Col-GAG, while completely dispensable in osteogenesis on MC-GAG.

**Disclosures:** Qi Zhou, None.

## SU0165

**Soybean Peroxidase Possesses Osteogenic Activity to Accelerate Bone Regeneration *In Vivo*.** Alexandra Shoubridge<sup>\*1</sup>, Vasilios Panagopoulos<sup>1</sup>, Peter Anderson<sup>2</sup>, John Field<sup>3</sup>, Siamak Saifzadeh<sup>3</sup>, Roland Steck<sup>3</sup>, Mark DeNichilo<sup>4</sup>, Irene Zinonos<sup>1</sup>, Shelley Hay<sup>5</sup>, Andreas Evdokiou<sup>1</sup>. <sup>1</sup>University of Adelaide, Australia, <sup>2</sup>Women's and Children's Hospital & University of Adelaide, Australia, <sup>3</sup>Queensland University of Technology, Australia, <sup>4</sup>University of South Australia, Australia, <sup>5</sup>Basil Hetzel Institute for Translational Health Research, Australia

Peroxidases are heme-containing enzymes which are normally released at sites of tissue injury and inflammation by infiltrating immune cells, and until recently, have been studied mainly in the context of providing oxidative defence against invading pathogenic microorganisms. Peroxidases catalyse the conversion of hydrogen peroxide and chloride ions into hypochlorous acid, which is one of the most reactive oxidants produced *in vivo* and is responsible for peroxidase anti-microbial actions. Our laboratory has uncovered a prominent and previously unrecognised role for this group of enzymes in bone biology that has great potential as a therapy for fracture repair. We described for the first time that mammalian and plant-derived peroxidases, (i) regulate fibroblast collagen extracellular matrix biosynthesis, (ii) inhibit osteoclast differentiation and bone resorption and (iii) drive angiogenesis. Here, we investigated the ability of soybean peroxidase (SBP) to effectively regulate osteoblast function *in vitro* and accelerate bone repair *in vivo*.

*In vitro* studies were performed by stimulating primary human osteoblasts with SBP. Collagen biosynthesis was assessed by an ELISA-based method, which quantitatively measures collagen levels. Mineralization was quantified by conducting Alizarin Red staining. In addition, quantitative real-time PCR was performed to determine the ability of SBP to regulate osteoblastic genes necessary for bone formation. Next, the ability of SBP to accelerate bone repair *in vivo* was determined by using a femoral defect model in sheep. A defect of 12 mm was created on the mid-medial aspect of the femoral condyles of both hind limbs (n=4). The defect was then filled with Mastergraft® biphasic granules pre-soaked in either SBP at 650 µg/mL or saline. Animals were sacrificed at 4 weeks and bone regeneration assessed by µCT.

Here, we report for the first time, the ability of SBP to stimulate collagen type-I secretion and increase matrix mineralization *in vitro*. SBP also increased expression of key osteogenic genes, including BMP-2, BSP, WNT-5A, CXCL5, CXCL6 and IL-8. µCT reconstructions and quantitative analysis revealed increased bone volume at the defect site in the SBP-treated hind limbs compared to control ( $p = 0.01$ ).

These findings suggest that peroxidases participate in bone dynamics, with prominent regulatory and effector functions and identify a new and cost effective therapeutic approach using SBP to accelerate fracture repair.

**Disclosures:** Alexandra Shoubridge, None.

## SU0166

**Impact of Wnt-induced changes in skeletal mass and of an anabolic PTH regime on circulating levels of periostin.** Christine Simpson<sup>\*1</sup>, Meiling Zhu<sup>1</sup>, Grace Lee<sup>1</sup>, Dinah Foer<sup>2</sup>, Joseph Belsky<sup>3</sup>, Rebecca Sullivan<sup>1</sup>, Elizabeth Streeten<sup>4</sup>, Karl Insogna<sup>1</sup>. <sup>1</sup>Yale University School of Medicine, United States, <sup>2</sup>Brigham and Women's Hospital, United States, <sup>3</sup>Danbury Hospital, United States, <sup>4</sup>University of Maryland School of Medicine, United States

Periostin is an extracellular matrix protein that appears to have an important role in regulating bone strength. Although widely expressed in extra-skeletal tissues, it is preferentially expressed in the periosteum of bone. Given the central role of the periosteum in cortical bone apposition it has been suggested that periostin impacts the function of this tissue. Calcitropic hormones that regulate periostin have not been fully defined, although it has been reported that states of continuous PTH excess are associated with higher levels of periostin transcript. Whether these changes are reflected in changes in circulating levels periostin, is unclear. Given that periostin is produced in multiple tissues circulating levels may not necessarily reflect changes in bone. We therefore explored the role of important signaling pathways in bone, the Wnt pathway and PTH-mediated bone anabolic pathways, in modulating circulating levels of periostin in humans and in a murine model.

We studied 14 individuals with LRP5 variants known to be associated with high bone mass (HBM), 12 unaffected kindred members, 11 individuals with OPG, and 7 relatives in the OPG kindred who were clinically unaffected but heterozygous for LOF in LRP5. There was no difference in the mean/median values in the affected individuals with HBM due to mutations in LRP5 and unaffected kindred members (mean ages 60 vs 43 yo; median/mean periostin levels: 1238/1340 vs 1021/1159 pmoles/L, affected vs. unaffected, n=14 vs. n= 12,  $p = 0.2$ ). Similarly, there were no significant differences in mean/median periostin levels in individuals with OPG and unaffected age-matched carriers



(mean ages 11 vs 7 yo; median/mean periostin levels: 1922/1841 vs 1763/1635 pmoles/L, affected vs. unaffected, n=11 vs. n=7, p=0.3).

To examine the effect of a PTH anabolic regimen on circulating periostin, normal mice were given single daily doses of hPTH (80 ng/kg) or vehicle for 30/d. Bone mass increased as expected in the PTH-treated animals (increase in L-spine BMD: 13.7% vs 3%, PTH-treated vs. vehicle-treated, n = 14 vs. 13, p < 0.01). However, there was no change in serum periostin in the treated animals vs controls (mean periostin levels 940 pmoles/L with PTH treatment vs 967 pmoles/L in controls, n=14 vs. 13, p=0.5).

In summary, it appears that dramatic alterations in the Wnt signaling pathway do not significantly affect circulating levels of periostin in humans, nor does an anabolic PTH regimen in a murine model.

**Disclosures:** Christine Simpson, None.

## SU0167

**Osteoblasts regulate type H endothelium via Schnurri-3-regulated production of proangiogenic factors.** Ren Xu<sup>\*1</sup>, Alisha Yallowitz<sup>1</sup>, Shawon Debnath<sup>1</sup>, Dong Yeon Shin<sup>1</sup>, Jung-Min Kim<sup>1</sup>, Na Li<sup>1</sup>, Sarfaraz Lalami<sup>1</sup>, Han Dong<sup>2</sup>, Chao Zhao<sup>3</sup>, Zhuohao Wu<sup>4</sup>, Michael G. Poulos<sup>5</sup>, Jason M. Butler<sup>5</sup>, Amanda Wach<sup>6</sup>, Jae-Hyuck Shim<sup>7</sup>, Laurie H. Glimcher<sup>2</sup>, Matthew B. Greenblatt<sup>8</sup>.

<sup>1</sup>Department of Pathology and Laboratory, Weill Cornell Medical College, Cornell University, United States, <sup>2</sup>Department of Cancer Immunology and Virology, Dana-Farber Cancer Institute and Harvard University Medical School, United States, <sup>3</sup>Institute for Computational Biomedicine, Weill Cornell Medical College, Cornell University, United States, <sup>4</sup>Laboratory of Brain Development and Repair, The Rockefeller University, New York, NY, USA, United States, <sup>5</sup>Department of Genetic Medicine, Ansary Stem Cell Institute, Weill Cornell Medical College, Cornell University, United States, <sup>6</sup>Department of Biomechanics, Hospital for Special Surgery, United States, <sup>7</sup>Department of Medicine/Division of Rheumatology, University of Massachusetts Medical School, United States, <sup>8</sup>Department of Pathology and Laboratory Medicine, Weill Cornell Medical College, Cornell University, United States

Recent studies have identified a specialized subset of vascular endothelium in bone termed type H endothelium as an important regulator of bone formation. However, it is currently unclear if and how levels of type H endothelium are coordinated with physiologic programs of bone formation by osteoblasts. Previously, we have demonstrated that the adaptor protein Schnurri3 (SHN3) is a suppressor of osteoblast activity, as mice lacking SHN3 display a progressive increase in postnatal bone mass due to augmented bone formation. Here, we show that the greatly elevated bone formation seen in mice lacking SHN3 (*Shn3*<sup>-/-</sup> mice) is accompanied by an increase in type H endothelium. Osteoblasts control type H endothelium levels, as seen in mice with an osteoblast-lineage specific *Shn3* deletion (*Shn3*<sup>dmp1</sup> mice and *Shn3*<sup>ocnert</sup> mice), whereas endothelial cell-lineage *Shn3* deletion in *Shn3*<sup>cd15</sup> mice produced no detectable phenotype. Further supporting that this increase in vasculogenesis is coordinated by osteoblasts, conditioned medium from *Shn3*<sup>-/-</sup> osteoblasts promoted endothelial cell migration and tube formation *in vitro*. RNA Seq. analysis identified multiple putative mediators of these proangiogenic effects that are increased in *Shn3*<sup>-/-</sup> osteoblasts. Mechanistically, this osteo-angio coupling occurs via SHN3-mediated regulation of ERK as shown by the recapitulation of both the vascular and bone phenotypes in mice with a knockin of a mutation in the ERK binding domain of SHN3. Targeting SHN3-regulated osteo-angio coupling may represent an attractive osteoanabolic therapeutic approach, as *Shn3*<sup>dmp1</sup> mice show protection from bone and type H endothelium loss in the ovariectomy model. Similarly, SHN3-deficient mice show greatly enhanced repair of femoral fractures alongside increased type H endothelium levels in the fracture callus. Collectively, these findings demonstrate that osteoblasts couple to type H endothelium levels via SHN3 to create a supportive milieu for bone formation.

**Disclosures:** Ren Xu, None.

## SU0168

**The Regulation of IL-17RD in IL-17A Mediated Bone Remodeling.** Xuehui Yang<sup>\*</sup>, Robert Friesel. MMCRI, United States

**Objective:** IL-17A is a proinflammatory cytokine that is involved in multiple inflammatory diseases, including diseases of bone. IL-17RD is a transmembrane protein that sharing a common SEFIR domain with other IL-17 receptors and the adaptor protein Act1. We have shown that IL-17RD regulates osteogenesis by modulating FGFR signaling, and osteoclastogenesis induced by RANKL. It is not known whether IL-17RD is also involved in IL-17A mediated bone remodeling. This study is aimed to investigate the role of IL-17RD in IL-17A mediated osteogenic and osteoclastogenic phenotypes, and communication between osteoblast and osteoclast during bone remodeling.

**Methods:** Primary cell culture-based differentiation models were used for examining the roles of IL-17RD in osteoclastogenesis and osteogenesis. RT-qPCR was used to examine potential molecules that may participate in the communication between osteoblast and osteoclast. Immunoblotting analyses were used to examine IL-17A mediated cellular signaling pathways.

**Results:** IL-17A inhibited osteogenic differentiation of periosteal derived cells (PDC) and bone marrow stromal cells (BMSC), while loss of IL-17RD diminished this effect. IL-17A had little effect on osteoclast differentiation of bone marrow derived monocytes (BMM) induced by RANKL, however IL-17A pre-treated BMM had accelerated osteoclastogenesis. Loss of IL-17RD alone increased RANKL induced osteoclastogenesis of BMM, however had little role on IL-17A mediated effect. By RT-qPCR analyses we observed that IL-17A increases the ratio of RANKL/OPG in osteoblast cells, while loss of IL-17RD eliminates this effect. Immunoblotting assays showed that loss of IL-17RD increased IL-17A induced p38MAPK phosphorylation in BMSC and differentiated osteoblastic cells.

**Conclusion:** IL-17A plays an important role in bone remodeling by inhibiting osteogenesis, and increasing the ratio of RANKL vs. OPG to induce osteoclastogenesis. IL-17RD regulates IL-17A mediated bone remodeling, and this effect may involve regulation of IL-17A induced p38MAPK.

**Disclosures:** Xuehui Yang, None.

## SU0169

**Glucocorticoids Suppress Notch Target Genes but not Notch Signaling in Osteoblasts.** Stefano Zanotti<sup>\*1</sup>, Suyash Adhikari<sup>2</sup>, Ernesto Canalis<sup>1</sup>.

<sup>1</sup>UConn Musculoskeletal Institute, UConn Health, United States,

<sup>2</sup>University of Connecticut, United States

Excessive levels of glucocorticoids suppress osteoblast function and cause osteoporosis. We demonstrated that osteoblastic cells exposed to glucocorticoids display increased expression of selected Notch receptors and cognate ligands such as Delta-like (Dll)1. These findings revealed a potential mechanism for the detrimental effects of glucocorticoids on skeletal integrity, since activation of Notch inhibits bone formation. However, an increase in the expression of Notch receptors and respective ligands does not imply that signaling activity is enhanced because induction of Notch requires cell-to-cell contact interactions. These lead to the release of the Notch intracellular domain (NICD), which translocates to the nucleus and binds to the DNA-associated protein Rbpjk to induce the expression of Notch target genes, such as *Hey1* and *HeyL*. To determine whether glucocorticoids modulate Notch signaling, the impact of glucocorticoid administration on Rbpjk-DNA interactions and on the expression of *Hey* genes was explored. In initial studies, 21-day release pellets containing 5 mg of prednisolone or placebo were implanted in wild-type C57BL/6J male mice at 1 month of age. Mice were sacrificed 72 h after implantation, and gene expression analyzed by qRT-PCR in total RNA from dissected femurs devoid of bone marrow. Prednisolone induced *Tsc22*, a glucocorticoid target gene, and suppressed *Hey1* and *HeyL* expression. This may represent an inhibition of Notch receptor activity or a direct downregulation of *Hey1* and *HeyL* expression by glucocorticoids. To clarify the nature of the *in vivo* findings, osteoblast-enriched cells from wild-type C57BL/6J mice were exposed to cortisol or vehicle and Notch signaling activated either by seeding on a Dll1-coated substrate or by transiently overexpressing the Notch1 NICD. Similarly to the observations *in vivo*, cortisol opposed the stimulatory effects of Dll1 on *Hey1* and *HeyL* expression. However, transactivation studies with a reporter construct driven by Rbpjk consensus sequences and electrophoretic mobility shift assays demonstrated that cortisol does not interfere with the ability of Rbpjk to induce transcription. In conclusion, glucocorticoids do not affect Notch receptor signaling but suppress *Hey1* and *HeyL* expression by Rbpjk-independent mechanisms.

**Disclosures:** Stefano Zanotti, None.

## SU0170

**In vivo Bone Formation by Osteoblasts Generated from Human Induced**

**Pluripotent Stem Cells under Fully Defined and Xeno-Free Conditions.**

Denise C. Zujewski<sup>\*1</sup>, Kosuke Kanke<sup>2</sup>, Hironori Hojo<sup>1</sup>, Shoko Onodera<sup>3</sup>,

Toshifumi Azuma<sup>3</sup>, Ung-il Chung<sup>4</sup>, Shinsuke Ohba<sup>4</sup>.

<sup>1</sup>Department of Bioengineering, The University of Tokyo, Japan, <sup>2</sup>Department of Oral and

Maxillofacial Surgery, The University of Tokyo Hospital, Japan,

<sup>3</sup>Department of Biochemistry, Tokyo Dental College, Japan, <sup>4</sup>Department of

Bioengineering, The University of Tokyo / Center for Disease Biology and

Integrative Medicine, The University of Tokyo, Japan

The latest progress in providing induced pluripotent stem cells (iPSCs) for use in clinical settings includes the establishment of an allogenic iPSC bank. Stored iPSCs will be matched to patients based on human leukocyte antigen haplotypes and processed in a reasonable time according to the application. The translation of the iPSC technology to various tissues depends largely on the efficacy of the differentiation treatments of the iPSCs, which must be safe while producing functional cells. Here we developed a fully defined, xeno-free strategy to direct human iPSCs (hiPSCs) toward osteoblasts for *in vivo* bone regeneration. We successfully achieved the osteogenic induction of four independently derived hiPSC lines within 21 days by a sequential use of combinations of small-molecule inducers. To manipulate the differentiation signals in a stage-specific manner, we used a GSK3 inhibitor, a hedgehog signaling activator and inhibitor, and the bone morphogenetic protein (BMP)-dependent osteogenic molecule that we identified previously (Ohba S. et al., Biochem Biophys Res Commun, 2007). The induction first generated mesodermal cells, and it subsequently recapitulated the developmental expression pattern of major osteoblast markers (*RUNX2*, *COL1A1*, *SP7*, and *BGLAP*) while gradually suppressing the expression of pluripotency markers (*REX1*, *NANOG*,

*POU5F1* and *SOX2*). Importantly, the resulting cell population formed calcified structures *in vitro* and exhibited a sustained expression of *BGLAP*, a bona fide marker of mature osteoblasts. When transplanted in critical-sized calvarial defects of immunodeficient mice, hiPSC-derived osteoblasts induced accelerated bone repair as indicated by MicroCT scans and histological analysis. In addition, the presence of human nuclear-positive cells in the regenerated sites suggested that the hiPSC-derived osteoblasts exerted their positive effect on bone repair by engraftment with the host tissue as well as via self-assembled bone-like tissue formation. Our findings thus demonstrate that we have developed a robust system to generate *in vivo* functional human iPSC-derived osteoblasts by a precise manipulation of signaling pathways involved in osteoblast commitment. The xeno-free condition, the short treatment period, and the stability of the inducers in the developed protocol together provide a new step toward the clinical applications of human iPSCs in skeletal regenerative medicine.

**Disclosures:** Denise C. Zujur, None.

## SU0171

**Orthopedic Particles Induce Inflammatory Osteolysis Through Transcriptional Inhibition of Regulatory T Cells.** Tim (Hung-Po) Chen\*, Gaurav Swarnkar, Amjad Nasir, Gabriel Mbalaviele, Yousef Abu-Amer. Washington University School of Medicine, United States

Inflammatory osteolysis is a major complication of orthopedic implants wherein wear particles trigger immune and inflammatory responses at the injury site. This cell- and cytokine-based pathologic response accelerates bone erosion around the implant leading to loosening and failure of implants. Despite recent progress, details of the cellular response to implant debris remain enigmatic. Previously, we have shown that polymethylmethacrylate (PMMA) particles directly target osteoclast precursors (OCPs; e.g. macrophages) and activate NF- $\kappa$ B pathway leading to osteolysis. It is further evident that immune cells, primarily T lymphocytes and dendritic cells are the first responders encountering orthopedic particles, yet the underlying mechanism of this response is unclear. T<sub>REG</sub> cells, which express the transcription factor Foxp3, are the chief immune-suppressive cells. Using an intratibial injection model, we show that PMMA particles affect T cells in either direct or indirect manner. First, we found that PMMA induce T<sub>REG</sub> instability evident by reduced number of Foxp3+ T<sub>REG</sub> and their Foxp3 protein. This phenomenon occurred both locally (bone marrow) and systemically (spleen, blood and lymph nodes). Importantly, while intratibial injection of PMMA initiated an acute and transient innate immune and inflammatory response evidenced by the increasing myelopoiesis and NF- $\kappa$ B reporter activity, the negative impact on T<sub>REG</sub> by PMMA remained persistent even 1 week after injection. We further show that PMMA induced T<sub>H</sub>17 response at the expense of other T effector cells (T<sub>EFF</sub>), particularly T<sub>H</sub>1. To encounter OCPs exacerbated by PMMA particles, T<sub>REG</sub> required direct cell-cell interaction with OCPs. Interestingly, anti-OCP property of T<sub>REG</sub> was only partially hindered by PMMA. Gene expression analysis on *in vivo* and *ex vivo* PMMA-encountered T<sub>REG</sub> and T<sub>EFF</sub> revealed that mechanistically, PMMA promoted mTOR signaling by regulating PI3K/AKT/Foxo3a axis to enhance T<sub>EFF</sub> function (T<sub>H</sub>17 cells in particular) and dampen T<sub>REG</sub> activity. PMMA also downregulated T<sub>H</sub>17 transcriptional factor ROR $\gamma$ T, T<sub>H</sub>1 Tbet and T<sub>H</sub>2 GATA3 expressions in Foxp3+ T<sub>REG</sub>, presumably to impair cell-specific suppressive function of T<sub>REG</sub>. Thus, myeloid and lymphoid cells may both contribute to PMMA-induced inflammatory osteolysis. The previously underappreciated impact of PMMA on lymphoid cells may represent one of the confounding mechanisms that contribute to prolonging disease progression of aseptic loosening.

**Disclosures:** Tim (Hung-Po) Chen, None.

## SU0172

**Novel Role For EZH2 Methyltransferase in Myeloma-Induced Abnormal Osteoclastogenesis.** Juraj Adamik\*<sup>1</sup>, Rebecca Silberman<sup>2</sup>, Konstantinos Lontos<sup>1</sup>, Peng Zhang<sup>1</sup>, Quanhong Sun<sup>1</sup>, Judy L Anderson<sup>2</sup>, Jolene J Windle<sup>3</sup>, G David Roodman<sup>4</sup>, Deborah L Galson<sup>5</sup>. <sup>1</sup>Department of Medicine, Hematology-Oncology Division, University of Pittsburgh Cancer Institute, United States, <sup>2</sup>Department of Medicine, Hematology-Oncology Division, Indiana University, Indianapolis, United States, <sup>3</sup>Department of Human and Molecular Genetics, Virginia Commonwealth University, United States, <sup>4</sup>Department of Medicine, Hematology-Oncology Division, Indiana University; Veterans Administration Medical Center, United States, <sup>5</sup>Department of Medicine, Hematology-Oncology Division, University of Pittsburgh Cancer Institute, McGowan Institute for Regenerative Medicine, United States

Multiple myeloma (MM) patients develop osteolytic bone lesions due to hyperactivation of osteoclast precursors (OCLp). The lesions rarely heal even after therapeutic remission due to MM-induced suppression of bone marrow stromal cell differentiation into osteoblasts. Pathological mechanisms associated with MM-induced OCL hyperactivity are not fully understood. We reported that expansion of bone marrow monocyte (BMM) OCLp in the presence of MM1.S-conditioned media (MMCM) significantly enhanced formation of TRAP-positive multinucleated OCL. We now find that MMCM significantly enhances RANKL-induction of the epigenetic modifier EZH2, which tri-methylates histone H3 at Lys-27 (H3K27me3) and plays a critical role during the initial 24h of

RANKL-induced osteoclastogenesis, silencing several OCL inhibitory factors such as *MafB*, *Irf8* and *Arg1*, and permitting OCL formation. Consistent with increased EZH2 levels and the rate of OCL formation, MMCM OCLp exhibit faster reduction of mRNA for these OCL inhibitory factors. The MMCM-amplified expression of OCL marker genes NFATc1, RANK, OSCAR, Cathepsin K, and DC-STAMP and the MM-supporting genes *Anxa2*, *Il6* and *MMP9* in OCLp is blocked when the EZH2 inhibitor GSK126 is present at RANKL addition. Interestingly, when GSK126 is present only during the M-CSF expansion and removed before RANKL addition, only MMCM amplification of OCL differentiation is inhibited. To better understand how MMCM primes and enhances OCL formation, we performed RNAseq transcriptome profiling to analyze the gene expression changes in the MMCM preconditioned FACS selected OCLp (CD45+Lin-CD115+). Using Ingenuity Pathway Analysis (IPA), we have identified several differentially expressed genes associated with various canonical and pro-inflammatory pathways. Among these are: TNF ligands and receptors APRIL/ TNFSF13, LIGHT/ TNFSF14, BAFF/ TNFSF13b, TNFRsf18, TNFRsf14, TNFRsf1b; calcium transport regulators ATP2A1, ATP2B3, TRPC1; and metalloproteinases MMP2, 8, 9, 27, important factors for supporting pro-inflammatory OCL. Additionally, we have identified Target Of Myb1 Membrane Trafficking Protein (TOM1), known to be a novel negative regulator of IL-1 and TNF signaling pathways, as a potential OCL inhibitory factor. Together, our studies reveal that MMCM enhances various pro-inflammatory signaling pathways that prime differentiation of OCLp. We further show that EZH2 as a critical mediator of the MM-amplified OCL differentiation.

**Disclosures:** Juraj Adamik, None.

## SU0173

**Intracellular Localization of *Staphylococcus aureus* in Osteoclasts.** Emily Goering\*, Jennifer Kraus, Deborah Novack. Washington University, United States

Osteomyelitis (OM) is infection-driven inflammatory disease of the bone primarily caused by *Staphylococcus aureus* (*S. aureus*) which causes pathological bone loss and can lead to prolonged hospitalization, amputation, and rarely death. Historically, *S. aureus* was thought to be an extracellular pathogen, but more recently, osteoblasts have been shown to harbor the bacteria, leading to inflammatory cytokine and RANKL production. We have now found that osteoclasts (OCs) also internalize *S. aureus*. However, unlike their macrophage precursors which show robust intracellular killing, OC support bacterial proliferation. The purpose of this study was to investigate how *S. aureus* evades the cellular defense system by studying the endocytic vesicles where *S. aureus* resides within OC over time. We hypothesized that *S. aureus* would be confined to acidified compartments (eg. lysosomes) in bone marrow macrophages (BMMs), while those within OCs would not be in acidified vesicles. To address this question, we used confocal microscopic imaging of BMMs and OCs infected with GFP-labeled *S. aureus* (MRSA strain USA300) and stained with the fluorescent dye LysoTracker, which marks acidified intracellular vesicles. Cells were fixed at 1.5 hours, 3 hours, 6 hours, and 18 hours post-infection for image analysis of the localization of intracellular *S. aureus* in lysosomes over time. We found that over half of *S. aureus* are localized to lysosomes in BMMs and OCs at 1.5 hours, 3 hours, and 6 hours of infection, with no significant differences in localization between cell types. However, 18 hours after infection the few remaining *S. aureus* in BMMs are localized to lysosomes while less than 5% of *S. aureus* is localized to lysosomes in differentiated OCs. This indicates that *S. aureus* may avoid intracellular killing in OCs by avoiding progression of endocytic vesicles to lysosomes or escaping the endocytic vesicle system in osteoclasts. To further assess the endocytic vesicular location of *S. aureus* in osteoclasts late in infection, we will next use antibodies for markers of earlier endocytic vesicles.

**Disclosures:** Emily Goering, None.

## SU0174

**Gpnmb/Osteoactivin Plays a Novel Role in Autophagy-Mediated Osteoclast Differentiation and Function.** Fatima Jaber\*<sup>1</sup>, Asaad Al-Adlaan<sup>1</sup>, Nazar Hussein<sup>1</sup>, Fayez Safadi<sup>2</sup>. <sup>1</sup>School of Biomedical Sciences, Kent State University, United States, <sup>2</sup>Northeast Ohio Medical University (NEOMED), United States

Autophagy plays an important role in bone homeostasis where it regulates both osteoblast (OB) and osteoclast (OC) differentiation and function. Autophagy is controlled by mTOR-independent and mTOR-dependent pathways. Glycoprotein nmb (Gpnmb), also called osteoactivin (OA) is a novel protein discovered in our lab that negatively regulates OC differentiation and positively regulates their function. In addition, our lab has shown that mutation in OA enhances OC differentiation but inhibits their function, while transgenic OA mice has decreased OC function. Previous literature has shown that autophagy is responsible for generating the OC-ruffled border. In this study, we investigated whether OA regulates OC differentiation and function by mediating the autophagy pathway. First, we induced autophagy in OC using bone marrow derived hematopoietic stem cells (BM-HSCs) from WT mice and found that OA expression was increased in a dose- and time-dependent manner. In addition, we and others showed that OA binds to microtubule associated protein light chain (LC3-II) in bone cells. Next, to determine if OA contributes to autophagy in OC, we generated OC derived from WT and D/2J mutant mice then treated them with either Trehalose (TH), an mTOR-independent pathway inducer or Rapamycin (R), mTOR-dependent autophagy pathway. We found that both treatments caused induction of autophagy. However, this induction was more profound in WT compared to D/2J OC. Next, we determined whether the role of OA in autophagy is mTOR dependent or independent on



OC differentiation and function. OC precursors from WT and D/2J mice were treated with either TH or R. OC differentiation and function were evaluated using TRAP staining, activity and resorption assays. Our data showed that R treatment inhibits RANKL-induced OC differentiation and function in D/2J OC, while TH treatment enhances OC differentiation and function in D/2J compared to WT OC. Next, we examined the expression of autophagy markers following treatment with either TH or R; and found that *Beclin-1*, *ATG5* and *LC3*, *OA* and *TRAP* expression were downregulated with R treatment while upregulated with TH treatment in D/2J compared to WT OC. Next, we assessed the effects of TH and R treatments on OC-ruffled border formation using electron microscopy. Our data showed that TH treatment causes a well-developed ruffled border compared to R-treated cultures in D/2J compared to WT mice. Next, we examined the contribution of OA-mediated autophagy during osteoclastogenesis in vivo. D/2J mutant and WT mice were subjected to calvarial osteolysis model. Mice were treated with either RANKL (positive control) or RANKL with TH or RANKL with R. Our data demonstrate that TH treatment increased osteoclastogenesis compared to R or RANKL treated groups in D/2J compared to control. These data suggest that OA regulates OC differentiation and function in part by mTOR-dependent pathway.

**Disclosures:** Fatima Jaber, None.

## SU0175

**Double Deletion of Ctsk and Mmp9 Exhibit a Severe Osteopetrosis Due to Impaired Osteoclast Differentiation and Activity from the Loss of Synergistic Functions of Ctsk and Mmp9.** Joel Jules\*, Hong Huang, Wei Chen, Guochun Zhu, Diep Nguyen, Yi-Ping Li. University of Alabama at Birmingham, United States

The lysosomal cysteine protease cathepsin K (*Ctsk*) and matrix metalloproteinase 9 (*Mmp9*) are two major proteolytic enzymes that are crucial for osteoclast (OC) function. It has been previously shown that *Ctsk* is not only markedly upregulated during OC differentiation and is selectively expressed by OCs, it can also promote the degradation of the organic matrix for bone resorption. Meanwhile, *Mmp9* is critical for bone collagen solubilization and OC migration as well as OC formation and activation. Whereas mice deficient in the *Ctsk* gene (*Ctsk*<sup>-/-</sup>) show a mild osteopetrotic phenotype, mice deficient in the *Mmp9* gene (*Mmp9*<sup>-/-</sup>) display a comparable bone density to the wild-type mice. Due to their compromised proteolytic activities, some functions of *Ctsk* and *Mmp9* in OCs may remain unknown. We hypothesized that *Ctsk* and *Mmp9* have synergistic functions in OCs. To address this issue, we generated a *Ctsk*<sup>-/-</sup>/*Mmp9*<sup>-/-</sup> double knockout (DKO) mouse model to examine their roles in OC biology. The DKO mice exhibited a severe osteopetrosis from defective OC differentiation and activation as well as impaired matrix protein degradation, which progressively accentuated as mice aged. Interestingly, the hypertrophic area was abnormally elongated by 3 and 2 folds in the *Ctsk*<sup>-/-</sup> and DKO, at day 1 of postnatal development, respectively, which remained constant in the *Ctsk*<sup>-/-</sup> group but continued to expand abnormally in the DKO group at 8 weeks. Notably, through *ex vivo* assays, we found that *Mmp9* and *Ctsk* exhibited a synergistic role in OC differentiation and activity. In addition, OC differentiated from cells isolated from the DKO mice, but not those from the wild-type, *Ctsk*<sup>-/-</sup>, or *Mmp9*<sup>-/-</sup> mice, showed enhanced cell apoptosis. By Western blot and qPCR, we showed that mechanistically, *Ctsk* and *Mmp9* synergistically induced the expression of NFATc1, a master regulator of osteoclastogenesis, but are dispensable to the upregulation of c-Fos, C/EBP $\alpha$  and PU.1, critical for OC differentiation and activity. Consistently, lack of *Ctsk* and *Mmp9* drastically repressed the expression of the tartrate-resistant acid phosphatase, a target gene of NFATc1 and a key marker gene of OC. Together, our results suggest that the severe osteopetrosis of the DKO mice stems from the drastic NFATc1 repression which affects OC formation and function and matrix protein degradation. This study provides a novel synergistic function(s) of *Mmp9* and *Ctsk* in bone homeostasis.

**Disclosures:** Joel Jules, None.

## SU0176

**Bisphosphonate inhibits bone resorption by blocking autophagy in osteoclasts.** Sol Kim\*, Vadim A. Goldshteyn<sup>1</sup>, Atsushi Arai<sup>2</sup>, No-Hee Park<sup>1</sup>, Reuben Kim<sup>1</sup>. <sup>1</sup>UCLA School of Dentistry, United States, <sup>2</sup>Matsumoto Dental University, Japan

Bisphosphonates (BPs), pharmacological agents for the treatment of bone-related diseases such as osteoporosis or cancer metastasis. Although BP is known to target osteoclasts (OCs) to inhibit bone resorption, the underlying molecular mechanism remain unclear. Matured OCs release a variety of proteases including cathepsin K (CtsK), TRAP, or metalloproteases (MMPs) in order to degrade bone matrices, and these proteases are required for further processing to be cleaved within a lysosome to achieve its active form. Here, we investigated the effect of BP on processing of proteases during osteoclastogenesis.

Bone marrow-derived macrophages (BMMs) were treated with M-CSF and RANKL to induce osteoclastic differentiation in the presence or absence of zoledronic acid (ZOL). We found that ZOL suppressed not only maturation and activity of bone-degrading protease but resorptive functions of osteoclasts in vitro. During osteoclastogenesis, RANKL-induced OCs diminished in protein expression of autophagy related (Atg) such as Atg4, 7, beclin1 or p62, whereas ZOL caused a delay in diminished expression of Atg proteins, suggesting an accumulation of non-degradative autophagosomes. Similar to ZOL treated OCs, the accumulation of Atg proteins was observed in autophagy inhibitor, bafilomycin A, treated osteoclast. Furthermore, the maturation of

proteases was also blocked by autophagy inhibitor. At the molecular level, BPs block the mevalonate pathway that leads to target protein prenylation including farnesylation and geranylgeranylation. Mechanistic studies revealed that BP inhibits osteoclastogenesis by interfering prenylation with small GTP-binding proteins of Rab family, specifically Rab7, and we confirmed that Rab7 is required for osteoclast differentiation in vitro. Conditional Rab7 knock-out mice which is specific Rab7-deficient in mature osteoclast displayed osteopetrotic phenotype by the failure of osteoclasts to resorb bone, and this impairment caused a significant inhibition of bone resorption in vitro.

Taken together, our study demonstrates that BPs inhibit bone-resorptive function of osteoclast by suppressing the maturation of bone-degrading enzymes to secrete into the ruffled border by interfering autophagy processing.

**Disclosures:** Sol Kim, None.

## SU0177

**Gulp1 deficiency impairs osteoclast function and results in high trabecular bone mass in mice.** Soon-Young Kim\*, Gunil Park<sup>1</sup>, Eun-Hye Lee<sup>2</sup>, Seong-Hwan Kim<sup>1</sup>, Suk-Hee Lee<sup>1</sup>, Yeon-Ju Lee<sup>2</sup>, Seung-Yoon Park<sup>3</sup>, Jung-Eun Kim<sup>4</sup>. <sup>1</sup>Kyungpook National University School of Medicine, BK21 Plus, Korea, Republic of, <sup>2</sup>Kyungpook National University School of Medicine, CMRI, Korea, Republic of, <sup>3</sup>School of Medicine, Dongguk University, Korea, Republic of, <sup>4</sup>Kyungpook National University School of Medicine, CMRI, BK21 Plus, Korea, Republic of

Engulfment adaptor phosphotyrosine-binding (PTB) domain containing 1 (GULP1) is an adaptor protein involved in the engulfment of apoptotic cells via phagocytosis. Although Gulp1 is widely expressed in various tissues, including the brain, muscle, testis, and bone, the function of Gulp1 has not been well studied. Here, we investigated whether Gulp1 plays a role in the regulation of bone remodeling and examined its expression in bone cells. Gulp1 knockout mice were prepared by crossing Gulp1 heterozygous mice generated by homologous recombination. The trabecular bone mass of the femur and tibia, as well as the lumbar vertebrae was significantly increased in Gulp1 knockout mice compared to their wild-type littermates. The dynamic bone formation of osteoblasts in Gulp1 knockout mice did not differ from that in wild-type mice. However, the number of fully differentiated osteoclasts and the surface area of the resorption pit in bone slices were lower in Gulp1 knockout mice than in wild-type mice. Furthermore, actin ring and microtubule formation in osteoclasts were inhibited in Gulp1 knockout mice. These results indicate that Gulp1 deficiency suppresses osteoclast differentiation and bone resorption, but does not alter the bone formation of osteoblasts, which ultimately increases bone mass. Taken together, these results suggest that Gulp1 may be a novel positive regulator of osteoclast differentiation and bone resorption.

**Disclosures:** Soon-Young Kim, None.

## SU0178

**Suppression of Osteoclastogenesis by Melatonin: A Melatonin Receptor-Independent Action.** Hyung Joon Kim\*, Yong Deok Kim<sup>2</sup>. <sup>1</sup>Department of Oral Physiology, BK21 PLUS Project, and Institute of Translational Dental Sciences, School of Dentistry, Pusan National University, Korea, Republic of, <sup>2</sup>Department of Oral and Maxillofacial Surgery, Dental Research Institute and Institute of Translational Dental Sciences, School of Dentistry, Pusan National University, Korea, Republic of

In vertebrates, melatonin is primarily secreted from pineal gland but it affects various biological processes including sleep-wake cycle, vasomotor control, immune system as well as bone homeostasis. Melatonin has been known to promote osteoblast differentiation and bone maturation, but a direct role of melatonin on osteoclast differentiation is still elusive. We report the direct inhibition of osteoclasts differentiation from mouse bone marrow-derived macrophages by melatonin. Interestingly, it seemed that the inhibitory action of melatonin on osteoclasts differentiation was MT1/MT2 melatonin receptor independent.

In the present study, the effect of melatonin on the differentiation of macrophages to osteoclasts was investigated. Data were obtained from at least three independent experiments. The Student's t-test was used to determine the significance of differences between melatonin treated and non-treated groups. Differences with p<0.01 were regarded as significant and denoted as an asterisk.

In the presence of melatonin, RANKL-induced osteoclastogenesis was significantly reduced and the siRNA-mediated knockdown of melatonin receptor failed to overcome the anti-osteoclastogenic effect of melatonin. Melatonin treatment did not affect the phosphorylation of ERK, p38 and JNK but the activation of NF- $\kappa$ B and subsequent induction of NFATc1 were markedly inhibited upon melatonin treatment. Thus, our results suggest that melatonin could suppress osteoclast differentiation through down-regulation of NF- $\kappa$ B pathway with concomitant decrease in the NFATc1 transcription factor induction. Furthermore, melatonin seems to have anti-osteoclastogenic effect independent of plasma membrane melatonin receptors. In addition to previously reported properties of melatonin, our study could also propose another aspect of melatonin and bone homeostasis.

**Disclosures:** Hyung Joon Kim, None.

## SU0179

**LRF/OCZF Regulates Survival of Osteoclasts via Sam68, a Splicing Regulator of Bcl-x.** Xianghe Xu<sup>1</sup>, Makoto Shiraki<sup>1</sup>, Asana Kamohara<sup>1</sup>, Takeo Shobuike<sup>1</sup>, Toshio Kukita<sup>2</sup>, Akiko Kukita<sup>1</sup>, <sup>1</sup>Department of Pathology and Microbiology, Faculty of Medicine, Saga University, Japan, <sup>2</sup>Department of Molecular Cell Biology & Oral Anatomy, Faculty of Dentistry, Kyushu University, Japan

LRF (leukemia/lymphoma-related factor), also known as Pokemon, OCZF in rat and FBI-1 in human is a member of the zBTB family of proteins. LRF/OCZF have been shown to be as a critical regulator of differentiation and commitment of hematopoietic cells and also implicated in human cancer. We previously reported that LRF/OCZF enhanced osteoclastogenesis and survival of osteoclasts using OCZF transgenic (OCZF-Tg) mice (Arthritis & Rheumatism 2011) and bone resorption with osteoclast-specific LRF deletion (PNAS 2012). Sam68 is a RNA-binding splicing regulator and involved in apoptosis. Sam68 affects alternative splicing of Bcl-x and cause the increase of proapoptotic Bcl-x<sub>s</sub> mRNA. Recent findings show that FBI-1 suppress Sam68-mediated Bcl-x alternative splicing thereby increasing antiapoptotic Bcl-x<sub>l</sub> mRNA and inhibiting apoptosis in cancer cell. In this study, we analyzed the function of LRF in the survival of osteoclasts using OCZF-Tg mice overexpressing OCZF under the control of the cathepsin K promoter.

Sam68 mRNA was increased transiently in BMM stimulated with RANKL and returned to a prior level. Expression of Sam68 mRNA in osteoclasts did not differ significantly between WT and OCZF-Tg mice. In contrast, immunofluorescence and Western analysis showed that the expression of Sam68 protein was markedly decreased in osteoclasts of OCZF-Tg in comparison with those of WT mice. In contrast, Bcl-x<sub>l</sub> mRNA was increased in osteoclasts of OCZF-Tg mice. Interestingly, the expression of LRF and Bcl-x<sub>l</sub> mRNA was increased in bone resorbing osteoclasts formed on dentine in comparison with osteoclasts formed on culture dish. These results suggest that bone resorbing osteoclasts have increased survival activity and LRF may enhance survival of bone surface osteoclasts by increasing Bcl-x<sub>l</sub> mRNA through regulating the stability of Sam68 protein. In addition, we found that ovariectomized-induced bone loss was accelerated in OCZF-Tg mice in comparison with that of WT mice. Currently, the study is in progress to analyze the mechanism of ovariectomized-induced bone loss of OCZF-Tg mice. Our study show that LRF/OCZF is a potential target for the regulation of bone-resorbing osteoclasts.

**Disclosures:** Xianghe Xu, None.

## SU0180

**Osteoclasts Formed under Stimulation by IL-1 $\beta$  Possess Extremely High Ability to Secrete Protons and to Resorb Dentin with Abnormal Adhesiveness, Imaged by pH-Sensitive Fluorescence Probes.** Takuma Shiratori<sup>1</sup>, Akiko Kukita<sup>2</sup>, Yukari Kyumoto-Nakamura<sup>1</sup>, Norihisa Uehara<sup>1</sup>, Jingqi Zhang<sup>1</sup>, Kinuko Koda<sup>3</sup>, Mako Kamiya<sup>3</sup>, Tamer Badawy<sup>1</sup>, Xianghe Xu<sup>4</sup>, Takayoshi Yamaza<sup>1</sup>, Yasuteru Urano<sup>3</sup>, Kiyoshi Koyano<sup>5</sup>, Toshio Kukita<sup>1</sup>, <sup>1</sup>Molecular Cell Biology & Oral Anatomy, Faculty of Dental Science, Kyushu University, Japan, <sup>2</sup>Microbiology, Faculty of Medicine, Saga University, Japan, <sup>3</sup>Chemical Biology & Molecular Imaging, Grad.Sch.Medicine; Chemistry & Biology, Grad.Sch.Pharm.Sci., The University of Tokyo, Japan, <sup>4</sup>Microbiology, Faculty of Medicine, Saga University ; Molecular Cell Biology & Oral Anatomy, Faculty of Dental Science, Kyushu University, Japan, <sup>5</sup>Implant Rehabilitation Dentistry, Faculty of Dental Science, Kyushu University, Japan

As osteoclasts have the central roles in normal bone remodeling, it is ideal to regulate only the osteoclasts performing pathological bone destruction without affecting normal osteoclasts. Based on a hypothesis that pathological osteoclasts form under the pathological microenvironment of the bone tissues, we here set-up optimum culture conditions to examine the entity of pathologically activated osteoclasts (PAOCs).

Through searching various inflammatory cytokines and their combinations, we found the highest resorbing activity of osteoclasts when osteoclasts were formed in the presence of M-CSF, RANKL and IL-1 $\beta$ . We have postulated that these osteoclasts are PAOCs. IL-1 $\beta$  is a cytokine having important roles in immune response and inflammation. We have previously demonstrated the expression of IL-1 receptor type 1 in osteoclasts present in the bone destruction sites in rat with adjuvant-induced arthritis, a model of human rheumatoid arthritis, and proposed a possibility that IL-1 directly regulates osteoclasts.

Analysis using confocal laser microscopy revealed that PAOCs showed extremely high proton secretion detected by the acid-sensitive fluorescence probe Rh-PM and bone resorption activity compared with normal osteoclasts. PAOC tended to form quite large multiple areas for proton secretion. PAOCs showed unique morphology bearing high-thickness and high motility with motile cellular processes in comparison to normal osteoclasts, suggesting some abnormality in cell adhesion. We further examined the expression of Kindlin-3 and Talin-1, essential molecules for activating integrin  $\beta$  chains. Although normal osteoclasts express high level of Kindlin-3 and Talin-1, expression of these molecules was markedly suppressed in PAOCs, suggesting the abnormality in the adhesion property. When whole membrane surface of mature osteoclasts was biotinylated and analyzed, the IL-1 $\beta$ -induced cell-surface protein was detected. PAOCs could form a subpopulation of osteoclasts which are derived from different osteoclast

precursors from that of normal osteoclasts. PAOC-specific molecules could be an ideal target for regulating pathological bone destruction.

**Disclosures:** Takuma Shiratori, None.

## SU0181

**$\alpha$ 7nAChR is required to regulate osteoclasts and bone mass via TNF $\alpha$ -dependent regulation of OPG and RANKL.** Kazuaki Mito<sup>\*</sup>, Takeshi Miyamoto, Kazuki Sato, Morio Matsumoto, Masaya Nakamura, Department of Orthopaedic Surgery, Keio University, Japan

[Introduction]

The nicotinic receptor  $\alpha$ 7nAChR reportedly regulates vagal nerve targets in brain and cardiac tissues, and the parasympathetic nervous system; however, its roles in bone metabolism were remained to be elucidated. Moreover, smoking is known as a risk of osteoporosis development, however, the mechanisms underlying have not been clarified.

[Methods and Results]

First, we found that *nAChR7<sup>-/-</sup>* mice exhibited significantly increased bone mass due to significantly decreased osteoclast formation than WT mice. To determine whether  $\alpha$ 7nAChR regulates osteoclastogenesis directly, we cultured osteoclast progenitors isolated from *nAChR7<sup>-/-</sup>* and WT mice, with or without the  $\alpha$ 7nAChR ligands, acetylcholine or nicotine. However, the osteoclastogenesis was not stimulated by either ligand. This result indicated that  $\alpha$ 7nAChR indirectly upregulates osteoclastogenesis. Next, we analyzed osteoprotegerin and RANKL levels in serum by ELISA, and found that osteoprotegerin/RANKL ratios was significantly elevated in serum of *nAChR7<sup>-/-</sup>* compared with WT mice. Significantly elevated bone mass and inhibited osteoclastogenesis seen in *nAChR7<sup>-/-</sup>* mice were completely rescued in *nAChR7<sup>-/-</sup>* and osteoprotegerin double knockout mice, suggesting that  $\alpha$ 7nAChR regulates serum OPG/RANKL ratios. Vagotomy in wild-type mice also significantly increased the serum osteoprotegerin/RANKL ratio, while nicotine administration in wild-type mice decreased the ratio.  $\alpha$ 7nAChR loss significantly increased TNF $\alpha$  expression in Mac1-positive macrophages, and TNF $\alpha$  increased the osteoprotegerin/RANKL ratio in osteoblasts. Targeting TNF $\alpha$  in *nAChR7<sup>-/-</sup>* mice normalized both serum osteoprotegerin/RANKL ratios and bone mass.

[Discussion and Conclusions]

Our study revealed that  $\alpha$ 7nAChR suppressed TNF $\alpha$  expression in macrophages, decreased osteoprotegerin/RANKL ratio via the parasympathetic nervous system and upregulated osteoclastogenesis, resulting in loss of bone mass. Nicotine, the ligand of  $\alpha$ 7nAChR, activated the system. We now clarified a novel mechanism underlying controlling bone metabolism by the parasympathetic nervous system, and how nicotine, a main bioactive substance taken by smoking, affected bone.

**Disclosures:** Kazuaki Mito, None.

## SU0182

**THOC5 is a positive regulator of human osteoclastogenesis.** Se Hwan Mun<sup>\*12</sup>, Seyeon Bae<sup>12</sup>, Kyung Hyun Parkmin<sup>12</sup>, <sup>1</sup>Hospital for Special Surgery, United States, <sup>2</sup>HOSPITAL FOR SPECIAL SURGERY, United States

THOC5 (suppressor of the transcriptional defects of hpr1 delta by overexpression complex 5) is a member of the TREX (TRanscription/EXport) complex that regulates the transcription and export of nuclear mRNA. THOC5 is identified as a c-FMS interacting protein (FMIP) and THOC5-deficient mice are embryonic lethal, indicating an important role in cell differentiation and development. Instead of targeting all mRNA, THOC5 targets and regulates only a small subset of genes in a cell-type specific manner. The targets and role of THOC5 in osteoclasts are unknown.

In this study, we examined the mechanisms by which THOC5 regulates osteoclastogenesis using signaling, proteomic, and bioinformatic approaches. We found that the knock-down (KD) of THOC5 in human osteoclast precursor cells (OCPs) using small interference RNA decreased osteoclast formation compared to control cells. Accordingly, the expression of osteoclast marker genes such as NFATc1, Cathepsin K, and Integrin  $\beta$ <sub>3</sub> was suppressed in THOC5 KD cells. Although THOC5 mRNA expression was not regulated by RANKL stimulation, subcellular localization of THOC5 protein was dynamically regulated during osteoclastogenesis and the majority of THOC5 was localized in the nucleus of human OCPs. Our proteomic analysis showed that THOC5 was co-localized with THOC3 and FICD (FMS intracellular domain), a recently identified positive regulator of osteoclastogenesis. Mechanistically, THOC5 deficiency suppressed the translocation of FICD into the nucleus and subsequently inhibited osteoclast formation.

In summary, our finding identified THOC5 as a positive regulator in osteoclastogenesis, in part, by shuttling FICD to the nucleus and regulating the gene expression. A better understanding of THOC5/FICD axis provides an insight into the regulation of gene expression during osteoclastogenesis.

**Disclosures:** Se Hwan Mun, None.



## SU0183

**Role of the lysosomal channel, Two Pore Channel 2, in osteoclast differentiation and bone remodeling under normal and low-magnesium conditions.** Takuya Notomi<sup>\*1</sup>, Miyuki Kuno<sup>2</sup>, Akiko Hiyama<sup>1</sup>, Yoichi Ezura<sup>3</sup>, Kiyoshi Ohura<sup>1</sup>, Masaki Noda<sup>3</sup>. <sup>1</sup>Osaka dental university, Japan, <sup>2</sup>Osaka City University, Japan, <sup>3</sup>Tokyo Medical and Dental University, Japan

The bone is the main storage site for  $\text{Ca}^{2+}$  and  $\text{Mg}^{2+}$  ions in the mammalian body. Although investigations into  $\text{Ca}^{2+}$  signaling to better understand bone biology have progressed rapidly, the  $\text{Mg}^{2+}$  signaling pathway and associated molecules remain to be elucidated. Here, we investigated the role of a potential  $\text{Mg}^{2+}$  signaling-related lysosomal molecule, two pore channel 2 (TPC2), in osteoclast differentiation and bone remodeling. Previously, we found that under normal  $\text{Mg}^{2+}$  conditions, TPC2 promotes osteoclastogenesis, and we now report that TPC2 inhibits, rather than promotes, osteoclast differentiation in low- $\text{Mg}^{2+}$  conditions (Low- $\text{Mg}^{2+}$ ) and that the  $\text{PI}(3,5)\text{P}_2$  signaling pathway plays a role in this functional conversion of TPC2 in Low- $\text{Mg}^{2+}$ . Under normal- $\text{Mg}^{2+}$  conditions, the deletion of TPC2 inhibited osteoclast differentiation in RAW267.4 and bone marrow cells, as determined by the TRAP activity and mRNA expression of osteoclast differentiation markers (*Calcr*, *Igfb3*, *Ctsk*). However, in Low- $\text{Mg}^{2+}$ , it promoted osteoclast differentiation. To further confirm that TPC2 plays a role in osteoclastogenesis under Low- $\text{Mg}^{2+}$ , we focused on  $\text{PI}(3,5)\text{P}_2$ , which is one of TPC2 ligands. The  $\text{PI}(3,5)\text{P}_2$  addition affected osteoclast differentiation only under Low- $\text{Mg}^{2+}$ , and the effect was diminished in TPC2 deletion cells. These findings indicated that the TPC2 activity was mediated via the  $\text{PI}(3,5)\text{P}_2$  signaling pathway only under Low- $\text{Mg}^{2+}$ .  $\text{PI}(3,5)\text{P}_2$  depolarized the membrane potential by increasing the intracellular  $\text{Na}^+$  levels, but not  $\text{Ca}^{2+}$  levels under Low- $\text{Mg}^{2+}$ . To investigate how membrane depolarization affects osteoclast differentiation, we generated a light-sensitive cell line and developed a system for light-stimulated depolarization of the membrane potential. The light-induced depolarization inhibited osteoclast differentiation, and TPC2 was involved in this membrane depolarization-induced inhibition. We then tested the effect of myo-inositol supplementation, which increased the  $\text{PI}(3,5)\text{P}_2$  levels in mice fed a low- $\text{Mg}^{2+}$  diet. The myo-inositol supplementation rescued the low- $\text{Mg}^{2+}$  diet-induced trabecular bone loss, and this rescue was accompanied by inhibition of osteoclastogenesis. These results indicate that low- $\text{Mg}^{2+}$ -induced osteoclastogenesis involves changes in the membrane potential and a functional conversion of TPC2 through the  $\text{PI}(3,5)\text{P}_2$  pathway. Our findings also suggest that myo-inositol consumption might provide beneficial effects on  $\text{Mg}^{2+}$  deficiency-induced skeletal diseases.

**Disclosures:** Takuya Notomi, None.

## SU0184

**MyD88-Dependent Signaling Impacts Skeletal Cell Biology and Antibacterial Defenses during *Staphylococcus aureus* Osteomyelitis.** Nicole Putnam<sup>\*1</sup>, Andrew Hendrix<sup>2</sup>, Jacob Curry<sup>2</sup>, Jim Cassat<sup>3</sup>. <sup>1</sup>Department of Pathology, Microbiology, and Immunology, Vanderbilt University Medical Center, United States, <sup>2</sup>Department of Pediatrics, Division of Pediatric Infectious Diseases, Vanderbilt University Medical Center, United States, <sup>3</sup>Department of Pathology, Microbiology, and Immunology, Vanderbilt University Medical Center; Department of Pediatrics, Division of Pediatric Infectious Diseases, Vanderbilt University Medical Center, United States

*Staphylococcus aureus* is the leading cause of invasive bone infection (osteomyelitis), leading to inflammation and dysregulated interactions between bone-forming osteoblasts and bone-resorbing osteoclasts. We have previously determined that alpha-type phenol soluble modulins (PSMs), which are abundantly produced by USA300 lineage *S. aureus* strains, mediate cell death of skeletal cells. However, alterations in bone remodeling may also be due to host factors that impact osteoclast physiology during osteomyelitis. We hypothesize that *S. aureus* or its secreted products can modulate osteoclast cell biology and bone homeostasis through ligation of pre-osteoclast pattern recognition receptors (PRRs) and the concomitant induction of inflammation. We discovered that stimulation with toxin-deficient bacterial supernatants can modulate differentiation of osteoclasts (osteoclastogenesis) from myeloid cells with and without the canonical osteoclast differentiation factor RANK-Ligand (RANKL). Importantly, skeletal cells express PRRs, but the contribution of osteoclast lineage PRRs towards pathogen clearance, inflammation, and bone remodeling during osteomyelitis has not yet been explored. To test the role of PRR signaling pathways in osteomyelitis pathogenesis, we utilized mice lacking the critical PRR and IL-1R signaling adaptor MyD88. *S. aureus* supernatant could no longer alter osteoclastogenesis in myeloid progenitor cells lacking MyD88. To address the contribution of MyD88-dependent signaling *in vivo*, we used a post-traumatic *S. aureus* murine osteomyelitis model. In this model, MyD88 was critical for control of *S. aureus* replication and dissemination during bone infection. Collectively, our data demonstrate that *S. aureus* modulates osteoclastogenesis in a MyD88-dependent manner, and innate sensing through MyD88 is important for limiting pathogenesis during osteomyelitis.

**Disclosures:** Nicole Putnam, None.

## SU0185

Withdrawn

## SU0186

**Lack of NLRP3 inflammasome increases osteoclast activity in vitro but does not affect inflammatory bone resorption in vivo.** Fernanda R G Rocha<sup>\*1</sup>, João A C Souza<sup>2</sup>, Marcell C Medeiros<sup>3</sup>, Shannon Walle<sup>1</sup>, Carlos Rossa Junior<sup>3</sup>. <sup>1</sup>University of Florida, United States, <sup>2</sup>Federal University of Goiás (UFG), School of Dentistry, Brazil, <sup>3</sup>Sao Paulo State University (UNESP), School of Dentistry at Araraquara, Brazil

NLRP3 inflammasome may be activated by a variety of stimuli, including microbial (MAMPs) and host-derived (DAMPs). Periodontal disease is a chronic inflammatory condition initiated and maintained by a complex biofilm of bacteria. Levels of inflammasome-processed cytokines IL-1 $\beta$  and IL-33 are associated with periodontal disease, suggesting a role for inflammasomes in its pathogenesis. We investigated the role of NLRP3 inflammasome on inflammation and bone resorption associated with periodontal disease in vivo and on osteoclast differentiation and activity in vitro. We used mice genetically deficient for NLRP3 in a C57BL/6 background and also wild-type mice of the same strain as controls. Periodontal disease was induced by injections of 3  $\mu\text{L}$  of PBS suspensions of heat-killed Gram-negative *Aggregatibacter actinomycetemcomitans* (Aa) ( $3 \times 10^8$  UFC/injection) in the palatal mucosa adjacent to the first molar. Controls received injections of the same volume of PBS diluent. Injections were performed 3x/week under inhalation anesthesia and all animals were killed after 30 days. Bone resorption was determined by  $\mu\text{CT}$ , osteoclast number was assessed by biochemical staining of TRAP, inflammation was assessed by immunofluorescence detection of leukocytes (CD45+ cells) and PMNs (Ly6G+ cells). Expression of IL-1 and IL-33 in the gingival tissues was studied by luminex assay. Primary bone marrow-derived macrophages were differentiated into osteoclasts in vitro with RANKL and M-CSF. Osteoclast differentiation was assessed by immunofluorescence (actin ring formation) and osteoclast activity by pit assay. Bacterial injections induced significant bone resorption and also significant increases in the number of osteoclasts and inflammatory cells, as well as in the production of IL-1 and IL-33 in the gingival tissues. These increases were similar in both WT and NLRP3-deficient animals. In vitro, osteoclast differentiation was not affected in NLRP3-deficient cells, however the resorbing activity was significantly increased in comparison with osteoclasts derived from BM macrophages from WT mice. We conclude that NLRP3 inflammasome does not play a significant role in inflammation and bone resorption in experimental periodontal disease in vivo; and that lack of functional NLRP3 increases osteoclast activity in vitro.

**Disclosures:** Fernanda R G Rocha, None.

## SU0187

**TBC1D25 is involved in autophagy in human osteoclasts.** Michèle Roy<sup>\*</sup>, Martine Bisson, Sophie Roux. Rheumatology, Sherbrooke University, Canada

Autophagy is a regulated process that is responsible for degrading defective or redundant cytosolic components through the lysosome pathway for recycling or energy production. Defects in autophagy could contribute to bone diseases, such as Paget's disease of bone or age-related bone loss. TBC1 domain family member 25 (TBC1D25) is a Rab GTPase-activating protein (Rab-GAP), which has been involved in vesicular trafficking and autophagy in other systems. In mouse fibroblasts, TBC1D25 directly interacts with LC3 on the autophagosome membrane and inactivates Rab33B through its GAP activity, resulting in delayed autophagosomal maturation. Rab proteins are small GTPases. Among those expressed in human osteoclasts, Rab34 and Rab33B may interact with TBC1D25. Because intracellular vesicular trafficking pathways play a major role in osteoclast resorption (ruffled border, transcytosis, and autophagy), our hypothesis is that TBC1D25 is a key player in osteoclast biology. Using a model of human osteoclasts generated from cord blood monocytes ( $n = 8$ ), this study was aimed to characterize TBC1D25 expression and its involvement in osteoclast autophagy. TBC1D25 location was studied by immunofluorescence. Although a diffuse cytoplasmic pattern was observed in basal conditions, aggregates of TBC1D25 formed in the presence of rapamycin, a potent autophagy inducer. We compared LC3-II/actin levels, which correlate with increased levels of autophagic vesicles, in the presence or absence of rapamycin in non-transfected cultures or in cells transfected with either specific DsiRNAs or with a negative control (scrambled DsiRNA). Compared to standard conditions, rapamycin-stimulated LC3-II/actin expression significantly increased in non-transfected osteoclasts and in scrambled DsiRNA transfected cells but did not increase in osteoclasts transfected with TBC1D25-specific DsiRNA. Finally, co-immunoprecipitation studies demonstrated interactions between TBC1D25 and Rab34 in osteoclasts. A significant decrease in these interactions was observed in rapamycin-induced autophagy compared to that in basal conditions. In conclusion, TBC1D25 appears as a new player in osteoclast biology. Here, we showed its potential role in osteoclast autophagy and its interaction with Rab34. Although the exact mechanism remains to be elucidated, our results suggest that TBC1D25 interferes with autophagic flux.

**Disclosures:** Michèle Roy, None.

## SU0188

**CD55 regulates survival and bone resorbing activity of osteoclasts by modulating Rac activity.** Bongjin Shin\*, Heeyeon Won, Sun-Kyeong Lee. University of Connecticut Health Center, United States

Factors that modify osteoclast differentiation and activity critically influence bone homeostasis and the development of bone disease. CD55 (decay accelerating factor, DAF) is a glycosylphosphatidylinositol(GPI)-anchored protein, which regulates complement mediated and innate and adaptive immune responses. Although CD55 is expressed in a variety of cells in the bone marrow, its role in bone has not been investigated. Furthermore, mice deficient for CD97, a receptor for CD55, had increased bone mass resulting from decreased osteoclast number. Hence, we used microCT and histomorphometry and bone marrow cultures to examine, respectively, the skeletal phenotype and osteoclastogenic potential of CD55-deficient (CD55KO) mice. We further analyzed the possible mechanism by which CD55 regulates osteoclastogenesis and bone mass.

Flow cytometry indicated that myeloid (CD11b<sup>+</sup>, 67%), dendritic (CD11c<sup>+</sup>, 66%), B-lymphoid (B220<sup>+</sup>, 70%) and T-lymphoid (CD3<sup>+</sup>, 64%) cells in bone marrow express CD55. Trabecular bone volume measured by  $\mu$ CT in the femurs of CD55KO female mice was increased by 95% ( $p < 0.05$ ) compared to WT at 8 weeks of age. Paradoxically, osteoclast number was increased by 54% ( $p < 0.05$ ) in CD55KO mice in vivo with no differences in osteoblast parameters. We found the number of osteoclast formed *in vitro* using BMM cultures was significantly fewer in CD55KO cells compared to WT (20 - 60% depending on the day of culture) without difference in c-Fos or NFATc1 protein levels, which are critical transcription factors for osteoclastogenesis. Osteoclasts formed from CD55KO mice exhibited abnormal actin-ring formation and reduced bone-resorbing activity (~35%). Moreover, M-CSF and RANKL treatment failed to activate Rac GTPase in CD55KO BMM cells. In addition, the activity of apoptotic caspases was enhanced during osteoclastogenesis in CD55KO cells, which led to the poor survival of mature osteoclasts.

Our results imply that CD55KO mice have increased bone mass due to defective osteoclast resorbing activity. It is likely that reduced Rac activity in CD55KO osteoclasts caused deficient actin formation and function, and a shortened osteoclast lifespan. The high bone mass phenotype of CD55KO mice with abundant osteoclast, indicates that CD55 is essential for function but is not required for osteoclast differentiation. Taken together, we conclude that CD55 plays an important role in the survival and bone resorbing activity of osteoclasts through regulation of Rac activity.

**Disclosures:** Bongjin Shin, None.

## SU0189

**YC-1 alleviates bone loss in ovariectomized rats by inhibiting bone resorption and inducing extrinsic apoptosis in osteoclasts.** Jia-Fwu Shyu<sup>1</sup>\*, Jin-Wen Wang<sup>2</sup>, Tzu-Hui Chu<sup>1</sup>, Tien-Hua Chen<sup>3</sup>, Lo-Wei Chen<sup>1</sup>, Jung-Ting Wu<sup>1</sup>.

<sup>1</sup>Department of Biology and Anatomy, National Defense Medical Center, Taiwan, Province of China, <sup>2</sup>Department of Orthopedics, Chiali Hospital, Chi Mei Medical Center, Taiwan, Province of China, <sup>3</sup>Institute of Anatomy and Cell Biology, School of Medicine, National Yang Ming University, Taiwan, Province of China

Osteoporosis is a major health problem in postmenopausal women and the elderly that leads to fractures associated with substantial morbidity and mortality. Current osteoporosis therapies have significant drawbacks, and the risk of fragility fractures has not yet been eliminated. There remains an unmet need for a broader range of therapeutics. Previous studies have shown that YC-1 has important regulatory functions in the cardiovascular and nervous systems. Many of the YC-1 effector molecules in platelets, smooth muscle cells and neurons, such as cGMP and u-calpain, also have important functions in osteoclasts. In this study, we explored the effect of YC-1 on bone remodeling and determined the potential of YC-1 as a treatment for postmenopausal osteoporosis. Microcomputed tomography of lumbar vertebrae showed that YC-1 significantly improved trabecular bone microarchitecture in ovariectomized rats compared with sham-operated rats. YC-1 also significantly reversed the increases in serum bone resorption and formation in these rats, as measured by enzyme immunoassay of serum CTX-1 and P1NP, respectively. Actin ring and pit formation assays and TRAP staining analysis showed that YC-1 inhibited osteoclast activity and survival. YC-1 induced extrinsic apoptosis in osteoclasts by activating caspase-3 and caspase-8. In osteoclasts, YC-1 stimulated u-calpain activity and inhibited Src activity. Our findings provide proof-of-concept for YC-1 as a novel antiresorptive treatment strategy for postmenopausal osteoporosis, confirming an important role of nitric oxide/cGMP/protein kinase G signaling in bone.

**Disclosures:** Jia-Fwu Shyu, None.

## SU0190

**NUMBL Negatively Regulates NF- $\kappa$ B Signaling via Interaction with TAK1/TRAF6/NEMO During Osteoclastogenesis.** Gaurav Swarnkar<sup>1</sup>\*, Tim Hung-Po Chen<sup>1</sup>, Manoj Arra<sup>1</sup>, Gabriel Gabriel Mbalaviele<sup>2</sup>, Yusef Abu-Amer<sup>3</sup>.

<sup>1</sup>Department of Orthopedic Surgery, Washington University School of Medicine, United States, <sup>2</sup>Bone and Mineral Division, Department of Medicine, Washington University School of Medicine, United States, <sup>3</sup>Department of Orthopaedic Surgery and Cell Biology & Physiology, United States

The transcription factor NF- $\kappa$ B is a family of proteins that mediate signaling pathways essential for normal osteoclast differentiation and function. We have shown recently, that NUMBL-like (NUMBL) protein modulates osteoclastogenesis by down regulating NF- $\kappa$ B activation. Other studies, have also shown that NUMBL suppresses NF- $\kappa$ B in different cell types. In this study, we set out to decipher the mechanism underlying this phenomenon. We found that TGF- $\beta$  activated kinase-1 (TAK1) deficiency is associated with increased NUMBL and decreased TRAF6 and NEMO expression during osteoclastogenesis. Further, expression of wild type-TAK1 but not catalytically inactive TAK1-K63W inhibits NUMBL and restores TRAF6 and NEMO expression in TAK1-null cells. In order to elucidate the interaction of NUMBL with TAK1/NF- $\kappa$ B signaling during osteoclastogenesis, we overexpressed NUMBL in wild-type (WT) bone marrow macrophages (BMMs). Our results show that NUMBL expression inhibits osteoclast differentiation as evident by reduced number of TRAP positive mature osteoclast and decreased mRNA expression of TRAP, MMP9, NFATc1, Cathepsin-K, DC-STAMP and  $\beta$ 3-Integrin. Under these conditions, protein expression of TRAF6, NEMO and NFATc1 were also reduced. Consistently, osteoclast bone resorbing function was diminished as evident by fewer pits and reduced actin ring formation. Conversely, NUMBL-null BMMs isolated from LysM-cre-NUMBL-knockout mice, show increased osteoclast differentiation and mRNA expression of osteoclast marker genes when compared with WT BMMs. This data present NUMBL as a negative regulator of osteoclastogenesis. Mechanistically, we found that regulation of NUMBL expression during RANKL-induced osteoclast differentiation is TAK1-dependent. In WT cells, NUMBL mRNA expression decreases upon RANKL stimulation but not in TAK1 null cells. Post-translationally, K48-linked poly-ubiquitination of NUMBL is diminished in TAK1-null BMMs compared to elevated K48-poly-ubiquitination in WT cells, indicating increased stability of NUMBL in TAK1-null conditions. Further, co-transfection and co-immunoprecipitation studies show that NUMBL acts as a negative regulator of NF- $\kappa$ B signaling, via directly interacting with TAK1, TRAF6 and NEMO, and by inducing their K48-poly-ubiquitination mediated proteasomal degradation. Collectively, our data suggest that NUMBL acts as an endogenous regulator of NF- $\kappa$ B signaling and osteoclastogenesis by targeting the TAK1/TRAF6/NEMO axis.

**Disclosures:** Gaurav Swarnkar, None.

## SU0191

**Basic research on anti-Siglec-15 antibody and characterization of humanized anti-Siglec-15 antibody (DS-1501a).** Eisuke Tsuda<sup>1</sup>\*, Yoshiharu Hiruma<sup>1</sup>, Chie Fukuda<sup>1</sup>, Akiko Okada<sup>1</sup>, Yumiko Fukushima<sup>2</sup>, Wada Naoya<sup>2</sup>,

Kazuishi Kubota<sup>2</sup>, Hiroyuki Hattori<sup>1</sup>, Megumi Miyamoto<sup>1</sup>, Reimi Kawaida<sup>1</sup>, Chigusa Yoshimura<sup>1</sup>, Yoshitaka Isumi<sup>1</sup>, Toshiaki Ohtsuka<sup>1</sup>, Toshinori Agatsuma<sup>1</sup>, Tohru Takahashi<sup>1</sup>, Seiichirou Kumakura<sup>1</sup>. <sup>1</sup>R&D Division, Daiichi Sankyo Co., Ltd., Japan, <sup>2</sup>Daiichi Sankyo RD Novare Co., Ltd., Japan

Siglecs are a family of cell-surface receptor proteins that recognize sialylated glycoconjugates as ligands. Sialic acid-binding immunoglobulin-like lectin (Siglec)-15 is one of the newly identified members of Siglecs.

Tissue distribution analysis of Siglec-15 mRNA revealed that Siglec-15 expression is highly specific in differentiated osteoclasts in both human and rat. The mRNA expression level of Siglec-15 increased in association with osteoclast differentiation in cultures of mouse RAW264.7 cells and human osteoclast precursors (hOCP). Siglec-15 protein was confirmed to be localized on plasma membrane of osteoclasts by immunostaining and flow cytometry analysis. Anti-Siglec-15 antibody inhibited osteoclast formation at the stage of cell fusion, regardless of the stage of osteoclast differentiation in both RAW264.7 cells and hOCPs. In addition, we generated Siglec-15-deficient mice. These mice had increased trabecular bone mass, causing mild osteopetrosis. Otherwise, Siglec-15-deficient mice had no significant abnormalities in appearance and organs/tissues, and grew normally until at least 12 months of age. These data support the probability that inhibition of Siglec-15 function by a new mechanism of action may be a safely available option for the treatment of osteoporosis.

DS-1501a is a humanized recombinant IgG2 antibody against human Siglec-15 protein among the human Siglec family proteins. The binding affinity (Kd values) of DS-1501a to Siglec-15 ortholog proteins were 29 ng/mL for human, 69 ng/mL for rat, 19 ng/mL for mouse, and 27 ng/mL for cynomolgus monkey. DS-1501a specifically bound to human Siglec-15 and did not bind to the other human Siglec family proteins including Siglec-2, Siglec-3, Siglec-5, and Siglec-7. DS-1501a significantly inhibited the receptor activator of nuclear factor  $\kappa$ B ligand-induced upregulation of tartrate-resistant acid phosphatase activity released from rat bone marrow-derived monocyte/macrophage and human osteoclast precursors with a 50% inhibitory concentration (IC50) of 19.1 ng/mL and 45.5 ng/mL, respectively.

Anti-Siglec-15 antibody inhibits maturation of osteoclast fusion but does not inhibit formation of mononuclear osteoclasts which are reported to have low bone-resorbing



activity and high potency to support osteoblast formation and activation, leading to the activity of DS-1501a as bone formation-sparing anti-bone resorptive agent as observed in a series of *in vivo* studies.

**Disclosures:** Eisuke Tsuda, None.

## SU0192

**Pmpa1 is Specifically Induced by Bone Components in Osteoclasts and Regulates Bone Resorption.** Xianghe Xu<sup>\*1</sup>, Makoto Shiraki<sup>1</sup>, Asana Kamohara<sup>1</sup>, Kenichi Nishioka<sup>2</sup>, Fumikazu Matsuhisa<sup>3</sup>, Shuji Kitajima<sup>3</sup>, Toshio Kukita<sup>4</sup>, Akiko Kukita<sup>1</sup>. <sup>1</sup>Department of Pathology and Microbiology, Faculty of Medicine, Saga University, Japan, <sup>2</sup>Department of Biomolecular Sciences, Faculty of Medicine, Saga University, Japan, <sup>3</sup>Division of Biological Resources and Development, Analytical Research Center for Experimental Sciences, Saga University, Japan, <sup>4</sup>Department of Molecular Cell Biology & Oral Anatomy, Faculty of Dentistry, Kyushu University, Japan

**Background & Objective:** Pmpa1 also called Tmpai is an adaptor protein to E3 ubiquitin ligase Nedd4 which is involved in intracellular trafficking, cell survival and autophagy through interacting with several proteins such as PTEN and LC3. We identified Pmpa1 as a highly expressing gene in rat preosteoclasts by DNA microarray. In this study, we investigated the expression and role of Pmpa1 in mouse osteoclast differentiation and functions.

**Methods:** Osteoclasts were formed from mouse bone marrow macrophage (BMM) in the presence of RANKL and M-CSF. Pmpa1 knockout mice were generated by Crispr/Cas9 system. Silencing of gene expression was also performed by infection of osteoclasts with shRNA lentiviruses.

**Results & Discussion:** Among Nedd4 adaptor proteins, only Pmpa1 was induced strongly by RANKL in mouse BMM. Pmpa1 was induced in preosteoclasts but decreased in osteoclasts formed from BMM. Surprisingly, the immunofluorescence staining of osteoclasts in bone tissue of adjuvant-induced arthritis rat revealed that Pmpa1 was expressed in osteoclasts on bone *in vivo*. We then examined the expression of Pmpa1 in osteoclasts cultured on dentine. In comparison with osteoclasts culturing on plastic dish, the expression of Pmpa1 was significantly increased in osteoclasts on dentine. Treatment of osteoclasts cultured on plastic dish with TGF- $\beta$  or osteopontin increased the expression of Pmpa1. Conversely, the inhibition of bone resorption by alendronate or bafilomycin A1 decreased the expression of Pmpa1. Bone resorption activity of osteoclasts was decreased by Pmpa1 knockdown and in Pmpa1 (+/-) osteoclasts. In osteoclasts, Pmpa1 was coexpressed with EEA1 (early endosome), GM130 (Golgi), calnexin (ER) and LC3. Knockdown of Pmpa1 in osteoclasts decreased the secretion of cathepsin K to extracellular space. In addition, the localization of cathepsin K within actin ring was greatly impaired in Pmpa1 mutant osteoclasts. On the other hand, Pmpa1 knockdown in osteoclasts decreased the expression of Nedd4 and increased the expression of PTEN which is a target of Nedd4 and also involved in intracellular trafficking. Collectively, these results show that Pmpa1 is specifically induced by bone components, and enhance bone resorption by regulating secretion of cathepsin K and protein level of PTEN. Our results suggest that Pmpa1 is a novel target for specifically affecting bone-resorbing osteoclasts.

**Disclosures:** Xianghe Xu, None.

## SU0193

**Increasing intracellular iron by Ferroportin deletion in murine myeloid precursors stimulates mitochondria metabolism and osteoclastogenesis and decreases trabecular bone mass.** Lei Wang<sup>\*1</sup>, Toshifumi Fujiwara<sup>2</sup>, Bin Fang<sup>3</sup>, Nukhet Aykin-burns<sup>4</sup>, Zhichang Zhang<sup>5</sup>, Xiaolin Li<sup>5</sup>, Stavros C Manolagas<sup>6</sup>, Michael L Jennings<sup>7</sup>, Jian Zhou<sup>1</sup>, Haibo Zhao<sup>6</sup>. <sup>1</sup>Department of Orthopedics, First Affiliated Hospital, Anhui Medical University, China, <sup>2</sup>Department of Orthopedic Surgery, Kyushu University, Japan, <sup>3</sup>Department of Dermatology, University of Arkansas for Medical Sciences, United States, <sup>4</sup>Division of Radiation Health, Department of Pharmaceutical Sciences, University of Arkansas for Medical Sciences, United States, <sup>5</sup>Department of Orthopedics, Shanghai Jiao Tong University Affiliated Sixth People's Hospital, China, <sup>6</sup>Division of Endocrinology and Metabolism, Department of Internal Medicine, University of Arkansas for Medical Sciences, United States, <sup>7</sup>Department of Physiology and Biophysics, University of Arkansas for Medical Sciences, United States

The presence of numerous mitochondria in osteoclasts (OCs) were observed as early as in 1930s (Chang H. Mitochondria in osteoclasts. *Anat Rec.* 1931;49), but the molecular pathways regulating mitochondrial biogenesis and metabolism during osteoclastogenesis and bone resorption remain largely unknown. Iron plays a fundamental role in mitochondrial metabolism and the biosynthesis of heme as well as a cluster of mitochondrial iron-sulphur (Fe-S) containing proteins which are critical components of the respiratory complexes. Iron chelation inhibits bone resorption and protects against ovariectomy-induced bone loss in mice. Iron overload, on the other hand, increases bone resorption and oxidative stress and exacerbates estrogen-deficiency bone loss.

Furthermore, osteoporosis is a frequent complication of iron-overload in diseases such as thalassemia and hemochromatosis. Iron is taken up by mammalian cells via transferrin (Tf), heme, and ferritins; and unutilized portion of intracellular iron is either stored in ferritin or exported via ferroportin (FPN). To investigate the role of cellular iron homeostasis in OC biology, we generated FPN myeloid and mature OC deficient mice in C57BL/6J129 mixed background, by crossing FPN-floxed mice with LysM-Cre (FPN<sup>fl/f</sup>; LysM-Cre) and Cathepsin K-Cre (FPN<sup>fl/f</sup>;CTSK-Cre) mice, respectively. FPN<sup>fl/f</sup>; LysM-Cre mice had decreased trabecular bone volume as compared to their littermate controls, but normal cortical thickness by micro-CT. FPN<sup>fl/f</sup>;CTSK-Cre mice had no bone phenotype. Consistent with the *in vivo* findings, *in vitro* mechanistic studies revealed that deletion of FPN resulted in a small increase in cellular iron levels in OC lineage cells as measured by a Tf-Fe<sup>59</sup> uptake assay. Loss of FPN in OC precursors accelerated osteoclastogenesis, as demonstrated by increased number of TRAP<sup>+</sup> multinucleated OCs and enhanced expression of NFATc1 and PGC1 $\beta$ , two transcription factors essential for osteoclast differentiation, in FPN-deficient OC lineage cells compared to the control cells. Mitochondrial metabolism, measured by Seahorse Extracellular Flux analyzer, showed significant increases in mitochondrial basal and ATP-linked respiration in FPN-deficient bone marrow monocytes and pre-osteoclasts, but not in mature cells. Collectively, these findings indicate that intracellular iron is critical for mitochondrial metabolism, osteoclastogenesis, and skeletal homeostasis.

**Disclosures:** Lei Wang, None.

## SU0194

**MLO-Y4 cells Modulate Human Peripheral Blood Mononuclear Cells Migration.** Daniel Aedo Martin<sup>\*1</sup>, Irene Buendia<sup>2</sup>, Jose Adolfo Orellana Gomez-Rico<sup>1</sup>, Francisco Javier Areta Jimenez<sup>1</sup>, Juan Antonio Ardura<sup>2</sup>, Arancha R. Gortazar<sup>2</sup>. <sup>1</sup>Hospital Universitario Central de la Defensa Gómez-Ulla, Spain, <sup>2</sup>Instituto de Medicina Molecular Aplicada (IMMA). Facultad de Medicina. Universidad San Pablo CEU, Spain

Osteocytes, the most abundant cell type in bone, are buried in the mineralized bone matrix but regulate bone remodeling by altering osteoblast and osteoclast function. The aim of the present study was to evaluate the response of peripheral blood mononuclear cells from patients with osteoporotic and non-osteoporotic fracture, to the factors secreted by MLO-Y4 osteocytic cells under static or mechanical conditions. We obtained 12ml of peripheral blood of non-osteoporotic patients older than 18 years with traumatic fracture of long bones and osteoporotic patients with hip fracture. Patients in treatment for osteoporosis, with a secondary osteoporosis state or a tumoral process were excluded from the study. The population was recruited in the last year in the Hospital Central de la Defensa Gómez Ulla (Madrid, Spain). Eighteen valid samples were obtained. 14 (78%) presented osteoporotic fracture and 4 (22%) presented traumatic long bone fracture without osteoporosis. We obtained the peripheral blood mononuclear cells and we evaluated their capacity to migrate under the presence of conditioned media from osteocytic cells. MLO-Y4 cells were subjected or not (static control) to mechanical stimulation by fluid flow (FF, 10 dyn/cm<sup>2</sup>, 15 min). Cell medium was changed and cells were cultured for additional 18 h and the conditioned medium (CM) was then collected. The migration assays were performed in Costar transwell cell culture chamber inserts (Corning Costar Corporation, Cambridge, MA) with an 8  $\mu$ m pore size. Briefly, 5  $\times$  10<sup>4</sup> cells were placed on the upper chamber in 20% of MLO-Y4 CM. After 6 hours, cells on the underside of the Transwell were fixed, stained with Crystal Violet and counted. We observed that CM from static MLO-Y4 cells increased monocyte migration (20.93 %). In contrast, CM from mechanically stimulated MLO-Y4 cells inhibited monocyte migration (53.98%). The CM from static condition cells favored the migration of monocytic cells (p < 0.001) with a correlation coefficient of 88%. The linear correlation coefficient of the regression line was 92%. The CM from mechanically stimulated cells inhibited the migration (p < 0.001) with a correlation coefficient of 79.2%. The linear correlation coefficient of the regression line was 58.8%. Our present data indicates that human monocytic cells can respond to factors secreted by MLO-Y4 cells modulating their migration.

**Disclosures:** Daniel Aedo Martin, None.

## SU0195

**Increased bone FGF23 production in CKD is associated with altered osteocyte development and bone mineralization.** Corey Dussold<sup>\*1</sup>, Samantha Neuburg<sup>1</sup>, Ying Liu<sup>2</sup>, Jian Q. Feng<sup>2</sup>, Xueyan Wang<sup>1</sup>, Valentin David<sup>1</sup>, Myles Wolf<sup>3</sup>, Aline Martin<sup>1</sup>. <sup>1</sup>Division of Nephrology and Hypertension, Center for Translational Metabolism and Health, Northwestern University, Chicago, IL, USA, United States, <sup>2</sup>Department of Biomedical Sciences, Baylor College of Dentistry, TXA&M University, Dallas, TX, USA, United States, <sup>3</sup>Division of Nephrology and Hypertension, Duke University, Durham, NC, USA, United States

Fibroblast growth factor (FGF)-23 is a hormone produced by osteocytes that regulates phosphate (Pi) homeostasis. Chronic kidney disease mineral and bone disease (CKD-MBD) leads to alterations of mineral and bone metabolism, including elevation of circulating intact FGF23 (iFGF23) levels that is associated with increased risk of cardiovascular mortality. The mechanism of increased FGF23 in CKD is poorly understood and the impact of CKD on osteocyte development and maturation has not been

described. We tested the hypothesis that CKD induces changes in osteocyte morphology that result in altered osteocyte network, bone mineralization and mineral metabolism.

We studied the bone and osteocyte phenotype of the Col4a3<sup>KO</sup> mouse, a validated model of progressive CKD. We analyzed femurs collected from 9 week-old Col4a3<sup>KO</sup> (advanced CKD) and wild-type (WT) littermates using 3D-microtomography, acid-etched scanning electron microscopy, whole bone FITC staining and Imaris modelisation. We assessed in vitro matrix mineralization by alizarin red S (ARS) staining and osteoblast differentiation by alkaline phosphatase (ALP) staining of WT and Col4a3<sup>KO</sup> isolated primary osteoblasts (BMSCs). In parallel, we also measured serum FGF23 and Pi levels, assessed renal function and measured FGF23 mRNA expression in vitro and in vivo.

Renal function was dramatically impaired in Col4a3<sup>KO</sup> mice (BUN: 100±12 vs 18±1 mg/dL) and we observed a 15-fold increase in bone FGF23 mRNA expression, a 70-fold increase in serum iFGF23 and a 50% increase in serum Pi levels ( $p < 0.05$  vs. WT for each). Col4a3<sup>KO</sup> mice displayed a 5% decrease in bone mineral density and a rounder, less polarized osteocyte morphology (osteocyte roundness index:  $0.43 \pm 0.17$  vs.  $0.34 \pm 0.12$ ) ( $p < 0.05$  vs. WT for each). The osteocyte network was significantly modified with an 80% reduction in number and length of the dendritic processes ( $p < 0.05$  vs. WT). In vitro, Col4a3<sup>KO</sup> BMSCs maintained intrinsic abnormalities in activity and mineralization (-40% ALP activity and ARS;  $p < 0.05$  vs. WT).

Our data suggest that CKD leads to impaired osteocyte morphology and function that is associated with defective bone mineralization and FGF23 overproduction. Whether altered osteocyte morphology is a cause of FGF23 over production and whether rescue of the bone mineralization and osteocyte morphology defects could prevent FGF23 elevation in CKD requires further investigation.

**Disclosures:** Corey Dussold, None.

## SU0196

**Sclerostin-Neutralizing Antibody Treatment Increases Serpinf1(PEDF) Expression In Mice Tibiae Independent of Mechanical Loading.** Tobias Thiele<sup>1</sup>, Catherine Julien<sup>2</sup>, Anne Seliger<sup>1</sup>, Annette Birkhold<sup>3</sup>, Michael Thelen<sup>1</sup>, François Lefebvre<sup>4</sup>, Martin Pellicelli<sup>2</sup>, René St-Arnaud<sup>2</sup>, Michael Ominsky<sup>5</sup>, Georg Duda<sup>1</sup>, Uwe Kornak<sup>6</sup>, Sara Checa<sup>1</sup>, Bettina M. Willie<sup>2</sup>. <sup>1</sup>Julius Wolff Institute, Universitätsmedizin Charité, Germany, <sup>2</sup>Shriners Hospital for Children, Canada, <sup>3</sup>University of Stuttgart, Germany, <sup>4</sup>Canadian Centre for Computational Genomics, Canada, <sup>5</sup>Amgen, United States, <sup>6</sup>Institute for Medical Genetics and Human Genetics, Charité-Universitätsmedizin, Germany

Bone adapts to mechanical stimuli to maintain an optimized structure. Mechanical loading causes decreased expression of sclerostin, an osteocyte-specific secreted glycoprotein encoded by the *Sost* gene, known to inhibit Wnt- $\beta$ -catenin signaling. However, it appears that load-induced formation can occur independent of sclerostin. Previous microCT analyses (1) of 78 wk old mice treated with sclerostin neutralizing antibody (Scl-Ab) and loaded for 2 wks showed a bone formation response to Scl-Ab and loading. Recent analyses of these data using time-lapse microCT registration (2) showed an additive formation response to loading and Scl-Ab. We aimed to examine the effect of load on gene expression after acute sclerostin inhibition. We performed a single bout of in vivo cyclic compressive loading to the left tibia of thirty, 78 wk old female C57Bl/6J mice, half of which were treated with 25 mg/kg of Scl-Ab, twice weekly for 2 weeks prior to loading ( $n=5$ /treatment/time point). The right limb was a nonloaded internal control. Mice were dissected at 1, 8 or 24 hours after loading and bone marrow was flushed. RNA was extracted, reverse-transcribed, and analyzed by microarray/qPCR. *Serpinf1* was found to be in the top ten regulated genes following Scl-Ab treatment (Fig 1A). *Serpinf1* expression levels were highly upregulated independent of loading. *Sost*, *Dkk1*, *Wif1* (Fig 1 B) were also highly upregulated in response to Scl-Ab, independent of loading. Results were validated by IHC in 2 wk loaded mice, which had higher sclerostin and *serpinf1* levels in osteocytes after Scl-Ab treatment. Osteocytic-like cell lines were also used to confirm the effect of Scl-Ab on Wnt inhibitors expression. Unpublished data shows *Serpinf1* is upregulated in *Sost* KO mice compared to littermates. Other recent studies have shown Scl-Ab treatment causes activation of Wnt target genes (3,4). *Serpinf1* and/or other Wnt pathway inhibitors might be responding to decreased tissue level strains due to increased bone mass. *Serpinf1* may also be upregulated due to increased mineralization (5), although we saw unchanged *serpinf1* expression after 2wks of load-induced bone formation in vehicle treated group. These data provide a possible explanation for the diminished bone formation response to Scl-Ab after longer-term treatment (6).

(1) Pflanz et al. ASBMR 2012, (2) Birkhold et al. Bone 2014, (3) Nioi et al. JBMR 2015, (4) Taylor et al. Bone, 2016 (5) Rajagopal et al. MGM, 2016 (6) McClung et al. NEJM 2014

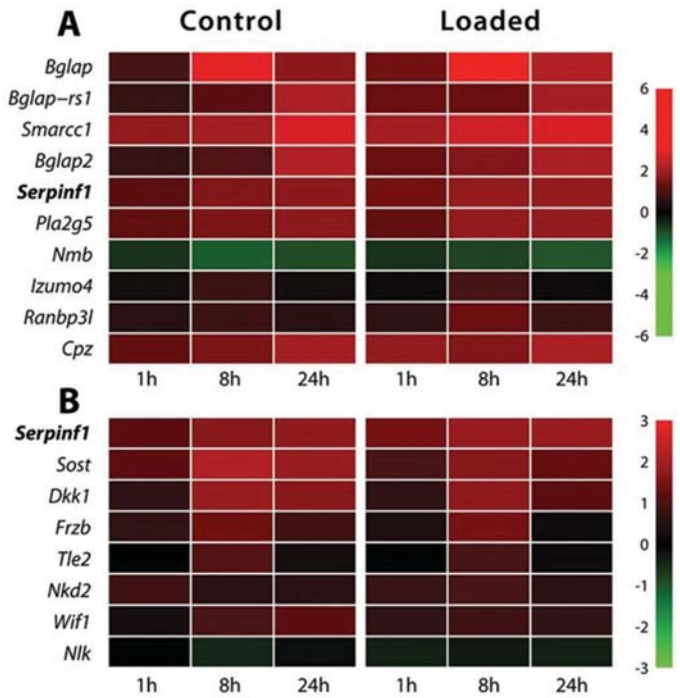


**Figure 1. A) Top 10 regulated genes following Scl-Ab treatment. B) Wnt inhibitors with significantly increased expression levels following Scl-Ab treatment.**

Figure 1

**Disclosures:** Tobias Thiele, None.

## SU0197

**Development and Characterization of Stably Transfected TOPFlash MLO-Y4 Cell Lines.** Nuria Lara\*, Mark L. Johnson. University of Missouri-Kansas City, United States

Activation of the Wnt/ $\beta$ -Catenin signaling pathway in osteocytes is critical for new bone formation in response to mechanical loading. Current methods for detection of  $\beta$ -catenin activity are laborious and are not easily quantifiable. We have developed several clonal MLO-Y4 osteocyte-like cell lines stably transfected with the TOPFlash luciferase reporter as a quick and sensitive assay to quantitate  $\beta$ -catenin signaling in osteocytes.

MLO-Y4 cells were stably transfected with the TOPFlash vector, pGL4.49[luc2P/TCF-LEF/Hygro] (Promega) which contains eight copies of the TCF-LEF response element promoter driving transcription of the luciferase gene and is used as a reporter for Wnt/ $\beta$ -catenin signaling. After hygromycin selection, single cell clones were screened for luciferase activity. Out of >250 clones tested, three clones showed robust induction of luciferase in response to LiCl and Wnt3a. Clones A3-F9, BB-B4 and H8-E1 were selected for further characterization. After 24 hours of treatment with 10mM LiCl, luciferase activity was determined using the Promega luminescence assay. LiCl increased luciferase activity by 16, 10 and 9-fold in clonal cell lines A3-F9, BB-B4 and H8-E1 respectively ( $p < 0.05$ ). The three cell lines were also responsive to 10ng/mL Wnt3a, showing a 17, 15 and 14-fold increase in A3-F9, BB-B4 and H8-E1 cells respectively ( $p < 0.01$ ). A dose response curve indicated activation in response to a range of Wnt3a concentrations (1–100 ng/ml) and time course analysis showed signaling activation as early as 4hrs post treatment with LiCl and Wnt3a. Clone A3-F9 was treated with 25% conditioned media from C2C12 myoblasts and myotubes. Consistent with previous studies, myotube but not myoblast CM induced luciferase activity by 2 fold ( $p < 0.05$ ) indicating activation of Wnt/ $\beta$ -catenin signaling. Similar to MLO-Y4 parental cells, the clonal cell lines maintained expression of mRNA for osteocyte markers *Dmp1* and *Pdpr*, although at 2-3 fold lower levels. *Phex* and *Fgf23* were not detected. *Gjal* and *Colla1* mRNA were 2-3 fold higher and *Alpl* mRNA was 3-5 lower in the clonal cell lines compared to parental MLO-Y4 cells.

In summary, we have developed 3 stable osteocyte-like cell lines that can be adapted for high throughput screening of potential drugs targeting the Wnt/ $\beta$ -catenin pathway for treatment of diseases of low bone mass.

**Disclosures:** Nuria Lara, None.



## SU0198

**PTEN deletion from osteocytes does not rescue the skeletal fragility phenotype induced by  $\beta$ -catenin deletion.** Kyung-Eun Lim\*, Phillip C. Witcher, Alexander Robling. Indiana University School of Medicine, United States

Selective hyperactivation of AKT in osteoblasts via deletion of PTEN (a PI3K phosphatase) increases bone mass. AKT activates a number of divergent pro-osteogenic signaling pathways (e.g., anti-apoptosis, cell survival, protein translation, proliferation, glucose import/transport). One of the cascades activated by AKT is the GSK3- $\beta$ / $\beta$ -catenin pathway, a key regulator of bone cell metabolism. Constitutive activation of  $\beta$ -catenin in osteoblasts/osteocytes increases bone mass, whereas selective deletion results in severe skeletal fragility and peripubertal lethality. We sought to determine whether the high bone mass phenotype associated with PTEN suppression is maintained when the downstream  $\beta$ -catenin signaling arm is selectively disabled. To do so, we hyperactivated AKT in osteocytes via Dmp1-Cre-mediated recombination of PTEN floxed alleles, and co-deleted  $\beta$ -catenin in the same cells using floxed CTNNB1 alleles. Mice were subjected to DXA scans at 6 wks of age, then sacrificed for  $\mu$ CT and histological evaluation at 7 wks. Surprisingly, the double mutants were generally more unhealthy than the single CTNNB1 mutants, and ~50% either died or required euthanasia due to veterinarian recommendation between 6 and 7 wks. None of the single mutant CTNNB1 mice died before the 7 wk termination point. Double mutants also exhibited an increase in spontaneous fractures. Compared to controls, DXA-derived whole body BMD was increased in PTEN mutants by ~9% ( $p < 0.05$ ) and was equally reduced in single CTNNB1 mutants and double mutants (~30% reduction in both genotypes,  $p < 0.05$ ).  $\mu$ CT analysis of the distal femur metaphyseal cancellous region was not possible due to the complete absence of cancellous bone in both CTNNB1 and double mutants. We therefore analyzed the total bone volume in the metaphyseal region. Total metaphyseal bone volume was increased by 11% ( $p < 0.05$ ) among PTEN single mutants, and was reduced by ~15% ( $p < 0.05$ ) in both single CTNNB1 and double mutants. Cortical/trabecular thickness was increased by 40% ( $p < 0.05$ ) in PTEN mutants but reduced by 30-33% ( $p < 0.05$ ) in CTNNB1 and double mutants. Our results suggest that AKT hyperactivation via PTEN deletion does not improve (and potentially worsens) the skeletal phenotype of CTNNB1 mutant mice, despite maintaining intact and hyperactive signaling through many other pathways that are beneficial to bone, including mTOR (protein translation), GLUT4 (glucose transport), CREB (cell survival) and BIM/BAX (anti-apoptosis).

**Disclosures:** Kyung-Eun Lim, None.

## SU0199

**Elevated osteocyte TNF- $\alpha$ , IL-6, and sclerostin in a rodent model of spinal cord injury correlates with altered bone turnover.** Corinne E. Metzger\*<sup>1</sup>, Sammy Gong<sup>2</sup>, Miriam Aceves<sup>2</sup>, Michelle A. Hook<sup>2</sup>, Susan A. Bloomfield<sup>1</sup>. <sup>1</sup>Texas A&M University, United States, <sup>2</sup>Texas A&M University Health Science Center, United States

In addition to muscle disuse and neural loss, spinal cord injury (SCI) is characterized by a protracted inflammatory response that may affect bone health. Even after the acute phase of injury (on average 10 years later), serum levels of a number of pro-inflammatory cytokines, including tumor necrosis factor- $\alpha$  (TNF- $\alpha$ ) and interleukin-6 (IL-6), are elevated in SCI patients indicating chronic systemic inflammation (Davis, Arch Phys Med Rehabil; 2007). Since TNF- $\alpha$  and IL-6 influence bone turnover and TNF- $\alpha$  activates sclerostin, we aimed to determine the osteocyte pro-inflammatory state in bone due to SCI and its relation to bone loss. We hypothesized that %positive osteocytes for TNF- $\alpha$ , IL-6, and sclerostin would be higher after SCI, coincident with lower bone formation rate (BFR) and higher osteoclast surface (%Oc.S/BS). To test this, male Sprague Dawley rats (2 mo old; n=6/group) received either a moderate contusion injury at T12 (SCI) or a Sham operation followed by recovery for 28 days. At 28 days post injury, all SCI rats regained weight-bearing on their hindlimbs, but locomotor ability remained lower in SCI subjects compared to Sham. Standard histomorphometry of proximal tibia cancellous bone revealed 52% lower cancellous bone volume, 25% lower trabecular thickness, 38% lower trabecular number, and 87% higher trabecular separation. %Oc.S/BS was 140% higher while cancellous BFR was 37% lower in SCI, due to 45% lower mineralized surface vs. Sham. IHC of the distal femur cancellous bone demonstrated large changes in %positive osteocytes for TNF- $\alpha$  (8-fold higher), IL-6 (2-fold higher), and sclerostin (65% higher) in SCI vs. Sham. Linear regression analyses showed that both locomotor scores and %TNF- $\alpha$ + osteocytes independently predicted %sclerostin+ osteocytes ( $R^2=0.716$ ,  $R^2=.770$ , respectively). Locomotor scores, %TNF- $\alpha$ + osteocyte, and %IL-6+ osteocytes were all independent predictors for cancellous osteoclast surface ( $R^2=.761$ ,  $R^2=.663$ ,  $R^2=.674$ , respectively). The high osteocyte prevalence of TNF- $\alpha$ , IL-6, and sclerostin in SCI bones coincident with increased bone resorption and decreased bone formation suggests a mechanistic role for inflammation in SCI-induced bone loss. In addition to weight-bearing activity, therefore, inflammatory factors influence bone turnover following an incomplete SCI. Treatments for minimizing fracture risk after SCI may need to address mitigating the chronically altered inflammatory state as well as disuse-induced bone loss.

**Disclosures:** Corinne E. Metzger, None.

## SU0200

**PPAR $\gamma$  and PPAR $\alpha$  regulate osteocyte activity by controlling expression of Sclerostin and DKK1 proteins.** Lance Stechschulte\*, Mathew Mazur, Dustin Marinelli, Zachary Rotter, Amit Chougule, Beata Lecka-Czernik. University of Toledo, United States

Osteocytes orchestrate bone remodeling through regulation of both osteoblast and osteoclast activities. Sclerostin, encoded by *Sost* gene, and DKK1 proteins are released from osteocytes and act as inhibitors of Wnt signaling pathway in osteoblasts. Recently we have showed that PPAR $\gamma$  is a positive regulator of both *Sost* and *Dkk1*, whereas PPAR $\alpha$  is a negative regulator of *Sost* expression. Decreased bone formation in mice treated with full PPAR $\gamma$  agonist, rosiglitazone, is associated with increased expression and protein production in osteocytes of both Sclerostin and DKK1. In contrast, mice treated with a new insulin sensitizer SR10171 which acts as PPAR $\gamma$  inverse agonist and PPAR $\alpha$  agonist, is associated with decreased expression and production of both Sclerostin and DKK1 resulting in increased bone formation and bone mass. Here we extended our studies by analyzing the mechanism by which PPAR $\gamma$  and PPAR $\alpha$  control expression of both genes. Using EpiTect software we have identified two PPRE sequences in *Sost* promoter located -1.8 kb ( $\alpha$ PPRE) and -7.0 kb ( $\gamma$ PPRE) from the transcription start site. ChIP analysis showed that PPAR $\alpha$  binds to  $\alpha$ PPRE in basal conditions. Treatment with WY14643 agonist results in augmentation of PPAR $\alpha$  binding which correlates with decreased promoter activity measured in luciferase gene reporter assay. In contrast, PPAR $\gamma$  is recruited to the *Sost* promoter only after activation with rosiglitazone, and this correlates with increased promoter activity. Similarly, PPAR $\gamma$  activation, but not PPAR $\alpha$ , increases *Dkk1* promoter activity and DKK1 protein production in osteocytes. To demonstrate that PPAR $\gamma$  and PPAR $\alpha$  regulate endocrine activities of osteocytes supporting of PBMC differentiation, we tested conditioned media (CM) from primary osteocytes treated with different PPARs selective modulators. CM collected from osteocytes with activated PPAR $\gamma$  increased adipocytic and decreased osteoblastic gene markers expressed in recipient PBMC, whereas CM from osteocytes with activated PPAR $\alpha$  decreased adipocytic and increased osteoblastic gene markers. PPAR $\alpha$  inhibitory effect on *Sost* expression was confirmed in animals deficient in PPAR $\alpha$  protein. Osteocytes derived from PPAR $\alpha$  knock-out mice are characterized with high expression of *Sost* and 2-fold increased Sclerostin protein levels. In conclusion, Sclerostin and DKK1 are directly regulated by PPAR $\gamma$  and PPAR $\alpha$  and these nuclear receptors can be pharmacological targets to control osteocyte-regulated bone remodeling.

**Disclosures:** Lance Stechschulte, None.

## SU0201

**Mechanical Forces Regulate Osteocytes Gene Expression through Gs $\alpha$ -independent Signaling Pathways.** Ningyuan Sun\*<sup>1</sup>, Yuhei Uda<sup>2</sup>, Chao Shi<sup>3</sup>, Keertik Fulzele<sup>4</sup>, Ehab Azab<sup>5</sup>, Paola Divieti Pajevic<sup>6</sup>. <sup>1</sup>PhD Candidate, United States, <sup>2</sup>Research Fellow, United States, <sup>3</sup>PhD Candidate, China, <sup>4</sup>Research Assistant Professor, United States, <sup>5</sup>DSc Student, United States, <sup>6</sup>Associate Professor, United States

It is well known that mechanical loading is important for skeletal development and maintenance. Reduced loading, such as prolonged bed rest, injuries, or space travel is always associated with bone loss. Osteocytes, the most abundant cells in bone are the mechano-sensors of bone. They control bone remodeling by altering the secretion of sclerostin/SOST, RANKL and other transcripts. Osteocytes express numerous G protein-coupled receptors that signal through Gs $\alpha$  such as parathyroid hormone receptor, prostaglandin receptors EP2 and 4 and others. Activation of these receptors regulates numerous transcripts, including SOST, DMP1 and RANKL. To investigate the role of Gs $\alpha$  signaling in osteocytes mechano-transduction we established osteocytic cell line Ocy454 lacking Gs $\alpha$  expression (Ocy454-Gs $\alpha$ KO cells) and exposed these cells to increased loading or simulated microgravity.

Ocy454 cells express high level of SOST/sclerostin and are responsive to hormonal, cytokine and mechanical stimuli. Using the CRISPR/Cas9 technique we generated Ocy454-Gs $\alpha$ KO cells and exposed them to fluid flow shear stress (FFSS) using a continuous laminar fluid flow system (8 dynes/cm<sup>2</sup>, 2h). For unloading experiments, cells were seeded into 3D scaffolds and subjected to simulated microgravity using NASA-developed slow rotating wall vessel system. At the end of FFSS or simulated microgravity, RNA was isolated and gene expression was analyzed by semi-quantitative realtime PCR.

FFSS regulated gene expression in Ocy454-Gs $\alpha$ KO cells similar to control. SOST was significantly down-regulated (~40% and ~60%) and RANKL (~2 folds and ~3 folds) and DMP1 (~2.5 folds) were up-regulated after exposure to FFSS, indicating that Gs $\alpha$  signaling was not required for responses to mechanical forces. Similarly, exposure to simulated microgravity induced significant suppression of RANKL (~40%) and increase in DMP1 (~2.4 and ~1.9 fold) in both control and Gs $\alpha$ KO cells. To investigate Gs $\alpha$  independent mechanisms of gene regulation we analyzed TGF- $\beta$  and Ca<sup>2+</sup> signaling pathways. The P-Smad3/Smad3 ratio (~30% and ~15%) significantly increased after FFSS in both Gs $\alpha$ KO and control cells. Preliminary studies demonstrated that treatment with nifedipine, a L-type Ca<sup>2+</sup> channel blocker, partially prevented FFSS down regulation of SOST expression (~30%). Here we demonstrated, for the first time, that mechanical forces suppress osteocytes SOST/sclerostin and up-regulated DMP1 and RANKL expression in a Gs $\alpha$ -independent mechanism.

**Disclosures:** Ningyuan Sun, None.

## SU0202

**Deletion of RANKL from Osteoblasts and Osteocytes in Osteogenesis Imperfecta Mice (oim) Increases Bone Mass but Does Not Rescue Bone Fragility or High Bone Turnover.** Sarah Zimmerman\*, Melissa Heard-Lipsmeier, Milena Dimori, Charles O'Brien, Roy Morello. University of Arkansas for Medical Sciences, United States

Osteogenesis imperfecta (OI) is characterized by osteopenia and bone fragility, and OI patients and animal models of OI often exhibit high bone turnover with the net result of low bone mass. The mechanisms driving this high bone turnover are unknown, although recent evidence shows that osteocytes can secrete many cytokines/factors that are able to regulate bone turnover under normal physiological conditions. Importantly, osteocytes have been shown to be the main source of RANKL for osteoclast formation in cancellous bone in adult mice. Therefore, we hypothesized that RANKL from osteocytes contributes to the increased osteoclast number and bone resorption in OI. To test this, we deleted RANKL from osteoblasts and osteocytes in a murine model of osteogenesis imperfecta (oim mice). This was accomplished by crossing mice carrying a floxed RANKL gene, a Cre transgene under the control of the Dmp1 promoter, and oim mice. This produced mice with the genotype Col1a2oim/oim; RANKL<sup>fl/fl</sup>; Dmp1-Cre (also called "oim-RANKL-cKO"). Compared to Col1a2oim/oim; RANKL<sup>fl/fl</sup> controls (which are not distinguishable from oim mice), oim-RANKL-cKO mice were similar in body weight and femoral biomechanical properties but had increased trabecular bone volume, trabecular number and trabecular thickness in the femur. Cortical thickness was also increased in the spine. Strikingly, serum CTX levels remained high in the oim-RANKL-cKO mice despite the deletion of RANKL in mature osteoblasts and osteocytes. This indicates that RANKL produced by osteocytes is not the main driver of the high bone turnover seen in oim mice, and that a likely cause may be RANKL produced by other cell types or perhaps the influence of other cytokines.

**Disclosures:** Sarah Zimmerman, None.

## SU0203

**FRAX is a robust predictor of baseline vertebral fractures in multiple myeloma patients.** Shebli Atrash\*, Amy Buros<sup>1</sup>, Frits van Rhee<sup>1</sup>, Larry J. Suva<sup>2</sup>, Sharmilan Thanendrarajan<sup>1</sup>, Carolina Schinke<sup>1</sup>, Faith Davies<sup>1</sup>, Gareth Morgan<sup>1</sup>, Maurizio Zangari<sup>1</sup>. <sup>1</sup>University of Arkansas for Medical Sciences, United States, <sup>2</sup>Texas A&M University, United States

FRAX is commonly used to predict the risk of major osteoporotic and hip fractures in the general population. The output is a 10-year probability of hip fracture and 10-year probability of a major osteoporotic fracture. Bone disease is considered a major player in multiple myeloma (MM) pathology with X-ray skeletal survey the standard of care in MM it is possible that such a survey might miss the presence of vertebral fractures. Therefore the risk factor identified by FRAX score algorithms in MM pts to predict their risk for having vertebral compression fractures at baseline presentation was tested.

Retrospectively, the data for patients enrolled in total therapy protocols (TT4 & TT5) between 8/2008 and 6/2014 was interrogated. FRAX scores were calculated, for every patient individually (<https://www.sheffield.ac.uk/FRAX/index.aspx>). Baseline bone status was obtained from PET and MRI imaging used for staging PET and MRI. Univariate and multivariate logistic regression determined the association between FRAX components and vertebral compression fractures. A logistic regression predictive model was built on 302 randomly selected patients, the model was also applied to the remaining 130 patients to assess validity. The results were internally cross validated to derive an accurate estimate of model prediction performance.

432 patients were identified (median age, 61 years old range (43-76); 37% female, 87% white). Median height was 173 cm, and median weight was 93 kg. Fractures were identified in 203 patients at baseline. Median Major osteoporotic score, and Hip fracture scores for TT4 pts were 5.6 and 0.5, respectively, while median Major osteoporotic score, and Hip fracture scores for TT5 pts were 6.2 and 0.7, respectively. Multivariate logistic regression confirmed age, race, sex, BMI, major osteoporotic score, and hip fracture score to be significant predictors of the presence of fractures at baseline. Estimates of individual model parameters are shown (Table 1). The model was highly accurate and discriminating, with an average area under the receiver operating characteristics (ROC) curve of 0.956 and average prediction accuracy of 88.5% when applied to the validation groups. In sum, an elevated baseline FRAX score is highly predictive of baseline vertebral fractures in MM pts at presentation. These findings support the notion that more sensitive imaging such as spinal MRI maybe beneficial in identifying MM patients at risk of vertebral fracture.

	$\beta$	Std. Error	p-value	Odds Ratio	95% CI for OR
Age at enrollment	-0.237	0.0358	<.0001	0.79	(0.73, 0.84)
Sex (Male)	2.86	0.5360	<.0001	17.4	(6.47, 53.7)
Race (White)	-3.72	0.704	<.0001	0.024	(0.006, 0.09)
BMI	0.087	0.031	0.005	1.09	(1.02, 1.16)
Major Osteoporotic	1.67	0.210	<.0001	5.32	(3.65, 8.34)
Hip Fracture	-2.05	0.353	<.0001	0.128	(0.061, 0.25)

Table 1

**Disclosures:** Shebli Atrash, None.

## SU0204

**Vitamin D Status of Highly Sun-exposed People: The "Surfer Study" Redux with Standardized 25(OH)D Data.** Neil Binkley\*, Diane Krueger<sup>1</sup>, Gretta Borchardt<sup>1</sup>, Gretta Borchardt<sup>1</sup>, Marc Drezner<sup>1</sup>, Chris Sempos<sup>2</sup>. <sup>1</sup>University of Wisconsin-Madison, United States, <sup>2</sup>Vitamin D Standardization Program, NIH-ODS, United States

**Objective:** Use of standardized vitamin D metabolite measurements is essential if we are ever to achieve clarity regarding vitamin D status. We previously reported 25(OH)D data in highly sun exposed adults (the "surfer study") measured by HPLC prior to the advent of 25(OH)D reference measurement standards.<sup>1</sup> Here we report surfer study serum total 25(OH)D results from stored sera using a LC-MS/MS methodology calibrated to the gold standard NIST, Ghent and CDC reference measurement procedures.

**Methods:** As previously reported,<sup>1</sup> we recruited 93 highly sun exposed adults in Honolulu, HI. All had self-reported sun exposure of  $\geq 3$  hours on  $\geq 5$  days per week for at least the prior 3 months. Serum aliquots had been stored at  $-80^{\circ}\text{C}$  until thawed for this analysis. Serum cholecalciferol (D<sub>3</sub>), 25(OH)D and 24,25(OH)<sub>2</sub>D were measured by LC-MS/MS. Thirty residual DEQAS sera with NIST-assigned 25(OH)D results were measured and a regression equation developed to standardize our current total 25(OH)D data. Prior HPLC 25(OH)D results were compared to the current LC-MS/MS NIST calibrated values by linear regression and Bland-Altman analysis; racial group differences were explored by factorial ANOVA.

**Results:** Data from 63 men and 30 women (37 White, 27 Asian, 18 multi-racial, 7 Hawaiian/Pacific Islander and 4 other) are reported. Calibrated 25(OH)D results were highly correlated ( $r^2 = 0.85$ ) with the originally reported 25(OH)D HPLC data but with a mean bias of  $+12.5$  ng/mL. As a result, use of calibrated 25(OH)D data reduced the prevalence of "low" vitamin D status, i.e.,  $< 30$  ng/mL, from 51% to 35% and  $< 20$  ng/mL from 9% to 6%. The overall mean 25(OH)D was 35.6 ng/mL. Race-based differences existed with serum D<sub>3</sub>, 25(OH)D and 24,25(OH)<sub>2</sub>D higher in Whites than other races (Table).

**Conclusion:** Retrospective calibration of 25(OH)D data is possible and can alter the prevalence of low vitamin D status, even when chromatography-based data were originally used. Data such as this calls into question the veracity of widely accepted cutpoints of 20 and 30 ng/mL that were developed using unstandardized 25(OH)D assays. Use of standardized 25(OH)D assays is essential in research studies to improve understanding of what truly constitutes vitamin D inadequacy. Though limited by small sample size, this study suggests race-based differences in vitamin D production may exist.

<sup>1</sup>Binkley, et. al., J Clin Endocrinol Metab. 2007;92:2130-2135.

Vitamin D metabolites in highly sun-exposed adults			
Race	D <sub>3</sub> (ng/mL)	25(OH)D (ng/mL)	24,25(OH) <sub>2</sub> D (ng/mL)
White (n=37)	15.5 (8.8)*	42.7 (12.1)*	6.6 (2.9)*
Asian (n=27)	4.7 (4.0)	26.6 (6.8)	3.0 (1.1)
HPI (n=7)	6.1 (3.4)	33.4 (7.9)	4.5 (1.4)
Multi (n=18)	7.4 (5.3)	32.7 (6.8)	4.8 (2.1)

Data as mean (SD); \* =  $p < 0.001$

**Figure**

**Disclosures:** Neil Binkley, None.

## SU0205

**Automated No-Dose Incidental Screening in the Context of Osteoporosis.** J. Keenan Brown\*, Wolfram Timm<sup>2</sup>, Reimer Andresen<sup>3</sup>. <sup>1</sup>Mindways Software, Inc., United States, <sup>2</sup>Mindways Software, Inc., Germany, <sup>3</sup>Institute of Diagnostic and Interventional Radiology/Neuroradiology, Westkuestenlinikum Heide, Academic Teaching Hospital of the Universities of Kiel, Luebeck and Hamburg, Heide, Germany, Germany

An automatic spine and femur analysis from existing CT scans, without the application of dose or manual work, has the potential to identify patients which should be forwarded to a standard procedure for the determination of the bone status.

A new screening module of the Mindways QCT Pro framework (Mindways Software, Inc., Austin, TX, USA) is under development and was applied to a set of native and contrast enhanced CT scans obtained for reasons other than bone densitometry. For 63 CT scans, the screening module automatically identified slices containing vertebrae, placed cylindrical ROIs, filtered out endplates and intervertebral discs based on the higher dispersion of density, and computed a calibrated mean volumetric bone mineral density, if the software classified the analysis as valid. Within the CT scans of 42 patients an automatic detection of the hip identified left and right femoral neck areal bone mineral density. All results were compared to a standard analysis by Mindways QCT Pro 6.1. Asynchronous 3D Spine and CTXA Hip modules.

For spine scans, a residual error of 7.94 mg/cm<sup>3</sup> was achieved when restricting the maximally allowed dispersion of the scan's slice-based densities to 8.33 mg/cm<sup>3</sup>. Results of 50 spine datasets showed a dispersion of slice-based densities below 15 mg/cm<sup>3</sup> and a residual error of 14.49 mg/cm<sup>3</sup>. Bland-Altman (BA) statistics (lower 95% CI, mean difference, upper 95% CI, [slope]) resulted in (-16.15, 0.72, 17.60, [0.10]) mg/cm<sup>3</sup> and (-25.43, 2.95, 31.33, [0.18]) mg/cm<sup>3</sup> for maximal dispersion of 8 and 15 mg/cm<sup>3</sup>, respectively. BA plots specific for the native, arterial and portal phase did not lead to clinically significant differences to the BA plots covering all phases.

For femoral neck results, 41 cases fulfilled a limit of 0.4 g/cm<sup>2</sup> applied to the difference between left and right side. Any further decrease of this limit did not decrease the corresponding residual error (mean 0.08 g/cm<sup>2</sup>). BA statistics did not show any



clinically significant differences (-0.07, 0.09, 0.24, [0.62]) g/cm<sup>2</sup> and (-0.07, 0.08, 0.23, [0.60]) g/cm<sup>2</sup> between the left and right side of the hip. BA plots specific for the native, arterial and portal phase did not lead to clinically significant differences to the BA plots covering all phases.

The new QCT Pro automatic screening module allowed to predict bone mineral density without any further dose and manual work. Further development is planned and validation on independent groups of patients required.

Phase	Left [g/cm <sup>2</sup> ]				Right [g/cm <sup>2</sup> ]			
	Lower 95% CI	Mean Diff.	Upper 95% CI	Slope	Lower 95% CI	Mean Diff.	Upper 95% CI	Slope
All	-0.07	0.09	0.24	0.62	-0.07	0.08	0.23	0.60
Native	-0.10	0.08	0.27	0.50	-0.09	0.08	0.25	0.53
Arterial	-0.07	0.08	0.22	0.78	-0.08	0.07	0.22	0.68
Portal	-0.04	0.10	0.24	0.67	-0.03	0.10	0.23	0.64

Bland-Altman statistics (femoral neck)

**Disclosures:** J. Keenan Brown, Mindways Software, Inc., Major Stock Shareholder.

## SU0206

**Comparison of Metaphyseal and Diaphyseal Microstructure of the Tibia in Elderly Men Measured by HR-pQCT.** Andrew Burgahrdt<sup>\*1</sup>, Andrew Yu<sup>1</sup>, Sharmila Majumdar<sup>1</sup>, Dennis Black<sup>1</sup>, Eric Orwoll<sup>2</sup>. <sup>1</sup>University of California, San Francisco, United States, <sup>2</sup>Oregon Health & Science University, United States

The most recent iteration of HR-pQCT (XtremeCT II, Scanco Medical) can image more proximal regions of the extremities, including the tibial diaphysis, and achieve a higher nominal resolution of 61µm. These advances make direct measurement of microstructural features of metaphyseal and diaphyseal cortical bone structure possible (Figure 1). Our objective was to (1) adapt a cortical bone analysis pipeline to measure the 30% diaphyseal tibia from second generation HR-pQCT images; and (2) evaluate the relationship to cortical bone measured at the standard distal metaphyseal position. We used data from a cohort of elderly men who attended the fourth visit of the Osteoporotic Fractures in Men (MrOS) study and had acceptable quality HR-pQCT scans of the distal and diaphyseal tibia. Associations between measures of bone density, geometry, structure, and µFEA estimates of strength were evaluated using Pearson correlations across the entire cohort, and within tibial length quintiles. Of the subjects studied with both distal and diaphyseal scans (N=1561), 98% had acceptable distal scans, 96% acceptable diaphyseal scans, and 95% had both (N=1475). A custom automated QA procedure determined segmentation error rates < 2% for the optimized diaphyseal tibia analysis pipeline. Cortical BMD was significantly higher at the diaphyseal site (Table 1). Porosity was approximately half at the diaphyseal site: the number of pores was lower, but pore diameter was not different. The correlation between metaphyseal and diaphyseal bone was moderate for integral BMD, total area, and cortical thickness ( $r^2=0.31-0.49$ ,  $p<0.0001$ ), and poor for porosity-related measures ( $r^2<0.10$ ,  $p<0.0001$ ). Inter-site correlations for To.Ar, Ct.Th, and Ct.Ar were minimally different when determined for tibial-length quintiles (data not shown), suggesting site-wise variance is not due to scan positioning variability associated with limb-length. This indicates that unique biological variability can be assessed by measuring both distal and diaphyseal sites. In conclusion, measurement of bone at the 30% diaphysis by second generation HR-pQCT likely provides complimentary information about skeletal status to traditional distal metaphyseal scan positions.

**Figure 1.** Scout view image illustrating the metaphyseal and 30% diaphyseal scan regions measured in the tibia by second generation HR-pQCT.



**Table 1.** Mean and standard deviations for bone measures at the standard distal metaphysis, 30% diaphysis, and the Pearson correlation coefficient between sites.

		Diaphyseal [mean (SD)]	Distal [mean (SD)]	r <sup>2</sup>
BMD	[mg/cm <sup>3</sup> ]	730.6 (78.3)	283.1 (55.2)	0.48
Ct.BMD	[mg/cm <sup>3</sup> ]	995.5 (35.2)	781.5 (79.8)	0.14
To.Ar	[mm <sup>2</sup> ]	440.4 (52.1)	881.2 (130.7)	0.42
Ct.Ar	[mm <sup>2</sup> ]	312.9 (40.4)	139.5 (31.3)	0.30
Tb.Ar	[mm <sup>2</sup> ]	132.0 (40.7)	747.8 (139.2)	0.25
Ct.Th	[mm]	6.2 (0.9)	1.5 (0.3)	0.31
CLPo	[%]	2.1% (1.2%)	4.3% (1.7%)	0.06
Po.Dm	[mm]	0.26 (0.0)	0.24 (0.0)	0.04
Stiffness	[kN/mm]	326 (57.4)	215 (50.1)	0.46
App.Mod	[MPa]	8098 (673.9)	2191 (526.1)	0.11

Figure 1 and Table 1

**Disclosures:** Andrew Burgahrdt, None.

## SU0207

**Addressing Bone Quality Loss After Renal Transplantation. A Systematic Assessment of the Evolution of Trabecular Bone Score (TBS) over the first one year following renal transplantation and its correlation with Bone Biochemical Parameters and Steroid Use in Asian Patients.** Manju Chandran<sup>\*</sup>, Ying Hao, David Ng, Pushan Bharadwaj. Singapore General Hospital, Singapore

**Introduction:** TBS gives an indirect index of trabecular microarchitecture. We aimed to evaluate its evolution over the 1<sup>st</sup> year after transplantation and correlations between this and bone parameters and steroid use in patients at the largest renal transplant centre in Singapore.

**Method:** Analysis of TBS on DXA scans performed at 0, 6 and 12 months post-transplant. BMD, parathyroid status, serum 25(OH)D, Calcium, iPTH, Phosphate, Bone Specific ALP, Osteocalcin levels and Cumulative steroid dose at 6 and 12 months were checked.

**Results:** Mean(SD) age of the 164 patients was 47.11(9.526). Mean TBS was 1.424 (0.098). Mean LS BMD(gm/cm<sup>2</sup>) was 0.935(0.183). TBS at baseline was lower in patients with tertiary (1.381(0.071)) vs those with secondary hyperparathyroidism (1.426(0.099)) and those who had parathyroidectomy (1.458(0.114)). TBS correlated positively with LS BMD at all 3 time points and at baseline, negatively with dialysis duration pre-transplant ( $\rho=-0.226$ ;  $p=0.005$ ). 6<sup>th</sup> month TBS was lower in patients with tertiary hyperparathyroidism (1.361 (0.077)) at baseline vs those with secondary hyperparathyroidism (1.405 (0.099)) and had parathyroidectomy (1.468 (0.076));  $p=0.007$ . TBS at 12 months correlated negatively with calcium level;  $\rho=-0.278$ ;  $p=0.005$ . TBS declined from baseline to 6 months (1.424->1.410 (95% CI: -0.03,0.01;  $p<0.001$ ) as did BMD. Mean TBS continued to decrease from 6<sup>th</sup> to 12<sup>th</sup> month; 1.410 -> 1.401; 95% CI: -0.021, 0.003;  $p=0.011$ ) though LS BMD did not. Overall, TBS decreased from baseline to 12<sup>th</sup> month (1.424 to 1.401; 95% CI: -0.039,0.016;  $p<0.001$ ). On Linear mixed model analysis, hypercalcemia and cumulative steroid dose correlated with the TBS decrease. Every unit increase in calcium and every doubling of cumulative steroid dose resulted in a decrease in TBS by 0.218 ( $p=0.031$ ) and 0.056 ( $p=0.05$ ) respectively at 12 months vs baseline.

**Conclusion:** In our knowledge, ours is the first systematic evaluation of the progression of TBS and its correlation with various bone parameters at multiple time points in the 1<sup>st</sup> year after renal transplantation. The fact that parathyroid status at the time of transplantation affected the TBS not only at baseline but also at 6 months after it underscores the detrimental effect of elevated PTH on bone quality. The continued decline of TBS in the 2<sup>nd</sup> half of the year following transplantation while BMD remained stable highlights the fact that relying on BMD alone in assessing bone loss in this population may be inadequate.

**Disclosures:** Manju Chandran, None.

## SU0208

**Inter-scanner Agreement of Trabecular Bone Score Data in Pre-peak Bone Mass Females, Compared to Intra-scanner Data Variability from Pre/peri/post-menopausal Adults.** Jodi Dowthwaite<sup>\*1</sup>, Renaud Winzenrieth<sup>2</sup>, Kristen Dunsmore<sup>3</sup>, Tamara Scerpella<sup>4</sup>. <sup>1</sup>SUNY Upstate Medical University, United States, <sup>2</sup>Med-Imaps, France, <sup>3</sup>Syracuse University, United States, <sup>4</sup>University of Wisconsin- Madison, United States

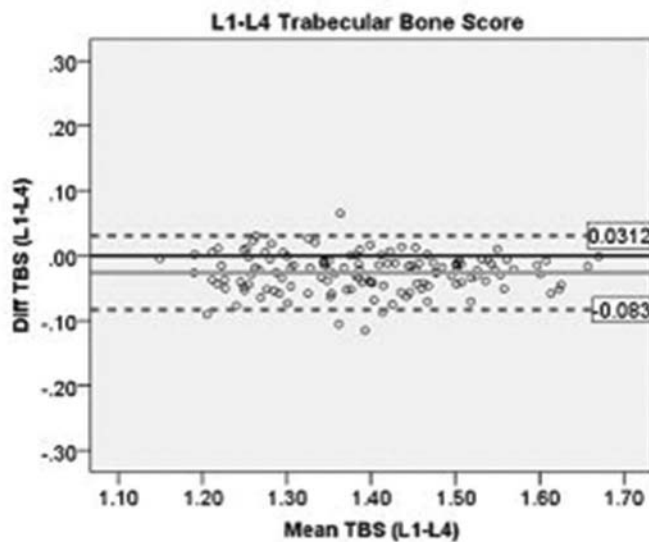
**Introduction:** Lumbar spine trabecular bone score (TBS) estimates trabecular microarchitectural traits using gray scale variation in postero-anterior DXA scans (TBS iNsight software, Med-Imaps, France). As scanner models may change during growth monitoring, we sought to evaluate how TBS assessments vary between DXA scanner models in maturing girls (pre-peak bone mass, PREPBM), relative to intra-scanner variation in adult women.

**Methods:** In a sample of PREPBM females, 7.8 to 23.9 years of age (mean 13.4, sd 4.9), we evaluated inter-scanner TBS variation using same-day, lumbar spine scans performed on two cross-calibrated DXA scanners (Hologic QDR 4500W and Discovery A, Waltham, MA). Intra-scanner variation was assessed using same-day, repositioned, duplicate Discovery A scans of 28 female ADULTS, 37.5 to 57.8 years of age (mean 45.9, 4.7: pre/peri/post-menopause). PREPBM TBS was determined for vertebrae L1-L4 using Med-Imaps custom software incorporating a pediatric soft tissue thickness correction. Root Mean Square Error coefficients of variation (RMSECV) were calculated in ADULTS (intra-scanner) and PREPBM subjects; the latter were subdivided into children (age 8 to 12) and adolescents (age 13 to 24). PREPBM inter-scanner agreement was evaluated using a Bland-Altman plot. Deming regression generated a reversible equation for PREPBM data conversion between scanners.

**Results:** For PREPBM participants, on both scanners, TBS minima and maxima were 1.15 and 1.67, respectively. QDR scans subtly, consistently and systematically overestimated TBS relative to Discovery A data, yielding a conversion equation with  $r^2 = 0.94$  (Discovery A =  $-0.0137963 + 0.993763 \times \text{TBS QDR}$ ). ADULT minimum and maximum TBS were 1.10 and 1.61, respectively; variability was almost as high as that observed across children, adolescents and young women of near-peak bone mass. The PREPBM inter-scanner RMSECV (1.95%) was lower than the ADULT intra-scanner RMSECV (2.08%); the ADOLESCENT RMSECV (1.34%) was particularly low compared to CHILDHOOD (2.31%). This finding is striking, because for all other standard DXA variables, we have reported ADULT RMSECV lower than PREPBM RMSECV in these same study participants (Dowthwaite et al. JCD 2017).

**Conclusion:** For TBS, in growing girls, inter-scanner hardware disparities are addressable using a conversion equation. TBS may vary more than other bone outcomes across peri-menopause, providing a more sensitive indicator of trabecular deterioration.

## Bland-Altman Plot:



Bland-Altman Plot

**Disclosures:** Jodi Dowthwaite, None.

## SU0209

**Vertebral Compression Deformities in Patients with Normal Bone Mineral Density.** Jay Ginther<sup>\*</sup>, Ann Ginther. Cedar Valley Bone Health Institute of Iowa, United States

**Introduction:** Last year our 1259 patient study revealed that adding VFA to DXA identified many additional patients at increased fracture risk. Some patients with normal

BMD had Genant grade 2 or 3 vertebral compression deformities. Were the deformities truly acute fractures, or natural kyphosis of age?

**Objectives:** This study attempts to determine how many of the apparent fracture deformities can be conclusively identified as acute fractures using VFA on a DXA machine. How does this compare to VFA by lateral x-ray required on patients with a high BMI? What are the implications for differentiating fractures from natural kyphosis of age on VFA by DXA machine?

**Methods:** The data of all 1259 patients was reassessed to identify patients with normal BMD, and VFA diagnosis of Clinical Osteoporosis. We found complete data on 79 patients. Each of the DXA/VFA studies performed on our Hologic Discovery SL machine was carefully reviewed on 2 separate occasions to identify which ones clearly showed the acute angles of acute fractures.

**Results:** Vertebral endplates were readily identified by our machine. 7 of 10 patients with grade 2 biconcave deformities showed acute fracture angles. 49 of 53 Wedge deformities had anterior cortices unreadable on DXA machine VFA. 4 showed definite anterior cortex buckles, and none of the 3 with multiple deformities showed more than 1. 2 wedge deformities were identified by an acute buckle of an endplate. Of 7 wedge patients with high BMI requiring x-ray: 1 had acute fracture, 4 anterior cortices showed remodeling, 1 had no acute fracture, and 1 (significant scoliosis) unreadable. 1 biconcave patient requiring x-rays had smoothly curved endplates.

**Conclusions:** Acute fracture angle endplate deformities were easily identified in 6 of 10 biconcave patients. 92% of anterior cortices were too fuzzy by DXA machine to analyze. By x-rays: 4 of 6 readable wedge deformity anterior cortices showed remodeling, 1 showed acute fracture, 1 showed no acute fracture. We can infer that the majority of wedge deformities would have shown acute or remodeling anterior cortex fracture deformities, if we had obtained lateral x-rays on all patients. These authors believe that the extra cost and radiation exposure cannot be justified. Therefore, we suggest that all wedge deformities may be considered the result of fracture. We suggest that natural kyphosis of age may be considered unrecognized fractures.

**Disclosures:** Jay Ginther, None.

## SU0210

**Will Free 25OH Vitamin D Measurement Replace The Current Total 25OH Vitamin D Test In IVD Laboratories?.** Nicolas Heureux<sup>\*</sup>. DIAsource Immunoassays, Belgium

The measurement of total 25OH Vitamin D is considered as the most accurate way to evaluate the individual's Vitamin D status or to detect and monitor Vitamin D deficiency amongst the worldwide population.

However, free 25OH Vitamin D has received increasing attention over the last three years and several studies have shown a better correlation to clinical markers and observations than total 25OH Vitamin D. The availability of a direct measurement method has greatly facilitated and improved the research in the field.

This poster will review the most recent evidence-based studies in the field of bone metabolism and in other areas and compare the use of total and free 25OH Vitamin D measurement. The current and potential future utility of the free 25OH Vitamin D test in IVD laboratories will also be discussed.

**Disclosures:** Nicolas Heureux, DIAsource Immunoassays, Other Financial or Material Support.

## SU0211

**Age-related changes in bone strength and microstructure in Asian: the Vietnam Osteoporosis Study.** Lan T Ho-Pham<sup>\*1</sup>, Tuan V. Nguyen<sup>2</sup>. <sup>1</sup>Ton Duc Thang University, Viet Nam, <sup>2</sup>Garvan Institute of Medical Research, Australia

Age-related changes in bone strength and microstructure in Asian: the Vietnam Osteoporosis Study

Lan T. Ho-Pham, Linh D. Mai, Truong X. Tran, Tuan V. Nguyen  
Bone and Muscle Research Laboratory, Ton Duc Thang University, Vietnam  
Pham Ngoc Thach University of Medicine, Vietnam  
Bone Biology Division, Garvan Institute of Medical Research, Australia  
University of Technology Sydney, Australia

**Background and aim:** Peripheral quantitative computed tomography (pQCT) allows the assessment of trabecular and cortical bone properties that are not possible by DXA technology. The present study sought to define the age-related changes in bone structural parameters and volumetric bone density in a Vietnamese population.

**Study Design and Methods:** The study was part of the large project called Vietnam Osteoporosis Study (VOS) that involved 1383 women and 828 men aged 18 years and older who were randomly recruited from the general population. pQCT measurements were performed at the distal radius and tibia using the CT bone scanner XCT 2000 (Stratec, Germany). Trabecular and cortical volumetric BMD (vBMD) were measured at the nondominant forearm at 4% and 38% point. Fracture load index, polar strength strain index (PSSI), and tibia strength strain index (SSI) were derived from the pQCT scan. Areal BMD was measured at the femoral neck and lumbar spine using a DXA system (Hologic Horizon, USA). Robust multiple linear regression was used to determine the rate of age-related changes in vBMD and aBMD.

**Results:** The relationship between age and vBMD largely followed a quadratic function, with peak level being reached at the age of 20-30 yr. The decline of vBMD started from the age of 50, with women having higher rate of loss than men. At the radius, the rate of loss in trabecular vBMD was 1.1%/yr in women which was significantly greater than that in men (0.2%/yr); the rate of loss in cortical vBMD was 0.3%/yr



compared with 0.1%/yr in men. Similar trends were also observed at the tibia. As expected, PSSI, SSI, and fracture load indices in men were greater than women, but the relative rate of decline in fracture load was not significantly different between men and women. The correlation between DXA aBMD and pQCT vBMD ranged between 0.10 and 0.35.

Conclusion: In normal individuals, vBMD reaches its peak at the age group of 20-30 yr, and starts declining at the age of 50. The rate of decline in trabecular vBMD was greater than cortical bone vBMD, and women have a greater rate of loss than men. The modest correlation between aBMD and vBMD suggests that vBMD can be a useful complementary tool for the assessment of bone health.

**Disclosures:** Lan T Ho-Pham, None.

## SU0212

**A New Device for Ultrasonic Assessment of the 1/3 Radius.** Emily Stein<sup>\*1</sup>, Gangming Luo<sup>2</sup>, Mariana Bucovsky<sup>3</sup>, Fernando Rosete<sup>3</sup>, Mafo Kamanda-Kosse<sup>3</sup>, Jonathan Kaufman<sup>2</sup>, Elizabeth Shane<sup>3</sup>, Robert Siffert<sup>4</sup>. <sup>1</sup>Hospital for Special Surgery, United States, <sup>2</sup>CyberLogic, Inc., United States, <sup>3</sup>Columbia University, United States, <sup>4</sup>The Mount Sinai School of Medicine, United States

Although x-ray methods can estimate BMD, osteoporosis remains one of the world's most undiagnosed diseases, in part because of inaccessibility of technologies to measure bone mass. The goals of this study were to evaluate the ability of a recently FDA-approved ultrasound device (*UltraScan 650*, CyberLogic, Inc., NY, USA, Fig. 1) to estimate BMD at the 1/3 radius (1/3R), and to investigate its ability to discriminate fragility fracture and non-fracture cases. The *UltraScan 650* (Fig. 1) is a portable desktop sonometer, that performs real-time evaluation of bone mineral density (BMD) at the radius. The device measures two net time delay (NTD) parameters, NTD<sub>DW</sub> and NTD<sub>CW</sub>. NTD<sub>DW</sub> is the difference between the transit time of an ultrasound pulse through soft-tissue, cortex and medullary cavity, and the transit time through soft tissue only of equal overall distance. NTD<sub>CW</sub> is the difference between the transit time of an ultrasound pulse through soft-tissue and cortex only, and the transit time through soft tissue only, again of equal overall distance. The square root of the product of these two parameters is a measure of the BMD at the 1/3R, as would be measured by DXA. We conducted a study in which ultrasound and DXA were performed at the 1/3R in 77 adults (age range 21-83, 75% female; DXA BMD range, 0.45-0.92 g/cm<sup>2</sup>). An age and sex-matched subset (28 fracture cases with 22 wrist, 5 ankle, 1 spine, and 16 controls) of these subjects was used to determine the capability of DXA and ultrasound to discriminate between fragility fracture and non-fracture cases. The controls were individually selected by sex and with subject closest in age of a fracture case. Linear regression showed that  $BMD_{US} = 0.19 * (NTD_{DW} * NTD_{CW})^{1/2} + 0.28$  and that the linear correlation between  $BMD_{US}$  and  $BMD_{DXA}$  was 0.93 ( $P < 0.001$ ). We found that forearm ultrasound measurements yield results that are very closely associated with those from DXA. These results on the ability of ultrasound to estimate radial bone mass are consistent with previous computer simulation and *in vitro* studies. In the case-control, cross-sectional fracture study, we found that mean  $BMD_{DXA}$  was lower in the fracture cases (0.61 g/cm<sup>2</sup>) compared to the controls (0.72 g/cm<sup>2</sup>) but the difference was not significant ( $P = 0.20$ ). In contrast, mean BMD by ultrasound was significantly lower in the fracture cases (0.61 g/cm<sup>2</sup>), compared to the non-fractured controls (0.73 g/cm<sup>2</sup>) ( $P = 0.05$ ), suggesting that  $BMD_{US}$  provides additional information on bone properties that track more consistently with fracture risk than  $BMD_{DXA}$ . This research study demonstrates that an ultrasonic desktop device can serve as a proxy for  $BMD_{DXA}$  at the 1/3R and should enable significant expansion of the identification of bone loss in patients at risk for osteoporosis. Larger studies will be required to confirm whether  $BMD_{US}$  can predict incident fracture risk with similar or greater accuracy than  $BMD_{DXA}$ .



UltraScan 650 Bone Sonometer

**Disclosures:** Emily Stein, None.

## SU0213

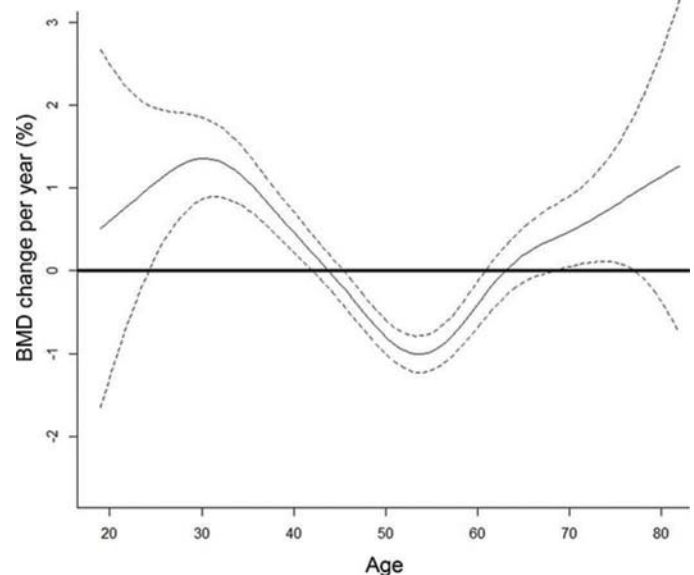
**Longitudinal Changes of Lumbar Bone Mineral Densities in Korean Women.** Young-Sang Kim<sup>\*1</sup>, Hyejin Chun<sup>2</sup>, Kunhee Han<sup>2</sup>, Soo-Hyun Lee<sup>2</sup>, Bo Youn Won<sup>2</sup>, Seung-Gun Park<sup>2</sup>. <sup>1</sup>CHA university, CHA Bundang Medical Center, Korea, Republic of, <sup>2</sup>CHA university, Korea, Republic of

The periods of acquisition of peak bone mass (PBM) in Korean adults have been reported in previous studies. PBM appeared to be reached later in the Korean women than in Caucasian population. However longitudinal changes have not been explored yet in Korean population.

We analyzed the lumbar bone mineral density (BMD) data of the female adults participated in the medical examination programs of CHA Bundang Medical Center from January 2005 to February 2016. BMD was measured by dual-energy X-ray absorptiometry from 12,942 women. A total of 4,502 images were obtained repeatedly with intervals of 1-3 years from 1,831 women. Age groups were stratified into 19-29, 30-34, 35-39, 40-44, 45-49, 50-54, 55-59, 60-64, 65-69, and 70 or older. BMDs and yearly changes of BMD were calculated in each age group. Using smoothing splines, the cross-sectional trends of BMD and longitudinal changes of BMD were evaluated with age.

According to the cross-sectional trends, BMD increased until the mid-40s. The highest BMD was  $0.999 \pm 0.117$  g/cm<sup>2</sup> in age group of 40-44. In age groups of 50 years or older, BMD began to decrease. Mean BMD was  $0.783 \pm 0.140$  g/cm<sup>2</sup> in age group of 70 years or older. According to the longitudinal analyses, the proportion of BMD change was peak (+1.99%/year) in age group of 30-34. After the age group of 45 years or older, the change of BMD inverted to decrease. The BMD change was bottom (-0.96%/year) in the age group of 50-54.

In conclusion, the PBM was reached at mid-40s in Korean women. The late reach of PBM may not be caused by the difference between generations, but by ethnic characteristics. Further considerations for the factors of the bone metabolism should be required.



Smoothing splines of BMD changes according to age

**Disclosures:** Young-Sang Kim, None.

## SU0214

**Leg Elevation Does Not Substantially Affect TBS Results.** Diane Krueger<sup>\*1</sup>, Ellen Siglinsky<sup>1</sup>, Doris Tran<sup>2</sup>, Luis Del Rio Barquero<sup>3</sup>, Neil Binkley<sup>1</sup>. <sup>1</sup>University of Wisconsin, United States, <sup>2</sup>Medimaps SASU, France, <sup>3</sup>CETIR Centre Medic, Spain

Objective: Lumbar spine DXA scans are typically acquired with a patient's legs elevated, thereby flattening lumbar lordosis. With GE densitometers it is possible to acquire spine scans with the legs down. BMD values do minimally differ between legs down vs. elevated, however it is unknown if positioning affects trabecular bone score (TBS). This study assessed the effect of leg position on TBS.

Methods: Lumbar spine (L1-L4) DXA scans were acquired with legs up and down positioning using GE Prodigy (3) and iDXA (1) densitometers at two centers. Scans were analyzed with enCORE software v 12.3 or 14.1 in routine clinical manner. Subsequently all scans were re-processed using Medimaps TBS Calculator v2.3 or TBS iNsite v3.0.2 to obtain TBS results on the same regions of interest as BMD analysis. Linear regression and Bland-Altman were performed to compare TBS with legs up vs. down. To evaluate potential leg elevation effects on single vertebrae due to parallax changes, a detailed manual analysis was performed. Bone edges were carefully defined using a zoom function and intervertebral markers were placed parallel to vertebral endplates, BMD and TBS were then computed.

Results: Sixty-four women, mean age 65.1 years (range 28.2-86.6) and BMI 26.4 kg/m<sup>2</sup> (range 18.1-34.8) were studied from Prodigys. Fifty women, mean age 68.6 years

(range 15.2-92.5) and BMI 26.2 kg/m<sup>2</sup> (range 19.9-35.1) were studied from an iDXA. On Prodigy with legs up positioning, the L1-4 BMD ranged from 0.738-1.549 g/cm<sup>2</sup> and was highly correlated with legs down positioning,  $R^2 = 0.99$ . TBS ranged from 1.072-1.632 and was also highly correlated,  $R^2 = 0.93$  with a mean bias of -0.005 TBS units between positions (Figure). On iDXA with legs up positioning, the L1-4 BMD ranged from 0.753-1.622 g/cm<sup>2</sup> and was highly correlated with legs down positioning,  $R^2 = 0.97$ . TBS results ranged from 1.040-1.455 and were also well correlated,  $R^2 = 0.90$  with a mean bias of 0.0 TBS between leg positions (data not shown). Results of detailed analysis were consistent with standard analysis; L1-4 TBS mean difference was 0.011 on Prodigy and 0.006 on iDXA. Single vertebral TBS mean difference varied from -0.005 to 0.023 with Prodigy and 0.0 to -0.017 with iDXA. Pearson correlation coefficient  $R^2$  was 0.89 on Prodigy and 0.86-0.87 on iDXA.

Conclusion: Leg positioning minimally affects TBS results with GE Healthcare Prodigy and iDXA densitometers but the difference from legs up to down is likely of no clinical significance.

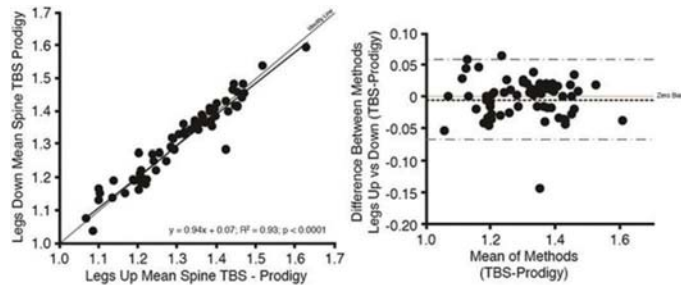


Figure 1

Disclosures: Diane Krueger, None.

## SU0215

**In Which Patient Populations Does Lumbar Spine Trabecular Bone Score (TBS) Have the Largest Effect on Fracture Prediction?** Patrick Martineau<sup>1</sup>, William Leslie<sup>2</sup>, Helena Johansson<sup>3</sup>, Anders Oden<sup>3</sup>, Eugene McCloskey<sup>3</sup>, John Kanis<sup>3</sup>, Didier Hans<sup>4</sup>. <sup>1</sup>University of Ottawa, Department of Radiology, Canada, <sup>2</sup>University of Manitoba, Canada, <sup>3</sup>University of Sheffield Medical School, United Kingdom, <sup>4</sup>Lausanne University Hospital, Switzerland

Background: Lumbar spine TBS enhances FRAX-based fracture prediction. No studies to date have identified which patients derive the greatest benefit from using TBS in the FRAX calculation.

Methods: Using the Manitoba BMD Registry, we identified 37,176 subjects with baseline DXA, FRAX-based fracture probability, lumbar spine TBS, and minimum 5 years of observation. Subgroups considered were based on sex, age, BMI, prior fracture, smoking proxy, high alcohol use, rheumatoid arthritis (RA), high glucocorticoid use, osteoporotic femoral neck T-score, number of comorbidities, diabetes mellitus (DM), secondary osteoporosis, and prior osteoporosis treatment. We compared TBS within subgroups using analysis of covariance (ANCOVA). Non-traumatic major osteoporotic fractures (MOF, n=3741) and hip fractures (HF, n=1008) were identified using population-based health services data. MOF and HF probability were estimated from FRAX with and without the TBS adjustment. Categorical net reclassification improvement (NRI) was estimated for all subjects and within each subgroup using FRAX-based intervention cutoffs (fixed MOF 20%, fixed HF 3%). FRAX-adjusted hazard ratios (HR) per SD reduction in TBS for MOF and HF were estimated and tested for interactions.

Results: Age- and BMI-adjusted TBS was significantly lower ( $p < 0.001$ ) for women (-4.0%), osteoporotic T-score (-4.0%), DM (-3.0%), smoking (-2.8%), high alcohol use (-2.3%), prior fracture (-2.2%), glucocorticoid use (-1.4%), RA (-0.8%) and secondary osteoporosis (-0.6%). NRI with TBS adjustment to FRAX for all subjects was 1.2% for MOF ( $p = 0.002$ ) and 1.7% for HF ( $p = 0.016$ ). NRI was greater in subjects age  $< 65$  y (MOF: 1.7%, HF: 5.6%), no prior fracture (HF: 2.4%), non-osteoporotic T-score (HF: 3.0%), and glucocorticoid use (MOF: 3.9%). Significant interactions were seen with larger effects for age  $< 65$  vs  $\geq 65$  (MOF  $p = 0.004$ , HF  $p < 0.001$ ), without vs with prior fracture (MOF  $p = 0.003$ , HF  $p = 0.048$ ), without vs with glucocorticoid use (HF  $p = 0.029$ ), lower vs higher ADG comorbidity score (HF  $p < 0.001$ ), and without vs with osteoporosis treatment (MOF  $p = 0.005$ ). No significant interactions were detected for sex, BMI, smoking proxy, RA, DM or secondary osteoporosis.

Conclusion: TBS adjusted fracture risk assessment resulted in significant improvements overall and in several subgroups. We saw larger benefits in terms of risk reclassification for age  $< 65$  y, no prior fracture, non-osteoporotic femoral neck T-score, and high glucocorticoid use.

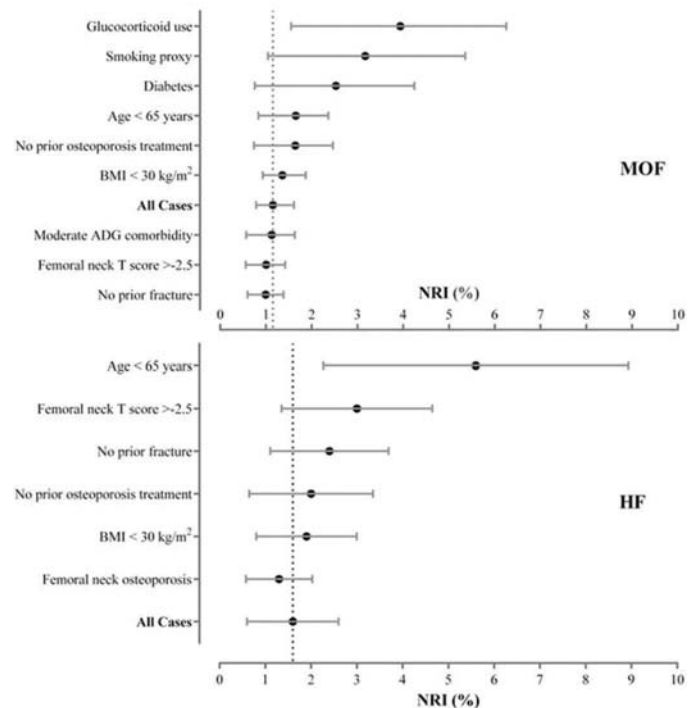


FIGURE: NRI for TBS-adjusted major osteoporotic (MOF) and hip fracture (HF). Dotted line all cases

Disclosures: Patrick Martineau, None.

## SU0216

**Comparison of volumetric density and microstructure between fixed offset and relative offset methods for HR-pQCT: relationships with lengths of forearm and lower leg.** Narihiro Okazaki\*, Ko Chiba, Kazuaki Yokota, Kazuteru Shiraishi, Makoto Osaki. Department of Orthopaedic Surgery, Nagasaki University Hospital, Japan

### Objective

Because the standard scan protocol for high-resolution peripheral quantitative computed tomography (HR-pQCT) does not take into account the lengths of the forearm or lower leg, concerns have been raised that scan sites might be shifted relatively more proximally when the bone length is short. We compared measurements obtained using the standard fixed offset method and the relative offset method determined by forearm and lower leg lengths in healthy Japanese subjects.

### Methods

Subjects comprised 116 healthy Japanese volunteers (75 females, 41 males). Mean age was 46.6 years; range, 21-87 years. The distal radius and tibia were scanned using HR-pQCT (XtremeCT II; Scanco Medical, Switzerland) with a voxel size of 61  $\mu$ m according to both the standard fixed offset method (radius: 9 mm, tibia: 22 mm) and the relative offset method (radius: 4%, tibia: 7.3%). We measured volumetric density and microstructure parameters, and compared differences in these parameters between the two methods using paired t-tests. In addition, differences between the two methods were calculated, and relationships with forearm and lower leg lengths were evaluated. Statistical significance was established at  $p < 0.01$ .

### Results

Mean body height was 162.1 cm (range, 141-185 cm), mean length of the forearm was 248.7 mm (range, 214-291 mm), and mean length of the lower leg was 342.2 mm (range, 281-405 mm). With the fixed offset method, as compared to the relative offset method, Ct.vBMD, Ct.Th, Tb.Th, and Tb.Sp were significantly higher, and BV/TV and Tb.N were significantly lower at the distal radius. Similarly, at the distal tibia, Ct.vBMD, Ct.Th, Tb.Th, and Tb.Sp were significantly higher, and Tb.vBMD, BV/TV, and Tb.N were significantly lower. Forearm length correlated with Ct.vBMD ( $r = -0.561$ ) and Ct.Th ( $r = -0.499$ ) ( $p < 0.001$  each) at the distal radius. At the distal tibia, lower leg length correlated with Ct.vBMD ( $r = -0.712$ ), Tb.vBMD ( $r = 0.699$ ), Ct.Th ( $r = -0.779$ ), BV/TV ( $r = 0.683$ ), Tb.N ( $r = 0.589$ ), and Tb.Sp ( $r = -0.491$ ) ( $p < 0.001$  each).

### Conclusion

At both the distal radius and tibia, significant differences in volumetric density and microstructure were evident between methods. Differences in parameters between the two methods changed depending on limb length, significantly affecting cortical bone parameters at the radius, and both cortical and trabecular bone parameters at the tibia.

Disclosures: Narihiro Okazaki, None.



## SU0217

**Densitometric lateral spine screening to detect vertebral fractures predicts incident osteoporotic fractures in elderly women in addition to bone density.** Richard L. Prince<sup>\*1</sup>, Joshua R. Lewis<sup>2</sup>, Wai H. Lim<sup>3</sup>, Germaine Wong<sup>2</sup>, Kevin E. Wilson<sup>4</sup>, Ben C. Khoo<sup>5</sup>, Kun Zhu<sup>1</sup>, Douglas P. Kiel<sup>6</sup>, John T. Schousboe<sup>7</sup>. <sup>1</sup>University of Western Australia, School of Medicine and Pharmacology, Australia, <sup>2</sup>Centre for Kidney Research, Children's Hospital at Westmead School of Public Health, Sydney Medical School, Australia, <sup>3</sup>Department of Renal Medicine, Sir Charles Gairdner Hospital, Australia, <sup>4</sup>Skeletal Health, Hologic, Inc., United States, <sup>5</sup>Medical Technology & Physics, Sir Charles Gairdner Hospital, Australia, <sup>6</sup>Institute for Aging Research, Hebrew Senior Life, Department of Medicine, Beth Israel Deaconess Medical Center, Harvard Medical School, United States, <sup>7</sup>Park Nicollet Osteoporosis Center and Health Partners Institute, United States

Vertebral fractures identified on lateral spine radiographs predict subsequent fractures independent of bone mineral density (BMD). However the use of low radiation lateral spine images (LSI) by bone densitometers at the time of areal bone density (aBMD) testing has not been established. To estimate the associations between prevalent vertebral fractures identified on densitometric LSI with incident fractures a prospective 14.5 year cohort study of 1,084 community dwelling women mean age 75 (SD 3) years living in Perth, Western Australia was completed. Baseline DXA imaging for hip aBMD and LSI was undertaken (Hologic, Marlborough, MA). The LSI scans were assessed for the presence of fracture by a single experienced clinician (JTS) blinded to the outcomes. Complete fracture ascertainment over the subsequent 14.5 yrs. was obtained from Health Department of WA hospital discharge records for hip and all fracture hospitalizations; clinical spine fractures were assessed by patient self-report and verified by x-ray report.

At baseline 100 women (9.2%) had a vertebral fracture (VF) identified on densitometric LSI. Incident clinical VF occurred in 73 (7%) of women; incident low-trauma hip fractures hospitalization occurred in 121 (11%) and all osteoporotic fracture hospitalization occurred in 305 (28%). Compared to those without baseline LSI VF, women with VF had higher risks of incident clinical VF of 19% vs 5.5% (RR 3.5, CI 2.2 – 5.6); hip fracture hospitalization of 18% vs 10.5 % (RR 1.7, CI 1.1 – 1.8,) and all osteoporotic fracture hospitalization of 38% vs 27% (RR 1.4, CI 1.1 – 1.8). Amongst those with femoral neck T score -1 to -2.5, who often do not meet criteria for pharmaceutical intervention, compared to those without baseline LSI VF those individuals with LSI VF were at higher absolute risk for incident clinical VF 21% vs 6% (RR 3.9 CI 2.2 – 6.9) and for all fracture hospitalizations 46% vs 29% (RR 1.6, CI 1.2 – 2.1) but not hip fracture hospitalization.

Women aged 70 years and older undergoing bone densitometry can receive additional information on future fracture risk by capturing densitometric lateral spine images at the time of aBMD measurement. Because pharmacologic therapy substantially reduces subsequent fractures in individuals with these fractures the identification of such individuals may lead to improved patient management.

**Disclosures:** Richard L. Prince, None.

## SU0218

**Fracture discrimination using cortical thickness and porosity index obtained with ultrasound.** Jean-Gabriel Minonzio<sup>\*1</sup>, Nicolas Bochud<sup>1</sup>, Quentin Vallet<sup>1</sup>, Donatien Ramiandrisoa<sup>1</sup>, Adrien Etcheto<sup>2</sup>, Karine Briot<sup>2</sup>, Sami Kolta<sup>2</sup>, Christian Roux<sup>2</sup>, Pascal Laugier<sup>1</sup>. <sup>1</sup>Sorbonne Universités, UPMC Univ Paris 06, CNRS, INSERM, Laboratoire d'Imagerie Biomédicale, France, <sup>2</sup>INSERM, U 1153, Rheumatology Department, Cochin Hospital, Paris Descartes University, France

Structural decay of bone is not fully assessed by current X-ray methods, and there is an unmet need in identifying women at risk of fracture who should receive a treatment. Recent axial transmission (AT) techniques exploit the multimode waveguide response of long bones such as the radius. The objective of this cross sectional study was to evaluate if a new AT device can discriminate between fractured and non-fractured postmenopausal women. Two hundred and five post-menopausal women were included, among whom 103 were non fractured (subgroup NF 62±7 years), 102 with one or more non-traumatic fractures (subgroup F 69±10 years), 19 with hip fractures (subgroup HF 65±11 years) and 28 with vertebral fractures only (subgroup VF 70±10 years). The cortical thickness (C.Th) and a cortical porosity index (C.PI) were estimated by using a prototype device (Azalée, Paris, France). The bone mineral density (BMD) was obtained using DXA at the femur and the spine. A weak but significant Spearman correlation was found between femoral BMD and ultrasound parameters (US): C.Th ( $R = -0.34, p < 0.001$ ), C.PI ( $R = 0.20, p < 0.001$ ).

Femoral BMD and US could discriminate the subgroup F from the control group ( $t$ -test,  $p < 0.05$  Table 1). Fracture prediction was significant for the subgroup F with C.PI and femoral BMD odds ratios [ORs] 1.36 and 1.53 and areas under the ROC curve [AUCs] 0.71 and 0.73 respectively. For the subgroup FF, C.Th OR was 1.86 and AUC was 0.70. For the subgroup VF, C.PI OR was 1.67 and AUCs was 0.77. All variables were age- and BMI-adjusted.

These results suggest that the multimode AT has the potential to yield cortical bone biomarkers to predict fracture risk in postmenopausal women. The study has to be confirmed by other clinical studies.

	non fractured (N = 103)	all non-traumatic fractures (N = 102)	hip fractures (N = 19)	vertebral fractures only (N = 28)
age	62 ± 7 years	69 ± 10 years ***	65 ± 11 years**	70 ± 10 years ***
C.Th	3.0 ± 0.3 mm	2.9 ± 0.3 mm*	2.7 ± 0.6 mm**	3.0 ± 0.5 mm
C.PI	10.1 ± 3.3 %	11.5 ± 1.6 % **	8.5 ± 3.0 %	12.1 ± 4.2 % **
BMD neck	0.66 ± 0.10	0.61 ± 0.08 ***	0.60 ± 0.10**	0.62 ± 0.09*
BMD femur	0.78 ± 0.12	0.73 ± 0.10 ***	0.70 ± 0.11 **	0.74 ± 0.12*
BMD spine	0.84 ± 0.19	0.82 ± 0.15	0.86 ± 0.16	0.81 ± 0.15
	AUC (95% CI)	OR (95% CI)	AUC (95% CI)	OR (95% CI)
C.Th	0.71 [0.63 – 0.77]	1.36 [1.01 – 1.85]*	0.70 [0.48 – 0.79]	1.86 [1.14 – 3.10]*
C.PI	0.73 [0.63 – 0.77]	1.53 [1.06 – 2.27]*	0.72 [0.49 – 0.79]	2.00 [1.05 – 4.17]*
BMD neck			0.72 [0.49 – 0.90]	2.20 [1.18 – 4.40]*
BMD femur				
BMD spine				
combination of an ultrasonic and a DXA measurements				
C.Th		1.37 [1.01 – 1.88]*		
BMD neck		0.74 [0.69 – 0.79]		
C.Th		1.54 [1.07 – 2.20]*		
BMD femur			0.74 [0.70 – 0.80]	1.76 [1.07 – 2.86]*
BMD spine				2.11 [1.09 – 4.42]*

Reference category is non fractured N = 103 (62 ± 7 yrs). CI: confidence interval, ROC: receiver operating characteristic. AUC and OR are adjusted for age and BMD (body mass index). \*p < 0.05 \*\*p < 0.01 \*\*\*p < 0.001. grey cells are non significant

Table 1

**Disclosures:** Jean-Gabriel Minonzio, Azalée, Consultant.

## SU0219

**The utility of trabecular bone score in evaluating bone quality in Hispanic population with type 2 diabetes.** Maryam Buni<sup>\*1</sup>, Catherine G Ambrose<sup>1</sup>, Joseph McCormick<sup>2</sup>, Susan Fisher-Hoch<sup>2</sup>, Nahid Rianon<sup>1</sup>. <sup>1</sup>UTHealth McGovern Medical School, United States, <sup>2</sup>UTHealth School of Public Health, United States

Fragility fractures are higher in subjects with type 2 diabetes (T2D) even in the presence of high or normal bone mineral density (BMD). Trabecular Bone Score (TBS), an indirect measure of bone microarchitecture, has been useful in indicating poor bone quality in T2D patients with non-osteoporotic BMD. However, there is a gap in knowledge about TBS in Hispanic populations, which have been shown to have the high rates of both T2D and osteoporosis in the US. The objective of this study was to compare TBS and BMD between Hispanic men and women of Mexican-American descent with T2D and without any history of diabetes. The current study participants were recruited from an ongoing cohort called the Cameron County Hispanic Cohort in Brownsville, Texas.

178 men (16 with and 44 without T2D) and women (48 with and 70 without T2D), 45 years or older (mean age 63, range 45-85) were included in the study. Body mass index, fasting plasma glucose, and HbA1C were all higher in the diabetic subjects compared to control subjects. TBS was assessed using existing lumbar spine BMD (LS-BMD) assessments and electronic medical records were reviewed to collect clinical and demographic information for each subject. Subjects with type 1 diabetes, cancer, known bone diseases or on dialysis were excluded from this study.

When both men and women were analyzed as a single group, there was no difference in LS-BMD comparing diabetic subjects to control (0.969 vs 0.931 g/cm<sup>2</sup>, p=0.173), but mean TBS was significantly lower in the diabetic group compared to control (1.20 vs 1.25, p=0.007). Area under (AUC) receiver operating characteristic (ROC) curves indicated that LS-TBS provided better ability than LS-BMD to discriminate between control subjects and those with diabetes (AUC TBS 0.630, p=0.004 vs AUC LS-BMD 0.448, p=0.249). When separated by gender, males with diabetes had higher LS-BMD (1.17 vs 0.98, p<0.001) but TBS was not different. Female subjects with diabetes had lower TBS (1.16 vs 1.24, p<0.001) but LS-BMD was not different.

TBS may help identify Hispanic men and women with T2D who are at high fracture risk due to poor bone quality even in the presence of non-osteoporotic BMD.

**Disclosures:** Maryam Buni, None.

## SU0220

**Assessment of Jawbone Quality as a Predictor of Lumbar Fracture Probability.** Yoshitomo Takaishi<sup>\*1</sup>, Megu Takaishi<sup>2</sup>, Takami Miki<sup>3</sup>, Akira Itabashi<sup>4</sup>, Aiko Kamada<sup>5</sup>, Takashi Ikeo<sup>5</sup>, Takuo Fujita<sup>6</sup>. <sup>1</sup>Takaishi Dental Clinic, Japan, <sup>2</sup>Center for the Special Needs Dentistry at Okayama University Hospital, Japan, <sup>3</sup>Izumi Otsu Municipal Hospital, Japan, <sup>4</sup>Saitama Center for Bone Research, Japan, <sup>5</sup>Osaka Dental University, Japan, <sup>6</sup>Kobe University professor emeritus, Japan

#### Background

Approximately 70 % of bone strength is predicted by bone density and the remaining 30% by bone quality. Atypical fracture, however, may occur at a high level of lumbar BMD presenting with problems. We developed a new jawbone quality evaluation method (International patent pending during the Patent Cooperation Treaty PCT/JP2017/61) based on the Jawbone Quality Score. In this method, the bone quality of the subjects is estimated based on the coefficient of the variation of each pixel in the predetermined area in the radiographic image of the alveolar bone using the Bone Right method.

#### Purpose

The aim of this study was to test the efficacy of measurement using the Bone Right Method to predict fracture incidence.

## Methods

In order to assess the usefulness of this method of osteoporosis screening, JQS of alveolar bone mineral density was measured in 30 postmenopausal women aged 50-69 years by the Bone Right System (Dental Graphic Com. Himeji, Japan) at a site lower than the neck of the right mandibular first premolar, along with lumbar BMD measurement by DXA by using Hologic 4500 type scanner made in USA, along with a survey of the history of fracture at Katsuragi Hospital under the Approval of The Institutional Review Board.

## Results

JQS was significantly and positively correlated with fracture ( $r=0.157$ ,  $p<0.05$ ) while al-BMD and L-BMD were significantly and negatively correlated with fracture ( $r = 0.614$ ,  $p < 0.01$ ,  $r = 0.472$ ,  $p < 0.01$ ). Age displays an apparent negative correlation with both al-BMD and L-BMD respectively ( $r = 0.456$   $p = 0.05$ ,  $r = 0.604$ ,  $p=0.01$ ), demonstrating a definite positive correlation with fractures ( $p = 0.479$ ,  $p < 0.05$ ). ROC analysis, JQS (AUC 0.760  $p = 0.016$ ) and L-BMD (AUC 0.792  $p=0.007$ ) revealed similar accuracy, while al-BMD (AUC 0.932,  $p = 0.00006$ ), provided an even higher one.

## Conclusion

Evaluation of JQS by the new bone mineral density device using dental X-ray film favorably compared with the conventional method using DXA. This would enlarge the range of subjects benefited by the osteoporosis detection and treatment tremendously. Effective osteoporosis treatment activates daily life and social activity, making them happier and more confident in themselves.

**Disclosures:** Yoshitomo Takaishi, None.

## SU0221

**Prescreening for Osteoporotic Hip BMD after Fracture with an accurate Pulse-Echo Ultrasound Device.** Peter van den Berg\*, Dave Schweitzer. Reinier de Graaf Gasthuis, Netherlands

## Introduction

Strategies to prevent osteoporotic fractures should be safe and cost-effective. Pulse-Echo Ultrasound (PE-US) is a small device non-ionizing tool, which has shown high prediction of osteoporosis at the hip. FLSs encourage prevention of new fractures (IOF "Capture the Fracture® Program"). PE-US was used for detection of hip osteoporosis and morphometric vertebral fractures.

## Methods

We studied 264 consecutive female fracture patients of mean age 67 (years (range, 50-94 years), referred to a single FLS. Prior to visit, each subject was seen at the trauma unit because of suspicion of fracture. Any confirmed new fracture led to an invitation to attend FLS. Patients with fractures (excluding skull) were first measured using PE-US (Bindex®, Bone Index Finland, Kuopio, Finland), which provides an estimate (Density Index, DI) for BMD at the hip. DI classifies patients to healthy (above upper threshold), intermediate (between the thresholds) or osteoporotic (below lower threshold) by applying previously determined thresholds. Second, a DXA Hologic® scan of the spine and hip for BMD and Vertebral Fracture Assessment. All these assessments were performed within 3 months. For screening purpose, the upper threshold of DI 0,844 g/cm<sup>2</sup>) was used as cut-off.

## Results

Sensitivity and specificity of DI for T-score  $\leq -2.5$  SD at the hip: 94% and 75%, resp. NPV and PPV at the hip: 97% and 54%, resp. Four out of 97 patients with a DI  $>0.844$  g/cm<sup>2</sup>, had a T-score of  $\leq -2.5$  SD. Twenty-two out of 264 patients had at least one spinal fracture (8%). Eight patients had a severe fracture (6 with DI  $<0.844$  g/cm<sup>2</sup>; 75%) and 14 patients a mild or moderate fracture (10 of them with DI  $<0.844$  g/cm<sup>2</sup>; 71%). Seven-teen out of 18 patients with a hip fracture had a DI  $< 0.844$  g/cm<sup>2</sup> (94%). Based on DI, 93 patients scored healthy (35%), 92 intermediate (35%) and osteoporosis (30%). Number of patients classified by DXA (lowest of T-Scores at neck or total hip) healthy were  $> -1.0$  SD:  $n=34$  (13 %); osteopenic from  $-1.0$  to  $-2.4$  SD;  $n=133$  (50%); osteoporosis  $\leq -2.5$  SD:  $n=97$  (37%).

## Conclusions

A healthy DI excluded a T-score of  $\leq -2.5$  SD at the femoral neck in nearly 100%. The PE-US could be used to refer only patients with a DI  $< 0.844$  g/cm<sup>2</sup> to further investigations at FLS.

**Disclosures:** Peter van den Berg, None.

## SU0222

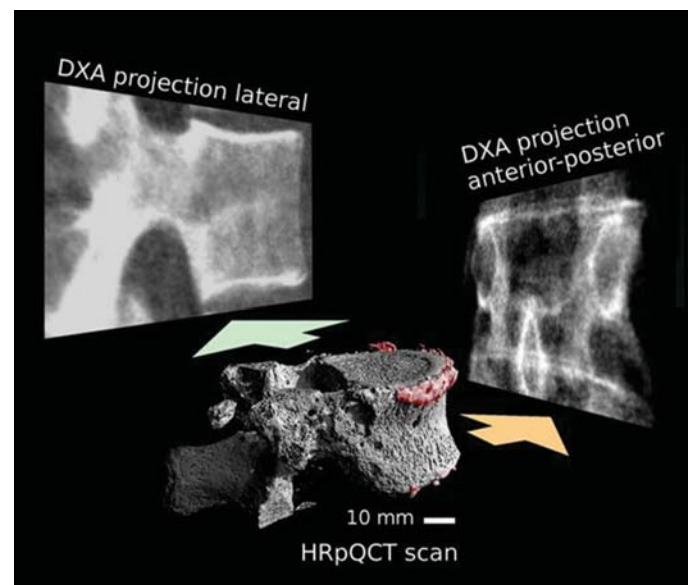
**Osteophyte-Induced Changes in Vertebral Microstructure in the Elderly Can Only Be Detected by DXA in Lateral but Not in Anterior-Posterior Projections.** Annika vom Scheidt\*, Carolin Pokrant<sup>1</sup>, Eric Flavio Grisolia Seifert<sup>1</sup>, Klaus Püschel<sup>2</sup>, Michael Amling<sup>1</sup>, Björn Busse<sup>1</sup>. <sup>1</sup>University Medical Center Hamburg-Eppendorf, Department of Osteology and Biomechanics, Germany, <sup>2</sup>University Medical Center Hamburg-Eppendorf, Department of Legal Medicine, Germany

Measurements of vertebral bone mineral density (BMD) can be obscured by large osteophytes, recognizable in low-resolution CT or 2D radiographs. However, to investigate if smaller osteophytes in early degenerative stages have similar influences on BMD, high-resolution CT and clinical evaluation of bone mineral density in young and aged patients is required. Our aim was to identify the effects of osteophytes on regional variations in bone volume and BMD.

We classified osteophytes in thoracic vertebrae of 22 women (ex vivo, Th12; 11 young:  $\bar{O} 32 \pm 6$  y; 11 aged:  $\bar{O} 72 \pm 5$  y) in three regions (superior, middle, inferior). We determined trabecular bone volume to tissue volume ratio (BV/TV) by high-resolution peripheral quantitative CT (resolution: 41  $\mu$ m) and bone mineral density (BMD) by dual energy x-ray absorptiometry in lateral and anterior-posterior (AP) projections, cf. Fig. 1. We normalized regional parameters to the whole vertebra average to limit the influence of inter-individual differences.

Whole vertebral BMD (lateral and AP) and BV/TV are significantly higher in young cases and osteophytes are less frequent (for all  $p \leq 0.001$ ). In young cases, BV/TV is significantly lower in the superior region compared to middle and inferior regions; BMD is also lower in superior than in inferior regions for both projections (for all  $p < 0.001$ ). Correlation between BV/TV and BMD is higher for the lateral projections and osteophytes show no influence on BV/TV or BMD in either projection in young cases. In sharp contrast, aged cases do not show a regional difference in trabecular BV/TV. In lateral projections, BMD is significantly lower in middle regions compared to superior and inferior regions ( $p = 0.001$ ), where most osteophytes are located. Thus, in aged cohorts lateral projections reveal a correlation between regional bone architecture and osteophyte presence, whereas regional osteophyte-related changes remain hidden in AP projections.

Bone mineral density from commonly used AP projections are less predictive of degenerative structural changes of the vertebrae. Our investigation shows that BMD in lateral projections represents trabecular bone volume most accurately in young cases, while the presence and influence of osteophytes is identifiable in aged cases. Clearly, since osteophytes are inversely correlated with vertebral fractures, information from lateral DXA projections are advantageous and of high relevance for diagnostics and vertebral fracture risk prediction.



Th12 vertebrae were scanned with HRpQCT (front, osteophytes: red) and DXA (left: lateral, right:AP)

**Disclosures:** Annika vom Scheidt, None.

## SU0223

**Comorbidities and medication use in patients with a recent clinical fracture at the Fracture Liaison Service.** Lisanne Vranken\*, Caroline E Wyers, Robert Y van der Velde, Irma J de Bruin, Heinrich M Janzing<sup>2</sup>, Sjoerd Kaarsemaker<sup>3</sup>, Piet P Geusens, Joop P van den Bergh. <sup>1</sup>Maastricht UMC+, NUTRIM, Department of Internal Medicine; VieCuri Medical Center, Department of Internal Medicine, Netherlands, <sup>2</sup>Department of Surgery and Trauma Surgery, VieCuri Medical Centre, Netherlands, <sup>3</sup>Department of Orthopedic Surgery and Trauma Surgery, VieCuri Medical Centre, Netherlands, <sup>4</sup>Maastricht UMC+, CAPHRI, Department of Internal Medicine subdivision of Rheumatology; University of Hasselt, Netherlands, <sup>5</sup>Maastricht UMC+, NUTRIM, Department of Internal Medicine; VieCuri Medical Center, Department of Internal Medicine; University of Hasselt, Netherlands

**Purpose:** To evaluate prevalence rates of comorbidities and medications associated with increased bone- and fall-related fracture (fx) risk in patients at the Fracture Liaison Service (FLS).

**Methods:** Cross-sectional cohort study of patients aged 50-90 yrs with a recent fx at the FLS. Comorbidities in medical history (MH) and laboratory tests (Lab) were categorized according to the ICD-10 and medications according to the ATC classification. Comorbidities and medications were further classified into those associated with a bone-related fx risk (BRR: bone-related comorbidity (BRC) and bone-related medication (BRM)) and fall-related fx risk (FRR: fall-related comorbidity (FRC) and fall-related medication (FRM)).



Results: Of 1282 patients (72% women; mean age 65±9 yrs), 66% had BRR or FRR (53% BRR (42% BRC (20% in MH and 30% in Lab), and 26% BRM), and 46% FRR (26% FRC, and 33% FRM)). The prevalence of at least one risk was similar for women and men, but increased significantly with decreasing BMD (normal 60% vs. osteopenia 66% vs. osteoporosis 70%,  $p=.039$ ), with increasing fx severity (minor 61% vs. major 71% vs. hip 79%,  $p<.001$ ), and with increasing age (50-59 yrs 55% up to 80+ yrs 81%,  $p<.001$ ). In multivariate analysis, age (OR (95% CI): 1.56 (1.18-3.18) per decade,  $p=.000$ ), major (1.43 (1.09-1.86),  $p=.000$ ), and hip fx (1.93 (1.18-3.18),  $p=.009$ ) remained associated with at least one BRR or FRR. The proportion of patients with only BRR ( $\pm 20\%$ ) and only FRR ( $\pm 10\%$ ) were similar among gender, BMD, fx type, and age subgroups. In contrast, the proportion of patients with a combination of BRR and FRR was similar for women and men, but increased significantly with decreasing BMD (normal 31% vs. osteopenia 30% vs. osteoporosis 40%,  $p=.002$ ), with increasing fx severity (minor 29% vs. major 40% vs. hip 41%,  $p<.001$ ) and increasing age (50-59 yrs 23% up to 80+ yrs 47%,  $p<.001$ ). These trends were observed for risks in MH only as well as in MH and Lab (Fig. 1). In multivariate analysis, age (OR (95% CI): 1.47 (1.30-1.68),  $p<.001$ ) and major fx (1.58 (1.21-2.04),  $p=.001$ ) remained associated with the combination of BRR and FRR.

Conclusion: Comorbidities and medications associated with increased BRR and FRR are common in all FLS patients and increase with age and fx severity, in particular the combination of BRR and FRR. Hence, systematic evaluation of comorbidities in MH and Lab and medications contributes to quantify the presence of bone- and fall-related risk factors.

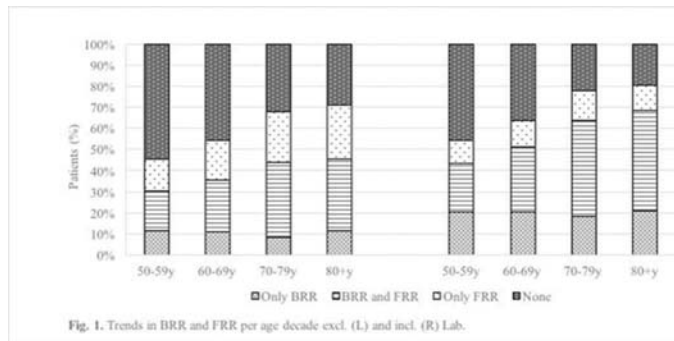


Figure 1: Trend in BRR and FRR per age decade excl. (L) and incl. (R) Lab

Disclosures: Lisanne Vranken, None.

## SU0224

**The Reproducibility of Measuring Trabecular Bone Parameters Using High-resolution Magnetic Resonance Imaging.** Sarah West<sup>\*1</sup>, Chamith Rajapakse<sup>2</sup>, Tammy Rayner<sup>3</sup>, Rhiannon Miller<sup>2</sup>, Michelle Slinger<sup>2</sup>, Greg Wells<sup>3</sup>. <sup>1</sup>Trent University, Canada, <sup>2</sup>University of Pennsylvania School of Medicine, United States, <sup>3</sup>SickKids Hospital, Canada

Bone loss is prevalent with aging, and non-invasive imaging is currently the best way to assess changes to bone. However, common imaging techniques such as high resolution peripheral quantitative computed tomography are associated with limitations. Magnetic resonance imaging (MRI) is a radiation-free imaging technique that can measure bone microarchitecture. However, published MRI bone assessment protocols often use specialized MRI coils and sequences and therefore have limited potential to be transferrable across institutions. We developed a protocol on a Siemens 3 Tesla MRI machine, using a commercially available coil (Siemens 15 CH knee coil), and manufacturer supplied sequences to acquire images at the tibia. We tested the reproducibility of the T1 TSE and the T2 FI3D Axial sequences and hypothesized that both would generate reproducible trabecular bone parameters. Eight healthy adults (age 25.5±5.4 years) completed three measurements of each MRI sequence at the tibia. Each of the images was processed for 8 different bone parameters (including volumetric bone volume fraction [BV/TV], trabecular thickness, trabecular number, average trabecular spacing, trabecular area, surface to curve ratio, erosion index, and stiffness). We computed the coefficient of variation (CV) and intraclass correlation coefficients (ICC) to assess reproducibility and reliability. Both the T1 TSE and the T2 FI3D sequences resulted in parameters that were reproducible (CV < 5% for most) and reliable (ICC > 80% for all). For example, BV/TV sequence 1 mean = 10.73%, CV = 3%, ICC = 0.88; sequence 2 mean = 15.53%, CV = 3.5%, ICC = 0.84. Our study is one of the first to report that a commercially available MRI protocol can result in reproducible data, and is significant as MRI may be an accessible method to measure bone microarchitecture in clinical or research environments. This requires further testing.

Disclosures: Sarah West, None.

## SU0225

**Prevalence of reduced renal function in the osteoporosis clinic and implications for the osteoporosis treatment gap - a study of 26,000 DXA referrals in a single-provider geographical area.** Bo Abrahamsen<sup>\*1</sup>, Daniel Prieto-Alhambra<sup>2</sup>, Martin T Ernst<sup>3</sup>, Mads Nybo<sup>4</sup>, Katrine H Rubin<sup>3</sup>, Pernille Hermann<sup>5</sup>.

<sup>1</sup>University of Southern Denmark and Holbæk Hospital, Denmark, <sup>2</sup>Centre for Statistics in Medicine and Nuffield Department of Orthopaedics, Rheumatology, and Musculoskeletal Sciences (NDORMS), University of Oxford, United Kingdom, <sup>3</sup>OPEN, Institute of Clinical Research, University of Southern Denmark, Denmark, <sup>4</sup>Dept of Clinical Biochemistry, Odense University Hospital, Denmark, <sup>5</sup>Dept of Endocrinology M, Odense University Hospital, Denmark

Introduction: Reduced renal function is a potential obstacle to treatment and could contribute to the treatment gap for osteoporosis. We therefore examined the demographics of renal function in DXA referrals and in patients newly diagnosed with osteoporosis.

Methods and study population: One clinical biochemistry service handles all samples (general practice and hospital) in one geographical area (pop 478,000) and provided eGFR estimates for the study. T-score was based on the first femoral neck BMD of all aged 40+ referred to routine clinical DXA 1999-2016 with current eGFR estimates. National data provided information on filled prescriptions for oral bisphosphonates (oBP). The distribution of renal function at presentation was examined for 1) DXA population, 2) femoral neck T-score <-2.5 and 3) patients who began oral bisphosphonates.

Results: Patients with CKD stage 3 (30-59 ml/min) accounted for 17% of patients with femoral neck T-score <-2.5 and 12.1% of those who began oBP treatment. The corresponding prevalence for CKD stage 4 (15-30 ml/min) was 1.5% and 0.6%.

Limitations: It is possible that less rigorous testing was done in persons whose BMD was normal and this could affect overall clinic prevalence, though routine blood tests are in the local clinical pathway and generally done ahead of exams. This is unlikely to affect estimates for those with osteoporosis and those beginning treatment.

Conclusions: Though moderate CKD (stage 3) is common (17%) among patients newly diagnosed with T<-2.5, the prevalence of severe (stage 4 or 5) CKD is very low (1.9% in osteoporosis, 0.6% if going on to oBP treatment). Though regular monitoring of eGFR levels during osteoporosis therapy will be required in a sizeable proportion of patients due to moderate CKD, only a small part of the treatment gap for osteoporosis can be justified by coexisting severe CKD.

eGFR ml/min	Osteoporosis clinic DXA referrals at presentation (N=26,354)	Osteoporosis clinic DXA population with femoral neck T-score <-2.5 at presentation (N=5,714)	oBP treated osteoporosis clinic population at presentation (N= 8,252 *)
>90	10,329 (39.2%)	1,647 (28.9%)	2,836 (34.4%)
60-89	13,102 (49.7%)	2,987 (52.3%)	4,359 (52.8%)
30-59	2,675 (10.2%)	973 (17.0%)	1,002 (12.1%)
15-29	195 (0.7%)	85 (1.5%)	52 (0.63%)
<15	53 (0.2%)	22 (0.4%)	3 (0.04%)

\*) Including low energy fracture indication or vertebral osteoporosis.

Table 1

Disclosures: Bo Abrahamsen, Novartis, Grant/Research Support.

## SU0226

**Oral bisphosphonate use and all-cause mortality in patients with advanced (stage IIIB+) chronic kidney disease: a population-based cohort study.** Dunia Alarkawi<sup>1</sup>, Sanni Ali<sup>2</sup>, Fergus Caskey<sup>3</sup>, Daniel Dedman<sup>4</sup>, Nigel Arden<sup>2</sup>, Yoav Ben-Shlomo<sup>5</sup>, Dana Bliuc<sup>6</sup>, Bo Abrahamsen<sup>7</sup>, Jacqueline Center<sup>6</sup>, Andrew Judge<sup>8</sup>, Cyrus Cooper<sup>9</sup>, Kassim Javaid<sup>9</sup>, Daniel Prieto-Alhambra<sup>10</sup>. <sup>1</sup>Bone Biology Division, Garvan Institute of Medical Research, University of New South Wales, Australia, <sup>2</sup>Centre for Statistics in Medicine and Nuffield Department of Orthopaedics, Rheumatology, and Musculoskeletal Sciences (NDORMS), University of Oxford, Oxford, UK, United Kingdom, <sup>3</sup>School of Social and Community Medicine, University of Bristol, Bristol, UK, <sup>4</sup>UK Renal Registry, Bristol, UK, United Kingdom, <sup>5</sup>Clinical Practice Research Datalink, MHR, London, UK, United Kingdom, <sup>6</sup>School of Social and Community Medicine, University of Bristol, Bristol, UK, United Kingdom, <sup>7</sup>Bone Biology Division, Garvan Institute of Medical Research, University of New South Wales, Sydney, Australia, Australia, <sup>8</sup>University of Southern Denmark, Odense, Denmark, Holbæk Hospital, Dept of Medicine, Holbæk, Denmark, Denmark, <sup>9</sup>Centre for Statistics in Medicine and Nuffield Department of Orthopaedics, Rheumatology, and Musculoskeletal Sciences (NDORMS), University of Oxford, Oxford, UK, MRC Lifecourse Epidemiology Unit, Southampton, UK, United Kingdom, <sup>10</sup>Centre for Statistics in Medicine and Nuffield Department of Orthopaedics, Rheumatology, and Musculoskeletal Sciences (NDORMS), University of Oxford, United Kingdom

**BACKGROUND** The risks and benefits of oral bisphosphonates (oBP) are unclear in patients with severe chronic kidney disease (CKD), and they are formally contraindicated in those with stage IV CKD. **OBJECTIVES** To study the association between oBP use and all-cause mortality in stage IIIB+ CKD. **METHODS** Design Cohort study including all subjects with an eGFR <45 at age 40 years or older, with 1+ years run-in data available. Previous and current users of anti-osteoporosis drugs other than oBP were excluded. **Setting** UK Primary Care computerised records in the Clinical Practice Research Datalink linked to Office for National Statistics (ONS) mortality data. **Exposure** GP prescriptions of oBP were identified using BNF codes. oBP use was modelled as a time-varying exposure to avoid immortal time bias. Treatment episodes (in BP users) were created by concatenating prescriptions until patients switched or stopped therapy (refill gap in prescriptions of 180+ days), or were censored (end of study or transfer out). A washout of 180 days was added to date of last prescription. **STATISTICAL ANALYSES** Cox regression models were fitted to estimate Hazard Ratios (HR) and 95% Confidence Intervals (95CI) for death according to oBP use. Multivariable models were adjusted for a priori defined confounders including age, gender, baseline eGFR, socio-economic status, co-morbidities (including Charlson Index), previous fracture, concomitant medications, and hospital admissions in the previous year. Interactions with gender, previous fracture and CKD stage were tested for using multiplicative terms. **RESULTS** Of 18,904 oBP users and 190,850 non-users, 4,581 (24%) and 85,178 (45%) deaths were recorded over 38,252 and 842,985 person-years of follow-up respectively. Multivariable adjusted HR for all-cause mortality in BP users was 0.85 (95CI 0.82-0.88). There were significant interactions ( $P < 0.0001$ ) between BP use and gender, history of previous fracture and CKD stage: HRs were 0.82 (95CI 0.79-0.85) in females and 0.96 (95CI 0.90-1.01) in males; 0.78 (95CI 0.73-0.83) in those with and 0.90 (95CI 0.87-0.93) in those without a previous fracture; and 0.88 (95CI 0.85-0.91) in CKD stage IIIB, compared to 0.71 (95CI 0.65-0.79) in CKD stage IV+. **CONCLUSION** BP use is associated with 15% reduced mortality amongst patients with severe (stage IIIB+) CKD, particularly in women, in secondary prevention, and in those with stage IV+ CKD. More data is needed on the risks and benefits of oBP in CKD patients.

**Disclosures:** Dunia Alarkawi, None.

## SU0227

**Fracture Incidence and Characteristics in Young Adults Age 18 to 49 years: A Population-Based Study.** Joshua Farr\*, L. Joseph Melton III, Sara Achenbach, Elizabeth Atkinson, Sundeep Khosla, Shreyasee Amin. Mayo Clinic, United States

While fractures in both the elderly and pediatric populations have been extensively investigated, comparatively little attention has been given to the age-group in between. Thus, we determined incidence rates for all fractures among young adult (age range, 18 to 49 years) residents of Olmsted County, Minnesota, USA, in 2009-11, and compared the distribution of fracture sites and causes in this young adult cohort with those for residents  $\geq 50$  years old.

Using the unique medical records linkage system of the Rochester Epidemiology Project, we identified all fractures that occurred among young adult Olmsted County residents during the 3-year period. Complete (inpatient and outpatient) community

medical records were reviewed by trained nurse abstractors to validate all fractures identified and to determine their antecedent cause (pathological process [e.g., metastatic malignancy], severe trauma [e.g., motor vehicle accidents, falls from greater than standing height] and those due to no more than moderate trauma [by convention, equivalent to a fall from standing height or less]). Comparable results that we previously reported in older residents (JBMR 29(3):581-589, 2014) were used for comparisons.

During 2009-2011, 2,482 Olmsted County residents age 18-49 years experienced one or more fractures. There were 1,730 fractures among 1,447 men compared to 1,164 among 1,035 women, and the age-adjusted incidence of all fractures was 66% greater among the men (1,882 vs. 1,135 per 100,000 person-years;  $p < 0.001$ ). Of all fractures, 80% resulted from severe trauma compared to 33% in Olmsted County residents age  $\geq 50$  years who sustained a fracture in 2009-11. Younger residents had a greater proportion of fractures than older residents of the hands and feet (40% vs. 18%) with relatively few fractures observed at traditional osteoporotic fracture sites (wrist, shoulder, spine or hip) (14% vs. 43%). Vertebral fractures were still more likely to be due to moderate trauma than at other sites in younger residents, especially in women (57% vs. 32% in men, 26% vs. 72% in women, for severe vs. moderate trauma vertebral fractures, respectively).

In conclusion, whereas elderly populations often fracture from no more than moderate trauma, young adults, and more commonly men, suffer fractures primarily at non-osteoporotic sites due to more significant trauma. The main exception is vertebral fractures in young women, which are still more likely to be secondary to moderate trauma.

**Disclosures:** Joshua Farr, None.

## SU0228

**Glycemic traits are related to phosphate metabolism: A double-edged sword.** Ching-Lung Cheung\*, Vincent Cheng, Victoria Wong, Grace Lee, Bernard Cheung. The University of Hong Kong, Hong Kong

Emerging evidence demonstrates that alteration in mineral metabolism is a risk factor of cardiometabolic diseases, in addition to its well-known role in bone metabolism, whereas phosphate is a biomarker implicating in cardiometabolic diseases. Randomized trials showed that colestilan, a phosphate binder and bile acid sequestrant, reduced glycated hemoglobin and LDL-cholesterol. However, the relationship and underlying mechanism between serum phosphate, glycemic control, and lipids, especially in people without diabetes and chronic kidney disease, remains unknown. We therefore evaluated the relationship of serum phosphate with glycated hemoglobin (HbA1c) and LDL-cholesterol in the the National Health and Nutrition Examination Survey III (NHANES III) and the Hong Kong Osteoporosis Study (HKOS).

We used data from 4,369 participants from the NHANES III and 284 participants from the HKOS. We studied the relationship of serum phosphate with HbA1c, fasting glucose, and LDL-cholesterol using multivariable linear regression with adjustment for age, sex, body mass index, blood pressure, serum calcium, triglycerides, eGFR, physical activity, and smoking and drinking status. Untargeted metabolomic profiling was performed to evaluate if metabolite plays a role in the relationship.

Serum phosphate was significantly associated with increased HbA1c levels in both cohorts and reduced fasting glucose levels in the NHANES III. No significant association with LDL-cholesterol was observed. A significant interaction was observed between phosphate and fasting glucose on HbA1c (Interaction term  $P = 0.003$ ). The beta estimate between fasting glucose (natural-log unit) and HbA1c (natural-log unit) increased from 0.151 in the lowest quartile of phosphate levels to 0.227 in the highest quartile of phosphate levels. Seven metabolites were found to be significantly associated with phosphate and HbA1c, with propionylcarnitine and carnitine being the most associated metabolites.

In conclusion, serum phosphate is associated with reduced fasting glucose but increased HbA1c. Inorganic phosphate is known to accelerate HbA1c synthesis through decreasing labile HbA1c dissociation and increasing Amadori rearrangement for stable HbA1c, which may explain the observation. In addition, several metabolites and metabolic pathways may be involved in the relationship between phosphate and HbA1c. Further study is required to confirm the findings.

**Disclosures:** Ching-Lung Cheung, None.



## SU0229

**Screening Young Postmenopausal Women for Osteoporosis: Comparison of Hip Fracture Risk Prediction by the Garvan and FRAX Risk Calculators in the Women's Health Initiative Observational Study and Clinical Trials.** Carolyn Crandall<sup>1</sup>, Joseph Larson<sup>2</sup>, Andrea LaCroix<sup>3</sup>, Jane Cauley<sup>4</sup>, Meryl LeBoff<sup>5</sup>, Wenjun Li<sup>6</sup>, Erin LeBlanc<sup>7</sup>, Beatrice Edwards<sup>8</sup>, JoAnn Manson<sup>5</sup>, Kris Ensrud<sup>9</sup>. <sup>1</sup>University of California, Los Angeles, United States, <sup>2</sup>Fred Hutchinson Cancer Research Center, United States, <sup>3</sup>University of California, San Diego, United States, <sup>4</sup>University of Pittsburgh, United States, <sup>5</sup>Harvard Medical School, United States, <sup>6</sup>University of Massachusetts Medical School, United States, <sup>7</sup>Kaiser Permanente Center for Health Research, United States, <sup>8</sup>The University of Texas MD Anderson Cancer Center, United States, <sup>9</sup>University of Minnesota Medical School, United States

**Background:** The optimal method of hip fracture risk assessment for young postmenopausal women is unknown.

**Objective:** To determine sensitivity, specificity, and area under the receiver operating characteristic curve (AUC) of the Fracture Risk Assessment Tool (FRAX®) and Garvan Fracture Risk Calculator for predicting hip fracture in postmenopausal women aged 50-64 years.

**Design:** Prospective observational study

**Setting:** Women's Health Initiative Observational Study and Clinical Trials at 40 U.S. clinical centers

**Participants:** 63,621 postmenopausal women aged 50 to 64 years

**Exposures:** FRAX- and Garvan-predicted 10-year risk of hip fracture

**Main Outcome and Measure:** Incident (observed) hip fracture during 10-year follow-up

**Results:** Observed 10-year hip fracture probability was 0.3% for women aged 50-54 yrs (n = 14768), 0.6% for women aged 55-59 yrs (n = 22442), and 1.1% for women aged 60-64 yrs (n = 25513). At sensitivity thresholds of  $\geq 80\%$ , the specificity of both tools for detecting incident hip fracture during 10 years of follow-up was low: Garvan 30.6% (95% confidence interval [CI] 30.3%-31.0%); FRAX 43.1% (95% CI 42.7%-43.5%). At maximal AUC values (0.58 for Garvan, 0.65 for FRAX), sensitivity was 16.0% (95% CI 12.7%-19.4%) for Garvan and 59.2% (95% CI 54.7%-63.7%) for FRAX. At maximal AUC values, sensitivity was lower in African American (Garvan 7.7%, 95% CI 0.0%-24.5%; FRAX 0%, 95% CI 0.0%-0.0%) and Hispanic (Garvan 12.5%, 95% CI 0.0%-42.1%; FRAX 0%, 95% CI 0.0%-0.0%) women than among white women (Garvan 16.2%, 95% CI 12.8%-19.7%; FRAX 62.2%, 95% CI 57.7%-66.8%), and lower in women aged 50-54 (Garvan 0.0%, 95% CI 0.0%-0.0%; FRAX 10.4%, 95% CI 1.5%-19.4%) than in women 60-64 years-old (Garvan 24.2%, 95% CI 19.1%-29.3%; FRAX 80.5%, 95% CI 75.8%-85.2%). Observed fracture probabilities were similar to FRAX-predicted probabilities but greater than Garvan-predicted probabilities.

**Conclusions and Relevance.** In postmenopausal women aged 50-64 years, the FRAX® and Garvan fracture risk calculators discriminate poorly between women who do and do not experience hip fracture during 10 years of follow-up. There is no useful threshold for either tool.

The WHI program is funded by the National Heart, Lung, and Blood Institute, National Institutes of Health, U.S. Department of Health and Human Services through contracts HHSN268201600018C, HHSN268201600001C, HHSN268201600002C, HHSN268201600003C, and HHSN268201600004C.

	Sensitivity (95% CI)	Specificity (95% CI)	AUC
<b>All participants (n=63621)</b>			
Garvan $\geq 0.462$	16.0 (12.7-19.4)	93.5 (93.3-93.7)	0.58 (0.55-0.60)
FRAX $\geq 0.706$	59.2 (54.7-63.7)	67.6 (67.2-67.9)	0.65 (0.62-0.67)
<b>Age</b>			
50-54 (n=14768)			
Garvan $\geq 0.462$	0.0 (0.0-0.0)	99.7 (99.7-99.8)	0.54 (0.49-0.60)
FRAX $\geq 0.706$	10.4 (1.5-19.4)	98.1 (97.9-98.3)	0.58 (0.52-0.65)
55-59 (n=22442)			
Garvan $\geq 0.462$	5.6 (1.8-9.4)	96.9 (96.7-97.1)	0.56 (0.52-0.60)
FRAX $\geq 0.706$	34.3 (26.4-42.1)	81.2 (80.7-81.7)	0.61 (0.56-0.65)
60-64 (n=25513)			
Garvan $\geq 0.462$	24.2 (19.1-29.3)	86.9 (86.5-87.3)	0.60 (0.57-0.63)
FRAX $\geq 0.706$	80.5 (75.8-85.2)	37.7 (37.1-38.3)	0.62 (0.59-0.65)
<b>HT Uses</b>			
No (n=27617)			
Garvan $\geq 0.462$	13.2 (8.8-17.7)	93.4 (93.1-93.7)	0.55 (0.52-0.58)
FRAX $\geq 0.706$	57.3 (50.8-63.8)	67.7 (67.1-68.2)	0.63 (0.60-0.67)
Yes (n=35065)			
Garvan $\geq 0.462$	18.7 (13.7-23.6)	93.6 (93.3-93.8)	0.60 (0.57-0.63)
FRAX $\geq 0.706$	61.0 (54.8-67.2)	67.5 (67.0-68.0)	0.66 (0.63-0.70)
<b>Years of HT Use</b>			
0 Years (n=12250)			
Garvan $\geq 0.462$	16.5 (8.7-24.3)	92.7 (92.3-93.2)	0.57 (0.53-0.62)
FRAX $\geq 0.706$	57.1 (46.8-67.5)	64.0 (63.2-64.9)	0.63 (0.57-0.68)
5+ Years (n=18762)			
Garvan $\geq 0.462$	21.8 (13.0-30.7)	93.1 (92.8-93.5)	0.61 (0.57-0.66)
FRAX $\geq 0.706$	64.4 (54.1-74.6)	65.8 (65.2-66.5)	0.67 (0.62-0.72)
<b>Race/Ethnicity</b>			
White (n=52536)			
Garvan $\geq 0.462$	16.2 (12.8-19.7)	93.2 (93.0-93.5)	0.57 (0.55-0.60)
FRAX $\geq 0.706$	62.2 (57.7-66.8)	62.9 (62.5-63.3)	0.64 (0.61-0.66)
African American (n=5475)			
Garvan $\geq 0.462$	7.7 (0.0-24.5)	97.5 (97.0-97.9)	0.61 (0.48-0.74)
FRAX $\geq 0.706$	0.0 (0.0-0.0)	96.4 (95.9-96.9)	0.63 (0.51-0.75)
Hispanic (n=2262)			
Garvan $\geq 0.462$	12.5 (0.0-42.1)	94.5 (93.5-95.4)	0.71 (0.58-0.83)
FRAX $\geq 0.706$	0.0 (0.0-0.0)	92.8 (91.7-93.8)	0.71 (0.61-0.81)
Other/Unknown: (n=2450)			
Garvan $\geq 0.462$	20.0 (0.0-50.2)	89.4 (88.2-90.6)	0.67 (0.56-0.78)
FRAX $\geq 0.706$	50.0 (12.3-87.7)	78.8 (77.1-80.4)	0.74 (0.62-0.86)

<sup>1</sup> Menopausal hormone therapy (HT) Status over the interval has varying definitions depending on whether the participant was enrolled in the Women's Health Initiative Observational Study (OS) or the HT Clinical Trials (CT): OS, Non-HT, CT Participants: Status determined by baseline current HT use (yes/no)

HT participants: Status determined by HT intervention arm (active/placebo)

<sup>2</sup> OS Participants: Participants who contributed data for at least 6 of the 8 possible years of self-report covered by WHI were divided into subgroups. Participants who reported  $\geq 50\%$  of study period using HT were included in the 5+ Years HT Use category. If the participant reported 0% of her time on HT, she was put into the No HT Use group

HT Participants: Active arm participants who were on intervention for 5+ years were put into the 5+ Years HT Use category. Placebo arm participants who were on placebo for 5+ years and then reported not starting hormones on their post-intervention form were put into the No HT Use group

Non-HT, CT participants: Not included in analysis.

<sup>3</sup> Other/Unknown category includes American Indian, Asian, and Unknown Race/Ethnicity participants

Table

**Disclosures:** Carolyn Crandall, None.

## SU0230

**Reasons for Stopping Osteoporosis Medications among Women with Previous Fractures.** Maria Danila<sup>1</sup>, Elizabeth Rahn<sup>1</sup>, Amy Mudano<sup>1</sup>, Ryan Outman<sup>1</sup>, Peng Li<sup>1</sup>, David Redden<sup>1</sup>, Fred Anderson<sup>2</sup>, Susan Greenspan<sup>3</sup>, Andrea LaCroix<sup>4</sup>, Jeri Nieves<sup>5</sup>, Stuart Silverman<sup>6</sup>, Ethel Siris<sup>7</sup>, Nelson Watts<sup>8</sup>, Sigrid Ladores<sup>1</sup>, Karen Meneses<sup>1</sup>, Jeffrey Curtis<sup>1</sup>, Kenneth Saag<sup>1</sup>.

<sup>1</sup>University of Alabama at Birmingham, United States, <sup>2</sup>University of Massachusetts Medical School, United States, <sup>3</sup>University of Pittsburgh, United States, <sup>4</sup>University of California, San Diego, United States, <sup>5</sup>Helen Hayes Hospital, United States, <sup>6</sup>Cedars-Sinai Medical Center, United States, <sup>7</sup>Columbia University Medical Center, United States, <sup>8</sup>Mercy Health Osteoporosis and Bone Health Services, United States

**Purpose:** High-consequence, albeit rare, adverse side effects of osteoporosis medication raise patients' risk perceptions and contribute to non-adherence. In the past decade, fears of osteonecrosis of the jaw (ONJ) and atypical femoral fractures (AFF) have been increasingly reported as barriers to both the initiation of and adherence to osteoporosis medications. We examined the temporal prevalence of self-reported concern about ONJ and AFF as reason for discontinuation of osteoporosis medication.

**Methods:** Activating Patients at Risk for Osteoporosis (APROPOS) enrolled US women from the Global Longitudinal Study of Osteoporosis (GLOW) with past self-reported fractures who were not currently using osteoporosis medication. Using mailed surveys in 2010 (T1), 2012 (T2) and 2013 (T3), women were asked whether they discontinued osteoporosis medication in the prior year because of concerns about ONJ at three time points (T1, T2, T3) and AFF at two time points (T2, T3). We calculated the proportion of women reporting fears of ONJ and AFF among those who discontinued their osteoporosis medication, and compared the proportions using chi-square tests.

**Results:** A total of 833 women discontinued osteoporosis treatment at three time points, T1 (N = 255), T2 (N = 471), and T3 (N = 107), respectively. The proportion of women reporting concerns of ONJ was 18.4% (T1), 26.7% (T2) and 64.5% (T3), while 23.5% (T2) and 60.7% (T3) reported fear of AFF as reason to discontinue osteoporosis treatment. These differences were statistically significant (p<0.0001) for all comparisons.

Conclusion: The proportion of women who reported concerns of ONJ and AFF increased over time among those women who discontinue osteoporosis medications. Strategies are needed to help patients balance risks and benefits given a significant and temporally growing concern of rare bisphosphonate side effects.

**Disclosures:** Maria Danila, None.

## SU0231

**Associations of Cognitive Dietary Restraint with Changes in Body Mass Index and Bone Mineral Density: A Population-based Cohort Study of Premenopausal Women and Men Aged 25-49 Years from CaMos.** Jenna C. Gibbs<sup>\*1</sup>, Lora M. Giangregorio<sup>1</sup>, Jerilynn Prior<sup>2</sup>, Susan I. Barr<sup>2</sup>, Claudie Berger<sup>3</sup>, Maryam S. Hamidi<sup>4</sup>, Jonathan D. Adachi<sup>5</sup>, K. Shawn Davison<sup>6</sup>, David Goltzman<sup>7</sup>, Robert G. Josse<sup>8</sup>, Stephanie M. Kaiser<sup>9</sup>, Christopher S. Kovacs<sup>10</sup>, William D. Leslie<sup>11</sup>, Suzanne N. Morin<sup>7</sup>, Alexandra Papaioannou<sup>5</sup>, Angela M. Cheung<sup>12</sup>. <sup>1</sup>University of Waterloo, Canada, <sup>2</sup>University of British Columbia, Canada, <sup>3</sup>McGill University Health Centre Research Institute, Canada, <sup>4</sup>Stanford University, United States, <sup>5</sup>McMaster University, Canada, <sup>6</sup>a priori medical science inc., Canada, <sup>7</sup>McGill University, Canada, <sup>8</sup>St. Michael's Hospital, Canada, <sup>9</sup>Dalhousie University, Canada, <sup>10</sup>Memorial University, Canada, <sup>11</sup>University of Manitoba, Canada, <sup>12</sup>University Health Network and University of Toronto, Canada

Cognitive dietary restraint (CDR) has been shown to contribute to weight change and lower bone mineral density (BMD). However, prior cross-sectional results are conflicting and few prospective studies have assessed CDR as a behavioral determinant of changes in body mass index (BMI) and BMD.

Purpose: The purpose of this study was to determine the associations between CDR and 10-year changes in BMI and BMD in premenopausal women and in men aged 25-49 years from the population-based prospective Canadian Multicentre Osteoporosis Study (CaMos).

Methods: CDR was assessed using three items from the 21-item CDR subscale of the Three Factor Eating Questionnaire at baseline (1995-1997). Height, weight, and total hip and lumbar spine (L1-L4) BMD were measured at baseline and year 10 (2005-2007). Socio-demographics, lifestyle behaviors, and health outcomes were determined from an interviewer-administered questionnaire at baseline. Multivariable linear regression models assessed the adjusted associations between CDR, BMI, and BMD stratified by sex, both cross-sectionally and longitudinally. Baseline BMI and BMD were included in all longitudinal analyses. Confounding variables included age, centre, employment status, smoking history, alcohol exposure, regular physical activity, history of weight loss >10 lb, prior fracture, caffeine intake, calcium intake, vitamin D intake, parental diagnosis of osteoporosis, estrogen use, age at menarche, and menopausal status, as relevant.

Results: The study included 697 men and 784 women (mean±SD age 40±7 years, BMI 26±5 kg/m<sup>2</sup>). Baseline CDR was associated with higher baseline BMI in women (estimate of 0.467 kg/m<sup>2</sup>, 95% CI: 0.159, 0.775) and in men (estimate of 0.692 kg/m<sup>2</sup>, 95% CI: 0.404, 0.979). However, CDR was not associated with lumbar spine BMD and total hip BMD in either sex at baseline. Baseline CDR was associated with a small increase in total hip BMD of 0.007 g/cm<sup>2</sup> (95% CI: 0.002, 0.011) in men, but not in women. Baseline CDR was not associated with changes in BMI or lumbar spine BMD in either sex (Table 1).

Conclusions: Our findings demonstrate non-significant or minor associations between CDR and 10-year changes in BMI and BMD in premenopausal women and men aged 25-49 years after adjusting for relevant confounding variables. Further examination of this data will determine whether higher CDR is associated with weight loss or weight cycling patterns, which may lead to bone loss over time.

**Table 1.** Longitudinal associations between baseline cognitive dietary restraint (CDR) and changes in body mass index (BMI) and bone mineral density (BMD) from baseline (1995-1997) to Year 10 (2005-2007) in premenopausal women and men aged 25-49 years from the Canadian Multicentre Osteoporosis Study (CaMos).

Exposure	Outcome	Adjusted Estimate (95% CI)
<i>Men</i>		
CDR	10-year change in BMI	-0.015 (-0.238, 0.208) <sup>a</sup>
	10-year change in total hip BMD	<b>0.007 (0.002, 0.011)<sup>b</sup></b>
	10-year change in L1-L4 BMD	0.004 (-0.002, 0.009) <sup>b</sup>
<i>Women</i>		
CDR	10-year change in BMI	0.024 (-0.167, 0.214) <sup>a</sup>
	10-year change in total hip BMD	0.001 (-0.004, 0.005) <sup>b</sup>
	10-year change in L1-L4 BMD	-0.002 (-0.008, 0.003) <sup>b</sup>

Note: Associations with 95% CI excluding the null effect are shown in bold.

<sup>a</sup> = Age, baseline BMI, employment status, centre, history of weight loss >10 lb, smoking history, regular physical activity, alcohol exposure, caffeine intake, estrogen use (women only), age at menarche (women only), menopausal status (women only).

<sup>b</sup> = Age, baseline BMI, 10-year change in BMI, baseline BMD, employment status, centre, prior fracture, parental diagnosis of osteoporosis, history of weight loss >10 lb, smoking history, regular physical activity, calcium intake, vitamin D intake, alcohol exposure, caffeine intake, estrogen use (women only), age at menarche (women only), menopausal status (women only).

Table 1

**Disclosures:** Jenna C. Gibbs, None.

## SU0232

**Temporal Trends in Length of Stay after Hip, Femur and Pelvic Fracture in Québec, Canada.** Sonia Jean<sup>\*1</sup>, Edward Harvey<sup>2</sup>, Etienne Belzile<sup>3</sup>, Jacques Brown<sup>3</sup>, Suzanne Morin<sup>2</sup>. <sup>1</sup>Institut national de santé publique du Québec, Canada, <sup>2</sup>McGill University, Canada, <sup>3</sup>Laval University, Canada

Purpose: The aim of this study consists to analyze temporal trends over 22 years in hospital length of stay (LOS) after hip, femur and pelvic fracture. We also investigated factors predicting LOS.

Methods: Using the hospital discharge database of the province of Québec, Canada, we performed a retrospective cohort study of individual aged 45 years and older who sustained an incident hip, femur or pelvic fracture between 1991 and 2014. Multiple hospital records with the same patient identifier (i.e. consecutive hospital stay with an admission date within +/- 1 day of the previous hospital stay) were combined into one single episode of care. Total hospital LOS was considered as the number of days from the first admission date to the discharge date of the last hospital admission. Competing Risk Analysis was used to assess the probability to be discharged (POD) within 30 days of first admission date.

Results: Over 22 years, 127,312 hip (73% women), 19,814 pelvic (72% women) and 10,090 femur (70% women) fractures were identified. For each fracture site, the mean hospital LOS significantly decreased over the study period. Compared to 1991-1995 period, the POD within 30 days of first admission date were significantly higher in 2011-2013 period (Table 1). Following a femur fracture, men had higher POD within 30 days of first admission date than women (aHR 1.12 [1.05-1.20]). Contrariwise, following a hip fracture, men had lower POD within 30 days of first admission date than women (aHR 0.94 [0.92-0.96]). Increasing age, having unfavorable material and social deprivation index and increasing number of comorbidities were all associated with lower POD within 30 days after hip, femur and pelvic fractures. Pelvic and femur fragility fractures (low intensity trauma) had higher POD within 30 days of first admission date than traumatic fractures; this relationship was reverse following a hip fracture. Patients with long term care residence (vs community dwelling) and those receiving care in a trauma center (vs those in non-trauma center) had higher POD within 30 days of first admission date.

Conclusion: In Québec, hospital LOS after hip, femur and pelvic fracture decreased substantially over the last quarter of century. This may suggest changes in access policy or bed management. Several factors affect LOS. These informations are useful for the implementation and evaluation of strategies to improve health care delivery.



Periods	Hospital Length of Stay					
	Pelvic		Femur		Hip	
	Mean (SD)	Risk ratio* [95% CI]	Mean (SD)	Risk ratio* [95% CI]	Mean (SD)	Risk ratio* [95% CI]
1991-1995	34.9 (41.3)	1.00 (ref)	49.2 (57.9)	1.00 (ref)	43.9 (83.0)	1.00 (ref)
1996-2000	28.0 (26.0)	1.43 [1.34-1.53]	34.0 (38.1)	1.44 [1.31-1.59]	30.5 (40.7)	1.42 [1.38-1.46]
2001-2005	27.5 (26.8)	1.64 [1.53-1.75]	32.3 (36.7)	1.75 [1.59-1.93]	29.0 (30.0)	1.85 [1.80-1.90]
2006-2010	25.8 (26.6)	1.96 [1.84-2.09]	28.8 (37.2)	2.19 [1.99-2.41]	27.1 (29.6)	2.29 [2.23-2.36]
2011-2013	23.4 (23.9)	2.34 [2.18-2.51]	27.1 (33.3)	2.47 [2.23-2.75]	25.6 (28.7)	2.51 [2.43-2.60]

\* adjusted for age, sex, material and social deprivation index, prior living arrangement, comorbidities, type of establishment, type of fracture, circumstance of fracture and surgical delay

Table: Hospital Length of stay related to hip, pelvic and femur fracture by periods

Disclosures: *Sonia Jean, None.*

## SU0233

**Testing an Evidence-based Theoretical Model of Imminent (1-year) Fracture Risk in Elderly Women: Results from the Canadian Multicentre Osteoporosis Study (CaMOS).** James S. McGinley<sup>\*1</sup>, George Ioannidis<sup>2</sup>, Christopher S. Kovacs<sup>3</sup>, Stephanie M. Kaiser<sup>4</sup>, David A. Hanley<sup>5</sup>, Jerilynn C. Prior<sup>6</sup>, K. Shawn Davison<sup>7</sup>, William D. Leslie<sup>8</sup>, Suzanne N. Morin<sup>9</sup>, Yawen Jiang<sup>10</sup>.

<sup>1</sup>Vector Psychometric Group, LLC, United States, <sup>2</sup>McMaster University, Canada, <sup>3</sup>Memorial University of Newfoundland, Canada, <sup>4</sup>Dalhousie University, Canada, <sup>5</sup>University of Calgary, Canada, <sup>6</sup>University of British Columbia, Canada, <sup>7</sup>A Priori Medical Sciences Inc., Canada, <sup>8</sup>University of Manitoba, Canada, <sup>9</sup>McGill University, Canada, <sup>10</sup>Amgen Inc., United States

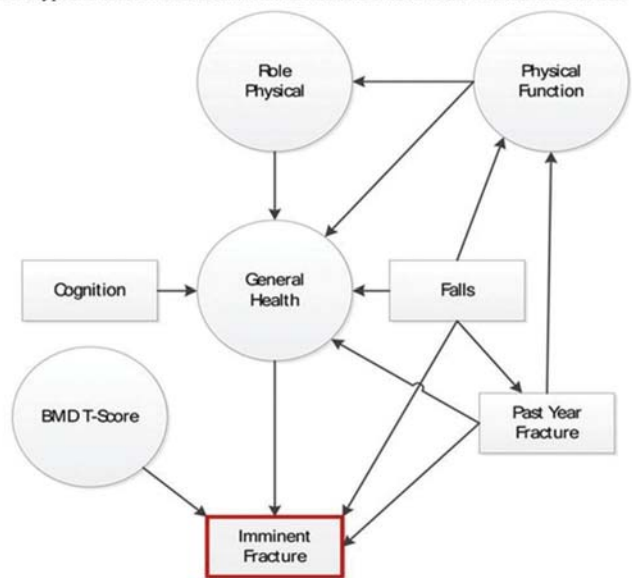
**Purpose:** This study builds on the existing literature by evaluating a theoretical model for imminent fracture risk using multiple years of data from the Canadian Multicentre Osteoporosis Study (CaMOS). The model examined both direct and indirect effects of several predictors on having one or more fractures in the immediate year after assessment (Figure).

**Methods:** Data from women age 65 and older from CaMOS were used for the current study. Study predictors were identified from study Years 5 and 10, and next year fracture data (imminent or 1-year fracture) came from Years 6 and 11 (Year 5 predicts Year 6, Year 10 predicts Year 11). A structural equation model (SEM) was used to test the theoretical model (Figure). General health, physical functioning, and role functioning physical were measured as latent variables using items from the SF-36 and areal bone mineral density (BMD) T-score was a latent variable based on observed site-specific BMD data (spine L1-L4, femoral neck, total hip). Observed variables were past year fractures (yes/no) and falls (yes/no), and cognition (Mark II: 1="unable to learn/remember" to 4="Learns/remembers normally"). Model fit was evaluated using Root Mean Square Error of Approximation (RMSEA), Tucker Lewis Index (TLI) and Comparative Fit Index (CFI).

**Results:** Analysis included 3,295 women, mean age (SD) of 74.7 (6.2) at Year 5, of which 58.3% (n=1,922) contributed two observations. Model fit tests showed that the SEM fit the data well;  $\chi^2(281) = 2349.12$ , RMSEA=.04, TLI=.98, CFI=.99. Results suggested that increased imminent fracture risk was directly predicted by having a prior year fracture, lower general health, and lower T-score ( $p < .001$ ). Falling did not have a significant direct effect on imminent fracture ( $p = .07$ ), but did have significant mediated effects on fracture through physical functioning, role functioning, and general health ( $p < .001$ ). Physical functioning, role functioning, and cognition indirectly predicted next year fractures, with better functioning predicting decreased fracture risk ( $p < .001$ ).

**Conclusions:** Our findings provide support for this model of imminent fracture risk. We have shown that SEM can test complex interrelations among multiple fracture risk factors. We found several direct and indirect pathways that predicted having an imminent fracture. Future studies should extend this work by examining other potentially important predictors and differences among fracture sites.

Figure. Hypothesized model of imminent fracture risk in older women in CaMOS



Figure

Disclosures: *James S. McGinley, Vector Psychometric Group, LLC., Other Financial or Material Support.*

## SU0234

**Risk of Hip Fracture After Recent Fracture – Comparison of Sentinel Fracture Sites (Reykjavik Study).** Helena Johansson<sup>\*1</sup>, Kristín Siggeirsdóttir<sup>2</sup>, Nicholas C Harvey<sup>3</sup>, Anders Odén<sup>4</sup>, Vilundur Gudnason<sup>5</sup>, Eugene McCloskey<sup>6</sup>, Gunnar Sigurdsson<sup>7</sup>, John A Kanis<sup>7</sup>. <sup>1</sup>Institute for Health and Aging, Australian Catholic University, Melbourne, Australia, Sweden, <sup>2</sup>Icelandic Heart Association, Kopavogur, Iceland, Iceland, <sup>3</sup>MRC Lifecourse Epidemiology Unit, University of Southampton, Southampton, UK, NIHR Southampton Biomedical Research Centre, University of Southampton and University, United Kingdom, <sup>4</sup>Centre for Metabolic Bone Diseases, University of Sheffield, Sheffield, UK, Sweden, <sup>5</sup>Icelandic Heart Association, Kopavogur, Iceland, University of Iceland, Reykjavik, Iceland, Iceland, <sup>6</sup>Centre for Metabolic Bone Diseases, University of Sheffield, Sheffield, UK, Centre for Integrated research in Musculoskeletal Ageing, Mellanby Centre for Bone Research, University of Sheffield, Sheffield UK, United Kingdom, <sup>7</sup>Institute for Health and Aging, Australian Catholic University, Melbourne, Australia, Centre for Metabolic Bone Diseases, University of Sheffield, Sheffield, UK, United Kingdom

**Purpose:** A history of fracture is a strong and well known risk factor for future fractures. The aim of the present study was to investigate whether the predictive value of a recent (sentinel) fracture for future hip fracture differed by site of fracture.

**Methods:** The analysis was based on an Icelandic population-based cohort of 18,872 men and women aged on average 53 years when recruited between 1967 and 1991 (range 33-81 years). Fractures were documented over a total follow-up of 510,265 person-years. An extension of Poisson regression was used to investigate the relationship between the first (sentinel) fracture and subsequent hip fractures. All associations were adjusted for age, sex and time since baseline.

**Results:** Sentinel hip, clinical vertebral, forearm and humeral fractures were identified in 2074, 1365, 2364 and 1092 individuals, respectively. Subsequent hip fractures arose in 352, 271, 479 and 236 individuals, respectively. The risk of hip fracture within 2 years after the sentinel fracture for a women aged 75 years varied from 1.6 to 5.0-fold higher than the risk of a hip fracture in the normal population depending on the site of the sentinel fracture (Table 1).

**Conclusions:** We conclude that the risk of hip fracture after a sentinel fracture depends in part on the site of the first fracture. The very high risk ratios underline the importance of treating patients as soon as possible after sustaining a fracture.

**Table.** Risk ratio between risk of hip fracture 2 year after a sentinel fracture at the sites shown and the risk of hip fracture in the normal population for a woman aged 75 years.

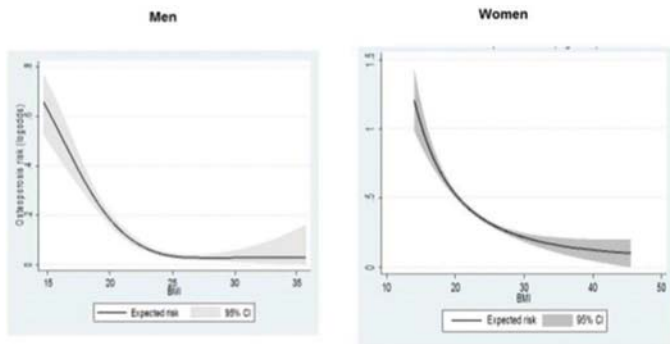
Sentinel fracture HR (95% CI) of hip fracture  
Clinical vertebral fracture 5.0 (3.8-6.6)  
Hip fracture 4.7 (3.7-6.0)  
Humeral fracture 2.9 (2.0-4.2)  
Distal forearm fracture 1.6 (1.2-2.2)

Disclosures: *Helena Johansson, None.*

## SU0235

**Association between osteoporosis and increased BMI in men and women: KNHANES 2008-2011.** Ji Hyun LEE\*, Jung Hee KIM, A Ram Hong, Sang Wan KIM, Chan Soo Shin. Internal Medicine, Seoul National University College of Medicine, Korea, Republic of

Several studies suggest that obesity is associated with increased bone mass. The aim of this study was to investigate an inflection point that increases osteoporosis (OP) as body mass index (BMI) increases in men and women. Our study was a cross-sectional investigation using data from KNHANES, 2008-2011. Lumbar spine, total hip, and femur neck bone mineral density (BMD) were measured using dual energy X-ray absorptiometry. We included 3,779 men aged 50 years or older and 5,367 postmenopausal women. Four categories of BMI were established: underweight (<18.5), normal weight (18.5-22.9), overweight (23.0-24.9), and obese ( $\geq 25$ ). Increasing BMI was associated with progressive increases in BMD at all skeletal sites after adjusting for age ( $P < 0.001$ ) in both men and women. The overall prevalence of OP was 8.6% for men and 36.4% for women. Underweight men was associated with a 23.4 folds increased prevalence of OP (OR = 23.39; 95% CI = 14.32-38.21) compared to obese men. This association was attenuated in the multivariable model (OR = 12.93, 95% confidence interval (CI) 6.05-27.63,  $P$  for trend  $< 0.001$ ). The relationship reached a plateau around a BMI of 25 kg/m<sup>2</sup>, with little additional increment with further increases in BMI. After multivariable adjustment, underweight women had odds ratios of 12.93 (95% confidence interval, 6.05-27.63,  $P$  for trend  $< 0.001$ ) for OP compared with obese women. Increasing BMI was linearly associated with decreases in OP in women. In conclusion, men with a BMI of less than 25 kg/m<sup>2</sup>, increasing BMI was associated with decreases in OP. However, higher BMI was significantly associated with a decreased prevalence of OP in postmenopausal women. Further studies on gender differences in the association between OP and BMI are warranted.



Associations of Body Mass Index With and Osteoporosis in men and women

**Disclosures:** Ji Hyun LEE, None.

## SU0236

**A cross-sectional study of osteoporosis in urban and rural areas of Shanghai.** Jinlong Li<sup>\*1</sup>, Chenguang Li<sup>2</sup>, Jing Wang<sup>2</sup>, Bing Shu<sup>2</sup>, Yan Zhang<sup>2</sup>, Lin Chen<sup>3</sup>, Qiang Wang<sup>3</sup>, Hao Zhang<sup>3</sup>, Nannan Sha<sup>3</sup>, Yin Zhu<sup>3</sup>, Zhenxing Luo<sup>3</sup>, Yongjun Wang<sup>4</sup>. <sup>1</sup>self, China, <sup>2</sup>workmate, China, <sup>3</sup>Student, China, <sup>4</sup>Professor, China

**Background:** Osteoporosis is becoming a serious problem in daily life with increasing life expectancy and aging of population in China. As is known, osteoporosis is closely related to living standard, living environment and life style which are extremely different between urban and rural areas due to the huge gap in development. Therefore, it is necessary to investigate whether morbidity of osteoporosis is different between urban and rural areas.

**Objective:** To investigate the difference in morbidity of osteoporosis between urban and rural areas among the elderly people.

**Methods:** 297 citizens (male 98 and female 109) and 153 villagers (male 99 and female 54) aged from 70 to 80 in Shanghai, China are involved. Lumbar spine bone mineral density (BMD) was measured by dual energy X-ray absorptiometry (DEXA).

**Result:** The morbidity of osteoporosis is much higher in the female citizens than in villagers (43.1% v.s 7.4%,  $P < 0.05$ ), but there is no significant difference between the two male groups. On the other hand, the general bone mass of citizens is higher than that of villagers with no relation to sex (male  $Z = -2.066$ ,  $P < 0.05$  and female  $Z = -3.091$ ,  $P < 0.05$ ), indicating more villagers are suffering a bone loss condition than citizens.

**Conclusion:** It is obvious that female citizens are more possible to suffer from osteoporosis. But it also shows that residents in the rural areas are more possible to suffer a loss of bone mass. In another word, they are easier to enter the osteopenia condition. Above all, it seems that rural life in Shanghai is a risk factor for osteopenia, but it is insufficient to drive the osteopenia to osteoporosis and has some interaction with sex, or it's just a bias. We need further study to confirm whether the interaction exists and what it is.

**Disclosures:** Jinlong Li, None.

## SU0237

**Acetabular Fractures in Patients Aged Over 60 Years.** Amanda Lorbergs\*, Jenny Thain, Richard Crilly. University of Western Ontario, Canada

Acetabular fractures in older adults are associated with increased risk of morbidity and mortality. Classification and surgical management of these fractures are well described; however, the risk factors predisposing older adults to acetabular fractures remain unknown. We conducted a retrospective cohort study to determine the characteristics of patients aged 60 years and older who sustained acetabular fracture.

We identified 79 patients (37 women, 42 men) admitted to acute care hospitals in southwestern Ontario who sustained a fracture of the acetabulum between 2013 and 2015. Mean age of patients was 81 years (range, 60-99y). Low-energy trauma, such as falls from standing height, was the most common mechanism of fracture, as reported in 58 (74%) patients. Eleven (14%) patients fell from greater than standing height, such as from a ladder, and nine (11%) reported high-energy trauma, such as motor vehicle accident. Eleven patients (14%) had metalwork in the hip on the same side as the acetabular fracture. Fifteen patients (80% women) had a diagnosis of osteoporosis prior to fracture incidence, of which twelve of were being treated pharmacologically for osteoporosis at the time of fracture.

The patients with fractures from low-energy trauma (27 women, 31 men) had a mean age of 85y, which was significantly older than those who fell from greater than standing height (mean 73y,  $p < 0.001$ ) or with high-energy trauma (mean 68y,  $p < 0.001$ ). In the low-energy trauma group, 10 patients (17%) had metalwork in the hip; however, most patients in this group (83%) had no prior hip fracture. The low-energy trauma group included all patients with osteoporosis ( $n = 15$ ), and all patients treated pharmacologically for osteoporosis prior to acetabular fracture (21%) or after acetabular fracture (9%).

These data suggest that older age and osteoporosis predispose to acetabular fractures. In contrast to hip fractures that predominantly occur in women, our findings showed that acetabular fracture incidence is higher in men. One explanation is variability in hip geometry that may influence risk of sustaining an acetabular fracture versus hip fracture. Alternatively, a relatively well-maintained BMD within the femoral cortex may transmit the fall force through to the acetabulum. Since availability of BMD data is limited for our cohort, investigating hip geometry may be useful for identifying risk factors for acetabular fracture.

**Disclosures:** Amanda Lorbergs, None.

## SU0238

**In-Hospital Mortality following Hip, Femur and Pelvic fractures in Québec, Canada.** Suzanne Morin<sup>\*1</sup>, Etienne Belzile<sup>2</sup>, Jacques Brown<sup>2</sup>, Sonia Jean<sup>3</sup>. <sup>1</sup>McGill University, Canada, <sup>2</sup>Laval University, Canada, <sup>3</sup>Institut national de santé publique du Québec, Canada

**Purpose:** We aim to describe in-hospital mortality rates following fractures of the hip, femur and pelvis over a 22-year period and characterize its predictors.

**Methods:** Using the hospital discharge database of the province of Québec, Canada, we performed a retrospective cohort study of men and women aged 45 years and older who sustained an incident hip, femur or pelvic fracture between 1991-2013. Fractures and trauma intensity were identified using ICD-9-CM or ICD-10-CM diagnosis codes. Annual crude in-hospital and 30-day in-hospital mortality rates per 1,000 patient days and adjusted hazard ratios (aHR) with 95% confidence intervals (95% CI) generated by Cox proportional regression analyses were estimated and stratified by fracture site, sex, time periods and age-categories.

**Results:** Over 22 years, we identified 127,312 hip (73% women), 19,814 pelvic (72% women) and 10,090 femur (70% women) fractures with a mean age of 79.7 (10.7), 77.1 (12.7) and 72.8 (13.7) years, respectively. The number of fractures and mean age of patients increased over time for all fracture sites. There were 12 084 in-hospital deaths (7.7%). In-hospital mortality rates per 1000 patient days were for hip fracture: 2.70 (2.64-2.75), pelvic fracture 1.63 (1.52-1.73) and femur fractures 1.51 (1.38-1.64). Adjusted HR for in-hospital mortality were highest for men (vs women;  $P < 0.0001$ ) following a hip fracture 1.88 (1.80- 1.96) and lowest following pelvic fractures (aHR 1.60 (1.38-1.86). The oldest age category (85+ y vs 45- 54 y;  $P < 0.0001$ ) had a higher mortality risk following a hip: aHR 9.03 (6.50-12.55), femur: aHR 10.38 (5.21-20.70) than a pelvic fracture: aHR 5.21 (3.07-8.83). In addition, dementia, long-term care residence, low trauma fracture and having more than 4 comorbidities were strongly associated with increased in-hospital mortality risk at all fracture sites (all  $P < 0.01$ ). 30 day-in hospital mortality risk was higher than in-hospital mortality risk in situations of non-surgical management of hip and femur fractures. Surgical delays and adjusted mortality rates decreased for hip and femur fractures over the study period.

**Conclusion:** Although much care has been devoted to the management of patients with hip fractures, we demonstrate that in-hospital mortality and its predictors are similar amongst patients who sustain a hip, femur or pelvic fractures, supporting that similar resources be allocated to all patients with fractures at these sites.

**Disclosures:** Suzanne Morin, Amgen, Grant/Research Support.



## SU0239

**Prospective Study of Proton Pump Inhibitor and H<sub>2</sub>-Receptor Antagonist Use and Risk of Vertebral Fracture in Women.** Julie M Paik<sup>\*1</sup>, Harold N Rosen<sup>2</sup>, Catherine M Gordon<sup>3</sup>, Gary C Curhan<sup>1</sup>. <sup>1</sup>Brigham and Women's Hospital, Harvard Medical School, United States, <sup>2</sup>Beth Israel Deaconess Medical Center, Harvard Medical School, United States, <sup>3</sup>Cincinnati Children's Hospital Medical Center, University of Cincinnati College of Medicine, United States

**Purpose:** Vertebral fractures (VF) are the most common type of osteoporotic fracture and associated with significant disability, morbidity, and mortality. Proton pump inhibitors (PPI) and histamine (H<sub>2</sub>) receptor antagonists, treatments for acid-related upper gastrointestinal disorders, are among the most commonly prescribed over-the-counter medications in the U.S. Prior studies suggest an increased risk of osteoporotic fracture with PPI use, but the studies have not demonstrated consistent results and the causative mechanism remains unclear. Potential etiologies include decreased calcium absorption or direct effects on osteoclast activity from the use of these acid-suppressing agents. The few prospective studies to date examining the relation between PPI use and risk of VF suggest an increased risk, but the magnitude of the effect has been inconsistent, which could be related to the assessment of VF by self-report or administrative codes. There are limited data on the association between H<sub>2</sub>-receptor antagonist use and risk of VF.

**Methods:** We conducted a prospective study of the relation between PPI use, H<sub>2</sub>-receptor antagonist use, and risk of VF in 60,120 women, 55-82 years of age (mean age 66.2 years) in 2002, with no history of prior fracture, who were participating in the Nurses' Health Study. Use of PPIs and H<sub>2</sub>-receptor antagonists was assessed by questionnaire every 4 years. Dietary intake and vitamin or supplement use were assessed from semi-quantitative food frequency questionnaires in the same years. All cases of self-reported VF were confirmed by medical record review.

**Results:** In 2002, there were 3,853 women (6.4%) using PPIs and 3,879 women (6.5%) using H<sub>2</sub>-receptor antagonists. Between 2002 and 2012, 443 incident VF cases were documented. After adjustment for other potential risk factors, including intakes of calcium, vitamin D, protein, caffeine and alcohol, body mass index, physical activity, smoking status, and history of hypertension and diabetes, the relative risk of VF for those women taking PPIs was 1.28 (95% CI 1.01 to 1.63) compared with women who were not receiving PPIs. After multivariate adjustment, the relative risk of VF for women taking H<sub>2</sub>-receptor antagonists was 1.25 (95% CI 0.89 to 1.75) compared with women who were not taking H<sub>2</sub>-receptor antagonists.

**Conclusion:** PPI use is associated with a modestly increased risk of vertebral fracture in women. The mechanism for this finding remains unclear and is an area for further research.

**Disclosures:** Julie M Paik, None.

## SU0240

**Impact of hip fracture on health-related quality of life and activities of daily living: the SPARE-HIP prospective cohort study.** Daniel Prieto-Alhambra<sup>\*1</sup>, Eduardo Vaquero-Cervino<sup>2</sup>, Isabel Sierra Setién<sup>3</sup>, Miguel Sanz Sainz<sup>4</sup>, Maria Dolores Sanz Amaro<sup>5</sup>, Mònica Salomó Domènech<sup>6</sup>, Pilar Sáez-López<sup>7</sup>, Leocadio Rodríguez Mañas<sup>8</sup>, Iván Pérez Coto<sup>9</sup>, Jesús Mora Fernández<sup>10</sup>, Damian Mifsut<sup>11</sup>, Jorge Martínez-Iníguez Blasco<sup>12</sup>, Miguel Martínez Ros<sup>13</sup>, Bartolomé Lladó Ferrer<sup>14</sup>, Paloma Gonzalez Garcia<sup>15</sup>, Miriam Garrido Clua<sup>16</sup>, Laura Ezquerro Herrando<sup>17</sup>, Iñigo Etxebarria-Foronda<sup>18</sup>, Pedro Carpintero Benítez<sup>19</sup>, José Ramón Caeiro Rey<sup>20</sup>, Gaspar Adrados Bueno<sup>21</sup>, Antonio Herrera<sup>22</sup>, Adolfo Díez-Pérez<sup>23</sup>. <sup>1</sup>Centre for Statistics in Medicine, Nuffield Department of Orthopaedics, Rheumatology, and Musculoskeletal Sciences (NDORMS), University of Oxford, United Kingdom, <sup>2</sup>Complejo Hospitalario Universitario de Pontevedra, Spain, <sup>3</sup>Departamento de Medicina Interna, Hospital Universitario M. Valdecilla-IDIVAL, Spain, <sup>4</sup>Hospital Universitario Miguel Servet, IIS Aragón, Spain, <sup>5</sup>Hospital Lluís Alcanyis, Spain, <sup>6</sup>Hospital Universitari Parc Tauli, Spain, <sup>7</sup>Geriatría Complejo Asistencial de Avila, Instituto de Investigación Hospital Universitario La Paz, Fundación Idi Paz, Spain, <sup>8</sup>Servicio de geriatría, Hospital Universitario de Getafe, Spain, <sup>9</sup>Hospital Universitario San Agustín, Spain, <sup>10</sup>Hospital Clínico San Carlos, Spain, <sup>11</sup>Hospital Clínico de Valencia, Spain, <sup>12</sup>Hospital San Pedro, Spain, <sup>13</sup>Hospital Universitario Virgen de la Arrixaca, Spain, <sup>14</sup>Unidad de Osteoporosis, Hospital Son Llàtzer, Spain, <sup>15</sup>Hospital Obispo Polanco, Spain, <sup>16</sup>Hospital Vall d'Hebron, Instituto de Recerca Vall d'Hebron (VHIR), Grupo de Recerca Aparato Locomotor, Spain, <sup>17</sup>Servicio de Cirugía Ortopédica y Traumatología, Hospital Clínico Universitario Lozano Blesa, Spain, <sup>18</sup>Alto Deba Hospital, Spain, <sup>19</sup>Hospital Reina Sofía, Spain, <sup>20</sup>Servicio de Cirugía Ortopédica y Traumatología, Complejo Hospitalario Universitario de Santiago de Compostela, Spain, <sup>21</sup>Servicio de Medicina Interna, Hospital Universitario Infanta Cristina, Spain, <sup>22</sup>Department of Surgery, University of Zaragoza, Aragon Health Research Institute, Spain, <sup>23</sup>Department of Internal Medicine, Hospital del Mar-IMIM and Autonomous University of Barcelona, Spain

**PURPOSE** There is a scarcity of prospectively collected data on functional and patient-reported outcomes following hip fracture. We therefore aimed to measure health-related quality of life (HRQoL) and activities of daily living activities (ADL) before, during index admission for a hip/proximal femur fracture, and at 1 and 4 months later.

## METHODS

**Design** Prospective cohort study including a consecutive sample of subjects aged 50 years or older, recruited in a representative sample of 38 Spanish hospitals at the time of admission for a hip or proximal femur fracture.

**Measurements** Baseline (pre-fracture) socio-demographics, fracture risk (FRAX), and clinical characteristics were collected at the time of admission. HRQoL (as measured using EuroQoL-5D) and ADLs (measured using Barthel index) were collected from patients (or carer in case of dementia/delirium) at time of admission and at 1 and 4 months following a hip/femur fracture.

**Statistical analyses** EQ-5D utility indices were estimated using national (Spanish) preferences. Barthel index was scored (maximum 100). Mean (standard deviation, SD) scores at each time point are described, and kernel density plots depicted for HRQoL. In addition, mean (SD) change in scores are also reported.

## RESULTS

A total of 997 subjects were consented and recruited, of mean (sd) age 83.6 (8.5) years, and 76.7% women. 828/997 (101 deaths, 68 lost or non-responders) completed the 4-month visit. ADLs dropped from 78.8/100 (23.8) pre-fracture to 43.6 (19.9) at admission, to partially recover at 54.9 (25.4) and 64.1 (27.2) at 1 and 4 months respectively. HRQoL dropped from 0.63/1 (0.39) to 0.06 (0.40) during admission, to then increase to 0.30 (0.43) and 0.46 (0.44) at 1 and 4 months post-fracture (see Figure). More than half participants (median -0.01) were reportedly 'worse than dead' at the time of fracture.

## CONCLUSION

Hip and proximal femur fractures have a striking impact on self-reported HRQoL and ADLs, with incomplete recovery at 1 and 4 months post-admission even amongst survivors (<90% of the patients). These data should inform future investment in acute and long-term care (including secondary fracture prevention) of hip fracture patients.

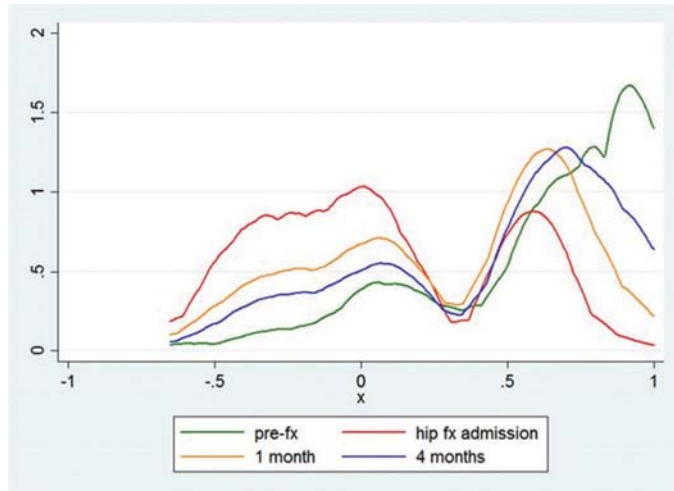


Figure 1. Kernel Density Plot: HRQoL (EQ5D utilities) at baseline (pre-fx), at admission for a hip f

**Disclosures:** Daniel Prieto-Alhambra, Amgen, Grant/Research Support.

## SU0241

**Serum osteoprotegerin concentration was positively associated with 25-OH Vitamin D and fibroblast growth factor 23 in the middle-aged and elderly people with different bone mass.** Bing Shu<sup>\*1</sup>, Jing Wang<sup>1</sup>, Chenguang Li<sup>1</sup>, Yan Zhang<sup>1</sup>, Jinlong Li<sup>1</sup>, Xiaofeng Qi<sup>1</sup>, Liang Qiao<sup>1</sup>, Yongjian Zhao<sup>1</sup>, Lin Chen<sup>1</sup>, Qiang Wang<sup>1</sup>, Hao Zhang<sup>1</sup>, Yongjun Wang<sup>2</sup>. <sup>1</sup>Longhua Hospital, Shanghai University of Traditional Chinese Medicine, China, <sup>2</sup>Longhua Hospital, Shanghai University of Traditional Chinese Medicine; School of Rehabilitation Science, Shanghai University of Traditional Chinese Medicine, China

**Background:** Disrupted calcium-phosphate homeostasis is considered an important risk factor in the pathogenesis of osteoporosis. Fibroblast growth factor 23 (FGF23), parathyroid hormone (PTH) and the active form of vitamin D are the most critical factors involved in the regulation of both calcium homeostasis and phosphate homeostasis. FGF23 was proved to induce osteoprotegerin (OPG) and prohibit osteoclast formation in vitro. No clinical observation was conducted to confirm the association between OPG and FGF23 as well as other parameters related to calcium-phosphate homeostasis.

**Objective:** to determine the association between serum OPG concentration and parameters related to calcium-phosphate homeostasis in the middle-aged and elderly people with different bone mass.

**Methods:** Residents (men aged from 50 to 79 and women aged from 45 to 79) from 2 sub-districts in Shanghai, China were included. Serum OPG, FGF23, Vitamin D, calcium and phosphate were detected and lumbar spine bone mineral density (BMD) was measured by dual energy X-ray absorptiometry (DEXA).

**Results:** No statistical significant relationship was found between serum OPG concentration and lumbar spine BMD in females and males. In both females and males with normal bone mass, osteopenia or osteoporosis, serum OPG concentration was positively associated with serum levels of 25-OH Vitamin D and FGF23. Serum OPG concentration was negatively associated with serum calcium concentration in females with osteoporosis and in males with osteopenia, and was positively associated with serum PTH concentration in females with osteopenia.

**Conclusions:** Serum OPG concentration was positively associated with 25-OH Vitamin D and FGF23 in the middle-aged and elderly people with different bone mass.

**Disclosures:** Bing Shu, None.

## SU0242

**Estimation of the Recommended Daily Allowance (RDA) for Vitamin D Intake Using Serum 25 Hydroxyvitamin D 20ng/ml As the End Point in two Randomized Trials.** Lynette Smith<sup>\*1</sup>, J Chris Gallagher<sup>2</sup>, Glenville Jones<sup>3</sup>, Martin Kaufmann<sup>3</sup>. <sup>1</sup>University of Nebraska Medical Center, United States, <sup>2</sup>Creighton univ, United States, <sup>3</sup>Queens univ, Canada

**Introduction:** Serum 25-hydroxyvitamin D (25OHD) is the best biomarker of vitamin D intake. The Institute of Medicine recommended daily allowance (RDA) that a serum 25OHD level of 20ng/ml (50nmol/l) is adequate to prevent fractures. Earlier we reported in a dosing study of older white women that vitamin D 800 IU daily would exceed 20ng/ml (50nmol/L) (Diasorin) in 97.5% of the population. We remeasured serum 25OHD using Liquid Chromatography/Mass Spectrophotometry (LCMS) in 2 trials of older and younger black and white women.

**Methods:** 163 older Caucasian and 110 black women (age 57-90 years) with vitamin D insufficiency defined as serum 25OHD  $\leq 20$  ng/ml were randomized to vitamin D3, 400, 800, 1600, 2400, 3200, 4000, 4800 IU/day or placebo for 1 year. 119 younger white and 79 black women age 25-45 years were randomized to placebo, 400, 800, 1600 and 2400 IU/day for 1 year. Serum 25OHD was remeasured by LCMS. Statistical analysis employed a mixed effects model for dose response curve estimation and bootstrapping resampling methodology to determine the 95% prediction limits for the 12-month value for 25OHD. Primary outcome was to estimate the RDA for a vitamin D intake that exceeded serum 25OHD 20ng/ml (50nmol/l).

**Results:** There was a curvilinear increase in serum 25OHD that best fit a quadratic model in white women and linear in black women. Using the bootstrap prediction intervals and a target serum 25OHD of 20ng/ml the RDA estimations are as follows; 400 IU/d in older white women, 800 IU in younger white women, 1600 IU/d in older and younger black women. The dropout rate was 10% in older and 35% in younger women. Differences in RDA can be partly explained by smaller numbers in black women and less dose groups. If all data is pooled on 343 white and black women completing study the RDA is estimated at 800 IU/d.

**Conclusion:** In estimating the RDA for vitamin D, a serum level of 20ng/ml is reached by a vitamin D dose of 400 IU/d in older white women and 800 IU/d in younger white women. In older and younger black women a vitamin D dose of 1600 IU/d exceeded serum 25OHD of 20ng/ml (50nmol/L).

Combining data in all groups the RDA for vitamin D is 800 IU. However, to best estimate the RDA, it is recommended that baseline serum 25OHD is  $< 20$  ng/ml (50nmol/L), use five vitamin D doses and larger numbers per group, especially larger studies of black women are needed to examine possible ethnic differences in RDA.

**Disclosures:** Lynette Smith, None.

## SU0243

**Extensive Undertreatment of Osteoporosis in Older Swedish Women.** Daniel Sundh<sup>\*1</sup>, Anna G Nilsson<sup>1</sup>, Helena Johansson<sup>2</sup>, Dan Mellström<sup>1</sup>, Mattias Lorentzon<sup>1</sup>. <sup>1</sup>Geriatric Medicine, Department of Internal Medicine and Clinical Nutrition, Institute of Medicine, University of Gothenburg, Gothenburg, Sweden, <sup>2</sup>Centre for Metabolic Bone Diseases, University of Sheffield Medical School, Sheffield, UK, Sweden

Fracture rates increase dramatically at old age and the incidence of hip fracture is among the greatest in the world in Swedish women. Although effective pharmacological treatment is available, treatment rates remain low. Only limited data is available regarding treatment rates in relation to a thoroughly evaluated fracture risk in a population based setting in older women. Swedish guidelines do not provide treatment recommendations based on risk of hip fracture according to FRAX. The aim of this study was to investigate the proportion of older women with treatment indication, according to National Osteoporosis Foundation (NOF) or Swedish Osteoporosis Society (SvOS) guidelines, and determine the proportion of these women, receiving osteoporosis treatment.

A population-based study was performed in Gothenburg in 3030 older women (77.8 $\pm$ 1.6 years [mean $\pm$ SD]). Bone mineral density (BMD) of the spine and hip was measured with DXA. Clinical risk factors for fracture and data regarding osteoporosis medication (current and previous use of p.o. bisphosphonates, zoledronic acid, denosumab, teriparatide) was collected with questionnaires. 2989 women had complete data. These women had a FRAX-score with BMD of 23.0 $\pm$ 11.8% for a major osteoporotic fracture (MOF) and 11.0 $\pm$ 11.0% for hip fracture. 1103 (36.9%) women had a previous fracture. NOF and SvOS guidelines were used to identify subjects who had treatment indication. NOF criteria included 1) diagnosis of osteoporosis at the spine, femoral neck, or total hip, 2) osteopenia, in combination with a FRAX-score  $\geq 20\%$  for a MOF or  $\geq 3\%$  for a hip fracture, and 3) self-reported hip or spine fracture. SvOS criteria included 1) previous hip or spine fracture, 2) osteoporosis, 3) low BMD (T-score  $\leq -2.0$  SD), prevalent fracture, and a FRAX-score  $\geq 20\%$  for a MOF, or 4) 5 mg of daily p.o. glucocorticoid treatment  $> 3$  months.

Using SvOS or NOF criteria, 1109 (37%) and 2416 (81%) women, respectively, had treatment indication. The proportion of these women receiving osteoporosis treatment was 21.8% and 12.6%, according to SvOS and NOF guidelines, respectively (Figure 1). 1701 women had osteopenia with a FRAX hip fracture risk of  $\geq 3\%$  (NOF).

This large population-based study demonstrates that a major proportion of older Swedish women should be considered for osteoporosis medication, given their high fracture risk, but that only a minority receives treatment. This undertreatment would be even more pronounced using NOF criteria in Sweden.



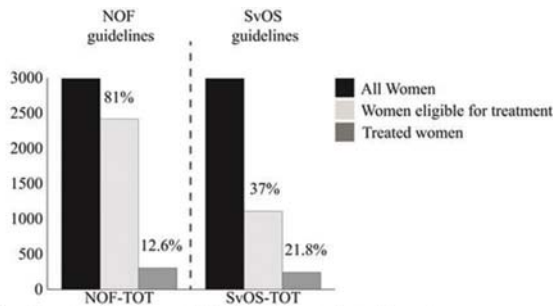


**Figure 1** Number of women with treatment indication and proportions with current or recent treatment. NOF-TOT=Subjects eligible for treatment due to any of the NOF treatment criteria. SvOS-TOT=Subjects eligible for treatment due to any of the SvOS treatment criteria.

Number of Women with Treatment Indication and Proportions with Current or Recent Treatment

**Disclosures:** Daniel Sundh, None.

## SU0244

**An association of a single missense nucleotide polymorphism in the ALDH2 gene with hip fracture.** Kenichiro Takeshima\*, Takeshi Miyamoto, Masaya Nakamura, Morio Matsumoto. Department of Orthopedic Surgery, Keio University School of Medicine, Japan

Osteoporosis is a systematic skeletal disease characterized by low bone mass, with a consequent increase in bone fragility fractures. Among osteoporotic injuries, hip fracture is the most severe bone fragility fracture, leading to morbidity and mortality. Parental history of hip fracture confers a risk factor for future fractures and was now included in the criteria for osteoporosis for treatment. However, genetic factors underlying family history remain to be clarified. We focused on a single nucleotide polymorphism (SNPs) in the alcohol dehydrogenase 2 (ALDH2) which is a member of a family of enzymes that catalyzes conversion of acetaldehyde to acetic acid. We enrolled 92 hip fracture patients (mean age, 77.4 years old) and 48 control groups (mean age, 72.8 years old) without any fragility fractures with higher than -2.5 S.D. bone mineral density. We investigated the presence of missense SNP in the ALDH2 gene, rs671, by direct sequencing, and found that rs671 frequency was 57.6% and 35.4%, respectively. These results indicated that missense SNP in the ALDH2 gene, rs671 (ALDH2\*2), is significantly associated with hip fracture (odds ratio=2.48,  $p=0.021$ ). We also enrolled 156 osteoporosis subjects diagnosed as below -2.5 S.D. in terms of bone mineral density without hip fractures. rs 671 SNP was also significantly associated with osteoporosis (odds ratio=2.04,  $p=0.040$ ). Our results indicate novel insight into the pathogenesis of hip fracture and osteoporosis.

**Disclosures:** Kenichiro Takeshima, None.

## SU0245

**Circulating steroid concentrations exhibit age-dependent associations with spinal muscle density: the Framingham Study.** Timothy Tsai<sup>1</sup>, Brett Allaire<sup>2</sup>, Robert McLean<sup>3</sup>, Marian Hannan<sup>3</sup>, Mary Bouxsein<sup>2</sup>, Kiel Douglas<sup>3</sup>, Thomas Trivison<sup>3</sup>. <sup>1</sup>Hebrew SeniorLife Institute for Aging Research, United States, <sup>2</sup>Beth Israel Deaconess Medical Center, United States, <sup>3</sup>Hebrew SeniorLife Institute for Aging Research and Harvard Medical School, United States

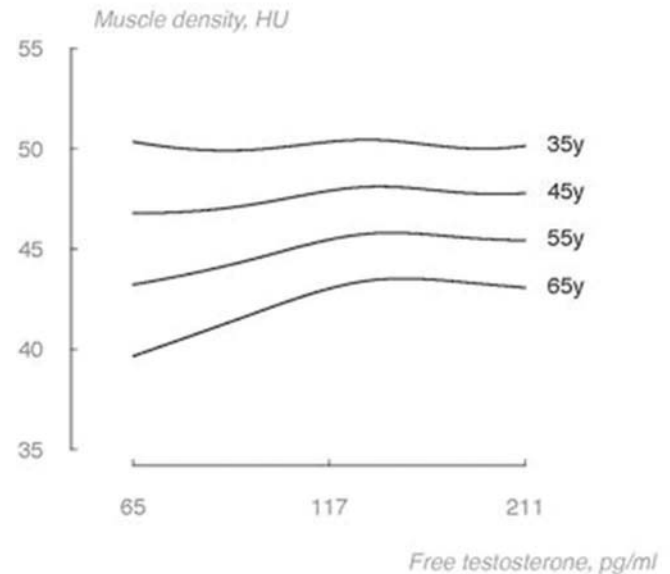
Maintenance of endogenous androgen concentrations is necessary for preservation of appendicular muscle mass and strength in aging. Less is known concerning the influence of sex steroids on spinal muscle quality, important for balance and physical functioning. In this cross-sectional study, we examined the roles of circulating total testosterone (TT) and estradiol (E2) on the combined density of eight muscles (rectus abdominus, latissimus dorsi, external oblique, internal oblique, erector spinae, transversospinalis, psoas major, quadratus lumborum) at the lumbar spine (L3). The influence of calculated free (unbound) testosterone (cFT) was also considered.

Data were obtained from 1,068 Framingham Study Generation 3 participants. Hormones were measured in morning fasting samples using tandem mass spectrometry. cFT was derived from steroid and sex hormone-binding globulin concentrations using mass action equations. Muscle density (in Hounsfield Units, HU) was measured using quantitative computed tomography. Multiple linear regression was used to quantify linear relationships and interactions. Hormone values were log-transformed and models scaled such that slope estimates represent mean trends in muscle density attending 50% cross-sectional increases in hormone concentrations. Separate models were fit for men ( $N = 629$ , ages 31 to 68 y); premenopausal women ( $N = 313$ , 33 to 55 years); and postmenopausal women ( $N = 126$ , 40 to 70 years).

Mean (standard deviation) TT was 485 (166), 21 (14) and 19 (26) ng/dl in men, premenopausal women and postmenopausal women, respectively; mean (SD) E2 concentrations were 28 (9), 127 (133) and 45 (71) pg/ml, respectively. Exploratory analysis suggested that there was little association between cFT and spinal muscle density among

younger men, but that the strength of this association increases with age (Figure). Linear models supported this observation of age-by-hormone interaction in men; for each successive decade of age, the magnitude of difference in muscle density apparently attributable to elevated cFT increased by 1.8 HU (95% confidence interval: -0.02 to 1.92 HU). Among women, TT and cFT had weaker associations with muscle density, but similar interactions between age and E2 were observed; the trend for muscle density to increase with E2 was observed to a greater extent in younger than older participants. These results suggest that sex steroid profiles affect spinal muscle quality in an age- and sex-specific fashion.

**Figure.** Model-estimated mean muscle density for hypothetical men of age 35y, 45y, 55y or 65y are displayed as a function of free testosterone concentration ( $N = 629$ ). Estimates are from a generalized additive model with nonlinear smoothing, and are displayed over a range comprising the middle 90% of observed cFT values. An increase in muscle density with increasing cFT is apparent for older, but not younger, participants.



**Figure**

**Disclosures:** Timothy Tsai, None.

## SU0246

**Cross-Sectional Association of BMAT Unsaturation Index (UI) with QCT Measures of Bone Density and Strength.** Gina Woods<sup>1</sup>, Kaipin Xu<sup>2</sup>, Sigurdur Sigurdsson<sup>3</sup>, Susan Ewing<sup>2</sup>, Deborah Kado<sup>1</sup>, Thomas Lang<sup>2</sup>, Thomas Link<sup>2</sup>, Gudny Eiriksdottir<sup>3</sup>, Trisha Hue<sup>2</sup>, Eric Vittinghoff<sup>2</sup>, Tamara Harris<sup>4</sup>, Clifford Rosen<sup>5</sup>, Vilundur Gudnason<sup>6</sup>, Ann Schwartz<sup>2</sup>, Xiaojuan Li<sup>2</sup>. <sup>1</sup>University of California, San Diego, United States, <sup>2</sup>University of California, San Francisco, United States, <sup>3</sup>Icelandic Heart Association, Iceland, <sup>4</sup>National Institute on Aging, NIH, United States, <sup>5</sup>Maine Medical Center Research Institute, United States, <sup>6</sup>University of Iceland, Iceland

Higher levels of bone marrow adipose tissue (BMAT) are associated with lower BMD and prevalent vertebral fracture (PVF) in older adults. The composition of BMAT, in addition to the amount, may also influence bone. Lipid composition can be evaluated with magnetic resonance spectroscopy (MRS). We hypothesize that a higher proportion of unsaturated lipid within the BMAT depot is associated with higher BMD and bone strength. This study aims to investigate the association between BMAT lipid unsaturation index (UI), expressed as the ratio of unsaturated lipids to all lipids (%), QCT measures of BMD, and PVF in 288 older adults from the AGES-Reykjavik study.

Participants were age 71+, not using medications known to affect BMAT or BMD. BMAT UI was measured by 1.5-T <sup>1</sup>H-MRS. BMD was assessed by QCT, and PVF by DXA VFA. Multivariable linear models were used to determine the association between average UI (L1-L4) and PVF or log-transformed QCT BMD.

Participants were 78.8 (SD 3.5) years, with mean BMI of 27.3 (SD 3.7) kg/m<sup>2</sup>, mean trabecular spine BMD of 0.066 (SD 0.029) g/cm<sup>3</sup>, and mean vertebral (L1-L4) BMAT content of 55.0 ± 8.3%. 19.2% (n=55) of participants had one or more prevalent vertebral fractures. The average lipid UI was 4.5 ± 1.3%. Lipid UI at the individual vertebral level increased from 3.9% at L1 to 4.7% at L4 (p for trend <0.0001). Higher UI was associated with younger age ( $r=-0.19$ ,  $p=0.002$ ), and higher BMAT content ( $r=0.17$ ,  $p=0.003$ ), but not with BMI ( $r=-0.004$ ,  $p=0.95$ ). Average UI was higher in men than women, but was not statistically significant (4.6% vs. 4.3%,  $p=0.06$ ). Average UI was no different in those with vs. without PVF (4.5% vs. 4.5%,  $p=0.95$ ), in fully adjusted models including age, gender, calendar time, trabecular spine BMD, diabetes status, and total

BMAT content. However, per SD increase in UI, spine integral BMD was 5.2% higher ( $p<0.0001$ ), femoral neck integral BMD was 3.0% higher ( $p=0.02$ ) and total hip integral BMD was 4.1% higher ( $p=0.0009$ ) in fully adjusted models (Table 1). Spine trabecular BMD, spine compressive strength, femoral neck cortical BMD and total hip trabecular and cortical BMD were also higher in those with higher UI. In conclusion our study showed that older adults with higher proportion of unsaturated lipids in BMAT have higher trabecular, cortical, and integral bone density, independent of the total amount of BMAT.

Percent Difference in Bone Density and Strength (QCT) per SD Increase in BMAT UI (n=288)		
	% Difference in Bone Measurement (95% CI)	P-value
<b>Spine</b>		
Trabecular BMD	10.0 (3.7, 16.8)	0.002
Integral BMD	5.2 (2.7, 7.8)	<0.0001
Compressive Strength	16.8 (8.6, 25.6)	<0.0001
<b>Femoral Neck</b>		
Trabecular BMD	1.5 (-3.0, 6.2)	0.52
Cortical BMD	1.5 (0.3, 2.7)	0.02
Integral BMD	3.0 (0.6, 5.6)	0.02
<b>Total Hip</b>		
Trabecular BMD	3.1 (0.1, 6.3)	0.04
Cortical BMD	1.4 (0.4, 2.3)	0.004
Integral BMD	4.1 (1.7, 6.6)	0.0009

Adjusted for age, gender, BMI, calendar time, diabetes and total BMAT content

Table 1

Disclosures: Gina Woods, None.

## SU0247

**Patient 'Self-Consultation' as a Novel Strategy to Combat the Osteoporosis Treatment Mismatch: Experience from a Single-Centre Pilot.** Emma Billington\*, Lynn Feasel, Greg Kline. University of Calgary, Canada

**Background:** Pharmacologic treatment reduces the risk of fragility fracture roughly by half, with those at the highest risk standing to benefit most. However, rates of uptake and adherence in high risk patients are low, and observational data suggest that many low risk patients are being initiated on therapy. A principal contributor to this treatment mismatch appears to be lack of patient access to sufficient, personally contextualized knowledge about fracture risk, fracture sequelae, and risks and benefits of anti-fracture therapies. Given the high prevalence of osteoporosis, it is not feasible for all individuals at risk of fracture to have a 1-on-1 consultation with an osteoporosis specialist. To address this care gap, we recently piloted a novel 'self-consultation session' (SCS), consisting of a specialist-led group medical visit designed to concurrently provide multiple participants with the education necessary to make an informed decision about osteoporosis treatment.

**Methods:** Patients referred for assessment of age-associated osteoporosis who agreed to participate in a group medical visit were evaluated. Participants attended a SCS (detailed in Figure 1) and data were collected regarding fracture risk factors, ten-year fracture risk (estimated with FRAX), and treatment decision. Patient experience was assessed using a validated questionnaire.

**Results:** Forty-four women were evaluated. Mean (SD) age was 61.8 (5.4)y. Estimated ten-year fracture risk was 12.2 (7.2)% for major osteoporotic fracture (MOF) and 2.6 (2.6)% for hip fracture. Following the SCS, 9 (20%) chose to commence pharmacologic therapy, 20 (46%) declined therapy, and 15 (34%) remained uncertain about treatment. Of those at low risk of MOF ( $<10\%$ ;  $n=19$ ), 4 (21%) chose to undergo therapy. Of those at high risk ( $\geq 20\%$ ;  $n=5$ ), none declined therapy. All 44 (100%) felt that the information provided in the SCS was useful, 38 (86%) felt that they were provided with enough information to make a treatment decision, and 42 (96%) reported overall satisfaction with the SCS. Mean (SD) per-patient time spent in consultation by the SCS physician was 22 (8)min.

**Conclusions:** The SCS appears to be an acceptable alternative to 1-on-1 specialist consultation for patients with uncomplicated, age-associated osteoporosis. The SCS can efficiently deliver specialized, person-centred care, empowering the majority of patients to make a treatment decision. Our findings support further evaluation of this novel program.

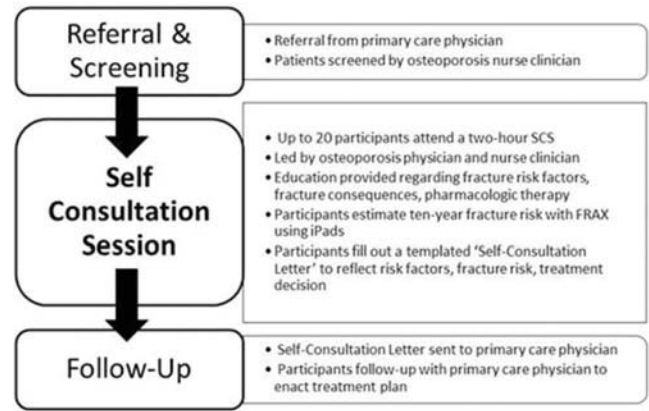


Figure 1. Patient flow through a self consultation session (SCS) for age-associated osteoporosis

Figure 1

Disclosures: Emma Billington, None.

## SU0248

**Novel Use of Telecarers in the Co-ordination of Secondary Osteoporosis Prevention in Hip Fracture Patients in a Regional Hospital Setting in Singapore.** Linsey Gani\*, Wen Hao Tan, Nicollette Pereira, Thomas King, Joan Khoo. Changi General Hospital, Singapore

**Background :** Globally, as much as 80% of patients with fragility fractures are not identified and treated. Our previous institution audit found similarly low rates of follow-up and treatment, with BMD being performed in 33-59%, vitamin D and calcium supplementation in 5-17% and anti-osteoporosis treatment rate of 10 -32%. The osteoporosis liaison service was started to bridge this gap. To reduce over-utilization of hospital visits and ensure commencement of appropriate osteoporosis investigation and treatment, we piloted the use of telecarers to follow up patients at specific time intervals post discharge from hip fracture to monitor osteoporosis treatment and compliance. Here we describe the service and first 3 months data of patient follow up.

**Methods :** Patients discharged with hip fracture from January 2017 were automatically enrolled in the Health Management Unit ( HMU). A multidisciplinary approach involving orthopaedic, ortho-geriatric and allied health teams were involved in scripting the telecaller questions for follow up post a hip fracture admission. The phonecall content included aspects of fracture healing, pain, functional assessment and osteoporosis treatment. Specific questions regarding osteoporosis treatment include calcium, vitamin D supplementation and anti osteoporosis medications, adherence and adverse effects. These were scheduled at 3-5 days post discharge, 3 months, 6 months and 1 year. Data from January to March 2017 for this new service were analyzed to assess the feasibility of this workflow.

**Results :** There were 165 hip fractures that were admitted to the hospital between December 2016 to March 2017. 20 fractures were managed conservatively and the rest were surgically managed. 87% of patients had BMD scheduled or performed by the time of discharge. 93% of patients who were discharged from the hip fracture pathway were contacted by the Healthcare Management Unit. 89% of patients were prescribed and were compliant with their vitamin D and calcium supplement at the time of calling.

**Conclusion :** Care co-ordination remains a challenge in closing the treatment gap in secondary fracture prevention in the setting of a regional hospital in Singapore. Telecarers may potentially be an effective way to follow up patients post discharge to ensure adequate investigation and treatment of osteoporosis. More longitudinal data is needed to see how effective the care co-ordination and follow up rate will be with this new service.

Disclosures: Linsey Gani, None.

## SU0249

**Cost-Utility Analysis of Fracture-Risk Assessment Using MicroRNAs Compared to Standard Tools and No-Monitoring in the Austrian Female Population.** Evelyn Walter\*, Hanna Dellago<sup>2</sup>, Johannes Grillari<sup>3</sup>, Hans Peter Dimai<sup>4</sup>, Matthias Hackl<sup>2</sup>. <sup>1</sup>Institute for Pharmacoeconomic Research, Austria, <sup>2</sup>TAmiRNA GmbH, 1190 Vienna, Austria, <sup>3</sup>Department of Biotechnology, BOKU - University of Natural Resources and Life Sciences, Vienna, Austria, <sup>4</sup>Medical University of Graz, Department of Internal Medicine, Division of Endocrinology and Diabetology, Graz, Austria, Austria

**Background:** Effective management of osteoporosis requires accurate diagnosis and assessment of fracture risk in order to set preventive measures. Respective approaches include utilization of FRAX®, a web-based country-specific fracture risk assessment



tool, and bone mineral density measurement by Dual Energy X-ray Absorptiometry (DXA). Recently, microRNAs have been recognized as important regulators of bone physiology and potential biomarkers for fracture risk assessment. A fracture risk assessment tool based on microRNAs (osteomiR™ test) is currently being developed.

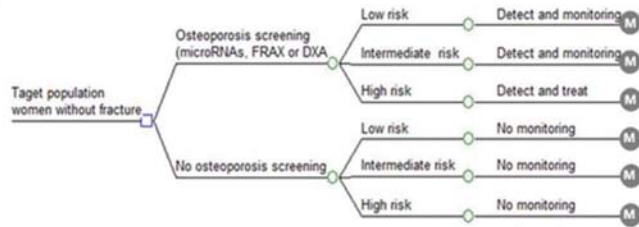
**Objective:** The aim of this study was to estimate the cost-effectiveness of fracture risk assessment and resulting treatment decisions for the Austrian female population using the osteomiR™ test compared against DXA, FRAX® or no screening/monitoring.

**Methods:** A cost utility model was developed to simulate long-term consequences of Austrian women from age 50 until age 100 or death with respect to osteoporosis. Markov-modelling techniques were used to calculate health state transitions of fracture incidence according to risk groups (high, intermediate, low). High-risk patients receive medical treatment. Probabilities were derived via systematic-literature-review; direct-costs (2015€) from published sources from the payer's perspective. QALYs, life-years (LYs) and costs were discounted (3% p.a). Results evaluate the incremental cost-effectiveness ratios (ICER) for osteomiR™ against the comparators, gains or losses of fractures, life years (LYs), quality-adjusted life years (QALYs), and direct costs.

**Results:** Fracture risk assessment and monitoring using the osteomiR™ test reduces fracture incidence compared with no monitoring, DXA and FRAX®. In the per-patient analysis, the ICER/QALY of osteomiR™ vs. no-monitoring was 13,103 €, vs. FRAX® 37,813 €, and vs. DXA -19,605 €, indicating that costs can be saved while gaining QALYs. Considering the total cohort over lifetime, the osteomiR™ test can avoid 57,919 fractures compared with DXA, 31,285 fractures compared with FRAX® and 133,394 fractures compared with no screening/monitoring. Sensitivity analysis confirmed the robustness of these findings.

**Conclusion:** Fracture-risk assessment using microRNAs dominates DXA-strategy and constitutes a cost-effective alternative to FRAX® and no screening/monitoring, respectively.

A



B

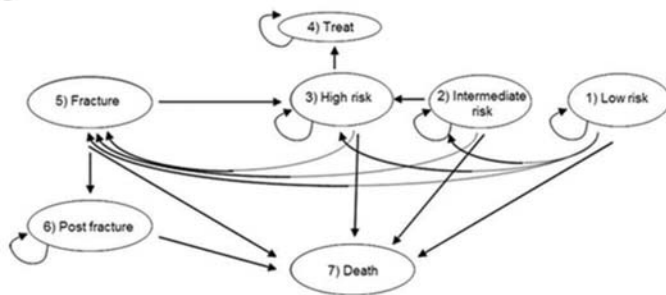


Figure: Markov Model. A) Decision tree for comparator strategies. B) Markov process

**Disclosures:** Evelyn Walter, None.

## SU0250

**Bone Mineral Density in the Osteopenic or Normal Range is a Disincentive to Treatment of Women at High Fracture Risk: Throwing Out the Baby, the Bathwater and Bathbub.** William Leslie<sup>1</sup>, Ego Seeman<sup>2</sup>, Suzanne Morin<sup>3</sup>, Lisa Lix<sup>1</sup>, Sumit Majumdar<sup>4</sup>. <sup>1</sup>University of Manitoba, Canada, <sup>2</sup>University of Melbourne, Australia, <sup>3</sup>McGill University, Canada, <sup>4</sup>University of Alberta, Canada

**Background:** Clinical practice guidelines for fracture prevention emphasize the need to identify and treat high risk individuals. However, fracture risk is continuous, not dichotomous. Given the Gaussian distribution of bone mineral density (BMD), most women sustaining fractures arise from the 'bell', not the 'tail', of the distribution. The WHO proposed a BMD T-score below -2.5 SD as a diagnostic threshold for defining the epidemiology of 'osteoporosis'. We hypothesized that this threshold serves, ironically, as a disincentive to initiation of treatment in those at high fracture risk should the BMD T-score not fall below -2.5 SD.

**Methods:** Using the population-based Manitoba BMD Registry, we identified untreated women age 50+ yr with baseline DXA in 2006-2012 and at least one year of follow up meeting one or more guidelines-based criteria for treatment: FRAX major fragility fracture (MFF) probability >20% or high-risk fracture equivalents (vertebral, hip or multiple non-hip/non-spine). The WHO category was assigned based upon the minimum BMD T-score for the femoral neck, total hip and lumbar spine. We identified initiation of new treatment in the year subsequent to BMD measurement using a

province-wide pharmacy database system and quantified the odds ratio (OR) of initiation of treatment using multivariable logistic regression with covariates of WHO T-score category (referent: osteoporotic), age (referent: 50-59 y), and calendar year (referent: 2006).

**Results:** Of 2517 eligible women, 1279 (51%) initiated treatment: 71% with osteoporotic, 14% osteopenic, 3% normal BMD. Non-osteoporotic BMD T-score was associated with a low OR (95% CI) for treatment: osteopenia 0.07 (0.05-0.09), normal BMD 0.01 (0.01-0.04). Similar results were seen in subgroups based on MFF probability >20% or >30%; hip fracture probability >3% or >6%; previous vertebral, hip or multiple non-hip/non-spine fractures (Table). Compared with women age 50-59 y, older women were more likely to initiate treatment: OR age 60-69 y 1.73 (1.15-2.59), age 70-79 y 1.82 (1.23-2.67), age 80+ y 1.47 (1.00-2.14). There was no effect of calendar year on odds of initiating treatment, despite publication of national guidelines in 2010 that highlighted the high risk criteria examined here.

**Conclusion:** A BMD T-score that does not fall below -2.5 SD appears to be a barrier to initiation of treatment, even among those at high fracture risk based upon other criteria.

	Treated %	Osteoporotic	Osteopenia	Normal BMD
All Women (N=2517)	51%	1.00 (REF)	0.07 (0.05-0.09)	0.01 (0.00-0.04)
MFF ≥ 20% (N=1939)	58%	1.00 (REF)	0.07 (0.05-0.09)	#
MFF ≥ 30% (N=449)	69%	1.00 (REF)	0.10 (0.05-0.20)	#
Hip ≥ 3% (N=1980)	59%	1.00 (REF)	0.08 (0.06-0.10)	#
Hip ≥ 6% (N=1614)	62%	1.00 (REF)	0.06 (0.04-0.09)	#
Prior vertebral fracture (N=417)	31%	1.00 (REF)	0.05 (0.03-0.09)	0.00 (0.00-0.04)
Prior hip fracture (N=302)	58%	1.00 (REF)	0.06 (0.03-0.12)	#
Multiple prior fractures (N=358)	40%	1.00 (REF)	0.05 (0.03-0.10)	0.04 (0.01-0.18)

Adjusted for age and calendar year. # = Insufficient numbers.

Table: Odds Ratios (95%CI) for Osteoporosis Treatment Initiation

**Disclosures:** William Leslie, None.

## SU0251

**Implementation of Fracture Liaison Service: a Mixed Methods Research Project.** Mireille Luc\*, Marie-Claude Beaulieu, Hélène Corriveau, Gilles Boire, Isabelle Gaboury. Université de Sherbrooke, Canada

### BACKGROUND

Fracture Liaison Services (FLS) have been proven clinically- and costly-effective. However, the factors that influence the success of their implementation are still poorly documented. An FLS, characterized by four main interventions (4i's) i.e. identification of patients with a new fragility fracture (FF), investigation of FF risk, initiation of medication and integration of a follow-up, was implemented in different sites of the Province of Quebec (CANADA). The aims of this project were to assess the implementation of the FLS interventions and to identify the factors that influenced their implementation.

### METHODS

A mixed methods research project was conducted, from January 2013 to March 2015, in the three implementation sites. Quantitative assessment of the interventions' implementation was calculated using FLS administrative database. Qualitative data were collected through semi-structured interviews with FLS stakeholders (coordinators, orthopaedic surgeons, and other team members), focus groups with the Implementation Steering Committee and minutes of the Committee meetings. The thematic analysis of interviews, focus groups and meeting minutes identified factors influencing the implementation, using Damschroder's Consolidated Framework for Implementation Research.

### RESULTS

A total of 457 patients were identified, and accepted to take part in the FLS interventions. Overall, 366 participants were investigated for their FF risk, and 299 initiated a medication. During the follow-up, communication with the family physicians was performed for 446 participants and 158 were referred to fall prevention activities. Both medication initiation and referencing to fall prevention interventions significantly varied between sites. Thirteen interviews and focus groups were conducted and analyzed, as well as minutes of 39 Committee meetings. Problematic accessibility hindered implementation of referencing to fall prevention. Most of the factors that greatly facilitated the implementation process were specific to dedicated coordinators e.g., full integration of their role and responsibilities, professional background and experience with FF. Stakeholders' leadership also played a catalytic role in implementing the FLS interventions successfully.

### CONCLUSION

This study highlights the relevance of consolidating the role of coordinators and involving leaders in a process to overcome access barriers, further promoting successful implementation of all FLS interventions.

**Disclosures:** Mireille Luc, None.

## SU0252

**Serum 25-hydroxyvitamin D Levels in Hospitalized Adults With Community-Acquired Pneumonia.** María Lorena Brance<sup>1</sup>, Julio Miljevic<sup>2</sup>, Raquel Tizziani<sup>3</sup>, Maria Eugenia Taberna<sup>4</sup>, Georgina P Grossi<sup>4</sup>, Pablo Toni<sup>4</sup>, Elina Valentini<sup>5</sup>, Andrea Trepac<sup>5</sup>, Julia Zaccardi<sup>6</sup>, Juan Moro<sup>6</sup>, Baltasar Finucci Curi<sup>7</sup>, Norberto Tamagnone<sup>7</sup>, Mariano Ramirez<sup>8</sup>, Javier Severini<sup>2</sup>, Pablo Chiarotti<sup>2</sup>, Francisco Consiglio<sup>9</sup>, Raúl Piñesky<sup>9</sup>, Albertina Ghelfi<sup>10</sup>, Jorge Kilstein<sup>10</sup>, Eduardo Street<sup>11</sup>, Dino Moretti<sup>12</sup>, Viviana Oliveto<sup>13</sup>, Marcelo Mariño<sup>14</sup>, Jorge Manera<sup>14</sup>, Lucas R Brun<sup>1</sup>. <sup>1</sup>Conicet, Argentina, <sup>2</sup>Hospital Juan Bautista Alberdi, Argentina, <sup>3</sup>Hospital Roque Saenz Peña, Argentina, <sup>4</sup>Hospital de Emergencias Clemente Alvarez, Argentina, <sup>5</sup>Sanatorio de la Mujer, Argentina, <sup>6</sup>Hospital Español, Argentina, <sup>7</sup>Hospital Provincial, Argentina, <sup>8</sup>Sanatorio Plaza, Argentina, <sup>9</sup>Sanatorio Laprida, Argentina, <sup>10</sup>Hospital Escuela Eva Perón, Argentina, <sup>11</sup>Sanatorio Rosendo García, Argentina, <sup>12</sup>Sanatorio Delta, Argentina, <sup>13</sup>Sanatorio IPAM, Argentina, <sup>14</sup>Sanatorio Británico, Argentina

Several studies have shown an association between vitamin D deficiency and increases susceptibility to respiratory tract infections. The aim of this study was to evaluate the serum 25-hydroxyvitamin D (25OHD) levels in hospitalized adults with community-acquired pneumonia (CAP) in Rosario city, Argentina. Materials and methods: An observational study with 207 hospitalized adults of both sex with CAP over 18 years from Rosario city (32°52'18"S) were carried out from July 2015 to June 2016. Exclusion criteria: CAP that was not the primary cause of hospitalization, patients hospitalized in the last 14 days, or who had oncological antecedents, AIDS, chronic renal or liver disease, autoimmune or connective diseases, or were treated with glucocorticoids, anticonvulsants or vitamin D. The results are expressed as mean±EE. Data distribution was analyzed using the Kolmogorov-Smirnov test and the comparison between groups was performed with parametric and non-parametric tests as appropriate. Results: 207 patients with CAP were recruited, and 167 were included in this study (59% women, 57.4±1.5 years, body mass index 27.1±0.8 kg/m<sup>2</sup> and 6.6±0.4 days of hospitalization). The most common clinical manifestations were: 81.8% fever, 77.1% cough with expectoration, 75.8% dyspnea and 40.2% chest pain. In the radiography, 62.5% showed unilobar infiltrate and in 37.5% were multilobar. Unilateral pleural effusion was found in 10.6% and only 4% was bilateral. The CURB65 index was 66.7% low risk, 16.0% intermediate risk and 17.3% high risk. According to Charlson comorbidity index (CCI) 53.5% had not comorbidity (CCI=0) and 46.5% showed CCI≥1. The 25OHD level (ng/ml) was: 11.92±0.58 (51.5%: <10 ng/ml, 33.5%: 10-20 ng/ml, 13.2%: 20-30 ng/ml, 1.8%: >30 ng/ml). 25OHD correlated with age (r= -0.17; p=0.02) and higher 25OHD were found in male (female: 10.83±0.67, male: 13.51±1.03, p=0.02). Due to the characteristics of the pathology under study, 54% were in winter, 28% spring, 2% summer and 15% autumn. 25OHD in winter-spring (11.05±0.55) were lower than summer-autumn (16.12±2.04, p=0.01). 25OHD correlated with CURB65 score (r= -0.13; p=0.049), CCI (r= -0.20, p=0.007) and with the 10 years life expectancy (%) calculated with age and CCI (r= 0.19; p=0.008). In addition, higher 25OHD were found with lower CCI (0= 13.04±0.89, <sup>3</sup>1= 10.50±0.79, p=0.009). It is concluded that hospitalized adults with CAP have lower 25OHD levels and would be associated with CAP severity.

**Disclosures:** María Lorena Brance, None.

## SU0253

**Short-Term Increased Physical Activity during Early Life Protects High Fat Diet-Induced Bone Resorption in Adult Mice.** Jin-Ran Chen<sup>1</sup>, Oxana P. Lazarenko<sup>1</sup>, Michael L. Blackburn<sup>1</sup>, Matthew E. Ferguson<sup>1</sup>, Eugenia Carvalho<sup>2</sup>, Kartik Shankar<sup>1</sup>, Elisabet Børshiem<sup>1</sup>. <sup>1</sup>Arkansas Children's Nutrition Center and the Department of Pediatrics, University of Arkansas for Medical Sciences, United States, <sup>2</sup>Department of geriatrics, University of Arkansas for Medical Sciences, United States

It has been recognized that mechanical stresses associated with physical activity (PA) have beneficial effects on increasing bone mineral density (BMD) and improving bone quality. On the other hand, high fat diet (HFD) and obesity increase bone marrow adiposity leading to increased excretion of pro-inflammatory cytokines that activate RANKL-induced bone resorption. In the current study, we investigated whether short-term increased PA via access to voluntary wheel running during early life has persistent and protective effects on HFD-induced bone resorption. Sixty (60) four-week-old male C57BL/6J mice were divided into two groups; without or with PA, access to voluntary running wheel (8 to 9 km per day) for 4 wks, with ad libitum access to control (17% fat) diet for all animals. After 4 wks with or without PA, mice were further subdivided into control diet or HFD [20% protein (casein), 35% carbohydrate (dextrose and maltodextrin), and 45% fat (corn oil)] groups for 8 wks, all animals were switched back to control diet for an additional 4 wks. Mice from the HFD groups were significantly heavier and obese, however, after 4 wks additional control diet, their body weights returned to levels of mice with control diet. Using peripheral quantitative CT (pQCT) and micro-CT scan on tibias *ex vivo*, we found that trabecular BMD and bone volume were significantly increased with PA in control diet animals compared to sedentary animals without access to wheels (102.8±3.5 vs. 91.5±4.2 mg/cm<sup>3</sup>, n=6, p<0.05). Early life PA protected HFD-induced trabecular bone loss (PA+HFD, 93.6±5.2 vs. HFD, 81.3±4.7 mg/cm<sup>3</sup>, n=6, p<0.05). Femur bone marrow cells were aspirated and cultured, and non-adherent hematopoietic cells collected the following day were used for RANKL-induced

osteoclastogenesis assay. We found that PA significantly blunted increases of HFD-induced osteoclastogenesis. In accordance with these data, signal transduction real-time PCR analysis showed that PA significantly inhibited HFD-induced Ezh2 and NFATc1 gene expression, and IRF8 expression was decreased in non-adherent hematopoietic cells from HFD mice. In conclusion, increased PA in early life is capable of altering the HFD-induced bone marrow hematopoietic cell differentiation program to protect against increased bone resorption. Supported in part by USDA-ARS Project 6026-51000-010-05S.

**Disclosures:** Jin-Ran Chen, None.

## SU0254

**Validity of Self-Reported Fractures in the VITamin D and Omega-3 Trial (VITAL).** Sharon Chou<sup>1</sup>, Catherine Donlon<sup>2</sup>, Nancy Cook<sup>3</sup>, Douglas Bauer<sup>4</sup>, Peggy Cawthon<sup>4</sup>, Dennis Black<sup>4</sup>, JoAnn Manson<sup>3</sup>, Julie Buring<sup>3</sup>, Meryl LeBoff<sup>5</sup>. <sup>1</sup>Brigham and Women's Hospital, Endocrinology, Diabetes and Hypertension Division, Instructor in Medicine, Harvard Medical School, United States, <sup>2</sup>Brigham and Women's Hospital, Endocrinology, Diabetes and Hypertension Division, United States, <sup>3</sup>Brigham and Women's Hospital, Division of Preventive Medicine, Professor of Medicine, Harvard Medical School, United States, <sup>4</sup>University of California, San Francisco, United States, <sup>5</sup>Brigham and Women's Hospital, Endocrinology, Diabetes and Hypertension Division, Professor of Medicine, Harvard Medical School, United States

Osteoporosis is the most common bone disease. Although vitamin D is widely used to benefit bone health, effects of supplemental vitamin D *alone* on fracture outcomes have been inconsistent. The parent VITamin D and Omega-3 Trial (VITAL) is a 2x2 factorial, double-blind, placebo-controlled study that is determining effects of supplemental vitamin D3 (2000 IU/day) and/or omega-3 fatty acid (1 g/day) on incident cancer and cardiovascular events in women ≥55 yrs and men ≥50 yrs. In an ancillary study to VITAL, we are testing in 25,874 US participants whether vitamin D supplements alone reduce risk of incident total, non-vertebral and hip fractures.<sup>1</sup> The goal of this analysis is to examine the validity of self-reported fractures in VITAL. Participants reported fractures on annual questionnaires or by phone and were then asked to consent to release medical records. Rigorous adjudication procedures were based on objective, masked review of radiographic and clinical records. Fractures were coded according to date of injury, location and level of trauma. Hip and femur fractures were further adjudicated by radiological image review by a radiologist. Fractures were confirmed, disconfirmed (determined not to be a fracture) or unconfirmed (lack of/insufficient medical records or assessment by a healthcare provider). After a mean of 2.5 yrs of follow-up, 1,623 participants reported a total of 1,727 fractures. Overall, 75.3% of all self-reported fractures were confirmed. Preliminary analyses show that 70.4%, 62.9%, 82.4% and 90% of spine, hip, wrist and humerus fractures have been confirmed, respectively. In multivariate analysis, predictors for confirmed fractures included age 75+, higher income and minor trauma. Compared with two prior studies (Women's Health Initiative,<sup>2</sup> Study of Osteoporotic Fractures<sup>3</sup>), there was a lower confirmation of self-reported hip fractures, driven by lack of available medical records. Among those with medical records, 91% of hip fractures were confirmed. Confirmation of total self-reported fractures was consistent with previous studies. VITAL also has access to CMS data, which will complement our ascertainment methods and allow for capture of unreported fractures among participants aged ≥65. The discrepancies in self-reported fractures support the rigorous adjudication methods for clinical studies. This study will resolve unanswered questions to inform clinical and public health guidelines on effects of supplemental vitamin D on fractures.

## References:

1. LeBoff MS, et al. Contemp Clin Trials. 2015;41:259-68.
2. Chen Z, et al. Menopause. 2004;11(3):264-74.
3. Nevitt MC, et al. Am J Epidemiol. 1992;135(5):490-9.

**Disclosures:** Sharon Chou, None.

## SU0255

**Build better bones with exercise: feasibility of a multicenter randomized controlled trial of 12 months of home exercise in women with a vertebral fracture.** Lora Giangregorio<sup>1</sup>, Lehana Thabane<sup>2</sup>, Jonathan Adachi<sup>2</sup>, Maureen Ashe<sup>3</sup>, Robert Bleakney<sup>4</sup>, Angela Cheung<sup>5</sup>, Jenna Gibbs<sup>1</sup>, Caitlin McArthur<sup>1</sup>, Keith Hill<sup>6</sup>, Jeffrey Templeton<sup>1</sup>, David Kendler<sup>3</sup>, Nicole Mittmann<sup>4</sup>, Sadhana Prasad<sup>2</sup>, Aliya Khan<sup>2</sup>, Sandra Kim<sup>7</sup>, Samuel Scherer<sup>8</sup>, John Wark<sup>8</sup>, Alexandra Papaioannou<sup>2</sup>. <sup>1</sup>University of Waterloo, Canada, <sup>2</sup>McMaster University, Canada, <sup>3</sup>University of British Columbia, Canada, <sup>4</sup>University of Toronto, Canada, <sup>5</sup>University Health Network, Canada, <sup>6</sup>Curtin University, Australia, <sup>7</sup>Women's College Hospital, Canada, <sup>8</sup>University of Melbourne, Australia

Clinical care guidelines recommend exercise for people with osteoporosis, including those with vertebral fractures, but there are few trials of efficacy, particularly in prevention of fractures, in those at high risk. However, a large sample size would be needed to detect the effect of exercise on fracture prevention. This pilot trial tested the feasibility of a definitive trial, focusing on recruitment concerns and effective methods for measuring adherence and harms in a home exercise program. Community-dwelling women



≥65 years old with at least one radiographically-confirmed vertebral compression fracture were recruited at 7 sites in 2 countries, randomized by computer (1:1) to 1 year of exercise and behavioral counseling, delivered by a physical therapist in 6 home visits over 8 months and monthly calls; participants were to exercise ≥3 times weekly. Controls received equal attention. Feasibility was defined by three criteria: 20 participants recruited/site, 75% of the sample remaining in the trial to complete the follow-up and 60% adherence to the intervention over the study. Recruitment reached the feasibility threshold, with 141 (71 intervention, 70 control) participants randomized, resulting in 20.14 participants being enrolled/site (range 6-32), though enrolment period nearly twice the 12 months planned. Only 11 participants (5 intervention, 6 control, 8% total) withdrew from the study. One remaining participant opted out of Visit 2, resulting in a completion rate of 91%. Overall adherence of 66% reached the feasibility threshold, despite a decrease toward the end of study. The intervention does not appear to confer extra risk to participants, with no significant increase in SAEs ( $U=2375$ ,  $p=.496$ ), falls ( $IRR=.967$ , 95%CI .575-1.625,  $p=.898$ ) or new vertebral fractures ( $IRR=1$ , 95%CI .424-2.356,  $p=1$ ) compared to controls, though as a pilot trial it was not designed to determine safety or efficacy of the intervention. This pilot trial demonstrates the feasibility of retention and adherence, but that recruitment was a challenge. Suggestions for future trials include having an active control group, having a large number of recruiting sites with multi-lingual support, selecting sites with a history of successful recruitment or a participant recruitment pool, having recruitment integrated with clinical visits instead of via referral and having a broader definition of high risk (e.g., history of any osteoporotic fracture, high fall risk plus osteoporosis).

**Disclosures:** Lora Giangregorio, None.

## SU0256

**Baseline Characteristics of the VITamin D and Omega-3 Trial (VITAL): Effects on Bone Structure and Architecture.** Catherine Donlon<sup>\*1</sup>, Sharon Chou<sup>2</sup>, Nancy Cook<sup>3</sup>, Trisha Copeland<sup>4</sup>, JoAnn Manson<sup>3</sup>, Julie Buring<sup>3</sup>, Meryl LeBoff<sup>5</sup>. <sup>1</sup>Brigham and Women's Hospital, Endocrinology, Diabetes and Hypertension Division, United States, <sup>2</sup>Brigham and Women's Hospital, Endocrinology, Diabetes and Hypertension Division, Instructor in Medicine, Harvard Medical School, United States, <sup>3</sup>Brigham and Women's Hospital, Division of Preventive Medicine, Professor of Medicine, Harvard Medical School, United States, <sup>4</sup>Brigham and Women's Hospital, Division of Preventive Medicine, United States, <sup>5</sup>Brigham and Women's Hospital, Endocrinology, Diabetes and Hypertension Division, Professor of Medicine, Harvard Medical School, United States

Vitamin D is widely used to support bone health, although effects of supplemental vitamin D alone on bone are inconsistent. While most previous randomized control trials (RCTs) have tested low doses of supplemental vitamin D (≤1000 IU/day) or vitamin D plus calcium, this ancillary study to the *VITamin D and Omega-3 Trial* (VITAL) aims to determine whether high-dose vitamin D<sub>3</sub> (2000 IU/d) affects bone health and body composition. The parent VITAL study is a 2x2 factorial designed RCT investigating effects of supplemental cholecalciferol and/or omega (ω)-3 fatty acids (1 g/d) for the primary prevention of cancer and cardiovascular disease. The study has a median of 5-yrs of treatment in 25,874 US men ≥50 yrs and women ≥55 yrs. Participants were enrolled in VITAL between Nov 2011 and Mar 2014. The intervention phase is slated to end on Dec 31, 2017, with an additional 2 yrs of post-intervention follow-up. In our ancillary study, *VITAL: Effects on Bone Structure and Architecture*,<sup>1</sup> in-person assessments were completed at baseline and 2-yrs post-randomization in a subcohort of 773 participants (46.8% women, 53.2% men). Medical histories were obtained by annual questionnaires. Body composition (fat and lean tissue) and bone mineral density (BMD) were determined by dual-energy X-ray absorptiometry. Baseline bone structure measures included Trabecular Bone Score and peripheral quantitative computed tomography. Physical performance was tested using grip strength and the Short Physical Performance Battery (SPPB; gait speed, standing balance, and chair stands). At baseline, participants had a mean age of 63.8±6.1 yrs and body mass index (BMI) of 28.31±5.14 kg/m<sup>2</sup>; 30% were obese. Mean BMD was greater in men than women at the spine (1.08±0.16 vs. 0.96±0.15 g/cm<sup>2</sup>), femoral neck (0.82±0.13 vs. 0.72±0.11 g/cm<sup>2</sup>), and whole body (1.23±0.13 vs. 1.08±0.10 g/cm<sup>2</sup>). Among participants, 25% had low muscle mass by appendicular lean mass/BMI (defined as men <0.789, women <0.512).<sup>2</sup> Few participants had sarcopenia by functional measures, including grip strength<sup>2</sup> and the SPPB. Most baseline characteristics were evenly distributed among treatment groups, suggesting that unidentified confounders will be similarly distributed. Sex differences among variables are being determined. At VITAL study completion, 2-yr follow-up data analyses will advance clinical and public health recommendations regarding the role of supplemental vitamin D<sub>3</sub> and/or ω-3 fatty acids on musculoskeletal outcomes.

### References:

1. LeBoff MS, et al. *Contemp Clin Trials*. 2015;41:259-68.
2. Studenski SA, et al. *J Gerontol A Biol Sci Med Sci*. 2014;69(5): 547-558.

**Disclosures:** Catherine Donlon, None.

## SU0257

**The Relationship of the Physical Performance and Osteoporosis Prevention with Vitamin D in Older African Americans (PODA).** John Aloia<sup>\*</sup>, Mageda Mikhail, Mageda Mikhail. Winthrop University Hospital, United States

**Background:** Vitamin D deficiency is associated with bone loss, poor physical performance and muscle strength. Older adults require higher intake of vitamin D to overcome secondary hyperparathyroidism related to aging. Little information is available on prevention or management of bone loss, or extra skeletal effects of vitamin D in older African Americans.

**Objective:** The study of relationship of Physical Performance and Osteoporosis Prevention with vitamin D in Older African Americans (PODA), is a randomized, double-blind, placebo-controlled trial designed to examine the effects of vitamin D on bone loss and physical performance in older African American women.

**Methods:** In this 3-year intervention trial, 260 healthy African American women older than 60 years of age, were assigned to receive either placebo or vitamin D3. Initial vitamin D3 dose was determined by the baseline serum 25OHD levels. The vitamin D3 dose was adjusted further at 3-month intervals, to maintain serum 25OHD level between 75-172 nmol/L. Subjects with baseline 25OHD < 20 nmol/L or > 65 nmol/L, were excluded from the study. Objective measures of anthropometric variables and neuromuscular strength [as measured by Short Physical Performance Battery (SPPB), grip strength and gait speed] were obtained. Total daily calcium intake of 1200 mg/d was ensured.

**Results:** No significant differences in baseline characteristics (demographics, BMD, grip strength, and serum total 25OHD) were noted between the active and placebo group. Overall, many participants were observed to have high physical assessment scores at baseline, which were well-preserved during follow-up. For example, 92% of participants in the active group and 91% of participants in the placebo group had a total balance score of 4/4 at baseline, which the vast majority maintained regardless of assigned treatment arm. For the 6-minute walk test and grip strength (continuous outcomes), no statistically significant interaction between treatment arms and time was observed ( $p$ -values 0.16 and 0.86, respectively). This means that although scores were observed to be declining over time ( $p$ -value < 0.001 for both assessments), there was no difference in this decline with respect to treatment arm.

**Conclusion:** The lack of vitamin D supplementation over a 3-year period did not differentially diminish physical performance in older African-American women with high physical assessment scores at baseline compared to those treated to maintain serum 25OHD above 75 nmol/L.

**Disclosures:** John Aloia, None.

## SU0258

**Risk Factors for Osteoporosis and Muscle Loss in Hemodialysis Patients.** Hiroyuki Tominaga<sup>\*1</sup>, Takao Setoguchi<sup>2</sup>, Manei Oku<sup>3</sup>, Akio Ido<sup>4</sup>, Setsuro Komiya<sup>1</sup>. <sup>1</sup>Department of Orthopaedic Surgery, Graduate School of Medical and Dental Sciences, Kagoshima University, Japan, <sup>2</sup>The Near-Future Locomotor Organ Medicine Creation Course (Kusunoki Kai), Graduate School of Medical and Dental Sciences, Kagoshima University, Japan, <sup>3</sup>Ikedo Hospital, Japan, <sup>4</sup>Digestive and Lifestyle Diseases, Kagoshima University, Japan

**Purpose:** Hemodialysis (HD) patients are at risk of bone loss and fracture. Sarcopenia, including reduced muscle mass and limited mobility/function, is also an important comorbidity in HD patients. Osteoporosis and sarcopenia both increase the risk of hospitalization and death in affected individuals. Malnutrition, which has been identified as a risk factor for osteoporosis and sarcopenia, also occurs as a complication in HD patients. In this study, we examined the relationship between osteoporosis, muscle volume and strength, and malnutrition.

**Methods:** Forty-six HD patients were evaluated. Bone mineral density and muscle volume were measured by dual-energy X-ray absorptiometry. Muscle volume and strength were evaluated based on lean mass index (LMI) and handgrip strength, respectively. The geriatric nutritional risk index (GNRI) was used to assess malnutrition.

**Results:** Multiple regression analysis showed that female sex (partial regression coefficient: -0.1209), low LMI (partial regression coefficient: 0.0429), and high total PINP (partial regression coefficient: -0.003) were risk factors for a low lumbar spine T-score. Female sex (partial regression coefficient: -0.1150) and low GNRI (partial regression coefficient: 0.0083) were risk factors for a low femoral neck T-score. Female sex (partial regression coefficient: -1.6822), long duration of HD (partial regression coefficient: -0.0045), and low GNRI (partial regression coefficient: 0.1834) were risk factors for low LMI. Advanced age (partial regression coefficient: -0.2392), female sex (partial regression coefficient: -9.7863), long duration of HD (partial regression coefficient: -0.0236), and low LMI (partial regression coefficient: 1.6748) were risk factors for low handgrip strength. Male sex (partial regression coefficient: -6.6305), short duration of HD (partial regression coefficient: 0.0147), and low LMI (partial regression coefficient: 2.6187) were risk factors for low GNRI.

**Conclusions:** In this study, the correlations of BMD with LMI and GNRI suggest that muscle preservation and nutritional management are required to maintain BMD. Similarly, the correlations of LMI and handgrip strength with GNRI and duration of HD suggest that nutritional management is necessary to maintain muscle strength and volume. Therefore, management of both muscle quality and nutrition are important for the prevention of osteoporosis and sarcopenia in HD patients.

**Disclosures:** Hiroyuki Tominaga, None.

## SU0259

**A Mechanism By Which Menopause Leads To Chronic Low-Grade Inflammation and Bone Loss.** Anna Cline-Smith\*, Elena Shashkova, Ariel Axelbaum, Rajeev Aurora. Saint Louis University School of Medicine, United States

It has been recognized for decades that estrogen (E<sub>2</sub>) is protective as the Framingham Study, Women's Health Initiative, among others, have documented the increase in risk of disease in the cardiovascular and skeletal systems as well as cancers, depression and autoimmunity postmenopause. We used ovariectomized (OVX) mice to study changes in cytokines that increase postmenopause. We found that IL-7 and IL-15 expression increased 10 d post-OVX in mice. IL-7 and IL-15 promote the development of memory T-cells (T<sub>MEM</sub>) and control their survival and expansion. T<sub>MEM</sub> develop during initial antigen exposure, and have long lifetimes to rapidly respond upon re-encounter with pathogen. To identify the source of IL-7 and IL-15 (abbreviated henceforth as IL-7+IL-15) we used reporter mice and flow cytometry, and independently immunofluorescence (IF) staining of bone sections. Both methods showed that dendritic cells (CD11c<sup>+</sup> DC) in the bone marrow express IL-7+IL-15 and that the increase in cytokines was due to an increase in the number of cells secreting IL-7 and IL-15, not an increase in the secretion per cell. We show that E<sub>2</sub> induces FasL and apoptosis in DC, so post-OVX DC lifespan increases leading to increase in IL-7+IL-15. Culturing T<sub>MEM</sub> with IL-7+IL-15, or DC in presence of absence of E<sub>2</sub> induced antigen-independent proliferation with secretion of IL-17A and TNF $\alpha$  in a subset of T<sub>MEM</sub>. Thus our results provide a novel mechanism by which E<sub>2</sub> depletion leads to a cytokine-dependent but antigen-independent low-grade activation of proinflammatory T-cells that promote bone loss and also most likely contribute to the multiple comorbidities observed in postmenopausal women.

**Disclosures:** Anna Cline-Smith, None.

## SU0260

**Characterization of the Remodeling Events Contributing to Trabecularization of Cortical Bone: A Study on Human Fibula Diaphysis.** Andreassen Christina M\*<sup>1</sup>, Jesper Skovhus Thomsen<sup>2</sup>, Lydia Peteva Bakalova<sup>3</sup>, Annemarie Br  l<sup>2</sup>, Ellen M. Hauge<sup>4</sup>, Gete Toft Eschen<sup>5</sup>, Birgitte Jul Kiil<sup>5</sup>, Jean-Marie Delaisse<sup>6</sup>, Mariana Elisabeth Kersh<sup>3</sup>, Thomas Levin Andersen<sup>6</sup>. <sup>1</sup>Orthopedic Research Laboratory, Department of Orthopedic Surgery & Traumatology, Odense University Hospital, Department of Clinical Institute, University of Southern Denmark, Denmark, <sup>2</sup>Dept. of Biomedicine, Aarhus University, Denmark, <sup>3</sup>Dept. of Mechanical Science and Engineering, University of Illinois, United States, <sup>4</sup>Dept. of Rheumatology, Aarhus University Hospital, Denmark, <sup>5</sup>Dept. of Plastic Surgery, Aarhus University Hospital, Denmark, <sup>6</sup>Dept. of Clinical Cell Biology, Vejle Hospital/Lillebaelt Hospital, Institute of Regional Health Research, University of Southern Denmark, Denmark

The trabecularization of cortical bone leads to a decrease of cortical thickness and to fragilization of the bones in the elderly. The present study investigates the characteristics of the intracortical remodeling events contributing to this trabecularization at the endosteal cortex.

The study was performed in bone specimens from the fibular diaphysis obtained from 20 patients (14 men and 6 women, 43–75 years) undergoing a jaw reconstruction. All specimens were embedded in plastic,  $\mu$ CT scanned and sectioned along the scanning plan, making it possible to investigate the same canals analyzed in 3D by  $\mu$ CT and in 2D by histology.

The 3D analysis by  $\mu$ CT showed a 3.5-fold higher porosity ( $p < 0.001$ ) and canals with a 3-fold larger diameter ( $p < 0.001$ ) at the endosteal half compared to the periosteal half, but no difference in the canal spacing. The 2D analysis of these canals as intracortical pores showed that pores with a diameter above 100  $\mu$ m were 3.3-fold more frequent in the endosteal half than in the periosteal half ( $p < 0.001$ ). It has been suggested that the generation of these enlarged pores in the endosteal half of the cortex is a key step in the ongoing trabecularization of the cortex. A detailed histological characterization of a total of 948 pores within these cortices revealed that these enlarged pores are preferentially resorptive pores overlapping with the pore of a preexisting parent osteon and with no bone formation. The odds of being such a resorptive pore were 1.6-fold higher in the endosteal half than in the periosteal half ( $p < 0.003$ ), and 6-fold higher in the enlarged pores ( $> 100 \mu$ m diameter) than in the smaller pores ( $p < 0.001$ ). Furthermore, the enlarged resorptive pores often resulted in coalescence of two or more pores of existing parent osteons. The odds of finding these enlarged coalescent resorptive pores were 1.9-fold higher in the endosteal half than in the periosteal half ( $p < 0.011$ ), and 8-fold higher in the enlarged pores ( $> 100 \mu$ m diameter) than in the smaller pores ( $p < 0.001$ ). Only 13.8% of the enlarged pores had signs of bone formation.

Collectively, both the 2D and 3D analyses showed that the trabecularization of the cortex may in part result from the accumulation of enlarged pores/canals in the endosteal part of cortex. These enlarged pores are preferentially enlarged coalescent resorptive pores with no signs of bone formation, suggesting that the bone formation is uncoupled from the bone resorption in these pores.

**Disclosures:** Andreassen Christina M, None.

## SU0261

**STRA6 as a possible candidate gene for pathogenesis of osteoporosis from RNA-seq analysis of human mesenchymal stem cells.** Insun Song\*<sup>1</sup>, Yong Jun Choi<sup>2</sup>, Ye-Yeon Won<sup>2</sup>, Yoon-Sok Chung<sup>2</sup>. <sup>1</sup>School of Biological Sciences, Seoul National University, Korea, Republic of, <sup>2</sup>Ajou University School of Medicine, Korea, Republic of

To explore novel candidate genes related to osteoporosis, we performed RNA-seq analysis of human mesenchymal stem cells (hMSCs) from subjects with osteoporosis (Group 3) and osteopenia (Group 2) and normal controls (Group 1) and identified differentially expressed genes (DEGs) from among the three human groups. DEGs were separated into 9 groups according to their gene expression patterns: UU (up and up), UF (up and flat), UD (up and down), FU (flat and up), FF (flat and flat), FD (flat and down), DU (down and up), DF (down and flat), and DD (down and down). Among the 42 DEGs, the Stimulated by Retinoic Acid 6 (STRA6) was highly expressed in the osteoporosis group and based on additional data with real-time PCR data, it was selected for further study. On whether STRA6 played a functional role in osteoblast or adipocyte differentiation, we examined the effects of forced STRA6 expression changes in pluripotent stem cell C3H10T1/2, preosteoblast cell MC3T3-E1 and stromal cell line ST2. Bone morphogenetic protein 2 enhanced STRA6 expression only at the early stage of osteoblast differentiation, and overexpression of STRA6 temporally inhibited the expression of osteoblastogenesis markers such as Runx2, bone sialoprotein and osteocalcin. Also, knockdown of STRA6 slightly enhanced nodule formation at the late stage of osteoblast differentiation, and overexpression of STRA6 in ST2 cells enhanced adipocyte differentiation. Taken together, STRA6 could be related to the pathogenesis of osteoporosis by promoting adipocyte differentiation over osteoblast differentiation in the hMSC population.

**Disclosures:** Insun Song, None.

## SU0262

**Supplementation with Calcium and Vitamin D prevents bone loss after Bariatric Surgery.** Katrien Corbeels\*<sup>1</sup>, Lieve Verlinden<sup>1</sup>, Mieke Verstuyf<sup>1</sup>, Matthias Lannoo<sup>1</sup>, Ann Mertens<sup>2</sup>, Christophe Matthys<sup>1</sup>, Ann Meulemans<sup>1</sup>, Geert Carmeliet<sup>1</sup>, Bart Van der Schueren<sup>1</sup>. <sup>1</sup>Laboratory Clinical and Experimental Endocrinology, KU Leuven, Belgium, <sup>2</sup>Department of Endocrinology, UZ Leuven, Belgium

Sleeve Gastrectomy (SG) and Roux-en-Y Gastric Bypass (RYGB) are the most commonly performed bariatric surgeries. However, after surgery, impaired calcium and vitamin D absorption can lead to metabolic bone disease. Therefore, we investigated whether dietary supplementation with calcium and vitamin D prevents bone loss. After 14 weeks on a high-fat diet, mice underwent sham surgery, SG or RYGB. After surgery, they received a standard diet (0.9% calcium, 4 units vitamin D/day) or diets containing extra calcium (2%) or extra calcium (2%) and vitamin D (40 units/day) for 8 weeks. In all mice, regardless of surgery and diet, serum calcium levels were within the normal range. Cortical thickness (Cort. Th.) and trabecular bone mass (Bone Volume/Total Volume, BV/TV) of the tibias decreased after SG or RYGB compared to sham-operated mice, all on standard diet (see table). Supplementation with calcium alone or calcium plus vitamin D almost completely prevented this bone loss. Additionally, the fractional calcium clearance showed a decreased trend after both SG and RYGB compared to sham-operated mice on a standard diet. With both supplementation strategies, fractional calcium clearance increased in sham-operated mice. However, in SG and RYGB, the calcium clearance remained low despite high supplementation of calcium and vitamin D. In conclusion, both SG and RYGB induced bone loss and both supplementation strategies were able to prevent this bone loss.

	Sham			SG			RYGB		
	Standard diet (n = 6)	+ Ca (n = 6)	+CaVitD (n = 6)	Standard diet (n = 6)	+ Ca (n = 4)	+CaVitD (n = 4)	Standard diet (n = 3)	+ Ca (n = 4)	+CaVitD (n = 3)
Cort. Th. (mm)	0.161 $\pm$ 0.003	0.173 $\pm$ 0.003	0.177 $\pm$ 0.003	0.121 $\pm$ 0.005 (1)	0.142 $\pm$ 0.006 (2)	0.162 $\pm$ 0.006 (2)	0.116 $\pm$ 0.007 (1)	0.162 $\pm$ 0.005 (3)	0.149 $\pm$ 0.006 (3)
BV/TV (%)	4.76 $\pm$ 0.45	5.79 $\pm$ 0.62 (2)	7.89 $\pm$ 0.87 (2,3,4)	2.50 $\pm$ 0.92	4.34 $\pm$ 1.05	4.85 $\pm$ 1.02	2.84 $\pm$ 0.96	5.19 $\pm$ 0.90	4.94 $\pm$ 0.16
Fractional calcium clearance (%)	0.54 $\pm$ 0.16	1.04 $\pm$ 0.15	1.35 $\pm$ 0.44	0.17 $\pm$ 0.16	0.36 $\pm$ 0.07	0.41 $\pm$ 0.08	0.16 $\pm$ 0.08	0.25 $\pm$ 0.08	0.15 $\pm$ 0.09

(1) significantly different from 'Sham on standard diet' ( $p < 0.0001$ )

(2) significantly different from 'SG on standard diet' ( $p < 0.05$ )

(3) significantly different from 'RYGB on standard diet' ( $p < 0.005$ )

(4) significantly different from 'SG on standard diet supplemented with calcium' ( $p < 0.05$ )

Table: Bone parameters and urinary excretion (mean  $\pm$  SEM). Statistical analysis: One-way ANOVA

**Disclosures:** Katrien Corbeels, None.



## SU0263

**Low bone mass and strength in juvenile rats with acquired epilepsy.** Hannah M. Davis<sup>1</sup>, Nicole D. Schartz<sup>2</sup>, Carmen Herrera<sup>1</sup>, Rafael Pacheco-Costa<sup>1</sup>, Season K. Wyatt<sup>2</sup>, Amy L. Brewster<sup>3</sup>, Lilian I. Plotkin<sup>1</sup>. <sup>1</sup>Indiana University School of Medicine, United States, <sup>2</sup>Purdue University, United States, <sup>3</sup>Purdue University, United Kingdom

Epilepsy is one of the most common neurological disorders and affects over 50 million people worldwide. Previous evidence indicates that individuals with a history of epilepsy are at higher risk for bone fractures compared to the general population. Further, individuals with epilepsy exhibit indicators of poor bone health, including hypocalcemia, hypophosphatemia, reduced vitamin D levels, increased PTH secretion, increased bone resorption, and reduced BMD. However, whether there is a direct effect of seizures on bone mass and strength is not known. To test this possibility, we used a Sprague Dawley rat model of acquired epilepsy in which 1-month-old male rats (150-200 g) subjected to a prolonged and continuous seizure (status epilepticus; SE) subsequently developed spontaneous recurrent seizures (epilepsy) 2 wks after. SE was induced with the chemoconvulsant pilocarpine (280–300 mg/kg, ip) and stopped with the anticonvulsant diazepam (10 mg/kg, ip) (n=5). Controls (n=6) were given saline. Five-six weeks after SE, the frequency of behavioral seizures was  $2.5 \pm 0.7$  every 48 h. Rats in this chronic epilepsy phase were sacrificed and tissue was collected.  $\mu$ CT analysis showed a 17% decrease in BA/TA in cortical bone of the femur middiaphysis, as well as increased marrow cavity area (25%) and periosteal perimeter (5%) in rats that had undergone SE compared to age-matched controls, suggesting decreased periosteal formation and increased endosteal resorption. Consistent with the changes in the femur geometry, structural parameters of mechanical strength were significantly decreased in the SE rats compared to controls. Specifically, the alterations in the femoral biomechanical properties included reductions in yield force (50%), ultimate force (8%), displacement to yield (35%), stiffness (16%), and work to yield (67%). Vertebra  $\mu$ CT analysis showed decreases in both the tissue volume (17%) and bone volume (21%), but BV/TV, or trabecular parameters were not changed in the SE rats. Both plasma CTX and alkaline phosphatase levels showed a tendency towards increase in SE rats compared to controls, without reaching significance ( $p=0.1/0.06$ ). A group of rats injected with pilocarpine but that did not develop SE showed values similar to controls for all parameters. Our results suggest that epileptic seizures deteriorate bone structure and strength, likely due to increased bone remodeling. Future studies will focus on the cellular and molecular basis of this bone phenotype.

**Disclosures:** Hannah M. Davis, None.

## SU0264

**Long non-coding RNAs and DNA methylation as regulators of mesenchymal stem cells (MSCs) of osteoporotic patients.** Alvaro del Real<sup>1\*</sup>, Jose A Riancho<sup>1</sup>, Leandro Castellano<sup>2</sup>, Maria Isabel Perez Nuñez<sup>3</sup>, Carolina Sañudo<sup>1</sup>, Carmen Garcia Ibarbia<sup>4</sup>, Esther Laguna<sup>3</sup>, Manuel Sumillera<sup>3</sup>, Mario F Fraga<sup>5</sup>, Agustin F Fernandez<sup>5</sup>. <sup>1</sup>Department of internal medicine, Hospital Universitario Marqués de Valdecilla-IDIVAL, University of Cantabria, Spain, <sup>2</sup>Department of Surgery and Cancer, Imperial College London, Imperial Centre for Translational and Experimental Medicine (ICTEM), Hammersmith Hospital, United Kingdom, <sup>3</sup>Department of Traumatology/Hospital Universitario Marqués de Valdecilla, University of Cantabria, Spain, <sup>4</sup>Department of internal medicine, Hospital Universitario Marqués de Valdecilla-IDIVAL, Universidad de Cantabria, Spain, <sup>5</sup>Nanomaterials and Nanotechnology Research Center (CINN-CSIC), Universidad de Oviedo-Principado de Asturias, Spain

Long non-coding RNAs (lncRNA) are important regulators of gene activity and cell function in a variety of tissues. The aim of this study was to determine the expression of lncRNAs in MSCs from osteoporotic patients and its relation with methylation marks and the expression of protein-coding genes.

MSCs were grown from the bone marrow of patients with osteoporotic hip fractures and controls with osteoarthritis. DNA and RNA were isolated from MSCs at first passage. Whole transcriptome analysis was done by RNAseq (n=20; Illumina HiSeq 2000), whereas DNA methylation was explored with the Human Methylation 450k array (n = 39; Illumina).

Transcriptome analysis showed that 118 nonprotein-coding genes and 778 protein-coding genes were differentially expressed (FDR<0.05); 98 and 665 of them, respectively, with fold-change >2. Among differentially expressed lncRNAs, most of them (72%) belonged to the antisense lncRNAs, followed by lncRNA and sense overlapping RNAs. There was a marked trend for association between differentially expressed lncRNAs and their cis protein-coding genes. In fact, 49% of the protein-coding genes situated in cis-position of a differentially expressed lncRNA were also differentially expressed. In line with this, Spearman correlation analysis showed R-values over 0.8 in 2135 coding-gene/lncRNAs pairs. In addition, enrichment analysis of the genes associated with lncRNAs showed significant overrepresentation in pathways related to bone metabolism, such as “regulation of ossification” ( $p=1.532E-5$ ) or “osteoblast differentiation” ( $p=5.861E-5$ ). On the other hand, we found 9038 differentially methylated CpGs (FDR<0.05, absolute Beta differences > 0.1) between patients with osteoporosis and controls. Interestingly, the frequency was similar in noncoding regions (946 out of 53084, 1.8%) and in other genomic regions (8092 out of 424625; 1.9%).

In conclusion, the majority of lncRNAs which are differentially expressed in MSCs obtained from patients with fractures are antisense-type. These lncRNAs are likely to play an important role in the regulation of gene transcription because they are correlated with cis protein-coding genes which are also differentially expressed and enriched in pathways related to bone formation. Differences in methylation marks are equally distributed between protein-coding and lncRNAs-coding regions, which suggests that interactions between these epigenetic mechanisms play a role in the differentiation of MSCs.

**Disclosures:** Alvaro del Real, None.

## SU0265

**Pyridinoline collagen cross-link content at actively forming trabecular surfaces is associated with fragility fracture incidence independent of BMD and the clinical diagnosis.** Sonja Gamsjaeger<sup>\*1</sup>, Erik Eriksen<sup>2</sup>, Francis Glorieux<sup>3</sup>, Frank Rauch<sup>4</sup>, David Dempster<sup>5</sup>, Hua Zhou<sup>6</sup>, Elizabeth Shane<sup>7</sup>, Adi Cohen<sup>8</sup>, John Bilezikian<sup>8</sup>, Mishaela Rubin<sup>9</sup>, Carolina Moreira<sup>10</sup>, Imre Pavo<sup>11</sup>, Jan Stepan<sup>12</sup>, Wolfgang Brozek<sup>13</sup>, Peter Fratzl<sup>14</sup>, Klaus Klaushofer<sup>13</sup>, Eleftherios Paschalis<sup>13</sup>. <sup>1</sup>Ludwig Boltzmann Institute of Osteology at the Hanusch Hospital of WGKK and AUVA Trauma Centre Meidling, 1st Medical Department, Hanusch Hospital, Vienna Austria, Austria, <sup>2</sup>Dept. of Endocrinology, Morbid Obesity and Preventive Medicine Oslo University Hospital Pb 4596 Nydalen N-0424 Oslo, Norway, <sup>3</sup>Shriners Hospital for Children-Canada, Canada, <sup>4</sup>Shriners Hospital for Children, Montreal, Canada, <sup>5</sup>College of Physicians and Surgeons Columbia university, New York, United States, <sup>6</sup>Regional Bone Center, Helen Hayes Hospital, United States, <sup>7</sup>Columbia University Medical Center, United States, <sup>8</sup>Division of Endocrinology, Columbia University Medical Center, United States, <sup>9</sup>Department of Medicine, Metabolic Bone Diseases Unit, College of Physicians & Surgeons Columbia University, United States, <sup>10</sup>Endocrinology Division, Federal University of Parana, Brazil, <sup>11</sup>Eli Lilly, Austria, <sup>12</sup>Institute of Rheumatology, Faculty of Medicine, Charles University, Prague, Czech Republic, Czech Republic, <sup>13</sup>Ludwig Boltzmann Institute of Osteology at the Hanusch Hospital of WGKK and AUVA Trauma Centre Meidling, 1st Medical Department, Hanusch Hospital, Austria, <sup>14</sup>Max Planck Institute of Colloids and Interfaces, Department of Biomaterials, Research Campus Golm, Germany

**Purpose:** Bone strength is dependent upon both the amount of bone present and the material properties of that bone. At the bone matrix level, bone material properties depend on bone turnover rate, patient age, tissue age within the same patient, as well as mineral and organic matrix composition. We recently reported on the variability in several of these parameters as a function of subject- and tissue-age in healthy women. The purpose of the present study was to test whether organic matrix quality is capable of identifying patients with fragile bone, as defined by fracture history, irrespective of the clinical diagnosis.

**Methods:** We used Raman microspectroscopy to compare iliac crest biopsies from 108 healthy women (H; ages 1 – 59) to biopsies from 130 women with a history of fragility fractures (Fx; ages 2 – 84) and 33 women with low BMD but no history of fragility fractures (No Fx; ages 23-74). The Fx group included women with mild osteogenesis imperfecta, idiopathic osteoporosis (IOP), postmenopausal osteoporosis, and postmenopausal osteoporosis coupled with chronic obstructive pulmonary disease (COPD). The NoFx group included women with low BMD values (premenopausal), COPD (postmenopausal), and hypoparathyroidism. We measured the following parameters at actively forming cancellous bone surfaces (as noted by the presence of distinct fluorescent double labels): mineral / matrix ratio (MM; affecting stiffness and brittleness), glycosaminoglycan (GAGs; known negative modulators of mineral homeostasis), and pyridinoline (pyd; trivalent enzymatic collagen cross-link, associated with fiber stiffness, ultimate stress and post-yield energy, bending strength, and post-yield strength) at actively forming cancellous bone surfaces (noted by the presence of distinct fluorescent double labels).

**Results:** Individual patient data were expressed as a function of patient- and tissue-age. By ANCOVA, MM did not differ among the 3 groups; GAGs discriminated between Fx and No Fx patients ( $p<0.05$ ), and pyd clearly ( $p<0.0001$ ) discriminated patients among the 3 groups.

**Conclusions:** The results of the present study indicate that bone matrix material properties are altered in patients with fragility fractures, independent of patient age and clinical etiology. These results may provide new insight into the pathogenesis and treatment of skeletal diseases, such as osteoporosis.

	AGE	Tissue Age	Skeletal Health	Sidak's post hoc
Mineral / Matrix	<0.0001	<0.0001	0.404	H vs Fx p=0.446 H vs. No Fx p=0.922 Fx vs. No Fx p=0.953
GAGs	<0.0001	0.524	0.017	H vs Fx p=0.990 H vs. No Fx p=0.051 Fx vs. No Fx p=0.016
Pyd	<0.0001	0.003	<0.0001	H vs Fx <0.0001 H vs. No Fx p<0.0001 Fx vs. No Fx <0.0001

Table

**Disclosures:** Sonja Gamsjaeger, None.

## SU0266

**A Randomized, Double-Blind, Placebo-Controlled, Multicenter 26-Week Study on the Effects of Dexlansoprazole and Esomeprazole on Bone Homeostasis in Healthy Postmenopausal Women.** Karen Hansen<sup>1</sup>, Jeri Nieves<sup>2</sup>, Sai Nudurupati<sup>3</sup>, David Metz<sup>4</sup>, Maria Claudia Perez<sup>5</sup>. <sup>1</sup>University of Wisconsin, United States, <sup>2</sup>Columbia University, United States, <sup>3</sup>AbbVie, Inc, United States, <sup>4</sup>University of Pennsylvania, United States, <sup>5</sup>Takeda Development Center Americas, Inc., United States

nivPurpose-Observational and epidemiologic data suggest an association between proton pump inhibitor (PPI) use and osteoporotic fractures. To evaluate potential mechanisms for this association, we randomized healthy postmenopausal women to two PPIs or placebo (PBO) and measured bone turnover, bone mineral density (BMD), true fractional calcium absorption (TFCA), and serum and urine mineral levels.

Methods-Postmenopausal women aged 45-75 were randomized to daily oral 60-mg dexlansoprazole (DEX), 40-mg esomeprazole (ESO) or PBO for 26 weeks with follow-up at week 52. Primary endpoints were 26-week % change in procollagen type 1 N-terminal propeptide (P1NP) and C-terminal telopeptide of type 1 collagen (CTX). Additional endpoints included changes in BMD (26 and 52 weeks) and serum and urine mineral levels (26 weeks). Fractures between baseline and week 26 were recorded as adverse events. TFCA (0 and 26 weeks) was measured in a subset (n=34) of patients.

Results-Excluding 1 disqualified site, 115 women were randomized and 93 completed the study. There were no substantial differences in age, BMI, baseline serum calcium, or vitamin D levels between groups. The bone turnover markers P1NP and CTX remained within normal range during 26 weeks of PPI therapy. Within each group, there was no statistically significant 26-week change in bone turnover, except a small increase in CTX levels with DEX (0.12 ng/mL, 95% CI 0.03-0.23). The 26-week median % increases in P1NP from baseline vs PBO were 19% (95% CI 7-30) for DEX and 18% (95% CI 7-30) for ESO. CTX levels increased vs PBO by 27% (95% CI 13-43) for DEX and 22% (95% CI 8-36) for ESO. PPI effects on BMD and serum and urine mineral levels were not statistically different vs PBO. Median % change from baseline in TFCA vs PBO was not statistically significant for DEX, but was significant for ESO (0.06, 95% CI 0.02-0.11). No spontaneous fractures occurred during treatment; 1 traumatic foot fracture (DEX) and 1 humerus fracture (circumstance unknown; ESO) occurred during follow-up.

Conclusions-Although bone turnover markers increased with PPI therapy, levels remained within the normal ranges. 26 weeks of DEX or ESO therapy did not reduce BMD, TFCA, or serum or urine mineral levels. ESO increased TFCA by <1%. Study results do not provide a clear explanation for the epidemiologic association between PPI therapy and fracture risk.

**Disclosures:** Karen Hansen, Takeda, Grant/Research Support.

## SU0267

**The Bone to Fat-free Mass Ratio—A reflector of the bone to muscle mass relationship.** Tom Sanchez<sup>1</sup>, Patrick Cunniff<sup>1</sup>, Jingmei Wang<sup>2</sup>. <sup>1</sup>Department of Research and Development, Norland at Swissray, United States, <sup>2</sup>Department of Research and Development, Norland at Swissray, China

Bone density is well known to respond to muscle activity or inactivity. If this is the case, we might consider monitoring bone within this mechanism by evaluating the ratio of total body bone mineral to fat free mass (TBMC/FFM) in a total body DXA study. To explore this we examined TBMC/FFM in male and female subjects.

Total body DXA studies were obtained during reference database studies in 100 male (6-58 years) and 100 female (7-68 years) subjects using a Norland scanner. Population statistics—including a Pearson normality test and the unpaired t-test—were computed for TBMC/FFM. Total body studies were then evaluated by regression analysis to examine the relationship between TBMC/FFM and total body lean or fat mass in male and female subjects. The study also examined the relationship between age and TBMC/FFM in males and females.

Population statistics showed TBMC/FFM for male (5.5±0.5) and female (6.5±0.8) subjects were normally distributed but differed significantly from each other (unpaired t-test, t = 10.71, p<0.0001). Regressions analysis between TBMC/FFM and total body lean mass showed significant positive relationships in male (Y = 9357X + 110369; Sy.x = 8888; r = 0.4837; p<0.0001) and female (Y = -5246X + 74931; Sy.x = 5574; r = 0.5921; p<0.0001) subjects. The relationship between TBMC/FFM and fat mass did not show

regressions different from zero in male (Y = 921.7X + 24189; Sy.x = 11680; r = 0.0414; p = 0.6826) or female (Y = 1789X + 17535; Sy.x = 9601; r = 0.1440; p = 0.1530). Finally, the relationship between age and TBMC/FFM indicates a significant negative relationship in male (Y = -0.0169X + 5.928; Sy.x = 0.4929; r = 0.3439; p = 0.0005) but no significant difference from zero in the female population (Y = 0.00397X + 6.324; Sy.x = 0.7786; r = 0.0723; p = 0.4745).

In conclusion, the study showed a significant positive relationship exists between TBMC/FFM and lean mass in both male and female subjects. The study also showed that TBMC/FFM in males and female populations differed significantly. The data suggest that subjects with a TBMC/FFM value better than two standard deviation below reference (male = 4.5 and female = 4.9) may increase bone density from increasing lean mass while TBMC/FFM values two standard deviations below reference (male = 4.5 and female = 4.9) may suggest low bone density originates outside the relationship to lean mass.

**Disclosures:** Tom Sanchez, None.

## SU0268

**Randomized controlled double blind trial: role of a putative  $\alpha$ -glucosidase inhibitor on bone turnover and GLP-1 after a mixed meal tolerance test.** Sue Shapses<sup>1</sup>, Alexandra Kreitman<sup>1</sup>, Lihong Hao<sup>1</sup>, Stephen Schneider<sup>2</sup>, Yvette Schlusser<sup>1</sup>. <sup>1</sup>Rutgers University, United States, <sup>2</sup>Robert Wood Johnson Medical Center, United States

Background: Studies show that  $\alpha$ -glucosidase inhibitors ( $\alpha$ -GIs) increase the postprandial secretion of glucagon-like peptide (GLP-1), in addition to attenuating serum glucose concentration. Evidence also indicates that the secretion of GLP-1 increases bone formation and may decrease bone resorption.

Purpose: This study was conducted to investigate whether a putative  $\alpha$ -GI, *Salacia chinensis*, would elevate GLP-1 and predict changes in markers of bone turnover.

Methods: Healthy volunteers were studied once monthly in a cross over design. Twenty overweight and obese individuals between the ages of 21-59 years were included (60% women). Fasting participants received either placebo or *Salacia* (500 mg) with a mixed breakfast meal. Blood was taken at baseline, 30, 60, 90, 120, and 180 minutes. Serum GLP-1, glucose, and bone markers, C-terminal telopeptide of type 1 collagen (CTX) and osteocalcin were analyzed.

Results: The average age was 34 ± 14 years, and body mass index was 28.7 ± 3.6 kg/m<sup>2</sup>. Serum glucose concentration was 93 ± 10 mg/dL. As expected, this compound with  $\alpha$ -GI properties attenuated the rise in postprandial glucose concentration after the meal (30 min) compared to placebo group (p < 0.05). The repeated measures analysis of variance indicated an interaction (time x treatment) for GLP-1 (p < 0.05) with higher values after treatment than placebo at 60 min. There was also an interaction (time x treatment) for CTX (p = 0.02) with lower concentrations at 90 and 120 minutes (p<0.01) in the treatment than placebo group. The integrated area under the curve for CTX was larger with treatment (p<0.01). A subset of subjects were measured for osteocalcin who demonstrated higher concentrations at 90 min with treatment than placebo (p < 0.01). Furthermore, there was an inverse correlation between GLP-1 and CTX in the treatment group at baseline (r = -0.59, p < 0.01), and after the meal (p < 0.05).

Conclusion: These findings show that a putative  $\alpha$ -GI attenuates peak serum glucose concentrations and increases GLP-1 after a mixed meal. GLP-1 agonists have been shown to reduce bone resorption and increase formation in previous intervention trials. In this study, the marked postprandial decrease in CTX and rise in OC after treatment indicates an acute response of bone turnover, and potential role for GLP-1.

**Disclosures:** Sue Shapses, None.

## SU0269

**Low-intensity repetitive blast injury results in long-term deleterious effects on bone.** Joshua Swift<sup>1</sup>, Aaron Hall<sup>1</sup>, Hanbing Zhou<sup>1</sup>, Drew Brown<sup>2</sup>, Sophia Kozlowski<sup>2</sup>, Matthew Allen<sup>2</sup>. <sup>1</sup>Naval Medical Research Center, United States, <sup>2</sup>Indiana University School of Medicine, United States

Mild traumatic brain injury (mTBI), due to blast exposure, has been a major cause of injury in recent wars. Evidence indicates that severe TBI results in dysregulation of bone metabolism within the axial skeleton, placing the affected individual at a higher risk of fracture. The purpose of this study was to expand on this evidence and determine the early and long-term effects of repeated low-intensity blast injury, inducing mTBI, on skeletal tissue distant to the injury site. To determine the timing and extent of potential damage to bone after blast overpressure (BOP), male Sprague-Dawley rodents (5-mos-old) were exposed to either BOP (74.5 kPa; n=30) or Sham (0 kPa; n=30) on 3 subsequent days. Femur bone properties and serum biomarkers were assessed 7, 30, and 90 days post-BOP and compared to Sham using microCT scans and serum ELISA, respectively. Mechanical testing was conducted by 4-point bending of femora to determine mechanical properties of cortical bone. No overt effects of repeated blast injury were detected on cancellous or cortical bone microarchitecture 7 or 30 days post-trauma. On D90, repeated BOP resulted in significantly lowered cancellous bone volume (BV/TV; -19%), trabecular thickness (Tb.Th; -8%), and trabecular number (Tb.N; -11%) as compared to sham animals. Cortical bone area (B.Ar) and cross-sectional thickness (Cs.Th) were 10% and 6% lower on D90 in BOP vs. Sham animals, respectively. Ultimate force of the femur mid-diaphysis was 9% lower (D7) and stiffness was 21% lower (D30) after blast injury with no differences in properties at D90. Circulating serum tartrate resistant acid phosphatase (TRAP 5b; biomarker for osteoclast number) was



significantly higher at all time points after BOP (+16% to +37%) vs. Sham. In addition, osteocalcin (biomarker of bone formation) was 6-8% lower after BOP (D30 and D90) as compared to Sham animals. Altogether, these data indicate that low-intensity repetitive blast injury has significant and long-term negative effects on cancellous bone structure and cortical bone strength at a site peripheral to the injury. This initial work demonstrates the skeletal injury may arise from early increases in bone resorption followed by latent reductions in formation activity, which persist for a minimum of 90 days post-injury.

**Disclosures:** Joshua Swift, None.

## SU0270

**Vitamin D level and calcium intake are related to PTH levels but not bone turnover in healthy young men at the age of peak bone mass.** Charlotte Verroken\*, Stefan Goemaere, Hans-Georg Zmierzak, Jean-Marc Kaufman, Bruno Lapauw. Unit for Osteoporosis and Metabolic Bone Diseases, Department of Endocrinology, Ghent University Hospital, Ghent, Belgium, Belgium

**OBJECTIVE:** In adult men after completion of growth, biochemical markers of bone turnover are remarkably high as compared to middle-aged men or young adult women. However, little is known about the determinants and biological significance hereof. The secretion of parathyroid hormone (PTH), a known determinant of bone turnover, is influenced by serum 25-hydroxyvitamin D [25(OH)D] levels and calcium intake. We investigated the relationship of 25(OH)D levels and calcium intake with biochemical markers of bone turnover in a cohort of young, healthy men.

**METHODS:** 994 healthy men aged 25-45 years were recruited in a cross-sectional, population-based sibling study. PTH, 25(OH)D, and bone turnover markers [procollagen type 1 amino-terminal propeptide (P1NP), osteocalcin (OC), C-terminal telopeptide of type 1 collagen (CTX)] were measured in fasting serum samples using electrochemoluminescence immunoassays. Mean daily calcium intake was estimated using a food questionnaire. Associations between PTH, 25(OH)D, calcium intake, and bone turnover markers were investigated using linear mixed-effects modeling.

**RESULTS:** Median PTH, 25(OH)D, P1NP, OC and CTX levels were 33.3 (25th-75th percentile 26.8-41.9) ng/L, 18.7 (14.2-23.9) ng/dL, 50.8 (41.7-63.7) µg/L, 21.7 (18.5-26.3) µg/L and 0.41 (0.31-0.52) µg/L, respectively. Seasonal variation was observed for 25(OH)D ( $p<0.001$ ) but not for PTH or bone turnover markers. Median calcium intake was 564 (427-743) mg/day and correlated positively with 25(OH)D ( $\beta=0.11, p<0.001$ ). PTH correlated inversely with 25(OH)D ( $\beta=-0.23, p<0.001$ ) and calcium intake ( $\beta=-0.07, p=0.028$ ) in unadjusted analyses, although the association with calcium intake lost significance when both 25(OH)D and calcium intake were included in the model. Moreover, a stronger association between PTH and 25(OH)D was observed in subjects with calcium intake below median as compared to subjects above median ( $\beta=-0.27$  vs.  $\beta=-0.16$ , both  $p<0.001$ ;  $p$  for interaction 0.065). In age-, height- and weight-adjusted analyses, P1NP, OC and CTX were positively associated with PTH ( $\beta=0.06, p=0.026$ ;  $\beta=0.12, p<0.001$ ;  $\beta=0.08, p=0.007$ ), whereas no associations were observed with 25(OH)D levels or calcium intake.

**CONCLUSION:** In healthy young men after completion of growth, low calcium intake and 25(OH)D levels are associated with higher PTH levels, and PTH is positively associated with bone turnover markers. However, 25(OH)D and calcium intake are not directly associated with bone turnover markers.

**Disclosures:** Charlotte Verroken, None.

## SU0271

**Renin-angiotensin system inhibition ameliorates bone fragility due to altered material properties in uremic rats with secondary hyperparathyroidism.** Suguru Yamamoto\*<sup>1</sup>, Takuya Wakamatsu<sup>1</sup>, Yoshiko Iwasaki<sup>2</sup>, Akemi Ito<sup>3</sup>, Ichiei Narita<sup>1</sup>, Masafumi Fukagawa<sup>4</sup>, Junichiro Kazama<sup>5</sup>. <sup>1</sup>Division of Clinical Nephrology and Rheumatology Niigata University Graduate School of Medical and Dental Sciences, Japan, <sup>2</sup>Department of Health Sciences, Oita University of Nursing and Health Sciences, Japan, <sup>3</sup>Ito Bone Histomorphometry Institute, Japan, <sup>4</sup>Tokai University, Japan, <sup>5</sup>Fukushima Medical University, Japan

**Background:** Chronic kidney disease (CKD) patients are at an extremely high risk of bone fracture, for which altered material properties has recently been considered to be a major mechanism besides the decrease of bone mineral density. Although we have recently reported that pharmacological use of renin-angiotensin system (RAS) inhibitors is associated with incident of fracture in hemodialysis patients, especially those with moderate secondary hyperparathyroidism (SHPT), the underlying mechanisms remain unknown.

**Methods:** Male Sprague-Dawley rats were divided into two groups, comprising only 5/6 nephrectomy (CKD with high turnover bone, HTB) or subtotal nephrectomy plus parathyroidectomy (CKD with low turnover bone, LTB) at 13 weeks of age. Each group was treated either with olmesartan (HTB-O and LTB-O) or hydralazine (HTB-H and LTB-H) to maintain comparable blood pressure for 6 weeks. Storage modulus by dynamic mechanical analysis and confocal Raman spectroscopy in femoral bone were measured. Empty lacunae in cancellous bone were measured to detect apoptosis of osteocytes.

**Results:** Comparable levels of kidney dysfunction, blood pressure and serum parathyroid hormone (PTH) level (HTB-O 907.6±414.1 pg/mL vs HTB-H 668.6±156.1 pg/

mL,  $p=0.14$ ) were observed in the HTB-O and HTB-H rats. HTB-O showed higher bone elasticity (storage modulus;  $3.01 \times 10^9 \pm 1.00 \times 10^9$  Pa vs HTB-H  $1.19 \times 10^9 \pm 0.79 \times 10^9$  Pa,  $p=0.046$ ), lower pentosidine-to-matrix ratio and higher crystallinity as compared to HTB-H. HTB-O also showed less osteocyte apoptosis (empty lacunae;  $36.6 \pm 12.2$  N/mm<sup>2</sup> vs Nx-H  $67.9 \pm 13.6$  N/mm<sup>2</sup>,  $p<0.01$ ) in cancellous bone.

In low turnover bone model, low serum PTH level was found both in LTB-O and LTB-H (LTB-O  $53.9 \pm 38.9$  pg/mL vs LTB-H  $22.1 \pm 4.2$  pg/mL,  $p=0.20$ ). LTB-O showed decrease of pentosidine-to-matrix ratio ( $0.41 \pm 0.07$  vs LTB-H  $0.75 \pm 0.24$ ,  $p=0.03$ ) while there were no significant difference between LTB-O and LTB-H in bone elasticity, as well as bone crystallinity.

**Conclusion:** Angiotensin II receptor blockade modulated physical property of bone mainly owing to improvement of material property in uremic rats with secondary hyperparathyroidism. The effect was disappeared in those with parathyroidectomy. Hence, the RAS inhibitor reduces fragility fracture risk specifically in CKD patients with secondary hyperparathyroidism.

**Disclosures:** Suguru Yamamoto, None.

## SU0272

**Severity of chronic obstructive pulmonary disease is associated with low muscle mass, osteoporosis and fragility fractures.** Roberta Graumam\*, Marcelo Pinheiro, Vera Szejnfeld, Aurora Cabral, Luis Eduardo Nery, Charles Castro. Universidade Federal de São Paulo - Escola Paulista de Medicina, Brazil

**Background/purpose:** Chronic Obstructive Pulmonary Disease (COPD) has been associated with different co-morbidities. The use of glucocorticoid and vertebral osteoporotic fractures in these patients may further impair respiratory function and impact negatively on prognosis. In the present study we assess the prevalence of osteoporosis and fragility fractures in patients with COPD as compared to healthy controls. Potential associations between bone fragility outcomes with clinical, demographic and epidemiological parameters were also investigated. **Methods:** A total of 97 patients with COPD answered a structured clinical questionnaire detailing disease variables and underwent bone densitometry (DXA), radiographic survey for morphometric vertebral fractures, pulmonary function and laboratorial tests. Patients with other comorbidities and medications (other than glucocorticoid) that could affect bone metabolism were excluded. **Results:** A total of 47 men ( $65 \pm 8$  years old) and 52 women ( $64 \pm 10$  years old) with COPD and 67 healthy controls matched by gender were included. Previous diagnosis of osteoporosis was reported in only 6.3% of the patients while densitometric osteoporosis and osteopenia was detected in 40.2% and 39.2%, respectively, and fragility fractures (vertebral and non-vertebral) were observed in about 23.7% of them. Only 5 patients (5.1%) were receiving treatment for osteoporosis. COPD severity measured by pulmonary function test was associated with worse bone outcomes: FEV1 and BMD were correlated in both men (total femur:  $r=0.451$ ;  $p=0.004$ ) and women (spine:  $r=0.561$ ;  $p<0.001$  and total femur:  $r=0.622$ ;  $p<0.001$ ). As compared to healthy controls, severe COPD (FEV1<50%) was associated with lower total skeletal lean mass ( $p=0.002$ ), skeletal lean mass index ( $p=0.005$ ) and lower BMD at spine and proximal femur ( $p=0.001$  for all sites). Multivariate linear regression analyses demonstrated that FEV1 was significantly associated with BMD at the lumbar spine, femoral neck and total femur either for men or women ( $p<0.05$ ). **Conclusion:** Osteoporosis and fragility fractures are highly prevalent in patients with COPD. Severity of the disease as measured by spirometry (FEV1) correlates significantly with bone mass and body composition parameters. These findings suggest that higher surveillance for osteoporosis is required in COPD patients, especially in those with severe disease.

**Disclosures:** Roberta Graumam, None.

## SU0273

**Longer duration of TSH suppression can affect Bone Mineral Density and Trabecular Bone Score in patients with Differentiated Thyroid Cancer.** Maria Luisa De Mingo\*, Sonsoles Guadalix, Maria Begoña Lopez Alvarez, Eduardo Ferrero Herrero, Guillermo Martinez Diaz-Guerra, Federico Hawkins. University Hospital 12 Octubre, Spain

There is still controversy about the effect of long-term TSH suppression to less than 0.1 µU/ml in high-risk well differentiated Thyroid Carcinoma (DTC) or maintenance of TSH slightly less (0.1-0.5 µU/ml for low and intermediate risk patients on bone density and quality). The aim of our study was to analyze the impact of longer TSH suppression in DTC patients followed in our Unit. **Patients and methods.** We studied 170 patients with DTC (age  $51.4 \pm 12$  yrs.; 60 pre and 101 postmenopausal women) followed in our Unit for a medium of  $12.2 \pm 6.2$  yrs. Patients treated with antiosteoporotic drugs or having diseases that affected bone metabolism were excluded. None had clinical secondary hypoparathyroidism. All patients had a DXA study at diagnosis, and at the last study; BMD was measured at L1-L4 using Discovery W Hologic and TBS using Medimaps (iN Sight software version 2.1). Blood samples were analyzed for TSH levels, thyroid hormones, bone markers at baseline and at the end. BMD and TBS results were adjusted by age, BMI, fracture history and menopausal status. **Results.** TSH suppression was <0.1 µU/ml in 26.8% of patients, between 0.1-0.5 µU/ml in 25.6% and non suppression >0.5 µU/ml in 47.6%. TSH suppression (<0.5 µU/ml;  $n=46$ ) >10 yrs. induced a decrease in TBS ( $1.411 \pm 0.158$  vs  $1.273 \pm 0.121$ ,  $p=0.01$ ), CL-BMD ( $0.978 \text{ g/cm}^2 \pm 0.116$  vs  $0.856 \text{ g/cm}^2 \pm 0.105$ ,  $p=0.00$ ) and CF-BMD ( $0.817 \text{ g/cm}^2 \pm 0.156$  vs  $0.809 \text{ g/cm}^2 \pm 0.122$ ,  $p=0.00$ ) and in TBS ( $1.371 \text{ g/cm}^2 \pm 0.128$  vs  $1.299 \text{ g/cm}^2 \pm 0.118$ ,  $p=0.00$ ), at 5-9 yrs. According to menopausal status, premenopausal women with >10 yrs. ( $n=39$ ) of TSH suppression,

had lower TBS, CL-BMD and CF BMD ( $p=0.00$ ) compared with  $< 10$  yrs. ( $n=30$ ). Postmenopausal women had only lower TBS after  $>5$  yrs. of duration of TSH suppression ( $1.321 \pm 0.113$  vs  $1.255 \pm 0.103$ ,  $p=0.00$ ). Conclusions: Our study demonstrate a decrease in TBS in DTC patients with suppression of TSH at  $>5$  yrs. BMD and TBS was significantly lower with a duration of  $>10$  yrs. of TSH suppression. Therefore bone density and bone quality should be studied in long-term ( $> 5$  yrs.) TSH suppressed DTC patients.

**Disclosures:** Maria Luisa De Mingo, None.

## SU0274

**Cumulative Epidural Steroid Dose is Associated with Lower Spine Volumetric Bone Density.** Yi Liu<sup>\*1</sup>, Lulu Yang<sup>2</sup>, John Carrino<sup>1</sup>, Huong Do<sup>1</sup>, Tariq Chukir<sup>3</sup>, Eric Holder<sup>1</sup>, Richard Bockman<sup>1</sup>, Joel Press<sup>1</sup>, Emily Stein<sup>1</sup>. <sup>1</sup>Hospital for Special Surgery, United States, <sup>2</sup>Rutgers School of Public Health, United States, <sup>3</sup>Weill Cornell Medical College, United States

Epidural steroid injections (ESI) are a common and effective treatment for low back pain. While the negative skeletal effects of oral and intravenous glucocorticoids are well established, little is known about whether and to what extent ESI impact bone quality. DXA, the standard tool for assessment of bone density is subject to substantial artifact in patients with spine pathology and may therefore have limited utility in the population receiving ESI.

The objective of the study was to investigate the relationship between ESI exposure and volumetric bone density (vBMD) at the lumbar spine (LS) using central quantitative computed tomography (cQCT). We hypothesized that patients who received a greater cumulative dose of ESI would have lower vBMD of the LS. We performed a retrospective study of all patients at our institution who had LS CT scans between 6/15 and 12/16 and who had received at least one ESI for low back pain in the 5 years prior to the CT. Cumulative ESI dose was calculated as the product of the number of ESI injections and the triamcinolone (or calculated equivalent) dose at each injection. vBMD was measured at T12 through L5 using QCTPro phantomless software (Mindways). Patients with a history of oral or intravenous glucocorticoid use were excluded. Of 141 subjects who met inclusion criteria, 106 had scans suitable for analysis. Mean age of subjects included was  $65 \pm 14$  years, mean BMI  $28 \pm 6$  kg/m<sup>2</sup>, 49% were women and 96% Caucasian. Median number of ESI injections over the study duration was 4, range 1 to 16. Median cumulative ESI dosage was 180 mg of triamcinolone, range 80 to 1300 mg. Higher cumulative ESI dose was associated with lower mean vBMD at L1-L2, the standard site for measurement ( $r = -0.35$ ;  $p < 0.0003$ ). Similarly, higher cumulative dose was associated with lower mean vBMD when all vertebrae (T12-L5) were included ( $r = -0.30$ ;  $p < 0.002$ ). There was no difference in the relationship between cumulative dose and vBMD according to sex. In summary, we found that there was a significant inverse relationship between cumulative ESI dose and vBMD at the LS. To our knowledge this is the first study to measure vBMD in patients treated with ESI. Given the high prevalence of ESI treatment for back pain, our preliminary findings of a negative relationship between ESI use and vBMD are of concern. Prospective, controlled studies are needed to confirm these findings and to help identify the best strategies for preventing bone loss in this population.

**Disclosures:** Yi Liu, None.

## SU0275

**Analysing the Effect of Multiple Sclerosis on Vitamin D Related Biochemical Markers of Bone Remodelling.** Malachi McKenna<sup>\*</sup>, Barbara Murray, Niall Tubridy, Mark Kilbane, St. Vincent's University Hospital, Ireland

**Background:** The Irish population is at risk of vitamin D deficiency during the winter months, but the secular trend over the past 40 years is for marked improvement. Multiple sclerosis (MS) is common in Ireland with a latitudinal pattern favouring high incidence in northern regions; MS is linked with vitamin D status as a causal factor. We sought firstly to study the relationship between vitamin D status and vitamin D-related bone biochemistry in the total group incorporating three different geographic regions in Ireland, and secondly to evaluate if MS had an independent effect on vitamin D related markers of bone remodelling.

**Methods:** Using a case-control design of 165 pairs (MS patient and matched control) residing in three different geographic regions during winter months, we measured serum 25-hydroxyvitamin D (25OHD), parathyroid hormone (PTH), C-terminal telopeptide of type I collagen (CTX) and total procollagen type I amino-terminal propeptide (PINP). Given the paired case-control design, associations were explored using mixed-effects linear regression analysis with the patient-control pair as a random effect and after log transformation of 25OHD; a two-way interaction effect for vitamin D status (25OHD  $< 30$  nmol/L) and presence of MS on PTH, CTX, and PINP was tested.

**Results:** In the total group, just over one-third (34.5%) had 25OHD  $< 30$  nmol/L; PTH was elevated in 7.6%; CTX was not elevated in any case; and, PINP was elevated in 4.5%. On mixed-effects linear regression analysis after adjusting for confounders (age, sex, renal function, and serum albumin), we demonstrated the principal determinant of 25OHD was location ( $p < 0.001$ ), of PTH was 25OHD ( $p < 0.001$ ), of CTX was PTH ( $p < 0.001$ ), and of PINP was PTH ( $p < 0.001$ ). MS did not have an independent effect on PTH ( $p = 0.921$ ), CTX ( $p = 0.912$ ), or PINP ( $p = 0.495$ ). As regards an interaction effect, the presence of MS and 25OHD  $< 30$  nmol/L was not significant but tended towards having lower PTH ( $p = 0.207$ ), lower CTX ( $p = 0.262$ ), and lower PINP ( $p = 0.473$ ).

**Conclusions:** Although vitamin D status has improved immensely in Ireland over the past 40 years, the population is still vulnerable to risk of vitamin D deficiency during the

winter months, but only a minority had abnormality in the secondary indices of vitamin D deficiency. MS had no independent effect on parathyroid status or bone remodelling activity, but the possibility of an interaction effect between MS and low 25OHD on these indices was suggested.

**Disclosures:** Malachi McKenna, None.

## SU0276

**Bone Histomorphometry in type 2 Diabetic Premenopausal Women.** Victoria Borba<sup>\*1</sup>, Carolina Moreira<sup>2</sup>, Vicente Andrade<sup>1</sup>, Cassio Ramos<sup>1</sup>, Cesar Boguszewski<sup>1</sup>, Cleber Rafael Da Costa<sup>3</sup>. <sup>1</sup>Endocrine Division of Federal University of Parana- SEMPR, Brazil, <sup>2</sup>Endocrine Division of Federal University of Parana- SEMPR; Laboratory PRO, Bone Histomorphometry Section, Pro Renal Foundation, Brazil, <sup>3</sup>Laboratory PRO, Bone Histomorphometry Section, Pro Renal Foundation, Brazil

Few studies have evaluated bone histomorphometry in type 2 diabetic patients (DM2) and none has established if the disease control plays a role on bone structure, remodeling and bone marrow adipocytes. The aim of this study is to present preliminary and descriptive data on bone histomorphometry in premenopausal women with DM2 with different levels of glucose control. Bone biopsy followed by tetracycline labelling was obtained for analysis of static and dynamic parameters of bone histomorphometry as well as adipocytes counting. To date, 11 bone biopsies with complete analysis have been performed in a group of patients with mean age of  $40.9 \pm 6.0$  years, mean duration of DM2 of  $6.8 \pm 2.6$  years and median glycosylated haemoglobin (HbA1c) of 7.6 % (range 5.5-12.3). Patients were divided in two groups: HbA1c lower than 7% (N:5) and greater than 7% (N:6). Initial results have shown a normal trabecular bone volume and cortical thickness with no difference between the groups. Mean bone formation rate is  $0.023 \pm 0.014 \mu\text{m}^3 \cdot \mu\text{m}^2 \cdot \text{day}$ . An increase in bone marrow adipocytes numbers and volume was observed in both groups. Our preliminary results suggest that premenopausal women with DM2 present normal bone microstructure, a trend to lower bone formation rate and increased marrow adiposity.

**Disclosures:** Victoria Borba, None.

## SU0277

**Long-term Effects of Severe Burn Injury on Bone Turnover and Micro-architecture.** Gabriela Katharina Muschitz<sup>\*1</sup>, Elisabeth Schwabegger<sup>2</sup>, Andreas Baierl<sup>3</sup>, Alexandra Fochtmann<sup>1</sup>, Roland Kocijan<sup>4</sup>, Judith Haschka<sup>4</sup>, Wolfgang Gruther<sup>5</sup>, Jakob Schanda<sup>6</sup>, Heinrich Resch<sup>4</sup>, Thomas Rath<sup>1</sup>, Peter Pietschmann<sup>7</sup>, Christian Muschitz<sup>4</sup>. <sup>1</sup>Division of Plastic and Reconstructive Surgery, Department of Surgery, Medical University Vienna, Austria, <sup>2</sup>Department of Plastic, Reconstructive and Aesthetic Surgery, Medical University of Innsbruck, Austria, <sup>3</sup>Department of Statistics and Operations Research, the University of Vienna, Austria, <sup>4</sup>St. Vincent Hospital - VINFORCE, Austria, <sup>5</sup>HealthPi Medical Center, Wollzeile 1, Austria, <sup>6</sup>AUVA Trauma Center Meidling, Austria, <sup>7</sup>Department of Pathophysiology and Allergy Research, Center for Pathophysiology, Infectiology and Immunology, Medical University of Vienna, Austria

**Purpose:** Severe burn injury triggers massive alterations in stress hormone levels. **Methods:** This study evaluated bone microarchitecture measured by non-invasive HR-pQCT. Changes of serum BTM as well as regulators of bone signaling pathways involved in skeletal health were assessed. Standardized effect sizes as a quantitative measure regarding the impact of serum changes and the prediction of these changes on bone microarchitecture were investigated. **Results:** In total 32 male patients with a severe burn injury (median total body surface area, TBSA, 40.5 %; median age 40.5 years) and 28 matched male controls (median age 38.3 years) over a period of 24 months were included. In patients who had sustained a thermal injury trabecular and cortical bone microstructure showed a continuous decline, whereas cortical porosity (Ct. Po) and pore volume increased. Initially elevated levels of BTM and C reactive protein (CRP) continuously decreased over time, but remained elevated. In contrast levels of sRANKL increased over time. Osteocalcin, BALP, PINP, and CTX acutely reflected the increase of Ct. Po at the radius ( $R^2 = 0.41$ ), followed by the reduction of trabecular thickness at the tibia ( $R^2 = 0.28$ ). **Conclusions:** Rapid and sustained changes of markers of bone resorption, formation and regulators of bone signaling pathways were observed in adult male patients. These alterations are directly linked to a prolonged deterioration of bone microarchitecture with unknown clinical outcome.

**Disclosures:** Gabriela Katharina Muschitz, None.



## SU0278

**Abnormal Microarchitecture and Stiffness in Postmenopausal Women Treated with Chronic Inhaled Glucocorticoids.** Yi Liu<sup>\*1</sup>, Emily Dimango<sup>2</sup>, Mariana Bucovsky<sup>2</sup>, Kyle Nishiyama<sup>2</sup>, Sanchita Agarwal<sup>2</sup>, X. Edward Guo<sup>2</sup>, Elizabeth Shane<sup>2</sup>, Emily Stein<sup>1</sup>. <sup>1</sup>Hospital for Special Surgery, United States, <sup>2</sup>Columbia University, United States

While oral glucocorticoids are well recognized to have destructive skeletal effects, far less is known about the effects of inhaled glucocorticoids (IGCs). This knowledge gap is important because of the prevalence and chronic nature of IGC use. Some studies have found an increased fracture risk in IGC users, but the mechanism is not known. The detrimental skeletal effects of IGCs may be greatest in postmenopausal (PM) women, in whom IGCs may augment negative effects of estrogen loss and aging. Despite this potential, few studies of IGCs have focused on PM women. This study used high resolution peripheral CT (HRpQCT) to characterize bone microarchitecture and stiffness in PM women on IGCs. We hypothesized that PM women using chronic IGCs have more pronounced abnormalities of bone microarchitecture and strength compared to controls. Eighty PM women were enrolled, 20 with chronic lung disease requiring IGCs for  $\geq 1$  year and 60 age-matched controls. Women who had used oral GCs for  $\geq 6$  weeks in the past 3 years were excluded. All had aBMD of lumbar spine (LS), total hip (TH), femoral neck (FN), and 1/3 radius (1/3R) by DXA. Trabecular (Tb) and cortical (Ct) volumetric BMD, and Tb microarchitecture were measured by HRpQCT (voxel size  $\sim 82 \mu\text{m}$ ) of the distal radius and tibia. Whole bone stiffness was estimated by finite element analysis. Mean age of subjects was  $69 \pm 7$  years. Groups were of similar race (68% Caucasian) and BMI ( $27 \pm 6 \text{ kg/m}^2$ ). Among IGC users, 80% were using fluticasone with a mean dose of 606 mcg daily. Mean duration of IGC use was 8 years. By DXA, mean T-scores in IGC subjects and controls were in the osteopenic range; aBMD tended to be lower in IGC subjects at the LS ( $p=0.07$ ), and was lower at the TH ( $p<0.04$ ), but did not differ at the FN or 1/3R. There were substantial microarchitectural differences between groups by HRpQCT (Table). IGC subjects had lower total, Ct and Tb vBMD at both radius and tibia. At the radius, IGC subjects had lower Ct thickness, Tb Number and greater Tb separation. Whole bone stiffness was lower in IGC subjects at the radius and tended to be lower at the tibia. In summary, PM women using IGCs had microarchitectural and biomechanical abnormalities compared to age-matched controls. Differences were most pronounced at the radius. That we were able to detect so many differences with this small sample suggests that there may be major, heretofore unrecognized, skeletal deficits in PM women using IGCs.

#### Microarchitecture in IGC subjects vs. Controls (%diff)

	RADIUS	p-value	TIBIA	p-value
Total Density	-25	<0.001	-15	<0.01
Ct Density	-9	<0.001	-6	<0.01
Ct Thickness	-19	<0.01	-7	0.41
Tb Density	-26	<0.01	-14	0.05
Tb Number	-15	<0.03	-9	0.14
Tb Thickness	-5	0.29	-7	0.14
Tb Separation	+42	<0.01	+12	0.10
Stiffness	-15	<0.02	-6	0.09

Table: Microarchitecture in IGC vs Control

**Disclosures:** Yi Liu, None.

## SU0279

**The Relationship between Severity of Chronic Obstructive Pulmonary Disease and Bone Metabolism Biomarkers.** Manabu Tsukamoto<sup>\*1</sup>, Toshiharu Mori<sup>1</sup>, Yasuaki Okada<sup>1</sup>, Hokuto Fukuda<sup>1</sup>, Ke-Yong Wang<sup>2</sup>, Kazuhiro Yatera<sup>3</sup>, Akinori Sakai<sup>1</sup>. <sup>1</sup>Department of Orthopaedic Surgery, University of Occupational and Environmental Health, Japan, <sup>2</sup>Shared-Use Research Center, University of Occupational and Environmental Health, Japan, <sup>3</sup>Department of Respiratory Medicine, University of Occupational and Environmental Health, Japan

**Introduction:** Many patients with chronic obstructive pulmonary disease (COPD) have osteopenia or osteoporosis. However, the influence of COPD on bone metabolism is still unclear. The aim of this study is to investigate the relationship between severity of COPD and bone metabolism biomarkers.

**Materials and Methods:** Thirteen males with COPD or healthy condition were enrolled. They underwent pulmonary function test, spinal x-ray, areal BMD (lumbar spine, femoral neck, distal radius) by DXA, and biochemical tests (ALP, Ca, P, PINP, TRACP-5b, uOC, MMP-9, RANKL, OPG, cathepsin K, DKK-1, sclerostin, FGF-23).

**Results:** The 13 subjects were classified the seriousness of COPD by the Global Initiative for Chronic Obstructive Lung Disease (GOLD) classification into five stages; 4 cases of stage 0, 4 cases of stage 1, 2 cases of stage 2, 2 cases of stage 3 and 1 case of stage 4. The number of vertebral fracture in each subject negatively correlated with forced expiratory volume in the first second (FEV<sub>1</sub>: % of predicted) ( $r^2 = 0.308$ ,

$p < 0.05$ ). The BMD in lumbar spine positively correlated with FEV<sub>1</sub> ( $r^2 = 0.407$ ,  $p < 0.05$ ), and the BMD in femoral neck and distal radius did not correlate with FEV<sub>1</sub>. On the other hands, the serum levels of ALP, PINP and sclerostin positively correlated with FEV<sub>1</sub> (respectively,  $r^2 = 0.449$ ,  $p < 0.05$ ,  $r^2 = 0.479$ ,  $p < 0.01$ ,  $r^2 = 0.529$ ,  $p < 0.05$ ). The other parameters of biochemical tests (Ca, P, TRACP-5b, uOC, MMP-9, RANKL, OPG, cathepsin K, DKK-1, FGF-23) did not correlate with FEV<sub>1</sub>.

**Discussion:** Previous reports showed the high prevalence of osteoporosis and the decreased value of bone formation markers in males with COPD. However, there is no evidence in relationship between the serum levels of sclerostin and severity of COPD. These two variables are correlated in our data. This result suggests that one of pathological mechanism of osteoporosis with COPD may be related to sclerostin.

**Conclusions:** The BMD in lumbar spine, the serum levels of ALP, PINP or sclerostin significantly correlated with FEV<sub>1</sub>.

**Disclosures:** Manabu Tsukamoto, None.

## SU0280

**Low Bone Mass among Aging HIV-infected patients Compared to HIV-uninfected controls in Thailand.** Lalita Wattanachanya<sup>\*1</sup>, Tanakorn Apornpong<sup>2</sup>, Tanya Do<sup>2</sup>, Supalak Klungklang<sup>2</sup>, Sarat Sunthornyothin<sup>1</sup>, Anchalee Avihingsanon<sup>2</sup>. <sup>1</sup>Division of Endocrinology and Metabolism, Department of Medicine, Faculty of Medicine, Chulalongkorn University, Thailand, <sup>2</sup>The HIV Netherlands Australia Thailand Research Collaboration (HIV-NAT), Thai Red Cross AIDS Research Centre, Thailand

**Introduction:** Low bone mineral density (BMD) has been commonly described among HIV-infected patients from many Western countries. However, there are limited studies regarding bone health in Asian people, especially in aging population. We therefore determined BMD in aging HIV-infected Thais (aged  $\geq 50$  years).

**Subjects and Methods:** This was a cross-sectional study among well suppressed HIV-infected patients who attended at our HIV clinic in Bangkok, Thailand from 2016 to 2017, compared to HIV-uninfected controls. BMD at the lumbar spine (LS), total hip (TH) and femoral neck (FN) were measured by dual-energy X-ray absorptiometry on the Hologic QDR 4500 bone densitometer. The BMD T- and Z-score were analyzed using Asian population reference databases.

**Results:** A total of 447 participants were enrolled (201 HIV+ men, 76 HIV- men, 122 HIV+ women and 48 HIV- women). HIV-infected subjects were about 3.5 years younger [men: 54.4 (51.6-59.1) vs. 57.9 (53.6-64.3) yr; women: 54.6 (52.1-59.4) vs. 57.9 (54.0-61.3) yr] and had lower body mass index [men: 23.2 (21.0-25.3) vs. 25.1 (22.1-27.2) kg/m<sup>2</sup>; women: 23.0 (20.8-25.2) vs. 24.7 (21.7-28.3) kg/m<sup>2</sup>]. Eighty-two percents of HIV-infected patients were on tenofovir for a median time of 7.6 (5.2-8.8) years. Median CD4 cell counts were 600 (453-789) cells/mm<sup>3</sup> in men and 675 (528-821) cells/mm<sup>3</sup> in women. Unadjusted BMD (g/cm<sup>2</sup>) was significantly lower in HIV+ men compared to controls at all sites. After adjustment for age and BMI, BMD remained significantly lower at the TH (5.8%). Prevalence of T scores below -1.0 was greater in HIV+ men at the TH (36 vs. 21%;  $P=0.017$ ) and the FN (62 vs. 45%;  $P=0.010$ ). Prevalence of osteoporosis was also greater in men with HIV infection. In women, there was a trend toward lower adjusted BMD at all sites in HIV+, but the difference was not statistically significant compared to controls. However, the prevalence of T scores below -1.0 was significantly higher in HIV+ women at FN (74 vs. 54%;  $P=0.015$ ). Z scores were also significantly lower in HIV+ women at all sites.

**Conclusion:** Aging ARV-treated HIV-infected patients had lower bone mineral density. Thus, careful monitoring and treatment of low BMD in these patients should not be overlooked to prevent further reduction in BMD and future fractures.

**Disclosures:** Lalita Wattanachanya, None.

## SU0281

**3D femur assessment using DXA in patients with primary hyperparathyroidism (PHPT) before and one year after parathyroidectomy.** Eugenie Koumakis<sup>\*1</sup>, Renaud Winzenrieth<sup>2</sup>, JC. Souberbielle<sup>3</sup>, E. Sarfati<sup>4</sup>, Catherine Cormier<sup>1</sup>. <sup>1</sup>Rheumatology Department A, Cochin Hospital, APHP, France, <sup>2</sup>Galgó Medical, Spain, <sup>3</sup>Service d'Explorations Fonctionnelles, Hôpital Necker-Enfants-malades, France, <sup>4</sup>Digestive and Endocrine Surgery, Hôpital de la Pitié-Salpêtrière, AP-HP, France

PHPT is a common endocrinological disease and considered as a frequent cause of cortical bone osteoporosis. An increase in areal bone mineral density (aBMD) following parathyroidectomy (PTX) has been reported in the literature. In this study, we examine effects of PTX at the femur in both trabecular and cortical compartment in PHPT women.

This longitudinal study involved 14 PHPT Caucasian postmenopausal women (aged  $= 62.6 \pm 8.0$  years). Before PTX, all patients had a measurement of serum total and ionized calcium, phosphate, PTH, CTX and the TRP. aBMD were evaluated at femoral neck, total femur and Spine (aBMDFN, aBMDTot, aBMDSpine) using a QDR 4500 (Hologic, USA) within 6 months before PTX, and one year after PTX. Using the same DXA acquisition, volumetric trabecular (vBMDTrab) and volumetric cortical (vBMDCort) BMD as well as the average cortical thickness (C.Th) have been evaluated using 3D-DXA software (Galgó Medical, Spain). This software registers a 3D appearance model of the femoral shape and density onto the DXA projection to obtain a 3D subject-specific model of the femur of the patient. Correlations were evaluated between

pre-Surgery aBMDs, vBMDs or aC.Th or their difference during the study period. Differences between pre-and post-PTX values were assessed using paired test.

Pre- and post-Surgery data are presented in Table below. Pre-PTX PTH and CTX were correlated ( $p=0.009$  &  $p=0.03$ ) with the aBMDFN gain one year post-PTX. Before PTX, vBMDTrab was correlated with 24-hour urine calcium ( $r=0.56$ ,  $p=0.048$ ). After PTX, aBMDTot, aBMDFN and vBMDTrab (consistent with aBMDSpine change) significantly increased by  $2.5\pm3.4\%$ ,  $4.2\pm3.1\%$  and  $3.8\pm4.6\%$  respectively while only a trend is observed in the cortical compartment vBMDCort ( $p=0.08$ ). A significant correlation (all  $p<0.02$ ) was obtained between vBMDTrab variation and PTH or serum Phosphate variations ( $r=-0.74$  &  $r=0.64$ ) while a negative correlation was observed between aBMDFN and CTX variations ( $r=-0.64$ ).

The present study is the first to report data on changes in femur vBMD in the trabecular and cortical compartments and in cortical thickness in PHPT women after PTX. Hip aBMD gain after PTX could be mainly explained by trabecular variation as well as cortical variations. This points to the need for the development of novel tools to discriminate between trabecular and cortical bone, in order to better understand bone changes in specific bone conditions.

	Pre-Surgery	Post-Surgery	p
Serum ionized calcium (mmol/l)	1.35 $\pm$ 0.04	1.21 $\pm$ 0.04	<0.0001
Serum Phosphate (mmol/l)	0.92 $\pm$ 0.09	1.03 $\pm$ 0.12	0.004
Serum PTH (pg/ml)	74,3 $\pm$ 32	45 $\pm$ 24	0.0002
Serum CTX (pmol/l)	5680 $\pm$ 2645	2315 $\pm$ 1410	0.0006
24-hour urine calcium (mmol/24h)	6.0 $\pm$ 3.2	3.1 $\pm$ 2.0	0.0001
TRP -	81 $\pm$ 7.5	82 $\pm$ 3.5	0.6
aBMDFN (g/cm <sup>2</sup> )	0.631 $\pm$ 0.09	0.656 $\pm$ 0.09	0.0006
aBMDTot (g/cm <sup>2</sup> )	0.749 $\pm$ 0.07	0.768 $\pm$ 0.08	0.011
aBMD Spine (g/cm <sup>2</sup> )	0.772 $\pm$ 0.10	0.802 $\pm$ 0.11	0.042
C.Th (mm)	1.750 $\pm$ 0.15	1.772 $\pm$ 0.19	0.31
vBMDTrab (mg/cm <sup>3</sup> )	263 $\pm$ 53	273 $\pm$ 57	0.02
vBMDcort (mg/cm <sup>3</sup> )	115 $\pm$ 44	123 $\pm$ 44	0.08

Table

Disclosures: Eugenie Koumakis, None.

## SU0282

**A randomized trial of Vitamin D3 in HIV+ postmenopausal women.** Michael Yin<sup>\*1</sup>, Arindam RoyChoudhury<sup>1</sup>, Mariana Bucovsky<sup>1</sup>, David Ferris<sup>2</sup>, Susan Olender<sup>1</sup>, Anajali Sharma<sup>3</sup>, Kyle Nishiyama<sup>1</sup>, Cosmina Zeana<sup>2</sup>, Barry Zingman<sup>3</sup>, Elizabeth Shane<sup>1</sup>. <sup>1</sup>Columbia University Medical Center, United States, <sup>2</sup>Bronx Lebanon Hospital Center, United States, <sup>3</sup>Albert Einstein College of Medicine, Montefiore Medical Center, United States

Background: In HIV+ postmenopausal women, we observed an association between lower total 25-hydroxy vitamin D (25OHD) levels and greater bone loss at the distal radius. Since VitD supplementation improves musculoskeletal outcomes in older women, we compared the effects of Low (1000 IU) vs Moderate (3000 IU) VitD3 supplementation on areal and volumetric bone mineral density (aBMD) in HIV+ postmenopausal women on stable antiretroviral regimens.

Methods: A 12-month prospective, randomized, double-blind, placebo-controlled study with change in aBMD measured by dual-energy X-ray absorptiometry (DXA) as the primary outcome, change in vBMD at the spine and hip by central QCT and tibia by HRpQCT, and bone turnover markers (P1NP and CTX) as secondary outcomes. 25OHD, parathyroid hormone (PTH) were also measured. A complete case analysis was performed on the 69 (31 Low and 38 Moderate) with complete 12 month DXA data. Regression analyses were used to test for associations between baseline 25OHD and percent change in BMD and bone turnover markers for each study arm.

Results: 82 participants were randomized (41 Low and 41 Moderate). The study arms were well-balanced at baseline: median age 56 years; 43% African American, 57% Hispanic; median CD4 count 724 cells/mm<sup>3</sup>; median total 25OHD 19.7 ng/mL (49.3 nmol/L). Baseline BMI was lower in the Moderate VitD group (29.6 vs 32.6 kg/m<sup>2</sup>,  $p=0.02$ ). Levels of total 25OHD were higher in the Moderate than Low VitD group at 6 months (33.1  $\pm$  10.3 vs 27.8  $\pm$  8.1 ng/mL,  $p=0.03$ ) and 12 months (30.2  $\pm$  9.6 vs 24.3  $\pm$  7.6 ng/mL,  $p=0.007$ ), but PTH levels did not differ between groups. Percent change in aBMD or vBMD and bone turnover markers did not differ between Low and Moderate VitD groups before or after adjustment for baseline aBMD and BMI (Table). In regression analyses, lower baseline 25OHD levels in the Moderate VitD group were associated with greater increase in aBMD at the femoral neck ( $p=0.04$ ) and ultra distal radius ( $p=0.045$ ) at 12 months.

Conclusion: VitD supplementation at 3000 IU daily increased mean total 25OHD levels to > 30 ng/ml in HIV+ postmenopausal women, but did not result in increases in BMD or suppression of bone turnover markers compared with 1000 IU daily. This suggests that VitD repletion is not sufficient to prevent bone loss in HIV+

postmenopausal women. Additional interventions are likely necessary to prevent or reverse bone loss in this population.

Table: Percent Change (unadjusted) in Areal and Volumetric BMD and Bone Turnover Markers			
Markers	Low VitD (1000 IU)	Mod VitD (3000 IU)	P value
Spine aBMD by DXA	0.1 +/- 0.7	-0.5 +/- 0.6	0.96
Total hip aBMD by DXA	-0.4 +/- 0.5	-0.8 +/- 0.5	0.96
Femoral neck aBMD by DXA	-1.4 +/- 0.7	-0.9 +/- 0.7	0.98
1/3 radius aBMD by DXA	-1.6 +/- 0.5	-1.4 +/- 0.5	0.99
L1 L2 vBMD by central QCT	0.0 +/- 7.8	0.4 +/- 5.3	0.87
Total hip vBMD by central QCT	-0.9 +/- 9.3	2.9 +/- 7.5	0.14
Tibia total vBMD by HRpQCT	-0.3 +/- 2.9	-0.9 +/- 2.4	0.34
P1NP (ng/ml)	-2.0 +/- 6.5	2.6 +/- 5.7	0.97
CTX (ng/ml)	-9.2 +/- 7.8	-13.9 +/- 6.9	0.97

Table

Disclosures: Michael Yin, None.

## SU0283

**Development and Validation of a LC-MS/MS Assay for Quantification of Parathyroid Hormone (PTH 1-34) in human Plasma.** Sulaiman Al Riyami<sup>\*1</sup>, Jonathan Tang<sup>1</sup>, John Dutton<sup>1</sup>, Christopher Washbourne<sup>1</sup>, Hillel Galitzer<sup>2</sup>, William Fraser<sup>3</sup>. <sup>1</sup>Bioanalytical Facility, University of East Anglia, Norwich Research Park, Norwich, United Kingdom, <sup>2</sup>Entera Bio Ltd, Hadassah Ein-Kerem, Jerusalem Bio Park, Jerusalem, Israel

Background: Teriparatide [recombinant human PTH (1-34)] is an osteoanabolic agent for treatment of osteoporosis. The effect on bone decreases the risk of vertebral and non-vertebral fractures and increases bone mineral density (BMD) in post-menopausal women with osteoporosis. Measurement of PTH (1-34) is valuable in assessing treatment response and concordance with therapy. Aim: To develop and validate a method for quantification of PTH (1-34) using Liquid chromatography tandem mass spectrometry (LC-MS/MS) and to perform comparison with a commercial immunoassay. Method: Sample extraction was developed using a Waters (Milford, MA, USA) Oasis<sup>®</sup> HLB  $\mu$ Elution solid phase extraction. Quantification m/z transition 589>656 was used on Waters/Micromass<sup>®</sup> Quattro Ultima<sup>™</sup> Pt mass spectrometer to measure PTH (1-34) in human plasma using rat PTH (1-34) as internal standard. Validation criteria were carried out against industry standards. PTH (1-34) results obtained from human subjects given Teriparatide (Fortteo, Eli Lilly, IN, USA) (n=390) were compared against results obtained from an immunoassay (IDS; Boldon Tyne and Wear, UK). Results and Discussion: LC-MS/MS produced a linear calibration curve from 10 to 2000 pg/mL ( $r^2 > 0.990$ ). The LLoQ and LLoD for PTH (1-34) were 10 pg/mL and 2.1 pg/mL respectively. The inter- /intra-assay precision (CV%) of the method were <9.8 and <7.8% and accuracy of >98.3% for four QC's (20, 100, 200, and 800 pg/mL). The mean recovery of PTH (1-34) was 107.2%. Method comparison between the LC-MS/MS and immunoassay using human EDTA plasma samples showed a high correlation ( $r^2 = 0.950$ ). A concentration-dependent, negative bias of 35.5% was observed across the range of 0 – 800 pg/mL. The immunoassay showed a 7% cross reactivity to human PTH (1-84) and 44% to rat PTH (1-34), no interference was observed in the LC-MS/MS method. Matrix effect and cross reactivity to human PTH (1-84) in the immunoassay were the likely contributing factors to the bias between the methods. The oxidised form of PTH (1-34) does not interfere with our LC-MS/MS method. Conclusion: Our LC-MS/MS method demonstrated linearity over the calibration range, good precision and accuracy, excellent analyte recovery, and negligible matrix effects. The method was successfully used for measurements of PTH (1-34) in rat and human plasma.

Disclosures: Sulaiman Al Riyami, None.

## SU0284

**Measurements of Osteoanabolic agents PTH (1-34) and PTHrP (1-36) in therapeutic studies and clinical diagnostics.** Sulaiman Al Riyami<sup>\*1</sup>, Jonathan Tang<sup>1</sup>, Hillel Galitzer<sup>2</sup>, William Fraser<sup>3</sup>. <sup>1</sup>Bioanalytical Facility, University of East Anglia, Norwich Research Park, Norwich, United Kingdom, <sup>2</sup>Entera Bio Ltd, Hadassah Ein-Kerem, Jerusalem Bio Park, Jerusalem, Israel, <sup>3</sup>Bioanalytical Facility, University of East Anglia, Norwich, United Kingdom

Background: Teriparatide PTH (1-34) is an osteoanabolic agent for treatment of osteoporosis. PTH (1-34) can also be used as replacement therapy in hypoparathyroidism and to accelerate fracture healing. Abaloparatide, PTHrP (1-36) analogue is a novel anabolic drug for treatment of osteoporosis. PTH (1-34) has also been used to assess response to PTH in conditions such as pseudohypoparathyroidism (PHP) (Ellsworth-Howard test (EHT))

Aims: To review the use of PTH (1-34) measurements in drug development studies, and in the diagnosis of patients with PHP. To highlight the potential use of measurement of PTHrP (1-36) using our LC-MS/MS method for measurement of intact PTHrP (1-36), intact PTH (1-34) and their respective oxidised forms simultaneously.





## SU0287

**Clinical Characteristics of Bisphosphonate Drug Holiday Patients.** Ammara Aziz<sup>1</sup>, Ziyue Liu<sup>2</sup>, Abby Church<sup>3</sup>, Jessica Weaver<sup>4</sup>, Andrea Kelley<sup>3</sup>, Erik Imel<sup>5</sup>. <sup>1</sup>Indiana University School of Medicine, United States, <sup>2</sup>Richard M. Fairbanks School of Public Health at IUPUI, United States, <sup>3</sup>Regenstrief Institute, Inc., United States, <sup>4</sup>Merck, Sharp & Dhome Corp., United States, <sup>5</sup>Indiana University School of Medicine; Regenstrief Institute, Inc., United States

Background: Bisphosphonates (BP) drug holidays (DH) have been recommended due to prolonged skeletal half-life and persistent skeletal benefits after cessation, along with the goal of decreasing adverse events. However scarce data exists to guide decisions about initiation or duration of DH.

Aim: To determine the incidence of the practice of DH, identify characteristics of DH patients, and assess fracture incidence during a DH.

Methods: Using electronic health records (EHR), we identified patients age  $\geq 40$  years receiving BP between Jan 1, 2005 to Mar 31, 2016. Patients receiving BP for Paget's disease, fibrous dysplasia, bone metastases, multiple myeloma, or other cancers were excluded. We used prescription dispensing records to identify patients with adherence to BP for  $\geq 2$  years (with  $\geq 50\%$  days covered, and no coverage gaps  $\geq 60$  days). Structured and unstructured data were extracted from the EHR. DH were defined when patients had gaps in dispensing records of  $\geq 180$  days plus clinical notes documenting intentional DH.

Results: A total of 48,116 patients having BP prescriptions were identified. 9,016 met inclusion criteria with adherence to BP for  $\geq 2$  years; 1,661 had BP treatment gaps of 6-12 months, and 4,956 had gaps of  $\geq 12$  months. During manual review of EHR, 299 patients had documented intentional DH. Mean ( $\pm$ SD) age of DH patients was  $71.1 \pm 10$  yrs; 89% were white; 95% were women. DH patients were generally healthy with Charlson Comorbidity Index of 0 in 71% and 1 in 22%. The most recent OP medications prior to initiating DH were alendronate (66%), zoledronic acid (14%), risendronate (12%), ibandronate (8%) and raloxifene (0.3%) (Some took both BP and raloxifene). Median duration of detected adherent BP treatment before DH was 3.07 years (min 2.07, max 7.52). DXA available for 64 patients prior to DH were: osteoporotic (20%), osteopenic (55%), and normal (25%). Fracture history was present in 10%, but only 6 (2%) had fractured in the 2 years preceding DH. Mean DH duration was 4.03 years. After initiating DH, 18 (6%) patients had fractures, including 6 femur neck and 2 other femoral fractures. Total hip DXA before and after DH in 38 patients (median 2.04 years apart) showed a mean % decline of 0.99%. Only 10.5% of subjects decreased BMD  $> 5\%$ .

Conclusion: DH in a generally healthy population appeared well tolerated. Most subjects started DH with osteopenic or better BMD. Few patients declined in BMD, and the fracture rate was similar before and during DH.

Disclosures: Ammara Aziz, None.

## SU0288

**Dual Therapy with Teriparatide and Denosumab in Severe Osteoporosis.** Paul Claffey<sup>1</sup>, Aoife Broderick<sup>2</sup>, Ronan O'Toole<sup>2</sup>, James Mahon<sup>1</sup>, Kevin McCarroll<sup>1</sup>. <sup>1</sup>St. James's Hospital, Ireland, <sup>2</sup>St James's Hospital, Ireland

Objective:

Recent studies have demonstrated combination therapy with teriparatide and denosumab to be effective and well tolerated in improving bone mineral density (BMD) at both the lumbar spine and hip compared with monotherapy(1). We set out to evaluate the utilisation of this therapy for individuals with severe osteoporosis at our bone health clinic and to examine its effects on biochemical markers of bone turnover.

Material and Methods:

We identified individuals (via our bone health clinic database) who had been commenced on combination therapy during 2015. Data were collected on pre-treatment DXA T-scores as well as baseline and follow-up bone markers, namely carboxyterminal collagen crosslinks (CTX) and procollagen type 1 amino-terminal propeptide (PINP).

Results:

Four individuals were identified and all were female. Mean age was 80 (range 70 to 88) and all completed at least 12 months of therapy. Mean baseline T-score for lumbar spine was -4.9 (range -3.5 to -5.9) and for hip was -3.8 (range -3.5 to -4.4). Mean baseline CTX and PINP was 0.39ng/mL and 106.5ng/mL respectively. Three patients had follow-up bone markers at 6 months, with a mean CTX of 0.081ng/mL (-79.2%) and PINP of 16.9ng/mL (-84.1%). All tolerated therapy well with no reported side effects.

Conclusion:

While our dataset was small, we observed a trend towards suppression in bone markers for patients on dual therapy in contrast to known effects of PTH alone, findings similar to previous studies(1). In our clinical practise, combination therapy was confined to those with both hip and spine T scores  $< -3.5$ .

References:

1. Response to Therapy With Teriparatide, Denosumab, or Both in Postmenopausal Women in the DATA (Denosumab and Teriparatide Administration) Study Randomized Controlled Trial. Leder BZ1, Tsai JN2, Neer RM2, Uihlein AV2, Wallace PM2, Burnett-Bowie SA2

J Clin Densitom. 2016 Jul-Sep;19(3):346-51. doi:10.1016/j.jocd.2016.01.004. Epub 2016 Feb 15.

Disclosures: Paul Claffey, None.

## SU0289

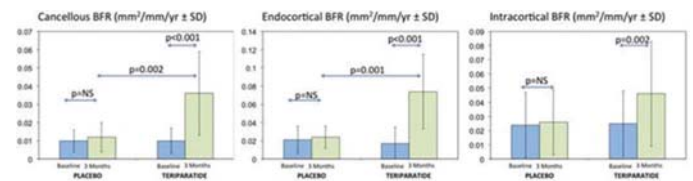
**Quadruple-Labeled Transiliac Crest Biopsies Quantify Bone Formation Response to Teriparatide in Premenopausal Women with Idiopathic Osteoporosis.** Adi Cohen<sup>1</sup>, David Dempster<sup>2</sup>, Hua Zhou<sup>3</sup>, Robert Recker<sup>4</sup>, Joan Lappe<sup>4</sup>, Mafo Kamanda-Kosseh<sup>1</sup>, Mariana Bucovsky<sup>1</sup>, Arindam RoyChoudhury<sup>1</sup>, Julie Stubby<sup>4</sup>, Emily Stein<sup>1</sup>, Thomas Nickolas<sup>1</sup>, Elizabeth Shane<sup>1</sup>. <sup>1</sup>Columbia University, United States, <sup>2</sup>Columbia University and Helen Hayes Hospital, United States, <sup>3</sup>Helen Hayes Hospital, United States, <sup>4</sup>Creighton University, United States

We previously reported that premenopausal women with idiopathic osteoporosis (IOP) have profound deficits in trabecular and cortical bone microstructure. In a pilot study of 21 women with IOP published in 2013, we reported marked increases in BMD at the spine and hip and dramatic microstructural improvements on paired transiliac biopsies (baseline and 18 months) in response to teriparatide (TPTD). However, 4 of 21 women had no response to TPTD. To investigate mechanisms of differential response to TPTD, we enrolled 41 additional otherwise healthy premenopausal women with IOP in an ongoing FDA-funded placebo-controlled study. Subjects are randomized to TPTD (n=28) or placebo (n=13) for the first 6 months, after which all receive TPTD. Transiliac biopsies are performed at 3 months on treatment or placebo after 2 sets of tetracycline labels administered before treatment and after 3 months on treatment. Two sets of bone remodeling measures were then calculated on a single biopsy specimen reflecting baseline and early treatment remodeling response.

Quadruple labeled biopsies were performed in 35 subjects (mean age  $38 \pm 7$  yrs; TPTD:placebo; 24:11). Dynamic indices of remodeling did not differ between TPTD and placebo treated subjects at baseline (baseline labels). At cancellous, endocortical and intracortical surfaces, there were substantial and significant increases in baseline vs 3 month mineralizing surface (MS/BS), mineral apposition rate (MAR) and bone formation rate (BFR; Figure) in the TPTD group, while no significant changes were seen in the placebo group. The absolute change in cancellous BFR on TPTD was quite variable, ranging from 0.001 to 0.61 mm<sup>3</sup>/mm<sup>2</sup>/year.

Dynamic remodeling parameters correlated directly but modestly with serum bone turnover markers both at baseline and during TPTD treatment. At baseline, cancellous BFR correlated with serum CTX, osteocalcin, and PINP ( $r=0.33-0.42$ ; all  $p<0.05$ ). In TPTD treated subjects, the absolute change in cancellous BFR correlated directly with 3 month absolute change in both CTX and PINP ( $r=0.43-0.48$ ; all  $p<0.5$ ), as well as with baseline BFR ( $r=0.45$ ;  $p=0.03$ ).

We conclude that quadruple-labeled transiliac bone biopsies capture the tissue level bone remodeling response to TPTD in three separate bone envelopes and that these data will allow us to examine mechanisms of differential long-term BMD response to TPTD in premenopausal women with IOP.



Figure

Disclosures: Adi Cohen, None.

## SU0290

**Correlations between Longitudinal Changes in the Bone Turnover Marker PINP and Bone Formation at the Tissue Level across 3 Envelopes with Teriparatide in the AVA Osteoporosis Study.** David Dempster<sup>1</sup>, Hua Zhou<sup>1</sup>, John Kregge<sup>2</sup>, Jahangir Alam<sup>2</sup>, Kathleen Taylor<sup>3</sup>, Valerie Ruff<sup>3</sup>. <sup>1</sup>Regional Bone Center, Helen Hayes Hospital, United States, <sup>2</sup>Lilly Research Laboratories, Eli Lilly and Company, United States, <sup>3</sup>Musculoskeletal and Men's Health, Lilly USA, LLC, United States

Bone turnover markers may be useful indicators of clinical response to osteoporosis treatment; however, to date, no study has correlated longitudinal changes in bone turnover markers with longitudinal changes in bone formation at the tissue level. In the AVA study of postmenopausal women with osteoporosis, we assessed serum procollagen type 1 N-terminal propeptide (PINP) and used quadruple tetracycline labeling to assess bone formation at baseline and after 3 months of treatment with teriparatide (TPTD) or denosumab in a single bone biopsy. Here we evaluated correlations among PINP, bone formation rate (BFR), or 3 types of bone forming units (BFUs): remodeling (RBF)-, modeling (MBF)-, or overflow modeling (oMBF)-based bone formation in the cancellous (Cn), endocortical (Ec), and periosteal (Ps) bone envelopes (envs) during TPTD therapy.

Biopsies were obtained from TPTD-treated (20 mcg/daily; subcutaneous injection) patients following double fluorochrome labeling at baseline and prior to the biopsy at 3 months. Bone formation was considered MBF if the underlying cement line was smooth, RBF if scalloped, and oMBF if smooth but adjacent to an RBF site. The referent for all indices was bone surface. Pearson correlation coefficient was used to assess correlations.



Following TPTD treatment, significant correlations were seen between  $\Delta$ PINP and  $\Delta$ BFR in Cn ( $r=.58$ ,  $p<.001$ ) and Ec ( $r=.61$ ,  $p<.001$ ) envs. At 3 months, correlations between BFR and different types of BFUs were strongest for RBF and oMBF in both Cn ( $r\geq .92$ ,  $p<.001$ ) and Ec ( $r\geq .85$ ,  $p<.001$ ) envs and for MBF in Ps env ( $r=.87$ ,  $p<.001$ ). By BFU type, significant correlations with  $\Delta$ PINP were also seen in Cn env for  $\Delta$ RBF,  $\Delta$ MBF, and  $\Delta$ oMBF (all  $r=.52$  to  $.53$ ,  $p<.01$ ); in Ec env for  $\Delta$ RBF ( $r=.54$ ,  $p=.002$ ) and  $\Delta$ oMBF ( $r=.67$ ,  $p<.001$ ); and in Ps env for  $\Delta$ MBF ( $r=.45$ ,  $p=.013$ ).

Quadruple labeling allowed the novel assessment of correlations among longitudinal changes in PINP, BFR, and BFU types across 3 bone envs. The results demonstrate a differential pattern of correlation between types of BFUs and changes in PINP or with BFR across envelopes, with RBF and oMBF significantly associated with these variables in the Cn and Ec envs and MBF in the Ps env. The data also suggest that TPTD is primarily a pro-remodeling agent as reflected by the predominance of remodeling-based formation units, RBF and oMBF, in Cn and Ec envs. This observation is supported by the significant correlations with measures of bone formation, PINP and BFR.

**Disclosures:** David Dempster, Eli Lilly and Company, Consultant.

## SU0291

**Association between Total Hip Bone Mineral Density at Baseline and Vertebral Fracture Incidence in the MOVER Study.** Hiroshi Hagino<sup>\*1</sup>, Toshitaka Nakamura<sup>2</sup>, Masako Ito<sup>3</sup>, Masato Tobinai<sup>4</sup>, Junko Hashimoto<sup>4</sup>, Seitaro Yoshida<sup>4</sup>. <sup>1</sup>School of Health Science & Rehabilitation Division, Tottori University Faculty of Medicine, Japan, <sup>2</sup>Aoba Hospital, Japan, <sup>3</sup>Center for Diversity & Inclusion, Nagasaki University, Japan, <sup>4</sup>Chugai Pharmaceutical Co. Ltd, Japan

**Purpose:** The phase III MOVER study compared the efficacy and safety of monthly intravenous (IV) ibandronate (IBN) with oral risedronate (RIS) in Japanese patients (pts) with primary osteoporosis. The study showed the non-inferiority of IBN to RIS in reducing the incidence of non-traumatic vertebral fractures over 3 years. Here we examine the association between total hip BMD T-score at baseline and the incidence of new vertebral fractures in the study.

**Methods:** 1265 pts were randomized to receive IV IBN 0.5 or 1mg/month + oral daily placebo, or oral RIS 2.5mg/day (licensed Japanese dose) + monthly IV placebo for 3 years. We divided the modified intent-to-treat population into four groups according to their total hip BMD T-score at baseline ( $\leq -3.0$ ,  $>-3.0$  and  $\leq -2.5$ ,  $>-2.5$  and  $\leq -2.0$ , and  $>-2.0$ ) and investigated the change in T-score in each treatment group over 3 years. We also analyzed the association between total hip BMD T-score at baseline and the cumulative incidence of new vertebral fractures in the four groups.

**Results:** The proportion of pts in the four BMD T-score groups at baseline was 17.5%, 18.0%, 21.7%, and 42.8% for IBN 0.5mg, 14.8%, 15.6%, 22.1%, and 47.5% for IBN 1mg, and 18.3%, 17.0%, 23.3%, and 41.4% for RIS. After 3 years of treatment, the proportion of pts in each group was 13.5%, 15.9%, 19.0%, and 51.6% for IBN 0.5mg, 11.1%, 11.1%, 20.1%, and 57.8% for IBN 1mg, and 14.4%, 16.8%, 24.6%, and 44.2% for RIS. The percentage of pts with a total hip BMD T-score  $>-2.5$  after 3 years increased by 6.1% in the IBN 0.5mg group, by 8.3% in the IBN 1mg group, and by 4.1% in the RIS group. In each treatment group, the cumulative incidence of new vertebral fractures was higher in pts with low baseline total hip BMD T-scores. The incidence of new vertebral fractures was lower with IBN 1mg than with IBN 0.5mg or RIS.

**Conclusions:** In the MOVER study, the proportion of pts who achieved a total hip BMD T-score of  $>-2.5$  (one index of the 'treat-to-target' analysis) increased in each treatment group with treatment duration. We found an association between total hip BMD T-score at baseline and future incidence of vertebral fractures, with the fracture incidence being lowest in the IBN 1mg/month group.

**Disclosures:** Hiroshi Hagino, Ono Pharmaceutical Co. Ltd., Consultant.

## SU0292

**Upper Gastrointestinal Safety with the Buffered Solution of Alendronate 70mg: Postmarketing Experience.** Josef Hruska<sup>\*1</sup>, Flemming Kjaer Jorgensen<sup>2</sup>, Erik Fink Eriksen<sup>3</sup>. <sup>1</sup>MeDACom GmbH, Switzerland, <sup>2</sup>KLIFO A/S, Denmark, <sup>3</sup>Oslo University Hospital, Norway

**Keywords:** osteoporosis, gastrointestinal effects, buffered alendronate

**Introduction:** Alendronate (ALN) and other bisphosphonates have been the mainstay in osteoporosis management and fracture prevention for over 20 years. While ALN reduces risk of vertebral, non-vertebral and hip fractures by 55%, 64% and 47% respectively<sup>1</sup>, adherence to treatment is problematic and  $>50\%$  discontinue within 12 months<sup>2,3</sup>. Upper gastrointestinal (GI) side effects are one of the most common reasons for treatment discontinuation<sup>4</sup>. ALN 70mg effervescent (ALN EX) was developed to improve the GI tolerability; it is ingested as a buffered solution of fully dissolved ALN to increase the pH in the stomach and to eliminate the contact of solid ALN particles with esophageal mucosa<sup>5</sup>.

**Objective:** To assess the impact of ALN EX on occurrence of upper GI adverse reactions (AR).

**Methods:** The post-marketing experience with ALN EX comprises of approximately 1 811 365 prescriptions, which translate into 150 947 patient years and 7 245 460 ingestions. Number of upper GI AR, descriptive of GI tolerability and associated with use ALN EX were extracted from the pharmacovigilance database.

**Results:** Three serious, erosive oesophagitis (1) and abdominal pain upper (2); and 29 non-serious upper GI AR were reported. Among the non-serious AR were abdominal

pain (7), nausea (6), dyspepsia (2), gastritis (1), abdominal distention (1), GI pain (1), dysphagia (1), vomiting (1). The reported frequency of esophagitis with ALN Tablets is 0.1 – 1%<sup>6</sup>. Assuming the same frequency for ALN EX in the 150 947 patient years, at least 150 cases of oesophagitis would be expected.

**Conclusion:** Even when considering that only 6-10% of all ARs are reported<sup>7</sup> post-marketing, the number of ALN EX cases is appreciably below the level expected for ALN Tablets. The available safety data suggest that ALN EX is associated with a lower frequency of upper GI AR than reported for ALN Tablets and that it is a well-tolerated oral bisphosphonate option in the management of osteoporosis.

**References:**

1. Black DM et al. *J Clin Endocrinol Metab* 2000;85:4118-4124.
2. Briesacher BA et al. *Pharmacotherapy* 2008;28(4):437-443.
3. Weycker D et al. *Osteoporos Int* 2006;17(11):1645-1652.
4. Invernizzi M et al. *Aging Clin Exp Res* 2015;27:107-113.
5. Hodges LA et al. *Int J Pharm* 2012;432:57-62.
6. Fosamax 70mg SPC. [www.ema.europa.eu](http://www.ema.europa.eu); accessed 7. April 2017.
7. Mazzitello C et al. *J Pharmacol Pharmacother* 2013;4:S20-S28.

	Reported ARs	ARs adjusted for under-reporting by 95% <sup>†</sup>	Reported frequency of AR tablet AR, % <sup>‡</sup>	Minimum expected cases if ALN Tbl AR frequency applied in 150 947 pt years
Oesophagitis†	1	20	0.1-1	150
Abdominal pain‡	10	200	1 -10	1509
Abdominal distention	1	20	1 -10	1509
Dyspepsia	2	40	1 -10	1509
Dysphagia	1	20	1 -10	1509
Nausea	6	120	0.1-1	150
Gastritis	1	20	0.1-1	150
Vomiting	1	20	0.1-1	150

<sup>†</sup>Serious AR

<sup>‡</sup>Include cases of abdominal pain upper, abdominal pain and GI pain. Two abdominal pain upper cases were serious ARs.

Reported GI ARs for ALN EX adjusted for under-reporting and expected cases in 150 947 patient years

**Disclosures:** Josef Hruska, EffRx Pharmaceuticals, Consultant.

## SU0293

**Indications for Drug Holiday among Japanese Patients after Long-term Bisphosphonate Treatment.** Yuji Kasukawa<sup>\*</sup>, Naohisa Miyakoshi, Michio Hongo, Koji Nozaka, Yoshinori Ishikawa, Hiroyuki Tsuchie, Daisuke Kudo, Yoichi Shimada. Department of Orthopedic Surgery, Akita University Graduate School of Medicine, Japan

**Introduction:** Bisphosphonates (BPs) are routinely used to treat osteoporosis; however, their long-term use can be associated with side effects or complications in some patients. The ASBMR task force has reported that post-menopausal women who have been treated with oral bisphosphonates for more than 5 years, who are without a history of fragility fracture before or during therapy, who do not have a high fracture risk or who have a hip bone mineral density of more than -2.5 SD should be considered for a drug holiday from BP therapy. However, it is unclear what proportion of such patients in Japan are eligible for a drug holiday. Thus, the purpose of present study was to determine the proportion of post-menopausal patients who have been treated with oral BPs for more than 5 years who would be eligible for a drug holiday from BP therapy among a Japanese cohort.

**Patients and Methods:** We enrolled 37 post-menopausal, Japanese women (mean age, 74.7 years) who were being treated for osteoporosis with BPs at our institute from October to December, 2016. For each patient, we evaluated the duration of BP treatment, the type of BP at the start of treatment and at the time of our survey; the incidence of fragility fracture during treatment; their history of fragility fracture; their risk of osteoporotic fracture, as evaluated with FRAX; and their eligibility for a drug holiday, as per the recommendations of the ASBMR task force report.

**Results:** Among the cohort, we found that 41% (15/37) of patients had been treated with BPs for more than 5 years. The mean age of these patients was 74.9 (60–83) years, and the mean duration of BP treatment was 103 (66–142) months. At the start of treatment, these patients had been prescribed alendronate ( $n = 10$ ), risendronate ( $n = 4$ ), and minodronate ( $n = 1$ ). At the time of our survey, alendronate was the least prescribed of the three drugs (alendronate,  $n = 2$ ; risendronate,  $n = 7$ ; minodronate,  $n = 6$ ). Four patients had a history or incidence of fragility fracture during BP treatment. The risk of major osteoporotic fracture was 21.6%, and the risk of proximal hip fracture was 8.7%. Only two subjects (13%) were eligible for a drug holiday as per the ASBMR task force report.

**Conclusion:** Of the 41% of post-menopausal osteoporotic patients who had been treated with BPs for more than 5 years, only 13% were eligible for a drug holiday from BP treatment, as per the recommendations of the ASBMR task force report.

**Disclosures:** Yuji Kasukawa, None.

## SU0294

**MRI for determining the treatment strategy in patients with apparently isolated greater trochanteric fractures.** Jai Hyung Park<sup>\*1</sup>, Ji Wan Kim<sup>2</sup>, Hyun Chul Shon<sup>3</sup>, Jae Suk Chang<sup>4</sup>, Seong-Eun Byun<sup>5</sup>, Kwang Hwan Jung<sup>6</sup>, Chul-Ho Kim<sup>4</sup>. <sup>1</sup>Kangbuk Samsung Hospital, Sungkyunkwan University, Korea, Republic of, <sup>2</sup>Haeundae Paik Hospital, Inje University, Korea, Republic of, <sup>3</sup>Chungbuk National University Hospital, Korea, Republic of, <sup>4</sup>Asan Medical Center, University of Ulsan, Korea, Republic of, <sup>5</sup>CHA Bundang Medical Center, CHA university, Korea, Republic of, <sup>6</sup>Ulsan University Hospital, Korea, Republic of

**Introduction:** The treatment methods for isolated greater trochanteric (GT) fractures still lack established guidelines. The purpose of this study was to investigate the use of MRI for formulating a treatment strategy in patients with isolated GT fractures on plain radiography. **Patients and Methods:** This retrospective cohort study reviewed 37 consecutive patients with isolated GT fractures on plain radiography. We decided on surgical or conservative treatment depending on the MRI findings. The clinical results, radiography findings, and magnetic resonance imaging findings were investigated. **Results:** We divided all the patients into 3 groups according to the extension of the fracture line. In group 1, the fracture line was within the lateral one-third in the coronal plane. In group 2, the fracture line extended from the lateral one-third to the medial one-third. In group 3, the fracture line extended over the medial one-third and/or to the medial cortex of the femur. Conservative treatment was performed in groups 1 and 2, and surgical treatment was performed in group 3. No displacement was found in groups 1 and 2. One patient from group 3 refused to undergo surgery. This patient presented 5 days later with increased hip pain, and radiography demonstrated displacement of the fracture, prompting surgical intervention. **Conclusions:** The evaluation of apparently isolated GT fractures using MRI can be useful to diagnose the extent of the occult fracture and determine the treatment strategy.

**Disclosures:** Jai Hyung Park, None.

## SU0295

**Uncertainty of Current Algorithm for Bisphosphonate-related Osteonecrosis of the Jaw in Population-based Studies.** Jin-Woo Kim<sup>\*</sup>, Hye-Yeon Kim, Sun-Jong Kim, Sang-Hwa Lee. Ewha Womans University, Korea, Republic of

**Introduction -** To assess the relevance of previous epidemiologic studies on bisphosphonate-related osteonecrosis of the jaw (BRONJ), we first conducted a systematic review of large population-based observational studies, and evaluated the validity of claims-based algorithms for the identification of BRONJ.

**Methods -** Studies containing primary observational epidemiologic data regarding bisphosphonate exposure and outcomes of osteonecrosis of the jaw were systematically reviewed. Using surrogates for identifying potential BRONJ cases from a population-based hospital registry, validation was performed through medical chart review. Positive predictive value (PPV) was estimated for each diagnostic code, and for the overall algorithm utilized. Various strategies to increase PPV were also performed.

**Results -** Seventeen studies were systematically reviewed and presented with variations in study quality as well as inconsistent findings. Moreover, there was a high level of methodological heterogeneity. A total of 1,920 patients were identified through the ICD-10 algorithm with potential BRONJ, though only 109 cases were confirmed, corresponding to an overall PPV of 5.68% (95% CI, 4.68-6.81). Only *K10.2* (inflammatory conditions of the jaw) exhibited a relatively high PPV of 26.18%, which increased to 74.47% after confinement to BP users. Other strategies to increase PPV value were not effective.

**Conclusion -** Our findings showed that the overall PPV for BRONJ identification was very low, indicating low validity of the current algorithm and possible overestimation of ONJ occurrence. There is an urgent need to develop more reliable and specific operational definitions for the identification of BRONJ cases in large population databases.

**Disclosures:** Jin-Woo Kim, None.

## SU0296

**Additional use of VitaminK2 (menatetelenon) reduces the elevation of ucOC/OC rate which administrated Teriparatides cause.** Yoichi Kishikawa<sup>\*</sup>. Kishikawa Orthopedics, Japan

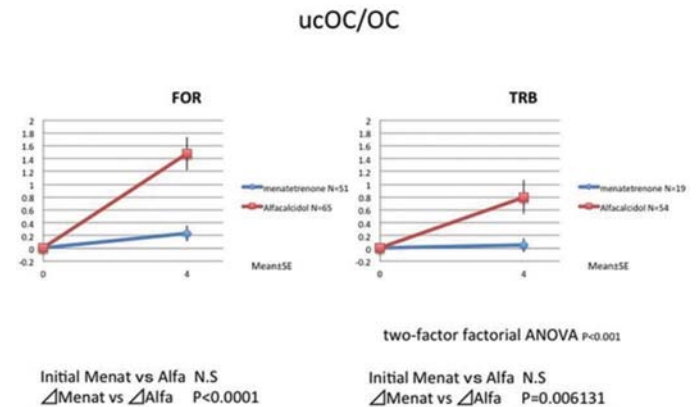
OC(Osteocalcin) is a major protein component of the bone matrix that represents the bone formation. Serum ucOC is a kind of OC not completely but an under carboxylated one that represents the lack of VitaminK. The cut off value of ucOC for vertebral fracture is reported at 4.5ng/ml, and high ucOC is known as one of the independent risk factors of femoral fracture in Japan.

Under administration of Teriparatide, ucOC elevation is more pronounced than OC elevation, and the ucOC/OC rate increases, while on the other hand under administration of Denosumab the ratio decreases. We investigated 2 groups in which Teriparatides were administered daily and weekly, and the groups were compared in this study. One group an additional use of VitaminD was administered and the other an additional use of VitaminK.

In daily Teriparatide (Forteo) group, additional use of VitaminK(menatetereone) N=51 and of VitaminD(alphacalcidol)N=65. In weekly Teriparatide(Teribone) group, additional use of VitaminK(menatetereone) N=19 and of VitaminD(alphacalcidol) N=54. Two factor factorial ANOVA was applied for statistical examination, and in daily Teriparatide group ucOC/OC elevation rate was lower in additional use of VitaminK rather than VitaminD(P<0.0001), and also in weekly Teriparatide group ucOC/OC elevation rate was lower in additional use of VitaminK rather than VitaminD.(P<0.006131)

In result an increasing rate of ucOC/OC rate was obviously suppressed in additional use of VitaminK group in both Teriparatide groups at the 4 month follow up. Bone mineral density was the same in both groups in the short term follow up of 4 months.

From the point of bone quality, additional use of VitaminK for Teriparatides means something good that can prevent osteoporotic fractures.



ucOC/OC

**Disclosures:** Yoichi Kishikawa, None.

## SU0297

**Bone Health TeleECHO to Address Disparities in Osteoporosis Care and Reduce the Treatment Gap: 18 Month Progress Report.** E. Michael Lewiecki<sup>\*</sup>, Natalie Weiss, Matthew Bouchonville II, David Chafey, Sanjeev Arora. University of New Mexico Health Sciences Center, United States

**Background.** Bone Health TeleECHO Clinic (Bone Health ECHO) was developed at the University of New Mexico Health Sciences Center through collaboration of the ECHO Institute and the Osteoporosis Foundation of New Mexico. It is a strategy for telementoring healthcare professionals in underserved communities to achieve advanced levels of knowledge in the care of skeletal diseases. ECHO uses videoconferencing technology for case-based interactive learning, with brief didactic presentations on topics of interest. This is a progress report of Bone Health ECHO since its launch on October 6, 2015.

**Methods.** Registration for Bone Health ECHO is processed at the ECHO Institute. Demographic information of learners is collected. Participation is logged for each session attended. Electronic queries record anticipated changes in clinical practice. A self-efficacy assessment questionnaire retrospectively evaluated the effect of ECHO for confidence in managing patients with osteoporosis.

**Results.** Over the first 18 months of weekly Bone Health ECHO, 202 individuals registered, with 143 attending at least 1 TeleECHO clinic. Of those who attended at least once, 77 (53.8%) were classified as physicians (MD, DO, DC), 35 (24.5%) advanced practice providers (PA, CNP, RN, CNM, etc.), 25 (17.5%) other (PT, OT, PhD, etc.), and 6 (4.2%) unknown. Number of TeleECHO clinics attended ranged from 1 to 59, with a mean of 10.5. There were 30 learners (faculty excluded) who attended more than 20 ECHO clinics and 18 who attended more than 30. Attendees were located in 33 US states plus 4 other countries. The self-efficacy questionnaire was administered online in August 2016, after 10 months of Bone Health ECHO. There were 16 responders, 10 of whom attended more than 10 clinics and had patient care responsibilities. In this group, there was a statistically significant overall improvement in confidence of caring for osteoporosis patients (Figure), with a significant effect size of 1.18 (p = 0.005).

**Conclusion.** Bone Health TeleECHO Clinic improves self-confidence of healthcare professionals treating patients with osteoporosis. This provides an opportunity for patients to receive better care, closer to home, with greater convenience, and lower cost than referral to a specialty center. Bone Health ECHO can be scaled to any level through replication in other US states and other countries, acting as a force multiplier to reduce disparities in osteoporosis care.



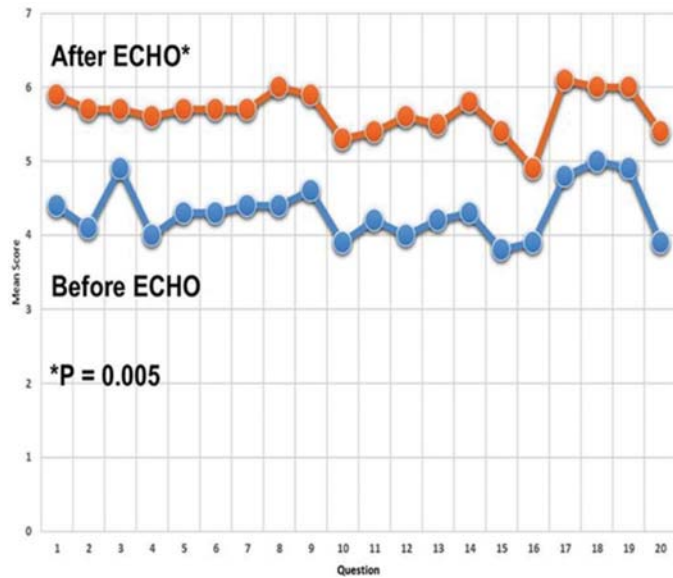


Figure. Self-efficacy assessment before and after ECHO for 20 domains of osteoporosis care

Disclosures: E. Michael Lewiecki, Shire, Consultant.

## SU0298

**Methodological considerations in evaluating treatment differences in fracture outcomes among female Medicare beneficiaries initiating osteoporosis medications.** Jiannong Liu<sup>\*1</sup>, Haifeng Guo<sup>1</sup>, Richard Barron<sup>2</sup>, Lionel Pinto<sup>2</sup>. <sup>1</sup>Minneapolis Medical Research Foundation, United States, <sup>2</sup>Global Health Economics, Amgen Inc., United States

There is significant variation in the baseline fracture risks of patients initiating different osteoporosis (OP) medications (meds). Patients at low risk of fracture tend to start on bisphosphonates (BP), whereas post-fracture patients, or those at high risk of fracture, tend to start on denosumab or teriparatide. We explore whether choice of specific pre- or post-index periods in retrospective claims analyses affect results when comparing fracture outcomes across various osteoporosis therapies.

Using the Medicare 100% OP patient files, we included female Medicare beneficiaries diagnosed with OP and aged  $\geq 66$  years who initiated OP meds (denosumab, oral BP, IV BP, raloxifene, teriparatide, or calcitonin) in 2009-2011 and used without discontinuation for  $\geq 1$  year and were covered by Medicare Parts A, B, and D for  $\geq 1$  year before the initiation date (index date). Patients with Paget's disease of bone, hypercalcemia, or cancer were excluded. Patients were followed from the index date to the earliest of death; diagnosis of Paget's disease, hypercalcemia, or cancer; loss of Medicare coverage; 18 months of follow-up; or end of 2012. The outcome was closed or pathologic fracture. A difference in difference (DiD) analysis was performed at the log scale of fracture rate using a Poisson regression model. Considering regression-to-the-mean issues and recognizing that treatment effects are usually delayed, we analyzed the data using different pre-index and follow-up periods (Table).

In all, 96,811 patients were included; 61.0% were on oral BP, 31.4% on IV BP, and percentages on other OP meds were 1.3%-2.9%. As anticipated, fracture rates preceding treatment initiation were relatively higher for teriparatide and denosumab users compared with users of other therapies (Table). Fracture rates decreased substantially during follow-up for users of all medications. Results of the DiD analysis varied depending on choice of baseline/follow-up periods. Significant variation in fracture reduction rates across treatments was observed; denosumab and teriparatide seemed to perform better.

In conclusion, while fracture rates were lower following treatment initiation for all medications, results of specific treatment comparisons may be influenced by choice of reference pre-index and follow-up periods. A pre-index period starting at month 7 to 12 and a follow-up period starting at month 4 onwards maybe less biased and serve as reasonable options to explore in future studies.

Pre-index Period	Follow-up Period	Denosumab	Teriparatide	Bisphosphonate
Month 1-12	Month 1-12	0.00	0.00	0.00
Month 1-12	Month 13-24	0.00	0.00	0.00
Month 1-12	Month 25-36	0.00	0.00	0.00
Month 1-12	Month 37-48	0.00	0.00	0.00
Month 1-12	Month 49-60	0.00	0.00	0.00
Month 13-24	Month 1-12	0.00	0.00	0.00
Month 13-24	Month 13-24	0.00	0.00	0.00
Month 13-24	Month 25-36	0.00	0.00	0.00
Month 13-24	Month 37-48	0.00	0.00	0.00
Month 13-24	Month 49-60	0.00	0.00	0.00
Month 25-36	Month 1-12	0.00	0.00	0.00
Month 25-36	Month 13-24	0.00	0.00	0.00
Month 25-36	Month 25-36	0.00	0.00	0.00
Month 25-36	Month 37-48	0.00	0.00	0.00
Month 25-36	Month 49-60	0.00	0.00	0.00
Month 37-48	Month 1-12	0.00	0.00	0.00
Month 37-48	Month 13-24	0.00	0.00	0.00
Month 37-48	Month 25-36	0.00	0.00	0.00
Month 37-48	Month 37-48	0.00	0.00	0.00
Month 37-48	Month 49-60	0.00	0.00	0.00
Month 49-60	Month 1-12	0.00	0.00	0.00
Month 49-60	Month 13-24	0.00	0.00	0.00
Month 49-60	Month 25-36	0.00	0.00	0.00
Month 49-60	Month 37-48	0.00	0.00	0.00
Month 49-60	Month 49-60	0.00	0.00	0.00

Table 1: Treatment Effect Comparison with Different Reference Periods and Follow-up Periods

Disclosures: Jiannong Liu, None.

## SU0299

**A Meta-Analysis of 4 Clinical Trials of Denosumab Compared With Bisphosphonates in Postmenopausal Women Previously Treated With Oral Bisphosphonates.** P Miller<sup>\*1</sup>, N Pannacciulli<sup>2</sup>, J Malouf-Sierra<sup>3</sup>, A Singer<sup>4</sup>, E Czerwinski<sup>5</sup>, HG Bone<sup>6</sup>, C Wang<sup>2</sup>, RB Wagman<sup>2</sup>, JP Brown<sup>7</sup>. <sup>1</sup>Colorado Center for Bone Research, United States, <sup>2</sup>Amgen Inc., United States, <sup>3</sup>Hospital de la Santa Creu i Sant Pau, Spain, <sup>4</sup>Georgetown University Medical Center, United States, <sup>5</sup>Krakow Medical Center, Poland, <sup>6</sup>Michigan Bone and Mineral Clinic, United States, <sup>7</sup>CHU de Québec Research Centre and Laval University, Canada

### Purpose

Four clinical trials have separately shown greater BMD gains with transitioning to denosumab (DMAb) compared with continuing on bisphosphonates (BP) in subjects previously treated with oral BPs (Kendler *JBM* 2010; Recknor *Obstet Gynecol* 2013; Roux *Bone* 2014; Miller *JCEM* 2016). The aim of this meta-analysis was to improve estimates of effect size and provide an integrated assessment of safety/efficacy of DMAb vs BPs with different dosing regimens (weekly, monthly, yearly) and administration routes (oral, IV), over 12 months in postmenopausal women pretreated with oral BPs.

### Methods

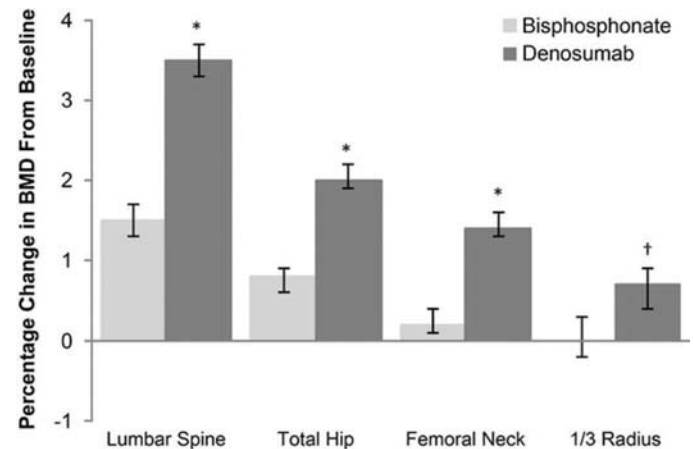
Data were pooled from 4 randomized studies in postmenopausal women with low bone mass or osteoporosis, aged  $\geq 55$  years, and pretreated with oral BPs, who were randomized 1:1 to DMAb (60mg every 6 months) or an oral (alendronate 70mg weekly, ibandronate 150mg monthly, risendronate 150mg monthly) or IV (zoledronic acid 5mg yearly) BP for 12 months. Percentage (%) change from baseline (BL) in BMD at the lumbar spine, total hip, femoral neck, and 1/3 radius (assessed in 2 studies) at month 12; % change from BL in serum CTX (sCTX, in a subset of 1058 subjects) at 1, 6, and 12 months (in 2 of the studies); and safety were assessed. Fractures were collected as adverse events (AEs) and not adjudicated.

### Results

A total of 2850 subjects were included (1426 DMAb; 1424 BP). Mean (SD) age was 68 (8) years, mean (SD) lumbar spine BMD T-score was -2.5 (1.0), and mean (SD) duration of prior oral BP use was 3.8 (3.6) years. BMD % change from BL at month 12 was significantly greater with DMAb vs BPs at all measured skeletal sites (Figure) and independent of length of prior BP use ( $<2$  or  $\geq 2$  years) at all sites measured (except for 1/3 radius for those with  $<2$  years of prior BP use). Median sCTX % decrease from BL was greater with DMAb than BPs at months 1 (-58% vs -12%), 6 (-36% vs -14%), and 12 (-26% vs 8%; all  $p<0.0001$ ). Overall AEs/serious AEs were similar between groups. There were no cases of osteonecrosis of the jaw. Three events consistent with the definition of atypical femoral fracture were observed (2 DMAb; 1 BP). Osteoporosis-related fractures were reported in 47 (3.3%) DMAb and 43 (3.1%) BP subjects.

### Conclusions

This integrated assessment shows greater clinical benefit with increases in BMD and reductions in bone turnover and similar safety profile in transitioning from oral BPs to DMAb, compared with continuing on or cycling through the same therapeutic class (from one BP to another).



\* $p<0.0001$  and † $p=0.001$  denosumab vs bisphosphonate.

Data are least-squared means and 95% confidence intervals based on an ANCOVA model adjusting for treatment, duration of prior bisphosphonate use, baseline BMD, study, DXA machine type, and baseline-BMD-value-by-machine-type interaction. 1/3 radius was assessed in 2 of the 4 studies.

Figure: Percentage Change in BMD From Baseline at Month 12

Disclosures: P Miller, Amgen, Alexion, Eli Lilly, Consultant.

## SU0300

**Observation of Discharge Destination Following Surgically Treated for Fragility Hip Fracture in Patients over 70-year old - A Single Surgeon Series at Urban Medical Center.** Kim Tae-Min\*, Seok-Tae Yun, Kwang-Jun Oh. Department of Orthopedic Surgery, Konkuk University Medical Center, Korea, Republic of

**Purpose:** The aim of this study was to observe the postoperative track in patients over 70-year old with intertrochanteric fracture treated by proximal femoral nailing and to review the clinical outcome including mortality and readmission according to each discharge destination. The study was done by single surgeon in urban medical center. **Methods:** 138 consecutive patients over 70 year-old (36 males, 102 females, mean age  $81.6 \pm 6.6$ ) with intertrochanteric femoral fractures who were treated by proximal femoral nail were observed and analyzed retrospectively. The patients were classified into three groups as discharge destination: those discharged to home (n=61) and those admitted rehabilitation institute (n=37) and admitted to nursing home (n=40). Using variables including age, postoperative functional outcome using Koval grade (from grade 1; independent community ambulation to grade 7; nonfunctional ambulation) at follow up, and mortality, readmission rate, re-fracture after postoperative 2 years according to discharge destination, statistical analyses were conducted. And it was checked whether taking osteoporosis medications for the estimation that how well the secondary hip fractures is being prevented. **Result:** Even though the preoperative Koval grade were not statistical difference between each groups ( $p=0.11$ ), the average age at operation date and Koval grade at last follow up of patients who discharge to nursing home was higher with statistical significance compared with other groups ( $p < 0.001$  and  $p < 0.002$  respectively). The re-fracture rate did not reveal the statistical difference between three groups. But, the mortality and re-admission rate within 2 years in patients who discharge to nursing home were higher than other groups ( $p < 0.0008$  and  $p < 0.03$  respectively). Low compliance with osteoporotic medications was observed, as only 27 out of 138 patients (19%) took the medications. However, it had no association with respective discharge destinations ( $p=0.852$ ). **Conclusion:** Information from this study is expected to be useful for determining discharge plans and for setting the treatment of goals and prognosis. And this study shows that it is important for orthopaedic surgeons to keep in mind with patient adherence for osteoporosis medication due to prevent secondary hip fractures. We propose the construction of a feedback system that aids in a discharge pass to improve the clinical outcome for fragile hip fractures in elderly.

**Disclosures:** Kim Tae-Min, None.

## SU0301

**DEXA areal BMD Measurement Underestimates the Bone Forming Effects of Teriparatide.** Eleftherios Paschalis\*<sup>1</sup>, John Krege<sup>2</sup>, Sonja Gamsjaeger<sup>1</sup>, Erik Eriksen<sup>3</sup>, David Burr<sup>4</sup>, Damon Disch<sup>2</sup>, Jan Stepan<sup>5</sup>, Astrid Fahrleitner-Pammer<sup>6</sup>, Klaus Klaushofer<sup>1</sup>, Imre Pavo<sup>7</sup>. <sup>1</sup>Ludwig Boltzmann Institute of Osteology, Hanusch Hospital of WGKK, AUA Trauma Centre Meidling, 1st Medical Department, Hanusch Hospital, Austria, <sup>2</sup>Eli Lilly and Company, United States, <sup>3</sup>Dept. of Clinical Endocrinology, Morbid Obesity and Preventive Medicine, Oslo University Hospital Institute of Clinical Medicine, Oslo University, Norway, <sup>4</sup>Dept of Anatomy and Cell Biology, Indiana Univ School of Medicine, United States, <sup>5</sup>Institute of Rheumatology, Faculty of Medicine 1, Charles University, Czech Republic, <sup>6</sup>Department of Internal Medicine, Division of Endocrinology and Metabolism, Medical University of Graz, Austria, <sup>7</sup>Eli Lilly and Company, Austria

Teriparatide (TPTD) increases bone mass primarily through the remodeling of older or damaged bone and over-replacement with new, initially less mineralized bone. We have investigated whether dual energy X-ray absorptiometry (DEXA) areal bone mineral density (aBMD) measurement adequately reflects changes of mineral and organic matrix in the cortical and trabecular bone compartments.

#### Methods

Paired biopsies and aBMD measurements were obtained prior to and at the end of two-years of TPTD treatment from postmenopausal women with osteoporosis who were either alendronate pre-treated or osteoporosis-treatment naïve. All biopsies with two intact cortices and cancellous structure were assessed by  $\mu$ CT (mean cortical width [MCW] and trabecular bone volume/total volume [BV/TV]). Fourier transformed infrared imaging (pixel size  $\sim 6.3 \times 6.3 \mu\text{m}^2$ ) was utilized to calculate the size as well as the average and total mineral and organic contents of the cortical and cancellous compartments. Effect of pre-treatment over time was analyzed using mixed model repeated measures (MMRM). Summary statistics and correlations were calculated.

#### Results

There was no alendronate pre-treatment effect ( $p > .09$ , either cortical or cancellous), so no adjustment for pre-treatment was performed.  $\mu$ CT derived MCW and cancellous BV/TV increased accompanied by similar increases in the respective overall mineral contents (Table). The average mineralization did not change (data not shown). The increases in cortical/trabecular mineral/organic matrix as well as  $\mu$ CT parameters consistently exceeded those of aBMD. Furthermore, we found that the increase in organic matrix exceeded the increase in mineral content in both the cortical and trabecular compartments. For percent changes, only MCW correlated to change in femoral neck

(FN) aBMD ( $r = .38$ ,  $p = .043$ ), while no other significant correlations of MCW or BV/TV with lumbar spine (LS), total hip (TH), or FN aBMD were demonstrable.

#### Conclusion

Our data indicate that 2 years of teriparatide treatment leads to an increased mineral content being distributed in an even larger bone volume in cortical as well as trabecular bone. This finding may help to explain why BMD measured by areal DEXA methodology underestimates the anabolic effects of teriparatide on the skeleton.

**Table. Summary of percent changes from baseline.**

Summary Statistic	BV/TV	Mean Cortical Width	LS BMD	TH BMD	FN BMD	Cortical Mineral Content	Cortical Matrix Content	Cancellous Mineral Content	Cancellous Matrix Content
N	31	27	31	31	31	31	31	31	31
Mean	21.6	28.9	5.97	-1.14	2.05	31.2	47.9	17.7	39.0
Standard Error	6.58	10.6	1.29	.84	1.07	9.84	12.5	6.04	8.82
p-Value*	.003	.011	<.001	.873	.065	.004	.001	.006	<.001

\* Two-sided t-test of whether the mean is zero

Table

**Disclosures:** Eleftherios Paschalis, None.

## SU0302

**Mineral and Organic Matrix Content at Bone Forming Surfaces in Postmenopausal Women Treated with Either Teriparatide or Zoledronic Acid for 6 Months.** Eleftherios P. Paschalis\*<sup>1</sup>, David W. Dempster<sup>2</sup>, Sonja Gamsjaeger<sup>1</sup>, Klaus Klaushofer<sup>1</sup>, Kathleen A. Taylor<sup>3</sup>. <sup>1</sup>Ludwig Boltzmann Institute of Osteology, Hanusch Hospital, Austria, <sup>2</sup>Regional Bone Center, Helen Hayes Hospital, New York State Department of Health, United States, <sup>3</sup>Lilly USA, United States

**Purpose:** Resistance of bone to fracture is dependent on the composite nature of its mineral (M) and organic matrix (OM) phases. Teriparatide (TPTD) and zoledronic acid (ZOL), approved anabolic and antiresorptive bone therapies, respectively, reduce the risk of fracture in women with postmenopausal osteoporosis. Raman microspectroscopy was used to analyze tetracycline-labeled iliac crest biopsies from postmenopausal women with osteoporosis treated with either TPTD 20mcg daily, subcutaneous injection (N = 28) or ZOL 5mg/year, intravenous infusion (N=25) for 6 months. Spatially resolved information on the M and OM phases, as well as their ratio (M/OM) was obtained to study effects of these drugs on number of forming sites and osteoblast activity.

**Methods:** Spectra were acquired at forming trabecular and intracortical surfaces (identified by double fluorescent labels [DLs]) to determine individual M and OM content, and M/OM at 3 distinct tissue ages (TA1=1-5 days; TA2=15 days; TA3  $\geq 25$  days). The total number of DLs per biopsy and anatomical envelope, and the interlabel (IrLD) distance were recorded. Two-way ANOVA and two-sample t-tests were used for statistical comparisons.

**Results:** At trabecular surfaces, TPTD therapy resulted in significantly higher OM across all tissue ages, and significantly lower M/OM at TA2 and TA3 compared to ZOL (Fig. 1). At intracortical forming surfaces, there were no differences in OM content between dose groups at any tissue age. However, treatment with ZOL compared with TPTD resulted in significantly higher M content and M/OM at TA1. IrLD was significantly higher in the TPTD group in both cancellous ( $p < 0.001$ ) and intracortical ( $p < 0.05$ ) envelopes. These results suggest that TPTD therapy results in increased osteoblast activity. TPTD-treated patients had significantly ( $p < 0.0001$ ) higher number of DLs, in both cancellous and intracortical envelopes. Multiplication of the M and OM content by the number of DLs showed that TPTD treatment results in significantly higher new M and OM synthesized compared to ZOL, in both cancellous and intracortical envelopes.

**Conclusions:** Our results show that: 1) TPTD and ZOL exert differential effects on newly synthesized M and OM content at identical tissue ages. 2) These effects are dependent on tissue age and bone envelope. 3) Compared to ZOL, TPTD increases bone matrix by modulating both the number of forming sites in both envelopes, as well as osteoblast activity at trabecular forming surfaces.



**Figure 1. Mineral and Organic Matrix Content, and their Ratios for Cancellous and Intracortical Bone in Tetracycline-labelled biopsies from Post-menopausal Women with Osteoporosis Treated with Teriparatide (TPD) or Zoledronic acid (ZOL) for 6 Months.**

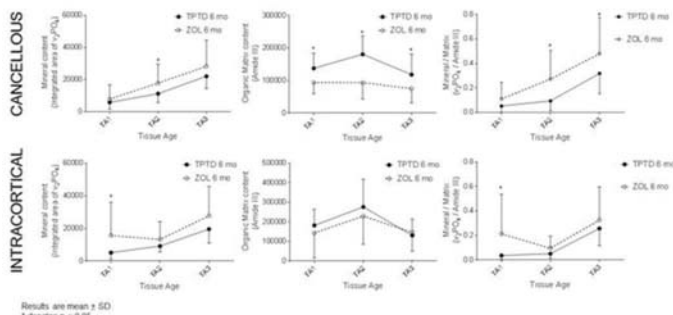


Figure 1

**Disclosures:** Eleftherios P. Paschalis, None.

## SU0303

**Differing Effects of Oral Conjugated Equine Estrogen and Transdermal Estradiol on Vitamin D Metabolism in Postmenopausal Women: A 4-Year Longitudinal Study.** Anna Maria Santoro<sup>1</sup>, Christine Simpson<sup>1</sup>, Elaine Cong<sup>2</sup>, Andrea Haas<sup>3</sup>, Karl Insogna<sup>1</sup>. <sup>1</sup>Yale University School of Medicine, United States, <sup>2</sup>Englewood Hospital, United States, <sup>3</sup>Brigham and Women's Hospital, United States

Despite the widespread use of low-dose transdermal estrogen for menopausal symptoms, the impact of these preparations on vitamin D metabolism has not been extensively studied. We therefore used data from KEEPS (Kronos Early Estrogen Prevention Study), a 4-year RCT that evaluated the effects of estrogen therapy on atherosclerosis endpoints in postmenopausal women, to evaluate the impact of estradiol on vitamin D homeostasis. Available samples included 25 participants who were treated with conjugated equine estrogen 0.45 mg/d (CEE; Premarin®) and 20 who received transdermal estradiol 50 mcg/wk (E<sub>2</sub>; Climara®). Participants also received micronized progesterone for 12 d/mo. No significant change was seen in total 25 hydroxyvitamin D (25D) levels assayed by chemiluminescence (IDS-iSYS®), in either group over four years, 30.1→31.2 ng/mL and 30.2→34.3 ng/mL respectively.

Vitamin D binding protein (DBP) levels were measured by ELISA (ALPCO®). There was a significant increase in mean DBP levels from baseline (BL) to 12 months in both the CEE and E<sub>2</sub> groups (34.0→51.8 mg/dL;  $p < 0.0001$ ) and (37.4→48.9 mg/dL;  $p = 0.003$ ), respectively, which was sustained to 36 months in both groups. There was a decline in DBP levels from 36 to 48 months in the CEE group (56.1→39.2 mg/dL;  $p < 0.0001$ ) and the E<sub>2</sub> group (47.7→36.6 mg/dL;  $p = 0.0004$ ). However, from BL to 48 months there was a significant change only in the CEE group (34.0→39.2 mg/dL;  $p = 0.01$ ) while there was no change in the E<sub>2</sub> group (37.4→36.6 mg/dL;  $p = \text{NS}$ ). Since DBP levels were unchanged from BL to 48 months in the E<sub>2</sub> group, free 25D levels were directly measured by ELISA (DIA Source®) in this group, and also calculated using available formulae. There was no difference in the BL free 25D values when directly measured or calculated. However, at 48 months, directly measured free 25D (10.9 pg/mL) was elevated when compared to the calculated value (7.3 pg/mL;  $p = 0.03$ ). Consistent with the rise in free 25D in the E<sub>2</sub> group, PTH, measured in a subset of E<sub>2</sub> subjects, declined slightly (26→23 nLeq/mL).

Although the reason for elevated free 25D levels with longer term E<sub>2</sub> treatment is unclear, these findings suggest that apart from its use in ameliorating menopausal symptoms, treatment with transdermal estradiol may result in more favorable vitamin D metabolism.

**Disclosures:** Anna Maria Santoro, None.

## SU0304

**Fracture healing is expedited via preferential upregulation of Wnt/β-catenin using targeted nanoparticle GSK3β inhibitor delivery.** Danielle Benoit<sup>1</sup>, Yuchen Wang<sup>1</sup>, Maureen Newman<sup>1</sup>, Tzong-Jen Sheu<sup>2</sup>, J. Edward Puzas<sup>2</sup>. <sup>1</sup>Biomedical Engineering and Center for Musculoskeletal Research, University of Rochester, United States, <sup>2</sup>Center for Musculoskeletal Research, University of Rochester Medical Center, United States

More than 10 million Americans suffer from fractures each year, of which ~20% have impaired fracture healing stemming from dysfunctional mesenchymal stem cell (MSC) osteogenesis. The Wnt/β-catenin pathway is a promising target to augment MSC osteogenesis during healing. However, systemic delivery of β-catenin agonists at doses necessary to affect bone results in myriad off-target effects. Therefore, fracture-targeted nanoparticles (NPs) were designed to provide greater solubility and selectivity of the β-catenin agonist, GSK3β inhibitor XXVII. Specifically, diblock copolymers of poly(styrene-alt-maleic anhydride)-b-poly(styrene) (PSMA-b-PS) were synthesized, self-assembled into NPs, and functionalized with a peptide with high affinity toward tartrate resistant acid phosphatase (TRAP), an enzyme selectively deposited by osteoclasts during the resorption phase of

bone remodeling. The TRAP-binding peptide (TBP, TPLSYLKGLTVG) and scrambled control peptide (SCP, VPVGTLSTYKLLTG) were conjugated to the NPs. Drug-loaded NP, TBP-NP, and SCP-NP showed uniform spherical morphology with sizes of  $50 \pm 2$  nm and surface charge of  $-26 \pm 1$  mV with 14% (w/w) β-catenin agonist loading capacity. NP, SCP-NP, and TBP-NP showed minimal biodistribution to liver and TBP-NP showed ~5-fold and 2-fold higher accumulation at fractured femur compared with SCP-NP and untargeted NPs, respectively, indicating that localization is specific to TBP. Fracture localized activation of β-catenin was also observed, with TBP-NP-β-catenin agonist resulting in robust β-galactosidase staining in LacZ reporter mice (Tg(Fos-LacZ)34Efu/J) compared with controls. X-ray showed enhanced callus formation of fractures treated with TBP-NP-β-catenin agonist at early stages (week 2) of healing versus controls with more rapid ossification of cartilage callus. Finally, torsional biomechanics of healing fractures were significantly greater (~2.5-4-fold) than controls 3 weeks after treatments. The development of targeted NPs for fracture-specific delivery of small molecule drugs, specifically, β-catenin agonists, improves bone regeneration with reduced off-target side effects, which is not currently possible via systemic delivery of small molecule drugs. Current experiments are focused on evaluating cellular targets of TBP-NP-β-catenin agonist within the fracture milieu to enable greater selectivity of drug delivery.

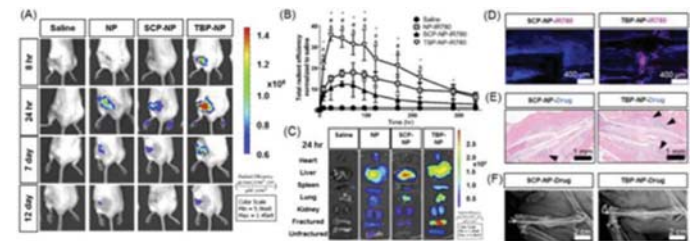


Figure 1: TBP functionalization results in preferential NP accumulation at fracture sites

**Disclosures:** Danielle Benoit, None.

## SU0305

**LIGHT/TNFSF14 deficiency affects basal bone remodeling through the regulation of osteoprotegerin expression.** Giacomina Brunetti<sup>1</sup>, Luciana Lippo<sup>2</sup>, Sara Bortolotti<sup>1</sup>, Giuseppina Storlino<sup>1</sup>, Isabella Gigante<sup>1</sup>, Graziana Colaianni<sup>1</sup>, Adriana Di Benedetto<sup>3</sup>, Paolo Pignataro<sup>1</sup>, Lindsay Ward-Kavanagh<sup>4</sup>, Mariasevera Di Comite<sup>1</sup>, Giorgio Mori<sup>2</sup>, Koji Tamada<sup>5</sup>, Janne E. Reseland<sup>6</sup>, Carl F Ware<sup>4</sup>, Silvia Colucci<sup>1</sup>, Maria Grano<sup>7</sup>. <sup>1</sup>Department of Basic and Medical Sciences, Neurosciences and Sense Organs, section of Human Anatomy and Histology, University of Bari, Italy, <sup>2</sup>Department of Basic Medical Sciences, Neurosciences and Sense Organs, Section of Human Anatomy and Histology, University of Bari, Italy, <sup>3</sup>Department of Clinical and Experimental Medicine, University of Foggia, Italy, <sup>4</sup>Infectious and Inflammatory Disease Center, Sanford Burnham Prebys Medical Discovery Institute, United States, <sup>5</sup>Department of Oncology, Johns Hopkins University School of Medicine, United States, <sup>6</sup>Department of Biomaterials, Institute for Clinical Dentistry, University of Oslo, Norway, <sup>7</sup>Department of Emergency and Organ Transplantation, Section of Human Anatomy and Histology, Italy

LIGHT (TNFSF14), expressed by different cells of the immune system, is known to play a major role in T-cell homeostasis. It is over-expressed in erosive rheumatoid arthritis and lytic myeloma-bone disease. Here, we investigated the bone phenotype in LIGHT-deficient mice (*Tnfsf14*<sup>-/-</sup>). Approximately 40% of newborn *Tnfsf14*<sup>-/-</sup> mice exhibit spinal deformity in the curvature of the spine at thoracic vertebrae compared to wild-type (WT) mice. The severity of the deformity continues to increase up to 12 months of age. MicroCT demonstrated that the femurs of *Tnfsf14*<sup>-/-</sup> mice exhibited a 30% ( $p < 0.001$ ) decrease in trabecular BV/TV due to a significant reduction in Tb.Th, Tb.N, Tb.Dm and the increase in Tb.Sp respect to WT mice. Furthermore, a five-fold increase of OC number/bone surface was found in femora from *Tnfsf14*<sup>-/-</sup> mice compared to WT ( $p < 0.008$ ), together with a slight significant reduction of osteoblast number/bone perimeter ( $p < 0.01$ ). Consistently, dynamic histomorphometry showed a significant decrease in bone formation parameters. To investigate the possible molecular mechanism responsible for this bone phenotype in *Tnfsf14*<sup>-/-</sup> mice we studied OPG levels in whole bone marrow (BM) samples from the femurs of these mice and demonstrated a significant reduction in OPG mRNA transcript and protein respect to WT. Further investigations showed that BM CD8+ T cells and B cell subpopulations from *Tnfsf14*<sup>-/-</sup> mice expressed lower levels of OPG compared to those from WT mice. Moreover, BM CD8+ T cells from *Tnfsf14*<sup>-/-</sup> expressed reduced levels of the pro-osteoblastogenic Wnt10b. Consistently, LIGHT treatment dose-dependently increased OPG expression in BM CD8+ T cells and B-cells as well as Wnt10b levels in CD8+ T cells. To further explore the B and T cell-mediated effects of LIGHT on bone, we evaluate the femoral microstructure of *Tnfsf14*<sup>-/-</sup> mice bred onto *Rag*-deficient mice, a strain that does not develop mature T or B cells, by microCT. Consistently, femur reconstructions from *Rag*-/*Tnfsf14*<sup>-/-</sup> mice showed a significant increase of trabecular bone with respect to *Rag*<sup>-/-</sup> mice. Indeed, we demonstrated a significant 33% increase in trabecular BV/TV in *Rag*-/*Tnfsf14*<sup>-/-</sup> mice resulting from a significant increase in Tb.Th, Tb.N, and Tb.Dm, as well as a decrease in Tb.Sp. Consistently, *Rag*-/*Tnfsf14*<sup>-/-</sup> displayed a 20-fold increase in

levels of OPG compared to *Rag-/-* mice. These results suggested that LIGHT effect on basal bone remodelling is mainly mediated by T- and B-cells through OPG.

**Disclosures:** *Giacomina Brunetti, None.*

## SU0306

**Ablation of IGF-1R in Osteochondroprogenitors Increases CXCL12 Expression in Bone Lining Cells.** Alessandra Esposito\*, Lai Wang, Tieshi Li, Joseph Temple, Anna Spagnoli. Rush University Medical Center, United States

The type 1 insulin-like growth factor ligand and receptor (IGF1/IGF1R) both have key anabolic roles in postnatal skeletal development. Because IGF1/IGF1R knockouts (KOs) mice die either early postnatally or prenatally, studying their downstream mediators has been difficult. Although periosteal/endosteal cells play critical roles in bone development and regeneration their nature still remain elusive and whether IGF1R signaling is involved in their function has never been investigated. We have previously reported that in bone regeneration, the regulation of the expression of C-X-C-motif-chemokine-ligand-12 (CXCL12) determines the fate of a population of CXCL12+, NG2+,  $\alpha$ SMA+ endosteal/perivascular cells either to osteogenic differentiation or to a supportive role in angiogenesis. To test the hypothesis that IGF1R signaling regulates CXCL12's expression to maintain bone homeostasis, we generated IGF1RKO mice by crossing Prx1-Cre+ with igf1r-floxed mice. First, we performed histomorphometric analyses using double labeling technique by intraperitoneally injecting 8 week-old IGF1RKO (n=3) and control females (n=3) with calcein at postnatal day 2 followed by alizarin red at day 7. Dynamic data of the tibiae showed that IGF1RKO mice had decreased MAR and BFR/BS in the midshaft endosteum (MAR=32% of control $\pm$ 0.012, p=0.049; BFR/BS=30 $\pm$ 0.05, p=0.05), in the periosteum (MAR=36% $\pm$ 0.013, p=0.0003; BFR/BS=33% $\pm$ 0.057, p=0.004) and in the trabecular bone (MAR=55% $\pm$ 0.11, p=0.0003; BFR/BS=45% $\pm$ 0.13, p=0.0004). Static data in the same regions, showed that IGF1R-KO had decreased Ob.Perimeter (45% $\pm$ 0.064, p=0.0042), Oc.Perimeter (16% $\pm$ 0.047, p<0.0001), N.Oc/BS (69% $\pm$ 0.05, p=0.0036) and increased N.Ob/BS (158% $\pm$ 0.05, p=0.003). IGF1RKO mice showed increased periosteal and endosteal cellularity and abnormal cortical bone neo-angiogenesis. IGF1RKO mice showed also an increase of bone lining CXCL12+/CXCR4+ expressing cells in the endosteum, as well as in the trabecular surface within the diaphyseal and metaphyseal regions. The abnormal cortical angiogenesis found in IGF1RKO was associated with an increase of CXCL12+/CXCR4+ cells, surrounding endothelial PECAM+ cells. Together, our results reiterate that IGF1R is essential to maintain bone homeostasis and uncover a new function of IGF1 signaling in regulating the expression of CXCL12 in bone lining cells. In vitro mechanistic studies are in progress to determine the function of this novel IGF1/CXCL12 axis in determining the fate of bone lining cells.

**Disclosures:** *Alessandra Esposito, None.*

## SU0307

**Stanniocalcin 1 inhibits RANKL-induced osteoclastogenesis.** Hanna Gu\*, Hwa Sung Chae, Kyung Mi Woo, Hyun-Mo Ryoo, Jeong-Hwa Baek. Department of Molecular Genetics, Seoul National University School of Dentistry, Korea, Republic of

Stanniocalcin 1 (STC1) is a mammalian homolog of STC, a glycoprotein hormone that regulates calcium and phosphate homeostasis in bony fish. STC1 gene is widely expressed in many tissues, including bone, cartilage and skeletal muscle. It has been previously demonstrated that STC1 stimulates osteoblast differentiation in rat calvarial cells. However, the function of STC1 in osteoclastogenesis has not been elucidated. In this study, we investigated the effect of STC1 in receptor activator of nuclear factor- $\kappa$ B ligand (RANKL)-induced osteoclast differentiation in RAW264.7 cells or primary cultured mouse bone marrow-derived macrophages (BMMs). Recombinant human STC1 protein (rhSTC1) did not affect cell viability or proliferation at the concentrations of 50 or 100 ng/ml. However, rhSTC1 significantly attenuated the formation of TRAP-positive multinucleated cells and mRNA expression levels of osteoclastogenic marker genes such as TRAP, c-src and cathepsin K. In addition, rhSTC1 suppressed cell migration and osteoclast fusion index. STC1 blocked RANKL-induced ROS production and transcriptional activity of NF- $\kappa$ B. These results suggest that STC1 functions as a negative regulator of osteoclastogenesis in bone tissues.

**Disclosures:** *Hanna Gu, None.*

## SU0308

**Bone phenotype in mouse models of obesity, insulin resistance and diabetes.** Xiaohong Bi\*<sup>1</sup>, Andrea Baker<sup>2</sup>, Guijin Lu<sup>1</sup>, Maria Mendoza-Rodriguez<sup>3</sup>, Vihang Narkar<sup>1</sup>, Rebecca Berdeaux<sup>3</sup>, Catherine Ambrose<sup>2</sup>. <sup>1</sup>The Institute of Molecular Medicine, UTHealth, United States, <sup>2</sup>Dept of Orthopaedic Surgery, UTHealth, United States, <sup>3</sup>Dept of Integrative Biology and Pharmacology, UTHealth, United States

In 2010, 27% of US residents age 65 and older had diabetes and 50% had prediabetes. While both conditions have detrimental effects on multiple organ systems, the effects on bone are not clear. We examined the bone phenotype in two common preclinical models

and compared the results to the available data from human studies. For prediabetes, male C57Bl6/J mice were fed a 60% high fat diet (HFD) for 13 weeks. These mice developed obesity, fasting hyperglycemia, and impaired glucose tolerance compared to isogenic lean animals (n=6, 4 mo old). For severe diabetes, male *db/db* mice which exhibit extreme obesity, hyperinsulinemia, hyperglycemia and impaired glucose tolerance, were compared to lean WT littermate controls (n=6, 4 mo old). After euthanasia, femurs were imaged using microCT and Raman spectroscopy, biomechanically tested, and subjected to advanced glycation end-products (AGE) assay. Data from experimental animals of each group were normalized to the respective controls and t-tests were used to determine how bone phenotypes were affected by diabetes of different severity.

In humans, diabetes results in a higher BMD as measured by DXA but reduced architectural integrity as measured by trabecular bone score. Raman spectroscopy showed increased mineralization in the *db/db* mice. MicroCT showed reduced BV/TV, Conn.D, SMI, TnN, and TbTh in *db/db* animals, while only Conn.D was reduced in the HFD animals. TbSp was increased in both models. Bone turnover is decreased in patients with type 2 diabetes. Although bone turnover was not measured specifically, the *db/db* animals demonstrated increased carbonate substitution, which has been associated with decreased turnover. It has been proposed that increased AGEs are responsible for the increased fragility in diabetic bone. The total AGE content increased over controls by 111% in *db/db* and 26% HFD mice. The ratio of Raman bands at 1660 and/ 1690 cm<sup>-1</sup>, a measure of collagen cross link maturity, was increased in the HFD animals. Mechanical testing showed no apparent differences in the HFD group compared to control, but the *db/db* mice demonstrated reduced ultimate load, stiffness, energy to failure, and ultimate strength.

The results from this analysis show that while some of the bone changes seen in subjects with diabetes are recapitulated in both *db/db* and HFD mice, the changes are more dramatic in *db/db* mice. These findings are consistent with HFD representing a prediabetes model, and the *db/db* mice severe diabetes.

**Disclosures:** *Xiaohong Bi, None.*

## SU0309

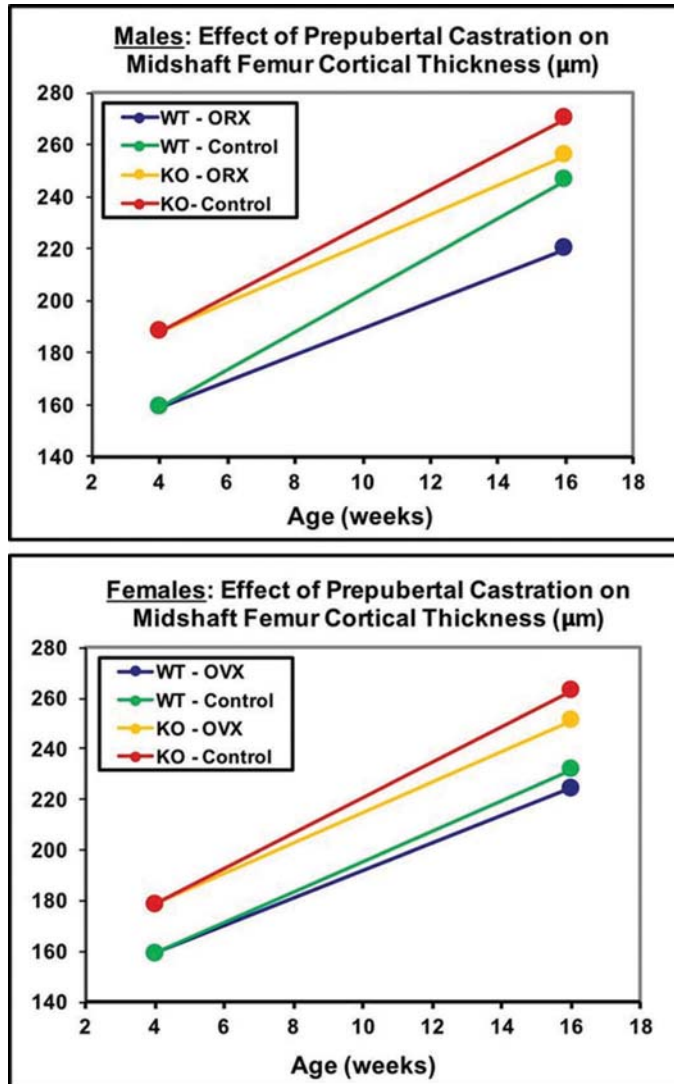
**Inhibiting the WNT Inactivating Lipase NOTUM Stimulates Endocortical Bone Formation Independently of Sex Hormones.** Robert Brommage\*, Faika Mseeh, David Potter, Jeff Liu, Melanie Shadoan, Andrea Thompson, Peter Vogel, Brian Zambrowicz, David Powell, Qingyun Liu. Lexicon Pharmaceuticals, United States

The secreted WNT lipase NOTUM inactivates WNTs by removing the palmitoleate essential for WNT binding to Frizzled receptors. Gene KO of *Notum* in mice results in elevated cortical bone thickness and strength. Both orally active small molecule and neutralizing antibody inhibitors of NOTUM lipase activity stimulate modeling-dependent endocortical bone formation, resulting in elevated cortical bone thickness and strength at multiple cortical bone sites.

Six studies were performed demonstrating that sex hormones do not have important roles in the anabolic skeletal actions of NOTUM inhibition. 1) Male and female *Notum* KO mice showed similarly elevated midshaft femur cortical bone thickness and strength from 14 through 52 weeks of age. 2) Ovariectomy of wild-type and *Notum* KO mice at 18 weeks of age resulted in similar losses of cortical bone thickness. 3) Pre-pubertal castration of male and female wild-type and *Notum* KO mice at 4 weeks of age resulted in similar reductions in cortical bone gain when assessed at 16 weeks of age. 4) Young adult male mice were routinely employed in pre-clinical pharmacology studies optimizing compound and antibody development. 5) Four weeks of treatment of both sham-surgery and ovariectomized adult mice with the NOTUM neutralizing antibody 2.78.33 produced similar gains in cortical bone mass in midshaft femur, femoral neck and vertebral body and endocortical bone formation rate in midshaft femur. 6) Eighteen weeks of treatment of both sham-surgery and ovariectomized adult rats with the orally active NOTUM small molecule inhibitor LP-922056 produced similar gains in cortical bone mass (midshaft femur, midshaft tibia, midshaft humerus, distal radius, distal ulna, distal tibia, vertebral body, femoral neck), strength (femur shaft, tibia shaft, vertebral body and femoral neck) and endocortical bone formation rate (distal tibia).

These findings suggest that inhibiting NOTUM with either orally active small molecules or neutralizing antibodies may provide potential anabolic therapies for preventing non-vertebral osteoporotic fractures in both men and women.





Study 3: Prepubertal Castration of Male and Female Mice

Disclosures: Robert Brommage, None.

## SU0310

**Abaloparatide, a Selective PTH1 Receptor Agonist, Reversed Bone Loss and Improved Trabecular Architecture in Orchiectomized Rats.** Heidi Chandler<sup>1,2</sup>, Tara Mullarkey<sup>1,2</sup>, Rachel Stewart<sup>3</sup>, Gary Hattersley<sup>1,2</sup>.

<sup>1</sup>Radius Health Inc, United States, <sup>2</sup>Radius Health inc, United States, <sup>3</sup>invicRO, United States

Androgens promote the acquisition and maintenance of bone mass. Hypogonadism and androgen deprivation therapy for prostate cancer contribute to bone loss and increased fracture risk in men. Anabolic therapy with PTH(1-34) can increase bone mineral density (BMD) in men with low bone mass, but concomitant stimulation of bone resorption with PTH(1-34) may limit its bone-building potential. Abaloparatide (ABL) is a selective PTH1 receptor agonist that increases bone formation and BMD with limited increases in bone resorption indices, suggesting potential for increasing BMD in states of androgen deficiency. ABL was therefore tested in castrated (orchiectomized; ORX) rats, an androgen deficiency model that may recapitulate some of the deleterious skeletal changes seen in men with androgen deficiency. Male Sprague-Dawley rats underwent ORX or sham surgery at ~3 months of age. After a 4-week bone depletion period, ORX rats were then treated by daily sc injection for 4 weeks with ABL (20 μg/kg/d, n = 8) or vehicle (Veh, n = 8). Sham controls (n = 8) received daily Veh sc. The 4<sup>th</sup> lumbar vertebra (L4) was collected at necropsy for micro-CT evaluation. After 8 total weeks of androgen deficiency, the ORX group had 13.2% lower L4 BMD (p < 0.005 vs sham) and 17.3% lower trabecular bone volume fraction (BVf; p = 0.067) compared with sham controls. Trabecular thickness (Tb.Th) was similar in the ORX and sham controls, but the ORX group showed a significant 133% increase vs sham controls for trabecular pattern factor (TPF), a morphometric index that is inversely related to the extent of trabecular disconnections and perforations. After 4 weeks of treatment, starting 4 weeks post-surgery, the ABL group had 16.6% greater L4 BMD, 50.2% greater BVf, and 32.6% greater Tb.Th compared with ORX controls (all p < 0.0001). The ABL group

showed a 39.3% lower TBF compared with ORX controls (p < 0.05) suggesting more robust and better-connected trabecular architecture. The ABL group also had 24.2% greater BVf and 29.0% greater Tb.Th compared with sham controls (both p < 0.01). These data indicate that ABL reversed vertebral bone loss and trabecular microarchitectural deterioration in ORX rats by increasing trabecular bone volume and thickness, with preliminary evidence that ABL may reduce the extent of trabecular perforations and disconnections.

Disclosures: Heidi Chandler, Radius Health, Other Financial or Material Support.

## SU0311

**Modulation of CD4<sup>+</sup> T Cell Osteogenic Cytokine Profile by the Probiotic *Lactobacillus reuteri* and its Secreted Factors.** Fraser Collins<sup>\*</sup>, A. Daniel Jones, Laura McCabe, Narayanan Parameswaran, Michigan State University, United States

Manipulation of the microbiome with the probiotic bacteria *Lactobacillus reuteri* 6475 (LR) has been demonstrated to increase bone density in intact male mice as well as protect against estrogen-deficiency-induced osteoporosis and type 1 diabetes-induced osteoporosis. However, the mechanism through which LR exerts its beneficial bone effect is not fully elucidated. Interestingly, when we treated male RAG-deficient mice with LR no bone effect was observed; suggesting that T cells may play a key role in conveying the beneficial bone effect. To investigate this we isolated CD3<sup>+</sup> cells from mesenteric lymph nodes (MLN) and naive CD4<sup>+</sup> T cells from the spleen of male C57BL/6 mice by magnetic isolation and measured their osteogenic cytokine response to treatment with live, dead or whole and fractionated conditioned media (CM) from *L. reuteri* (ATCC 6475). For live bacterial studies, cells were treated with multiplicity of infection (MOI) of 1, 10 or 100. For conditioned media studies cells were treated with whole CM or <3kD fraction; fractions based on water solubility; or fractions based on charge. After 4 days, cells were stained and analyzed by flow cytometry for expression of the osteogenic cytokines IL-10 and IL-17A. In both MLN and splenic T cell cultures live *L. reuteri* significantly increased expression of IL-10 and IL-17A in a dose-dependent manner. This effect was not induced by TLR signalling as inhibition of MyD88 did not suppress the response. Heat killed *L. reuteri* only affected expression of these cytokines at the highest dose. Compared to these studies, *L. reuteri* conditioned media significantly increased expression of IL-10 and IL-17A. Examination of fractionated conditioned media revealed that the active secreted component of LR is present in the <3kD fraction, is water soluble and has a positive charge. Taken together, our data demonstrate that live probiotic *L. reuteri* and a small, water soluble positively charged secreted factor is able to directly influence T cell cytokine profile. Dead bacteria only affected cytokine expression at high doses suggesting an important role for the secretory products of live *L. reuteri* in the regulation of T-cell differentiation and cytokine secretion. These results reveal an important potential mechanism through which intestinal *L. reuteri* can modulate distal bone health.

Disclosures: Fraser Collins, None.

## SU0312

**Chronic kidney disease and aging diminish both whole bone and microscale bone quality.** Chelsea Heveran<sup>1</sup>, Adam Rauff<sup>2</sup>, Eric Livingston<sup>3</sup>, Ted Bateman<sup>3</sup>, Moshe Levi<sup>4</sup>, Dana Carpenter<sup>3</sup>, Karen King<sup>5</sup>, Virginia Ferguson<sup>3</sup>. <sup>1</sup>Department of Mechanical Engineering, University of Colorado, United States, <sup>2</sup>Department of Bioengineering, United States, <sup>3</sup>Department of Mechanical Engineering, United States, <sup>4</sup>Department of Medicine, Division of Renal Diseases and Hypertension, University of Colorado School of Medicine, United States, <sup>5</sup>Department of Orthopaedics, University of Colorado School of Medicine, United States

Chronic Kidney Disease (CKD) increases the prevalence of bone fracture, yet the combined effects of aging and CKD on bone are unknown. The purpose of this study was to evaluate how whole bone and microscale bone quality are detrimentally affected with aging and CKD.

Male C57BL/6 mice aged 3 mo (young), 15 mo (middle-age) and 21 mo (old) underwent 5/6th nephrectomy to establish CKD or sham surgeries (N=48, n=6-10 per age/treatment group). Mice were aged three months and euthanized. MicroCT evaluated microarchitecture of the cortical femur and trabecular tibia. Femurs were broken *via* three-point bending then dehydrated, embedded, sectioned at the mid-diaphysis, and polished. Microscale mineral:matrix (v<sub>1</sub>PO<sub>4</sub>:amide III) and modulus (E) were mapped across the cortical thickness with site-matched Raman spectroscopy and nanoindentation. Mature enzymatic crosslinks (HP and LP) and pentosidine were evaluated for the humerus using high-performance liquid chromatography. Osteocyte lacunae were imaged *via* confocal microscopy from fuchsin-stained tibias and reconstructed in 3D to evaluate lacunar geometries.

CKD was confirmed with increased serum BUN (p<0.001). At the whole bone scale, bone quality was lower with both aging and CKD and most diminished in old mice with CKD. Age and CKD decreased cortical (e.g. thickness, tissue mineral density (Ct.TMD)) and trabecular (e.g. thickness (Tb.Th)) microarchitecture (p<0.05). Age and CKD also decreased stiffness and max load (p<0.05). CKD affected skeletal crosslinks, reducing LP (p<0.05). Further, HP and LP were -23.5% (p=0.054) and 13.7% (p=0.08) lower in old mice with CKD than sham, respectively.

At the microscale, age and CKD also decreased bone quality. *E* may be reduced (-6.8%,  $p=0.06$ ) while mineral:matrix was 18.4% higher in middle-age mice with CKD ( $p<0.05$ ). Osteocyte lacunar geometries also showed effects of age and CKD. In sham mice, osteocyte lacunae became smaller and more spherical with advancing age ( $p<0.05$ ). However, in CKD, lacunae had similar geometries across all ages, perhaps indicating disrupted perilacunar remodeling with kidney dysfunction.

Aging and CKD together reduce both whole bone and microscale bone quality. Less mature crosslinks and lower TMD suggest that both mineral and matrix changes occur with CKD and are most pronounced with advanced age. Also, the osteocyte may be implicated in bone quality changes in CKD. These findings may help explain the clinically-observed bone fragility in CKD.

	Young		Middle-age		Old	
	Sham	CKD	Sham	CKD	Sham	CKD
Ct.Th ( $\mu\text{m}$ )	198.1 $\pm$ 4.2	187.7 $\pm$ 5.3	189.4 $\pm$ 3.9	167.7 $\pm$ 4.7*	201.7 $\pm$ 5.6	162.4 $\pm$ 4.3*
Ct.TMD (mg HG/cm <sup>3</sup> )	1044.8 $\pm$ 8.88	1015.9 $\pm$ 4.09*	1056.1 $\pm$ 6.58	1037.7 $\pm$ 6.16*	1063.1 $\pm$ 3.05	1038.7 $\pm$ 6.40*
Tb.Th ( $\mu\text{m}$ )	50 $\pm$ 1.6	43 $\pm$ 1.3*	49 $\pm$ 1.0	45 $\pm$ 1.9	45 $\pm$ 1.3	40 $\pm$ 1.5*
Stiffness (N/mm)	97.96 $\pm$ 4.87	88.82 $\pm$ 5.01	92.30 $\pm$ 6.12	64.62* $\pm$ 6.41	83.28 $\pm$ 7.92	57.68* $\pm$ 3.24
Ln(mineral:matrix)	2.56 $\pm$ 0.056	2.67 $\pm$ 0.057	2.68 $\pm$ 0.056	2.85 $\pm$ 0.052*	2.67 $\pm$ 0.062	2.74 $\pm$ 0.058
(E (GPa)) <sup>2</sup>	735.2 $\pm$ 36.4	687.9 $\pm$ 37.5	634.0 $\pm$ 36.6	536.6 $\pm$ 34.3	506.0 $\pm$ 40.5	562.4 $\pm$ 38.1
mol LP/ mol collagen	0.27 $\pm$ 0.0079	0.23 $\pm$ 0.019	0.30 $\pm$ 0.020	0.30 $\pm$ 0.016	0.31 $\pm$ 0.015	0.26 $\pm$ 0.072*
Lacunar volume ( $\mu\text{m}^3$ )	454.9 $\pm$ 39.2	405.4 $\pm$ 55.2	365.1 $\pm$ 66.7	256.6 $\pm$ 32.1	269.7 $\pm$ 26.2	357.5 $\pm$ 54.9

Table 1: Bone quality is diminished with age and CKD. Mean  $\pm$  standard error. \* =  $p < 0.05$  for CKD vs sham within the same age.

Table 1

Disclosures: Chelsea Heveran, None.

## SU0313

**Phosphate Restriction Impairs Osteoblast Function in Growing Mice by attenuating mTOR Signaling.** Frank Ko\*, Marie Demay. Massachusetts General Hospital, United States

Hypophosphatemia is a common complication of drug therapy and numerous medical illnesses, including burn injury. Chronic hypophosphatemia leads to rickets, which is a consequence of impaired phosphate mediated hypertrophic chondrocyte apoptosis, and osteomalacia due to impaired mineralization of newly formed bone matrix. However, the effects of hypophosphatemia on osteoblast function are poorly understood. To define the effects of phosphate restriction on osteoblast differentiation and bone formation, 28 day old C57Bl6/J mice were fed a low phosphate diet. Histomorphometric analyses demonstrated a dramatic decrease in bone formation within 48 hours phosphate restriction, associated with an arrest in osteoblast differentiation between Runx2 and Osterix. These studies suggest that phosphate restriction impairs signaling pathways that promote bone matrix protein synthesis and osteoblast differentiation.

Nutrients and growth factors activate the mTOR signaling pathway, which promotes mRNA translation and protein synthesis. Within 72 hours of phosphate restriction of 28 day old mice, a dramatic decrease in phosphorylation of the ribosomal protein S6 (pS6) a downstream target of mTOR signaling, was observed by immunohistochemistry of trabecular and cortical osteoblasts, as well as by Western analyses of lysates from freshly isolated cortical osteoblasts. To evaluate whether phosphate restriction impairs mTOR signaling by interfering with the nutrient sensing or growth factor signaling pathways, their respective effectors were examined. Growth factor-dependent phosphorylation AKT promotes mTOR signaling, whereas nutrient stress impairs mTOR signaling by leading to phosphorylation AMP Kinase. Western analyses of lysates of primary cortical osteoblasts isolated from phosphate-restricted mice did not show a decrease in pAKT relative to osteoblasts from chow fed mice. However, pAMP Kinase, which inhibits mTOR signaling, was increased in primary osteoblasts isolated from phosphate-restricted mice. To determine if phosphate restriction acutely impairs mTOR signaling in osteoblastic cells, ST2 stromal cells and MC3T3-E1 osteoblastic cells were cultured in phosphate-restricted media. An increase in pAMP Kinase was observed with phosphate restriction, associated with a decrease in pS6. These studies suggest that acute dietary phosphate restriction of growing mice impairs osteoblast mTOR signaling by activating the AMP Kinase pathway.

Disclosures: Frank Ko, None.

## SU0314

**Role of Hematopoietic Cell  $\beta$ -glucuronidase in Bone-Specific Activation of Osteoprotective Turmeric-Derived Dietary Polyphenols.** Andrew G. Kunihiro\*, Jen B. Frye<sup>2</sup>, Julia A. Brickey<sup>1</sup>, Paula B. Luis<sup>3</sup>, Claus Schneider<sup>3</sup>, Janet L. Funk<sup>2</sup>. <sup>1</sup>Department of Nutritional Sciences, University of Arizona, United States, <sup>2</sup>Department of Medicine, University of Arizona, United States, <sup>3</sup>Department of Pharmacology, Vanderbilt University, United States

Most women with advanced breast cancer (BCa) develop incurable osteolytic bone metastases (BMETs). Our lab has shown that turmeric-derived curcuminoids (CURC): 1) hinder development of lytic bone lesions in a TGF $\beta$ -dependent, human-xenograft BCa (MDA-MB-231 [MDA]) BMET model in mice and 2) inhibit MDA tumor cell secretion of TGF $\beta$ -stimulated parathyroid-related protein (PTHrP), a pathway known to drive BMETs. In humans and mice, curcumin-glucuronide (G-CURC), a phase II metabolite thought to be biologically inactive, is the primary CURC metabolite detected in the circulation after consuming CURC-containing foods or supplements, while aglycone CURC is nearly undetectable. This has led to an untested postulate in the field that CURC is deconjugated at sites of action to form bioactive, aglycone (free) CURC. To test this hypothesis in the context of the BCa BMETs model, we assessed local deconjugation of CURC in the tumor-bone microenvironment.

G-CURC vs. CURC inhibition of TGF $\beta$ -stimulated Smad phosphorylation (Western) and PTHrP secretion (IRMA) by bone-tropic MDA cells *in vitro* was compared. *In vivo* G-CURC and CURC levels were quantified by LC-MS in plasma and bone marrow (BM) from CURC-treated female nude mice. Expression of enzymes with reported deglucuronidation activity ( $\beta$ -glucuronidase [GUSB], klotho [KL], and heparanase [HPSE]) were assessed in bone by Western blot, enzymatic assay, and/or immunohistochemistry (IHC).

In contrast to the inhibitory effects of CURC, G-CURC did not alter TGF $\beta$ -stimulated Smad signaling or PTHrP secretion, confirming its postulated lack of biologic activity. Whereas little free CURC was present (9%) in circulation, CURC in the BM was predominantly the aglycone form (56%,  $p < 0.01$ ). GUSB was the only deconjugating enzyme expressed in BM, as demonstrated by Western analysis. BM cells, and not MDA tumor cells, were the primary site of GUSB expression and activity in tumor bearing limbs, as determined by IHC and *ex vivo* assay of GUSB-specific enzyme activity.

These results suggest that CURC may act as a pro-drug that is activated within the tumor-bone microenvironment by GUSB-expressing hematopoietic cells, to limit the progression of TGF $\beta$ -dependent osteolytic lesion formation in a murine model of BCa BMETs.

Disclosures: Andrew G. Kunihiro, None.

## SU0315

**Identification of mouse cathepsin K structural elements that regulate its collagenase activity and the potency of odanacatib.** Simon Law\*, Pierre-Marie Andrault, Adeleke H Aguda, Andrew Yamroz, Marcus Lee, Gary D Brayer, Dieter Bromme. University of British Columbia, Canada

Cathepsin K (CatK) is the predominant bone-degrading protease and thus an ideal target for anti-osteoporotic drug development. Rodent models of osteoporosis are preferred due to their close reflection of the human disease and their ease of handling, genetic manipulation, and economic affordability. However large differences in the potency of CatK inhibitors for the mouse/rat versus the human protease orthologues made it difficult to use rodent models. Here, we elucidated the structural elements of the potency differences between mouse and human CatK. We determined and compared the structures of inhibitor-free mouse CatK (mCatK), human CatK (hCatK) and hCatK-odanacatib (ODN) complexes. Interestingly, rodent CatKs have a unique *N*-glycosylation site in an ectosteric site which blocks the collagenase activity of the protease whereas all other mammalian species lack this site. Removal of the *N*-glycosylation site restored the collagenase activity indicating that mCatK needs to be deglycosylated prior to its osteoclastic activity. The reduced susceptibility of mCatK toward ODN is due to two structural differences in the S2 and likely S3/4 substrate binding sites. Humanizing subsite 2 in mCatK led to a 5-fold improvement of ODN binding whereas the replacement of Tyr61 in mCatK with Asp resulted in mutant variant with a comparable ODN potency as hCatK. Combining both sites further improved the inhibition of the mCatK variant. These findings allow the generation of a mouse mutant CatK transgene that will facilitate the evaluation of CatK-inhibitor adverse effects and to explore routes to avoid them.

Disclosures: Simon Law, None.

## SU0316

**Calcitriol Treatment Rescues Osteopenia and Skeletal Fragility Outcomes in Goto-Kakizaki Type 2 Diabetes Rat Model.** Yanlong Liang\*, Yanzhi Liu, Minqun Du, Wenxiu Lai, Shuhui Li, Liao Cui. Guangdong Key laboratory for Research and Development of Natural Drugs, Guangdong Medical University, China

Aim Osteopenia and skeletal fragility are considered among the complications associated with type 2 diabetes. However, the underlying mechanisms of this



complications in diabetes are still not fully understood. Therefore, the profile of type 2 diabetes induced osteopenia and bone fragility should be further explored. In the present study, we used a genetic non-obese and non-insulin-dependent spontaneous diabetes rat model—Goto-kakizaki (GK) rat to investigate the profile of osteopenia and bone quality in type 2 diabetes rats. A vitamin D<sub>3</sub> treatment (Calcitriol) was also investigated in this type 2 diabetes induced osteopenia rat model.

Methods Ten-week-old male GK rats were monitored by oral glucose tolerance test (OGTT) to confirm the rats became diabetic. In vivo  $\mu$ -CT analysis was used to monitor bone mass and bone mineral density (BMD) every five weeks since diabetic GK rats were confirmed. The rats became diabetic five weeks thereafter. The diabetic GK rats were divided into 2 groups: diabetic model (GK) and calcitriol treatment (GK+Cal, calcitriol 0.045 $\mu$ g/kg/d to GK rats). Age-matched wistar rats were used as control. Calcitriol treatment was administered to GK rats for 20 weeks. Bone histomorphometry,  $\mu$ -CT and immunohistochemical analysis and biomechanical testing were used to evaluate the bone quality of rats at the endpoint.

Results The data from  $\mu$ CT, histomorphometry and BMD analysis demonstrated type 2 diabetes induced significant osteopenia and impaired bone microarchitecture in GK rats. Diabetics also significantly decreased bone formation parameters and increased bone resorption parameters from three region of rats (proximal, mid-shaft of tibia and lumbar vertebra), reduced AKP, OCN and increased CTX-I, TRAP in serum, decreased biomechanical properties and the expression of TXNIP in bone. Calcitriol treatment significantly rescued bone mass, BMD and improved bone microarchitecture and biomechanical properties in type 2 diabetes GK rats. Markers of bone formation and the expression of TXNIP in bone were also significantly increased after calcitriol treatment.

Conclusion These results suggest that type 2 diabetes induced significant osteopenia and increased skeletal fragility in GK rats, and GK rat could be a nice animal model to mimic non-obese type 2 diabetes induced osteopenia. Our results indicate that calcitriol treatment could rescue the osteopenia and impaired bone quality seen in the type 2 diabetes GK rats.

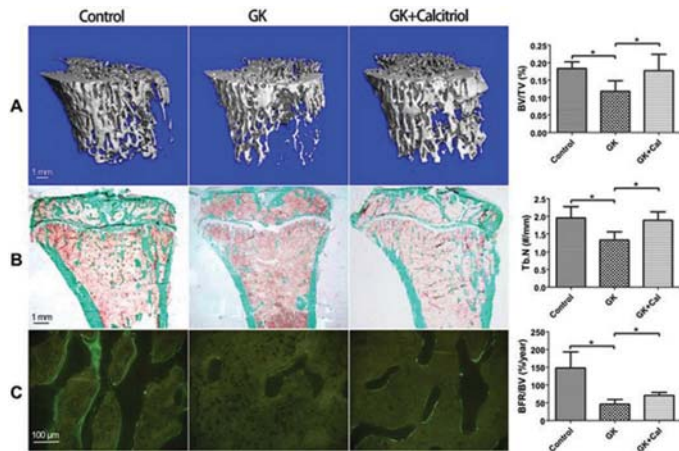


Figure 1 Calcitriol treatment rescues osteopenia outcomes in GK Diabetes Rats.

Disclosures: Yanlong Liang, None.

## SU0317

**PF708, a Therapeutic Equivalent and Biosimilar Candidate to FORTEO (Teriparatide), Demonstrates Nonclinical Efficacy Equivalence to the Reference Product in the Treatment of Established Osteopenia in Adult Ovariectomized Rats.** Jukka Morko<sup>1</sup>, Carrie Schneider<sup>2</sup>, Jukka Vääräniemi<sup>1</sup>, Jukka P Rissanen<sup>1</sup>, Jussi M Halleen<sup>1</sup>, Hubert Chen<sup>2</sup>.

<sup>1</sup>Pharmatest Services Ltd, Finland, <sup>2</sup>Pfenex Inc, United States

PF708 is a 34-amino acid recombinant analog of human parathyroid hormone that has the same route of administration, dosage form, formulation, and delivery device functionality as the branded reference product FORTEO (teriparatide). PF708 is being developed as a therapeutic equivalent in the U.S. and as a biosimilar outside the U.S. to provide an option for the reference product. The purpose of this study was to compare the nonclinical efficacy of PF708 to FORTEO in the treatment of established osteopenia in the rat ovariectomy (OVX) model of human postmenopausal osteoporosis. The study was conducted using female Sprague-Dawley rats. At 6 months of age, peripheral quantitative computed tomography (pQCT) measurements were performed in tibia, and the rats were ovariectomized. The development of osteopenia was confirmed by pQCT in tibia after 6 postsurgery weeks. Osteopenic rats were randomized into treatment groups by stratification according to trabecular bone mineral density (BMD) and body weight. After 7 postsurgery weeks, serum samples were harvested for bone turnover marker (BTM) measurements and the treatment of OVX rats was started. Rats were treated subcutaneously once a day with PF708 or FORTEO at 8  $\mu$ g/kg, or with vehicle. Treatment effects were studied on serum BTM levels after 2 treatment weeks and on tibia by pQCT after 6 treatment weeks. Both PF708 and FORTEO treatments increased serum levels of procollagen type I N-terminal propeptide (PINP) and N-terminal mid-fragment of osteocalcin (OC) and decreased serum activity of tartrate-resistant acid phosphatase isoform 5b (TRACP 5b) during the first 2 treatment weeks. There were no significant differences between the treatments indicating that both treatments enhanced bone formation similarly in adult OVX rats. Both PF708 and FORTEO

treatments increased total BMD and bone mineral content (BMC) and trabecular BMD and BMC in tibial metaphysis as well as total BMD, total and cortical BMC, cortical bone area and cortical thickness in tibial diaphysis during 6 treatment weeks. There were no significant differences in pQCT parameters between the treatments, indicating that PF708 and FORTEO treatments induced similar anabolic responses on metaphyseal, trabecular, diaphyseal and cortical bone in adult OVX rats. This study demonstrated that the nonclinical efficacy of PF708 is equivalent to FORTEO in the treatment of established osteopenia in the rat OVX model of human postmenopausal osteoporosis.

Disclosures: Jukka Morko, None.

## SU0318

**The influences of discontinuation of anti-resorptive agents on bone turnover in ovariectomized mice: a comparison between risedronate and anti-RANKL antibody.** Toshinobu Omiya<sup>1</sup>, Jun Hirose<sup>2</sup>, Takeshi Miyamoto<sup>3</sup>, Sakae Tanaka<sup>4</sup>. <sup>1</sup>oomiya9ort@yahoo.co.jp, Japan, <sup>2</sup>j.hirose513@gmail.com, Japan, <sup>3</sup>miyamoto@z5.keio.jp, Japan, <sup>4</sup>tanakas-ort@h.u-tokyo.ac.jp, Japan

Purpose: Bisphosphonate and anti-RANKL (receptor activator of nuclear factor  $\kappa$ B ligand) antibody are anti-osteoporosis drugs which suppress bone resorption. From the research of bone metabolism markers and bone mineral density, it is known that there are differences in resetting patterns after the discontinuation of these drugs. The purpose of this study was to analyze these differences in histological appearance using ovariectomized (OVX) mice.

Materials and Methods: Twelve-week-old female C57BL/6 mice were ovariectomized. Four weeks after the surgery, the OVX mice were subjected to one of the two following treatment options; risedronate (5  $\mu$ g/kg/day, 3 days a week) for 4 weeks followed by PBS for 4 weeks (RIS group), and anti-RANKL antibody (RANKL-MCA, a single injection of 5 mg/kg) for 4 weeks followed by PBS for 4 weeks (AB group). All mice were euthanized 12 weeks after the surgery. Hind limbs and lumbar spines were subjected to histomorphometric analysis.

Results: In the cancellous bone, histomorphometric analysis showed that there was no significant difference in the bone volume parameters (BV/TV, Tb. N). As for the bone resorption parameters, ES/BS increased significantly in AB group, but there was no significant difference in Oc. S/BS. Both bone formation parameters (OV/BV, Ob. S/BS) and bone formation speed parameters (BFR/BS, MARS) were significantly increased in AB group. On the periosteal surface of cortical bone, there was no significant difference in MAR and BFR/PS between two groups.

Conclusion: Our results showed that in AB group, the bone resorption and formation increase more rapidly after the discontinuation compared to those in RIS group in the cancellous bone. However, bone turnover speed on the periosteal surface was similar in both groups.

Disclosures: Toshinobu Omiya, None.

## SU0319

**Glucocorticoid Induced Osteoporosis is Prevented by Probiotic *Lactobacillus reuteri* 6475 Supplementation.** Jonathan Schepper<sup>\*</sup>, Fraser Collins, Regina Irwin, Naomi Rios, Narayanan Parameswaran, Laura McCabe. Michigan State University, United States

Glucocorticoids are important immune-modulating drugs used to manage inflammatory diseases of > 1.2% of the US population. However, glucocorticoid treatment is associated with significant detrimental side effects including glucocorticoid-induced osteoporosis (GIO), which is the underlying cause of nearly half of all fractures in treated patients. Past studies established that glucocorticoid treatment alters the gut microbiota, which has been shown to have an important role in bone health. Therefore, we investigated whether supplementation with the probiotic *Lactobacillus reuteri* 6475 (LR) or *Lactobacillus rhamnosus* GG (LGG) during the duration of glucocorticoid treatment could prevent the associated bone loss. C57BL/6J male (16-week-old) mice were treated with prednisolone (2.57 mg/kg/day, slow release pellet subQ) for 8 weeks. Mice were administered LR or LGG (10<sup>8</sup> CFU/ml) in the drinking water for the duration of the experiment and bone parameters analyzed. Glucocorticoid treatment without any probiotic supplementation significantly decreased trabecular bone volume fraction (~40%) in the distal femur metaphysis as determined by micro-computed tomography. In contrast, treated mice that received LR, but not LGG supplementation were protected from bone loss. Analysis of serum bone remodeling parameters revealed significantly lower osteocalcin levels (~45% of control) in the glucocorticoid treated mice, whereas no reduction was seen in the LR treated mice. In contrast, osteoclast (TRAP-5b) serum markers trended to increase in the glucocorticoid and glucocorticoid + LGG treated mice compared to controls, whereas the LR treated mice showed a significant decrease in TRAP-5b compared to controls. Together, these data suggest that modulation of the gut microbiota with the probiotic *L. reuteri* can prevent GIO.

Disclosures: Jonathan Schepper, None.

## SU0320

**Prior Focal Radiation Causes Atrophic Nonunion Healing in Mouse Long Bone Fracture.** Luqiang Wang<sup>\*1</sup>, Abhishek Chandra<sup>2</sup>, Robert Tower<sup>1</sup>, Jaimo Ahn<sup>1</sup>, Yejia Zhang<sup>1</sup>, Ling Qin<sup>1</sup>. <sup>1</sup>Department of Orthopaedic Surgery, Perelman School of Medicine, University of Pennsylvania, United States, <sup>2</sup>Department of Physiology and Biomedical Engineering, Division of Geriatric Medicine & Gerontology, Mayo Clinic, United States

Approximately 5-10% of bone fractures have delayed or nonunion healing. Among them, atrophic nonunion can be especially challenging representing a major clinical burden in skeletal trauma treatment. Cancer patients treated by radiotherapy are more prone to developing fracture nonunion within the irradiated area even several years later. To better understand the mechanism, we studied the fracture healing process in mouse long bones with prior focal radiation. Two-month-old C57BL/6 male mice received radiation at the midshaft of right tibiae (5 mm long) from a focal irradiator (SARRP, 8 Gy twice) and two weeks later, closed and transverse fractures within the irradiated area and contralateral legs. At this time point, bone marrow hematopoietic components had already recovered but the periosteal cellularity was significantly lower in the irradiated bone. Three days later, the periosteum in irradiated bones expanded significantly less compared to control at the proximal side of the fracture (the region close to the growth plate) and showed almost no notable expansion distal to the fracture site (the region close to the growth plate). Callus volume and bone volume were drastically decreased in irradiated bones at 1 and 2 weeks after fracture with virtually no bone detected distal to the fracture line. While the irradiated bones still healed through endochondral and intramembranous ossifications at the proximal side, albeit at a much less robust level compared to control, only cells with fibrotic morphology were detected at the distal side. Those cells failed to express osteogenic (osterix and osteocalcin) or chondrogenic (Sox9 and type 2 Collagen) markers. They also did not express VEGF with no vessel infiltration and no osteoclasts in the area. By 4 weeks, the bony callus at the proximal side draped over the fibrotic tissue of the distal side but they never consolidated. This resulted in a nonunion in all irradiated bones (n=11 mice/group). Mechanical testing at 6 weeks confirmed a drastically decreased peak load (-86%), stiffness (-75%), and energy to failure (-73%). This location-dependent healing in irradiated bones demonstrated that both periosteum insult and the lack of surrounding vasculature are critical elements for fracture nonunion. Furthermore, we establish a highly reliable, nonsurgical, and clinically relevant nonunion fracture model in mice for future studies of mechanisms and treatments of this disease.

**Disclosures:** Luqiang Wang, None.

## SU0321

**Gut Microbiome Contributes to Altered Bone Homeostasis in SCT and SCD Mice.** Liping Xiao<sup>\*1</sup>, Julia Oh<sup>2</sup>, Patience Meo Burt<sup>1</sup>, Kimberly Pantoja<sup>1</sup>, Marja Hurley<sup>1</sup>. <sup>1</sup>UConn Health, United States, <sup>2</sup>Jackson Laboratorty, United States

Sickle cell disease (SCD) is a hereditary disease arising when two parents are sickle cell trait (SCT) carriers. Eighty percent of adults with SCD have low bone mineral density (BMD). The mechanism(s) of bone loss in SCD subjects has not been fully investigated, and there are no targeted therapies to prevent or treat sickle cell bone disease. Recent studies showed the microbiome is involved in the development of chronic inflammation in SCD. Leukocytosis, in the absence of infection, is common in SCD subjects. Since inflammatory cytokines modulate bone remodeling, we hypothesize that gut microbiome contributes to underlying altered bone homeostasis in SCT and SCD mice. Four-month old control (Ctrl), SCT and SCD male mice were treated with H<sub>2</sub>O or broad-spectrum antibiotic (Abx) in drinking water for 7 weeks. Analysis of the gut microbiome showed a significant change in the composition following Abx treatment. Abx significantly decreased body weight in Ctrl mice. Interestingly, there is an increased trend in body weight in SCD mice after Abx treatment (p=0.07) (Fig.1A). DXA analysis revealed that Abx treatment increased leg BMD in SCD mice (Fig.1B) and increased leg bone mineral content (BMC) in both SCT and SCD mice (Fig.1C). There was no significant effect of Abx on leg BMD or BMC in Ctrl mice. Ex vivo bone marrow stromal cell cultures showed significantly decreased mineralization in cultures from SCT-H<sub>2</sub>O and SCD-H<sub>2</sub>O mice compared with Ctrl-H<sub>2</sub>O mice. Abx decreased mineralization in cultures from Ctrl mice but increased mineralization in cultures from SCT mice (Fig.1D,E). qPCR analysis of whole tibiae of 6-month old female mice showed increased IL1 $\beta$  mRNA in SCD-H<sub>2</sub>O group compared with Ctrl-H<sub>2</sub>O group (Fig.1F). Flow cytometry analysis of bone marrow of 2-month old male mice showed the numbers of aged neutrophils were expanded more than 1.4 and 1.5 fold in SCT-H<sub>2</sub>O and SCD-H<sub>2</sub>O mice compared with Ctrl-H<sub>2</sub>O, respectively (Fig.1G). Calvarial osteoblasts (OBs) of 3-day old Ctrl mice were co-cultured with neutrophils from Ctrl, SCT, and SCD mice. Alizarin Red staining showed decreased mineralization in OBs co-cultured with neutrophils from SCD mice (Fig.1H,I). We conclude that gut microbiome contributes to altered bone homeostasis in SCT and SCD male mice, and modulation of gut microbiome may act as potential therapies to prevent and treat bone loss in SCD or SCT subjects. Furthermore, increased aged neutrophils in bone marrow from SCD mice inhibit OB mineralization.

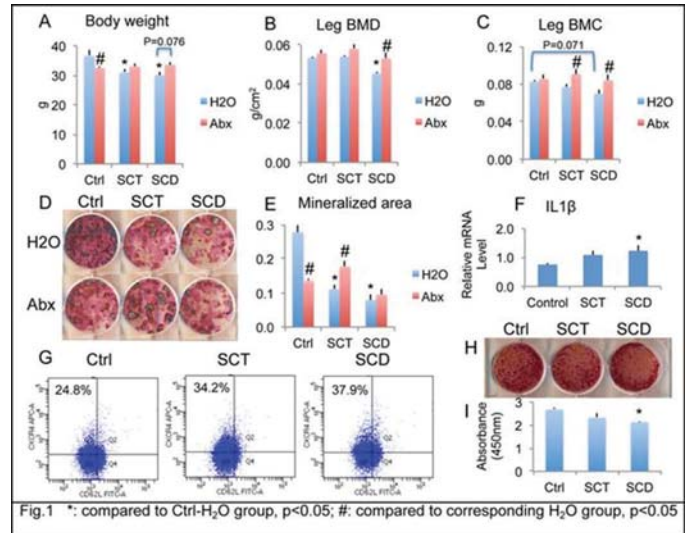


Fig.1

**Disclosures:** Liping Xiao, None.

## SU0322

**Hypoparathyroidism Presenting as Acute Cardiomyopathy.** Rahul Agarwal<sup>\*1</sup>, Lee R. Goldberg<sup>2</sup>, Mona Al Mukaddam<sup>1</sup>. <sup>1</sup>University of Pennsylvania, Division of Endocrinology, Diabetes and Metabolism, United States, <sup>2</sup>University of Pennsylvania, Division of Cardiovascular Medicine, United States

Hypoparathyroidism (HypoPT) is an orphan disease with an estimated prevalence of 37 per 100,000 person-years in the United States. The most common etiology of HypoPT is postsurgical (secondary to thyroid surgery) followed by autoimmune diseases and genetic syndromes and it usually presents with symptoms of hypocalcemia primarily neuromuscular irritability.

We present the case of a 34 year old healthy white female who was diagnosed with acute heart failure related to HypoPT. She presented to the ER with progressive symptoms of heart failure and was found to have anemia due to menorrhagia, hypocalcemia and hypoparathyroidism with an ejection fraction (EF) of 25-30%. Her labs revealed a hemoglobin of 6.4 g/dL, calcium < 5.0 mg/dL (8.5-10.2), albumin 3.4 g/dL (3.5-5.5), magnesium 1.3 mg/dL (1.7-2.2), phosphate 4.9 mg/dL (2.5-4.5), parathyroid hormone (PTH) of 9 pg/ml (14-64) and 25-hydroxyvitamin D of 31.9 ng/mL (30-79). The remaining data is listed in Table 1.

Other pertinent history included a full term birth with normal early development, no previous neck surgery or radiation, no family history of hypocalcemia, seizures, or intellectual disability. Notably the patient had been drinking 3-4 glasses of wine daily for the previous six months. Additionally, there were no signs of dysmorphic facies or palatal abnormalities on physical exam.

The patient's calcium and magnesium levels were repleted and by hospital day 4 the calcium levels were stably in the 7 mg/dL range and her EF had improved to 35% by hospital day 9. She was started on neurohormonal blockade. In follow-up, her EF was up to 50-55% at one month and then 60% at five months. The rapid recovery in her cardiac function after achieving normocalcemia and normal cardiac imaging suggested that alcohol, anemia, or viral infection were less likely etiologies of her acute heart failure.

The mechanism of hypoparathyroidism and heart failure is likely related to hypocalcemia and its effect on the cardiac muscle. During the cardiac action potential, calcium enters the cell which triggers calcium release from the sarcoplasmic reticulum followed by binding to the myofilament and activating the contractile machinery. Although rare as there have only been approximately 37 case reports of hypocalcemia related cardiomyopathy, it is crucial to recognize hypocalcemia as an etiology for heart failure given the rapid normalization of cardiac function with restoration of normocalcemia in almost all cases.



Table 1: Diagnostic work-up for hypocalcemia and hypoparathyroidism

Date	Calcium (8.5-10.2) mg/dL	Albumin (3.5-5.5) g/dL	Phosphate (2.5-4.5) mg/dL	PTH (14-64) pg/mL	Other Findings
4.18.16 Presented to ER	4.9	3.4		9	EF 25-30% EKG QTC 460-511 Imaging negative for pulmonary embolus Magnesium (Mg; 1.7-2.2) - 1.3 mg/dL Serum Creatinine (Cr; 0.50-1.10) - 0.58 mg/dL 25-hydroxy Vitamin D (30-74) - 31.9 ng/mL Thyroid studies normal Alcohol level undetectable
4.20.16	7.4		4.9		Mg 2.0 mg/dL Cortisol normal Coxsackie and Echovirus titers normal Esophagogastroduodenoscopy (EGD) and Colonoscopy normal
4.22.16	7.2				EF 30% Mg 1.6 mg/dL 1,25-dihydroxy Vitamin D (18-72) - 104 pg/mL
4.26.16					Cardiac MRI - EF 35%, no evidence of infiltrative/ ischemic/inflammatory disease Hemoglobin 9.5 g/dL; electrophoresis normal HIV negative Hepatitis B and C negative
4.28.16 Hospital Discharge	7.9				Mg 1.9 mg/dL Hemoglobin 8.5 g/dL Discharge Medications - Calcitriol 0.5 mcg daily, Calcium 500 mg three times daily
5.20.16					EF 50-55%
7.30.16 Initial Outpatient Endocrinology Visit	9.1	4.5	5.3	5	25-hydroxy Vitamin D - 40 Mg 1.8 mg/dL Hemoglobin 12.8 g/dL Screening for celiac disease, adrenal insufficiency, Wilson's disease, hemochromatosis, and pernicious anemia were all negative  Medication change - Calcitriol 0.25 mcg daily, Calcium 500 mg three times daily
8.27.16	8.5		4.7		Ionized calcium (4.8-5.6) - 4.6 mg/dL
9.29.16					EF 60%
10.8.16	8.2	4.5	4.7		24-hour urine calcium 232 mg/day
12.19.16	8.5	4.8	3.9		

Table 1: Diagnostic work-up for hypocalcemia and hypoparathyroidism

Disclosures: Rahul Agarwal, None.

## SU0323

**Trabecular Bone of the Appendicular and the Axial Skeleton Demonstrate Opposite Impairments in Adults with X-Linked Hypophosphatemic Rickets.** Thomas Funck-Brentano<sup>\*1</sup>, Agnès Ostertag<sup>2</sup>, Sylvie Fernandez<sup>2</sup>, Corinne Collet<sup>3</sup>, Martine Cohen-Solal<sup>2</sup>. <sup>1</sup>Department of Rheumatology, Lariboisière Teaching Hospital, Univ Paris Diderot, Université Sorbonne Paris Cité, France, <sup>2</sup>BIOSCAR UMRS 1132, Université Paris Diderot, Sorbonne Paris Cité, INSERM, France, <sup>3</sup>Department of Biochemistry, Lariboisière Teaching Hospital, Univ Paris Diderot, Université Sorbonne Paris Cité, France

X-Linked Hypophosphatemia (XLH) is the most common type of inherited rickets. Conventional therapy with activated vitamin D and phosphate improves radiographic abnormalities and skeletal deformities in children, and to some extent ameliorates osteomalacia-related pain in adults. However, mineralization impairments are poorly understood, with controversies regarding trabecular bone mass and mineralization at the spine or cortical BMD observed at the radial shaft. The presence of ossifications of the longitudinal ligaments add to the complexity of the analyses. Our aim was to analyze bone mineralization, geometry and architecture in the appendicular and axial skeleton of adults with XLH with non-invasive techniques.

Each of the 14 XLH patients (9 females, age  $49.8 \pm 14.5$  years, BMI  $27 \pm 6.6$ , 9 currently under therapy) were matched to a minimum of two controls (n= 34) adjusted for sex, age and Body Mass Index. DXA analyses revealed that lumbar spine BMD was elevated (mean Z-score L1-L4  $\pm$  SEM in XLH vs controls:  $+3.30 \text{ SD} \pm 0.56$  vs  $0.92 \text{ SD} \pm 0.20$ ) whereas the 1/3 distal radius BMD was reduced ( $-1.57 \text{ SD} \pm 0.24$  vs  $0.27 \text{ SD} \pm 0.30$ ). We analyzed the Trabecular Bone Score (TBS) at the lumbar spine in order to avoid lateral enthesophytes that may overestimate axial BMD. TBS was significantly higher in XLH patients compared to the controls ( $1.55 \pm 0.1$  vs  $1.35 \pm 0.1$ ,  $p < 0.001$ ) demonstrating an elevated trabecular bone mass and density regardless of the enthesophytes.

However, High Resolution peripheral Quantitative Computed Tomography (HRpQCT) of the radius demonstrated that total bone area was larger ( $+29.5\%$ ,  $p = 0.002$ ) in XLH. Cortical and trabecular volumetric BMD (vBMD) were reduced ( $-2.5\%$ ,  $p = 0.029$  and  $-22.4\%$ ,  $p = 0.014$ , respectively). Cortical thickness was however unchanged, unlike Trabecular Number (Tb.N  $-29.5\%$ ,  $p < 0.001$ ) and Trabecular Spacing (Tb.Sp  $+55.8\%$ ,  $p < 0.001$ ).

Similar results were observed at the tibia. Serum levels of PTH correlated negatively with trabecular vBMD and Tb.N and positively with Tb.Sp.

In conclusion, our study is the first to demonstrate that adult patients with XLH have reduced mineralization of trabecular bone of the appendicular skeleton while it is elevated in the axial skeleton. The underlying mechanisms for this site-specific regulation need to be investigated. We propose that the evaluation of the bone mineralization status under conventional or new therapies in XLH should include DXA measurements of the radius.

Disclosures: Thomas Funck-Brentano, None.

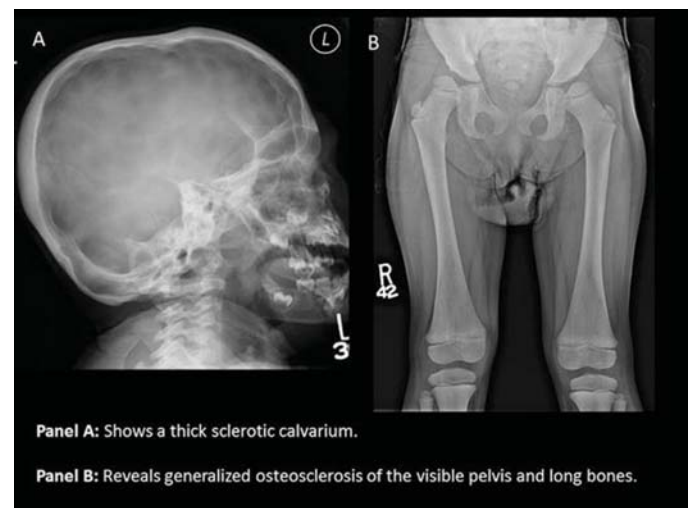
## SU0324

**Generalized Skeletal Sclerosis in a Two-Year Old Girl: Expanding the Phenotype of  $\alpha$ -Mannosidosis.** Gary S. Gottesman<sup>\*1</sup>, Philippe M. Campeau<sup>2</sup>, Margaret Huskey<sup>3</sup>, Angela Nenninger<sup>1</sup>, Deborah V. Novack<sup>3</sup>, William H. McAlister<sup>4</sup>, Steven Mumm<sup>3</sup>. <sup>1</sup>Center for Metabolic Bone Disease and Molecular Research, Shriners Hospital for Children, United States, <sup>2</sup>Department of Pediatrics, University of Montreal, Canada, <sup>3</sup>Division of Bone and Mineral Diseases, Washington University School of Medicine, United States, <sup>4</sup>Mallinckrodt Institute of Radiology, Washington University School of Medicine, United States

We report a 2-yr-old girl (now age 7) with a sclerosing bone disorder and mutational analysis consistent with  $\alpha$ -mannosidosis (OMIM#248500). Birth history was complicated by edema and cardiorespiratory problems requiring mechanical ventilation. Hearing loss was detected on newborn screen. Chronic sinus/ear infections led to myringotomy tubes and an adenoidectomy. Temporal bone CT revealed a diffusely thick and sclerotic skull. Gross motor and social developmental delay were present. Strabismus was corrected surgically at age 1 yr. The skeletal survey suggested sclerosteosis or other high bone mass (HBM) disorder. Physical exam showed normal growth, brachycephaly with biparietal prominence, lumbar scoliosis, exotropia, and hearing deficit. Serum biochemistries, ALP, PTH, 25(OH) and 1,25-(OH)<sub>2</sub>-vitamin D levels were normal. At age 4, despite radiographic HBM, tetracycline-labeled iliac crest biopsy revealed poor trabecular connectivity. However, tetracycline double labels were well-defined and normally spaced, and did not identify a specific disorder of bone formation.

Extensive genetic metabolic screening, karyotype, 22q11.2 deletion, and chromosomal microarray analyses were normal. Molecular tests were negative for HBM disorders (ANKK, CA2, CLCN7, CTSK, DLX3, FAM123B, LPR4, LRP5, LRP6, OSTMI, PLEKHM1, RANK, RANKL, SLC29A3, SNX10, SOST, TGFB1, TCIRG1, TYROBP). Mucopolysaccharidoses screen was negative. Trio exome sequencing revealed compound heterozygous missense mutations in the proband for MAN2B1, encoding  $\alpha$ -mannosidase. Sanger-sequencing confirmed the maternal c.2248C>T, p.Arg750Trp and paternal c.2426T>C, p.Leu809Pro alleles. These are the first and third most common MAN2B1 mutations, respectively, among 125 identified, causing  $\alpha$ -mannosidosis.

$\alpha$ -Mannosidosis is a lysosomal storage disease with intra-cellular accumulation and urinary excretion of mannose-containing oligosaccharides. The disorder affects many organ systems and is divided into 3 sub-types depending on age-of-onset and severity. Focal lytic or sclerotic lesions and osteonecrosis have been reported. Our patient with unique skeletal findings is best described as a Type 2 variant, but with generalized osteosclerosis. MAN2B1 defects should be considered as an etiology for HBM disease when the common HBM genes have been excluded.



Figure

Disclosures: Gary S. Gottesman, None.

## SU0325

**Effects of Burosumab (KRN23), a Human Monoclonal Antibody to FGF23, in Patients with Tumor-Induced Osteomalacia (TIO) or Epidermal Nevus Syndrome (ENS).** Suzanne Jan De Beur<sup>1</sup>, Paul D. Miller<sup>2</sup>, Thomas J. Weber<sup>3</sup>, Munro Peacock<sup>4</sup>, Mary D. Ruppe<sup>5</sup>, Karl Insogna<sup>6</sup>, Diana Luca<sup>7</sup>, Christina Theodore-Oklota<sup>7</sup>, Javier San Martin<sup>7</sup>, Thomas Carpenter<sup>6</sup>. <sup>1</sup>Johns Hopkins University School of Medicine, United States, <sup>2</sup>Colorado Center for Bone Research, United States, <sup>3</sup>Duke University, United States, <sup>4</sup>Indiana University School of Medicine, United States, <sup>5</sup>Houston Methodist Hospital, United States, <sup>6</sup>Yale University School of Medicine, United States, <sup>7</sup>Ultrasenx Pharmaceutical Inc., United States

Tumor-induced Osteomalacia (TIO) and Epidermal Nevus Syndrome (ENS) are rare conditions in which ectopic FGF23 production leads to decreased renal phosphate reabsorption, impaired 1,25(OH)<sub>2</sub>D synthesis, and osteomalacia with pain, weakness, and decreased mobility. An ongoing open-label Phase 2 study is evaluating the use of burosumab (KRN23), an investigational recombinant human antibody that inhibits FGF23, in adults with TIO or ENS. Burosumab (0.3-2.0 mg/kg) is administered SC every 4 weeks (w); interim data are presented for 16 subjects (15 TIO, 1 ENS) who completed ≥24w of burosumab treatment.

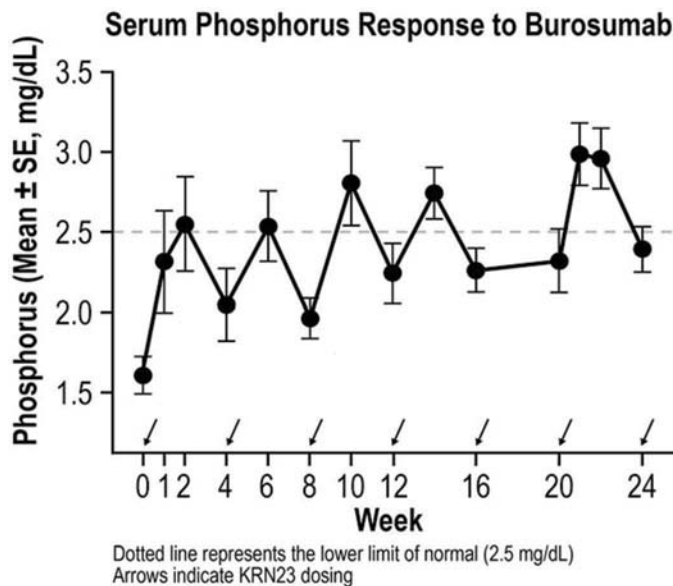
Mean age at study entry was 52 years, and median serum intact FGF23 was 289 pg/mL (normal: 10-62). Mean values for serum phosphorus (Pi) increased from below normal at baseline (BL: 1.6 mg/dL; normal: 2.5-4.0) to within normal range at all midpoint visits (2 weeks after a dose) (Figure). Increased serum Pi was accompanied by increases in both 1,25(OH)<sub>2</sub>D (Mean±SD; BL: 26±9 pg/mL; 24w: 43±17 pg/mL; p=0.0009) and renal Pi reabsorption (TmP/GFR, BL: 1.2±0.5 mg/dL; 24w: 2.0±0.7 mg/dL; p<0.0001).

Fatigue and pain were evaluated on 1-10 scales using the Brief Fatigue Inventory and Brief Pain Inventory. The worst fatigue mean score decreased from 7.1 (≥7 = severe) at BL to 5.4 (p=0.0018) at 24w. Although there was no significant change in worst pain at 24w from a mean BL score of 5.6 to 5.1 post-BL (p=0.4060), six subjects (37.5%) reported a ≥30% improvement in worst pain over 24w compared to BL. Subjects also reported improved physical health status as measured by the SF-36 physical component score (PCS, BL: 32.67; 24w: 37.32; p=0.0037) and the major domains that comprise the PCS: Physical Function (p=0.0413), Role Physical (p=0.0022), Bodily Pain (p=0.0614), and General Health (p=0.0235).

Strength and endurance also improved in study subjects, as measured by the number of sit-to-stand repetitions (reps) a subject can perform within 30 seconds (BL: 6.8 reps; 24w: 8.1 reps; p=0.0040).

Adverse events (AEs) were observed in all 16 subjects and were frequently musculoskeletal, related to underlying disease. One serious AE led to treatment discontinuation (neoplasm progression of preexisting metastatic sarcoma).

Burosumab administration increased serum Pi, TmP/GFR, and 1,25(OH)<sub>2</sub>D levels in adults with TIO or ENS. Treatment with burosumab over 24w led to reduced fatigue, enhanced strength, and improved physical health status.



Figure

**Disclosures:** Suzanne Jan De Beur, Ultrasenx Pharmaceutical Inc., Consultant.

## SU0326

**Uptake of Influenza Vaccine in UK Patients with Fibrodysplasia Ossificans Progressiva.** Richard Keen<sup>\*</sup>, Nataliya Gak, Jacqueline Vinton, Benjamin Jacobs, Royal National Orthopaedic Hospital, United Kingdom

Fibrodysplasia ossificans progressiva (FOP; OMIM #135100) begins in childhood and leads to irreversible restriction of movement, functional impairment, and shortened life-span. Individuals with FOP develop progressive limitations in chest expansion, resulting in restrictive lung disease. Current management guidelines published in 2011 (<http://www.ifopa.org/living-with-fop-menu/treatment-guidelines.html>) highlight that Influenza may be a causative factor for FOP flare-ups. Influenza can also cause potentially deadly cardiopulmonary complications, especially in individuals with severe restrictive chest wall disease. It is therefore recommended that patients with FOP should consider receiving influenza immunisations annually, and that unaffected household members of patients with FOP should also consider annual immunisations to decrease the risk of spreading the virus to highly susceptible FOP patients. The aim of this study is to investigate the vaccination rates of UK patients with FOP and their household contacts.

Telephone interviews were conducted with patients with FOP or their parents/guardians. All patients were resident in the UK and attended a single specialist centre.

We interviewed 17 of our 20 patients (85%). Of these 10 were children (age < 18 years) and 7 were adults (age > 18 years). Seasonal influenza vaccination rates were 23.5% in children (n=4) and 11.7% (n=2) in adults. The main reasons for not having the vaccine were: anxiety about the injection causing a flare of the disease (n=9, 52.9%), recurrent flares of the disease (n=3, 17.6%), and previous administration of influenza vaccine via the intramuscular route rather than subcutaneous, resulting in an acute flare (n=2, 11.7%). Influenza vaccination rates among household contacts (n=39), including parents, partners, children or siblings were 71.4% (n=5) in children and 31.2% (n=10) in adults.

This study highlights the need to provide education to individuals with FOP and their close contacts regarding the importance of influenza vaccination. There may also be an added role for education of the primary care/family physician involved in their care. In FOP individuals who are not vaccinated, consideration could be made to ensure access to antiviral medication if they develop influenza.

**Disclosures:** Richard Keen, None.

## SU0327

**Pulmonary Function in Adults with XLH who Display Kyphoscoliosis.** Greg Newman<sup>\*</sup>, Ilene Rosenberg<sup>1</sup>, Ramon Gonzalez<sup>1</sup>, Steven Tommasini<sup>2</sup>, Carolyn Macica<sup>1</sup>. <sup>1</sup>Quinnipiac University Frank H. Netter MD School of Medicine, United States, <sup>2</sup>Yale School of Medicine, United States

X-linked hypophosphatemia (XLH) is a phosphate wasting disorder that arises from an inactivating mutation of the PHEX gene resulting in elevated levels of the phosphatonin FGF23. Osteomalacia persists throughout adulthood and contributes to skeletal abnormalities characterized by defective calcification of cartilage, bone and entheses. Changes to thoracic structures in pediatric rickets have been described and include bulging of the costochondral joints (rachitic rosary) and a groove along the ribs at the diaphragmatic attachment (Harrison's groove). Here, we report that radiographs of a subset of patients with XLH display thoracic abnormalities similar to those seen in ankylosing spondylitis (AS), such as kyphosis, ossified spinal ligaments, and scoliosis. These same patients also present with widened ribs on x-ray, consistent with hypomineralization of rib osteoid in von Kossa (VK)-stained sections from Hyp mice, a murine XLH model. VK stain also revealed osteomalacia of thoracic structures including the spine and costochondral and costovertebral joints. However, the impact of thoracic structural abnormalities on pulmonary function has never been studied in adult XLH. Research from AS has shown that kyphosis can impede chest wall expansion and produce restrictive lung disease in some patients.

Pulmonary function tests (PFTs) were performed on 3 patients who showed severe thoracic structural abnormalities on x-ray. Tests included forced vital capacity (FVC), forced expiratory volume in one second (FEV<sub>1</sub>), maximum inspiratory flow volume loop, negative inspiratory pressure, lung volume by nitrogen washout, single breath diffusing capacity, maximum voluntary ventilation, and a six-minute walk test with pulse oximetry. Measurements of kyphosis, scoliosis, and rib width were obtained from radiographs.

PFTs revealed mild restrictive lung disease in Patient 3 whose x-rays showed the most severe skeletal abnormalities; Patients 1 and 2 were within the normal range. Cobb angles were measured from radiographs and showed moderate kyphosis and mild scoliosis.

We expected that restriction in these patients would have been greater than measured. Our study of three patients showed that only the most severely affected patient had restrictive lung disease with a total lung capacity of 77% predicted. Therefore, we hypothesize that osteomalacia of the rib cage allows greater compliance of the chest wall and compensates for restriction produced by kyphosis and scoliosis.



	FVC	FEV <sub>1</sub>	FEV <sub>1</sub> FVC	TLC	RV	FRC	DLCO	MIP	MEP	Kyphosis (°)	Scoliosis (°)
Patient 1	100	95	96	92	71	117	102	94	102	42	18
Patient 2	120	134	110	91	39	96	106	79	53	58	10
Patient 3	84	93	112	77	64	69	82	43	29	41	18

Table. PFT results given as % predicted values based on American Thoracic Society height, age, gender, and weight matched standards

PFT Results & Kyphoscoliosis Measurements

Disclosures: Greg Newman, None.

## SU0328

**A novel COL1A2 C-propeptide cleavage site mutation causing osteogenesis imperfecta with high bone mass.** Tim Rolvien<sup>\*1</sup>, Uwe Kornak<sup>2</sup>, Julian Stürznickel<sup>1</sup>, Stefan Mundlos<sup>2</sup>, Thorsten Schinke<sup>1</sup>, Michael Amling<sup>1</sup>, Ralf Oheim<sup>1</sup>. <sup>1</sup>Department of Osteology and Biomechanics, University Medical Center Hamburg-Eppendorf, Germany, <sup>2</sup>Institute of Medical Genetics and Human Genetics, Charité Universitätsmedizin Berlin, Germany

Osteogenesis imperfecta (OI) is a well described genetic skeletal disorder defined by low bone mass and increased bone fragility. Dominant mutations in two genes encoding collagen 1 (COL1A1/COL1A2) are present in most of the affected patients. Of note, there are reported cases in the literature, where specific COL1A1/COL1A2 mutations affecting the C-propeptide cleavage are associated with high bone mass. Here we report a case of OI in a 52-year-old woman, who experienced multiple non-vertebral and vertebral fractures with onset in early childhood. A full osteologic assessment including Dual Energy X-Ray absorptiometry (DXA), high-resolution peripheral quantitative computed tomography (HR-pQCT) and serum analyses revealed a high bone mass (BMD, DXA Z-score total hip +2.9) with increased trabecular thickness (Tb.Th) and elevated serum markers of bone formation and bone resorption. Whole exome sequencing identified a novel mutation in the COL1A2 gene causing a p.Asn1120Gly substitution at the protein level and affecting the type I procollagen C-propeptide cleavage site. In line with previously reported cases, our data independently proof the existence of an unusual phenotype of high BMD OI caused by a mutation in the procollagen C-propeptide cleavage.

Disclosures: Tim Rolvien, None.

## SU0329

**Determinants Of Impaired Quality Of Life In Patients With Fibrous Dysplasia.** Marlous Rotman<sup>\*</sup>, Bas Majoer, Cornelia Andela, Jens Bruggeman, Michiel van de Sande, Ad Kaptein, Neveen Hamdy, Sander Dijkstra, Natasha Appelman-Dijkstra. Leiden University Medical Center, Netherlands

**Background** Fibrous dysplasia is a rare bone disorder, commonly associated with pain, deformity and fractures, which may significantly have an impact on quality of life. In this study we evaluate quality of life in patients with fibrous dysplasia using the Short Form-36 and the Brief Pain Inventory questionnaires. Data were compared with those of the general Dutch population.

**Results** Out of 138 patients from a cohort of 255 patients with fibrous dysplasia that were sent questionnaires assessing quality of life and pain, the response rate was 70.3%, with 97 patients, predominantly female (65%), completing the questionnaires. Monostotic fibrous dysplasia was predominant (n=62, 64%). Fibrous dysplasia patients had significantly lower quality of life outcome scores than the general Dutch population for all tested domains of the Short Form-36 except for the "Mental health" and the "Role emotional" domains. More severe forms of fibrous dysplasia, had the more severe Short-Form-36 quality of life outcomes, but there was no significant difference in Brief Pain Inventory domains between different subtypes of fibrous dysplasia. Quality of life was lower in patients with higher disease burden, as reflected by high skeletal burden scores (p=0.003) and high levels of PAIN (p=0.002).

**Conclusion** We demonstrate impairments in all domains of quality of life, except for 'Mental health' and 'Role emotional' domains, across the wide spectrum of fibrous dysplasia including its milder forms. We identified high skeletal burden scores, reflecting disease severity, as the most consistent predictor of impaired quality of life. Our findings hold significant clinical implications as they draw attention to the clinically unmet need to address quality of life issues in the management of patients with all subtypes of fibrous dysplasia, including its milder forms.

Disclosures: Marlous Rotman, None.

## SU0330

**Long-Term Outcome of Patients Affected by Jansen's Disease and In Vitro Impact of an Inverse Agonist on Different Activating PTHR1 Mutations.** Hiroshi Saito<sup>\*1</sup>, Hiroshi Noda<sup>1</sup>, Thomas J Gardella<sup>2</sup>, Harald Jüppner<sup>2</sup>.

<sup>1</sup>Massachusetts General Hospital, Harvard University, United States, <sup>2</sup>Massachusetts General Hospital and Harvard Medical School, United States

Jansen metaphyseal chondrodysplasia (JMC) is a rare disorder caused by heterozygous activating mutations in the PTH/PTHrP receptor (PTHR1), and characterized by severe growth plate abnormalities that lead to short-limbed dwarfism with conditions of hypercalcemia and hypophosphatemia despite normal/low PTH levels. To better understand the natural history of JMC, we evaluated retrospectively the clinical findings for 24 patients. We also characterized the different known PTHR1 JMC variants in cell-based functional assays. Five different JMC mutations have so far been identified. The H223R mutation occurred in 18 cases; T410P, I458R and I458K were each identified in a single case, and T410R was found in a male and his two sons. Final adult heights (cm) were 127±6 (males) and 120±10 (females) in H223R, and 158±6 (males) for T410R. We compared the biochemical abnormalities between children (0-10 years) and adult (>17 years) in cases with each mutation. In children and adults serum Ca (mg/dL) was 12.0±0.4 vs 9.7±0.3 (P<0.001), respectively, urinary Ca to creatinine (mg/mg) was 0.81±0.13 vs 0.37±0.11 (P<0.05), serum PTH (pmol/L), was 0.52±0.16 vs 1.71±0.57 (P<0.05). Hypophosphatemia was observed to varying degrees at all ages. Serum 1.25 (OH)2D was normal. Five cases showed nephrocalcinosis and two H223R cases older than 50 years exhibited severe chronic kidney disease. Hypercalcemia, hypercalciuria and suppression of PTH secretion were pronounced during the first decade of life, but values moved closer to normal in young adults. Most cases continued to exhibit hypercalciuria after improvement of hypercalcemia. In glosensor cAMP assays performed in HEK-293 cells, the five different PTHR1-JMC variants showed varying levels of constitutive signaling activity, as I458K and I458R resulted in basal cAMP levels ~10-fold higher vs PTHR1-WT, while T410R resulted in levels that were indistinguishable from PTHR1-WT. Maximal response to PTH(1-34) also varied, as T410P, I458K and I458R exhibited responses higher than PTHR1-WT, while H223R and T410R exhibited responses lower than PTHR1-WT. The basal cAMP signaling of each variant was reduced by the inverse agonist [L11,dW12,W23]-PTHrP(7-36). These results suggest that the JMC phenotype varies with age and with the particular intrinsic signaling properties of the specific PTHR1 mutant allele. They also suggest that further study of PTHR1 inverse agonist ligands might offer a path towards potential therapy for JMC.

Disclosures: Hiroshi Saito, None.

## SU0331

**Improvement of physical function and bone marrow oedema in an adult patient with pediatric-onset hypophosphatasia after 16 weeks of asfotase alfa therapy.** Tobias Schmidt<sup>\*</sup>, Michael Amling, Florian Barvencik. Department of Osteology and Biomechanics, University Medical Center Hamburg Eppendorf, Germany

### Objective

Hypophosphatasia (HPP) is a rare bone disease caused by mutation of the gene that encodes for tissue-nonspecific isoenzyme of alkaline phosphatase (TNSALP). Asfotase alfa is a recombinant, bone targeted enzyme replacement which has been reported to show substantial beneficial effects in infantile and childhood HPP. The objective of this retrospective analysis was to study short term effects of asfotase alfa therapy on physical function, quality of life and bone quality in an adult patient with pediatric onset HPP.

### Methods

Diagnosis of the 24 years old HPP patient was established during childhood by typical clinical symptoms, decreased AP, elevated PLP and was genetically confirmed. MRI of left knee and right foot and were performed due to persistent pain. Bone quality was assessed by DXA, HR pQCT and Iliac crest bone biopsy which was analyzed by non-decalcified histology. MRI of left knee and right foot were repeated after 8 weeks of treatment. Laboratory values including alkaline Phosphatase, bone specific alkaline phosphatase, pyridoxal-5-phosphat, parathyroid hormone, calcium, phosphate and 25-OH-D were measured every two weeks. Functional tests including chair rising test, grip-strength and Tinetti test as well as general health assessment by SF-36 and Brief Pain Inventory were accomplished at therapy start and after 8 and 16 weeks of treatment.

### Results

In this retrospective analysis we evaluated the short term effects (16 weeks) of Asfotase alfa enzyme replacement therapy on muscle function and quality of life in an 24 year old female patient with pediatric onset HPP. Non-decalcified histology of iliac crest biopsy revealed massive accumulation of osteoid. On the contrary, DXA and HR-pQCT showed only slightly decreased parameters compared to age and gender matched reference values. At therapy initiation MRI displayed bone marrow oedema in the left tibial plateau and right talus which were strongly reduced after 8 weeks of treatment. Muscle function measured by chair rising test, grip-strength and Tinetti test improved in a time dependent manner. However, musculoskeletal pain was so far only slightly reduced after 16 weeks of treatment. Apart from local infection reactions within the first 4 weeks, no significant side effects occurred.

### Conclusion

Asfotase alfa enzyme replacement therapy can improve physical function within a short period of time in adults suffering from HPP.

Disclosures: Tobias Schmidt, None.

## SU0332

**Effect of Zoledronic acid treatment in cases of non-infectious osteomyelitis of the jaw.** Peter Schwarz\*. Department of Endocrinologi, Rigshospitalet and Copenhagen University, Denmark

In eight cases of diagnosed non-infectious osteomyelitis of the jaw we found five cases spontaneous and three cases in relation to surgery of the jaw. In all cases the diagnosis was confirmed by clinic and bone scintigraphy and supplemented by biochemistry and x-ray and in some MRI. One case of non-infectious osteomyelitis has been reported on earlier (1).

The five patients with spontaneous debut of non-infectious osteomyelitis were aged 9, 16, 28, 52 and 58 years at diagnosis. All patients had normal biochemistry including calcium metabolism. Clinical bone pain of the jaw and bone scintigraphy showed the active osteomyelitis. All patients were treated by antibiotics and painkillers before admission. None of the patients had any effect after 1 to 9 years of the initial treatment. The patients were all treated with Zoledronic acid 5 mg/year x 3. Four of five patients showed pain improvement after 1 year and after 2 years the four were clinically without pain. Follow-up since last zoledronic acid 1, 2, 4 and 5 years without any relapse (pain, activity at bone scintigraphy). One patient aged 52 at debut has been treated with 3 infusions of zoledronic acid without significant pain improvement. However, less bone activity has been observed at bone scintigraphy after 3 years.

Three cases of diagnosed osteomyelitis of the jaw were observed after tooth extraction. None of the three patients showed infection or responded to antibiotics or pain killers. The three patients were aged 35, 41 and 84 years at debut. Two women aged 41 and 84 were admitted for bisphosphonate treatment after 1 year without improvement in their disease and both have had zoledronic acid infusion of 4 mg once. No effect is yet observed. One 40 years old male was treated with antibiotics and pain killers for 5 years without effect and have had 2 infusions of Zoledronic acid. Eighteen months after initial Zoledronic acid treatment he was clinically without pain and bone scintigraphy showed significant improvement at 12 months.

None of the patients had severe side effects

In conclusion, Zoledronic acid treatment of non-infectious osteomyelitis seems promising.

1. Rasmussen AQ, Andersen UB, Jørgensen NR, Schwarz P. Non-infections osteomyelitis in the mandible of a young female, a case report. Case Reports 2014; 12(8): 44.

**Disclosures:** Peter Schwarz, None.

## SU0333

**Hypercalcemia of malignancy in a patient with hypoparathyroidism: a complicated but treatable condition.** Marielly Sierra\*<sup>1</sup>, Jillian Haddock<sup>2</sup>, Margarita Ramirez<sup>2</sup>, Milliet Alvarado<sup>2</sup>, Loida Gonzalez<sup>2</sup>. <sup>1</sup>University of Puerto Rico, Endocrinology Department, Puerto Rico, <sup>2</sup>University of Puerto Rico, Recinto de ciencias medicas. Endocrinology section, Puerto Rico

Hypercalcemia in a patient with primary hypoparathyroidism has rarely been described. Most of the cases reported have resulted from the treatment with excessive doses of calcium, vitamin D, or its derivatives. A 55-year-old male patient with primary hypoparathyroidism diagnosed when he was 12 years old, enucleation of the left eye due to retinal melanoma, hyperlipidemia, scoliosis, and Noonan's syndrome (NS), was referred to the endocrinology clinics for follow up of hypoparathyroidism. During initial evaluation, the patient referred intense pain in mid and lower back and at the right upper quadrant of the abdomen. Initial laboratories revealed calcium level at 8.0 mg/dl (nl 8-10.5), elevated phosphate 4.8 mg/dl (nl 2.5-4.3) and a calcium/phosphate product of 35, while using calcium carbonate 1200 mg and vitamin D3 600 IU daily. Calcitriol 0.25 mcg daily was added to therapy and calcium carbonate discontinued, although the patient was not compliant with treatment. Abdominopelvic CT scan and thoracolumbar MRI showed metastatic lesions to liver, pancreas, and pronounced osteolytic bone disease in vertebral bodies and ribs. Liver biopsy confirmed metastatic melanoma. Eight weeks after initial evaluation, serum calcium level increased to 12 mg/dl without calcium supplements. Parathyroid hormone (PTH), vitamin D 1,25-OH and PTHrP levels were within the lower range of normal compatible with hypercalcemia of malignancy, most likely secondary to osteolytic disease. Chemotherapy with ipilimumab and nivolumab was started, and zoledronic acid added to treat hypercalcemia and bone pain. Calcium levels decreased to 7.4 mg/dl three days after bisphosphonate therapy. Calcium levels reached normal range (8.3 mg/dl) 4 days after a monitored calcium carbonate and calcitriol therapy. The patient returned to daily calcitriol therapy after stabilization of calcium levels. Hypercalcemia of malignancy can be successfully treated with bisphosphonates. However, in patients with hypoparathyroidism this can be challenging due to a higher risk of hypocalcemia. Our case showed that patients with hypoparathyroidism presenting with increased plasma calcium levels should be assessed for malignancies and appropriate therapy given. Very few cases of hypercalcemia of malignancy have been reported in hypoparathyroid patients, and, to our knowledge, this is the first case secondary to osteolytic metastatic disease.

**Disclosures:** Marielly Sierra, None.

## SU0334

**Effect of Asfotase Alfa Treatment on Health States and Ambulatory Function Among Patients With Hypophosphatasia.** Andrew Lloyd\*<sup>1</sup>, Ioannis C Tomazos<sup>2</sup>, Katy Gallop<sup>1</sup>, Scott Moseley<sup>2</sup>, Bonnie MK Donato<sup>2</sup>, Gilbert L'Italien<sup>2</sup>. <sup>1</sup>AcasterLloyd Consulting Ltd., United Kingdom, <sup>2</sup>Alexion Pharmaceuticals, Inc., United States

Background: Hypophosphatasia (HPP) is a rare, genetic, complex, systemic, musculoskeletal disease with severe manifestations that impair mobility and substantially limit quality of life (QOL). The 6-Minute Walk Test (6MWT) is used to assess ambulatory capacity and has been documented to correlate with formal measures of QOL. Asfotase alfa, an enzyme replacement therapy approved for the treatment of HPP, has been shown in clinical studies to improve skeletal mineralization, physical functioning, and QOL. In this study, we sought to determine the effect of asfotase alfa on health states, defined based on 6MWT data, in patients with HPP aged ≥5 years. In addition, we assessed the transition of asfotase alfa-treated patients from one health state to another.

Methods: Patient-level data for the 6MWT from 2 clinical studies (NCT00952484/NCT01203826, NCT01163149) were used to identify 4 health states associated with HPP. Profiles for the 4 health states were created based on interviews with clinical experts who treat patients diagnosed with HPP. Three age cohorts (5–12 y, 13–17 y, and ≥18 y) were identified. The 6MWT results were described as a percent of normal function, with ≥80% defining the lower limit of normal. 6MWT clinical study data at baseline (or treatment initiation) and at 96 weeks of treatment were assigned to a corresponding health state.

Results: Health states, the distribution of patients (N=29), and age median values at baseline and 96 weeks of treatment are shown in the Table. Two nontreated adults did not change health state from baseline to 24 weeks, although their 6MWT percent predicted decreased from 79.1% to 70.4% and 92.4% to 88.7%.

Conclusion: Treatment with asfotase alfa was associated with no change or an improvement in health state as derived from the 6MWT and clinical expert classification, which was consistent across age cohorts. No patient experienced a decrease in health state while on treatment.

**Table: Health State Thresholds and Transition From Baseline to 96 Weeks of Treatment With Asfotase Alfa**

Asfotase Alfa		Age cohorts, y							
		5-12 (n=13)		13-17 (n=6)		≥18 (n=10)			
HPP health states		6MWT % predicted, % of normal function							
I (better)		>82.4 to ≤100		>82.6 to ≤100		>84.0 to ≤100			
II		>64.8 to ≤82.4		>65.2 to ≤82.6		>68.0 to ≤84.0			
III		>47.2 to ≤64.8		>47.8 to ≤65.2		>52.0 to ≤68.0			
IV (worse)		≤47.2		≤47.8		≤52.0			
		Patient distribution at baseline and 96 weeks of asfotase alfa treatment, n							
		Baseline <sup>a</sup>		Week 96 <sup>b</sup>		Baseline <sup>c</sup>		Week 96 <sup>d</sup>	
I (better)		0		2		3		6	
II		6		5		1		2	
III		3		0		1		4	
IV (worse)		2		0		1		0	
Transition between health states at 96 weeks of asfotase alfa treatment									
Transition to milder state, %		91 <sup>a</sup>				40 <sup>b</sup>		33 <sup>c</sup>	
Same state, %		9 <sup>a</sup>				60 <sup>b</sup>		67 <sup>c</sup>	
Worse state, %		0 <sup>a</sup>				0 <sup>b</sup>		0 <sup>c</sup>	
6MWT % predicted at baseline and 96 weeks of asfotase alfa treatment (group results)									
		Baseline <sup>e</sup>		Week 96 <sup>e</sup>		Baseline <sup>f</sup>		Week 96 <sup>f</sup>	
Median (min, max)		61 (29, 82)		83 (73, 92)		80 (63, 85)		86 (74, 90)	
						69 (42, 101)		92 (63, 121)	

<sup>a</sup>n=11; <sup>b</sup>n=5; <sup>c</sup>n=9; <sup>d</sup>n=13; <sup>e</sup>n=4; <sup>f</sup>n=10.

<sup>a</sup>n=11; <sup>b</sup>n=5; <sup>c</sup>n=9; <sup>d</sup>n=13; <sup>e</sup>n=4; <sup>f</sup>n=10.

Table: Health State Thresholds and Transition From Baseline to 96 Weeks of Treatment With Asfotase Alfa

**Disclosures:** Andrew Lloyd, Alexion Pharmaceuticals, Inc., Grant/Research Support.

## SU0335

**Atypical femoral fracture in autosomal dominant type II osteopetrosis.** Kyu Hyun Yang\*, Young Chang Park, Xuan Lin Zheng, Hyun Soo Moon. Yonsei University, Korea, Republic of

Background

Osteopetrosis is a heterogeneous group of heritable conditions involve a defect in bone resorption by osteoclasts. We observed three cases of subtrochanteric fractures in two patients with autosomal dominant type II osteopetrosis, and treated them surgically. Although the report from ASBMR task team excluded femoral fracture in patient with metabolic bone disease in defining atypical femoral fracture (AFF), clinical and radiographic features of osteopetrotic subtrochanteric fractures (OSF) resemble those of AFF.

Result

We reviewed two OSF patients who had been transferred to our hospital with history of trivial falls. Radiographs of these patients showed generally dense, sclerotic bone features, in addition to narrow medullary canal and thickening of lateral femoral cortex. Fracture pattern was unique as it consisted of transverse fractures without comminution, and beak-like callus formation in the lateral cortex. Both patients were treated with surgical intervention according to the treatment protocol of AFF. Patient 1 (26-year-old male) diagnosed with left OSF, was treated with closed reduction and internal fixation using a femoral nail (Fig.1-a,b). Patient 2 (70-year-old female) was diagnosed with right complete OSF, as well as contralateral incomplete OSF. Both femora had grade II anterolateral femoral bowing. Prophylactic IM nailing was performed for the left side,



while open reduction and internal fixation with a locking plate was needed for the right side (Fig. 1-c,d).

#### Discussion

AFF has been suggested to occur due to prolonged, decreased remodeling of the bone. It is known to cause bone brittleness as well as accumulation of microfracture in the femur, especially in the lateral cortex. In the context of pathogenesis, osteopetrosis has the same pathomechanism as AFF, due to defect in osteoclast function. We treated two osteopetrosis patients according to AFF treatment protocol, and covered the full length of their femur with IM nail or plate. IM nailing was quite difficult, due to hardness of bone and narrow medullary canal. As a result, we developed a reaming technique that was useful for this situation. Deformity of medullary canal is a main contraindication of IM nailing. However, IM nailing can be a treatment of choice in special conditions, such as osteogenesis imperfecta, AFF with excessive anterolateral femoral bowing, and osteopetrosis.

#### Conclusion

We recommend including OSF in the definition of AFF and treating it accordingly.

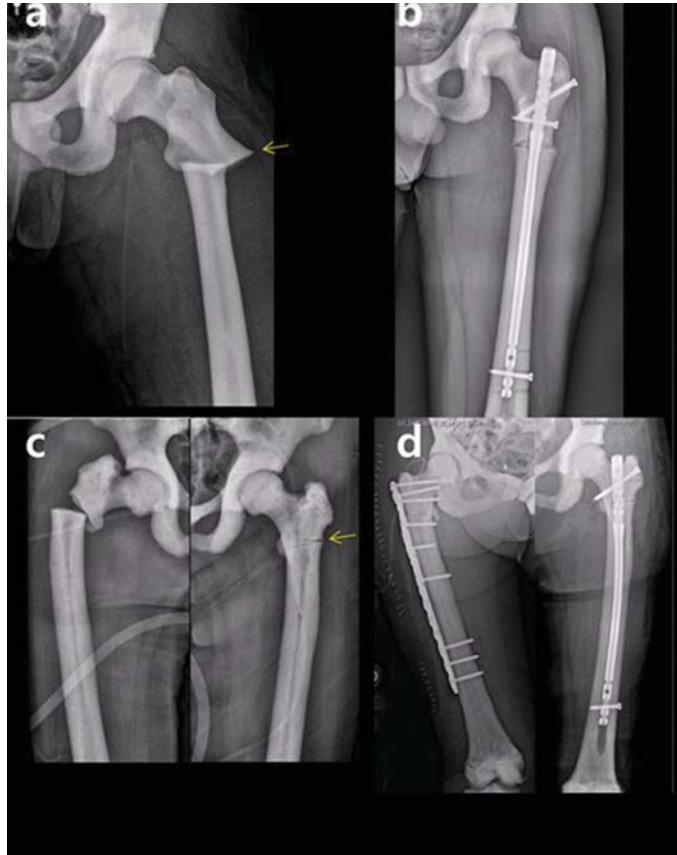


Figure 1

Disclosures: Kyu Hyun Yang, None.

## SU0336

**Automated segmentation and analysis of heterotopic ossification using *in vivo* micro-computed tomography ( $\mu$ CT).** Ali Behrooz<sup>\*1</sup>, Peter Waterman<sup>1</sup>, Julie Czupryna<sup>1</sup>, Thomas Backus<sup>2</sup>, Nikita Kondratiev<sup>2</sup>, Jennifer Lachey<sup>2</sup>.  
<sup>1</sup>PerkinElmer, United States, <sup>2</sup>Keros Therapeutics, United States

Heterotopic ossification (HO) is a condition in which bone forms outside of the normal skeleton in soft connective tissue. HO may result from several disease processes including genetic abnormalities and trauma.

*In vivo* micro-computed tomography (micro-CT) is an imaging modality capable of generating quantitative and longitudinal 3D anatomical images and has been found to be instrumental in the study of bone development, loss, and morphology. While micro-CT has been applied primarily to study the orthotopic skeleton, tracking the formation of calcification in soft tissues is possible. Morphometric analysis and density quantification of HO components *in vivo* enables longitudinal studies, analyses of HO formation, and evaluation of treatment efficacy.

While micro-CT provides a powerful means to visualize bone, analysis of the images has proven to be time consuming and technically challenging. Algorithms have been developed to automate analysis and have successfully detected and separated segments of orthotopic bone (Behrooz, et al, US Patent Application No. 14/812,483). However, analysis of heterotopic bone, where calcifications can be fused to the orthotopic skeleton or non-contiguous in nature analysis, remains a challenge.

To facilitate development of algorithms to segment and quantify HO, we induced ossification in the mouse hindlimb via intramuscular administration of bone

morphogenic protein (BMP). This model generates robust radiologically detectable HO within 14 days after BMP administration. Mice were imaged on a stand-alone gantry-based micro-CT system (Quantum<sup>®</sup> FX by Rigaku, Inc.).

An automated algorithm was developed to detect and separate HO from the orthotopic skeleton in micro-CT scans from the BMP-treated mice. A hybrid thresholding technique was applied to micro-CT images for detection of bone tissue including HO as shown in Fig. 1. Then, a watershed-based approach was applied to the bone mask to separate the HO from orthotopic skeleton automatically. The results are shown in Fig. 2. As shown, the HO separation algorithm performs successfully even in late-stage models where HO and orthotopic bone have become fused. Data from HO mouse models were acquired *in vivo* at different fields of view (24 and 30 mm) and voxel resolutions of 46 and 58 microns. We present results of HO analysis with various ASBMR morphometric parameters including volume, average thickness, porosity, and mineral density.

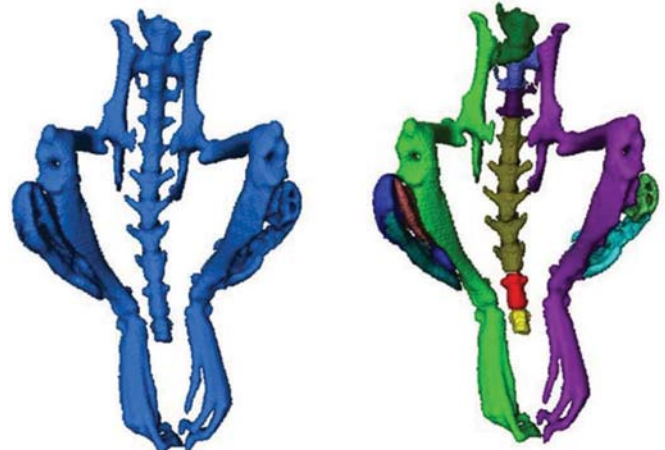


Fig 1. Detected bone mask of the hind limbs of an HO mouse model from a microCT scan at 30 mm field of view. The detection algorithm uses hybrid thresholding to segment bone and HO from soft tissue automatically.

Fig 2. HO components of the detected bone mask are segmented automatically from normal skeleton using watershed-based splitting. This allows for automated streamlined analysis of HO morphometric parameters and density separate from the skeletal bones.

Figures 1 and 2

Disclosures: Ali Behrooz, PerkinElmer, Inc., Grant/Research Support.

## SU0337

**Pharmacokinetics and Cardiovascular Assessment of TransCon CNP, a Sustained-Release C-type natriuretic Peptide Prodrug, for the Treatment of Achondroplasia.** Caroline Rasmussen<sup>\*1</sup>, Ulrich Hersel<sup>2</sup>, Tom Woods<sup>3</sup>, Thomas Wegge<sup>2</sup>, Frank Faltinger<sup>2</sup>, Albert Brenner<sup>3</sup>, Per Mygind<sup>1</sup>, Kennett Sprogøe<sup>1</sup>, Vibeke Miller Breinholt<sup>1</sup>. <sup>1</sup>Ascendis Pharma A/S, Denmark, <sup>2</sup>Ascendis Pharma GmbH, Denmark, <sup>3</sup>Ascendis Pharma GmbH, Germany

Currently, no FDA-approved therapy exists for achondroplasia (ACH), the most common form of dwarfism. Administration of C-type Natriuretic Peptide (CNP) to ACH patients and animals has been shown to stimulate endochondral bone growth and improve adverse skeletal manifestations of the disease. Given that continuous CNP exposure has demonstrated better efficacy than bolus administration, and that bolus administration has shown dose-limitation due to post-dose hypotension and reflex tachycardia (attributed to high  $C_{max}$  exposures), TransCon CNP, a prodrug of CNP, is being developed for the treatment of achondroplasia and could provide patients with a safe and effective treatment with once weekly dosing.

The aims of these nonclinical studies were to investigate the pharmacokinetics of TransCon CNP in cynomolgus monkeys and compare cardiovascular safety parameters to that of a daily administered CNP in cynomolgus monkeys and mice.

The pharmacokinetic profile was investigated in cynomolgus monkeys following a single dose of 146  $\mu$ g/kg TransCon CNP. The hemodynamic tolerability of subcutaneously administered TransCon CNP was investigated in telemetrized cynomolgus monkeys and Crl:CD1(ICR) mice. The effect of TransCon CNP was compared to dose-equivalent vosoritide or free CNP.

At equimolar doses, continuous vosoritide (a CNP analogue) administered to mice, showed better efficacy, resulting in increased right tibia growth compared to intermittent, daily injections. The half-life of TransCon CNP after single dose administration in monkeys was 79 hours, supporting once weekly dosing. In monkeys, no decrease in systolic arterial pressure (SAP) was detected at doses of up to 100  $\mu$ g/kg of TransCon CNP over a 48-hour monitoring period. In contrast, an equivalent dose of vosoritide led to a decrease on SAP at 0-1 hours post-dose. In mice (n=4), TransCon CNP doses up to 800  $\mu$ g/kg exhibited a hemodynamic profile comparable to control animals over a 48-hour monitoring period. In contrast, an equivalent dose of free CNP showed a decrease in SAP during the 0-2 hour post-dose interval.

TransCon CNP exhibits a substantial half-life extension compared to daily CNP analogues. Prolonged drug exposure of TransCon CNP, combined with low peak serum concentrations, may widen the therapeutic window and decrease the risk of hypotension,

thereby improving efficacy and tolerability; nonclinical studies in cynomolgus monkeys support weekly dosing in humans.

**Disclosures:** *Caroline Rasmussen, None.*

## SU0338

**Longitudinal micro-CT study assessing the development of enthesopathies and osteoarthritis in the murine model of X-Linked Hypophosphatemia.** Karine Briot<sup>1</sup>, Benjamin Salmon<sup>2</sup>, Carole-Anne Faraji-Bellé<sup>3</sup>, Olivier Fogel<sup>4</sup>, Aurélien Benoit<sup>5</sup>, Thorsten Schinke<sup>6</sup>, Agnès Linglart<sup>7</sup>, Corinne Miceli-Richard<sup>8</sup>, Christian Roux<sup>9</sup>, Catherine Chaussain<sup>10</sup>, Claire Bardet<sup>3</sup>. <sup>1</sup>AP-HP Service Rhumatologie B Hôpital Cochin, Paris, Reference Center for Rare Diseases of Calcium and Phosphorus Metabolism, France and Medical School Paris Descartes University, France, France, <sup>2</sup>EA 4462, Laboratory Orofacial Pathologies, Imaging and Biotherapies, School of Dentistry Paris Descartes University Sorbonne Paris Cité, France, AP-HP Department of Odontology, Bretonneau Hospital, Paris, France, France, <sup>3</sup>EA 4462, Laboratory Orofacial Pathologies, Imaging and Biotherapies, School of Dentistry Paris Descartes University Sorbonne Paris Cité, France, France, <sup>4</sup>AP-HP Service Rhumatologie B Hôpital Cochin, Paris, and Medical School Paris Descartes University, France, France, <sup>5</sup>EA 2496, URB2I, School of Dentistry University Paris Descartes Sorbonne Paris Cité, France, France, <sup>6</sup>Department of Osteology and Biomechanics, University Medical Center Hamburg Eppendorf, Hamburg, Germany., Germany, <sup>7</sup>Reference Center for Rare Diseases of Calcium and Phosphorus Metabolism, FranceAP-HP Department of Pediatric Endocrinology, Kremlin Bicêtre Hospital, School of Medicine University Paris Sud, France, France, <sup>8</sup>AP-HP Service Rhumatologie B Hôpital Cochin, Paris, and Medical School Paris Descartes University, France Pasteur Institute, Immunoregulation Unit, Paris, France, France, <sup>9</sup>AP-HP Service Rhumatologie B Hôpital Cochin, Paris, and Medical School Paris Descartes University, France. Reference Center for Rare Diseases of Calcium and Phosphorus Metabolism, France, France, <sup>10</sup>EA 4462, Laboratory Orofacial Pathologies, Imaging and Biotherapies, School of Dentistry Paris Descartes University Sorbonne Paris Cité, France. Reference Center for Rare Diseases of Calcium and Phosphorus Metabolism, France, France

X-linked hypophosphatemia (XLH) is characterized by rickets and osteomalacia because of an inactivating mutation of PHEX (phosphate-regulating gene with homology to endopeptidases on the X chromosome). Despite osteomalacia, paradoxical heterotopic calcifications form on tendon and ligament insertion sites limit functional range of motion of adult XLH patients. These features are associated with impaired quality of life although severities and locations of these complications are different. Understanding paradoxical heterotopic calcifications development will improve the management of XLH. Thus, we aimed at characterizing progression of enthesopathies, calcifications and osteoarthritis in Hyp mice, a murine model of XLH. Wild type (WT) and Hyp (#000528, Jackson Laboratory) male mice (n=5 per group) were scanned at age of 3, 6, 9 and 12 months using a high-resolution X-ray Micro-CT device (Quantum FX Caliper, Life Sciences, Perkin Elmer, Waltham, MA). The micro-CT allows 3D acquisitions with an isotropic voxel size of 20 µm (90 kV, 160 mA, 180s). Each micro-CT image was analyzing using Osirix software 5.8 (Pixmeo, Switzerland) (Skyscan, Belgium). Axial and coronal images of the sacroiliac joints, of the hip joints, sagittal images of the spine, and axial and lateral images of the feet were performed. Two blinded rheumatologists specialized in the field of rare bone diseases and bone inflammatory diseases assessed the presence of enthesopathies, ossifications (or calcifications) and bone erosions at calcaneum entheses, tarsis, sacroiliac joint (SIJ), hip joint and spine and score these parameters from M3 to M12, each ranging from 0 (normal) to 3. A composite score was built based on these parameters (from 0 to 18). Enthesopathies, erosions and ossifications were observed in each Hyp mouse and no abnormalities were observed in controls. These lesions were already present at 3 months and significantly increased from M3 to M12 (Figure 1). The pattern of lesions differs between Hyp mice. All the mice had a high score for bone erosions of SIJ with a mean score of 2.5 at M3 and of 2.85 at M12. Four out of five had a hip joint involvement and tarsis calcifications with a mean score of 0 and 1 at M3 and of 1.8 and 2.1 at M12, respectively. Two Hyp mice had a calcaneal enthesopathy and none of them developed spine enthesopathies. This longitudinal micro-CT follow-up of Hyp mice showed that peripheral enthesopathies, ossifications and osteoarthritis occur at early stages of the disease and further increase overtime. Our findings highlight the relevance of the Hyp murine model for pre-clinical studies aiming to test new therapies on the development of enthesopathies.

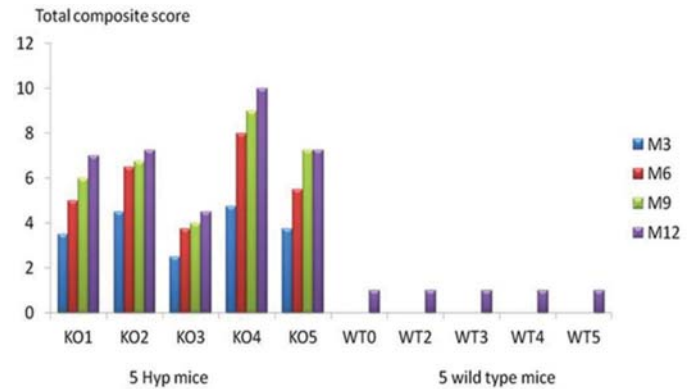


Figure 1: Longitudinal changes of the total composite score in Hyp and wild type mice over 12 months

**Disclosures:** *Karine Briot, None.*

## SU0339

**The Experience of XLH in Adulthood: Biopsychosocial Assessment, Needs, and Concerns.** Maya Doyle<sup>1</sup>, Carolyn Macica<sup>2</sup>. <sup>1</sup>Quinnipiac University, United States, <sup>2</sup>Quinnipiac University, Netter School of Medicine, United States

X-linked hypophosphatemia (XLH) is a rare renal phosphate wasting disorder that can result in lower limb deformities, short stature or slowed growth, waddling gait, fractures, dental abscesses, degenerative arthritis, bone spurs, bone and muscle pain, and weakness. An interprofessional team, including physicians, diagnostic imaging, physical therapy, occupational therapy and social work undertook a functional outcomes study to identify patient's health status and needs, with the goal of tailoring interventions for this population as they age. Prior studies have focused on management of the pediatric disorder; psychosocial research is limited as patients grow older and the disease progresses.

Qualitative semi-structured interviews were conducted regarding the experience of living with XLH as an adult. Quantitative data was also collected on daily activities, anxiety, stress, depression, quality of life, education, employment, insurance coverage and healthcare satisfaction. Interviews were audio-recorded and transcribed. Qualitative data was analyzed in the grounded theory tradition, including open coding to identify themes and categories, codebook creation, memoing, and focused coding to clarify emerging codes. Peer debriefing, triangulation, and prolonged engagement were used to support the rigor of qualitative analysis.

Eight individuals with XLH took part in interviews. A main concern expressed by all participants were expectations and worries about their future with XLH. Core categories emerged regarding perception of body by self and others, compensation for loss of mobility and range of motion, understanding of their condition by healthcare providers, and concerns about aging with XLH. Needs identified by participants included: improved physician and dentist awareness of XLH; improved genetic counseling; improved treatment now and for "next generation"; adequate health insurance including coverage for dental care; and access to and financial support for accommodations and equipment.

Adults with XLH face ongoing and progressive functional limitations and pain as they age which influences mental health, work, travel, and family life. Knowledgeable providers, psychosocial assessment, preparatory guidance, and peer support can be crucial to navigating the healthcare system and healthcare decision making. Advocacy for and access to knowledgeable providers and needed services could improve quality of life for individuals impacted by XLH in adulthood.

**Disclosures:** *Maya Doyle, None.*

## SU0340

**A Chaperone Complex Modulates Lysyl Hydroxylation of Type I Procollagen.** Ivan Duran<sup>\*</sup>, Deborah Krakow. UCLA, United States

Lysine hydroxylation of type I collagen telopeptides varies from tissue to tissue and these distinct hydroxylation patterns modulate collagen fibrillogenesis, crosslinking and mineralization to generate a unique extracellular matrix. Abnormalities in these patterns contribute to pathologies that include osteogenesis imperfecta (OI), tissue fibrosis, and cancer. Telopeptide procollagen modifications are carried out in the endoplasmic reticulum by lysyl hydroxylase 2 (LH2), however, little is known regarding how this enzyme regulates hydroxylation patterns. Through a series of experiments, we identified an ER complex of resident chaperones that includes HSP47, FKBP65 and BiP regulating the activity of LH2. Our findings show that FKBP65 and HSP47 modulate the activity of LH2 on telopeptide type I procollagen hydroxylation sites to either favor or repress its activity. Our in vitro data are also reflected in vivo in bone through studies on recessively inherited OI resulting from loss-of-function of either FKBP65 or HSP47 that produce altered bone specific cross-linking patterns. BiP was identified as a member of the complex, playing a role in enhancing the formation of the complex through its interactions with HSP47, adding a new function to its role in the ER. This newly identified ER chaperone complex contributes to our understanding of how LH2 regulates lysyl



hydroxylation of type I collagen telopeptides and when altered affects the quality of connective tissues, particularly bone.

**Disclosures:** Ivan Duran, None.

## SU0341

**Bone targeted bisphosphonate-antibiotic conjugates for the treatment of osteomyelitis biofilms.** Parish Sedghizadeh<sup>\*1</sup>, Frank Ebetino<sup>2</sup>, Shuting Sun<sup>2</sup>, Keivan Sadrerafi<sup>2</sup>, Adam Junka<sup>3</sup>, Susan Mahabady<sup>1</sup>, Jeffrey Neighbors<sup>4</sup>, Graham Russell<sup>5</sup>, Charles E. McKenna<sup>6</sup>. <sup>1</sup>Ostrow School of Dentistry, University of Southern California, United States, <sup>2</sup>BioVinc, United States, <sup>3</sup>Wroclaw Medical University, Poland, <sup>4</sup>Penn State University, United States, <sup>5</sup>University of Oxford, United Kingdom, <sup>6</sup>Dept. of Chemistry, University of Southern California, United States

The inadequate efficacy of current treatments for osteomyelitis has been ascribed to the limited access of systemically administered antibiotics to sites where causative bacteria (eg *S. aureus*) can reside in biofilms on bone, even within the osteocytic canalicular network, where bisphosphonates (BPs) can also gain access. We are investigating a "target and release" approach involving delivery of the fluoroquinolone antibiotic ciprofloxacin via bisphosphonate conjugates, utilizing serum-stable drug-BP linkers that metabolize and release the ciprofloxacin at the bone surface. Pharmacologically "inert" BPs were utilized to avoid confounding antiresorptive effects from the carrier. We recently reported impressive *in vivo* efficacy with a novel bisphosphonate-ciprofloxacin conjugate, BV600022. (*J Med Chem* 2017). Quantitative determination of the CFU of bacteria from resected peri-prosthetic osteomyelitis tissue showed that a single dose of 10 mg/kg of conjugate gave ca. 6 log units of greater suppression of bacteria relative to an untreated control, while multiple lower doses showed 2-3 (99% to 99.9%) log units of bacterial suppression. The single dose of 10 mg/kg of conjugate was highly significant ( $p=0.0005$ , unpaired t-test) compared to the control arm. Also, a non-cleavable linked conjugate was nearly inactive in osteomyelitis biofilms grown on hydroxyapatite (HA) surfaces *in vitro*. We now report further *in vitro* studies on this compound series to elucidate the effect of conjugate structure on the drug susceptibility of bacterial biofilms and to optimize efficacy by tuning the release rate under biofilms on simulated bone surfaces. A new carbamate-linked conjugate analog (BV600028) had an MIC of 3.8 µg/mL vs an MIC of 31.25 µg/mL for BV600022 against *S. aureus* strain ATCC-6538. This new carbamate analog at 50 µg/mL eradicated established *S. aureus* biofilms grown on HA *in vitro*, and prevented their formation with pretreatment prior to introduction of bacteria. As similar data has been demonstrated with carbamate linkages in osteoclast models *in vitro*, we suggest that enzymatic cleavage processes under bacteria may also be involved to release ciprofloxacin. Thus, this series of conjugates, incorporating an osteoadsorbent bisphosphonate and a fluoroquinolone antibiotic for bone-targeted delivery to treat osteomyelitis biofilm pathogens, constitute a promising approach to providing high antimicrobial potency in bone while minimizing systemic exposure.

**Disclosures:** Parish Sedghizadeh, BioVinc, Major Stock Shareholder.

## SU0342

**The Expansion of Heterotopic Bone in Fibrodysplasia Ossificans Progressiva is Activin A-Dependent.** Sarah Hatsell<sup>\*1</sup>, Jaymin Upadhyay<sup>1</sup>, LiQin Xie<sup>1</sup>, Lily Huang<sup>1</sup>, Nanditha Das<sup>1</sup>, Rachel Stewart<sup>2</sup>, Morgan Lyon<sup>2</sup>, Kervyn Palmer<sup>2</sup>, Saathyaki Rajamani<sup>1</sup>, Chris Graul<sup>2</sup>, Merryl Lobo<sup>2</sup>, Tyler Wellman<sup>2</sup>, Edward Soares<sup>2</sup>, Matt Silva<sup>2</sup>, Jacob Hesterman<sup>2</sup>, Kalyan Nannuru<sup>1</sup>, Vincent Idone<sup>1</sup>, Andrew Murphy<sup>1</sup>, Aris Economides<sup>1</sup>. <sup>1</sup>Regeneron Pharmaceuticals, Inc., United States, <sup>2</sup>INVICRO, United States

Fibrodysplasia Ossificans Progressiva (FOP) is a rare autosomal dominant disorder that is characterized by episodic, progressive, and cumulative heterotopic ossification (HO) in tendons, ligaments, and a subset of skeletal muscles over a patient's lifetime. FOP is caused by missense mutations in the type I Bone Morphogenetic Protein (BMP) receptor-encoding gene, *ACVRI*. We have shown that HO in FOP requires activation of mutant *ACVR1* by Activin A. Activin A – a BMP/TGFβ family member which is not osteogenic – induces formation of HO in FOP mice, whereas its inhibition blocks the formation of HO. Here we extend our previous studies by piecing together a 'natural history' of developing HO lesions, and determining where in the continuum of HO Activin A is required, using imaging (T2-MRI, µCT, <sup>18</sup>F-NaF PET/CT) coupled with pharmacologic inhibition of Activin A at different times during the progression of HO in FOP mice (MGI:5763014). As disease progresses, expansion of HO lesions comes about through growth and fusion of independent HO events that tend to arise within a neighborhood of existing lesions, indicating that already formed heterotopic bone lesions likely trigger the formation of new lesions. The process appears to be dependent on Activin A, as inhibition of this ligand not only suppresses the growth (and can even cause partial regression) of nascent HO lesions but also stops the emergence of new HO events. These results provide evidence for a model where HO is triggered by inflammation, and where existing or developing HO lesions become 'self-propagating' by a process that requires Activin A. This new data extends the potential utility of prophylactic treatment with inhibitors of Activin A as a therapy for FOP that might not only stop the emergence of new lesions but also limit the growth and expansion of the heterotopic bone field in subjects with ongoing disease activity.

**Disclosures:** Sarah Hatsell, Regeneron Pharmaceuticals, Inc., Other Financial or Material Support.

## SU0343

**Efficacy of Regulatory T Cell Transplantation in a Mouse Model of Osteogenesis Imperfecta.** Inhong Kang<sup>\*</sup>, Shilpak Chatterjee, Uday Baliga, Shikhar Mehrotra, Meenal Mehrotra. Medical University of South Carolina, United States

Osteogenesis imperfecta (OI), most common hereditary bone disease, is characterized by reduction in quantity of bone matrix that leads to repeated fractures and bone deformity. Incidence of OI in United States is estimated to be 1 per 20,000 live births, but there is no cure at present. Long-term treatment with drugs, to prevent fractures, have their own side effects; therefore several strategies are being tested to enhance bone remodeling. It is known that skeletal homeostasis can be dynamically influenced by the immune system. Recent studies have shown that T lymphocytes could be essential in regulating homeostasis, survival and function of not only osteoclasts but osteoblasts as well, thus playing an important role in bone turnover. Using mice lacking functional lymphocytes, it has been demonstrated that T cells play a role in bone regeneration with fracture calluses of deficient mice exhibiting lower levels of bone markers leading to poor bone quality. A previous study also demonstrated improved bone formation after delivery of anti-inflammatory regulatory T cells (Treg's) during mesenchymal stem cell based bone regeneration. However, whether T cells, specifically Treg's, play a role in OI, a disease with high turnover and high fracture rates, has never been investigated before. For our studies we used B6C3Fe a/a-Col1a2<sup>oim</sup>/J (*oim*) model, which resembles Type III OI, a non-lethal but severe form. Characterization of T lymphocytes demonstrated that splenic T cells derived from *oim* mouse exhibited a more activated phenotype as compared to wild type (WT) T cells, which also correlated with higher secretion of effector cytokines such as IFN-γ and TNF-α. Furthermore, we also determined that *oim* mouse exhibited a quantitative decrease in CD4<sup>+</sup>CD25<sup>+</sup>Foxp3<sup>+</sup> Treg's. Enhanced improvement in the trabecular parameters was observed by Micro-CT when the *oim* mice were transplanted with WT bone marrow (BM) + WT Treg's as compared to those transplanted with WT BM alone. To determine the mechanism of how Treg's mediated the healing of bone, we examined their effects on osteoblasts and osteoclasts. Conditioned media from *ex vivo* programmed iTreg's from WT mice not only suppressed osteoclast formation, but also caused an increase in osteoblast mineralization in *oim*. Thus, understanding the contribution of Treg's to osteogenesis in OI could help to develop immunotherapy based treatment modalities for OI.

**Disclosures:** Inhong Kang, None.

## SU0344

**Functional Analysis of a Candidate of Causal Gene for Ossification of the Posterior Longitudinal Ligament of the Spine, *CDC5L*.** Shingo Maeda<sup>\*1</sup>, Masahiro Nakajima<sup>2</sup>, Ichiro Kawamura<sup>3</sup>, Yuhei Yahiro<sup>1</sup>, Hiroyuki Tominaga<sup>3</sup>, Yasuhiro Ishidou<sup>1</sup>, Eiji Taketomi<sup>4</sup>, Shiro Ikegawa<sup>2</sup>, Setsumi Komiya<sup>3</sup>. <sup>1</sup>Department of Medical Joint Materials, Graduate School of Medical and Dental Sciences, Kagoshima University, Japan, <sup>2</sup>Laboratory for Bone and Joint Diseases, Center for Integrative Medical Sciences, RIKEN, Japan, <sup>3</sup>Department of Orthopaedic Surgery, Graduate School of Medical and Dental Sciences, Kagoshima University, Japan, <sup>4</sup>Japanese Red Cross Kagoshima Hospital, Japan

Ossification of the posterior longitudinal ligament of the spine (OPLL) is a common disease characterized by abnormal hypertrophy and ossification of the posterior longitudinal ligament in the spinal canal, which causes myelopathy and radiculopathy. We found six loci associated with OPLL in a previous genome-wide association study (Nakajima M *et al*, *Nature Genet*, 46, 1012-1016, 2014). However, little is known about the susceptibility genes in these loci responsible for pathogenesis of OPLL. Here, we found that a risk allele of single nucleotide polymorphism for OPLL in *CDC5L* (Cell division cycle 5 like), a gene located within one of the GWAS loci, was associated with the expression level in cultured fibroblasts obtained from 60 normal subjects. Immunohistochemistry on formalin-fixed paraffin-embedded OPLL specimens showed that *CDC5L* was strongly expressed by stromal cells located between ossified regions, osteoblasts residing on surface of OPLL, and chondrocytic cells in the degenerated ligaments, whereas it was not detected in mature osteocytes within the ossified ligaments. *In vitro*, siRNA-mediated knockdown of *Cdc5l* in mouse ATDC5 chondrocytes suppressed the bone morphogenetic protein (BMP)-2-induced chondrogenic differentiation, while the *Cdc5l* silencing significantly promoted osteoblast differentiation of ST-2 stromal cells triggered by BMP-2. *CDC5L* is known to regulate RNA splicing by forming a complex with CTNBNB1, however, the possible roles of CTNBNB1 in metabolism of bone or cartilage is totally unclear. Expression of *Ctnnb1* was down-regulated during chondrogenic differentiation of ATDC5 cells, while induction of *Ctnnb1* siRNA in ATDC5 increased expression of chondrocyte-specific Col2a1 gene to diminish the inhibitory action of *Cdc5l* siRNA in chondrogenesis. OPLL is believed to be formed through endochondral ossification-like process. Our results suggest that *CDC5L* drives differentiation of the degenerated ligament cells to chondrocytic, while inhibits the ossification of the ligament by suppressing the maturation of osteoblastic cells. The action of *CDC5L* in chondrocytic differentiation of the ligament cells may be antagonized by interaction with CTNBNB1.

**Disclosures:** Shingo Maeda, None.

## SU0345

**PLC $\gamma$ 2 differentially modulates pro-inflammatory macrophages through DAG and Calcium pathways in arthritic complications.** Sahil Mahajan<sup>\*1</sup>, Corinne Decker<sup>1</sup>, Elizabeth Mellins<sup>2</sup>, Roberta Faccio<sup>1</sup>. <sup>1</sup>Department of Orthopedics, Washington University, School of Medicine, United States, <sup>2</sup>Department of Pediatrics, Programme in Immunology, Stanford University, United States

Macrophage activation syndrome (MAS) is a lethal complication of systemic juvenile idiopathic arthritis (sJIA). For long MAS was thought to be induced by uncontrolled T cell activation. However, presence of macrophage (M $\Phi$ ) infiltrates in liver and spleen of MAS patients and elevated M $\Phi$ -produced cytokines suggested that M $\Phi$  might also be driving disease progression.

In order to understand the role of M $\Phi$  in MAS, we employed a model involving repeated TLR9 stimulations by injecting CpG every other day for 9 days into WT mice. Similarly to MAS patients, mice developed hepatosplenomegaly, drop in blood counts, cytopenia, and showed significant expansion of monocytes and M $\Phi$  in liver and spleen. Interestingly, depletion of M $\Phi$  by delivery of clodronate liposomes ameliorated all the symptoms, indicating that M $\Phi$  are important drivers of MAS. Next, to determine the signaling pathways activated in M $\Phi$  during MAS we turned to mice lacking phospholipase C gamma 2 (PLC $\gamma$ 2), a critical mediator of inflammation in arthritic conditions. Mice lacking PLC $\gamma$ 2 in myeloid cells were protected from development of MAS, showed normal spleen and liver size and architecture, lower inflammatory cytokine levels and reduced expression of M1 pro-inflammatory M $\Phi$  markers. To further dissect how PLC $\gamma$ 2 induces M $\Phi$  activation during MAS, we evaluated two PLC $\gamma$ 2 downstream pathways, namely Ca<sup>2+</sup> and diacylglycerol (DAG). First, we turned to Tmem178, a PLC $\gamma$ 2-dependent gene whose deletion leads to higher intracellular calcium levels in M $\Phi$ . Strikingly, Tmem178<sup>-/-</sup> mice receiving CpG developed a more severe MAS syndrome and showed increased numbers of M $\Phi$  in spleen and liver. *In vitro* Tmem178<sup>-/-</sup> M $\Phi$  expressed higher inflammatory cytokine levels and M1 markers, indicating that PLC $\gamma$ 2 controls M $\Phi$  responses via Ca<sup>2+</sup> signaling. Next, to analyze the role of DAG, we used mice lacking the diacylglycerol kinase  $\zeta$  (DGK $\zeta$ ) which leads to DAG accumulation in M $\Phi$ . Surprisingly, DGK $\zeta$ <sup>-/-</sup> injected with CpG showed partial protection from MAS and reduced pro-inflammatory M $\Phi$  responses, suggesting that DAG might be antagonizing the inflammatory effects of Ca<sup>2+</sup> downstream of PLC $\gamma$ 2. Highlighting the importance of a tight regulation of Ca<sup>2+</sup> and DAG levels, exposing M $\Phi$  to plasma from sJIA patients reduced Tmem178 while enhancing DGK $\zeta$  expression to promote M $\Phi$  activation. These data demonstrate the complexity of PLC $\gamma$ 2 pathway to activate pro-inflammatory M $\Phi$  and identify PLC $\gamma$ 2/Ca<sup>2+</sup> axis as a driver of inflammation in MAS.

**Disclosures:** Sahil Mahajan, None.

## SU0346

**Pin1 as a therapeutic target in craniosynostosis.** Hye-rim SHIN<sup>\*</sup>, Han-sol BAE, Bong-su KIM, Rabia Islam, Young-dan CHO, Won-joon YOON, Kyung-mi WOO, Jeong-Hwa Baek, Hyun-mo RYOO. Seoul National University, Korea, Republic of

Craniosynostosis (CS) is defined as the premature closure of one or more craniofacial sutures. In human, gain of function mutation in FGFRs cause various skeletal diseases including CS, and Apert syndrome (AS) is one of the severest form in CS. Previously we identified that Pin1 plays a critical role in mediating FGF signal-induced craniofacial bone development. In this study, we examined a preventing effect of a Pin1 inhibitor, juglone, in AS model mice. Systemic administration of juglone remarkably restored most of the calvaria abnormalities associated with AS. Juglone treatment in primary cultured osteoblast from AS mouse calvaria attenuates hyper-activated osteogenic differentiation pattern. Juglone administration in AS mice downregulated acetylation level of Runx2 protein, that subsequently lowered transacting activity and stability of Runx2. These results indicated the importance of Pin1 enzyme activity in FGF signaling-induced Runx2 activation and craniofacial suture morphogenesis. Moreover, juglone or other Pin1 inhibitor could open a new therapeutic avenue for the intervention of hyperostotic bone diseases instead of a surgical operation.

**Disclosures:** Hye-rim SHIN, None.

## SU0347

**Characterization of Osteofibrous Dysplasia-Causing MET Mutation in Osteoblast and Osteoclast Signaling.** Ralph Zirngibl<sup>\*1</sup>, Andrew Wang<sup>1</sup>, Raymond Poon<sup>2</sup>, Benjamin Alman<sup>3</sup>, Peter Kannu<sup>2</sup>, Irina Voronov<sup>1</sup>. <sup>1</sup>Faculty of Dentistry, University of Toronto, Canada, <sup>2</sup>The Hospital for Sick Children, Canada, <sup>3</sup>Duke University, United States

Osteofibrous Dysplasia (OFD) is characterized by the bowing/fracture involving mostly the tibia and fibula by the age of 10, with characteristic fibrous lesions in the affected bones. We have identified a mutation in Met, the hepatocyte growth factor (HGF) receptor, resulting in skipping of exon 14, as a common feature in four families with the OFD. To elucidate the role of MET in OFD, using the CRISPR/Cas9 system, we have generated a mouse model mimicking human point mutation (exon 15 deletion in mouse).

Heterozygous Met <sup>$\Delta$ E15</sup> (Met <sup>$\Delta$ E15</sup>) mice are indistinguishable from wild type (WT) in gross appearance. Interbreeding of heterozygous animals failed to generate homozygous

animals due to embryonic lethality at E9.5-E10.5. Gene expression analysis of bones from Met <sup>$\Delta$ E15</sup> mice showed reduced expression of early osteoblast markers *Runx2* and *Sp7* (Osterix), as well as late markers (*Ibsp*, *Ssp1*, *Sost*). Osteoblastic differentiation of mouse bone marrow mesenchymal stem cells (BMSCs) *in vitro* was decreased in Met <sup>$\Delta$ E15</sup> BMSCs to form CFU-ALP and CFU-O; however, this defect could be partially rescued by higher cell density. Expression of *Runx2*, *Sp7*, *Alp*, *Colla1*, and *Ssp1* was also decreased in the Met <sup>$\Delta$ E15</sup> BMSCs, confirming osteoblast differentiation defect. *In vitro* Met <sup>$\Delta$ E15</sup> osteoclast formation was increased; however, the resorptive ability of a bone-like substrate was not significantly affected in Met <sup>$\Delta$ E15</sup> osteoclasts compared to the WT cells. Gene expression of osteoclast markers tartrate resistant alkaline phosphatase (TRAP) and the  $\alpha$ 3 subunit of the V-ATPase was also increased in Met <sup>$\Delta$ E15</sup> cells, supporting the increased osteoclast numbers results. Both the osteoclasts and the osteoblasts expressed *Met* and *Hgf*, and the  $\Delta$ E15-causing mutation did not have an effect on their gene expression levels. Immunoblotting demonstrated that both the wild type (WT) and the  $\Delta$ E15 protein isoforms were expressed by the osteoblasts and the osteoclasts; however, the Met protein expression levels are lower in osteoclasts and osteoblasts derived from Met <sup>$\Delta$ E15</sup> mice. Examination of the signaling pathways downstream of Met, showed increased phosphorylation levels of mTOR and p65/NF- $\kappa$ B in Met <sup>$\Delta$ E15</sup> osteoblasts and osteoclasts, respectively, suggesting aberrant receptor signaling.

These results suggest that cMET lacking exon 15 causes abnormal receptor signaling in both osteoblast and osteoclasts, providing a possible explanation for reduced bone strength observed in OFD patients.

**Disclosures:** Ralph Zirngibl, None.

## SU0348

**Pathogenesis of the Inherited Skeletal Overgrowth Disorder Caused by Activating Mutations in Natriuretic Peptide Receptor B.** Keiko Yamamoto<sup>\*1</sup>, Masanobu Kawai<sup>1</sup>, Miwa Yamazaki<sup>1</sup>, Kanako Tachikawa<sup>1</sup>, Takuo Kubota<sup>2</sup>, Keiichi Ozono<sup>2</sup>, Toshimi Michigami<sup>1</sup>. <sup>1</sup>Department of Bone and Mineral Research, Research Institute, Osaka Women's and Children's Hospital, Osaka Prefectural Hospital Organization, Japan, <sup>2</sup>Department of Pediatrics, Osaka University Graduate School of Medicine, Japan

Natriuretic peptide receptor type B (NPRB) is a receptor-type of guanylate cyclase and produces cyclic GMP when bound by natriuretic peptide type C (CNP). We previously reported the first and second families with skeletal overgrowth caused by gain-of-function mutations in NPRB, and the condition has now been established as a new disease entity named epiphyseal chondrodysplasia, Miura type (ECDM, OMIM #615923). Here we aimed to clarify the mechanism for skeletal overgrowth in ECDM, using an animal model and chondrocytic cell models. We used a transgenic mouse line where the activating mutation in NPRB (p.V883M) was expressed specifically in chondrocytes (NPRB<sup>p.V883M</sup>-Tg). Tg mice exhibit an increased production of cGMP in the cartilage and skeletal overgrowth, recapitulating the phenotype in ECDM.

Detailed histological analysis of the tibial growth plates revealed longitudinal expansion of non-proliferative zone containing prehypertrophic and hypertrophic cells in Tg compared with the control. To uncover the reason, we measured the cell size (area) of the chondrocytes in this zone. We found that the rate of small cells (area < 200  $\mu$ m<sup>2</sup>) was increased in Tg compared to the controls, although the average areas were similar. To examine the effects of NPRB activation *in vitro*, we used ATDC5 and primary mouse chondrocytes. At 0, 2, 4, 6, 8 weeks of chondrogenic induction, ATDC5 cells were treated with CNP (1  $\mu$ M) or vehicle for 48 hours, and the gene expression was analyzed. In vehicle-treated ATDC5 cells, the expression of *Cyclin D1* was peaked at 4 weeks and was declined thereafter, reflecting the exit from the cell cycle as the cells stop proliferation and become hypertrophic. Interestingly, CNP treatment at 6 and 8 weeks of culture up-regulated *Cyclin D1* to the similar level to that at 4 weeks. Western blotting revealed that phosphorylation of CREB, a transcription factor regulating *Cyclin D1*, was enhanced by a 30-min CNP treatment, when added at 6 and 8 weeks of culture. Parallel results were obtained in primary chondrocytes isolated from control mice. To confirm these findings *in vivo*, we performed immunohistochemistry and found that signals of phosphorylated CREB and Ki67 in the zone of prehypertrophic and hypertrophic chondrocytes were stronger in Tg.

In conclusion, these results suggest that activated NPRB signaling in ECDM may modulate the cell cycle at the transition from proliferation to hypertrophic differentiation, leading to skeletal overgrowth.

**Disclosures:** Keiko Yamamoto, None.

## SU0349

**Association Between Vitamin D and Frailty in Community-Dwelling Older Women.** David Buchebner<sup>\*1</sup>, Fiona McGuigan<sup>2</sup>, Patrik Bartosch<sup>2</sup>, Kristina Akesson<sup>2</sup>. <sup>1</sup>Hallands Hospital, Department of Internal Medicine, Sweden, <sup>2</sup>Lund University, Department of Clinical Science Malmö, Clinical and Molecular Osteoporosis Research Unit, Sweden

Background: Vitamin D plays an important role in various physiological functions. Frailty is a recognized geriatric syndrome with a multisystem functional decline that embodies an increased risk for negative health outcomes, but this far mostly studied in institutionalized settings.

Objective: To investigate the association of vitamin D (25OHD) and frailty in community-dwelling women aged 75 and followed for 10 years.



Methods: In the OPRA cohort at 75 years (n=1044), 80 years (n=715) and 85 (n=382), frailty was quantified using a 10-variable frailty-index including physical activity, BMI, walking speed, number of steps, muscle strength, diabetes, cancer, medications, self-reported fall risk and diseases affecting balance. The index ranged from 0 (lowest) to 1 (highest). Women were categorized as being vitamin D insufficient (<50nmol/l) or sufficient (>50nmol/l).

Results: At both ages 75 and 80, women with insufficient 25OHD were more frail compared to women with sufficient 25OHD (0.23 vs 0.18;  $p<0.001$  and 0.32 vs 0.25;  $p=0.001$ ). Insufficient 25OHD at age 80 was also associated with subsequent frailty 5 years later (0.41 vs 0.32;  $p=0.011$ ). Interestingly, accelerated progression of frailty was not associated with lower 25OHD, neither was 25OHD >75nmol/l additionally beneficial with regards to frailty.

Within the frailty-index, variables that were associated with 25OHD were those related to muscle function. 25OHD insufficient women had higher odds of having lower muscle strength (OR=1.40 [1.01-1.95];  $p=0.042$ ), being in the need of walking aids (OR=1.67 [1.04-2.68];  $p=0.032$ ), being bedbound (OR=4.13 [1.67-10.22];  $p=0.002$ ), having a lower walking speed (OR=1.94 [1.43-2.63];  $p<0.001$ ) and taking more steps to cover the same distance (OR=1.74 [1.24-2.43];  $p=0.001$ ). No association between 25OHD and frailty was observed at age 85.

Conclusions: In this prospective observational community cohort study of women aged 75, vitamin D insufficiency was associated with higher frailty score in all but the oldest old. This study lends further evidence towards the importance of maintaining sufficient vitamin D levels in healthy aging.

**Disclosures:** David Buchebner, None.

## SU0350

**High Prevalence of Sarcopenia Among Binge Drinking Elderly Women: A Nationwide Population-Based Study.** Jun-Il Yoo<sup>\*1</sup>, Dong Won Byun<sup>2</sup>, Yong-Chan Ha<sup>1</sup>, Young-Kyun Lee<sup>3</sup>, Hana Choi<sup>4</sup>, Moon-Jib Yoo<sup>4</sup>, Kyung-Hoi Koo<sup>3</sup>. <sup>1</sup>Chung-Ang University College of Medicine, Korea, Republic of, <sup>2</sup>SoonChunHyang University Hospital, Korea, Republic of, <sup>3</sup>Seoul National University Bundang Hospital, Korea, Republic of, <sup>4</sup>Dankook University College of Medicine, Korea, Republic of

**BACKGROUND:** Alcohol consumption is considered a risk factor for sarcopenia, but the association between alcohol consumption and the prevalence of sarcopenia has not been evaluated in detail. This study was to identify the relationship between alcohol drinking patterns and the prevalence of sarcopenia in the elderly Korean population. **METHODS:** The cross-sectional study was performed using data from the Korea National Health and Nutrition Examination Survey. Participants were excluded if they were under the age of 65, or if data was not available regarding skeletal muscle mass or dietary intake. After these exclusions, a total of 4,020 participants (men: 1,698; women: 2,322) were analyzed in the present study. Sarcopenia is defined according to the criteria for the Asia Working Group for Sarcopenia (AWGS). Binge drinking was defined as consuming  $\geq 5$  standard alcoholic drinks ( $\geq 4$  drinks for women) consecutively on one occasion. This data was subcategorized into two groups based on presence of binge drinking: Social drinking ( $\leq 1$  time/month) and binge drinking ( $> 1$  time/month). **RESULTS:** Women binge drinkers with weekly or daily consumption had 2.8 times higher prevalence of sarcopenia than social drinkers (Odds Ratio [OR] = 2.84; 95% Confidence Interval [CI] = 1.12-7.29). However, there were no associations between binge drinkers and sarcopenia in men. After adjusting for age, body mass index (BMI), energy intake, moderate physical activity, and energy intake, women binge drinkers with weekly or daily alcohol consumption had 3.9 times higher prevalence of sarcopenia than social drinkers (OR = 3.88; 95% CI = 1.33-11.36). **CONCLUSIONS:** The prevalence of sarcopenia in elderly women was related to binge drinking frequency and amounts of drinking after adjusting for covariates. Elderly Korean women who binge drink once or more per week may be associated with sarcopenia, as seen with the observed 3.9 times higher prevalence compared to social drinkers.

**Disclosures:** Jun-Il Yoo, None.

## SU0351

**Does PROMIS29 correlate with Frailty in hip fracture patients?.** Omer Or<sup>\*1</sup>, Joseph M. Lane<sup>2</sup>, Omar Halawa<sup>1</sup>, Eric Marty<sup>1</sup>, Rehan Sayied<sup>1</sup>, Yi Liu<sup>1</sup>, Jackie Szymonifka<sup>1</sup>, Kirsten Grueter<sup>1</sup>, Ridhi Sachdev<sup>1</sup>, Lisa A. Mandl<sup>2</sup>. <sup>1</sup>Hospital for Special Surgery, United States, <sup>2</sup>Hospital for Special Surgery, Weill Cornell Medicine, United States

**Purpose:** Hand grip strength, a well examined marker of frailty and sarcopenia, is known to predict morbidity and mortality following hip fracture and correlates with level of appendicular osteoporosis. Studies assessing grip strength on functional recovery in this setting have thus far been inadequate, often limited to a measure of ADL, such as through the Barthel Index. The Patient-Reported Outcomes Measurement Information System (PROMIS) 29 score, developed by the NIH, is a reliable measure of seven important health status domains encompassing physical, mental, and social health. In contrast to grip strength, the PROMIS-29 can easily be administered to any hospitalized patient without need for equipment or special training. This study tests the hypothesis that physical function PROMIS-29 domains correlate with grip strength at baseline, and sought to examine if grip strength was independently predictive of 3 month functional recovery following hip fracture.

**Methods:** We prospectively enrolled consecutive patients admitted to a tertiary medical center from January 2016-January 2017 who underwent surgical repair of a

low-trauma hip fracture. Patients with active cancer, dementia, or age < 65 were excluded from the study. Hand grip strength was assessed 2 days post-operatively using the JAMAR Hydrolic Hand Dynamometer (Lafayette Instruments) with scores normalized for age and gender. PROMIS-29 and the Lower Extremity Activity Scale (LEAS) were collected upon admission and re-administered 3 months post-operatively. Linear regression and Spearman correlation were performed using SAS version 9.4. Two-tailed p-values < 0.05 were considered significant.

**Results:** Of 84 patients enrolled, 57 completed 3-month follow-up. Three patients had died, 5 withdrew consent, 6 were lost to follow up, 2 refused and 11 will be contacted at 12 months follow up. The mean age was 80 years and 75% were female. Mean BMI was 22.9 kg/m<sup>2</sup>. Median length of stay was 5 days. Mean grip strength Z score at 3-months was -2.65  $\pm$  0.65. There was no significant correlation between baseline grip strength to baseline PROMIS 29, change in PROMIS 29 domains or LEAS at 3 months: Physical Function ( $\rho=0.119$ ), Ability to Participate in Social Roles ( $\rho=0.073$ ), Fatigue ( $\rho=0.150$ ), Anxiety ( $\rho=0.255$ ), Depression ( $\rho=0.261$ ,  $p<0.059$ ), Pain Interference ( $\rho=0.143$ ), Sleep Disturbance ( $\rho=0.019$  or LEAS ( $\rho=-0.134$ ) (all  $p>0.059$ ).

**Conclusion:** No association was seen between grip strength and PROMIS-29 physical function domain at baseline. These findings suggest that the PROMIS-29 appear to measure different constructs than those encapsulated by grip strength. Additionally, there were no correlations between grip strength and change in any PROMIS29 functional domains or change in LEAS function. While hand grip strength is a known predictor of mortality and morbidity following hip fracture, it doesn't predict self-reported short-term functional recovery after surgical repair of low trauma hip fracture. The clinical utility of PROMIS-29 in the hip fracture setting requires further delineation. We will continue to study these patients up to 1-year post-operatively.

**Disclosures:** Omer Or, None.

## SU0352

Withdrawn

## SU0353

**A Multifaceted Intervention Improves Functional Fitness in Pre-frail/frail Seniors: Results from the TAPESTRY-TRIAGE Study.** Courtney Kennedy<sup>\*</sup>, George Ioannidis, Larkin Lamarche, Doug Oliver, Lisa Dolovich, Sarah Radcliffe, Aidan Giangregorio, Alexandra Papaioannou, McMaster University, Canada

**Introduction:** Functional movement (e.g. walking, standing up, climbing stairs) is critical to maintaining independence in everyday activities and requires sufficient reserves in underlying physiological parameters. In this analysis, we assessed changes in functional movement tasks that are required for everyday activities in older adults who completed a 6-month multifaceted frailty prevention intervention.

**Methods:** Tapestry-TRIAGE was a feasibility study aiming to delay frailty and improve quality of life in community-dwelling participants identified as at risk by primary care. The 6-month intervention consisted of several tailored components including an in-home exercise prescription incorporating endurance, resistance, and balance training with monthly visits that included cognitive-behavioural coaching. Medications and nutritional status were reviewed with follow-up appointments (pharmacist, family physician, dietitian) as indicated (e.g. stopping inappropriate medications, dose changes, nutrition counseling). Physical assessments performed at baseline and 6-months by a registered kinesiologist included the Senior Fitness Test (SFT; Rikli & Jones 2001), a well-validated and reliable tool that measures underlying physiological parameters (strength, endurance, balance, agility, flexibility) using functional movements (standing, bending, lifting, reaching and walking). We categorized our cohort based on SFT criterion-referenced cut-points with individuals falling above the threshold value considered in the "risk zone" for mobility loss.

**Results:** We enrolled 44 older adults; 33 individuals (aged 71 to 95 years, mean=79.8, SD=6.9; 61% women; mean BMI 28.2, SD=4.3) who completed both baseline/6-month assessments are included in this analysis. All individuals lived in a house/apartment and 47% lived alone. At baseline, 15% were frail and 73% pre-frail based on the Fried Frailty Phenotype. Improvements in the percentage of individuals categorized as at risk occurred over 6-months for 8-foot Up and Go, arm curls, chair stands, and steps in 2-min (Table).

**Conclusion:** Pre-frail/frail individuals are at high risk of further decline and are an important group to target interventions for maintaining independence in functional activities. The SFT provides detailed information for evaluating specific aspects of physical and functional fitness, which can assist in developing targeted interventions.

	Baseline	6-months
8-foot Up-and-Go (Agility/dynamic balance)	16 (49%)	11 (33%)
Number of arm curls in 30 sec (Upper body strength)	9 (27%)	1 (3%)
Number of chair stands in 30 sec (Lower body strength)	4 (12%)	1 (3%)
Number of steps in 2 min (Aerobic endurance)	11 (33%)	6 (19%)
Chair Sit-and-Reach (Lower body flexibility)	11 (34%)	14 (42%)

Number of participants in the Risk Zone for loss of functional mobility (n=33)

**Disclosures:** Courtney Kennedy, None.

## SU0354

**Spinal Alignment, Muscular Strength, and Quality of Life in Postmenopausal Osteoporosis: A Cross-sectional Comparative Study with Healthy Volunteers.** Naohisa Miyakoshi\*, Daisuke Kudo, Michio Hongo, Yuji Kasukawa, Yoshinori Ishikawa, Yoichi Shimada, Department of Orthopedic Surgery, Akita University Graduate School of Medicine, Japan

**Introduction:** Vertebral fractures, as the most common osteoporotic fractures, induce spinal kyphosis in patients with osteoporosis and increased spinal kyphosis leads to decreased quality of life (QOL). Muscular strengths are also an important factor for QOL in patients with osteoporosis. However, spinal kyphosis and muscle weakness also occur in healthy individuals with advancing age. Although QOL may differ between patients with osteoporosis and healthy individuals, no comparative studies focusing on spinal alignment and muscular strength in patients with osteoporosis and healthy individuals have been reported. The purpose of the present study was therefore to compare spinal alignment, muscular strength, and QOL between women with postmenopausal osteoporosis and healthy volunteer women.

**Methods:** Subjects comprised 236 consecutive patients with postmenopausal osteoporosis (osteoporosis group; mean age, 68.7 years), and 93 volunteer women who had willingly participated in this study (volunteer group; mean age, 71.0 years). Most participants in the volunteer group had been engaged in labor related to agricultural activities since they were young. Body mass index (BMI), angles of spinal kyphosis, back extensor strength, grip strength, and QOL were evaluated and compared between groups. QOL was assessed using the 36-Item Short-Form Health Survey (SF-36).

**Results:** BMI, back extensor strength, and grip strength were significantly higher in the volunteer group than in the osteoporosis group ( $p < 0.01$ ). Both thoracic kyphosis and lumbar lordosis were significantly higher in the osteoporosis group than in the volunteer group ( $p < 0.01$ ). The SF-36 subscale scores of role physical (RP), bodily pain (BP), general health (GH), role emotional (RE) were significantly lower in the osteoporosis group than in the volunteer group with both regular scoring and norm-based scaling ( $p < 0.05$ ). In the SF-36 summary score, physical component summary (PCS) was significantly lower in the osteoporosis group than in the volunteer group ( $p < 0.001$ ).

**Conclusions:** The results indicated that compared to healthy volunteers, the lower QOL (particularly in relation to pain, health, emotional status, and physical activity) in osteoporosis patients may be related to increased thoracic kyphosis, lean muscle mass, and generalized muscle weakness.

**Disclosures:** Naohisa Miyakoshi, None.

## SU0355

**Determinants of bone mineral density and insulin resistance: Area, strength or composition of muscle?** Hye-Sun Park<sup>\*1</sup>, JungSoo Lim<sup>2</sup>, Yumie Rhee<sup>3</sup>, Han Seok Choi<sup>4</sup>, Sung-Kil Lim<sup>1</sup>. <sup>1</sup>Division of Endocrinology and Metabolism, Department of Internal Medicine, Yonsei University College of Medicine, Korea, Republic of, <sup>2</sup>Division of Endocrinology and Metabolism, Department of Internal Medicine, Yonsei University Wonju College of Medicine, Korea, Republic of, <sup>3</sup>Department of Internal Medicine, Endocrine Research Institute, Severance Hospital, Yonsei University College of Medicine, Korea, Republic of, <sup>4</sup>Division of Endocrinology and Metabolism, Department of Internal Medicine, Dongguk University Ilsan Hospital, Korea, Republic of

Sarcopenia is a syndrome which is characterized by decreased muscle mass, strength and physical performance. It couples with functional deteriorations such as frailty, fracture, metabolic dysfunction, and high morbidity and mortality rate. And sarcopenia is also known to be related to osteoporosis and type 2 diabetes. However, it is unclear which muscle measurement is the main contributing factor. We measured muscle cross sectional area (CSA), attenuation (Hounsfield unit, HU) and strength, to get the insight of the relative importance of muscle measurements for development of low bone mass and insulin resistance. One hundred ninety-two postmenopausal women aged 60 years and older were enrolled and muscle CSA, attenuation and bone mineral density (BMD) were obtained from quantitative computed tomography. In addition, muscle strength was measured by hand grip test and physical performance by short physical performance battery (SPPB). The muscle CSA, handgrip strength and SPPB score revealed a positive correlation with spine and hip BMDs, but not with insulin resistance. In contrast, the muscle attenuation (HU) of gluteus or quadriceps was inversely related to HOMA-IR ( $r = -0.194$ ,  $p = 0.018$  and  $r = -0.292$ ,  $p < 0.001$ , respectively), but not related to BMD. Compared to the control group, muscle CSA, hand grip strength and SPPB score were significantly decreased in patients with osteoporosis; however, the HU of muscle was decreased only in patients with diabetes, which means high fat infiltration. Taken together, muscle mass, muscle strength and physical performance are associated with low bone mass, whereas the accumulation of intramuscular fat, a histological hallmark of persistently damaged and inflamed muscles, may play a major role in developing insulin resistance.

**Disclosures:** Hye-Sun Park, None.

## SU0356

**Vitamin D and Falls in Older African American Women - the PODA trial.** Rakhil Rubinova<sup>\*1</sup>, Mageda Mikhail<sup>1</sup>, Melissa Fazzari<sup>1</sup>, Ruban Dhaliwal<sup>2</sup>, Subhashini Katumuluwa<sup>1</sup>, John Aloia<sup>1</sup>. <sup>1</sup>NYU Winthrop Hospital, United States, <sup>2</sup>SUNY Upstate Medical University, United States

Falls are a major health problem in the elderly. The prevalence of fall rates varies and has been reported to be up to 46% annually in elderly women. Data suggests that fallers have a 52% chance of falling during the next year. Association studies have related the incidence of falls to reduced serum levels of vitamin D. African Americans are known to have reduced vitamin D levels.

We designed a randomized, double blind, placebo controlled trial PODA (Physical Performance and Osteoporosis prevention with Vitamin D in older African Americans) to assess the effects of vitamin D supplementation in African American elderly women on fall prevention.

Two hundred and sixty African American women with mean age of  $68.5 \pm 4.9$  years, were randomized to receive placebo ( $n=130$ ) or vitamin D ( $n=130$ ) supplementation and followed for 36 months. Serum vitamin D in the treatment group was maintained above 75 nmol/L with average serum level of  $94 \pm \text{nmol/L}$  vs  $51.7 \pm 20 \text{ nmol/L}$  in placebo group. Calcium supplements were provided to ensure a total calcium intake of 1200 mg/day in both groups. All participants at baseline were provided with fall questionnaires, which asked if they had fallen in the last year. For all subsequent visits, every 3 months, participants were asked if they had fallen since the previous visit.

Participants were classified as fallers or non-fallers based on whether they reported a fall at a particular visit. 14.2% of participants reported having fallen within the past year (13.1% in the placebo group, 15.4% in the vitamin D group). A total of 49.4% of participants reported one or more falls during follow up. Baseline faller status (fallen within the year prior to starting the study) was strongly associated with subsequent falls during the study ( $p \text{ value} = 0.001$ ). The fall rates were 35 per 100 patient years in the placebo group vs 31 per 100 patient years in the treatment group. A logistic regression model was estimated, adjusting for baseline fall status, treatment group, study time, and interaction between the group and time; there was no effect of vitamin D supplementation on the fall rate ( $p \text{ value} = 0.42$ ).

Higher serum concentrations of vitamin D 25OH have been associated with both decreased and increased risk of recurrent falls in the elderly. In our study we did not see any protection against falls in either group of elderly African American women.

**Disclosures:** Rakhil Rubinova, None.

## LB-SU0357

**Analysis of GCM2 Sequence Variants in Sporadic Parathyroid Adenomas.** Aaliyah Riccardi<sup>\*1</sup>, Taylor Brown<sup>2</sup>, Reju Korah<sup>2</sup>, Timothy Murtha<sup>2</sup>, Justin Bellizzi<sup>1</sup>, Kourosh Parham<sup>3</sup>, Tobias Carling<sup>2</sup>, Jessica Costa<sup>1</sup>, Andrew Arnold<sup>1</sup>. <sup>1</sup>Center for Molecular Medicine, University of Connecticut School of Medicine, United States, <sup>2</sup>Yale Endocrine Neoplasia Laboratory, Yale School of Medicine, United States, <sup>3</sup>University of Connecticut School of Medicine, United States

Sporadic (nonfamilial) solitary parathyroid adenoma is the most common cause of primary hyperparathyroidism (PHPT), and established pathogenetic drivers include somatic alterations in *MEN1* and *CCND1*. However, apart from germline variants in certain cyclin dependent kinase inhibitor genes, and occasionally *MEN1* or *CASR*, little is known about possible genetic variants in the population that may confer increased risk for development of typical sporadic adenoma. Transcriptionally activating germline variants in the C-terminal conserved inhibitory domain (CCID) of *GCM2*, encoding a transcription factor required for parathyroid gland development, were recently reported in familial isolated hyperparathyroidism (FIHP) (Guan et al., 2016), and appear to be especially enriched in FIHP kindreds of Ashkenazi Jewish background (Guan et al., 2017). Identical *GCM2* CCID variants were also identified in over 5% of patients with sporadic PHPT but this group included many cases of multiple gland disease; another study revealed a single *GCM2* variant among 30 sporadic adenomas (Mannstadt et al., 2011). To evaluate the potential role of *GCM2* CCID activating variants specifically in a large series of solitary sporadic parathyroid adenomas, we PCR amplified and Sanger sequenced the *GCM2* CCID-encoding region in genomic DNA from 385 tumors. Variants were identified in 3 of the 385 (.78%) adenomas, two containing the Y394S variant (confirmed as germline in the one patient with available matched germline DNA), and one with V382M, also confirmed as germline. This 0.78% frequency is not significantly different from 0.61%, the frequency in the unselected general population of the previously implicated CCID variants, according to the gnomAD database (Fisher Exact Test  $p = 0.51$ ). We conclude that variants in the *GCM2* CCID are rarely found in otherwise unselected patients with common solitary sporadic adenoma, and their frequency in this group may not exceed that in the general population. The potential roles of *GCM2* variants in sporadic adenomas may be different from those in sporadic multigland hyperparathyroidism and FIHP.

**Disclosures:** Aaliyah Riccardi, None.



## LB-SU0358

**Precision assessment of cortical thickness and volumetric bone mineral density derived from hip DXA scans using 3D DXA.** Ludovic Humbert<sup>\*1</sup>, Alejandro Hinojosa<sup>1</sup>, Edu Cortés<sup>1</sup>, Josep Potau Gines<sup>2</sup>, Luis Del Rio<sup>3</sup>, Renaud Winzenrieth<sup>1</sup>. <sup>1</sup>Galgo Medical SL, Spain, <sup>2</sup>Laboratorio de Anatomia, Hospital Clinic, Spain, <sup>3</sup>Cetir Grupo Medic, Spain

**Objective:** The aim of this study is to evaluate precision at the femur of the mean cortical thickness (Cth) and the volumetric BMD in the trabecular, cortical and integral compartments (vBMDtrab, vBMDint and vBMDcort) derived from hip DXA scans using cadaveric pieces and patients.

**Methods:** DXA scans were done at CETIR Centre Mèdic (Barcelona, Spain) using a GE-Lunar iDXA. 10 dried human femurs were obtained from the anatomical laboratory of the Hospital Clinic (Barcelona, Spain). The femurs were scanned using a soft tissue kit of 19cm water equivalent tissue thickness, 4 times a row without repositioning. In addition, 30 patients (90% women, mean age  $65 \pm 12$  years) were acquired two times a row with complete repositioning on the same DXA device. Finally, 55 post-menopausal women ( $66 \pm 5.7$  years) were recruited to evaluate the monitoring time intervals. DXA scans were obtained at baseline and at 12 months. 3D models were derived from hip DXA scans using 3D-DXA software (v2.3, Galgo Medical SL, Spain). The root-mean-square standard deviation (RMS-SD) and the LSC at 95% were computed for areal BMD at total femur (aBMDtot) and femoral neck (aBMDfn) and for the 3D measurements (Cth, vBMDtrab, vBMDcort, vBMDint). Monitoring time intervals were computed by dividing LSC values by the median change per annum.

**Results:** Ex- and in-vivo RMS-SD values are presented table 1. As expected, in-vivo RMS-SD were higher than those obtained ex-vivo. Interestingly, RMS-SD for Cth and vBMDcort are similar ex- and in-vivo. Monitoring time intervals were similar for DXA-derived [4.8 – 5.5 yrs] and 3D-DXA-derived measurements [3.6 – 7.0 yrs].

**Conclusions:** We observed minor differences between precision errors obtained with ex-vivo samples and in-vivo whatever the considered parameter. This implies that patient's positioning as well as soft tissues heterogeneity have few impacts on 3D-DXA measurements. These results suggest that 3D-DXA measurements could be used to monitor bone status in postmenopausal women.

RMS-SD	aBMDtot (g/cm <sup>2</sup> )	aBMDfn (g/cm <sup>2</sup> )	Cth (mm)	vBMDcort (g/cm <sup>3</sup> )	vBMDint (g/cm <sup>3</sup> )	vBMDtrab (g/cm <sup>3</sup> )
ex-vivo	0.0056 (0.0155)	0.0089 (0.0247)	0.02 (0.06)	0.0049 (0.0134)	0.0026 (0.0073)	0.0028 (0.0078)
in-vivo	0.0083 (0.0242)	0.0091 (0.0253)	0.02 (0.06)	0.0048 (0.0133)	0.0034 (0.0095)	0.0032 (0.0089)
in-vivo Monitoring Time Interval (yrs)	4.8	5.5	5.4	7.0	3.6	5.2

Table 1: Data are presented as RMS-SD (LSC 95%)

**Disclosures:** Ludovic Humbert, Galgo Medical, Major Stock Shareholder.

## LB-SU0359

**Bone phenotype of human immune system engrafted mice.** Tiina E Kähkönen<sup>\*1</sup>, Mari I Suominen<sup>1</sup>, Jussi M Halleen<sup>1</sup>, Azusa Tanaka<sup>2</sup>, Michael Seiler<sup>2</sup>, Jenni Bernoulli<sup>1</sup>, Jukka Morko<sup>3</sup>. <sup>1</sup>Pharmatest Services Ltd, Finland, <sup>2</sup>Taconic Biosciences, United States, <sup>3</sup>Pharmatest Services Ltd, United States

Human immune system engrafted mouse models have provided a promising opportunity to study therapeutic interventions requiring functional human immune system. These humanized mice are produced by myeloablation, reducing the number of mouse bone marrow cells and replacing them with human hematopoietic stem cells (hHSCs) that are progenitors of human immune cells, and also for example of bone resorbing osteoclasts. As the normal bone marrow homeostasis is disturbed in this process, concern arises if the bone phenotype is maintained. Though humanized mice have been widely used, there are no publications of their bone phenotype. The aim of this study was to characterize the bone phenotype of the humanized mice.

Twenty-five weeks old humanized female CIEA NOG mice (huNOG: HSCFTL-NOG-F, provided by Taconic Biosciences) were used in the study, and age-matched CIEA NOG mice served as controls. Maturation of hHSCs to CD45+ cells was confirmed by flow cytometry. The presence of T (CD3+) and B (CD20+) cells in the bone marrow of hind limbs was confirmed by immunohistochemistry accompanied by basic histological stainings. Cortical and trabecular bone volumes of tibia were analyzed by micro-computed tomography (μCT), and bone mineral density (BMD) and content (BMC) were analyzed by dual X-ray absorptiometry (DXA). Serum bone turnover markers were measured by ELISA methods.

Between 60-80% of circulating cells were CD45+, and these cells were also present in the bone marrow with T- and B-cells. Some mice had fibrotic areas in their bone marrow but this was observed only in a small proportion of the mice. Despite of the fibrosis, immune cells were present in the marrow. The humanized mice had unaltered BMD and BMC. Cortical bone volume was unchanged but trabecular bone volume, number and thickness showed a slight but non-significant increase in the humanized mice. Serum levels of the bone formation marker PINP were lower in humanized mice. The number of osteoclasts was slightly but non-significantly lower in humanized mice, correlating with serum levels of TRACP5b.

Human immune cells colonize the mouse bone marrow after myeloablation in the human immune system engrafted mice. Bones of the humanized mice did not exhibit significant changes compared to the immunodeficient NOG mice. These results support the use of humanized mice also in studies focusing on bone function.

**Disclosures:** Tiina E Kähkönen, None.

## LB-SU0360

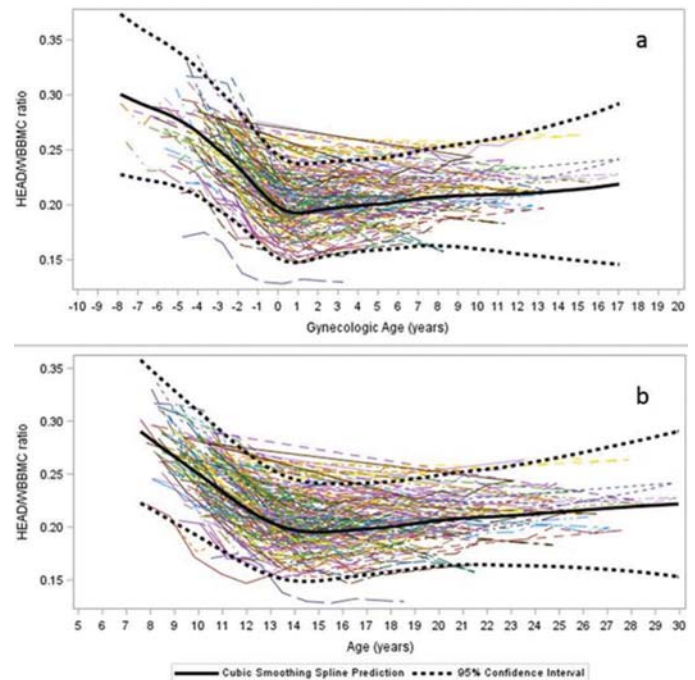
**In US Females, Adult Proportions of Head to Whole Body Bone Mass Ratio Stabilize Early, Allowing Evaluation of Whole Body BMC from Age 12 years, or Menarche, Onward.** Jodi N. Dowthwaite<sup>\*1</sup>, Stephanie A. Kliethermes<sup>2</sup>, Tamara A. Scerpella<sup>2</sup>. <sup>1</sup>SUNY Upstate Medical University, United States, <sup>2</sup>University of Wisconsin- Madison, United States

**Purpose:** In pediatrics, evaluation of DXA whole body bone mass “less head” (SUBBMC) is recommended to circumvent the problem of excessive contribution of HEADBMC to whole body bone mass (WBBMC) during childhood. However, use of SUBBMC inflates inter-scan variation and least significant change, due to subdivision variation. Thus, we evaluated female pediatric longitudinal data for HEAD/WBBMC ratios across growth to determine minimum appropriate age/maturity thresholds for transition to use of WBBMC based on achievement of adult proportions.

**Methods:** Whole body DXA scans were performed (Hologic, Waltham, MA: QDR 4500W (QDR) 1998 – 2010; Discovery A (DISCO) 2008-2017), using DISCO data preferentially. QDR data were converted to DISCO “equivalent” data for calculation of HEAD/WBBMC, using a developmentally appropriate regression equation (n=132: duplicate scans, age 8-24 years). Chronological and gynecological age-based curves for HEAD/WBBMC were generated using cubic smoothing spline functional mixed effects models.

**Results:** Girls with  $\geq 3$  annual scans were included (mean(SD)=8(3.3); range=3 to 19 scans), representing age 7 to 30 years (baseline age: mean(SD)=10.3(1.5); final age: mean(SD)=18.2(4.2) yrs). Individual and mean growth curves are presented by gynecological and chronological age [Figure 1a,b]. The mean of intra-individual means for HEAD/WBBMC ratio pre-menarche was 0.227 (n=129; 95% CI 0.223-0.232). The mean of intra-individual means post-menarche was 0.198 (n=125; 95% CI= 0.194-0.202). The mean of intra-individual means before age 10 years was 0.264 (n= 65; 95% CI= 0.257-0.271). From age  $\geq 18$  years, “adult” mean of means was 0.204 (n=66; 95% CI= 0.198-0.210). Adult intra- and inter-individual variation was high, with the mean ratio rising from 4 years post-menarche onward, such that the mean ratio at chronological age 22 years was 0.21 (n= 34; 95% CI=0.202-0.218). Overall, individual ratios stabilized to adult mean levels circum-menarche (closest scan to menarche +/-1 year gynecological age, n=124: mean= 0.198; 95% CI= 0.194-0.202), and the minimum age for which 95% CI overlapped broadly with adult values was 12 years (n= 120: mean=0.211; 95% CI= 0.207-0.216).

**Conclusion:** In girls, WBBMC may be used instead of SUBBMC from age 12 years or menarche onward, to minimize effects of scan subdivision on data quality. Continued longitudinal data collection for girls currently <10 years post-menarche (n>60) will improve adult pattern evaluation.



**Disclosures:** Jodi N. Dowthwaite, None.

## LB-SU0361

**Female mice are protected from the osteolytic effect of IAP antagonists, independent of estrogen.** Allahdad Zarei\*, Jesse Gibbs, Chang Yang, Jennifer Davis, Anna Ballard, Linda Cox, Deborah V. Novack. Washington University School of Medicine, United States

There are substantial differences in bone mass between male and female sexes, largely attributed to sex hormones. We have previously identified the alternative NF- $\kappa$ B pathway as a regulator of osteoclasts (OCs) that is stimulated by IAP antagonists, a class of drug with anti-cancer activity. In this study, we asked whether manipulation of alternative NF- $\kappa$ B, genetically or pharmacologically, has sexually dimorphic effects in mice.

Disruption of alternative NF- $\kappa$ B mediated by loss of NIK or RelB causes sexually dimorphic effects on bone mass. In both NIK and RelB KO, female mice (10 wk) possessed 2.5-fold higher BV/TV compared to female WT, whereas no differences were observed in males. *In vitro*, female RelB and NIK KO precursors showed a more severe OC differentiation defect than male in response to RANKL, while WT had no sex difference. We previously found that IAP antagonist BV6 increased OCs and reduced bone mass, and enhanced osteolytic metastasis in WT male mice. Based on the sex difference in the KO mice, we asked whether the effect of BV6 on bone was sex-dependent, treating cohorts (n=8) of male and female BALB/c mice with BV6 or vehicle for 4 weeks. Unlike male mice which lose bone, female mice on BV6 show no changes in osteoclast number or BV/TV. *In vitro*, marrow macrophages derived from both sexes show similar increases in OC number in response to BV6+ RANKL. Since estrogen suppresses NF- $\kappa$ B, we hypothesized that estrogen protects bone from BV6 effects *in vivo*. Thus, we performed ovariectomy (OVX) or sham surgery in female mice, treated with BV6 or vehicle for 4 weeks following surgery (n=10). Significant reduction in tibial BV/TV occurs in both OVX groups compared to sham. However, no significant differences in any bone parameters are observed between OVX/vehicle and OVX/sham groups, suggesting that the sexual dimorphism is not caused by estrogen.

In summary, the bone phenotype in models of alternative NF- $\kappa$ B modulation is distinct in male and female mice. Intriguingly, under basal conditions absence of signaling via ablation of NIK or RelB increases bone mass only in females, while pharmacologic stimulation of the pathway with BV6 causes bone loss only in males. Reduction of estrogen with OVX did not restore responsiveness to BV6 in females, suggesting that the observed sexual dimorphism has a unique mechanism, and further work is needed to determine the relative risk for bone metastasis in male and female patients treated with IAP antagonists.

**Disclosures:** Allahdad Zarei, None.

## LB-SU0362

**Measurement of lower extremity muscle by HR-pQCT: comparison between distal and diaphyseal sites, pQCT, lean mass by DXA, and physical performance.** Andrew Burghardt<sup>1</sup>, Nicolas Vilaythi<sup>2</sup>, Elsa S Strotmeyer<sup>3</sup>, Paolo Caserotti<sup>4</sup>, Deborah Kado<sup>5</sup>, Iva Miljkovic<sup>3</sup>, Peggy M Cawthon<sup>1</sup>, Dennis M Black<sup>1</sup>, Sharmila Majumdar<sup>1</sup>, Jane A Cauley<sup>3</sup>, Eric S Orwoll<sup>6</sup>. <sup>1</sup>University of California, San Francisco, United States, <sup>2</sup>Scanco Medical AG, Switzerland, <sup>3</sup>University of Pittsburgh, United States, <sup>4</sup>University of Southern Denmark, Denmark, <sup>5</sup>University of California, San Diego, United States, <sup>6</sup>Oregon Health & Science University, United States

High resolution peripheral quantitative computed tomography (HR-pQCT) has been used to measure myotendinous tissue volume and density at the distal extremity of the lower leg. The current iteration of HR-pQCT (XtremeCT II, Scanco Medical) can image more proximal regions, including the tibial diaphysis. The increased proximal coverage may allow measurement of a more reliable surrogate of muscle. Our objective was to (1) adapt a soft tissue analysis pipeline to measure muscle at the distal and 30% diaphyseal tibia from second generation HR-pQCT images; and (2) evaluate the relationship between soft tissue measures at the distal and diaphyseal sites, to other muscle and physical function measures, and to bone measures. We used data from the Osteoporotic Fractures in Men (MrOS) study, which included 118 subjects (age: 84.2±4.0yrs) who had acceptable HR-pQCT scans of the distal and diaphyseal tibia (Fig. 1), pQCT of the 66% tibia, DXA, and force-plate muscle power data. Pearson correlations were calculated to evaluate associations between muscle volume fraction (MVf; ratio of muscle volume (MV) to muscle plus inter- and intra-muscular fat volume) and muscle density (MD; mean intensity of the muscle and intra- and inter-muscular fat volume) by HR-pQCT with analogous measures from pQCT, leg lean mass % by DXA (LLM%=(Lean/(Lean+Fat))), and peak power (normalized by weight) for a jump test measured by force plate dynamometry. Bone density, structure, and failure load by  $\mu$ FEA were calculated for both scans. MVf ranged from 34 to 92% at the diaphysis, and from 27 to 88% at the distal site. Associations between pQCT and HR-pQCT measures of MVf and MD were stronger for the diaphyseal site (Table 1). MVf was more strongly associated with LLM% (r=0.58-0.70), while MD was moderately associated with muscle power (r=0.44-0.55). No significant correlations were observed between HR-pQCT muscle measures and bone microstructure. Weak correlations between MD and Ct.BMD were found (r=0.20-0.33), and between MV and Ct.Th (p=0.24-0.27). Distal tibial estimated failure load was also weakly correlated with diaphyseal muscle measures (r=0.25-0.34). In conclusion, measurement of muscle volume fraction and density is feasible using 2nd generation HR-pQCT. Muscle volume is strongly related to leg lean mass while density is more related to muscle power. Compared to the distal site, diaphyseal HR-pQCT muscle measures were generally better predictors of the reference muscle outcome measures.

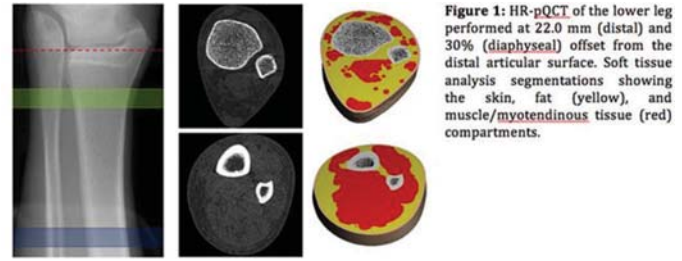


**Figure 1:** HR-pQCT of the lower leg performed at 22.0 mm (distal) and 30% (diaphyseal) offset from the distal articular surface. Soft tissue analysis segmentations showing the skin, fat (yellow), and muscle/myotendinous tissue (red) compartments.

**Table 1.** Mean HR-pQCT muscle volume fraction and density; Pearson correlation coefficients for comparisons of HR-pQCT muscle measures at the 30% diaphyseal (top rows) and distal (bottom rows) tibia, with pQCT at 66% tibia, leg lean mass by DXA, and peak power for a jump test. \*\* p<0.0001, \* p<0.001.

		Units	Mean $\pm$ SD	Distal HR-pQCT	pQCT 66% Tibia	DXA LLM%	Force Plate Peak Power/kg
Diaphyseal HR-pQCT	MVF	[%]	71 $\pm$ 10	0.69**	0.75**	0.70**	0.39**
	MD	[mg/cm <sup>3</sup> ]	10.7 $\pm$ 4.1	0.68**	0.58**	0.41**	0.44**
Distal HR-pQCT	MVF	[%]	60 $\pm$ 12	-	0.52**	0.58**	0.31*
	MD	[mg/cm <sup>3</sup> ]	-6.9 $\pm$ 6.3	-	0.49**	0.38**	0.55**

**Disclosures:** Andrew Burghardt, None.

## LB-SU0363

**Loss of sex steroids attenuates traumatic heterotopic ossification.** Semahat Serra Ucer\*, Charles Hwang, Anita Vaishampayan, Michael T. Chung, John Li, Chase Pagani, Joe Habbouche, Shuli Li, Benjamin Levi. University of Michigan, United States

Up to 20% of the patients who have experienced mechanical trauma, burns or hip replacement surgery develop pathologic extraskelatal bone formation or heterotopic ossification (HO). HO is an endochondral ossification process initiated by acute inflammation. Sex steroids are well-demonstrated to play role in different stages of heterotopic bone formation including inflammation, chondrogenesis and osteogenesis. Clinical observations demonstrated that male patients are more predisposed to formation of heterotopic ossification (HO) compared to female patients. This finding was also recapitulated in mouse models with trauma-induced HO formation (Ranganathan et al. PRSJ 2015). These observations raised the possibility of sex steroids contributing to HO formation. To explore the effects of estrogen on HO formation, 7-week old C57BL/6J male mice were sham-operated or orchidectomized (depletion of sex steroids). Two weeks after the surgery, mice underwent through Achilles' tendon transection and dorsal burn injury which causes trauma-induced HO formation (Agarwal et al. PNAS 2016). Mice were either sham (with vehicle injection) or orchidectomy operated (vehicle or estradiol injection) daily for nine weeks. In mice, loss of sex steroids attenuated burn tenotomy associated floating, but not bone associated ectopic bone formation. Administration of estrogen (30 ng/g) was sufficient to promote both floating and bone associated ectopic bone formation to at least pre-orchidectomy levels. These findings demonstrate that actions of androgens are only required for acting on a subpopulation of cells which give rise to floating HO, but not bone associated HO. Notably, these results suggest cellular and molecular mechanisms for the formation of floating versus bone associated HO are distinct.

**Disclosures:** Semahat Serra Ucer, None.

## LB-SU0364

**Wnt Signaling Inhibitor Characteristics According to Bone Status and Physical Activity Levels in Young and Middle-aged Premenopausal Women.** Pragya Sharma Ghimire\*, Samuel Buchanan<sup>1</sup>, Debra Bembel<sup>1</sup>, Michael Bembel<sup>1</sup>, Allen Knehans<sup>2</sup>, Jason Campbell<sup>1</sup>. <sup>1</sup>The University of Oklahoma, United States, <sup>2</sup>The University of Oklahoma Health Sciences Center, United States

Sclerostin and Dickkopf-1 (DKK-1) are the novel markers of bone metabolism and could be considered valuable tools to investigate the mechanisms of bone remodeling. Although the mechanism of the Wnt signaling pathway and its inhibitors on bone biology has been well studied, only sparse data are available in humans, especially related to age and physical activity differences in circulating levels of sclerostin and DKK-1. The primary purpose of this study was to compare serum concentrations of sclerostin and DKK-1 in young and middle-aged premenopausal women. These age groups were selected to allow comparisons between women who are still accruing bone mass versus those who have already achieved their peak bone mass. We also evaluated differences in sclerostin concentrations based on physical activity status assessed by the International Physical Activity Questionnaire: low- moderate and health enhancing physical activity (HEPA-active). In this non-randomized cross-sectional study, 50 young (n=25) and middle-aged (n=25) women participated and completed all protocols. Fasting morning blood samples were analyzed for serum sclerostin, DKK-1, and follicle-stimulating hormone (FSH). Total body, lumbar spine and dual femur aBMD



and BMC were measured using DXA, and tibia bone characteristics were assessed using pQCT at 4%, 38%, and 66% sites. Middle-aged women had significantly ( $p < 0.01$ ) higher ( $0.54 \pm 0.01$  ng/ml) serum sclerostin than young women ( $0.41 \pm 0.01$  ng/ml). No significant age and physical activity differences observed for DKK-1 levels. Sclerostin levels were significantly higher in HEPA-active women compared to low-moderately active women ( $p < 0.05$ ). Sclerostin and DKK-1 showed significant low positive relationships with spine BMD and several hip aBMD variables ( $r = 0.25$  to  $r = 0.44$ ,  $p < 0.05$ ). There was a significant moderate positive relationship between sclerostin and cortical vBMD at 38% tibia ( $r = 0.50$ ;  $p < 0.05$ ). In conclusion, middle-aged women have significantly higher sclerostin levels, which supports previous findings. We also found sclerostin concentrations were higher in women participating in a high volume of physical activity. Although Wnt signaling inhibitors are negative regulators of bone mass, the findings of a low positive association between sclerostin/DKK-1 with BMD were unexpected and deserves further investigation.

**Table 1. Serum Sclerostin and DKK-1 Based on Age and Physical Activity Levels (Mean  $\pm$  SD)**

Variables	Young (n=25)		Middle-Aged (n=25)	
	Low-Mod (n=13)	HEPA-Act (n=12)	Low-Mod (n=12)	HEPA-Act (n=13)
Sclerostin(ng/ml)**†	0.38 $\pm$ 0.77	0.44 $\pm$ 0.06	0.51 $\pm$ 0.09	0.56 $\pm$ 0.01
DKK-1 (pmol/l)	55.36 $\pm$ 17.14	53.05 $\pm$ 14.99	48.70 $\pm$ 17.95	48.84 $\pm$ 16.52

\*\*Significant age effect  $p < 0.01$ ; † Significant physical activity effect  $p < 0.05$ ; Low-Mod= Low to Moderate; HEPA-Act= HEPA Active

**Disclosures:** Pragna Sharma Ghimire, None.

## LB-SU0365

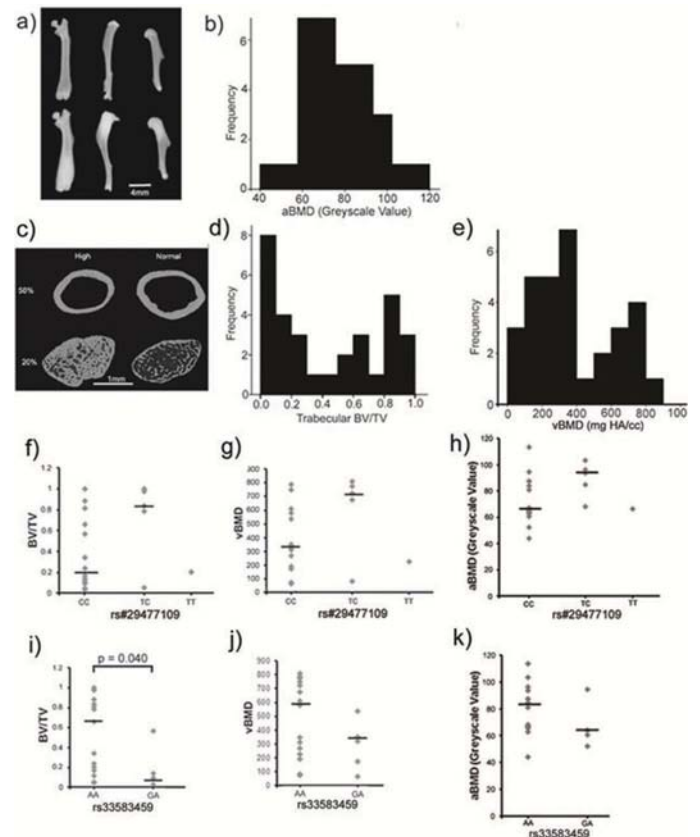
**Outbred CFW Mice Exhibit a Bimodal Bone Mass Distribution.** Meghan Moran<sup>1</sup>, Rick Sumner<sup>1</sup>, Abraham Palmer<sup>2</sup>, Maleeha Mashiatulla<sup>1</sup>. <sup>1</sup>Rush University Medical Center, United States, <sup>2</sup>UC San Diego, United States

Carworth Farms White (CFW) is a commercially available outbred mouse strain used for bone genetic studies<sup>1</sup>; 2. One study<sup>2</sup> found that some CFW mice have abnormally high aBMD. The current study sought to further characterize the CFW bone phenotype and to determine if two previously identified single-nucleotide polymorphisms (SNPs) associated with aBMD<sup>2</sup> were associated with this phenotype. We studied bones from 31 CFW mice that were 11, 16, 20, 24 or 28 weeks of age. Bone phenotyping was completed using contact radiography and micro-computed tomography ( $\mu$ CT) to examine frequency distributions and associations of the bone phenotype with SNPs rs29477109 and rs33583459.

Contact radiographs showed the existence of a high bone mass phenotype in femurs, tibiae and humeri (Fig. 1a) and the inferred aBMD had a unimodal frequency distribution (Fig. 1b), similar to the distribution previously reported<sup>2</sup>. However, when examined by  $\mu$ CT (Fig. 1c), we found a bimodal distribution in which ~45% of mice had high distal femoral trabecular bone volume (BV/TV, Fig. 1d) and volumetric BMD (vBMD, Fig. 1e). This high bone mass phenotype was evenly distributed among males (9 of 20 had high bone mass) and females (5 of 11) and across the ages (4 of 10 at 11 weeks, 3 of 6 at 16 weeks, 2 of 6 at 20 weeks, 2 of 5 at 24 weeks and 3 of 4 at 28 weeks). No age (2-way ANOVA,  $p = 0.581$ ) or sex ( $p = 0.799$ ) effects were present for BV/TV or vBMD ( $p = 0.161$  age and  $p = 0.534$  sex). A subset ( $n = 20$ ) of mice were genotyped for the selected SNPs. For rs29477109, 14 mice were CC, 5 were TC and 1 was TT. BV/TV ( $p = 0.139$ , Mann-Whitney test), vBMD ( $p = 0.096$ ) and radiograph-aBMD ( $p = 0.052$ ) was slightly higher in TC mice than in CC mice (Fig. 3f-h). For rs33583459, 15 mice were AA and 5 were GA. BV/TV was higher in AA mice than in GA mice ( $p = 0.040$ , Fig. 3i). Similar trends were found for vBMD ( $p = 0.176$ , Fig. 3j) and aBMD ( $p = 0.089$ , Fig. 3k). We also examined the bone mineral density distribution in the cortical and trabecular bone of 6 normal BV/TV and 4 high BV/TV mice using a new technique<sup>3</sup>. We found no significant differences in the mean bone tissue mineral density ( $p > 0.5$ ).

Our study shows that: 1) CFW mice are stratified into high and normal bone mass groups based on the frequency distribution of distal femoral BV/TV, 2) one of the two SNPs studied (rs33583459) is associated with this newly defined phenotype and 3)  $\mu$ CT has superior ability compared to planar radiographic techniques to characterize the bone phenotype. The data suggest that the use of screening methods such as dual energy x-ray absorptiometry may limit the ability of researchers to define the genetic basis of bone phenotypes in mouse models.

1. Nicod J, Davies RW, Cai N, et al. 2016. Genome-wide association of multiple complex traits in outbred mice by ultra-low-coverage sequencing. *Nat Genet* 48:912-918.
2. Parker CC, Gopalakrishnan S, Carbonetto P, et al. 2016. Genome-wide association study of behavioral, physiological and gene expression traits in outbred CFW mice. *Nat Genet* 48:919-926.
3. Mashiatulla M, Ross RD, Sumner DR. 2017. Validation of cortical bone mineral density distribution using micro-computed tomography. *Bone* 99:53-61.



**Disclosures:** Meghan Moran, None.

## LB-SU0366

**BMP2 Regulates Enthesal Bone Formation in Antigen-Induced Arthritis.** Yukiko Maeda\*, Catherine Manning, Ellen Gravalles. University of Massachusetts Medical School, United States

Ankylosing Spondylitis (AS) is a common rheumatic disease with a prevalence of ~0.5% in the general population. AS patients suffer from pain and disability due to inflammation and ossification at enthesal sites, the mechanism of which remains unclear. BMP2 is known to initiate endochondral bone formation and is reported to be upregulated in mesenchymal stem cells derived from AS patients. BMP2, 6 and 7 are also expressed early at sites of enthesal new bone formation (Lories, et al., *J Clin Invest* 2005). We have used the Antigen-Induced Arthritis (AIA) model, in which endochondral bone formation occurs at specific enthesal sites about the knee joint, to determine the role of BMP2 in this process. Since global deletion of BMP2 is embryonically lethal, we used limb mesenchymal cell-specific (Prx1-Cre) BMP2 knock out mice (KO) and induced AIA in knee joints of 8 and 14 week-old KO and littermate control mice (WT). At 8 and 14 weeks of age, both KO and WT mice showed similar inflammation in arthritic knees. Histologic analysis in 8 week-old WT mice revealed early chondrocytic endochondral bone formation at entheses by day 9. Chondrocytes and cartilage were absent from entheses in KO mice at this time point. After 15 days, angiogenesis, TRAP-positive osteoclasts and bone were observed at entheses in WT mice. In contrast, KO mice developed only cartilage, but not bone, and angiogenesis and osteoclasts were absent. To examine whether enthesal bone formation was simply delayed in KO mice, we prolonged AIA until day 36, at which time the endochondral sequence was complete in WT mice and bone alone was present at entheses. However, in KO mice, cartilage was retained and enthesal bone formation was not observed. To address the possibility that other BMPs compensated for the lack of BMP2 in young mice, we also induced AIA in 14 weeks-old KO and WT mice. Similar to younger mice, by day 15 of AIA WT mice developed enthesal bone formation. In contrast, KO mice did not develop cartilage or bone at the enthesis. We harvested enthesis cells and bone marrow stromal cells

(BMSCs) from WT and KO mice. After 3 weeks in osteoblast differentiation media, entheses cells and BMSCs from WT mice differentiated and were mineralized, but cells from KO mice were not mineralized. These results demonstrate that mesenchymal cell-derived BMP2 is essential for enthesal bone formation in the setting of inflammation and may have implications for the pathogenesis of enthesophytes in AS.

**Disclosures:** Yukiko Maeda, Abbvie, Grant/Research Support.

## LB-SU0367

**Imbalanced bone osteogenesis and adipogenesis in mice deficient of the chemokine Cxcl12 in the bone mesenchymal stem/progenitor cells.** Yi-shiuan Tzeng<sup>\*1</sup>, Ni-chun Chung<sup>2</sup>, Yu-ren Chen<sup>1</sup>, Yuan-ye Kuo<sup>1</sup>, Dar-ming Lai<sup>2</sup>. <sup>1</sup>Graduate Institute of Oncology, National Taiwan University, Taiwan, Province of China, <sup>2</sup>Department of Surgery, National Taiwan University Hospital, Taiwan, Province of China

Bone and bone marrow serve as an imperative ecosystem to various types of cells participating in critical body functions. The chemokine Cxcl12 is one of the communication factors in the marrow microenvironment that regulates hematopoietic stem/progenitor cell homeostasis. However, the function of Cxcl12 in other bone marrow cells *in vivo* is yet to be discovered. Here we report a novel function of Cxcl12 in postnatal bone development and homeostasis. Targeted deletion of *Cxcl12* in Prx1- or Osx-expressing mesenchymal stem/progenitor cells (MSPCs), but not in mature osteoblasts, resulted in marrow adiposity and reduced trabecular bone content. *In vivo* lineage tracing analyses revealed biased differentiation of MSPCs toward adipocytes. In contrast, adult-stage deletion of *Cxcl12* in Osx-expressing cells led to reduced bone content but not adiposity. Targeting the *Cxcl12* receptor *Cxcr4* in the Prx1-expressing cells also resulted in reduced trabecular bone content but not adiposity. Our study reveals a previously unidentified role of Cxcl12 signaling that regulates the MSPC osteogenesis and adipogenesis through the cell-autonomous and non-autonomous mechanism respectively; which could further influence the homeostatic control of the hematopoietic system.

**Disclosures:** Yi-shiuan Tzeng, None.

## LB-SU0368

**Effect of Yerba Mate (*Ilex paraguariensis*) on Osteoblastic Cells.** Lucas R Brun<sup>\*1</sup>, Laureana Villareal<sup>1</sup>, María J Rico<sup>2</sup>, Viviana R Rozados<sup>2</sup>, O. Graciela Scharovsky<sup>2</sup>, Verónica E Di Loreto<sup>1</sup>. <sup>1</sup>Laboratorio de Biología Ósea. Facultad de Ciencias Médicas UNR, Argentina, <sup>2</sup>Instituto de Genética Experimental, Argentina

Yerba mate (*I. paraguariensis*) infusion is frequently drank in several Latin American countries such as Uruguay, Argentina, Brazil and Paraguay. Several active phytochemicals including methyl xanthines (caffeine) and polyphenols have been identified in yerba mate. Caffeine has shown a negative impact on BMD in particular when it is associated with low calcium diet. Polyphenols have shown positive bone effects due to their antioxidant properties. An increased lumbar spine and femoral neck BMD have been demonstrated in postmenopausal women who drank at least 1 liter of *I. paraguariensis* infusion per day. Moreover, in rats the *I. paraguariensis* infusion increased the BMD and the trabecular bone volume with no effect on biomechanical properties. The aim of this study was to measure the content of *I. paraguariensis* components with potential effect on bone tissue and to evaluate the effect of these components on osteoblastic cells. Caffeine, total polyphenols, calcium, phosphate and fluoride content were measured in 12 commercial trademarks of *I. paraguariensis* infusion (triplicates). It was calculated the total polyphenols concentration that could scavenge 50% of the 2,2-difenil-1-picril-hidrazil radical (IC<sub>50</sub>) in order to measure the antioxidant activity. In addition, the effect of caffeine and polyphenols (rutin, quercetin and chlorogenic acid) on MC3T3E1 osteoblastic cells viability (Cell Proliferation Reagent WST-1, Roche) were evaluated. No differences in caffeine (95%CI 0.59-0.83 g/l), total polyphenols (14.5-16.0 g/l), calcium (13.3-16.7 mg/l), phosphate (101.3-135.7 mg/l) and fluoride (0.066-0.070 mg/l) content were found between the different commercial trademarks of *I. paraguariensis* evaluated. No differences were observed either in antioxidant activity (IC<sub>50</sub> 64.8-71.6 µg/ml). A significant increase in osteoblastic cells viability was observed at different concentrations (1 to 10 µg/ml) of rutin (~26%) and caffeine (~34%) compared with cells without treatment (controls). A significant increase on viability was also observed with 1 to 5 µg/ml of chlorogenic acid (~27%) and quercetin (~16%). Therefore, it is concluded that there were no significant differences between the different trademarks analyzed in their content of components with potential effect on bone tissue or its antioxidant activity. Our data suggest that the positive skeletal effects of *I. paraguariensis* could be attributed, at least in part, to stimulation of osteoblasts survival.

**Disclosures:** Lucas R Brun, None.

## LB-SU0369

**In vivo and In vitro Absence of 5-LO Gene Is Related to Higher Osteogenic Profile.** Flavia Amadeu de Oliveira<sup>\*1</sup>, Cintia Kazuko Tokuhara<sup>1</sup>, José Carlos Guareschi Filho<sup>1</sup>, Adriana Arruda Matos<sup>1</sup>, João Paulo Domezi<sup>1</sup>, Tania Mary Cestari<sup>1</sup>, Vimal Veeriah<sup>2</sup>, Camila Peres-Buzalaf<sup>3</sup>, Rodrigo Cardoso de Oliveira<sup>1</sup>. <sup>1</sup>University of Sao Paulo, Brazil, <sup>2</sup>The Kennedy Institute of Rheumatology- University of Oxford, United Kingdom, <sup>3</sup>University of Sagrado Coração, Brazil

Leukotrienes (LTs) are inflammatory mediators derived from arachidonic acid by 5-lipoxygenase (5-LO) enzyme produced by both osteoblasts and osteoclasts. However, it is unknown the impact of endogenously produced LTs in bone metabolism in the induction and/or inhibition of osteogenic differentiation. Thus, the objective was to evaluate the effect of LTs on osteogenesis from 129/Sv wild type (WT) and 5-LO Knockout (5-LO KO) mice. First, 2 month old WT and KO mice were sacrificed and femoral head was scanned and reconstructed into a 3D-structure using micro-CT with a voxel size of 6.6 µm at 50KV and 800µA. The bone volume density (BV/TV), trabecular number (Th. N), trabecular thickness (Th. Th) and trabecular separation (Tb. Sp) were evaluated using CTAn software. 3D images were reconstructed using CT-Vox software. The results showed that the femurs of the KO mice presented higher BV/TV (KO 52% ± 4.78 vs. WT 31% ± 3.37) and Tb.Sp (KO 10.1 mm ± 0.58 vs. WT 6.9 mm ± 0.41) accompanied by a lower Tb. N (KO 0.042 1/mm ± 0.003 vs. WT 0.059 1/mm ± 0.003) and Tb. Th (KO 7.33 mm ± 0.065 vs. WT 8.82 mm ± 0.46) compared to WT (p<0.05). Next, primary osteoblasts from 129/Sv and 5-LO KO mice were cultivated in osteogenic medium at 2, 4, 7, 10 and 14 days. Results from RT-PCR analysis demonstrated alkaline phosphatase (Alp) and Collagen type 1 (Col1A1) expression were upregulated in 5-LO KO mice osteoblasts at 7 days compared to WT (p<0.05). Alkaline phosphatase activity and matrix nodule formation was higher in 5-LO KO osteoblasts compared to WT in all time points (p<0.05). Moreover the kinetics of the Alox5 gene showed higher expression at 14 days of culture under osteogenic medium in WT osteoblasts (p<0.05). Thus, our results clearly showed that LTs modulate the bone metabolism, in which was evidenced by the bone profile of those different animal strains and by the increased bone formation markers and mineralization in 5-LO KO osteoblasts.

**Disclosures:** Flavia Amadeu de Oliveira, None.

## LB-SU0370

**Transcriptome profiling of stem cell-derived osteoblasts identifies genes associated with osteoblast differentiation.** Hui Zhu<sup>\*</sup>, Takaharu Kimura, Joy Wu. Stanford University School of Medicine, United States

Identification of genes and signaling pathways that are highly associated with osteoblast differentiation is important for better understanding bone development, homeostasis and regeneration. Traditional sources of osteoblasts including primary calvarial cells, bone marrow stromal cells and bone chip outgrowth are limited by heterogeneity of cell populations and low yield. 2.3ColGFP transgenic mice express green fluorescent protein (GFP) in osteoblasts. We reasoned that directed differentiation of embryonic stem cells (ESCs) from 2.3ColGFP mice could yield potentially unlimited numbers of relatively pure osteoblasts. To validate the osteoblast identity of ESC-derived 2.3ColGFP+ osteoblasts, we performed unbiased high-throughput RNA-sequencing to compare the global gene expression profile to two references populations: a) 2.3ColGFP+ osteoblasts freshly isolated from mouse long bone and b) 2.3ColGFP+ osteoblasts isolated from mouse bone chip culture. Gene Ontology Analysis shows that genes of 2.3ColGFP+ populations from all three sources are enriched in osteoblast differentiation, bone development, bone mineralization and ossification categories. Interestingly, in addition to major biological processes or signaling pathways known to be involved in osteogenesis, some novel pathway components, for example ER to Golgi vesicle-mediated transport and ErbB signaling, are observed. Comparison of the over 500 overlapping genes from the three sources reveals a highly representative candidate gene set associated with osteoblast differentiation and bone development. Comparing this candidate gene set with mouse transcription factor and mouse membrane protein database, we identified known and potential novel transcription factors and surface markers associated with osteoblast differentiation and bone development. We have previously reported that intensity of 2.3ColGFP expression correlates with osteoblast maturation stage. We therefore compared 2.3ColGFP(lo) and 2.3ColGFP(hi) populations, which represent preosteoblasts and mature osteoblasts, respectively, from mice long bone and bone chip sources to identify potential stage specific markers and/or regulators of osteogenesis. In summary, we provide genome-wide characterization of gene expression in more homogenous osteoblast populations of cells that may lead to novel regulators of osteoblast differentiation and bone development.

**Disclosures:** Hui Zhu, None.

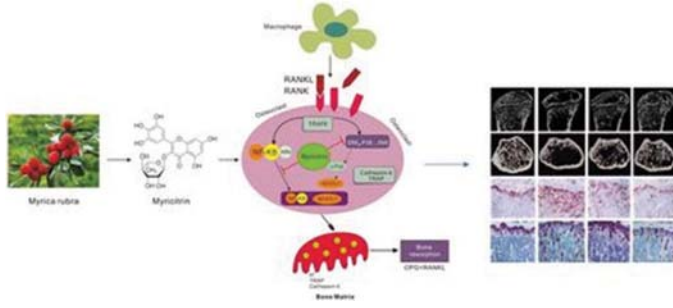
## LB-SU0371

**Myricitrin Inhibits Osteoclastogenesis by attenuating the NF-κB and MAPKs signaling pathway and Prevents Bone Loss in vivo.** lingbo kong<sup>\*</sup>, xiaobin yang, baorong he, dingjun hao. xi'an jiaotong university, China

**ABSTRACT:** Myricitrin is a natural flavonoid that inhibits nitric oxide (NO) transmission and has an atypical antipsychotic-like profile in animal models. The



present study was performed to define effects of myricitrin on nuclear factor-kappaB ligand (RANKL)-stimulated osteoclast differentiation and the underlying mechanisms. The bone marrow cells (BMMs) were harvested and induced with RANKL followed by treatment with myricitrin at several doses, and the differentiation of osteoclasts from these cells was evaluated by tartrate-resistant acid phosphatase (TRAP) staining and resorption pit formation assay. The effects of myricitrin on osteoclastogenesis were further studied by examining RANKL-induced osteoclast F-actin ring formation and osteoclast bone resorption. Moreover, we explored the mechanisms of these down-regulation effects by performed Western blotting and quantitative RT-PCR examination. Results demonstrated myricitrin strongly inhibited RANKL induced osteoclast formation when added during the early stage of BMMs cultures, suggesting that it acts on osteoclast precursors to inhibit RANKL/RANK signaling. Moreover, myricitrin markedly decreased the phosphorylation of p38, ERK, JNK, p65 and I- $\kappa$ B degradation, and significantly suppressed c-Fos and nuclear factor of activated T-cells cytoplasmic 1 (NFATc1), both the key transcription factors during osteoclastogenesis. The results demonstrating myricitrin inhibits RANKL-mediated osteoclastogenesis by attenuating the NF- $\kappa$ B and MAPKs signaling pathway. Furthermore, in vivo studies verified the bone protection effects of myricitrin. These results collectively suggested that myricitrin acted as an anti-resorption agent by blocking osteoclast activation.



**Disclosures:** lingbo kong, None.

## LB-SU0372

**Bone CLARITY reveals that anti-sclerostin antibody penetrates the lacunar canalicular system in mice under physiological loading conditions.** Alon Greenbaum<sup>\*1</sup>, Ken Chan<sup>2</sup>, Rogely Boyce<sup>3</sup>, Hossein Salimi-Moosavi<sup>4</sup>, Helen J. McBride<sup>3</sup>, Viviana Gradinaru<sup>1</sup>. <sup>1</sup>Division of Biology and Biological Engineering, California Institute of Technology, Pasadena, CA 91125, USA, United States, <sup>2</sup>Division of Biology and Biological Engineering, California Institute of Technology, Pasadena, CA 91125, USA., United States, <sup>3</sup>Comparative Biology and Safety Sciences, Amgen, Thousand Oaks, CA 91320, USA, United States, <sup>4</sup>Pharmacokinetics and Drug Metabolism, Amgen, Thousand Oaks, CA 91320, USA, United States

Anti-sclerostin antibody (Scl-Ab) neutralizes sclerostin activity, a secreted protein from osteocytes, resulting in WNT mediated increases in bone formation and decreases in bone resorption; this dual effect on bone results in rapid increases in bone mass and strength.

A recent study in rats has shown that the RNA expression profile dramatically changes in osteocytes as early as six hours after administration of Scl-Ab (Nioi et al 2015). This rapid response is surprising as it is hypothesized that Scl-Ab is too large (~150 kD) to penetrate into the lacunar canalicular system (LCS) to reach osteocytes directly and suggests this pharmacodynamic effect reflects effects of Scl-Ab on osteocytic processes at the bone surface. The sieving properties of the bone barrier having a 70 kD cutoff are based on previous studies frequently conducted in anesthetized animals using tracer dyes with euthanasia soon after dye injections.

By using our recently published tissue clearing method (Bone CLARITY; Greenbaum and Chan, et al 2017), we show that Scl-Ab is able to penetrate the LCS in mice, when the experiments were designed to more accurately model physiological conditions. Adult mice were administered either vehicle or fluorescent-labeled negative control or labeled Scl-Ab via the retro-orbital route and were allowed to resume normal movement and activity following dosing. After 48 hours, the animals were transcardially perfused with 0.01M PBS and 4% PFA, and bones were collected and fixed in 4% PFA overnight. Then the bones were cleared using Bone CLARITY, a method that retains the fluorescence signal, preserves the tissue morphology, minimizes photo-bleaching and allows for 3-dimensional imaging of labeled antibody using a light-sheet microscope. Labeled control antibody was detected in the liver as expected for large molecule clearance but not in the LCS. Labeled Scl-Ab was visualized in intact tibia, femur and vertebral body. We qualitatively observed that osteocytes labeled with Scl-Ab were located in the inner half of the cortex in contrast to minimal labeling of osteocytes in the sub-periosteal cortex. These findings demonstrate that Scl-Ab can access the LCS and illustrate how Bone CLARITY can be a valuable tool to characterize the bio-distribution of drugs at high resolution in intact samples.

**Disclosures:** Alon Greenbaum, AMGEN, Grant/Research Support.

## LB-SU0373

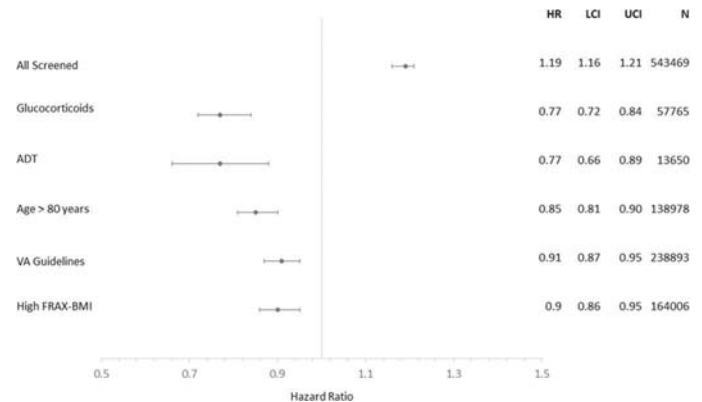
**Primary Osteoporosis Screening in U.S. Male Veterans is Effective in High Risk Subgroups, but not Overall.** Cathleen Colon-Emeric<sup>\*1</sup>, Carl Pieper<sup>1</sup>, Kenneth Lyles<sup>1</sup>, Courtney VanHoutven<sup>1</sup>, Joanne LaFleur<sup>2</sup>, Robert Adler<sup>3</sup>. <sup>1</sup>Duke University, United States, <sup>2</sup>University of Utah, United States, <sup>3</sup>Richmond VAMC, United States

**Background:** We reported in a previously submitted abstract that primary osteoporosis screening in men, as operationalized in the U.S. Veterans Health System, did not reduce fracture rates due to inefficient targeting and low treatment adherence rates. Here we report results of pre-planned subgroup analyses of men at high risk.

**Methods:** Propensity score matched case-control study using CMS and VA data among 2,539,812 men aged 65-99 years without prior fracture, osteoporosis diagnosis or treatment. Osteoporosis screening by dual energy x-ray absorptiometry (DXA) was identified from administrative codes and natural language processing. Propensity scores indicating the probability of screening within the next year were calculated for each of the 10 years of follow-up, incorporating 32 fracture risk factors. Screened cases were 1:3 matched with unscreened controls. Landmark analysis with competing risk compared time to fracture between cases and controls who survived at least 12 months after DXA without fracture. Interaction terms for pre-specified subgroups (glucocorticoid users, androgen deprivation therapy users (ADT), age >80 years, high FRAX-BMI risk, >1 VA Undersecretary Guideline risk factor) were tested, and separate models examined when significant.

**Results:** All subgroup interaction tests were significant ( $p < 0.001$ ). Screening was associated with a 9-25% lower hazard of fracture in the high-risk subgroups over a median of 4.7 years of follow-up (figure).

**Conclusion:** These results support primary osteoporosis screening for men >80 years, and for men >65 with risk factors. It remains unknown whether primary osteoporosis screening in average risk men would be effective if better treatment and adherence rates were achieved.



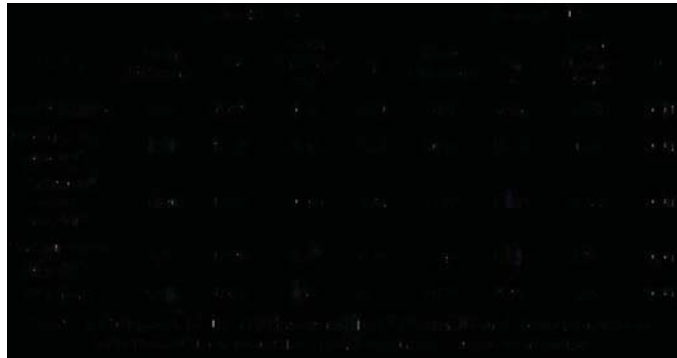
**Disclosures:** Cathleen Colon-Emeric, None.

## LB-SU0374

**Changes in volumetric BMD and cortical thickness measured by 3D-DXA in the lumbar spine after 24 months of Denosumab treatment.** Mirella Lopez Picazo<sup>\*1</sup>, Ludovic Humbert<sup>2</sup>, Miguel Angel Gonzalez Ballester<sup>3</sup>, Luis Del Rio<sup>4</sup>, Renaud Winzenrieth<sup>1</sup>, Silvana Di Gregorio<sup>5</sup>. <sup>1</sup>Galgó Medical, Spain, <sup>2</sup>Galgó Medical SL, Spain, <sup>3</sup>SIMBioSys, Universitat Pompeu Fabra, Spain, <sup>4</sup>CETIR Grup Mèdic, Spain, <sup>5</sup>CETIR Grup Mèdic, Spain

**Objective:** The objective of the study was to assess changes in trabecular and cortical volumetric BMD (vBMD) and mean cortical thickness (CTh) of L1-L4 vertebral bodies on a cohort of patients treated with Denosumab (Dmab). **Method:** We retrospectively analyzed a cohort of 18 patients (1 men and 17 women) treated with Dmab and 33 controls (6 men and 27 women) naive of treatment. Spine anteroposterior DXA scans were acquired at baseline and 24 months at CETIR Grup Mèdic using an iDXA scanner (GE Healthcare). Areal BMD (aBMD) at L1-L4 was measured using enCORE software (version 12.3 and 14.1, GE Healthcare). Integral, trabecular and cortical vBMD as well as CTh were assessed using 3D-DXA software (v2.3, Galgó Medical). The 3D-DXA algorithm estimates the vBMD and 3D shape of the lumbar spine from an anteroposterior DXA image by registering a statistical model onto the 2D-DXA image. Cortical and trabecular tissues at the vertebral body are differentiated by analyzing density variations along the bone cortex. Changes from baseline were analyzed using pair t-tests pair and differences between naive and Dmab groups were analyzed using unpair t-tests. **Results:** Mean (SD) age at baseline was  $61 \pm 8$  years in the naive group and  $61 \pm 6$  years in the Dmab group ( $p = 0.97$ ). Mean BMI was  $27.01 \pm 4.21$  kg/m<sup>2</sup> in the naive group and  $24.04 \pm 3.86$  kg/m<sup>2</sup> in the Dmab group ( $p = 0.02$ ). Mean T-score was  $-1.40 \pm 1.06$  in the naive group and  $-2.97 \pm 0.58$  in the Dmab group ( $p < 0.01$ ). Changes at 24 months in aBMD, vBMD and CTh in the naive group were not statistically significant (Table 1). In the Dmab group, a significant increase was observed in aBMD (9.12%,  $p < 0.01$ ), trabecular vBMD (12.31%,  $p < 0.01$ ), cortical vBMD (3.95%,

$p < 0.01$ ) and CTh (6.05%,  $p < 0.01$ ). Conclusion: As expected, no changes have been observed in the naive group after 24 months of follow-up but significant increases were observed in both cortical and trabecular compartments in patients treated with Dmab. vBMD and CTh measured by 3D-DXA could improve monitoring patient under pharmacological treatment. Further studies are needed to confirm these promising results.



**Disclosures:** Mirella Lopez Picazo, None.

## LB-SU0375

**Prevalence of morphologic femoral variants in a large single centre cohort; Implications for clinical application and therapeutic management.** Laurence Rubin<sup>1</sup>, Robert Josse<sup>1</sup>, Erin Norris<sup>1</sup>, Shabbir Mewa<sup>1</sup>, Karl Bruckmueller<sup>2</sup>, Angela Cheung<sup>3</sup>. <sup>1</sup>St. Michael's Hospital and the University of Toronto, Canada, <sup>2</sup>St. Michael's Hospital, Canada, <sup>3</sup>UHN and the University of Toronto, Canada

An increasing and worrisome "care gap" in the management of Osteoporosis and fracture reduction has been attributed to heightened concerns for adverse events (AE) associated with anti-resorptive therapy, specifically atypical femoral fractures (AFF). Clinical and imaging criteria have been developed to diagnosis AFF. The ability to detect and quantify morphologic changes which may predate AFF and track such changes over time presents an important option for AE reduction strategy. To achieve this, software analyzing Femoral shaft morphology (shape changes, extent and location) has now been developed for use with routine densitometry. We retrospectively analyzed all femoral DXA scans performed at a single academic Metabolic Bone Clinic Centre over the past 18 years ( $n=95,494$ ) with the GE Encore V17 software. We recorded the "Beaking Index (BI), a measure (in mm) that denotes the magnitude of the increase in the cortical width at the site of a localized periosteal reaction. It can be mapped and tracked over time<sup>1</sup>. 370 individual scans with a BI  $> 1$  (range 1-26.9) were detected, for an overall prevalence of 0.391%. The demographic status (age, self-reported ethnicity and gender) and Total FBMD of this subset, as well as total data cohort are shown in Table 1. 1/370 (with a BI 2.7) had been diagnosed with an AFF, but on the contralateral side. Additional subjects with morphologic variants likely went undetected (due to scan extent, lack of bilateral studies). These findings also require validation in an independent cohort. However, our results do inform, retrospectively, on the frequency of such structural changes in one large clinical sample. If BI is confirmed to be a useful biomarker of future risk for AFF, this may help clarify risk status and facilitate patient and physician acceptance of appropriate intervention for fracture reduction.

Table 1	BI $> 1$ ( $n=370$ )	Entire data set ( $n=95,495$ )
Age (yrs)	20-93	16-94
Female gender %	68.9	83.7
Ethnicity (W/B/H/A/O) * %	82/5/2/5/6	79/3/2/10/6
TFBMD gm/cm <sup>2</sup> – Median	0.8917	0.7578
TFBMD gm/cm <sup>2</sup> – Average	0.89584	0.7578

\*W=white, B=Black, H=Hispanic, A=Asian, O=Other

<sup>1</sup> <http://landing1.gehealthcare.com/rs/005-SHS-767/images/BMD-Global-AFF%20Whitepaper.pdf>

**Disclosures:** Laurence Rubin, None.

## LB-SU0376

**Parity and Lactation Are Not Associated with BMD Loss or Incident Major Fragility Fractures Over 15 Years of Follow-Up: Canadian Multicentre Osteoporosis Study (CaMos).** Sandra Cooke-Hubley<sup>1</sup>, Gao Zhiwei<sup>1</sup>, Gerald Mugford<sup>1</sup>, Stephanie M. Kaiser<sup>2</sup>, David Goltzman<sup>3</sup>, William D. Leslie<sup>4</sup>, K. Shawn Davison<sup>5</sup>, Jerilyn C. Prior<sup>6</sup>, Christopher S. Kovacs<sup>1</sup>. <sup>1</sup>Memorial University of Newfoundland, Canada, <sup>2</sup>Dalhousie University, Canada, <sup>3</sup>McGill University, Canada, <sup>4</sup>University of Manitoba, Canada, <sup>5</sup>A Priori Medical Sciences, Canada, <sup>6</sup>University of British Columbia, Canada

**Background:** Pregnancy and especially lactation cause loss of bone mass and micro-architectural changes that temporarily increase the risk of vertebral compression fractures. After weaning, BMD improves but skeletal microarchitecture may not be fully restored. With some exceptions, cross-sectional studies in older women have reported that parity and lactation are neutral or protective against fragility fractures. However, longitudinal or prospective data are sparse. CaMos is a randomly selected cohort that includes ~6,000 women who have been followed for up to 15 years, with annual, verified incident fractures, and 5-yearly bone density assessments.

**Objective:** To determine whether parity or lactation are related to BMD loss over 10 years or incident major fragility fractures over 15 years of follow-up.

**Methods:** The primary analyses included parity or lactation duration analyzed as continuous variables in predicting total incident fragility fractures, and change in BMD at the lumbar spine, total hip, and femoral neck. In secondary analyses, fractures at six skeletal sites were examined independently. Univariate analyses were performed for total fractures, fracture sites, 3 BMD sites, and 20 covariates, including age, BMI, menarche, age at menopause, baseline BMD, vitamin D intake, estrogen or oral contraceptive use, etc. Outcomes with  $p < 0.2$  were used to construct a stepwise multivariate regression model.

**Results:** Of 5,454 eligible women with baseline data, 3,437 completed the full 15 years of follow-up. Average age at entry was  $59 \pm 11$  (SD); menarche  $13 \pm 1.6$  yr; menopause  $47 \pm 6.8$  yr. 139 women were nulliparous; the remainder had mean parity of  $3 \pm 1.6$  with lactation duration  $11.8 \pm 12.2$  months. There were 633 fragility fractures, including 79 clinical spine, 84 hip, 33 pelvis, 188 forearm, 77 shoulder, and 114 rib. In the multivariate analysis, increasing parity (odds ratio [OR] 0.94, 95% confidence interval [CI] 0.86-1.02) and lactation duration (OR 1.01, CI 1.00-1.02) showed no relationship with total fragility fractures, nor any fracture site. Duration of lactation had no effect while parity showed trends to protect against loss of BMD of the lumbar spine and total hip (Table).

Strengths include the random cohort, duration, and verification of incident fractures. Limitations include the self-reporting of recalled breastfeeding duration.

**Conclusion:** Parity and lactation have no long-term association with fragility fracture risk or BMD loss in older women.

Site	Variable	Beta $\pm$ SE	p value
Lumbar spine	Breastfeeding	0.0007 $\pm$ 0.002	0.61
	Parity	-0.021 $\pm$ 0.011	0.06
Femoral neck	Breastfeeding	0.0016 $\pm$ 0.0015	0.32
	Parity	-0.012 $\pm$ 0.011	0.25
Total hip	Breastfeeding	-0.0008 $\pm$ 0.0016	0.61
	Parity	-0.019 $\pm$ 0.010	0.05

**Disclosures:** Sandra Cooke-Hubley, None.

## LB-SU0377

**Patients' Perceptions of Case-Managed Osteoporosis Care as Acceptable, Accessible and Appropriate: Qualitative Data from a Randomized Trial.** Lisa Wozniak<sup>\*</sup>, Lauren Beaupre, Brian Rowe, Finlay McAlister, Debbie Bellerose, Jeffrey Johnson, Sumit Majumdar. University of Alberta, Canada

**Purpose:** Few outpatients with fractures are treated for osteoporosis by their family physician. In previous randomized trials, we found a nurse case-manager could double rates of osteoporosis treatment; however, little is known about patients' perceptions of case-managed osteoporosis care.

**Therefore,** we collected qualitative data from patients with upper extremity fragility fractures enrolled in a randomized trial - Comparing Strategies Targeting Osteoporosis to Prevent recurrent Fractures (C-STOP). In the case-managed arm, nurses saw patients in clinics, arranged BMD tests, provided counseling and prescribed guideline-based treatments (i.e., bisphosphonates based on standardized algorithms) when indicated.

**Methods:** We used qualitative description methodology described by Sandelowski et al (Res Nurs Health; 2010) to elicit patients' perceptions in the quality dimensions of acceptability, accessibility and appropriateness of the case-managed approach. We purposefully sampled case-managed female patients whether or not offered bisphosphonate treatment until data saturation was reached. We conducted semi-structured



interviews which were transcribed and analyzed using content analysis and managed with ATLAS.ti 7 (Berlin, Germany, Scientific Software Development GmbH; 2017).

Results: We conducted interviews with 15 female case-managed patients, including 8 of whom were offered (6 accepted) and 7 not offered bisphosphonate treatment. Most (60%) were 60-years or older, 27% had a previous fracture, 80% had osteopenia or osteoporosis at one or more skeletal sites on BMD test and so were eligible for bisphosphonate treatment, and most (87%) had better than average osteoporosis knowledge when quantitatively surveyed.

Patients reported case-managed osteoporosis care as acceptable, accessible and appropriate. Table 1 provides results by these quality dimensions and direct patient quotes. This approach provided patients with high-quality, personalized information about bone health by a trusted expert in a respectful manner that helped inform treatment decisions. Most patients felt the amount of time required was reasonable and the approach provided both better coordinated care and easier access to follow-up care than seeing their family physicians. Patients also suggested it increased overall awareness, knowledge and confidence regarding osteoporosis and fractures, and considered it "absolutely necessary" (Table 1).

Conclusions: Patients report that case-managed osteoporosis care is acceptable, accessible and appropriate and that it is both proactive and patient-centred. These findings were not captured by quantitative data from the primary trial itself. Therefore, qualitative data should be collected from randomized trials, especially if one's goal is to also spread clinically effective interventions.

Results	Patient Quotes
Acceptable: Health services are respectful and responsive to user needs, preferences and expectations.	
Accessible: Health services are obtained in the most suitable setting in a reasonable time and distance.	
Appropriate: Health services are relevant to user needs and are based on accepted or evidence based practice.	

Disclosures: Lisa Wozniak, None.

## LB-SU0378

**Intra-individual changes in total versus free 25-hydroxyvitamin D associated with changes in 24,25-dihydroxyvitamin D and parathyroid hormone during 16 weeks of high-dose, daily supplementation with cholecalciferol or calcifediol.**

Albert Shieh<sup>1</sup>, Christina Ma<sup>1</sup>, Rene Chun<sup>1</sup>, Brandon Rafison<sup>1</sup>, Carter Gottlieb<sup>1</sup>, Martin Hewison<sup>2</sup>, John Adams<sup>1</sup>. <sup>1</sup>UCLA, United States, <sup>2</sup>University of Birmingham, United Kingdom

Purpose. It is unclear whether free 25-hydroxyvitamin D (25D) is physiologically active in either renal or extra-renal tissues in humans. The purpose of this study was to assess whether change in total (25Dt) versus free (25Df) 25D was more strongly associated with change in markers of vitamin D bioactivity in renal (24,25-dihydroxyvitamin D [24,25D]) and extra-renal (parathyroid hormone [PTH]) tissues following aggressive vitamin D supplementation.

Methods. 35 adults >18 years with vitamin D deficiency (25D <20 ng/ml) were previously randomized to receive 60 mcg/day of D3 or 20 mcg/day of 25D3 for 16 weeks. During that study, serum was collected at 0 (baseline), 4, 8 and 16 weeks. We measured 24,25D and PTH from stored serum collected at each time point. Using multivariable linear regression, we assessed the associations between change in 25Dt or 25Df (predictors) with change in 24,25D or PTH (outcomes) from 0-4 weeks, 4-8 weeks, and 8-16 weeks.

Results. At week 0, participants (D3 and 25D3 groups combined) were aged 35.1±10.6 years, and had 25Dt, 25Df, 1,25D, 24,25D, and PTH levels of 16.6±3.0 ng/ml, 4.6±1.0 pg/ml, 55.6±16.3 pg/ml, 1.3±0.5 ng/ml, and 37.2±16.3 pg/ml respectively. From 0-4 weeks, rise in 25Df was associated with rise in 24,25D (p=0.03, R<sup>2</sup>=0.20), whereas rise in 25Dt was not (p=0.3, R<sup>2</sup>=0.05) (adjusted for change in 1,25-dihydroxyvitamin D and supplementation regimen). Also from 0-4 weeks, rise in 25Df was associated with decline in PTH (p=0.008, R<sup>2</sup>=0.40), but rise in 25Dt was not (p=0.4, R<sup>2</sup>=0.18) (adjusted for change in serum calcium and phosphorus). From 4-8 weeks, rises in both 25Df (p=0.001) and 25Dt (p=0.01) were associated with rise in 24,25D; 25Df (R<sup>2</sup>=0.37) accounted for a greater proportion of the 24,25D response than 25Dt (R<sup>2</sup>=0.25). Rise in 25Df (p=0.7) and 25Dt (p=0.4) were not associated with decline in PTH during the same time. From 8-16 weeks, rises in both 25Df (p=0.04) and 25Dt (p=0.007) remained associated with rise in 24,25D; 25Dt (R<sup>2</sup>=0.29) accounted for a greater proportion of the 24,25D response than 25Df (R<sup>2</sup>=0.17). Rise in 25Df (p=0.4) and 25Dt (p=0.3) were not associated with change in PTH during the same time.

Conclusions. Early changes in 25Df during vitamin D repletion for vitamin D deficiency were more strongly associated with markers of vitamin D bioactivity in both renal and extra-renal tissues than 25Dt, suggesting a time-dependent, physiologic role for 25Df in humans.

Disclosures: Albert Shieh, None.

## LB-SU0379

**Bone Structure and Turnover Status in Women with and without Atypical Femur Fracture Following Long-term Bisphosphonate Therapy.** Ruban Dhaliwal<sup>1</sup>, Shijing Qiu<sup>2</sup>, Elizabeth Warner<sup>2</sup>, Donald Cibula<sup>3</sup>, Sudhaker D. Rao<sup>2</sup>. <sup>1</sup>Division of Endocrinology, Diabetes and Metabolism, State University of New York Upstate Medical University, United States, <sup>2</sup>Bone and Mineral Research Laboratory, Henry Ford Hospital, United States, <sup>3</sup>Department of Public Health, State University of New York Upstate Medical University, United States

Purpose: Atypical femur fracture (AFF), a serious complication of long-term bisphosphonate (BP) therapy, is considered to be a consequence of severe suppression of bone turnover (SSBT) thereby compromising bone biomechanical properties. The changes in bone structure and turnover with BP therapy in patients with AFF compared to those without AFF remain unknown.

Methods: We compared bone histomorphometry in postmenopausal women on BP therapy of >5 years: 19 with AFF and 32 without AFF; and in 43 healthy white premenopausal women. The measurements were performed separately in cancellous, intracortical and endosteal envelopes.

Results: Of the 19 histomorphometric variables in patients on BP, only the wall thickness (W.Th-volume of bone formed by osteoblasts per unit of cement surface), was significantly lower in subjects with AFF compared to those without AFF, and remained significant even after adjusting for the duration of BP use. Compared to the healthy premenopausal women, the trabecular bone volume, thickness and number, as expected, were all significantly lower in patients on BP. Osteoid indices (OS, O.Th. and OV) were lower in patients with AFF than those without AFF. Bone formation variables (MS/BS, MAR, BFR and Ac.f) were also significantly lower on all bone surfaces in subjects on BP compared to the healthy premenopausal women, and were more pronounced in those with AFF compared to those without AFF. However, the difference between the two patient groups did not reach statistical significance.

Conclusion: Compared to the healthy premenopausal women, bone turnover is severely suppressed in subjects on BPs. Our rather unique findings of significantly decreased W.Th. and a trend towards lower osteoid indices implies adverse effect of BPs on bone formation. These preliminary results suggest a progressive suppression of bone turnover and bone formation in those with compared to those without AFF, and may underlie the deterioration of bone material properties resulting in AFF. Further studies with larger sample of AFF patients are needed to fully understand the phenomenon of SSBT, reduced W.Th. and lower osteoid indices in the pathogenesis AFF.

Disclosures: Ruban Dhaliwal, None.

## LB-SU0380

**Serum Periostin is Positively Correlated with Leptin in Normal Weight and Obese Adults.** Amy Evans\*, Fatma Gossiel, Margaret Paggiosi, Richard Eastell, Jennifer Walsh. Academic Unit of Bone Metabolism, University of Sheffield, United Kingdom

Background: Obese (OB) adults have greater BMD and more favourable bone microarchitecture than normal weight (NW) adults, including thicker and denser cortices by HR-pQCT. However, cortical perimeter is not greater in obesity, which suggests that mechanical loading is not a major contributor to higher bone strength in obesity. Periostin is an extracellular matrix protein, and in bone is expressed most highly in the periosteum. It increases bone formation through osteoblast differentiation, cell adhesion, Wnt signalling and collagen cross-linking. Periostin expression increases with skeletal loading, and may also be a mediator of IGF-1 driven cortical consolidation in young adults. The aim of this study was to determine if circulating periostin concentration differs between normal weight and obese adults, and whether it is associated with areal BMD, cortical bone measures, bone turnover or hormones similarly in these two groups.

Methods: 200 healthy men and women age 25-40 or 55-75 years were recruited in individually-matched OB (BMI ≥30) and NW (BMI 18.5-24.9) pairs. Areal BMD of the lumbar spine and hip was measured with DXA. Cortical measures at the distal radius were determined by HR-pQCT. Periostin was measured in fasting serum using an ELISA optimised for human serum and plasma which recognises all known splice variants (Biomedica Gruppe). Bone turnover was assessed with CTX, PINP and sclerostin. Estradiol (totE2), leptin and IGF-1 were also measured.

Results: Periostin did not differ between NW and OB (953 vs 901 pmol/l, paired t-test p=0.2). There were no significant correlations between periostin and aBMD spine or hip, radius cortical measures, PINP, sclerostin, estradiol or IGF-1. Periostin was significantly correlated with leptin in NW and OB (Spearman's rho 0.322, <0.01 and 0.485 p<0.0001). In OB there was an inverse correlation between periostin and CTX (-0.216, p<0.05).

Discussion: Periostin has been shown experimentally to respond to intermittent PTH and loading, but it may not be responsive to the habitual passive loading in obesity. However, the correlation with leptin, and our previous observation that periostin is related to cortical bone measures and IGF-1 during skeletal maturation, suggest that it may respond to range of endocrine influences in different situations.

Disclosures: Amy Evans, None.

## LB-SU0381

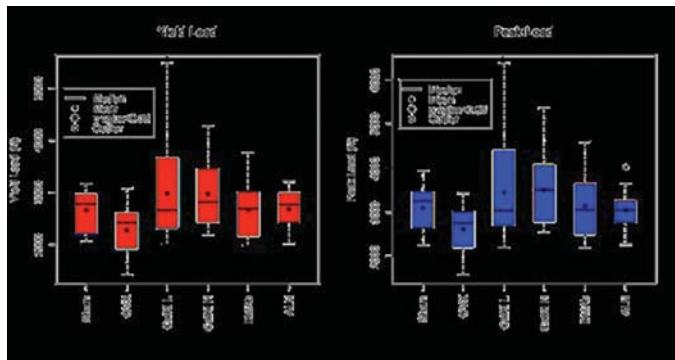
### After Two Years Of Bone Loss, Cathepsin K Inhibition Increases Lumbar Vertebral Strength Independent Of Changes In Trabecular Bone Morphology. Isabel Colon-Bernal<sup>1</sup>, Le Duong<sup>2</sup>, Kenneth Kozloff<sup>1</sup>, James Henderson<sup>3</sup>, Mark Banaszak Holl<sup>1</sup>.

<sup>1</sup>University of Michigan, United States, <sup>2</sup>Merck & Co. (retired), United States, <sup>3</sup>Center for Statistics, Computing and Analytics Research, United States

Anti-resorptive drugs can effectively treat bone loss by blocking osteoclast activity through a variety of independent mechanisms. However, once significant bone loss has occurred, the ability to restore biomechanical function is a primary challenge that may differ based on the drug mechanism. To assess this question, alendronate (ALN), denosumab (DMab), and a cathepsin K inhibitor (MK-0674, CatKi) were employed in treatment mode to explore the impact of varying biological mechanism of action on changes to cancellous bone microstructure and mechanical properties in ovariectomized (OVX) cynomolgus monkeys.

Lumbar vertebrae (LV) BMD values taken two years post-surgery prior to drug treatment show a significant 10-15% decrease for all OVX animals. OVX animals were then treated with vehicle (VEH), ALN (0.03 mg/kg weekly), DMab (2.5 mg/kg weekly), CatKi MK-0674 (CatKi-L, 0.6 mg/kg daily), or CatKi MK-0674 (CatKi-H, 2.5 mg/kg daily) for two years and compared to a control Sham surgery group. Ex-vivo micro-computed tomography (mCT) of LV2 and compression testing of LV4-6 were used to measure cancellous bone microstructure and changes in bone mechanics, respectively.

After two years of treatment, ALN and DMab-treated animals showed no difference in microCT or biomechanical parameters vs. OVX-VEH (DMab-treated monkeys developed anti-drug antibodies, which might reduce efficacy of this drug). However, treatment with CatKi-H resulted in a 30% increase in yield and peak load values as compared to OVX-VEH ( $p < 0.05$ ) and gave average mechanical values greater than the Sham sample. Treatment with CatKi-L exhibited similar trend of increase ( $p < 0.08$ ). Intriguingly, these changes were realized despite no significant detectable differences on mean values of trabecular bone morphologic parameters. Together, these data suggest matrix-level changes or alterations in bone composition that are unique to the mechanism of CatK inhibition, resulting in improving bone strength with treatment.



Disclosures: Isabel Colon-Bernal, None.

## LB-SU0382

**Rebound-associated bone loss after discontinuation of denosumab in 101 postmenopausal women: preliminary results of an observational study (Disco DMab).** Albrecht W Popp\*, Helene Buffat, Bita Yousefi, Christoph Senn, Sandra Grifone, Kurt Lippuner. Department of Osteoporosis, Inselspital, Bern University Hospital, University of Bern, Switzerland

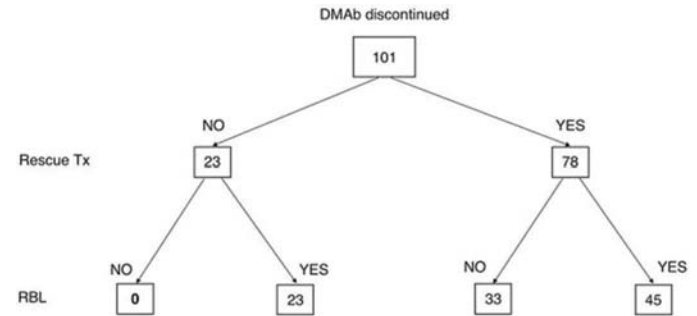
**Introduction:** Rebound-associated bone loss (RBL) after denosumab (DMab) non-renewal in postmenopausal women refers to the increase in bone turnover (BTM) and loss of bone mineral density (BMD) observed within the first year of follow-up (Miller PD et al, Bone, 43, 2008). In the absence of high quality scientific evidence, it has been suggested that follow-up therapy with a bisphosphonate may prevent RBL after DMab non-renewal (Anastasilakis AD et al, J Bone Miner Res, 32 (6), 2017). The aim of the present analysis was to document the occurrence of RBL in postmenopausal women who stopped DMab.

**Methods:** This observational study was conducted in all consecutive postmenopausal women (from 2015 to spring 2017) who discontinued subcutaneous DMab 60 mg every 6 months after at least two doses, i.e. in whom DMab has not been renewed within 6 to 18 months after the last injection. Based on earlier findings (Bone HG et al, JCEM, 96(4), 2011) RBL was defined as a BMD loss measured by DXA (Discovery<sup>TM</sup>, Hologic Inc., Bedford, MA, USA) that exceeds 5% at either the lumbar spine or the total hip and/or as BTM levels (CTX, PINP, osteocalcin or BAP) exceeding the upper limit of the premenopausal reference values. Women were categorized by having received rescue bisphosphonate (oral alendronate or intravenous ibandronate or zoledronate at recommended doses for the treatment of postmenopausal osteoporosis) treatment (rescue Tx) after discontinuation or not. The study was approved by the Cantonal Ethical Committee Bern, Switzerland.

**Results:** As shown in figure 1, between 2015 and spring 2017, 101 consecutive women (age 47 to 88 years, median 69 ys) had discontinued DMab. Mean interval until control DXA measurement was 24 (9 to 30) months since the last DMab injection. Of all women experiencing RBL, 39% had spine BMD loss >5%, 31% TH >5% and 60% BTM

increase above premenopausal normal range. In the absence of rescue Tx, all women experienced RBL after DMab non-renewal (23/23, 100%). Among women who received rescue Tx, 58% (45/78) had developed RBL.

**Conclusions:** Rebound-associated bone loss is frequent after DMab non-renewal. Rescue therapy with a bisphosphonate reduced RBL in less than half of all treated women. The predictors of response to bisphosphonates as well as the most effective dose and regimen remain unknown. The consequences in terms of fracture risk increase remain to be elucidated.



Disclosures: Albrecht W Popp, None.

## LB-SU0383

### Effect of Alendronic acid on fracture healing - A Randomised Clinical Trial.

Stuart Ralston\*, Andrew Duckworth, Christopher Tuck, Aryally Rodriguez, Gordon Murray, Margaret McQueen. University of Edinburgh, United Kingdom

**Background:** Bisphosphonates are often withheld immediately following the occurrence of a fracture due to the concerns that they may inhibit fracture union. The aim of this study was to determine if administration of bisphosphonate soon after a wrist fracture affects union or other clinical outcomes

**Methods:** A total of 421 patients age  $\geq 50$  years with radiologically confirmed low trauma wrist fractures, who were not currently being treated with bisphosphonates were included in a double blind randomised clinical trial of 26 weeks duration. Patients were randomised 1:1 to receive alendronic acid 70mg once weekly (n=215) or placebo (n=206) within 14 days of the fracture in addition to usual care. Fracture healing was assessed by evaluation of serial x-rays performed at weeks 2, 4, 6, 8 and 26 after the fracture by an observer blind to treatment allocation

**Main Outcomes and Measures:** The primary outcome measure was the percentage of fractures that were united at 4-weeks. Secondary outcome measures included patient reported upper limb specific Disability Arm Shoulder and Hand (DASH) questionnaire, range of wrist movement and grip strength, pain and analgesia requirements, the prevalence and the rate of malunion.

**Results:** Of the 421 randomised patients 362 (86%) patients were female. The mean  $\pm$  age was  $63 \pm 8.5$  years. There was no significant difference in the proportion of patients with a united between the treatment groups at 4 weeks (-4.1%; 95%CI -12.8 to 4.7%;  $p=0.53$ ) or any other time point and no difference in rate of healing using a time-to-event analysis. Adherence to medication was about 85% and did not differ between treatment groups. No significant differences were at any time point between the two groups in terms of DASH score, pain and grip strength.

**Conclusions:** Among patients aged 50 and above with a low trauma wrist fracture, early introduction of bisphosphonate therapy in the form of alendronic acid did not adversely affect fracture union or other clinical outcomes. This suggests that where clinically indicated, bisphosphonate therapy can be safely commenced almost immediately following a low trauma fracture.

Disclosures: Stuart Ralston, Novartis, Other Financial or Material Support.

## LB-SU0384

### Blackberry and raspberry attenuate angiotensin-II induced osteoclastogenesis.

Rafaela Feresin<sup>1</sup>, Ha-neui Kim<sup>2</sup>, Maria Almeida<sup>2</sup>, Shengyu Mu<sup>2</sup>, Christy Simecka<sup>2</sup>. <sup>1</sup>Georgia State University, United States, <sup>2</sup>University of Arkansas for Medical Sciences, United States

Evidence from cross-sectional studies indicate that hypertension is a negative predictor of bone mass in men and women. Animal and cell culture studies suggest that the renin-angiotensin system (RAS) plays a physiological role in bone remodeling, and angiotensin II (Ang II) may increase bone resorption resulting in decreased bone mass. Ang II is known to exert its deleterious effects on bone by increasing oxidative stress, thus, counteracting the production and/or accumulation of reactive oxygen species is an attractive approach to improving bone metabolism in the hypertensive state. Berries have been shown to have not only vascular but also bone-protective properties which have been attributed to their phytochemical content. To this end, we aimed to examine whether blackberry (BL) and/or raspberry (RB) attenuate Ang II-induced bone loss. Twelve-week male C57BL/6J mice were randomized to four groups: 1) Control, 2) Ang II, 3) Ang II + BL, and 4) Ang II + RB. Animals were implanted with minipumps containing Ang II (1000 ng/kg body weight/day) at week 4 and sacrificed at week 8. Ang II significantly increased blood pressure compared to control ( $185 \pm 11$  vs  $132 \pm 5$  mmHg,



$P < 0.000$ ) whereas BL ( $143 \pm 17$  mmHg,  $P = 0.001$ ) and RB ( $147 \pm 27$  mmHg,  $P = 0.002$ ) significantly attenuated this increase. While the analysis of bone phenotype is ongoing, *in vitro* studies using bone marrow-derived macrophages cultured in  $\alpha$ -MEM medium containing M-CSF (30 ng/ml), RANKL (30 ng/ml), Ang II (1  $\mu$ M) and BL and RB (500  $\mu$ g/ml) for five days revealed that Ang II significantly increased the number of TRAP-positive cells by 15% ( $P \leq 0.000$ ) compared to control. Treatment with BL and RB extracts significantly decreased the number of TRAP-positive cells by 98% and 96%, respectively, compared to Ang II alone ( $P \leq 0.000$ ) without exerting any cytotoxicity. Thus far, our results suggest a potential role for BL and RB in mitigating bone loss induced by Ang II. We also expect to demonstrate whether the favorable effects observed on bone phenotype, if any, will be due to the direct effects of BL and RB on Ang II signaling or a secondary effect of reduced blood pressure.

**Disclosures:** Rafaela Feresin, None.

## LB-SU0385

**Pharmacologically Targeting Aging Slows Age-Related Bone Loss.** Simon Melov<sup>\*1,4</sup>, Daniel Evans<sup>2</sup>, Ha-Neui Kim<sup>3</sup>, Monique O'leary<sup>1,4</sup>, Li Han<sup>3</sup>, Ryan Murphy<sup>1,4</sup>, Kristin Koenig<sup>1,4</sup>, Michael Presley<sup>1,4</sup>, Emmeline Academia<sup>1,4</sup>, Brittany Garrett<sup>1,4</sup>, Matt Lave<sup>1,4</sup>, Daniel Edgar<sup>1,4</sup>, Chris Zambatoro<sup>1,4</sup>, Tracey Barhydt<sup>1,4</sup>, Colleen Dewey<sup>1,4</sup>, Jarrot Mayfield<sup>1,4</sup>, Joy Wilson<sup>1,4</sup>, Silvestre Alvarez<sup>1,4</sup>, Brian Kennedy<sup>1,4</sup>, Julie Andersen<sup>1,4</sup>, Pankaj Kapahi<sup>1,4</sup>, Maria Schuller Almeida<sup>3</sup>, Gordon Lithgow<sup>1,4</sup>. <sup>1</sup>Buck Institute for Research on Aging, United States, <sup>2</sup>CPMC, United States, <sup>3</sup>University of Arkansas for Medical Sciences, United States, <sup>4</sup>Buck Institute for Research on aging, United States

There is considerable interest in determining whether chemical compounds or interventions shown to significantly increase longevity in invertebrate models will also affect aging in mammals. To explore this concept, we tested three compounds (HBX ((2-(2-hydroxyphenyl) benzoxazole); Beta Sito-Sterol (BS, Sterol (17-(5-Ethyl-6-methylheptan-2-yl)-10,13-dimethyl-2,3,4,7,8,9,11,12,14,15,16,17-dodecahydro-1H-cyclopenta[*z*]phenanthren-3-ol); Clotquinol (CQ, 5-chloro-7-iodo-quinolin-8-ol)) and one element (Li) for their ability to slow age-related bone micro-architecture and functional decline in older mice. Candidate compounds extended lifespan in either *C. elegans* or *Drosophila*, were efficacious in mouse models of neurodegenerative disease, or had been clinically approved for conditions unrelated to maintenance of bone. Using these four compounds, we chronically treated mice from 19 months of age through end of life, and used a repeated measures experimental design to evaluate a number of structural and functional indices over late life. We focused on the aging skeleton, particularly the femur, because it can be accurately observed by computed tomography (CT) in living animals. We observed that with age there was increased inter-animal variation in bone structure despite the genetically identical nature of the test population. Similar to prior studies, we also observed complex changes in femoral bone loss and architecture during late life; the latter, osteopenic changes being similar to those observed in humans. In addition, we were able to document that the incidence of spontaneous fractures in aged mice is similar to that for humans. Finally, we report that one of the four interventions tested (HBX) reduced the rate of bone loss in mice to a level similar to that seen with anti-osteoporotic drugs in humans. Additional *in vitro* studies in mouse cells indicate that the mechanism for late-life maintenance of bone in the HBX treated mice was due to decreased resorption from osteoclasts, unaccompanied by cell death. Our results demonstrate that selecting interventions on the basis of lifespan extension in invertebrates may be predictive of surprising positive healthspan effects, in tissues not even represented in the invertebrate model.

**Disclosures:** Simon Melov, None.

## LB-SU0386

**Improvements in Motor Function and Cognitive Development With Up to 6 Years of Treatment With Asfotase Alfa in Infants and Children Aged  $\geq 5$  Years With Hypophosphatasia.** Christine Hofmann<sup>\*1</sup>, Johannes Liese<sup>1</sup>, Paul Harmatz<sup>2</sup>, Jerry Vockley<sup>3</sup>, Wolfgang Högl<sup>4</sup>, Shanggen Zhou<sup>5</sup>, Andrew Denker<sup>6</sup>, Anna Petryk<sup>6</sup>, Cheryl Rockman-Greenberg<sup>7</sup>. <sup>1</sup>University Children's Hospital, University of Würzburg, Germany, <sup>2</sup>UCSF Benioff Children's Hospital Oakland, United States, <sup>3</sup>University of Pittsburgh School of Medicine and Graduate School of Public Health, United States, <sup>4</sup>Birmingham Children's Hospital and Institute of Metabolism and Systems Research, University of Birmingham, United Kingdom, <sup>5</sup>Chiltern International Inc., United States, <sup>6</sup>Alexion Pharmaceuticals, Inc., United States, <sup>7</sup>Children's Hospital Research Institute of Manitoba and University of Manitoba, Canada

Hypophosphatasia (HPP) is a rare, inherited, systemic, metabolic disease caused by tissue-nonspecific alkaline phosphatase (TNSALP) deficiency. Manifestations of HPP in infants and young children include impaired gait and ambulation, muscle weakness, and HPP rickets, as well as possible delays in motor and cognitive skills. Asfotase alfa, a human recombinant TNSALP, is indicated for the treatment of pediatric-onset HPP. We report data on cognitive development and motor function with up to 6 y of treatment with asfotase alfa 6 mg/kg/wk from a Phase 2, single-arm, multinational, open-label study (NCT01176266) in patients aged  $\leq 5$  y with potentially life-threatening HPP due to onset at age  $< 6$  mo. Cognitive, fine motor, and gross motor development were assessed as exploratory outcome measures using Bayley Scales of Infant and Toddler Development, 3rd Edition (BSID-III), Cognitive, Fine Motor, and Gross Motor sub-scale scaled scores (patient age:  $\leq 42$  mo), and the Peabody Developmental Motor

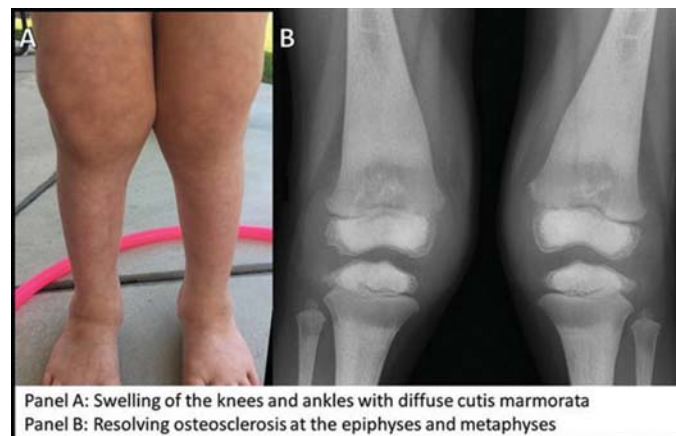
Scales, 2nd Edition (PDMS-2), Locomotion subtest standard score (age: 43–71 mo). The healthy, age-matched mean (standard deviation) for both scales is 10 (3). Both scales were administered by a licensed physical therapist. Unless otherwise specified, data are presented as median (min, max). In total, 69 patients were enrolled and treated (age: 69.1 [0.1–312.1] wk; male: 33 [47.8%]); 60 (87%) completed the study (discontinuations: adverse events, n=6; withdrew, n=3). Overall treatment duration was 2.3 (0.02, 5.8) y. On the BSID-III, the Cognitive scaled score increased from 5.0 (1, 18; n=43) at Baseline to 8.0 (1, 19; n=42) at Last Assessment. The Fine Motor scaled score increased from 7.0 (1, 14; n=43) at Baseline to 8.0 (1, 15; n=42) at Last Assessment, and the Gross Motor scaled score increased from 1.0 (1, 8; n=43) at Baseline to 3.0 (1, 10; n=42) at Last Assessment. On the PDMS-2, the Locomotion subtest standard score increased from 4.0 (1, 8; n=18) at Baseline to 6.5 (1, 13; n=30) at Last Assessment. All patients experienced adverse events, most commonly injection site reactions (62%; n=43). Most infants and young children with HPP generally had lower cognitive and motor scores than peers at Baseline, with improvements after asfotase alfa treatment.

**Disclosures:** Christine Hofmann, Alexion Pharmaceuticals, Inc., Grant/Research Support.

## LB-SU0387

**Severe 1,25-dihydroxyvitamin D-mediated hypercalcemia, polyarticular synovial thickening, and resolving generalized osteosclerosis associated with a heterozygous NOD2 mutation in a 3-year-old girl: a new disorder.** Michael P. Whyte<sup>\*1</sup>, Emilina Lim<sup>2</sup>, Gary S. Gottesman<sup>1</sup>, Lien Trinh<sup>2</sup>, William H. McAlister<sup>3</sup>, Deborah V. Novack<sup>4</sup>, Vinieth N. Bijanki<sup>5</sup>, Angela Nenninger<sup>1</sup>, Steven Mumm<sup>4</sup>, David Buchbinder<sup>2</sup>. <sup>1</sup>Shriners Hospital for Children, St. Louis, United States, <sup>2</sup>Children's Hospital of Orange County, United States, <sup>3</sup>St. Louis Children's Hospital, United States, <sup>4</sup>Washington University School of Medicine, United States, <sup>5</sup>Shriners Hospital for Children, United States

Extrarenal production of 1,25-dihydroxyvitamin D causes hypercalcemia in ~30 different disorders. Many feature granulomas (e.g., sarcoidosis) that express 1 $\alpha$ -hydroxylase activity. We report this pathogenesis in a non-consanguineous Caucasian 3-year-old girl with hypercalcemia/hypercalciuria that caused nephrocalcinosis and compromised renal function. She presented at 2 years-of-age with soft tissue swelling consistent with synovitis and synovial fluid, but without overt arthritis. Soft, spongy, non-tender, non-erythematous lesions were present over the dorsum of her hands, knees, and feet (fig A). Tapering fingers were noted with decreased mobility of her metacarpal phalangeal and interphalangeal joints. Height and weight were both 25<sup>th</sup> percentile whereas head circumference was 95<sup>th</sup> percentile. Frontal bossing was present. Additionally, she had generalized osteosclerosis, hyperostosis, and skeletal modeling abnormalities consistent with osteopetrosis (OPT), yet mutation analysis of 28 genes associated with OPT and dense bone dysplasias was negative, and bone marrow biopsy did not show the pathognomonic features of OPT or evidence of granulomas. The epiphyses at the knees and ankles were particularly osteosclerotic. Serum parathyroid levels were suppressed. Remarkably, over the past year, metaphyseal and apophyseal regions throughout her skeleton showed correction of osteosclerosis in the newly formed endochondral bone (fig B). Interestingly, her biopsy showed large amounts of unresorbed but largely superficial cartilage and relatively few osteoblasts (OBs) and osteoclasts (OCs) deep in the trabecular bone. There was less cartilage and normal appearing OBs and OCs near the cortex, likely reflecting more recently deposited bone. Markers of inflammation (serum C-reactive protein and ESR) and bone turnover (serum CTX and osteocalcin) were elevated. Family history was negative for this disorder. Infantile hypercalcemia was excluded by negative *CYP24A1* mutation analysis. Recently, rheumatoid factor was positive, circulating levels of IgG and neopterin were elevated, and a heterozygous *NOD2* mutation (R334Q), which causes Blau syndrome, was found. Blau syndrome typically features arthritis, uveitis, and dermatitis but not hypercalcemia or sclerotic bone disease. MRI of the swollen joints, synovial biopsy, and a course of prednisone are planned. Hence, our patient seems unique, presenting with Blau syndrome along with hypercalcemia and improving osteosclerosis.



**Disclosures:** Michael P. Whyte, None.

## MO0388

**Primary Hyperparathyroidism: Insights from Indian PHPT Registry.** Sanjay Bhadada<sup>1</sup>, Ashutosh Arya<sup>1</sup>, Satinath Mukhopadhyay<sup>2</sup>, Rajesh Khadgawat<sup>3</sup>, Suja Sukumar<sup>1</sup>, Sailesh Lodha<sup>4</sup>, Deependra N Singh<sup>4</sup>, Anjali Sathya<sup>1</sup>, Priyanka Singh<sup>1</sup>, Anil Bhansali<sup>1</sup>, Sudhaker D Rao<sup>5</sup>. <sup>1</sup>PGIMER, India, <sup>2</sup>IPGIMER, India, <sup>3</sup>AIIMS, India, <sup>4</sup>Fortis Hospital, India, <sup>5</sup>Henry Ford Hospital, United States

**Background and objective:** The presentation of Primary hyperparathyroidism (PHPT) is variable across the world. The present study explored retrospective data submitted in the Indian PHPT registry ([www.indianphptregistry.com](http://www.indianphptregistry.com)) (duration: July 2005–June 2015) from 5 centres covering four different geographical regions of the country.

**Method:** The clinical, biochemical, radiological and histopathological characteristics of PHPT patients across India were analysed for similarity and variability across the centres.

**Results:** Total of 464 subjects (137 men and 327 women) with histopathologically proven PHPT were analysed. The mean age was 41±14 years with the female: male ratio of 2.4:1. The majority (95%) of patients were symptomatic. Common clinical manifestations among all the centres were weakness and fatigability (58.7%), bone pain (56%), renal stone disease (31%), pancreatitis (12.3%) and gallstone disease (11%). Mean serum calcium, PTH and inorganic phosphorus levels were 11.9±1.6 mg/dL, 752.4±735.2 pg/mL and 2.8±0.9 mg/dL respectively. Asymptomatic PHPT patients (n = 23) had significantly lower plasma PTH (279±203 vs 760.4±740.7 pg/mL, p = 0.007) and serum ALP levels (211±99.6 vs 660.8±1181, p = 0.04) compared to symptomatic PHPT patients. Sestamibi scanning had better sensitivity than ultrasonography in the localization of parathyroid adenoma; also when these two modalities were combined, 93% of the cases were correctly localized. The most common histopathological diagnosis was adenoma (94.2%) followed by hyperplasia (n = 22, 4.8%) and parathyroid carcinoma (n = 5, 1%). Mean parathyroid adenoma weight was 5.6 ± 6.5 g (0.1 - 54g). Asymptomatic PHPT patients also had significantly lower tumor weight (2.1±1.6 vs 5.9±7.2 g, p = 0.02).

**Conclusion:** Majority of PHPT patients within India is still mainly symptomatic with more than 50% of patients presenting with bone disease and one-third with renal impairment. Compared to western countries, Indian patients with PHPT are younger, biochemical abnormalities are more severe and adenoma weight is higher. Our observation is largely derived from tertiary care hospital (no routine screening of serum calcium level). Therefore, our results do not reflect racial difference of susceptibility to PHPT.

**Disclosures:** Sanjay Bhadada, None.

## MO0389

**Paget's, Kidney Disease, and Denosumab: A Dangerous Combination.** Lila Chertman<sup>1</sup>, Violet Lagari-Libhaber<sup>2</sup>. <sup>1</sup>University of Miami Department of Endocrinology, Jackson Memorial Hospital, United States, <sup>2</sup>University of Miami Department of Endocrinology, Miami VA Healthcare System, Jackson Memorial Hospital, United States

**Introduction:** Paget's disease [PD] is characterized by increased bone turnover resulting in low-quality bone. Bisphosphonates are the mainstay of treatment resulting in biochemical remission in most cases (1, 2). Advanced chronic kidney disease [CKD] precludes the use of bisphosphonates. Case reports describe denosumab [D-mab], a monoclonal antibody against RANKL as an alternative. We describe a case in which 1 dose of 60 mg D-mab for PD produced clinically significant hypocalcemia for 5 months following injection.

**Case Report:** A 91-year-old male with CKD IV, secondary hyperparathyroidism (PTH 131 IU/L, calcium 8.8 mg/dl, 25-OH vitamin D [25(OH)D] 37 ng/ml, phosphorus 3.0 mg/dl, alkaline phosphatase 852 IU/L), PD (scintigraphy: increased uptake in skull, left humerus, right lower rib, thoracic & upper lumbar spine) and bone pain received D-mab 60 mg. He developed symptomatic hypocalcemia requiring hospitalization on 2 separate occasions (serum corrected calcium 6.4 mg/dl and 6.7 mg/dl respectively). He received high dose calcium and calcitriol until serum calcium normalized 5 months post injection. Bone pain minimally improved, GFR remained stable, while alkaline phosphatase improved and rose at 5 months (210-276 IU/L).

**Discussion:** Several case reports describe D-mab as second-line therapy for PD with temporizing results. An 86-year-old male with PD, GFR 11 ml/min, normal ionized calcium, PTH, and 25(OH)D levels received D-mab 60 mg with a decrease in markers of bone turnover within 1 month and rise to baseline by month 4, improvement in bone pain and bone scintigraphy with continued treatment (3). Reid et al describe a 75-year-old woman with PD intolerant of bisphosphonates and normalization of alkaline phosphatase 4-8 months following D-mab (2). CKD patients are at risk for hypocalcemia in the setting of D-mab despite normal 25(OH)D and baseline serum calcium (4, 5). The suspected mechanism of D-mab induced hypocalcemia involves decoupling of osteoclastic and osteoblastic activity with a net influx of calcium into bone. CKD and hyperparathyroid bone disease pose a greater risk of hypocalcemia due to a proposed hungry bone syndrome because of increased PTH-mediated bone turnover, such as what may have occurred with our patient.

**Conclusion:** Patients with CKD and PD are at risk of D-mab induced hypocalcemia despite normal baseline calcium and 25(OH)D levels. Hyperparathyroidism intensifies this risk. Caution should be used when using D-mab in this setting.

**Disclosures:** Lila Chertman, None.

## MO0390

**Comorbidities Associated with Hypoparathyroidism: An 8-Year Register-Based Study in Italy.** Cristiana Cipriani<sup>1</sup>, Jessica Pepe<sup>1</sup>, Rizieri Manai<sup>1</sup>, Luciano Nieldu<sup>2</sup>, Federica Biamonte<sup>1</sup>, Chiara Sonato<sup>1</sup>, Piergianni Biondi<sup>1</sup>, Luisella Cianferotti<sup>3</sup>, Maria Luisa Brandi<sup>3</sup>, Salvatore Minisola<sup>1</sup>. <sup>1</sup>Sapienza University of Rome, Italy, <sup>2</sup>UNINT University, Italy, <sup>3</sup>University of Florence, Italy

**Purpose.** To assess the prevalence of comorbidities associated with hypoparathyroidism among hospitalized patients in Italy during an 8-year period.

**Methods.** We retrieved data from the "Record of Hospital Discharge" (SDO) of the Italian Health Ministry, from the year 2006 to 2013 and analyzed the codes corresponding to hypoparathyroidism-related diagnoses. We observed a mean prevalence of hypoparathyroidism of 5.3/100,000 inhabitants/year among inpatients and retrieved the data corresponding to cardiovascular, infectious, urinary tract and psychiatric disease, cerebral calcifications, epilepsy, skin, cataract, fracture and cancer. The codes corresponding to cancer of the neck region were excluded as hypoparathyroidism can result from neck surgery in these cases.

**Results.** Table 1 shows the prevalence of diagnoses of the aforementioned complications, demographic data and days of stay in the period 2006-2013.

**Conclusions.** Our preliminary results demonstrate that there is a high prevalence of cardiovascular, infectious, urinary tract, psychiatric diseases and cancer in association with the diagnosis of hypoparathyroidism in Italy in the period 2006-2013. Comorbidities are more frequent in the sixth-seventh decade of life and in women than men. It is interesting to note the low rate of hospitalization for fracture among patients with hypoparathyroidism.

More data on factors possibly associated with the epidemiology and clinical manifestation of the comorbidities are needed. In particular, results need to be validated by the comparison with a control population in order to define the prevalence of the aforementioned comorbidities in association with hypoparathyroidism.

Table 1. Prevalence of diagnoses of any complication, demographic data and days of stay in the period 2006-2013

Comorbidities	n (%) of hospitalizations	Sex (F/M ratio)	Age (years; mean±SD)	Days of stay (mean±SD)
Cardiovascular	3600 (31.4)	2.8:1	64.4±16.7	11±11.4
Infectious	903 (7.9)	2.8:1	51.9±23.2	12.7±11.7
Urinary tract	955 (8.3)	2.2:1	64.6±16	10.9±10.3
Psychiatric	595 (5.2)	3.1:1	55±22.9	10.3±11.4
Epilepsy	252 (2.2)	2.1:1	52.2±23.4	12±11.8
Cerebral calcifications	46 (0.4)	1.4:1	57.5±18.7	14.5±11.3
Skin	197 (1.7)	3.5:1	51±25.4	10.8±12.5
Crampi e tetania	214 (1.9)	3.9:1	50±23	8.2±8.9
Cataract	18 (0.2)	1:1	58.2±16.9	8.3±8.5
Fracture	94 (0.8)	2.7:1	66.5±220.2	16.2±11.8
Cancer	898 (7.8)	2.2:1	59.5±15.7	9.2±9.8

Table 1

**Disclosures:** Cristiana Cipriani, None.

## MO0391

**Maintenance of Key Biochemical Parameters With Recombinant Human Parathyroid Hormone (1-84) in Patients With Hypoparathyroidism: An Analysis of a Long-Term, Open-Label, Single-Center Study.** Natalie E. Cusano<sup>1</sup>, Mishaella R. Rubin<sup>1</sup>, Rebecca Piccolo<sup>2</sup>, Alan Krasner<sup>2</sup>, John P. Bilezikian<sup>1</sup>. <sup>1</sup>College of Physicians and Surgeons, Columbia University, United States, <sup>2</sup>Shire Human Genetic Therapies, Inc., United States

Hypoparathyroidism is a rare disorder characterized by hypocalcemia and insufficient or undetectable parathyroid hormone (PTH). Recombinant human PTH, rhPTH (1-84), is available in the United States for the treatment of hypoparathyroidism. When hypoparathyroidism is established, long-term administration of rhPTH(1-84) is a treatment option. Thus, long-term safety and efficacy data for rhPTH(1-84) are needed. To this end, we evaluated data from adults with hypoparathyroidism who previously participated in a single-arm, single-center study known as HEXT (NCT00473265) and are now enrolled in a new phase 4 study (NCT02910466). Uninterrupted rhPTH(1-84) therapy has been maintained for 4.0–11.4 years.

Baseline was the last assessment before starting rhPTH(1-84). Visit windows, defined as once every 6±3 months from baseline, were used for summary of assessments collected over time from medical records. If multiple measurements were recorded within a visit window, the value closest to the target day was used. Data are presented as mean ± SD.

This cohort comprises 33 patients (53.4±12.4 years; 76% women; duration of hypoparathyroidism, 19.4±12.1 years). Mean duration of rhPTH(1-84) treatment was 7.5±2.3 years. Albumin-corrected serum calcium remained relatively stable during the treatment period and was near or within the target range for patients with hypoparathyroidism at most time points (Table: selected time points over 10 years). Urinary calcium, serum phosphate, and serum creatinine were maintained within the target or normal ranges at all time points during rhPTH(1-84) treatment (Table). Estimated glomerular filtration rate was between 60 and 89 mL/min/1.73 m<sup>2</sup> at baseline and at most time points over the course of rhPTH(1-84) treatment (Table). Calcium-phosphate



product was  $3.06 \pm 0.55 \text{ mmol}^2/\text{L}^2$  at baseline and remained  $<4.4 \text{ mmol}^2/\text{L}^2$  at all time points.

This analysis includes the longest reported experience with rhPTH(1-84) for the treatment of hypoparathyroidism. The results document that rhPTH(1-84) treatment is characterized by maintenance of biochemical parameters, including stable renal function, within normal or target ranges for this disease. These data provide strong support for the efficacy of rhPTH(1-84) in the long-term management of hypoparathyroidism.

Parameter, Mean (SD)	BL	2.5 y	5.0 y	7.5 y	10.0 y
Albumin-corrected serum calcium, mmol/L (target range, * 2.00–2.12 mmol/L)	n=30 2.10 (0.26)	n=29 2.08 (0.22)	n=26 2.01 (0.14)	n=12 1.97 (0.31)	n=6 1.99 (0.26)
Urinary calcium, mg/24 h (target range, * <300 mg/day)	n=17 290.9 (134.5)	n=21 214.1 (117.5)	n=24 237.0 (193.3)	n=10 242.5 (110.5)	n=5 178.6 (98.2)
Serum phosphate, mmol/L (normal range, 0.81–1.45 mmol/L)	n=32 1.43 (0.26)	n=29 1.32 (0.32)	n=25 1.31 (0.22)	n=12 1.34 (0.30)	n=6 1.26 (0.27)
Serum creatinine, $\mu\text{mol/L}$ (normal range, <115 $\mu\text{mol/L}$ )	n=31 83.1 (12.2)	n=29 78.7 (12.8)	n=26 80.5 (14.8)	n=13 80.6 (23.2)	n=6 76.6 (6.7)
Estimated GFR, mL/min/1.73m <sup>2</sup>	n=31 76.6 (16.6)	n=29 80.9 (15.9)	n=26 79.2 (13.2)	n=13 82.8 (19.5)	n=6 83.9 (12.9)

BL=baseline; GFR=glomerular filtration rate.

\*For patients with hypoparathyroidism.

Table

Disclosures: Natalie E. Cusano, Shire, Speakers' Bureau.

## MO0392

**A Case of Hypophosphatemic Rickets in Pregnancy.** Janet Lee<sup>\*1</sup>, Jeffrey Sperling<sup>2</sup>, Kirsten Salmeen<sup>2</sup>, Dolores Shoback<sup>3</sup>, Ingrid Block-Kurbisch<sup>2</sup>.

<sup>1</sup>Division of Endocrinology and Metabolism, Department of Medicine and Pediatrics, University of California, San Francisco, United States, <sup>2</sup>Department of Obstetrics, Gynecology, and Reproductive Sciences, Division of Maternal Fetal Medicine, University of California, San Francisco, United States, <sup>3</sup>Endocrine Research Unit, Department of Medicine, San Francisco Department of Veterans Affairs Medical Center, University of California, San Francisco, United States

Management of genetic disorders of phosphate wasting like X-linked hypophosphatemia (XLH) in adults is controversial, with no guidelines for pregnancy or lactation. We evaluated a 34-year-old G2P0 woman diagnosed with hypophosphatemic rickets in infancy. At age 2 years, she was initially thought to have XLH and later considered to have hypophosphatemic rickets with hypercalciuria (HHRH). No molecular diagnostic testing had been done. There was no family history of rickets, short stature, or bone disease. She was born full term via cesarean section and weighed 4366 g, had cardiomegaly with tricuspid and mitral valve insufficiency, all of which resolved after brief treatment with digoxin. She was of English, Welsh, and Native American descent with no known consanguinity. At diagnosis, she was treated with calcitriol and potassium phosphate for leg bowing and x-ray changes of rickets, with subsequent gradual healing and straightening of her legs. She did not have any early tooth loss or dental problems. She was treated with this regimen until age 15 years, when she reached her normal adult height. She had no orthopedic issues until age 22 years, when she suffered a right patellar dislocation and lateral tendon rupture. She also sustained a right foot stress fracture after climbing a ladder 2 to 3 years prior to presentation. She had no nephrolithiasis or renal dysfunction. At 27 years, while off all medications, her lab tests were consistent with HHRH [Table]. Bone density by DXA showed lower Z-scores at the hip (-0.8, -0.9). Potassium phosphate was initiated and titrated to 1500 mg by mouth 3 times daily, which was continued throughout pregnancy with serum phosphorus levels ranging from 1.7 to 2.7 mg/dL [Table]. Her pregnancy was uncomplicated until she developed foot pain after standing on a bus for 1.5 hours. X-rays showed stress fractures in her right foot. One published case report described bilateral atraumatic femoral fractures in the postpartum period in a woman with hypophosphatemia. Due to the lack of knowledge of her skeletal status pre-conception and the unknown risks of vaginal delivery in women with hypophosphatemia, an elective cesarean section was recommended. She underwent an uncomplicated primary cesarean delivery at 39 weeks and delivered a viable female weighing 3020 g. We recommended limited lactation. Genetic diagnosis and skeletal imaging will be pursued, and the infant will be evaluated for phosphate wasting and skeletal abnormalities.

Table. Labs before and during pregnancy				
	27 years*	1 <sup>st</sup> Trimester	2 <sup>nd</sup> Trimester**	3 <sup>rd</sup> Trimester
Serum Phosphorus (2.4-4.9 mg/dL)	1.9 mg/dL (2.5-4.5 mg/dL)	2.9 mg/dL	2.1 mg/dL	1.7 mg/dL*** 2.7 mg/dL
Serum Calcium (8.8-10.3 mg/dL)	8.5 mg/dL (8.5-10.6 mg/dL)	8.6 mg/dL	8.7 mg/dL	8.4 mg/dL*** 8.5 mg/dL
Serum Magnesium (1.8-2.4 mg/dL)		1.7 mg/dL		1.6 mg/dL*** 1.9 mg/dL
Intact PTH (12-65 pg/mL)	38 pg/mL (15-65 pg/mL)	78 pg/mL	41 pg/mL	
25-OH Vitamin D (20-50 ng/mL)	26 ng/mL (20-60 ng/mL)	21 ng/mL	19 ng/mL	22 ng/mL
Calcitriol (18-72 pg/mL)	39.7 pg/mL (10-75 pg/mL)	45 pg/mL	67 pg/mL	108 pg/mL
Alkaline phosphatase, Bone-specific (5.3-19.5 mcg/L)		23 mcg/L		
C-terminal fibroblast growth factor 23, FGF23 (<180 RU/mL)	<50 RU/mL	72 RU/mL	70 RU/mL	
Creatinine (0.44-1.00 mg/dL)		0.56 mg/dL	0.48 mg/dL	0.37 mg/dL
Tubular maximum reabsorption of phosphate to GFR, TmP/GFR (2.6-4.4 mg/dL)			1.9 mg/dL	
24 hour urine calcium (100-300 mg/day)	225.2 mg 202.5 mg		380.1 mg	

\*labs off all therapy for 12 years

\*\*labs taken after holding potassium phosphate for 5 days

\*\*\*viral illness, not consistently taking potassium phosphate

Table

Disclosures: Janet Lee, None.

## MO0393

**Clinical presentation and management of primary hyperparathyroidism in Italy.** Federica Saponaro<sup>\*1</sup>, Filomena Cetani<sup>2</sup>, Andrea Repaci<sup>3</sup>, Valentina Camozzi<sup>4</sup>, Salvatore Minisola<sup>5</sup>, Alfredo Scillitani<sup>6</sup>, Iacopo Chiodini<sup>7</sup>, Francesco Romanelli<sup>8</sup>, Bruno Madeo<sup>9</sup>, Laura Gianotti<sup>10</sup>, Antongiolio Faggiano<sup>11</sup>, Luisella Cianferotti<sup>12</sup>, Sabrina Corbetta<sup>13</sup>, Maria Laura De Feo<sup>14</sup>, Andrea Palermo<sup>15</sup>, Paolo Pozzilli<sup>15</sup>, Claudio Marcocci<sup>16</sup>.

<sup>1</sup>Department of Clinical and Experimental Medicine, University of Pisa, Italy, <sup>2</sup>University-Hospital of Pisa, Italy, <sup>3</sup>Endocrine Unit, Sant'Orsola Malpighi, Bologna, Italy, <sup>4</sup>Endocrine Unit, University of Padova, Italy, <sup>5</sup>Department of Internal Medicine and Medical Disciplines 'Sapienza' University, Rome, Italy, <sup>6</sup>Endocrinology Unit, "Casa Sollievo della Sofferenza," IRCCS, San Giovanni Rotondo, Italy, <sup>7</sup>Unit of Endocrinology and Metabolic Diseases Fondazione IRCCS Cà Granda-Ospedale Maggiore Policlinico, Milan, Italy, <sup>8</sup>Department of Experimental Medicine, Sapienza University of Rome, Italy, <sup>9</sup>Azienda USL of Modena, Unit of Endocrinology, Modena, Italy, <sup>10</sup>Division of Endocrinology, Diabetes and Metabolism, Santa Croce and Carle Hospital, 12100, Cuneo, Italy, <sup>11</sup>Endocrinology, Federico II University of Naples, Italy, <sup>12</sup>Department of Internal Medicine, University of Florence, Italy, <sup>13</sup>Area di Endocrinologia e Malattie Metaboliche, IRCCS Policlinico San Donato Milan, Italy, <sup>14</sup>Endocrinology Unit, Careggi Hospital and University of Florence, Italy, <sup>15</sup>Department of Endocrinology and Diabetes, University Campus Bio-Medico, Rome, Italy, <sup>16</sup>Department of Clinical and Experimental Medicine, University of Pisa, Italy

Aim of this study was to evaluate the clinical features of primary hyperparathyroidism (PHPT), the adherence to International Guidelines for parathyroidectomy (PTx) and the rate of surgical cure in Italy.

From January 2014 to January 2016, we conducted a prospective, multicenter study\* of patients with newly diagnosed PHPT.

Data were collected at baseline and during one-year follow-up.

The study group consisted of 604 patients with PHPT, with a mean age of  $61 \pm 14$  yrs (range 15-88), mostly women (n=502, 83%), who were referred from January 2014 to January 2015 for further evaluation and treatment advice. Most patients had sporadic PHPT [n=566 (93.7%), mean age  $63 \pm 13$  yrs]; the remaining 38 (6.3%, mean age  $41 \pm 17$  yrs) had familial forms. The majority of patients (358, 59%) were asymptomatic. Surgery was advised in 281 (46.5%).

Follow up data were available in 345 patients: 158 (45.8%) with symptomatic and 187 (54.2%) with asymptomatic PHPT. Eighty-six patients (54.4%) of the former group underwent PTx, mainly for nephrolithiasis (n=71, 82.6%). One hundred twenty-one asymptomatic patients (64.7%) met at least one criterion for PTx according to the 2008 International guidelines for parathyroidectomy and 65 patients (53.7%) underwent surgery. Criteria for PTx were: serum calcium levels 1 mg above the upper normal limit (n=37, 56.9%), osteoporosis (n=35, 53.8%) and age <50 yrs (n=14, 21.5%). Surgery was not performed in the remaining patients (n=56, 46.3%) despite the presence of serum calcium levels 1 mg above the upper normal limit (n=12, 21.4%), osteoporosis (n=44, 78.6%) and age <50 yrs (n=11, 19.6%). Surgery was also performed in 16 of the 66 (25.7%) patients who did not meet the criteria for surgery.

A total of 168 patients underwent PTx. The histological diagnosis was single adenoma in 89% of cases, hyperplasia in 9%, atypical adenoma in 1%, and carcinoma in 1%. The large majority (n=158, 94%) of patients were cured. Persistence of PHPT was observed in 10 patients with sporadic PHPT (7 single adenomas, 2 hyperplasia and 1 double adenoma).

Patients followed without surgery showed a stable clinical and biochemical disease over one year.

This is the first multicenter Italian study evaluating PHPT phenotype and therapeutic approach. International guidelines recommendations for surgery were followed in half of cases or either symptomatic or asymptomatic PHPT.

\*on the behalf of the Bone and Metabolic Bone disease Club of the Italian Society of Endocrinology

**Disclosures:** *Federica Saponaro, None.*

## MO0394

**Deterioration of Physical Function and Bone Mineral Density after Discontinuation of Asfotase Alfa Therapy in a Young Woman with Infantile Hypophosphatasia.** Mahshid Mohseni<sup>\*1</sup>, Katherine L. Madson<sup>2</sup>, Gary S. Gottesman<sup>2</sup>, Karen E. Mack<sup>2</sup>, Amy L. Reeves<sup>2</sup>, Michael P. Whyte<sup>1</sup>.

<sup>1</sup>Center for Metabolic Bone Disease and Molecular Research, Shriners Hospital for Children, and Division of Bone and Mineral Diseases, Department of Internal Medicine, Washington University School of Medicine, United States, <sup>2</sup>Center for Metabolic Bone Disease and Molecular Research, Shriners Hospital for Children, United States

Hypophosphatasia (HPP) is the inborn-error-of-metabolism caused by loss-of-function mutation(s) that deactivate the tissue-nonspecific isoenzyme of alkaline phosphatase. In 2015, asfotase alfa (AA) received multinational approval as a bone-targeted enzyme replacement treatment typically for pediatric-onset HPP. Whether continuation of AA therapy is necessary after completion of growth is unknown. We report a young woman survivor of infantile HPP, followed at our research center since age 6 months, who as a teenager responded well to AA over 3 years during an open-label clinical trial. After electing to discontinue the treatment, she then manifested deterioration to baseline in physical function and substantial decreases in bone mineral density (BMD). Early in life, she suffered failure to thrive, pneumonias, craniosynostosis, premature loss of deciduous teeth, delayed walking, gait abnormality, and lower extremity pain. At age 14 years, articulated ankle/foot orthoses (AFOs) helped her ambulate, but she could walk or stand for only 20 minutes before requiring a wheelchair. Then, six months after beginning AA treatment (NCT01163149), she discontinued her AFOs and use of a wheelchair. Within the first year of treatment, she could run, dance, walk, and stand for > 2 hours before developing foot pain. Nevertheless, after 39 months of AA therapy, she elected to stop the treatment because of injection site lipohypertrophy on her arms and abdomen known to sometimes complicate AA treatment. Six months later, decreased endurance and increased foot pain compromised her ambulation that gradually worsened so that she could walk for only 10 minutes. Two years after AA discontinuation, DXA showed 9.1% and 16.3% decreases in BMD in her lumbar spine and hip, respectively. Now, 21 years-of-age, our patient had resumed AA treatment accompanied once again by less pain and increased endurance. DXA 4 months later has shown 7% and 1% increases in her lumbar spine and hip BMD, respectively. Nevertheless, she reported that recovery was slower than during her first AA treatment. Thus, an adolescent girl with infantile HPP benefitted substantially from AA treatment, but deteriorated in physical function and BMD within months of stopping therapy. Other patients with HPP likely risk such deterioration if treatment ceases, and perhaps delayed improvement after reinitiating therapy.

**Disclosures:** *Mahshid Mohseni, None.*

## MO0395

**Geographic Heterogeneity in Health-Related Quality-of-Life Treatment Response to Recombinant Human Parathyroid Hormone (rhPTH[1-84]) in Patients With Chronic Hypoparathyroidism: Post Hoc Analysis of REPLACE.** Tamara J. Vokes<sup>\*1</sup>, Michael Mannstadt<sup>2</sup>, Michael A. Levine<sup>3</sup>, Bart L. Clarke<sup>4</sup>, Peter Lakatos<sup>5</sup>, Kristina Chen<sup>6</sup>, Rebecca Piccolo<sup>6</sup>, Alan Krasner<sup>6</sup>, Dolores M. Shoback<sup>7</sup>, John P. Bilezikian<sup>8</sup>. <sup>1</sup>University of Chicago Medicine, United States, <sup>2</sup>Massachusetts General Hospital and Harvard Medical School, United States, <sup>3</sup>Children's Hospital of Philadelphia, United States, <sup>4</sup>Mayo Clinic Division of Endocrinology, Diabetes, Metabolism, and Nutrition, United States, <sup>5</sup>Semmelweis University Medical School, Hungary, <sup>6</sup>Shire Human Genetic Therapies, Inc., United States, <sup>7</sup>SF Department of Veterans Affairs Medical Center, University of California, United States, <sup>8</sup>College of Physicians and Surgeons, Columbia University, United States

Health-related quality of life (HRQoL) was measured by the Short Form-36 (SF-36) health survey in 122 patients (n=83, rhPTH[1-84]; n=39, placebo [PBO]) with hypoparathyroidism from the randomized REPLACE study (NCT00732615/EudraCT2008-005063-34) conducted in Western Europe (WEU; Belgium, Denmark, France, Italy, UK), Central/Eastern Europe (Hungary), and North America (NA; Canada, USA). This post hoc analysis assessed the regional differences in baseline SF-36 scores and response to rhPTH(1-84) treatment.

SF-36 consists of 8 health domains including 2 composite scores. A mixed-effect model accounting for repeated measures was conducted to assess treatment effect and interaction between treatment and region on SF-36 score change at Wk24, adjusting for baseline (BL) characteristics (sex, age, and SF-36 scores).

BL SF-36 scores were balanced within regions, except in Hungary, where scores were numerically higher in rhPTH(1-84)-randomized patients (significant for physical functioning [PF,  $P=0.031$ ] and vitality [VT,  $P=0.025$ ]). Because we found a significant interaction between region and treatment effect, regional differences in response to rhPTH(1-84) were examined. rhPTH(1-84)-treated patients from Hungary (n=16)

showed trends (not significant) for worsened/unchanged scores. In contrast, rhPTH(1-84) treatment in NA/WEU (n=67) were associated with several improved scores: PF ( $P<0.001$ ), role-physical (RP;  $P<0.05$ ), bodily pain (BP;  $P<0.05$ ), general health (GH;  $P<0.05$ ), VT ( $P<0.001$ ), and mental health (MH;  $P<0.05$ ) domains and physical component summary (PCS;  $P<0.001$ ), with significant differences between rhPTH(1-84) and PBO for RP ( $P<0.05$ ), VT ( $P<0.05$ ), and PCS ( $P=0.01$ ). Temporal patterns of significant changes were as follows: for PF, GH, VT, and PCS, changes reported at Wk4 (first study time point) and maintained throughout the study; for BP, change reported at Wk4, then fluctuated mid-study until Wk24; for RP and MH, gradual increases observed (significant at Wk24). In patients receiving PBO, SF-36 scores did not change significantly for any domain.

This analysis found regional differences in SF-36 score at BL and after treatment with rhPTH(1-84). Differing results from Hungary may be due to unbalanced BL SF-36 scores, misunderstanding of questionnaires, lack of treatment response, or other factors. Among patients from WEU and NA on optimized conventional therapy, rhPTH(1-84) treatment improved several key HRQoL scores, particularly those in physical domains.

**Disclosures:** *Tamara J. Vokes, Shire, Consultant.*

## MO0396

**Is normal range of serum PTH really normal.** Junping Wen<sup>\*</sup>, Yinli Lin, Yuanyuan Zheng, Wei Lin, Jixing Liang, Huibin Huang, Liantao Li, Lixiang Lin, Gang Chen, Fujian Provincial Hospital, China

**Objective:** The aim of this study was to find upper limit of the PTH, considering the adverse effect of high PTH.

**Methods:** We provided 940 patients who visited at Fujian Provincial Hospital between September 2010 and December 2013 with a measured parathyroid hormone (PTH), calcium level and blood pressure. The blood pressure, serum calcium, creatinine, 25(OH)VitD, electrocardiogram, carotid artery plaque thickness, ventricular internal diameter and bone mineral were taken into analysis.

**Results:** There was a significant positive association between serum PTH and blood pressure ( $p<0.05$ ). The case with hypertension had higher level of PTH ( $50.24\pm54.80$  vs  $35.52\pm22.74$ ,  $P<0.01$ ) than the normotensive. After adjustment for all potential confounders, risks (odds ratios and 95% confidence interval) of PTH in hypertension was 1.007 (1.000, 1.013), respectively ( $P<0.05$ ). Within each PTH group there was a difference in systolic blood pressure of 1-7mmHg, but not in diastolic blood pressure. The area under the receiver operating characteristic curve for PTH was 57.5% ( $P<0.01$ ), the optimal threshold for PTH was 51.68pg/ml, sensitivity of 0.262, specificity of 0.884, which may therefore be considered a "fair" test, however, serum PTH is still insufficient for detecting hypertension. According to creatinine quartile, groups with PTH  $\geq 51.68$ pg/ml had higher mean blood pressure than those with PTH  $< 51.68$ pg/ml. The subjects with PTH  $\geq 51.68$ pg/ml had experienced significantly more undesirable hypertension than the PTH  $< 51.68$ pg/ml ( $P<0.01$ ), but the group differences were not significant in cardiovascular events or bone complication.

**Conclusions:** The subjects with PTH  $\geq 51.68$ pg/ml had experienced significantly more undesirable hypertension. The upper limit of PTH may less than 51.68pg/ml. It is considered that control the level of PTH  $< 51.68$ pg/ml may reduce the occurrence of hypertension.

**Disclosures:** *Junping Wen, None.*

## MO0397

**Exploring the Associations between Bone Composition and Clinical Measures of Fragility Fracture Risk: a Pilot Transcutaneous *in vivo* Raman Study.** Hao Ding<sup>\*</sup>, Andrea Baker, Ping Wang, Philip Orlander, William Ip, James Kellam, Catherine Ambrose, Nahid Rianon, Xiaohong Bi, University of Texas Health Science Center, United States

The fracture resistance of bone is determined by its quantity and quality. Bone tissue composition, as a key component of bone quality, has been investigated extensively *in vitro*. However, the relation between composition and the fracture risk is still unclear. The goal of the current study is to investigate the association between compositional bone quality indicators and fragility fracture risk in an aging population. We conducted a cross-sectional clinical study examining the relationship among bone composition using Raman spectroscopy (noninvasively determined) and clinical risk factors assessed by the Fracture Risk Assessment Tool (FRAX) and bone mineral density (BMD) in patients with or without fragility fracture.

A total of 17 patients were recruited to our pilot study including 9 with acute fracture (fragility fracture within the past 3 months) and 8 age-matched controls (no history of fracture). Raman spectra were collected transcutaneously from the mid-shaft of anterior tibia for each patient using a custom-designed *in vivo* Raman spectroscope. Raman signatures of bone were differentiated from that of the soft tissue using independent component analysis. Composition variables that were previously reported indicative of bone quality, including mineral-to-collagen ratio, carbonate content, and mineral crystallinity were calculated. All variables were compared between fractured and non-fractured groups using standard t-test. Spearman's correlation test was employed to determine the relationship between composition and clinical measures.

The fracture group demonstrated decreased mineral-to-collagen ratio and mineral crystallinity. No significant difference was observed between groups in carbonate content, BMD of spine or femoral neck, or T-score of spine. The mean T-score of femoral neck was -2.48 and -1.6 for fracture and non-fractured groups respectively with  $p=0.053$ . The FRAX score for hip fracture and major osteoporosis-related fracture didn't show



significant difference when the acute fracture was excluded, but was significantly higher after factoring in the fracture. There was no significant correlation between tissue composition and any of the clinical indices examined, indicating that tissue composition could be an independent risk factor for fragility fracture. The results from this study suggest the necessity of including compositional bone quality indicators for fracture risk prediction.

**Disclosures:** Hao Ding, None.

## MO0398

**Impact of Endurance Exercise on Bone Response to Continuous Low Dose-Rate Radiation during Hindlimb Unloading.** Rihana Bokhari<sup>\*1</sup>, Emily Sturgell<sup>1</sup>, Matthew Allen<sup>2</sup>, John Ford<sup>1</sup>, Susan Bloomfield<sup>1</sup>. <sup>1</sup>Texas A&M University, United States, <sup>2</sup>Indiana University School of Medicine, United States

The longest human experience with galactic cosmic radiation (GCR) is the 12-day Apollo mission. GCR is a major concern for human health outside of low earth orbit because its effective shielding does not yet exist. Most studies on the impact of low dose-rate radiation like GCR on bone deliver one acute dose within minutes. Combining continuous low dose-rate radiation (CIRR) exposure with hindlimb unloading (HU), we also tested exercise as a potential mitigant for harmful effects of radiation +/- HU. Endurance exercise can activate anti-oxidant defenses that may mitigate oxidative damage induced by radiation exposure. Female C57Bl6/J mice (17-wk-old) were randomly assigned to 8 groups (n=10/group): sham weight bearing (Sham-WB), irradiated weight bearing (CIRR-WB), sham HU (Sham-HU), irradiated HU (CIRR-HU), sham exercise (Sham-Ex), irradiated exercise (CIRR-Ex), sham exercise HU (Sham-ExHU) and irradiated exercise HU (CIRR-ExHU). Mice began treadmill running at 17 wks of age at 12 m/min for 45 min/day 3 days on 1 day off. After 3.5 wks of running, mice began HU. CIRR mice lived in the radiation field created with <sup>60</sup>Co sources for 28 days, for a total dose of 0.175 Gy (6.25 mGy/day). Extensive dosimetry confirmed a homogenous radiation field across the entire animal rack. All end-point data were analyzed by 3-way ANOVA; significance was set at p < .05. After 28 days, CIRR led to an increase in total body bone mineral density (Tb-BMD), fat and lean mass (by DEXA). CIRR also led to modest increases in  $\mu$ -CT measures of distal femur cancellous bone volume (%BV/TV) and trabecular thickness (Tb.Th). HU resulted in expected decreases in Tb-BMD, lean and fat mass, %BV/TV and Tb.Th. Exercise-trained mice exhibited higher %BV/TV and Tb.Th; negative impacts of HU on bone parameters were prevented in Sham-ExHU mice. However, the positive effects of CIRR did not mitigate HU losses in %BV/TV and Tb.Th. Interestingly, the positive effects of CIRR and Ex were not additive. Radiation exposure usually induces bone loss, even at low doses similar to that used in this study. However, our data illustrate a generally positive effect of very low dose-rate gamma radiation delivered over 28 days. To our knowledge, this is the first study to examine how continuous, low-dose rate radiation exposure modifies the bone response to HU in both sedentary and exercise trained mice.

**Disclosures:** Rihana Bokhari, None.

## MO0399

**Microgravity exposure diminishes trabecular microarchitecture and cortical bone morphology in skeletally mature mice.** Jennifer C. Coulombe<sup>\*1</sup>, Alicia M. Ortega<sup>1</sup>, Eric W. Livingston<sup>2</sup>, Ted A. Bateman<sup>2</sup>, Louis S. Stodieck<sup>1</sup>, Samuel M. Cadena<sup>3</sup>, Virginia L. Ferguson<sup>1</sup>. <sup>1</sup>University of Colorado, United States, <sup>2</sup>University of North Carolina at Chapel Hill, United States, <sup>3</sup>Novartis Institutes for Biomedical Research, Inc., United States

Microgravity causes bone loss in humans at rates that are greater than in postmenopausal osteoporosis. Spaceflight studies utilizing rodents have historically been of limited duration (~2 weeks), and many of these experiments utilized young mice where the influence of bone formation and resorption were not readily separated. Here we evaluate bone changes in skeletally mature mice flown for 21 days on the International Space Station (ISS) on Rodent Research-1, SpaceX-4.

Tibiae were collected from a separate study of skeletal muscle in wild type (WT) and muscle RING-finger protein-1 (MuRF1) knockout (KO) mice, a gene associated with skeletal muscle degradation. Thirty-two week-old female C57BL/6, WT and MuRF1 KO mice (n=10/group), were equally distributed into ground control (GC) and spaceflight (SF) groups. SF mice were housed on the ISS for 21 days, at which point they were euthanized and hindlimbs were removed. GC mice were maintained under matched conditions. Microcomputed tomography (microCT; 10 $\mu$ m; Scanco  $\mu$ CT80) was used to evaluate trabecular microarchitecture and cortical bone morphology within the proximal tibia.

Two-way ANOVA indicated no effect of MuRF1 deficiency on any microCT outcome measures ( $\alpha$ =0.05), thus WT and MuRF1 KO groups were pooled to subsequently compare GC vs. SF. Microgravity significantly reduced trabecular (Tb.) bone volume fraction Tb.BV/TV (-42.3%, p<0.01), thickness Tb.Th. (-24.0%, p<0.0001), and volumetric bone mineral density Tb.vBMD (-43.2%, p<0.01); however, no differences were observed in trabecular number and separation, connectivity density, or structure model index. In cortical (Ct.) bone, SF significantly reduced Ct.BV/TV (-5.4%, p<0.0001), thickness Ct.Th. (-15.9%, p<0.01), and polar moment of inertia (-13.7%, p<0.05). Correspondingly, porosity Ct.Po (+27.2%, p<0.0001) increased significantly in SF.

Overall, 21 days of microgravity exposure resulted in significantly decreased trabecular microarchitecture and cortical bone morphology in skeletally mature mice. As bone formation rates are low in skeletally mature bone, resorption is implicated as the dominant mechanism underlying these microgravity-induced changes. This phenomenon is similar to that which is observed in astronauts, where bone resorption outpaces formation. These results motivate the need for further study of bone changes following long-duration spaceflight and support the use of mice to study bone loss and potential countermeasures in microgravity.

	GC-WT	GC-KO	SF-WT	SF-KO	P-value
Tb.BV/TV	0.042 $\pm$ 0.008	0.045 $\pm$ 0.016	0.023 $\pm$ 0.008	0.027 $\pm$ 0.009	<0.01
Tb.Th (mm)	0.051 $\pm$ 0.003	0.053 $\pm$ 0.002	0.043 $\pm$ 0.008	0.036 $\pm$ 0.002	<0.0001
Tb.vBMD (mg HA/cm <sup>3</sup> )	66.7 $\pm$ 17.4	74.2 $\pm$ 24.9	36.1 $\pm$ 13.8	43.9 $\pm$ 14.3	<0.01
Ct.BV/TV	0.83 $\pm$ 0.02	0.84 $\pm$ 0.02	0.79 $\pm$ 0.01	0.79 $\pm$ 0.02	<0.0001
Ct.Th (mm)	0.14 $\pm$ 0.01	0.13 $\pm$ 0.01	0.12 $\pm$ 0.04	0.11 $\pm$ 0.02	<0.01
Ct.Po (%)	16.6 $\pm$ 1.8	16.4 $\pm$ 1.6	20.6 $\pm$ 1.5	21.3 $\pm$ 2.1	<0.0001
pMOI (mm <sup>4</sup> )	1.05 $\pm$ 0.14	1.06 $\pm$ 0.13	0.89 $\pm$ 0.03	0.93 $\pm$ 0.16	<0.05

**Table 1:** Bone microarchitecture is diminished with flight but not MuRF1 deficiency. P-values from 2-way ANOVA comparing Ground (GC) and Spaceflight (SF).

Table

**Disclosures:** Jennifer C. Coulombe, None.

## MO0400

**Bisphosphonate Pre-Treatments Protect Cancellous Bone Density and Strength in Unloaded Adult Rats.** Jon Elizondo<sup>\*1</sup>, Jeremy Black<sup>1</sup>, Jennifer Kosniewski<sup>1</sup>, Jessica Brezicha<sup>2</sup>, Scott Lenfest<sup>1</sup>, Susan Bloomfield<sup>3</sup>, Matthew Allen<sup>4</sup>, Harry Hogan<sup>5</sup>. <sup>1</sup>Dept. of Mechanical Engineering, Texas A&M University, United States, <sup>2</sup>Dept. of Biomedical Engineering, Texas A&M University, United States, <sup>3</sup>Dept. of Health and Kinesiology, Texas A&M University, United States, <sup>4</sup>Dept. of Anatomy and Cell Biology, Indiana University, United States, <sup>5</sup>Dept. of Mechanical Engineering and Dept. of Biomedical Engineering, Texas A&M University, United States

Bisphosphonates (BPs) mitigate negative effects of unloading on bone in astronauts and ground-based analogs for spaceflight. In all such cases, BPs were given throughout the unloading period. Because the anti-resorptive effects of BPs persist beyond treatment withdrawal, the current study was undertaken to test the efficacy of BPs when given only as a pre-treatment prior to unloading. We used the adult hindlimb-unloading (HU) rat model to simulate microgravity conditions, and we compared two BPs with different binding affinities: alendronate and risedronate.

Adult male Sprague Dawley rats were assigned to 4 groups: aging control (AC), HU control (HUC), alendronate pre-treated (ALN), and risedronate pre-treated (RIS). Pre-treatments were given for 4 weeks 3x/wk by injection. Following pre-treatment, all animals except the AC group were exposed to 4 weeks of HU, after which they were returned to ambulation for 8 weeks. Ex vivo pQCT scans were taken at the proximal tibia metaphysis (PTM) and distal femur metaphysis (DFM). Reduced platen compression (RPC) mechanical testing was performed on slice specimens from the PTM and DFM to estimate mechanical properties of the cancellous bone region.

Both BPs were effective in preventing negative effects of HU for most parameters. At the end of HU, cancellous vBMD for HUC was significantly lower than AC (-28% PTM; -17% DFM), but RIS and ALN were not different from AC, except for RIS at the DFM, which was significantly higher than AC. Thus, BP pre-treatment prevented negative effects of HU, and treatment even enhanced density in one case. Likewise, total vBMD at the DFM showed prevention of HU losses. Total vBMD at the PTM showed no significance between any groups. Compared to density, mechanical properties of HUC animals showed much more dramatic losses at the end of HU. Ultimate stress from RPC testing was 71.1% lower at the PTM and 63.4% lower (n.s.) at the DFM for HUC compared to AC. However, RIS and ALN groups still showed protection from HU losses at both bone sites. Similarly, elastic modulus at both sites showed drastic losses at the end of HU and protection with BP pre-treatment.

Overall, both BPs were effective in preventing HU losses in cancellous bone strength and density, despite the much greater losses in strength for untreated animals. This suggests that BP pre-treatment is a promising approach as a countermeasure for unloading-induced bone loss, and it may be a viable alternative to concurrent treatment.

**Disclosures:** Jon Elizondo, None.

## MO0401

**Age-related changes in the anabolic response to exercise.** Niloufar Rostami\*, Chunbin Zhang, Joseph Gardinier, Henry Ford Hospital, United States

Exercise is a key determinate of fracture risk and is often used to promote bone formation through dynamic loading. However, the efficacy of exercise to stimulate bone formation is often lost with age. The purpose of this study was to identify age-related differences in the response to exercise at the tissue and cellular level. The hypothesis states that osteocytes' response to exercise is diminished with age alongside the adaptation in tissue strength. Young (8-weeks of age) and old (36-weeks of age) male mice were weight-matched and assigned to baseline, sedentary and exercise groups with 20 mice per group. Exercise involved 30 minutes of treadmill running on 5° incline at speed of 12 m/min each day under approval by Henry Ford Health System Institutional Animal Care and Use Committee. After 6 days exercise, 5 mice from each group were sacrificed to measure early changes in gene expression based on qRT-PCR analysis of the tibia. The remaining mice from each group were sacrificed after 5 weeks of exercise to measure changes in the mechanical strength of the tibia alongside protein expression based on immunohistochemistry and serum analysis. At the cellular level, osteocytes' expression of sclerostin was significantly reduced during exercise in young mice based on mRNA expression by day 6 ( $0.64 \pm 0.08$  vs.  $1.0 \pm 0.12$ ,  $<0.05p$ ) and immunohistochemistry after 5 weeks of exercise. However, serum analysis of young mice did not reflect a decrease in circulating levels of sclerostin ( $182 \pm 30.8$  pg/ml vs.  $161 \pm 23.8$  pg/ml,  $>0.4p$ ). In aged mice, exercise had no effect on osteocytes' gene or protein expression of sclerostin. As expected, 5 weeks of exercise in young mice increased the ultimate load of the tibia compared with sedentary controls ( $20 \pm 2.97$  N vs.  $18 \pm 2.5$  N,  $<0.007p$ ), along with the post-yield deformation ( $440.5 \pm 328.1$   $\mu$ m vs.  $259.2 \pm 152.1$   $\mu$ m,  $<0.04p$ ). Despite significant differences in mechanical behavior, exercise in young mice had no effect on bone growth based on cortical area ( $0.71 \pm 0.051$  mm<sup>2</sup> vs.  $0.74 \pm 0.08$  mm<sup>2</sup>,  $>0.2p$ ) and moment of inertia ( $0.082 \pm 0.012$  mm<sup>4</sup> vs.  $0.085 \pm 0.018$  mm<sup>4</sup>,  $>0.6p$ ). In contrast, exercise in older mice had no significant effect on bone strength, but prevented age-related bone loss that was evident in sedentary mice when compared to baseline ( $0.67 \pm 0.03$  vs.  $0.75 \pm 0.06$ ,  $<0.05p$ ). Overall, these data suggest that osteocytes age-related differences in osteocytes' capacity to suppress sclerostin levels during exercise may explain the inefficacy of exercise to improve bone strength in aged mice.

**Disclosures:** Niloufar Rostami, None.

## MO0402

**Finite Element Models of Linear Microcracks in Trabecular Bone with Simulated Bisphosphonate and Raloxifene Treatment.** Max Hammond<sup>1</sup>, Joseph Wallace<sup>2</sup>, Matthew Allen<sup>3</sup>, Thomas Siegmund<sup>1</sup>. <sup>1</sup>Purdue University, United States, <sup>2</sup>Indiana University - Purdue University Indianapolis, United States, <sup>3</sup>Indiana University School of Medicine, United States

At the nanoscale bone is composed of aligned heterogeneously mineralized collagen fibrils. While raloxifene (Ral) and bisphosphonate (BP) treatment preserve bone mass, they also affect bone quality through changes in collagen hydration and mineral density/heterogeneity, respectively. It was hypothesized that the effects of pharmacological treatment on the tissue would alter linear microcracking in finite element (FE) models of trabeculae reflecting control (Ctrl), Ral and BP.

A FE mesh of a single canine vertebral body trabecula was generated from a micro-CT scan using ScanIP. A custom MATLAB code imposed tissue property heterogeneity and a collagen fibril orientation parallel to the trabecular surface. Ctrl was heterogeneous (based on vBMD) in both modulus and strength, and BP was homogenous (+25% of Ctrl mean modulus and strength). Ctrl and BP models had identical microcracking toughness. Ral had increased microcracking toughness (+25%) and the same modulus and strength heterogeneity as Ctrl. Transverse deflections were applied to simulate bending of the trabeculae, microcrack formation and propagation was simulated with the imposed orientation using the extended FE method in Abaqus/Standard, and the energy dissipated by the microcrack was assessed.

In all models microcracks initiated in the trabecular interior, and microcrack surfaces were aligned with collagen orientation. Therefore, the model correctly predicts the linear microcrack formation commonly observed in trabecular bone due to loading. Predicted deflection at crack initiation was similar for all models (BP at 7.3  $\mu$ m; Ctrl and Ral at 7.2  $\mu$ m). Microcracks advanced little until 9  $\mu$ m deflection, after which microcracks grew rapidly (Fig. 1). At 10  $\mu$ m deflection, the energy dissipation for BP was 2.5x greater than Ctrl, whereas there was no difference between Ctrl and Ral. Considering a constant energy dissipation value, Ctrl and Ral sustained about 15% more displacement than BP. The differences between BP and Ctrl demonstrate the important contribution of heterogeneity to resisting microcrack propagation. The present method automatically applied heterogeneity and orientation based on CT data. Therefore, the technique is readily scalable to model bone fragility and microdamage in larger trabecular samples and could use other data that estimates 3D geometry and mineral density (e.g., in vivo HRpQCT). In conclusion, altered microcracks were predicted with bisphosphonate but not raloxifene models.

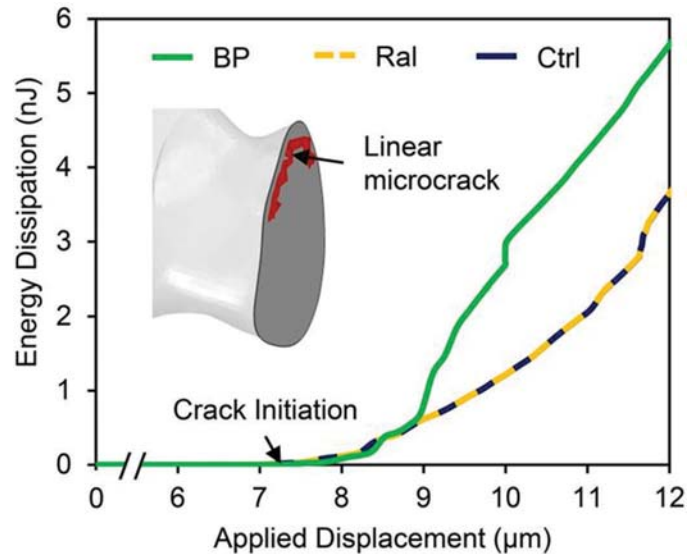


Figure 1: Predicted energy dissipation from microcracking was altered in the bisphosphonate model

**Disclosures:** Max Hammond, None.

## MO0403

**Fracture toughness and geometry-independent microscale material properties are improved with exercise for male but not female rats in diet-induced obesity.** Chelsea Heveran<sup>1</sup>, Rebecca Foright<sup>2</sup>, Ginger Johnson<sup>2</sup>, Virginia Ferguson<sup>1</sup>, Paul MacLean<sup>2</sup>, Vanessa Sherk<sup>2</sup>. <sup>1</sup>Department of Mechanical Engineering, University of Colorado, United States, <sup>2</sup>Department of Medicine, Division of Endocrinology, Metabolism & Diabetes, University of Colorado Anschutz Medical Campus, United States

Obesity increases bone fracture risk, yet combined effects of obesity, exercise, and sex differences on fracture toughness ( $K_{IC}$ ) are not understood. This study assessed whether diet-induced obesity (DIO) impairs  $K_{IC}$  and microscale bone quality, and whether exercise can mitigate negative effects of DIO. The study also tested whether DIO and/or exercise are sex-specific.

Female and male Wistar rats ( $N = 31$ ) were fed an ad libitum high fat diet (HFD) for 10 weeks, starting at 5 weeks of age. Within sex, obese and lean groups were defined as the highest and lowest tertiles of weight and fat gain. Obese and lean rats were randomized to exercise (EX) or sedentary (SED) controls for the last 4 weeks of HFD ( $n = 4$ /group; except female obese EX:  $n = 3$ ). EX was treadmill running at 15 m/min, 60 min/day, 5 days/week.

$K_{IC}$  was evaluated in notched femurs. Post-fracture, femurs were dehydrated, embedded, and polished to a 0.1  $\mu$ m finish. Nanoindentation was performed with 25 indents each for lamellar and woven bone in the medial quadrant. Nanoindentation modulus ( $E$ ) and plastic work ( $W$ , hysteresis of unloading curve) were averaged per lamellar/woven region. Three-way ANOVA evaluated how  $K_{IC}$ ,  $E$ , and  $W$  depended on sex, obesity status, and exercise status.

Bone radii and thickness were 36.0% ( $p < 0.01$ ) and 28.5% ( $p < 0.01$ ) larger, respectively, in males than females but did not differ with exercise or obesity. Male lean EX rats had 21% tougher (*i.e.*, higher  $K_{IC}$ ) bone than male lean SED ( $p = 0.05$ ). Male obese EX rats had 22% tougher bone than male obese SED ( $p = 0.04$ ). Female rats had less tough bone than males (-12.6%,  $p = 0.05$ ), and did not improve  $K_{IC}$  with exercise.

Diminished  $K_{IC}$  in SED males corresponded to decreased microscale bone material quality, but the location of lower quality bone depended on obesity status. Obese SED rats may have lower  $E$  in woven bone compared with obese EX (-9.1%,  $p = 0.07$ ). Lean SED rats may have lower  $W$  in lamellar bone compared with lean EX (-13.0%,  $p = 0.06$ ). For all lean EX rats, increased heterogeneity (*i.e.*, variance) of  $E$  in lamellar bone correlated with greater  $K_{IC}$  ( $r^2 = 0.57$ ). Meanwhile, variance in  $E$  did not change  $K_{IC}$  in obese or SED rats.

In summary,  $K_{IC}$  was preserved with EX for both lean and obese male rats fed HFD, but not for females. Lower  $K_{IC}$  in male SED rats corresponded with decreased microscale bone quality. These findings may help explain the effects of sex and exercise on obesity-related bone fragility.



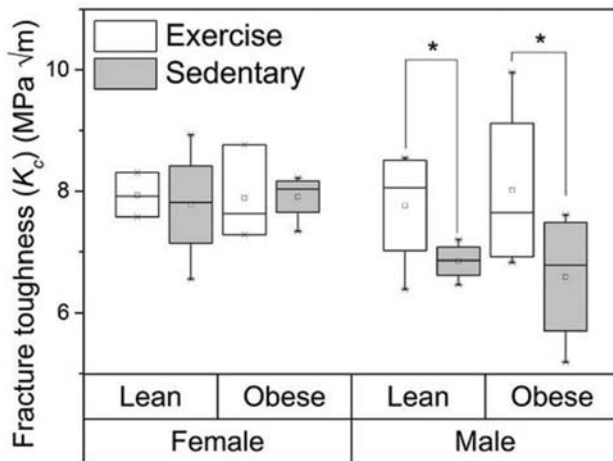


Fig 1:  $K_c$  is higher for EX vs SED for male rats. \*  $p \leq 0.05$

Figure 1

Disclosures: Chelsea Heveran, None.

## MO0404

**Long Term Effects of Omeprazole on Mouse Bone Quality and Mechanics.** Serra Kaya\*, Jessica Thomas, Tasnim Islam, Robert J Majeska, Mitchell B Schaffler. City College of New York, United States

Proton pump inhibitors (PPI) are widely used to reduce gastric acid and treat gastroesophageal reflux. Long term PPI use has been associated with bone fractures (Fx), which were widely assumed to result from drug-induced osteopenia. However, recent studies report no change in bone mineral density (BMD) with long-term PPI use suggesting that a different mechanism accounts for the observed fragility and Fx. This raises the intriguing question of whether long-term use of PPIs might contribute to Fx by directly affecting the quality of bone matrix. Here we tested whether long-term treatment with the PPI omeprazole (Omepr) altered structural and material properties of mouse bone.

Female C57Bl/6 mice ( $n = 20$ ) were treated with Omepr (5 d/wk, 20 mg/kg in DMSO, SQ) or vehicle (Veh). Mice were weighed weekly and drug doses adjusted accordingly. After 20 wk, mice were sacrificed.  $\mu$ CT studies on tibias assessed bone microstructure, BMD and TMD. Tissue-level elastic modulus (Ei) was measured by microindentation of femoral mid-diaphyseal cross-sections.

Trabecular bone volume (%), Tb.N, Tb.Th and Tb.Sp as well as BMD and TMD did not change with Omepr treatment. ( $p > 0.3$ , Table 1); nor did diaphyseal cortical bone area and structural rigidity (moment of inertia) ( $p > 0.4$ ). In contrast, Omepr caused a significant (6%) increase in tissue-level rigidity, Ei ( $p < 0.05$  vs Veh, Table 1). Omepr did not alter mean body weight.

These results reveal that long-term Omepr did not cause bone loss, but did alter local tissue material properties. We previously showed that indentation-based modulus measurements in mouse cortical bone are determined by bone matrix composition (particularly mineral content) and by the extent of osteocyte lacunar-canalicular space (LCS). Whether Omepr or other PPIs increase tissue rigidity by altering matrix mineralization or LCS volume is not yet known. It is also unclear whether Omepr acted directly or indirectly on osteocytes. PPIs block the  $H^+/K^+$  proton pump predominantly responsible for stomach acid production. However, osteoclasts, and now osteocytes as well, are thought to rely on different (vacuolar) proton pumps to acidify the pericellular space. The current data suggest that osteocytes in vivo may also utilize the  $H^+/K^+$  proton pumps that PPIs modulate. In any case, these initial studies reveal that long-term PPI use affects cortical bone quality. We posit that such changes long-term will adversely affect bone Fx resistance.

Table 1: Bone morphology and tissue-level material properties for mouse bone

	Control (n=10)	Omepr (n=10)
<b><math>\mu</math>CT-based trabecular bone microstructural parameters</b>		
BV / TV [%]	4.78 $\pm$ 0.84	5.26 $\pm$ 1.59
Tb.N [1/mm]	1.03 $\pm$ 0.20	1.12 $\pm$ 0.43
Tb.Th [mm]	0.05 $\pm$ 0.00	0.05 $\pm$ 0.00
Tb.Sp [mm]	0.24 $\pm$ 0.05	0.25 $\pm$ 0.05
BMD [mg HA/cm <sup>3</sup> ]	0.11 $\pm$ 0.02	0.11 $\pm$ 0.02
<b><math>\mu</math>CT-based cortical bone microstructural parameters</b>		
Tt.Ar [mm <sup>2</sup> ]	1.00 $\pm$ 0.06	1.02 $\pm$ 0.06
Ct.Ar [mm <sup>2</sup> ]	0.60 $\pm$ 0.03	0.57 $\pm$ 0.02 *
Ct.Th [mm]	0.18 $\pm$ 0.01	0.17 $\pm$ 0.01 *
Ct.Ar / Tt.Ar [%]	0.59 $\pm$ 0.02	0.56 $\pm$ 0.02 *
I <sub>max</sub> [mm <sup>4</sup> ]	0.08 $\pm$ 0.01	0.08 $\pm$ 0.01
J [mm <sup>4</sup> ]	0.14 $\pm$ 0.01	0.14 $\pm$ 0.01
TMD [mg HA/cm <sup>3</sup> ]	1.39 $\pm$ 0.03	1.39 $\pm$ 0.02
<b>Microindentation-based tissue-level mechanical parameter</b>		
Young's Modulus [GPa]	25.30 $\pm$ 1.72	26.82 $\pm$ 1.22 *

\*:  $p < 0.05$  Mann-Whitney

Trabecular and Cortical Bone Morphology and Tissue-Level Mechanical Properties of Mouse Bone

Disclosures: Serra Kaya, None.

## MO0405

**The Relationship between Stiffness and Strength in the Femur is Sex- and Age-Dependent.** Daniella Patton<sup>\*1</sup>, Erin Bigelow<sup>1</sup>, Steve Schlecht<sup>1</sup>, Todd Bredbenner<sup>2</sup>, Karl Jepsen<sup>1</sup>. <sup>1</sup>University of Michigan, United States, <sup>2</sup>Southwest Research Institute, United States

Estimating loss of whole bone strength in-vivo is critical in identifying individuals that would benefit from prophylactic therapy to reduce fracture risk. Whole bone strength is the maximum load bone sustains before failing, and only moderately correlates with BMD. Accurately estimating strength is difficult as failure is preceded by a complex, nonlinear phase, which is computationally taxing to model. Most in-vivo strength estimates report surrogates based on linear elastic beam theory and rely on an empirical stiffness-strength relationship. However, it is not known whether this relationship varies with age and sex.

We evaluated the relationship between femur stiffness and strength, stratified by sex, and examined how this relationship changes with age.

Cadaver proximal femora (36 M: 18–78 yr; 34 F: 24–95 yr) were loaded to failure in a sideways fall configuration and femoral diaphyses were loaded to failure in 4-point-bending (26 M: 18–89 yr; 17 F: 24–95 yr). Stiffness correlated highly with strength for diaphyses (M:  $R^2=0.77$ ; F:  $R^2=0.69$ ; both  $p < 0.001$ ) but less strongly for proximal femora (M:  $R^2=0.27$ ; F:  $R^2=0.27$ ; both  $p < 0.002$ ). Proximal femora were 39% ( $p < 0.001$ ) weaker for females than for males at a given stiffness.

To test for an age effect, residuals from the stiffness-strength regressions (Fig 1) were regressed with age, revealing a significant negative correlation for female ( $R^2=0.31$ ,  $p=0.0006$ ) but not male ( $R^2=0.26$ ,  $p=0.4$ ) proximal femora. In contrast, the stiffness-strength residuals declined with age for male ( $R^2=0.28$ ,  $p=0.007$ ) but not female ( $R^2=0.04$ ,  $p=0.4$ ) diaphyses. The average stiffness-strength residual for proximal femora was significantly less for older ( $>61$  yr) than younger women ( $\leq 60$  yr) (by 1006 N,  $p=0.006$ ) and this difference was 30.3% of the overall average strength for women. The average stiffness-strength residual for the diaphysis was significantly greater for older than younger men (by 1005 N,  $p=0.03$ ) at 10.2% of the average strength for men.

Mechanical testing of proximal femora revealed that whole bone strength degraded faster with age than stiffness in women compared to men. The discord in the rate of change in stiffness and strength suggests that estimates of strength based on stiffness may significantly underestimate actual losses in strength for women. Thus, our study identified a novel sex-specific difference in whole bone strength that may improve the accuracy of estimates in-vivo.

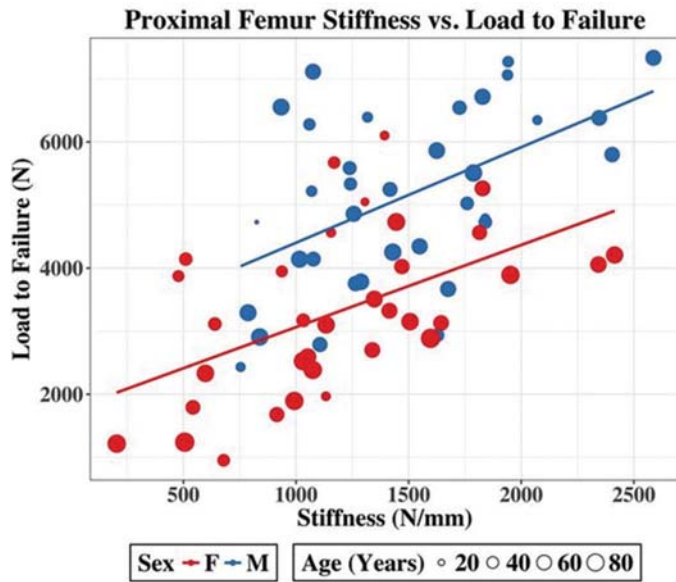


Figure 1: Proximal Femur Stiffness vs. Load to Failure

Disclosures: Daniella Patton, None.

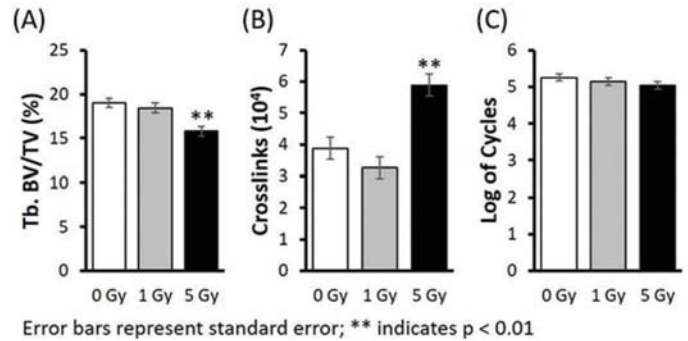
## MO0406

**Effect of Spaceflight-relevant Ionizing Radiation on Mechanical Properties of Mouse Vertebra for Repetitive Loading.** Megan Pendleton<sup>1</sup>, Saghi Sadoughi<sup>1</sup>, Alfred Li<sup>2</sup>, Jennifer Liu<sup>3</sup>, Grace O'Connell<sup>1</sup>, Joshua Alwood<sup>4</sup>, Tony Keaveny<sup>1</sup>. <sup>1</sup>University of California, Berkeley, United States, <sup>2</sup>SF VA Medical Center, University of California San Francisco, United States, <sup>3</sup>Washington University, St. Louis, United States, <sup>4</sup>NASA Ames Research Center, United States

Astronauts embarking on a deep-space mission to Mars will be exposed to high levels of ionizing radiation. This is of potential concern since ionizing radiation has been shown in other applications, such as radiotherapy treatment, to increase risk of fracture. While spaceflight-relevant radiation experiments so far have shown a quantitative degeneration of the tissue through loss of tissue mass, here we assessed the effects of such radiation on tissue quality. We hypothesized that radiation-induced changes in collagen crosslinks would decrease the ability of mouse vertebrae to withstand cyclic mechanical loading.

16-week old male mice were randomly assigned to one of three groups for *in vivo*, radiation-exposure: <sup>137</sup>Cs  $\gamma$ -radiation (1 Gy acute, whole-body), <sup>137</sup>Cs  $\gamma$ -radiation (5 Gy acute, whole-body), or a sham procedure (n=10 per group). After euthanasia at 11-days post-irradiation, the L5 vertebrae were extracted and  $\mu$ CT imaged (10- $\mu$ m resolution) without endplates. The specimens were then subjected to uniform compression cyclic loading (8 Hz) at room temperature in a saline-water bath, in force control, to approximately 50% of their estimated ultimate load, which was determined for each specimen by a  $\mu$ CT-based finite element analysis. The tests were stopped at imminent failure, defined as a rapid increase in strain; the main outcome was logarithmic number of cycles of loading to failure. Micro-architecture parameters and BV/TV for the tested vertebrae were assessed from the  $\mu$ CT images, and a fluorometric assay was used on the adjacent S1 vertebra to measure the number of non-enzymatic collagen crosslinks.

Consistent with previous literature, we observed a significant decrease in BV/TV (Figure; A) and micro-architecture for the 5 Gy-treated group. Additionally, we observed a small, yet significant increase in collagen crosslinks (Figure; B). There was no significant change in the number of cycles to failure, although there was a downward trend consistent with the other data (Figure; C). Typical space-induced levels of radiation are thought to be in the range of 1–2 Gy, with 5 Gy representing an upper bound. These results therefore suggest that typical doses of spaceflight-relevant ionizing radiation likely have no appreciable effect on tissue quality as it pertains to cyclic mechanical properties. However, different types of radiation (HZE ions) seen in space, and higher doses of radiation seen clinically in radiation therapy, may be cause for concern.

Error bars represent standard error; \*\* indicates  $p < 0.01$ 

Gamma-Radiation Effect on Mouse Vertebra

Disclosures: Megan Pendleton, None.

## MO0407

**A novel Raman parameter correlates with the fracture toughness of human cortical bone.** Mustafa Unal<sup>1</sup>, Selin Timur<sup>2</sup>, Sasidhar Uppuganti<sup>1</sup>, Ozan Akkus<sup>2</sup>, Jeffery S. Nyman<sup>1</sup>. <sup>1</sup>Vanderbilt University Medical Center, United States, <sup>2</sup>Case Western Reserve University, United States

Although age- and disease-related deterioration in bone matrix is an important contributor of impaired bone fracture resistance, there is currently no clinical tool that assesses the matrix. Raman spectroscopy (RS) is well suited to address this need, but to date, only one study showed RS parameters, namely crystallinity, significantly correlate with mechanical properties (tensile) of human cortical bone. Recently, we identified a new RS parameter, 1670/1640, as being sensitive to denatured collagen and related to toughness of bovine cortical bone. To establish the potential for RS in assessing the contribution of the matrix to the fracture resistance, we hypothesized that i) the new RS parameter correlates with fracture toughness of human cortical bone and ii) more importantly, RS adds value helping volumetric BMD (vBMD) and age predict fracture toughness properties.

Cadaveric femurs (28M/30F, age = 21-101 yrs) were machined into single-edge notched beam specimens. The intended crack path region was scanned by  $\mu$ CT and corresponding vBMD was determined. A non-linear fracture mechanics approach (R-curve testing) was used to determine crack initiation ( $K_{IC}$ ), crack growth toughness ( $\Delta K_{IC}/\Delta a$ ) and overall J-integral (J-int). Thirty-two Raman spectra per sample were each acquired by 12 accumulations (5 s), and distributed throughout the entire surface of bone (785 nm confocal RS, 20x obj). From the average spectrum per donor, we calculated traditional RS parameters (mineral to matrix ratios (MMRs), carbonate substitution, and crystallinity) as well as matrix maturity ratio (1670/1690) and the new 1670/1640 and 1610/1670 ratios (the intensities of Amide I shoulders were identified by the local maxima, not by band-fitting as guided by second derivative spectra) (Fig 1).

Matrix maturity and v1PO4/Pro did not correlate with any of the fracture toughness properties. Other traditional RS parameters and 1610/1670 only explained up to 18% of the variance for the fracture toughness properties (Table 1). The new parameter, 1670/1640, explained 48% of the variance in J-int and 35% of the variance for  $K_{IC}$  ( $R^2$ ). After including age and vBMD in multilinear regressions as covariates, 1670/1640 significantly improved the prediction of J-int (from adj- $R^2$ = 12.35 to 46.55) and the prediction of  $K_{IC}$  (from adj- $R^2$ = 40.73 to 50.49), suggesting RS assessment has potential to assist existing clinical tools in assessing an individual's fracture risk.

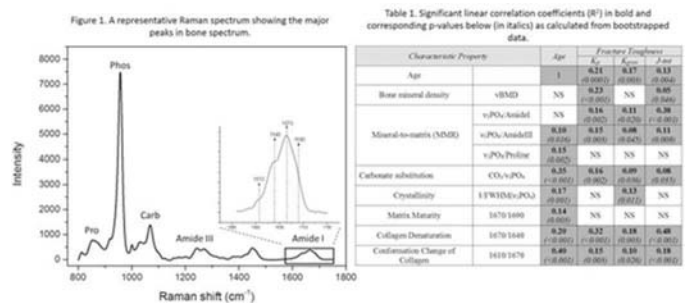


Figure 1

Disclosures: Mustafa Unal, None.



## MO0408

**Lactation-induced changes in mineral and matrix composition are site-specific.** Christina Vrahnas<sup>\*1</sup>, Christine Jun<sup>2</sup>, Ingrid Poulton<sup>1</sup>, Keith Bamberg<sup>3</sup>, Christopher Kovacs<sup>4</sup>, Jack Martin<sup>1</sup>, Natalie Sims<sup>1</sup>. <sup>1</sup>St. Vincent's Institute of Medical Research, Australia, <sup>2</sup>University of Melbourne, Australia, <sup>3</sup>Australian Synchrotron, Australia, <sup>4</sup>Memorial University of Newfoundland, St. John's, Australia

Mineral is removed from the maternal skeleton to provide calcium for milk by two processes: bone resorption by osteoclasts, and osteocytic osteolysis, when osteocytes remove mineral from the surrounding bone. The effects of lactation and recovery on material composition of the maternal skeleton have not been defined.

We analysed tibiae from 6 month old female mice after 21 days of lactation, during recovery (7 and 28 days post-weaning), and in unmat age-matched controls (n=5-11/group) by synchrotron-based Fourier-transform infrared microspectroscopy (sFTIRM). To account for differences due to bone maturity, spectra were collected in 15 x 15 micron regions spaced evenly from the periosteal to the endocortical surface. To account for differences in intrinsic mechanical loading, we assessed both medial and lateral cortices.

100 µm thick cross-sections of the femoral diaphysis were analysed by backscattered electron microscopy (BSEM) to confirm osteocytic osteolysis. Lactating mice showed a 25% increase in osteocyte lacunar size (p<0.008), which was not significantly recovered by 28 days after weaning.

As expected, sFTIRM detected mineral accumulation, carbonate incorporation and collagen compression in the most mature regions in the centre of the cortical bone compared to regions on the periosteal and endocortical edges. This was observed on both medial and lateral cortices in all treatment groups. In unmat controls, mineral:matrix ratio was 22% greater and amide I:II ratio 11% lower on lateral tibial cortices compared to medial (both p<0.0001), suggesting that bone subject to more compression has a higher mineral content.

In lactating mice, mineral:matrix ratio was greater in all regions measured across the medial cortices compared to unmat controls (p<0.0003); this difference was ameliorated as early as day 7 of recovery. Neither carbonate:mineral nor amide I:II ratio were altered. In the lateral cortices, while there was no significant change in mineral:matrix, newly deposited bone had a low carbonate:mineral ratio and high amide I:II ratio compared to controls.

In conclusion, we suggest the high mineral:matrix ratio in medial cortices of lactating mice is caused by retention of highly mineralised bone, and that during lactation and recovery, osteocytes preferentially remove and rapidly replace bone matrix with low mineral content in mature and immature cortical bone at the medial site which may be subject to less mechanical compression.

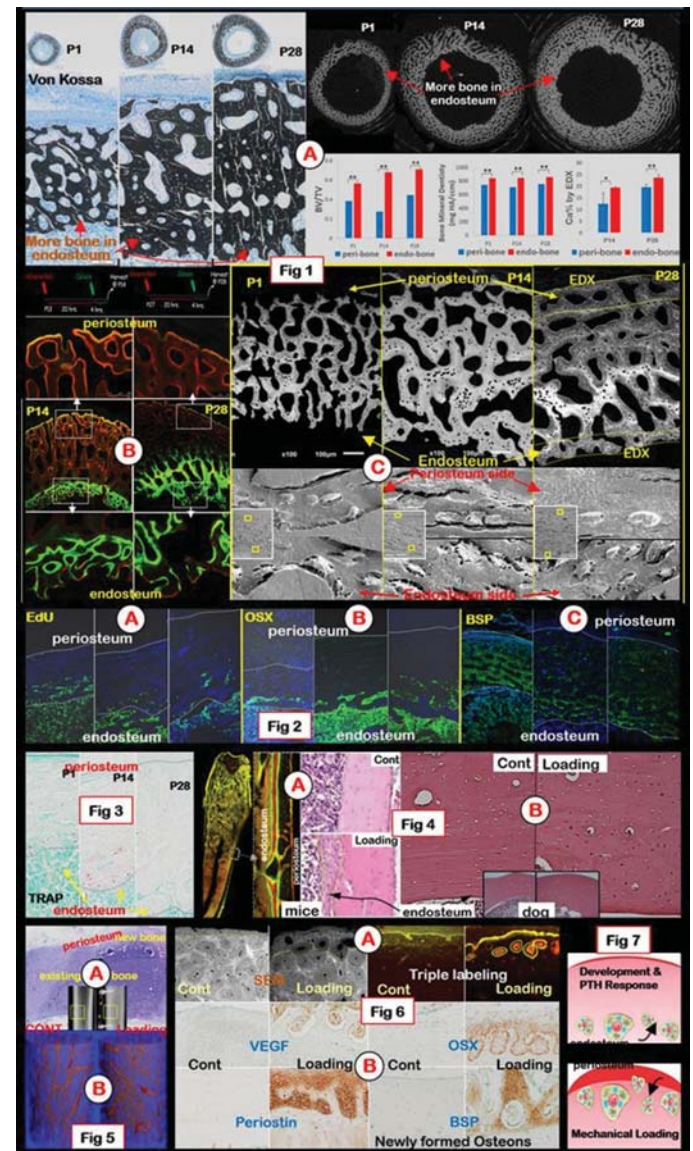
**Disclosures:** Christina Vrahnas, None.

## MO0409

**Distinct Roles of Periosteum and Endosteum during Long Bone Growth, Loading and Intermittent PTH Responses.** Ke Wang<sup>\*1</sup>, Yuan Hui<sup>1</sup>, Yingshi Ren<sup>1</sup>, Reuel Cornelia<sup>2</sup>, Harry Kim<sup>2</sup>, Xianglong Han<sup>3</sup>, Jian Feng<sup>1</sup>. <sup>1</sup>Department of Biomedical Science, Texas A&M Health Science Center, College of Dentistry, Dallas, TX; United States, <sup>2</sup>Department of Research, Texas Scottish Rite Hospital for Children, United States, <sup>3</sup>State Key Laboratory of Oral Diseases, West China Hospital of Stomatology, Sichuan University, China, China

The purpose of this study was to test the distinct roles of periosteum and endosteum cells in bone growth, PTH and loading responses. First, we demonstrated that the endosteum-derived bone cells play a key role in dog cortical bone growth (Fig 1): A. von Kossa and uCT data showed more endosteum-contributed bone mass, which is statistically significant; B. The double labeling assays display strong distinct lines in the endosteum layer but a faint and fused label line in the periosteum layer, indicating more active mineralization in the endosteum side; C. the backscattered SEM and EDX (for Ca %) analyses revealed high mineral/Ca contents in the endosteum-contributed bone (white color reflecting minerals). The acid-etched SEM images confirm more minerals produced in the endosteum side. The molecular mechanism studies in Fig 2 demonstrate more active cell proliferation and differentiation in the endosteum layer than in the periosteum layer: A. EdU/DAPI image; B. OSX/DAPI images; and C. BSP/DAPI images. Next, we found more osteoclast numbers in the endosteum layer (especially in P14) using the TRAP assay, reflecting active remodeling in the endosteum layer (Fig 3). Because of a positive relationship between the PTH level and pubertal and bone growth spurts reported in young people (Stagi, 2015), we tested bone responses to intermittent PTH injections in both mice and dogs (10 µg/kg per day for 2-wks), and showed active bone cell formation and strong bone mineralization occurred in the mouse endosteum (Fig 4A) and more osteon formation in the endosteum (Fig 4B). To address mechanical responses, we applied open-coil springs anchored miniscrew implants in the dog tibia with a force 0, and 200 g separately (Fig 5A). In the loading groups (6 adult dogs), there were sharp increases in Haversian canals by uCT (Fig 5B). The images of the back-scattered SEM and double labeling (with 10 days apart) displayed many newly formed osteons that were mainly derived from the expanded periosteum layer (Fig 6A). These newly formed osteons expressed high levels of VEGF, periostin, OSX and BSP (Fig 6B). Collectively, our data showed that the endosteum-derived bone cells play a key role in dog cortical bone growth, which is likely linked to PTH levels; and that the periosteum-derived bone cells mainly respond to mechanical loading. Thus, we propose that

bone cells in the periosteum and endosteum layers distinctly respond to different physiological needs (Fig 7).



Distinct Roles of Periosteum and Endosteum during Long Bone Growth, Loading and PTH Responses

**Disclosures:** Ke Wang, None.

## MO0410

**Association between vertebral cross-sectional area and vertebral wedging.** Tishya Wren<sup>\*</sup>, Skorn Ponrartana, Patricia Aggabao, Ervin Poorghasamians, Vicente Gilsanz. Children's Hospital Los Angeles, Keck School of Medicine, University of Southern California, United States

A small vertebral cross-sectional area (CSA) imparts a mechanical disadvantage that escalates the risk for vertebral fractures in elderly populations. We examined whether a small vertebral CSA is also associated with a greater degree of vertebral wedging in children. Using magnetic resonance imaging, measurements of vertebral CSA, vertebral wedging, and lumbar lordosis (LL) angle were obtained in 100 healthy adolescents (50 boys and 50 girls), 15 of which (all girls) had a follow-up examination one year later. The degree of postero-anterior vertebral wedging at L5 negatively correlated with the vertebral CSA of the lumbar vertebrae ( $r = -0.49$ ;  $P < 0.0001$ ); this was true whether all subjects were analyzed together or boys and girls independently. In contrast, we found a positive correlation between vertebral wedging and the degree of LL ( $r = 0.57$ ;  $P < 0.0001$ ). Multiple regression analysis showed that the association between vertebral wedging and CSA was independent of age and body mass. Follow-up examinations revealed a significant negative correlation between percent change (%Δ) in wedging and %Δ in vertebral CSA ( $r = -0.62$ ;  $P = 0.02$ ), and a strong positive correlation between %Δ in wedging and %Δ in LL ( $r = 0.88$ ;  $P < 0.0001$ ) – associations that persisted even after accounting changes in body mass. We conclude that smaller

vertebral CSA increases the stresses induced by asymmetric loading and accelerates the degree of vertebral wedging in LL.

**Disclosures:** Tishya Wren, None.

## MO0411

**Does Childhood and Adolescent Fat Mass Accrual Influence Trajectories of Bone Development in Emerging Adulthood?** Adam Baxter-Jones\*, Erin Barbour-Tuck, Saija Kontulainen, Marta Erlandson. University of Saskatchewan, Canada

**Background:** During childhood and adolescence, it is well known that lean tissue development confers skeletal benefits, which are carried into young adulthood. The effects of fat tissue during the same time-period are more controversial. Previous studies in the overweight and obese have documented equivocal results. The purpose of the present study was to investigate the role of fat accrual during childhood and adolescence on total body bone mineral content (TBBMC) and bone mineral density (TBBMD) development during emerging adulthood (18 to 28 years of age).

**Methods:** 157 (89 females) individuals were serially measured between 1991 and 2005 (age range 8 to 28 years). Annual measures included age, anthropometrics, body composition (DXA) and questionnaires of physical activity (PA) and diet (calcium intake, CI). From -6 to +7 years from peak height velocity, age specific z-scores for PA, CI and total body fat mass / lean mass (TBFM/TBLM) were calculated and yearly values averaged to provide individual childhood and adolescence mean z-scores. Multilevel random effects models were built to identify independent predictors (Estimates  $\pm$  Standard Error Estimate) of TBBMC/TBBMD trajectories in emerging adulthood.

**Results:** Once the confounders of adult age ( $1.2 \pm 0.9 \times 10^{-3}$ ), height ( $-1.0 \pm 0.9 \times 10^{-3}$ ), TBLM ( $2.2 \pm 0.6 \times 10^{-6}$ ), TBFM ( $1.1 \pm 0.3 \times 10^{-3}$ ) and PA ( $p > 0.05$ ) were controlled it was found that sex ( $0.08 \pm 0.02$ ) and childhood/adolescent TBLM z-scores ( $0.04 \pm 0.01$ ) predicted TBBMD. Childhood/adolescent z-scores for PA, CI and TBFM were not significant predictors ( $p > 0.05$ ) of BMD development. The model for TBBMC development showed the same results, once the confounders of adult age, height, TBLM, TBFM, and PA were controlled only sex ( $545.9 \pm 58.3$ ) and TBLM z-scores ( $215.4 \pm 26.1$ ) were significant predictors of TBBMC development.

**Discussion:** As seen in previous studies, once adjusted for age and size, males had greater TBBMD and TBBMC. The results also showed the strong relationship between bone parameters and adult and adolescent TBLM. Once the confounders of age, size and body composition were controlled, it was found that there was a negative relationship between emerging adulthood TBFM accrual and bone parameters. However, fat mass accrual in childhood and adolescence did not predict bone accrual in emerging adulthood. It is concluded that fat mass accrual during the growing years does not, independently, predict the trajectories of bone development in emerging adulthood.

**Disclosures:** Adam Baxter-Jones, None.

## MO0412

**Lumbar Spine Trabecular Bone Score: a Potential Screening Tool for the First Year Post-menarche?** Jodi Dowthwaite\*, Renaud Winzenrieth<sup>2</sup>, Tamara Scerpella<sup>3</sup>. <sup>1</sup>SUNY Upstate Medical University, United States, <sup>2</sup>Med-Imaps, France, <sup>3</sup>University of Wisconsin, Madison, United States

Trabecular bone score (TBS) grades lumbar spine trabecular texture from gray-scale DXA images. Silva et al. (2014) recommended TBS thresholds for post-menopausal women to be  $\geq 1.35$  (normal microarchitecture),  $>1.2$  to  $<1.35$  (partially degraded) and  $\leq 1.2$  (degraded). Numerous studies have evaluated pubertal lumbar spine BMC and BMD, but no studies have evaluated factors in TBS variation at initial reproductive maturity. Thus, for the first year post-menarche, we aimed to evaluate: 1) whether "normal" adult TBS ( $\geq 1.35$ ) has been reached; 2) the role of maturational timing (menarcheal age) and status (gynecological age) in TBS.

Participants were derived from a longitudinal DXA study of bone growth in healthy girls. For inclusion, a lumbar spine scan (LS: L1-L4), whole body scan and anthropometry were required between menarche and 1 year post-menarche. For some girls, 2 DXA sessions qualified; the scan closest to 0.5 years post-menarche was used. Custom software adjusted for soft tissue thickness (TBS iNsignit, Med-Imaps, France). We used linear and quadratic regressions to evaluate menarcheal age and gynecological age as factors in LS TBS, BMC and BMD, reporting beta semi-partial correlation coefficients (spcc) and significance.

Table 1 presents descriptive statistics. The lowest observed TBS was 1.362. For TBS, there were no significant linear or quadratic correlations with gynecological age, height, weight, BMI or fat mass ( $p > 0.15$ ); a significant negative linear correlation persisted with menarcheal age (spcc = -0.36,  $p = 0.015$ ), after accounting for gynecological age (spcc = +0.23,  $p = 0.111$ ). In contrast, gynecological age correlated positively with LSBMC and LSBMD (spcc = +0.37, +0.38;  $p < 0.015$ ), while menarcheal age did not (spcc = -0.09, -0.19;  $p > 0.18$ ). TBS linear correlations with both LSBMC and LSBMD were significant ( $r = +0.47, +0.63$ ;  $p < 0.001$ ).

"Normal" adult TBS appears to be achieved by menarche in healthy girls. Accordingly, TBS during the initial post-menarcheal year could assess trabecular structure to screen at-risk girls for intervention prior to "peak bone mass". TBS may reflect risk factors in trabecular structural development that are not reflected by lumbar spine BMC or BMD. Assessments may be particularly important in girls with delayed menarche; current gynecological age should be taken into account. Further longitudinal

study is needed to ascertain whether initial post-menarcheal TBS is a significant predictor of TBS at peak bone mass.

Variables	Mean	Standard Deviation	Minimum	Maximum
Age (years)	12.7	0.6	11.2	13.7
Menarcheal Age (years)	12.2	0.5	10.8	13.4
Gynecological Age (years)	0.50	0.25	0.03	0.93
Height (m)	1.61	0.06	1.49	1.72
Weight (kg)	52.2	8.3	40.8	83.3
Body Mass Index (kg/m <sup>2</sup> )	20.2	2.8	15.3	30.1
Lean Mass (kg)	35979.9	3828.2	25142.0	43623.0
Fat Mass (kg)	14471.2	5454.4	6799.0	37321.0
Whole Body Bone Mineral Content (BMC, g)	1939.2	218.63	1476.0	2437.0
Sub-head BMC (g)	1547.8	196.2	1088.0	2001.0
Lumbar Spine BMC (g)	46.05	7.34	32.4	67.0
Lumbar Spine Bone Mineral Density (g/cm <sup>3</sup> )	1.016	0.100	0.800	1.200
Lumbar Spine Trabecular Bone Score (TBS)	1.495	0.054	1.362	1.577

Table 1

**Disclosures:** Jodi Dowthwaite, None.

## MO0413

**Accuracy and Precision of estimated %FAT from Hologic Forearm and Lateral Distal Femur DXA Scans in children.** Bo Fan\*, Natasha Din<sup>1</sup>, Bennett Ng<sup>2</sup>, Amir Pasha Mahmoudzadeh<sup>1</sup>, Babette Zemel<sup>3</sup>, Heidi Kalkwarf<sup>4</sup>, Andrea Kelly<sup>3</sup>, James Heubi<sup>5</sup>, Kimberly Yoltos<sup>5</sup>, Leila Kazemi<sup>1</sup>, John Shepherd<sup>1</sup>. <sup>1</sup>UCSF, United States, <sup>2</sup>University of California Berkeley, United States, <sup>3</sup>CHOP, United States, <sup>4</sup>Cincinnati Children's Hospital, United States, <sup>5</sup>Cincinnati Children's Hospital, United States

**Objective:** To derive regional %fat measures from forearm acquisitions and validate against whole body DXA scans for both regional accuracy and whole body composition estimation. When infants and small children for whom whole body (WB) DXA scans are impractical due to motion and poor prediction from demographics.

**Design:** Forearm (FA), lateral distal femur (LDF) and WB DXA scans (Hologic systems) of healthy young children enrolled in Bone Mineral Accretion in Young Children Study were evaluated. FA and LDF scans, acquired using forearm scan mode were analyzed for body composition using the infant whole body analysis protocols. To meet the algorithmic conditions, additional background signal was added to some scans. FA and LDF ROI sizes were determined as half the limb length and positioned proximal to the distal growth plate. ROIs of similar size and location were also placed on WB scans. We compared estimates of %Fat from FA and LDF scans to sub-regional and total %Fat from matched WB scans using general linear regression. A second set of paired scans, acquired with interscan repositioning, were used to estimate the body composition precision as root mean square coefficients of variation (RMS-CV) and standard deviations (RMS-CV).

**Results:** A total of 69 participants [41 girls; mean ( $\pm$ SD) age:  $41.5 \pm 3.4$  months; BMI:  $15.6 \pm 1.0$  kg/m<sup>2</sup>] were included in the comparison study, and an additional 50 participants in the precision study. Regression analysis results are shown in Table 1. Age and BMI were not associated with WB %FAT. Regional scan %FAT measures were significantly associated with corresponding WB sub-region %FAT measures ( $R^2 = 0.31$  and  $0.65$  for FA and LDF scans, respectively) and total WB scan-derived measures ( $R^2 = 0.54$  and  $0.57$  for FA and LDF scans, respectively). Age and BMI adjustment did not improve associations. The %FAT precisions were 3.5% (RMSE=1.19) and 15.0% (RMSE=7.76) from converted FA and LDF scans respectively. Precision was limited by the size of the region of interests, lack of background signal, and position issues of the femur.

**Conclusion:** We found that %FAT estimates in FA and LDF scans were moderately associated with WB %FAT in children. It is unclear at this point if this limitation is due to the local analysis or from the poor estimation of body composition from subregions of whole body scans. Precision estimates from reasonable for FA but poor for LDF. More study is need to improve reproducibility and strengthen prediction models.

Table 1: Regression analysis comparing regional, WB sub-regional and WB total %FAT associations.

Models:	R <sup>2</sup>	RMSE
<b>Dependent variable: whole body Distal Femur % Fat</b>		
Age	0.03	7.01
BMI	0.05	6.97
Distal femur % FAT	0.65	4.22
<b>Dependent variable: whole body Forearm % Fat</b>		
Age	0.02	6.23
BMI	0.07	6.09
Forearm % FAT	0.31	5.24
<b>Dependent variable: whole body Total % Fat</b>		
Age	0.001	3.44
BMI	0.06	3.34
Distal femur % FAT	0.57	2.27
Forearm % FAT	0.54	2.33
Whole body sub-regional Distal femur % FAT	0.79	1.60
Whole body sub-regional Forearm % FAT	0.43	2.60

Table 1

**Disclosures:** Bo Fan, None.



## MO0414

**Do the Timing and Rate of Bone Mass Acquisition Differ Between Overweight and Healthy-Weight Adolescent Females? An 18-Month Prospective Study.** Joseph Kindler<sup>\*1</sup>, Kara Vogel<sup>1</sup>, Berdine Martin<sup>1</sup>, Linda McCabe<sup>1</sup>, Courtney Henry<sup>1</sup>, Munro Peacock<sup>2</sup>, Stuart Warden<sup>2</sup>, George McCabe<sup>1</sup>, Connie Weaver<sup>1</sup>. <sup>1</sup>Purdue University, United States, <sup>2</sup>Indiana University, United States

Childhood obesity is a major US public health concern, as nearly one in three children are overweight. Whereas obese adolescents are overrepresented in skeletal fracture cases, the manner in which excess adiposity influences bone development is still uncertain. Underpinning this debate is the paucity of longitudinal data examining the role of weight status in the timing and rate of pediatric skeletal development. This 18-month prospective study sought to examine differences in the timing and rate of total body bone mass acquisition in overweight versus healthy-weight adolescent females. This secondary analysis of a previously conducted 18-month randomized controlled dairy intervention includes 116 otherwise healthy females ages 8 to 15 years at baseline. Based on BMI-for-age percentile (%ile), participants were recruited to be either healthy-weight (5th-70th %ile) or overweight ( $\geq 85$ th %ile). The main outcome measure, assessed every 6 months, was total body bone mineral content (TBBMC) as measured via dual-energy X-ray absorptiometry. The original intervention had no effect on TBBMC. Statistical analyses were performed using SAS, version 9.3. At baseline, the overweight versus healthy-weight females were at a later stage of sexual maturation and had a greater TBBMC (both  $P < .05$ ). The peak rate of TBBMC accrual did not differ between the overweight ( $266.6 \pm 13.5$  g per year) versus healthy-weight ( $240.1 \pm 11.3$  g per year) females ( $P = .93$ ; Figure 1). However, the age at which the peak rate of TBBMC accrual was achieved was  $0.98 \pm 0.41$  years earlier in the overweight ( $10.8 \pm 0.4$  years of age) versus healthy-weight ( $11.8 \pm 0.1$  years of age) females ( $P = .01$ ). These results indicate that the timing, but not the rate, of total body bone mass acquisition differs between overweight and healthy-weight females. Specifically, the maximum rate of bone mass acquisition was achieved approximately one year earlier in overweight girls. These differences in bone mass accrual may have been attributed to the accompanying earlier maturation and accelerated longitudinal growth in overweight females. Whether or not these relationships involving weight status and bone development are consistent in males and are evident at specific regions of cortical and/or trabecular bone are currently under investigation.

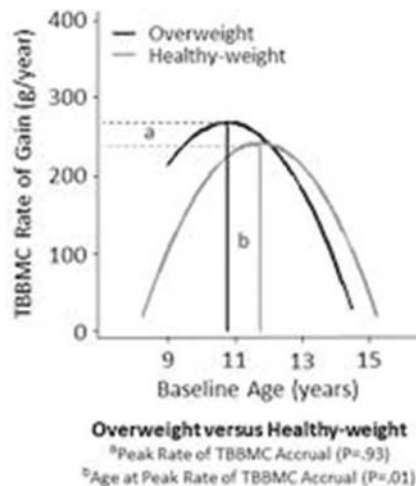


**Figure 1.** The peak rate of TBBMC accrual did not differ between overweight versus healthy-weight females ( $P = .93$ ). However, the age at which peak TBBMC accrual was achieved occurred approximately 1 year earlier in the overweight versus healthy-weight females ( $P = .01$ ). TBBMC, total body bone mineral content.

Figure 1

**Disclosures:** Joseph Kindler, None.

## MO0415

**Elevated IL-1 Expression in Mesenchymal Stem Cells Derived from Spondyloarthritis Patients Is Associated With an Increase in Their Capacity To Form Mineralizing Osteoblasts.** Gerlinde Layh-Schmitt<sup>\*</sup>, Breanna Nguven, Robert A. Colbert. Pediatric Translational Research Branch, NIAMS, NIH, United States

Axial spondyloarthritis (AxSpA) is characterized by inflammation of the axial skeleton, vertebral trabecular bone loss, and progressive bone formation in the spine. However, the root cause of osteoproliferation and aberrant bone formation is unknown. We evaluated, (i) whether bone progenitor cells (mesenchymal cells (MSCs) and osteoblasts (OBs)) derived from AxSpA patients (P) exhibit differences in their capacity to

form mineralizing osteoblasts in comparison to healthy controls (HC), and (ii) whether inflammatory cytokines alter osteoblastogenesis and gene expression patterns in MSCs. We used MSCs derived from induced pluripotent stem cells (iPSCs) generated from P and HC skin fibroblasts. MSCs from 3 HC and 6 P were differentiated into mineralizing osteoblasts. The influence of cytokines (IFN $\gamma$  & TNF $\alpha$ , and IL-1b) on MSCs and osteoblastogenesis was examined (1 HC, 1 P). The degree of calcification after 26 days of differentiation was measured by alizarin red stain. Whole transcriptome expression profiles were established for MSCs before and after cytokine treatments by applying RNAseq (3 HC and 4P). Standard approaches and statistical methods were used to analyze the data. On average, OBs derived from P ( $n = 6$ ) exhibited a 1.4 fold higher mineralization capacity compared to OBs from HC ( $n = 3$ ) ( $p < 0.05$ ; Mann Whitney test). In 2 P, elevated mineralization correlated with higher expression levels of alkaline phosphatase (ALPL), an enzyme crucial for osteoblast mineralization. Interestingly, in all tested P ( $n = 4$ ) IL-1 $\alpha$ , IL-1 $\beta$ , and COX2 mRNA levels were enriched compared to HC by 4-16 fold, 4-20 fold and 2-3 fold ( $q < 0.3$ ), respectively. Stimulation with IFN $\gamma$  & TNF $\alpha$  induced IL-1 $\alpha$  and IL-1 $\beta$  up to 20-fold and COX2 up to 15-fold. Treatment of P and HC MSC lines with IL-1 $\beta$  for 24h induced COX2 expression 3-5 fold ( $q < 0.3$ ) and led to an 1.5-time increase in mineralization ( $p < 0.05$ ). This suggests that, under certain conditions, IL-1 can enhance osteoblast mineralization. In summary, we found elevated IL-1 expression levels in P-derived MSCs associated with enhanced COX2 levels and OB mineralization. Exogenous IL-1 $\beta$  induced COX2 in MSCs lead to increased mineralization. COX2 is crucial for the synthesis of prostaglandin E2 (PGE2) which can mediate aberrant ossification through b-catenin stabilization. Further studies will evaluate whether IL-1 inhibition can abolish elevated mineralization capacity and whether PGE2 and b-catenin are increased in patient cell lines.

**Disclosures:** Gerlinde Layh-Schmitt, None.

## MO0416

**Pre-pubertal onset of type 1 diabetes mellitus (T1D) is associated with differences in bone microarchitecture in young adult males.** Roger Long<sup>\*</sup>, Ursula Heilmeyer, Ann Schwartz, Aenor Sawyer, Saleh Adi, Marie Nader, Courtney Pasco, Melis Yilmaz, Thomas Link, Galateia Kazakia. University of California, San Francisco, United States

**Background:** Fracture risk among adults with diabetes is higher than predicted by their areal BMD values. Increased fracture risk throughout life suggests that T1D during puberty may lead to lasting defects in bone. We performed this study to determine if the microarchitecture of bone as measured by high resolution peripheral quantitative computed tomography (HR-pQCT) differed between 18-30 yo males with T1D diagnosed prior to age 10 yrs and without T1D.

**Methods:** Sixteen subjects with T1D from the UCSF Pediatric Diabetes Clinic and 10 non-diabetic controls were enrolled. Data collection included clinical history, physical activity questionnaire, serum chemistries, hip and spine DXA and HR-pQCT scans of the radius and tibia. HR-pQCT analysis includes 7 additional matched controls from a UCSF reference database. Linear regression was used to compare BMD and HR-pQCT results across the two groups.

**Results:** No significant differences were observed between the two groups with respect to demographics, anthropometrics, activity levels, and biochemistries. The median duration of diabetes was 16.7 yrs (IQR:13.6,18.8). None had microvascular complications. DXA revealed significantly lower BMD at central sites in T1D (LS -11.4%  $p = .01$ , FN -11.9%  $p = .03$ , TH -10.7%  $p = .04$ ). HR-pQCT of the ultra-distal tibia revealed significantly lower Ct.TMD (-4%), Tb.BMD (-11%), inner Tb.BMD (-16%) and Tb.N (-11%), and higher Tb.Sp (+14%) and heterogeneity (+17%) in T1D (all  $p < .05$ ). At the ultra-distal radius, T1D was associated with significantly lower Ct.vBMD (7%) and Ct.TMD (6%) (both  $p < .01$ ). At the radius and tibia there were no observed differences in porosity or biomechanical indices by FE analysis. However, FE analysis with adjusted tissue modulus, scaled by mean Ct.TMD, revealed significantly lower app. modulus, stiffness, and failure load (-19 to -30%  $p < .001$ ) in T1D.

**Conclusion:** In males (median age 22.5 yrs), pre-pubertal onset of T1D is associated with lower central BMD accrual, lower trabecular BMD in weight bearing sites with vulnerability of the central trabecular compartment, and lower cortical mineral density (due to reduced tissue mineralization or increased sub-resolution porosity). These differences are associated with significant lowering of estimated strength when scaled for lower cortical TMD. These findings suggest that the observed increased fracture risk of T1D may in part be due to material or microarchitectural changes in bone which manifest in adolescence.

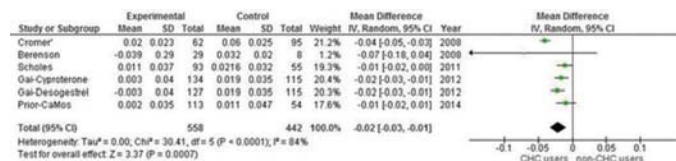
**Disclosures:** Roger Long, None.

## MO0417

**Adolescent use of Combined Hormonal Contraceptives and Peak Areal Bone Mineral Density Accrual in Prospective Studies: a meta-analysis.** Azita Goshtasebi\*<sup>1</sup>, Tatjana Subotic Brajic<sup>2</sup>, Delia Scholes<sup>3</sup>, Tamara Beres Lederer Goldberg<sup>4</sup>, Abbey Berenson<sup>5</sup>, Jerilyn Prior<sup>6</sup>. <sup>1</sup>University of British Columbia, Canada, <sup>2</sup>Centre for Menstrual Cycle and Ovulation Research, UBC, Canada, <sup>3</sup>Kaiser Permanente Washington Health Research Institute, United States, <sup>4</sup>Botucatu School of Medicine, São Paulo State University, Brazil, <sup>5</sup>University of Texas Medical Branch, United States, <sup>6</sup>Centre for Menstrual Cycle and Ovulation Research, Endocrinology and Metabolism, University of British Columbia, Canada

**Background**—for effectiveness, combined hormonal contraceptives (CHC, oral, patch or vaginal ring) include supraphysiological ethinyl estradiol that may suppress bone modeling necessary to gain peak areal bone mineral density (BMD). To our knowledge meta-analyses of adolescent CHC BMD change are lacking. We hypothesized adverse hip effects of CHC use on adolescent BMD accrual given skeletal site-specific ages at peak BMD. **Purpose**—to determine whether CHC use within-study centre compared with CHC non-use in healthy adolescent women was related to peak BMD accrual at the lumbar spine (LS), total hip (TH), femoral neck (FN) or whole body without head (WB) by DXA. **Methods**—a systematic literature search of prospective studies of BMD change over 12- or 24-month (m) by CHC use or not in healthy adolescents (ages 13-19). Studies could be RCTs or observational; if publications included non-teen data, we sought teen-specific data from authors. Analysis of eligible studies was by random-effects meta-analysis with sensitivity assessed by fixed effect models and sequential study removal. **Results**—the literature search yielded 83 data-sets of which 9 met eligibility criteria; 2 data-sets were RCTs comparing 2 CHC preparations and had non-randomized controls, the rest observational; 1 random population-based data-set was a 2014 ASBMR abstract. Adolescent-only data were obtained from 3 centres. The 12-m LS meta-analysis (8 studies, 9 paired comparisons) in 1645 adolescents showed a weighted mean difference for CHC-use versus (vs) non-exposed of -0.02 (95% CI: -0.04;-0.00) g/cm<sup>2</sup> (P=0.04). The 24-m LS meta-analysis (Figure) with 5 studies (6 comparisons) in 1000 adolescents showed a significant weighted mean difference for CHC use vs non-use of -0.02 (95%CI: -0.03;-0.01) g/cm<sup>2</sup> (P=0.0007). Both analyses were robust to fixed effects meta-analysis. The 24-m but not 12-m results were robust to sequential study removals. Heterogeneity by I<sup>2</sup> was 96 and 84% respectively consistent with the few available studies. Insufficient TH, FN and WB data were available for quantitative synthesis.

**Conclusions**—these first meta-analyses of BMD changes by CHC use or not in healthy adolescent women show significantly less 24-m LS BMD gain or BMD loss in CHC-users. As adolescent use of CHC is increasing, this information bears inclusion in counselling about contraception. These meta-analyses are of observational studies; randomized controlled trial data of adolescent BMD change on CHC are needed.



Meta-analysis of Lumbar Spine BMD 24-month Change in Adolescents by CHC use

**Disclosures:** Azita Goshtasebi, None.

## MO0418

**Relationship of total or calculated free 25-hydroxyvitamin D to metabolic indices in a cohort of healthy children.** Christine Simpson\*<sup>1</sup>, Jane Zhang<sup>2</sup>, Teresita Pennestri<sup>1</sup>, Lei Fu<sup>3</sup>, Dirk Vanderschueren<sup>4</sup>, Roger Bouillon<sup>4</sup>, David Cole<sup>3</sup>, Thomas Carpenter<sup>1</sup>. <sup>1</sup>Yale University School of Medicine, United States, <sup>2</sup>V.A. Connecticut Healthcare System, United States, <sup>3</sup>University of Toronto, Canada, <sup>4</sup>Katholieke Universiteit, Belgium

Vitamin D status represented by circulating total 25-hydroxyvitamin D (t25D) or calculated free 25-hydroxyvitamin D (cf25D) correlates with measures of calcium homeostasis. Whether these measures correlate with metabolic indices is less well established, particularly in children. We enrolled 225 healthy children, aged 7 mos. to 10 yrs. (115 girls/110 boys) from a largely Hispanic/Latino background (81% of subjects) into an interventional vitamin D trial, seeking significant associations of vitamin D status with candidate related variables. The cf25D was calculated using simultaneous measures of serum t25D, albumin, and vitamin D binding protein (DBP), and correlation analysis was performed.

Significant (P<0.05) correlates of t25D included height (spearman r = -0.17), BMI (r = -0.19), refractometer-determined skin pigmentation (r = -0.22), systolic blood pressure (r = -0.16), PTH (r = -0.28), insulin (r = -0.27), HOMA IR (r = -0.21), aldosterone (r = 0.16), and renin (r = 0.15). cf25D was associated with the same variables to a comparable degree. Similar correlations were observed when using the standard DBP dissociation constant for all subjects or when using dissociation constants specific to each subject's DBP genotype. In contrast, (total) 1,25-dihydroxyvitamin D (1,25D) correlated only with serum phosphate (r = 0.25) and the cytokines cathelicidin (r = -0.21) and CCL13 (r = -0.27), but with no other 25D-associated variables.

Analysis of subjects within each of the 6 common DBP genotype groups was comparable to that of the overall cohort.

These data support the findings of previously identified inverse correlations between circulating vitamin D status and metabolic parameters including BMI, and indices of insulin resistance (plasma insulin level and calculated HOMA-IR) in a childhood population. Furthermore, in this cohort vitamin D status correlates with blood pressure and its determinants (aldosterone and renin). As t25D and cf25D are comparably related to the metabolic variables examined in these pediatric subjects, we suggest that calculated methods do not appear to improve t25D as a marker for these measures. Moreover, we found comparable associations between 25D and associated variables within the six DBP genotype groups. Finally, we confirmed that 1,25D is not correlated with these variables, but is associated with levels of CCL13 and cathelicidin, as previously described in other populations.

**Disclosures:** Christine Simpson, None.

## MO0419

**Walking at 1 Year of Age Relates to Higher Lean Body Mass with Benefits to Bone Mineral Density Evident at 3 Years of Age.** Hope Weiler\*, Catherine Vanstone. McGill University, Canada

**Purpose:** Gross motor development is positively associated with bone mineral density in teenagers and is thought to be mediated by lean mass. Age at walking is an accepted milestone in motor development, achieved by 50% of infants by 12 mo of age according to the WHO Motor Development Study. We examined if walking within 12 mo of age is related to bone mineral density (BMD) at 36 mo of age and if this relationship is mediated by lean mass. In a subgroup we tested whether age at walking related to lean mass across infancy. **Methods:** Participants (35 girls; 46 boys) of a randomized dose-response trial of vitamin D (NCT00381914; approved by McGill University ethics) were assessed for anthropometry, whole body composition, bone mineral content (BMC) and BMD using dual-energy x-ray absorptiometry (Hologic 4500 APEX v13.3.3) at 1, 3, 6, 9, 12 and 36 mo. Children were term born, appropriate size for gestational age, born to healthy mothers and breastfed. Age at walking was parent-reported and categorized according to: ≤12 mo or >12 mo. Activity at 36 mo was surveyed using the Habitual Activity Estimation Scale. Mixed model ANOVA accounted for maternal education, gestational age at birth and age at follow-up. In a subgroup (n=58) with data at all time-points, differences between those walking by 12 mo vs after were also compared. **Results:** At follow-up, n=37 walked on their own before or at 12 mo of age compared to n=44 after 12 mo (mean ± SD: 10.8 ± 1.0 vs 14.6 ± 1.7 mo, p<0.0001). No differences were observed in weight or gestational age at birth, maternal characteristics, or BMI Z-score or activity level at 36 mo of age. After accounting for covariates, walking by 12 mo was associated with greater lean mass (10183 ± 1233 vs 9621 ± 1149 g, p=0.019), BMC (610.22 ± 46.53 vs 591.85 ± 46.61 g, p=0.023) and BMD (0.637 ± 0.040 vs 0.619 ± 0.036 g/cm<sup>2</sup>, p=0.023) at 36 mo. No differences were observed in fat mass or percent body fat. The relationships between walking by 12 mo and BMC (p=0.347) and BMD (p=0.195) at 36 mo were eliminated by including lean mass in the model. In the subgroup analysis with complete serial measurements available, only lean mass at 12 mo was different showing lower values in those with delayed walking (7573 ± 1122 vs 6974 ± 922 g, p=0.03). **Conclusion:** These data suggest that in healthy term born children, earlier attainment of walking relates to greater lean and bone mass by 3 y of age and that the relationships to bone are mediated by lean mass.

**Disclosures:** Hope Weiler, None.

## MO0420

**Limitations Associated with Bone Assessment by Dual-Energy X-ray Absorptiometry at the Distal Femur in Children with Cerebral Palsy.** Chuan Zhang\*<sup>1</sup>, Daniel Whitney<sup>1</sup>, Benjamin Conner<sup>1</sup>, Freeman Miller<sup>2</sup>, Christopher Modlesky<sup>1</sup>. <sup>1</sup>University of Delaware, United States, <sup>2</sup>A.I duPont hospital for children, United States

**Background:** Children with cerebral palsy (CP) have a high fracture rate at the distal femur. Studies examining the pattern of bone architecture suggest that the deficit in children with CP becomes more pronounced with increased distance proximally from the growth plate within the metaphysis. However, whether the same pattern is observed for areal bone mineral density (aBMD) and bone mineral content (BMC) from dual-energy X-ray absorptiometry (DXA) is unknown.

**Methods:** 32 children with CP (4-13 y; 18 M and 14 F; I-V on Gross Motor Function Classification System) and 32 sex- and age-matched typically developing children participated in this study. A lateral distal femur scan of the more affected side in children with CP and the non-dominant side in controls was acquired using DXA. The region of interest (ROI) was a 14 mm height box starting 2 mm above the growth plate. To determine the pattern of bone mineral and size, the ROI was evenly divided into 7 subregions. aBMD, BMC and bone area of the total ROI and each subregion were determined. Twenty magnetic resonance images (MRI; 0.7 mm thick per image) were used to assess bone area, the medial-lateral (ML) width and the anterior-posterior (AP) width of the distal femur at the same approximate ROI.

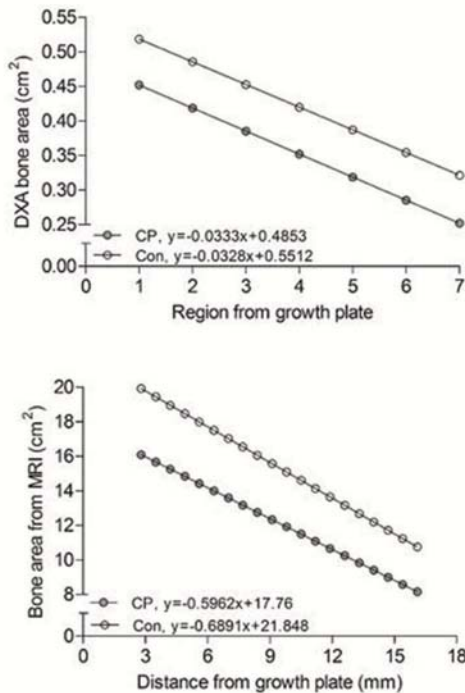
**Results:** Children with CP compared to controls had lower aBMD (26.9 %), BMC (32.7 %) and bone area (9.4 %) from DXA and lower bone area from MRI (21.5 %) (all p < 0.05). Linear random coefficients analysis indicated all four measurements decreased as distance from the growth plate increased (all p < 0.05). However, the rate of the decline was less steep for aBMD and BMC in children with CP than controls (both p < 0.05). While the rate of decline for bone area from DXA was not different (p = 0.897), the



rate of decline for bone area from MRI was less steep in the children with CP ( $p = 0.011$ ). Children with CP had a lower ML bone width and a lower ratio of ML to AP bone width (both  $p = 0.001$ ). Although AP bone width was lower in children with CP, the difference was not significant ( $p = 0.068$ ).

**Conclusion:** The decline in aBMD and BMC with distance from the growth plate in the distal femur is less pronounced in children with CP compared to their typically developing peers. The unusual pattern may be the result of the 2-D bone area data yielded by DXA in the AP plane, which failed to capture the more robust deficit in bone width in the ML plane in children with CP.

**Figure 1.** Estimated regression lines from linear random coefficient analysis for bone area changes with distance from the growth plate. Bone area from DXA showed virtually no difference for the rate of decline between groups as regions move away from the growth plate. However bone area from MRI showed that children with CP have a less steep rate of decline compared to controls.



Random coefficients analysis for bone areas

**Disclosures:** Chuan Zhang, None.

## MO0421

**Bone Marrow Adipose Tissue and Bone Turnover in Postmenopausal Osteoporotic Women and the Effects of Raloxifene.** Kerensa Beekman<sup>\*1</sup>, Annegreet Veldhuis-Vlug<sup>2</sup>, Martin den Heijer<sup>1</sup>, Mario Maas<sup>3</sup>, Paul Lips<sup>1</sup>, Susan Ott<sup>4</sup>, Rob van 't Hof<sup>5</sup>, Peter Bisschop<sup>2</sup>, Nathalie Bravenboer<sup>6</sup>. <sup>1</sup>VU University Medical Center, Department of Endocrinology, Netherlands, <sup>2</sup>Academic Medical Center/University of Amsterdam, Department of Endocrinology and Metabolism, Netherlands, <sup>3</sup>Academic Medical Center/University of Amsterdam, Department of Radiology, Netherlands, <sup>4</sup>University of Washington, Department of Metabolism, Endocrinology and Nutrition, United States, <sup>5</sup>University of Liverpool, Department of Musculoskeletal Biology, United Kingdom, <sup>6</sup>VU University Medical Center, Department of Clinical Chemistry and Leiden University Medical Center, Center for Bone Quality, Netherlands

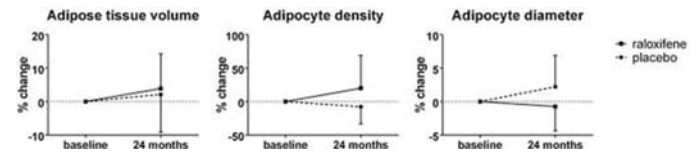
Marrow adipose tissue (MAT) is increased in postmenopausal osteoporosis and is associated with low bone mineral density and increased fracture risk, but the association with bone turnover remains unclear. If MAT is associated with bone turnover it could be a potential new target for treatment of osteoporosis. Hormone replacement therapy decreases marrow adiposity, but the effect of raloxifene, a selective estrogen receptor modulator, on MAT is not known. The aim of this study is 1] to determine the association between MAT and bone turnover and 2] to determine the effect of raloxifene on MAT in patients with osteoporosis.

We retrospectively analyzed 53 paired iliac crest biopsies of postmenopausal osteoporotic women, enrolled in the MORE-trial (NCT00670319). Biopsies were obtained at baseline and after 2 years of treatment with raloxifene (60-120mg/d,  $n=31$ ; age  $68.1 \pm 6.8$  years) or placebo ( $n=22$ ; age  $67.4 \pm 5.7$  years). MAT was quantified

semi-automatically using specially designed software based on ImageJ. Furthermore standardized bone histomorphometry was performed.

MAT was negatively associated with bone volume ( $r=-0.328$ ;  $p=0.01$ ) and positively with prevalent vertebral fracture (OR 1.09;  $p=0.02$ ). Surprisingly, MAT was negatively associated with osteoclast number ( $r=-0.352$ ;  $p=0.01$ ), but not with bone formation rate or osteoid surface. MAT increased in both placebo (2.2%) and raloxifene (3.9%) treated groups ( $p=0.56$ ), but the number of adipocytes decreased in the placebo ( $-7.7 \pm 25.6$  cells/mm<sup>2</sup>) and increased in the raloxifene ( $19.9 \pm 49.0$  cells/mm<sup>2</sup>) treated group ( $p=0.01$ ), whereas the adipocyte diameter increased in the placebo ( $2.2 \pm 4.7$  μm) and decreased in the raloxifene ( $-0.7 \pm 3.7$  μm) treated groups ( $p=0.01$ ).

In conclusion, MAT is negatively associated with osteoclast number in postmenopausal osteoporotic women, which suggests a role for MAT in bone turnover. Patients with prevalent vertebral fractures at baseline, have higher MAT volume compared to osteoporotic patients without prevalent vertebral fractures. Raloxifene increases the number of bone marrow adipocytes, while preventing an increase in size of bone marrow adipocytes in postmenopausal osteoporotic women, indicating that, besides BMD, raloxifene also affects MAT composition.



Changes in bone marrow adipose tissue parameters compared to baseline

**Disclosures:** Kerensa Beekman, None.

## MO0422

**Conditioned medium of Amniotic fluid derived mesenchymal stromal cells ameliorated ischemia induced bone loss in murine bone.** Sun Wook Cho<sup>\*1</sup>, Hyun Jin Sun<sup>1</sup>, Sang Eun Lee<sup>2</sup>, JoonHo Lee<sup>3</sup>, Young Joo Park<sup>1</sup>, Chan Soo Shin<sup>1</sup>. <sup>1</sup>Seoul National University Hospital, Korea, Republic of, <sup>2</sup>Asan medical center, Korea, Republic of, <sup>3</sup>YONSEI UNIVERSITY, COLLEGE OF MEDICINE, Korea, Republic of

Vascular insufficiency is one of the risk factors for fracture. The aim of this study was to investigate the effects of conditioned medium of human amniotic fluid-derived stromal cell (AFSC-CM) on bone metabolism and marrow vasculature. AFSCs were collected from mid-trimester (16-19 weeks) amniotic fluid, and conditioned media were harvested. To investigate the angiogenic effects of AFSC-CM, human microvascular endothelial cells (HMEC) were treated with AFSC-CM (0.5x) and transwell migration and tube formation assays were performed. Compared to control medium, AFSC-CM treatment enhanced cell migration and tube formation potentials in vitro. To evaluate whether the angiogenic effects of AFSC-CM could positively effects on bone metabolism or not, we established ischemic bone disease using chronic hind-limb ischemia model. C57Bl/6 mice (male, 12-week-old) underwent surgery for unilateral femoral artery ligation. Laser Doppler perfusion imaging (LDPI) analysis showed that peripheral blood flow was comparably recovered to that of sham operated limb at 3-4 weeks after operation. Bone mineral density (BMD), measured by DXA, was decreased by 8-10% than that of sham operated limb, during 3 weeks to 6 weeks after operation. AFSC-CMs were administrated via intraperitoneally from immediately after operation (3 days/week). Interestingly, 3 weeks after operation, CD31+ progenitor cells were increased in AFSC-CM than control group ( $34 \pm 8$  vs  $26 \pm 6$  %,  $P < 0.05$ ), and CD31+Endomucin+ were appeared in AFSC-CM ( $3.5 \pm 0.6$  %) while it was not detected in control group. Peripheral revascularization measured by LDPI demonstrated significantly increased vascularization in AFSC-CM than control group by 1.4-fold at 3 weeks, suggesting that AFSC-CM support angiogenesis in hind-limb ischemia model. Next, bone phenotypes were analyzed. BMD was significantly higher in AFSC-CM than control group ( $0.061$  vs  $0.057$  g/cm<sup>3</sup>,  $P < 0.05$ ). MicroCT analyses showed that trabecular bone volume (BV/TV), trabecular thickness and cortical bone volume (BV/TV) were significantly higher in AFSC-CM than control. Primary cultures of bone marrow-derived stromal cells in osteogenic medium (L-ascorbic acid and beta-glycerophosphate) showed that *alkaline phosphatase* and *collagen type 1* expressions were significantly decreased in operated limb than sham operated limb, while it was rescued by AFSC-CM treated group. Collectively, AFSC-CM attenuated ischemia induced bone loss in association with enhanced endothelial progenitor cells in marrows. These data pave the way to develop treatment strategies using angiogenic therapies to ischemia related bone disease such as peripheral artery disease or diabetic foot diseases.

**Disclosures:** Sun Wook Cho, None.

## MO0423

**MicroRNA-141 regulates SDF-1 $\alpha$  expression and osteogenic differentiation in mouse and human bone marrow derived stromal cells.** Sadanand Fulzele<sup>1</sup>, Sudharsan Periyasamy-Thandavan<sup>2</sup>, Galina Kondrikova<sup>2</sup>, John Burke<sup>3</sup>, Rajnikumar Sangani<sup>3</sup>, Bharati Mendhe<sup>4</sup>, Khaled Hussein<sup>2</sup>, Monte Hunter<sup>5</sup>, Carlos Isales<sup>6</sup>, Mark Hamrick<sup>2</sup>, William Hill<sup>7</sup>. <sup>1</sup>Department of Orthopedic Surgery, Medical College of Georgia, Augusta University, United States, <sup>2</sup>Department of Cell Biology and Anatomy, Medical College of Georgia, Augusta University, United States, <sup>3</sup>Medical College of Georgia, Augusta University, United States, <sup>4</sup>Department of Cell Biology and Anatomy, Medical College of Georgia, Augusta University, United States, <sup>5</sup>Department of Orthopedic Surgery, Medical College of Georgia, Augusta University, United States, <sup>6</sup>Department of Neuroscience and Regenerative Medicine, Medical College of Georgia, Augusta University, United States, <sup>7</sup>Department of Cell Biology and Anatomy Medical College of Georgia, Augusta University. Charlie Norwood VA Medical Center, United States

Stromal cell-derived factor 1 $\alpha$  (SDF-1 $\alpha$  or CXCL12), is a cytokine secreted by a number of cell types including bone marrow stromal/stem cells (BMSC). SDF-1 $\alpha$  plays a vital role in BMSC migration, survival and differentiation. Our group previously reported the role of SDF-1 $\alpha$  in in-vitro osteogenic differentiation and in-vivo bone formation. However, our understanding of the post-transcriptional regulatory mechanism of the SDF-1 $\alpha$  remains poor. MicroRNAs (miRNAs) are small non-coding RNAs that post-transcriptionally regulate the messenger RNAs of protein-coding genes. In this study, we demonstrated that mouse and human BMSCs expressed miR-141 and repressed SDF-1 $\alpha$  expression at the functional level (luciferase reporter assay) by targeting the 3'-untranslated region of SDF-1 mRNA. We determined that miR-141 expression increases with age in BMSCs, while SDF-1 $\alpha$  protein expression decreases. We also found that transfection with miR-141 mimetics decreased osteogenic markers in both mouse and human BMSCs. Our results also demonstrate that miR-141 expression increases with age in human BMSCs and SDF-1 $\alpha$  decreases in human bone marrow interstitial fluid. Taken together, these results indicate that miR-141 is a novel regulator of SDF-1 $\alpha$  and plays an important role in the age dependent pathophysiology of mouse and human bone marrow niche.

**Disclosures:** Sadanand Fulzele, None.

## MO0424

**B cell depletion by anti-CD20 antibodies entrains trabecular bone loss in mice.** Albert Kolomansky<sup>1</sup>, Naamit Deshet-Unger<sup>1</sup>, Alina Ostrovsky<sup>1</sup>, Sahar Hiram-Bab<sup>2</sup>, Nathalie Ben-Califa<sup>1</sup>, Tamar Liron<sup>2</sup>, Howard S Oster<sup>3</sup>, Moshe Mittelman<sup>3</sup>, Yankel Gabet<sup>2</sup>, Drorit Neumann<sup>1</sup>. <sup>1</sup>Department of Cell and Developmental Biology, Sackler Faculty of Medicine, Tel Aviv University, Israel, <sup>2</sup>Department of Anatomy and Anthropology, Sackler Faculty of Medicine, Tel Aviv University, Israel, <sup>3</sup>Department of Medicine A, Tel Aviv Sourasky Medical Center, Sackler Faculty of Medicine, Tel Aviv University, Israel

Targeted B cell therapy by anti-CD20 antibody has revolutionized the treatment of B cell malignancies and autoimmune disorders. A growing body of evidence links B cell homeostasis to bone metabolism, including reports indicating severe bone loss in a murine transgenic model of mature B cell depletion. Here we examined the effect of pharmacological depletion of mature B cells by anti-CD20 antibodies (Abs) on bone mass in mice.

Ten-week-old female C57BL/6J mice were treated with 150  $\mu$ g of anti-mouse CD20 Abs administered in two doses, two weeks apart. After 4 weeks, the efficiency of B cell depletion and immune-profiling of bone marrow (BM) cells were examined by flow cytometry. Bone morphometric analysis of distal femurs was performed using  $\mu$ CT. B cell subsets were flow-sorted and subjected to osteoclastogenic analysis *in-vitro*.

In mice with >90% splenic B cell depletion (5 out of 7), anti-CD20 treatment (compared to diluent controls) induced a significant trabecular bone loss, i.e. 25% decrease in bone mineral density ( $30.1 \pm 2.5$  vs  $40 \pm 3.7$  mg HA/cm<sup>3</sup>), 44% decrease in connectivity density ( $10.3 \pm 1.5$  vs  $18.9 \pm 2.8$  mm<sup>-3</sup>), 13% reduction in trabecular number ( $2.8 \pm 0.13$  vs  $3.24 \pm 0.13$  mm<sup>-1</sup>), and 14% increase in trabecular separation ( $p < 0.05$  for all parameters,  $n = 5-7$ ). Anti-CD20-treated mice had a compensatory 55% increase in BM pro-B cells ( $2.8 \pm 0.5\%$  vs  $1.8 \pm 0.1\%$ ) that also exhibited a 2.5-fold increase in macrophage colony-stimulating factor (M-CSF) receptor positivity (CD115+,  $p < 0.05$ ). To this end, *in-vitro* stimulation by M-CSF and receptor activator of nuclear factor  $\kappa$ -B ligand (RANKL) induced the transdifferentiation of pro-B cells (CD19+/CD43high/IgM-), but not pre-B cells (CD19+/CD43low/IgM-), nor immature B cells (CD19+/IgM+) into osteoclasts (OC) ( $16\% \pm 3.7$  vs  $0.8\% \pm 0.28$  and  $0.5\% \pm 0.1$  OC area, respectively). Moreover, only CD115+ pro-B cells, but not CD115- (negative) pro-B cells, gave rise to functional OC ( $18 \pm 6.5\%$  OC area vs none).

This is the first report demonstrating adverse skeletal outcomes of pharmacological mature B cell depletion, conceivably fueled by B cell-derived osteoclastogenesis. Since many patients treated with anti-CD20 already have other risk factors for bone loss, e.g. older age and glucocorticoid therapy, these data have immediate clinical implications.

**Disclosures:** Albert Kolomansky, None.

## MO0425

**Bone marrow phenotype in a murine model of cystic fibrosis.** Genevieve Mailhot<sup>\*</sup>, Safiétou Sankhe, Genevieve Morin, Valérie Orlando, Déborah Lénart. CHU Sainte-Justine Research Center, Canada

Background: Improvements in management and care have contributed to markedly extend the longevity of cystic fibrosis (CF) patients. However, this gain in lifespan is achieved at the expense of an increased occurrence of several comorbidities including CF bone disease (CFBD). Imbalanced bone remodeling caused by defective osteoblast differentiation and function is currently pointed out as the major CFBD pathophysiological mechanism in both humans and mice. Largely known for its role in hematopoiesis, the bone marrow (BM) also has a functional interdependence with bone due to its close anatomical proximity. The crosstalk between osteoblasts and the BM combined with the fact that CF osteoblasts are dysfunctional led us to postulate that CF bone marrow exhibits phenotypic alterations in its cellular composition. Objectives: The purpose of this study is to compare the leucocyte composition of the BM of non-infected CF and non-CF mice and to document the impact of gender, age, and genetic background on this outcome. Methods: BM was harvested from the femurs and tibiae of 6 and 12 week-old *Cftr*<sup>-/-</sup> and *Cftr*<sup>+/+</sup> males and females from two genetic backgrounds (i.e. BALB/c and C57BL/6) and leucocyte composition analyzed by flow cytometry. Leucocyte composition of the spleen and lymph nodes was also assessed. Results: BALB/c *Cftr*<sup>-/-</sup> mice displayed significantly reduced proportions of macrophages, dendritic cells and T lymphocytes compared to *Cftr*<sup>+/+</sup> mice. These changes were mainly attributed to males as only macrophages were significantly decreased in females. Age was not a contributing factor, as both 6 and 12-week mice exhibited the same phenotype. Immunophenotypic characterization of the spleen and lymph nodes revealed no difference between genotypes suggesting that no extramedullary compensation occurred in response to changes in the BM. Interestingly, C57BL/6 *Cftr*<sup>-/-</sup> mice exhibited distinct immunophenotypic profiles than BALB/c *Cftr*<sup>-/-</sup> mice with only a significant reduction in the proportion of dendritic cells in both sexes. BM cellular composition of the osteoblast conditional *Cftr* knockout mice was similar to that of *Cftr*<sup>+/+</sup> mice, indicating that the conditional absence of *Cftr* in the osteoblast did not influence the BM leucocyte composition. The fact that *Cftr* is expressed in the BM corroborates that its absence negatively impacts the BM through some unknown mechanisms. The consequences of such alterations for the bone and immune systems need to be clarified.

**Disclosures:** Genevieve Mailhot, None.

## MO0426

**The PEG Associated Solvent System (PEGASOS) Method Enables 3-Dimensional Visualization of Hard Tissue.** Shiwen Zhang<sup>1</sup>, Wenjing Luo<sup>2</sup>, Dian Jing<sup>1</sup>, Yi Men<sup>2</sup>, Quan Yuan<sup>3</sup>, Zhihe Zhao<sup>3</sup>, Hu Zhao<sup>3</sup>. <sup>1</sup>Texas A&M University College of Dentistry, USA; Sichuan University, China, United States, <sup>2</sup>Texas A&M University College of Dentistry, USA, United States, <sup>3</sup>Sichuan University, China, China

Purpose: Recent tissue-clearing approaches have become important alternatives to standard histology approaches. Tissue clearing techniques make tissue transparent while preserving endogenous fluorescent signals. 3-Dimensional visualization of whole organs at single cell resolution is becoming possible. However, progresses on the tissue clearing techniques have been mainly focusing on soft tissues. Although a few of clearing methods are involved in the application in hard tissue, they are still of limited tissue transparency or quenching of fluorescent protein [1, 2]. Here we are introducing the PEG Associated Solvent System (PEGASOS) method for clearing hard tissue while preserving endogenous fluorescent signal.

Method: Bone samples from adult mouse samples were processed following sequential steps including decalcification, decolorization, delipidation, dehydration and final clearing. Multiple transgenic models including  $\alpha$ SMA-CreERT2;A14, Wnt1-Cre;Ai14, CAG-EGFP, Tie2-Cre;Ai14 were used to label various structures of hard tissue. Samples were imaged with two photon microscope. Images were then processed with the Imaris 8.3.1 software.

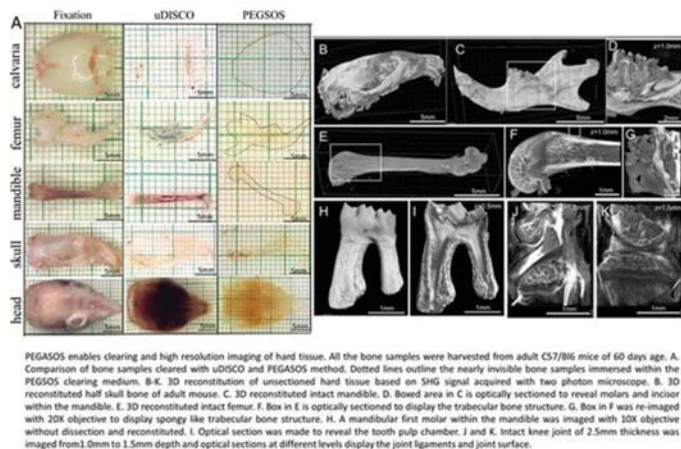
Results: The PEGASOS method efficiently clears hard tissue and provides superior fluorescence protection. Quantified comparison indicated PEGASOS provides better transparency and fluorescence preservation than uDISCO. Combining with transgenic mouse models, we were able to reconstruct the entire adult mouse head based on two photon microscope images. We also investigated the 3-dimensional organization of vasculatures and innervation within the bone marrow of femur. Interesting patterns were revealed from our analysis.

Conclusion: PEGASOS provides a powerful tool for visualizing and analyzing hard tissue in 3-dimension.

1. Pan C, Cai R, Quacquarelli FP, Ghasemigharagoz A, Loubopoulos A, Matryba P, Plesnila N, Dichgans M, Hellal F, Erturk A: Shrinkage-mediated imaging of entire organs and organisms using uDISCO. *Nature methods* 2016.

2. Richardson DS, Lichtman JW: Clarifying Tissue Clearing. *Cell*, 162(2):246-257, 2015





**Disclosures:** Shiwen Zhang, None.

## MO0427

**Selective Pharmacological Inhibition of Notch Receptor 3 Signaling Induces Myeloma Cell Death and Preserves Osteocyte Viability.** Emily G. Atkinson<sup>\*1</sup>, Teresita Bellido<sup>1</sup>, G. David Roodman<sup>2</sup>, Mark R. Kelley<sup>3</sup>, Jesus Delgado-Calle<sup>1</sup>. <sup>1</sup>Anatomy and Cell Biology, Indiana University School of Medicine, United States, <sup>2</sup>Department of Medicine, Indiana University School of Medicine, United States, <sup>3</sup>Department of Pediatrics, Herman B Wells Center for Pediatric Research, Indiana University School of Medicine, United States

Multiple myeloma (MM) cell growth and survival are highly dependent on interactions between MM cells and cells in the bone/bone marrow microenvironment. Earlier work demonstrated that osteocytes (Ot), major regulators of osteoblast and osteoclast activity and the most numerous cells in bone, contribute to MM growth and the associated bone disease. In addition, MM/Ot interactions activate bidirectional Notch signaling between MM cells and Ot, which in turn enhances MM growth and increases Ot apoptosis. Further, these effects were mediated by Notch receptor (R)3 and R4 and prevented *in vitro* by pharmacological inhibition of Notch using a  $\gamma$ -secretase inhibitor. Although systemic inhibition of Notch using  $\gamma$ -secretase inhibitors has anti-MM activity, it causes significant toxicity *in vivo*, thus limiting its use in patients. The goal of this study was to assess *in vitro* the effects of selective inhibition of Notch R3 signaling on Notch activation and viability of MM cells and Ot. Towards this end, we used APX3330, a novel, oral, first-in-class human Ref-1 inhibitor that downregulates Notch R3 expression in solid tumors. In murine 5TGM1 and human JJN3 MM cells, APX3330 (5-50  $\mu$ M) reduced Notch R3 mRNA expression by 50%, without affecting Notch R1, R2 or R4 levels, and decreased the expression of the Notch target gene *Hei1* by 40%. Further, APX3330 decreased the number of viable MM cells by 80%, measured by MTT, and increased the number of dead MM cells in a dose-dependent manner, measured by trypan blue exclusion. These results suggest that Notch R3 is required to maintain Notch signaling and MM cell survival. In MLO-A5 osteocytic cells, APX3330 also downregulated the expression of Notch R3 by 45%, but not Notch R1, R2 or R4, and reduced the mRNA levels of the Notch target gene *Hey1* by 60%. However, Ot viability and the number of dead Ot were not affected by APX3330, even when high concentrations were used. These results demonstrate that APX3330 effectively inhibits Notch signaling in both MM cells and Ot, and that induces MM cell death without altering Ot viability. Thus, APX3330 represents a novel pharmacologic approach to disrupt the bidirectional Notch signaling between Ot and MM and to inhibit Notch signaling in the MM microenvironment. These findings provide a basis for selective inhibition of Notch R3 signaling to treat MM patients and circumvent the deleterious side effects of systemic suppression of Notch using  $\gamma$ -secretase inhibitors.

**Disclosures:** Emily G. Atkinson, None.

## MO0428

**Characterizing Dose Dependent Effects of Estrogen in a Murine Model of Human Estrogen Receptor-Positive Breast Cancer Bone Metastasis.** Julia Cheng<sup>\*1</sup>, Jennifer Frye<sup>2</sup>, Susan Whitman<sup>2</sup>, Andrew Kunihiro<sup>3</sup>, Madison Egan<sup>4</sup>, Julia Brickey<sup>3</sup>, Janet Funk<sup>2</sup>. <sup>1</sup>Cancer Biology Graduate Interdisciplinary Program, University of Arizona, United States, <sup>2</sup>Department of Medicine, University of Arizona, United States, <sup>3</sup>Department of Nutritional Sciences, University of Arizona, United States, <sup>4</sup>Department of Molecular and Cellular Biology, University of Arizona, United States

Estrogen receptor  $\alpha$ -positive (ER+) breast cancers (BrCAs) have the greatest predilection for forming bone metastases (BMETs). Because most human xenograft models of BrCA BMET involve intracardiac injection of ER- tumors, we sought to develop an ER+ model using similar strategies to query ER $\alpha$ 's role in BMET progression. For these studies, naive or 17- $\beta$  estradiol ( $E_2$ )-treated female athymic mice aged 4 weeks (young) or 15 weeks (mature) were inoculated with  $1 \times 10^5$  human ER+ MCF-7 BrCA cells via the left cardiac ventricle 2-days post-placement of 60-day release  $E_2$  pellets (0.05, 0.10, 0.18, 0.36, & 0.72 mg  $E_2$ ). Osteolytic lesion formation was assessed by hind limb radiographs, and  $E_2$  effects on bone were assessed by DXA and  $\mu$ CT. BMET incidence and lesion size in young mice were  $E_2$  dose-dependent, achieving 100% incidence at the highest dose tested by day 14 post-inoculation, with intermediate doses falling below 100%, and zero incidence in the absence of  $E_2$  even after 8 months. Because radiographs suggested significant bone density increases with all  $E_2$  doses tested,  $E_2$  dose-dependent effects on bone, independent of lesion formation, were assessed in tumor cell-free mice. Notably, all  $E_2$  doses tested increased BMD in a non-dose dependent fashion, achieving peak levels by day 14, with BV/TV of trabecular bone, where lesions are located, increasing 3-4 fold by study end (day 42). Because increased age and  $E_2$  have been reported to have an inhibitory or neutral effect, respectively, on ER- BMET, effects of the highest  $E_2$  dose on bone and MCF-7 lesion development were determined in mature mice. In older mice,  $E_2$ -stimulated bone accrual was less marked, but lesion growth was analogous to young mice. In summary, osteolytic ER+ BMET development in young mice was  $E_2$  dose-dependent, despite non-dose-dependent increases in BMD, and comparable in young vs. mature mice, suggest that the dose dependent effects of estrogen on BMET development in this model are due to direct effects on the ER+ tumor cells. While the relative role of  $E_2$ -induced tumor cell proliferation vs osteolytic factor secretion cannot be distinguished here, the ability of MCF-7 cells to form osteolytic lesions similar in size to those reported in ER- BMET models is notable given the marked increase in bone volume. While further studies are required, these results suggest that estrogen may drive ER+ BMET progression via bone-specific effects mediated via the tumor as well as the bone microenvironment.

**Disclosures:** Julia Cheng, None.

## MO0429

**Conditioned Medium of the Osteosarcoma Cell Line Saos-2 Induces BMSCs to Exhibit Characteristics of Carcinoma-Associated Fibroblasts via TGF $\beta$  Pathway.** Ze Tang<sup>\*</sup>, Qiming Fan, Tingting Tang. Shanghai Key Laboratory of Orthopaedic Implants, Department of Orthopaedic Surgery, Shanghai Ninth People's Hospital, Shanghai Jiao Tong University School of Medicine (SJTUSM), China

Human bone marrow stromal cells (BMSCs) have been shown to have the abilities to actively home to the osteosarcoma (OS) site, promote osteosarcoma growth in local tumor microenvironment and increase remote osteosarcoma pulmonary metastasis. There are intense interactions between BMSCs and OS. However, the underlying molecular mechanisms remain elusive. So in the current study, we attempted to investigate the interaction pattern between BMSCs and OS. We deployed the BMSC/Saos-2 co-culture interaction model to test our hypothesis that BMSCs is the source of CAF in osteosarcoma microenvironment. By the data from microarray, GSEA (Gene Set Enrichment Analysis) showed that CAF marker gene set and TGF $\beta$  signaling pathway gene set had statistically significant and concordant differences between BMSCs under Saos2-CM and normal hBMSCs, which indicated that BMSCs under Saos-2-CM showed some characters of CAF and TGF $\beta$  signaling pathway might be the potential target signaling pathway that transformation from BMSCs into CAFs depended on. In order to verify the finding of GSEA, we used western immunoblotting / in cell western and Realtime RT-PCR to validate the upregulation of CAF marker gene expression and TGF $\beta$  signaling pathway in BMSCs under Saos2-CM. Furthermore, in order to discern whether the CAF characters that BMSCs possessed under Saos-2 were TGF $\beta$  signaling pathway depended, we evaluated the changes of CAF marker expression and CAF phenomenon in BMSCs under Saos-2 upon neutralizing TGF $\beta$  specific pan antibody and a specific inhibitor TGF $\beta$  signaling pathway SB431542. Line up GSEA and various verification, we suggested that the hBMSCs co-cultured with osteosarcoma acquired some CAF characteristics via the TGF $\beta$  signaling pathway and BMSCs under Saos-2-CM could enhance the proliferation and migration of Saos-2 in a feed back manner.

**Disclosures:** Ze Tang, None.

## MO0430

**Functional Comparison between CD44s and CD44v8-10 in Cancer Metastasis to Bone.** Toru Hiraga\*, Hiroaki Nakamura, Matsumoto Dental University, Japan

CD44, an adhesion molecule that interacts with extracellular matrices, primarily to hyaluronan, has been implicated in cancer progression and metastasis, as well as in cancer stem cells. Our previous study demonstrated that CD44 confers cancer stem-like properties to cancer cells and enhances their metastatic potential to bone. CD44 has numerous splice variants; however, little is known about their differential roles in bone metastasis. Thus, in the present study, we compared the roles of the standard isoform of CD44 (CD44s) and the variant isoform of CD44 (CD44v) in the development of bone metastases using a well-characterized mouse model. Among known isoforms, we focused mainly on CD44v8-10 (also known as CD44R1 or CD44E), whose expression has been shown to be correlated with metastasis of several types of cancer. For this purpose, MDA-MB-231 human breast cancer cells and A549 human lung cancer cells were stably transduced with epithelial splicing regulatory protein 1 (ESRP1), which regulates the alternative splicing of several genes, including CD44. Western blot and RT-PCR analyses showed that parental MDA-MB-231 and A549 cells endogenously express high levels of CD44s and low levels of CD44v. The introduction of ESRP1 induced a splicing switch from CD44s to CD44v, particularly to CD44v8-10, while the total amount of CD44 was barely influenced. However, WST-1 assay, wound healing assay, matrigel invasion assay, and suspension culture assay revealed that ESRP1 did not significantly affect cell proliferation, migration, invasion, or tumor sphere formation *in vitro*. Furthermore, ESRP1 did not cause significant differences in the development of bone metastases in mice. As an alternative approach, cancer cells stably transduced with the CD44v8-10 gene were also established. The overexpression of CD44v8-10 in MCF-7 human breast cancer cells, which rarely express any isoform of CD44, promoted cell migration and sphere formation *in vitro*. Similar effects were produced by CD44s. In contrast, CD44v8-10 overexpression in MDA-MB-231 cells, in which CD44s is constitutively and highly expressed, did not exert these effects. Bone metastasis of MDA-MB-231 cells was also not affected by CD44v8-10. These results collectively suggest that the ability of CD44v8-10 to promote tumor aggressiveness and bone metastases is similar to that of CD44s. Both CD44v8-10 and CD44s likely represent potential therapeutic targets for the treatment of bone metastases.

**Disclosures:** Toru Hiraga, None.

## MO0431

**Rare-earth-doped Luminescent Nanoparticles for Breast Cancer Detection and Potential Bone-targeting Contrast Agents.** Akhil Jain\*<sup>1</sup>, Fournier Pierrick<sup>2</sup>, Gustavo A Hirata<sup>1</sup>, Patricia Juarez<sup>2</sup>. <sup>1</sup>Center of Nanosciences and Nanotechnology-UNAM, Mexico, <sup>2</sup>Center for Scientific Research and Higher Education, Mexico

Breast cancer is the second leading cause of cancer death in women and it is estimated that more than 250,000 new cases will be diagnosed in the USA, in 2017. Breast cancer metastasizes to bone in more than 80% of patients with advanced disease, causing severe skeletal related events and bone metastases are incurable. The best chance for patients is to have their cancer detected as early as possible. The standard diagnosis method for breast tumor is mammography, which is often related with false-negative results leading to therapeutic delays and contributing indirectly to the development of metastasis to bone. Here, we have established a nanoparticle platform for the detection of breast cancer and bone metastasis by conjugating folic acid (FA) to rare-earth-doped luminescent nanoparticles (RE).

RE were synthesized using sucrose-assisted combustion synthesis and functionalized with FA using EDC-NHS coupling. Transmission electron microscopy analysis indicated an average nanoparticle diameter of 55 nm. FA-conjugated RE nanoparticles exhibited strong red emission at 613 nm with a 35% quantum yield. MTT analysis demonstrated that the nanoparticles had negligible cytotoxic effect on normal 293T cells and T47D breast cancer cells *in vitro*. Cellular uptake analysis showed significantly higher internalization of FA-conjugated RE nanoparticles into T47D cells (*Folr*<sup>hi</sup>) compared to MDA-MB-231 breast cancer cells (*Folr*<sup>lo</sup>).

*In vivo* studies in CD1 mice indicated that FA-conjugated RE nanoparticles are rapidly cleared from blood circulation after 2h post-injection thus minimizing the risk of toxic response. Additionally, these nanoparticles were well tolerated in mice even at doses as high as 300 mg/kg, after i.v. injection. We next evaluated the targeting ability of FA-conjugated RE nanoparticles in xenograft models of MDA-MB-231 and T47D breast cancer cells. Fluorescence imaging analysis showed that nanoparticles specifically accumulated at tumor site after a single intravenous dose. Overall, our results showed that our FA-conjugated RE nanoparticles have high tumor specificity and biocompatibility representing an advanced tool that can be applied for preclinical and clinical applications. Further studies are going on to evaluate bone targeting ability of surface functionalized RE nanoparticles in an *in vivo* model of bone metastasis.

**Disclosures:** Akhil Jain, None.

## MO0432

**Effects of estrogen removal by ovariectomy on growth of human MCF-7 breast cancer cells in bone.** Tiina E Kähkönen\*, Mari I Suominen, Jukka Morko, Jukka Vääräniemi, Jussi M Halleen, Jenni Bernoulli, Pharmatest Services Ltd, Finland

Hormone receptor positive cancers commonly metastasize to bone. Hormonal regulation in primary tumor and in bone is well established but poorly understood in the context of bone metastases. Our aim was to study the effects of hormone deprivation on growth of bone metastases in the early phases of outgrowth and on already growing metastases in bone.

Estrogen responsive, luciferase labelled MCF-7 human breast cancer cells (ATCC, labelled at DKFZ, Germany) were inoculated into the tibia of 7-8 week old athymic nude mice (Envigo, Netherlands). The mice were ovariectomized (OVX) one week before or four weeks after the cancer cell inoculation. Mice in the control group were left intact. Tumor growth and tumor-induced bone changes were studied by bioluminescence imaging (BLI) and radiography, respectively, at 2, 4, 6 and 9 weeks after the cancer cell inoculations. Changes in bone mineral density (BMD) was studied at endpoint by dual X-ray absorptiometry (DXA). Decalcified bone sections were evaluated by histology.

BLI in the control group revealed increased signal up to 6 weeks and then decreased towards endpoint at 9 weeks. Simultaneously, constant increase in osteoblastic bone lesion area was observed. Potentially, bone marrow was filled with cancer cells by 6 weeks from inoculation, and after that the newly formed bone started to decrease the amount of cancer cells in the marrow, seen as decrease in BLI signal. When OVX was performed prior to cancer cell inoculation, the BLI signal increased up to 4 weeks and disappeared at endpoint. By histological evaluation, there were no tumor cells in these mice, whereas viable tumor cells with osteoblastic bone reaction were observed in the control group. When OVX was performed 4 weeks after cancer cell inoculation, the osteoblastic bone reaction was observed but less cancer cells were found compared to the control group. Osteoblastic bone reaction was quantified by increased BMD in the tumor-bearing tibias.

Hormone regulation in bone metastasis is complex, consisting of hormone related changes in bone combined with tumor-induced changes. In the presence of endogenous estrogen, the tumors grew and induced major osteoblastic bone reaction. In the absence of estrogen the tumor cells disappeared from the bone marrow by time. In order to establish more predictive preclinical models for advanced breast cancer drug development, influence of hormonal microenvironment in the bone should be taken into account.

**Disclosures:** Tiina E Kähkönen, None.

## MO0433

**Association Between Mutations in a New Gene (*ZNF687*) and Neoplastic Degeneration of Paget's Disease of Bone in Giant Cell Tumor but not Osteosarcoma.** Materozzi Maria\*<sup>1</sup>, Daniela Merlotti<sup>2</sup>, Simone Bianciardi<sup>3</sup>, Domenico Rendina<sup>4</sup>, Vito Guarnieri<sup>5</sup>, Paolo Graziano<sup>6</sup>, Salvatore Minisola<sup>1</sup>, Alfredo Scillitani<sup>8</sup>, Pasquale Strazzullo<sup>4</sup>, Ranuccio Nuti<sup>3</sup>, Luigi Gennari<sup>3</sup>. <sup>1</sup>Department of Medicine, Surgery and Neurosciences, University of Siena, Italy; <sup>2</sup>Department of Medical, Biotechnologies, University of Siena, Italy, Italy, <sup>3</sup>Division of Genetics and Cell Biology, San Raffaele Scientific Institute, Milan, Italy; <sup>4</sup>Department of Medicine, Surgery and Neurosciences, University of Siena, Italy, Italy, <sup>5</sup>Department of Medicine, Surgery and Neurosciences, University of Siena, Italy, Italy, <sup>6</sup>Department of Medicine, Clinical and Experimental Medicine, Federico II University, Naples, Italy, Italy, <sup>7</sup>Unit of Medical Genetics, IRCCS Casa Sollievo della Sofferenza Hospital, San Giovanni Rotondo Italy, Italy, <sup>8</sup>Unit of Pathology, IRCCS Casa Sollievo della Sofferenza Hospital, San Giovanni Rotondo Italy, Italy, <sup>9</sup>Department of Internal Medicine, Sapienza University Rome, Italy, Italy, <sup>10</sup>Unit of Diabetology and Endocrinology, IRCCS Casa Sollievo della Sofferenza Hospital, San Giovanni Rotondo Italy, Italy

Paget's bone disease (PDB, OMIM 602080) is a focal disorder with a strong genetic component characterized by increased and disorganized bone remodeling, bone expansion and abnormal bone structure. Among the several complications, different reports clearly indicate that pagetic tissue may undergo neoplastic transformation in osteosarcoma and less frequently giant cell tumor (GCT). These tumors consistently arise in bones affected by PDB, and may present as multifocal lesions. Despite either GCT and osteosarcoma have been often described to occur in PDB families, the nature of the underlying genetic alterations and the molecular basis of tumorigenesis in pagetic bone remain to be defined. We recently identified a mutation in a new gene (*ZNF687*) as a monogenic cause of a severe, early-onset PDB associated with GCT degeneration in 2 large pedigrees and in 7 additional unrelated pagetic cases of GCT. In order to further explore the relationship between *ZNF687* and neoplastic degeneration we extended mutational screening to 3 new families with early onset, polyostotic PDB associated with GCT (n=2) or osteosarcoma (n=1), 3 additional osteosarcomas occurring in sporadic PDB cases, and 6 cases of GCT and 6 osteosarcomas occurring in non-pagetic patients. We confirmed the presence of a common missense mutation (P397R) of *ZNF687* in both the 2 families with PDB and GCT degeneration but not in all the 6 cases of GCT occurring in non pagetic patients. The mutation co-segregated with the



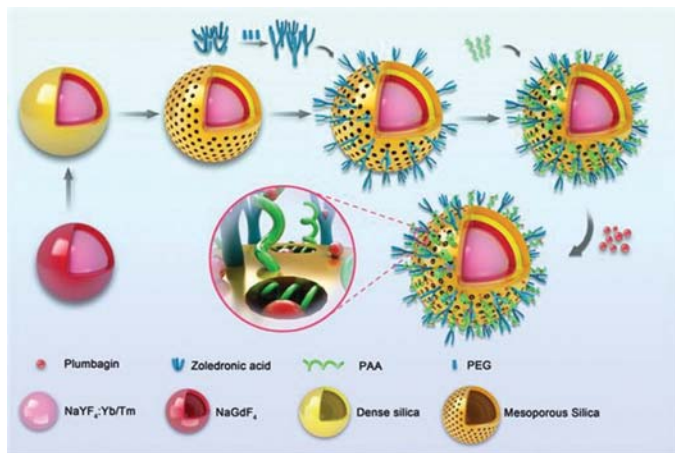
clinical phenotype in all affected family members. Conversely, we did not identify neither *SQSTM1* nor *ZNF687* mutations in pagetic and non-pagetic osteosarcomas. In particular, we identified a large PDB pedigree associated with sarcomatous degeneration in 2 affected members that were negative for mutational screening of *SQSTM1*, *ZNF687* or other genes associated with PDB-like syndromes (*TNFRSF11B*, *TNFRSF11A*, *VCP* and *hNRNP2B1*). All affected cases from this pedigree showed an early onset, polyostotic form of PDB requiring more than 1 course of treatment with zoledronic acid 5mg to suppress disease activity. Next generation sequencing analysis is ongoing in order to identify the causal gene. Taken together our results demonstrated that a rare mutation in *ZNF687* segregates with PDB associated with neoplastic degeneration in GCT (in all the familial and sporadic cases analysed to date) but not with PDB sarcomatous transformation or the occurrence of primary bone tumors in non-pagetic patients.

**Disclosures:** Materozzi Maria, None.

## MO0434

**Theranostic bone-targeting upconversion-nanoparticles with responsive plumbagin-release inhibit RANKL expression in osteocytes to attenuate early bone metastasis of breast cancer.** Han Qiao\*, Tingting Tang. Shanghai Ninth Hospital affiliated to Shanghai Jiaotong University School of Medicine, China

One big challenge in the treatment of bone metastasis of breast cancer is the early detection and targeting drug delivery. Previously, we have showed that combination of zoledronic acid (ZA) with plumbagin (PL) could synergistically alleviate cancer-induced bone destruction. The aim of this study is to develop a responsive bone-targeting drug delivery system, the ZA anchored bimodal imaging Gadolinium(III)-upconversion nanoparticles loaded with PL, to detect and treat the bone metastasis in the early stage. We demonstrated that this nanosystem could target osteocytes with pH-sensitive PL-release for decreasing osteocytic RANKL expression synergistically by structural simulation of adenosine phosphate to compete its binding against protein kinase-a (PKa), thereby inhibiting osteoclastogenesis both *in vitro* and *in vivo*. We further realized the high specific and high efficient theranostics of tiny bone metastasis in nude mice bearing breast cancer cells. Our work highlights the significance of theranostic nanomedicine and osteocyte targeting therapy in the treatment of early bone metastasis.



Scheme illustration of the synthesis of PL-Gd-UCNP@ZA-PAA

**Disclosures:** Han Qiao, None.

## MO0435

**Amlxanox inhibition of TBK1/IKKε Signaling Is a Novel Therapeutic Approach for Multiple Myeloma-Induced Bone Disease.** Quanhong Sun<sup>1</sup>, Peng Zhang<sup>1</sup>, Juraj Adamik<sup>1</sup>, Valentina Marchica<sup>2</sup>, Nicola Giuliani<sup>2</sup>, Rebecca Silbermann<sup>3</sup>, G. David Roodman<sup>3</sup>, Deborah L. Galson<sup>1</sup>.

<sup>1</sup>Department of Medicine, Hematology-Oncology Division, University of Pittsburgh Cancer Institute, McGowan Institute for Regenerative Medicine, University of Pittsburgh, PA, USA, United States, <sup>2</sup>Myeloma Unit, Department of Clinical and Experimental Medicine, University of Parma, Italy, Italy, <sup>3</sup>Department of Medicine, Hematology-Oncology Division, Indiana University, Indianapolis, IN, USA, United States

Multiple myeloma (MM) is the most frequent cancer to involve the skeleton and remains incurable for most patients, thus novel therapies are needed. MM bone disease is characterized by osteolytic lesions that contribute significantly to patient morbidity and mortality. We showed that TBK1 signaling is a novel pathway that increases osteoclast (OCL) formation in Paget's disease, an inflammatory bone disease. Therefore, we hypothesized that TBK1 plays a similar role in MM induction of OCL. We found that MM conditioned media (MM-CM) dose-dependently increased bone marrow monocyte

(BMM) expression of activated TBK1 protein and enhanced RANKL-driven OCL formation. The TBK1/IKKε inhibitor Amlxanox (Amlx) blocked normal and MM-enhanced OCL formation. Addition of Amlx for different windows of OCL formation revealed that the critical period for TBK1/IKKε function is the first 48 hrs. Importantly, TBK1 mRNA and protein expression in CD138+ plasma cells (PC) isolated from MM patients with active disease is significantly higher as compared to PC from patients with MM precursor states (MGUS, SMM). Therefore, we tested whether targeting the TBK1/IKKε signaling pathways would also affect MM cells. We found that Amlx strongly decreased the viability of several MM cell lines and primary MM cells *via* induction of apoptosis. Amlx treatment of MM cell lines also induced a G1/S blockade, increased translation of the dominant-negative C/EBPβ-LIP isoform and increased autophagy (detected by increased LC3II). The positive-acting C/EBPβ-LAP isoform was previously shown to be a critical transcription factor for MM viability. C/EBPβ-LIP might also be responsible for the increased autophagy. Importantly, Amlx also enhanced the effectiveness of the proteasome inhibitor bortezomib and the immunomodulatory drugs (IMiDs), Lenalidomide and Pomalidomide, to kill MM cells in culture. Amlx did not affect the viability of primary BMM, bone marrow stromal cells (BMSC), or splenocytes. Further, Amlx blocked primary BMSC expression of IL-6 and RANKL, thereby decreasing BMSC support of MM survival and OCL differentiation. Amlx pretreatment of BMSC and MC4 cells also decreased VCAM1 expression and reduced MM cell adhesion, another mechanism for reduced MM support. These data suggest that targeting TBK1/IKKε signaling may decrease MM bone disease by slowing MM growth, directly and indirectly, and preventing MM-induced osteolysis.

**Disclosures:** Quanhong Sun, None.

## MO0436

**Micro-environmental Features of the Bone and Bone Marrow Associated with Metastatic Colonization.** Maura Hartzman<sup>1</sup>, Amato Giaccia<sup>2</sup>, Colleen Wu<sup>1</sup>.

<sup>1</sup>Duke University, United States, <sup>2</sup>Stanford University, United States

The cellular and molecular mechanisms that regulate tissue specific metastatic organ tropism are incompletely understood. One unique feature of the bone microenvironment (BME) is that this region provides the niche for hematopoietic stem cells (HSCs). Interestingly, within the BME, metastatic tumor cells localize to niches occupied by HSCs and pharmacologic expansion of the HSC niche leads to an increase of tumor cell engraftment to this region. These observations led to the hypothesis that metastasizing tumor cells have the ability to "hijack and parasitize" the HSC niche. These discoveries highlight the importance of understanding the molecular underpinnings that drive metastatic engraftment and colonization of this shared region. The BME contains areas of vascular heterogeneity which contribute to regional areas of low oxygen tension, or hypoxia. HSCs localize to hypoxic regions within the BME as hypoxia inducible factor (HIF) signaling is required for HSC function and metabolism. In addition, HIF signaling regulates expression of genes that contribute to the initial homing and engraftment of malignant cells to the BME. However, the function of hypoxia and HIF signaling in regulating the later stages of bone metastasis is less clear. We hypothesize that hypoxia and HIF signaling within the BME contributes to metastatic colonization of the bone by malignant cells. Using a combination of *in vitro* studies and *in vivo* mouse models, we demonstrate that components of the HIF signaling pathway are expressed and HIF signaling is active in both bone marrow mesenchymal stromal cells and cancer cell lines that have a propensity to metastasize to the bone. In addition, our data reveals that upon intra-cardiac delivery, breast carcinoma and melanoma cell lines colonize to hypoxic regions in the BME. Taken together, we establish that hypoxia is associated with metastatic colonization to the bone.

**Disclosures:** Maura Hartzman, None.

## MO0437

**PARylation-mediated Activation of NF-κB by NAMPT in Chondrocytes Causes Catabolic Changes.** Manoj Arra<sup>1</sup>, Yousef Abu-Amer<sup>2</sup>, Gabriel Mbalaviele<sup>3</sup>.

<sup>1</sup>Department of Orthopedic Surgery, Washington University School of Medicine, United States, <sup>2</sup>Department of Orthopedic Surgery, Cell Biology and Physiology, Washington University School of Medicine, United States, <sup>3</sup>Bone and Mineral Disease, Department of Medicine, Washington University School of Medicine, United States

Adipokines, compounds secreted by adipocytes, have been identified as important mediators of homeostasis that play an important role in pathophysiology of arthritis. NAMPT (visfatin), an enzyme involved in the NAD<sup>+</sup> salvage pathway, is one such adipokine found throughout the body in both intracellular and extracellular forms. Secreted by several cell types, it has been shown to play a role in the pathogenesis of osteoarthritic cartilage degradation. Multiple studies have shown that eNAMPT upregulates the expression of catabolic enzymes in cartilage and promotes inflammation and that inhibition of this enzyme using compound FK866 reduces the severity of joint damage. This catabolic activity is believed to be mediated via activation of signaling pathways such as NF-κB and MAPK. However, the mechanism by which NAMPT mediates these changes in chondrocytes is not well elucidated. We propose that NAMPT activates the NF-κB pathway indirectly by modulating the function of NAD<sup>+</sup> dependent proteins via its effect on NAD<sup>+</sup> levels. One such group of proteins are PARPs, which are involved in the post-translational modification of proteins through the covalent attachment of ADP-ribose groups. This modification has previously been shown to play a role in modulation of the NF-κB pathway, leading us to believe that NAMPT might lead to

increased PARYlation of proteins in the NF- $\kappa$ B pathway. We use primary murine chondrocytes as well as inflammatory mouse models to study the mechanism of NAMPT-mediated cartilage damage. Our results indicate that NAMPT treatment increases PARYlation of proteins in primary chondrocytes, while FK866 inhibits this activity. NMN, an NAD<sup>+</sup> precursor and product of NAMPT activity, as well as NAD<sup>+</sup> itself, are able to reverse this FK866-mediated reduction in PARYlation, indicating that NAD<sup>+</sup> is the key factor needed for PARYlation activity, and unlikely to be due to physical interaction of NAMPT with PARP's. Our future work aims to identify proteins in the NF- $\kappa$ B pathway that are ADP-ribosylated, which PARPs are involved and whether the effect of NAMPT on PARYlation is cell specific. This study provides a mechanism by which NAMPT mediates its effects on chondrocytes as an inflammatory compound, providing a potential therapeutic target for treatment. In addition, it highlights the potential of NAD<sup>+</sup> to behave as a pro-inflammatory molecule in chondrocytes by increasing production of inflammatory mediators as well as an upstream modifier of NF- $\kappa$ B activity.

**Disclosures:** Manoj Arra, None.

## MO0438

**Anabolic Effects of Novel Small Molecular Weight Fibroblast Growth Factor Receptor (FGFR) 3 Agonists in Articular Chondrocytes.** Subburaman Mohan<sup>\*1</sup>, Karthikeyan Muthusamy<sup>2</sup>, Nikita Bajwa<sup>1</sup>, Chandrasekhar Kesavan<sup>1</sup>. <sup>1</sup>Musculoskeletal Disease Center, VA Loma Linda Healthcare System, United States, <sup>2</sup>Departments of Medicine and 3Orthopedic Surgery, Loma Linda University, India

Based on the established importance of the FGFR3 signaling pathway in articular cartilage (AC) development and in the pathogenesis of osteoarthritis, we undertook efforts to identify small molecular weight agonists to the FGFR3 using an *in silico* molecular docking approach with various chemical databases. Seven compounds showed potential binding affinity for FGFR3. Structural data from FGFR3 indicated that the  $\beta$ C'- $\beta$ E loop, located in the C-terminal of FGFR3 is involved in ligand binding and varied between FGFR family members. Our analysis found that the identified compounds bound to amino acids in this region through Hydrogen bonding, in particular to Glu322, which is specific to FGFR3 and falls within the  $\beta$ C'- $\beta$ E loop, thus suggesting that the identified compounds may bind specifically to FGFR3. Of the seven small molecules identified, compound 63818502 exhibited the highest docking score to the active site of FGFR3 followed by compound 14977614. In addition, the physicochemical properties predicted by ADMET analysis revealed that the partition coefficient (QP logP(o/w)), crucial for estimating the absorption and distribution of drugs within the body as well as the solubility of the identified compounds are well within the acceptable range. The predicted oral absorption rate of 50% and 65%, respectively, for compounds 63818502 and 14977614 are within the acceptable range of Lipinski's rule of five. To further validate the compound agonist effects predicted by the computational analysis, compound 14977614 was selected due to its availability and characteristics. We found that compound 14977614 at 10 $\mu$ M increased proliferation (15%,  $p < 0.05$ ) of chondrocytes-derived from AC as well as rib cartilage under serum-free conditions. To determine, if this anabolic effect occurred via FGFR3, we measured changes in FGFR3 phosphorylation using specific antibodies. In a dot blot analysis, we found that cells treated with 10 $\mu$ M 14977614 showed a 25% increase in phosphorylation of FGFR3 compared to vehicle treated control cells. Furthermore, ERK phosphorylation, as detected by immunofluorescence analysis, was increased after a 30 minute treatment with 10 $\mu$ M 14977614. No evidence of toxicity was found for compound 14977614 at 10 $\mu$ M based on a cytotoxicity assay. In conclusion, our computational analysis 1) identified multiple compounds that bind to the FGFR3 and 2) *in vitro* studies show that compound 14977614 promotes an agonist effect via FGFR3.

**Disclosures:** Subburaman Mohan, None.

## MO0439

**IL36 $\alpha$  enhances chondrocyte differentiation and maturation while promoting osteoarthritis.** Xin Jin<sup>\*1</sup>, Tieshi Li<sup>2</sup>, Lai Wang<sup>2</sup>, Alessandra Esposito<sup>2</sup>, Arnavaz Hakimiyan<sup>2</sup>, Joseph Temple<sup>2</sup>, Susan Chubinskaya<sup>2</sup>, Anna Spagnoli<sup>2</sup>. <sup>1</sup>Department of Pediatrics, Rush University Medical Center; Department of Orthopaedics, Union Hospital, Tongji Medical College, Huazhong University of Science and Technology, United States, <sup>2</sup>Department of Pediatrics, Rush University Medical Center, United States

We have reported that postnatal ablation of the TGF- $\beta$ -type-2 receptor in osteo-chondrogenic cells leads to aberrant joint development and spontaneous OA that occurs with up-regulation of IL36 $\alpha$  in the articular cartilage. This study aims to investigate the role of IL36 $\alpha$  in skeletogenesis with the ultimate goal to identify clues to understand the role of IL36 $\alpha$  in OA development. Hind paws of C57BL/6J wild type mice dissected at embryonic day (E) E12.5, E14.5, E16.5 and Postnatal day (P) P0, were histologically sectioned and subjected to immunohistochemistry analyses to evaluate expression of IL36 $\alpha$  during embryonic limb development. Isolated limb-bud mesenchymal progenitor cells from E11.5 embryos, cultured in micromasses, were treated with different dose of recombinant mouse IL36 $\alpha$  for respectively for 1,3,5,7 days. Chondrogenic differentiation was evaluated with Alcian Blue (AB) staining and RT-PCR. To assess the role of IL36 $\alpha$  on chondrocyte maturation, chondrocyte micromasses were treated with IL36 $\alpha$  respectively for 7 and 14 days and subjected to Alizarin Red (AR) staining and extracted mRNA to RT-PCR analyses. To assess the role of IL36 $\alpha$  to

maintain articular cartilage hemostasis in adulthood, intra-articular (IA) injections (daily injection for three days) of either IL36 $\alpha$  or PBS (negative control) were performed in 10 week-old mice. Animals were sacrificed 1 and 3 months after the last injection. We found that IL36 $\alpha$  expression was detected at E12.5, within the condensed mesenchymal cells (developing digit), at E14.5 expression was noted within the interphalangeal joint interzone and prehypertrophic zone of the growth plate. By P0 all kinds of chondrocytes expressed IL36 $\alpha$ . In micromass chondrogenic differentiation assay, IL36 $\alpha$  increased AB staining and the mRNA level of differentiation marker, Collagen2 at day5, Aggrecan at day 7, but not Sox9. In micromass chondrogenic maturation assay, IL36 $\alpha$  increased AR staining and the mRNA level of differentiation markers, such as Collagen10 at day7 and 14, Runx2 and Mmp13 at day14. IA injection of IL36 $\alpha$  induced increased Collagen 10 and Mmp13 expression in articular cartilage at 1 month and OA-like phenotype at 3 months indicated by loss of Safranin O staining in articular cartilage. In conclusion, IL36 $\alpha$  promoted the differentiation and maturation of chondrocytes and *in vivo* IL36 $\alpha$  induced OA. Our findings are supportive for a role for IL36 $\alpha$  in regulating skeletogenesis and contributing to OA development.

**Disclosures:** Xin Jin, None.

## MO0440

**Aggrecan Gene Expression in Chondrocytes is Controlled by Multiple DNA Regulatory Elements.** Ian M. H. Li<sup>\*1</sup>, Ke Liu<sup>1</sup>, Alice Neal<sup>2</sup>, Peter D. Clegg<sup>1</sup>, Sarah De Val<sup>2</sup>, George Bou-Gharios<sup>1</sup>. <sup>1</sup>University of Liverpool, United Kingdom, <sup>2</sup>University of Oxford, United Kingdom

Aggrecan (*Acan*) is a large aggregating proteoglycan, which is functionally important for the mechanical properties of cartilage. It is required for the development and maintenance of mature cartilage and loss of *Acan* is considered one of the first events in the development of osteoarthritis (OA). Little is understood about the transcriptional control of *Acan*. Moreover, consideration of how *Acan* is regulated by DNA regulatory elements, such as enhancers, in a tissue specific manner may identify disease relevant regions for future studies.

To this end we used the publically available ENCODE consortium data to identify regulatory elements of *Acan*. The criteria for selection included: evolutionary conserved sequences, histone modifications such as mono-methylation of histone H3 lysine 4 (H3K4me1) and acetylation of histone H3 lysine 27 (H3K27ac). Nine possible *cis*-acting sequences were identified that flanked the *Acan* gene, one of which was the known enhancer at -10kb identified by Han and Lefebvre in 2008. We inserted the sequences upstream of the HSP68 minimal promoter driving a LacZ reporter and generated transgenic mice. We found three upstream enhancer elements (-30, -62 and -80) and one intronic region (+28) expressed in chondrocytes. The -62 is active in hypertrophic regions in limbs but absent from the intervertebral disk (IVD). The -30 and +28 presented in all chondrocytes at E15.5, irrespective of the stage of the chondrocyte and remained active in adult mouse cartilage. The last element, the -80 region shows weak expression during development in the limbs, ribs and skull. At 8 weeks of age the expression progresses and becomes more robust in articular cartilage and the growth plate chondrocytes but is absent from the IVD.

To identify transcription factors that may play a role in activating these regions we examined the role of Sox9. Electromobility Shift Assays (EMSAs) reveals that Sox9 interacts at multiple sites in all enhancers. *In vivo* we introduced Sox9 binding site mutations into the -30 element. This resulted in a "shift" in the expression to areas other than the chondrocytes such as the fibroblasts. Suggesting Sox9 is required for the chondrocyte specificity but other factors act cooperatively for enhancer activity.

We have explored the function and importance of these enhancers during development, adulthood and showed that the *Acan* gene is under greater control than any other matrix genes studied up to date.

**Disclosures:** Ian M. H. Li, None.

## MO0441

**WNT16 Regulation of Articular Chondrocyte Proliferation and Differentiation.** Subburaman Mohan<sup>\*1</sup>, Siddhartha Pulli<sup>2</sup>, Chandrasekhar Kesavan<sup>1</sup>. <sup>1</sup>Musculoskeletal Disease Center, VA Loma Linda Healthcare System, Loma Linda, United States, <sup>2</sup>Departments of Medicine and 3Orthopedic Surgery, Loma Linda University, United States

Previous studies have shown that *Wnt16* is highly expressed in cortical bones during postnatal growth in mice and critically involved in the regulation of both periosteal bone formation and endocortical bone resorption. In addition, a recent study found that mice with targeted disruption of the *Wnt16* gene developed a severe osteoarthritis phenotype in response to injury. However, the issue of whether *Wnt16* is expressed in articular chondrocytes and exerts significant biological effects on cells of chondrocytic lineage is not known. We, therefore, evaluated expression levels of *Wnt* ligands by real time PCR in the RNA extracted from articular chondrocytes-derived from long bone epiphyses of 7 day old C57BL/6J mice and found that articular chondrocytes expressed a number of *Wnt* ligands including *Wnt1*, 3a, 4, 6a, 10b and 16. Treatment of serum-free cultures of articular chondrocytes with 100 ng/ml recombinant human (rh) WNT16 for 48 hrs increased proliferation by 24% ( $p < 0.01$ ) compared to vehicle treated control cultures. Furthermore, expression levels of *Sox5* ( $p = 0.06$ ), *Sox9* ( $p = 0.04$ ) and *Col2a1* ( $p < 0.01$ ) were increased while expression of *MMP9* ( $p < 0.01$ ) was decreased after 24 hrs of treatment with rhWNT16. After a 72 hr treatment with rhWNT16, expression levels of *Sox5* ( $p < 0.05$ ), *Col2a1* ( $p < 0.05$ ), *Acan* ( $p = 0.06$ ) and *Comp* ( $p = 0.06$ ) were increased while expression of *Mmp9* ( $p < 0.01$ ) was decreased. To determine if some of the



rhWNT16 effect on chondrocytes was through modulation of expression of other *Wnt* ligands, we measured expression levels of several *Wnts* that are found to be expressed in articular chondrocytes. We found that while expression of *Wnt5a* ( $p < 0.01$ ) was higher, levels of *Wnt1* ( $p = 0.08$ ), *Wnt3A* ( $p = 0.08$ ) and *Wnt10b* ( $p < 0.01$ ) were lower 24 hrs after rhWNT16 treatment. However, 72 hrs after rhWNT16 treatment, expression levels of *Wnt1*, 3A, 6A and 16b were increased ( $p < 0.05$ ). Based on these data, we conclude that *Wnt16* is expressed in articular chondrocytes and may be involved in the maintenance of immature chondrocyte status via its direct effect as well as through modulating expression of other *Wnt* ligands.

**Disclosures:** Subburaman Mohan, None.

## MO0442

**Tetrahedral DNA Nanostructure: A Potential Promoter for Cartilage Tissue Regeneration via Regulating Chondrocyte Phenotype and Proliferation.** Xiaoru Shao\*, Shiyu Lin. West China Hospital of Stomatology, Sichuan University, China

**Objectives:** Utilizing biomaterials to regulate the phenotype and proliferation of chondrocytes is a promising approach for effective cartilage tissue regeneration. Recently, a significant amount of effort has been invested into directing chondrocytes towards a desired location and function by utilizing biomaterials to control the dedifferentiation and phenotypic loss of chondrocytes during in vitro monolayer culture. Here, we exploited the transmission signals resulting from tetrahedral DNA nanostructures (TDNs) in the regulation of chondrocyte phenotype and proliferation.

**Methods:** TDNs were made up of four single-stranded DNA molecules via highly specific base pairing, and each single-stranded DNA was presented in equimolar amounts. Atomic force microscopy was used to observe the morphology of TDNs and particle size and distribution of TDNs were measured by dynamic light scattering. Real-time cell analysis and cell counting kit-8 were used to assess the effect of TDNs exposure on chondrocytes proliferation. Morphological changes of chondrocytes after exposure to TDNs were observed with fluorescence microscope. In addition, relevant biological mechanism involved in the regulation of chondrocytes proliferation and phenotype were demonstrated by quantitative real-time PCR, western blot, cell cycle assay and immunofluorescence.

**Results:** Upon exposure to TDNs, chondrocyte phenotype were significantly enhanced, accompanied by lower gene expression related to Notch signaling pathway and higher expression of type II collagen. In addition, the cell proliferation and morphology of chondrocytes were changed after exposure to TDNs.

**Conclusion:** This work demonstrated that TDNs, novel DNA nanomaterials, were able to regulate chondrocyte phenotype and promote chondrocyte proliferation. Further investigations found that TDNs at a concentration of 250 nM seemed to be more suitable for the maintenance of chondrocyte morphology and proliferation. Relevant biomechanism indicated that TDNs regulate cell functionalization by making adjustments in microtubules and regulating the Notch signaling pathway. This novel and noteworthy discovery may pave the way for the potential use of TDNs in regenerative medicine.

**Disclosures:** Xiaoru Shao, None.

## MO0443

**Cartilage ECM enhances chondrogenic differentiation of skeletal cells: formulation of a fracture callus mimetic for non-union repair.** Wollis Vas\*, Mittal Shah<sup>1</sup>, Thomas Blacker<sup>2</sup>, Michael Duchon<sup>2</sup>, Paul Sibbons<sup>3</sup>, Scott Roberts<sup>1</sup>. <sup>1</sup>Department of Materials and Tissue, University College London, United Kingdom, <sup>2</sup>Department of Cell and Developmental Biology, University College London, United Kingdom, <sup>3</sup>Northwick Park Institute for Medical Research, Northwick Park Hospital, United Kingdom

Fracture non-union is estimated to occur in approximately 5-10% of cases. Tissue engineering strategies that aim to replicate mature tissue may be unresponsive to the cues observed during the initiation of fracture repair, and as such have limited ability to integrate with the host tissues. As such, this study aims to develop an implant that mimics the cartilaginous callus, the initial reparative stage of the body's response to fracture through the development of decellularised xenogeneic hyaline cartilage in combination with skeletal (stem) cells.

An osmotic shock-based decellularization method was developed and optimized for hyaline cartilage. The resultant decellularized cartilage extracellular matrix scaffolds (dcECM) were assessed for cellular remnants, DNA and alpha-gal. Glycosaminoglycan (GAG) content was quantified, whilst matrix integrity was assessed by differential scanning calorimetry and fluorescence lifetime imaging microscopy. dcECM bioactivity was examined through combination with human chondrocytes or periosteum derived stem cells (hPDSC's), and monitored through analysis of marker genes. *In vivo* biocompatibility was assessed through subcutaneous implantation of dcECM or native tissue in immunocompetent mice for a period of 2 and 8 weeks.

The dcECM demonstrated effective clearance of the immunological components DNA and alpha-gal, whilst retaining GAG's and its native structure. Analysis of human chondrocyte seeded dcECM indicated that the matrix was able to promote *COL2A1* expression and cell migration. Furthermore, upon seeding with hPDSCs the dcECM enhanced chondrogenic differentiation, which was illustrated by the significant upregulation of *COL2A1*, *ACAN*, *SOX9*, *SOX5* and *SOX6*. Interestingly, the hypertrophic markers *COL10A1*, *RUNX2* and *VEGF-A* were also upregulated. *In vivo*

biocompatibility studies demonstrated a predominantly M2 macrophage-mediated immune response to dcECM, which was in contrast to native cartilage tissue.

These data indicate that dcECM is capable of enhancing chondrogenic differentiation of skeletal cells and elicits a regenerative response upon implantation in an immunocompetent host. The aforementioned characteristics demonstrate the potential of the produced constructs as biomimetic implants that replicate many features of the fracture callus. It is hypothesized that these constructs could enhance bone repair in cases of atrophic non-union fracture, where the failure of callus formation is a defining event.

**Disclosures:** Wollis Vas, None.

## MO0444

**Overexpression of human RANKL decreases skeletal muscle function, increases steatosis and engenders insulin resistance.** Julia Brun\*, Vagelis Rinos<sup>2</sup>, Eleni Douni<sup>3</sup>, Serge Ferrari<sup>1</sup>, Nicolas Bonnet<sup>1</sup>. <sup>1</sup>Service des Maladies Osseuses, Switzerland, <sup>2</sup>Biomedical Sciences Research Center "Alexander Fleming", Greece, <sup>3</sup>Biomedical Sciences Research Center "Alexander Fleming" Athens, Greece; <sup>3</sup>Department of Biotechnology, Agricultural University of Athens, Greece

The RANKL pathway is a key regulator of osteoclastogenesis, but is also expressed in many tissues, i.e. skeletal muscle and liver, with implication in Duchenne and diabetes model however it's role on glucose homeostasis in an integrative models remains. For this purpose we used transgenic mice carrying a high copy of human RANKL (Tg5519), treated with OPG-Fc (4mg/kg/week) or vehicle (Veh) for 4 weeks. Muscle function was investigated by treadmill exercise, handgrip and glucose by GTT, ITT and 2-[<sup>14</sup>C] deoxyglucose injection. Liver and muscle were assessed by histology and RT-qPCR.

Tg5519 have severe osteoporosis and lower maximal speed and force of the limb, respectively -41% and -11% vs WT ( $p < 0.05$ ). Although they exhibit a normal body weight, gastrocnemius and soleus mass is lower (-29% and -57% vs WT,  $p < 0.05$ ) and liver mass higher (+16% vs WT,  $p < 0.05$ ). Moreover, circulating myostatin levels are increased (+473% vs WT,  $p < 0.01$ ). ITT AUC is higher in Tg5519, +31% vs WT ( $p < 0.05$ ) whereas GTT is normal, indicating that insulin-resistance is compensated by a tissue up taking glucose independently of insulin. 2-[<sup>14</sup>C] indicates lower glucose uptake in soleus, and WATi of Tg5519 (-51.9%, -62.7% vs WT, all  $p < 0.05$ ), but higher uptake in the femur (+62.7% vs WT,  $p < 0.05$ ).

In the gastrocnemius, expression of Ppar $\alpha$ , LPL, Myh2 and Myh1 is decreased (-19.6%, -16.8%, -23% and -17.8% vs WT, all  $p < 0.05$ ). In the liver there is steatosis, and increased expression of CD36, LPL, ACC1, Ppar $\gamma$ , Fabp4, and Pgc1 $\alpha$  (+29%, +120%, +23%, +39%, +40% and +14% vs WT, all  $p < 0.05$ ). Hepatic glucose production is higher (+133% vs WT,  $p < 0.05$ ).

OPG-Fc increases the maximal speed and force of the limb (+36.7% and +25.6% vs Veh,  $p < 0.05$ ) and normalizes muscle gene expression (see above). In addition, OPG-Fc decreases GTT (AUC -20.8% vs Veh,  $p < 0.01$ ) and normalizes ITT (AUC 464 $\pm$ 25.1 in Veh vs 325.3 $\pm$ 6.8 in OPG-Fc,  $p < 0.01$ ). Steatosis and gluconeogenesis are partially rescued with a full normalization of fatty acid (FA) transport and synthesis.

In conclusion, overexpression of RANKL induces insulin-resistance with a decrease in mass, function, lipid oxidation and uptake of glucose in muscle; and an increase in mass, FA and glucose production in liver. These effects can be rescued by OPG-Fc. Hence RANKL could play a central role in the concomitant development of osteoporosis, sarcopenia and diabetes. However the role of RANKL on individual tissue or on the crosstalk between tissues remains to be determined.

**Disclosures:** Julia Brun, None.

## MO0445

**PPAR $\alpha$  nuclear receptor regulates osteoblast and osteoclast differentiation, and sclerostin protein levels in osteocytes.** Amit Chougule\*, Lance Stechschulte, Peter Czernik, Beata Lecka-Czernik. University of Toledo, United States

Many evidence provide strong support for the concept that bone and energy metabolism are integrated by common regulatory mechanisms. The nuclear receptor PPAR $\alpha$  is a major regulator of energy production and lipid metabolism, and pharmacologic target for fibrates, a class of drugs used to treat dyslipidemia. Mice deficient in PPAR $\alpha$  are metabolically impaired in response to fasting and high-fat diet, however their bone phenotype has not been analyzed in details. We have recently showed that Sclerostin transcript (*Sost*) and protein levels are under a negative control of PPAR $\alpha$ . As compared to WT animals, PPAR $\alpha$  KO mice have larger bone cavity and thinner cortex. Loss of PPAR $\alpha$  results in decreased bone formation and decreased number of osteoblasts (OB), and increased bone resorption accompanied with increased number of osteoclasts (OC), along with an increase in marrow fat volume. Consistently, OC differentiation from a pool of HSCs is increased. Surprisingly however, differentiation of MSCs toward OB and adipocytes (AD) is increased too, as measured *ex vivo* in Colony Forming Units assay. To address a discrepancy between *in vivo* and *ex vivo* results, we analyzed endosteal OB and cortical osteocytes (OT) freshly isolated from femur bone. OB from PPAR $\alpha$  KO mice have decreased expression of markers of Wnt signaling activity, including *Wnt10b* and *Wnt16*, while OT isolated from the same bone have increased expression of *Sost* and *Rankl* pro-osteoclastic cytokine. Consistently, there is 2-fold increase in Sclerostin protein levels in PPAR $\alpha$  KO femur bone. We have identified PPAR $\alpha$ -specific PPRE sequence ( $\alpha$ PPRE) in the *Sost* promoter located -1.8 kb from the transcription start site. ChIP assay confirmed that PPAR $\alpha$  binds to  $\alpha$ PPRE in basal conditions and this binding is increased upon activation PPAR $\alpha$  with WY14643 agonist,

while it is decreased in the presence of GW6471 antagonist. Increased PPAR $\alpha$  binding correlated with decreased promoter activity as measured in luciferase gene reporter assay. In summary, PPAR $\alpha$  acts as a negative regulator of OC differentiation and a negative regulator of MSCs commitment to OB and AD lineages. Most importantly, PPAR $\alpha$  is a negative regulator of Sclerostin production in OT, the activity which is responsible for decreased bone formation in PPAR $\alpha$  KO mice. These findings, provide additional evidence for common mechanisms regulating bone and energy metabolism, and position PPAR $\alpha$  as a potential target to control Sclerostin levels.

**Disclosures:** Amit Chougule, None.

## MO0446

**Marrow Adipose Tissue, Trabecular Bone Score and Osteocalcin as Parameters of Bone Quality in Type 2 Diabetes Mellitus.** Iana de Araújo\*, Carlos Salmon, Marcello Nogueira-Barbosa, Sergio Luchini, Francisco de Paula, Francisco de Paula. Ribeirao Preto Medical School, USP, Brazil

**Introduction:** Type 2 diabetes mellitus (T2D) combines high fracture risk with increased bone mineral density (BMD) and low bone formation. Therefore, BMD is unable to detect fracture risk in T2D. Recent studies suggested that the assessment of trabecular bone score (TBS) and marrow adipose tissue (MAT) may capture alterations in bone quality of T2DM. No study has evaluated the association between TBS, MAT, BMD and osteocalcin in T2DM.

**Objective:** The study was designed to evaluate the mutual relationship between BMD, TBS, MAT and osteocalcin in T2DM.

**Methods:** The study comprised 92 subjects divided in four groups: controls (C: 14F; 12M), overweight (Ov: 17F; 13M); obese (Ob: 9F; 5M) and T2D (11F; 11M). BMD was measured by DXA and MAT was assessed by MRI ( $^1\text{H}$  spectroscopy), OC was determined by Elisa.

**Results:** The groups were matched by sex, age (C:48 $\pm$ 10; Ov:49 $\pm$ 10; Ob:48 $\pm$ 13 and T2D:55 $\pm$ 10 years) and height (C:1.68 $\pm$ 0.1; Ov:1.66 $\pm$ 0.1; Ob:1.66 $\pm$ 0.1 e T2D:1.63 $\pm$ 0.1m). The BMI was higher in Ob and T2D than in C and Ov (C:22.6 $\pm$ 1.8; Ov:27.0 $\pm$ 1.5; Ob:33.6 $\pm$ 3.4; T2D:32.8 $\pm$ 7.5 Kg/m $^2$ ;  $p < 0.05$ ). T2D showed a trend to have higher BMD in lumbar spine than the C and Ov groups (C: 0.980 $\pm$ 0.152; Ov:0.985 $\pm$ 0.127; Ob:1.040 $\pm$ 0.177 e T2D:1.058 $\pm$ 0.140 g/cm $^2$ ). The TBS was higher in C and Ov than in Ob and T2D (TBS L1-L4: C:1.45 $\pm$ 0.1; Ov:1.39 $\pm$ 0.1; Ob:1.24 $\pm$ 0.14; T2D: 1.29 $\pm$ 0.17;  $p < 0.05$ ). The MAT was higher in T2D than in C and Ob (C:41 $\pm$ 11; Ov:43 $\pm$ 9; Ob:41 $\pm$ 9 and T2D:49 $\pm$ 11%  $p < 0.05$ ). OC was slightly lower in T2D (C:10.1 $\pm$ 5.1; Ov:8.9 $\pm$ 4.2; Ob:8.9 $\pm$ 7.5 e T2DM:6.7 $\pm$ 2.8 ng/mL). There was a negative association between TBS (L3) and MAT (L3) ( $r^2=0.11$ ;  $p < 0.05$ ), the association became stronger after adjustment for age and BMI ( $r^2=0.55$ ;  $p < 0.05$ ). The TBS (L1-L4) was positive associated with BMD (L1-L4) ( $r^2=0.68$ ;  $p < 0.05$ , adjusted for age and IMC). The serum levels of OC showed a positive association with MAT and a trend of negative association with BMD after adjustment for weight and BMI ( $r^2=0.61$ ;  $p=0.09$ ).

**Conclusion:** In T2D the TBS decreases, whereas it was observed an expansion in MAT. Moreover, it was observed a negative association between MAT and TBS. The present study was suggest that low bone turnover protects bone mass in T2D. The present study encourages further studies to evaluate the role of MAT and and OC on the prediction of fracture risk in T2D.

**Disclosures:** Iana de Araújo, None.

## MO0447

**Beyond the Skeletal Effects of PTH: Energy expenditure, body composition, gene expression and bone mass in PTH treated mouse models.** Victoria DeMambro\*<sup>1</sup>, David Maridas<sup>1</sup>, Elizabeth Rendina-Ruedy<sup>1</sup>, Beate Lanske<sup>2</sup>, Clifford Rosen<sup>1</sup>. <sup>1</sup>Maine Medical Center Research Institute, United States, <sup>2</sup>Harvard School of Dental Medicine, United States

Several *in vitro* studies have demonstrated that PTH can stimulate lipolysis in primary adipocytes and 3T3-L1 cells. More recently PTH1R (PPR) activation has been shown to lead to 'beiging' of white inguinal adipocytes (iWAT). Remarkably no clinical trials with PTH or abaloparatide have reported changes in total fat mass or compartmental fat. Notwithstanding we noted that PTH altered marrow stromal cell fate in mice and humans by reducing bone marrow adipose tissue (BMAT). Taken together we hypothesized that activation of the PPR might lead to changes in body composition and fat mass. To test this hypothesis we studied C57BL6J (B6) female and male mice treated with daily intermittent PTH (1-34) (80ug/kg/d) or vehicle 4 weeks after ovariectomy (OVX) or 4 weeks after calorie restriction (CR) (n=8/group). As expected, OVX'd, 20 wk old B6 mice treated with PTH had a 100% increase in femoral aBMD and a similar increase in femoral trabecular BV/TV ( $p < 0.0001$  vs vehicle). Fat mass increased in the vehicle group by 40% while in the PTH treated group there was a remarkable decline of 7% ( $p < 0.0001$  vs vehicle). Gene expression in the iWAT revealed a reduction in *AdipoQ* and *Pparg* with PTH ( $p < 0.05$ ), as well as a 40% decline in lysosomal acid lipase A (*Lal*). Gonadal (g)WAT also demonstrated a 50% reduction in *Lal* and a similar reduction in hepatic lipase (*Lipe*). Perilipin 2, a lipid-droplet protein, was markedly reduced in both iWAT and gWAT, while *Ucp1* and *DiO2*, markers of beiging, were increased 20 fold respectively ( $p < 0.05$  vs vehicle). As expected, body weight, fat mass, and resting energy expenditure (REE) declined significantly in the CR model without PTH. Areal BMD also declined significantly in the CR group. Of note, the change in both total body weight and % fat mass was greater with PTH than control ( $p < 0.01$  and  $p < 0.06$  respectively). Moreover, the PTH treated CR animals had

higher REE than the vehicle treated CR albeit lower than control mice fed a regular diet. Activity levels did not differ between control and vehicle treated mice. Multivariate analysis controlling for body weight, PTH had a positive effect on energy expenditure. In conclusion activation of PPR has significant effects on bone mass and body composition, likely through activation of the beige transcriptional network in adipocytes. Further studies are needed both in humans and in mice to define the translational importance in respect to anabolic therapies.

**Disclosures:** Victoria DeMambro, None.

## MO0448

**High fat, high protein diet increases nonshivering thermogenesis and serum leptin but is deleterious to trabecular bone in cold- and warm-housed mice.** Maureen Devlin\*, Amy Robbins, Christopher Tom, Miranda Cosman, Lillian Shipp, Katarina Alajbegovic. University of Michigan, United States

Previously we showed that chronic cold exposure impairs trabecular bone architecture despite increased nonshivering thermogenesis (NST) via uncoupling protein (UCP1) in mice. We hypothesize that a high fat, high protein diet, as was traditionally consumed by circumpolar humans, may protect against cold-induced bone loss by providing additional calories for NST. To test this hypothesis, we housed wildtype C57BL/6J male mice in pairs at 26°C (close to thermoneutrality), 22°C (standard housing temperature), and 20°C (mild cold stress) from 3-6 wks of age. Mice were fed a purified normal diet (N) or high fat, high protein diet (HFHP) ad libitum (N=6-8/group). Outcomes included body mass, body length, %body fat and whole body bone mineral density (BMD) via pDXA, UCP1 mRNA and protein expression in brown adipose tissue (BAT), and cortical and trabecular microarchitecture via  $\mu\text{CT}$ . Results indicate that HFHP mice at 20°C and 22°C gained 31.3% more body mass from 3-6 wks of age and had 4.7% longer body length vs. N ( $p < 0.05$  for both), while HFHP mice at 26°C did not have significant changes vs. N. At all temperatures, serum leptin levels were 40-48% higher in HFHP vs. N at 6 weeks of age ( $p < 0.05$  for all). In interscapular BAT, HFHP mice had higher UCP1 mRNA and protein expression vs. N at 6 wks of age ( $p < 0.05$  for both). There were no differences in BMD, but HFHP mice had higher %body fat at 6 wks of age vs. N ( $p < 0.05$ ). In distal femur trabecular bone, HFHP mice had markedly lower Tb.N at all temperatures (-14-21%,  $p < 0.007$  for all) and lower Conn.D at 22°C and 26°C (-39-52%,  $p < 0.009$  for both). There were no significant differences in cortical bone thickness or cross sectional geometry in HFHP vs. N mice. These data demonstrate that high fat, high protein diet increases nonshivering thermogenesis, body fat, and leptin levels, but is deleterious to trabecular bone architecture both during cold exposure and at thermoneutrality. These findings do not support our hypothesis that a diet-induced increase in nonshivering thermogenesis protects against cold-induced bone loss, and suggest high fat, high protein diets may actually be detrimental to bone health in humans.

**Disclosures:** Maureen Devlin, None.

## MO0449

**Increases in Gut Hormone PYY May Be Associated with Loss of Bone Mass After Gastric Bypass Surgery.** Tiffany Kim<sup>\*1</sup>, Dolores Shoback<sup>1</sup>, Dennis Black<sup>2</sup>, Stanley Rogers<sup>2</sup>, Lygia Stewart<sup>1</sup>, Jonathan Carter<sup>2</sup>, Andrew Posselt<sup>2</sup>, Nicole King<sup>2</sup>, Anne Schafer<sup>1</sup>. <sup>1</sup>University of California, San Francisco, and the San Francisco VA Health Care System, United States, <sup>2</sup>University of California, San Francisco, United States

Gut-derived hormones, including peptide YY (PYY) and ghrelin, are important in the metabolic benefits of Roux-en-Y gastric bypass (RYGB). However, both factors could also contribute to detrimental skeletal effects including BMD declines and heightened fracture risk. PYY, known to increase after RYGB, may act on central Y2 receptors and peripheral Y1 receptors on osteoblasts to decrease bone formation. Osteoblasts have ghrelin receptors, and a decrease in ghrelin after RYGB could also lead to decreased bone formation. We hypothesized that PYY increases and ghrelin decreases after RYGB are associated with BMD declines.

We studied 44 obese subjects (34 women, 10 men) within a longitudinal study of the skeletal effects of RYGB. Fasting serum total PYY and ghrelin were measured at baseline and 6 months after surgery. Other measures included procollagen type I N-terminal propeptide (PINP), C-terminal type I collagen telopeptide (CTX), areal BMD (aBMD) by DXA, and L3-L4 spine volumetric BMD (vBMD) by quantitative computed tomography (QCT).

Subjects had a mean  $\pm$  SD age of 45  $\pm$  12 years and preoperative body mass index (BMI) of 44  $\pm$  7 kg/m $^2$ . After RYGB, mean 6-month weight loss was 31 kg. There was a trend towards an increase in PYY level after surgery: +25 pg/mL (95% CI -3 to +53 pg/mL). Ghrelin levels increased after surgery: +192 (95% CI +119 to +264 pg/mL). Changes in PYY negatively correlated with spine vBMD changes, so that those with PYY increases had worse declines in vBMD ( $r = -0.36$ ,  $p = 0.02$ ) (Figure). Those with PYY increases had smaller increases in the bone formation marker PINP ( $r = -0.30$ ,  $p = 0.05$ ); a similar trend was seen for the resorption marker CTX ( $r = -0.25$ ,  $p = 0.10$ ). Proportionally, CTX increases were greater than PINP increases. There were not significant correlations between changes in PYY and aBMD. For change in ghrelin, there was only a significant correlation with change in spine aBMD ( $r = -0.34$ ,  $p = 0.03$ ).

In summary, PYY levels tended to increase after RYGB and correlated with worse declines in spine vBMD. Although ghrelin increased rather than decreased as hypothesized, changes correlated with spine aBMD declines. These results suggest that PYY and



ghrelin might contribute to bone loss after RYGB and may reveal insights into the relationship between the gut and bone.

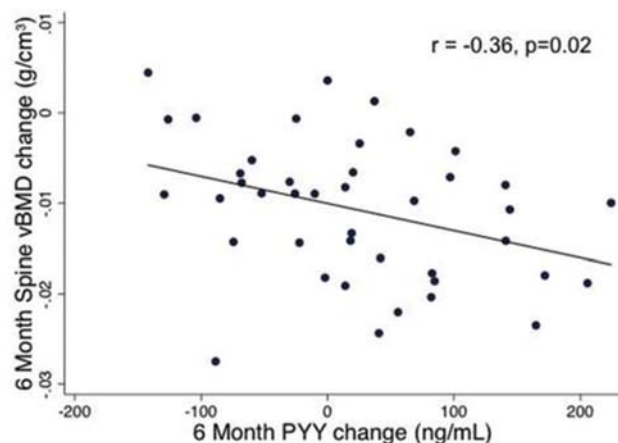


**Figure.** Change in PYY and spine vBMD after gastric bypass surgery.

Figure 1

**Disclosures:** Tiffany Kim, None.

## MO0450

**Rapid Marrow Adipogenesis Following Burns: Implications for Onset of Reduced Bone Formation.** Amina El Ayadi<sup>1</sup>, Ron Helderman<sup>2</sup>, David Herndon<sup>1</sup>, Celeste Finnerty<sup>1</sup>, Clifford Rosen<sup>2</sup>, Gordon Klein<sup>1</sup>. <sup>1</sup>University of Texas Medical Branch, United States, <sup>2</sup>Maine Medical Center Research Institute, United States

Low circulating PTH favors marrow adipogenesis over osteoblastogenesis. Pediatric burns patients have low circulating PTH and Ca due to inflammatory cytokine-mediated up-regulation of the parathyroid Ca sensing receptor. A large population of marrow adipocytes usually signifies reduced osteoblastogenesis and low bone formation originally reported in burned children by 2 wk post-burn. The aim of our study was to see if marrow adipogenesis is induced by burns and, if so, did this occur <2 wk post-burn. 8 wk old Sprague-Dawley rats weighing 325±17(SD)g were assigned randomly to burn (B) or control (C) groups. A 60% scald burn was effected under isoflurane anesthesia in the B group on day 2 of the study with sacrifice of both groups on day 5, day 3 post-burn. Tibias were collected in plastic vials and refrigerated overnight in 10% formalin before transfer to PBS. Specimens (n=2 per group) were decalcified and marrow adipocytes were quantified using a BioQuant 2016 software version 16.1.6M. Briefly, the area quantified included the proximal tibia, 1.0 mm distal from the growth plate and 0.5 mm from the endocortical surface and included an area approximately 3.0 mm. Adipocyte counts were expressed per mm<sup>2</sup>. The average adipocyte count in the B group was 61.7 and in the C group 9.5. Thus, preliminary data indicate that following a burn marrow adipogenesis occurs within 72h and possibly earlier suggesting that osteoblastogenesis is reduced much earlier than previously thought. Further studies are needed to confirm these findings and to identify the mechanisms of early adipogenesis and reduced osteoblastogenesis.

**Disclosures:** Amina El Ayadi, None.

## MO0451

**Vitamin D Regulates Adipocyte and Muscle Cells Differentiation in vitro and Muscle Fat Content in vivo.** Jiarong Li<sup>\*</sup>, Milton Mihalciou, Lifeng Li, Richard Kremer, McGill University, Canada

Low circulating 25-hydroxyvitamin D (25OHD) levels are associated with decreased muscle strength and an increased risk of falls in humans. Recently we reported that low 25OHD in young adolescent girls were associated with muscle fat accumulation using imaging techniques. In this study, we used both in vitro and in vivo models to examine the mechanism of this relationship. First we used human adipocyte (3T3L1) and muscle cell lines (C2C12) to test the effect of 1,25-dihydroxyvitamin D<sub>3</sub> (1,25(OH)<sub>2</sub>D<sub>3</sub>) on cellular differentiation and gene expression levels by qPCR and immunofluorescence (IF). Next we examined the effect of either a low (25 IU/Kg) vitamin D<sub>3</sub> diet or a normal (1000 IU/Kg) vitamin D<sub>3</sub> diet on muscle fat of FVB mice. All mice were bred in a room without UVB lighting and maintained on these specialized diets for 12 weeks. At sacrifice, total body fat was measured by DEXA and lower limb muscles were excised, fixed in formalin and embedded in paraffin or snapped frozen and kept at -80°C. Tissue were examined histologically with H&E, fat stained with Oil Red and perilipin-2 and PPAR $\gamma$  expression examined by IF. Mass spectrometry imaging (MSI) was performed to determine the content and distribution of fat on muscle.

In vitro effect of 1,25(OH)<sub>2</sub>D<sub>3</sub> addition (10<sup>-10</sup> to 10<sup>-7</sup>M) to 3T3-L1 cell line significantly inhibited differentiation into adipocytes in a dose dependent fashion as measured with Oil Red staining and decreased perilipin-2 and PPAR $\gamma$  expression

compared to vehicle treated cells (p< 0.005). Conversely, C2C12 cells treated with 1,25(OH)<sub>2</sub>D<sub>3</sub> showed a dose dependent increase in muscle cells differentiation together with a decrease in PPAR $\gamma$  and perilipin-2 expression by qPCR and IF whereas VDR knockdown blocked this effect.

In vivo studies showed a significant increase in total body fat by DEXA in mice fed a low vitamin D diet compared to mice fed a normal vitamin D diet. In addition, MSI analysis of vitamin D deficient mice showed increased lipid content of a wide array of lipid species known to be involved in fat metabolism with variable distribution. Furthermore, mice fed a low vitamin D diet showed a dramatic increase in lipid deposition within the muscle fibers as demonstrated by Oil Red staining and a dramatic increase in perilipin-2 and PPAR $\gamma$  by IF.

In summary, our data indicate that vitamin D is a strong regulator of adipocyte and muscle cells differentiation in vitro and of muscle fat content in vivo through PPAR $\gamma$  and perilipin-2 gene regulation.

**Disclosures:** Jiarong Li, None.

## MO0452

**Long-Term Exercise Restores Key Lipid Mediators in Muscle.** Chenglin Mo<sup>1</sup>, Julian Vallejo<sup>2</sup>, Zhiying Wang<sup>1</sup>, Liangqiao Bian<sup>3</sup>, Thomas O'Connell<sup>4</sup>, Lynda Bonewald<sup>4</sup>, Michael Wacker<sup>2</sup>, Marco Brotto<sup>1</sup>. <sup>1</sup>College of Nursing & Health Innovation, University of Texas-Arlington, United States, <sup>2</sup>School of Medicine, University of Missouri-Kansas City, United States, <sup>3</sup>Shimadzu Center for Advanced Analytical Chemistry, University of Texas-Arlington, United States, <sup>4</sup>School of Medicine, Indiana University, United States

Exercise has beneficial effects on many systems in the body such as neural, metabolic and musculoskeletal systems, but it is not clear if these benefits delay the effects of aging or if aging blunts the effects of exercise. Sarcopenia is a major hallmark of the aging skeletal muscle resulting in frailty, falls, fracture, and morbidity. Very few studies have investigated the effects of long-term voluntary exercise models, such as voluntary wheel running (VWR) on focused lipidomics and metabolomics profiling. Eight female C57BL/6 remained sedentary for life while eight female had continuous access to VWR for 6 mo from 12 mo to 18 mo of age. Gastrocnemius (GAS) muscles were used for the lipidomics profiling of 158 signaling lipid mediators using a new method we developed. The GAS main function is the plantar flexing of the foot at the ankle joint and flexing the leg at the knee joint, and is primarily involved in running, jumping and other fast movements of leg. Metabolomic profiling was also performed. GAS weight was 10% lower in VWR (P<0.05), but there was no difference in muscle weight to body weight ratio. Our new lipidomics profiling comparing 4 mo old mice with 18 mo old VWR and control mice revealed that with aging there is an overall decrease in the levels of key lipid signaling mediators. Particularly, levels of key lipid- signaling mediators of the arachidonic acid (AA) pathway decrease with aging. Remarkably, long-term voluntary exercise increased the levels of several lipid-signaling mediators in GAS muscles of the exercised mice, particularly of the AA, docosahexaenoic acid (DHA), eicosapentaenoic acid (EPA), linoleic acid (LA), and ethanolamide (EA) pathways (Fig. 1). These studies have identified specific lipid-signaling mediators such as 12-HHT; 11,12-DHET; 8-HETE; 10- and 11-HDoHE; 17,18-DiHETE; 13-KODE; 13-HpODE; and OEA, with known roles in wound-healing, anti-inflammatory, angiogenesis, insulin sensitivity, insulin resistance, and PPARs stimulation. Principal Component Analysis, PCA, of metabolic profiles showed significant differences between exercised and sedentary animals. We are refining our lipidomics and metabolomics approaches to measure the levels of these signaling mediators in a range of muscle types (i.e., oxidative, glycolytic, mixed) as well as heart, bone, and plasma, which will make this method highly applicable for aging biomarker discovery.

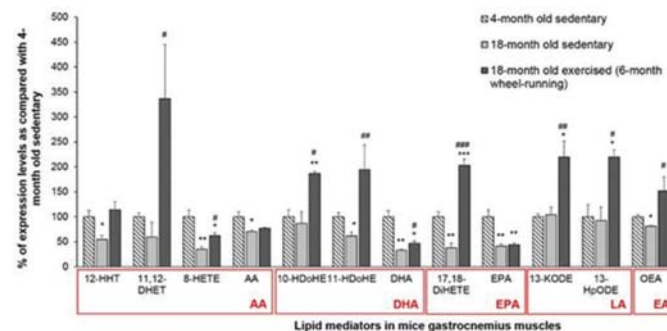


Figure 1

**Disclosures:** Chenglin Mo, None.

## MO0453

**Postprandial Regulation of Appetite by Lipocalin 2.** Ioanna Mosialou<sup>\*1</sup>, Steven Shikhel<sup>1</sup>, Elisabeth Sornay-Rendu<sup>2</sup>, Justine Bacchetta<sup>3</sup>, Blandine Laferriere<sup>4</sup>, Mishaella Rubin<sup>5</sup>, Cyrille B. Confavreux<sup>6</sup>, Stavroula Kousteni<sup>1</sup>.

<sup>1</sup>Department of Physiology, Columbia University, United States, United States, <sup>2</sup>INSERM UMR1033-Université de Lyon, 69008-Lyon, France, France, <sup>3</sup>INSERM UMR1033-Université de Lyon, 69008-Lyon, France and Department of Pediatrics, Hospices Civils de Lyon, 69500-Bron, France, France, <sup>4</sup>Department of Medicine Endocrinology, Columbia University, United States, <sup>5</sup>Department of Medicine Endocrinology, Columbia University, United States, United States, <sup>6</sup>INSERM UMR1033-Université de Lyon, 69008-Lyon, France, Department of Pediatrics, Hospices Civils de Lyon, 69500-Bron, France and Department of Rheumatology, Hospices Civils de Lyon, 69003-Lyon FRANCE, United States

Bone has emerged as an important endocrine regulator of energy metabolism through at least two hormones, osteocalcin and Lipocalin 2 (LCN2). The latter is an anorexigenic hormone secreted by osteoblasts that crosses the blood brain barrier (BBB), binds to the melanocortin 4 receptor (MC4R) in the paraventricular and ventromedial neurons of the hypothalamus and activates MC4R-dependent anorexigenic pathways. Here we examined the physiological role of LCN2 regulation with feeding and its involvement in acute appetite suppression after a meal or chronically in lean and obese states in mice and in humans. We found that circulating LCN2 levels increased 3-fold in wild-type (WT) mice within 1 hour of refeeding following an overnight fast. This effect was due to an increase in *Lcn2* expression specifically in osteoblasts. Intraperitoneal administration of recombinant LCN2 to fasted WT and *Lcn2<sup>ost/-</sup>* mice immediately after refeeding suppressed food intake within 1 hour and decreased body weight gain within 2 hours as efficiently as it does in WT mice. These observations suggested that upregulation of *Lcn2* expression by osteoblasts following feeding may be a physiological satiety signal and prompted us to address the question of whether such a mechanism is conserved in humans. To assess the relationship between LCN2 and postprandial regulation in humans, young normal weight (mean BMI  $\pm$  SD :  $20.8 \pm 0.5$  Kg/m<sup>2</sup>) and obese (BMI  $45.6 \pm 1.8$  Kg/m<sup>2</sup>) women were given a 200kcal mixed meal (55% carbohydrate) following an overnight fast. LCN2 serum levels were measured before and after ingestion of the test meal. LCN2 levels were significantly increased by over 50% within 1 h after meal ingestion in the normal weight group and remained significantly elevated by 40% for at least 2h. In contrast, LCN2 levels in obese women failed to increase in response to the 200kcal mixed meal. This was similar after a 600kcal mixed meal or 50gr (200kcal) of glucose during an oral glucose tolerance test. These results provide the first evidence that the anorexigenic function of LCN2 may be conserved in humans and that its postprandial response and function is impaired in obesity. Hence, correcting postprandial LCN2 levels may provide a mechanism to limit appetite after a meal to treat obesity.

**Disclosures:** Ioanna Mosialou, None.

## MO0454

**Specific Micro-RNA changes in healthy vitamin D deficient men before and after vitamin D supplementation.** Barbara Obermayer-Pietsch<sup>\*</sup>, Vito Francic, Sebastian Sonntagbauer, Roswitha Gumpold, Thomas R Pieber, Julia Münzker, Elisabeth Lerchbaum. Div. Endocrinology and Diabetology, Medical University Graz, Austria

#### Introduction:

MicroRNAs (miRNAs) are small, non-coding transcripts providing an important and pervasive layer of post-transcriptional gene regulation. Bone and vitamin D metabolism are important targets of miRNA research. As we previously found associations of bone and glucose parameters with vitamin D supplementation, we aimed to detect miRNA signatures, differentially expressed before and after 6 and 12 weeks of vitamin D or placebo (PBO) treatment in healthy vitamin D deficient men.

#### Methods:

Out of 100 healthy, but 25(OH)vitamin D (25OHD) deficient (<30 ng/ml) men treated with either 20,000 IU of vitamin D or PBO per week who participated in a randomized double-blind placebo controlled trial (NCT01748370), we randomly selected 4 men from the vitamin D group and 3 men from the PBO group for a pilot investigation. The volunteers were investigated for bone, hormonal and glucose parameters including oral glucose tolerance tests, DXA and body composition. By using the miRCURY LNA PCR panel 1 (Exiqon Inc.), we performed a targeted screening of miRNA expression.

#### Results:

While 25(OH) vitamin D increased significantly in the vitamin D group (from  $35 \pm 1.5$  to  $165 \pm 28$  nmol/L,  $p < 0.001$ ), we observed no changes in the PBO group. PTH levels were unaffected by supplementation. Out of 372 miRNAs tested, 111 were found to be present in all screened samples. Of these, 6 miRNAs showed a more than 2fold significant change in their expression pattern compared to baseline during 25OHD supplementation. Some of these miRNAs have already been associated with bone metabolism and  $\beta$ -cell-function in previous studies (e.g. miR-194-5p, miR-326).

#### Discussion:

In our pilot study, we demonstrate a significant change of miRNA patterns during vitamin D treatment in healthy vitamin D deficient men. Interestingly, some of these miRNAs have already been shown to be relevant in the regulation of bone and glucose metabolism. Further characterization and validation of these miRNA signatures in the study cohort is ongoing.

**Disclosures:** Barbara Obermayer-Pietsch, None.

## MO0455

**The effect of AdipoRon on osteogenesis and osteoclastogenesis *in vitro*.** Xingwen Wu<sup>\*12</sup>, Qisheng Tu<sup>12</sup>, Wei Qiu<sup>12</sup>, Jake Chen<sup>12</sup>, Youcheng Yu<sup>3</sup>. <sup>1</sup>Division of oral biology, Tufts university school of dental medicine, United States, <sup>2</sup>division of oral biology, Tufts university school of dental medicine, United States, <sup>3</sup>department of dentistry, zhongshan hospital, fudan university, China

**Background and objective:** Adiponectin, a primary adipokine, has insulin-sensitizing and anti-diabetic properties. Recent literature indicates a strong correlation between low levels of adiponectin and increased severity of periodontal disease, suggesting a role of adiponectin in these two prevalent diseases. AdipoRon, a recently found orally active small molecules, binds and activates both adiponectin receptors (AdipoR1, R2), with potent effects similar to adiponectin. In this study, we investigate whether AdipoRon can enhance osteogenesis, and inhibit osteoclastogenesis.

**Material and Method:** We initially used CCK-8 assay to investigate the proliferation, and wound closure assay to observe the effects of AdipoRon treatment on migration in MC3T3-E1 cells. Next, we investigated the effects of AdipoRon on the expression levels of osteogenic marker genes in MC3T3-E1 cells and inflammatory factors in RAW264.7 cells.

**Results:** AdipoRon treatment led to a significant promotion of MC3T3-E1 proliferation in short-time culture but an inhibition of proliferation in longer culture. High concentration of AdipoRon promoted cell horizontal migration after 24 hours incubation. Moreover, AdipoRon increased the expression level of Runx2 and BSP during osteogenic differentiation of MC3T3-E1 cells while the RANKL-enhanced expressions of NFAT-2 and TRAP were decreased by AdipoRon treatment in osteoclastic differentiation of RAW264.7 cells.

**Conclusion:** AdipoRon could promote the osteoblast proliferation in the early phase of differentiation but inhibit in late stage. Appropriate concentration of AdipoRon can increase cell horizontal migration and promote osteogenic differentiation of MC3T3-E1 cells as well as inhibit osteoclastogenesis of RAW264.7 cells.

**Disclosures:** Xingwen Wu, None.

## MO0456

**Generation of a mouse model overexpressing *Slc20a1*/*Pit1* in osteocytes to study the role this transporter in bone growth and phosphate homeostasis.** Sampada Chande<sup>\*1</sup>, Jonathan Fentene<sup>1</sup>, Nelli Mnatsakanyan<sup>2</sup>, Meiling Zhu<sup>3</sup>, Karl Insogna<sup>3</sup>, Clemens Bergwitz<sup>1</sup>. <sup>1</sup>Section of Endocrinology and Metabolism, Yale University School of Medicine, New Haven, CT 06519, USA., United States, <sup>2</sup>Internal Medicine, Yale University, New Haven, CT, USA, United States, <sup>3</sup>Yale Musculoskeletal Center, Yale University School of Medicine, New Haven, USA, United States

Phosphate has an essential role in signal transduction, metabolism and as structural component of membrane lipids and nucleic acids inside cells. Together with calcium it forms hydroxyapatite during mineralization of the extracellular bone matrix in higher species and humans. Phosphate is imported by cells via specialized co-transporters along with sodium. Expression of the type III sodium-phosphate co-transporter *Pit1* increases during osteoblast and osteocytes differentiation. Hypomorphic *Pit1* ablation was shown by Bourguine *et al* (2013) to reduce femur length in mice, but no significant changes of phosphate or calcium metabolism were reported, presumably due to residual *Pit1* expression and compensation by *Pit2*. Conversely, transgenic rats that overexpress *Pit1* globally using cytomegalovirus enhancer and chicken  $\beta$ -actin (CAG) promoter develop hyperparathyroidism, hyperphosphatemia and a low bone mass phenotype with reduced total bone area (Suzuki *et al*, 2010). To study the role of *Pit1* in bone growth and phosphate homeostasis we inserted the human influenza hemagglutinin (HA) epitope-tagged human *Pit1* transporter into pBT378.6 (Applied StemCell), which contains the cytomegalovirus enhancer and chicken  $\beta$ -actin (CAG) promoter and a stop-lox-stop cassette permitting expression using Cre-recombinase in a tissue specific/inducible fashion. Following pronuclear injection of the expression plasmid along with phi C31 integrase, integration into the transcriptionally inert H11 locus in the mouse genome was confirmed using PCR based genotyping of the transgenic offspring. Random integration was observed in seven lines and correct integration of the transgene into the H11 locus was observed in one line (*HPit1*). The *HPit1* line was crossed with *Dmp1-Cre* and robust expression of the *HA-hPit1* transporter over endogenous mouse *Pit1* mRNA in osteocytes was confirmed by qRT-PCR in the double transgenic offspring (*ocHPit1<sup>+/tg</sup>*). *ocHPit1<sup>+/tg</sup>* mice are viable and fertile and their phenotypic characterization is currently under way.

**Disclosures:** Sampada Chande, None.

## MO0457

**CRISPR/Cas9-Mediated Creation of Novel Mouse Strains Lacking the LRP5 LDLR Class A Repeats.** Bart Williams<sup>\*</sup>, Cassandra Diegel, Nicole Ethen, Jon Lensing. Van Andel Research Institute, United States

Loss of function mutations in the Low-density lipoprotein receptor-related protein 5 are the underlying cause of Osteoporosis pseudoglioma (OPPG) syndrome. OPPG



patients have extremely low bone mass leading to enhanced fracture risk. Lrp5-deficient mice model OPPG also displaying low bone mass and altered vasculature in the lens. LRP5 is a large, single-pass transmembrane protein containing four B-propeller motifs and three LDL Type A repeats in its extracellular domain. The B-propeller motifs mediate binding to many of the known effectors of LRP5 including Wnts, DKKs, and SOST. The role of the Type A repeats is less defined, but in other LDL family members they are known to bind lipoproteins. The three Type A repeats are entirely and uniquely encoded in two exons of LRP5. Conceptual evaluation of the genomic structure reveals that elimination of these two exons would not later the reading frame downstream. Based on this, we used the CRISPR/Cas9 system to create mouse lines carrying an approximately 7 kB deletion that encompassed these exons. We successfully created two independent lines carrying the desired modification and have begun to characterize mice homozygous for this alteration. Importantly, we can detect both mRNA and protein encoded by this altered allele of Lrp5. Our preliminary characterization of mice homozygous for this allele reveals substantially reduced bone mass. We are currently evaluating other Lrp5-associated phenotypes to assess whether this allele acts as a null allele in all contexts and are pursuing cell-based studies to evaluate localization and binding activity of this altered protein.

**Disclosures:** Bart Williams, Surrozen, Consultant.

## MO0458

**Phenomic analysis of zebrafish type I collagen mutants reveals a spectrum of skeletal phenotypes mimicking the clinical variability in human brittle bone disease.** Charlotte Gistelink<sup>\*1</sup>, Ronald Y. Kwon<sup>1</sup>, Fransiska Malfait<sup>2</sup>, Sofie Symoens<sup>2</sup>, Petra Vermassen<sup>2</sup>, Hanna De Saffel<sup>2</sup>, Katrin Henke<sup>3</sup>, Matthew P. Harris<sup>3</sup>, Anne De Paepe<sup>2</sup>, MaryAnn Weis<sup>1</sup>, David R. Eyre<sup>1</sup>, Andy Willaert<sup>2</sup>, Paul J. Coucke<sup>2</sup>. <sup>1</sup>Department of Orthopaedics and Sports Medicine, University of Washington, United States, <sup>2</sup>Center for Medical Genetics Ghent, Ghent University, Belgium, <sup>3</sup>Department of Genetics, Harvard Medical School, United States

**Objective:** The brittle bone disease osteogenesis imperfecta (OI) is a rare congenital disorder, mainly caused by defects related to type I collagen, which forms the structural protein scaffold of the bone extracellular matrix. Clinically, OI is characterized by a broad disease spectrum, ranging from mild forms with minimal fractures to severely deforming or even lethal forms. The underlying genetic basis of this variability between, but also within, different genetic types of OI remains one of the most puzzling questions in the field. In this study we illustrate the potential of zebrafish as a tool to better to understand and further dissect the underlying molecular basis of this phenotypic variability in human OI.

**Methods:** We generated a large set of zebrafish with similar mutations as human patients with different genetic forms of OI. Phenomic profiles were constructed by mapping and quantifying skeletal parameters, using a  $\mu$ CT-based pipeline.

**Results:** Our study revealed a remarkably high phenotypic reproducibility of the human disease features between zebrafish mutants and patients with comparable genetic forms of OI. Key features of OI, such as the occurrence of fractures, overmineralization, and bowing and kinking of the long bones, were noted in several mutant genotypes, often with variable penetrance.

**Summary and Conclusions:** Mice models are laborious and expensive for large scale genetic studies. Additionally, bone phenotypes in mice often cause (perinatal) lethality, making them unavailable for the study of later stages. Zebrafish overcomes these challenges as a model. With our study, we demonstrate that zebrafish models are able to both genocopy and phenocopy different forms of human OI, arguing for a similar genetic basis driving pathogenesis. We therefore propose zebrafish as a new tool to investigate unknown genetic modifiers and mechanism underlying the phenotypic variability in human OI.

<sup>1</sup> Hur, M., et al. (2017). "microCT-Based Skeletal Phenomics in Zebrafish Reveals Virtues of Deep Phenotyping at the Whole-Organism Scale." *bioRxiv*.

**Disclosures:** Charlotte Gistelink, None.

## MO0459

**Low Frequency Coding Variation in CYP2R1 has Large Effects on Vitamin D Level and Risk of Multiple Sclerosis.** Despoina Manousaki<sup>\*1</sup>, Tom Dudding<sup>2</sup>, Simon Haworth<sup>2</sup>, Yi-Hsiang Hsu<sup>3</sup>, Ching-Ti Liu<sup>4</sup>, Carolina Medina-Gomez<sup>5</sup>, Trudy Voortman<sup>6</sup>, Nathalie van der Velde<sup>5</sup>, Hakan Melhus<sup>7</sup>, Cassiane Robinson-Cohen<sup>8</sup>, Diana Cousminer<sup>9</sup>, Maria Nethander<sup>10</sup>, Liesbeth Vanderput<sup>10</sup>, Raymond Noordam<sup>11</sup>, Vincenzo Forgetta<sup>1</sup>, Celia Greenwood<sup>1</sup>, Mary Lou Biggs<sup>12</sup>, Bruce Psaty<sup>13</sup>, Jerome Rotter<sup>14</sup>, Babette Zemel<sup>15</sup>, Jonathan Mitchell<sup>15</sup>, Bruce Taylor<sup>16</sup>, Matthias Lorentzon<sup>10</sup>, Magnus Karlsson<sup>17</sup>, Vincent Jaddoe<sup>18</sup>, Henning Tiemeier<sup>18</sup>, Natalia Campos-Obando<sup>5</sup>, Oscar Franco<sup>6</sup>, Andre Uitterlinden<sup>5</sup>, Linda Broer<sup>5</sup>, Natasja van Schoor<sup>19</sup>, Annelies Ham<sup>5</sup>, M.Arfaan Ikram<sup>6</sup>, David Karasik<sup>3</sup>, Renee de Mutser<sup>20</sup>, Fritz Rosendaal<sup>20</sup>, Martin den Heijer<sup>21</sup>, Thomas Wang<sup>22</sup>, Lars Lind<sup>7</sup>, Eric Orwoll<sup>23</sup>, Dennis O Mook-Kanamori<sup>20</sup>, Karl Michaëlsson<sup>24</sup>, Bryan Kestenbaum<sup>8</sup>, Claes Ohlsson<sup>10</sup>, Dan Mellstrom<sup>10</sup>, Lisette de Groot<sup>25</sup>, Struan Grant<sup>9</sup>, Douglas Kiel<sup>3</sup>, Carola Zillikens<sup>5</sup>, Fernando Rivadeneira<sup>5</sup>, Stephen Sawcer<sup>26</sup>, Nicholas Timpson<sup>2</sup>, Brent Richards<sup>1</sup>. <sup>1</sup>Department of Human Genetics, McGill University, Montreal, Canada, Canada, <sup>2</sup>Medical Research Council Integrative Epidemiology Unit (IEU) at the University of Bristol, Bristol, UK, United Kingdom, <sup>3</sup>Institute for Aging Research, Hebrew SeniorLife, Boston, USA, United States, <sup>4</sup>Department of Biostatistics, Boston University School of Public Health, Boston, USA, United States, <sup>5</sup>Department of Internal Medicine, Erasmus Medical Center, Rotterdam, The Netherlands, Netherlands, <sup>6</sup>Department of Epidemiology, Erasmus Medical Center, Rotterdam, The Netherlands, Netherlands, <sup>7</sup>Department of medical sciences, Uppsala university, Uppsala, Sweden, Sweden, <sup>8</sup>Kidney Research Institute, Division of Nephrology, University of Washington, Seattle, WA, United States, <sup>9</sup>Division of Human Genetics, Children's Hospital of Philadelphia, Philadelphia, PA 19104, USA, United States, <sup>10</sup>Centre for Bone and Arthritis Research, Department of Internal Medicine and Clinical Nutrition, Institute of Medicine, Sahlgrenska Academy, University of Gothenburg, Gothenburg, Sweden, Sweden, <sup>11</sup>Department of Internal Medicine, Section of Gerontology and Geriatrics, Leiden University Medical Center, Leiden, the Netherlands, Netherlands, <sup>12</sup>Cardiovascular Health Research Unit, Departments of Medicine and Biostatistics, University of Washington, Seattle, WA, United States, <sup>13</sup>Cardiovascular Health Research Unit, Departments of Medicine, Epidemiology and Health Services, University of Washington, Seattle, WA, United States, <sup>14</sup>Institute for Translational Genomics and Population Sciences, Los Angeles Biomedical Research Institute and Department of Pediatrics at Harbor-UCLA Medical Center, Torrance, CA, USA, United States, <sup>15</sup>Department of Pediatrics, Perelman School of Medicine, University of Pennsylvania, Philadelphia, United States, <sup>16</sup>Menzies Research Institute Tasmania, University of Tasmania, Locked Bag 23, Hobart, Tasmania 7000, Australia, Australia, <sup>17</sup>Clinical and Molecular Osteoporosis Research Unit, Department of Clinical Sciences, Lund University, and Department of Orthopaedics, Skåne University Hospital, Malmö, Sweden, Sweden, <sup>18</sup>The Generation R Study Group, Erasmus Medical Center, Rotterdam, The Netherlands, Netherlands, <sup>19</sup>Department of Epidemiology and Biostatistics and the EMGO Institute of Health and Care Research, VU University Medical Center, Amsterdam, The Netherlands, Netherlands, <sup>20</sup>Department of Clinical Epidemiology, Leiden University Medical Center, Leiden, the Netherlands, Netherlands, <sup>21</sup>Department of Endocrinology, VU University Medical Center, Amsterdam, the Netherlands, Netherlands, <sup>22</sup>Division of Cardiovascular Medicine, Vanderbilt University Medical Center, Nashville, TN, USA, United States, <sup>23</sup>Bone & Mineral Unit, Oregon Health & Science University, Portland, USA, United States, <sup>24</sup>Department of surgical sciences, Uppsala university, Uppsala, Sweden, Sweden, <sup>25</sup>Department of Human Nutrition, Wageningen University, Wageningen, The Netherlands, Netherlands, <sup>26</sup>University of Cambridge, Department of Clinical Neurosciences, Box 165, Cambridge Biomedical Campus, Hills Road, Cambridge, CB2 0QQ, UK, United Kingdom

**Introduction:** Vitamin D insufficiency is common, correctable and influenced by genetic factors, and it has been associated to risk of several diseases. We sought to identify low-frequency genetic variants that strongly increased the risk of vitamin D insufficiency and tested their effect on risk of multiple sclerosis, a disease influenced by low vitamin D concentrations.

**Methods/Results:** We used whole-genome sequencing data from 2,619 individuals through the UK10K program and deep imputation data from 39,655 genome-wide

genotyped individuals. Meta-analysis of the summary statistics from 19 cohorts identified a low-frequency synonymous coding variant (rs117913124[A], minor allele frequency=2.5%) in the *CYP2R1* gene which conferred a large effect on 25-hydroxyvitamin D (25OHD) levels (-0.43 standard deviations of natural log-transformed 25OHD, per A allele,  $P$ -value =  $1.5 \times 10^{-88}$ ). The effect on 25OHD was four-times larger and independent of the effect of a previously described common variant near *CYP2R1*. By analyzing 8,711 individuals we showed that heterozygote carriers of this low-frequency variant have an increased risk of vitamin D insufficiency (OR=2.2, 95% CI 1.78-2.78,  $P=1.26 \times 10^{-12}$ ). Individuals carrying one copy of this variant had also an increased odds of multiple sclerosis (OR=1.4, 95%CI 1.19-1.64,  $P=2.63 \times 10^{-5}$ ) in a sample of 5,927 cases and 5,599 controls.

**Conclusions:** We describe a novel low-frequency coding variant in the *CYP2R1* gene, which exerts the largest effect upon 25OHD levels identified to date in the general European population. Since *CYP2R1* is known to encode a critical enzyme in the production of the active form of vitamin D, these findings implicate vitamin D in the etiology of multiple sclerosis.

**Disclosures:** Despoina Manousaki, None.

## MO0460

**Alterations in NFkB Signaling Contribute to the Bone Fragility in Osteogenesis Imperfecta type V.** Ronit Marom\*, Caressa D. Lietman, Abhirami Rajagopal, Mahim Jain, Ming-Ming Jiang, Yuqing Chen, Elda M. Munivez, Terry K. Bertin, Brendan Lee. Baylor College of Medicine, United States

Osteogenesis Imperfecta (OI) type V is characterized by increased bone fragility, bone deformities, hyperplastic callus formation and calcification of the interosseous membranes. It is caused by a common mutation in the 5' UTR of *IFITM5* gene (c.-14C>T), which introduces a new start codon adding 5 amino acid residues to IFITM5 protein. The purpose of this study was to identify downstream signaling cascades that may be altered by this mutant protein, which is known to have normal localization at the cell membrane. We utilized RNA sequencing and proteomic studies via reverse phase protein-array (RPPA) method in bone of mutant transgenic mice and cell culture models.

We have previously described a transgenic mouse model overexpressing the OI type V mutant *Ifitm5* in bone that showed severe bone deformities and perinatal lethality. Overexpression of the mutant *Ifitm5* caused abnormal mineralization, persistence of cartilage-like matrix throughout the limb, and altered cell morphology with chondrocyte-like cells in bone. RNA-sequencing in calvaria from transgenic mice suggested activation of NFkB signaling in the mutant model. The expression of *Ptgs2*, encoding the inflammatory mediator cyclooxygenase-2, was increased 6 fold in *Ifitm5*-mutant calvaria. In vitro mineralization assay in MC3T3 cells overexpressing mutant *Ifitm5* showed reduced alizarin red staining, and the application of an NFkB inhibitor partly rescued this phenotype. Interestingly, proteomic analysis using RPPA detected elevated levels of SOX9 in the mutant samples. NFkB signaling is reported to facilitate chondrogenic differentiation via regulation of SOX9 expression during endochondral bone ossification.

Inflammation is known to negatively affect bone formation, and this effect is, at least partly mediated via NFkB pathway. We suggest that altered NFkB signaling plays a role in the pathogenesis, and contributes to the development of bone fragility in OI type V.

**Disclosures:** Ronit Marom, None.

## MO0461

**Complete absence of calcitriol in *Cyp27b1* null fetal mice does not disturb mineral metabolism or skeletal development.** Brittany A. Ryan\*, K. Berit Sellars<sup>1</sup>, Kamal Alhani<sup>1</sup>, Beth J. Kirby<sup>1</sup>, René St-Arnaud<sup>2</sup>, Christopher S. Kovacs<sup>1</sup>. <sup>1</sup>Memorial University of Newfoundland, Canada, <sup>2</sup>McGill University, Canada

Does calcitriol play any role in regulating mineral metabolism or skeletal development *in utero*? Studies of Boston and Leuven vitamin D receptor ablation models reported that *Vdr* null fetuses have normal serum minerals, PTH, and skeletal morphology/mineralization. However, *Vdr* null fetuses have high calcitriol levels which conceivably could still act to regulate mineral metabolism. Parallel studies were also carried out in *Cyp27b1* null fetal mice, which do not make calcitriol. In those studies, *Cyp27b1*<sup>-/-</sup> dams were mated to generate pregnancies with WT, *Cyp27b1*<sup>+/-</sup>, and *Cyp27b1* null fetuses. However, passage of calcitriol from *Cyp27b1*<sup>+/-</sup> mothers to *Cyp27b1* null fetuses meant that they did not lack calcitriol.

In the present study, we generated *Cyp27b1* null and WT dams through heterozygous matings, and mated them to *Cyp27b1*<sup>+/-</sup> males. This generated *Cyp27b1* null and *Cyp27b1*<sup>+/-</sup> fetuses from null dams, which were also compared to *Cyp27b1*<sup>+/-</sup> and WT fetuses from WT dams.

Fetal serum was collected; intact fetuses were reduced to ash; ash mineral content was assessed by atomic absorption spectroscopy; tibiae and placentas were harvested.

We confirmed that calcitriol was undetectable in *Cyp27b1* null fetuses as compared to  $149 \pm 117$  pmol/l in *Cyp27b1*<sup>+/-</sup> fetal littermates and  $233 \pm 130$  pmol/l in WT fetuses ( $p < 0.001$ ). Therefore, *Cyp27b1* null fetuses truly lacked calcitriol.

*Cyp27b1* null fetuses had normal serum calcium ( $2.29 \pm 0.07$  vs.  $2.22 \pm 0.10$  mM), serum phosphorus ( $2.10 \pm 0.11$  vs.  $2.14 \pm 0.12$  mM), PTH ( $563 \pm 310$  vs.  $606 \pm 244$  pg/mL), skeletal ash weight ( $16.7 \pm 0.4$  vs.  $16.6 \pm 0.4$  mg), ash calcium ( $74.5 \pm 1.1$  vs.  $76.2 \pm 1.5$  mg/g),

and ash phosphorus ( $199.3 \pm 3.3$  vs.  $195.5 \pm 5.5$  mg/g). They also had normal tibial lengths, morphology, and mineral deposition. qPCR on placental RNA showed loss of *Cyp27b1* expression but no change in expression of key genes involved in placental mineral transport, including PTHrP, *Cyp24a1*, TRPV6, calbindin-D-9k,  $\text{Ca}^{2+}$ ATPase, and NaPi2a, NaPi2b, and NaPi2c. All comparisons are primarily to *Cyp27b1*<sup>+/-</sup> littermates ( $p = \text{NS}$ ) but there were also no differences compared with WT fetuses of WT dams.

In summary, loss of calcitriol in *Cyp27b1* null fetuses borne of *Cyp27b1* null dams did not significantly alter any measured parameter of mineral or bone homeostasis, confirming that neither maternal nor fetal calcitriol is required during fetal development. It is after birth that calcitriol becomes important to stimulate intestinal delivery of minerals to the neonatal skeleton.

**Disclosures:** Brittany A. Ryan, None.

## MO0462

**Reduction of *Gαs* expression in mice with maternal ablation of exon Nesp (*Nesp*<sup>tm</sup>) provides evidence for a potent *Gαs* silencing mechanism.** Olta Tafaj\*, Harald Juppner<sup>1</sup>, Lee S. Weinstein<sup>2</sup>. <sup>1</sup>Massachusetts General Hospital, United States, <sup>2</sup>Metabolic Diseases Branch, NIDDK, United States

Pseudohypoparathyroidism type 1a (PHP1A) is caused by mutations affecting *GNAS* exons 1-13, while pseudohypoparathyroidism type 1b (PHP1B) is caused by mutations affecting *GNAS* or *STX16*. The *GNAS* locus undergoes parent-specific methylation at different sites and it gives rise to several transcripts, including the alpha-subunit of the stimulatory G protein (*Gαs*), the signaling protein that mediates the actions of various hormones and neurotransmitters. *Gαs* is biallelically expressed with the exception of a few tissues/cells, such as brown adipose tissue, where its transcripts are derived predominantly from the maternal allele. Because of reduced paternal *Gαs* expression in these particular tissues, inactivating mutations on the maternal allele lead to little or no *Gαs* expression, thus hormonal resistance as observed in PHP1A patients. A similar *Gαs* reduction is also observed in PHP1B patients who show loss-of-methylation (LOM) at one or several differentially methylated regions (DMRs) within *GNAS*, which are sufficient to reduce *Gαs* levels and thus leading to hormonal resistance. In order to further investigate these observations, we took advantage of mouse models of PHP1A and PHP1B. We studied mice with global ablation of maternal *Gnas* exon 1 (*E1*<sup>tm</sup>) and animals with LOM at the three maternal methylation imprints due to ablation of *Gnas* exons Nesp and AS2-4 (*Nesp*<sup>tm</sup>). A slightly more severe reduction of *Gαs* mRNA and protein was observed in brown adipose tissue from *E1*<sup>tm</sup> than from *Nesp*<sup>tm</sup> mice ( $20 \pm 1$  vs  $31 \pm 3\%$  of wild type (wt)). Interestingly, *Nesp*<sup>tm</sup> mice also showed a mild, non-significant reduction in total *Gαs* transcript levels in kidney and liver ( $87 \pm 5$  vs  $84 \pm 8\%$  of wt), while these tissues from *E1*<sup>tm</sup> mice revealed the expected reduction ( $47 \pm 2$  vs  $40 \pm 2\%$  of wt). Quantification of the parental contribution to total *Gαs* transcripts in *Nesp*<sup>tm</sup> mice showed, in comparison to wild-type littermates, a robust reduction of maternal *Gαs* expression in all three investigated tissues leading to an about equal parental contribution. Thus LOM at the maternal DMRs upstream of the exons encoding *Gαs* leads to a major reduction of *Gαs* transcription from the maternal allele in BAT and, to a lesser extent, in kidney and liver. Taken together, our data suggest that regulatory proteins interact with non-methylated, paternal *Gnas* regions upstream of the exons encoding *Gαs*, and that these proteins are more abundantly expressed in tissues with predominantly maternal *Gαs* transcription.

**Disclosures:** Olta Tafaj, None.

## MO0463

**ADAMTS 18 plays an important role in murine endochondral ossification and fracture healing.** Sardar Uddin\*, Chuanju Liu<sup>2</sup>, David Komatsu<sup>1</sup>, Zong Dong Li<sup>3</sup>. <sup>1</sup>Department of Orthopaedics, Stony Brook University, United States, <sup>2</sup>Department of Orthopedic Surgery, New York University Medical Center, United States, <sup>3</sup>Dept. of Medicine, Stony Brook University, United States

ADAMTS 18 (a disintegrin and metalloproteinase with a thrombospondin type motif, AD18) is a member of a secreted Zn-metalloproteinase ADAMTS family. ADAMTS 18 was associated with low bone mass, hip fractures, and non/delayed unions in a recent genome-wide association study (GWAS). The objective of this project was to determine the role of ADAMTS18 in endochondral ossification using a femoral fracture model.

Our previous data showed runted growth in ADAMTS18 deficient mice, along with significantly reduced bone quality and quantity. Histological growth plate analyses were conducted to analyze cell morphology and patterning during endochondral ossification. The analyses revealed abnormal patterning in KO mice, with regions of delayed chondrocyte maturation, enlarged chondrocytes in the proliferative zone, and a disorganized columnar pattern in the proliferative zone. Abnormal trabecular bone patterning. Was also seen in metaphyseal bone. Femoral fractures were used to determine the effects of ADAMTS18 deficiency on fracture healing. Longitudinal radiographic analyses demonstrated delayed callus formation in ADAMTS18 deficient mice. Callus bone quantity was assessed using MicroCT at 10-micron resolution. MicroCT analysis at postfracture day 28 showed a significant increase in callus volume ( $p < 0.03$ ), as well as a decreased callus bone volume fraction and bone mineral density, indicative of large soft callus formation with impaired mineralization.

Collectively our data show that ADAMTS18 plays an important role in endochondral ossification, resulting in runted growth and delayed and/or impaired fracture healing. In future studies, we will further examine the cellular morphology and



patterning at different time-points during fracture healing and assess the mechanical integrity of healed fractures. In summary, the data from the current study indicate that ADAMTS18 is an important and novel regulator of skeletal maturity and bone remodeling with potential therapeutic implications for understanding and treating postnatal dwarfism, osteoporosis, and fracture healing.

**Disclosures:** Sardar Uddin, None.

## MO0464

**Histomorphometrical Analysis in Murine Hypophosphatasia.** Seiko Yamamoto-Nemoto<sup>\*1</sup>, Eri Yokoi<sup>1</sup>, Kei Ogawa<sup>1</sup>, Chika Endo<sup>2</sup>, Nao Ogawa<sup>1</sup>, Kunihiko Shimizu<sup>1</sup>, Takehiko Shimizu<sup>2</sup>. <sup>1</sup>Nihon Univ. School of Dentistry at Matsudo, Japan, <sup>2</sup>Nihon Univ. School of Dentistry at Mastudo, Japan

Hypophosphatasia (HPP) is caused by mutation of the gene (*ALPL* in humans, *Alpl* in mice) encoding tissue non-specific alkaline phosphatase (*TNSALP*). *TNSALP* has a large role in calcification since HPP develops rickets and osteomalacia by less function of *TNSALP*. Accumulation of inorganic pyrophosphate (PPi) known for one of *TNSALP* substrate inhibited bone calcification in the extracellular matrix. Physiological function of *TNSALP* has been investigated for years nevertheless the cellular mechanisms affecting calcification remain unclear.

Objectives: In this study we elucidated the bone metabolism of HPP model mice by bone morphometry to evaluate influence *TNSALP* in the cells involving ossification.

Methods: *Alpl*<sup>-/-</sup> mice develop skeletal disease at day 6-8 and usually die of their disease at postnatal day 20. The mice were injected with alizarin red 20mg/kg (Sigma-Aldrich, St. Louis, MO, USA) and calcein 20mg/kg (Sigma-Aldrich, St. Louis, MO, USA) at day 7 and day 9 via subcutaneous injection for the biological label. We performed the histomorphometrical analysis using the mice tibias collected at 10 days old. The samples obtained vilaneva staining.

Results: Cancellous bone and chondrocyte analysis were evaluated in comparison with *Alpl*<sup>+/+</sup> mice. The Osteoblasts decreased significantly in *Alpl*<sup>-/-</sup> mice. In regard to the osteoclasts there were no differences. Trabecular bone width and bone volume / tissue volume of *Alpl*<sup>-/-</sup> mice showed significant decrease in the value than those of *Alpl*<sup>+/+</sup> mice. Again the same numbers of type II osteoblasts were observed in both mice. The results showed that *Alpl*<sup>-/-</sup> mice had not only decreasing the bone volume but also reducing the number of osteoblasts. Thinning of hypertrophic chondrocytes layer was shown in *Alpl*<sup>-/-</sup> mice though the thick chondrocytes layer observed.

Conclusion: These results indicate that *TNSALP* effects the cell number of osteoblast and chondrocyte layer in *Alpl*<sup>-/-</sup> mice. Therefore the lack of *TNSALP* causes retarded bone mineralization in the HPP model mice.

**Disclosures:** Seiko Yamamoto-Nemoto, None.

## MO0465

**A Statistical Approach to the Identification of Potential Causal Variants Related to Bone Mineral Density.** Jonathan Greenbaum<sup>\*</sup>, Hong-Wen Deng, Tulane University, United States

Although GWAS have been able to successfully identify dozens of genetic loci associated with bone mineral density (BMD) and osteoporosis related traits, very few of these loci have been confirmed to be causal. This is due to the fact that in a given genetic region there may exist many trait-associated SNPs that are highly correlated. While this correlation is useful for discovering novel associations, the high degree of linkage disequilibrium that persists throughout the genome presents a major challenge to discern which among these correlated variants has a direct effect on the trait. In this study we apply a recently developed Bayesian fine mapping method, PAINTOR, to determine the SNPs that have the highest probability of causality for Femoral Neck (FNK) BMD and Lumbar Spine (LS) BMD. The advantage of this method is that it allows for the incorporation of information about GWAS summary statistics, linkage disequilibrium, and functional annotations to calculate a posterior probability of causality for SNPs across all loci of interest. We present a list of the top ten candidate SNPs for each BMD trait to be followed up in future functional validation experiments. The SNPs rs2566752 (*WLS*) and rs436792 (*ZNF621*) and *CTNNA1* are particularly noteworthy as they have more than 90% probability to be causal for both FNK and LS BMD. Using this statistical fine mapping approach we expect to gain a better understanding of the genetic determinants contributing to BMD at multiple skeletal sites.

**Disclosures:** Jonathan Greenbaum, None.

## MO0466

**A Case-Control Study of the Genetic Determinants of Atypical Femoral Fracture.** Roby Joehanes<sup>\*1</sup>, Emmanuel Biver<sup>2</sup>, Fredrick Kinyua<sup>1</sup>, Yi-Hsiang Hsu<sup>3</sup>, David Karasik<sup>3</sup>, Michelle Yau<sup>3</sup>, Serkalem Demissie<sup>4</sup>, Ching-Ti Liu<sup>4</sup>, Douglas Kiel<sup>3</sup>, Serge Ferrari<sup>2</sup>. <sup>1</sup>Hebrew SeniorLife, United States, <sup>2</sup>Geneva University Hospitals, Switzerland, <sup>3</sup>Hebrew SeniorLife / Harvard Medical School, United States, <sup>4</sup>Boston University, United States

Although there is a suggestion that genetic factors may influence the risk of atypical femur fractures (AFF), there have been no previous case control studies investigating

genetic determinants of AFF. In this study, we seek genetic variants that could be used to identify individuals at risk for AFF when taking antiresorptive therapy (ART), such as bisphosphonates (BP) or denosumab, and could lead to an understanding of the biology underlying these fractures.

Therefore we conducted a case-control genome-wide association study (GWAS) of 12 cases with AFF recruited from the Geneva University Hospitals and 54 controls who were currently or previously treated for osteoporosis and participating in the Geneva Retirees Cohort. All participants are females of European ancestry. All AFF cases were ascertained using the ASBMR AFF Task Force definition and were using ART at the time of fracture. Sixteen of the controls were taking ART at the time they were selected for this study, while the remaining controls were former users. Medication history was obtained during face-to-face questionnaires at the time of enrollment. Cases were older, more likely to have had past fractures, and had a longer duration of BP use. (Table 1). We performed genome wide genotyping using the Axiom Biobank array, imputed to the Haplotype Reference Consortium v1.1. We restricted the analysis to variants with minor allele frequency (MAF)  $\geq 5\%$ , yielding 5.58 million variants. Table 2 contains 20 variants most significantly associated with AFF based on allele distribution, with p-values estimated using Firth's logistic regression. These top variants had p-values in the  $10^{-6}$  range, and mapped to several genes not known to have roles in skeletal metabolism.

This case control study of common variants across the genome identified variants that were associated with AFF, although none reached genome wide significance. Nevertheless these suggestive associations merit further replication in larger studies. This study is a proof of concept that there may be genetic predisposition to this adverse effect of ART that could be leveraged in the future for personalized prescribing of osteoporosis therapy.

Table 1. Participant characteristics

	Control (n=54)	Cases (n=12)	P-value
Age (y)	68.3 $\pm$ 3.7	76.8 $\pm$ 7.0	<0.0001
Weight (kg)	62.4 $\pm$ 13.0	65.8 $\pm$ 14.2	0.4211
Height (cm)	161.3 $\pm$ 7.7	157.7 $\pm$ 8.2	0.1447
BMI (kg/cm <sup>2</sup> )	23.9 $\pm$ 4.2	26.6 $\pm$ 5.9	0.0732
Antiresorptive use	16 Current / 43 Former	12 Current	
Duration (y)	3.5 $\pm$ 3.1	8.1 $\pm$ 5.9	<0.0001
Prior fractures	22%	83%	<0.0001

Table 2. Most significant genetic variants associated with AFF

Variant	Gene	R <sup>2</sup>	MAF	Allele (Ref/Alt)	Avg. number of Alt allele in cases	Avg. number of Alt allele in controls	P
6:77937077	Intergenic	0.60	0.24	T/C	1.08	0.28	1.2x10 <sup>-6</sup>
7:206883171	ABCB5	0.74	0.43	G/C	1.83	0.98	2.2x10 <sup>-6</sup>
4:121270521	MAD2L1/PRDM5	0.63	0.44	T/C	0.25	1.17	4.2x10 <sup>-6</sup>
4:121272795	MAD2L1/PRDM5	0.63	0.45	G/C	0.25	1.17	4.7x10 <sup>-6</sup>
20:45567988	EYA2	0.44	0.12	T/G	0.67	0.11	4.7x10 <sup>-6</sup>
20:45568816	EYA2	0.44	0.12	G/A	0.67	0.11	4.8x10 <sup>-6</sup>
4:121274187	MAD2L1/PRDM5	0.65	0.46	T/C	0.25	1.17	4.8x10 <sup>-6</sup>
20:45568630	EYA2	0.44	0.12	A/G	0.67	0.11	4.8x10 <sup>-6</sup>
20:45567683	EYA2	0.44	0.12	C/T	0.67	0.11	4.8x10 <sup>-6</sup>
20:45568161	EYA2	0.44	0.12	A/G	0.67	0.11	4.9x10 <sup>-6</sup>
4:121276764	MAD2L1/PRDM5	0.64	0.46	A/T	0.25	1.17	6.0x10 <sup>-6</sup>
4:121277392	MAD2L1/PRDM5	0.64	0.46	T/C	0.25	1.17	6.2x10 <sup>-6</sup>
4:121278836	MAD2L1/PRDM5	0.65	0.47	T/C	0.25	1.17	7.3x10 <sup>-6</sup>
4:121279052	MAD2L1/PRDM5	0.65	0.47	T/C	0.25	1.17	7.5x10 <sup>-6</sup>
15:58568716	ALDH1A2	0.53	0.17	C/T	0.83	0.17	7.5x10 <sup>-6</sup>
15:58567786	ALDH1A2	0.53	0.17	A/G	0.83	0.17	7.7x10 <sup>-6</sup>
15:58567122	ALDH1A2	0.52	0.17	C/T	0.83	0.17	7.9x10 <sup>-6</sup>
15:58571401	ALDH1A2	0.62	0.16	A/T	0.83	0.19	8.9x10 <sup>-6</sup>
15:58576226	ALDH1A2	0.64	0.16	C/T	0.83	0.20	8.9x10 <sup>-6</sup>
14:70983001	COX16/ADAM21	0.85	0.22	C/T	1.08	0.26	9.2x10 <sup>-6</sup>

\*R<sup>2</sup> indicated variant imputation quality; Ref/Alt = Reference / Alternative

Tables

**Disclosures:** Roby Joehanes, None.

## MO0467

**Functional Effects of the p.Asp188Tyr Mutation in the Geranylgeranyl Diphosphate Synthase (GGPS1) Gene Associated with Bisphosphonate-related Atypical Femoral Fractures.** Neus Roca-Ayats<sup>\*1</sup>, James E. Dunford<sup>2</sup>, PeiYing Ng<sup>3</sup>, Natalia Garcia-Giral<sup>4</sup>, Monica Cozar<sup>5</sup>, Jose M Quesada-Gomez<sup>5</sup>, Xavier Nogués<sup>4</sup>, Daniel Prieto-Alhambra<sup>6</sup>, R Graham Russell<sup>2</sup>, Daniel Grinberg<sup>1</sup>, Adolfo Diez-Perez<sup>4</sup>, Roland Baron<sup>3</sup>, Susana Balcells<sup>1</sup>. <sup>1</sup>Dep of Genetics, University of Barcelona and CIBERER, Spain, <sup>2</sup>University of Oxford, United Kingdom, <sup>3</sup>Division of Bone and Mineral Research, Dept of Oral Medicine, Harvard School of Dental Medicine, United States, <sup>4</sup>Hospital del Mar Institute of Medical Investigation and CIBERFES, Spain, <sup>5</sup>Instituto Maimónides de Investigación, Cordoba, and CIBERFES, Spain, <sup>6</sup>Universitu of Oxford and GREMPAL CIBERFES, Spain

Background: A novel mutation in the GGPS1 gene was found in 3 sisters with atypical femoral fracture (AFF) after long-term bisphosphonates (N-BPs). This gene encodes the GGPPS protein, a key component of the mevalonate pathway. We have now performed functional studies to assess the impact of the mutation.

Methods: The cDNA for both wild type and Asp188Tyr GGPPS were cloned into a bacterial expression vector and the resulting his-tagged proteins were purified using Ni sepharose followed by gel filtration. Analysis of the oligomerisation of the GGPPS monomers was undertaken using a Sephadex S300 gel filtration column. Enzyme activity was assayed using both substrates, farnesyl pyrophosphate and C14-isopentenyl pyrophosphate (400KBq/uMol) at 20uM in buffer containing 100mM HEPES pH7.5, 2mM MgCl<sub>2</sub>, 0.1% Tween 20. Reactions were stopped after 10 mins at 37C by adding

acidified methanol. Products were extracted directly into water immiscible scintillation fluid and quantified by scintillation counting. The effect of shRNA-mediated GGPS1 depletion was also assessed in cells.

Results: Asp188 is an active site residue of GGPP synthase, involved in the binding of the substrate via a magnesium salt bridge. As predicted, disruption of this residue led to greatly reduced enzyme activity. In the recombinant enzyme the mutant had 5.7% of wildtype activity ( $0.72 \pm 0.09$  cpm/ng/min for the wildtype,  $0.04 \pm 0.013$  cpm/ng/min for the mutant ( $n=3$ )). Gel filtration experiments showed the wildtype enzyme to have a MW in excess of 200KDa suggesting that it is present as a hexamer in line with previous findings. The mutant enzyme consistently showed two peaks corresponding to the hexamer and the monomer (a peak around 38kDa), suggesting the mutant destabilises the oligomerisation of the enzyme.

Furthermore, shRNA-mediated GGPS1 depletion (>80%) in RAW 264.7 macrophages yielded significantly higher osteoclast numbers after mCSF-RANKL stimulation when compared to the corresponding non-target shRNA control. However, despite having higher osteoclast formation rates, osteoclasts with reduced GGPS1 expression had lower resorption activity when cultured on the bone-mimicking substrate Osteo Assay surface plates.

Conclusions: GGPS1 gene mutation greatly impairs the enzyme activity inducing biological effects that may contribute, along with other factors, possibly including exposure to BPs, to AFFs observed in patients carrying the mutation

**Disclosures:** *Neus Roca-Ayats, None.*

## MO0468

**Metabolomics of sarcopenia in Hong Kong Chinese.** Victoria Ho-Yee Wong\*, Grace Koon-Yee Lee, Ching-Lung Cheung. The University of Hong Kong, Hong Kong

Objective: Sarcopenia has recently been recognized as an independent condition by the International Classification of Disease, Tenth Revision, Clinical Modification (ICD-10-CM) Code. However, the pathophysiology of sarcopenia remains largely unknown. The aim of this study was to evaluate the role of metabolome in sarcopenia using untargeted metabolomics approach.

Materials and methods: Untargeted metabolomic profiling in serum sample was performed in 287 participants from the Hong Kong Osteoporosis Study. In total, 725 metabolites with known identity and missingness <50% were included in the final analysis. The sarcopenia phenotypes, gait speed, handgrip strength, and appendicular lean mass (ALM), were studied. Multivariable linear regression was used to evaluate the association between metabolites and sarcopenia phenotypes. Multivariate analysis of covariance (MANCOVA) was used to evaluate the association of metabolite with multiple correlated quantitative sarcopenia phenotypes. All analyses were adjusted for age, sex, height, and weight. Pathway analysis was performed using MetaboAnalyst 3.0.

Results: After correction for multiple testing using false-discovery rate, 1, 3, and 4 metabolites were significantly associated with gait speed, handgrip strength, and ALM, respectively. In MANCOVA analysis, 20 of them were significantly associated with the sarcopenia phenotype, with N-acetyl-1-methylhistidine being the most associated metabolite (FDR p-value:  $2 \times 10^{-5}$ ). The variance explained by these 20 metabolites in handgrip strength, gait speed, ALM was 12.6%, 11.4%, and 31%, respectively. Pathway analysis revealed that arginine and proline metabolic pathway was significantly enriched in the association (FDR p-value:  $9.3 \times 10^{-4}$ ).

Conclusion: The current study revealed a number of novel and known associated metabolites and provided novel targets for sarcopenia prediction and an improved understanding on the pathophysiology of sarcopenia.

**Disclosures:** *Victoria Ho-Yee Wong, None.*

## MO0469

**Aldosterone regulates FGF23 expression through WNK signaling in bone.** Olena Andrukhova\*<sup>1</sup>, Sibel Ada<sup>1</sup>, Jessica Bayer<sup>1</sup>, Kristopher Ford<sup>1</sup>, Nejla Katica<sup>1</sup>, Dario Alessi<sup>2</sup>, Reinhold G Erben<sup>1</sup>. <sup>1</sup>Department of Biomedical Sciences University of Veterinary Medicine, Austria, <sup>2</sup>College of Life Sciences, University of Dundee, United Kingdom

Chronic kidney disease (CKD) is associated with increased circulating fibroblast growth factor-23 (FGF23) and an activation of the renin-angiotensin-aldosterone system (RAAS). FGF23 is a bone-produced hormone regulating renal handling of minerals and vitamin D hormone production. Aldosterone (ALD) is known to up-regulate the with-no-lysine kinase (WNK) pathway in the kidney, activating renal sodium reabsorption which in turn may lead to hypernatremia and hypertension. To explore the hypothesis that ALD might stimulate bony FGF23 secretion via WNK activation, we treated wild-type (WT) mice with ALD or vehicle for 5 days. ALD treatment increased serum intact Fgf23 levels, and upregulated total and phosphorylated WNK1 protein in bone. Treatment of isolated primary osteoblasts with the ALD receptor blocker spironolactone or with the WNK pathway inhibitor closantel (Clos) blocked the ALD-induced increase in Fgf23 mRNA and protein expression, and the increase in Fgf23 secretion into the medium. To confirm the involvement of WNK in the regulation of Fgf23 expression we generated a WNK1 knockout (KO) cell line by CRISPR/Cas9 genome editing in U2OS osteoblast-like cells. WNK1-KO cells showed a blunted response to ALD treatment as evidenced by Fgf23 mRNA and protein expression, relative to WT U2OS cells. To test the pathophysiological relevance of this finding in vivo, we induced CKD by 5/6 nephrectomy in 3-month-old WT mice and orally treated the mice over 8 weeks post-surgery with vehicle or Clos (10 mg/kg).

Vehicle- and Clos-treated sham-operated mice served as controls. Serum ALD was increased in all groups of CKD mice. Importantly, the CKD-induced increase in circulating intact Fgf23 and in Fgf23 mRNA expression in bone was significantly reduced in Clos-treated CKD mice, relative to vehicle controls. Taken together, our study provides a novel mechanistic explanation for the regulation of Fgf23 secretion by ALD through activation of WNK signaling in bone cells. Our findings may lead to a better understanding of the molecular mechanisms behind the upregulation of FGF23 secretion in CKD, and may have important implications for the therapy of CKD patients in the future.

**Disclosures:** *Olena Andrukhova, None.*

## MO0470

**CKD-MBD in a model of targeted FGF23 deletion.** Erica L. Clinkenbeard\*, Pu Ni, Joseph C. Thomas, Megan L. Noonan, Julia M. Hum, Mohammad Aref, Matthew R. Allen, Kenneth E. White. Indiana University School of Medicine, United States

Fibroblast growth factor-23 (FGF23) is a bone-derived hormone central to the regulation of serum phosphate levels. The ability of FGF23 to control phosphate homeostasis is substantially hindered in the common disorder chronic kidney disease (CKD). Additionally, highly elevated levels of FGF23 in patients is associated with increased morbidity and mortality and is found to be associated with left ventricular hypertrophy (LVH). To test the role of FGF23 on CKD phenotypes during early and moderate disease states, a late osteoblast/osteocyte conditional Fgf23 knockout mouse (flox-Fgf23/Dmp1-Cre<sup>+/+</sup>) was placed on an adenine-containing diet to induce CKD. Adenine significantly induced serum intact FGF23 in the Cre- mice over casein fed mice (89-fold at 8 weeks,  $p < 0.01$ ), whereas Dmp1-Cre+ mice on adenine diet had a 90% reduction in serum intact and C-terminal FGF23 as well as bone Fgf23 mRNA ( $p < 0.01/0.05$ ). Serum biochemical analysis showed casein fed Cre+ mice had significantly higher serum phosphate at 8 weeks compared to the casein fed Cre- mice ( $p < 0.01$ ), whereas adenine diet fed Cre+ mice had higher serum phosphate versus Cre- mice on the same diet at both 4 and 8 weeks. Serum blood urea nitrogen (BUN), which is inversely related to kidney function, progressively rose in all adenine fed mice, yet the increase in Cre+ mice was significantly greater than Cre- mice at 8 weeks (1.75-fold;  $p < 0.001$ ). PTH was significantly elevated in the mice fed adenine diet regardless of genotype. Consistent with this finding, renal Cyp27b1 (vitamin D 1 $\alpha$ -hydroxylase) was significantly enhanced and midshaft cortical porosity was increased in all adenine fed groups compared to casein fed mice, with no effect of genotype. Echocardiographs of the adenine Cre+ hearts revealed profound calcification of the aortas. Additionally, pronounced LVH was observed in this group compared to adenine Cre- mice. Collectively, our results show that in an animal model of progressive CKD, a marked reduction of FGF23 could not block the hyperparathyroidism or metabolic bone disease, but the elevated FGF23 was sufficient to normalize serum phosphate and impart cardio-protective effects during mild and moderate disease.

**Disclosures:** *Erica L. Clinkenbeard, None.*

## MO0471

**Performance of Liaison immunoassays versus LC-MS/MS for measurement of serum 25OHD level and impact on clinical decision making.** Maya Rahme\*<sup>1</sup>, Laila Al Shaar<sup>1</sup>, Ravinder Singh<sup>2</sup>, Asma Arabi<sup>3</sup>, Rafic Baddoura<sup>3</sup>, Georges Halabi<sup>3</sup>, Robert Habib<sup>3</sup>, Rose Daher<sup>3</sup>, Darina Bassil<sup>1</sup>, Karim El Ferekh<sup>4</sup>, Maha Hoteit<sup>1</sup>, Ghada El-Hajj Fuleihan<sup>3</sup>. <sup>1</sup>Mrs, Lebanon, <sup>2</sup>Professor, United States, <sup>3</sup>Professor, Lebanon, <sup>4</sup>Mr, Lebanon

Context: Laboratories are increasingly shifting to new automated 25-hydroxyvitamin D (25OHD) assays, with reported large variability in their results, according to the International Vitamin D External Quality Assessment Scheme (DEQAS) quarterly reports. Liquid Chromatography Mass Spectroscopy (LC-MS/MS) is the gold standard method.

Objective/Setting: We compare the performance of a rapid automated immunoassays to measure serum 25OHD with tandem LC-MS/MS in subjects enrolled in a vitamin D RCT in the elderly (ClinicalTrials.gov identifier: NCT01315366).

Methods: The RCT enrolled 257 subjects of whom a total of 219 subjects had baseline 25-OHD levels measured in parallel, with the chemiluminescent Diasorin Liason Assay (Stillwater, MN, USA) at American University of Beirut, and the LC-MS/MS method at the Mayo clinic laboratories. Additional parallel measurements using both methods were done in subsets of patients at 6 months ( $N=171$ ) and 12 months ( $N=126$ ). Both laboratories pass the quality assurance standard requirements of DEQAS. Variability between the two methods was evaluated through t-tests, Bland-Altman plots, and linear regression analyses. Proportion of subjects who would be treated by the IOM cut-off (25OHD 20 ng/ml) according to 25OHD level whether run on platform or LC-MS/MS methods, and differences in patient proportions were tested ( $\chi^2$ ) at baseline and for all duplicates ( $N=516$ ).

Results: Study subjects were  $71.1 \pm 4.8$  yrs (mean  $\pm$  SD), included more women (55.4%), and were overweight or obese (BMI,  $30.2 \pm 4.5$  kg/m<sup>2</sup>). Serum 25OHD levels were significantly lower when measured with the Liaison assay as compared to LC-MS/MS ( $18.5 \pm 7.8$  vs  $20.5 \pm 7.6$  ng/ml;  $p < 0.001$ , Table). Examination of the Bland Altman graphs reveal the absolute bias was independent of average 25OHD values (at baseline, 6 and 12 months, and in the overall dataset). A larger number of subjects would have been allocated to vitamin D intervention based on Liaison as compared to LC-MS/MS



assay (38.2% vs. 27.1%;  $p < 0.001$ ). The proportions were 70% and 78%, respectively,  $p < 0.0001$ , if one considered the complete dataset. Linear regression: Diasorin (25OHD) =  $26 + 0.76 \text{ LC-MS/MS}(25\text{OHD})$ ,  $R^2 = 0.596$ .

Conclusion: Selection of assays has a significant impact on 25OHD results, patient classification, and treatment recommendations. Such variability cannot be ignored when deriving and applying vitamin D guidelines. It also renders universal assay standardization, as proposed by VDSP/CDC, a must.

Serum 25OHD levels by Assay Type, and Bias, in the Elderly Vitamin D Trial  
ClinicalTrials.gov Identifier: NCT01315366

Test	N	Mean $\pm$ SD	Median	Minimum	Maximum	p-value*
Baseline	Diasorin Liaison (ng/ml) <sup>a</sup>	219 18.51 $\pm$ 7.75	16.60	4.00	45.90	<0.0001
	LC-MS/MS (ng/ml) <sup>b</sup>	219 20.46 $\pm$ 7.58	19.00	6.00	45.00	
	Difference (ng/ml) <sup>b-a</sup>	219 1.95 $\pm$ 6.15	1.70	-30.90	19.20	
	Difference (%)	219 6.85 $\pm$ 29.28	10.00	-206.00	61.94	
Overall	Diasorin Liaison (ng/ml) <sup>a</sup>	516 24.13 $\pm$ 10.16	23.25	4.00	61.00	<0.0001
	LC-MS/MS (ng/ml) <sup>b</sup>	516 26.29 $\pm$ 10.38	25.00	6.00	68.00	
	Difference (ng/ml) <sup>b-a</sup>	516 2.17 $\pm$ 6.94	2.20	-30.90	28.40	
	Difference (%)	516 6.09 $\pm$ 26.65	9.79	-206.00	67.00	

\*p-value, by paired t-test, comparing Diasorin Liaison versus LC-MS/MS

Table

Disclosures: Maya Rahme, None.

## MO0472

**Quantification of soluble human Neuropilin-1 by sandwich ELISA.** Manfred Tesarz<sup>\*1</sup>, Elisabeth Gadermaier<sup>1</sup>, Thi Thuy Oanh Ho<sup>2</sup>, Gabriela Berg<sup>1</sup>, Gottfried Himmler<sup>1</sup>. <sup>1</sup>The Antibody Lab GmbH, Austria, <sup>2</sup>Biomedica Medizinprodukte GmbH & Co KG, Austria

Purpose: Neuropilin-1 (NRP1) functions as co-receptor for several extracellular ligands (e.g. members of the semaphorin family and specific VEGF isoforms). It exists as 103 kDa transmembrane NRP1 isoform 1, and as 72 and 68 kDa soluble NRP1 (sNRP1) isoforms 2 and 3, that are produced by alternative splicing. NRP1 is involved in multiple physiological processes. In bone, NRP1 is described to have a stimulatory role in osteoblast differentiation. It has further emerged as a promising target to inhibit prostate cancer metastasis. To investigate its potential as a biomarker in physiological and pathological conditions, there is a need for a highly specific and sensitive assay for the quantification of sNRP1 in peripheral blood.

Methods: We developed a sandwich ELISA employing polyclonal and monoclonal anti-human NRP1 antibodies. Linear epitopes were mapped with microarray technology and further compared between the soluble NRP1 isoforms. Assay parameters like specificity, dilution linearity, and spike recovery were assessed.

Results: The monoclonal detection antibody binds to a linear epitope located in the N-terminal CUB 1 domain of human NRP1. The multiple linear epitopes recognized by the polyclonal coating antibody are distributed over the whole NRP1 sequence. All mapped linear epitopes are conserved between the human sNRP1 isoforms. The assay is calibrated with sNRP1 isoform 2, and it detects sNRP1 in human serum and plasma (heparin, EDTA, citrate) samples. All assay characteristics (specificity, dilution linearity, spike recovery) meet the standards of acceptance.

Conclusion: This novel ELISA provides a reliable and accurate tool for the quantitative determination of human soluble Neuropilin-1 in healthy and diseased samples.

Disclosures: Manfred Tesarz, None.

## MO0473

**Measurement of (Free) 25OH Vitamin D in Saliva.** Christy Van Veenendaal<sup>\*1</sup>, Marsha Mersch<sup>1</sup>, Mike Martens<sup>1</sup>, Nicolas Heuvel<sup>2</sup>, Ernst Lindhout<sup>1</sup>. <sup>1</sup>Future Diagnostics Solutions, Netherlands, <sup>2</sup>DiaSource Immunoassays, Belgium

To measure Free 25OH Vitamin D in blood Future Diagnostics has developed a direct ELISA method<sup>1</sup>. The Free 25OH Vitamin D assay that reproducibly determines the level of Free 25OH Vitamin D in serum was also implemented and validated on an open ELISA platform<sup>2</sup>. With this assay a study was started to explore the possibility to use human saliva as matrix for the determination of (Free) 25OH Vitamin D concentration. Several literature articles suggest that in saliva 25OH Vitamin D is present in the free form only (no Vitamin D binding protein in Saliva). Saliva samples from healthy volunteers were tested in the Free 25OH vitamin D ELISA, a total 25OH Vitamin D ELISA and with LC/MS/MS for the concentration of 25OH Vitamin D. The results show that the concentration of Free 25OH Vitamin D in serum is within the normal range (J. Schwartz et al in prep), however the concentration of Free 25OH vitamin D in Saliva is below detection level (<1.9 pg/mL) or masked by Saliva constituents. When saliva samples were measured in a Total 25OH Vitamin D assay the concentration found is in the same order of magnitude as the Total 25OH Vitamin D concentration observed in serum. The results indicate that 25OH Vitamin D can be measured in saliva and that it is not as Free as supposed.

1) N. Heuvel et al ASBMR poster 2015

2) L. Swinkels et al ASBMR poster 2016

Disclosures: Christy Van Veenendaal, None.

## MO0474

**Free 25 (OH) vitamin D, but not total 25 (OH) vitamin D, is strongly correlated with gestational age and calcium in normal human pregnancy.** Oleg Tsuprykov<sup>\*1</sup>, Claudia Buse<sup>1</sup>, Roman Skoblo<sup>1</sup>, Berthold Hochozer<sup>2</sup>. <sup>1</sup>IFLB, Germany, <sup>2</sup>University of Potsdam, Germany

Basic science as well as epidemiological studies showed that vitamin D is causally involved in the pathogenesis of pregnancy related diseases such as gestational diabetes as well as pregnancy related hypertensive disorders short and long term outcome of the offspring. To translate this knowledge to clinical practice suitable tools to determine the vitamin D status during pregnancy are mandatory. Since 25(OH) vitamin D [25(OH)D] is mainly bound to vitamin D binding protein [VDBP] in the circulating blood and female sex steroids regulates hepatic VDBP synthesis, it is doubtful whether the determination of total vitamin D as it is current clinical practice does adequately reflect the vitamin D status of an individual pregnant women. We therefore compared the correlations of total serum 25(OH)D, free serum 25(OH)D, and 1,25(OH)2D in 475 apparently healthy pregnant women with gestational age, calcium, phosphorus, bone alkaline phosphatase and PTH. Free 25(OH)D was either measured directly using a novel assay system for direct measurements of free 25(OH)D as well as calculated free 25(OH)D based on measurements of VDBP, albumin and total 25(OH)D. There was a negative correlation between free 25(OH)D levels and gestational age ( $p < 0.0001$  for measured and calculated free 25(OH)D), whereas 1,25(OH)2D showed a strong positive correlation with gestational age ( $p < 0.0001$ ). Total 25(OH)D was not correlated with gestational age ( $p = 0.685$ ). Serum calcium was positively correlated with free 25(OH)D ( $p < 0.0001$  for measured and calculated free 25(OH)D) and not with total 25(OH)D ( $p = 0.065$ ). 1,25(OH)2D showed a negative correlation with calcium ( $p < 0.0001$ ). Phosphorus – on the other hand – was significantly associated with total 25(OH)D ( $p = 0.021$ ) only. Free and total 25(OH)D as well as 1,25(OH)2D were negatively correlate with PTH ( $p < 0.0001$  in all cases) and bone alkaline phosphatase ( $p < 0.01$  in all cases). Targets of vitamin D related gene activation such as albumin, LDL and vitamin B6 were correlated to free vitamin D, but not to total vitamin D. In conclusion, calculated and measured free 25(OH)D provide comparable data and correlates much better with components of the endocrine vitamin D system and targets of vitamin D induced gene expression. Free 25(OH)D concentrations decrease slightly during healthy pregnancy, whereas 1,25(OH)2D concentrations increase substantially during human pregnancy. Given the impact of vitamin D on maternal and offspring's health outcomes, an adequate monitoring of the vitamin D status during pregnancy might require measurements of both free 25(OH)D and 1,25(OH)2D at different time points of gestation.

Disclosures: Oleg Tsuprykov, None.

## MO0475

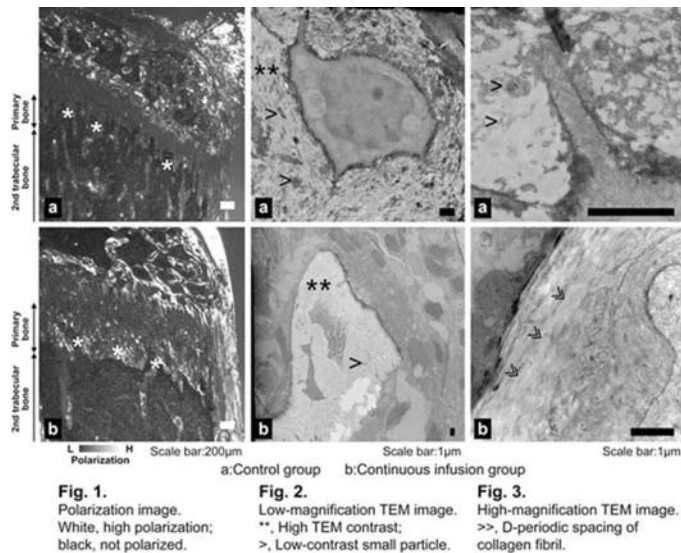
**The Primary Trabecular Bone Becomes Lamellar by Continuous Parathyroid Hormone Infusion.** Nobuhito Nango<sup>\*1</sup>, Shogo Kubota<sup>1</sup>, Yusuke Horiguchi<sup>1</sup>, Hidekazu Takano<sup>2</sup>, Wataru Yashiro<sup>2</sup>, Atsushi Momose<sup>2</sup>, Shizuko Ichinose<sup>3</sup>, Koichi Matsuo<sup>4</sup>. <sup>1</sup>Ratoc System Engineering Co., Ltd., Japan, <sup>2</sup>Institute of Multidisciplinary Research for Advanced Materials, Tohoku University, Japan, <sup>3</sup>Center for Stem Cell and Regenerative Medicine, Tokyo Medical and Dental University, Japan, <sup>4</sup>Laboratory of Cell and Tissue Biology, Keio University School of Medicine, Japan

Parathyroid hormone (PTH) is clinically used to accelerate bone formation, but the underlying mechanism remains obscure. We previously reported that continuous PTH infusion in mice reduces differentiation of osteoclasts, elongates primary trabecular bone, and delays osteoid mineralization in the primary trabecular bone. In the present study, we found that the elongated primary trabecular bone became lamellar after continuous PTH infusion.

Seven-week-old mice implanted with an osmotic pump were continuously administered with PTH at a dose of 40  $\mu\text{g/kg/day}$ , and after 72 and 144 h, tibiae were isolated. For each sample, the metaphysis was scanned using X-ray micro-computed tomography, mineralization of bone and cartilage matrices was visualized by synchrotron radiation multiscale X-ray microscopy, and the primary trabecular bone was observed by both transmission electron microscopy (TEM) and polarizing microscopy. The primary trabecular bone was polarized with the direction of polarization being parallel to the growth direction of the bone.

Polarization was stronger and wider in the continuous infusion group than in the control group (Fig. 1 \*). In the control group, many small particles with low TEM contrast were detected in the extracellular matrix (Fig. 2a >). TEM contrast in the matrix was homogeneous in the continuous infusion group than in control group (Fig. 2 \*\*). In the continuous infusion group, the D-periodic spacing structures (D-band) of collagen fibrils appeared (Fig. 3b >>), and the collagen fibers were aligned to the same direction, whereas in the control group, the D-band structure did not appear, and the orientation of the collagen fibers was unclear (Fig. 3a). Both the area and the intensity of polarization increased with the increase in the duration of PTH infusion. In the continuous infusion group, poorly mineralized primary trabecular bone was thickened.

Collagen fiber orientation is known to be random in the primary trabecular bone as seen in the control group. However, in the continuous infusion group, the orientation of the collagen fibers was not random. A plausible scenario is that the absorption of cartilage matrix by chondrocytes was inhibited by continuous PTH infusion, and primary trabecular bone were thickened, and the bone formation surface on the calcified cartilage was increased, and as a result, the primary trabecular bone became lamellar.



Fig

**Disclosures:** Nobuhito Nango, None.

## MO0476

**Steroid Orphan Receptor NR2C2 showed a osteopenia phenotype through regulation of RUNX2 function in osteoblast.** Maureen Newman<sup>\*1</sup>, Tzong-jen Sheu<sup>2</sup>, Edward Puzas<sup>2</sup>. <sup>1</sup>Department of Biomedical Engineering, University of Rochester, United States, <sup>2</sup>University of Rochester, United States

**BACKGROUND:** NR2C2 (nuclear receptor subfamily 2, group C, member 2) belongs to a nuclear receptor super family without an identified ligand. The DNA and protein domains of NR2C2 are closely related to those of testicular receptor 2 (TR2) and retinoid X receptors (RXRs). The protein expression of NR2C2 is found in several tissues including cerebellum, testis, prostate, and cardiovascular. NR2C2<sup>-/-</sup> mice have significant growth retardation and impaired cerebellar function. The bone density of NR2C2 deficient mice is significantly lower than that of littermate wild type mice. Although NR2C2 is highly expressed in macrophages, there is no detectable alteration of osteoclast formation or resorptive activity in knockout mice. Thus, it is hypothesized NR2C2 deficiency affects osteoblasts.

**RESULTS:** We generated several MC3T3-E1 stable cell lines: pBabe-NR2C2, pBabe-NR2C2 RNAi, and pBabe GFP. pBabe-NR2C2 MC3T3-E1 cells exhibited four-fold NR2C2 over-expression by real-time PCR and western blot. pBabe-NR2C2 RNAi MC3T3-E1 cells had 80% knock-down efficiency. pBabe-GFP MC3T3-E1 did not show a significant difference in NR2C2 expression level relative to non-stabilized MC3T3-E1 cells. Using an osteoblast differentiation assay, NR2C2 over-expression enhanced alkaline phosphatase activity and mineralization. On the contrary, NR2C2 RNAi led to decreased alkaline phosphatase activity and mineralization. In order to further understand the possible mechanism, we screened several osteogenic genes. Only osteocalcin and collagen I showed time-course changes with NR2C2 over-expression (increase) and NR2C2 RNAi (decrease), demonstrating a correlation between gene expression and osteoblast differentiation. Direct regulation of osteocalcin by NR2C2 was investigated using a reporter assay. In NR2C2 cells, NR2C2 and osteocalcin reporters both showed a 10-fold increase relative to control. However, NR2C2 RNAi cells showed a 60% decrease in both NR2C2 and osteocalcin reporters. Examining RNA and protein levels of Runx2 in both pBabe NR2C2 and NR2C2 RNAi cells, Runx2 RNA was similar between the two cell types, but Runx2 protein was enhanced by NR2C2 over-expression. Further, a Runx2 functional reporter gene assay (6XOSE2-OC-Luc) demonstrated that Runx2 protein stability is regulated by NR2C2 activity, subsequently altering osteocalcin levels. Finally, using NR2C2<sup>-/-</sup> knock-out mice, Runx2 immunoassay and osteocalcin ELISA confirmed these results in vivo.

**CONCLUSIONS:** Our data suggest that NR2C2 belongs to the steroid hormone family. NR2C2 regulates osteoblast gene and protein expression, with the loss of NR2C2 showing a significant bone loss phenotype. This receptor plays a pivotal role in fundamental bone formation through Runx2 stability and may be an interesting target for increasing bone formation in osteoporosis and other bone disorders.

**Disclosures:** Maureen Newman, None.

## MO0477

**Development of Long-Acting Antagonists for the PTH Receptor.** Hiroshi Noda<sup>\*1</sup>, Tomoyuki Watanabe<sup>1</sup>, Ashok Khatri<sup>2</sup>, Thomas J Gardella<sup>2</sup>. <sup>1</sup>Endocrine Unit, Massachusetts General Hospital, United States, <sup>2</sup>Endocrine Unit, Massachusetts General Hospital and Harvard Medical School, United States

Antagonists for the parathyroid hormone receptor (PTHr1) could potentially be used to treat diseases caused by excess PTHr1 signaling, such as hyperparathyroidism (HPT). Previous dW12-PTH(7-34)-based antagonists have limited efficacy in vivo, however, likely due, in part, to rapid receptor dissociation rates, as well as short pharmacokinetic (PK) profiles. We recently reported that certain PTH(1-14)/PTHrP(15-36) hybrid analogs exhibit slow PTHr1 dissociation rates and hence induce prolonged agonist actions in vitro and in vivo. We are now exploring N-terminal truncations of this hybrid scaffold for the development of new long-acting PTH antagonists, and here report on several such ligands, including dW12-LA-PTH(5-36) (IQLMHQRdWKWIQDARRRAWLHKLIAEIHAEI). In cell-based cAMP assays, dW12-LA-PTH(5-36) exhibited prolonged antagonism after wash out, confirming a slow receptor dissociation rate. Efficacy of dW12-LA-PTH(5-36) was then assessed in mice. To model HPT, we pre-injected mice with a PTH(1-34) analog containing a C-terminal 20kD PEG group (PEG-PTH), which induces prolonged hypercalcemia due to extended PK. At 24 hours after PEG-PTH injection (50 nmol/kg, IV), when blood Ca<sup>++</sup> was maximally elevated (~1.4 mM vs. ~1.2 mM at baseline), the mice were injected with vehicle, dW12-LA-PTH(5-36), or the previous antagonist, dW12-PTH(7-34) (peptide dose = 500 nmol/kg). By one hour post-injection, dW12-LA-PTH(5-36) reduced blood Ca<sup>++</sup> significantly (P < 0.05 vs. vehicle), whereas dW12-PTH(7-34) had no effect. The inhibitory effects of dW12-LA-PTH(5-36), however, waned by 4 hours. PK analyses, performed by injecting mice with TMR-labeled derivative peptides and measuring plasma TMR fluorescence at times after injection, revealed that TMR-dW12-LA-PTH(5-36) cleared rapidly from the blood (T<sub>1/2</sub> = 0.6 h vs. 0.9 h for TMR-PTH(1-34)). To extend the PK profile, we generated PEG-TMR, dW12-LA-PTH(5-37), which indeed exhibited improved PK (T<sub>1/2</sub> = 0.9 h), and inhibited the hypercalcemic response to co-injected PTH(1-34) even when injected at a dose only three-fold higher than the agonist (30 vs. 10 nmol/kg, respectively). The overall data suggest that more effective PTHr1 antagonists can be developed through strategies aimed at prolonging the ligand-receptor residence time, coupled with improving PK. Further studies of these analogs could lead to new antagonist-based modalities for treating diseases of excess PTHr1 signaling.

**Disclosures:** Hiroshi Noda, Chugai Pharmaceutical Co. Ltd., Grant/Research Support.

## MO0478

**Transient receptor potential melastatin 6 (TRPM6) as a Channel-kinase Regulator of Mineral Metabolism.** Nora Renthal<sup>\*</sup>, David Clapham. Boston Children's Hospital, United States

Magnesium is involved in most major metabolic processes, working as an enzymatic cofactor and playing a role in the stability of DNA and RNA. Despite this critical function, the mechanisms of magnesium homeostasis remain largely unknown. Much of our continued ignorance stems from the fact that, due to its critical role in the function of the cell and survival of the organism, evolution has ensured the rarity of disorders of magnesium homeostasis. Recently, an opportunity arose for elucidating the mystery of this basic biology in the discovery that patients with a rare defect in magnesium handling, known as Familial Hypomagnesemia with Secondary Hypocalcemia (HSH), were linked to mutations in the ion channel melastatin-related transient receptor potential 6 (TRPM6). In addition to being one of the few diseases of hypomagnesemia, HSH is one of few diseases linked to mutations in an ion channel. Furthermore, TRPM6 is exceptional among ion channels, as it is one of only two with an intrinsic kinase domain (the other being TRPM7). These unique features raise many questions, both of fundamental channel biology and the physiology of magnesium regulation.

Our studies are the first to methodically scrutinize the dual function of the TRPM6 channel and kinase, investigating the mechanism by which TRPM6 mutations produce the HSH phenotype in patients. Our data suggest TRPM6 produces cleaved kinases (M6CKs), which phosphorylate important downstream effectors of cell cycle regulation. This action is likely to be affected by TRPM6 channel conductance. We propose a mechanism whereby TRPM6 directs epithelial magnesium handling through localized ion signaling, triggering widespread kinase activity. These studies shed light on the signaling advantages of coupling both channel and kinase in the same polypeptide. It is our hope that an improved molecular understanding of TRPM6 will identify new mechanisms maintaining mineral balance in humans and better define the pathophysiology of Familial HSH.

**Disclosures:** Nora Renthal, None.

## MO0479

**Bidirectional Modulation of Adiponectin Signaling via APPL Proteins Interaction in Bone Cells.** Qisheng Tu<sup>\*</sup>, Liming Yu, Yuwei Wu, Tong Chen, wei Qiu, Dana Murray, Jake Chen. Tufts University School of Dental Medicine, United States

Adiponectin is important in maintaining the balance of energy metabolism, inflammatory responses, and bone formation. Our previous studies showed that adiponectin



inhibits osteoclastogenesis via adaptor protein APPL1-mediated suppression of Akt1, and promotes osteogenic differentiation. Yet, a few clinical studies have generated conflicting results. Many studies have been done to explain the discrepancies, but the results are still controversial. We have identified APPL1 as an adiponectin signaling protein in osteoclast cells. APPL2 is an isoform of APPL1 in cells. Our preliminary study showed that the ratio of APPL1/APPL2 expression in bones became lower in elder mice than in young mice. This study aimed to determine the bidirectional regulation of adiponectin signaling via APPL1/2 proteins interaction in osteoclastogenesis and osteoblast differentiation.

The results showed adiponectin inhibited RANKL-induced osteoclastogenesis, increased osteoclast apoptosis, and decreased osteoclast survival/proliferation. Moreover, the increase in APPL1/APPL2 ratio played a critical role in regulating the cross-talk between adiponectin and RANKL signaling pathways, which down-regulated RANKL-enhanced expressions of osteoclastogenic regulators including NFAT2, TRAF6, cathepsin K, and TRAP. Luciferase assays showed that the inhibitory effect of adiponectin on cathepsin K was antagonized by the siRNA specifically targeting APPL1 while APPL2 siRNA enhanced the adiponectin effects. In contrast, adiponectin strongly enhanced osteix and BSP promoter activity in osteoblasts via MAPK signaling pathways, which was regulated by modulation of APPL1/APPL2 expression in a similar way as in osteoclasts. Further, we found that APPL2 interacts with AdipoR1 by heterodimerizing with APPL1 and acts as a negative regulator of adiponectin signaling in bone cells. Adiponectin treatment stimulated APPL2 dissociating from AdipoR1 hence facilitated the binding of APPL1 to AdipoR1, which is a critical step for adiponectin signaling transduction.

Taken together, our results reveal that APPL1/2 isoforms exerted an opposite effects on adiponectin signaling, and balancing the interaction between APPL isoforms can precisely regulates the crosstalks between the adiponectin and MARK or RANKL signaling pathways in osteoblasts or osteoclasts during different stages of bone development, which may lead to more effective ways to prevent and treat diabetes associated bone diseases.

**Disclosures:** Qisheng Tu, None.

## MO0480

**Gene Expression Profiles of Selective Transcriptome Responses in the Intestine Reveal Novel 1,25(OH)<sub>2</sub>D<sub>3</sub> Targets and Suggest an Essential Role for the Vitamin D Receptor in Distal as well as Proximal Intestinal Segments.** Vaishali Veldurthy\*, Puneet Dhawan, Nishant Patel, Angela Porta, Shanshan Li, Alketa Stefa, Patricia Soteropoulos, Saleena Ghanny, Sylvia Christakos. Rutgers, New Jersey Medical School, United States

Vitamin D is critical for the integrity and function of the intestine and for controlling calcium homeostasis. However an understanding of vitamin D action in the intestine remains incomplete. To identify key genes involved in 1,25(OH)<sub>2</sub>D<sub>3</sub> action, RNA was isolated from the duodenum as well as from distal intestinal segments and studied by Affymetrix microarray. In studies using vitamin D deficient (-D) mice and -D mice injected with 1,25(OH)<sub>2</sub>D<sub>3</sub> (+D) [(1ng/g bw) 3 times over 48h] the genes most strongly affected by 1,25(OH)<sub>2</sub>D<sub>3</sub> in the intestine were CYP24A1, TRPV6 and calbindin-D<sub>9k</sub>. There was a 5 – 10 fold greater induction of TRPV6 and calbindin-D<sub>9k</sub> by 1,25(OH)<sub>2</sub>D<sub>3</sub> in the distal intestine compared to the duodenum. Transcript levels for S100A8 and S100A9 antibacterial proteins were induced 3 – 6 fold (2 fold greater induction in the distal intestine). Other novel genes induced by 1,25(OH)<sub>2</sub>D<sub>3</sub> (4 fold or greater in both proximal and distal intestine) include lipocalin 2 (an antibacterial peptide which has also been reported to be an anorexigenic hormone), FK506 BP5 (a co-chaperone for steroid receptor mediated transcription) and haptoglobin (which binds hemoglobin but also has anti-inflammatory activity). The transcript levels for claudin-2, claudin-12 and Cav1.3 voltage gated Ca<sup>++</sup> channel (suggested to be involved in vitamin D regulated calcium transport) were unaffected by 1,25(OH)<sub>2</sub>D<sub>3</sub>. In previous studies we showed that transgenic expression of VDR restricted to the distal ileum, cecum and colon of VDR KO mice rescues rickets. Microarray analysis indicated that the genes most strongly affected by VDR expression in the distal intestine are TRPV6 (100 -115 fold induction) and calbindin-D<sub>9k</sub> (10 – 71 fold vs. VDR KO). Transcript levels for claudin-2, 12, and Cav1.3 were similar in VDR KO and transgenic mice. In VDR KO mice that were fed a rescue diet (high in Ca, P and 20% lactose), which normalizes mineral homeostasis, TRPV6 and calbindin-D<sub>9k</sub> genes were down-regulated in the duodenum and genes for intra and intercellular matrix proteins including aquaporin 8 and claudin 8 were suppressed. In summary, our findings provide new insight into genes regulated by 1,25(OH)<sub>2</sub>D<sub>3</sub> and calcium/lactose in the intestine. Our study further emphasizes a role for 1,25(OH)<sub>2</sub>D<sub>3</sub> in the immune system as well as in calcium homeostasis and the importance of the distal as well as the proximal intestinal segments in order to understand intestinal effects of calcium and vitamin D.

**Disclosures:** Vaishali Veldurthy, None.

## MO0481

**Enpp1 regulates Klotho expression under phosphate overload conditions.** Ryuichi Watanabe\*, Takeshi Miyamoto<sup>1</sup>, Toshimi Michigami<sup>2</sup>, Seiji Fukumoto<sup>3</sup>, Masaya Nakamura<sup>1</sup>, Morio Matsumoto<sup>1</sup>. <sup>1</sup>Department of Orthopaedic Surgery, Keio University School of Medicine, Japan, <sup>2</sup>Department of Bone and Mineral Research, Osaka Medical Center and Research Institute for Maternal and Child Health, Japan, <sup>3</sup>Fujii Memorial Institute of Medical Sciences, Tokushima University, Japan

**Background:** Loss-of-function *Enpp1*<sup>tmw/tmw</sup> (*tmw*) mice exhibit aggravation of spinal ligamentous ossification and ectopic calcification on the Achilles tendons under phosphate overload condition. However, the precise mechanism underlying regulation of *Enpp1* gene expression was unclear. *Klotho* is a well-known anti-aging factor that regulates phosphate metabolism. It was reported that *Klotho* mutant mice exhibited phenotypes resembling human aging such as short life span, arteriosclerosis and osteoporosis. However, the upstream regulator of *Klotho* remains unclear. Thus, the primary objective of this study is to determine the factor(s) that is required for *Klotho* expression under phosphate overload conditions.

**Methods and Results:** 8-week-old *tmw* mice fed with high phosphate diet (HPD) became inactive and died within a couple of weeks after phosphate overloading. They exhibited ectopic calcification in aorta and kidney, and developed osteoporosis, all of which are the premature aging phenotypes resembling *klkl* mice. Next we analyzed serum FGF23 and 1,25(OH)<sub>2</sub>D levels in *tmw* mice fed with normal diet (ND) or HPD for two weeks. We found that both levels were upregulated significantly in *tmw* mice fed with HPD compared with ND. mRNA and protein expression level of *Klotho* in kidney were significantly lower in *tmw* than wild-type mice under phosphate overload condition, suggesting that the aging phenotypes in *tmw* mice fed with HPD are due to reduced renal *Klotho* expression. Furthermore, *cyp27b1*, which serves as a catalyst to convert 25(OH)D<sub>3</sub> to 1,25(OH)<sub>2</sub>D, was significantly upregulated in the *tmw* mice fed with HPD compared with ND. These results suggested that downregulation of renal *Klotho* expression by phosphate overload in *tmw* mice leads to excessive serum 1,25(OH)<sub>2</sub>D levels through increased *cyp27b1* expression. High 1,25(OH)<sub>2</sub>D levels were reportedly caused premature aging phenotypes in *klkl* mice. Thus, we asked whether the elevated serum 1,25(OH)<sub>2</sub>D levels promoted the aging phenotypes in *tmw* mice by phosphate overloading. 8-week-old *tmw* mice fed with high phosphate with low vitamin D diet (HPLD) alleviated premature aging phenotypes such as growth retardation, short life span, vascular calcification seen in *tmw* mice fed with HPD. In addition, the reduced renal *Klotho* expression in *tmw* mice fed with HPD was significantly restored by HPLD in *tmw* mice. Furthermore, we newly generated *Enpp1* and VDR double-knockout (*tmw/VDR KO*) mice. Surprisingly, all premature aging phenotypes in *tmw* mice were completely rescued in *tmw/VDR KO* mice even under phosphate overloading condition, and the renal expression of *Klotho* was significantly recovered in *tmw/VDR KO*.

**Conclusion:** Phosphate metabolism is crucial roles in regulating aging and ectopic calcification via FGF23-Klotho-vitamin D3 axis. In this study, we indicated that *Enpp1* might play as a regulator of this pathway under phosphate overload condition.

**Disclosures:** Ryuichi Watanabe, None.

## MO0482

**Fluoxetine use during pregnancy and lactation stimulates mammary-derived hormonal stimulation of bone turnover.** Samantha Weaver\*, Chad Vezina<sup>1</sup>, Julia Charles<sup>2</sup>, Laura Hernandez<sup>1</sup>. <sup>1</sup>University of Wisconsin-Madison, United States, <sup>2</sup>Brigham and Women's Hospital, United States

Lactation is characterized by bone turnover, freeing up calcium for milk. Cumulative time breastfeeding increases post-menopausal fracture risk. The antidepressant class Selective Serotonin Reuptake Inhibitors (SSRI) decrease bone mineral density (BMD) and increase fracture risk. As such, women using SSRI while pregnant and breastfeeding may be at increased risk for bone loss. During lactation, mammary gland (MG)-derived serotonin stimulates secretion of parathyroid hormone-related protein (PTHrP), a bone turnover hormone. We hypothesized that fluoxetine (a common SSRI) use during pregnancy and lactation would increase local serotonin activity, driving PTHrP release from the MG and shifting bone homeostasis. Beginning on embryonic d13 (E13), C57BL/6J mice were injected daily with saline (BS; n=8) or 20 mg/kg fluoxetine (BF; n=6) through d10 lactation. Serum was harvested on E13, d1, and d10 of lactation. On d10, mice were euthanized and MG, duodenum, and femur collected. One femur was analyzed by micro-computed tomography (microCT) (n=5 for BS, n=1 for BF), and one femur was evaluated for mRNA markers of bone resorption and formation. Serotonin content was elevated in the MG of BF compared to BS dams (P=0.04), but not in the duodenum. Total serum calcium was elevated in BF compared to BS dams on d1 lactation (P=0.03), but not on d10. There was reduced methylation at the PTHrP promoter (P=0.03) in BF dams compared to BS dams, although PTHrP mRNA was only slightly higher (P=0.09). At this early point in lactation, there were no significant differences in bone volume / total volume, BMD, or cortical thickness by microCT. While there were notable changes in mRNA abundance in femur, such as reduced osteocalcin (P=0.006) and increased macrophage colony stimulating factor (P=0.04) in BF compared to BS dams, the RANKL / OPG ratio was unaffected. These data are in line with recent reports by Ortuño et al. (2016) showing that detrimental effects on bone were only notable after 6 weeks of fluoxetine treatment. Collectively, this data suggests that fluoxetine administration during pregnancy and lactation increased serotonin content in the mammary gland, stimulating increased PTHrP production and shifts in expression of bone turnover markers. Given the widespread use of SSRI during

pregnancy and lactation, further research with a longer dosing regimen and extended follow-up is warranted to understand potential negative ramifications on women's bone health.

**Disclosures:** Samantha Weaver, None.

## MO0483

**Modulation of osteocyte membrane repair activity via Vitamin E alters the response of bone to mechanical loading.** Anoosh Bahraini<sup>\*1</sup>, Kanglun Yu<sup>1</sup>, Mackenzie Hagan<sup>1</sup>, Peyton Marshall<sup>1</sup>, Mark Hamrick<sup>1</sup>, Mohammed Elsalanty<sup>2</sup>, Anna McNeil<sup>1</sup>, Paul McNeil<sup>1</sup>, Meghan McGee-Lawrence<sup>1</sup>. <sup>1</sup>Medical College of Georgia, Augusta University, United States, <sup>2</sup>Dental College of Georgia, Augusta University, United States

We recently demonstrated that osteocytes experience plasma membrane disruptions (PMD) that initiate mechanotransduction during in vitro and in vivo loading, suggesting PMD are one way osteocytes detect and transduce a mechanical load. PMD repair is necessary for cell survival, and our in vitro studies show antioxidants like Vitamin E enhance osteocyte membrane repair. Reactive oxygen species (ROS), which accumulate during exercise, inhibit repair and can be counteracted by antioxidants in muscle, but this had not been explored in bone. The goal of this study was to determine whether modulating Vitamin E would impact osteocyte survival and bone adaptation with loading.

MLO-Y4 cells were mechanically wounded with glass beads in the presence of fluorescein-dextran (10 kDa) and stained after wounding with propidium iodide to detect repair failure (i.e., cell death). Addition of H<sub>2</sub>O<sub>2</sub> (1 mM) increased post-wounding necrosis (+40 fold) but pre-treatment with Vitamin E (220 µM) prevented wounding-associated cell death from ROS. For in vivo studies, male CD-1 mice (3 wk old) were fed a regular diet (RD) or vitamin E-deficient diet (VED) for up to 11 weeks. One group (n=5 RD, 5 VED) was run downhill to exhaustion to maximally induce osteocyte PMD after 6 weeks. Remaining mice performed osteogenic treadmill exercise (12 m/min, 30 min/day for 5 weeks) or were sedentary controls (n=10/group). Osteocyte PMD were measured histologically as intracellular exogenous Evans Blue and endogenous albumin. Empty lacunae quantified osteocyte viability, and ROS were detected by IHC for 4-HNE. VED mice showed more PMD-affected osteocytes (+50%) after a single exercise bout suggesting impaired PMD repair. After 5 weeks of training, VED mice failed to show exercise-induced osteocyte PMD formation, had more empty lacunae, and had increased ROS staining, suggesting loss of a wounded osteocyte population. Sedentary VED mice showed decreased cortical bone formation and mass compared to sedentary RD mice. While both VED and RD mice showed trends for increasing cortical bone with exercise, adaptation was more pronounced and significant in VED mice. This result may parallel changes in skeletal muscle, where PMD repair failure (e.g., muscular dystrophy) initially triggers hypertrophy but later leads to widespread degeneration. Our data support the idea that osteocyte membrane repair is an important aspect of bone mechanosensitivity in the osteocytic control of PMD-driven bone adaptation.

**Disclosures:** Anoosh Bahraini, None.

## MO0484

**Calcium Efflux from Diffuse Microdamaged Bone Matrix Enhances Osteoblastic Activity.** Hyungjin Jung<sup>\*</sup>, Ozan Akkus. Case Western Reserve University, United States

Daily physiological activities result in microdamage accumulation within bone matrix. Linear microcrack induced osteocyte apoptosis and resulting activation of basic multicellular unit was demonstrated in animal models [1]. However, mechanisms of repair for diffuse microdamage (MDx) remain to be elucidated. Calcium efflux was reported to occur from regions of bone undergoing MDx [2]. MDx induced calcium efflux to pericellular space was also shown to activate intracellular calcium signaling in osteoblasts specifically in the vicinity of MDx [3]. Such activation was abrogated by blockage of voltage-gated calcium channels (VGCC) [4]. The current study tested the hypotheses: 1) osteoblasts near actively forming MDx will display a greater anabolic response, 2) blockage of VGCC will reduce the enhancement of MDx induced anabolic response.

Calvarial murine primary osteoblasts were seeded on bone wafers and subjected to three-point bending to induce MDx. A VGCC blocker, bepridil, was used to evaluate the involvement of VGCC in the enhancement of anabolic responses of osteoblasts. Effect of MDx induced calcium efflux (DMICE) on anabolic function of osteoblasts was measured by evaluating changes in Runx2 and Osterix expressions (8H), osteocalcin synthesis (day 7) and mineralized nodule formation (day 14). Mann-Whitney test was used to test significant differences between groups at  $p < 0.05$ .

Runx2 and Osterix expressions of mechanically damaged samples were significantly greater than those of no-loaded control. Inhibition of VGCC significantly reduced the expressions (FIG.1A,B). Significantly higher amounts of osteocalcin and mineralized nodules were synthesized by osteoblasts on loaded bone wafers, while bepridil treatment resulted in a significant decrease in osteocalcin production and mineralized nodule formation (FIG.1C,D).

This study demonstrated that DMICE activates anabolic response of osteoblasts. Inhibition of VGCCs suppressed such enhancement of anabolism, indicating that VGCCs and the following activation of intracellular calcium signaling pathway is involved in the response. Future studies of osteoblast responses to DMICE in vivo will clarify how bone cells repair MDx. Insight gained from such studies also may help develop strategies for fracture healing.

[1] Cardose, *et al*, J Bone Miner Res, 24(4):597-605, 2009

[2] Sun, *et al*, Bone, 50:581-591, 2012

[3] Jung, *et al*, Bone, 76:88-96, 2015

[4] Jung, *et al*, Bonekey Rep, 5:778, 2016

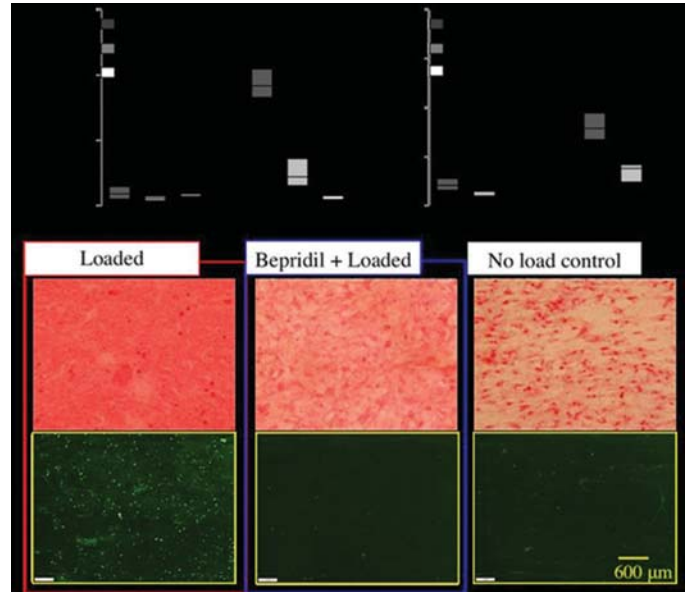


Fig.1 Activation of anabolic response in osteoblasts by diffuse microdamage induced calcium efflux.

**Disclosures:** Hyungjin Jung, None.

## MO0485

**Effect of IG9402 (Osteocyte Apoptosis Inhibitor) on Tooth Movement and Alveolar Bone.** Michelle Kaplan<sup>\*1</sup>, Sunil Wadhwa<sup>1</sup>, Imad Maleeh<sup>1</sup>, Jing Chen<sup>1</sup>, Zana Kalajic<sup>2</sup>. <sup>1</sup>Columbia University, United States, <sup>2</sup>University of Connecticut, United States

**Purpose:** We have previously shown in an in vivo mouse model of orthodontic tooth movement (OTM) that significant osteocyte apoptosis occurred on the compression side of the alveolar bone at 12, 24, and 72 hours after loading, peaking at 24 hours before osteoclast recruitment. However, the role of the osteocyte apoptosis in mediating the magnitude of orthodontic tooth movement is unknown. Recently, a bisphosphonate analog (IG9402) has been developed that effectively blocks osteocyte and osteoblast apoptosis in vitro. In this study we will assess the influence of osteocyte apoptosis using the IG9402 on orthodontic tooth movement in a mouse model.

**Methods:** 20 male 12-14 week old CD-1 mice were divided into 4 groups: 1) 5 mice with saline administration, 2) 5 mice with IG9402 administration, 3) 6 mice with Orthodontic tooth movement (OTM) and saline administration, 4) 4 mice with OTM and IG9402 administration. Tooth movement was achieved using Ultra Light (25g) Sentalloy Closed Coil Springs attached between the first maxillary molar and the incisors. Mice were administered daily subcutaneous injections of IG9402 (0.60 mg/kg/day) or the equivalent volume of saline for 10 consecutive days. On day 10, all mice were euthanized and mouse palates were scanned using a MicroCT scanner. The region of interest chosen for alveolar bone measurements was the furcation between the three roots of the maxillary first molar. A standard protocol was developed to trace the maximum three dimensional volume of the furcation while avoiding the roots and PDL. Measurements were analyzed on the tooth movement side as well as the contralateral side (no tooth movement). Linear measurements of tooth movement and alveolar bone volume fraction of the maxillary first molar furcation were recorded. T-tests were administered on all samples to determine statistical significance ( $P < 0.05$ ).

**Results:** There was a statistically significant ( $P < 0.05$ ) increase in alveolar bone volume fraction in mice undergoing tooth movement and injected with IG9402 compared to mice undergoing tooth movement and injected with saline. However, linear measurements of tooth movement displayed no statistically significant difference between the groups.

**Conclusion:** Our study displays the potential use of IG9402 during orthodontic treatment in individuals with compromised alveolar bone density, such as those with periodontal disease and osteoporosis.

**Disclosures:** Michelle Kaplan, None.



## MO0486

**Synergistic effect of remodeling and loading in aged mice.** Judith Piet<sup>1</sup>, Roland Baron<sup>2</sup>, Sandra Shefelbine<sup>3</sup>. <sup>1</sup>Bioengineering Department, Northeastern University, United States, <sup>2</sup>Oral Medicine, Infection, and Immunity, Harvard School of Dental Medicine, United States, <sup>3</sup>Mechanical and Industrial Engineering, Northeastern University, United States

**Introduction:** In mature bone, modeling and remodeling maintain healthy bone mass. Both processes are altered with aging as remodeling rates are skewed toward bone loss, and mechanosensitivity is reduced. We hypothesize that we can restore mechanosensitivity in aged bone by activating remodeling, thereby utilizing the synergistic effect of osteoclast/blast coupling and mechanical loading.

**Methods:** In aged (20 months) C57BL/6 female mice, we induced remodeling through 1) unilateral sciatic neurectomy (SN) of the right limb 2) pharmaceutical treatment (subcutaneous injection of hPTH(1-34) at a dose of 40µg/kg/day, 5 days/week). A week after surgery or beginning of PTH treatment, mice were subjected to *in vivo* uniaxial loading for 2 weeks (100 cycles/day, 3 days/week, 1s rest between cycles). A peak load of 9N was used in aged mice. A control group of mature mice (5 months) was loaded at a peak load of 10N, which matches the strain induced in old mice. After sacrifice, µCT images of right and left tibiae were analyzed for cortical cross sectional parameters. Within a pair, we quantified the amount of bone formed by the percent increase in cross sectional area (CSA) for the right tibia, compared to the left. Significance was tested with one-sample t-tests on CSA increase, with the null hypothesis that mean equals to zero.

**Results:** Loading promoted adaptation in mature mice ( $p < 0.01$ , Figure 1A), but similar strains were insufficient for bone formation in old mice (Figure 1B), which illustrates loss of mechanosensitivity with aging. Neurectomy induced resorption ( $p < 0.01$ , Figure 1B). However, combining neurectomy and loading promoted bone adaptation ( $p < 0.01$ , Figure 1B). Intermittent PTH increased the amount of bone compared to untreated legs (Student's t-test,  $p < 0.01$ ), and the combination of drug treatment and loading significantly promoted adaptation ( $p < 0.05$ , Figure 1C).

**Conclusions:** These results demonstrate lack of adaptation in aged bone and how mechanosensitivity can be restored through synergistic effect of remodeling and loading. Remodeling activity would provide cortical bone with a pool of responsive cells that can mediate adaptation.

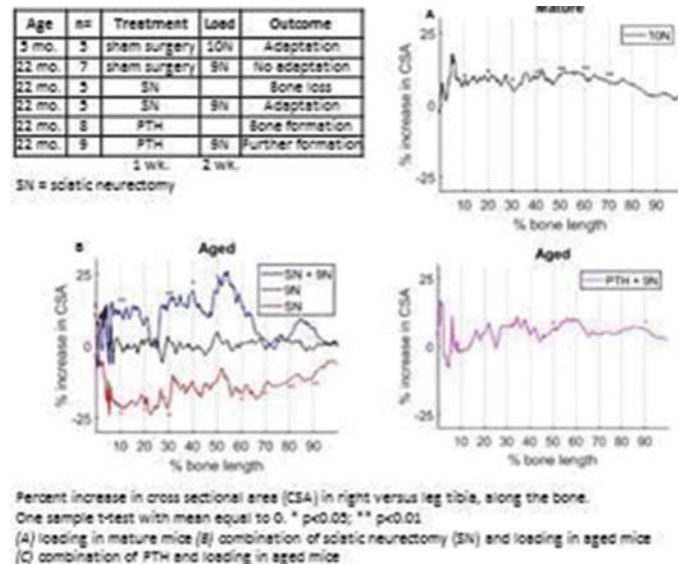


Figure 1: Experimental design and quantification of cortical bone formation

**Disclosures:** Judith Piet, None.

## MO0487

**Mechanical loading leads to bone formation in vivo in osteolytic Multiple Myeloma.** Maximilian Rummeler<sup>1</sup>, Fani Ziouti<sup>2</sup>, Anne Seliger<sup>3</sup>, Maureen Lynch<sup>4</sup>, Jundt Franziska<sup>2</sup>, Bettina Willie<sup>1</sup>. <sup>1</sup>Research Centre, Shriners Hospital for Children-Canada, Department of Pediatric Surgery, McGill University, Canada, <sup>2</sup>Medizinische Klinik und Poliklinik II-Hämatologie/Onkologie, Universitätsklinikum Würzburg, Germany, <sup>3</sup>Julius Wolff Institut, Charité- Universitätsmedizin Berlin, Germany, <sup>4</sup>University of Massachusetts, United States

Multiple myeloma (MM) is an incurable plasma cell derived neoplasia, characterized by aberrant growth of tumor cells within the bone marrow and pathological osteoclast activity resulting in increased bone resorption. Treating MM bone disease is a major goal in MM therapy. A previous study showed mechanical stimuli maintained bone mass during breast cancer bone metastasis (1). Thus, we hypothesized loading would maintain bone mass in a mouse model of MM. The left tibiae of 40, 10wk old female

BALB/c mice were either a) injected with PBS, b) injected with murine MM cells [MOPC315.BM, (2)], or c) not injected. 14 days after injection, 25 mice ( $n = 7-10$ /treatment) underwent 3 wks of *in vivo* cyclic tibial loading (3) (left limb,  $F_{max} = 10$  N;  $emax = 2000 \mu\epsilon$  determined by strain gauging, right limb was nonloaded), with the remaining 15 mice ( $n = 6$  PBS injected,  $n = 9$  tumor injected) serving as nonloaded control groups. *In vivo* microCT (10.5 µm resolution) was performed at day 0, 5, 10, 15 and 20 of loading, at proximal metaphysis and mid-shaft. Parameters measured included: cortical thickness (CtTh), mean cortical area (CtAr), mean total area (TtAr), cortical area per total area (CtAr/TtAr), mean porosity volume (PoV), mean cortical porosity (CtPo%) and mean tissue mineral density (TMD). An ANOVA assessed the effects of treatment, loading, and limb. After 20 days of loading, metaphyseal cortical bone formation (CtTh, CtAr, TAr, CtAr/TtAr, CtVTMD) was significantly greater and CtPo was lower compared to nonloaded right limbs and nonloaded groups. All right limbs had similar increases in cortical parameters over 20 days (+27-30% CtTh), indicating no systemic effects present. Left limbs of tumor-injected loaded group had +41% CtTh, while left limbs of tumor-injected nonloaded group increased by 1%. Interestingly, loading led to greater increases in the left limbs of PBS-injected loaded group (+64%) compared to non-injected loaded group (+51%). These data suggest the injection may have initiated a healing response. In conclusion, these data indicate mechanical loading can maintain bone mass in this model of MM bone disease. Histomorphometry and time-lapse imaging studies are underway to determine the relative contributions of formation and resorption to these bone mass gains.

1) Lynch et al. JBMR 2013, 2) Hofgaard et al. PLoS One 2012, 3) Willie et al. Bone 2013

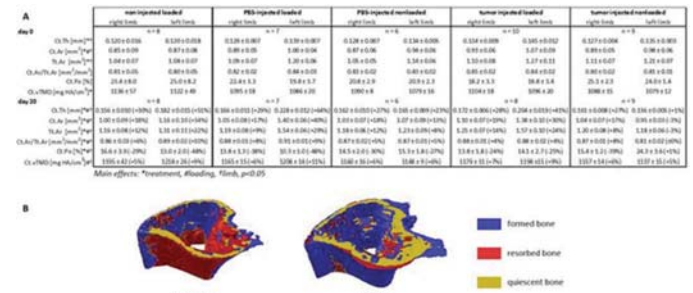


Fig. 1A Mean ± SD, % increase. B Formation & resorption between day 0 & 20 in tumor injected mice

**Disclosures:** Maximilian Rummeler, None.

## MO0488

**Age and Gender Does Not Influence All Biomechanical Properties of Femur and Ulna of C57BL/6 Mice.** Hammad Mumtaz<sup>1</sup>, Mark Dallas<sup>1</sup>, Mark Begonia<sup>2</sup>, JoAnna Scott<sup>1</sup>, Mark Johnson<sup>1</sup>, Ganesh Thiagarajan<sup>1</sup>. <sup>1</sup>University of Missouri Kansas City, United States, <sup>2</sup>Medical College of Wisconsin, United States

The effects of aging on femur and ulna biomechanical properties were determined in 6, 12, and 22 mo old C57BL/6 female ( $n=5-6$  per age) and male ( $n=6-7$  per age) mice. Using three-point bending, microCT, and ImageJ, we calculated the ultimate load to failure (UL), elastic stiffness (K), Young's Modulus (E), Moment of Inertia (MOI) and the tensile (TST) and compressive strengths (CST) for each bone. ANOVA with a Tukey post hoc test was used to analyze for differences between the age groups and paired t-tests were used to compare femurs and ulnas at each age for each sex.

In both males and females, the femur UL was significantly reduced at 22 mo compared to 6 mo ( $p < 0.05$ ). However, the ulna UL was significantly reduced in females at 22 mo of age ( $p < 0.05$ ) while the ulna UL in males did not change significantly. In female femurs, K did not change with aging, but male femurs exhibited a significantly lower K ( $p < 0.05$ ) at 22 mo vs. 6 mo. No significant changes in K were observed in the ulna of both sexes at any age group. E did not significantly change in male or female femurs across the age groups. However, female femurs had a significantly higher E than males ( $p < 0.05$ ), which was maintained across aging. No significant differences were observed in male or female ulna, either at different ages within or between sexes. Similarly, no significant differences were detected for MOI between the age groups or between sexes. Differences in MOI between femur and ulna were maintained at the different ages. Femur CST did not significantly change within males or females at the different ages, but males had a significantly lower CST compared to females at 22 mo ( $p < 0.05$ ). No significant changes were observed in CST at different ages or between sexes for the ulna. Similar findings were obtained for TST.

These data demonstrate that E, MOI, TST and CST are not changed significantly with aging in either gender or in either the ulna or the femur and hence may not play a role in the significant reductions in UL femur or female ulna with aging. Collectively, the data indicate that biomechanical properties are accompanied by compensatory mechanisms designed to maintain the strength of the femur and ulna. Additionally, these findings demonstrate that different bones (i.e., bone compartments) behave differently during aging and between sexes; therefore, caution must be taken to generalize findings in one bone to the rest of the skeleton.

**Disclosures:** Hammad Mumtaz, None.

## MO0489

**Osteoblast-Derived Nerve Growth Factor is Required for Skeletal Adaptation to Mechanical Loads.** Jino Park<sup>\*1</sup>, Liliana Minichiello<sup>2</sup>, Thomas Clemens<sup>3</sup>, Ryan Tomlinson<sup>1</sup>. <sup>1</sup>Thomas Jefferson University, United States, <sup>2</sup>Oxford University, United Kingdom, <sup>3</sup>Johns Hopkins University, United States

The periosteal and endosteal surfaces of mature bone are densely innervated by TrkA sensory nerves. We have previously shown that the invasion of these nerves during endochondral bone formation is necessary for the coordination of vascularization and ossification. Furthermore, we found that inhibition of TrkA signaling diminished load-induced bone formation in adult mice. During the course of this work, we observed that NGF expression is induced in mature osteoblasts in response to mechanical loading, both in vitro and in vivo. To directly test the role of osteoblast-derived NGF in skeletal adaptation to mechanical forces, we generated mice in which floxed NGF alleles have been selectively removed from the osteoblast lineage using Cre recombinase driven by the osteocalcin promoter ( $\Delta$ NGF mice). Although mice globally deficient in NGF die shortly after birth,  $\Delta$ NGF mice are born at normal Mendelian frequency, live to adulthood, and are indistinguishable from littermates. Furthermore,  $\Delta$ NGF mice displayed no significant skeletal defects in long bones as compared to wildtype littermates by microCT analysis. Therefore, we subjected adult  $\Delta$ NGF mice to three days of axial forelimb compression (100 cycles of 3.0N rest-inserted sinusoidal waveform). Calcitonin and alizarin were administered 3 and 8 days after the first bout of loading, and bone formation was assessed by dynamic histomorphometry. Axial compression produced the expected anabolic response in both  $\Delta$ NGF and wildtype littermates, with robust increases in bone formation evident on the periosteal and endosteal surfaces of loaded ulnae. However,  $\Delta$ NGF mice had a significantly diminished anabolic response, with a large reduction (~62%) in relative periosteal bone formation rate in loaded limbs. This effect was partially a result of diminished osteoblast bone formation activity, as  $\Delta$ NGF mice had smaller increases in mineral apposition rate (+12%) as compared to wildtype littermates (+35%). Furthermore, this effect was mediated by diminished osteoblast activation, as  $\Delta$ NGF mice had only a modest increase in mineralizing surface (+30%) as compared to wildtype littermates (+78%). There were no significant differences between genotypes in any parameter from non-loaded limbs. Because primary osteoblasts themselves do not express TrkA or respond to TrkA inhibition, these results indicate that activation of TrkA sensory nerves by osteoblast-derived NGF is required for optimal load-induced bone formation.

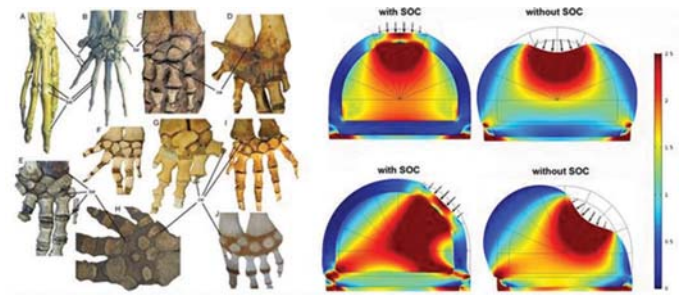
**Disclosures:** Jino Park, None.

## MO0490

**Evolutional Separation of Epiphyseal and Articular Cartilage is a Bone Adaptation to Terrestrial Growth.** Meng Xie<sup>\*1</sup>, Pavel Gol'din<sup>2</sup>, Jordi Estsfa<sup>3</sup>, Lei Li<sup>4</sup>, Irene Linares Arregui<sup>5</sup>, Christian Gasser<sup>5</sup>, Ekaterina Medvedeva<sup>6</sup>, Kotova Svetlana<sup>6</sup>, Peter Timashev<sup>6</sup>, Igor Adamevko<sup>4</sup>, Anders Eriksson<sup>7</sup>, Sophie Sanchez<sup>8</sup>, Andrei Chagin<sup>4</sup>. <sup>1</sup>Department of Physiology and Pharmacology, Karolinska Institute, Sweden, <sup>2</sup>Stockholm University, Sweden, <sup>3</sup>Department of Organismal Biology, Uppsala University, Sweden, <sup>4</sup>Department of Physiology and Pharmacology, Karolinska Institutet, Sweden, <sup>5</sup>Department of Solid Mechanics, KTH, Sweden, <sup>6</sup>Sechenov Medical University, Russian Federation, <sup>7</sup>Department of Mechanics, KTH, Sweden, <sup>8</sup>Department of Organismal Biology, Uppsala University, Sweden

Endochondral ossification describes the process of using cartilage as a template for long bone formation that involves appearance of primary and secondary ossification centers (POC and SOC). Unlike the POC that is formed prenatally in the diaphysis and is present in most species with a skeleton, the SOC is formed postnatally at the epiphysis and appears mainly in land animals. Despite the extensive understanding of the ossification process, the evolutionary role of SOC is poorly understood. Here we provide evolutionary observations combined with mathematical modeling and functional studies to show that the SOC is protecting the epiphyseal growth plate chondrocytes from mechanical stress allowing endochondral growth combined with weight bearing during juvenile growth of many amniotes. Specifically, SOC appears during evolution of many amniotes and disappears with migration back to water (e.g. whales). Mechanically, the SOC rendered the bone epiphysis more stiffness and reduced shear and normal stress within the epiphyseal growth plate. Modeling biological responses in 10-day-old rat bones (2 cm long, no SOC) and 1-month-old mouse bones (2 cm long, with SOC), we found that without SOC the growth plate chondrocytes undergo apoptosis upon minimal pressure application, whereas SOC allows chondrocytes to withstand 6 times higher pressure. Cell death was associated with activation of the YAP-p73 signaling pathway. Interestingly, the hypertrophic chondrocytes were the first to undergo apoptosis when the load increased beyond physiological range and more dead chondrocytes were found on the opposite side of the growth plate when load was applied angularly from the other side.

Our results demonstrate the functional importance of SOC for land animals and may provide indications on evolution of other bone structures. Moreover, revealing high sensitivity of epiphyseal chondrocytes to external pressure might improve our understanding of the causes to growth plate injuries in child and adolescent such as slippery epiphysis.



Gradual loss of bony epiphysis in whale and mathematical model of pressure distribution

**Disclosures:** Meng Xie, None.

## MO0491

**The Mechanism and an Alternative Method of Accelerated Bone Remodeling in Orthodontics after Maxillary Osteotomy.** Zoe (Xiaofang) Zhu<sup>\*1</sup>, Jake (Jinkun) Chen<sup>2</sup>, Qisheng Tu<sup>2</sup>, Guofang Shen<sup>3</sup>. <sup>1</sup>Tufts University, United States, <sup>2</sup>Division of Oral Biology, Tufts University, United States, <sup>3</sup>Ninth People's Hospital, Shanghai Jiao Tong University, China

**Objective:** In surgery-first accelerated orthognathic surgery (SFA), the clinical phenomenon of accelerated orthodontic bone remodeling and tooth movement after maxillary osteotomy is one of its superiorities compared with conventional approach. But there has no comprehensive study on mechanism of this phenomenon. We designed this study to explore the mechanism and find a replacement method without operative injury. 6-shogaol, a natural compound of ginger, may have the potential to be the assistant way of SFA or the alternatives for corticotomy in orthodontics. **Methods:** (1) 48 male adult SD rats were randomly divided into 2 groups. Le Fort I osteotomies were performed on left maxilla in LF Group. After surgery, an orthodontic appliance was ligated to deliver an initial mesial force of 0.5N. TM group were orthodontic treated only. The animals were sacrificed on day 3, 7, 14, and 28. The changes in alveolar bone near left upper first molar were evaluated. (2) Bone marrow macrophages (BMM) cells were cultured and induced to osteoclasts by M-CSF and RANKL. The effect of 6-shogaol on osteoclastogenesis is evaluated. (3) 6-shogaol were IP injected to the SD rats every 3 days for 2 weeks with orthodontic appliance. tooth movement were recorded after sacrificing. **Results:** (1) In LF group, the upper left first molars moved more rapidly ( $P < 0.05$ ). Micro-CT showed BV/TV, Tb.Th, Tb.SP were significantly lower in the early stage than in TM group. Histologic findings showed more active alveolar bone remodeling. The TRAP+ cells in LF group were 4fold higher than control group. The expression of RANKL was significantly increased, indicating significant osteoclast formation. TUNEL labeling notably increased in LF groups on day 3. (2) The CCK-8 assay and cell apoptosis analysis showed 6-shogaol did not affect BMMs at 6.25 $\mu$ M. The formation of osteoclasts was increased with 6-sho treatment. SEM image showed bone absorption pits. Staining of actin-ring with phalloidin-rodamine. The p-JNK was significantly increased by 6-shogaol at 60min. The expression of C-Jun and Nfatc1 are increased. (3) The tooth movement are remarkably rapid in the 6-shogaol injection group. **Conclusion:** Maxillary osteotomy can accelerate bone remodeling and orthodontic tooth movement by increasing osteocysts apoptosis and release of the RANKL. 6-Shogaol enhances osteoclastogenesis and has the potential for clinical use to accelerate bone remodeling during the orthodontics and/or orthognathic therapy.

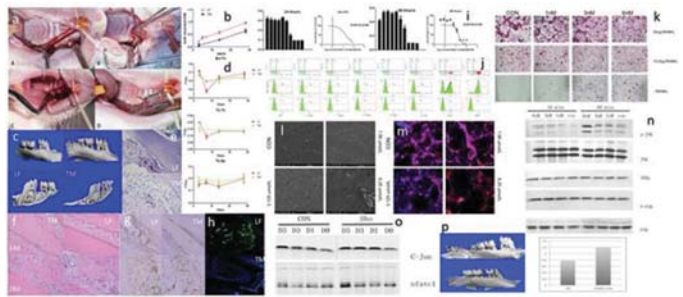


Figure 1

**Disclosures:** Zoe (Xiaofang) Zhu, None.



## MO0492

**Effects of 2g hypergravity on osteoarthritis-induced bone and muscle changes.** Benoit Dechaumet\*, Damien Cleret, Norbert Laroche, Arnaud Vanden-Bossche, Marie-Hélène Lafage-Proust, Laurence Vico. University of Lyon, INSERM, U1059, France

Knee osteoarthritis (OA) is a multifactorial disease that results from degradation of the articular cartilage, increased subchondral bone, decreased trabecular bone volume in epiphysis and metaphysis, increased vascularization in the subchondral bone. Mouse OA model of destabilization of the medial meniscus (DMM) reproduces these characteristics. OA protective effects of physical activity have been shown but compliance is often difficult to achieve. We previously showed that exposure to 2g hypergravity has beneficial effects on the skeleton of healthy mice. Our hypothesis is that 2g hypergravity could be used as a surrogate of resistance exercise.

Twenty-eight of the forty-two 16-week-old C57BL/6J male mice underwent right DMM inducing severe OA after 8 weeks. Mice are randomized into 3 groups (Ctrl, OA and OA 2g). OA 2g group (n=14) are subjected to continuous hypergravity 2 days after OA induction for a period of 8 weeks. In each group, 8 mice were used for bone analysis of right tibia (μCT, histomorphometry, bone vascular analysis after intracardiac perfusion with barium sulfate) and 6 mice for muscle analysis.

OA induces a thinning of articular cartilage and an increase in the OARSI score compared to the Ctrl. These characteristics tend to be less severe in OA 2g as compared to OA (OARSI score decreases by 20%). In the metaphysis, BV/TV decreases by 28% (p=0.02) in OA vs Ctrl. This loss is prevented by 2g. In OA the cortex is not affected, however, 2g decreases the thickness of the tibia cortex (9%, p<0.04, vs OA). As compared to Ctrl, OA increases Oc.S/BS (48%, p<0.0015) without affecting BFR/BS. These bone cell activities do not differ between OA and OA 2g. The vascular density of the tibia metaphysis is not affected in OA (but tends to increase), and decreases in OA 2g vs OA (15% p=0.015). In the soleus muscle, OA is not affecting muscle fiber size and type but decreases significantly (p<0.007) the number of vessels per fiber. Two-g increases the area of the fibers (p<0.001), favors a switch from type II (fast) to type I (slow) fibers, decreases soleus vascular density (vessel number per μm<sup>2</sup> p=0.02) but does not change the number of vessels per fiber vs. OA. Muscle changes with 2g are comparable to those describe with resistance exercises.

In conclusion, 2g improved the leg muscle in OA mice, alleviated OA severity at the tibia trabecular level but decreased the cortical thickness. The resulting biomechanical properties remain to be investigated.

**Disclosures:** Benoit Dechaumet, None.

## MO0493

**Delayed Bone Defect Healing In Dystrophin/Utrophin Double Knockout Mice Is Associated with Muscle Force and Decrease in Osteoblasts and Osteoclasts.** Xueqin Gao\*, Xuving Sun<sup>1</sup>, Sarah Amra<sup>1</sup>, Charles Huard<sup>1</sup>, Hazi Cheng<sup>1</sup>, David Mora-Boellstorff<sup>1</sup>, Bing Wang<sup>2</sup>, Johnny Huard<sup>1</sup>. <sup>1</sup>University of Texas Health Science Center at Houston, United States, <sup>2</sup>University of Pittsburgh, United States

Duchenne muscular dystrophy (DMD) is an X-linked recessive muscular disease caused by the mutation of dystrophin gene. DMD patients usually become wheelchair-bound in the third decade of life. Dystrophin/utrophin double knockout (DKO) mouse model was first described by Sanes' group and is a more useful model for DMD, as it more closely mimics human DMD. This study sought to explore the effect of muscle force on bone defect healing in DKO mice.

**Material and Methods:** 1. Four weeks old of C57BL/10J, dystrophin<sup>-/-</sup>(Mdx), Mdx/Utrophin<sup>+/-</sup>(Het) and Mdx/utrophin<sup>-/-</sup>(Homo) mice were used in this study. 2. Creation of 1 mm skull and tibial defects. A 1 mm defect was created in the right parietal bone and in the right proximal tibia of same mouse. 3. Bone defect healing was monitored at days 1, 7, 14, and 21 using Viva CT 40 lively. Mice were sacrificed on days 7 and 21 respectively. Bone defect healing was evaluated. 4. Histology: The skull and right tibia were harvested and fixed, and decalcified and paraffin-embedded. Herovici's staining was performed. Osteocalcin immunohistochemistry and tartrate-resistant acid phosphatase (TRAP) staining was performed to detect osteoclasts and osteoblasts respectively. 5. Statistical analysis: Student's t test or Wilcoxon rank sum test were used.

**Results:** (1) MicroCT results showed that the skull defects did not heal while the tibia defects were fully healed at 21 days. No differences were observed between the groups in new bone volume in the skull defect area. However, the bone density was lower in the Homo group than in the other groups. Healing of the tibial defect was delayed at day 7 in the Homo group, as shown by the lower bone volume of newly formed bone in the defect area, compared to other groups. The tibial defect was completely healed by day 21 in all the groups. No differences were observed in new bone volume at day 21. However, the newly formed bone density was lower in the Homo group than in the other groups on days 14 and 21. (2) New bone volume was significantly higher in the tibial defect than in the skull defect in all groups (p<0.0001 for all groups). (3) Histology: Herovici's staining showed that bone matrix collagen I (red color) was less dense in the Homo group compared to the other groups at days 7 and 21. (4) Osteocalcin staining showed fewer osteoblasts in the Mdx, Het, and Homo groups, in comparison with the B10 normal group (p<0.005). (5) TRAP staining also showed a decrease in osteoclasts in the defect area at day 21 in Mdx, Het, and homo groups compared to B10 group.

**Conclusion:** Our study indicated that long bone that are surrounded by muscle healed faster than skull bone that has no muscle support for both normal mice and DMD mice models. Furthermore, tibial defect healing was delayed in Homo mice. This

delayed defect healing was attributed to lower bone formation and bone remodeling in Homo mice. Further studies are needed to elucidate the underlying mechanism.

**Disclosures:** Xueqin Gao, None.

## MO0494

**Estrogen Modulates Musculoskeletal Physiology in Female Mice.** Saki Nagai\*, Kazuhiro Ikeda<sup>1</sup>, Kuniko Horie-Inoue<sup>1</sup>, Saya Nagasawa<sup>1</sup>, Satoru Takeda<sup>2</sup>, Satoshi Inoue<sup>3</sup>. <sup>1</sup>Division of Gene Regulation and Signal Transduction, Research Center for Genomic Medicine, Saitama Medical University, Japan, <sup>2</sup>Department of Obstetrics and Gynecology, Juntendo University School of Medicine, Tokyo, Japan, Japan, <sup>3</sup>Department of Functional Biogerontology, Tokyo Metropolitan Institute of Gerontology, Tokyo 173-0015, Japan, Japan

**[Objective]** It is suggested that estrogen deficiency is associated with musculoskeletal diseases in postmenopausal women as well as women with amenorrhea. Estrogen may play physiological roles in maintaining skeletal muscle strength and mass, although its precise mechanism remains to be elucidated. We thus assessed how estrogen modulates exercise performance and skeletal muscle activity in female mice. **[Methods]** Ovariectomized C57BL/6 mice were administered with estradiol benzoate (OVX + E) or vehicle (OVX + V) every 4 days. As a control, sham-operated mice were administered with vehicle (Sham + V). Mice were exercised on a treadmill and gene expression in muscles was examined by microarray analysis. Next, we performed microarray analysis using mouse C2C12 myoblastic cells infected with a recombinant adenovirus expressing constitutively active ERα (Ad-caERα). **[Results]** Mean bone mineral density of OVX + V group was significant lower compared to Sham + V group, whereas that of OVX + E group was higher than OVX + V group. In treadmill test, OVX + V group exhibited a significant shorter running duration than Sham + V group, whereas OVX + E group exhibited almost the same running duration as Sham + V group. Microarray analysis of soleus muscle showed that genes involved in mitochondrial and muscle functions were differentially expressed among groups. Notably, expression levels of uncoupling protein 3 (UCP3) were significantly upregulated by estrogen deficiency and downregulated by estrogen administration. Downregulated Ucp3 along with increase in cellular ATP content was also observed in differentiated myoblastic C2C12 cells infected with Ad-caERα. Microarray analysis of differentiated myoblastic C2C12 cells showed that Ad-caERα infection upregulated expression of a transcriptional factor, which is known as a regulator of oxidative metabolism and mitochondrial activity in skeletal muscle. **[Conclusion]** Estrogen could regulate energy expenditure and exercise endurance in female via modulation of gene expression in muscles.

**Disclosures:** Saki Nagai, None.

## MO0495

**Myostatin Inhibition of Osteoblastic Differentiation by Suppression of Osteocyte-derived Exosomal miR-218 in Vitro: A Novel Mechanism of Muscle-Bone Communication.** Weiping Qin\*, Yuanzhen Peng<sup>1</sup>, Wei Zhao<sup>1</sup>, Paola Divieti Pajevic<sup>2</sup>, Lynda F. Bonewald<sup>3</sup>, William A. Bauman<sup>1</sup>. <sup>1</sup>James J. Peters VA Medical Center, United States, <sup>2</sup>Boston University, United States, <sup>3</sup>Indiana University School of Medicine, United States

Muscle and bone are closely associated in anatomy and function, but the mechanisms to coordinate their synergistic action remain poorly defined. Myostatin, a myokine secreted by muscles, has been shown to inhibit muscle growth while the disruption of the myostatin gene has been reported to cause muscle hypertrophy and high bone mass. Extracellular vesicle-exosomes carrying microRNA (miRNA), mRNA, and proteins are recognized to perform an important role in cell-cell communication. We report herein that myostatin promotes expression of SOST, DKK1, and RANKL in cultured osteocytic (Ocy454) cells, concomitant with the suppression of miR-218 in both the parent Ocy454 cells and derived exosomes. Exosomes produced by Ocy454 cells that are pretreated with myostatin are able to be taken up by osteoblastic MC3T3 cells, resulting in marked reduction of Runx2 and osteoblastic differentiation by the down-regulation of the Wnt signaling pathway. Importantly, the inhibitory effect of myostatin-modified osteocytic exosomes on differentiation of osteoblasts is completely reversed by expression of exogenous miR-218 through down-regulation of SOST. Together, our findings indicate that myostatin directly influences osteocyte function and thereby inhibits osteoblastic differentiation, at least in part, through the suppression of osteocyte-derived exosomal miR-218, suggesting a novel mechanism of muscle-bone communication.

**Disclosures:** Weiping Qin, None.

## MO0496

**Lack of a direct effect of FGF23 on skeletal muscle contractility,  $\text{Ca}^{2+}$  handling and development.** Julian A. Vallejo<sup>\*1</sup>, Keith G. Avin<sup>2</sup>, Neal X. Chen<sup>3</sup>, Kun Wang<sup>4</sup>, Chad D. Touchberry<sup>5</sup>, Marco Brotto<sup>6</sup>, Sarah L. Dallas<sup>4</sup>, Sharon M. Moe<sup>3</sup>, Michael J. Wacker<sup>5</sup>. <sup>1</sup>Department of Biomedical Science, School of Medicine, University of Missouri-Kansas City; Department of Biomedical Sciences, School of Medicine, University of Missouri-Kansas City, United States, <sup>2</sup>Department of Physical Therapy, School of Health & Rehabilitation Sciences, Indiana University; Division of Nephrology, School of Medicine, Indiana University, United States, <sup>3</sup>Division of Nephrology, School of Medicine, Indiana University, United States, <sup>4</sup>Department of Oral & Craniofacial Sciences, School of Dentistry, University of Missouri-Kansas City, United States, <sup>5</sup>Department of Biomedical Science, School of Medicine, University of Missouri-Kansas City, United States, <sup>6</sup>College of Nursing and Health Innovation, University of Texas-Arlington, United States

Skeletal muscle dysfunction accompanies the clinical disorders of chronic kidney disease (CKD) and hereditary hypophosphatemic rickets/osteomalacia. In both disorders serum fibroblast growth factor 23 (FGF23), a bone-derived hormone regulating vitamin D and phosphate metabolism, becomes chronically elevated. Elevated FGF23 has been shown to play a direct role in cardiac muscle dysfunction in CKD, however, it is unknown whether FGF23 can also directly induce dysfunction of skeletal muscles. Therefore, we assessed functional parameters of isolated murine fast twitch (extensor digitorum longus, EDL) or slow-twitch (soleus) muscle groups, as well as  $[\text{Ca}^{2+}]_i$  handling properties, markers of cellular proliferation, muscle fiber development and oxidative stress in C2C12 cells after treatment with various amounts of FGF23. Gene expression of FGF receptors (1-4) and *α-Klotho* was first verified in CD1 mice and the 2-Cy/+ rat (a naturally occurring rat model of CKD-mineral bone disorder) and cell-based models via real time-PCR. Acute FGF23 (9 ng/ml) administration had no effect upon isolated EDL or soleus muscle contractile force or kinetics, force-frequency relationship, or rate of fatigue and recovery from fatigue (n=6-8 mice per group). In C2C12 myotubes, FGF23 exposure (20 ng/ml) did not directly increase  $[\text{Ca}^{2+}]_i$ , nor did C2C12 cells treated with FGF23 for 24 hours or six days during myotube development show a difference in myotube  $\text{KCl}$  and caffeine-induced  $\text{Ca}^{2+}$  release properties measured using the  $\text{Ca}^{2+}$  indicator dye Fluo-4 (n=3-6 dishes per group with 5-11 averaged cells per dish). Moreover, FGF23 (2.5-100 ng/ml) did not alter C2C12 myoblast proliferation, expression of myogenic genes or oxidative stress marker 8-OHdG in C2C12 myotubes (n=3). In conclusion, although skeletal muscles express the components involved in FGF23-mediated signaling, in vitro FGF23 treatments failed to directly alter skeletal muscle function or development under the conditions tested. It is possible that downstream targets of FGF23 signaling such as phosphorous/vitamin D metabolism, parathyroid hormone level, uremia and/or inflammatory state may be central to muscle dysfunction in hereditary hypophosphatemic rickets/osteomalacia and CKD.

**Disclosures:** Julian A. Vallejo, None.

## MO0497

**Innate IgM Natural Antibodies against oxidized phospholipids decline with age in mice: a putative contributor to the declining bone formation and a novel target for bone anabolic therapy.** Elena Ambrogini<sup>\*1</sup>, Michela Palmieri<sup>1</sup>, Li Han<sup>1</sup>, Stuart B Berryhill<sup>1</sup>, Xuchu Que<sup>2</sup>, Sotirios Tsimikas<sup>2</sup>, Stavros C Manolagas<sup>1</sup>, Joseph L Witztum<sup>2</sup>, Robert L Jilka<sup>3</sup>. <sup>1</sup>Center for Osteoporosis and Metabolic Bone Diseases, University of Arkansas for Medical Sciences and the Central Arkansas Veterans Healthcare System, United States, <sup>2</sup>Department of Medicine, University of California San Diego, United States, <sup>3</sup>Center for Osteoporosis and Metabolic Bone Diseases, University of Arkansas for Medical Sciences, United States

Lipid peroxidation leads to the formation of highly reactive molecules, such as 4-hydroxynonenal (4-HNE) and oxidized phospholipids that form adducts with amino groups of proteins and other lipids, collectively known as oxidation specific epitopes (OSEs). OSEs have strong proinflammatory properties and, unless they are removed, can cause extensive cell damage. Persistent and/or excessive generation of OSEs has been implicated in the pathogenesis of several age-associated diseases. B-1 lymphocytes of the innate immune system produce germline encoded anti-OSE Natural Antibodies (NABs) that are predominantly of the IgM class. By binding to OSEs, these NABs can protect against the adverse effects of OSEs. We have previously reported that loss of cancellous bone with age in mice is associated with increased lipid peroxidation as evidenced by increased levels of 4-HNE in bone extracts. Moreover, overexpression of the antigen-binding domain of E06 – a prototypic mouse anti-OSE IgM that recognizes the phosphocholine of oxidized phospholipids (PC-OxPL) – increased vertebral and femoral cancellous bone mass in 5-month-old mice. In addition, PC-OxPL decreased the replication, differentiation and survival of osteoblast progenitors in vitro; and all these effects were reversed by purified E06 IgM as well as serum from mice overexpressing the antigen-binding domain of E06. Hence, lipid peroxidation restrains bone formation even under physiologic conditions; and endogenous levels of anti-OSE antibodies are insufficient to fully prevent the adverse effects of PC-OxPL on the skeleton. In view of the above, and evidence that the B-1 cells that produce anti-OSE antibodies decline with age in humans, we measured serum levels of anti-OSE antibodies in aging mice using an

ELISA. We found that the level of anti-PC IgM antibodies decreased to practically undetectable levels in serum from 21-26 month old female C57BL/6J mice, as compared to 6-month old females. This antibody decrease was associated with decreased vertebral cancellous bone mass, decreased femoral cortical thickness, and increased femoral cortical porosity, as determined by microCT. We conclude that diminished B-1 cell number or function leads to a decrease in IgM NABs, which decreases the defense against the anti-osteogenic effects of OSEs and contributes to age-related decrease of bone formation. Synthetic anti-OSEs, therefore, may represent a novel bone anabolic therapy for involutional osteoporosis.

**Disclosures:** Elena Ambrogini, None.

## MO0498

**Kynurenine, an endogenous ligand of the aryl hydrocarbon receptor that accumulates with age, stimulates expression of the senescence-associated microRNA miR-183 in bone marrow-derived mesenchymal stem cells.** Andrea Lambert<sup>\*</sup>, Sadanand Fulzele, Bharati Mendhe, William Hill, Carlos Isaacs, Meghan McGee-Lawrence, Xingming Shi, Mark Hamrick, Medical College of Georgia, United States

The tryptophan metabolite kynurenine has been observed to accumulate with age in various organs and tissues. Elevated kynurenine relative to tryptophan is also associated with increased age-related mortality, and the kynurenine pathway is implicated in age-associated diseases such as neurodegeneration and immunosenescence. Moreover, kynurenine is an endogenous ligand of the aryl hydrocarbon receptor (Ahr), and previous studies indicate that mice lacking Ahr have increased bone mass. We tested the hypothesis that kynurenine may play a role in senescence of bone marrow derived mesenchymal (stromal) stem cells (BMSCs) by activating Ahr and modifying expression of Ahr-responsive microRNAs. We focused on miR-183 since we and others have found that members of the miR-183 family can induce cell senescence, inhibit osteogenesis, and stimulate osteoclastogenesis. We first examined age-related changes in miR-183-5p expression from bone marrow cell lysates of young (4-6 mo) and aged (20-24 mo) mice using qRT-PCR, and quantified Ahr expression from cell lysates using ELISA. Results demonstrate that miR-183 expression increases with age by approximately 3-fold in mouse bone marrow, and ELISA assays show that normalized protein levels of Ahr are on average 50% higher in bone cell lysates from aged mice. Primary BMSCs from humans and mice were then treated with increasing concentrations of kynurenine (0-50  $\mu\text{M}$ ) and miR-183-5p expression assayed by qPCR. Mir-183-5p expression was found to increase significantly in a dose-dependent fashion, with 50  $\mu\text{M}$  kynurenine yielding a 5-fold increase in miR-183-5p expression. These data suggest that age-associated increases in kynurenine levels contribute directly to bone loss by activating Ahr and stimulating miR-183 expression in BMSCs.

**Disclosures:** Andrea Lambert, None.

## MO0499

**Kynurenine and SDF-1 $\alpha$  Derived Bone Marrow Mesenchymal Stem Cells in Age-Related Bone Loss: Potential Role of Aryl Hydrocarbon Receptor.** Khaled Hussein<sup>\*1</sup>, Xue Jiang<sup>2</sup>, Ke-Hong Ding<sup>3</sup>, Sadanand Fulzele<sup>4</sup>, Wendy Bollag<sup>5</sup>, Mohammed Elsalanty<sup>6</sup>, Qing Zhong<sup>3</sup>, Xing-ming Shi<sup>7</sup>, Maribeth Johnson<sup>8</sup>, Monte Hunter<sup>9</sup>, Mark Hamrick<sup>1</sup>, Carlos Isaacs<sup>10</sup>, William Hill<sup>11</sup>. <sup>1</sup>Department of Cell Biology and Anatomy Medical College of Georgia, Augusta University, United States, <sup>2</sup>Department of Cell Biology and Anatomy Medical College of Georgia, Augusta University, United States, <sup>3</sup>Department of Cell Biology and Anatomy Medical College of Georgia, Augusta University, United States, <sup>4</sup>Department of Orthopedic Surgery, Medical College of Georgia, Augusta University, United States, <sup>5</sup>Department of Neuroscience and Regenerative Medicine, Medical College of Georgia, Augusta University, United States, <sup>6</sup>Department of Orthopedic Surgery, Medical College of Georgia, Augusta University, United States, <sup>7</sup>Department of Biostatistics and Epidemiology, Medical College of Georgia, Augusta University, United States, <sup>8</sup>Department of Orthopedic Surgery, Medical College of Georgia, Augusta University, United States, <sup>9</sup>Department of Orthopedic Surgery, Medical College of Georgia, Augusta University, United States, <sup>10</sup>Department of Neuroscience and Regenerative Medicine, Department of Orthopedic Surgery, Medicine and Cellular Biology and Anatomy, Medical College of Georgia, Augusta University, United States, <sup>11</sup>Department of Cell Biology and Anatomy Medical College of Georgia, Augusta University, Charlie Norwood VA Medical Center, United States

Aging is associated with significant changes in multiple organ systems, including the proliferative and the osteoprogenitor capacity of bone marrow-derived mesenchymal stem cells (BMMSCs). Recently, high levels of kynurenine (KYN), a Tryptophan (Trp) metabolite, have been linked to many age-associated diseases. The aryl hydrocarbon receptor (Ahr) is a KYN activated transcription factor. Previous studies have



highlighted that mice lacking Ahr have increased bone mass. Stromal cell-derived factor-1 (SDF-1 $\alpha$ /CXCL12 is a member of the pro-inflammatory CXC chemokine family. Our group previously reported the role of SDF-1 $\alpha$  in in-vitro osteogenic differentiation and in-vivo bone formation. In addition, SDF-1 $\alpha$  is an essential factor for migration and homing of BMMSCs. Thus, we hypothesized that KYN induces age-related bone loss by attenuating BMMSCs SDF-1 $\alpha$  levels via activation of Ahr. First we examined changes of KYN/Trp ratio in serum in Old (22 months) versus Young (3 months) mice using HPLC. SDF-1 $\alpha$  levels were also measured in serum and bone marrow interstitial fluid of old versus young mice and in serum of old (> 60 years) versus Young (< 40 years) humans using ELISA. Subsequently, Twelve-month-old, male C57BL/6 mice were fed with high KYN diet compared to high Trp and high protein diet for 8 wks. Bone mineral density (BMD), content (BMC) and morphometric parameters were analyzed using  $\mu$ Ct. In vitro, serial doses of KYN (25, 50, 100, 200  $\mu$ M) were used to treat BMMSCs, in both normoxic and acute hypoxic (3% O<sub>2</sub>) conditions. Levels of SDF-1 $\alpha$  were evaluated in supernatant of these cells using ELISA at 24 and 48 hours. Using WB, AHR translocation into the nucleus of BMMSCs and indoleamine-(2,3)-dioxygenase (IDO1) levels were evaluated at 30 mins and 48 hours, respectively. Our results show that KYN/Trp ratio was increased in serum of old versus young mice. In addition, SDF-1 $\alpha$  levels were significantly decreased in bone marrow of old mice and human subjects. BMD, BMC and bone morphometric parameters were significantly altered in high KYN fed mice. In vitro, KYN induced a decrease in SDF-1 $\alpha$  levels secreted by BMMSCs mainly in hypoxic conditions. Meanwhile, KYN induced activation and translocation of AHR and increased levels of IDO1. These results suggest that elevated levels of KYN might contribute to age related bone loss by attenuating levels of SDF-1 $\alpha$  in BMMSCs via an Ahr dependent pathway.

**Disclosures:** Khaled Hussein, None.

## MO0500

**Kynurenine, a Tryptophan Oxidation Product That Accumulates With Age, Interferes With Fracture Healing.** Kehong Ding<sup>1</sup>, Ariana Reyes<sup>1</sup>, Jianrui Xu<sup>1</sup>, Qing Zhong<sup>1</sup>, Wendy Bollag<sup>1</sup>, Meghan McGee-Lawrence<sup>1</sup>, William Hill<sup>1</sup>, Xingming Shi<sup>1</sup>, Monte Hunter<sup>1</sup>, Sadanand Fulzele<sup>1</sup>, Eileen Kennedy<sup>2</sup>, Ranya Elsave<sup>1</sup>, Mohammed Elsalanty<sup>1</sup>, Maribeth Johnson<sup>1</sup>, Mark Hamrick<sup>1</sup>, Carlos Isales<sup>1</sup>. <sup>1</sup>Medical College of Georgia, United States, <sup>2</sup>University of Georgia, United States

Age dependent accumulation of reactive oxygen species has been proposed to play a pathogenic role in development of osteoporosis. We previously reported that aromatic amino acids (AAs) function as antioxidants and are anabolic for bone. In contrast, oxidation products of these aromatic AAs lead to bone loss because of their detrimental effects on bone marrow derived mesenchymal stem cells (MSCs). We have also reported that kynurenine, the tryptophan oxidation product, accumulates with age and feeding kynurenine to younger mice (3 month old C57BL/6) results in an accelerated aging bone phenotype. The initial step in fracture healing is MSC dependent callus formation and in aging models, fracture callus is smaller and less dense. We hypothesized that the kynurenine metabolite would interfere with skeletal repair. To test this hypothesis, in an IACUC-approved protocol, the right fibulae of twenty 3-month-old C57BL/6 mice were fractured while under anesthesia. The groups were then divided in half, with ten mice receiving treated drinking water containing 1mM kynurenine. In contrast, the control group was provided untreated drinking water. The daily drinking rates of both groups were observed over a 30-day period and found to be about equal, there were no significant differences in weight or body composition after 30 days of kynurenine treatment. At the end of the study period, the right fibula of both groups was harvested and analyzed by micro-CT and histology. We report that the fracture callus in the kynurenine-treated group was significantly smaller than control (22.4 $\pm$ 1.7 vs 17.8 $\pm$ 0.9 %Cntrl vs Kyn; Mean $\pm$ SEM; p<0.02) and less dense (0.23 $\pm$ 0.02 vs 0.19 $\pm$ 0.01 g/cm<sup>3</sup>, Cntrl vs Kyn; Mean $\pm$ SEM; p=0.05). These data suggest that catabolic oxidation products of normally anabolic nutrients can impact fracture healing in the elderly.

**Disclosures:** Kehong Ding, None.

## MO0501

**Mutation of the glycan binding domain of galectin-3 in mice enhances cortical bone mass in males, but trabecular bone mass in females.** Kevin Maupin<sup>1</sup>, Daniel Dick<sup>2</sup>, Tristan Kempston<sup>2</sup>, Audra Guikema<sup>2</sup>, Tina Meringa<sup>2</sup>, Bryn Eagleson<sup>2</sup>, Bart Williams<sup>2</sup>. <sup>1</sup>Indiana University School of Medicine, United States, <sup>2</sup>Van Andel Research Institute, United States

Galectin-3 (Gal3) is a chaperone protein which functions both intracellularly via protein-protein interactions and extracellularly by binding specific glycans on glycoproteins. Our previous studies showed that the global deletion of the Gal3 gene enhanced cortical bone expansion in both male and female mice during aging and in response to gonadectomy. In addition, female Gal3-null mice were protected against age-related loss of trabecular bone. Determining the mechanism driving these phenotypes is complicated by the ability of Gal3 to function both intracellularly and extracellularly. While the mechanism of Gal3 secretion remains to be fully elucidated, studies show that the mutation of a highly conserved arginine to a serine in human Gal3 (Gal3-R186S) blocks glycan binding and secretion. In order to best distinguish between extracellular and intracellular functions of Gal3, we generated mice with the equivalent mutation (Gal3-R200S) using CRISPR/Cas9 directed homologous recombination. Like Gal3-null mice, aged Gal3-R200S females, but not males, had significantly increased trabecular bone mass.

However unlike Gal3-null mice, only male Gal3-R200S mice replicated the increased cortical bone expansion. These results suggest that the trabecular bone phenotype of Gal3-null female mice was driven primarily by loss of extracellular Gal3. However loss of intracellular Gal3 may be necessary for female cortical expansion. Understanding the role of extracellular vs. intracellular Gal3 in enhancing bone mass could lead to improved drug development and better understanding of how Gal3 influences cellular function.

**Disclosures:** Kevin Maupin, None.

## MO0502

**Ephrin Ligand and Receptor Expression during Bone Fracture Repair Indicates Ephrin Regulation of Chondrogenesis and Bone Formation.** Amandeep Kaur<sup>\*</sup>, Weirong Xing, Subburaman Mohan, Charles H Rundle. Loma Linda VA Medical Center, United States

The ephrin families of ligands (efn) and receptors (Eph) are cell surface molecules that regulate the development of diverse type of tissues, including bone. They control proliferation and establish tissue boundaries through cell-to cell signaling with forward (ligand to receptor) and reverse (receptor to ligand) signaling functions. The developmental potential and bone formation functions of ephrin signaling suggest a role for ephrins in endochondral bone fracture repair. Because the ephrins are widely expressed in many developing tissues, we evaluated efn and Eph for changes in their gene expression in fracture tissues that might suggest a regulatory role in fracture repair.

Fracture calluses from 3 to 4 wild-type mice were harvested at weekly intervals from 7 to 28 days post-closed femur fracture, and the total RNA compared by real-time RT-PCR with gene-specific primers. The fold-change in ephrin gene expression was quantified by a dCt comparison with a housekeeping gene, and then normalized for femur expression by a ddCt comparison with the unfractured contralateral diaphysis.

ANOVA determined that the expression of *efnA2* (1.5  $\pm$  0.2 fold at 7 days post-fracture), *efnB1* (1.4  $\pm$  0.1-fold at 14 days) and *EphA4* (1.4  $\pm$  0.1-fold at 7 and 14 days) were significantly up-regulated, while *EphB4* was significantly down-regulated (0.6  $\pm$  0.1-fold at 14 days). *EphB2* trended toward up-regulation at 21 days (2.0  $\pm$  0.4-fold). Immunohistochemistry with ephrin-specific antibodies in the developing callus at weekly intervals revealed the expression of efnA2 in callus fibroblasts, efnB1 and EphB2 in fibroblasts, prehypertrophic chondrocytes and osteoblasts, and EphB4 in endothelial cells, prehypertrophic chondrocytes and osteoblasts. The expression of these efn ligands and Eph receptors during endochondral bone repair indicates a role for efnA2 and efnB1 signaling in chondrocyte development and osteoblast functions. EphA4 has been associated with osteoclast functions, and EphB4 expression in endothelial cells could regulate fracture angiogenesis, as well as chondrogenesis and osteoblast functions. The unique ability of these efn and Eph to elicit forward and reverse signaling could provide additional layers of complexity for regulating fracture healing.

**Disclosures:** Amandeep Kaur, None.

## MO0503

**Prenatal Exposure to Acetaminophen Affects Tissue Mineral Density and Microarchitecture of Young Adult Murine Bone.** Jessica Lavery<sup>\*</sup>, Katelyn Langford, Patricia Hoffman, Tyler Milewski, Patrick T. Orr, Maria E. Squire. The University of Scranton, United States

Acetaminophen affects the cannabinoid system through the metabolite AM404, and previous studies have shown interactions between bone cells (osteoblasts and osteoclasts) and the cannabinoid system that may be influenced by factors including age, genetics, and the site examined. Use of acetaminophen by adults has been associated with an increased risk of fracture, whereas former users of acetaminophen exhibit a decreased fracture risk. To our knowledge, the effects of acetaminophen exposure at earlier stages of bone development are not well known. In this study, we sought to determine if prenatal exposure to acetaminophen affected bone quantity, microarchitecture, and tissue mineral density in the skeleton of young adult (16-week old) female C57BL/6J mice. We used high-resolution (10mm) micro-computed tomography scanning to assess cortical and trabecular bone regions in the femora and tibiae of mice that had been exposed prenatally to acetaminophen (ACET) versus those that had not been exposed prenatally (CTR) to acetaminophen (n=10 each). Trabecular BV/TV was not different in either the metaphyseal or epiphyseal regions of the distal femur or proximal tibia of ACET vs. CTR mice. However, tissue mineral density (TMD) was 5% greater in the femoral and tibial epiphyses, 3% greater in the tibial metaphysis, and 2% greater in the femoral metaphysis of ACET vs. CTR mice (p<0.05 each). Tb.Th was 12% greater in the femoral epiphysis and 30% greater in the tibial epiphysis of ACET mice as compared to CTR (p<0.05 each). In cortical bone, ACET mice had 3% and 4% higher cortical TMD in the femoral and tibial mid-diaphysis, respectively, as compared to CTR mice (p<0.05 each). Ct.Th was also 4% greater in the femoral (but not tibial) mid-diaphysis of ACET vs. CTR mice (p<0.05). Finally, Ct.BV was 5% greater in the tibia of ACET vs. CTR mice (p<0.05). In summary, with the exception of the tibial mid-diaphysis, bone quantity was unaffected in ACET vs. CTR mice, yet young adult female ACET mice had greater tissue mineral density in all regions examined and some, but not all, regions saw an increase in trabecular or cortical bone thickness. These findings suggest an increase in mineralization despite similar tissue quantity following prenatal exposure to acetaminophen and that the effects on bone may vary depending on the site examined. Additional work is needed in order to further understand how bone may respond to exposure to acetaminophen during development and growth.

**Disclosures:** Jessica Lavery, None.

## MO0504

**Molecular changes triggered in local osteoprogenitors at the onset of bone remodeling.** Pia Rosgaard Jensen<sup>1</sup>, Thomas Levin Andersen<sup>1</sup>, Tanja Tvistholm Sikiær<sup>2</sup>, Lars Reinmark<sup>2</sup>, Charlotte Ejersted<sup>3</sup>, Jean-Marie Delaisse<sup>1</sup>. <sup>1</sup>Clinical Cell Biology, Lillebaelt/Vejle Hospital, Institute of Regional Health Research, University of Southern Denmark, Denmark, <sup>2</sup>Institute of Clinical Medicine, Aarhus University Hospital, Denmark, <sup>3</sup>Department of Endocrinology, Odense University Hospital, Denmark

The flat osteoblast lineage cells interposed between the quiescent bone surfaces (QS) and the bone marrow have been recognized as an important source of bone forming osteoblasts – both based on cell tracing in mouse and on human bone histology. At an early stage of remodeling, some of these cells spread over the eroded surface generated by osteoclasts, and become so-called reversal cells. Others form a continuous canopy of osteoprogenitors covering the osteoclasts, reversal cells and osteoblasts, and establish close contacts with capillaries at the bone marrow side. Later, both reversal and canopy cells transform into bone forming osteoblasts. Here we address the early molecular changes occurring in these cells when they switch from their quiescent environment to either the eroded surface or the canopy. Immunostainings and in situ hybridizations of specific markers were performed on iliac crest bone biopsies from 11 healthy women (age 36-71 years). The nerve growth factor receptor CD271, reported to define a subtype of mesenchymal cells with dendritic features, stains virtually all cells over the QS and in the canopy but significantly less reversal cells on eroded surfaces (Odd Ratio (OR) vs. QS 0.4,  $p < 0.01$ ). Smooth muscle actin (SMA) and PDGF-R $\alpha$  which are early osteoblast lineage markers related with migration, are strongly induced in canopy cells (for both markers OR vs. QS  $> 11$ ,  $p < 0.01$ ), but much less (SMA: OR 1.2,  $p < 0.05$ ) or not (PDGF-R $\alpha$ ) in reversal cells. Furthermore, MMP-13 and fibronectin, also early osteoblast lineage markers, are uniquely induced upon contact with osteoclasts, whether in canopy cells (OR vs. away of osteoclasts 18.6 and 4.2, respectively,  $p < 0.005$ ) or reversal cells (for both markers OR vs. away of osteoclasts 6.8,  $p < 0.001$ ). The proliferation marker Ki67 is induced both in some canopy and reversal cells (for both cell types OR vs. QS  $> 2.2$ ,  $p < 0.002$ ). FZD9, a WNT receptor, stains most of the cells over the QS and this prevalence of FZD9-positive cells does not vary in the canopies but drops a little on reversal surfaces (OR vs. QS 0.75,  $p < 0.01$ ). These diverse specific changes in expression/immunoreactivity reflect the onset of osteoblast differentiation as it occurs in vivo respectively in the canopy and on the eroded surfaces. Thereby, the present study is first to define the osteoblast differentiation program in relation with spatiotemporal features of remodeling sites, and it highlights the critical role of osteoclast contacts.

**Disclosures:** Pia Rosgaard Jensen, None.

## MO0505

**IL-4, but not IL-6 and IL-17F, Significantly Inhibits Osteogenic Differentiation of Human Adipose Stem Cells under Hypoxia.** Angela P. Bastidas-Coral<sup>1</sup>, Astrid D. Bakker<sup>1</sup>, Jolanda M.A. Hogervorst<sup>1</sup>, Cees J. Kleverlaan<sup>2</sup>, Tim Forouzanfar<sup>3</sup>, Jenneke Klein-Nulend<sup>1</sup>. <sup>1</sup>Department of Oral Cell Biology, Academic Centre for Dentistry Amsterdam (ACTA), University of Amsterdam and Vrije Universiteit Amsterdam, Amsterdam Movement Sciences, Amsterdam, The Netherlands, Netherlands, <sup>2</sup>Department of Dental Materials Science, Academic Centre for Dentistry Amsterdam (ACTA), University of Amsterdam and Vrije Universiteit Amsterdam, Amsterdam, The Netherlands, Netherlands, <sup>3</sup>Department of Oral and Maxillofacial Surgery, VU University Medical Center / Academic Centre for Dentistry Amsterdam (ACTA), Amsterdam Movement Sciences, Amsterdam, The Netherlands, Netherlands

**Introduction:** Increased understanding of the inflammatory phase of bone healing is important to improve strategies using mesenchymal stem cells (MSCs) for the treatment of large bone defects. The cytokines IL-4, IL-6, and IL-17F are expressed in the first three days of bone healing when hypoxia prevails. They are known to differentially affect MSC proliferation and osteogenic differentiation in vitro under normoxia. The cytokine and hypoxia-activated pathways, as occur in vivo, may have additive or even synergistic effects in MSCs. To better predict the effects of cytokines on MSC-aided bone healing, we investigated the effect of IL-4, IL-6, and IL-17F on MSC proliferation and osteogenic differentiation under hypoxia.

**Methods:** Human adipose stem cells (hASCs) were stimulated with or without 1 or 10 ng/ml IL-4, IL-6, or IL-17F, under hypoxia (1% O<sub>2</sub>) for 3 days. Quantification of proliferation (DNA, Ki67 gene expression), osteogenic differentiation (RUNX2, COL1, osteocalcin gene expression), alkaline phosphatase (ALP) activity, bone nodule formation (alizarin red staining), and vasculogenic stimulation potential (VEGF protein and gene expression) was performed up to day 14.

**Results:** IL-4 decreased RUNX2 expression at day 2 (3.5-fold; 10 ng/ml), and at day 7 (2.7-5.3-fold; 1 and 10 ng/ml). IL-4 (10 ng/ml) decreased COL1 expression (3.6-fold) at day 7. In contrast to IL-6 and IL-17F, IL-4 enhanced osteocalcin expression at day 2 (5.4-6.3-fold; 1 and 10 ng/ml), and at day 7 (2.3-fold; 10 ng/ml). IL-4 at 1 and 10 ng/ml decreased ALP activity (12.0-13.3-fold), VEGF gene expression (6.2-7.9-fold), and protein concentration (2.0-fold) at day 7. IL-4 at 1 and 10 ng/ml strongly decreased bone nodule formation at day 14. IL-6 at 10 ng/ml decreased DNA content (1.25-fold), but increased RUNX2 expression (3.2-fold) at day 2, while decreasing its expression

(5.8-fold) at day 7. IL-6 at 1 ng/ml decreased VEGF expression (1.7-fold) at day 7. Finally, IL-17F at 10 ng/ml decreased VEGF expression (2.3-fold) at day 7.

**Conclusion:** IL-4, IL-6, and IL-17F reduced rather than enhanced proliferation and osteogenic differentiation of hASCs under hypoxia. Specifically IL-4 strongly inhibited osteogenic differentiation of hASCs. This suggests that IL-4 may delay the bone healing process using MSCs as a strategy for bone regeneration procedures.

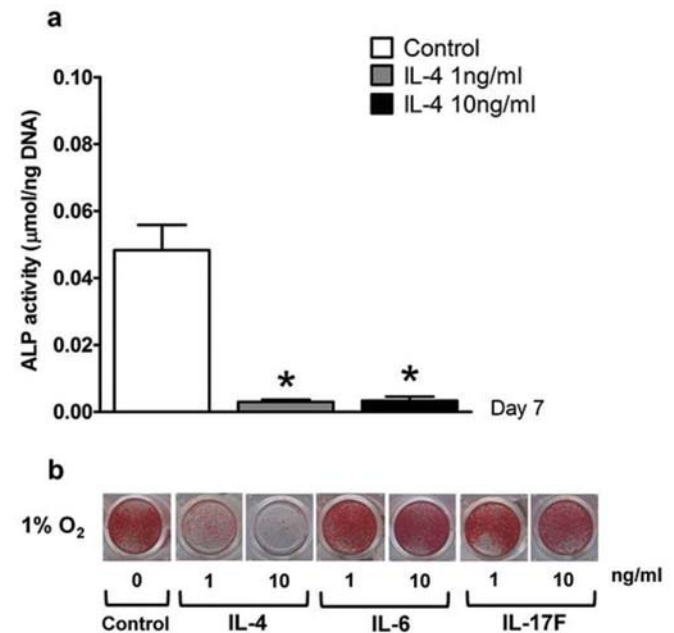


**Figure 1. a)** IL-4 at 1 and 10 ng/ml decreased ALP activity under hypoxia at day 7. Results are mean  $\pm$  SD,  $n = 6$ . \*Significant effect of cytokine treatment,  $p < 0.05$ . **b)** IL-4 at 1 and 10 ng/ml decreased mineralization of hASCs (alizarin red staining) under hypoxia at day 14 compared to untreated control. IL-6 and IL-17F did not affect mineralization.

Bastidas Coral attachment

**Disclosures:** Angela P. Bastidas-Coral, None.

## MO0506

**Inducible Cre Targeting of Bone and Vascular Cells during Various Modes of Fracture Repair.** Evan Buettmann<sup>\*</sup>, Nicole Migotsky, Jennifer McKenzie, Matt Silva. Washington University in St. Louis, United States

Osteogenesis in response to bone injury occurs through endochondral or intramembranous ossification and requires angiogenesis. We are interested in the mechanisms by which angiogenesis and osteogenesis are coordinated *in vivo* during bone healing. In recent years Osterix (Ox), Dentin Matrix Protein-1 (Dmp1), and Cadherin-5 (Cdh5) CreERT2 drivers have been generated to inducibly target bone and vascular cells. These tools have great value to address bone-vascular interactions, although their targeting specificity in mouse models of bone repair remains unclear. We completed an observational study of their expression patterning in established mouse models of intramembranous healing (stress fracture) and endochondral healing (full fracture). We hypothesized that Ox targets all osteoblast lineage cells, Dmp1 targets only osteocytes, and Cdh5 targets only endothelial cells. To test our hypothesis, 12-week old male and female transgenic mice carrying Ox<sup>-</sup>, Dmp1<sup>-</sup>, or Cdh5-CreERT2 crossed with Ai9 were subjected to cyclic axial forelimb compression (stress fracture,  $n = 12$ /strain) or three-point bending of the femur (full fracture,  $n = 9$ /strain). Mice were given tamoxifen chow starting 1 week before fracture and continuously until death at day 10 (stress fracture) or 14 (full fracture). Cre positive mice not given tamoxifen were used to assess non-inducible Cre activation. Histological sections (decalcified, frozen) showed that Ox labeled the majority of cells on periosteal, endosteal and woven bone surfaces as well as intracortically (osteocytes). Hypertrophic chondrocytes within the soft full fracture callus were also labeled by Ox. In contrast, Dmp1 was less effective at targeting all osteocytes and was activated in muscle. Cdh5 labeled vessels were seen only in newly formed woven bone, cortical bone and surrounding muscle. Contrary to our hypothesis, neither Ox nor Dmp1 are effective at exclusively targeting osteoblasts and osteocytes when dosed continuously with tamoxifen during fracture healing, although Ox targeted a greater proportion of osteocytes and did not target muscle. Cdh5 appears to be a good candidate for assessing endothelial cellular contributions to healing, but caution must be taken as Cdh5 is non-inducibly expressed in muscle (not shown). This study highlights the benefits and drawbacks of inducible Cre lines in fracture healing and reinforces the need for investigators to confirm which cell types may be targeted in each model.



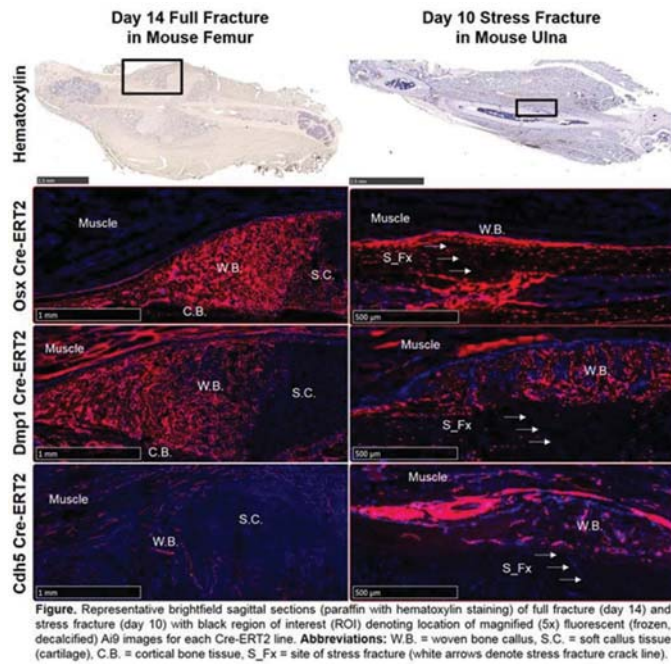


Figure: A19 Bone Fracture

Disclosures: Evan Buettmann, None.

## MO0507

**Status of the Blood-Nerve Barrier is Critical for Both Neuroma Formation and Heterotopic Ossification.** Eleanor Davis<sup>\*1</sup>, Austin Dickerson<sup>1</sup>, Dustin Neubauer<sup>1</sup>, Zbigniew Gugala<sup>2</sup>, Elizabeth Salisbury<sup>2</sup>, Elizabeth Olmsted-Davis<sup>1</sup>, Alan Davis<sup>1</sup>. <sup>1</sup>Baylor College of Medicine, United States, <sup>2</sup>University of Texas Medical Branch, United States

Studies identifying the earliest stages of heterotopic ossification (HO) after BMP2 induction in the mouse demonstrate the presence of  $\beta$ 3-adrenergic receptor (ADRB3)-expressing cells in peripheral nerves. Activation of ADRB3 in cells within the perineurium causes them to undergo replication, mitochondrial expansion, and expression of uncoupling protein 1 (UCP1). Cells in the perineurium migrate towards the new bone formation and a subset express the glutamate aspartate transporter (GLAST) normally found associated with astrocytes. We recently identified similar cells in human tissues associated with HO. These ADRB3+, GLAST+, UCP1+ cells localize near PGP9.5+ cells (neurons) and express the neural guidance molecule reelin, suggesting involvement in directing nerve growth for innervation of the newly forming bone. We propose that these glial-like cells function like astrocytes and coordinately regulate vascular and neural ingrowth. Addition of cromolyn, a blocker of mast cell degranulation and cell egress from the perineurium, results in total suppression of UCP1 expression and a significant decrease in HO. These same cells also expand during neuroma formation. Using a rat model of neuroma, we have shown that both perineurial cells and nerve fibers undergo expansion. Selective suppression of the perineurial cells through inclusion of an ADRB3 antagonist (L-748,337), leads to complete suppression of neuroma formation. Studies are underway to identify whether the antagonist blocks blood-nerve barrier opening, which is associated with neuroma formation. Since perineurial cells play a key role in maintaining the BNB, studies are also underway to determine if the BNB remains closed because of L-748,337 treatment, which ultimately suppresses axonal growth. Surprisingly, studies in the rat using a similar model of HO show that bone formation will only occur when the BNB is open, indicating a relationship between these processes. Finally, we are currently measuring the changes in UCP1 expression and cell replication in the presence of this antagonist during HO. Our findings demonstrate suppression of both HO and neuroma formation through blocking expansion of the ADRB3+ cells by delivering L-748,337. Hence, peripheral nerve trauma leading to neuroma formation in combination with skeletal damage may trigger HO.

Disclosures: Eleanor Davis, None.

## MO0508

**Nerve Injury is a Prerequisite for Neurogenic Heterotopic Ossification.** Austin Dickerson<sup>\*1</sup>, Dustin Neubauer<sup>1</sup>, Eleanor Davis<sup>1</sup>, Corinne Sonnet<sup>1</sup>, Zbigniew Gugala<sup>2</sup>, Alan Davis<sup>1</sup>, Elizabeth Olmsted-Davis<sup>1</sup>. <sup>1</sup>Baylor College of Medicine, United States, <sup>2</sup>University of Texas Medical Branch, United States

Heterotopic ossification (HO) is the de novo formation of bone in extraskeletal soft tissue. Our studies in rodents have shown that peripheral nerves house osteogenic

progenitors. Attempts to induce HO in a rat model proved to be more complex than in a mouse model, likely due to the multi-fascicled structure and epineurium of rat peripheral nerves, which provide a much greater blood nerve barrier (BNB). However, if the rat nerves are injured in the presence of low dose BMP-2, the BNB opens, leading to rapid bone formation.

Wistar rat skin fibroblasts were transduced with Ad5BMP-2 and injected into the hind limb near the sciatic nerve. Rats (n=4) received a peripheral nerve injury (PNI) consisting of either a stretch, crush, loose constriction with chronic gut, or sham exposure (control). The status of the BNB was then determined at 1 day and 2 weeks by measuring Evans blue dye, which will only enter the nerve when the barrier is open. The nerve was harvested and the dye concentration within the nerve was quantified using spectrophotometry at 620 nm. Bone formation was analyzed using radiography and histology.

In the rat model, HO is not induced by intramuscular injection of BMP-2- producing cells. Bone formation was only achieved when a PNI accompanied the injection of the cells. Spectrophotometric readings demonstrated significantly higher levels of dye in the nerves that sustained injuries versus the contralateral control nerve in the same animal. Interestingly, small amounts of HO were observed in the crush injury model, where we observe the lowest level of dye uptake by the nerve, while alternatively, the largest amounts of HO were observed in the samples that correlated with high levels of dye uptake.

Our findings indicate that PNI plays a critical role in the induction of BMP-2 mediated HO. Previous studies have implicated neuroinflammation in HO. The complexity of the nerve in larger species like the rat necessitates an additional mechanical or chemical opening of the barrier, either for the entrance of BMP-2 into the nerve or exit of osteogenic progenitors. In the mouse, peripheral nerves have only a single fascicle and the nerve sheath is far less substantial. Rat peripheral nerves are multi-fascicled and have a fully developed epineurium. The confirmation of a neural origin and role of the BNB in HO indicates a mechanistic link between the two processes that has yet to be clearly defined, but appears vital to the understanding of neurogenic HO.

Disclosures: Austin Dickerson, None.

## MO0509

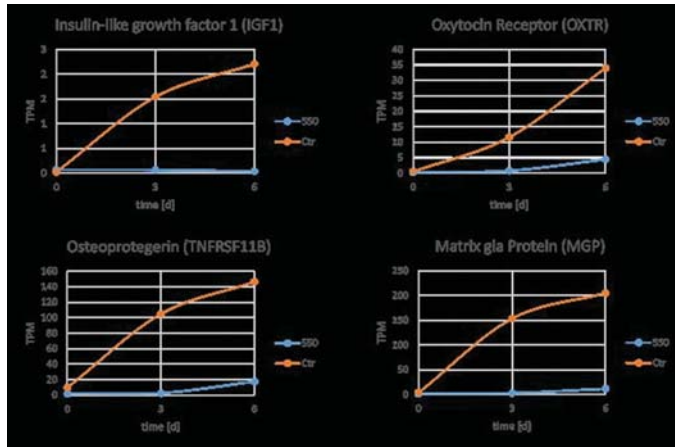
**miR-550a-5p inhibits osteogenic differentiation of immortalized human mesenchymal stem cells.** Matthias Hackl<sup>\*1</sup>, Viktoria Wiedemann<sup>1</sup>, Susanna Skaliky<sup>1</sup>, Elisabeth Geiger<sup>1</sup>, Moustapha Kassem<sup>2</sup>, Jamie Soul<sup>3</sup>, Jean-Marc Schwartz<sup>3</sup>, Tina Schleicher<sup>4</sup>, Yadhu Kumar<sup>4</sup>, Johannes Grillari<sup>5</sup>. <sup>1</sup>TAmiRNA GmbH, 1190 Vienna, Austria, Austria, <sup>2</sup>Department of Endocrinology, University Hospital of Odense and University of Southern Denmark, DK-5000, Denmark, <sup>3</sup>University of Manchester, Manchester, UK, United Kingdom, <sup>4</sup>GATC Biotech, Konstanz, Germany, Germany, <sup>5</sup>Department of Biotechnology, BOKU - University of Natural Resources and Life Sciences, Vienna, Austria

**Purpose:** Circulating microRNAs (miRNAs) are promising biomarkers for bone diseases, such as osteoporosis. Information whether miRNAs can impact bone metabolism is, however, only partially available. We have previously identified miR-550a, a primate-specific microRNA, as a specific and sensitive biomarker for fracture-risk in postmenopausal women, and observed that miR-550a inhibits osteogenic and adipogenic differentiation of telomerase-immortalized primary human adipose tissue derived stem cells (hASC-TERT). In this study, we aimed to confirm these results using telomerase-immortalized bone marrow-derived stromal (mesenchymal) stem cells (hMSC-TERT), to identify potential target genes of miR-550a, and to explore the mechanism by which miR-550a regulates osteogenic differentiation.

**Methods:** hASC-TERT and hMSC-TERT were transfected with miR-550a miRNA mimics or a negative control, and osteogenic differentiation was induced. Total RNA from hASC-TERT was harvested after transfection but prior to osteogenic differentiation as well as on day 3 and day 6 during differentiation. RNA-Seq was used to identify up- and downregulated genes following transfection, and observed changes were confirmed by qPCR.

**Results:** Human miR-550a-5p is a strong negative regulator of osteogenic differentiation of both hASC-TERT and hMSC-TERT, which was clearly established on the basis of reduced ALP activity and mineralized matrix calcium deposition as well as osteoblast biomarker expression. Whole transcriptome sequencing (RNA-Seq) was used to explore the underlying mechanism. The analysis was focused on 71 genes that were significantly regulated upon osteogenic differentiation in hASC-TERT at day 3 (log<sub>2</sub>FC>2), 35 of which were negatively regulated by miR-550a overexpression, compared to the control. Among these genes, Matrix Gla protein (MGP), Oxytocin receptor, Osteoprotegerin and IGF1 were selected for further analysis, since they contain putative binding sites and were downregulated after miR-550a overexpression. qPCR and luciferase-reporter assays in hMSC-TERT transfected with miR-550a confirmed the interaction with these genes.

**Conclusion:** These results shed light on putative mRNA targets of miR-550a-5p, which could mediate its strong inhibitory effect on osteogenic differentiation. Through the inhibition of osteoprotegerin, the soluble decoy-receptor of RANK-Ligand, miR-550a might indirectly affect osteoclast differentiation and tilt the balance of bone homeostasis.



Downregulated genes upon miR-550a overexpression

**Disclosures:** Matthias Hackl, None.

## MO0510

**H3K9MTase G9a regulates tooth development in mice.** Hisashi Ideno<sup>\*1</sup>, Taichi Kamiunten<sup>2</sup>, Akemi Shimada<sup>1</sup>, Tatsuo Terashima<sup>3</sup>, Kazuhisa Nakashima<sup>1</sup>, Yasuhiro Tomooka<sup>4</sup>, Yoshiki Nakamura<sup>2</sup>, Hiroshi Kimura<sup>5</sup>, Makoto Tachibana<sup>6</sup>, Akira Nifuji<sup>1</sup>. <sup>1</sup>Department of Pharmacology, Tsurumi University School of Dental Medicine, Japan, <sup>2</sup>Department of Orthodontics, Tsurumi University School of Dental Medicine, Japan, <sup>3</sup>Department of Biochemistry and Molecular Biology, Tsurumi University School of Dental Medicine, Japan, <sup>4</sup>Biological Science & Technology, The Tokyo University of Science, Japan, <sup>5</sup>School of Life Science and Technology, Tokyo Institute of Technology, Japan, <sup>6</sup>Institute for Enzyme Research, The University of Tokushima, Japan

The expression of cell lineage specific genes during cell differentiation or tissue development is subjected to the epigenetic as well as genetic regulation. Posttranslational modifications of histone tails are important epigenetic marks. Among them, methylation at histone 3 lysine 9 (H3K9) is a crucial modification that indeed affects gene expression and cell differentiation. The methylations of H3K9 are catalyzed by H3K9 methyltransferase, such as G9a. Previously, we showed specific localization of G9a in the dental mesenchyme during tooth development (Kamiunten et al. 2014), and in the hypertrophic chondrocytes during chondrogenesis (Ideno et al. 2013). Therefore, we hypothesized G9a plays a role in hard tissue formation. G9a-null mice, however, show embryonic lethality, and the function in hard tissue development are unclear. In this study, we used G9a conditional knockout (cKO) mice to elucidate the function of G9a in hard tissue formation in vivo. We used Sox9-Cre mice to delete G9a in cranial neural crest-derived hard tissue. G9a cKO mice showed smaller skull, and tooth germs after embryonic day (E) 15.5. At 3 weeks after birth, small first molars with smaller cusps and unseparated roots were formed. Organ culture of tooth germ derived from cKO mice at E15.5 embryo resulted impaired tooth development, suggesting that tooth development per se is affected independently of skull development. BrdU-labeling experiments revealed that the proliferation rates were decreased in the mesenchyme in G9a cKO mice. In situ hybridization analysis revealed altered localization of genes associated with tooth development. In cKO mice, intensively localized expression of mRNAs encoding bone morphogenic protein (BMP2 and BMP4), Shh, and related Shh signaling components, including gli1, ptc1, and ptc2, in the tooth mesenchyme of cKO mice was generally similar to that at earlier stages in control mice. In addition, expressions of Fgfs, including Fgf-3, Fgf-9, and Fgf-10 were decreased in the mesenchyme in G9a cKO mice. Thus, the expression of genes associated with tooth development was delayed in cKO mice. Our results suggested that the H3K9MTase G9a regulated cell proliferation and timing of differentiation in tooth and that G9a expression in the neural crest was required for proper tooth development.

**Disclosures:** Hisashi Ideno, None.

## MO0511

**Whole transcriptome analysis of MSCs derived from different types of tissue reveals unique profiles.** Satoru Onizuka<sup>\*1</sup>, Yasuhiro Yamazaki<sup>2</sup>, Takayuki Sugimoto<sup>2</sup>, Yumiko Sone<sup>2</sup>, Akira Takeda<sup>2</sup>, Sung-Joon Park<sup>3</sup>, Kenta Nakai<sup>3</sup>, Takanori Iwata<sup>1</sup>, Masayuki Yamato<sup>3</sup>, Teruo Okano<sup>3</sup>. <sup>1</sup>Institute of Advanced Biomedical Engineering and Science, Tokyo Women's Medical University, Japan, <sup>2</sup>Department of Plastic and Aesthetic Surgery, Kitasato University School of Medicine, Japan, <sup>3</sup>Human Genome Center, The Institute of Medical Science, The University of Tokyo, Japan

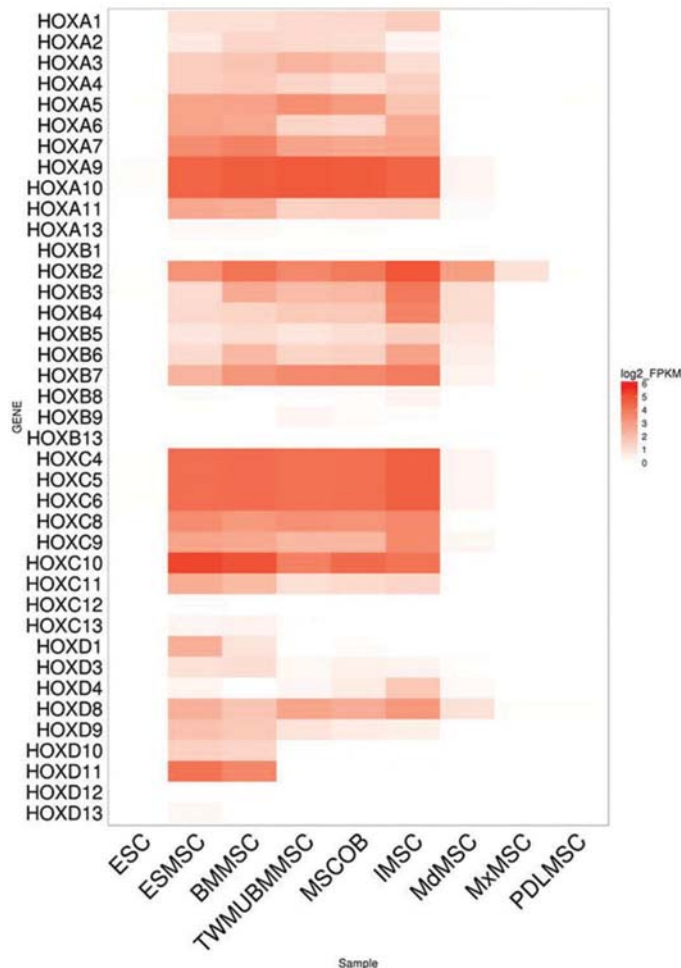
[Background] Multipotent mesenchymal stromal cells (MSCs) possess the ability to differentiate into cells of the mesodermal lineage. In addition to the multipotency, MSCs have self-renewal ability and specific surface marker expression. Although cells possessing these characteristics are commonly categorized as the same cell type ("MSCs"), in reality, it is known that their differentiation capabilities vary depending on the origin tissues. However, the molecular basis of these variations in differentiation potential are not well understood. The purpose of this study was to investigate the variation of gene expression profile among MSCs from several anatomical locations with next-generation sequencing.

[Materials and methods] The experimental protocol was approved by the ethics committee of Tokyo Women's Medical University and Kitasato University. We used MSCs isolated from ilium (I-MSCs), jaw bone (Maxilla and Mandible; Mx-MSCs, Md-MSCs), periodontal ligament (PDL-MSCs), and bone marrow (BM-MSCs), respectively. RNA-sequencing using IonProton system was performed under standard conditions. Sequenced reads were mapped to the human reference genome (hg19) using the TopHat-Cufflinks pipeline. The pipeline quantified FPKM (fragments per kilobase of exons per million) values as the expression levels of coding genes. Differentially expressed genes (DEGs) between MSCs derived from different tissues were defined as fold changes of FPKMs >2.0 and *q*-value (Benjamini-Hochberg correction) <0.05.

[Results] We compared I-MSCs to Mx-MSCs or Md-MSCs, and identified 973 and 365 DEGs, respectively. In these DEGs, we chose the top 20 DEGs that were up-regulated in I-MSCs compared with Mx-MSCs/Md-MSCs. The majority of these DEGs specifically expressed in I-MSCs were HOX gene family. Furthermore, although expression of HOX genes in BM-MSCs were at a similar level to I-MSCs, these genes were rarely expressed in PDL-MSCs, Mx-MSCs, and Md-MSCs.

[Conclusions] Our analysis suggested that gene expression pattern of I-MSCs possessed HOX-positive profile in comparison with Md-/Mx-MSCs. Moreover, BM-MSCs were also HOX-positive profile, but not PDL-MSCs. Hence it follows that MSCs derived from non-craniofacial sites possess HOX-positive profile. Although stromal cells from different anatomical sources are generally categorized as MSCs, differentiation potential and biological function vary, and MSCs may retain memory from the developmental process, including gene expression profile.





Gene expression profile of HOX among various cells

Disclosures: Satoru Onizuka, None.

## MO0512

**WISP-1 associated osteochondral differentiation in heterotopic ossification.** Carolyn Meyers<sup>1</sup>, Semahet Ucer<sup>2</sup>, Michael Chung<sup>2</sup>, David Cholok<sup>2</sup>, John Li<sup>2</sup>, Greg Asatrian<sup>3</sup>, Catherine Ding<sup>3</sup>, Paulina Giacomelli<sup>3</sup>, Edward McCarthy<sup>1</sup>, Benjamin Levi<sup>2</sup>, Aaron James<sup>1</sup>. <sup>1</sup>Johns Hopkins University, United States, <sup>2</sup>University of Michigan, United States, <sup>3</sup>University of California, Los Angeles, United States

**Purpose.** Heterotopic ossification (HO) is the formation of extra-skeletal bone in muscle and soft tissues. Better characterization of the signaling pathways in HO is critical to identifying therapies directed against this common condition. WISP-1 (WNT1-inducible-signaling pathway protein 1) is a CCN family member and is expressed in osteoprogenitor cells, either during skeletal development or fracture repair. The significance of WISP-1 within heterotopic ossification is entirely unknown.

**Methods.** The transcriptome of an experimental, post-traumatic HO model in the mouse limb was examined. Here, combined local Achilles tenotomy coupled with a cutaneous burn injury incites HO development. Next, the temporospatial pattern of WISP-1 protein expression was examined across mouse and human HO. First, Wisp-1 protein expression was examined among genetic (constitutively active *Acvr1*, *Nfate1-Cre*; *caAcvr1*<sup>fl/wt</sup>) and post-traumatic mouse models of HO. Next, the surgical pathology case files of ten human HO specimens were examined for WISP-1 expression. Finally, the effects of siRNA mediated *WISP1* knockdown were examined in human perivascular MSC.

**Results.** RNA Sequencing results showed a ~10 fold enrichment for *Wisp1* during early HO development, which was one of the most highly up-regulated genes. Next, the temporospatial pattern of WISP-1 upregulation was examined in mouse models of HO. Among a post-traumatic HO model and an *Acvr1* driven genetic model, WISP-1 was robustly expressed across multiple cells types giving rise to HO, including cells within cartilage anlagen, osteoblasts, and osteocytes. These findings were next extended to the human patient. Across ten samples of human HO, immunohistochemical staining again showed extensive WISP-1 staining in areas of cartilage, fibrocartilage, and bone. Next, we returned to cell culture studies to determine if *WISP1* antagonism could prevent the process of osteogenic differentiation *in vitro*. Using siRNA, *WISP1* knockdown

significantly inhibited the osteogenic differentiation among human adipose-derived MSC with BMP signaling inhibition.

**Conclusions.** These results demonstrate a dramatic upregulation in WISP-1 expression to the pathophysiology of HO across mouse and human models. WISP-1 antagonism may represent a future therapeutic strategy for the prevention or treatment for this common condition. Ongoing studies are examining the extent to which heterotopic ossification is diminished among *Wisp1* null mice.

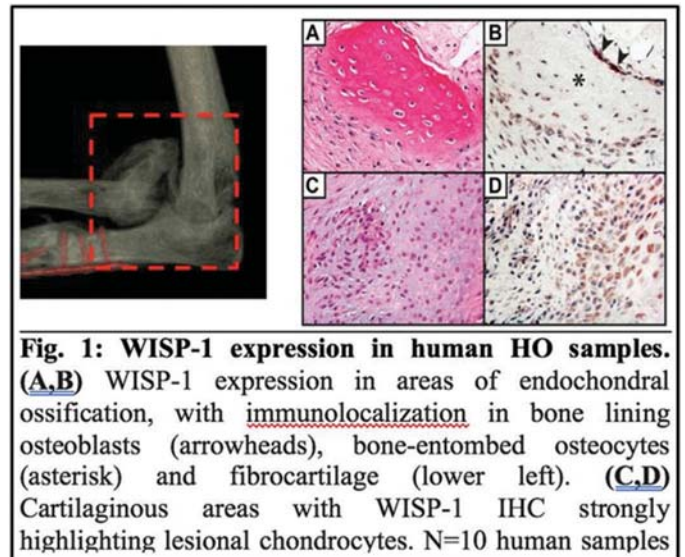


Figure 1

Disclosures: Carolyn Meyers, None.

## MO0513

**Multilayered Nanofiber Mimetic as a Functional Periosteum for Bone Tissue Repair and Reconstruction.** Tao Wang\*, Marc Nuzzo, Yunpeng Yang, Xinping Zhang. University of Rochester Medical Center, United States

Periosteum harbors osteogenic and chondrogenic progenitors and demonstrates remarkable regenerative capacity in repair and reconstruction of injured bone. While an indispensable role of periosteum has been established, engineering of a flexible, transplantable periosteum that simulates the multilayered tissue structure of periosteum have not yet been realized. Utilizing a composite electrospun nanofiber mesh made of polycaprolactone, collagen and hydroxylapatite nanoparticles, we devised a layer-by-layer bottom-up approach to construction of a flexible 3D cellularized tissue graft that could function as a periosteum replacement for successful bone defect repair and reconstruction. Using an established segmental bone graft transplantation model in mice, we showed that the bone-marrow-stromal-cell (BMSC)-seeded, nanofiber-enabled tissue construct developed multiple-layered bone formation at the periosteum sites and further restored the inferior biomechanics of structural bone allograft healing after 6 week of implantation. Interestingly, depending upon the sites of implantation, donor BMSCs initiated either intramembraneous or endochondral bone formation and further recruited host cells to form chimeric bone. Using a windowed cranial defect chamber model that allows real-time, three-dimensional and longitudinal analyses of osteogenesis and angiogenesis of the multilayer periosteum mimetic at the site of defect via multiphoton laser scanning microscopy (MPLSM) in mice, we further showed that nanofiber constructs blocked exuberant angiogenesis and arteriogenesis originated from dura, facilitating host bone formation from the surrounding periosteum. Further seeding of nanofiber with BMSC reversed the aberrant vascular pattern and spatiotemporal changes associated with the chronic inflammatory responses elicited by electrospun nanofibrous materials, leading to marked bone formation and rapid defect closure. Taken together, our study demonstrated an effective engineering platform for construction of a multifunctional and multi-scaled periosteum mimetic for bone defect repair. Our data further revealed an intricate balance between osteogenesis and angiogenesis during nanofiber-mediated repair, underscoring the importance of development smart biomaterials capable of modifying host vascular microenvironment at multiple time scales for effective repair and regeneration.

Disclosures: Tao Wang, None.

## MO0514

**Fibromodulin Reprogrammed Cells: A Safe Source for Musculoskeletal Regeneration.** Pin Ha<sup>1</sup>, Chenshuang Li<sup>2</sup>, Wenlu Jiang<sup>3</sup>, Emily Berthiaume<sup>4</sup>, Zane Mills<sup>5</sup>, Jony Kil Kim<sup>2</sup>, Joyce Wang<sup>6</sup>, Eric Chen<sup>2</sup>, Xinli Zhang<sup>2</sup>, Kang Ting<sup>2</sup>, Chia Soo<sup>7</sup>, Zhong Zheng<sup>2</sup>. <sup>1</sup>Department of Cleft Lip and Palate Surgery, West China Stomatology Hospital, Sichuan University, China, <sup>2</sup>Division of Growth and Development, School of Dentistry, University of California, Los Angeles, United States, <sup>3</sup>State Key Laboratory of Oral Diseases, Department of Orthodontics, West China Hospital of Stomatology, Sichuan University, China, <sup>4</sup>David Geffen School of Medicine, University of California, Los Angeles, United States, <sup>5</sup>Department of Ecology and Evolutionary Biology, University of California, Los Angeles, United States, <sup>6</sup>Department of Emergency Medicine, Highland General Hospital, United States, <sup>7</sup>Department of Orthopaedic Surgery and the Orthopaedic Hospital Research Center, University of California, Los Angeles, United States

Pluripotent or multipotent cell-based therapeutics are vital to the regeneration of non-healing, critical-sized musculoskeletal defects. To date, a major challenge is the generation or isolation of safer and readily available regenerative cell sources *via* a consistent process that bypasses ethical concerns and allogeneic immune rejection. Previously, we established a novel technology platform to reprogram the easily obtainable and expandable human dermal fibroblast to a multipotent state using a single extracellular matrix molecule, fibromodulin (FMD), while circumventing genome integration essential for iPSC generation. Here, we compare the efficacy and safety of yield FMD reprogrammed (FReP) cells and iPSCs for *in vivo* application. In SCID mouse critical-sized calvarial defects, although the spatial co-localization of human markers with osteogenic markers characterized the osteogenic differentiation and engraftment of both iPSCs and FReP cells *in vivo*, FReP cell implantation resulted in new bone formation throughout the entire defects, while bone regeneration was limited to the edge of the defects in the iPSC group (Fig. 1A). Meanwhile, iPSC implantation into the tibialis anterior (TA) muscle of SCID mice led to tumor formation in 25% of the animals (2/8), while none of the FReP cell-implanted animals showed evidence of tumor formation. Instead, the FReP cell-implanted animals had significant increases in skeletal muscle mass (Fig. 1B), as noted by increased spatial overlap of human markers with a skeletal muscle marker on a broad range of the TA muscles demonstrating the differentiation and engraftment of FReP cells (Fig. 1C). Additionally, compared to iPSCs, FReP cells had lower oncogene levels and formed significantly fewer colonies in a soft agar colony formation assay *in vitro*. Because, in comparison with subcutaneous and intramuscular microenvironments, intratesticular stromal cells have an increased propensity to produce a milieu of supportive factors that can foster implanted cells, intratesticular injection was used to further validate the safety of FReP cells *in vivo*. As expected, intratesticular injection of  $1 \times 10^6$  iPSCs resulted in 100% (10/10) teratoma formation. Excitingly, all animals implanted with FReP cells (10/10) were devoid of tumor formation in the 4-month experimental period. Therefore, our data collectively constitute strong evidence that FReP cells are a safe source for inducing musculoskeletal tissue regeneration.

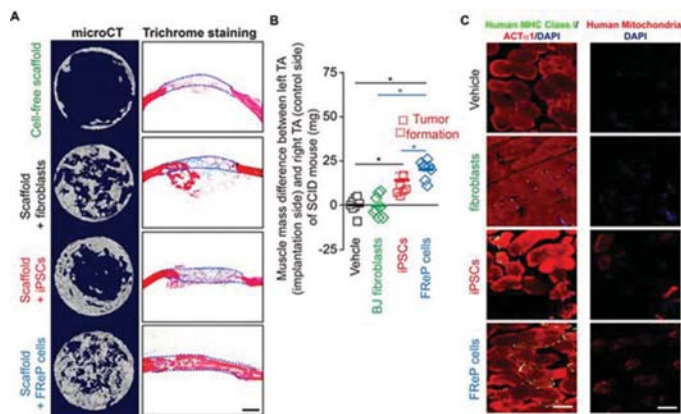


Figure 1: FReP cells for musculoskeletal tissue regeneration.

**Disclosures:** Pin Ha, None.

## MO0515

**Increased migration of cementless acetabular cups in female THR patients with low osteogenic capacity of their bone marrow MSCs.** Jessica Alm<sup>\*</sup>, Sami Finnilä, Niko Moritz, Hannu Aro. Orthopaedic Research Unit, University of Turku, Finland

Bone marrow osteoprogenitor cells (mesenchymal stromal cells, MSCs) are responsible for biological fixation of cementless implants to the surrounding bone, although little is known about how MSC properties of patients correlate with bone healing

capacity *in vivo*. We therefore investigated how the *in vitro* osteogenic capacity of MSCs from female patients undergoing cementless total hip replacement (THR) correlate with the magnitude of migration of uncemented acetabular cups.

A cohort of 16 women with primary hip osteoarthritis (mean age 66 years, range 55-78) underwent successful preoperative analysis of iliac crest bone marrow MSCs as well as two-year radiostereometric analysis (RSA) of acetabular cup migration. Cup migration was analyzed as cumulative micromotions between follow-up time points as a measure of total distance of migration. Osteogenic capacity of MSCs was evaluated as alkaline phosphatase (ALP) expression and mineralization after culturing in osteogenic medium. For analyzing the relationship between *in vitro* osteogenic differentiation and cup migration, patients were classified as having MSCs with high (n=4) or low (n=12) osteogenic (OB) capacity, based on the combined ALP and mineralization outcome (based on tertiles). The two OB-capacity groups were compared for cup migration and demographic parameters using Mann-Whitney U test.

Patients with MSC of low osteogenic capacity displayed increased cumulative distance of cup migration at 2 years compared to patients with high OB capacity MSCs. This was seen for three dimensional (x, y, z vectors) translational (mm) (p=0.006) and rotational (degrees) (p=0.031) movements. This was due to a prolonged period of micro-migration in the low OB-capacity group following the 3 months settling period. While no differences were found in cup movements (translational or rotational) at 3 months, cumulative translational migration from 3 to 24 months was greater in the low OB-capacity group (mean 0.32, SD 0.14 mm) compared to the high OB-capacity group (mean 0.14, SD 0.03 mm, p=0.001). A similar trend was seen for cumulative rotational movements, with 1.2 degrees (SD 0.7) movement in the low OB-capacity and 0.8 degrees (SD 0.1) movement in the high OB-capacity group (p=0.073). There were no difference in basic demographic parameters between the groups.

By applying RSA, this study demonstrated the impact of decreased osteogenic function of MSCs on the biological process of acetabular cup osseointegration.

**Disclosures:** Jessica Alm, None.

## MO0516

**Distinct expression of adipokines and cartilage degradation markers in obese patients with knee osteoarthritis.** Friederike Behler-Janbeck<sup>\*</sup>, Tobias Schmidt, Nicola Oehler, Andreas Niemeier. Department of Orthopedics, Institute of Biochemistry and Molecular Cell Biology, University Medical Center Hamburg Eppendorf, Hamburg 20246, Germany., Germany

Objective: Growing evidence suggests that not only mechanical overload but also systemic metabolic factors contribute to articular cartilage degradation in obesity. The role of adipokines in this context remains incompletely understood. We here analyze the expression of various adipokines in intra- and extra-articular tissues in patients with end-stage knee OA, stratified according to BMI < 25 and BMI > 35, and correlate the adipokine expression with cartilage degeneration markers. Methods: Blood serum, s.c. fat, synovial fluid, synovium and articular cartilage were obtained from 30 TKA patients (primary OA). Cartilage was obtained from the medial compartment and qRT-PCR TaqMan gene expression analysis was performed for the adipokines leptin, adiponectin, visfatin, resistin, the inflammatory markers TNF $\alpha$ , IL6 and IL1 $\beta$ , the cartilage degradation and hypertrophy markers Col2a, ADAMTS 5, ColXa and MMP13 as well as the nuclear receptors liver X receptors  $\alpha$  and  $\beta$  (LXR $\alpha$ ,  $\beta$ ). Protein levels of adipokines and inflammatory markers in serum and synovial fluid were measured by ELISA. Results: There was a significant relationship of BMI (35) with the expression of inflammatory markers in s.c. adipose tissue, confirming adipose tissue inflammation in obesity. In contrast to the inflammatory markers TNF $\alpha$  and IL1 $\beta$  that were not detectable in serum or synovial fluid, the expression levels of adipokines in s.c. fat were reflected in both serum and synovial fluid (lower adiponectin levels in serum and higher leptin levels with BMI>35). Also gene expression of leptin in s.c. fat was significantly higher in obese patients (BMI>35). There were no differences in adipokine expression in articular cartilage or synovial tissue, indicating that adipose tissue inflammation and obesity-induced altered extra-articular adipokine expression has a direct effect on the intra-articular milieu via alteration of synovial fluid protein composition. Interestingly, BMI correlated significantly with cartilage expression of ADAMTS5 but not with COL2, COLXa and MMP13 expression, suggesting a potential direct and specific effect of synovial fluid adipokines on ADAMTS5 expression. In addition, there was an up-regulation of the pharmacologically targetable, lipid activated nuclear receptor LXR $\beta$  in obese cartilage. Conclusion: In obese patients with OA, distinct pathogenic mechanisms begin to evolve and may offer specific therapeutic options for pharmacological interventions in the future.

**Disclosures:** Friederike Behler-Janbeck, None.



## MO0517

**Boldine Inhibits Bone Resorption by Suppressing the Osteoclast Differentiation in Collagen-induced Arthritis.** Zhao Hongyan<sup>1</sup>, Xu Huihui<sup>2</sup>, Qiao Senyan<sup>3</sup>, Lu Cheng<sup>4</sup>, Wang Gui<sup>2</sup>, Liu Meijie<sup>1</sup>, Guo Baosheng<sup>5</sup>, Tan Yong<sup>6</sup>, Xiao Cheng<sup>7</sup>. <sup>1</sup>Experimental research center, China Academy of Chinese Medical Science, China, <sup>2</sup>Institute of Clinical Medicine, China-Japan Friendship Hospital, Beijing University of Chinese Medicine, China, <sup>3</sup>Department of Pathology, the Third People's Hospital of Zhengzhou, China, <sup>4</sup>Institute of Basic Research in Clinical Medicine, China Academy of Chinese Medical Science, China, <sup>5</sup>Institute for Advancing Translational Medicine in Bone & Joint Diseases, School of Chinese Medicine, Hong Kong Baptist University, China, <sup>6</sup>Institute of Basic Research in Clinical Medicine, China Academy of Chinese Medical Science, China, <sup>7</sup>Institute of Clinical Medicine, China-Japan Friendship Hospital, China

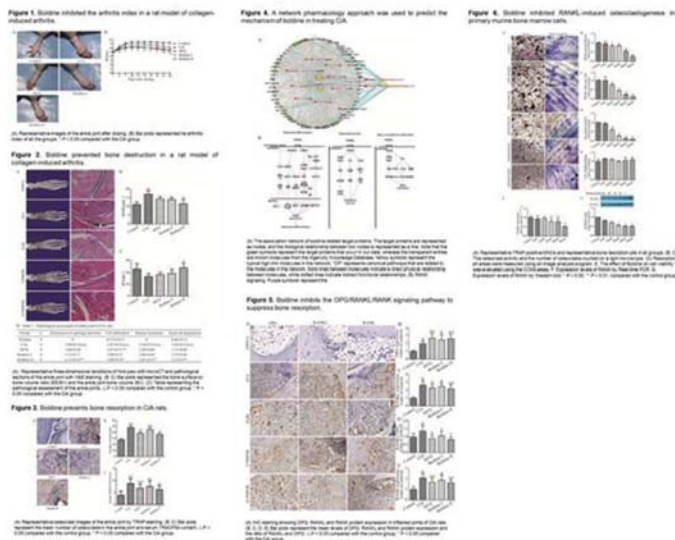
**Introduction:** *Litsea cubeba* (Lour.) Pers. has long been applied in traditional Chinese medicine for the treatment of rheumatism, traumatic injury, common cold, stomach pain. Boldine is an aporphine isoquinoline alkaloid extracted from the root of *Litsea cubeba* and possesses these properties, such as antioxidant, anti-inflammatory, and cytoprotective effects. Our preliminary results showed that boldine significantly improved the bone micro-architecture of the lumbar spine and proximal femur in collagen-induced arthritis (CIA) rats. These results suggested that boldine is at least partly responsible for the pharmacological function and might have a potential role in the prevention of osteoporosis and bone resorption in arthritis. We therefore used CIA rats as the research model to explore the effect of boldine on RA and the molecular mechanism predicted by network pharmacology.

**Material and methods:** CIA rats were orally administered with boldine. The bone destruction of paws was analyzed by histologic examination, TRACP staining and microCT. Prediction of signal pathway associated with boldine network molecules and CIA genes was applied by the network pharmacology analysis. The expressions of osteoprotegerin (OPG), receptor activator of nuclear factor-kappaB (RANK) and its ligand (RANKL) in the ankle were detected by immunohistochemistry. In vitro osteoclasts were cultured in the presence of variable doses of boldine and the RANK expressions were evaluated using RT-PCR and western blot.

**Results:** Boldine reduced ankle swelling, alleviated pathological damage, and significantly prevented bone destruction in CIA rats (Figure 1 and 2). Consistent with this, enzyme linked immunosorbent assay revealed boldine decreased serum TRACP 5b levels and osteoclast number in the ankle region by TRACP staining from CIA rats (Figure 3). The network pharmacology analysis indicated that RANK signaling in osteoclasts was the most significant canonical pathway associated with boldine network molecules and CIA genes, which was verified by the increased expression of OPG, reduced expression of RANK and RANKL, and the ratio of RANKL and OPG in boldine-treated CIA rats (Figure 4 and 5). The in vitro study further confirmed that boldine inhibited osteoclastogenesis by inhibiting the RANKL/RANK signaling pathway (Figure 6).

**Conclusion:** Boldine suppresses osteoclastogenesis by down-regulating the OPG/RANKL/RANK signal pathway and might be a potential therapeutic agent for RA.

## Figures and Tables



Figures and Tables

**Disclosures:** Zhao Hongyan, None.

## MO0518

**Inhibition of the FoxA family of transcription factors ameliorates Osteoarthritis (OA) progression following destabilization of the medial meniscus.** Kailing Ho<sup>1</sup>, Lin Xu<sup>1</sup>, Elena Kozhemyakina<sup>2</sup>, yefu Li<sup>1</sup>, Andrew Lassar<sup>2</sup>, Klaus Kaestner<sup>3</sup>, Malcolm Whitman<sup>1</sup>, Steven Pregizer<sup>1</sup>, Shek Man Chim<sup>1</sup>, Laura Gamer<sup>1</sup>, Vicki Rosen<sup>1</sup>, Andreia Ionescu<sup>1</sup>. <sup>1</sup>HSDM, United States, <sup>2</sup>HMS, United States, <sup>3</sup>Upenn, United States

With initiation of OA, articular cartilage cells leave their quiescent state and acquire a phenotype resembling that of hypertrophic chondrocytes found in the growth plate. Recently, we discovered a new family of transcription factors (FoxA) as important regulators of epiphyseal cartilage hypertrophy. Immunohistochemistry revealed that FoxA1, FoxA2 and FoxA3 are highly expressed in the hypertrophic zone of newborn mouse growth plate, but they are absent from the articular cartilage primordium. In adult knee joints, FoxA1 and FoxA2 were restricted to the calcified zone (below the tidemark) of the articular cartilage but absent from the non-calcified layer (above the tidemark). Next, we wanted to examine FoxA expression in mice challenged with surgical destabilization of the medial meniscus (DMM) which triggers Osteoarthritic cartilage degeneration. We collected RNA from the non-calcified region of the articular cartilage from either sham- or DMM- operated mice at 1week post-surgery via Laser capture microscopy. Quantitative PCR revealed a 5-fold increase in FoxA2 expression in DMM-operated knees as compared to controls. There was no change in FoxA3 expression between sham- and DMM- operated knees, while FoxA1 expression was too low to be detected. This suggests that DMM surgery induced expression of FoxA2 above the tidemark, a place where it's not normally expressed in healthy cartilage. We next asked whether loss of FoxA2 would alter the progression of Osteoarthritis. We employed a mouse line in which tamoxifen-inducible CRE recombinase is driven by the Prg4 (Lubricin) regulatory sequences. We conditionally removed FoxA2 alone (tamoxifen treated Prg4Cre/+;FoxA2fl/fl mice) or in combination with FoxA3 (tamoxifen treated Prg4Cre/+;FoxA2fl/fl;FoxA3-/- mice). While control mice displayed significant cartilage destruction following DMM (average OARSI score 24.7), tamoxifen treated Prg4Cre/+;FoxA2fl/fl mice had an average OARSI score of 18.3, while combined deletion of both FoxA2/3 resulted in an OARSI score of 13.9 (Fig.1). Loss of FoxA2 and FoxA3 expression in either Prg4- or Agg- positive chondrocytes had a similar effect on cartilage degradation caused by DMM. Prg4-driven deletion of FoxA1/2/3 did not further ameliorate cartilage resistance to degradation as compared to Prg4-driven deletion of FoxA2/3 (Fig.2-3). Altogether this suggests that loss of FoxA2 and FoxA3 (but not FoxA1) can slow the progression of cartilage destruction following joint destabilization.

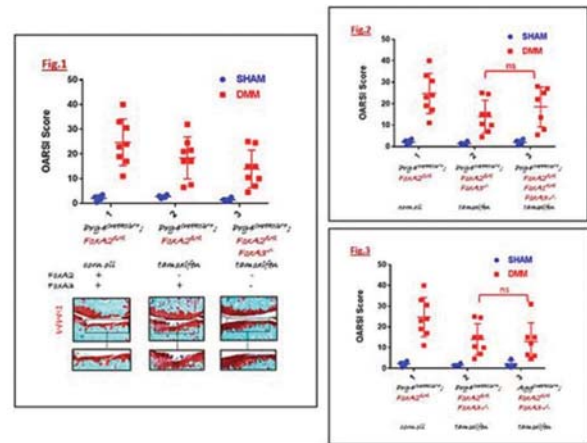


**Fig.1 Loss of FoxA2 and FoxA3 in articular cartilage attenuates cartilage degradation caused by DMM.** Safranin O/ Fast green staining and OARSI scoring of knees 16 weeks after sham or DMM surgery in control mice, tamoxifen treated Prg4<sup>Cre/+</sup>; FoxA2<sup>fl/fl</sup> mice and tamoxifen treated Prg4<sup>Cre/+</sup>; FoxA2<sup>fl/fl</sup>; FoxA3<sup>-/-</sup> mice. **Fig.2 Additional deletion of FoxA1 did not further ameliorate cartilage degradation caused by DMM.** OARSI scoring of knees 16 weeks after sham or DMM surgery in control mice, tamoxifen treated Prg4<sup>Cre/+</sup>; FoxA2<sup>fl/fl</sup>; FoxA3<sup>-/-</sup> mice and tamoxifen treated Prg4<sup>Cre/+</sup>; FoxA1<sup>fl/fl</sup>; FoxA2<sup>fl/fl</sup>; FoxA3<sup>-/-</sup> mice. **Fig.3 Loss of FoxA2 and FoxA3 expression in either Prg4- or Agg- positive chondrocytes had a similar effect on cartilage degradation caused by DMM.** OARSI scoring of knees 16 weeks after sham or DMM surgery in control mice, tamoxifen treated Prg4<sup>Cre/+</sup>; FoxA2<sup>fl/fl</sup>; FoxA3<sup>-/-</sup> mice and tamoxifen treated Agg<sup>Cre/+</sup>; FoxA2<sup>fl/fl</sup>; FoxA3<sup>-/-</sup> mice.

Figure supplement

**Disclosures:** Kailing Ho, None.

## MO0519

**HR-pQCT-Based Individual Trabecula Segmentation: Potentials in *in Vivo* Monitoring of Subchondral Microstructural Changes in Human Knee Osteoarthritis.** Yizhong Hu<sup>\*1</sup>, Y. Eric Yu<sup>1</sup>, Xingjian Zhang<sup>1</sup>, William Macaulay<sup>2</sup>, X. Edward Guo<sup>1</sup>. <sup>1</sup>Bone Bioengineering Laboratory, Department of Biomedical Engineering, Columbia University, United States, <sup>2</sup>Department of Orthopaedic Surgery, New York University Langone Hospital for Joint Disease, United States

Osteoarthritis (OA) is a prevalent joint disease, yet its pathogenesis remains unclear. Studies have shown that detecting and blocking acute subchondral bone loss associated with traumatic injuries may prevent OA. By applying Individual Trabecula Segmentation (ITS) to  $\mu$ CT scans, we previously identified a loss of trabecular rods in the subchondral trabecular bone as an early and consistent microstructural marker of OA in animal and in human. To examine the potentials of rod loss as a quantitative and reliable biomarker to monitor OA *in vivo*, the sensitivity of ITS to detect these changes clinically was tested using the second-generation HR-pQCT, a valuable clinical scanner that permits *in vivo* quantification of trabecular microstructure in the knee.

OA (n = 4) and control (n = 4) tibial plateaus were collected from total knee replacement patients and cadavers with no history of metabolic bone disease or fracture. Samples were scanned by  $\mu$ CT at 26- $\mu$ m voxel size and by HR-pQCT at 61- $\mu$ m voxel size. Images were registered and thresholded by matching BV/TV between the two resolutions. Cubic trabecular regions were selected from the subchondral bone beneath intact and severely damaged cartilage in OA samples and from corresponding control regions. ITS was used to analyze and compare trabecular morphology between OA and control at both resolutions.

High correlation in morphological parameters was found in  $\mu$ CT and HR-pQCT scans. Furthermore, ITS analyses of  $\mu$ CT images and HR-pQCT images consistently reported significant increases in PR ratio in the OA subchondral bone beneath both intact and damaged cartilage. Interestingly, this increase was due to a simultaneous loss of trabecular rods by number and thickening of trabecular plates beneath intact cartilage, while solely due to plate thickening beneath damaged cartilage. Most importantly, despite the reduced resolution of HR-pQCT, ITS was still sensitive to these subtle but dynamic changes in trabecular microstructure.

We previously showed that rod loss may be an early signature of OA. This study demonstrates the first attempt to correlate ITS based on 2<sup>nd</sup> generation HR-pQCT with gold standard  $\mu$ CT, and confirms the sensitivity of ITS to this rod loss at clinical resolution. The combination of ITS and HR-pQCT may serve as a useful tool in identifying early signs of bone loss quantitatively, monitoring microstructural changes in disease progression and identifying the best time window for preventative treatments.

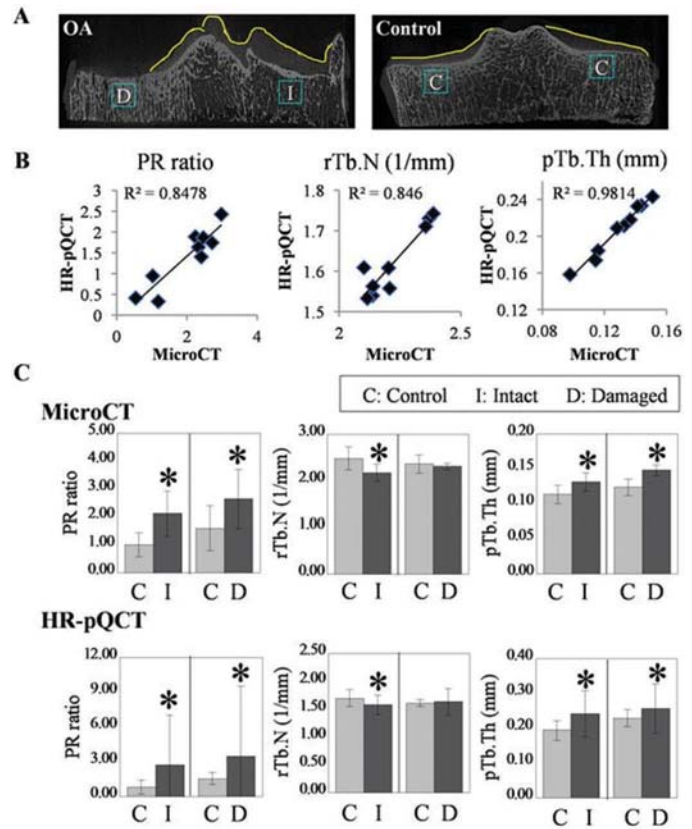


**Figure 1.** (A) Reconstructed slice from CT images of control and OA tibial plateaus indicating regions of interest. (B) Correlation of ITS morphological parameters based on MicroCT and HR-pQCT images. (C) Changes in PR ratio, rod trabecular number (rTb.N) and plate trabecular thickness (pTb.Th) from ITS analyses detected at MicroCT (top row) and HR-pQCT (bottom row) resolution.

Figure

**Disclosures:** Yizhong Hu, None.

## MO0520

**Establishment of an autoinflammatory disease model in mice.** Takatsugu Oike<sup>\*</sup>, Takeshi Miyamoto, Hiroya Kanagawa, Yasuo Niki, Morio Matsumoto, Masaya Nakamura. Department of Orthopaedic Surgery, Keio University School of Medicine, Japan

**BACKGROUND.** Recently, IL-1 is implicated in the pathogenesis of auto-inflammatory syndrome. To date, several animal rheumatoid arthritis models such as Collagen-Induced Arthritis/Adjuvant-Induced Arthritis (CIA/AIA) were established, however, no animal models for IL-1 diseases were reported.

**METHODS.** We newly generated conditional human IL-1 transgenic mice (IL-1 cTg), in which human IL-1 $\alpha$  was driven under a Cre/loxP system, in a C57/BL6 background. We crossed the IL-1 cTg mice with inducible Cre mice, Mx1 Cre mice, to yield Mx1 Cre/IL-1 cTg mice. PolyIpolyC was administrated to 8-week old Mx1 Cre/IL-1 cTg mice, and the phenotypes were observed. Mx1 Cre/IL-1 cTg mice were also crossed with IL-6 knockout (IL-6 KO), IL-17 knockout (IL-17KO) or Stat3 conditional knockout (Stat3cKO) to yield Mx1 Cre/IL-1 cTg/IL-6 KO, Mx1 Cre/IL-1 cTg/IL-17 KO or Mx1 Cre/IL-1 cTg/Stat3cKO, respectively.

**RESULTS.** Arthritis development was seen in all Mx1 Cre/IL-1 cTg mice one week after polyIpolyC administration. Elevated white blood cell counts, dermatitis, and splenomegaly were detected in these mice. These phenotypes were rescued by crossing them with either IL-6 KO, IL-17 KO or Stat3cKO. Deleting Stat3 was the most effective to improve symptoms seen in the Mx1 Cre/IL-1 cTg mice.

**CONCLUSION.** We successfully generated a new IL-1 disease model, and show that either IL-6, IL-17 or Stat3 may represent a therapeutic target, and Stat3 was considered as the best, to treat this disease.

**Disclosures:** Takatsugu Oike, None.



**MO0521**

Withdrawn

**MO0522**

**Mechanical loading regulates endoplasmic reticulum stress in a mouse model of osteoarthritis.** Xinle Li<sup>1</sup>, Daquan Liu<sup>1</sup>, Jie Li<sup>1</sup>, Zhaonan Wang<sup>1</sup>, Hiroki Yokota<sup>2</sup>, Ping Zhang<sup>1</sup>. <sup>1</sup>Department of Anatomy and Histology, School of Basic Medical Sciences, Tianjin Medical University, China, <sup>2</sup>Department of Biomedical Engineering, Indiana University-Purdue University Indianapolis, United States

Osteoarthritis (OA) is characterized by cartilage degradation leading to functional impairment in synovial joints, in which the stress to the endoplasmic reticulum (ER) is associated with OA progression. While knee loading is reported to promote bone formation and reduce p38 MAPK signaling as well as MMP13 activity in the mouse cartilage, the intriguing question is whether the chondroprotective effect of knee loading is associated with the ER stress in OA. Using a surgery-induced mouse model of OA, we examined the hypothesis that mechanical loading prevents chondrocyte degradation by reducing ER stress through eIF2 $\alpha$  signaling.

Forty-eight C57BL/6 female mice (~16 weeks) were divided into 8 groups (n=6): the sham control and seven OA groups at different time points (from 3 h to 8 weeks post-operatively). In addition, thirty mice were randomly divided into 3 groups (n=10): the sham control, OA control, and knee-loaded OA. To induce OA, the medial collateral ligament was transected and the medial meniscus was removed on the right knee. For the knee-loaded group, daily dynamic knee loading (1 N at 5 Hz) was applied 5min/day for 8 weeks. Knee joints were harvested for histomorphometry analysis and imaging with transmission electron microscopy (TEM). Protein samples were isolated from knee cartilage for Western blotting to examine eIF2 $\alpha$  signaling.

The Safranin-O staining showed that the cartilage surface was superficially fibrillated in the OA group, and the number of chondrocytes in the proximal tibia was reduced with an increase in vacuoles. However, knee loading significantly improved the OA-linked lesion. OARS1 scores revealed the degeneration of articular cartilage in OA group compared to the sham control, knee loading significantly reduced the OARS1 scores. In the OA group, TEM imaging showed the expansion of rough ER and the decreased number of ribosomes on the ER membrane. Knee loading exhibited a statistically significant recovery of the rough ER. Compared to the sham control, the OA group first increased the levels of Bip, p-eIF2 $\alpha$  and ATF4 within 7 post-surgery days and later decreased them after 7 days. Knee loading significantly restored the expression of eIF2 $\alpha$  signaling in late stage OA. Furthermore, knee loading attenuated cartilage apoptosis through regulating the phosphorylation of eIF2 $\alpha$ .

Collectively, the ER stress plays an important role in the surgery-induced OA. Knee loading contributes to preventing cartilage degeneration via eIF2 $\alpha$  signaling, which might support its possibility as a new potential therapy for OA.

**Disclosures:** Xinle Li, None.

**MO0523**

**PiT2 is Essential for Normal Endochondral and Intramembranous Ossification, Tooth Development and the Maintenance of Adult Bone Structure and Strength.** Sarah Beck<sup>\*1</sup>, John Logan<sup>2</sup>, David Tino-Lafont<sup>3</sup>, Laure Merametdjian<sup>1</sup>, Nina Bon<sup>1</sup>, Sophie Source<sup>1</sup>, Jérôme Guicheux<sup>1</sup>, Laurent Beck<sup>1</sup>, Graham Williams<sup>2</sup>, Chris Lelliott<sup>3</sup>, J. H. Duncan Bassett<sup>2</sup>. <sup>1</sup>Inserm U1229-RMeS, Université de Nantes, France, <sup>2</sup>Molecular Endocrinology Laboratory, Department of Medicine, Imperial College London, United Kingdom, <sup>3</sup>Wellcome Trust Sanger Institute, Hinxton, UK, United Kingdom

Uptake of inorganic phosphate (Pi) by osteoblasts and mineralizing chondrocytes is considered a pre-requisite for mineralization that is facilitated by unknown membrane proteins. In vertebrates, the type III co-transporters (*PiT1/SLC20A1* and *PiT2/SLC20A2*) are the only sodium-Pi co-transporters known to be expressed in skeletal tissues, and are thought to be essential for Pi delivery during mineralization. *In vitro* studies have demonstrated that *PiT1*, but not *PiT2*, expression is regulated by osteogenic factors and we previously demonstrated that *PiT1* hypomorphic adult mice surprisingly have normal bone mineralization. Here, we investigate the skeletal phenotype of *PiT2* knock-out (*PiT2KO*) mice to determine the role of *PiT2* during skeletogenesis (n=3-6 *PiT2KO* and wild type mice per age, per sex). Analyses of tibial growth plate sections demonstrated a decreased height at 3 and 16 weeks (p<0.01) showing impaired endochondral ossification in *PiT2KO* mice. Similarly, cranial morphometry showed reduced cranial length (p<0.001), zygomatic width (p<0.01) and mandibular length (p<0.01) indicating disrupted intramembranous ossification. X-ray microradiography, micro-computed tomography ( $\mu$ CT), quantitative back-scattered electron-scanning electron microscopy (BSE-SEM) and confocal imaging in 16 week old *PiT2KO* mice showed reduced bone length (p<0.001), reduced trabecular and cortical volumes (p<0.05 and p<0.001, respectively) and impaired trabecular and cortical mineralization (p<0.001). Furthermore, biomechanical testing, revealed reduced bone stiffness and strength in long bones from *PiT2KO* mice (p<0.001 and p<0.01, respectively).  $\mu$ CT, SEM and histological analysis of teeth in 4 week and 32 week old *PiT2KO* mice demonstrated increased pre-dentine but reduced dentine volumes (p<0.001 and p<0.0001) indicating that *PiT2* is also required for normal dentin mineralization and morphology. Despite the

profound skeletal phenotype in *PiT2KO* mice, primary osteoblast and chondrocyte cultures showed no defect in either cellular differentiation or mineralization indicating that the skeletal effects of *PiT2* deficiency are indirect. Taken together these results indicate that, contrary to the commonly admitted idea, *PiT2* is essential for endochondral and intramembranous ossification, tooth development and the maintenance of adult bone structure and strength.

**Disclosures:** Sarah Beck, None.

**MO0524**

**Female Protein Kinase D1 Osteoprogenitor-specific Conditional Knockout Mice Show Reduced Bone Mineral Density with No Further Decrease upon Ovariectomy.** Wendy Bollag<sup>\*</sup>, Ke-Hong Ding, Jianrui Xu, Vivek Choudhary, Qing Zhong, Ranya Elsayed, Kanglun Yu, Mohammed El-Salanty, Meghan McGee-Lawrence, Carlos Isales, Augusta University, United States

The serine-threonine protein kinase D1 (Prkd1) has been reported to play a role in a number of cellular functions, including proliferation and differentiation, cell survival, autophagy, and Golgi trafficking. We previously found that 3- and 6-month-old male conditional knockout (cKO) mice with Prkd1 ablated in osteoprogenitor cells by osterix promoter-driven Cre recombinase exhibited significantly reduced bone mineral density (BMD) and alterations in bone microarchitecture. Here we examined the effect of ovariectomy (OVX) on ~6-month-old female mice, comparing BMD, microarchitectural parameters, histomorphometric measures and serum PYD levels in floxed control and cKO mice. Femoral and tibial BMD values were significantly reduced (by ~9 and 11%, respectively) in the sham-operated cKO female mice compared to the sham-operated control animals. OVX of the control mice resulted in a significant ~9 and ~7% decrease in femoral and tibial BMD values, respectively, but no significant change in the cKO mice. MicroCT analysis showed that the cKO mice had significantly lower femoral BMD, decreased trabecular number and increased trabecular separation. There was also a trend towards reduced bone volume fraction (%BV/TV) in the sham-operated cKO mice relative to the sham control mice, and in the OVX control relative to the sham control mice, but none of these differences achieved statistical significance. There were also no significant changes in trabecular thickness or any significant effect of OVX on any trabecular architecture parameter either in control or cKO mice. Histomorphometric analysis of calcein labeling indicated that the mineral apposition rate was significantly decreased (by about 20%) in the sham-operated cKO mice in comparison to the sham-operated control females, suggesting a mineralizing defect in the Prkd1 cKO mice. Two-factor ANOVA also indicated a significant effect of genotype (with control greater than cKO mice) and a trend that approached significance for an effect of OVX (with OVX greater than sham operation). In the sham-operated mice there was no significant differences in serum PYD levels observed between the two genotypes. Serum PYD levels in the floxed control animals increased upon OVX; however, this OVX-induced increase was not seen in the cKO mice. Our results suggest a potentially important role for Prkd1 in bone formation/mineralization basally and in bone loss associated with estrogen deficiency.

**Disclosures:** Wendy Bollag, None.

**MO0525**

**PDGFR $\beta$ -Expressing Osteoprogenitors and PDGFR $\beta$  Signaling Contribute to Fracture Healing by Promoting Callus Formation and Vascularization.** Naomi Dirckx<sup>\*1</sup>, Robert J. Tower<sup>2</sup>, Matthias Van Hul<sup>1</sup>, Christa Maes<sup>1</sup>. <sup>1</sup>Laboratory of Skeletal Cell Biology and Physiology (SCEBP), Skeletal Biology and Engineering Research Center (SBE), Department of Development and Regeneration, KU Leuven, Leuven, Belgium, <sup>2</sup>Laboratory of Skeletal Cell Biology and Physiology (SCEBP), Skeletal Biology and Engineering Research Center (SBE), Department of Development and Regeneration, KU Leuven, Leuven, Belgium, United States

Osteoprogenitors (OPs) and blood vessels (BVs) co-invade fracture calluses and are crucial for bone repair, but the angiogenic-osteogenic crosstalk is poorly understood molecularly. Platelet-derived growth factor (PDGF)-B is angiogenic as well as chemotactic and mitogenic for osteoblasts *in vitro* and promotes bone repair in animal models and clinical orthopedics. Its main receptor PDGFR $\beta$  is expressed on osteolineage cells and perivascular progenitors in bone, but their contribution to fracture healing has not been characterized.

Here, we first studied the role of PDGFR $\beta$  in the crosstalk between OPs and endothelial cells (ECs) *in vitro*. We found that EC-secreted factors promoted OP migration and that OPs were rapidly recruited to EC tubules, with both processes mitigated by PDGFR $\beta$  inhibitors. Next, we visualized PDGFR $\beta$ <sup>+</sup> cells and their descendants in semi-stabilized fractures applied to PDGFR $\beta$ -Cre;mTmG mice. These *in vivo* reporter studies revealed abundant mGFP<sup>+</sup> cells during periosteal expansion (post fracture day (PFD)3) and comprising fibroblasts, stromal cells, chondrocytes and osteoblasts contributing to the callus over the course of repair (PFD7,14,28), including ample cells located close to BVs. In addition, all PDGF family members were upregulated during soft and hard callus formation (qRT-PCR). These findings suggest a broad functional involvement of PDGF-PDGFR signaling in bone repair. To assess specifically the role of PDGFR $\beta$  in osteogenic cells we deleted PDGFR $\beta$  using *Oss-Cre*:GFP mice, targeting an OP population known to be partly pericytic. Analysis by  $\mu$ CT and histology evidenced that PDGFR $\beta$ -deficient mice displayed significantly altered fracture healing, characterized

by delayed periosteal cell expansion (reduced periosteal thickness and BrdU incorporation, PFD3), impaired callus formation (2.5-fold reduced callus volume, PFD14,  $p < 0.001$ ,  $n = 6-8$ ), and altered tissue composition (reduced cartilage, bone and marrow, but 2-fold increased callus fibrotic tissue, and increased adipogenesis). Co-immunostaining for Osx-Cre:GFP<sup>+</sup> cells and CD31<sup>+</sup> ECs revealed decreased association between OPs and BVs ( $n = 6-7$ ,  $p < 0.001$ ), as well as reduced BV size and number.

Altogether, these data show that PDGFR $\beta$ <sup>+</sup> cells contribute extensively to fracture repair and that osteogenic PDGFR $\beta$  signaling is crucial for proper periosteal cell proliferation, callus formation and angiogenesis, elucidating some of the mechanisms behind the beneficial effects of PDGF in bone regeneration.

**Disclosures:** Naomi Dirckx, None.

## MO0526

**Investigating *Zbtb40* and its Role in Osteoblast-Mediated Bone Formation.** Madison Doolittle<sup>\*1</sup>, Robert Maynard<sup>1</sup>, Gina Calabrese<sup>2</sup>, Charles Farber<sup>2</sup>, Cheryl Ackert-Bicknell<sup>1</sup>. <sup>1</sup>Center for Musculoskeletal Research, University of Rochester, United States, <sup>2</sup>Center for Public Health Genomics, University of Virginia, United States

Bone Mineral Density (BMD), the surrogate trait used to diagnose osteoporosis, is influenced by a myriad of genes leading to a composite phenotype shown to have high heritability. Genome-Wide Association Studies (GWASs) for BMD in humans have been used in an attempt to uncover additional genetic determinants and have repeatedly identified a significantly associated locus on chromosome 1p36.12, located in an intergenic region upstream of Zinc Finger And BTB Domain Containing 40 (*ZBTB40*). In mice, GWAS for *in vitro* mineralized nodule formation by primary calvarial osteoblasts uncovered an associated locus upstream of the mouse ortholog of *ZBTB40* (*Zbtb40*), suggesting a role in osteoblast-mediated bone formation. Since the genomic associations are only correlative, the objective of this study was to determine if *Zbtb40* plays a role in the regulation of osteoblast activity. The mouse transcript for *Zbtb40* contains 19 exons and we have determined experimentally that there are no alternative splice variants. *ZBTB40* is predicted to be a transcription factor, but little is known regarding its exact function. The protein is predicted to have both a BTB domain, shown to be involved in protein-protein interactions, and multiple C2H2 Zinc-Finger domains, which contain DNA-binding motifs. We have found that *Zbtb40* is expressed in a wide array of mouse tissues including long bones, calvaria, and osteoblasts. During differentiation of the MC3T3-E1 preosteoblast cell line for 21 days, *Zbtb40* has a surge in both transcript and protein expression early in osteogenesis, reaching a peak at Day 3 and progressively declining over the subsequent days. This expression pattern is conserved during *in vitro* osteogenesis of primary calvarial osteoblasts from wild type C57BL/6 mice. Using siRNA-mediated gene silencing, we demonstrate that knocking down *Zbtb40* in MC3T3-E1 cells significantly decreases alkaline phosphatase staining at day 10, and drastically decreases mineralized nodule formation measured by Alizarin Red staining at day 21. In summary, the above data indicates that *Zbtb40* is expressed in osteoblasts, shows increased expression early in osteogenesis, and is involved in the regulation of both osteoblast differentiation and mineralization.

**Disclosures:** Madison Doolittle, None.

## MO0527

**Vitamin E-stabilized UHMWPE: evaluation of biological response on human osteoblasts to wear debris.** Emanuela Galliera<sup>\*1</sup>, Vincenza Ragone<sup>2</sup>, Francesca Selmin<sup>3</sup>, Massimiliano Corsi Romanelli<sup>4</sup>. <sup>1</sup>Department of Biomedical Sciences for Health, Università degli Studi di Milano, Milan, Italy, <sup>2</sup>IRCCS Galeazzi Orthopaedic Institute, Milan, Italy, <sup>3</sup>Research and Development Department, Permedica S.p.A. via como, 38 Merate (LC), Italy, <sup>4</sup>Department of Pharmaceutical Science, Università degli Studi di Milano, Milan, Italy, <sup>5</sup>Department of Biomedical Sciences for Health, Università degli Studi di Milano, Milan, Italy and U.O.C SMEL-1 Patologia Clinica IRCCS Policlinico San Donato, San Donato, Milan, Italy., Italy

**Background:** Wear particles from prosthetic bearings surfaces can be released in the interface between implant and surrounding bone, leading to periprosthetic osteolysis. Ultra High Molecular Weight Polyethylene (UHMWPE) wear debris stimulated a chronic inflammatory response, mainly mediated by infiltrating macrophages which are responsible of the phagocytosis of wear particles. UHMWPE doped with vitamin E was introduced as a method to provide oxidation resistance upon sterilization, without modifying UHMWPE mechanical property. During osteolytic process, in addition to the macrophage mediated phagocytosis and the consequent inflammation, osteoblasts have been shown to produce not only inflammatory mediators, but also osteoimmunological factors, such as RANKL and OPG and the inhibitors of Wnt pathway DKK-1 and Sclerostin. This study aimed to investigate *in vitro* how vitamin E-blended UHMWPE wear debris might modulate osteoblast mediated osteolysis, focusing in particular on the production of osteoimmunological markers RANKL, OPG, Sclerostin and DKK-1 compared to conventional UHMWPE wear debris.

**Methods:** Human osteoblastic cell line SaOS2 were incubated with wear particles derived from HMWPE doped and not doped and cellular response was evaluated in terms of gene expression and protein production of IL-6, RANKL; OPG, DKK-1, Sclerostin, compared to not treated cells.

Results: RANKL, a bone erosion marker, resulted reduced, while OPG, DKK-1 and Sclerostin, as bone protective markers, resulted increased by the presence of vitamin E-blended UHMWPE compared to HMWPE treatment.

**Conclusion:** vitamin E-blended UHMWPE induced an osteoimmunological response in bone cells that positively affect the osteolysis induced by wear debris, thereby reducing the aseptic loosening of the implants.

**Disclosures:** Emanuela Galliera, None.

## MO0528

**Overexpression of MitoNEET in osteoblasts leads to impaired bone mass and energy metabolism in mice.** Phuong Le<sup>\*</sup>, Sheila Bornstein, Victoria Demambro, Clifford Rosen, Anyonya Guntur. MMCR, United States

Osteoblasts during *in vitro* differentiation increase glycolytic ATP production rates in response to exogenous glucose supply (glycolysis 67% vs Oxidative phosphorylation 43%). To study the role of the two major ATP generating pathways *in vivo* in osteoblasts we overexpressed MitoNEET an outer mitochondrial membrane protein generating a novel osteoblast specific overexpression mouse model. Previous work shows that overexpression of MitoNEET in adipocytes specifically leads to decreased oxidative phosphorylation and a concomitant increase in glycolysis. In our overexpression model, mice containing the tetracycline responsive element (TRE) fused to the MitoNEET open reading frame were crossed to Runx2 reverse-tetracycline trans-activator (rtTA) to generate osteoblast specific overexpression. Two groups of 4 week old male mice were generated and Doxycycline+Saccharin (Dox), and Saccharin (controls) were introduced through drinking water for 12 weeks. Tibiae from mice positive and negative for TRE MitoNEET on Dox were isolated and qRT-PCR analysis performed showing a significant increase in MitoNEET expression in bone. Trabecular bone microarchitecture was assessed in the distal femoral metaphysis, whereas cortical bone morphology was assessed at the femoral mid-shaft with  $\mu$ CT analysis at 16 weeks of age. Dox treated male mice had significantly lower trabecular bone mineral density (Tb. BMD,  $n = 8-10$ ,  $p = 0.04$ ) and trabecular thickness (Tb.Th,  $p = 0.0001$ ), along with lower cortical tissue mineral density (Ct.TMD, -0.7%), medullary area (Ma.Ar, -11.8%), total area (Tt.Ar, -10.7%), and minimum moment of inertia (Imin, -22%) compared to controls. In contrast female mice, showed no differences in the trabecular bone volume or architecture. At the femoral mid-shaft, Dox treated female mice had greater cortical thickness (Ct.Th, +12.5%), cortical area (Ct.Ar, +16.4%), total area (Tt.Ar, +10.8%), and moments of inertia (pMOI, Imax, Imin, +21 to 33.8%). The Dox treated mice had greater body weight than the control mice (+27.8%) potentially explaining the greater cortical bone thickness and area. Next, we performed indirect calorimetry to obtain energy expenditure (EE) and respiratory quotient (RQ) data. We did not observe any differences in female mice. We found a significant increase in day time energy expenditure even though body weight in the Dox group animals was slightly higher compared to controls. Interestingly, 24 hour RQ was significantly lower in the MitoNEET overexpressing animals, suggesting oxidation of fat ( $n = 8-10$ ,  $p = 0.03$ ). There was no difference in food consumption with the Dox group drinking significantly less amount of water ( $n = 8-10$ ,  $p = 0.009$ ). In sum, manipulating MitoNEET expression specifically in the osteoblast impairs bone mass and leads to decreased, energy expenditure and respiratory quotient in male mice potentially affecting whole body energy metabolism.

**Disclosures:** Phuong Le, None.

## MO0529

**Usp53, a novel target gene of the PTH-activated  $\alpha$ NAC transcriptional coregulator.** Hadla Hariri<sup>\*1</sup>, William Addison<sup>2</sup>, Martin Pellicelli<sup>1</sup>, René St-Arnaud<sup>1</sup>. <sup>1</sup>Shriners Hospitals for Children - Canada, Canada, <sup>2</sup>Shriners Hospitals for Children, Canada

Upon PTH treatment of osteoblasts, cAMP accumulates to activate PKA, which in turn phosphorylates Nascent-polypeptide-associated complex and coregulator alpha ( $\alpha$ NAC) on residue Ser99. This leads to nuclear translocation of the  $\alpha$ NAC protein. Little is known about potential transcriptional targets of the PTH-activated, PKA-phosphorylated  $\alpha$ NAC protein in osteoblasts. In order to identify such targets, we performed ChIP-seq against  $\alpha$ NAC and RNA-seq experiments in PTH-treated MC3T3-E1 osteoblastic cells. Genes showing differential responses in both data sets were further validated using conventional ChIP and RT-qPCR. These experiments identified *Usp53* as a potential  $\alpha$ NAC target gene. Conventional ChIP assays in PTH-treated MC3T3-E1 cells confirmed a 4-fold enrichment of  $\alpha$ NAC binding at the *Usp53* promoter region. PTH treatment also increased the mRNA expression of *Usp53* by 3-fold. We then established shRNA-mediated *Naca* ( $\alpha$ NAC) knockdown in MC3T3-E1 cells. Interestingly, PTH-driven transcriptional induction of *Usp53* was completely blunted following  $\alpha$ NAC knockdown. *Usp53* promoter fragments were subsequently cloned upstream of a luciferase reporter vector. In transiently transfected MC3T3-E1 cells, PTH treatment stimulated transcription from the *Usp53* promoter and  $\alpha$ NAC knockdown abrogated the response. In order to understand the role of USP53 in osteoblastic differentiation, we established shRNA-mediated *Usp53* knockdown in ST2 stromal cells and MC3T3-E1 cells. *Usp53* knockdown enhanced the differentiation of ST2 into osteoblasts and inhibited their differentiation into adipocytes. Increased differentiation was also observed in *Usp53* knockdown MC3T3-E1 cells. *Usp53* knockdown up-regulated the expression level of osteoblastic differentiation markers such as: *Bglap* (*Osteocalcin*) and *Alpl* (Alkaline phosphatase) and down-regulated expression of regulators of adipogenesis such as *Pparg* and *Cebpa*. *In vivo* osteogenesis assays performed in immunocompromised mice using *Usp53*-knockdown bone marrow stromal



cells (BMSCs) have also shown an increase in osteoblast number (osterix immunostaining) and a decrease in adipocyte counts (perilipin immunodetection). These experiments identify *Usp53* as a novel target of  $\alpha$ NAC downstream of PTH signal transduction. Future studies will address the mechanism through which USP53 affects mesenchymal cell lineage-making decisions and differentiation.

**Disclosures:** Hadla Hariri, None.

## MO0530

**The Unfolded Protein Response plays an important role in osteoblastogenesis and its aberrations adversely affect skeletal homeostasis.** Srividhya Iyer\*, Kanan Vyas, Annick Deloese, Michela Palmieri, Ha-neui Kim, Marilina Piemontese, Maria Almeida, Charles O'Brien, Stavros Manolagas, Robert Jilka. Center for Osteoporosis and Metabolic Bone Diseases, Univ. Arkansas for Medical Sciences, and Central Arkansas Veterans Healthcare System, United States

It has been shown earlier that osteoblasts and osteocytes rely extensively on their endoplasmic reticulum (ER) to properly fold and secrete the proteins that they produce; and protein misfolding negatively impacts bone formation. Accumulation of misfolded proteins in the ER engages the unfolded protein response (UPR), a signaling cascade that has three arms apexed by the ER stress activated proteins PERK, IRE1 $\alpha$ , and ATF6. Here, we report that all three arms of the UPR were activated during osteoblast differentiation of cultured bone marrow stromal cells. These changes were accompanied by increased expression of ERO1, ERdj4 and EDEM1, genes that are induced by ER stress and encode proteins which promote protein folding. Nonetheless, consistent with evidence that failure to relieve ER stress and sustained activation of the UPR activates inflammation and/or cell death, addition of tunicamycin – a pharmacologic ER stress inducer – to calvaria-derived osteoblast cultures induced UPR and increased apoptosis. Osteoblast and osteocyte apoptosis stimulates RANKL expression in neighboring live cells. In line with this evidence, short term (4 h) tunicamycin treatment increased the expression of osteoclastogenic cytokines RANKL, TNF, VEGF and in neonatal calvarial organ cultures. Furthermore, calvaria treated with tunicamycin for a 4 h period/day for a total of 4 days exhibited increased resorption, as indicated by increased cathepsin K expression and calcium release into the culture medium. Moreover, administration of tunicamycin (0.3ug/g body weight) to C57Bl6 mice increased expression of several UPR genes, including the Perk target CHOP – a pro-apoptotic transcription factor, as well as VEGF and RANKL in the femoral bone shafts. Additionally, tunicamycin administration increased osteoclast number in femoral cancellous bone. In contrast, osteocyte enriched femoral bone shafts obtained from C57Bl6 mice receiving prednisolone for 28 days had reduced expression of UPR genes, such as the ATF6 target Xbp1 and CHOP. These results demonstrate that UPR induction is an important cellular adaptation during osteoblastogenesis and inadequate or sustained UPR adversely affects skeletal homeostasis. Specifically, excessive UPR activation in osteoblast-lineage cells diminishes their viability and promotes the expression of pro-osteoclastogenic cytokines. Conversely, suppression of the UPR by glucocorticoid excess in osteocytes may contribute to their deleterious effect on bone.

**Disclosures:** Srividhya Iyer, None.

## MO0531

**Interrelationship Between c-src and SIT in the Regulation of Osteoblast Differentiation.** Sydney Kauffman\*<sup>1</sup>, Candace Morales-Wilde<sup>1</sup>, David Cifelli<sup>1</sup>, Samuel Sanchez<sup>1</sup>, Alyssa Rosa<sup>1</sup>, Joseph Tarr<sup>2</sup>, Nicole Rodstrom<sup>1</sup>, Steven Popoff<sup>2</sup>, Thomas Owen<sup>1</sup>. <sup>1</sup>Ramapo College of New Jersey, United States, <sup>2</sup>Temple University School of Medicine, United States

Deletion of the c-src gene results in decreased osteoclast and increased osteoblast activity. Inhibition of c-src family kinases in calvarial osteoblasts or MC3T3 cells by the c-src inhibitor compound PP2 increases their differentiation. In Ros 17/2.8 osteosarcoma cells and in primary bone marrow cells though, PP2 results in a diminution of osteoblast phenotype markers, suggesting a differential role for the src family kinases in osteoblast function depending on the developmental origin. More recently, SIT (SHP2-interacting transmembrane adaptor) was described as a potential target for phosphorylation by src-family kinases in osteoblasts. When the SIT gene is deleted in mice, they show increased trabecular number, bone volume fraction, and connectivity density, as well as decreased trabecular thickness and spacing. The intracellular portion of the SIT protein has three tyrosines in motifs which are known to mediate phosphorylation-dependent interaction with the SH2 domains of c-src family kinases. In T-cells, these tyrosines are phosphorylated following activation of the T-cell receptor and mediate binding to proteins including Grb2, SHP2, and Csk. Since the deletion of both c-src and SIT in mice results in increased osteoblast activity and they are known to interact in the immune system, it is reasonable to hypothesize that in osteoblasts, they interact to influence signaling pathways and ultimately regulate bone mass. We used the crispr-Cas9 system to independently target c-src and SIT in Ros 17/2.8 cells. Preliminary analysis of osteoblast phenotype marker expression in the antibiotic resistant pools following transfection of either c-src or SIT crispr-Cas9 shows that the levels of gene expression for OC, OP, DMP, and AP decrease as does AP enzyme activity. These data are consistent with our previous observations using PP2 in Ros 17/2.8 cells but also demonstrate that it is c-src itself and not a family member that is responsible for this activity. We are currently cloning cell lines from the c-src crispr pool but interestingly, have not been able to clone any cell lines from either the SIT crispr pool or from a similar

experiment done with SIT shRNA. We are also performing parallel work in the MC3T3 cell line as well as generating lentivirus crispr-Cas9 constructs in order to delete c-src and/or SIT in primary osteoblasts. This work allows us to begin to address on the molecular level the interactions of SIT and c-src in regulating bone formation.

**Disclosures:** Sydney Kauffman, None.

## MO0532

**Analysis of the miR-101/Ezh2 axis during osteoblast differentiation by Crispr/Cas9 and scalable over-expression technology.** Farzaneh Khani\*<sup>1</sup>, Roman Thaler<sup>1</sup>, Janet Denbeigh<sup>1</sup>, Christopher Paradise<sup>1</sup>, Endre Soreide<sup>1</sup>, Gary S. Stein<sup>2</sup>, Amel Dudakov<sup>1</sup>, Andre J van Wijnen<sup>1</sup>. <sup>1</sup>Departments of Orthopedic Surgery & Biochemistry and Molecular Biology, Mayo Clinic, United States, <sup>2</sup>Departments of Biochemistry & Surgery, University of Vermont Cancer Center, Burlington, VT, United States

Bone development and homeostasis is controlled by chromatin and RNA-mediated epigenetic mechanisms including microRNA regulated gene expression. The chromatin regulator Ezh2 plays a major role in osteoblastic differentiation and bone development, and suppression of its intrinsic H3K27 methyltransferase activity promotes osteoblast differentiation. Because miR-101 is predicted to suppress expression of Ezh2, we examined the physiological significance of the link between miR-101 and Ezh2 during bone cell maturation. Using Crispr/CAS9 technology, we created MC3T3-E1 cells in which miR-101 is inactivated or that stably overexpress scalable levels of miR-101. Furthermore, transient inactivation experiments were performed using miR-101 mimics. During differentiation of MC3T3-E1 osteoblasts, Ezh2 expression significantly decreases while miR-101 expression increases over time. Compared to control cells, miR-101 negative MC3T3-E1 cells show clearly reductions in cell proliferation, extra cellular matrix (ECM) deposition, Alpl activity and ECM mineralization at day 28 of differentiation. Accordingly, mRNA expression of primary osteoblastic transcription factors like Runx2 and Mef2c, as well as ECM related genes like Bglap2 and Phospho1 are repressed by miR-101 knock out in MC3T3-E1 cells. Scalable stable overexpression of miR-101 negatively affects cell proliferation and correlates with the amount of miR-101 being overexpressed. However, ECM deposition increases with increasing levels of miR-101 in MC3T3-E1 cells. Cells expressing highest levels of miR-101 typically show a higher degree of ECM mineralization at day 28. At the mRNA level, Ezh2 expression is suppressed at day 3 of differentiation in MC3T3-E1 subclones over-expressing low to high amounts of miR-101, while Bglap2 expression is accelerated after day 14. Transient depletion using miR-101 mimics for 3 days confirms the functional linkage between miR-101 and Ezh2 in osteoblasts and reveals clearly reduced expression of Ezh2 and levels of H3K27me3 methylation. Collectively, our data indicate that miR-101 functionally controls osteoblast differentiation of MC3T3-E1 and may form a mechanistic regulatory circuit with Ezh2 that epigenetically controls progression of osteoblast maturation.

**Disclosures:** Farzaneh Khani, None.

## MO0533

**Interleukin-6 Inhibits Osteoblastic Differentiation of Bone Marrow Stromal Cells and Decreases Bone Formation Following Ischemic Osteonecrosis.** Gen Kuroyanagi\*, Naga Suresh Adapala, Ryosuke Yamaguchi, Harry K.W. Kim. Texas Scottish Rite Hospital for Children, United States

Legg-Calvé-Perthes disease (LCPD) is a childhood form of ischemic osteonecrosis (ON) of the femoral head which produces pain and stiffness, femoral head deformity, and early arthritis. A recent study of LCPD patients showed a significant elevation of a pro-inflammatory cytokine, interleukin-6 (IL-6), in their synovial fluids, and a chronic persistent hip synovitis on serial MRIs. In patients with LCPD, bone formation is also remarkably decreased and delayed during healing. Given these observations, we hypothesized that IL-6 elevation inhibits osteoblastic differentiation of bone marrow stromal cells (BMSCs) and decreases bone formation following ischemic ON. To test this hypothesis, we first analyzed the necrotic bone for the presence of IL-6. Western blot analysis and ELISA showed a significant elevation of IL-6 protein levels in the necrotic bone fluid obtained after a surgical induction of ischemic ON in a well-established piglet model of LCPD ( $p < 0.01$ ). *In-vitro* BMSC culture studies showed that a soluble fraction of the necrotic bone significantly decreased gene expression of Runx2, Osterix and ALP ( $p < 0.01$ ), and significantly decreased alkaline phosphatase (ALP) and alizarin red staining. These inhibitory effects of the soluble necrotic bone fraction were rescued by an IL-6 receptor blocker, tocilizumab ( $p < 0.01$ ). *In vivo* studies using a mouse model of ischemic ON (N=15, 12-week-old mice) also showed increased IL-6 expression after the induction of ischemic ON on immunohistochemistry. Furthermore, significantly decreased osteoblast number/bone surface, mineral apposition rate and bone volume were observed ( $p < 0.05$ ) in the necrotic bone on histomorphometric and micro-CT analyses. In contrast, IL-6 KO mice (B6.129S2-Il6<sup>tm1Kopf</sup>/J, N=19) showed increased osteoblast number/bone surface ( $p < 0.05$ ), bone formation ( $p < 0.01$ ) and bone volume % ( $p < 0.001$ ) compared to the wild-type mice following ischemic ON. Lastly, treatment of wild-type mice (N=15) with an IL-6 receptor blocker (cMR16-1) significantly increased osteoblast number/bone surface and bone volume % compared to the saline control group (N=15) following ischemic ON ( $p < 0.01$ ). Taken together, these findings indicate that IL-6 plays an important role in osteoblast differentiation and bone formation following ischemic ON. These results suggest that anti-IL-6 therapy could be a potential treatment to increase bone formation following ischemic ON.

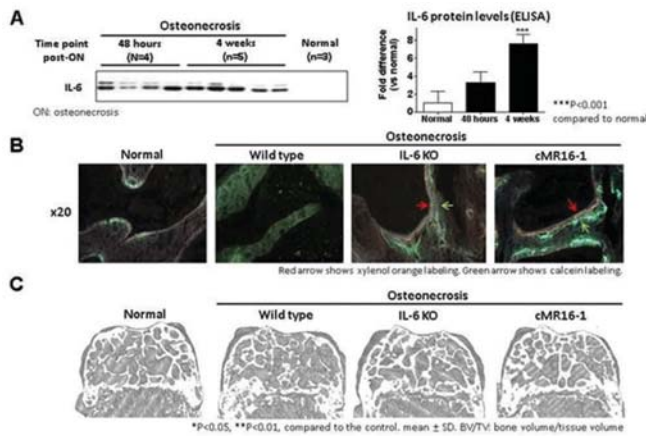


Figure 4. IL-6 expression levels in the necrotic bone fluid after osteonecrosis induction.  
Figure 5. Dynamic histomorphometric analysis of bone formation parameters at 4 weeks following ischemic osteonecrosis of the distal femoral epiphysis.  
Figure 6. Micro CT analysis of the influence of the lack of IL-6 in IL-6 KO mice and IL-6 blocker (cMR16-1) at 4 weeks following ischemic osteonecrosis of the distal femoral epiphysis.

Figure

Disclosures: Gen Kuroyanagi, None.

## MO0534

**Nuclear Factor I-C Regulates Calvarial Bone Formation via Control of *Fgfr1* Expression and Cell Proliferation.** Song Yi Roh\*, Dong-Seol Lee, Joo-Cheol Park. School of Dentistry, Seoul National University, Korea, Republic of

The nuclear factor I (NFI) gene family encodes site-specific transcription factors essential for the development of number of organ systems. Our previous studies that NFI-C is required for tooth root development and endochondral ossification, but the exact function of NFI-C in calvarial intramembranous bone formation remains unknown. Here, we show that disruption of *Nfic* exhibited defects in intramembranous bone formation with decreased osteogenic proliferative activity and reduced osteoblast differentiation during postnatal osteogenesis. Moreover, *Nfic*-deficient mice showed incomplete suture closure. However, *Nfic* disruption has no influence on prenatal calvarial bone development. Expression of *Fgfr1* and *Fgfr2* was decreased in primary calvarial mesenchymal cells of *Nfic*-deficient mice, but it was significantly increased by *Nfic* overexpression in hBMSCs. Furthermore, NFI-C regulates *Fgfr1* expression by direct binding to its promoter. These results indicate that NFI-C plays a key role in the regulation of calvarial bone formation and suture closure via control of *Fgfr1* expression and proliferation.

Disclosures: Song Yi Roh, None.

## MO0535

**The Critical Role of Peroxiredoxin-1 for the Estrogen Protects Osteoblast from Oxidative Stress.** Di Liu\*, Juan Du, Minqi Li. Shandong Provincial Key Laboratory of Oral Biomedicine, Shandong University, China

Oxidative damage is an important contributor to the morphological and functional changes in osteoporotic bone. Estrogen closely relates to antioxidant system in bone remodelling during osteoporosis. As a family of peroxidases, Peroxiredoxin (PRX) is associated with various biological processes such as the detoxification of oxidants and cell apoptosis. This study aimed to investigate whether PRX1 as one of the major oxidative stress-inducible proteins from MC3T3-E1 played a great part in antioxidative mechanism of estrogen in vitro. The wild-type, PRX-1 knockout and over-expression MC3T3-E1 cells generated by CRISPR/Cas9 technology and Integration operation system respectively, which were pretreatment with 17 $\beta$ -estradiol (E2) and N-acetyl cysteine followed by oxidative injury induced with H2O2. Western blot and real time-PCR were applied to clarify the expression of PRX1, caspase-3, cleaved caspase-3, JNK and p-p66Shc. Cell immunofluorescence was used to evaluate the apoptosis of MC3T3-E1 cells after treated with H2O2 and the anti-apoptosis effect of E2, to verify the location of the expression of PRX1 by the Hoechst33342 staining. The results of Hoechst33342 staining showed H2O2 induced apoptosis and the PRX1 nuclei accumulation in cells. Furthermore, preconditioning with E2 and NAC could attenuate upregulation of PRX1, caspase-3, cleaved caspase-3, JNK and p-p66Shc expression at both the mRNA and protein levels induced by H2O2. Also, a decrease/increase of caspase-3, cleaved caspase-3, JNK and p-p66Shc expression was observed in PRX1 knockout/over-expression cells with or without H2O2 in comparison to wild-type cells respectively. These findings suggested that PRX may play important roles in protective effects of estrogen on osteoblasts from oxidative stress.

Disclosures: Di Liu, None.

## MO0536

**Comparative Study of the Effect of Different Tea Types on Mineral Deposition in an Osteoblast Cell Model.** Michael McAlpine\*, Wendy Ward, Adam MacNeil, William Gittings. Faculty of Applied Health Sciences, Brock University, Canada

Epidemiological literature suggests a positive correlation between tea consumption and bone mineral density. Thus, consumption of tea, possibly due to its abundance of polyphenols, may be part of a dietary strategy that supports bone health. Recently, research from our lab has shown higher mineral deposition following supplementation with traditional green or black tea or green rooibos tea in an osteoblast cell model. The purpose of this study was to build upon this previous research and determine the ability of a wider variety of whole leaf tea, including white tea and red rooibos tea, to promote mineral deposition. Saos-2 cells were cultured and differentiated for 8 days at 37°C in 5% CO<sub>2</sub>. Following this, mineralization was induced for 5 days in the presence or absence of 1  $\mu$ g/mL of tea polyphenols. White (WT, Bai Hao Yin Zhen), green (GT, Dragonwell), black (EB, English Breakfast), green rooibos (GR), and red rooibos (RR) loose leaf teas were steeped according to manufacturer's recommendations. Total polyphenol content (TPC) of each tea was determined using Folin-Ciocalteu's reagent with gallic acid as a standard; and antioxidative capacity was determined by the ability of 1  $\mu$ g/mL of polyphenols from each tea to scavenge the free radical 2, 2-diphenyl-1-picrylhydrazyl (DPPH). Mineral deposition was quantified using alizarin red stain (n=6, where each 'n' represents an independent plating of four replicate wells that were averaged). TPC of black tea was greater (p<0.05) than other teas (mg of gallic acid equivalents/g, EB:64 $\pm$ 13 > GT:46 $\pm$ 11, GR:41 $\pm$ 6, RR:26 $\pm$ 5, WT:10 $\pm$ 3). The ability of each tea to inhibit the free radical DPPH also differed (WT and GT>RR, p<0.05), possibly due to their different polyphenols. Each tea increased (p<0.05) mineral deposition (% of control, RR:150 $\pm$ 7, GR:144 $\pm$ 7, EB:144 $\pm$ 11, GT:141 $\pm$ 11, WT:130 $\pm$ 10). Specifically, RR resulted in greater (p<0.05) mineral deposition compared to WT. Interestingly, the data regarding mineral deposition does not follow the same trend as anti-oxidative capacity and suggests other potential mechanisms. The findings also suggest that the effectiveness of tea to promote mineral deposition may depend on both the quantity and the specific profile of polyphenols within a tea. Differential quantitative gene expression analysis, as well as cell viability measurements, are ongoing to elucidate potential molecular mechanisms and will be presented.

Disclosures: Michael McAlpine, None.

## MO0537

**Regulation of Bone Mass by FGF Signaling Pathways.** Jennifer McKenzie\*, Kannan Karuppaiah, Craig Smith, Matthew Silva, David Ornitz. Washington University in St. Louis, United States

Fibroblast Growth Factor (FGF) signaling is important for skeletal growth and development; however, the functions of FGF receptor (FGFR) signaling in postnatal bone growth and homeostasis are not known. To investigate FGFR signaling in mature osteoblasts and osteocytes *Osteocalcin-Cre* (OC-Cre) was used to inactivate *Fgfr1* and *Fgfr2*. We hypothesize that loss of FGFR1 and FGFR2 signaling will increase osteoblast anabolic activity and differentiation into osteocytes. This animal study was approved by our IACUC. At 24 wk, *Fgfr1*<sup>fl/fl</sup> *Fgfr2*<sup>fl/fl</sup> (DFF) and OC-Cre; *Fgfr1*<sup>fl/fl</sup> *Fgfr2*<sup>fl/fl</sup> double conditional knockout (DCKO) mice show no significant difference in body weight (females: 25  $\pm$  1.0 g, n=8; 24  $\pm$  1.7, n=6, respectively). Lineage tracing analysis of OC-Cre, ROSA<sup>TdTomato</sup> mice demonstrated targeting of trabecular and cortical osteoblasts (endosteal and periosteal) and osteocytes. *In vivo* microCT analysis of DCKO mice revealed a progressive accrual of cortical bone occurring after 6 wk in both male and female mice (Figure, n=3-10). Metaphyseal cancellous bone volume also increased as the mice reached skeletal maturity. mRNA expression analysis showed decreased levels of *Sost* and increased levels of *Runx2* and *Pthlh* at 24 wk (n=3, p<0.05), consistent with increased bone formation. Furthermore, dynamic histomorphometry at 12 wk (n=3) suggested increased anabolic activity in DCKO compared to DFF control mice, with increased endocortical MAR (p<0.005) and periosteal MS/BS (p<0.005). Both the histology and dynamic histomorphometry exhibit an increase in the cortical porosity of DCKO mice, consistent with increased numbers of osteoclasts by TRAP staining (n=3, 12 wk). Mechanical testing (femur three-point bending, n=6, 24 wk) demonstrated increased structural mechanical properties in DCKO mice (stiffness, max load, p<0.001), but inferior material properties (Young's modulus, maximum stress, p<0.001). Taken together, these data suggest an important postnatal role for FGFR signaling. In agreement with our hypothesis, when FGFR signaling is inactivated, there is an increase in late stage osteoblast and osteocyte activity leading to increased bone formation. Knowledge of these signaling mechanisms will provide new targets that can be used to develop therapies aimed at preventing bone loss or restoring bone mass.



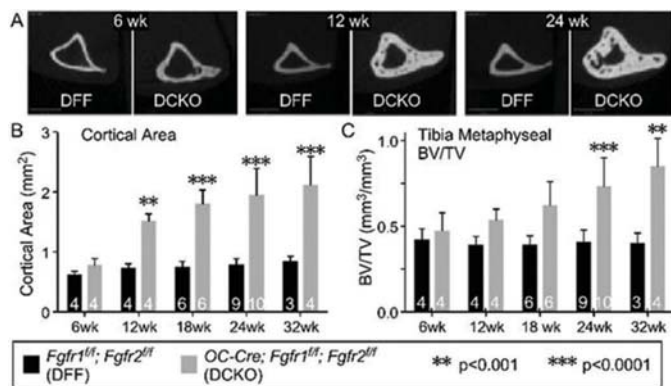


**Figure.** (A) *In vivo* micro CT of serial tibial midshaft sections in control *Fgfr1<sup>fl</sup>; Fgfr2<sup>fl</sup>* (DFF) and OC-Cre; *Fgfr1<sup>fl</sup>; Fgfr2<sup>fl</sup>* (DCKO) mice. (B) Cortical area increases dramatically over time in DCKO mice. (C) Tibia metaphyseal BV/TV similarly increases over time. Number of mice is indicated on each bar. Statistics, 2-way ANOVA.

Figure

**Disclosures:** Jennifer McKenzie, None.

## MO0538

**Runx2 mediated autophagy promotes osteoblast and chondrocyte differentiation.** Ahmad Othman<sup>1</sup>, Manish Tandon<sup>1</sup>, Ryan Ross<sup>1</sup>, Lifan Liao<sup>1</sup>, Rick Sumner<sup>1</sup>, Amjad Javed<sup>2</sup>, Di Chen<sup>1</sup>, Jitesh Pratap<sup>1</sup>. <sup>1</sup>Rush University Medical Center, United States, <sup>2</sup>University of Alabama at Birmingham, United States

Autophagy, an evolutionary conserved catabolic process, recycles amino acids after lysosomal degradation of cytoplasmic proteins and organelles. To meet the high metabolic demand of protein synthesis during bone synthesis and remodeling, the autophagy pathway is induced in chondrocyte, osteoblast, osteocyte and osteoclast. However, the crosstalk which integrates the autophagy pathway and regulators of differentiation is surprisingly not clear. Previously, we and others have reported that Runx2 is necessary for osteoblast and chondroblast differentiation. To examine the role of Runx2 in autophagy, we utilized multiple cell types including primary osteoblasts, chondrocytes and fibroblasts from Runx2 conditional or global knockout mice. The expression levels of autophagy marker microtubule associated light chain protein (LC3B) were examined in both basal conditions and during differentiation. We demonstrate that gene expression of both Runx2 and LC3B is peaked at day 14 of osteoblast differentiation. Runx2 gene deletion or RNAi-mediated knockdown of Runx2, leads to a two-fold reduction in autophagic flux. A critical stage of autophagy involving autophagosome trafficking and fusion with the lysosome relies on their interaction with microtubules (MTs). A time-dependent increase in LC3B-II and acetylated  $\alpha$ -tubulin protein levels was detected during differentiation. We found that Runx2 deficiency reduces acetylation levels of MTs concomitant to loss of autophagic flux. Furthermore, punctate LC3B staining, indicating autophagosomes, colocalized with acetylated tubulin in immunofluorescence analysis. The electron microscopy of Runx2 knockdown cells revealed an increase in number of autophagic vesicles and a concomitant decrease in number of mitochondria. Autophagy is also known to facilitate glycolysis and oxidative phosphorylation. Both oxidative phosphorylation and glycolysis were reduced following Runx2 knockdown and inhibition of autophagy. Taken together, our results reveal a novel mechanism of Runx2-mediated autophagy via acetylated- $\alpha$ -tubulin that could be important for bone formation, remodeling, regeneration and metabolic disorders.

**Disclosures:** Ahmad Othman, None.

## MO0539

**Unexpected and controversial role of Lipocalin 2 in bone and energy metabolism.** Nadia Rucci<sup>\*</sup>, Mattia Capulli, Marco Ponzetti, Antonio Maurizi, Sara Gemini-Piperni, Anna Teti. Department of Biotechnological and Applied Clinical Sciences, Italy

Lipocalin 2 (LCN2) is an adipokine carrying out various functions in different organs. However, its role in bone metabolism is controversial and a recent report suggests that global or osteoblast (OB)-specific LCN2 deletion has no effect on bone mass. In this study, we observed a very faint LCN2 expression in OBs in basal conditions, while we did observe an unexpected osteopenia in *Lcn2<sup>-/-</sup>* mice, with 40% lower bone volume, and 50% and 21% lower trabecular number and thickness vs WT at 3 months of age ( $p < 0.05$ ), which worsened at 12 months, reducing also cortical thickness

by 25% ( $p < 0.001$ ). *Lcn2<sup>-/-</sup>* mice had lower OB number and surface and 50% lower bone formation rate ( $p < 0.05$ ), while osteoclast variables were unremarkable. Despite this strong *in vivo* osteopenia, we found no difference in alkaline phosphatase (ALP) activity or nodule mineralization in 21 days OB cultures, while only *Osteocalcin* expression was lower (~70%) in *Lcn2<sup>-/-</sup>* vs WT OBs ( $p = 0.003$ ). Intriguingly, bone marrow-derived ALP-positive colonies were 30% less in *Lcn2<sup>-/-</sup>* mice, portraying the *Lcn2<sup>-/-</sup>* bone phenotype as environment-derived, which would reconcile our controversial *in vivo* and *in vitro* results. As reported, *Lcn2<sup>-/-</sup>* mice were heavier, suggesting that altered energy metabolism was the culprit. In fact, we observed higher glucose tolerance in *Lcn2<sup>-/-</sup>* vs WT mice (1.2fold,  $P = 0.003$ ), likely due to higher serum insulin levels (ng/ml, *Lcn2<sup>-/-</sup>*: 3.67; WT, 2.25;  $p = 0.036$ ). Insulin tolerance was similar at 3 months of age, while 12 month-old *Lcn2<sup>-/-</sup>* mice had lower insulin sensitivity (~20%,  $P = 0.036$ ). Food intake and glycosuria were higher at 3 and 12 months of age ( $p < 0.05$ ). This was even more baffling because insulin is anabolic for OBs, while lower blood glucose means cells are well fed, and OBs rely on glucose uptake for collagen deposition and Runx2 stabilization. To clear the fog, we performed short term (4 days) OB cultures, to retain at least part of the effects caused by *in vivo* environment. Interestingly, transcriptional expression of the *glucose transporter-1* and glucose uptake were 40% lower in *Lcn2<sup>-/-</sup>* OBs compared to WT ( $p < 0.05$ ). Insulin signaling was also impaired in *Lcn2<sup>-/-</sup>* since *Insulin receptor* expression was 50% lower ( $p = 0.04$ ) in bone, and GSK3B and AKT were over- and under-activated, respectively, after *in vitro* insulin treatment. Our results contradict recent report and prompt us to conclude that LCN2 is able to flip upside-down everything we know about bone and energy metabolism.

**Disclosures:** Nadia Rucci, None.

## MO0540

**Systems Genetics Identifies Novel Genes and Gene Networks Influencing Osteoblast Activity.** Olivia L Sabik<sup>1</sup>, Gina M Calabrese<sup>2</sup>, Cheryl L Ackert-Bicknell<sup>3</sup>, Charles R Farber<sup>4</sup>. <sup>1</sup>Department of Biochemistry and Molecular Genetics and Center for Public Health Genomics, School of Medicine, University of Virginia, United States, <sup>2</sup>Center for Public Health Genomics, School of Medicine, University of Virginia, United States, <sup>3</sup>Center for Musculoskeletal Research, University of Rochester Medical Center, University of Rochester, United States, <sup>4</sup>Department of Public Health Sciences and Center for Public Health Genomics, School of Medicine, University of Virginia, United States

Osteoporosis is a disease characterized by low bone mineral density (BMD) and increased risk for fracture. Identifying novel modulators of bone formation remains a goal in the pursuit of safe, effective therapies that promote bone anabolism. While many of the critical signaling pathways impacting bone formation by the osteoblast are known, our knowledge is incomplete, and it is unclear how osteoblast activity is regulated at a systems-level. BMD is a "snap shot in time" measure—it is the sum of bone formation and resorption and cannot be used as surrogate phenotype for bone formation alone. Similarly, serum markers of bone formation can be confounded by other physiologic and pathologic factors from a genetics point of view. In this study, we used an innovative systems genetic approach to identify novel genes and gene networks modulating osteoblast activity in the Collaborative Cross (CC), a transformative new murine genetic reference population. We measured *in vitro* mineralization of primary calvarial osteoblasts in 48 CC strains. Levels of *in vitro* mineralization were highly heritable ( $H^2 = 0.52$ ;  $p = 1.4 \times 10^{-52}$ ) in the CC. Additionally, we observed a positive correlation between *in vitro* mineralization and cortical bone area/total area (BA/TA) of the femur (0.43,  $p = 0.008$ ), supporting the physiological relevance of *in vitro* osteoblast activity. To identify genetic drivers of *in vitro* mineralization we performed a genetic analysis in the CC and identified one quantitative trait locus (QTL) on Chromosome 10. Calvarial osteoblasts from CC strains homozygous for the CAST/EIJ (CAST) haplotype in the QTL region displayed lower levels of mineralization. To determine the gene responsible for the association we identified colocalizing local expression QTL (eQTL). Cytoskeleton Associated Protein 4 (*Ckap4*) was the only gene whose expression was significantly associated with the CAST haplotype, which increased *Ckap4* expression in osteoblasts. *Ckap4* is a known receptor of WNT antagonist Dickkopf1 (*Dkk1*), in the context of cancer. We also constructed a weighted gene co-expression network using transcriptomic data on the osteoblasts from 42 CC strains and identified three modules of genes associated with *in vitro* mineralization. We are currently prioritizing hub genes from these modules for mechanistic follow up. This work has provided us with new insight into the molecular mechanisms that regulate osteoblast activity.

**Disclosures:** Olivia L Sabik, None.

## MO0541

**A footstep to figuring out the difference between alveolar bone and long bone.** Chul Son<sup>\*</sup>, Yeoung Hyun Park, Joo Cheol Park. Department of Oral Histology-Developmental Biology, School of Dentistry, Seoul National University, Korea, Republic of

The alveolar bone is both morphologically and functionally different from the other bones of the axial or peripheral skeleton. It also arises from a different embryonic germ layer (neuroectoderm) compared with bone of the axial and appendicular skeleton, which arises from mesoderm. Unlike long bone, alveolar bone is still poorly studied. We aim to elucidate the difference in mechanisms underlying the development and

remodeling of alveolar bone and long bone. In order to elucidate the difference between alveolar bone and long bone *in vitro*, we isolated cell from alveolar, femurs and tibia bone tissue. When we analyzed the cell morphology under the light microscope, mouse alveolar bone derived cells (mABDC) and long bone derived cells (mLBDC) looked similar to calvaria osteoblast cell line (MC3T3-E1). To figure out whether alveolar and long bone derived cells have the osteoblastic traits, we analyzed the expressions of Bsp, Alp and OC, known as osteoblast markers. We used mouse dermal fibroblast (mDF) as a negative control. These marker genes were expressed much higher in bone derived cells than in mDF. Moreover, when the cells were cultured in osteogenic differentiation media for 10 and 20 days, the bone derived cells manifested more mineralized nodule formation than mDF. These results suggest that mABDC and mLBDC showed osteoblast-like characteristics. Focusing on the difference between mABDC and mLBDC, the expressions of two of the intramembranous ossification-associated markers, *Msx* and *Dlx* gene families, were expressed higher in mABDC than in mLBDC. *CPNE7* and *Nfic*, which were found to be associated with epithelial-mesenchymal interaction (EMI) in our previous studies, were expressed higher in mABDC than in mLBDC. Tissue samples showed a consistent result. Interestingly, *Bmp* family genes, *Bmp2* and *Bmp4*, also increased in mABDC. Our data suggest that different mechanisms underlie the development and remodeling of alveolar bone and long bone. Particularly, factors involved in EMI signaling such as *cpne7*, *nfic*, and *bmp* families, seem to affect alveolar bone more than they affect long bone. In the near future, we plan to explore the difference between alveolar bone and long bone by systemic analysis such as RNA sequencing.

**Disclosures:** Chul Son, None.

## MO0542

**The role of Tet1 and Tet2 and active DNA demethylation for osteoblastic differentiation.** Roman Thaler<sup>\*1</sup>, Farzaneh Khani<sup>1</sup>, Janet Denbeigh<sup>1</sup>, Markus Schreiner<sup>1</sup>, Amel Dudakovic<sup>1</sup>, Xianhu Zhou<sup>1</sup>, David Deyle<sup>2</sup>, Andre J van Wijnen<sup>1</sup>. <sup>1</sup>Departments of Orthopedic Surgery & Biochemistry and Molecular Biology, Mayo Clinic, United States, <sup>2</sup>Departments of Medical Genetics, Mayo Clinic, United States

Bone development and homeostasis is controlled by several mechanisms including epigenetic control of gene expression. As we have shown before, osteoblastic differentiation is epigenetically regulated on the histone as well as on the DNA level. For example, the natural isothiocyanate sulforaphane promotes osteoblastic differentiation and has bone anabolic effects via the promotion of active DNA demethylation via the DNA hydroxymethylases Tet1 and Tet2. Based on this dataset, we aim to better understand the role of these two epigenetic regulators and of active DNA demethylation during osteoblastic differentiation.

Interestingly, treatment of human adipose derived mesenchymal stem cells with sulforaphane stimulates Tet expression along with active DNA demethylation shifting the differentiation potential of these cells towards the osteogenic lineage. This is reflected by the increased expression of *RUNX2*, *COL1A1* and *ALPL*, and increased extra cellular matrix mineralization during osteoblastic differentiation as well as decreased fat droplet formation and suppressed expression of the adipose tissue related genes like PPARG, PLIN1 or CEBPA during adipogenic differentiation. Tet1 expression is highest in embryonic stem cells, however in bone marrow stem cells and osteoblastic cells, Tet2 expression exceeds Tet1 expression. Tet1 and Tet2 expression patterns remain rather constant during osteoblastic differentiation and stable knock down of these two genes by shRNAs strongly de-regulates osteoblastic differentiation of MC3T3-E1 cells. In fact, knock down of Tet1 as well as of Tet2 expression strongly reduces the expression of primary osteoblastic transcription factors like Runx2, Sp7 or Mef2c as well as of extra cellular matrix (ECM) related genes like Alpl, Col1a1, Smpd3, Lox, Sparc or Ifitm5. Furthermore, Tet1 and as well as Tet2 suppression hinders ECM deposition and mineralization. Of note, knock down of Tet2 but not of Tet1 primarily affects global DNA hydroxymethylation levels during osteoblastic differentiation of MC3T3-E1 cells. This might be due to the higher expression levels of Tet2 in osteoblastic cells. Functionally, DNA hydroxymethylation patterns accumulate on promoters of osteoblastic genes during osteoblastic differentiation as for the *Dlx3* promoter.

In summary, here we show that Tet1 and Tet2 enzymes, and thus active DNA demethylation plays a major role for osteoblastic differentiation.

**Disclosures:** Roman Thaler, None.

## MO0543

**MiR-23a Cluster – RUNX2 – EZH2 Axis Controls Bone Formation In-Vivo.** Benjamin Wildman<sup>\*1</sup>, Mohammad Hassan<sup>1</sup>, Tanner Godfrey<sup>1</sup>, Harunur Rashid<sup>1</sup>, Chris Lengner<sup>2</sup>, Amjad Javed<sup>1</sup>. <sup>1</sup>UAB, United States, <sup>2</sup>UPenn, United States

Epigenetic regulation is critical to the differentiation and renewal of stem cell populations. Important to this endeavor, EZH2, the enzymatic subunit of the PRC2 complex, is a potent epigenetic inhibitor of gene expression. There is a gap in knowledge of how epigenetics impacts the differentiation of mesenchymal stem cells to mature osteoblasts. To fulfill this need, our lab previously identified that the miR-23a cluster is a potent inhibitor of osteogenesis.

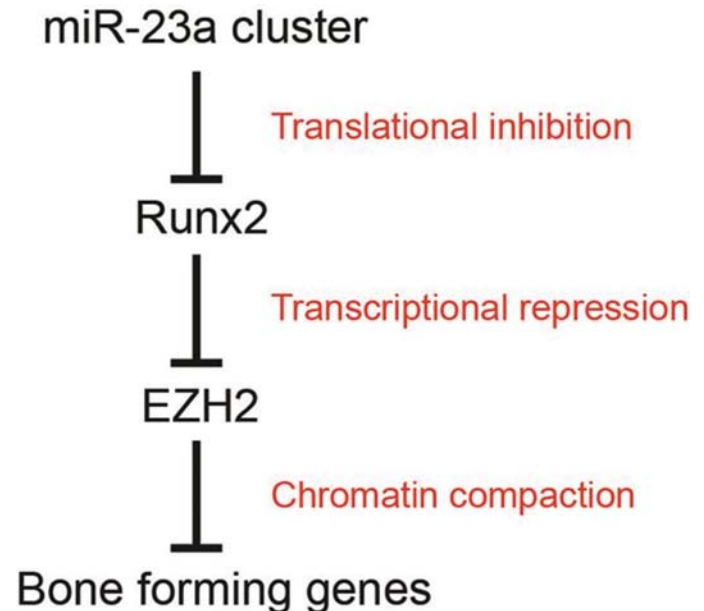
Due to the critical nature of the miR-23a cluster in bone development, we have recently developed an anti-miRNA strategy to knock down this cluster in mouse. With this novel tool, we have discovered that knockdown of the miR-23a cluster results in high trabecular and cortical bone, using Micro CT at 2 months of age. To elucidate the

mechanism behind this observation, we performed RNA sequencing on calvarial cells which revealed significantly increased Runx2 expression and a significant decrease Ezh2 expression. Additionally, ChIP assays revealed decreased H3K27 trimethylation at bone specific promoters, correlating with increased expression. These results demonstrate the miR-23a cluster inhibition of bone formation is mediated by posttranscriptional down-regulation of Runx2 along with EZH2 mediated repression of osteoblast specific promoters.

To demonstrate that miR-23a cluster mediated regulation of EZH2 is RUNX2 dependent, RT-PCR of Runx2 null cells identified a significant increase in Ezh2 expression. Additionally, ChIP analysis revealed a higher occupancy of EZH2 at bone specific promoters. Importantly, miR-23a cl overexpression in Runx2 null cells did not impact EZH2 expression. These findings indicate that the miR23-a cluster modulates EZH2 in a RUNX2 dependent manner.

Recently, we developed a stably expressing chimeric protein composed of EZH2 fused to a promiscuous biotin ligase (EZH2-BioID). This technology is able to identify proximal interacting proteins to EZH2. EZH2-BioID will allow us to determine the bone specific composition of the EZH2 led PRC2 complex temporally through osteoblast development. Additionally, we will be able to identify PRC2 associated complexes that facilitate physiological epigenetic regulation of osteogenesis.

Taken together, these findings reveal an epigenetic axis wherein the miR-23a cluster regulates Runx2 to modulate physiological EZH2 expression. This study elucidates a novel regulatory system to better understand the epigenetic drivers of bone formation *in-vivo*.



miR-23a cluster - Runx2 - Ezh2 Axis

**Disclosures:** Benjamin Wildman, None.

## MO0544

**Inhibition of CaMKK2 accelerates bone fracture healing.** Justin Williams<sup>\*</sup>, Anu Valiya Kambrath, Roshni Patel, Yinghua Chen, Alexander Robling, Uma Sankar, Melissa Kacena. Indiana University School of Medicine, United States

Fractures associated with osteoporosis and acute trauma result in significant medical costs, loss of productivity and patient quality of life. Currently, there are no effective pharmacological treatments that promote efficient healing of bone fractures. Here we describe a novel therapeutic target which accelerates bone healing by a whole week.  $\text{Ca}^{2+}$ /calmodulin (CaM)-dependent protein kinase kinase 2 (CaMKK2) has roles in the anabolic and catabolic pathways of bone remodeling. Its pharmacological inhibitor STO-609 protects from post-menopausal and age-dependent osteoporosis. We hypothesized that inhibition of CaMKK2 with STO-609 will result in accelerated fracture healing and efficient recovery from bone fracture.

Unilateral femoral fractures were generated in 10 week old C57BL6 mice using a three-point bending device. Location and quality of the fractures were confirmed by radiography. Fractures were stabilized with a 24 gauge stainless steel rod. Tri-weekly intraperitoneal injections of saline (n=30) or STO-609 (n=30; 10 µmol/kg) were administered for 4 weeks post-fracture. Fractured calluses were analyzed by micro-CT before being processed for histology or immunohistochemistry. Torsional biomechanical testing was performed to assess strength.

STO-609 treatment resulted in a significant increase in callus area, and also contained significantly more bone by 2 weeks post-fracture, implying that CaMKK2 inhibition stimulates early bone formation within the callus. By 4 weeks, STO-609 treated calluses possessed a significantly higher percent of mature bone that translated into improved strength. Mechanistic investigations revealed an acceleration of early molecular events associated with bone healing. During normal fracture healing in mice, hypertrophic



chondrocytes appear around day 14, produce VEGF which serves as a chemoattractant for migration of stem and osteoprogenitor cells into primary ossification centers. Our observations reveal a marked elevation in hypertrophic chondrocytes and VEGF, as well as an influx of mesenchymal stem cells in the callus by day 7 in STO-609 treated mice. By day 14, these calluses possessed significantly higher levels of osteocalcin and calcified matrix compared to controls. Our studies indicate that CaMKK2 inhibition with STO-609 accelerates the healing process by a whole week such that drug-treated mice possess more mature and stronger secondary bone in their calluses indicating faster repair of the fracture.

**Disclosures:** Justin Williams, None.

## MO0545

**Cbfb Governs Osteoblast-Adipocyte Lineage Commitment through Enhancing  $\beta$ -Catenin Signaling and Suppressing Adipogenesis Gene Expression.** Mengrui Wu<sup>\*1</sup>, Wei Chen<sup>1</sup>, Jue Wang<sup>2</sup>, Yi-Ping Li<sup>2</sup>. <sup>1</sup>Department of Pathology, University of Alabama at Birmingham, United States, <sup>2</sup>University of Alabama at Birmingham, United States

The majority of conditions associated with bone loss (e.g. aging, glucocorticoid treatment, and thiazolidinedione treatment) stem from a decreased number of osteoblasts and an increased number of adipocytes in the bone marrow. Both osteoblasts and adipocytes derive from bone marrow mesenchymal stem cells upon specific stimulation during cell differentiation. However, the mechanism underlying how transcription factors regulate mesenchymal stem cell lineage commitment remains unclear. Core-binding factor subunit beta (Cbfb) is a non-DNA-binding partner of Runt-related transcription factors (Runx1, 2 and 3) that is involved in skeletal development, osteoblast and chondrocyte differentiation as well as fracture healing. To determine the role of Cbfb in osteoblast lineage commitment, we utilized the cre-lox system to generate three tissue-specific *Cbfb* conditional knockout mouse models at different osteoblast-lineage stages. Radiological and histological analyses demonstrated that the *Cbfb*<sup>fl/fl</sup>*Prx1-Cre*, *Cbfb*<sup>fl/fl</sup>*Col2a1-Cre* and *Cbfb*<sup>fl/fl</sup>*Osx-Cre* mice exhibited severe osteoporosis with substantial accumulation of marrow adipocytes resembling aged bone from enhanced adipogenesis, indicating that mesenchymal stem cells and osteoblasts can be programmed and reprogramed into adipocytes. Gene expression analysis revealed that *Cbfb*-deficient calvarial cells and bone marrow mesenchymal stem cells displayed strong adipogenic potential with 5~70-fold increased adipocyte gene expression, which can be rescued by Cbfb overexpression. Canonical Wnt signaling was impeded in the *Cbfb*-deficient cells, with ~80% decrease of Wnt10b expression. Accordingly, ChIP and luciferase assays demonstrated that *Cbfb*/RUNX2 binds to *Wnt10b* promoter driving *Wnt10b* expression. Furthermore, Wnt3a suppressed adipogenesis but did not rescue osteoblastogenesis in *Cbfb*-deficient cells. Notably, mixing culture of Cbfb-deficient with normal cells demonstrates that Cbfb functions not only through WNT paracrine pathway but also endogenous signaling. Further analysis shows that *Cbfb*/RUNX2 inhibits *clebpa* expression at transcriptional level. Our results show that besides its osteogenic role, Cbfb governs osteoblast-adipocyte lineage commitment both cells non-autonomously through enhancing  $\beta$ -catenin signalling and cell-autonomously through suppressing adipogenesis gene expression to maintain osteoblast-lineage commitment, indicating Cbfb may be a new therapeutic target for osteoporosis.

**Disclosures:** Mengrui Wu, None.

## MO0546

**AFF1 and AFF4 differentially regulate the osteogenic differentiation of human MSCs.** chenchen zhou<sup>\*</sup>, QiuChan Xiong. NO.14, 3rd Section of Ren Min Nan Rd, China

AFF1 and AFF4 belong to the AFF (AF4/FMR2) family, which functions as scaffolding proteins linking the two different transcription elongation factors, positive elongation factor b (P-TEFb) and ELL1/2 in Super Elongation Complexes (SECs). Studies have shown that both AFF1 and AFF4 regulate gene transcription through elongation and chromatin remodeling. However, their function in osteogenic differentiation of mesenchymal stem cells (MSCs) is unclear. In this study, we first knocked down AFF1 in human MSCs by siRNA. Depletion of AFF1 led to a more intensive staining of alkaline phosphatase (ALP) and Alizarin red S (ARS). The expression of osteogenic-related genes, such as *RUNX2*, *SP7* and *BGLAP* was significantly upregulated. On the contrary, overexpression of AFF1 with lentiviruses expressing HA-AFF1 particles decreased the ALP activity and mineralization of MSCs. In addition, the expression of *RUNX2*, *SP7* and *BGLAP* was significantly diminished after osteogenic induction for 5 days. Next, we sought to evaluate if AFF4 has the similar function as AFF1. Surprisingly, depletion of AFF4 significantly inhibited the osteogenic potential of MSCs, which is opposite to AFF1. We then infected the MSCs with lentiviruses expressing HA-AFF4 and confirmed that overexpression of AFF4 enhanced osteoblastic differentiation. Next, we examined whether the overexpression of AFF1 and AFF4 differentially affected MSC-mediated bone formation *in vivo*. To this end, MSCs stably overexpressed with HA-AFF1 or HA-AFF4 were seeded on  $\beta$ -TCP scaffolds and implanted into immunocompromised mice subcutaneously. After 3 and 6 weeks, cells overexpressed with HA-AFF1 formed much less bone tissues, while those overexpressed with HA-AFF4 led to a significant increase in bone formation. Mechanically, we found that AFF1, but not AFF4, regulated the expression of DKK1, an antagonistic inhibitor of the Wnt/ $\beta$ -Catenin signaling pathway. ChIP assay demonstrated that AFF1 bound on the promoter region of *DKK1*. In addition, depletion of DKK1 in stable HA-AFF1 MSCs rescued the impaired capability of osteogenic differentiation. Finally, we observed that AFF4 bound on the promoter region of *ID1*. BRE luciferase assay showed that AFF4 depletion markedly restricted BMP2-induced

responses. Knockdown of AFF4 also blunted the expression of *SP7* and ALP activity induced by BMP2 treatment. In conclusion, our data demonstrated that AFF1 and AFF4 differentially regulate the osteogenic differentiation of human MSCs.

ASBMR

**Disclosures:** chenchen zhou, None.

## MO0547

**Novel Cytoplasmic Roles of EZH2 Methyltransferase During RANKL Signaling, Cytoskeletal Organization and Resorption of Osteoclasts.** Juraj Adamik<sup>\*1</sup>, Peng Zhang<sup>1</sup>, Qianhong Sun<sup>1</sup>, Jolene J Windle<sup>2</sup>, Philip E Auron<sup>3</sup>, Deborah L Galson<sup>1</sup>. <sup>1</sup>Department of Medicine, Hematology-Oncology Division, University of Pittsburgh Cancer Institute, McGowan Institute for Regenerative Medicine, University of Pittsburgh, United States, <sup>2</sup>Department of Human and Molecular Genetics, Virginia Commonwealth University, United States, <sup>3</sup>Department of Biological Sciences Duquesne University, United States

EZH2, the methyltransferase subunit of Polycomb Repressive Complex 2, methylates histones on lysine residues, which induces gene repression. Using EZH2 knockdown and the small molecule inhibitor GSK126, we showed that EZH2 plays a critical epigenetic role during the first 24 hours of RANKL activation in osteoclast precursors (OCLp). Here we reveal that EZH2 changes its cellular partitioning and plays distinct roles during OCL differentiation.

Immunofluorescence microscopy revealed that EZH2 in OCLp is primarily associated with large punctate cytoplasmic structures. Consistent with cytoplasmic localization, EZH2 methyltransferase activity is required during early RANKL signaling for phosphorylation of cytoplasmic Akt (pSer473 and pThr 308), resulting in downstream activation of both cytoplasmic and nuclear mTOR complexes that are required for induction of OCL differentiation. Inhibition of pmTOR-pS6RP signaling by GSK126 altered the ratio of C/EBP $\beta$ -LAP and LIP alternative translation isoforms, reducing the inhibitory LIP that is necessary for transcriptional repression of OCL negative regulatory factor MafB. RANKL treatment induced most of EZH2 to translocate to the nucleus. Surprisingly, this was blocked by GSK126. Inhibition of EZH2 during the initial phase of RANKL activation of OCLp prevented OCL fusion and formation, but not TRAP expression, and the cells exhibited impaired shape and actin morphology. While EZH2 in multinucleated OCL on glass was primarily cytoplasmic, EZH2 in OCL differentiated on bone was distributed between nuclei and the cytoplasm. We noted that EZH2 remained nuclear in mononuclear OCL in the same cultures. Mature OCL on bone treated with GSK126 (day 6-8) exhibited condensed cytoskeletal architecture with impaired sealing zone formation, impaired migration and reduced resorptive activity. Cytoplasmic EZH2 has been reported to methylate LIM domain kinase 1 (LIMK1) and inactivate its Ser/Thr kinase in megakaryocyte precursors, which results in increased remodeling of the actin cytoskeleton. As LIMK1 was reported to regulate OCL shape, future studies will examine EZH2 regulation of this protein's function in osteoclasts. Here we present new evidence that EZH2 plays multiple novel non-histone roles during OCL differentiation by regulating early phases of p-Akt mediated-RANKL signaling and also cytoskeletal dynamics during OCL fusion and resorption.

**Disclosures:** Juraj Adamik, None.

## MO0548

**Osteomacs express higher levels of MCSF, MCSF-R and Galectin3 and show increased osteoclastogenesis compared to bone marrow-derived macrophages.** Alexandra Aguilar-Perez<sup>\*</sup>, Angela Bruzzaniti, Melissa Kacena, Edward Srouf, Safa Mohamad, Joydeep Ghosh, Marta Alvarez, Paul Jeffrey Childress, Korbin Davis, Lin Lin Xu, Hao Wu. Indiana University, United States

Bone formation is a coordinated event that requires the contribution of hematopoietic and mesenchymal stem cells. Loss of homeostasis between the cells in the bone marrow niche could result in bone loss and osteoporosis. We previously reported that megakaryocytes increase osteoblast precursor proliferation by up to 6-fold in calvarial cells (CC) derived from 2 day neonates and augment bone deposition *in vivo*. As described by others and confirmed here, CC are a heterogeneous cell population that contain ~95% osteoblasts and 3-5% osteomacs (OM) which are phenotypically CD45<sup>+</sup>F4/80<sup>+</sup> cells (also known as osteal macrophages). Megakaryocyte-induced osteoblast proliferation and mineralization is abrogated with the removal of OM from the CC population, demonstrating a key function of OM in bone metabolism. Since OM and bone marrow-derived macrophages (BMMF) are both CD45<sup>+</sup>F4/80<sup>+</sup> hematopoietic lineage cells we characterized the functional differences between these cell types. Fluorescence activated cell sorting was used to isolate OM from collagenase-digested CC or BMMF from crushed femur/tibia of 2 day-old neonates. We found that proliferation was significantly higher in OM than BMMF as determined by MTS assay. Using single-cell genomics we also demonstrated significantly increased levels of MCSF and MCSF-R in OM compared to BMMF. In addition, OM, but not BMMF, formed osteoclasts in the presence of RANKL (without exogenous MCSF). Moreover, when cultured with MCSF+RANKL, OM showed a significant increase in the formation of

TRAP+ osteoclasts compared to BMMF. Next we examined signaling differences in OM and BMMF by focusing on the carbohydrate binding lectin, galectin 3 (Gal3, also known as Mac2) which is a surface marker for OM (Mac2/Gal3<sup>low</sup>). Gal3 is known to bind CD45, a regulator of osteoclastogenesis and Gal3-deficient mice exhibit high bone mass. We found that OM endogenously express and secrete higher levels of Gal3 than BMMF when cultured with either RANKL alone, MCSF+RANKL or VitaminD<sub>3</sub>+PGE<sub>2</sub>. These data suggest that Gal3 may be part of the mechanism leading to increased osteoclastogenesis in OM cultures compared to BMMF. Thus OM, which are intimately associated with bone surfaces, may contribute to bone turnover in the bone marrow niche by both promoting osteoblastic bone formation/mineralization and acting as a source of osteoclast progenitors that can undergo osteoclastogenesis in the absence of paracrine MCSF signaling.

**Disclosures:** Alexandra Aguilar-Perez, None.

## MO0549

**Rapid Effects of Low Extracellular Sodium on Osteoclasts: Molecular Mechanisms.** Julia Barsony\*, Qin Xu, Joseph Verbalis, Georgetown University, United States

Chronic hyponatremia (CH) has become appreciated as a secondary cause of osteoporosis and increased fracture frequency in the elderly population, but still remains largely untreated. CH is frequently caused by comorbidities, medication use and the syndrome of inappropriate antidiuretic hormone secretion, and its potential impact on mortality, loss of bone mineral density, increased falls due to gait impairments and fractures requires identification of effective treatment strategies. Our prior studies in cell culture models demonstrated that reducing sodium concentration ([Na<sup>+</sup>]) in the culture media markedly activates osteoclastogenesis and osteoclastic bone resorption, but the mechanism(s) by which osteoclasts sense and respond to low extracellular [Na<sup>+</sup>] remained to be elucidated. We used mature murine primary osteoclasts and RAW264.7-derived osteoclasts cultured in normal media or in low [Na<sup>+</sup>] with osmolality normalized by the addition of mannitol to define the low [Na<sup>+</sup>] sensing and signaling cascade. Western blot analyses and phosphor-kinase array studies indicated that reducing [Na<sup>+</sup>] triggers rapid and sustained phosphorylation events in osteoclastic cells involving the PI3K/Akt/RANKL pathway. The low [Na<sup>+</sup>] induced phosphorylation of Src and GSK were significant after 5 min, and peaked at 30 min. Low [Na<sup>+</sup>] also triggered significant gene expression changes downstream to the PI3K/Akt/RANKL pathway using a dedicated RT-PCR profiling array (Qiagen). Microscopy showed signs of osteoclast activation within minutes after reducing media [Na<sup>+</sup>] indicated by changes in cell shape, reorganization of actin cytoskeleton, and production of acidic lysosomes and their shift to the ruffled border membrane. Fluorometric lysosomal acidity measurements in a 96-well assay using LysoSensor DND-189 demonstrated that the onset of acidification of mature osteoclasts was significant within 3 min (p<0.001) and was sustained over 60 min. This lysosomal response was not prevented by compensating for low [Na<sup>+</sup>]-induced membrane hyperpolarization by the addition of choline chloride or N-Methyl-D-glucamine. These results indicate that an early osteoclastic response to reduced [Na<sup>+</sup>] is specific, perhaps involving a G-protein coupled membrane receptor mediated signaling. Thus, osteoclasts provide the first cell model to define the process of low [Na<sup>+</sup>] sensing and to understand the signaling transduction cascade responsible for cellular adaptation to reduced sodium in the environment.

**Disclosures:** Julia Barsony, None.

## MO0550

**Unraveling the molecular determinants of continuous long-term bone resorption by osteoclasts.** Xenia G Borggaard\*, Dinisha C Pirapaharan, Anais MJ Moeller, Jean-Marie Delaissé, Kent Soe, Vejle Hospital/University of Southern Denmark, Denmark

We have shown that osteoclasts (OCs) can resorb in two distinct resorption modes: pit- (intermittent) and trench-mode (continuous). We have also shown that OCs making trenches generally start in pit- and switch to trench-mode and that a balance between collagenolysis and demineralization is critical for enabling this transition. Here we address in more detail the importance of collagenolysis and proper intracellular processing of collagen fragments. Resorption assays were done using human OCs cultured on bone for 72h. We found a positive linear correlation (r<sup>2</sup> = 0.68, p = 0.0003, n = 14 donors) between the IC50 (trench surface/ES) of odanacatib (specific CatK-inh) and the extent of trench surface/ES in controls, demonstrating that CatK-collagenolysis is the rate limiting factor of trench-formation. To evaluate the respective contribution of extra- and intra-cellular acidic compartments in the processing of collagen fragments, we specifically raised the pH of the intra-cellular ones by using chloroquine. Effective targeting of intra- and not extra-cellular compartments was supported by immunolocalizations of chloroquine and by unreduced demineralization depths in presence of chloroquine (reflecting no extracellular pH-rise). Interestingly, time-lapse of resorption events showed that chloroquine doesn't change erosion speeds, up to initiation of trench formation, but induces a premature arrest of trenches thus leading to overall decreased trench-erosion. So, trench-erosion was 3.1 fold (n=4) more sensitive to chloroquine-treatment than pit-erosion. Time-lapse using lysosome and collagen labelling (n=3) showed the presence of large lysosomes at the resorptive site of OCs in trench-mode coinciding with labelled collagen uptake and their subsequent transport to the rear of the OC. Large lysosomes were not observed in pit-mode. These data suggest a more stringent need for intra-cellular collagen fragment processing in trench-mode. This would also require an efficient uptake of collagen fragments. A characteristic apical

co-localization of clathrin (n=2) with septin-9 (flotation-barrier protein) in trench-compared to pit-mode and a 3.3-fold (n=3) higher sensitivity of trench-mode to inhibition of septins may suggest a unique spatiotemporal organization of collagen uptake in trench-mode. We conclude that the generation of trenches is strictly determined by CatK activity and is more dependent on intracellular processing of collagen fragments compared with pit formation.

**Disclosures:** Xenia G Borggaard, None.

## MO0551

**Slit-ROBO Rho GTPase Activating Protein 2 (SRGAP2) Regulates Osteoclast and Osteoblast Differentiation.** Henry Hrdlicka\*, Bongjin Shin, Anne Delany, Sun-Kyeong Lee, UConn Health, United States

Signaling pathways regulated by the Rho family GTPases are critical for osteoclast formation, motility and function. When GTP-bound, small GTPases activate downstream effectors; when in their GDP-bound form, they are inactive. SRGAP2 is a Rac-specific GTPase activating protein, which limits the duration of Rac signaling. By regulating actin dynamics, SRGAP2 induces filopodia formation and inhibits migration in neurons. We identified Srgap2 as a novel gene induced 20 fold by RANKL during osteoclastogenesis. In contrast, SRGAP2 protein levels are gradually induced as osteoclasts differentiate. Like Srgap2 RNA, levels of miR-29 family members also increase during osteoclastogenesis, and Srgap2 is a miR-29 target. It is likely miR-29 fine tunes SRGAP2 protein levels, to ensure optimal Rac signaling and osteoclast differentiation.

Although Rac signaling is important for osteoclast function, the impact of SRGAP2 on osteoclast differentiation and function is unexplored. Therefore, we examined global Srgap2-null mice. Srgap2-null mice were obtained at 3 fold lower rate compared with WT or haploinsufficient littermates, and were smaller at birth. microCT showed that femurs from 4 week old Srgap2-null mice displayed a 45% decrease in trabecular bone, driven by decreased trabecular thickness and number, with a 40% decrease in cortical thickness (p<0.01). By 8 weeks, trabecular bone volume in Srgap2-null mice was essentially normalized, although femoral length remained shorter and periosteal perimeter was decreased compared with WT littermates (p<0.02).

When cultured in osteoblast differentiation medium, bone marrow stromal cells from Srgap2 haploinsufficient mice displayed decreased mineralized matrix deposition. Similarly, bone marrow macrophages (BMMs) from Srgap2-null mice treated with MCSF and RANKL formed fewer TRAP(+) osteoclasts compared to WT, with decreased levels of NFATc1 and c-FOS. Further, BMMs from Srgap2-null mice had reduced RhoA activity in response to MCSF and RANKL, suggesting cross talk between the RhoA and Rac signaling pathways. These data indicate that adequate levels of SRGAP2 are needed to support both osteoclast and osteoblast differentiation.

Overall, we show Srgap2-null mice have cell-autonomous defects in osteoblastogenesis and osteoclastogenesis, likely contributing to growth delay and decreased trabecular bone volume. These studies underscore the importance of appropriately regulated Rac signaling in bone.

**Disclosures:** Henry Hrdlicka, None.

## MO0552

**The nuclear receptor AhR controls bone homeostasis by regulating osteoclast differentiation via the RANK/c-Fos signaling axis.** Takashi Izawa\*<sup>1</sup>, Eiji Tanaka<sup>1</sup>, Naozumi Ishimaru<sup>2</sup>, <sup>1</sup>Tokushima University Grad School, dept of Orthod, Japan, <sup>2</sup>Tokushima University Grad School, dept of Oral Pathol, Japan

The aryl hydrocarbon receptor (AhR) pathway plays a key role in receptor activator of nuclear factor (NF)-κB ligand (RANKL)-mediated osteoclastogenesis. However, the mechanism underlying the regulation of AhR expression in osteoclasts and the signaling pathway through which AhR controls osteoclastogenesis remain unclear. We found that the expression of AhR in bone marrow-derived osteoclasts was upregulated by RANKL at an earlier stage than the expression of signature osteoclast genes such as those encoding cathepsin K and nuclear factor of activated T cells, cytoplasmic, calcineurin-dependent 1. In response to RANKL, bone marrow macrophages isolated from AhR<sup>-/-</sup> mice exhibited impaired phosphorylation of Akt and mitogen-activated protein kinase as well as NF-κB, while their response to the macrophage colony-stimulating factor remained unchanged. Osteoclast differentiation mediated by the AhR signaling pathway was also regulated in a RANKL/c-Fos-dependent manner. Further, ligand activation of AhR by the smoke toxin benzo [a] pyrene (BaP) accelerated osteoclast differentiation in a receptor-dependent manner, and AhR-dependent regulation of mitochondrial biogenesis in osteoclasts was observed. Moreover, AhR<sup>-/-</sup> mice exhibited impaired bone healing with delayed endochondral ossification. Taken together, the present results suggest that the RANKL-AhR-c-Fos signaling axis plays a critical role in osteoclastogenesis, thereby identifying the potential of AhR in treating pathological, inflammatory, or metabolic disorders of the bone.

**Disclosures:** Takashi Izawa, None.



## MO0553

**C/EBP $\alpha$  Binds to the Androgen Receptor Cofactor MEP50, a Novel Inhibitor of Osteoclast formation, to Release the Inhibitory Effect by Promoting Early Stages of Osteoclastogenesis.** Joel Jules\*, Wei Chen, Yi-Ping Li. University of Alabama at Birmingham, United States

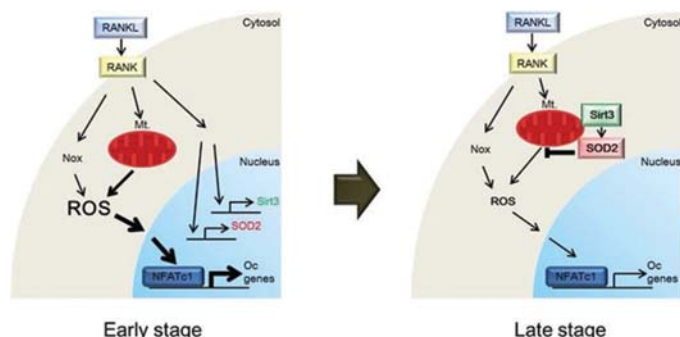
Binding of the receptor activator of NF- $\kappa$ B ligand (RANKL) to its receptor RANK on mouse bone marrow cells upregulates the transcription factor CCAAT/enhancer binding protein- $\alpha$  (C/EBP $\alpha$ ) during osteoclastogenesis. We have recently shown that C/EBP $\alpha$  can not only appoint mouse bone marrow cells to the osteoclast (OC) lineage, but is also important for OC differentiation and activity. While C/EBP $\alpha$  functions in other cells by forming complexes with other factors, it is unknown whether C/EBP $\alpha$  also interacts with other factors in OC. Herein, we used an immuno-affinity purification combined with quantitative mass spectrometry analysis to identify the proteins with which C/EBP $\alpha$  interacts to promote OC formation and activity. We identified methylome protein 50 (MEP50), one of the cofactors of androgen receptor, as a binding partner for C/EBP $\alpha$ , and confirmed that MEP50 interacted with C/EBP $\alpha$  in OC. We found that MEP50 was downregulated by RANKL during osteoclastogenesis, and revealed that MEP50 was a potent inhibitor of osteoclastogenesis. MEP50 silencing strongly enhanced OC formation and upregulated the expressions of the OC genes encoding the nuclear factor of activated T-cells, C1 (NFATc1), cathepsin K (Ctsk), and tartrate-resistant acid phosphatase (TRAP). Consistently, MEP50 overexpression strongly abrogated osteoclastogenesis and repressed the expressions of NFATc1, Ctsk, and TRAP. However, MEP50 was dispensable to RANKL-induced activation of the NF- $\kappa$ B and MAPK signaling pathways, indicating that MEP50 abrogated osteoclastogenesis by repressing gene expression. Mechanistically, we revealed that C/EBP $\alpha$  could release the inhibitory effect of MEP50 on OC formation and gene expression by promoting the early stage of osteoclastogenesis, and MEP50 silencing could mediate OC formation with permissive levels of RANKL. Accordingly, we showed that whereas dihydrotestosterone (DHT) could inhibit osteoclastogenesis in a dose-dependent manner, MEP50 silencing significantly abrogated DHT-induced OC inhibition, indicating that MEP50 is a key cofactor for androgen receptor signaling in OC. Furthermore, we investigated the roles of MEP50 in the late stage of osteoclastogenesis and OC activity. The data showed that MEP50 was dispensable to OC maturation and osteoclastic bone resorption. Collectively, our results suggest that C/EBP $\alpha$  binds to MEP50 to regulate early-stage osteoclastogenesis, but this complex is dispensable to late-stage osteoclastogenesis and OC activity.

**Disclosures:** Joel Jules, None.

## MO0554

**Mitochondrial proteins SOD2 and Sirt3 play a crucial role in ROS regulation during osteoclast differentiation.** Haemin Kim\*, Hong-Hee Kim<sup>1</sup>, Yong Deok Lee<sup>1</sup>, Hyung Joon Kim<sup>2</sup>, Zang Hee Lee<sup>1</sup>. <sup>1</sup>Seoul National University School of Dentistry, Korea, Republic of, <sup>2</sup>Pusan National University, Korea, Republic of

Several studies have shown that reactive oxygen species (ROS) have a role in the differentiation and activation of various cell types including bone cells. Particularly, osteoclasts employ ROS as second messengers during receptor activator of NF- $\kappa$ B ligand (RANKL)-induced differentiation. In addition, osteoclasts contain large amounts of mitochondria in order to support the high energy demands of bone-resorbing activity. Therefore, it is expected that ROS from mitochondria, the major source of intracellular ROS, might play pivotal roles in RANKL-induced osteoclastogenesis. In this study, we report the involvement of mitochondrial SOD2 and Sirt3 in the regulation of osteoclast differentiation. RANKL up-regulated the expression of both SOD2 and Sirt3 during osteoclastogenesis. Manipulation of expression levels of SOD2 or Sirt3 affected intracellular ROS levels and subsequently osteoclast formation. Moreover, we found that Sirt3 deacetylated lysine 68 of SOD2 in response to RANKL. Furthermore, in vivo administration of SOD2 or Sirt3 siRNA into mouse calvariae decreased calvarial bone volume and increased osteoclast surface. These in vitro and in vivo findings suggest that the Sirt3-SOD2 axis of ROS regulation is important for the control of osteoclast differentiation program by RANKL.



Suggested model figure of Sirt3-SOD2 axis of ROS regulation in osteoclastogenesis

**Disclosures:** Haemin Kim, None.

## MO0555

**TNF Induction of Deubiquitinases Polarize Inflammatory Macrophages via NF- $\kappa$ B RelB.** Wei Lei\*, Xiaoxiang Yin<sup>2</sup>, Zhijun Zhao<sup>2</sup>, Xiaodong Hou<sup>2</sup>, Rong Duan<sup>1</sup>, Brendan Boyce<sup>1</sup>, Zhenqiang Yao<sup>1</sup>. <sup>1</sup>University of Rochester Medical Center, United States, <sup>2</sup>Henan University First Affiliated Hospital, China

Rheumatoid arthritis (RA) is a chronic inflammatory disease characterized by inflamed invasive pannus containing blood vessels and inflammatory cells that lead to erosion of the articular cartilage and adjacent bone. Macrophages (Macs) play a central role in these pathological process. They are classified as classical (M1) and alternative (M2) activated Macs, with inflammatory and anti-inflammatory functions, respectively. We recently reported that TNF increases NF- $\kappa$ B RelB protein levels to switch M-CSF-induced M2s to M1s. However, the mechanisms by which TNF increases RelB protein to regulate M1 polarization and invasive pannus formation remains unknown. Ubiquitination (Ub) is an important step in protein degradation, mediated by E3 ligases; deubiquitinases (DUBs) remove ubiquitin from substrate proteins to prevent their degradation. We found that TNF induced the expression of several DUBs, including OTUD7b, and decreased Ub of a broad-range of proteins in Macs. OTUD7b underwent constitutive Ub and degradation while TNF prevented its degradation, associated with reduced expression of the E3 ubiquitin ligases, cIAP1/2. Importantly, the DUB inhibitor, PR-619, reduced TNF-induced OTUD7b and RelB to basal levels in Macs and reduced TNF-induced F4/80+Ly6C+ M1s (11% vs.32%) in cultured mouse bone marrow cells. Interestingly, TNF-induced M1s have 5-fold increased expression of VEGF-A, which induces angiogenesis. Immunostaining showed that CD31 was highly expressed and co-localized in F4/80+ cells, and CD31+ blood endothelial cells (BECs) also highly expressed M-CSF, which is essential for Mac expansion, in the inflamed invasive pannus of TNF-Tg mice. Finally, 7-day short-term treatment of TNF-Tg mice with PR-619 reduced CD11b+F4/80+Gr1-Ly6C+ M1s in PBMCs (6.1% vs. 15.5%) and in inflamed joints (6.2% vs. 13.4%), OC numbers (34 $\pm$ 5 vs. 83 $\pm$ 13/mm<sup>2</sup> inflamed tissue area, p<0.05) as well as M-CSF expression by BECs in the inflamed joints of TNF-Tg mice. In summary, 1) TNF increases DUBs to prevent RelB degradation and thus polarizes Macs as M1s to enhance OC formation; 2) TNF-induced M1s produce VEGF-A to promote angiogenesis, and BECs in turn produce M-CSF to expand the Mac pool in the inflamed tissues; 3) Inhibition of DUBs prevents TNF induction of RelB proteins and subsequent M1 polarization, angiogenesis, Mac expansion and OC differentiation. We conclude that DUB inhibitors could be novel therapeutic agents to block inflammation and joint erosion in RA.

**Disclosures:** Wei Lei, None.

## MO0556

**Effects of Retinoids on Physiological and Inflammatory Osteoclastogenesis in vitro.** Vikte Lionikaite\*, Anna Westerlund<sup>1</sup>, Howard H Conaway<sup>2</sup>, Ulf H Lerner<sup>1</sup>, Petra Henning<sup>1</sup>. <sup>1</sup>University of Gothenburg, Sweden, <sup>2</sup>University of Arkansas for Medical Sciences, United States

Increased intake of vitamin A (retinoids) is associated with decreased bone mass and increased fracture risk in humans and rodents. These effects are attributed to increased formation of periosteal osteoclasts and decreased numbers of endocortical osteoclasts. In addition, it has been reported that retinoids can inhibit osteoclast formation under inflammatory conditions such as experimentally induced arthritis in mice.

In the present study, we have compared the effect of all-*trans* retinoic acid (ATRA; the biologically active form of vitamin A) on physiologically- and inflammatory-induced osteoclastogenesis *in vitro* using osteoclast progenitors isolated from human peripheral blood and mouse bone marrow stimulated by RANKL, or either TNF $\alpha$  or LPS.

ATRA inhibited physiologically-induced (RANKL) osteoclast formation in human monocytes. Retinoic acid receptor (RAR) agonists and an antagonist indicated that inhibition occurred by activation of RAR $\alpha$ . ATRA also inhibited osteoclastogenesis in human monocytes stimulated with the pro-inflammatory compounds TNF $\alpha$  and LPS, indicating that inhibition with ATRA is not specific for RANKL-induced osteoclast formation. The expression of osteoclastic genes *ACP5* and *CTSK*, and of the osteoclastogenic gene *NFATc1*, induced by RANKL and TNF $\alpha$  were decreased by ATRA, indicating that retinoids inhibit differentiation, rather than fusion, of mononucleated progenitor cells. Analyses of the mRNA expression of genes encoding for RANKL and TNF $\alpha$ -receptors indicate that inhibition of osteoclast formation by ATRA is not due to early decreased expression of the receptors for RANKL or TNF $\alpha$ . ATRA also inhibited osteoclastogenesis induced by RANKL, TNF $\alpha$  and LPS in murine bone marrow macrophages (BMM). These observations indicate that retinoids inhibit intracellular signaling machinery in osteoclast progenitors downstream of receptors involved in physiologically and pathologically induced osteoclast formation. In agreement with this view, inhibition of osteoclastogenesis with ATRA was also noted when *Tnfrsf11a* (which encodes for RANK) was overexpressed in BMM.

The data suggest that ATRA inhibits both physiological and inflammatory osteoclast differentiation of progenitors from the bone marrow or peripheral blood, observations which could help explain why there is reduced osteoclast formation at endocortical bone surfaces and in arthritis.

**Disclosures:** Vikte Lionikaite, None.

## MO0557

**Bone healing in response to *S. aureus* infection is associated with rapid initiation of neutrophil and osteoclast invasion, and bone resorption prior to aberrant bone healing.** Cameron Martin\*, Alyssa Falck, Sofia Lopez Gelston, Chris Litwin, Larry Suva, Dana Gaddy. Texas A&M University College of Veterinary Medicine, United States

Osteomyelitis is a serious bone infection typically caused by *Staphylococcus aureus*, the pathogenesis of which is poorly understood; cellular host responses of bone to the infection are especially lacking. We sought to determine the time course and extent of the host hematopoietic responses of immune cell invasion, development of osteoclasts, and the onset of bone healing following infection with a clinical *S. aureus* isolate, UAMS1. A unicortical femoral diaphyseal defect was created in 8 week old female mice that were infected with either vehicle Control (Con) or UAMS1. On days 3, 7 and 14, serum was collected and infected limbs harvested and formalin fixed, imaged by microCT, and processed for immunohistochemistry. Serum PINP progressively increased in Con bones over the 14 days of complete uninfected bone healing. In contrast, significantly lower levels of serum PINP levels were observed in infected mice, despite increased reactive bone formation by microCT. Increased serum CTX levels in infected animals did not reach significance although bone destruction across time was significantly and progressively increased in UAMS1 infected mice. To determine and compare the time course of hematopoietic cell invasion, immunohistochemistry of Con and infected bones was performed to measure the number of Myeloperoxidase + (MPO+) neutrophils, F4/80 macrophages and TRAP+ differentiated osteoclasts in the site. MPO+ cells were consistently detected across 14 days in Con, whereas MPO+ cells were first detected in infected bones at d3 and significantly increased by d14. Macrophages and TRAP+ cells were observed on d3 in both groups. TRAP+ cells increased by d7, and were maintained at high levels through d14 in both groups. TRAP+ cells in d14 Con bones was associated with significantly increased bone remodeling of the woven bone formed during normal bone repair. However, TRAP+ cells in infected bones were localized to the eroding cortices, consistent with the significant and progressive increases in bone destruction observed by microCT. In sum, these data demonstrate a similar extent of neutrophil invasion in both groups, consistent with an overall inflammatory response and suggesting that the cells are not mediating the enhanced bone formation response observed in the infected animals. The rapid invasion of macrophages and differentiation of osteoclasts occurs during bone healing and their presence is maintained in the presence of infection to further bone destruction.

**Disclosures:** Cameron Martin, None.

## MO0558

**Def6 restrains osteoclastogenesis and inflammatory bone resorption.** Nikolaus Binder\*<sup>1</sup>, Christine Miller<sup>2</sup>, Masaki Yoshida<sup>2</sup>, Kazuki Inoue<sup>2</sup>, Shinichi Nakano<sup>2</sup>, Xiaoyu Hu<sup>2</sup>, Lionel B. Ivaskiv<sup>2</sup>, Georg Schett<sup>3</sup>, Alessandra Pernis<sup>2</sup>, Steve R. Goldring<sup>2</sup>, F. Patrick Ross<sup>2</sup>, Baohong Zhao<sup>2</sup>. <sup>1</sup>Hospital for Supecial Surgery, United States, <sup>2</sup>Hospital for Special Surgery, United States, <sup>3</sup>Erlangen university, Germany

Inflammatory osteoclastic bone resorption is a major cause of morbidity and disability in many inflammatory disorders, including rheumatoid arthritis (RA). The mechanisms that regulate osteoclastogenesis and bone resorption in inflammatory settings are complex and are far from well understood. In this study, we identify the immunoregulator Def6 as a novel inhibitor of osteoclastogenesis in both physiological and inflammatory conditions. Def6, a novel type of guanine nucleotide exchange factor (GEF), plays an important role in the activation of lymphocytes by regulating IRF4 activity and/or exerting its function in conjunction with Swap70, the only other molecule with high homology to Def6. Recent studies show that IRF4 and Swap70 negatively regulate physiological osteoclast differentiation and function, respectively. In addition, Def6 deficiency leads to the development of RA like joint disease with bone erosion in a mouse model. These findings stimulated us to explore the role of Def6 in osteoclastogenesis and inflammatory osteolysis, as well as to investigate its underlying mechanisms of action. Osteoclast precursors from Def6 deficient mice (*Def6*<sup>-/-</sup>) demonstrated enhanced sensitivity to RANKL in the early differentiation phase. Unlike Swap70, *Def6*<sup>-/-</sup> osteoclasts formed actin rings. As TNF- $\alpha$  is a key pathogenic factor driving inflammatory bone resorption in RA, we next investigated the role of Def6 in TNF-mediated osteoclastogenesis. We found that lack of Def6 markedly enhanced TNF- $\alpha$ -induced osteoclastogenesis both in vitro and in vivo and resulted in increased bone resorption in a TNF- $\alpha$ -induced inflammatory osteolysis mouse model. In the human system, Def6 levels were decreased in osteoclast precursors obtained from RA patients and were elevated after TNF blockade therapy. Furthermore, the osteoclastogenic capacity of the RA cells was significantly inversely correlated with Def6 expression levels, indicating that Def6 functions as an inhibitory factor in limiting enhanced osteoclast formation and bone destruction in RA. Mechanistically, we found that Def6 suppressed osteoclastogenesis and the expression of key osteoclastogenic factors NFATc1 and c-Fos by regulating an endogenous IFN- $\beta$  mediated autocrine feedback loop. The Def6-dependent pathway may represent a novel therapeutic target to prevent pathological bone destruction.

**Disclosures:** Nikolaus Binder, None.

## MO0559

**Elucidation of the role of DC-STAMP heterogeneity and calcium signaling in osteoclastogenesis.** Ananta Paine\*<sup>1</sup>, Maria De La Luz Garcia-Hernandez<sup>1</sup>, Nelson Huertas<sup>1</sup>, Dongge Li<sup>1</sup>, Minsoo Kim<sup>2</sup>, Larry E. Wagner<sup>3</sup>, David Yule<sup>3</sup>, Christopher Ritchlin<sup>4</sup>. <sup>1</sup>Division of Allergy/Immunology and Rheumatology, School of Medicine and Dentistry, University of Rochester Medical School, United States, <sup>2</sup>Microbiology and Immunology, University of Rochester, United States, <sup>3</sup>Department of Pharmacology and Physiology, University of Rochester, United States, <sup>4</sup>Division of Allergy/Immunology and Rheumatology, School of Medicine and Dentistry, United States

**Background:** Osteoclasts (OC) are bone resorbing multinuclear cells that originate from myeloid progenitor cells through repetitive cycles of cell fusion. DC-STAMP, a transmembrane protein, is essential for cell-cell fusion and formation of fully functional OC although the molecular mechanisms are not well understood. We previously reported that when exposed to receptor activator of nuclear factor kappa-B ligand (RANKL), mouse leukemic monocyte-macrophage RAW 264.7 cells showed significant heterogeneity in terms of intracellular and membranous DC-STAMP expressions which further correlated with their ability to form multinuclear OCs. Most interestingly, optimal cell fusions were observed when DC-STAMP<sup>low</sup> and DC-STAMP<sup>high</sup> cells interacted. Herein, we further examined how complete absence of DC-STAMP in the primary osteogenic progenitor cells (OCs) affects their ability to fuse and to mount calcium (Ca<sup>2+</sup>) flux in response to appropriate stimulus.

**Methods:** We isolated bone marrow macrophages (BMMs) from wild type (WT) and DC-STAMP knockout (KO) mice. To analyze cell fusion, we labeled DC-STAMP<sup>+/+</sup> and DC-STAMP<sup>-/-</sup> BMMs obtained from WT and KO mice respectively with red and green membrane dyes, cultured them in OCgenic condition and monitored cell-cell fusion using live cell imaging. Moreover, we examined the expression dynamics of DC-STAMP protein in forming OC employing retroviral mediated expression of GFP-tagged DC-STAMP protein in DC-STAMP<sup>-/-</sup> cells. In addition, to investigate if DC-STAMP alters Ca<sup>2+</sup> flux during OCgenesis, we have measured calcium Ca<sup>2+</sup> flux in WT and KO cells using Fura-2 AM to compare their differential response by exposing the cells to RANKL and trypsin.

**Results:** We find that DC-STAMP<sup>-/-</sup> BMMs are incorporated into forming OC, however, DC-STAMP<sup>+/+</sup> cells are essential to initiate such cell fusion events. Following retroviral vector mediated complementation of GFP-tagged DC-STAMP protein expression in DC-STAMP<sup>-/-</sup> BMMs, we noted that during OC formation, DC-STAMP expression levels remained high but progressively declined during several rounds of cell-cell fusion and levels were low or absent in mature OCs. Lastly, we found that in response to RANKL and trypsin treatment, the induced Ca<sup>2+</sup> flux was significantly lower in DC-STAMP<sup>-/-</sup> BMMs compared to DC-STAMP<sup>+/+</sup> BMMs.

**Conclusion:** Our findings indicate that DC-STAMP expression levels are high in OCs during the early cell-cell fusion events but progressively decline and are absent or low in mature OCs. Our findings also indicates that while DC-STAMP<sup>-/-</sup> OCs cannot form multinuclear OCs, they still can fuse with DC-STAMP<sup>+/+</sup> OCs and in maturing OCs. Eventual fate and the mechanisms underlying such fusion events will now be studied. Finally, our data demonstrate an effect of DC-STAMP on Ca<sup>2+</sup> signaling in OCs. Further studies are in progress to elucidate the events promoting cell-cell fusion during OCgenesis.

**Disclosures:** Ananta Paine, None.

## MO0560

**Blockade of Osteoclast-Mediated Bone Resorption with a RANKL Inhibitor Enhances Spinal Fusion in a Rat Model.** Karin Payne\*, Christopher Erickson, Nichole Shaw, Peter Yarger, Todd Baldini, Christopher Kleck, Vikas Patel, Evalina Burger. University of Colorado Anschutz Medical Campus, United States

Bone allograft is often used during spinal fusion to provide a scaffold for bone remodeling, with osteoclasts and osteoblasts working to incorporate allograft into the spine. The former resorbs existing bone, then the latter secretes new matrix. Osteoprotegerin (OPG) is a RANKL inhibitor that blocks osteoclast differentiation and activation. Inhibiting osteoclast-mediated bone resorption may allow for more matrix deposition, thereby promoting improved spinal fusion. OPG does not incorporate into bone matrix and has a quick and reversible effect, thus making it a potential candidate to control the remodeling process and enhance bone formation. Interestingly, the administration of OPG as an enhancer of spinal fusion has not been studied previously. This study aimed to determine whether administration of an antiresorptive agent such as OPG after spinal fusion in a rat model will lead to greater bone at the fusion site, and whether a timing-dependent dosing regimen would allow for a more targeted control. Forty-eight male Sprague-Dawley (SD) rats received a one-level posterolateral intertransverse fusion of L4-L5 with bone allograft. Rats were divided into 4 groups according to initiation of OPG or saline administration: (1) saline at day 0, (2) OPG initiated at Day 0, (3) OPG at Day 10, or (4) OPG at Day 21 post-surgery. Rats received weekly subcutaneous injections of rat OPG-Fc (10 mg/kg) and were euthanized at 6 weeks post-surgery. Quantitative microCT analysis of the fusion revealed a greater bone volume fraction and a greater mean trabecular thickness in the groups that received OPG injections starting at Day 0 and Day 10 after surgery when compared to the group receiving saline (p<0.05). Quantitative histological analysis revealed a smaller percentage of trabecular bone surface lined with osteoclasts in the groups that started receiving OPG injections at post-surgical Days 0, 10 and 21 when compared to the group that



received saline (Fig. 1, \* $p < 0.05$ ). Initiation of OPG at Day 0 and 10 after surgery led to an even greater decrease when compared to OPG initiated on Day 21 (Fig. 1, # $p < 0.05$ ). This study indicates success of OPG in inhibiting osteoclast bone resorption, which led to greater bone at the spinal fusion site. It also demonstrates that early administration of OPG after spinal fusion is critical to enhance fusion mass. Thus, OPG is an attractive therapy to improve spinal fusion and warrants further investigation.

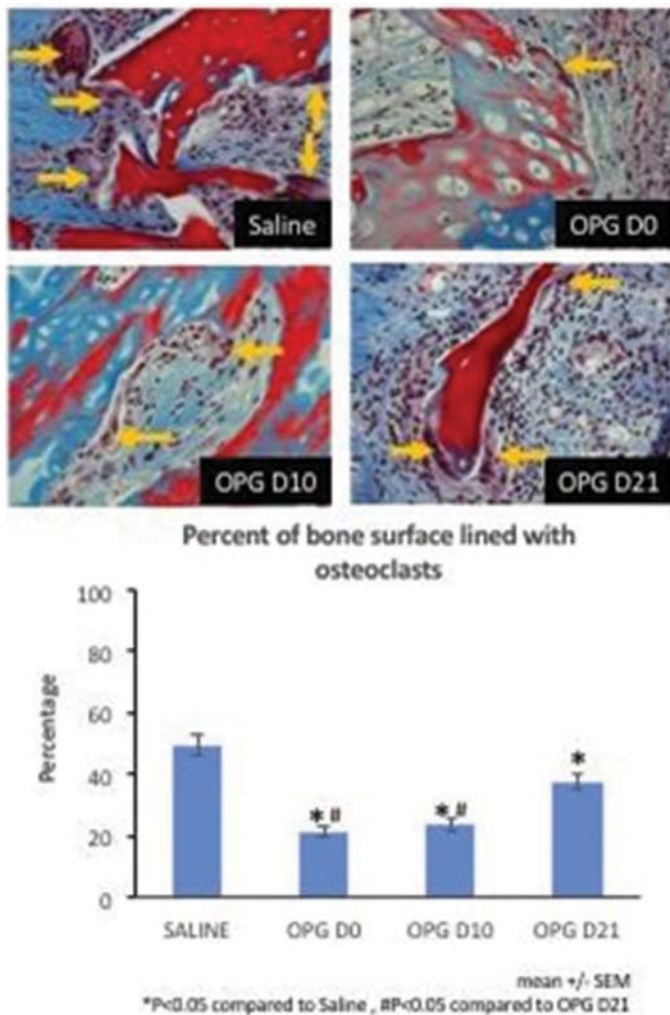


Figure 1: Images of bone surface lined with osteoclasts (yellow arrows) and quantification

Disclosures: Karin Payne, None.

## MO0561

**Nupr1/p8, a Key Player of Stress Response, Regulates Autophagy and Apoptosis of Osteoclasts.** Makoto Shiraki<sup>1</sup>, Xianghe Xu<sup>2</sup>, Asana Kamohara<sup>2</sup>, Juan Iovanna<sup>3</sup>, Yasushi Kubota<sup>4</sup>, Masaaki Mawatari<sup>5</sup>, Akiko Kukita<sup>2</sup>. <sup>1</sup>Department of Orthopaedic Surgery, Faculty of Medicine, Saga University, Japan, <sup>2</sup>Department of Pathology and Microbiology, Faculty of Medicine, Saga University, Japan, <sup>3</sup>Center de Recherche en Cancerologie de Marseille, INSERM U1068, France, France, <sup>4</sup>Division of Hematology, Respiratory Medicine and Oncology, Department of Internal Medicine, Faculty of Medicine, Saga University, Japan, <sup>5</sup>Department of Orthopaedic Surgery, Faculty of Medicine, Saga University, Japan

Nuclear protein(Nupr1)/p8 is a small nuclear protein induced by multiple stress stimuli, including LPS and nutrient starvation. Nupr1 is increased in some cancer types and pathological conditions and regulates apoptosis and autophagy. We identified Nupr1 as a highly expressed gene in mature osteoclasts by DNA microarray analysis of rat bone marrow culture system. We hypothesized that Nupr1 may play an important role in osteoclast (OC) differentiation and function by regulating autophagy and apoptosis induced in multiple adverse environments. We first examined the expression of Nupr1 in mouse osteoclastogenesis, and found that Nupr1 mRNA and protein levels were greatly increased in OCs formed by RANKL and M-CSF from bone marrow macrophages (BMMs). Nupr1 was co-localized with NFATc1 in the nucleus of OCs. Promoter region of Nupr1 gene contains several putative NFATc1 binding sites and an NFATc1 inhibitor, FK506, dose-dependently inhibited the expression of Nupr1. Both

BMMs derived from Nupr1 KO and wild-type (WT) mice similarly differentiated into OCs after 2 days in nutritious culture. Intriguingly, when the culture was prolonged to 7 days without medium change, the number of survived OCs was significantly increased in KO mice in comparison with that of WT mice. In addition, more resorption pits were detected in Nupr1 KO OCs. When OCs were cultured under amino acids free or RANKL and M-CSF depleted condition, Nupr1 expression was dramatically upregulated. One hour amino acids starvation significantly increased mRNA levels of autophagy regulator FOXO3 which is a target of Nupr1 and Bcl2 family member BNIP3 in Nupr1 KO but not in WT OCs. Furthermore, bafilomycin A1 increased an autophagy marker LC3-II protein levels in amino acids starved Nupr1 KO OCs. On the other hands, Bim expression was enhanced in Nupr1 KO mice in cytokine starved condition. These results show that Nupr1 is induced by several stress stimuli in OCs and inhibits autophagy. Nupr1 is a potential candidate regulator of longevity and bone resorption of OCs.

Disclosures: Makoto Shiraki, None.

## MO0562

**Anti-Siglec-15 antibody inhibits bone-resorbing activity of osteoclasts and stimulates osteoblast differentiation.** Nobuyuki Udagawa<sup>1</sup>, Shunsuke Uehara<sup>1</sup>, Masanori Koide<sup>2</sup>, Atsushi Arai<sup>2</sup>, Toshihide Mizoguchi<sup>2</sup>, Midori Nakamura<sup>1</sup>, Yasuhiro Kobayashi<sup>2</sup>, Naoyuki Takahashi<sup>2</sup>, Chie Fukuda<sup>3</sup>, Eisuke Tsuda<sup>3</sup>. <sup>1</sup>Department of Biochemistry, Institute for Oral Science, Matsumoto Dental University, Japan, <sup>2</sup>Institute for Oral Science, Matsumoto Dental University, Japan, <sup>3</sup>Rare Disease & LCM Laboratories, R&D Division, Daiichi Sankyo Co., Ltd., Japan

We previously identified sialic acid-binding immunoglobulin-like lectin 15 (Siglec-15) as a gene product expressed in giant cell tumor of bone. The expression of Siglec-15 was increased with osteoclast formation in mouse bone marrow (BM) cultures. Treatment of BM macrophage cultures with anti-Siglec-15 antibody (Siglec-15 Ab) inhibited TRAP-positive multinucleated cell formation induced by RANKL and M-CSF. However, Siglec-15 Ab failed to suppress TRAP-positive mononuclear cell (mononuclear osteoclast) differentiation. We then examined the effects of Siglec-15 Ab on the appearance of osteoclast precursors, which express RANK and c-Fms but not TRAP, in mouse co-cultures of osteoblasts and BM cells. Siglec-15 Ab showed no effects on the appearance of osteoclast precursors in the co-culture. Osteoclasts prepared from mouse co-cultures were further cultured on dentin slices in the presence or absence of Siglec-15 Ab. Pit-forming activity of osteoclasts was inhibited by Siglec-15 Ab. The actin rings in osteoclasts on dentin slices almost disappeared within 3 hours in the presence of Siglec-15 Ab. Finally, we examined effects of Siglec-15 Ab on osteoblast differentiation associated with osteoclast differentiation in whole BM cultures treated with RANKL and M-CSF. Siglec-15 Ab suppressed TRAP-positive multinucleated cell formation, but not TRAP-positive mononuclear cell differentiation. Interestingly, Siglec-15 Ab treatment stimulated the appearance of alkaline phosphatase-positive osteoblasts in those cultures. Siglec-15 Ab failed to stimulate osteoblast differentiation in the whole BM cultures treated without RANKL and M-CSF. Our findings suggest that Siglec-15 plays important roles in the induction of both bone-resorbing activity of mature osteoclasts and osteoblast differentiation, and that mononuclear osteoclasts may play an important role in the coupling between bone resorption and formation.

Disclosures: Nobuyuki Udagawa, Daiichi Sankyo Co., Ltd., Grant/Research Support.

## MO0563

**A Role for Cathepsin K in the Periosteal Response to Bone Repair.** Bhavita Walia<sup>1</sup>, Elizabeth Lingenheld<sup>2</sup>, Le Duong<sup>3</sup>, Archana Sanjay<sup>4</sup>, Hicham Drissi<sup>5</sup>. <sup>1</sup>Department of Genetics and Genome Sciences, UConn Health, United States, <sup>2</sup>Department of Orthopaedic Surgery, UConn Health, United States, <sup>3</sup>Bone Biology Group, Merck Research Laboratories, United States, <sup>4</sup>Department of Orthopaedic Surgery, United States, <sup>5</sup>Department of Orthopaedics, Emory University School of Medicine, United States

The mechanisms by which periosteal osteoclasts (OC) and OC precursors (OCP) contribute to augmented periosteal bone formation upon Cathepsin K (CatK) inhibition are unknown and elucidating these mechanisms will provide a new function for CatK inhibitors to manage fracture repair. Here we studied the impact of periosteum derived OCPs on bone modeling/remodeling in the context of fracture repair. We hypothesized that CatK deficient OCPs directly enhance bone formation.

Control mice and CatK<sup>-/-</sup> mice (CatKO) were fractured and limbs harvested at 3, 5 and 7 days post fracture for histological and immunohistochemical analyses. Histological analysis of intact femur sections revealed increased periosteal TRAP<sup>+</sup> cells in CatKO mice relative to WT. Flow cytometry analyses of periosteal cells from intact bones showed a decrease in OCPs from CatKO mice compared to WT. In vitro culture and differentiation OCPs into OCs showed decreases in TRAP<sup>+</sup> mononuclear cells in day 2 cultures and mature multinucleated TRAP<sup>+</sup> OCs at day 5 cultures in CatKO vs. WT. Expression of OC markers, TRAP, RANK, Calcitonin receptor and DC-STAMP were also decreased. TRAP staining of day 3, 5 and 7 fractured femur sections revealed more TRAP<sup>+</sup> cells in the periosteum of fractured CatKO femurs relative to WT. Flow cytometry analysis of the periosteum from 5 days post fracture showed increased numbers of OCPs in CatKO compared to WT. Characterization of mesenchymal populations (MSCs) by flow cytometry showed significantly decreased

populations of CD45<sup>+</sup>CD31<sup>+</sup>Ter119<sup>+</sup>CD29<sup>+</sup> and CD45<sup>+</sup>CD31<sup>+</sup>Ter119<sup>+</sup>Sca1<sup>+</sup> cells but increased CD45<sup>+</sup>CD31<sup>+</sup>Ter119<sup>+</sup>CD105<sup>+</sup> cells in intact CatKO periosteum relative to WT. Analysis of these MSC populations in response to fracture showed decreases in CD29<sup>+</sup>, Sca1<sup>+</sup> and CD105<sup>+</sup> cells in CatKO mice relative to WT. Immunohistochemical analysis to detect PDGF-BB expression in fracture activated periosteum revealed increased PDGF-BB expression in the periosteum of CatKO fractured femurs relative to WT at day 3 post-fracture. PDGF-BB expression progressively decreased in CatKO fracture callus whilst increasing in WT at days 5 and 7 post fracture.

Cumulatively, these findings point to a new role for Cathepsin K in regulating the periosteal response to fracture by modulating PDGF-BB temporal expression. The augmented PDGF-BB expression in CatKO fractured periosteum may enhance osteogenic differentiation and callus mineralization.

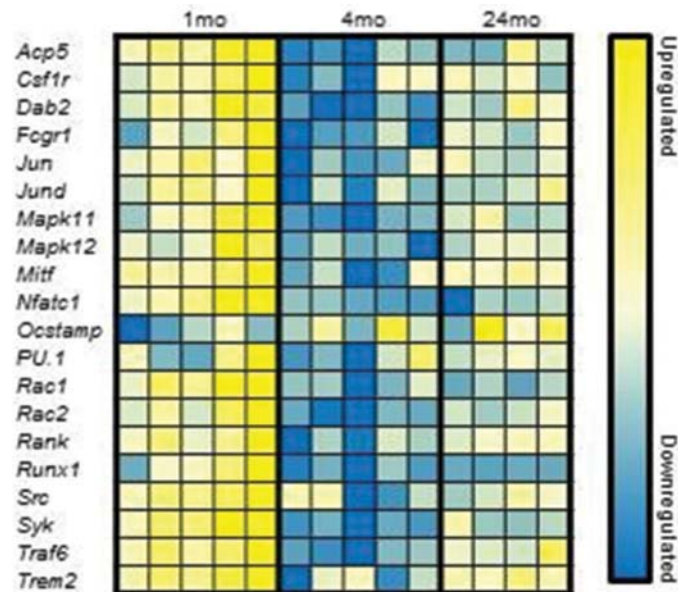
**Disclosures:** Bhavita Walia, Merck, Grant/Research Support.

## MO0564

### Differential effects of Wnt signaling on osteoclast differentiation with aging.

Megan Weivoda\*, Ming Ruan, Christine Hachfeld, Glenda Evans, Stephanie Youssef, Joshua Farr, David Monroe, Sundee Khosla, Jennifer Westendorf, Merry Jo Oursler, Mayo Clinic, United States

Canonical and non-canonical Wnt signaling are crucial for skeletal homeostasis. Activation of canonical versus non-canonical signaling is determined by the presence of Wnt ligands and receptor complexes. Importantly, changes in Wnt receptor complex composition affect the responses to specific Wnt ligands. While both canonical and non-canonical Wnt pathways promote osteoblastogenesis, they have differential effects on osteoclastogenesis, with canonical signaling reducing and non-canonical signaling increasing differentiation of osteoclast progenitors (pOCs). Because marrow pOC numbers increase during aging, we hypothesized that pOCs exhibit changes in Wnt receptor expression leading to reduced canonical Wnt signaling and increased osteoclastogenic potential with age. To test our hypothesis, we used magnetic activated cell sorting to isolate pOCs (Rank+ monocytes) from the bone marrow of young, adult, and aged (1, 4, and 24 months) female mice. The RNA was immediately isolated to obtain a "snapshot" of the *in vivo* transcriptome by RNA-Sequencing (Seq). A subset of total marrow cells were cultured overnight in M-CSF to obtain an enriched population of pOCs which were then cultured in osteoclast differentiation medium (10ng/mL M-CSF, 100ng/mL RANKL) in the presence of vehicle or 10ng/mL Wnt3a. RNA was obtained on Day 1 and mature osteoclasts were fixed on Day 4 and TRAP stained. RNA-Seq revealed that *Fzd1* and *8* significantly increased and *Fzd10* decreased with age. In addition, the non-canonical receptors *Ryk* and *Kremen1* were significantly increased, whereas the canonical Wnt target genes *Lef1*, *Tcf7*, *Apc2*, *Tcf7l2*, *Bcl9*, *Wisp3*, and *Sox4* were significantly decreased in the pOCs isolated from aged mice. Wnt3a had differential effects on gene expression in young, adult, or aged pOCs. While Wnt3a significantly increased osteoclast differentiation genes in young pOCs, it significantly reduced expression of these genes in the adult pOCs, with a lesser effect on the pOCs from aged mice (see Figure). The gene expression changes correlated with significant inhibition of osteoclast differentiation by Wnt3a only in the adult pOCs. Overall, our data show that aging alters pOC Wnt receptor expression *in vivo*, as well as the responsiveness of pOCs to Wnt3a-mediated inhibition of osteoclast differentiation. These data suggest that altering the responsiveness to canonical Wnt signaling may be an effective strategy to reduce pOC numbers in patients at risk for bone loss.



Fold activation or repression of osteoclast differentiation genes in pOCs by Wnt3a

**Disclosures:** Megan Weivoda, None.

## MO0565

### TMEM178 is a novel negative regulator of store-operated calcium entry in osteoclasts by affecting STIM1 oligomerization. Zhengfeng Yang\*, Roberta Faccio, Department of Orthopaedic Surgery, School of Medicine, Washington University in St. Louis, United States

We recently identified Tmem-178 as a novel negative regulator of RANKL-induced calcium ( $\text{Ca}^{2+}$ ) fluxes, NFATc1 activation and osteoclastogenesis. We also reported that Tmem178 expression is reduced in monocytes treated with plasma of juvenile arthritis patients, and its downregulation correlates with the extent of erosive disease. These findings suggested that changes in Tmem178 expression lead to aberrant osteoclastogenesis by affecting  $\text{Ca}^{2+}$  signaling.

Maintenance of  $\text{Ca}^{2+}$  fluxes during osteoclastogenesis is dependent on extracellular  $\text{Ca}^{2+}$  entry through activation of store-operated  $\text{Ca}^{2+}$  entry (SOCE) followed by  $\text{Ca}^{2+}$  re-uptake into the endoplasmic reticulum. SOCE activation requires oligomerization of STIM1 and its interaction with ORAI1, however the dynamic regulation of this complex in osteoclasts (OC) is not well defined. To investigate whether Tmem178 negatively regulates  $\text{Ca}^{2+}$  fluxes by affecting SOCE, we performed  $\text{Ca}^{2+}$  imaging in WT and Tmem178<sup>-/-</sup> pre-OCs. We found that Tmem178 deficiency has no major effects on ER  $\text{Ca}^{2+}$  release in response to ATP or thapsigargin (Tg), but enhances SOCE-mediated  $\text{Ca}^{2+}$  entry compared with WT cells. By contrast, Tmem178 overexpression significantly reduces SOCE and limits OC differentiation.

To evaluate how Tmem178 modulates SOCE, we analyzed the interaction of Tmem178 with STIM1 and ORAI1, two integral components of SOCE. Co-IP and FRET imaging showed that Tmem178 associates with STIM1 but not ORAI1. Structure/function analysis revealed that neither the C- nor the N-terminal domain of Tmem178 is required for Tmem178/STIM1 binding, but two of the four transmembrane (TM) regions, specifically TM2 and TM3, are required for this interaction and to modulate SOCE activation and osteoclastogenesis. Consistently, molecular docking analysis predicted six potential binding sites in the TM domain of STIM1 interacting with Tmem178. We identified STIM1G225 to modulate STIM1/TMEM178 association, calcium fluxes and osteoclastogenesis. These findings led to the hypothesis that Tmem178-STIM1 association prevents STIM1 oligomerization thus reducing SOCE. To examine this possibility, we overexpressed STIM1-YFP in WT and Tmem178<sup>-/-</sup> cells. STIM1 puncta formation, representing STIM1 oligomerization, in response to Tg was enhanced in Tmem178<sup>-/-</sup> cells compared with WT.

These data demonstrate that Tmem178 acts as an anchor limiting STIM1 oligomerization and provide novel insights into tight regulation of  $\text{Ca}^{2+}$  fluxes during osteoclastogenesis.

**Disclosures:** Zhengfeng Yang, None.

## MO0566

### Osteocytic Proteins Upregulated by Mechanical Signals Display Increased Functional Specificity. Graeme Murray\*, Fanchi Meng<sup>2</sup>, Lukasz Kurgan<sup>3</sup>, Henry Donahue<sup>1</sup>.

<sup>1</sup>Biomedical Engineering, Virginia Commonwealth University, United States, <sup>2</sup>Electrical and Computer Engineering, University of Alberta, Canada, <sup>3</sup>Computer Science, Virginia Commonwealth University, United States

Signal transduction pathways involved in osteocyte mechanotransduction are only partially understood. To address this, we completed an *in silico* analyses of gene array, liquid chromatography-mass spectrometry, and RNA-seq data previously obtained. In the original study, samples were cultured on collagen I-coated glass slides for 2 days and exposed to 2hrs oscillating (1Hz) fluid flow inducing 10 dynes/cm<sup>2</sup> shear stress. Sham controls were maintained in identical, static chambers. Cells were collected following post-incubation in fresh medium for 2hr. We found that 99 genes were significantly differentially expressed in response to flow and they were annotated and identified using UniGene IDs. These genes were mapped to corresponding proteins, for which sequences and identifiers were collected from UniProt. Evolutionary conservation was estimated with relative entropy computed from evolutionary profiles generated with HHblits using the UniProt-20 database. Interconnectedness was quantified with the number of protein-protein interactions collected from the mentha database. Putative intrinsic disorder was annotated using a consensus of five predictors: three versions of the Espritz method and two versions of the IUPred method.

Proteins upregulated by flow displayed less conservation, lower levels of intrinsic disorder and a smaller degree of interconnectedness than average proteins in the murine proteome. Our results suggest that proteins upregulated by flow are more "functionally specific" than most proteins in the mouse proteome. That is, they are not as evolutionarily conserved (they include fewer functional residues and thus they potentially interact with fewer protein partners) and are more structured and not as widely connected within and between signaling networks as opposed to being more promiscuous with their binding protein partners. Thus, targeting these signaling pathways, for instance to mimic the anabolic effect of mechanical signals, would have fewer off target effects given their lower degree of connectivity. Moreover, the above average amount of defined tertiary structure allows for easier protein modeling and rational design of potential bone anabolic agents. Pathway and network analysis predicted flow-induced downregulation of proteins associated with osteoclast differentiation, including NOS2, TLR2, and PTGS2. Consistent with the inflammatory nature of this pathway, gene ontology analysis found an increase in extracellular signaling.



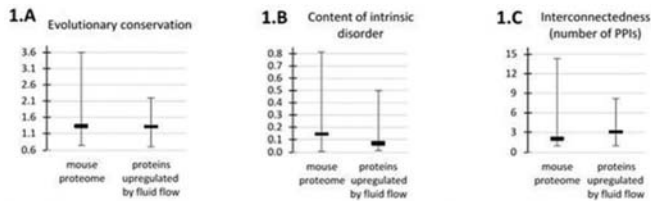


**Figure 1:** Comparison of the distributions of the evolutionary conservation quantified with relative entropy (Panel A), content (fraction) of intrinsic disorder (Panel B) and the number of protein-protein interactions (PPIs) that are used to quantify interconnectedness (Panel C) between mouse proteins upregulated by the fluid flow and proteins from the complete mouse proteome. Distributions are represented by median and 5<sup>th</sup> and 95<sup>th</sup> percentiles.

Figure

**Disclosures:** Graeme Murray, None.

## MO0567

**Deletion of CaMKK2 in Osteocytes Elicits Gender-Specific Effects on Bone Mass.** Mavis Irwin<sup>\*</sup>, Uma Sankar, Indiana University Purdue University of Indianapolis, United States

Intracellular calcium complexed with its receptor calmodulin (CaM) binds to and activates a plethora of downstream proteins including the multifunctional serine-threonine protein kinase Ca2+/CaM dependent protein kinase 2 (CaMKK2). We previously reported a potent bone anabolic response following either the global deletion (*Camkk2*<sup>-/-</sup>) or pharmacological inhibition of CaMKK2 in mice. Mesenchymal stem cells isolated from these mice generate significantly higher numbers of osteoblasts (OBs) in vitro, indicating a cell-intrinsic role for CaMKK2. We hypothesized that the loss of CaMKK2 in each of the three bone cell types contributes to the overall bone phenotype following its global deletion.

To further understand cell-intrinsic function(s) of CaMKK2, we deleted its expression in osteocytes (OCY) by mating *Dmp1*-8kb-Cre transgenic mice with *CaMKK2*<sup>fllox/flox</sup> mice to generate the *Camkk2Δ<sup>OCY</sup>* mice. Long bones collected from 3 month-old male and female *Camkk2Δ<sup>OCY</sup>* (n=7 and 6), *Camkk2*<sup>-/-</sup> (n=3 and 4) and control (n=4 per) mice were analyzed for trabecular and cortical bone parameters using micro-computed tomography (micro-CT) and subsequently processed for un-decalcified dynamic and static histomorphometry. Quantitative real-time RT-PCR analyses were performed on RNA isolated from long bones.

Deletion of CaMKK2 in OCY resulted in significant increases in trabecular bone volume (2.6-fold higher in males and 1.7-fold higher in females) compared to sex-matched control mice. Interestingly, male *Camkk2Δ<sup>OCY</sup>* mice possessed similar trabecular bone volume as male *Camkk2*<sup>-/-</sup> mice. In contrast, female *Camkk2Δ<sup>OCY</sup>* mice possessed a significant 1.6-fold lower bone volume compared to female *Camkk2*<sup>-/-</sup> mice, although these parameters were significantly higher than those in female control mice. Similar trends were observed in trabecular number and separation as well as cortical bone thickness, suggesting a gender-specific effect of CaMKK2 deletion from OCY. The cortical bone mean polar moment of inertia in *Camkk2Δ<sup>OCY</sup>* mice was significantly higher compared to sex-matched control and *Camkk2*<sup>-/-</sup> mice.

In conclusion, our results indicate that the deletion of CaMKK2 from OCY potentiates an anabolic effect on trabecular and cortical bone that is more pronounced in male than female mice. Further analyses are currently underway to identify the cellular and molecular mechanisms underlying the anabolic phenotype and its potential regulation in a gender-specific manner.

**Disclosures:** Mavis Irwin, None.

## MO0568

**DMP1-conditional YAP/TAZ ablation impairs bone matrix organization and reduces bone accrual differentially in load-bearing compared to non-bearing bones.** Chris Kegelman<sup>\*</sup><sup>1</sup>, Devon Mason<sup>1</sup>, Teresita Bellido<sup>2</sup>, Alexander Robling<sup>2</sup>, Joel Boerckel<sup>1</sup>. <sup>1</sup>University of Notre Dame, United States, <sup>2</sup>Indiana University, United States

Osteocytes are the primary mechanosensor cells in bone, but the underlying molecular mechanisms remain poorly understood. Yes-associated protein (YAP) and transcriptional co-activator with PDZ-binding motif (TAZ) have emerged as key mediators of cellular mechanotransduction, but their roles in osteocyte control of bone adaptation have not been studied. We previously demonstrated a critical positive role of both YAP and TAZ in bone development by combinatorial deletion from all cells of the skeletal lineage [1]. Here, we interrogated their functions late in the skeletal cell sequence, targeting YAP and/or TAZ deletion in mature osteoblasts and osteocytes using Cre-recombination under control of the 8kb-DMP1-promoter [2]. We hypothesized that YAP/TAZ ablation in DMP1-expressing cells would impair bone accrual, preferentially in loaded bones compared to bones with minimal loading. All animal experiments were approved by the IACUC. We generated allele dosage-dependent DMP1-conditional YAP/TAZ knockouts, but only double homozygotes, *YAP<sup>fl</sup>/fl;TAZ<sup>fl</sup>/fl;DMP1-Cre*, (cDKO) had deficits in long bone growth, which were rescued by a single copy of either gene, suggesting molecular compensation. Compared to WT littermates, 12 week-old cDKO mice had reduced femoral trabecular number and cortical thickness (Fig.1A,B), characterized by decreased periosteal bone. Correlation of bending stiffness with moment of inertia demonstrated significantly reduced intrinsic matrix elastic

properties in cDKO cortical bone (Fig.1C). DMP1-conditional YAP/TAZ deletion had no effect on cortical tissue mineral density but significantly decreased collagen content and organization (Fig.1D,E) and collagen I mRNA expression (Fig.1F). To test whether osteocyte YAP/TAZ play a role in mechanical adaptation to functional loads during development, we compared the relative morphology of two craniofacial bones, both of intramembranous origin, but with different load histories: the dynamically loaded mandible and the minimally loaded parietal bone (Fig.1G). We found that DMP1-conditional YAP/TAZ deletion significantly reduced mandibular, but not parietal thickness (Fig.1H). Together, these data demonstrate that YAP and TAZ have positive compensatory roles in osteoblast/osteocyte function in vivo, regulating bone quality, and promoting bone accrual in a manner dependent on load history, suggesting a role in mechanotransduction.

1. Kegelman+ ASBMR 2016. #1053.

2. Bivi+ JBMR 2012, 27(2):374-89

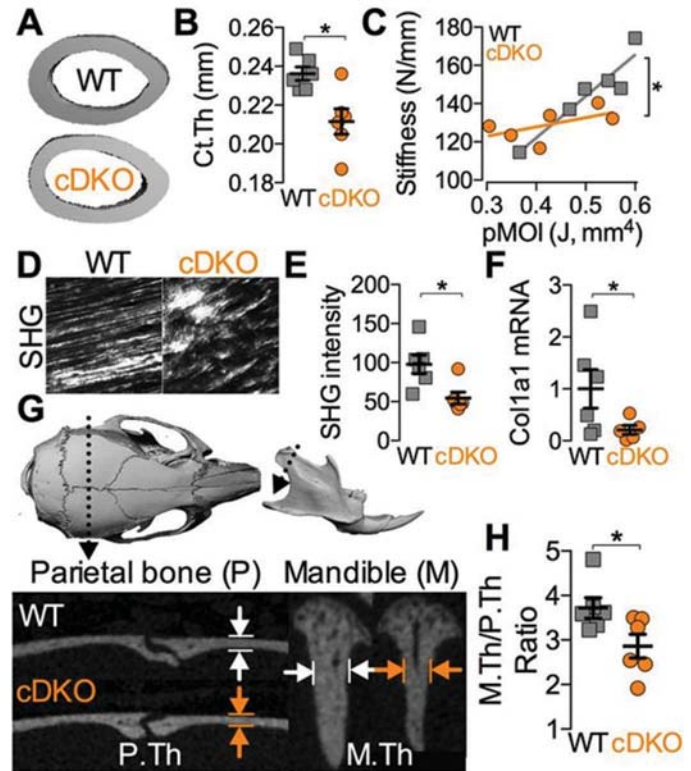


Figure 1

**Disclosures:** Chris Kegelman, None.

## MO0569

**Differential expression of Dickkopf-1 (DKK1) and wntless-type MMTV integration site family, member 3A (Wnt3a) in BALB/c and C57BL/6J axial spondyloarthritis models.** Michael Schirmer<sup>\*</sup><sup>1</sup>, Tobias De Zordo<sup>2</sup>, Sandra Kemmerling<sup>3</sup>, Christian Kremser<sup>2</sup>, Christoph Ammann<sup>4</sup>, Volker Kuhn<sup>5</sup>. <sup>1</sup>Medical University Innsbruck, Internal Medicine II, Austria, <sup>2</sup>Medical University Innsbruck, Radiology, Austria, <sup>3</sup>Medical University Hospital Innsbruck, Austria, <sup>4</sup>Medical University Innsbruck, Austria, <sup>5</sup>Medical University Innsbruck, Trauma Surgery, Austria

**Purpose:** The hallmarks of axial spondyloarthritis (axSpA) are inflammation and new bone formation, leading to ankylosis of the sacroiliac joint and spine. Little is known about the complex network of inflammatory and osteogenic factors: In brief, bone formation and erosions are associated with Wnt proteins and the natural Wnt inhibitor Dickkopf-1 (DKK1); TNF- $\alpha$  and IL-17 are important pro-inflammatory cytokines in axSpA and negatively associated with osteogenesis in rheumatoid arthritis (RA). In RA TNF- $\alpha$ , which induces the expression of DKK1, leads to inhibition of Wnt signaling and further to joint destruction. However, axSpA is characterized by low DKK1 levels and new bone formation.

**Methods:** Mice were immunized subcutaneously with human proteoglycan in Freund's adjuvant. Magnetic resonance imaging (MR) of the sacroiliac joints was performed and levels of cytokines were determined in heparin-plasma by Luminex ProcartaPlex Mouse Panel 1, and Wnt3a and DKK1 were quantified by ELISA kits.

**Results:** Direct comparison showed that DKK1 levels were increased in C57 compared to their non-immunized controls. BALB/c mice tended to have lower levels of DKK1 and wnt3a compared to C57 mice. DKK1 negatively correlated with Wnt3a in BALB/c and positively with IL-17A in both. IL-17A tended to correlate negatively with wnt3a in BALB/c. Subgrouping in bone marrow edema positive (MR<sup>+</sup>) and negative

(MR<sup>+</sup>) mice revealed that MR<sup>+</sup> BALB/c mice tended to have higher *wnt3a* and lower *DKK1* levels compared to MR<sup>-</sup> mice.

**Discussion:** Expression patterns of inflammatory cytokines and osteogenic factors differ between BALB/c and C57 mice, also depending on sacroiliac edema. These data suggest that expression of *DKK1* is inhibited in the presence of bone marrow edema while *Wnt3a* is highly expressed. *DKK1* positively correlates with IL-17A but not with TNF- $\alpha$  in both immunized mice strains, indicating a major role of IL-17A in the murine axSpA models.

**Conclusion:** These data suggest different expression patterns of inflammatory cytokines and osteogenic factors in a Th1-prone murine axSpA model (C57BL/6J) compared to BALB/c), even depending on MR edema. *DKK1* positively correlates with IL-17A but not with TNF- $\alpha$  in both immunized mice strains, indicating a major role of IL-17A in the late stages of murine axSpA models.

#### References:

Diarrar, D. et al. Dickkopf-1 is a master regulator of joint remodeling. *Nature medicine* 13, 156-163 (2007)

Rossini, M. et al. Focal bone involvement in inflammatory arthritis: the role of IL17. *Rheumatology International* 36(4), 469-82 (2016)

**Acknowledgement:** This work is funded by a grant of the Austrian Research Fund - FWF (P-253380).

**Disclosures:** Michael Schirmer, None.

## MO0570

**miR-145 overexpression impairs osteocytes structure and function in Adolescent Idiopathic Scoliosis.** Wayne Yuk-wai Lee<sup>\*1</sup>, Jiajun Zhang<sup>1</sup>, Yujia Wang<sup>1</sup>, Ross KK Leung<sup>2</sup>, Tsz-ping Lam<sup>1</sup>, Yong Qiu<sup>3</sup>, Jack Chun-yiu Cheng<sup>1</sup>. <sup>1</sup>Department of Orthopaedics and Traumatology, SH Ho Scoliosis Research Laboratory, The Chinese University of Hong Kong, Shatin, NT, Hong Kong SAR, China, Hong Kong, <sup>2</sup>School of Public Health, The University of Hong Kong, Hong Kong SAR, China, Hong Kong, <sup>3</sup>Spine Surgery, Nanjing Drum Tower Hospital, Nanjing University, Nanjing, China, China

Adolescent Idiopathic Scoliosis (AIS) is a three-dimensional spinal deformity of unclear etiopathogenesis with the prevalence of 1-4% worldwide. Systemic low bone mineral density (BMD) was found to be one of the significant prognostic factors for curve progression. Better understanding of how bone quality is affected will help to advance prognosis and therapeutic strategies as current treatment regime is mainly targeting on the anatomical abnormality. Osteocytes are specialised cell type for mechanosensing and orchestrating bone metabolism. We have reported abnormal osteocytes structure in AIS bone biopsies (Fig. 1a). This work investigated further the underlying mechanism and explored the potential clinical implication.

In this case-control study, iliac crest trabecular bone biopsies were harvested intraoperatively from 9 AIS patients undergoing posterior spinal fusion and from 5 age-matched control subjects undergoing respective orthopaedic surgery requiring iliac crest autografts with informed consent and then divided for microRNA microarray for identification of miR candidates and osteoblasts isolation. Osteocyte culture was derived from primary osteoblasts seeding in type I collagen gel and validated by co-immunostaining of osteocyte markers (sclerostin and E11) and secreted sclerostin in conditioned medium. The biological roles of the identified miR target on osteocyte differentiation were evaluated with loss-of-function test. The serum levels of osteocyte secreted cytokines and the miR target in another cohort of 100 subjects were measured with Multiplex and qPCR. Mann-Whitney test and Spearman's rank correlation were used for statistical analysis.

Compared with the control, primary AIS osteocytes (Fig. 1b) was found to have significantly lower transcriptional level of osteocytic markers (*E11*, *Fg23* and *Sost*) and cell gap junction protein (Connexin 43, *Gja1*), and secreted less sclerostin. Microarray and miRWalk analysis identified miR-145-5p as a potential upstream regulator via b-catenin signalling pathway. miR-145-5p expression was significantly and positively correlated with *Ctmb1*. Knockdown of miR-145-5p could significantly down-regulate active b-catenin expression in AIS osteoblasts, up-regulate *E11* and *Sost* mRNA expression and rescue sclerostin secretion. Correlation analysis showed a negative correlation between miR-145-5p and sclerostin in AIS which was absent in the control.

This study provided new evidence of structural and functional abnormalities of osteocyte, and its link to aberrant miR-145-5p/ $\beta$ -catenin signalling in the pathogenesis of AIS. Our findings shed light on the potential role of epigenetic-related factors like miRNA on the etiopathogenesis of AIS and the development of circulating miRNAs as potential biomarkers.

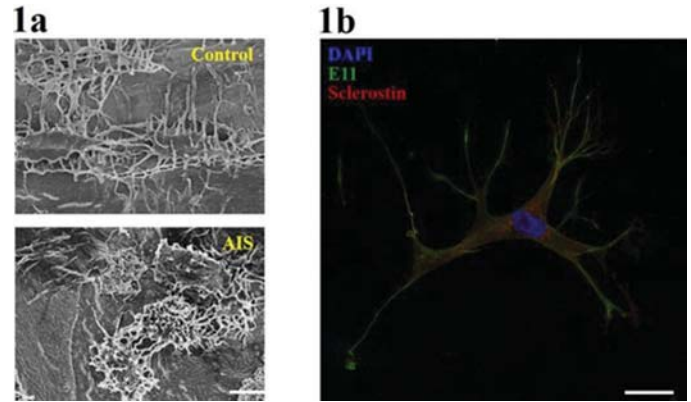


Figure 1: Abnormal osteocytes structure in AIS by SEM and Confocal image of primary osteocytes.

**Disclosures:** Wayne Yuk-wai Lee, None.

## MO0571

**A 3D collagen-hydroxyapatite tissue culture model for studying bone formation and osteocyte differentiation.** Brian Golz<sup>\*1</sup>, Sherry Harbin<sup>1</sup>, Eric Nauman<sup>1</sup>, Teresita Bellido<sup>2</sup>, Fredrick Pavalko<sup>2</sup>, Russell Main<sup>1</sup>. <sup>1</sup>Purdue University, United States, <sup>2</sup>Indiana University School of Medicine, United States

Osteocytes reside within the skeleton as a 3D cellular syncytium encased in mineralized bone matrix. If we hope to study osteocyte biology in a controlled environment, optimize drug delivery methods, or develop osteocyte-driven methods for bone healing and regeneration, we must be able to capture the unique features of the osteocyte's 3D extra-cellular matrix environment and cellular syncytium *in vitro*. Here, we combine porcine skin collagen (PSC) and hydroxyapatite (HA) as components of the extracellular matrix in a 3D tissue culture model. The cellular component of the model consists of primary osteoblasts from mT/mG x DMP1-8kb-Cre mice that express membrane-bound tdTomato fluorescent protein in all cells, except those expressing DMP1 promoter-driven Cre recombinase, which express EGFP (including osteocytes). Osteoblasts ( $3 \times 10^6$  cells) from 6-8wk old mT/mG x DMP1-8kb-Cre mice were combined with a mixture of PSC (at fibril density corresponding 500Pa shear modulus) and HA (14mg/mL or 28mg/mL) and cultured for 3d, 28d or 56d in osteogenic media. Following the culture period, cell membrane fluorescence was assayed by confocal microscopy and unconfined compression testing was used to measure the compressive modulus (from 50%-70% strain) at the different time points for the different culture compositions (N=2-3 for each condition).

From 3d to 56d, the percentage of red cells (osteoblasts) in the 14mg/mL cultures decreased (44% vs. 16%) and the percentage of yellow cells (transitioning between osteoblast and DMP1 expressing osteocyte) increased (54% vs. 69%). The number of green cells (mature osteocytes) increased from 3% to 26% of the cells counted, but this increase did not reach statistical significance. In the 28mg/mL cultures, similar patterns were observed for the red and yellow cells between 3d and 56d cultures, but at this higher HA concentration, the increase in the percentage of green cells in the cultures was significant (3% vs. 16%). By 28d, only the 14mg/mL cultures had become significantly stiffer than at 3d (403kPa vs. 170kPa). By 56d, both the 14mg/mL and 28mg/mL cultures were stiffer (618kPa and 1,053kPa, respectively) than they were at 3d (170kPa and 420kPa, respectively). In conclusion, the mineral-collagen constructs were able to induce differentiation of seeded osteoblasts to osteocytes, which coincided with increased construct compressive stiffness over the 28d and 56d culture periods, presumably due to the formation of new bone matrix.

**Disclosures:** Brian Golz, None.

## MO0572

**Metabolic Labelling of Osteocyte Pericellular Matrix in vitro and in vivo.** Shaopeng Pei<sup>\*</sup>, Jerahme Martinez, Shubo Wang, Shongshan Fan, Catherine Kirm-Safran, X.Lucas Lu, Liyun Wang. University of Delaware, United States

#### Introduction

In bone, the pericellular matrix (PCM) surrounding osteocytes [1] is hypothesized to form a mechanosensing complex for bone mechanotransduction [2]. Yet, there are very limited data on the dynamics of osteocyte PCM. In this study, we developed a novel metabolic labeling method using click chemistry [3] to label the osteocyte PCM and track the labeled PCM components in vitro as in a classic "Pulse-Chase" experiment [4]. Our overall goal is to track and quantify the composition of the osteocyte PCM and the changes under various mechanical environments.

#### Methods

MLO-Y4 cells in  $\alpha$ -MEM (5% FBS, 1% PS) were fed with a modified sugar (Ac4GalNAz) for 3days before "click reaction" with fluorescent dye MB 488 DBCO



on day 4. The labeled PCM was imaged at 1-5 days post click to track the PCM turnover in cultured cells.

Male B6 mT/mG transgenic mice were injected with Ac4GalNAz or vehicle (DMSO) for 7 consecutive days. MB 488 DBCO was injected on day 8. Tibiae were harvested and imaged under confocal microscope without sectioning. The image area was located at the relatively flat anterior-medial surface 30-40% distal from the proximal end.

#### Results

For *in vitro* PCM visualization, we observed a nicely labeled fibrous matrix (green) outside the cell bodies (labeled red, Fig. 1A). For *in vivo* labeling, most of the osteocytes showed "halo" like labeling surrounding the cell bodies (with the red membrane transgene expression), while negligible green signals were seen in vehicle-treated group (Fig. 1B). 5-day consecutive confocal images (Fig. 1C) and plate reader readings (Fig. 1D) of MLO-Y4 cells PCM labeling showed a rapid loss of the newly synthesized PCM with a half-life time of approximately 24 hrs.

#### Conclusion

In this study, we provided the very first quantification of the osteocyte PCM turnover rate *in vitro*, which was surprisingly fast (half-time of 24 hours). This may be due to the fact that PCM was exposed to a large amount of media (faster diffusion) compared to the confined environment *in vivo*. The successful labelling of osteocyte PCM *in vivo* will help us further study the turnover rate of osteocyte PCM in their native environment and the components of the PCM mechanosensing complex, which will greatly enhance our understanding of osteocyte's responses to mechanical stimulations.

#### References

1. You, Anat Rec A Discov Mol Cell Evol Biol. 2004.
2. Wang, J Bone Miner Res. 2014.
3. Nwe K, Cancer Biother Radiopharm. 2009.
4. Simon E, Vol 536. 1st ed. Elsevier Inc. 2014.

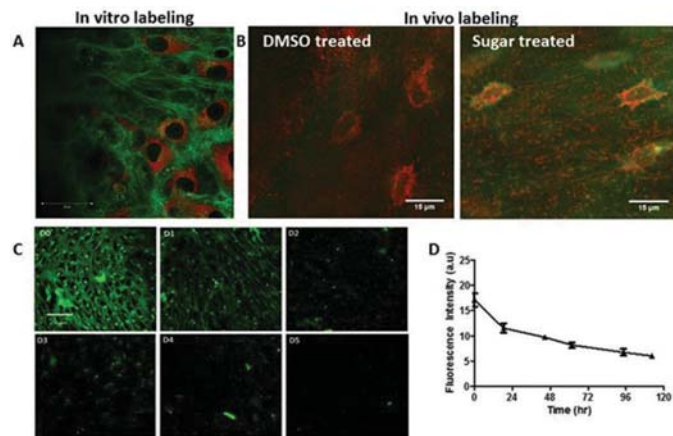


Fig. 1. (A) MLO-Y4 cells stained with cell-tracker and MB 488 DBCO; (B) Tibia anterior-medial surface osteocyte imaging of vehicle treated group and Ac<sub>4</sub>GalNAz treated group; (C) 5-day consecutive imaging of MLO-Y4 cells under confocal microscope; (D) 5-day consecutive reading from plate reader of MLO-Y4 cells treated with Ac<sub>4</sub>GalNAz supplemented media for 3 days prior metabolic labelling and plater reading.

Figure. 1 Osteocyte PCM labeling and turnover quantification

Disclosures: Shaopeng Pei, None.

## MO0573

**Accelerated bone aging in human auditory ossicles is accompanied by excessive hypermineralization, osteocyte death and micropetrosis.** Tim Rolvien<sup>1</sup>, Christoph Riedel<sup>1</sup>, Petar Milovanovic<sup>1</sup>, Anke Jeschke<sup>1</sup>, Sebastian Butscheidt<sup>1</sup>, Klaus Puschel<sup>2</sup>, Michael Amling<sup>1</sup>, Björn Busse<sup>1</sup>. <sup>1</sup>Department of Osteology and Biomechanics, University Medical Center Hamburg-Eppendorf, Germany, <sup>2</sup>Department of Legal Medicine, University Medical Center Hamburg-Eppendorf, Germany

Osteocytes, the most abundant bone cells, form a multifunctional network within the mineralized bone that orchestrates bone remodeling by osteoclasts and osteoblasts. A preserved osteocyte population is seen as a crucial determinant of maintained bone quality. The reduction of osteocyte numbers due to pronounced osteocyte apoptosis, as it occurs in aging and osteoporosis, increases bone fracture risk. Hitherto, in-depth investigation of the auditory ossicles' osteocytic lacuno-canalicular system and its morphology has not been performed. Here we analyzed the frequency, size and composition of osteocyte lacunae in the auditory ossicles of 22 individuals from early postnatal period to old age. Furthermore, overall mineralization of the bone matrix was determined using backscattered electron imaging. While signs of bone modeling and bone remodeling were found in newborns, no bone remodeling processes were observed above the age of 1 year. We detected signs of premature and excessive bone aging, such as an age-related decrease in number of osteocytes, as well as lower total lacunar density and lacunar area. Other indicators of accelerated bone aging were high matrix mineralization and prominent accumulation of micropetrotic lacunae. The majority of these changes took place in the first months and years of life, while afterwards only minor reorganization of ossicles was present. With osteocyte apoptosis potentially being a consequence of low

mechanical stimuli present in auditory ossicles, the early loss of osteocytes without initiation of bone remodeling indicates an adaptive response conserving the architecture of the auditory ossicles and ensuring stable sound transmission throughout life.

Disclosures: Tim Rolvien, None.

## MO0574

**Histone deacetylases HDAC4 and HDAC5 participate in osteocyte mechanotransduction and are required for loading-induced bone formation.** Tadatoshi Sato<sup>1</sup>, Maureen J. Omeara<sup>1</sup>, Nia Campbell<sup>1</sup>, Henry M. Kronenberg<sup>1</sup>, Ted S. Gross<sup>2</sup>, Marc Wein<sup>1</sup>. <sup>1</sup>Massachusetts General Hospital Endocrine unit, Harvard Medical School, United States, <sup>2</sup>University of Washington, Department of Orthopaedics and Sports Medicine, United States

**Background:** Osteocytes are the primary mechanosensors in bone. Loading-induced bone formation requires SOST down-regulation. The intracellular signaling pathways through which loading suppresses SOST suppression are unknown. HDAC4 and HDAC5 control SOST expression in osteocytes, and are required for PTH-induced SOST regulation. The goal of this study was to determine if class IIa HDACs participate in mechanical loading induced osteocyte mechanotransduction.

**Methods:** 20 week old wild type, HDAC4 conditional knockout (cKO, HDAC4 f/f; DMPI-Cre), HDAC5 knockout, and double knockout (DKO, HDAC4 f/f; HDAC5 -/-; DMPI-Cre) female mice were subjected to *in vivo* cantilever bending of the right tibia. Each mouse underwent a 3 wk regimen (3 d/wk, 100 cycles/d, 2500  $\mu$ -epsilon peak normal strain), and dynamic histomorphometry was performed on the tibia mid-shaft. Ocy454 cells were subjected to fluid flow stress (FFSS, 8 dynes/cm<sup>2</sup>). Gene expression was measured by RT-qPCR, and HDAC4/5 phosphorylation was measured with phospho-specific antibodies. HDAC4/5-deficient Ocy454 cells were generated using CRISPR/Cas9.

**Results:** *In vivo* loading studies showed that HDAC4 and HDAC5 are required for loading-induced periosteal bone formation. In WT mice, periosteal bone formation rate (p.BFR) significantly increased in response to loading (0.022 $\pm$ 0.029 vs 0.285 $\pm$ 0.244  $\mu$ m/d, p=0.0055). Similar increases were observed in HDAC4 cKO (0.007 $\pm$ 0.013 vs 0.112 $\pm$ 0.082  $\mu$ m/d, p=0.022) and HDAC5 knockout mice (0.0154 $\pm$ 0.009 vs 0.2432 $\pm$ 0.196  $\mu$ m/d, p=0.032). In contrast, DKO mice failed to increase periosteal BFR in response to loading (0.006 $\pm$ 0.008 vs 0.022 $\pm$ 0.031  $\mu$ m/d, p=0.298). In Ocy454 cells, FFSS led to time-dependent reductions in HDAC4 S246 and HDAC5 S259 phosphorylation, with peak reductions at 90 minutes. Control Ocy454 cells showed 77.4 $\pm$ 4.9% SOST down-regulation in response to FFSS compared to static treatment. In contrast, HDAC5-deficient cells reduced SOST by 58.8 $\pm$ 3.4%, and double HDAC4/5-deficient cells only reduced SOST by 37.1 $\pm$ 4.4% (p<0.05 comparing FFSS-induced SOST suppression in WT vs HDAC5 KO and HDAC5 KO vs DKO cells).

**Conclusions:** Combined deletion of HDAC4 and HDAC5 in osteocytes *in vivo* inhibited loading-induced periosteal bone formation. *In vitro*, flow induced mechanotransduction in osteocytes reduced HDAC4/5 phosphorylation. Finally, HDAC4/5 were required for optimal SOST FFSS-induced down-regulation. Therefore, class IIa HDACs are key determinants of osteocyte mechanotransduction.

Disclosures: Tadatoshi Sato, None.

## MO0575

**Second-generation HR-pQCT: Reproducibility of *in vivo* Bone Microarchitecture and Strength Measurements.** Sanchita Agarwal<sup>1</sup>, Kyle Nishiyama<sup>1</sup>, Fernando Rosete<sup>1</sup>, Mariana Bucovsky<sup>1</sup>, Ivelisse Colon<sup>1</sup>, X. Edward Guo<sup>2</sup>, Elizabeth Shane<sup>1</sup>. <sup>1</sup>Division of Endocrinology, Department of Medicine, Columbia University, United States, <sup>2</sup>Department of Biomedical Engineering, Columbia University, United States

High-resolution peripheral quantitative computed tomography (HR-pQCT) permits three-dimensional measurement of bone microarchitecture and can be combined with finite element (FE) modeling to estimate bone strength. Second generation HR-pQCT scanners (XtremeCTII) offer improved isotropic voxel size (61  $\mu$ m), which allows for direct measurements of cortical and trabecular microstructure using distance transform methods.

The purpose of this study was to assess the short- and long-term reproducibility of XtremeCTII measurements in a heterogeneous cohort of healthy men and women (N=30, age: 42 $\pm$ 15) scanned at two sites (standard and contiguous proximal). Participants were scanned 3 times: twice on the same day with repositioning and again 1 month later. Precision error was assessed by root mean squared coefficient of variation (RMSCV%) and intraclass correlation coefficient (ICC). Least significant change (LSC) was calculated as 2.77\*RMSCV.

After eliminating scans with motion score>3 (distal radius 6, proximal radius 5), short-term RMSCV ranged from 0.0-3.0% at radius and tibia for most measurements (Table). Exceptions included trabecular number (Tb.N; radius: 4.5%; tibia: 4.2%) and cortical porosity (Ct.Po; radius: 15.6%; tibia: 9.9%). Findings at the proximal location were similar. Precision error in estimated stiffness at the distal radius was also high (RMSCV: 6.8%). ICC correlation values were excellent for all measurements, with lowest correlations for Tb.N and Ct.Po. Findings for long-term reproducibility were similar, with RMSCV between 0.0-1.0% for geometry, 0.0-1.6% for density, 0.8-5.4% for trabecular microstructure, 0.7-1.4% for Ct.Th and 9.5-20.0% for Ct.Po (20.0% at the radius).

The higher precision error observed for Ct.Po and stiffness in the distal radius scans could be related to higher variability in motion between scans. As 50% of our cohort was < 40 years old, values for mean Ct.Po were low (radius: 0.4%; tibia: 2.0%). Hence, small changes in detection of these fewer and smaller pores may also have contributed to higher Ct.Po precision error. Despite high RMSCV for Ct.Po, the LSC was small (radius: 0.18%; tibia: 0.55%), thereby providing high sensitivity in detection of small changes in porosity. However, further improvements of precision error for Ct.Po are needed. In conclusion, measurements from XtremeCTII have good reproducibility for most measurements and moderate precision for Ct.Po across all sites.

Parameter	LSC (RMSCV%)			ICC	LSC (RMSCV%)			ICC
	Mean $\pm$ SD	Mean $\pm$ SD	Mean $\pm$ SD		Mean $\pm$ SD	Mean $\pm$ SD	Mean $\pm$ SD	
	Distal Radius				Proximal Radius			
Tot.vBMD (mg HA/cm <sup>3</sup> )	335 $\pm$ 64	8 (0.9%)	0.99		506 $\pm$ 76	6 (0.4%)	0.99	
Tb.vBMD (mg HA/cm <sup>3</sup> )	159 $\pm$ 50	3 (0.6%)	0.99		126 $\pm$ 63	3 (0.8%)	1	
Tb.N (1/mm)	1.46 $\pm$ 0.24	0.18 (4.5%)	0.92		1.10 $\pm$ 0.29	0.11 (3.5%)	0.98	
Ct.vBMD (mg HA/cm <sup>3</sup> )	920 $\pm$ 57	15 (0.6%)	0.99		1030 $\pm$ 46	10 (0.4%)	0.99	
Ct.Po (%)	0.41 $\pm$ 0.29	0.18 (15.6%)	0.95		1.20 $\pm$ 0.54	0.26 (7.8%)	0.97	
Ct.Po.Dm (mm)	0.155 $\pm$ 0.029	0.03 (6.5%)	0.88		0.170 $\pm$ 0.033	0.02 (3.9%)	0.95	
Ct.Th (mm)	1.03 $\pm$ 0.17	0.04 (1.3%)	0.99		1.61 $\pm$ 0.20	0.03 (0.7%)	0.99	
Stiffness (N/mm)	38743 $\pm$ 15260	7283 (6.8%)	0.97		47661 $\pm$ 11989	2414 (1.8%)	0.99	
	Distal Tibia				Proximal Tibia			
Tot.vBMD (mg HA/cm <sup>3</sup> )	311 $\pm$ 62	3 (0.4%)	1		372 $\pm$ 78	4 (0.4%)	1	
Tb.vBMD (mg HA/cm <sup>3</sup> )	162 $\pm$ 47	2 (0.4%)	1		131 $\pm$ 57	2 (0.6%)	1	
Tb.N (1/mm)	1.27 $\pm$ 0.23	0.15 (4.2%)	0.98		1.06 $\pm$ 0.27	0.09 (3.2%)	0.98	
Ct.vBMD (mg HA/cm <sup>3</sup> )	919 $\pm$ 75	9 (0.4%)	0.99		980 $\pm$ 57	8 (0.3%)	0.99	
Ct.Po (%)	2.00 $\pm$ 1.18	0.55 (9.9%)	0.98		1.40 $\pm$ 0.9	0.46 (11.9%)	0.97	
Ct.Po.Dm (mm)	0.229 $\pm$ 0.039	0.03 (5.4%)	0.93		0.218 $\pm$ 0.042	0.02 (3.9%)	0.95	
Ct.Th (mm)	1.53 $\pm$ 0.30	0.03 (0.7%)	0.99		2.02 $\pm$ 0.39	0.03 (0.6%)	0.99	
Stiffness (N/mm)	110721 $\pm$ 33483	8463 (2.8%)	0.99		114310 $\pm$ 31448	4340 (1.4%)	0.99	

Table: Short-term reproducibility of bone microstructure measurements

**Disclosures:** Sanchita Agarwal, None.

## MO0576

**Volumetric Hip DXA Indicates Rapid Deterioration Of Both Cortical And Trabecular Bone Compartments After Allogeneic Hematologic Stem Cell Transplant.** Mohammed Almohaya<sup>\*1</sup>, Naveen Sami<sup>2</sup>, David Kendler<sup>3</sup>, Renaud Winzenrieth<sup>4</sup>, Ni Bai<sup>2</sup>, Stephen Robertson<sup>2</sup>, Raewyn Broadb<sup>3</sup>. <sup>1</sup>King Fahad Medical City, Saudi Arabia, <sup>2</sup>Prohealth Clinical Research, Canada, <sup>3</sup>University of British Columbia, Canada, <sup>4</sup>Galgo Medical, Spain

Allogeneic stem cell transplant (aHSCT) is being utilized more frequently for hematologic malignancy. Bone loss leading to osteoporosis is common after aHSCT with reported significant decreases in bone density greater at hip than spine 100 days after aHSCT. There are no reports differentiating trabecular from cortical bone loss by specific imaging of the cortical and trabecular compartments.

From DXA capture at proximal femur, volumetric integral (vBMD Int), volumetric trabecular (vBMD Trab) and volumetric cortical (vBMD Cort) BMD as well as the average cortical thickness (vBMD cortthick) can be evaluated using 3D-DXA software (Galgo Medical, Spain). This software (3D-DXA) registers a 3D appearance model of the femoral shape and density onto the DXA projection to obtain a 3D subject-specific model of the femur of the patient and quantify both volumetric trabecular and cortical compartments [Humbert et al., IEEE Trans Med Imaging, 2016].

We retrospectively reviewed 93 consecutive patients undergoing aHSCT for hematologic malignancy, who were not given osteoporosis medications. Average age was 48.5 yr (Female n=41, Male n=52). DXA hip (Hologic Discovery) on the same equipment was captured prior to aHSCT and 100 days after aHSCT. Hip DXA scan captures were analysed to determine hip integral, cortical and trabecular volumetric parameters as well as the usual areal BMD (aBMD).

At day 100, total hip and femoral neck aBMD declined 4.3% and 4.3% respectively. vBMD Int declined by 0.36 SD (21.4 mg/cm<sup>3</sup>), vBMD Trab loss was 0.41 SD (18.1 mg/cm<sup>3</sup>) and vBMD Cort loss was 0.33 SD (13.4 mg/cm<sup>3</sup>). Mean vBMD cortthick declined by 0.28 SD (0.055 mm) (P<0.0001 for all). The highest correlation was between changes in total hip aBMD and vBMD Int (Pearson r=0.85). Femoral neck aBMD changes showed stronger correlations to vBMD Trab (r=0.70), as compared to changes in femoral neck aBMD correlation with vBMD Cort (r=0.50).

These data suggest that DXA software-derived parameters of cortical and trabecular bone may be helpful in determining compartmental bone loss in aHSCT patients. Adverse interactions between the transplanted stem cells and host bone cells may rapidly deteriorate both trabecular and cortical compartments. Bisphosphonate may afford incomplete protection of cortical bone after aHSCT; bone protective therapies with greater effectiveness on both cortical and trabecular bone compartments may be more beneficial in this patient population.

**Disclosures:** Mohammed Almohaya, None.

## MO0577

**Peripheral bone microstructure and strength improve the prediction of incident clinical low-trauma fractures beyond DXA and FRAX in postmenopausal women.** Emmanuel Biver<sup>\*1</sup>, Claire Durosier-Izart<sup>1</sup>, Thierry Chevalley<sup>1</sup>, Bert van Rietbergen<sup>2</sup>, René Rizzoli<sup>1</sup>, Serge Ferrari<sup>1</sup>. <sup>1</sup>Division of Bone Diseases, Geneva University Hospitals and Faculty of Medicine, Switzerland, <sup>2</sup>Department of Biomedical Engineering, Eindhoven University of Technology, Netherlands

### Purpose

A majority of clinical fractures (cFx) occurs in subjects with osteopenia suggesting that alterations in bone "quality" contribute to bone fragility in addition to areal bone mineral density (aBMD). Whereas bone microstructure and estimated strength have been associated with prevalent fractures, it remains unclear whether they may improve the prediction of incident fractures. We investigated the contribution of aBMD, trabecular bone score (TBS), FRAX, as well as cortical (Ct) and trabecular (Tb) volumetric BMD (vBMD), bone microstructure and estimated strength at the peripheral skeleton to incident cFx risk in a cohort of community-dwelling postmenopausal women.

### Methods

Seven hundred and forty women (age 65.0  $\pm$  1.4 yrs), enrolled in the Geneva Retirees Cohort (GERICO), were prospectively evaluated over 5.0  $\pm$  1.8 yrs for the occurrence of low-trauma cFx. At baseline, we evaluated aBMD and TBS by DXA, Ct and Tb vBMD and microstructure at distal radius and tibia by HR-pQCT, as well as bone strength by micro-finite element analysis. We assessed Cox model discrimination using Harrell's C index.

### Results

Incident low-trauma cFx occurred in 68 (9%) women. Radius and tibia Ct and Tb vBMD and most microstructure parameters, as well as failure load (FL), stiffness and modulus, were associated with cFx. The highest hazard ratios [HR] were observed with radius total vBMD, Tb vBMD, Ct area and FL (HR 1.69, 1.70, 1.68 and 1.71 respectively, p<0.001 for all). These HR remained significant after adjustment for femoral neck (FN) aBMD and FRAX (with or without BMD and TBS). However, they were markedly attenuated after adjustment for ultra-distal radius aBMD (adjusted HR 1.44, 1.39, 1.35 and 1.56, p=0.093, 0.100, 0.164 and 0.085, respectively). The combination of FN aBMD with radius FL showed the highest discrimination between women with and without cFx: C-index (95%CI) 0.667 (0.594, 0.740), vs 0.570 (0.487, 0.653) for FN aBMD (p=0.024). Tb vBMD combined with Ct area, as well as FL or ultra distal aBMD at the radius, significantly improved cFx prediction compared to FN aBMD (Table).

### Conclusion

Peripheral Ct and Tb vBMD, microstructure and derived bone strength predict incident low-trauma cFx independently of FN aBMD and FRAX (with TBS). The prediction of cFx is improved by the combination of a Ct with a Tb parameter, as well as by estimated bone strength at the distal radius, which are partially captured in aBMD measured by DXA at the same bone site (ultra-distal radius).

Table: Harrell's C indices showing ability of various models to predict incident clinical low-trauma fractures				
Covariate	Covariate	Covariate + FN aBMD	Covariate + spine aBMD	Covariate + FN + spine aBMD
FN aBMD	0.570	0.570		
spine aBMD	0.625		0.625	
FN + spine aBMD	0.625			0.625
Tb.vBMD	0.631	0.634	0.641	0.641
Ct.area	0.640	0.646	0.654	0.655
Tb.BMD	0.642	0.645	0.653	0.655
Tb.vBMD + Ct.area	0.665*	0.668*	0.661	0.664
Failure load	0.666*	0.667*	0.660	0.665
Ultra distal radius aBMD	0.659*	0.635*	0.645	0.645

\*Harrell's C index significantly different from that for femoral neck aBMD at p<0.05

Table

**Disclosures:** Emmanuel Biver, None.

## MO0578

**Spatial Assessment of Bone Microarchitecture in Postmenopausal Women With a Recent Colles' Fracture.** Andrew Burghardt<sup>\*1</sup>, Sundeep Khosla<sup>2</sup>, Julio Carballido-Gamio<sup>3</sup>. <sup>1</sup>University of California, San Francisco, United States, <sup>2</sup>Mayo Clinic, United States, <sup>3</sup>University of Colorado Denver, United States

The spatial assessment of bone with data-driven image analysis techniques, including statistical parametric mapping (SPM), could identify biologically-relevant regions and bone features that distinguish clinical populations. We applied SPM to a case-control study of forearm fracture. The forearms of postmenopausal women with (N=84) and without (N=98) recent Colles' fractures were imaged using HR-pQCT. The distal radius was segmented and spatially normalized to a template effectively aligning corresponding anatomical regions across the study population. These transformations were applied to voxel-based maps of local bone volume fraction (BV/TV), homogenized volumetric bone mineral density (vBMD), strain energy density (SED) from  $\mu$ FEA, and inter-trabecular distances (Tb(1/N)). Surface-based maps of cortical thickness (Ct.Th), Ct. vBMD, and Ct.SED were used to study the cortex, in whole and in three laminar zones: sub-periosteal, central, and endocortical. Voxel/vertex-wise comparisons between cases



Figure 1 and 2

**Disclosures:** Andrew Burghardt, None.

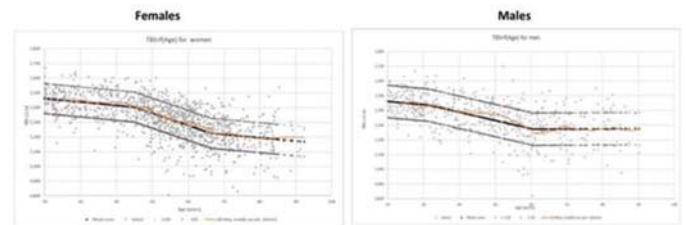
## MO0579

**Age-related normative values of trabecular bone score (TBS) for Spanish population. SEIOMM-TBS project.** Antonio Cano<sup>\*1</sup>, Javier del Pino<sup>2</sup>, Luis Del Rio<sup>3</sup>, Silvana Di Gregorio<sup>4</sup>, Jesus Garcia-Vadillo<sup>5</sup>, Carlos Gomez<sup>6</sup>, Jesus Gonzalez-Macias<sup>7</sup>, Nuria Gualañabens<sup>8</sup>, Federico Hawkins<sup>9</sup>, Jorge Malouf<sup>10</sup>, Eduardo Kanterewicz<sup>11</sup>, Esteban Martinez<sup>8</sup>, Ana Monegal<sup>12</sup>, Maria Jose Montoya<sup>13</sup>, Manuel Muñoz<sup>14</sup>, Xavier Nogues<sup>15</sup>, Joan Miquel Nolla<sup>16</sup>, Jose Maria Olmos<sup>17</sup>, Ramon Perez-Cano<sup>18</sup>, Jose Luis Perez-Castrillon<sup>19</sup>, Pilar Peris<sup>12</sup>, Manuel Rodriguez<sup>20</sup>, Daniel Roig<sup>21</sup>, Manuel Sosa<sup>22</sup>, Elena Valassi<sup>10</sup>. <sup>1</sup>Hospital Clínico Universitario, Spain, <sup>2</sup>Hospital Univ. De Salamanca, Spain, <sup>3</sup>CETIR Centre Medic, Spain, <sup>4</sup>ERESA Centro Médico Quirúrgico el Campanar, Spain, <sup>5</sup>Hospital de la Princesa, Spain, <sup>6</sup>Hospital Central de Asturias, Spain, <sup>7</sup>Hospital Univ. Marques de Valdecilla, Spain, <sup>8</sup>Hospital Clinic, Spain, <sup>9</sup>Hospital Universitario 12 Octubre, Spain, <sup>10</sup>Hospital de Santa Creu i Sant Pau, Spain, <sup>11</sup>Hospital general de Vic, Spain, <sup>12</sup>Hospital Clinic, Spain, <sup>13</sup>Departamento de Medicina. Universidad de Sevilla, Spain, <sup>14</sup>Hospital Universitario San Cecilio, Spain, <sup>15</sup>Hospital del Mar, Spain, <sup>16</sup>Hospital Universitari de Bellvitge, Spain, <sup>17</sup>Hospital Univ.Marques de Valdecilla, Spain, <sup>18</sup>Hospital Univ. Virgen Macarena, Spain, <sup>19</sup>Hospital Universitario Rio Horta, Spain, <sup>20</sup>Hospital Regional Univ. de Málaga, Spain, <sup>21</sup>Hospital Sant Joan Despi Moises Broggi, Spain, <sup>22</sup>Hospital Univ. Insular, Spain

TBS is a method that analyzes the texture of gray-level image generates in a DXA spine scan. TBS has been shown to discriminate patients with fractures from healthy subjects independently of BMD. Although conceptually TBS does not depend directly of ethnic or geographical origin of the subjects, the phenotype and more specifically the amount of abdominal soft tissue could be explained by potential differences among population in different countries. The aim of this study was to establish age-adjusted normative curves to be used as reference values for Spanish population. Subjects and Methods: A cross-sectional study was conducted among volunteers of both sexes, from 19 to 90 years old, recruited from 17 medical centers based in 9 autonomic communities in Spain. Data obtained from these centers were cross calibrated for TBS and BMD. All participants completed a detailed questionnaire on pathological conditions, treatments, bone fractures, gynecological history (in females) and lifestyle factors. Participants with history of such conditions with potential influence on bone metabolism were excluded from the analysis. BMD measurements were obtained using different DXA models devices from GE-Healthcare and Hologic Inc., manufacturers (Prodigy, iDXA, Discovery, QDR 4500). BMD was calculated from L1 to L4 lumbar vertebrae. TBS was calculated at the same regions of interest used for BMD measurements. A cohort of 1863 healthy subjects of both genders was selected from a 3007 participants in the study (66,5%), a total of 1349 woman and 514 males. Results: Values of TBS in young women and young men (20-30 years) were similar. TBS values decreased with age in both sexes. In females a three-piece regression line fitted at the values scattered TBS maximum values were observed at 20-30 decade and decline at the 40-50 years as BMD. The TBS change between 45 and 85 years old have two piecewise linear parts, and the averaged TBS decrease compared to TBS values of young women was 18%. In males, TBS decreases 11% from 20's decade to 80's decade. TBS values at L1-L4 were poorly correlated with BMI ( $r=-0.1$ ), weight ( $r=-0.1$ ), and sBMD ( $r=0.2$ ). In women, the values were similar to those previously reported in Caucasian population.

**Conclusion:** Robust reference age- and sex-specific curves for TBS are provided in Spanish population. This could improve the management of patients with osteoporosis and help to monitor microarchitectural changes in clinical practice

### Age -TBS curves in healthy Spanish population



**Disclosures:** Antonio Cano, None.

## MO0580

**Fractal-based Assessment of Bone-antiresorptive Treatment Effects at the Lumbar Spine Using Conventional Radiographs; Results from a Pilot Study in a Sub-cohort of Postmenopausal Women who Participated in the FREEDOM Pivotal Trial and its Extension Phase\***. Hans Peter Dimai<sup>1</sup>, Richard Ljuhar<sup>2</sup>, Davul Ljuhar<sup>3</sup>, Benjamin Norman<sup>3</sup>, Tobias Haftner<sup>3</sup>, Stefan Nehrer<sup>4</sup>, Astrid Fahrleitner-Pammer<sup>1</sup>. <sup>1</sup>Medical University of Graz, Department of Internal Medicine, Division of Endocrinology & Diabetology, Austria, <sup>2</sup>Image Biopsy Lab, R & D, Austria, <sup>3</sup>Braincon Technologies, Austria, <sup>4</sup>Danube University Krems, Department for Health Services and Biomedicine, Center for Regenerative Medicine, Austria

## Background

Fractal mathematics, a form of nonlinear mathematics, have been shown to offer the ability of exploiting textural information as present on plain bone radiographs. Accordingly, it has been demonstrated earlier that such models, e.g., if applied to trabecular bone radiographs of the calcaneus, can discriminate between patients with prevalent osteoporotic fractures and those without (1).

## Subjects and Methods

A fractal-based method was developed to extract textural information from plain lumbar spine radiographs, using state-of-the-art computer hardware and software together with a specific machine-learning algorithm. The obtained parameter, referred to as Bone Structure Value (BSV), was then tested in plain lumbar spine radiographs taken in lateral projection, obtained from a sub-cohort of postmenopausal women treated with denosumab 60mg subcutaneously every 6 months, within the framework of FREEDOM, a large 3-year international randomized controlled trial, and its 5-year open label extension phase. Radiographs were digitally archived in 16-bit DICOM format. Semi-automatically placed regions-of-interest (ROI), sized 28x14mm, were used for each vertebra from L1 to L4 (depending on eligibility). Bone mineral density (BMD) was assessed in the same study population by using dual energy x-ray absorptiometry (DXA). Differences between baseline values, and 3 and 8 years of treatment were analyzed for both BSV and DXA using Repeated Measures ANOVA.

## Results

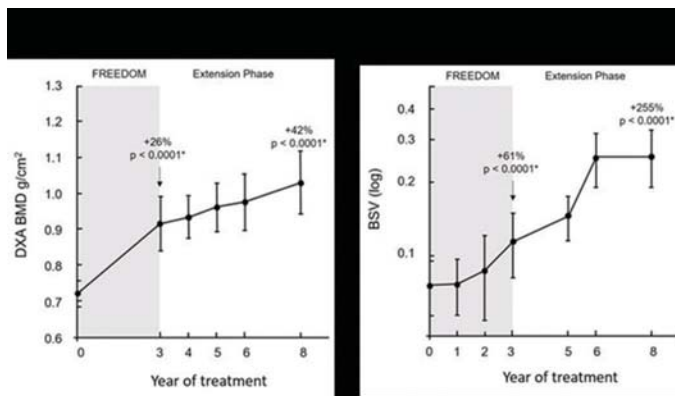
Nineteen treatment-group subjects were included in the analyses, yielding a total of 110 lumbar spine radiographs (of 133 possible), and 87 lumbar spine DXA reports (of 114 possible). After 3 and after 8 years of treatment with denosumab, mean BMD as well as mean BSV were significantly different from their respective baseline values at study entry (DXA:  $F=108.2$ ,  $p < 0.00001$ ; BSV:  $F=84.3$ ,  $p < 0.00001$ ). The overall increase in DXA-derived BMD at year 8 was +42% ( $0.725 \pm 0.038$  g/cm<sup>2</sup> to  $1.031 \pm 0.092$  g/cm<sup>2</sup>,  $p < 0.0001$ ), and the overall increase of BSV was 255% ( $0.076 \pm 0.022$  to  $0.270 \pm 0.09$ ,  $p < 0.0001$ ) (Fig. 1 & Fig. 2). BMD and BSV showed a highly significant correlation ( $R = 0.51$ ;  $p < 0.0001$ ).

## Conclusion

This study provides strong evidence that BSV as obtained from conventional spine radiographs constitutes a highly responsive means in the assessment of bone-specific, treatment-related effects in osteoporotic postmenopausal women treated with denosumab.

1) Benhamou CL et al; J Bone Miner Res 2001; 697 – 704

\* Supported by AMGEN Inc. (Thousand Oaks, California, USA) and the Medical University of Graz (MedUniGraz, AUSTRIA) including a Data Sharing Agreement.



Effect of denosumab on DXA (Fig.1) and BSV (Fig.2)

Disclosures: Hans Peter Dimai, None.

## MO0581

**Quantification of the effects of tissues thickness and fat content on the experimental variogram, the basic algorithm of TBS.** Franck Michelet<sup>1</sup>, Didier Hans<sup>2</sup>. <sup>1</sup>Medimaps, France, <sup>2</sup>Center of Bone diseases, Bone and Joint Department, Lausanne University Hospital, Switzerland

**Purposes:** TBS is derived from the initial slope of the log-log experimental variogram of the DXA bone image, and the TBS computation process includes a soft tissue compensation. The aim of this study was to quantify the influence of soft tissues on the variogram, and provide background information on how tissues could influence TBS, to better implement corrective adjustments if necessary.

**Material & Method:** We used a set of 15 dried lumbar or low thoracic human vertebrae, set in AP position. Soft tissues were simulated by a mix of homogeneous layers of HDPE and PVC, achieving tissue thickness and fat percent compatible with normal human variation. First, all vertebrae were scanned at a constant fat percent of 30%, with thickness varying from 13cm to 25cm. Then, all vertebrae were scanned at a constant thickness of 17cm, with fat percent varying from 4% to 45%. Vertebrae were scanned on GE-Lunar Prodigy device, using Standard mode. We called rawTBS the initial slope of the log-log variogram. As opposed to TBS, rawTBS does not include any soft tissue compensation algorithm. For each vertebra, rawTBS was computed over the largest rectangular region inside the vertebral body. RawTBS values for all vertebrae were averaged for each tissue configuration and plotted against the relevant variable.

**Results:** A positive relationship was observed between rawTBS and fat percent, with an almost flat slope of 0.0012 per percent of fat ( $r^2=0.97$ ). A negative relationship was observed between TBS and tissue thickness, with a slope of -0.055 per cm of tissue ( $r^2=0.99$ ). These results are presented in Figure 1.

**Discussion / Conclusion:** This study showed that the effect of soft tissues on rawTBS depends mainly on the thickness of soft tissues and to a smaller extent on the tissue fat percent. Indeed, a change of 45% in fat percent had an equivalent absolute impact on rawTBS as a change of 1cm of tissue thickness. These compensations are notably dependent on the DXA device brand and model, as well as on the scan mode but also on the gender. All these findings are already integrated in TBS iNsite version 2.1 and higher, as the TBS computation process includes soft tissue compensation techniques.

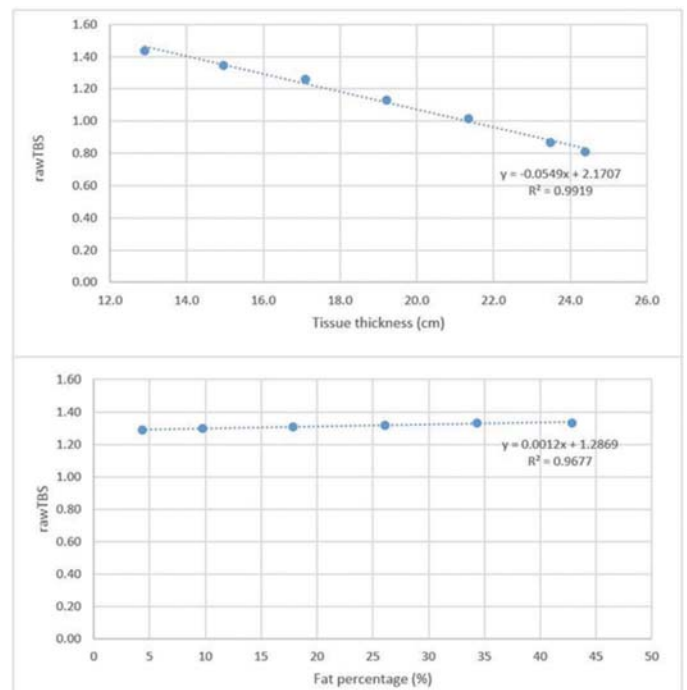


Figure1: rawTBS variations depending on tissue thickness and fat percent (GE Prodigy)

Figure: Soft Tissues

Disclosures: Franck Michelet, Medimaps, Other Financial or Material Support.



## MO0582

**Commercial Laboratory Reproducibility of Serum CTX in Clinical Practice.**

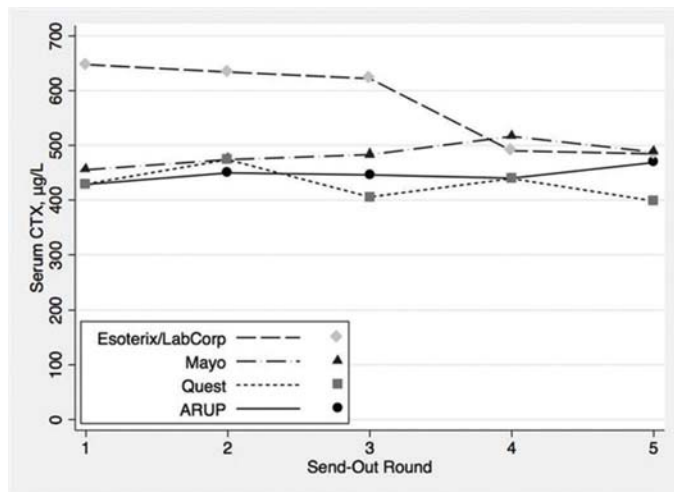
Sahar M. Hindi<sup>1</sup>, Eric Vittinghoff<sup>2</sup>, Anne L. Schafer<sup>1</sup>, Stuart Silverman<sup>3</sup>, Douglas C. Bauer<sup>4</sup>. <sup>1</sup>Division of Endocrinology and Metabolism, Department of Medicine, University of California, San Francisco, United States, <sup>2</sup>Department of Epidemiology and Biostatistics, University of California, San Francisco, United States, <sup>3</sup>Cedars Sinai Medical Center, UCLA School of Medicine, United States, <sup>4</sup>Department of Epidemiology and Biostatistics and Division of General Internal Medicine, Department of Medicine, University of California, San Francisco, United States

**Introduction:** The use of bone turnover markers (BTM) in clinical practice has been limited by several factors, including assay heterogeneity. In 2011, the IOF/IFCC selected serum collagen Type-I cross-linked C-peptide (s-CTX) as the reference standard for bone resorption. This study aims to determine the within- and between-laboratory reproducibility for s-CTX assays performed under routine clinical conditions.

**Methods:** To create standardized pools, serum was collected from ten premenopausal women and ten postmenopausal women. Premenopausal sera were pooled to approximate a population with low bone-turnover; postmenopausal sera were pooled to approximate a population with high bone-turnover; and a third pool was created by evenly mixing sera from pre- and postmenopausal women. Multiple identical aliquots from each pool were created and frozen; all were labeled as routine clinical specimens with fictitious patient identifiers. To evaluate longitudinal reproducibility, an aliquot from each of the 3 pools was sent to 4 US commercial laboratories on 5 dates over a 6-month period. To evaluate within-run reproducibility, on the 5th date, each lab received 5 aliquots from each pool. Three labs (Mayo, ARUP, and Quest) used the Roche Diagnostics Elecsys assay, and one (Esoterix/LabCorp) used the IDS-iSYS assay. Reproducibility was assessed using the coefficient of variation (CV) with 95% confidence intervals (CI). Labs were unaware of the investigation.

**Results:** Across labs, mean s-CTX values were 423, 533, and 480 for the premenopausal, postmenopausal, and mixed pools, respectively. The premenopausal pool longitudinal CVs ranged from 5.0% to 18.8%; postmenopausal pool CVs ranged from 3.4% to 19.3%; and mixed-pool CVs ranged from 3.3% to 16.0%. Between-lab patterns were similar for each pool, so results from all 3 pools are combined for this analysis. The longitudinal reproducibility for Esoterix/LabCorp (IDS assay) was higher (CV=18.0%, CI: 13.0-28.9) than for the other labs (Roche assay)(Figure). Within-run reproducibility was also highest for Esoterix/LabCorp (CV=16.3%, CI: 11.9-26.2) compared to the other labs (CVs 9.2-12.3%).

**Conclusion:** Longitudinal and within-run reproducibility of s-CTX varies across US commercial labs. Reproducibility was poorer for Esoterix/LabCorp, which uses the IDS assay, compared to the other 3 labs, which use the Roche assay. Our results indicate that better commercial lab s-CTX assay calibration is needed.



Longitudinal reproducibility of s-CTX among 4 US commercial labs over 6 months

**Disclosures:** Sahar M. Hindi, None.

## MO0583

**Quantification of Age-Related Changes in Whole-Skeleton Bone Metabolism using <sup>18</sup>F-NaF PET/CT.**

Alyssa Johncola<sup>\*</sup>, Jonathan Guntin, Christian McHugh, Austin Alecxih, Sun Kim, Rishika Sharma, Shivali Patel, Sheenali Patel, Thomas Werner, Poul Flemming, Abass Alavi, Chamith Rajapakse. University of Pennsylvania, United States

<sup>18</sup>F-NaF Positron Emission Tomography/Computer Tomography, or PET/CT, is a recently developed imaging tool capable of detecting bone turnover in human subjects. While conventional bone imaging modalities such as DXA and HR-pQCT can detect structural changes in bone, NaF PET/CT can provide functional information about bone sooner than any structural manifestations of bone disease or in response to therapy.

The goal of this study was to explore the use of Standard Uptake Value (SUV) of NaF PET/CT in subjects lacking skeletal abnormalities, other than age related metabolic bone diseases such as osteoporosis.

Most metabolic bone diseases are characterized by an imbalance of bone forming osteoblastic activity and bone reabsorbing osteoclastic activity, leading to osseous degeneration. The relationship between osteoblastic and osteoclastic activity can be determined by incorporation, or uptake of <sup>18</sup>F-NaF into the bone matrix. NaF passes extracellular fluid and is absorbed onto hydroxyapatite and exchanges rapidly for OH, which is on the surface of the hydroxyapatite matrix. The SUV, or NaF uptake value, can be detected and anatomically localized through PET/CT.

This study included 68 female and 71 male subjects (age 21-75 years, BMI 18-43 kg/m<sup>2</sup>). The subjects were scanned using NaF PET/CT at 90 minutes after NaF injection. Image analysis was completed using Pmod software (Pmod Technologies LLC, Switzerland). First, the whole skeleton was segmented from the CT image using Hounsfield value 100 as the lower threshold. Then, the PET and CT images were fused to calculate the SUV at each voxel in the segmented region (outlined in green, in Figure 1) and the average SUV for the whole skeleton was recorded. The completely automatic image analysis approach result in perfect inter-operator reproducibility (i.e., intra-class correlation coefficient = 1).

Average SUV decreased with age across females ( $p=0.01$ ) and males ( $p=0.04$ ), indicating approximately 3.8% and 2.3% decrease in bone metabolism per decade after 30 years of age, for females and males, respectively.

NaF PET/CT has the potential to be complementary to structural imaging modalities for the management of metabolic bone diseases.

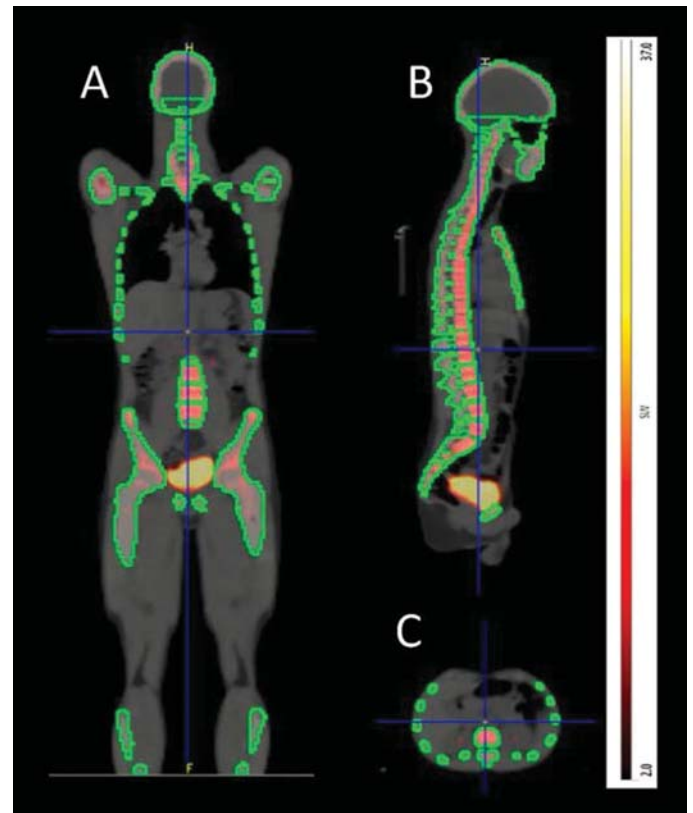


Figure 1

**Disclosures:** Alyssa Johncola, None.

## MO0584

**Shift in narrow neck centre-of mass influences neck of femur fracture prediction.**

Ben Khoo<sup>1</sup>, Matthew Miller<sup>2</sup>, Keenan Brown<sup>3</sup>, Joshua Lewis<sup>2</sup>, Kathy Zhu<sup>1</sup>, Richard Prince<sup>2</sup>. <sup>1</sup>Sir Charles Gairdner Hospital, Australia, <sup>2</sup>University of Western Australia, Australia, <sup>3</sup>Mindways Software, United States

Femoral neck (FN) fracture risk can be calculated from hip aBMD obtained from 2D DXA imaging of the proximal femur. Two geometric mechanisms of failure of FN have been suggested, bending and buckling. Using fracture data from a 14.5 y cohort study (LSAW), commenced as a 5 yr. RCT of calcium or placebo, the role of structural variables derived from DXA hip images were evaluated for predictive benefit (Fig). These variables can be related to failure in bending or buckling. Cross-sectional moment of inertia (CMSI) and section modulus (Z) relate to bending resistance, and r calculated as sum of  $\Delta$  (the displacement between centre-of-mineral mass (CoM)) and the geometric centre calculated as half the periosteal width (W/2) and  $\sigma$  (the SD of mineral-mass projection profile distribution) related to bone distribution and cortical thickness, are considered as measures of propensity to buckling failure (calculated as cortical thickness/r).

1159 women, mean age 75 y, had a hip DXA (Hologic, MA) in 1998/9. Derived narrow neck (NN) structural variables were cross sectional aBMD, CMSI, Z, W, d and  $\sigma$ . Over a total 14.5 y FN fracture hospitalisation was determined from WA Health Dept. hospital morbidity data. Statistical analysis used logistic regression and ROC area under curves (AUC).

The Table shows the data for the fracture and non-fracture cases. Neither CMSI nor Z was different in the two groups and both had the lowest AUC's for fracture. However comparison of W and d together with the derived variable r identified substantial differences supported by high AUC's,  $\sigma$  was also different between two groups and also had a high AUC. Because r includes both w and d and its role in computing failure in buckling it was entered into a stepwise logistic regression with age and treatment to identify the most important structural variables in resistance to FN fracture. The most parsimonious model consisted of age and r and  $\sigma$  (M2) which was then compared to the base model M1 (NN aBMD, age and calcium treatment) in ROC. The resultant C-statistic AUC's were M1 0.62 and M2 0.71,  $P=0.005$ .

These data support the hypothesis that FN fractures may occur as a result of structural changes in parameters related to buckling. It further suggests a way that the prediction of FN fracture may be improved by use of  $\Delta$  and r calculated from W/2 and  $\sigma$  in addition to aBMD, that together are related to determinants of buckling.

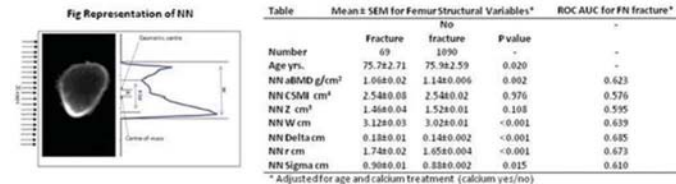


Figure and Table

Disclosures: Ben Khoo, None.

## MO0585

**Plasma MicroRNAs Might Be Related to Trabecular Bone Score in Postmenopausal Women.** Tilen Kranjc<sup>1</sup>\*, Barbara Ostanek<sup>1</sup>, Tomaz Kocjan<sup>2</sup>, Janez Prezelj<sup>2</sup>, Janja Marc<sup>1</sup>. <sup>1</sup>University of Ljubljana, Faculty of Pharmacy, Slovenia, <sup>2</sup>Dept. of Endocrinology, Diabetes and Metabolic Diseases, University Medical Centre Ljubljana, Slovenia

Objective:

Decreased lumbar spine trabecular bone score (TBS) is an indicator of poor bone quality and an independent risk factor for osteoporotic fractures. However, TBS measurement is not universally available and a plasma marker related to TBS would be clinically useful. Our objective was to establish if plasma microRNAs (miRNAs), novel biological markers in osteoporosis, might be used for this purpose.

Methods:

Initial screening included 4 postmenopausal women with normal TBS (>1.350) and 6 women with decreased TBS (<1.350). TBS was measured using DXA (Discovery, Hologic, Waltham, MA, USA) upgraded with TBS measurement software (Medimaps Group, Geneva, Switzerland). Their plasma samples were screened for 800 miRNA molecules by nCounter technology (Nanostring, Seattle, WA, USA). The selected miRNA molecules were then validated using miRNA specific primers and qPCR (Exiqon, Vedbaek, Denmark). The validation cohort consisted of 85 postmenopausal women with normal TBS and 25 postmenopausal women with decreased TBS. Missing values were imputed by choosing a random number from the representative normal distribution. The t-test was used for comparison of plasma levels of the selected miRNAs between the two subgroups.

Results:

Plasma levels of twenty miRNA molecules differed between decreased TBS group and normal TBS group. We further validated 6 miRNA molecules with the highest fold changes between the two subgroups and additional 7 miRNA molecules that were previously shown to have different plasma levels in osteoporotic population in comparison to controls. Analysis of non-imputed data showed significantly higher plasma levels of miR-93, miR-30d and miR-21 in patients with decreased TBS when compared to patients with normal TBS ( $p<0.05$ ). When using data with imputed missing values, plasma levels of miR-148a and miR-125b were significantly higher in the decreased TBS subgroup ( $p<0.05$ ).

Conclusions:

Plasma miRNAs might be related to TBS in postmenopausal women. Further studies are needed to establish their role in clinical practice.

Disclosures: Tilen Kranjc, None.

## MO0586

**Bone Mineral Density Measurement Intervals for Rheumatoid Arthritis Patients Not Treated for Osteoporosis.** Seung Yun Lee<sup>\*</sup>, Min-jae Jo, Kyong-Hee Jung, Seong-Ryul Kwon, Won Park. Division of Rheumatology, Departments of Internal Medicine, Inha University Hospital, Inha University School of Medicine, Korea, Republic of

Background/Aims: Osteoporosis occurs more frequently in rheumatoid arthritis (RA) patients than in healthy individuals. This study investigated the appropriate

bone mineral density (BMD) measurement interval and risk factors associated with osteoporosis for RA patients.

Methods: A retrospective study was performed on 511 RA patients aged more than 40 years old who had undergone BMD testing more than once and who had normal BMD or osteopenia at the baseline BMD test and no history of any fracture of the spine or femur. The subjects were categorized into four subgroups: normal BMD (T-score > -1), mild (-1 ≥ T-score > -1.5), moderate (-1.5 ≥ T-score > -2), and advanced (-2 ≥ T-score > -2.5) osteopenia. The BMD testing interval was defined as the estimated time for 10% of the RA patients to make the transition to osteoporosis without osteoporotic fracture or the administration of any osteoporosis drug.

Results: The observation period was 2,214 patient-years, with an average of 4.3 years. The estimated BMD testing interval was more than 10 years for normal, 4.3 years for mild, 2.5 years for moderate, and 1.5 years for advanced osteopenia in each of the RA patient groups.

Conclusions: Our study indicated that in normal or osteopenic RA groups, a baseline BMD T-score is the most important factor in estimating the interval in which osteoporosis is predicted to occur. In addition, we recommend that the BMD measuring interval should be greater than 10 years in normal BMD RA patients, 4 years in mild, 2 years in moderate, and 1 year in advanced osteopenic RA patients on the basis of L-spine BMD.

Disclosures: Seung Yun Lee, None.

## MO0587

**Assessing Intervention Thresholds for Osteoporotic Fracture Using FRAX® in Patients Following a Hematopoietic Stem Cell Transplantation.** Huifang Lu<sup>\*</sup>, William A Murphy Jr, Srishti Manocha, Data Don-Pedro, Gabriela Rondon, Cheuk Hong Leung, Liu Suyu, Richard E Champlin, Xerxes Pundole. The University of Texas MD Anderson Cancer Center, United States

Background: Osteoporotic fractures occur commonly following a hematopoietic stem cell transplantation (HSCT). In the general population, different intervention thresholds of the calculated FRAX probability are used to make treatment decisions in clinical practice. Intervention thresholds based on FRAX probabilities have not been evaluated in patients following HSCT.

Methods: We conducted a retrospective chart review of patients >18 years that received a HSCT at The University of Texas MD Anderson Cancer Center, between January 1, 2001 and December 31, 2010. Patients were considered to have entered the cohort at the time of HSCT. Osteoporotic fractures identified using ICD-9 codes were assessed until December 31, 2013, and confirmed by radiology and physician documentation. FRAX probabilities were calculated for each patient from baseline information obtained by chart review. We evaluated age dependent, fixed intervention thresholds for osteoporotic fractures using the FRAX tool major osteoporotic fracture probabilities.

Results: In the 10 year study period a total of 5,170 patients received a HSCT. Of these 527 (10%) patients developed an osteoporotic fracture, during an average of 3.3 years of follow up. Multivariate Cox regression models were built using FRAX score thresholds of low risk <10, medium risk 10 to 20, and high risk >20% probability of major fracture; and HSCT specific factors (underlying disease, type of HSCT and type of preparatory regimen). In patients > 65 years of age, those with medium risk had a 2.38 (95% confidence interval (CI): 1.27-4.47) times greater risk of fracture and patients with high risk had a 3.41 (95% CI: 1.73-6.75) times greater risk of osteoporotic fracture compared to those at low risk. In patients between 50 and 65 years of age, those with medium risk had a 1.3 (95% CI: 1.01-1.67) times greater risk and those at high risk had a 1.9 (95% CI: 1.21-2.94) times greater risk of osteoporotic fracture compared to those at low risk, while adjusting for the underlying indication and type of HSCT. In patients < 50 years, the FRAX score risk groups were not statistically significantly related with osteoporotic fracture and those with underlying multiple myeloma had a 4.12 (95% CI: 3.03-5.60) time risk of developing a fracture compared to patients without multiple myeloma.

Conclusion: In patients older than years at the time of HSCT, FRAX score risk groups can be potentially used in treatment decision making.

Disclosures: Huifang Lu, None.

## MO0588

**Multi-Centre Cross-Calibration for First and Second Generation HR-pQCT.** Sarah L Manske<sup>\*</sup>, Lauren A Burt<sup>1</sup>, Kyle K Nishiyama<sup>2</sup>, Sanchita Agarwal<sup>2</sup>, Elizabeth Shane<sup>2</sup>, Steven K Boyd<sup>1</sup>. <sup>1</sup>McCaig Institute for Bone and Joint Health, Department of Radiology, Cumming School of Medicine, University of Calgary, Canada, <sup>2</sup>Division of Endocrinology, Department of Medicine, Columbia University, United States

Bone microarchitectural imaging with high-resolution peripheral quantitative computed tomography (HR-pQCT) has emerged as useful tool for the investigation of bone quality. In vivo studies have demonstrated good agreement between first and second scanner generations for most outcomes after cross-calibration using participants scanned on both scanners at a single center. Appropriate cross-calibration for multi-center HR-pQCT studies remains a challenge. We sought to determine whether cross-calibration equations to relate multi-generation HR-pQCT outcomes, derived from a single center, can be applied to data acquired at another center.

The Calgary cohort included 62 participants (71% F), aged 55 to 70, scanned on both XtremeCT (XCTI) and XtremeCTII (XCTII) at two timepoints (6- and 12-mo) in an



ongoing clinical trial. The Columbia cohort included 51 participants (69% F), aged 25 to 81, scanned on XCTI and XCTII. Linear regression equations relating XCTI to XCTII outcomes were developed for cross-calibration on the 6-mo data on the Calgary cohort (Manske et al. JBMR 2017), and then tested on the same cohort at 12-mo and the Columbia cohort (XCTII\*). We compared 95% limits of agreement (LOA) using Bland-Altman plots.

Fig 1 shows Bland-Altman plots for Tb.BV/TV and Ct.Po. Estimated XCTII\* for the Columbia cohort fell within the same 95% LOA as the Calgary cohort for Tb.N, Tb.Th, Tb.Sp and Ct.Po at both the radius and tibia. For Ct.BMD, Ct.Th, Tb.BMD and Tb.BV/TV at the radius and tibia, the 95% LOA for the Columbia cohort fell outside the 95% LOA for the Calgary cohort.

We found that cross-calibration equations for multi-generation HR-pQCT developed at a single center were best when applied to the same center. They could be applied at a second center for some, but not all outcomes. There are two possible explanations for outcomes that did not show strong multi-center agreement. First, Calgary and Columbia chose different reference line locations on XCTII. The outcomes with the weakest agreement are more dependent on the relative positioning of the reference line, and agreement could be improved by selecting only the common XCTII region scanned at both centers. Second, multi-center calibration will likely be improved by adjusting density with a common density calibration phantom. These strategies should be explored for successful utilization of multiple scanner generations at different centers as this will expand the utility of HR-pQCT in large trials.

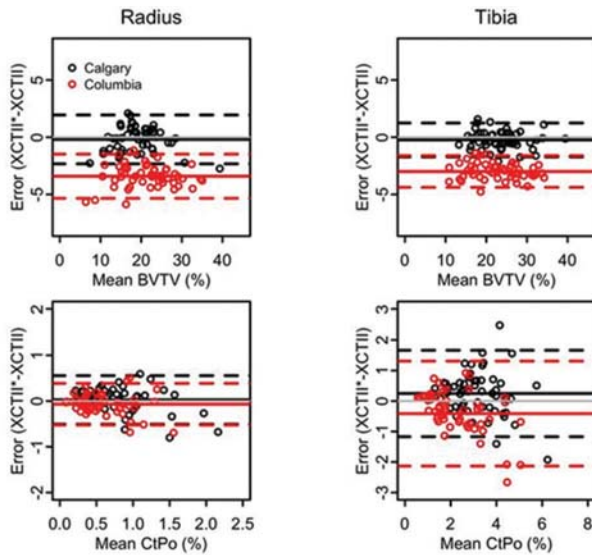


Figure 1. Bland-Altman plots after XCTI/XCTII cross-calibration with equations developed on Calgary cohort (6-mo) and tested on Calgary cohort (12-mo) and Columbia cohort.

Figure 1

Disclosures: Sarah L Manske, None.

## MO0589

**Comparisons of Hip Fractures Rates for a New Fracture Risk Scale in Adults Living in Long-term Care Across Canada.** Ahmed NEGM<sup>\*1</sup>, Micaela Jantzi<sup>2</sup>, George Ioannidis<sup>1</sup>, Jenn Bucek<sup>2</sup>, Jonathan Adachi<sup>1</sup>, Lora Giangregorio<sup>2</sup>, Laura Pickard<sup>1</sup>, John Hirdes<sup>2</sup>, Alexandra Papaioannou<sup>1</sup>. <sup>1</sup>McMaster University, Canada, <sup>2</sup>University of Waterloo, Canada

### Purpose

To compare hip fracture rates over one-year period among individuals living in long-term care (LTC) from three Canadian provinces for the eight fracture risk levels of our New Fracture Risk Scale (FRS).

### Methods

A retrospective cohort study design was used. Long-term care residents were included if they were: 1) Adults admitted to LTC homes in Ontario (ON), British Columbia (BC) and Manitoba (MB) Canada; and 2) Received a Resident Assessment Instrument Minimum Data Set Version 2.0 (RAI-MDS 2.0). One-year hip fracture risk was evaluated using the FRS, an eight level risk scale (level 8 represents the highest hip fracture risk). We previously used decision tree analysis to develop the FRS, using Ontario residents' data from the RAI-MDS 2.0, the Canadian Discharge Abstract Database (DAD) and the National Ambulatory Care Reporting System (NACRS). Population characteristics, fracture incidence, and other categorical variables are expressed as mean (SD) or counts and percentages. To assess the discriminative properties of the FRS for each province, we used the C-statistic.

### Results

Provinces with adequate DAD/NACRS links and adequate resident sample sizes were analyzed, and included ON (n=29,848), BC (n=3,129) and MB (n=2,293). Descriptive statistics on the LTC populations in ON, BC and MB are as follows: age mean (SD) 82 (10), 83 (10), and 84 (9), gender (female %) 66%, 64, and 70%, resident with prior fall in last 180 days (34%, 33%, 30%), and resident with prior hip fracture in last 180 days (6%, 6%, 3%) respectively. A total of 1553 (5.2%), 154 (4.9%) and 100 (4.4%) new

fractures were reported over the one year time period in ON, BC, and MB, respectively. Of these, 959 (3.2%), 124 (4%) and 92 (4%) were hip fractures in ON, BC, and MB. Our scale's one-year absolute hip fracture risk levels were similar among the three provinces and ranged from 0.6 to 19.2 % (Table 1). The overall discriminative properties of the FRS were similar between ON (c-statistic= 0.673), BC (c-statistic= 0.644) and MB (c-statistic= 0.649) samples.

### Conclusion

FRS is a valid tool for identifying adults at highest risk of hip fracture. Having a fracture risk assessment tool that is tailored to the LTC context may have significant implications for policy, service delivery, and care planning, and may improve care for residents of LTC across Canada.

**Table 1. Incident Hip Fracture Rates (%) by Hip Fracture Risk Levels for Three Canadian Provinces.**

Hip Fracture Risk Levels	Ontario	British Columbia	Manitoba
Hip fracture risk level 1	0.6	0.6	1.2
Hip fracture risk level 2	1.8	1.6	1.4
Hip fracture risk level 3	2.5	4.5	4.3
Hip fracture risk level 4	3.1	3.9	4.7
Hip fracture risk level 5	5.0	5.2	5.3
Hip fracture risk level 6	6.8	7.4	8.3
Hip fracture risk level 7	7.8	6.6	8.3
Hip fracture risk level 8	12.6	19.2	11.8

Table 1: Incident Hip Fracture Rates (%) by Hip Fracture Risk Levels for Three Canadian Provinces

Disclosures: Ahmed NEGM, None.

## MO0590

**Analysis of the evolution of cortical and trabecular bone compartments in the proximal femur after spinal cord injury by 3D-DXA.** Laia Gifre<sup>\*1</sup>, Ludovic Humbert<sup>2</sup>, Africa Muxi<sup>3</sup>, Luis del Rio<sup>4</sup>, Joan Vidal<sup>5</sup>, Enric Portell<sup>5</sup>, Ana Monegal<sup>1</sup>, Nuria Gunañens<sup>1</sup>, Pilar Peris<sup>1</sup>. <sup>1</sup>Rheumatology Department, Hospital Clinic of Barcelona, University of Barcelona, Spain, <sup>2</sup>Galgo Medical, Spain, <sup>3</sup>Nuclear Medicine Department, Hospital Clinic of Barcelona, Spain, <sup>4</sup>CETIR, Spain, <sup>5</sup>Guttmann Neurorehabilitation Institute, Universitat Autònoma de Barcelona, Spain

Spinal cord injury (SCI) is associated with a marked increase in bone loss and risk of osteoporosis development short-term after injury. 3D-DXA is a new imaging analysis technique providing 3D analysis of the cortical and trabecular bone from DXA scans. The aim of this study was to assess the evolution of trabecular macrostructure and cortical bone using 3D-DXA in patients with recent SCI followed over 12 months.

Methods: 16 males with recent SCI (< 3 months since injury) and without antiosteoporotic treatment were included. Clinical assessment, bone mineral density (BMD) measurements by DXA and 3D-DXA evaluation at proximal femur (analyzing the integral, trabecular and cortical volumetric BMD [vBMD] and cortical thickness) were performed at baseline and at 6 and 12 months of follow-up.

Results: vBMD significantly decreased at integral, trabecular and cortical compartments at 6 months (-8.8%, -11.6% and -2.4%), with a further decrease at 12 months, resulting in an overall decrease of -16.6%, -21.9% and -5.0%, respectively. Cortical thickness also decreased at 6 and 12 months (-8.0% and -11.4%), with the maximal decrease being observed during the first 6 months. The mean BMD loss by DXA at femoral neck and total femur were -17.7% and -21.1%, at 12 months, respectively.

Conclusions: Marked trabecular and cortical bone loss was observed at the proximal femur short-term after SCI. 3D-DXA provided measurement of vBMD evolution at both femoral compartments and cortical thinning, thereby suggesting that this technique could be useful for bone analysis in these patients.

Disclosures: Laia Gifre, None.

## MO0591

**Relationship between Bone Structural Variables from bone biopsy and Bone Mineral Density (BMD) in Patients on long term Bisphosphonate (BP) Therapy.** Christopher Little<sup>\*1</sup>, Elizabeth Warner<sup>2</sup>, Mahalakshmi Honasoge<sup>2</sup>, Loren Safta<sup>3</sup>, Shiri Levy<sup>2</sup>, Sudhakar Rao<sup>2</sup>, Saroj Palnitkar<sup>2</sup>, Pooja Kulkarni<sup>2</sup>. <sup>1</sup>Wayne State University School of Medicine, United States, <sup>2</sup>Henry Ford Hospital, United States, <sup>3</sup>High School Student, United States

BMD is a 2D measurement of a 3D structure that has been the cornerstone to diagnose osteoporosis, monitor progression, and response to therapy. Bone volume in biopsy is also a 3D estimate of a 2D measurement. Intuitively it is expected to correlate with each other. A few studies showed significant correlations between bone biopsy and BMD variables in a group of patients with various metabolic bone diseases. However, the strengths of correlations were modest or not significant in a more homogenous subset. Our aim was to understand if there were correlations between the bone structural variables and BMD in a group of post-menopausal women on long-term BP therapy.

Methods: Trans-Iliac bone biopsies were obtained from 25 postmenopausal women (mean age 66.8 ± 6.6y) treated with BP for 6.1 ± 4.3 y. Using standard methods cortical bone volume, mean cortical thickness, trabecular bone volume, and trabecular thickness were measured. BMD of both proximal femurs (femoral neck, total hip, and trochanter) was measured by DEXA about 1-2 months before biopsy. Correlations among proximal femur measures and among biopsy variables, as well as between BMD and biopsy structural variables were performed using SigmaPlot.

Results: Mean right and left femoral neck BMDs were 0.636 ± 0.068 and 0.637 ± 0.072 with highly significant correlation between the sides ( $r=0.77$ ;  $P<0.0001$ ). As expected, there were statistically significant correlations among various BMD parameters ( $r=0.46$  to  $0.87$ ;  $p=0.02$  to  $<.0001$ ) with much stronger relationship between the sides (left Vs. right;  $r=0.62$  to  $0.84$ ;  $p<0.001$  for all). In contrast, bone structural measurements showed variable correlations ranging from strongest correlation between trabecular thickness and volume ( $r=0.83$ ;  $p<0.001$ ) to lack of correlation between cortical and trabecular bone volumes. There was a trend for a relationship between cortical thickness and trabecular bone volume ( $r=0.36$ ;  $p=0.06$ ). Finally, there were very few, if any, correlations between BMD and bone structural measurements.

Conclusion: We confirmed strong correlation between the right and left femoral neck, trochanter, and total hip BMDs. However, weak to poor correlation between BMD and bone structural measurements implies that the two methods assess different aspects of bone biology. Alternatively, BPs may have differential effects on BMD and bone structure. Further research is needed to elucidate underlying pathophysiologic mechanism for these observations.

**Disclosures:** Christopher Little, None.

## MO0592

**Urinary N-telopeptide and rate of decline in femoral neck strength across the menopause transition: Results from the Study of Women's Health Across the Nation (SWAN).** Albert Shieh<sup>\*1</sup>, Shinya Ishii<sup>2</sup>, Gail Greendale<sup>1</sup>, Jane Cauley<sup>3</sup>, Arun Karlamangla<sup>1</sup>. <sup>1</sup>UCLA, United States, <sup>2</sup>University of Tokyo, United States, <sup>3</sup>University of Pittsburgh, United States

The bone resorption marker, urinary N-telopeptide (U-NTX), measured in women during their 40s, can be used to gauge the rate of areal bone mineral density (aBMD) decline over the menopause transition (MT) in the lumbar spine (LS) but not in the femoral neck (FN). One possible explanation is that the FN is composed mostly of cortical bone, and aBMD measurements by DXA do not adequately capture the effects of increased endocortical bone resorption on the cortical compartment. One such effect is the compensatory increase in bone formation at the periosteal surface, and the corresponding increase in bone size. In contrast to aBMD, composite indices of FN strength combine DXA-based measurements of FN aBMD and FN size with body size, and are independently associated with fracture risk. They also decline over the MT: indices of FN strength in compression (CSI) and impact (ISI) failure modes begin to decrease rapidly ~1 year prior to the final menstrual period (FMP), and continue to decline at a rapid rate for 3-4 years. We hypothesized that U-NTX, measured in pre- or early perimenopause, would predict the rate of FN strength decline during its rapid phase of MT-related loss. U-NTX was measured in 42-52 year-old, pre- or early perimenopausal women at the baseline visit of the Study of Women's Health Across the Nation (SWAN). FN aBMD was measured by DXA (Hologic) at baseline and annually thereafter. CSI and ISI were calculated from FN aBMD, FN size, and body size. A total of 696 women had measurements of both U-NTX and CSI or ISI decline over the MT. Among these participants, after adjusting for relevant clinical covariates (MT stage at baseline, age, body mass index, race/ethnicity, SWAN study site) in multivariable linear regression, every standard deviation (SD) increase in U-NTX was associated with 0.34% ( $p=0.02$ ) and 0.36% ( $p=0.01$ ) per year faster declines over the MT in CSI and ISI, respectively. We conclude that U-NTX, measured during pre- and early perimenopause, is strongly associated with rate of CSI and ISI decline during their rapid phase of MT-related loss, and may aid early identification of women who will experience the greatest loss in femoral neck strength during this critical period.

**Disclosures:** Albert Shieh, None.

## MO0593

**Region-Specific Assessment of Bone Mineral Density and Trabecular Bone Score in Lateral Projection Identifies Local Decay in Trabecular Bone Microstructure of the Vertebral Body.** Petar Milovanovic<sup>\*1</sup>, Annika vom Scheidt<sup>1</sup>, Eric Flavio Grisolia Seifert<sup>1</sup>, Klaus Püschel<sup>2</sup>, Michael Amling<sup>1</sup>, Björn Busse<sup>1</sup>. <sup>1</sup>University Medical Center Hamburg-Eppendorf, Department of Osteology and Biomechanics, Germany, <sup>2</sup>University Medical Center Hamburg-Eppendorf, Department of Legal Medicine, Germany

Clinical assessment of osteoporosis is based on anterior-posterior (AP) Dual-Energy X-Ray Absorptiometry (DXA) scans of the spine, offering 2D information on global Bone Mineral Density (BMD) and Trabecular Bone Score (TBS) for the entire vertebra. However, recent research showed regional heterogeneity in 3D trabecular microarchitecture of the vertebral body, which could explain the particular vulnerability of certain regions for fracture. Our aim was to determine whether DXA-based 2D parameters (BMD, TBS) can reflect regional differences in 3D bone volume ratio (BV/TV), which could improve clinical fracture risk assessment.

We examined the 12<sup>th</sup> thoracic vertebrae from 24 women postmortem (12 young: 32 ± 6 y, 12 aged: 71 ± 5 y). DXA was performed in anterior-posterior (AP) and lateral projections, providing global BMD and TBS values for both. BMD and TBS were also determined for three horizontal regions (superior, middle, inferior – on AP and lateral scans) and three vertical regions (anterior, middle, posterior – on lateral scans) of the vertebra. Trabecular BV/TV was based on high-resolution peripheral quantitative computed tomography (HR-pQCT, 41 µm) of the vertebra.

BMD and TBS did not correlate significantly, indicating that TBS captures information partly independent of BMD data. In aged cases, mean BV/TV of the whole vertebral body correlated strongly with global BMD (lateral:  $\rho=0.960$ ,  $p<0.001$ ; AP:  $\rho=0.834$ ,  $p<0.001$ ), lateral TBS ( $\rho=0.632$ ,  $p=0.028$ ), but not AP TBS ( $p>0.05$ ). In young cases, correlations were similar but slightly weaker. Mean BV/TV is best predicted in aged cases based on lateral BMD and lateral TBS (96%,  $p<0.001$ ). Regional distinction revealed significant differences in trabecular BV/TV among horizontal and vertical regions in both age groups. Yet, BMD in AP projection differed only among horizontal regions in young cases, while AP TBS did not vary among the regions in both age groups. Lateral scans were advantageous in detecting regional variations: BMD differed among both vertical and horizontal regions in both age groups, whereas TBS was region-dependent only in aged cases.

In summary, combination of BMD and TBS in lateral and AP scans provides additional insights into bone structural integrity, where lateral BMD and TBS are valuable for detecting local decay in bone structure, especially in aged cases. Our findings offer a new possibility for improving the assessment of region-specific vertebral defects in clinical diagnostics.

**Disclosures:** Petar Milovanovic, None.

## MO0594

**Racial Dimorphism in the Assembly of Bone Microstructure in Chinese resident in Hong Kong and Melbourne.** Xiao-Fang Wang<sup>\*1</sup>, Ka Yee Cheuk<sup>2</sup>, Tsz Ping Lam<sup>2</sup>, Ali Ghasem-Zadeh<sup>1</sup>, Roger Zebaze<sup>1</sup>, X. Edward Guo<sup>3</sup>, Jack Chun-Yiu Cheng<sup>2</sup>, Ego Seeman<sup>1</sup>. <sup>1</sup>Departments of Endocrinology and Medicine, Austin Health, University of Melbourne, Australia, <sup>2</sup>Department of Orthopaedics and Traumatology, The Chinese University of Hong Kong, China, <sup>3</sup>Bone Bioengineering Laboratory, Department of Biomedical Engineering, Columbia University, United States

Chinese have lower hip and forearm fracture rates than Caucasians. We hypothesized that bone microstructure in Chinese lifelong resident in Hong Kong differ from Chinese lifelong resident in Melbourne, and relative to Caucasians in Melbourne. We compared bone microstructure in 206 Chinese girls aged between 7 and 17 years living in Hong Kong with 57 Chinese and 62 age-comparable Caucasian girls living in Melbourne. The distal radius was scanned using high-resolution peripheral quantitative computed tomography. Total cross sectional area (CSA), porosity of the total cortex (TC), compact-appearing cortex (CC) and outer and inner transitional zones (TZ) were quantified using StrAx1.0. Trabecular plate and rod microarchitecture were quantified by Individual Trabecula Segmentation (ITS). The results were age-adjusted.

There were no racial differences pre-puberty but during puberty, total CSA was 8.3% lower in Hong Kong Chinese than in Melbourne Chinese ( $p=0.1$ ) and 15.5% lower than in Caucasians ( $p=0.003$ ). Puberty occurred earlier in Hong Kong Chinese so that they were 0.9 years younger, 2.3 cm shorter and 5.1 kg lighter with 12.7-15.7% smaller total CSA, ~5% larger cortical area with a smaller medullary canal than the Melbourne groups ( $p<0.05$ ). Chinese in Hong Kong had lower porosity than Chinese in Melbourne and both had lower porosity than Caucasians. Hong Kong Chinese had lower trabecular rod volume fraction due to fewer rods than both groups in Melbourne. Plate/rod ratio was greater in Hong Kong Chinese than Caucasians. No differences in matrix mineral density were present.

Hong Kong Chinese have earlier age of menarche that probably contributes to the finding of smaller bone CSA, lower porosity and greater trabecular plate to rod ratio after puberty compared to Caucasians. The smaller appendicular bone has a relatively thicker and less porous cortex perhaps attributed to earlier cessation of growth with excavation of a smaller medullary canal and fewer osteons. These morphological features may contribute to racial differences in fracture risk.

**Disclosures:** Xiao-Fang Wang, None.



## MO0595

**Systematic Evaluation of Abdominal Aortic Calcification Reveals Unknown Cardiovascular Disease Risk in Patients Visiting a Fracture Liaison Service.**

Caroline E Wyers<sup>\*1</sup>, Lisanne Vranken<sup>1</sup>, John T Schousboe<sup>2</sup>, Robert Y van der Velde<sup>1</sup>, Irma J de Bruin<sup>1</sup>, Heinrich M Janzing<sup>3</sup>, Sjoerd Kaarsemaker<sup>4</sup>, Piet P Geusens<sup>5</sup>, Joop P van den Bergh<sup>6</sup>. <sup>1</sup>Maastricht UMC+, NUTRIM, Department of Internal Medicine; VieCuri Medical Center, Department of Internal Medicine, Netherlands, <sup>2</sup>Park Nicollet Clinic, St. Louis Park, MN, Division of Health Policy & Management, University of Minnesota, Minneapolis, MN, United States, <sup>3</sup>Department of Surgery and Trauma Surgery, VieCuri Medical Centre, Netherlands, <sup>4</sup>Department of Orthopedic Surgery and Trauma Surgery, VieCuri Medical Centre, Netherlands, <sup>5</sup>Maastricht UMC+, CAPHRI, Department of Internal Medicine subdivision of Rheumatology; University of Hasselt, Netherlands, <sup>6</sup>Maastricht UMC+, NUTRIM, Department of Internal Medicine; VieCuri Medical Center, Department of Internal Medicine; University of Hasselt, Netherlands

**Purpose:** Abdominal aortic calcification (AAC) is associated with higher risk of fracture (fx) and cardiovascular disease (CVD) related mortality. We analyzed the prevalence of AAC in patients with a recent clinical fx visiting a Fracture Liaison Service (FLS).

**Methods:** Cross-sectional cohort study in patients with a recent clinical fx (aged 50-90 years) at the FLS (VieCuri Medical Centre, Venlo, The Netherlands). Fx risk evaluation consisted of a questionnaire regarding clinical risk factors for fx including medical history (e.g. CVD), bone mineral density (BMD) measurements and lateral spine imaging by DXA (Hologic QDR 4500). Vertebral fxs (Vfx) were assessed using the Genant semiquantitative approach. AAC was assessed by a single reader using the 8-point semiquantitative score (AAC-8) developed by Schousboe et al. (2006) and categorized as no, low (AAC-8=1), moderate (AAC-8=2), and severe AAC (AAC-8≥3). Fxs were categorized as hip fx, major (vertebra, pelvis, distal femur, proximal tibia, multiple rib, and proximal humerus), minor (all others), finger/toe fx (Center et al. 2007).

**Results:** From October 2013 until May 2016, 1952 patients visited the FLS. Of 1775 patients, lateral spine images were assessable (69% women, mean age 66±9 years), 10% presented with finger/toe fx, 56% minor, 27% major, and 7% with hip fx. Osteoporosis was diagnosed in 27%, osteopenia in 51% and 22% normal BMD. In total, 27% had AAC (8% low, 13% moderate and 6% severe AAC). Prevalence rates of AAC were similar for men and women (26% vs. 28%; p=NS), but were associated with age (11% in 50-59 years vs. 54% in 80+; p≤.001), with decreasing BMD (22% normal vs. 27% osteopenia vs. 32% osteoporosis; p≤.001), with fx type (21% finger/toe vs. 24% minor vs. 34% major vs. 40% hip fx; p≤.001). Vfx was present in 30% of patients. The prevalence of AAC was significantly higher in patients with Vfx (24% vs. 35%, p≤.001). In multivariate analyses only age remained a significant predictor for the presence of AAC (p≤.001). In patients with known CVD, 38% had AAC on lateral spine imaging as compared to 26% of those without CVD (p=.002).

**Conclusion:** One out of four patients with a recent fx visiting a FLS presented with AAC, which was associated with age, but not with fracture location or BMD. Moreover, in one out of four patients AAC was present while CVD were not reported in medical history, which points at an unknown increased CVD risk in patients with a recent fx.

**Disclosures:** Caroline E Wyers, None.

## MO0596

**Bone turnover in postmenopausal women with hyponatremia.** Caroline Chiu<sup>\*1</sup>, Philip Orlander<sup>1</sup>, Kelly Wirfel<sup>1</sup>, Jeena Varghese<sup>2</sup>, Catherine G Ambrose<sup>1</sup>, Nahid Rianon<sup>1</sup>. <sup>1</sup>UTHealth McGovern Medical School, United States, <sup>2</sup>University of Texas M.D. Anderson Cancer Center, United States

Hyponatremia is the most common electrolyte disorder seen in clinical practice and is associated with increased risk of morbidity and mortality. Prior epidemiological studies suggest that hyponatremia affects the bone as demonstrated by increased risk of osteoporosis and fracture in patients with hyponatremia. It has been proposed that prolonged hyponatremia mobilizes the sodium storage from the bone. We present associations between serum sodium levels and bone turnover in postmenopausal women with compromised skeletal health.

A cross-sectional data analysis was conducted using data collected by retrospective chart review from inpatient acute fracture (within past 2 weeks) and outpatient osteoporosis clinic patients seen between 2010 and 2015. Patients seen in osteoporosis clinic were referred due to some degree of compromised skeletal health and did not have any acute fracture. Osteocalcin was used to indicate bone turnover in our study. Multivariate linear regression analysis was conducted to determine associations between serum sodium and osteocalcin. The regression model was adjusted for creatinine, serum calcium, 25OH-vitamin D and fracture status.

193 postmenopausal women were included in our analysis of which 96 from outpatient and 97 from inpatient. Mean age (standard deviation) of women was 78 (10) years. Mean serum sodium was 139 (3.7). Twenty patients had hyponatremia defined as serum sodium less than 135 (60% of them had acute fracture). In the 20 women with hyponatremia, serum sodium had a significant positive association with serum osteocalcin (beta coefficient 0.28, 95% confidence interval 0.02 to 0.54, p<0.05). The significant association persisted after adjustment for creatinine, serum calcium, 25OH-vitamin D and fracture status (acute fracture for in-patient vs. no or past history for outpatient). The association became non-significant after adjustment for age. However, in

the hyponatremic group, age was negatively associated (p<0.05) with serum sodium. There were no associations between serum sodium and fracture state in our study.

Increase in bone sodium content has been reported with increasing age. However, older age was also associated with decreased mobilization of sodium out of bone when needed, e.g., hyponatremia. It is unclear why age changed associations between sodium and bone turnover in our study. Further understanding of the mechanism through which hyponatremia decreases bone quality is warranted.

**Disclosures:** Caroline Chiu, None.

## MO0597

**Prevalence of osteoporosis and rate of bone loss in Korean adults.** Kihyun Baek<sup>\*</sup>, Je-Ho Han, Moo-Il Kang. Division of Endocrinology and Metabolism, Department of Internal Medicine, College of Medicine, The Catholic University of Korea, Korea, Republic of

**Context**

The rate of age-dependent bone loss has been shown to be an important risk factor of fracture. However, longitudinal rates of bone mineral density (BMD) loss in Korea have not yet been reported.

**Objective**

The objective of the study was to evaluate the longitudinal changes in BMD in Korea.

**Design**

This was a community-based cohort study. The 2nd examination was conducted approximately 4 years after the baseline examination.

**Setting**

The study was conducted in the rural area of Chungju City, Korea.

**Participants**

A total of 3,379 of the 6,007 subjects 40 years of age or older completed the follow-up visit, corresponding to rates of 60.68% and 53.51% in males and females, respectively.

**Results**

The age-standardized osteoporosis prevalence was 12.81% in males and 44.35% in females. In males, the average annual BMD loss at the total hip increased from 0.25% per year in their 40s to -1.12% per year in their 80s (p for trend < 0.001). In females, the average annual BMD loss at the total hip increased from -0.69% per year in their 40s to -1.51% per year in their 80s (p for trend = 0.001). However, the average annual percentage change in spine BMD in females increased from -0.91% per year in their 40s to +1.39% per year in their 80s (p for trend < 0.001).

**Conclusions**

A substantial number of subjects had osteoporosis. The spine BMD may not be recommended when assessing BMD change in adults because it was relatively stable

**Disclosures:** Kihyun Baek, None.

## MO0598

**Osteoporosis diagnosed with distal forearm addition is better at identifying osteoporosis, but does not increase the predictive value for incidental clinical fracture in older adults. Preliminary data from the SARCOS study.** Sheila Ingham<sup>\*</sup>, Alberto Frisoli, Jairo Borges, Angela Paes, Antonio Carvalho. Federal University of Sao Paulo, Brazil

There is a huge increase of incidental clinical fractures in older adults in the 60ies decade to 80ies decade, but the decrease of BMD is not enough to justify it. Osteoporosis is the main risk factor for fractures, even in older adults, however, difficulties in the evaluation of lumbar spine BMD due to aortic calcification and osteophytosis may underestimate the diagnosis of osteoporosis and consequently, the risk of fracture. Based on this, we hypothesized that the addition of distal forearm in the screening of DXA analyses will improve the detection of the osteoporosis and consequently in the risk for clinical fractures in older adults.

**Methods:** Longitudinal analyses of data from SARCOS study, an observational study of the epidemiology of Sarcopenia and Osteoporosis in older outpatients from Cardiology Division of Federal University of Sao Paulo-Brazil. All subjects were underwent DXA of total body and bone sites at base line. Demographic data, habits, medications, physical function, falls, co morbidities and others risk factors were evaluated. Osteoporosis was diagnosed by WHO criteria, i.e. (BMD <-2.5SD at lumbar spine and/or proximal femur) and by WHO criteria plus distal forearm (BMD <-2.5SD at lumbar spine and/or proximal femur and/or distal forearm). Incidental clinical fractures of any bone site were evaluated by phone call each 6 months and documented by medical services.

**Results:** at this moment, from 468 subjects, only 129 have finished the follow up. Osteoporosis by WHO was prevalent in 33.7% (n=32) and WHO plus DF 55% (n=43) (McNemar test <0.001). Clinical fracture occurred in 17.9%(n=22) of them, with mean age 78.5(±7.25), 54.5% were female, 68.2%(n=15) were Caucasian, 68.2% (n=15) had previous fractures (p<0.001), 13.6%(n=3)(p=0.058) was taking bisphosphonate and there were no significant differences in the BMD from lumbar spine, femoral neck and total femur compared to subjects with no fracture. Among subjects with new fractures, 75% (n=15) (p=0.027) of them presented osteoporosis WHO plus DF and 50% (n=11) (p= 0.085) with osteoporosis WHO at baseline. In the logistic regression analyses for incidental clinical fractures, Osteoporosis by WHO presented OR: 2.99 (95% CI 1.08-8.26; p=0.034) and WHO plus distal forearm OR: 5.011 (95% CI:1.44-17.38; p=0.011). However, after the adjustment for female gender, age, bisphosphonate use, previous

fractures and falls, the osteoporosis by WHO criteria and by WHO plus DF have become very similar with OR: 3.29(1.05-10.30;p=0.040) and OR: 4.08(1.08-15.38;p=0.038), respectively.

Conclusion: The addition of distal forearm BMD in screening for osteoporosis significantly increases the sensitivity of the method, however, it does not improve the predictive value for incidental clinical fracture compared to diagnosis of osteoporosis based on only at the lumbar spine and proximal femur in older adults.

**Disclosures:** Sheila Ingham, None.

## MO0599

**Bone Turnover Markers in Men with Dysglycemia.** Kara Holloway\*, Lelia de Abreu, Mark Kotowicz, M. Amber Sajjad, Julie Pasco. Deakin University, Australia

Background: Diabetes is associated with increased fracture risk but we have been unable to detect an increased fracture risk in impaired fasting glycemia (IFG). We have reported lower trabecular bone score in diabetes and others have shown differences in bone material strength, suggesting abnormalities in bone microarchitecture and material properties. The aim of this study was to investigate whether bone turnover is altered in IFG and diabetes compared to normoglycemia in Australian men.

Methods: Participants were 1129 men aged 59.6±18.3 years, enrolled in the Geelong Osteoporosis Study. IFG was defined as fasting plasma glucose (FPG) ≥5.5mmol/L and diabetes as FPG ≥7.0mmol/L, use of antihyperglycemic medication and/or self-report. Fasting blood samples were analysed for serum C-terminal telopeptide (CTX) and procollagen type 1 N-terminal propeptide (PINP). After natural log transformation to normalise the data, multivariable regression was used to examine the relationship between dysglycemia and bone turnover markers (BTM), before and after adjusting for age, weight, height, physical activity, smoking, alcohol intake, glucocorticoid and bisphosphonate use.

Results: There were 664 men with normoglycemia, 364 IFG and 101 men with diabetes. In an unadjusted model, mean ln(CTX) and ln(PINP) were lower for IFG and diabetes compared to normoglycemia (Table).

Men with IFG and diabetes also had lower age-adjusted ln(CTX) and ln(PINP) compared to normoglycemia.

An age\*dysglycemia interaction term indicated a between group differences in BTM that diminished with increasing age. Thus, the percentage differences in CTx between normoglycemia compared to IFG and diabetes at age 40 yr were 16.7% and 44.3%, respectively. At age 60 yr, the differences were 10.1% and 27.4% and at age 80 yr; 3.0% and 5.5%. Results were similar for PINP; the percentage difference for IFG and diabetes compared to normoglycemia were 16.4% and 38.6% at 40 yr, 7.2% and 23.8% at 60 yr and 2.9% and 5.5% at 80 yr. No other confounders were identified.

Conclusion: Bone turnover is lower in men with either IFG or diabetes compared to normoglycemia, consistent with data reported by others in women. Furthermore, reduced BTM in IFG may be indicative of increased fracture risk in this population. Altered bone turnover, possibly related to alterations in bone structural proteins associated with hyperglycemia, may be a potential mechanism for altered bone microarchitecture in diabetes.

Table: Values for ln(CTX) and ln(PINP) in men with normoglycemia, impaired fasting glucose and diabetes. Data presented as mean (95%CI).

	Normoglycemia (n=664)	IFG (n=364)	P value*	Diabetes (n=101)	P value†
<b>Unadjusted</b>					
ln(CTX) (ng/L)	5.83 (5.79-5.87)	5.69 (5.64-5.75)	<0.001	5.57 (5.47-5.67)	<0.001
ln(PINP) (µg/L)	3.66 (3.63-3.70)	3.56 (3.51-3.61)	0.002	3.43 (3.33-3.53)	<0.001
<b>Adjusted for age</b>					
ln(CTX) (ng/L)	5.81 (5.77-5.85)	5.72 (5.66-5.77)	0.010	5.63 (5.52-5.73)	0.001
ln(PINP) (µg/L)	3.64 (3.60-3.68)	3.58 (3.53-3.63)	0.002	3.49 (3.39-3.59)	0.003

CTX = C-terminal telopeptide; PINP = procollagen type 1 N-terminal propeptide; IFG = Impaired fasting glucose

\* P value for difference between IFG and normoglycaemia

† P value for difference between diabetes and normoglycaemia

Table: Values for ln(CTX) and ln(PINP) in men

**Disclosures:** Kara Holloway, None.

## MO0600

Withdrawn

## MO0601

**Is hyperkyphosis associated with incident falls in older men?** Corinne McDaniels-Davidson<sup>\*1</sup>, Lynn Marshall<sup>2</sup>, Jeanne Nichols<sup>1</sup>, Florin Vaida<sup>1</sup>, John Schousboe<sup>3</sup>, Jane Cauley<sup>4</sup>, Peggy Cawthon<sup>5</sup>, Deborah Kado<sup>1</sup>. <sup>1</sup>University of California, San Diego, United States, <sup>2</sup>Oregon Health Sciences University, United States, <sup>3</sup>Health Partners Institute for Education and Research, U. Minnesota, United States, <sup>4</sup>University of Pittsburgh, United States, <sup>5</sup>California Pacific Medical Center, United States

Purpose: To determine whether older men with kyphotic posture, measured via two different methods, may be at increased risk for incident falls.

Methods: Within the Osteoporotic Fractures in Men Study (MrOS), we conducted two three-year prospective analyses of 2,346 and 2,928 men. The first group of men had kyphosis measured by Cobb angle derived from x-rays obtained in the lying position at visit 1 (2000-2002), while the second group of men had kyphosis assessed with the blocks method at visit 3 (2007-09); both groups self-reported falls tri-annually for three years after the kyphosis assessment. Poisson regression with GEE was used to obtain relative risks (RR) of falls that were categorized as number of falls experienced over the entire 3-year follow-up period.

Results: The fall rate over three years among the visit 1 sample (mean age 74±6 years) was 651/1,000 person-years. There was no association between Cobb angle at visit 1 and subsequent falls. In multivariable models adjusted for age, weight and hip BMD, the relative risk (RR) per SD increase in Cobb angle was 1.04 (95% CI: 0.95, 1.14). The fall rate among the visit 3 sample (mean age 79±5 years) was 839/1,000 person-years. In multivariable analyses adjusted for age, weight, and hip BMD, the risk of falls was increased by 11% for each standard deviation increase (1.4 blocks) in the number of blocks required to achieve a neutral head and neck position (RR=1.11, 95% CI: 1.06, 1.17).

Conclusion: Although Cobb angle did not predict falls in community-dwelling older men over three years, the blocks method of measuring kyphosis was associated with incident falls in this population. This difference could be due to the Cobb angle's focus on thoracic kyphosis only, whereas the blocks method may capture abnormal thoracic and cervical spine curvature.

**Disclosures:** Corinne McDaniels-Davidson, None.

## MO0602

**The Relation Between Radiographic Vertebral Fractures And Trabecular Bone Score In Elderly Women: A Meta- Analysis Of Prospective Studies.** Fjorda Koromani<sup>\*1</sup>, Ling Oei<sup>1</sup>, Biljana Atanasovska<sup>2</sup>, Carolina Medina-Gomez<sup>1</sup>, Enisa Shevroja<sup>3</sup>, Josje Schoufour<sup>1</sup>, Berengere Aubry-Rozier<sup>3</sup>, Carola Zillikens<sup>1</sup>, Andre Uitterlinden<sup>1</sup>, Edwin Oei<sup>1</sup>, Didier Hans<sup>3</sup>, Fernando Rivadeneira<sup>1</sup>. <sup>1</sup>Erasmus MC, Netherlands, <sup>2</sup>Groningen University, Netherlands, <sup>3</sup>University of Lausanne, Switzerland

Vertebral fractures (VFs) are a hallmark for osteoporosis. Trabecular bone score (TBS) is a technique applied to dual-energy X-ray absorptiometry (DXA) images of the lumbar spine to assess micro architecture. We aimed to examine the association between lumbar spine (LS) TBS in relation to: a) prevalent VFs b) severity of VFs and c) independence from LS- BMD, in a meta-analysis of two female population-based cohorts. Cross-sectional radiographies and DXA scans of the LS were available for participants of the Rotterdam Study (RS) and Osteolaus. VFs cases were defined as a vertebral height reduction above 20% and graded according to Genant's classification for vertebral fractures. Odds ratios (OR) were derived from logistic regression models per SD decrease adjusted for age, visit and LS- BMD. Results were meta-analyzed using random effect models. We calculated continuous net reclassification improvement (NRI) to assess the improvement in VF risk when adding LS- TBS to a model with Age and LS-BMD. The pooled study population comprised 4,720 participants of which, 730 had a prevalent VF classified as mild (58.3%) or moderate to severe (41.7%). Every SD decrease in LS-TBS was associated with 39% increased risk of prevalent VF (OR= 1.39, 95%CI [1.15; 1.69]). LS- TBS was more strongly associated with moderate and severe fractures (OR= 1.56, 95% [CI 1.02; 2.61]) than with mild (OR=1.26, 95%CI [1.13; 1.40]). In RS, the addition of LS- BMD to the model with age showed an improvement of the overall NRI by 0.038, 95%CI [0.004;0.07] an improvement in the event NRI (sensitivity) of 2.2% 95%CI [0.007; 0.03] but no significant improvement in the non-event NRI (specificity) 0.017, 95%CI [-0.013; 0.048]. After adding TBS to the model with age and LS-BMD, the overall NRI was 0.13, 95%CI [0.10; 0.17], with an improvement in the non-event NRI (specificity) 12.6% 95%CI [0.09;0.15] but no significant improvement in the event NRI (sensitivity) 0.01, 95%CI [-0.004;0.023]. In Osteolaus the addition of LS- TBS to a model with age and LS-BMD resulted in an overall NRI of 0.16, 95%CI [0.11;0.21], with an improvement in the non-event NRI of 14%, 95%CI[0.09;0.19] and in the event NRI of 2.2%, 95%CI [0.005; 0.04]. In conclusion LS-TBS is strongly associated with prevalent VFs and progressively with increased severity independent of LS-BMD. LS- TBS can contribute to the assessment of VFs risk by increasing the specificity of the evaluations achieved by using age and LS- BMD alone.

**Disclosures:** Fjorda Koromani, None.



## MO0603

**Machine Learning Principles Can Improve Hip Fracture Prediction.** Christian Kruse<sup>1</sup>, Eiken Pia<sup>2</sup>, Peter Vestergaard<sup>1</sup>. <sup>1</sup>Aalborg University Hospital, Denmark, <sup>2</sup>University of Copenhagen, Denmark

## INTRODUCTION:

We applied machine learning principles to predict hip fractures and estimate predictor importance in Dual-energy X-ray absorptiometry (DXA)-scanned men and women.

## METHODS:

Dual-energy X-ray absorptiometry data from two Danish regions between 1996 and 2006 were combined with national Danish patient data to comprise 4722 women and 717 men with 5 years of follow-up time (original cohort n = 6606 men and women). Twenty-four statistical models were built on 75% of data points through k-5, 5-repeat cross-validation, and then validated on the remaining 25% of data points to calculate area under the curve (AUC) and calibrate probability estimates. The best models were retained with restricted predictor subsets to estimate the best subsets.

## RESULTS:

For women, bootstrap aggregated flexible discriminant analysis ("bagFDA") performed best with a test AUC of 0.92 [0.89; 0.94] and well-calibrated probabilities following Naïve Bayes adjustments. A "bagFDA" model limited to 11 predictors (among them bone mineral densities (BMD), biochemical glucose measurements, general practitioner and dentist use) achieved a test AUC of 0.91 [0.88; 0.93]. For men, eXtreme Gradient Boosting ("xgbTree") performed best with a test AUC of 0.89 [0.82; 0.95], but with poor calibration in higher probabilities. A ten predictor subset (BMD, biochemical cholesterol and liver function tests, penicillin use and osteoarthritis diagnoses) achieved a test AUC of 0.86 [0.78; 0.94] using an "xgbTree" model.

## CONCLUSION:

Machine learning can improve hip fracture prediction beyond logistic regression using ensemble models. Compiling data from international cohorts of longer follow-up and performing similar machine learning procedures has the potential to further improve discrimination and calibration.



Predictive Capability for Hip Fractures in the Female Cohort

**Disclosures:** Christian Kruse, None.

## MO0604

**Sleep disorders are associated with trabecular bone score and osteoporotic fractures, not with bone mineral density.** Nadege Lambert<sup>1</sup>, Didier Hans<sup>1</sup>, Raphael Heinzer<sup>2</sup>, José Haba-Rubio<sup>2</sup>, Pedro Marques-Vidal<sup>3</sup>, Olivier Lamy<sup>1</sup>. <sup>1</sup>Bone Unit, Switzerland, <sup>2</sup>Sleep Disorder Center, Switzerland, <sup>3</sup>internal medicine department, Switzerland

**Context:** Sleep disorders and osteoporosis increase with age and are associated with high morbidity, mortality and economic burden. Poor sleep quality is associated with increased risk of fall and inconsistently with low bone mineral density (BMD), but the mechanisms are unknown. Our study aimed to assess if sleep characteristics are associated with markers of bone health: BMD, trabecular bone score (TBS), and osteoporosis (OP) and non-OP fractures.

**Methods:** OsteoLaus is a population-based cohort of 1500 women (50 to 80 y old) living in Lausanne. All women had lumbar spine BMD and TBS, hip BMD, vertebral fracture assessment, and questionnaire about OP and non OP fractures. A random selection of 660 women was included in the HypnoLaus Sleep cohort study and had a polysomnography. Total sleep time (TST), sleep onset latency (SOL), slow-wave sleep (SWS), rapid eye movement sleep (REM) quantity, apnoea-hypopnoea index (AHI), oxygen desaturation index (ODI) and sleep efficiency were evaluated.

**Results:** Sleep parameters were not associated with BMD (age- and BMI-adjusted). AHI and ODI were inversely associated with TBS (age-adjusted). Results for fractures were adjusted for age, BMI and psychoactive drugs. SOL was associated with OP fractures ( $p < 0.001$ ). REM was associated with OP and non-OP fractures ( $p < 0.05$ ). We create a score of "efficient long sleep" including 6 parameters: TST, SOL, SWS,

REM sleep, AHI, and sleep efficiency. This score was significantly lower for women with prevalent OP fracture ( $-0.25 \pm 0.09$  vs  $0.05 \pm 0.04$ ,  $P = 0.003$ ).

**Conclusion:** We found no association between BMD and sleep characteristics. Our study demonstrates for the first time that TBS is altered in women with high AHI or ODI. The "efficient long sleep" score was lower for women with OP fracture. Further studies are needed to: 1) explain how some sleep characteristics affect TBS; and 2) validate the score of "efficient long sleep" in other studies.

**Disclosures:** Nadege Lambert, None.

## MO0605

**The bone-vascular hypothesis: relationship between abdominal aortic calcification, bone mineral density and fractures in elderly women.** Joshua Lewis<sup>1</sup>, Celeste Eggermont<sup>2</sup>, John Schousboe<sup>3</sup>, Wai Lim<sup>2</sup>, Germaine Wong<sup>1</sup>, Ben Khoo<sup>4</sup>, MingXiang Yu<sup>5</sup>, Kun Zhu<sup>2</sup>, Kevin Wilson<sup>6</sup>, Douglas Kiel<sup>7</sup>, Richard Prince<sup>2</sup>. <sup>1</sup>School of Public Health, University of Sydney, Australia, <sup>2</sup>School of Medicine and Pharmacology, University of Western Australia, Australia, <sup>3</sup>Park Nicollet Osteoporosis Center and Institute for Research and Education, United States, <sup>4</sup>Medical Technology and Physics, Sir Charles Gairdner Hospital, Australia, <sup>5</sup>Department of Endocrinology & Metabolism, Shanghai Zhongshan Hospital, Fudan University, China, <sup>6</sup>Skeletal Health, Hologic, Inc, United States, <sup>7</sup>Institute for Aging Research, Hebrew SeniorLife, Beth Israel Deaconess Medical Center, Harvard Medical School, United States

The abdominal aorta is the major artery supplying oxygenated blood to the lumbar spine, abdominal organs, pelvis and lower limbs. Studies using standard radiographs suggest abdominal aortic calcification (AAC) may influence bone fragility. We examined the vascular disease – bone relationship, using AAC measured on images from a bone densitometer with hip bone mineral density (BMD) by DXA, heel bone broadband ultrasound attenuation (BUA) by ultrasonography and fracture occurrence in a prospective study of 1,024 elderly women. Lateral spine images were captured in 1998 or 1999 and analyzed for vertebral fractures graded using the Genant semi-quantitative method and AAC score 0-24 categorized into low AAC (score 0 and 1,  $n = 459$ ); moderate AAC (score 2-5,  $n = 373$ ) and severe AAC (score  $> 5$ ,  $n = 192$ ). Ten-year osteoporotic fracture incidence was identified by x-ray verified self-report and hospital discharge data. The participants mean age was  $75.0 \pm 2.6$  SD years while the median AAC24 score was 2 (range 0-18). AAC24 scores were inversely correlated to total hip BMD (Spearman's  $\rho = -0.077$ ,  $P = 0.013$ ) and heel bone BUA (Spearman's  $\rho = -0.074$ ,  $P = 0.020$ ). Increasing severity of AAC was associated with increases in the presence and number of prevalent osteoporotic fractures from the age of 50 and prevalent vertebral fractures ( $P < 0.05$  for tests of trend). A nonlinear relationship was observed between AAC severity category and incident fracture risk, thus the moderate and severe AAC categories were combined. Compared to women with low AAC (0-1), women with moderate to severe AAC (AAC24 score  $> 1$ ) had increases in relative hazards for 10-year self-reported verified fracture and fracture hospitalization before (HR 1.48 [1.15-1.91],  $P = 0.002$  and HR 1.46 [1.07-1.99],  $P = 0.019$  respectively) and after adjustment for estimated fracture risk without BMD (HR 1.45 [1.12-1.87],  $P = 0.005$  and HR 1.39 [1.01-1.90],  $P = 0.048$  respectively). However after adjustment for estimated fracture risk with BMD only verified fractures by self-report remained significant HR 1.40 (1.08-1.81),  $P = 0.011$ . These findings support the hypothesis that AAC is inversely related to BMD and BUA as well as increased long-term fracture risk. Identifying the underlying cell biological basis of increasing vascular calcification and impaired bone structure in older women may lead to therapy that could prevent both vascular disease and osteoporosis.

**Disclosures:** Joshua Lewis, None.

## MO0606

**Is microangiopathy an independent risk factor of vertebral fracture? A prospective study from Chinese population.** Jixing Liang<sup>\*</sup>, Junping Wen, Kaka Tang, Huibin Huang, Liantao Li, Wei Lin, Lixiang Lin, Gang Chen. Fujian Provincial Hospital, China

**Objective:** The aim of this study is to clarify whether microangiopathy is an independent risk factor of vertebral fractures.

**Methods:** This prospective study derived from REACTION study. 2176 premenopausal women, 2633 postmenopausal women, 2998 men under 65 years old ( $< 65$ ) and 737 men age 65 or older ( $\geq 65$ ) were included. Baseline population was categorized into two groups (microangiopathy and without microangiopathy) and then follow up three years to find out the relationship between microvascular disease and vertebral fractures.

**Results:** After full adjustment, presence of microangiopathy was related to risk of low BMD only in men  $> 65$  [ORs (95%CI) = 2.506 (1.454 to 4.321),  $P = 0.001$ ]. After adjusting confounding factors, microangiopathy was related to risk of vertebral fractures in men  $> 65$  [ORs (95%CI) = 2.341 (1.042 to 5.258),  $P = 0.039$ ] and the risk of vertebral fractures was higher in microangiopathy group than that in without microangiopathy group when men were older than 65 [Pearson chi-square (4.225),  $P = 0.04$ ]. However, no associations were found between microangiopathy and vertebral fractures in men age  $< 65$ , premenopausal women and postmenopausal women.

Conclusion: Microangiopathy is an independent risk factor of vertebral fractures in men >65.

*Disclosures: Jixing Liang, None.*

## MO0607

**Burden of fractures attributable to low bone mineral density.** Thao Ho-Le<sup>\*1</sup>, Thach Tran<sup>2</sup>, Jacqueline Center<sup>2</sup>, John Eisman<sup>2</sup>, Tuan Nguyen<sup>2</sup>. <sup>1</sup>University of Technology Sydney, Australia, <sup>2</sup>Garvan Institute of Medical Research, Australia

Although bone mineral density (BMD) is causally related to fracture, the burden of fractures attributable to low BMD has not been systematically studied. In this study, we sought to estimate the fraction of different fracture types occurring in old people that can be attributed to low BMD.

The study involved 2264 women and 1339 men aged 50 years and older, whose bone health has been continuously monitored for up to 20 years. During the follow-up period, the incidence of total fracture, hip fracture, clinical vertebral fracture, and wrist fracture was ascertained by X-ray report. Femoral neck BMD was measured at baseline, and was converted to T-scores. We defined "low BMD" by using a series of thresholds -2.5, -2.0, -1.5 for femoral neck BMD T-scores. The estimation of time-dependent attributable fraction (AF) was based on the Cox's proportional hazards model which allows for confounding factors to be taken into account.

During the follow-up period, the incidence rate of fracture was 3.8% (n=687) and 1.7% (n=240) per 100 person-years for women and men, respectively. For total fractures, in women, the proportion of fracture attributable to low BMD during the first year was 20%, but declined to 16% at year 10 and 12% at year 20. In men, the overall attributable fraction was 13% for total fracture, but was also gradually declined to 10% at year 20. For hip fracture, the 5-year AF was 55% in women and 40% in men, while 20-year AF was 42% in women and 30% in men. For clinical vertebral fracture, the 5-year AF was 27% in women and 20% in men; 20-year AF was 20% in women and 17% in men. For wrist fracture, the 5-year AF was 14% in women and 15% in men; 20-year AF was 13% in women and 15% in men.

Thus, the burden of fractures occurring in older individuals attributable to osteoporosis is modest. The decline in the attributable fraction with time implies that repeat BMD measurements can be valuable in accounting for a substantial proportion of hip fractures.

*Disclosures: Thao Ho-Le, None.*

## MO0608

**Multi-Modal Intervention for Improving Osteoporosis Treatment Initiation and Adherence.** Ryan Outman<sup>\*1</sup>, Paul Muntner<sup>1</sup>, Andrew Bradlyn<sup>2</sup>, Jeffrey Curtis<sup>1</sup>, Lee Cromwell<sup>2</sup>, Douglas Wilmot Roblin<sup>3</sup>, Dennis Tolsma<sup>2</sup>, Doraina Walker-Williams<sup>2</sup>, Kenneth Saag<sup>1</sup>. <sup>1</sup>University of Alabama at Birmingham, United States, <sup>2</sup>Kaiser Permanente, United States, <sup>3</sup>Georgia State University, United States

Purpose: Clinical trials have demonstrated bisphosphonates reduce the risk for osteoporotic fractures. In clinic populations, however, low adherence to bisphosphonates is common.

Methods: We conducted a pilot trial comparing bisphosphonate adherence among women randomized to a group with nurse consultation plus Internet-based video education ("nurse+video", n=21) to a group with Internet-based video education alone ("video-alone", n=28). Eligible participants were Kaiser Permanente Georgia patients who were English speaking, 55 years or older, with Internet access and an initial bisphosphonate prescription in 30-days prior to enrollment. The video included information on the risk reduction benefits of osteoporosis treatment (both groups) and patient stories (nurse+video). Nurse consultation was conducted by phone and focused on possible barriers to initiation of therapy. The primary outcomes were: 1) filling the order ("initiation"), 2) days of bisphosphonate supply in the 180-day period following enrollment. Comparisons of outcomes were made between the two study groups, and with a group of eligibles who did not respond to the invitation to participate ("passive refusals", n=110).

Results: The mean age for the nurse+video, video-alone and passive refusals was 69.3, 69.6 and 69.3 years, respectively; and, 19.1%, 32.1% and 28.2% were black, respectively. In the 180 days following the initial bisphosphonate order date, 90.5% of nurse+video participants, 85.7% of video-alone participants, and 90.9% of passive refusals had at least one fill (p-value > 0.4 for all pairwise comparisons). Among participants with at least one bisphosphonate fill, 71% in the nurse+video group, 68% of participants in the video-alone group, but only 37% of passive refusals had 180 days of bisphosphonate supply. The difference in days supply between the nurse+video and video-alone groups was not statistically significant; however, days supply in each of these two groups was greater than that among passive refusals (p < 0.01).

Conclusions: Neither a video intervention alone nor a video intervention with a nurse consultation appeared to reduce primary non-adherence among older women following an initial bisphosphonate prescription. An educational video, with or without nurse consultation, did improve bisphosphonate refill adherence.

*Disclosures: Ryan Outman, None.*

## MO0609

**Low peak bone mineral density of lumbar spine in Korean women of Korea National Health and Nutrition Examination Survey (2008-2010).** Ye Soo Park<sup>\*1</sup>, Sangmo Hong<sup>2</sup>, Woong Hwan Choi<sup>3</sup>. <sup>1</sup>Department of Orthopaedic Surgery, Guri Hospital, Hanyang University College of Medicine, Korea, Republic of, <sup>2</sup>Division of Endocrinology, Department of Internal Medicine Hallym University Dongtan Sacred Heart Hospital, Korea, Republic of, <sup>3</sup>Division of Endocrinology, Department of Internal Medicine, College of Medicine, Hanyang University, Korea, Republic of

Background: Increasing peak bone mineral density (BMD) in young people may help to reduce the incidence of osteoporosis.

Objective: We aimed to determine the age of the peak BMD and associated factors with peak BMD.

Design: We analyzed body composition and BMD data of 20-39 years old men (n=1768) and women (n=1959) from KNHANES 2008-2010 who had not liver, kidney, pulmonary, metabolic disease, cancer, pregnancy or breastfeeding. Body composition and bone mineral density (BMD) of femur neck were measured by DXA.

Results: Femur neck and spine BMD in men and femur neck BMD in women were negative correlated with age (all p < 0.001) even after adjusting body weight, vitamin D level, exercise, smoking, and nutritional intake. Interestingly, spine BMD in women was positive correlated with age (p < 0.001) even after adjusting. BMD of young adult also had positive association with exercise, vitamin D level, EQ-5D, and body weight but negative correlated with recent weight change (all p < 0.05).

Conclusion: Korean young adult attained the peak BMD around early 20 years, but the lumbar BMD of women not. Low lumbar BMD in early 20 years old women might be associated bad life style (diets and no exercise) but further studies needed.

*Disclosures: Ye Soo Park, None.*

## MO0610

**Bisphosphonates and Age-Related Macular Degeneration: A Propensity-Matched Cohort and Nested Case-Control Analysis.** Cesar Garriga<sup>\*1</sup>, Andy Judge<sup>2</sup>, Samuel Hawley<sup>1</sup>, Antonella Delmestri<sup>1</sup>, Daniel Prieto-Alhambra<sup>1</sup>, Cyrus Cooper<sup>3</sup>, Michael Pazianas<sup>1</sup>. <sup>1</sup>NIHR Musculoskeletal Biomedical Research Unit, Nuffield Department of Orthopaedics, Rheumatology and Musculoskeletal Sciences, Nuffield Orthopaedic Centre, University of Oxford, United Kingdom, <sup>2</sup>NIHR Musculoskeletal Biomedical Research Unit, Nuffield Department of Orthopaedics, Rheumatology and Musculoskeletal Sciences, Nuffield Orthopaedic Centre, University of Oxford, Oxford and MRC Lifecourse Epidemiology Unit, University of Southampton, United Kingdom, <sup>3</sup>NIHR Musculoskeletal Biomedical Research Unit, Nuffield Department of Orthopaedics, Rheumatology and Musculoskeletal Sciences, Nuffield Orthopaedic Centre, University of Oxford, and MRC Lifecourse Epidemiology Unit, University of Southampton, United Kingdom

Objective. To investigate the association between oral bisphosphonate (BP) use and the risk of developing age-related macular degeneration (AMD).

Methods. *Design:* a propensity score-matched hip fracture cohort. We also used a nested case control design to study dose-response according to medication possession ratio (MPR). *Setting:* UK primary care, using data from the Clinical Practice Research Datalink. *Participants:* Patients ≥ 50 years old with an incident hip fracture in 1999-2013, without previous history of AMD at hip fracture (index) date or in the following year. *Exposure:* BP use with a first prescription after follow-up initiation. BP use was further categorised according to medication possession ratio (MPR) in quartiles. *Outcomes:* Primary outcome was AMD. *Statistical methods:* Propensity scores were used to match 1:1 non-users and BP users. Covariates in the propensity score were index year, age, gender, BMI, smoking, alcohol drinking, region, drug confounders and comorbidities. Risk of AMD was analysed using subhazard ratios (sHR) and their 95% confidence intervals (CI), accounting for a competing risk with death. A nested matched 1:20 case-control was analysed using conditional logistic regression according to MPR quartiles.

Results. The 1:1 matched cohort had 6,208 BP-users and non-users, with 57 (1.8%) vs 39 (1.3%) AMD cases respectively. The sHR (CI) was 1.60 (0.95, 2.72) (P=0.08). BP-users in the top quartile of MPR had the highest risk of AMD, with OR 5.70 (3.43-9.50) (P<0.01) compared to non-users.

Conclusions. Overall, oral BP use was not associated with increased risk of AMD in a cohort of hip fracture patients, although the risk increased with higher MPR. More data are needed to confirm these findings.

*Disclosures: Cesar Garriga, None.*



## MO0611

**Young adult muscle strength is not associated with middle-age fracture risk in men: a cohort study using Swedish conscription data linked to the National Patient Register.** Daniel Prieto-Alhambra<sup>\*1</sup>, Aleksandra Turkiewicz<sup>2</sup>, Björn Rosengren<sup>3</sup>, Martin Englund<sup>2</sup>. <sup>1</sup>Centre for Statistics in Medicine and Nuffield Department of Orthopaedics, Rheumatology, and Musculoskeletal Sciences (NDORMS), University of Oxford, United Kingdom, <sup>2</sup>Clinical Epidemiology Unit, Orthopaedics, Department of Clinical Sciences Lund, Lund University, Sweden, <sup>3</sup>Clinical and Molecular Osteoporosis Research Unit, Departments of Clinical Sciences and Orthopedics Malmö, Skåne University Hospital, Lund University, Sweden

## PURPOSE

There is a lack of data on the determinants of fracture risk in young and middle-aged male adults. We aimed to study the relationship between grip strength measured at conscription examination (age 18 years old) and middle-age (34 to 59 years old) fracture risk in Swedish men.

## METHODS

Design Cohort study including all Swedish men undergoing conscription examination between September 1969 and May 1970 at age 17-18 years old.

Setting Conscription data (muscle strength, height/weight, socio-economics, and lifestyle) were linked to the National Patient Register (hospital contacts and procedures) for 1987-2010

Exposure The conscription examination was performed at six centres including standardised physical tests as well as evaluations by a physician. Grip strength was our main study exposure.

Outcome All fractures (except face/skull and digits) as recorded in the Swedish National Patient Register were the study outcome.

Statistical Analyses Cox regression models were fitted to estimate Hazard Ratios (HR) and 95% Confidence Intervals (95% CI) according to grip strength as a continuous variable (per 1 SD), with quartiles as a secondary analysis. Sensitivity analyses were conducted to analyse these same associations with site-specific fractures using a marginal model for unordered events of different type. All models were adjusted for weight, height, parental education, smoking and alcohol consumption.

## RESULTS

Of 41,516 potentially eligible, 40,112 subjects were included (1,404 died or migrated before 1987) contributing 892,572 person-years of follow-up. Overall, 3974 of the men fractured, corresponding to an incidence rate of 44.5/1,000 person-years (95% CI 43.2-45.9). Adjusted HR was 1.01 (95% CI 0.97-1.05) per SD lower grip strength [Figure 1]. No association was seen between quartiles of grip strength and fracture risk. Similarly, no significant association was observed between grip strength and site-specific fractures.

## CONCLUSIONS

Our data do not support an association between young adult/adolescent grip strength and middle-age fractures in men. More data are needed on the impact of training/exercise (and potentially other interventions) during young adulthood and fracture risk at later stages of life.

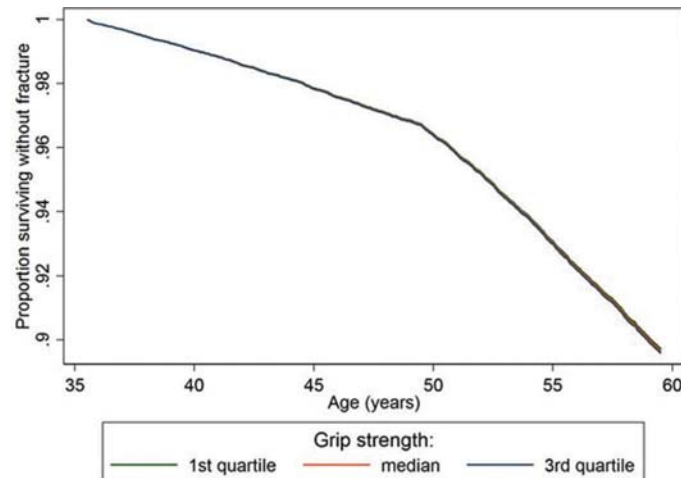


Fig. 1: Probability of survival without fracturing (Kaplan-Meier estimates) from age 34 to 59 years

**Disclosures:** Daniel Prieto-Alhambra, Amgen, Grant/Research Support.

## MO0612

**Bone Attenuation on Computed Tomography (CT) is Inversely Associated with All-cause Mortality in Elderly Women in the National Lung Screening Trial.** Thomas Register<sup>\*1</sup>, Robert Boutin<sup>2</sup>, Stephen Kritchevsky<sup>1</sup>, Haifying Chen<sup>1</sup>, Caroline Chiles<sup>1</sup>, Barton Wise<sup>2</sup>, Cyrus Bateni<sup>2</sup>, Ahmed Bayoumi<sup>2</sup>, Leon Lenchik<sup>1</sup>. <sup>1</sup>Wake Forest School of Medicine, United States, <sup>2</sup>University of California, Davis, United States

Purpose: To examine the association between CT trabecular bone attenuation at baseline and at year-2 follow-up with all-cause mortality in older women and men in the National Lung Screening Trial (NLST).

Methods: Association of trabecular bone attenuation and all-cause mortality was examined in 672 women and 1176 men, age 70-74 years, from the CT arm of the NLST. Analysis of low-dose chest CTs at baseline and year-2 follow-up was performed. Using a clinical PACS workstation, a 1cm region of interest was used to measure trabecular bone density of T12 vertebra. Associations between baseline bone attenuation and change in bone attenuation with all-cause mortality were determined using logistic regression models. Four models were used, stratified by sex: 1) unadjusted; 2) adjusted for age, race and BMI; 3) Model 2 plus smoking; 4) Model 3 plus chronic conditions (cancer, COPD, emphysema, heart disease, hypertension, and stroke).

Results: At a mean 6 years of follow-up, 81 (12.1%) women and 201 (17.1%) men were deceased. In women, mean (SD) bone attenuation was 115.3HU (42.4) at baseline and 111.6HU (44.0) at year-2. In men, mean (SD) bone attenuation was 114.6HU (36.9) at baseline and 112.3HU (39.1) at year-2. In women, baseline bone attenuation was inversely associated with all-cause mortality: Model 2: OR=0.72 (95%CI: 0.54, 0.97), p=0.03; Model 3: OR=0.72 (95%CI: 0.54, 0.96), p=0.03; Model 4: OR=0.70 (95%CI: 0.52, 0.94), p=0.02. In men, the association did not reach significance. In men and women, the change in bone attenuation from baseline to year-2 was not associated with all-cause mortality.

Conclusion: In older women, decreased T12 trabecular bone attenuation was associated with increased all-cause mortality. Two-year change in bone attenuation was not associated with mortality. Opportunistic measurement of bone attenuation on chest CT exams may help improve the accuracy of health-related outcome prediction models in older adults.

**Disclosures:** Thomas Register, None.

## MO0613

**Low femur neck BMD is associated with CAD in elderly women not on statins.** Olasimbo Chiadika<sup>\*</sup>, Fisayomi Shobayo, Syed Naqvi, Catherine G Ambrose, Nahid Rianon. UTHealth McGovern Medical School, United States

Low bone mineral density (BMD) has been associated with presence of coronary artery disease (CAD). There is evidence supporting protective effects of statins on bone loss. Most of these studies were conducted in relatively younger (<50) adults. Estrogen deficiency puts postmenopausal women at a higher risk of both CAD and osteoporosis (OP). It is unknown if CAD should be considered a risk factor for OP or vice versa in these women. A cross-sectional analysis was conducted to determine associations between femur neck (FN) BMD and CAD with or without statin use in a high risk group of elderly women who were referred to the Geriatric Osteoporosis clinic for OP, osteopenia or fragility fractures.

Retrospective chart review identified 185 women, ≥60 years old, who visited the clinic between 10/2010 and 03/2015. Age, body mass index (BMI), racial/ethnic background, any history of smoking, history of CAD, hypertension, atrial fibrillation and congestive heart failure, use of statins, steroids, medications for OP, serum levels of calcium, 25 hydroxy-vitamin D, creatinine were risk variables in our analysis. A combined variable with 4 categories (no history of CAD and no use of statin [control], history of CAD and statin use, history of CAD and no statin use and no history of CAD with statin use) was created as an independent variable to determine associations between CAD with or without influence of statin and FN BMD (outcome variable) for a multi-variable regression analysis. The regression model was adjusted for the variables mentioned above.

Mean (standard deviation) age of women was 80+/-8 years, mean BMI was 25+/-5; 27 (14%) had CAD and 76 (41%) were on statins. Greater percentages of women with CAD were on statins (74% in CAD vs 34% in non-CAD groups). Compared to those without CAD and without statin use, patients with CAD and no statin use were more likely to have decreased FN BMD ( $\beta$  -0.47, 95% confidence interval -0.77 to -0.18). There was no significant associations between low femur neck BMD and either having CAD with statins or no CAD with statins.

Statins may have a protective role in preventing bone loss in elderly women suffering from CAD. Longitudinal studies will help determine if statin use in elderly women with CAD would continue to prevent bone loss as seen in younger adults.

**Disclosures:** Olasimbo Chiadika, None.

## MO0614

**Evaluation of Current Screening and Treatment Patterns in Males at the Veteran Affairs Healthcare System.** David Smith<sup>1</sup>, Nicola Berman<sup>2</sup>, Craig Tenner<sup>3</sup>, Virginia Pike<sup>4</sup>, Michael Pillinger<sup>4</sup>, Stephen Honig<sup>4</sup>. <sup>1</sup>NYU School of Medicine, United States, <sup>2</sup>NYU Rheumatology, United States, <sup>3</sup>NYU Department of Medicine, United States, <sup>4</sup>NYU Department of Rheumatology, United States

## Background

By 2050 the worldwide incidence of hip fractures in men is projected to increase by 310%. It has been proposed that this increase will be due, in part, to the number of undiagnosed and untreated cases of osteoporosis in this population. Existing literature suggest that men may be under-screened, and screening recommendations for men lag behind those for women. The aim of this study was to identify the need for screening and appropriate follow up in this population by identifying the number of fractures that preceded screening, and assess whether these patients had appropriate treatment and follow up.

## Methods

A retrospective chart review using the Computerized Patient Record System was performed on 1848 males aged 20-80, who had undergone DEXA scanning at the VA NY Harbor Healthcare System between 2011 and 2016. The primary endpoint for assessment was whether the DEXA scan was ordered in response to a fracture event. Among patients who suffered a fracture, a further assessment was performed to evaluate whether these patients were treated for osteoporosis and whether they suffered subsequent fractures. Time to follow up DEXA was also measured. Data was collected by three investigators using a standardized extraction algorithm.

## Results

1848 DEXA scans were performed on males from 2011 and 2016, including 485 individuals with a history of fracture. Average age at time of first fracture was 75. The 485 patients were assessed in two groups – those who had DEXA scans ordered in response to a fragility fracture (Group A: N=170) and those who had fractures following their first DEXA (Group B: N=315). In Group A, 30% received treatment for osteoporosis following their fracture and 40% of patients sustained another fracture (46% of the untreated patients and 23% of the treated patients). In Group B, 63% received treatment following the fracture. A further 25% sustained another fracture (13% of the treated patients, and 24% of the untreated patients). 47% of all patients had a follow up DEXA.

## Conclusion

Given the high prevalence of fractures among males without a known history of osteoporosis, there is need for routine screening of this demographic of patients in order to prevent fractures. Fewer than half the patients had a follow up DEXA. Further, our data suggest that appropriate treatment can reduce the risk of subsequent fractures by 50%. We conclude that physicians should be educated on appropriate management of osteoporosis following fractures.

**Disclosures:** David Smith, None.

## MO0615

**A Retrospective Study on the Relationship between Spinal Fragility Fracture and Bone Mineral Density.** Kwang-Sup Song<sup>1</sup>, Hyun Kang<sup>2</sup>, Geun-Wu Chang<sup>1</sup>. <sup>1</sup>Department of Orthopaedic Surgery, Chung-Ang University School of Medicine, Korea, Republic of, <sup>2</sup>Department of Anesthesiology, Chung-Ang University School of Medicine, Korea, Republic of

## Purpose

Fragility fracture is an important criterion of osteoporosis treatment, but some fragility fracture patients do not show sufficient bone mineral density (BMD) score for the diagnosis of osteoporosis. Authors attempted to understand the relationship between fragility fracture and BMD, further investigating other risk factors of fragility fracture in the process.

## Methods

Between January 2005 and February 2016, patients over 50 years old who were diagnosed with vertebral compression fracture were selected for this study. 1867 patients remained after excluding patients without DEXA scan result. Chart review revealed patients' age, sex, trauma mechanism, DEXA scan results, BMI. Patients were then divided into fragility fracture and non-fragility fracture group according to their trauma mechanism. We analyzed differences among the two fracture groups and the age groups using SPSS.

## Results

Amongst 1867 patients with vertebral fracture, 1631 patients were verified as fragility fracture, with 427 patients being male and 1440 patients being female. Mean age of the group was 72 years old (ranging from 50 to 97).

Compared to non-fragility fracture, fragility fracture patients were predominantly elderly female who had lower BMI and BMD. In detail, female composed 80.13% of fragility fracture patients. Within age groups, 61.6% of 5<sup>th</sup> decade, 79.6% of 6<sup>th</sup> decade, 93.3% of 7<sup>th</sup> decade and 99% of patients over 80 years old were fragility fracture [②]. As for BMD, female had lower score than male and elderly had lower score than young. Also evaluated BMDs in compartmental regions, lumbar area had highest and femur neck area had lowest density, leaving total hip area in-between.

Authors calculated risk ratio for vertebral fragility fracture occurrence in comparison to BMD results of divisional areas. Osteopenia patients had 1.57 times and osteoporosis patients had 2.62 times more chance to get fragility fracture than patients with normal range BMD. This risk ratio of overall BMD matched best with total hip area BMD than other areas.

## Conclusions

We found that as patients get older, BMD decreases and fragility fracture proportion increases. However, considerable number of patients under 60 years old without osteoporosis also suffered from fragility fracture, suggesting a firm necessity of assertive osteoporosis management in younger age group especially for women. And total hip BMD could be a useful tool in fragility fracture prediction than other areas.

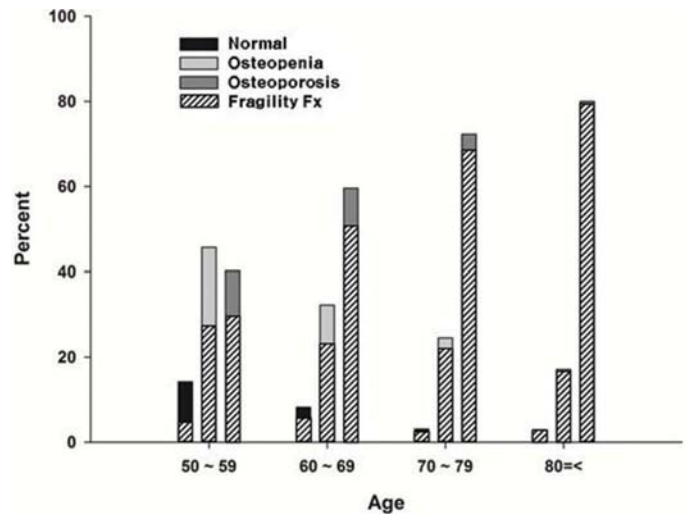


Figure: bone mineral density and fragility fracture in age groups

**Disclosures:** Kwang-Sup Song, None.

## MO0616

**Relationship between bilateral muscle strength and lumbar spine bone mineral density in postmenopausal women- a cross sectional study.** Jing Wang<sup>\*</sup>, Chenguang Li, Yan Zhang, Xiaofeng Qi, Liang Qiao, Jinlong Li, Lin Chen, Qiang Wang, Hao Zhang, Yongjian Zhao, Yongjun Wang, Bing Shu. Longhua Hospital, Shanghai University of Traditional Chinese Medicine, China

**Background:** Both low bone mineral density (BMD) and muscle weakness are risk factors for bone fracture in postmenopausal women, and muscle strength has potential effects on bone mass. The purpose of this study was to evaluate the association between handgrip strength and BMD in postmenopausal women. **Methods:** In this cross-sectional study, 2020 postmenopausal women (amenorrhea > 12 months and age ≥ 45 years) were included and divided into normal, osteopenia and osteoporosis groups according to the lumbar spine BMD measured by dual energy X-ray absorptiometry (DXA). Women with neurological or musculoskeletal disorders, uncorrected visual deficit or taking medicine that could affect muscle strength were excluded. Handgrip strength was evaluated with a hand dynamometer and body mass index (BMI) was calculated. Wilcoxon's Test and Chi-Square Test and logistic regression method were used for statistical analysis. **Results:** Women in normal group were younger compared to those in osteopenia and osteoporosis groups ( $p < 0.05$ ). Bilateral handgrip strength and BMI of women with osteoporosis were significantly lower compared with women with normal bone mass or osteopenia. Handgrip strength below 21.5kg was a risk of osteoporosis (OR 2.113; CI 95% 1.456-3.066). In contrast, higher BMI was significantly associated with lower rate of osteoporosis (OR 0.783; CI 95% 0.749-0.819). **Conclusions:** In postmenopausal women, muscle strength of women with osteoporosis was significantly lower. Low handgrip strength could be a risk indicator for osteoporosis.

**Disclosures:** Jing Wang, None.

## MO0617

**Trends in Self-Reported and Measured Osteoporosis Among US Adults, 2005-2014.** Qing Wu<sup>1</sup>, Yingke Xu<sup>1</sup>, William Leslie<sup>2</sup>. <sup>1</sup>University of Nevada, Las Vegas, United States, <sup>2</sup>University of Manitoba, Canada

**Background:** Studies examining trends in osteoporosis among US adults are limited, and have not described self-reported osteoporosis as a measure of perceived risk. We examined recent trends in self-reported osteoporosis prevalence between 2005-2006 and 2013-2014, and compared this with trends in osteoporosis defined by T-score in the same period. **Method:** Data from the last 4 cycles of the National Health and Nutritional Examination Survey (NHANES), from 2005-2006 to 2013-2014, were analyzed. Self-reported osteoporosis was ascertained if an individual had ever been told he/she had osteoporosis/brittle bones or had ever been treated for osteoporosis. Separate analyses were conducted for osteoporosis defined by T-score of the femoral neck (T-score < -2.5). Sampling weights accounted for unequal probabilities of selection. Prevalence was calculated with 95% confidence intervals (CIs), overall and for sex, age and race subgroups. Prevalence ratios (2013-2014 versus 2005-2006) with 95% CIs were estimated



as a measure of the overall increase or decrease. Results: Overall prevalence of self-reported osteoporosis was around 5% between 2005-2006 and 2009-2010, then increased to 6.49% in 2013-2014. Prevalence in women increased from 8.43% to 11.75%, but in men decreased from 1.34% to 0.76% for the same period. Self-reported osteoporosis prevalence increased with age for all survey cycles. Among the four race groups, Non-Hispanic White men and women had the highest prevalence in the first and final cycles. Prevalence ratios for self-reported osteoporosis indicated an increase between 2005-2006 and 2013-2014 for women but not for men. Compared with self-reported osteoporosis, the prevalence of T-score defined osteoporosis was consistently lower among women but not among men. The overall prevalence of T-score defined osteoporosis increased from 2005-2006 to 2013-2014 (ratio 1.56, 95% CI 1.24-1.96), and this was seen in both men (1.78, 95% CI 1.18-2.68) and women (1.47, 95% CI 1.10-1.96). Among the four race groups, Non-Hispanic Other had the highest prevalence of T-score defined osteoporosis in the last three cycles, while Non-Hispanic White had the highest prevalence in 2005-2006. Summary: The prevalence of self-reported osteoporosis was stable between 2005-2006 and 2009-2010, but increased in 2013-2014 for women but not men. Self-reported and T-score defined osteoporosis showed very different prevalence and trends.

**Disclosures:** Qing Wu, None.

## MO0618

### Impact of Primary Osteoporosis Screening in a National Sample of Older Men.

Cathleen Colon-Emeric<sup>\*1</sup>, Carl Pieper<sup>1</sup>, Courtney VanHoutven<sup>2</sup>, Kenneth Lyles<sup>1</sup>, Joanne LaFleur<sup>3</sup>, Janet Grubber<sup>2</sup>, Robert Adler<sup>4</sup>. <sup>1</sup>Duke University, United States, <sup>2</sup>Durham VA Medical Center, United States, <sup>3</sup>Salt Lake City VA, United States, <sup>4</sup>Hunter Holmes McGuire VAMC, United States

**Background:** There is no consensus on whether primary osteoporosis screening in older men is beneficial.

**Methods:** Propensity score matched case-control study using CMS and VA data among 2,539,812 men aged 65-99 years without prior fracture, osteoporosis diagnosis or treatment. Osteoporosis screening by dual energy x-ray absorptiometry (DXA) was identified from administrative codes and natural language processing. Across each of the 10 years of follow-up, propensity scores indicating the probability of screening within the next year were calculated, incorporating 32 fracture-related risk factors. Screened cases were 1:3 matched with unscreened controls. Landmark analysis with and without competing risk was used to compare time to fracture and mortality between cases and their matched controls who survived at least 12 months after DXA without fracture.

**Results:** Known fracture risk factors were well balanced between the 183,943 screened men and their 475,449 controls. During an average follow-up of 4.7 years, 9.4% fractured and 20.6% died. Among cases with available results, 36% had osteoporosis and 37% had osteopenia. After deletion of those with fractures or censoring prior to the 1-year landmark, 13.9% of cases met treatment guidelines and received osteoporosis medication, 67.6% were appropriately untreated, 7.1% were potentially over-treated, and 11.5% were untreated or were treated outside VA. Screening was associated with a higher hazard of fracture in all groups; for example, the HR in cases who met treatment guidelines and received at least 1 bisphosphonate prescription was 1.45 (1.39-1.52). These results are counterintuitive and suggest unmeasured confounders. However, for such an effect the confounding factor would have to have to independently increase fracture risk by 100% and be 2.5 times as prevalent in the screened group to have resulted in missing a 10% decrease in fracture attributable to screening. For those starting treatment, osteoporosis medication use occurred during only 12% of follow-up time, with less than 10% of use occurring 1 year after screening or later.

**Conclusion:** Osteoporosis screening as currently operationalized in this large national health system is unlikely to have a clinically important impact on fracture rates. Low treatment and adherence rates and inefficient selection for screening should be addressed to improve screening effectiveness.

**Disclosures:** Cathleen Colon-Emeric, Biscardia Inc, Major Stock Shareholder.

## MO0619

### Delirium and Operatively-Managed Fragility Fracture: an Intervention to Educate Providers and Improve Detection and Outcomes.

Jamie Confino<sup>\*1</sup>, John Roe<sup>2</sup>, Sara Merwin<sup>2</sup>, Vafa Tabatabaie<sup>2</sup>, Stephanie Kim<sup>2</sup>, Yungtai Lo<sup>2</sup>, Wanda Horn<sup>2</sup>. <sup>1</sup>Albert Einstein College of Medicine, United States, <sup>2</sup>Montefiore Medical Center, United States

**Background:** Delirium in geriatric patients with operatively managed hip fractures (fx) is associated with increased hospital stay, mortality, and complications. Delirium is under-recognized, and consequently under-managed, by providers despite proven screening tools such as the confusion assessment method (CAM) and prevention strategies. We hypothesized that targeted education to providers caring for at-risk patients would result in enhanced practice.

**Methods:** Multiphase quality initiative to detect and prevent delirium at an urban tertiary care teaching hospital. Chart review of pre and post-implementation patient cohort of age  $\geq 60$  with operative management hip fx. Current delirium knowledge assessed by survey from evidence-based methods, administered to orthopedic residents, RNs, and PAs caring for patients on the ortho-geriatrics co-management service. Education continues to providers and staff on the CAM, with checklist methodology for daily bedside implementation.

**Results:** In pre-implementation cohort of 100 patients, 46% had dementia at baseline, 27% had documented delirium; odds ratio for delirium diagnosis given dementia was 12.5 ( $p < 0.0001$ ). Delirium vs no delirium age was  $87.1 \pm 6.5$  vs  $83.0 \pm 8.3$ ,  $p = 0.01$ . Gender and pre-op opioids were not associated with delirium. 59 providers completed survey. 22 residents reported: 45% rarely evaluated polysubstance abuse (PSA), 73% rarely raised shades, 95% rarely placed assistive devices. 91% very often/always assessed pain and removed Foleys, 42% very often/always got patients out of bed (OOB) daily. 8 PAs reported: 50% rarely evaluated PSA, 38% rarely raised shades, 93% rarely placed assistive devices. 100% very often/always assessed pain, 63% very often got patients OOB daily and removed Foleys. 29 RNs reported: 59% very often/always evaluated PSA, 66% very often/always raised shades, 55% very often/always placed assistive devices, 86% very often/always got patients OOB daily, 72% very often/always removed Foleys.

**Conclusion:** Understanding the characteristics associated with delirium in our cohort will enhance education efforts to direct attention to the patients at highest risk. A significant proportion of providers were uninformed about delirium prevention and management. RNs reported more consistently implementing best practices to prevent and manage delirium than PAs or residents. Future efforts will focus on targeting the professions most in need of acquiring delirium detection and management skills.

**Disclosures:** Jamie Confino, None.

## MO0620

### Training the Next Generation of Musculoskeletal Investigators: A Report on the Activity of the USBJI's Young Investigator Initiative.

Edward Puzas<sup>\*1</sup>, Toby King<sup>2</sup>, Nancy Lane<sup>3</sup>. <sup>1</sup>University of Rochester School of Medicine and Dentistry, United States, <sup>2</sup>United States Bone and Joint Initiative, United States, <sup>3</sup>University of California Davis Health System, United States

Developing the skills to become an effective grant writer for the purpose of establishing a funded independent research career can often require a long learning curve. Mastering the art of posing hypotheses, writing high-information-content aims, responding to critiques, etc. can be a formidable undertaking. Many grant writing seminars exist, and although most provide valuable information, few include a mentoring process that continues throughout the learning curve. To address this issue the United States Bone and Joint Initiative (USBJI) launched a different type of program that has met with excellent success in training new scientists. This program, the Young Investigators Initiative (YII) is now completing its 12<sup>th</sup> year.

Young scientists (from both the US and Canada) are assigned two or more seasoned mentors and over the course of two weekends, usually separated by 12-18 months, and ongoing mentoring the scientists learn how to construct a hypothesis-driven research project and submit it for competitive funding. Of note, early stage investigators who are members of ASBMR have taken particular advantage of the program. We now present our data for the first time.

The YII is a competitive program. Since 2005, 736 young investigators have applied to enter the program and 364 have been accepted (i.e. 49.5%). 51% of the attendees are female. 83% are American and 17% are Canadian. Most are between the ages of 30 and 40 (72%).

The YII attendees are from a wide spectrum of disciplines and belong to a number of related specialty societies, including ASBMR. Attendees from the top five societies are:

Amer. Academy of Orthopaedics 73  
Amer. College of Rheumatology 64  
Amer. Society for Bone and Mineral Research 61  
Orthopaedic Research Society 51  
American Physical Therapy Association 30

202 of the 364 participants (56%) have received funding during the program. The total grant monies awarded is \$269,935,403. The top four awarding agencies are NIH (177 grants), Canadian Institutes of Health Research (64 grants), Orthopaedics Research and Education Foundation (26 grants) and the Department of Defense (14 grants).

In summary, although the YII faculty (13 of which are ASBMR members) are pleased with the success of the program, they continue to evolve the content of the curriculum to respond to the changing climate of biomedical research funding. More information on the YII can be found at: <https://www.usbji.org>.

**Disclosures:** Edward Puzas, None.

## MO0621

### Evaluating Racial Differences in Medical Experiences Among Women with Osteoporosis.

Nicole Wright<sup>\*1</sup>, Mary Melton<sup>2</sup>, Ivan Herbey<sup>3</sup>, Susan Davies<sup>4</sup>, Emily Levitan<sup>1</sup>, Kenneth Saag<sup>2</sup>, Nataliya Ivankova<sup>5</sup>. <sup>1</sup>Department of Epidemiology, University of Alabama at Birmingham, United States, <sup>2</sup>Division of Clinical Immunology & Rheumatology, University of Alabama at Birmingham, United States, <sup>3</sup>Department of Nursing Family, Community & Health Systems, University of Alabama at Birmingham, United States, <sup>4</sup>Department of Health Behavior, University of Alabama at Birmingham, United States, <sup>5</sup>Department of Health Services Administration, University of Alabama at Birmingham, United States

**Purpose:** Although more prevalent in non-Hispanic White women than Non-Hispanic Black women, inequities exist in outcomes associated with osteoporosis that cannot be explained after adjusting for other important variables. The goal of our study

was to qualitatively explore and compare knowledge and health care experiences among Black and White women with osteoporosis.

Methods: We conducted race-specific focus groups with Black and White women who had an osteoporosis diagnosis within the last five years, based on bone density results from the University of Alabama at Birmingham Health Care system. Focus group questions were based on the following domains: 1) osteoporosis and bone health concerns, 2) knowledge about osteoporosis, 3) utilization of medical services for osteoporosis, 4) facilitators to performing osteoporosis prevention activities (prescribed therapies, non-prescribed therapies, physical activity), and 5) barriers to doing the osteoporosis prevention activities. We recorded and transcribed the focus groups, and analyzed the transcripts using an inductive thematic approach with the help of NVivo 10 software.

Results: We completed eight focus groups with White women (n=36) and seven groups with Black Women (n=13). The mean (SD) age was 73.2 (9.4) years, with no difference in age between the two groups. Overall, we identified 10 unique themes. The themes and subthemes that differed by race included: knowledge about osteoporosis (lower in Black women), types of physical activity performed (Black: walking vs. White: other strength-based activities), coping with multimorbidity (osteoporosis lower priority in Black women), physician trust, and benefits of religion (positive for Black women). White women displayed more activation around the doing positive bone health activities such as taking prescribed medications and physical activity.

Conclusions: We qualitatively observed racial differences in the medical experiences of our sample of women with osteoporosis. The findings can be used to assist health care professionals to tailor their approaches to the specific barrier a patient may be facing, as well as assist researchers in developing educational tools to address barriers to improving care.

**Disclosures:** Nicole Wright, Pfizer, Consultant.

## MO0622

**Dancing on Broadway with Irregular Periods and a Femoral Neck Stress Fracture.** Dorothy Fink<sup>\*1</sup>, David Weiss<sup>2</sup>, Ryan Turner<sup>3</sup>, Marijeanne Liederbach<sup>2</sup>. <sup>1</sup>Hospital for Special Surgery, United States, <sup>2</sup>Harkness Center for Dance Injuries, NYU Hospital for Joint Diseases, United States, <sup>3</sup>Top Balance Nutrition, United States

The female athlete triad/ hypothalamic amenorrhea and polycystic ovarian syndrome (PCOS) are both common causes of irregular periods in young women. A 26-year-old woman presented with right hip pain after performing for 2 months in her first Broadway show. She was diagnosed with a left inferior (compression) femoral neck stress fracture by MRI scan. Because she had no history of fracture but had irregular periods, she was sent to endocrinology for evaluation.

Her menarche was at 13-years-old. She had irregular periods throughout high school and she reported missing approximately 2-3 menstrual cycles a year. She took isotretinoin (Accutane) for acne in college and reported excess body hair, but was never worked up for PCOS. She denied weight changes and any eating disorder. Her food journal revealed an average intake of 1395 kcal per day with restriction of carbohydrates. Her food intake did not increase during periods of intense activity because of not taking time to plan ahead for meals and not wanting to eat before performing.

Her weight was 98 pounds with a BMI of 19.83 kg/m<sup>2</sup>. Her exam showed mild hirsutism (Ferriman-Gallwey score of 12) and cystic acne. Her blood work was unremarkable except her total testosterone was 40 ng/dL (nl: 9-55) and her dehydroepiandrosterone sulfate (DHEAS) was elevated at 428 ug/dL (nl: 65-380). Her bone density revealed an AP spine Z-score of -3.0, left femoral neck Z-score of -2.6, and right femoral neck Z-score of -2.9, all consistent with low bone mass for age.

Her irregular periods provided a clue for underlying hormonal dysfunction and eating patterns that resulted in her low bone mass and fracture. While she did not have an overt eating disorder with anorexia or bulimia, long term exposure to restrictive eating patterns led to poor bone health and affected her accrual of peak bone mass. Her case also highlights that biochemical and physical evidence of elevated androgen levels often seen in PCOS may occur simultaneous with the female athlete triad and these symptoms may lead to challenges in the appropriate diagnosis.

**Disclosures:** Dorothy Fink, None.

## MO0623

**Participation in Varsity Sports is Associated with Tibial Bone Health as Assessed by Peripheral QCT.** Katelyn Guerriere<sup>\*</sup>, Caitlin Dillon, Kathryn Taylor, Julie Hughes, Anna Nakayama, Erin Gaffney-Stomberg, USARIEM, United States

Background: Mechanical loading has been associated with positive effects on bone parameters such as increased fatigue resistance in animal models. Areas of the bone that are subject to high stress and strain, such as at the midshaft of the tibia, are of particular interest when examining the effect of physical activity on bone. While greater physical fitness has been associated with lower injury rates in military recruits, it is not known whether a reported history of specific types of activity influences this relationship. We hypothesized that recruits who participated in varsity sports, particularly those involving multiaxial loading, would have greater indices of bone health at that start of military training. Methods: U.S. Marine recruits completed a background survey and a peripheral QCT (pQCT) (Stratec XCT 2000L or XCT 3000) scan of the non-dominant tibia during the first week of training. Participation in a varsity sport was treated as a

dichotomous (sport status=yes/no) variable and then further categorized into multiaxial loading sports and non-multiaxial loading sports. Associations between sport status and vBMD, total CSA, and estimated bone strength (polar stress strain index; SSIP) at 66% the length of the tibia, were analyzed using multiple linear regression with age, sex, race, ethnicity and BMI as covariates. Results: Participants included 144 men (age, 18.9(1.9) yrs, mean(SD); BMI, 24.4(3.0)kg/m<sup>2</sup> 60.8% varsity athletes) and 140 women (age, 18.9 (1.9)yrs; BMI, 23.1(2.1)kg/m<sup>2</sup> 61.2% varsity athletes). Although participation in varsity sports was not associated with vBMD (p=0.142), a significant 19.71mm<sup>2</sup> increase in CSA and a 138.06mm<sup>3</sup> increase in SSIP were observed for varsity athletes (p<.0001, 0.022, respectively). The association between sport status and vBMD and SSIP differed by sex with significant effects observed for women but not for men. However, sport status and CSA were associated in both men and women (Table 1). There were no additive effects of participation in multiaxial loading sports on any bone outcomes. Conclusion: Participation in varsity sports was associated with more favorable vBMD, CSA, and SSIP at the midshaft tibia in women, and greater CSA at the same site in men. Multiaxial loading did not confer additional benefit in this population. History of participation in a competitive sport regardless of multiaxial loading status may be a simple but important indicator of bone health prior to entering military training.

Bone Parameters of the Midshaft (66%) Tibia	Men*			Women*		
	$\beta$	95% CI	p-value	$\beta$	95% CI	p-value
vBMD, mg/ccm	-0.167	-7.12, 6.78	0.962	-6.56	-13.15, 0.031	0.051
CSA, mm <sup>2</sup>	21.16	5.06, 37.26	0.010	17.79	6.42, 29.17	0.002
SSIP, mm <sup>3</sup>	72.44	-129.06, 273.93	0.478	198.40	75.73, 321.06	0.002

\*Models adjusted for age, race, ethnicity, and BMI.

Effect of varsity sport status on vBMD, CSA, and SSIP at 66% of tibia length in men and women

**Disclosures:** Katelyn Guerriere, None.

## MO0624

**The effects of endurance exercise and dietary restriction on zoledronic acid caused quiescence of bone turnover in male adult rats.** Tsang-Hai Huang<sup>\*1</sup>, Rong-Sen Yang<sup>2</sup>, Ming-Shi Chang<sup>1</sup>. <sup>1</sup>National Cheng Kung University, Taiwan, Province of China, <sup>2</sup>National Taiwan University Hospital, Taiwan, Province of China

Purpose: To investigate the effects of endurance exercise training under conditions of bisphosphonate induced down regulation of bone turnover. Methods: Adult male Sprague Dawley rats (age: 6 month) were body weight matched and assigned to one of the following six groups, which were 1) the CON group: fed *ad libitum* control group; 2) the EE group: animals were subjected to a 9-week treadmill endurance running training; 3) the DR group, animals were fed under 40% dietary restriction. Moreover, zoledronic acid (ZOL, dose: 100mg/kg b.w.) was used as a functional inhibitor to reduce bone turnover for three similar group, which were the 4) CON+ZOL, 5) EE+ZOL and 6) DR+ZOL groups. Histomorphometry, densitometry and serum assays were conducted for the current study. Two-way (ZOL\*interventions) ANOVA was used for statistical analyses. Results: After the 10-week experimental periods, the DR and EE significantly reduced body weight gain as well as epididymis fat mass (p<0.05). ZOL demonstrated a significant main effects as shown by higher bone mineral as well as structural accumulation in spongy bone of ZOL treated animals (p<0.05). However, no difference shown in densitometry and histomorphometry between two endurance exercise groups suggested EE could reverse the effect of ZOL. In serum bone markers, while ZOL treatment showed main effect in down-regulating serum bone resorption marker (e.g. TRACP 5b), EE demonstrated significant main effect in up-regulating bone resorption (e.g. TRACP 5b and CTX-1) and bone formation (e.g. PINP) serum markers (p<0.05). And, two EE groups showed no difference in serum bone markers, which suggested endurance training is capable to reverse ZOL induced down-regulation of bone turnover. Conclusion: By using bisphosphonate as a functional inhibitor for bone turnover, endurance exercise showed counteractive efficacies. Further human study will be valuable to determine whether endurance exercise could show reverse efficiencies on bone turnover for those bisphosphonate-treated patients.

**Disclosures:** Tsang-Hai Huang, None.



## MO0625

**Changes of Trabecular Bone Score (TBS) in Asian Females: Comparison of 1990's and 2010's.** Young-Seong Kim<sup>1</sup>, Taeyong Lee<sup>2</sup>, Jin-Hwan Kim<sup>3</sup>, Dong Gyu Hwang<sup>2</sup>. <sup>1</sup>Dongguk University, Korea, Republic of, <sup>2</sup>Ewha womans University, Korea, Republic of, <sup>3</sup>Inje University Ilsan Paik Hospital, Korea, Republic of

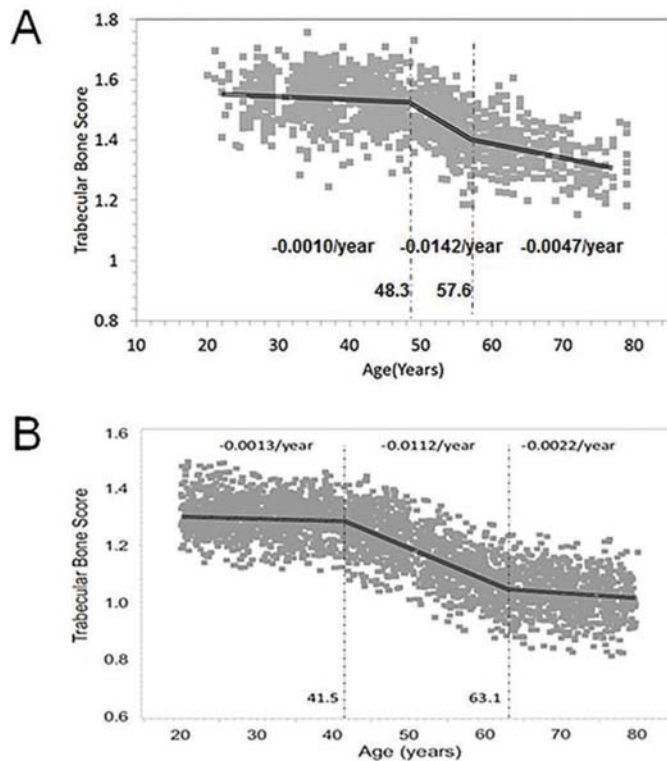
The purpose of this study is to understand the changes of TBS scores in Asian females by comparing 1990's and 2010's DXA images. Moreover, we want to examine the difference in the change of TBS between Korean and Japanese due to aging.

We have compared the DXA images of 1,726 Korean females (Age: 20~79) to Japanese (Age: 20~79). While Korean DXA images were obtained in 2014 and 2015, Japanese data were obtained in 1996. We excluded participants who have abnormal DXA images or lumbar disease.

We used TBS iNsight software (version 2.1.1, Med-Imaps, Bordeaux, France) to calculate lumbar spine TBS. DXA images was used for the BMD and TBS measurements. Statistical analysis was performed using piecewise linear regression.

Korean showed higher values of height and weight than Japanese in all age groups. However, they showed similar BMI, which are 22.4kg/m<sup>2</sup> for Koreans and 22.9kg/m<sup>2</sup> for Japanese. Korean showed higher TBS than Japanese in all age group. On average, TBS of Koreans are 0.281 higher than that of Japanese and the difference is bigger in the elderly. There is a significant difference in the slope and breaking points of TBS values between Korean and Japanese. Japanese showed drastic reduction of TBS in 21.6 years but only 9.3 years in Korean data.

In conclusion, we have observed the higher TBS values in all age groups of Korean population, which might be explained by the time-difference of data acquisition (1990's vs. 2010's) as well as different iron consumptions in the diet. Higher level of iron in Korean may explain the later onset of TBS decrease (48.3 yrs) and shorter duration (9.3 yrs). Dietary iron may be a more important factor in bone mineralization than originally thought.



Piecewise linear regression of TBS with aging (A : Korean, B : Japanese)

**Disclosures:** Young-Seong Kim, None.

## MO0626

**A dietary pattern rich in calcium, potassium, and protein is associated with tibia bone mineral content and strength in young adults entering initial military training.** Anna Nakayama<sup>\*</sup>, Laura Lutz, Adela Hruby, J. Philip Karl, James McClung, Erin Gaffney-Stomberg. USARIEM, United States

Calcium (Ca), potassium (K) and protein intake are associated with bone health in both adolescents and older adults but has not been studied in young adults. Stress fracture risk is elevated for young adults during initial military training (IMT). One commonly fractured site is the tibia. While the etiology of stress fractures is multifactorial, lower bone strength increases risk. The objective of this study was to assess whether adherence to a dietary pattern rich in Ca, K and protein is associated with bone indices using peripheral quantitative computed tomography (pQCT) in young adults

entering IMT. A cross-sectional analysis was performed using baseline data from 3 randomized controlled trials assessing the efficacy of Ca and vitamin D on bone health during IMT in Army, Air Force, and Marine recruits (N=401; 179 males, 222 females). Dietary intake was estimated from a semi-quantitative food frequency questionnaire (Block FFQ). A dietary pattern characterized by Ca, K, and protein was derived from 27 food groups using reduced-rank regression (SAS, v9.4) and a pattern z-score was computed, where higher z-scores indicate greater adherence to the pattern. At the 4% site (metaphysis) and 14% site (diaphysis) of the tibia, BMC, vBMD, and strength parameters [bone strength index (BSI) at the 4% site and stress strain index (SSI) at the 14% site] were evaluated. Associations between adherence to the dietary pattern as the predictor variable and bone parameters as the response variables were evaluated by multiple linear regression (see Table). The dietary pattern explained 44% of the variability in Ca, K, and protein intake and was positively correlated with all 3 nutrients (r=0.58, 0.63 and 0.52, respectively). The pattern had high positive factor loadings for milk, dark green vegetables, and yogurt, and high negative loadings for added sugars, refined grains and discretionary oils. The pattern z-score was positively associated with BMC (P=0.004) and strength (BSI; P=0.01) at the metaphysis, and with BMC (P=0.0002), strength (SSI Polar, P=0.0006), and robustness (P=0.02) at the diaphysis in model 1. Further adjusting for BMI in model 2 attenuated the associations except with BMC (P=0.005) and strength (P=0.01) at the diaphysis. A dietary pattern rich in Ca, K, and protein is positively associated with measures of tibia BMC and strength in recruits entering IMT. Adherence to this dietary pattern prior to IMT may potentially decrease injury susceptibility.

Relationship between Dietary Pattern Z-scores and Tibia Parameters

Bone Parameters	Model 1*			Model 2*		
	$\beta$	SE	p-value	$\beta$	SE	p-value
<b>4% Site</b>						
Total BMC (mg/mm)	8.702	3.00	<b>0.004</b>	5.378	2.79	0.055
Total vBMD (mg/ccm)	2.571	2.22	0.248	1.170	2.19	0.594
Total BSI <sup>1</sup> (mg/mm <sup>4</sup> )	4.157	1.65	<b>0.012</b>	2.445	1.55	0.116
Robustness	0.031	0.02	0.092	0.017	0.02	0.344
<b>14% site</b>						
Cortical BMC (mg/mm)	5.806	1.56	<b>0.0002</b>	4.132	1.46	<b>0.005</b>
Cortical vBMD (mg/ccm)	-0.027	1.03	0.979	0.240	1.04	0.817
SSI Polar <sup>1</sup> (mm <sup>3</sup> )	56.377	16.31	<b>0.0006</b>	39.418	15.28	<b>0.010</b>
Robustness	0.022	0.01	<b>0.017</b>	0.013	0.01	0.128

\*Model 1 controlled for age, sex, race, energy, smoking, education, self-reported physical activity; model 2 = model 1 plus BMI. BSI = bone strength index; SSI Polar = polar stress index. Bolded values indicate statistical significance <0.05.

Table

**Disclosures:** Anna Nakayama, None.

## MO0627

**Relationship between dietary calcium intake and biomarkers of bone and vascular health in healthy postmenopausal women.** Angel Ong<sup>\*</sup>, Hope Weiler<sup>1</sup>, Shubhabrata Das<sup>1</sup>, Michelle Wall<sup>2</sup>, Stella Daskalopoulou<sup>2</sup>, David Goltzman<sup>2</sup>, Suzanne Morin<sup>2</sup>. <sup>1</sup>McGill University, Canada, <sup>2</sup>Research Institute of McGill University Health Centre, Canada

**Purpose:** Concerns exist regarding calcium intake and vascular health in postmenopausal (PM) women. We aim to describe the relationship between dietary calcium intake (dCa<sub>i</sub>) and selected serum bone and vascular biomarkers in this population.

**Methods:** Cross-sectional data from 79 healthy PM women were analyzed. Usual daily dCa<sub>i</sub> (previous month) was estimated using a validated semi-quantitative food frequency questionnaire, and categorized into 3 levels of dCa<sub>i</sub> (<600, 600-1000, and >1000 mg/d) and sources of dietary calcium (dairy and non-dairy). No participants used supplements. Body mass index (BMI), physical activity level (PAL) (International Physical Activity Questionnaire), and concentrations of bone (25-hydroxyvitamin D, bone specific alkaline phosphatase [BSAP] and C-terminal telopeptide [CTx]), parathyroid hormone [PTH] and vascular (total cholesterol [TC], low-density lipoprotein [LDL-C], and apolipoprotein B [Apo B]) biomarkers were analyzed. One-way ANOVA and Kruskal-Wallis tests with post-hoc comparisons tested for differences in biomarker levels across dCa<sub>i</sub> levels and sources of dCa<sub>i</sub>, and for differences in categories and sources of dCa<sub>i</sub> across tertiles of biomarker levels. Multivariable linear regression models tested for relationships between dCa<sub>i</sub> levels and bone and vascular health biomarkers.

**Results:** Participants were 60 (SD 6) years with a median of 10 (interquartile range [IQR] 5-15) years post-menopause. BMI was 25.7 (SD 3.8) kg/m<sup>2</sup>. Mean dCa<sub>i</sub> was 860 (SD 337) mg/d; there were no differences in bone or vascular health biomarkers across levels of dCa<sub>i</sub>. Milk derived dCa<sub>i</sub> was higher in the middle tertile of TC (P=0.01), LDL-C (P=0.001), and Apo B levels (P=0.01) compared to the lowest and highest tertiles of each. Higher dCa<sub>i</sub> from cheese was associated with the highest TC tertile compared to the middle tertile (dCa<sub>i</sub> 192 [IQR 120-354] vs. 123 [IQR 75-159] mg/d, P=0.01). In fully adjusted models, there was no relationship between total dCa<sub>i</sub>, or dairy Ca intake, and any biomarkers of bone or vascular health (Table). In these models, Apo B, LDL-C and TC levels were inversely associated with CTx levels (P<0.01).

Conclusion: In this cross-sectional study in healthy PM women, we found no relationship between dCa<sub>i</sub> and selected biomarkers of bone and vascular health. However, we observed an association between serum CTX and serum lipids suggesting an interaction between bone resorption and risk factors for vascular disease.

Table: Multiple linear regression models for selected bone and vascular health biomarkers in healthy postmenopausal women

Bone health biomarkers			Vascular health biomarkers		
Models	$\beta$ (SE)	P-value	Models	$\beta$ (SE)	P-value
<b>25(OH)D (nmol/L)</b>			<b>TC (mmol/L)</b>		
Intercept	92.129±16.031	<0.001	Intercept	5.606±0.822	<0.001
dCa <sub>i</sub> group 1 (<600 mg/d <sup>2</sup> )	-5.139±5.855	0.38	dCa <sub>i</sub> group 1 (<600 mg/d <sup>2</sup> )	0.129±0.243	0.60
dCa <sub>i</sub> group 3 (>1000 mg/d <sup>2</sup> )	-1.657±5.438	0.76	dCa <sub>i</sub> group 3 (>1000 mg/d <sup>2</sup> )	0.303±0.230	0.19
Time since menopause (y)	0.906±0.342	0.01	Time since menopause (y)	0.014±0.014	0.30
BMI (kg/m <sup>2</sup> )	-1.533±0.602	0.01	BMI (kg/m <sup>2</sup> )	0.027±0.028	0.34
Season*	3.377±4.883	0.49	CTX (ng/mL)	-1.463±0.536	0.009
FAL (MET-b/wk)	0.038±0.041	0.36	hsCRP (mg/L)	0.067±0.056	0.24
<b>CTx (ng/mL)</b>			<b>LDL-C (mmol/L)</b>		
Intercept	0.850±0.153	<0.001	Intercept	2.525±0.736	<0.001
dCa <sub>i</sub> group 1 (<600 mg/d <sup>2</sup> )	0.001±0.050	1.00	dCa <sub>i</sub> group 1 (<600 mg/d <sup>2</sup> )	0.033±0.218	0.88
dCa <sub>i</sub> group 3 (>1000 mg/d <sup>2</sup> )	0.024±0.047	0.61	dCa <sub>i</sub> group 3 (>1000 mg/d <sup>2</sup> )	0.342±0.206	0.54
Time since menopause (y)	0.002±0.003	0.44	Time since menopause (y)	0.015±0.012	0.22
BMI (kg/m <sup>2</sup> )	-0.003±0.006	0.59	BMI (kg/m <sup>2</sup> )	0.053±0.025	0.04
Apo B (g/L)	-0.297±0.098	0.004	CTX (ng/mL)	-1.304±0.480	0.01
PTH (pmol/L)	0.020±0.021	0.34	hsCRP (mg/L)	0.034±0.050	0.50
<b>BSAP (pg/L)</b>			<b>Apo B (g/L)</b>		
Intercept	48.054±10.074	<0.001	Intercept	0.903±0.187	<0.001
dCa <sub>i</sub> group 1 (<600 mg/d <sup>2</sup> )	3.784±2.473	0.19	dCa <sub>i</sub> group 1 (<600 mg/d <sup>2</sup> )	-0.023±0.053	0.67
dCa <sub>i</sub> group 3 (>1000 mg/d <sup>2</sup> )	3.854±2.684	0.16	dCa <sub>i</sub> group 3 (>1000 mg/d <sup>2</sup> )	0.015±0.052	0.78
Time since menopause (y)	0.053±0.177	0.77	Time since menopause (y)	0.004±0.003	0.16
BMI (kg/m <sup>2</sup> )	-0.372±0.314	0.24	BMI (kg/m <sup>2</sup> )	0.014±0.006	0.03
25(OH)D (nmol/L)	-0.227±0.059	<0.001	CTX (ng/mL)	-0.408±0.123	<0.001
PTH (pmol/L)	-0.086±1.173	<0.001	hsCRP (mg/L)	0.024±0.013	0.07
FAL (MET-b/wk)	0.044±0.021	0.04			

$\beta$ , unstandardized beta coefficient; SE, standard error; 25(OH)D, 25-hydroxyvitamin D; dCa<sub>i</sub>, dietary calcium intake; BMI, body mass index; FAL, physical activity level; CTx, cross-linked C-terminal peptide; Apo B, apolipoprotein B; PTH, parathyroid hormone; BSAP, bone-specific alkaline phosphatase; TC, total cholesterol; hsCRP, high-sensitivity C-reactive protein; LDL-C, low-density lipoprotein cholesterol.

\*Referent group was moderate dietary calcium intake level of 600-1000 mg/d.

\*Season = warm season (October to March). Referent group was cold season (April to September).

Table: Multiple linear regression models for selected bone and vascular health biomarkers

Disclosures: Angel Ong, None.

## MO0628

**Effect of Maintenance of Serum Ionized Calcium during Treadmill Walking on Parathyroid Hormone and C-Terminal Telopeptides of Type I Collagen in Older Adults.** Sarah Wherry\*, Christine Swanson, Pamela Wolfe, Toby Wellington, Andrew Overstreet, Jane Quick, Rebecca Boxer, Robert Schwartz, Wendy Kohrt. University of Colorado, United States

Exercise is often recommended to improve or maintain bone mass in older adults, but several studies have shown that vigorous exercise increases parathyroid hormone (PTH) and markers of bone resorption (c-terminal telopeptides of type I collagen (CTX)) in healthy adults. We believe that this catabolic response is driven by decreases in serum ionized calcium (iCa) seen at the onset of exercise. Work from our lab has demonstrated that preventing the decline in iCa during exercise attenuates increases in PTH and CTX during vigorous cycling exercise in younger adults. However, it is unknown if there are any age-related differences that may influence this relationship in older adults. Therefore, the purpose of this study was to determine if preventing the decline in iCa during vigorous treadmill exercise attenuates increases in PTH and CTX in older adults. Women (n=4) and men (n=1) aged 64-78 years performed two identical treadmill exercise bouts for 60 minutes at ~75% of VO<sub>2peak</sub> under conditions of calcium gluconate (C) versus half-normal saline (S) infusion. Blood samples were taken every 5 minutes during exercise to adjust the calcium infusion rate, with a goal of maintaining iCa at 0.1-0.2 mg/dL over the pre-exercise baseline value. The S condition was volume-matched to the C condition. PTH and CTX were measured every 15 minutes during exercise, 15 and 30 minutes after exercise, and hourly thereafter for 4 hours. Serum iCa was successfully maintained above baseline in the C condition and was significantly different than the S condition at all time points beginning 30 minutes into exercise (all p<0.05). The changes in PTH (C: 6.9 ± 5.8 pg/mL; S: 23.3 ± 8.1 pg/mL) and CTX (C: 0.04 ± 0.08 ng/mL; S: 0.08 ± 0.03 ng/mL) from the beginning to the end of exercise were not different between conditions. The area under the curve (AUC) during recovery was not significantly different between conditions for either CTX or PTH. Even though iCa was significantly higher during the C condition versus S for half of the exercise session, there was no effect of Ca infusion on the increases in PTH and CTX during exercise or during the 4 hour recovery. Future research with larger sample sizes is needed to determine the role of iCa on PTH and CTX during vigorous treadmill walking in older adults. To investigate if there are any sex-related differences, greater numbers of men should also be included.

Disclosures: Sarah Wherry, None.

## MO0629

**Overexpression of WNT16 does not Rescue the Bone Loss due to Glucocorticoid Treatment in Mice.** Imranul Alam\*, Dana Oakes, Shahed Sbata, Caylin Billingsley, Dena Acton, Austin Reilly, Rita Gerard-O'Riley, Michael Econs. Indiana University School of Medicine, United States

Glucocorticoid (GC) is commonly used for the treatment of a wide variety of autoimmune, pulmonary and gastrointestinal conditions as well as in post-transplant and malignancy conditions. One of the devastating side effects of GC use is a significant risk (30-50%) of osteoporotic fractures, particularly in the spine and hip as a result of the development of GC-induced osteoporosis (GIO). GC influences skeletal health by decreasing bone formation, increasing bone resorption as well as promoting apoptosis of osteoblasts and osteocytes. Bisphosphonates (BP) are the current pharmacological gold standard for the prevention and treatment of GIO; however, GIO is marked by reduced bone formation and BP serves merely to decrease bone resorption. Therefore,

it is crucial to identify an anabolic treatment for GIO. The WNT signaling pathway plays a major role in bone and mineral homeostasis. Several studies have demonstrated that WNT16 is a critical regulator for bone development and maintenance. One of the mechanisms by which GC suppress bone formation is through their effects on WNT-signaling pathway. Previously, we demonstrated that over-expression of *WNT16* in mice led to higher bone density, improved bone microarchitecture and strength. We hypothesized that *WNT16* overexpression would rescue bone loss and prevent bone fragility due to glucocorticoid treatment in mice. To test our hypothesis we treated adult wild-type and WNT16-transgenic mice with vehicle and GC (prednisolone; 2.1 mg/kg body weight) via slow-release pellets for 28 days. We measured bone mass and microarchitecture by DXA and micro-CT and performed gene expression and serum biochemical analysis. We found that GC treatment compared to the vehicle significantly decreased femoral aBMD and BMC and femur mid-shaft cortical bone area and thickness in both wild-type and transgenic female mice. In contrast, the trabecular bone parameters at distal femur were not significantly changed by GC treatment in male and female mice for both genotypes. In addition, we observed significantly lower level of serum P1NP and a tendency of higher level of serum TRAP in wild-type and transgenic mice due to GC treatment in both sexes. Gene expression analysis showed lower mRNA levels of *Opg* and *Opg/Rankl* ratio in GC-treated female mice for both genotypes compared to the sex-matched vehicle-treated mice. These data suggest that WNT16 overexpression was insufficient to prevent bone loss in mice due to glucocorticoid treatment.

Disclosures: Imranul Alam, None.

## MO0630

**Changes in Macrophage and Inflammatory Response During Fracture Healing in an Ovariectomized Mice Model.** Lin Chen\*, Chunxun Xue, Yongjian Zhao, Yan Zhang, Yongjun Wang, Bing Shu. Spine Research Institute, Shanghai University of T.C.M., Shanghai, China, 200032, China

Background:

Macrophage and inflammatory cytokines plays important roles in bone fracture healing. However, the influence of osteoporosis on macrophage and inflammatory cytokine expressions during fracture healing has not been revealed. The objective of this study was to observe the changes in macrophage and inflammatory cytokine expressions during osteoporotic fracture in an ovariectomized mice model.

Methods:

Tibia open fracture was established in mice 12 weeks after ovariectomy (OVX) or sham-operation (sham). Tibias were harvested before fracture and 1, 3, 5, 7, 14, 21, 28 days after fracture for X-ray, micro-computed tomography (CT), histological examinations and real-time polymerase chain reaction (PCR) analysis.

Results:

Fracture healing was delayed in OVX mice radiographically. Alcian Blue/Orange G staining showed that endochondral ossification and callus remodeling were impaired in OVX mice. TRAP positive osteoclasts in callus of OVX mice were significantly increased compared with that of sham mice during the middle and late stages of fracture healing except Day 21. Immunohistochemical and immunofluorescence staining demonstrated that there were two peaks (Day 1, Day 14) in TNF- $\alpha$  and IL-1 $\beta$  expression levels and one peak (Day 1) in expression levels of IL-6, M1 macrophage and M2 macrophage during fracture healing in both OVX mice and sham mice. The expression levels of TNF- $\alpha$  in OVX mice were lower at Day 1, 14, 21 than that in sham mice, and were higher at Day 3, 5, 7. There was no significant difference in IL-1 $\beta$  expression levels at different time points between these two groups. IL-6 expression levels were higher at Day 1, 3, 21 in OVX mice than that in sham mice. OVX mice also showed lower expressions of both M1 and M2 macrophages at Day 1 compared with sham mice. Inflammatory macrophages (F4/80<sup>+</sup> Mac-2<sup>+</sup>) were highly expressed in the early stage of fracture healing (Day 1, 3, 5, 7) in both OVX mice and sham mice. During the late stage of fracture healing (Day 14, 21, 28), both inflammatory macrophages and osteomacrophages (F4/80<sup>+</sup> Mac-2<sup>neg</sup>) were expressed in sham mice, while only inflammatory macrophage was expressed in OVX mice.

Conclusions:

Macrophage activity and inflammatory response were impaired in OVX mice, which might contribute to delayed fracture healing.

Disclosures: Lin Chen, None.

## MO0631

**$\alpha$ -Klotho is Associated with Bone Fractures and Arterial Stiffness in Dialysis Patients.** Louis-Charles Desbiens\*, Aboubacar Sidibe, Roth-Visal Ung, Michaël Munger, Catherine Fortier, Yue-Pei Wang, Mohsen Agharazi, Karine Marquis, Fabrice Mac-Way. CHU de Québec Research Center, L'Hôtel-Dieu-de-Québec Hospital, Endocrinology and Nephrology axis, Faculty and Department of Medicine, Laval University, Canada

Introduction

Mineral and bone disorders in Chronic Kidney Disease (CKD) are associated with increased fractures rate and arterial stiffness. This study aims to determine whether new bone markers (Sclerostin, DKK1,  $\alpha$ -Klotho, FGF23) are associated with bone metabolism parameters, fractures and arterial stiffness in a dialysis population.

Design and methods

Cross-sectional and retrospective study of hemodialysis patients at CHU de Québec, Canada. Demographic, clinical, pharmacological, biochemical parameters and fractures were identified through clinical records. Pre-dialytic plasma levels of Sclerostin,



DDK1,  $\alpha$ -Klotho, FGF23, P1NP and TRAP5b were measured by ELISA. Each fractured patient was matched 1:4 with non-fractured patients for sex and age. Central and peripheral arterial stiffness were measured at baseline. Linear and Cox regression analyses were used to assess factors associated with bone parameters, fractures and arterial stiffness.

#### Results

We included 130 (26 fractured, 104 non-fractured) hemodialysis patients with a median follow-up of 1290 (864) days (Table 1). The population is composed of 47% male with a mean age of 72 (14) years and a mean dialysis vintage of 545 (117) days. 56% had coronary artery disease, 51% had diabetes and 89% suffered from hypertension. In univariate analysis, high FGF23 and P1NP were associated with fractures. In a multivariate stepwise model built by forward elimination,  $\alpha$ -Klotho levels were inversely associated with fractures (Table 2).  $\alpha$ -Klotho was also positively correlated with alkaline phosphatase and P1NP levels, but not with PTH and TRAP5b levels (Table 3). In multivariate models adjusting for demographic, biochemical and mineral parameters,  $\alpha$ -Klotho was positively associated with peripheral but not central arterial stiffness. (Table 4)

#### Conclusion

In a dialysis population, high plasma levels of  $\alpha$ -Klotho are associated with parameters of increased bone formation, lower fractures and increased peripheral arterial stiffness. These results suggest a central role of  $\alpha$ -Klotho in bone-vessels axis anomalies in CKD.

Table 1. Population characteristics

	Non-fractured (n = 104)	Fractured (n = 26)
<b>Demography</b>		
Age (years)	72 (14)	70 (15)
Dialysis vintage (days)	457 (1136)	827 (1204)
Sex (Male)	50 (48.1)	11 (42.3)
<b>Comorbidities</b>		
Coronary artery disease	59 (56.7)	14 (53.8)
Peripheral artery disease	93 (89.4)	17 (65.4)*
High blood pressure	93 (89.4)	22 (84.6)
Diabetes mellitus	55 (52.9)	11 (42.3)
<b>Biochemistry</b>		
Calcium (mmol/L)	2.18 (0.12)	2.14 (0.12)
Phosphate (mmol/L)	1.41 (0.29)	1.47 (0.37)
PTH (ng/L)	304 (173)	440 (309)*
Alkaline phosphatase (U/L)	89.1 (49.8)	94.7 (41.0)
<b>Arterial parameters</b>		
Carotid-femoral PWV (m/s)	13.3 (5.0)	13.7 (4.6)
Carotid-radial PWV (m/s)	8.4 (2.0)	8.5 (2.0)
<b>Bone markers</b>		
$\alpha$ -Klotho (pg/ml)	314 (153)	292 (149)
DKK1 (pg/ml)	231 (149)	223 (182)
FGF23 (RU/L)	711 (1496)	863 (940)
P1NP (pg/ml)	3565 (1581)	4291 (4060)*
Sclerostin (ng/ml)	1.49 (0.79)	1.41 (0.71)
TRAP5b (U/L)	4.35 (3.18)	3.77 (2.00)

Continuous variables are expressed as either mean  $\pm$  SD if normally distributed or as median (IQR) if non-normally distributed. Categorical variables are expressed as number (percentage).  
PWV, pulse wave velocity;  
\* p < 0.05

Table 2. Factors associated with fractures in a multivariate model

	Unit	HR	95% CI
Peripheral artery disease	Y vs N	0.018**	0.086 0.073
Ferritin (ug/L)	1 ug/L	0.995*	0.991 0.999
PTH (ng/L)	< 150	1.000 (ref)	
	150 - 300	0.048*	0.005 0.516
	300 - 600	0.574	0.189 1.750
	> 600	1.084	0.282 4.168
Haemoglobin <sup>a</sup> (g/L)	< 108	1.000 (ref)	
	108 - 112	0.051**	0.010 0.271
	112 - 116	0.620	0.193 1.997
	> 116	0.206*	0.056 0.755
$\alpha$ -Klotho	Above vs below median	0.284*	0.104 0.773

<sup>a</sup> Patients were separated in four equal groups according to quartile values

\* p < 0.05

\*\* p < 0.001

Table 3. Correlation between  $\alpha$ -Klotho levels and bone metabolism parameters

	rho	p
PTH	-0.073	0.434
Alkaline phosphatase	0.200	0.031
P1NP	0.285	0.005
TRAP5b	0.155	0.100

Rho is computed from the Spearman correlation

Table 4. Association between bone markers and arterial stiffness parameters

	$\alpha$ -Klotho	DKK1	FGF23	Sclerostin
<b>Central stiffness (Carotid-femoral PWV, adjusted for mean arterial blood pressure)</b>				
Univariate	0.252 (0.041, 0.463)*	0.096 (-0.123, 0.314)	-1.138 (-1.724, -0.552)*	-0.671 (-2.056, 0.714)
Model 1 <sup>†</sup>	-0.161 (-0.629, 0.307)	0.360 (-0.107, 0.828)	0.009 (-0.593, 0.575)	-0.319 (-1.523, 0.884)
Model 2 <sup>‡</sup>	-0.265 (-0.740, 0.210)	0.326 (-0.149, 0.802)	0.071 (-0.536, 0.679)	-0.497 (-1.716, 0.721)
Model 3 <sup>§</sup>	-0.262 (-0.760, 0.235)	0.412 (-0.093, 0.917)	0.088 (-0.575, 0.751)	-0.530 (-1.947, 0.888)
<b>Peripheral stiffness (Carotid-radial PWV, adjusted for mean arterial blood pressure)</b>				
Univariate	0.252 (0.041, 0.463)*	0.096 (-0.123, 0.314)	0.007 (-0.206, 0.221)	0.856 (0.401, 1.311)*
Model 1 <sup>†</sup>	0.214 (0.016, 0.413)*	0.100 (-0.108, 0.309)	-0.060 (-0.303, 0.183)	0.465 (-0.040, 0.970)
Model 2 <sup>‡</sup>	0.191 (-0.010, 0.392)	0.089 (-0.119, 0.298)	-0.044 (-0.293, 0.206)	0.390 (-0.117, 0.897)
Model 3 <sup>§</sup>	0.174 (-0.030, 0.378)	0.104 (-0.109, 0.316)	-0.106 (-0.368, 0.156)	0.322 (0.246, 0.889)

Associations are presented as  $\beta$ -coefficient (95% confidence interval) for an increase of 1 quartile (in  $\alpha$ -Klotho, DKK1 and FGF23) or from the below median to the above median group (Sclerostin)

PWV: Pulse wave velocity

<sup>†</sup> Model 1 adjusted for age, sex, dialysis vintage, weight, cardiovascular disease, diabetes and smoking

<sup>‡</sup> Model 2 adjusted for Model 1 + calcium, phosphate and PTH

<sup>§</sup> Model 3 adjusted for Model 2 + statin, ASA, ACE and ARBs,  $\beta$ -blockers, atypical/citric, phosphate binders and calcium

\* p < 0.05

Annex

Disclosures: Louis-Charles Desbiens, None.

## MO0632

**Recombinant Soluble Betaglycan as a Potent Bone Remodeling Agent in Osteoporosis and Cancer Induced Bone Disease.** Fernando M Guerra-Olvera<sup>\*1</sup>, Cinthia N Cuero-Antolin<sup>1</sup>, Fernando López-Casillas<sup>2</sup>, Pierrick Fournier<sup>1</sup>, Patricia Juárez<sup>1</sup>. <sup>1</sup>Center for Scientific Research and Higher Education, Mexico, <sup>2</sup>Cellular Physiology Institute, Mexico

Osteoporosis is characterized by increased bone fragility due to bone loss and altered bone microarchitecture. TGF- $\beta$  is one of the most abundant cytokine in bone and a main regulator of bone remodeling. TGF- $\beta$  receptor III or Betaglycan (BG) modulates the biological function of bone morphogenetic protein 2 (BMP2) associated with low bone mineral density (BMD), and BG knockout mice have severe skeletal defects. Moreover, BG levels are significantly lower in patients with normal skeletal fracture compared to patients with nonunion fracture. These data suggest that low levels of BG contribute to low BMD and osteoporosis risk. Soluble BG (SolBG) is the hydrolyzed extracellular domain of BG, and is known for its ability to inhibit TGF- $\beta$  and BMP signaling. We hypothesized that SolBG reduces bone resorption and increases bone remodeling.

We developed an *ex vivo* model where hemicalvarias from 4-5d BALB/C mice (n=4) were cultured in the presence of insulin, as a positive control of new bone formation, and in the presence or absence of SolBG (5-10  $\mu$ g/ml). After one week, tissues were homogenized and expression of bone remodeling genes was analyzed by RT-qPCR. Bone structural characteristics were assessed by histomorphometric analysis. SolBG induced

new bone formation in mouse calvarias, as showed by a significant increase in bone thickness, in a dose-dependent manner ( $p < 0.01$ ) compared to untreated bones. SolBG (10  $\mu$ g/ml) increased mRNA levels of *Alpl* and *Runx2* and *Rankl/Opg* ratio and reduced *Col1a1*. To mimic bone metastasis conditions, MDA-MB-231 cancer cells were co-cultured with the hemicalvarias leading to osteolysis as shown by histology. In these conditions, SolBG reduced bone destruction as well as levels of *Rankl* mRNA and markers of bone metastases.

Our results show that the *ex vivo* model implemented can be used to study the conditions of bone remodeling and related mechanisms. Further studies to validate the effect of SolBG on BMD and mechanical bone properties in an *in vivo* model of osteoporosis and bone metastasis are ongoing. With more than 200 million persons affected by osteoporosis worldwide, uncontrolled bone resorption represents a serious public health problem. Soluble Betaglycan is a potential novel agent for the treatment of osteoporosis as well as cancer-induced bone loss.

Disclosures: Fernando M Guerra-Olvera, None.

## MO0633

**High serum Erythropoietin Predicts Incident Fractures in Men.** MrOS Sweden. Hallgerdur Lind Kristjansdottir<sup>\*1</sup>, sten Ljunggren<sup>2</sup>, Magnus Karlsson<sup>3</sup>, Mattias Lorentzon<sup>4</sup>, Ulf Lerner<sup>5</sup>, Claes Ohlsson<sup>5</sup>, Catharina Lewerin<sup>1</sup>, Dan Mellström<sup>4</sup>. <sup>1</sup>Section of Hematology and Coagulation, Department of Internal Medicine, Institute of Medicine, Sahlgrenska Academy, University of Gothenburg, Gothenburg, Sweden, Sweden, <sup>2</sup>Department of Medical Sciences, University of Uppsala, Uppsala, Sweden, Sweden, <sup>3</sup>Department of Clinical Sciences and orthopaedics, Lund University, Lund, Sweden, Sweden, <sup>4</sup>Department of Geriatric Medicine, Institute of Medicine, Sahlgrenska Academy, University of Gothenburg, Gothenburg, Sweden, Sweden, <sup>5</sup>Centre for Bone and Arthritis Research (CBAR), Sahlgrenska Academy, University of Gothenburg, Gothenburg, Sweden, Sweden

**Purpose** Erythropoietin (EPO) activates erythropoiesis in the bone marrow. It has been suggested to be involved in the cross talks between hematopoietic cells and bone forming osteoblasts exist. Data regarding associations between circulating erythropoietin and areal bone density (BMD) in older men are sparse. The aim of this study was to investigate the association between EPO and BMD as well as incident fractures in men.

**Population and methods** The Gothenburg part of the Swedish MrOS study examined BMD at hip sites and lumbar spine (n=1010) with (Hologic QDR 4500). Serum EPO concentrations were measured with an immune enzymatic assay (Quantikine IVD Human EPO; R&D Systems with a total CV of 6.2%). Fibroblast growth factor (intact FGF23) was measured with a two-site monoclonal antibody-based ELISA and intact parathyroid hormone (PTH) was measured by an immunometric assay. Estimated glomerular filtration rate was calculated with serum cystatin C and hand grip strength was measured with a Jamar hand dynamometer. Incident fractures were assessed in computerized X-ray archives during a 10 year period from baseline. The risk for incident fractures was calculated with a Cox proportional hazard model

**Results** The number of all fractures was 242, vertebral fractures 91, hip fracture 61 and major osteoporotic fractures 172. EPO was associated to age ( $r=0.11$ ,  $p < 0.001$ ) but also age adjusted to BMI, BMD (both hip sites and lumbar spine), iFGF23, iPTH and estimated GFR below 60 ml (all associations  $p < 0.01$ ). The association between EPO and fractures was not strictly linear and we, therefore, divided EPO in tertiles. Age adjusted Hazard Ratio (HR) for all fractures with trend test of tertiles of EPO was 1.24 (95% CI 1.06-1.46). HR for all fractures in a multivariate model with trend test of tertiles of EPO was 1.32 (CI 1.11-1.58), adjusting for age, BMI, BMD hip, iPTH, iFGF23, estimated GFR, falls last year and hand grip strength. Age adjusted HR for vertebral fractures with trend test of tertiles of EPO was 1.33 (1.03-1.73). HR for vertebral fractures in a multivariate model with trend test of tertiles of EPO was 1.42 (CI 1.07-1.88). HR for major osteoporotic fractures in an age adjusted model of trend test of tertiles of EPO was 1.19 (CI 0.99-1.43) and in a multivariate model 1.28 (1.4-1.58). The HR for hip fracture in relation to trend test of EPO was not significant.

**Conclusion** High serum EPO is associated with BMD and increased risk of fractures in Men.

Disclosures: Hallgerdur Lind Kristjansdottir, None.

## MO0634

**Low serum vitamin D and high parathyroid hormone are not associated with cortical porosity in postmenopausal women, but are associated with non-vertebral fracture independent of cortical porosity: the Tromsø Study.** Marit Osima<sup>\*1</sup>, Tove Tveitan Borgen<sup>1</sup>, Marko Lukic<sup>1</sup>, Guri Grimnes<sup>2</sup>, Ragnar Joakimsen<sup>2</sup>, Erik F Eriksen<sup>2</sup>, Åshild Bjørnerem<sup>2</sup>. <sup>1</sup>MD, Norway, <sup>2</sup>MD, PhD, Norway

Vitamin D deficiency leads to secondary hyperparathyroidism, increased bone turnover, bone loss, and fracture. However, it is less clear whether serum vitamin D and parathyroid hormone (PTH) are associated with cortical porosity, and if so, whether the association with fracture is mediated through increasing cortical porosity. We therefore tested (i) whether serum 25-hydroxyvitamin D (25(OH)D) and PTH were associated with cortical porosity, and (ii) whether associations with fracture risk were dependent on cortical porosity. We measured serum 25(OH)D, PTH, procollagen type I N-terminal

propeptide (PINP), C-terminal cross-linking telopeptide of type I collagen (CTX), and femoral neck areal bone mineral density (FN aBMD) using DXA in 211 postmenopausal women aged 54-94 years with non-vertebral fractures and 232 controls from the Tromsø Study. Femoral subtrochanteric cortical porosity and thickness were quantified using CT and StrAx1.0 software. Women with fracture exhibited lower serum 25(OH)D (76.4 vs. 82.9 nmol/L), higher PTH (4.58 vs. 4.13 pmol/L), PINP (49.7 vs. 43.5 ng/mL), and CTX (0.49 vs. 43.5 ng/mL) than controls ( $p < 0.05$ ). They exhibited increased femoral subtrochanteric cortical porosity (43.8 vs. 41.7%), reduced cortical thickness (4.06 vs. 4.36 mm) and reduced FN aBMD (794 vs. 860 mg/cm<sup>2</sup>,  $p < 0.05$ ). Serum 25(OH)D and PTH were not associated with cortical porosity or thickness ( $p > 0.10$ ). Each standard deviation (SD) decrease in 25(OH)D and each SD increase in PTH was associated with increased odds for fracture (OR 1.26; 95% confidence interval (CI) (1.00-1.58) and 1.31 (1.04-1.65) respectively), after adjustment for age, height, weight, supplementation of calcium, season, and cortical porosity. Serum 25(OH)D, not PTH, remained associated with fracture after further adjustment for FN aBMD. This data suggests that serum vitamin D and PTH are not associated with cortical porosity in postmenopausal women, and that vitamin D and PTH associations with fracture risk are independent of cortical bone architecture. We infer that this fracture risk may be mediated through other mechanisms than increased cortical porosity.

**Disclosures:** Marit Osima, None.

## MO0635

**New bone biopsy sectioning approach for histomorphometry and molecular biology.** Sylvain Picard\*, Roth-Visal Ung, Sarah-Kim Bisson, Fabrice Mac-Way. Research Center of CHU de Quebec, Hôtel-Dieu de Quebec Hospital, Faculty and Department of Medicine, Université Laval, Canada

Bone histomorphometry analysis is the gold standard for determination of bone turnover activities from undecalcified iliac crest bone biopsy. The bone specimen is classically embedded in methylmetacrylate (MMA) in order to preserve the double fluorochrome calcium labelling that is essential for evaluation of bone formation and mineralisation. However MMA embedding causes loss in enzymatic activity and protein antigenicity which makes immunohistological and other molecular biology methods challenging. Our goal was to evaluate the possibility of dividing the bone specimen in order to allow histomorphometric, immunohistological and molecular analyses within the same biopsy.

We tested a low speed precision saw (Isomet®, Buehler, Illinois, USA), designed for cutting different materials with minimal deformation, on iliac crest bone specimens. A first 3mm segment was cut, snap frozen and stored at -80°C. A second section was fixed in buffered formalin, decalcified under EDTA and embedded in paraffin. The rest of the biopsies were embedded in MMA. Immunohistochemical and histomorphometry staining were performed on the paraffin and MMA sections, respectively. qPCR and Western blot analyses were assessed following mRNA and protein extractions on the frozen sections.

Our results show that standard bone histomorphometry analysis, immunohistochemical staining, qPCR and Western blot analyses are successfully performed from a single iliac crest bone biopsy specimen. Our cutting technique produces quality data without compromising the architectural and molecular integrity of the specimen.

In conclusion, our simple approach allows to widen the analysis possibilities from a single iliac crest biopsy by allowing molecular biology assessment in addition to the standard bone histomorphometry.

**Disclosures:** Sylvain Picard, None.

## MO0636

Withdrawn

## MO0637

**Targeted Massively Parallel Sequencing of 128 Candidate Genes Reveals a Potential Molecular Cause in 75% of Cases with Idiopathic, Severe or Familial Osteoporosis.** Manuela Rocha-Braz\*, Monica França<sup>2</sup>, Adriana Fernandes<sup>1</sup>, Regina Martin<sup>2</sup>, Antonio Lerario<sup>2</sup>, Berenice Mendonça<sup>2</sup>, Bruno Ferraz-de-Souza<sup>1</sup>. <sup>1</sup>Endocrinology/LIM-25, Hospital das Clínicas, University of Sao Paulo School of Medicine, Brazil, Brazil, <sup>2</sup>SELA/LIM-42, Hospital das Clínicas, University of Sao Paulo School of Medicine, Brazil, Brazil

Osteoporosis (OP) is a multifactorial disorder with high heritability. Incorporating molecular information in clinical practice could lead to better identification of individuals at risk, decreasing disease burden. Several candidate genes for bone fragility have arisen, but the contribution of pathogenic variants in these genes to the pathophysiology of OP is still poorly understood. Our objective was to perform mutational analysis of candidate genes in a cohort of patients with idiopathic, severe or familial OP.

We selected 28 cases (7 families, 21 sporadic) of men or premenopausal women with idiopathic OP or low bone density, or post-menopausal women with a T-score  $\leq -4.0$ . Secondary causes of OP were excluded. Through a systematic review of monogenic diseases with altered bone mass phenotypes, reports of idiopathic or familial OP, and GWAS for OP, 128 candidate genes for bone fragility were identified and included in a customized massively parallel sequencing panel. Coding regions and 25-bp boundaries were captured with Agilent SureSelectXT and sequenced in Illumina NextSeq. Reads

were aligned with BWA, variant detection and copy-number variation analysis were performed with Platypus and CONTRA. Rare (MAF<0.005) stop-gain, frameshift, splice site, or missense variants predicted to alter protein function were considered potentially pathogenic variants (PPVs).

Thirty-three heterozygous PPVs were identified, 24% of which in well-established candidate genes (*COL1A1*, *COL1A2*, *WNT1*, *LRP5*, *PLS3*), and 76% in new candidate genes (e.g. *NBR1*, *AXIN1*, *WLS*, *LRP4*). Only 1 PPV was found in *LRP5*, previously associated with several cases of idiopathic OP. In 7 cases (25%) no PPV was found. In 29% of the cohort, a combination of 2 or more PPVs were found, including a young woman with severe OP and PPVs on *WNT1*, *PLS3* and *NOTCH2*. PPVs were also found in GWAS candidate genes *NBR1* and *GPR68*, associated with mineralization and osteoclast defects in mice, respectively, but without association with human OP phenotypes so far.

In conclusion, a targeted massively parallel sequencing strategy was able to identify potential molecular causes of OP in 75% of this cohort of extreme OP cases. Novel genes were associated to human OP, and digenic/oligogenic interactions were uncovered, expanding our knowledge of the molecular bases of bone strength. The identification of pathogenic variants associated with OP may allow individualized clinical management of patients and relatives in the future.

**Disclosures:** Manuela Rocha-Braz, None.

## MO0638

**The effect of hyperbaric oxygen therapy on bone metabolism.** Zaida Salmón\*, Juan Carlos Borregan, Mayte García Unzueta, José Antonio Riancho, Carmen Valero. Department of Internal Medicine. University Hospital Marqués de Valdecilla. University of Cantabria. IDIVAL. Santander. Spain, Spain

Oxygen is critical for maintaining cellular functions. In line with this, changes in oxygen supply have been suggested to influence bone cell activity in a number of experimental models, but their clinical consequences are still unclear. Therefore, the aim of this study was to determine the effects of hyperbaric oxygen therapy (HBOT) on bone metabolism in humans.

The study population included 44 patients (62% men), aged 57±13 years (range 30-81). They received HBOT in 90-minute sessions with 100% oxygen and 2.3 atmospheres of pressure. The reasons for treatment were chronic anal fissure (57%) and complications due to radiotherapy (cystitis 12%, proctitis 12% and radionecrosis 19%). The average number of sessions was 24±6. We measured plasma levels of aminoterminal propeptide of type I collagen (PINP), C-terminal telopeptide of type I collagen (CTX), intact parathyroid hormone (PTH) and 25-hydroxyvitamin D3 (25OHD) by chemiluminescent immunoassays at baseline and twice after HBOT (at an average of 38±13 and 127±33 days).

There were no significant variations after treatment with respect to baseline biochemical parameters, but there was a non-significant decreasing tendency in the parameters of bone formation (PINP -15.4%;  $p=0.33$ ) and resorption CTX -51.7%;  $p=0.18$ ) at the second post-therapy measurement. However, 25OHD levels increased after treatment (35%;  $p=0.01$ ), despite no patient took vitamin D supplements.

These results do not provide evidence for a significant effect of hyperbaric oxygen therapy on bone turnover markers. The increase in vitamin D levels could reflect the improvement of patients' general condition.

	Baseline (n=44)	First analysis after HBOT (n=35)	Second analysis after HBOT (n=18)
<b>Creatinine mg/dl</b>	0.84±0.22	0.82±0.22 -2.3%(p=0.38)	0.89±0.25 5.6%(p=0.56)
<b>P1NP ng/ml</b>	46.1±26.6	44.0±26.5 -4.5%(p=0.31)	39.0±12.6 -15.4%(p=0.33)
<b>CTX ng/ml</b>	0.201±0.184	0.161±0.119 -19.9%(p=0.32)	0.104±0.075 -51.7%(p=0.18)
<b>PTH pg/ml</b>	37.1±24.8	37.0±23.5 -0.2%(p=0.14)	34.2±18.9 -7.8%(p=0.15)
<b>25OHD ng/ml</b>	19.4±12.3	19.9±12.1 2.5%(p=0.71)	26.2±13.7 35%(p=0.01)

Mean±SD; p value for percentage of change with respect to baseline

Figure

**Disclosures:** Zaida Salmón, None.



## MO0639

**Identification of Enhancer-SNPs Associated with Osteoporosis.** Chuan Qiu\*, Hui Shen, Hongwen Deng. Tulane University, United States

## Background

Osteoporosis is an increasingly serious public health problem, affecting over 200 million people worldwide. To date, over 100 osteoporosis-associated loci have been identified, however, all these loci together account for ~6% of bone mineral density (BMD) variation. Recent studies suggest that most of the disease-associated SNPs located in noncoding intragenic and intergenic regions. Enhancers are short (50-1500 bp) noncoding segments of DNA that can be bound with proteins to regulate gene transcription, often in a cell-type specific manner. In this study, we aimed to identify novel and potential functional enhancer SNPs associated with osteoporosis by conducting a targeted meta-analysis of genome-wide association studies (GWAS).

## Methods

We retrieved common and rare genomic variants from the 1000 Genomes Project and downloaded the enhancer regions in osteoblast from Functional Annotation of Mammalian Genome (Fantom5) project. SNPs that were mapped to osteoblast enhancers were genotyped/imputed in five GWAS cohorts with a total of 11,140 subjects. Then, meta-analysis was carried out by using the program METAL.

## Results

A total of 8659 candidate SNPs were mapped to osteoblast enhancers. Meta-analysis identified 16 enhancer SNPs significantly ( $p$ -value  $< 5 \times 10^{-4}$ ) associated with BMD. Interestingly, most of the identified enhancer-SNPs were mapped to candidate genes which have been significantly associated with BMD in previous GWAS and/or have known functional roles in bone biology. For example, BMD-associated enhancer SNPs rs9748916 ( $p$ -value  $= 2.37 \times 10^{-4}$ ) was detected in an enhancer region of NFATC1, which directly links inflammation with differentiation of osteoblasts. In addition, several BMD-associated enhancer SNPs were clustered into the same or neighboring enhancers, which may interactively influence enhancer activity.

## Conclusion

In this study, we identified a number of osteoblast-enhancer SNPs associated with osteoporosis risk and provided novel insights into the pathogenesis of osteoporosis.

**Disclosures:** Chuan Qiu, None.

## MO0640

**Cortical Porosity is not Synonymous with Microstructural Deterioration.** Roger Zebaze\*, Roland Charpulat\*, Elizabeth Sornay-Rendu\*, ego Seeman\*. <sup>1</sup>Department of Medicine, Austin Health, Australia, <sup>2</sup>Inserm Lyon, France

Osteoporosis is defined as a femoral neck bone mineral density (BMD) T score  $\leq -2.5$  SD with microstructural deterioration. The morphological basis of 'deterioration' has not been formally quantified but commonly refers to cortical porosity and thinning, trabecular thinning, perforation and loss of connectivity. The absolute trait values are used to predict fracture risk but, like BMD, these values are the net result of growth-related assembly of microstructural and its age-related deterioration.

However, the variance in microstructure at completion of growth determines its strength and accounts for most of the trait variance during aging. For example, about 80% of cortical 'porosity' is void volume formed by Haversian canals (seen in cross section). The canals contain extracellular water which confers strength and each canal is part of an osteon with its cement line and concentric lamellae. This microstructure forms 'edges' or 'discontinuities'. The greater the osteonal number, the greater the canal number, the greater the 'porosity' but the greater the resistance to crack propagation because discontinuities increase the energy needed to propagate a crack. Intersecting trabecular plates and sheets form scaffolds supporting cortical bone.

We propose that the growth-related components of variance obscure the microstructural basis of bone fragility produced by unbalanced remodelling which enlarges and coalesces the canals forming stress risers, and produces loss of trabecular number and connectivity.

We quantified baseline cortical and trabecular deterioration as a structural deterioration score (SFS), the trait deviation from its mean in premenopausal women in an attempt to capture the morphological basis of bone fragility free of its contribution to bone strength. We hypothesized that the SFS will identify women in the OFELY cohort of 562 women having incident fractures during 10 years prospective follow-up, and will do so more accurately than the absolute trait values.

The predictive strength of the traits was expressed as a relative risk with sensitivity and specificities of 38%/76% for cortical porosity, 38%/78% for trabecular density giving respective ORs of 1.64 (95%CI 1.05-2.56;  $p=0.03$ ) and 1.83 (95%CI 1.17-2.85;  $p=0.001$ ). The SFS had a sensitivity and specificity of 44.3%/78% with OR of 2.80 (95%CI 1.81-4.33;  $p<0.0001$ ). We infer that fracture risk assessment is more sensitive when microstructural deterioration is quantified.

**Disclosures:** Roger Zebaze, None.

## MO0641

**Fractures in Adults with Type 1 Diabetes: Results from the T1D Exchange Clinic Registry.** Ruban Dhaliwal\*, Claire Boyle<sup>2</sup>, Mona Al Mukaddam<sup>3</sup>, Ruth Weinstock<sup>1</sup>, Michael Rickels<sup>4</sup>, Viral Shah<sup>5</sup>, Linda DiMeglio<sup>6</sup>. <sup>1</sup>SUNY Upstate Medical University, United States, <sup>2</sup>Jaeb Center for Health Research, United States, <sup>3</sup>University of Pennsylvania School of Medicine, United States, <sup>4</sup>University of Pennsylvania Perelman School of Medicine, United States, <sup>5</sup>Barbara Davis Center for Diabetes, United States, <sup>6</sup>Indiana University School of Medicine, United States

**Background:** Type 1 diabetes (T1D) is associated with a high fracture risk due to adverse effects on the skeleton. **Purpose:** To determine the prevalence and determinants of participant-reported fracture in the T1D Exchange Clinic Registry. **Methods:** Participants aged  $>18$  yrs diagnosed with T1D prior to age 45 with T1D for  $\geq 5$  yrs completed a comprehensive fracture history questionnaire. Demographic and clinical characteristics were gathered from registry update data obtained  $\leq 15$  mos prior to questionnaire completion. Only fractures reported as occurring after T1D diagnosis were considered for analyses. Chi-square and t-tests were used to compare characteristics between those with and without reported fracture history. Data are reported as mean  $\pm$  SD. **Results:** 756 adults (age  $39 \pm 16$  yrs (range 18-82 yrs, 28%  $\geq 50$  yrs), 63% female, 90% non-Hispanic White, T1D duration  $24 \pm 14$  yrs) completed the questionnaire. 48% reported  $>1$  fracture after T1D diagnosis (61% female). Among those with fracture after diagnosis, the number of broken bones was  $4 \pm 2$ , and age and T1D duration at fracture were  $31 \pm 16$  and  $17 \pm 14$  yrs, respectively. Of the 659 reported fractures, 24% involved feet/ankles, 21% hands/wrists, 12% fibula/tibia, 3% hip/pelvis and 3% vertebral fractures were reported. Those with fracture were more likely to be older ( $43 \pm 16$  vs.  $36 \pm 14$  yrs), have longer T1D duration ( $28 \pm 14$  vs.  $20 \pm 12$  yrs), be diagnosed with T1D prior to peak bone mass (defined as age  $<20$  yrs) (79% vs. 71%), and have at least one parent diagnosed with osteoporosis or osteopenia (22% vs. 10%) compared to those without fracture (all  $p$ -values  $<0.01$ ). They were also more likely to have microvascular T1D complications (retinopathy 27% vs. 14% and neuropathy 22% vs. 14%), have received treatment for osteopenia or osteoporosis (8% vs. 2%), and used calcium and vitamin D supplements (63% vs. 50%) (all  $p$ -values  $<0.01$ ). Limitations include the inherent cross-sectional nature of the data, and a possible recall bias in participant-reported fractures. **Conclusion:** Fractures in adults with T1D are common. Older age, longer T1D duration, and T1D diagnosis prior to peak bone mass are notable risk factors for fracture. Additionally, the rates of retinopathy and neuropathy were higher among those with fractures. Prospective studies are needed to explore the impact of these determinants on fracture risk in T1D.

**Disclosures:** Ruban Dhaliwal, None.

## MO0642

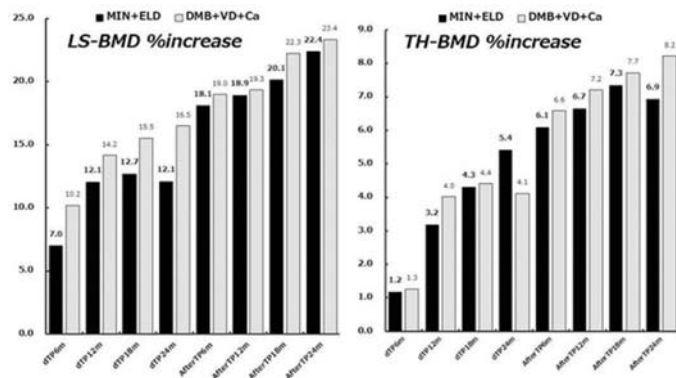
**Comparative Study between "Minodronate with Eldecalcitol" and "Denosumab" as Treatment after 2-year Daily Teriparatide in Osteoporosis in Patients with Rheumatoid Arthritis - Results in 24 Months.** Yuji Hirano\*, Kyosuke Hattori<sup>1</sup>, Takayasu Ito<sup>2</sup>. <sup>1</sup>Department of Rheumatology, Toyohashi Municipal Hospital, Japan, <sup>2</sup>To Orthopaedic Clinic, Japan

**Background:** Although daily teriparatide (dTP) treatment increases bone mineral density (BMD), increase of BMD is not enough after 2-year dTP treatment in some osteoporosis (OP) patients. This prospective study compared minodronate (a bisphosphonate developed in Japan) with eldecalcitol (activated vitamin D developed in Japan) (MIN/ELD) and denosumab (DMB) as the treatment after 2-year dTP treatment in OP in patients with rheumatoid arthritis (RAOP). Results in 6 months and 12 months were reported in ASBMR 2015 in Seattle and ASBMR 2016 in Atlanta 2017, respectively. This study investigated 24-months results.

**Methods:** Female RAOP patients treated with MIN/ELD ( $n=20$ ) or DMB ( $n=9$ ) for 24 months after dTP were used. Change of BMD (lumbar spine and total hip: LSBMD and THBMD) measured by DEXA at every 6 month from the initiation of dTP and change of bone turnover markers (BTM) (P1NP and TRACP5b) at every 6 month from the initiation of dTP were compared between two groups. DMB (60mg) was injected every 6 month with prescribing of native vitamin D and calcium. MIN (50mg) was administered every 4 weeks and ELD (0.75µg) was administered every day.

**Results:** Patients' characteristics (MIN/ELD: DMB): Mean age (70.3: 70.2). Body mass index (20.5: 21.0). PSL use (75.0%: 76.7%). %increase of BMD was expressed as the value at the initiation of dTP was standard. Increase of LSBMD (dTP6m/12m/18m/24m/AfterTP6m/12m/18m/24m): dTP7.0/12.1/12.7/12.1/AfterTP18.1/18.9/20.1/22.4 in MIN/ELD and dTP10.2/14.2/15.5/16.5/AfterTP19.0/19.3/22.3/23.4 in DMB. No significant differences were observed at all time points. % increase of THBMD: dTP1.2/3.2/4.3/5.4/AfterTP6.1/6.7/7.3/6.9 in MIN/ELD and dTP1.3/4.0/4.4/4.1/AfterTP6.6/7.2/7.7/8.2 in DMB. No significant differences were also observed at all time points. % change of BTM was expressed as the value at the initiation of dTP was 100. P1NP: dTP100/405/343/251/214/AfterTP38/52/52/61 in MIN/ELD. dTP100/524/414/290/248/AfterTP59/64/70/67 in DMB. TRACP-5b: dTP100/150/159/141/146/AfterTP50/65/70/84 in MIN/ELD. dTP100/205/229/193/193/AfterTP98/96/109/110 in DMB. There were no significant differences in BTM between two groups except TRACP-5b at 6m after dTP treatment ( $p=0.02$ ).

**Conclusions:** This study suggests that 4-year treatment with 2-year dTP followed by 2-year MIN/ELD mostly equals to 4-year treatment with 2-year dTP followed by 2-year DMB in RAOP. Bone turnover tended to be more decreased in MIN/ELD group after dTP treatment than that in DMB group.



LSBMD &amp; THBMD

Disclosures: Yuji Hirano, None.

## MO0643

**Lower bone mass and higher bone resorption in pheochromocytoma: Clinical evidence for the effect of the sympathetic nervous system on bone.** Beom-Jun Kim<sup>1</sup>, Mi Kyung Kwak<sup>1</sup>, Seong Hee Ahn<sup>2</sup>, Hyeonmok Kim<sup>3</sup>, Seung Hun Lee<sup>1</sup>, Kee-Ho Song<sup>4</sup>, Sunghwan Suh<sup>5</sup>, Jae Hyeon Kim<sup>6</sup>, Jung-Min Koh<sup>1</sup>.

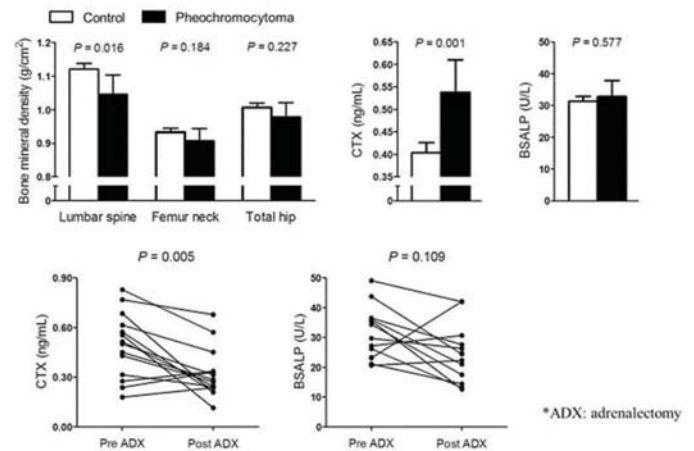
<sup>1</sup>Division of Endocrinology and Metabolism, Asan Medical Center, University of Ulsan College of Medicine, Korea, Republic of, <sup>2</sup>Department of Endocrinology, Inha University School of Medicine, Korea, Republic of, <sup>3</sup>Department of Internal Medicine and Institute of Health Sciences, Gyeongsang National University Hospital, Gyeongsang National University School of Medicine, Korea, Republic of, <sup>4</sup>Division of Endocrinology and Metabolism, Konkuk University Medical Center, Konkuk University School of Medicine, Korea, Republic of, <sup>5</sup>Division of Endocrinology and Metabolism, Department of Internal Medicine, Dong-A University Medical Center, Dong-A University College of Medicine, Korea, Republic of, <sup>6</sup>Division of Endocrinology and Metabolism, Department of Medicine, Samsung Medical Center, Sungkyunkwan University School of Medicine, Korea, Republic of

**Objective:** Despite the apparent biological importance of sympathetic activity on bone metabolism in rodents, its role in humans remains questionable. To clarify the link between the sympathetic nervous system and the skeleton in humans, we investigated the association of catecholamine excess with osteoporosis-related phenotypes, especially focusing on bone mineral density (BMD), in a Korean cohort consisting of patients with pheochromocytoma and controls.

**Methods:** Among 620 consecutive subjects with newly diagnosed adrenal incidentaloma, 31 patients with histologically confirmed pheochromocytoma (a catecholamine-secreting neuroendocrine tumor) and 280 patients with nonfunctional adrenal incidentaloma were defined as cases and controls, respectively.

**Results:** After adjustment for confounders, subjects with pheochromocytoma had 7.2% lower bone mass at the lumbar spine and 33.5% higher serum C-terminal telopeptide of type I collagen (CTX) than those without pheochromocytoma ( $P = 0.016$  and  $0.001$ , respectively), whereas there were no statistical differences between groups in bone mineral density (BMD) at the femur neck and total hip and in serum bone-specific alkaline phosphatase (BSALP) level. The odds ratio (OR) for lower BMD at the lumbar spine in the presence of pheochromocytoma was 3.31 (95% confidence interval, 1.23–8.56). However, the ORs for lower BMD at the femur neck and total hip did not differ according to the presence of pheochromocytoma. Serum CTX level decreased by 35.2% after adrenalectomy in patients with pheochromocytoma, while serum BSALP level did not change significantly.

**Conclusions:** This study provides the first clinical evidence showing that sympathetic overstimulation in pheochromocytoma can contribute to adverse effects on human bone through the increase of bone loss (especially in trabecular bone) as well as bone resorption.



Pheochromocytoma and Osteoporosis-related Phenotypes

Disclosures: Beom-Jun Kim, None.

## MO0644

**The increased risk of fractures after treatment of aromatase inhibitors in patients with breast cancer: The National Health Insurance System Data (NHIS 2005-2015).** Sujin Lee<sup>1</sup>, Yumie Rhee<sup>2</sup>, Jung Wha Hong<sup>3</sup>, Soojung Hong<sup>3</sup>, Kyoung Hye Park<sup>1</sup>, Sun Ok Song<sup>1</sup>, Ju Young Nam<sup>1</sup>, Kyoungmin Kim<sup>1</sup>, Eun Young Lee<sup>4</sup>, Ho Hur<sup>1</sup>, Namki Hong<sup>2</sup>. <sup>1</sup>Department of Internal Medicine, National Health Insurance Service Ilsan Hospital, Korea, Republic of, <sup>2</sup>Yonsei University College of Medicine, Endocrine Research Institute, Yonsei University College of Medicine, Korea, Republic of, <sup>3</sup>Research Institute, National Health Insurance Service Ilsan Hospital, Korea, Republic of, <sup>4</sup>Seoul St. Mary's Hospital, College of Medicine, The Catholic University of Korea, Korea, Republic of

Aromatase inhibitors (AI) are well known to negatively affect bone strength. We aimed to estimate the incidence of fractures in early breast cancer women treated with AI and fracture risk in Korea. We performed nationwide population-based retrospective study in women with breast cancer (ICD code: C50) over 55-year-old who received mastectomy using the National Health Insurance System (NHIS) data from 2005 to 2015. The patients who had distant metastasis, tamoxifen treatment, double primary cancer and previous bisphosphonate treatment were excluded. Logistic regression analysis was used to compute the odds ratios (OR) of major osteoporotic fractures. A total of 28,905 women with breast cancer were finally evaluated. Five hundred twenty two cases (1.8%) of the major osteoporotic fractures were detected. We also evaluated the risk of fractures according to the duration of AI treatment. After adjusting age, the fracture risk increased in breast cancer patients treated with AI over 3 years compared to the patients treated with AI less than 3 years (OR=1.286; 95% CI 1.063-1.557,  $P = 0.0096$ ). Our findings suggest a significant increased risk of fracture after the treatment of AI in breast cancer patients. Based on this population-base data, the regular check-up and proper management for bone metabolism are needed in breast cancer patients with AI treatment.

Disclosures: Sujin Lee, None.

## MO0645

**17 Patients with Monoclonal Gammopathy of Undetermined Significance (MGUS) Presenting with Symptomatic Vertebral Compression Fractures (SVCF).** Michael Lovy<sup>1</sup>, Jack Hodgkins<sup>1</sup>, Nir Ben-Shlomo<sup>2</sup>, Brian Hodgkins<sup>1</sup>. <sup>1</sup>Desert Oasis Healthcare, United States, <sup>2</sup>Ben-Gurion Medical School, Israel

### Background

The presence of MGUS has been associated with vertebral fracture (1), is more prevalent among patients with SVCF (2), and is associated with an increased risk of fracture (3). Changes in cytokine profiles and bone microarchitecture that may explain this risk have been found and the skeletal significance of MGUS has been emphasized (4). Clinical description of patients with MGUS and SVCF is lacking.

### Purpose

To describe the clinical details and circumstances of fracture in a cohort of patients with MGUS who presented with SVCF and compare that to patients with SVCF and no MGUS.

### Methods

17 patients with MGUS were identified among 150 patients presenting with SVCF in our community based outpatient fracture clinic. All patients had a complete history and physical, review of past medical records and radiographs, CBC, sedimentation rate,



chemistry profile, TSH, urinalysis, vitamin B12, PTH, 25-OH vitamin D, and serum protein electrophoresis. We performed testosterone level and immunofixation of serum and urine in select patients.

#### Results

There were 9 females and 8 males ranging in age from 70-94 (mean 80.5 years), with a BMI of 20-32 (mean 26.4) and an average of 1.23 comorbid conditions. 3 patients were on steroids. 9 fractures occurred after falling, 5 spontaneously, 2 while lifting and 1 with bending. 1 patient each with Schnitzler, CAPS, Kaposi sarcoma, pernicious anemia, and hepatitis C were diagnosed at the time of presentation. 9 patients had peripheral neuropathy. There were a total of 22 fractures including 5 patients with 2 fractures-12 thoracic and 10 lumbar. 59% of fractures were distributed from T10-L2. M-spike ranged from 0.1-1.6% comprised of IgG 72%, IgM 22% and IgA 6% and kappa and lambda light chains each 50%. Vitamin D insufficiency and deficiency were each present in 2 patients. There were more men ( $p=0.081$ ) and fewer falls ( $p=0.067$ ) among the MGUS patients but these and all other clinical comparisons did not reach statistical significance.

#### Conclusion

The circumstances of fracture and patient characteristics of this cohort of MGUS patients with SVCF did not differ from those with SVCF and no MGUS. Even with the understanding of the deleterious effect of MGUS on bone, the fact that MGUS is asymptomatic makes preemptive therapeutic intervention a challenge.

1) Bida, et al, Mayo Clin Proc. 2009;84:685-693, 2) Golombick, et al, Acta Hematol. 2008;120:87-90, 3) Melton, et al, J Bone Miner Res. 2004;19:25-30, 4) Drake, J Bone Miner Res. 2014;29:29-2533.

**Disclosures:** Michael Levy, None.

## MO0646

**Evolution of Serum Sclerostin Six Months After Liver Transplantation: Different Response Compared With Bone Turnover Markers.** Gonzalo Allo Miguel<sup>\*1</sup>, Soledad Librizzi<sup>1</sup>, Mercedes Aramendi Ramos<sup>2</sup>, Carlos Jiménez<sup>3</sup>, Federico Hawkins<sup>4</sup>, Guillermo Martínez Díaz-Guerra<sup>1</sup>. <sup>1</sup>Endocrinology Service, 12 de Octubre University Hospital, Spain, <sup>2</sup>laboratory Service, 12 de Octubre University Hospital, Spain, <sup>3</sup>Surgery Service, 12 de Octubre University Hospital, Spain, <sup>4</sup>Endocrinology Service, 12 de Octubre University Hospital, Spain

**INTRODUCTION:** Increased risk of fracture and low bone mineral density (BMD) are common findings in patients with liver transplantation. Sclerostin (SCL, a negative regulator of bone formation) could have an important role in the increased risk of fracture after transplantation. The aim of our study is to evaluate serum SCL and other bone turnover markers in a cohort of patients with liver transplantation (LT).

**PATIENTS AND METHODS:** This is a prospective, single-center study. 42 patients with LT were enrolled. Serum sclerostin, beta cross-laps ( $\beta$ -CTX) and osteocalcin (OC) were measured at baseline (24 hours before transplantation) and 1, 3 and 6 months after the procedure. Data are expressed as mean $\pm$ s.d. for continuous variables. Pearson's correlation coefficient was employed to test correlations among bone turnover markers. Student's t-test was used to compare bone markers levels (from baseline to 6 months). A p-value  $<0.05$  was considered as statistically significant.

**RESULTS:** 28/14 (male/female) patients were included in the study. Mean age was 58.6 $\pm$ 12.5 years. Bone markers levels at baseline were: SCL: 0.73 $\pm$ 0.26 ng/ml;  $\beta$ -CTX: 0.43 $\pm$ 0.25 ng/ml; OC 15.83 $\pm$ 7.02 ng/ml. Sclerostin levels decreased significantly during the study (1st month: 0.48 $\pm$ 0.14  $p<0.001$ ; 3rd month 0.52 $\pm$ 0.14,  $p=0.002$ ; 6th month: 0.55 $\pm$ 0.14,  $p=0.035$ ). OC increased significantly after one month (18.6 $\pm$ 14.4;  $p<0.001$ ) and three months (40.2 $\pm$ 36.2;  $p=0.01$ ). There was also an increase after six months, but this was non-significant.  $\beta$ -CTX increased throughout the study and after three months there was a significant increase compared to baseline (0.79 $\pm$ 0.57;  $p<0.001$ ), which persisted after six months (0.68 $\pm$ 0.33;  $p=0.01$ ). There were no significant correlations between SCL and other bone markers during the study.

**CONCLUSIONS:** Our study is the first to show consistent serum SCL decrease after liver transplantation. Also, our results showed that OC and  $\beta$ -CTX increased significantly six months after liver transplantation. More studies are necessary to evaluate the association of bone marker levels with BMD and fracture risk in patients with liver transplantation, to confirm if their measurement may have a future role in clinical practice.

**Disclosures:** Gonzalo Allo Miguel, None.

## MO0647

**One-year Changes in Bone Mineral Density with High-Dose Prednisone in Patients with Rheumatoid Arthritis.** Linda Rasch<sup>\*1</sup>, Lilian van Tuyt<sup>1</sup>, Martijn Kremer<sup>1</sup>, Irene Bultink<sup>1</sup>, Maarten Boers<sup>2</sup>, Willem Lems<sup>1</sup>. <sup>1</sup>Amsterdam Rheumatology and immunology Center | VU University Medical Center, Netherlands, <sup>2</sup>Epidemiology and Biostatistics, VU University Medical Center, Netherlands

**Background:** Recently, we showed that treatment with COBRA-light therapy including prednisone with initially 30 mg/day, was as effective as the original COBRA scheme, with initially 60 mg/day [1], in the treatment of rheumatoid arthritis (RA). Since high-dose glucocorticoids are associated with bone loss and vertebral and nonvertebral fractures, we investigated the differences in bone mineral density (BMD) after one year of treatment in both arms.

**Objectives:** To compare 1-year changes in BMD (lumbar spine L1-L4, total hip, and femoral neck) between the treatment groups.

**Methods:** An open-label, randomised controlled, non-inferiority trial of patients with active, newly diagnosed RA following a treat-to-target protocol.

**Results:** BMD data were determined in 144 out of 164 included RA patients, all randomized to either COBRA (n=71) or COBRA-light (n=73) therapy. Overall bone loss was very limited, and no significant difference in change in BMD between COBRA and COBRA-light was found at any site (Table 1). However, in secondary analyses, COBRA-light showed a significant decrease in BMD in the lumbar spine and total hip after 52 weeks, whereas the femoral neck and the COBRA group did not.

**Conclusions:** During the trial, overall bone loss was very limited and not significantly different between the treatments. These findings strengthen the hypothesis that positive effects associated with the large reduction in disease activity as a result of combination therapy and tight control treatment counteract the negative effects of (high-dose) prednisone on bone.

**References:** [1] Ter Wee MM, et al. Ann Rheum Dis 2015

**Table 1. Changes in bone mineral density between baseline and week 52 during COBRA and COBRA-light therapy**

	COBRA (n=71)			COBRA-light (n=73)		
	baseline	week 52	change	baseline	week 52	change
Lumbar spine	1.12 (0.17)	1.12 (0.17)	0.01%	1.10 (0.15)	1.09 (0.15)	-1.02%*
Total hip	0.95 (0.14)	0.95 (0.14)	0.05%	0.95 (0.12)	0.94 (0.13)	-1.16%*
Femoral neck	0.90 (0.16)	0.89 (0.17)	-0.59%	0.88 (0.12)	0.87 (0.11)	-0.98%

\* Significant change between baseline and week 52 ( $p<0.05$ ); Values are reported as mean (SD), unless otherwise specified.

Table 1

**Disclosures:** Linda Rasch, None.

## MO0648

**Combined treatment with Growth Hormone and Anastrozole in a pubertal male with Growth Hormone Deficiency and Low Bone Density Due To Chronic Steroids Use.** Marielly Sierra<sup>\*1</sup>, Lillian Haddock<sup>1</sup>, Milliette Alvarado<sup>2</sup>, Margarita Ramirez<sup>3</sup>, Loida Gonzalez<sup>4</sup>, Francisco Nieves<sup>5</sup>, Anette Garces<sup>6</sup>. <sup>1</sup>University of Puerto Rico, Recinto de Ciencias Medicas. Endocrinology section, Puerto Rico, <sup>2</sup>University of Puerto Rico, Recinto de Ciencias Medicas. Endocrinology department, Puerto Rico, <sup>3</sup>University of PR. Recinto de Ciencias Medicas. Endocrinology department., Puerto Rico, <sup>4</sup>Universidad de Puerto Rico. Recinto de Ciencias Medicas, Endocrinology department, Puerto Rico, <sup>5</sup>University of Puerto Rico, Pediatric Endocrinology department, Puerto Rico, <sup>6</sup>University of Puerto Rico, Puerto Rico

Growth delay and short stature are typical manifestations of chronic glucocorticoid exposure during childhood. Therapeutic strategies directed to improve the final stature of these patients are needed. A 21-year-old male patient with Systemic Lupus Erythematosus (SLE) diagnosed at 5 years old, was referred to endocrinology clinics to evaluate for short stature. After SLE was diagnosed, the patient received oral prednisone 5mg daily and solumedrol 200mg intravenously weekly. Initial hormonal workup prior to treatment was within normal parameters and he was started on prophylactic bisphosphonate therapy from 6 to 10 years of age. He was lost to follow up until he was 18 when was evaluated at our clinics and found with pronounced growth failure. Found with height at 53 inches, much less than the expected height of 69, and a bone age of 10 years despite adequate pubertal development. Initial bone mineral density (BMD) revealed a Z-score at spine of -4.5 and total hip of -4.4. He was started on growth hormone (GH) therapy and vitamin D supplementation with gradual weaning from glucocorticoids as tolerated. After one year of therapy, the patient's height increased 1.5 inches and bone age advanced to 14 years. Follow up BMD showed a significant decrease (6.1%) in spine BMD and a low Trabecular Bone Score of 1.14. To optimize height prior to closure of epiphyses, combination therapy with anastrozole 1mg orally daily was added to therapy, maintaining estradiol and testosterone levels within the reference range for an adult male. After a year of combined therapy the patient was able to increase linear growth to a total of 3.4 inches with further bone age advancement to 15 years. He has not suffered bone fractures and has continued growing albeit at a slow rate, since corticosteroids have not been able to be discontinued. Once closure of epiphyses ensues, anabolic bone therapy can be considered. Growth hormone therapy in combination with anastrozole has been recently introduced as a viable therapeutic approach for patients with idiopathic short stature. Our case report demonstrates that this treatment could be an option for pubertal patients with growth delay secondary to chronic glucocorticoid exposure.

**Disclosures:** Marielly Sierra, None.

## MO0649

**A meta-analysis of the risk of ankle and wrist fractures in diabetes.** Tatiane Vilaca<sup>\*</sup>, Jennifer Walsh, Richard Eastell. Academic Unit of Bone Metabolism Department of Oncology and Metabolism University of Sheffield, United Kingdom

There is evidence for an increase in the risk of hip fractures in diabetes (type 1 and 2), but the risk is not established for other skeletal sites. This increase is not captured by bone mineral density (BMD), the main tool used to evaluate the risk of fractures in the

clinical setting. Usually, the higher the BMD, the lower the fracture risk, however, people with diabetes have fractures on a higher BMD than people without the disease.

Microarchitecture studies using high-resolution peripheral computed tomography have reported an increase in cortical porosity at the tibia and radius in this population. The corresponding clinical picture would be an increase in the risk of fractures of the ankle and wrist. To evaluate this hypothesis, a meta-analysis was conducted.

The aim of this study is to estimate the risk of ankle and wrist fractures in patients with diabetes compared with non-diabetic controls.

Medline and Embase were searched using the terms "diabetes mellitus", "fracture", "ankle", "radius", "forearm" and "wrist". Relative risks and 95% confidence intervals were calculated using random effects model.

For ankle fractures, 6 studies were eligible (5 cohorts, 1 case-control) including 2,137,223 participants and 15,395 fractures. For wrist fractures, 10 studies were eligible (all cohorts) resulting in 2,768,694 subjects and 37,123 fractures. The studies included men and women, from 20 to 97 years, the vast majority with type 2 diabetes.

Diabetes was associated with a significant increase in the risk of ankle fractures (RR 1.31 95%CI 1.15 – 1.49) and a non-significant decrease at the wrist (RR 0.89 95%CI 0.79 – 1.00). In the three studies that reported body mass index (BMI), the mean values were 10% higher in the diabetic group.

If the effect of the increase in cortical porosity was clinically significant we would expect to find an increase in the risk of fractures in both sites. However, ankle fractures are associated with obesity, that is highly prevalent among type 2 diabetes.

In conclusion, the risk of fractures is increased in diabetes at the ankle, but not at the wrist. The finding is probably associated with the higher BMI in this population and not with microarchitectural features.

**Disclosures:** Tatiane Vilaca, None.

## MO0650

**Cross-sectional evaluation of bone metabolism in male patients with type 2 diabetes.** Reiko Watanabe\*, Nobuyuki Tai, Junko Hirano, Yoshiyuki Ban, Daisuke Inoue, Ryo Okazaki. Third Department of Medicine, Teikyo University Chiba Medical Center, Japan

**Background & Aim:** Type 2 diabetes (T2DM) is a risk for osteoporosis independent of bone mineral density (BMD). However, the mechanism of bone fragility is unclear. We thus investigated determinants of bone metabolic changes and skeletal fragility in T2DM.

**Subject & Method:** In this cross-sectional study, we recruited 91 Japanese male patients with T2DM (63.7±11.7 years old, duration: 14.0±10.3 years, BMI: 24.5±3.8 kg/m<sup>2</sup>). BMD, trabecular bone score (TBS), 25-hydroxyvitamin D (25D) and bone turnover markers, and serum sclerostin (Scl), inflammatory cytokines were examined.

**Result:** HbA1c was 7.14±1.58%. Prevalence of insulin use, retinopathy, nephropathy, past or current pioglitazone (PIO) use was 15.4%, 34.1%, 41.0%, 23.1%, respectively. HbA1c showed no correlation with any bone markers. Femoral neck BMD (FN-BMD) T-score was -0.93 ± 0.90 (osteoporosis: 5.6%, osteopenia: 36.0%) and TBS was 1.399±0.081. Mean 25D levels were 20.0±6.9 ng/ml and were not correlated with intact PTH (45.1±17.3 pg/ml). Scl levels were 51.4±22.8 pmol/ml and Tracp5b levels were 220.3±89.5 mU/dl. FN-BMD was positively correlated with BMI, 25D and TBS. In multivariate linear regression analysis, 25D was an independent determinant of FN-BMD besides BMI after adjustment for age. TBS was positively correlated with BMD and negatively with age. Moreover, pioglitazone (PIO) users showed significantly lower levels of TBS compared to non users. In multilogistic regression analysis, PIO use was associated with lower TBS in addition to age and BMD after adjustment for BMI and creatinine. Scl was positively correlated with age, diabetic duration, retinopathy, nephropathy, creatinine, calcium, PTH, bone metabolic markers, and lumbar spine BMD (LS-BMD). In multivariate regression analysis, Tracp-5b was found to be an independent determinant of Scl after adjustment for age, BMI, creatinine, PTH and LS-BMD.

**Conclusion:** Vitamin D deficiency was shown to be an independent risk for BMD loss in T2DM males. The current study also demonstrated, for the first time, impaired trabecular quality in PIO users. Finally, circulating Scl was associated with increased resorption rather than decreased formation at least in Japanese T2DM males in the present study. Ongoing longitudinal studies will further elucidate contribution of various biochemical parameters including Scl to deregulated bone metabolism in T2DM.

**Disclosures:** Reiko Watanabe, None.

## MO0651

**Cinacalcet hydrochloride increases Sharpey fiber in patients with renal hyperparathyroidism.** Aiji Yajima\*, Ken Tsuchiya<sup>2</sup>, David Burr<sup>1</sup>, Kosaku Nitta<sup>3</sup>. <sup>1</sup>Indiana University, School of Medicine, Anatomy and Cell Biology, United States, <sup>2</sup>Tokyo Women's Medical University, Blood Purification, Kidney Center, Japan, <sup>3</sup>Tokyo Women's Medical University, Medicine, Kidney Center, Japan

**Introduction** Skeletal muscle interaction is one of the important factors which determines bone volume. In patients receiving maintenance hemodialysis (HD), both cortical thinning and increased cortical porosity (Co.Po) are causes of severe bone fragility in these patients. We evaluated the impact of cinacalcet hydrochloride (HCl) on Sharpey fiber and cortical porosity (Ct.Po) by obtaining the transiliac bone biopsy specimens in HD patients with renal hyperparathyroidism. We could find that Sharpey

fiber connects periosteal surface of the iliac bone with gluteus medius muscle at the time of the iliac crest bone biopsies.

**Methods:** Ten cotex were obtained before and after the treatment with cinacalcet HCl from seven HD patients with renal hyperparathyroidism (female;2, male;5, Age 60.0 ± 4.9 years). Serum intact parathyroid hormone (i-PTH) levels were measured before and after 1 year of treatment. Both Sharpey fiber area (Sharpey fiber area/periosteal surface; %) and Co.Po (%) were also measured before and after the treatment.

**Results:** Serum i-PTH levels were decreased from 803.4 ± 360.9 to 144.9 ± 68.5 pg/ml (P<0.001) after 1 year of treatment. Sharpey fiber area was increased from 53.0 ± 13.4 to 69.0 ± 18.5 % (P=0.040) and Co.Po was changed from 28.2 ± 19.9 to 19.9 ± 16.2 % (P=0.160), but the change was not significant.

**Discussion and Conclusion:** Skeletal muscle interaction through the osteocyte is important and increases bone volume (Tatsumi S. Cell Metab 2017). And (mini)modeling formation at the endocortical surface and intracortical resorption spaces is important to reduce the rate of cortical bone loss (Yajima A. Am J Kidney Dis 2007). and it is likely that Sharpey fiber supports the skeletal muscle interaction. One year treatment with cinacalcet HCl increased Sharpey fiber, but did not reduce Co.Po in these patients. A long-term treatment is required, because the changes of cortical bone lag behind those of cancellous bone (Nephrol Dial Transplant 2007).

**Disclosures:** Aiji Yajima, None.

## MO0652

**Cardiovascular Safety of zoledronic acid compared with oral bisphosphonates and untreated population controls: an observational cohort study using Danish and Swedish National Health registries.** Bo Abrahamsen<sup>1</sup>, Katrine H Rubin<sup>2</sup>, Sören Möller<sup>2</sup>, Anup Choudhury<sup>3</sup>, Erik F Eriksen<sup>4</sup>, Morten Andersen<sup>5</sup>. <sup>1</sup>University of Southern Denmark and Holbæk Hospital, Denmark, <sup>2</sup>OPEN, University of Southern Denmark, Denmark, <sup>3</sup>Global Drug Development, Novartis, India, <sup>4</sup>Department of Health, University of Oslo, Norway, <sup>5</sup>Karolinska Institute Stockholm and Department of Drug Design and Pharmacology, University of Copenhagen, Sweden

**Background:** The study examined the incidence of specified safety-related outcomes in patients treated with annual zoledronic acid (ZA) and matched control subjects (using oral bisphosphonates - oBP - or untreated) in accordance with the post-marketing commitment to the EMA. This abstract reports the cardiovascular events.

**Methods:** Retrospective five-year propensity score matched cohort study using nation-wide health registries in two Nordic countries. Exposure was determined using national prescription registers (SE and DK) and claims for hospital infusions of zoledronic acid (DK). The outcomes were hospital contacts for atrial fibrillation, arrhythmias, heart failure, myocardial infarction and stroke. Each incident ZA user (numbers below) in the years 2007 to 2012 was propensity-score matched up to 3 oBP treated users and up to 3 untreated control subjects. The analysis comprised 21,520 person years in zoledronic acid users, 63,020 person years in oBP users and 63,880 person years in untreated subjects. The median observation time was 2.4y.

**Results:** Compared with users of oBP, the risk of heart failure was significantly higher in the ZA group (table 1) with no significant difference for other cardiovascular outcomes. Compared with untreated control subjects, the risk of atrial fibrillation, and other arrhythmias, and heart failure was significantly higher in the ZA group. There was no difference in the risk of stroke irrespective of comparator group.

**Discussion:** A higher risk of heart failure was observed in ZA users compared with users of oBPs, and an increased risk of heart failure and arrhythmias including atrial fibrillation observed in ZA users compared with untreated matched control subjects. Because of the observational nature of the study it was not possible to determine with certainty whether the observed higher rates of cardiovascular events represents a drug effect, a difference in base risk or both. It is possible that ZA was targeted to a frailer subset of patients than oBP. Though propensity score matching and confounder adjustment was employed to reduce the influence of confounding, information on confounders such as smoking, alcohol, exercise and BMI is not available in national registers.

Cardiovascular outcome events	ZA vs oBP HR (95% CI) N <sub>ZA</sub> =8,739 N <sub>oBP</sub> =25,577	ZA vs untreated HR (95% CI) N <sub>ZA</sub> =8,731 N <sub>UT</sub> =25,924
Atrial fibrillation	1.02 (0.93;1.12)	1.17 (1.07;1.28)
Arrhythmias	1.05 (0.96; 1.14)	1.18 (1.08; 1.28)
Heart failure	1.21 (1.09;1.34)	1.39 (1.25;1.55)
Myocardial infarction	0.94 (0.78; 1.12)	1.13(0.94; 1.39)
Stroke	0.88 (0.77;1.01)	1.13 (0.98;1.30)

Table 1 Cox proportional hazards analyses with adjustment for major comorbid conditions and medications.

Table 1

**Disclosures:** Bo Abrahamsen, UCB, Grant/Research Support.



## MO0653

**CT-guided cement sacroplasty (CSP) as pain therapy in non-dislocated insufficiency fractures.** Reimer Andresen<sup>\*1</sup>, Sebastian Radmer<sup>2</sup>, Mathias Wollny<sup>3</sup>, Julian Ramin Andresen<sup>4</sup>, Urs Nissen<sup>5</sup>, Hans-Christof Schober<sup>6</sup>.

<sup>1</sup>Institute of Diagnostic and Interventional Radiology/Neuroradiology, Westkuestenlinikum Heide, Academic Teaching Hospital of the Universities of Kiel, Luebeck and Hamburg, Heide, Germany, Germany, <sup>2</sup>Centre for Orthopaedics, Berlin, Germany, Germany, <sup>3</sup>Medimbursement, Tarmstedt, Germany, Germany, <sup>4</sup>Medical School Sigmund Freud University, Vienna, Austria, Austria, <sup>5</sup>Department of Neurosurgery and Spine Surgery, Westkuestenlinikum Heide, Academic Teaching Hospital of the Universities of Kiel, Luebeck and Hamburg, Heide, Germany, Germany, <sup>6</sup>Department of Internal Medicine I, Municipal Hospital Suedstadt Rostock, Academic Teaching Hospital of the University of Rostock, Rostock, Germany, Germany

#### Introduction:

In elderly patients with reduced bone quality, insufficiency fractures of the sacrum are relatively common and are typically associated with severe, disabling pain. The objective of the present study was to examine the feasibility of cement augmentation by CSP, to determine postinterventional leakages and to present the outcome of pain over the course of 18 months.

#### Material and method:

In 23 patients with an average age of 81.3 (71-92) years, a total of 41 sacral fractures were detected by MRI. Conservative treatment initially performed over a period of 3 weeks did not bring any satisfactory reduction of the disabling pain. The intervention was performed under intubation anaesthesia. Under sterile conditions, a Jamshidi needle was then advanced into the respective fracture zone in the sacrum from dorsal to ventral or from lateral to medial transiliac. After removing the inner needle, a flexible osteotome was inserted through the positioned hollow needle and used to extend the spongy space in the fracture zone and thus prepare a cavity for the cement filling. Viscous PMMA cement (StabilIT MX Vertebral Augmentation System – DFINE/Merit Medical) was then inserted discontinuously with the aid of a pressure gauge under low dose CT control. Cement leakages were determined in the CT image on the day after the intervention. Pain was documented on a VAS on the day before the intervention, on the second day, and 6, 12 and 18 months after the intervention. Additionally the patients were asked to rate their satisfaction after 6 and 18 months.

#### Results:

CSP was technically feasible in all patients. In the control CT scan, sufficient cement distribution and interlocking with vital bone was found along the course of the fracture in the sacrum. An average of 6.0 +/- 0.83 ml of cement was inserted per fracture. Leakage was found in 12.2% of the fractures treated, although none were symptomatic. The mean pain score on the VAS was 8.8 +/- 0.59 before the intervention, a significant pain reduction ( $p < 0.001$ ) was seen on the second postoperative day, with an average value of 2.1 +/- 0.36, and this was stable at 2.2 +/- 0.28 after 6, 2.3 +/- 0.31 after 12, and 2.2 +/- 0.41 after 18 months. All of the patients were fully re-mobilised and discharged back home. A high patient satisfaction was found.

#### Conclusion:

As a minimally invasive procedure, CSP is an effective treatment method for rapid, significant and sustained pain reduction.

**Disclosures:** Reimer Andresen, None.

## MO0654

**Bisphosphonate Prescriptions May Reduce Fracture Risk in Older Nursing Home (NH) Residents.** Sarah Berry<sup>\*1</sup>, Andrew Zullo<sup>2</sup>, Tingting Zhang<sup>2</sup>, Yoojin Lee<sup>2</sup>, Geetanjoli Banerjee<sup>2</sup>, Lori Daiello<sup>2</sup>, Kevin McConeghy<sup>2</sup>, David Dosa<sup>2</sup>, Vincent Mor<sup>2</sup>, Douglas Kiel<sup>1</sup>. <sup>1</sup>Hebrew SeniorLife, Institute for Aging Research, United States, <sup>2</sup>Brown University School of Public Health, United States

Bisphosphonates increase BMD in NH residents, but no studies have examined whether these drugs prevent fracture (fx) in this setting. Our objective was to determine whether bisphosphonates reduce the incidence of non-vertebral fx in long-stay NH residents over two yrs.

Medicare Parts A, B, and D claims were linked with patient and facility level information for all long-stay NH residents in the U.S. enrolled in fee-for-service Medicare between 1/2008-12/2009. We restricted our retrospective cohort to residents aged  $\geq 65$  yrs, not enrolled in hospice, and without advanced dementia ( $n=851,300$ ). We identified all new users of an oral bisphosphonate, defined as a resident with a bisphosphonate prescription and no osteoporosis drug prescription in the prior yr. In order to minimize confounding by indication, we compared the incidence of fx in new bisphosphonate users ( $n=22,480$ ) with incidence in new calcitonin users ( $n=11,132$ ). New bisphosphonate and calcitonin users were matched according to the date of drug prescription (index date) and length of stay in the NH. We then 1:1 matched new bisphosphonate and calcitonin users according to propensity scores (PS). Fx events were ascertained using Medicare Parts A and B claims, and included all sites except vertebral, face, skull, hand, foot, and ribs. We used an intention-to-treat approach: residents were followed from the index date until the first event of fx, death, Medicare disenrollment, or study end (12/2011). Competing risk regression was used to model the

association between new bisphosphonate vs calcitonin use and the incidence of non-vertebral fx.

We included 9,896 new users of an oral bisphosphonate and the same number of new calcitonin users in our analysis. Mean age was 85.7 yrs ( $\pm 7.4$ ) and 90.7% were women. After PS matching, both groups were similar with regards to patient and facility level characteristics. During a mean follow-up of 1.5 yrs, 3.3% of new bisphosphonate users and 3.8% of calcitonin users experienced a non-vertebral fx. 44.4% of residents died. In regression models, new users of a bisphosphonate had a decreased risk of non-vertebral fx (HR=0.85, 95% CI 0.73, 0.98)

Using an active comparator approach to minimize confounding by indication, we found that oral bisphosphonate prescriptions may reduce the risk of non-vertebral fx in older NH residents. Future research should determine whether the efficacy and safety of bisphosphonates differs according to absolute fx risk.

**Disclosures:** Sarah Berry, Amgen, Grant/Research Support.

## MO0655

**Bone Mineral Density and Bone Turnover Marker Changes with Sequential Abaloparatide/Alendronate: Results of ACTIVEExtend.** John P Bilezikian<sup>\*1</sup>, Lorraine A Fitzpatrick<sup>2</sup>, Gregory C Williams<sup>2</sup>, Ming-yi Hu<sup>2</sup>, Gary Hattersley<sup>2</sup>, Rene Rizzoli<sup>3</sup>. <sup>1</sup>Columbia University Medical Center, United States, <sup>2</sup>Radius Health, Inc., United States, <sup>3</sup>Geneva University Hospitals and Faculty of Medicine, Switzerland

**Introduction:** In the ACTIVE trial of 2463 postmenopausal women with osteoporosis randomized 1:1:1 to abaloparatide (ABL), blinded placebo (PBO) or open-label teriparatide, ABL significantly reduced vertebral, nonvertebral, clinical, and major osteoporotic fractures vs PBO. Women in the ABL and PBO arms who completed ACTIVE were eligible to receive alendronate (ALN) 70 mg weekly for up to 2 years in ACTIVEExtend. We report final BMD and BTM results following 2 years of ALN treatment in ACTIVEExtend.

**Methods:** 558 women from the ABL arm and 581 from the PBO arm of ACTIVE enrolled in ACTIVEExtend. BMD, PINP and CTX were measured from the beginning of ACTIVE to the end of ACTIVEExtend (18 months of ABL or PBO, 1 month for reconstituted and 24 months of ALN for a total of 43 months).

**Results:** In the group treated with ABL followed by ALN (ABL/ALN), BMD increased at the lumbar spine (LS) by 14.4% from ACTIVE baseline to the end of ACTIVEExtend. Over this same time period, increases in BMD at the total hip (TH) and femoral neck (FN) were 6.4% and 5.3%, respectively. In the group treated with PBO followed by ALN (PBO/ALN), the increases in LS, TH, and FN BMD from ACTIVE baseline to the end of ACTIVEExtend were 6.5%, 2.8%, and 1.6%, respectively. BMD increases at all three sites were significantly greater with ABL/ALN vs PBO/ALN (all  $p < 0.0001$ ). At the distal radius, BMD decreased by 1.5% in the ABL/ALN group vs 0.9% in the PBO/ALN group ( $p=NS$ ). BMD increased at the ultradistal radius by 1.3% in the ABL/ALN group vs 0.5% in the PBO/ALN group ( $p=NS$ ).

Initially, PINP increased with ABL treatment in ACTIVE at 1 month and returned toward baseline at the end of ACTIVE. During the 2-year extension phase, PINP was reduced below the baseline levels observed in ACTIVE in both the ABL/ALN and PBO/ALN groups. Results with CTX were similar; the initial rise at month 3 with ABL treatment returned to baseline by month 18 of ACTIVE, with further reductions in the ABL/ALN and PBO/ALN groups throughout ACTIVEExtend until month 43.

The incidence of AEs was similar for both arms, with a safety profile consistent with ALN treatment and no cases of AFF or ONJ.

**Conclusions:** ABL followed by ALN resulted in sustained increases in lumbar spine, total hip and femoral neck BMD and increased followed by decreased levels of CTX and PINP. The results provide a model by which benefits observed during treatment with ABL can be sustained during subsequent administration with an antiresorptive agent.

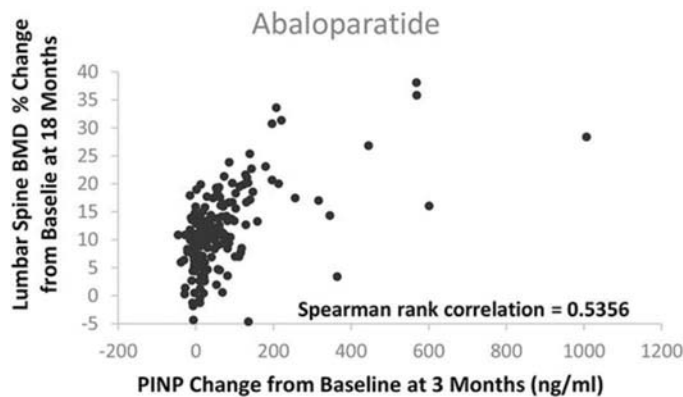
**Disclosures:** John P Bilezikian, Shire, Consultant.

## MO0656

**Early Change in Serum PINP During Treatment with Abaloparatide is Correlated with Lumbar Spine BMD: Results from the ACTIVE Trial.** Dennis M Black<sup>\*1</sup>, Bruce H Mitlak<sup>2</sup>, Yamei Wang<sup>2</sup>, Ming-yi Hu<sup>2</sup>, Lorraine A Fitzpatrick<sup>2</sup>, Richard Eastell<sup>3</sup>. <sup>1</sup>University of California San Francisco, United States, <sup>2</sup>Radius Health, Inc., United States, <sup>3</sup>University of Sheffield, United States

Abaloparatide is a selective activator of the PTH1 receptor signaling pathway that stimulates bone formation. Treatment with abaloparatide results in a rapid and sustained increase in serum PINP. The relationship between serum PINP and subsequent change in lumbar spine BMD in patients receiving abaloparatide 80 micrograms/day was evaluated in the ACTIVE trial which enrolled postmenopausal women with osteoporosis at 28 sites in 10 countries. Blood samples were taken for measurement of BTMs at baseline, 1, 3, 6, 12 and 18 months in 189 abaloparatide-treated patients who were randomly selected from study participants. Patients were excluded if they had received treatment with bisphosphonates, fluoride or strontium for more than 3 months in the past five years. PINP was assayed on a Roche Cobas analyzer. Lumbar spine BMD was measured by DXA at baseline, 6, 12 and 18 months. The correlation of absolute PINP concentration, change in PINP concentration, and percentage change in PINP concentration at 3 months was compared with percentage change in lumbar spine BMD at 18 months using Spearman rank correlation. In these patients, the median pretreatment PINP concentration at baseline was approximately 50 ng/ml. The serum concentration

of PINP increased during abaloparatide treatment with a median increase of 29 ng/ml at 3 months. Mean lumbar spine BMD increased by 11.3% after 18 months. The Spearman rank correlation between absolute change in PINP from baseline to 3 months and percent change in lumbar spine BMD at 18 months is 0.5356 ( $p < 0.0001$ ), and between PINP absolute value at 3 months and percent change in lumbar spine BMD at 18 months was 0.5226 ( $p < 0.0001$ ). The absolute change in PINP after 3 months of abaloparatide treatment correlated most strongly with the percentage increase in lumbar spine BMD at 18 months. The correlation of the absolute value of PINP at 3 months was nearly as strong and could be useful when a baseline value is not available.



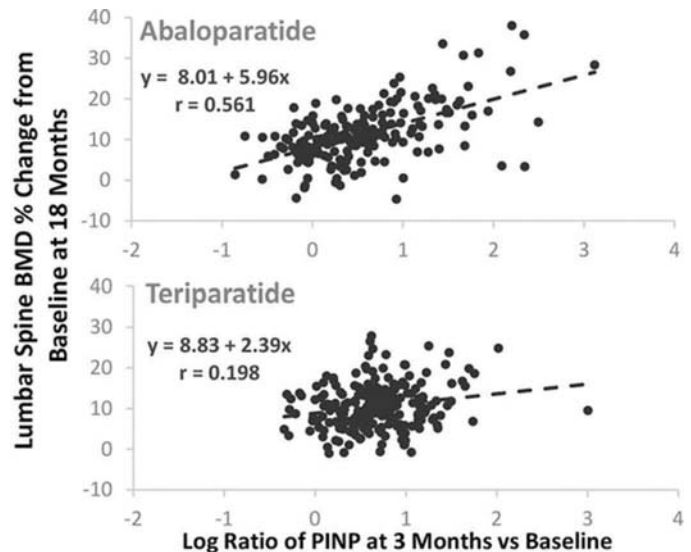
Figure

Disclosures: Dennis M Black, Merck, Other Financial or Material Support.

## MO0657

**Early Change in PINP Correlates with Lumbar Spine BMD More Strongly with Abaloparatide than with Teriparatide: Results of the ACTIVE trial.** Richard Eastell<sup>\*1</sup>, Bruce H Mitlak<sup>2</sup>, Yamei Wang<sup>2</sup>, Ming-yi Hu<sup>2</sup>, Lorraine A Fitzpatrick<sup>2</sup>, Dennis M Black<sup>3</sup>. <sup>1</sup>University of Sheffield, United Kingdom, <sup>2</sup>Radius Health, Inc., United States, <sup>3</sup>University of California San Francisco, United States

Abaloparatide and teriparatide both activate the PTH1 receptor signaling pathway and stimulate bone formation. Treatment with abaloparatide and teriparatide for 18 months increases lumbar spine BMD to a similar extent and yet the increment of PINP with teriparatide is greater than with abaloparatide. The aim of this analysis was to evaluate the relationship between early changes in serum PINP and subsequent changes in lumbar spine BMD in response to these two anabolic treatments. The ACTIVE trial, which enrolled postmenopausal women with osteoporosis at 28 sites in 10 countries, included patients receiving abaloparatide 80 micrograms/day and teriparatide 20 micrograms/day by daily subcutaneous injection. Blood samples were taken for measurement of BTMs at baseline, 1, 3, 6, 12, and 18 months from 189 patients assigned to treatment with abaloparatide and 227 assigned to treatment with teriparatide who were randomly selected from all participants who completed the study. These groups were well matched for race, age, BMI, geographic location and fracture history. Patients were excluded from study enrollment if they had received treatment with bisphosphonates, fluoride or strontium for more than 3 months in the past five years. PINP was assayed on a Roche Cobas analyzer. Lumbar spine BMD was measured by DXA at baseline, 6, 12 and 18 months. Because the distribution of PINP data was skewed, we evaluated the correlation of log ratio of PINP at 3 months with percent change in lumbar spine BMD at 18 months. To compare between treatments, Pearson correlation coefficients were assessed using the Z score test after Fisher's Z transformation and the slopes from linear regression were assessed using a t-test. The correlation coefficient in the abaloparatide group ( $r = 0.561$ ) was greater than that in the teriparatide group ( $r = 0.198$ );  $p < 0.0001$  for the comparison of correlation coefficients. The slope of the correlation was greater for abaloparatide (slope = 5.96) than teriparatide (slope = 2.39);  $p < 0.001$  for the comparison of the slopes. These analyses demonstrate that a steeper slope of the relationship between early change in PINP and lumbar spine BMD exists for abaloparatide and teriparatide such that for a given increase in PINP there is a greater increase in spine BMD.



Figure

Disclosures: Richard Eastell, Teijin Pharma, Consultant.

## MO0658

**QCT Demonstrates Long-Term Proximal Femur Trabecular Density Increases in Osteoporotic Women Following Treatment with a Minimally-Invasive Local Osteo-Enhancement Procedure Involving Injection of a Resorbable, Triphasic Calcium-Based Implant Material.** Klaus Engelke<sup>\*1</sup>, Dominique Favell<sup>2</sup>, Ronald Hill<sup>2</sup>, Thomas Fuerst<sup>3</sup>, Bryan Huber<sup>4</sup>, James Howe<sup>2</sup>, Harry Genant<sup>5</sup>. <sup>1</sup>Bioclinica Germany, Germany, <sup>2</sup>AgNovos Healthcare, United States, <sup>3</sup>Bioclinica, United States, <sup>4</sup>Copley Hospital, United States, <sup>5</sup>Bioclinica; University of California, San Francisco, United States

Fragility hip fractures significantly impact quality of life and are associated with high mortality rates. These fractures often occur due to failure of trabecular bone in the proximal femur. Individuals with osteoporosis have reduced trabecular density in the proximal femur, resulting in reduced structural integrity and bone strength. A new investigational treatment uses a minimally-invasive local osteo-enhancement procedure (LOEP) to inject a unique, resorbable triphasic calcium sulfate/calcium phosphate implant material (AGN1) into the proximal femur to rebuild lost trabecular bone and increase bone strength. In canine studies, AGN1 was resorbed and replaced with integrated bone with normal humeral bone strength. In this IRB-approved clinical study, 12 postmenopausal women (age range 56-89; T-score (mean±sd) left hip  $-3.1 \pm 0.5$ ; right hip  $3.0 \pm 0.7$ ) underwent AGN1 LOEP on left proximal femurs; the right served as an untreated control. Total hip integral BMD (intBMD), trabecular (trBMD) and implant volume were measured by QCT (MIAF, U. of Erlangen) pre-LOEP, 12 and 24 weeks and 5-7 years (average 315 weeks) post LOEP in 10 of 12 patients. The initial implant volume (estimated  $15.3 \pm 4.9$  cm<sup>3</sup>) was 78%, 95% and 100% resorbed at 12, 24 and 315 weeks, respectively. Compromised bone strength before AGN1 LOEP was confirmed in all femurs by their low trBMD (Table) and was lowest in the implant area. IntBMD and trBMD increased significantly in treated femurs at all timepoints (Table). These increases were due to changes in the implant area as trBMD surrounding the implant area was not increased at 315 weeks compared to control (data not shown). Similar to pre-clinical observations, qualitative evaluation showed that bone formed in the implant area was integrated with surrounding bone. In conclusion, AGN1 LOEP significantly increased trBMD in the implant area, resulting in rapid and durable increases in proximal femur BMD. By increasing proximal femur BMD in osteoporotic femurs, it would be expected that bone strength improves, increasing fracture resistance.



Total Hip (TH) BMD: Integral and Trabecular Density<sup>1</sup> (mg/cm<sup>3</sup>)

Week	N	TH intBMD		TH trBMD		BMD Implant Area
		Control	Treated	Control	Treated	
0	10	177±35	176±32	21±20	22±21	7±38
12	10	172±28	290±35*	21±18	217±56*	52±79
24	8 <sup>2</sup>	174±33	257±21*	22±20	161±18*	418±50
315	10	169±28	235±33*	17±15	121±37*	536±78

<sup>1</sup>excludes femoral head <sup>2</sup>two subjects missing axial reconstructions \*p<0.001 by paired t-test vs. control

Table

**Disclosures:** Klaus Engelke, AgNovos Healthcare, Consultant.

## MO0659

**Offset of Effect of Oral Bisphosphonates on Tartrate-Resistant Acid Phosphatase in Postmenopausal Osteoporosis: the TRIO Study.** Fatma Gossiel<sup>1</sup>, Lucy Flinham<sup>1</sup>, Kim Naylor<sup>1</sup>, Jennifer Walsh<sup>1</sup>, Nicola Peel<sup>2</sup>, Eugene McCloskey<sup>1</sup>, Richard Eastell<sup>1</sup>. <sup>1</sup>University of Sheffield, United Kingdom, <sup>2</sup>Sheffield Teaching Hospital, United Kingdom

Serum 5b isoenzyme of tartrate-resistant acid phosphatase (TRACP5b) is a bone turnover marker that reflects the number and activity of osteoclasts. We have shown that oral bisphosphonates suppress bone turnover markers and osteoclast precursor cells, in postmenopausal women with osteoporosis. Last year we reported that there is partial return to baseline of bone turnover markers two years after stopping oral bisphosphonate therapy. Our current aim was to determine whether there was also a return of osteoclast number (as assessed by TRACP5b) to baseline.

Postmenopausal osteoporotic women were randomized to receive ibandronate (Bonviva, Roche, 150mg monthly), alendronate (Fosamax, Merck, 70mg weekly), or risendronate (Actonel, Warner Chilcott, 35mg weekly) for 2 years in the TRIO study. At the end of the study women with >80% compliance with their treatment, in whom it was clinically appropriate to discontinue BP, were invited to participate in a further 2 year offset of effect study (n=31 women age 56 to 81y). Participants received daily calcium (1200 mg/day) and vitamin D (800IU/day) throughout. Fasting blood samples were collected at 24, 48, 72 and 96 weeks after the end of treatment and were compared to the pre-bisphosphonate treatment baseline when women were already taking calcium and vitamin D. TRACP 5b was measured by automated assay (IDS-iSYS, Immunodiagnostic Systems, UK).

The decrease from baseline in levels of TRACP5b during treatment was 40% (95% CI 46 to 36) and was similar between the 3 bisphosphonates. Levels increased during the offset period back towards baseline levels, see table.

All three drugs showed evidence of offset of effect as assessed by levels of TRACP 5b. The offset after alendronate and risendronate appears to be earlier than for ibandronate. This may indicate that with ibandronate there may be fewer osteoclasts two years after stopping therapy.

	Week 48 offset	Week 96 offset
Ibandronate	-24 (-37 to -10)	-23 (-34 to -13)
Alendronate	-15 (-30 to -0.5)	5 (-13 to 22)
Risendronate	-13 (-30 to 3.0)	-16 (-27 to -5)

Mean %change (95% CI) from baseline in TRACP5b during the 2 year offset period

**Disclosures:** Fatma Gossiel, None.

## MO0660

**Bone density, microarchitecture and tissue quality after 1 year of treatment with Tenofovir Disoproxil Fumarate.** Robert Güerri-Fernández<sup>1</sup>, Xavier Nogués<sup>2</sup>, Alicia Gonzalez-Mena<sup>3</sup>, Ana Guelar<sup>2</sup>, Leonardo Mellibovsky<sup>4</sup>, Natalia Garcia-Giral<sup>2</sup>, Hernando Knobel<sup>2</sup>, Adolfo Díez-Pérez<sup>3</sup>. <sup>1</sup>Infectious Diseases. Hospital del Mar., Spain, <sup>2</sup>Infectious Diseases, Spain, <sup>3</sup>Infectious Diseases. Hospital del Mar Research Institute, Spain, <sup>4</sup>Infectious Diseases. Hospital del Mar Research Institute., Spain, <sup>5</sup>IMIM., Spain

Bone mineral density (BMD) measured by dual-energy x-ray absorptiometry (DXA) is used to assess bone health in HIV patients. Besides DXA, other techniques, Trabecular Bone Score (TBS) and in vivo microindentation measure trabecular microarchitecture and mechanical properties of bone at a tissue level, respectively.

**Objectives**

We tested the bone status after 1 year of treatment with Tenofovir Disoproxil Fumarate (TDF) using BMD, TBS and microindentation.

### METHODS:

Longitudinal study from January 2014 to June 2015; we included 40 HIV naïve patients that were to start antiretroviral treatment (ART). BMD by DXA (DXA-Hologic QDR4500SL) was measured at lumbar spine and the hip. TBS was obtained from DXA-scan (Medimetrics inc.) Microindentation test were performed using a handheld Osteoprobe (Active-Life-Scientific, Santa Barbara, CA, US) at the anterior tibial face with a reference-point indenter device.

The BMD, BMSi and measurements at baseline and after treatment were compared using paired samples Student's t-test. Multivariable (age, gender and body mass index-adjusted) linear regression models were fitted to study the association between TDF treatment and changes in BMD/TBS/BMSi.

### Results

Forty HIV patients were included (33 men (82%) and 7 women (18%). Median age at baseline was 38 years (IQR 31.7-44.2). Median time since diagnosis of HIV infection was 1 year (IQR 0-4). All included patients received Elvitegravir/cobicistat QD as main treatment with TDF + Emtricitavine as backbone.

Changes in DMO (g/cm<sup>2</sup>) were: lumbar spine (0.987±0.022 vs 0.953±0.022; p=0.001; -3.4%), total hip (0.936±0.026 vs 0.930±0.025; p=0.56; -0.3%) and femoral neck (0.823±0.021 vs 0.796 ± 0.023; p=0.001; -2.7%) at baseline and after 1 year of TDF treatment respectively.

When analysing bone microarchitecture with TBS at spine level a significant reduction of TBS was observed (1.359±0.016 vs 1.322±0.01; p=0.0059; -2.5%).

On the other side, when studying the other component of bone strength, bone tissue quality with microindentation, the BMSi was significantly higher (85.5±1.1 vs 88.5±1.2; p=0.03; +3.8%), showing better bone material properties after 1 year of treatment with TDF.

### CONCLUSION:

Significant decrease in spine and hip BMD and in trabecular microarchitecture at spine was observed after 1 year of TDF therapy with DXA and TBS respectively. However, tissue quality significantly improved after 1 year of treatment, suggesting a recovery of bone material properties following the control of the infection despite the significant reduction of BMD. These three techniques provide additional and necessary information to DXA about bone health in treated HIV patients, and due to its convenience and feasibility they could be routinely apply to assess bone in clinical practice.

This work was supported by a grant of Fondos FEDER and Fondo de Investigaciones Sanitarias (PI13/00589) of the ISCIII Spanish Ministry of Health.

**Disclosures:** Robert Güerri-Fernández, None.

## MO0661

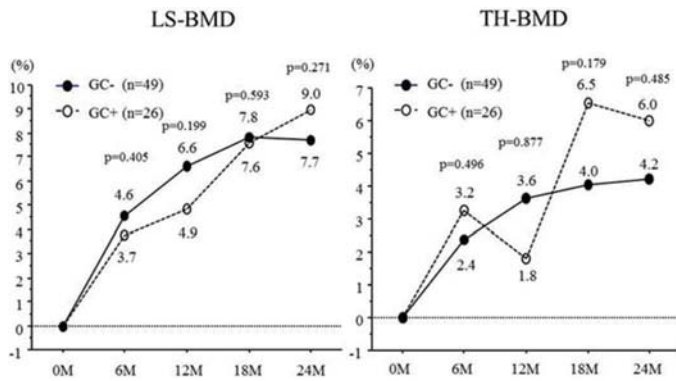
**Influence of glucocorticoids on effect of denosumab on osteoporosis in patients with Japanese rheumatoid arthritis; 24 months of follow-up ~a Multicenter Registry Study~.** Yasuhide Kanayama<sup>1</sup>, Yuji Hirano<sup>2</sup>, Nobunori Takahashi<sup>3</sup>, Shuji Asai<sup>3</sup>, Naoki Ishiguro<sup>3</sup>, Toshihisa Kojima<sup>3</sup>. <sup>1</sup>Toyota Kosei Hospital, Japan, <sup>2</sup>Toyohashi Municipal Hospital, Japan, <sup>3</sup>Nagoya University Graduate school of Medicine, Japan

**[Objectives]** To investigate the efficacy of DMB for 24 months on glucocorticoid-induced OP in Japanese RA patients.

**[Methods]** Patients with a diagnosis of RA according to the 2010 ACR/EULAR criteria who had been prescribed DMB from Tsurumi Biologics Communication Registry (TBCR)-BONE between October 2013 and February 2015 were enrolled. The final study cohort of 75 patients received continuous DMB therapy more than 24 months. The DMB dose was 60mg at once every 6 months. In all cases native or activated vitamin D has been used. We reviewed the results for 24 months about the increase and decrease of bone mineral density (BMD) of lumbar spine (LS) and total hip (TH) by DEXA and bone turnover markers, intact n-terminal propeptide type I procollagen (PINP) and tartrate-resistant acid phosphatase form 5b (TRACP-5b).

**[Results]** In the patients receiving oral prednisolone group (n=26, GC+) and not receiving group (n=49, GC-), the number of female was each 24(92%) and 47(96%) cases (p=0.508). The mean age was 69.1 ± 8.1 and 71.0 ± 7.4 years old (p=0.469); disease duration was 16.3 ± 10.0 and 16.9 ± 13.4 years (p=0.859); the body mass index was 20.8 ± 3.4 and 19.8 ± 2.9 (p=0.249) and the FRAX was 35.6 ± 18.6 and 23.8 ± 13.6 (p=0.008). Clinical findings related to RA and OP at baseline were as follows; CRP 1.3 ± 1.5 and 0.5 ± 1.0 mg/dl (p=0.007); DAS-CRP 3.14 ± 1.18 and 2.50 ± 1.18 (p=0.016); HAQ-DI 1.21 ± 0.89 and 0.82 ± 0.81 (p=0.058); PINP 59.4 ± 37.3 and 54.4 ± 32.2 µg/l (p=0.497); TRACP-5b 500 ± 256 and 487 ± 196 mU/dL (p=0.772); LS-BMD 0.87 ± 0.17 and 0.81 ± 0.16 g/cm<sup>2</sup> (p=0.080) and TH-BMD 0.60 ± 0.11 and 0.60 ± 0.08 g/cm<sup>2</sup> (p=0.716). The rate of decreased PINP from baseline to 6, 12 and 24 months were each -25.6% vs -39.6% (p=0.245) at 6 month, -5.8% vs -40.5% (p=0.085) at 12 month and -17.0% vs -32.3% (p=0.281) at 24 month and TRAC-5b were -29.1% vs -33.9% (p=0.874) at 6 month, -17.9% vs -30.8% (p=0.303) at 12 month and -18.8% vs -24.3% (p=0.800) at 24 month in the GC+ group vs GC- group. The rate of increased LS-BMD from baseline to 6, 12 and 24 months were each 3.7% vs 4.6% (p=0.405) at 6 month, 4.9% vs 6.6% (p=0.199) at 12 month and 9.0% vs 7.7% (p=0.271) at 24 month and TH-BMD were 3.2% vs 2.4% (p=0.496) at 6 month, 1.8% vs 3.6% (p=0.877) at 12 month and 6.0% vs 4.2% (p=0.485) at 24 month in the GC+ group vs GC- group (Fig.1).

**[Conclusion]** DMB was effective in OP of RA patients. Glucocorticoids use did not influence the efficacy of DMB for 24 months.



Figure

Disclosures: Yasuhide Kanayama, None.

## MO0662

**The Change of Injected Cement after Percutaneous Vertebroplasty(PVP) and Percutaneous Balloon Kyphoplasty(KP) on Osteoporotic Vertebral Fractures.** Jin Hwan Kim<sup>1</sup>, Tae Yong Lee<sup>2</sup>, Ji Woong Yeom<sup>1</sup>. <sup>1</sup>Department of Orthopedic Surgery, Inje University, Ilsan Paik Hospital, Korea, Republic of, <sup>2</sup>Ewha woman's university, Division of Mechanical and Biomedical engineering, Korea, Republic of

### Purpose

There are few study data on the change of injected cements after percutaneous vertebroplasty (PVP) and balloon kyphoplasty (KP) on osteoporotic vertebral fractures. This study is to compare the radiologic results of the change of vertebral bodies and injected cements between PVP and KP.

### Material and method

We targeted 103 patients (171 vertebrae) who were available for more than 5-year follow-up time point, from a total group of 436 patients who were treated with PVP and KP for osteoporotic vertebral fracture between January 2000 and December 2009; 69 patients (121 vertebrae) were treated by PVP, 34 patients (50 vertebrae) by KP. We analyzed the radiologic outcomes focused on the changes of injected cements and vertebral bodies as well as anterior vertebral height and kyphotic angle on pre- and post-operation.

### Result

The mean follow-up period was 7.2 years.

After PVP, 63 patients (91.3%) among 69 patients were stable. But we found 2 cases of radiolucent line with decreased bone density in the adjacent area of cement and 4 cases of cement cracks accompanied with vertebral collapse. Anterior vertebral height was improved 0.3mm, (from 17.4mm to 17.7mm), kyphotic angle was reduced 0.6° (from 12.3° to 11.7°). New fractures were documented in 22 patients (33 vertebrae, (31.8%); adjacent fractures were observed in 11 vertebrae (33%), nonadjacent fractures in 22 vertebrae(67%).

After KP, 21 patients (61.8%) in 34 patients were stable. But we found 7 cases of radiolucent line with decreased bone density in the adjacent area of cement and 6 cases of cement cracks accompanied with vertebral collapse. Anterior vertebral height was improved 1.0mm(from 18.4mm to 19.4mm), while kyphotic angle was reduced 2.0°(16.1° ? 14.1°). New fractures were documented in 14 patients(21 vertebrae, 42%); adjacent fractures were observed in 11 vertebrae(52.4%), nonadjacent fractures in 10 vertebrae(47.6%).

### Conclusion

As the radiologic results, the vertebral bodies and injected cement were maintained more stable after PVP compared to KP.

Disclosures: Jin Hwan Kim, None.

## MO0663

**Effective treatment of severe pregnancy and lactation- associated osteoporosis with denosumab:case report.** Shigeki Nishida\*. M.D. Ph.D., Japan

Pregnancy and lactation-associated osteoporosis (PLO) is a rare condition with little known pathophysiology. we report a case of PLO successfully treated with denosumab. 35-year -old woman suffered acute low back pain after her first pregnancy. started after three month postpartum an acute increase in the low back pain led to a MRI which showed recent deformity in Th8,9,11, L3,4. She had five vertebral fracture. She had low bone mineral density (BMD, DXA) 0.645g/cm<sup>2</sup> (-3.1SD) YAM64 %. Laboratory evaluation did not reveal metabolic derangements. She was diagnosed to have PLO and started with active Vitamin D3 analog(Eldecalcitol). after 6 month still she had low back pain and lumbar bone mineral density (BMD) was unchanged. The lactation was stopped. And treatment was switched to subcutaneous denosumab, 60 mg every

6 months, and daily active Vitamin D3 analog(Eldecalcitol) was begun. There was slowly improvement in pain. after 3 months serum alkaline phosphatase and osteocalcin had not increased. After one year, lumbar BMD had increased and the pain had almost completely subsided. Denosumab treatment improve severe back pain and quality of life and prevent further occurrence of vertebral fractures.

Disclosures: Shigeki Nishida, None.

## MO0664

**Effects of Romosozumab in Postmenopausal Women With Osteoporosis After 2 and 12 Months Assessed by MicroCT on Iliac Crest Bone Biopsies.** Jean-Paul Roux<sup>\*1</sup>, Pascale Chavassieux<sup>1</sup>, Roland Chapurlat<sup>1</sup>, Nathalie Portero-Muzy<sup>1</sup>, Pedro Garcia<sup>2</sup>, Jacques P Brown<sup>3</sup>, Cesar Libanati<sup>4</sup>, Rogely Boyce<sup>5</sup>, Andrea Wang<sup>5</sup>, Andreas Grauer<sup>5</sup>. <sup>1</sup>INSERM UMR 1033, Université de Lyon, France, <sup>2</sup>Hospital Universitario de Monterrey, Mexico, <sup>3</sup>CHU de Quebec Research Centre and Laval University, Canada, <sup>4</sup>UCB BioPharma, Belgium, <sup>5</sup>Amgen Inc., United States

**Purpose:** Romosozumab, a humanized sclerostin antibody, induces an increase in bone formation, a reduction in bone resorption, improves BMD, and reduces fracture risk. The aim of this analysis from the multicenter, international, randomized, double-blind, placebo-controlled FRAME study was to evaluate the effects of romosozumab on bone mass and microarchitecture assessed by microCT (Skyscan 1174 with a nominal isotropic voxel size of 19 µm) on iliac crest bone biopsies from postmenopausal women with osteoporosis.

**Methods:** Patients received romosozumab 210 mg or placebo monthly for 12 months and underwent transiliac biopsies at months 2 and 12. For microCT assessment, 28 (14 placebo, 14 romosozumab) patients were evaluable at month 2 and 71 (32 placebo, 39 romosozumab) were evaluable at month 12. Between-group comparisons at month 2 and month 12 were based on Wilcoxon rank sum test.

**Results:** Already at month 2 of romosozumab treatment, trabecular separation (Tb.Sp) was significantly lower than placebo, and at month 12, parameters reflecting mineral density (Tb.BMD and Tb.TMD) and bone volume (Tb.BV/TV) were significantly increased (Table). These changes were associated with improvement of the microarchitecture (Figure) as shown by significant increase in trabecular thickness (Tb.Th) and decrease in trabecular bone pattern factor (Tb.Pf) in the romosozumab group compared with the placebo group. An effect of romosozumab on cortical BMD and cortical porosity was not observed at month 2 or 12.

**Conclusion:** Twelve months of romosozumab treatment improved bone volume and microarchitecture with a beneficial effect on trabecular spacing observed as early as month 2, consistent with the rapid fracture risk reductions observed clinically.

	Month 2 median (Q1, Q3)			p-value*	Month 12 median (Q1, Q3)			p-value*
	Placebo n = 14	Romosozumab n = 14			Placebo n = 32	Romosozumab n = 39		
<b>Cancellous bone</b>								
Tb BMD (mg/cm <sup>3</sup> )	185 (150, 210)	225 (140, 250)	0.36		170 (140, 235)	230 (170, 300)	0.03	
Tb TMD (mg/cm <sup>3</sup> )	701 (689, 723)	716 (667, 749)	0.75		704 (678, 722)	727 (699, 744)	0.01	
Tb BV/TV (%)	17.10 (15.17, 18.66)	20.42 (12.91, 23.54)	0.42		15.97 (13.92, 21.13)	22.04 (17.92, 28.61)	0.006	
Tb N (/mm)	0.79 (0.70, 0.99)	0.87 (0.74, 0.98)	0.70		0.85 (0.69, 0.95)	0.89 (0.77, 0.98)	0.21	
Tb Th (mm)	0.191 (0.164, 0.233)	0.222 (0.198, 0.231)	0.35		0.204 (0.180, 0.232)	0.241 (0.215, 0.293)	0.001	
Tb Sp (mm)	0.858 (0.807, 0.894)	0.762 (0.710, 0.809)	0.046		0.788 (0.717, 0.838)	0.793 (0.732, 0.860)	0.86	
SMI (#)	1.32 (1.15, 1.53)	1.42 (1.16, 1.65)	0.42		1.49 (1.33, 1.80)	1.36 (1.20, 1.69)	0.22	
TbPF (/mm)	3.51 (2.93, 4.58)	3.68 (2.74, 5.07)	0.84		3.99 (3.25, 5.61)	3.24 (2.11, 4.34)	0.03	
<b>Cortical bone</b>								
Ct BMD (mg/cm <sup>3</sup> )	774 (733, 803)	780 (736, 795)	0.98		789 (754, 812)	770 (748, 794)	0.15	
Ct Th (mm)	0.854 (0.585, 1.016)	0.719 (0.565, 0.810)	0.42		0.661 (0.535, 0.837)	0.786 (0.621, 0.977)	0.06	
Ct Po (%)	5.07 (3.31, 7.12)	3.74 (3.40, 6.82)	0.73		3.87 (2.28, 5.74)	3.39 (2.34, 4.93)	0.47	

n = number of biopsies analyzed; \*based on the Wilcoxon rank sum test without multiplicity adjustment; Tb: trabecular; BMD: bone mineral density; TMD: tissue bone mineral density; BV: bone volume; TV: tissue volume; N: number; Th: thickness; Sp: separation; SMI: structure model index; Tb.Pf: trabecular bone pattern factor; Ct: intracortical; Po: porosity



Figure: Bone samples representative of the median observed results at Month 12

Table: MicroCT Parameters – Months 2 and 12

Disclosures: Jean-Paul Roux, None.



## MO0665

**Effects of vitamin D compounds on intestinal calcium absorption and calcium regulating hormones.** Makio Tokiwa<sup>\*1</sup>, Masataka Shiraki<sup>2</sup>. <sup>1</sup>IDD Inc. Clinical Development Dept, Japan, <sup>2</sup>Department of Internal Medicine, Research Institute and Practice for Involuntal Diseases, Japan

Sufficient calcium intake and appropriate serum vitamin D concentration are essential factors for treatment of osteoporosis. However, native D supplementation to osteoporosis has not been approved in Japan. Instead of native vitamin D, pro-active or active forms of vitamin D such as alfacalcidol (ALF) and eldecalcitol (ELD), both calcitriol analogues, are approved and be widely used for the treatment of osteoporosis. Therefore, the present study aimed to determine the effect of vitamin D compounds on intestinal calcium absorption in postmenopausal osteoporosis using a double isotope method.

This randomized open-label study aimed to investigate the effect of vitamin D compounds on intestinal fractional calcium absorption (FCA) in Japanese postmenopausal osteoporosis. A total of 40 eligible patients (mean, 74.6 years) were allocated randomly into four groups: ELD (0.75 µg/day), ALF (1 µg/day), native vitamin D (800 IU/day) and controls. Before and after the 4-week treatment, the intestinal calcium absorption was estimated by the double isotope method. The net calcium balance before and after treatment was calculated using the values of calcium intake, intestinal FCA and urinary calcium excretion.

FCA in four groups were approximately 20% at baseline. After the treatment for one month, the FCA expressed significantly increased 22.6% to 33.7% in the ELD group ( $p < 0.0001$  vs baseline) and 22.7% to 30.2% in the ALF group ( $p = 0.0029$  vs baseline). Although, in the native D groups, the changes in serum concentrations of 25(OH)D (24 ng/mL to 37 ng/mL) and 1,25(OH)<sub>2</sub>D (46.6 pg/mL to 63.6 pg/mL) from the baseline were increased significantly, the FCA did not show significant change (21.5% to 24.7%). There was no case with hypercalcemia after the intervention. The mean calcium balance in the ELD group increased 13.4 mg/day ( $p = 0.034$  vs ALF group). Those for the other groups did not show the positive balance.

These results indicated that ELD and ALF stimulated intestinal calcium absorption but native vitamin D did not, despite of increasing 1,25(OH)<sub>2</sub>D concentration. Active vitamin D administration is more efficient than native vitamin D supplementation in order to increase calcium absorption in postmenopausal osteoporotic patients.

**Disclosures:** Makio Tokiwa, None.

## MO0666

**Clinical efficacy and safety of bazedoxifene (Viviant®) in postmenopausal women with osteoporosis and osteopenia.** Hee-Dong Chae<sup>\*</sup>, Ji-Won Song, Sung-Hoon Kim, Chung-Hoon Kim, Byung-Moon Kang. Asan medical center, Korea, Republic of

**Objective :** Bazedoxifene is a selective estrogen receptor modulator that decreases fracture risk and bone turnover in postmenopausal women. The objective of this study was to evaluate the efficacy and safety of bazedoxifene in women with postmenopausal osteoporosis or osteopenia.

**Materials and Methods :** A prospective pilot study was performed in Asan Medical Center from 2014 to 2016 and the eligible patients were followed up for up to 15 months. Patients were screened and women with osteoporosis or osteopenia were included. Subjects received bazedoxifene 20 mg per day, followed by visits at months 1, 3, 9, and 15. Bone mineral density (BMD) of lumbar spine and hip was measured using DXA (Dual X-ray absorptiometry) at months -24 and -12, at the start of the study, and at month 12. Safety and tolerability evaluations included adverse event reports, physical examinations and clinical laboratory tests, including chemical and lipid assessments. Other safety monitoring included breast examination, mammography, and gynecologic ultrasound.

**Results :** Sixty-seven patients were enrolled, and 65 patients completed the study in 15 months. Five patients (8%) showed significant improvement in lumbar spine BMD at month 12 ( $p < 0.03$ ), however total hip BMD showed no statistically significant improvement. Fourty of the 65 patients (61%) maintained the lumbar spine BMD, and 50 patients (78%) had no significant change in femur BMD. Fifteen patients (23%) showing a decrease in lumbar spine BMD and 5 patients (8%) showing a decrease in femur BMD prior to administration of bazedoxifene obtained sustained BMD after medication. Ten of the 65 patients (15%) complained of dyspepsia, the other 10 patients (15%) showed an increase in liver enzymes, and 5 patients (8%) had shoulder pain, but these events did not lead to discontinuation of medication. There were no serious adverse events including venous thromboembolism, coronary heart disease, cerebrovascular accidents, breast cancer, or endometrial carcinoma.

**Conclusions:** Treatment with bazedoxifene prevented bone loss and reduced bone turnover and was generally safe and well tolerated in postmenopausal women with osteoporosis or osteopenia.

**Disclosures:** Hee-Dong Chae, None.

## MO0667

**Incidence Rates of Acute Events Leading to Hospitalization or Emergency Room Visit Among Postmenopausal Women Receiving Treatment for Osteoporosis.** Leslie Spangler<sup>\*1</sup>, Florence T Wang<sup>2</sup>, Vera Ehrenstein<sup>3</sup>, Henrik T Sørensen<sup>3</sup>, Susan Yue<sup>4</sup>, Xiang Yin<sup>5</sup>, J Michael Sprafka<sup>6</sup>, Shawna Smith<sup>7</sup>, Jeffrey R Curtis<sup>8</sup>. <sup>1</sup>Center for Observational Research, Amgen Inc, United States, <sup>2</sup>Optum Epidemiology, United States, <sup>3</sup>Department of Clinical Epidemiology, Aarhus University, Denmark, <sup>4</sup>Global Development, Amgen Inc., United States, <sup>5</sup>Global Biostatistics, Amgen Inc., United States, <sup>6</sup>Center for Observational Research, Amgen Inc., United States, <sup>7</sup>Global Safety, Amgen Inc., United States, <sup>8</sup>Division of Clinical Immunology and Rheumatology, University of Alabama at Birmingham, United States

Pharmacovigilance is important to ensure safe and effective use of medicines. Using a large US data system, we present results from an interim analysis of a post-marketing study of denosumab (DMAb) for osteoporosis<sup>1</sup> reporting incidence rates (IRs) of events with expected early onsets including hypocalcemia, dermatologic events, hypersensitivity, serious infection, and acute pancreatitis.

Women with postmenopausal osteoporosis (PMO) were identified in the administrative data from US Medicare (2010-2013), using an algorithm based on age, osteoporosis diagnosis or treatment, or fracture. Exposure cohorts (DMAb only, oral bisphosphonate (BP) only (alendronate, ibandronate, risendronate), or IV BP only (zoledronic acid, ibandronate)) were created based on use of osteoporosis treatment(s) during follow-up. Age-standardized (to the 2010 US census age distribution) IRs (per 100,000 person-years) for outcomes (based on ICD 9 code algorithms) leading to hospitalization or emergency room visit by therapy received are reported.

This analysis included 3,973,567 women with PMO; 58% were  $\geq 75$  years old, with mean follow-up of 2.5 years. Hypocalcemia was noted in 217 women in the DMAb or BP only cohorts; 23% of these women had baseline chronic kidney disease (55% and 11% of the women with hypocalcemia in the DMAb and BP cohorts respectively). The IR of hypocalcemia was highest in the DMAb-treated population (IR 74 (95% CI 55-98)) whereas hypersensitivity (IR 307 (95% CI 286-329)) and serious infection (IR 10,825 (95% CI 10,695-10,956)) were highest among the IV BP cohort. Of the remaining rates for the other adverse events (dermatologic events, acute pancreatitis), the CIs for the IRs across the three cohorts overlapped (Table 1).

With the exception of hypocalcemia, IRs in the DMAb treated population were comparable to those in the BP treated population. The IR of hypocalcemia was higher in the DMAb cohort, consistent with the labeled risk.<sup>2</sup> Estimated IRs in this descriptive analysis did not account for differential distribution of risk factors that may contribute to variations in IR across exposure cohorts.

1. Xue, F., et al. (2013). "Design and methods of a postmarketing pharmacoepidemiology study assessing long-term safety of Prolia (denosumab) for the treatment of postmenopausal osteoporosis." *Pharmacoepidemiol Drug Saf.* Oct;22(10):1107-14.

2. Prolia US Product Information (PI) Version 16.0, Date Modified : Jan 31, 2017 www.prolia.com

**Table 1. Number of Patients and Age-Standardized Incidence Rate\* for ICD 9 Code Algorithms Identified Acute Events Leading to Hospitalization or Emergency Room Visit Among Postmenopausal Women Receiving Treatment for Osteoporosis**

Exposure Cohorts	Hypocalcemia N IR (95% CI)	Dermatologic Events N IR (95% CI)	Hypersensitivity N IR (95% CI)	Infection N IR (95% CI)	Acute Pancreatitis N IR (95% CI)
Oral BP only <sup>1</sup>	134 6 (5-7)	4,933 233 (226-240)	4,628 220 (213-227)	192,041 9,286 (9,243-9,329)	2,663 116 (111-121)
IV BP only <sup>1</sup>	23 9 (6-14)	774 255 (236-274)	917 307 (286-329)	29,342 10,825 (10,695-10,956)	402 128 (115-142)
DMAb only <sup>2</sup>	60 74 (55-98)	196 231 (197-269)	195 234 (199-273)	7,663 10,017 (9,777-10,261)	128 135 (111-162)

N = Number of patients with acute events; IR = Incidence Rate; IV = Intravenous; BP = Bisphosphonate

<sup>1</sup> Exposed to any oral BP without concomitant treatment with Denosumab (DMAb) or IV BP

<sup>2</sup> Exposed to any IV BP without concomitant treatment with DMAb or oral BP

<sup>\*</sup> Exposed to DMAb without concomitant BP treatment (oral or IV)

<sup>\*</sup> Rate per 100,000 Person-years (95% CI), age standardized to the 2010 US census

Table: Age-Standardized Incidence Rate **Disclosures:** Leslie Spangler, Major Stock

Shareholder: Employment & Major Stockholder: Amgen, Inc

## MO0668

**The Safety and Efficacy of Monthly Intravenous Ibandronate Injections in a Prospective, Post-Marketing Observational Study in Japanese Patients with Osteoporosis.** Yasuhiro Takeuchi<sup>\*1</sup>, Junko Hashimoto<sup>2</sup>, Chiemi Yamagiwa<sup>3</sup>, Takashi Tamura<sup>3</sup>, Ryouyusuke Harada<sup>3</sup>, Yosuke Nishida<sup>3</sup>, Akihide Atsumi<sup>3</sup>. <sup>1</sup>Endocrine Center, Toranomon Hospital, Japan, <sup>2</sup>Project & Lifecycle Management Unit, Chugai Pharmaceutical Co. Ltd, Japan, <sup>3</sup>Drug Safety Division, Chugai Pharmaceutical Co. Ltd, Japan

**Purpose:** The safety and efficacy of monthly intravenous (IV) ibandronate (IBN) injections were evaluated in Japanese patients with osteoporosis in a Japanese real world setting.

**Methods:** In this large-scale, post-marketing observational study (BON1301), osteoporotic patients received monthly IV IBN 1mg for 1 year. The following outcomes were evaluated: adverse drug reactions (ADRs) and adverse events of interest during treatment with intermittent bisphosphonates, the incidence of new vertebral and non-vertebral fractures, increases in bone mineral density (BMD), and suppression of bone turnover markers. The values at 1 year were compared with those at baseline using matched t-test analysis.

**Results:** In total, 1,062 patients were enrolled and 1,025 patients (887 women, 138 men) were assessed. The mean patient age was 77 years. Overall, 50% of patients were pretreated with other osteoporosis agents prior to IBN and 55% of patients received osteoporosis agents concurrently. The 1-year adherence rate was 82%. A total of 75 ADRs were reported in 54 patients (5.26%) (5.74% women, 2.17% men). The most common, all non-serious, adverse events were malaise (0.48%), injection site pain, dizziness, headache, feeling abnormal, and hepatic function abnormalities (0.29% each). There were four (0.39%) serious ADRs, including one case of osteonecrosis of the jaw. This case occurred in a man who had been receiving long-term treatment with another bisphosphonate prior to IBN and had poor oral hygiene. Acute phase reactions were reported in 21 patients (2.04%), half of which had occurred after the first injection. The cumulative incidence of non-traumatic new vertebral and non-vertebral fractures was 3.16% (95% CI 2.12, 4.70) at 1 year. Significant increases in BMD relative to baseline were observed at the lumbar spine (4.84%, 187 patients, 95% CI 3.47, 6.21), femoral neck (2.73%, 166 patients, 95% CI 1.46, 4.01), and total hip (1.93%, 133 patients, 95% CI 0.80, 3.07). Significant reductions were observed in all bone turnover markers.

**Conclusions:** No new safety concerns were identified with monthly IV IBN in this observational study. These findings confirm the favorable safety profile and consistent efficacy of IBN, and indicate that monthly IBN injections would be clinically beneficial in daily practice for the treatment of Japanese patients with osteoporosis.

**Disclosures:** Yasuhiro Takeuchi, Chugai, Speakers' Bureau.

## MO0669

**Antiresorptive activity of a cathepsin K inhibitor ONO-5334 and its relationship to BMD increase in a phase II trial for postmenopausal osteoporosis.** Makoto Tanaka<sup>\*1</sup>, Yoshitaka Hashimoto<sup>1</sup>, Chihiro Hasegawa<sup>1</sup>, Steve Deacon<sup>2</sup>, Richard Eastell<sup>3</sup>. <sup>1</sup>Ono Pharmaceutical Co., Ltd., Japan, <sup>2</sup>Ono Pharma UK Ltd., United Kingdom, <sup>3</sup>University of Sheffield, United Kingdom

**Background:** ONO-5334, a cathepsin K inhibitor, induced bone mineral density (BMD) gain in a phase II study with postmenopausal osteoporosis patients. Even though the antiresorptive effect could only be monitored in the morning during the study, simulation can allow the antiresorptive effect to be assessed throughout 24 h and may assessment of its relationship to BMD gain.

**Methods:** Inhibition of serum C-telopeptide of type I collagen (sCTX) level for 100 mg once daily (QD), 300 mg QD and 50 mg twice daily (BID) was simulated by plasma ONO-5334 pharmacodynamic (PK) data of repeated dose in phase I study and corresponding sCTX inhibition on the PK-pharmacodynamic (PK/PD) relationship to the PK value. The parameter sCTX was selected because it has high signal-to-noise ratio than other telopeptide. The negative sigmoidal shape of PK/PD relationship between plasma ONO-5334 concentration of and sCTX levels was obtained in our previous study.

**Results:** The simulated sCTX inhibition reached over 99% of the maximal inhibitory effect (*E<sub>max</sub>*) at 0.5 h in all treatment groups, and decreased to below 80% *E<sub>max</sub>* at 8 and 12 h with 50 mg BID and 100 mg QD, respectively. However the sCTX inhibition with 300 mg QD was maintained 82% *E<sub>max</sub>* or more throughout 24 h. The mean sCTX inhibitions during 24 h for 100 mg QD, 300 mg QD and 50 mg BID were 63%, 95% and 80% *E<sub>max</sub>*, respectively. There was a positive linear relationship by treatment group between the mean sCTX inhibition during 24 h and observed BMD gain in the phase II study.

**Conclusion:** The dose response for BMD with 100 and 300mg QD and higher BMD gain with 50 mg BID versus 100 mg QD can be explained by the sCTX inhibition during 24 h. The simulation provides antiresorptive activity of ONO-5334 during 24 h, and improved prediction of BMD gain by ONO-5334.

**Disclosures:** Makoto Tanaka, Ono Pharmaceutical Co.,Ltd, Grant/Research Support.

## MO0670

**A dedicated Telephone program and use of a single Bone Turnover Marker for individual Persistence to Oral Bisphosphonates: A single center Fracture Liaison Service (FLS) study.** Peter Van den Berg<sup>\*1</sup>, Paul Van Haard<sup>1</sup>, Eveline Van der Veer<sup>2</sup>, Piet Geusens<sup>3</sup>, Joop Van den Bergh<sup>3</sup>, Dave Schweitzer<sup>1</sup>. <sup>1</sup>Reinier de Graaf Gasthuis, Netherlands, <sup>2</sup>University Medical Center Groningen, Netherlands, <sup>3</sup>Maastricht University Medical Center, Netherlands

#### Introduction

One of the main goals of the Fracture Liaison Service (FLS) is to prevent subsequent fractures. Unfortunately persistence to prescribed oral bisphosphonates treatment is generally low. In the current study we evaluated the influence of telephone call intervention on persistence and the predictive value of changes in Bone Turnover Markers (BTMs) for Persistence to alendronate once-weekly in FLS patients.

#### Methods

Postmenopausal women with a recent fracture and osteoporosis that started treatment with alendronate were randomized to receive Phone Calls (PC) or No Phone Calls (no PC) intervention. Each patient was followed during 12 months including 5 BTMs assessments at baseline and at 3,6,9 and 12 months. Additionally, 30 postmenopausal osteopenic patients with a recent fracture were analyzed as Reference group for BTM changes during fracture repair. Persistence was assessed using the Dutch National Switch Point Pharmacies-GPs (LSP) database; a score of 1 = persistent and 0 = non-persistent at 12 months. LSP offers actual information on Pharmacies' deliveries to healthcare professionals with legal access to a persistence monitor. BTM changes were cross-referenced with identifiable LSP monitored deliveries. Defined cut-off values were derived from Least Significant Change (LSC) and underrunning the Median of BTM values retrieved from the Reference group. Both cut-off values were tested for individual Pharmacies' deliveries.

#### Results

Out of 119 patients, 93 (78 %) completed 12 months follow-up (45 PC and 48 No PC, mean age 69 yrs (range 53-86)). There was no difference in persistence between PC vs. No PC intervention (persistence in both groups: 75%). The cut-off value for LSC of s-CTX was > 29%. This was < 415 ng/L with use of underrunning the Median of s-CTX from the Reference group. Cut-off values were optimal at 3 months and predicted 93 and 96% of persistence (LSP=1) at 12 months. PINP (at 3 months) showed less individual agreements, resp. 85% (LSC >36%) and 88% (underrunning Median <53,1 µg/L).

#### Conclusions

Telephone calls intervention did not improve alendronate persistence. LSC of s-CTX in the individual fracture patient showed a practically useful prediction of individual alendronate persistence. Nationwide use of Pharmacies' deliveries was used as alendronate persistence indicator showing usefulness of BTM's in FLS patients.

**Disclosures:** Peter Van den Berg, None.

## MO0671

**Comparison between daily and weekly Teriparatide treatments for Osteoporosis after 3 years from the start of injection.** Tsuyoshi Watanabe<sup>\*1</sup>, Emi Konno<sup>2</sup>. <sup>1</sup>National Center for Geriatrics and Gerontology, Japan, <sup>2</sup>Minami Seikyo Hospital, Japan

**Background:** Teribone™ is a weekly Teriparatide (wTPTD) developed in Japan. Daily Teriparatide (dTPTD) is well known as a great useful treatment medication in osteoporosis (OP). Head to head comparison between these medications is not well addressed previously.

**Object:** In this retrospective study, we compared BMD changes, fracture event and fracture event with dTPTD and wTPTD in 3 years.

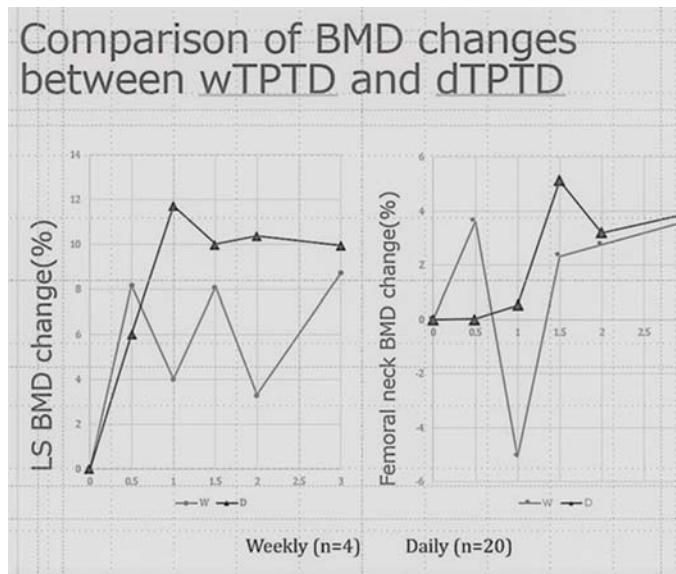
**Methods:** Two centers were included in this study from January 2011 to December 2014. All patients are women. dTPTD (n=20) and wTPTD (n=4) were enrolled. The patients who couldn't continue teriparatide medications during a prescribed periods were excluded, (dTPTD 104weeks, wTPTD 72 weeks). BMD, bone markers, fracture events are recorded from their medical records.

#### Results:

Patients' characteristics (dTPTD : wTPTD): Mean age (70.1: 68.5). Body mass index (22.4: 20.5). All patients are treated with several medications after finishing TPTD (denosmab, bisphosphonate, SERM, or VitD3). % increase of BMD are equal to lumbar spine (LS) BMD (9.9 %: 8.7%) and femoral neck (FN) BMD (3.9%: 3.6%) at the final observational time. Two fracture events were happened in dTPTD group. No fracture events was happened in wTPTD group. No significant differences were observed.

**Conclusions:** This study shows that weekly PTH injection seems to be almost equal to dTPTD about BMD changes and fracture prevention rate.





BMD changes between wTPTD and dTPTD

Disclosures: Tsuyoshi Watanabe, None.

## MO0672

**Atypical Femoral Fractures and Bisphosphonates Exposure among Patients Participating in a Fracture Liaison Service- A Case Control Study.** Uri Yoel<sup>1</sup>, Lior Baraf<sup>1</sup>, Vitaly Medvedovsky<sup>1</sup>, Tamar Eshkoli<sup>1</sup>, Dayana Cohen<sup>1</sup>, Victor Novack<sup>2</sup>, Poliana Shamgar<sup>3</sup>, Michal Lamberger<sup>3</sup>, Avital Blum<sup>4</sup>, Vera Polischuk<sup>5</sup>, Dvora Lieberman<sup>6</sup>, Viktoria Makarov<sup>7</sup>, Ethel Siris<sup>8</sup>, Merav Fraenkel<sup>9</sup>. <sup>1</sup>Endocrinology, Soroka University Medical Center, Faculty of Health Sciences, Ben-Gurion University of the Negev, Israel, <sup>2</sup>Clinical Research Center, Soroka University Medical Center, Faculty of Health Sciences, Ben-Gurion University of the Negev, Israel, <sup>3</sup>Clinical Research Center, Soroka University Medical Center, Israel, <sup>4</sup>Clinical Research Center, Faculty of Health Sciences, Ben-Gurion University of the Negev, Israel, <sup>5</sup>Internal medicine, Soroka University Medical Center, Faculty of Health Sciences, Ben-Gurion University of the Negev, Israel, <sup>6</sup>Geriatrics, Soroka University Medical Center, Faculty of Health Sciences, Ben-Gurion University of the Negev, Israel, <sup>7</sup>Clinical Image Institution, Soroka University Medical Center, Faculty of Health Sciences, Ben-Gurion University of the Negev, Israel, <sup>8</sup>Division of Endocrinology, Columbia University Medical Center, New York, USA, United States, <sup>9</sup>Endocrinology, Soroka University Medical Center, the Faculty of Health Sciences, Ben-Gurion University of the Negev, Israel

### Aim

It was our aim to characterize atypical femoral fractures (AFF) among our cohort of patients participating in a tertiary university medical center, Fracture Liaison Service (FLS).

### Methods

From July 2014 to October 2016, patients over age 50 admitted to our institution with osteoporotic hip fracture were offered investigation, follow up and treatment by the FLS. The computerized medical records were reviewed for ICD-9 codes for subtrochanteric and femoral shaft fractures. Radiology films of the selected patients were reviewed together by an endocrinologist and a radiologist. AFFs were defined using the revised American Society for Bone and Mineral Research (ASBMR) criteria. Patients with typical hip fractures and those with AFF were compared according to demographic and biochemical data, and exposure to anti-osteoporotic medications prior to the index fracture.

### Results

During the study period 608 patients with hip fracture were evaluated and treated by the FLS. Following evaluation, 19 patients (3%) were judged to fulfill the revised ASBMR task force criteria for an AFF. Patients with AFF were younger than patients with typical osteoporotic hip fracture (73±35 vs. 79±10 years, p=0.009) and the majority were female (89% vs. 73%, p=0.175). Patients with AFF had lower mean creatinine levels (mg/dL, 0.72±0.24 vs. 0.97±0.54, p=0.042) and higher mean 25(OH)-vitamin D level (nmol/L, 57±29 vs. 43±23, p=0.01) compared with patients with typical hip fracture. There was no difference between groups in parathyroid hormone (PTH) levels. Patients with AFF compared to those with typical hip fracture had higher rates of any exposure to bisphosphonates (BPs) (73.7% vs. 42.5%, p=0.007), longer duration of exposure (median {Q1,Q3}, 85 months {59-145} vs. 42 months {9-92}, p=0.003), and higher rates of patients treated for more than 5 years with BPs (79% vs. 41%, p=0.005).

The association between the occurrence of AFF and BPs use for more than 5 years, was proven statistically significant in multivariate analysis corrected for age and gender, odds ratio (OR)= 5.2 (95% CI, 1.32 to 20.26).

### Conclusions

In our cohort of patients with osteoporotic hip fractures treated by the FLS, 3% presented with AFF. Our results support the association between BPs treatment and AFF, especially when this treatment is prolonged.

Disclosures: Uri Yoel, None.

## MO0673

**Damage-Associated Molecular Patterns (DAMPs) Released Following Ischemic Osteonecrosis of the Femoral Head.** Harry Kim\*, Ryosuke Yamaguchi, Naga Suresh Adapala, Matthew Phipps, Olumide Aruwajoye. Texas Scottish Rite Hospital for Children, United States

Legg-Calvé-Perthes disease (LCPD) is a childhood form of ischemic osteonecrosis (ON) characterized by extensive cell death in the femoral head, chronic hip joint synovitis, and femoral head collapse. Cell death releases endogenous molecules called damage-associated molecular patterns (DAMPs) or alarmins which activate pattern recognition receptors (PRRs) on immune and other cells, such as toll-like receptors (TLR2,4) and receptor for advanced glycosylation end products (RAGE). The types of DAMPs released, their effects on synovial and invading repair cells (macrophages and endothelial cells), and PRRs involve in the repair process following ischemic ON have not been investigated. To better understand the DAMPs associated with ischemic ON, we first analyzed synovial fluid samples from patients with LCPD (n=8). Western blotting analysis revealed elevation of prototype DAMPs, HMGB1 and HSP90. To further investigate DAMPs associated with ischemic ON, we used a well established piglet model of ischemic ON (N=18). Necrotic bone fluid (NBF) and synovial fluid samples were obtained at 48 hrs, 2 and 4 wks following the induction of ischemic ON which represent ischemic, necrotic, and early revascularization phases of the model, respectively. Increasing levels of DAMPs (HMGB1, S100A6, NADH, cytochrome B) were detected by western blotting in the NBF and synovial fluid samples compared to unoperated control samples. NBF also contained elevated levels of lipid peroxidation product 4-hydroxynonenal (4-HNE), biglycan (matrix alarmin), mitochondrial DNA and uric acid. NBF and SF samples also showed elevated levels of pro-inflammatory cytokines (TNF-, IL-1β, IL6, IL12) on multiplex-ELISA analysis. Immunohistochemistry of the femoral heads revealed the recruitment of endothelial cells (CD31) and macrophages (CD163) in the femoral head at 4 weeks following ischemic ON, which expressed TLR2/4, and RAGE. Blockade of TLR4 and RAGE receptors using chemical inhibitors reduced the in-vitro migration of these cells in response to NBF. In primary synovial cells, the synovial fluid samples increased cell proliferation and inflammatory cytokine production (TNF-α, IL-1β, IL-6) which were abrogated by a blockade of TLR4 and RAGE. These results indicate that ischemic ON produces increased levels of DAMPs and inflammatory cytokines in the necrotic bone and synovial fluid which stimulate repair cell migration and further production of inflammatory cytokines.

Disclosures: Harry Kim, Genentech, Other Financial or Material Support.

## MO0674

**Adiponectin Enhances Osteogenic Differentiation in Human Adipose-derived Stem Cells by Activating the APPL1-p38 MAPK Signaling Pathway.** Tong Chen\*, Qisheng Tu, Jake Chen. Division of Oral Biology, Tufts University School of Dental Medicine, United States

Human adipose-derived stem cells (hASCs) are multipotent progenitor cells with multi-lineage differentiation potential including osteogenesis and adipogenesis. While significant progress has been made in understanding the transcriptional control of hASC fate, little is known about how hASC differentiation is regulated by the autocrine loop. The most abundant adipocytokine secreted by adipocytes, adiponectin (APN) plays a pivotal role in glucose metabolism and energy homeostasis. Growing evidence suggests a positive association between APN and bone formation yet little is known regarding the direct effects of APN on hASC osteogenesis. Therefore, this study was designed to investigate the varied osteogenic effects and regulatory mechanisms of APN in the osteogenic commitment of hASCs. hASCs were obtained from the primary culture of human adipose tissue and treated with or without APN (1 µg/ml). Osteogenesis related gene expression was evaluated by real-time polymerase chain reaction (PCR), alkaline phosphatase (ALP) activity assay, and alizarin red S (AR-S) staining and mineralization assays. To further investigate the signaling pathway, mechanistic studies were performed using western blotting, immunofluorescence and lentiviral transduction. We found that the expression of osteoblast-related genes in hASCs, such as osteocalcin (OCN), alkaline phosphatase (ALP), runt-related transcription factor-2 (Runx2, also known as Cbfa1) and bone sialoprotein (BSP) were up-regulated in APN-treated cells compared to untreated controls (Fig 1B). This was further confirmed by the higher ALP activity and increased formation of mineralization nodules (Fig 1A). Mechanistically, we found for the first time that APN increased nuclear translocation of adaptor protein containing pleckstrin homology domain, phosphotyrosine domain, and leucine zipper motif (APPL) 1 in those cells (Fig 1C). Additionally, the phosphorylation of p38 mitogen-activated protein kinase (MAPK) increased over time with APN treatment. Moreover, knockdown of APPL1 blocked the expression of APN-induced osteogenic transcription factor Runx2 (Fig 1D). Our results indicate that APN promotes the osteogenic

differentiation of hASCs by activating APPL1-p38 MAPK signaling, suggesting that manipulation of APN may be a novel therapeutic target for bone loss diseases.

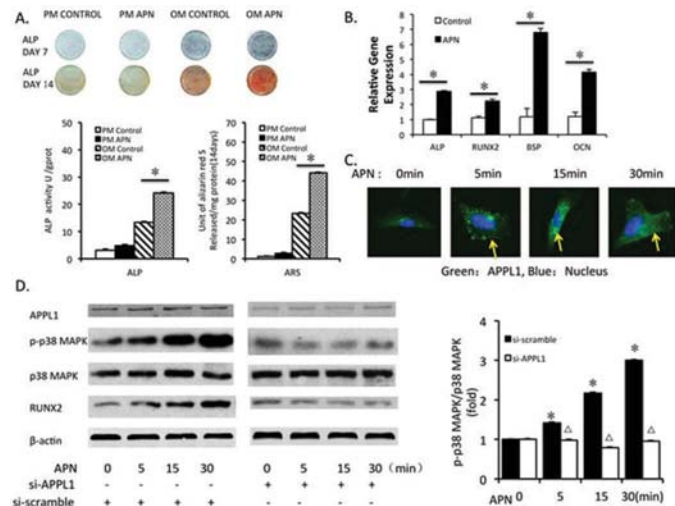


Figure 1

Disclosures: Tong Chen, None.

## MO0675

**Identification of commercially available antibodies that block ligand binding by BMPR2.** Laura Schoerning\*, Ruthann Gorrell, Jordan Newby, Julia Hum, Jonathan Lowery, Marian University College of Osteopathic Medicine, United States

Osteoporosis, a disease of low bone mineral density, affects 10 million Americans and is a significant health problem and a considerable socioeconomic burden. Current treatments for osteoporosis have significant limitations, necessitating identifying new treatment strategies via building a better understanding of the endogenous mechanisms regulating bone mass. We recently demonstrated that removal of the BMP type 2 receptor, BMPR2, in skeletal progenitor cells of *Bmpr2*-cKO mice during embryonic development leads to reduced age-related bone loss due to a sustained elevation in bone formation rate (Lowery et al, 2015); the molecular mechanism underlying this phenotype is being pursued in other work. In the present study, we sought to advance the translational potential of our genetic model by identifying antibodies that neutralize the ligand-binding function of the BMPR2 extracellular domain. We first established a modified, cell-free immunoprecipitation assay wherein the ligand BMP2 (R&D Systems) is pulled-down by BMPR2-ECD (Sino Biological) conjugated to Protein G beads; the unbound BMP2, which is found in the supernatant, is subsequently quantified by ELISA. This yielded a standard assay wherein approximately 2  $\mu$ g BMPR2-ECD leads to a 70% reduction in BMP2 signal. Next, we examined the neutralizing ability of 3F6 (Thermo Fisher Scientific), which is a mouse monoclonal antibody raised against the ligand-binding region of BMPR2, and found a dose-dependent inhibition of BMPR2-ECD ligand-binding. Given that the commercial availability of this antibody is as an ascites preparation, specificity of this assay was confirmed by demonstrating that ligand-binding activity of BMPR2-ECD is unchanged in the presence of non-specific, negative control ascites. Using these results as a guide, we then evaluated 1F12 (Thermo Fisher Scientific), which is another mouse monoclonal antibody raised against the ligand-binding region of BMPR2, and found that this antibody is also capable of neutralizing the ligand-binding function of BMPR2-ECD. In contrast, no effect on ligand-binding function of BMPR2-ECD was observed with the mouse monoclonal antibody 9A10 (Abcam) even though antibody is also raised against the ligand-binding region of BMPR2. These results provide proof-of-concept data for future studies evaluating inhibition of BMPR2 function *in vivo* as a means to reduce age-related bone loss.

Disclosures: Laura Schoerning, None.

## MO0676

**BMP2 encapsulated within exosomes bypasses its cell surface plasma membrane receptors to signal directly from inside the cell. Does this represent a new signaling paradigm?** Saigopalakrishna Yerneni<sup>1</sup>, Lee Weiss<sup>1</sup>, Theresa Whiteside<sup>2</sup>, Phil Campbell<sup>1</sup>. <sup>1</sup>Carnegie Mellon University, United States, <sup>2</sup>University of Pittsburgh, United States

Exosomes are involved in intercellular communication, locally and systemically, from early development onward, and across physiological and pathophysiological conditions. Exosomes contain diverse cargo, including lipids, nucleic acids, peptides, proteins and proteoglycans, enveloped within the exosome lumen and/or associated with its external surface. Exosomes directly interact with cells, either through signaling at the cell surface or via trafficking of their cargo across the plasma membrane into the cell. Growth factors on the surface of exosomes appear to signal target cells via cell surface

receptors, whereas the signaling mechanisms of exosome luminal confined growth factors remains unknown. Using BMP2 as a prototypical growth factor, we present data suggesting that BMP2 contained within exosomes and not on the exosome surface is trafficked directly into cells without the involvement of BMP2 cell surface receptors. And, this BMP2 delivered within exosomes exhibits BMP2-directed cellular biological activity. For these experiments we loaded exogenous BMP2 into exosomes derived from unstimulated macrophage exosomes (BMP2-exosomes). Cell experiments were conducted with BMP2-exosomes delivered in both the 'liquid phase' (soluble) and in the 'solid-phase' (immobilized) to extracellular matrix (ECM) substrates. For the solid-phase experiments, we used an inkjet-based bioprinting technology to create microenvironments consisting of specified patterns of BMP2-exosomes immobilized via native binding affinities between elements on the exosome surface and ECM (BMP2-exosomes/ECMs). Both soluble BMP2-exosomes and immobilized BMP2-exosomes/ECMs induced stem cell differentiation toward osteogenesis *in vitro*. Immobilized BMP2-exosomes/ECMs induced heterotopic bone formation *in vivo* in a mouse muscle pocket assay in registration to printed patterns. Using fluorescent- and 125I-labeling, we observed that BMP2-exosomes were trafficked directly into cells via exosome-directed endocytic pathway(s), bypassing BMP2 cell surface receptors. Overall, these data not only demonstrate that exosomes can be a delivery vehicle for BMP2, but it also challenges one of the central dogmas of endocrinology whereby growth factors, as proteins, are presumed to bind to their surface receptors on target cells as a prerequisite to the initiation of their intracellular signaling cascades. The intracellular signaling pathway(s) of BMP2-exosomes remains to be determined.

Disclosures: Saigopalakrishna Yerneni, None.

## MO0677

**Initiating Zoledronic Acid in Rice Rats with Established Periodontitis Shortens Time to First Occurrence of Osteonecrosis of the Jaw-like Lesions.**

Jose Aguirre<sup>1</sup>, Jonathan Messer<sup>1</sup>, Jessica Jiron<sup>1</sup>, Evelyn Castillo<sup>1</sup>, Jorge Mendieta<sup>1</sup>, Jorge Mendieta<sup>1</sup>, Indraneel Bhattacharyya<sup>2</sup>, Catherine van Poznak<sup>3</sup>, Donald Kimmel<sup>1</sup>. <sup>1</sup>Department of Physiological Sciences, University of Florida, United States, <sup>2</sup>Department of Oral & Maxillofacial Diagnostic Sciences, College of Dentistry, University of Florida, United States, <sup>3</sup>Oncology Division, Department of Medicine, College of Medicine, University of Michigan, United States

**Introduction:** Zoledronic acid (ZOL) is a potent anti-resorptive (pAR) therapy associated with osteonecrosis of the jaw (ONJ). Periodontitis (PD) and poor oral health are risk factors for the development of ONJ. We hypothesize that ONJ occurs when PD-related infection causes jaw bone necrosis and pARs slow the removal of necrotic bone causing abnormally extended persistence and eventual exposure. Rice rats naturally develop PD by ages 16-22 wks. We previously established a dose/time relationship between ZOL and ONJ in rice rats when ZOL is started at age 4 wks, before PD has developed. In the current study, we designed an experiment to test the working hypothesis that onset of ONJ is more rapid when initiating ZOL after moderate/severe PD is established (age 16-22 wks), compared to ZOL initiated in rats with no PD (age 4 wks). ZOL starting times were ages 4 wks (no PD) or 16-22 wks (established PD).

**Methods:** Rats received either 0 (VEH) or 80 $\mu$ g/kg intravenous ZOL monthly; were necropsied in groups (N=16-51) at 6, 12, and 18 weeks after starting ZOL; and underwent oral exams at necropsy. High-resolution photos of all four jaw quadrants taken at necropsy were independently examined by three blinded observers, and gross severe PD/ONJ-like lesions were diagnosed. Histological characterization of these lesions is underway.

**Results:** We found that initiating ZOL at 4 wks old (no PD) resulted in ONJ-like lesions in 20% of rats by age 16-22 wks, while only 6% of rats developed lesions in VEH control. Initiating ZOL at 16-22 wks (established PD) resulted in ONJ-like lesions in 14% of rats after only 6 wks ZOL, and 33% of rats after only 12 wks ZOL, compared to only 4% of rats in each of the VEH control groups for the same time points. 13% of rats developed lesions after 18 wks when ZOL was initiated at 16-22 weeks, compared to 11% of VEH.

**Conclusion:** These data demonstrate that the presence of PD both increases the risk of developing ONJ and decreases the time to ONJ onset in rice rats treated with ZOL. Although this animal model can spontaneously develop an ONJ-like lesion, the prevalence ONJ in ZOL treated rats was > 3 times VEH rats at age 34 wks or less. These data support the use of this animal model in experiments designed to elucidate the etiology of ONJ.

Disclosures: Jose Aguirre, None.

## MO0678

**Strontium treatment has synergistic effects with PTH as evaluated in OVX rats.** Patrick Ammann\*. Division of Bone Diseases, Switzerland

Most of the anti-fracture efficacy of strontium treatment is related to an improvement of bone material level properties. Strontium is also known to stimulate bone formation during skeletal growth and bone healing process. An obvious question is to understand if strontium could improve bone material level properties under PTH treatment and influence the PTH stimulating effect on bone formation.

The aims of this study are (i) to evaluate whether the association of strontium with PTH or Alendronate can be synergistic and able to better prevent the decrease of bone strength in OVX rats than either drug administered alone and (ii) to investigate whether



its potential synergistic effects are dependent on the in vivo stimulation of new bone formation. OVX rats were treated with strontium ranelate (SR, 625 mg/kg day po) alone, with a stimulator of bone formation (PTH 8 microg/kg\*day SC) or treatment decreasing bone remodeling, i.e. formation, (Alendronate 18 microg/kg twice a week, SC) with or without strontium ranelate (625 mg/kg day po). Seven groups of 12 rats (SHAM, OVX, SR, PTH, Alendronate, SR-PTH, SR-Alendronate) received treatments or respective vehicles for 8 weeks. At the end of the experiment, vertebrae were removed for biomechanics, microCT and nanoindentation testing. A curative protocol was also performed.

PTH and Alendronate, but not strontium, fully prevent the deleterious effect of OVX on bone strength; values obtained under PTH are significantly higher as compared to SHAM. This was associated with the preservation of bone volume in Alendronate treated animals but not in strontium treated rats, and further significant increment under PTH as compared to SHAM. Combined therapy with strontium resulted in a further significant increase of maximum load as compared with PTH treatment alone. The addition of strontium improved intrinsic bone tissue quality. In SR-PTH treated rats and corrected the impaired intrinsic tissue quality observed under PTH treatment. Furthermore it resulted in a significant increment of trabecular thickness reflecting the positive influence of strontium on bone formation. No effect was observed in the case of the association with Alendronate. Similar effects were observed in a curative protocol.

Together, these data suggest that strontium treatment maximizes the in vivo effect of PTH by improving the intrinsic bone quality of the new formed bone and potentially by a synergistic effect on bone formation.

**Disclosures:** Patrick Ammann, *servier, Grant/Research Support.*

## MO0679

**Addition of Diabetes Aggravates Deleterious Effects of Metabolic Syndrome on Bone.** Cedo Bagi\*, Edwin Berryman, Kristin Edwards, David Zakur, Chang-Ning Liu, Pfizer, Inc, United States

**Rationale.** Metabolic syndrome (MSy) and osteoporosis share the same risk factors. Patients with type 1 and 2 diabetes, have a higher risk of osteoporosis and fractures. Occurrence of diabetes in patients with MSy signals the point at which time the disease follows an increasingly malignant path with the worsening of symptoms caused by liver failure. Nonalcoholic fatty liver disease (NAFLD), and its more serious form nonalcoholic steatohepatitis (NASH), are known manifestations of obesity and MSy. To determine the long-term influence of a westernized diet on bone we combined streptozotocin treatment with this westernized diet to create a rat model of human MSy.

**Methods.** Mature male rats were fed and watered with either standard chow and RO water (controls), or a high fat, high cholesterol diet and sugar water containing 55% fructose and 45% glucose (HFTFX). A third group of rats also received the HFTFX diet and a single dose of streptozotocin (30 mg/kg; ip) to induce diabetes (HFTFX STZ). Body weight was done twice weekly. Glucose tolerance tests were conducted several times during the course of the study. Serum chemistry, liver enzymes and biomarkers of bone metabolism were evaluated at 10 and 28 weeks. Shear wave elastography (SWE) was deployed to assess liver fibrosis. The liver and pancreas were evaluated by histology. Cancellous bone was evaluated by mCT, and cortical bone by pQCT and by 3-point bending method.

**Results.** Body mass and fat was significantly greater in HFTFX and HFTFX STZ rats compared to Controls. Rats in both HFTFX and the HFTFX STZ group showed clear signs of NASH. The HFTFX STZ rats were insulin resistant at 10 and 28 weeks, although the insulin resistance diminished over time. Both HFTFX and HFTFX STZ rats exhibited deterioration of cancellous bone at the proximal tibia, however the change was more dramatic in HFTFX STZ rats. Despite the fact that obese rats had somewhat larger bones the cortical bone thickness was diminished and contributed to significant deterioration of bone strength. Diminished cortical bone strength in HFTFX fed rats was further aggravated by diabetes.

**Conclusion.** The HFTFX and HFTFX STZ rats provide pre-clinical model of NAFLD and NASH and can be easily manipulated to mimic various aspects of MSy in humans. The addition of diabetes even at a very mild form significantly aggravates the symptoms of MSy and NASH, and significantly contributes to the deterioration of bone structure and strength.

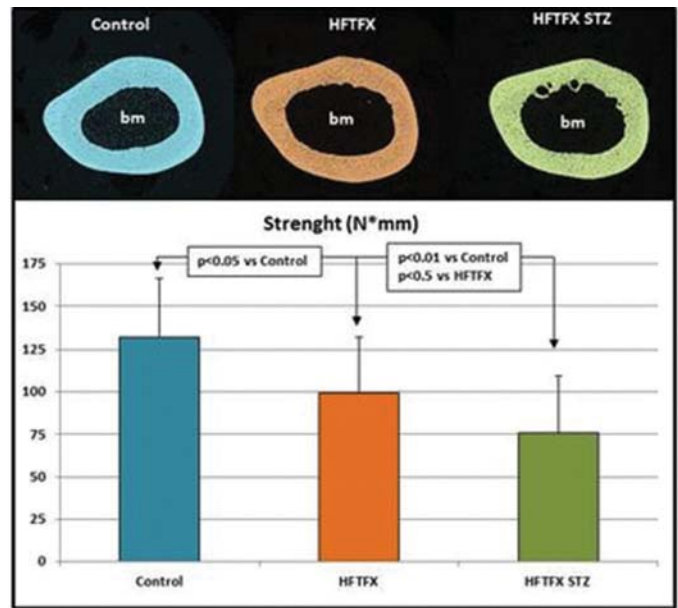


Figure 1

**Disclosures:** Cedo Bagi, *None.*

## MO0680

**Abaloparatide Increased Bone Mass in a Rabbit Glucocorticoid-Induced Osteopenia Model.** Heidi Chandler\*, Allen Pierce, Jeffery Brown, Michael Ominsky, Gary Hattersley, Radius Health Inc, United States

Estrogen deficiency and glucocorticoid (GC) therapy are the main causes of postmenopausal and secondary osteoporosis, respectively. Abaloparatide (ABL), a selective PTH1 receptor agonist, increased BMD and bone formation in estrogen-deficient ovariectomized (OVX) animals and in postmenopausal women with osteoporosis, with limited increases in bone resorption indices. The ability of ABL to reverse established bone loss caused by glucocorticoid excess was studied in New Zealand White rabbits. Forty rabbits underwent OVX (n=32) or sham surgery (n=8) at ~6 months of age, with 24 OVX rabbits receiving GC methylprednisolone (OVX + GC) for 6 weeks post-surgery. After a 6-week bone depletion period, the OVX + GC rabbits continued to receive GC and treatment was initiated with ABL at 5 or 25 µg/kg (n=8/group) or vehicle (Veh) sc once daily, while the other OVX (n=8) and sham groups received Veh sc. GC treatment resulted in robust bone loss at the end of the bone depletion period in OVX rabbits, with lumbar spine DXA BMD that was 28% lower in the Veh-treated OVX+GC group compared to OVX controls at week 0 (p<0.05), an effect which persisted through the treatment period. After 8 weeks of ABL, bone mass was dose-dependently increased in OVX+GC rabbits, with 35% greater lumbar spine BMD in the ABL-25 µg/kg group compared with OVX+GC Veh (p<0.05). The GC-mediated loss of lumbar spine BMD in OVX rabbits was predominantly restored in the ABL-25 µg/kg group, which had a similar mean BMD to that of the OVX control group at week 8. These preclinical findings demonstrate that ABL increases bone mass in a glucocorticoid-induced osteopenia model.

**Disclosures:** Heidi Chandler, *Radius Health, Other Financial or Material Support.*

## MO0681

**PAI-1 inhibitor treatment attenuate bone loss through stimulating bone formation in a mouse model of postmenopausal osteoporosis.** Guangwen Jin<sup>\*1</sup>, Jinying Piao<sup>2</sup>, Zulipiya Aibibula<sup>2</sup>, alkebaier aobulikasimu<sup>2</sup>, Daisuke Koga<sup>2</sup>, Hiroki Ochi<sup>3</sup>, Kunikazu Tsuji<sup>4</sup>, Toshio Miyata<sup>5</sup>, Atsushi Okawa<sup>2</sup>, Yoshinori Asou<sup>2</sup>. <sup>1</sup>Department of Orthopaedics Surgery, Tokyo Medical and Dental University, Japan, <sup>2</sup>Department of Orthopedics Surgery, Tokyo Medical and Dental University, Japan, <sup>3</sup>Department of Physiology and Cell Biology, Tokyo Medical and Dental University, Japan, <sup>4</sup>Department of Cartilage Regeneration, Tokyo Medical and Dental University, Japan, <sup>5</sup>Department of Molecular Medicine and Therapy, United Centers for Advanced Research and Translational Medicine, Tohoku University Graduate School of Medicine, Japan

Osteoporosis is a progressive bone disease caused by an imbalance between bone resorption and formation. Plasminogen activator inhibitor-1 (PAI-1), a serine (serine protease inhibitor), is a 50-kDa single-chain glycoprotein that inhibits urokinase/ tissue plasminogen activator. Recently, PAI-1 has been shown to play important roles in the bone metabolism using PAI-1 deficient mice. In this study, we relied on an orally

available small molecule PAI-1 inhibitor, iPAI-1, and evaluated its therapeutic benefits in the estrogen deficiency-induced osteoporosis model. C57BL/6J female mice in eight weeks old were divided into three groups, such as sham+vehicle (Sham), OVX+vehicle (OVX+v) and OVX+iPAI-1 (OVX+i). The PAI-1 inhibitor iPAI-1 was resuspended in 200  $\mu$ L of 0.5% carboxymethylcellulose (MP Biomedicals) and orally administered (10 mg/kg body weight) daily for six weeks from the day after the operation. Micro-CT analysis of femoral bone and histological analysis of lumbar spine indicated BV/TV was decreased in OVX+v as expected. Six weeks of iPAI-1 treatment prevented ovx-induced trabecular bone loss both in femoral bone and lumbar spine. By bone histomorphometry of lumbar spine, OVX+v resulted in significant increases in MAR and BFR/BS, compared to Sham group. OVX+i group exhibited further increase in these osteoblastic parameters, compared with OVX+v group. ES/BS, N.Oc/BS and Oc.S/BS were similarly increased in OVX-i group and OVX-v group. Urinal CTX-1 level was increased in OVX+v group, compared with Sham group. OVX+i group exhibited similar levels of CTX-1 concentration with OVX+v group, indicating iPAI-1 had no effect on bone resorption activity. FACS analysis indicated the number of MSC in bone marrow was increased in OVX+i group compared to OVX+v group. To verify anabolic effect of iPAI-1 on bones, bone marrow ablation analysis was performed. Femoral bones were ablated by K-wire and iPAI-1 or vehicle were administered orally from the day after the operation. Micro-CT analysis indicated remodeled trabecular bone volume was significantly elevated in the iPAI-1-treated group than in the control group at twelve days after the procedure. In conclusion, our results suggest PAI-1 blockade by a small molecule inhibitor is a new therapeutic approach for the anabolic treatment of postmenopausal osteoporosis.

**Disclosures:** Guangwen Jin, None.

## MO0682

**TransCon PTH, a Sustained-Release PTH Prodrug for the Treatment of Hypoparathyroidism: Proof-of-Principle in Cynomolgus Monkeys and TPTx Rats.** Lars Holten-Andersen<sup>\*1</sup>, Martin Guillot<sup>2</sup>, Felix Cleemann<sup>3</sup>, Melanie Felix<sup>2</sup>, Susanne Pihl<sup>1</sup>, Kennett Sprogø<sup>1</sup>, David Karpl<sup>4</sup>, Aurore Valera<sup>2</sup>, Vibeke Miller Breinholt<sup>1</sup>. <sup>1</sup>Ascendis Pharma A/S, Denmark, <sup>2</sup>Charles River Laboratories, Canada, <sup>3</sup>Ascendis Pharma GmbH, Germany, <sup>4</sup>Ascendis Pharma Inc., United States

Ascendis Pharma is developing TransCon PTH, a prodrug releasing unmodified teriparatide, PTH (1-34), via non-enzymatic hydrolysis of the proprietary TransCon linker, for the treatment of hypoparathyroidism (HP). Natpara, PTH (1-84), is approved for once-daily subcutaneous injection as an adjunct to vitamin D and calcium in patients with HP. However, it has not demonstrated the ability to reduce the incidence of hypercalcemia, hypocalcemia, or hypercalciuria relative to conventional therapy, likely due to its relatively short half-life resulting in little-or-no exposure over at least 12 hours per day. TransCon PTH, a once-daily prodrug formulation of PTH (1-34), is designed to maintain a steady concentration of PTH in the blood stream within the normal range, and thereby overcome the fundamental limitations of short-acting PTH molecules.

Single doses of TransCon PTH were administered at 1 or 5  $\mu$ g/kg to male cynomolgus monkeys. Pharmacokinetics was assessed together with selected pharmacodynamics endpoints; serum calcium (sCa) and serum phosphorus (sP) levels and urinary calcium. Moreover, the pharmacology of TransCon PTH was investigated in rats subjected to thyroparathyroidectomy (TPTx), a model of HP. The study was performed as a head-to-head comparison to PTH (1-84), administered as daily subcutaneous injections.

Following single subcutaneous injection of TransCon PTH to male cynomolgus monkeys, TransCon PTH plasma levels increased in a dose-dependent manner with corresponding increases in sCa. In monkeys dosed with TransCon PTH at 1  $\mu$ g/kg, sCa levels remained stable within the upper end of the normal range for 96 hours post dose. There was a clear trend for decreased urinary calcium levels at 1  $\mu$ g/kg over the first 24 hours after dosing.

Once-daily administration of TransCon PTH at 5  $\mu$ g/kg/day for 28 days to TPTx rats normalized sCa and sP levels (compared to sham) by day 6, and was maintained within the normal range throughout the study. In contrast, hypocalcemia was not corrected in PTH (1-84) 70  $\mu$ g/kg/day and vehicle-dosed TPTx rats. After 28 days, bone density measured by pQCT in TPTx rats treated with TransCon PTH was similar or slightly lower compared to sham-operated rats, whereas vehicle-dosed TPTx rats exhibited increased bone density, and PTH (1-84)-treated TPTx rats showed a further increase in bone density.

In conclusion, these nonclinical data suggest that TransCon PTH may be a safe and efficacious treatment for HP patients.

**Disclosures:** Lars Holten-Andersen, None.

## MO0683

**YKL-05-099 uncouples bone formation and resorption by blocking M-CSF-driven osteoclastogenesis.** Maureen Omeara<sup>\*1</sup>, Janaina Da Silva Martins<sup>1</sup>, Nathanael Gray<sup>2</sup>, Henry Kronenberg<sup>1</sup>, Marc Wein<sup>1</sup>. <sup>1</sup>MGH Endocrine Unit, United States, <sup>2</sup>Dana Farber Cancer Institute, United States

Background: We recently reported that PTH signaling in osteocytes blocks the activity of the kinase, salt inducible kinase 2 (SIK2). Accordingly, small molecule SIK inhibitors, such as YKL-05-099, mimic PTH action. Treatment of mice with YKL-05-099 once daily (single dose, 6 mg/kg) for 2 weeks led to effects similar to those of intermittent PTH: increased osteoblast numbers, increased bone formation, and

increased bone mass. However, unlike PTH, YKL-05-099 treatment led to reductions in osteoclast numbers despite increased levels of RANKL. The goal of the current study is to understand how YKL-05-099 regulates osteoclast differentiation.

Methods: 8-week-old male C57BL/6 mice were treated with vehicle or different doses of YKL-05-099 (2 mg/kg, 6 mg/kg, 18 mg/kg) once daily for two weeks. Static and dynamic histomorphometry was performed. Previous results of *in vitro* kinase profiling (DiscoverX) for YKL-05-099 were examined. Murine bone marrow-derived macrophages were differentiated into osteoclasts in the presence of 10 different doses of YKL-05-099. Effects on osteoclast differentiation were assessed by TRAP secretion assays and counting multi-nucleated TRAP-positive cells. M-CSF signaling in primary macrophages, was assessed by immunoblotting for MCSF-receptor Y723 phosphorylation and ERK1/2 phosphorylation.

Results: Compared to vehicle-treated mice, YKL-05-099 treatment caused dose-dependent increases in trabecular bone volume (veh 10.3 $\pm$ 1.9 vs 18 mg/kg 16.3 $\pm$ 2.0, p<0.01), increases in Ob.S/BS (veh 11.9 $\pm$ 0.8 vs 18 mg/kg 16.8 $\pm$ 1.3, p<0.01), and reductions in Oc.S/BS (veh 2.79 $\pm$ 0.8 vs 18 mg/kg 1.59 $\pm$ 0.4, p<0.05). We hypothesized that YKL-05-099 might directly block osteoclastogenesis. M-CSF+RANKL-primed osteoclastogenesis was inhibited by YKL-05-099 treatment *in vitro* with an IC<sub>50</sub> of 52 nM. In addition to SIK2, DiscoverX profiling data indicated that this compound could also target the M-CSF receptor. Acute YKL-05-099 pre-treatment (15  $\mu$ M) of bone marrow-derived macrophages blocked M-CSF-induced M-CSF receptor Y723 auto-phosphorylation and downstream ERK phosphorylation.

Conclusions: YKL-05-099 targets bone formation and bone resorption by two distinct mechanisms. In osteocytes, this compound blocks SIK2 and boosts bone formation, in part, by reducing sclerostin production. In pre-osteoclasts, this compound blocks M-CSF receptor signaling. By boosting bone formation and inhibiting bone resorption, YKL-05-099 represents a promising osteoporosis treatment strategy.

**Disclosures:** Maureen Omeara, None.

## MO0684

**Naproxen, but not Aspirin, Increases Risk and Impairs Repair of Stress Fractures.** Jino Park<sup>\*1</sup>, Camilo Restrepo<sup>2</sup>, Javad Parvizi<sup>2</sup>, Ryan Tomlinson<sup>1</sup>. <sup>1</sup>Thomas Jefferson University, United States, <sup>2</sup>Rothman Institute, United States

Stress fractures are debilitating and surprisingly common in athletes, military recruits, and performers. These individuals are among the 30 million daily users of non-steroidal anti-inflammatory drugs (NSAIDs), which reduce pain by preventing the synthesis of PGE<sub>2</sub> through COX1 and/or COX2. However, the effect of chronic NSAID usage on bone health remains controversial. Previous work found that US soldiers prescribed any NSAID have a 2.5 fold increased risk of future stress fracture. Similarly, we found that patients treated at the Rothman Institute for a stress fracture had a history of NSAID usage about twice the national average. Thus, we hypothesized that chronic NSAID use may predispose habitually loaded bones to stress fracture. To test this hypothesis, C57BL/6J mice were subjected to six bouts of axial forelimb compression (3 N, 100 cycles) over two weeks, starting at 16 weeks of age. Drinking water was used to administer naproxen (68 mg/L), aspirin (624 mg/L), or vehicle (control) starting 24 hours before loading. The number of loading bouts was associated with modest decreases in apparent forelimb stiffness in all groups (p < 0.01); only naproxen-treated mice (-8.5%) were significantly different than control. By dynamic histomorphometry, naproxen-treated mice had a sharply diminished rPs.BFR/BS (-74%) but aspirin-treated mice were not different than control. However, RANKL/OPG ratio was not significantly different between groups. In total, these results indicate that naproxen, but not aspirin, increases stress fracture risk by limiting skeletal adaptation to repetitive loads. Separately, C57BL/6J mice were subjected to an ulnar stress fracture generated by a single bout of fatigue loading at 16 weeks of age. Drinking water with naproxen, aspirin, or vehicle was provided 24 hours before loading. MicroCT analysis after 7 days indicated a significant decrease in woven bone volume (-27%) in the naproxen-treated group, but not in the aspirin-treated group. Behavioral analysis in the week after stress fracture revealed normal forelimb use in both aspirin- and naproxen-treated mice (p > 0.05 vs. baseline) whereas control mice favored the injured forelimb until day 7 (p < 0.05). Thus, aspirin and naproxen had similar analgesic efficacy following stress fracture, but only naproxen impaired stress fracture repair. In summary, the substitution of aspirin for naproxen in patients at-risk for stress fracture may reduce injury rates and improve recovery times.

**Disclosures:** Jino Park, None.

## MO0685

**Chondroprotective effects of orally consumed hydrolyzed type 1 collagen in osteoarthritis are associated with shifts in the gut microbiome.** Eric Schott<sup>\*1</sup>, Sarah Soniwalla<sup>2</sup>, Christopher Farnsworth<sup>1</sup>, Alex Grier<sup>1</sup>, Sarah Catheline<sup>1</sup>, Quratul-Ain Dar<sup>2</sup>, John Ketz<sup>1</sup>, Cheryl Ackert-Bicknell<sup>1</sup>, Jennifer Jonason<sup>1</sup>, Steven Gill<sup>1</sup>, Robert Mooney<sup>1</sup>, Janne Prawitt<sup>3</sup>, Michael Zuscik<sup>1</sup>. <sup>1</sup>University of Rochester Medical Center, United States, <sup>2</sup>University of Rochester, United States, <sup>3</sup>Rousselot BVBA, Belgium

Purpose: Over the past two decades, nutraceutical products consisting of cartilage and connective tissue matrix components have been marketed as effective in mitigating OA with no consensus on efficacy or mechanism of action. A recent agent with a reported positive influence on joint health and potential disease modifying capability in human OA



is hydrolyzed type I collagen (hColI). Given emerging data indicating that dietary supplements have profound effects on the gut microbiome that support positive health effects in numerous disease conditions, we hypothesized that hColI is protective against OA progression in a manner that is linked with alterations in the gut microbiome.

**Methods:** Male C57BL/6J mice consuming a standard chow diet ad libitum were supplemented with daily bolus doses of hColI (38mg/day) or vehicle (Nutella). After 4 weeks of supplementation, mice were administered a meniscal-ligamentous injury (MLI) to the right knee to induce OA and a sham surgery to the left knee (control). Supplements were continued until tissue harvest at 12 weeks post-surgery, when knee joints were collected for histology/histomorphometry to study cartilage structure, and fecal samples were collected for rDNA sequencing to determine relative abundance of microbial species in the gut.

**Results:** Mice administered hColI showed chondroprotection 12 weeks post-MLI (Fig. 1A). Total (not shown) and uncalsified tibial cartilage area (Fig. 1B) were increased, correlating with increased chondrocyte cell number (Fig. 1C) and chondrocyte pericellular proteoglycan deposition (Fig. 1D) in the hColI supplemented group. rDNA sequencing revealed that supplementation with hColI led to significant shifts in resident microbes of the gut. Of note, *Bifidobacterium pseudolongum* and *Lactobacillus sp* were reduced in the hColI-supplemented mice, with two unidentified species in the Lachnospiraceae family and the *Tenericute Anaeroplasmata sp* increased (Fig. 1E).

**Conclusion:** In addition to providing chondroprotection in OA, hColI induces a shift in the gut microbiome characterized by changes in several species whose role in human biology has not been determined. Given the debate about how oral nutraceuticals impact the joint and support positive clinical reporting of reduced symptoms in OA, we propose the novel concept that hColI and agents like it influence joint degeneration indirectly through an alteration in the gut microbiome, begging deeper study of cause and effect in this context.

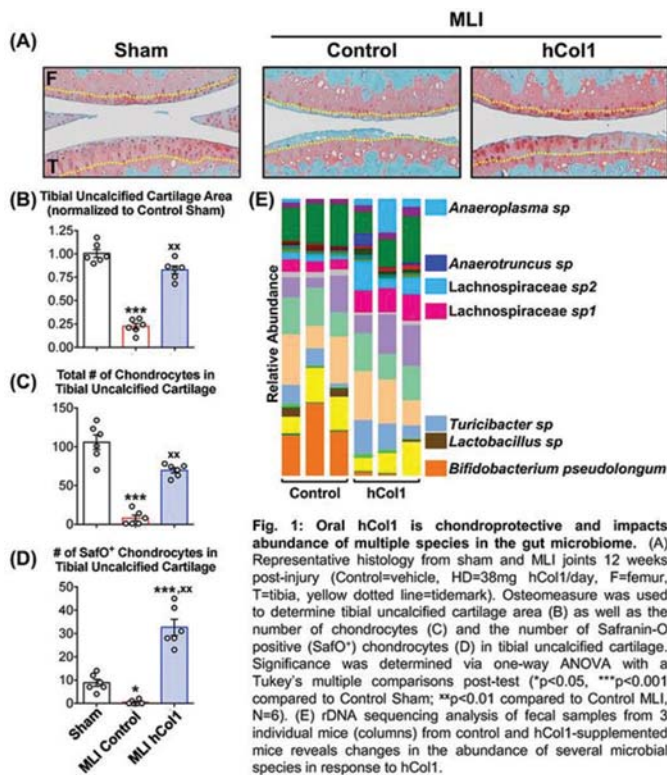


Figure 1

**Disclosures:** Eric Schott, None.

## MO0686

**Maternal phosphate loading during pregnancy does not alter fetal FGF23, PTH, or phosphorus parameters.** K. Berit Sellars\*, Brittany A. Ryan, Beth J. Kirby, Christopher S. Kovacs. Memorial University of Newfoundland, Canada

Fibroblast growth factor-23 (FGF23) plays a significant role in regulating phosphorus metabolism in the child or adult. Genetic loss of FGF23 action causes hyperphosphatemia with hypophosphaturia, while excess action of FGF23 has the opposite effects. FGF23 also increases in response to an increased dietary load of phosphorus, thereby inducing hyperphosphaturia. However, during fetal development, neither genetic loss of FGF23 action nor excess FGF23 action disturbed phosphorus parameters. These findings suggest that FGF23 plays no role in regulating fetal phosphorus metabolism.

The present studies were undertaken to determine if increased dietary phosphorus intake during pregnancy would alter fetal phosphorus parameters and invoke a fetal FGF23 response.

A 1.6% phosphorus diet has been previously shown to cause hyperphosphatemia and increased FGF23 in adult mice. Twenty normal C57BL/6 female mice were mated and

separated into two groups to receive either a normal phosphate (NP) (0.7%) or high phosphate (HP) (1.6%) diet (Envigo/Harlan Teklad). One day before expected birth, maternal blood was taken, fetal blood was collected, carcasses were reduced to ash, mineral content of ash was determined, placental RNA was extracted, and qPCR was performed to analyze relevant calcium and phosphorus transporting genes.

The HP diet increased maternal FGF23 (1,166±50 vs. 560±104 pg/ml) and PTH (6.5±2.3 vs. 4.0±0.0 pg/ml) but did not alter maternal phosphorus (3.02±0.20 vs. 3.16±0.40 mmol/l). In turn, there were no differences between fetuses raised on the HP vs. NP diet, including serum phosphorus (4.31±0.11 vs. 4.46±0.11 mmol/l), FGF23 (51.3±15.0 vs. 68.7±18.1), and PTH (65.7±8.2 vs. 62.8±11.4 pg/ml). There were also no differences in fetal ash weight; ash content of phosphorus, calcium, or magnesium; or in placental expression of Fgf23, Klotho, Cyp27b1, NaPi2a/2b/2c, Ca2+-ATPase, calbindin-9K, or TRPV6.

In summary, FGF23 normally doubles during pregnancy, and maternal phosphate loading caused a further doubling in maternal FGF23. However, the maternal phosphate load did not alter fetal FGF23, PTH, serum or bone phosphorus content, or the expression of placental genes relevant to phosphorus metabolism.

In conclusion, FGF23 appears to work more efficiently in pregnant females to clear absorbed dietary phosphorus, thereby protecting fetuses from exposure to an increased phosphorus load.

**Disclosures:** K. Berit Sellars, None.

## MO0687

**The Chemotherapeutic Trabectedin Negatively Impacts Osteal Macrophages, Bone Formation and Bone Healing.** Benjamin Sinder\*, Justin Do\*, Amy Koh\*, Megan Michalski\*, Jose Aguirre\*, Hernan Roca\*, Laurie McCauley\*. <sup>1</sup>University of Michigan, United States, <sup>2</sup>University of Florida, United States

Osteal macrophages have emerged as key regulators of bone mass and inhibition of macrophages compromises bone formation. Trabectedin is an FDA approved chemotherapeutic that induces apoptosis in cancer cells and macrophages. The purpose of this study was to investigate the role of macrophages and trabectedin on bone homeostasis and bone healing. Sixteen wk old C57BL/6 male mice were treated with trabectedin or vehicle (0.15mg/kg i.v., n=8-12/gp) in short(1wk)- and long(6wk)- term treatment regimes followed by flow cytometry, microCT, serum biomarkers, RT-PCR, and static and dynamic histomorphometry. Trabectedin significantly reduced F4/80+ (-16%) and CD68+ (-23%) bone marrow macrophages. The macrophage function of apoptotic cell clearance (efferocytosis) was reduced with trabectedin in vitro, and marrow from trabectedin treated mice had reduced gene expression of MFG-E8 - a key efferocytic factor. Correspondingly, trabectedin treated mice had compromised bone formation as evidenced by significant reductions in serum PINP (-27%), as well as MS/BS (-42%) and BFR/BS (-48%) in metaphyseal tibial trabecular bone, which collectively resulted in lower BV/TV (-56%). While serum TRAcP5b was decreased, OcS/BS was unchanged by trabectedin. An established fatigue loading protocol was used to induce a stress fracture (sFx) in the left ulna of 16wk male C57BL/6 mice followed by 1wk of vehicle or trabectedin treatment (0.15mg/kg i.v., n=7-8/gp) with microCT, flow cytometry and immunofluorescent outcomes. Immediately (~3hr) after sFx fatigue loading in a separate cohort of mice (n=3/gp), significantly elevated levels (+60%) of apoptotic AnnexinV+PI+ cells were observed in ulnae with sFx. Given the increase in apoptotic cells, the presence of macrophages in the sFx was evaluated by F4/80 immunostaining at multiple time points. Robust macrophage presence was observed 4d after sFx induction and continued throughout healing. MicroCT analysis revealed that trabectedin significantly reduced total sFx callus size (-52%) as well as callus bone volume (-57%) after 1wk of healing. A corresponding trend (p=.10) towards reduced macrophage (F4/80) density within the stress fracture callus was observed in immunostained cryosections. In conclusion, trabectedin significantly compromises osteal macrophages and bone formation with a negative impact on bone healing. Results of this study may have immediate clinical relevance for patients receiving trabectedin treatment.

**Disclosures:** Benjamin Sinder, None.

## MO0688

**Suitability of Various Non-Invasive Imaging Techniques to Analyze Bone, Muscle and Fat Tissues in Ovariectomized Mice.** Jukka Vääräniemi\*, Thomas Delale\*, Tiina E Kähkönen\*, Jussi M Halleen\*, Thierry Abribat\*, Jukka Morko\*. <sup>1</sup>Pharmatest Services Ltd, Finland, <sup>2</sup>Alizé Pharma III SAS, France

Preclinical evaluation of drug candidates for treating musculoskeletal diseases could benefit from an integrated approach analyzing the pharmacological effects on both bone, muscle and fat tissues. A broad range of non-invasive imaging techniques are now available in animal models to address this evaluation, from dual-energy X-ray absorptiometry (DXA), peripheral quantitative computed tomography (pQCT), echo magnetic resonance imaging (MRI) to micro-computed tomography (μCT). Currently, mice are used increasingly in studies of musculoskeletal diseases. In this study, we evaluated the suitability of non-invasive DXA, pQCT, EchoMRI and μCT to measure bone, muscle and fat tissues in mice using the ovariectomy (OVX) model of human postmenopausal osteoporosis. This study was conducted using female C57BL/6J mice that were ovariectomized at 8 weeks of age. OVX-induced effects on bone, muscle and fat tissues were analyzed 9 weeks after the surgery. The effects were determined by DXA using Faxitron UltrafocusDXA, pQCT using Norland Stratec XCT Research SA+,

EchoMRI using EchoMRI-700 Quantitative Magnetic Resonance, and  $\mu$ CT using SkyScan 1072 equipment. Surgical ovariectomy increased body weight after 9 postsurgery weeks. EchoMRI and DXA demonstrated that this OVX-induced increase in body weight was due to an increase in fat mass without apparent changes in lean mass, resulting in increased fat percentage in OVX mice. Similar OVX-induced effects were observed by pQCT in fat and muscle cross-sectional areas in calf. The OVX-induced reduction in areal bone mineral density (BMD) was demonstrated by DXA in whole body, long bones and lumbar vertebrae, in volumetric BMD by pQCT, and in trabecular bone volume and microarchitecture by  $\mu$ CT in long bone metaphysis. This study demonstrated that also in mice, DXA can be used to analyze effects on bone, muscle and fat both in whole body and specific regions, pQCT on bone, muscle and fat in specific regions, EchoMRI on muscle and fat in whole body, and  $\mu$ CT on bone in specific regions. These non-invasive imaging techniques enable follow-up of effects. Due to the small size of murine bones, the follow-up of treatment effects in trabecular bone by *in vivo*  $\mu$ CT would improve the analysis of preclinical efficacy in skeletal diseases studied extensively in mice, such as in rare bone diseases.

**Disclosures:** Jukka Vääräniemi, None.

## MO0689

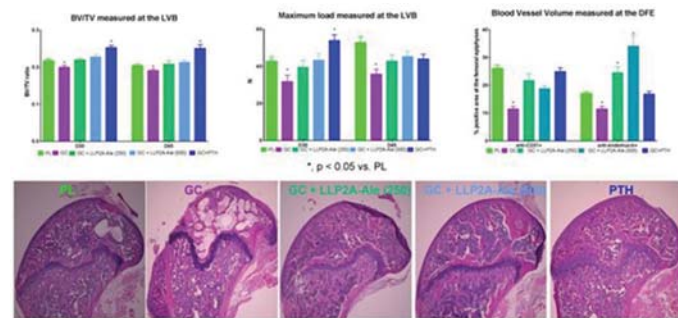
**Prevention of glucocorticoid induced osteonecrosis with either parathyroid hormone or LLP2A-Ale.** Wei Yao<sup>\*1</sup>, Geetha Mohan<sup>1</sup>, Yu-An Lay<sup>1</sup>, Alexander Kot<sup>1</sup>, MieJin Lim<sup>1</sup>, Donald Kimmel<sup>2</sup>, Nancy Lane<sup>1</sup>. <sup>1</sup>UC Davis Medical Center, United States, <sup>2</sup>University of Florida, United States

**Introduction.** A traumatic osteonecrosis (ON) results from reduced bone vascularity. Glucocorticoids (GC) are a major risk factor for ON as GCs reduce vascular endothelial growth factor, vascular density, and bone mass [Mohan et al CTI 2017]. GC-treated mice co-treated with either LLP2A-Ale, a bone targeted therapy that directs mesenchymal stem cells to bone surfaces, or PTH, showed significantly fewer GC-induced bone changes. This study's aim was to determine if PTH or LLP2A-Ale co-treatment prevents GC-induced ON.

**Methods.** Seven-week-old male BALB/c mice were randomized into Placebo (PL), PL+GC (4 mg/L dexamethasone in drinking water), GC+250  $\mu$ g/kg or GC+500  $\mu$ g/kg LLP2A-Ale (SC, 1X/2 wks), or GC+40  $\mu$ g/kg PTH (hPTH(1-34), 5x/wk, SC) (n=8 for PL and 16 for all GC groups). Mice were sacrificed on Day 30 or Day 45. Both distal femurs (DF) from each mouse were decalcified, sectioned frontally, and stained with H&E. ON was identified in the DF epiphysis (DFE) using modified criteria [Yang et al., JOR, 2009]: presence of empty osteocyte lacunae, nuclear pyknosis, ghost osteocytes in trabeculae bone, bone marrow/stromal necrosis, > 30% fat in marrow, and fibrin thrombi in blood vessels, particularly in the middle and lateral DFE. ON was diagnosed when three or more of the above features were seen, by three independent, blinded observers with >80% agreement. Immunohistochemical staining for blood vessels with CD31 and Endomucin antibodies was performed at the DFE. Bone volume (BV/TV) and bone strength were measured at the LVB.

**Results.** PL+GC mice had 15-20% lower BV/TV and bone strength than PL (p<0.05), which were prevented by concurrent treatment of LLP2A-Ale or PTH. At Day 30, ON prevalence was 18%, 6%, 0% and 6%, respectively, in PL+GC, GC+LLP2A-Ale (250), GC+LLP2A-Ale (500) and GC+PTH groups. At Day 45, ON prevalence was 81%, 25%, 18% and 12%, respectively, in GC, GC+LLP2A-Ale (250), GC+LLP2A-Ale (500), or PTH. Blood vessels (anti-CD31/endomucin) appeared more intact in GC+LLP2A-Ale and GC+PTH groups than in PL+GC at both times (p<0.05).

**Conclusion.** Co-treatment of murine GC-induced ON with PTH or LLP2A-Ale reduced the prevalence of ON after 45 days. Additional studies to ascertain the mechanism by which these agents prevent GC-induced ON are warranted.



GC-ON

**Disclosures:** Wei Yao, None.

## MO0690

**Bodyweight Supported Treadmill Training and Testosterone Produce Additive Bone Anabolic and Antiresorptive Benefit after Spinal Cord Injury.** Joshua Yarrow<sup>\*1</sup>, Ean Phillips<sup>1</sup>, Hui Jean Kok<sup>2</sup>, Christine Conover<sup>1</sup>, Taylor Bassett<sup>1</sup>, Hannah Prock<sup>1</sup>, Andrea Catter<sup>1</sup>, Carol Buydos<sup>1</sup>, Jessica Jiron<sup>2</sup>, J. Ignacio Aguirre<sup>2</sup>, Stephen Borst<sup>2</sup>, Fan Ye<sup>1</sup>. <sup>1</sup>VA Medical Center, United States, <sup>2</sup>University of Florida, United States

Bone loss after spinal cord injury (SCI) is influenced by disuse and other factors resulting from the neurologic insult, including testosterone (T) deficiency. In our rodent SCI model, bodyweight supported treadmill training (TM) partially prevents cancellous/cortical bone loss. In contrast, T treatment produces a near-complete preservation of cancellous bone, but does not prevent cortical bone deficits after SCI. Our purpose was to analyze whether a multimodal therapy involving T+TM prevents cancellous/cortical bone deficits after SCI. 16-week old male Sprague-Dawley rats (n=39) received: 1) SHAM surgery (T9 laminectomy), 2) severe (250 kdynes) contusion SCI, 3) SCI+T (7.0 mg/week, i.m.), or 4) SCI+T+TM. 50% bodyweight supported TM training was initiated 1-week post-SCI and consisted of two 20 min bouts/day, during which the hindlimbs were manually positioned into plantar stepping position, performed 5 days/week for 7 weeks. Severe cancellous bone loss was present after SCI, characterized by 54% lower proximal tibial BV/TV, reduced Tb.N, and increased Tb.Sp vs SHAM (p<0.01). These changes were accompanied by directionally higher Oc.S/BS and Ob.S/BS in SCI, suggestive of high-turnover osteopenia. T treatment minimized bone loss, evidenced by 43% higher BV/TV (non-significant) and lower Tb.Sp vs SCI (p<0.05). In comparison, T+TM completely prevented cancellous bone loss, producing 122% higher BV/TV, higher Tb.Th, and lower Tb.Sp vs SCI (p<0.01). The effects of T were primarily antiresorptive, indicated by lower Oc.S/BS (trend, p=0.076) and lower histomorphometric indices of cancellous bone formation vs SCI (p<0.05). In contrast, T+TM produced bone anabolic effects, evidenced by higher Ob.S/BS (trend, p=0.052) and higher histomorphometric bone formation indices vs T-alone (p<0.05), along with lower Oc.S/BS vs SCI (p<0.05). T+TM also produced 20% higher Ct.Th at the tibial diaphysis vs all other groups (p<0.01).  $\mu$ CT of femur indicated similar cancellous morphologic results. Interestingly, T+TM also exhibited the highest tissue mineral density at the distal femur and femoral diaphysis (p<0.01 vs SCI and SHAM), indicating improved cortical bone material density. Our findings suggest that T+TM is a viable therapy to prevent bone loss after SCI because 1) T reduced bone resorption and TM stimulated bone formation, resulting in additive benefit to cancellous bone and 2) cortical bone responded beneficially to the multimodal T+TM therapy.

**Disclosures:** Joshua Yarrow, None.

## MO0691

**Effect of Lowering Dietary Calcium and Vitamin D on Bone Development in Female CD-1 Mice.** Jenalyn L. Yumol<sup>\*1</sup>, C. Brent Wakefield<sup>2</sup>, Sandra M. Sacco<sup>2</sup>, Philip J. Sullivan<sup>2</sup>, Elena M. Comelli<sup>3</sup>, Wendy E. Ward<sup>4</sup>. <sup>1</sup>Health Sciences, Brock University, Canada, <sup>2</sup>Kinesiology, Brock University, Canada, <sup>3</sup>Nutritional Sciences, University of Toronto; Kinesiology, Brock University, Canada, <sup>4</sup>Health Sciences, Brock University; Kinesiology, Brock University; Nutritional Sciences, University of Toronto, Canada

The AIN93G control diet is a widely used reference diet for rodent studies to allow for comparison within and between research groups. With respect to bone development, studies in rodents suggest current levels of dietary vitamin D (vit D, 1000 IU/kg diet) and calcium (Ca, 5 g/kg diet) may be higher than required. For the AIN93G diet, lowering dietary vit D has little effect while lower levels of Ca (2.5 g Ca/kg diet or lower) compromise bone development. However, the effect of lowering both dietary Ca and vit D on bone structure has not been thoroughly studied. While sex-specific responses are possible, due to differences in growth rates and absolute growth, this study focused on bone development in females as a first step. Objective: To determine if lowering the level of Ca and vit D of the AIN93G diet supports normal bone development in female CD-1 mice at 2 and 4 months of age. Methods: Weanling females (n=118) were randomized to 1 of 2 trials that studied 100 or 400 IU vit D/kg diet, respectively. Within a trial, mice were randomized to 1 of 3 Ca levels (3.5, 3 or 2.5g Ca/kg diet) until 4 months of age. A group fed reference AIN93G diet (REF, 1000 IU vit D, 5g Ca/kg diet) was also included in each trial. At 2 and 4 months of age, *in vivo* bone structure and bone mineral density (BMD) were assessed using microCT at the proximal and midpoint tibia. *Ex vivo* lumbar vertebrae (L4) structure was also analyzed. Results: For both trials, there were bone developmental changes between 2 and 4 months. In regards to the effect of dietary interventions, there were no differences (p>.05) in trabecular (proximal tibia) or cortical (tibia midpoint) bone morphology or BMD, except at 2 months in the 400 IU trial, mice fed 2.5g Ca/kg diet had lower (p<.05) cortical area fraction than the REF group and lower (p<.05) cross sectional thickness than the REF and 3.5g Ca/kg diet groups. In the 400 IU trial, bone volume fraction of L4 was lower (p<.05) in the 3.0g Ca/kg diet group compared to REF. Conclusion: There are modest effects to bone development with lowering the level of both Ca and vit D in AIN93G diet. That an effect at L4 occurs at 400 IU and not 100 IU vit D (at the same Ca levels) requires further investigation. Because AIN93G diet may provide Ca and vit D in excess, benefits of novel dietary interventions to support bone health may be masked. Refinement of Ca and vit D levels for studies investigating diet to support bone development is warranted.

**Disclosures:** Jenalyn L. Yumol, None.



## MO0692

**Serum Inflammatory Biomarkers and Monocyte Responses in Fibrodysplasia Ossificans Progressiva.** Emilie Barluet<sup>\*1</sup>, Blanca M Morales<sup>1</sup>, Tea Chan<sup>1</sup>, Katherine Bigay<sup>1</sup>, Jennifer Ho<sup>1</sup>, Mary Nakamura<sup>2</sup>, Edward C Hsiao<sup>1</sup>.  
<sup>1</sup>University of California, San Francisco, United States, <sup>2</sup>UCSF/SFVAMC, United States

Heterotopic ossification (abnormal bone formation in soft tissue) is known to be triggered in inflammatory settings, although the underlying mechanisms are poorly understood. Diseases of heterotopic bone formation such as fibrodysplasia ossificans progressiva (FOP) give valuable insights into human-specific mechanisms of increased bone formation. FOP is associated with mutations in the Activin A type I receptor (ACVR1), a BMP receptor increases ACVR1 signaling activity and response to both BMP and Activin A ligands. FOP is characterized by progressive and debilitating heterotopic ossification, often occurring in inflammatory flares with pain, erythema, swelling, and localized edema. The forming bone lesions contain multiple cell types, including large numbers of macrophages that may play a key role in modulating osteogenesis. We hypothesized that patients with FOP are in a pro-inflammatory state that increases their sensitivity to inflammatory insults. Using carefully-obtained samples of blood from 8 FOP subjects without a flare, 6 FOP patients with ongoing flare, and 6 control subjects, we found elevated levels of pro-inflammatory and myeloid cytokines IL-3 ( $0.42 \pm 0.1$  pg/ml vs  $0.13 \pm 0.02$  pg/ml,  $p < 0.05$ ), IL-7 ( $4.06 \pm 0.85$  pg/ml vs  $0.91 \pm 0.21$  pg/ml,  $p < 0.05$ ), and IL-8 ( $48.38 \pm 12.75$  pg/ml vs  $11.55 \pm 2.03$  pg/ml,  $p < 0.05$ ) in the serum of FOP patients with no flare compared to WT. These elevations were not present in FOP subjects treated with standard-of-care prednisone for a flare. We also found that IL-10 (FOP  $8.09 \pm 2.30$  pg/ml vs WT  $0.96 \pm 0.73$  pg/ml,  $p < 0.05$ ) was increased in FOP patients at baseline with no flare. Increased IL-10 has been described as a negative feedback mechanism to counteract excessive activation of immune cells in inflammatory and auto-immune disease. We also analyzed the different subtypes (classical, intermediate and non-classical) of monocytes present in whole blood of FOP patients. We found a significant increase in the intermediate monocyte population that is thought to be pro-inflammatory. Sorted CD14<sup>+</sup> primary monocytes from FOP subjects showed increased gene expression of CCL5 ( $p < 0.01$ ), CCR7 ( $p < 0.05$ ), and CXCL10 ( $p < 0.05$ ) in response to lipopolysaccharide (LPS) treatment. Together, these results suggest a pro-inflammatory state at baseline in FOP patients that can be detected in serum and FOP monocytes. The insights gained from these studies indicate that modulation of the inflammatory state may be a key strategy for mitigating the devastating progression of FOP. In addition, the results suggest a significant role for monocyte-lineage cells in heterotopic ossification. Further study of the inflammatory responses will help identify how disruptions of the normal bone-regulating roles of monocytes and macrophages trigger heterotopic bone formation, and whether these immune targets may be amenable to modulation as part of a comprehensive treatment strategy.

**Disclosures:** Emilie Barluet, None.

## MO0693

**Improvement of severe bone pain from fibrous dysplasia of bone with tocilizumab treatment - A case report.** Nadia Mehseu-Cetre<sup>\*1</sup>, Deborah Gensburger<sup>2</sup>, Johanna Benhamou<sup>2</sup>, Roland Chapurlat<sup>2</sup>. <sup>1</sup>Bordeaux University Hospital, FHU ACRONIM, France, <sup>2</sup>Lyon University Hospital, Rheumatology department, France

#### Introduction :

Fibrous dysplasia of bone (FD) is a rare genetic disease, characterized by bone pain, fractures and bone deformity.

This disease is due to a somatic mutation of GNAS, leading to fibrous tissue proliferation in the bone marrow by undifferentiated pre-osteoblastic cells. These cells produce excess of interleukin 6 (IL6), with increased bone resorption and creation of osteolytic lesions as a result. Bisphosphonate (BP) therapy is the usual first line to treat bone pain of FD, but a small subset of patients do not respond or relapse after an initial favorable response. Therefore, we reasoned that an IL-6 inhibitor, tocilizumab, may rescue those patients not responding to BPs.

#### Case Report :

A 54-year-old man was admitted to our hospital for severe cervical pain associated with right C8 cervicobrachial neuralgia in March 2015.

The diagnostic of fibrous dysplasia was confirmed after histological examination of the first rib resected in 1989. Neither the surgery in 1999, nor repeated bisphosphonate infusions (pamidronate, then zoledronate), nor denosumab (60 mg twice a year) could relieve his intense pain.

Given this intractable pain, and the inability to perform a complete surgical resection, we proposed a tocilizumab treatment (8mg/kg once a month), i.e., the same dosage that for rheumatoid arthritis.

The patient gave informed consent.

Before the first infusion, the pain visual analog scale (VAS) was 8/10, while on pregabalin (600mg/day), acetaminophen (3g/day) and morphin (sometimes 20 mg/day) treatments. Bone pain decreased after the 5<sup>th</sup> infusion and complete pain relief was obtained after six months of therapy with a pain VAS at 0/10 and no pain medication. Tocilizumab was stopped after the ninth infusion. Eighteen months after the treatment withdrawal, no relapse has been noted without any pain medication needed. In parallel, we observed that biochemical markers of bone turnover (serum CTX and bone alkaline phosphatase), which were low at study entry, did not increase substantially, i.e., without any rebound after denosumab cessation.

#### Discussion

To our knowledge, this was the first experience of tocilizumab therapy in fibrous dysplasia in a patient with inadequate response to both bisphosphonates and denosumab. A placebo-controlled randomized trial is currently ongoing to establish the value of this drug in FD.

**Disclosures:** Nadia Mehseu-Cetre, None.

## MO0694

**Bone Involvement in Gaucher Disease is Related to Late Diagnosis and Treatment.** Diana Gonzalez<sup>\*1</sup>, Felisa Quiroga<sup>2</sup>, Claudio Silva<sup>2</sup>, Paula Rozenfeld<sup>3</sup>, Beatriz Oliveri<sup>4</sup>. <sup>1</sup>Mautalen, Salud e Investigación, Argentina, <sup>2</sup>Diagnóstico Maipú, Argentina, <sup>3</sup>LISIN Departamento de Ciencias Biológicas Facultad de Ciencias Exactas Universidad Nacional de La Plata, Argentina, <sup>4</sup>Laboratorio de Osteoporosis y Enfermedades Metabólicas Oseas INIGEM UBA Conicet Hospital de Clínicas Jose de San Martín, Argentina

Gaucher disease (GD) is the most prevalent lysosomal storage disease. Even asymptomatic patients may have bone complications that impair quality of life

Purpose: Evaluating bone involvement in type 1GD patients receiving enzymatic replacement treatment (ERT) with velaglucerase (VG).

Methods: observational, transversal and prospective analysis. Demographic data and antecedents of GD (clinical presentation, time from diagnosis and under ERT) were recorded. Skeletal involvement was evaluated by X-rays (spine and lower limbs) bone densitometry (BMD) and magnetic resonance imaging (MRI) of lumbar spine (LS), femur and total skeleton. Laboratory: hemogramme, ferritin (FT), angiotensin converting enzyme (ACE), chitotriosidase (CHIT), intact parathormone (iPTH), 25hydroxyvitamin D (25OHD) and in adults patients  $\beta$  cross laps [CTX] and bone alkaline phosphatase (BAP)

Results: 27 patients were included (11 males; age:  $24.7 \pm 14$  years; 33% <20 years-old). Age at diagnosis was  $\leq 20$  in 74% of patients. Reason for consultation included bone symptoms in 22% of the patients. Sixteen patients had received VG as first ERT (naïve).

Although all subjects met therapeutic goals (TG) for visceromegalies and 26/27 for hematological parameters, X-ray alterations were detected in 55% of patients included irreversible lesions: avascular necrosis (AVN), bone infarction (BI) and vertebral fractures. MRI showed bone infiltration in femur (52%), spine (15%) and in other bones (44%) and also showed AVN (n=10), BI (n=8) and edema (n=6). LS BMD Z-score was  $< -1$  in 6 patients, without correlation with fractures.

Insufficient (n=11) or deficient (n=5) 25OH-D levels were found and 5 patients had elevated PTH levels. CHIT, ACE and FT were elevated in 81 %, 44% and 28% respectively. In 7 adults with bone infiltration, CTX levels were elevated.

Time from diagnosis correlated with the presence of fractures and skeletal involvement in MRI ( $p < 0.05$ ). Bone marrow infiltration did not significantly correlate neither with ferritin, CHIT or ACE levels nor with BAP but highly correlated with CTX levels ( $p = 0.0004$ ). Naïve patients had lower incidence of bone marrow infiltration, AVN and BI ( $p < 0.01$ )

Conclusions: Even after reaching TG, 44% had irreversible bone lesions. Prevalence of bone involvement was lower among subjects who started velaglucerase therapy soon after diagnosis of GD. The relevance of early diagnosis and ERT to avoid skeletal complications is highlighted

**Disclosures:** Diana Gonzalez, Shire , Speakers' Bureau.

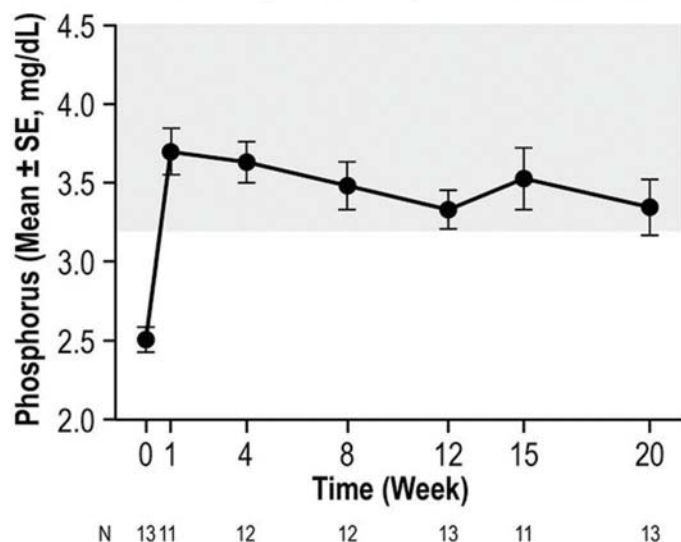
## MO0695

**The Effects of Burosumab (KRN23), a Fully Human Anti-FGF23 Monoclonal Antibody, on Phosphate Metabolism and Rickets in 1 to 4-Year-Old Children with X-linked Hypophosphatemia (XLH).** Erik Imel<sup>\*1</sup>, Thomas Carpenter<sup>2</sup>, Gary S Gottesman<sup>3</sup>, Javier San Martin<sup>4</sup>, Meng Mao<sup>4</sup>, Alison Skrinar<sup>4</sup>, Michael P Whyte<sup>3</sup>. <sup>1</sup>Indiana University School of Medicine, United States, <sup>2</sup>Yale University School of Medicine, United States, <sup>3</sup>Shriners Hospitals for Children, United States, <sup>4</sup>Ultragenyx Pharmaceutical Inc., United States

In XLH, hypophosphatemia is mediated by elevated circulating levels of fibroblast growth factor 23 (FGF23). The resulting skeletal abnormalities, including rickets and lower extremity deformity, can impair ambulation and quality of life. Burosumab, an investigational human monoclonal antibody, binds FGF23 and inhibits its action. Interim results from a Phase 2 study of burosumab in 5 to 12-yr-old children with XLH showed improved serum phosphorus (Pi) and improvement of rickets. In an ongoing, open-label, multicenter trial, children 1-4 yrs old with XLH began burosumab treatment at 0.8 mg/kg SC every 2 weeks (Q2W), titrated to 1.2 mg/kg if serum Pi remained below the target range. We evaluated safety and efficacy based on serum Pi, 1,25(OH)<sub>2</sub>D, and alkaline phosphatase (ALP) levels, and a radiographic rickets severity score (RSS). Biochemical data for 13 children treated with burosumab for 24 weeks are reported here, and changes in rickets severity at Week 40 will be presented. Mean age at BL (N=13) was 2.9 yrs; 9/13 (69%) were boys. Radiographic rickets (RSS $\geq 2.0$ ) was present in 11/13 (85%) children despite prior conventional therapy for a mean of 17 months. All had low serum Pi levels (mean[SE]= $2.5[0.08]$  mg/dL; normal: 3.2-6.1). ALP was elevated in 11/13 (85%) children. During burosumab treatment, mean serum Pi increased by  $+1.2$  (0.08) mg/dL and  $+1.1$  (0.09) mg/dL at Weeks 1 and 4, respectively, and was maintained through Week 20 ( $+0.8$  [0.14] mg/dL). Normal serum Pi levels were

achieved in 82%, 83%, and 62% of children at Weeks 1, 4, and 20. Mean (SE) ALP levels decreased from 549 (54) U/L at BL to 389 (23) U/L at Week 20. Mean (SE) serum 1,25 (OH)<sub>2</sub>D levels increased from 45 (5.1) pg/mL at BL to 94 (9.2) pg/mL, 68 (4.4) pg/mL, and 61 (3.9) pg/mL at Weeks 1, 12, and 20. During 24 weeks of burosumab therapy, no serious AEs were reported. All adverse events (AEs) were mild or moderate, except for a Grade 3 food allergy considered unrelated to study drug. The most common AEs were pyrexia and upper respiratory tract infection (each in 39% of children), and injection site reactions (23% of children). There were no meaningful increases in calcium or PTH. Initial results in 1 to 4-yr-old children with XLH treated with burosumab confirm that pharmacodynamic responses and the safety profile are similar to those findings in older children with XLH. The significant decrease in ALP suggests healing of rickets, and the radiographic findings will be presented at the meeting.

### Serum Phosphorus Response to Burosumab



Figure

Disclosures: Erik Imel, Ultragenyx Pharmaceutical Inc., Consultant.

## MO0696

**High-Turnover Bone Disease Due to a Novel 27-Base Pair Tandem Duplication in *TNFRSF11A* Leading to Constitutively Active RANK.** Sean J. Iwamoto<sup>\*1</sup>, Micol S. Rothman<sup>1</sup>, Shenghui Duan<sup>2</sup>, Steven Mumm<sup>2</sup>, Kelsey Burr<sup>1</sup>, Michael P. Whyte<sup>3</sup>. <sup>1</sup>Division of Endocrinology, Metabolism & Diabetes, University of Colorado School of Medicine, United States, <sup>2</sup>Division of Bone and Mineral Diseases, Washington University School of Medicine at Barnes-Jewish Hospital, United States, <sup>3</sup>Center for Metabolic Bone Disease and Molecular Research, Shriners Hospital for Children, United States

**Purpose:** Rare genetic bone diseases include the monogenic disorders of receptor activator of nuclear factor kappa-B (RANK). Several result from heterozygous autosomal dominant tandem duplications within exon 1 of *TNFRSF11A*, the gene that encodes the signal peptide of RANK. Depending on duplication length, these mutations seem to cause different skeletal diseases (1-4) related to constitutive RANK activity causing high-turnover bone disease via accelerated osteoclast formation and activation. We have identified a novel 27-base pair tandem duplication causing what has been called early-onset Paget disease of bone (PBD2).

**Case:** A 48-year-old Mexican man infected with HIV was evaluated for very low BMD and multiple atraumatic fractures starting in adulthood, including bilateral femur fractures. Transient hypercalcemia followed hip surgery. His viral load was suppressed on HAART. He had adult-onset tooth and hearing loss. He did not report familial bone disease, but his father had short stature and multiple fractures. Physical exam revealed a height of 5'2", edentulous mouth, subjective right > left hearing loss, white sclerae, thoracic kyphosis, widened fingers, and anteriorly bowed tibias. Serum alkaline phosphatase (ALP) was 330 U/L (n: 39-117) and bone-specific ALP was 87.6 ug/L (n: 6.5-20.1), whereas parathyroid hormone, calcium, 25-OH vitamin D and phosphorus were normal. Bone turnover markers were strikingly elevated: serum C-terminal telopeptide 2477 pg/mL (n: 60-700) and osteocalcin 281 ng/mL (n: 11-50). DXA spine BMD Z-score was -5.5. Skeletal survey showed lucent bones with vertebral compression fractures, trabecular coarseness, calvarial lucencies, and thinned long bone cortices (Figure 1). We identified a unique, heterozygous 27-base pair duplication (77dup27) in exon 1 of *TNFRSF11A*. Alendronate, 70 mg/week, modestly decreased bone turnover markers at 6 weeks.

**Conclusions:** Our patient's high-turnover bone disease involves a novel 27-base pair duplication in *TNFRSF11A*, elongating the signal peptide of RANK. Similar 27-base pair duplications have been identified in Japanese (75dup27) and Chinese (78dup27) PBD2 cohorts, predicting the same 9-amino acid extension (4). Our patient shares features of PBD2 with presentation in his late 20s, painless enlarged fingers, transient post-op hypercalcemia, and absence of childhood tooth or hearing loss. Our experience

supports mutation analysis in the diagnosis and understanding of high-turnover bone diseases.

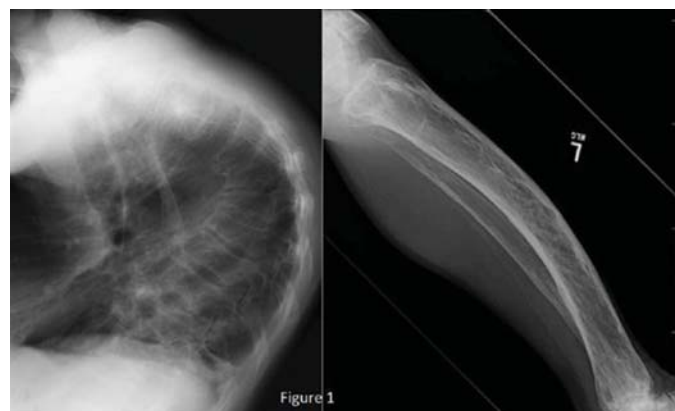


Figure 1 High-Turnover Bone Disease Due to a Novel 27-Base Pair Tandem Duplication in *TNFRSF11A*

Disclosures: Sean J. Iwamoto, None.

## MO0697

**Earlier onset age of p.R179 than p.R176 mutation of *FGF23* gene in autosomal dominant hypophosphatemic rickets: Analysis of 6 Chinese pedigrees and review of the literature.** Zhen Zhao\*, Chang Liu, Ou Wang, Mei Li, Xiaoping Xing, Yue Sun, Yan Jiang, Weibo Xia. Department of Endocrinology, Key Laboratory of Endocrinology, The Ministry of Health, Peking Union Medical College Hospital, Chinese Academy of Medical Sciences, China

**Objective:** To compare the clinical features between autosomal dominant hypophosphatemic rickets (ADHR) patients with p.R176 mutation and p.R179 mutation, as well as to explore the additional contribution of c.716C>T, p.T239M mutation in *FGF23* gene on occurrence and progression of ADHR.

**Methods:** 6 Chinese kindreds of ADHR were collected with their manifestations and lab examinations, genetic analysis were performed using Sanger sequence. Literatures about ADHR in pubmed were reviewed. Statistical analyses were performed using IBM SPSS 23.

**Results:** Of the 11 ADHR patients, patients with p.R179 mutation tended to have earlier onset than patients with p.R176 mutation (1.3(1.0,37.0)year-old versus 28.5 (19.0,44.0)year-old). More patients with p.R179 mutation have a history of rickets with low extremity deformity and growth retardation (3/5, 60%) than patients with p.R176 mutation (1/15, 6.6%), ( $p<0.05$ ). The serum phosphate of patients with p.R179 and p.R176 mutation were  $0.82\pm0.33$ mmol/L versus  $0.68\pm0.30$ mmol/L. Together with other ADHR patients in the world, earlier onset was found in patients with p.R179 than those with p.R176 mutation (1.0(0.9, 36) year-old versus 27.0(1.2, 54) year-old,  $p<0.01$ ). Patients with p.R179 mutation revealed more severe manifestation than those with p.R176 mutation (rickets: 84.6% versus 11.5%,  $p=0.000$ ; low extremity deformity: 83.3% versus 16%,  $p=0.000$ ; growth retardation: 77.7% versus 4.3%,  $p=0.000$ ). ADHR patients with p.T239M mutation tended to have more severe hypophosphatemia and higher *FGF23* than other ADHR patients.

**Conclusions:** Patients with p.R179 mutation have earlier onset of ADHR and more severe syndromes than those with p.R176 mutation. Most patients with p.R179 mutation have history of rickets with growth retardation and low extremity deformity. Patients with p.T239M mutation reveal more severe condition than patients without this mutation, which might explain the variable expressivities of ADHR patients.



**Table 1.** Clinical manifestations and laboratory findings of ADHR patients with p.R176 and p.R179 mutation.

	Mutation in p.R176	Mutation in p.R179
No. of female/male	11/4	5/0
Onset age	28.5 (19.0, 44.0)	1.3 (1.0, 37.0)
Rickets	0	3/5*
Growth retardation	0/15	3/5*
Low extremity deformity	1/15	3/5*
Iron deficiency anemia	5/15	4/5
Hypophosphatemia	7/15	4/5
Serum P(mmol/L)	0.82±0.33	0.68±0.30
Serum Ca(mmol/L)	2.42±0.17	2.29±0.08
ALP (U/L)	130±70	224±194
i-PTH (pg/ml)	76.5(19.5,222.0)	39.2(36.1,81.8)
TmP/GFR(mmol/L)	0.44(0.26,2.00)	0.21(0.08,0.34)
i-FGF23(pg/ml)	130.4(19.8,1034.01)	82.2(23.2,474.9)

Values with normal distribution are expressed as mean ± SD, values with asymmetric distribution are expressed as Median(range). Reference values: serum phosphate(P), 0.81–1.45mmol/l in adults; serum total Ca, 2.13–2.70mmol/l; serum alkaline phosphatase (ALP), 35–100 U/l; serum i-PTH,12–65pg/ml; TmP/GFR, 0.8–1.35 mmol/L; serum intact fibroblast growth factor (FGF)23, 10–50 pg/ml in our laboratory

i-PTH, intact parathyroid hormone; TmP/GFR, ratio of phosphorus tubule maximum (TmP) to glomerular filtration rate (GFR).

\*: p<0.05, compared with p.R176 group

Clinical manifestations and laboratory findings of ADHR patients with p.R176 and p.R179 mutation

**Disclosures:** Zhen Zhao, None.

## MO0698

### Gestational Gigantomastia Complicated By PTHrP-mediated Hypercalcemia.

Taher Modarressi<sup>\*1</sup>, Michael A. Levine<sup>2</sup>, Amna N. Khan<sup>1</sup>. <sup>1</sup>Department of Endocrinology, Hospital of the University of Pennsylvania, United States, <sup>2</sup>Division of Endocrinology and Diabetes, Children's Hospital of Philadelphia, United States

PTHrP-mediated hypercalcemia in gestational gigantomastia has only been reported once previously: a 24-year-old female experienced resolution of hypercalcemia after bilateral mastectomy, subsequently delivering a healthy infant at term (1). We present the first case of PTHrP-mediated hypercalcemia in gestational gigantomastia with resolution on termination of pregnancy.

A 33-year-old female was transferred to our institution at 17 weeks' gestation for management of hypercalcemia and bilateral mastitis. She had presented at week 13 with sepsis, suspected from mastitis. She reported a two month-history of fatigue, headache and constipation corresponding with development of gigantomastia. Initial labs had revealed serum calcium 14 mg/dL, undetectable 25(OH)D and mildly elevated PTHrP. There was no history of hypercalcemia during previous pregnancies. Whole body MRI failed to disclose evidence of malignancy and a breast biopsy revealed only hyperplasia.

Our initial laboratory evaluation revealed Ca 11.1 mg/dL (albumin-corrected 12.8 mg/dL), ionized Ca 1.63 mmol/L (nl 1.00-1.25), 25(OH)D 14 ng/mL (nl 25-80), 1,25(OH)2D 142 pg/mL (2nd trimester nl 72-160), PTH 0.7 pmol/L (nl 1.6-6.9), PTHrP 19.2 pmol/L (nl <3.4), and normal phosphate, prolactin, ACE level, SPEP and UPEP. She was initially treated with prednisone and thereafter switched to calcitonin and cinacalcet. Corrected Ca levels improved to the upper limit of normal, but soon climbed due to suspected calcitonin tachyphylaxis. The patient declined bilateral mastectomy and requested termination of pregnancy, which was performed at week 20 of gestation. She experienced rapid resolution of hypercalcemia: corrected Ca decreased from 12.8 to 10.9 and 9.5 mg/dL on post-op days 1 and 2, respectively. PTH increased from 0.7 to 2.0 pmol/L and PTHrP decreased from 29.7 to 5.0 and 2.9 pmol/L on post-op days 1 and 4, respectively. Unfortunately, she was lost to follow-up until six months later when she presented for bilateral mastectomy; two months post-op, labs showed Ca 9.4 mg/dL, PTH 4.0 pmol/L and PTHrP <2.0 pmol/L.

This rare case, which demonstrated resolution of hypercalcemia and PTHrP excess after termination of pregnancy in a patient with gestational gigantomastia, suggests either a pathologic placental source of PTHrP or excessive breast PTHrP due to oversensitivity or over-production of placental hormones.

1) Pseudohyperparathyroidism Secondary to Gigantic Mammary Hypertrophy, Arch.Surg. 123:80, 1988.



Pre-bilateral mastectomy

**Disclosures:** Taher Modarressi, None.

## MO0699

### Assessment Tools of Physical and Functional Disability in Fibrodysplasia Ossificans Progressiva (FOP).

Frederick S. Kaplan<sup>\*1</sup>, Edward C. Hsiao<sup>2</sup>, Genevieve Baujat<sup>3</sup>, Maja Di Rocco<sup>4</sup>, Matthew A. Brown<sup>5</sup>, Carmen De Cunto<sup>6</sup>, Richard Keen<sup>7</sup>, Mona Al Mukaddam<sup>8</sup>, Donna R. Grogan<sup>9</sup>, Robert J. Pignolo<sup>10</sup>. <sup>1</sup>The University of Pennsylvania, Perelman School of Medicine, United States, <sup>2</sup>Institute of Human Genetics and the Division of Endocrinology & Metabolism, University of California, San Francisco, United States, <sup>3</sup>Departement de Genetique, Institut IMAGINE and Hôpital Necker-Enfants Malades, France, <sup>4</sup>Unit of Rare Diseases, Department of Pediatrics, Gaslini Institute, Italy, <sup>5</sup>Queensland University of Technology, Faculty of Health, School - Biomedical Sciences, Australia, <sup>6</sup>Department of Pediatrics/Hospital Italiano de Buenos Aires, Argentina, <sup>7</sup>The Royal National Orthopaedic Hospital (Stanmore), United Kingdom, <sup>8</sup>The University of Pennsylvania, United States, <sup>9</sup>Clementia Pharmaceuticals Inc., United States, <sup>10</sup>Geriatric Medicine & Gerontology, Mayo Clinic College of Medicine, United States

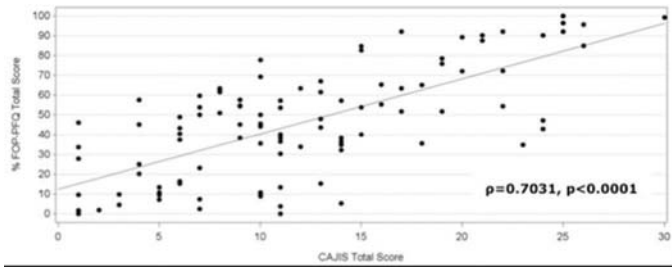
FOP is a rare, genetic disease of congenital skeletal malformations and progressive heterotopic ossification that irreversibly restricts movement and physical function. One aim of a cross-sectional analysis of baseline data from an on-going, 3-year, global, natural history study (NHS) of FOP is to evaluate progression of functional disability using the Cumulative Analogue Joint Involvement Scale for FOP (CAJIS) and the FOP-Physical Function Questionnaire (FOP-PFQ).

The CAJIS is a physician-administered measure that categorizes range of motion across 12 joints (left/right shoulder, elbow, wrist, hip, knee, and ankle) and three body regions (jaw, cervical spine, and thoraco-lumbar spine) as 0=uninvolved; 1=partially involved; 2=completely ankylosed (total score range of 0 [normal] to 30 [all joints/regions ankylosed]). The FOP-PFQ is a disease-specific patient-reported outcome measure of physical impairment. Age-appropriate forms assess activities of daily living and physical performance; data were analyzed as a percent of the total possible score (higher percentages represent greater impairment).

The cross-sectional analyses were derived from baseline data in 114 subjects ranging from 4 to 56 yrs; with good representation across age categories (2 to <8 yrs: 15%; 8 to <15 yrs: 32%; 15 to <25 yrs: 30%, ≥25 to ≤65 yrs: 24%). Subject age was strongly correlated with worsening CAJIS total scores ( $p=0.65$ ,  $p<0.0001$ ) with an estimated average change per year, based on a linear regression model, of 0.47 units. A weaker correlation was observed between age and FOP-PFQ ( $p=0.41$   $p<0.0001$ ), with an estimated average change per year of 1.2%. The findings were corroborated in a subset of subjects (N=57) with assessments at baseline and 12 months in which the observed mean changes were 0.40 units for the CAJIS and 3.0% for the FOP-PFQ. The CAJIS and FOP-PFQ were highly correlated with each other ( $p=0.70$ ,  $p<0.0001$ ), indicating that patient reports of functional impairment are closely related to physician-assessed functional disability (see figure).

In conclusion, the NHS cross-sectional findings demonstrate that these assessment tools can measure progression of functional and physical disability over a patient's lifetime. However, they are not sensitive to detect this progression over a 12-month period.

Acknowledgments: the authors wish to thank the FOP patient community and the clinical research teams for their participation and support of this study.



Correlation of Two Assessment Tools of Physical and Functional Disability in FOP

**Disclosures:** Frederick S. Kaplan, None.

## MO0700

**Diagnosis and Management of Osteopetrosis: Consensus Guidelines from the Osteopetrosis Working Group.** Calvin Wu<sup>\*1</sup>, Michael J. Econs<sup>2</sup>, Linda A. DiMeglio<sup>2</sup>, Karl L. Insogna<sup>3</sup>, Michael A. Levine<sup>4</sup>, Paul J. Orchard<sup>5</sup>, Weston P. Miller<sup>5</sup>, Anna Petryk<sup>6</sup>, Eric T. Rush<sup>7</sup>, Dolores M. Shoback<sup>8</sup>, Leanne M. Ward<sup>9</sup>, Lynda E. Polgreen<sup>1</sup>. <sup>1</sup>Los Angeles Biomedical Research Institute at Harbor-UCLA Medical Center, United States, <sup>2</sup>Indiana University School of Medicine, United States, <sup>3</sup>Yale School of Medicine, United States, <sup>4</sup>University of Pennsylvania Perelman School of Medicine, United States, <sup>5</sup>University of Minnesota, United States, <sup>6</sup>Alexion Pharmaceuticals, Inc., United States, <sup>7</sup>University of Nebraska Medical Center, United States, <sup>8</sup>University of California, San Francisco, United States, <sup>9</sup>University of Ottawa, Canada

**Background.** The term osteopetrosis encompasses a group of rare metabolic bone diseases characterized by impaired osteoclast activity or failure of osteoclast development, resulting in high bone mineral density. Existing guidelines for the management of osteopetrosis focus on treatment of the severe “malignant” forms with hematopoietic cell transplantation (HCT), which is not the standard-of-care treatment for the less severe forms of the disease. There are currently no published guidelines on the management of patients with osteopetrosis who have not been treated with HCT. Therefore, the objective of this project was to develop expert consensus guidelines that would address the management of this group of patients.

**Methods.** A modified Delphi method was used to build consensus. This involved anonymous online surveys sent by email to participants of the Osteopetrosis Working Group. After the first survey was completed, areas of agreement and conflict were identified and used in developing a follow up survey. The strength of recommendations and quality of evidence was graded using the Grading of Recommendations, Assessment, Development, and Evaluation (GRADE) system.

**Results.** Consensus was found in the areas of diagnosis, monitoring, and treatment. We recommend relying upon characteristic radiographic findings of osteopetrosis to make the diagnosis, and that genetic testing adds important information by identifying mutations associated with unique disease complications but is not required for the diagnosis. We recommend ongoing monitoring for changes in mineral metabolism and other complications of osteopetrosis such as cranial nerve impingement, anemia, leukopenia, and dental disease every 6-12 months depending on disease severity. We suggest that calcitriol should not be used in high doses for treatment of osteopetrosis and instead recommend symptom-based supportive therapy for disease complications since there is currently no established effective medical treatment for osteopetrosis.

**Conclusions.** Scarcity of published studies on osteopetrosis reduce the ability to develop evidence-based guidelines for the clinical management of these patients. Despite this, expert opinion-based guidelines for this rare condition are important to enable improved care and optimized patient outcomes.

**Disclosures:** Calvin Wu, None.

## MO0701

**Passive Coping Strategies Are Associated With Higher Impairment In Quality Of Life In Patients With Fibrous Dysplasia.** Marlous Rotman<sup>\*</sup>, Cornelia Andela, Bas Majoer, Ad Kaptein, Sander Dijkstra, Neveen Hamdy, Neveen Hamdy, Natasha Appelman-Dijkstra. Leiden University Medical Center, Netherlands

**Introduction** Fibrous dysplasia (FD) is a chronic, rare bone disease with a wide spectrum of skeletal and extraskeletal manifestations, all impacting to various degrees on quality of life (QoL), with bone pain being the major determinant. Earlier analysis of QoL, using the Short Form 36 (SF-36), suggests that FD patients may have adequate coping strategies. In this study we further explore this premise by using the Utrecht Coping List (UCL).

**Methods** The SF-36 and the UCL were sent to 138 consecutive patients, aged >16 years, who attended the FD clinic of the Leiden University Medical Center between 2013-2016. Data on age, gender, age at diagnosis, FD type, Skeletal Burden Scores (SBS) and relevant serum biochemistry were retrieved from electronic medical records. Coping

strategies of FD patients were compared to reference data from a population of patients with chronic pain of multiple origin, and 700 healthy individuals.

**Results** There were 61 women and 31 men, response rate was 67%. Median age was 47 years (range 16-80 years). FD patients reported seeking more distraction ( $p<0.01$ ), being more avoidant ( $p<0.01$ ) and fostering more reassuring thoughts ( $p=0.01$ ), but seeking less social support ( $p<0.01$ ) compared to healthy individuals. FD patients further reported using more active coping strategies ( $p<0.01$ ), seeking more distraction ( $p=0.01$ ) and social support ( $p<0.01$ ), but using less passive coping strategies ( $p=0.02$ ) compared to patients with chronic pain. FD-type and clinical severity did not influence any coping domain. Using more passive coping strategies correlated with a higher impairment in the SF-36 domains: social function, physical role, mental health, vitality and general health ( $p<0.01$  in all), but using more active coping strategies correlated with better mental health ( $r=0.235$ ;  $p=0.04$ ).

**Conclusion** Our findings suggest that in FD patients coping is independent of type or clinical severity of FD, with passive coping significantly decreasing most aspects of QoL, whereas active coping beneficially influences mental health. FD patients appear to have significantly different coping strategies to deal with their illness than patients with chronic pain. We believe that our findings shed an important light on the so far little known ability of patients with FD to cope with their chronic illness.

**Disclosures:** Marlous Rotman, None.

## MO0702

**PTH treatment activates intracortical bone remodeling in patients with hypoparathyroidism.** Tanja Sikjaer<sup>\*1</sup>, Lars Reinmark<sup>1</sup>, Jesper Skovhus Thomsen<sup>2</sup>, Annemarie Brül<sup>2</sup>, Ellen Margrethe Hauge<sup>3</sup>, Jean-Marie Delaïsse<sup>4</sup>, Thomas Levin Andersen<sup>4</sup>. <sup>1</sup>Department of Internal Medicine and Endocrinology, Aarhus University Hospital, Denmark, <sup>2</sup>Department of Biomedicine, Aarhus University, Denmark, <sup>3</sup>Department of Rheumatology, Aarhus University hospital, Denmark, <sup>4</sup>Department of Clinical Cell Biology, Vejle Hospital – Lillebaelt Hospital, Institute of Regional Health Research, University of Southern Denmark, Denmark

Hypoparathyroidism (hypoPT) is characterized by a state of low bone turnover and high BMD. We have previously shown that hypoPT patients treated with PTH(1-84) for six months have highly increased bone turnover markers and a decrease in aBMD at the hip and spine(1).

The present study aims to investigate the effect of PTH(1-84) on cortical bone and intracortical bone remodeling in hypoPT.

The study was conducted on 20 transiliac bone biopsies from hypoPT patients after six months of treatment with either PTH(1-84) 100 µg s.c./day N=10 or placebo N=10. The groups were age- (±6 years) and gender-matched. Age, duration of disease, and etiology of hypoPT did not differ between groups. A comprehensive analysis of the cortical bone was performed including estimates of cortical porosity, and pore density (# of pores/mm<sup>2</sup>). The remodeling stage of all intracortical pores was evaluated, and pore area and diameter were measured.

Cortical porosity and pore density did not differ between groups, but PTH treatment had a marked effect on the remodeling status of the pores. The percentage of pores undergoing remodeling was higher in the PTH-group than in placebo-group reported as median values (IQR[25-75%]) (52% [45-59%] vs. 18% [12-34%] of pore number,  $p<0.001$ ). Interestingly, this PTH-induced increase was mainly due to a higher proportion of formative pores (27% [23-40%] vs. 6% [3-7%];  $p<0.001$ ) and mixed resorptive/formative pores (15% [9-16%] vs. 4% [1-8%];  $p=0.004$ ), whereas the percentage of resorptive pores (9% [5-11%] vs. 11% [6-19%], ns) did not differ between the PTH- and the placebo-group, respectively. The PTH-induced change was even greater when assessing the cortical porosity (% of pore area) rather than the pore number; PTH- vs. placebo-treated: resorptive pores 10% [3-20%] vs. 37% [8-74%] ( $p=0.02$ ); mixed resorptive and formative pores 48% [36-61%] vs. 7% [1-17%] ( $p<0.001$ ); formative pores 24% [16-32%] vs. 1% [1-3%] ( $p<0.001$ ).

Collectively, these data suggest an increased activation of intracortical bone remodeling with a change in the relative proportion of resorptive and formative pores, which may be due to a shortening of the intracortical resorptive/reversal phase in response to PTH treatment of hypoPT. Furthermore, the PTH-treatment did not increase cortical porosity or pore density.

1. Sikjaer et al. Changes in 3-dimensional bone structure indices in hypoparathyroid patients treated with PTH(1-84): a randomized controlled study. 2012J Bone Miner Res 27:781

**Disclosures:** Tanja Sikjaer, Shire Pharmaceuticals, Speakers' Bureau.



## MO0703

**Frequency and Time of Clinical Symptom Onset Impacting Health-Related Quality-of-Life Dimensions in Patients With Hypophosphatasia.** Shelagh M Szabo<sup>\*1</sup>, Ioannis C Tomazos<sup>2</sup>, Lauren C Stewart<sup>1</sup>, Sanjesh C Roop<sup>1</sup>, Bonnie MK Donato<sup>2</sup>, Anna Petryk<sup>2</sup>, Yuri A Zarate<sup>3</sup>, Anatoly Tiulpakov<sup>4</sup>, Gabriel Angel Martos-Moreno<sup>5</sup>. <sup>1</sup>Broadstreet HEOR, Canada, <sup>2</sup>Alexion Pharmaceuticals, Inc., United States, <sup>3</sup>University of Arkansas for Medical Sciences, United States, <sup>4</sup>Endocrinology Scientific Center, Russian Federation, <sup>5</sup>Hospital Infantil Universitario Niño Jesús, Universidad Autónoma de Madrid, CIBEROBN, ISCIII, Spain

Hypophosphatasia (HPP) is a rare, inherited, systemic, metabolic disease characterized by low serum alkaline phosphatase activity and poor skeletal mineralization. Health-related quality of life (HRQOL) in HPP is poorly characterized. Disease burden may be related to clinical symptoms, and subsequent complications may impact HRQOL. Frequency and timing of clinical signs/symptoms potentially affecting HRQOL in HPP patients were assessed. A systematic review of the literature (MEDLINE, Embase 1946–2016) identified HPP cases with longitudinal ( $\geq 1$  y) follow-up. Data were extracted by age of onset: infancy, childhood, adolescence, adulthood. Clinical signs/symptoms with an important impact on activities of daily living and functional and emotional status were identified by consultation with clinical experts. Frequency of the identified symptoms and time to onset were determined by Kaplan-Meier analysis. Of 3040 screened abstracts, full data were extracted from 268 (patient age at presentation: in utero to 90 y). Median follow-up was 11 (range: 9–15) years. The majority of patients (89.9%) experienced clinical signs/symptoms that can impact HRQOL; most frequent were premature tooth loss (50.4%), fractures (35.4%; almost half had  $\geq 3$ ), ambulation difficulties (33.5%), pain (30.6%), cranial abnormalities (28.4%), and surgeries (23.9%). In infancy/childhood, cranial abnormalities, cranial surgery, premature tooth loss, and ambulation difficulties were most frequent; in adolescence/adulthood, fractures, extremity surgeries, pain, and ambulation difficulties were most frequent. Median (range) years to clinical signs/symptoms that can impact HRQOL (listed by increasing age): respiratory difficulties, 0.3 (0–2); cranial abnormalities, 1 (0–12); premature tooth loss, 14 (1–60); pain, 44 (0–64); fracture, 46 (0–75); ambulation difficulties, 54 (0–90); surgery, 59 (0–83). Kaplan-Meier analysis showed the probability of clinical signs/symptoms that could impact HRQOL increased with age, except respiratory and cranial problems. Clinical signs/symptoms associated with HPP can impact HRQOL across all ages. Cranial abnormalities and tooth loss were common in younger patients, fractures and pain were common in older patients; ambulation difficulties and surgeries were common across all ages. These clinical symptoms are frequent and can have substantial HRQOL impacts that generally increase with age. The full burden of HPP as a systemic disease is not yet fully understood.

**Disclosures:** Shelagh M Szabo, Alexion Pharmaceuticals, Inc., Grant/Research Support.

## MO0704

**Bone Indices in Patients with Non-Surgical Hypoparathyroidism and Pseudohypoparathyroidism.** Line Underbjerg<sup>\*1</sup>, Tanja Sikjaer<sup>2</sup>, Lars Rejnmark<sup>3</sup>. <sup>1</sup>MD/Ph.D.-student, Denmark, <sup>2</sup>MD, Ph.D., Denmark, <sup>3</sup>Clinical professor, consultant, PhD, DMSc, Denmark

**Objective:** Both non-surgical hypoparathyroidism (NS-HypoPT) and pseudohypoparathyroidism (Ps-HypoPT) are rare diseases. As patients with NS-HypoPT lack PTH they have an elevated BMD compared to normal background population. Patients with Ps-HypoPT on the other hand have despite peripheral resistance against PTH and a constant elevated level of PTH which may decrease their bone strength.

**Methods:** 52 patients with NS-HypoPT and 20 with Ps-HypoPT were scanned by DXA and high-resolution pQCT scanner (XtremeCT, Scanco Medical AG, Switzerland). Bone mineral density in the lumbar spine, hip and ultra-distal forearm were measured by DXA, whereas cortical and trabecular architecture were measured by HRpQCT in the distal radius and tibia. All calculations were performed with an independent t-test.

**Results:** Patients with Ps-HypoPT have a significantly increased BMI compared with patients with NS-HypoPT. Nevertheless, they have a significantly reduced BMD in the neck of the hip ( $p=0.02$ ), whereas the groups were compatible in the lumbar spine, total hip, ultra-distal forearm and whole body ( $p_{all}>0.05$ ).

There are a significant difference between groups when investigation the HRpQCT data. Patients with Ps-HypoPT a significant higher cortical volumetric density at the distal radius ( $p=0.02$ ) borderline significant in the distal tibia ( $p=0.07$ ). However, patients with NS-HypoPT have an increased trabecular microarchitecture with significant increased trabecular bone density ( $p_{radius}=0.02$ ;  $p_{tibia}=0.03$ ), trabecular number ( $p_{radius}=0.05$ ;  $p_{tibia}<0.01$ ) and bone volume ratio ( $p_{radius}=0.03$ ;  $p_{tibia}=0.02$ ).

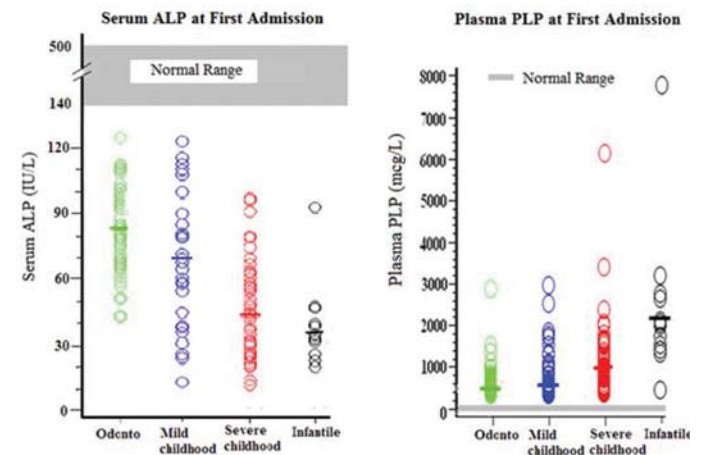
**Summary and conclusion:** Ps-HypoPT mainly affects the trabecular bone compared to patients with NS-HypoPT, whereas it seems like patients with NS-Hypo have a slightly reduced cortical bone.

**Disclosures:** Line Underbjerg, NPS pharmaceuticals, Shire, Speakers' Bureau.

## MO0705

**Hypophosphatasia: Principal Biochemical Features Validate The Clinical Nosology for Affected Children.** Michael P. Whyte<sup>\*1</sup>, Fan Zhang<sup>2</sup>, Stephen P. Coburn<sup>3</sup>, Karen L. Ericson<sup>3</sup>. <sup>1</sup>Center for Metabolic Bone Disease and Molecular Research, Shriners Hospital for Children; and Division of Bone and Mineral Diseases, Department of Internal Medicine, Washington University School of Medicine, United States, <sup>2</sup>Center for Metabolic Bone Disease and Molecular Research, Shriners Hospital for Children, United States, <sup>3</sup>Indiana University-Purdue University Fort Wayne, United States

Hypophosphatasia (HPP) is the heritable dento-osseous disease characterized by deficient activity of the tissue non-specific isoenzyme of alkaline phosphatase (ALP). Consequently, its natural substrates inorganic pyrophosphate (PPi) and pyridoxal 5'-phosphate (PLP) accumulate extracellularly. PPi inhibits mineralization and its excess in HPP can cause rickets or osteomalacia and dental disease. Here, we support our clinical nosology for pediatric HPP by contrasting these principal biochemical features captured in data from the first admission of 165 pre-teenage HPP patients to our research center. Data were acquired using consistent testing methods. Our nosology comprises "infantile HPP" ( $n=12$ ), "severe childhood HPP" ( $n=53$ ), "mild childhood HPP" ( $n=38$ ), and "odonto HPP" ( $n=62$ ). Fasting serum ALP and bone-specific ALP (BAP) were invariably below published reference ranges and our in-house control values. Serum BAP was highly correlated with ALP ( $r=0.97$ ,  $P<0.0001$ ). ALP and BAP both reflected HPP severity captured in this nosology, with the values distinguishing the HPP groups except the two groups at either extreme of HPP severity. Similarly, plasma PLP concentration was elevated in virtually all patients, and discriminated ( $P<0.05$ ) among the four patient groups except between odonto/mild childhood HPP and mild/severe childhood HPP (Figure). As an exception, mean serum inorganic phosphate (Pi) levels at referral were elevated to a similar degree in all patient groups ( $P<0.001$ ), although serum ionized calcium levels did not differ from controls. Hyperphosphatemia from enhanced renal reclamation of Pi is a recognized feature of HPP. Plasma PLP correlated inversely ( $r=0.41$ ,  $P<0.001$ ) with serum ALP. Height Z-scores correlated positively with ALP ( $r=0.32$ ,  $P<0.0001$ ) and negatively with PLP ( $r=0.34$ ,  $P<0.001$ ). Hence, as we have previously reported for demographic and DXA parameters, the principal biochemical aberrations of HPP too reflect our clinical nosology for pediatric HPP.



Figure

**Disclosures:** Michael P. Whyte, Alexion Pharmaceuticals, New Haven, CT USA, Grant/Research Support.

## MO0706

**Type I Collagen C-propeptide Cleavage Deficiency Increases Bone Mineralization and Alters Bone Cell Differentiation.** Aileen M. Barnes<sup>\*1</sup>, Joseph E. Perosky<sup>2</sup>, Basma Khoury<sup>2</sup>, Stephane Blouin<sup>3</sup>, M. Helen Rajpar<sup>1</sup>, MaryAnn Weis<sup>4</sup>, Klaus Klaushofer<sup>3</sup>, Paul Roschger<sup>3</sup>, David Eyre<sup>5</sup>, Nadja Fratzl-Zelman<sup>3</sup>, Kenneth M. Kozloff<sup>2</sup>, Joan C. Marini<sup>1</sup>. <sup>1</sup>NICHD/NIH, United States, <sup>2</sup>University of Michigan, United States, <sup>3</sup>Ludwig Boltzmann Institute of Osteology, Austria, <sup>4</sup>University of Washington, United States, <sup>5</sup>University of Washington, United States

High Bone Mass (HBM) osteogenesis imperfecta (OI), caused by dominant mutations in the C-propeptide cleavage site of *COL1A1* or *COL1A2*, is characterized by bone hypermineralization. To elucidate the role of C-propeptide processing in bone mineralization and development, we generated heterozygous HBM mice with both residues of the *COL1A1* cleavage site substituted to prevent processing by BMP1.

Two, 6- and 12-month WT and HBM bones were examined for histology, mineralization, mechanics, and cell differentiation.

HBM mice are smaller than WT in weight and length throughout life. Their femoral extracts contain pC-collagen and increased monomeric *COL1A1* C-propeptide, resulting in a "barbed-wire" appearance to bone collagen fibrils, thin cortices and decreased

BV/TV. By 6 months, HBM mice hind limb joints show severe contractures. HBM femora have decreased stiffness, yield and fracture load, which did not improve with age. Their femora are also extremely brittle; post-yield displacement is ~15% of WT ( $p < 0.001$ ). HBM femora have decreased collagen content (59% of WT) with an increase in mature (HP) and total (HP+LP) crosslinks. Femoral aBMD is decreased at 2-months but is near normal (93%) at 1 year. On  $\mu$ CT, HBM cortical and trabecular TMD are normalized at 1 year. Giemsa staining of 2 month femurs confirmed that the increase in mineralization is not due to an increased amount of retained mineralized cartilage. Using quantitative backscattered electron imaging (qBEI) to assay mineral content, HBM cortical bone had increased CaMean, CaPeak and CaHigh at 2- and 6- and 12-months compared to WT. HBM CaPeak increased significantly between 6- to 12-months, although WT levels peaked at 6 months. There is a complementary decrease in HBM percent body fat at 6- and 12-months. Bone cell differentiation was also affected in HBM. Femoral *Bglap* transcripts are decreased, as was osteoblast collagen secretion. HBM femora had fewer osteocyte lacunae ( $p < 0.01$ ) but increased lacunar area at 2-, 6- and 12-months ( $p < 0.001$ ). HBM serum TRAP and PINP were significantly increased, consistent with increased femoral transcripts of *Ctsk*, *Acp5* and the *Rankl/Op* ratio.

Murine HBM bone mineralization is increased throughout life and increases with age, even after WT mineralization has peaked, raising concerns for long-term patient status. Alterations in multiple bone cell populations support a putative C-propeptide trimer signaling function, influencing bone matrix and mineralization.

**Disclosures:** Aileen M. Barnes, None.

## MO0707

### TransCon CNP, a sustained-release prodrug of C-type natriuretic peptide, prevents premature synchondrosis closure in an achondroplasia mouse model.

Vibeke Miller Breinholt<sup>1</sup>, Maxence Cornille<sup>2</sup>, Nabil Kaci<sup>3</sup>, Kennett Sprogoc<sup>1</sup>, Laurence Legeai-Mallet<sup>2</sup>. <sup>1</sup>Ascendis Pharma A/S, Denmark, <sup>2</sup>Imagine Institute, France, <sup>3</sup>Imagine Institute, France

Activating gain-of-function mutations in FGFR3 cause achondroplasia, one of the most common and disabling human skeletal dysplasias. In this disorder, spinal and foramen magnum stenosis caused by premature synchondroses closure, can result in serious neurologic complications, including pain, muscle weakness, apnea, and paralysis. Symptoms can be so severe that surgical enlargement of the foramen magnum may be required.

The aim of this nonclinical study was to investigate the ability of TransCon CNP, a peptide capable of inhibiting FGFR3 downstream signaling, to reverse abnormal cranial bone formation in *Fgfr3*<sup>Y367C/+</sup> mice. This mouse strain exhibits a severe dwarfism phenotype similar to achondroplasia, including reduction in appendicular and axial skeletal length, dome-shaped skull, cranial skull base anomalies, and disorganized growth plate chondrocytes. The focus of this investigation was to investigate the impact of TransCon CNP on calvaria ossification and the synchondroses in the skull.

TransCon CNP (5.6 mg CNP/kg) was administered daily, by the subcutaneous route, from birth through two weeks of life to *Fgfr3*<sup>Y367C/+</sup> mice ( $n = 9$ ). Body, and selected long bones were measured by radiography/ $\mu$ CT and/or with a caliper. Ossification of the skull bones, and the presence of synchondroses were measured by radiography and  $\mu$ CT (Skyscan).

In addition to elongation of the long bones, we observed that TransCon CNP increased occipital and frontal bone ossification in TransCon treated *Fgfr3*<sup>Y367C/+</sup> mice compared to untreated mice. In *Fgfr3*<sup>Y367C/+</sup> mice, without treatment, the anterior intra-occipital (IOSA), sphenoid-occipital (SOS) and inter-sphenoidal synchondroses (ISS) were fused. TransCon CNP of *Fgfr3*<sup>Y367C/+</sup> mice partially prevented fusion of the three synchondroses. The effect on IOSA is particularly interesting, because the shape of the foramen magnum is controlled by IOSA. The administration of TransCon CNP, initiated at birth, resulted in modification of the size and the shape of the foramen magnum.

In conclusion, TransCon CNP exerted a positive effect on membranous and endochondral ossification in a severe model of achondroplasia. TransCon CNP counteracted premature fusion of both IOSA, SOS, and ISS, evidenced by flattening of the skull and modification of the shape of the foramen magnum. These results suggest that early administration of TransCon CNP may ameliorate some of the more disabling achondroplasia traits, including foramen magnum stenosis.

**Disclosures:** Vibeke Miller Breinholt, None.

## MO0708

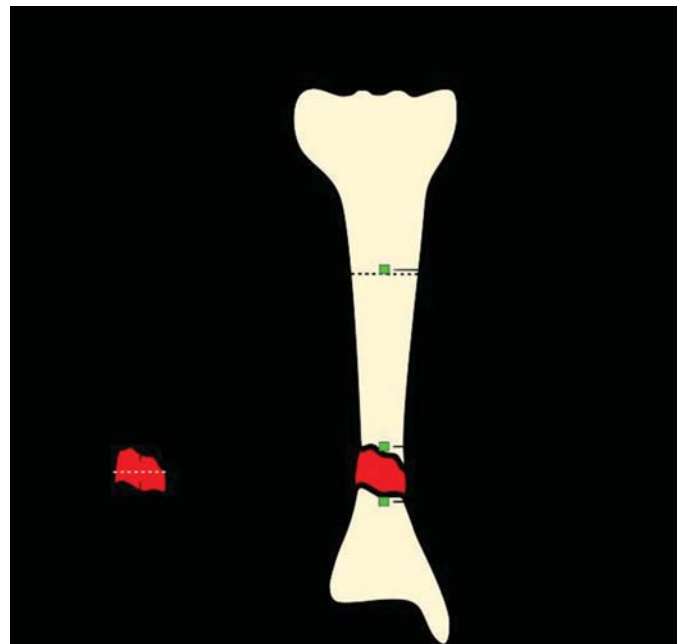
**NF1-Related Pseudarthrosis: Beyond the Pseudarthrosis Site.** Carlijn Brekelmans<sup>1</sup>, Silke Hollants<sup>2</sup>, Caroline De Groote<sup>2</sup>, Marijke Spaepen<sup>2</sup>, Natalie Sohler<sup>2</sup>, Marina Marechal<sup>1</sup>, Frank Luyten<sup>2</sup>, Johan Lammens<sup>2</sup>, Eric Legius<sup>1</sup>, Hilde Brems<sup>1</sup>. <sup>1</sup>KU Leuven, Belgium, <sup>2</sup>UZ Leuven, Belgium

Neurofibromatosis type 1 (NF1) is an autosomal dominant disorder affecting 1 in 2,700 individuals. NF1 is caused by an inactivating mutation in the *NF1* gene that encodes neurofibromin, a negative regulator of the RAS-MAPK pathway. Around 5% of NF1 children present with congenital bowing of a long bone, which upon fracture often progresses to a pseudarthrosis (PA). Current treatment methods for NF1-PA are often unsatisfactory, and if union of the affected limb remains elusive, it is amputated. For the development of better treatment options, improved understanding of NF1-PA is crucial.

We performed *NF1* mutation analysis on cultured cells from the pseudarthrosis site and, if available, periosteum of NF1-PA patients. Mutation analysis was performed using Sanger sequencing on cDNA. Identified mutations were confirmed on gDNA. Intragenic deletions and duplications were examined using multiplex ligation-dependent probe amplification. The germline mutation was confirmed on cultured blood lymphocytes or buccal swabs.

We found bi-allelic *NF1* inactivation in cultured cells of primary PA-tissue in 8/8 NF1 patients and in cells of later PA-tissue in 3/6 NF1 patients. Three patients (primary PA) were sampled more extensively. In the PA of these patients we found a mixture of *NF1*<sup>+/+</sup> and *NF1*<sup>-/-</sup> cells, with different relative percentages of *NF1*<sup>-/-</sup> cells even between fragments derived from the same PA site. Periosteum surrounding the PA contained  $\pm 20\%$  (proximal) to  $\pm 100\%$  (distal) *NF1*<sup>-/-</sup> periosteal-derived cells (PDCs). Surprisingly one patient even had 30% *NF1*<sup>-/-</sup> PDCs at the osteotomy site, just below the knee and far above the PA site.

The uncovered *NF1* inactivation in PA tissue proves the necessity of *NF1* inactivation for a pseudarthrosis to develop (primary PA), but not to persist (later PA). The *NF1*<sup>-/-</sup> cells found in the periosteum hint to the involvement of periosteum. Furthermore, we hypothesize that a large percentage of remaining *NF1*<sup>-/-</sup> cells (in the PA and/or surrounding periosteum) might be one of the factors negatively influencing union of the PA. The observation that *NF1*<sup>-/-</sup> PDCs are present far from the PA and the fact that NF1-PA is always localized in the same region of the tibia, suggests the involvement of additional local factors in the mechanism causing non-union. Our results indicate that NF1-PA is a multifactorial problem. However, to uncover the full pathogenetic sequence of NF1-PA more research is needed, especially on factors influencing non-union.



Extensive pseudarthrosis and periosteum sampling

**Disclosures:** Carlijn Brekelmans, None.

## MO0709

**IFITM5 (BRIL) p.S40L mutation causing atypical type VI OI results in unique bone material phenotype impacting both endochondral ossification and chondrocyte development.** Nadja Fratzl-Zelman<sup>1</sup>, Ingo Schmidt<sup>2</sup>, Andreas Roschger<sup>2</sup>, Francis H. Glorieux<sup>3</sup>, Wolfgang Wagermaier<sup>2</sup>, Klaus Klaushofer<sup>1</sup>, Frank Rauch<sup>3</sup>, Peter Fratzl<sup>2</sup>, Paul Roschger<sup>1</sup>, Joan C. Marini<sup>4</sup>. <sup>1</sup>Ludwig Boltzmann Institute of Osteology at Hanusch Hospital of WGKK and AUA Trauma Centre Meidling, 1st Med. Dept. Hanusch Hospital, Austria, <sup>2</sup>Max Planck Institute of Colloids and Interfaces, Department of Biomaterials, Germany, <sup>3</sup>Genetics Unit, Shriners Hospital for Children and McGill University, Canada, <sup>4</sup>Bone and Extracellular Matrix Branch, NICHD, NIH, United States

**Introduction:** BRIL is an osteoblast specific protein highly expressed during early stages of bone mineralization and encoded by *IFITM5*. Heterozygous mutations in the 5'-UTR cause gain of function, leading to autosomal dominant Osteogenesis imperfecta (OI) type V with exuberant hypertrophic callus formation and interosseous membrane calcification. Recently, a *de novo* mutation causing p.S40L substitution in *IFITM5* was described as a very severe form of OI. The proband has increased osteoid formation and minimal PEDF secretion by osteoblasts, similar to OI type VI with null mutation in *SERPINF1*. While typical OI type VI bone tissue shows coexistence of hypo- and hyper-mineralized areas and abnormal osteoblast-osteocyte development, bone tissue properties have not been reported for atypical OI type VI. **Patient and Methods:** We analyzed transiliac bone biopsies from the same patient at 7 and 25 years, using histology,



histomorphometry, quantitative and high-resolution backscattered electron imaging to assess bone mineralization density distribution, as well as synchrotron small-angle x-ray scattering to evaluate mineral particle size.

Results: The fractions of highly mineralized and poorly mineralized bone areas were both strongly increased in the childhood biopsy. Matrix mineralization was unevenly distributed, in that the most frequent calcium concentration (CaPeak) varied between 25.1 and 29.8 weight% calcium, the higher values being typical for mineralized cartilage. Bone matrix appeared disorganized in polarized light. Osteocytes with atypical size and mineralization pattern were viewed by high-resolution backscattered electron imaging. In addition, we observed remnants of non-mineralized proliferating cartilage and abnormally mineralizing chondrocytes with unusually small (2.6 nm thick) and disorientated mineral particles, as well as chondrocyte lacunae that showed features of trans-differentiation into osteoblasts. In the young adult biopsy, however, most bone appears remodeled with high indices of osteoid formation and nearly absent mineralized cartilage. CaPeak was similar to what the value in typical OI type VI (24.9 as compared to  $25.5 \pm 1.3$  weight% calcium).

In conclusion, our data suggest that PEDF appears necessary for a proper bone matrix mineralization and for osteocyte differentiation. Moreover, the dominant negative effect of the S40L mutation severely impacts chondrocyte development and endochondral ossification causing a unique OI phenotype.

**Disclosures:** Nadja Fratzl-Zelman, None.

## MO0710

**Bone morphology in *IKBK*G (NEMO) mutation positive women. A case-control study.** Morten Frost<sup>\*1</sup>, Michaela Tencerova<sup>2</sup>, Charlotte Ejersted<sup>1</sup>, Dea Svaneby<sup>3</sup>, Thomas Levin Andersen<sup>4</sup>, Moustapha Kassem<sup>2</sup>, William H McAlister<sup>5</sup>, Deborah V Novack<sup>6</sup>, Michael P Whyte<sup>7</sup>, Anja L Frederiksen<sup>8</sup>.

<sup>1</sup>Endocrine Research Unit, Odense University Hospital, Denmark, <sup>2</sup>Molecular Endocrinology Laboratory (KMEB), Department of Endocrinology, Odense University Hospital & University of Southern Denmark, Denmark, <sup>3</sup>Department of Clinical Genetics, Vejle Hospital, Denmark, <sup>4</sup>Clinical Cell Biology (KCB), Institute of Regional Health Research, University of Southern Denmark, Denmark, <sup>5</sup>Department of Pediatric Radiology, Mallinckrodt Institute of Radiology, Washington University School of Medicine at St. Louis Children's Hospital, United States, <sup>6</sup>Division of Bone and Mineral Diseases, Department of Internal Medicine, Washington University School of Medicine at Barnes-Jewish Hospital, United States, <sup>7</sup>Center for Metabolic Bone Disease and Molecular Research, Shriners Hospital for Children, United States, <sup>8</sup>Department of Clinical Genetics, Odense University Hospital, Denmark

Purpose: The ubiquitous nuclear factor kappa-light-chain-enhancer of activated B cells (NF- $\kappa$ B) functions importantly in skeletal homeostasis. NF- $\kappa$ B subunits p50/p52<sup>-/-</sup> knockout mice have impaired osteoclast (OC) differentiation and an osteopetrosis (OPT) bone phenotype. NF- $\kappa$ B activation requires the regulator subunit of NF- $\kappa$ B essential modulator (NEMO) encoded by *IKBK*G. In humans, *IKBK*G deactivating mutations cause incontinentia pigmenti (IP), a rare X-linked disease featuring linear hypopigmentation, alopecia, hypodontia, dystrophic nails, and immunodeficiency. Animal studies suggest NEMO is essential for NF- $\kappa$ B mediated bone homeostasis but this has not been thoroughly studied in humans. Single case-reports describe OPT in boys carrying hypomorphic *IKBK*G mutations. Accordingly, we investigated whether women with IP have an abnormal bone phenotype.

Methods: A cross-sectional age-, sex- and BMI-matched case-control study that evaluated: lumbar spine and femoral neck aBMD using DXA, plain X-ray skeletal survey of the spine, non-dominant arm and leg, bone turnover markers (CTX, PINP, OC), and circulating sclerostin, RANKL OPG, Ca<sup>2+</sup>, PTH, and 25OH-D. Bone marrow aspiration and isolation of bone marrow skeletal (stromal) stem cells (BMMSC). X-chromosome inactivation was measured in whole blood and in BMMSC by a PCR method with methylation of HpaII sites. NF- $\kappa$ B activity was measured in BMMSC employing a Luciferase NF- $\kappa$ B reporter assay.

Results: Seven Caucasian *IKBK*G mutation positive women with IP (age: 24-67 years and BMI: 20.0-35.2 kg/m<sup>2</sup>) were contrasted to age- and BMI matched control women. Carrier genotypes encompassed *IKBK*G, del exon 4-10 (n=4) and c.460C>Y (n=3). No differences in aBMD and plain x-ray morphology was observed between cases and controls. Furthermore, no differences were noted in circulating CTX, PINP, OC, sclerostin, RANKL, OPG, Ca<sup>2+</sup>, PTH or 25OH-D. Cases had extremely skewed X-inactivation (>90:10%) in blood but not in BMMSC. NF- $\kappa$ B activity was reduced in BMMSC obtained from *IKBK*G mutation positive females (n=5) compared to controls (3094±679 vs. 5422±1038/μg protein, p<0.01).

Conclusion: No skeletal phenotype was identified in *IKBK*G mutation positive females despite a significant decrease in NF- $\kappa$ B activity in their BMMSC. A selection against BMMSC lines carrying activated mutated alleles could theoretically favour cell lines with activated normal alleles and hence the development of mature bone cells with normal NF- $\kappa$ B activity.

**Disclosures:** Morten Frost, None.

## MO0711

**Increased circulating FGF23 does not lead to cardiac hypertrophy in the Hyp mouse model of XLH.** Eva Liu<sup>\*1</sup>, Robrecht Thoonen<sup>2</sup>, Elizabeth Petit<sup>2</sup>, Binglan Yu<sup>2</sup>, Marielle Scherrer-Crosbie<sup>3</sup>, Emmanuel Buys<sup>2</sup>, Marie Demay<sup>4</sup>.

<sup>1</sup>Brigham and Women's Hospital and MGH, United States, <sup>2</sup>Massachusetts General Hospital, United States, <sup>3</sup>University of Pennsylvania, United States, <sup>4</sup>Massachusetts General Hospital, Harvard Medical School, United States

Fibroblast growth factor 23 (FGF23) is secreted by osteocytes to regulate phosphate homeostasis. FGF23 has also been shown to activate the calcineurin signaling pathway, inducing cardiac remodeling and leading to left ventricular (LV) hypertrophy. Increased circulating FGF23 correlates with mortality and LV hypertrophy in chronic kidney disease. Despite the increased circulating FGF23 levels in X-linked hypophosphatemia (XLH), no consistent cardiac phenotype has been reported. Thus, studies were performed to evaluate the cardiac phenotype in the Hyp mouse, a model of XLH.

Cardiac ultrasound demonstrated that the hearts of Hyp mice are smaller than those of wild type (WT) mice and exhibit a significant decrease in LV anterior and posterior wall thickness, end diastolic diameter, and mass. However, when normalized for body weight, LV weight was not significantly different from that of WT mice (WT vs Hyp: 4.8±0.7 vs 4.5±0.4 mg/g). Fractional shortening and ejection fraction (EF) were decreased in the LV of Hyp mice (EF WT vs Hyp: 76±3% vs 71±4%), whereas blood pressure and heart rate did not differ from that of WT mice. Consistent with the lack of LV hypertrophy in Hyp mice, mRNA expression of the cardiomyocyte hypertrophy markers beta-myosin heavy chain (beta-MHC), atrial natriuretic peptide (ANP), and B-type natriuretic peptide (BNP) in either the LV or right ventricle (RV) did not differ between Hyp and WT mice.

FGF23 can activate several signaling pathways, including the MAPK and calcineurin signaling pathways. A significant increase in expression of calcineurin signaling target genes NFATc1 and RCAN1 was observed in the LV of Hyp mice. However, MAPK signaling, evaluated by immunohistochemistry for p-Erk1/2, was not altered in the hearts of Hyp mice, nor was there an increase in fibrosis, based on Sirius red staining.

These findings demonstrate that an increase in circulating FGF23 does not lead to cardiac hypertrophy when renal function is normal. This suggests that other metabolic disturbances are important in the pathogenesis of the cardiac hypertrophy in the setting of chronic kidney disease and increased circulating FGF23.

**Disclosures:** Eva Liu, None.

## MO0712

**CLCN7-dependent Autosomal Dominant Osteopetrosis type 2 (ADO2): more than a bone disease.** Antonio Maurizi<sup>\*1</sup>, Mattia Capulli<sup>1</sup>, Rajvi Patel<sup>1</sup>, Juliana Cortes<sup>2</sup>, Nadia Rucci<sup>1</sup>, Anna Teti<sup>1</sup>. <sup>1</sup>University of L'Aquila, Italy, <sup>2</sup>University of L'Aquila, Israel

The *Cln7* gene encodes for the lysosomal proton/chloride antiporter CIC7 that plays a pivotal role in bone resorption. Heterozygous dominant negative mutations of *Cln7* cause ADO2, a genetic bone disease characterized by impaired acidification of the osteoclast lysosomes and resorption lacuna, which reduces bone degradation. RNA deep sequencing of osteoclasts from mice carrying the ADO2 mutation *Cln7*<sup>G213R</sup> revealed upregulated pathways of cellular activities involving *Jak-Stat* (p=0.001), cytokines-cytokine receptors (p<0.001) and interaction with ECM (p<0.001). Intriguingly, the mRNA of the pro-fibrotic cytokine, *Tgfb* (p<0.05), was also upregulated and the molecular classification revealed an enrichment of transcripts encoding for ECM components (p<0.05). These data and the pleiotropic expression of the *Cln7* in the organism, prompted us to hypothesize that ADO2 is more than simply a bone disease. Indeed, in-depth phenotyping of ADO2 mice showed multiorgan dysfunctions: perivascular fibrosis was observed in lung (+1.5fold;p=0.005), kidney (+4.4fold;p=0.01) and muscle (+1.8fold;p=0.04), with an increased number of macrophages in ADO2 organs (+7.5fold;p<0.05 vs. WT). Furthermore, ADO2 brains exhibited higher β-amyloid aggregates in hippocampus (+3.64fold), thalamus (+4.6fold) and amygdala (+2.28fold; p<0.05), representing a landmark of protein accumulation and brain damage. Additionally, ADO2 mice showed increased anxiety and depression (+1.4fold;p<0.05), while cognitive functions were normal. To elucidate the underlying cellular mechanisms we first analyzed the lysosomal pH, which was increased in ADO2 cells (+1.64 pH units, p<0.001) and in purified ADO2 lysosomes (p<0.05). This was due to an altered vesicular trafficking that impaired CIC7 lysosomal localization (-0.52%;p=0.02). In fact, in monocytes, osteoclasts and neurons, CIC7 accumulated in the Golgi (+2fold;p<0.05) and in the clathrin-coated vesicular network (+8.5fold;p=0.01) that appeared expanded (+4fold;p=0.01). Furthermore, no UPR or ER stress was observed, suggesting an impairment of the Golgi exit pathway rather than an altered ER response. Finally, a targeted therapy using *Cln7*<sup>G213R</sup>-specific siRNA that rescued the bone phenotype cured also the fibrosis in kidney, lung and muscle (-78%;-41%;-57% respectively vs scrambled siRNA;p<0.05) and restored the canonical lysosomal CIC7 localization and acidic pH. Results suggest that ADO2 is not only a bone disease but also a complex systemic disorder.

**Disclosures:** Antonio Maurizi, None.

## MO0713

**High Diagnostic Yield and Higher Proportion of Non-Collagen Defects in Adults with Osteogenesis Imperfecta Analyzed Using Targeted Massively Parallel Sequencing.** Adriana M Fernandes<sup>\*1</sup>, Manuela GM Rocha-Braz<sup>1</sup>, Monica M Franca<sup>2</sup>, Regina M Martin<sup>1</sup>, Antonio M Lerario<sup>3</sup>, Berenice B Mendonca<sup>3</sup>, Bruno Ferraz-de-Souza<sup>1</sup>. <sup>1</sup>Endocrinology/LIM-25, Hospital das Clinicas, University of Sao Paulo School of Medicine, Brazil, <sup>2</sup>SELA/LIM-42, Hospital das Clinicas, University of Sao Paulo School of Medicine, Brazil, <sup>3</sup>SELA/LIM-42, Hospital das Clinicas, University of Sao Paulo School of Medicine, Brazil, Brazil

Osteogenesis imperfecta (OI) is clinically and genetically heterogeneous. Several new candidate genes have recently been associated with OI, but ~85% of cases are still considered to be due to *COL1A1/COL1A2*. Digenic/oligogenic contribution to the pathogenesis of OI is presently poorly understood, but the advent of massively parallel sequencing (MPS) offers an opportunity for comprehensive analysis of OI genes simultaneously. Our objective was to obtain the molecular diagnosis of OI through targeted MPS in a single tertiary center cohort of Brazilian adults with OI.

After informed consent, DNA samples were obtained from 38 cases of OI (8 families and 30 sporadic; total of 49 individuals). Sixty-five percent of the cohort had moderate to severe OI, and consanguinity was common (26%). Coding regions and 25-bp boundaries of 16 OI genes (*COL1A1*, *COL1A2*, *IFITM5* [plus 5'UTR], *SERPINF1*, *CRTAP*, *LEPRE1*, *PPIB*, *SERPINH1*, *FKBP10*, *PLOD2*, *BMP1*, *SP7*, *TMEM38B*, *WNT1*, *CREB3L1*, *PLS3*) were captured with Agilent SureSelectXT, sequenced in Illumina NextSeq, and analyzed using Platypus and CONTRA. Identified variants were classified according to ACMG/AMP guidelines and those considered to be disease-causing were confirmed by Sanger sequencing and segregation analysis.

A molecular diagnosis was obtained in 97% of cases. Variants in *COL1A1* or *COL1A2* were identified in 71%, whereas 26% had variants in other candidate genes. Amongst these, variants in *SERPINF1*, *FKBP10* and *PLOD2* were more prevalent. Only one case had the previously described *IFITM5* c.-14C>T variant. A homozygous exonic deletion of *TMEM38B* was detected in one case, and a combination of four heterozygous *P3H1* and *WNT1* variants was detected in a peculiar non-consanguineous case. Surprisingly, in three consanguineous families the molecular cause was still related to *COL1A1* or *COL1A2*, and two non-consanguineous cases had compound heterozygous *PLOD2* variants.

In conclusion, targeted massively parallel sequencing is very effective in diagnosing the molecular cause of OI. In 26% of cases the cause was not related to *COL1A1* or *COL1A2*, and defects in *P3H1*, *FKBP10*, *PLOD2* and *SERPINF1* were more common than previously reported. In this cohort, inferring the molecular diagnosis from a family history of consanguinity was misleading. Interestingly, a potentially digenic defect was identified in one case. A precise molecular diagnosis of OI obtained through comprehensive MPS may allow better and personalized care in the future.

**Disclosures:** Adriana M Fernandes, None.

## MO0714

**Pathological Analysis and Drug Discovery for Osteogenesis Imperfecta using Patient-specific induced Pluripotent Stem Cells and Fibroblasts.** Shinji Takeyari<sup>\*1</sup>, Makoto Fujiwara<sup>1</sup>, Ohata Yasuhisa<sup>1</sup>, Takuo Kubota<sup>1</sup>, Yuki Taga<sup>2</sup>, Kazunori Mizuno<sup>2</sup>, Keichi Ozono<sup>1</sup>. <sup>1</sup>Department of Pediatrics, Osaka University Graduate School of Medicine, Japan, <sup>2</sup>Nippi Research Institute of Biomatrix, Japan

**Introduction:** Osteogenesis Imperfecta (OI) is a heritable brittle bone disease mainly caused by mutation of *COL1A1* or *COL1A2* encoding type I collagen. Treatment with bisphosphonate is not effective enough in patients with severe OI. The accumulation of mutant type I procollagen in endoplasmic reticulum (ER) leading to ER stress was demonstrated in OI model mouse. In the present study, we aimed at drug discovery for OI by focusing on collagen production and ER stress in patient-specific induced pluripotent stem cells (iPSCs) and fibroblasts.

**Methods:** Dermal fibroblasts were obtained from 6 patients with OI: 1 had a non-sense mutation, 2 had a glycine substitution mutation and 3 had an exon skipping mutation in *COL1A1* or *COL1A2*. ER retention of type I procollagen was observed by immunofluorescent staining. ER stress was evaluated from the expression of ER stress markers quantified by real-time PCR. The molecular weight of secreted type I collagen was analyzed by SDS-PAGE. Post-translational modifications of type I collagen were analyzed by LC-MS. Normal and patient-specific iPSCs were established from fibroblasts, and induced to mature osteoblasts. Mineralization was assessed by staining with Alizarin Red S. We evaluated the effects of several drugs on the ER stress.

**Results:** Immunofluorescent staining showed excessive amount of type I procollagen in ER by over 2 times more in OI fibroblasts than normal. Drug X addition decreased the retention in a dose-dependent manner. The expression of BiP, a marker of ER stress, was increased by about 2 times and decreased by drug X. SDS-PAGE showed the retarded band of type I collagen with a glycine substitution. LC-MS analysis showed overglycosylation of type I collagen with a glycine substitution. Drug X did not change the retarded band and overglycosylation, but 3-hydroxyproline in type I collagen was increased by drug X. Osteoblasts differentiated from patient-specific iPSCs exhibited less calcification than normal, but drug X improved the calcification as normal.

**Discussions:** We detected ER accumulation of type I procollagen, increased ER stress and overglycosylation of type I collagen in fibroblasts taken from OI patients. In addition, we showed impaired mineralization of osteoblasts differentiated from patient-

specific iPSCs. Drug X decreased the accumulation and ER stress and improved mineralization. Since drug X has already been approved for other indication, we may reposition drug X for the treatment of OI.

**Disclosures:** Shinji Takeyari, None.

## MO0715

**Estimation of ground reaction forces by accelerometer in healthy youth and youth with osteogenesis imperfecta type I.** Louis-Nicolas Veilleux<sup>\*1</sup>, Bahare Samadi<sup>2</sup>. <sup>1</sup>Université de Montréal; Shriners Hospital for Children-Canada, Canada, <sup>2</sup>École Polytechnique de Montréal; Sainte-Justine University Hospital Research Center, Canada

**Context:** Vertical accelerations are closely related to ground reaction forces (GRF), both of which are seen as a valid estimates of mechanical loads imposed on the lower limbs. For this reason, accelerometers are considered as valuable tool to understand the mechanisms underlying bone adaptation to mechanical loading outside laboratory settings. This is of utmost importance to implement therapeutic intervention for growing children, especially those with bone fragility disorders such as osteogenesis imperfecta. However, the current state of knowledge indicates that accelerometer data are highly noisy resulting in over/underestimation of GRFs. **Objectives:** To optimize the filtering processes of raw acceleration signal and to validate accelerometer as a tool to estimate GRFs. Two different filtering techniques (Butterworth 20Hz vs. wavelet transformation) will be compared to raw acceleration signal and to force plate's GRFs, the gold standard. **Patients and Other Participants:** Twelve youths with a diagnosis of osteogenesis imperfecta type I (5 males; mean age [SD]: 15.2 years [4.6]) and 12 healthy youths (4 males; mean age [SD]: 13.5 years [4.2]) took part in the study. **Main Outcome Measures:** Participants performed three repetitions of 10 multiple two-legged hops on a force platform while wearing the accelerometer at the right hip. Raw vertical acceleration signals were transformed into GRFs according Newton's second law. The Bland and Altman method was used to establish the agreement between peak GRFs recorded by the force plate and those estimated from acceleration signals. The limits of agreement were established for the raw acceleration-, Butterworth 20Hz- and wavelet transformation plate's comparisons. **Results:** Limits of agreement obtained for raw data accounted for 27% of the average measured forces, and was reduced to 17% for both the Butterworth and wavelet filtered data sets ( $p < 0.01$ ). The average differences between accelerometer estimated force compared with the force platform was of 11% for raw data but was reduced to 5% and 0.8% when treated with the Butterworth and wavelet filters, respectively ( $p = 0.01$ ; Figure 1). These results were not influenced by the populations under study. **Conclusion:** The filtering of the accelerometer data increased the level of agreement with the force platform data and is considered as a valid tool to estimate the ground reaction forces in everyday life settings.

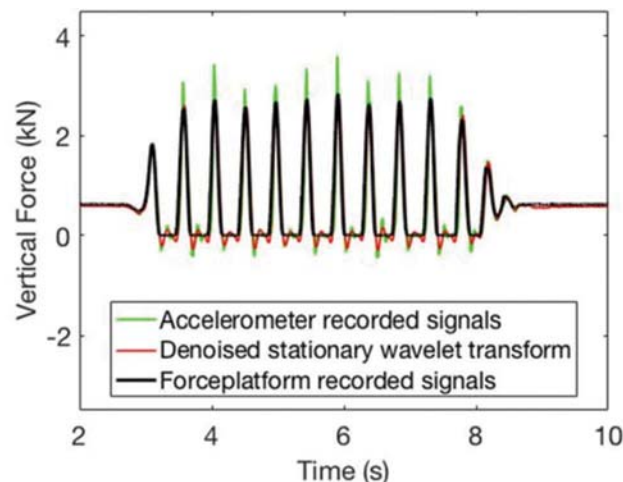


Figure 1. Comparison of 3 force-time curves for the multiple two-legged hopping test. Black line: force-time curve recorded from the force plate; Green line: force-time curve based on raw accelerometer signal; Red line: force-time curve based on wavelet transform accelerometer signal. Note how the raw accelerometer signal (green line) overestimate peak forces and how the wavelet filtering process (red line) removed this overestimation.

Figure 1

**Disclosures:** Louis-Nicolas Veilleux, None.



## MO0716

**Genetic engineering a sheep model of Hypophosphatasia.** Diarra K. Williams\*, Jane H. Pryor, Shannon Huggins, Hannah M. Georges, Carlos A. Pinzon, Forrest Hermann, James Oldeschulte, Mark E. Westhusin, Charles R. Long, Dana Gaddy, Larry J. Suva. Texas A&M University College Veterinary Medicine and Biomedical Science, United States

Hypophosphatasia (HPP) is a rare inherited disorder that affects the development of bones and teeth. The disease is caused by mutations in the tissue-nonspecific alkaline phosphatase (TNSALP) gene (*ALPL*) and accompanied by a highly variable clinical presentation. Although HPP patient studies have advanced our understanding of HPP, as well as documented disease severity, the rarity of the disease combined with a lack of sufficient animal models has significantly delayed mechanistic understanding and therapeutic development. As a result, HPP is one of the last Rarich diseases to receive a medical treatment. Similar to other human disease models, current HPP models have been engineered virtually exclusively in rodents – specifically mice harboring null or loss-of-function mutations. Although useful for modeling many features of HPP, these murine models do not faithfully represent the broad spectrum of human HPP clinical bone, muscle and tooth (odonto-HPP) phenotypes. However, in sheep both Haversian bone remodeling and tooth development are analogous to humans with sheep TNSALP amino acid sequence sharing 89% identity with human. Our objective was to generate a sheep model of HPP and we posit that *ALPL* mutation-specific replacements in the sheep genome using CRISPR/Cas9 will produce a model that accurately phenocopies the bone, muscle and tooth pathophysiology of HPP. To this end, we developed, cloned and validated CRISPR/Cas9 single guide RNAs targeting four distinct *ALPL* mutation loci [Alanine → Threonine in exon 5 (c.346 G>A), Glutamine → Lysine at exon 6 (c.571G>A), Isoleucine → Methionine (c.1077 C>G) and Aspartic Acid → Valine (c.1133A>T) at exon 10] of the sheep genome in addition to sequencing these target regions. *In vivo* produced sheep zygotes were surgically collected and microinjected with the validated exon 10 CRISPR/Cas9 mRNAs, mutation-specific DNA repair template and Cas9 protein (n=41) and WT (n=11). Microinjected zygotes were surgically transferred (3-4 per ewe) into the oviducts of 17 female synchronized recipients resulting in a 52.9% (9/17) pregnancy rate. Additionally, Sanger sequencing from 7 microinjected *in vitro* cultured sheep embryos from exon 10 revealed a high mutation incorporation rate of 57.1% (4/7). These results demonstrate the utility of CRISPR/Cas9 for efficiently editing the sheep *ALPL* gene and represent a major advance in the development of a large animal platform for the examination of rare bone diseases such as HPP.

**Disclosures:** Diarra K. Williams, None.

## MO0717

**Comparison of PET-based Imaging Tracers and MRI in Monitoring HO Progression and the Efficacy of anti-Activin A Antibody Treatment in FOP Mice.** Liqin Xie\*, Jaymin Upadhyay<sup>1</sup>, Lily Huang<sup>1</sup>, Nanditha Das<sup>1</sup>, Lauren Singletary<sup>1</sup>, Xialing Wen<sup>1</sup>, Rachel Stewart<sup>2</sup>, Morgan Lyon<sup>2</sup>, Kervyn Palmer<sup>2</sup>, Saathyak Rajamani<sup>1</sup>, Chris Graul<sup>2</sup>, Merry Lobo<sup>2</sup>, Tyler Wellman<sup>2</sup>, Ed Soares<sup>2</sup>, Matt Silva<sup>2</sup>, Jacob Hesterman<sup>2</sup>, Kalyan Nannuru<sup>1</sup>, Vincent Idone<sup>1</sup>, Andrew Murphy<sup>1</sup>, Sarah Hatsell<sup>1</sup>, Aris Economides<sup>1</sup>. <sup>1</sup>Regeneron, United States, <sup>2</sup>InviCRO, United States

Fibrodysplasia ossificans progressiva (FOP) is a rare genetic disorder characterized by episodes of heterotopic ossification (HO), which are often preceded by injury-induced soft tissue swelling referred to as “flare-ups”. FOP is driven by mutations in the type I BMP receptor ACVR1. Our *Acvr1*<sup>R206H/Flex</sup> ‘conditional-on’ knock-in mice (MGI: 5763014) mimic the clinical symptoms of FOP, including the growth of HO lesions at locations such as the pelvis, femur, tibia and neck. In this mouse model, FOP disease activity is initiated using ubiquitously expressed CreERT2 and tamoxifen, thereby enabling careful longitudinal studies of the process of HO, and ascertainment of the ‘age’ of any given lesion. We have previously shown that HO in FOP requires activation of the *Acvr1*<sup>R206H</sup> by Activin A, in part by demonstrating that prophylactic treatment with a neutralizing antibody highly specific for Activin A inhibits HO in these mice. In this study, we implemented T2-MRI (for inflammation, edema, and cartilage) and PET/CT (<sup>18</sup>F-NaF for bone formation and <sup>18</sup>F-FDG for glucose metabolism) and investigated the utility of these imaging modalities in detecting early HO lesions, and for monitoring the efficacy of Activin A antibody treatment. MRI could readily detect pre-osseous lesions as early as Day 9. ~90% of these MRI lesions progressed to HO. Notably, on Day 9, there were no signs of an active mineralization process. This data is consistent with the idea that inflammation and edema precede HO in FOP. By Day 15, lesions progressed towards mineralization, and HO was accompanied by <sup>18</sup>F-NaF and <sup>18</sup>F-FDG uptake suggesting active bone remodeling and a high metabolic rate. Activin A antibody treatment of nascent HO resulted in a significant reduction in MRI lesion severity, MRI lesion volume and <sup>18</sup>F-NaF signals but not <sup>18</sup>F-FDG uptake compared to the isotype antibody control. MRI gave the most rapid significant readout of treatment effect followed by <sup>18</sup>F-NaF PET and finally CT suggesting that MRI or PET imaging modalities could enable more sensitive monitoring of HO lesion formation and treatment effect than CT. These results also demonstrate that Activin A plays a role in the development of heterotopic bone lesions at the level of the initial inflammation-driven process that leads to HO, to the emergence of edema, cartilage formation, and into the early stages of mineralization.

**Disclosures:** Liqin Xie, None.

## MO0718

**Balance Assessment in Older Adults Using Novel Methodologies.** Bjoern Buehring\*, Ellen Siglinsky, Diane Krueger, Neil Binkely. UW-Madison, United States

**Introduction:** Falls are a major cause of fragility fractures. Impaired balance increases fall risk. Various traditional methods exist to assess balance including the step-wise (Romberg stance (ROM), semi-tandem stance (ST) and tandem stance (TAN)) approach to measure static balance used in the Short Physical Performance Battery (SPPB). Recently, novel, computerized methods have been developed to assess balance that might be an improvement over classical approaches. The aim of this study is to compare two novel methods; Leonardo Mechanography (LEO) and Mobility Lab (ML) in older adults with and without falls.

**Methods:** Static balance was assessed using the SPPB protocol performed on a LEO force plate (Novotec, Germany) while the participants were wearing ML wireless sensors (Portland, OR). Both the LEO and the ML systems record body sway, the former through changes in force on the platform, the latter through changes in sensor position. Body sway was expressed as sway area. Additionally, participants were asked how often they fell in the last 12 months and completed the Activity Measure for Post-Acute Care™ (AM-PAC™) questionnaire, a validated tool to assess mobility.

**Results:** 112 older adults (23 men, 89 women, mean age (SD) 80.6 (6.04)) were studied. 46 reported ≥ 1 falls in the last year. 95 had the maximal SPPB balance score of 4 (i.e. able to perform tandem stance ≥ 10s). Mean Elliptical Area (cm<sup>2</sup>) for the LEO system was 3.9 (3.97), 4.8 (3.55) and 6.4 (6.59) for ROM, ST and TAN respectively. ML Sway Area (RMS degrees) were 0.67 (0.398), 0.76 (0.418) and 1.34 (1.47). Correlation between LEO and ML was good ranging from R = 0.59 (TAN) to R = 0.74 (ROM and ST). Both LEO and ML TAN sway area correlated very well with TAN time (R = 0.88 and 0.97). There were small but significant relationships between number of falls and AM-PAC™ mobility score and LEO and ML sway area during ROM (all p< 0.05) but not with TAN time or SPPB balance score.

**Conclusion:** Two novel, computerized methods to assess body sway (LEO and ML) correlate well with each other and the SPPB balance score. Importantly, body sway measured with these computerized systems related to outcomes (number of historical falls and AM-PAC™ questionnaire measured mobility), whereas the SPPB balance score was not. These tools promise to be valid, quantitative tools to assess balance that might prove to be more sensitive than current methods such as the SPPB.

**Disclosures:** Bjoern Buehring, None.

## MO0719

**Altered Physical Performance Tests are Risk Factors for Falls and Osteoporotic Fractures.** Adriana Graciela Diaz\*, Sabrina Paola Lucas<sup>1</sup>, Maria Gabriela Torres<sup>1</sup>, Claudia Martinez<sup>1</sup>, Felipe Silva Pavon<sup>1</sup>, Reynaldo Gomez<sup>1</sup>, Beatriz Oliveri<sup>2</sup>. <sup>1</sup>Division Endocrinología, Hospital de Clínicas-UBA, Argentina, <sup>2</sup>Laboratorio Osteoporosis y Enfermedades Metabólicas Oseas (INIGEM, UBA-CONICET), Argentina

**Purpose :** To describe associations of falls and osteoporotic fractures with physical performance in ambulatory adults ≥ 60 years.

**Methods:** A cohort of 405 adults ≥60 years who attended a community activity to evaluate risk factors for osteoporotic fractures and muscle health at the University Hospital. Evaluation included anthropometric measurements, physical performance tests: 4-meter walking speed (WS) [(Normal value (NV) < 5 s), 3-meter Timed Get-Up-and-Go Test (NV ≤ 10 s) and Chair sit-to-stand test (NV < 11.2s). Grip strength assessed by dynamometry (NV > 20kg for women and > 30kg for men). All participants answered a questionnaire about falls in the last year and history of osteoporotic fractures. Weekly physical activities (scored as none, mild and moderate activity), spontaneous loss of weight (>4.5Kg in the last year) and obesity (BMI > 30kg/m<sup>2</sup>) were considered as possible modifiers of physical performance tests.

**Results:** 321 women aged 69.9 ± 7.23yo and 82 men aged 71.96 ± 7.56 yo, with similar BMI in both sexes. Women had worse performance in all tests evaluated than men (p< 0.001). Falls were associated with loss of weight (p=0.004) and altered Grip strength (p=0.026). In women, previous falls were also associated with worse Get-Up-and-Go and Walking Speed tests (p=0.007, 0.003, respectively). Considering obesity, men with BMI > 30, showed worse Get-Up-and-Go (p=0.033) and Walking Speed test (p=0.0001) than non obese men. History of osteoporotic fractures was associated with falls, with one or more altered physical performance tests and particularly with altered Chair sit-to-stand test (p=0.023). Physical activity was associated significantly with better physical performance tests (p=0.015-0.001) and Grip strength (p=0.005).

**Conclusions:** Worse physical performance tests were associated with falls and history of osteoporotic fractures. Obesity and sedentary lifestyle were deleterious for physical performance while spontaneous loss of weight seems to be a risk factor for falls.

**Disclosures:** Adriana Graciela Diaz, None.

## MO0720

**Combined efficacy of different exercise interventions in osteosarcopenic men.** Franca Genest<sup>1</sup>, Sarah Lindström<sup>1</sup>, Nicole Luksche<sup>1</sup>, Franz Jakob<sup>2</sup>, Lothar Seefried<sup>1</sup>. <sup>1</sup>Clinical trial Unit department of orthopedic surgery University of Wuerzburg, Germany, <sup>2</sup>Musculoskeletal Center Wuerzburg, Germany

**Introduction:** Osteoporosis and sarcopenia both are critical determinants of impaired health outcomes and functional decline in aging. Clinical significance of a combined occurrence, i.e. osteosarcopenia might be even worse. Various exercise interventions have been proven beneficial but comparative evaluations of distinct exercise modalities are lacking.

**Methods:** Prospective randomized controlled trial to compare efficacy and feasibility of 4 different exercise modalities over 6 months in men aged 65-90y at risk for osteoporosis and sarcopenia. Interventions comprised Resistance Training (RT), Whole Body Vibration Exercise (VE), Qi Gong (QG) or wearing a Lumbar Orthosis (LO). Primary endpoint was isometric trunk strength (TS) for Extension (E) and Flexion (F), secondary endpoints included key diagnostic parameters for osteosarcopenia: BMD, Appendicular Lean Mass (ALM), Grip Strength and the Short Physical Performance Battery (SPPB). Results: n=47 men were equally randomized. RT resulted in sig. improvements for TS-E (p=0,009) and TS-F (p=0,013). VE improved TS-E (p=0,014) and performance in CRT (p=0,005), LO improved CRT (p=0,003) and GS (p=0,027), while QG did not yield any sig. improvements. Subgroup analyses revealed outstanding improvements in those subjects at increased risk, irrespective of the type of exercise, i.e. participants  $\geq 80y$  showed improvements in both LS-BMD (p=0,01) and ALM (p=0,016) and sig. enhanced performance for TS-E (p=0,029) and CRT (p=0,017). Presarcopenic subjects improved in TS-E (p=0,003), CRT (p=0,001) and GS (p=0,016). Participants with multiple ( $\geq 3$ ) chronic diseases achieved sig. improvements in TS-E (p<0,001), TS-F (p=0,002), GS (p=0,036) and Grip Strength (p=0,046). Discussion: In osteosarcopenic men, different exercise modalities elicited sig. improvements in key diagnostic criteria for both osteoporosis and sarcopenia. Overall efficacy was primarily restricted to parameters specifically addressed by an exercise and did not elicit improvement outside the focus of the intervention. However, subgroup analyses revealed pronounced improvements beyond the scope of a specific intervention for high risk subjects even with low-impact interventions (QG,LO). In conclusion, exercise intervention is effective in elderly males, primarily to improve those parameters specifically addressed. However, in subjects with reduced health status, even low threshold interventions may be beneficial, actually beyond exercise-specific improvements.

**Disclosures:** Franca Genest, None.

## MO0721

**Comparison of calf skeletal muscle composition among rural south Indian, US Caucasian and Afro-Caribbean older men.** Guru Rajesh Jammy<sup>1</sup>, Iva Miljkovic<sup>1</sup>, Robert M Boudreau<sup>1</sup>, Tushar Singh<sup>1</sup>, Pawan Kumar Sharma<sup>2</sup>, Kristine E Ensrud<sup>3</sup>, Joseph M Zmuda<sup>1</sup>, P S Reddy<sup>2</sup>, Anne B Newman<sup>1</sup>, Jane A Cauley<sup>1</sup>. <sup>1</sup>Department of Epidemiology, University of Pittsburgh, United States, <sup>2</sup>SHARE INDIA - Medciti Institute of Medical Sciences, India, <sup>3</sup>Division of Epidemiology & Community Health, University of Minnesota; Department of Medicine, University of Minnesota; Center for Chronic Disease Outcomes Research, VA Health Care System, Minneapolis., United States

Current demographic trends towards an aging society have become a global health issue. With aging, there are decreases in muscle mass and increases in skeletal muscle adipose tissue infiltration. This is associated with decreased strength, mobility loss, insulin resistance, fractures, and diabetes. The geographical/racial differences in muscle composition have been less studied. We compared the peripheral Quantitative Computed Tomography (pQCT) (Stratec XCT-2000) measured skeletal muscle parameters in the calf among (i) Indian men aged 60 years and older enrolled in the Mobility and Independent Living among Elders Study (MILES) in rural south India (N=243), (ii) US Caucasian men aged 65 years and older enrolled in Osteoporotic Fractures in Men Study (MrOS) in the US (N=1119), and (iii) Afro-Caribbean men aged 60 years and older enrolled in the Tobago Bone Health Study, in Trinidad and Tobago (N=828).

Indian [Mean (SD) = 68.3 (6.7)] and Afro-Caribbean [68.8 (6.8)] men were significantly younger compared to US Caucasian men [77.4 (5.3)]. The BMI ( $\text{kg/m}^2$ ) of Indian men [21.6 (3.9)] was significantly lower compared to US Caucasian [28.1 (3.7)] and Afro-Caribbean men [27 (4.5)]. Though not harmonized, diabetes was higher among Indian (19%) and Afro-Caribbean men (30%) compared to US Caucasians (10%). Muscle cross-sectional area (CSA), muscle density, intermuscular adipose tissue (IMAT) and subcutaneous adipose tissue (SAT) were compared with US Caucasians as the referent population adjusting for age, BMI and tibia length (Figure 1). Using SDs in US Caucasians, SD differences were calculated. Among Indian men, IMAT (+0.6 SD) and SAT (+0.3 SD) were significantly higher compared to US Caucasians. Afro-Caribbean men had significantly higher IMAT (+0.6 SD) but significantly lower SAT (-0.5 SD) compared to US Caucasians. Muscle density (-1.7 SD) and muscle CSA (-1.6 SD) were significantly lower among Indian men compared to US Caucasians. Afro-Caribbean men also had significantly lower muscle density (-0.3 SD) and muscle CSA (-0.6 SD) compared to US Caucasians. Despite having low general adiposity (BMI), Indian men had higher muscle adipose tissue infiltration, lower muscle CSA and muscle density. Similar observations were observed among the Afro-Caribbean men despite similar BMI as US Caucasians. Further research is needed to better understand the

physiologic causes and clinical consequences of these geographical/racial differences in the skeletal muscle composition.

Figure 1:

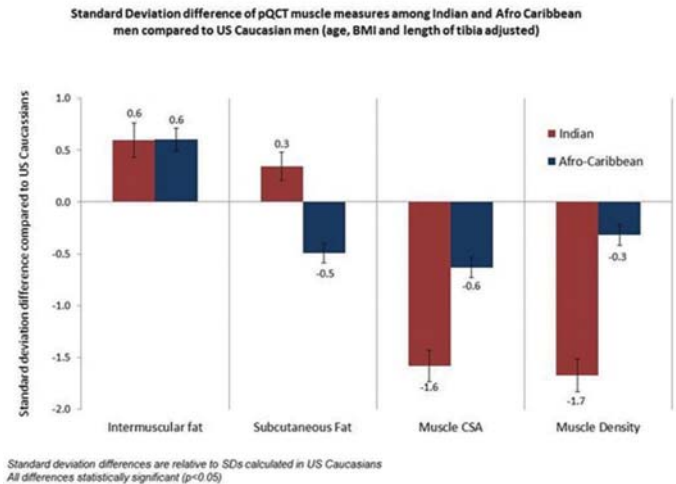


Figure 1: Standard Deviation difference of pQCT muscle measures

**Disclosures:** Guru Rajesh Jammy, None.

## MO0722

**Sarcopenia and Estimates of Fracture Risk.** Julie Pasco<sup>\*</sup>, Kara Holloway, Pamela Rufus, Natalie Hyde, Monica Tembo, Sophia Sui, Lana Williams, Mark Kotowicz, Deakin University, Australia

**Purpose:** The decline of the musculoskeletal system is manifested as sarcopenia and osteoporosis. Fracture risk increases with decreasing BMD but it is not clear whether sarcopenia is associated with increased fracture risk. We aimed to compare estimates of fracture risk for older women with and without sarcopenia.

**Methods:** Lean mass and BMD were assessed by DXA (Lunar) for 324 women aged 60-90 years as part of the Geelong Osteoporosis Study (GOS). Sarcopenia was identified by relative lean mass ( $\text{kg/m}^2$ ) T-score <-1 and timed up-&-go >10s for 3m. Ten-year probabilities for hip and major osteoporotic fractures were calculated using FRAX(Aus) with and without femoral neck BMD. Differences in FRAX scores for women with and without sarcopenia were identified using the Mann-Whitney test for non-parametric data.

**Results:** The 23 (7.1%) women with sarcopenia were older (mean $\pm$ SD), 77.5 $\pm$ 7.3 vs 72.3 $\pm$ 8.1 yr (p=0.003), had lower BMI, 23.3 $\pm$ 4.0 vs 27.9 $\pm$ 4.9  $\text{kg/m}^2$  (p<0.001) and lower BMD, 0.765 $\pm$ 0.099 vs 0.832 $\pm$ 0.142  $\text{kg/m}^2$  (p=0.005) than those without sarcopenia. Sarcopenia was associated with higher FRAX scores for hip fracture calculated with BMD (median(IQR)), 4.7(2.5-6.5) vs 2.0(0.6-5.2) (p=0.004) and without BMD, 11.0 (5.0-21.0) vs 4.7(1.4-11.0), (p<0.001). A similar pattern was observed for major osteoporotic fractures, both with BMD, 13.0(11.0-16.0) vs 8.1(4.2-15.0) (p=0.01) and without BMD, 24.0(13.0-33.0) vs 11.0(5.1-22.0), (p<0.001).

**Conclusion:** We report that sarcopenia is associated with higher FRAX scores for hip and major osteoporotic fractures among older women. Sarcopenia was associated with higher fracture risk estimates that are based on age and BMD. This finding underscores the need to investigate the risk of fracture attributable to osteosarcopenia.

**Disclosures:** Julie Pasco, None.

## MO0723

**Sarcopenia is Associated with Low Bone Mineral Density in Japanese Elderly Women.** Shinjiro Takata<sup>\*</sup>. Department of Orthopedics and Rehabilitation, Tokushima National Hospital, National Hospital Organization, Japan

The term sarcopenia was proposed by Irwin Rosenberg to describe an age-related decrease of muscle mass (Am J Clin Nutr 1989; 59:1231-3). The European Working Group on Sarcopenia in Older People (EWG-SOP) recommends using the presence of both low muscle mass and low muscle function (strength or performance) to make a diagnosis of sarcopenia (Age and Ageing 2010; 39:412-423). This study was designed to clarify the characteristics of regional bone mineral density (BMD) and soft tissue composition in Japanese elderly women with sarcopenia.

Three hundred and ten Japanese elderly women aged 65 years or more were divided into two groups, sarcopenia group (n=79) and control group (n=231). There were no significant differences of age, body height, body weight, and body mass index between these two groups. The mean BMD of the second to fourth lumbar vertebrae (L2-4BMD), total body BMD, and soft tissue composition were measured by DXA using Hologic Discovery W (Waltham, MA, USA). Skeletal mass index (SMI) is the appendicular skeletal mass in kilograms measured by dual energy X-ray absorptiometry divided by the square of the height in meters ( $\text{kg/m}^2$ ). SMI of the sarcopenia group was less than 5.4 ( $\text{kg/m}^2$ ).



The BMDs of the arms, legs, and femoral neck as well as the L2-4BMD of the sarcopenia group were significantly lower than those of the control group ( $p < 0.05$ ). The lean masses of the arms, trunk, and legs of the sarcopenia group were significantly lower than those of the control group ( $p < 0.05$ ), whereas the fat masses of the arms and legs of the sarcopenia group were significantly greater than those of the control group ( $p < 0.05$ ).

The results obtained in this study show that sarcopenia in Japanese women aged 65 years or more is associated with osteopenia or osteoporosis in addition to reduced muscle mass.

**Disclosures:** Shinjiro Takata, None.

## MO0724

**Prevalence of sarcopenia and characterisation of the muscle bone unit in a rural population in Sub-Saharan Africa.** Ayse Zengin<sup>\*1</sup>, Ann Prentice<sup>2</sup>, Landing Jarjou<sup>3</sup>, Peter Ebeling<sup>1</sup>, Kate Ward<sup>4</sup>. <sup>1</sup>Monash University, Australia, <sup>2</sup>MRC Elsie Widdowson Laboratory, United Kingdom, <sup>3</sup>MRC The Gambia Unit, Gambia, <sup>4</sup>MRC Lifecourse Epidemiology, University of Southampton, United Kingdom

By 2050 over 60% of the world's ageing population will live in low and middle income countries. Characterising musculoskeletal ageing is therefore a growing need in Sub-Saharan Africa. This study aimed to estimate the prevalence of sarcopenia, to describe age-related differences in muscle and to assess the muscle-bone unit using DXA, jumping mechanography and pQCT in a rural subsistence farming community from The Gambia, West Africa.

249 women (W) and 239 men (M) mean[SD] age 61.1[12.5] and 60.8[12.3] years respectively were recruited. Muscle outcomes were whole body lean mass (kg), muscle force (kN) and power (kW) and muscle density and cross-sectional area. Bone outcomes from the 14% tibia were cortical content (BMC), cortical area, and cross-sectional area. The European Working Group on Sarcopenia definition was used to assess sarcopenia prevalence in the population. Linear regression was used to test associations between muscle parameters with age, including a sex-age interaction, muscle force and bone outcomes, including a sex-muscle interaction, adjusting for height and weight. Data are presented as mean [95%CI] difference per unit increase in age (10y) or muscle (1kN).

Sarcopenia prevalence was greatest in men, 18% compared to 10% in women ( $p < 0.0001$ ). Whole body lean mass (M -2[-3,-1], F -1[-1,-0.2]); force (M -10[-12,-8], F -10[-12,-7]) power (M -27[-31,-24], F -20[-25,-16]) and density (M -1[-2,-1], F -2[-2,-1]) declined with age ( $p$ -interaction 0.002 to 0.05). Jump force was positively associated with BMC (M 11[3,26], F 44[26,63]), cortical area (M 10[2,22], F 34[18,49]) and cross sectional area (M 11[1,22], F 34[19,49]), with women greater differences in bone outcome for a given force than men ( $p < 0.0001$  for all).

Using several methods to assess muscle mass, function and anatomy we have shown negative associations with age in this population. Importantly, men have greatest differences with age than women, and the highest sarcopenia prevalence. Some of these differences could be methodological, though there is consistency across different measures. The associations between bone and muscle highlight the importance of maintaining muscle function during ageing. In a population that is rapidly transitioning to a Western lifestyle it is important to better characterise musculoskeletal outcomes to prevent NCDs of ageing.

**Disclosures:** Ayse Zengin, None.

## MO0725

**Does sarcopenia and osteoporosis increase the risk of occurrence of frailty?**

**Four-year observations between the second and third ROAD study surveys.**

Noriko Yoshimura<sup>\*1</sup>, Shigeyuki Muraki<sup>1</sup>, Hiroyuki Oka<sup>2</sup>, Toshiko Iidaka<sup>1</sup>, Rie Kodama<sup>3</sup>, Hiroshi Kawaguchi<sup>4</sup>, Kozo Nakamura<sup>5</sup>, Toru Akune<sup>5</sup>, Sakae Tanaka<sup>3</sup>. <sup>1</sup>Department of Prevention Medicine for Locomotive Organ Disorders, 22nd Century Medical and Research Center, The University of Tokyo, Japan, <sup>2</sup> Department of Medical Research and Management for Musculoskeletal Pain, 22nd Century Medical and Research Center, The University of Tokyo, Japan, <sup>3</sup>Department of Orthopaedic Surgery, Sensory and Motor System Medicine, Graduate School of Medicine, The University of Tokyo, Japan, <sup>4</sup>JCHO Tokyo Shinjuku Medical Center, Japan, <sup>5</sup> National Rehabilitation Center for Persons with Disabilities, Japan

**Purpose:** To clarify the contribution of sarcopenia (SP) and osteoporosis (OP) to the occurrence of frailty.

**Methods:** The second survey of the Research on Osteoarthritis/Osteoporosis Against Disability (ROAD) study—a large-scale population-based cohort study—was conducted between 2008 and 2010. Among 1,099 participants of the second survey of the ROAD study, 1,083 subjects (aged  $\geq 60$  years, 372 men, 711 women) completed the all examinations of frailty, SP and OP. Frailty was defined using the Fried's definition with following five variables: unintentional weight loss, self-reported exhaustion, low physical activity, weakness (grip strength,  $< 26$  kg in men and  $< 18$  kg in women), and slowness (slow walking speed, usual gait speed was  $\leq 0.8$  m/s). Those with three or more of the five factors were judged to be frailty. The third survey was conducted between 2012 and 2013; 767 of the 1,083 individuals who were enrolled from the second survey (70.8%, 253 men, 514 women) had completed assessments identical to those in the

second survey. SP was defined as per the algorithm of the Asian Working Group for Sarcopenia, whereas OP was defined based on the World Health Organization criteria.

**Results:** The cumulative annual incidence of frailty was 1.2%/yr. After adjustment for confounding factors, a logistic regression analysis using the occurrence of frailty as the objective variable and the presence of OP as the explanatory variable indicated that the presence of OP was significantly associated with the occurrence of frailty in the near future (odds ratio (OR), 3.24; 95% confidence interval (CI), 1.38-7.63;  $p < 0.01$ ). Again, the logistic regression revealed occurrence of frailty significantly increased according to the number of OP and SP present (OR vs. neither OP nor SP: OP or SP, 2.50; OP and SP, 5.80).

**Conclusions:** This prospective study suggests that OP and SP prevention may be useful in reducing future frailty risk.

**Disclosures:** Noriko Yoshimura, None.

## LB-MO0726

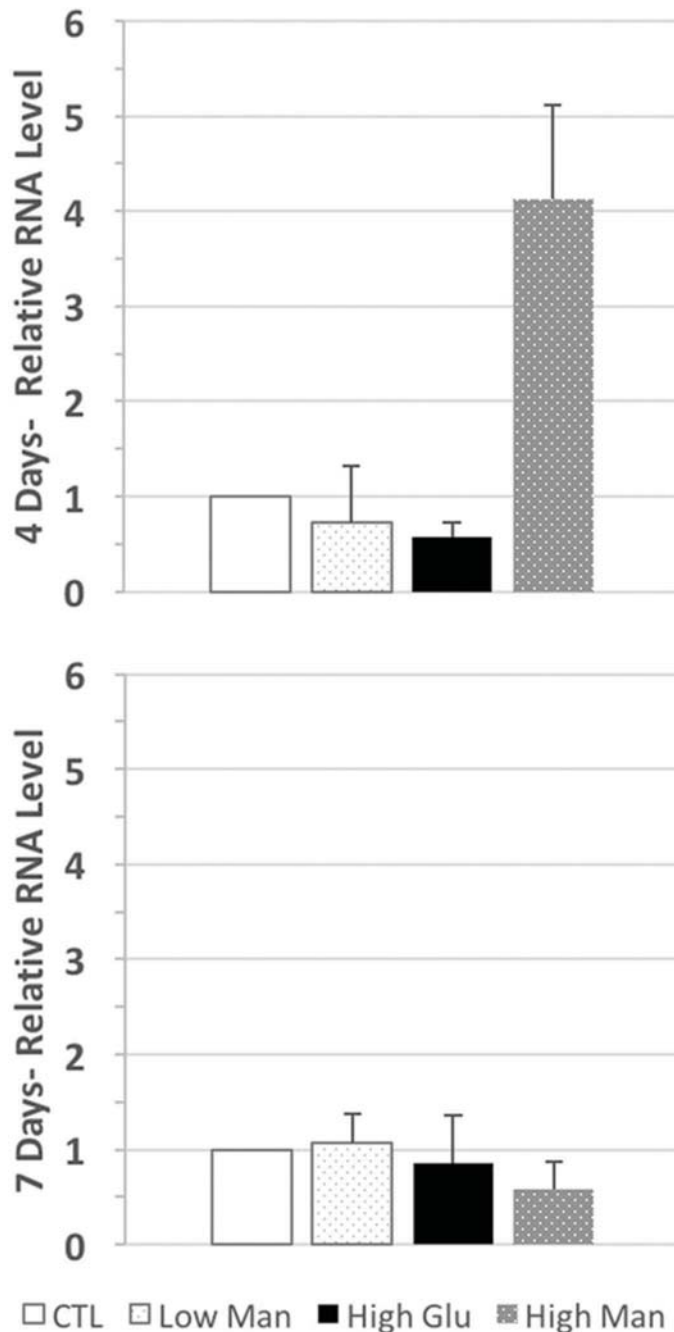
**Human osteoblast VEGF-A expression after short-term exposure to hyperglycemic conditions.** Jesse Hernandez<sup>\*1</sup>, Zachary Child<sup>1</sup>, Todd Bredbenner<sup>2</sup>, Roberto Fajardo<sup>1</sup>. <sup>1</sup>UT Health San Antonio, United States, <sup>2</sup>Southwest Research Institute, United States

The role of vascular complications and vascular endothelial growth factor (VEGF-A) signaling in diabetic skeletal fragility is gaining more interest, with some data suggesting that VEGF-A expression is low in diabetic human bone tissue. VEGF-A signaling is critical for angiogenesis and bone remodeling. Murine data suggest that chronic ( $> 21$  days), as opposed to short-term ( $< 21$  days), exposure to hyperglycemic conditions suppresses VEGF-A expression in osteoblasts. The impact of high glucose (Glu) conditions on human osteoblast VEGF-A expression is unknown. We performed 4 and 7 day in-vitro experiments using a human osteoblast cell line to determine the impact of relatively short term hyperglycemic conditions on VEGF-A expression.

Adult human osteoblasts (Cell Applications, San Diego, CA) were seeded at 20,000 cells/well and proliferated for 7 days in a-MEM containing 10% FBS and 1% Pen/Strep. Then, cells were differentiated in a-MEM containing 50  $\mu$ g/mL ascorbic acid and 10mmol/L beta-glycerol phosphate. After 24hrs, four different treatment groups were created: 5mM Glu/0 mannitol, 5mM Glu/5mM mannitol, 25mM Glu/0 mannitol, 5mM Glu/ 20mM mannitol. At 4 and 7 day time points, extractions were performed using Direct Zol MiniPrep kit. Synthesis of cDNA was performed with qScript cDNA SuperMix and PerfeCTa SYBR Green SuperMix, ROX.

Relative VEGF-A RNA expression in human osteoblasts treated for 4 days with 25mM glucose trended lower than controls but the differences were not significant. A similar pattern occurred after 7 days of treatment (Fig. 1). No significant differences were observed in the mannitol controls compared to the normal glucose group. A 4-fold increase in VEGF-A expression occurred in the high mannitol group. This result was not significant due to high variation; the relative expression decreased dramatically by day 7.

Results suggest that osteoblast RNA expression is normal after 4 and 7 day treatments in hyperglycemic conditions. These results contrast with limited data suggesting that VEGF-A expression is low in human diabetic bone tissue. However, these results are consistent with patterns observed by Botolin and McCabe in murine osteoblast cultures where VEGF-A expression was unchanged in cultures treated for less than 21 days with high glucose. More experiments are necessary to determine whether longer-term (chronic) exposures to hyperglycemic conditions result in alteration in VEGF-A expression by osteoblasts in vitro.



Disclosures: Jesse Hernandez, None.

## LB-MO0727

**Change in BMD over 12 to 24 Months Is Strongly Associated with Fracture Reductions in Randomized Trials: A Study-Level Meta-Regression using the FNIH Bone Quality Study Project Database.** Dennis Black<sup>1</sup>, Richard Eastell<sup>2</sup>, Douglas Bauer<sup>1</sup>, Li-Yung Lui<sup>3</sup>, Charles McCulloch<sup>1</sup>, Anne de Papp<sup>4</sup>, Sundeep Khosla<sup>5</sup>, Steven Hoffmann<sup>6</sup>, Mary Bouxsein<sup>7</sup>. <sup>1</sup>University of California, San Francisco, United States, <sup>2</sup>University of Sheffield, United Kingdom, <sup>3</sup>California Pacific Medical Center, United States, <sup>4</sup>Merck and Co., Inc. Kenilworth, NJ, USA, United States, <sup>5</sup>Mayo Clinic College of Medicine, United States, <sup>6</sup>Foundation for National Institute of Health, United States, <sup>7</sup>Harvard Medical School, United States

There is a great need to decrease the size and cost of clinical trials for new osteoporosis therapies. To determine if change in BMD can be used as a surrogate for fracture (Fx) for drug development, the FNIH Bone Quality Project is compiling individual patient data from as many randomized osteoporosis trials as possible. Data compilation

is in progress and we are obtaining data on >150,000 patients (>85,000 with DXA BMD) from >50 trials of 11 osteoporosis treatments, including 4 bisphosphonates, 3 SERMS, Denosumab, ERT, Teriparatide and PTH(1-84). Study durations range from 1 to 5 years.

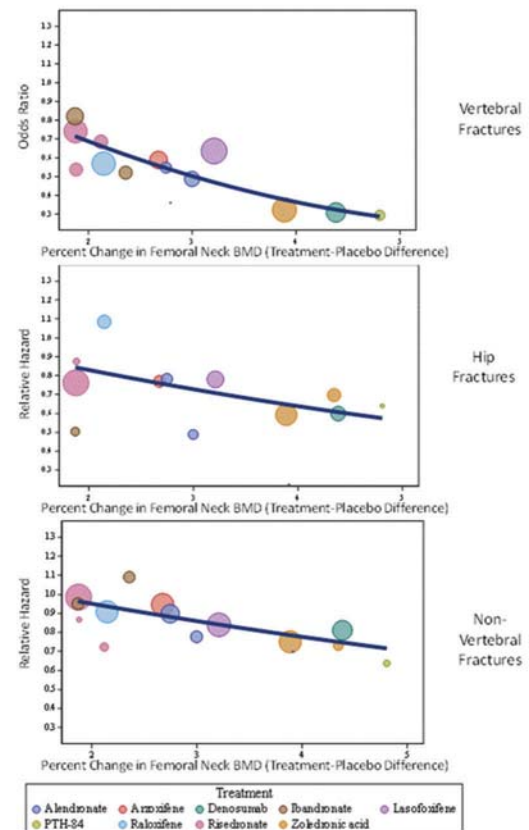
Previous meta-regressions of BMD and Fx relied on published data, could not control for study duration and used inconsistent statistical methods. To address the BMD-Fx association more rigorously, we used FNIH BQ data (from all placebo-controlled trials), varying BMD follow-up times, and applying consistent methods, including uniform Fx definitions. We analyzed mean % BMD changes (total hip, femoral neck (FN) and spine) over 12, 18 and 24 months. We plotted % BMD change (treatment-placebo) for each study vs. the log of relative risk for Fx and used weighted linear regression to describe the relationship. We calculated  $r^2$  and p-value for each BMD-Fx combination and estimated the % reduction in Fx risk associated with a given % BMD, spanning the min and max BMD changes observed in the trials.

The relationships between % change in FN BMD over 24 months and Fx reduction for vertebral (VFx), hip and non-vertebral (NVFx) Fx are shown in figures. For 24 month FN BMD change, the analysis included 4033 VFx, 829 hip and 6111 NVFx. The relationship was most striking for VFx: 1.8% BMD difference predicted a 27% VFx reduction, while a 4.9% BMD difference predicted 72% reduction ( $r^2=0.74, p<0.0001$ ). In comparison, a 1.8% and 4.9% BMD difference predicted 15% and 43% reductions in hip Fx ( $r^2=0.20, p=0.09$ ) and 3% and 29% reductions in NVFx ( $r^2=0.60, p=0.0007$ ).

Relationships were similar but somewhat weaker for BMD changes over 12 or 18 vs. 24 months. Analyses with total hip BMD showed similar results while spine BMD showed weaker associations.

We conclude that change in hip BMD in 24 month trials robustly predicts Fx reductions in those trials. We expect that when data collection is complete and analyses are finalized, our results will support the possibility that shorter BMD endpoint trials with fewer patients may be sufficient for future approvals of new osteoporosis treatments.

Figure: Relationship of 24-Month Change in Femoral Neck BMD and Reduction in Fractures



Disclosures: Dennis Black, Radius Pharmaceuticals, Asahi-Kasei, Consultant.

## LB-MO0728

**Myogenic Autoregulation in Bone Marrow Arterioles and *In Vivo* Intramedullary Pressure in Femora of Conscious Female Long Evans Rats.** Seungyong Lee<sup>1</sup>, Rhonda Prisby<sup>1</sup>, Sophie Guderian<sup>2</sup>. <sup>1</sup>University of Texas at Arlington, United States, <sup>2</sup>University of Delaware, United States

The Myogenic Response is the inherent ability of blood vessels to dilate and constrict to low and high intraluminal pressures, respectively, and provides local regulation of blood flow. Few studies have been conducted on isolated bone marrow arterioles. Further, intraluminal pressure in bone marrow arterioles have not been measured and



reported recordings of bone intramedullary pressure are variable. The purpose was to assess *in vivo* intramedullary pressure in the femoral canal of conscious rats and assess Myogenic Autoregulation in bone marrow arterioles. *Experiment 1*: Female Long Evans rats (~5 months; n=13) were anesthetized (3% isoflurane to O<sub>2</sub> balance) and the femoral shafts were catheterized. Subsequent to 1 hour of recovery, the catheter was hooked to a pressure transducer and *in vivo* intramedullary pressure (mmHg) was recorded (PowerLab, AD Instruments), whereby the last 5 minutes were averaged. *Experiment 2*: Right femora were dissected from female Long Evans rats (~5 months; n=11). Bone marrow arterioles were isolated and cannulated to conduct active (with Ca<sup>2+</sup>) and passive (without Ca<sup>2+</sup>) Myogenic Responses to step-wise increases and decreases (0 to 135 to 0 cmH<sub>2</sub>O) in intraluminal pressure. For comparison, active and passive Myogenic Responses were normalized to maximal diameters recorded in Ca<sup>2+</sup> free conditions at pressures of 20 cmH<sub>2</sub>O (15 mmHg), 30 cmH<sub>2</sub>O (22 mmHg), 45 cmH<sub>2</sub>O (33 mmHg) and 60 cmH<sub>2</sub>O (44 mmHg). Repeated Measures ANOVAs with pair-wise comparisons were performed. Alpha level was set at  $p < 0.05$  *a priori*. Values represent Means  $\pm$  S.E. Body masses were 293 $\pm$ 9 g and 307 $\pm$ 7 g for Experiments 1 and 2, respectively. *In vivo* intramedullary pressure averaged 33 $\pm$ 3 mmHg. Maximal diameter and wall thickness of the bone marrow arterioles were 96 $\pm$ 7 mm and 17 $\pm$ 2 mm, respectively. Active Myogenic Responses were observed at all normalized pressures; i.e., 15 mmHg, 22 mmHg, 33 mmHg and 44 mmHg ( $p < 0.016$ ,  $p < 0.011$ ,  $p < 0.002$  and  $p < 0.000$  vs. passive Myogenic Responses, respectively). This is the first report of Myogenic Autoregulation in bone marrow arterioles, which occurred at the following range of normalized pressures: 15-44 mmHg. This range is consistent with recorded intramedullary pressures (i.e., range: 15-51 mmHg and average: 33 mmHg) within the femur. Thus, Myogenic Autoregulation may serve as a mechanism by which bone marrow arterioles participate in the regulation of blood flow to bone and bone marrow.

**Disclosures:** Seungyong Lee, None.

## LB-MO0729

**Dietary fat and *de novo* derived lipid trafficking in bone *in vivo*.** Vanessa Sherk\*, David Presby, Janine Higgins, Matthew Jackman, Julie Houck, Paul MacLean. University of Colorado Anschutz Medical Campus, United States

The bioenergetics of skeletal tissue *in vivo* are poorly understood, despite an awareness that bone remodeling expends energy and that marrow is an adipose depot. This study was conducted to determine whether lipid in bone is derived from dietary fat accumulation or from *de novo* (DN) lipogenesis, and whether an increase in whole body fat oxidation is associated with decreased dietary fat retention in bone. Mice overexpressing lipoprotein lipase (mLPL) in skeletal muscle were used to mimic the bioenergetics effects of exercise. mLPL and WT (6 wks old; n=5-6/grp) were fed a high fat + sucrose diet for 8 weeks, and then switched to a medium fat diet for 3 weeks. <sup>3</sup>H<sub>2</sub>O was injected 2 hours prior to providing food treated with <sup>14</sup>C labelled oleate and palmitate (3:1) for 24 hours to trace DN derived (<sup>3</sup>H) and dietary fat (<sup>14</sup>C) lipids. Lipids were extracted from the gastrocnemius and the hind limb bones (femurs and tibiae) with marrow, and tested for 1) dietary fat retention, and 2) the presence of DN-derived lipids. Data are expressed as mean $\pm$ SE. <sup>3</sup>H was detected in lipid from bone in all mice (% plasma <sup>3</sup>H retained per g of lipid: 0.946 $\pm$ 0.100%), and to a greater relative extent than lipid in muscle (%plasma <sup>3</sup>H retained per g of lipid in muscle: 0.659 $\pm$ 0.064%), indicating that lipid in bone is partly derived from non-dietary-fat sources. Group differences in <sup>3</sup>H retention in bone lipid neared significance (WT: 1.073 $\pm$ 0.157% mLPL: 0.794 $\pm$ 0.103%;  $p=0.076$ ). Dietary fat accumulation (<sup>14</sup>C) in hind limb bones was 258 $\pm$ 59  $\mu$ g/24h, which was 65 $\pm$ 8% less than in muscle (874 $\pm$ 200  $\mu$ g/24h). Exogenous fat accumulation in bone did not differ between groups. The proportion of bone lipid that consisted of new dietary fat was similar to muscle and tended to be lower in LPL mice (1.67 $\pm$ 0.45% g vs 0.90 $\pm$ 0.21%,  $p=0.073$ ). Trends for group differences were consistent with greater <sup>14</sup>C expiration (i.e., greater meal fat oxidation) in the mLPL mice. This is the first direct evidence of DN-derived lipid in bone *in vivo*. Further, whole body fat oxidation affects total bone fat accumulation, both DN and meal-derived.

**Disclosures:** Vanessa Sherk, None.

## LB-MO0730

**Long-term response to intrauterine stress induced by teratogen 5-deoxy-2'-cytidine differs in adult offspring of C3H/HeJ and C57BL/6J mice.** Deepak Kumar Khajuria\*<sup>1</sup>, Maria Raygorodskaya<sup>2</sup>, Yankel Gabet<sup>3</sup>, Sahar Hiram Bab<sup>3</sup>, Chen Shochat<sup>1</sup>, David Karasik<sup>1</sup>. <sup>1</sup>The Musculoskeletal Genetics Laboratory, Faculty of Medicine in the Galilee, Bar Ilan University, Safed, Israel, Israel, <sup>2</sup>The Musculoskeletal Genetics Laboratory, Faculty of Medicine in the Galilee, Bar Ilan University, Safed, Israel; <sup>3</sup>SRC BioClinicum, Moscow, Russia, Israel, <sup>3</sup>Department of Anatomy & Anthropology, Sackler Faculty of Medicine, Tel Aviv University, Tel-Aviv, Israel, Israel

The long-term skeletal effects of antenatal exposure to teratogen 5-deoxy-2'-cytidine (5-AZA) was studied using two inbred strains, C3H/HeJ (C3H, with inherently stronger bones) and C57BL/6J (C57, with weaker bones). We previously reported that bone structure and bone mineral density (BMD) of the 3- and 6-month-old offspring's femora differed by strain (Raygorodskaya et al. *Bone* 2016: 114-119). *In-utero* exposure to 5-AZA resulted in loss of bone quality in 6-mo-old C3H offspring but not in their C57 counterparts. Gestational 5-AZA treatment also caused decreased expression of *Colla1* in adult C3H offspring, but decreased expression of *Sox9* in the C57 strain.

In this study, we further examined whether the long-term effects of an acute teratogenic exposure are still evident in older mice. Mice exposed to a single injection of 5-AZA on day 10 of their mother's pregnancy were evaluated by micro-computed tomography ( $\mu$ CT, Bruker 1172) after one year. The main observation of this study is a reduced bone mass in 12-mo-old C57 males that were exposed to 5-AZA *in-utero*. Table 1 provides a comparison of the bone structure and BMD of the femur of treated and untreated, male and female mice. There were statistically significant lower BV/TV and Tb.N in 5-AZA treated C57 males, as well as a marginally significant increase in Ct. Th of C3H females. As expected, we did not find differences in the 3<sup>rd</sup> lumbar vertebra since *in-utero* exposure to 5-AZA was shown to affect the limb buds but not the axial skeleton.

In summary, by characterizing teratogen-exposed C57 and C3H mice, we further confirmed the differences in adaptive response to antenatal insults between the strain inherently exhibiting a low bone mass (C57) and the strain exhibiting a high bone mass (C3H), as well as sex-specificity of these responses.

**Table 1: Bone morphometry and density of the femur measured by  $\mu$ CT at the age of 12 months (presented as group mean  $\pm$  S.E.M)**

			Cortical		Trabecular			
			Ct.Th [mm]	TMD [mg HA/cm <sup>3</sup> ]	BV/TV [%]	Tb.Th [mm]	Tb.N [mm <sup>-3</sup> ]	Tb.Sp. [mm]
C57	Males [n=7]	untreated	0.188±0.007	1245±60.5	4.15± 0.40	0.047±0.001	0.87±0.07	0.392±0.010
		treated	0.178±0.008	1202±27.4	1.78±0.20	0.045±0.003	0.40±0.05	0.431±0.049
		p-value	>0.05	>0.05	<0.0001	>0.05	<0.0001	>0.05
	Females [n=6]	untreated	0.182±0.018	1295±81.2	1.25±0.41	0.053±0.009	0.23±0.06	0.564±0.054
		treated	0.166±0.005	1321±22.1	0.90±0.20	0.046±0.002	0.20±0.06	0.652±0.071
		p-value	>0.05	>0.05	>0.05	>0.05	>0.05	>0.05
C3H	Males [n=7]	untreated	0.296±0.024	1310±169	9.28±1.81	0.056±0.001	1.67±0.34	0.249±0.027
		treated	0.277±0.014	1318±123	6.60±1.29	0.054±0.005	1.22±0.21	0.268±0.006
		p-value	>0.05	>0.05	>0.05	>0.05	>0.05	>0.05
	Females [n=6]	untreated	0.354±0.037	1302±72	10.41±6.38	0.075±0.003	1.41±0.91	0.40±0.01
		treated	0.426±0.028	1310±44	9.96±0.78	0.079±0.001	1.27±0.09	0.42±0.01
		p-value	>0.05	>0.05	>0.05	>0.05	>0.05	>0.05

**Disclosures:** Deepak Kumar Khajuria, None.

## LB-MO0731

**The Bone Phenotype of the Klotho Mutant Mouse Does Not Reflect Changes in Skeletal Architecture that occur with Aging.** Lieve Verlinden\*<sup>1</sup>, Vaishali Veldurthy<sup>2</sup>, Geert Carmeliet<sup>1</sup>, Sylvia Christakos<sup>2</sup>. <sup>1</sup>KU Leuven, Belgium, <sup>2</sup>Rutgers, New Jersey Medical School, United States

Aging is associated with alterations in calcium homeostasis that contribute to age-related bone loss. To understand the mechanisms that contribute to bone loss with aging we previously examined age-related changes in genes involved in calcium homeostasis in intestine and kidney (22- 24 month old mice compared to 6 month old mice). We also compared the phenotype with the premature aging phenotype that has been described in mice deficient in klotho, a cofactor for FGF23 involved in phosphate and calcium homeostasis. However, we found that alterations in vitamin D targets genes in the klotho mutant mice are in contrast to changes observed in aging mice; more precisely, levels of TRPV6 and calbindin-D<sub>9k</sub> mRNAs were increased compared to the decline observed in aging mice. These findings may reflect over production of 1,25(OH)<sub>2</sub>D<sub>3</sub> rather than changes in calcium homeostasis that contribute to bone loss with aging. In the present study we compared the bone phenotype of the klotho deficient mice (from M. Kuro-o) and aging mice by  $\mu$ CT and histomorphometry. Trabecular bone volume (BV/TV) significantly decreased with age in the tibia of both male and female C57BL/6 mice analyzed at 6 and 22-24 months of age. Females had lower BV/TV than males throughout life. A similar pattern of age related changes in trabecular bone has been reported in humans, showing a decrease in BV/TV that is more pronounced in females. In contrast to aging mice, trabecular bone volume was increased in both male and female klotho mutant mice (6 – 7 weeks of age; compared to age matched WT controls and to aged mice). The decline in BV/TV in the aging mice was accompanied by a decrease in trabecular number in males and females. Findings in the aging mice are in contrast to the increase in trabecular number observed in both male and female klotho mutant mice. Thus, although the klotho mutant mouse shows features of premature aging that include atherosclerosis and infertility, the bone phenotype of the klotho mutant mice does not reflect pathophysiological changes in bone mass and architecture that occur with aging.

**Disclosures:** Lieve Verlinden, None.

## LB-MO0732

**Corin is a key regulator of endochondral ossification and bone development via modulation of VEGF-A expression.** Rachel Nordberg\*<sup>1</sup>, Hao Wang<sup>2</sup>, Qingyu Wu<sup>2</sup>, Elizabeth Loba<sup>3</sup>. <sup>1</sup>North Carolina State University, United States, <sup>2</sup>Cleveland Clinic, United States, <sup>3</sup>University of Missouri, United States

Corin has been studied extensively within the vascular system, and is known to regulate blood pressure and sodium homeostasis. We have shown that corin is one of the most highly upregulated genes during osteogenic differentiation of human adipose

derived stem cells (hASC). The goal of this study was to test the hypothesis that, through modulation of angiogenic signaling pathways, corin is a critical regulator of osteogenic differentiation and endochondral ossification. We investigated this hypothesis both in vitro and in vivo. In vitro, hASC were obtained from liposuction aspirate of three female donors (ages 25-36). Corin expression in hASC was suppressed via siRNA knockdown. Vascular endothelial growth factor A (VEGF-A) expression was quantified via RT-PCR. In vivo, a murine corin knockout model (female, 10 week) was used to determine corin's effect on long bone development. Wildtype (n=5) and corin knockout (n=8) tibiae were sectioned for histology and stained via hematoxylin and eosin for tissue characteristics and cellular organization. Three-point-bending was used to assess mechanical properties of the knockout femurs. Immunohistochemistry was used to visualize VEGF-A expression in wild type and corin knockout tibiae. We found that corin expression was highly upregulated (over 200-fold) throughout osteogenic differentiation in hASC of all three donors. Corin knockdown significantly ( $p<0.05$ ) increased VEGF-A mRNA expression during osteogenic differentiation. In vivo, corin knockout resulted in abnormal tibial development patterns. In addition, thickness of the growth plate was significantly reduced ( $p<0.01$ ); and, the hypertrophic region of the growth plate was absent in corin knockout mice. Corin knockout femurs had significantly increased stiffness ( $p<0.01$ ) and maximum loads ( $p<0.01$ ) but also reduced post-yield deflections ( $p<0.01$ ), indicating that corin knockout femur were more brittle. In corin knockout mice, VEGF-A expression was increased near the growth plate, but was reduced throughout the tibial shaft and distal head of the tibiae. This is the first study to show that corin is a key regulator of bone development by modulation of VEGF-A expression. Further elucidation of this mechanism will aid in the development of optimized bone tissue engineering and regenerative medicine therapies and potentially facilitate the development of pharmaceutical interventions for osteoarthritis by targeting corin to prevent cartilage ossification.

**Disclosures:** Rachel Nordberg, None.

## LB-MO0733

**The Perichondrium is Enriched for Mesenchymal Progenitors that Initiate Canal Formation during the Development of the Secondary Ossification Center.** Robert Tower<sup>\*1</sup>, Wei Tong<sup>2</sup>, Chider Chen<sup>1</sup>, Motomi Enomoto-Iwamoto<sup>1</sup>, Songtao Shi<sup>1</sup>, Ling Qin<sup>1</sup>. <sup>1</sup>University of Pennsylvania, United States, <sup>2</sup>Huazhong University of Science and Technology, China

Long bone development progresses through the formation of the embryonic primary ossification center (POC) and the postnatal secondary ossification center (SOC). Several studies have elucidated the mechanisms behind POC formation, while much remains unknown regarding SOC development. Using Col2-Cre;tdTomato transgenic mice and in vitro techniques, we demonstrate the presence of an undifferentiated mesenchymal stem cell population enriched in the highly fluorescent (tomato<sup>H</sup>) perichondrium of the epiphyseal cartilage prior to SOC initiation. In vitro, these tomato<sup>H</sup> cells possess increased proliferative ( $p<0.05$ ), as well as osteogenic ( $p<0.001$ ) and adipogenic ( $p<0.001$ ) differentiation potentials. In vivo, perichondrial cells were found to show increased proliferation, visualized by Edu injection, and contained the stem and progenitor markers PDGFR $\beta$ , CD44 and CD105 only after becoming part of the advancing SOC canal, which was also found to be populated by GDF5<sup>+</sup> progenitor cells (observed using the GDF5-Cre;confetti transgenic mice) typically associated with cells lining the joints. These cells were able to give rise to several cell types within the formed epiphyseal bone, including osteoblasts, osteocytes, adipocytes and pericytes, along with their known role in the formation of the articular cartilage. In contrast to the POC, our results also demonstrate that it is the perichondrium, and not invading blood vessels, driven by hypertrophic chondrocyte-derived VEGF, which initiates and forms the invading SOC canal, coinciding with a cleavage of the chondrogenic matrix, visualized by VDIPEN and NITGE staining. This perichondrium-derived canal was found to be the main source of VEGF, resulting in immature, filipodia-rich blood vessels (visualized by CD31 and endomucin staining) trailing behind the leading canal front. Later, epiphyseal chondrocytes outside the canal began expressing VEGF, driving angiogenesis and resulting in a shift to blood vessel invasion now leading bone cavity expansion. Our results suggest the presence of undifferentiated mesenchymal stem cells populating the perichondrium of the epiphyseal cartilage of developing bones with a unique ability to initiate the formation of the SOC canal. These results support an important role for the perichondrium and highlight its potential use as a source of multipotent progenitor cells which could be used in the treatment of bone and cartilage-related disease such as osteoarthritis.

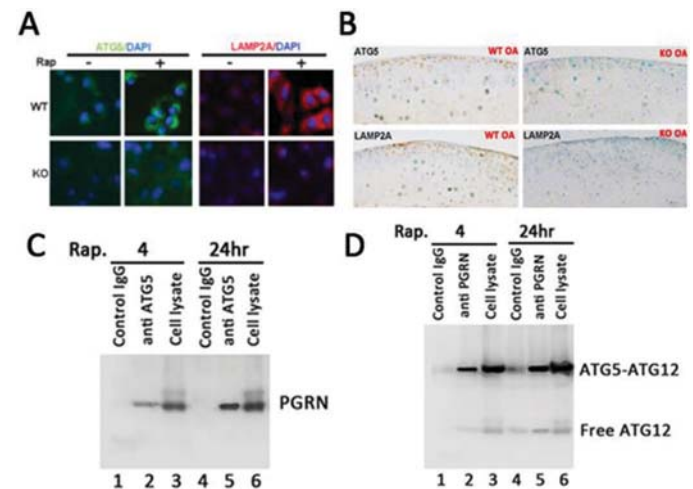
**Disclosures:** Robert Tower, None.

## LB-MO0734

**Progranulin associates with ATG5-ATG12 conjugate and is required for autophagy activation in osteoarthritis.** Fengjin Guo<sup>\*</sup>, Chuan-Ju Liu. Departments of Orthopaedic Surgery and Cell Biology, New York University School of Medicine, New York, NY10003, USA, United States

Osteoarthritis (OA) is the most common degenerative joint disease, but the pathogenesis of OA is not fully understood. Our genome-wide screen for novel genes in OA isolated progranulin (PGRN) as an OA-associated growth factor (Guo, et al, *Arthritis Rheum.*, 2010), and genetic screen for PGRN binding partners identified TNFR as the PGRN-binding receptor (Tang, et al, *Science*, 2011). We have shown that PGRN/TNFR2 pathway mediates anabolic metabolism in chondrocytes and protects against

OA (Zhao, et al, *Ann Rheum Dis.*, 2015). Our recent reports demonstrated that PGRN also regulates autophagy and PGRN deficiency causes autophagy defect in macrophages (Jian, et al, *EBioMedicine*, 2016). These previous reports prompted us to determine whether PGRN also regulates autophagy in chondrocytes and OA. We observed that autophagy was activated in both human OA chondrocytes and surgically induced mouse OA models. We first examined whether PGRN is important for Rapamycin-induced autophagy in chondrocytes. Rapamycin effectively induced the expressions of autophagy marker genes, including ATG5 and LAMP2A, but Rapamycin-stimulated expressions of ATG5 and LAMP2A were significantly lower in PGRN null chondrocytes (Fig.1A). We next examined autophagy in a surgically induced OA in 3-month-old WT and PGRN-KO mice (Fig.1B). We observed clear expression of ATG5 and LAMP2A in the articular chondrocytes of wildtype mice under the DMM OA model; however, their levels were markedly reduced in the articular chondrocytes of KO OA mice. These data indicate that endogenous PGRN is required for autophagy activation in chondrocytes and OA. Yeast two-hybrid screen identified ATG12 as one of the PGRN-binding partners, and Co-immunoprecipitation confirmed the interactions between PGRN and ATG5-ATG12 conjugate (Fig.1C,D). In addition, interactions between PGRN with ATG proteins were also observed in human OA chondrocytes. Further protein-protein interactions assays with a series of PGRN deletion mutants identified the C-terminal granulin E domain is required for the binding to ATG5-ATG12 in chondrocytes. We are currently testing whether PGRN-mediated regulation of chondrocyte autophagy is important for PGRN's chondroprotective role in OA by using recombinant PGRN, autophagy inhibitors and chondrocyte-specific ATG5-deficient OA models. In brief, these studies provide new insights into the pathogenesis of OA in general, and PGRN associated autophagy in chondrocyte homeostasis in particular.



**Disclosures:** Fengjin Guo, None.

## LB-MO0735

**Establishing the functional role of *Cped1* in the osteoblast.** Robert Maynard<sup>\*1</sup>, Madison Doolittle<sup>1</sup>, Michael-John Beltejar<sup>1</sup>, Kwangbom Choi<sup>2</sup>, Cheryl Ackert-Bicknell<sup>1</sup>. <sup>1</sup>Center for Musculoskeletal Research, University of Rochester, United States, <sup>2</sup>The Jackson Laboratory, United States

Human genome-wide association studies for BMD have repeatedly identified a significant locus on chromosome (Chr) 7 that contains the genes *WNT16*, *FAM3C*, and *CPED1*. *WNT16* and *FAM3C* have defined roles in bone biology, but *CPED1* cannot be ruled out as a possible candidate gene for this locus. *CPED1* is an uncharacterized gene with no known function. The protein putatively contains an N-terminal signal peptide for translocation to the cell surface where it may be secreted and interact with the extracellular matrix (ECM). We have determined that in mouse cells, *Cped1* expression increases throughout osteoblast maturation and correlates with expression of the ECM proteins osteonectin (*Sparc*,  $R^2=0.99$ ) and type I collagen (*Col1a1*,  $R^2=0.83$ ). Additionally, *Cped1* is alternatively spliced whereby exon 3 is removed from a portion of the transcripts. To understand the role of *Cped1* in osteoblast function, siRNAs against *Cped1* exon 1-containing transcripts were delivered to differentiating MC3T3-E1 pre-osteoblasts. We observed a decrease in total cell number due to decreased proliferation but no change in cell death. Our data show that *Cped1* knockdown leads to the immediate suppression of *Sp7* transcript and protein, but not *Runx2* expression. Similar to a loss of *Sp7*, *Cped1* knockdown leads to decreased expression and production of the ECM proteins osteonectin and bone sialoprotein (BSP II). However, *Cped1* knockdown did not change *Col1a1* expression, suggesting these cells are capable of reaching a later stage of maturation. Ultimately, failure to make a sufficient ECM resulted in a 50-87% decrease in mineralized nodule formation. Overexpression of full-length *Cped1* transcript containing exon 1, yet lacking exon 3, leads to increased expression of *Sp7*, *Sparc*, and *Ibsp*. Contrary to siRNA targeting exon 1, siRNAs against exon 3-containing transcripts resulted in elevated *Sp7*, a significant increase in osteonectin, and enhanced mineralized nodule formation. In summary, our data show that knockdown of *Cped1* exon 1-containing transcripts interferes with the critical window for differentiation of pre-osteoblasts into immature osteoblasts, whereas removal of



exon 3-containing transcripts accelerates maturation, increases the production of osteonectin, and enhances mineralization. Overall, these *Cped1* transcripts diametrically oppose each other and function to regulate maturation. In conclusion, our data establish that *Cped1* could be a candidate gene for this human Chr 7 locus.

**Disclosures:** Robert Maynard, None.

## LB-MO0736

**Leukotriene B<sub>4</sub> Is Related to Lower Osteogenic Profile.** Flávia Oliveira<sup>1</sup>, Cintia Tokuhara<sup>1</sup>, José Guareschi Filho<sup>1</sup>, João Domezi<sup>1</sup>, Vimal Veeriah<sup>2</sup>, Camila Peres-Buzalaf<sup>3</sup>, Rodrigo Oliveira<sup>1</sup>. <sup>1</sup>Bauru School of Dentistry, University of Sao Paulo, Brazil, <sup>2</sup>Kennedy Institute of Rheumatology, University of Oxford, United Kingdom, <sup>3</sup>Pró-Reitoria de Pesquisa e Pós-Graduação, Universidade do Sagrado Coração, Brazil

Leukotriene B<sub>4</sub> (LTB<sub>4</sub>) is a bone degrading factor, involved in various inflammatory conditions and constitutes one of the major target of many inflammatory diseases including bone loss in arthritis like condition, osteoarthritis and periodontitis. They are secreted by various cell types including bone cells such as osteoblast and osteoclast. Although most of knowledge is based on LTs-mediated osteoclasts bone resorbing activity, the mechanism of action of LTB<sub>4</sub> in osteoblast is poorly understood. Thus, the objective was to evaluate the effect of LTB<sub>4</sub> on osteogenesis. For this, primary osteoblasts from C57BL/6j mice calvaria were cultured in osteogenic medium and treated with LTB<sub>4</sub> at the doses of 0 (control group), 10<sup>-9</sup> M, 10<sup>-8</sup> M and 10<sup>-7</sup> M, at 4, 7 and 14 days for the differentiation analysis such as gene expression bone markers: receptor activator of NF-κB ligand (RANKL), osteoprotegerin (OPG); and alkaline phosphatase (ALP) activity and 21 days for mineralization assay by alizarin red. Results from RT-PCR analysis demonstrated no modulation on RANKL-OPG ratio by LTB<sub>4</sub>, though OPG expression was upregulated (p<0.05) at 14 days' time point. The ALP activity was decreased by LTB<sub>4</sub> at 10<sup>-7</sup> M in the initial periods of osteoblastic differentiation, 4 and 7 days (p<0.05), and the matrix nodule formation was lower in cells treated with low doses (10<sup>-9</sup> M, 10<sup>-8</sup> M) of LTB<sub>4</sub> when compared to control group (p<0.05). Therefore, our results showed that LTB<sub>4</sub> can modulate the osteogenic profile, evidenced by the decreased ALP activity and mineralization at all doses tested.

**Disclosures:** Flávia Oliveira, None.

## LB-MO0737

**Bmp and Canonical Wnt Signaling Are Required at Separate Stages of Mature Chondrocytes to Osteoblasts Differentiation in Endochondral Bone Formation.** Xin Zhou<sup>1</sup>, Ailing Huang<sup>1</sup>, Andrew Gladden<sup>1</sup>, Yuji Mishina<sup>2</sup>, Klaus von der Mark<sup>3</sup>, Benoit de Crombrughe<sup>1</sup>. <sup>1</sup>UT MD Anderson Cancer Center, United States, <sup>2</sup>University of Michigan, United States, <sup>3</sup>University of Erlangen-Nuremberg, Germany

Type X collagen (Col10a1) expressing-mature chondrocytes are a major source of osteoblasts in mouse endochondral bone formation. Since a significant population of bone marrow skeletal mesenchymal progenitor cells are derived from mature chondrocytes, we postulated that mature chondrocytes may first dedifferentiate into bone marrow skeletal mesenchymal progenitor cells (step 1), which later differentiate into osteoblasts (step 2). To test whether Bmp and/or canonical Wnt pathways play critical roles in these two steps either Bmpr1a or β-catenin were genetically inactivated in chondrocytes of cre/reporter mice. Inactivation of Bmp signaling in chondrocytes of Col10a1-Cre/Bmpr1a-/-/TdTomato mice completely blocked formation of cre mediated tomatopos bone marrow skeletal mesenchymal progenitor cells (CDPCs). Similarly, injection of tamoxifen in P13 Agc1-CreERT2/Bmpr1a-/-/TdTomato mice followed by a 10 day and a 3 months chase led to a complete absence of cre mediated tomatopos bone marrow CDPCs and a lack of trabecular tissue. In these mutant mice, the entire cartilaginous epiphyseal region including the growth plate was gradually completely converted into type I collagen producing bone matrix, suggesting that Bmp signaling in growth plate chondrocytes is essential for the maintenance of their chondrocyte identity and their development into bone marrow CDPCs. In contrast deletion of β-catenin in chondrocytes by Col10a1-Cre or tamoxifen activated Agc1-CreERT2 led to a 2 to 3-fold increase in bone marrow CDPCs and resulted in a marked decrease in chondrocyte-derived mature osteoblasts and a reduced bone volume. At postnatal day 14 in Col10a1-Cre/β-catenin-/-/TdTomato mice, only tomatopos bone marrow CDPCs, no tomatopos osteoblasts were observed on trabecular and endosteal surfaces, and no tomatopos osteocytes within the cortex. Unlike the wild-type bone marrow CDPCs, which exhibited osteogenic capacity, the Col10a1-Cre/β-catenin-/- and Agc1-CreERT2/β-catenin-/- CDPCs completely failed to differentiate into mature osteoblasts. Lentiviral infection of the cre induced β-catenin-/- CDPCs restored their osteogenic capacity. Furthermore, the β-catenin-/- CDPCs displayed enhanced adipogenic capacity. Thus, Bmp signaling is required for step 1: mature chondrocytes to bone marrow CDPCs differentiation, whereas Wnt/β-catenin signaling is essential for step 2: bone marrow CDPCs to mature osteoblast differentiation.

**Disclosures:** Xin Zhou, None.

## LB-MO0738

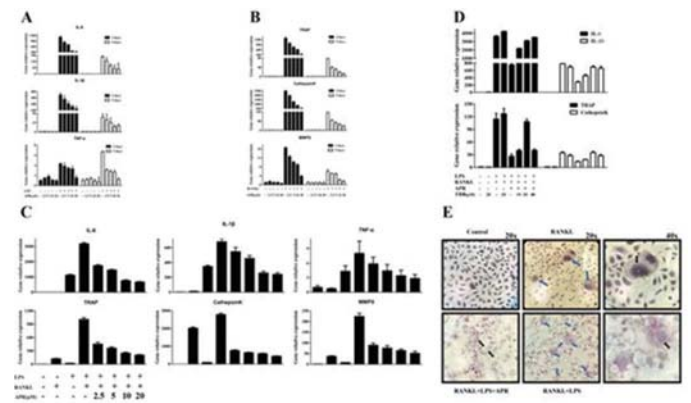
**AdipoRon Inhibits Inflammation-Induced Osteoclastogenesis.** Wei Qiu<sup>1</sup>, Qisheng Tu<sup>1</sup>, Xingwen Wu<sup>1</sup>, Jake Chen<sup>1</sup>, Xuedong Zhou<sup>2</sup>. <sup>1</sup>Tufts Univ.School of Dental Medicine, United States, <sup>2</sup>West China School of Stomatology, Sichuan University, China

**Background and objective:** AdipoRon, a recently found orally active small molecule, binds and activates both adiponectin receptors (AdipoR1, R2), with potent effects of anti-diabetes and prolonging shortened life of diabetic mice. However, its effects on bone metabolism and homeostasis are unknown. Lipopolysaccharide (LPS) is derived from Gram-negative bacteria and stimulates inflammatory environment in chronic infection, is recognized as a major mediator during osteoclastic differentiation by triggering Toll-like receptor 4 signaling. In this study, we for the first time report that AdipoRon can inhibit osteoclastogenesis induced by LPS suggesting a promising approach for the treatment of bone resorptive diseases particularly in diabetes patients.

**Material and Method:** We used TRAP stain assay to observe osteoclastic differentiation of RAW264.7 cells stimulated by LPS and treated by AdipoRon. The effects of AdipoRon on the expression levels of inflammatory factors and osteoclastic marker genes in RAW264.7 cells were determined by real time RT-PCR and Western blotting. To explore the potential crosstalk between AdipoRon and LPS signal pathway via casein kinase 2 (CK2), an intracellular interacting partners of AdipoR1, cells were pretreated with a highly selective ATP/GTP competitive CK2 inhibitor 4, 5, 6, 7-tetrabromobenzotriazole (TBB) (20 μM).

**Results:** LPS strongly promoted osteoclastogenesis and significantly increased inflammatory cytokine expression from RAW264.7 cells. AdipoRon treatment led to a significant inhibition of the expression level of LPS-induced osteoclastic marker genes (TRAP, CathepsinK, MMP9) and inflammatory cytokines genes (IL-6, IL-1β, TNF-α) in RAW264.7 cells, in a CK2-dependent manner.

**Conclusion:** AdipoRon reverses LPS-stimulated inflammatory environment and inhibits the osteoclastogenesis in the early phase of differentiation of RAW264.7 cells in a CK2-dependent manner. AdipoRon represents a potential molecule for inhibiting bone resorption in diabetic bone disorders.



A-E: Effects of AdipoRon on LPS-induced osteoclastogenesis in RAW264.7 cells. (A-D) mRNA expressions of inflammatory cytokine genes and osteoclast-related genes in RAW264.7 cells treated with RANKL, LPS, AdipoRon and TBB, separately or in different combinations. (E) TRAP staining in RANKL- or RANKL/LPS-stimulated RAW 264.7 cells treated with AdipoRon.

**Disclosures:** Wei Qiu, None.

## LB-MO0739

**Nutrient Sensing by Tas1R Proteins is Required for Normal Bone Resorption.** Nicholas Weinstein<sup>1</sup>, Michael Eaton<sup>2</sup>, Stephen Shively<sup>2</sup>, Jonathan Lowery<sup>1</sup>. <sup>1</sup>Marian University College of Osteopathic Medicine- Division of Biomedical Science, United States, <sup>2</sup>Marian University College of Osteopathic Medicine- Division of Biomedical Sciences, United States

Current therapies for diseases of low bone mass consist of inhibiting osteoclast activity or increasing the PTH or Wnt signaling pathways. While largely effective, these approaches have significant drawbacks that limit their use in specific patient populations and/or negatively impact patient compliance with therapy. Thus, there is a need to identify new therapeutic targets and, we contend, this requires diversifying our understanding of the mechanisms underlying postnatal bone remodeling by examining lesser-known signaling pathways. One such pathway is the taste receptor type 1 (TAS1R) family of heterotrimeric G protein-coupled receptors, which participates in monitoring energy and nutrient status. Simon et al. (2015) reported that global deletion of TAS1R member 3 (TAS1R3), which is a bi-functional protein that recognizes amino acids or sweet molecules when dimerized with TAS1R member 1 (TAS1R1) or TAS1R member 2 (TAS1R2), respectively, leads to increased cortical bone mass. But, the underlying cellular mechanisms leading to this phenotype remain unclear. Here, we independently corroborate the increased thickness of cortical bone in femurs of 20-week-old male *Tas1r3* knockout mice and confirm that *Tas1r3* is expressed in the bone environment. Quantification of serum bone turnover markers indicate that this phenotype is likely due to uncoupled bone remodeling, with levels of the bone resorption

marker CTx being reduced greater than 60% in *Tas1R3* mutant mice; no changes were observed in levels of the bone formation marker PINP. Consistent with this, *Tas1R3* and its putative signaling partner *Tas1R2* are expressed in primary osteoclasts and the osteoclast precursor RAW264.7 following RANKL-mediated differentiation. Moreover, the responsiveness of RAW264.7 cells to the TAS1R2:TAS1R3 ligand saccharin, as indicated by phosphorylation of ERK1/2 and AKT, is increased in RANKL-treated RAW264.7 cells. These findings suggest that osteoclast function and/or differentiation may be altered in the absence of *Tas1R3* expression. To test this, we quantified bone-specific expression of *Rankl* and determined the *Rankl:Opg* ratio; however, no differences were observed between control and *Tas1R3* knockout mice in these analyses. Studies involving *in vitro* functional assays in control versus *Tas1R3*-deficient osteoclasts are currently underway. Collectively, our findings provide the first demonstration that nutrient monitoring by TAS1R3 is essential for normal bone resorption *in vivo*.

**Disclosures:** Nicholas Weinstein, None.

## LB-MO0740

**Potential Novel Mediators of PTH Signaling in Osteocytes.** Matthew Prideaux<sup>\*1</sup>, Gerald Atkins<sup>2</sup>, Lynda Bonewald<sup>1</sup>. <sup>1</sup>Indiana University, United States, <sup>2</sup>The University of Adelaide, Australia

PTH is a known modulator of bone remodeling, however its mechanism of action on osteocytes has not been fully elucidated. To investigate potential mediators of PTH, we utilized the IDG-SW3 cell line, which differentiates into a mature osteocyte phenotype. RNA Seq was performed on day 28 IDG-SW3 cells treated with 50nM PTH or vehicle for 24 hrs. Mature osteocyte markers, and particularly mineralization-associated genes were strongly downregulated by PTH. Additionally, Dmp1-GFP expressing cells acquired a highly motile phenotype. Further RNA Seq analysis showed that factors known to regulate differentiation and motility but not previously identified in osteocytes, such as *Sema4d* and *Abi3* were downregulated by PTH (10 and 35 fold,  $P < 0.001$ ) and *Sna1* was upregulated (6 fold,  $P < 0.001$ ) in the mature IDG-SW3 cells. To further investigate the link between PTH and these genes, IDG-SW3 cells were cultured over a 28 day time course and treated with 50nM PTH for 24 hrs at day 1, 7, 14, 21 and 28. *Sema4d* and *Abi3* expression increased with differentiation and was downregulated by PTH in the mature cultures ( $P < 0.001$ ). *Sna1* expression peaked at day 8 in the control cells before decreasing with further differentiation. PTH induced *Sna1* mRNA expression at all time points but particularly in mature cells (5 fold at day 28,  $P < 0.001$ ). As *Sna1* is a mediator of TGF- $\beta$  signaling, members of this family were investigated by RNA Seq analysis. The expression of TGF $\beta$ RI, TGF $\beta$ RII and TGF $\beta$ RIII were all upregulated by 24hrs PTH treatment ( $P < 0.001$ ). Furthermore, the TGF $\beta$  antagonist Bambi and latent TGF $\beta$  binding protein were strongly downregulated by PTH and Tgf $\beta$  was upregulated (60 fold,  $P < 0.001$ ) in mature IDG-SW3 cells, suggesting activation of the TGF $\beta$  pathway.

To investigate the effects of continuous PTH administration on osteocyte differentiation, IDG-SW3 cells were cultured for 28 days with 50nM PTH. Continuous PTH inhibited osteocyte differentiation and maturation as assessed by decreased matrix mineralization, Dmp1-GFP expression and mRNA expression of *Sost*, *Mepe*, *PheX* and *Dmp1* ( $P < 0.001$ ). *Sna1* and Tgf $\beta$  mRNA expression remained significantly elevated in the day 28 IDG-SW3 cells and Bambi was downregulated compared to control ( $P < 0.001$ ). Altogether, our results identify *Sna1*, *Sema4d* and *Abi3* as novel targets of PTH signaling. Further analysis using knockdown and overexpression of these genes will determine their role in PTH signaling in osteocytes.

**Disclosures:** Matthew Prideaux, None.

## LB-MO0741

**Differences of Bone Mineral Density and Fatty Degeneration of Thigh Muscles in Hip Fracture Patients over 65 years old.** Myung Hoon Hahn<sup>\*1</sup>, ye yeon Won<sup>2</sup>, Jun Han<sup>2</sup>. <sup>1</sup>Department of Orthopaedics, Cheil General Hospital and Women's Healthcare Center, Dankook University College of Medicine, Korea, Republic of, <sup>2</sup>Department of Orthopaedics, Ajou University school of Medicine, 1, Korea, Republic of

**Background:** As an independent fracture factor from bone mineral density, muscle weakness due to the fatty degeneration of thigh muscles have been attracting attentions as causes of hip fracture. The purpose of this study is to investigate the correlation between the body composition and BMD and fatty degeneration of thigh muscle of the female patients over 65 years old with osteoporotic hip fracture.

**Methods:** this study was conducted with 178 female osteoporotic hip fracture patients. Total hip BMD was measured using dual energy X-ray absorptiometry. Cross sectional area (CSA), Cross sectional muscle area (CSmA), Muscle attenuation coefficient (MAC) and intramuscular adipose tissue (IMAT) of gluteus maximus, hip abductor, quadriceps and hamstring muscle were measured with computed tomography. Normalized IMAT (nIMAT) was calculated by dividing the fat area in the muscle into the size of each muscle. The correlation between each measurement is examined then the differences between the intertrochanteric fracture group and the femoral neck fracture group were analyzed.

**Results:** CSmA and MAC of quadriceps were the largest and nIMAT was the lowest. CSA and CSmA of the four muscles showed a statistically significant positive correlation with weight, height, body mass index and BMD. MAC of 2 gluteal muscles was positively

correlated with weight, BMI and BMD. nIMAT of all four muscles was positively correlation with weight and BMI but nIMAT of 2 mid thigh muscles was positively correlation with BMD

**Conclusions:** Muscle size and fatty degeneration in the thigh muscles were most positively correlated with the body weight. BMD was positively correlation with cSA and cSmA of all thigh muscles, and MAC of 2 gluteal muscles and fatty degeneration of 2 mid thigh muscle. There was no statistically significant difference in the size of the femoral muscle and the degree of fatty degeneration between the two fracture groups

**Disclosures:** Myung Hoon Hahn, None.

## LB-MO0742

**Bone microarchitecture, density, and geometry predict incident fracture independently of DXA BMD in older women and men: The Bone Microarchitecture International Consortium (BoMIC).** Elizabeth Samelson<sup>\*1</sup>, Serkalem Demissie<sup>2</sup>, Jonathan Adachi<sup>3</sup>, Shreyasee Amin<sup>4</sup>, Elizabeth Atkinson<sup>4</sup>, Claudia Berger<sup>5</sup>, Emmanuel Biver<sup>6</sup>, Steven Boyd<sup>7</sup>, Kerry Broe<sup>8</sup>, Lauren Burt<sup>7</sup>, Roland Chapurlat<sup>9</sup>, Thierry Chevalley<sup>6</sup>, Serge Ferrari<sup>6</sup>, David Goltzman<sup>10</sup>, David Hanley<sup>11</sup>, Marian Hannan<sup>1</sup>, David Karasik<sup>1</sup>, Sundeep Khosla<sup>4</sup>, Ching-Ti Liu<sup>2</sup>, Mattias Lorentzon<sup>12</sup>, Robert McLean<sup>1</sup>, Dan Mellstrom<sup>13</sup>, Blandine Merle<sup>14</sup>, Maria Nethander<sup>15</sup>, Claes Ohlsson<sup>16</sup>, René Rizzoli<sup>6</sup>, Elisabeth Sornay-Rendu<sup>14</sup>, Daniel Sundh<sup>12</sup>, Pawel Szulc<sup>17</sup>, Bert Van Rietbergen<sup>18</sup>, Andy Wong<sup>19</sup>, Hanfei Xu<sup>2</sup>, Laiji Yang<sup>8</sup>, Mary Bouxsein<sup>20</sup>, Douglas Kiel<sup>1</sup>. <sup>1</sup>Institute for Aging Research, Hebrew SeniorLife, Harvard Medical School, United States, <sup>2</sup>Department of Biostatistics, Boston University School of Public Health, United States, <sup>3</sup>Department of Medicine, Michael G. DeGroote School of Medicine, St Joseph's Healthcare - McMaster University, Canada, <sup>4</sup>Mayo Clinic College of Medicine, United States, <sup>5</sup>Research Institute of the McGill University Health Centre, Canada, <sup>6</sup>Division of Bone Diseases, Geneva University Hospitals and Faculty of Medicine, Switzerland, <sup>7</sup>McCaig Institute for Bone and Joint Health, Canada, <sup>8</sup>Institute for Aging Research, Hebrew SeniorLife, United States, <sup>9</sup>INSERM UMR 1033, Université de Lyon, Hospices Civils de Lyon, Lyon, France, <sup>10</sup>Departments of Medicine, McGill University and McGill University Health Centre, Canada, <sup>11</sup>McCaig Institute for Bone & Joint Health, Canada, <sup>12</sup>Geriatric Medicine, Centre for Bone and Arthritis Research, Institute of Medicine, University of Gothenburg, Sweden, <sup>13</sup>Geriatric Medicine, Centre for Bone and Arthritis Research, Institute of Medicine, Sahlgrenska Academy, University of Gothenburg, Sweden, <sup>14</sup>INSERM UMR 1033, Pavillon F, Hôpital E Herriot, France, <sup>15</sup>Bioinformatics Core Facility, Sahlgrenska Academy, University of Gothenburg, Gothenburg, Sweden, <sup>16</sup>Centre for Bone and Arthritis Research, Institute of Medicine, Sahlgrenska Academy, University of Gothenburg, Gothenburg, Sweden, <sup>17</sup>INSERM UMR1033, University of Lyon, Hôpital Edouard Herriot Place d'Arsonval, France, <sup>18</sup>Department of Biomedical Engineering, Eindhoven University of Technology, Netherlands, <sup>19</sup>Toronto General Hospital, Canada, <sup>20</sup>Dept of Orthopedic Surgery, Harvard Medical School, Center for Advanced Orthopedic Studies, BIDMC, United States

Although DXA assessed BMD is the clinical standard for determining fracture risk, the majority of older adults who sustain a fracture do not have osteoporosis (T-Score  $< -2.5$ ). Importantly, bone fragility results not only from low BMD, but also deterioration in bone structure. Although prior cross-sectional studies found associations between history of fracture and deficits in bone structure, prospective studies are limited. Therefore, we combined 6 cohorts to conduct a prospective study of bone microarchitecture, evaluated by HR-pQCT, and fracture incidence. Further, we evaluated whether HR-pQCT indices were associated with fracture risk independently of DXA assessed femoral neck areal BMD (FN aBMD).

Participants included 4,911 individuals (2578 women, 2333 men) from the Framingham Osteoporosis Study, Geneva Retirees, Mayo Clinic, MrOS Sweden, OFELY, and STRAMBO cohorts. Participants underwent HR-pQCT scanning (XtremeCT, Scanco Medical AG) at the distal radius and tibia, and were followed for incident fracture for a mean ( $\pm$ SD) of  $4.8 \pm 2.9$  yr. We performed a meta-analysis of log-hazard ratios (HR) from Cox proportional HR models for the association between FN aBMD and HR-pQCT bone measures and incidence of fracture, adjusted for age, sex, and cohort. Based on preliminary findings, we *a priori* selected 6 HR-pQCT bone measures for analysis.

Mean age was  $69 \pm 9.5$  yr (range, 40-96). Cumulative incidence of fracture was 11% (563/4911). Fractures included 154 (27%) spine, 80 (14%) wrist, 60 (11%) rib, 54 (10%) hip, 48 (9%) upper arm, and 167 (29%) other. Adjusted HR for fracture was 1.57 per SD decrease in DXA FN aBMD (Table). For each SD decrease in CtBMD, CtAr, TbBMD, and TbN, risk for fracture was increased 30% to 50%, and remained increased 10% to 40% after accounting for FN aBMD. In contrast, CtPo was weakly or not associated with incident fracture. Failure load was associated with 2-fold increased risk of fracture (per SD decrease in  $\mu$ FEA), with HR=1.8 after adjustment for FN aBMD.



Our results from this large international cohort of women and men confirm and extend prior studies showing that deficits in trabecular and cortical bone density and structure contribute to fracture risk independently of DXA assessed aBMD. Assembly of this large cohort will allow us to examine in the future whether bone microarchitecture is important in those with osteopenia, and whether bone microarchitecture predicts fracture independent of FRAX.

**Disclosures:** Elizabeth Samelson, Amgen, Grant/Research Support.

## LB-MO0743

**Dietary patterns and longitudinal change in hip bone mineral density in older men.** Tara Rogers<sup>\*1</sup>, Stephanie Harrison<sup>2</sup>, Suzanne Judd<sup>3</sup>, Eric Orwoll<sup>4</sup>, Lynn Marshall<sup>4</sup>, Jackilen Shannon<sup>4</sup>, Lisa Langsetmo<sup>5</sup>, Nancy Lane<sup>1</sup>, James Shikany<sup>3</sup>.

<sup>1</sup>Center for Musculoskeletal Health and Department of Internal Medicine, University of California at Davis, United States, <sup>2</sup>California Pacific Medical Center Research Institute, United States, <sup>3</sup>University of Alabama at Birmingham, United States, <sup>4</sup>Oregon Health & Science University, United States, <sup>5</sup>University of Minnesota Epidemiology and Community Health, United States

**Background:** Many nutrients work synergistically and are present together in foods, and free-living people generally eat a variety of foods in combination. Therefore, studying dietary patterns (rather than individual nutrients or foods) is often more informative in relation to health outcomes. "Prudent" dietary patterns (i.e. higher in healthier foods such as fruit and vegetables) have been associated with increased bone mineral density (BMD) and lower fracture risk in older men and women in some, but not all, studies [Langsetmo et al. 2010, Fung et al. 2015, Tucker et al. 2002; Langsetmo et al. 2011]. We hypothesized that a Prudent dietary pattern would be associated with reduced BMD loss over time.

**Methods:** We studied the ongoing Osteoporotic Fractures in Men (MrOS) prospective cohort, which follows ambulatory men  $\geq 65$  years of age at baseline (3/2000-4/2002) at 6 U.S. clinics (n=5994). Men with dietary data at baseline, and BMD at baseline and Visit 2 (3/2005-5/2006), were included in this analysis (n=4398, mean age 73 $\pm$ 5 years). Dietary intake was assessed with a brief Block food frequency questionnaire (FFQ); BMD was measured by dual energy x-ray absorptiometry (DXA), and percent change (% $\Delta$ ) in total hip and femoral neck BMD was calculated from baseline to Visit 2. We used factor analysis to derive dietary patterns based on FFQ data, and we used generalized linear regression to estimate least square (LS) means of % $\Delta$ BMD in quartiles of dietary pattern factor scores adjusted for potential confounding factors.

**Results:** Two major dietary patterns were identified: Prudent (characterized by higher intake of carrots, broccoli, spinach, green beans, green salad, cabbage, baked beans, tomatoes, non-fried fish and vegetable soup) and Western (characterized by higher intake of hamburger, fries, processed meats, gravy, cheese dishes, ice cream, butter, doughnuts/pastries and mayonnaise). There was a significant inverse association between factor score for the Prudent dietary pattern and total hip % $\Delta$ BMD, independent of covariates (Table). There were no associations between the Western dietary pattern and % $\Delta$ BMD at the total hip (Table) or between either dietary pattern and % $\Delta$ BMD at the femoral neck (data not shown).

**Conclusion:** Greater adherence to a Prudent dietary pattern was associated with attenuated total hip BMD loss over 4-5 years in older men.

Table. Associations between dietary patterns and % $\Delta$ BMD at the total hip in older men

	Model 1 (n=4398)		Model 2 (n=4236)	
	LS Means (95% CI)	p-trend	LS Means (95% CI)	p-trend
Prudent dietary pattern		0.028		0.049
Q1(ref)	-1.94 (-2.17, -1.70)		-1.93 (-2.17, -1.68)	
Q2	-1.63 (-1.86, -1.40)		-1.55 (-1.78, -1.31)	
Q3	-1.57 (-1.80, -1.34)		-1.59 (-1.83, -1.36)	
Q4	-1.56 (-1.79, -1.34)		-1.53 (-1.78, -1.29)	
Western dietary pattern		0.197		0.454
Q1(ref)	-1.64 (-1.87, -1.41)		-1.62 (-1.89, -1.36)	
Q2	-1.49 (-1.72, -1.26)		-1.50 (-1.74, -1.26)	
Q3	-1.76 (-1.99, -1.53)		-1.76 (-1.99, -1.52)	
Q4	-1.79 (-2.02, -1.55)		-1.71 (-2.00, -1.42)	

Model 1 adjusted for age and clinic site

Model 2 adjusted for age, clinic site, smoking, calcium supplement use and total energy intake

**Disclosures:** Tara Rogers, None.

## LB-MO0744

**The contribution of AP-1 and TCF binding sites in the proximal promoter of the endogenous Tnfrsf11b (OPG) gene to basal expression and suppression by glucocorticoids.** Keisha Cawley\*, Charles O'Brien. University of Arkansas for Medical Sciences, United States

Glucocorticoids stimulate bone resorption and this is associated with suppression of the Tnfrsf11b gene, which encodes osteoprotegerin (OPG). The mechanisms by which glucocorticoids suppress OPG production remain unclear. Wnt/beta-catenin/TCF signaling has been shown to stimulate OPG promoter-reporter constructs via a TCF binding site -776 bp upstream from exon 1. Importantly, some studies suggest that glucocorticoids suppress canonical Wnt signaling. Other promoter-reporter studies suggest that a binding site for the AP-1 transcription factor located 530 bp upstream from exon 1 contributes to basal OPG expression and that glucocorticoids suppress OPG by blocking AP-1 action at this site. To determine whether the TCF or AP-1 binding site is important for regulation of the endogenous Tnfrsf11b gene expression, or its suppression by glucocorticoids, we used the CRISPR/Cas9 system to delete each site from the Tnfrsf11b gene in MC3T3-E1 cells. This was accomplished by transfecting CRISPR/Cas9 components, targeting either the TCF or AP-1 site, and green fluorescent protein (GFP) into MC3T3-E1 cells and flow sorting for pools of GFP+ cells. This process was repeated a total of three times resulting in a pool of cells in which there was at least an 80% reduction in the DNA encoding either the TCF site or the AP-1 site, as measured by PCR. These pools, or a pool resulting from transfections with GFP+ alone, were expanded and treated with vehicle or dexamethasone for 3 hr, after which expression of Tnfrsf11b mRNA was analyzed by Taqman RT-PCR. A control gene, GILZ, was used as a positive control for dexamethasone action. Dexamethasone stimulated GILZ to a similar extent in all genotypes. MC3T3-E1 cells lacking the AP-1 site showed no significant change in basal Tnfrsf11b mRNA levels, which were suppressed by dexamethasone to a similar extent as in parental cells. In cells lacking the TCF site, basal Tnfrsf11b mRNA was lower than in parental cells. Dexamethasone suppressed Tnfrsf11b mRNA in both genotypes, but the fold suppression was lower in cells lacking the TCF site compared to the GFP+ pool. These results suggest that the AP-1 site at -530 bp does not contribute to basal expression of Tnfrsf11b or its suppression by glucocorticoids. In contrast, the TCF site at -776 bp contributes to basal expression of Tnfrsf11b and may mediate part of the negative effect of glucocorticoids on OPG production.

**Disclosures:** Keisha Cawley, None.

## LB-MO0745

**Multiple Vertebral Fractures Following Osteoporosis Treatment Discontinuation: A Case-Report with Odanacatib.** Neil Binkley\*, Diane Krueger. University of Wisconsin Osteoporosis Clinical Research Program, United States

**Background:** Case reports of women sustaining multiple vertebral fractures (VF) soon after denosumab discontinuation are accumulating. It may be that rapid resolution of anti-resorptive effect with rebound bone remodeling elevation and resultant rapid bone loss may lead to a syndrome of vertebral fragility. It is plausible that a similar phenomenon occurs when other bone-active agents that do not have prolonged skeletal residence are discontinued. Here we report, to our knowledge, the first such case following odanacatib (ODN) discontinuation. **Methods:** A 67-year old white female entered an ODN clinical trial in 2000. At baseline, her L1-L4, total femur and femoral neck T-scores were -1.2, -1.5 and -1.7 respectively. Her L1-L4 TBS was 1.297 and spine

x-ray demonstrated mild T8, T9 and T11 VF. She received ODN 50 mg once weekly from Sept 2000 to Sept 2016.

Results: While receiving ODN, her L1-L4, FN and TF BMD increased (Table). Retrospective lumbar spine trabecular bone score (TBS) analysis also demonstrated an increase (Table). In Jan 2017 she developed bronchitis, treatment included 11 days of prednisone. With coughing she developed back pain, which led ultimately to spine MRI demonstrating acute VFs at T6, T7, T10 and L1. Lab evaluation (Mar 2017) found normal PTH, TSH, 25(OH)D, SPEP, salivary cortisol, creatinine, calcium and alk phos. Teriparatide was subsequently prescribed. BMD and VFA on the research DXA in June 2017 demonstrated known VFs at T6-T11, L1 and a new VF at L3. In the ~8 months since discontinuing ODN L2, L4 BMD and TBS (excluded L1 & L3 as VFs elevate BMD results) declined by 11.9% and 9.4% respectively.

Conclusion: We report a 74 year old female whose lumbar spine BMD and TBS declined by ~12% and ~9% respectively and who sustained multiple VFs in ~8 months following ODN discontinuation. This mimics observations following denosumab discontinuation, but, to our knowledge, is the first reported with ODN. While not directly clinically relevant as ODN is no longer being developed, this case raises the possibility that a multiple vertebral fracture syndrome could follow discontinuation of all potent osteoporosis therapies that produce major BMD increases but do not have persisting bone effects (i.e., all non-bisphosphonates). Use of therapies to prevent rapid bone loss following discontinuation of potent bone active agents seems appropriate. Clarification of those who are at risk for the multiple VF syndrome is needed.

Table: BMD and TBS change with ODN treatment and discontinuation

	9/17/09	9/17/10	9/20/11	9/13/12	10/2/13	9/23/14	9/29/15	9/26/16	6/6/17
L1-L4 BMD	1.072	1.096	1.140	1.152	1.141	1.177	1.149	1.215	1.211
L1-L4 TBS	1.308	1.331	1.386	1.374	1.352	1.375	1.292	1.439	1.299
L1-L4 BMD % change	0.0	2.2	6.3	7.5	6.4	9.8	7.2	13.3	13.0
L1-L4 TBS % change	0.0	1.8	6.0	5.0	3.4	5.1	-1.2	10.0	-0.7
LFN BMD	0.820	0.824	0.848	0.873	0.872	0.882	0.879	0.893	0.891
LFN % Change	0.0	0.5	3.4	6.5	6.3	7.6	7.2	8.9	8.7
LTF BMD	0.823	0.830	0.854	0.874	0.878	0.890	0.886	0.911	0.891
LTF % ChangeBMD	0.0	0.9	3.8	6.2	6.7	8.1	7.7	10.7	8.3

Effect of ODN discontinuation excluding L1 and L3 to remove effect of new vertebral fractures on BMD and TBS									
L2-4 (L3) BMD								1.256	1.107
L2-4 (L3) TBS								1.457	1.320
L2-4 (L3) BMD % change								0.0	-11.9
L2-4 (L3) TBS % change								0.0	-9.4

Disclosures: Neil Binkley, None.

## LB-MO0746

### Bone Matrix Mineralization After Denosumab Treatment Discontinuation.

Jacques Brown<sup>\*1</sup>, David Dempster<sup>2</sup>, Susan Yue<sup>3</sup>, Sebastien Rizzo<sup>4</sup>, Delphine Farlay<sup>4</sup>, Rachel Wagman<sup>3</sup>, Xiang Yin<sup>3</sup>, Georges Boivin<sup>4</sup>. <sup>1</sup>Laval University and CHU de Quebec-(CHUL) Research Centre, Canada, <sup>2</sup>Columbia University, United States, <sup>3</sup>Amgen Inc., United States, <sup>4</sup>INSERM, UMR 1033, Univ Lyon, Université Claude Bernard Lyon 1, France

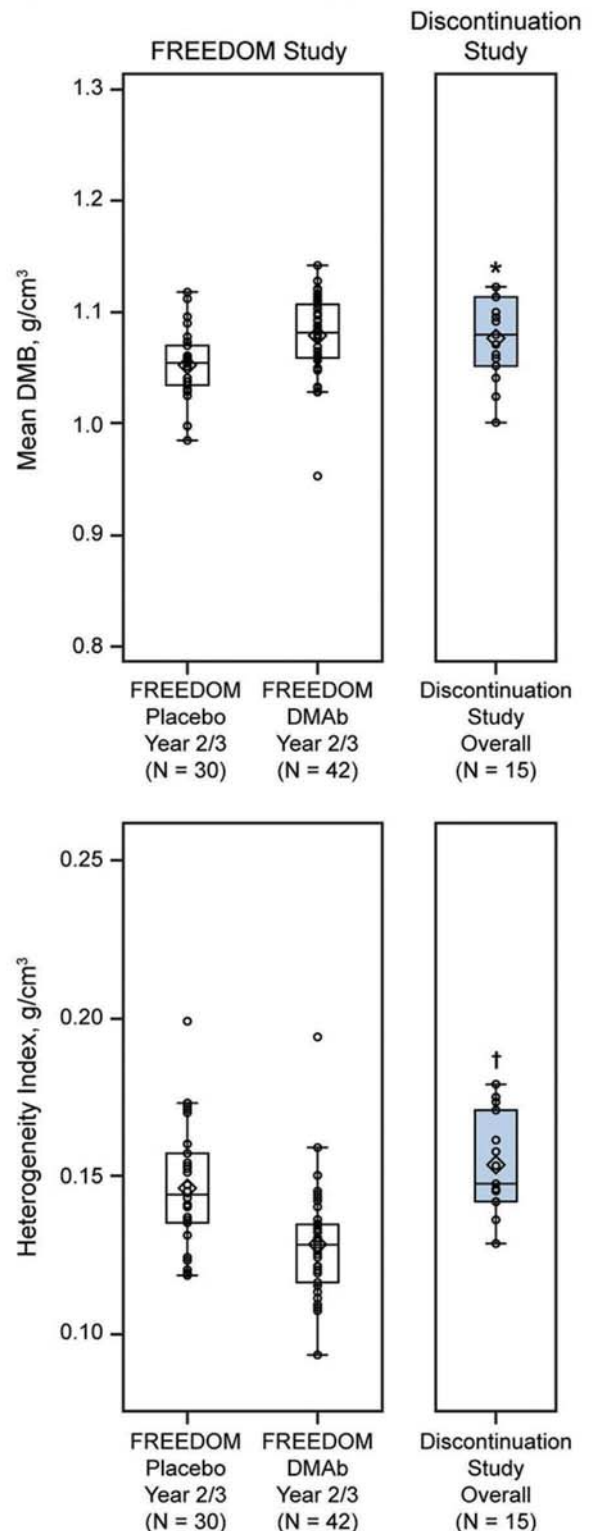
Purpose: In postmenopausal women with osteoporosis, denosumab (DnAb) therapy through 10 years is associated with bone mineral density (BMD) gains and low fracture incidence [1] which correlate with gains in mean degree of mineralization of bone (DMB) that reaches a maximum by 5 years [2]. DnAb discontinuation is associated with reversibility of BMD and bone turnover markers [3-5]. To understand the effects of reversibility on mineralization, we evaluated bone matrix mineralization in transiliac bone biopsy samples.

Methods: A non-interventional cohort study enrolled subjects who received 12 months of DnAb in one of two parent clinical trials and agreed to undergo bone biopsy after ≥12 and ≤36 months off-treatment [4]. Subjects could not have received any commercially available osteoporosis treatment, with the exception of calcium and vitamin D. Mean DMB and the heterogeneity index (HI) were calculated [6] for cancellous bone, cortical bone, the endocortical + periosteal cortical sub-compartments, and total bone (cancellous + cortical). Bone biopsy samples at 2 or 3 years in the FREEDOM trial from 30 placebo-treated (PBO) and 42 DnAb-treated subjects [2] were used as comparator groups in this analysis.

Results: A total of 15 subjects were enrolled from two parent trials (10 and 5 subjects, respectively). Mean (min, max) age: 62.1 (54, 73) years; years since menopause: 15.8 (6, 30); and time since discontinuation of DnAb: 25 (21, 29) months. Median (min, max) total bone DMB was 1.080 g/cm<sup>3</sup> (1.001, 1.123) vs 1.055 g/cm<sup>3</sup> (0.985, 1.118) in the FREEDOM PBO group, *p*-value = 0.029, and 1.081 g/cm<sup>3</sup> (0.953, 1.142) in the FREEDOM DnAb group, *p*-value = 0.89 (Figure). Median (min, max) total bone HI was 0.147 g/cm<sup>3</sup> (0.128, 0.179) vs 0.144 g/cm<sup>3</sup> (0.118, 0.199) in the FREEDOM PBO group, *p*-value = 0.11 and 0.128 g/cm<sup>3</sup> (0.093, 0.194) in the FREEDOM DnAb group, *p*-value <0.0001 (Figure). Similar results were observed in all bone compartments assessed.

Conclusion: After stopping DnAb for an average of 25 months, the DMB was similar to that observed after 2 or 3 years of DnAb treatment in FREEDOM, indicating a sustained benefit of DnAb treatment after discontinuation. The HI was higher than that observed after 2 or 3 years of DnAb treatment, which may reflect a transient increase in remodeling activity. These data suggest that significant changes in the degree of mineralization were not observed after DnAb cessation as bone remodeling returned to pretreatment levels.

Figure: Mean DMB and HI in Total Bone



\**p* < 0.05 vs FREEDOM Placebo Year 2/3; †*p* < 0.0001 vs FREEDOM DnAb Year 2/3; ‡*p*-value of 2-sided Wilcoxon rank-sum test for between-group comparisons. Data are shown as box-and-whisker plots with the interquartile range as the box, the median as a line, and the mean as a diamond. Outliers are indicated as circles. DnAb, denosumab; DMB, degree of mineralization of bone.

[1] Bone HG, et al. *Lancet Diabetes Endocrinol* 2017. [2] Dempster DW, et al. *ASBMR* 2016. [3] Bone HG, et al. *J Clin Endocrinol Metab* 2011. [4] Brown JP, et al. *J Bone Miner Res* 2011. [5] Brown JP, et al. *ASBMR* 2016. [6] Montagnier F, et al. *J X-Ray Sci Technol* 2015.

Disclosures: Jacques Brown, Amgen, Speakers' Bureau.



## LB-MO0747

**A selective p38 MAPK-MK2 axis inhibitor dampens inflammasome priming signals and causes remarkable efficacy in disease models.** Chun Wang<sup>1</sup>, Yael Allipe<sup>1</sup>, Jianqiu Xiao<sup>1</sup>, Susan Hockerman<sup>2</sup>, Jon Jacobsen<sup>2</sup>, Heidi Hope<sup>2</sup>, Jeff Hirsch<sup>2</sup>, Steve Mnich<sup>2</sup>, Matt Saabye<sup>2</sup>, Sheri Bonar<sup>2</sup>, Hal Hoffman<sup>3</sup>, Joseph Monahan<sup>2</sup>, Gabriel Mbalaviele<sup>1</sup>. <sup>1</sup>Washington University School of Medicine, United States, <sup>2</sup>Confluence Life Sciences, Inc, United States, <sup>3</sup>University of California, San Diego, United States

NF- $\kappa$ B is viewed as the gatekeeper of the so-called priming signals that produce pro-IL-1 $\beta$ , which is processed into IL-1 $\beta$  by the inflammasomes. We discovered a unique inhibitor of p38 MAPK-MK2 signaling that spares p38 MAPK interactions with other substrates, and used it to test a novel hypothesis that p38 MAPK-MK2 contributes to pro-IL-1 $\beta$  abundance. We found that this inhibitor markedly promoted IL-1 $\beta$  mRNA instability, thereby, decreased cytokine levels in various cell systems. As a result, this compound prevented the onset of IL-1 $\beta$ -driven systemic inflammation and bone resorption in a mouse model of aberrant NLRP3 inflammasome activity. We also found that this inhibitor decreased rodent arthritis, consistent with the broad inflammatory actions of p38 MAPK. From a translational perspective, we demonstrated that p38 MAPK-MK2 inhibitor decreased cytokine production in cells isolated from patients with cryopyrinopathies or rheumatoid arthritis. Thus, this work expands the mechanisms actions of p38 MAPK-MK2 on inflammatory pathways whose blockade by our drug candidate provides efficacy in disease relevant models.

**Disclosures:** Chun Wang, None.

## LB-MO0748

**Co-treatment with PTH and propranolol causes a site-specific improvement in trabecular and cortical microarchitecture while reducing marrow adiposity in C57BL/6J mice.** Annika Treyball<sup>1</sup>, Daniel Brooks<sup>2</sup>, Anyonya R Guntur<sup>1</sup>, Katherine J Motyl<sup>1</sup>. <sup>1</sup>Maine Medical Center Research Institute, United States, <sup>2</sup>Beth Israel Deaconess Medical Center, United States

PTH receptor (PTHR) signaling promotes a shift in mesenchymal stem cell fate from the adipogenic to osteogenic lineage, whereas the effect of  $\beta$ -adrenergic receptor ( $\beta$ AR) signaling on bone marrow adiposity is unclear. In previous studies, sequential-combined treatment with  $\beta$ -blockers enhanced the anabolic effects of PTH in ovariectomized (OVX) mice, which have high marrow adiposity. We were interested in determining whether the positive effects of combined treatment were driven by changes in bone marrow adiposity and whether these effects would be observed in intact mice. We treated 16-wk-old C57BL/6J female, intact mice with vehicle (VEH), PTH, the non-selective  $\beta$ -antagonist propranolol (PRO), or a combination of PTH and PRO. We hypothesized that PRO would enhance PTH-induced bone anabolism while decreasing marrow adiposity. Interestingly, the positive effect of PTH on total aBMC was only significant when combined with PRO. As expected, PTH alone improved total and femur aBMD. Co-treating with PRO enhanced the effect on total, but not femur, aBMD. Consistent with this, we observed site-specific variations in bone microarchitecture. Whereas improvements in vertebral trabecular bone volume fraction (Tb.BV/TV) and Tb.BMD were greater with co-treatment compared to PTH alone, PTH improved trabecular and cortical parameters to the same extent with or without PRO in the femur. In the tibia, co-treatment, but not PTH alone, decreased cortical porosity and increased Tb.BV/TV relative to VEH. Tibia marrow adipocyte number was reduced in PTH-PRO versus VEH-treated mice and this was recapitulated with *Fabp4* expression. Gene expression suggests that co-treatment with PRO may stimulate osteoblast maturation and mineralization while simultaneously blocking PTH-induced resorption. While neither PTH nor PRO alone affected *Omdn*, the combination caused a significant increase compared to VEH; *Dmp1* was upregulated by PTH alone and was further elevated with co-treatment. The PTH-induced upregulation of the osteoclast marker *Trap5* was also blocked by co-treatment with PRO. The absence of changes in early osteoblast markers suggests lineage shift may be less relevant in this case, however, the reduction of marrow adiposity may promote osteoblast maturation through paracrine pathways, and this is currently under investigation. Collectively, our data suggest that co-treatment with PRO may enhance the anabolic effects of PTH by increasing mineralization and decreasing resorption.

**Disclosures:** Annika Treyball, None.

## LB-MO0749

**The small molecule SIK inhibitor YKL-05-099 increases trabecular bone mass and bone formation in hypogonadal female mice.** Maureen Omeara<sup>1</sup>, Janaina Da Silva Martins<sup>1</sup>, Michael Armanini<sup>1</sup>, Daniel Brooks<sup>1</sup>, Jinhua Wang<sup>2</sup>, Nathanael Gray<sup>2</sup>, Mary Bouxsein<sup>1</sup>, Henry Kronenberg<sup>1</sup>, Marc Wein<sup>1</sup>. <sup>1</sup>MGH Endocrine Unit, United States, <sup>2</sup>Dana Farber Cancer Institute, United States

Background: PTH signaling in osteocytes blocks the activity of salt inducible kinase 2 (SIK2). Accordingly, small molecule SIK inhibitors, such as YKL-05-099, mimic PTH some actions in young, eugonadal mice. However, whether YKL-05-099 boosts bone mass in oophorectomized (OVX) animals remains unknown. Furthermore, side-by-side

comparison of PTH and YKL-05-099 treatment *in vivo* has not been performed. Here, we determined if YKL-05-099 increases bone mass in OVX mice, and compared the skeletal effects of these two bone anabolic agents.

Methods: 48 female C57B/6 mice were subjected to sham (n=24) or oophorectomy (n=24) at 12 weeks of age. 8 weeks later, mice were treated with either vehicle (n=8), YKL-05-099 (18 mg/kg, n=8), or PTH (1-34, 100 mcg/kg, n=8) once per day for 4 weeks. Effects of OVX and drug treatments were assessed by micro-CT of the femur and L5 vertebrae, and static/dynamic histomorphometry of the tibia.

Results: Neither PTH nor YKL-05-099 altered growth or peripheral blood counts. OVX reduced trabecular BMD in the distal femur (sham/veh vs OVX/veh p=0.041, see accompanying table for all quantitative data) and L5 vertebrae (p=0.00043), and reduced trabecular L5 BV/TV (p=0.00089). In OVX mice, PTH and YKL-05-099 treatment increased trabecular bone mass at both skeletal sites (for example, distal femur Tb.BMD p=0.0047 veh vs PTH, p=0.00036 veh vs YKL). Both PTH and YKL-05-099 increased osteoblast numbers and bone formation rate in OVX mice. Treatment effects of PTH and YKL-05-099 differed in two significant regards. First, while PTH tended to increase osteoclast activity, YKL-05-099 reduced eroded surfaces (p=0.41 veh vs PTH, p=0.0129 veh vs YKL). Second, while PTH increased amounts of non-mineralized osteoid, YKL-05-099 did not (p=0.00071 veh vs PTH, p=0.64 veh vs YKL).

Conclusions: In OVX mice, both YKL-05-099 and PTH increase trabecular bone mass and bone formation. Potential therapeutic advantages of YKL-05-099 may include its ability to reduce bone resorption and promote efficient osteoid mineralization.

	Sham/VEH	OVX/VEH	OVX/PTH	OVX/YKL
<b>Micro-CT</b>				
Femur Tb.BMD	90.1±14.8	73.6±16.4*	96.7±9.5*	106.6±10.1*
Femur BV/TV	6.50±1.71	6.27±1.24	7.36±1.05*	9.25±1.03*
L5 Tb.BMD	222.5±17.4	179.0±16.4*	201.1±23.8*	200.3±15.4*
L5 BV/TV	23.21±1.96	18.72±1.87*	22.20±2.84*	22.03±1.44*
<b>Histo-morphometry</b>				
Ob.S/BS	9.80±2.38	13.48±2.93*	27.07±4.56*	18.52±2.71*
BFR/BS	0.0098±0.005	0.0059±0.0042*	0.02084±0.012*	0.0188±0.0062*
OS/BS	2.20±1.27	2.91±1.17	6.82±2.27*	3.23±1.49
ES/BS	3.75±1.26	4.19±1.36	4.75±1.26	2.61±0.78*

\*, p<0.05 sham versus OVX  
\*, p<0.05 treatment versus VEH

**Disclosures:** Maureen Omeara, None.

## LB-MO0750

**Enhanced bioavailability and reduced pharmacokinetic variability of Oral PTH (1-34) in man.** Gregory Burstien<sup>1</sup>, Jonathan C.Y. Tang<sup>2</sup>, Ariel Rothner<sup>1</sup>, Hillel Galitzer<sup>1</sup>, Phillip Schwartz<sup>1</sup>, William D. Fraser<sup>2</sup>, Yoseph Caraco<sup>3</sup>.

<sup>1</sup>Entera Bio Ltd., Israel, <sup>2</sup>University of East Anglia, United Kingdom, <sup>3</sup>Hadassah University Hospital, Israel

An orally administered PTH may have prodigious advantages in the treatment of hypoparathyroidism and osteoporosis. Unfortunately, the oral delivery of biologic macromolecules is characterized by a negligible bioavailability and a high dose-to-dose variability in absorption, resulting in difficulty in accurately titrating the drug effect. We present clinical study data of a novel oral peptide delivery technology demonstrating an enhanced bioavailability with reduced Cmax variability.

Methods:

A Phase I, open label crossover pharmacokinetic (PK) study to assess the safety and PK of oral PTH (1-34) in ten healthy male adult volunteers was conducted. The PK profile of a fixed dose - 1.5mg PTH (1-34) of three different oral formulations was compared. PTH (1-34) levels in the plasma of subjects was analyzed at a number of time points post administration, utilizing a PTH (1-34) immunoassay (IDS; Bolden, UK). In parallel, to assess the pharmacodynamic (PD) effect, serum calcium of subjects receiving the different formulations of oral PTH (1-34) was analyzed.

Results:

PK profiles of all oral PTH (1-34) formulations were characterized by a rapid absorption and elimination. The systemic exposure (AUC) of the basic oral formulation and two modified formulation versions were 3481 ±1843 pg\*min/mL, 7976 ±2556 pg\*min/mL and 11369 ±3719 pg\*min/mL (mean ± SE). The maximal plasma concentration (Cmax) of these formulations were 145 ±56pg/mL, 375 ±108pg/mL, and 481 ±101pg/mL, respectively. Cmax coefficients of variation (CV%) of the same formulations were 123%, 91% and 67%, respectively. Similarly to the drug absorption, PD

response of the modified formulations, presented as the maximal relative increase in albumin adjusted calcium, was improved from  $0.07 \pm 0.29\text{mg/dL}$  to  $0.32 \pm 0.24\text{mg/dL}$ .

#### Discussion:

Inherent to oral drug delivery of biopharmaceuticals is the extremely low bioavailability and high absorption variability. The current results indicate that Entera's delivery technology can overcome these two principal obstacles by achieving repeatable, clinically relevant systemic drug exposure. Entera's proprietary delivery platform was optimized and achieved an enhancement in drug bioavailability in parallel with the significant decrease in its absorption variability. Similarly, its effect on blood calcium was enhanced by the novel oral formulation of PTH (1-34) pointing out the potential of the drug to be a first line treatment of hypoparathyroidism and osteoporosis.

**Disclosures:** Gregory Burstien, None.

## LB-MO0751

### Improvements in Skeletal Manifestations and Growth With Up to 6 Years of Treatment With Asfotase Alfa in Infants and Children Aged $\leq 5$ Years With Hypophosphatasia.

Christine Hofmann<sup>\*1</sup>, Johannes Liese<sup>1</sup>, Paul Harmatz<sup>2</sup>, Jerry Vockley<sup>3</sup>, Wolfgang Högl<sup>4</sup>, Shanggen Zhou<sup>5</sup>, Andrew Denker<sup>6</sup>, Anna Petryk<sup>6</sup>, Cheryl Rockman-Greenberg<sup>7</sup>. <sup>1</sup>University Children's Hospital, University of Würzburg, Germany, <sup>2</sup>UCSF Benioff Children's Hospital Oakland, United States, <sup>3</sup>University of Pittsburgh School of Medicine and Graduate School of Public Health, United States, <sup>4</sup>Birmingham Children's Hospital and Institute of Metabolism and Systems Research, University of Birmingham, United Kingdom, <sup>5</sup>Chiltern International Inc., United States, <sup>6</sup>Alexion Pharmaceuticals, Inc., United States, <sup>7</sup>Children's Hospital Research Institute of Manitoba and University of Manitoba, Canada

Hypophosphatasia (HPP) is a rare, inherited, systemic, metabolic disease caused by tissue-nonspecific alkaline phosphatase (TNSALP) deficiency. HPP characteristics in infants and young children include impaired skeletal mineralization, craniosynostosis, respiratory failure, seizures, HPP rickets, and failure to thrive. Asfotase alfa is a human recombinant TNSALP indicated for treatment of pediatric-onset HPP. We report data on HPP-related skeletal manifestations and growth with up to 6 y of treatment with asfotase alfa 6 mg/kg/wk from a Phase 2, single-arm, multinational, open-label study (NCT01176266) in patients (pts) aged  $\leq 5$  y with potentially life-threatening HPP due to onset at age  $< 6$  mo. The primary outcome measure was change in Radiographic Global Impression of Change (RGI-C) score at Wk 24 and 48 of treatment ( $-3$ =severe worsening,  $+3$ =complete or near-complete healing). Pts were responders if their average RGI-C score at the visit was  $\geq 2$ . Secondary measures included Rickets Severity Scale (RSS) score (0=absence of rickets, 10=severe rickets), growth (length/weight Z-scores), and safety. Unless otherwise specified, data are presented as median (min, max). In total, 69 pts were enrolled and treated (age: 69.1 [0.1, 312.1] wk; male: 33 [47.8%]; 60 (87%) completed the study (discontinuations: adverse events [AEs], n=6; withdrew, n=3). Overall treatment duration was 2.3 (0.02, 5.8) y. Significant ( $P<0.0001$ ) improvements in RGI-C from Baseline (BL) were observed at Wk 24 (2.0 [-1.7, 3.0]; n=69; responders: 58%; last observation carried forward [LOCF]) and Wk 48 (2.0 [-2.3, 3.0]; n=69; responders: 72%; LOCF) and were sustained at Last Assessment (2.3 [-2.7, 3.0]; n=67;  $P<0.0001$ ; responders: 73%). Significant ( $P<0.0001$ ) changes from BL were also observed in RSS scores at Wk 24 ( $-1.5$  [-9.0, 4.5]; n=61) and Wk 48 ( $-2.5$  [-10.0, 6.0]; n=52) and were sustained at Last Assessment ( $-2.5$  [-10.0, 6.0]; n=65). BL length Z-score was  $-2.7$  ( $-10$ , 1; n=67) and improved by 0.3 ( $-2$ , 6; n=62) at Wk 24 and 0.5 ( $-4$ , 4; n=66) at Last Assessment. BL weight Z-score was  $-2.5$  ( $-24$ , 0; n=68), and improved by 0.5 ( $-5$ , 6; n=63) at Wk 24 and 1.0 ( $-5$ , 6; n=67) at Last Assessment. All pts experienced AEs, most commonly injection site reactions (62%; n=43). Nine pts died; majority (n=8) were unlikely related to study drug. Long-term improvements in HPP-related skeletal manifestations and growth were sustained up to Last Assessment with asfotase alfa in infants and young children with HPP.

**Disclosures:** Christine Hofmann, Alexion Pharmaceuticals, Inc., Grant/Research Support.